

B. V. Babu · Atulya Nagar  
Kusum Deep · Millie Pant  
Jagdish Chand Bansal · Kanad Ray  
Umesh Gupta *Editors*

Proceedings of the  
Second International  
Conference on Soft  
Computing for Problem  
Solving (SocProS 2012),  
December 28–30, 2012

# **Advances in Intelligent Systems and Computing**

Volume 236

*Series editor*

Janusz Kacprzyk, Warsaw, Poland

For further volumes:

<http://www.springer.com/series/11156>

## *About this Series*

The series “Advances in Intelligent Systems and Computing” contains publications on theory, applications, and design methods of Intelligent Systems and Intelligent Computing. Virtually all disciplines such as engineering, natural sciences, computer and information science, ICT, economics, business, e-commerce, environment, healthcare, life science are covered. The list of topics spans all the areas of modern intelligent systems and computing.

The publications within “Advances in Intelligent Systems and Computing” are primarily textbooks and proceedings of important conferences, symposia and congresses. They cover significant recent developments in the field, both of a foundational and applicable character. An important characteristic feature of the series is the short publication time and world-wide distribution. This permits a rapid and broad dissemination of research results.

## *Advisory Board*

### Chairman

Nikhil R. Pal, Indian Statistical Institute, Kolkata, India  
e-mail: [nikhil@isical.ac.in](mailto:nikhil@isical.ac.in)

### Members

Emilio S. Corchado, University of Salamanca, Salamanca, Spain  
e-mail: [escorchado@usal.es](mailto:escorchado@usal.es)

Hani Hagrais, University of Essex, Colchester, UK  
e-mail: [hani@essex.ac.uk](mailto:hani@essex.ac.uk)

László T. Kóczy, Széchenyi István University, Győr, Hungary  
e-mail: [koczy@sze.hu](mailto:koczy@sze.hu)

Vladik Kreinovich, University of Texas at El Paso, El Paso, USA  
e-mail: [vladik@utep.edu](mailto:vladik@utep.edu)

Chin-Teng Lin, National Chiao Tung University, Hsinchu, Taiwan  
e-mail: [ctlin@mail.nctu.edu.tw](mailto:ctlin@mail.nctu.edu.tw)

Jie Lu, University of Technology, Sydney, Australia  
e-mail: [Jie.Lu@uts.edu.au](mailto:Jie.Lu@uts.edu.au)

Patricia Melin, Tijuana Institute of Technology, Tijuana, Mexico  
e-mail: [epmelin@hafsamx.org](mailto:epmelin@hafsamx.org)

Nadia Nedjah, State University of Rio de Janeiro, Rio de Janeiro, Brazil  
e-mail: [nadia@eng.uerj.br](mailto:nadia@eng.uerj.br)

Ngoc Thanh Nguyen, Wroclaw University of Technology, Wroclaw, Poland  
e-mail: [Ngoc-Thanh.Nguyen@pwr.edu.pl](mailto:Ngoc-Thanh.Nguyen@pwr.edu.pl)

Jun Wang, The Chinese University of Hong Kong, Shatin, Hong Kong  
e-mail: [jwang@mae.cuhk.edu.hk](mailto:jwang@mae.cuhk.edu.hk)

B. V. Babu · Atulya Nagar  
Kusum Deep · Millie Pant  
Jagdish Chand Bansal  
Kanad Ray · Umesh Gupta  
Editors

Proceedings of the Second  
International Conference on  
Soft Computing for Problem  
Solving (SocProS 2012),  
December 28–30, 2012

*Editors*

B. V. Babu  
Institute of Engineering and Technology  
JK Lakshmipat University  
Jaipur  
Rajasthan  
India

Atulya Nagar  
Department of Computer Science  
Liverpool Hope University  
Liverpool  
UK

Kusum Deep  
Department of Mathematics  
Indian Institute of Technology Roorkee  
Roorkee  
Uttaranchal  
India

Millie Pant  
Department of Paper Technology  
Indian Institute of Technology Roorkee  
Roorkee  
India

Jagdish Chand Bansal  
Department of Applied Mathematics  
South Asian University  
New Delhi  
India

Kanad Ray  
Umesh Gupta  
Institute of Engineering and Technology  
JK Lakshmipat University  
Jaipur  
Rajasthan  
India

ISSN 2194-5357

ISBN 978-81-322-1601-8

DOI 10.1007/978-81-322-1602-5

Springer New Delhi Heidelberg New York Dordrecht London

ISSN 2194-5365 (electronic)

ISBN 978-81-322-1602-5 (eBook)

Library of Congress Control Number: 2013955048

© Springer India 2014

This work is subject to copyright. All rights are reserved by the Publisher, whether the whole or part of the material is concerned, specifically the rights of translation, reprinting, reuse of illustrations, recitation, broadcasting, reproduction on microfilms or in any other physical way, and transmission or information storage and retrieval, electronic adaptation, computer software, or by similar or dissimilar methodology now known or hereafter developed. Exempted from this legal reservation are brief excerpts in connection with reviews or scholarly analysis or material supplied specifically for the purpose of being entered and executed on a computer system, for exclusive use by the purchaser of the work. Duplication of this publication or parts thereof is permitted only under the provisions of the Copyright Law of the Publisher's location, in its current version, and permission for use must always be obtained from Springer. Permissions for use may be obtained through RightsLink at the Copyright Clearance Center. Violations are liable to prosecution under the respective Copyright Law. The use of general descriptive names, registered names, trademarks, service marks, etc. in this publication does not imply, even in the absence of a specific statement, that such names are exempt from the relevant protective laws and regulations and therefore free for general use.

While the advice and information in this book are believed to be true and accurate at the date of publication, neither the authors nor the editors nor the publisher can accept any legal responsibility for any errors or omissions that may be made. The publisher makes no warranty, express or implied, with respect to the material contained herein.

Printed on acid-free paper

Springer is part of Springer Science+Business Media (www.springer.com)

# Foreword



I am delighted that the Second International Conference on “Soft Computing for Problem Solving (SocProS 2012)” was organized by the Institute of Engineering and Technology of our University from December 28–30, 2012.

1. Zadeh, founder of soft computing had stated that soft computing differs from conventional (hard) computing in that, unlike hard computing, it is tolerant of imprecision, uncertainty, partial truth and approximation. In effect, the role model for soft computing is the human mind. The guiding principle of soft computing being: Exploit the tolerance for imprecision, uncertainty, partial truth and approximation to achieve tractability, robustness and low solution cost. Every single one of these methods can be called soft computing method.

The soft computing models are based on human reasoning and are closer to human thinking. Soft computing is not a melange; it can be viewed as a founding component for the emerging field of conceptual intelligence. It is the fusion of methodologies assigned to model and enable solutions to real-world problems which are not modelled or too difficult to model mathematically. The core of soft computing comprises neural networks, fuzzy logic and genetic computing. In the coming years, soft computing will play a more important role in many areas, including software engineering. Soft computing is still growing. It is still somewhat in the formative stage and the definite components that comprise soft

computing have not yet been designed. More new sciences are still merging into soft computing. SocProS 2012 was aimed to reach out to such development.

I am happy to know that Springer is publishing the Proceedings of this conference as AISC book series. I am confident that the readers will be benefited by the research inputs provided by delegates during the conference. This book will certainly provide an enriching and rewarding experience to all for academic networking.

I congratulate the editorial team and Springer for meticulously working on all the details of the book. I also congratulate all the authors of research papers for their contribution to SocProS 2012.

A handwritten signature in black ink, appearing to read 'Upinder Dhar', with a horizontal line underneath the name.

Jaipur, September 27, 2013

Upinder Dhar

# About JK Lakshmipat University



Set up in the pink city of Jaipur, India and spread over a sprawling 30 acre campus, JK Lakshmipat University (JKLU) offers state-of-the-art academic infrastructure and world class faculty for conducting Graduate, Post Graduate and Ph.D. programmes in the mainstream disciplines of Management and Engineering. Promoted by JK Organisation, one of India's leading industrial conglomerates with a rich heritage of over 100 years, the University offers students an open, green and high-tech learning environment, combining the serene settings of the Gurukuls of yesteryears with the technological advancements of the new age.

The Institute of Management offers MBA (Full-Time Residential), MBA (Family Business and Entrepreneurship), MEA (Master of Educational Administration), a 5-year integrated dual degree (BBA + MBA) and Ph.D. programme in Management, besides PG Diploma in Tourism Administration and PG Diploma in Family Business & Entrepreneurship. Specializations include Finance and Accounting, Marketing, HRM, International Business and Information Technology. In order to balance conceptual framework with the industry practices, the delivery of each course is done in close consultation with the corporate world.

The University has also set up a 'Management Development Centre' for practicing Managers aiming to build capabilities through short-term programmes. It also organizes faculty development programmes for the benefit of academia.

The Institute of Engineering and Technology offers 4 year B.Tech, 2 year M.Tech, 5 year integrated dual degree (B.Tech + MBA) and (B.Tech + M.Tech), and Ph.D. programme in Chemical Engineering, Civil Engineering, Computer Science Engineering, Electrical Engineering, Electronics and Communications Engineering, Information Technology and Mechanical Engineering.



The curriculum is designed to enrich the students with the knowledge and relevant skills to prepare them not only to face the contemporary world but also to make them future ready to effectively perform in leadership roles assigned to them. The curriculum is updated to integrate changes that are taking place in the business environment.

JKLU is visualized to emerge as a premier institution of higher learning with global standards; it has tied up with a few renowned universities, such as University of Houston (USA), Hanyang University (South Korea), St. Cloud State University (USA), University of Wales (UK) and Szechenyi Istvan University (Hungary) for cooperation in the field of Faculty Development, Students Exchange and Research. The University has also signed an MoU with IBM India Ltd. for establishing a 'Centre of Technology Excellence' for undertaking technology development projects involving faculty members and students.

JKLU has been set up under Rajasthan Private Universities Act by 'Lakshmipat Singhania Foundation for Higher Learning'.

# Preface

Unlike hard computing, the guiding principle of soft computing is exploiting the tolerance for imprecision, uncertainty, partial truth, and approximation to achieve tractability, robustness, and low solution cost, the role model being the human mind. The areas that come under the purview of Soft Computing include Fuzzy Logic, Neural Computing, Evolutionary Computation, Machine Learning and Probabilistic Reasoning, with the latter subsuming belief networks, chaos theory and parts of learning theory. The successful applications of soft computing and its rapid growth suggest that the impact of soft computing will be felt increasingly in the coming years. Soft computing is likely to play a very important role in science and engineering, but eventually its influence may extend much farther.

After the successful completion of the First International Conference on Soft Computing for Problem Solving in 2011 (SocProS 2011) at IIT Roorkee, the 2nd of the series, Second International Conference on Soft Computing for Problem Solving (SocProS 2012), was held in JK Lakshmipat University (JKLU), Jaipur, during December 28–30, 2012. It had been a matter of great privilege and pleasure to organize SocProS 2012 at JKLU, Jaipur. The response had been overwhelming and heartwarming. We had received 312 paper submissions of which 200, i.e., 64 % had been accepted for presentation. The review process included double review of submitted papers by an International team of reviewers using Easy Chair as online conference management software. There were 20 Technical Sessions including two Special Sessions, besides five Keynote Addresses by eminent Academicians and Scientists from different parts of the world that made SocProS 2012 an enriching experience to all the participants. In addition, there was one Workshop on Game Programming and one Special Tutorial on Brain like computing as a part of this conference. There were 144 Programme Committee members and 20 International Advisory Committee members from across the world associated with SocProS 2012.

We would like to express our sincere gratitude to Dr. Madhukar Gupta, Divisional Commissioner, Government of Rajasthan for gracing the occasion as the Chief Guest for the Inaugural Session.

We would also like to extend our heartfelt gratitude to all Programme Committee and International Advisory Committee members. We sincerely thank the Keynote Speakers Prof. Dipankar Dasgupta from University of Memphis—USA,

Prof. Anirban Bandyopadhyay from National Institute of Material Sciences (NIMS)—Japan, Prof. Ravindra Gudi from IIT Bombay—Mumbai, Prof. D. Nagesh Kumar from IISc—Bangalore and Prof. Ajoy Ray from Bengal Engineering and Science University (BESU)—Howrah.

We are grateful to Prof. Anirban Bandyopadhyay for conducting a Special Tutorial also in addition to delivering Keynote Address. We thank Mr. Arijit Bhattacharyya from Virtual Infocom—Kolkata for conducting the Workshop.

We thank the invited guests for accepting our invitation and also for chairing the technical sessions. We thank Dr. Kannan Govindan and Dr. P. C. Jha for delivering the Invited Talks. We express sincere thanks to the entire national and local organizing committee members for their continuous support and relentless cooperation right from the conception to execution in making SocProS 2012 a memorable event. We thank all the participants who had presented their research papers and attended the conference. A special mention of thanks is due to our student volunteers for the spirit and enthusiasm they had shown throughout the duration of the event, without which it would had been difficult for us to organize such a successful event.

Thanks are due to Springer for Publishing the Conference Proceedings. We hope that the Proceedings will prove helpful towards understanding about Soft Computing in teaching as well as in their research and will inspire more and more researchers to work in this interesting, challenging and ever growing field of Soft Computing.

We are thankful to the JKL family for the support given in making this mega event successful. We sincerely hope that the delegates had certainly taken home several pleasant memories of SocProS 2012 with them.

We are honoured and it has been a proud privilege to be associated with this Second International Conference on SocProS 2012 as its General Chairs.

Dr. B. V. Babu  
Dr. Atulya Nagar  
Dr. Kusum Deep  
Dr. Millie Pant  
Dr. Jagdish Chand Bansal  
Dr. Kanad Ray  
Dr. Umesh Gupta

# Committees

## Organizing Committee

Patron	Dr. Upinder Dhar, JK Lakshmipat University, Jaipur, India
General Chairs	Dr. B. V. Babu, JK Lakshmipat University, Jaipur, India Dr. Atulya Nagar, Liverpool Hope University (LHU), Liverpool, UK
Programme Committee Chairs	Dr. Kusum Deep, IIT Roorkee, Roorkee, India Dr. Millie Pant, IIT Roorkee, Roorkee, India Dr. Jagdish C. Bansal, South Asian University, New Delhi, India
Local Organizing Chairs	Dr. Kanad Ray, JK Lakshmipat University, Jaipur, India Dr. Umesh Gupta, JK Lakshmipat University, Jaipur, India
Special Session Chairs	Dr. Millie Pant, IIT Roorkee, Roorkee, India Dr. Jagdish C. Bansal, ABV-IIITM, Gwalior, India Mr. Alok Agarwal, JK Lakshmipat University, Jaipur, India
Publicity Chairs	Dr. Sandeep Kumar Tomar, JK Lakshmipat University, Jaipur, India Dr. Sonal Jain, JK Lakshmipat University, Jaipur, India
Best Paper Chairs	Dr. Ravidra Gudi, IIT Bombay, Mumbai, India Dr. D. Nagesh Kumar, IISc, Bangalore, India Dr. P. C. Jha, Delhi University, New Delhi, India
Steering Committee	Dr. Atulya Nagar Dr. B. V. Babu Dr. Kusum Deep Dr. Millie Pant Dr. Jagdish C. Bansal

## International Advisory Committee

Prof. Zbigniew Michalewicz	University of Adelaide, Adelaide, Australia
Dr. Gurvinder S. Baicher	University of Wales, UK
Prof. Lipo Wang	Nanyang Technological University, Singapore
Prof. Patrick Siarry,	Université de Paris, France
Prof. Michael N. Vrahatis	University of Patras, Greece
Prof. Helio J. C. Barbosa	Federal University of Juiz de Fora, Brazil
Prof. S. K. Singh	CSIR—Central Building Research Institute, Roorkee, India
Prof. Wei-Chiang Samuelson Hong	Oriental Institute of Technology, Taiwan
Prof. P. K. Kapur	Amity University, Noida, India
Prof. Samrat Sabat	University of Hyderabad, India
Prof. S. S. Rao	University of Miami, Florida, USA
Prof. Pramod Kumar Singh	ABV-IIITM, Gwalior, India
Prof. Montaz Ali	Witwatersrand University, Johannesburg, South Africa
Prof. Andries P. Engelbrecht	University of Pretoria, South Africa
Prof. Suresh Chandra	Indian Institute of Technology New Delhi, New Delhi, India
Prof. Kalyanmoy Deb	Indian Institute of Technology Kanpur, Kanpur, India
Prof. D. Nagesh Kumar	Indian Institute of Science, Bangalore, India
Prof. Nirupam Chakraborti	Indian Institute of Technology Kharagpur, Kharagpur, India
Prof. K. C. Tan	National University of Singapore, Singapore
Prof. Roman R. Poznanski	Universiti Tunku Abdul Rahman (UTAR), Malaysia

## Programme Committee

Dr. Abhijit Sanyal	Dr. K. K. Shukla
Dr. Abhay Jha	Dr. K. P. Singh
Dr. Abhijit Sarkar	Dr. Kusum Deep
Dr. Abhinay Pandya	Dr. Lalit Awasthi
Dr. Adel Aljumaily	Dr. Laxman Tawade

Dr. Aitorrodriguez Alsina	Dr. Leonard Barolli
Dr. A. J. Umbarkar	Dr. Manjaree Pandit
Dr. Akila Muthuramalingam	Dr. Manoj Saxena
Dr. Amit Pandit	Dr. Manoj Thakur
Dr. Andres Muñoz	Dr. Mansaf Alam
Dr. Anil Parihar	Dr. Manu Augustine
Dr. Antonio Jara	Dr. Mario Koeppen
Dr. Anupam Singh	Dr. Mehul Raval
Dr. Anuradha Fukane	Dr. Millie Pant
Dr. Aram Soroushian	Dr. Mohammad Ahoque
Dr. Arnab Nandi	Dr. Mohammad Reza Nouri Rad
Dr. Arshin Rezazadeh	Dr. Mohammed Abdulqadeer
Dr. Ashish Gujarathi	Dr. Mohammed Rokibul Alam Kotwal
Dr. Ashraf Darwish	Dr. Mohdabdul Hameed
Dr. Ashwani Kush	Dr. Mourad Abbas
Dr. AsokeNath	Dr. Mrutyunjaya Panda
Dr. Atulya Nagar	Dr. Munawar A. Shaik
Dr. Ayoub Khan	Dr. Musrrat Ali
Dr. B. V. Babu	Dr. Ninansajeeth Philip
Dr. Balaji Venkatraman	Dr. Nitin Merh
Dr. Balakrishna Maddali	Dr. O. P. Vyas
Dr. Banani Basu	Dr. Philip Moore
Dr. Bharanidharan Shanmugam	Dr. Poonam Sharma
Dr. Bratin Ghosh	Dr. Pramod Kumar Singh
Dr. Carlos Fernandezllatas	Dr. Punam Bedi
Dr. Chu-Hsing Lin	Dr. Pushpinder Patheja
Dr. Ciprian Dobre	Dr. Radha Thangaraj
Dr. D. Nagesh Kumar	Dr. Rajesh Sanghvi
Dr. Dante Tapia	Dr. Ram Ratan
Dr. Dipika Joshi	Dr. Ramesh Babu
Dr. Dipti Gupta	Dr. K. C. Raveendranathan
Dr. Eduard Babulak	Dr. Ravi Sankar Vadali
Dr. Farhad Nematy	Dr. Razibhayat Khan
Dr. Francesco Marcelloni	Dr. Ritu Agarwal
Dr. G. Shivaprasad	Dr. Rodger Carroll
Dr. G. R. S. Murthy	Dr. Sami Habib
Dr. Gauri S. Mittal	Dr. Sandeep Kumar Tomar
Dr. Gendelman Oleg	Dr. Sanjeev Singh
Dr. Gurvinder Singh-Baicher	Dr. Shaojing Fu

Dr. Hadushmebrahtu Adane	Dr. Shashi Barak
Dr. Hariganesh Shanmugam	Dr. Shashibhushan Kotwal
Dr. Harris Michail	Dr. Shirshu Varma
Dr. Hemant Mehta	Dr. Shyam Lal
Dr. Hitesh Shah	Dr. S. M. Sameer
Dr. Hugo Proença	Dr. Sonal Jain
Dr. Ivica Boticki	Dr. Sotirios Ziavras
Dr. Jagdish Chand Bansal	Dr. Soumyabrata Saha
Dr. Javier Bajo	Dr. Sucheta Datt
Dr. Jayant M. Modak	Dr. Sudepto Bhattacharya
Dr. Jerlang Hong	Dr. Sudhir Warier
Dr. Joanna Kolodziej	Dr. Sumithra Devika
Dr. Jose Molina	Dr. Sunilkumar Jha
Dr. J. T. Pal Singh	Dr. Suparna Dasgupta
Dr. Juan Mauricio	Dr. Suresh Sankaranarayanan
Dr. K. Mustafa	Dr. Surya Prakash
Dr. Kadian Davis	Dr. Sushil Kulkarni
Dr. Kamal Kant	Dr. Thanga Raj
Dr. Kanad Ray	Dr. Trilochan Panigrahi
Dr. Kannammal Sampath Kumar	Dr. Tzungpei Hong
Dr. Karthik Sindhya	Dr. Umesh Chandra Pati
Dr. Katheej Parveen	Dr. Umesh Gupta
Dr. Kavita Burse	Dr. Uzay Kaymak
Dr. Kazumi Nakamatsu	Dr. Vidya Dhamdhare
Dr. Kedarnath Das	Dr. Vivek Tiwari
Dr. Khaled Abdullah	Dr. Wei-Chiang Samuelson Hong
Dr. Khushboo Hemnani	Dr. Yoseba Penya
Dr. Kishanrao Kalitkar	Dr. Yusuke Nojima

# Contents

## Part I Genetic Algorithm for Problem Solving (GAPS)

<b>Insulin Chart Prediction for Diabetic Patients Using Hidden Markov Model (HMM) and Simulated Annealing Method . . . . .</b>	<b>3</b>
Ravindra Nath and Renu Jain	
<b>A Single Curve Piecewise Fitting Method for Detecting Valve Stiction and Quantification in Oscillating Control Loops. . . . .</b>	<b>13</b>
S. Kalaivani, T. Aravind and D. Yuvaraj	
<b>Feed Point Optimization of Fractal Antenna Using GRNN-GA Hybrid Algorithm . . . . .</b>	<b>25</b>
Balwinder Singh Dhaliwal and Shyam S. Pattnaik	
<b>Diversity Maintenance Perspective: An Analysis of Exploratory Power and Function Optimization in the Context of Adaptive Genetic Algorithms. . . . .</b>	<b>31</b>
Sunanda Gupta and M. L. Garg	
<b>Use of Ant Colony System in Solving Vehicle Routing Problem with Time Window Constraints . . . . .</b>	<b>39</b>
Sandhya Bansal, Rajeev Goel and C. Mohan	
<b>Energy Saving Model for Sensor Network Using Ant Colony Optimization Algorithm. . . . .</b>	<b>51</b>
Doreswamy and S. Narasegouda	
<b>Multi-Objective Optimization of PID Controller for Coupled-Tank Liquid-Level Control System Using Genetic Algorithm. . . . .</b>	<b>59</b>
Sanjay Kr. Singh, Nitish Katal and S. G. Modani	
<b>Comparative Performance Analysis of Particle Swarm Optimization and Interval Type-2 Fuzzy Logic-based TCSC Controller Design . . . .</b>	<b>67</b>
Manoj Kumar Panda, G. N. Pillai and Vijay Kumar	



**Improved Parallelization of an Image Segmentation Bio-inspired Algorithm . . . . . 75**  
 Javier Carnero, Hepzibah A. Christinal, Daniel Díaz-Pernil,  
 Raúl Reina-Molina and M. S. P. Subathra

**A Novel Hardware/Software Partitioning Technique for System-on-Chip in Dynamic Partial Reconfiguration Using Genetic Algorithm . . . . . 83**  
 N. Janakiraman and P. Nirmal Kumar

**Solving School Bus Routing Problem Using Hybrid Genetic Algorithm: A Case Study . . . . . 93**  
 Bhawna Minocha and Saswati Tripathi

**Taguchi-Based Tuning of Rotation Angles and Population Size in Quantum-Inspired Evolutionary Algorithm for Solving MMDP . . . . . 105**  
 Nija Mani, S. Gursaran, A. K. Sinha and Ashish Mani

**Part II Soft Computing for Mathematics and Optimization (SCMO)**

**Simultaneous Feature Selection and Extraction Using Fuzzy Rough Sets . . . . . 115**  
 Pradipta Maji and Partha Garai

**A Fuzzy Programming Approach for Bilevel Stochastic Programming . . . . . 125**  
 Nilkanta Modak and Animesh Biswas

**Implementation of Intelligent Water Drops Algorithm to Solve Graph-Based Travelling Salesman Problem . . . . . 137**  
 Roli Bansal, Hina Agrawal, Hifza Afaq and Sanjay Saini

**Optimization of Complex Mathematical Functions Using a Novel Implementation of Intelligent Water Drops Algorithm . . . . . 145**  
 Maneet Singh and Sanjay Saini

**A New Centroid Method of Ranking for Intuitionistic Fuzzy Numbers . . . . . 151**  
 Anil Kumar Nishad, Shailendra Kumar Bharati and S. R. Singh

**Solution of Multi-Objective Linear Programming Problems in Intuitionistic Fuzzy Environment . . . . . 161**  
 S. K. Bharati, A. K. Nishad and S. R. Singh

**Analyzing Competitive Priorities for Machine Tool Manufacturing Industry: ANP Based Approach** . . . . . 173  
 Deepika Joshi

**A Modified Variant of RSA Algorithm for Gaussian Integers** . . . . . 183  
 Sushma Pradhan and Birendra Kumar Sharma

**Neural Network and Statistical Modeling of Software Development Effort** . . . . . 189  
 Ruchi Shukla, Mukul Shukla and Tshilidzi Marwala

**On  $\alpha$ -Convex Multivalent Functions Defined by Generalized Ruscheweyh Derivatives Involving Fractional Differential Operator** . . 199  
 Ritu Agarwal and J. Sokol

**A New Expected Value Model for the Fuzzy Shortest Path Problem** . . . . . 209  
 Sk. Md. Abu Nayeem

**Existence and Uniqueness of Fixed Point in Fuzzy Metric Spaces and its Applications** . . . . . 217  
 Vishal Gupta and Naveen Mani

**Variable Selection and Fault Detection Using a Hybrid Intelligent Water Drop Algorithm** . . . . . 225  
 Manish Kumar, Srikant Jayaraman, Shikha Bhat, Shameek Ghosh and V. K. Jayaraman

**Air Conditioning System with Fuzzy Logic and Neuro-Fuzzy Algorithm** . . . . . 233  
 Rajani Kumari, Sandeep Kumar and Vivek Kumar Sharma

**Improving the Performance of the Optimization Technique Using Chaotic Algorithm** . . . . . 243  
 R. Arunkumar and V. Jothiprakash

**New Reliable Algorithm for Fractional Harry Dym Equation** . . . . . 251  
 Devendra Kumar and Jagdev Singh

**Floating Point-Based Universal Fused Add–Subtract Unit** . . . . . 259  
 Ishan A. Patil, Prasanna Palsodkar and Ajay Gurjar

**New Analytical Approach for Fractional Cubic Nonlinear Schrödinger Equation Via Laplace Transform . . . . .** 271  
 Jagdev Singh and Devendra Kumar

**An Investigation on the Structure of Super Strongly Perfect Graphs on Trees . . . . .** 279  
 R. Mary Jeya Jothi and A. Amutha

**A Novel Approach for Thin Film Flow Problem Via Homotopy Analysis Sumudu Transform Method . . . . .** 287  
 Sushila and Y. S. Shishodia

**Buckling and Vibration of Non-Homogeneous Orthotropic Rectangular Plates with Variable Thickness Using DQM . . . . .** 295  
 Renu Saini and Roshan Lal

**A Dual SBM Model with Fuzzy Weights in Fuzzy DEA . . . . .** 305  
 Jolly Puri and Shiv Prasad Yadav

**Ball Bearing Fault Diagnosis Using Continuous Wavelet Transforms with Modern Algebraic Function . . . . .** 313  
 R. Sharma, A. Kumar and P. K. Kankar

**Engineering Optimization Using SOMGA . . . . .** 323  
 Kusum Deep and Dipti Singh

**Goal Programming Approach to Trans-shipment Problem . . . . .** 337  
 Om Prakash Dubey, Kusum Deep and Atulya K. Nagar

**An Efficient Solution to a Multiple Non-Linear Regression Model with Interaction Effect using TORA and LINDO . . . . .** 345  
 Umesh Gupta, Devender Singh Hada and Ankita Mathur

**On the Fekete–Szegő Problem for Certain Subclass of Analytic Functions . . . . .** 353  
 Ritu Agarwal and G. S. Paliwal

**Part III Soft Computing for Operations Management (SCOM)**

**Bi-Objective Scheduling on Parallel Machines in Fuzzy Environment . . . . .** 365  
 Sameer Sharma, Deepak Gupta and Seema Sharma

**Inventory Model for Decaying Item with Continuously Variable Holding Cost and Partial Backlogging . . . . .** 373  
 Ankit Prakash Tyagi, Shivraj Singh and Rama Kant Pandey

**The Value of Product Life-Cycle for Deteriorating Items in a Closed Loop Under the Reverse Logistics Operations . . . . .** 383  
 S. R. Singh and Neha Saxena

**A Fuzzified Production Model with Time Varying Demand Under Shortages and Inflation . . . . .** 397  
 Shalini Jain and S. R. Singh

**A Partial Backlogging Inventory Model for Decaying Items: Considering Stock and Price Dependent Consumption Rate in Fuzzy Environment . . . . .** 407  
 S. R. Singh and Swati Sharma

**Efficient Protocol Prediction Algorithm for MANET Multimedia Transmission Under JF Periodic Dropping Attack . . . . .** 419  
 Avita Katal, Mohammad Wazid and R. H. Goudar

**New Placement Strategy for Buffers in Critical Chain . . . . .** 429  
 Vibha Saihpal and S. B. Singh

**Inducing Fuzzy Association Rules with Multiple Minimum Supports for Time Series Data . . . . .** 437  
 Rakesh Rathi, Vinesh Jain and Anshuman Kumar Gautam

**RGA Analysis of Dynamic Process Models Under Uncertainty . . . . .** 447  
 Amit Jain and B. V. Babu

**Part IV Applications of Soft Computing in Image Analysis and Pattern Recognition (SCIAPR)**

**Steps Towards Web Ubiquitous Computing . . . . .** 459  
 Manu Ram Pandit, Tushar Bhardwaj and Vikas Khatri

**Estimation of Uncertainty Using Entropy on Noise Based Soft Classifiers . . . . .** 465  
 Rakesh Dwivedi, Anil Kumar and S. K. Ghosh

**Location Management in Mobile Computing Using Swarm Intelligence Techniques . . . . .** 481  
 Nikhil Goel, J. Senthilnath, S. N. Omkar and V. Mani

<b>Fingerprint and Minutiae Points Technique . . . . .</b>	491
Karun Verma and Ishdeep Singla	
<b>Optimization Problems in Pulp and Paper Industries . . . . .</b>	501
Mohar Singh, Ameya Patkar, Ankit Jain and Millie Pant	
<b>Integrating ERP with E-Commerce: A New Dimension Toward Growth for Micro, Small and Medium-Scale Enterprises in India. . . . .</b>	507
Vinamra Nayak and Nitin Jain	
<b>A New Heuristic for Disassembly Line Balancing Problems With AND/OR Precedence Relations . . . . .</b>	519
Shwetank Avikal, Rajeev Jain, Harish Yadav and P. K. Mishra	
<b>A New Approach to Rework in Merge Production Systems. . . . .</b>	527
S. Kannan and Sadia Samar Ali	
 <b>Part V Applications of Soft Computing in Image Analysis and Pattern Recognition (SCIAPR)</b>	
<b>An Iterative Marching with Correctness Criterion Algorithm for Shape from Shading under Oblique Light Source . . . . .</b>	535
Gaurav Gupta and Manoj Kumar	
<b>Enhancement of Mean Shift Tracking Through Joint Histogram of Color and Color Coherence Vector . . . . .</b>	547
M. H. Sidram and N. U. Bhajantri	
<b>A Rubric Based Assessment of Student Performance Using Fuzzy Logic. . . . .</b>	557
G. Meenakshi and V. Manisharma	
<b>Representation and Classification of Medicinal Plants: A Symbolic Approach Based on Fuzzy Inference Technique . . . . .</b>	565
H. S. Nagendraswamy and Y. G. Naresh	
<b>Fractal Image Compression Using Dynamically Pipelined GPU Clusters . . . . .</b>	575
Munesh Singh Chauhan, Ashish Negi and Prashant Singh Rana	
<b>Person Identification Using Components of Average Silhouette Image . . . . .</b>	583
Rohit Katiyar, K. V. Arya and Vinay Kumar Pathak	

**Modified LSB Method Using New Cryptographic Algorithm for Steganography** . . . . . 591  
 R. Boopathy, M. Ramakrishnan and S. P. Victor

**TDAC: Co-Expressed Gene Pattern Finding Using Attribute Clustering** . . . . . 601  
 Tahleen A. Rahman and Dhruba K. Bhattacharyya

**An Introduction to Back Propagation Learning and its Application in Classification of Genome Data Sequence** . . . . . 609  
 Medha J. Patel, Devarshi Mehta, Patrick Paterson and Rakesh Rawal

**Sobel-Fuzzy Technique to Enhance the Detection of Edges in Grayscale Images Using Auto-Thresholding** . . . . . 617  
 Jesal Vasavada and Shamik Tiwari

**Part VI Soft Computing for Classification (SCC)**

**Hesitant k-Nearest Neighbor (HK-*nn*) Classifier for Document Classification and Numerical Result Analysis** . . . . . 631  
 Neeraj Sahu, R. S. Thakur and G. S. Thakur

**Lower Bound on Naïve Bayes Classifier Accuracy in Case of Noisy Data** . . . . . 639  
 Karan Rawat, Abhishek Kumar and Anshuman Kumar Gautam

**A Neuro-Fuzzy Approach to Diagnose and Classify Learning Disability** . . . . . 645  
 Kavita Jain, Pooja Manghirmalani Mishra and Sushil Kulkarni

**A Review of Hybrid Machine Learning Approaches in Cognitive Classification** . . . . . 659  
 Shantipriya Parida and Satchidananda Dehuri

**“A Safer Cloud”, Data Isolation and Security by Tus-Man Protocol** . . . . . 667  
 Tushar Bhardwaj, Manu Ram Pandit and Tarun Kumar Sharma

**Poem Classification Using Machine Learning Approach** . . . . . 675  
 Vipin Kumar and Sonajharia Minz

**Novel Class Detection in Data Streams** . . . . . 683  
 Vahida Attar and Gargi Pingale

**Analyzing Random Forest Classifier with Different Split Measures . . .** 691  
Vrushali Y. Kulkarni, Manisha Petare and P. K. Sinha

**Text Classification Using Machine Learning Methods-A Survey . . . . .** 701  
Basant Agarwal and Namita Mittal

**Weka-Based Classification Techniques for Offline Handwritten Gurmukhi Character Recognition . . . . .** 711  
Munish Kumar, M. K. Jindal and R. K. Sharma

**Part VII Soft Computing for Security (SCS)**

**An Efficient Fingerprint Indexing Scheme . . . . .** 723  
Arjun Reddy, Umarani Jayaraman, Vandana Dixit Kaushik and P. Gupta

**Gait Biometrics: An Approach to Speed Invariant Human Gait Analysis for Person Identification. . . . .** 729  
Anup Nandy, Soumabha Bhowmick, Pavan Chakraborty and G. C. Nandi

**XML-Based Authentication to Handle SQL Injection . . . . .** 739  
Nitin Mishra, Saumya Chaturvedi, Anil Kumar Sharma and Shantanu Choudhary

**Observation Probability in Hidden Markov Model for Credit Card Fraudulent Detection System . . . . .** 751  
Ashphak Khan, Tejpal Singh and Amit Sinhal

**Comparative Study of Feature Reduction and Machine Learning Methods for Spam Detection . . . . .** 761  
Basant Agarwal and Namita Mittal

**Generation of Key Bit-Streams Using Sparse Matrix-Vector Multiplication for Video Encryption . . . . .** 771  
M. Sivasankar

**Steganography-based Secure Communication . . . . .** 781  
Manjot Bhatia, Sunil Kumar Muttoo and M. P. S. Bhatia

**Part VIII Soft Computing and Web Technologies (SCWT)**

**Heirarchy of Communities in Dynamic Social Network . . . . .** 795  
S. Mishra and G. C. Nandi

**SLAOCMS: A Layered Architecture of SLA Oriented Cloud Management System for Achieving Agreement During Resource Failure** . . . . . 801  
 Rajkumar Rajavel and Mala T

**Semantic Search in E-Tourism Services: Making Data Compilation Easier** . . . . . 811  
 Juhi Agarwal, Nishkarsh Sharma, Pratik Kumar, Vishesh Parshav, Anubhav Srivastava, Rohit Rathore and R. H. Goudar

**Deep Questions in the “Deep or Hidden” Web** . . . . . 821  
 Sonali Gupta and Komal Kumar Bhatia

**Combined and Improved Framework of Infrastructure as a Service and Platform as a Service in Cloud Computing** . . . . . 831  
 Poonam Rana, P. K. Gupta and Rajesh Siddavatam

**Web Site Reorganization Based on Topology and Usage Patterns** . . . . 841  
 R. B. Geeta, Shashikumar G. Totad and P. V. G. D. Prasad Reddy

**Web Search Personalization Using Ontological User Profiles** . . . . . 849  
 Kretika Gupta and Anuja Arora

**Autonomous Computation Offloading Application for Android Phones Using Cloud** . . . . . 857  
 Mayank Arora and Mala Kalra

**Optimizing Battery Utilization and Reducing Time Consumption in Smartphones Exploiting the Power of Cloud Computing** . . . . . 865  
 Variza Negi and Mala Kalra

**Part IX Algorithms and Applications (AA)**

**On Clustering of DNA Sequence of Olfactory Receptors Using Scaled Fuzzy Graph Model** . . . . . 875  
 Satya Ranjan Dash, Satchidananda Dehuri, Uma Kant Sahoo and Gi Nam Wang

**Linear Hopfield Based Optimization for Combined Economic Emission Load Dispatch Problem** . . . . . 885  
 J. P. Sharma and H. R. Kamath



<b>Soft Computing Approach for VLSI Mincut Partitioning: The State of the Arts . . . . .</b>	895
Debasree Maity, Indrajit Saha, Ujjwal Maulik and Dariusz Plewczynski	
<b>Multimedia Classification Using ANN Approach . . . . .</b>	905
Maiya Din, Ram Ratan, Ashok K. Bhateja and Aditi Bhateja	
<b>Live Traffic English Text Monitoring Using Fuzzy Approach . . . . .</b>	911
Renu, Ravi and Ram Ratan	
<b>Digital Mammogram and Tumour Detection Using Fractal-Based Texture Analysis: A Box-Counting Algorithm . . . . .</b>	919
K. C. Latha, S. Valarmathi, Ayesha Sulthana, Ramya Rathan, R. Sridhar and S. Balasubramanian	
<b>Approaches of Computing Traffic Load for Automated Traffic Signal Control: A Survey . . . . .</b>	931
Pratishtha Gupta, G. N. Purohit and Adhyana Gupta	
<b>Comparative Analysis of Neural Model and Statistical Model for Abnormal Retinal Image Segmentation . . . . .</b>	947
D. Jude Hemanth and J. Anitha	
<b>An Efficient Training Dataset Generation Method for Extractive Text Summarization . . . . .</b>	955
Esther Hannah and Saswati Mukherjee	
<b>Online Identification of English Plain Text Using Artificial Neural Network . . . . .</b>	965
Aditi Bhateja, Ashok K. Bhateja and Maiya Din	
<b>Novel Approach to Predict Promoter Region Based on Short Range Interaction Between DNA Sequences . . . . .</b>	973
Arul Mugilan and Abraham Nartey	
<b>“Eco-Computation”: A Step Towards More Friendly Green Computing . . . . .</b>	983
Ashish Joshi, Kanak Tewari, Bhaskar Pant and R. H. Goudar	
<b>A Comparative Study of Performance of Different Window Functions for Speech Enhancement . . . . .</b>	993
A. R. Verma, R. K. Singh and A. Kumar	

**Methods for Estimation of Structural State of Alkali Feldspars . . . .** 1003  
 T. N. Jowhar

**Iris Recognition System Using Local Features  
 Matching Technique . . . . .** 1015  
 Alamdeep Singh and Amandeep Kaur

**Part X Soft Computing for Image Analysis (SCIA)**

**Fast and Accurate Face Recognition Using SVM and DCT. . . . .** 1027  
 Deepti Sisodia, Lokesh Singh and Sheetal Sisodia

**Multi-Temporal Satellite Image Analysis Using Gene  
 Expression Programming. . . . .** 1039  
 J. Senthilnath, S. N. Omkar, V. Mani, Ashoka Vanjare  
 and P. G. Diwakar

**An Advanced Approach of Face Alignment for Gender Recognition  
 Using PCA . . . . .** 1047  
 Abhishek Kumar, Deepak Gupta and Karan Rawat

**Analysis of Pattern Storage Network with Simulated Annealing  
 for Storage and Recalling of Compressed Image Using SOM . . . . .** 1059  
 Manu Pratap Singh and Rinku Sharma Dixit

**Nonrigid Image Registration of Brain MR Images  
 Using Normalized Mutual Information. . . . .** 1069  
 Smita Pradhan and Dipti Patra

**Part XI Soft Computing for Communication, Signals  
 and Networks (CSN)**

**A Proposal for Deployment of Wireless Sensor Network in  
 Day-to-Day Home and Industrial Appliances for a Greener  
 Environment . . . . .** 1081  
 Rajat Arora, Sukhdeep Singh Sandhu and Paridhi Agarwal

**Energy-Aware Mathematical Modeling of Packet Transmission  
 Through Cluster Head from Unequal Clusters in WSN . . . . .** 1087  
 Raju Dutta, Shishir Gupta and Mukul Kumar Das

<b>Evaluation of Various Battery Models for Bellman Ford Ad hoc Routing Protocol in VANET Using Qualnet . . . . .</b>	1101
Manish Sharma	
<b>A Comparative Analysis of Emotion Recognition from Stimulated EEG Signals . . . . .</b>	1109
Garima Singh, Arindam Jati, Anwasha Khasnobish, Saugat Bhattacharyya, Amit Konar, D. N. Tibarewala and R Janarthanan	
<b>Propagation Delay Analysis for Bundled Multi-Walled CNT in Global VLSI Interconnects . . . . .</b>	1117
Pankaj Kumar Das, Manoj Kumar Majumder, B. K. Kaushik and S. K. Manhas	
<b>Improvement in Radiation Parameters Using Single Slot Circular Microstrip Patch Antenna . . . . .</b>	1127
Monika Kiroriwal and Sanyog Rawat	
<b>A <math>\Pi</math>- Slot Microstrip Antenna with Band Rejection Characteristics for Ultra Wideband Applications . . . . .</b>	1135
Mukesh Arora, Abha Sharma and Kanad Ray	
<b>A Technique to Minimize the Effect On Resonance Frequency Due to Fabrication Errors of MS Antenna by Operating Dielectric Constant . . . . .</b>	1145
Sandeep Kumar Toshniwal and Kanad Ray	
<b>Part XII Soft Computing for Industrial Applications (SCI)</b>	
<b>Artificial Neural Network Model for Forecasting the Stock Price of Indian IT Company . . . . .</b>	1153
Joydeep Sen and Arup K. Das	
<b>V/f-Based Speed Controllers for an Induction Motor Using AI Techniques: A Comparative Analysis. . . . .</b>	1161
Awadhesh Gupta, Lini Mathew and S. Chatterji	
<b>Part XIII Soft Computing for Information Management (SCIM)</b>	
<b>Enhanced Technique to Identify Higher Level Clones in Software . . .</b>	1175
S. Mythili and S. Sarala	

<b>Privacy Protected Mining Using Heuristic Based Inherent Voting Spatial Cluster Ensembles . . . . .</b>	1183
R. J. Anandhi and S. Natarajan	
<b>Smart Relay-Based Online Estimation of Process Model Parameters . . . . .</b>	1195
Bajarangbali and Somanath Majhi	
<b>Software Cost Estimation Using Similarity Difference Between Software Attributes . . . . .</b>	1205
Divya Kashyap and A. K. Misra	
<b>Mining Knowledge from Engineering Materials Database for Data Analysis . . . . .</b>	1217
Doreswamy and K. S. Hemanth	
<b>Rule Based Architecture for Medical Question Answering System . . .</b>	1225
Sonal Jain and Tripti Dodiya	
 <b>Part XIV Soft Computing for Clustering (SCCL)</b>	
<b>Adaptive Mutation-Driven Search for Global Minima in 3D Coulomb Clusters: A New Method with Preliminary Applications . . . . .</b>	1237
S. P. Bhattacharyya and Kanchan Sarkar	
<b>A New Rough-Fuzzy Clustering Algorithm and its Applications . . . .</b>	1245
Sushmita Paul and Pradipta Maji	
<b>A Novel Rough Set Based Clustering Approach for Streaming Data . . . . .</b>	1253
Yogita and Durga Toshniwal	
<b>Optimizing Number of Cluster Heads in Wireless Sensor Networks for Clustering Algorithms . . . . .</b>	1267
Vipin Pal, Girdhari Singh and R. P Yadav	
<b>Data Clustering Using Cuckoo Search Algorithm (CSA). . . . .</b>	1275
P. Manikandan and S. Selvarajan	

**Search Result Clustering Through Expectation Maximization Based Pruning of Terms . . . . . 1285**  
 K. Hima Bindu and C. Raghavendra Rao

**Intensity-Based Detection of Microcalcification Clusters in Digital Mammograms using Fractal Dimension . . . . . 1293**  
 P. Shanmugavadivu and V. Sivakumar

**Part XV General Soft Computing Approaches and Applications**

**Palmpoint Recognition Using Geometrical and Statistical Constraints . . . . . 1303**  
 Aditya Nigam and Phalguni Gupta

**A Diversity-Based Comparative Study for Advance Variants of Differential Evolution . . . . . 1317**  
 Prashant Singh Rana, Kavita Sharma, Mahua Bhattacharya, Anupam Shukla and Harish Sharma

**Computing Vectors Based Document Clustering and Numerical Result Analysis . . . . . 1333**  
 Neeraj Sahu and G. S. Thakur

**Altered Fingerprint Identification and Classification Using SP Detection and Fuzzy Classification. . . . . 1343**  
 Ram Kumar, Jasvinder Pal Singh and Gaurav Srivastava

**Optimal Advertisement Planning for Multi Products Incorporating Segment Specific and Spectrum Effect of Different Medias . . . . . 1351**  
 Sugandha Aggarwal, Remica Aggarwal and P. C. Jha

**Two Storage Inventory Model for Perishable Items with Trapezoidal Type Demand Under Conditionally Permissible Delay in Payment . . . . . 1369**  
 S R Singh and Monika Vishnoi

**Development of an EOQ Model for Multi Source and Destinations, Deteriorating Products Under Fuzzy Environment . . . . . 1387**  
 Kanika Gandhi and P. C. Jha

**A Goal Programming Model for Advertisement Selection on Online News Media . . . . . 1401**  
 Prerna Manik, Anshu Gupta and P. C. Jha

**An Integrated Approach and Framework for Document Clustering Using Graph Based Association Rule Mining** . . . . . 1421  
 D. S. Rajput, R. S. Thakur and G. S. Thakur

**Desktop Virtualization and Green Computing Solutions** . . . . . 1439  
 Shalabh Agarwal and Asoke Nath

**Noise Reduction from the Microarray Images to Identify the Intensity of the Expression** . . . . . 1451  
 S. Valarmathi, Ayesha Sulthana, K. C. Latha, Ramya Rathan, R. Sridhar and S. Balasubramanian

**A Comparative Study on Machine Learning Algorithms in Emotion State Recognition Using ECG**. . . . . 1467  
 Abhishek Vaish and Pinki Kumari

**Fault Diagnosis of Ball Bearings Using Support Vector Machine and Adaptive Neuro Fuzzy Classifier** . . . . . 1477  
 Rohit Tiwari, Pavan Kumar Kankar and Vijay Kumar Gupta

**Designing a Closed-Loop Logistic Network in Supply Chain by Reducing its Unfriendly Consequences on Environment**. . . . . 1483  
 Kiran Garg, Sanjam, Aman Jain and P. C. Jha

**Optimal Component Selection Based on Cohesion and Coupling for Component-Based Software System**. . . . . 1499  
 P. C. Jha, Vikram Bali, Sonam Narula and Mala Kalra

**Some Issues on Choices of Modalities for Multimodal Biometric Systems**. . . . . 1513  
 Mohammad Imran, Ashok Rao, S. Nousath and G. Hemantha Kumar

**An Adaptive Iterative PCA-SVM Based Technique for Dimensionality Reduction to Support Fast Mining of Leukemia Data** . . . . . 1525  
 Vikrant Sabnis and Neelu Khare

**Social Evolution: An Evolutionary Algorithm Inspired by Human Interactions** . . . . . 1537  
 R. S. Pavithr and Gursaran

**A Survey on Filter Techniques for Feature Selection in Text Mining** . . . . . 1545  
 Kusum Kumari Bharti and Pramod kumar Singh

**An Effective Hybrid Method Based on DE, GA, and K-means for Data Clustering** . . . . . 1561  
Jay Prakash and Pramod Kumar Singh

**Studies and Evaluation of EIT Image Reconstruction in EIDORS with Simulated Boundary Data** . . . . . 1573  
Tushar Kanti Bera and J. Nagaraju

**Coverage of Indoor WLAN in Obstructed Environment Using Particle Swarm Optimization** . . . . . 1583  
Leena Arya and S. C. Sharma

**Stereovision for 3D Information.** . . . . . 1595  
Mary Ann George and Anna Merine George

**About the Editors** . . . . . 1603

**Part I**  
**Genetic Algorithm for Problem Solving**  
**(GAPS)**



# Insulin Chart Prediction for Diabetic Patients Using Hidden Markov Model (HMM) and Simulated Annealing Method

Ravindra Nath and Renu Jain

**Abstract** Most of the diabetic patients need to take insulin before every meal. The doctors have to decide insulin doses for every patient according to the patient's previous records of doses and sugar levels measured at regular intervals. This paper proposes a hidden Markov model to predict the insulin chart for a patient and uses simulated annealing search algorithm to efficiently implement the model. The one-month chart maintained by the patient has been used to train the model, and the prediction for next fifteen days is done on the basis of the trained data. We discussed the results with the university medical doctor; he was very pleased to see to the result obtained.

**Keywords** Hidden Markov model (HMM) · Randomized algorithm (RA) · Simulated annealing (SA) · Diabetic patient chart prediction (DPCP)

## 1 Introduction

Hidden Markov model has various applications in the area of speech recognition, bioinformatics (DNA sequences and gene recognitions) [1–4], climatology, acoustics [1, 5], etc. In addition to this, HMM has been applied for prediction problems like stock marketing [6–8] and forecasting. Mostly researches have to work with the third problem of HMM for training and prediction of the data. Out of many probabilistic models, HMM is most popular due to its mathematical foundation of model.

---

R. Nath · R. Jain (✉)

Department of Computer Science and Engineering, University Institute of Engineering and Technology, Chattrapati Shahuji Maharaj University, Kanpur, Uttar Pradesh 208024, India

e-mail: rnkatiyar@gmail.com

R. Jain

e-mail: jainrenu@gmail.com

In this paper, we have taken the application of medical science, i.e., preparation of insulin chart for diabetic patients. We have used HMM to predict the insulin chart taking the data of a diabetic patient. We have used simulated annealing as a randomized algorithm. Training is done taking one-month chart maintained by the patient.

Simulated annealing [9–11] is a randomized search method that can perform global search within the defined searching space giving local maxima or global maxima. In our previous paper [12, 13], we modeled HMM learning problem as a discrete search problem and solved that discrete problem using different randomized search algorithms. In this paper, insulin chart prediction is modeled as HMM, and HMM learning problem is solved using simulated annealing algorithm. Experimental results show that SA evaluates HMM parameters quite fast and accurately on the basis of previous data giving good prediction results.

The organization of the paper is as follows. Section 2 briefly describes the data set taken. Section 3 explains HMM, and Sect. 4 explains in detail the HMM used and results obtained. Section 5 is about results and discussions.

## 2 Data Set Information

The data set used in this paper was taken from <http://archive.ics.uci.edu/ml/> called UCI Repository. Diabetics patient records can be obtained from two sources: an automatic electronic recording device and paper records. The automatic device has an internal clock to timestamp events, whereas paper records provide ‘logical time’ slots (breakfast, lunch, dinner, bedtime). Diabetic files consist of four fields per record: (1) date in MM-DD-YYYY format, (2) time in XX:YY format, (3) code, and (4) value.

The code field is deciphered as follows: 33 = Regular insulin dose, 34 = NPH insulin dose, 35 = Ultralente insulin dose, 48 = Unspecified blood glucose measurement, 57 = Unspecified blood glucose measurement, etc.

We have taken two-month data (insulin chart) for code 33, i.e., regular insulin dose of a patient. Assuming first-month data as training data, next one-month chart is predicted and compared with the actual data.

## 3 The Hidden Markov Model

HMM is a probabilistic model useful for finite-state stochastic sequence structures. Stochastic sequences are called observation sequences, i.e.,  $O = O_1 O_2 \dots O_T$ , where  $T$  is the length of the observed sequence. HMM with  $N$  states ( $S_1, S_2, \dots S_N$ ) can be characterized by a set of parameters  $(A, B, \pi)$  is called the model of HMM  $\lambda = (A, B, \pi)$

In order to characterize an HMM completely, following elements are needed [8–10, 14, 15]

$N$ : The number of states in the model

$M$ : The number of distinct observation symbols  $M$  per state

$A$ : The state transition probability distribution

$$A = \{a_{ij}\}, a_{ij} = p(q_t = s_j | q_{t-1} = S_i)$$

$$\sum_{i=1}^j a_{ij} = 1 \text{ where } a_{ij} \geq 0, 1 \leq i \leq N \text{ and } 1 \leq j \leq N$$

$B$ : The observation symbol probability distribution in state  $j$

$$B = b_j(k) = P(V_k \text{ at } t | q_t = S_j)$$

$$\sum_{k=1}^M b_j(k) = 1 \quad b_j(k) \geq 0$$

$\pi$ : The initial-state distribution  $\pi_i = P(q_1 = S_i)$

The three main problems of HMM are as follows: evaluation problem, decoding, problem, and learning problem.

- (1) HMM evaluation problem: Compute  $P(O|\lambda)$ , the probability of the observation sequence  $O = O_1 O_2 O_3 \dots O_T$ , given the model  $\lambda = (A, B, \pi)$ .
- (2) HMM decoding problem: Uncover the hidden part of the model, i.e., find the optimal state sequence, for the given observation sequences  $O = O_1 O_2 O_3 \dots O_T$ , given the model  $\lambda = (A, B, \pi)$ .
- (3) HMM learning problem: Model parameters  $(A, B, \pi)$  are adjusted such that  $P(O|\lambda)$  is maximized.

In this paper, we have considered the third problem of HMM, i.e., the learning problem or training problem and tried to solve it.

### 3.1 Hidden Markov Model for a Diabetic Patient

To completely define a problem of HMM, we need to define three probabilities: state transition probabilities, observation symbols probabilities, and initial-state probabilities. It was observed that a patient takes the medicine at breakfast (08:00), lunch

**Table 1** Actual input of doses for one month

Date	Code	Breakfast	Lunch	Dinner	Bedtime
21-Apr-91	33	9	0	7	0
22-Apr-91	33	10	2	7	0
23-Apr-91	33	11	0	7	0
24-Apr-91	33	10	4	0	5
25-Apr-91	33	9	4	7	2
26-Apr-91	33	9	5	7	0
27-Apr-91	33	10	0	8	0
28-Apr-91	33	10	0	7	0
29-Apr-91	33	9	5	8	0
30-Apr-91	33	10	4	7	0
1-May-91	33	10	4	7	0
2-May-91	33	10	5	7	0
3-May-91	33	10	5	7	0
4-May-91	33	10	5	7	0
5-May-91	33	10	5	7	2
6-May-91	33	10	5	7	0
7-May-91	33	10	5	7	0
8-May-91	33	10	5	7	0
9-May-91	33	9	4	7	0
.	.	.	.	.	.
.	.	.	.	.	.

(12:00), dinner (18:00), and bedtime (22:00) or morning, noon, evening, and night, and the amount of insulin (code=33) varies from value 2 to 11. The data set contains 4 values per day corresponding to 4 slots, i.e., breakfast, lunch, dinner, and bedtime. We have taken these four slots as four states where  $S_1$  corresponds to breakfast,  $S_2$  corresponds to lunch,  $S_3$  corresponds to dinner, and  $S_4$  corresponds to bedtime. In addition to this, we have taken 10 observation symbols on the basis of insulin dose values given to the patient. Table 1 shows the actual amount of insulin give to the patient for thirty days.

Further, whole one-month data were divided into slots of three days and training is done taking three-day data repeatedly. For training, simulated annealing algorithm is used, and at the end of the process, a model  $\lambda$  is obtained. Hence, our model  $\lambda$  has four states ( $S_1$ ,  $S_2$ ,  $S_3$ , and  $S_4$ ), and we assume that the patient starts his doses from morning, i.e., there is a very high probability that the patient will be in state 1. So, we take initial probability as:

$$\pi = [0.925 \ 0.025 \ 0.025 \ 0.025]$$

After examining the patient's previous data, we roughly initialize the state transition probabilities and symbol emitting probabilities generating initial  $A = a_{ij}$  and  $B = B_j(k)$  as follows:

$$A = a_{ij} = \begin{bmatrix} 0.025 & 0.325 & 0.625 & 0.025 \\ 0.025 & 0.025 & 0.925 & 0.025 \\ 0.925 & 0.025 & 0.025 & 0.025 \\ 0.250 & 0.250 & 0.250 & 0.250 \end{bmatrix}$$

$$B = b_j(k) = \begin{bmatrix} .0090 & .0091 & .0091 & .0091 & .0091 & .0091 & .0091 & .0091 & .3391 & .3391 & .2491 \\ .6090 & .3091 & .0091 & .0091 & .0091 & .0091 & .0091 & .0091 & .0091 & .0091 & .0091 \\ .0090 & .0091 & .0091 & .0091 & .0091 & .0091 & .9000 & .0091 & .0091 & .0091 & .0091 \\ .9090 & .0091 & .0091 & .0091 & .0091 & .0091 & .0091 & .0091 & .0091 & .0091 & .0091 \end{bmatrix}$$

The observation sequence for first three days will be:

$$O = [O_1 \ O_2 \ O_3 \ O_4 \ O_5 \ O_6 \ O_7 \ O_8 \ O_9 \ O_{10} \ O_{11} \ O_{12}]$$

Taking the initial model, we keep training using simulated annealing [11, 16, 17] method for every three days and get a model  $\lambda$ , and then, it is again trained taking all the previous observation sequences getting a  $\lambda_{\text{Final}}$ . Taking  $\lambda_{\text{Final}}$  as model, observation sequence is predicted by matching  $P(O|\lambda)$  values with previous model values, and these processes are shown as follows.

### 3.2 HMM Training by Simulated Annealing Algorithm

The HMM training is performing in the following steps.

- (a) Take an initial values  $A$ ,  $B$ , and  $\pi$ .
- (b) Using simulated annealing method and adjusting the values of  $A$  and  $B$ , a set of values of  $A$  and  $B$  is found having maximum values say  $\lambda_1$ .
- (c) for the next sequence, initial values of  $A$  and  $B$  are taken for the model  $\lambda_1$ , and then, step 'b' is repeated to get a new model  $\lambda_2$ . This way we continue and  $\lambda_1, \lambda_{12} \dots, \lambda_{10}$  models are created as shown in the Table 2.
- (d) To further refine the model, we took the model  $\lambda_{10}$  as a starting model and using simulated annealing, got refined new model  $\lambda_{\text{new1}}, \lambda_{\text{new2}}, \dots, \lambda_{\text{new10}}$  as shown in Table 3 and corresponding values of  $A_{10}, B_{10}$ , and  $\pi_{10}$  are given in the Table 3.

**Table 2** Observation sequence and corresponding  $p(O|\lambda)$  values

S.no.	Training sequence	HMM	Log10 ( $p(O \lambda_i)$ )
1	9 1 7 1 10 2 7 1 11 1 7 1	$\lambda_1$	-9.6952
2	10 4 1 5 9 4 7 2 9 5 7 1	$\lambda_2$	-10.797
3	10 1 8 1 10 1 7 1 9 5 8 1	$\lambda_3$	-8.7954
4	10 4 7 1 10 4 7 1 10 5 7 1	$\lambda_4$	-7.3351
5	10 5 7 1 10 5 7 1 10 5 7 2	$\lambda_5$	-3.0548
6	10 5 7 1 10 5 7 1 10 5 7 1	$\lambda_6$	-6.4811
7	9 4 7 1 10 4 8 1 10 4 7 1	$\lambda_7$	-8.9516
8	9 4 7 1 10 4 8 1 10 4 7 1	$\lambda_8$	-9.8487
9	10 6 7 1 10 1 7 1 9 5 7 1	$\lambda_9$	-10.7967
10	10 5 7 1 10 4 7 1 9 5 7 1	$\lambda_{10}$	-8.1579

**Table 3** Training sequence and corresponding  $p(O|\lambda)$  values (second iteration values)

S.no.	Training sequence	HMM	log10( $p(O \lambda_{max})$ )
1	9 1 7 1 10 2 7 1 11 1 7 1	$\lambda_{new1}$	-12.5923
2	10 4 1 5 9 4 7 2 9 5 7 1	$\lambda_{new2}$	-13.5613
3	10 1 8 1 10 1 7 1 9 5 8 1	$\lambda_{new3}$	-8.9966
4	10 4 7 1 10 4 7 1 10 5 7 1	$\lambda_{new4}$	-6.6894
5	10 5 7 1 10 5 7 1 10 5 7 2	$\lambda_{new5}$	-3.1633
6	10 5 7 1 10 5 7 1 10 5 7 1	$\lambda_{new6}$	-2.8713
7	9 4 7 1 10 4 8 1 10 4 7 1	$\lambda_{new7}$	-10.6096
8	9 4 7 1 10 4 8 1 10 4 7 1	$\lambda_{new8}$	-6.7935
9	10 6 7 1 10 1 7 1 9 5 7 1	$\lambda_{new9}$	-8.5143
10	10 5 7 1 10 4 7 1 9 5 7 1	$\lambda_{new10}$	-6.619

$$\begin{aligned}
 \Pi_{10} &= [0.9250 \ 0.0250 \ 0.0250 \ 0.0250] \\
 &[0.0130 \ 0.0091 \ 0.0091 \ 0.0091 \ 0.0091 \ 0.0091 \ 0.0091 \ 0.0091 \ 0.0091 \ 0.0131 \\
 &\quad 0.0091 \ 0.0091 \\
 &0.0090 \ 0.0091 \ 0.0091 \ 0.0111 \ 0.9031 \ 0.0131 \ 0.0091 \ 0.0091 \ 0.0091 \\
 &\quad 0.0091 \ 0.0091 \\
 B_{10} &= 0.0090 \ 0.0091 \ 0.0091 \ 0.0091 \ 0.0091 \ 0.0091 \ 0.0091 \ 0.0091 \ 0.6071 \ 0.0111 \\
 &\quad 0.0091 \ 0.0091 \\
 &0.6051 \ 0.3031 \ 0.0091 \ 0.0131 \ 0.0091 \ 0.0091 \ 0.0091 \ 0.0091 \ 0.0091 \\
 &\quad 0.0151 \ 0.0091 \\
 &0.0270 \ 0.9170 \ 0.0290 \ 0.0270 \\
 A_{10} &= 0.0250 \ 0.0330 \ 0.9170 \ 0.0250 \\
 &0.6170 \ 0.0330 \ 0.0350 \ 0.3150 \\
 &0.9110 \ 0.0270 \ 0.0330 \ 0.0290
 \end{aligned}$$

(e)  $\lambda_{new10}$  is assumed as  $\lambda_{final}$ , which we used for prediction of sequence.

### 4 Prediction

After training the HMM [18], the procedure can be described as for the predicting the observation sequence. For predicting  $O_i + 1$ , we use  $P(O_i|\lambda_{\text{final}})$  ( $O_i$  is  $i$ th the observation sequence) to find those events which have closest  $P(O_i|\lambda_{\text{final}})$  value. If we assume there are two closest values  $O_{k1}$  and  $O_{k2}$ ; then, we evaluate two possible predicting values  $O_{p1} = O_i + (O_{k1+1} - O_{k1})$  and  $O_{p2} = O_i + (O_{k2+1} - O_{k2})$ . For example, for predicting  $O_{11}$ , we use the following steps:

(a) For predicting  $O_{11}$ , we found  $P(O_4/\lambda_{\text{final}})$  and  $P(O_8/\lambda_{\text{final}})$ , which are the closest observation sequences. (b) We find the differences of  $O_5 - O_4$  and  $O_9 - O_8$ , and then, these differences are added to  $O_{10}$  giving two predicted observation sequences  $O_{p1}$  and  $O_{p2}$ .

Predicted Observation

$$(O_{p1} = 10\ 7\ 7\ 0\ 10\ 0\ 7\ 0\ 9\ 5\ 7\ 2) \text{ and } (O_{p2} = 10\ 8\ 7\ 0\ 10\ 5\ 6\ 0\ 9\ 5\ 7\ 0)$$

(c) We again evaluate the  $P(O_{p1}|\lambda_{\text{Final}})$  and  $P(O_{p2}|\lambda_{\text{Final}})$  values, and  $O_{p2}$  chosen because it is observed that  $P(O_{p2}|\lambda_{\text{Final}})$  is higher value than  $P(O_{p1}|\lambda_{\text{Final}})$ . Therefore,  $O_{p2}$  observation sequence because the predicted sequence.

Similarly using steps a, b, and c, we predict  $O_{p11}$ ,  $O_{p12}$ ,  $O_{p13}$ ,  $O_{p14}$  and  $O_{p15}$  as follows.

$$\begin{aligned} O_{p11} &= 10\ 6\ 7\ 0\ 10\ 5\ 6\ 0\ 9\ 5\ 7\ 0 & O_{p12} &= 9\ 3\ 8\ 0\ 10\ 7\ 8\ 0\ 9\ 4\ 7\ 0 & O_{p13} \\ &= 10\ 2\ 7\ 0\ 10\ 6\ 6\ 0\ 9\ 5\ 7\ 0 \\ O_{p14} &= 10\ 6\ 7\ 0\ 10\ 9\ 6\ 0\ 9\ 5\ 7\ 0 & O_{p15} &= 9\ 3\ 7\ 0\ 10\ 7\ 8\ 0\ 9\ 4\ 7\ 0 \end{aligned}$$

Actual observation sequences are  $O_{a11}$ ,  $O_{a12}$ ,  $O_{a13}$ ,  $O_{a14}$  and  $O_{a15}$  as follows (Table 4):

**Table 4** Comparison between actual data and predicted data

Date	Code	Actual data				Predictable data			
		Breakfast	Lunch	Dinner	Bedtime	Breakfast	Lunch	Dinner	Bedtime
21-May-91	33	9	2	7	0	10	6	7	0
22-May-91	33	9	4	8	0	10	5	6	0
23-May-91	33	10	0	7	0	9	5	7	0
24-May-91	33	10	3	8	0	9	3	8	0
25-May-91	33	10	7	2	0	10	7	8	0
26-May-91	33	11	0	7	2	9	4	7	0
27-May-91	33	11	2	7	0	10	2	7	0
28-May-91	33	9	4	7	0	10	6	6	0
29-May-91	33	10	4	7	0	9	5	7	0
30-May-91	33	9	3	7	0	10	6	7	0
31-May-91	33	10	3	7	0	10	9	6	0
1-Jun-91	33	11	3	7	0	9	5	7	0
2-Jun-91	3	9	0	7	0	9	3	7	0
3-Jun-91	33	9	4	7	0	10	7	8	0
4-Jun-91	33	10	4	7	0	9	4	7	0

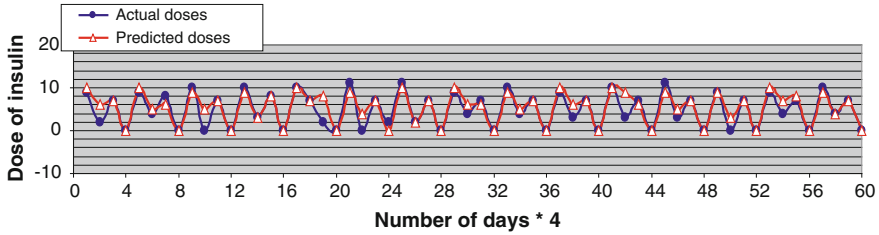


Fig. 1 Graph between actual doses and predicted doses for fifteen days

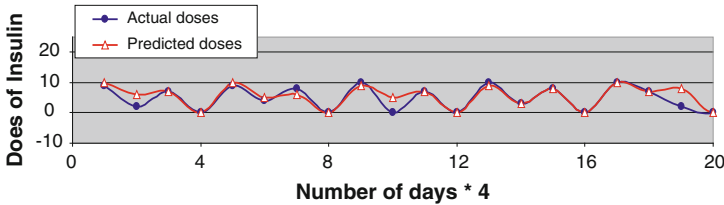


Fig. 2 Graph between actual doses and predicted doses for five days

$$\begin{aligned}
 O_{a11} &= 9\ 2\ 7\ 0\ 9\ 4\ 8\ 0\ 10\ 0\ 7\ 0 & O_{a12} &= 10\ 3\ 8\ 0\ 10\ 7\ 2\ 0\ 11\ 0\ 7\ 2 \\
 O_{a13} &= 11\ 2\ 7\ 0\ 9\ 4\ 7\ 0\ 10\ 4\ 7\ 0 \\
 O_{a14} &= 9\ 3\ 7\ 0\ 10\ 3\ 7\ 0\ 11\ 3\ 7\ 0 & O_{a15} &= 9\ 0\ 7\ 0\ 9\ 4\ 7\ 0\ 10\ 4\ 7\ 0
 \end{aligned}$$

## 5 Results and Discussions

In this study, we have taken the problem of predicting insulin chart for diabetic patients. Figures 1 and 2 show the comparison between predicted data and actual data, and it can be observed that results are very encouraging. We have discussed our results with our university medical doctor Dr. Chaman Kumar; he was very enthusiastic to see the results. To start with, the results obtained can be very useful to guide the junior doctors who prepare the complete chart for the patients. However, we need to make it user friendly before it can be tested in actual practice by the doctors. The solution of third problem, i.e., the learning problem has exponential complexity ( $N^T$ ) and HMM learning problem is solved using randomized search algorithm in polynomial time. We would like to compare the results by implementing other randomized algorithms.



**Acknowledgments** The authors of the paper are highly grateful to Dr. Chaman Kumar (MBBS, MD), CSJM University, Kanpur, for discussing the results with us and encouraging us to do more work in this direction.

## Appendix A

<http://archive.ics.uci.edu/ml/> called UCI Repository.

## References

1. Durbin, R., Eddy, R., Krogh, A.: Graeme Mitchison. Cambridge University Press, Biological Sequence Analysis (2005)
2. Dan, E. Krane., Michael, L. Raymer.: Fundamental Concepts of Bioinformatics. Pearson Education first edition (2000)
3. Antequera, F., Bird, A.: CpG islands as the genomic footprints of promoters that are associated with replication origins. *Curr Biol.* **9**(17), 661–667 (1999)
4. Larsen, F., Gundersen, G., Lopez, R., Prydz, H.: CpG islands as gene markers in the human genome. *Genomics* **13**(4), 1095–1107 (1992)
5. Eren, Akdemir., Tolga.: The use of articulator motion information in automatic speech segmentation., Science Direct Received 5 October 2007; received in revised form 7 March 2008; accepted 17 April (2008)
6. Md. Rafiul, Hassan., Baikunth, Nath.: Stock market forecasting using HMM: a new approach. In: Proceeding of international conference on intelligent systems design and applications (ISDA) (2005)
7. Behrooz, Nobakht., Cart-Edward, Joseph., Babak, Loni.: Stock market analysis and prediction Using HMM LIACS
8. Sundararajan, R.: Stock market trend and prediction using Markov models. RTCSP 09, Department of ECE, Amrita Vishwa vidyapeeth, Coimbatore
9. Kwong, S., Chau, C.W., Man, K.F., Tang, K.S.: Optimization of HMM topology and its model parameters by genetic algorithm. *Pattern Recognitions* **34**, 509–522 (2001)
10. The Metropolis Algorithm, Statistical systems and simulated annealing
11. Mantawy, A.H., Abdul Mazid, L., Selim, Z.: Integrating genetic algorithms. Tabu search and Simulated Annealing for the unit commitment problem. *IEEE Trans Power Syst* **14**(3) August (1999)
12. Ravindra, Nath., Renu, Jain.: Estimating HMM learning parameters using genetic algorithm. In: International conference on computational intelligence applications (2010)
13. Ravindra, Nath., Renu, Jain.: Using randomized search algorithms to estimate HMM learning parameters. In: IEEE international advanced computing conference (IACC) (2009)
14. Rabiner, L.R.: A tutorial on HMM and selected applications in speech recognition. *Proc IEEE* **77**(2), 267–296 (1977)
15. Liu, Y., Lin, Y., Chen Z.: Using hidden markov model for information extraction based on multiple templates. In: Porch of the international conference on natural language processing and knowledge engineering pp. 394–399, (2003)
16. Coleman, C. M.: Investigation of simulated annealing, Ant-colony optimization, and genetic algorithms for self-structuring antennas. **52**(4), April (2004)
17. Pirlot, Mark: General local search method. *European J. Opera. Res.* **92**, 493–511 (1996)
18. Wegener, I.: Randomized search heuristics as an alternative to exact optimization. University of Dortmund, Department of the Computer Science, Technical report February 2004

# A Single Curve Piecewise Fitting Method for Detecting Valve Stiction and Quantification in Oscillating Control Loops

S. Kalaivani, T. Aravind and D. Yuvaraj

**Abstract** Stiction is one of the most common problems in the spring-diaphragm type control valves, which are widely used in the process industry. In this paper, a procedure for single curve piecewise fitting stiction detection method and quantifying valve stiction in control loops based on ant colony optimization has been proposed. The single curve piecewise fitting method of detecting valve stiction is based on the qualitative analysis of the control signals. The basic idea of this method is to fit two different functions, triangular wave and sinusoidal wave, to the controller output data. The calculation of stiction index (SI) is introduced based on the proposed method to facilitate the automatic detection of stiction. A better fit to a triangular wave indicates valve stiction, while a better fit to a sinusoidal wave indicates non-stiction. This method is time saving and easiest method for detecting the stiction. Ant colony optimization (ACO), an intelligent swarm algorithm, proves effective in various fields. The ACO algorithm is inspired from the natural trail following behaviour of ants. The parameters of the Stenman model estimated using ant colony optimization, from the input–output data by minimizing the error between the actual stiction model output and the simulated stiction model output. Using ant colony optimization, Stenman model with known nonlinear structure and unknown parameters can be estimated.

---

S. Kalaivani (✉)

Electronics and Instrumentation Engineering, Muthayammal Engineering College,  
Namakkal, India  
e-mail: instrokalai@gmail.com

T. Aravind

Computer Science Engineering, Muthayammal Engineering College, Namakkal, India  
e-mail: aravindnkl@gmail.com

D. Yuvaraj

Instrumentation and Control Engineering, Tamilnadu College of Engineering, Coimbatore, India  
e-mail: pciyuvaraj@gmail.com

**Keywords** Control valve stiction · Stenman model · Single curve piecewise fitting · Ant colony optimization

## 1 Introduction

Large-scale, highly integrated processing plants include some hundreds or even thousands of control loops. The aim of each control loop is to maintain the process at the desired operating conditions, safely and efficiently. A poorly performing control loop can result in disrupted process operation, degraded product quality, higher material or energy consumption and thus decreased plant profitability.

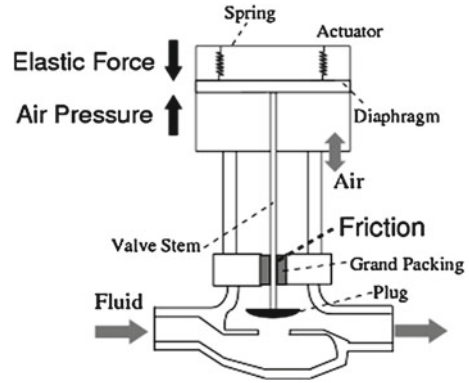
Nonlinearities such as stiction, backlash and dead band cause oscillations in the process output. They may be present in the process itself or in the control valves. Among the many types of nonlinearities in control valves, stiction is the most common problem in the control valves, which are widely used in the process industry. It hinders the proper movement of the valve stem and consequently affects control loop performance. As the presence of oscillation in a control-loop increases the variability of the process variables, thus causing inferior quality products and larger rejection rates, it is important to detect and quantify stiction. The single curve piecewise fitting method involves fitting the single curve of OP to both triangular and sinusoidal waves using least square estimation (LSE). A better fit to a triangular wave indicates valve stiction, while a better fit to a sinusoidal wave indicates nonstiction. This method is time saving and easiest method for detect the stiction. All valves are sticky to some extent, it is important to quantify stiction. The quantification is implemented by an ant colony optimization procedure. The ant colony optimization procedure involves certain steps to estimate the parameter values. The parameter estimation is done by minimizing the objective function. The error ( $e$ ) is the difference between actual stiction model output ( $y$ ) and the dynamic stiction model output ( $y_m$ ). It is used as the criterion to correct the model parameters, so as to identify the parameters of the actual process.

## 2 Valve Stiction Model

The present work focuses on pneumatic control valves, which are widely used in the process industry. The general structure of pneumatic control valve is shown in Fig. 1.

Stiction is a portmanteau word formed from the two words static friction. Stiction is the static friction that prevents an object from moving and when the external force overcomes the static friction the object starts moving [1]. The presence of stiction impairs proper valve movement, i.e. the valve stem may not move in response to the output signal from the controller or the valve positioner. To check the behaviour

**Fig. 1** Structure of pneumatic control valve



of valve moment by modelling, the stiction detection made by physical model and Stenman model used to quantification process.

## 2.1 Physical Model of Valve Friction

The purpose of this section is to understand the physics of valve friction and reproduce the behaviour seen in real plant data. For a pneumatic sliding stem valve, the force balance equation based on Newton's second law can be written as,

$$M \frac{d^2x}{dt^2} = \sum \text{Force} = F_a + F_r + F_f + F_p + F_i \quad (1)$$

where,

$M$  = Mass of the moving parts,  $x$  = Relative stem position.

$F_a = Au$  = Force applied by pneumatic actuator ( $A$  = Area of the diaphragm,  $u$  = Actuator air pressure or the valve input signal).

$F_r = -kx$  = Spring force ( $k$  = Spring constant).

$F_p = -\alpha \Delta P$  = Force due to fluid pressure drop ( $\alpha$  = plug unbalance area,  $\Delta P$  = Fluid pressure drop across the valve).

$F_i$  = Extra force required to force the valve to be into the seat.

$F_f$  = Friction force includes static and moving friction.

where

$$F_f = \begin{cases} F(v) & \text{if } v \neq 0 \\ -(F_a + F_r) & \text{if } v = 0 \text{ and } |F_a + F_r| \leq F_s \\ -F_s \text{ sign}(F_a + F_r) & \text{if } v = 0 \text{ and } |F_a + F_r| > F_s \end{cases} \quad (2)$$

**Table 1** Values of  $F_s$  and  $F_c$  for different levels of stiction

Magnitude of stiction	$F_s$ (lbf)	$F_c$ (lbf)
Weak stiction	384	320
Strong stiction	600	500

$$F(v) = -F_c \text{sgn}(v) - vF_v - (F_s - F_c) \exp(-v/vs)2\text{sgn}(v) \quad (3)$$

The expression for the moving friction is in the first line of equation and comprises a velocity independent term  $F_c$  known as Coulomb friction and a viscous friction term  $vF_v$  that depends linearly upon velocity. Both act in opposition to the velocity, as shown by the negative signs.

The second line in equation is the case when the valve is stuck.  $F_s$  is the maximum static friction. The velocity of the stuck valve is zero and not changing; therefore, the acceleration is zero also. Thus, the right-hand side of Newton's law is zero, so  $F_f = -(F_a + F_r)$ .

The third line of the model represents the situation at the instant of breakaway. At that instant, the sum of forces is  $(F_a + F_r) - F_s \text{sgn}(F_a + F_r)$ , which is not zero if  $|F_a + F_r| > F_s$ . Therefore, the acceleration becomes nonzero and the valve starts to move. Here,  $F_i$  and  $F_p$  assumed to be zero because of their negligible contribution in the model Table 1.

### 3 Proposed Single Curve Piecewise Fitting Detection Method

Single curve piecewise fitting method of detecting valve stiction is based on the qualitative analysis of the control signals [2]. The basic idea of this method is to fit two different functions, triangular wave and sinusoidal wave, to the controller output (OP) data. The response of physical model is considered as the valve stiction, the stiction detection method is based on the single curve piecewise fitting results of the output signal of first integrating processes, and finally, according to the calculation of stiction index, it is introduced based on the proposed method to facilitate the automatic detection of stiction [3].

#### 3.1 Method Description

The single curve piecewise fitting based identification algorithm can be summarized in the following steps:

- Step 1: Simulated the closed-loop stiction model in pneumatic control valves.
- Step 2: M output data points are generated from the system to be identified [4].

- Step 3: In the case of stiction-induced oscillations, the valve position switches back and forth periodically, which results in a rectangular wave.
- Step 4: The first integrator after the valve in the control loop converts it into a triangular wave.
- Step 5: A sinusoidal external disturbance results in sinusoidal controller output (OP) and process variable (PV), as the integration of a sine wave results in a sinusoidal wave with phase shift.
- Step 6: A marginally stable control loop also results in smooth sinusoidal-shaped controller output (OP) and process variable (PV) for the same reason as for a sinusoidal external disturbance.
- Step 7: Random initial values for parameters of the nonlinearities in the appropriate range are generated. Choose the any single curve from the controller output [5].
- Step 8: Generate the single sine wave and triangular wave and fit with controller output, the objective function for each particle in the initial population is evaluated.
- Step 9: Judge end of the iteration and output the best solution, while a better fit to a sinusoidal wave indicates nonstiction. A better fit to a triangular wave indicates valve stiction.
- Step 10: According to the stiction index, value used to find the magnitude of stiction.

### 3.2 Stiction Index

The stiction index (SI) is defined as the ratio of the MSE of the sinusoidal fit to the summation of the MSEs of both sinusoidal and triangular fits: SI is bounded to the interval [0, 1]. The mathematical expression for SI can be written as

$$SI = \frac{MSE_{sin}}{MSE_{sin} + MSE_{tri}} \quad (4)$$

SI = 0 indicates nonstiction, where S(t) fits a sinusoidal wave perfectly (MSE<sub>sin</sub> = 0), SI = 1 indicates stiction, where S(t) fits a triangular wave perfectly (MSE<sub>tri</sub> = 0). For real process data, an SI close to 0 would indicate nonstiction, while an SI close to 1 would indicate stiction. SI is around 0.5, which means MSE<sub>sin</sub> = MSE<sub>tri</sub>, and it is undetermined.

Based on the experience, the following rules are recommended:

$$\begin{aligned} SI \leq 0.4 &= \text{no stiction} \\ 0.4 < SI < 0.6 &= \text{undetermined} \\ SI \geq 0.6 &= \text{stiction} \end{aligned} \quad (5)$$

## 4 Data-Driven Stiction Model

Stenman et al.[1] with reference to a private communication with Hagglund reported a one-parameter data-driven stiction model. Stenman proposed a single-parameter data-driven stiction model based on  $d$ . Since physical model has certain disadvantages, a single-parameter data-driven model is used for quantifying stiction.

The model is described as follows:

$$x(t) = \begin{cases} x(t-1) & \text{if } |u(t) - x(t-1)| \leq d \\ u(t) & \text{otherwise} \end{cases} \quad (6)$$

where  $u$  and  $x$  are the valve input and output,  $x(t-1)$  and  $x(t)$  represent past and present stem positions,  $u(t)$  is the actual controller output, and  $d$  is the valve stiction band. The model compares the difference between the current input ( $u(t)$ ) to the valve and the previous output ( $x(t-1)$ ) of the valve with the dead band. A real valve can stick anywhere whenever the input reverses direction.

## 5 Ant Colony Optimization

Ant colony algorithm was first introduced by E. Bonabeau and M. Dorigo in 1991, and the algorithm is a simulation-based evolution process of the real ant seeking food. In 1992, ant colony optimization (ACO) takes inspiration from the foraging behaviour of some ant species. A foraging ant deposits a chemical (pheromone) on the ground which increases the probability that the other ant will follow the same path. This type of communication is also known as stigmergy [6].

The basic procedure of ACO involves certain steps to estimate the unknown parameters of the system. The flowchart of the basic ant colony optimization is shown in Fig. 2.

The main principle of ACO is to minimize the objective function which is also represented as fitness function. If this objective function does not reach the minimum value, the next iteration starts by updating the pheromones. The pheromone is updated till the objective function reaches the minimum value [7].

## 6 Principle and Implement of Parameter Estimation Using ACO

The framework of ACO-based parameter estimation of the Stenman stiction model is illustrated in Fig. 3. The quantification of process nonlinearity can help decide whether to implement a nonlinear controller or not. It is important to measure the degree of nonlinearity of a process under various input excitation signals or operating

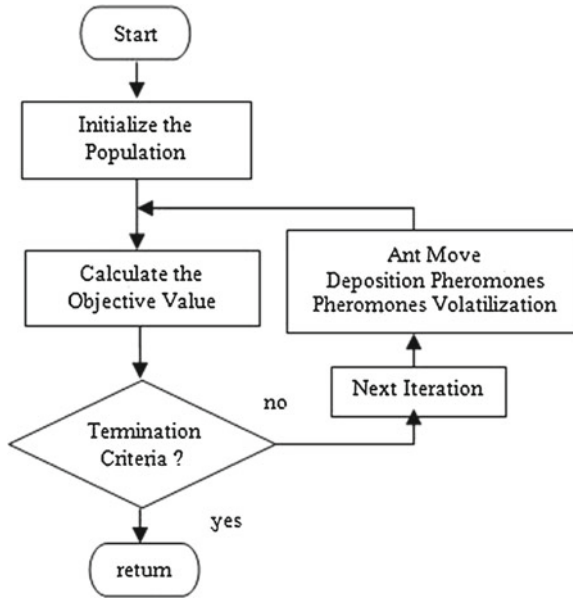


Fig. 2 Flowchart of the basic ant colony optimization

conditions [6]. The quantification is implemented by an ant colony optimization procedure. The open-loop response is obtained for Stenman stiction model.

Since, Stenman model is a single-parameter model, the valve stiction band ( $d$ ) is to be estimated by obtaining the difference between the actual stiction model output  $y(t)$  and simulated stiction model output  $y_m(t)$ ,  $u(t)$  is the system input signal that can be used in common to both the actual stiction model and simulated stiction model

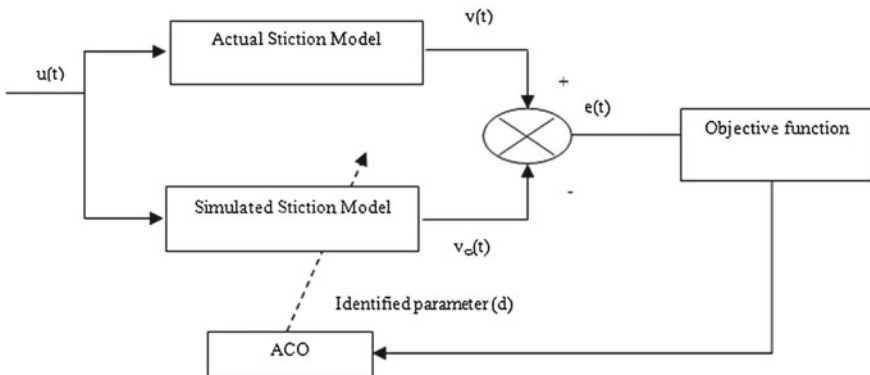


Fig. 3 ACO-based parameter estimation procedure



The following objective function (fitness function) can be defined so as to determine how well the estimates fit the system [8].

$$F = \sum_{t=1}^M (y(t) - y_m(t))^2 \quad (7)$$

The ant colony optimization automatically adjusts the parameters of the simulated stiction model. The ACO procedure is used to minimize the objective function which is the difference between the actual stiction model output  $y(t)$  and the simulated stiction model output  $y_m(t)$ .

## 6.1 Algorithm for Parameter Estimation

### 6.1.1 Initialize the Pheromone

For constructing a solution, an ant chooses at each construction step  $t = 1, \dots, m$ , a value for decision variable  $x_i$  in  $m$  dimensional problem. While termination condition not met, do [10].

---

```

Procedure ACO
begin
  Initialize the pheromone
  while (stopping criterion not satisfied) do
    Position each ant in a starting point
    while (stopping when every ant has
      build a solution) do
  for each ant do
    Chose position for next task by
    pheromone trail intensity
  end for
  end while
  update the pheromone
end while
end

```

---

### 6.1.2 Ant Solution Construction

The tour length for the  $k$ th ant,  $L_k$ , the quantity of pheromone added to each edge belonging to the completed tour is given by the following equation

$$\Delta\tau_{ij}^k(t) \begin{cases} \frac{Q}{L_k} & \text{where edge } (i, j) \in T_k(t) \\ 0 & \text{if edge } (i, j) \notin T_k(t) \end{cases} \quad (8)$$

where  $\tau_{ij}$  is the trail intensity which indicates the intensity of the pheromone on the trail segment (ij), and  $Q$  represents the pheromone quantity [10].

### 6.1.3 Pheromone Update

After performing local searching, the pheromone table is updated by using the former ants. The pheromone decay in each edge of a tour is given by

$$\tau_{ij}(t+1) = (1 - \rho) \tau_{ij}(t) + \Delta\tau_{ij}(t) \quad (9)$$

where  $\rho \in (0, 1)$  is the trail persistence or evaporation rate. The greater the value of  $\rho$  is, the less the impact of past solution is. When the ant completes its tour, the local pheromone updating is done. The value of  $\Delta\tau_j$  is defined as follows:

$$\Delta\tau_j = \frac{1}{T_{ik}} \quad (10)$$

where  $T_{ik}$  is the shortest path length that searched by  $k$ th ant at  $i$ th iteration. When the ant completes its tour, if it finds the current optimal solution, it can lay a larger intensity of the pheromone on its tour, and the global pheromone updating is applied and the value of  $\Delta\tau_j$  is given by

$$\Delta\tau_j = \frac{D}{T_{op}} \quad (11)$$

where  $T_{op}$  is the current optimal solution, and  $D$  is the encouragement coefficient.

## 7 Results and Discussion

In this section, several simulations are performed for detecting pneumatic control valve stiction in the closed loop of a physical model using MATLAB/Simulink software. The control valve stiction is detected by obtaining the closed-loop response of valve stiction. To study the effect of stiction, a first-order process with a time-delay was simulated using a pneumatic control valve modelled using Newton's second law.

$$G(s) = \frac{1.54e^{-1.07s}}{5.93s + 1} \quad (12)$$

The model parameters used in the simulation are given below. The values of  $f_s$  and  $f_c$  are as per Table 3.1.  $A = 1,000 \text{ in}^2$ ,  $k = 300 \text{ lbf.in}^{-1}$ ,  $M = 3 \text{ lb}$ ,  $F_v = 3.5 \text{ lbf.s.in}^{-1}$ ,  $v_s = 0.01$ . Figures 4a and 4b show the variations of controller output, plant output and valve output in the presence of weak stiction and strong stiction, respectively.

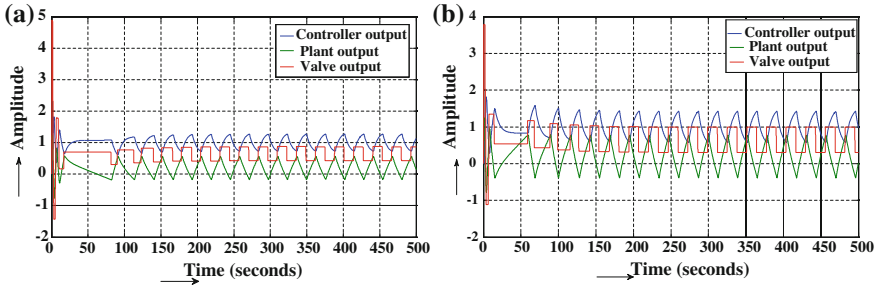


Fig. 4 **a** Closed-loop response of physical model in the case of weak stiction, **b** closed-loop response of physical model in the case of strong stiction

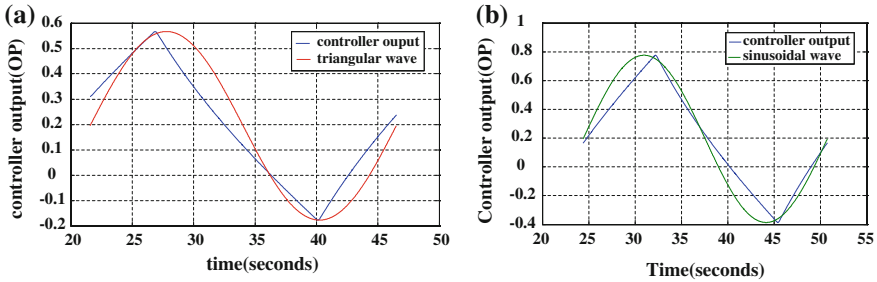


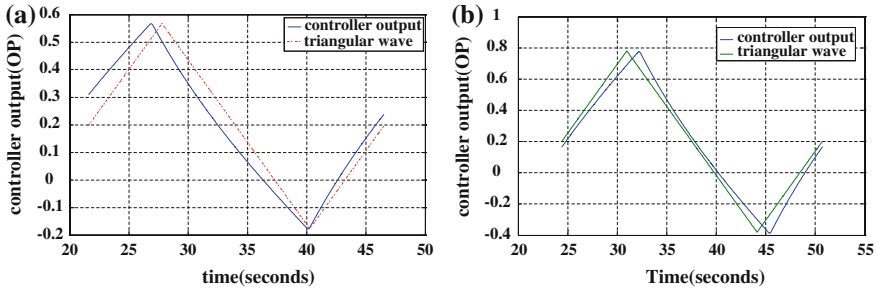
Fig. 5 **a** Response of curve fitting method for weak stiction, **b** response of curve fitting method for strong stiction

Table 2 Stiction index for different levels of stiction for curve fitting method

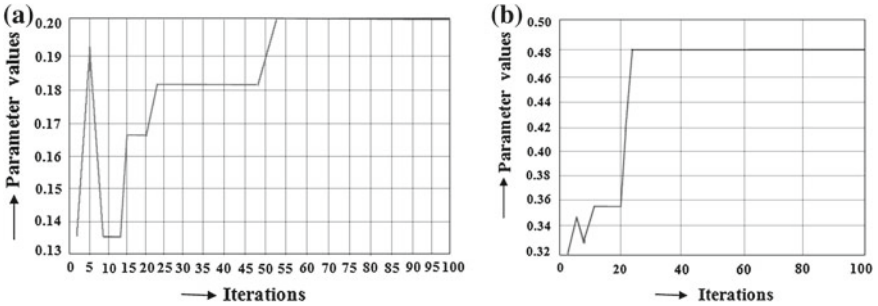
Magnitude of stiction	Stiction index
Weak stiction	0.5342
Strong stiction	0.8008

The above figure shows the process output and plant output produces triangle wave and the stiction valve produce the rectangular-shaped output. The above figs. 6a and 6b show the variations of controller output for weak stiction and strong stiction using sinusoidal fitting.

The single curve controller output is fitting with single curve triangular wave form, and the mean square error (MSE) value was calculated in weak stiction and strong stiction, the mean square error value was calculated in weak and strong stiction. The figs. 7(a) and 7(b) show the variations of controller output for weak stiction and strong stiction using triangular fitting. Stenman model is a single parameter model, the valve stiction band ( $d$ ) is to be estimated by obtaining the difference between the actual stiction model output  $y(t)$  and simulated stiction model output  $y_m(t)$ , and  $u(t)$  is the system input signal that can be used in common to both the actual stiction model and simulated stiction model. The trajectories of estimated parameters for weak stiction and strong stiction shown in figs. 7(a) and 7(b)



**Fig. 6** **a** Response of curve fitting method for weak stiction, **b** response of curve fitting method for strong stiction



**Fig. 7** **a** Trajectories of estimated parameters for weak stiction ( $d = 0.2$ ), **b** trajectories of estimated parameters for strong stiction ( $d = 0.5$ )

The population and iteration values are 20 and 100, respectively. The parameter ‘d’ is initialized from 0.01 and is increased up to 10. The evaporation rate  $\rho$  is 0.2, and the parameter Q is 100. A control valve stiction model with weak stiction ( $d = 0.2$ ), and strong stiction ( $d = 0.5$ ) cases are simulated in the control loop.

Due to the presence of stiction the quantification of stiction is essential. The quantification of stiction is done by using ant colony optimization procedure [9]. By using ACO algorithm, the stiction parameters are estimated, when the objective function reaches the minimum value and the process is repeated for 100 iterations Table 3.

**Table 3** ACO-based optimization

Magnitude of stiction	Actual stiction model parameter (d) value	Simulated stiction model parameter (d) value
Weak stiction	0.2	0.2
Strong stiction	0.5	0.48

It shows the parameter estimation is done by minimizing the objective function. The error,  $e(t)$ , is the difference between actual strong stiction model output  $y(t)$  and the simulated strong stiction model output  $y_m(t)$ . It is used as the criterion to correct the model parameters, so as to estimate the parameters of the actual process. Here, 50 seconds time is taken to find the optimal value. The estimates of the recovered stiction model are very close to the true values.

## 8 Conclusion

In this paper, the dynamics of the stiction phenomenon found in the pneumatic control valve is understood by the physical model. The stiction found in the pneumatic control valve is modelled using first principles and implemented using MATLAB/Simulink software environment. The physical model involves several parameters, but the magnitude of stiction is based on the two parameters such as maximum static friction ( $f_s$ ) and Coulomb friction ( $f_c$ ). The closed-loop response for the physical model is obtained and the various detection methods such as the single curve piecewise fitting method implemented in the controller output. Due to the presence of stiction, the quantification of stiction is essential. The quantification of stiction is done by using ant colony optimization procedure. The ant colony optimization procedure involves certain steps to estimate the parameter values. The parameter estimation is done by minimizing the objective function. The error ( $e$ ) is the difference between actual stiction model output ( $y$ ) and the dynamic stiction model output ( $y_m$ ). It is used as the criterion to correct the model parameters, so as to estimate the parameters of the actual process.

## References

1. Choudhury, M.A.A.S., Thornhill, N.F., Shah, S.L.: Modelling valve stiction. *Control Eng. Pract.* **13**, 641–658 (2004)
2. Rossi, M., Scali, C.: A comparison of techniques for automatic detection of stiction: simulation and application to industrial data. *J. proc. control* **15**, 505–514 (2005)
3. Horch, A.: A simple method for detection of stiction in control valves. *Control Eng. Pract.* **7**, 1221–1231 (1999)
4. He, Q.p., Pottmann.: Detection of valve stiction using curve fitting. Internal Report, Process Dynamics and Control. Dupont Engineering, (2003).
5. He, Q.P., Wang, J., Pottmann, M., Qin, S.J.: A curve fitting method for detecting valve stiction in oscillating control loops. *Ind. Eng. Chem. Res.* **46**, 4549–4560 (2007)
6. Dorigo, M., Maniezzo, V., Colorni, A.: Ant system: optimization by a colony of cooperating agents. *IEEE Trans. Syst. Man Cybern. B* **26**(1), 29–41 (1996)
7. Dorigo, M., Stützle, T.: *Ant Colony Optimization*. MIT Press, Cambridge (2004)
8. Toliyat, H.A., Levi, E., Raina, M.: A review of RFO induction motor parameter estimation techniques. *IEEE Trans. Ene. Conv.* **18**, 271–283 (June 2003)
9. Sivagamasundari, S., Sivakumar, D.: Estimation of valve stiction using particle swarm optimization. *J. Sens. Transducers* **129**, 149–162 (2011)
10. Kim, J.-W., Kim, S.W.: Parameter identification of induction motors using dynamic encoding algorithm for searches (DEAS). *IEEE Trans. Ene. Conv.* **20**, 16–24 (2005)

# Feed Point Optimization of Fractal Antenna Using GRNN-GA Hybrid Algorithm

Balwinder Singh Dhaliwal and Shyam S. Pattnaik

**Abstract** The design of miniaturized and efficient patch antennas has been a main topic of research in the past two decades. The fractal patch antennas have provided a good solution to this problem. But, in fractal antennas, finding the location of optimum feed point is a very difficult task. In this chapter, a novel method of using GRNN-GA hybrid model is presented to find the optimum feed location. The results of this hybrid model are compared with the simulation results of IE3D which are in good agreement.

**Keywords** Fractal antenna · Generalized regression neural networks · Genetic algorithm · Hybrid algorithm

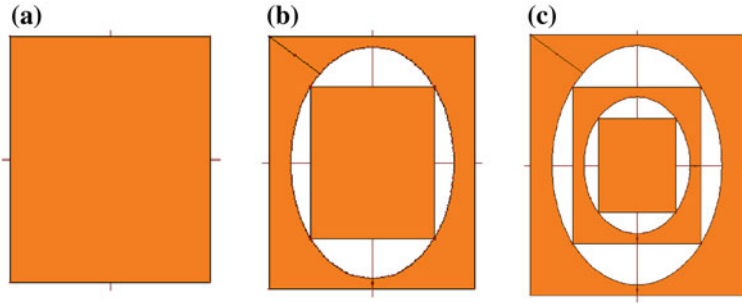
## 1 Introduction

A fractal antenna is one that has been shaped in a fractal fashion, either through bending or shaping a volume, or through introducing holes. They are based on fractal shapes such as the Sierpinski triangle, Mandelbrot tree, Koch curve, and Koch island etc. [1]. There has been a considerable amount of recent interest in the possibility of developing new types of antennas that employ fractal rather than Euclidean geometric concepts in their design. Sierpinski gasket is an example of mostly explored fractal antenna. Other geometries used for fractal antennas include Sierpinski carpet, Hilbert, Koch, and Crown square antenna [2].

---

B. S. Dhaliwal (✉)  
Guru Nanak Dev Engineering College, Ludhiana, Punjab, India  
e-mail: bs\_dhaliwal@gndec.ac.in

S. S. Pattnaik  
National Institute of Technical Teachers Training and Research, Chandigarh, India



**Fig. 1** **a** Base geometry (zeroth iteration), **b** first iteration geometry, **c** second iteration geometry

A fractal antenna based on rectangular base shape is proposed in this presented work. The base geometry or zeroth iteration is a rectangle with side lengths of 39.3 and 48.4 mm as shown in Fig. 1a. To obtain the first iteration geometry shown in Fig.1b, an ellipse is cut from the base shape of Fig. 1a. The primary axis radius of the ellipse is 16 mm, and secondary axis radius of ellipse is 22.62mm. Then, a rectangle is inserted in the area from where the ellipse is cut, such that all four corners of inserted rectangle are connected with the boundary of ellipse cut. The side lengths of the inserted rectangle are 24.18 and 29.64 mm. The dimensions of the ellipse and rectangle are selected so that the inserted rectangle is 60 % of size of the base rectangle. To obtain the second iteration geometry shown in Fig.1c, the same procedure is applied on the first iteration geometry i.e., an ellipse is cut, and then a rectangle is inserted. The primary axis radius of the ellipse cut is 10 mm, and secondary axis radius is 12.92 mm. The side lengths of the inserted rectangle are 14.5 and 17.78 mm. The dimensions of the ellipse and rectangle are selected so that the inserted rectangle is 60 % of size of the first iteration rectangle. The height of substrate used is 3.175 mm with dielectric constant and loss tangent of 2.2 and 0.0009, respectively.

In antenna design, feeding techniques are very important as they ensure that antenna structure operates at full power of transmission. Especially at high frequencies, designing of feeding techniques becomes a more difficult process. One of the most common techniques used for feeding antennas is coaxial probe feed technique. The location of feed (i.e., feed point) is very important in antenna performance. The feed point must be located at that point on the patch, where the input impedance is 50ohms for the resonant frequency. But, it is not an easy task to achieve specially for small-size antennas. This problem is further complex in case of fractal antennas because of the complex geometry of different iterations.

In this chapter, a novel method of finding feed point using hybrid GRNN-GA model is proposed. The following section describes GRNN, GA, and proposed hybrid algorithm. The results are given in Sect. 3, and present work is concluded in Sect. 4.

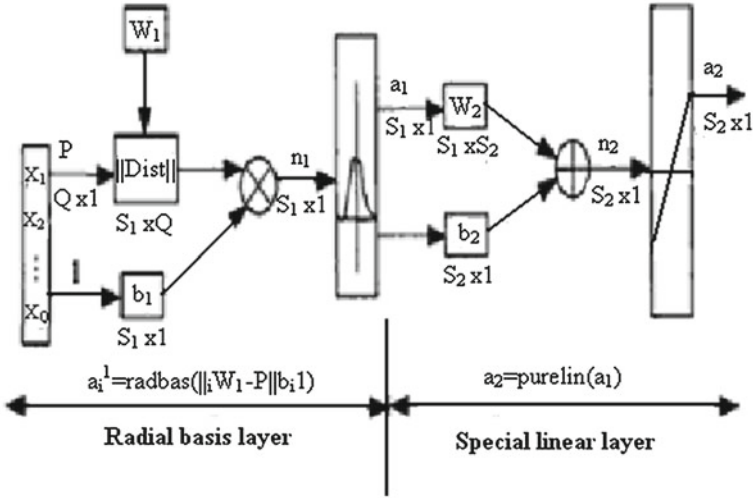


Fig. 2 Generalized regression neural network model

## 2 Hybrid GRNN-GA Model for Feed Point Calculation

### 2.1 Generalized Regression Neural Networks

Back-propagation neural networks (BPNN) is a widely used model of the neural network paradigm and has been applied successfully in applications in a broad range of areas. However, BPNN, in general, has slow convergence speed, and there is no guarantee at all that the absolute minima can be achieved. This disadvantage can be overcome by using generalized regression neural networks (GRNN).

The GRNN were first proposed by Sprecht in 1991, which are feed-forward neural network model based on nonlinear regression theory. The network structure is shown in Fig. 2. GRNN consists of a radial basis function network layer and a linear network layer. The transfer function of hidden layer is radial basis function. The basis function of hidden layer nodes in network adopts Gaussian function, which is a non-negative and nonlinear function of local distribution and radial symmetry attenuation for central point, and generates the responses to input signal locally. GRNN employs the smoothing factor as a parameter in learning phase. The single smoothing factor is selected to optimize the transfer function for all nodes. To reduce computational time, GRNN performs one-pass training through the network [3].



## 2.2 Genetic Algorithms

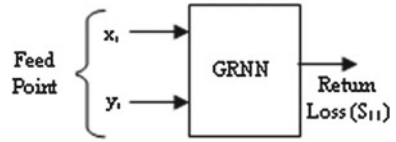
Genetic algorithm belongs to a class of probabilistic methods called “Evolutionary Algorithms” based on the principles of selection and mutation. GA was introduced by J. Holland, and it is based on natural evolution theory of Darwin. It is a population-based algorithm, and they find their application in various engineering problems. Usually, a simple GA consists of the following operations: selection, crossover, mutation, and replacement. First, an initial population composed of a group of chromosomes is generated randomly. These chromosomes represent the problem’s variables. The fitness values of the all chromosomes are evaluated by calculating the objective function in a decoded form. A particular group of chromosomes is selected from the population to generate the offspring by the defined genetic operations such as crossover and mutation. The fitness of the offspring is evaluated in a similar fashion to their parents. The chromosomes in the current population are then replaced by their offspring, based on a certain replacement strategy. Such a GA cycle is repeated until a desired termination criterion is reached (for example, a predefined number of generations are produced). If all goes well throughout this process of simulated evolution, the best chromosomes in the final population can become a highly evolved solution to the problem. To overcome the possibility of being trapped in local minima, in GA, the mutation operation in the chromosomes is employed. GA has been applied in a large number of optimization problems in several domains, telecommunication, routing, and scheduling, and it proves its efficiency to obtain a good solution. It has also been extensively used for a variety of problems in antenna design during the last decade [4–6].

## 2.3 Proposed Hybrid Algorithm

The genetic algorithm (GA) technique uses the objective function for the optimization and without which the optimization technique has no meaning. But in case of fractal antennas, closed-form mathematical formulation for finding the optimum feed location is not available. Thus, a novel method of objective function formulation has been presented, in which generalized regression neural networks are used as the fitness function. This technique can be used everywhere, particularly in those cases where the objective function formulation is difficult, or the objective function is improper. The procedure adopted to find the optimum feed location of the proposed fractal antenna is given below.

- **Data Set Generation:** Data set for the training of GRNN has been prepared by using IE3D software. The antenna is simulated for different feed locations  $(x_i, y_i)$ , and the return loss for the corresponding feed location points has been taken as output. The center of antenna is considered at  $(0, 0)$  all cases.

**Fig. 3** Training model of GRNN



- Training the ANN: The above data set has been used to train the GRNN in MATLAB. Sufficient number of training samples has been used to train the network. Fig. 3 shows the model for the training of GRNN network.
- The genetic algorithm optimization technique has been implemented using MATLAB, and the trained GRNN network has been used as objective function for the GA algorithm. The GA minimizes the objective function, and it gives the feed location where return loss is minimum, as output.
- The optimum feed points given by GA have been simulated using IE3D software, and return loss ( $S_{11}$ ) is found. The simulation values are compared with the hybrid model results in order to check the accuracy of the results.

### 3 Results and Discussion

Three different models have been trained, one for each geometry. For the training of GRNN, the spread constant is required to be set, and it is taken as 0.1 for all the 3 models. These trained GRNN models have been then used as objective functions for the genetic algorithm. The parameters of GA are as follows: The population size is 50 and the crossover probability is 0.8. GA is run for 500 iterations for each model. The optimum feed locations provided by this hybrid GRNN-GA model along with the minimized return loss are given in Table 1.

The feed locations obtained from hybrid algorithm are simulated using IE3D software. The return loss ( $S_{11}$ ) for all geometries is found. The simulated values of return loss are almost same as given by hybrid algorithm for base geometry and second iteration geometry, and it is better than hybrid model value for first iteration geometry. The comparison of hybrid model results and simulation results is given in Table 2 which shows a reasonable match.

**Table 1** Results of hybrid GRNN-GA model

Geometry	Minimized return loss ( $S_{11}$ ) in dB	Optimized feed location	
		$x_i$	$y_i$
Base geometry	-34.370	8.152	13.326
First iteration	-36.142	8.348	9.005
Second iteration	-40.349	-9.432	12.466

**Table 2** Comparison of hybrid model and simulation results

Geometry	$S_{11}$ (dB) Hybrid model value	$S_{11}$ (dB) Simulation value	Resonant frequency $f_r$ (GHz)
Base geometry	-34.370	-33.816	2.34
First iteration	-36.142	-43.535	1.85
Second iteration	-40.349	-40.351	1.82

## 4 Conclusion

The optimum feed points of the three geometries are different. As the iterations of fractal antenna increases, the optimum feed location changes, thus affecting the performance of the antenna. A novel approach based on GRNN-GA hybrid algorithm has been implemented successfully to locate the optimum feed point for each generation of fractal geometry. The results obtained using GRNN-GA hybrid algorithm are in good agreement with the simulation results obtained using IE3D software. This approach can be used for any other geometry.

## References

1. Puente, C., Romeu, J., Pous, R., Cardama, A.: On the behavior of the sierpinski multiband fractal antenna. *IEEE Trans. Antenna Propagation* **46**(4), 517–524 (1998)
2. Dehkhoda, P., Tavakoli, A.: A crown square microstrip fractal antenna. *IEEE Antennas and Propagation Society International Symposium* **3**, 2396–2399 (2004)
3. Jeatrakul, P., Wong, K.W.: Comparing the performance of different neural networks for binary classification problems. *International Symposium on Natural Language Processing*. 111–115 (2009)
4. Cengiz, Y., Tokat, H.: Linear antenna array design with use of genetic, memetic and tabu search optimization algorithms. *Prog Electromagnetics Res C*. **1**, 63–72 (2008)
5. Pattnaik, S.S., Khuntia, B., Panda, D.C., Neog, D.K., Devi, S.: Calculation of optimized parameters of rectangular microstrip patch antenna using genetic algorithm. *Microwave Optical Technol Lett* **23**(4), 431–433 (2003)
6. Johnson, J.M., Rahmat, S.Y.: Genetic algorithms and method of moments (GA/MOM) for the design of integrated antennas. *IEEE Trans. Antennas Propagation* **47**(10), 1606–1614 (1999)

# Diversity Maintenance Perspective: An Analysis of Exploratory Power and Function Optimization in the Context of Adaptive Genetic Algorithms

Sunanda Gupta and M. L. Garg

**Abstract** In order to increase the probability of finding optimal solution, GAs must maintain a balance between the exploration and exploitation. Maintaining population diversity not only prevents premature convergence but also provides a better coverage of the search space. Diversity measures are traditionally used to analyze evolutionary algorithms rather than guiding them. This chapter discusses the applicability of updation phase of binary trie coding scheme [BTCS] in introducing as well as maintaining population diversity. Here, the robustness of BTCS is compared with informed hybrid adaptive genetic algorithm (IHAGA), which works by adaptively changing the probabilities of crossover and mutation based on the fitness results of the respective offsprings in the next generation.

**Keywords** Genetic algorithm · Multidimensional knapsack problem · Diversity maintenance

## 1 Introduction

Genetic algorithms (GAs) have been successfully applied to various optimization problems where one intends to find an optimum or approximate solution to a problem that has a huge size of solution space. However, one of the major concerns in using evolutionary algorithms to search a complex state space is the problem of premature convergence, especially for combinatorial optimization problems like multidimensional knapsack problem (MKP), where the landscape is multipeaked; the probability of search sticking to local optima is all the more high. Because genetic

---

S. Gupta (✉) · M. L. Garg  
School of Computer Science and Engineering, S.M.V.D.U, Katra, India  
e-mail: sunanda.gupta@smvdu.ac.in; gupta.sunanda@gmail.com

M. L. Garg  
e-mail: garg.ml@smvdu.ac.in

programming is highly stochastic, we do not expect to obtain clear rules about exact levels of diversity. We aim to draw general conclusions and “rules of thumb” from the investigation of evolving populations with different measures of diversity. Given a specific landscape structure—defined by the search space, objective function, then relying on problem-specific knowledge for navigating this structure in order to extract helpful information from the search space, would make the optimization faster and more effective. This paper investigates the characteristic issues of BTCS [1] (which incorporates this strategy) and compares it with IHAGA [2] for solving test instances of combinatorial optimization problem on MKP. The simulation results show that the proposed strategy significantly improves the computational efficiency of GAs. The rest of the chapter is organized as follows. In the section that follows, a brief review of the BTCS scheme and the research work going on in the field of using adaptive crossover and mutation operators for achieving diversity is provided. Section 3 describes the BTCS bucket updation phase vis-a-vis population diversity. Experimental results are presented in Sect. 4. Section 5 summarizes the main contributions of the chapter.

## **2 Related Work**

### ***2.1 Binary Trie Coding Scheme***

Binary trie coding scheme [BTCS] creates and maintains a diverse population of highly fit individuals capable of adapting quickly to fitness landscape change [1]. BTCS provides three major contributions related to duplicate elimination and premature convergence in a steady-state GA. The first contribution of BTCS is the virtually compressed binary trie structure (VCBT). VCBT when integrated with GA proves to be beneficial in determining duplicates among all the generations and replacing them with unique individuals [1, 3]. The second contribution is to demonstrate that preventing duplicates results in improved performance. It effectively avoids what is usually a difficult trade-off between achieving fast search and sustaining diversity and thereby provides means to avoid premature convergence. The third contribution of BTCS is that it relies on problem-specific knowledge in fragmenting the search space into feasible and infeasible regions and then pruning the infeasible regions. This chapter discusses as to how bucket updation phase of BTCS incorporates the effective measures pertaining to population diversity without using adaptive crossover and mutation operators.

### ***2.2 Adaptive Crossover and Mutation Rate***

The significance of crossover operator in controlling GA performance has long been acknowledged in GA research which can be dated back to 1980s [4]. A number

of guidelines exist in the literature for setting the values of crossover probability [5]. Some studies particularly focused on finding optimal crossover rates [6]. These heralded the need for self-adaption of the crossover or mutation rates. In [7], an adaptive genetic algorithm was proposed, in which crossover and mutation probabilities were varied according to the fitness values of the solutions. There were also works on devising adaptive crossover operators instead of varying the crossover rates [8]. Several operators were employed, and the probabilities of applying each operator were adapted according to the performance of the offsprings generated by the operator. Since then, several similar works have also been done [9].

The choice of mutation rate is also critical to GA's performance [10]. Various researchers have come up with novel approaches to implement the adaptive mutation into a GA. Some approaches to adaptive mutation control employ parent fitness in determining mutation probability [11]. If selected, highly fit individuals undergo low levels of mutation (minimal disruption), while low-fitness individuals are subjected to large rates of disruptive mutation. A measure of population diversity is employed by [12] and [13] in adapting mutation probabilities. In a similar vein, Zhang et al. [14] adapt crossover and mutation according to parameters extracted from a K-means clustering algorithm. Thus, many researchers have emphasized on using adaptive mutation so as to improve GA's performance as it facilitates the finding of global optimum more efficiently [15].

Although the adaptive crossover and mutation rates are hot spots in the study of genetic search, the BTCS scheme proposed by us [1] does not explicitly employ any scheme to adaptively mutate or crossover. For analyzing the robustness of BTCS, we compare it with informed hybrid adaptive genetic algorithm (IHAGA). This scheme works by adjusting its cross-adaptive rate and mutation rate according to the situation surrounding the fitness of the individual [2]. In the course of crossover and mutation, the probabilities of crossover and mutation are adjusted adaptively according to the following formulas:

$$P_c = \begin{cases} \frac{P_{c_{\max}} - P_{c_{\min}}}{1 + \exp\left(Ax\left(\frac{2(f' - f_{\text{avg}})}{f_{\max} - f_{\text{avg}}} - 1\right)\right)} + P_{c_{\min}} & f' \geq f_{\text{avg}} \\ P_{c_{\min}} & f' \leq f_{\text{avg}} \end{cases}$$

$$P_m = \begin{cases} \frac{P_{m_{\max}} - P_{m_{\min}}}{1 + \exp\left(Ax\left(\frac{2(f' - f_{\text{avg}})}{f_{\max} - f_{\text{avg}}} - 1\right)\right)} + P_{m_{\min}} & f' \geq f_{\text{avg}} \\ P_{m_{\min}} & f' \leq f_{\text{avg}} \end{cases}$$

where  $P_{c_{\max}}$  and  $P_{c_{\min}}$  denote the lower limit and the upper limit of probability of crossover, respectively.  $f_{\max}$  and  $f_{\text{avg}}$  denote the maximal fitness and the average fitness of population, respectively,  $f'$  denotes the higher fitness of two crossover individuals,  $f$  denotes the fitness of the individuals, and  $A = 9.903438$  [2].

### 3 BTCS Bucket Updation Phase

#### 3.1 Buckets and Their Significance

The buckets correspond to the leaf nodes in a VCBT [1, 3]. The aim of buckets is to maintain a continuous presence on as many peaks as possible. Population's spatial information is obtained with computationally inexpensive buckets. It provides important information in addition to the address of the trie structure existing under it. This information is used to identify potentially local convergence. Buckets are significant in dividing the population into an exploration section and exploitation section. It monitors and measures diversity at synchronized time intervals and accordingly attempts to control or promote diversity during the evolution. Identifying such measures allows better prediction for run performance and improved understanding of the population and enables the design of efficient operators.

#### 3.2 Bucket Updation

The contribution of updation phase in the BTCS scheme is twofold [1, 3]. The first contribution of updation phase is to manage the size of VCBT structure. The size of VCBT structure can be kept small by pruning fully explored regions of the search space. The second contribution is to monitor convergence and introduce diversity so as to avoid local entrapment.

##### 3.2.1 Guided Crossover Operator

The proposed procedure works by randomly selecting buckets with criterion value 1, and then exchanges information by copying their best strings [1, 3]. The copying of best feasible boundary solution of one to another is done only if ( $new\_bucket\_sum + old\_bucket\_best\_sum$ ) are feasible and  $new\_bucket\_sum$  is greater than  $old\_bucket\_sum$ . Doing this restricts the copying of strings between any two selected buckets randomly.  $Bucket\_sum$  and  $bucket\_best\_sum$  are two variables that are unique to each bucket. They are used for storing the sum of included objects from root to  $bucket\_position$  and sum of  $bucket + 1$  position till  $n$  (the number of objects), respectively. GA with the proposed method distributes the individuals more widely compared to simple GA, where the individuals represent the local optima for that region. The aim is to identify feasible regions in the landscape that could replace less fit individuals by more promising samples from the unexplored sections of the search space. This prevents entrapment in local optima by including new individuals from the unexplored regions of the search space.

**Table 1** Average execution time of BTCS in comparison with IHAGA

<i>n</i>	<i>m</i>	$\alpha$	Simple GA		BTCS_IMO		IHAGA	
			A.B.S.T	A.E.T	A.B.S.T	A.E.T	A.B.S.T	A.E.T
100	5	0.25	9.6	345.9	10.85	109.47	8.14	<b>31.13</b>
		0.5	23.5	347.3	26.32	120.23	19.92	<b>76.41</b>
		0.75	26.9	361.7	33.36	123.02	23.19	<b>90.43</b>
	10	0.25	97.5	384.1	104.20	<b>115.12</b>	83.33	192.05
		0.5	97.3	418.9	111.90	143.6	84.61	<b>129.86</b>
		0.75	16.8	462.6	19.15	159.56	14.36	<b>129.53</b>
	30	0.25	177.4	604.5	198.69	202.68	150.00	<b>199.49</b>
		0.5	118	782.1	130.98	247.74	113.90	<b>218.99</b>
		0.75	90	904.2	80.10	315.34	80.10	<b>253.18</b>
250	5	0.25	50.7	682	34.19	<b>216.03</b>	34.48	265.98
		0.5	276.7	709.4	191.59	<b>257.54</b>	185.39	333.42
		0.75	195.9	763.3	127.12	<b>241.78</b>	137.13	534.31
	10	0.25	359	870.9	258.16	<b>290.65</b>	290.43	566.09
		0.5	342.2	931.5	249.91	<b>295.06</b>	281.63	596.16
		0.75	129.1	1011.2	95.91	<b>320.3</b>	104.44	455.04
	30	0.25	582.9	1499.5	332.51	<b>493.45</b>	472.73	794.74
		0.5	901.5	1980	601.20	<b>643.14</b>	720.30	1207.80
		0.75	1059.3	2441.4	754.22	<b>815.23</b>	840.02	1440.43
500	5	0.5	291.3	1345.9	142.10	<b>416.09</b>	236.83	969.05
		0.75	386.2	1412.6	188.40	<b>499.32</b>	317.84	974.69
	10	0.5	562.2	1728.8	274.20	<b>615.35</b>	490.24	1383.04
		0.75	937.6	1931.7	457.40	<b>715.34</b>	792.27	1564.68
	30	0.5	1121.6	3198.9	547.10	<b>1334.56</b>	923.08	2600.71
		0.75	1903.3	3888.2	928.40	<b>1231.49</b>	1545.48	3110.56

### 3.2.2 Adaptive Selection Parameter Control

This takes place when there is some form of feedback from the search that serves as input to the mechanism used to determine the change in the strategy parameters. During this phase, the *avg* corresponding to the worst and best individuals within that bucket is checked. It is computed as the average of all the individuals within that bucket. The *new avg* value will drop if more boundary solutions between the worst and average interval are generated and would increase if more boundary solutions between average and best interval are generated. During this phase, that bucket is selected, whose *new avg* has increased and at least approximately more than 60% of the region within that bucket has already been explored. The aim of phase 2 in bucket updation is to prevent the unnecessary delay caused in exploring those regions of search space where the probability of best solution to exist is very limited. The phase 2 describes the buckets' solution space diversity from a fitness perspective, i.e., a measure of diversity of healthy individuals. *BDS Bucket Updation* employs ASPC



**Table 2** Percentage gaps for BTCS and IHAGA

$n$	$m$	$\alpha$	GA	BTCS_IMO	IHAGA
100	5	0.5	0.4564	0.4613	0.46200
		0.75	0.3212	0.2884	0.32119
	10	0.5	0.7982	0.7774	0.79838
		0.75	0.4813	0.4697	0.48100
	30	0.5	1.3457	1.3145	1.36953
		0.75	0.8321	0.8296	0.81546
250	5	0.5	0.1253	0.1183	0.12525
		0.75	0.0811	0.0752	0.08759
	10	0.5	0.2543	0.2362	0.25429
		0.75	0.1572	0.1513	0.15710
	30	0.5	0.5321	0.5267	0.54877
		0.75	0.3112	0.2972	0.32431
500	5	0.5	0.0441	0.0443	0.04631
		0.75	0.0378	0.0429	0.04271
	10	0.5	0.1134	0.0946	0.11907
		0.75	0.0712	0.0501	0.07903
	30	0.5	0.2635	0.2387	0.26908
		0.75	0.1747	0.1738	0.17905

to regulate selection pressure. ASPC's objective is to create a diversity of health in the population, i.e., the diversity of high-fitness individuals.

## 4 Experimental Results

Tables 1 and 2 illustrate the comparison of results of BTCS with those of IHAGA [2] for solving the MKP. The results of BTCS and IHAGA are based on our own computations. Table 1 provides the average best solution time (ABST) and the average execution time (AET) for both BTCS and IHAGA. The bold highlights in Table 1 show the optimal average execution time among the two for varying  $n$  and  $m$  values, where  $n$  is the number of objects and  $m$  is the number of constraints. It is clear from Table 1 that IHAGA outperforms BTCS computationally, for smaller values of  $n$ . The cost of constructing VCBT results in an increase in the average execution time. However, for larger instances, despite the time utilized in the construction of VCBT structure, BTCS is effective in reaching the optimal solution in comparison with IHAGA. The ability to work with unique boundary individuals facilitates faster convergence. The probability of recurrence of individuals in the subsequent generations results in deviation from path, leading to optimality, for larger set of individuals in the case of IHAGA despite its ability to guide the search. Table 2 further provides the average percentage gaps for the two approaches. For both, the BTCS and IHAGA, the percentage gaps ( $100 \times (\text{optimum LP} - \text{optimum GA})/\text{optimum LP}$ ) relative to

the solution of LP relaxation were computed. Here GA refers to special cases of GA, i.e., BTCS and IHAGA. It can be inferred from the results of Table 2 that BTCS outperforms IHAGA for all test instances under consideration. BTCS has provided better coverage of the search space and has been found to be successful in providing solutions of better quality in comparison with IHAGA.

## 5 Conclusion

The aim of updation phase in the BTCS scheme has been the exploring of promising regions while concentrating the search on hyperplanes that are likely to contain good solutions. The GCO and ASPC focus on extracting information about the selected buckets before deciding on the introduction of diversity. Its advantage is that at the point of near convergence, late in a GA run, such diversion reduces the probability of GA to entrap in local convergence and thus provides better solutions.

In our approach, we have not used a mutation parameter, which should be adapted explicitly. Instead, it is the principle of working with unique chromosomes (or individuals) in the VCBT structure, which guarantees automatic mutation. Furthermore, our approach still concentrates on using one-point crossover operator with a fixed probability of 0.70. This is attributed to the deeper nature of BTCS scheme, which permits only good optimal solutions from the search space to participate in the process of evolution. Working with unique boundary solutions assists in maintaining an optimum level of diversity among the individuals.

## References

1. Sunanda, Garg M.L.: Binary trie coding scheme—An intelligent genetic algorithm avoiding premature convergence. *Int. J. Comput. Math.* Taylor & Francis. (2012). doi:[10.1080/00207160.2012.742514](https://doi.org/10.1080/00207160.2012.742514).
2. Yanqin, M., Jianchen W.: Improved hybrid adaptive genetic algorithm for solving knapsack problem. In: *Proceedings of the 2nd International Conference and Information Processing*, pp. 644–647 IEEE, (2011)
3. Sunanda, Garg, M.L.: GA implementation of the multi dimensional knapsack problem using compressed binary tries. *Advances in computational research* (ISSN: 0975–3273), 43–46 (2009)
4. Goldberg, D.: *Genetic Algorithms in Search, Optimization and Machine Learning*. Addison Wesley Publishing Company Inc, Massachusetts (1989)
5. Schaffer, J.D., Carvana, R.A., Eshelman, L.J.: R. A study of control parameters affecting online performance of genetic algorithms for function optimization. In: *Proceedings of the Third International Conference on Genetic Algorithms*, Das (1989)
6. Ochoa, G., Harvey, I., Buxton, H.: On recombination and optimal mutation rates. In: *Proceedings of Genetic and Evolutionary Computation Conference*, pp. 488–495 (1999)
7. Srinivas, M., Parnaik, L.: Adaptive probabilities of crossover and mutation in genetic algorithms. *IEEE Trans. Syst. Man. Cybern.* **3**, 1841–1844 (2003)

8. Vekaria, K., Clark, C.: Biases introduced by adaptive recombination operators. In: Proceedings of Genetic and Evolutionary Computation Conference, 670–677 (1999)
9. Ono, I., Kita, H., Kobayashi, S.: A robust real coded genetic algorithm using unimodal normal distribution crossover augmented by uniform crossover: Effects of self-adaptation of crossover probabilities. In: Proceedings of Genetic and Evolutionary Computation Conference, pp. 496–503 (1999)
10. Cervantes, J., Stephens, C.R.: Limitations of existing mutation rate heuristics and how a rank GA overcomes them. *IEEE Trans. evol. comput.* **13**(2), 369–397 (2009)
11. Liu, D., Feng, S.: A novel adaptive genetic algorithms. *Proc. Int. Conf. Mach. Learn. Cybern.* **1**, 414–416 (2004)
12. Zhu, K.: A diversity controlling adaptive genetic algorithm for the vehicle routing Problem with time windows. In: Proceedings. 15th IEEE International Conference on Tools with Artificial Intelligence, pp. 176–183 (2003)
13. Hagnas, H., Pounds-Cornish, A., Cooley, M., Callaghan, V., Clarke, G.: Evolving spiking neural network controllers for autonomous robots. In: Proceedings IEEE International Conference on Robotics and Automation, vol. 5, pp. 4620–4626 (2004)
14. Zhang, J., Chung, H., Lo, W., et al.: Clustering based adaptive crossover and mutation probabilities for genetic algorithms. *IEEE Trans. Evol. Comput.* **11**(3), 326–335 (Jun. 2007)
15. Lobo, F. G., Lima, C. F., Michalewicz, Z (eds.): Parameter setting in evolutionary algorithms. volume 54 of *Studies in Computational Intelligence* Springer, (2007)

# Use of Ant Colony System in Solving Vehicle Routing Problem with Time Window Constraints

Sandhya Bansal, Rajeev Goel and C. Mohan

**Abstract** Vehicle routing problem with time window constraints (VRPTW) is an extension of the original vehicle routing problem (VRP). It is a well-known NP-hard problem which has several real-life applications. Meta-heuristics have been often tried to solve VRTPW problem. In this paper, an attempt has been made to develop a suitable version of Ant colony optimization heuristic to efficiently solve VRPTW problem. Experimentation with the developed version of Ant colony optimization has shown that it succeeds in general in obtaining results obtained with earlier version and often even better than the results that are better than the corresponding results available in literature which have been obtained using even previously developed hybridized versions of ACO. In many cases, the obtained results are comparable with the best results available in literature.

**Keywords** Vehicle routing problem · Ant colony optimization · Heuristics · Optimization

## 1 Introduction

Vehicle routing problem (VRP) [21, 22] lies at the heart of logistics and distribution management that is presently being used by the companies engaged in delivery and collection of goods. Since the conditions and constraints vary from one situation to another, several variants [3, 11, 18] of basic problem have been proposed in

---

S. Bansal (✉)  
Maharishi Markandeswar University, Mullana, India  
e-mail: Sandhya12bansal@gmail.com

R. Goel · C. Mohan  
Ambala College of Engineering and Applied Research, Ambala, India  
e-mail: rajiv\_2709@rediffmail.com

literature. This paper addresses itself to developing an efficient Ant-colony-system-based heuristic for solving VRPTW.

VRPTW [23, 26] problem consists of finding the minimum set of routes for identical capacity vehicles originating and terminating at a central depot such that each customer is served once and only once, given that the exact number of customers and their demands are known. There are also constraints of time windows in that each customer must be served in a specified slot of time. Objective of VRPTW is to find the minimum of total distance travelled and/or the minimum number of vehicles required which can accomplish this job. It is a NP-hard problem where the number of feasible solutions grows exponentially as the number of customer's increases. The work on this problem available in literature can be divided into two classes: exact optimization techniques and heuristic-based (approximate) algorithms. In the first category, the works by [21, 24, 27] can be cited. The methods developed in these papers have been able to efficiently solve some of the Solomon benchmark problems [5, 20, 31]. In the second category, a very large number of heuristic approaches such as tabu search, genetic algorithms, ant colony algorithms, simulated annealing, large neighborhood search, variable neighborhood based algorithms, and multi-phase approaches have been tried [6, 7, 20, 26, 29].

Among heuristic-based optimization techniques, ACO is a more recent optimization heuristic proposed by Dorigo et al. [4, 12–16]. ACO imitates real ant behavior to search for optimal solutions. ACO-based optimization techniques tried thus far for solving VRPTW problem generally use distance and pheromone as search guide parameters. This paper proposes a version of ACO which incorporates besides these two parameters waiting time, urgency to serve and the bias factor also as search guide parameters. Our objective has been to see whether inclusion of these additional parameters can further improve the performance of ACO algorithm for solving VRPTW.

The rest of the paper is organized as follows. Section 2 presents mathematical model of VRPTW problem. Conventional use of ACO heuristic in solving VRPTW problem is presented in Sect. 3. Proposed modifications in this algorithm are presented in Sect. 3.2. Computational experimentation using the modified ant colony system (ACS) algorithm is presented in Sect. 4. Comparison of the obtained results with those earlier available in literature obtained through is done Sect. 5 and certain conclusions drawn.

## 2 Mathematical Description of VRPTW

In this section, we briefly describe the mathematical model of VRPTW.

The VRP is a complicated combinatorial optimization problem. It has received considerable attention in the past decades because of its practical importance in the fields of transportation, distribution, and logistics. VRPTW is a generalization of the classical VRP with the additional restriction of time window constraints. The

VRPTW can be modeled in mathematical terms through a complete weighted digraph as follows.

Let  $G = (V, A)$  where  $V = \{v_0, v_1, v_2 \dots v_n\}$  be a set of nodes, where  $v_0$  represents the depot that holds a fleet of vehicles and  $v_1, v_2 \dots v_n$  denote a set of  $n$  customers which are to be served by these vehicles. Each customer has an associated demand  $q_i$ , service time  $s_i$ , a service time window  $[e_i, l_i]$ . Also  $A = [\{v_i, v_j\} (i, j = 0, 1, 2, \dots, n, i \neq j)]$  is the set of arcs connecting various nodes, having distance  $d_{ij}$  as weights. If a vehicle reaches a customer  $v_i$  before specified time  $e_i$ , it needs to wait until  $e_i$  in order to service the customer. The service has to be provided before close time of window at  $l_i$ . The depot has also time window  $[e_0, l_0]$ . No vehicle is to leave the depot before  $e_0$  and all should come back before  $l_0$ . The load-carrying capacity of all vehicles is same and all travel with identical constant speed. The objective of the VRPTW is to service all the customers without violating vehicle capacity constraints and time window constraints using minimum number of vehicles that travel minimum possible total distance.

Mathematically, the problem is usually expressed as:

Minimize

$$F = \sum_{i=0}^N \sum_{j=0}^N \sum_{K=1}^V c_{ij} x_{ij}^v \quad (1)$$

Subject to:

$$\sum_{v=1}^V \sum_{j=1}^N x_{ij}^v \leq V \quad \text{for } i = 0 \quad (2)$$

$$\sum_{v=1}^V x_{ij}^v = \sum_{j=1}^N x_{ji}^v \leq 1 \quad \text{for } i = 0 \text{ and } v \in \{1, \dots, V\} \quad (3)$$

$$\sum_{v=1}^V \sum_{j=0}^N x_{ij}^v = 1 \quad \text{for } i \in \{1, \dots, N\} \quad (4)$$

$$\sum_{v=1}^V \sum_{i=0}^N x_{ij}^v = 1 \quad \text{for } j \in \{1, \dots, N\} \quad (5)$$

$$\sum_{i=0}^N c_i \sum_{j=0}^N x_{ij}^v \leq q_v \quad \text{for } v \in \{1, \dots, V\} \quad (6)$$

$$\sum_{v=1}^V \sum_{i=0}^N x_{ij}^k (t_i + t_{ij} + s_i + w_i) = t_j \quad \text{for } j \in \{1, \dots, N\} \quad (7)$$

$$e_i \leq (t_i + w_i \leq l_i) \quad \text{for } i \in \{1, \dots, N\} \quad (8)$$

$$t_0 = w_0 = s_0 = 0 \quad (9)$$

$x_{ij} = 1$  if vehicle  $k$  travels from customer  $i$  to customer  $j$ , and 0 otherwise ( $i \neq j$ ;  $i, j = 0, 1, \dots, N$ ).

Here,

$V$  denotes total number of vehicles,

$N$  total number of customers,

$c_i$  customer  $i$  ( $i = 1, 2, \dots, N$ ) and  $c_0$  delivery depot,

$d_{ij}$  traveling distance between customer  $i$  and customer  $j$ ,

$t_{ij}$  travel time between customer  $i$  and customer  $j$ ,

$q_i$  demand of customer  $i$ ,

$q_v$  loading capacity of each vehicle, (loading capacity of all vehicles are identical).

$e_i$  earliest permitted arrival time of vehicle at customer  $i$ ;

$l_i$  latest permitted arrival time of vehicle at customer  $i$ ;

$s_i$  service time of customer  $i$ ;

This is an optimization problem in which, (1) is the objective function of the problem which is to be minimized subject to constraints (2)–(9).

In this optimization model, decision variables are as follows:

$V$  total number of vehicles required;

$t_i$  arrival time of vehicle  $V$  at customer  $i$ ;

$w_i$  waiting time of vehicle at customer  $i$  before service can be started;

Objective function (1) ensures that total distance travelled by all the vehicles is minimized. The first constraint (2) specifies that there are at the most  $V$  vehicles going out of the depot. The set of constraint (3) ensures that every vehicle starts from and ends at the delivery depot. The next two sets of constraints (4) and (5) restrict the assignment of each customer to exactly one vehicle route. The next set of constraints (6) ensures that the loading capacity of no vehicle is exceeded. The constraints of

set (7) are the maximum travel time constraint. Remaining constraints (8) guarantee schedule feasibility with respect to time windows.

In formulating the above mathematical model, the following assumptions have been made:

- Identical vehicles with known capacities  $Q$  are used.
- All vehicles travel with identical constant velocity.
- Every vehicle leaves the depot and returns to the depot within specified time window  $[l_0, s_0]$ .
- Demand of each customer is  $q_i$  is known.
- Each customer is serviced by one and only one vehicle.
- The total demand of any customer is not more than the capacity of the vehicle.

### 3 Use of ACS in Solving VRPTW

VRPTW being an NP-hard problem, its exact solution is not known in general. Therefore, large numbers of alternative algorithms have been proposed for solving it. In this section, we first present conventional ACS-based approach for solving VRPTW problem and then present our proposed modification in it. The basic philosophy of ACS approach is to use a suitable positive feedback mechanism to reinforce those arcs of the graph that belong to a good solution. This mechanism is implemented associating pheromone levels with each arc which are then updated in proportion to the goodness of solutions found.

While presenting ACS-based algorithm, for solving VRPTW, we shall use the term ‘tour’ to denote a set of routes followed by all ants (vehicles) which are able to serve all the nodes of the graph as per their requirements under specified conditions. Our problem is to determine an optimal tour. The ACS algorithm commonly used for solving VRPTW is given below.

#### 3.1 ACS Algorithm for Solving VRPTW:

Step 1. Construction of an initial feasible route:

- (a) Each ANT starts from the depot and the set of customers included in its route is empty.
- (b) The ant selects the next customer to visit from the list of feasible customers based upon the probabilistic formula (10).
- (c) After serving the customer storage capacity and the time used thus far of the Ant is updated and the process continued. Ant returns to the depot when either of the capacity constraint or time window constraint of the depot is satisfied.



- (d) We next check whether all the customers have been served or not. If all the customers have been served, stop else send a new ant (vehicle) to visit the remaining destinations.
- (e) Continue till all customers served.
- (f) Calculate total distance travelled and the number of vehicles used and compute the objective function value for the complete route using (1) (which gives total distance travelled by all used vehicles).

Step 2. Construct a specified number of feasible tours as in step 1.

Step 3. From among these constructed feasible tours, choose the tour which uses minimum number of ants (vehicles). In case of a tie, choose the tour in which total travelled distance is minimum (or vice-versa depending upon whether greater priority is to be given to minimize the number of vehicles used or total distance travelled).

### 3.1.1 Selection of Next Customer

In setting up of a feasible tour, each ant constructs a path that visits certain customer before returning back to depot. In the previous studies using ACO/ACS for solving VRPTW, the ant (vehicle), currently located at node  $i$ , selects the next node  $j$  to move to using the transition rule,

$$j = \begin{cases} \arg \max_{j \in \phi_i} \left\{ \tau_{ij}^\alpha \eta_{ij}^\beta \right\} & \text{if } q \leq q_o \\ J & \text{otherwise} \end{cases} \quad (10)$$

where

$$\eta_{ij} = 1/d_{ij} \text{ is a heuristic-based parameter.} \quad (11)$$

and  $J \in \phi_i$  is randomly chosen according to the probability

$$p_{ij}^k = \frac{\tau_{ij}^\alpha \eta_{ij}^\beta}{\sum_{u \in \phi_i} \tau_{iu}^\alpha \eta_{iu}^\beta} \quad (12)$$

Here, set  $\phi_i$  contains the cities not visited so far.

In (10),  $q \sim U(0, 1)$ , and  $q_o \in [0, 1]$  is a user-specified value of parameter  $q$ .

In (11),  $d_{ij}$  is Euclidian distance between  $i$  and  $j$  and  $\tau_{ij}$  is the amount of pheromone on the path between current location  $i$  and next possible location  $j$ . Also  $\alpha, \beta$  are the positive constants that determine the importance of  $\eta$  verses  $\tau$ .

The transition rule (10) creates a bias toward customers connected by short distances and having large amount of pheromone. The parameter  $q_o$  balances exploration and exploitation. if  $q \leq q_o$ , the algorithm exploits (favoring the best nearest customer). Otherwise if  $q > q_o$ , the algorithm explores selecting node  $j \in \phi_i$  randomly.

### 3.1.2 Pheromone Update for New Tour

After construction of a complete feasible route, the pheromones are laid for the next path depending upon the total traveled distance ( $L$ ) of that route. For each arc  $v_i \rightarrow v_j$  that was used in the previous feasible route, the pheromone trail is increased by  $\Delta\tau_{ij}$ . Furthermore, part of existing pheromone is also allowed to evaporate [4, 11, 14, 17, 34]. Thus in the next route, pheromones are updated according to the following

$$\tau_{ij} = \tau_{ij} (1 - \rho) + \Delta\tau_{ij} \quad (13)$$

$$\text{where } \Delta\tau_{ij} = Q/L \quad (14)$$

Here,  $\rho$  is parameter that controls rate of evaporation of pheromone.

### 3.2 Proposed Modifications in ACS Algorithm

Following modifications have been introduced in the conventional algorithms for solving VRPTW problem using ACS heuristics.

1. Whereas earlier approaches using ant colony technique for solving VRPTW problem have primarily given importance to distance and pheromone only to guide the heuristic [3, 32, 34], we in our present study have used besides these two parameters such as urgency to serve, waiting time and bias parameter also for this purpose. In (11), heuristic-based parameter  $\eta_{ij}$  only gives importance to the distance in determining the heuristic parameter. However, it was observed on experimentation that in addition to the distance waiting time, urgency to serve, and biasing should also be given importance in deciding the choice of next customer [11, 32].

As a result in our present study choice of  $\eta_{ij}$  defined in (11) has been modified as:

$$\eta_{ij} = \frac{1}{(d_{ij} + w_j)^\lambda} * \frac{1}{(l_j - a_j)^\gamma} * \frac{1}{(I_{\max} - I_j)} \delta \quad (15)$$

In (13),  $a_j$  is arrival time of vehicle at customer  $j$  and  $w_j$  defined as

$$w_j = \begin{cases} e_j - a_j & \text{if } e_j > a_j \\ 0 & \text{otherwise} \end{cases} \quad (16)$$

is the waiting time at customer  $j$  before service can be started. Also  $l_j - a_j$ ,  $a_j < l_j$ , is the difference between the latest arrival time  $l_j$  and actual arrival time  $a_j$  at customer  $j$ . It is a measure of urgency of customer  $j$  to be served, emphasizing that those customers whose time window is going to expire soon be given priority. Also  $I_{\max} - I_j$ , (where  $I_j$  is the number of consecutive times the customer  $j$  who could be next visited from the present customer has not been visited and  $I_{\max}$  is a user-specified maximum permissible value of  $I_j$  ( $I_j < I_{\max}$ ) is a measure of bias factor).

2. In order to prevent the slow convergence of the algorithm when specified number of initial tours have been generated, we update the pheromone for the next tour using the best solution among the solution provided by  $m$  feasible routes [17]. In order to prevent local optimization and increase the probability of obtaining higher quality of solution upper and lower values of pheromone have been specified as  $1/\sum 2d_{0i}$  and  $1/\min(d_{ij})$  respectively, where  $d_{0i}$  is distance from the depot to the customer.
3. In conventional studies, total travelled distance has been minimized irrespective of vehicles needed. However keeping in view the fact that cost of obtaining a vehicle and its maintenance is generally much more than fuel cost we have tried to minimize total number of vehicles required as a first priority and total travelled distance as a second priority.

## 4 Implementation of the Modified ACS Algorithm

In this section, we summarize our computational experience of using the modified ACS algorithm for solving some of the Solomon benchmark [5] problems.

Solomon generated a set of 56 problems which have been frequently used in literature to check the performance of the developed algorithm. This set is divided into three categories namely C, R, and RC. In C category problems, customers are clustered either geographically or according to the time windows. R types of problems have uniform distribution of customers. Category RC is hybrid of problems of R and C set. In our present study, we have chosen 15 problems of 25 customers, 10 problems of 50 customers, and 10 problems of 100 customers from all these three sets. To solve these problems, the proposed algorithm was coded in MATLAB 7.0 at Intel Core 2 Duo 2.0 GHz. After experimentation, it was observed that the following values of parameters proved most suited for solving these problems. The number of initial feasible tours = 10,  $\alpha = 1$ ,  $\beta = 1$ ,  $\lambda = 5.5$ ,  $\gamma = 3.5$ ,  $\delta = 1$ ,  $Q = 250$  and  $q_0 = 0.9$ . All problems were run for maximum of 2,500 iterations, Tables 1, 2 and 3 present a summary of our results and their comparison with the best-known routing solutions compiled from different heuristics available in literature as per our information.

It may be noticed that whereas in our study, we have used only ACS, most of the earlier studies with ACO/ACS usually are hybrid in the sense that after completion of search with ACO/ACS, search is further carried out with some other optimization

**Table 1** Comparison of best-known results with the results generated by proposed algorithms for Solomon's 25 customers set problem

Problem	Best	Worst	Using conventional ACO's	Best known [Ref.]
C201	215.54/2	215.54/2	222.53/2	214.7/2 [10]
R101	618.33/8	619.17/8	625.23/8	617.1/8 [20]
R102	563.35/7	573.15/7	605.45/7	547.1/7 [20]
R105	556.72/5	556.72/5	600.13/5	530.5/6 [20]
R109	442.63/5	448.54/5	510.31/5	441.3/5 [20]
RC101	462.15/4	462.15/4	507.87/4	461.4/4 [20]
RC105	416.16/4	416.88/4	435.97/4	411.3/4 [20]
RC106	346.51/3	346.51/3	402.11/3	345.5/3 [20]
RC201	432.30/2	432.30/2	412.34/3	360.2/3 [10]
RC202	376.61/2	381.75/2	400.72/2	338.0/3 [18]
RC203	433.94/1	433.94/1	454.78/2	326.9/3 [19]
RC204	331.29/1	333.36/1	370.56/1	299.7/3 [8]
RC205	386.15/2	386.15/2	413.37/3	338.0/3 [23]
RC207	358.92/2	367.92/2	387.16/2	298.3/3 [19]
RC208	309.85/1	309.85/1	313.76/1	269.1/2 [8]

**Table 2** Comparison of best-known results with the results generated by proposed algorithms for Solomon's 50 customers set problem

Problem	Best	Worst	Using conventional ACO's	Best known [Ref.]
C101	363.25/5	363.25/5	363.25/5	362.5/5 [20]
C201	444.96/2	444.96/2	402.43/3	360.2/3 [20]
C205	444.57/2	444.57/2	407.58/2	360.2/3 [20]
R101	1053.04/12	1054.84/12	1107.18/12	1044/12 [20]
R201	882.32/2	893.56/3	900.72/3	791.9/6 [20]
R202	869.42/2	870.06/2	898.68/3	791.9/6 [20]
R203	741.3/2	764.3/2	612.32/5	605.3/5 [20]
R206	711.6/2	711.6/2	645.56/4	632.4/4 [20]
R209	722.24/2	735.20/2	619.23/4	600.6/4 [20]
RC101	951.07/8	962.80/8	987.97/8	944/8 [20]

heuristic also (such as local search, genetic algorithm [7, 21, 27]). In order to compare our present results with performance of earlier versions of ACO only (without use of any hybrid), we repeated our experimentation with those versions without using any other add on optimization heuristic. The results of this study are also presented in the Table 1 (column 4) for comparison.

The proposed algorithm has produced some improved results with lesser number of vehicles used (however, with some increase in routing length compared to the best available in literature. This is due to the priority that we assigned to minimize the total number of vehicles used visa vis total distance travelled).

**Table 3** Comparison of best-known results with the results generated by proposed algorithms for Solomon's 100 customers set problem

Problem	Best	Worst	Using conventional ACO's	Best known [Ref.]
C101	828.94/10	828.94/10	830.37/10 (828.94/10)* [9]	828.94/10 [30]
C102	874.20/10	875.36/10	917.53/10 (828.94/10)* [34]	828.94/10 [30]
C105	828.94/10	828.94/10	830.37/10 (828.94/10)* [9]	828.94/10 [30]
C106	856.18/10	857.91/10	875.71/10 (828.94/10)* [9]	828.94/10 [30]
C107	830.60/10	838.42/10	842.67/10 (828.94/10)* [34]	828.94/10 [30]
C201	591.56/3	591.56/3	594.23/3 (591.56/3)* [34]	591.56/3 [20]
C205	591.5/3	595.33/3	598.28/3 (588.88/3)* [25]	588.88/3 [20]
R101	1714.26/19	1725.65/19	1845.12/19 (1670.66/19)* [25]	1645.79/19 [30]
R102	1558.19/17	1575.69/17	1613.34/18 (1535.52/17)* [25]	1486.12/17 [30]
R105	1519.55/14	1544.86/14	1853.45/18 (1365.23/15)* [25]	1377.11/14 [30]

Note \* indicates results available in literature using hybrid versions of ACO's

## 5 Conclusions

In this paper, a modified version of ACS is proposed.

In our proposed algorithm, we have modified the heuristic-based parameter and pheromone update rules, used in conventional ACO for solving VRPTW. An extensive computational study on a set of benchmark test problems has been conducted. The experimental results show that the proposed algorithm even when used by itself is competitive with the earlier versions of ACO even when these are hybridized with certain other heuristics. We have obtained certain results in which lesser number of vehicles are needed than those reported in literature. However, in most of such cases, total distance travelled is slightly greater. Lesser number of vehicles means less initial investment in purchase of vehicles and less maintenance cost. (However, there is slight increase in fuel cost if total distance travelled is more).

The results are encouraging and we propose to direct further study toward use of proposed algorithm for solving the dynamic VRPTW

## References

1. Andres, F.M.: An iterative route construction and improvement algorithm for the vehicle routing problem with soft time windows. *Transp. Res. Part B* **43**, 438–447 (2010)
2. Azi, N., Gendreau, M., Potvin, J.Y.: An exact algorithm for a vehicle routing problem with time windows and multiple use of vehicles. *Eur. J. Oper. Res.* **202**(3), 756–763 (2010)
3. Balseiro, S.R., Loiseau, I., Ramone, J.: An ant colony algorithm hybridized with insertion heuristics for the time dependent vehicle routing problem with time windows. *Comput. Oper. Res.* **38**, 954–966 (2011)
4. Bell, J.E., McMullen, P.R.: Ant colony optimization techniques for the vehicle routing problem. *Adv. Eng. Inform.* **18**, 41–48 (2004)
5. Best solutions to Solomon problems identified by heuristics. (SINTEF VRP page): <http://www.sintef.no/static/am/opti/projects/top/vrp/bknown.html>

6. Bianchessi, N., Righini, G.: Heuristic algorithms for the vehicle routing problem with simultaneous pick-up and delivery. *Comput. Oper. Res.* **34**, 578–594 (2007)
7. Bräysy, O.: Local search and variable neighborhood search algorithms for the vehicle routing problem with time windows. University of Vaasa, Finland, Doctoral Dissertation (2001)
8. Chabrier, A.: Vehicle routing problem with elementary shortest path based column generation. *Comput. Oper. Res.* **33**(10), 2972–2990 (2006)
9. Chen, C.-H., et al.: A hybrid ant colony system for vehicle routing problem with time windows. *J. East. Asia Soc. Transp. Stud.* **6**, 2822–2836 (2005)
10. Cook, W., Rich, J.L.: A parallel cutting plane algorithm for the vehicle routing problem with time windows. Working Paper of Computational and Applied Mathematics, Rice University, Houston, TX (1999)
11. Donati, A.V., et al.: Time dependent vehicle routing problem. *Eur. J. Oper. Res.* (2006). doi:[10.1016/j.ejor.06.047](https://doi.org/10.1016/j.ejor.06.047)
12. Dorigo, M., Birattari, M., Stützle, T.: Ant colony optimization: Artificial ants as a computational intelligence technique. *IEEE Comput. Intell. Mag.* **1**, 28–39 (2006)
13. Dorigo, M., Blum, C.: Ant colony optimization theory: A survey. *Theor. Comput. Sci.* **334**, 243–278 (2005)
14. Dorigo, M., Gambardella, L.M.: Ant colony system: A cooperative learning approach to the traveling salesman problem. *IEEE Trans. Evol. Comput.* **1**, 53–66 (1997)
15. Dorigo, M., Maniezzo, V., Colomi, A.: Ant system: Optimization by a colony of cooperating agents. *IEEE Trans. Syst. Man Cybern. Part B. Cybern.* **26**, 29–41 (1996)
16. Gambardella, L.M., Taillard, E., Agazzi, G.: MACS-VRPTW: A Multiple Ant Colony System for Vehicle Routing Problems with Time Windows *New Ideas in Optimization*. McGraw-Hill, London (1999)
17. Garcia-Najera, A., Bullinaria, J.A.: An improved multi-objective evolutionary algorithm for the vehicle routing problem with time windows. *Comput. Oper. Res.* **38**(1), 287–300 (2011)
18. Irnich, S., Villeneuve, D.: The shortest path problem with k-cycle elimination ( $k > 3$ ): Improving a branch-and-price algorithm for the VRPTW *INFORMS. J. Comput.* **18**(3), 391–406 (2003)
19. Kallehauge, B., Larsen, J., Madsen, O.B.G.: Lagrangean duality and non-differentiable optimization applied on routing with time windows. *Comput. Oper. Res.* **33**(5), 1464–1487 (2006)
20. Kohl, N., Desrosiers, J., Madsen, O.B.G., Solomon, M.M., Soumis, F.: 2-path cuts for the vehicle routing problem with time windows. *Transp. Sci.* **33**(1), 101–116 (1999)
21. Laporate, G.: The vehicle routing problem: An overview of exact and approximate algorithms. *Eur. J. Oper. Res.* **59**, 345–358 (1997)
22. Laporte, G.: Fifty years of vehicle routing. *Transp. Sci.* **43**, 408–416 (2011)
23. Larsen J.: Parallelization of the vehicle routing problem with time windows. Ph.D. thesis IMM-PHD-1999-62, Department of Mathematical Modelling, Technical University of Denmark, Lyngby, Denmark (1999)
24. Lau, H.C., et al.: Vehicle routing problem with time windows and a limited number of vehicles. *Eur. J. Oper. Res.* **148**, 559–569 (2003)
25. Ma, X.: Vehicle routing problem with time windows based on improved ant colony algorithm. In *Proceedings of IEEE Computer Society Second International Conference on Information Technology and Computer Science*, Washington, DC, USA, pp. 94–97 (2010)
26. Masrom, S., Nasir, A.M., Abidin, S.Z., Rahman, A.S.A.: Software framework for vehicle routing problem with hybrid metaheuristic algorithms. In *Proceedings of the Applied Computing Conference*, Angers, pp. 55–61 (2011)
27. Mester, D.: An evolutionary strategies algorithm for large scale vehicle routing problem with capacitate and time windows restrictions. In *Proceedings of the Conference on Mathematical and Population Genetics*, University of Haifa, Israel (2002)
28. Qi, C., Sun, Y.: An improved ant colony algorithm for VRPTW. In *IEEE International Conference on Computer Science and Software Engineering* (2008)
29. Rizzoli, A.E., Montemanni, R., Lucibello, E., Gambardella, L.M.: Ant colony optimization for real-world vehicle routing problems. *Swarm Intell* **1**(2), 135–151 (2007)

30. Rochat, Y., Taillard, E.: Probabilistic diversification and intensification in local search for vehicle routing. *J. Heuristics* **1**, 147–167 (1995)
31. Solomon, M.M.: Algorithms for vehicle routing and scheduling problems with time window constraints. *Oper. Res.* **35**, 254–265 (1987)
32. Yu, B., Yang, Z.Z., Yao, B.: An improved ant colony optimization for vehicle routing problem. *Eur. J. Oper. Res.* **196**, 171–176 (2009)
33. Yuichi, N., Olli, B.: A powerful route minimization heuristic for the vehicle routing problem with time windows. *Oper. Res. Lett.* **37**, 333–338 (2009)
34. Zhang, X., Tang, L.: A new hybrid ant colony optimization algorithm for the vehicle routing problem. *Pattern Recogn. Lett.* **30**, 848–855 (2009)

# Energy Saving Model for Sensor Network Using Ant Colony Optimization Algorithm

Doreswamy and S. Narasegouda

**Abstract** In this paper, we propose an energy saving model for sensor network by finding the optimal path for data transmission using ant colony optimization (ACO) algorithm. The proposed model involves (1) developing a relational model based on the correlation among sensors both in spatial and in temporal dimensions using DBSCAN clustering, (2) identifying a set of sensors which represents the network state, and (3) finding the best path for transmission of data using ACO algorithm. Experimental results show that the proposed model reduces the energy consumption by reducing the amount of data acquiring and query processing using the representative sensors and ensures that the transmission is done on the best path which minimizes the probability of retransmission of data.

**Keywords** Ant colony optimization · DBSCAN · Data mining · Sensor network

## 1 Introduction

Revolution in technology has made sensors an integral part of our life. Sensors are used in various applications to make human life safer, comfortable, and profitable. In many areas such as agriculture, smart parking, structural health, traffic control, fire detection, air and/or water pollution monitoring, environmental monitoring, surveillance, sensor nodes are deployed to collect and process the data to aid users in decision making. These tiny sensor nodes are equipped with limited battery supply. And the performance, life span of the network, depends on the energy of the

---

S. Narasegouda (✉)

Department of P.G. Studies and Research in Computer Science,  
Mangalore University, Mangalagangothri, Mangalore, India  
e-mail: srinivasnpatil@gmail.com

Doreswamy

e-mail: doreswamyh@yahoo.com



sensor nodes. Due to the limited battery power, sensor networks' life span rapidly decreases resulting in the failure of the applications. Researchers have observed that data processing and data transmission are the main causes for the decline in sensor node energy. Hence, various methodologies have been proposed in order to reduce query processing and data transmission.

In a densely deployed sensor network, correlated data are frequently generated by different sensors. In the past, data mining technique such as clustering has been exploited [1–3] to analyze the correlation among sensors both in spatial and in temporal dimensions to reduce the amount of data acquiring and query processing. Other methodologies such as data aggregation, clustering, efficient routing protocols have also been applied to reduce the energy consumption in sensor networks.

The rest of the paper is organized as follows. An overview of the literature survey is given in Sect. 2. Section 3 presents the proposed model. Experimental results are discussed in Sect. 4, and conclusion is given in Sect. 5.

## 2 Literature Review

Energy-efficient routing strategy using nonlinear min–max programming problem with convex product was proposed in [4]. The selection of sensor representatives to reduce query processing and save energy was first proposed by [5], where selection was made by exchanging the messages between the neighboring nodes. In [1], clustering techniques were exploited to select a set of representative sensor nodes for query processing, resulting in the reduction in the data collection and energy consumption. Energy-efficient data gathering algorithm Energy-efficient Routing Algorithm to Prolong Lifetime (ERAPL) was proposed by [6]. SeReNe framework was proposed by [2] to develop energy saving model for wireless sensor networks. SeReNe framework exploited the clustering technique to select the set of sensor representatives. Using traveling salesman problem concept, an efficient transmission path is estimated. In [3], a technique was developed for the selection of cluster heads to reduce energy consumption called Cluster-based Routing for Top k Querying (CRTQ). Chong et al. [7] proposed a rule-based framework called Context Awareness in Sensing Environments (CASE) to save energy in sensor networks. In [8], an energy-efficient routing protocol for acquiring correlated data in sensor network by considering the issues such as energy of the sensor node, multi-hop data aggregation was developed. To reduce the number of message exchange between source and destination, data aggregation technique was designed by [9].

Another approach to save energy in sensor network is to select the best transmission path which minimizes the retransmission rate. But selecting the optimal path from a finite set sensor node is a combinatorial optimization problem. Hence, in this paper, we have proposed to develop energy saving model for sensor network by finding an optimal path for transmission by applying ant colony optimization (ACO) algorithm on a subset of sensor nodes, which best represents the network state. The ant colony

optimization was proposed in [10, 11] and is used in the past for finding an optimal solution in many combinatorial problems such as traveling salesman problem, assignment problems, scheduling problems. [12].

### 3 Proposed Model

The proposed model works on the phenomena of finding the optimized data transmission path using ACO algorithm on the relational model of sensor network to reduce query processing, data retransmission, and energy consumption.

In relational model, clustering techniques are exploited to find correlation among the sensor observations in both spatial and temporal dimensions. Among clustering techniques, partitioning clustering algorithms such as k-means are only capable of finding circle-shaped clusters, whereas density-based clustering algorithms such as DBSCAN is capable of identifying non-spherical-shaped clusters and DBSCAN is very less sensitive in the presence of outliers. Hence, DBSCAN is used in our model. By applying the DBSCAN algorithm [13], different clusters are formed. In each cluster, representative sensors are selected based on the measurement tendency strategy as explained in [1, 2]. These set of representative sensors symbolize the entire sensor network. Hence, query processing is reduced by querying only the set of representative sensors instead of querying all sensor nodes in the network.

In any sensor network, sensor nodes consume more energy to transmit a packet than to collect the data. Due to lack of connectivity strength, packet may not reach the destination. In such cases, retransmission of lost packet results in excessive energy consumption. In order to minimize the loss of packets, we propose to find the optimized transmission path among the representative sensors by applying ACO algorithm. To estimate the best transmission path, we have considered the probability of packets reaching from source to destination as a parameter. In [14], ACO algorithm is explained in detail. The pseudo-code for ACO algorithm is given below.

```

Set parameters: alpha, beta, rho, Q, ant_num, Max_time.
Initialize: Sensor_Distance_Graph,
Ant_to_random_trail,
Determine initial best path and its length
Initialize pheromone trails
While Max_time
  Update Ants
  Update pheromones
  Construct Ant Solutions
  If current solution is better than previous
    Initialize: Best solution=current solution
End While

```

The proposed model is summarized as follows:

1. Calculate spatiotemporal measures using DBSCAN.
2. Select representative sensors.
3. Calculate optimized transmission path using ACO algorithm.

## 4 Experimental Results

The proposed model is implemented using Visual Studio 2010 with C#. Experiment has been conducted on publicly available [15] dataset. It contains 2.3 million observations and three tables, namely *location table* containing information about  $x$  and  $y$  coordinates of sensors, *aggregate connectivity table* containing information about probability of a packet reaching from source to destination, and *data table* containing information about features such as date, time, epoch, sensor id, temperature, humidity, light, voltage. By applying the data mining preprocessing techniques such as data cleaning, data smoothing using binning, dataset has been reduced to 6.5 lakhs.

In our experiment, before applying clustering technique, entire dataset has been divided into three parts. Each part contains readings taken for 12 days. DBSCAN is applied on each part separately. And DBSCAN parameters are set as, epsilon value  $\text{eps} = 1.75$  and minimum point to form cluster  $\text{minPts} = 25$ . In our experiment, we found that cluster 1 contains measurements from all sensors and most of the other clusters formed were containing faulty data; hence, they were discarded. After clusters are formed, representative sensors and set of sensors it representing are obtained using measuring tendency. Twenty-three representative sensors have been identified, which can be used to represent the network state. In Fig 1, purple rectangle

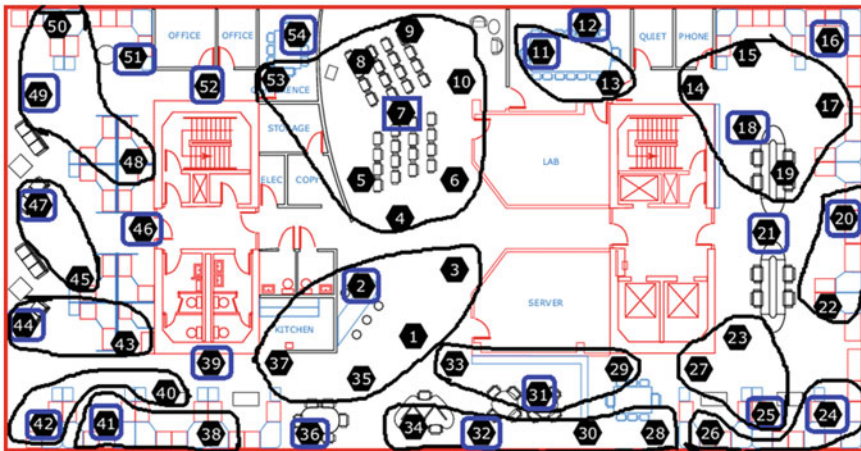


Fig. 1 Intel Berkeley research lab

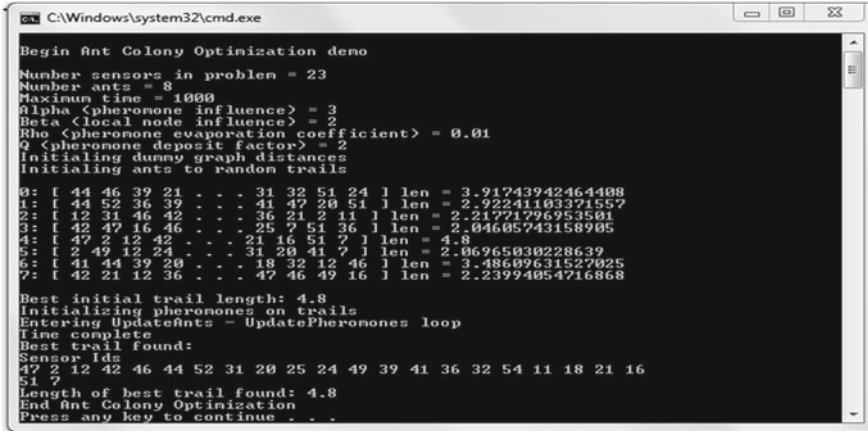


Fig. 2 Result of ACO

Table 1 Default values of ACO

Parameter	Default value
Influence of pheromone on direction ( <i>alpha</i> )	3
Influence of adjacent node distance ( <i>beta</i> )	2
Pheromone decrease factor ( <i>rho</i> )	0.01
Pheromone increase factor ( <i>Q</i> )	2.0
Number of ants ( <i>Ant_num</i> )	8
Maximum time ( <i>Max_time</i> )	1000

represents the representative sensors, and a boundary is drawn to show the set of correlated sensors they represent and representative sensors without any boundary indicates that they represent only themselves.

The optimal transmission path among the representative sensors is calculated using ACO algorithm where the best solution is defined as the transmission path whose connectivity strength is higher than other transmission paths. The default parameter set for ACO algorithm is given in Table 1. The optimal transmission path found by the ACO algorithm is {47, 2, 12, 42, 46, 44, 52, 31, 20, 25, 24, 49, 39, 41, 36, 32, 54, 11, 18, 21, 16, 51, 7}, and the strength of the best trail found is 4.8 (result is shown in Fig. 2).

From experimental results, we observed that (1) out of 54 only 23 sensor nodes need to be queried to model the network state, i.e., energy required to collect the data can be reduced since query processing is reduced by 57.40 %. (2) Optimized path for data transmission is obtained.

## 5 Conclusion

In any sensor network, the main reason for energy consumption is data acquiring, query processing, and data transmission. Furthermore, an excessive energy is consumed when data are retransmitted due to failure in reaching the destination. Data acquiring and query processing can be reduced by analyzing the correlation among the sensors, and data retransmission can be reduced by selecting the best transmission path which increases the possibility of packet being delivered to destination successfully.

A relational model is developed using DBSCAN to analyze the correlation among sensors both in spatial and in temporal dimensions. Using relational model, a set of representative sensors are selected, which best represents the network's state. Instead of using all sensor nodes, only representative sensors are used for querying the sensor network, resulting in the reduction in amount of data acquiring and query processing. In order to reduce the retransmission of data, we applied ACO algorithm to find the best transmission path which increases the probability of data being delivered from source to sink successfully.

Experimental results show that the proposed model reduces the energy consumption by reducing the amount of data collection and query processing using the representative sensors and ensures that the transmission is done on the best path which minimizes the need for retransmission of data. In future, we wish to address the other issues such as estimation of missing data, prediction of data, developing a visualization model for sensor networks.

## References

1. Baralis, E., Cerquitelli, T., D'Elia, V.: Modeling a sensor network by means of clustering. In: Proceedings of the 18th International Workshop on Database and Expert Systems Applications, pp. 177–181 (2007)
2. Apiletti, D., Baralis, E., Cerquitelli, T.: Energy saving models for wireless sensor networks. *Knowl. Inf. Syst.* **28**, 615–644 (2010)
3. Mo, S., Chen, H., Li, Y.: Clustering based routing for top k query in wireless sensor networks. *EURASIP J. Wireless Commun. Netw.* 1–13 (2011)
4. Shiou, C.W., Lin, Y.S., Cheng, H.C., Wen, Y.F.: Optimal energy efficient routing for wireless sensor networks. In: Proceedings of 19th International Conference on Advanced Information Networking and Applications, pp. 325–330 (2005)
5. Kotidis, Y.: Snapshot queries towards data centric sensor networks. In: IEEE Proceedings of 21st International Conference on Data, Engineering. pp. 131–142 (2005)
6. Zhu, Y., Wu, W., Pan, J., Tang, Y., et al.: An energy efficient data gathering algorithm to prolong lifetime of wireless sensor. *Networks* **33**, 639–647 (2010)
7. Chong, S.K., Gaber, M.M., Krishnaswamy, S., Loke, S.W., et al.: Energy conservation in wireless sensor networks a rule based approach. *Knowl. Inf. Syst.* **28**(3), 579–614 (2011)
8. Zeydan, E., Tureli, D.K., Comaniciu, C., Tureli, U.: Energy efficient routing for correlated data in wireless sensor networks. *Ad Hoc Netw.* **10**, 962–975 (2011)
9. Hung, C.C., Peng, W.C.: Optimizing in-network aggregate queries in wireless sensor networks for energy saving. *Data Knowl. Eng.* **70**, 617–641 (2011)

10. Dorigo, M., Maniezzo, V., Coloni, A.: Positive feedback as a search strategy. Technical Report, Dipartimento di Elettronica, Politecnico di Milano, Italy, pp. 91–016 (1991)
11. Dorigo, M., Maniezzo, V., Coloni, A.: Ant system optimization by a colony of cooperating agents. *IEEE Trans. Syst. Man Cybern. B Cybern.* **26**, 29–41 (1996)
12. Dorigo, M., Blum, C.: Ant colony optimization theory a survey. *Theor. Comput. Sci.* **344**, 243–278 (2005)
13. Han, J., Kamber, M.: *Data Mining concepts and techniques*. Morgan Kaufmann Publishers, San Francisco (2006)
14. Dorigo, M., Birattari, M., Stutzle, T.: Ant colony optimization. *IEEE Comput. Intell. Mag.* 28–39 (2006)
15. Intel Berkeley Research Lab.: <http://db.csail.mit.edu/labdata/labdata.html>

# Multi-Objective Optimization of PID Controller for Coupled-Tank Liquid-Level Control System Using Genetic Algorithm

Sanjay Kr. Singh, Nitish Katal and S. G. Modani

**Abstract** The main aim of this chapter is to obtain optimal gains for a PID controller using multi-objective genetic algorithm used in a coupled-tank liquid-level control system. Liquid level control system is a nonlinear system and finds a wide application in petrochemical, food processing, and water treatment industries, and the quality of control directly affects the quality of products and safety. This chapter employs the use of multi-objective genetic algorithm for the optimization of the PID gains for better plant operations in contrast to conventional tuning methods and GA. The simulations indicate that better performance is obtained in case of multi-objective genetic algorithm-optimized PID controller.

**Keywords** PID controller · Multi-objective genetic algorithm · PID optimization · Liquid level control

## 1 Introduction

Coupled-tank liquid-level control is the center to many diverse industrial applications ranging from petrochemical, food processing to nuclear power generation [1]. The main objective of this system is to control the flow of liquid between tanks so that optimum levels are maintained in both the tanks [2].

---

S. K. Singh  
Department of ECE, Anand International College of Engineering, Jaipur,  
Rajasthan, India  
e-mail: sksingh.mnit@gmail.com

N. Katal (✉)  
Department of ECE, ASET, Amity University, Jaipur, Rajasthan, India  
e-mail: nitishkatal@gmail.com

S. G. Modani  
Malaviya National Institute of Technology, Jaipur, Rajasthan, India

In this chapter, coupled-tank liquid-level system has been considered, and the PID controller is implemented for either maintaining the liquid level at a desired set point, disturbance rejection or to be used for moving the liquid set point. For designing the PID controller, classical method of Ziegler Nichols has been used, followed by the optimization using multi-objective genetic algorithm. The gain parameters have been tuned with respect to the objective function, stated as “Sum of integral of the squared error and the sum of integral of absolute error”. According to the results obtained, considerably better results have been obtained in case of multi-objective genetic algorithm-optimized PID controllers when compared to Ziegler-Nichols method in their respective step response on the system.

## 2 Mathematical Modeling of Coupled-Tank Liquid-Level System

Considering the coupled-tank system, is in Fig. 1. The dynamic equations of the system, by considering the flow balances for each tank, the equations for rate of change of fluid volume in tanks are as [3, 4]:

$$\text{For Tank 1 : } Q_i - Q_1 = A \frac{dH_1}{dt} \tag{1}$$

$$\text{For Tank 2 : } Q_1 - Q_0 = A \frac{dH_2}{dt} \tag{2}$$

where

$H_1, H_2$  Height of tank 1 and 2

$A$  Cross sectional area of tank 1 and 2

$Q_1, Q_2$  Flow rate of the fluid

$Q_i$  Pump flow rate

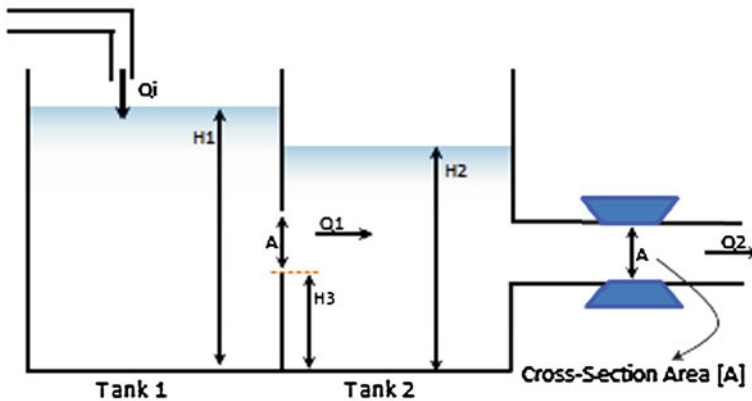


Fig. 1 Schematic representation of the coupled-tank system



The steady-state representation of the coupled-tank system can be given as follows:

$$\begin{bmatrix} \dot{h}_1 \\ \dot{h}_2 \end{bmatrix} = \begin{pmatrix} -k_1/A & k_1/A \\ k_1/A & -\frac{(k_1+k_2)}{A} \end{pmatrix} \begin{bmatrix} h_1 \\ h_2 \end{bmatrix} + \begin{bmatrix} 1/A \\ 0 \end{bmatrix} q_i \quad (3)$$

Taking the Laplace transformation of Eq. 3, the transfer function is obtained in Eq. 4.

$$G(s) = \frac{1/k_2}{\left(\frac{A^2}{k_1 k_2}\right) \cdot s^2 + \left(\frac{A(2k_1+k_2)}{k_1 k_2}\right) \cdot s + 1} = \frac{1/k_2}{(sT_1 + 1)(sT_2 + 1)}$$

where

$$\begin{aligned} T_1 T_2 &= A^2/k_1 k_2 \\ T_1 + T_2 &= \frac{A(2k_1 + k_2)}{k_1 k_2} \\ k_1 &= \frac{\alpha}{2\sqrt{H_1 - H_2}} \\ \text{and } k_2 &= \frac{\alpha}{2\sqrt{H_2 - H_3}} \end{aligned}$$

Using;  $H_1 = 18$  cm,  $H_2 = 14$  cm,  $H_3 = 6$  cm,  $\alpha = 9.5$  (constant for coefficient of discharge),  $H = 32$ ; the transfer function can be obtained in Eq. 4.

$$G(s) = \frac{0.002318}{s^2 + 0.201 \cdot s + 0.00389} \quad (4)$$

### 3 Designing and Optimization of PID Controllers

PID controllers are the most widely used controllers in the industrial control processes [5], and 90 % of the controllers today used in industry are alone PIDs. The general equation for a PID controller can be given by Eq. 5.

$$C(s) = K_p \cdot R(s) + K_i \int R(s) dt + K_d \frac{dR(s)}{dt} \quad (5)$$

where  $K_p$ ,  $K_i$  and  $K_d$  are the controller gains,  $C(s)$  is output signal, and  $R(s)$  is the difference between the desired output and output obtained [6].

### 3.1 PID Tuning Using Ziegler Nichols

Ziegler Nichols is the most operative method for tuning the PID controllers. But, this method is limited for application till ratio of 4:1 for the first two peaks in closed-loop response, leading to an oscillatory response [7]. Initially, unit-step response is derived (Fig. 2) followed by the computation of the PID gains as suggested by Ziegler-Nichols as in Table 1.

### 3.2 PID Optimization Using Genetic Algorithm

Genetic algorithms have vanguard advantage of wider adaptability to any constraints and hence are considered as one of the most robust optimization algorithms [8]. Optimization of the PID controllers with genetic algorithms focuses on obtaining the best possible solution for the three PID gains [ $K_p$ ,  $K_i$ ,  $K_d$ ] by minimizing the objective function. For the optimal tuning of the controller, the minimization of the integral square error (ISE) has been carried out.

$$ISE = \int_0^{T_s} e^2(t) dt$$

The optimization has been carried out using Global Optimization Toolbox and Simulink [9] with a population size of 20, scattered crossover, both-side migration and roulette-wheel-based selection. The PID gains obtained by optimal tuning using GA are represented in Table 2, and Fig. 3 shows the closed-loop response of the GA-optimized controllers. Figure 4 represents the plot for best and mean fitness

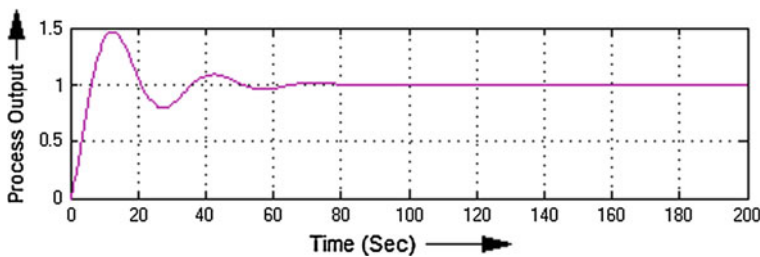


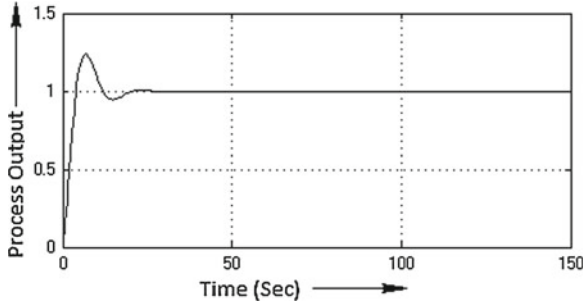
Fig. 2 Closed-loop step response of the system with ZN-PID controller

Table 1 PID parameters estimated by Ziegler-Nichols

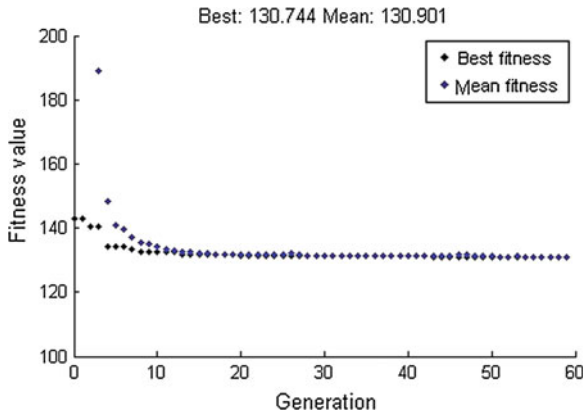
PID gains	Value
$K_p$	28.214
$K_i$	4.155
$K_d$	47.89

**Table 2** PID parameters estimated by genetic algorithm

PID gains	Value
$K_p$	79.9820
$K_i$	1.2042
$K_d$	83.4625



**Fig. 3** Closed-loop step response of the system with GA-PID controller

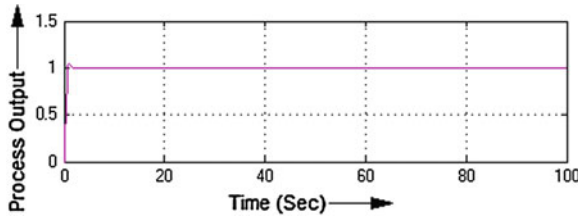


**Fig. 4** Plot for the best and average fitness values of the genetic algorithm optimization

values across various generations obtained while optimizing the PID controller using Genetic Algorithm.

### 3.3 PID Optimization Using Multi-Objective Genetic Algorithm

Since the Ziegler-Nichols tuned PID controllers give an oscillatory response, they are not optimum for implementation for plant. PID optimization using multi-objective genetic algorithm aims at obtaining an optimal Pareto solution, simultaneously



**Fig. 5** Closed-loop response using Mobj-GA-optimized PID controllers

**Table 3** PID parameters estimated by multi-objective genetic algorithm

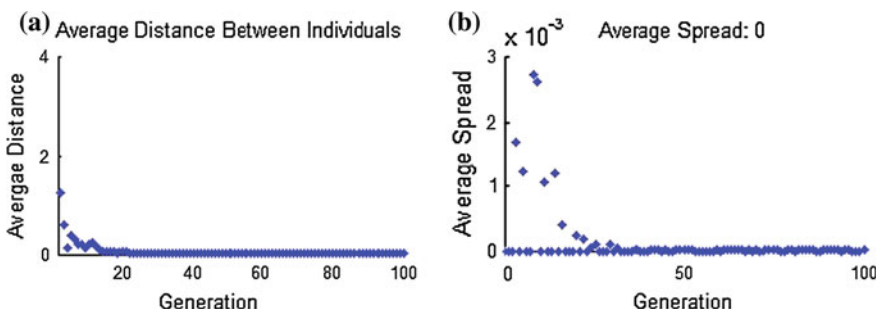
PID gains	Value
$K_p$	255.1
$K_i$	5.5
$K_d$	1249.96

improving the objective function of both the objectives  $O_1$  and  $O_2$ , given as follows:

First objective function is integral square error (ISE) which discards the large amplitudes, and second objective function is integral absolute error (IAE) which gives the measure of the systems performance. ISE tends to suppress the larger errors, while IAE tends to suppress the smaller errors [10]. The algorithm used here is NSGA-II, which using the controlled elitist genetic algorithm boosts obtaining the better fitness value of the individuals; and if the value is less, it still favors increasing the diversity of the population [11, 12]. Diversity of the populations/gains is controlled by the elite members of the population, while elitism is controlled by Pareto fraction and at Pareto Front also bound the number of individuals.

$$ISE = O_1 = \int_0^{T_s} e^2(t) dt \quad \text{and} \quad IAE = \int_0^{T_s} |u(t)| dt$$

The system implementation and optimization have been carried out in MATLAB and Simulink [9] environment using Global Optimization Toolbox. The population

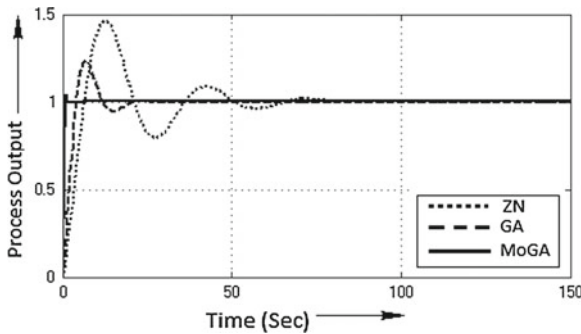


**Fig. 6** Plot for the **a** Average distance **b** Average spread between individuals

size of 45 has been considered with adaptive feasible mutation function, heuristic crossover, and the selection of individuals on the basis of tournament with a tournament size of 2. A hybrid function of Fitness Goal Attain (*fgoalattain*) is used, which further minimizes the function after GA terminates. Figure 5 shows the closed-loop response, and the optimized PID parameters are shown in Table 3. In Fig. 6a, distance between members of each generation is shown, and Fig. 6b gives the plot for average Pareto spread, which is the change in distance measure with respect to the previous generations.

### 4 Results and Discussion

In this chapter, the implementation and simulations of the system has been carried out in Simulink. Initially, the gains of the PID have been estimated using Ziegler Nichols rules [13] which give an oscillatory response, followed by the optimization by genetic algorithm and multi-objective genetic algorithm. The computed parameters are implemented for obtaining the closed-loop response of the system. Figure 7 shows the compared closed-loop step response graph, clearly indicating that better results are obtained in case of multi-objective genetic algorithm-optimized PID controller with decreased overshoot percentage and rise and settling time values. Table 4 represents the numerical data of the results obtained.



**Fig. 7** Comparative closed-loop response of the ZN, GA, and MoGA-optimized PID controllers

**Table 4** Comparison of the results

Method of design	Overshoot percentage	Rise time (s)	Settling time (s)
Ziegler-Nichols	46.4	4.83	62.4
Genetic algorithm	23.7	2.93	18.5
Multi-objective GA	4.47	0.504	1.41

## 5 Conclusion

The use of multi-objective genetic algorithm for the optimization of PID controller offers better results in terms of decreased overshoot percentage and rise and settling times as compared to Ziegler Nichols and genetic algorithm-tuned PIDs, thus offering better operation for the coupled-tank liquid-level control and better plant safety and performance.

## References

1. Bhuvaneswari, N. S., G. Uma, and T. R. Rangaswamy. "Adaptive and optimal control of a non-linear process using intelligent controllers." *Applied Soft Computing* 9.1 (2009): 182–190. Elsevier Ltd.
2. Capón-García, Elisabet, Espuña, Antonio, Puigjaner, Luis: Statistical and simulation tools for designing an optimal blanketing system of a multiple-tank facility. *Chemical Engineering Journal* **152**(1), 122–132 (2009)
3. B. Seth, D.S. J, "Liquid Level Control", Control System Laboratory (ME413), IIT Bombay (2006–07).
4. Elke Laubwald, "Coupled Tanks Systems 1", [www.control-systems-principles.co.uk](http://www.control-systems-principles.co.uk).
5. Åström, K. J., Albertos, P. and Quevedo, J. 2001. PID Control. *Control Engineering Practice*, 9,159–1161.J.
6. Norman S. Nise, 2003, *Control System Engineering*, 4<sup>th</sup> Edition.
7. Goodwin, G.C., Graebe, S.F., Salgado, M.E.: *Control System Design*. Prentice Hall Inc., New Jersey (2001)
8. Larbes, C., Aït Cheikh, S. M., Obeidi, T., & Zerguerras, A. (2009). Genetic algorithms optimized fuzzy logic control for the maximum power point tracking in photovoltaic system. *Renewable Energy*, Elsevier Ltd. 34(10), 2093–2100.
9. MATLAB and SIMULINK Documentation.
10. Corriou, Jean-Pierre. *Process Control: Theory and Applications*. Springer. 2004. Page132-133.
11. Grefenstette, J.J.: Optimization of Control Parameters for Genetic Algorithms. *IEEE Trans. Systems, Man, and Cybernetics* **SMC-16**(1), 122–128 (1986)
12. Konak, Abdullah, Coit, David W., Smith, Alice E., et al.: Multi-objective optimization using genetic algorithm. *Reliability Engineering and Safety System* **91**, 992–1007 (2006). Elsevier Ltd
13. Ziegler, J.G., Nichols, N.B.: Optimum settings for automatic controllers. *Transactions of the ASME*. **64**, 759–768 (1942)

# Comparative Performance Analysis of Particle Swarm Optimization and Interval Type-2 Fuzzy Logic-Based TCSC Controller Design

Manoj Kumar Panda, G. N. Pillai and Vijay Kumar

**Abstract** In this paper, an interval type-2 fuzzy logic controller (IT2FLC) is proposed for thyristor-controlled series capacitor (TCSC) to improve power system damping. It has been tested on the single-machine infinite-bus (SMIB) system. The proposed controller performance is compared with particle swarm optimization (PSO) and type-1 fuzzy logic controller (T1FLC)-based TCSC. In this problem, the PSO algorithm is applied to find out the optimal values of parameters of lead-lag compensator-based TCSC controller. The comparative performance is analyzed based on the simulation results obtained for rotor speed deviation and power angle deviation plot, and it has been found that for damping oscillations of SMIB system, the proposed IT2FLC is quite effective. The proposed controller is also robust subjected to different operating conditions and parameter variation of the power system.

**Keywords** Particle swarm optimization · Type-2 fuzzy system · TCSC · Fuzzy logic controller

## 1 Introduction

The particle swarm optimization (PSO) algorithm is a population-based, stochastic and multi-agent parallel global search technique [1]. The PSO algorithm is based on the mathematical modeling of various collective behaviors of the living creatures that

---

M. K. Panda (✉) · V. Kumar  
Department of Electronics and Computer Engineering, I. I. T Roorkee, Roorkee, India  
e-mail: pandadec@iitr.ernet.in

V. Kumar  
e-mail: vijecfec@iitr.ernet.in

G. N. Pillai  
Department of Electrical Engineering, I. I. T Roorkee, Roorkee, India  
e-mail: gnathfee@iitr.ernet.in

display complex social behaviors. In the PSO algorithm, while a particle is developing a new situation, both the cognitive component of the relative particle and the social component generated by the swarms are used. This situation enables the PSO algorithm to effectively develop the local situations into global optimum solutions [2]. PSO is a computational intelligence-based technique that is not largely affected by the size and nonlinearity of the problem and can converge to the optimal solution in many problems where most analytical methods fail to converge. It can therefore be effectively applied to different optimization problems in power systems [1]. The PSO is successfully applied in almost all areas of power system engineering like reactive power and voltage control, economic dispatch, power system reliability and security [1]. Very few applications of type-2 fuzzy logic to power system problems were reported in literature [3–6].

Thyristor-controlled series capacitor (TCSC) is one of the important members of flexible AC transmission systems (FACTS) family for damping the power oscillations also to enhance the transient stability [7, 8]. Over the years, artificial intelligence techniques [9–11] being used in developing TCSC models.

In this paper, a comparison has been made between the performance of three types of TCSC controller, i.e., PSO optimized lead lag compensator based TCSC (PSOLLC) in which the time constants and gain of LLC are optimized, a fuzzy logic control (FLC)-based TCSC controller, and the proposed IT2FL-based TCSC controller. Simulation is carried out for single-machine infinite-bus (SMIB) system. The effectiveness of the proposed controller is also tested at all loading conditions with transmission line reactance variation.

Section 2 of this paper describes about basic theory of PSO and its application in TCSC controller design. Type-2 fuzzy logic controller (IT2FLC)-based TCSC is presented in Sect. 3. Results are given and discussed in Sect. 4 and finally conclusion is presented in Sect. 5.

## 2 Particle Swarm Optimized Lead-Lag Compensator-based TCSC

In this paper, the PSO technique is applied to find out the optimal values of TCSC controller gain  $K_T$  and time constants  $T_{1T}$  and  $T_{3T}$  as shown in Fig. 1.

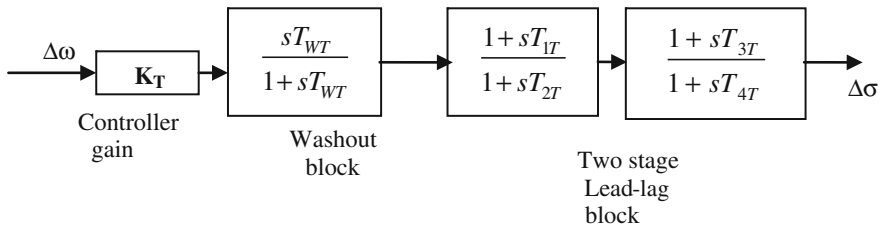


Fig. 1 TCSC controller block diagram



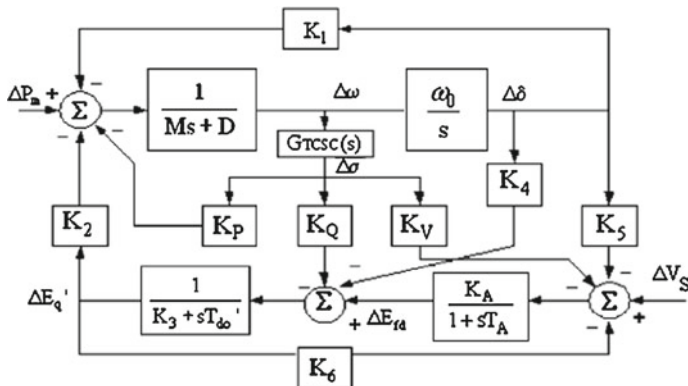


Fig. 2 Modified Phillips–Heffron model of SMIB system using TCSC [12]

### 2.1 TCSC Controller Description

The TCSC controller consists of a gain block having gain  $K_T$ , a washout block, which is a high-pass filter to allow signals associated with oscillations in input signal to pass unchanged and a two-stage phase-compensation block to compensate for the phase lag between the input and output signal.

The transfer function of the TCSC controller is

$$y = K_T \left( \frac{sT_{wT}}{1 + sT_{wT}} \right) \left( \frac{1 + sT_{1T}}{1 + sT_{2T}} \right) \left( \frac{1 + sT_{3T}}{1 + sT_{4T}} \right) x \tag{1}$$

where  $y$  is the output signal and  $x$  is the input signal of the TCSC controller, respectively. The TCSC controller is connected in the SMIB system model as shown in the Fig. 2. The objective of the TCSC controller is to minimize the power system oscillations after a disturbance to improve the stability by contributing a damping torque [10].

### 2.2 Application of PSO for Computing Optimum TCSC Controller Parameter

The problem is formulated as an optimization problem for the TCSC controller (as shown in Fig. 1). In this case, the washout time constant  $T_{wT}$  and the time constant of the two-stage lead-lag block  $T_{2T}$  and  $T_{4T}$  are prespecified. The controller gain  $K_T$  and time constant  $T_{1T}$  and  $T_{3T}$  of lead-lag compensator are to be determined applying PSO. As mentioned earlier, the aim of the TCSC-based controller is to minimize the power system oscillations after a disturbance to improve the stability. These oscillations are reflected in the deviation in the generator rotor speed ( $\Delta\omega$ ).

The objective function considered here is an integral time absolute error of the speed deviations, i.e.,

$$J = \int_{t=0}^{t=t_1} |\Delta\omega| \cdot t \cdot dt \quad (2)$$

The aim is to minimize this objective function to improve the system response in terms of the settling time and overshoot. In this optimization problem, the different parameters chosen are as follows:

Swarm size = 20, maximum number of generations = 100,  $C_1 = C_2 = 2.0$ ,  $w_{\text{start}} = 0.9$  and  $w_{\text{end}} = 0.4$  [15]. The optimized values of TCSC-based controller parameters obtained by PSO are as follows:

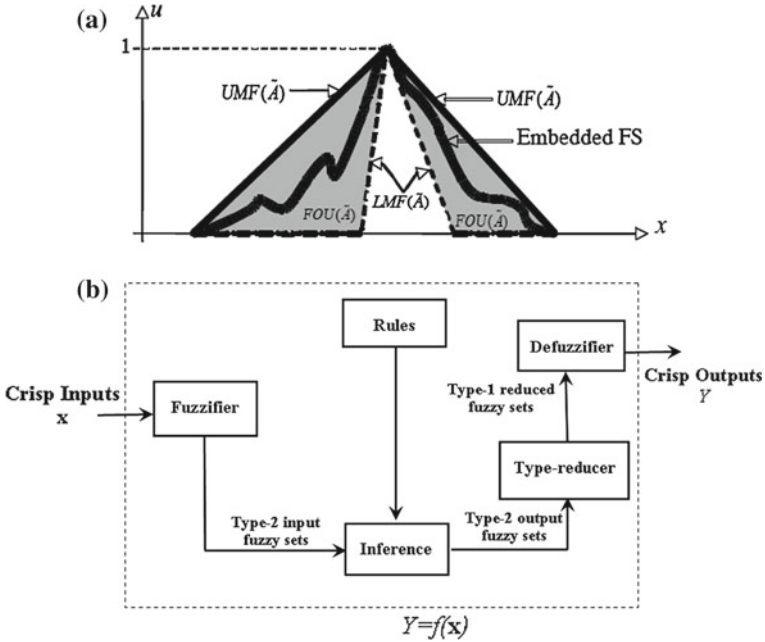
$$K_T = 62.9343, T_{1T} = 0.1245 \text{ and } T_{3T} = 0.1154.$$

### 3 Interval Type-2 Fuzzy Logic-based TCSC Controller

It is a well-known fact that the conventional fuzzy logic controller (type-1 FLC) has the limitations that, it cannot handle or accommodate the linguistic and numerical uncertainties associated with dynamical systems because its membership grade is crisp in nature. Type-2 fuzzy logic systems outperformed the type-1 fuzzy logic systems because of the membership functions of an IT2FLS are fuzzy and also contain a footprint of uncertainty (Fig. 3). IT2FLC design is based on the concept of interval type-2 fuzzy logic system. The structure of IT2FLC is same as the conventional fuzzy logic controller structure except, one type reducer block is introduced between the inference engine and defuzzifier block because the output of the inference engine is a type-2 output fuzzy set and before applying it to the defuzzifier for getting the crisp input, it has to be converted to a type-1 fuzzy set.

The block diagram of an IT2FLC is shown in Fig. 3b which contains five interconnected blocks, i.e., fuzzifier, rules, inference, type reducer, and defuzzifier. There is a mapping exist between crisp inputs to crisp outputs of the IT2FLS and is expressed as  $Y = f(X)$ . The principle of working of the IT2FLC is very much similar to the type-1 fuzzy logic controller (T1FLC). It is important to note that increasing the type of fuzzy system only enhances the degree of fuzziness of the system and all other principles of conventional fuzzy logic like inferencing procedure, defuzzification techniques holds good for both type [6].

In this problem, the conventional lead-lag compensator-based TCSC is used in the modified Phillips–Heffron model block diagram, and GTCSC(s) is replaced by an IT2FLC. First, the SMIB system model is simulated using a conventional T1FLC and then with IT2FLC. The rule base is same for both FLC and IT2FLC. The inputs considered here are speed ( $\Delta\omega$ ) and its derivative ( $\Delta\omega'$ ). The output is the change in conduction angle ( $\Delta\sigma$ ). Triangular and gaussian type membership functions have been used for the mamdani-type FLC and IT2FLC, respectively. Centroid-type



**Fig. 3** a FOU (shaded), LMF (dashed), UMF (solid) and an embedded FS (wavy line) for IT2FS $\tilde{A}$ . b Block diagram of IT2FLC [6]

**Table 1** Rule base table for both FLC and IT2FLC

$\Delta\sigma$		$\Delta\omega \rightarrow$				
		NB	NS	ZO	PS	PB
↓	NB	NB	NB	NB	NM	NS
	NS	NM	NS	NS	ZE	PS
	ZO	NM	NS	ZE	PS	PM
	PS	NS	ZE	PS	PS	PM
	PB	PS	PM	PB	PB	PB

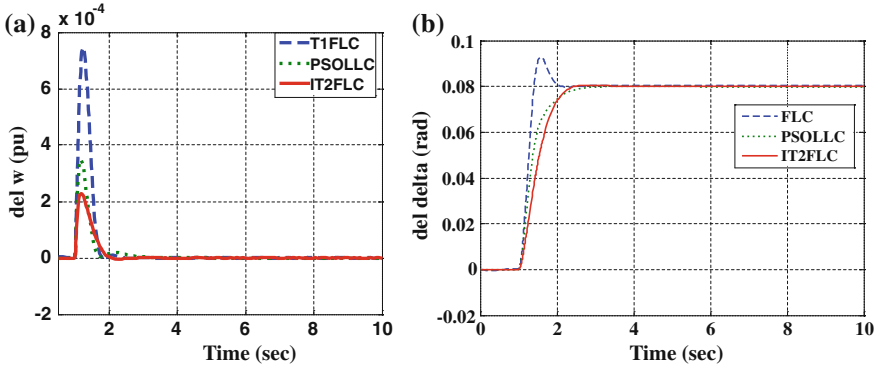
Where NB-Negative Big, NS-Negative Small, ZO-Zero Error, PS-Positive Small and PB-Positive Big are the name of the membership functions

defuzzification method is used for the FLC design. The performance of the SMIB system is analyzed.

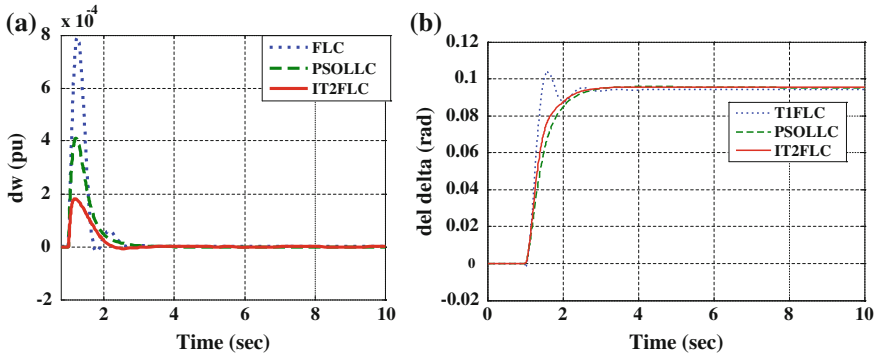
The performance of the controller is studied and is also validated at different operating conditions.

### 4 Results and Discussion

First, the SMIB power system model is simulated using the lead-lag compensator-based TCSC. The PSO algorithm was used to find the optimal values  $K_T = 62.9343$ ,  $T_{1T} = 0.1245$  and  $T_{3T} = 0.1154$ . Washout time constant  $T_{WT}$  and the time



**Fig. 4** a Rotor speed deviation. b Power angle deviation plot for 5% step increase in mechanical power at nominal loading condition

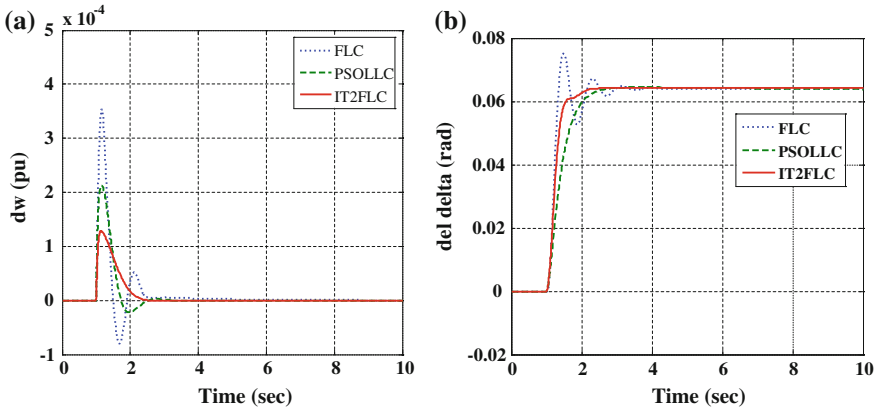


**Fig. 5** a Rotor speed deviation. b Power angle deviation plot for 5% step increase in mechanical power input with 50% increase in line reactance at nominal loading

constant of the two-stage lead-lag block  $T_{2T}$  and  $T_{4T}$  are prespecified. These values are considered in the TCSC structure for simulation. Three loading conditions are taken, i.e., nominal, light, and heavy loading. The real (P) and reactive power (Q) values for the two loading conditions are as follows.

- (1) Nominal loading (pu)  $\rightarrow P=0.9$  and  $Q=0.469$
- (2) Heavy loading (pu)  $\rightarrow P=1.02$  and  $Q=0.5941$ .

Second, the GTCSC(S) block of SMIB model is replaced by the conventional fuzzy logic controller designed with the principle as discussed in the Sect. 3. Third, the GTCSC(S) block of SMIB system is replaced by the IT2FLC designed with the procedure as depicted in previous section. The rule base as shown in Table 1 is designed based on the generalized performance of power system oscillations employing TCSC. The effectiveness and robustness of the controllers are also evaluated at (1) different loading conditions (2) disturbance of 5% step increase in reference mechanical power input (3) variation of transmission line reactance.



**Fig. 6** a Rotor speed deviation. b Power angle deviation plot for 5 % step increase in mechanical power input at heavy loading with 10 % decrease in line reactance

Figures 4, 5 and 6 shows the rotor speed deviation and power angle deviation plots at disturbance of 5% step increase in mechanical power input at different loading conditions and varying the transmission line reactance. It is analyzed from all the responses that the magnitude of overshoot and the settling time in all the speed deviation plots is less in case of IT2FLC compared to both PSOLLC and FLC. For the same condition, it is observed from the power angle deviation plots that there is no overshoot contributed by the PSOLLC and IT2FLC, but the IT2FLC response is faster compared to other two. FLC contributed some overshoot, but all are settling approximately at the same time.

It is found from all three results that the proposed controller is an effective and robust one compared to PSOLLC and FLC-based TCSC in providing good damping of low-frequency oscillations and to improve the system voltage profile. Although PSO-based algorithms are simple concept, easy to implement and computationally efficient, but there is possibility of trapped in local minima when handling more constrained problems due to the limited searching capacity.

## 5 Conclusion

In this paper, the performance of IT2FLC and FLC-based TCSC controllers are compared with a PSO optimized lead-lag compensator-based TCSC controller. The IT2FL-based TCSC controller surpasses the FL- and PSO-tuned TCSC controller performance at different loading conditions.

## Appendix

All data are in per unit (pu) unless specified. Generator:  $M = 9.26$  s,  $D = 0$ ,  $X_d = 0.973$ ,  $X_q = 0.55$ ,  $X'_d = 0.19$ ,  $T'_{do} = 7.76$ ,  $f = 60$  Hz,  $X = 0.997$ , Exciter:  $K_A = 50$ ,  $T_A = 0.05$  s, TCSC:  $X_{TCSC0} = 0.2169$ ,  $X_C = 0.2X$ ,  $X_P = 0.25X_C$ .

## References

1. Valle, Y.D., Venayagamoorthy, G.K., Mohagheghi, S., Hernandez, J.C., Harley R.G.: Particle swarm optimization: basic concepts, variants and applications in power systems. In: IEEE transaction on evolutionary computation. vol. 12(2), pp. 171–195 (2008)
2. Civicioglu, P., Besdok, E.: A conceptual comparison of the Cuckoo search, particle swarm optimization, differential evolution and artificial bee colony algorithm. *Artif Intell Rev.* (2011). doi:[10.1007/s10462-011-9276-0](https://doi.org/10.1007/s10462-011-9276-0)
3. Aguero, J.R., Vargas, A.: Calculating functions of interval type-2 fuzzy numbers for fault current analysis. *IEEE Trans. Fuzzy Syst.* **15**(1), 31–40 (2007). February
4. Lin, P.Z., Lin, C.M., Hsu, C.F., Lee, T.T.: Type-2 fuzzy controller design using a sliding-mode approach for application to DC-DC converters. *IEE Proc. Electr. Power Appl.* **152**(6), 1482–1488 (2005). Nov
5. Tripathy, M., Mishra, S.: Interval type-2 based thyristor controlled series capacitor to improve power system stability. *IET Gener. Transm. Distrib.* **5**(2), 209–222 (2011)
6. Panda, M.K., Pillai, G.N., Kumar, V.: Design of an Interval Type-2 Fuzzy Logic Controller for Automatic Voltage Regulator System. *Electric Power Compon. Syst.* **40**(2), 219–235 (2012)
7. Hingorani, N.G., Gyugyi, L.: *Understanding FACTS: Concepts and Technology of Flexible ac Transmission Systems*. IEEE Press, New York (2000)
8. Mathur, R.M., Verma, R.K.: *Thyristor-based FACTS Controllers for Electrical Transmission Systems*. IEEE Press, Piscataway (2002)
9. Panda S., Padhy, N.P., Patel, R.N.: Genetically optimized TCSC controller for transient stability improvement. *Int. J. Comput. Inf. Syst. Sci. Eng.* 1(1) 2008
10. Panda, S., Padhy, N.P.: Comparison of particle swarm optimization and genetic algorithm for FACTS-based controller design. *Electric Power Syst. Res.* (2008)
11. Hameed, S., Das, B., Pant, V.: A self tuning PI controller for TCSC to improve power system stability. *Electric Power Syst. Res.* **78**, 1726–1735 (2008)
12. Padiyar, K.R.: *Power System Dynamics: Stability and Control*. Wiley, New York (1996)

# Improved Parallelization of an Image Segmentation Bio-Inspired Algorithm

Javier Carnero, Hepzibah A. Christinal, Daniel Díaz-Pernil,  
Rául Reina-Molina and M. S. P. Subathra

**Abstract** In this paper, we give a solution for the segmentation problem using membrane computing techniques. There is an important difference with respect to the solution presented in Christinal et al. [6], we use multiple membranes. Hence, the parallel behavior of the algorithm with respect to the previous works has been improved.

**Keywords** Image segmentation · Digital topology · Membrane computing · Tissue-like P systems · Parallel computing

## 1 Introduction

Membrane systems [8] are distributed and parallel computing devices processing multisets of objects in compartments delimited by membranes. Computation is carried out by applying given rules to every membrane content, in a maximally parallel non-deterministic way, although other semantics are being explored.

---

J. Carnero · D. Díaz-Pernil · R. Reina-Molina  
Research Group on Computational Topology and Applied Mathematics, Department  
of Applied Mathematics, University of Sevilla, Sevilla, Spain  
e-mail: javier@carnero.net

D. Díaz-Pernil  
e-mail: sbdani@us.es

R. Reina-Molina  
e-mail: raureimol@alum.us.es

H. A. Christinal (✉) · M. S. P. Subathra  
Karunya University, Coimbatore, India  
e-mail: hepzia@yahoo.com

M. S. P. Subathra  
e-mail: sumiolivia@gmail.com

Segmentation [11] is the process of splitting a digital image into sets of pixels in order to make it simpler and easier to analyze. Segmentation is typically used to locate region of interest (ROI) in medical images or in satellite image by finding the frontiers among regions. Segmentation has shown its utility in bordering tumors and other pathologies, computer-guided surgery or the study of anatomical structure, but also in techniques which are not thought to produce images, but it produces positional information as electroencephalography (EEG), or electrocardiography (ECG). Locating a ROI is a hard task even for the expert human eye, mainly due to problems such as noise and the degradation of colors. Technically, the process consists of assigning a label to each pixel, in such way that pixels with the same labels form a meaningful region.

Here, a solution is given for the segmentation problem using a membrane computing device: tissue-like P systems. Initially, systems with only one working cell were used (see Carnero et al. [2], Christinal et al. [6]). Formally, membrane computing was used, but the key of these models was not considered: the membranes. In order to address this, return the membranes to their previous role and to improve the inherent parallelism of these models (see Christinal et al. [6]) using multiple membranes, increase the scalability for future parallel software implementations of the algorithm. A brief proof has been added for the ideas which are shown in Reina-Molina et al. [9]. Also a software tool implemented in Python showing the use of this algorithm is presented.

In the literature, one can find several attempts for bridging problems from digital imagery with membrane computing. The following are a few examples: the works done by Subramanian et al. [3, 4] and a few more problems from digital imagery have been solved in the framework of membrane computing (see Christinal et al. [5, 6]).

The paper is organized as follows: First, a family of tissue-like P systems is designed to obtain a segmentation of a 2D digital image using multiple cells. Moreover, an overview of the computation of this algorithm and a complexity study are presented in the following section. Next, an implementation of the algorithm using Python and some examples are shown. Finally, future work is presented.

## 2 Image Processing: Segmentation Problem

The *m-D Segmentation Problem with  $k$  auxiliary cells (mDSP- $kC$ )* can be described as follows: Given a *m-D Digital Image  $I$* , of size  $n^m$ , to determine the edge pixels of this image using  $k$  auxiliary cells.

There are two usual problems when we work with real images, the noise and degradation of colors. The former arises when we process or analyze an image whose color has no relation with those in its environment. The later takes place when we look at a digital image and we can see different colors connecting two adjacent regions, blurring the common edge of them. Our aim is to define the boundaries of these regions. These boundaries are considered as small regions where the colors of pixels gradually change from one side to another side of each region.



The usual definition of edge pixel presents problems from a practical point of view, when noise and degradation of colors are taken into account, because a lot of border pixels that are not edge pixels are considered. Hence, some cleaning processes must be applied to our image in order to obtain better results in edge pixels detection.

Next, we will show that *mDSP-kC* can be solved in constant time (with respect to the number of pixels of the image) by a family of tIP systems.

Formally, a *tissue-like P system (tIP System)* of degree  $q \geq 1$  with input is a tuple of the form  $\Pi = (\Gamma, \Sigma, \xi, w_1, \dots, w_q, R, i_\Pi, o_\Pi)$  where

(a)  $\Gamma$  is a finite *alphabet*, whose symbols will be called *objects*,  $\Sigma \subset \Gamma$  is the input alphabet and  $\xi \subseteq \Gamma$  is the alphabet of objects in the environment. (b)  $w_1, \dots, w_q$  are strings over  $\Gamma$  representing the multisets of objects associated with the cells at the initial configuration. (c)  $R$  is a finite set of communication rules of the following form:  $(i, u/v, j)$ , for  $i, j \in \{0, 1, 2, \dots, q\}$ ,  $i \neq j$ ,  $u, v \in \Gamma^*$  and (d)  $i_\Pi \in \{1, 2, \dots, q\}$  is the input cell and  $o_\Pi \in \{0, 1, 2, \dots, q\}$  is the output cell.

A tIP system of degree  $q \geq 1$  can be seen as a set of  $q$  cells labeled by  $1, 2, \dots, q$ . We will use 0 to refer to the label of the environment,  $i_\Pi$  and  $o_\Pi$  denote the input region and the output region (which can be the region inside a cell or the environment), respectively.

Let us construct a family  $\pi = \{p(n, m, k): n, m, k \in \mathbb{N}\}$  where each system of the family will process every instance  $u$  of the problem given by a  $m$ -D image  $I$  with  $n^m$  pixels and using  $k$  auxiliary cells. More formally, we define  $s(u) = \langle n, m, k \rangle = \langle n, \langle m, k \rangle \rangle$ , where  $\langle x, y \rangle = (x + y)(x + y + 1)/2 + x$  is the Gödel mapping. In order to provide a suitable encoding of this instances into the systems, we will use the objects  $a_{i_1}, \dots, a_{i_m}$  with  $1 \leq i_1, \dots, i_m \leq n$ , to represent the pixels of the image, and we will provide  $cod(u)$  as the initial multiset for the system, where  $cod(u)$  is the multiset  $a'_{i_1}, \dots, a_{i_m}$ .

Then, given an instance  $u$  of the *mDSP-kC* problem, the system  $\pi(s(u))$  with input  $cod(u)$  gives a solution to this problem, implemented in the following stages:

- Cleaning noise.
- Homogenizing colors using a general thresholding in color space.
- Segmenting image process.

The family  $\pi = \{\pi(n, 2, k): n, k \in \mathbb{N}\}$  of tIP systems of degree  $k + 1$  is defined as follows: for each  $n, k \in \mathbb{N}$ ,  $\pi(n, 2, k) = (\Gamma, \Sigma, \xi, w_1, \dots, w_{k+1}, R, i_\Pi, o_\Pi)$ , defined as follows:

- $\Gamma = \Sigma \cup \left\{ a_{ij}a''_{ij}, \bar{a}_{ij}, A_{ij}, A'_{ij}, A''_{ij}, \bar{A}_{ij}: 1 \leq i, j \leq n, a \in C \right\}$ ,  
 $\Sigma = \left\{ a'_{ij}: 1 \leq i, j \leq n, a \in C \right\}$ ,  $\xi = \Gamma - \Sigma$ ,
- $w_1 = *_{ij}; *_{ji}$  with  $i = 0, n + 1, 0 \leq j \leq n + 1$ ,  $w_2 = \dots = w_{k+2} = T^{\lfloor n^2/k \rfloor}$ ,
- $R$  is the following set of communication rules:  
 –  $\left( 1, a'_{ij}/a_{ij}^8 A_{ij}, 0 \right)$  for  $0 \leq i, j \leq n + 1$  and  $a \in C \cup \{*\}$

$$- \left( \begin{array}{cccc} c_{i-1j-1} & d_{i-1j} & e_{i-1j+1} & \\ 1, & b_{ij-1} & A_{ij} & f_{ij+1} \\ o_{i+1j-1} & h_{i+1j} & g_{i+1j+1} & \end{array} \middle/ \begin{array}{l} T, t \end{array} \right)$$

for  $1 \leq i, j \leq n$ ,  $a, b, c, d, e, f, g, h, o \in C \cup \{*\}$  and  $2 \leq t \leq k + 1$  indicating an auxiliary working cell.

$$- \left( \begin{array}{cccc} c_{i-1j-1} & d_{i-1j} & e_{i-1j+1} & \\ t, & b_{ij-1} & A_{ij} & f_{ij+1} \\ o_{i+1j-1} & h_{i+1j} & g_{i+1j+1} & \end{array} \middle/ \begin{array}{l} z'_{ij}, 0 \end{array} \right)$$

for  $1 \leq i, j \leq n$ ,  $a, b, c, d, e, f, g, h, o \in C \cup \{*\}$ . We take  $\mu$  as the number of pixels adjacent to the  $ij$  position with colors in  $C$  and  $* = 0$ . Then,  $av = (b + c + d + e + f + g + j + o)/\mu$  and  $z = \max\{s \in C: s \leq av\}$  and  $|z - av| > \rho_1$ , where  $\rho_1 \in (, +\infty)$ .

$$- \left( \begin{array}{cccc} c_{i-1j-1} & d_{i-1j} & e_{i-1j+1} & \\ t, & b_{ij-1} & A_{ij} & f_{ij+1} \\ o_{i+1j-1} & h_{i+1j} & g_{i+1j+1} & \end{array} \middle/ \begin{array}{l} a'_{ij}, 0 \end{array} \right)$$

for  $1 \leq i, j \leq n$ ,  $a, b, c, d, e, f, g, h, o \in C \cup \{*\}$ . We take  $\mu$  as the number of pixels adjacent to the  $ij$  position with colors in  $C$  and  $* = 0$ .  $av = (b + c + d + e + f + g + j + o)/\mu$  and  $z = \max\{s \in C: s \leq av\}$  and  $|a - av| \leq \rho_1$ , where  $\rho_1 \in (, +\infty)$ .

$$- (t, b'_{ij}/A'_{ij}, 0) \text{ for } 1 \leq i, j \leq n, \nu = (|C|/\rho_2), l = 0, 1, 2, \dots, \rho_2. \text{ If } b \in C \text{ then } a \in C$$

( $a < b \leq a + (\nu - 1)$  and  $a = \nu \cdot l$ ) or ( $b = a = \nu \cdot l$ ) and, if  $b = *$  then  $A = *$ .

$$- (t, A'_{ij}/T, 1) \text{ for } a \in C, 0 \leq i, j \leq n + 1 \text{ and } 2 \leq t \leq k + 1.$$

$$- (t, A'_{ij}/A'_{ij}, \bar{a}^8_{ij}, 0) \text{ for } a \in C, \cup \{*\} \text{ and } 0 \leq i, j \leq n + 1.$$

$$- \left( \begin{array}{cccc} \bar{c}_{i-1j-1} & \bar{d}_{i-1j} & \bar{e}_{i-1j+1} & \\ 0, & \bar{b}_{ij-1} & \bar{A}_{ij} & \bar{f}_{ij+1} \\ i_{i+1j-1} & \bar{h}_{i+1j} & \bar{g}_{i+1j+1} & \end{array} \middle/ \begin{array}{l} T, t \end{array} \right)$$

For  $1 \leq i, j \leq n$  and  $a, b, c, d, e, f, g, h, i \in C \cup \{*\}$ .

$$- (t, A'_{ij} \bar{b}_{kl} / \bar{A}_{ij}, 0) \text{ for } 1 \leq i, j, k, l \leq n, (i, j), (k, l) \text{ adjacent pixels; i.e. } (i, j) \in \Delta \text{ and } a, b \in C \text{ and } a < b.$$

$$- (t, \bar{A}_{ij}/T, 1) \text{ for } a \in C \text{ and } 1 \leq i, j \leq n.$$

$$- i_{\Pi} = o_{\Pi} = 1.$$

## 2.1 Overview

The input data of the system are given by the set  $\{a'_{ij}: a' \in C, 1 \leq i, j \leq n\}$ , which consists of the pixels of an image.

The computation starts in cell 1 which contains the initial image encoded by the objects  $a'_{ij}$ , along the edge pixels  $*_{ij}$ . Cells 2, 3, ...,  $k + 1$  contain enough copies of objects  $T$  called workflow markers. The unique rule that can be applied to this initial configuration is the first one, which is designed to mark non-edge pixels ( $a'_{ij}, a \in C$ ) with  $A_{ij}$  and to create enough copies of objects  $a'_{ij}$  and  $*_{ij}$ , which will be used later in workflow distribution. This step will be called *copies creation*.

Then, the only rule that can be applied is the second one, which sends one object  $A_{ij}$  and its neighborhood represented by adjacent objects  $a_{kl}$  to one working cell (cells 2, 3, ...,  $k + 1$ ) to be processed later. This step will be called *object distribution*.

After these two initial steps, for the third configuration of the system, only rules of the third and fourth type can be applied. These rules transform one object  $A'_{ij}$  into one object  $z''_{ij}$ , where  $z$  is the nearest color in  $C$  to the average color in the neighborhood of object  $A_{ij}$  and  $a$  is considered as noise, or color  $a$  itself in other cases.

Next, only the fifth rule can be applied, which transforms objects  $b''_{ij}$  into objects  $A'_{ij}$ , where  $a$  is a color in a subset of  $C$  defining a general thresholding with respect to the colors. Subsequently, the sixth rule is the one available, for obtaining the sixth configuration of the system, with the original image preprocessed (noise cleaned and thresholded) in order to improve the segmentation process.

Once all the preprocessing work is done, the image to be segmented is represented as objects  $A'_{ij}$ , where  $a$  is either a color in  $C$  or  $*$ . The next two steps consist in applying seventh and eighth rules, respectively, which send to the working cells an object  $A''_{ij}$  and its neighborhood represented by adjacent pixels  $\bar{a}_{kl}$ . From these steps, we get the eighth configuration.

The next configuration of the system is obtained by applying the rules in the ninth scheme, marking with  $\bar{A}_{ij}$  the edge pixels  $A''_{ij}$  with respect to an adjacent pixel  $\bar{b}_{kl}$  with greater color. The last configuration is got by sending the edge pixels  $\bar{A}_{ij}$  back to the cell 1.

## 2.2 Complexity Aspects

A little study of the complexity aspects of this solution is given by Fig. 1 showing this is an efficient algorithm from a theoretical point of view (Table 1).

**Fig. 1** Test image (on the left) and its segmented one (on the right). Next, we will show that  $mD$



### 3 Implementation of the Algorithm

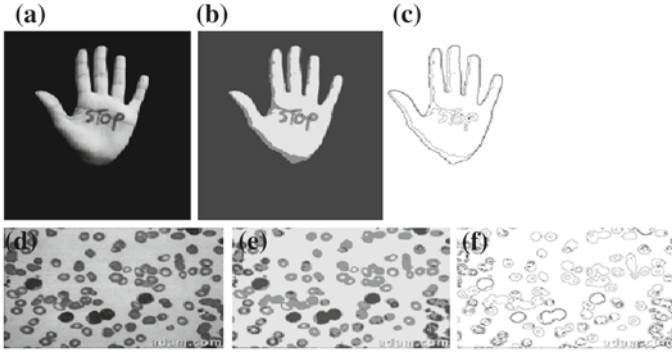
The algorithm proposed in this paper is implemented in Python Rossum et al. [10], an interpreted multiparadigm programming language which is powerful and easy to learn, read, and write. We have focused our implementation in the use of matrices as every alphabet object is represented by a matrix. This approach allows us to use the Numpy library (Ascher et al. [1]) for working effectively with large arrays of numbers. This way of facing the implementation of membrane objects seems to make available an easy adaptation of the algorithm to parallel architectures as GPU or multicores CPU.

The segmentation algorithm is implemented through the definition of the following functions:

- *BioSeg*. This function achieves the full segmentation process by calling other auxiliary functions described below. First of all, it creates a dictionary for storing the initial state of the computation. Next, a new computation is performed by distributing the work flow through the auxiliary cells. Then, cleaning and thresholding stages are performed into each auxiliary cell, following which a new computation is carried out by integrating all the information processed by the auxiliary cells into the first one. Next, the image cleaned and thresholded is distributed among the auxiliary cells to be segmented. Finally, the processed information is returned to the initial cell to be returned.
- *createInitialState*. This function creates the initial structure for storing the initial state of the P system.
- *distributionWork*. This function distributes every column and its adjacent ones to the corresponding auxiliary cell. In the P system design, this task is non-deterministically carried out. However, in the current implementation, the auxiliary cell for every pixel and its adjacent is deterministically chosen.
- *integrationWork*. This function integrates the processed pixels back into the first cell, forgetting the surrounding ones.
- *cleaningStep*. This function performs the image cleaning in every auxiliary cell.
- *thresholdingStep*. This function achieves the color thresholding in every auxiliary cell.

**Table 1** Complexity aspects, where the size of the input data is  $O(n^2)$ ,  $|C| = h$  is the number of colors of the image, and  $k$  is the number of working cells

mDSP-kC Problem	
<i>Complexity</i>	
Number of steps of computation	9
<i>Resources needed</i>	
Size of the alphabet	$8n^2 + 4n + 5$
Initial number of cells	$k + 1$
Initial number of objects	$(n + 2)^2$
Number of rules	$O(n^2 \cdot h^9 \cdot k)$
Upper bound for the length of the rules	10



**Fig. 2** Examples of images at the beginning of the algorithm (a) and (d), after cleaning and thresholding steps (b) and (e) and after segmentation step (c) and (f)

- *segmentationStep*. This function makes the segmentation process in every auxiliary cell.

The algorithm design implemented allows us to rewrite the code in order to take advantage of massively parallel devices as GPUs. However, in the current development stage, we have not implemented it yet and the code executes sequentially.

On the other hand, both cleaning, thresholding and segmentation steps can be developed using different approaches than those selected by us. Hence, the segmentation algorithm can evolve from the easier one in this work to more complex one, also designed to be executed in parallel. These changes do not alter the behavior of the complete algorithm, but they can improve the final result.

### 3.1 Examples

We present in this section several examples of the application of the implementation proposed in this paper.

The process is illustrated in Fig. 2, where two images are shown in the initial state, after cleaning, thresholding and segmentation. Both processes have been carried out using 1 as cleaning threshold, 3 as color threshold, and 5 as segmentation threshold.

## 4 Future Work

Our next step in this research line will be the real parallel implementation of the algorithm using the massive parallelism present in current GPUs. It is also planned to study other noise cleaning algorithms and also more elaborated segmentation algorithms, aiming for better results.

## References

1. Ascher, D., Dubois, P.F., Hinsen, K., Hugunin, J., Oliphant, T.: Numerical Python, Lawrence Livermore National Laboratory, Livermore, California, USA, 2001. Available at <http://numpy.scipy.org/>
2. Carnero, J., Diaz-Pernil, D., Molina-Abril, H., Real, P.: Image segmentation inspired by cellular models using hardware programming. *Image-A* **2**(4), 25–28 (2010)
3. Ceterchi, R., Gramatovici, R., Jonoska, N., Subramanian, K.G.: Tissue-like P systems with active membranes for picture generation. *Fundam. Inf.* **56**(4), 311–328 (2003)
4. Ceterchi, R., Mutyam, M., Paun, G., Subramanian, K.G.: Array-rewriting P systems. *Nat. Comput.* **2**(3), 229–249 (2003)
5. Christinal, H.A., Diaz-Pernil, D., Real, P.: P systems and computational algebraic topology. *J. Math. Comput. Model.* **52**(11–12), 1982–1996 (2010)
6. Christinal, H.A., Diaz-Pernil, D., Real, P.: Region-based segmentation of 2D and 3D images with tissue-like P systems. *Patt. Recogn. Lett.* **32**(16), 2206–2212 (2011)
7. Diaz-Pernil, D., Gutierrez-Naranjo, M.A., Molina-Abril, H., Real, P.: A bio-inspired software for segmenting digital images. In: Nagar, A.K., Thamburaj, R., Li, K., Tang, Z., Li, R. (eds.) Proceedings of the 2010 IEEE Fifth International Conference on Bio-Inspired Computing: Theories and Applications BIC-TA, IEEE Computer Society, vol. 2, pp. 1377–1381 (2010)
8. Paun, G.: Computing with membranes. Tech. Rep. 208, Turku Centre for Computer Science, Turku, Finland (November 1998).
9. Reina-Molina, R., Carnero, J., Diaz-Pernil, D.: Image segmentation using tissue-like P systems with multiple auxiliary cells. *Image-A* **1**(3), 143–150 (2010)
10. Rossum, G. Van and Drake, F.L. (eds.) Python Reference Manual, PythonLabs, Virginia, USA, 2001. Available at <http://www.python.org>
11. Shapiro, L.G., Stockman, G.C.: Computer Vision Upper Saddle River. Prentice Hall PTR, NJ (2001)

# A Novel Hardware/Software Partitioning Technique for System-on-Chip in Dynamic Partial Reconfiguration Using Genetic Algorithm

Janakiraman N. and Nirmal Kumar P.

**Abstract** Hardware/software partitioning is a common method used to reduce the design complexity of a reconfigurable system. Also, it is a major critical issue in hardware/software co-design flow and high influence on the system performance. This paper presents a novel method to solve the hardware/software partitioning problems in dynamic partial reconfiguration of system-on-chip (SoC) and observes the common traits of the superior contributions using genetic algorithm (GA). This method is stochastic in nature and has been successfully applied to solve many non-trivial polynomial hard problems. It is based on the appropriate formulation of a general system model, being therefore independent of either the particular co-design problem or the specific partitioning procedure. These algorithms can perform decomposition and scheduling of the target application among available computational resources at runtime. The former have been entirely proposed by the authors in previous works, while the later have been properly extended to deal with system-level issues. The performance of all approaches is compared using benchmark data provided by MCNC standard cell placement benchmark netlists. This paper has shown the solution methodology in the basis of quality and convergence rate. Consequently, it is extremely important to choose the most suitable technique for the particular co-design problem that is being confronted.

**Keywords** Hardware/software partitioning · Genetic algorithm · Dynamic partial reconfiguration · System-on-chip

---

N. Janakiraman (✉)  
Anna University, Chennai, India  
e-mail: janakiramanforu@yahoo.com

P. N. Kumar  
Anna University, Chennai, India  
e-mail: nirmal.p@annauniv.edu

## 1 Introduction

Hardware/software partitioning is a method of dividing a complex heterogeneous system into hardware co-processor functions and its compatible software programs. It is a prominent practice that can realize results greater than the software-only or hardware-only solutions in system-on-chip (SoC) design. This technique can improve the system performance [1] and reduce the total energy consumption [2]. The proposed partial dynamic reconfiguration method does not depend on any tool. It uses a set of algorithms to detect crucial code regions, compilation/synthesize of hardware/software modules, and updating of communication logic. Hence, it could tune up the system to give full efficiency without disruption of other SoC-related operations. Here, the genetic algorithm (GA) is used for optimization process. This is essential in system-level design, since decision-making process affects the total performance of system. This paper presents a novel system partitioning technique with in-depth analysis. The paper is organized as follows. Section 2 briefs about the previous works in this field. Section 3 presents the proposed system model for partitioning problem. Section 4 gives the results and its analysis. Section 5 concludes the paper and discusses about the future work. Last section provides the list of references.

## 2 Related Works

When compared to dynamic partitioning using standard software, the run-time (or) partial dynamic reconfigurable systems had attained superior performance with manually specified predetermined hardware regions. Multiple choices of preplanned reconfigurations were rapidly executed in a run-time reconfigurable system using PipeRench architecture [3] and dynamically programmable gate arrays (DPGA) [4]. The binary-level partitioning technique [5] was provided a good solution compared to source-level partitioning methods due to the functionality of any high-level language and software compiler. Since the satisfaction of performance was not considered for the cost function of this system, it may be failed to find out local minima. A mapping technique for nodes and hardware/software components was developed in [6] called GCLP algorithm. The hardware cost was minimized by the incorporation of hill-climbing heuristic algorithm with the hardware/software partitioning algorithm [7].

## 3 System Model for Partitioning

The problem resolution requires the system model definition to represent the important issues in the hardware/software co-design for a specific problem [8]. The system partitioning problem model is represented by the task graph (TG) flow diagram. TG is a model of directed and acyclic graph (DAG) flow with weight vectors. Formally,



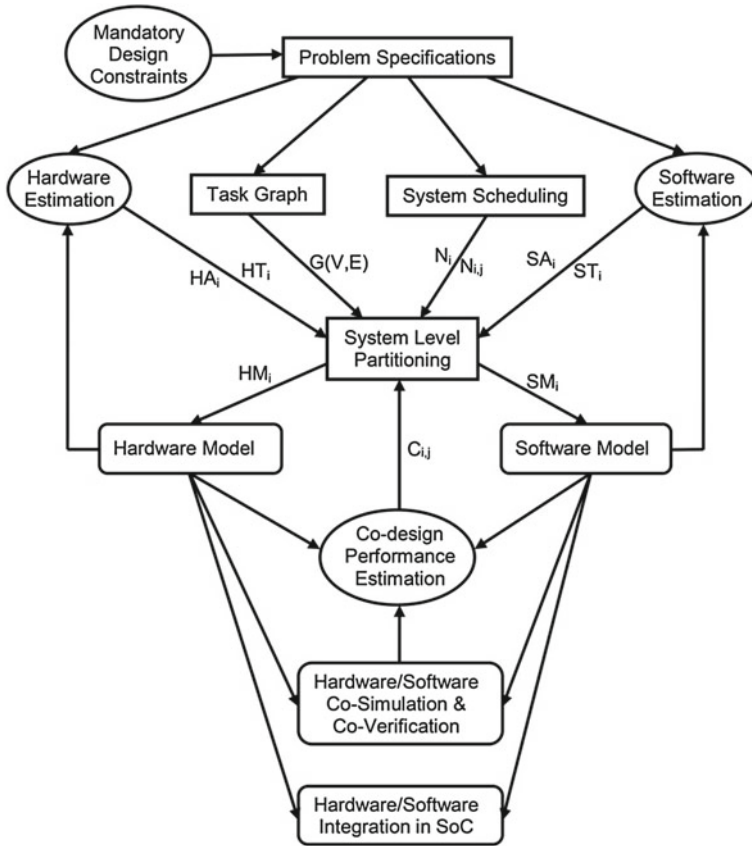


Fig. 1 System model for partitioning

it is defined as  $G = (V, E)$ , where ‘ $V$ ’ represents the nodes and ‘ $E$ ’ represents the edges. The flow direction is represented by each edge. Due to reducing the complexity of TG, it can be modified as one starting node and one ending node. Figure 1 represents the overview of the partitioning procedure. Design constraints and design specifications are given as the input to the partitioning process as a high-level specification language. The nodes can act as giant pieces of information like tasks and processes of coarse granularity or tiny types like instructions and operations of fine granularity approach.

After the system space estimation, every node is tagged with some attributes. Giant pieces of data for a node ( $V_{i,j}$ ) are represented by 5 attributes as follows:

- (1) Hardware area ( $HA_{i,j}$ ).
- (2) Hardware implementation time ( $HT_{i,j}$ ).
- (3) Software memory size ( $SS_{i,j}$ ).
- (4) Software execution time ( $ST_{i,j}$ ).

(5) The average execution time in numbers ( $N_{i,j}$ ).

Shortly,

$$\begin{aligned} \text{Hardware module (HM}_{i,j}\text{)} &= (\text{HA}_{i,j}) + (\text{HT}_{i,j}) + (N_{i,j}) \\ \text{Software module (SM}_{i,j}\text{)} &= (\text{SS}_{i,j}) + (\text{ST}_{i,j}) + (N_{i,j}) \end{aligned}$$

Communication values ( $C_{i,j}$ ) of every node are represented by three components as follows:

- (1) Transfer time ( $\text{TT}_{i,j}$ )
- (2) Synchronization time ( $\text{SynT}_{i,j}$ )
- (3) The average communication time in numbers ( $M_{i,j}$ )

Shortly,

$$\text{Communication value of node (C}_{i,j}\text{)} = (\text{TT}_{i,j}) + (\text{SynT}_{i,j}) + (M_{i,j})$$

$$C_{i,j} = \frac{(N_i * \Delta\text{TT}_i) + (N_j * \Delta\text{TT}_j) + (\text{SynT}_{i,j})}{(\text{HT}_i) + (\text{HT}_j)}$$

where  $(\Delta\text{TT}_i) = (\text{ST}_i) - (\text{HT}_i)$  and  $(\Delta\text{TT}_j) = (\text{ST}_j) - (\text{HT}_j)$ .

Efficiency of the hardware/software system partitioning process is based on the target architecture and its mapping technique. Hence, this work considers the ‘Dynamically Reconfigurable Architecture for Mobile Systems’ (DReAM) as target architecture. Execution of hardware and software processes should be concurrently in the standard processor and the application-specific co-processor. This partitioning process concludes the assignment of modules to implement the hardware and software stages, implementation schedule (timing), and the communication interface between software and hardware modules. In general, this partitioning solution can be validated by the measurement of eminent attributes like performance and cost parameters. Hence, this paper used as three quality attributes related to design elements as follows:

- (1) The estimated hardware area is  $A_E$ , and the maximum available area is  $A$ .
- (2) The estimated design latency is  $T_E$ , and the maximum allowed latency is  $T$ .
- (3) The estimated software (or) memory space is  $M_E$ , and the maximum available space is  $M$ .

Static-list scheduling method is used for the scheduling process [9]. It is a subtype of resource-constrained scheduling algorithm. This scheduler considers the timing estimation of every vertex and its interconnections. This scheduler unit provides the design latency ( $T_E$ ) and the cost of communication for hardware–software co-design. Based on the hardware and software implementations, another four parameters are considered for co-design realization.

When the entire system is implemented in hardware,

- (1) The minimum design latency is  $\text{MinT}$ .
- (2) The maximum hardware area is  $\text{MaxA}$ .

When the entire system is implemented in software,

- (1) The maximum design latency is MaxT.
- (2) The maximum memory space is MaxM.

These parameters are used to create the bounding constraints for the design space.

$$0 \leq A \leq \text{MaxA}; 0 \leq M \leq \text{MaxM}; \text{MinT} \leq T \leq \text{MaxT}.$$

### 3.1 System Operations

The design specifications are given in the format of ISPD98 benchmark suite [10] circuit netlist. This partitioning process has three stages.

In first stage, the processing of design specifications is divided into three subtasks. The first subtask is the separation of hardware ( $HA_i$  and  $HT_i$ ) and software ( $SS_i$  and  $ST_i$ ) estimations from the design specifications. The second subtask is to translate the design specifications into a hypergraph-based control data flow graph (CDFG) representation  $G = (V, E)$ . The third subtask is scheduling ( $N_i$  and  $N_{i,j}$ ) of each operations in the CDFG with satisfaction of the design constraints and the priority of operations.

In second stage, the outputs of these three tasks are given into the system-level partitioning module through the registers. It has three functionalities. The operational-level analysis is the first process, used to classify the tasks whether it is suitable for hardware realization or software execution. Next, the allocation process is used to allocate the required supporting entities like functional units, interconnections, and storage elements for the scheduled hardware and software systems. This allocation is based on the speed constraint (i.e., parallel processing) and the area constraint (i.e., dynamic partial reconfiguration). Finally, an absolute data path is generated by integrating components in the basis of hardware and software partitions. Then, the partitioning data are given to the specific hardware ( $HM_i$ ) and software ( $SM_i$ ) models.

In third stage, the hardware and software models are executed separately and the outcomes are compared with their estimated values (i.e., first stage). If any controversy arises, the feedbacks are given to the second-stage process. This looping process is continued till the satisfaction of all criterions.

Next, the performance ( $C_{i,j}$ ) of hardware–software co-design is estimated and compared with target performance metrics. If any misalignment arises, the feedback is indicated to the system-level partitioning stage. Then, the entire second and third stages are recompiled, till the achievement of target performance measures. Finally, the hardware/software co-simulation and co-verification is performed, and then, the SoC is realized.

### 3.2 Hardware/Software Estimation

The CDFG file is given to the input of both hardware and software estimations with the settings of target technology files and processor specifications. The hardware execution is a parallel process since the specifications are modeled in VHDL library. The software execution is a sequential process since the specifications are modeled in C code. The GA technique is used to optimize these parallel and sequential processes.

Hardware estimation is based on the high-level synthesizable components, to share the control and data path between hardware and software processes. GA is used to optimize this resource sharing process [11]. The quality measures are closely associated with performance metrics like execution, implementation, transfer, and synchronization times commonly called reaction time. This reaction time is associated with each node in each execution of local DFG. For convenient, the CDFG is split into several small DFGs called local DFGs.

The response times for

Routine statements,  $T_{RS} = T_{DFG}$

Conditional statements,  $T_{CS} = \sum_n P_n T_{DFGn}$  ;

n—Number of iterations

$P_n$ —Probabilities of iterations of outcomes

Looping statements,  $T_{LS} = nT_{DFG}$  ;

$$T_{CDFG} = F(T_{DFG1}, F_{DFG1}, \dots, T_{DFGi}, F_{DFGi}) \\ + F(T_{DFG1}, F_{DFG1}, \dots, T_{DFGj}, F_{DFGj})$$

$$\text{MinT} = \alpha[(\text{MaxA} * C_{i,j}) + \sum_i T_i N_{i,j}]$$

$T_i$ —Time delay for each node

$\alpha$ —Co-estimation factor

$$\text{MaxT} = \text{MinT} + \beta \sum_i [T_i \sum_{j=1}^{R_i} N_{i,j}]$$

$R_i$ —Required components of each node ‘i’

$\beta$ —Constant, since MaxT is a higher-order term

$F_i$ —Number of fixed components for each node ‘i’

$$T_{CDFG} = \text{MinT} + \beta \sum_i \left[ \frac{T_i}{F_i} \sum_{j=F_i+1}^{R_i} N_{i,j} \right]$$

Register Estimation: [12]

Many input multiplexers = (i\*MUXs)

State machine-based control logic is used to control lines,  $\log_2 i$   
 ROM size,  $(STA * [(1 + \log_2 i) \left( \text{REG} + \sum_i F_i \right) + \log_2 S])$ bits

STA—Number of states  
 REG—Number of registers

Software estimation is based on the calculation of memory space occupied by instruction set and user-defined data types and data structures. The average queuing time for each memory access can be modeled as  $T_q$ , and the number of access is represented by  $N_{\text{mem}}$ . This calculation is necessary to estimate  $(TT_{i,j})$  and  $(\text{Syn}T_{i,j})$ .

Hardware estimation  $(T_{\text{HM}}) = (T_{(\text{CDFG, HM})}) + \alpha T_q (N_{\text{mem, HM}})$

Software estimation  $(T_{\text{SM}}) = (T_{(\text{CDFG, SM})}) + T_q (N_{(\text{mem, SM})})$

Co-estimation  $(T_{\text{HM/SM}}) = \sigma (T_q) + \varphi (\frac{N_{\text{mem}}}{T_q})$ ; where  $\sigma$  and  $\varphi$  are complex structures.

### 4 Analyses of Results

All the hardware/software partitioning algorithms have been experimented in a set of benchmark suites provided by ISPD’98, whose characterization is shown in Table 1. Size and values of the system graph should bound within the design space. All these examples are illustrated in the form of directed and acyclic graphs to specify the certain coarse-grain tasks. Every example has been tested in different constraints, but it always within the specified boundary conditions. The results are summarized in Table 2. These results will be analyzed from both qualitative and quantitative perspectives. The qualitative aspects will be mainly represented by the resulting cost of the solutions obtained from each method, under different constraints. The quantitative issues will be shown by means of the computation time resulting from each technique.

**Table 1** Design characteristics for ISPD’98 benchmark suite

Circuit	# Cells	# Pads	# Modules	# Nets	# Pins
ibm01	12,506	246	12,752	14,111	50,566
ibm02	19,342	259	19,601	19,584	81,199
ibm03	22,853	283	23,136	27,401	93,573
ibm04	27,220	287	27,507	31,970	105,859
Ibm05	28,146	1,201	29,347	28,446	126,308

**Table 2** Results acquired with the ISPD'98 examples

Example	Constraints			Genetic algorithm			Fitness
	Area (CLBs)	Time (ns)	Memory (Bytes)	$A_E$	$T_E$	$M_E$	
ibm01	121,800	10,200	52,670	118,146	9,384	46,350	0.9233
	103,080	8,670	44,770	101,637	8,020	41,189	0.9437
ibm02	154,700	12,600	55,980	140,170	11,230	49,823	1.0000
	193,375	15,750	48,980	172,104	15,435	51,429	0.9733
ibm03	171,200	14,200	48,090	154,896	12,040	38,953	1.0000
	111,280	9,230	57,708	103,521	8,769	54,823	1.0000
ibm04	182,200	15,900	56,460	173,090	14,469	62,106	0.9866
	258,724	19,239	50,814	234,597	16,546	46,749	0.9600
ibm05	198,300	16,800	62,210	180,453	13,776	58,478	0.8900
	97,167	12,432	81,495	92,309	10,940	84,755	0.9566

## 5 Conclusion and Future Work

In this paper, the commonly used biologically inspired optimization algorithm, which addresses the hardware/software partitioning problem for SOC designs, is implemented using clustering approach as well as their performance is evaluated. This evaluation process does not have any constraints on the cluster size and the number of clusters. Hence, this evaluation approach is quiet suitable to be used in reducing the design complexity of systems. This paper had shown how this problem can be solved by means of very different partitioning techniques at runtime of the system (dynamic partial reconfiguration). The problem resolution has been based on the definition of a common system model that allows the comparison of different procedures. These extensions have improved previous implementations, because they include some issues previously not considered. The constraints of these algorithms have been integrated into the cost function in a general and efficient way. This genetic algorithm-based dynamic partitioning technique has produced an average of 16.19 % accuracy in hardware/software partitioning compared to [13] and [14].

A future study could extend the system model to encompass other quality attributes, like power consumption, influence of communications, and the degree of parallelism. Also, the hybrid algorithms of these biologically inspired algorithms and their compilation are currently under study.

**Acknowledgments** This work was supported in part by All India Council for Technical Education —Quality Improvement Programme scheme 2010. Access to research and computing facilities was provided by the Anna University and K.L.N. College of Engineering.

## References

1. Gajski, D.D., Vahid, F., Narayan, S., Gong, J.: SpecSyn—an environment supporting the specify-explore-refine paradigm for Hardware/Software system design. *IEEE Trans. VLSI Syst.* **6**(1), 84–100 (1998)
2. Henkel, J.: A low power Hardware/Software partitioning approach for core-based embedded systems. In: *Proceedings of the 36th ACM/IEEE Conference on Design Automation*, pp. 122–127 (1999)
3. Goldstein, S.C., Schmit, H., Budiu, M., Moe, M., Taylor, R.R.: PipeRench—a reconfigurable architecture and compiler. *IEEE Computer* **33**, 70–77 (2000)
4. DeHon, A.: DPGA-coupled microprocessors-commodity ICs for the early 21st century. In: *Proceedings of FCCM* (1994)
5. Stitt, G., Vahid, F.: Hardware/Software partitioning of software binaries. In: *IEEE/ACM International Conference on Computer Aided Design*, pp. 164–170 (2002)
6. Karypis, G., Aggarwal, R., Kumar, V., Shekhar, S.: Multilevel hypergraph partitioning—application in VLSI domain. *IEEE Trans. VLSI Syst.* **20**(1) (1999)
7. Alpert, C. J.: The ISPD98 circuit benchmark suite. In: *Proceedings of the 1998 International Symposium on Physical Design*, pp. 80–85 (1998)
8. Jiang, Y., Zhang, H., Jiao, X., Song, X., Hung, W.N.N., Gu, M., Sun, J.: Uncertain model and algorithm for Hardware/Software partitioning. *IEEE Comp. Soc. Annu. Symp. VLSI* 243–248 (2012)
9. Al-Wattar, A., Areibi, S., Saffih, F.: Efficient on-line Hardware/Software task scheduling for dynamic run-time reconfigurable systems. In: *26th International Parallel and Distributed Processing Symposium Workshops & PhD, Forum*, pp. 401–406 (2012)
10. Goldberg, D.E.: *Genetic Algorithms in Search, Optimization and Machine Learning*. Pearson Education (2004)
11. Sheng, W., He, W., Jiang, J., Mao, Z.: Pareto optimal temporal partition methodology for reconfigurable architectures based on multi-objective genetic algorithm. In: *26th International Parallel and Distributed Processing Symposium Workshops and PhD, Forum*, pp. 425–430 (2012)
12. Mazumder, P., Rudnik, E.M.: *Genetic Algorithms for VLSI Design, Layout and Test Automation*. Pearson Education (2003)
13. Luo, L., He, H., Dou, Q., Xu, W.: Hardware/Software partitioning for heterogeneous multicore SoC using genetic algorithm. In: *Second International Conference on Intelligent System Design and Engineering Application*, pp. 1267–1270 (2011)
14. Su, L., Zhang, X.: Research on an SOC Software/Hardware partition algorithm based on undirected graphs theory. In: *IEEE International Conference on Computer Science and Automation Engineering*, pp. 274–278 (2012)

# Solving School Bus Routing Problem Using Hybrid Genetic Algorithm: A Case Study

Bhawna Minocha and Saswati Tripathi

**Abstract** School bus routing involves transporting students from predefined locations to school using a fleet of buses with varying capacity. This paper describes a real-life problem of the school bus routing. The overall goal of this study is to develop a route plan for the school bus service so that it is able to serve the students in an efficient and economical manner with maximum utilization of the capacity of buses using hybrid genetic algorithm.

**Keywords** School bus routing problem · Genetic algorithm · Vehicle routing problem with time windows

## 1 Introduction

Approximately 23 million public school students travel through 400,000 school buses twice daily for going to school and back from the school. It has been estimated that out of these one to two million students travel in school buses (National Association of State Directors of Pupil Transportation Services 1998).

School bus routing and scheduling is a transportation area which needs an in-depth study for improving the service quality and reducing operating costs. The school bus routing problem consists of a set of students dispersed in a region who have to travel to and back from their schools every day. The main goal of any school transportation system is to provide safe efficient and reliable transportation for its students. It is therefore necessary to efficiently assign students to designated bus

---

B. Minocha (✉)  
Amity School of Computer Sciences, Noida, India  
e-mail: bminocha@amity.edu

S. Tripathi  
Indian Institute of Foreign Trade, Kolkata, India  
e-mail: saswati@iift.ac.in



stops and determine the appropriate locations of different bus stops and routes and the bus schedules to minimize the total operating cost while satisfying requirements of the school and the children.

According to Swersey et al. [8], “In school bus transportation the two most visible problems are routing and scheduling. In the routing problem every student is assigned to a bus stop and those particular stops are sum up to form routes. In the morning a bus follows these routes, from one stop to another, picking up the students and carrying them to school. In the scheduling problem, particular buses are assigned to particular routes.”

According to Spasovic et al. [7], “School Bus Routing is a version of the traveling salesman problem, normally referred to the group of vehicle routing problems (VRP), also with or with no time window constraints. Three factors that make School Bus Routing unique are: (1) Efficiency (the cost to run a school bus) (2) Effectiveness (how well the demand for service is fulfilled) (3) Equity (fairness of the school bus for each student).”

Ke et al. [3] present a variety of model formulations of school bus routing problem. Li et al. [4] solved a case study treating the problem as multi-objective combinatorial optimization problem. Thangiah et al. [9] discuss the routing of school buses in rural areas. Recently, a complete review of school bus routing problems has been provided by Park et al. [6].

Bus routing has gained the attention of many researchers in different fields. Whereas some researchers are focusing on the designing new algorithms, others are advancing existing algorithms and applying existing algorithms to the real-world problems. These have been discussed by Toth et al. [10] and Golden et al. [1] in their respective books.

The aim of school bus routing is to transport students in the safest, most economical, and convenient manner such that the following objectives and constraints are met:

Objectives:

- Minimize the total number of buses required.
- Minimize the total distance traveled by the buses.

Constraints:

- The number of students must not exceed the number of seats on each bus.
- The time taken by buses must not exceed the specified limit.
- Each bus stop is to be allocated to only one bus.
- Each bus must pick all the students allocated on that route within specified time windows and must reach the school before it starts.

Thus, school bus routing is essentially vehicle routing problem with time window (VRPTW). In VRPTW, a set of vehicles with fixed and identical capacity is to be routed from a central depot to a set of geographically scattered locations (cities, stores, schools, customers, warehouses, etc.), which have varying demands and predefined time windows. The vehicle can visit the location in this specified time window only.

The objective of VRPTW is to service all the customers as per their requirement while minimizing the number of vehicles required as well as the total travel distance by all the vehicles used without violating capacity constraints of the vehicles and the location's time window requirement such that each location is visited once and only once by one of the vehicles. All the routes are to start and ultimately end at the depot. In the present study, we deal with routing the buses to appropriate bus stops.

The genetic algorithm (GA) approach was proposed by Holland [2] in 1975. It is an adaptive heuristic search method that mimics evolution through natural selection. It works by combining selection, crossover, and mutation operations of genes. The selection procedure drives the population toward a better solution, while crossover uses genes of selected parents to produce new offsprings that form the next generation. The genetic algorithm approach has now become popular as it helps in finding reasonably good solutions for complex mathematical problems and NP-hard problems like vehicle routing problem.

## **2 Optimal Allocation of School Buses in Vehicle Routing Planning of Blooming Dales School: A Case Study**

The case study considered by us is the school bus routing problem of Blooming Dales School situated in Ganga Nagar, Rajasthan, India. The school has primary wing and high school wing in which presently students from nursery grade to grade X study. Students from all over the town come there for schooling as it is very famous school in the city imparting quality education to the students. An important problem before the school management is to provide transport the students to and from the school which is safe, economical, and convenient to the students who do not have their own means of travel to the school.

Students travel to the school by different modes of transports. However, a large number of them depend upon school buses. Presently, the school has a fleet of six buses each with a seating capacity of 60 seats. The school starts at 8:00 am, so all the buses have to reach the school campus by 7:50 am. The students go to their allocated bus stop from their respective homes and board the school buses from there. The students have been clustered into groups. Each group is associated with one of 50 bus stops. The buses are required to depart and return to the school within an allotted fifty minutes time period. Table 1 shows the data provided by the school.

The travel plan currently being followed by the school management is shown in Table 2. The currently running routes have been established intuitively and providing the bus facility to 286 students. Every single route is serviced by a single vehicle. All routes start and end at 0 indicate that all buses start their journey from school and ends at school. Each bus stop is represented by a unique number, and all students at a particular bus stop are serviced by a single bus.

**Table 1** Distance and demands of case study

Bus stop	No. of students boarding at bus stop	Distance of bus stop from school (in km)	Scheduled arrival time of bus at bus stop
0	0	0	7:00
1	12	5.1	7:33
2	4	7.9	7:22
3	9	9.5	7:17
4	4	5.7	7:33
5	10	7.2	7:28
6	6	6.7	7:24
7	4	4.2	7:34
8	8	4.7	7:32
9	6	9.7	7:19
10	4	7.9	7:26
11	6	6.3	7:30
12	3	8.9	7:20
13	6	8.3	7:17
14	4	8.9	7:21
15	3	4.9	7:36
16	9	8.4	7:21
17	3	5.9	7:33
18	6	7.4	7:25
19	8	6.2	7:26
20	7	9.4	7:20
21	6	6.4	7:31
22	4	6.9	7:29
23	3	7.8	7:24
24	3	7.9	7:26
25	8	6.7	7:28
26	8	6.9	7:27
27	4	9	7:16
28	6	8.9	7:23
29	2	10.1	7:19
30	4	5.2	7:31
31	3	4.4	7:38
32	4	3.9	7:40
33	7	4.1	7:38
34	12	5.9	7:31
35	2	8.5	7:24
36	5	5.4	7:35
37	8	7.2	7:22
38	4	5.2	7:34
39	7	4.9	7:35
40	8	7.4	7:25
41	4	5.7	7:28
42	2	9.3	7:22
43	4	7.5	7:27

(continued)

**Table 1** (continued)

Bus stop	No. of students boarding at bus stop	Distance of bus stop from school (in km)	Scheduled arrival time of bus at bus stop
44	16	8.4	7:18
45	9	8.5	7:23
46	8	6.1	7:30
47	3	8.8	7:16
48	2	9.9	7:18
49	6	7.7	7:00
50	2	4.1	7:37

**Table 2** Current bus route plan

Bus	Route	Start time (am)	Return time (am)
1	0-29-28-35-10-5-21-17-15-31-0	7:00	7:46
2	0-48-20-14-24-43-22-4-39-33-0	7:00	7:46
3	0-3-12-16-23-40-25-34-38-0	7:00	7:45
4	0-47-13-49-37-6-19-41-8-7-0	7:00	7:43
5	0-27-44-2-18-26-46-1-0	7:00	7:45
6	0-9-42-45-11-30-36-50-32-0	7:00	7:44

## 2.1 Problem Identification

We analyzed the data provided by the school management and calculated the capacity utilization of each bus, which is shown in Table 3. The table shows details for each bus route which includes the starting time from the school and time at which bus return to the school, the number of stops it covers and total number of students it served during the entire trip. The capacity utilization (students/capacity) has also been computed and listed in the Table 3. This shows that some of the buses are under utilized.

## 2.2 Design of More Efficient Bus Routes

The goal of this study is to develop a route plan for the school bus service so that it is able to serve all the students efficiently with maximum utilization of the buses. For this, we have first transformed the problem into the format of a VRPTW. In order to convert the given school bus routing problem into VRPTW problem, we need the latest arrival time of bus and required service time at each stop. We have added four minutes to the scheduled arrival time of bus at each stop to determine the latest acceptable arrival time of bus at a designated stop. Service time is actually the

**Table 3** Current bus routes with their capacity utilization

Bus	Route	Start time (am)	Return time (am)	No. of stops	No. of students	Vehicle capacity	Capacity utilization (%)
1	0-29-28-35-10-5-21-17-15-31-0	7:00	7:46	9	39	60	65
2	0-48-20-14-24-43-22-4-39-33-0	7:00	7:46	9	42	60	70
3	0-3-12-16-23-40-25-34-38-0	7:00	7:45	8	56	60	93.33
4	0-47-13-49-37-6-19-41-8-7-0	7:00	7:43	9	53	60	88.33
5	0-27-44-2-18-26-46-1-0	7:00	7:45	7	58	60	96.66
6	0-9-42-45-11-30-36-50-32-0	7:00	7:44	8	38	60	63.33
Total				50	286	360	79.44

stoppage time of bus at each stop. This is equal to total time required by all students to board the bus. This has been taken to be the number of students boarding the bus from that stop multiplied by ten. (We are assuming here that each student needs about 10 s to board the bus.)

The buses depart from the school to the farthest bus stop points and start picking up students from various bus stops in their return journey to the school. The travel time  $t_{0i}$  is computed as  $d_{oi}/v$ , where  $d$  is the distance of bus stop  $i$  from school, and  $v$  is the average running speed of the bus (we have assumed the average speed of the bus to be 30km/h). The present problem in reality is a VRPTW problem with some constraints. Buses cannot travel randomly from one stop to another. They have to follow the roads available. For instance, there is no direct path between many bus stops such as 45 and 35, 3 and 29, 42 and 48, 47 and 27, 18 and 19, 16 and 37. Similarly, one can reach bus stop 42 only from bus stop nine.

### 3 Use of Genetic Algorithm to Solve School Bus Routing Problem

Keeping all points in view, we developed a VRPTW-based model for this problem. A genetic algorithm is developed to solve it. After building the initial population, all individuals are evaluated according to the fitness criteria. The evolution continues with a three-way tournament selection in which good individuals are selected for reproduction. In each generation, two best individuals are preserved for the next generation without being subjected to genetic operations. The problem-specific route-exchange crossover and mutation operations have been designed and applied to modify the selected individuals to form new feasible individuals for the population. Details of the algorithm are available in Minocha et al. [5]. The proposed algorithm has been coded in C++.

The travel plan obtained by genetic algorithm is shown in Table 4. All the bus departs and arrives at the school within the time window. Now, bus no. 1 and bus no. 2 cover more bus stops, but bus No. 6 covers lesser bus stops than the original route plan. The overall capacity utilization of the buses though remains same. But if we replace the bus no. 6 with a bus with half the capacity, it will increase the overall capacity utilization to 86.67 %.

### 4 Use of Hybrid Genetic Algorithm to Solve School Bus Routing Problem

Although genetic algorithms can rapidly locate the region in which the global optimum exists, they take a relatively long time to locate the exact local optimum in the region of convergence. On contrary, local searches (valid in a small region of search

**Table 4** New bus routes by genetic algorithm

Bus	Route	Start time (am)	Return time (am)	No. of stops	No. of students	Vehicle capacity	Capacity utilization (%)
1	0-29-9-42-28-35-10-5-21-17-15-31-0	7:00	7:48	11	47	60	78.34
2	0-48-20-14-24-43-22-11-4-39-33-0	7:00	7:47	10	42	60	80
3	0-3-12-16-23-40-25-34-38-0	7:00	7:45	8	56	60	93.33
4	0-47-13-49-37-6-19-41-8-7-0	7:00	7:43	9	53	60	88.33
5	0-27-44-2-18-26-46-1-0	7:00	7:45	7	58	60	96.66
6	0-45-30-36-50-32-0	7:00	7:44	5	24	60	40
Total				50	286	360	79.44

**Table 5** New bus routes by hybrid genetic algorithm

Bus Route	Start time (am)	Return time (am)	No. of stops	No. of students	Vehicle capacity	Capacity utilization (%)
1 0-29-9-42-28-35-10-5-21-17-36-15-31-32-0	7:00	7:49	13	56	60	93.33
2 0-48-20-14-45-24-43-22-11-4-39-33-0	7:00	7:48	11	57	60	95
3 0-3-12-16-23-40-25-34-38-50-0	7:00	7:46	9	58	60	96.66
4 0-47-13-49-37-6-19-41-30-8-7-0	7:00	7:44	10	57	60	95
5 0-27-44-2-18-26-46-1-0	7:00	7:45	7	58	60	96.66
Total			50	286	300	95.33



space) are quick in finding an optimal solution. A combination of a genetic algorithm and a local search method can speed up the search to locate the exact or near-exact global optimum. These are now properly known as hybridized GAs. In such an algorithm, applying a local search to the solutions that are guided by a genetic algorithm to the most promising region can accelerate convergence to the global optimum.

In this study, we incorporate two new local search heuristics to search for better routing solutions of VRPTW. These searches are as follows:

1. *Changing next neighbor (CNN)*: In this case having selected an individual randomly from the population, a node says  $C_j$  is randomly chosen from one of its routes. An effort is now made to replace its next neighbor  $C_{j+1}$  by some alternative acceptable node, say  $C_k$ . If it is possible, then we terminate the selected route at  $C_{j+1}$  and all the nodes from  $C_{j+2}$  onwards are reinserted in suitable places in other existing routes. The route from which new  $C_{j+1}$  was picked up is joined together at the next node of that route. If such an arrangement of routes is not possible, then the same individual is returned.
2. *Reinserting random node (RRN)*: In this case again after selecting an individual randomly from the population, a customer  $C_j$  is randomly selected from one of its routes. An attempt is made to insert it in another existing route at an appropriate place. If that becomes possible we join the route from where  $C_j$  was taken at the next node of that route. This creates a new feasible solution. If it is not possible, then the same individual is returned.

The genetic algorithm used in previous section is combined with these local searches to yield hybridized genetic algorithm. Any one of the alternative local search heuristics is applied randomly. The travel plan obtained by hybrid genetic algorithm is shown in Table 5. All the bus departs and arrives at the school within the time window, but covers more bus stops. Hence, the overall requirement of buses is reduced by one, and thus, capacity utilization of buses is increased.

## 5 Conclusion

In the present study, we have solved a practical real-life situation using hybrid genetic algorithm. New travel plan obtained yields a better solution as compared to the currently used one both in the terms of number of buses required and in terms of the overall capacity utilization of the buses. This has motivated the school management to use the suggested route plan. Less number of buses indicates saving in terms of cost of bus, its maintenance, running expanses (including fuel, salary of driver, conductor). In fact with the increase in fuel prices, transportation schedules should be planned efficiently.

## References

1. Golden, B., Raghavan, S., Wasil, E.: *The Vehicle Routing Problem: Latest Advances and New Challenges*. Springer, Berlin (2008)
2. Holland, J.H.: *Adaptation in Natural and Artificial System*. The University of Michigan Press, Michigan (1975)
3. Ke, X., Caron, R.J., Aneja, Y.P.: The school bus routing and scheduling problem with homogenous bus capacity: formulations and their solutions. <http://www.uwindsor.ca/math/sites/uwindsor.ca.math/files/05-06.pdf> (2006)
4. Li, L.Y., Fu, Z.: The school bus routing: a case study. *J. Oper. Res. Soc.* **53**, 552–558 (2002)
5. Minocha, B., Tripathi S., Mohan, C.: Solving vehicle routing and scheduling problems using hybrid genetic algorithm. In: *IEEE Proceedings of 3rd International Conference on Electronics Computer Technology-ICECT 2011*, vol. 2, pp. 189–193. IEEE. [http://ieeexplore.ieee.org/xpl/freeabs\\_all.jsp?arnumber=5941682&reason=concurrency](http://ieeexplore.ieee.org/xpl/freeabs_all.jsp?arnumber=5941682&reason=concurrency)
6. Park, J., Kim, B.: The school bus routing problem: a review. *Eur. J. Oper. Res.* **202**(2), 311–319 (2010)
7. Spasovic, L., Chien, S., Kelnhofer-Feeley, C., Wang, Y., Hu, Q.: A methodology for evaluating of school bus routing-a case study of riverdale, New Jersey. Transportation Research Board 80th Annual Meeting Washington, D.C. Springer, Berlin. <http://transportation.njit.edu/nctip/publications/No01-2088.pdf> (2001)
8. Swersey, A.J., Wilson, B.: Scheduling school buses. *Manag. Sci.* **30**(7), 844–853 (1984)
9. Thangiah, S.R., Fergany, A., Wilson, B., Pitluga, A., Mennell, W.: School bus routing in rural school districts. computer-aided systems in public transport. *Lecture Notes in Economics and Mathematical Systems*, vol. 600(II), pp. 209–232, Springer, Berlin (2008)
10. Toth, P., Vigo. D.: *The Vehicle Routing Problem. Monographs on Discrete Mathematics and Applications*. SIAM, Philadelphia, (2002)

# Taguchi-Based Tuning of Rotation Angles and Population Size in Quantum-Inspired Evolutionary Algorithm for Solving MMDP

Nija Mani, Gursaran, A. K. Sinha and Ashish Mani

**Abstract** Quantum-inspired evolutionary algorithms (QEAs) have been successfully used for solving search and optimization problems. QEAs employ quantum rotation gates as variation operator. The selection of rotation angles in the quantum gate has been mostly performed intuitively. This paper presents tuning of the parameters by designing experiments using well-known Taguchi's method with massively multimodal deceptive problem as the benchmark.

**Keywords** Robust design · Multimodal · Deceptive · Optimization

## 1 Introduction

Quantum-inspired evolutionary algorithms (QEAs) have been successfully applied in solving wide variety of real-life difficult optimization problems, where near-optimal solutions are acceptable and efficient deterministic techniques are not known [1]. QEAs are EAs inspired by the principles of quantum mechanics. They are developed by drawing some ideas from quantum mechanics and integrating them in the current framework of EA. QEAs have performed better than classical evolutionary

---

N. Mani (✉) · Gursaran · A. K. Sinha  
Department of Mathematics, Dayalbagh Educational Institute, Dayalbagh, Agra, India  
e-mail: nijam@acm.org

Gursaran  
e-mail: gursaran.db@gmail.com

A. K. Sinha  
e-mail: arunsinha47@gmail.com

A. Mani  
USIC, Dayalbagh Educational Institute, Dayalbagh, Agra, India  
e-mail: ashish.mani@ieee.org

algorithms (EAs) on many complex problems [1] as they provide better balance between exploration and exploitation due to probabilistic representation of solutions.

The canonical QEA proposed by Han and Kim [2] employs Q-bit as the smallest unit of information, which is essentially a probabilistic bit. The Q-bit is modified by using quantum gates, which are implemented as unitary matrix [2]. A quantum gate known as rotation gate has been widely used in many QEA implementations [1]. It acts as the main variation operator that rotates Q-bit strings to obtain good candidate solutions for the next iteration. It takes into account the relative current fitness level of the individual and the attractor and also their binary bit values for selecting the magnitude and direction of rotation. The magnitude of rotation is a tunable parameter and is selected from a set of eight rotation angles. The value of the rotation angles are problem dependent and require tuning.

The other parameters that require tuning in QEA are population size, group size, and migration period. The effect of population size, group size, and migration period on the performance of QEA have been studied in some detail [2]; however, the eight rotation angles have been mostly set by ad hoc experimentation, which is not a best practice as per [3]. It has also been recommended in [3] that proper design of experimentation should be employed for determining the parameter values.

Taguchi had proposed fractional design of experiments which have been very successful in identifying the parameters that have maximum influence on the process. Though Taguchi's method was developed primarily for improving quality of the product by incorporating it in design and manufacturing process, it has been used in some efforts for tuning of evolutionary algorithms [4] as the process of search in EAs is analogous to industrial process affected by set of tunable parameters with the objective function fitness as the quality characteristics [4]. Taguchi's design of experiment are based on a special set of orthogonal arrays that does not guarantee optimality (unlike factorial design of experiments) but has been shown to find better parameters values than ad hoc experimentation [3]. Further, it does not suffer from curse of dimensionality as in case of factorial design of experiments, in which number of experiments quickly become impractical to execute, e.g., in this study, nine parameters with five levels each have been considered, so according to factorial design of experiments, the total number experiments to be conducted is  $9^5$ , which is a whopping 59,049 experiments. It can be argued that even after considering more than 59,000 experiments, the optimality is not guaranteed in principle as it is dependent on choice of levels, which is determined subjectively. Taguchi's fractional design of experiment reduces the number experiments to a manageable 50 experiments only, which is a reduction by a factor of about 1,200.

## 2 Quantum-Inspired Evolutionary Algorithm

The potential advantages offered by quantum computing [1] have led to the development of approaches that suggest ways to integrate aspects of quantum computing with evolutionary computation [5]. The first attempt was made by Narayan and Moore [6]

to use quantum interpretation for designing a quantum-inspired genetic algorithm. A number of other hybridizations have also been proposed, of which the most popular proposal has been made by Han and Kim [2], which primarily hybridizes the superposition and measurement principles of quantum computing in evolutionary framework by implementing qubit as Q-bit.

A qubit is the smallest information element in quantum computer, which is quantum analog of classical bit. The classical bit can be either in state ‘zero’ or in state ‘one,’ whereas a quantum bit can be in a superposition of basis states in a quantum system [2]. The Q-bit string acts as genotype of the individual and the binary bit string formed by collapsing Q-bit forms the phenotype of the individual. The process of measuring or collapsing Q-bit is performed by generating a random number between 0 and 1 and comparing it with  $|\alpha|^2$ . If the random number is less than  $|\alpha|^2$ , then the Q-bit collapses to 0 or else to 1 and this value is assigned to the corresponding binary bit. Further, the Q-bit is modified by using quantum gates or operators, which are also unitary in nature [7]. The quantum gates are implemented in QEA as unitary matrix, and further details are available in [2].

A quantum gate known as rotation gate has been employed in [2]. It acts as the main variation operator that rotates Q-bit strings to obtain good candidate solutions for the next iteration. It requires an attractor [8] toward, which the Q-bit would be rotated. It further takes into account the relative current fitness level of the individual and the attractor and also their binary bit values for determining the magnitude and direction of rotation. The magnitude of rotation is a tunable parameter and is selected from a set of eight rotation angles viz.,  $\theta_1, \theta_2, \dots, \theta_8$ . The value of the rotation angles is problem dependent and require tuning [2].

The quantum-inspired evolutionary algorithm is as follows [2]:

- (a)  $t = 0$ ; Define Group Size;
- (b) initialize  $Q(t)$ ;
- (c) make  $P(t)$  by observing the states of  $Q(t)$ ;
- (d) evaluate  $P(t)$ ;
- (e) store the best solutions among  $P(t)$  into  $B(t)$ ;
- (f) while (termination condition is not met) {
- (g)      $t = t + 1$ ;
- (h)     make  $P(t)$  by observing the states of  $Q(t-1)$ ;
- (i)     evaluate  $P(t)$ ;
- (j)     Determine the attractors  $Atr(t)$ ;
- (k)     update  $Q(t)$  according to  $P(t)$  and  $Atr(t)$  using Q-gate;
- (l)     store the best solutions among  $B(t-1)$  and  $P(t)$  into  $B(t)$ ;
- (m)     store the best solution  $b$  among  $B(t)$ ;
- (n)     if(migration condition)
- (o)     migrate  $b$  or  $b^i$  to  $B(t)$  globally or locally, respectively
- }

In step (b), the qubit register  $Q(t)$  containing Q-bit strings for all the individuals is initialized randomly. In step (c), the binary solutions in  $P(0)$  are constructed by

observing the states of  $Q(0)$ . In a quantum computer, the act of observing a quantum state collapses it to a single state. However, collapsing into a single state does not occur in QEA, since QEA runs on a digital computer, not on a quantum computer. In step (d), each binary solution is evaluated to give a measure of its fitness. In step (e), the initial best solutions are then selected among the binary solutions  $P(0)$ , and stored into  $B(0)$ . In steps (f) and (g), iteratively, the binary solutions in  $P(t)$  are formed by observing the states of  $Q(t - 1)$  as in step (c), and each binary solution is evaluated for the fitness value. In step (j), the attractors are determined for each individual according to the strategy. In step (k), Q-bit individuals in  $Q(t)$  are updated by applying Q-gates by taking into account  $Atr(t)$ ,  $b$  and  $P(t)$ , which is defined as a variation operator of QEA. The variation operator is rotation gate. In steps (l) and (m), the best solutions among  $B(t - 1)$  and  $P(t)$  are selected and stored into  $B(t)$ , and if the best solution stored in  $B(t)$  is better fitted than the stored best solution  $b$ , the stored solution is replaced by the new one.

In step (n), a migration condition is checked and if satisfied, the best solution  $b$  is migrated to  $B(t)$  or the best among some of the solutions in  $B(t)$ ,  $b_j^t$ , is migrated to them. The migration condition and local groups are taken to be design parameters and have to be chosen appropriately for the problem at hand.

It is suggested that QEA should have a local migration in every iteration and global migration after every 100 iterations. The group size is taken as five.

### 3 Design of Experiments

The design of experiment follows guidelines given in [3] and is outlined below:

1. The process objective describing the quality of the algorithm is the objective fitness function value.
2. The design parameters are the eight rotation angle parameters ( $\theta_1$  to  $\theta_8$ ) in the Q-gate and the population size. The number of levels has been taken as five for each parameter so that we can investigate them thoroughly. The value of each level for all the parameters is shown in Table 1.
3. There are a total of nine parameters and five levels, so the orthogonal array listed in L50 has been selected [9] for deciding the experiments; hence, a total of fifty experiments have been conducted.
4. Thirty runs of QEA with different sets of random numbers have been conducted for each experiment. The experiments data have been collected for mean and variance of objective fitness value.
5. The primary interest in design of EAs is to have better mean value rather than signal to noise ratio. Therefore, data analysis has been reported in this work for the mean value only.

The experimentation is performed by using massively multimodal deceptive problem as benchmark, with size  $k = 40$ , which is a large instance [10]. This problem

**Table 1** Parameter levels

Parameters	L1	L2	L3	L4	L5
$\theta_1$	0	$-0.0025 \pi$	$-0.005 \pi$	$-0.01 \pi$	$-0.05 \pi$
$\theta_2$	0	$-0.0025 \pi$	$-0.005 \pi$	$-0.01 \pi$	$-0.05 \pi$
$\theta_3$	0	$+0.005 \pi$	$+0.01 \pi$	$+0.05 \pi$	$+0.1 \pi$
$\theta_4$	0	$-0.0025 \pi$	$-0.005 \pi$	$-0.01 \pi$	$-0.05 \pi$
$\theta_5$	0	$-0.005 \pi$	$-0.01 \pi$	$-0.05 \pi$	$-0.1 \pi$
$\theta_6$	0	$+0.0025 \pi$	$+0.005 \pi$	$+0.01 \pi$	$+0.05 \pi$
$\theta_7$	0	$+0.0025 \pi$	$+0.005 \pi$	$+0.01 \pi$	$+0.05 \pi$
$\theta_8$	0	$+0.0025 \pi$	$+0.005 \pi$	$+0.01 \pi$	$+0.05 \pi$
Population size	10	15	25	35	50

is difficult for EAs as the numbers of local maxima are very large as compared with global maxima. Further, the fitness landscape is such that EA finds it very convenient to reach the local maxima, but searching global maxima is extremely difficult as it is located at the extreme ends of subproblem string.

## 4 Results and Analysis

The results of the experiments conducted by employing Taguchi’s method are summarized in Table 2. The results show that best set of parameters values identified from the experiments are  $-0.005 \pi$  for  $\theta_1$ ,  $-0.01 \pi$  for  $\theta_2$ ,  $+0.1 \pi$  for  $\theta_3$ ,  $-0.05 \pi$  for  $\theta_4$ ,  $-0.005 \pi$  for  $\theta_5$ ,  $+0.01 \pi$  for  $\theta_6$ ,  $+0.005 \pi$  for  $\theta_7$ ,  $+0.0025 \pi$  for  $\theta_8$ , 25 for population size. Table 3 shows comparison between the performance of QEA with parameters’ value tuned with Taguchi’s method and the performance of QEA with parameters’ value at recommended setting derived by ad hoc experimentation as reported in the literature [1, 2]. The result in Table 3 indicates the superiority of the Taguchi’s method over ad hoc experimentation for finding suitable values of parameters.

**Table 2** Results of parameter optimization

L	$\theta_1$	$\theta_2$	$\theta_3$	$\theta_4$	$\theta_5$	$\theta_6$	$\theta_7$	$\theta_8$	Pop size
1	37.13	35.38	32.23	35.74	37.43	33.34	36.23	33.83	33.52
2	36.25	36.64	36.02	34.95	<b>38.63</b>	37.87	36.28	<b>37.59</b>	36.64
3	<b>37.49</b>	35.12	37.76	36.00	35.33	35.06	<b>36.79</b>	37.42	<b>37.17</b>
4	32.74	<b>37.09</b>	35.65	35.70	32.88	<b>37.92</b>	34.47	35.19	36.98
5	36.49	35.87	<b>38.77</b>	<b>36.29</b>	35.96	35.64	36.32	35.88	35.68

**Table 3** Comparison between Adhoc-tuned and Taguchi-tuned QEAs

	Adhoc-tuned QEA	Taguchi-tuned QEA
Optimal		40
Best	40	40
Median	39.64058	40
Worst	38.5623	40
Mean	39.4968	40
SD	0.418	0.0
Percentage success runs	26.67	100

The ad hoc-tuned QEA had all  $\theta$ s set to zero except  $\theta_3(= 0.01\pi)$  and  $\theta_5(= -0.01\pi)$  and with population size as 25, and the comparison has been made over 30 independent runs.

## 5 Conclusion

QEAs are evolutionary algorithms, which provide better balance between exploration and exploitation and have been widely used for solving difficult problems. This paper highlights issues in tuning of parameters and shows the utility of Taguchi-based method for tuning of parameters, especially the eight rotation angles and population size.

Further studies will include more comprehensive study by including other parameters on a suite of difficult problems.

## References

1. Zhang, G.: Quantum-inspired evolutionary algorithms: a survey and empirical study. *J Heuristics* **17**, 303–351 (2011)
2. Han, K.H., Kim, J.H.: Quantum-inspired Evolutionary Algorithm for a Class of Combinatorial Optimization. *IEEE Trans. on Evo. Comp.* **6**(6), 580–593 (2002)
3. Adenso-Diaz, B., Laguna, M.: Fine-Tuning of Algorithms using Fractional Experimental Designs and Local Search. *Op. Res.* **54**(1), 99–114 (2006)
4. Hippolyte, J.L., Bloch, C., Chatonnay P., Espanet, C., Chamagne, D., and Wimmer, G.: Tuning an Evolutionary Algorithm with Taguchi Methods and Application to the dimensioning of an Electrical Motor. *Proc. CSTST-2008*, 265–272 (2008).
5. Sofge, D. A.: *Prospective Algorithms for Quantum Evolutionary Computation*. Proc. QI-2008, College Publications, UK, 2008.
6. Narayanan, A. and Moore M. : Quantum-inspired genetic algorithms. *Proc. IEEE CEC-1996*, 61–66, (1996).
7. Nielsen, M.A. and Chuang, I.L.: *Quantum Computation and Quantum Information*. Cambridge University Press, Cambridge.



8. Platelt, M.D., Schliebs, S., Kasabov, N.: A Verstaile Quantum-inspired Evolutionary Algorithm. Proc. of IEEE CEC **2007**, 423–430 (2007)
9. Design of experiments via Taguchi methods: orthogonal arrays available at [https://controls.engin.umich.edu/wiki/index.php/Design\\_of\\_experiments\\_via\\_taguchi\\_methods:\\_orthogonal\\_arrays](https://controls.engin.umich.edu/wiki/index.php/Design_of_experiments_via_taguchi_methods:_orthogonal_arrays)
10. Alba, E., Dorronsoro, B.: The exploration / exploitation tradeoff in dynamic cellular genetic algorithms. IEEE Trans. Evo. Co. **8**(2), 126–142 (2005)

**Part II**  
**Soft Computing for Mathematics**  
**and Optimization (SCMO)**

# Simultaneous Feature Selection and Extraction Using Fuzzy Rough Sets

Pradipta Maji and Partha Garai

**Abstract** In this chapter, a novel dimensionality reduction method, based on fuzzy rough sets, is presented, which simultaneously selects attributes and extracts features using the concept of feature significance. The method is based on maximizing both relevance and significance of the reduced feature set, whereby redundancy therein is removed. The chapter also presents classical and neighborhood rough sets for computing relevance and significance of the feature set and compares their performance with that of fuzzy rough sets based on the predictive accuracy of nearest neighbor rule, support vector machine, and decision tree. The effectiveness of the proposed fuzzy rough set-based dimensionality reduction method, along with a comparison with existing attribute selection and feature extraction methods, is demonstrated on real-life data sets.

## 1 Introduction

Dimensionality reduction is a process of selecting a map by which a sample in an  $m$ -dimensional measurement space is transformed into an object in a  $d$ -dimensional feature space, where  $d < m$ . The problem of dimensionality reduction has two aspects, namely formulation of a suitable criterion to evaluate the goodness of a feature set and searching the optimal set in terms of the criterion. The major mathematical measures so far devised for the estimation of feature quality can be broadly classified into two categories, namely feature selection in measurement space and feature selection in a transformed space. The techniques in the first category generally reduce the

---

P. Maji (✉) · P. Garai  
Machine Intelligence Unit, Indian Statistical Institute, 203, BT Road,  
Kolkata 700108, India  
e-mail: pmaji@isical.ac.in

P. Garai  
e-mail: parthagarai\_r@isical.ac.in

dimensionality of measurement space by discarding redundant or least information-carrying features. On the other hand, those in second category utilize all information contained in the measurement space to obtain a new transformed space, thereby mapping a higher dimensional pattern to a lower dimensional one. This is referred to as feature extraction [1].

An optimal feature subset selected or extracted by a dimensionality reduction method is always relative to a certain feature evaluation criterion. In general, different criteria may lead to different optimal feature subsets. However, every criterion tries to measure the discriminating ability of a feature or a subset of features to distinguish different class labels. One of the main problems in real-life data analysis is uncertainty. Some of the sources of this uncertainty include incompleteness and vagueness in class definitions. In this background, the rough set theory [2] has gained popularity in modeling and propagating uncertainty. Rough sets can be used to find most informative feature subset of original attributes from a given data with discretized attribute values [3, 4]. However, there are usually real-valued data and fuzzy information in real-world applications. In rough sets, the real-valued features are divided into several discrete partitions, and the dependency or quality of approximation of a feature is calculated. The inherent error that exists in discretization process is of major concern in the computation of the dependency of real-valued features. Combining fuzzy and rough sets provides an important direction in reasoning with uncertainty for real-valued data [5]. They are complementary in some aspects. The generalized theories of rough fuzzy computing have been applied successfully to feature selection of real-valued data set [5–7]. Also, neighborhood rough sets [8] are found to be suitable for both numerical and categorical data sets.

On the other hand, a feature extraction technique such as principal component analysis (PCA), linear discriminant analysis, and independent component analysis [1] generates a new set of features using a mapping function that takes some linear or nonlinear combination of original features. While PCA uses a linear orthogonal transformation to project a sample space containing possibly correlated variables into a different space with uncorrelated variables, independent component analysis decomposes a multidimensional feature vector into statistically independent components to reveal the hidden factors from a set of random variables [1]. In general, a feature extraction technique provides a richer feature subset than that obtained using a feature selection algorithm with a higher cost. Hence, it is very difficult to decide whether to select a feature from original measurement space or to extract a new feature by transforming the existing features for a given data set. A dimensionality reduction algorithm needs to be formulated, which can simultaneously select or extract features depending upon the criteria, integrating the merits of both feature selection and extraction techniques.

In this regard, a novel dimensionality reduction algorithm is proposed based on fuzzy rough sets, which simultaneously selects and extracts features from a given data set. Using the concept of feature significance, the feature set in each iteration is partitioned into three subsets, namely insignificant, dispensable, and significant feature sets. The insignificant feature set is discarded from the current feature set, while significant feature set is used to select or extract a feature in the next iteration.

Depending on the quality of features present in the dispensable set of current iteration, a new feature is extracted or an existing feature is selected from the dispensable set for reduced feature set. In effect, the final reduced feature set may simultaneously contain some original features of measurement space and extracted new features of transformed space, which are both relevant and significant. The effectiveness of the proposed fuzzy rough dimensionality reduction method, along with a comparison with other methods, is demonstrated on a set of real-life data.

## 2 Proposed Dimensionality Reduction Method

In this section, a new dimensionality reduction method is presented, integrating fuzzy rough sets and the merits of feature selection and extraction techniques.

### 2.1 Fuzzy Rough Sets

A crisp equivalence relation induces a crisp partition of the universe and generates a family of crisp equivalence classes. Correspondingly, a fuzzy equivalence relation generates a fuzzy partition of the universe and a series of fuzzy equivalence classes or fuzzy knowledge granules. This means that the decision and condition attributes may all be fuzzy [9]. Let  $\langle \mathbb{U}, \mathbb{A} \rangle$  represents a fuzzy approximation space and  $X$  is a fuzzy subset of  $\mathbb{U}$ . The fuzzy  $\mathbb{P}$ -lower and  $\mathbb{P}$ -upper approximations are then defined as follows [9]:

$$\mu_{\underline{\mathbb{P}}X}(F_i) = \inf_x \{\max\{(1 - \mu_{F_i}(x)), \mu_X(x)\}\} \quad \forall i \quad (1)$$

$$\mu_{\overline{\mathbb{P}}X}(F_i) = \sup_x \{\min\{\mu_{F_i}(x), \mu_X(x)\}\} \quad \forall i \quad (2)$$

where  $F_i$  represents a fuzzy equivalence class belonging to  $\mathbb{U}/\mathbb{P}$ , the partition of  $\mathbb{U}$  generated by  $\mathbb{P} \subseteq \mathbb{A}$ , and  $\mu_X(x)$  represents the membership of object  $x$  in  $X$ . These definitions diverge a little from the crisp upper and lower approximations, as the memberships of individual objects to the approximations are not explicitly available. As a result of this, the fuzzy lower and upper approximations can be defined as [5]

$$\mu_{\underline{\mathbb{P}}X}(x) = \sup_{F_i \in \mathbb{U}/\mathbb{P}} \min\{\mu_{F_i}(x), \mu_{\underline{\mathbb{P}}X}(F_i)\} \quad (3)$$

$$\mu_{\overline{\mathbb{P}}X}(x) = \sup_{F_i \in \mathbb{U}/\mathbb{P}} \min\{\mu_{F_i}(x), \mu_{\overline{\mathbb{P}}X}(F_i)\}. \quad (4)$$

The tuple  $\langle \underline{\mathbb{P}}X, \overline{\mathbb{P}}X \rangle$  is called a fuzzy rough set. This definition degenerates to traditional rough sets when all equivalence classes are crisp. The membership of an object  $x \in \mathbb{U}$  belonging to the fuzzy positive region is

$$\mu_{\text{POS}_{\mathbb{C}}(\mathbb{D})}(x) = \sup_{X \in \mathbb{U}/\mathbb{D}} \mu_{\underline{\mathbb{C}}X}(x) \quad (5)$$

where  $\mathbb{A} = \mathbb{C} \cup \mathbb{D}$ . Using the definition of fuzzy positive region, the dependency function can be defined as follows [5]:

$$\gamma_{\mathbb{C}}(\mathbb{D}) = \frac{|\mu_{\text{POS}_{\mathbb{C}}(\mathbb{D})}(x)|}{|\mathbb{U}|} = \frac{1}{|\mathbb{U}|} \sum_{x \in \mathbb{U}} \mu_{\text{POS}_{\mathbb{C}}(\mathbb{D})}(x). \quad (6)$$

## 2.2 Feature Significance

Let  $\mathbb{U} = \{x_1, \dots, x_i, \dots, x_n\}$  be the set of  $n$  samples and  $\mathbb{C} = \{\mathcal{A}_1, \dots, \mathcal{A}_j, \dots, \mathcal{A}_m\}$  denotes the set of  $m$  features of a given data set. Define  $\gamma_{\mathcal{A}_i}(\mathbb{D})$  as the relevance of the feature  $\mathcal{A}_i$  with respect to the class label or decision attribute  $\mathbb{D}$ . The relevance represents the quality of a feature or degree of dependency of decision attribute  $\mathbb{D}$  on condition attribute  $\mathcal{A}_i$ . To what extent a feature is contributing to calculate the joint relevance or dependency can be calculated by the significance of that feature. The change in dependency when a feature is removed from the set of features is a measure of the significance of the feature.

**Definition 1** The significance of a feature  $\mathcal{A}_j$  with respect to another feature  $\mathcal{A}_i$  can be defined as follows:

$$\sigma_{\{\mathcal{A}_i, \mathcal{A}_j\}}(\mathcal{A}_j, \mathbb{D}) = \gamma_{\{\mathcal{A}_i, \mathcal{A}_j\}}(\mathbb{D}) - \gamma_{\mathcal{A}_i}(\mathbb{D}). \quad (7)$$

Hence, the significance of a feature  $\mathcal{A}_j$  is the change in dependency when the feature  $\mathcal{A}_j$  is removed from the set  $\{\mathcal{A}_i, \mathcal{A}_j\}$ . The higher the change in dependency, the more significant feature  $\mathcal{A}_j$  is. If significance is 0, then feature  $\mathcal{A}_j$  is dispensable. The following properties can be stated about the measure:

1.  $\sigma_{\{\mathcal{A}_i, \mathcal{A}_j\}}(\mathcal{A}_j, \mathbb{D}) = 0$  if and only if the feature  $\mathcal{A}_j$  is dispensable in the set  $\{\mathcal{A}_i, \mathcal{A}_j\}$ .
2.  $\sigma_{\{\mathcal{A}_i, \mathcal{A}_j\}}(\mathcal{A}_j, \mathbb{D}) < 0$  if the feature  $\mathcal{A}_i$  is more relevant than the feature set  $\{\mathcal{A}_i, \mathcal{A}_j\}$ .
3.  $\sigma_{\{\mathcal{A}_i, \mathcal{A}_j\}}(\mathcal{A}_j, \mathbb{D}) > 0$  if the feature  $\mathcal{A}_j$  is significant with respect to another feature  $\mathcal{A}_i$ .
4.  $\sigma_{\{\mathcal{A}_i, \mathcal{A}_j\}}(\mathcal{A}_j, \mathbb{D}) \neq \sigma_{\{\mathcal{A}_i, \mathcal{A}_j\}}(\mathcal{A}_i, \mathbb{D})$  (asymmetric).

## 2.3 Simultaneous Feature Selection and Extraction

The high-dimensional real-life data set generally may contain a number of nonrelevant and insignificant features. The presence of such features may lead to a reduction

in the useful information. Ideally, the reduced feature set obtained using a dimensionality reduction algorithm should contain features those have high relevance with the classes, while the significance among them would be as high as possible. The relevant and significant features are expected to be able to predict the classes of the samples. Hence, to assess the effectiveness of the features, both relevance and significance need to be measured quantitatively. The proposed dimensionality reduction method addresses the above issues through the following three phases:

1. computation of the relevance of each feature present in original feature set;
2. determination of the insignificant, dispensable, and significant feature sets; and
3. extraction of a relevant feature from the dispensable set.

The fuzzy rough set is used to compute both relevance and significance of features. The insignificant feature set is discarded from the whole feature set, while the significant feature set is used to select or extract significant features for reduced feature set. Let  $\gamma_{\mathcal{A}_i}(\mathbb{D})$  represents the relevance of feature  $\mathcal{A}_i \in \mathbb{C}$ . The proposed algorithm starts with a single feature  $\mathcal{A}_i$  that has the highest relevance value. Based on the significance values of all other features, the feature set  $\mathbb{C}$  is then partitioned into three subsets, namely insignificant set  $I_i$ , dispensable set  $D_i$ , and significant set  $S_i$ , which are defined as follows:

$$I_i = \{\mathcal{A}_j | \sigma_{\{\mathcal{A}_i, \mathcal{A}_j\}}(\mathcal{A}_j, \mathbb{D}) < -\delta_i; \mathcal{A}_j \neq \mathcal{A}_i \in \mathbb{C}\} \quad (8)$$

$$D_i = \{\mathcal{A}_j | -\delta_i \leq \sigma_{\{\mathcal{A}_i, \mathcal{A}_j\}}(\mathcal{A}_j, \mathbb{D}) \leq \delta_i; \mathcal{A}_j \neq \mathcal{A}_i \in \mathbb{C}\} \quad (9)$$

$$S_i = \{\mathcal{A}_j | \sigma_{\{\mathcal{A}_i, \mathcal{A}_j\}}(\mathcal{A}_j, \mathbb{D}) > \delta_i; \mathcal{A}_j \neq \mathcal{A}_i \in \mathbb{C}\} \quad (10)$$

where  $\mathbb{C} = I_i \cup D_i \cup S_i \cup \{\mathcal{A}_i\}$  and  $\delta_i$  is a predefined threshold value corresponding to the feature  $\mathcal{A}_i$ .

The insignificant set  $I_i$  represents the set of features those are insignificant with respect to the candidate feature  $\mathcal{A}_i$  of the current iteration. Hence, the insignificant set  $I_i$  should be discarded from the whole feature set  $\mathbb{C}$  as the presence of such insignificant features may lead to a reduction in the useful information. If insignificant features are present in the reduced feature set, they may reduce the classification or clustering performance. The significant set  $S_i$  consists of a set of features those are significant with respect to the feature  $\mathcal{A}_i$ . In other words, the set  $S_i$  represents the set of features of  $\mathbb{C}$  those have the significance values with respect to the feature  $\mathcal{A}_i$  greater than the threshold  $\delta_i$ . This set is considered in the next iteration to select or extract a new feature.

On the other hand, the dispensable set  $D_i$  is used for extracting a new feature in the current iteration. As the significance values of the features present in the dispensable set are very low, they form a group of similar features. These features may be considered to generate a new feature. However, the similar features of dispensable set may be in phase or out of phase with respect to each other. Hence, the following definition can be used to extract a new feature  $\overline{\mathcal{A}_i}$  from the dispensable set of features  $D_i$ :

$$\overline{\mathcal{A}}_i = \frac{\mathcal{A}_i + \sum \lambda_j \mathcal{A}_j}{1 + \sum |\lambda_j|} \text{ where } \lambda_j \in \{-1, 0, 1\} \text{ and } \mathcal{A}_j \in D_i. \quad (11)$$

To find out the value of  $\lambda_j$  for each feature  $\mathcal{A}_j \in D_i$ , the following greedy algorithm can be used. Let  $\mathcal{A}_i$  be the initial representative of the set  $D_i$ . The representative of  $D_i$  is refined incrementally. By searching among the features of set  $D_i$ , the current representative is merged and averaged with other features, both in phase and out of phase, such that the augmented representative  $\overline{\mathcal{A}}_i$  increases the relevance value. The merging process is repeated until the relevance value can no longer be improved. If a feature  $\mathcal{A}_j \in D_i$  in phase (respectively, out of phase) with the feature  $\mathcal{A}_i$  increases the relevance value, then  $\lambda_j = 1$  (respectively,  $\lambda_j = -1$ ). On the other hand, the value of  $\lambda_j = 0$  if feature  $\mathcal{A}_j$  does not increase the relevance value, irrespective of the phases.

After extracting the feature  $\overline{\mathcal{A}}_i$  from the dispensable set  $D_i$  using (11), the insignificant feature set  $I_i$  and used features of  $D_i$  are discarded from the whole feature set  $\mathbb{C}$ . From the remaining features of  $\mathbb{C}$ , another feature  $\mathcal{A}_j$  is selected by maximizing the following condition:

$$\gamma_{\mathcal{A}_j}(\mathbb{D}) + \frac{1}{|\mathbb{S}|} \sum_{\overline{\mathcal{A}}_i \in \mathbb{S}} \sigma_{\{\overline{\mathcal{A}}_i, \mathcal{A}_j\}}(\mathcal{A}_j, \mathbb{D}) \quad (12)$$

where  $\mathbb{S}$  is the already selected or extracted feature set. The process is repeated to select or extract more features. In the proposed dimensionality reduction method, both relevance and significance of a set of features are computed using fuzzy rough sets. If  $\lambda_j = 0$  for all  $\mathcal{A}_j \in D_i$ , then the extracted feature  $\overline{\mathcal{A}}_i$  at a particular iteration is actually the candidate feature  $\mathcal{A}_i$  of the original feature set  $\mathbb{C}$ . Hence, the proposed dimensionality reduction method generates a reduced feature set  $\mathbb{S}$  that may simultaneously contain some selected features of original measurement space and some extracted features of transformed feature space, which are both relevant and significant.

### 3 Experimental Results

The performance of the proposed fuzzy rough simultaneous attribute selection and feature extraction method is extensively studied and compared with that of some existing feature selection and extraction algorithms, namely maximal-relevance (Max-Relevance) and maximal-relevance maximal-significance (MRMS) [4] frameworks with classical, neighborhood, and fuzzy rough sets, quick reduct (Max-Dependency and rough sets) [3], fuzzy rough quick reduct (Max-Dependency and fuzzy rough sets) [5], neighborhood quick reduct (Max-Dependency and neighborhood rough sets) [8], minimal-redundancy maximal-relevance (mRMR) framework [10], fuzzy rough set-based mRMR framework (fuzzy rough mRMR) [7], and PCA [1].



### 3.1 Performance of Various Rough Set Models

In dimensionality reduction method, the reduced feature set is always relative to a certain feature evaluation index. In general, different evaluation indices may lead to different reduced feature subsets. To establish the effectiveness of fuzzy rough sets over Pawlak’s or classical and neighborhood rough sets, extensive experiments are done on various data sets. Table 1 presents the comparative performance of different rough set models for simultaneous attribute selection and feature extraction tasks. The results and subsequent discussions are presented in this table with respect to the classification accuracy of the K-NN, SVM, and C4.5 on test samples considering the optimum parameter values.

From the results reported in Table 1, it can be seen that the proposed dimensionality reduction method based on fuzzy rough sets attains maximum classification accuracy of the K-NN, SVM, and C4.5 in most of the cases. Out of 12 cases of training–testing, the proposed method with fuzzy rough sets achieves highest classification accuracy in 10 cases, while that with classical or Pawlak’s rough sets attains it only in 2 cases. The better performance of the fuzzy rough sets is achieved due to the fact that it can capture uncertainties associated with the data more accurately.

### 3.2 Performance of Different Algorithms

Finally, Table 2 compares the performance of the proposed fuzzy rough simultaneous feature selection and extraction algorithm with that of different existing feature selection and extraction algorithms on various data sets.

From the results reported in Table 2, it is seen that the proposed dimensionality reduction method achieves highest classification accuracy of SVM, C4.5, and K-NN in 11 cases out of total 12 cases, while the PCA attains highest classification accuracy in only 1 case. The proposed method also provides higher classification accuracy than the max-Relevance, max-Dependency, and MRMS criteria in all cases, irrespective of the classifiers, rough sets, and data sets used.

Hence, all the results reported in Table 2 confirms that the proposed fuzzy rough dimensionality reduction method selects a set of features having highest classification

**Table 1** Performance of various rough set models on different data sets

Different data sets	Test accuracy of K-NN			Test accuracy of SVM			Test accuracy of C4.5		
	Classical	Neighbor	Fuzzy	Classical	Neighbor	Fuzzy	Classical	Neighbor	Fuzzy
Satimage	84.65	87.50	87.55	84.45	83.60	87.35	82.40	83.95	87.20
Segmentation	87.61	85.76	86.24	91.38	91.38	92.33	90.90	89.98	90.33
Leukemia II	91.07	91.07	94.64	91.07	90.17	93.75	91.07	90.17	93.75
Breast II	84.21	94.73	94.73	89.47	94.73	94.73	100	100	100

**Table 2** Comparative performance analysis of different methods

Methods/ algorithms	Different rough sets	Satimage			Segmentation			Leukemia II			Breast II		
		K-NN	SVM	C4.5	K-NN	SVM	C4.5	K-NN	SVM	C4.5	K-NN	SVM	C4.5
Max-relevance	Classical	69.20	67.25	67.45	63.16	57.89	63.16	81.25	81.25	81.25	67.90	78.86	77.48
	Neighborhood	77.70	74.65	79.60	78.95	73.68	73.68	83.04	80.36	80.36	76.81	78.86	77.48
	Fuzzy	77.90	76.40	80.00	78.95	78.95	78.95	83.04	82.14	82.14	82.10	80.86	78.76
Max-dependency	Classical	70.40	67.30	67.45	63.16	57.89	68.42	82.14	82.14	82.14	67.90	82.48	81.78
	Neighborhood	83.20	81.70	81.45	78.95	73.68	73.68	85.71	83.03	83.03	81.45	82.48	82.80
	Fuzzy	83.20	83.00	82.80	78.95	78.95	78.95	85.71	84.82	84.82	84.19	83.76	82.76
MRMS	Classical	74.00	73.85	74.10	72.67	74.10	74.67	84.82	85.71	85.71	84.21	84.21	84.21
	Neighborhood	83.40	85.00	85.15	80.52	82.57	83.24	87.50	89.29	88.39	84.21	89.47	89.47
	Fuzzy	84.10	84.10	84.10	80.76	83.95	85.14	88.39	90.18	89.29	89.47	94.74	94.74
Classical mRMR		75.45	75.40	75.35	72.81	73.76	74.33	84.82	84.82	84.82	84.21	84.21	89.47
	Fuzzy rough mRMR	83.95	84.60	83.70	80.33	84.10	84.71	87.50	89.29	90.18	89.47	89.47	94.74
	PCA	82.55	83.95	82.00	78.94	89.47	94.73	80.35	78.59	79.46	77.30	79.50	74.10
Proposed fuzzy rough		87.55	87.35	87.20	86.24	92.33	90.33	94.64	93.75	93.75	94.73	94.73	100

accuracy of the K-NN, SVM, and C4.5 in most of the cases, irrespective of the data sets. Also, the proposed method can potentially yield significantly better results than the existing algorithms. The better performance of the proposed method is achieved due to the fact that it provides an efficient way to simultaneously select and extract features for classification. In effect, a reduced set of features having maximum relevance and significance is being obtained using the proposed method.

## 4 Conclusion

This chapter presents a novel dimensionality reduction method, integrating judiciously the theory of fuzzy rough sets and merits of both attribute selection and feature extraction. An efficient algorithm is introduced by performing simultaneous feature selection and extraction. It uses the concept of fuzzy rough feature significance for finding significant and relevant features of real-valued data sets. Finally, the effectiveness of the proposed method is presented, along with a comparison with other related algorithms, on a set of real-life data sets.

**Acknowledgments** This work is partially supported by the Indian National Science Academy, New Delhi (grant no. SP/YSP/68/2012). The work was done when one of the authors, P. Garai, was a DST-INSPIRE Fellow of the Department of Science and Technology, Government of India.

## References

1. Duda, R.O., Hart, P.E., Stork, D.G.: Pattern Classification and Scene Analysis. Wiley Inc., New York (2000)
2. Pawlak, Z.: Rough Sets: Theoretical Aspects of Reasoning About Data. Kluwer, Dordrecht (1991)
3. Chouchoulas, A., Shen, Q.: Rough set-aided keyword reduction for text categorisation. *Appl. Artif. Intell.* **15**(9), 843–873 (2001)
4. Maji, P., Paul, S.: Rough set based maximum relevance-maximum significance criterion and gene selection from microarray data. *Int. J. Approximate Reasoning* **52**(3), 408–426 (2011)
5. Jensen, R., Shen, Q.: Semantics-preserving dimensionality reduction: rough and fuzzy-rough-based approach. *IEEE Trans. Knowl. Data Eng.* **16**(12), 1457–1471 (2004)
6. Maji, P., Pal, S.K.: Rough-Fuzzy Pattern Recognition: Applications in Bioinformatics and Medical Imaging. Wiley, New Jersey (2012)
7. Maji, P., Pal, S.K.: Feature selection using  $f$ -information measures in fuzzy approximation spaces. *IEEE Trans. Knowl. Data Eng.* **22**(6), 854–867 (2010)
8. Hu, Q., Yu, D., Liu, J., Wu, C.: Neighborhood rough set based heterogeneous feature subset selection. *Inf. Sci.* **178**, 3577–3594 (2008)
9. Dubois, D., Prade, H.: Rough fuzzy sets and fuzzy rough sets. *Int. J. Gen. Syst.* **17**, 191–209 (1990)
10. Peng, H., Long, F., Ding, C.: Feature selection based on mutual information: criteria of max-dependency, max-relevance, and min-redundancy. *IEEE Trans. Pattern Anal. Mach. Intell.* **27**(8), 1226–1238 (2005)

# A Fuzzy Programming Approach for Bilevel Stochastic Programming

Nilkanta Modak and Animesh Biswas

**Abstract** This article presents a fuzzy programming (FP) method for modeling and solving bilevel stochastic decision-making problems involving fuzzy random variables (FRVs) associated with the parameters of the objectives at different hierarchical decision-making units as well as system constraints. In model formulation process, an expectation model is generated first on the basis of the fuzzy random variables involved with the objectives at each level. The problem is then converted into a FP model by considering the fuzzily described chance constraints with the aid of applying chance constrained methodology in a fuzzy context. After that, the model is decomposed on the basis of tolerance ranges of fuzzy numbers associated with the parameters of the problem. To construct the fuzzy goals of the decomposed objectives of both decision-making levels under the extended feasible region defined by the decomposed system constraints, the individual optimal values of each objective at each level are calculated in isolation. Then, the membership functions are formulated to measure the degree of satisfaction of each decomposed objectives in both the levels. In the solution process, the membership functions are converted into membership goals by assigning unity as the aspiration level to each of them. Finally, a fuzzy goal programming model is developed to achieving the highest membership degree to the extent possible by minimizing the under deviational variables of the membership goals of the objectives of the decision makers (DMs) in a hierarchical decision-making environment. To expound the application potentiality of the approach, a numerical example is solved.

**Keywords** Bilevel programming · Stochastic programming · Fuzzy random variable · Fuzzy goal programming

---

N. Modak · A. Biswas (✉)  
Department of Mathematics, University of Kalyani, Kalyani 741235, India  
e-mail: nmodak9@gmail.com

A. Biswas  
e-mail: abiswaskln@rediffmail.com

## 1 Introduction

Bilevel programming (BLP) is considered as a hierarchical decision-making problem in which decision makers (DMs) locating at two hierarchical levels independently controls a vector of decision variables for optimizing his/her own pay off by taking serious attention to the benefit of the other. In the decision-making situation, although the execution of decision is sequential from higher level to lower level, the decision for optimizing the objective of the upper level DM (leader) is often affected by the reaction of the lower level DM (follower) due to his/her dissatisfaction with the decision. In such cases, the problem for proper distribution of decision power to the DMs is often encountered and decision deadlock arises.

To solve BLP problems (BLPPs), several approaches are developed by some pioneer researchers in the field, viz. Kuhn–Tucker approach [1], kth best solution approach [2], penalty function approach [3], complementary pivot approach [4]. But the use of classical approaches developed so far often leads to the paradox that the decision of the follower dominates the decision of leader and the methods do not always provide satisfactory decision in a highly conflicting hierarchical decision situation.

Considering uncertainties involved with most of the mathematical programming, probabilistic programming and fuzzy programming (FP) advanced to deal with different inexact parameters values and inherent uncertain characteristic of decision parameters. The stochastic programming (SP) is a field of probabilistic programming where the parameters associated with the objectives are random variables. The methodology to solve this kind of problem was introduced by Charnes and Cooper [5] for its potential applications in various real-life planning problems [6]. SP is further classified as chance constrained programming (CCP) if some or more constraints are probabilistic in nature following some sort of probability distribution. Different aspects of CCP were studied [7] in the past.

In model formulation process, it is often found that the parameters involved with the model cannot be defined precisely. Under this situation, FP is appeared as a powerful technique to solve optimization problem, which was developed by Zimmermann [8], Klir and Yuan [9], and others based on fuzzy set theory [10]. The main difficulty with conventional FP approach is that re-evaluation of the problem again and again by redefining membership values of the objectives is involved to reach satisfactory decision.

To avoid such computational difficulties, fuzzy goal programming (FGP) [11] for solving BLPP has been presented by Biswas and Bose [12] in the recent past. Considering fuzziness involved with different CCP or SP problems, Luhadjula and Joubert [13] developed some technique by using fuzzy random variable (FRV) to solve CCP problems in fuzzy environment. A methodology for solving CCP problems through expectation model by using FGP technique has been recently studied by Biswas and Modak [14].

In real-life decision-making context, it is often found that the probability of occurrence of the objective of the DM at higher level is not the same as that of lower level,

and also, the parameters involved with the objectives as well as system constraints are not defined precisely. To capture this type of uncertainties, stochastic BLP is considered in this article.

In the present study, FGP approach is adopted to solve fuzzy stochastic BLPP where the parameters associated with the objectives as well as with system constraints are FRVs and fuzzy numbers. In model formulation process, the objectives of the problem is first approximated by using expectation model (E-Model) [14] and the system constraints are converted into fuzzy constraints by applying general CCP methodology. Then, the model is decomposed on the basis of the tolerance ranges of the fuzzy numbers associated with the objectives as well as with the system constraints by the concept of  $\alpha$ -cut of fuzzy numbers in order to defuzzify the problem. Individual objective values are obtained to construct the membership functions of each of the decomposed objectives within the extended feasible region. The membership functions are then converted into membership goals by assigning unity as the aspiration level of each of them. Lastly, an FGP model is constructed to achieving the highest membership degree to the extent possible by the DM by minimizing the group regret consisting of under deviational variables in decision-making environment.

## 2 Formulation of Bilevel Stochastic Programming Problem

In a stochastic bilevel decision-making situation, let  $F_1$  and  $F_2$  be the objective function of leader and follower respectively. Also, let  $x_1$  be the controlling vector of leader and  $x_2$  be the controlling vector of follower. Then, a bilevel SP problem with chance constraints is stated as

Find  $X(x_1, x_2)$  so as to

$$\text{Max}_{x_1} F_1 = \tilde{c}_{11}x_1 + \tilde{c}_{12}x_2 \text{ and for given } x_1, x_2 \text{ solves } \text{Max}_{x_2} F_2 = \tilde{c}_{21}x_1 + \tilde{c}_{22}x_2$$

subject to  $\Pr(\tilde{a}_{11}x_1 + \tilde{a}_{12}x_2 \leq \tilde{b}_1) \geq p_1$ ;  $\Pr(\tilde{a}_{21}x_1 + \tilde{a}_{22}x_2 \leq \tilde{b}_2) \geq p_2$ ;  $x_1, x_2 \geq 0$  (1)

where  $\tilde{c}_{11}, \tilde{c}_{12}, \tilde{c}_{21}, \tilde{c}_{22}$ , and  $\tilde{b}_2$  are the vectors of normally distributed independent FRVs with fuzzily defined mean and variance;  $\tilde{a}_{11}, \tilde{a}_{12}$  are the matrices of normally distributed independent FRVs;  $\tilde{b}_1$  is a vector of right-sided fuzzy number;  $\tilde{a}_{21}, \tilde{a}_{22}$  are matrices of triangular fuzzy numbers;  $p_1, p_2$  are vectors of real numbers. With the consideration of the above model, the FP model is derived in the next section.

## 3 FP Model Construction

Considering the FRVs associated with the objectives at each level DM, an E-model is generated in the following subsection.

### 3.1 Fuzzy E-model of Objective Function

Since  $\tilde{c}_{11}, \tilde{c}_{12}, \tilde{c}_{21}, \tilde{c}_{22}$  are the vectors of normally distributed independent FRVs, let  $E(\tilde{c}_{11}), E(\tilde{c}_{12}), E(\tilde{c}_{21}),$  and  $E(\tilde{c}_{22})$  are the respective mean values of the FRVs  $\tilde{c}_{11}, \tilde{c}_{12}, \tilde{c}_{21}, \tilde{c}_{22}$  associated with objective functions of leader and follower. Then, the objectives of equivalent E-model of the given problem (1) are presented as

$$\begin{aligned} \text{Max}_{x_1} E(F_1) &= E(\tilde{c}_{11})x_1 + E(\tilde{c}_{12})x_2 \text{ where for given } x_1, x_2 \text{ solves } \text{Max}_{x_2} \\ E(F_2) &= E(\tilde{c}_{21})x_1 + E(\tilde{c}_{22})x_2. \end{aligned} \tag{2}$$

Since  $E(\tilde{c}_{11}), E(\tilde{c}_{12}), E(\tilde{c}_{21}),$  and  $E(\tilde{c}_{22})$  are vectors of fuzzy numbers, introducing  $\tilde{M}_{11}, \tilde{M}_{12}, \tilde{M}_{21},$  and  $\tilde{M}_{22}$  are vectors of fuzzy numbers with the assigned values  $\tilde{M}_{11} = E(\tilde{c}_{11}), \tilde{M}_{12} = E(\tilde{c}_{12}), \tilde{M}_{21} = E(\tilde{c}_{21}),$  and  $\tilde{M}_{22} = E(\tilde{c}_{22}).$

In a fuzzy decision-making situation, it is to be assumed that the mean associated with the vectors of FRVs  $\tilde{c}_{11}, \tilde{c}_{12}, \tilde{c}_{21}, \tilde{c}_{22}$  are triangular fuzzy numbers.

A triangular fuzzy number  $\tilde{a}$  can be represented by a triple of three real numbers as  $\tilde{a} = (a^L, a, a^R).$  The membership function of a triangular fuzzy number is of the form

$$\mu_{\tilde{a}}(x) = \begin{cases} 0 & \text{if } x < a^L \text{ or } x > a^R \\ \frac{x - a^L}{a - a^L} & \text{if } a^L \leq x \leq a \\ \frac{a^R - x}{a^R - a} & \text{if } a \leq x \leq a^R \end{cases}$$

where  $a^L$  and  $a^R$  denote, respectively, the left and right tolerance values of the fuzzy number  $\tilde{a}.$  Now considering the following triangular fuzzy numbers associated with the mean values of the vectors FRVs of the objectives of the DMs with the form  $\tilde{c}_{11}, \tilde{c}_{12}, \tilde{c}_{21}, \tilde{c}_{22}$  as  $\tilde{M}_{11} = (M_{11}^L, M_{11}, M_{11}^R), \tilde{M}_{12} = (M_{12}^L, M_{12}, M_{12}^R), \tilde{M}_{21} = (M_{21}^L, M_{21}, M_{21}^R), \tilde{M}_{22} = (M_{22}^L, M_{22}, M_{22}^R),$  the objective functions in (2) are decomposed as

$$\left. \begin{aligned} \text{Max}_{x_1} E(F_1)^L &= \{M_{11}^L + (M_{11} - M_{11}^L)\alpha\} x_1 + \{M_{12}^L + (M_{12} - M_{12}^L)\alpha\} x_2 \\ \text{Max}_{x_1} E(F_1)^R &= \{M_{11}^R - (M_{11}^R - M_{11})\alpha\} x_1 + \{M_{12}^R - (M_{12}^R - M_{12})\alpha\} x_2 \end{aligned} \right\} \text{(Leader's problem)} \tag{3}$$

$$\left. \begin{aligned} \text{Max}_{x_2} E(F_2)^L &= \{M_{21}^L + (M_{21} - M_{21}^L)\alpha\} x_1 + \{M_{22}^L + (M_{22} - M_{22}^L)\alpha\} x_2 \\ \text{Max}_{x_2} E(F_2)^R &= \{M_{21}^R - (M_{21}^R - M_{21})\alpha\} x_1 + \{M_{22}^R - (M_{22}^R - M_{22})\alpha\} x_2 \end{aligned} \right\} \text{(Follower's problem)} \tag{4}$$

### 3.2 Conversion of Fuzzy Chance Constraints into Fuzzy Constraints

The parameters involved with the chance constraints are treated here as FRVs following normal distribution. Under this consideration, it is assumed that  $E(\tilde{a}_{11})$ ,  $\text{Var}(\tilde{a}_{11})$ ,  $E(\tilde{a}_{12})$ ,  $\text{Var}(\tilde{a}_{12})$  and  $E(\tilde{b}_2)$ ,  $\text{Var}(\tilde{b}_2)$  be the respective mean and variance of the matrices  $\tilde{a}_{11}$ ,  $\tilde{a}_{12}$ , and the vector  $\tilde{b}_2$  whose entries are normally distributed FRVs.

Now applying CCP methodology in fuzzy environment, the constraints in (1) is converted into the equivalent fuzzy constraints as

$$\begin{aligned}
 E(\tilde{a}_{11})x_1 + E(\tilde{a}_{12})x_2 + \Phi^{-1}(p_1)\sqrt{\text{Var}(\tilde{a}_{11})x_1^2 + \text{Var}(\tilde{a}_{12})x_2^2} &\leq \tilde{b}_1 \\
 \tilde{a}_{21}x_1 + \tilde{a}_{22}x_2 &\leq E(\tilde{b}_2) + \Phi^{-1}(1-p_2)\sqrt{\text{Var}(\tilde{b}_2)}, x_1, x_2 \geq 0
 \end{aligned}
 \tag{5}$$

Here,  $\Phi(\cdot)$  represents cumulative distribution function of the standard normal variate.

Since  $\tilde{a}_{11}$ ,  $\tilde{a}_{12}$  are the matrices of normally distributed FRVs and the decision variables  $x_1, x_2 \geq 0$  are unknowns, then two FRVs,  $\tilde{d}_1, \tilde{d}_2$ , are introduced by  $\tilde{d}_1 = \tilde{a}_{11}x_1$ , and  $\tilde{d}_2 = \tilde{a}_{12}x_2$  whose respective mean and variance are given by  $m_{\tilde{d}_1} = E(\tilde{a}_{11})x_1$ ,  $m_{\tilde{d}_2} = E(\tilde{a}_{12})x_2$ ,  $\sigma_{\tilde{d}_1}^2 = \text{Var}(\tilde{a}_{11})x_1$ ,  $\sigma_{\tilde{d}_2}^2 = \text{Var}(\tilde{a}_{12})x_2$ . Also, let  $m_{\tilde{b}_2} = E(\tilde{b}_2)$  and  $\sigma_{\tilde{b}_2}^2 = \text{Var}(\tilde{b}_2)$  be the respective mean and variance of the normally distributed FRV  $\tilde{b}_2$ .

Now applying mean and variance to the elements of the matrices of FRVs, the above constraints in (5) is converted into the following form

$$\begin{aligned}
 m_{\tilde{d}_1} + m_{\tilde{d}_2} + \Phi^{-1}(p_1)\{\sigma_{\tilde{d}_1} + \sigma_{\tilde{d}_2}\} &\leq \tilde{b}_1, \tilde{a}_{21}x_1 + \tilde{a}_{22}x_2 \leq m_{\tilde{b}_2} + \Phi^{-1} \\
 (1-p_2)\sigma_{\tilde{b}_2}, x_1, x_2 &\geq 0
 \end{aligned}
 \tag{6}$$

In a fuzzy decision-making situation, it is to be assumed that the mean and variance associated with the elements of matrices of the FRVs  $\tilde{d}_1, \tilde{d}_2$ , and the vectors of FRVs  $\tilde{b}_2$  are the matrices of triangular fuzzy numbers. With the form

$$\begin{aligned}
 m_{\tilde{d}_1} &= (m_{\tilde{d}_1}^L, m_{\tilde{d}_1}, m_{\tilde{d}_1}^R); \quad \sigma_{\tilde{d}_1}^2 = (\sigma_{\tilde{d}_1}^{2L}, \sigma_{\tilde{d}_1}^2, \sigma_{\tilde{d}_1}^{2R}); \quad m_{\tilde{d}_2} = (m_{\tilde{d}_2}^L, m_{\tilde{d}_2}, m_{\tilde{d}_2}^R); \\
 \sigma_{\tilde{d}_2}^2 &= (\sigma_{\tilde{d}_2}^{2L}, \sigma_{\tilde{d}_2}^2, \sigma_{\tilde{d}_2}^{2R}) \\
 m_{\tilde{b}_2} &= (m_{\tilde{b}_2}^L, m_{\tilde{b}_2}, m_{\tilde{b}_2}^R); \quad \sigma_{\tilde{b}_2}^2 = (\sigma_{\tilde{b}_2}^{2L}, \sigma_{\tilde{b}_2}^2, \sigma_{\tilde{b}_2}^{2R}), \\
 \tilde{a}_{21} &= (a_{21}^L, a_{21}, a_{21}^R), \tilde{a}_{22} = (a_{22}^L, a_{22}, a_{22}^R).
 \end{aligned}$$



Further, the fuzzy numbers  $\tilde{b}_1$  are considered as one-sided fuzzy numbers as

$$\mu_{b_1}(x) = \begin{cases} 1 & \text{if } x \leq b_1 \\ [8.5 - x]/0.5 & \text{if } b_1 \leq x \leq b_1 + \delta_1 \\ 0 & \text{if } x \geq 8.5 \end{cases}$$

On the basis of the lower and upper tolerance limits of the triangular fuzzy numbers, the constraints in (6) can be expressed as

$$\begin{aligned} & \left\{ m_{\tilde{d}_1}^L + (m_{\tilde{d}_1}^- m_{\tilde{d}_1}^L)\alpha \right\} + \left\{ m_{\tilde{d}_2}^L + (m_{\tilde{d}_2}^- m_{\tilde{d}_2}^L)\alpha \right\} \\ & + \Phi^{-1}(p_1) \sqrt{\left\{ \sigma_{\tilde{d}_1}^{2L} + (\sigma_{\tilde{d}_1}^2 - \sigma_{\tilde{d}_1}^{2L})\alpha \right\} + \left\{ \sigma_{\tilde{d}_2}^{2L} + (\sigma_{\tilde{d}_2}^2 - \sigma_{\tilde{d}_2}^{2L})\alpha \right\}} \\ & \leq \{E(b_1) + \delta_1 - \alpha\delta_1\} \\ & \left\{ m_{\tilde{d}_1}^R - (m_{\tilde{d}_1}^R - m_{\tilde{d}_1}^-)\alpha \right\} + \left\{ m_{\tilde{d}_2}^R - (m_{\tilde{d}_2}^R - m_{\tilde{d}_2}^-)\alpha \right\} \\ & + \Phi^{-1}(p_1) \sqrt{\left\{ \sigma_{\tilde{d}_1}^{2R} - (\sigma_{\tilde{d}_1}^{2R} - \sigma_{\tilde{d}_1}^2)\alpha \right\} + \left\{ \sigma_{\tilde{d}_2}^{2R} - (\sigma_{\tilde{d}_2}^{2R} - \sigma_{\tilde{d}_2}^2)\alpha \right\}} \\ & \leq \{E(b_1) + \delta_1 - \alpha\delta_1\} \\ & \left\{ a_{21}^L + (a_{21} - a_{21}^L)\alpha \right\} x_1 + \left\{ a_{22}^L + (a_{22} - a_{22}^L)\alpha \right\} x_2 \leq \left\{ m_{b_2}^L + (m_{b_2} - m_{b_2}^L)\alpha \right\} \\ & + \Phi^{-1}(1 - p_2) \left\{ \sigma_{b_2}^L + (\sigma_{b_2} - \sigma_{b_2}^L)\alpha \right\} \\ & \left\{ a_{21}^R - (a_{21}^R - a_{21})\alpha \right\} x_1 + \left\{ a_{22}^R - (a_{22}^R - a_{22})\alpha \right\} x_2 \leq \left\{ m_{b_2}^R - (m_{b_2}^R - m_{b_2})\alpha \right\} \\ & + \Phi^{-1}(1 - p_2) \left\{ \sigma_{b_2}^R + (\sigma_{b_2}^R - \sigma_{b_2})\alpha \right\} \\ & 0 \leq \alpha \leq 1 \end{aligned} \tag{7}$$

Hence, the BLPP model under the decomposed set of system constraints is presented as

Find  $X(x_1, x_2)$  so as to

$$\begin{aligned} & \left. \begin{aligned} \text{Max}_{x_1} E(F_1)^L &= \{M_{11}^L + (M_{11} - M_{11}^L)\alpha\} x_1 + \{M_{12}^L + (M_{12} - M_{12}^L)\alpha\} x_2 \\ \text{Max}_{x_1} E(F_1)^R &= \{M_{11}^R - (M_{11}^R - M_{11})\alpha\} x_1 + \{M_{12}^R - (M_{12}^R - M_{12})\alpha\} x_2 \end{aligned} \right\} \text{(Leader's problem)} \\ & \left. \begin{aligned} \text{Max}_{x_2} E(F_2)^L &= \{M_{21}^L + (M_{21} - M_{21}^L)\alpha\} x_1 + \{M_{22}^L + (M_{22} - M_{22}^L)\alpha\} x_2 \\ \text{Max}_{x_2} E(F_2)^R &= \{M_{21}^R - (M_{21}^R - M_{21})\alpha\} x_1 + \{M_{22}^R - (M_{22}^R - M_{22})\alpha\} x_2 \end{aligned} \right\} \text{(Follower's problem)} \end{aligned}$$

subject to the constraints given in (7);

$$x_1, x_2 \geq 0 \tag{8}$$

### 3.3 Construction of Membership Functions

In a bilevel decision-making context, the DMs are very much interested to optimize their own payoffs to the extent possible by paying serious attention to the benefit of the others. To assess the fuzzy goals of the objectives of the DMs, the independent optimal solutions are determined first.

Let  $E(F_1)_B^L, E(F_1)_B^R$  and  $E(F_1)_W^L, E(F_1)_W^R$  be the respective best and worst achieved expected decomposed objective values of the leader when the above model (8) is solved only by considering leader's problem independently.

Similarly, let the independent best and worst achieved expected decomposed objective values of the follower are appeared as  $E(F_2)_B^L, E(F_2)_B^R$  and  $E(F_2)_W^L, E(F_2)_W^R$ .

Hence, the fuzzy goals of the expected values of the decomposed objectives of leader and follower are appeared as

$$E(F_1)^L \gtrsim E(F_1)_B^L, E(F_1)^R \gtrsim E(F_1)_B^R, E(F_2)^L \gtrsim E(F_2)_B^L, E(F_2)^R \gtrsim E(F_2)_B^R$$

On the basis of upper and lower tolerance values of the fuzzy goals, the following membership functions are developed to measure the degree of satisfaction of the each level DMs.

$$\mu_{E(F_1)^L}(x) = \begin{cases} 0 & \text{if } E(F_1)^L \leq E(F_1)_W^L \\ \frac{[E(F_1)^L - E(F_1)_W^L] / [E(F_1)_B^L - E(F_1)_W^L]}{1} & \text{if } E(F_1)_W^L \leq E(F_1)^L \leq E(F_1)_B^L \\ 1 & \text{if } E(F_1)^L \geq E(F_1)_B^L \end{cases}$$

$$\mu_{E(F_1)^R}(x) = \begin{cases} 0 & \text{if } E(F_1)^R \leq E(F_1)_W^R \\ \frac{[E(F_1)^R - E(F_1)_W^R] / [E(F_1)_B^R - E(F_1)_W^R]}{1} & \text{if } E(F_1)_W^R \leq E(F_1)^R \leq E(F_1)_B^R \\ 1 & \text{if } E(F_1)^R \geq E(F_1)_B^R \end{cases}$$

The membership functions corresponding to  $E(F_2)^L$  are to be defined similarly.

## 4 FGP Model Formulation

In FGP, the membership functions are considered as flexible goals by assigning unity as the aspiration level and introducing under- and over-deviational variables to each of them. Then, the FGP model is formulated by considering each membership function of the fuzzy goals of the DMs as follows

Find  $X(x_1, x_2)$  so as to

$$\text{Min } D = w_1^- d_1^- + w_2^- d_2^- + w_3^- d_3^- + w_4^- d_4^-$$

and satisfy

$$\begin{aligned} \frac{E(F_1)^L(x_1, x_2) - E(F_1)_W^L}{E(F_1)_B^L - E(F_1)_W^L} + d_1^- - d_1^+ = 1; & \frac{E(F_1)^R(x_1, x_2) - E(F_1)_W^R}{E(F_1)_B^R - E(F_1)_W^R} + d_2^- - d_2^+ = 1 \\ \frac{E(F_2)^L(x_1, x_2) - E(F_2)_W^L}{E(F_2)_B^L - E(F_2)_W^L} + d_3^- - d_3^+ = 1; & \frac{E(F_2)^R(x_1, x_2) - E(F_2)_W^R}{E(F_2)_B^R - E(F_2)_W^R} + d_4^- - d_4^+ = 1 \end{aligned}$$

subject to the system constraints in (8)

$$x_1, x_2 \geq 0, d_k^-, d_k^+ \geq 0, \text{ with } d_k^- \cdot d_k^+ = 0 \text{ for } k = 1, 2, 3, 4 \tag{9}$$

where  $d_k^-, d_k^+$  represent the under- and over-deviational variables, respectively, and the fuzzy weights  $w_k, (k \in N_4)$  are determined as [14]:

$$\begin{aligned} w_1 = \left[ E(F_1)_B^L - E(F_1)_W^L \right]^{-1}, w_2 = \left[ E(F_1)_B^R - E(F_1)_W^R \right]^{-1}, \\ w_3 = \left[ E(F_2)_B^L - E(F_2)_W^L \right]^{-1}, w_4 = \left[ E(F_2)_B^R - E(F_2)_W^R \right]^{-1}. \end{aligned}$$

The *minsum* GP technique is used to solve the problem (9).

### 5 A Numerical Example

To illustrate the proposed methodology, the following fuzzy stochastic BLPP is solved. The problem is presented as

$$\begin{aligned} \text{Find } X(x_1, x_2) \text{ so as to Max}_{x_1} F_1 = \tilde{c}_{11}x_1 + \tilde{c}_{12}x_2 \text{ and for given } x_1, x_2 \text{ solves} \\ \text{Max}_{x_2} F_2 = \tilde{c}_{21}x_2 \end{aligned}$$

$$\text{subject to } \Pr(\tilde{a}_{11}x_1 + \tilde{a}_{12}x_2 \leq \tilde{b}_1) \geq 0.95; \Pr(\tilde{a}_{21}x_1 + \tilde{a}_{22}x_2 \leq \tilde{b}_2) \geq 0.10; x_1, x_2 \geq 0 \tag{10}$$

Now, the E-model of the above problem with fuzzy constraints is written as

$$\begin{aligned} \text{Find } X(x_1, x_2) \text{ so as to} \\ \text{Max}_{x_1} E(F_1) = E(\tilde{c}_{11})x_1 + E(\tilde{c}_{12})x_2 \text{ and for given } x_1, x_2 \text{ solves } \text{Max}_{x_2} E(F_2) = \\ E(\tilde{c}_{21})x_2 \end{aligned}$$

$$\begin{aligned} \text{subject to } E(\tilde{a}_{11})x_1 + E(\tilde{a}_{12})x_2 + 1.645\sqrt{\text{var}(\tilde{a}_{11})x_1^2 + \text{var}(\tilde{a}_{12})x_2^2} \leq \tilde{b}_1, \\ \tilde{a}_{21}x_1 + \tilde{a}_{22}x_2 \leq E(\tilde{b}_2) + 1.28\sqrt{\text{var}(\tilde{b}_2)}, x_1, x_2 \geq 0 \end{aligned} \tag{11}$$

where  $\tilde{c}_{11}, \tilde{c}_{12}, \tilde{c}_{21}$  are normally distributed FRVs with respective mean represented by the following triangular fuzzy numbers

$$E(\tilde{c}_{11}) = (6.5, 7, 7.5); E(\tilde{c}_{12}) = (2.8, 3, 3.2); E(\tilde{c}_{21}) = (4.6, 5, 5.6);$$

Also,  $\tilde{a}_{11}, \tilde{a}_{12}, \tilde{b}_2$  are normally distributed independent FRVs with the mean and variance of these variables that are considered as  $E(\tilde{a}_{11}) = (0.95, 1, 1.05), E(\tilde{a}_{12}) = (2.95, 3, 3.05), Var(\tilde{a}_{11}) = (24.95, 25, 25.05), Var(\tilde{a}_{12}) = (15.95, 16, 16.05), E(\tilde{b}_2) = (6.95, 7, 7.05), Var(\tilde{b}_2) = (8.95, 9, 9.05)$ . Again  $\tilde{a}_{21}, \tilde{a}_{22}$  are considered as triangular fuzzy numbers with the form  $\tilde{a}_{21} = (3.95, 4, 4.05), \tilde{a}_{22} = (2.95, 3, 3.05)$ .

Here,  $\tilde{b}_1$  is considered as right-sided fuzzy number which is given by

$$\mu_{b_1}(x) = \begin{cases} 1 & \text{if } b_1 \leq 8 \\ [8.5 - b_1] / 0.5 & \text{if } 8 \leq b_1 \leq 8.5 \\ 0 & \text{if } b_1 \geq 8.5 \end{cases}$$

Now, the FP model using the above defined fuzzy numbers takes the form as Find  $X(x_1, x_2)$  so as to

$$\begin{aligned} \text{Max}_{x_1} E(F_1)^L &= (6.5 + 0.5\alpha)x_1 + (2.8 + 0.2\alpha)x_2, \text{Max}_{x_1} E(F_1)^R \\ &= (7.5 - 0.5\alpha)x_1 + (3.2 - 0.2\alpha)x_2 \text{Max}_{x_2} E(F_2)^L = (4.6 + 0.4\alpha)x_2, \\ \text{Max}_{x_2} E(F_2)^R &= (5.6 - 0.6\alpha)x_2 \end{aligned}$$

Subject to

$$\begin{aligned} (0.95 + 0.05\alpha)x_1 + (2.95 + 0.05\alpha)x_2 \\ + 1.645\sqrt{(24.95 + 0.05\alpha)x_1^2 + (15.95 + 0.05\alpha)x_2^2} &\leq (8.5 - 0.5\alpha) \\ (1.05 - 0.05\alpha)x_1 + (3.05 - 0.05\alpha)x_2 \\ + 1.645\sqrt{(25.05 - 0.05\alpha)x_1^2 + (16.05 - 0.05\alpha)x_2^2} &\leq (8.5 - 0.5\alpha) \\ (3.95 + 0.05\alpha)x_1 + (2.95 + 0.05\alpha)x_2 &\leq (6.95 + 0.05\alpha) + 1.28\sqrt{(8.95 + 0.05\alpha)} \\ (4.05 - 0.05\alpha)x_1 + (3.05 - 0.05\alpha)x_2 &\leq (7.05 - 0.05\alpha) + 1.28\sqrt{(9.05 - 0.05\alpha)} \\ x_1, x_2 \geq 0, 0 \leq \alpha \leq 1. \end{aligned} \tag{12}$$

The individual best and worst decision of the leader when calculated in isolation are obtained as  $E(F_1)_B^L = 6.003, E(F_1)_B^R = 6.922, E(F_1)_W^L = 0, E(F_1)_W^R = 0$

Again the follower's best and worst solution are found as  $E(F_2)_B^L = 4.132, E(F_2)_B^R = 4.938, E(F_2)_W^L = 0, E(F_2)_W^R = 0$ .

The fuzzy goals of the DMs are appeared as

$$E(F_1)^L \gtrsim 6.003, E(F_1)^R \gtrsim 6.922, E(F_2)^L \gtrsim 4.132, E(F_2)^R \gtrsim 4.938.$$

Now developing the membership functions and assigning highest achievement level (unity) to the membership goals, the *minsum* FGP model is formulated as

Find  $X(x_1, x_2)$  so as to

$$\text{Min } D = d_1^-/6.003 + d_2^-/6.922 + d_3^-/4.132 + d_4^-/4.938$$

and satisfy

$$\begin{aligned} [(6.5 + 0.5\alpha)x_1 + (2.8 + 0.2\alpha)x_2]/6.003 + d_1^- - d_1^+ &= 1; [(7.5 - 0.5\alpha)x_1 \\ &+ (3.2 - 0.2\alpha)x_2]/6.922 + d_2^- - d_2^+ = 1; \\ [(4.6 + 0.4\alpha)x_2]/4.132 + d_3^- - d_3^+ &= 1; [(5.6 - 0.6\alpha)x_2]/4.938 + d_4^- - d_4^+ = 1 \end{aligned}$$

subject to same system constraints in (12)

$$x_1, x_2 \geq 0, 0 \leq \alpha \leq 1, d_k^- \geq 0, d_k^+ \geq 0, \text{ with } d_k^- \cdot d_k^+ = 0 \text{ for } k = 1, 2, 3, 4. \quad (13)$$

The software LINGO (6.0) is used to solve the problem.

The achieved solutions of problem (13) are found as  $x_1 = 0.31$ ,  $x_2 = 0.786$  with the expected decomposed objective values  $E(F_1)^L = 4.528$ ,  $E(F_1)^R = 4.84$  of the leader and  $E(F_2)^L = 3.93$ ,  $E(F_2)^R = 4.402$  for the follower. Hence, it may be concluded that for different tolerance values of the objectives of the fuzzy parameters, the expected objectives value of the leader lies in the interval  $[4.528, 4.84]$  and that of the follower lies in the interval  $[3.93, 4.402]$ . The achieved solution is most satisfactory from the view point of achieving desired goal levels of the objectives of both the leader and follower in a hierarchical decision-making context.

## 6 Conclusions

The methodology developed in this paper captures the simultaneous occurrence of probabilistic and imprecise nature of the parameters associated with the model under one roof. The solution approach can be extended to solve multiobjective stochastic BLPP, fuzzy stochastic nonlinear BLPPs and multilevel stochastic linear programming problem, multilevel multiobjective stochastic linear programming problem in some large hierarchical decision-making organization without any computational difficulties. Finally, it is hoped that the approach may open up new look into the way of solving stochastic hierarchical decision-making problems.

**Acknowledgments** The authors are grateful to the anonymous reviewers for their comments and suggestions.

## References

1. Bard, J., Falk, J.: An explicit solution to the multilevel programming problem. *Comput. Oper. Res.* **9**, 77–100 (1982)
2. Bialas, W., Karwan, M.: Two level linear programming. *Manage. Sci.* **30**, 1004–1020 (1984)
3. Aiyoshi, E., Shimizu, K.: Hierarchical decentralized systems and its new solution by barrier method. *IEEE Trans. Syst. Man Cybern.* **11**, 444–449 (1981)
4. Bialas, W., Karwan M., Shaw, J.: A parametric complementary pivot approach for two level linear programming. *Operations Research Programme, State University of New York, Buffalo*, p. 80 (1980).
5. Charnes, A., Cooper, W.W.: Chance-constrained programming. *Manage. Sci.* **6**, 73–79 (1959)
6. Feiring, B.R., Sastri, T., Sim, L.S.M.: A stochastic programming model for water resource planning. *Math. Comput. Model.* **27**(3), 1–7 (1998)
7. Kataoka, S.: A stochastic programming model. *Econometric* **31**, 181–196 (1963)
8. Zimmermann, H.J.: Fuzzy programming and linear programming with several objective functions. *Fuzzy Sets Syst.* **1**, 45–55 (1978)
9. Klir, G.J., Yuan, B.: *Fuzzy Sets and Fuzzy Logic: Theory and Applications*. Prentice-Hall Inc, New Jersey (1995)
10. Zadeh, L.A.: Fuzzy sets. *Inf. Control* **8**, 338–353 (1965)
11. Biswas, A., Pal, B.B.: Application of fuzzy goal programming technique to land use planning in agricultural system. *Omega* **33**, 391–398 (2005)
12. Biswas, A., Bose, K.: A fuzzy programming approach for solving quadratic bilevel programming problems with fuzzy resource constraints. *Int. J. Oper. Res.* **12**, 142–156 (2011)
13. Luhandjula, M.K., Joubert, J.W.: On some optimization models in a fuzzy stochastic environment. *Eur. J. Oper. Res.* **207**, 1433–1441 (2010)
14. Biswas, A., Modak, N.: A fuzzy goal programming approach for fuzzy multiobjective stochastic programming through expectation model. *Commun. Comput. Inf. Sci.* **283**, 124–135 (2012)

# Implementation of Intelligent Water Drops Algorithm to Solve Graph-Based Travelling Salesman Problem

Roli Bansal, Hina Agrawal, Hifza Afaq and Sanjay Saini

**Abstract** The travelling salesman problem (TSP) is one of the most sought out NP-hard, routing problems in the literature. TSP is important with respect to some real-life applications, especially when tour is generated in real time. The objective of this paper is to apply the intelligent water drops algorithm to solve graph-based TSP (GB-TSP). The intelligent water drops (IWD) algorithm is a new meta-heuristic approach belonging to a class of swarm intelligence-based algorithm. It is inspired from observing natural water drops that flow in rivers. The idea of path finding of rivers is used to find the near-optimal solution of the travelling salesman problem (TSP).

**Keywords** Intelligent water drops (IWD) · Travelling salesman problem (TSP) · Swarm intelligence · Graph-based TSP (GB-TSP)

## 1 Introduction

Soft computing is a term applied to a field within computer science which is used to obtain near-optimal solutions to NP-complete problems in polynomial time. Swarm intelligence is a relatively new field of soft computing [1] which is inspired by nature. Swarm intelligence is based on the collective behavior of decentralized, self-

---

R. Bansal (✉) · H. Agrawal · H. Afaq · S. Saini  
Department of Physics and Computer Science, Dayalbagh Educational Institute, Agra, India  
e-mail: dei.rolibansal@gmail.com

H. Agrawal  
e-mail: hinaagrawal29@gmail.com

H. Afaq  
e-mail: hifza.afaq@gmail.com

S. Saini  
e-mail: sanjay.s.saini@gmail.com

organized systems. It refers to algorithms such as ant colony optimization (ACO) [9], particle swarm optimization (PSO) [4], artificial bee colony [3], bat algorithm [11], and many more. Intelligent water drops (IWD) is an upcoming swarm intelligence-based algorithm. IWD was proposed by Hamed Shah-Hosseini [7] in 2007. IWD algorithm is based on the dynamics of river system, action, and reactions that takes place among the water drops in rivers [6]. A water drop prefers the path having low soil to the path having high soil. In this way, it finds best possible path for itself. This behavior of IWD is used to optimize the tour for travelling salesman problem (TSP).

In the TSP [2], a map of cities is given to the salesman and he is required to visit all the cities to complete his tour such that no city is visited twice except the city it starts with, which it has to visit in the end again to complete its tour. In real-life situation, all cities may not be completely interconnected with direct paths and so paths may not exist between some of the cities, so the map of cities is not completely interconnected. The goal in the TSP is to find the tour with the minimum total length, among all possible tours for the given map.

## 2 Behavior of Intelligent Water Drops

The behavior of the natural water drop is observed with some properties such as

- Velocity (with which a drop moves)
- Soil (which is carried by the drop)

IWD is based on these two properties of water drops. These properties change with time according to the environment of water drop when IWD flows from source to destination. Initially, IWD has zero amount of soil and nonzero velocity. It carries more soil with high velocity and unloads the soil with low velocity of IWD.

A water drop prefers an easier path to a harder path in an obvious way when it has to choose between several paths that exist in the path from source to destination. Each IWD has a number of possible paths to choose from when it goes from one position to another position. It chooses the path with the low soil and maximum probability.

Every IWD flows in finite length steps from one location to another location. The IWD's velocity depends on the soil between two locations. The IWD's velocity increases on less soil path and decreases on high soil path. Thus, IWD's velocity is inversely proportional to the soil between two locations. An IWD removes some amount of soil from the path and carries it while travelling through that path. It removes the soil from the path depending upon the time it takes to cover the distance between two locations. More soil is removed from the path if the time taken by IWD is high and vice versa. Thus, IWD's soil is inversely proportional to time taken in travelling from current location to next location. This time is calculated by the simple laws of physics linear motion.



### 3 Solving GB-TSP Using IWD

In this section, steps for solving the graph-based TSP (GB-TSP) are discussed. For geographical problems, where location of cities is given by their Cartesian coordinates and path from any node to any other node exists necessarily (which is simply the Euclidean distance between the two nodes), solution using IWD to such TSP has been given by Hamed Shah-Hosseini as MIWD [5]. In our case, a GB-TSP is represented by a graph  $(N, E)$ , where the node set  $N$  denotes the  $n$  cities of the TSP, and the edge set  $E$  denotes the paths between the two cities. The considered graphs are non-complete, i.e., it is not necessary that a direct edge exists between every pair of nodes. In fact, we consider graphs where a direct edge may not exist between certain two nodes. This formulation of the problem is much more realistic than the earlier problems. The cost associated with the edges represents distance between cities. However, for the sake of simplicity and similarity with earlier problems, in this paper, the location of cities is given by their Cartesian coordinates and the distance between them is their Euclidean distance. For GB-TSP, we start with a graph which is not completely interconnected. For this, we create an adjacency matrix depicting distances between cities, and then, we remove the edges where there is no path between the cities. In this way, we have a subset of edge set which represent a graph which is not completely interconnected. A solution of the GB-TSP having the graph  $(N, E)$  is then an ordered set of  $n$  distinct cities.

Now, the following IWD strategy for the GB-TSP is used. Each link of the edge set  $E$  has an amount of soil. An IWD visits nodes of the graph through the links. The IWD is able to change the amount of soil on the links. An IWD starts its tour from a random node. The IWD changes the soil of each link that it flows on while completing its tour.

Since there are no standard problems available where the graph is not complete, we have created such test graphs for our experiments. For this, we convert a completely connected graph into a non-complete graph. This conversion of complete graph into non-complete graph is done using the X nearest neighbor (XNN) algorithm [8]. In this method, the links, depicting distances, from one node to all other nodes are taken, and then, a certain percentage of those links are dropped. The dropped links are those which are the largest in that set of links. We repeat the same process for all the nodes in our graph. By converting the complete graph into a non-complete graph, the search space of the problem is reduced.

This algorithm takes a complete graph and drops a given percentage of links from it. For our experiments, a few standard problems are considered and 20% links are dropped from it.

The IWD algorithm that is used for the GB-TSP is as follows:

1. Initialization of static parameters:

- Set the number of water drops  $N_{IWD}$ , the number of cities  $N_C$ , and the Cartesian coordinate of each city  $i$  such that  $c(i) = [x_i, y_i]^T$  to their chosen constant values. The number of cities and their coordinate values depends on the prob-

lem at hand, while the  $N_{IWD}$  is set by the user. We choose  $N_{IWD}$  to be equal to or greater than the number of cities.

- Set the parameter number of neighbor cities called `neighbor_city`. For instance, if we have to drop 20% links from each node, then `neighbor_city` is 80% of  $N_C - 1$ .
- Parameters for velocity updating:  $a_v = c_v = 1$  and  $b_v = 0.01$ .
- Parameters for soil updating:  $a_s = c_s = 1$  and  $b_s = 0.01$ .
- Initial soil on each link is denoted by the constant `InitSoil` such that the soil of the link between every two cities  $i$  and  $j$  is set by  $\text{soil}(i, j) = \text{InitSoil}$ . Here, we choose `InitSoil` = 10,000.
- Initial velocity of IWD is denoted by the constant `InitVel`. Velocity of each drop with which they start their tour. Here, `InitVel` = 200.
- The best tour with minimum tour length ( $\text{Len}(T_B)$ ) is denoted by  $T_B$ . Initially, it is set as  $\text{Len}(T_B) = \text{infinity}$ .
- The termination condition is met when maximum number of iterations is reached.

## 2. Initialization of dynamic parameters:

- For every IWD, we create an empty visited city list  $V_c(\text{IWD}) = \{\}$ .
- Initially, each IWD has velocity equal to `InitVal` and soil equal to zero.

## 3. Non-complete graph is generated using XNN algorithm [8] along with its adjacency matrix.

- Initialize the number of neighbors of each city with the constant `neighbor_city`.
- Create the adjacency matrix for new city links.

## 4. For every IWD, select a city randomly and place that IWD on that city.

## 5. Update the visited city lists of all IWDs to include the cities just visited.

## 6. Select the next city:

- For each IWD, choose the next city  $j$  to be visited by IWD when it is in city  $i$  with the probability  $P_i^{\text{IWD}}(j)$  as given in (1).

$$P_i^{\text{IWD}}(j) = \frac{f(\text{soil}(i, j))}{\sum_{k \notin v_c} f(\text{soil}(i, k))} \quad (1)$$

such that  $f(\text{soil}(i, j)) = 1/\varepsilon_s + g(\text{soil}(i, j))$

where

$$g(\text{soil}(i, j)) = \begin{cases} \text{soil}(i, j) & \text{if } \min_{l \notin v_c(\text{IWD})}(\text{soil}(i, l)) \geq 0 \\ \text{soil}(i, j) - \min_{l \notin v_c(\text{IWD})}(\text{soil}(i, l)) & \text{else} \end{cases}$$

Here,  $\varepsilon_s = 0.01$ . Where  $v_c(\text{IWD})$  is the visited city list of the IWD.

The probability depends on the soil between the path. IWD selects the city with maximum probability.

7. Update the soil and velocity:

- An IWD in city  $i$  wants to go to next city  $j$ ; then, the amount of soil on this path, i.e., soil  $(i, j)$  is used to update the velocity as given by (2).

$$\text{vel}^{\text{IWD}}(t+1) = \text{vel}^{\text{IWD}}(t) + \frac{a_v}{b_v + c_v \cdot \text{soil}(i, j)} \quad (2)$$

- Each IWD, carries some amount of the soil,  $\Delta\text{soil}(i, j)$ , that the current IWD alters in its current path while travelling between the cities  $i$  and  $j$  is given by (3).

$$\Delta\text{soil}(i, j) = \frac{a_s}{b_s + c_s \cdot \text{time}(i, j; \text{vel}^{\text{IWD}})} \quad (3)$$

where time taken to travel from city  $i$  to city  $j$  with velocity  $\text{vel}^{\text{IWD}}$  is given by  $\text{time}(i, j; \text{vel}^{\text{IWD}}) = c(i) - c(j)/\max(\varepsilon_v, \text{vel}^{\text{IWD}})$

- For each IWD, update the soil of the path traversed by that IWD by removing certain soil from the path as in (4)

$$\text{soil}(i, j) = (1 - \rho) \cdot \text{soil}(i, j) - \rho \cdot \Delta\text{soil}(i, j) \quad (4)$$

Here,  $\rho = 0.9$ .

Update the soil of each IWD by adding soil removed from the path in present soil of the IWD

$$\text{soil}^{\text{IWD}} = \text{soil}^{\text{IWD}} + \Delta\text{soil}(i, j) \quad (5)$$

soil  $(i, j)$  represents the soil of the path between  $i$  and  $j$ .  $\Delta\text{soil}(i, j)$  represents the soil that IWD carries from that path, and soil<sup>IWD</sup> represents total soil carried by the drop.

- Each IWD completes its tour by using steps 5 to 8 repeatedly. Then, length of the tour (Tour<sup>IWD</sup>) traversed by the IWD is calculated. Then, the tour with minimum length among all IWD tours in this iteration is found. Test the correctness of the minimum path from the adjacency matrix.
- If iteration best tour (current minimum tour) exists then:
  - Update the soil of the paths included in the current minimum tour of the IWD denoted by  $T_M$  by (6).

$$\text{soil}(i, j) = (1 - \rho) \cdot \text{soil}(i, j) + \rho \cdot \frac{2 \cdot \text{soils}^{\text{IWD}}}{N_c(N_c - 1)} \forall (i, j) \in T_M \quad (6)$$

- If the minimum tour  $T_M$  is shorter than the best tour  $T_B$  found so far, then  $T_B$  is updated by (7).

$$T_B = T_M \text{ and } \text{Len}(T_B) = \text{Len}(T_M) \tag{7}$$

10. Otherwise discard the current minimum tour.
11. Go to step 2 unless the maximum number of iterations is reached.
12. If the maximum number of iterations is reached, then the algorithm stops with the best tour  $T_B$  with tour length  $\text{Len}(T_B)$ .

### 4 Experimental Result

In this section, we present computational results obtained. We evaluated the performance of IWD algorithm for some TSP benchmark problems form TSPLIB [10]. We applied IWD algorithm on self-generated network like a pentagon. Firstly, a five node layout is taken as a complete graph, which then is converted to a non-complete graph using XNN algorithm. This network and its optimal path are shown in Fig. 1.

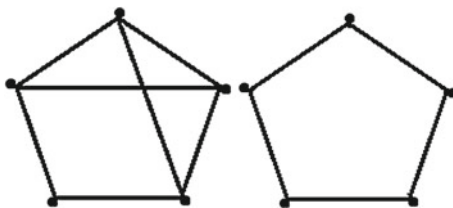
We also apply this on some benchmark problems such as eil51, eil76, st70, and kroA100 after converting them to non-complete graphs.

The experimental result of benchmark problem is shown in the Table 1.

**Table 1** Experimental results for benchmark problems (10 run)

Problems	Optimum length	Average length by IWD
Eil51	426	445
Eil76	538	550
St70	675	748
Kroa100	21,282	24,344

**Fig. 1** *Left* the non-complete graph and *right* the optimal path



## 5 Conclusion

The intelligent water drops algorithm or the IWD algorithm is one of the recent bio-inspired swarm-based optimization algorithms. It gives the optimal solution to various optimization problems. The experimental results show that this algorithm is capable of finding the near-optimal solution. In this paper, we apply IWD on graph-based TSP (non-complete graphs) which gives the near-best optimal solution. We used XNN algorithm to convert the complete TSP graph to non-complete graph. GB-TSP represents the real-life transportation problem.

The IWD algorithm can also be used for solving multiple knapsack problem,  $n$ -Queen problem, multilevel thresholding problem, etc.

## References

1. Bonabeau, E., Dorigo, M., Therault, G.: *Swarm Intelligence: From Natural to Artificial Systems*. Oxford University Press, New York (1999)
2. Greco, F.: *Travelling Salesman Problem*. In-Teh is Croatian Branch of I-Tech Education and Publishing KG, Vienna, Austria (2008)
3. Karaboga, D., Akay, B.: A comparative study of artificial bee colony algorithm. *Appl. Math. Comput* **214**(1), 108–132 (2009)
4. Kennedy, J., Eberhart, R.C.: Particle swarm optimization, pp. 1942–1948. *Proceedings of the Fourth IEEE International Conference on Neural Networks*, IEEE Service Center, Perth, Australia (1995)
5. Shah-Hosseini, H.: Optimization with the Nature-Inspired Intelligent Water Drops Algorithm. In: Sentos E.W (ed.) *Evolutionary Computation*, p. 572. I-Tech, Vienna, Austria (2009).
6. Shah-Hosseini, H.: Problem solving by intelligent water drops. *Proceedings on IEEE Congress on Evolutionary Computation*, pp. 3226–3231. Singapore (2007).
7. Shah-hosseini, H.: The intelligent water drops algorithm : a nature-inspired swarm-based optimization algorithm. *Compu. Eng.* **1**(1), 71–79 (2009)
8. Taba, M.S.: *Solving Traveling Salesman Problem With a Non-complete Graph*. Waterloo, Ontario, Canada (2009)
9. Toksari, M.D.: Ant colony optimization for finding the global minimum. *Appl. Math. Comput.* **176**(1), 308–316 (2006)
10. TSPLIB. (n.d.). Retrieved 08 23, 2012, from <http://comopt.ifl.uni-heidelberg.de/software/TSPLIB95/>
11. Yang, X.-S.: A new metaheuristic bat-inspired algorithm. In: *Nature Inspired Cooperative Strategies for Optimization (NICSO 2010)* 284, 65–74 (2010).

# Optimization of Complex Mathematical Functions Using a Novel Implementation of Intelligent Water Drops Algorithm

Maneet Singh and Sanjay Saini

**Abstract** The intelligent water drops (IWD) algorithm was introduced by Hamed Shah Hosseini in 2007, which has been used to solve some of the discrete optimization problems. This chapter introduces a simplified version of the basic IWD algorithm and uses it to find the global minimum of some of the complex mathematical functions. The parameter settings have a very important role in the efficiency of the algorithm. The results demonstrated that the simplified IWD algorithm gave better results as compared to other techniques in less number of iterations.

**Keywords** Complex mathematical functions · Global minimum · Intelligent water drops

## 1 Introduction

The optimization problems can be classified into two broad categories namely discrete optimization problems and continuous optimization problem. Discrete optimization problems are those that involve finding values for discrete variables such that constructing an optimal solution for the given objective function. Traveling salesman problem, multi-knapsack problem, and  $n$ -queen problem are some of the examples of combinatorial or discrete optimization problems. Continuous optimization problems are those that involve finding real values of the parameters of a given problem. Function minimization and maximization are the examples of continuous optimization problems.

---

M. Singh (✉) · S. Saini

Department of Physics and Computer Science, Dayalbagh Educational Institute, Agra, India  
e-mail: maneetsingh88@gmail.com

S. Saini

e-mail: sanjay.s.saini@gmail.com

## 2 Global Minimum

Each function has two kinds of extremes, commonly known as maxima and minima. The maxima corresponds to the largest value of the function, whereas minima corresponds to the smallest value of the function. Global minimum is the term which is used in place of minima to refer to the point where the function takes on the smallest value. The point where the function has the smallest value with respect to its neighborhood and not to the whole function is known as local minima.

## 3 Recent Work

Intelligent water drops (IWD) algorithm follows the principle of swarm intelligence. Using Swarm Intelligence for optimization problems as specified by Blum et al. [1], has become a very popular and widely used technique. IWD algorithm was proposed by Hosseini [2, 3]. Various problems have been solved using this technique. Kamkar et al. [4] used IWD to solve an NP\_hard combinatorial optimization problem i.e., vehicle routing problem. Rayapudi [5] solved economic dispatch problem using IWD. Ochoa et al. [6] used IWD algorithm along with the cultural algorithm (hybrid approach) to improve a shoal in FishVille. Msallam et al. [7] improved the IWD algorithm using adaptive schema to prevent it from premature convergence. Hosseini [8] reviewed various optimization problems (traveling salesman problem,  $n$ -queen puzzle, multidimensional knapsack problem and automatic multilevel thresholding) that can be solved using IWD.

## 4 IWD Algorithm

IWD algorithm is a nature-inspired optimization algorithm proposed by Hamed Shah Hoseini. Shah Hoseini simulated the behavior of water drops flowing in the natural river. The moving water drops all together in the form of a group creates path for the natural river. The water drops affect the environment in which they move, and the environment also effects the movement of water drops. Artificial water drops retain two important properties of natural water drops—velocity and soil. The velocity with which an IWD moves and the soil an IWD carries may change as an IWD flows in the environment. The path containing less soil is considered to be the easiest path to traverse. An IWD may load or unload soil from the path it traverses.

## 5 Complex Mathematical Functions Taken for Finding Global Minimum

The following mathematical functions are considered for applying IWD to find the global minimum:

1. Rastrigin’s Function: This function is defined as:

$$f(x) = 10n + \sum_{i=1}^n \left( x_i^2 - 10 \cos(2\pi x_i) \right)$$

In this function, there are two number of variables, several local mimima, and the global minima is  $x = (0, 0, \dots, 0)$ , with  $f(x) = 0$ .

2. Rosenbrock’s Function: This function is defined as:

$$f(x) = \sum_{i=1}^{n-1} \left[ 100 \left( x_{i+1}^2 - x_i \right)^2 + \left( 1 - x_i \right)^2 \right]$$

In this function, there are two number of variables, several local mimima, and the global minima is  $x = (1, 1, \dots, 1)$ , with  $f(x) = 0$ .

3. Griewank’s Function: This function is defined as:

$$f(x) = \sum_{i=1}^n \frac{x_i^2}{4,000} - \prod_{i=1}^n \cos\left(\frac{x_i}{\sqrt{i}}\right) + 1$$

In this, the global minima is  $x = (0, 0, \dots, 0)$ , with  $f(x) = 0$ .

4. Sphere Function: This function is defined as:

$$f(x) = \sum_{i=1}^n x_i^2$$

In this function, the global minima is  $x = (0, 0, \dots, 0)$ , with  $f(x) = 0$ .

## 6 Simplified Intelligent Water Drops Algorithm for Finding Global Minimum

The basic IWD algorithm is being modified and implemented on some of the complex mathematical functions. The simplified IWD algorithm is as follows:

1. Initializing static parameters:  $n_{iwd}$  for number of water drops,  $G_B$  represents the quality of the total best solution—initially set to worse,  $max\_iter$  for maximum number of iterations,  $count\_iter$  for counting the number of iterations—initially set to zero.
2. Initializing dynamic parameters: velocity of each IWD is initially set to  $start\_vel$ , but as the iteration proceeds, the velocity decreases, soil of each IWD is set to the function value at the point in the space where IWD lies.
3. Every IWD is randomly placed in the two-dimensional space.



4. Each IWD randomly selects some theta values. If the lowest function value for all the directions is less than the current soil of the IWD, then IWD is moved in that particular direction with the distance equal to the velocity of the IWD; otherwise, the IWD will not move for the current iteration.
5. The velocity is reduced by some fixed ratio each time.
6. Compute the iteration best solution  $I_B$  from the given solution by all  $IWD_B$ , where  $IWD_B = \text{soil}_{iwd}$ .
7. Update the total best solution as the current best solution if the current best solution is better than total best solution; otherwise, the total best solution will remain unchanged.
8. The *count\_iter* is incremented by one, and if *count\_iter* is less than *max\_iter*, then go to step 2 (initializing dynamic parameters).
9. The algorithm gets terminated with  $G_B$  as the optimal solution.

## 7 Results

The results that were obtained after applying the simplified IWD algorithm on complex mathematical functions are compared with the performance of GA and PSO as specified by Valdez et al. [9] and are shown in the Table 1. From the table, we can say that the performance of the simplified IWD algorithm is better than GA and PSO. The performance of the proposed algorithm on Rosenbrock function was compared with the ARSET and ACO algorithms as specified by Toksari [10] (Table 2).

## 8 Conclusion

In this chapter, a simplified version of IWD algorithm is proposed. The proposed algorithm is tested on some of the benchmark problems, the results are compared with the results of genetic algorithm and particle swarm optimization algorithm, and it has been observed that the performance of the proposed algorithm is better than the GA and PSO. The efficiency of the simplified IWD algorithm was tested in terms of epoch number by comparing with ARSET and ACO. The results clearly depicts

**Table 1** Comparison of the performance of simplified IWD with GA and PSO

Mathematical functions	Minima by GA	Minima by PSO	Minima by simplified IWD	Global minimum
Rastrigin	7.36E-07	3.48E-05	0	0
Rosenbrock	2.35E-05	2.46E-03	0	0
Sphere	1.62E-04	8.26E-11	1.5831e-046	0
Griewank	2.552E-05	2.56E-02	0	0

**Table 2** Comparison of the performance of simplified IWD with ARSET and ACO for Rosenbrock function

Algorithms	X	y	F(x, y)	Epoch number
ARSET	0.99401	0.997	3.58E-005	10,000
ACO	1.00021	1.00004	1.73E-006	
<i>Simplified IWD</i>	1	1	0	
ARSET	1.0001	1.0001	2.03E-008	30,000
ACO	1	1	5.68E-12	
<i>Simplified IWD</i>	1	1	0	
ARSET	1	1	4.02E-16	50,000
ACO	1	1	0	
<i>Simplified IWD</i>	1	1	0	

that the proposed algorithm is much better also in the case of number of iterations required to produce good results.

## References

- Blum, C., Li, X.: Swarm intelligence in optimization. In: Blum, C., Merkle, D. (eds.) *Swarm Intelligence — Introduction and Applications*, pp. 43–85. Springer (2008)
- Hosseini, H.S.: Problem solving by intelligent water drops. In: *Proceeding of IEEE Congress on Evolutionary Computation* (2007)
- Hosseini, H.S.: The intelligent water drops algorithm: a nature inspired swarm based optimization algorithm. *Int. J. Bio-Insp. Comput.* **1**(1/2) (2009)
- Kamkar, I., Akbarzadeh-T, M.-R., Yaghoobi, M.: Intelligent water drops a new optimization algorithm for solving the vehicle routing problem. In: *Proceedings of IEEE International Conference on Systems Man and Cybernetics* (2010)
- Rayapudi, S.R.: An intelligent water drop algorithm for solving economic load dispatch problem. *Int. J. Electric. Electron. Eng.* **5**, 1 (2011)
- Ochoa, A., Hernández, A., Bustillos, S., Zamarrón, A.: Water on the water : A hybrid approach using to intelligent water drops algorithm and cultural algorithm to improve a shoal in FishVille. In: *Proceedings of 3rd Workshop of Hybrid Intell. Syst. at MICIA* (2010)
- Msallam, M.M., Hamdan, M.: Improved intelligent water drops algorithm using adaptive schema. *Int. J. Bio-Inspir. Comput.* **3**, 103–111 (2011)
- Hosseini, H.S.: Optimization with the nature-inspired intelligent water drops algorithm. *Evol. Comput.* (2009)
- Valdez, F., Melin, P.: Comparative study of particle swarm optimization and genetic algorithms for complex mathematical functions. *J. Autom. Mob. Robot. Intell. Syst.* **2**, 43–51 (2008)
- Toksari, M.D.: Ant colony optimization for finding the global minimum. *Appl. Math. Comput.* 308–316 (2006)

# A New Centroid Method of Ranking for Intuitionistic Fuzzy Numbers

Anil Kumar Nishad, Shailendra Kumar Bharati and S. R. Singh

**Abstract** In this paper, we proposed a new ranking method for intuitionistic fuzzy numbers (IFNs) by using centroid and circumcenter of membership function and non-membership function of the intuitionistic fuzzy number. The method utilizes the midpoint of the circumcenter of membership and non-membership function of intuitionistic fuzzy number to define the ranking function for IFN satisfying the general axioms of ranking functions. The developed method has been illustrated by some examples and is compared with some existing ranking method to show its suitability.

**Keywords** Intuitionistic fuzzy sets (IFS) · Trapezoidal intuitionistic fuzzy number · Triangular intuitionistic fuzzy number (TIFN) · Membership function · Non-membership function · Ranking function

## 1 Introduction

Decision-making problems need the processing of information for getting an optimal solution of a problem in a specific situation. But in general the information available is often imprecise and vague and many times contains uncertainty, and thus, such situation demands its handling by non-traditional methods. The fuzzy set theory developed by Zadeh [14] immersed as a potential tool in theory of optimization to deal with imprecision and vagueness in parameters. Further dealing with sociometric

---

A.K. Nishad (✉) · S. K. Bharati · S. R. Singh  
Department of Mathematics, Banaras Hindu University, Varanasi 221005, India  
e-mail: anil.k.nishad16@gmail.com

S. K. Bharati  
e-mail: skmaths.bhu@gmail.com

S. R. Singh  
e-mail: singh\_shivaraj@rediffmail.com

problems of decision-making one is encountered by a situation where information available also contains hesitation factor in addition to belonging and non-belonging. Intuitionistic fuzzy set theory was developed by Atanassov [1, 2] to deal with such situations in an effective way. Such optimization problems in general involve the intuitionist fuzzy numbers. Here, while defining arithmetic operations on intuitionistic fuzzy number (IFN), its ranking is needed to have comparison among IFNs. Unlike to ranking of fuzzy numbers, one has also to take the cognition of non-membership functions in ranking of IFNs. Thus, this ranking becomes an interesting property of intuitionistic fuzzy number, and various workers have proposed several methods of ranking. In order to develop a standard for raking methods, Wang and Kerre [13] proposed six axioms which a reasonable ranking method is desired to satisfy. Further, Grzegorzewski [5] studied distances and ordering in a family of IFNs. A significant work on ranking method was carried out by Michell [7] for fuzzy numbers. Theory of ranking methods for IFN was further enriched by Su [12], Nayagam [10], Abbasbandy [3], and Nan and Li [8]. Recently, Rao and Shanker [11], Dubey and Mehra [4], Nagoorgani and Ponnalagu [9] proposed some ranking methods for normal IFNs. In the present study, we have studied the various aspects of some ranking methods on six standard axioms and have proposed a general method for ranking of IFNs satisfying the six standard axioms for its application to decision-making problems.

## 2 Preliminaries

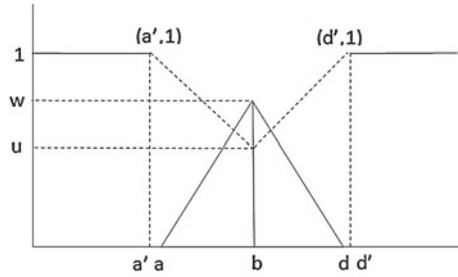
**Definition 1** (*Fuzzy Set*) If  $X$  is a collection of objects denoted generically by  $x$ , then a fuzzy set  $\tilde{A}$  in  $X$  is a set of ordered pairs:  $\tilde{A} = \{(x, \mu_{\tilde{A}}(x)) | x \in X\}$ , where  $\mu_{\tilde{A}}(x)$  is called the membership function or grade of membership of  $x$  in  $\tilde{A}$  that maps  $X$  to the membership space  $M [0, 1]$ .

**Definition 2** (*Intuitionistic Fuzzy Set*) If  $X$  is a collection of objects, then an intuitionistic fuzzy set  $\tilde{A}$  in  $X$  is defined as :  $\tilde{A} = \{(x, \mu_{\tilde{A}}(x), \nu_A(x)) | x \in X\}$ , where  $\mu_{\tilde{A}}(x), \nu_A(x)$  is called the membership and non-membership function of  $x$  in  $\tilde{A}$  respectively.

**Definition 3** [*Trapezoidal Intuitionistic Fuzzy Number (TFN)*] An intuitionistic fuzzy set (IFS)  $\tilde{A} = \{(x, \mu_{\tilde{A}}(x), \nu_A(x)) | x \in X\}$  of  $\mathbb{R}$  is said to be an intuitionistic fuzzy number if  $\mu_A$ , and  $\nu_A$  are fuzzy numbers with  $\nu_A \leq \mu_A^c$ , where  $\mu_A^c$ , denotes the complement of  $\mu_A$ . A TFN with parameters  $a' \leq a \leq b \leq c \leq d \leq d'$  denoted by  $\tilde{A} = \langle (a, b, c, d, \mu_A, \nu_A), (a', b, c, d', \nu_A) \rangle$  is a IFS on real line  $\mathbb{R}$  whose membership function and non-membership function are defined as follows:

$$\mu_{\tilde{A}}(x) = \begin{cases} \frac{(x-a)w}{(b-a)} & \text{if } a \leq x < b \\ w & \text{if } b \leq x < c \\ \frac{(d-x)w}{(d-c)} & \text{if } c \leq x < d \end{cases}$$

**Fig. 1** Membership and non-membership function of triangular intuitionistic fuzzy number



and

$$v_A(x) = \begin{cases} \frac{(x-a')u+(b-x)}{(b-a')} & \text{if } a' \leq x < b \\ u & \text{if } b \leq x < c \\ \frac{(x-d')u+(c-x)}{(c-d')} & \text{if } c \leq x < d' \end{cases}$$

respectively. The values  $w$  and  $u$  represent the maximum degree of membership and the minimum degree of non-membership function, respectively, such that  $\mu_A : X \rightarrow [0, 1]$  and  $\nu_A : X \rightarrow [0, 1]$  and  $0 \leq w + u \leq 1$ .

**Definition 4** (*Triangular Intuitionistic Fuzzy Number (TIFN)*) If in a trapezoidal IFN we take ( $b=c$ ), then it becomes a triangular IFN with the parameters  $a' \leq a \leq b \leq d \leq d'$  and denoted by  $\tilde{A} = \langle (a, b, d, \mu_A, \nu_A) \rangle$  Fig. 1.

### 3 Ranking of Intuitionistic Fuzzy Numbers

Ranking of fuzzy numbers is an important arithmetic property of IFNs. It provides comparison between two IFNs. This property of ranking is used in decision-making problems in uncertain environment. In view of belonging, non-belonging and hesitations factor of an IFN several ranking methods have been developed. Thus, in order to standardize these methods, Wang and Kerre [13] proposed six axioms. Let  $M$  be an ordering method and  $S$  the set of fuzzy quantities for which the method  $M$  can be applied and  $A$  be finite subset of  $S$ .

- A<sub>1</sub>. For any arbitrary finite subset  $\tilde{A}$  of  $S$  and  $\tilde{a} \in \tilde{A} \succsim \tilde{a}$  by  $M$  on  $\tilde{A}$ .
- A<sub>2</sub>. For an arbitrary finite subset  $\tilde{A}$  of  $S$  and  $(\tilde{a}; \tilde{b}) \in \tilde{A}^2, \tilde{a} \succsim \tilde{b}$ , and  $\tilde{b} \succsim \tilde{a}$  by  $M$  on  $\tilde{A}$ , we should have  $\tilde{a} \sim \tilde{b}$  by  $M$  on  $\tilde{A}$ .
- A<sub>3</sub>. For an arbitrary finite subset  $\tilde{A}$  of  $S$  and  $(\tilde{a}; \tilde{b}; \tilde{c}) \in \tilde{A}^3, \tilde{a} \succsim \tilde{b}$  and  $\tilde{b} \succsim \tilde{c}$  by  $M$  on  $\tilde{A}$  we should have  $\tilde{a} \succsim \tilde{c}$  by  $M$  on  $\tilde{A}$ .
- A<sub>4</sub>. For an arbitrary finite subset  $\tilde{A}$  of  $S$  and  $(\tilde{a}, \tilde{b}) \in \tilde{A}^2 \inf \sup (\tilde{a}) \geq \sup \sup (\tilde{b})$ , we should have  $\tilde{a} \geq \tilde{b}$  by  $M$  on  $\tilde{A}$ .

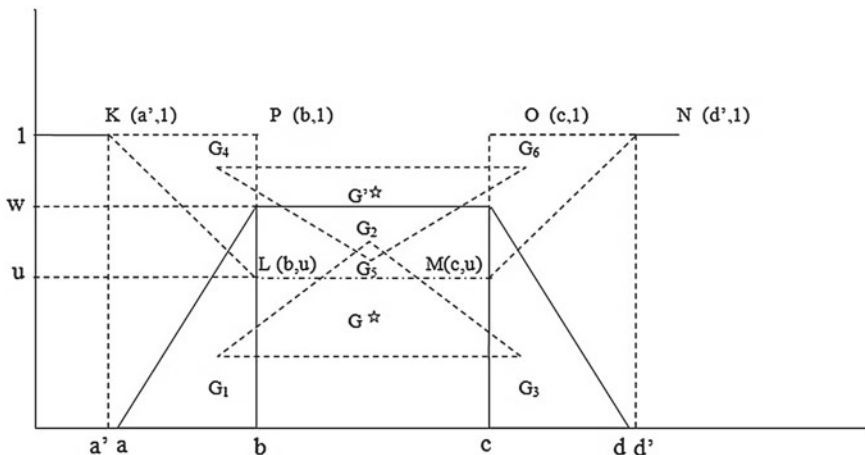


Fig. 2 Centroids of membership function and non-membership function

A<sub>5</sub>. Let  $S$  and  $S'$  be two arbitrary finite sets of fuzzy quantities in which  $M$  can be applied and  $\tilde{a}$  and  $\tilde{b}$  are in  $s \cap s'$ . We obtain the ranking order  $\tilde{a} > \tilde{b}$  by  $M$  on  $S'$  iff  $\tilde{a} > \tilde{b}$  by  $M$  on  $S$ .

A<sub>6</sub>. Let  $\tilde{a}, \tilde{b}, \tilde{a} + \tilde{c}, \tilde{b} + \tilde{c}$  be element of  $S$ , If  $\tilde{a} \gtrsim \tilde{b}$  by  $M$  on  $\{\tilde{a}, \tilde{b}\}$ , then  $\tilde{a} + \tilde{c} \gtrsim \tilde{b} + \tilde{c}$  by  $M$  on  $\{\tilde{a} + \tilde{c}, \tilde{b} + \tilde{c}\}$ .

### 3.1 Proposed Ranking Method

Centroid of TIFN is considered as the balancing point of trapezoidal IFN for membership function and non-membership function are shown Fig. 2. Midpoints of circumcenters of centroid of membership function and non-membership function is taken as point of references to define the ranking of generalized trapezoidal IFN, and these points (circumcenters) are considered as balancing point of each individual membership function and non-membership function.

Consider a generalized trapezoidal IFN,  $\tilde{A} = \langle (a, b, c, d, \mu_A), (a', b, c, d', \nu_A) \rangle$  as shown in Fig. 2.

In which centroid of the three plain figures of membership function are  $G_1 = (\frac{(a+2b)}{3}, \frac{w}{3})$ ,  $G_2 = (\frac{(b+c)}{2}, \frac{w}{2})$ , and  $G_3 = (\frac{(2c+d)}{3}, \frac{w}{3})$ , respectively. These centroids are non-collinear and they form a triangle whose circumcenter is  $C_{\tilde{A}}(x_0, y_0)$  with vertices  $G_1, G_2$  and  $G_3$  of membership function of generalized trapezoidal IFN. Let  $\tilde{A} = \langle (a, b, c, d, w), (a', b, c, d', u) \rangle$  is a intuitionistic fuzzy number whose circumcenter is given as:

$$C_{\tilde{A}}(x_0, y_0) = \left( \frac{(a + 2b + 2c + d)}{6}, \frac{(2a + b - 3c)(c + 2d - 3b) + 5w^2}{12w} \right)$$

And centroid points of non-membership function are  $G_4 = (\frac{(a'+2b)}{3}, \frac{u+2}{3})$ ,  $G_5 = (\frac{(b+c)}{2}, \frac{1+u}{2})$ , and  $G_6 = (\frac{(2c+d')}{3}, \frac{2+u}{3})$ , respectively forms a triangle  $G_4, G_5, G_6$  whose circumcenters is given as:

$$C'_{\tilde{A}}(x_0, y_0) = \left( \frac{(a'+2b+2c+d')}{6}, \frac{(-2a' - b + 3c)(c + 2d' - 3b) + 7 - 2u - 5u^2}{12(1 - u)} \right) \tag{1}$$

Thus, we have two circumcenters  $C_{\tilde{A}}(x_0, y_0)$  and  $C'_{\tilde{A}}(x_0, y_0)$ , now take the midpoint of these circumcenters of generalized trapezoidal IFNs  $S_{\tilde{A}}(\tilde{x}_0, \tilde{y}_0)$  which is given as :

$$S_{\tilde{A}}(\tilde{x}_0, \tilde{y}_0) = \left( \frac{(a' + a + 4b + 4c + d' + d)}{12}, \frac{(1 - u)[(2a + b - 3c)(c + 2d - 3b) + 5w^2] + w[(-2a' - b + 3c)(c + 2d' - 3b) + (7 - 2u - 5u^2)]}{24w(1 - u)} \right)$$

**Definition 5** For a generalized trapezoidal IFN  $\tilde{A} = \langle (a, b, c, d, w), (a', b, c, d', u) \rangle$  with midpoint of circumcenters of membership and non-membership function  $S_{\tilde{A}}(\tilde{x}_0, \tilde{y}_0)$ , we define index associated with the ranking as  $I_{\alpha} = \alpha \tilde{y}_0 + (1 - \alpha) \tilde{x}_0 I$ , where  $\alpha \in [0, 1]$  is the index of optimism which represent the degree of optimism of decision maker. If  $\alpha = 0$ , we have a pessimistic decision maker, and if  $\alpha = 1$ , then we have optimistic decision maker or a neutral with  $\alpha = .5$ . The ranking function of trapezoidal IFN  $\tilde{A} = \langle (a, b, c, d, w), (a', b, c, d', u) \rangle$  is a function which maps the set of all IFNs to a set of real number and is defined as  $R(\tilde{A}) = \sqrt{\tilde{x}_0^2 + \tilde{y}_0^2}$ , which is the Euclidean distance of midpoint of circumcenters of centroids of membership function and non-membership function of trapezoidal IFN. Now using above definition, we define ranking between IFNs as follows :

Let  $\tilde{A}$  and  $\tilde{B}$  be two IFNs then

1.  $\tilde{A} > \tilde{B}$ , if  $(R(\tilde{A}) > R(\tilde{B}))$
2.  $\tilde{A} < \tilde{B}$ , if  $(R(\tilde{A}) < R(\tilde{B}))$

But if  $R(\tilde{A}) = R(\tilde{B})$ , then this definition of ranking fails.

For such situation, we use second ranking function defined as  $I_{(\alpha, \beta)}(\tilde{A}) = \beta (\frac{\tilde{x}_0 + \tilde{y}_0}{2}) + (1 - \beta) I_{\alpha}(\tilde{A})$  where  $\beta \in [0, 1]$  and represent the weight of central value and  $(1 - \beta)$  is the weight associated with the extreme values of  $\tilde{x}_0$  and  $\tilde{y}_0$ . This ranking function of trapezoidal IFN also holds for the triangular IFN since triangular IFNs are special case of trapezoidal IFN, i.e., let  $\tilde{A} = \langle (a, b, c, d, w), (a', b, c, d', u) \rangle$  be a trapezoidal IFN and if take  $b = c$  it becomes triangular IFN, the midpoint of circumcenters of membership and non-membership function of triangular IFN is given by

$$S_{\tilde{A}}(\tilde{x}_0, \tilde{y}_0) = \left( \frac{(a' + a + 8b + d' + d)}{12}, \frac{(1 - u) [4(a - b)(d - b) + 5w^2] + w[4(b - a')(d' - b) + (7 - 2u - 5u^2)]}{24w(1 - u)} \right)$$

and holds for ranking function defined above.

*Example 1* Let  $\tilde{A} = \langle (0.4, 0.5, 0.7; 0.8), (0.3, 0.5, 0.8; 0.1) \rangle$ ,  $\tilde{B} = \langle (0.4, 0.6, 0.7; 0.6), (0.5, 0.6, 0.9; 0.3) \rangle$ ,  $\tilde{C} = \langle (0.2, 0.6, 0.7; 0.9), (0.1, 0.6, 0.8; 0.3) \rangle$ , are three IFNs which are to be compared

Here, using the above ranking method, we get

$$S_{\tilde{A}}(\tilde{x}_0, \tilde{y}_0) = (0.516, 0.486), S_{\tilde{B}}(\tilde{x}_0, \tilde{y}_0) = (0.608, 0.475), S_{\tilde{C}}(\tilde{x}_0, \tilde{y}_0) = (0.55, 0.511).$$

This on further computation gives

$$R(\tilde{A}) = 0.7088 \quad R(\tilde{B}) = 0.771 \quad R(\tilde{C}) = 0.750 \Rightarrow \tilde{B} > \tilde{C} > \tilde{A}$$

*Example 2* Let  $\tilde{A} = \langle (0.1, 0.3, 0.5; 1), (0.1, 0.3, 0.5; 0) \rangle$  and  $\tilde{B} = \langle (-0.5, -0.3, -0.1; 1), (-0.5, -0.3, -0.1; 0) \rangle$  are two IFNs.

The above method gives  $S_{\tilde{A}}(\tilde{x}_0, \tilde{y}_0) = (0.3, 0.5)$ ,  $S_{\tilde{B}}(\tilde{x}_0, \tilde{y}_0) = (-0.3, 0.5)$  and hence  $R(\tilde{A}) = R(\tilde{B}) = \frac{\sqrt{34}}{10}$

Thus, we use second definition for its ranking

1. For a pessimistic decision maker, i.e.,  $\alpha = 0$

$$I_{(0,\beta)}(\tilde{A}) = \beta(0.4) + (1 - \beta)0.3$$

$$I_{(0,\beta)}(\tilde{B}) = \beta(0.1) - (1 - \beta)0.3 \Rightarrow \tilde{A} > \tilde{B}$$

2. For an optimistic decision maker, i.e.,  $\alpha = 1$

$$I_{(1,\beta)}(\tilde{A}) = \beta(0.4) + (1 - \beta)0.5$$

$$I_{(1,\beta)}(\tilde{B}) = \beta(0.1) + (1 - \beta)0.5 \Rightarrow \tilde{A} > \tilde{B}$$

3. For a neutral decision maker, i.e.,  $\alpha = 0$ .

$$I_{(0.5,\beta)}(\tilde{A}) = \beta(0.4) + (1 - \beta)0.4$$

$$I_{(0.5,\beta)}(\tilde{B}) = \beta(0.1) + (1 - \beta)0.4 \Rightarrow \tilde{A} > \tilde{B}$$

$\Rightarrow \tilde{A} > \tilde{B}$  Thus, we see that the ranking order of IFN is same for all cases

*Example 3* Let  $\tilde{A} = \langle (0.1, 0.3, 0.5; 1), (0.1, 0.3, 0.5; 0) \rangle$ ,  $\tilde{B} = \langle (-0.5, -0.3, -0.1; 1), (-0.5, -0.3, -0.1; 0) \rangle$  are two IFNs.



Then,  $-\tilde{A} = \langle(-0.5, -0.3, -0.1; 1), (-0.5, -0.3, -0.1; 0)\rangle$  and

$$-\tilde{B} = \langle(0.1, 0.3, 0.5; 1), (0.1, 0.3, 0.5; 0)\rangle, \text{ and } S_{\tilde{A}}(\bar{x}_0, \bar{y}_0) = (-0.3, 0.5), \\ S_{\tilde{B}}(\bar{x}_0, \bar{y}_0) = (0.3, 0.5),$$

Thus,  $R(\tilde{A}) = R(\tilde{B}) = \frac{\sqrt{34}}{10}$  and discrimination of triangular IFN is not possible. Thus, for this case, we use the second definition of ranking function and get the following,

1. For a pessimistic decision maker, i.e.,  $\alpha = 0$

$$I_{(0,\beta)}(-\tilde{A}) = \beta(0.1) - (1 - \beta)0.3 \\ I_{(0,\beta)}(-\tilde{B}) = \beta(0.1) - (1 - \beta)0.3 \Rightarrow -\tilde{A} < -\tilde{B}$$

2. For an optimistic decision maker, i.e.,  $\alpha = 1$

$$I_{(1,\beta)}(-\tilde{A}) = \beta(0.1) + (1 - \beta)0.5 \\ I_{(1,\beta)}(-\tilde{B}) = \beta(0.4) + (1 - \beta)0.5 \Rightarrow -\tilde{A} < -\tilde{B}$$

3. For a neutral decision maker, i.e.,  $\alpha = 0.5$

$$I_{(0.5,\beta)}(-\tilde{A}) = \beta(0.1) + (1 - \beta)0.4 \\ I_{(0.5,\beta)}(-\tilde{B}) = \beta(0.4) + (1 - \beta)0.4 \Rightarrow -\tilde{A} < \tilde{B}$$

Now from the above Example 2 and Example 3, we see that  $\tilde{A} > \tilde{B} \Rightarrow -\tilde{A} < -\tilde{B}$

### 3.1.1 Comparison with Dubey and Mehra Method

*Example 4* Let  $\tilde{A} = \langle(9, 10, 20; 1), (9, 10, 20; 0)\rangle$ ,  $\tilde{B} = \langle(8.7, 8.8, 8.9; 1), (8.7, 8.8, 8.9; 0)\rangle$  are two IFNs, then Dipty ranking method fails to satisfy axiom  $A_4$  (For an arbitrary finite subset  $\tilde{A}$  of  $S$  and  $(\tilde{a}, \tilde{b}) \in \tilde{A}^2$   $\inf \sup (\tilde{a}) \geq \sup \sup (\tilde{b})$ , we should have  $\tilde{a} \geq \tilde{b}$  by M on  $\tilde{A}$ ) and rank as  $\tilde{A} < \tilde{B}$  .

But proposed ranking method satisfy axiom  $A_4$  and rank this IFN, i.e., by getting  $S_{\tilde{A}}(\bar{x}_0, \bar{y}_0) = (18.66, 0.5)$ ,  $S_{\tilde{B}}(\bar{x}_0, \bar{y}_0) = (14.66, 0.5)$ ,  $R(\tilde{A}) = 18.17$ ,  $R(\tilde{B}) = 14.67 \Rightarrow \tilde{A} > \tilde{B}$

which is correct according to axiom  $A_4$ .

### 3.1.2 Comparison with Hassan Method

Let  $\tilde{A} = \langle (a_1, a_2, a_3, a_4), (b_1, b_2, b_3, b_4, ) \rangle$  be a triangular IFN, then characteristic values of membership and non-membership for IFN  $\tilde{A}$  with parameter  $(k)$  denoted by  $C_\mu^k(\tilde{A}), C_\nu^k(\tilde{B})$ , respectively, are defined by

$$C_\mu^k(\tilde{A}) = \frac{a_1 + a_3}{2} + \frac{(a_1 - a_2) + (a_4 - a_3)}{2(k + 2)}, C_\nu^k(\tilde{B}) = \frac{b_1 + b_4}{2} + \frac{(b_2 - b_1) + (b_3 - b_4)}{2(k + 2)}$$

and according to the two IFNs,  $\tilde{A}$  and  $\tilde{B}$  are compared as follows :

1. For a given  $k$ , compare ordering of  $\tilde{A}$  and  $\tilde{B}$  according to relative position of  $C_\mu^k(\tilde{A})$  ,and  $C_\mu^k(\tilde{B})$ ,
2. If  $C_\mu^k(\tilde{A})$  and  $C_\mu^k(\tilde{B})$  are equals, then conclude that  $\tilde{A}$  and  $\tilde{B}$  are equals. Otherwise, rank  $\tilde{A}$  and  $\tilde{B}$  according to relative position of  $-C_\nu^k(\tilde{A})$  and  $-C_\nu^k(\tilde{B})$

*Example 5* Let  $\tilde{A} = \langle (0.4, 0.5, 0.7; 0.8), (0.3, 0.5, 0.8; 0.1) \rangle$  and  $(\tilde{B}) = \langle (0.4, 0.5, 0.7; 0.7), (0.3, 0.5, 0.8; 0.1) \rangle$  are two IFNs, then by Hassan as well as Nagoorgani methods it is clear that these two IFNs are equal. But using the proposed method, we have  $S_{\tilde{A}}(\bar{x}_0, \bar{y}_0) = (0.516, 0.486)$ ,  $S_{\tilde{B}}(\bar{x}_0, \bar{y}_0) = (0.516, 0.464)$ ,

$$R(\tilde{A}) = 0.7088, R(\tilde{B}) = 0.6939 \Rightarrow R(\tilde{A}) > R(\tilde{B}), \Rightarrow \tilde{A} > \tilde{B}.$$

## 4 Conclusion

Thus, we proposed a more general method for ranking of IFNs to provide an appealing and logically interpretation of comparison in IFNs in view of ambiguity. The proposed method satisfy the standard axioms given by Wang and Kerre [13] which is commonly used standard for ranking method of IFNs. We have clearly illustrated with suitable examples that even those specific cases where Dubey and Mehra [4], Hassan [6], and Nagoorgani [9] methods for ranking do not give clear conclusion, the proposed method provides a better comparison to such IFN. Thus, the proposed method of ranking may be suitably used in optimization problems in intuitionistic fuzzy environment for better understanding under ambiguity.

**Acknowledgments** The authors are thankful to University Grants Commission (UGC), Government of India, and DST-CIMS, Banaras Hindu University, for financial support to carry out this research work.

## References

1. Atanassov, K.T.: Intuitionistic fuzzy sets. *Fuzzy Sets Syst.* **20**, 87–96 (1986)
2. Atanassov, K.T.: interval valued intuitionistic fuzzy sets. *Fuzzy Sets Syst.* **31**, 343–349 (1989)
3. Abbasbandy S, Ranking of fuzzy numbers, some recent and new formulas, in IFSA-EUSFLAT (2009), pp. 642–646
4. Dipti, Dubey, Aparna, Mehra: Fuzzy linear programming with triangular intuitionistic fuzzy number, EUSFLAT-LFA 2011. *Advances in intelligent System Research*, Atlantis Press, vol. 1, issue 1, pp. 563–569 (2011)
5. Grzegorzewski P, Distances and orderings in a family of intuitionistic fuzzy numbers, in *Proceedings of the Third Conference on Fuzzy Logic and Technology (Eusflat03)*, pp. 223–227, (2003)
6. Hassan, M.N.: A new Ranking Method for Intuitionistic Fuzzy Numbers. *Int. J. Fuzzy Syst.* **12**(1), 80–86 (2010)
7. Mitchell H.B., Ranking Intuitionistic fuzzy numbers, *Int. J. Uncertainty Fuzziness Knowl. Based Syst.* **12**(3), 377–386 (2004)
8. Nan, J.X., Li, D.-F.: A lexicographic method for matrix games with payoffs of triangular intuitionistic fuzzy numbers. *Int. J. Comput. Intell. Syst.* **3**, 280–289 (2010)
9. Nagoorgani, A.: Ponnalagu K. A New Approach on Solving Intuitionistic Fuzzy Linear Programming Problem, *Appl. Math. Sci.* **6**(70), 3467–3474 (2012)
10. Nayagam V.L., Vankateshwari G, and SivaramanG, Ranking of intuitionistic fuzzy numbers. *IEEE International Conference on Fuzzy Systems*, pp. 1971–1974 (2008)
11. Rao P.H.B., Shankar N.R., Ranking fuzzy numbers with a distance method using circumcenter of centroids and an index of modality. *Adv. Fuzzy Syst.* Article ID 178308, (2011). doi:[10.1155/2011/178308](https://doi.org/10.1155/2011/178308)
12. Su, J.S.: Fuzzy programming based on interval valued fuzzy numbers and ranking. *Int. J. Contemp. Math. Sci.* **2**, 393–410 (2007)
13. Wang, X.: Kerre E.E., Reasonable properties for the ordering of fuzzy quantities (I). *Fuzzy Sets Syst.* **118**, 375–385 (2001)
14. Zadeh, L.: A. Fuzzy sets. *Inf. Control* **8**, 338–353 (1965)

# Solution of Multi-Objective Linear Programming Problems in Intuitionistic Fuzzy Environment

S. K. Bharati, A. K. Nishad and S.R. Singh

**Abstract** In the paper, we give a new method for solution of multi-objective linear programming problem in intuitionistic fuzzy environment. The method uses computation of the upper bound of a non-membership function in such way that the upper bound of the non-membership function is always less than the upper bound of the membership function of intuitionistic fuzzy number. Further, we also construct membership and non-membership function to maximize membership function and minimize non-membership function so that we can get a more efficient solution of a probabilistic problem by intuitionistic fuzzy approach. The developed method has been illustrated on a problem, and the result has been compared with existing solutions to show its superiority.

**Keywords** Multi-objective programming · Positive ideal solution · Intuitionistic fuzzy sets · Intuitionistic fuzzy optimization

## 1 Introduction

Atanassov [1] generalized the fuzzy sets to intuitionistic fuzzy sets to deal with imprecision, vagueness, and uncertainty for a class of problems in a better way. In fuzzy sets, we consider only belonging of an element to a set, whereas in intuitionistic fuzzy set theory, we consider both the belonging and the non-belonging as membership and non-membership functions. Intuitionistic fuzzy set, with this

---

S. R.Singh · S. K. Bharati (✉) · A. K. Nishad  
Department of Mathematics, Banaras Hindu University, Varanasi 221005, India  
e-mail: srsingh\_mathbhu@rediffmail.com

S. K. Bharati  
e-mail: skmaths.bhu@gmail.com

A. K. Nishad  
e-mail: anil.k.nishad16@gmail.com

property, emerged as more powerful tool in dealing with vagueness and uncertainty than fuzzy set. Angelov [3] proposed a method for solving multi-objective programming problems in intuitionistic fuzzy environment. Further, Atanassov and Gargov in [2] generalized intuitionistic fuzzy sets and proposed several new properties to intuitionistic fuzzy sets which made IFS suitable to deal with problems of optimizations. De et al. [4], Mondal and Samanta [12] proposed some properties of intuitionistic fuzzy sets to make it more suitable for various applications. For dealing with multi-objective programming, goal programming emerged as more powerful to provide its solutions, and Mohamed [11] studied relationship in goal programming and fuzzy programming. Etoh et al. [8] considered a probabilistic problem in fuzzy environment for its solution, and this problem was further studied by Garg and Singh [7] for suitability of fuzzy solution of a probabilistic problem. Jana and Roy [9] considered a multi-objective intuitionistic fuzzy linear programming approach for solution of transportation problem, and Mahapatra et al. [13] studied intuitionistic fuzzy mathematical programming on reliability optimization model. Another direction in optimization under interval-valued intuitionistic fuzzy emerged with the work of Li [10] who considered linear programming method for MADM with interval-valued intuitionistic fuzzy sets. Dubey et al. [5, 6] considered the linear programming problems with triangular intuitionistic fuzzy number interval uncertainty in intuitionistic fuzzy set (IFS). Recently Nachammai and Thangaraj [14], Nagoorani, Ponnalagu and Shahroki et al. [16] have also studied the solutions of linear programming problems in intuitionistic fuzzy environment. Here, we construct the membership and non-membership functions and have applied the developed algorithm for solution of a probabilistic problem by intuitionistic fuzzy approach.

## 2 Preliminaries

Since Zadeh [17] generalized the set theory as fuzzy set theory to deal with information available in imprecise form, many new properties have been developed for fuzzy set and numerous applications have been developed. It was Zimmermann [18] who considered a fuzzy programming with several objectives. As Atanassov [1, 2] theories are considered the generalization of fuzzy set to intuitionistic fuzzy set, it is needed to study the basics of intuitionistic fuzzy to develop an application of this IFS. Thus, here we reproduce some of its fundamentals to make the study self-sufficient.

*Definition 1* An intuitionistic fuzzy set  $\tilde{A}$  assigns to each element  $x$  of the universe  $X$  a membership degree  $\mu_{\tilde{A}}(x) \in [0, 1]$  and non-membership degree  $\nu_{\tilde{A}}(x) \in [0, 1]$  such that  $\mu_{\tilde{A}}(x) + \nu_{\tilde{A}}(x) \leq 1$ . A IFS is mathematically represented as  $\{ \{x, \mu_{\tilde{A}}(x), \nu_{\tilde{A}}(x)\} | x \in X \}$  where  $1 - \mu_{\tilde{A}}(x) - \nu_{\tilde{A}}(x)$  is called hesitancy margin.

*Example* Let  $A$  be set of countries with elected government, and let  $x$  be a member of  $A$ . Let  $M(x)$  be the percentage of the electorate that voted for the government,  $N(x)$  the percentage that voted against. If we take  $\mu_{\tilde{A}}(x) = \frac{M(x)}{100}$ ,  $\nu_{\tilde{A}}(x) = \frac{N(x)}{100}$

then  $\mu_{\tilde{A}}(x)$  gives the degree of support,  $\nu_{\tilde{A}}(x)$  the degree of opposition and  $h_{\tilde{A}}(x) = 1 - \mu_{\tilde{A}}(x) - \nu_{\tilde{A}}(x)$  stand for indeterminacy which is the portion that cast bad votes: invalid votes, abstinent.

### 2.1 Intuitionistic Fuzzy Number

An IFS  $\tilde{A} = (\mu_{\tilde{A}}, \nu_{\tilde{A}})$  of real numbers is said to be an intuitionistic fuzzy number if  $\mu_{\tilde{A}}$  and  $\nu_{\tilde{A}}$  are fuzzy numbers. Hence,  $A = (\mu_{\tilde{A}}, \nu_{\tilde{A}})$  denotes an intuitionistic fuzzy number if  $\mu_{\tilde{A}}$ , and  $\nu_{\tilde{A}}$  are fuzzy numbers with  $\nu_{\tilde{A}} \leq \mu_{\tilde{A}}^C$ , where  $\mu_{\tilde{A}}^C$  denotes the complement of  $\mu_{\tilde{A}}$ .

Some operations on intuitionistic fuzzy sets are as follows:

$$\begin{aligned} \tilde{A} \cap \tilde{B} &= \{ \{x, \min(\mu_{\tilde{A}}(x), \mu_{\tilde{B}}(x)), \max(\nu_{\tilde{A}}(x), \nu_{\tilde{B}}(x)) \} | x \in X \} \\ \tilde{A} \cup \tilde{B} &= \{ \{x, \max(\mu_{\tilde{A}}(x), \mu_{\tilde{B}}(x)), \min(\nu_{\tilde{A}}(x), \nu_{\tilde{B}}(x)) \} | x \in X \} \end{aligned}$$

### 3 Optimization in Intuitionistic Fuzzy Set

Various studies of optimization problems in fuzzy environment showed the suitability of considering optimization problems in fuzzy environment. The reason for the success was quite obvious that a small violation in constraints leads to more efficient solution. Further studies revealed that fuzzy optimization formulations are more flexible and allow better range of solutions especially when boundaries are not sharp. As a matter of fact in case of multi-objective programming problem, we search an optimal compromise solution rather than optimal solution. This idea of getting compromise solution in intuitionistic fuzzy environment needs to maximize the degree of acceptance to objective functions and constraints and to minimize the rejection of objective functions and constraints.

Consider the intuitionistic fuzzy optimization problem as generalization of fuzzy optimization problem under taken by Angelov [3] and is given as

$$\min f_i(x), \quad i = 1, 2, \dots, m$$

Such that

$$g_j(x) \leq 0, \quad j = 1, 2, \dots, n$$

where  $x$  is decision variables,  $f_i(x)$  denotes objective functions, and  $g_j(x)$  denotes the constraint functions.  $m$  and  $n$  denote the number of objective(s) and constraints, respectively.

**Theorem 1** *For objective function of maximization problem, the upper bound for non-membership function is always less than that of the upper bound of membership function.*

*Proof* From definition of IFS, sum of the degree of rejection and acceptance is less than unity.

If,  $U_k^\mu$  and  $L_k^\mu$  are upper and lower bound, respectively, for the membership function and similarly  $U_k^v$  and  $L_k^v$  are upper and lower bound, respectively, for the non-membership function, then

$$\mu_k(f_k(x)) + \nu_k(f_k(x)) < 1 \quad \text{for all } k = 1, 2, \dots, K$$

or

$$\frac{f_i(x) - L_k^\mu}{U_k^\mu - L_k^\mu} + \frac{U_k^v - f_k(x)}{U_k^v - L_k^v} < 1$$

*Case 1* If possible, let  $U_k^v = U_k^\mu$ , then we have

$$\frac{f_k(x) - L_k^\mu}{U_k^\mu - L_k^\mu} + \frac{U_k^v - f_k(x)}{U_k^\mu - L_k^v} < 1$$

this gives  $L_k^v < L_k^\mu$  which is contradicting the fact that lower bound of the membership and non-membership is equal; hence,  $U_k^v \neq U_k^\mu$ .

*Case 2* Let us consider  $L_k^v = L_k^\mu$ , then we have

$$\frac{f_k(x) - L_k^\mu}{U_k^\mu - L_k^\mu} + \frac{U_k^v - f_k(x)}{U_k^v - L_k^\mu} < 1$$

Which imply that  $U_k^v < U_k^\mu$ .

*Case 3* Let us consider  $L_k^v = L_k^\mu + \varepsilon_k, \varepsilon_k > 0$  for all  $k = 1, 2, \dots, K$ .

$$\frac{f_k(x) - L_k^\mu}{U_k^\mu - L_k^\mu} + \frac{U_k^v - f_k(x)}{U_k^v - L_k^\mu} < 1$$

$$U_k^\mu > U_k^v + \varepsilon_k \frac{U_k^v - f_k(x)}{f_k(x) - L_k^\mu - \varepsilon_k}$$

i.e.,  $U_k^\mu > U_k^v$  hence  $U_k^\mu > U_k^v$ .

### 3.1 Computational Algorithm

Using the above-mentioned theorem and with the method by Anglev [3], we develop the following algorithm for getting solution of a multi-objective programming problem in intuitionistic fuzzy environment:

- Step 1: Take one objective function out of given k objectives and solve it as a single objective subject to the given constraints. From obtained solution vectors, find the values of remaining (k - 1) objective functions.
- Step 2: Continue the step 1 for remaining (k - 1) objective functions. If all the solutions are same, then one of them is the optimal compromise solution.
- Step 3: Tabulate the solutions thus obtained in step 1 and step 2 to construct the positive ideal solution (PIS) as given in Table 1.
- Step 4: From PIS, obtain the lower bounds and upper bounds for each objective functions, where  $f_k^*$  and  $f_k'$  are the maximum and minimum values, respectively.
- Step 5: Set upper and lower bounds for each objective for degree of acceptance and degree of rejection corresponding to the set of solutions obtained in step 4.

For membership functions:

$$U_k^\mu = \max(Z_k(X_r)) \quad \text{and} \quad L_k^\mu = \min(Z_k(X_r)), \quad 1 \leq r \leq k.$$

For non-membership functions:

$$U_k^\nu = U_k^\mu - \lambda(U_k^\mu - L_k^\mu) \quad \text{and} \quad L_k^\nu = L_k^\mu \quad 0 < \lambda < 1.$$

Step6: Consider the membership function  $\mu_k(f_k(x))$  and non-membership function  $\nu_k(f_k(x))$  as following linear functions:

$$\mu_k(f_k(x)) = \begin{cases} 0 & \text{if } f_k(x) \leq L_k^\mu \\ \frac{f_k(x) - L_k^\mu}{U_k^\mu - L_k^\mu} & \text{if } L_k^\mu \leq f_k(x) \leq U_k^\mu \\ 1 & \text{if } f_k(x) \geq U_k^\mu \end{cases}$$

**Table 1** Positive ideal solution

	$f_1$	$f_2$	$f_3$	.....	$f_k$	$X$
max $f_1$	$f_1^*$	$f_2(X_1)$	$f_3(X_1)$	...	$f_k(X_1)$	$X_1$
max $f_2$	$f_1(X_2)$	$f_2^*$	$f_3(X_2)$	...	$f_k(X_2)$	$X_2$
max $f_3$	$f_1(X_3)$	$f_2(X_3)$	$f_3^*$	...	$f_k(X_3)$	$X_3$
⋮	⋮					⋮
⋮	⋮					⋮
max $f_k$	$f_1(X_k)$	$f_2(X_k)$	$f_3(X_k)$	...	$f_k^*(X_k)$	$X_k$
	$f_1'$	$f_2'$	$f_3'$	...	$f_k'$	



$$v_k(f_k(x)) = \begin{cases} 0 & \text{if } f_k(x) \geq U_k^v \\ \frac{U_k^v - f_k(x)}{U_k^v - L_k^v} & \text{if } L_k^v \leq f_k(x) \leq U_k^v \\ 1 & \text{if } f_k(x) \leq L_k^\mu \end{cases}$$

Figure of the membership function and non-membership function for maximization type objective function are shown in Fig. 1.

Step 7: An intuitionistic fuzzy optimization technique for MOLP problem as taken in this section with such membership and non-membership functions can be written as

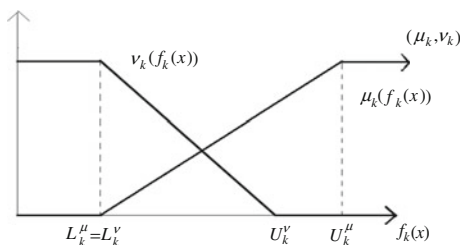
$$\begin{aligned} &\text{Maximize } \mu_k(f_k(x)) \\ &\text{Minimize } v_k(f_k(x)) \\ &\text{Subject to } \mu_k(f_k(x)) + v_k(f_k(x)) \leq 1, \\ &\quad \mu_k(f_k(x)) \geq v_k(f_k(x)), \\ &\quad v_k(f_k(x)) \geq 0, \\ &\quad g_j(x) \leq b_j, \quad x \geq 0, \\ &\text{for } k = 1, 2, \dots, K; \quad j = 1, 2, \dots, m. \end{aligned}$$

Now the above problem may be equivalently written in a linear programming problem as

$$\begin{aligned} &\text{Maximize } (\alpha - \beta) \\ &\text{Subject to } \alpha \leq \mu_k(f_k(x)), \\ &\quad \beta \geq v_k(f_k(x)), \\ &\quad \alpha + \beta \leq 1, \\ &\quad \alpha \geq \beta, \\ &\quad \beta \geq 0, \\ &\quad g_j(x) \leq b_j, x \geq 0, \quad k = 1, 2, \dots, K; \quad j = 1, 2, \dots, m. \end{aligned}$$

This linear programming problem can be easily solved by a simple method.

**Fig. 1** Membership and non-membership functions



### 4 Numerical Illustration

In this section, the developed algorithm is implemented by a numerical example. We consider the problem as undertaken by Garg and Singh [7], Itoh [8] in which a farmer has to grow carrot, radish, cabbage, and Chinese cabbage in a season under areas  $x_1, x_2, x_3,$  and  $x_4$  (unit 10 acres = 1000 m<sup>2</sup>), respectively. The farmer has a total land of 10 acres and a max labor work time available to him is 260 h. The profit coefficients (unit 10,000 Japanese Yen) and work time for the crops are given in the Table 2 .

The complete mathematical formulation of the above problem is as follows:

$$\begin{aligned}
 &\text{Maximize } z_1 = 29.8x_1 + 10.4x_2 + 13.8x_3 + 19.8x_4 \\
 &\text{Maximize } z_2 = 23.9x_1 + 21.4x_2 + 49.2x_3 + 32.8x_4 \\
 &\text{Maximize } z_3 = 37x_1 + 16x_2 + 3.6x_3 + 9.7x_4 \\
 &\text{Maximize } z_4 = 19.3x_1 + 26.6x_2 + 48.4x_3 + 75.6x_4
 \end{aligned} \tag{1}$$

Subject to the constraints

$$\begin{aligned}
 &x_1 + x_2 + x_3 + x_4 \leq 10 \\
 &6.9x_1 + 71x_2 + 2x_3 + 33x_4 \leq 260, \\
 &x_1, x_2, x_3, x_4 \geq 0.
 \end{aligned}$$

The solution procedure of the above problem involves the following steps:

Step 1: The solution choosing one by one objective as single objective function programming problem

$$\begin{aligned}
 &\text{Maximize } z_1 = 29.8x_1 + 10.4x_2 + 13.8x_3 + 19.8x_4 \\
 &\text{Subject to the constraints}
 \end{aligned}$$

$$\begin{aligned}
 &x_1 + x_2 + x_3 + x_4 \leq 10 \\
 &6.9x_1 + 71x_2 + 2x_3 + 33x_4 \leq 260 \\
 &x_1, x_2, x_3, x_4 \geq 0.
 \end{aligned}$$

**Table 2** Values of various parameters available to the problem

Random variable	Carrot	Radish	Cabbage	Chinese cabbage	Probability percentage of profit coefficients
	$c_{i1}$	$c_{i2}$	$c_{i3}$	$c_{i4}$	
$c_1$	29.8	10.4	13.8	19.8	10
$c_2$	23.9	21.4	49.2	32.8	50
$c_2$	37.0	16.0	3.6	9.7	10
$c_2$	6.9	26.6	48.4	75.6	30
Work time	6.9	71	2	33	

The optimal solution to this linear programming problem is

$$x_1 = 10, x_2 = 0, x_3 = 0, x_4 = 0, (z_1)_1 = 298.$$

And with this solution vectors, the value of other objective functions are as

$$(z_2)_1 = 239, (z_3)_1 = 370 \text{ and } (z_4)_1 = 193.$$

Step 2: Solve linear programming problem for  $z_2, z_3, z_4$  subject to constraints and find values of remaining objective functions.

Step 3: Tabulate the values as given below to form PIS as given in Table 3.

Step 4: Find lower and upper bounds for each case of  $\max z_1, \max z_2, \max z_3, \max z_4$  which are

$$U_1^\mu = 298, L_1^\mu = 138; U_2^\mu = 492, L_2^\mu = 239; U_3^\mu = 370, L_3^\mu = 36; \\ U_4^\mu = 694.58, L_4^\mu = 193.$$

Step 5: Set the upper and lower bounds of each objective for degree of rejections as

$$L_k^\mu = L_k^\nu \\ U_k^\nu = U_k^\mu + \lambda(U_k^\mu - L_k^\mu) = (1 - \lambda)U_k^\mu + \lambda L_k^\mu, \quad k = 1, 2, 3, 4.$$

Which for  $\lambda = 0.6$  becomes

$$U_k^\nu = (1 - 0.6)U_k^\mu + 0.6L_k^\mu = 0.4U_k^\mu + 0.6L_k^\mu \\ U_1^\nu = 202, L_1^\nu = 138, U_2^\nu = 340.2, L_2^\nu = 239, U_3^\nu = 169.6, L_3^\nu = 36, \\ U_4^\nu = 393.63, L_4^\nu = 193.$$

Step 6: Construction of membership functions:

**Table 3** Positive ideal solution

	$z_1$	$z_2$	$z_3$	$z_4$	
Max $z_1$	298	239	370	484	$X_1$
Max $z_2$	138	492	36	484	$X_2$
Max $z_3$	298	239	370	193	$X_3$
Max $z_4$	184.44	365.06	83.21	694.85	$X_4$

$$\begin{aligned}\mu_1(x) &= \frac{29.8x_1 + 10.4x_2 + 13.8x_3 + 19.8x_4 - 138}{(298 - 138)}, \\ \mu_2(x) &= \frac{23.9x_1 + 21.4x_2 + 49.2x_3 + 32.8x_4 - 239}{(492 - 239)}, \\ \mu_3(x) &= \frac{37x_1 + 16x_2 + 3.6x_3 + 9.7x_4 - 36}{(370 - 36)}, \\ \mu_4(x) &= \frac{19.3x_1 + 26.6x_2 + 48.4x_3 + 75.6x_4 - 139}{(694.58 - 193)}.\end{aligned}$$

Construction of non-membership functions:

$$\begin{aligned}v_1(x) &= \frac{202 - 29.8x_1 - 10.4x_2 - 13.8x_3 - 19.8x_4}{(202 - 138)}, \\ v_2(x) &= \frac{340.2 - 23.9x_1 - 21.4x_2 - 49.2x_3 - 32.8x_4}{(340.2 - 239)}, \\ v_3(x) &= \frac{169.6 - 37x_1 - 16x_2 - 3.6x_3 - 9.7x_4}{(169.6 - 36)}, \\ v_4(x) &= \frac{393.63 - 19.3x_1 - 26.6x_2 - 48.4x_3 - 75.6x_4}{(393.63 - 193)}.\end{aligned}$$

Step 7: The above problem (1) is now equivalently written to a linear programming problem as

$$\begin{aligned}&\text{Maximize } (\alpha - \beta), \\ &\text{Subject to } 29.8x_1 + 10.4x_2 + 13.8x_3 + 19.8x_4 - 138 \geq 160\alpha, \\ &\quad 23.9x_1 + 21.4x_2 + 49.2x_3 + 32.8x_4 - 239 \geq 253\alpha, \\ &\quad 37x_1 + 16x_2 + 3.6x_3 + 9.7x_4 - 36 \geq 334\alpha, \\ &\quad 19.3x_1 + 26.6x_2 + 48.4x_3 + 75.6x_4 - 193 \geq 501.58\alpha, \\ &\quad 202 - 29.8x_1 - 10.4x_2 - 13.8x_3 - 19.8x_4 \leq 64\beta, \\ &\quad 340.2 - 23.9x_1 - 21.4x_2 - 49.2x_3 - 32.8x_4 \leq 101.2\beta, \\ &\quad 169.6 - 37x_1 - 16x_2 - 3.6x_3 - 9.7x_4 \leq 133.6\beta, \\ &\quad 393.63 - 19.3x_1 - 26.6x_2 - 48.4x_3 - 75.6x_4 \leq 200.63\beta, \quad (2) \\ &\quad x_1 + x_2 + x_3 + x_4 \leq 10, \\ &\quad 6.9x_1 + 71x_2 + 2x_3 + 33x_4 \leq 260, \\ &\quad \alpha + \beta \leq 1, \\ &\quad \alpha \geq \beta, \quad \beta, x_1, x_2, x_3, x_4 \geq 0\end{aligned}$$

The above problem (2), a linear programming problem is solved by MATLAB and the solutions obtained are

$$x_1 = 4.14$$

**Table 4** Profit in different probabilistic cases

Probability cases for profit coefficients (%)	Profit by proposed intuitionistic fuzzy optimization technique	Profit by Garg and Singh method [7]	Profit by Itoh method [8]
10	216.46	207.37	268.4
50	352.98	348.58	280.4
10	186.80	181.07	303.5
30	419.07	410.54	274.8
Weighted profit	342.53	336.29	280.08

$$x_2 = 0.00$$

$$x_3 = 3.79$$

$$x_4 = 2.06$$

$$\alpha = 0.45$$

$$\beta = 0.00$$

Putting these values in the problem, the profit obtained are as in (Table 4).

## 5 Conclusion

The objective of this paper was to develop a method to solve a probabilistic programming problem in an intuitionistic fuzzy optimization environment. Here, the developed method first considers the conversion of the probabilistic programming problem into a multi-objective programming problem. This is done by considering the objective function corresponding to probabilistic cases as one objective function of the said multi-objective programming. Thus, such converted multi-objective programming problem is solved with one objective at a time to construct the PIS. Thus, in order to obtain a best compromise solution of the situation, we construct the membership function and non-membership functions for the solutions, and thus, we introduce intuitionistic fuzzy parameters. Using the intuitionistic fuzzy optimization approach, the problem is transformed into an equivalent linear programming problem. The linear programming problem thus obtained has been solved by using MATLAB. The result thus obtained has been compared with the existing solution, and clearly, the proposed method gives a better solution than existing solutions.

**Acknowledgments** Authors are thankful to University Grants Commission (UGC), Government of India, for financial support to carry out this research work.

## References

1. Atanassov, K.T.: Intuitionistic fuzzy sets. *Fuzzy Sets and Systems*. **20**, 87–96 (1986)
2. Atanassov, K.T., Gargov, G.: interval valued intuitionistic fuzzy sets. *Fuzzy Sets and Systems*. **31**, 343–349 (1989)
3. Angelov, P.: P Optimization in an intuitionistic fuzzy environment. *Fuzzy Sets and Systems*. **86**, 299–306 (1997)
4. De, S.K., Biswas, R.A.: Ray R. Some operations on intuitionistic fuzzy sets, *Fuzzy Sets and Systems*. **114**, 474–487 (2000)
5. Dipti, Dubey, Mehra, Aparna: Linear programming with Triangular Intuitionistic Fuzzy Number, *EUSFLAT-LFA 2011. Advances in Intelligent Systems Research* **1**(1), 563–569 (2011). Atlantis Press
6. Dipti, Dubey, Suresh, Chandra, Aparna, Mehra: Fuzzy linear programming under interval uncertainty based on IFS representation. *Fuzzy Sets and Systems*. **188**(1), 68–87 (2012)
7. Garg, A., Singh, S.R.: Optimization under uncertainty in agricultural production planning. *iconcept pocket journal: Computational Intelligence for Financial Engineers* **1**(1), 1–12 (2010)
8. Itoh, T., Ishii, H., Nanseki, T.: Fuzzy crop planning problem under uncertainty in agriculture management. *Int. J. Production Economics*. **81–82**, 555–558 (2003)
9. Jana, B., Roy, T.K.: Multiobjective intuitionistic fuzzy linear programming and its application in transportation model *NIFS–13–1–34–51*, 1–18 (2007)
10. Li, D.F.: Linear programming method for MADM with interval valued intuitionistic fuzzy sets. *Expert Systems and Applications*. **37**, 5939–5945 (2010)
11. Mohamed, R.H.: The relationship between goal programming and fuzzy programming. *Fuzzy Sets and Systems* **89**, 215–222 (1997)
12. Mondal, T.K., Samanta, S.K.: Generalized intuitionistic fuzzy set. *Journal of Fuzzy Math* **10**, 839–861 (2002)
13. Mahaparta, G.S., Mitra, M., Roy, T.K.: Intuitionistic fuzzy multiobjective mathematical programming on reliability optimization model. *International Journal of Fuzzy Systems*. **12**(3), 259–266 (2010)
14. Nachamani, A.L., Thangaraj, P.: Solving Intuitionistic fuzzy linear programming problems by using similarity measures. *European Journal of Scientific Research* **72**(2), 204–210 (2012)
15. Nagoorgani, A., Ponnalagu, K.: A new approach on solving intuitionistic fuzzy linear programming problem. *Applied Mathematical Sciences* **6**(70), 3467–3474 (2012)
16. Shahrokhi M, Bernard A, Shidpour H, An integrated method using intuitionistic fuzzy set and linear programming for supplier selection problem, *18<sup>th</sup> IFAC World congress Milano(Italy)Aug18-Sept2, 2011*, 6391–6395.
17. Zadeh, L.: A Fuzzy Sets. *Information and Control* **8**, 338–353 (1965)
18. Zimmermann, H.: J. Fuzzy programming and linear programming with several objective functions. *Fuzzy Sets and Systems* **1**, 45–55 (1978)

# Analyzing Competitive Priorities for Machine Tool Manufacturing Industry: ANP Based Approach

Deepika Joshi

**Abstract** In an attempt to study the success factors for the competitiveness of machine tool manufacturing (MTM) industry an in-depth study of 10 manufacturers located in India was carried out. Performance measures, especially which are related to supply chain (SC) activities, are also the part of competitive priorities [16, 17]. It can be seen that systematic identification and prioritization of SC performance indicators would help managers to integrate them into corporate strategy. An ANP approach is used to analyze the dynamic, large, and complex attribute decision. To perform the related computations, a programming platform of MATLAB™ software suite was operated. Research findings unveiled that flexibility and quality dimensions are of foremost significance in the development of sector under study, followed by delivery indicators. However, the companies believed that cost constituents need to be focused to achieve overall SC competitiveness.

**Keywords** Analytic network process (ANP) · Supply chain performance indicators · Competitiveness · Machine tool manufacturing industry · India

## 1 Introduction

Machine tool manufacturing (MTM) industry in India is performing a vital role in advancing national competitiveness. In particular, it is instrumental in promoting the output of Indian manufacturing industry and in general, the Indian economy. Typically, growth of any industry depends on the ability to manage its supply chain (SC) activity [28]. SC of MTM industry is composed of large number of firms. Consequently, it necessitates concerted efforts to overcome the overwhelming complexity and associated challenges of this developing sector. It will not only bring structural

---

D. Joshi (✉)

Research/Faculty Associate, Gautam Buddha University, Greater Noida, India  
e-mail: joshi.deepikaa@gmail.com

transformation in business operations but will also compel engineers and managers to inculcate strategic thinking while managing value chain elements.

The spurred industry reforms have radically shifted the significance of competitive priorities in SC management activity. For example, in auto-component manufacturing, cost and flexibility drives the SC performance whereas in retail sector delivery leads to successful business operations [16, 17]. Thus, there are always some sector specific performance indicators leading to overall SC competitiveness. A systematic identification of performance indicators and their priorities is necessary in order to plan and implement suitable strategies for industrial competitiveness. Most of the previous studies on MTM sector were conducted considering the whole gamut of competitive priorities and factors affecting these priorities. Few of such studies, which are exclusively considered competitive priorities, were nation specific like China, US, and Japan [33]. It has been noted, however, that there is hardly any research study which reports the prioritization of competitive priorities specific to Indian MTM industry. On the whole, this perceived gap among existing research studies shapes the main ground of the work presented in this paper.

In Sect. 2 a review of literature is presented to disseminate knowledge regarding SC performance indicators. Section 3 presents a research methodology exclusively designed to attain the research objective. Section 4 portrays the research findings. Section 5 discusses the results and strategies for its managerial implications. Section 6 concludes the paper while providing avenues for future research.

## 2 Review of Literature

In the present era of globalization and industrialization, competitive priorities like cost, delivery, flexibility, and quality (CDFQ) which are critical to operation's success of the firm [31]. Neely et al., Ho et al. and Singh et al. are few of the numerous proponents who suggested the need of competitive priorities for SC competitiveness building [14, 21, 28]. Identifying competitive priorities for industrial application lead to overall competitiveness.

### 2.1 *Competitive Priorities*

Traditional operations management literature considers cost as the simplest measure of competitiveness. Herein, labor cost, raw material cost, R&D cost, manufacturing cost, etc., are found to be important ones [1, 9] and [18]. With the objective of SC responsiveness, inventory control is another major concern for manufacturing based industries [2]. Fuss and Waverman highlighted the impact of variation in inter-country costs such as costs related to labor and raw material, toward cost competitiveness [10]. Due to increased distances the costs related to distribution have become a major concern for managers [2]. Managers control it by focusing on storage



facilities at client's location. Flexibility as a determinant of competitiveness has been discussed. It effects the business operations to capture global market opportunities [30]. The various types of flexibilities discussed in literature are—volume flexibility, process flexibility, product-mix, delivery flexibility, distribution flexibility, new product development, and design flexibility [27]. However, the type of flexibility which would best make a business competitive depends on available resources, goals and objectives of a particular firm.

Similarly, researchers mentioned that specific quality norms reduce the defects and enhance the perceived quality level of a product. This also advocates the consistency of process and product design. Durability, performance, conformance, reliability, and design characteristics are various commonly used dimensions of quality [11]. Quality parameters are reflected in higher value of returns on investment, defect-free products, goodwill, strong brand loyalty, and higher chance of repeat purchase. Fulfilling customer demand through on-time delivery leads to competitiveness [13]. Today all major business activities, right from procurement of raw material to distribution of finished goods, mark delivery as a distinctive indicator of their performance. The delivery capability of a firm depends on factors like delivery speed, vehicle speed, delivery date and time [12, 13]. Considering delivery decision as a significant part of SC strategy leads to strategic and operational competitiveness.

Literature review emphasizes the significance in SC performance for competitiveness building. The mentioned performance indicators comprise of internal as well as external performance indicators. Executing these competitive priorities firms can realizes its business goals and objectives. Literature also unveiled the majority of research on SC competitiveness are aimed at competitive priorities [32, 33]. The targeted sectors were auto component firms [16, 17, 20, 22] and grocery and retail [5], PC manufacturing company [24]. But dynamic business environment calls for most up-to-date industry specific Key Performance Indicators [15]. Thus a realistic and easy-to-implement framework is crucial to any SC management activity.

## ***2.2 Multi-Criteria Decision-Making Technique***

The survey of literature unveiled a variety of MCDM methods which are universally recognized approaches for MCDM problems. Taking into account both outranking methods and multi attribute utility theory (MAUT), these methods are: analytic hierarchy process (AHP) [25], data envelopment analysis (DEA) [4], GRA [7], rough set approach (RSA) [23], and analytic network process (ANP) [26]. Choice among these to be used would depend on the type of available data, ease of understanding, and nature of the required decision.

Literature review unveiled that in real life business situations, business elements are dependent on each other. Unlike AHP, it is not compulsory to have such dependence in hierarchical form, where the lower level is dependent on the upper one [3, 19, 25]. Similarly, the technique like RSA, which simply classifies the attributes on the basis of 'if-then' decision rules, is least suited, especially for the task of

prioritization in modern business environment [29]. Moreover, with information complexity in various business facets, the DEA technique falls short in dealing with fuzzy and imprecise information [8]. MCDM techniques like GRA, DEA, and RSA involves rigorous mathematical calculations which require that managers spend a great deal of time to learn and understand the functioning and implementation of a chosen approach. Thus, a technique which can lead to weights of individual attributes is the need of industrial decision makers.

An apparent technique which can overcome the limitations associated with the above mentioned MCDM techniques was the need of strategists and managers. Such a technique should be clear and precise and most importantly, it should be time bound and easy to implement by managers. To overcome such limitations of AHP, GRA, DEA, and RSA techniques, ANP technique was established. It addresses the issue of prioritization while considering the nature of interdependence.

### **3 Research Methodology**

The current section presents an overview of the overall research approach adopted to discover the fact and accuracy behind the performance of competitive priorities for SC competitiveness.

#### ***3.1 Designing of Research Instrument***

A well-structured questionnaire was prepared using sixteen performance indicators. These indicators are the dimensions of competitive priorities. For the ease of study symbols were assigned to each criterion. Refer column 3 of Table 2. Questionnaire was divided into two different sections. Section 1 contains a pairwise comparison matrices designed while Sect. 2 is composed of a large number of open-ended questions. Section I was designed on the basis of Satty 9-point scale (2001). The significance of numerical rating is mentioned in Table 1. Section 2 contained questions related to the cost, quality delivery flexibility, business category, and impact of business environment. Unlike few of the research studies, the present research uses open-ended questions to help in gathering the rationale behind the responses of pairwise comparison matrices. During the entire study, the dynamic nature of machine tool industry was discussed in detail with the respondents.

#### ***3.2 Profile of the Respondents and Responding Organization***

In order to select the responding firms, the directory of India Machine Tool Manufacturers' Association was used. In all, 30 organizations were selected, of which only 10 showed their positive response to participate in research process.

**Table 1** Satty 9-point scale [26]

Comparison scale	Verbal scale
1	Equal importance of both elements
3	Moderate importance of one element over another
5	Strong importance of one element over another
7	Very strong importance of one element over another
9	Extreme importance of one element over another
2, 4, 6, 8	Intermediate values

These firms have an annual turnover between 30 million USD to 25 billion USD. In India, these firms are listed in Bombay stock exchange (BSE) and National stock exchange (NSE). Approved firms were considered as the representative section of Indian MTM industry. Managers having minimum experience of 5 years with MTM industry were considered for administering the questionnaire. With the aim of concealing respondent's identity, the firms'/respondents names are not divulged in the paper.

### 3.3 ANP Technique of Prioritization

As defined by Saaty [26], "ANP is a theory of measurement generally applied to the dominance of influence among several stakeholders, or alternatives with respect to an attribute or a criterion." It is based on the theory of relative measurement. It allows prioritization without making assumptions about the dependence among considered set of elements. Generic steps followed for ANP implementation are: (a) carry out pairwise comparison between the criteria on the basis of the nature of being influenced and influencing, (b) obtain the super-matrix by calculating the weights from pairwise comparison matrices, (c) obtain limit super-matrix by matrix multiplication, and (d) analyze the results based on final assessment. For this research paper, MATLAB<sup>TM</sup> programming platform was used for ANP computations. Two different programs were written to obtain the final Priority Vector (PV). The first program helped to generate the eigenvectors. The second program was used to obtain the limit super-matrix.

Once the filled pairwise questionnaires were received, these were processed with the first program on the programming platform of MATLAB<sup>TM</sup> software suite. In all twenty-five eigenvectors were obtained. These eigenvectors were then arranged under the respective control criterion, to obtain the un-weighted super-matrix. The un-weighted super-matrix so obtained was normalized to obtain the weighted super-matrix. This ANP super-matrix reveals the local-priority information of the considered network by representing the overall impact of one criterion on a group of criteria and vice-versa. In this representation, the zeros in the matrix indicate nondependence. Positive numerical values indicate the strength of *being influenced and influencing*

**Table 2** Priority vector for competitive priorities

Competitive priorities	Performance indicators	Symbols	Priority vector	Competitive priority contribution
Cost	Labour cost	CPC1	0.04112	0.183197
	Material cost	CPC2	0.04268	
	Manufacturing cost	CPC3	0.03761	
	Inventory cost	CPC4	0.03603	
	Distribution cost	CPC5	0.02575	
Delivery	Delivery dependability	CPD1	0.05312	0.096214
	Delivery speed	CPD2	0.04309	
Flexibility	Product mix	CPF1	0.08818	0.411823
	Volume flexibility	CPF2	0.07407	
	Design flexibility	CPF3	0.12387	
	New product development flexibility	CPF4	0.12571	
Quality	Durability	CPQ1	0.06056	0.308767
	Working condition and safety	CPQ2	0.0608	
	Environmental damage	CPQ3	0.05575	
	Defect rate	CPQ4	0.06274	
	Reliability	CPQ5	0.06892	

(dependence) the criteria by each other. Then, the second program was used to repeatedly multiply the weighted super-matrix by itself, until the entities in the matrix become regularized. The converged matrix so obtained is called a limit super-matrix. The limit super-matrix indicates the final priorities for all the considered elements. The values in any column of the limit super-matrix represent the priority vector for the responding firm.

## 4 Survey Results

The quantitative results of qualitative variables were obtained by using ANP approach. The priorities so obtained in form of PV elicit the relative weights of each performance indicator in overall SC competitiveness of Indian machine tool industry.

The PV unveiled that:

1. Flexibility (41 % weight) is the most important among all competitive priority. Herein, new product development and design flexibility drives the business growth. Flexibility indicators get affected by almost all cost and quality variables.
2. Quality being the major concern for all manufacturers carries a significant weight of 0.308767. It affects and gets affected by cost and flexibility variables. It gets hold of existing buyers and draws the newer customer demand.

3. Cost falls short to gain the highest contribution in overall SC competitiveness. It is because of the fact that cost advantage associated with labor, manufacturing, and material are higher than other European and American manufacturers.
4. Delivery as competitive priority contributed 10% weight. Firms' ideal decision regarding both the delivery indicators reduces distribution cost, inventory cost, environmental damage, and enhances the volume flexibility and reliability whereby making Indian machine tool industry a competitive sector.

## 5 Discussion for Managerial Implications

The questionnaire-based survey of MTM firms of India was carried out. The obtained responses were analyzed to generate priority vectors. Study revealed that all the considered performance indicators are important for SC competitiveness of the sector under study. Based on firm's capability to harness such competitive priorities, the business strategies are planned and implemented [16, 17]. In the following points, the PV and the imperative strategies are discussed for managerial implication.

- Flexibility is found to be the key competitive priority for SC performance of Indian tool manufacturing companies. It is justified by dynamic demand of customers like auto and auto component manufacturers, capital goods industry, consumer durables, and aviation industry. Tool manufacturers are implementing strategies like customization, rapid response, and postponement. It is found that new product development and design flexibility is among the critical dimensions of flexibility. Due to variation in process technology at customers end, the large product mix drives the customer demand.
- The machine tool manufacturers deliver their finished goods to component manufacturers. Their quality in turn determines the production of quality equipment. Presently, Indian machine tool industry is manufacturing its products with ISO certification and international standard of quality/precision and reliability. Companies have entered into joint ventures and alliances with Swiss, German and Chinese counterparts to bring in the state-of-art technology. Computer numerically controlled (CNC) technology is among the most commonly used technique for quality improvement in tool manufacturing. For process improvement companies are executing soft strategies like 5S, Kaizen, and quality circles. Moreover, companies are utilizing third party services for trouble shooting, accurate measurement and adjustment for CNC machines, laser cutter, gas and oil turbine manufacturing, and many more.
- In dynamic business environment, customer responsiveness has become the prime measure of performance. Respondents found delivery as one of the component for fulfilling such responsiveness. Most of the companies were found to be dependable on third-party logistic providers for tools delivery. The advent of information technology had eased the logistic facility, for both national and international

customers. However, respondents mentioned delivery speed as an indicator dependent on other factors like infrastructure, plant location, and vehicle conditions.

- Insignificant variation was observed among the five cost dimensions. Due to major contribution of material cost in overall cost composition, manufacturers are struggling to reduce it. Respondents from studied firms believed that any re-engineering to reduce material cost leads to cost advantage with their immediate competitors. It can also be lowered by reducing the procurement cost and cost of product redesign. Labor cost was found to be the least significant. It is rationalized by the availability of low cost labor with Asian countries especially with India and China. Firms are implementing latest techniques like INVENTORIA to manage the inventory of small-sized tools. However, least effort can be exercised to reduce the inventory cost raised due to storage of heavy machines. It was also found that due to extreme locations of machine tool manufacturers distribution cost needs a greater attention in overall cost structure.

## 6 Conclusion and Avenues for Future Research

This study highlights the significance of competitive priorities in development of Indian machine tool industry. The findings will guide SC managers in aligning SC strategy with their firm's corporate strategy. It will also help strategy managers in improving their SC competitiveness in global market. Further studies with the aim of considering the impact of other performance indicators like business environment, buyer-supplier relationship, technology, location and infrastructure on competitive priorities are required for more comprehensive insights.

In contrast to the work done by Dangayach and Deshmukh [6] and Joshi et al. [16, 17] on complete Indian manufacturing companies and auto-component sector respectively, the presented work was targeted exclusively for machine tool manufacturing industry. Instead of considering the entire range of manufacturing strategy and related issues, herein the focus was kept on competitive priorities. Similarly, the survey conducted by Zhao [33] was entirely targeted toward the competitiveness of manufacturing enterprises in China. In order to study the SC competitiveness of Indian machine-tool manufacturers, few performance indicators were added. While studying the Indian strategies, it was found that they are rarely different from the ones implemented at China except for greater focus on quality enhancement parameters and cost reduction tactics. With the Indian market strategy of importing technologies from international market like Germany and Switzerland, specially related to CNC will lead to the place of Indian MTM industry in global canvas. Moreover, changing management style at public limited companies and concentration of Department of Heavy Engineering on private firms is boosting the competition. Surely this will lead to the development of Indian manufacturing industry as a whole. It was also found those small and middle scale tool manufacturing firms are still unorganized in their management and technological deals. Prospective research is suggested for the unorganized tool manufacturers in India.

## References

1. Balakrishnan, K., Seshadri, S., Sheopuri, A., Iyer, A.: Indian auto-component supply chain at the crossroads. *Interfaces* **37**(4), 310–323 (2007)
2. Beamon, B.M.: Measuring supply chain performance. *Int. J. Oper. Prod. Manage.* **19**(3), 275–292 (1999)
3. Buyukyazien, M., Sueu, M.: The analytic hierarchy and analytic network processes. *Haceteppe J. Math. Stat.* **32**, 65–73 (2003)
4. Charnes, A., Cooper, W.W., Rhodes, E.: Measuring the efficiency of decision making units. *Eur. J. Oper. Res.* **2**, 429–444 (1978)
5. Chou, C.: Development of comprehensive supply chain performance measurement system: A case study in grocery retail industry. <http://dspace.mit.edu/bitstream/handle/1721.1/29520/57308003.pdf> (2004)
6. Dangayach, G.S., Deshmukh, S.G.: Evidence of manufacturing strategies in Indian industry: A survey. *Int. J. Prod. Econ.* **83**(3), 279–298 (2003)
7. Deng, J.L.: The introduction to grey system theory. *J. Grey Syst.* **1**(1), 1–24 (1989)
8. Dolabi, H., Radfar, R., Nasr, M.: Applied imprecise data envelopment analysis for selecting the efficient method of technology transfer: A case study in automotive parts manufacturing industry corporation. *Contemp. Eng. Sci.* **4**(1), 13–24 (2011)
9. Edwards, L., Golub, S.: South Africa's international cost competitiveness and exports in manufacturing. *World Dev.* **32**(8), 1323–1339 (2004)
10. Fuss, M.A., Waverman, L.: Cost and productivity in automobile production: The challenges of Japanese efficiency, Cambridge (2006)
11. Garvin, D.A.: Competing on the eight dimension of quality. *Harv. Bus. Rev.* **65**(6), 101–109 (1987)
12. Gunasekaran, A., Kobu, B.: Performance measures and metrics in logistics and supply chain management: A review of recent literature (1995–2004) for research and applications. *Int. J. Prod. Res.* **45**(12), 2819–2840 (2006)
13. Gunasekaran, A., Patel, C., McGaughey, R.E.: A framework for supply chain performance measurement. *Int. J. Prod. Econ.* **87**(3), 333–347 (2004)
14. Ho, D.C.K., Au, K.F., Newton, E.: Empirical research on supply chain management: A critical review and recommendations. *Int. J. Prod. Res.* **40**(17), 4415–4430 (2002)
15. Jamil, C.M., Mohamed, R.: Performance measurement system (PMS) in small and medium enterprises (SMES): A practical modified framework. *World J. Soc. Sci.* **1**(3), 200–212 (2011)
16. Joshi, D., Nepal, B., Rathore, A.P.S., Sharma, D.: On supply chain competitiveness of India automotive component manufacturing industry. *Int. J. Prod. Eco.* **143**(1), 151–161 (2013)
17. Joshi, D., Rathore, A.P.S., Sharma, D., Nepal, B.: Determinants of competitiveness and their relative importance: A study of Indian auto-component industry. *Int. J. Serv. Oper. Manage.* **10**(4), 426–448 (2011)
18. Majumdar, S.: How do they plan for growth in auto component business? - A study on small foundries of western India. *J. Bus. Venturing* **25**(3), 274–289 (2010)
19. Navarro, T.G., Melon, M.G., Martin, D.D., Dutra, S.A.: Evaluation of urban development proposals: An ANP approach. *World Acad. Sci. Eng. Tech.* **44**, 498–508 (2008)
20. Neely, A., Mills, J., Platts, K., Richard, H., Gregory, M., Bourne, M., Kennerley, M.: Performance measurement system design: Developing and testing a process-based approach. *Int. J. Oper. Prod. Manage.* **20**(10), 1119–1145 (2000)
21. Neely, A.D., Gregory, M., Platts, K.: Performance measurement system design: A literature review and research agenda. *Int. J. Oper. Prod. Manage.* **15**(4), 80–116 (1995)
22. Olugu, E.U., Wong, K.Y., Shaharoun, A.M.: A comprehensive approach in assessing the performance of an automobile closed-loop supply chain. *Sustainability* **2**(4), 871–889 (2010)
23. Pawlak, Z.: Rough sets. *Int. J. Comput. Inf. Sci.* **11**(5), 341–356 (1982)
24. Ravi, V., Shankar, R., Tiwari, M.K.: Analyzing alternative in reverse logistics for end-of-life computers: ANP and balanced scorecard approach. *Comput. Ind. Eng.* **48**(2), 327–356 (2005)

25. Saaty, T.L.: *The Analytic Hierarchy Process*. New York (1980)
26. Saaty, T.L.: *Decision Making with Dependence and Feedback: The Analytic Network Process*. 2nd edn. Pittsburgh (2001)
27. Sangwan, K.S., Digalwar, A.K.: Evaluation of world-class manufacturing systems: A case of Indian automotive industries. *Int. J. Serv. Oper. Manage.* **4**(6), 687–708 (2008)
28. Singh, R.K., Garg, S.K., Deshmukh, S.G.: Strategy development for competitiveness: A study on Indian auto component sector. *Int. J. Prod. Perform Manage.* **56**(4), 285–304 (2007)
29. Tzeng, G.-H., Huang, J.-J.: *Multiple Attribute Decision Making: Methods and Applications*. CRC Press, USA (2011)
30. Upton, D.: The management of manufacturing flexibility. *California Manage. Rev.* **36**(2), 72–89 (1994)
31. Van Dierdonck, R., Miller, J.G.: Designing production planning and control systems. *J. Oper. Manage.* **1**(1), 37–46 (1980)
32. Ward, P.T., Duray, R.: Manufacturing strategy in context: Environment, competitive strategy and manufacturing strategy. *J. Oper. Manage.* **18**(6), 123–138 (2000)
33. Zhao, X., Yeung, J.H.Y., Zhou, O.: Competitive priorities of enterprises in mainland China. *Total Qual. Manage.* **13**(3), 285–300 (2002)



# A Modified Variant of RSA Algorithm for Gaussian Integers

Sushma Pradhan and Birendra Kumar Sharma

**Abstract** A Gaussian prime is a Gaussian integer that cannot be expressed in the form of the product of other Gaussian integers. The concept of Gaussian integer was introduced by Gauss [4] who proved its unique factorization domain. In this paper, we propose a modified RSA variant using the domain of Gaussian integers providing more security as compared to the old one.

**Keywords** RSA public-key cryptosystem · Gaussian integers · Multiprime RSA

## 1 Introduction

RSA system is the one of most practical public-key password systems. In addition to other domain, it has successfully provided security to the electronic-based commerce. Encryption of plaintext in asymmetric key encryption is based on a public key and a corresponding private key. Document authentication and digital signature are other advantages of RSA public-key cryptosystem. RSA provides security to the plaintext based on factorization problem [5]. There are PKCs other than RSA. Those are Elgamal and Rabin's PKCs. These PKCs provide security-based discrete logarithm problem.

The classical RSA cryptosystem is described in the setting of the ring  $Z_n$ , the ring of integers modulo a composite integer  $n = pq$ , where  $p$  and  $q$  are two distinct odd prime integers. Many aspects of arithmetics over the domain of integers can be carried out to the domain of Gaussian integers  $Z[i]$ , the set of all complex numbers of the form  $a + bi$ , where  $a$  and  $b$  are integers [6]. The RSA cryptosystem was extended

---

S. Pradhan (✉) · B. K. Sharma  
School of Studies in Mathematics, Pt. Ravishankar Shukla University, Raipur, India  
e-mail: sushpradhan@gmail.com

B. K. Sharma  
e-mail: shramabk07@gmail.com

domain of Gaussian integers in the papers [2] and [3]. In [2] and [3], the advantages of such extension of RSA were briefly stated in these papers.

Now in this paper, another fast variants of RSA cryptosystems is proposed using arithmetic's modulo of Gaussian integers. Proposed scheme provides more security with same efficiency. Before doing so, in next section, we review the classical RSA PKC. Next, we introduced Gaussian integers and its properties in Sect. 3. In Sect. 4, we present a variant of RSA scheme based on factorization of Gaussian integers with a suitable example. Finally, we conclude with security analysis and comparison with the standard method.

## 2 Classical RSA Public-Key Cryptosystem

The classical RSA cryptosystem is described as follows: entity  $A$  generates the public key by first generating two large random odd prime integers  $p$  and  $q$ , each roughly of the same size. Then, entity  $A$  computes the modulus  $n = pq$  and  $\phi(n) = (p-1)(q-1)$ , where  $\phi$  is Euler's phi function. Next, entity  $A$  selects the encryption exponent  $e$  to be any random integer in the interval  $(1, \phi(n))$ , and which is relatively prime to  $\phi(n)$ . Using the extended Euclidean algorithm for integers, entity  $A$  finds the decryption exponent  $d$ , which is the unique inverse of  $e$  in  $\mathbb{Z}_n$ . The public key is the pair  $(n, e)$  and  $A$ 's private key is the triplet  $(p, q, d)$ .

To encrypt a message, entity  $B$  first represents the message as an integer  $m$  in  $\mathbb{Z}_n$ . Then, entity  $B$  obtains  $A$ 's public-key  $(n, e)$ , uses it to compute the cipher text  $c = m^e \pmod{n}$ , and sends  $c$  it to entity  $A$ . Now, to decrypt  $c$ , entity  $A$  computes  $m = c^d \pmod{n}$  and recovers the original message  $m$ .

## 3 Gaussian Integers

Gaussian integer is a complex number  $a + bi$  where both  $a$  and  $b$  is integers:

$\mathbb{Z}[i] = a + bi : a, b \in \mathbb{Z}$ . Gaussian integers, with ordinary addition and multiplication of complex numbers, form an integral domain, usually written as  $\mathbb{Z}[i]$ . The norm of a Gaussian integer is the natural number defined  $|a + bi| = a^2 + b^2$ .

Gaussian primes are Gaussian integer's  $z = a + bi$  satisfying one of the following properties:

1. If both  $a$  and  $b$  are nonzero, then  $(a + bi)$  is a Gaussian prime iff  $(a^2 + b^2)$  is an ordinary prime.
2. If  $a = 0$ , then  $bi$  is a Gaussian prime iff  $|b|$  is an ordinary prime and  $|b| \equiv 3 \pmod{4}$ .
3. If  $b = 0$ , then  $a$  is a Gaussian.

J.T. Cross [1] gave a full description for complete residue systems modulo prime powers of Gaussian integers.

## 4 RSA Algorithms Over the Field of Gaussian Integers

In paper [2], the RSA is extended into the field of Gaussian integers. It is presented as follows:

**Key Generation:** Generate two large Gaussian primes  $P$  and  $Q$ . Compute  $N = PQ$ . Compute  $\phi(N) = (|p| - 1)(|q| - 1)$ . Select a random integer  $e$  such that  $1 < e < \phi(N)$  and  $\gcd(e, \phi(N) = 1)$ . Compute  $d = e^{-1} \pmod{\phi(N)}$ . Pair  $N$  and  $e$  is a public key, and  $d$  is the private key.

**Encryption:** Given a message  $M$  (represented as a Gaussian integer), compute ciphertext

$$C := m^e \pmod{n}.$$

**Decryption:** Compute the original message  $M := c^d \pmod{n}$ .

Now, we propose the algorithms for the variant of RSA cryptosystem in  $Z[i]$  as below:

**Key Generation:**  
 Generate  $b$  distinct large Gaussian primes  $\alpha$ ,  $\beta$ , and  $\gamma$  each  $n/b$  bits long.  
 Compute  $N = \alpha\beta\gamma$ .  
 Compute  $\phi(N) = (|\alpha| - 1)(|\beta| - 1)(|\gamma| - 1)$ .  
 Select a random integer  $e$  such that  $1 < e < \phi(N)$  and  $\gcd(e, \phi(N) = 1)$ .  
 Compute  $d = e^{-1} \pmod{\phi(N)}$ .  
 Pair  $(N, e)$  is a public key, and  $(\alpha, \beta, \gamma, d)$  is the private key.

**Encryption:**  
 Given a message  $M$  (represented as a Gaussian integer) compute cipher text

$$C = m^e \pmod{N}$$

**Decryption:**  
 Compute the original message  $M = c^d \pmod{N}$ .  
 Following is the example in support of proposed algorithm.

### Example

**Key generation**  
 Let us select  $\alpha = 19$  and  $\beta = 5$  and  $\gamma = 3$ ,  
 Compute the product  $N = \alpha\beta\gamma = 285$ ,

$$\phi(N) = (19^2 - 1)(5^2 - 1)(3^2 - 1) = 69, 120.$$

Choose  $e = 3,331$ .  
 Then,  $d = e^{-1} \pmod{\phi(N)} = 3331^{-1} \pmod{69,120} = 29,611$   
 The public key is  $n = 285, e = 3,331$

*Encryption*

Let message  $M = m_1; m_2 = (555, 444)$

$$\begin{aligned} C &= (c_1; c_2) = m^e \pmod{N} \\ &= (555, 444)^{3331} \pmod{285} \\ &= (270, 159) \end{aligned}$$

*Decryption*

$$\begin{aligned} M &= c^d \pmod{N} \\ &= (270, 159) \pmod{285} \\ &= (555, 444) \end{aligned}$$

## 5 Security Analyses

The comparison of the classical RSA [7], its Gaussian integer domain in  $Z[i]$  [2], and our proposed scheme is as follows:

- The generation of primes  $p, q$  in classical scheme and Gaussian primes  $a, b$  in  $Z[i]$  require the same amount of computation. Same in the case with our proposed scheme where an additional prime  $g$  in the form of  $4k + 3$  would be generated with the same computation.
- The modified Gaussian variant provides more security than the classical method since the number of elements which are chosen to represent the message  $m$  is about square of those used in the classical case. scheme would provide security as compared to Gaussian variant, because domain  $Z[i]$  in our proposed scheme provides a more extension to the range of chosen messages, which make trails more complicated as compared to the Gaussian integer domain [2].
- In [2], Euler's phi function is  $\phi = (p^2 - 1)(q^2 - 1)$ , whereas in proposed scheme, it is  $\phi = (\alpha^2 - 1)(\beta^2 - 1)(\gamma^2 - 1)$ . This make the attempt to find the private key  $d$  from the public key more complicated as compared to the Gaussian variant [2] in  $Z[i]$ . Thus, our proposed scheme provides more security than the [2]. More so, the computations involved in the Gaussian variant do not require computational procedures different from those of the classical method. Same would be the case with our scheme.
- It is noted that the complexity for programs depends on the complexity of generating the public key. Thus, the classical and proposed algorithms are equivalent since their public-key generation algorithms are identical when restricting the choice of primes to those of the form  $4k + 3$ . However, our scheme is recommended since it provides a better extension to the message space and the public exponent range as compared to classical one.

## 6 Conclusion

We modify the computational methods in the domain of Gaussian integers. Lastly, we show how the modified computational methods can be used to extend the RSA algorithm to the domain  $Z[i]$ . Also, we show that the modified algorithm requires a little additional computational effort than the classical one and accomplishes much greater security.

## References

1. Cross, J.T.: The Eulers  $f$ -function in the Gaussian integers. *Amer. Math.* **55**, 518–528 (1995)
2. Elkamchouchi, H., Elshenawy, K., Shaban, H.: Extended RSA cryptosystem and digital signature schemes in the domain of Gaussian integers. *The 8th International Conference on Communication Systems*, vol. 1 (ICCS'02), pp. 91–95 (2002).
3. El-Kassar, A.N., Haraty, R., Awad, Y., Debnath, N.C.: Modified RSA in the domains of Gaussian integers and polynomials over finite fields. In: *Proceedings of international conference computer applications in industry and engineering—CAINE*, pp. 298–303 (2005).
4. Gauss, C.F.: *Theoria residuorum biquadraticorum*. *Comm. Soc. Reg. Sci. Gottingen* **7**, 1–34 (1832)
5. Menezes, A., Van Oorshot, J., Vanstone, P.C.S.A.: *Handbook of Applied Cryptography*. CRC Press, Boca Raton, FL (1997)
6. Niven, I., Zukerman, H.S., Montgomery, H.L.: *An Introduction to the Theory of Numbers*. John Wiley, New York (1991)
7. Rivest, R., Shamir, A., Adleman, L.: A method for obtaining digital signatures and public key cryptosystems. *Commun. ACM* **21**, 120–126 (1978)

# Neural Network and Statistical Modeling of Software Development Effort

Ruchi Shukla, Mukul Shukla and Tshilidzi Marwala

**Abstract** Many modeling studies that aimed at providing an accurate relationship between the software project effort (or cost) and the involved cost drivers have been conducted for effective management of software projects. However, the derived models are only applicable for a specific project and its variables. In this chapter, we present the use of back-propagation neural network (NN) to model the software development (SD) effort of 18 SD NASA projects based on six cost drivers. The performance of the NN model was also compared with a multi-regression model and other models available in the literature.

**Keywords** Neural network · Software development · Effort estimation · Regression

---

R. Shukla (✉)

Department of Electrical and Electronic Engineering Science, University of Johannesburg,  
Johannesburg, South Africa  
e-mail: ruchishuklamtech@gmail.com

M. Shukla

Department of Mechanical Engineering Technology, University of Johannesburg,  
Johannesburg, South Africa

M. Shukla

Department of Mechanical Engineering, MNNIT, Allahabad, UP, India  
e-mail: mukulshukla2k@gmail.com

T. Marwala

Faulty of Engineering and Built Environment, University of Johannesburg,  
Johannesburg, South Africa  
e-mail: tmarwala@uj.ac.z

## 1 Introduction

Software companies today are outsourcing a wide variety of their jobs to offshore organizations, for maximizing returns on investments. Estimating the amount of effort, time, and cost required for developing any information system is a critical project management issue. In view of the above, long-term, credible, and optimum forecast of software project estimates in the early stages of a project's life cycle is an almost intractable problem. Often, key information of real-life projects regarding size, complexity, system documentation, vocabulary, annual change traffic, client attitude, multilocation teams, etc. is unavailable. In spite of the availability of more than 100 estimation tools in the market, experience-based reasoning still remains the commonly applied estimation approach owing to some fundamental estimation issues which software developers have struggled with [1].

## 2 Literature Review

A review of studies on expert estimation of SD effort was presented by [2, 3]. An exploratory analysis of the state of the practice on schedule estimation and software project success prediction is presented in [4]. It was found that the data collection approach, role of respondents, and analysis type had an important impact on software estimation error [5]. Soft-computing- or artificial intelligence (AI)-based approaches are of late being used for more accurate prediction of software effort/cost. Artificial neural networks (ANN) offer a powerful computing architecture capable of learning from experimental data and representing complex, nonlinear, multivariate relationships [6, 7]. Kumar et al. compared the effectiveness of the variants of wavelet neural network (WNN) with many other techniques to forecast the SD effort [8]. Genetic algorithms (GAs) were used for the estimation of COCOMO model parameters of NASA SD projects in [9] while different fuzzy logic-based studies have been conducted [10–12]. Many hybrid schemes (neuro-GA, neuro-fuzzy, grey-GA, fuzzy-grey, etc) have also been investigated [13–15]. Many studies on software prediction have focused on the development of regression models based on historical data [16, 17].

## 3 Statistical Modeling

This modeling study is based on the SD effort dataset of Bailey and Basili [18] (Table 1—shown partly for brevity reasons). The six input factors are the total lines of code, new lines of code, developed lines of code (DL) (all in kloc), total methodology (ME), cumulative complexity, and cumulative experience, and the output is effort (in man months). Preliminary statistical analysis of the dataset was conducted

**Table 1** SD effort dataset [18]

Project no.	Project attributes			Project attributes				Response
	Total lines (kloc)	New lines (kloc)	Developed lines (kloc)	Total method-ology	Cumulative complexity	Cumulative ex-pertence	Effort (man months)	
1	111.9	84.7	90.2	30	21	16	115.8	
2	55.2	44	46.2	20	21	14	96	
-	-	-	-	-	-	-	-	
17	14.8	11.9	12.5	27	23	18	23.9	
18	110.3	98.4	100.8	34	33	16	138.3	
Correlation Coef-ficient	0.94	0.97	0.96	0.03	0.65	-0.02		
Covariance	1593.7	1319.3	1456.3	6.98	134.4	-2.82		
Kurtosis	-1.25	-0.38	-0.73	-0.83	-0.27	3.55	-1.26	
R-Square	0.88	0.95	0.92	0.00	0.42	0.00		



beforehand including the following: (1) correlation coefficient, (2) covariance, (3) kurtosis, and (4) R-square as presented in Table 1. Initially, from Minitab [19]-based ANOVA, a multivariable linear regression model (Eq. 1) has been fitted. The goodness of this developed model is validated with two other models (Eqs. 2 and 3) given by Sheta and Al-Afeef [15] in Table 2. Based on the high T (or low P) values, the following ranking (in a decreasing order) of the 6 effort drivers has been established: (1) methodology, (2) new LoC, (3) total LoC, (4) cumulative experience, (5) developed LoC, and (6) cumulative complexity. The high R-squared value of 98.3% and R-Sq(adjusted) values of 97.4% justify the correctness of the ANOVA.

$$\text{Effort} = 41.6 + 0.314 \text{ Tot\_LoC} + 0.986 \text{ New\_LoC} + 0.116 \text{ Develop\_LoC} - 1.57 \text{ Meth} - 0.112 \text{ Cum\_Complex} + 0.376 \text{ Cum\_Exper} \tag{1}$$

$$E = 1.75992 \times DL - 4.56 \times 10^{-3} \times DL^2 \tag{2}$$

$$E = 2 \times DL - 0.59 \times 10^{-3} ME^2 \times DL \tag{3}$$

The main effect plots for the 6 effort drivers are shown in Fig. 1.

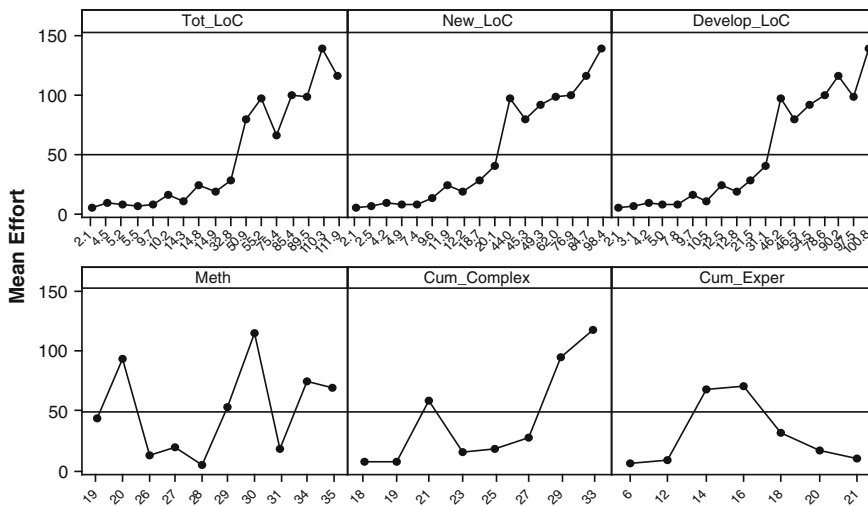


Fig. 1 Main effects plot

### 4 Neural Network Modeling

Back-propagation (BP) NN modeling for effort estimation has been carried out in this work using the MATLAB (2007b) NN toolbox options. Initially, a simple two-layer BP (6-6-1) NN was employed. The number of hidden nodes in the hidden layer was kept equal to the number of inputs (6 here). The number of hidden neurons was then suitably increased in an orderly hit and trial manner, to decide the final structure of the NN by keeping a check on the convergence rate of training, testing, and validation errors as well as the average percentage error. The learning rate and momentum can also be adjusted for the above purpose (although not varied in the present work).

Before the network is made ready to make estimates, we input the combinations of data inputs and outputs [18] through the network for training (60%), validation (20%), and testing (20%). In our case, the activation functions of both the hidden and output layers were initially chosen to be tan-sigmoid. The same was later changed to the purelin(ear) function in the output layer. We used the two most popular training algorithms i.e., the Levenberg-Marquardt (LM) and the Bayesian regularization (BR) algorithms. The training performance and linear regression analysis (between the network outputs and the corresponding targets) are shown in Figs. 2 and 3. For the LM algorithm, the output tracks the targets reasonably well, and the regression coefficient (R) value is over 0.97 mostly. Similarly, for the BR algorithm-based training with purelin output function, the R values are over 0.99 in nearly all the cases (Fig. 3).

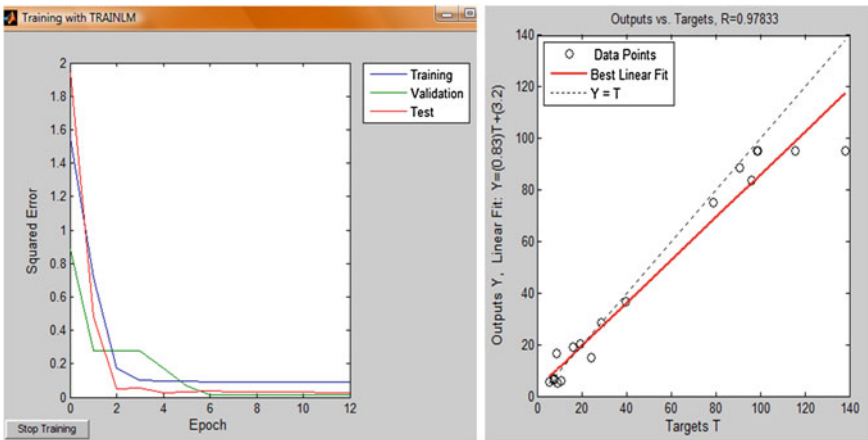


Fig. 2 Levenberg-Marquardt training with tansigmoid function in output layer

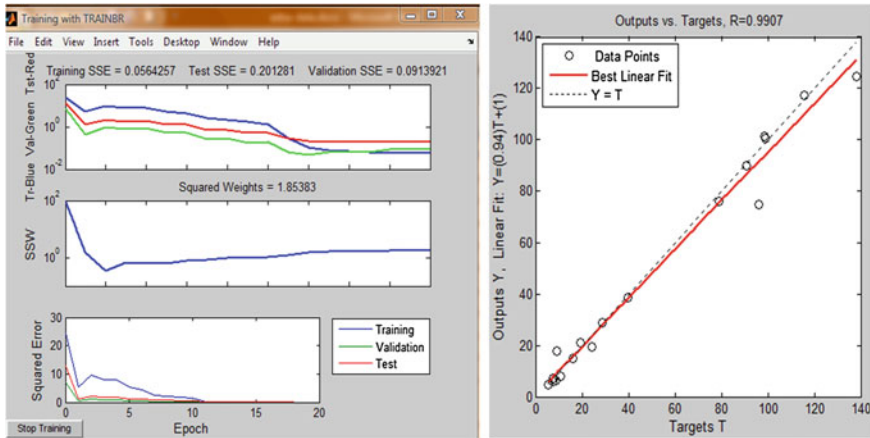


Fig. 3 Bayesian regularization training with purelin(ear) function in output layer

### 4.1 NN Modeling Tips

Listed underneath are some practical tips for efficient NN modeling.

- NNs are rather sensitive to the number of neurons in the hidden layers. Too few neurons often lead to underfitting, while too many neurons can contribute to overfitting. In this case, in spite of all the training points being well fitted, the fitted curve oscillates largely between these points [20].
- The NN dataset is generally divided in the following ratios: training (50–60), validation (20–25), and testing (20–25).
- Learning rate (alpha) represents how quickly an NN learns ranges from 0 to 1 and is initialized randomly. As with linear networks, a learning rate that is too large leads to unstable learning. Contrarily, a too small learning rate results in much longer training times. Typical values are 0.01–0.05.
- Momentum is a variable, which helps NN to break out of local minima. It may range from 0 to 1. Typical values are around 0.5.
- The threshold function (logsig, tansig, purelin, etc) selection is critical and determines when a node fires propagating a value further through the network. The choice is essentially based on the range and sign of inputs/outputs.
- The BR algorithm which is a modification of the LM algorithm is often used, as it generalizes well and reduces the difficulty of determining the optimum network architecture.
- LM training would normally be used for small- and medium-size networks, if enough memory is available. If memory is a problem, then there are a variety of other fast algorithms available. For large networks, one would probably want to use trainsec (conjugate gradient) or trainrp (resilient BP) algorithms.

- Overfitting is one of the most common problems that occurs in NN training. The training set error becomes a very small value, but the error turns to a large value when new data are presented to the network. An attempt at collecting more data and increasing the size of the training set must be made to prevent the situation of overfitting [20].
- One suggested method to improve network generalization is the use of a just large enough network that provides an adequate fit. Larger is the network used, more complex can be the functions the network can create. A small enough network will not have enough power to overfit the data. The two methods for improving generalization and implemented in MATLAB NN toolbox are regularization and early stopping [20].

## 5 Results and Discussion

The degree to which a model's estimated effort ( $MM_{est}$ ) matches the actual or target effort ( $MM_{act}$ ) is estimated by a percentage relative error. Magnitude of relative error (MRE), which accounts for under and overestimates along with its mean magnitude of relative error (MMRE) is often used in effort estimation analysis.

$$MRE = \left| \frac{MM_{act} - MM_{est}}{MM_{act}} \right| \quad (4)$$

Table 2 (in brief) presents a comparison of the empirical models (Eqs. 1–3) fitted effort and NN effort (for different configurations) with the target effort of [19]. It can be concluded that the present NN framework is able to successfully model the dataset with nearly the following percentage relative error and percentage mean relative error:

1.  $-10.58$  to  $8.36$  and  $4.68\%$ , respectively, for `trainlm` with `tansig` function in output layer and hidden neurons varied from 6 to 20.
2.  $-12.5$  to  $-9.62$  and  $-10.3\%$ , respectively, for `trainbr` with `tansig` function in output layer and hidden neurons varied from 6 to 20.
3.  $0.65$  to  $-3.12$  and  $0.79\%$ , respectively, for `trainbr` with `purelin` function in output layer and hidden neurons varied from 6 to 20.

The relative error obtained from the developed multi-regression model (Eq. 1) is comparable to other models (Eqs. 2 and 3). A comparison between the mean relative error of the developed NN and regression models and the MMRE of Halstead, Walston-Felix, Bailey-Basili, and Doty models are shown in Table 3 [16].

**Table 2** Comparison of empirical model fitted and NN effort with target effort

Project number	Target effort [18]	Predicted effort (Eq. 1)	Percentage error = $(1-C3/C2) * 100$	Predicted effort (Eq. 2)	% error = $(1-C5/C2) * 100$	Percentage error (Predicted effort from Eq. 3)	LM	BR	Percentage error NN output
							tansig	purelin	
1	115.8	127.28	-9.91	121.64	-5.05	-14.42	17.8	19.2	-1.1
6	98.4	98.63	-0.23	128.24	-30.33	-49.01	9.0	-54.2	-2.8
18	138.3	133.89	3.19	131.07	5.23	3.94	31.2	31.9	10.0
		Percentage mean error	-5.41		-8.66	-2.76	4.68	-10.3	0.79

**Table 3** Comparison of different models

Model name	Model equation	MMRE
Halstead	$E = 5.2(DL)1.50$	0.1479
Walston-Felix	$E = 0.7(DL)0.91$	0.0822
Bailey-Basili	$E = 5.5 + 0.73(DL)1.16$	0.0095
Doty (for $DL > 9$ )	$E = 5.288(DL)1.0$	0.1848
		Mean relative error
Present work—(1) LM-based BPNN	–	0.0468
(2) BR-based BPNN – 1		–0.1030
(3) BR-based BPNN – 2		0.0079
(4) Multilinear regression	Eq. 1	–0.0541

## 6 Conclusions

Effort estimation is a complex task, and research studies indicate that results in general vary a lot. The market potential for SD and maintenance is huge and constantly growing mainly for financial and online applications. In this work, a twofold approach based on NN and multilinear regression has been carried out for more accurate SD effort estimation

**Acknowledgments** The authors would like to acknowledge the financial support extended by the Faculty of Engineering and Built Environment, University of Johannesburg.

## References

1. Shukla, R. Misra, A.K.: Estimating software maintenance effort - a neural network approach. 1st India, Software Engineering Conference. 107–112 (2008).
2. Jorgensen, M.: A review of studies on expert estimation of software development effort. *J Syst. Software*. **70**(1–2), 37–60 (2004)
3. Jorgensen, M., Shepperd, M.: A systematic review of software development cost estimation studies. *IEEE T. Software Eng.* **33**(1), 33–53 (2007)
4. Verner, J.M., Evanco, W.M., Cerpa, N.: State of the practice: an exploratory analysis of schedule estimation and software project success prediction. *Inform. Software Tech.* **49**(2), 181–193 (2007)
5. Jorgensen, M., Ostvold, K.M.: Reasons for software effort estimation error: impact of respondent role, information collection approach, and data analysis method. *IEEE T. Software Eng.* **30**(12), 993–1007 (2004)
6. Huang, X., Ho, D., Ren, J., Capretz, L.F.: A soft computing framework for software effort estimation. *Soft Comput.* **10**, 170–177 (2006)
7. Tronto, I.F.B., Silva, J.D.S., Anna, N.S.: An investigation of artificial neural networks based prediction systems in software project management. *J Syst. Software*. **81**(3), 356–367 (2008)
8. Kumar, K.V., Ravi, V., Carr, M., Kiran, N.R.: Software development cost estimation using wavelet neural networks. *J Syst. Software*. **81**(11), 1853–1860 (2008)
9. Sheta, A.: Estimation of the COCOMO model parameters using genetic algorithms for NASA software projects. *J. Comput. Sci.* **2**(2), 118–123 (2006)

10. Xu, Z.W., Khoshgoftaar, T.M.: Identification of fuzzy models of software cost estimation. *Fuzzy Set. Syst.* **145**(1), 141–163 (2004)
11. Ahmed, M., Saliu, M.O., Alghamdi, J.: Adaptive fuzzy logic-based framework for software development effort prediction. *Inform. Software Tech.* **47**(1), 31–48 (2005)
12. Kazemifard, M., Zaeri, A., Ghasem-Aghaee, N., Nematbakhsh, M.A., Mardukhi, F.: Fuzzy emotional COCOMO II software cost estimation (FECSCCE) using multi-agent systems. *Appl. Soft Comput.* **11**(2), 2260–2270 (2011)
13. Shukla, K.K.: Neuro-genetic prediction of software development effort. *Inform. Software Tech.* **42**, 701–713 (2000)
14. Huang, S.J., Chiu, N.H.: Optimization of analogy weights by genetic algorithm for software effort estimation. *Inform. Software Tech.* **48**, 1034–1045 (2006)
15. Sheta, A. F., Al-Afeef, A.: A GP effort estimation model utilizing line of code and methodology for NASA software projects. 10th International Conference on Intelligent Systems Design and Applications. 290–295 (2010).
16. Jorgensen, M.: Regression models of software development effort estimation accuracy and bias. *Empir. Softw. Eng.* **9**, 297–314 (2004)
17. Shukla, R., Misra, A.K.: Software maintenance effort estimation-neural network vs regression modeling approach. *Int. J. Comput. Applic.* **1**(29), 83–89 (2010)
18. Bailey, J.W., Basili, V.R.: A metamodel for software development resource expenditures. 5th IEEE International Conference on, Software Engineering. 107–116 (1981).
19. [www.minitab.com](http://www.minitab.com) (2012).
20. [www.mathworks.com/access/helpdesk/help/pdf\\_doc/nnet/nnet.pdf](http://www.mathworks.com/access/helpdesk/help/pdf_doc/nnet/nnet.pdf) (2012).

# On $\alpha$ -Convex Multivalent Functions Defined by Generalized Ruscheweyh Derivatives Involving Fractional Differential Operator

Ritu Agarwal and J. Sokol

**Abstract** In the present investigation, we introduce a class of  $\alpha$ -convex multivalent functions defined by generalized Ruscheweyh derivatives introduced by Goyal and Goyal (J. Indian Acad. Math. 27(2):439–456, 2005) which involves a generalized fractional differential operator. The necessary and sufficient condition for functions to belong to this class is obtained. We study properties of this class and derive a theorem about image of a function from this class through generalized Komatu integral operator. Also, the integral representation for the functions of this class has been obtained.

## 1 Introduction

Let  $A$  denote the class of analytic  $p$ -valent functions defined on unit disk  $U = \{z : |z| < 1\}$  of the form

$$f(z) = z^p + \sum_{k=p+1}^{\infty} a_k z^k. \quad (1)$$

The function  $f(z) \in A$  is said to be  $p$ -valent starlike of order  $\delta$  if and only if

$$\operatorname{Re} \left( \frac{zf'(z)}{f(z)} \right) > \delta, \quad (z \in U; 0 \leq \delta < p) \quad (2)$$

---

R. Agarwal (✉)

Malaviya National Institute of Technology, Jaipur, Rajasthan, India  
e-mail: ritugoyal.1980@gmail.com

J. Sokol

Institute of Mathematics, University of Rzeszów, ul. Rejtana 16A, 35-310 Rzeszów, Poland  
e-mail: jsokol@prz.edu.pl



The class of starlike functions of order  $\delta$  is denoted by  $S_\delta^*$ . On the other hand, a function  $f(z) \in A$  is said to be *p-valent convex of order  $\delta$*  if and only if

$$\operatorname{Re} \left( 1 + \frac{zf''(z)}{f'(z)} \right) > \delta, \quad (z \in U; 0 \leq \delta < p). \tag{3}$$

The class of convex functions of order  $\delta$  is denoted by  $K_\delta$ . It is observed that  $f(z) \in K_\delta \Leftrightarrow zf'(z) \in S_\delta^*$ .

For  $\alpha \in [0, 1]$ , let  $K_\delta(\alpha)$  denote the family of functions  $f(z) \in A$  with  $f'(z)f(z)/z \neq 0$  in  $U$  such that

$$\operatorname{Re} \left\{ (1 - \alpha) \frac{zf'(z)}{f(z)} + \alpha \left( \frac{(zf'(z))'}{f'(z)} \right) \right\} > \delta, \quad (z \in U) \tag{4}$$

The functions in class  $K_\delta(\alpha)$  are said to be  $\alpha$ -convex functions of order  $\delta$  (see e.g. [1, 2]). We recall the definition of subordination ([3], p. 190). For two functions  $f$  and  $g$  analytic in  $U$ , we say that  $f(z)$  is subordinate to  $g(z)$  in  $U$  and write  $f \prec g$  or  $f(z) \prec g(z)$ , if there exists a Schwarz function  $w(z)$ , analytic in  $U$  with  $w(0) = 0$  and  $|w(z)| < 1$  such that  $f(z) = g(w(z))$ ,  $z \in U$ .

The generalized Ruscheweyh derivative operator  $\mathcal{J}_p^{\lambda, \mu}$  defined by the author (see e.g. [5, 10]) is given by

$$\mathcal{J}_p^{\lambda, \mu} f(z) = \frac{\Gamma(\mu - \lambda + \nu + 2)}{\Gamma(\nu + 2)\Gamma(\mu + 1)} z^p J_{0,z}^{\lambda, \mu, \nu} (z^{\mu-p} f(z)) \tag{5}$$

where the fractional differential operator  $J_{0,z}^{\lambda, \mu, \nu}$  is given by (see e.g. [16])

$$J_{0,z}^{\lambda, \mu, \nu} f(z) = \begin{cases} \frac{1}{\Gamma(1-\lambda)} \frac{d}{dz} \left\{ z^{\lambda-\mu} \int_0^z (z-\zeta)^{-\lambda} \times {}_2F_1 \left( \mu - \lambda, -\nu; 1 - \frac{\zeta}{z} \right) f(\zeta) d\zeta \right\}, & (0 \leq \lambda < 1) \\ \frac{d^n}{dz^n} J_{0,z}^{\lambda-n, \mu, \nu} f(z), & (n \leq \lambda < n+1, n \in \mathbb{N}) \quad (k > \max\{0, \mu - \nu - 1\} - 1) \end{cases} \tag{6}$$

provided further that

$$f(z) = O(|z|^k), \quad (z \rightarrow 0)$$

The generalized Ruscheweyh derivative of  $f \in A$ , introduced by Goyal and Goyal [5], is defined as

$$\mathcal{J}_p^{\lambda, \mu} f(z) = z^p + \sum_{k=p+1}^{\infty} a_k B_p^{\lambda, \mu}(k) z^k, \tag{7}$$

where

$$B_p^{\lambda, \mu}(k) = \frac{\Gamma(k - p + 1 + \mu)\Gamma(v + 2 + \mu - \lambda)\Gamma(k + v - p + 2)}{\Gamma(k - p + 1)\Gamma(k + v - p + 2 + \mu - \lambda)\Gamma(v + 2)\Gamma(1 + \mu)} \tag{8}$$

For  $\mu = \lambda$ , this generalized Ruscheweyh derivative operator reduces to Ruscheweyh derivative operator of order  $\lambda$  (see, e.g. [13]). Further, for  $p = 1$ , it reduces to ordinary Ruscheweyh derivative of univalent functions [14].

**Definition 1** Let  $q$  be a univalent function in  $U$  with  $q(0)=1$  and such that  $D = q(U)$  is a convex domain from right half-plane. We define a subclass  $\mathcal{M}_\alpha^p(\lambda, \mu, q)$  of  $\alpha$ -convex functions  $f$  in  $A$  for  $0 \leq \alpha \leq 1$  and  $\lambda > -1$ , satisfying the subordination condition

$$\mathcal{J}(\alpha, \lambda, \mu, f; z) = \left[ \frac{(1 - \alpha) z (\mathcal{J}_p^{\lambda, \mu} f(z))'}{p \mathcal{J}_p^{\lambda, \mu} f(z)} + \frac{\alpha}{p} \left( 1 + \frac{z (\mathcal{J}_p^{\lambda, \mu} f(z))''}{(\mathcal{J}_p^{\lambda, \mu} f(z))'} \right) \right] \prec q(z) \tag{9}$$

Subclasses of  $\mathcal{M}_\alpha^p(\lambda, \mu, q)$  were studied by several authors. To mention a few are:

$$\begin{aligned} \mathcal{M}_0^1(0, 0, q) &= S^*(q) \\ \mathcal{M}_\alpha^1(0, 0, q) &= \mathcal{M}_\alpha(q) \\ \mathcal{M}_0^1(0, 0, q_\gamma) &= S^*(\gamma) \text{ where } q_\gamma(z) = \frac{1 + (1 - 2\gamma)z}{1 - z}, 0 \leq \gamma < 1 \\ \mathcal{M}_\alpha^1(0, 0, q) &= \mathcal{M}_\alpha \text{ for } q(z) = \frac{1 + z}{1 - z} \\ \mathcal{M}_\alpha^1(m, m, q) &= \mathcal{M}_\alpha(m, 0, q), m \in \mathbb{N}^* \end{aligned}$$

The class  $S^*(\gamma)$  is the well-known class of starlike functions of order  $\gamma$ . The class  $S^*(q)$  was introduced by Ma and Minda [7], the class  $\mathcal{M}_\alpha(q)$  was studied by Ravichandran and Darus [12],  $\mathcal{M}_\alpha$  is the class of  $\alpha$ -convex functions introduced by Mocanu [9], and  $\mathcal{M}_\alpha(m, 0, q)$  makes the object of the papers of Raducanu and Nechita [11]. For  $\alpha = 0$ , we shall denote the following subclass of functions  $f \in A$  as  $S_p^*(\lambda, \mu, q)$ .

$$\begin{aligned} S_p^*(\lambda, \mu, q) &= \mathcal{M}_0^p(\lambda, \mu, q) \\ &= \left\{ f \in A : \mathcal{J}(0, \lambda, \mu, f; z) = \frac{z (\mathcal{J}_p^{\lambda, \mu} f(z))'}{p \mathcal{J}_p^{\lambda, \mu} f(z)} \prec q(z), z \in U \right\} \end{aligned} \tag{10}$$

## 2 Preliminaries

In our present investigation, we shall need the following results concerning Briot–Bouquet differential subordinations.

**Theorem 1** [4] *Let  $\beta, \gamma \in \mathbb{C}, \beta \neq 0$  and consider the convex function  $h$ , such that  $\operatorname{Re}[\beta h(z) + \gamma] > 0, z \in U$ . If  $p \in \mathcal{H}[h(0), n]$ , then*

$$p(z) + \frac{zp'(z)}{\beta p(z) + \gamma} \prec h(z) \Rightarrow p(z) \prec h(z)$$

**Theorem 2** [8] *Let  $q$  be an univalent function in  $U$  and consider  $\theta$  and  $\phi$  to be analytic functions in a domain  $q(U)$ . We denote by  $Q(z) = zq'(z) \cdot \phi[q(z)]$ ,  $h(z) = \theta[q(z)] + Q(z)$  and assume that*

1.  $h$  is convex, or
  2.  $Q$  is starlike.
- Further suppose that
- 3.

$$\operatorname{Re} \frac{zh'(z)}{Q(z)} = \operatorname{Re} \left[ \frac{\theta'[q(z)]}{\phi[q(z)]} + \frac{zQ'(z)}{Q(z)} \right] > 0$$

*If  $p$  is an analytic function in  $U$ , with  $p(0) = q(0), p(U) \subseteq D$  and such that*

$$\theta[p(z)] + zp'(z)\phi[p(z)] \prec \theta[q(z)] + zq'(z)\phi[q(z)] = h(z)$$

*then  $p(z) \prec q(z)$  and  $q$  is the best dominant.*

## 3 Main Results

**Theorem 3** *Let  $\alpha \in [0, 1], \lambda \geq 0, \mu > -1$ . Then  $f \in \mathcal{M}_\alpha^p(\lambda, \mu, q)$  if and only if the function  $g$  defined by*

$$g(z) = \mathcal{J}_p^{\lambda, \mu} f(z) \left[ \frac{z(\mathcal{J}_p^{\lambda, \mu} f(z))'}{\mathcal{J}_p^{\lambda, \mu} f(z)} \right]^\alpha, \quad z \in U \tag{11}$$

*belongs to  $S_p^*(\lambda, \mu, q)$ . the branch of the power function is chosen such that*

$$\left[ \frac{z(\mathcal{J}_p^{\lambda, \mu} f(z))'}{\mathcal{J}_p^{\lambda, \mu} f(z)} \right]^\alpha \Big|_{z=0} = 1.$$

*Proof* Calculating the logarithmic derivative of  $g$ , we obtain

$$\begin{aligned} \frac{zg'(z)}{pg(z)} &= \frac{z(\mathcal{J}_p^{\lambda,\mu} f(z))'}{p \mathcal{J}_p^{\lambda,\mu} f(z)} + \frac{\alpha}{p} \left[ 1 + \frac{z(\mathcal{J}_p^{\lambda,\mu} f(z))''}{(\mathcal{J}_p^{\lambda,\mu} f(z))'} - \frac{z(\mathcal{J}_p^{\lambda,\mu} f(z))'}{\mathcal{J}_p^{\lambda,\mu} f(z)} \right] \\ &= \mathcal{J}(\alpha, \lambda, \mu, f; z) < q(z) \end{aligned}$$

The equivalence from the hypothesis follows immediately.

**Theorem 4** *If the function  $f$  belongs to the class  $\mathcal{M}_\alpha^p(\lambda, \mu, q)$ , for a given  $\alpha \in [0, 1]$ ,  $\lambda \geq 0$ ,  $\mu > -1$ , then  $f \in S_p^*(\lambda, \mu, q)$ .*

*Proof* Let us denote

$$p(z) = \frac{z \left( \mathcal{J}_p^{\lambda,\mu} f(z) \right)'}{p \left( \mathcal{J}_p^{\lambda,\mu} f(z) \right)}$$

The logarithmic derivative of  $p(z)$  is

$$\frac{zp'(z)}{p(z)} = 1 + \frac{z \left( \mathcal{J}_p^{\lambda,\mu} f(z) \right)''}{\left( \mathcal{J}_p^{\lambda,\mu} f(z) \right)'} - \frac{z \left( \mathcal{J}_p^{\lambda,\mu} f(z) \right)'}{\left( \mathcal{J}_p^{\lambda,\mu} f(z) \right)}$$

Since  $f \in \mathcal{M}_\alpha^p(\lambda, \mu, q)$ ,

$$p(z) + \frac{\alpha zp'(z)}{p(z)} = \mathcal{J}(\alpha, \lambda, \mu, f; z) < q(z)$$

It has been assumed that the function  $q$  is convex and that the image  $q(U)$  is in the right half-plane. We have  $\alpha \in [0, 1]$ , therefore,

$$\operatorname{Re} \left[ \frac{q(z)}{\alpha} \right] > 0 \quad z \in U$$

By applying Theorem 1 for  $\beta = \frac{p}{\alpha}$  and  $\gamma = 0$ , we conclude that  $p(z) < q(z)$  and hence  $f \in S_p^*(\lambda, \mu, q)$ .

**Theorem 5** *Let  $q$  be convex function in  $U$  with  $q(0)=1$  and  $\operatorname{Re} q(z) > 0$ . Also consider  $Q(z) = \alpha \frac{zq'(z)}{p q(z)}$  and  $h(z) = q(z) + Q(z)$ ,  $z \in U$ . If  $Q$  is a convex function in  $U$  and  $f \in \mathcal{M}_\alpha^p(\lambda, \mu, h)$  for an  $\alpha \in [0, 1]$ ,  $\lambda \geq 0$ ,  $\mu > -1$ , then  $f \in S_p^*(\lambda, \mu, q)$ .*

*Proof* Define the functions  $\theta(w) = w$  and  $\phi(w) = \frac{\alpha}{pw}$  and notice that the hypothesis of the Theorem 2 are satisfied. It follows that

$$p(z) = \frac{z \left( \mathcal{J}_p^{\lambda,\mu} f(z) \right)'}{p \left( \mathcal{J}_p^{\lambda,\mu} f(z) \right)} < q(z)$$

and  $q$  is the best dominant. Therefore,  $f \in S_p^*(\lambda, \mu, q)$ .

The generalized Komatu integral operator  $K_{c,p}^\sigma : A \rightarrow A, c + p > 0, \sigma \geq 0$  introduced by Komatu [6] is defined as

$$\begin{aligned}
 K_{c,p}^\sigma f(z) &= \frac{(c+p)^\sigma}{\Gamma(\sigma)z^c} \int_0^z t^{c-1} \log\left(\frac{z}{t}\right)^{\sigma-1} f(t) dt \\
 &= z^p + \sum_{k=p+1}^\infty \left(\frac{c+p}{c+p+k}\right)^\sigma a_k z^k
 \end{aligned}
 \tag{12}$$

**Theorem 6** If  $K_{c,p}^\sigma f \in \mathcal{M}_\alpha^p(\lambda, \mu, q)$ , then  $K_{c,p}^{\sigma+1} f \in S_p^*(\lambda, \mu, q), \lambda \geq 0, \mu > -1$ .

*Proof* Komatu integral operator satisfies the recurrence relation

$$(c+p)K_{c,p}^\sigma f(z) = z \left( K_{c,p}^{\sigma+1} f(z) \right)' + cK_{c,p}^{\sigma+1} f(z) \tag{13}$$

Applying generalized Ruscheweyh derivative operator, defined by (5), on both sides of (13), we obtain

$$(c+p) \mathcal{J}_p^{\lambda,\mu}(K_{c,p}^\sigma f(z)) = \mathcal{J}_p^{\lambda,\mu} \left( z K_{c,p}^{\sigma+1} f(z) \right)' + c \mathcal{J}_p^{\lambda,\mu}(K_{c,p}^{\sigma+1} f(z)) \tag{14}$$

Observe that  $\mathcal{J}_p^{\lambda,\mu} \left( z K_{c,p}^{\sigma+1} f(z) \right)' = z \left( \mathcal{J}_p^{\lambda,\mu}(K_{c,p}^{\sigma+1} f(z)) \right)'$ . Therefore, for  $f \in A$ , Eq. (14) result becomes

$$(c+p) \mathcal{J}_p^{\lambda,\mu}(K_{c,p}^\sigma f(z)) = z \left( \mathcal{J}_p^{\lambda,\mu}(K_{c,p}^{\sigma+1} f(z)) \right)' + c \mathcal{J}_p^{\lambda,\mu}(K_{c,p}^{\sigma+1} f(z)) \tag{15}$$

Differentiating (15) w.r.t.  $z$  and multiplying by  $z$ , we obtain

$$\begin{aligned}
 (c+p)z \left[ \mathcal{J}_p^{\lambda,\mu}(K_{c,p}^\sigma f(z)) \right]' & \\
 &= (c+1)z \left[ \mathcal{J}_p^{\lambda,\mu}(K_{c,p}^{\sigma+1} f(z)) \right]' + z^2 \left[ \mathcal{J}_p^{\lambda,\mu}(K_{c,p}^{\sigma+1} f(z)) \right]''
 \end{aligned}
 \tag{16}$$

Divide (16) by (15) to obtain

$$z \frac{\left( \mathcal{J}_p^{\lambda,\mu}(K_{c,p}^\sigma f(z)) \right)'}{\mathcal{J}_p^{\lambda,\mu}(K_{c,p}^\sigma f(z))} = z \frac{\left( \mathcal{J}_p^{\lambda,\mu}(K_{c,p}^{\sigma+1} f(z)) \right)'}{\mathcal{J}_p^{\lambda,\mu}(K_{c,p}^{\sigma+1} f(z))} \left[ \frac{c+1+z \frac{\left( \mathcal{J}_p^{\lambda,\mu}(K_{c,p}^{\sigma+1} f(z)) \right)''}{\left( \mathcal{J}_p^{\lambda,\mu}(K_{c,p}^{\sigma+1} f(z)) \right)'}}{c+z \frac{\left( \mathcal{J}_p^{\lambda,\mu}(K_{c,p}^{\sigma+1} f(z)) \right)'}{\mathcal{J}_p^{\lambda,\mu}(K_{c,p}^{\sigma+1} f(z))}} \right] \tag{17}$$

Using the notations

$$P(z) = \frac{z \left( \mathcal{J}_p^{\lambda, \mu} (K_{c,p}^{\sigma+1} f(z)) \right)'}{p \left( \mathcal{J}_p^{\lambda, \mu} (K_{c,p}^{\sigma+1} f(z)) \right)} \quad \text{and} \quad p(z) = \frac{z \left( \mathcal{J}_p^{\lambda, \mu} (K_{c,p}^{\sigma} f(z)) \right)'}{p \left( \mathcal{J}_p^{\lambda, \mu} (K_{c,p}^{\sigma} f(z)) \right)}$$

in (15), we get

$$p(z) = P(z) \frac{c + p P(z) + \frac{zP'(z)}{P(z)}}{c + p P(z)} = P(z) + \frac{zP'(z)}{c + p P(z)}$$

Let  $K_{c,p}^{\sigma} f \in \mathcal{M}_{\alpha}^p(\lambda, \mu, q)$ , then by Theorem 4,  $K_{c,p}^{\sigma} f \in S_p^*(\lambda, \mu, q)$  and hence the subordination

$$p(z) < q(z) \Rightarrow P(z) + \frac{zP'(z)}{c + p P(z)} < q(z)$$

holds. As  $q$  is a convex function and  $\text{Re}[c + p P(z)] > 0$ , from Theorem 1, with  $\beta = p$  and  $\gamma = c$ , we conclude that  $P(z) < q(z)$ . Thus,

$$P(z) = \frac{z \left( \mathcal{J}_p^{\lambda, \mu} (K_{c,p}^{\sigma+1} f(z)) \right)'}{p \left( \mathcal{J}_p^{\lambda, \mu} (K_{c,p}^{\sigma+1} f(z)) \right)} < q(z),$$

that is,  $K_{c,p}^{\sigma+1} f \in S_p^*(\lambda, \mu, q)$ .

Put  $\sigma = 0$  in the above theorem and denote  $K_{c,p}^1 \equiv L_{c,p}$ , which is generalized Libera integral operator, to obtain the important result contained in the following theorem:

**Theorem 7** *If  $f \in \mathcal{M}_{\alpha}^p(\lambda, \mu, q)$ , then  $L_{c,p} f \in S_p^*(\lambda, \mu, q)$ .*

### 4 A Representation Theorem

**Theorem 8** *A function  $f \in \mathcal{M}_{\alpha}^p(\lambda, \mu, q)$  for an  $\alpha \in [0, 1]$ ,  $\lambda \geq 0$ ,  $\mu > -1$  if and only if*

$$\frac{\mathcal{J}_p^{\lambda, \mu} f(z)}{z^p} \left( \frac{z \left( \mathcal{J}_p^{\lambda, \mu} f(z) \right)'}{\left( \mathcal{J}_p^{\lambda, \mu} f(z) \right)} \right)^{\alpha} = \exp \left( p \int_0^z \frac{q(w(z)) - 1}{z} dz \right) \quad (18)$$

where  $w(z)$  is analytic in  $U$  satisfying  $w(0) = 0$  and  $|w(z)| \leq 1$ .

*Proof* Since  $f \in \mathcal{M}_\alpha^p(\lambda, \mu, q)$ , (9) holds, and therefore, there exists a Schwarz function  $w(z)$  such that  $w(0) = 0$  and  $|w(z)| \leq 1$  and

$$\left[ \frac{(1 - \alpha) z (\mathcal{J}_p^{\lambda, \mu} f(z))'}{p \mathcal{J}_p^{\lambda, \mu} f(z)} + \frac{\alpha}{p} \left( 1 + \frac{z (\mathcal{J}_p^{\lambda, \mu} f(z))''}{(\mathcal{J}_p^{\lambda, \mu} f(z))'} \right) \right] = q(w(z))$$

Rewriting the above equation in the form

$$\left[ \frac{(1 - \alpha)}{p} \left( \frac{(\mathcal{J}_p^{\lambda, \mu} f(z))'}{\mathcal{J}_p^{\lambda, \mu} f(z)} \right) + \frac{\alpha}{p} \left( \frac{1}{z} + \frac{(\mathcal{J}_p^{\lambda, \mu} f(z))'}{(\mathcal{J}_p^{\lambda, \mu} f(z))'} \right) - \frac{1}{z} \right] = \frac{q(w(z)) - 1}{z}$$

On integrating from 0 to  $z$ , we obtain the desired expression upon exponentiation. The converse follows directly by differentiation.

Putting  $\mu = \lambda$  in Theorem 8, we obtain the following corollary.

**Theorem 9** A function  $f \in \mathcal{M}_\alpha^p(\lambda, q)$  for an  $\alpha \in [0, 1]$ ,  $\lambda \geq 0$  if and only if

$$\frac{D_p^\lambda f(z)}{z^p} \left( \frac{z (D_p^\lambda f(z))'}{(D_p^\lambda f(z))} \right)^\alpha = \exp \left( p \int_0^z \frac{q(w(z)) - 1}{z} dz \right) \tag{19}$$

where  $w(z)$  is analytic in  $U$  satisfying  $w(0)=0$  and  $|w(z)| \leq 1$ .

Further, on taking  $p = 1$  in the Theorem 9, we can find the corresponding result for univalent functions.

## References

1. Acu, M., et al.: On some  $\alpha$ -convex functions. *Int. J. Open Problems Comput. Sci. Math* 1(1), 1–10 (2008).
2. Ali, R.M., Ravichandran, V.: Classes of meromorphic  $\alpha$ -convex functions. *Taiwanese J. Math.* **14**(4), 1479–1490 (2010)
3. Duren, P.L.: *Univalent funct.* Springer Verlag, New York (1983)
4. Eenigenburg, P.J., Miller, S.S., Mocanu, P.T., Reade, M.O.: On a Briot-Bouquet differential subordination. *General inequalities, 3. Int. Series of Numerical Math*, pp. 339–348. Birkhauser Verlag, Basel (1983).
5. Goyal, S.P., Goyal, R.: On a class of multivalent functions defined by generalized Ruscheweyh derivatives involving a general fractional derivative operator. *J. Indian Acad. Math.* **27**(2), 439–456 (2005)
6. Komatu, Y.: On analytic prolongation of a family of operators. *Mathematica (Cluj)* **32**(55), 141–145 (1990)
7. Ma, W., Minda, D.: A unified treatment of some special classes of univalent functions, proceedings of the conference on complex analysis, Tianjin, China. *Int. Press. Conf. Proc. Lect. Notes Anal.* 1, 157–169 (1994).

8. Miller, S.S., Mocanu, P.T.: On some classes of first-order differential subordinations. *Michig. Math. J.* **32**, 185–195 (1985)
9. Mocanu, P.T.: Une propriete de convexite geneealisee dans la theorie de la representation conforme. *Mathematica (Cluj)* **11**(34), 127–133 (1969)
10. Parihar, H.S., Agarwal, R.: Application of generalized Ruscheweyh derivatives on p-valent functions. *J. Math. Appl.* **34**, 75–86 (2011)
11. Raducanu, D., Nechita, V.O.: On  $\alpha$ -convex functions defined by generalized Ruscheweyh derivatives operator, *Studia Univ. "Babes-Bolyai". Mathematica* **53**, 109–118 (2008)
12. Ravichandran, V., Darus, M.: On class of  $\alpha$ -convex functions. *J. Anal. Appl.* **2**(1), 17–25 (2004)
13. Ravichandran, V., Seenivasagan, N., Srivastava, H.M.: Some inequalities associated with a linear operator defined for a class of multivalent functions. *J. Inequal. Pure and Appl. Math.* **4**(4), 1–7 (2003). Art. 70.
14. Ruscheweyh, S.T.: New criterion for univalent functions. *Proc. Amer. Math. Soc.* **49**, 109–115 (1975)
15. Sokol, J.: On a condition for alpha-starlikeness. *J. Math. Anal. Appl.* **352**, 696–701 (2009)
16. Srivastava, H.M., Saxena, R.K.: Operators of fractional integration and their applications. *Appl. Math. Comput.* **118**, 1–52 (2001)



# A New Expected Value Model for the Fuzzy Shortest Path Problem

Sk. Md. Abu Nayeem

**Abstract** Here, we consider a network, whose arc lengths are intervals or triangular fuzzy numbers. A new comparison technique based on the expected value of intervals and triangular fuzzy numbers is introduced. These expected values depend on a parameter which reflects the optimism/pessimism level of the decision-maker. Moreover, they can be used for negative intervals or triangular fuzzy numbers.

## 1 Introduction

Shortest path problem on a network with fuzzy parameters is one of the most studied problems in fuzzy set theory. A wide range of variations in the study of the fuzzy shortest path problem (FSPP) is found in the literature [1–3]. In a recent development, Nayeem and Pal [4] proposed an algorithm to find a fuzzy optimal path to which the decision-maker always satisfies with different grades of satisfaction. Hernandez et al. [5] proposes an iterative algorithm that assumes a generic ranking index for comparing the fuzzy numbers involved in the problem. But, neither of the above works addressed the problem when the arc lengths are imprecise numbers of mixed type. Tajdin et al. [6] gave an algorithm to find a fuzzy shortest path in a network with mixed fuzzy arc lengths using  $\alpha$ -cuts. But, this  $\alpha$ -cuts are not applicable for intervals, which can be considered as equipossible fuzzy numbers.

Recently, Liu [7, 8] developed a credibility theory including credibility measure, pessimistic value, and expected value as fuzzy ranking methods. Yang and Iwamura [9] introduced the  $m_\lambda$  measure as the linear combination of possibility measure and necessity measure and employed that measure to construct the fuzzy chance-constrained programming models. In this chapter, we have introduced the  $\lambda$ -expected

---

S. M. A. Nayeem (✉)

Department of Mathematics, Aliah University, DN-41, Sector-V, Salt Lake  
City, Kolkata 700091, India  
e-mail: nayeem.math@aliah.ac.in

value of a fuzzy variable. Using this  $\lambda$ -expected values, Dijkstra's [10] algorithm for classical graphs can be applied to solve the FSPP.

## 2 Preliminaries and $m_\lambda$ Measures

In this section, we give the arithmetic and ranking methods of intervals and triangular fuzzy numbers. Also we give a brief introduction to the  $m_\lambda$  measure and define the  $\lambda$ -expected value of fuzzy variables.

An interval number is defined as  $A = [a, b] = \{x : a \leq x \leq b\}$ , where  $a$  and  $b$  are real numbers called the left end point and the right end point of the interval  $A$ . or, alternatively,  $A = \langle m(A), w(A) \rangle$ , where  $m(A)$  = midpoint of  $A = \frac{a+b}{2}$ , and  $w(A)$  = half width of  $A = \frac{a-b}{2}$ . or, an interval  $A = [a, b]$  is an equipossible fuzzy variable, whose membership function is given by  $\mu_1(x) = \begin{cases} 1, & \text{if } a \leq x \leq b \\ 0, & \text{otherwise.} \end{cases}$

A crisp real number  $k$  may be considered as a degenerate interval  $[k, k] = \langle k, 0 \rangle$ .

The sum of two interval numbers  $A = [a_1, b_1]$  and  $B = [a_2, b_2]$  is given by  $A \oplus B = [a_1 + a_2, a_2 + b_2]$ . Alternatively, in mean-width notations, if  $A = \langle m_1, w_1 \rangle$  and  $B = \langle m_2, w_2 \rangle$ , then  $A \oplus B = \langle m_1 + m_2, w_1 + w_2 \rangle$ .

In the following, we give the definition of *acceptability index* in connection with the ranking two intervals, due to Sengupta and Pal [11].

**Definition 1** The acceptability index ( $\mathcal{A}$ -index) of the proposition ‘ $A = \langle m_1, w_1 \rangle$  is preferred to  $B = \langle m_2, w_2 \rangle$ ’ is given by  $\mathcal{A}(A < B) = \frac{m_2 - m_1}{w_1 + w_2}$ .

Using this  $\mathcal{A}$ -index, we may define the following ranking orders.

**Definition 2** If  $\mathcal{A}(A < B) \geq 1$ , then  $A$  is said to be totally dominating over  $B$  in case of minimization, and the case is converse in case of maximization, and this is denoted by  $A < B$ .

**Definition 3** If  $0 < \mathcal{A}(A < B) < 1$ , then  $A$  is said to be ‘partially dominating’ over  $B$  in the sense of minimization and  $B$  is said to be ‘partially dominating’ over  $A$  in the sense of maximization. This is denoted by  $A <_P B$ .

A triangular fuzzy number is given by a triplet  $\tilde{A} = (a, b, c)$  with the membership function  $\mu_2(x) = \begin{cases} \frac{x-a}{b-a}, & \text{if } a \leq x \leq b \\ \frac{x-c}{b-c}, & \text{if } b \leq x \leq c \\ 0, & \text{otherwise.} \end{cases}$

i.e.,  $b$  is the point whose membership value is 1, and  $b - a$  and  $c - b$  are the left-hand and right-hand spreads, respectively.

In fuzzy optimization theory, the most important fuzzy ranking methods are based on the possibility and necessity measures. The possibility theory was proposed by Zadeh [12] and developed by many researchers such as Dubois and Prade [13]. Let  $\xi$  be a fuzzy variable with membership function  $\mu_\xi(x)$  and  $B$  be an arbitrary subset of  $R$ , then the possibility measure of fuzzy event  $\{\xi \in B\}$  is defined as  $\text{Pos}\{\xi \in B\} = \sup_{x \in B} \mu_\xi(x)$ . The necessity of this fuzzy event is defined as  $\text{Nec}\{\xi \in B\} = 1 - \text{Pos}\{\xi \in B^c\} = 1 - \sup_{x \in B^c} \mu_\xi(x)$ .

Liu [7] introduced the credibility measure of a fuzzy event as an average of the possibility and necessity measure as below.

**Definition 4** The credibility measure for the chance of a fuzzy event is defined as  $\text{Cr}\{\xi \in B\} = \frac{1}{2}(\text{Pos}\{\xi \in B\} + \text{Nec}\{\xi \in B\})$ .

Liu and Liu [8] show that the expected value of a fuzzy variable can be defined in terms of the credibility measure as follows.

**Definition 5** Let  $\xi$  be a fuzzy variable. The expected value of  $\xi$  is defined as  $E[\xi] = \int_0^\infty \text{Cr}\{\xi \geq r\}dr - \int_{-\infty}^0 \text{Cr}\{\xi \leq r\}dr$ , provided that at least one of the two integrals is finite.

But, in reality, most decision-makers are neither absolutely optimistic/ optimistic, nor absolutely neutral. To balance between the optimism and pessimism, a convex combination of the possibility measure, and the necessity measure is introduced by Yang and Iwamura [9]. It gives scope to the decision-maker to set the degree of optimism/ pessimism. Thus,  $m_\lambda$  measure is a generalization of the credibility measure.

**Definition 6** Formally, the  $m_\lambda$  measure for the chance of a fuzzy event is defined as  $m_\lambda\{\xi \in B\} = \lambda\text{Pos}\{\xi \in B\} + (1 - \lambda)\text{Nec}\{\xi \in B\}$ , where the parameter  $\lambda \in [0, 1]$  is predetermined by the decision-maker according to the degree of optimism or pessimism.

Clearly, when  $\lambda = 0.5$ , the  $m_\lambda$  measure reduces to the credibility measure. Based on the  $m_\lambda$  measure, the  $\lambda$ -expected value of a fuzzy variable is defined as follows [14]:

**Definition 7** Let  $\xi$  be a fuzzy variable. The  $\lambda$ -expected value of  $\xi$  is defined as,  $E_\lambda[\xi] = \int_0^\infty m_\lambda\{\xi \geq r\}dr - \int_{-\infty}^0 m_\lambda\{\xi \leq r\}dr$ , provided that at least one of the two integrals is finite, and the parameter  $\lambda \in [0, 1]$  is predetermined by the decision-maker according to the degree of optimism or pessimism.

*Example 1* Let  $\xi$  be the equipossible fuzzy variable  $(a, b)$ , i.e., the interval  $[a, b]$ , then the  $\lambda$ -expected value of  $\xi$  is given by  $E_\lambda[\xi] = \begin{cases} \lambda b + (1 - \lambda)a, & \text{if } a \geq 0 \\ \lambda(a + b), & \text{if } a < 0 < b \\ \lambda a + (1 - \lambda)b, & \text{if } b \leq 0. \end{cases}$

*Example 2* Let  $\eta$  be the triangular fuzzy variable  $(a, b, c)$ , then the  $\lambda$ -expected value

$$\text{of } \eta \text{ is given by } E_\lambda[\eta] = \begin{cases} \frac{a+b}{2} + \frac{\lambda}{2}(c-a), & \text{if } a \geq 0 \\ \frac{b^2 + \lambda(bc - ab - ac - a^2)}{2(b-a)}, & \text{if } a < 0 \leq b < c \\ \frac{b^2 + \lambda(ab - bc - ac - c^2)}{2(b-c)}, & \text{if } a < b \leq 0 < c \\ \frac{b+c}{2} - \frac{\lambda}{2}(c-a), & \text{if } c \leq 0. \end{cases}$$

Liou and Wang [15] considered an ordinance method of fuzzy numbers with integral values. This definition involves the areas relating to the left-hand spread and right-hand spread, and the index is the convex combination of those two.

*Remark 1* If  $\xi$  is a positive triangular fuzzy number, then the Liou and Wang index of  $\xi$  coincides with  $E_\lambda[\xi]$ .

It can be shown that the  $\lambda$ -expected value operator is linear as like the ordinary expected value operator.

**Lemma 1** *Let  $\xi$  and  $\eta$  be two independent fuzzy variables, then for any real numbers  $a$  and  $b$ , we have  $E_\lambda[a\xi + b\eta] = aE_\lambda[\xi] + bE_\lambda[\eta]$ .*

Using the  $\lambda$ -expected value operator, we can define the following functions to find the fuzzy minimum of two independent fuzzy variables.

**Definition 8** Let  $\xi$  and  $\eta$  be two independent fuzzy variables, then we say that the fuzzy minimum between  $\xi$  and  $\eta$  is  $\xi$  if  $E_\lambda[\xi] \leq E_\lambda[\eta]$  and denote this by ' $\xi \ll \eta$ '.

**Theorem 1** *Let  $A$  and  $B$  be two positive intervals, then  $A \ll B$  if  $A < B$ .*

*Proof* Let  $A = [a_1, b_1]$  and  $B = [a_2, b_2]$ , then  $A < B$  gives  $\frac{\frac{a_2+b_2}{2} - \frac{a_1+b_1}{2}}{\frac{b_1-a_1}{2} + \frac{b_2-a_2}{2}} \geq 1$ , i.e.,  $a_2 \geq b_1$ .

Now,  $E_\lambda[A] = a_1 + (b_1 - a_1)\lambda \leq a_1 + (b_1 - a_1)$  (since,  $\lambda \leq 1$ ) =  $b_1 \leq a_2 \leq a_2 + \lambda(b_2 - a_2)$  (since  $\lambda \geq 0$ ) =  $E_\lambda[B]$ .

Hence the theorem follows. □

**Theorem 2** *Let  $A = [a_1, b_1]$  and  $B = [a_2, b_2]$  be two positive intervals, then  $a_1 < a_2$  and  $w(A) \leq w(B)$  imply  $A <_P B$  and  $A \ll B$ .*

*Proof*  $w(A) \leq w(B)$  gives  $b_1 - a_1 < b_2 - a_2$ . So,  $a_1 < a_2$  and  $w(A) \leq w(B)$  together give  $b_1 < b_2$ . Thus,  $m(A) < m(B)$ , and hence,  $A <_P B$ .

Again,  $E_\lambda[A] = a_1 + \lambda(b_1 - a_1) < a_2 + \lambda(b_1 - a_1) \leq a_2 + \lambda(b_2 - a_2) = E_\lambda[B]$ , and hence,  $A \ll B$ . □

### 3 Expected Value Model of FSPP

Let us consider a directed network  $G = (V, E)$ , where  $V$  is the set of vertices and  $E$  is the set of arcs. Each arc is denoted by an ordered pair  $(i, j)$ , where  $i, j \in V$ . We consider that there is only one directed arc  $(i, j)$  from  $i$  to  $j$ . Let the node 1 be the source node and let us assume  $t$  as the destination node. We define a path  $p_{ij}$  as a sequence  $p_{ij} = \{i, (i, i_1), i_1, \dots, i_k, (i_k, j), j\}$  of alternating nodes and arcs. The existence of at least one path  $p_{si}$  in  $G = (V, E)$  is assumed for every node  $i \in V - \{s\}$ . Let  $\xi_{ij}$  be an imprecise number (either an interval or a triangular fuzzy number) associated with the arc  $(i, j)$ , corresponding to the length necessary to traverse  $(i, j)$  from  $i$  to  $j$ , then the FSPP is formulated as the following linear programming problem:

$$\begin{aligned} \min f(x) &= \sum_{(i,j) \in E} E_\lambda[\xi_{ij}]x_{ij} \\ \text{subject to } \sum_j x_{ij} - \sum_j x_{ji} &= \begin{cases} 1, & \text{if } i = 1 \\ 0, & \text{if } i \in \{1, 2, \dots, |V|\} \setminus \{1, t\} \\ -1 & \text{if } i = t, \end{cases} \\ &x_{ij} = 0 \text{ or } 1, \text{ for } (i, j) \in E. \end{aligned}$$

To solve this expected value model of FSPP, we replace each  $\xi_{ij}, (i, j) \in E$  with the corresponding  $\lambda$ -expected value  $E_\lambda[\xi_{ij}]$  and then we apply the classical shortest path algorithms, like that of Dijkstra [10]. We illustrate this with the help of the following examples.

*Example 3* We consider a small-sized network as shown in Fig. 1 having mixed arc lengths with four nodes and five arcs, of which two arcs are of triangular fuzzy length and the other three are of interval length.  $\lambda$ -expected values of the arc lengths for different  $\lambda$  are listed in Table 1. Different fuzzy shortest paths obtained for different  $\lambda$  are shown in Table 2.

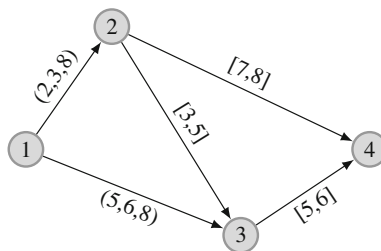


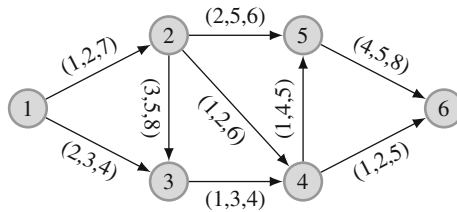
Fig. 1 A small-sized network

**Table 1** Arc lengths and expected values

Arc	Length	$\lambda$ -expected value		
		$\lambda = 0.25$	$\lambda = 0.50$	$\lambda = 0.75$
(1, 2)	(2, 3, 8)	3.25	4.00	4.75
(1, 3)	(5, 6, 8)	5.88	6.25	6.63
(2, 3)	[3, 5]	3.50	4.00	4.50
(2, 4)	[7, 8]	7.25	7.50	7.75
(3, 4)	[5, 6]	5.25	5.50	5.75

**Table 2** Different fuzzy shortest paths of the network in Fig 1

$\lambda$	Path	Expected length
0.25	1 $\rightarrow$ 2 $\rightarrow$ 4	10.50
0.50	1 $\rightarrow$ 2 $\rightarrow$ 4	11.50
0.75	1 $\rightarrow$ 3 $\rightarrow$ 4	12.38



**Fig. 2** Another network

*Remark 2* It is evident that, as  $\lambda$  increases, the expected length of the FSPP is also increased. So, in a maximization problem,  $\lambda$  would be considered as an index of optimism, whereas in case of minimization, it would be considered as an index of pessimism.

*Example 4* For the sake of a comparative study, we consider the network shown in Fig. 2 with same arc lengths as considered by Tajdin et al. [6]. Using our method, we get the FSPP 1  $\rightarrow$  2  $\rightarrow$  4  $\rightarrow$  6 for  $\lambda < 0.5$ , and the FSPP 1  $\rightarrow$  3  $\rightarrow$  4  $\rightarrow$  6 for  $\lambda > 0.5$ . For  $\lambda = 0.5$ , there is tie between those two FSPP with the expected length 8.25. The FSPP 1  $\rightarrow$  3  $\rightarrow$  4  $\rightarrow$  6 has the  $\lambda$ -expected value 5.93 (the distance value obtained by Tajdin et al.) for  $\lambda = 0.19$ , which clearly reflects a highly optimistic view of the decision-maker.

### 4 Conclusion

In this chapter, we have considered the fuzzy shortest path problem on a network with mixed arc lengths. Replacing each imprecise arc length by the corresponding  $\lambda$ -expected value, we may apply the Dijkstra’s algorithm to solve the problem. If

some of the arc lengths are crisp real numbers, then also the method works. It is also worth mentioning that instead of Dijkstra's algorithm, if we use Ford-Moore-Bellman's algorithm [16], then the presence of a negative circuit can be detected, since the  $\lambda$ -expected value of negative intervals or negative triangular fuzzy numbers can also be computed.

## References

1. Klein, C.M.: Fuzzy shortest paths. *Fuzzy Sets and System* **39**, 27–41 (1991)
2. Okada, S., Gen, M.: Order relation between intervals and its application to shortest path problem. *Comput. Ind. Eng.* **25**, 147–150 (1993)
3. Okada, S., Gen, M.: Fuzzy shortest path problem. *Comput. Ind. Eng.* **27**, 465–468 (1994)
4. Nayeem, S.M.A., Pal, M.: Shortest path problem on a network with imprecise edge weight. *Fuzzy Optim. Decis. Making* **4**, 293–312 (2005)
5. Hernandez, F., Lamata, M.T., Verdegay, J.L., Yamakami, A.: The shortest path problem on networks with fuzzy parameters. *Fuzzy Sets and Syst.* **158**, 1561–1570 (2007)
6. Tajdin, A., Mahdavi, I., Mahdavi-Amiri, N., Sadeghpour-Gildeh, B.: Computing a fuzzy shortest path in a network with mixed fuzzy arc lengths using  $\alpha$ -cuts. *Comput. Math. Appl.* **60**, 989–1002 (2010)
7. Liu, B.: *Theory and Practice of Uncertain Programming*. Physica-Verlag, Heidelberg (2002)
8. Liu, B.: *Uncertainty theory: An introduction to its axiomatic foundations*. Springer-Verlag, Berlin (2004)
9. Yang, L., Iwamura, K.: Fuzzy chance-constrained programming with linear combination of possibility measure and necessity measure. *Appl. Math. Sci.* **2**, 2271–2288 (2008)
10. Dijkstra, E.W.: A note on two problems in connection with graphs. *Numerische Mathematik* **1**, 269–271 (1959)
11. Sengupta, A., Pal, T.K.: On comparing interval numbers. *Eur. J. Oper. Res.* **127**, 28–43 (2000)
12. Zadeh, L.A.: Fuzzy sets as a basis for a theory of possibility. *Fuzzy Sets and Syst.* **1**, 3–28 (1978)
13. Dubois, D., Prade, H.: *Possibility theory*. Plenum, New York (1988)
14. Nayeem, S.M.A.: An expected value model of quadratic clique problem on a graph with fuzzy parameters. *Proceedings of 12th international conference on intelligent systems design and applications (ISDA)*, Kochi, India, (to appear).
15. Liou, T.-S., Wang, M.-J.: Ranking fuzzy numbers with integral interval. *Fuzzy Sets and Syst.* **50**, 247–255 (1992)
16. Bellman, R.E.: On a routing problem. *Quart. Appl. Math.* **16**, 87–90 (1958)

# Existence and Uniqueness of Fixed Point in Fuzzy Metric Spaces and its Applications

Vishal Gupta and Naveen Mani

**Abstract** The main aim of this paper is to prove some fixed point theorems in fuzzy metric spaces through rational inequality. Our results extend and generalize the results of many other authors existing in the literature. Some applications are also given in support of our results.

**Keywords** Fuzzy metric space · Rational expression · Integral type · Control function

## 1 Introduction

The foundation of fuzzy mathematics is laid by Zadeh [1] with the introduction of fuzzy sets in 1965. This foundation represents a vagueness in everyday life. Subsequently, several authors have applied various form general topology of fuzzy sets and developed the concept of fuzzy space. In 1975, Kramosil and Michalek [2] introduced concept of fuzzy metric spaces. In 1988, Mariusz Grabiec [3] extended fixed point theorem of Banach and Eldestien to fuzzy metric spaces in the sense of Kramosil and Michalek. In 1994, George et al. [4] modified the notion of fuzzy metric spaces with the help of continuous t-norms. A number of fixed point theorems have been obtained by various authors in fuzzy metric space by using the concept of compatible map, implicit relation, weakly compatible map, R weakly compatible map. (See Section-: [5–13]). Also Saini and Gupta [10, 11] proved some fixed points theorems, on expansion type maps and common coincidence points of

---

V. Gupta (✉) · N. Mani  
Department of Mathematics, Maharishi Markandeshwar University, Mullana  
Ambala, Haryana 133001, India  
e-mail: vishal.gmn@gmail.com  
N. Mani  
e-mail: naveenmani81@gmail.com



R weakly commuting fuzzy maps, in fuzzy metric space. The present paper extends and generalizes the results of Grabeic [3] and also many other authors existing in the literature.

## 2 Preliminaries

In this section, we define some important definition and results which are used in sequel.

**Definition 1** [1] Let  $X$  be any set. A fuzzy set  $A$  in  $X$  is a function with domain  $X$  and values in  $[0, 1]$ .

**Definition 2** [14] A binary operation  $*$  :  $[0, 1] \times [0, 1] \rightarrow [0, 1]$  is a continuous t-norms if  $([0, 1], *)$  is an abelian topological monoid with the unit 1 such that  $a * b \leq c * d$  whenever  $a \leq c$  and  $b \leq d$  for all  $a, b, c, d \in [0, 1]$ .

**Definition 3** [2] A triplet  $(X, M, *)$  is a fuzzy metric space if  $X$  is an arbitrary set,  $*$  is continuous t-norm and  $M$  is a fuzzy set on  $X^2 \times (0, \infty)$  satisfying the following conditions, for all  $x, y, z \in X$ , such that  $t, s \in (0, \infty)$

1.  $M(x, y, t) > 0$ .
2.  $M(x, y, t) = 1$  iff  $x = y$ .
3.  $M(x, y, t) = M(y, x, t)$ .
4.  $M(x, y, t) * M(y, z, s) \leq M(x, z, t + s)$ .
5.  $M(x, y, \cdot) : [0, \infty) \rightarrow [0, 1]$  is continuous.

Then,  $M$  is called a fuzzy metric on  $X$ , and  $M(x, y, t)$  denotes the degree of nearness between  $x$  and  $y$  with respect to  $t$ .

**Definition 4** [3] Let  $(X, M, *)$  is a fuzzy metric space then a sequence  $\{x_n\} \in X$  is said to be convergent to a point  $x \in X$  if  $\lim_{n \rightarrow \infty} M(x_n, x, t) = 1$  for all  $t > 0$ .

**Definition 5** [3] Let  $(X, M, *)$  is a fuzzy metric space then a sequence  $\{x_n\} \in X$  is called a Cauchy sequence if  $\lim_{n \rightarrow \infty} M(x_{n+p}, x_n, t) = 1$  for all  $t > 0$  and  $p > 0$ .

**Definition 6** [3] Let  $(X, M, *)$  is a fuzzy metric space then an fuzzy metric space in which every Cauchy sequence is convergent is called complete. It is called compact, if every sequence contains a convergent subsequence.

**Lemma 1** [3] For all,  $x, y \in X$ ,  $M(x, y, \cdot)$  is non-decreasing.

**Lemma 2** [9] If there exist  $k \in (0, 1)$  such that  $M(x, y, kt) \geq M(x, y, t)$  for all  $x, y, \in X$  and  $t \in (0, \infty)$ , then  $x = y$

Now, we prove our main result.

### 3 Main Results

**Theorem 1** *Let  $(X, M, *)$  be a complete fuzzy metric space and  $f : X \rightarrow X$  be a mapping satisfying*

$$M(x, y, t) = 1 \tag{1}$$

and

$$M(fx, fy, kt) \geq \lambda(x, y, t) \tag{2}$$

where

$$\lambda(x, y, t) = \min \left\{ \frac{M(x, fx, t) M(y, fy, t)}{M(x, y, t)}, M(x, y, t) \right\} \tag{3}$$

for all  $x, y, \in X$  and  $k \in (0, 1)$ . Then  $f$  has a unique fixed point.

*Proof* Let us consider  $x \in X$  be any arbitrary point in  $X$ . Now construct a sequence  $\{x_n\} \in X$  such that  $fx_n = x_{n+1}$  for all  $n \in N$

**Claim:**  $\{x_n\}$  is a Cauchy sequence.

Let us take  $x = x_{n-1}$  and  $y = x_n$  in (2), we get

$$M(x_n, x_{n+1}, kt) = M(fx_{n-1}, fx_n, kt) \geq \lambda(x_{n-1}, x_n, t) \tag{4}$$

Now

$$\begin{aligned} \lambda(x_{n-1}, x_n, t) &= \min \left\{ \frac{M(x_{n-1}, x_n, t) M(x_n, x_{n+1}, t)}{M(x_{n-1}, x_n, t)}, M(x_{n-1}, x_n, t) \right\} \\ &= \min \{M(x_n, x_{n+1}, t), M(x_{n-1}, x_n, t)\} \end{aligned}$$

Now if  $M(x_n, x_{n+1}, t) \leq M(x_{n-1}, x_n, t)$ , then from Eq. (4)

$$M(x_n, x_{n+1}, kt) \geq M(x_n, x_{n+1}, t)$$

Thus, our claim is immediately follows. Now suppose  $M(x_n, x_{n+1}, t) \geq M(x_{n-1}, x_n, t)$  then again from Eq. (4),

$$M(x_n, x_{n+1}, kt) \geq M(x_{n-1}, x_n, t)$$

Now by simple induction, for all  $n$  and  $t > 0$ , we get

$$M(x_n, x_{n+1}, kt) \geq M\left(x, x_1, \frac{t}{k^{n-1}}\right) \tag{5}$$

Now for any positive integer  $q$ , we have

$$M(x_n, x_{n+q}, t) \geq M\left(x_n, x_{n+1}, \frac{t}{q}\right) * \dots^{(q)} \dots * M\left(x_{n+p-1}, x_{n+p}, \frac{t}{q}\right)$$

By using Eq. (5), we get

$$M(x_n, x_{n+q}, t) \geq M\left(x, x_1, \frac{t}{qk^n}\right) * \dots^{(q)} \dots * M\left(x, x_1, \frac{t}{qk^n}\right)$$

Now taking  $\lim_{n \rightarrow \infty}$  and using (1), we get

$$\lim_{n \rightarrow \infty} M(x_n, x_{n+q}, t) = 1 \tag{6}$$

This implies,  $\{x_n\}$  is a Cauchy sequence. Call the limit  $z$ .

**Claim:**  $z$  is a fixed point of  $f$ .

Consider

$$M(fz, z, t) \geq M(fz, fx_n, t) * M(x_{n+1}, z_n, t) \geq \lambda\left(z, x_n, \frac{t}{2k}\right) * M(x_{n+1}, z_n, t) \tag{7}$$

Now

$$\lambda\left(z, x_n, \frac{t}{2k}\right) = \min\left\{\frac{M\left(z, fz, \frac{t}{2k}\right) M\left(x_n, fx_n, \frac{t}{2k}\right)}{M\left(z, x_n, \frac{t}{2k}\right)}, M\left(z, x_n, \frac{t}{2k}\right)\right\}$$

Taking  $\lim_{n \rightarrow \infty}$  in above inequality and using (1), we get

$$\lambda\left(z, z, \frac{t}{2k}\right) = \min\left\{M\left(z, fz, \frac{t}{2k}\right), 1\right\}$$

Now if  $M\left(z, fz, \frac{t}{2k}\right) \geq 1$  then  $\lambda\left(z, z, \frac{t}{2k}\right) = 1$ . Therefore, from (7) and using Definition 3, we get  $z$  is a fixed point of  $f$ . Now if  $M\left(z, fz, \frac{t}{2k}\right) \leq 1$ , then  $\lambda\left(z, z, \frac{t}{2k}\right) = M\left(z, fz, \frac{t}{2k}\right)$  Hence, from Eq. (7), we get

$$M(fz, z, t) \geq M\left(z, fz, \frac{t}{2k}\right) * M(x_{n+1}, z_n, t) \tag{8}$$

Now taking  $\lim_{n \rightarrow \infty}$  in (8) and using lemma 2, we get  $fz = z$ . That is  $z$  is a fixed point of  $f$ .

**Uniqueness:** Now, we show that  $z$  is a unique fixed point of  $f$ . Suppose not, then there exist a point  $v \in X$  such that  $fv = v$ . Consider

$$1 \geq M(z, v, t) = M(fz, fv, t) \geq \lambda\left(z, v, \frac{t}{k}\right) \geq M\left(fz, fv, \frac{t}{k}\right) \tag{9}$$

Again

$$M\left(fz, fv, \frac{t}{k}\right) \geq M\left(fz, fv, \frac{t}{k^2}\right) \geq \dots \geq M\left(fz, fv, \frac{t}{k^n}\right) \tag{10}$$

Taking  $\lim_{n \rightarrow \infty}$  in (10) and use it in (9), we get  $z = v$ . Thus,  $z$  is unique fixed point of  $f$ . This completes the proof of Theorem 1. □

let us define  $\Phi = \{\phi/\phi : [0, 1] \rightarrow [0, 1]\}$  is a continuous function such that  $\phi(1) = 1, \phi(0) = 0, \phi(a) > a$  for each  $0 < a < 1$ .

**Theorem 2** *Let  $(X, M, *)$  be a complete fuzzy metric space and  $f : X \rightarrow X$  be a mapping satisfying*

$$M(x, y, t) = 1 \tag{11}$$

and

$$M(fx, fy, kt) \geq \phi\{\lambda(x, y, t)\} \tag{12}$$

where

$$\lambda(x, y, t) = \min\left\{\frac{M(x, fx, t)M(y, fy, t)}{M(x, y, t)}, M(x, y, t)\right\} \tag{13}$$

for all  $x, y, \in X, k \in (0, 1), \phi \in \Phi$ . Then,  $f$  has a unique fixed point.

*Proof* Since  $\phi \in \Phi$ , this implies that  $\phi(a) > a$  for each  $0 < a < 1$ . Thus, from (12)

$$M(fx, fy, kt) \geq \phi\{\lambda(x, y, t)\} \geq \lambda(x, y, t)$$

Now, applying Theorem 1, we obtain the desired result. □

### 4 Applications

In this section, we give some applications related to our results. Let us define  $\Psi : [0, \infty) \rightarrow [0, \infty)$ , as  $\Psi(t) = \int_0^t \varphi(t) dt \quad \forall t > 0$ , be a non-decreasing and continuous function. Moreover, for each  $\epsilon > 0, \varphi(\epsilon) > 0$ . Also implies that  $\varphi(t) = 0$  iff  $t = 0$ .

**Theorem 3** *Let  $(X, M, *)$  be a complete fuzzy metric space and  $f : X \rightarrow X$  be a mapping satisfying*

$$M(x, y, t) = 1$$

$$\int_0^{M(fx, fy, kt)} \varphi(t) dt \geq \int_0^{\lambda(x, y, t)} \varphi(t) dt$$

where

$$\lambda(x, y, t) = \min \left\{ \frac{M(x, fx, t) M(y, fy, t)}{M(x, y, t)}, M(x, y, t) \right\}$$

for all  $x, y, \in X, \varphi \in \Psi$  and  $k \in (0, 1)$ . Then,  $f$  has a unique fixed point.

*Proof* By taking  $\varphi(t) = 1$  and applying Theorem 1, we obtain the result. □

**Theorem 4** Let  $(X, M, *)$  be a complete fuzzy metric space and  $f : X \rightarrow X$  be a mapping satisfying

$$M(x, y, t) = 1$$

$$\int_0^{M(fx, fy, kt)} \varphi(t) dt \geq \phi \left\{ \int_0^{\lambda(x, y, t)} \varphi(t) dt \right\}$$

where

$$\lambda(x, y, t) = \min \left\{ \frac{M(x, fx, t) M(y, fy, t)}{M(x, y, t)}, M(x, y, t) \right\}$$

for all  $x, y, \in X \varphi \in \Psi, k \in (0, 1)$  and  $\phi \in \Phi$ . Then,  $f$  has a unique fixed point. Then,  $f$  has a unique fixed point.

*Proof* Since  $\phi(a) > a$  for each  $0 < a < 1$ , therefore, result follows immediately from Theorem 3. □

*Remark 1* Our paper extends and generalizes the result of Grabeic [3] and also many other authors existing in the literature.

**Acknowledgments** The authors would like to express their sincere appreciation to the referees for their helpful suggestions and many kind comment.

## References

1. Zadeh, L.A.: Fuzzy sets. Inform. Control **8**, 338–353 (1965)
2. Kramosil, O., Michalek, J.: Fuzzy metric and statistical metric spaces. Kybernetika **11**, 326–334 (1975)
3. Grabeic, M.: Fixed points in fuzzy metric spaces. Fuzzy Sets Syst. **27**, 385–389 (1988)
4. George, A., Veermani, P.: On some results in fuzzy metric spaces. Fuzzy Sets Syst. **64**, 395–399 (1994)
5. Balasubramaniam, P., Murlisankar, S., Pant, R.P.: Common fixed points of four mappings in a fuzzy metric space. J. Fuzzy Math. **10**(2), 379–384 (2002)
6. Cho, S.H.: On common fixed point theorems in fuzzy metric spaces. Int. Math. Forum **1**(9–12), 471–479 (2006)
7. Cho, Y.J., Sedghi, S., Shobe, N.: Generalized fixed point theorems for compatible mappings with some types in fuzzy metric spaces. Chaos, Solitons and Fractals **39**, 2233–2244 (2009)

8. Gregori, V., Sapena, A.: On fixed point theorems in fuzzy metric spaces. *Fuzzy Sets Syst.* **125**, 245–252 (2002)
9. Mishra, S.N., Sharma, S.N., Singh, S.L.: Common fixed point of maps on fuzzy metric spaces. *Internat. J. Math. Sci.* **17**, 253–258 (1994)
10. Saini, R.K., Gupta, V.: Common coincidence points of R-Weakly commuting fuzzy maps, *thai journal of mathematics, mathematical assoc. of Thailand*, 6(1):109–115, (2008) ISSN 1686–0209.
11. Saini, R.K., Gupta, V.: Fuzzy version of some fixed points theorems on expansion type maps in fuzzy metric space. *Thai J. Math., Math. Assoc. Thailand* **5**(2), 245–252 (2007). ISSN 1686–0209
12. Vasuki, R.: A common fixed point theorem in a fuzzy metric space. *Fuzzy Sets and Syst.* **97**, 395–397 (1998)
13. Vasuki, R.: Common fixed point for R-weakly commuting maps in fuzzy metric space. *Indian J. Pure. Appl. Math.* **30**, 419–423 (1999)
14. Schweizer, B., Sklar, A.: Probabilistic metric spaces, North-Holland series in probability and applied mathematics. North-Holland Publishing Co., New York (1983), ISBN: 0-444-00666-4 MR0790314 (86g:54045).

# Variable Selection and Fault Detection Using a Hybrid Intelligent Water Drop Algorithm

Manish Kumar, Srikant Jayaraman, Shikha Bhat, Shameek Ghosh  
and V. K. Jayaraman

**Abstract** Process fault detection concerns itself with monitoring process variables and identifying when a fault has occurred in the process workflow. Sophisticated learning algorithms may be used to select the relevant process state variables out of a massive search space and can be used to build more efficient and robust fault detection models. In this study, we present a recently proposed swarm intelligence-based hybrid intelligent water drop (IWD) optimization algorithm in combination with support vector machines and an information gain heuristic for selecting a subset of relevant fault indicators. In the process, we demonstrate the successful application and effectiveness of this swarm intelligence-based method to variable selection and fault identification. Moreover, performance testing on standard machine learning benchmark datasets also indicates its viability as a strong candidate for complex classification and prediction tasks.

---

M. Kumar  
Bioinformatics Center, University of Pune, Pune, India  
e-mail: rishimanish123@gmail.com

S. Jayaraman · S. Bhat  
Centre for Modelling and Simulation, University of Pune, Pune, India  
e-mail: srikant@cms.unipune.ac.in

S. Bhat  
e-mail: shikha@cms.unipune.ac.in

S. Ghosh · V. K. Jayaraman (✉)  
Evolutionary Computing and Image Processing, Centre for Development of Advanced Computing, Pune, India  
e-mail: jayaramanv@cdac.in

S. Ghosh  
e-mail: shameekg@cdac.in

V. K. Jayaraman  
Informatics Centre, Shiv Nadar University, Chithera Village, Dadri District, UP, India

**Keywords** Fault detection · Swarm intelligence · Intelligent water drop optimization · Information gain · Support vector machines

## 1 Introduction

Fault detection and isolation are associated with monitoring a process and identifying when a fault may occur [1, 2]. Generally, a large set of sensor readings may be collected over a long period of time by a process monitoring module. As part of this process, a system can inject faults into the process by random variation of variable measures. A log of all such process data may thus be treated as a training dataset by a learning algorithm for building fault prediction models. However, a limitation of this technique is that it generates a vast amount of complex data. Constructing classification models from such data thus turns out to be very tedious and the resulting model is normally quite inferior due to inclusion of irrelevant and redundant variables in the model. To get around this problem, we can select a small subset of relevant variables from the data. This process is known as variable selection and it helps in reducing the computational load and in increasing the overall classification performance.

Variable selection algorithms may typically be categorized as: wrappers and filters. Wrappers [3–5] use a learning algorithm to estimate the suitability of a subset of variables. In contrast, filters evaluate the capability of a variable considering their inherent characteristics using techniques based on statistical tests and mutual information.

In the following study, we present a recently proposed swarm intelligence-based learning technique known as intelligent water drop (IWD) optimization [6] in conjunction with an entropy-based heuristic ranking and support vector machines as a filter-wrapper algorithm for variable subset selection and simultaneous fault detection.

## 2 Intelligent Water Drop Algorithm

Natural phenomena are a huge source of inspiration for building swarm intelligence-based techniques. A particular instance of a natural process is found in the optimal selection of path by flowing water sources, while converging to a bigger source of water, say a sea or an ocean. The paths followed by rivers exemplify this nature. At a finer level, the flowing water is basically built up of a swarm of natural water drops. The behaviour of a single water drop thus turns to be of significant importance in the construction and movement of a swarm of water drops. Shah-Hosseini, consequently, extended this concept to introduce the IWD algorithm for the travelling salesman problem (TSP) [6].



The IWD algorithm involves employing a swarm of IWDs characterized by two important properties. These are (1) the IWD's soil content denoted as  $soil(IWD)$  and (2) the velocity of an IWD denoted by  $vel(IWD)$ . The  $soil(IWD)$  and  $vel(IWD)$  dynamically keep changing based on the path taken by an IWD while flowing through the problem landscape. It is thus pertinent that as an IWD moves, it removes soil from the traversed path and the path soil is also updated dynamically in the process. This joint action may thus contribute to lowering of soil content of certain routes in the problem environment which is associated with the fitness landscape. It has been consequently posited that the paths with lesser soil content are thus the most important for the search of a near optimal solution. The emergent behaviour of a swarm of IWDs therefore governs the construction of an optimal solution for the concerned problem.

Accordingly, when an IWD moves in discrete time steps from its current location  $i$  to its next location  $j$ , the IWD velocity is increased by a  $\Delta vel$  component which is given by

$$\Delta vel^{IWD}(t) = \frac{a_v}{b_v + c_v \times soil^{2\alpha}(i, j)} \quad (1)$$

Here,  $a_v$ ,  $b_v$ ,  $c_v$ , and  $\alpha$  are algorithm specific parameters. Similarly the soil content of an IWD is also increased by a  $\Delta soil$  given as

$$\Delta soil(i, j) = \frac{a_s}{b_s + c_s \times time^{2\theta}(i, j)} \quad (2)$$

Here,  $\Delta soil$  indicates the soil content removed by the IWD while moving from location  $i$  to  $j$ .  $time^{2\theta}(i, j)$  denotes the amount of time required for the IWD to move from  $i$  to  $j$  which is given as

$$time(i, j) = \frac{HUD(i, j)}{vel(IWD)} \quad (3)$$

HUD is characterized as a heuristic function which can be used to measure the undesirability of an IWD to select a path from  $i$  to  $j$ .

Once the IWD properties are updated, the soil content of the concerned solution paths also need to be updated which is possible by following-

$$soil(i, j) = \rho_o \times soil(i, j) - \rho_n \times \Delta soil(i, j) \quad (4)$$

where  $\rho_o$  and  $\rho_n$  are between 0 and 1. According to the original IWD algorithm for the TSP,  $\rho_o = 1 - \rho_n$ .

The most important behavioural characteristic of an IWD lies in its probabilistic selection of a partial solution component where the transition function is given by

$$P(i, j) = \frac{f(soil(i, j))}{\sum_{k \text{ is unvisited}} f(soil(i, k))} \quad (5)$$

$$f(\text{soil}(i, j)) = \frac{1}{\varepsilon + g(\text{soil}(i, j))} \quad (6)$$

$$g(\text{soil}(i, j)) = \begin{cases} \text{soil}(i, j) & \text{if } \text{minsoil} \geq 0 \\ \text{soil}(i, j) - \text{minsoil} & \text{if } \text{minsoil} < 0 \end{cases} \quad (7)$$

Here, *minsoil* indicates the least soil available on a path between any location *i* and *j*. As illustrated in Eqs. (5–7), the transition probability of an IWD is thus proportional to the soil content available in a path between component *i* and *j*. Thus, the lower the soil content of a path, the more the probability of selection of the corresponding solution component.

A discussion of the IWD algorithm for the simultaneous variable selection and fault detection problem is provided in the next section.

### 3 Hybrid IWD-Based Variable Selection and Fault Detection

The IWD algorithm had earlier been used for solving a variety of discrete combinatorial optimization problems, viz. TSP [6], vehicle routing [7], robot path planning [8]. For the variable selection problem, a solution may be represented as a set of variable indices [4, 5]. For example, if the fault detection dataset is composed of 100 variables/attributes, then a possible solution could be a variable subset comprising of {10, 21, 32, 57, 84} with subset size as 5. Any variable index could thus be a part of the complete solution vector, where the vector size is specified by the user.

Therefore, we initially position each IWD randomly on different variables, from where they commence their flow. Each IWD moves to the next variable by employing the transition probability given by Eq. 5. Once a variable has been visited, a local soil update between variables *i* and *j* are performed by Eq. 4 as mentioned before. This process, continues till a complete solution vector is constructed by the IWD, updating the path soil content, the IWD soil and velocity in the process. When a variable subset of the required size is obtained, a corresponding reduced dataset with the given variables is generated. The reduced dataset is thus fed as input to a classifier like SVM [9], which reports back a 10-fold classification cross-validation accuracy (10-fold CVA). The 10-fold CVA is assigned as the fitness function value for the corresponding variable subset. Subsequent IWDs also build up their solution vectors in a similar manner.

At the end of one iteration, the solution vector with the maximum 10-fold CVA is selected as the iteration-best solution ( $T_{IB}$ ). Subsequently, a certain amount of soil on the edges of the iteration-best solution is decreased based on the quality of the solution. For example, if  $T_{IB}$  is given as (5, 11, 18, 21, 76), then the edges to be updated are 5–11, 11–18, 18–21 and 21–27. This can be done according to Eq. 8.

$$\text{soil}(i, j) = \rho_s \times \text{soil}(i, j) - \rho^{\text{IWD}} \times \frac{1}{(N_{\text{IB}} - 1)} \times \text{soil}_{\text{IB}}^{\text{IWD}} \quad (8)$$

where  $\text{soil}_{\text{IB}}^{\text{IWD}}$  represents the soil of the iteration-best IWD.  $N_{\text{IB}}$  is the number of variables in the solution vector  $T_{\text{IB}}$ .  $\rho^{\text{IWD}}$  is the global soil updating parameter, which may be selected from  $[0, 1]$ .  $\rho_s$  is normally set as  $(1 + \rho^{\text{IWD}})$ .

In addition, we also maintain a global best solution which is given by the maximum of all the iteration-best solutions. The above process is thus repeated till a termination criterion is reached. At this stage, the global best solution is reported as the most optimal solution to the variable selection problem.

### 3.1 Information-Gain-Based Heuristic Function

Owing to a massive search space, it might be advantageous and useful to incorporate additional intelligent information in the form of a variable ranking. We thus employ the information gain (IG) filter as heuristic ranking in the computation of time taken by an IWD (Eq. 3) to move from location  $i$  to  $j$  as given in (Eq. 9).

$$\text{time}(i, j) = \frac{1}{\text{Infogain}(j) + \text{vel}(\text{IWD})} \quad (9)$$

IG records the ‘information content’ of a variable in correlation to the class label for the problem under consideration. So, a higher IG value (corresponding to a relevant variable) aids in minimizing the time taken to traverse from  $i$  to  $j$  and consequently initiating increased soil removal from the corresponding path given by  $\Delta\text{soil}(i, j)$  in Eq. (2). IG thus greatly helps in faster convergence by probabilistically favouring soil updates to higher-ranked variables.

## 4 Results and Discussion

The IWD algorithm has been used to solve the problem of fault detection in the benchmark tennessee eastman process (TEP) [2, 10, 11]. There are 51 variables in the system comprising different pressures, temperatures, etc. monitored over a certain period of time. The data dimensions, variability and dynamics of the process add to the complexity of constructing an efficient classification model. Earlier, several methods have been suggested to solve this problem [2, 10, 11]. We approach this problem typically as a joint subset selection and classification problem by first obtaining an optimal variable subset of a much reduced size and then using SVM to build a binary fault classification model. The faults considered in this case are due to the step in D feed temperature and reactor cooling water inlet temperature as given in [12]. In addition to fault detection, we also considered the ionosphere (34 features) and the

**Table 1** Algorithm parameters

Parameters	Values
Number of IWDs	25
Number of iterations	30
$\rho_0, \varepsilon$	0.1, 0.5

**Table 2** 10-fold cross-validation results

Dataset	SVM	Infogain-SVM	Hybrid IWD
Fault detection	80.89	78.23(15)	92.02(15)
Ionosphere	95.60	95.44(15)	96.86(15)
Wisconsin breast cancer	95.76	94.90(15)	95.95(15)

Wisconsin breast cancer (32 features) datasets for performance benchmarking [13]. The parameters of the hybrid IWD algorithm are as given in Table 1.

We carried out numerous simulations for all cases before arriving at the estimates provided in Table 2. The subset sizes are reported in brackets.

Based on the results, we can infer that the hybrid IWD filter–wrapper technique is clearly more powerful in the selection of important fault detection variables. In contrast, the base SVM without any variable selection and with a filter solely does not help to get the best performances for classification.

## 5 Conclusion

The IWD algorithm utilizes both filter and wrapper methods to obtain smaller informative subset of variables important for fault detection. The information gain heuristic also provided more possibilities for an effective search space exploration that seems to have helped in the selection of important variables. The algorithm is also simple to implement, flexible and robust since we can adapt it to a given problem and related domain constraints.

**Acknowledgments** VKJ gratefully acknowledges the Council for Scientific and Industrial Research (CSIR) and Department of Science and Technology (DST), New Delhi, India, for financial support in the form of Emeritus Scientist Grant. The authors also acknowledge the Centre for Modeling and Simulation, University of Pune and C-DAC, Pune, for their kind support.

## References

1. Kulkarni, A.J., Jayaraman, V.K., Kulkarni, B.D.: Support vector classification with parameter tuning assisted by agent based technique. *Comput. Chem. Eng.* **28**, 311–318 (2004)

2. Downs, J.J., Vogel, E.F.: A plant-wide industrial-process control problem. *Comput. Chem. Eng.* **17**, 245–255 (1993)
3. John, G.H., Kohavi, R., Pfleger, K.: Irrelevant features and the subset selection problem. *Proceedings of the Eleventh International Conference on Machine Learning*. 121–129(1994).
4. Gupta A., Jayaraman V. K., Kulkarni. B. D.: Feature selection for cancer classification using ant colony optimization and support vector machines. In *Analysis of Biological Data : A Soft Computing Approach*. ser. World Scientific, Singapore. 259–280(2006).
5. Nikumbh S., Ghosh S., Jayaraman V. K.: Biogeography-Based Informative Gene Selection and Cancer Classification Using SVM and Random Forests. In *Proceedings of IEEE World Congress on Computational Intelligence (IEEE WCCI 2012)*. 187–192(2012).
6. Hosseini, H.S.: The intelligent water drops algorithm: a nature-inspired swarm-based optimization algorithm. *International Journal of Bio-Inspired Computation* **1**, 71–79 (2009)
7. Kamkar, I.: Intelligent water drops a new optimization algorithm for solving the Vehicle Routing Problem, pp. 4142–4146. In *Proceedings of IEEE International Conference on Systems Man and Cybernetics* (2010).
8. Haibin, D., Liu S., Lei, X.: Air robot path planning based on Intelligent Water Drops optimization. In *Proceedings of IEEE World Congress on Computational Intelligence*. 1397–1401(2008).
9. Boser, B.E., Guyon, I.M., Vapnik, V. N.: A training algorithm for optimal margin classifiers. In *Proceedings of the fifth annual workshop on Computational learning theory*, ser. COLT '92. 144–152(1992).
10. Lyman, P.R., Georgakis, C.: Plant-wide control of the Tennessee Eastman problem. *Comput. Chem. Eng.* **19**, 321–331 (1995)
11. Kulkarni, A., Jayaraman, V.K., Kulkarni, B.D., et al.: Knowledge incorporated support vector machines to detect faults in Tennessee Eastman Process. *Comput. Chem. Eng.* **29**, 2128–2133 (2005)
12. Ricker, N.L.: Tennessee Eastman Challenge Archive <http://depts.washington.edu/control/LARRY/TE/download.html>
13. UCI Repository <http://archive.ics.uci.edu/ml/>

# Air Conditioning System with Fuzzy Logic and Neuro-Fuzzy Algorithm

Rajani Kumari, Sandeep Kumar and Vivek Kumar Sharma

**Abstract** Fuzzy logic controls and neuro-fuzzy controls are accustomed to increase the performance of air conditioning system. In this paper, we are trying to provide the new design air conditioning system by exploitation two logics, namely fuzzy logic and neuro-fuzzy management. This paper proposes a set of rule and uses 2 inputs specifically temperature and humidness and 4 outputs specifically compressor speed, fan speed, fin direction and mode of operation. These outputs are rule-based output. At last, compare simulation results of each system exploitation fuzzy logic and neuro-fuzzy management and notice the higher output.

**Keywords** Fuzzy logic controls · Neuro-fuzzy controls · Air conditioning system · Membership function

## 1 Introduction

The air conditioning systems are usually found in homes and publicly capsulated areas to make snug surroundings. Air conditioners and air conditioning systems are integral part of nearly each establishment. It includes atmosphere, energy, machinery, physical science and automatic management technology [1, 2].

---

R. Kumari (✉) · S. Kumar · V. K. Sharma  
Jagannath University, Chaksu, Jaipur 303901, India  
e-mail: sweetugdd@gmail.com

S. Kumar  
e-mail: sandpoonia@gmail.com

V. K. Sharma  
e-mail: vivek.kumar@jagannathuniversity.org

## ***1.1 Conventional System***

Conventional style strategies need the event of a mathematical model of the control system then use of this model to construct the controller that is represented by the differential equations. The task of dehumidification and temperature decrease goes hand in hand just in case of typical AC. Once target temperature is reached AC ceases to perform sort of a dehumidifier. Within the typical methodology, it is very troublesome to interaction between user preferences, actual temperature and humidity level and it is too nonlinear [3]. Typical AC system controls humidity in its own means while not giving the users any scope for ever changing the point for the targeted humidity. However, this limitation has been overcome by exploitation of fuzzy logic management. It is the power to handle nonlinear systems.

## ***1.2 Problem Definition***

The optimum limit of temperature that is marked as temperature is 25 °C and saturation point is 11 °C. Standard AC system controls set the target purpose by its own approach. This drawback takes 3 input variables user temperature preference, actual temperature and space saturation point temperature. Fuzzy logic algorithmic program is applied on these variables and finds the ultimate result. User temperature is deducted from actual temperature and then sent it for fuzzification, once this fuzzy arithmetic and criterion is applied on these variables and also the consequence is shipped for defuzzification to urge crisp result.

## ***1.3 Fuzzy Logic Control***

Fuzzy logic may be a straightforward however very powerful drawback solving technique with in-depth relevancy. It is presently employed in the fields of business, systems management, physical science and traffic engineering. A fuzzy logic deals with uncertainty in engineering by attaching degrees of certainty to the solution to a logical question. A fuzzy logic system (FLS) will be outlined as the nonlinear mapping of an information set to a scalar output data. Fuzzy logic is employed for management machine and shopper merchandize. Several applications have successfully used fuzzy logic management, for example environmental management, domestic merchandize and automotive system [4].

The fuzzy sets are quantitatively outlined by membership functions. These functions are generally very straightforward functions that cover a fixed domain of the worth of the system input and output. Fuzzy logic management is primarily rule-based system, and therefore, the performance of it depends on its control rules and membership functions (Fig. 1).

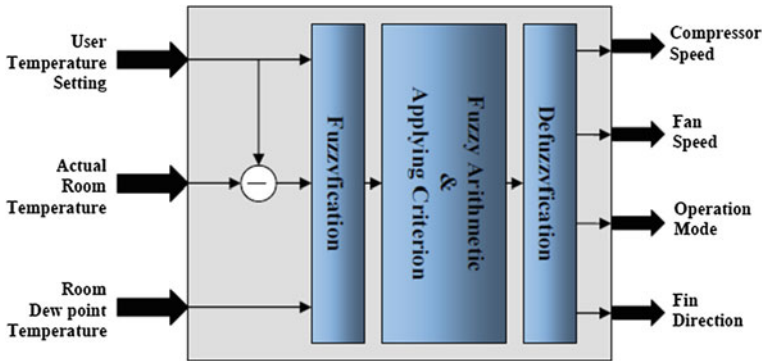


Fig. 1 Block diagram of controller

### 1.4 Neuro-Fuzzy Logic Control

One of the key issues of the fuzzy logic management is that the problem of selection and style of membership functions for a given downside. Neural networks provide the likelihood of finding the matter of standardization. Neural fuzzy systems will generate formal logic rules and membership functions for advanced systems that a standard fuzzy approach could fail. Hence, combining the adaptive neural networks and formal logic management forms a system known as neuro-fuzzy system. Neuro-fuzzy system is based on the neural network that learned from fuzzy if-then rules. Neural network performance is dependent on the quality and quantity of training samples presented to the network. Neural nets can solve many problems that are either unsolved or inefficiently solved by existing techniques, including fuzzy logic [5, 6].

## 2 Fuzzy Logic Control Algorithm

Fuzzy logic management primarily based on air conditioning system consists of two inputs that are actual temperature and room temperature dew point (humidity). When measuring actual temperature, the user temperature ( $U_t$ ) is subtracted from actual temperature for realize the temperature distinction ( $T_d$ ) and sent it for fuzzification. Fuzzy arithmetic and criterion is applied on the input variables, outcome is defuzzified to induce output, and these output signals are distributed to manage the compressor speed. During this case, the range of actual temperature is taken to be 15–50 °C and range of its taken to be 18–30 °C; therefore, the temperature distinction arises between  $-3$  and 32 °C. The input has 2 membership functions. The size over that membership functions for temperature is represented as 0–50 °C and membership functions for humidness is represented as 0–100 %. The output additionally has four



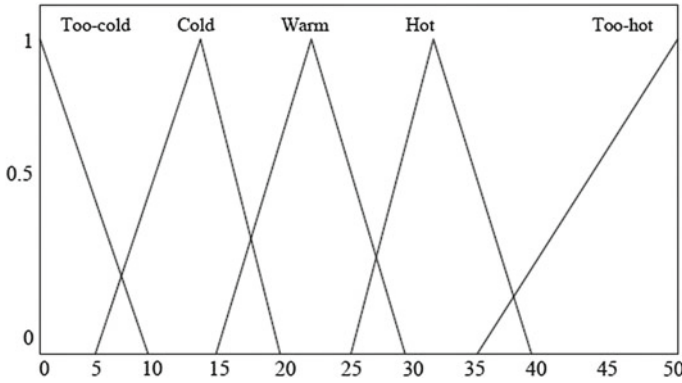


Fig. 2 Temperature membership functions

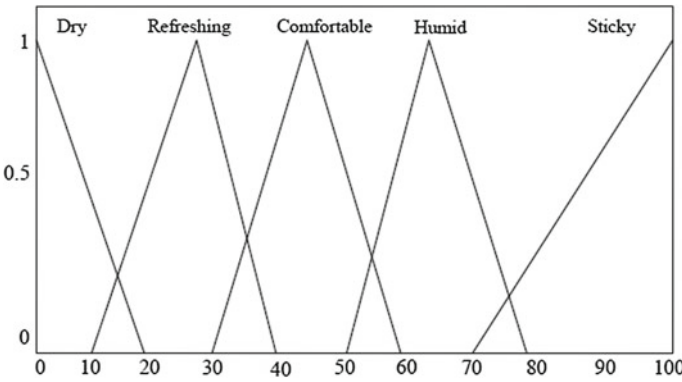


Fig. 3 Humidity membership functions

membership functions particularly compressor speed, fin direction, fan speed and operation mode. The principles base for coming up with is as “IF Temperature is just too cold AND humidness is dry THEN compressor speed is Off, Fin direction is Away, Fan speed is Off and Operation mode is AC” and so on [7, 8] (Table 1).

### 3 Neuro-Fuzzy Algorithm

Neuro-fuzzy management primarily based on air conditioning system additionally consists of 2 inputs that are actual temperature and space room (humidity). The input, temperature takes the name “input1” (In1) and range is taken to be 0–40 °C for membership function. Similarly, the input, humidness takes the name “input2” (In2) and range is taken to be 5–85 % for membership function. The output, compressor speed amendment the name as “output1” (Out1), fin direction named as “output2”

**Table 1** Fuzzy rules for proposed design

Rules	Input		Output			
	Temperature	Humidity	Compressor speed	Fin direction	Fan speed	Operation mode
1	Too cold	Dry	Off	Away	Off	AC
2	Too cold	Refreshing	Off	Away	Off	AC
3	Too cold	Comfortable	Off	Away	Off	AC
4	Too cold	Humid	Off	Away	Very low	AC
5	Too cold	Sticky	Very low	Towards	Low	Dehumidifier
6	Cold	Dry	Off	Away	Off	AC
7	Cold	Refreshing	Off	Away	Off	AC
8	Cold	Comfortable	Very low	Away	Very low	AC
9	Cold	Humid	Very low	Towards	Low	AC
10	Cold	Sticky	Low	Towards	Low	Dehumidifier
11	Warm	Dry	Very low	Away	Very low	AC
12	Warm	Refreshing	Very low	Away	Very low	AC
13	Warm	Comfortable	Low	Away	Low	AC
14	Warm	Humid	Medium	Towards	Medium	Dehumidifier
15	Warm	Sticky	Medium	Towards	Medium	Dehumidifier
16	Hot	Dry	Low	Away	Low	AC
17	Hot	Refreshing	Medium	Away	Medium	AC
18	Hot	Comfortable	Medium	Towards	Medium	AC
19	Hot	Humid	Fast	Towards	Fast	Dehumidifier
20	Hot	Sticky	Fast	Towards	Fast	Dehumidifier
21	Too hot	Dry	Medium	Away	Medium	AC
22	Too hot	Refreshing	Medium	Towards	Medium	AC
23	Too hot	Comfortable	Fast	Towards	Fast	Dehumidifier
24	Too hot	Humid	Fast	Towards	Fast	Dehumidifier
25	Too hot	Sticky	Fast	Towards	Fast	Dehumidifier

(Out2), fan speed named as “output3” (Out3) and operation named as “output4” (Out4). The principles are applied consequently in Table 2.

### 4 Experimental Results

Result of this experiment is predicated on fuzzy rules and neuro-fuzzy rules. Figures 2 and 3 show input values for fuzzy logic management, and Figs. 4 and 5 show input values for neuro-fuzzy management. Supported these inputs acquire results when simulation of fuzzy logic management is based on air conditioning system that are shown in the following figures. Figure 6 shows the compressor speed memberships of air conditioning system. Compressor speed may be either off or may be varied between 10 and 100 % (Fig. 7).

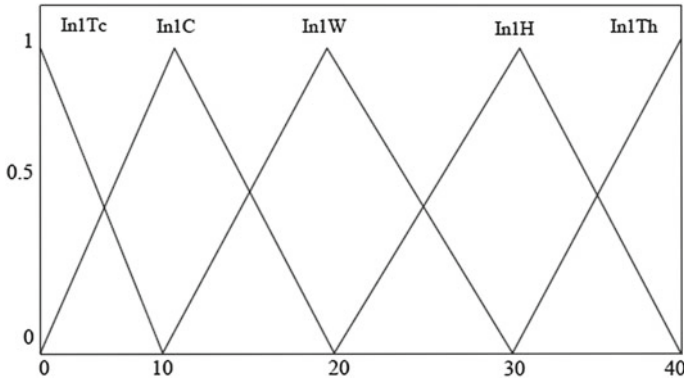


Fig. 4 Input1 membership functions

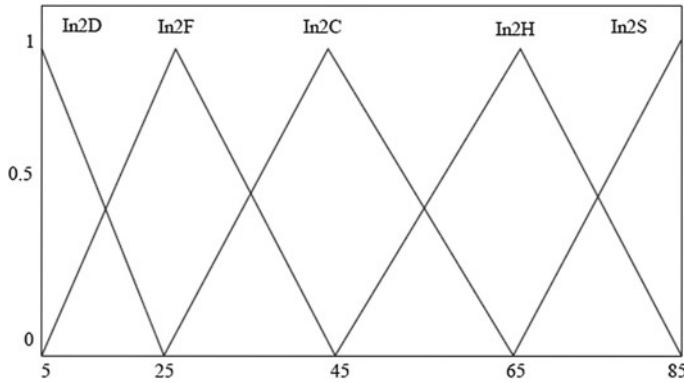


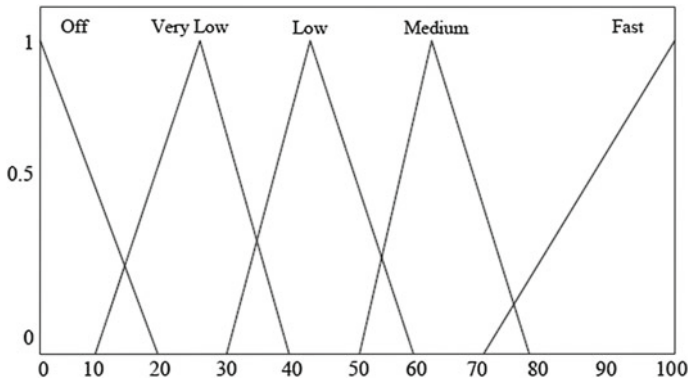
Fig. 5 Input2 membership functions

Figure 8 shows the operation mode memberships of air conditioning system. Mode of operation decides whether AC works like a dehumidifier only or normal. Figure 9 shows the fin direction memberships of air conditioning system. Fin direction directs air from the AC towards or away from occupants.

Figure 10 shows compressor speed with respect to temperature by using fuzzy rules. Figure 11 shows compressor speed with respect to humidity by using fuzzy rules. Figure 12 shows the output1 with respect to input1 by using neuro-fuzzy rules. Figure 13 shows the output1 with respect to input2 by using neuro-fuzzy rules.

**Table 2** Neuro-fuzzy rules for proposed design

Rules	Input		Output			
	Temperature (Input1)	Humidity	Compressor speed	Fin direction	Fan speed	Operation mode
1	In1Tc	In2D	Out1Of	Out2A	Out3Of	Out4AC
2	In1Tc	In2R	Out1Of	Out2A	Out3Of	Out4AC
3	In1Tc	In2C	Out1Of	Out2A	Out3Of	Out4AC
4	In1Tc	In2H	Out1Of	Out2A	Out3Vl	Out4AC
5	In1Tc	In2S	Out1Vl	Out2To	Out3L	Out4D
6	In1C	In2D	Out1Of	Out2A	Out3Of	Out4AC
7	In1C	In2R	Out1Of	Out2A	Out3Of	Out4AC
8	In1C	In2C	Out1Vl	Out2A	Out3Vl	Out4AC
9	In1C	In2H	Out1Vl	Out2To	Out3L	Out4AC
10	In1C	In2S	Out1L	Out2To	Out3L	Out4D
11	In1W	In2D	Out1Vl	Out2A	Out3Vl	Out4AC
12	In1W	In2R	Out1Vl	Out2A	Out3Vl	Out4AC
13	In1W	In2C	Out1L	Out2A	Out3L	Out4AC
14	In1W	In2H	Out1M	Out2To	Out3Of	Out4D
15	In1W	In2S	Out1M	Out2To	Out3M	Out4D
16	In1H	In2D	Out1L	Out2A	Out3L	Out4AC
17	In1H	In2R	Out1M	Out2A	Out3M	Out4AC
18	In1H	In2C	Out1M	Out2To	Out3M	Out4AC
19	In1H	In2H	Out1F	Out2To	Out3F	Out4D
20	In1H	In2S	Out1F	Out2To	Out3F	Out4D
21	In1Th	In2D	Out1M	Out2A	Out3M	Out4AC
22	In1Th	In2R	Out1M	Out2To	Out3M	Out4AC
23	In1Th	In2C	Out1F	Out2To	Out3F	Out4D
24	In1Th	In2H	Out1F	Out2To	Out3F	Out4D
25	In1Th	In2S	Out1F	Out2To	Out3F	Out4D



**Fig. 6** Compressor speed membership functions

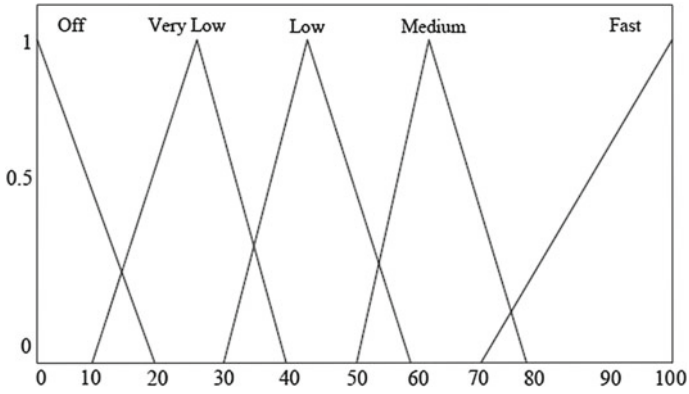


Fig. 7 Fan speed membership functions

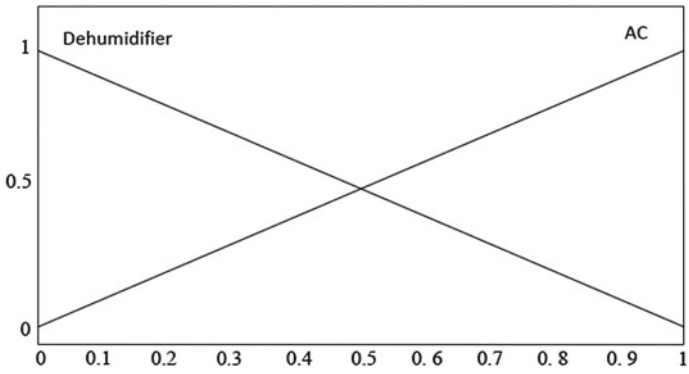


Fig. 8 Operation mode membership functions

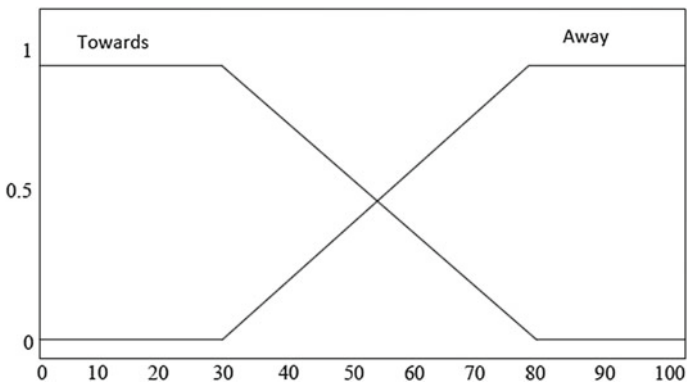


Fig. 9 Fin direction membership function

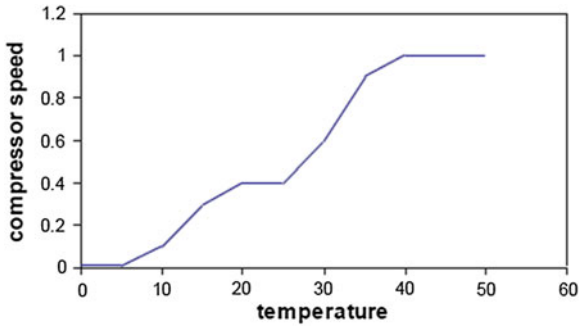


Fig. 10 Compressor speed with temperature

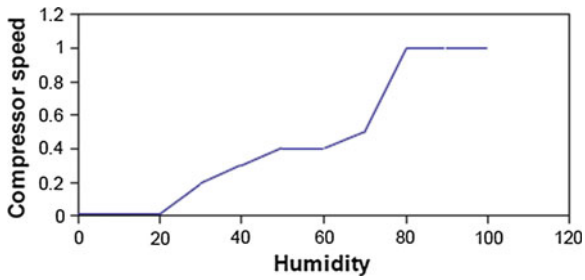


Fig. 11 Compressor speed with humidity

Fig. 12 Output with Input1 (temp)

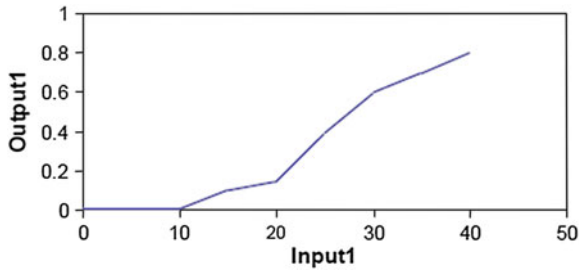
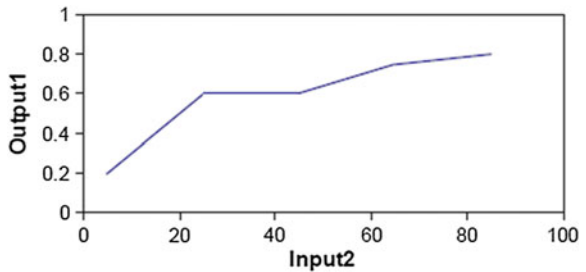


Fig. 13 Output with Input2 (humidity)



## 5 Conclusion

Neuro-fuzzy algorithm is better than fuzzy logic algorithm in air conditioning system. Neuro logic algorithm gives a better control than fuzzy logic. In neuro logic algorithm, performance of compressor speed is much better than fuzzy logic algorithm. In fuzzy logic control design, the compressor speed remains constant for temperature range from 35 °C onwards, but in neuro-fuzzy control design, it increases consistently with respect to temperature. By this, it provides proper output and save energy. It controls the room environment and weather.

## References

1. Nasution, H., Jamaluddin, H., Syeriff, J.M.: Energy analysis for air conditioning system using fuzzy logic controller. *TELKOMNIKA* **9**(1), 139–150 (2011)
2. Du, M., Fan, T., Su, W., Li, H.: Design of a new practical expert fuzzy controller in central air conditioning control system. *IEEE Pacific-Asia workshop on computational intelligence and industrial application* (2008)
3. Passino, K.M., Yurkovich, S.: *Fuzzy control*, Addison Wesley (1998)
4. Isomursu, P., Rauma, T.: A self-tuning fuzzy logic controller for temperature control of super-heated steam. *Fuzzy systems, IEEE world congress on computational intelligence, proceedings of the third IEEE conference*, vol. 3 (1994)
5. Islam, M.S., Sarker, Z., Ahmed Rafi, K.A., Othman, M.: Development of a fuzzy logic controller algorithm for air conditioning system. *ICSE proceedings* (2006)
6. Batayneh, W., Al-Araidah, O., Bataineh, K.: Fuzzy logic approach to provide safe and comfortable indoor environment. *Int. J. Eng. Sci. Technol.* **2**(7) (2010)
7. Abbas, M., Khan, M.S., Zafar, F.: Autonomous room air cooler using fuzzy logic control system. *Int. J. Sci. Eng. Res.* **2**(5), 74–81 (2011)
8. Hamidi, M., Lachiver, G.: A fuzzy control system based on the human sensation of thermal comfort. *Fuzzy systems proceedings, 1998. IEEE world congress on computational intelligence, the IEEE international conference*, vol. **1** (1998)

# Improving the Performance of the Optimization Technique Using Chaotic Algorithm

R. Arunkumar and V. Jothiprakash

**Abstract** Optimizing the operations of a multi-reservoir systems are complex because of their larger dimension and convexity of the problem. The advancement of soft computing techniques not only overcomes the drawbacks of conventional techniques but also solves the complex problems in a simple manner. However, if the problem is too complex with hardbound variables, the simple evolutionary algorithm results in slower convergence and sub-optimal solutions. In evolutionary algorithms, the search for global optimum starts from the randomly generated initial population. Thus, initializing the algorithm with a better initial population not only results in faster convergence but also results in global optimal solution. Hence in the present study, chaotic algorithm is used to generate the initial population and coupled with genetic algorithm (GA) to optimize the hydropower production from a multi-reservoir system in India. On comparing the results with simple GA, it is found that the chaotic genetic algorithm (CGA) has produced slightly more hydropower than simple GA in fewer generations and also converged quickly.

**Keywords** Optimization · Genetic algorithm · Chaotic algorithm · Multi-hydropower system.

## 1 Introduction

The last decade had witnessed several optimization techniques from conventional linear programming to recently soft computing techniques. Among the soft computing techniques, the genetic algorithm (GA) had been widely used for optimization of

---

R. Arunkumar (✉) · V. Jothiprakash  
Department of Civil Engineering, Indian Institute of Technology Bombay, Mumbai 400076, India  
e-mail: arunkumar.r@iitb.ac.in

V. Jothiprakash  
e-mail: vprakash@iitb.ac.in



reservoir operation [1–3]. Application of simple GA technique to solve real-life water resources problems, especially optimizing multi-hydropower system is always cumbersome because of the complex nature, large number of variables and nonlinearity of the problem. Some recent studies reported that simple optimization techniques often succumb to premature convergence and results in local optimal solution for complex water resources problems [4–6]. Hence, still researches are emerging to introduce new techniques and also to improve the performance of the existing techniques to achieve global optimum and faster convergence.

The search for global optimal solution in evolutionary algorithms begins from the randomly generated initial population. Thus, a better initial population leads to faster convergence and not only saves substantial computational time but also results in global optimal solution. Hence, to generate a good initial population, chaotic algorithm is used, since chaos is highly sensitivity to the initial value, ergodic, and randomness in nature [7]. Yuan et al. [4] proposed a hybrid chaotic genetic algorithm (HCGA) model to prevent premature convergence for a short-term hydropower scheduling problem. Cheng et al. [5] optimized the hydropower reservoir operation using HCGA and reported that the long-term average annual energy production was the best in HCGA and also it converges faster than the standard GA. It was also reported that the combination of chaotic characteristics along with general optimization algorithm would more likely result in global optimal solution. Han and Lu [6] proposed a mutative scale chaos optimization algorithm (MSCOA) for the economic load dispatch problem. Huang et al. [8] optimized the hydropower reservoir with ecological consideration using chaotic genetic algorithm (CGA) approach. These studies show that GA results better when coupled with chaotic algorithm and also escapes premature convergence. Hence in this study, in order to improve the performance of GA, chaotic algorithm is used to generate initial population and tested for a real-life hydropower system. The proposed algorithm is applied to maximize the hydropower production from a multi-reservoir system, namely Koyna hydroelectric project (KHEP).

The KHEP consists of two reservoirs, namely Koyna and Kolkewadi, which has four powerhouses to a total capacity of 1,960 MW [9]. Earlier, Jothiprakash and Arunkumar [10] optimized the operation of Koyna reservoir alone considering it as a single reservoir system. However, in the present study, both the reservoirs are considered and optimized as multi-reservoir system. Apart from hydropower production, it also serves multiple purposes such as irrigation and flood control. In this system, the major powerhouses of the Koyna reservoir and Kolkewadi reservoir are in the western side and the irrigation releases are in the eastern side. The diversion of large quantity of water toward the western side for power production has resulted in disputes from the eastern side stakeholders, and hence, it was limited by Krishna water dispute tribunal [11]. This limiting constraint on the discharge for power production from the western side powerhouses made the system more complex by making the variables hard bound. This hard-binding constraint is considered in this study.

## 2 Chaotic Genetic Algorithm

GA is a search and optimization algorithm based on the principles of natural genetics [12]. In contrast to traditional optimization technique, GA searches the optimal solution from a randomly generated population within the upper and lower bounds of the variables. Each solution is represented through group of genes (sub-string) called chromosome (string) in the population space (search space). Each gene controls one or more features of the chromosomes. In the present study, the chaotic logistic mapping method is used to generate the initial population. Chaos often exists in nonlinear systems [13] and exhibits many good properties such as ergodicity, stochasticity, and irregularity [7]. May [7] proposed a one-dimensional logistic mapping equation to generate a chaotic sequence. It is given as:

$$Y_{j+1} = \lambda Y_j(1 - Y_j) \quad j = 1, 2, 3 \dots \quad (1)$$

where  $\lambda$  is a control parameter and varies between  $0 \leq \lambda \leq 4$ . The chaotic sequence is produced when  $\lambda$  is equal to 4. The initial random variable ( $Y_1$ ) is generated in the range between 0 and 1; however, it should not be equal to 0.25, 0.5, and 0.75, since it leads to a deterministic sequence [7]. Thus, the generated sequence using the logistic Eq. (1) is highly irregular and possesses chaotic characteristics. Each variable in the sequence is dependent on initial variable, and a small change in initial value causes a large difference in its long-time behavior, which is the basic characteristic of chaos. This can be correlated with the releases in reservoir operation, such that the releases in the subsequent months depend on previous month releases. Hence in the present study, the initial population is generated as floating-point chaotic values within the upper ( $UB_j$ ) and lower bounds ( $LB_j$ ) of the variables using the equation:

$$X_{i,j} = Y_{i,j} \times (UB_j - LB_j) + LB_j \quad i = 1, 2, \dots, N_p; j = 1, 2, \dots, N_v \quad (2)$$

where  $X_{i,j}$  is the ' $j^{\text{th}}$ ' sub-string of ' $i^{\text{th}}$ ' string,  $N_p$  is the population size,  $Y_{i,j}$  is the chaotic variable, and  $N_v$  is the number of variables. Once the initial population is generated, the fitness of each string is evaluated using an appropriate fitness function. Based on the fitness value, the strings are selected for crossover and mutation to create a new population for the next generation. The tournament selection is used in the present study, since it provides selective pressure by holding a tournament among the selected individuals [12]. In the tournament selection, the fitness of the randomly selected strings from the population is compared with each other and the string having with higher fitness value will be copied to the mating pool. This process is repeated until the mating pool is filled with strings for generating new offspring for the next generation. The mating pool comprising the winners of the tournament will have higher average fitness value. Then, the strings in the mating pool are made to cross each other to create a new population. The simulated binary crossover (SBX) [14] is applied to create new population. The following steps were performed during SBX operation [12]. In the first step, a random number ( $u_i$ ) between 0 and 1 is generated.

Then, the spread factor ( $\beta_{qi}$ ) is computed using the equation

$$\beta_{qi} = \begin{cases} (2u_i)^{\frac{1}{(\eta_c+1)}}, & \text{if } u_i < 0.5 \\ \left(\frac{1}{2(1-u_i)}\right)^{\frac{1}{(\eta_c+1)}}, & \text{otherwise} \end{cases} \quad (3)$$

where  $\eta_c$  is the distribution index for crossover. Deb [12] reported that larger value of  $\eta_c$  produces ‘near-parent’ offspring’s and vice versa. Then, the off-springs  $x_i^{1,t+1}$  and  $x_i^{2,t+1}$  are computed from  $x_i^{1,t}$  and  $x_i^{2,t}$  using the equations,

$$x_i^{1,t+1} = 0.5 \left[ (1 + \beta_{qi}) x_i^{1,t} + (1 - \beta_{qi}) x_i^{2,t} \right] \quad (4)$$

$$x_i^{2,t+1} = 0.5 \left[ (1 - \beta_{qi}) x_i^{1,t} + (1 + \beta_{qi}) x_i^{2,t} \right] \quad (5)$$

where  $x_i^{1,t}$  and  $x_i^{2,t}$  are the parent string with  $i$ th sub-string in the  $t$ th generation. If the created offsprings are not within the upper and lower limits, the probability distribution needs to be adjusted accordingly. The new two offsprings are symmetric about the parent to avoid bias toward any particular parent solution in a single crossover operation. After crossover, the strings are subjected to mutation. The mutation operator introduces random changes into the characteristic of the offsprings. Mutation is generally applied at the sub-string level at a very small rate and depends on the length of the string. The mutation reintroduces the genetic diversity into the population and assists the search to escape from the local optima [12]. Then, the fitness of the newly created population is evaluated, and the procedure is continued until the termination criteria are reached.

### 3 Hydropower Model Development

The objective of the present study is to maximize the power production from all the four powerhouses of the KHEP and is expressed as:

$$\text{Max } Z = \sum_{t=1}^{12} \sum_{n=1}^4 \text{PH}_{n,t} \quad (6)$$

where  $\text{PH}_{n,t}$  is the power production from the powerhouse ‘ $n$ ’ during the time period ‘ $t$ ’ in terms of kWh. The hydropower production from the power plant [15] is given by

$$\text{PH}_{n,t} = K \times R_{n,t} \times \text{HN}_{n,t} \times \eta \quad (7)$$

where  $K$  is the constant for converting hydropower production in terms of kilo Watt hour (kWh),  $R_{n,t}$  is discharge to the powerhouse ‘ $n$ ’ during the time period ‘ $t$ ’,  $\text{HN}_{n,t}$

is the net head available for the powerhouse 'n' during the time period 't', and  $\eta$  is the plant efficiency.

The above objective function is subjected to various constraints. They are:

$$H_{n,t} \geq \text{MDDL}_{n,t} \quad t = 1, 2 \dots 12; n = 1, 2, 3, 4 \quad (8)$$

$$\text{PH}_{n,t} \leq P \max_{n,t} \quad t = 1, 2 \dots 12; n = 1, 2, 3, 4 \quad (9)$$

$$R_{4,t} \geq \text{ID}_t \quad t = 1, 2 \dots 12 \quad (10)$$

$$S_{x,\min} \leq S_{x,t} \leq S_{x,\max} \quad t = 1, 2 \dots 12; x = 1, 2 \quad (11)$$

$$S_{1,(t+1)} = S_{1,t} + I_{1,t} - \sum_{n=1}^{1,3,4} R_{n,t} - O_{1,t} - E_{1,t} \quad t = 1, 2 \dots 12 \quad (12)$$

$$S_{2,(t+1)} = S_{2,t} + I_{2,t} + R_{1,t} + R_{3,t} - R_{2,t} - O_{2,t} - E_{2,t} \quad t = 1, 2 \dots 12 \quad (13)$$

$$O_{x,t} = S_{x,(t+1)} - S_{x,\max} \quad t = 1, 2 \dots 12 \quad (14)$$

$$O_{x,t} \geq 0 \quad t = 1, 2 \dots 12 \quad (15)$$

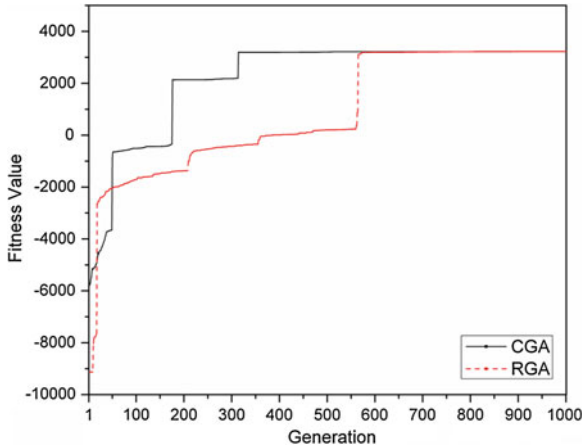
where  $\text{MDDL}_{n,t}$  is the minimum drawdown level (m) for the powerhouse 'n';  $P \max_{n,t}$  is the maximum generation capacity (kWh) for the powerhouse 'n';  $R_{4,t}$  is the irrigation release ( $10^6 \text{ m}^3$ );  $\text{ID}_t$  is the monthly irrigation demand ( $10^6 \text{ m}^3$ );  $S_{x,\min}$  is the minimum storage of the reservoir 'x' ( $10^6 \text{ m}^3$ );  $S_{x,\max}$  is the maximum storage of the reservoir 'x' ( $10^6 \text{ m}^3$ );  $S_{x,t}$  is the storage in the reservoir 'x' ( $10^6 \text{ m}^3$ );  $S_{x,(t+1)}$  is the final storage in the reservoir 'x' ( $10^6 \text{ m}^3$ );  $I_{x,t}$  is the inflow into the reservoir 'x' ( $10^6 \text{ m}^3$ );  $O_{x,t}$  is the overflow from the reservoir 'x' ( $10^6 \text{ m}^3$ );  $E_{x,t}$  is the evaporation losses from the reservoir ( $10^6 \text{ m}^3$ );  $t$  is the time period.

As already stated, the diversion of water to the western side powerhouses are limited by KWDT [11]. This constraint is given by:

$$\sum_{t=1}^{12} \sum_{n=1,3} R_{n,t} \leq R_{w,\max} \quad (16)$$

$$\sum_{t=1}^{12} R_{4,t} \leq \text{AID}_{\max} \quad (17)$$

where  $R_{w,\max}$  is the maximum water that can be diverted to the western side for power production, and  $\text{AID}_{\max}$  is the water to be released annually for irrigation to the eastern side.  $R_{4,t}$  is the monthly irrigation release on the eastern side of the reservoir. These constraints make the system more complex by limiting the discharge to the powerhouses.



**Fig. 1** Comparison of CGA and simple GA technique

## 4 Results and Discussion

The proposed CGA is applied to a complex multi-powerhouse system, namely KHEP to maximize its power production. The KHEP is one of the largest hydropower projects in India and consists of two reservoirs with various stages of development. The constraint on diverting large quantity of water for power production on the western side powerhouses makes the problem complex. This hard-binding constraint on discharge restricts the operation of the powerhouses on the western side to its full potential. Evaporation is one of the important components of reservoir operation studies, since a considerable amount of water is lost, especially from large reservoirs. Hence in the present study, the regression equation developed by Arunkumar and Jothiprakash [16] for estimating reservoir evaporation is considered and directly incorporated in the continuity equation. Both the CGA and simple GA used in the study employ tournament selection, simulated binary crossover, and random mutation for comparison. The crossover probability of CGA and simple GA is varied from 0.5 to 0.95 with an increment of 0.05 and found that 0.80 resulted better. The mutation probability is fixed as the ratio of the number of variable ( $1/n$ ) [12]. The elitism is also applied to preserve the best strings in the population. The algorithm is evaluated for 1,000 generation for a population size of 250. The constraints of the problems are handled by penalty function approach. Thus, heavy penalties are imposed on fitness function, if the constraints are violated. For each constraint different values of penalties are assumed. The total annual power production shows that CGA has resulted slightly higher power production of  $3,225.71 \times 10^6$  kWh than simple GA ( $3,224.23 \times 10^6$  kWh). However, the convergence of these techniques over the generation varied largely and is given in Fig. 1. From the figure, it can be observed that the convergence to an optimal solution by CGA is faster than simple GA. It can also be noted that due to hard-binding constraints on releases, both the

techniques have resulted in sub-optimal solution for first few generations. Thus imposing heavy penalty on fitness function leads to negative fitness value and results in sub-optimal solution. However, the CGA has satisfied all the constraints and reaches the optimal solution in lesser generations than simple GA. This also shows that when hard-binding constraints are imposed strictly, the simple GA takes more generations for convergence. The time taken by CGA is 1,790.753 s where as simple GA took 2,418.966 s.

## 5 Conclusion

In the present study, the chaotic algorithm is combined with genetic algorithm to maximize the power production from a multi-powerhouse system. Based on the performances, it is found that the chaotic genetic algorithm resulted slightly higher power production than simple GA within fewer generations and also converged quickly. This shows that coupling the chaotic algorithm with evolutionary algorithm has enriched the global search of the optimization technique by having better initial population. Thus, it may be concluded that the chaotic algorithm with general optimizer converges quickly to global optimum in lesser generation compared to simple optimization technique.

**Acknowledgments** The authors gratefully acknowledge the Ministry of Water Resources, Government of India, New Delhi, for sponsoring this research project. The authors also thank Chief Engineer, KHEP, Executive Engineer, Koyna Dam and Executive Engineer, Kolkewadi Dam for providing the necessary data.

## References

1. Wardlaw, R., Sharif, M.: Evaluation of genetic algorithms for optimal reservoir system operation. *J. Water Resour. Plann. Manage.* **125**(1), 25–33 (1999)
2. Sharif, M., Wardlaw, R.: Multireservoir systems optimization using genetic algorithms: case study. *J. Comput. Civ. Eng.* **14**(4), 255–263 (2000)
3. Jothiprakash, V., Shanthi, G., Arunkumar, R.: Development of operational policy for a multi-reservoir system in India using genetic algorithm. *Water Resour. Manage.* **25**(10), 2405–2423 (2011)
4. Yuan, X., Yuan, Y., Zhang, Y.: A hybrid chaotic genetic algorithm for short-term hydro system scheduling. *Math. Comput. Simul.* **59**(4), 319–327 (2002)
5. Cheng, C.T., Wang, W.C., Xu, D.M., Chau, K.: Optimizing hydropower reservoir operation using hybrid genetic algorithm and chaos. *Water Resour. Manage.* **22**(7), 895–909 (2008)
6. Han, F., Lu, Q.S.: An improved chaos optimization algorithm and its application in the economic load dispatch problem. *Int. J. Comput. Math.* **85**(6), 969–982 (2008)
7. May, R.M.: Simple mathematical models with very complicated dynamics. *Nature* **261**(5560), 459–467 (1976)
8. Huang, X., Fang, G., Gao, Y., Dong, Q.: Chaotic optimal operation of hydropower station with ecology consideration. *Energy Power Eng.* **2**(3), 182–189 (2010)

9. KHEP: Koyna hydro electric project stage-IV. Irrigation Department, Government of Maharashtra, (2005)
10. Jothiprakash, V., Arunkumar, R.: Optimization of hydropower reservoir using evolutionary algorithms coupled with chaos. *Water Resour. Manage.* (2013). doi:10.1007/s11269-013-0265-8, (Published online)
11. KWDT: Krishna water disputes tribunal: The report of the Krishna water disputes tribunal with the decision. Ministry of water resources, Government of India. New Delhi (2010)
12. Deb, K.: *Multi-objective Optimization Using Evolutionary Algorithm*. Wiley, New Jersey (2001)
13. Williams, G.P.: *Chaos Theory Tamed*. Joseph Henry Press, Washington, D.C (1997)
14. Deb, K., Agrawal, R.B.: Simulated binary crossover for continuous search space. *Complex Syst.* **9**, 115–148 (1995)
15. Loucks, D.P., Stedinger, J.R., Haith, D.A.: *Water Resources Systems Planning and Analysis*. Prentice Hall Inc, Englewood Cliffs, New Jersey (1981)
16. Arunkumar, R., Jothiprakash, V.: Optimal reservoir operation for hydropower generation using non-linear programming model. *J. Inst. Eng. (India)* **93**(2), 111–120 (2012)

# New Reliable Algorithm for Fractional Harry Dym Equation

Devendra Kumar and Jagdev Singh

**Abstract** In this paper, a new reliable algorithm based on homotopy perturbation method using Laplace transform, named homotopy perturbation transform method (HPTM), is proposed to solve nonlinear fractional Harry Dym equation. The numerical solutions obtained by the HPTM show that the approach is easy to implement and computationally very attractive.

**Keywords** Fractional Harry Dym equation · Laplace transform · Homotopy perturbation transform method · He's polynomials · Maple code.

## 1 Introduction

Fractional differential equations have gained importance and popularity, mainly due to its demonstrated applications in science and engineering. For example, these equations are increasingly used to model problems in fluid mechanics, acoustics, biology, electromagnetism, diffusion, signal processing, and many other physical processes [1–6].

In this paper, we consider the following nonlinear time-fractional Harry Dym equation of the form:

$$D_t^\alpha u(x, t) = u^3(x, t) D_x^3 u(x, t), \quad 0 < \alpha \leq 1, \quad (1)$$

---

D. Kumar (✉)

Department of Mathematics, JaganNath Gupta Institute of Engineering and Technology,  
Jaipur, Rajasthan 302022, India  
e-mail: devendra.maths@gmail.com

J. Singh

Department of Mathematics, Jagan Nath University, Village-Rampura, Tehsil-Chaksu,  
Jaipur, Rajasthan 303901, India  
e-mail: jagdevsinghrathore@gmail.com



with the initial condition

$$u(x, 0) = \left( a - \frac{3\sqrt{b}}{2}x \right)^{2/3}. \tag{2}$$

where  $u(x, t)$  is a function of  $x$  and  $t$ . The derivative is understood in the Caputo sense. In the case of  $\alpha = 1$ , the fractional Harry Dym equation reduces to the classical nonlinear Harry Dym equation. The exact solution of the Harry Dym equation is given by [7]

$$u(x, t) = \left( a - \frac{3\sqrt{b}}{2}(x + bt) \right)^{2/3}, \tag{3}$$

where  $a$  and  $b$  are suitable constants. The Harry Dym is an important dynamical equation which finds applications in several physical systems. The Harry Dym equation first appeared in Kruskal and Moser [8] and was discovered by H. Dym in 1973–1974. Harry Dym is a completely integrable nonlinear evolution equation. The Harry Dym equation is very interesting because it obeys an infinite number of conservation laws; it does not possess the Painleve property. It has strong links to the Korteweg-de Vries equation, and applications of this equation were found in the problems of hydrodynamics [9]. Recently, a fractional model of Harry Dym equation was presented by Kumar et al. [10] and approximate analytical solution was obtained by using homotopy perturbation method (HPM).

The HPM was first introduced by He [11]. In a recent paper, a new approach, named homotopy perturbation transform method (HPTM), is introduced by Khan and Wu [12] to handle nonlinear equations. The HPTM is a combination of Laplace transform method, HPM, and He’s polynomials.

In this paper, we apply the HPTM to solve the nonlinear time-fractional Harry Dym equation. It provides the solutions in terms of convergent series with easily computable components in a direct way without using linearization, perturbation, or restrictive assumptions.

## 2 Basic Definitions of Fractional Calculus

In this section, we mention the following basic definitions of fractional calculus.

**Definition 2.1** The Riemann–Liouville fractional integral operator of order  $\alpha > 0$ , of a function  $f(t) \in C_\mu, \mu \geq -1$  is defined as [2]

$$J^\alpha f(t) = \frac{1}{\Gamma(\alpha)} \int_0^t (t - \tau)^{\alpha-1} f(\tau) d\tau, (\alpha > 0), \tag{4}$$

$$J^0 f(t) = f(t). \tag{5}$$

For the Riemann–Liouville fractional integral, we have

$$J^{\alpha} t^{\gamma} = \frac{\Gamma(\gamma + 1)}{\Gamma(\gamma + \alpha + 1)} t^{\alpha + \gamma}. \tag{6}$$

**Definition 2.2** The fractional derivative of  $f(t)$  in the Caputo sense is defined as [3]

$$D_t^{\alpha} f(t) = J^{m-\alpha} D^n f(t) = \frac{1}{\Gamma(n-\alpha)} \int_0^t (t-\tau)^{m-\alpha-1} f^{(m)}(\tau) d\tau, \tag{7}$$

for  $m - 1 < \alpha \leq m, m \in N, t > 0$ .

**Definition 2.3** The Laplace transform of the Caputo derivative is given as [6]

$$L[D_t^{\alpha} f(t)] = s^{\alpha} L[f(t)] - \sum_{r=0}^{m-1} s^{\alpha-r-1} f^{(r)}(0+), (m - 1 < \alpha \leq m). \tag{8}$$

### 3 Basic Idea of HPTM

We consider a general fractional nonlinear nonhomogeneous partial differential equation with the initial condition of the form:

$$D_t^{\alpha} u(x, t) + Ru(x, t) + Nu(x, t) = g(x, t), \tag{9}$$

$$u(x, 0) = f(x), \tag{10}$$

where  $D_t^{\alpha} u(x, t)$  is the Caputo fractional derivative of the function  $u(x, t)$ ,  $R$  is the linear differential operator,  $N$  represents the general nonlinear differential operator, and  $g(x, t)$  is the source term.

Applying the Laplace transform (denoted in this paper by  $L$ ) on both sides of Eq. (9) and using result (8), we have

$$L[u(x, t)] = \frac{f(x)}{s} + \frac{1}{s^{\alpha}} L[g(x, t)] - \frac{1}{s^{\alpha}} L[Ru(x, t) + Nu(x, t)]. \tag{11}$$

Operating with the Laplace inverse on both sides of Eq. (11) gives

$$u(x, t) = G(x, t) - L^{-1} \left[ \frac{1}{s^{\alpha}} L[Ru(x, t) + Nu(x, t)] \right], \tag{12}$$

where  $G(x, t)$  represents source term and initial conditions separately. Now, we apply the homotopy perturbation method

$$u(x, t) = \sum_{n=0}^{\infty} p^n u_n(x, t), \tag{13}$$

and the nonlinear term can be decomposed as

$$N u(x, t) = \sum_{n=0}^{\infty} p^n H_n(u), \tag{14}$$

for some He’s polynomials  $H_n(u)$  [13, 14] that are given by

$$H_n(u_0, u_1, \dots, u_n) = \frac{1}{n!} \frac{\partial^n}{\partial p^n} \left[ N \left( \sum_{i=0}^{\infty} p^i u_i \right) \right]_{p=0}, \quad n = 0, 1, 2, \dots \tag{15}$$

Substituting Eqs. (13) and (14) in Eq. (12), we get

$$\sum_{n=0}^{\infty} p^n u_n(x, t) = G(x, t) - p \left( L^{-1} \left[ \frac{1}{s^\alpha} L \left[ R \sum_{n=0}^{\infty} p^n u_n(x, t) + \sum_{n=0}^{\infty} p^n H_n(u) \right] \right] \right), \tag{16}$$

which is the coupling of the Laplace transform and the homotopy perturbation method using He’s polynomials. Comparing the coefficients of like powers of  $p$ , the approximations  $u_0, u_1, u_2$ , and so on are obtained.

### 4 Solution of the Problem

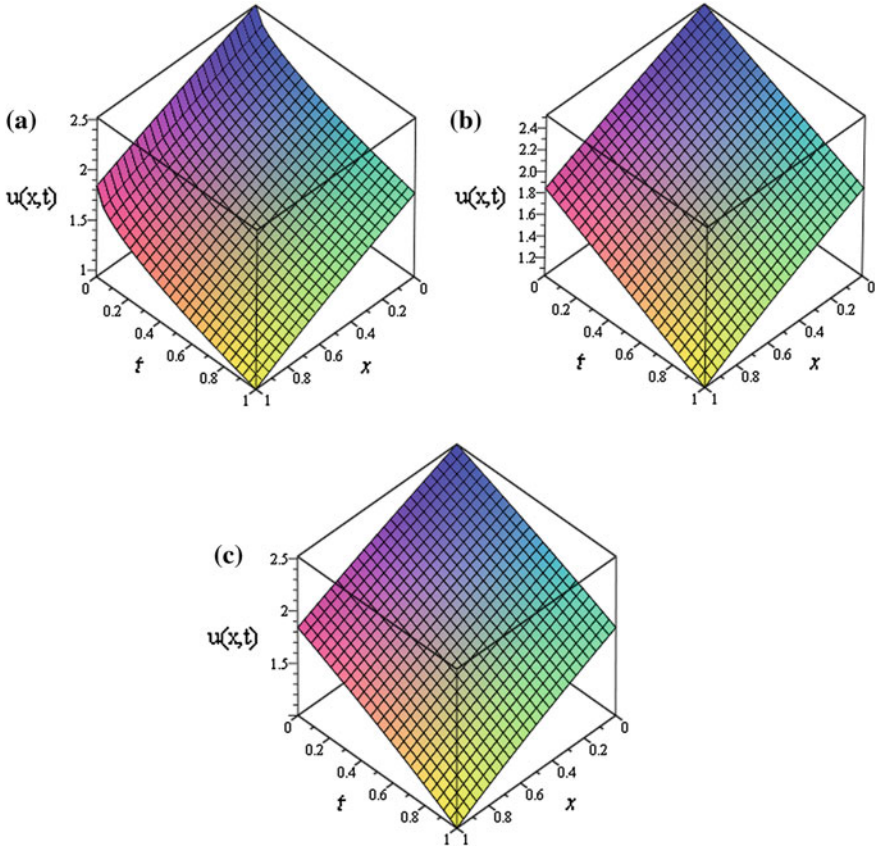
In this section, we use the HPTM to solve the time-fractional Harry Dym Eqs. (1)–(2). Applying the Laplace transform on both sides of Eq. (1) and using result (8), we get

$$L[u(x, t)] = \frac{1}{s} \left( a - \frac{3\sqrt{b}}{2} x \right)^{2/3} + \frac{1}{s^\alpha} L \left[ u^3(x, t) D_x^3 u(x, t) \right]. \tag{17}$$

The inverse Laplace transform implies that

$$u(x, t) = \left( a - \frac{3\sqrt{b}}{2} x \right)^{2/3} + L^{-1} \left[ \frac{1}{s^\alpha} L \left[ u^3(x, t) D_x^3 u(x, t) \right] \right]. \tag{18}$$

Now applying the homotopy perturbation method, we get



**Fig. 1** The behavior of the  $u(x, t)$  w.r.t  $x$  and  $t$  are obtained, when **a**  $\alpha = 1/2$  **b**  $\alpha = 1$  **c** exact solution

$$\sum_{n=0}^{\infty} p^n u_n(x, t) = \left( a - \frac{3\sqrt{b}}{2} x \right)^{2/3} + p \left( L^{-1} \left[ \frac{1}{s^\alpha} L \left[ \sum_{n=0}^{\infty} p^n H_n(u) \right] \right] \right), \quad (19)$$

where  $H_n(u)$  are He's polynomials [13, 14] that represent the nonlinear terms.

The first few components of He's polynomials are given by

$$\begin{aligned} H_0(u) &= u_0^3 D_x^3 u_0, \\ H_1(u) &= u_0^3 D_x^3 u_1 + 3u_0^2 u_1 D_x^3 u_0, \\ &\vdots \end{aligned} \quad (20)$$

Comparing the coefficients of like powers of  $p$ , we have

$$p^0 : u_0(x, t) = \left( a - \frac{3\sqrt{b}}{2}x \right)^{2/3},$$

$$p^1 : u_1(x, t) = L^{-1} \left[ \frac{1}{s^\alpha} L [H_0(u)] \right] = -b^{3/2} \left( a - \frac{3\sqrt{b}}{2}x \right)^{-1/3} \frac{t^\alpha}{\Gamma(\alpha + 1)}, \tag{21}$$

$$p^2 : u_2(x, t) = L^{-1} \left[ \frac{1}{s^\alpha} L [H_1(u)] \right] = -\frac{b^3}{2} \left( a - \frac{3\sqrt{b}}{2}x \right)^{-4/3} \frac{t^{2\alpha}}{\Gamma(2\alpha + 1)},$$

⋮

and so on. Thus, the solution  $u(x, t)$  of the Eq. (1) is given as

$$u(x, t) = u_0(x, t) + u_1(x, t) + u_2(x, t) + \dots \tag{22}$$

The numerical results for the approximate solution obtained by using HPTM and the exact solution given by Mokhtari [7] for constant values of  $a = 4$  and  $b = 1$  for various values of  $t, x$ , and  $\alpha$  are shown in Fig. 1a–c. Figure 1b and c clearly shows that when  $\alpha = 1$ , the approximate solution obtained by the present method is very near to the exact solution.

## 5 Conclusions

In this paper, the HPTM is successfully applied for solving nonlinear time-fractional Harry Dym equation. It is worth mentioning that the HPTM is capable of reducing the volume of the computational work as compared to the classical methods while still maintaining the high accuracy of the numerical result; the size reduction amounts to an improvement in the performance of the approach. In conclusion, the HPTM may be considered as a nice refinement in existing numerical techniques and might find the wide applications.

## References

1. Hilfer, R. (ed.): Applications of Fractional Calculus in Physics, pp. 87–130. World Scientific Publishing Company, Singapore-New Jersey-Hong Kong (2000)
2. Podlubny, I. (ed.): Fractional Differential Equations. Academic Press, New York (1999)
3. Caputo, M.: Elasticita e Dissipazione. Zani-Chelli, Bologna (1969)
4. Miller, K.S., Ross, B.: An Introduction to the fractional Calculus and Fractional Differential Equations. Wiley, New York (1993)
5. Oldham, K.B., Spanier, J.: The Fractional Calculus Theory and Applications of Differentiation and Integration to Arbitrary Order. Academic Press, New York (1974)

6. Kilbas, A.A., Srivastava, H.M., Trujillo, J.J.: Theory and Applications of Fractional Differential Equations. Elsevier, Amsterdam (2006)
7. Mokhtari, R.: Exact solutions of the Harry-Dym equation. *Commun. Theor. Phys.* **55**, 204–208 (2011)
8. Kruskal, M.D., Moser, J.: Dynamical Systems, Theory and Applications, Lecturer Notes Physics, p. 310. Springer, Berlin (1975)
9. Vosconcelos, G.L., Kaclanoff, L.P.: Stationary solution for the Saffman Taylor problem with surface tension. *Phys. Rev. A* **44**, 6490–6495 (1991)
10. Kumar, S., Tripathi, M.P., Singh O.P.: A fractional model of Harry Dym equation and its approximate solution. *Ain Shams Eng. J.* (2012). <http://dx.doi.org/10.1016/j.asej.2012.07.001>
11. He, J.H.: Homotopy perturbation technique. *Comput. Methods Appl. Mech. Eng.* **178**, 257–262 (1999)
12. Khan, Y., Wu, Q.: Homotopy perturbation transform method for nonlinear equations using He's polynomials. *Comput. Math. Appl.* **61**(8), 1963–1967 (2011)
13. Ghorbani, A.: Beyond Adomian's polynomials: He polynomials. *Chaos Solitons Fractals* **39**, 1486–1492 (2009)
14. Mohyud-Din, S.T., Noor, M.A., Noor, K.I.: Traveling wave solutions of seventh-order generalized KdV equation using He's polynomials. *Int. J. Nonlinear Sci. Numer. Simul.* **10**, 227–233 (2009)

# Floating Point-based Universal Fused Add–Subtract Unit

Ishan A. Patil, Prasanna Palsodkar and Ajay Gurjar

**Abstract** This paper describes fused floating point add–subtract operations and which is applied to the implementation of fast fourier transform (FFT) processors. The fused operations of an add–subtract unit which can be used both radix-2 and radix-4 butterflies are implemented efficiently with the two fused floating point operations. When placed and routed using a high-performance standard cell technology, the fused FFT butterflies are about may be work fast and gives user-defined facility to modify the butterfly’s structure. Also the numerical results of the fused implementations are more accurate, as they use rounding modes is defined as per user requirement.

**Keywords** Floating point · Fused · Addition · Subtraction · Universal · Different types of rounding

## 1 Introduction

Traditionally, most DSP applications have used fixed-point arithmetic to reduce delay, chip area, and power consumption. Fixed-point arithmetic has serious problems of overflow, underflow, scaling, etc. Single-precision floating point arithmetic is a potential solution because of no overflow or underflow, automatic scaling [3].

---

I. A. Patil (✉) · P. Palsodkar  
Electronics Engineering Department, Yeshwantrao Chavan College of Engineering,  
Nagpur, Maharashtra, India  
e-mail: ishanpatil29@gmail.com

P. Palsodkar  
e-mail: palsodkar.prasanna@ieee.org

A. Gurjar  
Electronics Engineering Department, Sipna College of Engineering Amravati,  
Amravati, Maharashtra, India  
e-mail: prof\_gurjar1928@rediffmail.com





1. Round to nearest even: default rounding mode increment result if: rs = “11” or (rs = “10” and fln = ‘1’). Otherwise, truncate result significant to 1. flf2...fln
2. Round toward +∞: result is rounded up Increment result if sign is positive and r or s = ‘1’
3. Round toward −∞: result is rounded down Increment result if sign is negative and r or s = ‘1’
4. Round toward 0: always truncate result.

### 3 Normal Addition–Subtraction Rule

$$\begin{array}{r}
 +1.1234 \quad -1.1234 \\
 +1.2456 \quad -1.2456 \\
 \hline
 +2.4690 \quad -2.4690
 \end{array}$$

If we take normal addition or subtraction, consider a two numbers [Greater (G) and Lesser (L)] magnitude wise then only 4 combination are possible which are given in Table 1 [2].

After watching all examples, we came to conclusion that in addition and subtraction when there same sign number added or substrate then only add or subtract, respectively. Similarly, when two numbers have different signs, then we can use opposite function, i.e., subtract or add.

### 4 Study of FP Arithmetic Algorithms

Floating Point addition steps

Assume 32 bit binary number and then by applying algorithm for normal addition by calculator and by using FP addition algorithm stepwise.

$$\begin{aligned}
 A &= 32'b0\_0111\_1000\_1011\_1010\_0000\_1111\_0110\_110; \\
 B &= 32'b0\_0111\_0011\_0101\_0000\_0000\_0011\_1111\_111;
 \end{aligned}$$

**Table 1** Signed addition or subtraction rules

Sr. no	Numbers	Operations	Sign used
1	+G    +L	(+G) + (+L) ⇒ G + L	+
2	−G    −L	(−G) + (−L) ⇒ −G − L ⇒ −(G + L)	+
3	+G    −L	(+G) + (−L) ⇒ G − L	−
4	−G    +L	(−G) + (+L) ⇒ L − G OR −(G − L)	−
1	+G    +L	(+G) − (+L) ⇒ G − L	−
2	−G    −L	(−G) − (−L) ⇒ −G + L ⇒ −(G + L)	−
3	+G    −L	(+G) − (−L) ⇒ G + L	+
4	−G    +L	(−G) − (+L) ⇒ −G − L OR −(G + L)	+

$$A = 1.3490607 * E-2, B = 3.2044944 * E-4.$$

### 4.1 Calculation From Calculator

1st step align decimal point

2nd step add

$$\begin{aligned} &1.3490607 * E-2 \\ &+0.032044944 * E-2 \\ &+1.381105644 * E-2 \end{aligned}$$

3rd Normalize result

### 4.2 Detailed Bitwise Example

<i>S EXP</i>	<i>Mantissa(M)</i>	(1)
0 01111000	1011_1010_0000_1111_0110_110	
0 01110011	0101_0000_0000_0011_1111_111	

Find Greater no. and lesser no. and assign it [6].

$$\begin{aligned} G &= 0 01111000 1011_1010_0000_1111_0110_110 \\ L &= 0 01110011 0101_0000_0000_0011_1111_111 \end{aligned}$$

- **1st step**

Align radix point by using True exponent value difference

$$G\_exp\_t = 0111\_1000(120) - 0111\_1111 = 1111\_1001(-7)$$

$$L\_exp\_t = 0111\_0011(115) - 0111\_1111 = 1111\_0100(-12)$$

$$Ed = G\_exp - L\_exp = 5$$

Shift Lesser no. to right by Ed value

$$\text{Shift\_L\_m} = 1.0101\_0000\_0000\_0011\_1111\_111(0)$$

$$\text{Shift\_L\_m} = 0.10101\_0000\_0000\_0011\_1111\_111(1)$$

$$\text{Shift\_L\_m} = 0.010101\_0000\_0000\_0011\_1111\_111(2)$$

$$\text{Shift\_L\_m} = 0.0010101\_0000\_0000\_0011\_1111\_111(3)$$

$$\text{Shift\_L\_m} = 0.00010101\_0000\_0000\_0011\_1111111(4)$$

$$\text{Shift\_L\_m} = 0.0000\_1010\_1000\_0000\_0001\_111\_111(5)$$

- **2nd step** addition of mantissa depend on signs of both no. (Table 1) and store last bits for rounding

$$1.1011\_1010\_0000\_1111\_0110\_110$$

$$+0.0000\_1010\_1000\_0000\_0001\_111\_111$$

$$01.1100\_0100\_1000\_1111\_1000\_101\_111$$

$$\text{Result\_m} = 01.1100\_0100\_1000\_1111\_1000\_101\_111$$

- **3rd step** normalize mantissa result

n\_Result\_m = 01.1100\_0100\_1000\_1111\_1000\_101\_111  
 (For if result is m = 00.0010\_0100\_1000\_1111\_1000\_101\_111  
 Normalize now m = 01.0010\_0100\_0111\_1100\_0101\_111\_000)  
 (For if result is m = 10.0010\_0100\_1000\_1111\_1000\_101\_111  
 Normalize now m = 01.00010\_0100\_1000\_1111\_1000\_101\_111)

- **4th step** Rounding (Round toward 0: always truncate result)

Round\_Result\_m = 01.1100\_0100\_1000\_1111\_1000\_101

- **5th Step** After rounding normalize

n\_Result\_m = 01.1100\_0100\_1000\_1111\_1000\_101  
 Final Result sig\_G, G\_exp, n\_Result\_m  
 Sum = 0 0111\_1000 1100\_0100\_1000\_1111\_1000\_101  
 +1.3811056 \* E - 2  
 +1.381105644 \* E - 2 (From actual calculation)

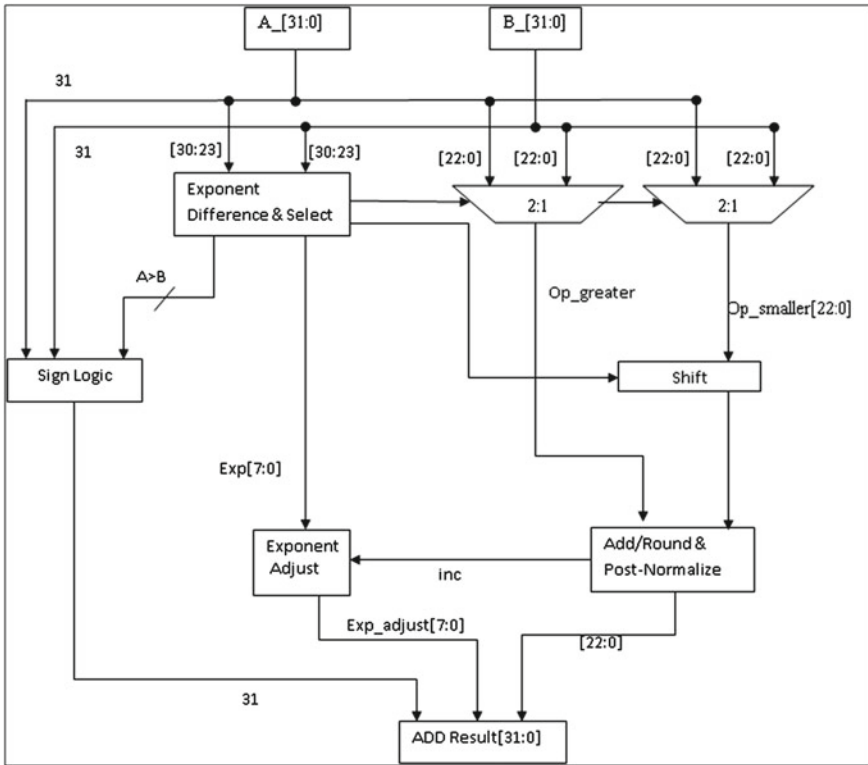
## 5 Floating Point Adders

This contains original floating point adder and proposed floating point adder. Due three limitations like it will also work on invalid floating point, rounding mode, inefficient swap in greater and lesser number when both number have same sign and same exponent. To remove all limitations, we can see their proposed model satisfied in all three manners.

### 5.1 Traditional Floating Point Adder

**Basic Floating Point Addition Algorithm** [1, 3, 8]: The straightforward basic floating point addition algorithm requires the most serial operations. It has the following steps: (Fig. 2)

1. Exponent subtraction: Perform subtraction of the exponents to form the absolute difference  $|E_a - E_b| = d$ .
2. Alignment: Right shift the significant of the smaller operand by d bits. The larger exponent is denoted  $E_f$ .
3. Significant addition: Perform addition or subtraction according to the effective operation. The result is a function of the op-code and the signs of the operands.
4. Conversion: Convert a negative significant result to a sign-magnitude representation. The conversion requires a two’s complement operation, including an addition step.



**Fig. 2** Traditional floating point adder

5. Leading one detection: Determine the amount of left shift needed in the case of Subtraction yielding cancellation. For addition, determine whether or not a 1-bit right shift is required. Then priority-encode the result to drive the normalizing shifter.
6. Normalization: Normalize the significant and update Exponent appropriately.
7. Rounding: Round the final result by conditionally adding as required by the IEEE standard. If rounding causes an overflow, perform a 1-bit right shift and increment  $E_f$ .

### 5.2 Proposed Floating Point Adder

**Proposed Floating Point Addition Algorithm:** The straightforward derived floating point addition algorithm requires the most serial operations. It has the following steps: (Fig. 3)

1. Check given number is floating point number or invalid floating point enable other operation or enable not a FP no to show given data is invalid.

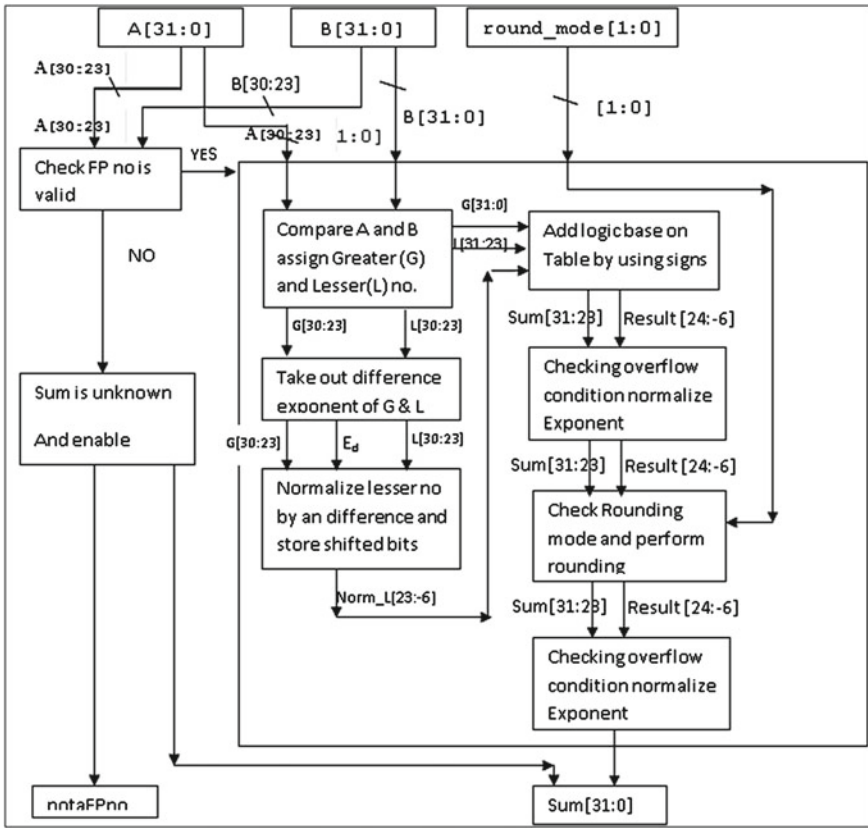


Fig. 3 Proposed floating point adder

2. If given number is valid floating point number then sort out greater and lesser number from data comparing its magnitude.
3. Exponent subtraction: Perform subtraction of greater exponents to lesser exponent  $E_G - E_L = d$ .
4. Alignment: Right shift the significant of the lesser mantissa by d bits and store last 3 shifted bits.
5. Significant addition: Perform addition according to their signs take decision.
6. Normalize result: check result is overflow or not and then according to condition adjust exponent.
7. Rounding: Check the rounding mode and perform rounding on the result with the help of last 3 stored bits.
8. Normalize result: Check result is overflow or not and then according to condition adjust exponent and Display the result.

To remove all limitation in this, we have use 1st check valid floating point or not then for selective rounding, we have given choice to user mode, i.e., user-defined rounding modes to select round mode by giving signals to round\_mode pins, and

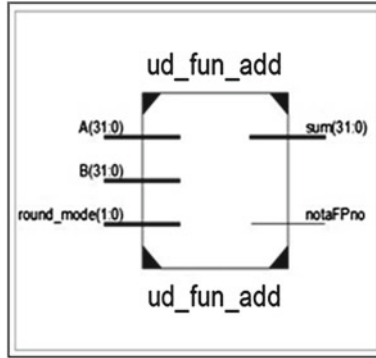


Fig. 4 Adder

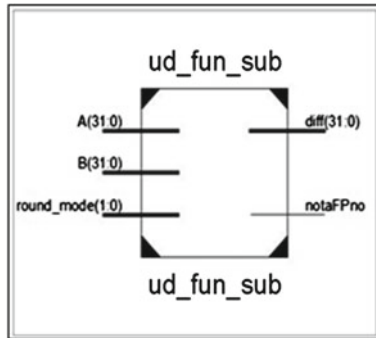


Fig. 5 Subtractor

finally, we have to check exact greater or lesser number by comparing all 31 bits. Similarly, we can create substrater module referring Table 1 and then, we serially and parallel combination of adder and substrater finally we made fuse model of one adder and one substrater and we have advantage that fused required less numbers of LUT's and less delay to get final output as if we use both different models of adder and subtract.

## 6 Proposed Floating Point Work Result

This shows all main modules implementations in RTL and outputs waveforms with respect to Xilinx SPARTAN 6 kit [7] stimulation on Xilinx software.

### 6.1 Proposed Models RTL View

Figures 4, 5 and 6.

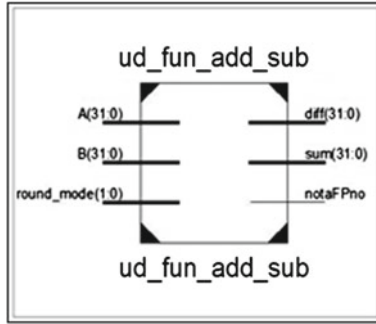


Fig. 6 Add-subtracter

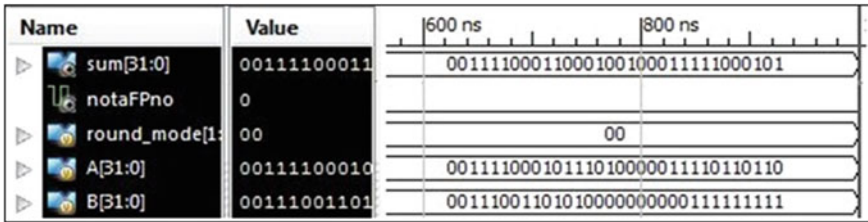


Fig. 7 Adder output waveform

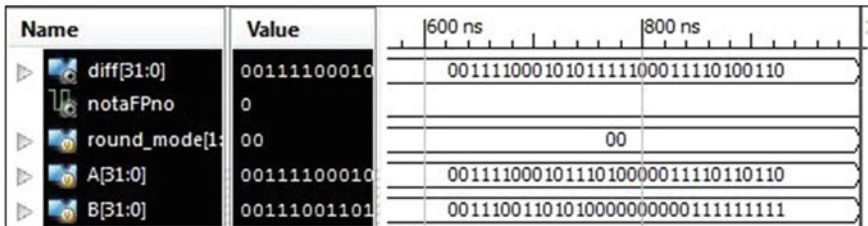


Fig. 8 Subtracter output waveform

### 6.2 Proposed Models Output Waveform

Figures 7, 8 and 9.

## 7 Comparisons of all Modules

See Table 2.

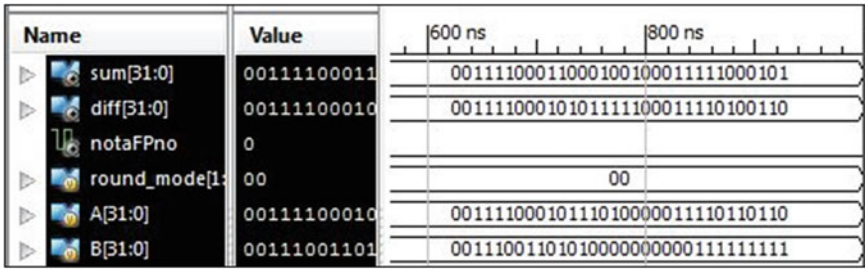


Fig. 9 Add–subtractor output waveform

Table 2 All modules details of implementations

Types	No of LUT used(Area %)	IOBs %	Delay (ns)
<i>FP adder</i>	381 of 9112 (4.18)	99 of 232 (42.67)	35.418
<i>FP subtracter</i>	381 of 9112 (4.18)	99 of 232 (42.67)	35.513
<i>FP Serial AS</i>	762 of 9112 (8.36)	131 of 232 (56.47)	70.518
<i>FP parallel AS</i>	808 of 9112 (8.86)	131 of 232 (56.47)	37.213
<i>Fused FP add–subtract unit</i>	678 of 9112 (7.44)	131 of 232 (56.47)	39.876

Table 3 All modules comparisons in terms of percentage w.r.t. adder

Types	No of LUT used (Area %)	IOBs (%)	Delay (ns)
<i>FP adder</i>	100	100	100
<i>FP subtracter</i>	100	100	100.27
<i>FP serial AS</i>	200	132.32	200
<i>FP parallel AS</i>	212	132.32	105
<i>Fused FP add–subtract unit</i>	177.95	132.32	112.58

Table 4 Basic comparison of programming styles in Verilog on demo floating point adder

Types of programming	Time (ns)	LUTs
<i>Normal adder</i>	26.468	254
<i>Task adder</i>	27.727	308
<i>Function adder</i>	24.533	249

## 8 Conclusions

In proposed floating point adder have two different functions from traditional floating point adder to provide user-defined adder. First is to check the given data are valid floating point number or not. Second is to give privilege to select rounding modes (i.e., user-defined rounding mode selection and default is truncating). While programming, we used different methods like by using TASK, function, and normal programming. After comparing all types of models of floating point adder, we came to conclusion that we modified traditional adder and able to prove that when we use functions in programming has good result at cost of saving 2 % number of LUTs and 7.8 %



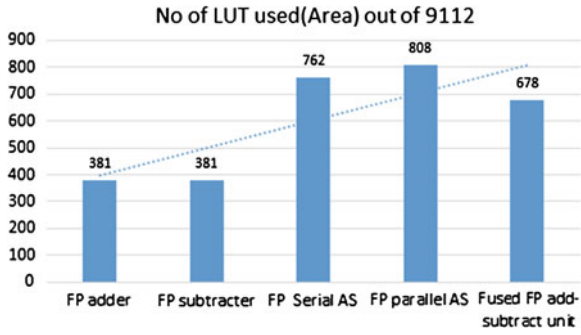


Fig. 10 LUT

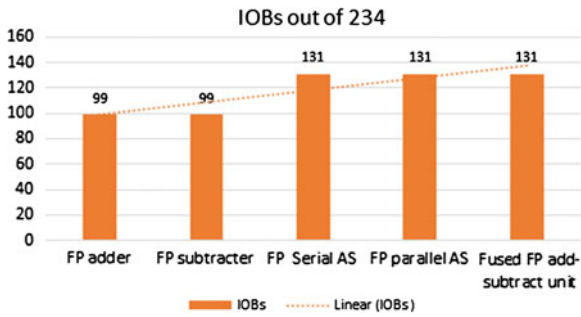


Fig. 11 IOB

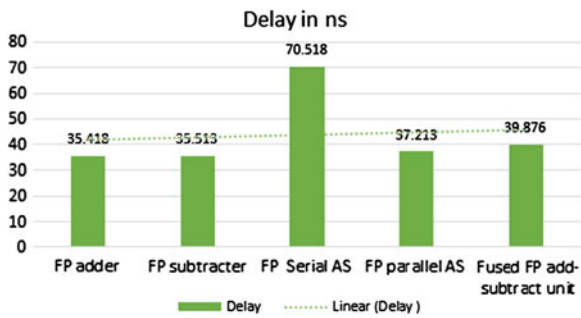


Fig. 12 Delay

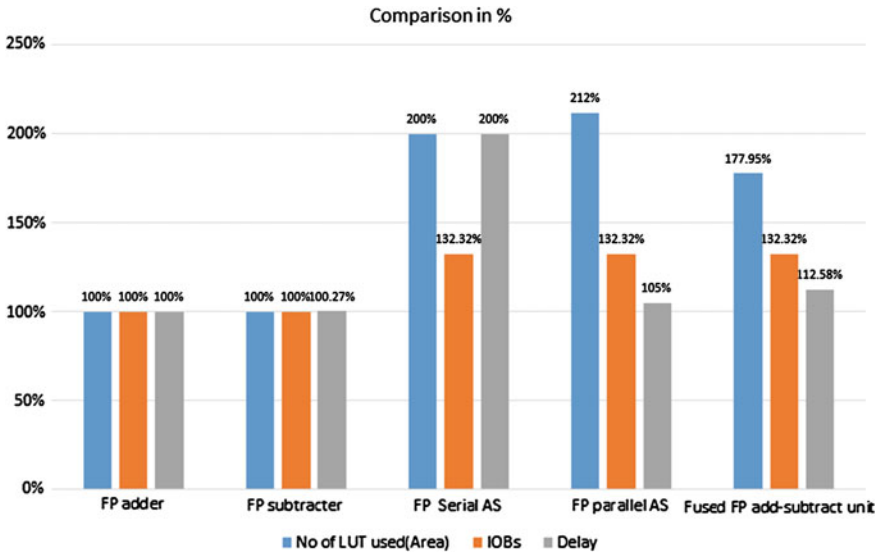


Fig. 13 Comparison in percentage

reduce delay (referring Table 4 Basic comparison of programming styles in Verilog on demo floating point adder). So we finally decided that we are using functions in all Verilog design programs to give best output.

After watching results from Tables 2, 3 and Figs. 10, 11, 12, 13, we came to know that we are saving in proposed floating point add-subtract model is 68 % decrease in IOBs, saving 23 % number of LUTs and 88 % reduce delay as compared to the single adder, single subtracter, serial adder and subtracter, Parallel adder and subtracter.

## References

1. Swartzlander Jr, E.E., Saleh, H.H.: FFT Implementation with Fused Floating-Point Operations. IEEE Transactions on Computers, Feb (2012)
2. Jongwook Sohn and Earl E. Swartzlander, Jr., "Improved Architectures for a Fused Floating-Point Add-Subtract Unit" IEEE Transactions on circuits and systems-I, Vol. 59, no. 11, 2012
3. H. Saleh and E.E. Swartzlander, Jr., "A Floating-Point Fused Add-Subtract Unit", Proc. IEEE Midwest Symp. Circuits and Systems (MWSCAS), pp. 519-522, 2008
4. IEEE Standard for Floating-Point Arithmetic, ANSI/IEEE Standard 754-2008, Aug. 2008
5. [http://www.xilinx.com/FPGA\\_series](http://www.xilinx.com/FPGA_series)
6. Lecture notes - Chapter 7 - Floating Point Arithmetic: <http://pages.cs.wisc.edu/smoler/x86text/lect.notes/arith.flpt.html>
7. All o/p are w.r.to XILINX Spartan-6 XC6SLX16 -CSG324C
8. Stuart Franklin Oberman: Design Issues in High Performance Floating Point Arithmetic Units. Stanford University, Ph. D. Dissertation (1996)

# New Analytical Approach for Fractional Cubic Nonlinear Schrödinger Equation Via Laplace Transform

Jagdev Singh and Devendra Kumar

**Abstract** In this paper, a user-friendly algorithm based on new homotopy perturbation transform method (HPTM) is proposed to obtain approximate solution of a time-space fractional cubic nonlinear Schrödinger equation. The numerical solutions obtained by the HPTM indicate that the technique is easy to implement and computationally very attractive.

**Keywords** Fractional cubic nonlinear Schrödinger equation · Laplace transform · Homotopy perturbation transform method · He's polynomials · Maple code

## 1 Introduction

Fractional differential equations have found applications in many problems of physics and engineering. For example, these equations are increasingly used to model problems in research areas as diverse as dynamical systems, mechanical systems, control, chaos, chaos synchronization, continuous-time random walks, anomalous diffusive and subdiffusive systems, unification of diffusion and wave propagation phenomenon, and others [1–6]. It is difficult to get the exact analytical solution of fractional order problems especially nonlinear cases. The homotopy perturbation method (HPM) was first introduced by the Chinese mathematician J.H. He in 1998 and was further developed by He [7–9]. This method was applied to handle various problems

---

J. Singh (✉)

Department of Mathematics, Jagannath University, Village- Rampura, Tehsil-Chaksu, Jaipur, Rajasthan 303901, India  
e-mail: jagdevsinghrathore@gmail.com

D. Kumar

Department of Mathematics, Jagannath Gupta Institute of Engineering and Technology, Jaipur, Rajasthan 302022, India  
e-mail: devendra.maths@gmail.com

arising in science and engineering [10–14]. In recent years, many authors have paid attention to study the solutions of linear and nonlinear partial differential equations by using various methods combined with the Laplace transform. Among these are Laplace decomposition method (LDM) [15, 16] and homotopy perturbation transform method (HPTM) [17, 18].

In this article, we consider the following time-space fractional cubic nonlinear Schrödinger equation of the form:

$$i \frac{\partial^\alpha u}{\partial t^\alpha} + \frac{\partial^{2\beta} u}{\partial x^{2\beta}} + 2|u|^2 u = 0, \quad t > 0, 0 < \alpha, \beta \leq 1, \tag{1}$$

with the initial condition

$$u(x, 0) = e^{ix}, \quad i = \sqrt{-1}. \tag{2}$$

where  $u(x, t)$  is a function of  $x$  and  $t$ . The derivative is considered in the Caputo sense. In the case of  $\alpha = 1$  and  $\beta = 1$ , the fractional cubic nonlinear Schrödinger equation reduces to the classical cubic nonlinear Schrödinger equation. The time-space fractional cubic nonlinear Schrödinger equation has been previously studied by Herzallah and Gepreel [19] and Hemida et al. [20].

In this paper, we apply the HPTM to solve the time-space fractional cubic nonlinear Schrödinger equation. The HPTM is a combination of Laplace transform method, HPM, and He’s polynomials. It provides the solutions in terms of convergent series with easily computable components in a direct way without using linearization, perturbation, or restrictive assumptions.

## 2 Basic Idea of HPTM

To illustrate the basic idea of this method, we consider a general fractional nonlinear nonhomogeneous partial differential equation with the initial condition of the form:

$$D_t^\alpha u(x, t) + R u(x, t) + N u(x, t) = g(x, t), \tag{3}$$

$$u(x, 0) = f(x), \tag{4}$$

where  $D_t^\alpha u(x, t)$  is the Caputo fractional derivative of the function  $u(x, t)$ ,  $R$  is the linear differential operator,  $N$  represents the general nonlinear differential operator and  $g(x, t)$ , is the source term.

Applying the Laplace transform on both sides of Eq. (3), we get

$$L [u(x, t)] = \frac{f(x)}{s} + \frac{1}{s^\alpha} L [g(x, t)] - \frac{1}{s^\alpha} L [R u(x, t) + N u(x, t)]. \tag{5}$$

Operating with the Laplace inverse on both sides of Eq. (5) gives

$$u(x, t) = G(x, t) - L^{-1} \left[ \frac{1}{s^\alpha} L[Ru(x, t) + Nu(x, t)] \right], \tag{6}$$

where  $G(x, t)$  represents the term arising from the source term and the prescribed initial condition. Now, we apply the HPM

$$u(x, t) = \sum_{n=0}^{\infty} p^n u_n(x, t), \tag{7}$$

and the nonlinear term can be decomposed as

$$Nu(x, t) = \sum_{n=0}^{\infty} p^n H_n(u), \tag{8}$$

for some He’s polynomials  $H_n(u)$  [21, 22] that are given by

$$H_n(u_0, u_1, \dots, u_n) = \frac{1}{n!} \frac{\partial^n}{\partial p^n} \left[ N \left( \sum_{i=0}^{\infty} p^i u_i \right) \right]_{p=0}, \quad n = 0, 1, 2, \dots \tag{9}$$

Using (7) and (8) in (6), we get

$$\sum_{n=0}^{\infty} p^n u_n(x, t) = G(x, t) - p \left( L^{-1} \left[ \frac{1}{s^\alpha} L \left[ R \sum_{n=0}^{\infty} p^n u_n(x, t) + \sum_{n=0}^{\infty} p^n H_n(u) \right] \right] \right), \tag{10}$$

which is the coupling of the Laplace transform and the HPM using He’s polynomials. Comparing the coefficients of like powers of  $p$ , the components  $u_0, u_1, u_2$  and so on are obtained.

### 3 Solution of the Problem

In this section, we use the HPTM to solve the time-space fractional cubic nonlinear Schrödinger Eqs. (1), (2). Applying the Laplace transform on both sides of Eq. (1), we get

$$L[u(x, t)] = \frac{e^{ix}}{s} + \frac{i}{s^\alpha} L \left[ \frac{\partial^{2\beta} u}{\partial x^{2\beta}} + 2u^2 \bar{u} \right], \tag{11}$$

where  $u^2 \bar{u} = |u|^2 u$  and  $\bar{u}$  is the conjugate of  $u$ .

The inverse Laplace transform implies that

$$u(x, t) = e^{ix} + L^{-1} \left[ \frac{i}{s^\alpha} L \left[ \frac{\partial^{2\beta} u}{\partial x^{2\beta}} + 2u^2 \bar{u} \right] \right]. \tag{12}$$

Now applying the HPM, we get

$$\sum_{n=0}^{\infty} p^n u_n(x, t) = e^{ix} + p \left( L^{-1} \left[ \frac{i}{s^\alpha} L \left[ \frac{\partial^{2\beta}}{\partial x^{2\beta}} \left( \sum_{n=0}^{\infty} p^n u_n(x, t) \right) + \left( \sum_{n=0}^{\infty} p^n H_n(u) \right) \right] \right] \right), \tag{13}$$

where  $H_n(u)$  are He’s polynomials that represent the nonlinear terms.

The first few components of He’s polynomials are given by

$$\begin{aligned} H_0(u) &= 2u_0^2 \bar{u}_0, \\ H_1(u) &= 2(u_0^2 \bar{u}_1 + 2u_0 u_1 \bar{u}_0), \\ &\vdots \end{aligned} \tag{14}$$

Comparing the coefficients of like powers of  $p$ , we have

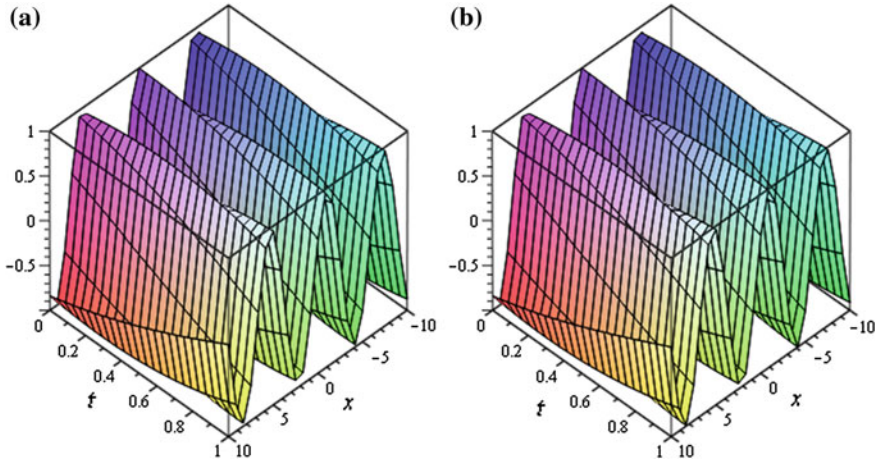
$$\begin{aligned} p^0 : u_0(x, t) &= e^{ix}, \\ p^1 : u_1(x, t) &= L^{-1} \left[ \frac{i}{s^\alpha} L \left[ \frac{\partial^{2\beta}}{\partial x^{2\beta}} u_0 + H_0(u) \right] \right] = c_1 e^{ix} \frac{t^\alpha}{\Gamma(\alpha+1)}, \\ p^2 : u_2(x, t) &= L^{-1} \left[ \frac{i}{s^\alpha} L \left[ \frac{\partial^{2\beta}}{\partial x^{2\beta}} u_1 + H_1(u) \right] \right] = c_2 e^{ix} \frac{t^{2\alpha}}{\Gamma(2\alpha+1)}, \\ p^3 : u_3(x, t) &= L^{-1} \left[ \frac{i}{s^\alpha} L \left[ \frac{\partial^{2\beta}}{\partial x^{2\beta}} u_2 + H_2(u) \right] \right] = c_3 e^{ix} \frac{t^{3\alpha}}{\Gamma(3\alpha+1)}, \\ &\vdots \end{aligned} \tag{15}$$

and so on. After some calculation, we get

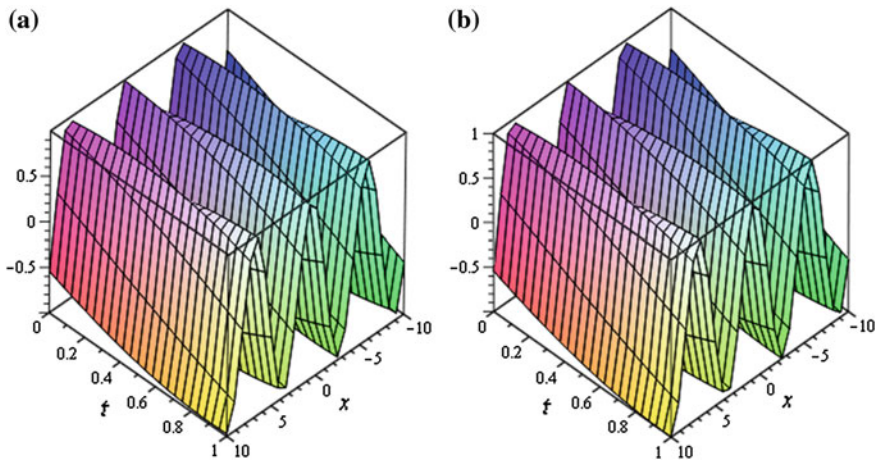
$$\begin{aligned} c_1 &= i(e^{i\pi\beta} + 2), \\ c_2 &= i(e^{i\pi\beta} c_1 + 2\bar{c}_1 + 4c_1), \\ c_3 &= i \left( e^{i\pi\beta} c_2 + 2 \left[ \bar{c}_2 + 2c_2 + \frac{\Gamma(2\alpha + 1)}{(\Gamma(\alpha + 1))^2} (2|c_1|^2 + c_1^2) \right] \right), \\ &\vdots \end{aligned} \tag{16}$$

Therefore, the HPTM series solution is

$$u(x, t) = e^{ix} \left( 1 + \frac{c_1 t^\alpha}{\Gamma(\alpha + 1)} + \frac{c_2 t^{2\alpha}}{\Gamma(2\alpha + 1)} + \frac{c_3 t^{3\alpha}}{\Gamma(3\alpha + 1)} + \dots \right). \tag{17}$$



**Fig. 1** The behavior of the real part of  $u(x, t)$  w.r.t.  $x$  and  $t$  is obtained, when **a**  $\alpha = 1$  and  $\beta = 1$   
**b** Exact solution



**Fig. 2** The behavior of the imaginary part of  $u(x, t)$  w.r.t.  $x$  and  $t$  is obtained, when **a**  $\alpha = 1$  and  $\beta = 1$   
**b** Exact solution

Setting  $\alpha = 1$  and  $\beta = 1$  in (16) and (17), we reproduce the solution of the problem as follows:

$$u(x, t) = e^{ix} \left( 1 + it + \frac{(it)^2}{2!} + \frac{(it)^3}{3!} + \dots \right). \tag{18}$$

This solution is equivalent to the exact solution in closed form

$$u(x, t) = e^{i(x+t)}. \quad (19)$$

The numerical results for the approximate solution obtained by using HPTM at  $\alpha = 1$  and  $\beta = 1$  and the exact solution for various values of  $t$  and  $x$  are shown by Figs. 1 and 2. Figs. 1 and 2 clearly show that, when  $\alpha = 1$  and  $\beta = 1$ , the approximate solution obtained by the HPTM is very near to the exact solution.

## 4 Conclusions

In this paper, the HPTM is successfully employed for solving time-space fractional cubic nonlinear Schrödinger equation. It is worth mentioning that the HPTM is capable of reducing the volume of the computational work as compared to the classical methods while still maintaining the high accuracy of the numerical result; the size reduction amounts to an improvement of the performance of the approach. Finally, we can conclude the HPTM may be considered as a nice refinement in existing numerical techniques and might find the wide applications.

## References

1. Hilfer, R. (ed.): Applications of Fractional Calculus in Physics, pp. 87–130. World Scientific Publishing Company, Singapore, New Jersey, Hong Kong (2000)
2. Podlubny, I.: Fractional Differential Equations. Academic Press, New York (1999)
3. Caputo, M.: Elasticita e Dissipazione. Zani-Chelli, Bologna (1969)
4. Miller, K.S., Ross, B.: An Introduction to the fractional Calculus and Fractional Differential Equations. Wiley, New York (1993)
5. Oldham, K.B., Spanier, J.: The Fractional Calculus Theory and Applications of Differentiation and Integration to Arbitrary Order. Academic Press, New York (1974)
6. Kilbas, A.A., Srivastava, H.M., Trujillo, J.J.: Theory and Applications of Fractional Differential Equations. Elsevier, Amsterdam (2006)
7. He, J.H.: Homotopy perturbation technique. Comput. Methods Appl. Mech. Eng. **178**, 257–262 (1999)
8. He, J.H.: Homotopy perturbation method: a new nonlinear analytical technique. Appl. Math. Comput. **135**, 73–79 (2003)
9. He, J.H.: New interpretation of homotopy perturbation method. Int. J. Mod. Phys. B **20**, 2561–2568 (2006)
10. Abbasbandy, S.: Application of He's homotopy perturbation method to functional integral equations. Chaos, Solitons Fractals **31**, 1243–1247 (2007)
11. Ganji, D.D., Sadighi, A.: Application of He's homotopy perturbation method to nonlinear coupled system of reaction-diffusion equations. Int. J. Nonlinear Sci. Numer. Simul. **7**, 411–418 (2006)
12. Rafei, M., Ganji, D.D.: Explicit solutions of Helmholtz equation and fifth-order KdV equation using homotopy perturbation method. Int. J. Nonlinear Sci. Numer. Simul. **7**, 321–328 (2006)
13. Rafei, M., Ganji, D.D., Daniali, D.: Solution of epidemic model by homotopy perturbation method. Appl. Math. Comput. **187**, 1056–1062 (2007)
14. Ozis, T., Yildirim, A.: Travelling wave solution of KdV equation using He' homotopy perturbation method. Int. J. Nonlinear Sci. Numer. Simul. **8**, 239–242 (2007)



15. Khuri, S.A.: A Laplace decomposition algorithm applied to a class of nonlinear differential equations. *J. Appl. Math.* **1**, 141–155 (2001)
16. Khan, Y.: An effective modification of the Laplace decomposition method for nonlinear equations. *Int. J. Nonlinear Sci. Numer. Simul.* **10**, 1373–1376 (2009)
17. Khan, Y., Wu, Q.: Homotopy perturbation transform method for nonlinear equations using He's polynomials. *Comput. Math. Appl.* **61**(8), 1963–1967 (2011)
18. Singh, J., Kumar, D., Rathore, S.: Application of homotopy perturbation transform method for solving linear and nonlinear Klein-Gordon equations. *J. Inf. Comput. Sci.* **7**(2), 131–139 (2012)
19. Herzallah Mohamed, A.E., Gepreel, K.A.: Approximate solution to time-space fractional cubic nonlinear Schrödinger equation. *Appl. Math. Model.* **36**(11), 56–78 (2012)
20. Hemida, K.M., Gepreel, K.A., Mohamed, M.S.: Analytical approximate solution to the time-space nonlinear partial fractional differential equations. *Int. J. Pure Appl. Math.* **78**(2), 233–243 (2012)
21. Ghorbani, A.: Beyond adomian's polynomials: He polynomials. *Chaos, Solitons Fractals* **39**, 1486–1492 (2009)
22. Mohyud-Din, S.T., Noor, M.A., Noor, K.I.: Traveling wave solutions of seventh-order generalized KdV equation using He's polynomials. *Int. J. Nonlinear Sci. Numer. Simul.* **10**, 227–233 (2009)

# An Investigation on the Structure of Super Strongly Perfect Graphs on Trees

R. Mary Jeya Jothi and A. Amutha

**Abstract** A graph  $G$  is super strongly perfect graph if every induced subgraph  $H$  of  $G$  possesses a minimal dominating set that meets all the maximal cliques of  $H$ . In this paper, we have characterized the super strongly perfect graphs on trees. We have presented the results on trees in terms of domination and codomination numbers  $\gamma$  and  $\bar{\gamma}$ . Also, we have given the relationship between diameter, domination, and codomination numbers in trees.

**Keywords** Super strongly perfect graph · Minimal dominating set · Domination and codomination numbers and tree

## 1 Introduction

Graph theory is a growing area in mathematical research and has a large specialized vocabulary. It is rapidly moving into the mainstream of mathematics mainly because of its applications in diverse fields which include biochemistry (genomics), electrical engineering (communications networks and coding theory), computer science (algorithms and computations), and operations research (scheduling) [1].

A tree is a mathematical structure that can be viewed either as a graph or as a data structure. The two views are equivalent, since a tree data structure contains not only a set of elements, but also connections between elements, giving a tree graph. Trees were first studied by Cayley [2, 3]. A tree is a special kind of graph and follows a particular set of rules. It is a simple, undirected, connected, acyclic graph. A tree does not have a specific direction. Depending on how it is to be used, the tree may branch outward while going [4].

---

R. Mary Jeya Jothi (✉)

Research Scholar, Department of Mathematics, Sathyabama University, Chennai 600119, India  
e-mail: jeyajothi31@gmail.com

A. Amutha

Assistant Professor, Department of Mathematics, Sathyabama University, Chennai 600119, India  
e-mail: amudhajo@gmail.com

## 2 Basic Concepts

In this paper, graphs are finite and simple, that is, they have no loops or multiple edges. Let  $G = (V, E)$  be a graph. A *clique* in  $G$  is a set  $X \subseteq V(G)$  of pairwise adjacent vertices. A subset  $D$  of  $V(G)$  is called a *dominating set* if every vertex in  $V-D$  is adjacent to at least one vertex in  $D$ . A subset  $S$  of  $V$  is said to be a *minimal dominating set* if  $S-\{u\}$  is not a dominating set for any  $u \in S$ . The domination number  $\gamma(G)$  of  $G$  is the smallest size of a dominating set of  $G$ . The domination number of its complement  $\bar{G}$  is called the codomination number of  $G$  and is denoted by  $\gamma(\bar{G})$  or simply  $\bar{\gamma}$  [5]. A shortest  $u-v$  path of a connected graph  $G$  is often called a geodesic. The diameter denoted by  $\text{diam}(G)$  is the length of any longest geodesic. A vertex of degree zero in  $G$  is called an isolated vertex of  $G$ . The minimum degree of a graph is denoted by  $\delta(G)$ .

## 3 Our Results on Super Strongly Perfect Graph

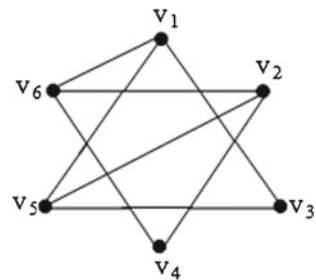
In this paper, we have characterized the super strongly perfect graphs on trees. We have presented the results on trees in terms of domination and codomination numbers  $\gamma$  and  $\bar{\gamma}$ . Also, we have found the relationship between diameter, domination, and codomination numbers of super strongly perfect graph in trees.

### 3.1 Super Strongly Perfect Graph (SSP)

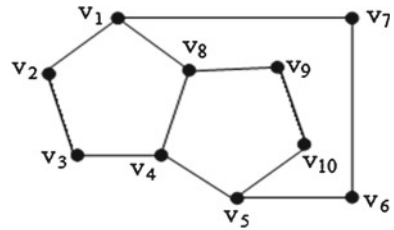
A Graph  $G = (V, E)$  is super strongly perfect if every induced subgraph  $H$  of  $G$  possesses a minimal dominating set that meets all the maximal cliques of  $H$ . Figures 1 and 2 illustrates the structures of SSP and Non-SSP

*Example 1*  $\{v_1, v_2\}$  is a minimal dominating set which meets all maximal cliques of  $G$ .

**Fig. 1** Super strongly perfect graph



**Fig. 2** Non-super strongly perfect graph



*Example 2*  $\{v_1, v_3, v_6, v_9\}$  is a minimal dominating set which does not meet all maximal cliques of  $G$ .

### 4 Cycle Graph

A closed path is called a cycle. A path is a walk in which all vertices are distinct. A walk on a graph is an alternating series of vertices and edges, beginning and ending with a vertex, in which each edge is incident with the vertex immediately preceding it and the vertex immediately following it. An odd cycle is a cycle with odd length, that is, with an odd number of edges. An even cycle is a cycle with even length, that is, with an even number of edges. The number of vertices in a cycle equals the number of edges.

#### 4.1 Theorem

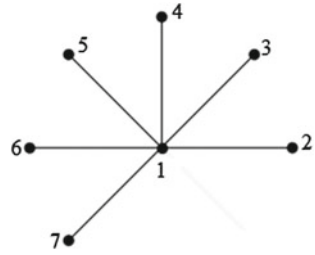
Let  $G = (V, E)$  be a graph with number of vertices  $n$ , where  $n \geq 5$ . Then,  $G$  is super strongly perfect if and only if it does not contain an odd cycle as an induced subgraph [6].

### 5 Tree

An acyclic graph is a graph which contains no cycle. A tree is a connected acyclic graph. Every tree on  $n$  vertices has exactly  $n - 1$  edges. Any two vertices of a tree are connected by exactly one path. Figure 3 illustrates the tree structure which is SSP.

*Example 3*  $\{1\}$  is a minimal dominating set which meets all maximal cliques of  $G$ .

Fig. 3 Tree



**5.1 Theorem**

Every tree is super strongly perfect.

*Proof* Let  $G$  be a tree.

$\Rightarrow G$  does not contain an odd cycle as an induced subgraph.

Now, by the Theorem 4.1,  $G$  is super strongly perfect.

Hence, every tree is super strongly perfect.

**5.2 Theorem**

Let  $G$  be a tree which is super strongly perfect with number of vertices  $n$ , where  $n \geq 2$ , then  $\gamma(G) = 1$  if and only if  $\text{diam}(G) = 2$ .

*Proof* Let  $G$  be a tree which is super strongly perfect with  $n \geq 2$ .

Assume that  $\gamma(G) = 1$ .

$\Rightarrow$  There exists a vertex  $v \in G$  which is adjacent to all the remaining vertices in  $G$ .

To prove  $\text{diam}(G) = 2$ .

Suppose  $\text{diam}(G) > 2$ , then there exists at least two vertices  $a$  and  $b$  with  $\text{diam}(a, b) \geq 3$ .

$\Rightarrow$  There does not exist a vertex in  $G$  which is adjacent to both  $a$  and  $b$ .

$\Rightarrow \gamma(G) > 1$ .

which is a contradiction to the assumption, hence  $\text{diam}(G) = 2$ .

Conversely assume that  $\text{diam}(G) = 2$ .

To prove  $\gamma(G) = 1$ .

Suppose  $\gamma(G) \neq 1$ ,

$\Rightarrow \gamma(G) \geq 2$ , then there does not exist a vertex in  $G$  which is adjacent to all the remaining vertices.

$\Rightarrow$  There exists at least two vertices  $a$  and  $b$  such that  $\text{diam}(a, b) \geq 3$ .

$\Rightarrow \text{diam}(G) \geq 3$ .

Which is a contradiction to the assumption, hence  $\gamma(G) = 1$ .

### 5.3 Theorem

Let  $G$  be a tree which is super strongly perfect with number of vertices  $n$ , where  $n \geq 2$  with  $\gamma(G) = 1$ , then  $\gamma(\overline{G}) = 2$  if and only if  $\text{diam}(\overline{G})$  is not defined.

*Proof* Let  $G$  be a tree which is super strongly perfect,  $n \geq 2$  with  $\gamma(G) = 1$ .

Assume that  $\gamma(\overline{G}) = 2$ .

To prove  $\text{diam}(\overline{G})$  is not defined.

Since  $\gamma(G) = 1$ , there exists a vertex  $v \in G$  which is adjacent to all the vertices in  $G$ .

$\Rightarrow v$  is an isolated vertex in  $(\overline{G})$ .

Since  $\gamma(\overline{G}) = 2$  and  $v$  is an isolated vertex in  $\overline{G}$ , hence  $v$  must be one of the vertex of the minimum dominating set of  $\overline{G}$ .

Let  $u \in \overline{G}$  such that  $\{u, v\}$  be a minimum dominating set of  $\overline{G}$ .

$\Rightarrow \text{diam}(u, v)$  is not defined in  $\overline{G}$ , since  $v$  is an isolated vertex in  $\overline{G}$ .

$\Rightarrow \text{diam}(\overline{G})$  is not defined.

Conversely assume that  $\gamma(G) = 1$  and  $\text{diam}(\overline{G})$  is not defined.

To prove  $\gamma(\overline{G}) = 2$ .

Since  $\text{diam}(\overline{G})$  is not defined, there exists a vertex  $v \in \overline{G}$  which is an isolated vertex such that  $\text{diam}(u, v)$  is not defined for some  $u \in \overline{G}$ .

Since  $\gamma(G) = 1$ ,  $\{v\}$  will be the minimum dominating set of  $G$ .

Since  $G$  is a tree, there exists at least one pendent vertex  $u^1$  incident with a pendent edge, let it be  $e = u^1v^1 \in G$ .

$\Rightarrow u^1$  is a pendent vertex in  $G$ , it is adjacent with all the remaining vertices except  $v^1$  in  $\overline{G}$ .

$\Rightarrow$  There exists a vertex  $u^1$  which is adjacent with all the remaining vertices in  $\overline{G}$  and  $v$  is an isolated vertex in  $\overline{G}$ .

$\Rightarrow \{u^1, v\}$  is a minimum dominating set of  $\overline{G}$ .

$\Rightarrow \gamma(\overline{G}) = 2$ .

Hence proved.

### 5.4 Theorem

Let  $G$  be a tree which is super strongly perfect with number of vertices  $n$ , where  $n \geq 2$ , then  $\gamma(G) > 1$  if and only if  $\text{diam}(G) \geq 3$ .

*Proof* Let  $G$  be a tree which is super strongly perfect with  $n \geq 2$ .

Assume that  $\text{diam}(G) \geq 3$ .

To prove  $\gamma(G) > 1$ .

By the assumption,  $\text{diam}(G) \geq 3$ .

Then, there exists at least two vertices  $u$  and  $v$  of  $G$  such that  $\text{diam}(u, v) \geq 3$ .

$\Rightarrow$  There does not exist a vertex in  $G$  which is adjacent to both  $u$  and  $v$ .

$\Rightarrow \gamma(G) > 1$ .

Conversely assume that  $\gamma(G) \geq 1$ .

$\Rightarrow \gamma(G) \neq 1$ .

By the Theorem 5.2,  $\text{diam}(G) \neq 2$ .

$\Rightarrow \text{diam}(G) > 2$ .

$\Rightarrow \text{diam}(G) \geq 3$ .

Hence proved.

### 5.5 Theorem

Let  $G$  be a tree which is super strongly perfect with number of vertices  $n$ , where  $n \geq 2$  and  $\text{diam}(G) = 2$  then  $\gamma(G) = \delta(G)$ .

*Proof* Let  $G$  be a tree which is super strongly perfect,  $n \geq 2$  and  $\text{diam}(G) = 2$ .

Since  $G$  is a tree,  $\delta(G) = 1$ .

To prove  $\gamma(G) = \delta(G)$ .

It is enough to prove  $\gamma(G) = 1$ .

Suppose  $\gamma(G) > 1$

Then, by the Theorem 5.4,  $\text{diam}(G) \geq 3$ .

which is a contradiction to the hypothesis.

Hence, our assumption is wrong.

$\Rightarrow \gamma(G) = 1$ .

$\Rightarrow \gamma(G) = \delta(G)$ .

Hence proved.

### 5.6 Theorem

Let  $G$  be a tree which is super strongly perfect with number of vertices  $n$ , where  $n \geq 2$ , then  $\text{diam}(G)$  and  $\text{diam}(\overline{G})$  cannot be 1.

*Proof* Let  $G$  be a tree which is super strongly perfect with  $n \geq 2$ .

To prove  $\text{diam}(G) \neq 1$  and  $\text{diam}(\overline{G}) \neq 1$ .

Suppose  $\text{diam}(G) = 1$ .

$\Rightarrow$  All the vertices are pairwise adjacent in  $G$ .

$\Rightarrow G$  is complete, which is a contradiction to the hypothesis.

Hence, our assumption is wrong

$\Rightarrow \text{diam}(G) \neq 1$ .

Now to prove  $\text{diam}(\overline{G}) \neq 1$ .

Suppose  $\text{diam}(\overline{G}) = 1$ .

$\Rightarrow$  All the vertices are pairwise adjacent in  $\overline{G}$ .

$\Rightarrow$  All the vertices are isolated in  $G$ .

$\Rightarrow G$  is not connected.

Which is a contradiction to the hypothesis.

Hence, our assumption is wrong.

$\Rightarrow \text{diam}(\overline{G}) \neq 1$ .

Hence,  $\text{diam}(G) \neq 1$  and  $\text{diam}(\overline{G}) \neq 1$ .

### 5.7 Proposition

Let  $G$  be a tree which is super strongly perfect with number of vertices  $n$ , where  $n \geq 2$ , then  $\text{diam}(G) \geq 3$  if and only if  $\gamma(\overline{G}) = 2$ .

### 5.8 Proposition

Let  $G$  be a tree which is super strongly perfect with number of vertices  $n$ , where  $n \geq 2$ , then  $\text{diam}(\overline{G}) \leq 3$  if and only if  $\gamma(\overline{G}) = 2$ .

## 6 Conclusion

We have investigated the characterization of super strongly perfect graphs on trees. Also, we have given the relationship between diameter, domination, and codomination numbers of super strongly perfect graph in trees. This investigation can be applicable for the well known architectures like bipartite graphs, butterfly graphs, Benes butterfly graphs, and chordal graphs.

## References

1. Foulds, R.: Graph theory applications. Springer, New York (1994)
2. Cayley, A.: On the theory of analytic forms called trees. *Philos. Mag.* **13**, 19–30 (1857)
3. Cayley, A.: On the theory of analytic forms called trees. *Mathematical Papers (Cambridge)* **3**, 242–246 (1891)
4. Bondy, J.A., Murty, U.S.R.: Graph theory with applications. Elsevier Science Publishing Company Inc., New York (1976)
5. Haynes, T.W., Hedetniemi, S.T., Slater, P.J.: Domination in graphs advanced topic. Marcel Dekker, Inc., New York (1998)
6. Amutha, A., Mary Jeya Jothi, R.: Characterization of super strongly perfect graphs. In: Bipartite graphs, proceedings of an international conference on mathematical modelling and scientific computation, 1, 183–185 (2012).



# A Novel Approach for Thin Film Flow Problem Via Homotopy Analysis Sumudu Transform Method

Sushila and Y. S. Shishodia

**Abstract** In this paper, a numerical algorithm based on new homotopy analysis sumudu transform method (HASTM) is proposed to solve a nonlinear boundary value problem arising in the study of thin flow of a third-grade fluid down an inclined plane. The homotopy analysis sumudu transform is a combined form of sumudu transform and homotopy analysis method. The proposed technique finds the solution without any discretization or restrictive assumptions and avoids the round-off errors. The numerical results show that the proposed approach is very efficient and simple and can be applied to other nonlinear problems.

**Keywords** Thin flow problem · Third-grade fluid · Nonlinear boundary value problem · Homotopy analysis sumudu transform method · Maple code

## 1 Introduction

Nonlinear phenomena that appear in many areas of scientific fields, such as solid state physics, plasma physics, fluid mechanics, population models, and chemical kinetics, can be modeled by nonlinear differential equations. Most of the science and engineering problems, especially some heat transfer and fluid flow equations, are nonlinear; therefore, some of these problems are solved by computational fluid dynamic (numerical) method, and some are solved by analytical perturbation method.

---

Sushila (✉)

Department of Physics, Jagan Nath University, Village-Rampura, Tehsil-Chaksu, Jaipur, Rajasthan 303901, India  
e-mail: sushila.jag@gmail.com

Y. S. Shishodia

Pro-Vice-Chancellor, Jagan Nath University, Village- Rampura, Tehsil-Chaksu, Jaipur, Rajasthan 303901, India  
e-mail: yad.shi@gmail.com

Recently, for solving the linear and nonlinear boundary value problems, the analytical techniques have become an ever-increasing interest of the scientists and engineers. These techniques have been dominated by the perturbation methods and have found many applications in physical problems. However, perturbation methods, like other analytical techniques, have their own limitations. For example, all perturbation methods require the presence of a small parameter in the equation, and approximate solutions of the equation are expressed in the form of series expansion containing this parameter. Selection of small parameter also requires special skill. Therefore, an analytical method is welcomed which does not require a small parameter in the equation modeling the phenomenon. Unlike perturbation methods, the homotopy analysis method (HAM) [1] does not require the existence of a small parameter in terms of which a perturbation solution is developed and is thus valid for both weakly and strongly nonlinear problems. In recent years, determining approximate analytical solutions using the homotopy analysis method has generated a lot of interest due to its applicability and efficiency, and this technique has been successfully applied to a number of nonlinear problems [2–6]. Very recently, Sushila et al. [7] have introduced a new approximate method, named homotopy analysis sumudu transform method (HASTM) to handle nonlinear partial differential equations. The homotopy analysis sumudu transform method is a combined form of sumudu transform and homotopy analysis method.

In this paper, we apply the homotopy analysis sumudu transform method (HASTM) to obtain the approximate solutions of nonlinear equation governing the thin flow of a third-grade fluid down an inclined plane. The HASTM provides the solution in a rapid convergent series which may lead to the solution in a closed form. The advantage of this method is its capability of combining two powerful methods for obtaining exact and approximate solutions for nonlinear equations.

## 2 Sumudu Transform

The sumudu transform [8] is defined over the set of functions

$$A = \{f(t) | \exists M, \tau_1, \tau_2 > 0, |f(t)| < M e^{|t|/\tau_j}, \text{ if } t \in (-1)^j \times [0, \infty)\}$$

by the following formula

$$\tilde{f}(u) = S[f(t)] = \int_0^{\infty} f(ut) e^{-t} dt, \quad u \in (-\tau_1, \tau_2). \quad (1)$$

Some of the properties of the sumudu transform were established by Asiru [9]. Further, fundamental properties of this transform were established by Belgacem et al. [10]. The sumudu transform has scale and unit preserving properties, so it can be used to solve problems without resorting to a new frequency domain.

### 3 Governing Equation

The thin film flow of a third-grade fluid down an inclined plane of inclination  $\alpha \neq 0$  is governed by the following nonlinear boundary value problem [11, 12]

$$\frac{d^2U}{dy^2} + \frac{6(\beta_2 + \beta_3)}{\mu} \left(\frac{dU}{dy}\right)^2 \frac{d^2U}{dy^2} + \frac{\rho g \sin \alpha}{\mu} = 0, \tag{2}$$

$$U(0) = 0, \quad \frac{dU}{dy} = 0 \quad \text{at } y = \delta. \tag{3}$$

Introducing the parameters

$$y = \delta y^*, \quad U = \frac{\delta^2 \rho g \sin \alpha}{\mu} U^*,$$

$$\beta^* = \frac{3\delta^2 \rho^2 g^2 \sin^2 \alpha}{\mu^3} (\beta_2 + \beta_3) \tag{4}$$

the problem in Eqs. (2) and (3), after omitting asterisks, takes the following form

$$\frac{d^2U}{dy^2} + 6\beta \left(\frac{dU}{dy}\right)^2 \frac{d^2U}{dy^2} + 1 = 0, \tag{5}$$

$$U(0) = 0, \quad \frac{dU}{dy} = 0 \quad \text{at } y = 1, \tag{6}$$

where  $\mu$  is the dynamic viscosity,  $g$  is the gravity,  $\rho$  is the fluid density, and  $\beta > 0$  is the material constant of a third-grade fluid. We note that Eq. (5) is a second-order nonlinear and inhomogeneous differential equation with two boundary conditions; therefore, it is a well-posed problem.

Through integration of Eq. (5), we have

$$\frac{dU}{dy} + 2\beta \left(\frac{dU}{dy}\right)^3 + y = C_1, \tag{7}$$

where  $C_1$  is a constant of integration. Employing the second condition of (6) in Eq. (7), we obtain  $C_1 = 1$ . Thus, the system (5)–(6) can be written as

$$\frac{dU}{dy} + 2\beta \left(\frac{dU}{dy}\right)^3 + (y - 1) = 0, \tag{8}$$

$$U(0) = 0. \tag{9}$$

It should be noted that for  $\beta = 0$ , Eq. (5) corresponds to that of Newtonian fluid whose exact solution subjected to the boundary conditions (6) is given by

$$U(y) = -\frac{1}{2} [(y - 1)^2 - 1]. \tag{10}$$

In what follows, we will obtain the approximate analytic solution of the nonlinear system (8)–(9) by using the HASTM.

### 4 Basic Idea of HASTM

To illustrate the basic idea of this method, we consider an equation  $N[U(x, t)] = g(x, t)$ , where  $N$  represents a general nonlinear ordinary or partial differential operator including both linear and nonlinear terms. The linear terms are decomposed into  $L + R$ , where  $L$  is the highest order linear operator, and  $R$  is the remaining of the linear operator. Thus, the equation can be written as

$$LU + RU + NU = g(x, t), \tag{11}$$

where  $NU$  indicates the nonlinear terms.

Applying the sumudu transform on both sides of Eq. (11) and using the differentiation property of the sumudu transform, we have

$$S[U] - u^n \sum_{k=0}^{n-1} \frac{U^{(k)}(0)}{u^{(n-k)}} + u^n [S[RU] + S[NU] - S[g(x)]] = 0. \tag{12}$$

We define the nonlinear operator

$$N[\phi(x, t; q)] = S[\phi(x, t; q)] - u^n \sum_{k=0}^{n-1} \frac{\phi^{(k)}(x, t; q)(0)}{u^{(n-k)}} + u^n [S[R\phi(x, t; q)] + S[N\phi(x, t; q)] - S[g(x)]], \tag{13}$$

where  $q \in [0, 1]$  and  $\phi(x, t; q)$  is a real function of  $x, t$  and  $q$ . We construct a homotopy as follows:

$$(1 - q)S[\phi(x, t; q) - U_0(x, t)] = \hbar q H(x, t) N[U(x, t)], \tag{14}$$

where  $S$  denotes the sumudu transform,  $q \in [0, 1]$  is the embedding parameter,  $H(x, t)$  denotes a nonzero auxiliary function,  $\hbar \neq 0$  is an auxiliary parameter,  $U_0(x, t)$  is an initial guess of  $U(x, t)$ , and  $\phi(x, t; q)$  is a unknown function. Obviously, when the embedding parameter  $q = 0$  and  $q = 1$ , it holds

$$\phi(x, t; 0) = U_0(x, t), \quad \phi(x, t; 1) = U(x, t), \tag{15}$$

respectively. Thus, as  $q$  increases from 0 to 1, the solution  $\phi(x, t; q)$  varies from the initial guess  $U_0(x, t)$  to the solution  $U(x, t)$ . Expanding  $\phi(x, t; q)$  in Taylor series with respect to  $q$ , we have

$$\phi(x, t; q) = U_0(x, t) + \sum_{m=1}^{\infty} U_m(x, t)q^m, \tag{16}$$

where

$$U_m(x, t) = \frac{1}{m!} \frac{\partial^m \phi(x, t; q)}{\partial q^m} \Big|_{q=0}. \tag{17}$$

If the auxiliary linear operator, the initial guess, the auxiliary parameter  $\hbar$ , and the auxiliary function are properly chosen, the series (16) converges at  $q = 1$ , then we have

$$U(x, t) = U_0(x, t) + \sum_{m=1}^{\infty} U_m(x, t), \tag{18}$$

which must be one of the solutions of the original nonlinear equations. According to the definition (18), the governing equation can be deduced from the zero-order deformation (14). Define the vectors

$$\vec{U}_m = \{U_0(x, t), U_1(x, t), \dots, U_m(x, t)\}. \tag{19}$$

Differentiating the zero-order deformation Eq. (14)  $m$ -times with respect to  $q$  and then dividing them by  $m!$  and finally setting  $q = 0$ , we get the following  $m$ th-order deformation equation:

$$S[U_m(x, t) - \chi_m U_{m-1}(x, t)] = \hbar H(x, t) \mathfrak{R}_m(\vec{U}_{m-1}). \tag{20}$$

Applying the inverse sumudu transform, we have

$$U_m(x, t) = \chi_m U_{m-1}(x, t) + \hbar S^{-1}[H(x, t) \mathfrak{R}_m(\vec{U}_{m-1})], \tag{21}$$

where

$$\mathfrak{R}_m(\vec{U}_{m-1}) = \frac{1}{(m-1)!} \frac{\partial^{m-1} N[\phi(x, t; q)]}{\partial q^{m-1}} \Big|_{q=0}, \tag{22}$$

and

$$\chi_m = \begin{cases} 0, & m \leq 1, \\ 1, & m > 1. \end{cases} \tag{23}$$

### 5 Solution of the Problem

According to HASTM, we take the initial guess as

$$U_0(y) = y - \frac{y^2}{2}. \tag{24}$$

Applying sumudu transform on both sides of Eq. (8), we have

$$S[U] - u + u^2 + 2\beta u S \left[ \left( \frac{dU}{dy} \right)^3 \right] = 0. \tag{25}$$

We define the nonlinear operator

$$N [\phi(y; q)] = S [\phi(y; q)] - u + u^2 + 2\beta u S \left[ \left( \frac{d\phi(y; q)}{dy} \right)^3 \right] \tag{26}$$

and thus

$$\mathfrak{R}_m(\vec{U}_{m-1}) = S \left[ \vec{U}_{m-1} \right] - (1 - \chi_m)(u - u^2) + 2\beta u S \left[ \sum_{i=0}^{m-1} \sum_{l=0}^i \frac{dU_l}{dy} \frac{dU_{i-l}}{dy} \frac{dU_{m-1-i}}{dy} \right]. \tag{27}$$

The  $m$ th -order deformation equation is given by

$$S [U_m(y) - \chi_m U_{m-1}(y)] = \hbar \mathfrak{R}_m(\vec{U}_{m-1}). \tag{28}$$

Applying the inverse sumudu transform, we have

$$U_m(y) = \chi_m U_{m-1}(y) + \hbar S^{-1}[\mathfrak{R}_m(\vec{U}_{m-1})]. \tag{29}$$

Solving the above Eq. (29), for  $m = 1, 2, 3, \dots$ , we get

$$U_1(y) = -\frac{\beta \hbar}{2} [(y - 1)^4 - 1], \tag{30}$$

$$U_2(y) = -\frac{\beta \hbar}{2} (1 + \hbar) [(y - 1)^4 - 1] - 2\beta^2 \hbar^2 [(y - 1)^6 - 1], \tag{31}$$

$$\begin{aligned}
 U_3(y) = & -\frac{\beta\hbar}{2}(1+\hbar)^2\left[(y-1)^4-1\right]-4\beta^2\hbar^2(1+\hbar)\left[(y-1)^6-1\right] \\
 & -12\beta^3\hbar^3\left[(y-1)^8-1\right], \\
 & \vdots
 \end{aligned}
 \tag{32}$$

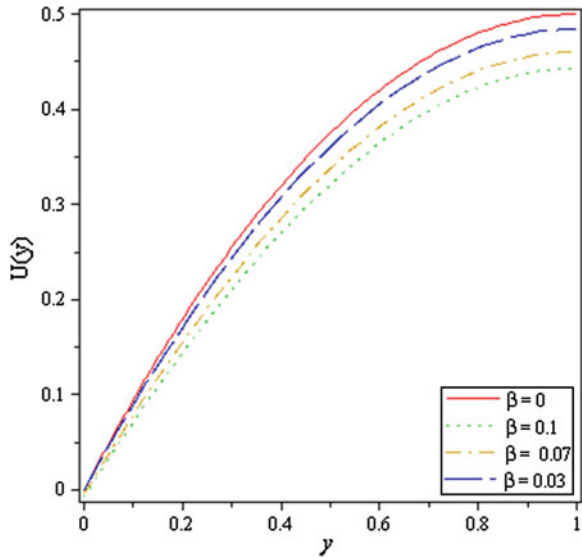
The series solution is given by

$$U(y) = U_0(y) + U_1(y) + U_2(y) + U_3(y) + \dots
 \tag{33}$$

If we put  $\hbar = -1$  in Eqs. (30)–(33), we can recover the solutions obtained by using HPM [9], VIM [10], and ADM [10].

In the solution (33), the terms involving the powers of  $\beta$  gives the contribution of the non-Newtonian fluid. It is worth noting that by setting  $\beta = 0$  in the above approximations, we recover the exact solution for the case of Newtonian fluid. Thus, the first approximation of the nonlinear system (8)–(9) obtained by HASTM is identical with the exact solutions of the corresponding linear problem. This indicates that the HASTM can be equally applied to linear equations. The effects of the non-Newtonian parameter  $\beta$  on the velocity given in (33) are shown in Fig. 1. It is depicted that as we decrease the non-Newtonian parameter  $\beta$ , the solution converges to the Newtonian case.

**Fig. 1** Variations in velocity with  $y$  for different values of  $\beta$



## 6 Conclusions

In this paper, the homotopy analysis sumudu transform method (HASTM) is employed for solving the nonlinear equation governing the thin flow of a third-grade fluid down an inclined plane. The numerical results reveal that the HASTM is a very effective method and might find wide applications to solve many types of nonlinear differential equations in science, engineering, and finance. Maple has been used for computation in this paper.

## References

1. Liao, S.J.: *Beyond Perturbation: Introduction to homotopy analysis method*. Chapman and Hall / CRC Press, Boca Raton (2003)
2. Liao, S.J.: On the homotopy analysis method for nonlinear problems. *Appl. Math. Comput.* **147**, 499–513 (2004)
3. Liao, S.J.: A new branch of solutions of boundary-layer flows over an impermeable stretched plate. *Int. J. Heat Mass Trans.* **48**, 2529–2539 (2005)
4. Qi, W.: Application of homotopy analysis method to solve relativistic Toda-Lattice system. *Commun. Theor. Phys.* **53**, 1111–1116 (2010)
5. Shidfar, A., Molabrahimi, A.: A weighted algorithm based on the homotopy analysis method: application to inverse heat conduction problems. *Commun. Nonlinear Sci. Numer. Simul.* **15**, 2908–2915 (2010)
6. Kheiri, H., Alipour, N., Dehgani, R.: Homotopy analysis and Homotopy-Pade methods for the modified Burgers-Korteweg-de-Vries and the Newell Whitehead equation. *Math. Sci.* **5**(1), 33–50 (2011)
7. Sushila, Kumar, D., Singh, J., Gupta, S.: Homotopy analysis sumudu transform method for nonlinear equations. *Int. J. Ind. Math.* **4**, 301–314 (2012)
8. Watugala, G.K.: Sumudu transform- a new integral transform to solve differential equations and control engineering problems. *Math. Engg. Indust.* **6**(4), 319–329 (1998)
9. Asiru, M.A.: Further properties of the Sumudu transform and its applications. *Int. J. Math. Educ. Sci. Tech.* **33**, 441–449 (2002)
10. Belgacem, F.B.M., Karaballi, A.A., Kalla, S.L.: Analytical investigations of the Sumudu transform and applications to integral production equations. *Math. Prob. Engg.* **3**, 103–118 (2003)
11. Siddique, A.M., Mahmood, R., Ghori, Q.K.: Homotopy perturbation method for thin film flow of a third grade fluid down an inclined plane. *Chaos Solitons Fractals* **35**(1), 140–147 (2008)
12. Siddique, A.M., Farooq, A.A., Haroon, T., Rana, M.A., Babcock, B.S.: Application of He's variational iterative method for solving thin flow problem arising in non-Newtonian fluid mechanics. *World J. Mech.* **2**, 138–142 (2012)



# Buckling and Vibration of Non-Homogeneous Orthotropic Rectangular Plates with Variable Thickness Using DQM

Renu Saini and Roshan Lal

**Abstract** The present work analyzes the buckling and vibration behavior of non-homogeneous orthotropic rectangular plates of variable thickness and subjected to constant in-plane force along two opposite simply supported edges on the basis of classical plate theory. The other two edges may be clamped, simply supported, and free. For non-homogeneity of the plate material, it is assumed that Young's moduli and density vary exponentially along one direction. The governing partial differential equation of motion of such plates has been reduced to an ordinary differential equation using the sine function for mode shapes between the simply supported edges. This has been solved numerically employing DQM. The effect of various parameters has been studied on the natural frequencies for the first three modes of vibration. Critical buckling loads by allowing frequencies to approach zero have been computed. Comparison has been made with the known results.

**Keywords** Non-homogeneous · Orthotropic · Rectangular · Buckling · DQM

## 1 Introduction

Plates of various geometries are key components in many structural and machinery applications, particularly in aerospace, civil, mechanical, and automotive industries. In various engineering applications, plates are often subjected to in-plane stresses arising from hydrostatic, centrifugal, and thermal stresses [1–3], which may induce buckling, a phenomenon that is highly undesirable. A lot of work has been carried out to study the vibration of rectangular plates and reported in references [4, 5]. Orthotropic plates are often non-homogeneous either by design or because of the

---

R. Saini (✉) · R. Lal  
Department of Mathematics, Indian Institute of Technology Roorkee,  
Roorkee 247667, India  
e-mail: renusaini189@gmail.com

physical composition and imperfection in the underlying materials. Very few models representing the behavior of non-homogeneous materials have been proposed in the literature, and some recent references are [6–8]. The present paper analyzes the behavior of non-homogeneous orthotropic rectangular plates whose two opposite edges are assumed to be simply supported and are subjected to constant in-plane force on the basis of classical plate theory. For non-homogeneity of the plate material, it is assumed that Young’s moduli and density vary exponentially along one direction. The governing differential equation for such plates reduces to fourth-order differential equation with variable coefficients whose analytical solution is not feasible. DQM has been employed to obtain the natural frequency for C-C, C-S, and C-F boundary conditions.

## 2 Formulation

Consider a non-homogeneous orthotropic rectangular plate of dimension  $a \times b$  and thickness  $h(x, y)$ . The  $x$  and  $y$  axes are taken along the principal directions of orthotropy, and axis of  $z$  is perpendicular to the  $xy$  plane. The plate that is simply supported at  $y = 0$  and  $b$  is taken to be under constant in-plane force  $N_y$  along these two edges (Fig. 1). The differential equation of motion is given by

$$\begin{aligned}
 D_x \frac{\partial^4 w}{\partial x^4} + D_y \frac{\partial^4 w}{\partial y^4} + 2H \frac{\partial^4 w}{\partial x^2 \partial y^2} + 2 \frac{\partial H}{\partial x} \frac{\partial^3 w}{\partial x \partial y^2} + 2 \frac{\partial H}{\partial y} \frac{\partial^3 w}{\partial y \partial x^2} \\
 + 2 \frac{\partial D_x}{\partial x} \frac{\partial^3 w}{\partial x^3} + 2 \frac{\partial D_y}{\partial y} \frac{\partial^3 w}{\partial y^3} + \frac{\partial^2 D_x}{\partial x^2} \frac{\partial^2 w}{\partial x^2} + \frac{\partial^2 D_y}{\partial y^2} \frac{\partial^2 w}{\partial y^2} \\
 + \frac{\partial^2 D_1}{\partial x^2} \frac{\partial^2 w}{\partial y^2} + \frac{\partial^2 D_1}{\partial y^2} \frac{\partial^2 w}{\partial x^2} + 4 \frac{\partial^2 D_{xy}}{\partial x \partial y} \frac{\partial^2 w}{\partial x \partial y} + \rho h \frac{\partial^2 w}{\partial t^2} - N_y \frac{\partial^2 w}{\partial y^2} = 0,
 \end{aligned}
 \tag{1}$$

where  $D_x = E_x^* h^3 / 12$ ,  $D_y = E_y^* h^3 / 12$ ,  $D_{xy} = G_{xy} h^3 / 12$ ,  $D_1 = E^* h^3 / 12$ ,

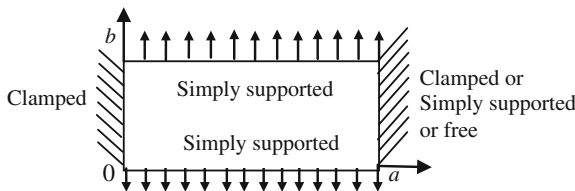


Fig. 1 Geometry of the plate and boundary conditions

$H = D_1 + 2D_{xy}$ ,  $E^* = \nu_y E_x^* = \nu_x E_y^*$ ,  $(E_x^*, E_y^*) = (E_x, E_y)/(1 - \nu_x \nu_y)$ ,  $w(x, y, t)$  is the transverse deflection,  $t$  is the time, and  $E_x, E_y, \nu_x, \nu_y, G_{xy}$  are material constants.

Let us assume that  $h = h(x)$ , i.e., independent of  $y$ . For harmonic solution, the deflection  $w$  is assumed to be

$$w(x, y, z) = \bar{w}(x) \sin(p\pi y/b)e^{i\omega t} \tag{2}$$

where  $p$  is a positive number and  $\omega$  is the frequency in radians. Further, for elastically non-homogeneous material, it is assumed that the  $E_x, E_y$ , and  $\rho$  are the functions of  $x$  only, i.e.,  $E_x = E_1 e^{\mu X}$ ,  $E_y = E_2 e^{\mu X}$ ,  $\rho = \rho_0 e^{\beta X}$  and the shear modulus is  $G_{xy} = \sqrt{E_x E_y}/2(1 + \sqrt{\nu_x \nu_y})$ . Using (2) and introducing the non-dimensional variables  $X = x/a, Y = y/b, \bar{h} = h/a, W = \bar{w}/a$  where  $\bar{h} = h_0 e^{\alpha X}$ , Eq. (1) reduces to  $A_0 W^{iv} + A_1 W''' + A_2 W'' + A_3 W' + A_4 W = 0$ , where  $A_0 = 1$

$$\begin{aligned} A_1 &= 2(\mu + 3\alpha), A_2 = (\mu + 3\alpha)^2 - 2\sqrt{E_2/E_1}\lambda^2, A_3 = -2(\mu + 3\alpha)\sqrt{E_2/E_1}\lambda^2 \\ A_4 &= \lambda^4 E_2/E_1 - \nu_y(\mu + 3\alpha)^2 \lambda^2 - \Omega^2 e^{(\beta - \mu - 2\alpha)X} + \lambda^2 \bar{N}_y e^{(-\mu - 3\alpha)X} \end{aligned} \tag{3}$$

$\lambda^2 = \pi^2 a^2 p^2 / b^2$ ,  $\Omega^2 = 12 \rho_0 (1 - \nu_x \nu_y) a^2 \omega^2 / E_1 h$ ,  $N_0^* = 12 N_y (1 - \nu_x \nu_y) / a E_1 h_0^3$  and prime denotes the differentiation with respect to  $X$ . Here,  $(h_0, \rho_0) = (h, \rho)_{X=0}$ ,  $\mu$  is the non-homogeneity parameter,  $\alpha$  is the taper parameter,  $\beta$  is the density parameter, and  $E_1, E_2$  are Young's moduli. Equation (3) is a fourth-order differential equation with variable coefficients whose approximate solution is obtained by DQM.

### 3 Method of Solution and Boundary Conditions

Let  $X_1, X_2 \dots X_N$  be the  $N$  grid points in the applicability range  $[0, 1]$  of the plate. According to DQM, the  $n$ th-order derivative of  $W(X)$  with respect to  $X$  can be expressed discretely at the point  $X_i$  as

$$\frac{d^n W(X_i)}{dX^n} = \sum_{j=1}^N c_{ij}^{(n)} W(X_j), \quad i = 1, 2, \dots, N$$

where  $c_{ij}^{(n)}$  are the weighting coefficients at  $X_i$  and given by

$$\begin{aligned} c_{ij}^{(n)} &= M^{(1)}(X_i)/(X_i - X_j)M^{(1)}(X_j), \quad i = 1, 2 \dots N (i \neq j), \\ M^{(1)}(X_i) &= \prod_{j=1, j \neq i}^N (X_i - X_j) \end{aligned}$$

$$c_{ij}^{(n)} = n \left( c_{ii}^{(n-1)} c_{ij}^{(1)} - \frac{c_{ij}^{(n-1)}}{(X_i - X_j)} \right) \quad i, j = 1, 2 \dots N, j \neq i \text{ and } n = 2, 3, 4$$

$c_{ii}^{(n)} = -\sum_{j=1, j \neq i}^N c_{ij}^{(n)}$ ,  $i = 1, 2, \dots, N$  and  $n = 1, 2, 3, 4$ . Discretizing Eq. (3) and substituting for  $W(X)$  and its derivative at the  $i$ th grid point

$$\sum_{j=1}^N \left( A_0 c_{ij}^{(4)} + A_1 c_{ij}^{(3)} + A_2 c_{ij}^{(2)} + A_3 c_{ij}^{(1)} \right) W(X_j) + A_{4,i} W(X_i) = 0 \quad (4)$$

For  $i = 3, 4 \dots (N - 2)$ , ones obtain a set of  $(N - 4)$  equations in terms of unknowns  $W_j (\equiv W(X_j))$ ,  $j = 1, 2, \dots, N$ , which can be written in the matrix form as

$$[B][W^*] = [0], \quad (5)$$

where  $B$  and  $W^*$  are matrices of order  $(N - 4) \times N$  and  $(N \times 1)$ , respectively. The  $(N - 2)$  internal grid points are the zeroes of shifted Chebyshev polynomial in the range  $[0, 1]$  given by  $X_{k+1} = 1/2[1 + \cos((2k - 1)\pi/2(N - 2))]$ ,  $k = 1, 2, \dots, N - 2$ .

The three sets of boundary conditions, namely C-C, C-S, and C-F, have been considered. By satisfying the relations, a set of four homogeneous equations are obtained.

$$\begin{aligned} W = dW/dX = 0; \quad W = (d^2W/dX^2) - (E^*/E_x^*)\lambda^2 W = 0 \text{ and} \\ W = (d^2W/dX^2) - (E^*/E_x^*)\lambda^2 W \\ = (d^3W/dX^3) - \lambda^2(E^* + 4G_{xy})/E_x(dW/dX) = 0. \end{aligned}$$

This set together with field Eq. (5) gives a complete set of  $N$  equations in  $N$  unknowns, which is expressed as

$$\begin{bmatrix} A \\ B^{CC} \end{bmatrix} \{B\} = 0 \quad (6)$$

For a non-trivial solution of Eq. (6), the frequency determinant must vanish, and hence,

$$\left| \begin{matrix} A \\ B^{CC} \end{matrix} \right| = 0, \quad (7)$$

Similarly for C-S and C-F plates

$$\left| \begin{matrix} A \\ B^{CS} \end{matrix} \right| = 0, \quad (8)$$

$$\left| \begin{matrix} A \\ B^{CF} \end{matrix} \right| = 0. \quad (9)$$

### 4 Numerical Results and Discussions

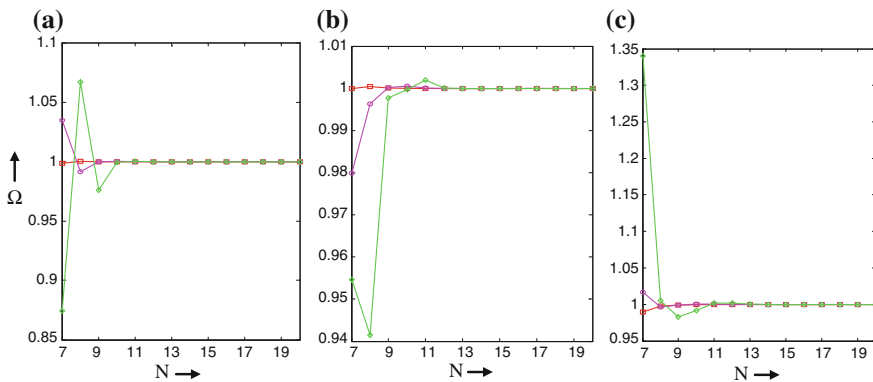
The frequency Eqs. (7–9) provide the values of frequency parameter  $\Omega$  for various values of  $\bar{N}_y = -50$  (20) 50, 0,  $\beta = -0.5$  (0.2) 0.5, 0.0, 0.1,  $\alpha = -0.5$  (0.2) 0.5, 0.0, 0.1,  $\mu = -0.5$  (0.2) 0.5, 0.0, 0.1 and  $a/b = 0.25$  (0.25) 2.0 for  $p = 1$ . The values of elastic constants for plate material ‘ORTH01’ are taken as  $(E_1, E_2) = (1 \times 10^{10}, 0.5 \times 10^{10})$  MPa,  $\nu_x = 0.2, \nu_y = 0.1$ . To choose the appropriate number of grid points  $N$ , a convergence study has been carried out and graphs are shown in Fig. 2. The value of  $N$  has been fixed as 17, for all the three plates.

The results are presented in Figs. (3, 4, 5, 6 and 7) and Table 1. In Fig. 3a, it is observed that  $\Omega$  increases with the increasing values of  $\bar{N}_y$  for all three boundary conditions. The rate of increase in  $\Omega$  with  $\bar{N}_y$  increases in the order of boundary conditions C-C, C-S, and C-F. In Fig. 3b, c, the behavior of  $\Omega$  with  $\bar{N}_y$  is the same except the rate of increase in  $\Omega$  with  $\bar{N}_y$  decreases with the increase in the number of modes.

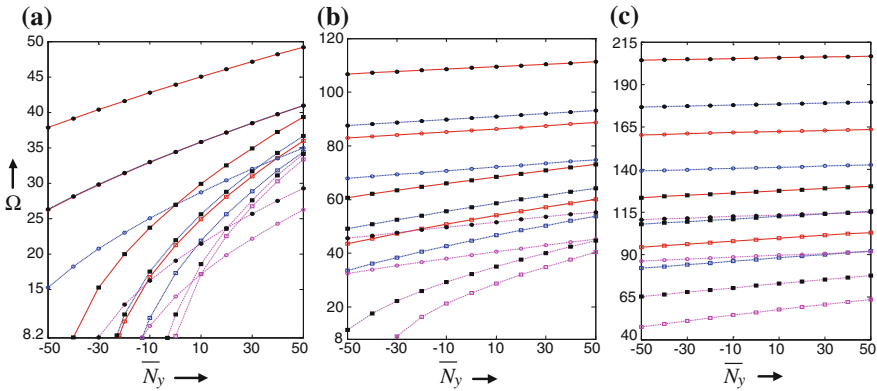
In Fig. 4a, it is observed that  $\Omega$  increases with the increasing values of  $\mu$  for all three plates. The rate of increase in  $\Omega$  with  $\mu$  increases in the order of boundary conditions C-F, C-S, and C-C. In Fig. 4b, c, the rate of increase in  $\Omega$  with increasing values of  $\mu$  increases with the increase in the number of modes.

From Fig. 5a, it is clear that  $\Omega$  decreases with increasing value of  $\beta$ . The rate of decrease in  $\Omega$  with  $\beta$  for a C-S plate is higher than that for a C-F plate but lower for a C-C plate. For II and III modes of vibration, this rate of decrease in  $\Omega$  further increases in the same order of boundary conditions as shown in Fig. 5b, c.

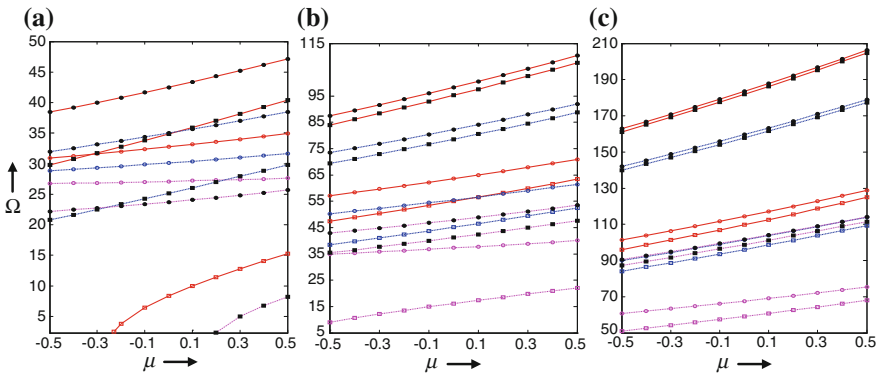
From Fig. 6a, it is observed that  $\Omega$  increase with the increasing values of  $\alpha$  when  $\bar{N}_y < 0$  for all three plates. In Fig. 6b, c, the value of  $\Omega$  increases with the increasing values of  $\alpha$  for all three plates.



**Fig. 2** Normalized frequency parameter  $\Omega/\Omega^*$ : **a** C-C plate, **b** C-S plate, and **c** C-F plate, for  $a/b = 1, \beta = -0.5, \mu = -0.5, \bar{N}_y = 30$ , square, I mode circle, II mode lozenge, III mode.  $\Omega^*$ -result using 20 grid points



**Fig. 3** Frequency parameter: **a** I mode, **b** II mode, and **c** III mode for  $\beta = -0.5, a/b = 1$ . —C-C; - - -, C-S; -.-., C-F; *square*,  $\mu = \alpha = -0.5$ ; *blacksquare*,  $\mu = 0.5, \alpha = -0.5$ ; *circle*,  $\mu = -0.5, \alpha = 0.5$ ; *blackcircle*,  $\mu = \alpha = 0.5$



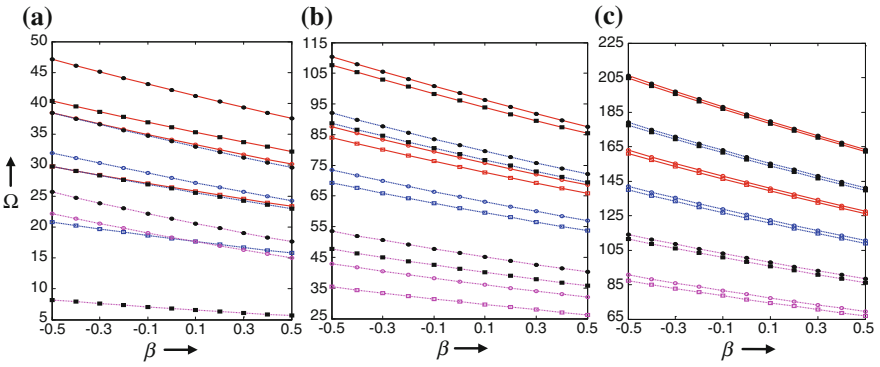
**Fig. 4** Frequency parameter: **a** I mode, **b** II mode, and **c** III mode for  $\beta = -0.5, \dots$ —C-C; - - -, C-S; -.-., C-F; *square*,  $\bar{N}_y = 30, \alpha = -0.5$ ; *blacksquare*,  $\bar{N}_y = 30, \alpha = -0.5$ ; *circle*,  $\bar{N}_y = 30, \alpha = 0.5$ ; *blackcircle*,  $\bar{N}_y = 30, \alpha = 0.5$

In Fig. 7a, it is found that  $\Omega$  increases with the increasing values of  $a/b$  for all three plates. The rate of change of  $\Omega$  with  $a/b$  increases for  $\bar{N}_y = -30$  and decreases for  $\bar{N}_y = 30$  with the increase in the number of modes as shown in Fig. 7b, c. By allowing the frequency to approach zero, the critical values  $\bar{N}_{cr}$  of  $\bar{N}_y$  have been computed for all the three plates (Table 1).

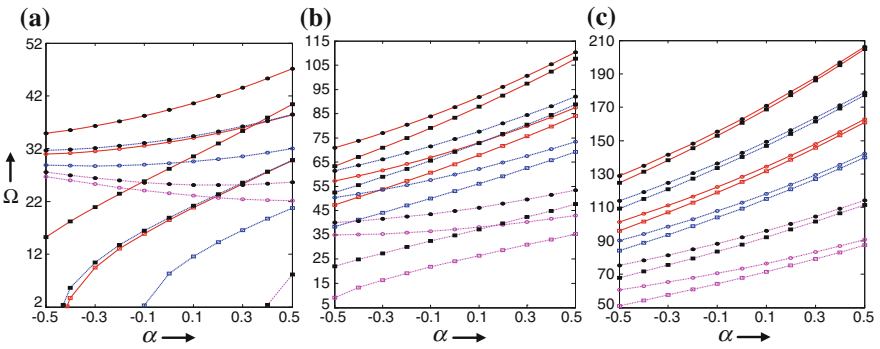
A comparison of result by other methods has been given in Tables 2 and 3.

**Table 1** Values of critical buckling loads  $\overline{N}_{cr}$  for  $\beta = -0.5$ ,  $E_2/E_1 = 0.5$ ,  $\nu_y = 0.1$

$\alpha$	$\mu/\text{Mode}$	C-C			C-S			C-F		
		I	II	III	I	II	III	I	II	III
-0.5	-0.5	-26.4422	-163.114	-579.019	-16.6631	-116.046	-445.942	-3.48216	-34.4576	-179.265
	-0.3	-29.3030	-181.174	-643.859	-18.4300	-128.690	-495.404	-3.89020	-38.1689	-198.872
	0	-34.1661	-211.872	-754.077	-21.4265	-150.132	-579.353	-4.59909	-44.4753	-232.124
0	0.3	-39.8103	-247.480	-881.885	-24.8952	-174.931	-676.519	-5.44568	-51.7942	-270.589
	0.5	-44.0663	-274.303	-978.119	-27.5056	-193.567	-749.564	-6.10067	-57.3151	-299.498
	-0.5	-56.7337	-353.962	-1263.60	-35.2560	-248.717	-965.732	-8.13189	-73.7733	-385.074
0.5	-0.3	-62.7361	-391.602	-1398.31	-38.9216	-274.687	-1067.49	-9.13560	-81.5918	-425.390
	0	-72.9123	-455.248	-1625.80	-45.1300	-318.487	-1239.01	-10.8950	-94.8847	-493.419
	0.3	-84.6849	-528.608	-1887.53	-52.3074	-368.817	-1435.90	-13.0172	-110.332	-571.656
0.5	0.5	-93.5380	-583.585	-2083.33	-57.7042	-406.439	-1582.91	-14.6717	-122.002	-630.191
	-0.5	-119.785	-745.634	-2658.80	-73.7176	-516.929	-2013.68	-19.8536	-156.906	-802.402
	-0.3	-132.175	-821.662	-2927.96	-81.2905	-568.588	-2214.57	-22.4353	-173.551	-883.095
0.5	0	-153.122	-949.546	-3379.54	-94.1220	-655.266	-2550.85	-26.9843	-201.947	-1018.77
	0.3	-177.273	-1096.04	-3895.12	-108.971	-754.272	-2933.73	-32.5003	-235.095	-1174.20
	0.5	-195.383	-1205.26	-4278.41	-120.150	-827.922	-3217.70	-36.8162	-260.241	-1290.18

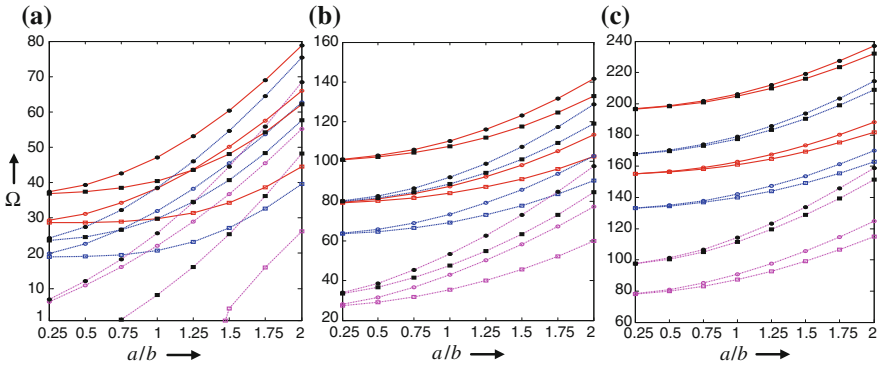


**Fig. 5** Frequency parameter: **a** I mode, **b** II mode, and **c** III mode for  $a/b = 1$ . —C-C; - - -, C-S; -.-, C-F; square,  $\bar{N}_y = -30, \mu = -0.5$ ; blacksquare,  $\bar{N}_y = -30, \mu = 0.5$  circle,  $\bar{N}_y = 30, \mu = -0.5$ ; blackcircle,  $\bar{N}_y = 30, \mu = 0.5$



**Fig. 6** Frequency parameter: **a** I mode, **b** II mode, and **c** III mode for  $\beta = -0.5$ . —C-C; - - -, C-S; -.-, C-F; square,  $\bar{N}_y = -30, \mu = -0.5$ ; blacksquare,  $\bar{N}_y = -30, \mu = 0.5$  circle,  $\bar{N}_y = 30, \mu = -0.5$ ; blackcircle,  $\bar{N}_y = 30, \mu = 0.5$





**Fig. 7** Frequency parameter: **a** I mode, **b** II mode, and **c** III mode for  $\alpha = 0.5$ . —C-C; - - -, C-S; -.-. C-F; square,  $\bar{N}_y = -30, \mu = -0.5$ ; blacksquare,  $\bar{N}_y = -30, \mu = 0.5$ , circle,  $\bar{N}_y = 30, \mu = -0.5$ ; blackcircle,  $\bar{N}_y = 30, \mu = 0.5$

**Table 2** Comparison of frequency parameter  $\Omega$  for homogeneous ( $\mu = 0, \beta = 0$ ), isotropic ( $E_x = E_y = E$ ), plates for  $\nu = 0.3$

		I Mode				II Mode			
$a/b$		0.5		1		0.5		1	
$\alpha$	$a/b$	0.0	0.5	0.0	0.5	0.0	0.5	0.0	0.5
C-C	0.0	23.8156	30.7594	28.9509	37.2761	63.5345	81.6107	69.3270	88.9922
	0.5	23.8204 <sup>a</sup>	30.7573 <sup>a</sup>	28.9499 <sup>a</sup>	37.2675 <sup>a</sup>	63.6027 <sup>a</sup>	81.6757 <sup>a</sup>	69.3796 <sup>a</sup>	89.0385 <sup>a</sup>
	1.0	—	—	28.946 <sup>b</sup>	—	—	—	69.320 <sup>b</sup>	—
C-S	0.0	23.8156 <sup>c</sup>	30.7594 <sup>c</sup>	28.9508 <sup>c</sup>	37.2761 <sup>c</sup>	63.6345 <sup>c</sup>	81.6101 <sup>c</sup>	69.3270 <sup>c</sup>	88.9921 <sup>c</sup>
	0.5	17.3318	21.2621	23.6463	30.1345	52.0979	65.6981	58.6464	74.5075
	1.0	17.3350 <sup>a</sup>	21.2595 <sup>a</sup>	23.6468 <sup>a</sup>	30.1282 <sup>a</sup>	52.0978 <sup>a</sup>	65.7417 <sup>a</sup>	58.6880 <sup>a</sup>	74.5381 <sup>a</sup>
C-F	0.0	—	—	23.646 <sup>b</sup>	—	—	—	58.641 <sup>b</sup>	—
	0.5	17.1614 <sup>c</sup>	21.2621 <sup>c</sup>	23.6463 <sup>c</sup>	30.1345 <sup>c</sup>	52.0978 <sup>c</sup>	65.6999 <sup>c</sup>	58.6463 <sup>c</sup>	74.5102 <sup>c</sup>
	1.0	5.70387	6.86986	12.6874	17.2586	24.9438	30.1903	33.0651	42.0484
C-F	0.5	5.7031 <sup>a</sup>	6.8682 <sup>a</sup>	12.6838 <sup>a</sup>	17.2545 <sup>a</sup>	24.949 <sup>a</sup>	30.194 <sup>a</sup>	33.064 <sup>a</sup>	42.045 <sup>a</sup>
	1.0	—	—	12.69 <sup>b</sup>	—	—	—	33.06 <sup>b</sup>	—
	2.0	5.7039 <sup>c</sup>	6.8677 <sup>c</sup>	12.6873 <sup>c</sup>	17.2583 <sup>c</sup>	24.9438 <sup>c</sup>	30.1922 <sup>c</sup>	33.0652 <sup>c</sup>	42.0566 <sup>c</sup>

<sup>a</sup> values from quintic spline [7], <sup>b</sup> exact values [9] and <sup>c</sup> values from Chebyshev collocation technique [10]. A comparison of  $\bar{N}_{cr}$  has been presented in Table 3

**Table 3** Comparison of critical buckling loads  $\bar{N}_{cr}$  for homogeneous ( $\mu = 0, \beta = 0$ ), isotropic ( $E_x = E_y = E$ ), C-C plates for  $\nu = 0.3$

Ref. $a/b$	0.4	0.5	0.6	0.7	0.8	0.9	1
Present	93.247	75.910	69.632	69.095	72.084	77.545	84.922
[7, 11]	93.209	75.887	69.604	69.072	72.067	77.533	75.877
	93.247	75.91	69.632	69.095	72.084	77.545	75.91

## 5 Conclusions

The DQM has been used to study the effect of in-plane force together with non-homogeneity of the material on the transverse vibrations of orthotropic rectangular plates of exponentially varying thickness on the basis of classical plate theory. The frequency parameter  $\Omega$  is found to be increased with the increasing values of  $\bar{N}_y$ ,  $\mu$ ,  $a/b$  and decreased with the increasing values of  $\beta$  keeping all other parameters fixed. Critical buckling load  $\bar{N}_{cr}$  for a C-S plate is higher than that for a C-F plate but less than that for a C-C plate keeping all other plate parameters fixed. An excellent agreement of the results with those obtained by other methods shows the high accuracy and computational efficiency of the present approach.

## References

1. Brayan, G.H.: On the stability of a plane plate under thrust in its own plane with application to the buckling of the sides of a ship. Proc. London Math. Soc. **22**, 54–67 (1890)
2. Timoshenko, S., Gere, J.: Theory of Elastic Stability, 2nd ed. McGraw-Hill, New York (1963)
3. Gorman, D.G.: Vibration of thermally stressed polar orthotropic annular plates. Earthquake Eng. Struct. Dynam. **11**, 843–855 (1983)
4. Gorman, D.J.: Free vibration and buckling of in-plane loaded plates with rotational elastic edge support. J. Sound Vib. **229**(4), 755–773 (2000)
5. Dhanpati.: Free transverse vibrations of rectangular and circular orthotropic plates. Ph.D. thesis, Indian Institute of Technology Roorkee, Roorkee, India (2007)
6. Chakraverty, S., Jindal, R., Agarwal, V.K.: Vibration of nonhomogeneous orthotropic elliptic and circular plates with variable thickness. J. Sound Vib. **129**, 256–259 (2007)
7. Lal, R.: Dhanpati.: Quintic splines in the study of buckling and vibration of non-homogeneous orthotropic rectangular plates with variable thickness. Int. J. Appl. Math. Mech. **3**(3), 18–35 (2007)
8. Lal, R., Kumar, Y.: Buckling and vibration of orthotropic nonhomogeneous rectangular plates With bilinear thickness variation. J. Appl. Mech. **78**(06), 1011–1012 (2011)
9. Leissa, A.W.: Vibration of Plates. NASA SP-160 Washington, DC. Govt. Office (1969)
10. Lal, R., Gupta, U.S., Goel, C.: Chebyshev polynomials in the study of transverse vibrations of non-uniform rectangular orthotropic plates. S. V. Digest. **33**(2), 103–112 (2001)
11. Leissa, A.W., Kang, J.H.: Exact solution for vibration and buckling of an SS-C-SS-C rectangular plate loaded by linearly varying in plane stresses. Int. J. Mech. Sci. **44**, 1925–1945 (2002)

# A Dual SBM Model with Fuzzy Weights in Fuzzy DEA

Jolly Puri and Shiv Prasad Yadav

**Abstract** The dual part of a SBM model in data envelopment analysis (DEA) aims to calculate the optimal virtual costs and prices (also known as weights) of inputs and outputs for the concerned decision-making units (DMUs). In conventional dual SBM model, the weights are found as crisp quantities. However, in real-world problems, the weights of inputs and outputs in DEA may have fuzzy essence. In this paper, we propose a dual SBM model with fuzzy weights for input and output data. The proposed model is then reduced to a crisp linear programming problem by using ranking function of a fuzzy number (FN). This model gives the fuzzy efficiencies and the fuzzy weights of inputs and outputs of the concerned DMUs as triangular fuzzy numbers (TFNs). The proposed model is illustrated with a numerical example.

**Keywords** Fuzzy DEA · Fuzzy SBM model · Fuzzy efficiency · Fuzzy weights

## 1 Introduction

Data envelopment analysis (DEA) [1] is a nonparametric and linear programming-based technique which evaluates the relative efficiency of homogeneous DMUs on the basis of multiple inputs and multiple outputs. Since the time DEA was proposed, it has got comprehensive attention both in theory and in applications. The beauty of DEA is its ability to measure relative efficiencies of DMUs without assuming prior weights on the inputs and outputs. The first model in DEA is the CCR model [1] which deals with proportional changes in inputs and outputs. The CCR efficiency score reflects the proportional maximum input reduction (or output augmentation)

---

J. Puri (✉) · S. P. Yadav

Department of Mathematics, I.I.T. Roorkee, Roorkee 247667, India  
e-mail: puri.jolly@gmail.com

S. P. Yadav

e-mail: yadavfma@iitr.ernet.in

rate which is common to all inputs (outputs). But it neglects the slacks corresponding to inputs and outputs. To overcome this shortcoming of CCR model, Tone presented Slack-based Measure (SBM) model [15] in DEA, which puts aside the assumption of proportionate changes in inputs and outputs, and deals with slacks directly. The primal part of the SBM model directly deals with input excesses and output shortfalls of the concerned DMUs. On the other hand, the dual part of the SBM model can be interpreted as profit maximization model and it aims to calculate the optimal virtual costs and prices (also known as weights) of inputs and outputs for the concerned DMUs. Other theoretical extensions of SBM model can be seen in [4, 13].

The conventional DEA models are limited to only crisp input/output data and also their weights take only crisp values. However, in real-world problems, two situations can be possible: (1) Input/output data may have imprecision or fuzziness and (2) the weights of data may have fuzzy essence. To deal with imprecise data, the notion of fuzziness has been introduced in DEA. The DEA is extended to fuzzy DEA (FDEA) in which the imprecision is represented by fuzzy sets or FNs [7, 14]. The SBM efficiency in DEA is extended to fuzzy settings in [6, 11, 12]. Several approaches have been developed to deal with fuzzy data in FDEA. These approaches are as follows: (1) tolerance approach [14], (2)  $\alpha$ -cut approach [7], (3) fuzzy ranking approach [5], and (4) possibility approach [8]. However, very less emphasis has been given to FDEA models with fuzzy weights. Mansourirad et al. [10] are the first who introduced fuzzy weights in fuzzy CCR model and proposed a method based on  $\alpha$ -cut approach to evaluate weights for outputs in terms of TFNs. In this paper, we propose a dual SBM model with fuzzy weights corresponding to crisp input and output data. We reduce the proposed model into crisp linear programming problem (LPP) by using ranking function of an FN. The proposed model gives the fuzzy efficiencies and the fuzzy weights corresponding to inputs and outputs of the concerned DMUs as TFNs.

The paper is organized as follows: Section 2 presents preliminaries which include basic definitions. Section 3 presents the description of primal and dual parts of the SBM model. Section 4 presents the dual SBM model with fuzzy weights and its reduction to a crisp LPP. Section 5 presents the results and discussion of a numerical example to illustrate the proposed model. The last Section 6 concludes the findings of our study.

## 2 Preliminaries

The basic definitions in the fuzzy set theory can be seen from [16]. This section includes the definition of TFN and arithmetic operations on TFNs [2]. It also includes ranking function which maps FN to the real line [9].

### 2.1 Triangular Fuzzy Number

A TFN  $\tilde{A}$ , denoted by  $(a_1, a_2, a_3)$ , is defined by the membership function  $\mu_{\tilde{A}}$  given by

$$\mu_{\tilde{A}}(x) = \begin{cases} \frac{x - a_1}{a_2 - a_1}, & a_1 < x \leq a_2, \\ 1, & x = a_2, \\ \frac{x - a_3}{a_2 - a_3}, & a_2 \leq x < a_3, \\ 0, & \text{otherwise,} \end{cases}$$

$\forall x \in R$ . In the present study,  $\tilde{0} = (0, 0, 0)$ ,  $\tilde{1} = (1, 1, 1)$  and  $\tilde{a} = (a, a, a)$  where  $a \in R$ .

### 2.2 Arithmetic Operations on TFNs

Let  $\tilde{A} = (a_1, a_2, a_3)$  and  $\tilde{B} = (b_1, b_2, b_3)$  be two TFNs. Then,

Addition:  $\tilde{A} \oplus \tilde{B} = (a_1 + b_1, a_2 + b_2, a_3 + b_3)$ .

Subtraction:  $\tilde{A} \ominus \tilde{B} = (a_1 - b_3, a_2 - b_2, a_3 - b_1)$ .

Scalar multiplication:  $k\tilde{A} = \begin{cases} (ka_1, ka_2, ka_3), & k \geq 0, \\ (ka_3, ka_2, ka_1), & k < 0. \end{cases}$

Multiplication:  $\tilde{A} \otimes \tilde{B} = (\min(a_1b_1, a_1b_3, a_3b_1, a_3b_3), a_2b_2, \max(a_1b_1, a_1b_3, a_3b_1, a_3b_3))$ .

### 2.3 Ranking Function

Let  $F(R)$  be the set of all FNs. A ranking function [9]  $\mathfrak{R}$  is a mapping from  $F(R)$  to the real line. The FNs can easily be compared by using ranking functions. The rank of TFN  $\tilde{A} = (a_1, a_2, a_3)$ , represented by  $\mathfrak{R}(\tilde{A})$ , is defined by  $\mathfrak{R}(\tilde{A}) = (a_1 + 2a_2 + a_3)/4$ .

Let  $\tilde{A} = (a_1, a_2, a_3)$  and  $\tilde{B} = (b_1, b_2, b_3)$  be two TFNs in  $F(R)$ . Then,

1.  $\tilde{A}$  is said to be equal to  $\tilde{B}$  based on ranking function  $\mathfrak{R}$ , written as  $\tilde{A} \stackrel{\mathfrak{R}}{=} \tilde{B}$ , iff  $\mathfrak{R}(\tilde{A}) = \mathfrak{R}(\tilde{B})$ .
2.  $\tilde{A}$  is said to be less than or equal to  $\tilde{B}$  based on ranking function  $\mathfrak{R}$ , written as  $\tilde{A} \stackrel{\mathfrak{R}}{\leq} \tilde{B}$ , iff  $\mathfrak{R}(\tilde{A}) \leq \mathfrak{R}(\tilde{B})$ .
3.  $\tilde{A}$  is said to be greater than or equal to  $\tilde{B}$  based on ranking function  $\mathfrak{R}$ , written as  $\tilde{A} \stackrel{\mathfrak{R}}{\geq} \tilde{B}$ , iff  $\mathfrak{R}(\tilde{A}) \geq \mathfrak{R}(\tilde{B})$ .

4.  $\tilde{A}$  is said to be less than or equal to  $\tilde{O}$  based on ranking function  $\mathfrak{R}$ , written as  $\tilde{A} \leq_{\mathfrak{R}} \tilde{O}$ , iff  $\mathfrak{R}(\tilde{A}) \leq \mathfrak{R}(\tilde{O})$ .

**Theorem:**  $\mathfrak{R}(c\tilde{A} + \tilde{B}) = c\mathfrak{R}(\tilde{A}) + \mathfrak{R}(\tilde{B})$ ,  $c$  is any constant. (*Linearity property* [11]).

### 3 Slack-based Measure Model

Assume that the performance of a set of  $n$  homogeneous DMUs ( $DMU_j$ ;  $j = 1, \dots, n$ ) is to be measured. The performance of  $DMU_j$  is characterized by a production process of  $m$  inputs ( $x_{ij}$ ;  $i = 1, \dots, m$ ) to yield  $s$  outputs ( $y_{rj}$ ;  $r = 1, \dots, s$ ). Let  $y_{rk}$  be the amount of the  $r$ th output produced by the  $k$ th DMU and  $x_{ik}$  be the amount of the  $i$ th input used by the  $k$ th DMU. Assume that input and output data are positive. The primal of SBM model [15] of the  $k$ th DMU, represented by SBM-P $_k$ , is defined as

$$\begin{aligned}
 \text{SBM-P}_k \quad \rho_k &= \min \frac{1 - (1/m) \sum_{i=1}^m s_{ik}^- / x_{ik}}{1 + (1/s) \sum_{r=1}^s s_{rk}^+ / y_{rk}} \\
 &\text{subject to } x_{ik} = \sum_{j=1}^n x_{ij} \lambda_{jk} + s_{ik}^- \quad \forall i, \\
 &y_{rk} = \sum_{j=1}^n y_{rj} \lambda_{jk} - s_{rk}^+ \quad \forall r, \\
 &\lambda_{jk} \geq 0 \quad \forall j, s_{ik}^- \geq 0 \quad \forall i, s_{rk}^+ \geq 0 \quad \forall r,
 \end{aligned}$$

where  $s_{rk}^+$  is the slack in the  $r$ th output of the  $k$ th DMU;  $s_{ik}^-$  is the slack in the  $i$ th input of the  $k$ th DMU;  $\lambda_{jk}$ 's, i.e.,  $(\lambda_{j1}, \lambda_{j2}, \dots, \lambda_{jn})$  are non-negative variables for  $j = 1, 2, \dots, n$ . The  $k$ th DMU is SBM efficient if  $\rho_k = 1$  and all  $s_{ik}^- = 0, s_{rk}^+ = 0$ , i.e., no input excesses and no output shortfalls in any optimal solution.

SBM-P $_k$  can be transformed into LPP using Charnes–Cooper transformation given in [1]. Multiply a scalar  $t_k > 0$  to both the denominator and the numerator of SBM-P $_k$ . This causes no change in the value of  $\rho_k$ . The value of  $t_k$  can be adjusted in such a way that the denominator becomes 1. The SBM-P $_k$  model in LPP form becomes

$$\begin{aligned}
 \text{LPP-SBM-P}_k \quad \tau_k &= \min t_k - \frac{1}{m} \sum_{i=1}^m S_{ik}^- / x_{ik} \\
 &\text{subject to } 1 = t_k + \frac{1}{s} \sum_{r=1}^s S_{rk}^+ / y_{rk}, \\
 &t_k x_{ik} = \sum_{j=1}^n x_{ij} \Lambda_{jk} + S_{ik}^- \quad \forall i, \\
 &t_k y_{rk} = \sum_{j=1}^n y_{rj} \Lambda_{jk} - S_{rk}^+ \quad \forall r,
 \end{aligned}$$

$$\Lambda_{jk} \geq 0 \forall j, S_{ik}^- \geq 0 \forall i, S_{rk}^+ \geq 0 \forall r, t_k > 0,$$

where  $\rho_k = \tau_k, \lambda_{jk} = \Lambda_{jk}/t_k \forall j, s_{ik}^- = S_{ik}^-/t_k \forall i$  and  $s_{rk}^+ = S_{rk}^+/t_k \forall r$ .

The dual of LPP-SBM-P<sub>k</sub>, represented by SBM-D<sub>k</sub>, can be expressed as follows:

$$\begin{aligned} \text{SBM-D}_k \quad E_k &= \max \xi_k \\ \text{subject to } \xi_k + \sum_{i=1}^m x_{ik} v_{ik} - \sum_{r=1}^s y_{rk} u_{rk} &= 1, \\ \sum_{r=1}^s y_{rj} u_{rk} - \sum_{i=1}^m x_{ij} v_{ik} &\leq 0 \forall j, \\ v_{ik} &\geq \frac{1}{m x_{ik}} \forall i, u_{rk} \geq \frac{\xi_k}{s y_{rk}} \forall r. \end{aligned}$$

where  $\xi_k \in R, v_{ik} \forall i$ , and  $u_{rk} \forall r$  are the dual variables corresponding to LPP-SBM-P<sub>k</sub>. The dual variables  $v_{ik}$  and  $u_{rk}$  are the weights associated with the  $i$ th input and the  $r$ th output, respectively. The  $E_k$  is the SBM efficiency of the  $k$ th DMU.

### 4 Dual SBM Model with Fuzzy Weights

In conventional SBM-D<sub>k</sub> model, the weights of inputs and outputs are found as crisp quantities. However, in real-world problems, the weights may have fuzzy essence. Therefore, in this paper, weights of inputs and outputs are taken as TFNs, and thus, the SBM-D<sub>k</sub> model becomes fuzzy SBM-D<sub>k</sub> (FSBM-D<sub>k</sub>) model given by

$$\begin{aligned} \text{FSBM-D}_k \quad \tilde{E}_k &= \max_{\mathfrak{R}} \tilde{\xi}^k \\ \text{subject to } \tilde{\xi}^k \oplus \sum_{i=1}^m x_{ik} \tilde{v}^{ik} \ominus \sum_{r=1}^s y_{rk} \tilde{u}^{rk} &= \tilde{1}, \\ \sum_{r=1}^s y_{rj} \tilde{u}^{rk} \ominus \sum_{i=1}^m x_{ij} \tilde{v}^{ik} &\leq \tilde{0} \forall j, \\ \tilde{v}^{ik} &\geq \frac{1}{m x_{ik}} \tilde{1} \forall i, \tilde{u}^{rk} \geq \frac{1}{s y_{rk}} \tilde{\xi}^k \forall r, \\ v_1^{ik} \leq v_2^{ik} \leq v_3^{ik} \forall i, u_1^{rk} \leq u_2^{rk} \leq u_3^{rk} \forall r, \xi_1^k \leq \xi_2^k \leq \xi_3^k. \end{aligned}$$

where  $\tilde{v}^{ik}$  and  $\tilde{u}^{rk}$  are the triangular fuzzy weights associated with the  $i$ th input and the  $r$ th output, respectively. The  $\tilde{E}_k$  is the fuzzy SBM efficiency of the  $k$ th DMU which is also found as a TFN. By using the ranking function of TFN, FSBM-D<sub>k</sub> model reduces to Model 1, which is as follows:

$$\begin{aligned} \text{Model-1} \quad \mathfrak{R}(\tilde{E}_k) &= \max \mathfrak{R}(\tilde{\xi}^k) \\ \text{subject to } \mathfrak{R}(\tilde{\xi}^k) + \sum_{i=1}^m x_{ik} \mathfrak{R}(\tilde{v}^{ik}) - \sum_{r=1}^s y_{rk} \mathfrak{R}(\tilde{u}^{rk}) &= \mathfrak{R}(\tilde{1}), \\ \sum_{r=1}^s y_{rj} \mathfrak{R}(\tilde{u}^{rk}) - \sum_{i=1}^m x_{ij} \mathfrak{R}(\tilde{v}^{ik}) &\leq \mathfrak{R}(\tilde{0}) \forall j, \\ \mathfrak{R}(\tilde{v}^{ik}) &\geq \frac{1}{m x_{ik}} \mathfrak{R}(\tilde{1}) \forall i, \mathfrak{R}(\tilde{u}^{rk}) \geq \frac{1}{s y_{rk}} \mathfrak{R}(\tilde{\xi}^k) \forall r, \\ v_1^{ik} \leq v_2^{ik} \leq v_3^{ik} \forall i, u_1^{rk} \leq u_2^{rk} \leq u_3^{rk} \forall r, \xi_1^k \leq \xi_2^k \leq \xi_3^k. \end{aligned}$$

**Table 1** Input and output data of six DMUs

Inputs and outputs	A	B	C	D	E	F
I <sub>1</sub>	4	14	24	20	48	50
I <sub>2</sub>	3	6	3	2	4	7.5
O <sub>1</sub>	1	2	3	2	4	5
O <sub>2</sub>	2	6	12	6	16	30

Source The input and output data are taken from [3]

**Table 2** Fuzzy efficiencies  $\tilde{\xi}^k = (\xi_1^k, \xi_2^k, \xi_3^k)$  and  $\Re(\tilde{\xi}^k)$

$\tilde{\xi}^k$	A	B	C	D	E	F
$\xi_1^k$	0.3429	0.2930	0.6720	0.2733	0.2172	0.3247
$\xi_2^k$	0.8964	0.6113	0.7671	0.6183	0.4434	0.7321
$\xi_3^k$	1.8644	1.2535	1.7939	1.5758	2.2292	2.2112
$\Re(\tilde{\xi}^k)$	1.0000	0.6923	1.0000	0.7714	0.8333	1.0000

By putting the values of  $\Re(\tilde{\xi}^k)$ ,  $\Re(\tilde{v}^{ik}) \forall i$ , and  $\Re(\tilde{u}^{rk}) \forall r$ , the Model-1 reduces to Model-2, which is crisp LPP.

$$\begin{aligned}
 \text{Model-2 } E_k &= \max(\xi_1^k + 2\xi_2^k + \xi_3^k)/4 \\
 \text{subject to } &(\xi_1^k + 2\xi_2^k + \xi_3^k) + \sum_{i=1}^m x_{ik}(v_1^{ik} + 2v_2^{ik} + v_3^{ik}) \\
 &\quad - \sum_{r=1}^s y_{rk}(u_1^{rk} + 2u_2^{rk} + u_3^{rk}) = 4, \\
 &\sum_{r=1}^s y_{rj}(u_1^{rk} + 2u_2^{rk} + u_3^{rk}) - \sum_{i=1}^m x_{ij}(v_1^{ik} + 2v_2^{ik} + v_3^{ik}) \leq 0 \forall j, \\
 &\frac{v_1^{ik} + 2v_2^{ik} + v_3^{ik}}{4} \geq \frac{1}{m x_{ik}} \forall i, u_1^{rk} + 2u_2^{rk} + u_3^{rk} \geq \frac{\xi_1^k + 2\xi_2^k + \xi_3^k}{s y_{rk}} \forall r, \\
 &v_1^{ik} \leq v_2^{ik} \leq v_3^{ik} \forall i, u_1^{rk} \leq u_2^{rk} \leq u_3^{rk} \forall r, \xi_1^k \leq \xi_2^k \leq \xi_3^k.
 \end{aligned}$$

### 5 Results and Discussion of a Numerical Example

In this section, we provide a numerical example to illustrate the proposed dual SBM model with fuzzy weights. Table 1 presents the performance evaluation problem of six DMUs with two inputs I<sub>1</sub> and I<sub>2</sub>, and two outputs O<sub>1</sub> and O<sub>2</sub>.

The fuzzy efficiencies of all DMUs are evaluated from Model-2, which are shown in Table 2. The results reveal that the rank of each fuzzy efficiency score lies between 0 and 1, i.e.,  $0 < \Re(\tilde{\xi}^k) \leq 1$ . The fuzzy weights corresponding to inputs and outputs of the concerned DMU are also evaluated by using Model-2, which are shown in Tables 3 and 4, respectively. These fuzzy weights provide additional information to the decision maker, which is not provided by crisp weights in crisp dual SBM model.



**Table 3** Fuzzy weights corresponding to inputs

Fuzzy weights		A	B	C	D	E	F
$\tilde{v}^{1k}$	$v_1^{1k}$	4.4466	0.0220	3.8200	0.0080	0.0034	2.2823
	$v_2^{1k}$	10.6011	0.0543	8.4805	0.0203	0.0079	6.0048
	$v_3^{1k}$	35.0495	0.1515	26.6735	0.0514	0.0224	27.9433
$\tilde{v}^{2k}$	$v_1^{2k}$	4.1217	0.0262	10.2804	16.3350	33.8386	6.0896
	$v_2^{2k}$	10.0303	0.0645	23.4940	39.3018	78.3524	16.3315
	$v_3^{2k}$	31.1839	0.1781	61.7977	96.1473	175.6625	54.6475

**Table 4** Fuzzy weights corresponding to outputs

Fuzzy weights		A	B	C	D	E	F
$\tilde{u}^{1k}$	$u_1^{1k}$	28.6998	0.1356	24.3567	16.7974	12.9102	11.6846
	$u_2^{1k}$	62.6096	0.3327	55.0749	40.0764	32.2595	32.5052
	$u_3^{1k}$	129.3616	0.8657	115.9649	93.9072	80.8491	89.4276
$\tilde{u}^{2k}$	$u_1^{2k}$	4.6918	0.0181	5.1196	0.0197	3.5286	3.6698
	$u_2^{2k}$	11.0246	0.0443	11.1800	0.0490	10.2253	10.0071
	$u_3^{2k}$	36.0650	0.1241	34.5782	0.1394	28.0860	42.3709

## 6 Conclusion

In this paper, we proposed a dual SBM model with fuzzy weights (FSBM- $D_k$ ) for crisp inputs and outputs. The FSBM- $D_k$  model is then reduced to crisp LPP by using ranking function. The proposed model evaluates the components of fuzzy efficiencies and fuzzy weights corresponding to inputs and outputs as TFNs. These fuzzy efficiencies and fuzzy weights provide additional information to the decision maker, which helps to deal with uncertainty in real-life problems.

**Acknowledgments** The first author is thankful to the University Grants Commission (UGC), Government of India, for financial assistance.

## References

1. Charnes, A., Cooper, W.W., Rhodes, E.: Measuring the efficiency of decision making units. *Eur. J. Oper. Res.* **2**, 429–444 (1978)
2. Chen, S.M.: Fuzzy system reliability analysis using fuzzy number arithmetic operations. *Fuzzy Set. Syst.* **66**, 31–38 (1994)
3. Cooper, W. W., Seiford, L. M., Zhu, J.: *Handbook on Data Envelopment Analysis*. 2nd edn. International Series in Operations Research and Management Science, Springer, **164**, p. 200 (2011)
4. Goudarzi, M.R.M.: A slack-based model for estimating returns to scale under weight restrictions. *Appl. Math. Sci.* **6**(29), 1419–1430 (2012)

5. Hatami-Marbini, A., Saati, S., Makuui, A.: An application of fuzzy numbers ranking in performance analysis. *J. Appl. Sci.* **9**(9), 1770–1775 (2009)
6. Jahanshahloo, G.R., Soleimani-damaneh, M., Nasrabadi, E.: Measure of efficiency in DEA with fuzzy input-output levels: A methodology for assessing, ranking and imposing of weights restrictions. *Appl. Math. Comput.* **156**, 175–187 (2004)
7. Kao, C., Liu, S.T.: Fuzzy efficiency measures in data envelopment analysis. *Fuzzy Sets Syst.* **113**, 427–437 (2000)
8. Lertworasirikul, S., Fang, S.C., Joines, J.A., Nuttle, H.L.W.: Fuzzy data envelopment analysis: A possibility approach. *Fuzzy Set. Syst.* **139**(2), 379–394 (2003)
9. Mahdavi-Amiri, N., Nasseri, S.H.: Duality in fuzzy number linear programming by use of a certain linear ranking function. *Appl. Math. Comput.* **180**, 206–216 (2006)
10. Mansourirad, E., Rizam, M.R.A.B., Lee, L.S., Jaafar, A.: Fuzzy weights in data envelopment analysis. *Int. Math. Forum* **5**(38), 1871–1886 (2010)
11. Puri, J., Yadav, S.P.: A concept of fuzzy input mix-efficiency in fuzzy DEA and its application in banking sector. *Expert Syst. Appl.* **40**, 1437–1450 (2013)
12. Saati, S., Memariani, A.: SBM model with fuzzy input-output levels in DEA. *Aust. J. Basic Appl. Sci.* **3**(2), 352–357 (2009)
13. Saen, R.F.: Developing a nondiscretionary model of slacks-based measure in data envelopment analysis. *Appl. Math. Comput.* **169**, 1440–1447 (2005)
14. Sengupta, J.K.: A fuzzy systems approach in data envelopment analysis. *Comput. Math. Appl.* **24**(8–9), 259–266 (1992)
15. Tone, K.: A slacks-based measure of efficiency in data envelopment analysis. *Eur. J. Oper. Res.* **130**, 498–509 (2001)
16. Zimmermann, H.J.: *Fuzzy Set Theory and its Applications*, 3rd edn. Kluwer-Nijhoff Publishing, Boston (1996)

# Ball Bearing Fault Diagnosis Using Continuous Wavelet Transforms with Modern Algebraic Function

R. Sharma, A. Kumar and P. K. Kankar

**Abstract** Ball bearing plays a very crucial part of any rotating machineries, and the fault diagnosis in rotating system can be detected at early states when the fault is still small. In this paper, a ball bearing fault is detected by using continuous wavelet transform (CWT) with modern algebraic function. The reflected vibration signals from ball bearing having single point defect on its inner race, outer race, ball fault, and combination of these faults have been considered for analysis. The features extracted from a non-stationary multi-component ball bearing signal are very difficult. In this paper, a CWT with selected stretching parameters is used to analyze a signal in time–frequency domain and extract the features from non-stationary multi-component signals. The algebraic function norms are calculated from the matrix which can be generated with the help of wavelet transforms. The norms lookup table is used as a reference for fault diagnosis. The experimental results show that this method is simple and robust.

**Keywords** Bearing faults · Norms · CWT

---

R. Sharma (✉) · A. Kumar · P. K. Kankar

Department of Electronic and Communication Engineering, PDPM Indian Institute of Information Technology Design and Manufacturing Jabalpur, Jabalpur, Madhya Pradesh 482005, India  
e-mail: rahul.ece23@gmail.com

A. Kumar  
e-mail: anil.dee@gmail.com

P. K. Kankar  
e-mail: pavankankar@gmail.com

## 1 Introduction

Rolling element bearings are used in wide variety of rotating machineries from small devices to heavy industrial systems. Ball bearing defect may be categorized as point of local defect and distribution defects. These defects are generated at the time of manufacturing due to geometrical imperfection bearing components. Literature review reveals that an extensive work has been done on fault diagnosis in ball bearing system. Chiang et al. [1] have been used Fisher discriminate analysis and support vector machines for fault diagnosis. Lei et al. [2] have proposed an intelligent classification method to mechanical fault diagnosis based on wavelet packet transform (WPT), empirical mode decomposition (EDM), dimensionless parameters, a distance evolution technique, and radial basis function network. It becomes difficult to diagnosis the fault when the amplitude of noise is high and also affects the system performance. Hidden Markov model (HMM), support vector machine (SVM), and artificial neural network (ANN) methods are used for fault classifications [3–5].

Wigner–Ville distribution and wavelet decomposition have been used for their excellent time frequency analysis. Generally, it is difficult to analyze model-based technique of a nonlinear system or non-stationary multi-component signals. Phakde et al. [6] have used a set of coefficients based on the sequence current and voltage phasor components to calculate the apparent impedance. Staszewski [7] have proposed a wavelet-based method for fault detection in mechanical system. The energy-confined DWT is used for fault detection by Prabhakar et al. [8]. Wavelet transform gives the better solution than any other known method; however, the problem is for selecting the parameter for wavelet analysis. The Gaussian correlation of vibration signal and wavelet coefficients for fault diagnosis has been used in [9]. Yuan and Chu [10] have used the particle swarm optimization (PSO) technique for feature selection of wavelet function. Kankar et al. [11] have used the maximum relative wavelet energy criterion and maximum energy to Shannon entropy ratio criterion for fault diagnosis. Adaptive wavelet filter with the selection of wavelet parameter on the basis of amplitude and frequency has been used for fault diagnosis in ball bearing system [12].

In this paper, the algebraic norms are used for fault classification, which can be calculated with the help of continuous wavelet transform. For the selection of the suitable parameter, the sensitive analysis technique is used. The fast Fourier transform (FFT) of healthy as well as non-healthy ball bearing is taken, and only those frequencies will be considered where there is appropriate difference in the magnitude of FFT of the signals and these frequencies are called pseudo-frequencies. These pseudo-frequencies are used to find out the scales of wavelet. With the help of selected scales, the matrix is generated and from that matrix the energy confine norms can be calculated, which are essentially used for fault diagnosis in ball bearing system.

## 2 Overview of CWT

Wavelet transform is a powerful tool that provides the analysis of signal at transient’s state. The continuous wavelet transform (CWT) of  $x(t)$  by  $\Psi$  (both belong to real domain) is a projection of a function  $x(t)$  onto a particular wavelet  $\Psi(t)$ . The wavelet analogy of the spectrogram is the scalogram since CWT behaves like orthonormal basis decomposition. It is energy preserving transformation [13, 14].

$$(W_{\Psi}^x)(a, b) = \frac{1}{\sqrt{a}} \int_{-\infty}^{\infty} x(t)\Psi\left(\frac{t-b}{a}\right) dt \tag{1}$$

where  $a > 0$  and  $b$  are scale and translation parameters, respectively.  $\Psi$  is the mother wavelet.

$$(W_{\Psi}^x)x(a, b) = \int x(l)\Psi_{(a,b)}(l)dl \tag{2}$$

Equation (2) is called wavelet equation or the inner product of  $x(t)$  with the scaled and translation versions of the basis function  $\psi_{(a,b)}(l)$ . The scale ‘a’ is assumed to be restricted to  $\mathbb{R}^+$ , although tenuously interpreted as a reciprocal of frequency. When ‘a’ decreases, the oscillation becomes more intense and shows high-frequency behavior. Similarly, when ‘a’ increases, the oscillations become drawn out and show low-frequency behavior.

$$x(t) = \frac{1}{C_{\Psi}} \int_0^{\infty} \int_{-\infty}^{\infty} (W_{\Psi}^x)(a, b)\Psi\left(\frac{t-b}{a}\right)\frac{da}{a^2}db \tag{3}$$

Square magnitude of CWT is defined as wavelet spectrogram or scalogram. It is distribution of signal in timescale plane and is expressed in power per frequency unit.

$$\int_{-\infty}^{\infty} |x(t)|^2 dt = \frac{1}{C_{\Psi}} \int_{-\infty}^{\infty} \int_{-\infty}^{\infty} |(W_{\Psi}^x)(a, b)|^2 \frac{da}{a^2} db \tag{4}$$

$C_{\Psi}$  is the constant that depends on  $\Psi$  and  $W_{\Psi}^x(a, b)$  is the CWT. Equation (4) is called the scalogram of CWT. It is also called an energy preserving transformation as Eq. (4) has only constraint, that is, the mother wavelet  $\Psi \in L^2(\mathbb{R})$  satisfies:

$$C_{\Psi} = \int_{-\infty}^{\infty} \frac{|\Psi(w)|^2}{w} dw < \infty \tag{5}$$

Equation (5) is called admissibility condition, which leads to define the wavelet spectrogram. Sensitivity analysis can be viewed as to remove distracting variance from the dataset. Therefore, in this work, we are analyzing those sensors' data which are most sensitive and discard other.

### 3 Norms

The norm is used to quantify the size of a matrix or the distance between two matrices. If  $K$  denotes the field of real or complex numbers. Let  $K^{m \times n}$  denote the vector space containing all matrices with 'm' rows and 'n' columns with entries in  $K$ .

Let 'A' be any real matrix then  $\|A\|$  represents the norm of a real matrix 'A' in vector space  $K^{m \times n}$ . The norm can be defined as follows:

- $\|A\| > 0$  If  $A \neq 0$  and  $\|A\| = 0$  iff  $A = 0$ , say null matrix.
- $\|\alpha A\| = |\alpha| \|A\|$ , for all ' $\alpha$ ' in  $K$  and all matrices 'A' in  $K^{m \times n}$ .
- $\|A + B\| \leq \|A\| + \|B\|$ , for all matrices 'A' and 'B' in  $K^{m \times n}$ .

Incase of square matrices ( $m = n$ ), some (but not all) matrix norms satisfy the following condition:

- $\|AB\| \leq \|A\| \|B\|$ , for all matrices 'A' and 'B' in  $K^{m \times n}$  also called a submultiplicative norm.

Let  $\lambda_1, \lambda_2, \dots, \lambda_n$  be the eigenvalues of 'A', then

- $\frac{1}{\|A^{-1}\|} \leq |\lambda| \leq \|A\|$ ,

If the vector norms treat a matrix as a vector of size and use one of the familiar vector norms. The norms can be defined as follows:

$$\|A\|_p = \left( \sum_{i=1}^m \sum_{j=1}^m |a_{ij}|^p \right)^{1/p} \tag{6}$$

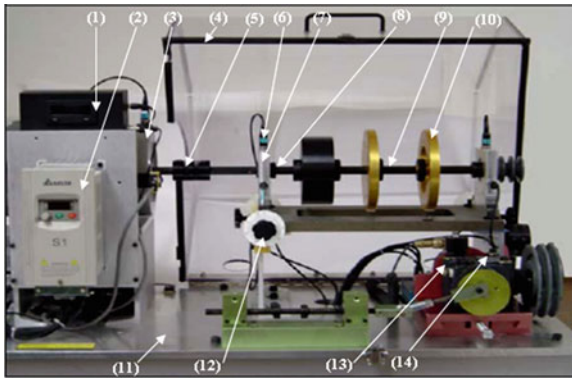
Equation (6) is called p-norms of a vector. Depending on the value of  $p$ , norms can be defined in various way such as 1-norm, 2-norm, and  $\infty$ -norm for  $p=1, 2,$  and  $\infty$ , respectively.

$$\|A\|_2 = \sqrt{\sum_{i=1}^m \sum_{j=1}^m |a_{ij}|^2} = \sqrt{\text{trace}(A^*A)} = \sqrt{\sum_{i=1}^{\min\{m,n\}} \sigma_i^2} \tag{7}$$

where  $A^*$  denoted the conjugate transpose of  $A$  and are defined as the singular values of. The 2-norm can also be defined as the square root of confined matrix energy [15, 16].

**Table 1** Parameters specification of experimental setup

Parameters	Values
Outer race diameter	28.2 mm
Inner race diameter	18.738 mm
Ball diameter	4.762 mm
Contact angle	0°
Radial clearance	10 μm
Ball number	8



**Fig. 1** Experimental setup: 1 Digital encoder; 2 Variable speed control; 3 Motor; 4 Enclosure; 5 Flexible coupling; 6 Accelerometer; 7 Bearing housing; 8 Tested bearing; 9 Rotor; 10 Load disk; 11 Base; 12 Alignment adjuster; 13 Magnetic load system; 14 Gearbox Ref. [11]

## 4 Experimental Setup

The problem of predicting the degradation of working conditions of bearings before they reach the alarm or failure threshold is extremely important in industries to fully utilize the machine production capacity and to reduce the plant downtime. Figure 1 shows the experimental setup which is used for extracting vibration signals. In the present study, an experimental test rig is used and vibration response for healthy bearing and bearing with faults is obtained. Table 1 shows dimensions of the ball bearings taken for the study. Accelerometers are used for picking up the vibration signals from various stations on the rig. As a first step, the machine was run with healthy bearing to establish the baseline data.

Table 1 shows the test bearing characteristics like diameter of inner race, outer race, ball diameter, number of balls, contact angle, and radial clearance. For the study point of view, collection of vibration data of healthy as well as faulty ball bearing at different loading conditions (no loader, one loader, and two loader) and bearings are simulated on the rig at different rotor speed 1,000, 1,500, and 2,000 rpm Ref. [11].

The following five bearing conditions are considered for the study:

1. Healthy bearings (HB).
2. Bearing with spall on inner race (BSIR).
3. Bearing with spall on outer race (BSOR).
4. Bearing with spall on ball (BSB).
5. Combined bearing component defects (CBD).

## 5 Methodology

In this methodology, first all reflected signals from ball bearing at different rotating speeds and different loading conditions are collected via the most sensitive sensors, but these signals are contaminated by the noise and other unwanted variance.

The following steps explain the proposed methodology for fault diagnosis in ball bearing system:

- Step 1: Collect all the signals which reflect the faults in ball bearing system as an occurrence of fault in a signal introduces distinctive and detectable change in the energy distribution of the sensor data.
- Step 2: As the reflected signals are not faulty at all time with respect to non-faulty signal, those part of signal is analyzed, where the probability of fault is more.
- Step 3: For applying CWT, the selection of stretching parameters plays a very important roll. In this paper, the sensitivity analysis technique is used for the analysis of noise-contaminated reflected signal features.
- Step 4: Fast Fourier transform (FFT) of both faulty as well as non-faulty reflected signals is taken, and only those values of signals will be considered, where there is an appropriate difference in the magnitude of fast Fourier transforms (FFT) of the signals as shown in Fig. 2.
- Step 5: Collect all those frequencies at which there are appropriate differences of faulty and non-faulty data and these frequencies are called pseudo-frequencies.
- Step 6: Calculate the scales by using Eq. (8).

$$a = \frac{F_c}{F_a} \quad (8)$$

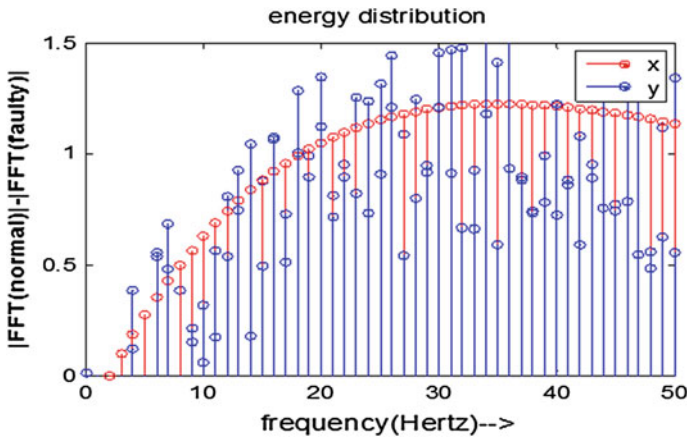
where  $a$  scales,  $F_c$  center frequency of wavelet, and  $F_a$  pseudo-frequency corresponding to scales.

- Step 7: Calculate the big matrices of wavelet coefficients corresponding to reference and faulty signals. The first one is called as signature matrix and the other is known as indicator matrix.
- Step 8: Estimate the norms of these big matrices and make a lookup table with some tolerance. This is the reference table of norms. The sample version of lookup table is shown in Table 2.



**Table 2** Sample version of lookup table

2-Norm	Speed (rpm)	Loading	Fault
0.1219	1,000	No	BFB
0.2622	1,000	One	HEL
0.5211	2,000	One	IRD
0.1912	2,000	Two	HEL
0.2312	1,500	One	MFB
0.2365	1,500	Two	IRD
0.3564	2,000	One	BFB
0.0932	1,500	No	ORD
0.1168	1,000	No	ORD



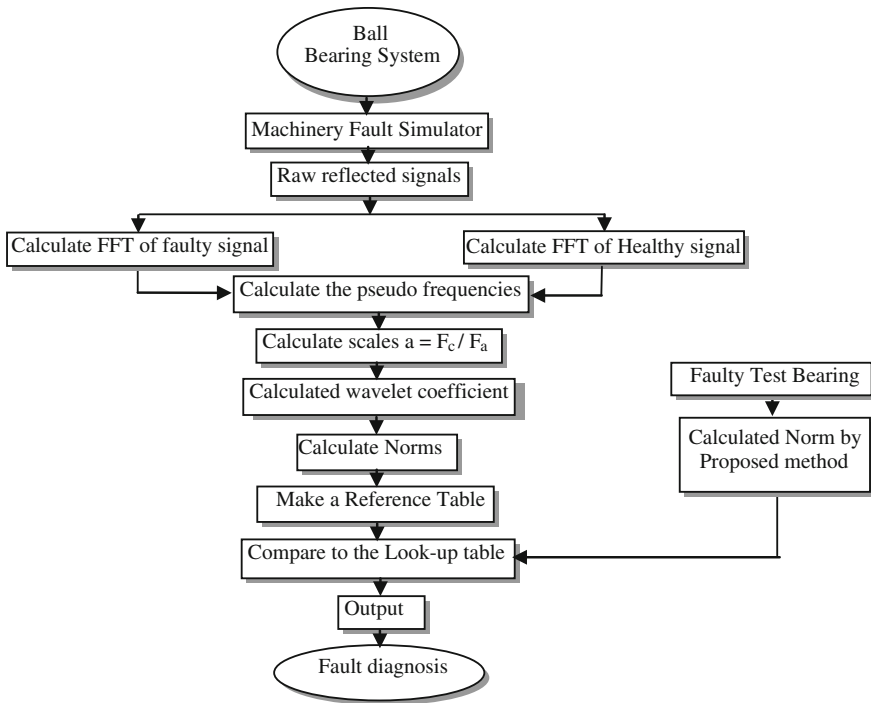
**Fig. 2** Variation in amplitude difference between faulty or non-faulty bearing versus frequency

Step 9: Now take a test signal from a faulty test bearing and calculate the norms by using above-mentioned steps and compare that norms with the reference lookup Table 2 to diagnosis the fault that which type of fault occurs in test bearing.

A complete flowchart for the proposed method is depicted in Fig. 3.

## 6 Results and Discussion

In this paper, the study is carried out on total of 72 instances (36 for horizontal response and 36 for vertical response) at different loading conditions and at different speeds. The square root of energy-confined matrix or second norm can be calculated



**Fig. 3** Flowchart of the proposed method

for horizontal and vertical responses. The sample version of these norms is shown in Table 2. This table is called reference table or look-up table.

### Example

1. Take a reflected signal from the faulty test ball bearing (already known that which type of fault occurs in bearing by which one can test the proposed methodology).
2. Calculate FFT of that reflected signal ball bearing.
3. Compare that test signal FFT to the healthy bearing FFT.
4. Calculate those frequencies at which there is an appropriate difference in their FFT magnitude (in this example, 100 frequency points can be taken as the number of points increases, the accuracy will be increased)
5. Calculate the stretching parameters with the help of Eq. (8) (100 stretching parameters can be calculated as the number of stretching parameters is equal to the number of selected frequency points).
6. Apply the wavelet transform on that stretching parameters and calculate the big matrix of wavelet coefficients.
7. Calculate the norms from that coefficient matrix with some  $\pm 0.0010$  tolerance.
8. Compare that norm to the reference lookup table norms and predict the type of fault occurring in the test bearing as from the result one can see that the result is 100% true.

The evaluation of success by using wavelet transform (selected stretching parameters) with modern algebraic function methods for analyzing of non-stationary multi-component faulty reflected signals. With the help of the lookup table, one can figure out the type of fault. The method is very simple and gives out magnificent result.

## 7 Conclusions

In this paper, the fault diagnosis in ball bearing system is done by using CWT with modern algebraic function. As the complete data are not faulty at all its limit, in this paper only those part of signal has been considered, where the probability of fault is more for which the sensitivity analysis technique is used. The proposed method is useful for extracting features from the original data, and dimension of original data can be reduced by removing irrelevant features. The stretching parameters for the wavelet are calculated with the help of proposed technique. The energy-confined norms are used for the fault classification from the matrix that would be generated by WT at selected stretching parameters. Experimental results included in this paper clearly show the key advantageous features of the proposed methodology. It is evident from the experimental results that the proposed method shows better performance. The example taken in this study shows that this methodology gives the effectively accurate result. This process shows the potential application for developing knowledge-based system. Therefore, the proposed technique can be effectively used for developing online fault diagnosis.

## References

1. Chiang, L.H., Kotanchek, M.E., Kordon, A.K.: Fault diagnosis based on Fisher discriminant analysis and support vector machines. *28*, 1389–1401 (2004)
2. Lei, Y., He, Z., Zi, Y.: Application of an intelligent classification method to mechanical fault diagnosis. *Expert Syst. Appl.* **36**, 9941–9948 (2009)
3. Li, Z., Wu, Z., He, Y., Fulei, C.: Hidden Markov model-based fault diagnostics method in speed-up and speed-down process for rotating machinery. *Mech. Syst. Sign. Process.* **19**, 329–339 (2005)
4. Widodo, A., Yang, B.S.: Review on a vector support machine in machine condition monitoring and fault diagnosis. *Mech. Syst. Sign. Process.* **21**, 2560–2574 (2007)
5. Vyas, N.S., Satishkumar, D.: Artificial neural network design for fault identification in a rotor bearing system. *Mech. Syst. Sign. Process.* **36**, 157–175 (2001)
6. Phadke, A.G., Ibrahim, M., Hlibka, T.: Fundamental basis for distance relaying with symmetrical components. *IEEE Trans. Power Apparatus Syst.* **96**, 635–646 (1977)
7. Staszewski, W.J.: Structural and mechanical damage detection using wavelets. *Shock Vib. Dig.* **30**, 457–472 (1998)
8. Prabhakar, S., Mohanty, A.R., Sekhar, A.S.: Application of discrete wavelet transforms for detection of ball bearing race faults. *Tribol. Int.* **35**, 793–800 (2002)

9. Galli, A.W., Heyd, G.T.: Comments on power quality assessment using wavelets. The 27 Annual NAPS. Bozeman, MT, U.S.A
10. Yuan, F.S., Chu, F.L.: Fault diagnosis based on particle swarm optimization and support vector machines. *Mech. Syst. Sign. Process.* **20**, 1787–1798 (2007)
11. Kankar, P.K., Sharma, S.C., Harsha, S.P.: Fault diagnosis of ball bearing using continuous wavelet transforms. *Appl. Soft Comput.* **11**, 2300–2312 (2011)
12. Lin, J., Zuo, M.J.: Gearbox fault diagnosis using adaptive wavelet filter. *Mech. Syst. Sign. Process.* **17**, 1259–1269 (2003)
13. <https://ewhdbks.mugu.navy.mil/wavelet.htm>
14. Daubechies, I.: Ten Lectures on Wavelets. Regional Conference Series in Applied Mathematics. SIAM, Philadelphia (1992)
15. Watrous, J.: Theory of Quantum Information, 2.4 Norms of operators, lecture notes, University of Waterloo (2008)
16. Meyer, C.D.: Matrix Analysis and Applied Linear Algebra. SIAM (2000)

# Engineering Optimization Using SOMGA

Kusum Deep and Dipti Singh

**Abstract** Many real-life problems arising in science, business, engineering, etc. can be modeled as nonlinear constrained optimization problems. To solve these problems, population-based stochastic search methods have been frequently used in literature. In this paper, a population-based constraint-handling technique C-SOMGA is used to solve six engineering optimization problems. To show the efficiency of this algorithm, the results are compared with the previously quoted results.

**Keywords** SOMGA · C-SOMGA · Optimization

## 1 Introduction

Constraint handling is considered to be challenging and difficult task in optimization. Many real-life problems in engineering can be modeled as nonlinear constrained optimization problems. In view of their practical utility, there is a need to develop efficient and robust computational algorithms, which can numerically solve problems in different fields irrespective of their size. These days a number of probabilistic techniques are available for obtaining the global optimal solution of nonlinear optimization problems. Though GAs are very efficient at finding the global optimal solution of unconstrained or simply constrained (i.e., box constraints) optimization problems but encounter some difficulties in solving highly constraint nonlinear optimization problems, because the operators used in GAs are not very efficient in dealing with the constraints. Several methodologies have been developed to handle constraints when

---

K. Deep (✉)

Indian Institute of Technology, Roorkee, India  
e-mail: kusumfma@iitr.ernet.in

D. Singh

Gautam Buddha University, Greater Noida, India  
e-mail: diptipma@rediffmail.com

GAs are used to solve constrained optimization problems refer Kim and Myung [12], Michalewicz [13], Myung and Kim [14], Orvosh and Davis [15]. Deep and Dipti [8] proposed a penalty parameter free hybrid approach C-SOMGA for solving the nonlinear constrained optimization problems. It is not only easy to implement but also does not require any parameter to be fine-tuned for constraint handling. It works with a very low population size, hence uses low function evaluations where the term “function evaluations” represents the number of times an objective function is evaluated in the entire run. In this paper, six engineering optimization algorithms has been solved using C-SOMGA. The results obtained are compared with the previously quoted results. On the basis of the results, it is concluded that the C-SOMGA is efficient to solve these problems.

The paper is organized as follows: in Sect. 1, introduction is given; in Sect. 2, methodology of C-SOMGA is presented; in Sect. 3, mathematical models of the problems are given and results obtained using C-SOMGA are discussed and compared with the previously quoted results; and Sect. 4 summarizes the conclusions based on the present study.

## 2 Methodology of C-SOMGA

The algorithm C-SOMGA is an extension of SOMGA [7] for solving the constraint nonlinear optimization problems in which SOMGA is combined with constraint-handling tournament selection scheme, and as a result of this, C-SOMGA has been proposed. The methodology of C-SOMGA algorithm is as follows:

First, the individuals are generated randomly. These individuals compete with each other through constraint tournament selection method: Create new individuals via single-point crossover and bitwise mutation. Then, the best individual among them is considered as leader and all others are considered as active. For each active individual, a new population of size  $N$  is created, where  $N$  is the ratio of path length and step size. This population is nothing but the new positions of the active individual proceeds in the direction of the leader in  $n$  steps of the defined length. The movement of this individual is given by

$$x_{i,j}^{MLnew} = x_{i,j,start}^{ML} + \left( x_{L,j}^{ML} - x_{i,j,start}^{ML} \right) tPRTVector_j \quad (1)$$

where  $t \in <0, \text{ by Step to, PathLength}>$ ,

- ML is actual migration loop.
- $x_{i,j}^{MLnew}$  is the new positions of an individual.
- $x_{i,j,start}^{ML}$  is the positions of active individual.
- $x_{L,j}^{ML}$  is the positions of leader.

PRT vector is created before an individual proceeds toward leader. This parameter has the same effect as mutation in GA. It is defined in the range  $<0, 1>$ . Then, sort

this population according to the fitness value in decreasing order. Starting from the best one of the new population, evaluate the constraint violation function described by Eq. 2.

$$\psi(x) = \sum_{m=1}^M [h_m(x)]^2 + \sum_{k=1}^K G_k [g_k(k)]^2 \quad (2)$$

where  $G_k$  is the Heaviside operator such that  $G_k = 0$  for  $g_k(x) \geq 0$  and  $G_k = 1$  for  $g_k(x) < 0$ .

If  $\psi(x) = 0$ , replace the active individual with the current position and move to the next active individual and if  $\psi(x) > 0$ , then move to the next best position of the sorted new population. In this way, all the active individuals are replaced by the new updated feasible position. If no feasible solution is available, then active individual remains the same. At last, the best individuals (number equal to population size) from the previous and current generations are selected for the next generation. The computational steps of this approach are given below:

- Step 1: Generate the initial population.
- Step 2: Evaluate all individuals.
- Step 3: Apply tournament selection for constrained optimization on all individuals to select the better individuals for the next generation.
- Step 4: Apply crossover operator on all individuals with crossover probability  $P_c$  to produce new child individuals.
- Step 5: Evaluate the new child individuals.
- Step 6: Apply mutation operator on every bit of every individual of the population with mutation probability  $P_m$ .
- Step 7: Evaluate the mutated individuals.
- Step 8: Find leader (best fit individual) of the population and consider all others as active individuals of the population.
- Step 9: For each active individual, a new population of size  $N$  is created. This population is nothing but the new positions of the active individual toward the leader in  $n$  steps of the defined length. The movement of this individual is given in Eq. (1).
- Step 10: Sort new population with respect to fitness in decreasing order.
- Step 11: For each individual in the sorted population, check feasibility criterion.
- Step 12: If feasibility criterion is satisfied, replace the active individual with the new position, else move to next position in sort order, and go to Step 11.
- Step 13: Select the best individuals (in fitness) of previous and current generation for the next generation via tournament selection.
- Step 14: If termination criterion is satisfied go to 15 else go to Step 3.
- Step 15: Report the best chromosome as the final optimal solution.

### 3 Mathematical Models of Engineering Optimization Problems

In this section, mathematical model of six engineering optimization problems has been given and the results obtained using C-SOMGA are compared with the available results. These models have been taken from the literature to see the performance of the C-SOMGA on constrained optimization problems. Many researchers used these models to demonstrate the performance of their techniques [2, 16–18]. The experimental setup for C-SOMGA is given in Table 1.

#### 3.1 Gas Transmission Compressor Design

This problem is taken from Beightler and Phillips [2]. This is a real-life problem in which the values of design parameters  $P_1, x_1, x_2, x_3$  are to be determined that will deliver 100 million cu. Ft. of gas per day with minimum cost for a gas pipe line transmission system. Here,

- $P_1$  Compressor discharge pressure,
- $Q$  Flow rate,
- $x_1$  Length between compressor stations (in miles),
- $x_2$  Compressor ratio =  $P_1/P_2$ ,
- $x_3$  Pipe inside diameter (in inches).

The mathematical model of the problem is

$$\text{Minimize } g_0 = 8.61 \times 10^5 x_1^{1/2} x_2 x_3^{-2/3} x_4^{-1/2} + 3.69 \times 10^4 x_3 + 7.72 \times 10^8 \times 10^8 x_1^{-1} x_2^{0.219} - 765.43 \times 10^6 x_1^{-1}$$

subject to  $x_4 x_2^{-2} + x_2^{-2} \leq 1$ , where  $x_1, x_2, x_3, x_4 > 0$ .

Bounds on the variables are as follows:

$$20 \leq x_1 \leq 50, 1 \leq x_2 \leq 10, 20 \leq x_3 \leq 50, 0.1 \leq x_4 \leq 60$$

**Table 1** Experimental setup

Population size	20
$P_c$	0.85
$P_m$	0.009
Step size	0.31
Path length	3
String length	20



**Table 2** Optimal solution to the design of a gas transmission compressor

	Value of objective	Values of variables
Solution obtained by C-SOMGA	$296.490 \times 10^4$	$x_1 = 49.9996, x_2 = 1.17834,$ $x_3 = 24.5996, x_4 = 0.388482$
Solution given in Pant [16]	$296.528 \times 10^4$	$x_1 = 50.000, x_2 = 1.183,$ $x_3 = 24.347, x_4 = 0.339$
Solution given in Beightler and Phillips [2]	$299 \times 10^4$	$x_1 = 28.760, x_2 = 1.109,$ $x_3 = 25.030, x_4 = 0.230$

The problem turns out to be a constrained geometric programming problem. This problem is earlier solved by Beightler and Phillips [2], Verma [18], Thanh [17], and Pant [16]. The results obtained using C-SOMGA and those given in source are shown in Table 2. It is evident with the Table 2 that the cost obtained by C-SOMGA in deliver the gas per day that is 2964900 is lesser than the cost obtained by Pant, i.e., 2965280 and by Beightler and Phillips, i.e., 2990000. In other words, C-SOMGA provides far better results than previously quoted results.

### 3.2 Optimization of a Riser Design

This problem is taken from Gaindhar et al. [9]. The objective of this problem is to determine the optimal volume of the riser. Any metal will shrink in volume when it is allowed to cool and solidify from a molten state. A riser is a device by which the location of a shrinkage cavity is shifted from within the casting to the riser, which is an extraneous portion cast as an integral but distinct portion of the casting. After the casting is solidified, all extraneous parts are cut off leaving behind the desired casting free of any shrinkage cavity.

The basic requirement for the riser design is that the solidification time of the riser must not be less than the solidification time of the casting. From the practical point of view, it is considered advantageous to have top riser connected to the casting through a neck. The molding sand in the neck region gets up more heated as compared to the rest of the region surrounding the riser. This ensures molten metal in the region of the neck. This also facilitates cutting off of the riser from the casting after the casting has been solidified.

The mathematical modal of the problem, as given in Gaindhar et al. [9] is

$$\begin{aligned} \text{Minimize } f(x) &= (1/4) \pi x_1 x_2^2 + (1/12) \pi x_4 \left( 3 - 3x_4/x_3 + x_4^2/x_3^3 \right) x_2 \\ \text{subject to } 2E &\left( 5 + (x_4/x_3) (2 - x_4/x_3) \left( 1 + x_3^2 \right)^{1/2} \right) x + 4E x_2^{-1} \\ &- (x_4/3) \left( 3 - 3x_4/x_3 + x_4^2/x_3^3 \right) \leq 1 \end{aligned}$$

$$x_1, x_2, x_3, x_4 > 0.$$

where

- $x_1$  height of riser
- $x_2$  diameter of the riser
- $E$  riser modulus constant ( $E = 10 / 7$ )
- $x_3$   $\tan\theta$  and
- $x_4$  height of the neck riser.

The variable bounds are as follows:

$$1 \leq x_1 \leq 8; 1 \leq x_2 \leq 10; 0 \leq x_3 \leq 1; 0 \leq x_4 \leq 1$$

This problem is earlier solved by Gaindhar et. al [9] and by Pant [16]. The numerical results obtained are compared with the available results and are presented in Table 3. It is evident with the Table 3 that the result obtained by C-SOMGA that is 290.78142 is better than the result obtained by Pant [16] i.e 290.8532 and by Gaindhar et al. [9] i.e. 290.8069.

### 3.3 Optimum Design of a Welded Beam

Optimum design of a welded beam problem is a well-known problem. The formulation of this problem is available in literature with two models. In model (a), the number of constraints is six and in model (b), it is seven. Both the models are described below:

**Model (a):**

This problem is taken from Beightler and Phillips [2]. In this problem, the assembly of the welded structure as is being considered for mass production. Outside considerations fix the material of the bar  $A$  as well as the design parameters  $F$  and  $L$ . Assuming that the design engineer has fixed the specifications,  $F = 6,000$  lb,  $L = 14$  in and bar  $A = 1,010$  steel; the objective function is to find a feasible combination of  $x_1, x_2, x_3$  and  $x_4$  such that the total cost assembly construction is minimum.

**Table 3** Optimal design of a riser

	Value of objective	Values of variables
Solution obtained by C-SOMGA	290.78142	$x_1 = 4.276, x_2 = 8.7510,$ $x_3 = 1, x_4 = 0.1001$
Solution given in Pant [16].	290.8532	$x_1 = 4.2233, x_2 = 8.6055,$ $x_3 = 1.0000, x_4 = 0.1000$
Solution given in Gaindhar et al. [9]	290.8069	$x_1 = 4.266, x_2 = 8.5710,$ $x_3 = 1.000, x_4 = 0.1000$

The mathematical model of the problem is

$$\text{Minimize } g_0(X) = 1.1047x_1^2x_2 + 0.6735x_3x_4 + 0.04811x_2x_3x_4$$

Subject to

$$g_1(X) = 16.8x_4^{-1}x_3^{-2} \leq 1, \quad g_2(X) = x_1x_4^{-1} \leq 1, \quad g_3(X) = 0.125x_1^{-1} \leq 1,$$

$$g_4(X) = 9.08x_3^{-3}x_4^{-1} \leq 1, \quad g_5(X) = 0.09428x_3^{-1}x_4^{-3} + 0.02776x_3 \leq 1$$

$$g_6(X) = \left[ \left( \frac{F^2x_1^{-2}x_2^{-2} + \frac{F^2x_2^{-1}(L+x_2/12)}{2\left(\frac{x_2^2}{12} + \frac{(x_3+x_1)^2}{4}\right)^{-1}}}{F^2(L+x_2/2)^2\left(\frac{x_2^2+(x_3+x_1)^2}{4}\right)} + \frac{2x_1^2x_2^2\left(\frac{x_2^2}{12} + \frac{(x_3+x_1)^2}{4}\right)^2} \right)^{1/2} \right] \leq 13,000$$

$$(x_1, x_2, x_3, x_4) > 0.$$

The variable bounds are as follows:

$$0.1 \leq x_1 \leq 1; 5 \leq x_2 \leq 7; 7 \leq x_3 \leq 9; 0.1 \leq x_4 \leq 1$$

### Model (b):

This model is taken from Xiaohui et al. [19]. The objective is to minimize the cost of a welded beam subject to constraints on shear stress, bending stress in the beam, bucking load on the bar, end deflection of the beam, and side constraints. The problem can be stated as follows:

$$\text{Minimize } f(X) = 1.10471x_1^2x_2 + 0.04811x_3x_4(14.0 + x_2)$$

subject to

$$g_1(X) = \tau(X) - \tau_{\max} \leq 0$$

$$g_2(X) = \sigma(X) - \sigma_{\max} \leq 0$$

$$g_3(X) = x_1 - x_4 \leq 0$$

$$g_4(X) = 0.10471x_1^2 + 0.04811x_3x_4(14.0 + x_2) - 5.0 \leq 0$$

$$g_5(X) = 0.125 - x_1 \leq 0,$$

$$g_6(X) = \delta(X) - \delta_{\max} \leq 0$$

$$g_7(X) = P - P_c(X) \leq 0$$

where

$$\tau(X) = \sqrt{(\tau')^2 + 2\tau'\tau''\frac{x_2}{2R} + (\tau'')^2}$$

$$\tau' = \frac{P}{\sqrt{2}x_1x_2}, \quad \tau'' = \frac{MR}{J}, \quad M = P\left(L + \frac{x_2}{2}\right), \quad R = \sqrt{\frac{x_2^2}{4} + \left(\frac{x_1 + x_3}{2}\right)^2}$$

$$J = 2 \left\{ \sqrt{2}x_1x_2 \left[ \frac{x_2^2}{12} + \left( \frac{x_1 + x_3}{2} \right)^2 \right] \right\}, \sigma(X) = \frac{6PL}{x_4x_3^2}, \delta(X) = \frac{4PL^3}{Ex_3^3x_4}$$

$$P_c(X) = \frac{4.013E\sqrt{x_3^2x_4^6/36}}{L^2} \left( 1 - \frac{x_3}{2L}\sqrt{\frac{E}{4G}} \right)$$

$$P = 6,000\text{ lb}, \quad L = 14\text{ in}, \quad E = 30 \times 10^6\text{ psi}, \quad G = 12 \times 10^6\text{ psi},$$

$$\pi_{\max} = 13,600\text{ psi}, \quad \sigma_{\max} = 30,000\text{ psi}, \quad \delta_{\max} = 0.25\text{ in}$$

The following ranges of the variables were used:

$$0.1 \leq x_1 \leq 2, \quad 0.1 \leq x_2 \leq 10, \quad 0.1 \leq x_3 \leq 10, \quad 0.1 \leq x_4 \leq 2$$

Both the models are solved by C-SOMGA. The numerical results obtained and the results given in source are presented in Table 4 for model (a) and Table 5 for model (b).

In Table 4, although the results available in source are lesser than the results obtained by C-SOMGA, but the solutions are not satisfying the feasibility conditions. Hence, these solutions cannot be accepted. The result obtained by C-SOMGA is a feasible solution. Therefore, C-SOMGA is best in this problem.

In Table 5, the result attained by C-SOMGA is superior to Coello [5] and Deb [6] but slightly inferior at fifth place to Xiaohui et al. [19]. It shows that the results are comparable.

### 3.4 Optimal Capacity of Gas Production Facilities

This problem is taken from Beightler and Phillips [2]. This is the problem of determining the optimum capacity of production facilities that combine to make an oxygen

**Table 4** Optimal design of a welded beam based on model (a)

	Value of objective	Value of variables	Feasibility
Solution obtained by C-SOMGA	2.45694	$x_1 = 0.244241, x_2 = 6.4712,$ $x_3 = 8.43726, x_4 = 0.244364$	Satisfied
Solution given in Pant [16]	1.9786	$x_1 = 0.1489, x_2 = 5.000,$ $x_3 = 8.2736, x_4 = 0.2454$	Not Satisfied
Solution given in Beightler and Phillips [2]	2.3860	$x_1 = 0.2455, x_2 = 6.1960,$ $x_3 = 8.2730, x_4 = 0.2455$	Not Satisfied

**Table 5** Optimal design of a welded beam based on model (b)

	Value of objective	Value of variables
Solution obtained by C-SOMGA	1.72486	$x_1 = 0.205731, x_2 = 3.47048,$ $x_3 = 9.03669, x_4 = 0.20573$
Solution given in Xiaohui [19]	1.72485084	$x_1 = 0.20573, x_2 = 3.47049,$ $x_3 = 9.03662, x_4 = 0.20573$
Solution given in Coello [5]	1.74830941	$x_1 = 0.2088, x_2 = 3.4205,$ $x_3 = 8.9975, x_4 = .2100$
Solution given in Deb [6]	2.43311600	$x_1 = 0.2489, x_2 = 6.1730,$ $x_3 = 8.1739, x_4 = 0.2533$

**Table 6** Optimal capacity of gas production facilities

	Value of objective	Value of variables
Solution obtained by C-SOMGA	169.844	$x_1 = 17.500, x_2 = 600.000,$
Solution given in Pant [16]	169.844	$x_1 = 17.500, x_2 = 600.000,$
Solution given in Beightler and Phillips [2]	173.760	$x_1 = 17.500, x_2 = 465.000,$

producing and storing system. Oxygen for basic oxygen furnace is produced at a steady-state level. The demand for oxygen is cyclic with a period of one hour, which is too short to allow an adjustment of level of production to the demand. Hence, the manager of the plant has two alternatives:

1. He can keep the production at the maximum demand level; excess production is lost in the atmosphere.
2. He can keep the production at lower level; excess production is compressed and stored for use during the high demand period. The mathematical model of the problem is

$$\text{Minimize } g_0(X) = 61.8 + 5.72x_1 + .2623 \left[ (40 - x_1) \ln \frac{x_2}{200} \right]^{-0.85} + .087 (40 - x_1) \ln \frac{x_2}{200} + 700.23x_2^{-.75}$$

subject to  $x_1 \geq 17.5, x_2 \geq 200, x_1, x_2 > 0$ .

The variable bounds are as follows:  $17.5 \leq x_1 \leq 40; 300 \leq x_2 \leq 600$

The numerical results obtained using C-SOMGA and the numerical results given in source are presented in Table 6. In this problem, C-SOMGA produced better results than Beightler and Philips [2] but similar results as obtained by Pant [16] using GRST.

**Table 7** Minimization of the weight of a tension/compression Spring

	Value of objective	Value of variables
Solution obtained by C-SOMGA	.0126656	$x_1 = .0516216, x_2 = 0.355094,$ $x_3 = 11.385$
Solution given in Xiaohui [19]	0.0126661409	$x_1 = 0.05147, x_2 = .35138394,$ $x_3 = 11.60865920$
Solution given in Coello [5]	.0127047834	$x_1 = .051480, x_2 = .351661,$ $x_3 = 11.632201$
Solution given in Arora [1]	.127302737	$x_1 = .053396, x_2 = .399180,$ $x_3 = 9.185400.$

### 3.5 Minimization of the Weight of a Tension/Compression Spring

This problem was described by Arora [1] and Belegundu [3]. The problem consists of minimizing the weight of a tension/compression spring subject to constraints on minimum deflection, shear stress, surge frequency, limits on outside diameter and on design variables. The design variables are the mean coil diameter  $D$ , the wire diameter  $d$ , and the number of active coils  $N$ . The problem can be expressed as follows:

$$\text{Minimize } f(X) = (N + 2) Dd^2$$

subject to

$$g_1(X) = 1 - \frac{D^3 N}{71785d^4} \leq 0$$

$$g_2(X) = \frac{4D^2 - dD}{12566(Dd^3 - d^4)} + \frac{1}{5108d^2} - 1 \leq 0$$

$$g_3(X) = 1 - \frac{140.45d}{D^2 N} \leq 0$$

$$g_4(X) = \frac{D + d}{1.5} - 1 \leq 0.$$

The following ranges of the variables were used:

$$0.05 \leq x_1 \leq 2, \quad 0.25 \leq x_2 \leq 1.3, \quad 2.0 \leq x_3 \leq 15.$$

The numerical results of the solution obtained using C-SOMGA and the numerical results given in source are presented in Table 7. The result attained by C-SOMGA is superior to Coello and Mezura [4] and Arora [1] at the fourth place and at the sixth place to Xiaohui et al. [19]. Hence, the results are comparable.

### 3.6 Himmelblau’s Nonlinear Optimization Problem

This problem has been taken from Xiaohui [19]. This problem was proposed by Himmelblau [10], and it has been used before as a benchmark for several evolutionary algorithm-based techniques. In this problem, there are five design variables, six nonlinear inequality constraints, and ten boundary conditions. The problem can be stated as follows:

$$\text{Minimize } f(X) = 5.3578547x_3^2 + 0.8356891x_1x_5 + 37.2932239x_1 - 40792.141$$

subject to

$$\begin{aligned} 0 &\leq 85.334407 + .0056858x_2x_5 + .00026x_1x_4 - .0022053x_3x_5 \leq 92 \\ 90 &\leq 80.51249 + 0.0071317x_2x_5 + 0.00026x_1x_2 + 0.0021813x_3^2 \leq 110 \\ 20 &\leq 9.300961 + 0.0047026x_3x_5 + 0.0012547x_1x_3 + 0.0019085x_3x_4 \leq 25 \\ 78 &\leq x_1 \leq 102, \quad 33 \leq x_2 \leq 45, \quad 27 \leq x_3 \leq 45, \quad 27 \leq x_4 \leq 45, \quad 27 \leq x_5 \leq 45. \end{aligned}$$

The results obtained by C-SOMGA and available from the other source are presented in Table 8. C-SOMGA gives better results than Coello and Mezura [4] and Homaifar et al [11] and results are comparable to Xiaohui et al. [19].

**Table 8** Himmelblau’s Nonlinear Optimization Problem

	Value of objective	Value of variables
Solution obtained by C-SOMGA	-31025.6	$x_1 = 78, x_2 = 33.0001,$ $x_3 = 27.071, x_4 = 45,$ $x_5 = 44.969$
Solution given in Xiaohui [19]	-31025.56142	$x_1 = 78.0, x_2 = 33.0,$ $x_3 = 27.070997, x_4 = 45,$ $x_5 = 44.96924255$
Solution given in Coello [5]	-31020.859	$x_1 = 78.0495, x_2 = 33.0070,$ $x_3 = 27.0810, x_4 = 45,$ $x_5 = 44.9400$
Solution given in Homaifar et al. [11]	-30665.609	$x_1 = 78.0000, x_2 = 33.0000,$ $x_3 = 29.9950, x_4 = 45,$ $x_5 = 36.7760.$

## 4 Conclusions

In this paper, six real-life constrained optimization problems arising in various fields of engineering have been solved. For solving these constrained optimization problems, a population-based hybridized algorithm C-SOMGA has been used. In four problems, C-SOMGA provides better results than the previously quoted results, and in two problems, results are comparable. The algorithm requires only 20 population size for solving these problems. It is therefore concluded that C-SOMGA is well suited for obtaining the global optimal solution of engineering optimization problems.

## References

1. Arora, J.S.: Introduction to Optimum Design, 2nd edn. Academic Press, New Delhi (2006)
2. Beightler, C.S., Phillips, D.T.: Applied Geometric Programming. Wiley, New York (1976)
3. Belegundu, A.D.: A Study of Mathematical Programming for Structural Optimization. University of Iowa, Iowa, Department of Civil and Environmental Engineering (1982)
4. Coello, C.A., Mezura, M.E.: Constraint-handling in genetic algorithms through the use of dominance-based tournament selection. *Adv. Eng. Inf.* **16**, 193–203 (2002)
5. Coello, C.A.: Use of a self-adaptive penalty approach for engineering optimization problems. *Comput. Ind.* **41**, 113–127 (2000)
6. Deb, K., Gene AS: A Robust Optimal Design Technique for Mechanical Component Design. In Dasgupta, D., Michalewicz, Z.: (eds). *Evolutionary Algorithms in Engineering Applications*, pp. 497–514. Springer, Berlin (1997b)
7. Deep, K., and Dipti: A New Hybrid Self Organizing Migrating Genetic Algorithm for Function Optimization. *IEEE Congress on Evolutionary Computation*, pp. 2796–2803 (2007)
8. Deep, K., and Dipti: A self organizing migrating genetic algorithm for constrained optimization. *Appl. Math. Comput.* **198**(1), 237–250 (2008)
9. Gaiindhar, J.L., Mohan, C., Tyagi, S.: Optimization of riser design in metal casting. *J. Eng. Optim.* **14**, 1–26 (1988)
10. Himmelblau, D.M.: *Applied Nonlinear Programming*. McGraw-Hill, New York (1972)
11. Homaifar, A.A., Lai, S.H.Y., Qi, X.: Constrained optimization via genetic algorithms. *Simulation* **62**, 242–254 (1994)
12. Kim, J.H., Myung, H.: A Two Phase Evolutionary Programming for General Constrained Optimization Problem. *Proceedings of the Fifth Annual Conference on Evolutionary Programming*, San Diego (1996)
13. Michalewicz, Z.: Genetic Algorithms, Numerical Optimization and Constraints. In: Echelman, L.J. (ed.) *Proceedings of the Sixth International Conference on Genetic Algorithms*, pp. 151–158 (1995)
14. Myung, H., Kim, J.H.: Hybrid evolutionary programming for heavily constrained problems. *Bio-Systems* **38**, 29–43 (1996)
15. Orvosh, D., Davis, L.: Using a Genetic Algorithm to Optimize Problems with Feasibility Constraints. In: Echelman, L.J. (ed). *Proceedings of the Sixth International Conference on Genetic Algorithms*, pp. 548–552 (1995)
16. Pant, M.: *Genetic Algorithms for Global Optimization and their Applications*. Ph.D. Thesis, Department of Mathematics, IIT Roorkee, Formerly University of Roorkee (2003)
17. Thann, N.H.: *Some Global Optimization Techniques and their use in solving Optimization Problems in Crisp and Fuzzy Environments*. University of Roorkee, Roorkee, India, Department of Mathematics (1996)



18. Verma, S.K.: Solution of Optimization Problems in Crisp Fuzzy and Stochastic Environments. Ph.D. Thesis, Dept. of Mathematics, University of Roorkee, Roorkee (1997)
19. Xiaohui, H., Eberhart, R.C., Shi, Y.: Engineering Optimization with Particle Swarm. IEEE Swarm Intelligence Symposium, Indianapolis, USA (2003)

# Goal Programming Approach to Trans-shipment Problem

Om Prakash Dubey, Kusum Deep and Atulya K. Nagar

**Abstract** The technocrats put their efforts regularly to minimize the total cost/budget of transportation problem. However, the proper effort has not been put for minimizing the total cost of trans-shipment problem. A goal programming approach has been developed to obtain the minimum budget for trans-shipment problem. The trans-shipment problem is regarded as the extended transportation problem and hence be solved by the transportation techniques. In the present algorithm, trans-shipment problem is transferred to suitable transportation problem and further modified as a proper goal programming problem. The priorities of goal programming explore the wider impact for decision maker. Therefore, the solution obtained is more suitable for decision makers. Hence, it is widely acceptable for any organization. At the end, a numerical example is solved in support of the procedure.

**Keywords** Trans-shipment problem · Transportation problem · Lexicographic goal programming · Priority level · Decision maker

## 1 Introduction

A transportation problem (TP) allows only shipments which go directly from a supply/source point, acts only as a shipper of the goods, to a demand point/destination, acts only as receiver of the goods. Transportation models deal with problems

---

O. P. Dubey (✉)

Department of Mathematics, Bengal College of Engineering and Technology, Durgapur, India  
e-mail: omprakashdubeymaths@gmail.com

K. Deep

Department of Mathematics, Indian Institute of Technology, Roorkee, India  
e-mail: kusumfma@iitr.ernet.in

A. K. Nagar

Department of Computer Science, Liverpool Hope University, Liverpool L 169 JD, UK  
e-mail: nagara@hope.ac.uk

concerned with the effectiveness function when each of a number of origins associates with each of a possibly different number of destinations. In many situations, shipments are allowed between supply points or between demand points. Sometimes there may also be trans-shipment points through which goods can be transhipped on their journey from a supply point to a demand point. Shipping problems with any or all of these characteristics are Trans-shipment Problems. Thus, the optimal solution to a Trans-shipment Problem can be found by solving a Transportation problem [1–3].

Goal programming (GP) is a decision-making technique generally used to solve multiple objective problems, which provides a best compromise solution according to the DM's needs and desires. The concept was originally developed by Charnes and Cooper [4]. In GP, instead of trying to optimize the objective function directly, the deviation between the goals and what can be achieved under a given set of constraints are to be minimized. In the priority-based GP, the priorities/weights are assigned to the goals according to their importance as specified by the DM. Sometimes it happens that the DM is not satisfied with the solution(s) and DM wants some other solutions to suit his desires; then, set of alternate solutions can be provided using interactive GP techniques [5, 6]. The GP formulations ordered the unwanted deviations into a number of priority levels, with the minimization of a deviation in a higher priority level being of infinitely more important than any deviations in lower priority levels, known as Lexicographic or Pre-emptive GP [7]. It should be used when there exists a clear ordering among the decisions.

## 2 Methodology

The TP assumes that direct routes exist from each source to each destination. However, there are situations in which units may be shipped from one source to another or to other destinations before reaching their final destination, known as Trans-shipment Problem.

In generalized trans-shipment model, items are supplied from different sources to different destination. It is sometimes economical if the shipment passes through some transient nodes in between sources and destinations. Unlike in TP, in trans-shipment problem, the objective is to minimize the total cost of shipments, and thus, the shipment passes through one or more intermediate nodes before it reaches its desired destination.

For the purpose of trans-shipment, the distinction between a source and destination is dropped so that a TP with  $m$  sources and  $n$  destinations gives rise to a trans-shipment problem with  $m + n$  sources and  $m + n$  destinations. The basic feasible solution to such a problem will involve  $[(m + n) + (m + n) - 1]$  or  $2m + 2n - 1$  basic variables, and if we omit the variables appearing in the  $(m + n)$  diagonal cells, we have  $m + n - 1$  basic variables.

Here, as each source or destination is a potential point of supply as well demand, the total supply (say of  $K$  units) is added to the actual supply of each source as

well as to the actual demand at each destination. Also, the ‘demand’ at each source and ‘supply’ at each destination are set equal to  $K$ . It may assume the supply and demand of each location to be fictitious one. These quantities ( $K$ ) may be regarded as buffer stocks, and each of these buffer stocks should at least be equal to the total supply/demand in the given problem.

Therefore, construct a transportation tableau creating a row for each supply point and trans-shipment point, and a column for each demand point and trans-shipment point. Each supply point will have a supply equal to its original supply, and each demand point will have a demand equal to its original demand [3].

The general TP with  $m$  production sites and  $n$  destinations is given by the cost matrix  $[C_{ij}]$ ,  $i = 1, 2, \dots, m$  and  $j = 1, 2, \dots, n$ , together with production capacity  $a_i$  and demand  $b_j$ . The problem is said to be balanced if total supply = total demand, i.e.,  $\sum_{i=1}^m a_i = \sum_{j=1}^n b_j$ , otherwise unbalanced. TP can be expressed mathematically as,

$$\begin{aligned} \text{Minimize } Z &= \sum_{i=1}^m \sum_{j=1}^n C_{ij}x_{ij} \\ \text{subject to, } \sum_{j=1}^n x_{ij} &= a_i \quad i = 1, 2, \dots, m \\ \sum_{i=1}^m x_{ij} &= b_j \quad j = 1, 2, \dots, n \\ \sum_{i=1}^m a_i &= \sum_{j=1}^n b_j, \quad x_{ij} \geq 0. \end{aligned}$$

where  $x_{ij}$  is the amount of goods to be transported.

Now, the GP version of the above TP model can be written as,

$$\begin{aligned} \text{Minimize } F(d) \\ \text{subject to,} \end{aligned}$$

$$\text{supply constraints, } \sum_{j=1}^n x_{ij} + d_j^- - d_j^+ = a_i, \quad i = 1, 2, \dots, m; \quad j = 1, 2, \dots, k.$$

$$\text{demand goals, } \sum_{i=1}^m x_{ij} + d_j^- - d_j^+ = b_i, \quad j = 1 + k, 2 + k, \dots, n + k.$$

$$\text{and, budget goal, } \sum_{i=1}^m \sum_{j=1}^n C_{ij}x_{ij} + d_{k+n+1}^- - d_{k+n+1}^+ = B; d_j^- \cdot d_j^+ = 0, \text{ for all } j; x_{ij}, d_j^-, d_j^+ \geq 0$$

where  $B$  represents budget aspiration level as fixed by the DM [8].

### 3 Case Study

To support the algorithm, a sample problem is considered as follows.

A firm has two factories X and Y and three retail stores A, B, and C. The numbers of units of a product available at factories X and Y are 200 and 300, respectively, while demanded at retail stores are 100, 150, and 250, respectively. Rather than shipping directly from sources to destinations, it is decided to investigate the possibility of trans-shipment. Find the optimal shipping schedule. The transportation costs in rupees per unit are given in Table 1.

**Table 1** Sample problem

		Factory		Retail store		
		X	Y	A	B	C
Factory	X	0	6	7	8	9
	Y	6	0	5	4	3
Retail store	A	7	2	0	5	1
	B	1	5	1	0	4
	C	8	9	7	6	0

#### Solution

For this trans-shipment problem, buffer stock = total supply = total demand = 500 units. Adding 500 units to each supply/demand point, we get Table 2.

**Table 2** Trans-shipment problem as transportation problem

		Factory		Retail store			Supply
		X	Y	A	B	C	
Factory	X	0 (500)	6	7 (200)	8	9	700
	Y	6	0 (500)	5	4 (50)	3 (250)	800
Retail store	A	7	2	0 (400)	5 (100)	1	500
	B	1	5	1	0 (500)	4	500
	C	8	9	7	6	0 (500)	500
Demand		500	500	600	650	750	

Following is the initial solution obtained by the Vogel’s approximation method (Table 3).

Factory X supplies 100 units each to retail stores A and B, whereas factory Y supplies 50 units to retail store B and 250 units to C.

Goal programming formulation of the transportation problem obtained from the given trans-shipment problem is as follows in two models.

#### Model -1

Minimize  $F(d)$   
 subject to,

**Table 3** Solution by Vogel’s approximation method

		Factory		Retail store			Supply
		X	Y	A	B	C	
Factory	X	0 (500)	6	7 (100)	8 (100)	9	700
	Y	6	0 (500)	5	4 (50)	3 (250)	800
Retail store	A	7	2	0 (500)	5	1	500
	B	1	5	1	0 (500)	4	500
	C	8	9	7	6	0 (500)	500
Demand		500	500	600	650	750	

$$x_1 + x_6 + x_{11} + x_{16} + x_{21} \geq 500 \tag{1}$$

$$x_2 + x_7 + x_{12} + x_{17} + x_{22} \geq 500 \tag{2}$$

$$x_3 + x_8 + x_{13} + x_{18} + x_{23} \geq 600 \tag{3}$$

$$x_4 + x_9 + x_{14} + x_{19} + x_{24} \geq 650 \tag{4}$$

$$x_5 + x_{10} + x_{15} + x_{20} + x_{25} \geq 750 \tag{5}$$

$$\begin{aligned}
 &0 \cdot x_1 + 6 \cdot x_2 + 7 \cdot x_3 + 8 \cdot x_4 + 9 \cdot x_5 \\
 &\quad + 6 \cdot x_6 + 0 \cdot x_7 + 5 \cdot x_8 + 4 \cdot x_9 + 3 \cdot x_{10} \\
 &\quad + 7 \cdot x_{11} + 2 \cdot x_{12} + 0 \cdot x_{13} + 5 \cdot x_{14} \\
 &\quad + 1 \cdot x_{15} + 1 \cdot x_{16} + 5 \cdot x_{17} + 1 \cdot x_{18} + 0 \cdot x_{19} \\
 &\quad + 4 \cdot x_{20} + 9 \cdot x_{21} + 9 \cdot x_{22} + 7 \cdot x_{23} + 6 \cdot x_{24} + 0 \cdot x_{25} \leq 10,000
 \end{aligned} \tag{6}$$

$$x_1 + x_2 + x_3 + x_4 + x_5 \leq 700 \tag{7}$$

$$x_6 + x_7 + x_8 + x_9 + x_{10} \leq 800 \tag{8}$$

$$x_{11} + x_{12} + x_{13} + x_{14} + x_{15} \leq 500 \tag{9}$$

$$x_{16} + x_{17} + x_{18} + x_{19} + x_{20} \leq 500 \tag{10}$$

$$x_{21} + x_{22} + x_{23} + x_{24} + x_{25} \leq 500 \tag{11}$$

$$x_i \geq 0, \quad i = 1, 2, 3, \dots, 25. \tag{12 to 36}$$

where  $F(d)$  is a function of deviational variables.

In the present trans-shipment problem, for  $F(d)$ , the authors consider demand goal as 1st priority level, budget goal as 2nd priority level, supply goal as 3rd priority level, and non-negative constraints as 4th priority level (Table 4).

Here, factory X supplies 100 units to retail store A and B each, whereas factory Y supplies 50 units to retail store B. However, C received 250 units from A in the processing of the solution.

**Model - 2**

Minimize  $F(d)$

subject to,

**Table 4** Initial solution obtained by the goal programming technique

		Factory		Retail store			Supply
		X	Y	A	B	C	
Factory	X	0	6	7 (600)	8 (100)	9	700
	Y	6	0 (250)	5	4 (550)	3	800
Retail store	A	7	2 (56.25)	0	5	1 (443.75)	500
	B	1 (500)	5	1	0	4	500
	C	8	9 (193.75)	7	6	0 (306.25)	500
Demand		500	500	600	650	750	

$$x_1 + x_6 + x_{11} + x_{16} + x_{21} \geq 500 \tag{1}$$

$$x_2 + x_7 + x_{12} + x_{17} + x_{22} \geq 500 \tag{2}$$

$$x_3 + x_8 + x_{13} + x_{18} + x_{23} \geq 600 \tag{3}$$

$$x_4 + x_9 + x_{14} + x_{19} + x_{24} \geq 650 \tag{4}$$

$$x_5 + x_{10} + x_{15} + x_{20} + x_{25} \geq 750 \tag{5}$$

$$0 \cdot x_1 + 6 \cdot x_2 + 7 \cdot x_3 + 8 \cdot x_4 + 9 \cdot x_5 + 6 \cdot x_6 + 0 \cdot x_7 + 5 \cdot x_8 + 4 \cdot x_9 + 3 \cdot x_{10} + 7 \cdot x_{11} + 2 \cdot x_{12} + 0 \cdot x_{13} + 5 \cdot x_{14} + 1 \cdot x_{15} + 1 \cdot x_{16} + 5 \cdot x_{17} + 1 \cdot x_{18} + 0 \cdot x_{19} + 4 \cdot x_{20} + 9 \cdot x_{21} + 9 \cdot x_{22} + 7 \cdot x_{23} + 6 \cdot x_{24} + 0 \cdot x_{25} \leq 1000 \tag{6}$$

$$x_1 + x_2 + x_3 + x_4 + x_5 \leq 700 \tag{7}$$

$$x_6 + x_7 + x_8 + x_9 + x_{10} \leq 800 \tag{8}$$

$$x_{11} + x_{12} + x_{13} + x_{14} + x_{15} \leq 500 \tag{9}$$

$$x_{16} + x_{17} + x_{18} + x_{19} + x_{20} \leq 500 \tag{10}$$

$$x_{21} + x_{22} + x_{23} + x_{24} + x_{25} \leq 500 \tag{11}$$

$$x_i \geq 0, i = 1, 2, 3, \dots, 25. \tag{12 to 36}$$

where  $F(d)$  is a function of deviational variables.

In the present trans-shipment problem, for  $F(d)$ , the authors consider demand goal as 1st priority level, budget goal as 2nd priority level, supply goal as 3rd priority level, and non-negative constraints as 4th priority level (Table 5).

Factory X supplies 7.1429 units to retail store A and 92.86 units generated to A in the processing, whereas factory Y supplies 50 units to retail store B and 250 to C. However, B received 100 units from A in the processing of the solution.

These two models show the impact of assigning the budget value. Hence, care should be taken in this situation.

**Table 5** Initial solution obtained by the goal programming technique

		Factory		Retail store			Supply
		X	Y	A	B	C	
Factory	X	0 (500)	6	7 (7.1429)	8	9	700
	Y	6	0 (500)	5	4 (50)	3 (250)	800
Retail store	A	7	2	0 (592.86)	5 (100)	1	500
	B	1	5	1	0 (600)	4	500
	C	8	9	7	6	0 (500)	500
Demand		500	500	600	650	750	

### 4 Conclusion

The beauty of this algorithm is that DM may select priority level as per his/her own choice suitable for the concern organization interchanging demand, budget, supply or different levels of demand, different levels of supply and budget. In the above-mentioned case study, the algorithm minimizes the budget compared to available traditional techniques. Hence, it is better and the obtained results may be more realistic and useful for the organization in view of the DM. Care should be taken in assigning the budget value, because under-budget as well as over-budget explores bad impact on solution. Further, set of solutions may be generated for each model (priority-wise formulation) formulated by the DM.

### References

1. Srinivasan, P.: A trans-shipment model for cash management decisions. *Manage. Sci.* **20**, 1350–1363 (1974)
2. Mohan, C.: Kusum Deep: Optimization techniques. New Age International Publishers, UK (2009)
3. Gupta, P.K., Hira, D.S.: Operations Research. S. Chand and Co. Ltd., India (2007)
4. Charnes, A., Cooper, W.W.: Management models and industrial application of linear programming. Wiley, New York (1961)
5. Dyer, J.S.: Interactive goal programming. *Manage. Sci.* **19**, 62 (1972)
6. Masud, A.S.M.: Interactive goal Programming- A Survey. Times/ORSA Meeting, Chicago (1983)
7. Ignizio, J.P.: Generalized Goal Programming- An overview. *Comput. Oper. Res.* **10**, 277–289 (1983)
8. Dubey, O.P., Singh, M.K., Dwivedi, R.K., Singh, S.N.: Interactive Decisions for transport management—Application in the coal transportation sector. *IUP J. Oper. Manage.* **10**(2), 7–21 (2011)



# An Efficient Solution to a Multiple Non-Linear Regression Model with Interaction Effect using TORA and LINDO

Umesh Gupta, Devender Singh Hada and Ankita Mathur

**Abstract** Goal programming (GP) has been proven a valuable mathematical programming form in a number of venues. GP model serves a valuable purpose of cross-checking answers from other methodologies. Different software packages are used to solve these GP models. Likewise, multiple regression models can also be used to more accurately combine multiple criteria measures that can be used in GP model parameters. Those parameters can include the relative weighting and the goal constraint parameters. A comparative study on the solutions using TORA, LINDO, and least square method has been made in this paper. The objective of this paper is to find out a method that gives most accurate result to a nonlinear multiple regression model.

**Keywords** Goal programming · Multiple regression · Least square method · TORA · LINDO

## 1 Introduction

Regression analysis is used to understand the statistical dependence of one variable on other variables. Linear regression is the oldest and most widely used predictive model in decision making in managerial sciences, environmental science, and all the

---

U. Gupta (✉)

Institute of Engineering and Technology, JK Lakshmipat University, Jaipur, India  
e-mail: umeshindian@yahoo.com

D. S. Hada

Kautilya Institute of Technology and Engineering, Jaipur, India  
e-mail: dev.singh1978@yahoo.com

A. Mathur

Jaipur Institute of Technology and Group of Institutions, Jaipur, India  
e-mail: ankita25jaipur@gmail.com

areas wherever it is required to describe possible relationships between two or more variables. This technique can show what proportion of variance between variables is due to the dependent variable, and what proportion is due to the independent variables. The earliest form of regression was the method of least squares, which was published by Legendre [1] and by Gauss [2]. The linear regression can be classified into two types, simple linear regression and multiple linear regression (MLR). The simple linear regression describes the relationship between two variables and MLR analysis describes the relationship between several independent variables and a single dependent variable. A number of methods for the estimation of the regression parameters are available in the literature. These include methods of minimizing the sum of absolute residuals, minimizing the maximum of absolute residuals, and minimizing the sum of squares of residuals [3], where the last method of minimizing the sum of squares of residuals popularly known as least square methods is commonly used. Alp et al. [4] explained that linear goal programming (GP) can be proposed as an alternative of the least square method. For this, he took an example of vertical network adjustment. Hessonpour et al. [5] proposed a linear programming model based on GP to calculate regression coefficient.

An interaction occurs when the magnitude of the effect of one independent variable on a dependent variable varies as a function of a second independent variable. This is also known as a moderation effect, although some have more strict criteria for moderation effects than for interactions. Nowadays, interaction effects through regression models are a widely interested area of investigation as there has been a great deal of confusion about the analysis of moderated relationships involving continuous variables. Alken and West [6] have analyzed such interaction effects; further, this method was applied into several models by the researchers, for example, Curran et al. [7] applied into hierarchical linear growth models.

Multiple objective optimization techniques provide more realistic solutions for most of the problems as it deals with multiple objectives, whereas single objective optimization techniques provide solutions to the problems that deals with single objective. GP is a type of multiple objective optimization technique that converts a multi-objective optimization model into a single objective optimization model. GP model has been proven a valuable tool in support of decision making. The first publication using GP as the form of a constrained regression model was used by Charnes et al. [8]. There have been many books devoted to this topic over past years (Ijiri [9]; Lee [10]; Spronk [11]; Ignizio [12]). This tool often represents a substantial improvement in the modeling and analysis of multi-objective problems (Charnes and Cooper [13]; Eiselt et al. [14]; Ignizio [15]). By minimizing deviation, the GP model can generate decision variable values that are the same as the beta values in some types of multiple regression models. Tamiz et al. [16] presents the review of current literature on the branch of multi-criteria decision modeling known as GP. Machiel Kruger [17] proposed a GP approach to efficiently managing a bank's balance sheet while maximizing returns and at the same time taking into account the conflicting goals such as minimizing risk, subject to regulatory and managerial constraints. Gupta et al. [18] solved a multi-objective investment management planning problem using fuzzy min sum weighted fuzzy goal programming technique.

Application of a multi-objective programming model like GP model is an important tool for studying various aspects of management systems (Sen and Nandi [19]). As an extension to the findings of Sharma et al. [20], this paper is focused on comparative study of the results obtained through different software packages like LINDO and TORA.

## 2 Regression and Goal Programming Formulation

The regression equation used to analyze and interpret a two-way interaction is:

$$y_{ir} = b_0 + b_1X_i + b_2Z_i + b_3X_i^2 + b_4Z_i^2 + b_5X_iZ_i + e_i, \quad i = 1, 2, \dots, m.$$

where  $b_0, b_1, b_2, b_3, b_4$  and  $b_5$  are the parameters to be estimated, and  $e_i$  is the error components which are assumed to be normally and independently distributed with zero mean and constant variance. The linear absolute residual method requires us to estimate the values of these unknown parameters so as to minimize  $\sum_{i=1}^m |y_{io} - y_{ir}|$ .

Let  $y_i$  be the  $i$ th goal,  $d_i^+$  be positive deviation from the  $i$ th goal, and  $d_i^-$  be the negative deviation from the  $i$ th goal. Then, the problem of minimizing  $\sum_{i=1}^m |y_i - y_{ir}|$  may be reformulated as

$$\text{Minimize } \sum_{i=1}^m (d_i^+ + d_i^-)$$

Subject to:

$$a_0 + a_1X_{i1} + a_2X_{i2} + a_3X_{i3} + a_4X_{i4} + a_5X_{i5} + d_i^+ - d_i^- = y_{iG},$$

$$d_i^+ \geq 0$$

$$d_i^- \geq 0$$

and  $a_0, a_1, a_2, a_3, a_4, a_5$  are unrestricted.

$$i = 1, 2, \dots, m.$$

where  $X_i^2, Z_i^2,$  and  $X_iZ_i$  are taken as  $X_{i3}, X_{i4},$  and  $X_{i5},$  respectively, to formulate the multiple nonlinear regression problem into linear GP model.

### 3 Mathematical Modeling and Solution

#### 3.1 Mathematical Modeling

Relationship between two methods can be established by taking a simple example. We consider a regression equation of Y on X and Z. The data for illustration are:

y	x	z
7.88	3	2
7.43	2	1
8.38	4	3
7.42	2	1
7.97	3	2
7.49	2	2
8.84	5	3
8.29	4	2

Reformulating the above problem into linear GP model:

$$\text{Minimize } \sum_{i=1}^8 (d_i^+ + d_i^-)$$

Subject to:

$$a_0 + 3a_1 + 2a_2 + 9a_3 + 4a_4 + 6a_5 + d_1^+ - d_1^- = 7.88$$

$$a_0 + 2a_1 + a_2 + 4a_3 + a_4 + 2a_5 + d_2^+ - d_2^- = 7.43$$

$$a_0 + 4a_1 + 3a_2 + 16a_3 + 9a_4 + 12a_5 + d_3^+ - d_3^- = 8.38$$

$$a_0 + 2a_1 + a_2 + 4a_3 + a_4 + 2a_5 + d_4^+ - d_4^- = 7.42$$

$$a_0 + 3a_1 + 2a_2 + 9a_3 + 4a_4 + 6a_5 + d_5^+ - d_5^- = 7.97$$

$$a_0 + 2a_1 + 2a_2 + 4a_3 + 4a_4 + 4a_5 + d_6^+ - d_6^- = 7.49$$

$$a_0 + 5a_1 + 3a_2 + 25a_3 + 9a_4 + 15a_5 + d_7^+ - d_7^- = 8.84$$

$$a_0 + 4a_1 + 2a_2 + 16a_3 + 4a_4 + 8a_5 + d_8^+ - d_8^- = 8.29$$

$$d_i^+ \geq 0, \quad i = 1, 2, \dots, 8$$

$$d_i^- \geq 0, \quad i = 1, 2, \dots, 8$$

$a_i$  are unrestricted,  $i = 0, 1, 2, \dots, 5$ .

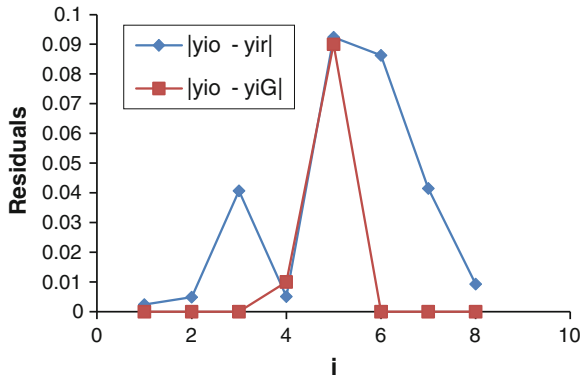


Fig. 1 Comparative results of residuals through different algorithms

### 3.2 Solution

The values of coefficients in the above problem through different methods are tabulated in Table 1

Final results are tabulated in Table 2:

### 4 Discussion

It is clear from Table 1 that all software packages give the same results to linear GP formulation with zero difference in the results.

It is observed from the above-tabulated results of Table 2 and Fig. 1 that  $\text{Minimize } \sum_{i=1}^m |y_{io} - y_{iG}| < \text{Minimize } \sum_{i=1}^m |y_{io} - y_{ir}|$ , where  $y_{iG}$  be the estimate of the  $i$ th response using GP technique, and  $y_{ir}$  be the estimate using the least square method. Hence, it is concluded that the GP technique provide better estimate of the multiple nonlinear regression parameters with two-way interaction effect than the least square method.

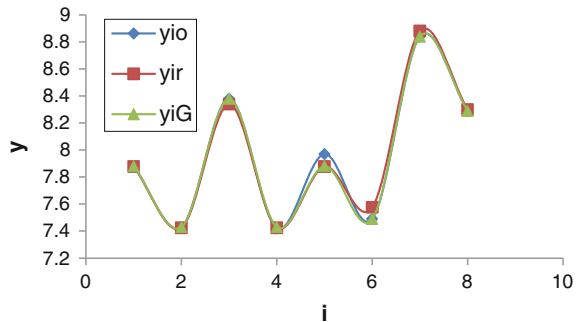
Table 1 The values of coefficients using different methods

Coefficients	Least square method	TORA	LINDO
$a_0$	6.9215	6.74	6.74
$a_1$	0.00001	0.28	0.28
$a_2$	0.3181	0.045	0.045
$a_3$	0.0602	0.01	0.01
$a_4$	-0.0557	-0.015	-0.015
$a_5$	0.0001	0.03	0.03

**Table 2** Values of  $y$  for paired values of  $x$  and  $z$

$y_i$	Observed value ( $y_{io}$ )	Expected values		
		Least square method ( $y_{ir}$ )	TORA ( $y_{iG}$ )	LINDO ( $y_{iG}$ )
$y_1$	7.88	7.8776	7.88	7.88
$y_2$	7.43	7.4251	7.43	7.43
$y_3$	8.38	8.3393	8.38	8.38
$y_4$	7.42	7.4251	7.43	7.43
$y_5$	7.97	7.8776	7.88	7.88
$y_6$	7.49	7.5763	7.49	7.49
$y_7$	8.84	8.8815	8.84	8.84
$y_8$	8.29	8.2993	8.29	8.29
	$\sum_{i=1}^8  y_i - y_{ir} $	0.2826	0.1	0.1

**Fig. 2** Comparative results of  $y$  through different algorithms



It is clear from Fig. 2 that the data are best fitted into the curve when we get the values of coefficients through solutions of the GP formulation comparative to the solutions using least square method.

## 5 Conclusion

1. The software packages TORA and LINDO both give similar results to a linear GP problem.
2. GP formulation gives better and best-fitted results than the traditional least square method.
3. The error is minimized when we solve regression model using GP formulation.

## References

1. Legendre, A.M.: Nouvelles méthodes pour la détermination des orbites des comètes. “Sur la Méthode des moindres carrés” appears as an appendix (1805)
2. Gauss, C.F.: *Theoria Motus Corporum Coelestium in Sectionibus Conicis Solem Ambientum* (1809)
3. Weisberg, s: *Applied Linear Regression*, 2nd edn. Wiley, Inc, New York (1985)
4. Alp, S., Yavuz, E., Ersoy, N.: Using linear goal programming in surveying engineering for vertical network adjustment. *Int. J. Phys. Sci.* **6**(8), 1982–1987 (2011)
5. Hassanpour H., Maleki R.H., Yaghoobi A.M.: Fuzzy linear regression model with crisp coefficients: a goal programming approach. *Int. J. Fuzzy Syst.* **7**(2), 19–39 (2010)
6. Alken, L.S., West, S.G.: *Multiple Regression: Testing and Interpreting Interactions*. Sage Publications, Thousand Oaks (1991)
7. Curran, P.J., Bauer, D.J., Willoughby, M.T.: Testing main effects and interactions in hierarchical linear growth models. *Psychol. Methods* **9**(2), 220–237 (2004)
8. Charnes, A., Cooper, W.W., Ferguson, R.: Optimal estimation of executive compensation by linear programming. *Manage. Sci.* **1**(2), 138–151 (1955)
9. Ijiri, Y.: *Management Goals and Accounting for Control*. North-Holland Publishing Company, Amsterdam (1965)
10. Lee, S.M.: *Goal Programming for Decision Analysis*. Auerbach Publishers Inc., Philadelphia (1972)
11. Spronk, J.: *Interactive Multiple Goal Programming: Application to Financial Planning*. Martinus Nijhoff, Amsterdam (1981)
12. Ignizio, J.P.: *Introduction to Linear Goal Programming*. Sage Publications, Thousand Oaks, CA (1986)
13. Charnes, A., Cooper, W.W.: Goal programming and multiple objective optimizations. *Eur. J. Operat. Res.* **1**, 39–54 (1977)
14. Eiselt, H.A., Pederzoli, G., Sandblom, C.L.: *Continuous Optimization Models*. W De G, New York (1987)
15. Ignizio, J.P.: A review of goal programming—a tool for multiobjective analysis. *J. Opl. Res. Soc.* **29**(11), 1109–1119 (1978)
16. Tamiz, M., Jones, D., Darzi, E.: A review of goal programming and its applications. *Ann. Oper. Res.* **58**(1), 39–53 (1995)
17. Machiel, K.: A goal programming approach to strategic bank balance sheet management. SAS Global Forum 2011, Centre for BMI, North-West University, South Africa, Paper 024–2011 (2011)
18. Gupta, M., Bhattacharjee, D.: Min sum weighted fuzzy goal programming model in investment management planning: a case study. *Int. Res. J. Fin. Econ. Issue* **56** (2010)
19. Sen, N., Nandi, M.: Goal programming, its application in management sectors—special attention into plantation management: a review. *Int. J. Sci. Res. Pub.* **2**(9) (2012)
20. Sharma, S.C., Hada, D.S., Gupta, U.: A goal programming model for the interaction effects in multiple nonlinear regression. *J. Comp. Math. Sci.* **1**(4), 477–481 (2010)

# On the Fekete–Szegő Problem for Certain Subclass of Analytic Functions

Ritu Agarwal and G. S. Paliwal

**Abstract** The purpose of the present investigation is to derive several Fekete–Szegő-type coefficient inequalities for certain subclasses of normalized analytic function  $f(z)$  defined in the open unit disk. Various applications of our main results involving (for example) the operators defined using generalized fractional differential operator are also considered. Thus, as one of these applications of our result, we obtain the Fekete–Szegő-type inequality for a class of normalized analytic functions, which is defined here by means of the convolution and the fractional differential operators.

**Keywords** Starlike functions · Fekete–Szegő problem · Fractional derivatives · Generalized Ruscheweyh derivative · Convolution

## 1 Introduction and Definitions

Let  $\mathbf{A}$  denote the class of functions  $f(z)$  of the form

$$f(z) = z + \sum_{n=2}^{\infty} a_n z^n, \quad (1)$$

which are analytic in the open unit disk

---

R. Agarwal (✉)

Malviya National Institute of Technology, J.L.N. Marg, Jaipur 302017, India  
e-mail: ritugoyal.1980@gmail.com

G. S. Paliwal

JECRC UDML College of Engineering, Kukas, Jaipur 302028, India  
e-mail: gaurishankarpaliwal@gmail.com



$$\Delta = \{z : z \in C \text{ and } |z| < 1\}. \tag{2}$$

Also, let **S** be the subclass of **A** consisting of all univalent functions in  $\Delta$ . A function  $f(z)$  in **A** is said to be in class **S\*** of *starlike functions* of order zero in  $\Delta$ , if  $\text{Re} \left\{ \frac{zf'(z)}{f(z)} \right\} > 0$  for  $z \in \Delta$ . Let **K** denote the class of all functions  $f \in \mathbf{A}$  that are convex. Further,  $f$  is convex if and only if  $zf'(z)$  is starlike.

**Definition 1.1** Let  $(f * g)(z)$  denote the *convolution* of two functions  $f(z)$  given by (1) and  $g(z) = z + \sum_{n=2}^{\infty} b_n z^n$ , then

$$(f * g)(z) = z + \sum_{n=2}^{\infty} a_n b_n z^n. \tag{3}$$

We shall be requiring the following fractional differential operator in the present investigations:

**Definition 1.2** Let  $f(z)$  is an analytic function in a simply connected region of the  $z$  plane containing the origin, and the multiplicity of  $(z - \zeta)^\lambda$  is removed by requiring that  $\log(z - \zeta)$  to be real when  $(z - \zeta) > 0$ . Then, the generalized fractional derivative of order  $\lambda$  is defined for a function  $f(z)$  by (see, e.g., [16])

$$J_{0,z}^{\lambda,\mu,\nu} f(z) = \left\{ \begin{array}{l} \frac{1}{\Gamma(1-\lambda)} \frac{d}{dz} \left\{ z^{\lambda-\mu} \int_0^z (z-\zeta)^{-\lambda} \right. \\ \left. {}_2F_1 \left( \mu - \lambda, -\nu; 1 - \lambda; 1 - \frac{\zeta}{z} \right) f(\zeta) d\zeta \right\}, (0 \leq \lambda < 1) \\ \frac{d^n}{dz^n} J_{0,z}^{\lambda-n,\mu,\nu} f(z), (n \leq \lambda < n + 1, n \in N) \end{array} \right.$$

and  $f(z) = O(|z|^k)$ ,  $(z \rightarrow 0, k > \max \{0, \mu - \nu - 1\} - 1)$ .

It follows at once from the above definition that  $J_{0,z}^{\lambda,\lambda,\nu} f(z) := D_z^\lambda f(z)$ ,  $(0 \leq \lambda < 1)$  which is fractional derivative of  $f$  of order  $\lambda$  (see, e.g., [10, 11]). Furthermore, in terms of gamma function, we have:

$$J_{0,z}^{\lambda,\mu,\nu} z^\rho := \frac{\Gamma(\rho + 1)\Gamma(\rho - \mu + \nu + 1)}{\Gamma(\rho - \mu + 1)\Gamma(\rho - \lambda + \nu + 2)} z^{\rho-\mu},$$

$$(0 \leq \lambda; \rho > \max \{0, \mu - \nu - 1\} - 1)$$

**Definition 1.3** Let  $f$  and  $g$  analytic in  $\Delta$ . We say that the function  $f$  is subordinate to  $g$  if there exists a Schwarz function  $w(z)$ , analytic in  $\Delta$  with  $w(z) = 0$  and  $|w(z)| < 1$ , such that  $f(z) = g(w(z))$  for  $z \in \Delta$ . We denote this subordination by  $f \prec g$  or  $f(z) \prec g(z)$ .

Let  $\phi(z)$  be an analytic function in  $\Delta$  with  $\phi(0) = 1, \phi'(0) > 0$  and  $\text{Re}(\phi(z)) > 0, (z \in \Delta)$ , which maps the open unit disk  $\Delta$  onto a region starlike with respect

to 1 and is symmetric with respect to the real axis. Motivated by the class  $R_{\lambda}^{\tau}(\phi)$  in paper [1], we introduce the following class.

**Definition 1.4** Let  $0 \leq \alpha < 1, 0 \leq \gamma < 1, 0 \leq \rho < 1, \tau \in C \setminus \{0\}$ . A function  $f \in A$  is in the class  $R_{\alpha, \gamma, \rho}^{\tau}(\phi)$  if

$$1 + \frac{1}{\tau} (\rho \{(f * S_{\alpha})(z)\}' + \gamma z \{(f * S_{\alpha})(z)\}'' - \rho) \prec \phi(z), \quad (z \in \Delta) \tag{4}$$

where  $\phi(z)$  is defined same as above.

The function

$$S_{\alpha}(z) = \frac{z}{(1-z)^{2(1-\alpha)}} = z + \sum_{n=2}^{\infty} C(\alpha, n)z^n, \tag{5}$$

is the well-known extremal function (see, e.g., [9]). It is observed that  $C(\alpha, n), n = 2, 3, \dots$  is decreasing in  $\alpha$ . Also,

$$C(\alpha, n) = \frac{\prod_{k=2}^n (k - 2\alpha)}{(n - 1)!} \quad \text{and} \quad \lim_{n \rightarrow \infty} C(\alpha, n) = \begin{cases} \infty & (\alpha < 1/2) \\ 1 & (\alpha = 1/2) \\ 0 & (\alpha > 1/2) \end{cases} \tag{6}$$

If we set  $\phi(z) = \frac{1+Az}{1+Bz}, (-1 \leq B < A \leq 1, z \in \Delta)$ , in (4), we get

$$R_{\alpha, \gamma, \rho}^{\tau}(A, B) = \left\{ f \in A : \left| \frac{\rho \{(f * S_{\alpha})(z)\}' + \gamma z \{(f * S_{\alpha})(z)\}'' - \rho}{\tau(A - B) - B(\rho \{(f * S_{\alpha})(z)\}' + \gamma z \{(f * S_{\alpha})(z)\}'' - \rho)} \right| < 1 \right\},$$

which is again a new class. The classes discussed recently by Bansal [1], Swaminathan [17], Ponnusamy and Ronning [12], Ponnusamy [14] and Li [4] follow as special cases of our class.

To prove our main results, we need the following Lemma:

**Lemma 1.1** [5] *If  $p(z) = 1 + c_1z + c_2z^2 + c_3z^3 + \dots (z \in \Delta)$  is a function with positive real part, then for any complex number  $\varepsilon, |c_3 - \varepsilon c_2^2| \leq 2 \max\{1, |2\varepsilon - 1|\}$ . The result is sharp for the functions given by  $p(z) = \frac{1+z^2}{1-z^2}$  and  $p(z) = \frac{1+z}{1-z}$ .*

## 2 Fekete–Szegő Problem

In this section, we shall be finding the Fekete–Szegő coefficient inequalities for the class of functions  $R_{\alpha, \gamma, \rho}^{\tau}(\phi)$ . Our main result is contained in the following theorem:

**Theorem 2.1** Let  $\phi(z) = 1 + B_1z + B_2z^2 + B_3z^3 + \dots$ , where  $\phi(0) = 1$  with  $\phi'(0) > 0$ . If  $f(z)$  given by (1) belongs to  $R_{\alpha, \gamma, \rho}^{\tau}(\phi)$  ( $\alpha, \gamma, \rho \in [0, 1], \tau \in C \setminus \{0\}, z \in \Delta$ ), then for any complex number  $v$

$$|a_3 - va_2^2| \leq \frac{2B_1|\tau|}{3(\rho + 2\gamma)(2 - 2\alpha)(3 - 2\alpha)} \max \left\{ 1, \left| \frac{B_2}{B_1} - \frac{3v\tau B_1(\rho + 2\gamma)(3 - 2\alpha)}{8(\rho + \gamma)^2(2 - 2\alpha)} \right| \right\} \tag{7}$$

The result is sharp.

*Proof* If  $f(z) \in R_{\alpha, \gamma, \rho}^{\tau}(\phi)$ , then there exists a Schwarz function  $w(z)$  analytic in  $\Delta$  with  $w(z) = 0$  and  $|w(z)| < 1, (z \in \Delta)$  such that

$$1 + \frac{1}{\tau} (\rho \{(f * S_{\alpha})(z)\}' + \gamma z \{(f * S_{\alpha})(z)\}'' - \rho) = \phi(w(z)) \tag{8}$$

Define the function  $p_1(z)$  by

$$p_1(z) = \frac{1 + w(z)}{1 - w(z)} = 1 + c_1z + c_2z^2 + c_3z^3 + \dots \tag{9}$$

Since  $w(z)$  is a Schwarz function, we see that  $Re(p_1(z)) > 0$  and  $p_1(0) = 1$ . Define the function  $p(z)$  by

$$p(z) = 1 + \frac{1}{\tau} (\rho \{(f * S_{\alpha})(z)\}' + \gamma z \{(f * S_{\alpha})(z)\}'' - \rho) \tag{10}$$

In view of (8), (9) and (10),

$$p(z) = \varphi \left( \frac{p_1(z) - 1}{p_1(z) + 1} \right) = \varphi \left( \frac{1}{2}c_1z + \frac{1}{2} \left( c_2 - \frac{c_1^2}{2} \right) z^2 + \dots \right) \tag{11}$$

$$= 1 + \frac{B_1c_1z}{2} + \frac{B_1}{2} \left( c_2 - \frac{c_1^2}{2} \right) z^2 + \frac{B_2c_1^2}{4} z^2 + \dots \tag{12}$$

Using (6) in (5), we get

$$S_{\alpha}(z) = z + (2 - 2\alpha)z^2 + \frac{(2 - 2\alpha)(3 - 2\alpha)}{2} z^3 + \dots$$

which on substitution in (10) gives

$$p(z) = 1 + \frac{1}{\tau} \left( 2a_2(2 - 2\alpha)(\rho + \gamma)z + 3a_3 \frac{(2 - 2\alpha)(3 - 2\alpha)(\rho + 2\gamma)}{2} z^2 + \dots \right) \tag{13}$$

Comparing (12) and (13)

$$a_2 = \frac{B_1 c_1 \tau}{4(2 - 2\alpha)(\rho + \gamma)}$$

and

$$a_3 = \frac{\tau}{3(2 - 2\alpha)(3 - 2\alpha)(\rho + 2\gamma)} \left( B_1 \left( c_2 - \frac{c_1^2}{2} \right) + \frac{B_2 c_1^2}{2} \right).$$

Therefore, we have

$$a_3 - \nu a_2^2 = \frac{\tau B_1}{3(2 - 2\alpha)(3 - 2\alpha)(\rho + 2\gamma)} (c_2 - \varepsilon c_1^2)$$

where

$$\varepsilon = \frac{1}{2} \left\{ 1 - \frac{B_2}{B_1} + \frac{3\nu\tau B_1(3 - 2\alpha)(\rho + 2\gamma)}{8(2 - 2\alpha)(\rho + \gamma)^2} \right\}.$$

Our result is followed by application of Lemma (1.1).

Also, by the application of Lemma (1.1), equality in (7) is obtained when

$$p_1(z) = \frac{1 + z^2}{1 - z^2} \quad \text{or} \quad p_1(z) = \frac{1 + z}{1 - z}.$$

For the class  $R_{\alpha, \gamma, \rho}^\tau(A, B)$ ,  $\phi(z) = \frac{1 + Az}{1 + Bz} = 1 + (A - B)z - (AB - B^2)z^2 + \dots$ . Thus, putting  $B_1 = A - B$  and  $B_2 = -B(A - B)$  in Theorem 2.1, we get the following corollary:

**Corollary 2.2** *If  $f(z)$  given by (1) belongs to  $R_{\alpha, \gamma, \rho}^\tau(A, B)$ , then*

$$\left| a_3 - \nu a_2^2 \right| \leq \frac{2|\tau|(A - B)}{3(2 - 2\alpha)(3 - 2\alpha)(\rho + 2\gamma)} \max \left\{ 1, \left| B - \frac{3\nu\tau(A - B)(3 - 2\alpha)(\rho + 2\gamma)}{8(2 - 2\alpha)(\rho + \gamma)^2} \right| \right\}.$$

### 3 Applications to Functions Defined Using Fractional Derivative

For fixed  $g \in A$ , we define the class  $R_{\alpha, \gamma, \rho}^{\tau, g}(\phi)$  of functions  $f \in A$  for which  $(f * g) \in R_{\alpha, \gamma, \rho}^\tau(\phi)$ . Suppose that  $g(z) = z + \sum_{n=2}^\infty g_n z^n (g_n > 0)$ . Then,  $f(z) = z + \sum_{n=2}^\infty a_n z^n \in R_{\alpha, \gamma, \rho}^{\tau, g}(\phi)$  if and only if  $(f * g)(z) = z + \sum_{n=2}^\infty g_n a_n z^n \in R_{\alpha, \gamma, \rho}^\tau(\phi)$ .

By applying Theorem (2.1) to the convolution  $(f * g)(z) = z + g_2 a_2 z^2 + g_3 a_3 z^3 + \dots$ , we get Theorem (3.1) below after an obvious change of the parameter  $\nu$ .

**Theorem 3.1** Let  $\phi(z) = 1 + B_1z + B_2z^2 + B_3z^3 + \dots$  where  $\phi(0) = 1$  with  $\phi'(0) > 0$ . If  $f(z)$  given by (I) belongs to  $R_{\alpha,\gamma,\rho}^{\tau,g}(\phi)$  ( $\alpha, \gamma, \rho \in [0, 1], \tau \in C \setminus \{0\}, z \in \Delta$ ), then for any complex number  $v$

$$\left| a_3 - va_2^2 \right| \leq \frac{2B_1|\tau|}{3g_3(\rho + 2\gamma)(2 - 2\alpha)(3 - 2\alpha)} \max \left\{ 1, \left| \frac{B_2}{B_1} - \frac{g_3}{g_2^2} \frac{3v\tau B_1(\rho + 2\gamma)(3 - 2\alpha)}{8(\rho + \gamma)^2(2 - 2\alpha)} \right| \right\}$$

The result is sharp.

We, now, discuss some applications of the above theorem to the subclasses defined using fractional derivatives.

1. In terms of generalized Ruscheweyh derivative operator, we now introduce the function class  $R_{\alpha,\gamma,\rho}^{\tau,\lambda,\mu}(\phi)$  in the following way:

$$R_{\alpha,\gamma,\rho}^{\tau,\lambda,\mu}(\phi) := \left\{ f : f \in A \text{ and } J^{\lambda,\mu} f \in R_{\alpha,\gamma,\rho}^{\tau}(\phi) \right\}, \tag{14}$$

where the generalized Ruscheweyh derivative introduced by Goyal and Goyal [2], Parihar and Agarwal [13] is defined as

$$\begin{aligned} J^{\lambda,\mu} f(z) &= \frac{\Gamma(\mu - \lambda + v + 2)}{\Gamma(\mu + 1)\Gamma(v + 2)} z J_{0,z}^{\lambda,\mu,v} \left( z^{\mu-1} f(z) \right) \\ &= z + \sum_{n=2}^{\infty} a_n B^{\lambda,\mu}(n) z^n = (f * g)(z) \end{aligned} \tag{15}$$

where

$$B^{\lambda,\mu}(n) := \frac{\Gamma(n + \mu)\Gamma(v + 2 + \mu - \lambda)\Gamma(n + v + 1)}{\Gamma(n)\Gamma(n + v + 1 + \mu - \lambda)\Gamma(v + 2)\Gamma(1 + \mu)} \tag{16}$$

It is easily seen that the function class  $R_{\alpha,\gamma,\rho}^{\tau,\lambda,\mu}(\phi)$  is a special case of the function class  $R_{\alpha,\gamma,\rho}^{\tau,g}(\phi)$  when  $g(z) = z + \sum_{n=2}^{\infty} B^{\lambda,\mu} z^n = z \cdot {}_2F_1(\mu + 1, v + 2; v + 2 + \mu - \lambda; z)$ .

Thus, we obtain the coefficient estimates for functions in the subclass  $R_{\alpha,\gamma,\rho}^{\tau,\lambda,\mu}(\phi)$  from the corresponding estimates for functions in the class  $R_{\alpha,\gamma,\rho}^{\tau,g}(\phi)$ .

**Theorem 3.2** Let  $\phi(z) = 1 + B_1z + B_2z^2 + B_3z^3 + \dots$ , where  $\phi(0) = 1$  with  $\phi'(0) > 0$ . If  $f(z)$  given by (I) belongs to  $R_{\alpha,\gamma,\rho}^{\tau,\lambda,\mu}(\phi)$  ( $\alpha, \gamma, \rho \in [0, 1], \tau \in C \setminus \{0\}, z \in \Delta$ ), then for any complex number  $v$

$$|a_3 - \nu a_2^2| \leq \frac{4(\nu + 2 + \mu - \lambda)(\nu + 3 + \mu - \lambda)B_1 |\tau|}{3(\mu + 1)(\mu + 2)(\nu + 2)(\nu + 3)(\rho + 2\gamma)(2 - 2\alpha)(3 - 2\alpha)} \max \left\{ 1, \left| \frac{B_2}{B_1} - \frac{(\mu + 2)(\nu + 3)(\nu + 2 + \mu - \lambda)}{2(\mu + 1)(\nu + 2)(\nu + 3 + \mu - \lambda)} \frac{3\nu\tau B_1(\rho + 2\gamma)(3 - 2\alpha)}{8(\rho + \gamma)^2(2 - 2\alpha)} \right| \right\}$$

The result is sharp.

2. In terms of generalized Owa–Srivastava operator, we now introduce the function class

$$S_{\alpha, \gamma, \rho}^{\tau, \lambda, \mu}(\phi) := \left\{ f : f \in A \text{ and } \Omega_v^{\lambda, \mu} f \in R_{\alpha, \gamma, \rho}^{\tau}(\phi) \right\} \tag{17}$$

where we define the generalized Owa–Srivastava operator as

$$\begin{aligned} \Omega_v^{\lambda, \mu} f(z) &= \frac{\Gamma(2 - \mu)\Gamma(3 - \lambda + \nu)}{\Gamma(3 - \mu + \nu)} z^\mu J_{0, z}^{\lambda, \mu, \nu} f(z) \\ &= z + \sum_{n=2}^{\infty} \frac{\Gamma(n + 1)\Gamma(2 - \mu)\Gamma(n - \mu + \nu + 2)\Gamma(3 - \lambda + \nu)}{\Gamma(n - \mu + 1)\Gamma(3 - \mu + \nu)\Gamma(n - \lambda + \nu + 2)} a_n z^n \end{aligned}$$

For  $\mu = \lambda$ ,  $\Omega_v^{\lambda, \mu}$  reduces to the Owa–Srivastava operators  $\Omega^\lambda$  [10].

It is easily seen that the function class  $S_{\alpha, \gamma, \rho}^{\tau, \lambda, \mu}(\phi)$  is a special case of the function class  $R_{\alpha, \gamma, \rho}^{\tau, g}(\phi)$  when

$$g(z) = z + \sum_{n=2}^{\infty} \frac{\Gamma(n + 1)\Gamma(2 - \mu)\Gamma(n - \mu + \nu + 2)\Gamma(3 - \lambda + \nu)}{\Gamma(n - \mu + 1)\Gamma(3 - \mu + \nu)\Gamma(n - \lambda + \nu + 2)} z^n \tag{18}$$

The coefficient estimates for functions in the subclass  $S_{\alpha, \gamma, \rho}^{\tau, \lambda, \mu}(\phi)$  are given by

**Theorem 3.3** Let  $\phi(z) = 1 + B_1z + B_2z^2 + B_3z^3 + \dots$ , where  $\phi(0) = 1$  with  $\phi'(0) > 0$ . If  $f(z)$  given by (1) belongs to  $S_{\alpha, \gamma, \rho}^{\tau, \lambda, \mu}(\phi)$  ( $\alpha, \gamma, \rho \in [0, 1], \tau \in C \setminus \{0\}, z \in \Delta$ ), then for any complex number  $\nu$

$$|a_3 - \nu a_2^2| \leq \frac{(3 - \mu)(2 - \mu)(\nu + 3 - \lambda)(\nu + 4 - \lambda)B_1 |\tau|}{9(\nu + 4 - \mu)(\nu + 3 - \mu)(\rho + 2\gamma)(2 - 2\alpha)(3 - 2\alpha)} \max \left\{ 1, \left| \frac{B_2}{B_1} - \frac{3(\nu + 4 - \mu)(\nu + 3 - \lambda)(2 - \mu)}{2(3 - \mu)(\nu + 4 - \lambda)(\nu + 3 - \mu)} \frac{3\nu\tau B_1(\rho + 2\gamma)(3 - 2\alpha)}{8(\rho + \gamma)^2(2 - 2\alpha)} \right| \right\}$$

3. In terms of Najafzadeh operator, we now introduce the function class

$$S_{\alpha, \gamma, \rho}^{\tau, \lambda, k}(\phi) := \left\{ f : f \in A \text{ and } \Omega_\lambda^k f \in R_{\alpha, \gamma, \rho}^{\tau}(\phi) \right\}. \tag{19}$$

For  $k \in N \cup \{0\}$  and  $\lambda \geq 0$ , the operator  $\Omega_\lambda^k f : N \rightarrow N$  is defined by Najafzadeh [8] as

$$\Omega_\lambda^k f(z) = (1 - \lambda)S^k f(z) + \lambda R^k f(z), z \in \Delta, \tag{20}$$

where  $S^k f$  is the Salagean differential operator [15] and  $R^k f$  is the Ruscheweyh differential operator [9].

For  $f(z) \in A$  given by (1), we have respectively

$$S^k f(z) = z + \sum_{n=2}^\infty n^k a_n z^n \quad \text{and} \quad R^k f(z) = z + \sum_{n=2}^\infty \binom{k+n-1}{k} a_n z^n \tag{21}$$

and hence

$$\Omega_\lambda^k f(z) = \sum_{k=2}^\infty \left[ (1 - \lambda)n^k + \lambda \binom{k+n-1}{k} \right] a_n z^n, z \in \Delta \tag{22}$$

It is easily seen that the function class  $S_{\alpha, \gamma, \rho}^{\tau, \lambda, k}(\phi)$  is a special case of the function class  $R_{\alpha, \gamma, \rho}^{\tau, g}(\phi)$  when

$$g(z) = z + \sum_{n=2}^\infty \left[ (1 - \lambda)n^k + \lambda \binom{k+n-1}{k} \right] z^n \tag{23}$$

The coefficient estimates for functions in the subclass  $S_{\alpha, \gamma, \rho}^{\tau, \lambda, k}(\phi)$  is given by:

**Theorem 3.4** *Let  $\phi(z) = 1 + B_1 z + B_2 z^2 + B_3 z^3 + \dots$ , where  $\phi(0) = 1$  with  $\phi'(0) > 0$ . If  $f(z)$  given by (1) belongs to  $S_{\alpha, \gamma, \rho}^{\tau, \lambda, k}(\phi)$  ( $\alpha, \gamma, \rho \in [0, 1], \tau \in C \setminus \{0\}, z \in \Delta$ ), then for any complex number  $v$*

$$\begin{aligned} |a_3 - v a_2^2| \leq & \frac{2B_1 |\tau|}{3(3^k(1 - \lambda) + \lambda(k + 2)(k + 1)/2)(\rho + 2\gamma)(2 - 2\alpha)(3 - 2\alpha)} \\ & \max \left\{ 1, \left| \frac{B_2}{B_1} - \frac{(3^k(1 - \lambda) + \lambda(k + 2)(k + 1)/2) 3v\tau B_1(\rho + 2\gamma)(3 - 2\alpha)}{(2^k(1 - \lambda) + \lambda(k + 1))^2 8(\rho + \gamma)^2(2 - 2\alpha)} \right| \right\} \end{aligned}$$

For  $\lambda = 0$  and  $\lambda = 1$ , Najafzadeh operators  $\Omega_\lambda^k f$  reduce to Salagean differentiation of  $f$  and Ruscheweyh derivative of  $f$ , respectively. Hence, the Fekete–Szegő inequality for these functions follows immediately from the Theorem 3.4.

### References

1. Bansal, D.: Fekete -Szegő problem for a new class of analytic function. Int. J. Math. Math. Sci., article ID 143096, 5 pp (2011)
2. Goyal, S.P., Goyal, R.: On a class of multivalent functions defined by generalized Ruscheweyh derivatives involving a general fractional derivative operator. J. Indian Acad. Math. **27**(2), 439–456 (2005)

3. Koepf, W.: On the Fekete-Szegő problem for close-to-convex functions. *Archiv der Mathematik* **49**(5), 420–433 (1987)
4. Li, J.L.: On some classes of analytic functions. *Mathematica Japonica* **40**(3), 523–529 (1994)
5. Libera, R.J., Zlotkiewicz, E.J.: Coefficient bounds for the inverse of a function with derivative in  $\rho$ . *Proc. Am. Math. Soc.* **87**(2), 251–257 (1983)
6. London, R.R.: Fekete-Szegő inequalities for close-to-convex functions. *Proc. Am. Math. Soc.* **117**(4), 947–950 (1993)
7. Ma, W., Minda, D.: A unified treatment of some special classes of univalent functions. In: Li, Z., Ren, F., Yang, L., Zhang, S. (eds.) *Proceedings of the Conference on Complex Analysis*, pp. 157–169. *Conference Proceedings and Lecture Notes in Analysis*, vol. I. International Press, Cambridge, Massachusetts (1994)
8. Najafzadeh, S.: Application of Salagean and Ruscheweyh operators on univalent holomorphic functions with finitely many coefficients. *Fractional Calculus Appl. Anal.* **13**(5), 517–520 (2010)
9. Owa, S., Uralegaddi, B.A.: A class of functions  $\alpha$ -prestarlike of order  $\beta$ . *Bull. Korean Math. Soc.* **21**(4), 77–85 (1984)
10. Owa, S., Srivastava, H.M.: Univalent and starlike generalized hypergeometric functions. *Canad. J. Math.* **39**, 1057–1077 (1987)
11. Owa, S.: On the distortion theorems I. *Kyungpook Math. J.* **18**, 53–58 (1978)
12. Ponnusamy, S., Ronning, F.: Integral transforms of a class of analytic functions. *Complex Variables Elliptic Equ.* **53**(5), 423–434 (2008)
13. Parihar, H.S., Agarwal, R.: Application of generalized Ruscheweyh derivatives on  $p$ -valent functions. *J. Math. Appl.* **34**, 75–86 (2011)
14. Ponnusamy, S.: Neighborhoods and Carathéodory functions. *J. Anal.* **4**, 41–51 (1996)
15. Salagean, G.S.: Subclasses of univalent functions. *Lect. Notes Math.* **1983**, 362–372 (1013)
16. Srivastava, H.M., Saxena, R.K.: Operators of fractional integration and their applications. *Appl. Math. Comput.* **118**, 1–52 (2001)
17. Swaminathan, A.: Certain sufficiency conditions on Gaussian hypergeometric functions. *J. Inequalities Pure Appl. Math.* **5**(4), article 83, 6 pp (2004)



**Part III**  
**Soft Computing for Operations**  
**Management (SCOM)**

# Bi-Objective Scheduling on Parallel Machines in Fuzzy Environment

Sameer Sharma, Deepak Gupta and Seema Sharma

**Abstract** The present chapter pertains to a bi-objective scheduling on parallel machines involving total tardiness and number of tardy jobs (NT). The processing time of jobs are uncertain in nature and are represented by triangular fuzzy membership function. The objective of the chapter is to find the optimal sequence of jobs processing on parallel identical machines so as to minimize the secondary criteria of NT with the condition that the primary criteria of total tardiness remains optimized. The bi-objective problem with total tardiness and NT as primary and secondary criteria, respectively, for any number of parallel machines is NP-hard. Following the theoretical treatment, a numerical illustration has also been given to demonstrate the potential efficiency of the proposed algorithm as a valuable analytical tool for the researchers.

**Keywords** Fuzzy processing time · Average high ranking · Total tardiness · Due date · Tardy job.

## 1 Introduction

Scheduling is a very common activity in both industry and non-industry settings. Everyday meetings are scheduled, deadlines are set for projects, vacations and work periods are set, maintenance and upgrade operations are planned, operation rooms are

---

S. Sharma (✉) · S. Sharma  
Department of Mathematics, D.A.V. College, Jalandhar, Punjab, India  
e-mail: samsharma31@yahoo.com

S. Sharma  
e-mail: seemasharma7788@yahoo.com

D. Gupta  
Department of Mathematics, M.M. University, Mullana, Ambala, India  
e-mail: guptadeepak2003@yahoo.co.in

booked, and sports games are scheduled and arenas are booked. Proper scheduling allows various activities, jobs or tasks to be executed in an organized manner, while preventing resource conflicts. The parallel machine scheduling problem is a widely studied optimization problem. It is a kind of important multi-machine scheduling in which every machine has same work function and every job can be processed by any available machine. Scheduling problems in real-life applications generally involve optimization of more than one criterion. A large number of deterministic scheduling algorithms have been proposed in last decades to deal with scheduling problems with various objectives and constraints. However, in real-world applications, it is usually difficult to set exact processing times for jobs. More often, the processing time of a job may vary within an interval. Thus, it is natural and realistic to represent this kind of uncertainties by fuzzy numbers.

A survey of the literature has revealed little work reported on the bi-objective scheduling problems on parallel machines. Most of the work done in the bi-objective problems has been on the single machine. Anghinolfi and Paolucci [1] studied total tardiness scheduling problems on parallel machines. Azizoglu et al. [2] discussed bi-criteria scheduling problem involving total tardiness and total earliness penalties. Parkash [9] studied the bi-criteria scheduling problems on parallel machines. Shim and Kim [10] dealt with scheduling on parallel identical machines to minimize the total tardiness. Gupta and Sharma [6] studied the scheduling on parallel machines with bi-objective function  $NT/T_{\max}$  in fuzzy environment. Some of the noteworthy approaches are due to Chand and Schneerbrg [4], Moore [8], and Singh and Sunita [11].

The present chapter addresses the bi-objective scheduling problems on identical parallel machines involving total tardiness and number of tardy jobs (NT) with bi-objective function as  $NT/\text{Total Tardiness}$ . Two approaches can be used to address the bi-objective problems: Both the criteria are optimized simultaneously by using suitable weights for the criteria, and secondly, the criteria are optimized sequentially by first optimizing the primary criterion and then the secondary criterion subject to the value obtained for the primary criterion. In this research paper, we have used the second approach. A practical application of this paper can be taken as to minimize the cost of production or production time given the penalty for delaying the product.

## 2 Problem Formulation

The following assumptions are made for the problem formulation

1. The jobs are available at time zero.
2. The jobs are independent of each other.
3. No preemption of jobs is allowed.
4. The machines are identical in all respects.
5. No machine can handle more than one job at a time.

The following notations will be used all the way through out the chapter

- i*: Designate the *i*th job,  $i = 1, 2, 3, \dots, n$
- k*: Machine on which *i*th job is assigned at the *j*th position
- j*: Location of *i*th job on machine *k*, where  $j = 1, 2, 3, \dots, n$
- d<sub>i</sub>*: Due date of the *i*th job
- c<sub>i</sub>*: Completion time of *i*th job
- T<sub>i</sub>*: Tardiness of the *i*th job =  $\max(c_i - d_i, 0)$
- T*: Total tardiness
- n*: Total number of jobs to be scheduled
- NT: Number of tardy jobs.
- $X_{ijk} = 1$ ; if job *i* is located at the *j*th position on *k*th machine and 0; otherwise.

Chen and Bulfin [5] studied the scheduling on a single machine to minimize the two criteria of maximum tardiness and NT. Akker et al. [3] discussed the minimization of NT. Lawer et al. [7] described the minimization of maximum lateness in a two-machine open shop scheduling. Before formulating the bi-criteria problem, the formulation for the single criterion is represented first. They are as follows:

**Criterion: Total Tardiness**

Tardiness is given by  $\max(0, c_i - d_i)$ , where *c<sub>i</sub>* and *d<sub>i</sub>* are the completion and due date of job *i*. This function is a nonlinear function but can be linearized. The formulation is as follows:

$$\text{Min } Z = \sum_{i=1}^n T_i$$

Subject to:

$$\sum_{j=1}^n \sum_{k=1}^n X_{ijk} = 1 \quad \forall i \quad \text{(i)}, \quad \sum_{i=1}^n X_{ijk} \leq 1 \quad \forall j, k \quad \text{(ii)},$$

$$X_{ijk} \text{ is Binary} \quad \forall i, j, k \quad \text{(iii)}, \quad T_i \geq c_i - d_i \quad \forall i \quad \text{(iv)};$$

along with non-negativity constraint.

**Criterion: Number of Tardy Jobs**

A job is considered to be late only if its tardiness is strictly positive. Let *Y<sub>i</sub>* be a binary variable that depict whether or not the job *i* is late. It assumes a value 1 when the job *i* is late and 0 otherwise. The  $\sum_{i=1}^n Y_i$  gives the total number of the tardy jobs. The formulation is as follows:

$$\text{Min } Z = \sum_{i=1}^n Y_i$$

Subject to: Constraint set (i), (ii), (iii) and (iv)

$$Y_i \geq MT_i \quad \forall i \quad \text{(v)}, \quad Y_i \text{ binary} \quad \forall i \quad \text{(vi)};$$

where *M* is a very large number.

The formulation of the bi-criteria problems is similar to that of single criterion problems but with some additional constraints requiring that the optimal value of the primary objective is not violated. The two parts of the bi-criteria problem formulation are as follows:

**Primary Objective Function**

Subject to: Primary problem constraints

**Secondary Objective Function**

Subject to:

1. Secondary problem constraint.
2. Primary objective function value constraint.
3. Primary problem constraint.

In the present work, we consider the parallel machines bi-criteria scheduling problem in which the objective is to schedule jobs on parallel identical machines so as to minimize primary and secondary criteria. So here, the problem is distributed in two steps: first, the primary criterion in which total tardiness of jobs is minimized, and in secondary step, the NT is minimized under the objective function value of primary criterion.

### 3 Algorithm

The following algorithm is proposed to optimize the bi-objective function NT/Total Tardiness by considering total tardiness and number of tardy jobs as primary and secondary criteria.

- Step 1: Arrange all the jobs in early due date (EDD) order, and find the tardiness of each job (if any). Let  $L$  be the set of late jobs in the current schedule and  $T$  be the total tardiness. Initialize a set of jobs,  $C = \varphi$ . It contains the jobs that cannot be switched.
- Step 2: Calculate  $T_i, \forall i \in L$ . If  $T_i < 1 \forall i \in L$ , then exit; else go to step 3.
- Step 3: Select the first late job  $i \in L$  and  $i \notin C$ . If none exist then exit; else go to step 4.
- Step 4: Check if  $c_i = d_j$  for some late job  $j \in L$ . If so, then exchange jobs  $i$  and  $j$ ; Set  $L = L - \{j\}$ , else set  $C = C + \{i\}$ . Go to step 3, in any case.

### 4 Theorems

The following theorems have been developed to optimize the bi-criteria scheduling on parallel machines involving total tardiness and NT.

## 4.1 Theorem

The proposed algorithm 3 optimizes the bi-objective function  $NT/Total\ tardiness$ .

*Proof* To prove the optimality of proposed, we need to prove the optimality of steps 2, 3, and 4 of the proposed algorithm. As we know that the EDD rule optimizes total tardiness, further, the completion time of any job  $i$  is the location number of that job in the schedule. Hence, the completion time of a job can be determined by its new location after it is switched with another job.

**For Optimality of Step 2:** By assumption,  $T_i < 1 \forall i \in L$ . If there exist a better schedule than that of schedule obtained by EDD rule and can be obtained by moving jobs, we shall show that the movement of any job from EDD schedule does not lead to a better schedule.

**Case I:** If a job  $i$  moves to an earlier position from its position in the EDD schedule, then it delays all the intermediate jobs by at least one unit each. Hence, irrespective of whether job  $i$  is early or late in the EDD schedule, the value of  $NT$  and total tardiness at best remain the same and could possibly deteriorate from their values in the EDD schedule.

**Case II:** If a job  $i$  moves to a late position (delaying) from its position in the EDD schedule, then again two subcases arises:

If job  $i$  is late in the EDD schedule, then every unit of time that is delayed, its tardiness increases by a unit, while the tardiness of already late  $j$  improves only by the amount  $T_j (< 1$ , by assumption). Hence, the net effect is an increment in total tardiness.

If job  $i$  is not late in the EDD schedule, then two situations may further arise. If job  $i$  is delayed to a position where it is still early, then both tardiness and  $NT$  remain the same. However, if it is moved to a position where it becomes late, for unit increment in its tardiness, the reduction in tardiness of already late job  $j$  is  $T_j (< 1$ , by assumption). Hence, the net effect is an increment in total tardiness.

Therefore, if  $T_i < 1 \forall i \in L$ , no improvement in the job scheduling is possible.

**For optimality of Steps 3 and 4:** Here, we shall show that the conditions mentioned in steps 3 and 4 of the proposed algorithm are the only conditions under which an improved schedule can be obtained.

First, we observe that for these steps  $T_i \geq 1$  for all  $i \in L$  with strict inequality holding for at least one  $i$ . Further, switching either the early jobs or jobs with the same due date will not result in a better schedule. In fact, it may make the number of late jobs and total tardiness worse. Thus, we consider the switching of a late job with a job that is either late or early job. Pick any two jobs  $i$  and  $j$  from the EDD schedule. Let job  $j$  be the late job. The following cases may arise:

**Case I: Job  $i$  is late and  $d_i < d_j$**

In this case, we have either  $c_i = c_j$  or  $t_i < t_j$ .

If  $c_i = c_j$ , then the switching of these jobs will not improve the solution.

If  $c_i < c_j$ , then the tardiness  $T$  and  $T'$  before and after the exchange are

$$T_i = \max(0, c_i - d_i) + c_j - d_j, T'_i = \max(0, c_i - d_j) + c_j - d_i$$

In case if  $c_i > d_j$ , then switching job  $i$  and job  $j$  will worsen the primary criterion.

In case if  $c_i < d_j$ , then switching job  $i$  and job  $j$  does not change the total tardiness and NT values. Hence, the only case in which the primary criterion is not violated and NT improves is, if  $c_i = d_j$ .

**Case II: If job  $i$  is not late and  $d_i < d_j$**

In this case, the total tardiness before and after switching job  $i$  and  $j$  is  $T = c_j - d_j, T' = c_i - d_j$ . Here, we have  $T < T'$ .

Hence, the primary criterion of total tardiness is violated.

**Case III: If job  $i$  is not late job  $d_i > d_j$**

In this case, the total tardiness before and after switching job  $i$  and job  $j$  is  $T = c_j - d_j, T' = c_i - d_j$ . Here, we have  $T < T'$ .

Hence, the primary criterion of total tardiness is again violated.

**Case IV: If job  $i$  is late and  $d_i > d_j$**

In this case, we get the similar result as we get in case I, discussed above.

Hence, we have shown that a switching among any two jobs will worsen the EDD schedule except that made under the exchange condition  $c_i = d_j$  as stated in the algorithm. Hence, the proposed algorithm optimizes the bi-objective function NT/Total tardiness.

## 4.2 Theorem

*If the problem of single criterion, total tardiness, is NP-hard, the scheduling problem on parallel machines optimizing the bi-objective function NT/Total Tardiness will also be NP-hard.*

**Solution:** We shall prove the result by the method of contradiction:

Let if possible the bi-objective function NT/Total Tardiness is not NP-hard. Therefore, there must exist a polynomial algorithm which can solve the problem of optimizing the bi-objective function NT/Total Tardiness on parallel processing machines.

This implies that single criterion of total tardiness can be optimized in polynomial time, i.e., total tardiness is not NP-hard. This is a contradiction as total tardiness is NP-hard.

Hence, the scheduling problem optimizing the bi-objective function NT/Total Tardiness on parallel processing machines is NP-hard.

## 5 Numerical Illustration

Optimize the NT with condition of total tardiness, whenever the processing times of jobs are in fuzzy environment with due time on parallel machines are as follows (Tables 1, 2):

**Solution:** The AHR of the processing time by using Yagers [12] formula of the given jobs is as shown in Table 2.

**Table 1** Processing time of jobs in fuzzy environment

Jobs ( <i>i</i> )	1	2	3	4	5	6
Processing time	(6,7,8)	(5,6,7)	(9,10,11)	(7,8,9)	(5,6,7)	(10,11,12)
Due date ( <i>d<sub>i</sub></i> )	20/3	27/3	32/3	26/3	25/3	35/3

**Table 2** AHR of processing time of jobs

Jobs ( <i>i</i> )	1	2	3	4	5	6
Processing time	29/3	20/3	32/3	26/3	20/3	35/3
Due date ( <i>d<sub>i</sub></i> )	20/3	27/3	32/3	26/3	25/3	35/3

On arranging the jobs in EDD order on parallel machines  $M_1, M_2$  and  $M_3$ , we have (Table 3).

Therefore, total tardiness = 75/3 units and NT = 4.

Set of late jobs =  $L = \{1, 2, 3, 6\}$  and set of jobs that cannot be switched  $C = \varphi$ .

On considering the 1<sup>st</sup> late job  $i = 1 \in L$  and  $1 \notin C$ . Here, for the late job  $j = 2 \in L$ , we have  $c_i = d_j$ . Therefore, on exchanging jobs  $i = 1 \in L$  and  $j = 2 \in L$ , setting  $L = L - \{2\}$ , the jobs schedule becomes (Table 4).

Therefore, total tardiness = 75/3 units and NT = 3.

Here, we observe that no further improvement in scheduling of jobs is possible.

Hence, the optimal sequence of jobs processing optimizing the bi-objective function NT/Total Tardiness on parallel machines is 2–5–4–1–3–6 with minimum total tardiness = 75/3 units and minimum NT as 3.

**Table 3** Job scheduling with EDD order

Jobs ( <i>i</i> )	1	5	4	2	3	6
$M_1$	0–29/3	–	–	–	–	29/3–64/3
$M_2$	–	0–20/3	–	20/3–40/3	–	–
$M_3$	–	–	0–26/3	–	26/3–58/3	–
$d_i$	20/3	25/3	26/3	29/3	32/3	35/3
$T_i$	9/3	–	–	11/3	26/3	29/3

**Table 4** Reduced job scheduling table

Jobs ( <i>i</i> )	2	5	4	1	3	6
$M_1$	0–20/3	–	–	20/3–49/3	–	–
$M_2$	–	0–20/3	–	–	20/3–52/3	–
$M_3$	–	–	0–26/3	–	–	26/3–61/3
$d_i$	29/3	25/3	26/3	20/3	32/3	35/3
$T_i$	–	–	–	29/3	20/3	26/3



## 6 Conclusion

The present chapter is aimed at developing heuristic algorithm to solve the bi-objective problem with total tardiness and NT as primary and secondary criteria more efficiently, in reasonable amount of time and with little conciliation on the optimality of the solution on parallel machines. In past, the processing time for each job was usually assumed to be exactly known. But, in many real-life situations, processing times may vary dynamically due to human factors or operating faults, and hence, the concept of fuzziness in processing time of jobs is introduced. For a given set of jobs initially arranged in EDD order, a late job needs to be considered for being exchanged only with another job or a job having the same due date in order to potentially improve the value of a secondary criteria, given the primary criteria of minimum total tardiness. The study may further be extended by generalizing the number of parallel machines and by introducing trapezoidal fuzzy membership function to represent the fuzziness in processing time.

## References

1. Anghinolfi, D., Paolucci, M.: Parallel machine total tardiness scheduling problem. *Comput. Oper. Res.* **3**, 3471–3490 (2007)
2. Azizoglu, M., Kondacki, S., Omer, K.: Bicriteria scheduling problem involving total tardiness and total earliness penalties. *Int. J. Prod. Econ.* **23**, 17–24 (1991)
3. Akker Vanden, J.M., Hoogeveen, J.A.: Minimizing the number of tardy jobs. *Hand Book of Scheduling*. Chap-man and Hall/CRC, Boca Raton, Florida (2004)
4. Chand, S.: Schneerberger: A note on single machine scheduling problem with minimum weighted completion time and maximum allowable tardiness. *Naval Res. Logistic* **33**, 551–557 (1986)
5. Chen, C.L., Bulfin, R.L.: Scheduling a single machine to minimize two criteria: Maximum tardiness and number of tardy jobs. *IIE Trans.* **26**, 76–84 (1994)
6. Gupta, D., Sharma, S., Aggarwal, S.: Bi-objective parallel machine scheduling with uncertain processing time. *Adv. Appl. Sci. Res.* **3**, 1020–1226 (2012)
7. Lawler, E.L., Lenstra, J.K., Rinnooy Kan, A.H.G.: Minimizing maximum lateness in a two machine open shop. *Math. Oper. Res.* **6**, 153–158 (1981)
8. Moore, J.M.: Sequencing n jobs one machine to minimize the number of tardy jobs. *Manage. Sci.* **77**, 102–109 (1968)
9. Parkash, D.: Bicriteria scheduling problems on parallel machine. Ph.D. thesis. University of Birekshurg. Virginia (1997)
10. Shin, S.O., Kim, Y.D.: Scheduling on parallel machines to minimize total tardiness. *J. Oper. Res.* **177**, 629–634 (2007)
11. Singh, T.P.: Bi-objective in fuzzy scheduling on parallel machines. *Arya Bhatta J. Math. Inf.* **2**, 149–152 (2011)
12. Yager, R.R.: A procedure for ordering fuzzy subsets of unit interval. *Inf. Sci.* **24**, 143–161 (1981)
13. Zadeh, L.A.: Fuzzy sets. *Inf. Control* **8**, 78–98 (1965)

# Inventory Model for Decaying Item with Continuously Variable Holding Cost and Partial Backlogging

Ankit Prakash Tyagi, Shivraj Singh and Rama Kant pandey

**Abstract** Holding costs are determined from the investment in physical stocks and storage facilities for items during a cycle. In most of the research papers, holding cost rate per unit time for perishable inventory is assumed as constant. However, this is not necessarily the case when items in stock are decaying. In this work, paying better attention on the holding cost, we present a deteriorating inventory model in which the unit holding cost is continuously based on the deterioration of the inventory with the time the item is in stock. The deterioration rate is assumed as a Weibull distribution function. Declining market demand is considered in this paper. Shortages are allowed and partial backlogged. The partial backlogging rate is a continuous exponentially decreasing function of waiting time in purchasing the item during stock out period. Conditions for uniquely existence of global minimum value of the average total cost per unit time are carried out. Numerical illustration and sensitivity analysis are presented.

**Keywords** Inventory · Weibull deterioration · Partial backlogging · Continuously variable holding cost

---

A. P. Tyagi (✉) · R. K. Pandey  
Department of Mathematics, D.B.S. (PG) College, Dehradun, Uttarakhand, India  
e-mail: ankitprakashtyagi88@gmail.com

R. K. Pandey  
e-mail: rkpandey0055@gmail.com

S. Singh  
Department of Mathematics, D.N. (PG) College, Meerut, Uttar Pradesh, India  
e-mail: shivrajpundir@gmail.com

## 1 Introduction

In daily life, deteriorating goods cannot use for long time. Foods, vegetables, fruits and pharmaceuticals are a few examples of such items. So, the loss due to deterioration is needed to give a better consideration of inventory managers. First, Ghare and Schrader [1] considered continuously deteriorating inventory model with a constant demand. Later, Cover and Philip [2] assumed variable deterioration rate. In this study, they considered two-parameter Weibull distributive deterioration rate. Since then, a great deal of research has focused on variable deterioration rate in models.

The assumption of constant demand rate is not always applicable for decaying inventory. In reality, market demand of an item goes up in the growth phase of its life cycle. On the other hand, on introducing more attractive products consumer's preference may change. This causes demand of some items to decline. The consumer's confidence on quality of such products loses due to the age of the product. Therefore, the age of inventory has a negative pressure on demand. This phenomenon attracted numerous researchers to developed deteriorating models with time varying demand pattern.

Hollier and Mak [3] were first presented the consideration of exponentially decreasing demand. They also developed optimal policies under both conditions where replenishment intervals are constant and variable. In developing such inventory models, Goyal and Giri [4] provided a detail review of deteriorating inventory literatures.

In the mention above, most researchers assumed that shortage are completely backlogged. In practice, during the shortage period a few customers would like to wait for backlogging but the other would not. In daily life, a common observation is that, in the event of shortage, the proportion of consumers who will to purchase the item decreases as the waiting time increases. Therefore, backlogging rate should be variable and dependent on the waiting time for the next replenishment. Chang and Dey [5] investigated an inventory model with shortage. They assumed a variable backlogging rate which depends on the length of waiting for the next replenishment. Recently, Pentico and Drake [6] provide a prominent survey of deterministic models for the EOQ with partial backlogging.

In the consideration above, most researchers assumed that holding cost rate per unit time is constant. However, more sophisticated storage facilities and services may be needed for holding perishable items if they are kept for longer periods of time. So, in holding of decaying items, the assumption of constant holding cost rate is not always suitable. Weiss [7] noted that variable holding cost is appropriate when the value of an item decreases the longer it is in stock. Ferguson et al. [8] indicated that this type of model is suitable for perishable items in which price markdowns and removal of ageing product are necessary. Recently, Mishra and Singh [9] developed the inventory model for deteriorating items with time dependent linear demand and holding cost. To give attention on the concept of variability of the holding cost of decaying item, Tyagi et al. [10] developed an inventory lot-size model for decaying item following the power patterns of demand of item. In that

study, shortages were allowed and partial backlogged inversely with the waiting time for the next replenishment.

On the basis of the discussion above, a question crops up that what optimal policy will be adopted by the inventory managers when demand of item follows the exponentially declining path and partial backlogging rate is also a exponentially decreasing function of the waiting time for the next replenishment? To give optimal policy in this situation, in this paper, an Economic Order Quantity (EOQ) inventory model of deteriorating item is considered with declining market demand. To extend such EOQ models, it is assumed continuously variable holding cost rate per unit per unit time based on deterioration. The deterioration rate of item is considered as two-parameter Weibull distribution function. Partial backlogging is allowed. The backlogging rate is an exponentially decreasing function of the waiting time for the next replenishment. In this paper, the primary problem is to minimize the average total cost per unit time by optimizing the shortage point per cycle. We also show that minimized objective function is convex and the obtained solution is uniquely determined. A numerical example is proposed to illustrate the model and the solution procedure. The sensitivity analysis of major parameters is performed in the last, here.

## 2 Notations and Assumptions

The following notations and assumptions are used throughout the whole paper.

### 2.1 Notations

$I(t)$  the inventory level at any time  $t$ ,  $t \geq 0$ ;  $T$  constant prescribed scheduling period or cycle length (time units);  $I_{\max}$  maximum inventory level at the start of a cycle (units);  $S$  maximum amount of demand backlogged per cycle (units);  $t_1$  duration of inventory cycle when there is positive inventory;  $Q$  order quantity (units/cycle);  $c_1$  cost of the inventory item (\$);  $c_2$  fixed order cost (\$/per order);  $c_3$  shortage cost per unit backordered per unit time (\$/unit/unit time);  $c_4$  opportunity cost due to lost sales (\$/unit).

### 2.2 Assumptions

In developing the mathematical model of the inventory system, the following assumptions are made: (1) the replenishment rate is infinite; (2) lead time is negligible; (3) the replenishment quantity and cycle length are constant for each cycle; (4) there is no replacement or repair of deteriorated items during a given cycle; (5) the time to deterioration of the item is Weibull distributed. So, the rate of deterioration is

$d(t) = \alpha\beta t^{\beta-1}$ , where  $\alpha$  and  $\beta$  are shape and scale parameters; (6) the demand rate  $R_1(t)$  is known and decreases exponentially as  $R_1(t) = De^{-\lambda t}$  for  $I(t) > 0$  and  $R_1(t) = D$  for  $I(t) \leq 0$  where  $D(> 0)$  is initial demand and  $\lambda(> 0)$  is a constant governing the decreasing rate of the demand; (7) shortage are allowed. Unsatisfied demand is partially backlogged. The backlogging rate  $B(t)$  which is a decreasing function of the waiting time  $t$  for next replenishment, we here assume that  $B(t) = e^{-\delta t}$ , where  $1 > \delta \geq 0$  is backlogging parameter and  $t$  is the waiting time; (8) the holding cost rate per unit time is assumed continuously variable with storage period of the item. The holding cost  $h(t)$  consists of fix holding charges and variable handling charges of item due to its deterioration. So, we here assume that  $h(t) = R + He^{dt}$  which is increasing function of storage period  $t$  of item, where  $R(> 0)$  is fix holding charge per unit,  $H(> 0)$  is handling charge per unit time and  $d(> 0)$  is deterioration rate governing the increasing path of handling charges.

### 3 Model Formulations

The inventory system goes like this: At  $t = 0$ , initial replenishment  $Q$  units are made, of which  $S$  units are delivered towards backorders, leaving a balance of  $I_{\max}$  units in the initial inventory. From  $t = 0$  and  $t = t_1$  time units, the inventory level depletes due to both demand and deterioration. At  $t_1$ , the inventory level is zero. During the time  $(T - t_1)$  the shortage is partially backlogged at the rate of  $B(t)$  after receiving next lot and left part of demand during shortage is lost. That is, only the backlogging items are replaced by the next replenishment.

The inventory function with respect to time can be determined by evaluating the differential equations

$$\frac{dI(t)}{dt} + d(t)I(t) = -R_1(t); \quad 0 \leq t \leq t_1, \tag{1}$$

and

$$\frac{dI(t)}{dt} = -DB(t); \quad t_1 \leq t \leq T. \tag{2}$$

with the boundary conditions  $I(0) = I_{\max}$  and  $I(t_1) = 0$ .

The solutions of (1) and (2) are

$$I(t) = D \left[ (t_1 - t) - \lambda \left( \frac{t_1^2}{2} - \frac{t^2}{2} \right) + \frac{\alpha}{\beta + 1} (t_1^{\beta+1} - t^{\beta+1}) \right] (1 - \alpha t^\beta); \quad 0 \leq t \leq t_1, \tag{3}$$

and

$$I(t) = -\frac{D}{\delta} \left[ e^{-\delta(T-t)} - e^{-\delta(T-t_1)} \right]; \quad t_1 \leq t \leq T. \tag{4}$$

The maximum inventory level at the starting point of the cycle is

$$I_{\max} = I(0) = I(t) = D \left[ t_1 - \frac{\lambda t_1^2}{2} + \frac{\alpha t_1^{\beta+1}}{\beta+1} \right]. \quad (5)$$

The maximum amount of demand backlogged per cycle can be obtained as

$$S = -I(T) = \frac{D}{\delta} \left[ 1 - e^{-\delta(T-t_1)} \right]. \quad (6)$$

So, from (5) and (6), the order quantity per cycle is

$$Q = I_{\max} + S = D \left( t_1 - \frac{\lambda t_1^2}{2} + \frac{\alpha t_1^{(1+\beta)}}{(1+\beta)} \right) + \frac{D}{\delta} \left[ 1 - e^{-\delta(T-t_1)} \right]. \quad (7)$$

The average total cost per unit time per cycle consists of ordering cost per cycle, holding cost per cycle, deterioration cost per cycle, shortage cost per cycle and opportunity cost per cycle. Now, the ordering cost (*OC*) per order is  $c_2$ .

The inventory holding cost (*HC*) per cycle is

$$= \int_0^{t_1} h(t)I(t)dt \quad (8)$$

The deterioration cost (*DC*) per cycle is

$$= \int_0^{t_1} c_1 d(t)I(t)dt \quad (9)$$

The shortage cost (*SC*) per cycle is

$$= \int_{t_1}^T c_3 \{-I(t)\}dt \quad (10)$$

And, the opportunity cost (*OPC*) due to lost sales per cycle is

$$= \int_{t_1}^T [1 - B(t)]Ddt \quad (11)$$

The objective of this model is to determined the optimal value ( $t_1^*$ ) of  $t_1$  in order to minimize the average total cost per unit time is

$$ATC(t_1) = \frac{[OC + HC + DC + SC + OPC]}{T} \tag{12}$$

The necessary condition for average total cost per unit time  $ATC(t_1)$  to be minimized is

$$\frac{dATC(t_1)}{dt_1} = \frac{Df(t_1)}{T} = 0, \tag{13}$$

where

$$f(t_1) = \left[ (R + H) (t_1 - \lambda t_1^2) + \frac{\alpha\beta(R + 2H)t_1^{\beta+1}}{(1 + \beta)} + \frac{\{R - H(\beta - 1)\} \alpha\lambda t_1^{\beta+2}}{(1 + \beta)} \right] + c_1\alpha \left[ t_1^\beta - \lambda t_1^{\beta+1} \right] - \frac{(c_4\delta - c_3e^{-\delta(T-t_1)})}{\delta} - (T - t_1)c_3e^{-\delta(T-t_1)} - \frac{(c_3 - \delta c_4) e^{-\delta(T-t_1)}}{\delta}.$$

Now, our main concern is to know about the existence of the solution of (13) that will be the inner point in the interval  $[0, T]$  at which average total cost per unit time is at minimum value, globally. This is analogous to show that the solution of  $f(t_1) = 0$  uniquely exists.

**Theorem 1** *If  $R > H(\beta - 1)$  and  $1 > \lambda T$ , then the solution of  $f(t_1) = 0$  not only exists but also is uniquely determined as an inner point of  $[0, T]$ .*

**Theorem 2** *If  $R + H + \alpha\beta(R + 2H)t_1^\beta + \frac{\alpha\lambda R(\beta+2)t_1^{\beta+1}}{(1+\beta)} + (c_3 + \delta c_4)e^{-\delta(T-t_1)} + c_1\alpha[\beta t_1^{\beta-1} - \lambda(1 + \beta)t_1^\beta] > \frac{\alpha\lambda H(\beta-1)(\beta+2)t_1^{\beta+1}}{(\beta+1)} + 2(R + H)\lambda t_1 + \delta(T - t_1)c_3e^{-\delta(T-t_1)}$ , the average total cost per unit time  $ATC(t_1)$  is convex and reaches its global minimum at point  $t_1^*$ .*

Next, by using  $t_1^*$ , we can obtain the optimal maximum inventory level, the optimal order quantity and the minimum average total cost per unit time from (5), (7) and (12).

### 4 Numerical Illustrations

To illustrate the preceding discussion we consider the following example.

*Example 1* We consider an inventory system which verifies the assumptions described above. The randomly chosen input data of parameters are  $T = 1, \alpha = 0.8$

$$R = 2, H = 0.4, \delta = 0.1, \lambda = 0.4, D = 100, \beta = 2, c_1 = 3, c_2 = 10, c_3 = 3$$

and  $c_4 = 7$ .

The optimal value  $t_1^* = 0.516906$  unit time of  $t_1$  are calculated by MATHEMATICA 8.0 for the proposed model. By using the optimal value  $t_1^*$ , the minimum average total cost per unit time  $ATC(t_1^*) = \$91.7083$  is obtained and Theorem 2 is satisfied. We can obtain the optimal value  $Q^* = 97.1908$  units of ordering quantity  $Q$  per cycle.

### 5 Sensitivity Analysis

Here, taking one parameter at a time and keeping the remaining parameters unchanged, we have studied the effect of changes ( $\pm 5\%$  and  $\pm 10\%$ ) in the values of some parameters  $\alpha, \beta, R$  and  $H$  on optimal shortage point  $t_1^*$ , optimal order quantity  $Q^*$  and

**Table 1** Effect of changes in the parameters of the inventory model

Parameters	% Change	% Change in the value of		
		$t_1^*$	$Q^*$	$ATC(t_1^*)$
$R = 2$	+10	-2.38	-0.06	+2.67
	+5	-1.20	-0.03	+1.35
	-5	+1.23	+0.03	-1.38
	-10	+2.49	+0.07	-2.80
$H = 0.4$	+10	-0.54	-0.015	+0.57
	+5	-0.27	-0.007	+0.29
	-5	+0.27	+0.007	-0.29
	-10	+0.54	+0.015	-0.58
$\alpha = 0.8$	+10	-1.74	+0.31	+1.29
	+5	-0.88	+0.15	+0.65
	-5	+0.91	-0.16	-0.67
	-10	+1.87	-0.31	-1.36
$\beta = 2$	+10	+2.14	-0.64	-2.33
	+5	+1.09	-0.33	-1.21
	-5	-1.15	+0.35	+1.32
	-10	-2.36	+0.74	+2.75



the minimum average total cost per unit  $ATC(t_1^*)$ . Example 1 is used and results are shown in Table 1. From Table 1, it is clearly observed that when the values of parameters  $R$  and  $H$  of holding cost rate increase or decrease, the optimal value of  $ATC(t_1^*)$  increase or decrease. But this trend is reversed for the solutions  $t_1^*$  and  $Q^*$ . The main reason is that when  $R$  and  $H$  increase, the holding cost will increase. Therefore, inventory managers reduce the order quantity and consequently the shortage point is reduced. Finally, it also increases the average total cost for the inventory system.

## 6 Conclusion

In this paper we study an inventory model where the inventory level is depleted not only by exponentially decreasing demand but also by Weibull distributive deterioration, in which holding cost per unit time is considered a continuously variable function depends upon item's deterioration nature. Shortages are allowed and partially backlogged. Therefore, the proposed model can be used in inventory controlling of certain perishable items like food items, electronic components and other fashionable products. Moreover, the advantage of the proposed inventory model is that the behavior of the model illustrated by the help of given example is easy to understand by sensitivity analysis due to major parameters. From sensitivity analysis, it is shown that the optimal order quantity is highly sensitive to changes in the value of  $\alpha$  and  $\beta$ , on the other hand the optimal value of average total cost per unit time is highly sensitive to changes in the value of  $R$ ,  $\alpha$  and  $\beta$  as well as slightly sensitive to changes in the value of  $H$ . According this situation, inventory managers have to take decision to place an order on the basis of decaying nature of goods after setting a justifying level of average total cost that can be accepted by their organization. As far as the future researches biased on this study are concerned, this paper can be extended with stochastic demand and permissible delay in payment.

## References

1. Ghare, P.M., Schrader, G.H.: A model for exponentially decaying inventory system. *Int. J. Prod. Econ.* **21**, 449–460 (1963)
2. Covert, R.B., Philip, G.S.: An EOQ model with weibull distribution deterioration. *AIIE Trans.* **5**, 323–326 (1973)
3. Hollier, R.H., Mak, K.L.: Inventory replenishment policies for deteriorating items in a declining market. *Int. J. Prod. Econ.* **21**, 813–826 (1983)
4. Goyal, S.K., Giri, B.C.: Recent trends in modeling of deteriorating inventory. *Eur. J. Oper. Res.* **134**, 1–16 (2001)
5. Chang, H.J., Dye, C.Y.: An EOQ model for deteriorating items with time varying demand and partial backlogging. *J. Oper. Res. Soc.* **50**, 1176–1182 (1999)
6. Pentico, D.W., Drake, M.J.: A survey of deterministic models for the EOQ and EPQ with partial backlogging. *Eur. J. Oper. Res.* **214**(2), 179–198 (2011)

7. Weiss, H.J.: Economic order quantity models with nonlinear holding costs. *Eur. J. Oper. Res.* **9**(1), 56–60 (1982)
8. Ferguson, M., Hayaraman, V., Souza, G.C.: Note: an application of the EOQ model with nonlinear holding cost to inventory management of perishables. *Eur. J. Oper. Res.* **180**(1), 485–490 (2007)
9. Mishra, V.K., Singh, L.S.: Deteriorating inventory model for time dependent demand and holding cost with partial backlogging. *Int. J. Manage. Sci. Eng. Manage.* **6**(4), 267–271 (2011)
10. Tyagi, A.P., Pandey, R.K., Singh, S.R.: Optimization of inventory model for decaying item with variable holding cost and power demand. *Proceedings of National Conference on TAME*, pp 774–781 (2012). ISBN: 978-93-5087-574-2

# The Value of Product Life-Cycle for Deteriorating Items in a Closed Loop Under the Reverse Logistics Operations

S. R. Singh and Neha Saxena

**Abstract** Owing to its strategic implications, reverse logistics has received much attention in recent years. Growing green concerns and advancement of reverse logistics concepts make it all the more relevant who can be achieved through the End-of-Life (EoL) treatment. In the proposed model, we develop a production inventory model with the reverse flow of the material. Here we determined the value of product life cycle with EoL scenario where the reverse logistics operations deal with the collection, sorting, cleaning, disassembling, and remanufacturing of the buyback products. The purpose of this paper is to develop an effective and efficient management of product remanufacturing. As a result, in this article, we establish a mathematical formulation of the model to determine the optimal payment period and replenishment cycle. Illustrative examples, which explain the application of the theoretical results as well as their numerical verifications, are also given. Finally, the sensitivity analysis is reported.

**Keywords** Production · Reverse operations · Deterioration · Short life cycle products · Collection investment

## 1 Introduction

Supply chain management has received remarkable attention both from the business world and from academic researchers. Most of the research concentrates on the forward movement of supply chain and transformation of the materials from the suppliers to the end consumer. However, rapid developments in technology, the

---

S. R. Singh · N. Saxena (✉)  
D. N. College, Meerut, India  
e-mail: shivrajpundir@gmail.com

N. Saxena  
e-mail: nancineha.saxena@gmail.com

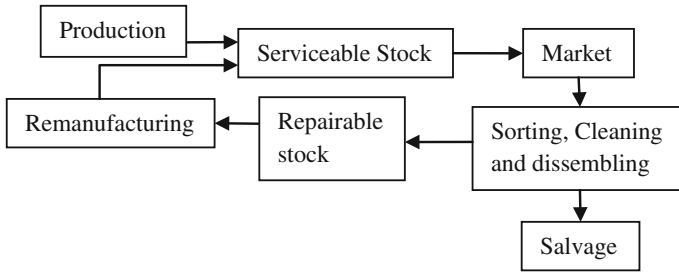
emergence of new industrial products and shortened product life cycles have resulted in an increasing number of discarded products and caused growing environmental problems in the developed world. Due to the governmental regulations and consumer concerns regarding these environmental issues, an increasing number of companies have focused on reduction efforts in the amount of waste stream, diversion of the discarded products and disposition of the retired products properly. Enforced legislation and customer expectations increasingly force manufacturers to take back their products after use, which can be achieved through the collection investment. The collection investment represents the monetary amount of effort (e.g., promotion, marketing) that the recycled-material supplier applies to the end-user market to create the necessary incentive to receive targeted returns. This subject is related to the concept of reverse logistics. Due to this awareness manufacturers and researchers in many countries have been paid much attention to the reverse flow of products from consumers to upstream businesses interest. The Reverse logistics is the process of retrieving the product from the end consumer for the purposes of or proper disposal. A Reverse Production System includes collection, sorting, and remanufacturing processes for end-of-life products. Reverse distribution can take place through the original forward channel, through a separate reverse channel, or through combinations of the forward and the reverse channel.

The green supply chain, which links the natural environment both with the forward and reverse supply chain, has a growing stream of research and is quickly becoming a well-established field of its own. This development has stimulated a number of companies to explore options for take-back and recovery of their products. There are two types of reverse logistics (RL) classified on the basis of the degree of the openness in its network. One of the two classifications is Open-loop structure and the other one is Closed-loop System. In the open-loop RL system, the products from the end user do not return to the original manufacturers or suppliers. The products are taken away by the third logistics party for the purpose of waste reduction, resale etc. while in case of closed-loop RL system products get returned to the original manufacturers or suppliers, for the purpose of repair, reformation or reuse. In need of repair or renovation it usually points the original source, belonging to the closed-loop structure.

In the past recent years, a growing environmental consciousness enforce the researchers to be more environmental responsible. A lot of work has been done in the field of RL. There are very few models treating forward and reverse distribution simultaneously. Schrady [16] was the first who determined both of the system, reverse flow of material with forward system. He considers the traditional Economic Order Quantity (EOQ) model for repairable items assuming that the manufacturing and recovery (repair) rates are instantaneous. This model was generalized by Nahmias and Rivera [13] for the case of finite repair rate and limited storage in the repair and production shops. Another extension of the model of Schrady [16] was made by Mabini et al. [12]. Ishii et al. [8] developed a model and demonstrate the need of life-cycle design to maximize the life-cycle value of a product at the initial stages of design. Koh et al. [10] generalized the model of Nahmias and Rivera [13] by assuming a limited repair capacity. Dobos and Richter [5] explore a RL inventory system

with non instantaneous production and remanufacturing rate. Dobos and Richter [6] generalized their earlier work (2003) to the case of multiple remanufacturing and production cycle. Dobos and Richter [7] extended their previous model and assumed that the quality of collected returned items is not always suitable for further repairing [14]. In a further study a closed-loop supply chain for the returned items is developed by Savaskan et al. [15] assuming that the returned rate depends on the Collection investment. Dekker et al. [4] proposed a quantitative model for closed loop supply chain. He investigated that the amount of returns is highly uncertain and this uncertainty greatly affect the collection and inventory decisions. Bayındır et al. [2] investigated the level of the desired recovery effort with the imperfect recovery process. King et al. [9] defined the term repair as the correction of specified faults in a product, where the quality of repaired products is inferior to those of remanufactured. Srivastava [19] generalized an overview in green supply chain. He showed that RL is a complex process to achieve greater economic benefits. El Saadany and Jaber investigated the model by assuming that the collection rate of returned items is dependent on the purchasing price and the acceptance quality level of these returns. That is, the flow of buyback items increases as the purchasing price increases, and decreases as the corresponding acceptance quality level increases. Konstantaras and Skouri [11] generalized the model by considering a general cycle pattern in which a variable number of reproduction lots of equal size are followed by a variable number of manufacturing lots of equal size. They also have studied the case where shortages are allowed in each manufacturing and reproduction cycle. Alamri [1] proposed a general reverse Logistics inventory model for the optimal returned quantity with deteriorated items. Singh and Saxena [18] developed a RL inventory model for stock out situation. Along the same line Singh et al. [17] developed there model for the flexible manufacturing under the stock out situation. Green supply chain inventory model with short life cycle product is developed by Chung and Wee [3]. This paper differs from the previous research, since in this study a closed loop system in reverse logistics is considered. In this article, we have developed the model for the short life cycle products.

In this paper, a closed loop system for integrated production of new items and remanufacturing of returned items is presented for an infinite planning horizon. The effect of deterioration is taken as under consideration. We developed a model assuming the coordination of joint production and reproduction options by producing new items and reproducing the returned items to quality standards that are “as-good-as” those of new products. In this model, the demand of customer is satisfied by the serviceable stock which is either produced or remanufactured items from the market the buyback products are subjected to the sorting, cleaning, and disassembling from where a constant ratio of the products (repairable stock) that confirms the certain quality standard are collected to be remanufactured and the rest is salvaged. The process is going on. A general framework of such a system is depicted in Fig. 1. The next section is for assumption and notations. Section 3 is for the formulation of the model. In Sect. 4 we have determined the solution procedures for the model. The numerical example to illustrate the model and sensitivity analysis is presented



**Fig. 1** Material flow in a reverse logistics inventory model

in Sect. 5. Concluding remarks are derived and future research topics are suggested in Sect. 6.

## 2 Assumption and Notations

### *Notations for the forward logistics*

- $I_m(t)$  = Inventory level at time  $t$  in manufacturing stock.
- $P_m$  = The production rate.
- $d$  = The demand rate (satisfied from the newly produced and reproduced items).
- $\delta_m$  = Deterioration rate.
- $\alpha$  = Scaling parameter, production formulation.
- Cost parameters for the manufacturing stock are as follows.

$C_m$  = Unit item cost.  
 $K_m$  = Fixed unit production cost.  
 $S_m$  = Variable unit production cost.  
 $H_m$  = Unit holding cost.

### *Notations for reverse logistic*

- $I_r(t)$  = Inventory level at time  $t$  in remanufacturing process.
- $I_m(t)$  = Inventory level at time  $t$  in production process.
- $P_r$  = The reproduction rate.
- $R$  = The returned rate.
- $\beta$  = Scaling parameter, remanufacturing formulation.
- $\gamma$  = Scaling parameter, collection investment formulation.
- $\eta$  = Scaling parameter, salvage formulation.
- The cost parameters for the reproduced stock are as follows.

$F_r$  = Fixed unit reproduction cost.  
 $S_r$  = Variable unit reproduction cost.  
 $H_r$  = Unit holding cost.

- $\delta_r$  = Deterioration cost.
- The cost parameters for the returned stock are as follows.

$C_R$  = Unit returned item cost.

$H_R$  = Unit holding cost.

- $\delta_R$  = Deterioration cost.
- $S_{av}$  = Salvage.
- $M$  = number of the life cycles before the component is recycled or disposed off.
- $CI$  = Collection investment.
- $F_{cl}$  = fixed cost including cleaning and disassembly cost during the collecting process.
- $C_{cl}$  = variable cost including cleaning and disassembly cost during the collecting process.
- $A_{df}$  = fixed component life-cycle design cost ratio for the green design.
- $B_{dv}$  = variable component life-cycle design cost ratio for the green design.
- $C_d$  = component life-cycle design cost for the green design.
- $r_j$  = reliability of the sub function  $j$ .

### Assumptions

- Production and remanufacturing rate taken to be demand dependent as

$$P_r = \alpha d, \quad \alpha > 1$$

$$P_m = \beta d, \quad \beta > 1$$

- Returned items are collected at a rate  $R$  determined by the collection investment  $CI$  and demand. The collection investment represents the economical amount of effort (e.g., promotion, marketing) that the supplier applies to the end-user to create the necessary incentive to receive targeted returns.  $R = (\sqrt{CI/\gamma})d$  where  $\gamma$  is a scaling parameter and  $\sqrt{CI/\gamma} < 1$ .

## 3 Formulation of the General Model

The change in inventory of Production and Remanufacturing house is depicted in Fig. 2. In the remanufacturing house the reproduction starts at time  $T_0$  and the inventory level rises up at a rate  $P_r - d - \delta_r I_r(t)$ . At the time  $T_1$  reproduction stops then the stock level wind up at a rate  $-d - \delta_r I_r(t)$  to the time  $T_2$ . At the same time due to the production the stock level rises up at a rate  $P_m - d - \delta_m I_m(t)$  in the Production house and at the time  $T_3$  when the production stops the stock level starts to decrease at a rate  $-d - \delta_m I_m(t)$  up to the time  $T_4$ . Now the stock level of the returned items assumed to be remanufactured is start to decreasing at a rate  $\eta R - P_r - \delta_R I_R(t)$  up

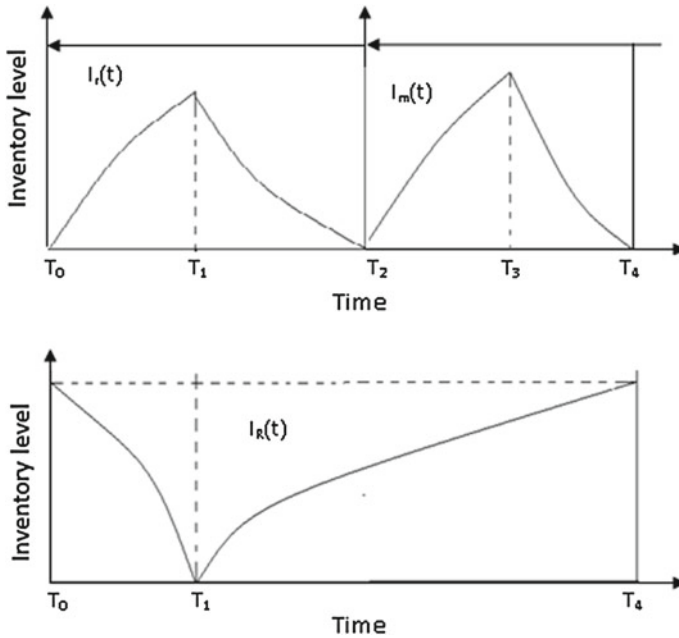


Fig. 2 Inventory variation of an EPQ model for reverse logistics system

to the time  $T_1$  and after the end of the reproduction the stock level is raising at a rate up to the time  $T_4$

The changes in the inventory levels depicted in Fig. 2 are governed by the following differential equations:

$$I'_r(t) + \delta_r I_r(t) = P_r - d, \quad \text{With the ending condition } I_r(T_0) = 0 \quad 0 \leq t \leq T_1 \tag{1}$$

$$I'_r(t) + \delta_r I_r(t) = -d, \quad \text{With the ending condition } I_r(T_2) = 0 \quad T_1 \leq t \leq T_2 \tag{2}$$

$$I'_m(t) + \delta_m I_m(t) = P_m - d, \quad \text{With the initial condition } I_m(T_2) = 0 \quad T_2 \leq t \leq T_3 \tag{3}$$

$$I'_m(t) + \delta_m I_m(t) = -d, \quad \text{With the ending condition } I_m(T_4) = 0 \quad T_3 \leq t \leq T_4 \tag{4}$$

$$I'_R(t) + \delta_R I_R(t) = \eta R - P_r, \quad \text{With the ending condition } I_R(T_1) = 0 \quad 0 \leq t \leq T_1 \tag{5}$$

$$I'_R(t) + \delta_R I_R(t) = \eta R, \quad \text{With the initial condition } I_R(T_1) = 0 \quad T_1 \leq t \leq T_4 \tag{6}$$

The solution of the above differential equations is as follows:

$$I_r(t) = \left\{ \frac{P_r - d}{\delta_r} \right\} (1 - e^{-\delta_r t}) \quad 0 \leq t \leq T_1 \tag{7}$$



$$I_r(t) = \left\{ \frac{d}{\delta_r} \right\} (e^{\delta_r(T_2-t)} - 1) \quad T_1 \leq t \leq T_2 \tag{8}$$

$$I_m(t) = \left\{ \frac{P_m - d}{\delta_m} \right\} (1 - e^{\delta_m(T_2-t)}), \quad T_2 \leq t \leq T_3 \tag{9}$$

$$I_m(t) = \left\{ \frac{d}{\delta_m} \right\} (e^{\delta_m(T_4-t)} - 1) \quad T_3 \leq t \leq T_4 \tag{10}$$

$$I_R(t) = \left\{ \frac{P_r - \eta R}{\delta_R} \right\} (e^{\delta_R(T_1-t)} - 1) \quad 0 \leq t \leq T_1 \tag{11}$$

$$I_R(t) = \left\{ \frac{\eta R}{\delta_R} \right\} (1 - e^{\delta_R(T_1-t)}), \quad T_1 \leq t \leq T_4 \tag{12}$$

Now the per cycle cost components for the given inventory system are as follows.

Item cost:  $C_m \int_{T_2}^{T_3} P_m du + C_R \int_0^{T_4} R du$  this cost includes the deterioration cost

Production cost:  $K_m + S_m \int_{T_2}^{T_3} P_m du$

Holding cost =  $h_r [I_r(0, T_1) + I_r(T_1, T_2)] + h_m [I_m(T_2, T_3) + I_m(T_3, T_4)] + h_R [I_R(0, T_1) + I_R(T_1, T_4)]$

Remanufacturing cost =  $K_r + \frac{F_r}{M} + MS_r \int_0^{T_1} P_r du + F_{cl} + C_{cl} \int_0^{T_4} R du$

Salvage =  $\int_0^{T_4} (1 - \eta) R du$

Design life cost =  $C_D \left\{ \frac{ADF}{M} + MB_{DV} \prod_{j=1}^2 r_j \right\}$

Total cost = cost for the forward supply chain + cost for the reverse supply chain

$$\begin{aligned} Z(T_1, T_2, T_3, T_4, M) = & \frac{1}{T_4} \left[ C_m \int_{T_2}^{T_3} P_m du + C_R \int_0^{T_4} R du + K_m + S_m \int_{T_2}^{T_3} P_m du \right. \\ & + K_r + \frac{F_r}{M} + MS_r \int_0^{T_1} P_r du + F_{cl} + C_{cl} \int_0^{T_4} R du \\ & - \int_0^{T_4} (1 - \eta) R du + CI + C_D \left\{ \frac{ADF}{M} + MB_{DV} \prod_{j=1}^2 r_j \right\} \\ & \left. + h_R \left\{ \int_{T_0}^{T_1} \left\{ \frac{P_r - \eta R}{\delta_R} \right\} (e^{\delta_R(T_1-t)} - 1) dt \right. \right. \end{aligned}$$

$$\begin{aligned}
 & + \int_{T_0}^{T_1} \left\{ \frac{\eta R}{\delta_R} \right\} (1 - e^{\delta_R(T_1-t)}) dt \Bigg\} \\
 & + h_m \left[ \int_{T_2}^{T_3} \left\{ \frac{P_m - d}{\delta_m} \right\} (1 - e^{\delta_m(T_2-t)}) dt \right. \\
 & \left. + \int_{T_3}^{T_4} \left\{ \frac{d}{\delta_m} \right\} (e^{\delta_m(T_4-t)} - 1) dt \right] \\
 & + h_r \left[ \int_{T_0}^{T_1} \left\{ \frac{P_r - d}{\delta_r} \right\} (1 - e^{-\delta_r t}) dt \right. \\
 & \left. + \int_{T_1}^{T_2} \left\{ \frac{d}{\delta_r} \right\} (e^{\delta_r(T_2-t)} - 1) dt \right] \Bigg]
 \end{aligned}$$

$$\begin{aligned}
 Z(T_1, T_2, T_3, T_4, M) = & \frac{1}{T_4} \left[ d \left\{ \frac{H_r \beta}{\delta_r} - \frac{H_R \beta}{\delta_R} + M S_r \beta \right\} T_1 \right. \\
 & + d \left\{ -C_m \alpha - S_m \alpha - \frac{H_r}{\delta_r} - \frac{H_m (\alpha - 1)}{\delta_m} \right\} T_2 \\
 & + d \left\{ C_m \alpha + S_m \alpha + \frac{H_m}{\delta_m} + \frac{H_m (\alpha - 1)}{\delta_m} \right\} T_3 \\
 & + d \left\{ \left( -1 + \eta + C_R + C_{cl} + \frac{H_r}{\delta_r} \right) \sqrt{\frac{CI}{\gamma}} - \frac{H_m}{\delta_m} \right\} T_4 \\
 & \left. + \left[ K_m + K_r + CI + F_{cl} + \frac{F_r}{M} + C_D \left( \frac{A_{DF}}{M} + M B_{DVR} r_2 \right) \right] \right] \tag{13}
 \end{aligned}$$

The total cost can be rewriting the cost function as follows:

$$Z(T_1, T_2, T_3, T_4, M) = \frac{1}{T_4} [AT_1 + BT_2 + CT_3 + DT_4 + E] \tag{14}$$

Now we have to find the value of  $T_1, T_2, T_3$  and  $T_4$  that minimize  $Z(T_1, T_2, T_3, T_4)$ . But there are some relations between the variables as follows:

$$0 < T_1 < T_2 < T_3 < T_4 \tag{15}$$

$$\left\{ \frac{P_r - d}{\delta_r} \right\} (1 - e^{-\delta_r T_1}) = \left\{ \frac{d}{\delta_r} \right\} (e^{\delta_r(T_2-T_1)} - 1) \tag{16}$$

$$\left\{ \frac{P_m - d}{\delta_m} \right\} (1 - e^{\delta_m(T_2 - T_3)}) = \left\{ \frac{d}{\delta_m} \right\} (e^{\delta_m(T_4 - T_3)} - 1) \tag{17}$$

$$\left\{ \frac{P_r - \eta R}{\delta_R} \right\} (e^{\delta_R(T_1)} - 1) = \left\{ \frac{\eta R}{\delta_R} \right\} (1 - e^{\delta_R(T_1 - T_4)}) \tag{18}$$

Thus our purpose is to minimize the total cost  $Z(T_1, T_2, T_3, T_4, M)$  subject to the Eqs. (15), (16), (17) and (18).

### 4 Solution Procedure

Let  $Q$  be the acceptable returned quantity for used items in the interval  $[0, T_4]$  then

$$Q = \int_0^{T_4} R dt \tag{19}$$

From (19), we note that  $T_4$  can be determined as a function of  $Q$ , say

$$T_4 = f_4(Q) = \frac{Q}{D\sqrt{\frac{CI}{\gamma}}} \tag{20}$$

From which and (18) we find that  $T_1$  can be determined as a function of  $T_4$ , hence of  $Q$ , say

$$T_1 = f_1(Q) = \frac{1}{\delta_r} \left[ \log \left\{ \frac{\beta}{\beta - \eta\sqrt{CI/\gamma} (1 - e^{\delta_r T_4})} \right\} \right] \tag{21}$$

From which and (16),  $T_2$  can be determined as a function of  $T_1$ , hence of  $Q$ , say

$$T_2 = f_2(Q) = \frac{1}{\delta_r} \left[ \log \left\{ \beta e^{\delta_r T_1} - \beta + 1 \right\} \right] \tag{22}$$

From which, (17),  $T_3$  can be determined as a function of  $T_2$  and  $T_4$  hence of  $Q$ , say

$$T_3 = f_3(Q) = \frac{1}{\delta_m} \left[ \log \left\{ \frac{1}{\alpha} \left( e^{\delta_m T_4} + (\alpha - 1) e^{\delta_m T_2} \right) \right\} \right] \tag{23}$$

Thus, if we substitute (20), (21), (22), (23) in (14) then the problem will be converted to the following unconstrained problem with the variable  $Q$ .

$$W(Q, M) = \frac{1}{f_4} [Af_1 + Bf_2 + Cf_3 + Df_4 + E] \tag{24}$$

$$\frac{\partial W(Q, M)}{\partial Q} = [A (f_4 f'_1 - f_1 f'_4) + B (f_4 f'_2 - f_2 f'_4) + C (f_4 f'_3 - f_3 f'_4) - E f'_4] = 0 \tag{25}$$

By which

$$f'_4 = \frac{1}{d} \sqrt{\frac{\gamma}{CI}} \tag{26}$$

$$f'_1 = \left\{ \frac{\eta \sqrt{CI/\gamma}}{\beta - \eta \sqrt{CI/\gamma} (1 - e^{-\delta_R f_4})} \right\} f_4 e^{-\delta_R f_4} \tag{27}$$

$$f'_2 = f'_1 \beta e^{\delta_r (f_1 - f_2)} \tag{28}$$

$$f'_3 = \frac{1}{\alpha} \left\{ f'_4 e^{\delta_m (f_4 - f_3)} + (\alpha - 1) f'_2 e^{\delta_m (f_2 - f_3)} \right\} \tag{29}$$

Here  $f'_i$  is the differentiation of  $f_i$

Now

$$\frac{\partial W(Q, M)}{\partial M} = \frac{-F_r}{M^2} + S_r d f_1 \beta + C_D \left\{ \frac{-A_{DF}}{M^2} + B_{DV} (r_1 r_2) \right\} = 0 \tag{30}$$

From Eq. (24) we can see that the total cost function is the function of  $M$  and  $Q$  only. While the value of  $M$  and  $Q$  can be find from the Eqs. (25) and (26). Since  $M$  is a discrete variable therefore the optimal value of  $M$  is find by satisfying the equation  $W(Q^*, M - 1) \leq W(Q^*, M) \leq W(Q^*, M + 1)$  where  $Q^*$  is the optimal value of  $Q$ . Therefore, now our aim is to find the optimal values of  $M$  and  $Q$  such that

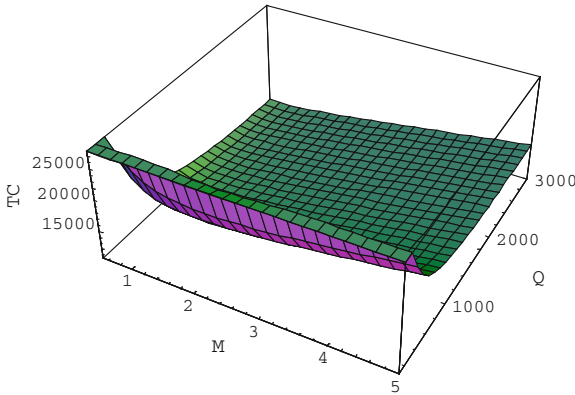
Minimize  $W(Q, M)$

$$\text{Subject to: } W(Q^*, M - 1) \leq W(Q^*, M) \leq W(Q^*, M + 1). \tag{31}$$

### 5 Numerical Example and Sensitivity Analysis

The above theoretical results are illustrated through the numerical verification. The example is based on the following parametric values. We have considered the input parameters in appropriate units:

$$d = 2500, \quad C_m = 2.5, \quad C_R = 1, \quad K_m = 800, \quad H_m = 1.5, \quad H_r = 1, \quad H_R = 1, \\ S_m = 2, \quad \alpha = 1.5, \quad \beta = 1.8, \quad \gamma = 196, \quad \eta = 0.9, \quad \delta_m = 0.1, \quad \delta_r = 0.1, \\ \delta_R = 0.1, \quad C_{cl} = 0.25, \quad F_{cl} = 500, \quad F_r = 100, \quad S_r = 1, \quad A_{df} = 8, \quad B_{dv} = 1, \quad C_d = 50, \\ r_1 = 0.99, \quad r_2 = 0.98, \quad S_{av} = 3, \quad CI = 100.$$



**Fig. 3** Convexity of the green supply chain

**Table 1** Sensitivity analysis for the scaling parameter (production formulation)  $\alpha$

$\alpha$	$M$	$T_1$	$T_2$	$T_3$	$T_4$	$Q$	$TC$
1.3	1	0.569041	1.00205	1.52977	1.6828	3005	10829.3
1.4	1	0.561878	0.989702	1.47332	1.6604	2965	10865.9
1.5	1	0.555961	0.979495	1.42595	1.664192	2932	10897.3
1.6	1	0.550935	0.970821	1.38546	1.62624	2904	10924.5
1.7	1	0.546622	0.963377	1.35048	1.6128	2880	10948.4

**Table 2** Sensitivity analysis for the scaling parameter (remufacturing formulation)  $\beta$

$\beta$	$M$	$T_1$	$T_2$	$T_3$	$T_4$	$Q$	$TC$
1.6	1	0.65162	1.02314	1.48488	1.708	3050	10747.6
1.7	1	0.599931	0.999445	1.45291	1.67216	2986	10827.8
1.8	1	0.555961	0.979495	1.42595	1.664192	2932	10897.3
1.9	1	0.518284	0.962829	1.40347	1.61672	2887	10958.2
2.0	1	0.485444	0.948409	1.384	1.59488	2848	11012.1

Under the given values of the parameters in above section, the optimal acceptable returned quantity for the used items is  $Q^* = 2932$  units and the optimal number of life-cycles  $M = 1$  which is accumulated by the time  $T_1^* = 0.555961$ ,  $T_2^* = 0.979495$ ,  $T_3^* = 1.42595$  and  $T_4^* = 1.64192$  by which the minimum relevant cost is as  $TC^* = 10897.3$ . The convexity of the problem is shown in Fig. 3.

*Sensitivity Analysis*

In order to study the effect of various parameters on the optimal policy, a sensitivity analysis is done and results are presented in the following tables.

*Observations*

When the parameters fluctuate, the following observations have been made during the sensitivity analysis.

**Table 3** Sensitivity analysis for the scaling parameter (returned formulation)  $\eta$ 

$\eta$	$M$	$T_1$	$T_2$	$T_3$	$T_4$	$Q$	$TC$
0.88	1	0.545717	0.961814	1.42566	1.64976	2946	10896.5
0.89	1	0.552093	0.970678	1.42581	1.64584	2939	10896.9
0.90	1	0.555961	0.979495	1.42595	1.664192	2932	10897.3
0.91	1	0.561045	0.988264	1.42608	1.638	2925	10897.8
0.92	1	0.566286	0.997303	1.42668	1.63464	2919	10898.4

- From Tables 1, 2 and 3 it is observed that as the production, remanufacturing and returned rate increase, total profit increases.
- It is observed from the above tables that as the production, remanufacturing and returned rate increase, the acceptable returned quantity and the cycle length decreases.
- The analysis shows that the deviation in the value of  $M$  is negligible according to the deviation of the parameters.
- The cost function is stable for all the parameter but more stable for the returned formulation parameter.

## 6 Conclusion

This study develops a closed loop supply chain inventory model for the short life cycle products with deterioration. In the development of inventory models, most of the previous researchers have considered that an item can be repaired an indefinite number of times but in practical it is not always possible. We have studied a supply chain system from an End of Life perspective for the decaying items where the whole life-cycle of the product is considering. In this process, returned products are collected, cleaned, dismantling, make some re-use value be re-applications or create “new” products, the “new” products has the performance of original product. This paper develops a model where an item is recovered a finite number of times. Examples, which explain the application of the theoretical results, are given here and these illustrative examples are numerically verified too. Further, the effects of production, remanufacturing and return rates are compared.

## References

1. Alamri, A.A.: Theory and methodology on the global optimal solution to a general reverse logistics inventory model for deteriorating items and time-varying rates. *Comput. Ind. Eng* **60**, 236–247 (2010)

2. Bayındır, Z.P., Dekker, R., Porras, E.: Determination of recovery effort for a probabilistic recovery system under various inventory control policies. *Omega* **34**, 571–584 (2006)
3. Chung, C.-J., Wee, H.-M.: Short life-cycle deteriorating product remanufacturing in a green supply chain inventory control system. *Int. J. Prod. Econ.* **129**, 195–203 (2011)
4. Dekker, R., Fleischmann, M., Inderfurth, K.: *Reverse logistics: quantitative models for closed-loop supply chains*. Springer-Verlag, Heidelberg (2004)
5. Dobos, I., Richter, K.: A production/recycling model with stationary demand and return rates. *CEJOR* **11**(1), 35–46 (2003)
6. Dobos, I., Richter, K.: An extended production/recycling model with stationary demand and return rates. *Int. J. Prod. Econ.* **90**(3), 311–323 (2004)
7. Dobos, I., Richter, K.: A production/recycling model with quality considerations. *Int. J. Prod. Econ.* **104**(2), 571–579 (2006)
8. Ishii, K., Eubanks, C.F., Marco, P.D.: Design for product retirement and material life-cycle. *J. Mater. Des.* **15**(4), 225–233 (1994)
9. King, A.M., Burgess, S.C., Ijomah, W., McMahon, C.A.: Reducing waste: repair, recondition, remanufacture or recycle? *Sustain. Dev.* **14**(4), 257–267 (2006)
10. Koh, S.G., Hwang, H., Sohn, K.I., Ko, C.S.: An optimal ordering and recovery policy for reusable items. *Comput. Ind. Eng.* **43**, 59–73 (2002)
11. Konstantaras, I., Skouri, K.: Lot sizing for a single product recovery system with variable setup numbers. *Eur. J. Oper. Res.* **203**(2), 326–335 (2010)
12. Mabini, M.C., Pintelon, L.M., Gelders, L.F.: EOQ type formulations for controlling repairable inventories. *Int. J. Prod. Econ.* **28**(1), 21–33 (1992)
13. Nahmias, N., Rivera, H.: A deterministic model for a repairable item inventory system with a finite repair rate. *Int. J. Prod. Res.* **17**(3), 215–221 (1979)
14. El Saadany, A.M.A., Jaber, M.Y.: A production/remanufacturing inventory model with price and quality dependant return rate. *Comput. Ind. Eng.* **58**(3), 352–362 (2010)
15. Savaskan, R.C., Bhattacharya, S., van Wassenhove, L.N.: Closed-loop supply chain models with product remanufacturing. *Manage. Sci.* **50**(2), 239–252 (2004)
16. Schrady, D.A.: A deterministic inventory model for repairable items. *Naval Res Logistics Q.* **14**, 391–398 (1967)
17. Singh, S.R., Prasher, L., Saxena, N.: A centralized reverse channel structure with flexible manufacturing under the stock out situation. *Int. J. Ind. Eng. Comput.* **4**, 559–570 (2013)
18. Singh, S.R., Saxena N.: An optimal returned policy for a reverse logistics inventory model with backorders. *Adv. Decis. Sci.* **2012**, 21 (2012). Article ID 386598
19. Srivastava, S.K.: Green supply-chain management: a state-of-the-art literature review. *Int. J. Manage. Rev.* **9**(1), 53–80 (2007)

# A Fuzzified Production Model with Time Varying Demand Under Shortages and Inflation

Shalini Jain and S. R. Singh

**Abstract** We develop an inventory model with time-dependent demand rate and deterioration, allowing shortages. The production rate is assumed to be finite and proportional to the demand rate. The shortages are partially backlogged with time-dependent rate. Inflation is also taken in this model. Inflation plays a very significant role in inventory policy. We developed the model in both fuzzy and crisp sense. The model is solved logically to obtain the optimal solution of the problem. It is then illustrated with the help of numerical examples. Sensitivity of the optimal solution with respect to changes in the values of the system parameters is also studied.

**Keywords** Time-dependent demand · Shortages · Deterioration · Fuzzy

## 1 Introduction

Inventory control involves human capability to deal with uncertainty of future demand of stock items. Hence, the application of fuzzy reasoning models in inventory control systems is quite important as fuzzy inferring procedures are becoming essential in managing uncertainties. In the past, a great deal of research has been done in the areas of inventory control systems. But, only few of the researchers have contributed in the applications of fuzzy logic. [29] first developed a inventory model in fuzzy sense. [24] fuzzified the ordering cost into trapezoidal fuzzy number in the total cost of an inventory without backordering and obtained the fuzzy total cost. Later, they used the centroid method and gained the total cost in the fuzzy sense. [7] fuzzified the

---

S. Jain (✉)

Centre of Mathematical Sciences, Banasthali University, Banasthali, Rajasthan, India  
e-mail: shalini.shalini2706@gmail.com

S. R. Singh

Department of Mathematics, D.N. College, Meerut, India  
e-mail: shivrajpundir@gmail.com



ordering cost, inventory cost, and backordering cost into trapezoidal fuzzy numbers and used the functional principle to obtain the estimate of the total cost in the fuzzy sense. [14] proposed an inventory model without shortages by fuzzifying the order quantity into a triangular fuzzy number. [28] generalized an inventory model without any backlogging for fuzzy order quantity and fuzzy total demand quantity. [5] considered the fuzzy problems for the mixture of backorders and lost sales in inventory model. The total expected annual cost is obtained in the fuzzy sense. [6] considered the mixture inventory model involving a fuzzy variable and obtained the total cost in the fuzzy sense. [22] consider inflation and apply discounted cash flow in a inventory model and formulated the total cost of the system using genetic algorithm. [18] presented solution changed model to a crisp multipurpose problem using defuzzification of fuzzy constraints and fuzzy chance-constrained programming methods.

Production is a process whereby raw material is converted into semifinished products and then converted into finished products. The main purpose of production function is to produce the goods and services demanded by the customers in the most efficient and economical way. So efficient management of the production function is of utmost importance in order to achieve this objective. An optimal production quantity model for a deteriorating item was developed by [15]. [25] proposed economic production quantity (EPQ) deteriorating inventory with partial backordering. [11] introduced an EPQ model with marketing policies and a deteriorating item. [23] developed a model with price and stock-dependent demand considering a production model for deteriorating items. [20] introduced a model that generates an economic run quantity solution and the total production solution simultaneously. Economic run quantity is an extended model of production model. The objective of production planning, and control, like that of all other manufacturing controls, is to contribute to the profits of the industry. As with inventory management and control, this is accomplished by keeping the customers satisfied during the meeting of delivery schedules.

Usually, it is assumed that lifetime of an item is immeasurable when it is in storage. However, there are abundant types of items such as food grains, highly volatile substances, radioactive materials, films, drugs, blood, fashion goods, electronic components, and high-tech products in which there is gradual loss of potential or value with a passage of time. Therefore, the effect of deterioration cannot be ignored in inventory models. [10] were the first to consider deterioration of inventory with constant demand. As time passed, several researchers developed inventory models by assuming either instantaneous or finite production with different assumptions on the patterns of deterioration. In this connection, researchers may refer to work by [4, 8, 9, 13, 15]. Also, some researchers [26, 27] have studied the chances and effect of integration and co-operation between the buyer and the producer of deteriorating items. Interested readers may review the articles by [19] and [12]. Lin and Gong assumed varying production rate and deteriorating inventory.

Inflation plays a very significant role in inventory models. Inflation refers to the movement in the general level of prices. It does not refer to changes in one price relative to other prices. Rather than measure inflation by using the actual rate at which prices are rising, some economists prefer a measure of inflation that reflects primarily only the systematic factors that act to raise prices. [3] developed the first

EOQ model taking inflation into the model. [1] developed the inventory decisions under inflationary condition. [2] proposed an economic order quantity under variable rate of inflation and mark-up prices. [17] criticized a net present value. [16] studied the inflation effects on inventory system. Yang et al. presented a deterministic inventory lot-size models under inflation with shortages and deterioration for fluctuating demand. [21] presented a fuzzy inventory model under inflation.

In the present paper, we assume the production model with time-dependent demand and deterioration. As a result, the finite production rate is also time dependent. Shortages are allowed and are partially backlogged. The model developed in both fuzzy and crisp sense. An analytical solution of the model is discussed and is illustrated with the help of numerical examples. Sensitivity of the optimal solution with respect to changes in different parameter values is also examined.

## 2 Assumptions and Notations

The following assumptions and notations have been used throughout the paper:

1. The demand rate is deterministic and is a function of time.
2. The rate of production is finite.
3. Production rate depends on the demand rate.
4. Inflation and time value of money are considered.
5. Shortages are allowed.
6. Holding cost is taken to be variable in nature

The following notations are used in our study:

- D(t) Demand rate (units/unit time),  $D(t) = a + bt$ , a and b are positive constants,  $a > b$ .
- P(t) Production rate (units/unit time),  $k > 1$ ,  $P(t) = kD(t)$  for any t.
- $\theta(t)$  Rate of deterioration where  $\theta(t) = \theta t$ ,  $\theta$  is a positive constant.
- $I_i(t)$  Inventory level at any time t.
  - s Per unit selling price of the item.
- B Backlogging rate,  $B = e^{-\delta t}$ ,  $\delta$  is a positive constant.
- r Constant representing the difference between the discount rate and inflation rate.
- c Production cost per unit item.
- $c_3$  Set up cost per unit item.
- $c_2$  Shortage cost per unit item.
- $c_1 + \alpha t$  Inventory holding cost per unit item per unit time,  $\alpha > 0$ .

### 3 Model Illustration

The problem has been formulated in two steps. In the first step, we formulate a crisp model and then in the next step, we extend the model into a fuzzy sense. The crisp formulation of the model has been presented here:

$$I_1'(t) + \theta t I_1(t) = k(a + bt) - (a + bt), 0 \leq t \leq T_1 \quad (1)$$

$$I_2'(t) + \theta t I_2(t) = -(a + bt), T_1 \leq t \leq T_2 \quad (2)$$

$$I_3'(t) = -e^{-\delta t}(a + bt), T_2 \leq t \leq T_3 \quad (3)$$

$$I_4'(t) = k(a + bt) - (a + bt), T_3 \leq t \leq T_4 \quad (4)$$

With the boundary conditions:

$$I_1(0) = 0, I_2(T_2) = 0, I_3(T_2) = 0, I_4(T_4) = 0 \quad (5)$$

Solutions of (1)–(4) are

$$I_1(t) = (k - 1) \left[ \left( at + \frac{bt^2}{2} + \frac{a\theta t^3}{6} + \frac{b\theta t^4}{8} \right) \right] e^{-\frac{\theta t^2}{2}} \quad (6)$$

$$I_2(t) = \left[ a(T_2 - t) + \frac{b}{2} (T_2^2 - t^2) + \frac{a\theta}{6} (T_2^3 - t^3) + \frac{b\theta}{8} (T_2^4 - t^4) \right] e^{-\frac{\theta t^2}{2}} \quad (7)$$

$$I_3(t) = \left[ a(T_2 - t) + \frac{b}{2} (T_2^2 - t^2) \right] \quad (8)$$

$$I_4(t) = (k - 1) \left[ a(t - T_4) + \frac{b}{2} (t^2 - T_4^2) \right] \quad (9)$$

At  $t = T_1$ ,  $I_1(T_1) = I_2(T_1)$ . From Eqs. (6) and (7), we get

$$T_1 = f(T_2) \quad (10)$$

At  $t = T_3$ ,  $I_3(T_3) = I_4(T_3)$ . From Eqs. (8) and (9), we get

$$T_3 = f(T_2, T_4) \quad (11)$$

The present worth of holding cost for the period under consideration

$$HC = \int_0^{T_1} (c_1 + \alpha t)I_1(t)e^{-rt}dt + c_1 \int_{T_1}^{T_2} (c_1 + \alpha t)I_2(t)e^{-rt}dt \tag{12}$$

Production has been taking place in the period  $[0, T_1]$  and  $[T_3, T_4]$ , hence, the present worth of the production cost is:

$$PC = \left( \int_0^{T_1} k(a + bt)e^{-rt}dt + \int_{T_3}^{T_4} k(a + bt)e^{-rt}dt \right) \tag{13}$$

Before the start of a production run, the fixed cost to be borne by the producer is:

$$SPC = c_3 + c_3e^{-rT_3} \tag{14}$$

Shortages are accumulated in the system during  $[T_2, T_4]$ . The maximum level of shortages are present at  $t = T_4$ . The total present worth of shortages during this time is

$$SC = \left( \int_{T_2}^{T_3} -I_3(t)e^{-rt}dt + \int_{T_3}^{T_4} -I_4(t)e^{-rt}dt \right) \tag{15}$$

Inventory is present and sold during  $[0, T_4]$ . The present worth of the generated revenue is given by

$$SP = s \left( \int_0^{T_1} D(t)e^{-rt}dt + \int_{T_1}^{T_2} D(t)e^{-rt}dt + \int_{T_2}^{T_3} D(t)e^{-\delta t}e^{-rt}dt + \int_{T_3}^{T_4} D(t)e^{-rt}dt \right) \tag{16}$$

So, the net profit of the system is represented by:

$$NP = \frac{s.SP - c_1.HC - c.PC - c_3 - c_2.SC}{T_4} \tag{17}$$

### 4 Fuzzy Modeling

In order to develop the model in a fuzzy environment, we consider the Production cost per inventory unit per unit time  $c^{\vee}$  and Shortage cost per inventory unit per unit time  $c_2^{\vee}$  as the triangular fuzzy numbers  $\tilde{c} = (c - \Delta_1, c, c + \Delta_2)$  and  $\tilde{c}_2 = (c_2 - \Delta_3, c_2, c_2 + \Delta_4)$  such that that  $0 < \Delta_1 < c, 0 < \Delta_2, 0 < \Delta_3 < c_2, 0 < \Delta_4$

and where  $\Delta_1, \Delta_2, \Delta_3, \Delta_4$  are determined by the decision maker based on the uncertainty of the problem. Thus, the Production cost  $c$  and the shortage cost  $c_2$  are considered as the fuzzy numbers  $\tilde{c}$  and  $\tilde{c}_2$  with membership functions.

$$NP = \frac{s.SP - c_1.HC - \hat{c}.PC - c_3.SPC - \hat{c}_2.SC}{T_4} \tag{18}$$

$$\tilde{c} = [c - \Delta_1, c, c + \Delta_2] \tag{19}$$

$$\tilde{c}_2 = [c_2 - \Delta_3, c_2, c_2 + \Delta_4] \tag{20}$$

By Centroid Method, we get

$$\tilde{c} = c + \frac{1}{3}(\Delta_2 - \Delta_1) \tag{21}$$

$$\tilde{c}_2 = c_2 + \frac{1}{3}(\Delta_4 - \Delta_3) \tag{22}$$

$$F_1 = \frac{s.SP - c_1.HC - (c + \Delta_2).PC - c_3.SPC - (c_2 + \Delta_4).SC}{T_4} \tag{23}$$

$$F_2 = \frac{s.SP - c_1.HC - c.PC - c_3.SPC - c_2.SC}{T_4} \tag{24}$$

$$F_3 = \frac{s.SP - c_1.HC - (c - \Delta_1).PC - c_3.SPC - (c_2 - \Delta_3).SC}{T_4} \tag{25}$$

By the method of Defuzzification,

$$NP = \frac{F_1 + 2F_2 + F_3}{4} \tag{26}$$

we find out Net profit in fuzzy sense.

### 5 Solution Procedure

To maximize total average profit per unit time (NP), the optimal values of  $t_2$  and  $t_4$  can be obtained by solving the following equations simultaneously

$$\frac{\partial NP}{\partial T_2} = 0 \tag{27}$$

and

$$\frac{\partial NP}{\partial T_4} = 0 \tag{28}$$

Provided, they satisfy the following conditions

$$\frac{\partial^2 NP}{\partial T_2^2} < 0, \frac{\partial^2 NP}{\partial T_4^2} < 0 \text{ and } \left(\frac{\partial^2 NP}{\partial T_2^2}\right)\left(\frac{\partial^2 NP}{\partial T_4^2}\right) - \left(\frac{\partial^2 NP}{\partial T_2 \partial T_4}\right)^2 > 0$$

Equation (16) is our objective function which needs to be maximized. For this, we use the classical optimization techniques. The Eqs. (27) and (28) obtained thereafter are highly nonlinear in the continuous variable  $T_2$ ,  $T_4$  and the discrete variables  $T_1$ ,  $T_3$ . However, if we give particular values to the discrete variable  $T_1$ ,  $T_3$ , our objective function becomes the function of two variables  $T_2$  and  $T_4$ . We have used the mathematical software MATHEMATICA 8.0 to arrive at the solution of the system in consideration. We can obtain the optimal values of different values of the time with the help of software. With the use of these optimal values, Eq. (17) provides maximum total average profit per unit time of the system in consideration.

### 6 Numerical Example

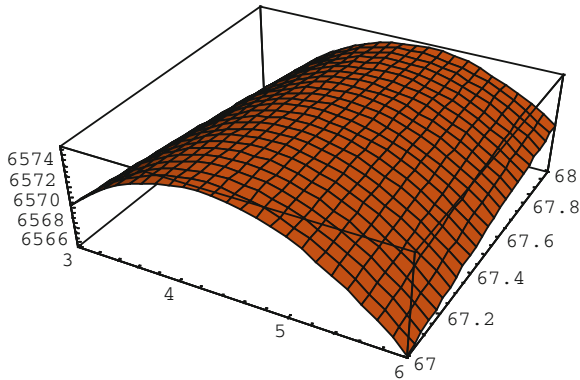
To illustrate the results, let us apply the proposed method to efficiently solve the following numerical example. For convenience, the values of the parameters are selected randomly.

$$k = 1.5, a = 80, b = 0.2, \alpha = 0.02, c = 1.6, c_1 = 0.9, c_2 = 10, c_3 = 40, s = 22, r = 0.03, \theta = 0.05, T_1 = 2, T_3 = 26.5472$$

#### Optimal Solution of the Proposed Model

$T_2$	$T_4$	Total profit (NP)
4.49286	67.5452	6575.58

The graph shows the variation of the system cost with  $T_2$  and  $T_4$ . From the figure, it is very clear that the total profit function is concave with respect to the two variables.

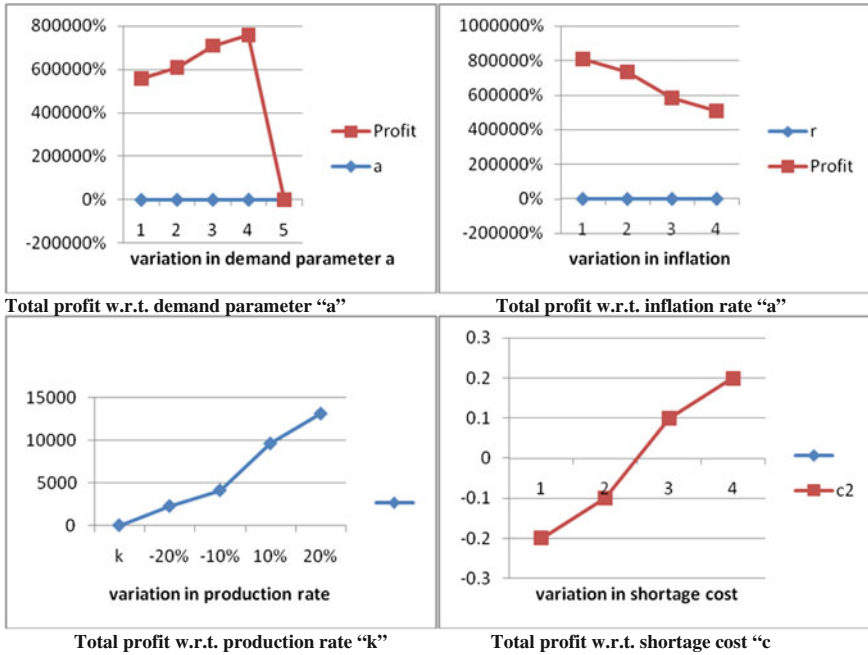


### 7 Sensitivity Analysis

We now study the effects of changes in the values of the system parameters  $a, b, k, \alpha, c, c_1, c_2, c_3, s, r, \theta$  on the total system cost in consideration. The sensitivity analysis is performed by changing each of the parameters by  $-10-20\%$ , taking one parameter at a time and keeping the remaining parameters unchanged. The analysis is based on the familiar results obtained from Example.

Parameter	Change in parameter			
	$-20\%$	$-10\%$	$10\%$	$20\%$
$a$	5579.61	6077.65	7073.41	7571.17
$b$	6255.86	6415.76	6735.3	6894.94
$k$	2257.36	4105.75	9606.43	13106.3
$\alpha$	6575.99	6575.99	6575.98	6575.97
$c$	6583.38	6579.44	6571.67	6571.67
$c_1$	6578.17	6576.87	6574.28	6584.65
$c_2$	5409.32	5992.45	7158.71	7741.83
$c_3$	6575.75	6575.66	6576.49	6575.4
$s$	6416.06	6495.82	6655.33	6735.09
$r$	8082.49	7325.72	5831.22	5091.93
$\theta$	6575.37	6575.47	6575.68	6575.78

Graphical representation of the sensitivity results with respect to different system parameters have been plotted in figures shown below.



## 8 Conclusion

The model has been developed for time-dependent demand with time-dependent deterioration in inventory. In this model, production rate is dependent on the demand rate. The average net profit function is the objective function in the case of crisp model. The same function extends to give the fuzzy model of the situation. This model is later defuzzified to a crisp model. Both the crisp as well as the fuzzy models have been solved numerically. In this study, shortages in inventory are allowed and the backlogging rate is taken as time dependent. The proposed model can be extended in numerous ways. For example, we may extend the inflation-dependent demand to inflation. Also, we could extend the model to incorporate some more features, such as quantity discount, and permissible delay in payment.

## References

1. Bierman, H., Thomas, J.: Inventory decisions under inflationary condition. *Deci. Sci.* **8**(1), 151–155 (1977)
2. Brahmabhatt, A.C.: Economic order quantity under variable rate of inflation and mark-up prices. *Productivity* **23**, 127–130 (1982)
3. Buzacott, J.A.: Economic order quantities with inflation. *Oper. Res. Quart.* **26**(3), 553–558 (1975)



4. Chakrabarti, T., Giri, B.C., Chaudhuri, K.S.: An EOQ model for items weibull distribution deterioration shortages and trended demand: an extension of philip's model. *Comp. Oper. Res.* **25**, 649–657 (1998)
5. Chang, H.C., Yao, J.S., Ouyang, L.Y.: Fuzzy mixture inventory model with variable lead-time based on probabilistic fuzzy set and triangular fuzzy number. *Math. Comp. Mode.* **39**(2–3), 287–304 (2004)
6. Chang, H.C., Yao, J.S., Ouyang, L.Y.: Fuzzy mixture inventory model involving fuzzy random variable lead time demand and fuzzy total demand. *Euro. J. Oper. Res.* **169**(1), 65–80 (2006)
7. Chen, S.H., Wang, C.C.: Backorder fuzzy inventory model under functional principle. *Inf. Sci.* **95**, 71–79 (1996)
8. Covert, R.P., Philip, G.C.: An EOQ model for items with weibull distribution deterioration. *AIIE Trans.* **5**, 323–326 (1973)
9. Dave, U.: On a discrete-in-time order-level inventory model for deteriorating items. *Oper. Res.* **30**, 349–354 (1979)
10. Ghare, P.M., Schrader, S.F.: A model for exponentially decaying inventory. *J. Ind. Eng.* **14**, 238–243 (1963)
11. Goyal, S.K., Gunasekaran, A.: An integrated production-inventory-marketing model for deteriorating items. *Comp. Ind. Eng.* **28**(4), 755–762 (1995)
12. Goyal, S.K., Giri, B.C.: Recent trends in modeling of deteriorating inventory. *Euro. J. Oper. Res.* **134**, 1–16 (2001)
13. Kang, S., Kim, I.: A study on the price and production level of the deteriorating inventory system. *Int. J. Prod. Res.* **21**, 899–908 (1983)
14. Lee, H.M., Yao, J.S.: Economic order quantity in fuzzy sense for inventory without backorder model. *Fuzzy Sets Syst.* **105**, 13–31 (1999)
15. Misra, R.B.: Optimum production lot-size model for a system with deteriorating inventory. *Int. J. Prod. Res.* **13**(5), 495–505 (1975)
16. Misra, R.B.: A study of inflation effects on inventory system. *Logi. Spect.* **9**(3), 260–268 (1997)
17. Moon, I., Yun, W.: A note on evaluating inventory systems: a net present value frame work. *Eng. Econ.* **39**(1), 93–99 (1993)
18. Nayebi, M.A., Sharifi, M., Shahriari, M.R., Zarabadipour, O.: Fuzzy-chance constrained multi-objective programming applications for inventory control model. *App. Math. Sci.* **6**(5), 209–228 (2012)
19. Raafat, F.: Survey of literature on continuously deteriorating inventory models. *J. Oper. Res. Soci.* **42**, 27–37 (1991)
20. Simmons, D., Cheng, J.: An alternative approach to computing economic run quantity. *Int. J. Prod. Res.* **56**(3), 837–847 (2008)
21. Singh, S.R., Bhatia, D.: Fuzzy inventory model for non-instantaneous perishable products under inflation. *Int. J. Man. Res. Tech.* **4**(2), 261–270 (2010)
22. Singh, S.R., Kumar, T., Gupta, C.B.: Optimal replenishment policy for ameliorating item with shortages under inflation and time value of money using genetic algorithm. *Int. J. Comp. App.* **27**(1), 5–17 (2011)
23. Teng, J.T., Chang, C.T.: Economic production quantity models for deteriorating itemswith price- and stock-dependent demand. *Comp. Oper. Res.* **32**(2), 297–308 (2005)
24. Vojosevic, M., Petrovic, D., Petrovic, R.: EOQ formula when inventory cost is fuzzy. *Int. J. Prod. Eco.* **45**, 499–504 (1996)
25. Wee, H.M.: Economic production lot-size model for deteriorating items with partial backordering. *Comp. Ind. Eng.* **20**(2), 187–197 (1993)
26. Wee, H.M., Jong, J.F.: An integrated multi-lot-size production inventory modelfor deteriorating items. *Manage. Syst.* **5**, 97–114 (1998)
27. Yang, P.C., Wee, H.M.: Economic order policy of deteriorated item for vendor and buyer: an integrated approach. *Prod. Plan. Cont.* **11**, 474–480 (2000)
28. Yao, J.S., Chang, S.C., Su, J.S.: Fuzzy inventory without backorder for fuzzy order quantity and fuzzy total demand quantity. *Comp. Oper. Res.* **27**, 935–962 (2000)
29. Zadeh, L.: Fuzzy sets. *Inf. control* **8**, 338–353 (1965)

# A Partial Backlogging Inventory Model for Decaying Items: Considering Stock and Price Dependent Consumption Rate in Fuzzy Environment

S. R. Singh and Swati Sharma

**Abstract** In this article, an inventory model is developed to deal with the impreciseness present in the market demand and the various cost parameters. The presented model is developed in crisp and fuzzy environments. Signed distance method is used for defuzzification. In most of the classical models, constant demand rate is considered. But in practice purchasing deeds of the customers is affected by the selling price and inventory level. In this study, we have considered demand rate as a function of stock-level and selling price. Two parameters Weibull distribution deterioration is considered. It is assumed that shortages are allowed and are partially backordered with the time dependent backlogging rate. A numerical experiment is provided to illustrate the problem. Sensitivity analysis of the optimal solution with respect to the changes in the value of the system parameters is also discussed.

**Keywords** Inventory model · Triangular fuzzy numbers · Signed distance · Partial backlogging · Stock and price dependent demand rate

## 1 Introduction

In most of the inventory models, it is assumed that the inventory parameters like demand rate and ordering cost, etc., are precisely known. But in actual living situations, the nature of these parameters is imprecise, so it is important to consider them as fuzzy numbers. The concept of fuzzy set theory first introduced by Zadeh [1], after that Park [2] extended the classical EOQ model by introducing the fuzziness

---

S. R. Singh · S. Sharma (✉)  
Department of Mathematics, D.N. College, Meerut, India  
e-mail: shivrajpundir@gmail.com

S. Sharma  
e-mail: jmlashi0@gmail.com

of ordering cost and holding cost. Recently, Chang [3] and Wang et al. [4] presented an inventory model under fuzzy demand.

Deterioration is a natural phenomenon in many real situations so it plays an important role in developing an inventory model. Generally, deterioration is defined as damage, spoilage, decay and obsolescence, vaporization, etc., that result in decrease of value of the original one. The first model for decaying items was presented by Ghare and Schrader [5]. It was extended by Covert and Philip [6] considering Weibull distribution deterioration. A complete survey for deteriorating inventory models was presented by Raafat [7]. Some other papers relevant to this topic are Teng et al. [8] and Bakker et al. [9].

Various researchers considered the situation in which shortages are either completely backlogged or completely lost which is not realistic. Many practical experiences disclose that some but not all customers will wait for backlogged items during a shortage period, such as for fashionable supplies and the products with short life cycle. According to such phenomenon, backlogging rate should not be disregarded. Thus, it is necessary to consider the backlogging rate. Researchers, such as Park [10] and Wee [11] developed inventory models with partial backorders. Some recent work in this direction is done by Singh [12] and Hsieh et al. [13].

In many classical research articles, it is assumed that demand rate is constant during the sales period. In real life, the demand may be inspired if there is a large pile of goods displayed on shelf. Gupta and Vrat [14] developed the first models for stock-dependent consumption rate. Mandal and Phaujdar [15] then developed a production inventory model for deteriorating items with uniform rate of production and linearly stock-dependent demand. Other papers related to this research area are Ray et al. [16], Goyal and Giri [17], and Chang et al. [18].

All the above-cited papers reveal that many research articles are developed in which demand is considered as the function of stock level or selling price, shortages are allowed and partially backlogged, but there is no such research paper which is partially backlogged assuming demand rate as the function of selling price and inventory level in fuzzy environment. In lots of business practices, it is observed that several parameters in inventory system are imprecise. Therefore, it is necessary to consider them as fuzzy numbers while developing the inventory model.

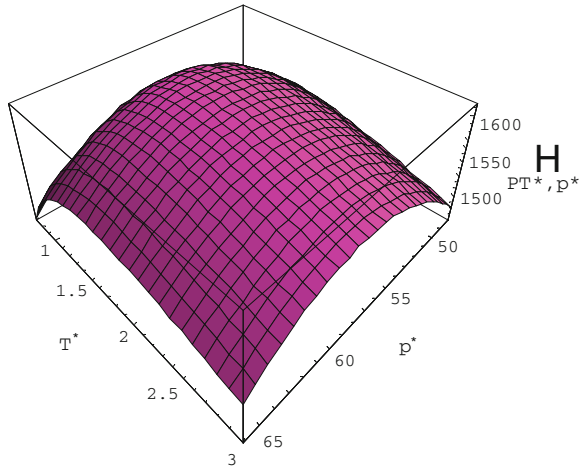
In this study, we have developed a partial backlogging inventory model for deteriorating items considering stock and price sensitive demand rate in crisp and fuzzy surroundings. A numerical example to prove that the optimal solution exists and is unique is provided and the sensitivity analysis with respect to system parameters is discussed. The concavity is also shown through the figure (Fig. 1).

## 2 Assumptions and Notations

The notations and basic assumptions of the model are as follows:

- (1) The demand rate is a function of stock and selling price considered as  $f(t) = (a + bQ(t) - p)$  where  $a > 0$ ,  $0 < b < 1$ ,  $a > b$  and  $p$  is selling price.

**Fig. 1** Concavity of the profit function



- (2) Holding cost  $h(t)$  per item per time-unit is time dependent and is assumed to be  $h(t) = h + \delta t$  where  $\delta > 0, h > 0$ .
- (3) Shortages are allowed and partially backlogged and rate is assumed to be  $1/(1 + \eta t)$ , which is a decreasing function of time,  $\eta \geq 0$ .
- (4) The deterioration rate is time-dependent.
- (5)  $T$  is the length of the cycle.
- (6) Replenishment is instantaneous and lead time is zero.
- (7) The order quantity in one cycle is  $Q$ .
- (8) The selling price per unit item is  $p$ .
- (9)  $A$  is the ordering cost per order.
- (10)  $c_1$  is the purchasing cost per unit per unit time.
- (11)  $c_2$  is the backordering cost per unit per unit time.
- (12)  $c_3$  is the opportunity cost per unit.
- (13)  $c_4$  is the deterioration cost per unit.
- (14)  $P(T, t_1, p)$  the total profit per unit time.
- (15) The deterioration of units follows the two parameter Weibull distribution (say)  $\theta(t) = \alpha\beta t^{\beta-1}$  where  $0 < \alpha < 1$  is the scale parameter and  $\beta > 0$  is the shape parameter.
- (16) During time  $t_1$ , inventory is depleted due to deterioration and demand of the item. At time  $t_1$  the inventory becomes zero and shortages start going on (Fig.2).

### 3 Mathematical Formulation and Solution

Let  $Q(t)$  be the inventory level at time  $t (0 \leq t \leq T)$ . During the time interval  $[0, t_1]$  inventory level decreases due to the combined effect of demand and deterioration

both and at  $t_1$  inventory level depletes up to zero. The differential equation to describe immediate state over  $[0, t_1]$  is given by

$$Q'(t) + \alpha\beta t^{\beta-1}Q(t) = -(a + bQ(t) - p) \quad 0 \leq t \leq t_1 \tag{1}$$

Again, during time interval  $[t_1, T]$  shortages starts occurring and at  $T$  there are maximum shortages, due to partial backordering some sales are lost. The differential equation to describe instant state over  $[t_1, T]$  is given by

$$Q'(t) = -\frac{(a - p)}{[1 + \eta(T - t)]} \quad t_1 \leq t \leq T \tag{2}$$

With condition  $Q(t_1) = 0$ . Solving Eqs. (1) and (2) and neglecting higher powers of  $\alpha$ , we get

$$Q(t) = (a-p) \left[ t_1 - t + \frac{b}{2}(t_1^2 - t^2) + \frac{\alpha}{(\beta + 1)}(t_1^{\beta+1} - t^{\beta+1}) \right] e^{-bt - \alpha t^\beta} \quad 0 \leq t \leq t_1 \tag{3}$$

$$Q(t) = \frac{(a - p)}{\eta} [\log 1 + \eta(T - t) - \log 1 + \eta(T - t_1)] t_1 \leq t \leq T \tag{4}$$

At time  $t = 0$  inventory level is  $Q(0)$  and is given by

$$Q(0) = (a - p) \left( t_1 + \frac{bt_1^2}{2} + \frac{\alpha t_1^{\beta+1}}{\beta + 1} \right)$$

At time  $T$  maximum shortages ( $Q_1$ ) occurs and is given by

$$Q_1 = \frac{(a - p)}{\eta} [\log \{1 + \eta(T - t_1)\}]$$

The order quantity is  $Q$  and is given by

$$Q = (a - p) \left( t_1 + \frac{bt_1^2}{2} + \frac{\alpha t_1^{\beta+1}}{\beta + 1} + \frac{1}{\eta} \log (1 + \eta(T - t_1)) \right) \tag{5}$$

The purchasing cost is

$$PC = c_1(a - p) \left( t_1 + \frac{bt_1^2}{2} + \frac{\alpha t_1^{\beta+1}}{\beta + 1} + \frac{1}{\eta} \log (1 + \eta(T - t_1)) \right) \tag{6}$$

Ordering cost is given by

$$OC = A \tag{7}$$

Holding cost during the period  $[0, t_1]$  is given by

$$\begin{aligned} \text{IHC} &= \int_0^{t_1} (h + \delta t) Q(t) dt \\ &= \int_0^{t_1} (h + \delta t)(a - p) \left[ t_1 - t + \frac{b}{2}(t_1^2 - t^2) + \frac{\alpha}{(\beta + 1)}(t_1^{\beta+1} - t^{\beta+1}) \right] \\ &\quad \times e^{-bt - \alpha t^\beta} dt \end{aligned} \tag{8}$$

Deterioration cost during the period  $[0, t_1]$  is given by

$$\text{DC} = c_4 \left\{ Q(0) - \int_0^{t_1} (a + bQ(t) - p) dt \right\} \tag{9}$$

Shortage cost due to backordered is

$$\begin{aligned} \text{BC} &= c_2 \int_{t_1}^T [-Q(t)] dt \\ &= -c_2 \int_{t_1}^T \frac{(a - p)}{\eta} [\log \{1 + \eta(T - t)\} - \log \{1 + \eta(T - t_1)\}] dt \end{aligned} \tag{10}$$

Lost sales cost due to lost sales is

$$\text{LS} = c_3(a - p) \int_{t_1}^T \left[ 1 - \frac{1}{(1 + \eta(T - t))} \right] dt \tag{11}$$

Sales revenue is given by

$$\text{SR} = p \int_0^{t_1} (a + bQ(t) - p) dt + p \int_{t_1}^T \frac{(a - p)}{[1 + \eta(T - t)]} dt \tag{12}$$

From Eqs. (6), (7), (8), (9), (10), (11), and (12) total profit per unit time is given by

$$P(T, t_1, p) = \frac{1}{T} \text{SR} - \text{OC} - \text{PC} - \text{IHC} - \text{BC} - \text{LS} - \text{DC} \tag{13}$$

Let  $t_1 = \gamma T, 0 < \gamma < 1$ . Hence we get the profit function is

$$P(T, p) = \frac{1}{T} [p(a - p)\gamma T + b(a - p)pK_1 - b(a - p)pK_2 + p(a - p)K_3 - A - c_1(a - p)K_4 - \frac{c_2(a - p)K_5}{\eta} - c_3(a - p)K_5 - c_4(a - p)K_6 - (a - p)K_7] \tag{14}$$

Where,

$$K_1 = \left( \gamma T + \frac{b\gamma^2 T^2}{2} + \frac{\alpha\gamma^{\beta+1} T^{\beta+1}}{\beta + 1} \right) \left( \gamma T - \frac{b\gamma^2 T^2}{2} - \frac{\alpha\gamma^{\beta+1} T^{\beta+1}}{\beta + 1} \right)$$

$$K_2 = \left[ \frac{\gamma^2 T^2}{2} + \frac{b\gamma^3 T^3}{6} + \frac{\alpha\gamma^{\beta+2} T^{\beta+2}}{(\beta + 1)(\beta + 2)} - b \left\{ \frac{\gamma^3 T^3}{3} + \frac{b\gamma^4 T^4}{8} + \frac{\alpha\gamma^{\beta+3} T^{\beta+3}}{(\beta + 1)(\beta + 3)} \right\} - \alpha \left\{ \frac{\gamma^{\beta+2} T^{\beta+2}}{\beta + 2} + \frac{b\gamma^{\beta+3} T^{\beta+3}}{2(\beta + 3)} + \frac{\alpha\gamma^{2\beta+2} T^{2\beta+2}}{2(\beta + 1)^2} \right\} \right]$$

$$K_3 = \frac{\{\log \{1 + \eta(T - \gamma T)\}\}}{\eta}, \quad K_4 = \left( \gamma T + \frac{b\gamma^2 T^2}{2} + \frac{\alpha\gamma^{\beta+1} T^{\beta+1}}{\beta + 1} + \frac{1}{\eta} \log (1 + \eta(T - \gamma T)) \right), \quad K_5 = \frac{1}{\eta} \left\{ \eta(T - \gamma T) - \log (1 + \eta(T - \gamma T)) \right\},$$

$$K_6 = \left( \frac{b\gamma^2 T^2}{2} + \frac{\alpha\gamma^{\beta+1} T^{\beta+1}}{\beta + 1} - b \left( \frac{\gamma^2 T^2}{2} + \frac{b\gamma^3 T^3}{6} - \frac{b^2\gamma^4 T^4}{8} - \frac{2\alpha\gamma^{\beta+2} T^{\beta+2}}{(\beta + 1)(\beta + 2)} - \frac{b\alpha\gamma^{\beta+3} T^{\beta+3}}{2(\beta + 1)} - \frac{\alpha^2\gamma^{2\beta+2} T^{2\beta+2}}{2(\beta + 1)^2} \right) \right)$$

$$K_7 = \left\{ \frac{h\gamma^2 T^2}{2} + \frac{\delta\gamma^3 T^3}{6} + \frac{bh\gamma^3 T^3}{6} + \frac{b\delta\gamma^4 T^4}{24} - \frac{b^2 h\gamma^4 T^4}{8} - \frac{b^2 \delta\gamma^5 T^5}{15} + \frac{\alpha h\gamma^{\beta+2} T^{\beta+2}}{\beta + 2} - \frac{\alpha h\gamma^{\beta+2} T^{\beta+2}}{(\beta + 1)(\beta + 2)} + \frac{3\alpha\delta\gamma^{\beta+3} T^{\beta+3}}{2(\beta + 3)} - \frac{\alpha b h\gamma^{\beta+3} T^{\beta+3}}{2(\beta + 1)} - \frac{\alpha\delta\gamma^{\beta+3} T^{\beta+3}}{(\beta + 2)} + \frac{\alpha\delta b\gamma^{\beta+4} T^{\beta+4}}{6(\beta + 4)} - \frac{\alpha\delta b\gamma^{\beta+4} T^{\beta+4}}{2(\beta + 2)} - \frac{\alpha^2 h\gamma^{2\beta+2} T^{2\beta+2}}{2(\beta + 1)^2} - \frac{\alpha^2 \delta\gamma^{2\beta+3} T^{2\beta+3}}{(\beta + 2)(2\beta + 3)} \right\}$$

Our objective is to maximize the profit function  $P(T, p)$ . The necessary conditions for maximizing the profit are

$$\frac{\partial P(T, p)}{\partial T} = 0 \quad \text{and} \quad \frac{\partial P(T, p)}{\partial p} = 0$$

Using the software Mathematica-8.0, from these two equations, we can determine the optimum values of  $T^*$  and  $p^*$  simultaneously and the optimal value  $P^*(T^*, p^*)$  of the average net profit can be determined by (14) provided they satisfy the sufficiency conditions for maximizing  $P^*(T^*, p^*)$  are

$$\frac{\partial^2 P(T, p)}{\partial T^2} < 0, \frac{\partial^2 P(T, p)}{\partial p^2} < 0 \text{ and } \frac{\partial^2 P(T, p)}{\partial T^2} \frac{\partial^2 P(T, p)}{\partial p^2} - \left( \frac{\partial^2 P(T, p)}{\partial T \partial p} \right)^2 > 0$$

### 4 Numerical Example

To illustrate the theory of the model, we consider the following data on the basis of the previous study.

$A = 200, a = 100, b = 0.02, c_1 = 12, \gamma = 0.6, c_2 = 8, c_3 = 15, c_4 = 0.4, \alpha = 0.1, h = 0.6, \beta = 0.01, \eta = 0.5, \delta = 0.02.$

Based on these input data, the findings are as follows:  $p^* = 57.2434, t_1^* = 0.896826, Q^* = 64.8475, T^* = 1.49471$  and  $P^*(T^*, p^*) = 1612.65.$

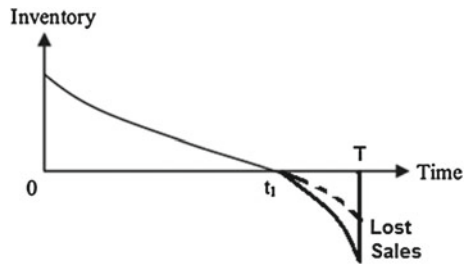
### 5 Sensitivity Analysis

See Table 1.

### 6 Fuzzy Mathematical model

In this study, we consider  $a, A, c_1, c_2, c_3$  and  $c_4$  as fuzzy numbers, i.e.,  $\tilde{a}, \tilde{A}, \tilde{c}_1, \tilde{c}_2, \tilde{c}_3$  and  $\tilde{c}_4$ . Then  $\tilde{P}(T, P)$  is regarded as the estimate of total profit per unit time in the

Fig. 2 Graphical representation of the inventory system





**Table 1** Sensitivity analysis is performed by changing (increasing or decreasing) the parameters by 10 and 20% and considering one parameter at a time, keeping the left over parameters at their original values

Changing parameter	% change in system	Change in $T^*$	Change in $p^*$	Change in $t_1^*$	Change in $Q^*$	Change in $P^*(T^*, p^*)$
A	-20	1.30930	57.1406	0.785580	53.1966	1641.20
	-10	1.40364	57.1932	0.842184	61.1014	1626.45
	+10	1.58302	57.2914	0.949812	68.4592	1599.65
	+20	1.66899	57.3376	1.001390	71.9558	1587.35
a	-20	1.89826	47.4582	1.138960	62.1062	896.308
	-10	1.67136	52.3388	1.002820	63.6073	1229.32
	+10	1.35289	62.1650	0.811734	65.8912	2046.22
	+20	1.23631	67.0994	0.741786	66.7825	2529.98
b	-20	1.48084	57.2373	0.888504	64.2087	1610.57
	-10	1.48771	57.2403	0.892626	64.5252	1611.61
	+10	1.50184	57.2464	0.901104	65.1760	1613.70
	+20	1.50910	57.2496	0.905460	65.5101	1614.76
c <sub>1</sub>	-20	1.45761	55.9485	0.874566	65.2108	1718.40
	-10	1.47591	56.5958	0.885546	65.0308	1665.12
	+10	1.51403	57.8912	0.908418	64.6609	1561.00
	+20	1.53389	58.5394	0.920334	64.4704	1510.15
c <sub>2</sub>	-20	1.53379	57.1790	0.920274	66.5816	1619.58
	-10	1.51388	57.2115	0.908328	65.6983	1616.09
	+10	1.47623	57.2747	0.885738	64.0271	1609.25
	+20	1.45842	57.3054	0.875052	63.2361	1605.88
c <sub>3</sub>	-20	1.53126	57.1831	0.918756	66.4694	1619.14
	-10	1.51266	57.2135	0.907596	65.6442	1615.88
	+10	1.47737	57.2727	0.886422	64.0778	1609.46
	+20	1.46061	57.3016	0.876366	63.3334	1606.30
α	-20	1.49451	57.1739	0.896706	64.1849	1618.36
	-10	1.49461	57.2086	0.896766	64.5166	1615.50
	+10	1.49480	57.2781	0.896880	65.1776	1609.80
	+20	1.49488	57.3128	0.896928	65.5067	1606.95
h	-20	1.50387	57.2314	0.902322	65.2491	1614.03
	-10	1.49926	57.2374	0.899556	65.0318	1613.34
	+10	1.49020	57.2493	0.894120	64.6499	1611.97
	+20	1.48574	57.2552	0.891444	64.4543	1611.28

(continued)

fuzzy sense. In this study, we considered the signed distance method as proposed by Chang [3].

$$\tilde{a} = (a - \Delta_1, a, a + \Delta_2) \text{ where } 0 < \Delta_1 < a \text{ and } \Delta_1 \Delta_2 > 0, \tilde{A} = (A - \Delta_3, A, A + \Delta_4) \text{ where } 0 < \Delta_3 < A \text{ and } \Delta_3 \Delta_4 > 0.$$

$$\tilde{c}_1 = (c_1 - \Delta_5, c_1, c_1 + \Delta_6) \text{ where } 0 < \Delta_5 < c_1 \text{ and } \Delta_5 \Delta_6 > 0, \tilde{c}_2 = (c_2 - \Delta_7, c_2, c_2 + \Delta_8) \text{ where } 0 < \Delta_7 < c_2 \text{ and } \Delta_7 \Delta_8 > 0.$$

**Table 1** (continued)

Changing parameter	% change in system	Change in $T^*$	Change in $p^*$	Change in $t_1^*$	Change in $Q^*$	Change in $P^*(T^*, p^*)$
$\eta$	-20	1.59373	57.2295	0.956238	69.6239	1634.32
	-10	1.54094	57.2358	0.924564	67.0794	1623.19
	+10	1.45381	57.2518	0.872286	62.8699	1602.62
	+20	1.41731	57.2609	0.850386	61.1021	1593.04

$\tilde{c}_3 = c_3 - \Delta_9, c_3, c_3 + \Delta_{10}$  where  $0 < \Delta_9 < c_3$  and  $\Delta_9 \Delta_{10} > 0, \tilde{c}_4 = c_4 - \Delta_{11}, c_4, c_4 + \Delta_{12}$  where  $0 < \Delta_{11} < c_4$  and  $\Delta_{11} \Delta_{12} > 0$ .

And the signed distance of  $\tilde{a}$  to  $\tilde{0}$  is given by the relation  $d(\tilde{a}, \tilde{0}) = a + 1/4(\Delta_2 - \Delta_1)$  where  $d(\tilde{a}, \tilde{0}) > 0$  and  $d(\tilde{a}, \tilde{0}) \in [a - \Delta_1, a + \Delta_2]$ . Similarly, for other parameters signed distance can be defined as above.

Now, by the fuzzy triangular rule fuzzy total profit per unit is  $FP(\tilde{a}, \tilde{A}, \tilde{c}_1, \tilde{c}_2, \tilde{c}_3, \tilde{c}_4) = (F_1, F_2, F_3)$ .

And  $F_1, F_2, F_3$  are obtained as

$$F_1 = \frac{1}{T} [p(a - \Delta_1 - p)\gamma T + b(a - \Delta_1 - p)pK_1 - b(a + \Delta_2 - p)pK_2 + p(a - \Delta_1 - p)K_3 - (A + \Delta_4) - (c_1 + \Delta_6)(a + \Delta_2 - p)K_3 - \frac{(c_2 + \Delta_8)(a + \Delta_2 - p)K_5}{\eta} - (c_3 + \Delta_{10})(a + \Delta_2 - p)K_5 - (c_4 + \Delta_{12})(a + \Delta_2 - p)K_6 - (a + \Delta_2 - p)K_7] \tag{15}$$

$$F_2 = \frac{1}{T} [p(a - p)\gamma T + b(a - p)pK_1 - b(a - p)pK_2 + p(a - p)K_3 - A - c_1(a - p)K_4 - \frac{c_2(a - p)K_5}{\eta} - c_3(a - p)K_5 - c_4(a - p)K_6 - (a - p)K_7] \tag{16}$$

$$F_3 = \frac{1}{T} [p(a + \Delta_2 - p)\gamma T + b(a + \Delta_2 - p)pK_1 - b(a - \Delta_1 - p)pK_2 + p(a + \Delta_2 - p)K_3 - (A - \Delta_3) - (c_1 - \Delta_5)(a - \Delta_1 - p)K_4 - \frac{(c_2 - \Delta_7)(a - \Delta_1 - p)K_5}{\eta} - (c_3 - \Delta_9)(a - \Delta_1 - p)K_5 - (c_4 - \Delta_{11})(a - \Delta_1 - p)K_6 - (a - \Delta_1 - p)K_7] \tag{17}$$

Now, defuzzified average profit using the signed distance method is given by

$$\tilde{P}(T, p) = (F_1 + 2F_2 + F_3)/4 \tag{18}$$

Also, the defuzzified order quantity is  $Q$  and is given by

$$Q = \left( a + \frac{(\Delta_2 - \Delta_1)}{4} - p \right) \left( t_1 + \frac{bt_1^2}{2} + \frac{\alpha t_1^{\beta+1}}{\beta+1} + \frac{1}{\eta} \log(1 + \eta(T - t_1)) \right) \tag{19}$$

The necessary conditions for maximizing the average profit are  $\partial \tilde{P}(T, p) / \partial T = 0$  and  $\partial \tilde{P}(T, p) / \partial p = 0$ .

Using the software Mathematica-8.0, from the above two equations, the optimum values of  $\tilde{T}$  and  $\tilde{p}$  can be determined simultaneously and the optimal value of the average net profit ( $\tilde{P}(T, p)$ ) can be obtained by (18).

### 7 Numerical Example

$A = 200, \Delta_3 = 10, \Delta_4 = 20, a = 100, \Delta_1 = 5, \Delta_2 = 10, b = 0.02, c_1 = 12, \Delta_5 = 0.60, \Delta_6 = 1.2, c_2 = 8, \Delta_7 = 0.4, \Delta_8 = 0.8, c_3 = 15, \Delta_9 = 0.75, \Delta_{10} = 1.5, c_4 = 0.4, \Delta_{11} = 0.02, \Delta_{12} = 0.04, \alpha = 0.1, \beta = 0.01, \gamma = 0.6, h = 0.6, \eta = 0.5, \delta = 0.02.$

Based on these input data, the findings are as follows:

$p_f^* = 58.0034, T_f^* = 1.48131, t_{1f}^* = 0.888786, Q_f^* = 65.0234$  and  $\tilde{P}(p_f^*, T_f^*) = 1646.53.$

### 8 Sensitivity Analysis

See Table 2.

#### 8.1 Observations

- (1) When  $\Delta_1 > \Delta_2$ , i.e., demand parameter  $\mathbf{a}$  decreases then the optimal profit  $\tilde{P}(p_f^*, T_f^*)$  decreases and when  $\Delta_1 < \Delta_2$  i.e.,  $\mathbf{a}$  increases then  $\tilde{P}(p_f^*, T_f^*)$  increases.
- (2) When  $\Delta_3 > \Delta_4$ , i.e., ordering cost  $\mathbf{A}$  decreases then  $\tilde{P}(p_f^*, T_f^*)$  slightly increases and when  $\Delta_3 < \Delta_4$  i.e.,  $\mathbf{A}$  increases then profit decreases. Similarly, profit increases and decreases as  $\Delta_5 > \Delta_6, \Delta_7 > \Delta_8, \Delta_9 > \Delta_{10}$  and  $\Delta_5 < \Delta_6, \Delta_7 < \Delta_8, \Delta_9 < \Delta_{10}$  respectively.
- (3) There is a small decline in profit  $\tilde{P}(p_f^*, T_f^*)$ , as  $\Delta_{11} < \Delta_{12}$  i.e., deterioration cost  $c_4$  increases and profit increases as  $\Delta_{11} > \Delta_{12}$  i.e.,  $c_4$  decreases.

**Table 2** Sensitivity table with respect to system parameters

Changing parameter	Change in parameter	Change in $T_f^*$	Change in $p_f^*$	Change in $t_{1f}^*$	Change in $Q_f^*$	Change in $\tilde{P}(p_f^*, T_f^*)$
$\Delta_1, \Delta_2$	(40, 20)	1.57895	54.9325	0.947370	64.0666	1387.46
	(10, 5)	1.52093	56.7755	0.912558	64.7378	1545.21
	(5, 10)	1.48131	58.0034	0.888786	65.0234	1646.53
	(20, 40)	1.42152	59.8449	0.852912	65.2461	1792.81
$\Delta_3, \Delta_4$	(80, 40)	1.42603	57.9725	0.855618	62.7247	1655.13
	(20, 10)	1.45933	57.9912	0.875598	64.1103	1649.93
	(10, 20)	1.48131	58.0034	0.888786	65.0234	1646.53
	(40, 80)	1.51398	58.0216	0.908388	66.3780	1641.53
$\Delta_5, \Delta_6$	(4.8, 2.4)	1.47188	57.5999	0.883128	65.2270	1670.29
	(1.2, 0.6)	1.47660	57.8415	0.885960	65.0666	1660.11
	(0.6, 1.2)	1.48131	58.0034	0.888786	65.0234	1646.53
	(2.4, 4.8)	1.49085	58.2477	0.894510	65.0577	1615.99
$\Delta_7, \Delta_8$	(3.3, 1.6)	1.49001	57.9809	0.894006	65.4258	1648.17
	(0.8, 0.4)	1.48605	57.9957	0.891630	65.2357	1647.42
	(0.4, 0.8)	1.48131	58.0034	0.888786	65.0234	1646.53
	(1.6, 3.3)	1.47002	58.0139	0.882012	64.5295	1644.42
$\Delta_9, \Delta_{10}$	(6, 3)	1.48900	57.9833	0.893400	65.3794	1647.98
	(1.5, 0.75)	1.48576	57.9961	0.891456	65.2228	1647.36
	(0.75, 1.5)	1.48131	58.0034	0.888786	65.0234	1646.53
	(3, 6)	1.47135	58.0124	0.882810	64.5881	1644.67
$\Delta_{11}, \Delta_{12}$	(0.16, 0.08)	1.48134	58.0018	0.888804	65.0271	1646.63
	(0.04, 0.02)	1.48133	58.0028	0.888798	65.0252	1646.59
	(0.02, 0.04)	1.48131	58.0034	0.888786	65.0234	1646.53
	(0.08, 0.16)	1.48128	58.0044	0.888768	65.0206	1646.41

## 9 Conclusion

In this study, the model is proposed in the following two senses: (1) crisp and (2) fuzzy. In fuzzy situation, demand rate, ordering cost, purchasing cost, deterioration cost, backordering cost, and opportunity cost are considered as triangular fuzzy numbers. It is assumed that the demand rate is a function of price and stock both, shortages are allowed and are partially backlogged. The proposed model is more practical as real life businesses are affected by the stock and price dependent demand. If there is a large pile of stock and a suitable selling price of the products is sustained in a business then it attracts the customers to buy more. In real life situations, all the shortages cannot be fully backlogged as some sales will be lost due to interruption of time, therefore partial backlogging is more realistic. In today’s market due to the impreciseness of the inventory costs and demand, it is more useful to consider them as fuzzy numbers since the business strategy will be able to face the upper and down conditions of the market. Moreover, from sensitivity table, it is observed that the model is enough stable toward the changes in the system parameters.

**Acknowledgments** The second author wish to thank to Council of Scientific and Industrial Research (New Delhi) for providing financial help in the form of JRF vide letter no. 08/017(0017)/2011-EMR-I.

## References

1. Zadeh, L.: Fuzzy sets. *Inf. Control* **8**, 338–353 (1965)
2. Park, K.S.: Fuzzy-set theoretic interpretation of economic order quantity. *IEEE Trans. Syst. Man Cybern. SMC-17*, 1082–1084 (1987)
3. Chang, H.C.: An application of fuzzy sets theory to the EOQ model with imperfect quality items. *Comput. Oper. Res.* **31**, 2079–2092 (2004)
4. Wang, J., Fu, Q.L., Zeng, Y.R.: Continuous review inventory models with a mixture of back-orders and lost sales under fuzzy demand and different decision situations. *Expert Syst. Appl.* **39**, 4181–4189 (2012)
5. Ghare, P.M., Schrader, G.F.: A model for exponential decaying inventory. *J. Ind. Eng.* **14**, 238–243 (1963)
6. Covert, R.P., Philip, G.C.: An EOQ model for items with Weibull distribution deteriorating. *AIIE Trans.* **5**, 323–326 (1973)
7. Raffat, F.: Survey of literature on continuously deteriorating inventory model. *Eur. J. Oper. Res. Soc.* **42**, 27–37 (1991)
8. Teng, J.T., Chang, H.J., Dye, C.Y., Hung, C.H.: An optimal replenishment policy for deteriorating items with time-varying demand and partial backlogging. *Oper. Res. Lett.* **30**, 387–393 (2002)
9. Bakker, M., Riezebos, J., Teunter, R.H.: Review of inventory systems with deterioration since 2001. *Teunter.* **221**, 275–284 (2012)
10. Park, K.S.: Inventory models with partial backorders. *Int. J. Syst. Sci.* **13**, 1313–1317 (1982)
11. Wee, H.M.: A deterministic lot-size inventory model for deteriorating items with shortages and a declining market. *Comput. Oper. Res.* **22**, 345–356 (1995)
12. Singh, S.R., Singh, T.J.: Perishable inventory model with quadratic demand, partial backlogging and permissible delay in payments. *Int. Rev. Pure Appl. Math.* **1**, 53–66 (2008)
13. Hsieh, T.P., Dye, C.Y., Ouyang, L.Y.: Optimal lot size for an item with partial backlogging rate when demand is stimulated by inventory above a certain stock level. *Math. Comput. Model.* **51**, 13–32 (2010)
14. Gupta, R., Vrat, P.: Inventory model with multi-items under constraint systems for stock dependent consumption rate. *Oper. Res.* **24**, 41–42 (1986)
15. Mandal, B.N., Phaujdar, S.: An inventory model for deteriorating items and stock-dependent consumption rate. *J. Oper. Res. Soc.* **40**, 483–488 (1989)
16. Ray, J., Goswami, A., Chaudhuri, K.S.: On an inventory model with two levels of storage and stock-dependent demand rate. *Int. J. Syst. Sci.* **29**, 249–254 (1998)
17. Goyal, S.K., Giri, B.C.: The production-inventory problem of a product with time varying demand, production and deterioration rates. *Eur. J. Oper. Res.* **147**, 549–557 (2003)
18. Chang, C.T., Chen, Y.J., Tsai, T.R., Wu, S.J.: Inventory models with stock-and price dependent demand for deteriorating items based on limited shelf space. *Yugoslav J. Oper. Res.* **20**, 55–69 (2010)

# Efficient Protocol Prediction Algorithm for MANET Multimedia Transmission Under JF Periodic Dropping Attack

Avita Katal, Mohammad Wazid and R H Goudar

**Abstract** Mobile ad hoc network is prone to denial of service attack. Jellyfish is a new denial of service attack and is categorized as JF Reorder Attack, JF Periodic Dropping Attack, JF Delay Variance Attack. In JF Periodic Dropping Attack, intruder node intrudes into forwarding group and starts dropping packets periodically. Due to JF Periodic Dropping attack, the delay in the network increases and throughput decreases. In this paper a comparative performance analysis of three reactive routing protocols i.e. AODV, DSR and TORA used in mobile ad hoc network under JF Periodic Dropping attack is done. This work is specially done for multimedia transmission i.e. video and voice. If we have a mobile ad hoc network in which probability of occurrence of JF Periodic Dropping attack is high and also if it requires time efficient network multimedia service for information exchange then TORA protocol is to be chosen. If it requires high multimedia throughput and consistent service in the network then AODV protocol is recommended. An algorithm has been proposed depending upon the analysis done particularly for multimedia transmission in MANET which will help in choosing the best suited protocol for the required network parameters under JF Periodic Dropping attack.

**Keywords** JF periodic dropping attack · Multimedia transmission · AODV · DSR · TORA

---

A. Katal (✉) · M. Wazid · R. H. Goudar  
Department of CSE, Graphic Era University, Dehradun, India  
e-mail: avita207@gmail.com

M. Wazid  
e-mail: wazidkec2005@gmail.com

R. H. Goudar  
e-mail: rhgoudar@gmail.com

## 1 Introduction

An intruder can easily access mobile ad hoc network because of weak defense mechanism and high mobility of nodes. Multimedia transmission includes streaming of multimedia to an end user by the provider. It mainly includes voice and video transmission. MANET assailable to JF Periodic Dropping attack increases the end to end delay between selected packets in a flow with any lost packets being ignored. This is called Jitter which increases under the above mentioned attack leading to degradation in the quality of the media being transmitted. In this paper the impact of presence of JF Periodic Dropping attack on the performance of network transmitting multimedia is analyzed. Comparative analysis of the three routing protocols i.e. AODV, DSR and TORA used for the transmission of multimedia for various network parameters is done. Section 2 includes the literature review about different kinds of work done by various authors in area related to JellyFish attacks. The novelty of the proposed idea is discussed in Sect. 3. In Sect. 4 a brief introduction to JellyFish attack is given. The methodology and experiment design of this work is discussed in Sect. 5. Section 6 contains performance parameters and results. Section 7 includes the algorithm for protocol prediction designed on the basis of results obtained followed by conclusion, future work and application of the work done in Sect. 8.

## 2 Literature Review

Paper [1] discusses about techniques for resilience of denial of service attacks on a mobile ad hoc network focusing on JellyFish attacks. The throughput of network under JellyFish attacks introduced here is calculated. Techniques to protect MANET i.e. flow-based route access control (FRAC), Multi-Path Routing Source-Initiated Flow Routing, Sequence Numbers etc are discussed. In [2] authors calculate the performance of MANET under black hole attack using AODV routing protocol with HTTP traffic load. In [4] authors explain various attacks on a mobile ad hoc network corresponding to different MANET layers and they also discuss some available attack detection techniques. They give a brief idea about JellyFish attack. In [5] the performance of different routing protocols for multimedia data transmission over vehicular ad hoc networks is done. The focus was put on the performance evaluation metrics that were used in simulations. Three popular routing protocols were selected for the evaluation: two reactive (AODV, DSR) and one proactive (OLSR). In [6] authors develop an algorithm that detects the Jellyfish attack at a single node and that can be effectively deployed at all other nodes. A novel metric depending on reorder density is proposed and comparison table is given which shows the effectiveness of novel metric which helps protocol designers to develop the counter strategies for JF attack. The main objective of [7] is to analyze and compare the performance of Preemptive DSR and temporarily ordered routing algorithm (TORA). It discusses the effect of variation in number of nodes and average speed on protocol performance.

It concludes that PDSR outperforms TORA in terms of the number of MANET control packets used to maintain or erase routes. TORA is a better choice than PDSR for fast moving highly connected set of nodes. In [8] an attempt has been made to compare the performance of two prominent on demand reactive routing protocols for MANETs: ad hoc on demand distance vector (AODV), dynamic source routing (DSR) protocols. It concludes that if the MANET has to be setup for a small amount of time then AODV should be preferred due to low initial packet loss. If we have to use the MANET for a longer duration then both the protocols can be used, because after sometime both the protocols may have same ratio of packet delivering. But AODV have very good packet receiving ratio in comparison to DSR. In [10] the performance of DSR and TORA routing protocols is calculated using the OPNET simulator. It concludes that delay experienced with mobile nodes employing DSR routing is higher than that of fixed nodes. Delay experienced with fixed nodes employing TORA routing is higher than that of mobile nodes. In [12] authors discuss the most common types of attacks on MANET, namely Rushing attack, Blackhole attack, Neighbor attack and JellyFish attack. They simulate these attacks and calculate parameters such as Average end-to-end delay, Average throughput etc. In Paper [13] JellyFish and Black hole attacks are discussed. Authors calculate the impact of JF on the system performance i.e. Throughput etc. They introduce three factors: mobility, node density and system size and calculate the effect of these factors on fairness to receive packets under the presence of various number of JF attackers. They observe that the effect of mobility is more under the absence of JF attackers and fairness reduces when we increase mobility.

### **3 Problem Definition and Novelty**

Previously many authors have analyzed the performance of various MANET protocols for multimedia transmission. In this paper the performance analysis of the most popular reactive routing protocols in the multimedia transmission under JF Periodic Dropping attack is done followed by an algorithm used for selecting the best suited routing protocol for transmitting multimedia with the desire network parameters.

### **4 JellyFish Attack**

JellyFish attack is related to transport layer of MANET stack. The JF attacker disrupts the TCP connection which is established for communication. JellyFish (JF) attacker needs to intrude into forwarding group and then it delays data packets unnecessarily for some amount of time before forwarding them. Due to JF attack, high end to end delay takes place in the network. So the performance of network (i.e. throughput etc) decreases substantially. JF attacker disrupts the whole functionality of TCP, so performance of real time applications become worse. JF attack is further divided into



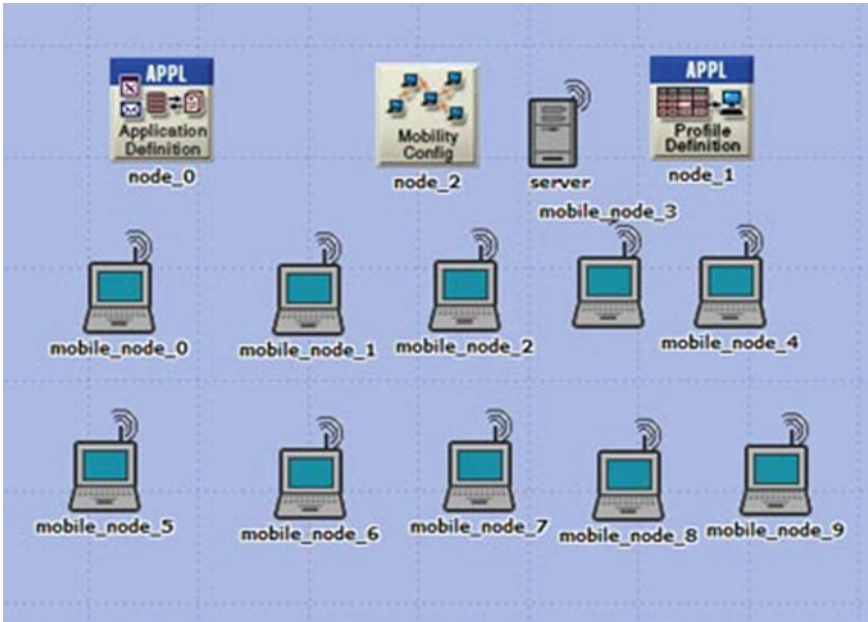


Fig. 1 MANET under normal flow

three categories- JF Reorder Attack, JF Periodic Dropping Attack, JF Delay Variance Attack.

### 4.1 JF Periodic Dropping Attack

In this attack the JF attackers drop all packets for a short duration of time. Thus JF nodes seem passive in nature and do not generate traffic themselves. JF nodes drop packets for only a small fraction of time due to dropping of packets the performance becomes worse [1].

## 5 Methodology and Experiment Design

For experimental purpose we simulate a mobile ad hoc network under JF Periodic Dropping attack for three reactive routing protocols i.e. AODV, DSR and TORA using Opnet modeler. We are using the following two simulation scenarios in this paper:

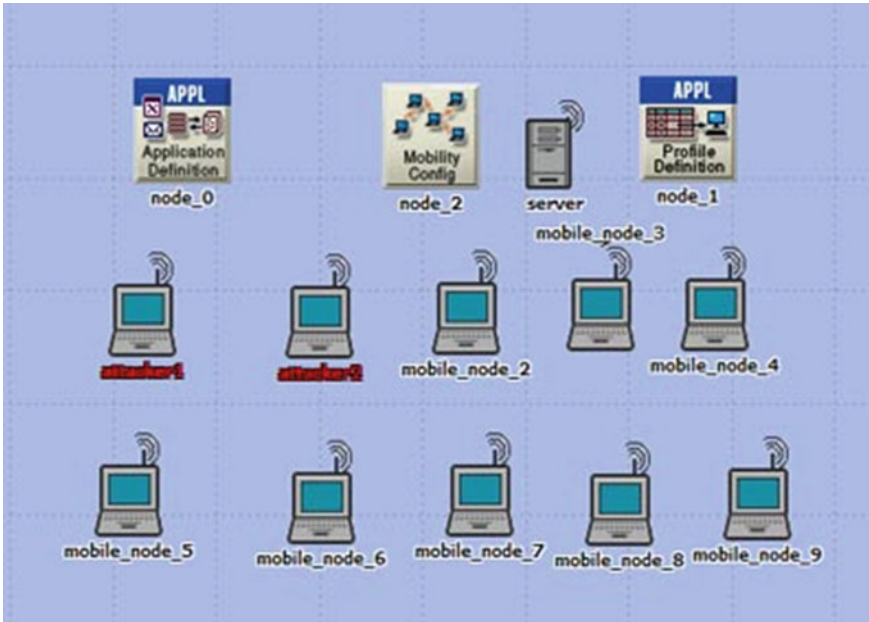


Fig. 2 MANET under jellyfish attack

In Fig. 1 we use 10 mobile nodes and build a scenario without any JF attacker showing a normal flow of traffic. In Fig. 2 we use 10 mobile nodes and build a scenario with two JF Periodic Dropping attackers. JF attackers are shown in red label i.e. attacker 1 and attacker 2. All scenarios are simulated using AODV, DSR and TORA protocols.

The experimental design setup is used to examine the performance of three reactive routing protocols under JF Periodic Dropping attack in MANET transmitting multimedia data.

### 5.1 Experiment Design Parameters

#### 5.1.1 Common Parameters

##### Implementations of JF Periodic Dropping Attack

The normal packet forwarding rate is 100,000 packets per second and simulation time is ten minutes. To simulate JF Periodic Dropping attack the time of periodic dropping is taken to five minutes. During other five minutes there is normal flow. Given two scenarios are simulated under routing protocols i.e. AODV, DSR and TORA (Table 1).

**Table 1** Common parameters used in simulation

Parameter	Value
Platform	Windows XP SP2
Simulator	Opnet modeler 14.5
Area	500 × 500 m (Fix)
Network size	10 nodes
Mobility model	20 m/s (Fix)
Traffic type	Video and Voice both
Simulation time	10 min
Address mode	Only IPv4
Ad Hoc routing protocol	AODV, DSR, TORA
AODV, DSR, TORA, TCP parameters	Default
JellyFish attackers	Zero attacker for normal flow (Scenario 1) Two attackers (Scenario 2)
Attacking scenario	For 5 min, normal flow For 5 min, flow under JF packet dropping
Packet size (bits)	Exponential (1024)

**Table 2** End-to-end delay and throughput

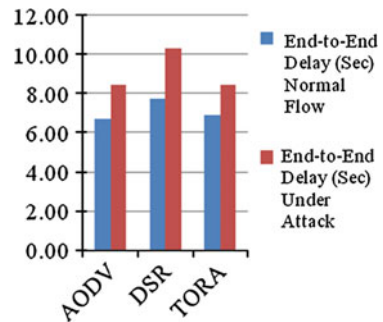
Parameters	End-to-end delay (s)		Throughput (bps)	
	Normal flow	Under attack	Normal flow	Under attack
AODV	6.72	8.47	51573.91	41517.39
DSR	7.74	10.32	25832.07	19263.31
TORA	6.87	8.47	21714.92	16903.32

### 5.2 Results

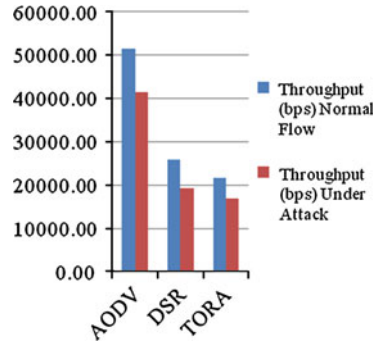
In simulation we take following statistics of the network: End-to-end Delay (msec), Throughput (bps).

Figure 3 shows end-to-end delay with normal flow (zero attackers) and also in the presence of JF attackers for all given three protocols. Figure 4 shows throughput

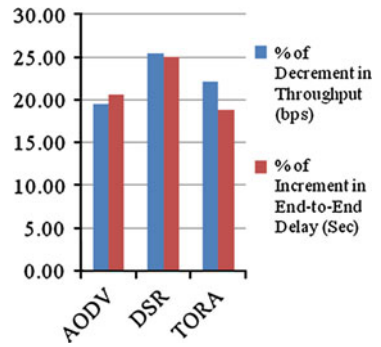
**Fig. 3** End-to-end delay



**Fig. 4** Throughput (bps)



**Fig. 5** Impact of JF periodic dropping attack



**Table 3** Impact of JF periodic dropping attack on end-to-end delay and throughput

Protocol	% of Decrement in throughput (bps)	% of Increment in end-to-end delay (Sec)
AODV	19.50	20.66
DSR	25.43	25.00
TORA	22.16	18.89

(bps) with normal flow (zero attackers) and also in the presence of JF attackers for all given three protocols.

Figure 5 shows impact of JF Periodic Dropping attack on end-to-end delay and throughput for all given three protocols.

## 6 Protocol Prediction Algorithm

```

enum protocol set => {AODV,TORA,DSR}
enum service set => {Throughput Efficient, In Time}
if service = Throughput Efficient then
    
```

```

select_protocol = AODV
otherwise if service = In Time then
  select_protocol = TORA
otherwise
  select_protocol = DSR

```

#### *Complexity Analysis:*

The complexity of protocol prediction algorithm comes to be  $\Theta(1)$  in combination with the complexity of AODV, TORA or DSR. We can say the complexity of the above algorithm comes in the order of the complexity of the AODV, TORA or DSR.

The above algorithm designed is basically used for choosing the appropriate reactive routing protocol out of the set of three protocols i.e. AODV, DSR and TORA for efficient multimedia transmission depending upon the network parameter requirements that is throughput efficiency and in time delivery.

## 7 Key Findings

Here, we try to evaluate the performance of three reactive protocols i.e. AODV, DSR and TORA which are implemented in mobile ad hoc network under the presence of JF Periodic Dropping attack for multimedia transmission. Some of the observations are as:

- The performance of DSR is worst for both the network parameters i.e. throughput and delay in multimedia transmission (as shown in Table 2).
- In multimedia transmission a throughput efficient service is provided by AODV protocol as compared to DSR and TORA. The % of decrement in throughput for AODV is 19.50 as compared to DSR and TORA which are having a decrement of 25.43 and 22.16 respectively (as shown in Table 3).
- Multimedia time demanding service must use TORA protocol as TORA proves to be more efficient under JF Periodic Dropping attack with a % increment of end-to-end delay of 18.89 as compared to AODV and DSR which are having 20.66 and 25.00 respectively (as shown in Table 3).

## 8 Conclusion

If we have a mobile ad hoc network in which probability of occurrence of JF Periodic Dropping attack is high and we want a good time efficient network multimedia service then we have to choose TORA protocol whereas good throughput multimedia

service should make use of AODV protocol (as shown in Table 3). Depending upon these results the protocol prediction algorithm is proposed which efficiently chooses the required protocol for multimedia transmission.

Here we take mobility and system size as constant, if we change these two factors then performance may vary. So this work can be further extended to calculate the performance of MANET under varying mobility and system size.

There are certain applications which can bear the time inefficiency but require high throughput service as in case of virtual classrooms where the student can attend lectures even when they are not sitting in the campus class whereas in case of Warfield the time efficiency would be important as compared to throughput. Depending upon these different requirements for different scenarios we recommend AODV for virtual classrooms and TORA for Warfield applications.

## References

1. Begum, S. A., Mohan, L., Ranjitha, B.: Techniques for resilience of denial of service attacks in mobile ad hoc networks. In: Proceedings published by International Journal of Electronics Communication and Computer Engineering, Vol. 3(1), NCRTCST, ISSN 2249–071X National Conference on Research Trends in Computer Science and Technology (2012)
2. Barkhodia, E., Singh, P., Walia, G. K.: Performance analysis of AODV using HTTP traffic under Black Hole Attack in MANET. *Comput. Sci. Eng. Int. J. (CSEIJ)*. **2**(3), (2012)
3. Jan, V. M., Welch, I., Seah, W. K. G: Security threats and solutions in MANETs: A case study using AODV and SAODV. *Elsevier J. Netw. Comput. Appl.* **35**, 1249–1259 (2012)
4. Wazid, M., Singh, R. K., Goudar, R. H.: A survey of attacks happened at different layers of mobile ad-hoc network and some available detection techniques. In: Proceedings published by International Journal of Computer Applications (IJCA) International Conference on Computer Communication and Networks CSI- COMNET, Hawaii, December (2011)
5. Adam, G., Kapoulas, V., Bouras, C., Kioumourtzis, G., Gkamas, A., Tavoularis. N.: Performance evaluation of routing protocols for multimedia transmission over mobile ad hoc networks. In: IEEE International Conference on Wireless and Mobile Networking Conference (WMNC), (2011)
6. Jayasingh, B. B., Swathi, B.: A novel metric for detection of jellyfish reorder attack on ad hoc network. *BVICAM'S Int. J. Inf. Technol. (BIJT)* **2**(1), ISSN 0973–5658 (2010)
7. Ramesh, V., Subbaiah, P., Koteswar Rao, N., Subhashini, N., Narayana.D.: Performance comparison and analysis of preemptive-DSR and TORA. *Int. J. Ad hoc, Sens. and Ubiquitous Comput. (IJASUC)* **1**(4) (2010)
8. Thakare, A. N., Joshi, M. Y.: Performance analysis of AODV & DSR routing protocol in mobile ad hoc networks. *IJCA Special Issue on Mobile Ad-hoc Networks MANETs* (2010)
9. Cai, J., Yi, P., Tian, Y., Zhou, Y., Liu, N.: The simulation and comparison of routing attacks on DSR protocol. In: IEEE International Conference on Wireless Communications, Networking and Mobile Computing (WiCom), Beijing, September (2009)
10. Amer, S. H., Hamilton, J. A.: DSR and TORA in fixed and mobile wireless networks. In: Proceedings of ACM-SE, ACM, Auburn, March (2008)
11. Alshanyour, A. M., Baroudi, U.: Bypass AODV: improving performance of ad hoc on-demand distance vector (AODV) routing protocol in wireless ad hoc networks. In: Proceedings of ACM Ambi-sys, ACM Digital Library, Quebec city, 11–14 February (2008)

12. Nguyen, H. L., Nguyen, U. T.: A study of different types of attacks on multicast in mobile ad hoc networks. Elsevier J. Ad Hoc Netw. **6**, 32–46 (2008)
13. Aad, I., Hubaux, J.-P., Knightly, E. W.: Denial of service resilience in ad hoc networks. In: Proceedings of ACM MobiCom, Philadelphia, Sept. 26–Oct.1 (2004)

# New Placement Strategy for Buffers in Critical Chain

Vibha Saihjpal and S. B. Singh

**Abstract** With the introduction of Critical chain by Goldratt in 1997, there has been a lot of research in the field of resource constraint project scheduling problems (RCPSP) and Buffer Sizing techniques. This paper suggests a Buffer management technique which aims at reducing the make span time yet maintaining the stability of the project. In the theory of CCPM it is suggested to reduce the duration of all the activities by half to remove the excess safety time in each activity. The trimmed duration is collected and made available at the end of the project in the form of project buffer which could be used if the project gets delayed. Another buffer called the feeding buffer is added whenever a noncritical chain joins a critical chain. This increases the project duration if the slack of the last activity in the feeding chain is smaller than the feeding buffer. In such cases, this paper suggests the division of the project buffer into parts, fitting each part at the junction of critical and noncritical chains so that the delay occurred because of addition of feeding buffer can be utilized and the duration of project buffer is shortened. The use of the proposed technique has reduced the project duration by a significant value.

**Keywords** Buffer · Feeding buffer · Project buffer · Buffer sizing technique · CCPM

---

V. Saihjpal (✉)  
University College, Chunni Kalan, Punjab, India  
e-mail: saihjpal.vibha@gmail.com

S. B. Singh  
Department of Mathematics, Punjabi University, Patiala, India  
e-mail: sbsingh69@yahoo.com



# 1 Introduction

In most simple terms, project scheduling means the planned dates for performing activities and the planned dates for meeting milestones. It is a plan of procedure, usually written for a proposed objective, specially, with reference to the sequence of activities satisfying certain constraints such as the precedence relations and resource constraints and time allotted for each activity or operation necessary to its completion. PERT and CPM have been the most basic tools used for project scheduling for years. Considering the probabilistic time durations, the longest path (called the critical path) in the network of activities is determined which marks the project duration. The critical path however does not recognize the resource constraints. Considering the role of resource constraints in a practical project schedule, Goldratt in 1997 introduced the concept of critical chain project management (CCPM).

## 1.1 PERT/CPM

PERT was devised in 1958 for the POLARIS missile program by the Program Evaluation Branch of the Special Projects office of the U.S. Navy, helped by the Lockheed Missile Systems division and the Consultant firm of Booz-Allen and Hamilton [1]. One key element to PERT's application is that three estimates are required because of the element of uncertainty and to provide time frames for the PERT network. These three estimates are classed as optimistic, most likely and pessimistic time durations, and are predicted for each activity of the overall project. Generally, the optimistic time estimate is the minimum time the activity would take, considering that all goes right the first time. The reverse is the pessimistic estimate, or maximum time estimate for completing the activity. This estimate takes into account Murphy's Law, i.e., whatever can go wrong will and all possible negative factors are considered when computing this estimate. The third is the most likely estimate, or the normal or realistic time an activity requires. It lies anywhere in the interval  $(a, b)$ , where  $a$  represents the optimistic time and  $b$  represents the pessimistic time. Two other elements that comprise the PERT networks are the path, or critical path, and slack time. The critical path is a combination of the critical activities, i.e., the activities which if delayed, would delay the project.

The primary goal of a CPM analysis of a project is the determination of the critical path, which determines the completion time of a project [2, 3]. However, the schedule defined by CPM does not consider the resource constraints, hence giving rise to the development of the theory of critical chain.

## 1.2 CCPM

In 1997, Dr. Eliyahu Goldratt introduced a new significant approach to project management, in over 30 years, with the publication of his best selling business novel, Critical Chain [4]. Critical chain is the theory of constraints (TOC) philosophy

for project management which is considered an innovation that would be useful to organizations [5, 6]. Goldratt's approach introduced a new era in the world of project management by merging, for the first time, both the human side and the algorithmic methodology side of project management in a unified discipline. It considers factors such as

- Parkinson's Law: Work expands to fill the available time.
- Student Syndrome: People start to work in full fledge when deadline is near.
- Bad Multitasking: Bad multitasking can delay start of the successor tasks.

As the activity duration is defined, the project manager tends to keep some safety time in the duration of each activity which increases the project duration unnecessarily and as suggested by Parkinson's Law, each activity consumes all the duration allotted to it. Considering this, it is suggested in CCPM to cut the duration in every activity so as to minimize this wastage. However, buffers are added at specific stages of the project so that any delay in any of the activities does not affect the total project duration. Various methods have been proposed to manage buffer sizing. The C&P, i.e., Cut and Paste Method and RSE, i.e., Root Square Error Method are the most traditional ones. Xie et al. suggested improved root square error (IRSE), a method based on critical chain theory for buffer sizing majorly suitable for software projects and the results claim to have a direct effect in shortening the project duration [7]. Tukel et al. suggested two methods for determining feeding buffers, one incorporates resource tightness while the other uses network complexity resulting in smaller buffer sizes [8]. Fuzzy numbers have also been used in methods to determine the project buffers [9]. It has been observed that through Critical Chain Project Management, projects are completed in significantly shorter time than traditional Critical Path project management techniques. Importantly, Critical Chain Project Management is also simpler to use and requires less work for the project team in both the planning and tracking phases of project [10]. Bevilacqua et al. applied the Theory of Constraints and Risk Assessment to develop a prioritization method for Work Packages, using the critical chain concept and concluded that the proposed method allowed the company to maximize the quality and safety of work and minimized the turnaround time and cost [11].

Another important aspect of CCPM is to start each activity at the latest possible starting time. This helps the project manager gain experience on the project till the time the activity starts and also reduces the WIP time. However it is argued that this makes each activity critical. But the presence of buffers compensates any delays in the activity completion. The following steps are used to modify the critical path into the critical chain [8].

- Step 1. Reduce duration of each activity by 50%.
- Step 2. Push all the tasks to as late as possible subject to the precedence relations. ( i.e., determine the late finish network).
- Step 3. Eliminate the resource constraints by resequencing the tasks. Though Goldratt has not offered any specific procedure to resolve resource constraints this has given rise to a research problem marked as RCPSP (Resource

constraint Project Scheduling Problem) and a lot of research has been done on these problems.

Step 4. Identify the critical chain as the longest chain of dependent events for feasible schedule that was identified in step 3.

There could be ties in longest chain, in that case an arbitrary choice can be made between them [12].

Step 5. Add the project buffer to the end of the critical chain.

Step 6. Add the feeding buffers wherever a noncritical chain feeds the critical chain and offset the tasks on the feeding chain by the size of the buffer.

## 2 Buffers

The reduction of activity durations by 50% as suggested by Goldratt is compensated by the insertion of buffers at various stages of the project. A buffer is a cushion provided at different stages of a project schedule so as to absorb the delays that occur during the execution of the project up to a maximum possible extent. In the development of the project plan the duration of each activity will be coupled with a lot of security time. Even if a task is ahead of schedule, the security time will not accumulate to the next activity. This problem is tackled by the use of buffers. CCPM suggests that duration of each activity is halved and the duration trimmed from each activity is accumulated and added at the end of the project as project buffer and at various other stages in the form of feeding buffer and resource buffer. A project buffer is inserted to protect the project delivery date. Resource buffers are inserted at every point where work passes from one resource to another on the critical chain. Feeding buffers are inserted to protect the critical chain from delays in the noncritical chain. [13] suggested that the project buffer size is the more appropriate robustness measure regardless of the network complexity.

## 3 The Placing of Buffers

This paper suggests that whenever the project duration is forced ahead because of the insertion of a feeding buffer (Fig. 1b), there is a void or a gap created in the critical chain. In such a case a part of the project buffer is suggested to be removed from the project buffer and inserted at this point (Fig. 1c), since the activities before this point have got extra time and any delays can be absorbed by this extra time and same is the role of a buffer. This part of the critical chain has got its share of the protection at this point only and hence the project buffer placed in the end of the project need not contribute to its protection. Hence this part of the project buffer is taken out and placed in the gap created in the critical chain. The contribution of project buffer to this part of the chain is given by:

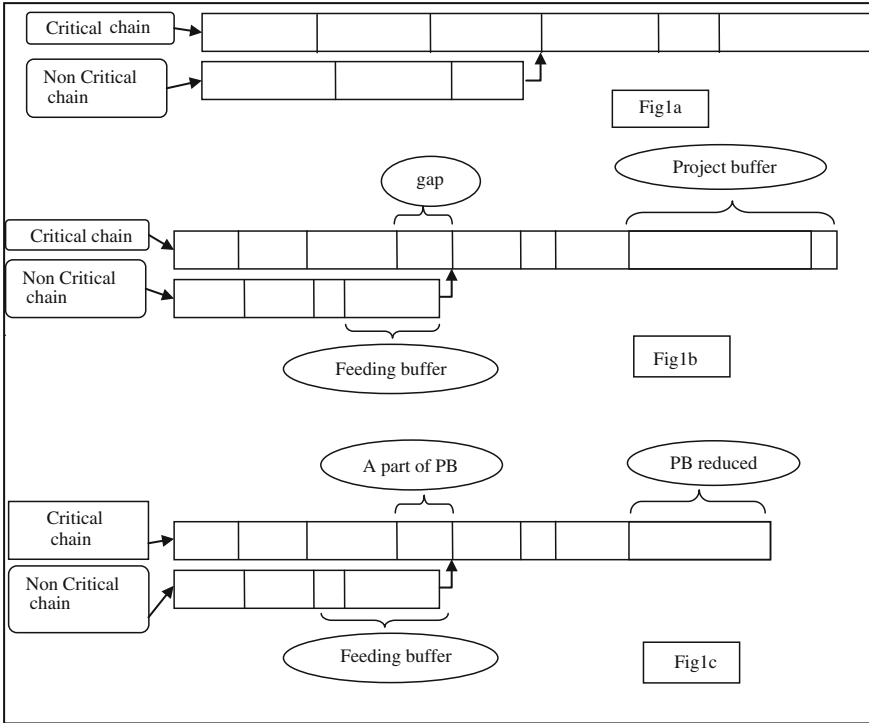


Fig. 1 Use of buffers

$$PB_i = \frac{\sum_{j \in C_i} t_j}{T} (PB) \tag{1}$$

where  $PB_i$  is  $i$ th part of the project buffer;  $C_i$  is the set of activities in  $PB_i$ ;  $t_j$  is the duration of activities;  $T$  is the project duration, i.e., length of the critical chain and  $PB$  is the project buffer duration.

If the buffer required by part of the critical chain preceding the gap is less than the gap, the part of project buffer can fit into it. This would decrease the project duration by  $\sum_i PB_i$ . Else the project would be reduced by difference between the gap and the slack.

### 4 Numerical Example

The validation of the procedure suggested in Sect. 2 is done here through a numerical example. Consider the project scheduling problem as given in Table 1.

Table 2 shows the results obtained.

**Table 1** Numerical example

Activity	Preceded by	Activity durations		
		Optimistic	Most likely	Pessimistic
A		45	51	60
B	A	19	23	30
C	A	27	32	43
D	A	38	42	52
E	A	28	32	39
F	A	23	27	34
G	B	33	40	47
H	B	43	47	54
I	E	31	39	52
J	D, H	24	30	38
K	C, G, F, I	39	43	50
L	C, G, F, I	25	31	42
M	K	16	20	25
N	M, J, L	43	49	60

### 4.1 Results from the Numerical Example

The critical chain is  $A \rightarrow E \rightarrow I \rightarrow K \rightarrow M \rightarrow N$ . The feeding chains are  $A \rightarrow B \rightarrow G \rightarrow K$ ,  $A \rightarrow C \rightarrow K$ ,  $A \rightarrow F \rightarrow K$ , etc. Feeding chains are joining the critical chain at activity  $K$  and  $N$ . The corresponding feeding buffer sizes are shown in Table 2. Buffer size for the feeding chain  $A \rightarrow B \rightarrow G$  is greater than the slack of activity  $G$ . Hence the next activity on the critical chain, i.e., activity  $K$  is shifted by  $(34.38749773-8)$  27 units (approximately). Hence there exists a gap of 27 units in the critical chain. Hence a part from the project buffer which is the **share of the  $A \rightarrow E \rightarrow I$**  part of the critical chain given by (1) is added in this gap. If this share is less than the gap, the final project duration is reduced by these many units of time. Similarly share of buffer for the part  $K \rightarrow M \rightarrow N$  of the critical chain is added after activity  $N$ , i.e., as the project buffer.

Directly adding the project buffer would have increased the project duration by nearly **49.4873** units of time while using the suggested procedure where the project duration is increased by nearly 24 units only.

Also since the buffer consumption is less than 100 % for all the buffers the schedule is stable. The buffer consumption rate is calculated using the formula  $(a + b - e)/b$  where  $a$  is the most likely time of activity duration,  $b$  is the buffer size and  $e$  is the estimated duration which is calculated using the Beta distribution.

**Table 2** Results of the numerical example

Activity	Expected duration (unit of time)	Slack for activity	Buffer size (units of time)	Buffer utilization
A	51.5	0		
B	23.5	8		
<i>Buffer for A → C</i>				
C	33	39	30.104	95.02%
D	43	62		
E	32.5	0		
<i>Buffer for A → F</i>				
F	27.5	44	28.8531	96.53%
<i>Buffer for A → B → G</i>				
G	40	8		
H	47.5	34	34.388	97.092%
I	39.833	0		
<i>Buffer for A → B → H → J</i>				
J	30.333	34	39.493	A → B → H → J 44.72%
K	43.5	0	25.801	92.89%
<i>Buffer for A → E → I → L</i>				
L	31.833	32	39.074	95.308%
M	20.166	0		
N	49.833	0	23.686	93.667%
<i>Project buffer</i>			49.4873	<i>Project buffer utilisation</i> 93.264%

## 5 Conclusion

The suggested procedure reduces the project duration while maintaining the project stability. The division of the project buffer into parts and each part being used at the gap which otherwise was being wasted has reduced the project duration. Since the buffer is only reshuffled and not reduced, there is no harm to the stability.

## References

1. Reference for Business Encyclopedia of Business, 2nd ed. Per-Pro Program Evaluation and Review Technique (PERT) <http://www.referenceforbusiness.com/encyclopedia/Per-Pro/Program-Evaluation-and-Review-Technique-PERT.html#ixzz0mVjkm5k2>
2. Badiru, A.B.: Activity resource assignments using critical resource diagramming. *Proj. Manage. J.* **XXIV**, 15–21 (1993)
3. Gemmill, D.D., Tsai, Y.-W.: Using a simulated annealing algorithm to schedule activities of resource constrained projects. *Proj. Manage. J.*, pp. 8–20 (1997)
4. Goldratt, E.: *Critical Chain*, 1st edn. North River Press, Barrington (1997). ISBN 0-88425-153-6
5. Steyn, H.: An investigation into the fundamentals of critical chain project scheduling. *Int. J. Proj. Manage.* **19**(6), 363–369 (2001)
6. Steyn, H.: Project management applications of the theory of constraints beyond critical chain scheduling. *Int. J. Proj. Manage.* **20**(1), 75–80 (2002)
7. Xie, X, Yang, G., Lin, C.: Software development projects IRSE buffer settings and simulation based on critical chain. *J. China Univ. Posts Telecommun.* **17**(Suppl 1), 100–106 (2010)
8. Tukul, O.I., Rom, W.O., Eksioğlu, S.D.: An investigation of buffer sizing techniques in critical chain scheduling. *Eur. J. Oper. Res.* **172**(2), 401–416 (2006)
9. Long, L.D., Ohsato, A.: Fuzzy critical chain method for project scheduling under resource constraints and uncertainty. *Int. J. Proj. Manage.* **26**(6), 688–698 (2008)
10. <http://www.civiles.org/publi/Gestion/Critical-Chain-Concepts.pdf>
11. Bevilacqua, M., Ciarapica, F.E., Giacchetta, G.: critical chain and risk analysis applied to high-risk industry maintenance. A case study. *Int. J. Proj. Manage.* **27**(4), 419–432 (2009)
12. Herroelen, W., Leus, R.: On the merits and pitfalls of critical chain scheduling Original Research Article. *J. Oper. Manage.* **19**(5), 559–577 (2001)
13. Hazir, O., Haouari, M., Erel, E.: Robust scheduling and robustness measures for the discrete time/cost trade-off problem. *Eur. J. Oper. Res.* **207**, 633–643 (2010)

# Inducing Fuzzy Association Rules with Multiple Minimum Supports for Time Series Data

Rakesh Rathi, Vinesh Jain and Anshuman Kumar Gautam

**Abstract** Technological changes have occurred at an exponential rate in recent years leading to the generation of large amount of data in various sectors. Several database and data warehouse is built to store and manage the data. As we know the data which are relevant to us should be extracted from the database for our task. Earlier different mining approaches are proposed in which items are collected at same minimum support value. In this paper we propose a fuzzy data mining algorithm which generates the fuzzy association rules from time series data having different minimum support values. The temperature varying dataset is used to generate fuzzy rules. The proposed algorithm also predicts the variation of temperature. Experiments are also performed to get the desired result.

**Keywords** Association rule · Data mining · Different minimum support · Fuzzy set

## 1 Introduction

Data mining plays a vital role in today's application. So, researchers are paying more attention toward the new tricks and techniques which can be evolved in it. It covers a large domain where it is frequently applied such as business, medical, biometrics. Fuzzy concepts have a great impact on data dredging methodology. Various data warehouses are managed to store and use the data efficiently through different domain. Time series data is a collection of data points which has some specific value

---

R. Rathi (✉) · V. Jain · A. K. Gautam  
Government Engineering College Ajmer, Ajmer, Rajasthan, India  
e-mail: rakeshrathi4@rediffmail.com

V. Jain  
e-mail: vineshjain1280@gmail.com

A. K. Gautam  
e-mail: er.anshuman2011@gmail.com



at that instant of time. It varies with respect to time. This paper proposes an algorithm which induce fuzzy association rule with multiple minimum support value. Earlier many algorithms have been proposed but they follow only single support value condition. Sometimes itemset has different minimum support. To explain this we applied a fuzzy concept on time series data more specifically temperature varying data. As we know that time series data comes under the category of Sequence data which has some trend or pattern in it. So algorithm would predict the near temperature using the trend analysis. The proposed algorithm has two advantages:—First, the result would be easier to understand as we are using fuzzy theory which is quite familiar with natural language. Second, it also helps to determine the sudden change in temperature of a place.

The remaining parts of this paper are assembled as follows: review of fuzzy set theory is given in Sect. 2. The related work of the paper is explained in Sect. 3. The proposed algorithm is explained in given in Sect. 4. Further experimental results are shown in Sect. 5. Finally conclusion and future work is discussed in Sect. 6.

## 2 Fuzzy Set Theory

Fuzzy set theory was pointed out in 1965 by Zadeh in his seminal paper entitled “Fuzzy sets” which played a vital role in human thinking, focusing in the domains of pattern recognition, communication of information and abstraction. Fuzzy set theory consists of fuzzy membership functions. Fuzzy set expresses the degree to which an element belongs to a set called as characteristic function. For a given crisp set B, the function assigns a value  $\mu_B(x)$  to every  $x \in X$  such that

$$\begin{aligned}\mu_B(x) &= \{1 \text{ iff } x \in B \\ \mu_B(x) &= \{0 \text{ iff } x \text{ does not } \in B\end{aligned}$$

Assume that  $x_1$  to  $x_k$  are the elements in fuzzy set B, and  $\mu_1$  to  $\mu_k$  are respectively their grades of membership function in B. B is usually represented as follows:

$$B = \mu_1/x_1 + \mu_2/x_2 + \dots + \mu_k/x_k \quad (1)$$

## 3 Related Work

Data mining is frequently used in inducing association rules from large itemsets. The association rules describes the effects of presence and absence of an item in a transaction with other items in terms of two measures support and confidence.

Hong proposed an algorithm which induces association rules with multiple minimum supports using maximum constraints on general items. Au and Chan

proposed a fuzzy dredging approach to find fuzzy rules for time series data. Das proposed a dredging algorithm for time series data prediction. Das used the clustering method to extract basic shapes from time series and applied Apriori method to induce the association rules on it.

### 4 The Proposed Algorithm with Multiple Minimum Support

**Input:** A time series TS with n data points, a list of m membership functions for data points, a predefined minimum support threshold for each fuzzy item  $ms_i, i = 1$  to z, a predefined minimum confidence threshold  $\lambda$ , and a sliding window size ws.

- Step 1: Convert the time series TS into a list of subsequences W(TS) according to the sliding-window size ws. That is,  $W(TS) = \{s_b | s_b = (d_b, d_{b+1}, \dots, d_{b+ws-1}), b = 1 \text{ to } n - ws + 1\}$ , where  $d_b$  is the value of the b-th data point in TS.
- Step 2: Transform the k-th ( $k = 1$  to ws) quantitative value  $v_{bk}$  in each subsequence  $s_b$  ( $b = 1$  to  $n - ws + 1$ ) into a fuzzy set  $f_{bk}$  represented as  $(f_{bk1}/R_{k1} + f_{bk2}/R_{k2} + \dots + f_{bkn}/R_{kn})$  using the given membership functions, where  $R_{kl}$  is the l-th fuzzy region of the k-th data point in each subsequence, m is the number of fuzzy memberships, and  $f_{bkl}$  is  $v_{bk}$ 's fuzzy membership value in region  $R_{kl}$ . Each  $R_{kl}$  is called a fuzzy item.
- Step 3: Compute the scalar cardinality of each fuzzy item  $R_{kl}$  as

$$Count_{kl} = \sum_{b=1}^{n-ws+1} f_{bkl}$$

- Step 4: Check whether the support value ( $= count_{kl}/n - ws + 1$ ) of each  $R_{kl}$  in  $C_1$  is greater than or equal to its predefined minimum support threshold value  $ms_{R_{kl}}$ . If  $R_{kl}$  satisfies the above condition, collect it in the set of large 1-itemsets ( $L_1$ ). That is:

$$L_1 = \{R_{kl} | count_{kl} \geq ms_{R_{kl}}, 1 \leq k \leq b + ws - 1 \text{ and } 1 \leq l \leq m\}.$$

- Step 5: IF  $L_1$  is not null, then perform the next step; otherwise, terminate the algorithm.
- Step 6: Set  $t = 1$ , where t is used to represent the number of fuzzy items in the current itemsets to be processed.
- Step 7: Join the large t-itemsets  $L_t$  to obtain the candidate (t + 1)-itemsets  $C_{t+1}$  in the same way as in the Apriori algorithm provided that two items obtained from the same order of data points in subsequences cannot exist in an itemset in  $C_{t+1}$  at the same instant provided the minimum support of all the large t-itemsets must be greater than or equal to the maximum of the minimum supports of fuzzy items in theses large t-itemsets.

Step 8: Now, perform the following steps for fuzzy items in  $C_{t+1}$ :

- (a) Compute the fuzzy value of I in each subsequence  $s_b$  as  $f_I^{sb} = f_{I1}^{sb} \wedge f_{I2}^{sb} \wedge \dots \wedge f_{I_{t+1}}^{sb}$  where  $f_{I_k}^{sb}$  is the membership value of fuzzy item  $I_k$  in  $S_b$ . If the minimum operator is used for the intersection, then:

$$f_{Ib}^s = \text{Min}_{k=1}^{t+1} f_{I_k}^s.$$

- (b) Compute the count of I in all the subsequences as:

$$\text{Count}_I = \sum_{b=1}^{n-ws+1} f_I^{sb}$$

Step 9: If the support ( $= \text{count}_I/n - ws + 1$ ) of I is greater than or equal to maximum of the minimum support value, put it in  $L_{t+1}$ .

$$L_{t+1} = \{I_k \mid \text{count}_I \geq \text{ms}_{I_k}, \}$$

Step 10: STEP 13: If  $L_{t+1}$  is null, then do the next step; otherwise, set  $t = t + 1$  and repeat STEPs 6–9.

Step 11: Generate the association rules for each large h-itemset I with items  $(I_1, I_2, \dots, I_h)$ ,  $h \geq 2$ , using the following substeps:

- (a) Form each possible association rule as follows:  $I_1^{\wedge} \dots \wedge I_{n-1}^{\wedge} I_{n+1}^{\wedge} \dots \wedge I_h \rightarrow I_n$ ,  $n = 1$  to  $h$ .
- (b) Calculate the confidence values of all association rules by the following formula:

$$= \sum_{b=1}^{n-ws+1} f_I^{sb} \setminus \sum_{b=1}^{n-ws+1} \left( (f_I^{sb} \wedge \dots \wedge f_{I_P}^s) \right)$$

**Output:** A set of association rules which satisfies the condition of the maximum values of minimum supports.

## 5 An Example

This section explains the working of the proposed algorithm and generates fuzzy association rule (Table 1).

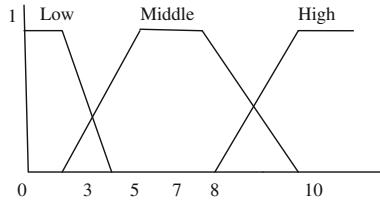
Assume the membership function used in the example as Fig. 1 (Table 2).

Step 1: The window size is assumed as 5. Using the formula we get  $(15 - 5 + 1) = 11$  subsequences

Step 2: The data values are then converted into fuzzy item sets using the membership function shown in fig no.

**Table 1** Set of data points

Time Series
3, 4, 6, 1, 8, 6, 3, 9, 3, 6, 1, 5, 8, 1, 9



**Fig. 1** Membership function used in this example

**Table 2** Predefined minimum support value of all fuzzy itemset

Fuzzy item	Minimum support	Fuzzy item	Minimum support
Q1.Low	3.90	Q4.low	4.00
Q1.Middle	3.80	Q4.Middle	3.00
Q1.High	3.50	Q4.High	5.00
Q2.Low	2.00	Q5.Low	4.90
Q2.Middle	2.30	Q5.Middle	3.03
Q2.High	2.00	Q5.High	2.00
Q3.Low	2.10	Q3.High	4.00
Q3.Middle	4.50		

**Table 3** Sequence generated,  $ws = 5$

$S_b$	Subsequence	$S_b$	Subsequence
$S_1$	(3, 4, 6, 1, 8)	$S_7$	(3, 9, 3, 6, 1)
$S_2$	(4, 6, 1, 8, 6)	$S_8$	(9, 3, 6, 1, 5)
$S_3$	(6, 1, 8, 6, 3)	$S_9$	(3, 6, 1, 5, 8)
$S_4$	(1, 8, 6, 3, 9)	$S_{10}$	(6, 1, 5, 8, 1)
$S_5$	(8, 6, 3, 9, 3)	$S_{11}$	(1, 5, 8, 1, 9)
$S_6$	(6, 3, 9, 3, 6)		

Step 3: Add all the value of fuzzy region of the subsequences called as its count. For example-Assume a fuzzy item  $Q_1$ .Middle.count is  $(0 + 0.33 + 1 + 0 + 0.33 + 1 + 0 + .2 + 0 + 1 + 0) = 3.86$

Step 4: Now,compare the count of all fuzzy item with its individual minimum support count which is predefined. Fuzzy items whose count is greater than minimum support value of itself put the fuzzy item in the table  $L_1$  (Table 3).

Step 5: If  $L_1$  consists of fuzzy item, proceed to step 6, else terminate.

**Table 4** Converted fuzzy set

$S_t$	$Q_1$			$Q_2$			$Q_3$			$Q_4$			$Q_5$		
	Low	Mid	High	Low	Mid	High	Low	Mid	High	Low	Mid	High	Low	Mid	High
$S_1$	0.67	0	0	0.67	0.33	0	0	1	0	1	0	0	0	0.33	0.67
$S_2$	0.67	0.33	0	0	1	0	1	0	0	0	0.33	0.67	0	1	0
$S_3$	0	1	0	1	0	0	0	0.33	0.67	0	1	0	0.67	0	0
$S_4$	1	0	0	0	0.33	0.67	0	1	0	0.67	0	0	0	0.2	1
$S_5$	0	0.33	0.67	0	1	0	0.67	0	0	0	2	1	0.67	0	0
$S_6$	0	1	0	0.67	0	0	0	0.2	1	0.67	0	0	0	1	0
$S_7$	0.67	0	0	0	0.2	1	0.67	0	0	0	1	0	1	0	0
$S_8$	0	0.2	1	0.67	0	0	0	1	0	1	0	0	0	1	0
$S_9$	0.67	0	0	0	1	0	1	0	0	0	1	0	0.33	0.33	0.67
$S_{10}$	0	1	0	1	0	0	0	1	0	0.33	0.33	0.67	1	0	0
$S_{11}$	1	0	0	0	1	0	0	0.33	0.67	1	0	0	0	0.2	1
Count	4.68	3.86	1.67	4.01	4.86	1.67	3.34	4.68	2.34	4.34	3.68	2.34	2.34	2.70	3.34

Step 6: Candidate set  $C_{t+1}$  is generated from  $L_t$ . Fuzzy items in  $L_1$  are ( $Q_1$ .Low,  $Q_1$ .Middle,  $Q_2$ .Low,  $Q_2$ .Middle,  $Q_3$ .Low,  $Q_3$ .Middle,  $Q_4$ .Low,  $Q_5$ .Low,  $Q_5$ .High) .

Step 7:  $L_1$  is joined to generate  $C_2$ . The new fuzzy items in  $C_2$  are as follows ( $Q_1$ .Low,  $Q_2$ .Mid), ( $Q_1$ .Low,  $Q_3$ .Mid), ( $Q_1$ .Low,  $Q_5$ .High), ( $Q_1$ .Low,  $Q_2$ .Mid), ( $Q_1$ .Low,  $Q_3$ .Mid), ( $Q_1$ .Low,  $Q_5$ .Low), ( $Q_2$ .Low,  $Q_3$ .Low), ( $Q_2$ .Low,  $Q_4$ .Low), ( $Q_2$ .Low,  $Q_5$ .High), ( $Q_2$ .Low,  $Q_1$ .Mid), ( $Q_2$ .Low,  $Q_3$ .Mid), ( $Q_2$ .Low,  $Q_5$ .Low), ( $Q_3$ .Low,  $Q_4$ .Low), ( $Q_3$ .Low,  $Q_5$ .High), ( $Q_3$ .Low,  $Q_1$ .Mid), ( $Q_3$ .Low,  $Q_2$ .Mid), ( $Q_3$ .Low,  $Q_5$ .Low), ( $Q_4$ .Low,  $Q_1$ .Mid), ( $Q_4$ .Low,  $Q_2$ .Mid), ( $Q_4$ .Low,  $Q_5$ .High), ( $Q_4$ .Low,  $Q_5$ .Low), ( $Q_5$ .High,  $Q_1$ .Mid), ( $Q_5$ .High,  $Q_2$ .Mid), ( $Q_5$ .High,  $Q_3$ .High).

**Table 5** Candidate set  $C_2$

Fuzzy itemset	Count	Fuzzy itemset	Count
$Q_1$ Low, $Q_2$ Mid	4.68	$Q_2$ Low, $Q_5$ Low	2.34
$Q_1$ Low, $Q_3$ Mid	4.68	$Q_3$ Low, $Q_5$ High	3.34
$Q_1$ Low, $Q_5$ High	3.34	$Q_3$ Low, $Q_1$ Mid	3.34
$Q_1$ Low, $Q_2$ Low	4.01	$Q_3$ Low, $Q_2$ Mid	3.34
$Q_1$ Low, $Q_3$ Low	3.34	$Q_3$ Low, $Q_5$ Low	2.34
$Q_1$ Low, $Q_5$ Low	2.34	$Q_4$ Low, $Q_1$ Mid	3.86
$Q_2$ Low, $Q_3$ Low	3.34	$Q_4$ Low, $Q_2$ Mid	4.34
$Q_2$ Low, $Q_4$ Low	4.01	$Q_4$ Low, $Q_5$ High	3.86
$Q_2$ Low, $Q_3$ Low	3.34	$Q_4$ Low, $Q_2$ Mid	4.34
$Q_2$ Low, $Q_4$ Low	4.01	$Q_4$ Low, $Q_5$ High	3.86
$Q_2$ Low, $Q_5$ High	3.34	$Q_4$ Low, $Q_5$ Low	2.34
$Q_2$ Low, $Q_1$ Mid	3.86	$Q_5$ High, $Q_1$ Mid	3.34
$Q_2$ Low, $Q_3$ Mid	4.01	$Q_5$ High, $Q_2$ Mid	3.34
$Q_3$ Low, $Q_4$ Low	3.34	$Q_5$ High, $Q_3$ High	2.34

**Table 6** Fuzzy itemset  $L_2$

---

(Q1Low, Q2Low)(Q1Low, Q2Mid)(Q1Low, Q3Mid)(Q2Low, Q3Low)
(Q2Low, Q4Low)(Q2Low, Q5High)(Q1.Low, Q4.Low)
(Q3.Low, Q2.Mid)(Q4.Low, Q1.Mid)(Q5.High, Q2.Mid)(Q4.Low, Q5.High)

---

Step 8: Now compute the count of all the fuzzy items of  $C_2$ .

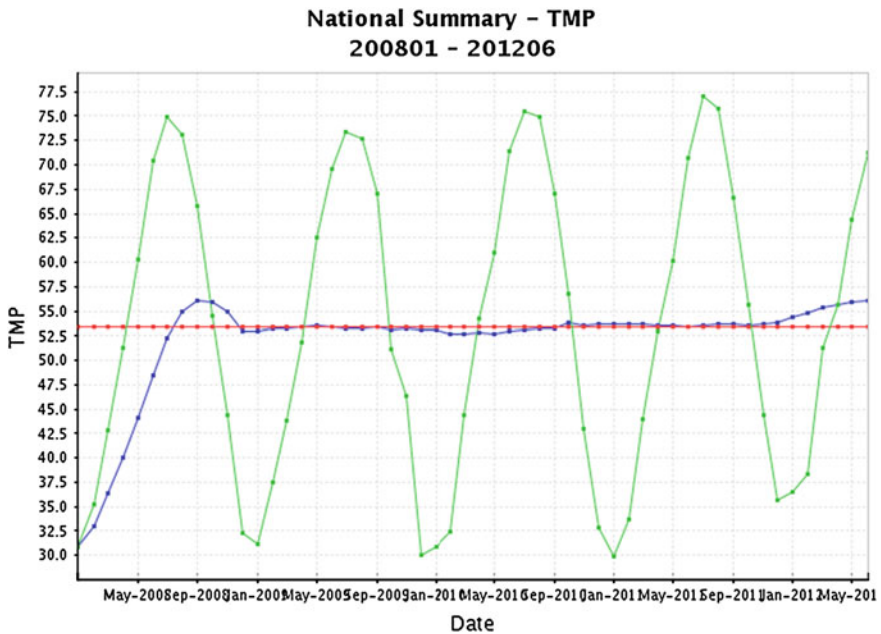
Step 9: Compare the  $C_2$  itemset count with minimum support count of Fuzzy itemset.  $C_2$  items whose count is greater or equal to minimum support of maximum of the two itemset is stored in  $L_2$ .

Step 10: Since  $L_2$  is not null, repeat step no 6–9 until  $L_t$  is null (Tables 4, 5, 6).

Step 11: (a) In this example, only (Q3.Low Q2.Mid) exists. It means association rules formed are

If  $Q_3 = \text{Low}$  then  $Q_2 = \text{Mid}$ . If  $Q_2 = \text{Mid}$  then  $Q_3 = \text{Low}$ .

(b) Calculation of confidence of (Q3.Low Q2.Mid) =  $3.34 \setminus 3.34 = 1$ . It means if the value of a data point is mid at time2 then value of a data point is low at time3 with a confidence factor of 1.



**Fig. 2** Temperature varying data

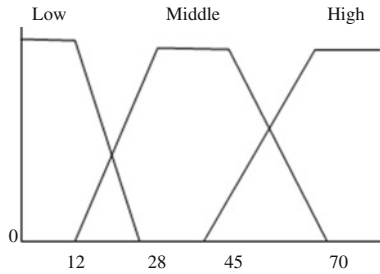


Fig. 3 Membership function used in experiment

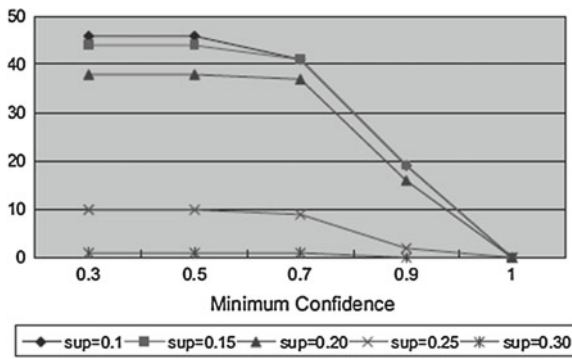


Fig. 4 Relation between support value and confidence

## 6 Experimental Results

The proposed algorithm is implemented in a programming language C. The dataset points consisted of temperature varying points between year 2008–2012. The dataset is taken from National Data Center (NDC) US (Figs. 2 and 3).

In Fig. 4 as the support value of fuzzy itemset is increased, number of fuzzy association rule decreased. This means change in temperature is effected with change in support value. It means that if the temperature of a day at second day of a month is moderate, then it may be high at third day of the month.

## 7 Conclusion and Future Work

In this paper, the proposed algorithm provided the best way to induce efficient fuzzy association rule as there is predefined minimum support for all the fuzzy items. The temperature prediction would be more accurate than earlier proposed approaches. Future work suggests that the membership function can be set dynamically. In this

paper membership functions are known in advance. More complex operations could be made in near future. It also provided us another view point for defining minimum support of fuzzy items.

## References

1. Aggrawal, R.: Mining association rules between sets of items inlarge database ACM
2. Stepnicka, M.: Time series analysis and prediction based on fuzzy rules and the fuzzy transform
3. Dr.Sivatsa S.K.: Inaccuracy minimization by partitioning fuzzy data sets—validation of an analytical methodology(IJCSIS). *Int. J. Comput. Sci. Inf. Secur.* **8**(1), (2010)
4. Das, G.: Rule discovery from time series. In: Proceedings of the 4 the International Conference
5. Pongracz, R.: Application of fuzzy rule-based modeling technique to regional drought. *J. Hydrol.* **224**, 100–114 (1999)
6. Mueen, A.A.: Exact primitives for time series data mining. University of California, Riverside (2012)
7. Zhu, Y.: High performance data mining in time series: techniques and case studies. New work University, New York (2004)
8. Herrera, Francisco: Learning the membership function contexts for mining fuzzy association rules by using genetic algorithms. *Fuzzy Sets Syst.* **160**, 905–921 (2009)
9. Han, J.: *Data Mining concepts and Techniques*
10. Hong, T.P.: Mining association rules with multiple minimum supports. *Int. J. Approximate reasoning.* **3**, 38–42 (2005)



# RGA Analysis of Dynamic Process Models Under Uncertainty

Amit Jain and B. V. Babu

**Abstract** The aim of this paper is to gain insights into how process dynamics can affect control configuration decision based on relative gain array (RGA) analysis in the face of model uncertainty. Analytical expressions for worst-case bounds of uncertainty in steady-state and dynamic RGA are derived for two inputs two outputs (TITO) plant models. A simulation example which has been used in several prior studies is considered here to demonstrate the results. The obtained bounds of uncertainty in RGA provide valuable information pertaining to the necessity of robustness and accuracy in the model of decentralized multivariable systems.

**Keywords** Relative gain array · Parametric uncertainty · Control configuration selection · Worst-case bounds · Multivariable plants

## 1 Introduction

It has been almost five decades since the introduction of the relative gain array (RGA) in 1966 [1]. It has found to be a promising tool for determination of control loop pairings and in the analysis of the level of the interaction exist in such pairings. Because of its inherent simplicity, the RGA is still popular among industries and academia, particularly after the use of the Niederlinski Index [2] as a complementary tool for analyzing closed-loop stability. The RGA has many useful algebraic properties with

---

B. V. Babu (✉)

Institute of Engineering and Technology, JK Laxmipat University (JKLU),  
Jaipur 302026, India  
e-mail: director.iet@jklu.edu.in

A. Jain

Chemical Engineering Department, Birla Institute of Technology and Science,  
Pilani, Rajasthan 333031, India  
e-mail: amitjain@bits-pilani.ac.in

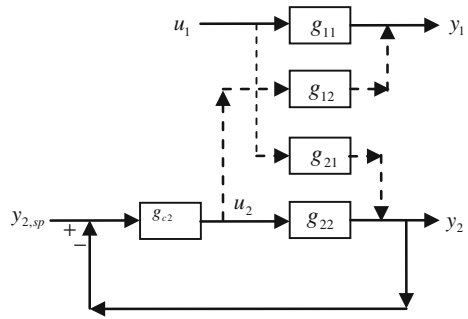
strong control impositions [3]. The applications of RGA are thoroughly discussed in a book written by McAvoy [4] and Shinskey [5]. However, it is clearly indicated [6–13] that the RGA is not just a tool for choosing input/output pairings for decentralized control but also a measure of attainable control quality. It is associated with many elementary properties; robustness, stability, tolerance to the failure of actuators and sensors, decentralized integral controllability (DIC) etc., defined for closed loop systems.

Despite many advantages, the RGA also suffers from certain disadvantages. Since it depends on the steady-state gain information alone, a due consideration has not been given to the process dynamic behavior which leads to incorrect conclusions in certain cases. The dynamic extension of RGA to nonzero frequencies is presented in many ways by different authors [4, 14–19]. The originate work in this field is presented for two inputs two outputs (TITO) plants. Early methods of dynamic RGA employed the transfer function matrix in the definition of RGA as an alternative to the steady-state matrix of gains [14–16]. McAvoy et. al. [18] has offered a novel approach to define a dynamic RGA. It is assumed in this computationally complicated approach that a dynamic model of the process exists and a proportional output optimal controller has been designed using state-space approach. Finally, based on the matrix of consequential controller gains a dynamic RGA is defined. However, these methods [16, 18] have lost the controller independency, which is a valuable property in a pairing criterion. To give a more complete description of control-loop interaction, both the steady-state gain and the process dynamic behavior in terms of bandwidth of the elements of transfer function has been adopted by some authors in a controller independent framework [19, 20].

Although for years, in most of the studies on the analysis of RGA and its properties, the availability of a process model is frequently assumed, still the sensitivity of the RGA analysis to model uncertainty is in nascent stage. However, in practice, the models of real systems always have some uncertainty associated with them. Thus, process models can never be perfect. For plants with uncertain process models, an incorrect pairing decision may result if the RGA analysis carried out based only on a nominal model of the process. The problem further aggravates when a sensitivity analysis of RGA elements to model uncertainty is carried out based on steady-state process model alone.

In this paper, analytical expressions are derived for worst-case bounds of uncertainty in steady-state and dynamic RGA considering TITO plant models. The parametric model uncertainty is considered and is presented here with the aim to identify the possible input–output selection changes resulting from the parameter changes. The transfer function model ( $2 \times 2$ ) used here to demonstrate the results has also been used by many authors before.

**Fig. 1** Block diagram of loop interaction in  $2 \times 2$  plant model



## 2 Relative Gain Array: Definitions and Properties

The RGA, a measure of interaction for the multivariable control system was formerly proposed by Bristol [1]. Each element in the RGA matrix has been defined as the ratio of gains, i.e., open-loop gain to the gain obtained between the similar variables keeping all other loops under “perfect” control (Fig. 1):

$$\lambda_{ij} = \frac{(\partial y_i / \partial u_j)_u}{(\partial y_i / \partial u_j)_y} = \frac{\text{open-loop gain}}{\text{closed-loop gain}} \tag{1}$$

The elements  $\lambda_{ij}$  forms the RGA  $\Lambda$ . Writing definition (1) in the transfer matrix form as,

$$\Lambda(G) = G(s) \otimes G^{-1}(s)' \tag{2}$$

where  $\otimes$  denotes element-by-element multiplication or Schur product. The substitution of  $(s = j\omega)$  in (2) computes RGA at different frequencies [9]. The steady-state ( $s = 0$ ) version of the RGA is found by substituting the transfer function matrix  $G(s)$  of (2) with the corresponding matrix of steady-state gains,  $K$ . In addition to its numerous algebraic properties, the RGA is also a good gage of sensitivity to uncertainty. The relative gain  $\lambda_{ij}$  provides a direct estimate of the sensitivity of the plant model to independent element-by-element uncertainty.  $G(j\omega)$  turn out to be singular if any element  $g_{ij}(j\omega)$  changes by  $-1/\lambda_{ij}(j\omega)$  [8–10]. Since the steady-state RGA matrix is a function of open loop gains only, thus any uncertainty in open-loop gain leads to the uncertainty in RGA.

## 3 Analyzing $2 \times 2$ Plant Model Control Problem

Let a multivariable system  $G(s)$  with two controlled variables and two manipulated variables:

$$G(s) = \begin{bmatrix} g_{11}(s) & g_{12}(s) \\ g_{21}(s) & g_{22}(s) \end{bmatrix} \tag{3}$$

For the given control problem the steady-state gain matrix is,

$$G(0) = K = \begin{bmatrix} g_{11}(0) & g_{12}(0) \\ g_{21}(0) & g_{22}(0) \end{bmatrix} = \begin{bmatrix} K_{11} & K_{12} \\ K_{21} & K_{22} \end{bmatrix} \tag{4}$$

and the subsequent matrix of RGA elements is,

$$\Lambda = \begin{bmatrix} \lambda_{11} & \lambda_{12} \\ \lambda_{21} & \lambda_{22} \end{bmatrix} = \begin{bmatrix} \lambda_{11} & 1 - \lambda_{11} \\ 1 - \lambda_{11} & \lambda_{11} \end{bmatrix} \tag{5}$$

here,  $\lambda_{11}$  is the relative gain between output-1 and input-1, i.e.,

$$\lambda_{11} = \frac{(\partial y_1 / \partial u_1)_{u_2}}{(\partial y_1 / \partial u_1)_{y_2}} = \frac{1}{1 - \hat{k}}; \tag{6}$$

where,

$$\hat{k} = (-1)^n \frac{|K_{12}| |K_{21}|}{|K_{11}| |K_{22}|} \tag{7}$$

$\hat{k}$ , here is referred to as the interaction quotient and  $n$ , is the number of negative elements in  $G(s)$ . Obviously  $\hat{k} = 1$  is a singular point for RGA matrix. Note here that for odd number of negative elements (i.e.,  $n = \text{odd number}$ ) the RGA matrix can never be singular as  $\hat{k} \neq 1$ .

### 3.1 Analyzing Uncertainty Bounds for Steady-State Process Model

Assume lower bounds of uncertainty in all the elements of the steady-state gain matrix  $K$  to be symmetrical with that of higher bounds. Thus, the nominal steady-state gain element,  $K_{ij}$  varies within  $K_{ij} \pm \Delta K_{ij}$ . Let  $|\Delta K_{ij}| \leq \alpha |K_{ij}|$  represents the uncertainty bound to the every element of  $K$ , then,

$$\hat{k}_{uc} = \hat{k} \left( \frac{1 \pm \alpha}{1 \mp \alpha} \right)^2 \tag{8}$$

where  $\hat{k}_{uc}$  is the interaction quotient under model uncertainty. The respective limits of the  $\hat{k}_{uc}$  are represented as,

$$\hat{k}^l \leq \hat{k}_{uc} \leq \hat{k}^h \tag{9}$$

where,

$$\hat{k}^l \left( = \min \left( \hat{k}_{uc} \right) \right) = \hat{k} \left( \frac{1 + \alpha}{1 - \alpha} \right)^2 \quad \forall n = \text{odd number} \quad (10)$$

$$= \hat{k} \left( \frac{1 - \alpha}{1 + \alpha} \right)^2 \quad \forall n = \text{even number} \quad (11)$$

$$\hat{k}^h \left( = \max \left( \hat{k}_{uc} \right) \right) = \hat{k} \left( \frac{1 - \alpha}{1 + \alpha} \right)^2 \quad \forall n = \text{odd number} \quad (12)$$

$$= \hat{k} \left( \frac{1 + \alpha}{1 - \alpha} \right)^2 \quad \forall n = \text{even number} \quad (13)$$

For  $\hat{k} \neq 1$ , the RGA element  $\lambda_{11}$  changes within the uncertainty limits:

$$\frac{1}{1 - \hat{k}^l} \leq \lambda_{11} \leq \frac{1}{1 - \hat{k}^h} \quad (14)$$

For  $\hat{k} = 1$  (singular point), the sign of  $\lambda_{11}$  changes. Thus the  $\lambda_{11}$  changes within the uncertainty limits:

$$-\infty \leq \lambda_{11} \leq \frac{1}{1 - \hat{k}^h} \quad (15)$$

and

$$\frac{1}{1 - \hat{k}^l} \leq \lambda_{11} \leq \infty \quad (16)$$

The application of above methodology will be demonstrated with the help of examples available in open literature.

### 3.2 Worst-Case Bounds for Dynamic Process Model

In order to assimilate both the static and dynamic behavior of the plant in the interaction measure, we encourage the use of the elective gain,  $e_{ij}$  as defined in Xiong et al. [19] for a given element  $g_{ij}(\omega)$  of transfer function model at the critical frequencies. Approximating the effective gain integration with a rectangular area, the effective gain  $e_{ij}$  can simply be given as,

$$e_{ij} \approx g_{ij}(0) \omega_{c.ij} \quad (17)$$

Therefore, the matrix of effective gains is defined as,

$$E = G(0) \otimes \Omega; \tag{18}$$

where,

$$\Omega = \begin{bmatrix} \omega_{c,11} & \omega_{c,12} \\ \omega_{c,21} & \omega_{c,22} \end{bmatrix} \tag{19}$$

Based on (4) and (19), the dynamic interaction quotient can be defined as:

$$\hat{k}_{dy} = (-1)^n \frac{|K_{12}|(\omega_{c,12}) \times |K_{21}|(\omega_{c,21})}{|K_{11}|(\omega_{c,11}) \times |K_{22}|(\omega_{c,22})} = \hat{k}\varpi; \tag{20}$$

where,

$$\varpi = \frac{(\omega_{c,12})(\omega_{c,21})}{(\omega_{c,11})(\omega_{c,22})} \tag{21}$$

Equations (9)–(15), defined for steady-state system are all directly applicable to dynamic process model after replacing  $\hat{k}$  in (8) by  $\hat{k}_{dy}$  of (20).

### 4 Examples

*Example 1* Consider a process model [21]:

$$G(s) = \begin{bmatrix} \frac{5}{4.s+1} & \frac{2.5e^{-5s}}{(2.s+1)(15.s+1)} \\ \frac{-4e^{-6s}}{20.s+1} & \frac{1}{3.s+1} \end{bmatrix} \tag{22}$$

*For steady-state system:*

The steady-state RGA matrix and interaction quotient  $\hat{k}$  for  $n = 1$  are:

$$\hat{\Lambda} = \begin{bmatrix} 0.3333 & 0.6667 \\ 0.6667 & 0.3333 \end{bmatrix} \& \hat{k} = -2 \tag{23}$$

which suggest the 1-2/2-1 (off-diagonal) pairing. Taking into consideration the different values for model uncertainty  $\alpha$ . The range of  $\lambda_{11}$  for given  $\alpha$  value can be found.

*Case 1*  $\alpha = 0.01$ . According to (10)–(13), the bounds for  $\hat{k}$  are  $\hat{k}^l = -2.08$  and  $\hat{k}^h = -1.92$ , the corresponding bounds for  $\lambda_{11}$  are given by (14):

$$0.32 \leq \lambda_{11} \leq 0.34$$

Since,  $\lambda_{11} < 0.5$  thus, the suggested control-loop pairing based on the RGA analysis is 1-2/2-1 (off-diagonal).

*Case 2*  $\alpha = 0.1$ . The bounds are  $\hat{k}^l = -2.99$  and  $\hat{k}^h = -1.34$  and

$$0.25 \leq \lambda_{11} \leq 0.43$$

Thus, suggested pairing is still 1-2/2-1 (off-diagonal).

*Case 3*  $\alpha = 0.2$ . Now  $\hat{k}^l = -4.55$  and  $\hat{k}^h = -0.88$ . The range of  $\lambda_{11}$  can be obtained using (14):

$$0.18 \leq \lambda_{11} \leq 0.53$$

Still in its range,  $\lambda_{11} \leq 0.5$ . Thus, the suggested control-loop pairing based on the RGA analysis is 1-2/2-1 (off-diagonal).

*Case 4*  $\alpha = 0.5$ . Now  $\hat{k}^l = -18.18$  and  $\hat{k}^h = -0.22$  and

$$0.05 \leq \lambda_{11} \leq 0.82$$

For the obtained range of  $\lambda_{11}$  the pairing decision is quite ambiguous.

*Case 5*  $\alpha = 0.9$ . Now  $\hat{k}^l = -666.7$  and  $\hat{k}^h = -0.006$  and

$$0.001 \leq \lambda_{11} \leq 0.99$$

In the obtained range of  $\lambda_{11}$  the pairing decision remained ambiguous. As was discussed, for odd number of negative elements in given matrix of the transfer function the RGA matrix will never be singular as  $\hat{k} \neq 1$ , within the whole uncertainty range.

*For Dynamic Systems:*

The critical frequency quotient  $\varpi$  and dynamic interaction quotient  $\hat{k}_{dy}$  can be obtained using (20) and (21) respectively, as:

$$\varpi = 0.04 \tag{24}$$

and,

$$\hat{k}_{dy} = -0.08 \tag{25}$$

The range of  $\lambda_{11}$  corresponding to the same  $\alpha$  values that was used for steady-state analysis could be found.

*Case 1*  $\alpha = 0.01$ . In accordance to (10)–(13), the bounds for  $\hat{k}_{dy}$  are  $\hat{k}_{dy}^l = -0.083$  and  $\hat{k}_{dy}^h = -0.077$ , consequently the  $\lambda_{11}$  varies within the bounds as per (14):

$$0.92 \leq \lambda_{11} \leq 0.93$$

Thus, the suggested control-loop pairing based on the RGA analysis is 1-1/2-2, i.e., diagonal.

Case 2  $\alpha = 0.1$  Now  $\hat{k}_{dy}^l = -0.12$  and  $\hat{k}_{dy}^h = -0.05$  and

$$0.89 \leq \lambda_{11} \leq 0.95$$

Thus, the suggested control-loop pairing based on the RGA analysis is 1-1/2-2, i.e., diagonal.

Case 3  $\alpha = 0.5$ ; The bounds are given as  $\hat{k}_{dy}^l = -0.73$  and  $\hat{k}_{dy}^h = -0.01$  and

$$0.58 \leq \lambda_{11} \leq 0.99$$

Thus, the suggested control-loop pairing based on the RGA analysis is 1-1/2-2, i.e., diagonal.

Case 4  $\alpha = 0.9$ . Now  $\hat{k}_{dy}^l = -28.88$  and  $\hat{k}_{dy}^h = -0.0002$  and

$$0.03 \leq \lambda_{11} \leq 0.999$$

For the obtained range of  $\lambda_{11}$  the pairing decision is quite ambiguous.

Table 1 compares the outcome of uncertainty analysis of steady-state and dynamic RGA for Example 1. As is clearly shown, the uncertainty analysis of steady-state gain matrix gives ambiguous results and no unique control loop-pairing is favored within the whole range of uncertainty whereas dynamic RGA analysis clearly suggest diagonal pairing. The results obtained are in complete agreement with the results of Grosdidier and Morari [21], whose analysis of interaction between the loops was based on frequency response characteristics. The example under considerations illustrates: (i) The uncertainty in process model may have a severe effect on the selection of control configuration if the RGA analysis based on steady-state alone is utilized. (ii) In order to ensure robustness in the system pertaining to decentralized

**Table 1** Uncertainty analysis results of Example 1 for different  $\alpha$  values

$\alpha$	Uncertainty range of static RGA Elements	Uncertainty range of dynamic RGA Elements
0.01	$0.32 \leq \lambda_{11} \leq 0.34$	$0.92 \leq \lambda_{11} \leq 0.93$
0.10	$0.25 \leq \lambda_{11} \leq 0.43$	$0.89 \leq \lambda_{11} \leq 0.95$
0.50	$0.05 \leq \lambda_{11} \leq 0.82$	$0.58 \leq \lambda_{11} \leq 0.99$
0.90	$0.001 \leq \lambda_{11} \leq 0.99$	$0.03 \leq \lambda_{11} \leq 0.999$



control, the uncertainty in model parameters should be infused in the RGA analysis under a dynamic framework.

## 5 Conclusions

In this paper, analytical expressions are derived for bounds of uncertainty (worst-case) in steady-state and dynamic RGA for TITO plant models. On the analysis of considered example it is thus reasoned that the steady-state RGA analysis leads to incorrect conclusions about worst-case bounds and tolerable uncertainty. It is thus recommended to use dynamic RGA uncertainty analysis to approximate the highest degree of uncertainty in the model parameters such that the suggested control-loop pairing will remain unaffected. Such analysis provides an idea about how much change in the operating parameter values are tolerable so as to keep the control-loop pairing decision unchanged.

The method presented is introductory in essence that it is applicable to  $2 \times 2$  plant models with uncertainty in steady-state gains only.

## References

1. Bristol, E.H.: On a new measure of interactions for multivariable process control. *IEEE Trans. Autom. Control* **AC-11**, 133–134 (1966)
2. Niederlinski, A.: A heuristic approach to the design of linear multivariable interacting control systems. *Automatica* **7**, 691–701 (1971)
3. Skogestad, S., Postlethwaite, I.: *Multivariable feedback control: analysis and design*. Wiley, Chichester (2005)
4. McAvoy, T.J.: *Interaction Analysis*. Instrument Society of America, Research Triangle Park (1983a)
5. Shinskey, F.G.: *Distillation Control*, 2nd edn. McGraw-Hill, New York (1984)
6. Grosdidier, P., Morari, M., Holt, B.R.: Closed-loop properties from steady-state gain information. *Ind. Eng. Chem. Fundam.* **24**, 221–235 (1985)
7. Yu, C.C., Luyben, W.L.: Robustness with respect to integral controllability. *Ind. Eng. Chem. Res.* **26**, 1043–1045 (1987)
8. Skogestad, S., Morari, M.: Implications of large rga elements on control performance. *Ind. Eng. Chem. Res.* **26**, 2323–2330 (1987)
9. Chiu, M.S., Arkun, Y.: A new result on relative gain array, niederlinski index and decentralized stability condition: 2x2 plant cases. *Automatica* **27**, 419–421 (1991)
10. Hovd, M., Skogestad, S.: Simple frequency-dependent tools for control system analysis, structure selection and design. *Automatica* **28**, 989–996 (1992)
11. Chen, J., Freudenberg, J.S., Nett, C.N.: The role of the condition number and the relative gain array in robustness analysis. *Automatica* **30**, 1029–1035 (1994)
12. Zhu, Z.X., Jutan, A.: Loop decomposition and dynamic interaction analysis of decentralized control systems. *Chem. Eng. Sci.* **51**, 3325–3335 (1996)
13. Lee, J., Edgar, T.F.: Computational method for decentralized integral controllability of low dimensional processes. *Comput. Chem. Eng.* **24**, 847–852 (2000)
14. Witcher, M., McAvoy, T.J.: Interacting control systems: steady-state and dynamic measurement of interaction. *ISA Trans.* **16**, 35–44 (1977)

15. Bristol, E.H.: Recent results on interactions in multivariable process control. Presented at 71st Annual AIChE Meeting, Houston, TX (1979)
16. Tung, L., Edgar, T.: Analysis of control-output interactions in dynamic systems. *A.I.Ch.E. J.* **27**, 690–693(1981)
17. Gagnepain, J.P., Seborg, D.E.: Analysis of process interactions with application to multiloop control system design. *Ind. Eng. Chem. Pro. Des. Dev.* **21**, 5–11 (1982)
18. McAvoy, T.J., Arkun, Y., Chen, R., Robinson, D., Schnelle, P.D.: A new approach to defining a dynamic relative gain. *Cont. Eng. Pract.* **11**, 907–914 (2003)
19. Xiong, Q., Cai, W., He, M.: A practical loop pairing criterion for multivariable processes. *J. Process Control* **15**, 741–747 (2005)
20. Monshizadeh-Naini, N., Fatehi, A., Khaki-Sedigh, A.: Input-output pairing using effective relative energy array. *Ind. Eng. Chem. Res.* **48**, 7137–7144 (2009)
21. Grosdidier, P., Morari, M.: Interaction measures for systems under decentralized control. *Automatica* **22**, 309–319 (1986)

**Part IV**  
**Soft Computing in Industrial**  
**and Management Applications**  
**(SCIMA)**

# Steps Towards Web Ubiquitous Computing

Manu Ram Pandit, Tushar Bhardwaj and Vikas Khatri

**Abstract** With evasion of digital convergence [1], computing has by and large pervaded into our environment. WWW has enhanced day-to-day life by utilizing information such as Location awareness, User-context awareness; touch API, mutation observer [2], and many more. The future [3] trends in ubiquitous computing [4] provide a great scope for innovation and value-added services. With approach of “computing being embedded,” the future sees its usage more pervasive and appealing. Web is evolving and so are supporting technologies (in terms of hardware technologies). Many real-life examples including augmented-reality, wearable technologies, gesture-based recognition systems, etc., are already in place illustrating its high-end usage. Such diverse future targeting billions of people and devices need streamlined approach. Some steps have already been taken care by World Wide Web consortium (W3C) to provide standards relating to API usage. In this paper, we highlight various aspects of web-ubiquitous computing and how they can be dealt w.r.t to their implementation.

**Keywords** Web ubiquitous computing · Ubiquitous computing recommendation · WWW pervasive computing · Future trends in web ubiquitous computing

---

M. R. Pandit (✉)  
Pursuing M.S. from BITS, Pilani, India  
e-mail: manupandit123@gmail.com

T. Bhardwaj  
Pursuing M.Tech, Pilani, India  
e-mail: tusharbhardwaj19@gmail.com

V. Khatri  
M.Tech(K.U.), Pilani, India  
e-mail: khatrivikas.mit@gmail.com

## 1 Introduction

With evasion of digital convergence [1] computing has by and large pervaded into our environment. WWW has enhanced day-to-day life by utilizing information such as Location awareness, User-context awareness; touch API, mutation observer [2] and many more. The future [3] trends in ubiquitous computing [4] provide a great scope for innovation and value-added services. With approach of “computing being embedded,” the future sees its usage more pervasive and appealing.

Today, much of user data can be seen on internet. This provides an opportunity for better services in ubiquitous computing domain. Some strategic approach is already taken in this prospect by World Wide Web consortium (W3c) to make standards for upcoming devices. This paper provides insight of web usage of ubiquitous computing domain. We first describe classifying requirements for enforcement of web ubiquitous domain followed by in-depth strategies to be taken care off during their implementation.

## 2 Context Scenarios and Recommendations

In lieu of the same, requirements of ubiquitous systems may be categorized into- (Fig. 1)

- (a) Need of high-end computing devices
- (b) Seamless network integration
- (c) Contextual awareness(User, Social, cultural and location-specific)
- (d) Security
- (e) Policy enforcement

### 2.1 Need of Computing Devices

Computing devices are important ingredient of this system. Devices may be hand-held devices or might be embedded in others like cloth. Some recommendation for making them suitable w.r.t. web-ubiquitous computing are:

- (a) They should conform to Device API specification.
- (b) Should expose themselves through *<meta>* [5] tag. This will help in self-discovery of the devices. We recommend every device to have a local information server at its ephemeral port (called as discovery port). Other devices within the device ‘X’ periphery would discover with help of : <http://www.device-x:portNo/> Similar page would turn up:
- (c) Data transfer format should be preferably HTTP.
- (d) Conformance to W3.org API specification [6].

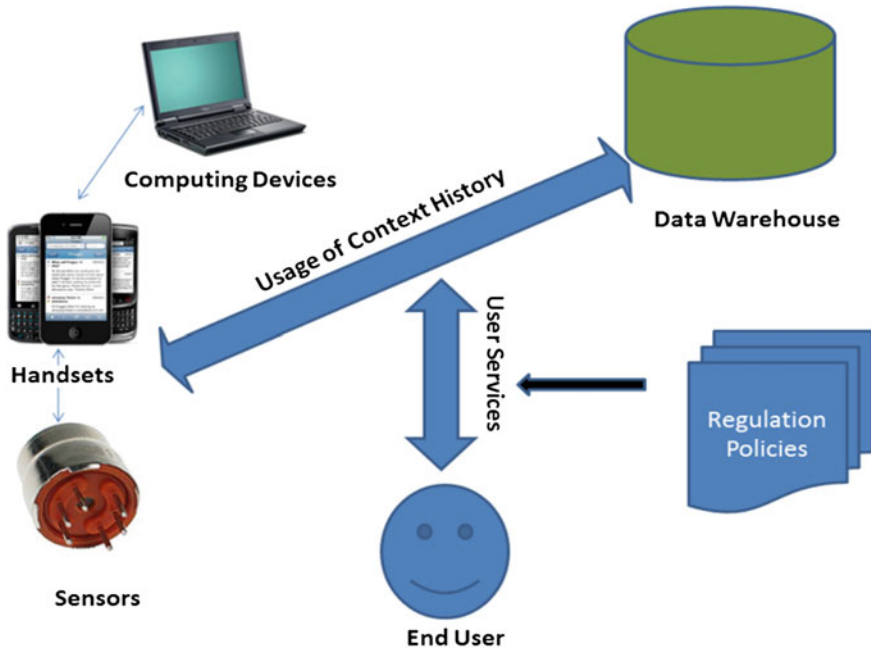


Fig. 1 The complete picture of ubiquitous computing

### 2.2 Seamless Network Integration

Underlying network technologies should be seamlessly accessible whether it is Bluetooth, wireless, connected or RF-based, etc. Frequency interference should be taken care of which are typically catered by some regulation committee such as FCC (Fig. 2).

### 2.3 Contextual Awareness

Contextual awareness is one of the most sighted features in ubiquitous computing with the help of which surrounding devices (environment) makes decision thereby adding value services to the subject. This contextual data has to be stored and regularly updated. Since contextual data will be huge, we recommend use of data warehousing technique. To add a further step, we recommend use of *data-warehousing as a service* ('daas') [7] for particular user. This service can be categorized into particular subsections like user travel information, health information, hobbies information, etc. As it involves complex performance requirements, a centralized cloud-based server typically fit into this context (Fig. 3).

```
Service_Discovery.html 88
1 <!DOCTYPE html>
2 <html lang="en">
3 <head>
4 <title>Service Discovery Page</title>
5 <meta name="description" value="Android smart phone">
6 <meta name="id" value="And_Sams_114x">
7 </head>
8 <body>
9 <<!--Content Home Page-->
10 </body>
11 </html>
```

Fig. 2 Service discovery page

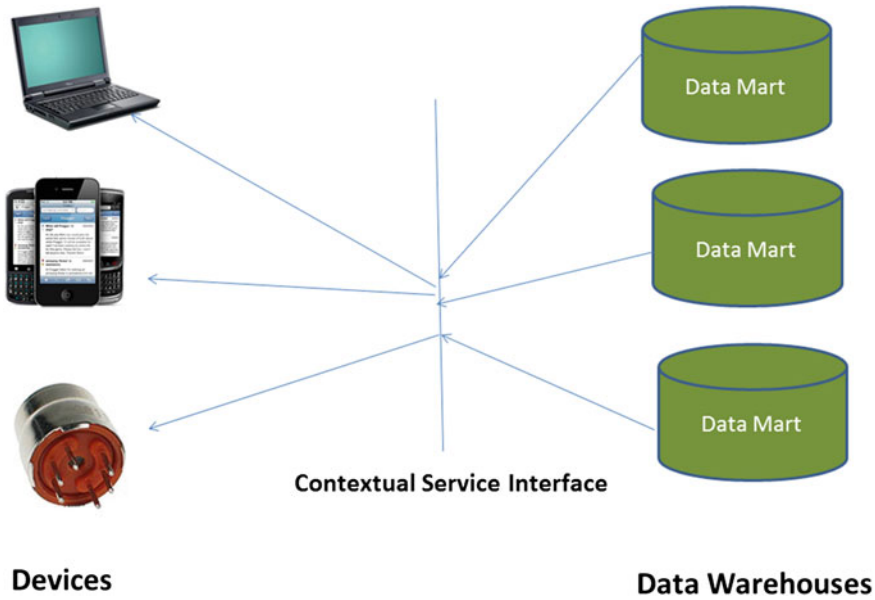


Fig. 3 Contextual service scenario

For fast performance, the data warehouse repository and underlying web-service can be deployed on cloud based server.

### 2.4 Security

While the above-mentioned services provide lucrative services, it provides vulnerabilities to personal life. User data can be hacked and details may be compromised. Basic cryptographic property viz. confidentiality, integrity, and nonrepudiation needs

to be dealt with. One possible recommended strategy to deal with is to allow user data to be shared only with devices/environment which user trust. This may be based on preconfigured security certificates or user passed tokens based on RFID [8] /other master configurable interface (e.g., Open Id-based authentication [9], Facebook/twitter/Google authentication, etc.)

## 2.5 Regulatory Policies

We highly recommend enforcement of environment policies before the devices provides user some contextual service. For instance, recommending medical aid (drugs that may be banned in some geographies), automatic software downloads (handling IP issues), purchasing some product from customer e-wallet (automatically cater new sales/revenue tax), etc. This can be easily achieved by having some centralized web-service exposed to the devices. Based on the parameters achieved, the devices can make valuable decisions. With the help of a centralized policy server, it will be effective for government/regulatory bodies to make/change decision on-the-fly.

## 3 Conclusion

With a huge user data on web, web ubiquitous computing provides a great deal of scope for innovation and development. Supporting technologies and standards will provide smoother gateway for its success. We propose some changes in classical model of ubiquitous domain (viz. intelligent devices, network, and contextual information) to suit web followed by two new parameters of security and regulatory policies.

## References

1. Infosys SETLabs Briefings. Vol 8, No 5 (2010)
2. Mozilla, Mutation Observers. [https://developer.mozilla.org/en-US/docs/DOM/DOM\\_Mutation\\_Observers](https://developer.mozilla.org/en-US/docs/DOM/DOM_Mutation_Observers)
3. Wireless Future: Ubiquitous Computing. Friedemann Mattern, ETH Zürich
4. Ubiquitous Web Domain group. <http://www.w3.org/UbiWeb/>
5. World Wide Web Consortium, Meta Tag Description. <http://www.w3.org/TR/html401/struct/global.html#h-7.4.4.2>
6. Device API Working Group. <http://www.w3.org/2009/dap/> (2009)
7. Example of Data-Warehousing as a Service. [http://www.kognitio.com/data\\_warehousing\\_as\\_a\\_service\\_daas](http://www.kognitio.com/data_warehousing_as_a_service_daas)
8. Lee, Y.K., Verbaughede, I.: Secure and Low-cost RFID Authentication Protocols
9. Open Id Authentication Specification. [http://openid.net/specs/openid-authentication-1\\_1.html](http://openid.net/specs/openid-authentication-1_1.html)



# Estimation of Uncertainty Using Entropy on Noise Based Soft Classifiers

Rakesh Dwivedi, Anil Kumar and S. K. Ghosh

**Abstract** In remote sensing noise is some kind of ambiguous data that occurs due to some inadequacy in the sensing, digitization or data recording process. This paper examines the effect of noise clustering algorithm of image classification. In remotely sensed data the easiest and usual assumption is that each pixel represents a homogeneous area on the ground. However in real world, it is found to be heterogeneous in nature. For this reason, it has been proposed that fuzziness should be accommodated in the classification procedure and preserves the extracted information. Classification of satellite images are complex process and accuracy of the output is dependent on classifier parameters. This paper examines the effect of various parameters like weighted exponent ' $m$ ' as well as resolution parameter ' $\partial$ ' for noise clustering (NC) classifier. The prime focus in this work is to select suitable parameters for classification of remotely sensed data which improves the accuracy of classification output to study the behaviour of associated learning parameters for optimization estimation using noise clustering classifier. A concept of "Noise Cluster" is introduced such that noisy data points may be assigned to the noise class. In this research work it has been tried to generate, a fraction outputs of noise clustering based classifier. The remote sensing data used has been from AWiFS, LISS-III and LISS-IV sensors of IRS-P6 satellite. This study proposes the entropy, as a special criterion for visualising and evaluating the uncertainty and it has been used as an absolute uncertainty indicator from output data. From the resultant aspect, while monitoring entropy of fraction images for different values, optimum weighting exponent ' $m$ ' and resolution parameter ' $\partial$ ' has been obtained for AWiFS, LISS-III and LISS-IV images and that is ' $m$ ' = 2.9

---

R. Dwivedi (✉) · S. K. Ghosh  
Indian Institute of Technology Roorkee, Roorkee, Uttarakhand, India  
e-mail: r\_dwivedi2000@yahoo.com

S. K. Ghosh  
e-mail: scangfce@iitr.ernet.in

A. Kumar  
Indian Institute of Remote Sensing, Dehradun, Uttarakhand, India  
e-mail: anil@iirs.gov.in

and ‘ $\partial$ ’ =  $10^6$ , providing highest degree of membership value with minimum entropy value as shown in Table 1.

**Keywords** Entropy · Noise clustering (NC) · Fuzzy c-mean (FCM) · Possibilistic c-mean (PCM) · All wide field sensor (AWiFS) · Linear imaging self scanning (LISS).

## 1 Introduction

A traditional hard classification technique does not take into account that continuous spatial variation in land cover classes. To incorporate the gradual boundary change problem researchers had been proposed the ‘soft’ classification techniques that decompose the pixel into class proportions. Fuzzy classification is a soft classification technique, which deals with vagueness in class definition. Therefore, it can model the gradual spatial transition between land cover classes.

Fuzzy c-Means (FCM) [4–6] is an unsupervised clustering algorithm which has been widely used to find fuzzy membership grades between zero and one. The aim of FCM is to find cluster centers in the feature space that minimize an objective function. The objective function is associated with the optimization problem, which minimizes within class variation and maximizes variation between two classes. Standard FCM algorithm considers the spectral characteristics.

FCM clustering algorithm has been widely used to classify Satellite images with vague land cover classes. It is a popular fuzzy set theory based soft classifier, which handles the vagueness of a pixel at sub-pixel level. FCM has been successful in assigning the membership ( $u_{ij}$ ) of a pixel to multiple classes but this assignment is relative to total number of classes defined and not absolute [16, 17]. This is because of the constraint on the membership values as given by Eq. (1)

$$\sum_{i=1}^c u_{ij} = 1 \text{ for all } j \quad (1)$$

i.e. the sum of membership values for a pixel in all the classes should be equal to one [5, 17] hence a new variation of FCM, called Possibilistic c-Means(PCM) which relaxes the constraint on membership value in Eq. (1) and gives absolute membership value, as stated by Eq. (2)

$$\max_i u_{ij} > 0 \text{ for all } j \quad (2)$$

In case of PCM, this membership value represents the “degree of belongingness or compatibility or typicality”, contrary to that represented by FCM, where it is, “degree of sharing”.

The bias due to noise is a classical problem affecting all clustering algorithms. A good solution to this problem does not exist, although the field of clustering has

been in existence for decades. An ideal solution would be one where the noise points get automatically identified and removed from the data. The concept of having an approach where one can define one cluster as the noise cluster is also promising, provided there is a way by which all the noise points could be dumped into one single cluster.

A concept of “Noise Cluster” is introduced such that noisy data points may be assigned to the noise class. The approach is developed for objective functional type (K-means or fuzzy K-means) algorithms, and its ability to detect ‘good’ clusters amongst noisy data is demonstrated. The approach presented is applicable to a variety of fuzzy clustering algorithms as well as regression analysis [9].

It is believed that cluster validity plays a pivotal role in robust clustering because without the concept of validity, it is not possible to separate the good points from the noise points and outliers and verify that our solution is good. The solution to the robust clustering problem requires that a fuzzy subset of the data set is rejected before the parameter estimates are computed. However, it is possible to optimize the objective function very trivially by excluding all points. Therefore, an additional constraint such as, cluster validity to avoid the trivial solution, is required. Hence, the solution to the general clustering problem appears to be inalienable from the notion of validity. Ideally, the objective function should be the same as the cluster validity [10].

The purpose of study of noise clustering without entropy is not only to establish a connection between fuzzy set theory and robust statistics, but also to discuss and compare several popular clustering methods from the point of view of robustness [8].

The aim of this paper is to study the behaviour of associated learning parameters of FCM, PCM and noise clustering without entropy for optimization estimation, with different fuzzy based functions, which is used for classification of multi-spectral remote sensing data in sub-pixel mode. In the next section, the details of parameters considered in FCM, PCM and noise clustering without entropy are provided. After that the remote sensing data used to produce optimization estimation based soft classification. After this experimental setup, results and their analysis are described. In last conclusion of this work is mentioned. This work has been done using in-house developed Sub-Pixel Multi-Spectral Image Classifier (SMIC) package using JAVA programming language [18].

## **2 Classifiers and Accuracy Assessment Approaches**

### ***2.1 Fuzzy C-Means Approach (FCM)***

Fuzzy c-means (FCM) was originally introduced by J. C. Bezdek in [7]. In this clustering technique, each data point belongs to a cluster to some degree that is specified by a membership grade, and the sum of the memberships for each pixel must

be equal to unity. This can be achieved by minimizing the generalized least-square error objective function,

$$J_m(U, V) = \sum_{i=1}^N \sum_{j=1}^c (\mu_{ij})^m \|X_i - x_j\|_A^2 \tag{3}$$

Subject to constraints, that

$$\sum_{j=1}^c \mu_{ij} = 1 \text{ for all } i$$

and

$$\begin{aligned} \sum_{i=1}^N \mu_{ij} &> 1 \text{ for all } j \\ 0 \leq \mu_{ij} &\leq 1 \text{ for all } i, j \end{aligned} \tag{4}$$

where  $X_i$  is the vector denoting spectral response of a pixel  $i$ ,  $x$  is the collection of vector of cluster centers  $x_j$ ,  $\mu_{ij}$  are class membership values of a pixel,  $c$  and  $N$  are number of clusters and pixels respectively, and  $m$  is a weighting exponent ( $1 < m < \infty$ ), which controls the degree of fuzziness,  $\|X_i - x_j\|_A^2$  is the squared distance ( $d_{ij}$ ) between  $X_i$  and  $x_j$ , and is given by,

$$d_{ij}^2 = \|X_i - x_j\|_A^2 = (X_i - x_j)^T A (X_i - x_j) \tag{5}$$

where  $A$  is the weight matrix.

Amongst a number of A-norms, three namely Euclidean, Diagonal and Mahalanobis norm, each induced by specific weight matrix, are widely used. The formulations of each norm are given as [7],

$$\begin{aligned} A &= I \text{ Euclidean Norm} \\ A &= D_j^{-1} \text{ Diagonal Norm} \\ A &= C_j^{-1} \text{ Mahalanobis Norm} \end{aligned} \tag{6}$$

where  $I$  is the identity matrix,  $D_j$  is the diagonal matrix having diagonal elements as the eigen values of the variance covariance matrix,  $C_j$  given by,

$$C_j = \sum_{i=1}^N (X_i - x_j)(X_i - x_j)^T \tag{7}$$

The class membership matrix  $\mu_{ij}$  is obtained by:

$$\mu_{ij} = \frac{1}{\sum_{k=1}^c \left(\frac{d_{ij}^2}{d_{ik}^2}\right)^{1/(m-1)}} \tag{8}$$

where

$$d_{ik}^2 = \sum_{j=1}^c d_{ij}^2; \tag{9}$$

### 2.2 Possibilistic C-Means Approach (PCM)

The basic change in PCM in comparison to FCM is that one would like the memberships for representative feature points to be as high as possible, while unrepresentative points should have low membership in all clusters [17]. The objective function, which satisfies this requirement, may be formulated as:

$$J_m(U, V) = \sum_{i=1}^N \sum_{j=1}^c (\mu_{ij})^m \|X_i - v_j\|_A^2 + \sum_{j=1}^c \eta_j \sum_{i=1}^N (1 - \mu_{ij})^m \tag{10}$$

Subject to constraints;

$$\max_j \mu_{ij} > 0 \text{ for all } i$$

$$\sum_{i=1}^N \mu_{ij} > 0 \text{ for all } j$$

$$0 \leq \mu_{ij} \leq 1 \text{ for all } i, j$$

here  $\mu_{ij}$  is calculated from Eq. (8).

In Eq. (10) where  $\eta_j$  is the suitable positive number, the first term demands that the distances from the feature vectors to the prototypes be as low as possible, whereas the second term forces the  $\mu_{ij}$  to be as large as possible, thus avoiding the trivial solution. Generally,  $\eta_j$  depends on the shape and average size of the cluster  $j$  and its value may be computed as:

$$\eta_j = K \frac{\sum_{i=1}^N \mu_{ij}^m d_{ij}^2}{\sum_{i=1}^N \mu_{ij}^m} \tag{11}$$

where  $K$  is a constant and is generally kept as one. After this, class memberships,  $\mu_{ij}$  are obtained as:

$$\mu_{ij} = \frac{1}{1 + \left(\frac{d_{ij}^2}{\eta_j}\right)^{1/(m-1)}} \tag{12}$$

### 2.3 Noise clustering without Entropy

A concept of ‘‘Noise Cluster’’ is introduced such that all noisy data points may be assigned to the noise class. The approach has been developed for objective functional type (K-means or fuzzy K-means) algorithms, and its ability to detect ‘good’ clusters amongst noisy data is demonstrated. Clustering methods need to be robust if they are to be useful in practice. Uncertainty is imposed simultaneously with multispectral data acquisition in remote sensing. It grows and propagates in processing, transmitting and classification processes. This uncertainty affects the extracted information quality. Usually, the classification performance is evaluated by criteria such as the accuracy and reliability. These criteria can not show the exact quality and certainty of the classification results. Unlike the correctness, no special criterion has been propounded for evaluation of the certainty and uncertainty of the classification results.

$$\mu_{i,j} = \left[ \sum_{k=1}^c \left(\frac{d_{ij}^2}{d_{ik}^2}\right)^{\frac{1}{m-1}} + \left(\frac{d_{ij}^2}{\delta}\right)^{\frac{1}{m-1}} \right]^{-1} \tag{13}$$

where  $1 \leq k \leq c$   
 where  $1 \leq j \leq c$   
 and

$$\mu_{i,c+1} = \left[ \sum_{j=1}^c \left(\frac{\delta}{d_{ik}^2}\right)^{\frac{1}{m-1}} + 1 \right]^{-1} \tag{14}$$

Resolution parameter  $\delta > 0$ , any float value greater than zero.

This study proposes the entropy, as a special criterion for visualizing and evaluating the uncertainty of the results. This paper follows the uncertainty problem in multispectral data classification process. In addition to entropy, several uncertainty criteria are introduced and applied in order to evaluate the classification performance.

The objective function, which satisfies this requirement, may be formulated as:

$$U(u_{ij}|d) = \left[ \sum_{i=1}^N \sum_{j=1}^c u_{ij} d_{ij} + \sum_{i=1}^N (u_{k,c+1})^m \vartheta \right] \tag{15}$$

and

Resolution parameter  $\delta > 0$ , any float value greater than zero  
 where  $\infty > m > 1$ , (any constant float value more than 1)

$N$  = row \* column (image size)

$i$  = stands for pixel position at  $i$ th location distance between  $X_i$  and  $V_j$

$$d_{ij}^2 = \|X_i - v_j\|_A^2 = (X_i - v_j)^T A (X_i - v_j)$$

$V_j$  = Mean Vector for each cluster centers.

### 2.4 Accuracy Assessment Approach

With the availability of IRS-P6 satellite data, it is possible to acquire spectrally same and spatial different data sets of same area with same acquisition time. Due to the uniqueness of availability of these data sets, soft fraction images generated from coarser resolution data set (e.g. LISS-III, IRS-P6) can be evaluated from fraction images generated from finer resolution data sets (e.g. LISS-IV, IRS-P6) as reference data set is acquired at same time.

In any closed system, the entropy of the system will either remain constant or increase. This is known as the second law of thermodynamics from where the concept of entropy evolves. In information technology, entropy is measure of the uncertainty Dehghan et al. Further, Entropy is also considered to be a measure of disorder, or more precisely unpredictability Shannon.

This study envisages the usage of entropy, as a special criterion for visualizing and evaluating the uncertainty of the classified results of noise clustering classifiers. This criterion is able to purely and completely reflect the uncertainty from the classified image Congalton and Goodchild M. F. For the uncertainty visualization and evaluation of the classification results, the entropy criterion is proposed. This measure expressed by the following equation:

$$Entropy(x) = \sum_{i=1}^M -\mu(w_i/x) \log_2(\mu(w_i/x)) \tag{16}$$

where “ $M$ ” denotes no. of classes and  $(\mu(\frac{w_i}{x}))$  is the estimated membership function of class  $i$  for pixel  $x$ .

For high uncertainty, the calculated value of entropy (Eq. 16) is high and inverse. Therefore, this criterion may be able to visualize the pure uncertainty in the classification results.

### 3 Study Area And Data Used

The study area for the present research work belongs to Sitarganj Tehsil, Udham Singh Nagar District, Uttarkhand, India. It is located in the southern part of the state. In terms of Geographic lat/long, the area extends from 28°52'29"N to 28°54'20"N and 79°34'25"E to 79°36'34"E. The area consists of agricultural farms with sugarcane and paddy as one of the few major crops with two reservoirs namely, Dhora and Bhagul reservoir.

The images for this research work have been taken from two different sensors namely LISS-III and LISS-IV belonging to satellite IRS-P6. The LISS-III dataset used here for classification and LISS -IV for referencing purposes.

### 4 Methodology

All three datasets (AWiFS, LISS-III, and LISS-IV) were geometrically corrected with RMSE less than 1/3 of a pixel and resampled using nearest neighbour resample method at 20m, and 5 m spatial resolution respectively to maintain the correspondence of a LISS-III pixel with specific number of LISS-IV pixels (here four pixels will corresponding to 1 LISS-III pixel) with respect to sampling during accuracy assessment. The flow chart of the methodology adopted is shown in Fig. 1 (Figs. 2 and 3).

The six classes of interest, namely Agriculture land with crop, Sal forest, Eucalyptus plantation, Agriculture dry land without crop, Agriculture moist land without crop, and water body have been used for this study work.

### 5 Results And Discussions

The ambiguity and uncertainty is one of the major issue in the classification of remote sensing data. The estimation of uncertainty in the classification results is important and is necessary to evaluate the performance of any classifier. This study addresses the evaluation of entropy, based on noise clustering classifier which estimates uncertainty in classification results. In varying spatial resolution of classification and reference soft outputs, entropy gives the true reflectance of uncertainty ratio among various classes. The uncertainty criteria have been estimated from computed entropy based on actual output of classifier.

In this research work it has been tried to generate fraction outputs from NC classifiers. These outputs have been generated from AWiFS, LISS-III and LISS-IV images of IRS-P6 data. Entropy has been used as assessment parameters of accuracy for various land cover classes i. e. water bodies, Sal forest, Eucalyptus plantation,



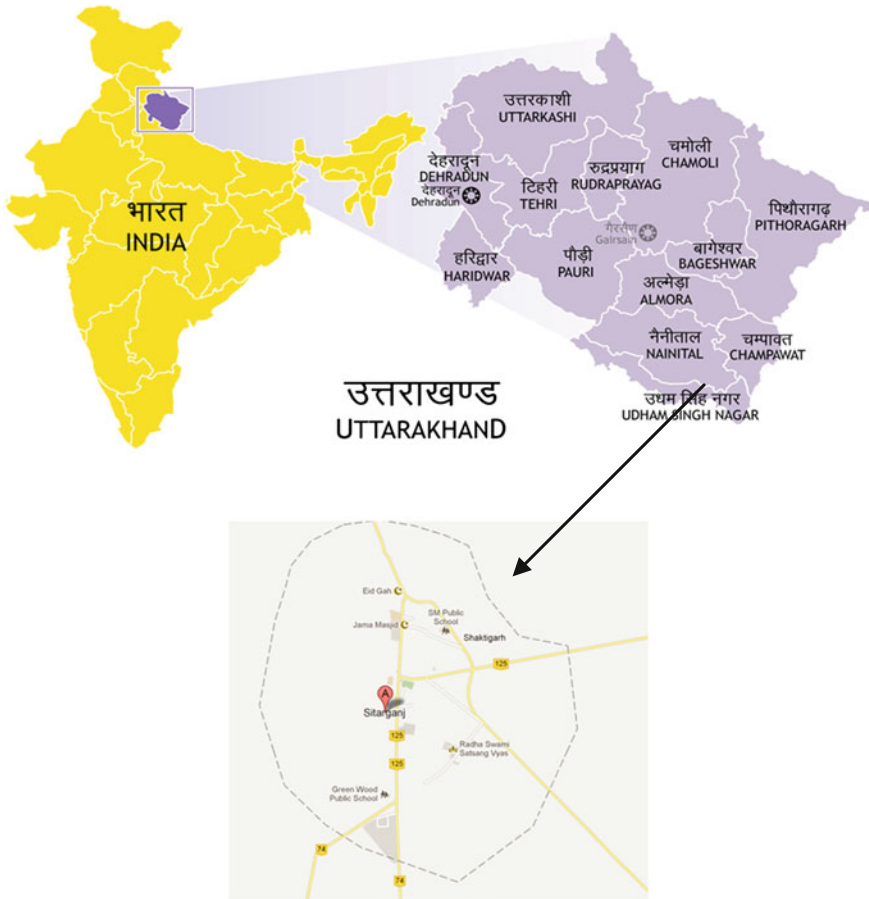


Fig. 1 Location map of study area

agriculture land with crop, agriculture moist land without crop, agriculture dry land without crop.

To investigate the effect of uncertain pixels in noise clustering classifiers, Euclidean norm has been chosen for noise clustering classifiers whereas, for fixed optimized weighting exponent  $m = 2.9$ , resolution parameter  $\theta$  varies from 1 to  $10^9$  for Sal forest, Eucalyptus plantation, water bodies, agriculture land with crop, agriculture moist land without crop, and agriculture dry land without crop. It is observed from the result Tables 1, 2, and 3, that uncertainty ratio is almost less to referential value 2.585, for noise classifiers using Euclidean norm. This reflects that noise based soft classifier is producing higher classification accuracy with minimum level of uncertainty. The computation of entropy is an absolute reflector of an uncertainty and this study identifies that entropy criterion provides stable results for noise, classifier for optimized value of  $m$  and  $\theta$ .

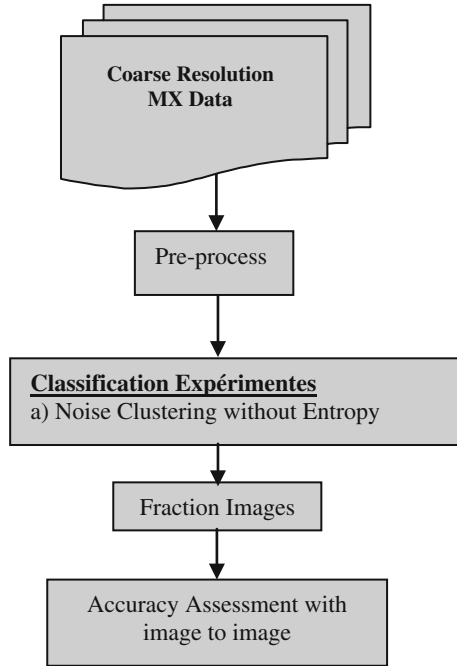


Fig. 2 Methodology adopted



Fig. 3 Location of study area

For setting the optimized value of  $m$  and ‘ $\vartheta$ ’, a number of experiments have been conducted individually for noise classifier for fixed optimized value of ‘ $m$ ’ = 2.9 and varying ‘ $\vartheta$ ’ from 1 to  $10^9$ . It has been observed from the resultant Tables 1, 2, and 3 that is for homogenous classes like Agriculture land with crop, Agriculture dry land without crop Agriculture moist land without crop, and Water Body for noise classifiers the optimized value of ‘ $\vartheta$ ’ is  $10^6$ . Similarly for heterogeneous classes like

Sal forest and Eucalyptus plantation, the optimized value of ' $\partial$ ' for noise classifier is also  $10^6$ . These findings suggest that using these optimized values of weighting exponent ' $m$ ' and resolution parameter ' $\partial$ ' for noise classifier on homogenous and heterogeneous land cover classes the range of the computed entropy varies between the range of [0, 2] as shown in resultant Tables 2, 3, and 4. This in turn states that the information uncertainty is not exceeding more than 2 %.

In this research entropy has been used to measure the accuracy in terms of uncertainty without using any kind of ground reference data. This classification accuracy is directly measured by entropy. Measuring the spatial statistics of a satellite image using an entropy, of six land cover classes can be measured using Eq. (16) i. e.  $6 * (-1/6 * \log_2(1/6)) = 2.585$  [21]. This states that if the computed entropy values of classified images are lying within this range; then indirectly this reflects better classification results. It is shown in Table 2, 3, and 4, where AWIFS, LISS-III and LISS-IV entropy of noise classifiers for six land cover classes have been computed and, found that the entropy values are approximately lying within the specified range wherein the value of weighting exponent ' $m$ ' = 2.9 and resolution parameter ' $\partial$ ' is varying from 1 to  $10^9$ .

## 6 Conclusion

In this research work entropy has been used as an assessment parameters of accuracy for various land cover classes i. e. water bodies, Sal forest, Eucalyptus plantation, agriculture land with crop, agriculture moist land without crop, agriculture dry land without crop. Entropy is used as an uniform measure to quantify the total spatial data uncertainty and fuzzy mixture uncertainty. In nutshell this study on spatial variation has identified that total uncertainty which is not exceeding the referential value, 2.585; mentioned in Table 1 for any of the above mentioned six classes of homogenous and heterogeneous categories. This mathematical model of entropy computation is used as an absolute indicator of measuring uncertainty among various land cover classes, without using any ground reference data. Accuracy assessment of a classified image is an integral part of image classification and in this research two things were involved first optimization of weighting exponent ' $m$ ' and resolution parameter ' $\partial$ ' and secondly computation of entropy. From the resultant Tables 2, 3, and 4, it shows that the optimum values of ' $m$ ' and ' $\partial$ ' for NC classifier on homogenous and heterogeneous classes are 2.9 and  $10^6$  respectively; wherein the membership values are varying from 0.9 to 1.0 with lesser entropy values, i. e. 0.86. From the Table 1, it can be observed that when the value of weighting exponent ' $m$ ' = 2.9 and resolution parameter ' $\partial$ ' =  $10^6$ , the uncertainty is almost stable for all six land cover classes.

**Table 1** Entropy variation for NC classifier

Classifiers used for various land cover classes	AWIFS Entropy		LISS-III Entropy		LISS-IV Entropy	
	Min	Max	Min	Max	Min	Max
Agriculture land with crop	0.69 at $m = 2.9$ & $\partial = 10^6$	1.21 at $m = 2.9$ & $\partial = 1$	1.15 at $m = 2.9$ & $\partial = 10^6$	1.47 at $m = 2.9$ & $\partial = 1$	1.25 at $m = 2.9$ & $\partial = 10^6$	1.67 at $m = 2.9$ & $\partial = 100$
Sal forest	0.16 at $m = 2.9$ & $\partial = 10^6$	0.87 at $m = 2.9$ & $\partial = 1$	1.11 at $m = 2.9$ & $\partial = 10^6$	1.59 at $m = 2.9$ & $\partial = 10$	0.63 at $m = 2.9$ & $\partial = 10^6$	1.31 at $m = 2.9$ & $\partial = 1$
Eucalyptus plantation	0.87 at $m = 2.9$ & $\partial = 10^6$	1.32 at $m = 2.9$ & $\partial = 100$	0.55 at $m = 2.9$ & $\partial = 10^6$	1.79 at $m = 2.9$ & $\partial = 1$	0.75 at $m = 2.9$ & $\partial = 10^6$	1.35 at $m = 2.9$ & $\partial = 1$
Agriculture dry land without crop	0.84 at $m = 2.9$ & $\partial = 10^6$	1.33 at $m = 2.9$ & $\partial = 100$	1.19 at $m = 2.9$ & $\partial = 10^6$	1.40 at $m = 2.9$ & $\partial = 100$	1.20 at $m = 2.9$ & $\partial = 10^6$	1.65 at $m = 2.9$ & $\partial = 100$
Agriculture moist land without crop	1.13 at $m = 2.9$ & $\partial = 10^6$	1.52 at $m = 2.9$ & $\partial = 100$	0.92 at $m = 2.9$ & $\partial = 10^6$	1.31 at $m = 2.9$ & $\partial = 10$	1.16 at $m = 2.9$ & $\partial = 10^6$	1.56 at $m = 2.9$ & $\partial = 1$
Water Body	0.19 at $m = 2.9$ & $\partial = 10^6$	1.04 at $m = 2.9$ & $\partial = 10$	0.67 at $m = 2.9$ & $\partial = 10^6$	1.22 at $m = 2.9$ & $\partial = 10$	1.13 at $m = 2.9$ & $\partial = 10^6$	1.51 at $m = 2.9$ & $\partial = 1$

**Table 2** AWIFS entropy of various land cover classes from NC classification output

Value of 'm' = 2.9 and varying Resolution Parameter 'θ'	Agriculture land with crop	Sal forest	Eucalyptus plantation	Agriculture dry land without crop	Agriculture moist land without crop	Water Body
θ = 1	1.21	0.87	0.93	0.51	0.61	0.93
θ = 10	1.25	0.52	1.21	1.06	1.20	1.04
θ = 10 <sup>2</sup>	0.98	0.30	1.32	1.33	1.52	0.76
θ = 10 <sup>3</sup>	0.76	0.20	1.08	1.19	1.44	0.45
θ = 10 <sup>4</sup>	0.70	0.16	0.95	0.99	1.31	0.29
θ = 10 <sup>5</sup>	0.69	0.16	0.87	0.92	1.22	0.23
θ = 10 <sup>6</sup>	0.69	0.16	0.87	0.84	1.13	0.19
θ = 10 <sup>7</sup>	0.69	0.16	0.87	0.84	1.13	0.19
θ = 10 <sup>8</sup>	0.69	0.16	0.87	0.84	1.13	0.19
θ = 10 <sup>9</sup>	0.69	0.16	0.87	0.84	1.13	0.19

**Table 3** LISS-III entropy of various land cover classes from NC classification output

Value of 'm' = 2.9 and varying Resolution Parameter 'θ'	Agriculture land with crop	Sal forest	Eucalyptus plantation	Agriculture dry land without crop	Agriculture moist land without crop	Water Body
θ = 1	1.47	1.45	1.193	0.90	1.109	0.99
θ = 10	1.66	1.59	1.013	1.22	1.31	1.22
θ = 10 <sup>2</sup>	1.51	1.40	0.80	1.40	1.128	1.09
θ = 10 <sup>3</sup>	1.33	1.25	0.66	1.37	0.99	0.90
θ = 10 <sup>4</sup>	1.22	1.174	0.58	1.30	0.91	0.79
θ = 10 <sup>5</sup>	1.16	1.11	0.55	1.24	0.91	0.68
θ = 10 <sup>6</sup>	1.15	1.11	0.55	1.19	0.92	0.67
θ = 10 <sup>7</sup>	1.15	1.11	0.55	1.19	0.92	0.67
θ = 10 <sup>8</sup>	1.157	1.11	0.55	1.19	0.92	0.67
θ = 10 <sup>9</sup>	1.157	1.11	0.55	1.19	0.92	0.67

**Table 4** LISS-IV entropy of various land cover classes from NC classification output

Value of ' $m$ ' = 2.9 and varying Resolution Parameter ' $\theta$ '	Agriculture land with crop	Sal forest	Eucalyptus plantation	Agriculture dry land without crop	Agriculture moist land without crop	Water Body
$\theta = 1$	1.37	1.31	1.35	0.96	1.11	1.03
$\theta = 10$	1.66	1.076	1.19	1.51	1.57	1.49
$\theta = 10^2$	1.67	0.83	1.04	1.65	1.56	1.51
$\theta = 10^3$	1.54	0.74	0.89	1.49	1.35	1.32
$\theta = 10^4$	1.40	0.68	0.81	1.35	1.36	1.19
$\theta = 10^5$	1.30	0.64	0.77	1.29	1.20	1.16
$\theta = 10^6$	1.25	0.63	0.75	1.20	1.16	1.14
$\theta = 10^7$	1.25	0.63	0.75	1.20	1.16	1.13
$\theta = 10^8$	1.25	0.63	0.75	1.20	1.16	1.13
$\theta = 10^9$	1.25	0.63	0.75	1.20	1.16	1.135

## References

1. Binaghi, E., Rampini, A.: Fuzzy decision making in the classification of multisource remote sensing data. *Opt. Eng.* **6**, 1193–1203 (1993)
2. Binaghi, E., Rampini, A., Brivio, P.A., Schowengerdt, R.A. (eds.): Special Issue on Non-conventional Pattern Analysis in Remote Sensing. *Pattern Recogn. Lett.* **17**(13) (1996)
3. Binaghi, E., Brivio, P.A., Chessi, P., Rampini, A.: A fuzzy set based accuracy assessment of soft classification. *Pattern Recogn. Lett.* **20**, 935–948 (1999)
4. Bezdek, J.C.: A convergence theorem for the fuzzy ISODATA clustering algorithms. *IEEE Trans. on Pattern Anal. Machine Intell. PAMI-2*(1), 1–8 (1980)
5. Bezdek, J.C., Ehrlich, R., Full, W.: FCM: the fuzzy c-means clustering algorithm. *Comput. Geosci.* **10**(2–3), 191–203 (1984)
6. Bezdek, J.C., Hathaway, R.J., Sabin, M.J., Tucker, W.T.: Convergence theory for fuzzy c-means: counterexamples and repairs. *IEEE Trans. Syst., Man, Cybern. SMC-17*(5), 873–877 (1987)
7. Bezdek, J.C.: *Pattern recognition with fuzzy objective function algorithms*. Plenum, New York, USA (1981)
8. Dav'e, R.N.: Fuzzy-shell clustering and applications to circle detection in digital images. *Int. J. Gen. Syst.* **16**, 343–355 (1990)
9. Dave, R.N.: Characterization and detection of noise in clustering. *Pattern Recogn. Lett.* **12**, 657–664 (1991)
10. Dav'e, R.N., Krishnapuram, R.: Robust clustering methods: a unified view. *IEEE Trans. Fuzzy Syst.* **5**(2), 270–293 (1997)
11. Fisher, P.: The pixel: a snare and a delusion. *Int. J. Remote Sens.* **18**(3), 679–685 (1997)
12. Foody, G.M.: Cross-entropy for the evaluation of the accuracy of a fuzzy land cover classification with fuzzy ground data. *ISPRS J. Photogrammetry Remote Sens.* **50**, 2–12 (1995)
13. Foody, G.M.: Approaches for the production and evaluation of fuzzy land cover classifications from remotely sensed data. *Int. J. Remote Sens.* **17**(7), 1317–1340 (1996)
14. Foody, G.M., Arora, M.K.: Incorporating mixed pixels in the training, allocation and testing stages of supervised classification. *Pattern Recogn. Lett.* **17**, 1389–1398 (1996)
15. Foody, G.M., Lucas, R.M., Curran, P.J., Honzak, M.: Non-linear mixture modelling without end-members using an ANN. *Int. J. Remote Sens.* **18**(4), 937–953 (1997)
16. Foody, G.M.: Estimation of sub-pixel land cover composition in the presence of untrained classes. *Comput. Geosci.* **26**, 469–478 (2000)
17. Krishnapuram, R., Keller, J.M.: A possibilistic approach to clustering. *IEEE Trans. Fuzzy Syst.* **1**(2), 98–110 (1993)
18. Kumar, A., Ghosh, S.K., Dadhwal, V.K.: Study of sub-pixel classification algorithms for high dimensionality data set. In: *IEEE International Geoscience and Remote Sensing Symposium and 27th Canadian Symposium on Remote Sensing*, Denver, Colorado, USA, 31 July–04 August (accepted), (2006)
19. Okeke, F., Karnieli, A.: Methods for fuzzy classification and accuracy assessment of historical aerial photographs for vegetation change analyses. Part I: algorithm development. *Int. J. Remote Sens.* **27**(1–2), 153–176 (2006)
20. Pontius, Jr, R.G., Cheuk, M.L.: A generalized cross tabulation matrix to compare soft classified maps at multiple resolutions. *Int. J. Geogr. Inf. Sci.* **20**(1), 1–30 (2006)
21. Verhoeye, J., Robert, D.W.: Sub-pixel mapping of sahelian wetlands using multi-temporal SPOT vegetation images. Laboratory of Forest Management and Spatial Information Techniques, Faculty of Agricultural and Applied Biological Sciences, University of Gent, Belgium, (2000)



# Location Management in Mobile Computing Using Swarm Intelligence Techniques

Nikhil Goel, J. Senthilnath, S. N. Omkar and V. Mani

**Abstract** Location management is an important and complex issue in mobile computing. Location management problem can be solved by partitioning the network into location areas such that the total cost, i.e., sum of handoff (update) cost and paging cost is minimum. Finding the optimal number of location areas and the corresponding configuration of the partitioned network is NP-complete problem. In this paper, we present two swarm intelligence algorithms namely genetic algorithm (GA) and artificial bee colony (ABC) to obtain minimum cost in the location management problem. We compare the performance of the swarm intelligence algorithms and the results show that ABC give better optimal solution to locate the optimal solution.

**Keywords** Location management · Genetic algorithm · Artificial bee colony

## 1 Introduction

The aim of location management is to track where the subscribers are in order to route incoming calls to appropriate mobile terminals. Location Management strategies can be divided into always-update strategy and never-update strategy. In the

---

N. Goel (✉)

Department of Information Technology, National Institute of Technology Karnataka,  
Surathkal, India  
e-mail: nikhil8877@gmail.com

J. Senthilnath · S. N. Omkar · V. Mani

Department of Aerospace Engineering, Indian Institute of Science, Bangalore, India  
e-mail: snrj@aero.iisc.ernet.in

S. N. Omkar

e-mail: omkar@aero.iisc.ernet.in

V. Mani

e-mail: mani@aero.iisc.ernet.in

always-update strategy, as soon as mobile terminals enter new cells, it performs location update. Using this strategy you can get accurate location information and hence save resources spent on searching (paging). But this frequent location update will require high resource (overhead). In the never-update strategy, location update is never performed. Instead, when an incoming call comes, a search operation is conducted to route the call to appropriate mobile terminals. Here, no resources would be used for location update, overhead for search operation (paging) would be very high. Hence, there is need to have balance between location update and paging so as to minimize the total cost of mobile communication [1–3].

The location area scheme is another location management technique that is commonly used in existing networks [4–6]. In this scheme, the network is partitioned into regions known as location areas (LA), with each region consisting of one or more cells. The update operation is performed only when any user moves from one location area to another. When a call arrives, searching (paging) operation is performed for cells in specific LA. Optimal LA partitioning is NP-complete problem [7].

Genetic algorithm with modified genetic operators was used to solve this optimization problem in [8]. Another swarm intelligence algorithm—ant colony optimization was discussed in [1]. Minimizing the location update subject to a paging bound constraint is studied in [9]. A polynomial time approximate algorithms with the objective of minimizing the sum of handoff traffic cost and paging cost are presented in [10].

*Contributions of this paper:* In this paper, we consider the location area scheme model and try to minimize the cost per arrival presented in earlier studies [1, 11]. We obtain the optimal cost per arrival using swarm intelligence techniques namely GA and artificial bee colony (ABC). Call per cost arrival is defined as total cost divided by total call arrivals in given network in time  $T$ , and obtains optimal number of location areas. Previous study [2] on location management using GA has been carried out using reporting cell model [3]. Here, we present GA for location management problem but using location area scheme [1]. We also apply ABC algorithm to minimize cost per call arrival and compare our results with results of earlier study [1, 2].

## 2 Problem Formulation

Let us assume a network with  $n$  cells. With each cell  $i$  we associate call movement weight  $W_{mi}$  and call arrival weight  $W_{ci}$ . Movement weight represents total number of movement into the cell. Call arrival weight represents total number of call arrivals within a cell. Paging Cost for a cell in  $K$ th location area is

$$a_j = \sum_{j \in k}^n W_{cj}, \quad \text{for all } j = 1, 2, \dots, n \quad (1)$$

Total paging cost for location area  $k$ , if there are  $NLA_k$  cells in  $k$ th location area is

$$PC_k = NLA_k * a_j \tag{2}$$

Hence total paging cost is:

$$N_P = \sum_{k=1}^m PC_k \tag{3}$$

Whenever there is movement among two adjacent cells in different two location areas, cost is incurred for updating its location. Total handoff cost is:

$$N_{LU} = \sum_{i=1}^n \sum_{j=1}^n (1 - Y_{ij}) * h(i, j) \tag{4}$$

We know from [1] that:

$$\text{Total cost} = N_p + C * N_{LU} \tag{5}$$

Therefore,

$$\text{Total cost} = \sum_{k=1}^m NLA_k * \left\{ \sum_{j \in k}^n W_{cj} \right\} + C * \sum_{i=1}^n \sum_{j=1}^n (1 - Y_{ij}) * h(i, j) \tag{6}$$

$Y_{ij} = 1$ , if both cell  $i$  and cell  $j$  are assigned to the same location area;  
 $Y_{ij} = 0$  otherwise.

where  $h(i, j)$  is cost per unit time handoff occur between cell  $i$  and cell  $j$  and depends upon the movement weight of cell  $i$  and cell  $j$ .  $C$  is a constant representing the cost ratio of location update and paging. It was studied in [12] that cost of location update is much higher than paging cost and it was also concluded in [8] that  $C$  value is approximately 10. Cost per call arrival is calculated by dividing total cost by total number of call arrivals. For a given network, total number of call arrivals is calculated using

$$\text{Total number of call arrivals} = \sum_{j \in k}^n W_{cj} \tag{7}$$

Hence,

$$\text{Cost per call arrival} = (\text{total Cost}) / \text{total number of call arrivals} \tag{8}$$

### 3 The Methodology

This section gives brief introduction to swarm intelligence algorithms [13–22] used in our study, the way they are used to solve combinatorial optimization and the pseudocode for the algorithms.

#### 3.1 Genetic Algorithm

Genetic algorithm is a population based evolutionary computation technique [13]. This algorithm takes a predetermined number of random solutions (population) in the search space called chromosomes. At each iteration the chromosomes are made to crossover. At any random point, chromosomes undergo mutation based on mutation rate and the fitness of each chromosome is calculated using Eq. (8). The fitness is calculated and the best solutions carry-on till termination criteria is reached. Thus, optimal distribution of cells among different LA can be determined using this algorithm.

#### 3.2 Artificial Bee Colony

In the ABC algorithm [14], all the population is considered as employed bee and onlooker bee, i.e., they checked for food source in their neighbor region. Solutions consisting of cells belonging to specific LA are changed to get a new solution given by Eq. (9).

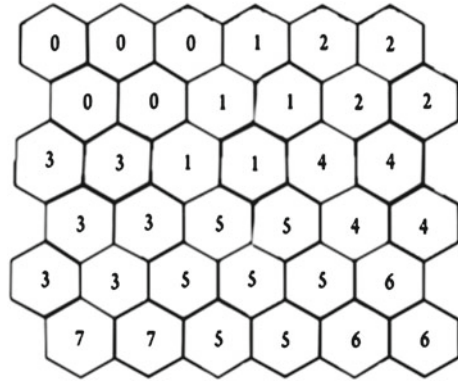
$$V [ij] = x [ij] + phi [ij] * (x [kj] - x [ij]) \quad (9)$$

where  $x [ij]$  represents LA of  $j$ th cell in  $i$ th solution and  $x [kj]$  represents LA of  $j$ th cell in  $k$ th solution ( $k$  is randomly selected).  $Phi [ij]$  ensures that new LA assigned to  $j$ th cell in  $i$ th solution already exists. New LA value is stored in  $V [ij]$ .

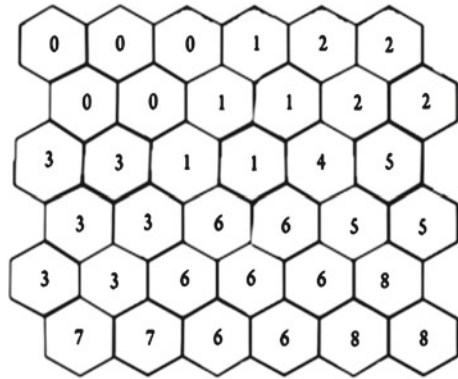
### 4 Results and Discussion

In this section, the results and the performance evaluation are shown. A discussion is carried out at the end of this section pertaining to the results obtained. Here, we have considered two networks (i)  $6 \times 6$  and (ii)  $8 \times 8$  with the values of movement weight  $W_{mi}$  and call arrival weight  $W_{ci}$  for all the cells in the networks [2]. For each network we found the optimal number of LA so that cost per call arrivals is minimum using GA and ABC and compare our results with ant colony optimization method given in [1]. We run the code for 10 times for each of the algorithm mentioned above and

**Fig. 1** Configuration with optimal number of LA using GA



**Fig. 2** Configuration with optimal number of LA using ABC



**Table 1** 6 × 6 network

Method	Minimum fitness	Number of LA	Maximum	Mean	SD
ACO [1]	11.1147	8	–	–	–
GA	11.1147	8	11.586426	11.3098419	0.1554
ABC	11.0943	9	11.545944	11.2829718	0.1393

maximum, minimum, mean, and deviation are calculated. We also made the graph for fitness value versus number of iterations for the run where we get optimal fitness.

In first case, we consider 6 × 6 (36 cells) network. For 6 × 6 network we have search space of size  $2^{36} = 68,719,476,736$ . In all the methods used in this study we use population of 10 and maximum generation of 10,000. In GA, the best 20 % of the parent are reproduced and the remaining 80 % undergoes crossover and mutation for the next generation. Parameter in ABC such as limit value is set to be 50. Best results of GA and ABC have been shown in Figs. 1 and 2, respectively and corresponding regions have been assigned to the same value. From Table 1, we observe after 10 runs for this network, ABC provides better optimal solution compared to ACO and GA.

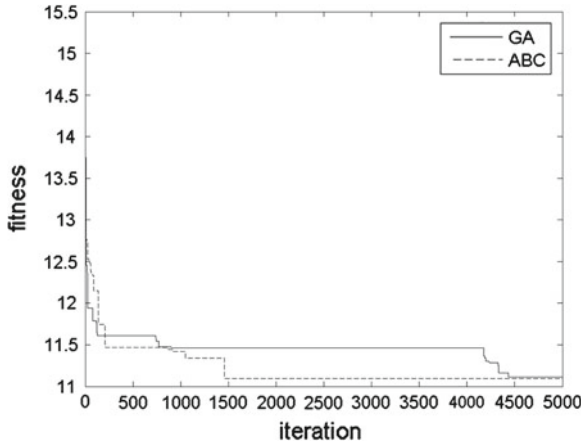


Fig. 3  $6 \times 6$  network

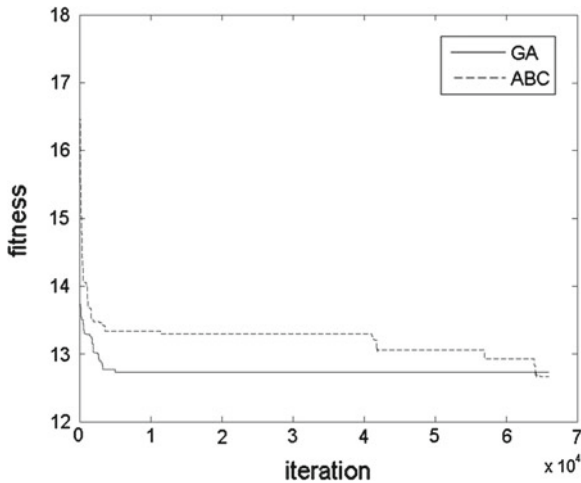


Fig. 4  $8 \times 8$  network

ABC shows minimum standard deviation. From Fig. 3, we can observe GA converges faster in comparison to ABC.

In second case, we consider  $8 \times 8$  (64 cells) network. For  $8 \times 8$  network we have search space of size  $2^{64} = 18,446,744,073,709,551,616$ . The parameters such as population size and maximum generation are kept constant which is 20 and 1,00,000. Here also in GA, the best 20% of the parent are reproduced and the remaining 80% undergoes crossover and mutation for the next generation, whereas in ABC limit value is set to be 1,000. From Fig. 4 we can once again observe GA converges faster in comparison to ABC. Again best result obtained using GA and ABC has been shown in Figs. 5 and 6, respectively and corresponding regions have been assigned

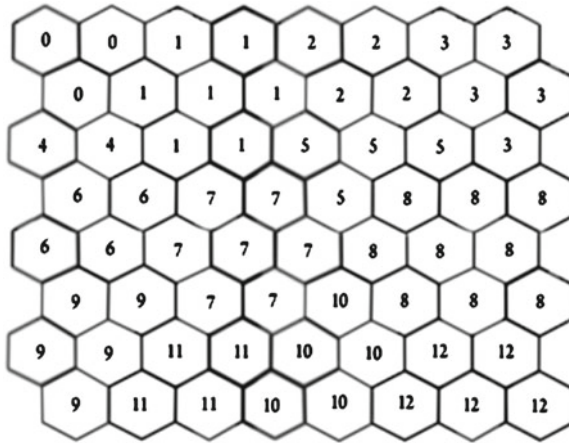


Fig. 5 Configuration with optimal number of LA using GA

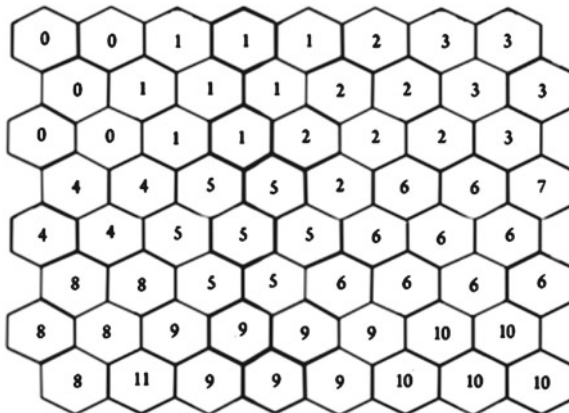


Fig. 6 Configuration with optimal number of LA using ABC

Table 2 8 × 8 network

Method	Minimum fitness	Number of LA	Maximum	Mean	SD
ACO [1]	12.86895	13	–	–	–
GA	12.731830	13	13.266327	12.926776	0.1596
ABC	12.668662	13	13.158280	12.842936	0.1255

to the same value. From Table 2, we observe that after 10 runs for this network, ABC provides better optimal solution compared to ACO and GA. ABC shows minimum standard deviation.

## 5 Conclusion

In this paper, we have implemented and analyzed two nature inspired techniques for location management problem and compared it with earlier studied method. The optimal partitions of  $6 \times 6$  and  $8 \times 8$  networks are presented. Results of the experiments show that ABC and GA can be effectively implemented for location management scheme. While ABC show best performance in terms of optimal value of cost per call arrival and standard deviation, GA converges faster in both the network.

## References

1. Kim, S.S., Kim, I.H., Mani, V., Kim, H.J., Agarwal, D.P.: Partitioning of mobile network into location areas using ant colony optimization. *ICIC Express Lett. Part B: Appl.* **1**(1), 39–44 (2010)
2. Subrata, R., Zomaya, A.Y.: A comparison of three artificial life techniques for reporting cell planning in mobile computing. *IEEE Trans. parallel Distrib. Syst.* **14**(2), 142–153 (2003)
3. Bar, N.A., Kessler, I.: Tracking mobile users in wireless communications networks. *IEEE Trans. Inf. Theory* **39**, 1877–1886 (1993)
4. Okasaka, S., Onoe, S., Yasuda, S., Maebara, A.: A new location updating method for digital cellular systems. In: *Proceedings of 41st IEEE Vehicular Technology Conference* (1991)
5. Plassmann, D.: Location management strategies for mobile cellular networks of 3rd generation. In: *Proceedings of IEEE 44th Vehicular Technology Conference* (1994)
6. Yeung, K.L., Yum, T.S.P.: A comparative study on location tracking strategies in cellular mobile radio systems. In: *Proceedings of IEEE Global Telecommunication Conference* (1995)
7. Gondim, P.R.L.: Genetic algorithms and the location area partitioning problem in cellular networks. In: *Proceedings of IEEE 46th Vehicular Technology Conference* (1996)
8. Taheri, J., Albert Y.Z.: A genetic algorithm for finding optimal location area configurations for mobility management. *IEEE Conference on Local Computer Networks 30th Anniversary* (2005)
9. Yannis, M., Magdalene, M., Michael, D., Nikolaos, M., Constantin, Z.: A hybrid stochastic genetic-GRASP algorithm for clustering analysis. *Oper. Res. Int. J.* **8**, 33–46 (2008). doi: [10.1007/s12351-008-0004-8](https://doi.org/10.1007/s12351-008-0004-8)
10. Bejerano, Y., Smith, M.A., Naor, J.S., Immorlica, N.: Efficient location area planning for personal communication systems. *IEEE/ACM Trans. Netw.* **14**, 438–450 (2006)
11. Subrata, R., Zomaya, A.Y.: Evolving cellular automata for location management in mobile computing networks. *IEEE Trans. Parallel Distrib. Syst.* **14**, 13–26 (2003)
12. Imielinski, T., Badrinath, B.R.: Querying locations in wireless environments. In: *Proceedings of Wireless Communication and Future Directions* (1992)
13. Goldberg, D.E.: *Genetic Algorithms in Search Optimization and Machine Learning*. Addison-Wesley, Reading (1989)
14. Karaboga, D., Basturk, B.: On the performance of artificial bee colony (ABC) algorithm. *Appl. Soft Comput.* **8**(1), 687–697 (2008)
15. Senthilnath, J., Omkar, S.N., Mani, V., Tejovanth, N., Diwakar, P.G., Archana Shenoy, B.: Hierarchical clustering algorithm for land cover mapping using satellite images. *IEEE J. Sel. Topics Appl. Earth Obs. Remote Sens.* **5**(3), 762–768 (2012)
16. Craig, D., Omkar, S.N., Senthilnath, J.: Pickup and delivery problem using metaheuristics. *Expert Syst. Appl.* **39**(1), 328–334 (2012)
17. Senthilnath, J., Omkar, S.N., Mani, V.: Clustering using firefly algorithm: performance study. *Swarm Evol. Comput.* **1**(3), 164–171 (2011)



18. Omkar, S.N., Senthilnath, J., Khandelwal, R., Narayana Naik, G., Gopalakrishnan, S.: Artificial Bee Colony (ABC) for multi-objective design optimization of composite structures. *Appl. Soft Comput.* **11**(1), 489–499 (2011)
19. Omkar, S.N., Senthilnath, J.: Artificial bee colony for classification of acoustic emission signal sources. *Int. J. Aerosp. Innov.* **1**(3), 129–143 (2009)
20. Omkar, S.N., Senthilnath, J., Suresh, S.: Mathematical model and rule extraction for tool wear monitoring problem using nature inspired techniques. *Indian J. Eng. Mater. Sci.* **16**, 205–210 (2009)
21. Omkar, S.N., Senthilnath, J.: Mudigere, D., Manoj Kumar, M.: Crop classification using biologically inspired techniques with high resolution satellite image. *J. Indian Soc. Remote Sens.* **36**(2), 172–182 (2008)
22. Omkar, S.N., Senthilnath, J.: In: Dehuri, S., et al. (eds.) *Integration of Swarm Intelligence and Artificial Neural Network, Neural Network and Swarm Intelligence for Data Mining*, chap. 2. World Scientific Press, Singapore, pp. 23–65 (2011)

# Fingerprint and Minutiae Points Technique

Karun Verma and Ishdeep Singla

**Abstract** This paper will extensively dictate the whole basic details of fingerprint and its techniques. Moreover one of the most important and widely used techniques that is minutiae point extraction technique is also covered in detail. The minutiae points are extracted with the help of cross-number algorithm. Cross-number algorithm also helps for the rejection of false minutiae point's extraction

**Keywords** Biometrics · Fingerprint · Minutiae points

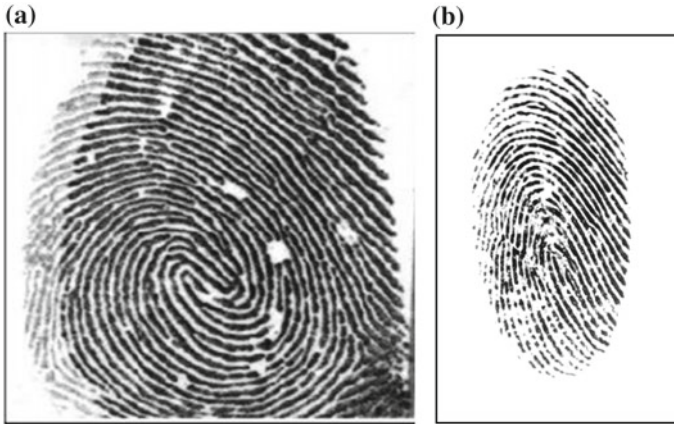
## 1 Introduction

In an increasingly digital world, the control over entry of authorized person has become a vital thing. From the personal computer to National security, there is big use of identity checking that is Authentication. And biometrics provide automated access to the security systems. It's always better to use some automated methods instead of remembering and filling passwords. In biometrics, fingerprint technology is widely used technology, using this technology we need not to carry any identity card. Fingerprint works as identity card, meaning there are no tension of forgetting and losing identity cards [1].

---

K. Verma · I. Singla (✉)  
Computer Science and Engineering Department, Thapar University, Patiala, India  
e-mail: ishdeep.singla@gmail.com

I. Singla  
e-mail: karun.verma@thapar.edu



**Fig. 1** Fingerprint images: **a** inked fingerprint and **b** live-scan fingerprint [3]

## 2 What is Fingerprint?

Fingerprint is the graphical flow-like ridges. It is present on each and every finger of every human's fingers as shown in Fig. 1. Ridges are embedded on all fingers from the very first day of our birth and do not change throughout the life. It may only change if a serious accident such as bruises and cuts or surgery on the fingertips occurs. This property makes fingerprints a very attractive biometric identifier and point of research. Basically, there are two resources for getting fingerprint pattern [2]:

- (i) Scanning an inked impression of a finger is shown in Fig. 1a.
- (ii) Using a live-scan fingerprint scanner shown in Fig. 1b.

In Fig. 1, dark lines are called ridges and the white area that exists between the ridges are called valley or furrow.

## 3 Fingerprint Features

Fingerprint features are those attributes of a fingerprint that may be useful either to classify or to uniquely identify the fingerprint. There are two main types of features, namely, the local features and the global features. Figure 2a shows the local features and Fig. 2b shows the global features.

### 3.1 Global Features

The fingerprint global features are identified by means of the local orientation of the fingerprint ridges, that is, the Orientation Field Curves (OFCs). As shown in Fig. 2b the core and the delta are the features which have been located in central position of

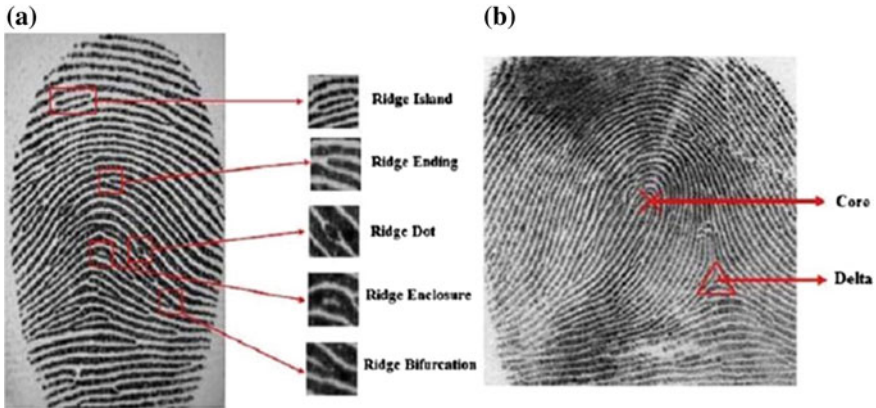


Fig. 2 a Local Features: Minutiae; b global features: core and delta [3]

fingerprint. A Core is the area around the center of the fingerprint loop and a Delta is the area where the fingerprint ridges tend to triangulate. Due to their unique property, both plays an important role to compare one fingerprint with other fingerprints [4].

### 3.2 Local Features

The fingerprint local features are those attributes that give the minutiae details about the fingerprint pattern. Minutiae further provide various ways that the ridges can be discontinuous. A ridge can suddenly end (termination), or can divide into two ridges (bifurcation) as shown in Fig. 2a. There are 40–100 minutiae point in a good quality image [8]. And in a fingerprint image of  $300 \times 300$  pixels the distance between two fingerprints vary between 1-113 pixels. With these features and numerical figures, local features have become more suitable to compare fingerprints [4]. There are many methods like cross number are available to extract the minutiae points.

## 4 Fingerprint Classification

It is obvious that with the increase database size complexity and automatic comparison time will also increase. So to reduce the search time and computational complexity, there is a need to classify fingerprint in a precise and consistent manner which will help to reduce search time with less number of comparisons. According to Galton–Henry classification (Galton, 1892 and Henry, 1900) classification, we classify fingerprint images into five major classes: plain arch, tented arch, left-loop, right-loop, and whorl (a plain and twin loop, respectively).

**Arch:** In whole fingerprint arch covers only 5% of the portion. These consist of ridges that run major in horizontal manner can say from left to right as shown in Fig. 3. There are two types of arches: plain arches and tented arches. Generally, plain arch has no singular points. While tented arch have one core and one delta.

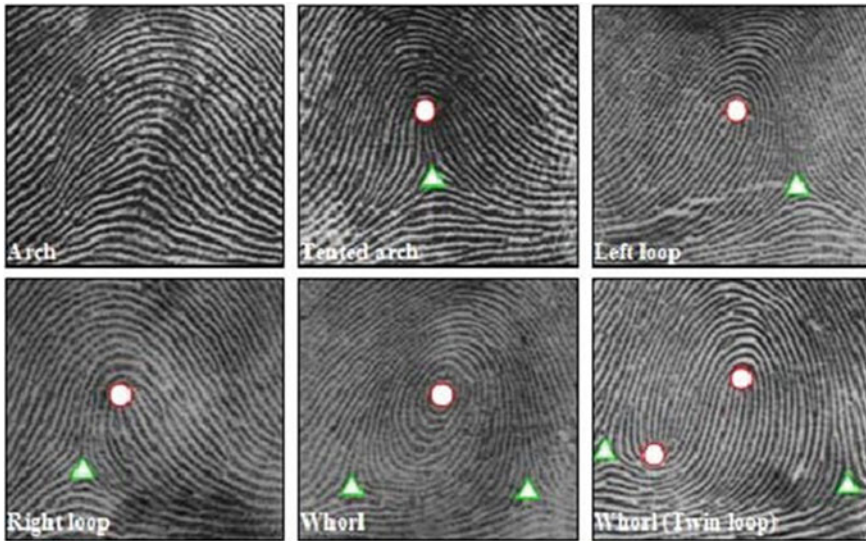


Fig. 3 Fingerprint classes [5]

**Loop:** Loops cover 60–70% of whole fingerprint pattern. As the name suggests set of the ridges enters on either side of the fingerprint, bends, touches, or crosses the line running from the delta to the core and run back in same direction of the side where the ridge or ridges entered as shown in Fig. 3. Each loop pattern has one delta and one core. There can be left loop or right loop.

**Whorl:** 25–35% of fingerprint pattern is covered by whorl. In a whorl, more than one ridges moves through at least one circuit. A whorl pattern always consists of two or more deltas. There are two types of whorl plain whorl and double whorl. A plain whorl is the pattern which consists of some ridges which make or partially make a complete circuit with two deltas. Double loop whorl consists of two separate and distinct loops.

## 5 Fingerprint Matching Techniques

There a lot of techniques for matching a fingerprint. There are three most popular methods for matching fingerprints [2] described below.

### 5.1 Correlation-based Matching

In this method one fingerprint image is superimposed on other. The correlation between corresponding pixels is computed for different alignments and on the basis of these correlations and computations decision is made.

## 5.2 *Pattern-based (or Image-based) Matching*

In pattern-based algorithms, the basic fingerprint patterns (arch, whorl, and loop) are used to compare fingerprints, between a previously stored template and a candidate fingerprint. This requires that the images are aligned in the same orientation. To do this, the algorithm finds a central point in the fingerprint image and centers on that. In a pattern-based algorithm, the template contains the type, size, and orientation of patterns within the aligned fingerprint image. The candidate fingerprint image is graphically compared with the template to determine the degree to which they match.

## 5.3 *Minutiae-based Matching*

This is the most popular and widely used technique, being the basis of the fingerprint comparison made by fingerprint examiners. Minutiae are extracted from the two fingerprints and stored as sets of points in the two-dimensional plane. Minutiae-based matching essentially consists of finding the alignment between the template and the input minutiae sets that result in the maximum number of minutiae pairings. In this thesis we have implemented a minutiae-based matching technique. This approach has been intensively studied, also is the backbone of the current available fingerprint identification products.

# 6 Minutiae Extraction

Minutiae points matching is the best approach for the matching of fingerprints. The work of minutiae extraction includes some important steps that are Ridge Thinning, Minutiae Marking, False Minutiae Removal, and Minutiae Representation.

## 6.1 *Ridge Thinning*

The main aim of this step is to convert the redundant pixels of ridge into one pixel wide. This will be very helpful in finding minutiae points and to implement minutiae point algorithm. In Matlab there has been one very popular morphological thinning function to perform this task.

**bwmorph(binaryImage,'thin',Inf)**

The thinned image is then filtered, again using MATLAB's three morphological functions to remove some H breaks, isolated points, and spikes (see Fig. 4).

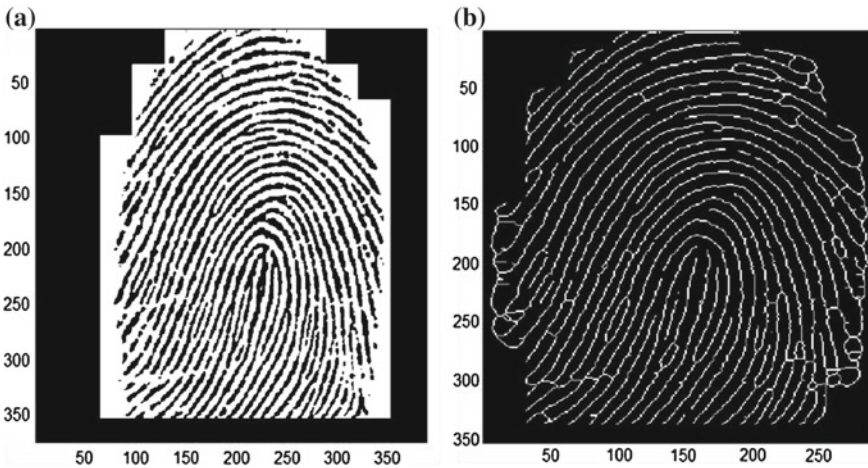


Fig. 4 a Binarize image; b Thinning image

**bwmorph(binaryImage,'hbreak',k) → For H breaks**  
**bwmorph(binaryImage,'clean',k) → For isolated points**  
**bwmorph(binaryImage,'spur',k) → Spikes**

### 6.2 Minutiae Marking

The name of this algorithm is crossing number (CN). It is implemented thinned image. Iteratively a  $3 \times 3$  pixels wide picture is selected from thinned image then check that if the central pixel is a ridge branch and the central pixel is 1 and has exactly three neighbors of 1's, then its *bifurcation* (see Fig. 5).

If there one central 1 with exactly one 1 in its neighbourhood, then its a *ridge ending* (see Fig. 6).

Fig. 5 Ridge bifurcation

0	1	0
0	1	0
1	0	1

Fig. 6 Ridge termination

0	0	0
0	1	0
0	0	1

### 6.3 False Minutiae Removal

As fingerprint sample maybe taken from ink impression (paper, thing) or it may be taken by using fingerprint scanner. But in case of ink impression the fingerprint quality may suffer. The quality of ink impression fingerprint image may be low which creates false minutiae points. So in most of the cases it need to be eliminated. To remove false minutiae points first calculate the inter ridge distance  $D$  (say) which is the average distance between two neighboring ridges. For this scan each row calculate the inter ridge distance using the formula [6]:

$$\text{Inter ridge distance} = \frac{\text{sum all the pixels in the row whose value is one}}{\text{row length}}$$

Calculate an average of all the inter ridge distance  $D$ . A MATLAB morphological operation ‘BWLABEL’ is helpful in this task. There have been seven different cases studied of false minutiae point’s patterns. Follow the steps to remove these seven erogenous patterns (see Fig. 7) [6, 7].

- If  $d$  (bifurcation, termination)  $< D$  and the two minutia are in the same ridge then remove both of them (case  $m1$ ).
- If  $d$  (bifurcation, bifurcation)  $< D$  and the two minutia are in the same ridge then remove both of them (cases  $m2, m3$ ).

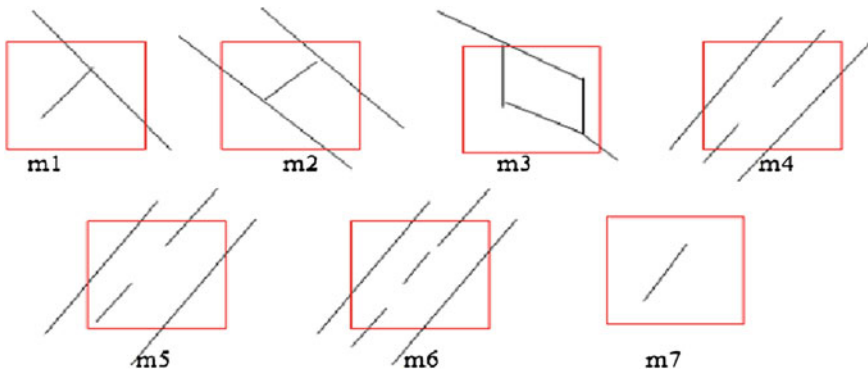
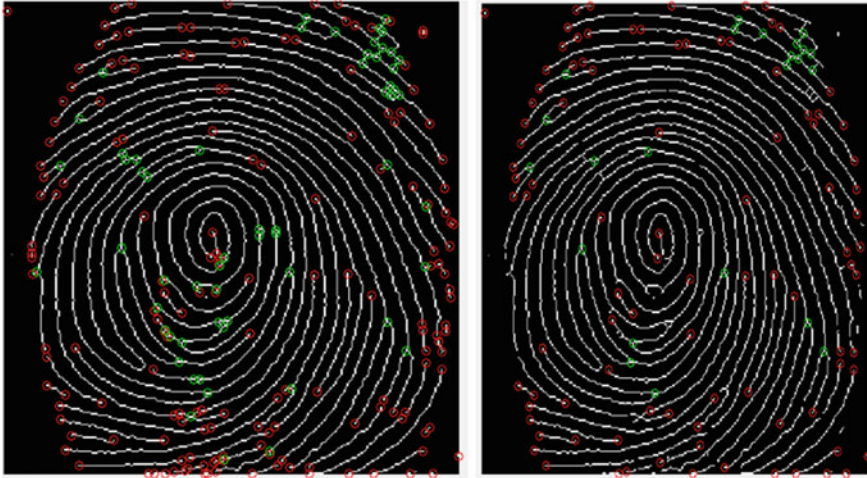


Fig. 7 False minutia structures





**Fig. 8** Remove spurious minutiae

- If  $d$  (termination, termination)  $\approx D$  and the their directions are coincident with a small angle variation and no any other termination is located between the two terminations then remove both of them (cases  $m4$ ,  $m5$ ,  $m6$ ).
- If  $d$  (termination, termination)  $< D$  and the two minutia are in the same ridge then remove both of them (case  $m7$ ) (Fig. 8).

## 7 Conclusion

Fingerprint technique is good biometric technique for identification. Most of the time fingerprint is not of good quality. Due to low quality image false minutiae points get increases. But low quality image needs to preprocessed. Preprocessing to increase contrast, and reduce different types of noises. When some background region is included in the segmented regions of interest, noisy pixels also generate many spurious minutiae because these noisy pixels are also enhanced during preprocessing and enhancement steps. There is a scope of further improvement in terms of efficiency and accuracy, which can be achieved by improving the image enhancement techniques or by improving the hardware to capture the image. So that the input image to the thinning stage could be made, better this could improve the future stages and the outcome.

## References

1. Mehtre, B.M., Chatterjee, B.: Segmentation of fingerprint images—a composite method. *Pattern Recogn.* **22**(4), 381–385 (1989)
2. Maltoni, D., Maio, D., Jain, A.K., Prabhakar, S.: *Handbook of Fingerprint Recognition*, 2nd edn. Springer, London (2009)
3. Hong, L.: Automatic personal identification using fingerprints. Ph.D. Thesis (1998).
4. Msiza, I.S., Leke-Betechuoh, B., Nelwamondo, F.V., Msimang, N.: A fingerprint pattern classification approach based on the coordinate geometry of singularities. In: *Proceedings of the IEEE International Conference on Systems, Man, and Cybernetics*, San Antonio, TX, USA, October 2009.
5. Cappelli, R., Lumini, A., Maio, D., Maltoni, D.: Fingerprint classification by directional image partitioning. *IEEE Trans. Pattern Anal. Mach. Intell.* **21**(5), 402–421 (1999)
6. Ratha, N., Chen, S., Jain, A.K.: Adaptive flow orientation based feature extraction in fingerprint images. *Pattern Recogn.* **28**, 1657–1672 (1995)
7. Demuth, H., Beale, M.: *Neural Network Toolbox for Use with MATLAB*. The MathWorks Inc, Natick (1998)

# Optimization Problems in Pulp and Paper Industries

Mohar Singh, Ameya Patkar, Ankit Jain and Millie Pant

**Abstract** Pulp and paper industry plays an important role in Indian as well world economy. These are large scale process industries working round the clock. The focus of the present paper is on optimization problems encountered in pulp and paper industries. Different areas where optimization has been applied are identified and methods available for dealing with such problems are discussed.

**Keywords** Optimization · Pulp and paper industry · Classical methods · Non-traditional methods

## 1 Introduction

Pulp and paper industry is one of the most important process industries. It is not just a one industry but is an integration of several processes. Each process is to be carefully dealt for the smooth functioning of the industry. Some facts about these industries are:

---

M. Singh (✉) · A. Jain  
Department of Paper Technology, Indian Institute of Technology Roorkee, Roorkee, India  
e-mail: moharsingh.iitr@gmail.com

A. Jain  
e-mail: ankitjain.iitr@gmail.com

A. Patkar  
Department of Polymer and Process Engineering, Indian Institute  
of Technology Roorkee, Roorkee, India  
e-mail: ameya1991.iitr@gmail.com

M. Pant  
Department of Applied Sciences and Engineering, Indian Institute  
of Technology Roorkee, Roorkee, India  
e-mail: millifpt@iitr.ernet.in

- Paper industry accounts for nearly 3.5 % of world's industrial production and 2 % of world trade.
- Current annual consumption of paper is of the order of 270 million tones.
- This industry is 10th major section in India.
- Pulp and paper production is a critical part of the global economy with annual revenues of US\$ 500 billion from sales of over 300 million tonnes of products [5].
- A modern pulp and paper mill with a production capacity of 300,000 tonnes per year is estimated to cost more than a billion dollars to construct [23].
- In terms of energy use, pulp and paper production accounts for 11 % of the total manufacturing sector, standing in the third place behind the petroleum (24 %) and chemicals (19 %) production industries [6].
- Although the projection of consumption trends towards year 2015 show approximately 2 % annual growth in the demand for pulp and paper products [12].

From the above listed facts it can be easily seen that these are highly capital incentive industries and a proper planning will be beneficial in terms of product/profit maximization and loss minimization. Mathematically speaking many situations in a pulp and paper industry may be modeled as optimization problems which require suitable methods for their solution. The objective of the present study is to discuss various areas where optimization tools can be applied for improving the various processes of a pulp and paper mill.

Besides introduction, this paper has three more sections. In Sect. 2 we give the general optimization model used in the present study. Section 3, gives a very brief review of optimization problems arising in paper and pulp industries. In Sect. 4, methods available for solving such problems are discussed. The paper concludes with Sect. 4.

## 2 Definition of an Optimization Problem

Optimization is the art of selecting the best alternative among a given set of options. The process of finding the largest or the smallest possible value, which is a given function can attain in its domain of definitions, is known as optimization. The function to be optimized could be linear, non-linear, fractional or geometric. Sometimes even the explicit mathematical formulation of the function may not be available often the function has to be optimized in a prescribed domain which is specified by a number of constraints in the form of inequalities and equalities.

The general non-linear optimization problem is defined as:

*Minimize / Maximize*  $f(\bar{x})$ , where  $f : R^n \rightarrow R$

*Subject to:*  $x \in S \subset R^n$

where  $S$  is defined by:

$$\begin{aligned}
 g_j(\bar{x}) &\leq 0, j = 1, 2, \dots, p \\
 h_k(\bar{x}) &= 0, k = 1, 2, \dots, q \\
 a_i &\leq x_i \leq b_i (i = 1, \dots, n).
 \end{aligned}$$

where  $p$  and  $q$  are the number of inequality and equality constraints respectively,  $a_i$  and  $b_i$  are lower and upper bounds of the decision variable  $x_i$ .

Any vector  $x$  satisfying all above constraints is called feasible solution. The best of the feasible solution is called an optimal solution.

- If the objective function and all constraints are linear then the model is called linear programming problem (LPP).
- If the solution has an additional requirement that the decision variables are integers then the model is called integer programming problem (IPP).
- If some variables are integers and other variables are real then the problem is called Mixed integer programming problem (MIPP).
- If the objective function and/or constraints are nonlinear then the problem is called non-Linear programming problem (NLPP).
- If besides nonlinearity, the model also has integer restrictions imposed on it then it called a mixed integer nonlinear programming problem (MINLPP).

### 3 Common Optimization Problems in Paper and Pulp Industries

In general, industrial processes are defined as large scale, high dimensional, non-linear and highly uncertain. Conventional methods such as ‘trial and error’ are often used to solve complex optimization problems. These methods often result in sub-optimal solutions due to inherent limitations in representing and exploiting the provided problem information. The exploration of design space is also inhibited. Paper and pulp industry is an integration of several processes that need to be optimized to improve the qualitative and quantitative working of the industry. In pulp and paper industry, optimization is applied during different phases of paper making. There are a number of studies in the literature that address the optimization of the unit operations in pulp and paper mills:

For example:

Some common optimization problems can be identified as:

- Minimizing energy cost and production rate with constrained environment [22].
- Optimizing paper making process [6, 21].
- Controlling the kappa number and pulp yield [16].
- Energy optimization in a pulp and paper mill cogeneration facility [25].
- Energy management technology [17, 19].
- Economic optimization of Kraft pulping process [19].
- Trim loss minimization [4, 10, 11, 14, 19, 26, 27].

- Continuous digester process [13].
- Biological treatment of waste water in pulp and paper industry [15].
- Optimization of a Kraft digester process [2].
- Optimization of refining process for fiber board production [20].
- Optimization of a broke recirculation system [3].

Mathematical model of these problems can be continuous or discrete. It can be as simple as a linear model (optimization of Kraft pulping process) or can be nonlinear, non-convex subject to ordinary or binary variable constraints/restrictions (trim loss optimization). The models can be put under the category of assignment or transshipment. Also, to make the model more realistic, authors have considered multi-objective formulation.

## 4 Methods Available

The methods available for dealing with optimization problems can be classified as traditional/classical and nontraditional.

### 4.1 *Traditional/Classical Methods*

Traditional methods or classical methods are the ones that rely on the mathematical characteristics of the problem. These methods are often slow and are restricted to a particular class of problems. However these techniques have an advantage of having a strong theoretical proof. Some examples of classical optimization methods include: Simplex Method for linear programming models; Branch and Bound method for integer programming problems etc.

### 4.2 *Nontraditional Methods*

Nontraditional methods on the other hand are more user friendly as they do not depend upon the nature of the problem and can thus be applied to a broader range of problems. A major drawback of these algorithms is however that there is no concrete theoretical proof. Some examples are: genetic algorithms (GA) [9], and differential evolution (DE) [24] and algorithms based on systematic and interactive behavior of various species like ant colony optimization (ACO) [7], particle swarm optimization (PSO) [8] and artificial bee colony (ABC) [16] etc. the algorithms mentioned here are also known as nature inspired meta-heuristics as they are based on some natural concept or phenomena.

## 5 Conclusions

Optimization methods are potential tools that can be applied in almost all the real life scenarios where the situation can be modeled/ formulated in terms of an optimization problem. The objective of the present work is to discuss various areas of a pulp and paper industry where optimization can be applied. This work will help the researchers and industrialists working in this field.

## References

1. Borairi, M., Wang, H., Roberts, J.C.: Dynamic modelling of a paper making process based on bilinear system modelling and genetic neural networks. Presented at UKACC international Conference on, control, pp. 1277–1282 (1998)
2. Cristina, H., Aguiar, I.L., Filho, R.M.: Modeling and optimization of pulp and paper processes using neural networks. *Comput. Chem. Eng.* 22(Suppl.), S981–S984 (1998)
3. Dabros, M., Perrier, M., Forbes, F., Fairbank, M., Stuart, P.R.: Model based direct search optimization of the broke recirculation system in a newsprint mill. *J. Cleaner Prod.* **13**, 1416–1423 (2005)
4. Deep, K., Chauhan, P., Bansal, J.C.: Solving nonconvex trim loss problem using an efficient hybrid particle swarm optimization. In: *IEEE Xplore Proceedings of the World Congress on Nature and Biologically Inspired Computing Coimbatore, India*, pp. 1608–1611, 9–11 Dec 2009
5. DeKing, N. (ed.): *Pulp and paper global fact & price book 2003–2004*, Boston: Paperloop, Inc. (2004)
6. DoE Annual Energy Review. Report No. DOE/EIA-0384 (2004)
7. Dorigo, M., Maniezzo, V., Colomi, A.: The ant system: optimization by a colony of cooperating agents. *IEEE Trans. Syst. Man. Cybern. B.* **26**(1), 29–41 (1996)
8. Eberhart, R.C., Kennedy, J.A.: New optimizer using particle swarm theory. In: *IEEE Service Center Proceedings of the 6th International Symposium on Micro Machine and Human Science*, pp. 39–43, Piscataway, NJ, Japan, 4–6 Oct 1995
9. Goldberg, D.E.: *Genetic Algorithms Search. Optimization and Machine Learning*, Addison-Wesley, Reading (1989)
10. Harjunkoski, I., Porn, R., Westerlund, T., Skrifvars, H.: Different transformations for solving nonconvex trim loss problems with MINLP. *Eur. J. Oper. Res.* **105**, 594–603 (1998)
11. Harjunkoski, I., Westerlund, T.: Enlarging the trim-loss problem to cover the raw paper mill. *Comput. Chem. Eng.* 22(Suppl.), 1019–1022 (1998)
12. Consulting, Jaakko Poyry Management: *World paper markets up to 2015: what drives the global demand?* *Tappi Solutions* **86**(8), 64 (2003)
13. Jin, F.J., Wang, H., Li, P.: Cleaner production for continuous digester processes based on hybrid Pareto genetic algorithm. *J. Environ. Sci.* **15**(1), 129–135 (2003)
14. Johnson, M.P., Rennick, C., Zak, E.: Skiving addition to the cutting stock problem in the paper industry. *SIAM Rev.* **39**(3), 472–483 (1997)
15. Juuso, E.K.: Hybrid models in dynamic simulation of a biological water treatment process. In: *International Conference on Computational Intelligence, Modelling and, Simulation*, pp. 30–35 (2009)
16. Karaboga, D.: *An idea based on honey bee swarm for numerical optimization*. Technical Report. Erciyes University, Engineering Faculty, Kayseri (2005)
17. Kaya, A., Keyes, M.A.: IV. Energy management technology in pulp, paper, and allied industries. *Automatica* **19**(2), 11–130 (1983)

18. Marshman, D.J., Chmelyk, T., Sidhu, M.S., Gopaluni, R.B., Dumont, G.A.: Energy optimization in a pulp and paper mill cogeneration facility. *Appl. Energy* **87**, 3514–3525 (2010)
19. Pant, M., Thangaraj, R., Singh, V.P.: The Economic optimization of pulp and paper making processes using computational intelligence. In: *Proceedings of AIP Conference*, 1146(1), p. 462 Agra July 2009
20. Runklera, T.A., Gerstorfer, E., Schlang, M., Junnemann, E., Hollatz, J.: Modeling and optimisation of a refining process for fibre board production. *Control Eng. Pract.* **11**, 1229–1241 (2003)
21. Santos, A., Dourado, A.: Global optimization of energy and production in process industries: a genetic algorithm application. *Contr. Eng. Pract.* **7**, 549–554 (1999)
22. Silva, C.M., Biscaia Jr, E.C.: Multiobjective optimization of a continuous pulp digester. *Comput. Aided Chem. Eng.* **14**, 1055–1060 (2003)
23. Smook, G.A.: *Handbook of pulp and paper Technology*, 2nd edn. Angus Wilde Publications, Vancouver (1992)
24. Storn R., Price K: *Differential evolution—a simple and efficient adaptive scheme for global optimization over continuous*. Technical Report TR-95-012, Spaces, Berkeley 1995
25. Wang, H., Borairi, M., Roberts, J.C., Xiao, H.: Modelling of a paper making process via genetic neural networks and first principle approaches. Presented at the IEEE International Conference on Intelligent Processing Systems, ICIPS, pp. 584–588. Beijing, China (1997)
26. Westerlund, T., Isaksson, J.: Some efficient formulations for the simultaneous solution of trim-loss and scheduling problems in the paper-converting industry. *Chem. Eng. Res. Des.* **76**, 677–684 (1998)
27. Westerlund, T., Isaksson, J., Harjunkoski, I.: Solving a two-dimensional trim loss problem with MILP. *Eur. J. Oper. Res.* **104**, 572–581 (1998)



# Integrating ERP with E-Commerce: A New Dimension Toward Growth for Micro, Small and Medium-Scale Enterprises in India

Vinamra Nayak and Nitin Jain

**Abstract** In the developing economy like India Micro, Small and Medium Enterprises (MSMEs) play a very important role as they are the engines of growth in development, upliftment, and transition of economy to the next level. The MSME's in India have played a critical role in generation of employment, providing goods and services at affordable costs by offering innovative solutions in very unstructured and unorganized manner. With the increase in the growing competition and its complexity it is essential for today's business enterprises to work in structured manner by changing its functioning environment dynamically by integrating internal information resources to the platform of ERP systems which will assist in optimizing potential of utilizing resources efficiently and determining growth. Moreover, with the exponential growth of Internet technology and the emergence of e-business, MSME's can unify the external information resources with internal functional areas within an organization. Use of e-commerce solutions will help enterprises to expand their business through broader product exposure, better customer service, accurate order entry processes and faster product fulfillment. It is expected that in MSME's implementation of an ERP system can facilitate an e-business effort of an organization to optimize its overall functioning. In order to serve as a platform for e-business, it is essential that an ERP system must also be able to be extended to support a range of external constituents for a firm. This paper focuses on that how the challenges faced by MSME's can be overcome by implementing ERP system in an organisation with the efficient integration of e-commerce to optimize its functioning. Further, the paper will highlight the add-on benefits to the companies for using integrated e-commerce platforms with ERP systems. The paper is based on the in-depth study of publicly available information collected from the published articles, journals, reports, websites, blogs, and academic literatures in context with the economy of India.

---

V. Nayak (✉) · N. Jain

Department of MBA, Gyan Ganga Institute of Technology and Sciences, Jabalpur, India  
e-mail: vinamra.lucky@gmail.com

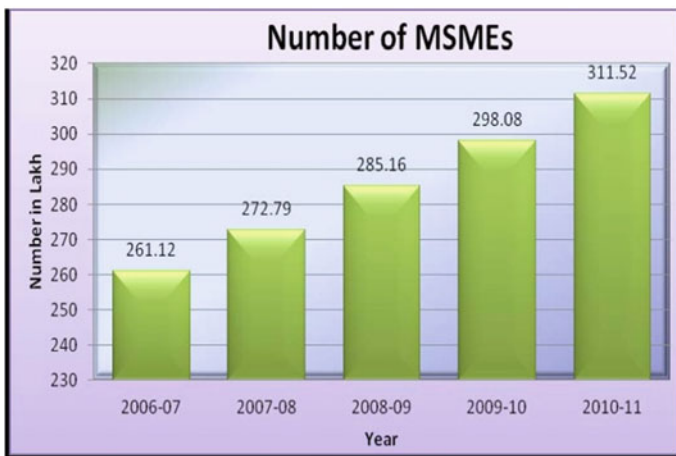
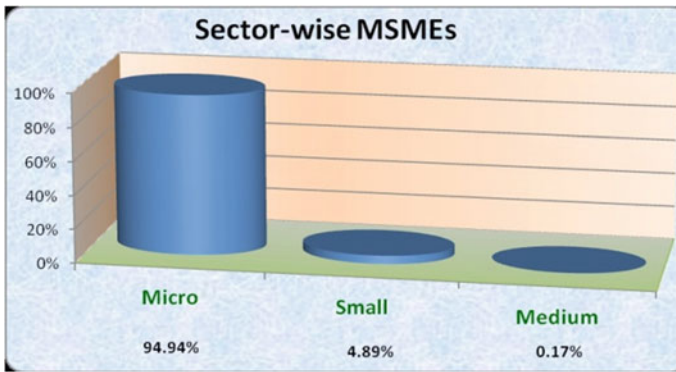
N. Jain

e-mail: nitinjain\_abc@yahoo.co.in

**Keywords** ERP · MSME's · E-commerce · Indian economy

## 1 Introduction

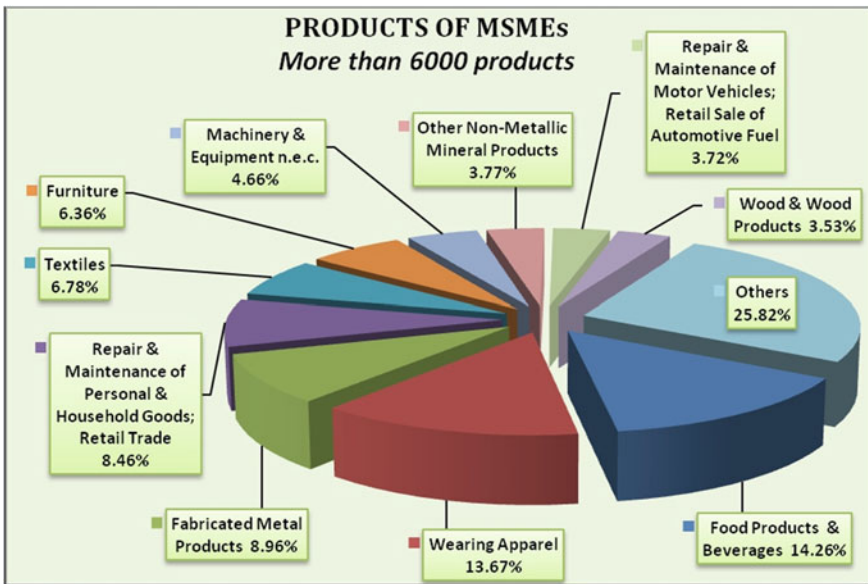
Micro, Small, and Medium-sized Enterprises (MSMEs) are the backbone of all economies and are a key source of economic growth, dynamism, and flexibility in advanced industrialized countries, as well as in emerging and developing economies. Micro, Small, and Medium businesses are particularly very important for bringing innovative products or techniques to the market. For the sustainability of this kind of growth, proper nurturing of MSME sector is imperative. There are around 31 million MSME's units in India, of which 99 % are Micro and small-scale units, contributing nearly 40 % of India domestic production, almost 50 % of total exports, and 45 % of industrial employment.



**Source:** - Final Report of the Fourth All India Census of Micro, Small & Medium Enterprises 2006-07: Registered Sector.

The MSME's in India are mostly in the unorganized sector though have had played a critical role in generation of employment, providing goods and services at affordable costs by offering innovative solutions. The need of the hour is to empower the MSME Sector so that it is able to take its rightful place as the growth engine of the economy.

However, one of the known bottlenecks to the growth of the MSME sector is its lack of adequate access to finance, despite the tremendous efforts laid down by the government and the corporative banks. Focusing on the other challenges will make MSE's more vibrant in managing many new uncharted areas such as infrastructure, nonavailability of suitable technology, ineffective marketing due to limited resources and nonavailability of skilled manpower, and optimum utilization of available resources. These factors are critically affecting the pace at which the micro, small, and medium businesses should prosper and develop.



**Source:** - Final Report of the Fourth All India Census of Micro, Small & Medium Enterprises 2006-07: Registered Sector.

Enterprise Resource Planning (ERP) is an outcome of Information Technology and is a way to integrate the data and processes of an organization into one single system, using subsystems that include hardware, software, and a unified database in order to achieve integration, to store the data for various functions found throughout the organization. Today, ERP is used in almost any type of organization; it does not matter whether it is large, small, or what industry it falls in. The main aim of implementing ERP is to integrate data and processes from all areas of the organization and unify it to provide ease of access and an efficient work flow. ERP systems usually accomplish this through one single database that employs multiple software modules.

According to Karunakaran (2001), Enterprise resource planning or ERP is a method of effective planning of all the resources like money, manpower, materials, and other things that are required to run the enterprise. It comprises management of functional and related areas in SMEs like manufacturing, materials, sales and distribution, human resource, finance, strategy and operations, quality, logistics, and maintenance.

ERP implementation is not just installation and configuration of the software but is the process of defining the way an organization should work; it involves defining the process flows within different departments and across the departments, imposing the checks and controls at different points and implementing the authorization levels in all departments, which requires certain important and stern decisions to be taken for successful execution.

Every business now has the opportunity to take advantage of the Internet's geographical reach and potential for profit. Thus, the Internet has made it possible for MSMEs to compete effectively with the larger organizations. The enabling potential of the Internet guarantees that MSMEs are appropriately represented and active participants in the globalized marketplace.

According to the Internet and Mobile Association of India Report, the total e-commerce market in India was estimated at around Rs. 46,000 crore (US \$8.28 billion) at the end of 2011 and is growing at around 40% year on year.

## **2 Aims and Objectives**

This paper focuses on how the challenges faced by MSME's can be overcome by implementing the ERP system in an organization with the efficient integration of e-commerce to optimize its functioning. Further, paper will highlight the add-on benefits to the companies for using integrated e-commerce platforms with ERP systems.

## **3 Rationale**

The purpose of the research is to identify the challenges and constraints faced by Indian MSME's, and how by integrating the concept of ERP and its strategies they are overcome efficiently. Moreover, to understand the advantages to MSME's for using e-commerce platform with integrated ERP systems in today's competitive environment.

## 4 Research Methodology

In order to achieve the research objectives, the blend of deductive and inductive research approach is selected, whereas qualitative research method is utilized. The research is based on only publically available information which has been taken into account. In order to fulfill proposed objectives data on various facts related to the concept of ERP and e-commerce is been presented with the help of the literature review. The data is collected using secondary method to fulfill different issues related to research topic from the published articles, journals, reports, websites, blogs, and academic literatures.

## 5 Literature Review

The factors like opening up of the economy business era in the postliberalization, ease in international trade barriers, globalization, privatization, disinvestments, and deregulation have thrown several challenges to MSMEs in the fast developing economies like India. Economic downturns, compressed product development cycles, cut-throat domestic and global competition, rapidly changing customer demands, and volatile financial markets have all increased the pressure on MSMEs to come up with effective and competitive capabilities to survive and succeed. ERP is often considered as one of the solutions for their survival [1].

SMEs sector in India had operated under a much-protected economic regime characterized by limited competition and a highly regulated business environment. This business atmosphere had resulted in limited focus on process efficiencies, centralized control structures, highly formalized business settings, and lack of professional business practices [2]. However, following the economic liberalization and opening up of the economy to foreign Multi-National Companies (MNCs), Indian SMEs have been forced to adopt modern business practices and strategies, which in turn can provide SMEs a cutting edge over its competitors.

In recent time, many MSME's implement ERP to increase internal efficiency and external competitiveness. Once ERP is established at all levels of the organization catering all the possible needs necessary to optimize its potentiality to face the challenges of the outside competitive environment ensures desired growth. The enterprise-wide data sharing in SMEs has many benefits like automation of the procedures, availability of high quality information for better decision making, faster response time, and so on Karunakaran (2001).

According to industry reports, the total cost of deploying ERP has ranged between 1 and 2% of companies' gross sales. Lower cost solutions are available for comparatively smaller-sized companies. Though the market seems to be very encouraging for ERP implementation, the time frame for deployment may be an issue.

While many new MSMEs start each year, nearly 50% cease to exist in the first 3 years of business itself. Though it is assumed that all MSMEs desire growth,

only 40 % survive beyond 10 years. Majority of the firms do not think of long-term business strategy but focus only on survival. They think of change only when the business begins to fail as a result of not keeping track of the changing market scenario. The firms who survive and grow are the ones who have the ability to take risks and respond to the changing circumstances [3].

An ERP system would allow MSMEs to integrate their business functions. MSMEs would be able to increase their efficiency and productivity by implementing a suitable ERP system. Over the next 5 years, the ERP market in India is expected to reach Rs. 1,550 crore (\$341 million), according to International Data Corporation (IDC), a market research and analysis firm. Of this, the SME potential in India for the enterprise class is projected to be Rs. 728 crore (\$160 million) 47 % of the overall market [4] (Table 1).

According to Gattiker and Goodhue (2005), ERP vendors have developed and customized the ERP software for the use of all types of industries. This has created a great demand on the use of ERP among business entities to integrate and maximize their resources. The growing demand for ERP applications among business firms has several reasons:

- Competitive pressures to become a low cost producer.
- To increase the revenue growth.
- Ability to compete globally.
- Maximizing the resources and the desire to re-engineer the business to respond to market challenges.

According to Gattiker and Goodhue (2005), ERP implementation failure rate is from 40 %, yet companies try to implement these systems because they are absolutely essential to responsive planning and communication. The competitive pressure unleashed by the process of globalization is driving implementation of ERP projects in increasingly large numbers, so a methodological framework for dealing with complex problem of evaluating ERP projects is required. It has been found that, unique risks in ERP implementation arises due to tightly linked interdependencies of

**Table 1** Projected growth rate overall industrial sector

Year	Growth rates of SSI sector (2001–2002) base IIP (%)	Over all industrial sector growth rate (%) <sup>a</sup>
2004–2005	10.88	8.40
2005–2006	12.32	8.00
2006–2007	12.60	11.90
2007–2008	13.00 <sup>b</sup>	8.70
2008–2009	c	3.20
2009–2010	c	10.50
2010–2011	c	7.80

<sup>a</sup> Source M/o Statistics and PI website [www.mospi.nic.in](http://www.mospi.nic.in)

<sup>b</sup> Projected, IIP Index of Industrial Production

<sup>c</sup> Due to revised definition of MSMEs Sector, figures not available

business processes, relational databases, and process reengineering [5]. According to Gordon [6], three main factors that can be held responsible for failure of ERP system: (a) Poor planning or poor management, (b) Change in business goals during project, and (c) Lack of business management support.

According to Gordon [6], a careful use of communication and change management procedures is required to handle the often business process re-engineering impact of ERP systems which can alleviate some of the problems, but a more fundamental issue of concern is the cost feasibility of system integration, training and user licenses, system utilization, etc. need to be checked. A design interface with a process plan is an essential part of the system integration process in ERP.

The pressure of staying ahead in a competitive environment by reduction of costs and product development time is compelling SMEs to leverage technology and enterprise applications like ERP application, as adapted by their large counterparts [7].

Sharma and Bhagat [8] in their study of information system (IS)-related practices in 210 MSMEs of western part of India concluded that though MSMEs understand and acknowledge the importance of the IS in day-to-day operations management in the present dynamic and heterogeneous business environment, but these are yet to implement, operate, and exploit it fully in a formal and professional manner so as to enable them to derive maximum business gains out of it.

According to Mishra et al. [9], in an increasingly competitive and globalized world, MSMEs need to compete more effectively to boost domestic economic activities and contribute toward increasing export earnings. E-commerce is emerging as a new way of helping business enterprises to compete in the marketplace and thereby contributing to their economic success. MSMEs also continue to play an important role in increasing employment and thus contributing to poverty reduction on a sustainable basis. With spread of technology and infrastructure, rural businesses will be the biggest beneficiaries of e-commerce.

## 6 Research Analysis

The boom in the ERP business segment is accompanied by a lot of challenges. One of the key challenges faced by solution providers is that the MSME sector is poor paymasters. Considering the concept is just a decade old in India, MSMEs are reluctant to invest in an ERP replacement as they lack domain-specific knowledge, technical know-how, and monetary resources to implement solutions.

Moreover, the MSME's are fighting with the problems and challenges faced to survive in this competitive environment but for sure adopting the strategies to optimize its overall business through ERP which will be the key to success. On the basis of the literature review, critical success factors are highlighted which assist in identifying and stating the key elements required for the success of a business operation. Furthermore, these critical success factors and key variables can be described in more details as a small number of easily identifiable operational goals shaped

by the industry, the firm, the manager, and the environment that assures the success of an organization. In this research paper, some key success factors and variables are identified which will be helpful to MSME’s after integrating ERP systems with e-commerce (Table 2):

Looking into the growing need of business enterprises to optimize its resources and meeting their upcoming problems and challenges for the better functioning in the present competitive environment, ERP tool is one of the most important and complete business software for any organization today, but if you do business through e-commerce and your ERP is not integrated with your e-commerce website then it would not consider that you are using a complete package.

Here are the most important benefits of integrated ERP software with your e-commerce website which will assist MSMEs to overcome the business constraints in present scenario:

1. **Improves Inventory Management:** ERP e-commerce integration allows you to check your inventory in real time, Products uploaded in the ERP system can be automatically published on your e-commerce website which helps enterprises to maintain level of inventory.
2. **Increases Self-Service Functionality:** The availability of real-time data from the ERP system on to the store front, allows customers to view available inventory, latest order status, and track shipments with tracking numbers. This helps in reducing the cost of operations and improves customer experience with store front of the enterprises.
3. **Quick Updates:** On purchases or sales of inventory in business ERP system as well as on online stores, which further helps in making quick decisions and necessary corrections.

**Table 2** Success criteria and key variables

ERP	E-commerce
Business process re-engineering	Customer satisfaction
Reduced inventory level	Online product catalogue
Reduced logistic cost	Tight integration with ERP system
Reduced procurement cost	Secure electronic payment
Order fulfillment performance	Reduced cost
Increased productivity and flexibility	Online customer service
Standardization of computing platforms	
Global sharing of information	
Improved responsiveness to the customer	
<i>Key variables</i>	
Top management commitment	
Consultant skills	
Schedule reliability	
Budget reliability	
Implementation team skills	



4. **Less Manual Process:** ERP and e-commerce integration allows businesses to have less manual intervention as every part or entry is taken care with the help of system integration. Automatically uploading of all the entries in the ERP system or vice versa help to reduce re-entry.
5. **Increased Internal Productivity:** ERP integrated system streamlines multiple business processes, helps in reducing human resource involvement in these processes. Web sales orders will be integrated to the ERP system in real time, back office ERP user can instantly track the order, and start the further processing. Thus, the order fulfillment cycle is reduced through this integration.
6. **Reduced Human Involvement, Data Redundancy and Error:** By integration, web customer details, web orders, payment and shipping information to ERP system, similarly Item and Inventory details can be uploaded from ERP to e-commerce portal, eliminating the need of re-entering the data. Thus, the integration solution will reduce human involvement, data redundancy, and error over two platforms.
7. **No Duplication of Entries:** ERP integration with e-commerce website eliminates the re-entering or rekeying process which further allows to have more accuracies in accounting, data processing, billing, and other modules of business enterprises.
8. **Generating Financial Reports in ERP, based on Web Transactions:** E-commerce applications are able to generate financial reports on sales. But integration with ERP provides the merchant the ability to produce Balance Sheet, P/L Statement, Trial Balance, Cash Flow, etc. which gives the transparency in financial information across the organization.
9. **Increase Customer Satisfaction:** Easy availability of up to date product information, inventory availability details, order tracking detail, etc in the web from ERP system; customer satisfaction level raises a lot and it reduces operational hassle for the business.
10. **Reduced Overall Cost:** Adopting the platform of ERP system with e-commerce helps business to cut down its logistics and procurement cost whereas also eliminates the possibility of underutilization of resources by efficiently streamlining the distribution process.
11. **Reduces Process Time:** E-commerce platform gives an opportunity to the business to serve multiple customers by streamlining the efficient distribution process through integrated ERP implementation.
12. **Better Control of Business Enterprise:** Integration of e-commerce and ERP business processes provides the business owners with a better control of their business and there by getting competitive advantage.

## 7 Conclusion

E-commerce solutions are a big support for business today. The demands and the expectations of the customers are high and so is the level of competition in the industry. E-commerce solution provides assistance to streamline business processes

efficiently and covers all the gaps that might have gone unseen. ERP Investments has been top IT spending priorities for MSME's off late. Most business organizations which are MSME in nature have complex ERP environments consisting of customized packages from multiple vendors, as well as an array of internally developed software that must integrate with the packages.

Any information system implementation is a complex task and hence complex ERP environments present several solutions to overcome challenges which are met by the MSMEs. The findings hold significance for any organization in the micro, small, and medium-scale sector which wishes to leverage the benefits of integration of business processes by implementing an ERP system in their organization.

The data analysis presented in this paper clearly specifies the way in which the constraints and challenges commonly encountered by MSMEs in managing the business house can be effectively dealt with the efficient use of integrated ERP system platform with e-commerce to gain competitive position over the conditions in which they are operating.

## References

1. Rao, S.S.: Enterprise resource planning: Business needs and technologies. *Ind. Manage. Data. Syst.* **100**(2), 81–86 (2000)
2. Ranganathan, C., Kannabiran, J.: Effective management of information systems function: An exploratory study of Indian organizations. *Int. J. Inf. Manage.* **25**, 247–266 (2004)
3. Levy, M., Powell, P.: Strategies for growth in SMEs: The role of information and information systems. *Inf. Proc. Manage. Int. J.* **42** (2006).
4. Munjal, S.: Small is beautiful: ERP for SMEs. [http://www.domainb.com/infotech/itfeature/20060601\\_beautiful.htm](http://www.domainb.com/infotech/itfeature/20060601_beautiful.htm) (2006)
5. Wright, S., Wright, A.M.: Information system assurance for enterprise resource planning systems : Unique risk considerations. *J. Inf. Sci.* **16**, 99–113 (2002)
6. Gordon, A.: ERP applications: Myth and misconceptions, *ezinearticles*. [www.ezinearticles.com](http://www.ezinearticles.com) (2006)
7. Goswami, S., Sarangdevot S.S.: Study of critical success factors for enterprise system in Indian SMEs. *Refeered Q. J.*, **4**(1) (2010).
8. Sharma, K.M., Bhagat, R.: Practice of information systems evidence from select Indian SMEs. *J. Manufact. Technol. Manage.* **17**(2), 199–223 (2006)
9. Mishra, B.B., Mishra, U.S., Mishra, P.K., et al.: Perception and adoption of e-commerce in Indian SMEs : A study in the state of Orissa. *Int. J. Adv. Comput. Math. Sci.* **3**(2), 227–236 (2012) (ISSN 2230–9624)
10. Anonymous., Benefits of having an integrated ERP with an e-commerce store front. Online <http://www.sboconnect.com/blog/e-commerce/benefits-of-having-an-integrated-erp-with-an-e-commerce-store-front.html>
11. Anonymous., Companies are benefiting from integrating ERP with e-commerce. Online <http://www.erpsoftwareblog.com/2012/03/companies-are-benefiting-from-integrating-erp-with-e-commerce/>
12. Anonymous., ERP and e-commerce. Online <http://www.managementstudyguide.com/erp-and-e-commerce.htm>
13. Anonymous., What is the difference between e-commerce and e-business? Online <http://www.eresourceerp.com/What-is-the-difference-between-E-commerce-and-E-Business.html>

14. Bajaj, K.K., Nag, D.: E-Commerce-the cutting edge of business, 2nd edn. Tata McGraw Hill Publishing Company Ltd., New Delhi (2009)
15. Dixit, A., Prakash, O.: A study of issues affecting ERP implementation in SME's. *J. Arts Sci. Commer.*, **2**(2), 77–85 (2011) (E-ISSN 2229–4686, ISSN 2231–4172) Available at [www.researchersworld.com](http://www.researchersworld.com)
16. Final report of the fourth all India census of micro, small and medium enterprises 2006–07: Registered sector
17. Kale, P.T., Banwait, S. S., Laroia S. C.: Enterprise resource planning implementation in Indian SMEs: issues and challenges
18. Kale, P.T., Banwait, S.S.: Evaluation of ERP implementation in an Indian company: a case department of mechanical engineering, national institute of technical teachers, training and research. Available Online
19. Leon, A.: Enterprise resource planning, 2nd edn. Tata McGraw Hill Publishing Company Ltd., New Delhi (2008)
20. Lewis, A.: E-commerce application in India : an emperical study. Welingkar Institute of Management Development and Research, Mumbai (2008)
21. Rayport, J.F., Jaworski, B.J.: Introduction to e-commerce, 2nd edn. Tata McGraw Hill Publishing Company Ltd., New Delhi (2007)
22. Thapliyal, M.P., Vashishta. P.: ERP software implementation in Indian small and medium enterprises. *Int. J. Emerg. Trends Technol. Comput. Sci.* **1**(2), 107 (2012) [www.ijettcs.org](http://www.ijettcs.org) Accessed 15 Oct 2012
23. The integration strategy of E-commerce platform and ERP based on cooperative application. <http://ieeexplore.ieee.org/xpl/articleDetails.jsp?reload=true&arnumber=5593163&contentType=Conference+Publications>
24. Upadhyay, P.: ERP in Indian SME's: a post implementation study of the underlying critical success factors. *Int. J. Manage. Innovation Syst.* **1**(2), E1 (2009). ISSN 1943–1384
25. Whiteley, D.: E-commerce-strategy, technologies and applications, 1st edn. Tata McGraw Hill Publishing Company Ltd., New Delhi (2009)

# A New Heuristic for Disassembly Line Balancing Problems with AND/OR Precedence Relations

Shwetank Avikal, Rajeev Jain, Harish Yadav and P. K. Mishra

**Abstract** Disassembly operations are inevitable elements of product recovery with the disassembly line as the best choice to carry out the same. The product recovery operations are fully based on disassembly line balancing and because of this, disassembly lines have become the chaise of automated disassembly of returned product. It is difficult to find the optimal balance of a disassembly line because of its N-P hard nature. In this paper a new heuristic is proposed to assign the parts to the disassembly workstations under AND/OR precedence constraints. The heuristic solutions are known as intrinsically optimal/suboptimal solutions of the N-P hard problems. The solution obtained by proposed heuristic has been compared with other heuristic solutions. The heuristic tries to minimize the number of workstations and the cycle time of the line while addressing the different criteria. The methodology of the proposed heuristics has been illustrated with the help of examples and it has been observed that the heuristic generates significantly better result.

**Keywords** Line balancing · Disassembly · Product recovery · Heuristic

---

S. Avikal (✉) · R. Jain · H. Yadav · P. K. Mishra  
Department of Mechanical Engineering, Motilal Nehru National Institute of Technology,  
Allahabad, India  
e-mail: avi.shwetank@gmail.com

R. Jain  
e-mail: jainrajeev@rediffmail.com

H. Yadav  
e-mail: harishivri@gmail.com

P. K. Mishra  
e-mail: pkm@mnnit.ac.in

## 1 Introductions

The impact of industrial and domestic waste on the environment has been overwhelming. Extensive diffusion of consumer goods and reduction in product lifecycles have led to a large number of used products being discarded due to chaotic transition and drastic changes in demand for a product during the past decade, which is due to globalization [1].

Disassembly has proven its role in material and product recovery by allowing selective separation of desired parts and materials [2]. Disassembly is defined as the methodical extraction of valuable parts/subassemblies and materials from discarded products through a series of operations. After disassembly, reusable parts/subassemblies are cleaned, refurbished, tested, and directed to inventory for remanufacturing operations. The recyclable materials can be sold to raw-material suppliers, while the residuals are sent to landfills [3].

End-of-life processing of complex products such as electronic products is becoming increasingly important, because they contain a large variety of hazardous, useful, as well as valuable components and materials. Disassembly is often used to separate such components and materials. A disassembly precedence graph (DPG) is frequently used to describe a disassembly process. The box in this graph refers to operations, typically the detachments of components. Arcs represent the precedence relationships. Both yield and costs are associated with every operation [4].

In order to minimize the amount of waste sent to landfills, product recovery seeks to obtain materials and components from old or outdated products through recycling and remanufacturing—this includes the reuse of components and products. There are many attributes of a product that enhance product recovery; examples include ease of disassembly, modularity, type and compatibility of materials used, material identification markings, and efficient cross-industrial reuse of common parts/materials. The first crucial step of product recovery is disassembly [3].

In this paper an analysis of U-shaped disassembly line has been carried out using proposed heuristic. In Sect. 2, the relevant literature has reviewed. The proposed heuristic has been described in Sect. 3, a practical example and computational results have been shown in Sect. 4. while the conclusions are drawn in Sect. 5.

## 2 Literature Review

The problem of disassembly line balancing (DLBP) can be defined as the assignment of disassembly tasks to workstations such that all the disassembly precedence relations are satisfied and some measure of effectiveness is optimized. Gungor and Gupta [5–7] presented the first introduction to the disassembly line-balancing problem and developed an algorithm for solving the DLBP in the presence of failures with the goal of assigning tasks to workstations in a way that probabilistically minimizes the cost of defective parts. Tiwari et al. [8] presents a Petri Net-based approach to determine the

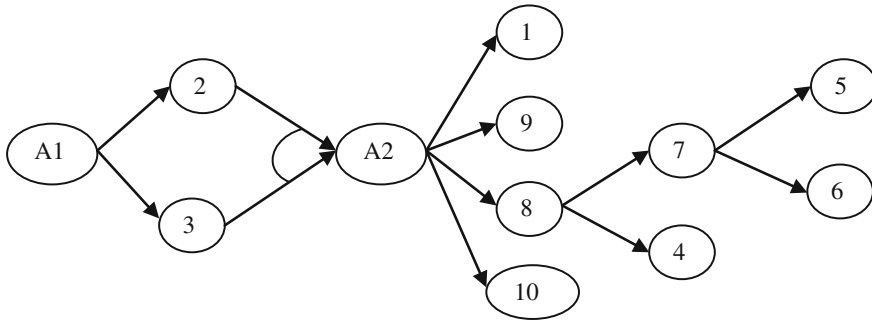
disassembly strategy of a product; it was a cost-based heuristic analysis for the circuit board. McGovern and Gupta [3] presented a disassembly solution which was found first by greedy modal, then improving the solution with the help of 2-opt heuristic. Later, various combinatorial optimization techniques to solve DLBP were compared by McGovern and Gupta [9]. Recently, the fact that even a simple disassembly line balancing problem is NP-complete that has been proven in the literature and a genetic algorithm was presented by McGovern and Gupta [10] for obtaining optimal solutions for DLBP. In order to solve the profit-oriented DLBP, Altekin et al. [11] developed the mixed integer programming algorithm for the DLBP. Koc et al. [12] proposed two exact formulations for disassembly line balancing problems with task precedence diagram construction using an AND/OR graph Ding et al. [13] proposed a multiobjective disassembly line balancing problem and then solved this by an ant colony algorithm.

### 3 Proposed Heuristic

In this paper a heuristic has been proposed for the assignment of tasks to the workstations under consideration of some criteria such as task time, part demand, part hazardousness, and part removal cost. The proposed heuristic has been developed to achieve some objectives such as minimize the total minimum number of disassembly workstations to decrease total idle time and balance the disassembly line. Remove hazardous parts/components early in the disassembly sequence, remove high demand components before low demand components, remove low disassembly cost components before high disassembly cost components, and remove the parts which have large part removal time before the parts which have small part removal time. In this proposed heuristic a rank has been provided to all the tasks according to the described objectives which has been done by taking the sum score of their criteria. The ranking of all tasks has been done by normalizing the data for each criteria and adding them together. Now assign the rank to all the tasks according to summation of their criteria, and then assign the task to the workstations on the bases of their rank and precedence relations and cycle time constraints.

### 4 Computational Example

The developed algorithm has been investigated on a variety of test cases to confirm its performance and to optimize parameters. The proposed heuristic has been used to provide a solution to the disassembly line balancing problem based on the modified disassembly sequencing problem presented by McGovern and Gupta [3], where the objective is to completely disassemble a given product (see Fig. 1) consisting of  $n = 10$  components and several precedence relationships. The problem and its data were modified with a disassembly line operating at a speed which allows  $CT = 40$  s



**Fig. 1** Modified precedence diagram of McGovern and Gupta [3] example

**Table 1** Tasks data set of McGovern and Gupta [3]modified example

Part	Time	Hazardous	Demand	Cost
1	14	0	0	27
2	10	0	500	63
3	12	0	0	48
4	18	0	0	62
5	23	0	0	24
6	16	0	485	18
7	20	1	295	83
8	36	0	0	77
9	14	0	360	93
10	10	0	0	10

for each workstation to perform its required disassembly tasks with AND/OR precedence relations. This provided an application to a previously explored disassembly problem. This practical and relevant example consists of the data for the disassembly of a product as shown in Table 1. It consists of ten subassemblies with part removal times of  $T_k = \{14, 10, 12, 18, 23, 16, 20, 36, 14, 10\}$ , hazardousness as  $h_k = \{0, 0, 0, 0, 0, 0, 0, 1, 0, 0, 0\}$ , part demand  $d_k = \{0, 500, 0, 0, 0, 750, 295, 0, 360, 0\}$ , and part removal cost as  $C_k = \{27, 63, 48, 62, 24, 18, 83, 77, 93, 10\}$ . The disassembly line is operated at a speed that allows 40s for each workstation.

### 4.1 Determination the Rank of Tasks

After applying proposed heuristic, the normalization of data (see Table 2) has been done and, by adding the normalized value of each criterion, the final ranking of tasks has been done. The final ranking of tasks is given in Table 2.

**Table 2** Ranking of tasks

Part	Time	Hazardous	Demand	Cost	Total	Rank
1	0.1111	0	0	0.7097	0.8208	8
2	0.0000	0	1	0.3226	1.3226	3
3	0.0556	0	0	0.4839	0.5394	10
4	0.2222	0	0	0.3333	0.5556	9
5	0.3611	0	0	0.7419	1.1030	4
6	0.1667	0	0.97	0.8065	1.9431	2
7	0.2778	1	0.59	0.1075	1.9753	1
8	0.7222	0	0	0.1720	0.8943	5
9	0.1111	0	0.72	0.0000	0.8311	7
10	0.0000	0	0	0.8925	0.8925	6

In this list part number 7 is ranked first because it has hazardous property and also, it has some demand; after this part number 6 is assigned at rank 2 because it has no hazardous property but has maximum demand over all the parts. Then part number 2 is assigned at rank 3 and part number 9 at rank 7, because part number 2 has much more demand and requires a minimum of 8 removed parts to remove it; part 9 does not require any removed part to remove it. Parts 10 and 5 are also assigned at ranks 6 and 4, as these tasks also do not have hazardous property and demand, so here, their part removal cost is considered as decision variable and according to their part removal cost they are assigned the ranking. This process is also repeated for part numbers 1, 2, 3, 4, and 8 and they are assigned their respective ranks.

### 4.2 Assignment of Tasks to the Workstations

The assignment of tasks to the workstation is performed with the help of ranks assigned to the tasks according to the proposed heuristic. In the assignment procedure the cycle time of the workstation is taken as 40 s and only four workstations are required for the complete disassembly of the product. The tasks assigned to the workstation are as follows:  $W1 = \{2, 10, 9\}$ ;  $W2 = \{8\}$ ;  $W3 = \{7, 6\}$ ;  $W4 = \{5, 1\}$ ; and  $W5 = \{4, 3\}$ . The idle times of the workstations are:  $I_1 = 6$  s;  $I_2 = 4$  s;  $I_3 = 4$  s;  $I_4 = 3$  s;  $I_5 = 10$  s. The overall idle time of the disassembly line  $I = 27$  s. The performance of the heuristic in terms of minimization of number of workstation required and idle time per workstation is examined because the heuristic is designed for the minimization of the number of workstation and cycle time of the line for complete disassembly. The proposed heuristic balances the line for the given problem and reduces the cycle time up to 3 s and minimizes it up to 37 s, while the compared heuristic can reduce the cycle time by only one unit and minimize up to only 39 s. Now it can be said that the proposed heuristic performs better than the compared heuristic. The results of tasks assignment are given in Table 3.



**Table 3** Solution by proposed heuristic

W/S No.	Part assigned	Part removal time	Idle time
1	2	10	30
	10	10	20
	9	14	6
2	8	36	4
3	7	20	20
	6	16	4
4	5	23	17
5	1	14	3
	4	18	22
	3	12	10

## 5 Conclusion

However, the use of disassembly lines generates the demand to balance the disassembly line [11]. As environmental regulations come into lime light and producers are gratified to collect their end-of-life products and recover the parts and materials, the problem of disassembling them in large volumes arises. In the presence of costs of performing disassembly associated with disposal, and the presence of hazardous material, the discarded products should be disassembled safely, efficiently, environment friendly, and cost-effectively [7]. An efficient, near optimal, multiobjective heuristic is presented for deterministic disassembly line balancing.

## References

1. Zhang, H.C., Kuo, T.C., Lu, H., Huang, S.H.: Environmentally conscious Design and Manufacturing: a state-of-the-art survey. *J. Manuf. Syst.* **16**(5), 352–371 (1997)
2. Gupta, S.M., Taleb, K.N.: Scheduling disassembly. *Int. J. Prod. Res.* **32**, 1857–1866 (1994)
3. McGovern, S.M., Gupta, S.M.: 2-opt heuristic for the disassembly line balancing problem. Iris Northeastern University, Boston (2003)
4. Gupta, S.M., Lambert, A.J.D.: A heuristic solution for disassembly line balancing problem incorporating sequence dependent costs. Iris Northeastern University, Boston (2005)
5. Gungor, A., Gupta, S.M.: Issues in environmentally conscious manufacturing and product recovery: a survey. *Comput. Ind. Eng.* **36**(4), 811–853 (1999a)
6. Gungor, A., Gupta, S. M.: Disassembly line balancing. In: Proceedings of the 1999 Annual Meeting of the Northeast Decision Sciences Institute, Newport, Rhode Island, 193–195 March 1999b
7. Gungor, A., Gupta, S.M.: Disassembly line in product recovery. *Int. J. Prod. Res.* **40**(11), 2569–2589 (2002)
8. Tiwari, M.K., Sinha, N., Kumar, S., Rai, R., Mukhopadhyay, S.K.: A petri net based approach to determine strategy of a product. *Int. J. Prod. Res.* **40**(5), 1113–1129 (2001)
9. McGovern, S.M., Gupta, S.M.: Combinatorial optimization methods for disassembly line balancing. In: Proceedings of the 2004 SPIE International Conference on Environmentally Conscious Manufacturing, Philadelphia, Pennsylvania, 53–66 (2004)

10. McGovern, S.M., Gupta, S.M.: A balancing method and genetic algorithm for disassembly line balancing. *Eur. J. Oper. Res.* **179**, 692–708 (2007)
11. Altekin, F.T., et al.: Profit-oriented disassembly-line balancing. *Int. J. Prod. Res.* **46**, 2675–2693 (2008)
12. Koc, A., Sabuncuoglu, I., Erel, E.: Two exact formulations for disassembly line balancing problems with task precedence diagram construction using an AND/OR graph. *IIE Trans. Oper. Eng.* **41**, 866–881 (2009)
13. Ding, L.-P., et al.: A new multi-objective ant colony algorithm for solving the disassembly line balancing problems. *Int. J. Adv. Manuf. Technol.* **48**, 761–771 (2010)

# A New Approach to Rework in Merge Production Systems

S. Kannan and Sadia Samar Ali

**Abstract** This paper introduces and incorporates the concept of rework in modelling of a merge production system under random conditions. Merge and split production stages are common in assembly lines. Merging of components can be performed correctly or otherwise. If not done properly, a merging operation can be redone, i.e. the merging operation can be reworked. This paper explains the modelling of a two stage merge production system subject to rework using semi-regenerative stochastic processes. The modelling has been done to obtain various busy period durations over finite time duration for transient state analysis. Also, the modelling and analysis has been carried out without any particular assumption on the distributions of processing times. All the processing times involved have been assumed to be arbitrarily distributed.

**Keywords** System performance · Expected duration · Design stage of transfer-line production systems · System over a finite horizon of time

## 1 Introduction

Production system modelling and analysis is a field as old as industrial engineering itself. Research is being carried out for a long time, over the years and decades, under varied assumptions [10]. In the initial stages, research has been carried out under deterministic assumptions. Later, randomness has been incorporated but confined to

---

S. Kannan (✉)  
Management Department, BITS, Pilani 333031, India  
e-mail: rnskannan@gmail.com

S. S. Ali  
Operations Management, Fortune Institute of International Business, Vasant Vihar,  
New Delhi 110057, India  
e-mail: sadiasamarali@gmail.com

exponential distribution only. There is quite an amount of literature on modelling and analysis of production systems under Markovian assumption, that is, the processing times involved in the analysis are assumed to follow an exponential distribution. The present model makes no assumption about the distributions of any processing times involved and provides transient state solution and analysis. A general framework is developed and for particular cases one can substitute desired distributions for various processing times involved. A system can be defined as a collection of interacting elements or processes that operate in a coordinated and combined fashion to achieve a predefined common goal. A production system can be defined as the means by which resource inputs are transformed to create goods and services. In manufacturing industries, the inputs are various raw materials such as energy, labour, machine, etc. In service industries, the inputs are likely to be dominated by labour [2]. The focus of analysis of this paper is discrete part manufacturing systems, where each item processed is distinct and the processing times are non-Markovian. Such systems can be found in mechanical, electrical and electronic industries making components possibly for *cars, refrigerator, computers*, etc. While the 'production line' plays an important role in a manufacturing industry, very little research on the interactions between the stages in a line is reported [3, 11]. The analysis of production systems, though not given importance to the extent it deserves, is one of the oldest problems in industrial engineering [1, 6]. Analysis of two-stage systems provides useful hints to describe generalised  $n$ -stage systems and such an analysis is getting a great deal of attention over the last few years. This is because any multi " $n$ -stage" system can be analysed by formulating the system as a series of two-stage systems [4].

A variety of applications particularly those arising out of computers and communication systems lead to the consideration of an input queue of unlimited capacity. This concept is applied in many a serial production systems [5]. Though the assumption of initial buffer of infinite capacity sounds artificial in production lines, it only implies that an input is always available, meaning that the initial stage is never starved [7]. Recently, [4] have analysed a production system taking into account the concept of rework but the model is of deterministic type. Merge production systems have been analysed without taking into account the concept of rework in [8] and [9].

Consider the following quality control problem in a Merge production system. In the first stage, components are made/ processed. In the second stage, the components are assembled. Assembled products coming out of stage II are inspected at an inspection point and the good ones are transferred out of the system while the bad ones are further classified as products that can be reworked (say minor defects) and otherwise (i.e. scraps). This is because not all the rejects can be reworked (major defects). A diagram of this system is given in Fig. 1.

The production system under study is modelled using a semi-regenerative process. This modelling requires knowledge over the concept of renewal processes. These equations, which are of convolution type, have been solved using the numerical method suggested by Jones [6]. Usage of this numerical method provides means to use distributions like Erlang (two-stage), which can be used in practical situations, unlike the traditional Laplace Transform technique, which can only be used when the processing times follow an exponential distribution.

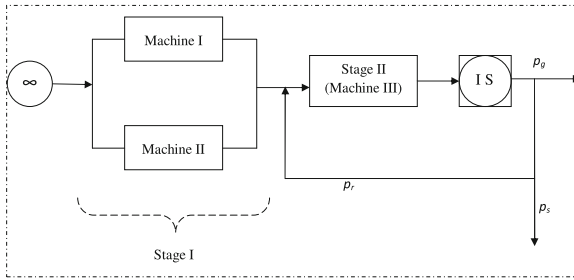


Fig. 1 Schematic diagram of the production system I.S.: inspection station

## 2 Assumptions

Following is a list of assumptions made to model the system under consideration.

1. Transfer of units from the initial buffer to Machines in stage I to Stage II is of instantaneous type.
2. Inspection is instantaneous.
3. Whenever a merge operation is to be reworked, then the Stage II machine will immediately start reworking the merge operation.
4. Processing times at both the stages are independent, random and arbitrarily distributed.
5. Products from Stage I will be inspected at the inspection station only when Stage II is free.
6. Stage II (i.e. machine 3) is never blocked.
7. Reworked jobs are always perfect.
8. Machine 1/2/3 is perfect (i.e. reliable)
9. Setup time is of instantaneous type.

## 3 Notations

pdf : Probability density function

cdf : Cumulative distribution function

sf : Survivor function

$f(\cdot) / g(\cdot)$  : pdf of processing time of machine I/machine II in Stage I

$F(\cdot) / G(\cdot)$  : cdf of processing time of machine I/machine II in Stage I

$\bar{F}(\cdot) / \bar{G}(\cdot)$  : sf of processing time of machine I/machine II in Stage I

$h(\cdot) / r(\cdot)$  : pdf of merge processing time and that of rework time in Stage II

$H(\cdot) / R(\cdot)$  : cdf of merge processing time and that of rework time in Stage II

$\bar{H}(\cdot) / \bar{R}(\cdot)$  : sf of merge processing time and that of rework time in Stage II

$p_g$  : Probability of a merge operation completed by Stage II is good

$p_r$  : Probability of a merge operation completed by Stage II is not good but can be reworked

$p_s$  : Probability of a merge operation completed by Stage II is neither good nor can be reworked. Clearly,  $p_g + p_r + p_s = 1$

: Convolution :  $f(t) * g(t) = \int_0^t f(u)g(t - u)du = g(t) * f(t)$

### 4 System Modelling

The system under consideration is modelled by identifying the state of the system at any instant t. The exhaustive list of possible states of the system is given in Table 1.

### 5 Evolution of System Characteristics

In this Section, analytical expressions for various measures of system performance such as busy period durations have been obtained. See Fig. 1.

The following system characteristics have been obtained under the assumption that the distributions of all the random variables involved in the analysis (including the processing times of rework) are arbitrary.

1. Expected duration Machine 1 in Stage I is busy in  $[0, t]$ .
2. Expected duration Machine 2 in Stage I is busy in  $[0, t]$ .
3. Expected duration both Machines in Stage I is busy in  $[0, t]$ .
4. Expected duration Machine 1 in Stage I is blocked in  $[0, t]$ .
5. Expected duration Machine 2 in Stage I is blocked in  $[0, t]$ .
6. Expected duration Stage II (i.e. Machine 3) is busy in  $[0, t]$ .

**Table 1** State space

State	Machine 1 in Stage I	Machine 2 in Stage I	Machine 3 in Stage II
1	Busy	Busy	Free
2	Blocked	Busy	Free
3	Busy	Blocked	Free
4	Busy	Busy	Busy
5	Blocked	Busy	Busy
6	Busy	Blocked	Busy
7	Blocked	Blocked	Busy
8	Busy	Busy	Busy with rework
9	Blocked	Busy	Busy with rework
10	Busy	Blocked	Busy with rework
11	Blocked	Blocked	Busy with rework

7. Expected duration Stage II is idle in  $[0, t]$ .
8. Expected duration Stage II is busy with rework in  $[0, t]$ .
9. Expected duration Stage II is busy with rework of type “ $i$ ” in  $[0, t]$ .

In this paper, the modelling of a two stage merge production system subject to rework using semi-regenerative stochastic processes is explained where all the processing times involved have been assumed to be arbitrarily distributed. The finished components from machines I and II are transferred to machine III for merging). The expected duration for various machines in both stages during  $[0, t]$ , are found following the expected duration of Stage II is busy with rework and idle, in  $[0, t]$ .

In case of Expected duration of Machine I in Stage I is busy in  $[0, t]$  when there are two types of rework, we shall extend the number of types of defects from one to two. Later, we shall generalise the number of defects to “ $M$ ” ( $M = 2$ ). Assume that a merging operation can result in two types of defects. The assembled product has a defect of type 1. The expected duration for type 1 and type 2 in Stage II, is busy with rework is then found during  $[0, t]$ . We shall extend and generalise the number of types of defects from two to “ $M$ ” ( $M = 2$ ). The completed merging operation is of type 1 defect with probability  $p_{r1}$  and is of type 2 defect with probability  $p_{r2}$  and so on. Clearly,  $p_g + p_s + p_{r1} + p_{r2} + \dots + p_{rM} = 1$ , i.e. after merging in Stage II, products are inspected at the inspection station and the merging operation clears inspection with probability  $p_g$ , could be defective of type 1 with probability  $p_{r1}$  or could be defective of type 2 with probability  $p_{r2}$ , . . . , could be defective of type  $M$  with probability  $p_{rM}$  and the operation is neither good nor can be reworked (i.e. a scrap) with probability  $p_s$ . Finally, expected duration of Stage II is busy with rework of type “ $i$ ” in  $[0, t]$  is expressed with:

$$Av_1^{Ri}(t) = [f(t)G(t) + g(t)F(t)] * Av_4^{Ri}(t) \tag{1}$$

$$Av_4^{Ri}(t) = \{f(t)[h(t)G(t) + g(t)H(t)] + g(t)[f(t)H(t) + h(t)F(t)] + h(t)[f(t)G(t) + g(t)F(t)]\} \left( p_g Av_4^{Ri}(t) + \sum_{i=1}^M p_{r1} Av_8^{Ri}(t) + p_s Av_4^{Ri}(t) \right) \tag{2}$$

$$Av_{8(i)}^{Ri}(t) = \{f(t)[r_i(t)G(t) + g(t)R_i(t)] + g(t)[f(t)R_i(t) + r_i(t)F(t)] + r_i(t)[f(t)G(t) + g(t)F(t)]\} Av_4^{Ri}(t) + \bar{F}(t); 1 \leq i \leq M; \tag{3}$$

The expected duration Stage II is busy with rework of type 1, is then given by, in  $[0, t]$ ,

$$\mu^{Ri}(t) = \int_0^t Av_1^{Ri}(u)du \quad (4)$$

## 6 Conclusion

When the number of types of defects is taken to be 2, i.e. merging operation, when not correct, can result in an item having one of two types of defect. As the time progresses the proportion of blocked duration also increases. If these proportions are measured in terms of % value of the time, the blocked durations are actually decreasing. Similarly it happens for busy, blocked/idle durations of Machines 2 and 3. One can test the sensitivity of various durations with respect to changes in processing rates of Machines 1, 2 and 3. Such a sensitivity analysis can be useful in two ways. First is to fix the desired busy/blocked/idle durations (including that of rework) and experiment on processing rates of various machines until the desired durations are obtained. Another way is to fix the processing times of machines and experiment on the sensitivity of changes in busy/blocked/idle durations. Such a transient state analysis will be highly useful at the design stage of transfer-line production systems under random conditions and also when it is decided to monitor the system over a finite time horizon.

## References

1. Birolini, A.: On the use of stochastic processes in modeling reliability problems. Springer-Verlag, Lecture Notes in Economics and Mathematical Systems (1985)
2. Buffa, E.S.: Modern production/operations management, 7th edn. Wiley Eastern Ltd., New Delhi (1983)
3. Buzacott, J.A., Shanthikumar, J.G.: Stochastic models of manufacturing systems. Prentice Hall Inc., New Jersey (1993)
4. De Koster, M.B.M., Wigngaard, J.: On the equivalence of multi-stage production lines and two-stage lines. *IIE Trans.* 19, 351–354 (1987).
5. Yang, L., Jingshan, L.: Performance analysis of split and merge production systems. In: Proceedings of 2009 American Control Conference, pp. 2190–2195 (2009).
6. Jones, J.G.: On the numerical solution of convolution integral equations and systems of such equations. *Math. Comput.* 15, 131–142 (1961)
7. Neuts, M.F.: Matrix-geometric solutions in stochastic models: an algorithmic approach. The John Hopkins University Press, Baltimore and London (1981)
8. Gopalan, M.N.: Dinesh Kumar, U.: On the production rate of a merge production system. *Int. J. Qual. Reliab. Manage.* 11(1994), 66–72 (1994)
9. Koneigsberg, E.: Production lines and internal storages : a review. *Manage. Sci.* 5, 410–433 (1959)
10. Shanthikumar, J.G., Tien, C.C.: An algorithmic solution to two-stage transfer lines with possible scrapping of units. *Manage. Sci.* 29, 1069–1086 (1993)
11. Buscher, U., Lindner, G.: Optimizing a production system with rework and equal sized batch shipments. *Comput. Oper. Res.* 34, 515–535 (2007)



**Part V**  
**Applications of Soft Computing in Image**  
**Analysis and Pattern Recognition**  
**(SCIAPR)**

# An Iterative Marching with Correctness Criterion Algorithm for Shape from Shading Under Oblique Light Source

Gaurav Gupta and Manoj Kumar

**Abstract** In this paper, a fast and robust Shape from Shading (SfS) algorithm by iterative marching with corrections criterion under oblique light source is presented. Usually, SfS algorithms are based on the assumption that image radiance is a function of normal surface alone. SfS algorithms solve first-order nonlinear Hamilton Jacobi equation called image irradiance equation. Both Fast Marching Method (FMM) and Marching with Correctness Criterion (MCC) basically work for the frontal light illumination direction, in which the image irradiance equation is an Eikonal equation. The problem task is to recover the surface from the image—which amounts to finding a solution to the Eikonal equation. FMM copes better the image irradiance iteratively under oblique light sources with the cost of computational complexity  $O(N \log N)$ . One prominent solution is the Marching with MCC of Mauch which solves the Eikonal equation with computational complexity  $O(N)$ . Here, we present a new iterative variant of the MCC which copes better with images taken under oblique light sources. The proposed approach is evaluated on two synthetic real images and compared with the iterative variant of FMM. The experimental results show that the proposed approach, iterative variant of MCC is more efficient than the iterative variant of FMM.

**Keywords** SfS · FMM · MCC · Complexity

---

G. Gupta (✉)  
ITM University, Gurgaon, India  
e-mail: guptagaurav.19821@gmail.com

M. Kumar  
Babasaheb Bhimrao Ambedkar University, Lucknow, India  
e-mail: mkjnuiitr@gmail.com

## 1 Introduction

Shape from Shading (SfS) is a well-known problem of Computer Vision. SfS was first introduced by Horn [11] in 1970s, where the 3D shape of the object is reconstructed by exploiting the shading information contained in its single shaded image. After the introduction of this field, various techniques have been reported to solve the SfS problems. Zhang et al. [16] categorized the reported techniques on SfS into four categories, viz. *local*, *linear*, *minimization*, and *propagation* approach.

Rouy et al. [10] introduced a viscosity solution and used dynamic programming to solve the SfS problem. Dupis et al. [14] formulated SfS as an optimal control problem and solved it by numerical methods. Bichel et al. [12] improved Dupis and Oliensis approach and proposed a fast converging, minimum downhill approach for SfS. All these propagation methods are guaranteed to converge; however, they are iterative and the convergence speed is uncertain. To deal with this problem, Kimmel and Sethian [15] reported a deterministic, non-iterative single pass algorithm known as Fast Marching Method of complexity  $O(N \log N)$  for unique surface reconstruction, where  $N$  is the number of pixels in the image. Various algorithms [1–4, 9, 8, 17, 18] have been derived from Fast marching method to solve the SfS problem. Tankus [3, 4] and Yuen et al. [18] have reported the FMM-based methods for perspective SfS. However, Sean Mauch [19] observed that more than one point can be selected as the best solution at each iteration and hence reported a greedier algorithm namely Marching with Correctness Criterion (MCC) to solve Hamilton Jacobi equation. The MCC is faster and more efficient algorithm than FMM algorithm as its computational complexity is  $O(N)$ . FMM uses binary heap to store and search the minimum data points but MCC uses the array or list, so the space complexity of MCC is also less than FMM. The MCC algorithm produces almost same result as FMM but with less space and time complexity. Both FMM and MCC basically work for the frontal light illumination direction, in which the image irradiance equation is an Eikonal equation.

In order to solve the SfS problem using FMM approach for oblique light source direction, Sethian [15] suggested to rotate the image coordinate system to the light source coordinate system. The rotation of image coordinate system yields the image irradiance equation as an almost Eikonal equation and hence the problem is solved similar to the case of vertical light source direction. However, the rotation of image coordinate system requires the depth values of the surface which are not known in priori and basically the goal of the algorithm is to obtain them. Hence to accomplish this, the way is to use the initial approximation of the depth values, which leads toward the erroneous shape reconstruction of the surface. To deal with this problem, Tankus et al. [4] proposed an iterative scheme, in which the rotation of co-ordinate system is not used. In this scheme, the image irradiance equation is approximated into the series of Eikonal equations and each equation approximation refines the approximation of previous equation. Numerical tests performed in [6, 7, 13] clearly show that the PSFS algorithm is not able to catch discontinuities of the surface. In fact, it tries to reconstruct a continuous surface with the same brightness function as the original one.

In this paper, an iterative Marching with Correctness Criterion algorithm for SfS problem under oblique light source direction has been reported. The Lambertian reflectance map is used to model the SfS problem as it is simple and almost fair approximation of most of the real world objects. Rest of the paper is organized as follows. Section 2.1 describes the mathematical formulation of SfS problem and its solution using FMM for oblique light source direction. The solution of SfS problem of oblique light source directions by MCC is described in Sect. 3. Experimental results, error analysis, and time complexity are discussed in Sect. 4. The proposed work is concluded in Sect. 5.

## 2 Shape from Shading

Let  $z(x, y)$  denotes the depth function in a real world Cartesian coordinate system whose origin is at camera plane. The real world coordinate system  $(x, y, z(x, y))$  of a surface is projected orthographically onto image point  $(x, y)$ . The surface normal and the image intensity at the point  $(x, y)$  are denoted by  $\vec{N}(x, y)$  and  $I(x, y)$  respectively. If the object is assumed to be Lambertian and illuminated by a point light source at infinity with the direction  $\vec{L}(p_s, q_s, -1)$ , then the orientation of the object surface and image intensity are related by the image irradiance equation which is given as follows:

$$I(x, y) = \vec{L} \cdot \vec{N}(x, y) = \frac{p_s p + q_s q + 1}{\sqrt{(p_s^2 + q_s^2 + 1)(p^2 + q^2 + 1)}} \quad (1)$$

where  $p = \frac{\partial z}{\partial x}$  and  $q = \frac{\partial z}{\partial y}$ .

If the light source direction is vertical, i.e.,  $\vec{L} = (0, 0, -1)$ , then the above equation becomes an Eikonal equation which can be written as:

$$p^2 + q^2 = f^2 \text{ or } |\nabla z(x, y)| = f \quad (2)$$

where  $f = \sqrt{\frac{1}{I^2(x, y)} - 1}$ .

### 2.1 Fast Marching Method

The previously existing methods to solve the Eikonal equation are boundary value methods and are iterative. The Marching methods allow to solve the boundary value problem in a single pass, i.e., without iterations. Therefore these methods are based on an optimal ordering of the grid points in the solution domain. The FMM produces

a solution which satisfies the discrete version of the Eikonal equation. The first-order approximations of  $\frac{\partial z}{\partial x}$  and  $\frac{\partial z}{\partial y}$  in forward and backward directions can be written as:

$$D_{i,j}^{+x} z = \frac{z_{i+1,j} - z_{i,j}}{\Delta x}, \quad D_{i,j}^{-x} z = \frac{z_{i,j} - z_{i-1,j}}{\Delta x}$$

$$D_{i,j}^{+y} z = \frac{z_{i,j+1} - z_{i,j}}{\Delta y}, \quad D_{i,j}^{-y} z = \frac{z_{i,j} - z_{i,j-1}}{\Delta y}$$

The Fast Marching Method is a upwind direction scheme and information always flows from small values to large values of the solution  $z$ . This information is encoded into the first-order, adjacent difference scheme:

$$\left( \max(D_{i,j}^{-x} z, -D_{i,j}^{+x} z, 0) \right)^2 + \left( \max(D_{i,j}^{-y} z, -D_{i,j}^{+y} z, 0) \right)^2 = f_{i,j}^2 \tag{3}$$

In this scheme, the  $z$  values at all grid points are set to  $\infty$  and the correct  $z$  values at the local minimum points are assigned. The solution propagates from these points to all other points. Assuming without loss of generality  $\Delta x = \Delta y = 1$ , the solution of the above Equation at point  $(i, j)$  is given as:

$$z_{i,j} = \begin{cases} \frac{z_1+z_2+\sqrt{2f_{i,j}^2-(z_1-z_2)^2}}{2}, & \text{if } |z_1 - z_2| < f_{i,j} \\ \min \{z_1, z_2\} + f_{i,j}, & \text{otherwise} \end{cases} \tag{4}$$

Here two input arrays namely solution array and status array of size  $N$  (size of the image) are used. Initially, in status array, the minimum singular points are set to *Known* and at the corresponding points in solution array, the true depth values are assigned. The rest points in status array are set to be *Unknown* and their values are set as  $\infty$  in solution array. The trial (neighbors of *Known*) points are pushed in a minimum binary heap. The minimum  $z$  value vertex with its indices is removed from heap and the corresponding status in status array is set to be *Known*. While updating the value at *Trial* points, value of a point can be decreased which increases its priority in the heap. On the basis of priority, the position of this point is adjusted in the heap.

For oblique light source (non-vertical), Eq. (2) takes the following form

$$p^2 + q^2 = f^2(p, q) \tag{5}$$

where,  $f(p, q) = \sqrt{1 - \left( \frac{p_s p + q_s q + 1}{(p_s^2 + q_s^2 + 1)I(x,y)} \right)}$ .

Thus the difference between vertical and oblique light source is the dependency of  $f$  on  $p$  and  $q$  in the right-hand sides of Eqs. (2) and (5). Sethian’s Fast Marching Method [15] solves these Equations in “upwind” fashion in a single pass. Tankus et al. [4] analyzed that due to the dependence of  $f$  on  $p$  and  $q$  in case of oblique light source direction, the Sethian’s single pass FMM method may not solve this case efficiently and proposed an iterative use of Fast Marching Method. The Eq. 5

is written in iterative fashion as follows:

$$p_{n+1}^2 + q_{n+1}^2 = f^2(p_n, q_n) \tag{6}$$

where  $p_n$  and  $q_n$  are the values of  $p$  and  $q$  at the  $n$ th iteration. The algorithm is as follows:

1. Initialize  $(p_0, q_0)$  on the basis of Sethian’s FMM.
2. Calculate the value of  $f^2(p_n, q_n)$  using the approximated  $(p_n, q_n)$ .
3. As the  $f^2(p_n, q_n)$  is obtained, Eq. 6 becomes an Eikonal equation. Use Eq. (4) to calculate the  $z$  values and hence the values of  $p_{n+1}, q_{n+1}$ .
4.  $n = n + 1$ , go to the step 2 and repeat the above process for  $n$  steps.

FMM uses a finite difference scheme to label the adjacent neighbors of the *Known* grid point. If there are  $N$  grid points, the computational complexity of labeling operation of these points is  $O(N)$ . Since there may be atmost  $N$  *Trial* grid points, the maintenance of the binary heap and choosing the minimum labeled grid points add a cost of  $O(N \log N)$ . Hence the total complexity of the FMM is  $O(N \log N)$ . Sethian proved that the solution by FMM satisfies the discrete version of Eikonal. In this iterative scheme, series of Eikonal equations are used. Therefore the iterative version of FMM is also convergent.

### 3 Marching with Correctness Criterion (MCC)

Sean Mauch [19] improved the Fast Marching Method and proposed a faster method to solve the Hamilton Jacobi equation named as Marching with Correctness Criterion (MCC). The MCC is similar to FMM as both are based on Dijkstra’s single source shortest path algorithm but dissimilar to FMM in the way of storing and freezing the vertices. In MCC, the labeled adjacent neighbors are not stored in the heap and instead of selecting a single vertex from the heap to become *Known* at each iteration, it tries to make the multiple vertices to known at each iteration. To examine whether a *Trial* point could be converted to a *Known* point, the future labeling operations are observed. If the future labeling does not decrease the value of a *Trial* point then the point can be converted to the known point at the same label. To accomplish this task, a lower bound is defined in which the future labeling operations are incorporated. If the value of a *Trial* vertex is less than or equal to the lower bound then the *Trial* vertex is moved from *Trial* set to the *Known* set at the same step. Let  $z_{i,j}$  be the value of a trial vertex then the lower bound is defined as follows:  $\text{lowerbound} = \min(z_{i,j}, \min(z_{k,l} + f_{k,l}))$  where  $(k, l)$  are the unknown neighbors of  $(i, j)$ . MCC is also used for ordering an upwind finite difference scheme to solve the static Hamilton Jacobi equation. In this method, difference scheme is used in coordination as well as in diagonal directions. Hence a *Trial* point can be possible in three directions of a *Known* point viz. adjacent, diagonal, and adjacent-diagonal directions. The first-order

approximation of  $\frac{\partial z}{\partial x}$  and  $\frac{\partial z}{\partial y}$  is obtained also in diagonal direction and is written as follows:

$$\frac{z_{i,j} - z_{i-1,j-1}}{\Delta x} \approx \frac{\partial z}{\partial x} + \frac{\partial z}{\partial y} \tag{7}$$

If  $\frac{\partial z}{\partial x} + \frac{\partial z}{\partial y}$  is obtained from diagonal directions and  $\frac{\partial z}{\partial x}$  from differencing in horizontal direction, then  $\frac{\partial z}{\partial y}$  can be obtained from these two. Thus  $\frac{\partial z}{\partial x}$  and  $\frac{\partial z}{\partial y}$  are calculated by differencing in horizontal and diagonal direction. Without loss of generality, we can assume that  $\Delta x = \Delta y = 1$  throughout the grid. If  $z_{i,j}$  is a trial point then the value at this point is updated as follows:

1. If the points at adjacent position to  $z_{i,j}$  are *Known* then  $z_{i,j} = z_a + f_{i,j}$ , where  $z_a$  is the minimum of all *Known* points adjacent to  $z_{i,j}$ .
2. If the points at diagonal position to  $z_{i,j}$  are *Known* then  $z_{i,j} = z_d + f_{i,j}$ , where  $z_d$  is the minimum of all *Known* points diagonal to  $z_{i,j}$ .
3. If the points at both adjacent and diagonal positions to  $z_{i,j}$  are *Known* then

$$z_{i,j} = \begin{cases} z_a + \sqrt{(2)} f_{i,j}, & \text{if } 0 \leq D \leq \sqrt{2} f_{i,j} \\ \infty \text{ (large value),} & \text{otherwise;} \end{cases}$$

where,  $D = z_a - z_d$ .

The corresponding algorithms for vertical and oblique light sources are written as follows:

**For Vertical Light Source**

1. Label the minimum singular point as *Known*.
2. Label all other grid points as *Far*.
3. Label all the neighbors of *Known* points as *Trial*, compute the  $z$  value on these points and add them in the *Trial* set.

Marching Forward:

1. If a point is in *Trial* set, examine it for its possible conversion into the *Known* point on the basis of lower bound.
2. If the *Trial* point converts into the *Known* point, label the neighbors of this *Known* point as *Trial*, compute the  $z$  value, and add them in the New *Trial* set.
3. Remove the converted *Known* points from the *Trial* set.
4. Add the points of New *Trial* set in the *Trial* set.
5. Make the New *Trial* set empty.
6. Return to step 1.

The marching forward steps are repeated until all the *Trial* points are converted to the *Known* points.

### For Oblique Light Source

In case of oblique light source direction, image irradiance equation takes the form of Eq. (5), in which the right-hand side is depending on  $p$  and  $q$ . We have used the same iterative fashion of Eq. (5) as by Tankus et al. [4] and which is shown in Eq. (6).

1. After one iteration of the algorithm of MCC for Vertical Light Source, obtain the values of  $p$  and  $q$ , and initialize them as  $p_0$  and  $q_0$  for this algorithm.
2. Calculate the value of  $f^2(p_n, q_n)$  as in Eq. (5), using the above values of  $p$  and  $q$ .
3. As the  $f^2(p_n, q_n)$  is obtained, Eq. 6 becomes an Eikonal Equation. Use the algorithm of MCC for Vertical Light Source to calculate the  $z$  values and hence the values of  $p_{n+1}, q_{n+1}$ .
4. increase  $n$  by one unit and go to the step 2. Repeat the above process for  $n$  steps.

The MCC algorithm is convergent because at each iteration at least one vertex (minimum value vertex) converts to a *Known* point. In SfS formulation, the MCC algorithm is basically used to solve the Eikonal equation  $|\nabla z(x, y)| = f$ . Let  $f_{\min} \leq f \leq f_{\max}$  and  $K = f_{\max}/f_{\min}$ . Let  $z_m$  be the minimum solution of the *Trial* points and the solution at all *Trial* points lie in the range  $[z_m, z_m + \frac{\sqrt{2}\Delta x}{f_{\min}}]$ . On applying the correctness criterion, vertices with  $z$  value less than  $z_m + \frac{\Delta x}{\sqrt{2}f_{\max}}$  become *Known*.

At each step, the minimum solution at *Trial* points increase by at least  $\frac{\Delta x}{\sqrt{2}f_{\max}}$ . This implies that a point can stay in the *Trial* set by at most  $\frac{\sqrt{2}\Delta x}{f_{\min}} / \frac{\Delta x}{\sqrt{2}f_{\max}} = \frac{2f_{\max}}{f_{\min}} = 2K$  steps. Hence, if there are  $N$  grid points then the computational complexity of correctness criterion is  $O(KN)$ . The cost of labeling is  $O(N)$ , the cost of adding and removing *Trial* points is  $O(N)$ . Hence the total computational complexity of MCC algorithm is  $O(KN)$ .

## 4 Results and Discussions

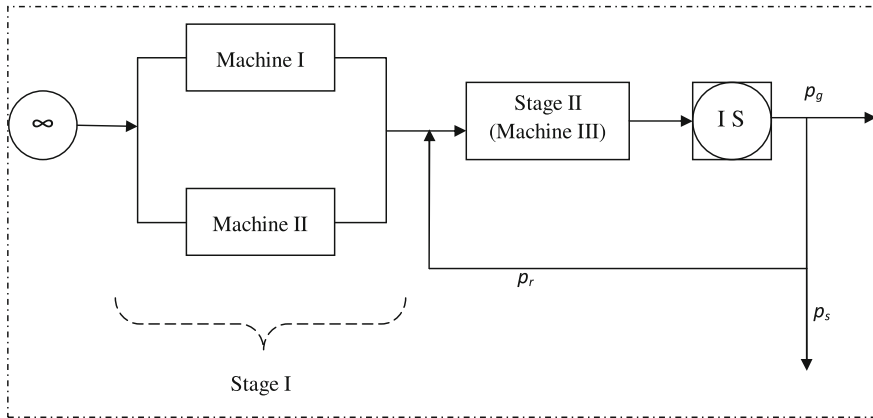
### 4.1 Synthetic Images

The proposed algorithm is tested on two synthetic images: sphere and vase are used to test the proposed scheme. The first test image is sphere, as the sphere has only one minimum depth point. The sphere is generated by using the formula.

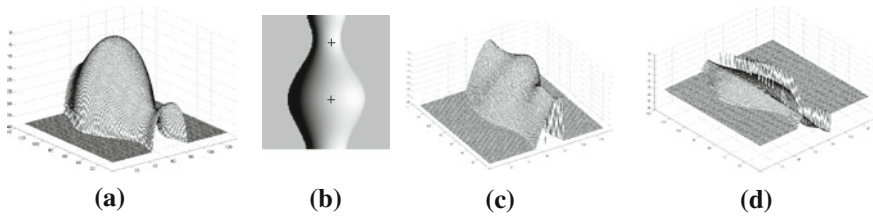
$$z(x, y) = \sqrt{r^2 - (x - 64)^2 - (y - 64)^2} \quad (8)$$

where  $r$  is the radius and  $0 \leq x, y \leq 127$ . The surface of the sphere is shown in Fig. 1a. The second test image is the synthetic vase. The vase is generated using the formula provided by Ascher et al. [5] as follows:





**Fig. 1** **a** The original depth map **b** Shaded image generated from true depth map in Oblique light source direction **c** Reconstructed depth map **d** Error depth map for oblique light source



**Fig. 2** **a** The original depth map **b** Shaded image generated from true depth map in Oblique light source direction **c** Reconstructed depth map **d** Error depth map for oblique light source

$$z(x, y) = \sqrt{(f(y))^2 - x^2}, \tag{9}$$

where  $f(y) = 0.15 - 0.1y(6y + 1)^2(y - 1)^2(3y - 2)$ ,  $-0.5 \leq x \leq 0.5$  and  $0 \leq y \leq 1.0$ . For the proper size and scale of the depth map,  $x$  and  $y$  are mapped in the range  $[0, 127]$  and  $z$  is scaled by a factor of 128. The synthetic surface of vase is shown in Fig. 2a.

In order to obtain the shaded images (of these surfaces), the surfaces are assumed to be Lambertian, and illuminated by a point light source in the direction  $(0, 0, 1)$  (vertical) and  $(0, -1, 1)$  (oblique). The surfaces gradients  $p$  and  $q$  are obtained by the discrete approximation of depth values in  $x$  and  $y$  directions. The surfaces are projected orthographically on  $z = 0$  plane and the intensities at each pixel in the image are calculated by using Eq. (1). The obtained shaded images of sphere and vase under oblique light source direction are shown in Figs. 1b and 2b. The obtained shaded images under oblique light source direction are used as the input in MCC algorithm for the possible 3D shape reconstruction. However, the images are synthetic and the known true depth values are assigned on the minimum singular points. In sphere image, only one minimum singular point (center point) and vase image for

two minimum singular points are chosen respectively. The minimum singular points in the shaded images are shown by + marks. These minimum singular points are taken as the initial points and the  $z$  values at all the grid points are calculated. The minimum singular points in the image are shown by + marks as shown in Fig. 1b and 2b.

The iterative MCC algorithm is used under oblique light source direction and the  $z$  values are computed using three iterations for each image. The reconstructed surfaces of sphere and vase under oblique light source direction are shown in Figs. 1c and 2c. Reconstructed depth values are normalized in the range of true data and the error maps are calculated which is the difference of true  $z$  values and reconstructed  $z$  values. The error maps of synthetic images are shown in Figs. 1d and 2d.

### 4.2 Real Images

We have tested the proposed scheme on two real images: pepper and real vase. The size of both the images is  $256 \times 256$ . However, the light source directions for real images are not known, by perception the light source directions for both the images are assumed as vertical. We have taken two minimum singular points for pepper image and one minimum singular point for vase image. The minimum singular points are taken on the basis of human perception. The minimum singular points in the image are shown by + marks as shown in Figs. 3a and 4a. On these points, the constant values are assigned according to the perception of relative heights. Algorithm starts from these points and calculates the  $z$  value at each point of the image. The reconstructed depth maps of pepper and vase are shown in the Figs. 3b and 4b. As the true data were not available for real images, is not available hence to show the efficiency of the proposed scheme, the reconstructed depth maps are projected orthographically on  $z = 0$  plane, surface gradients  $p$  and  $q$  are calculated from the obtained  $z$  values, and intensity at each point is calculated using Eq. (1). Thus the shaded images from

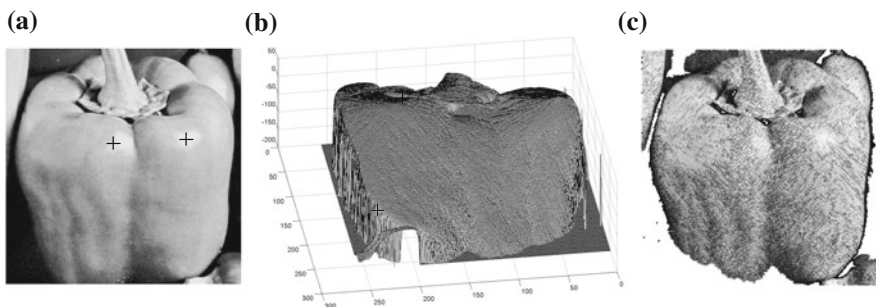
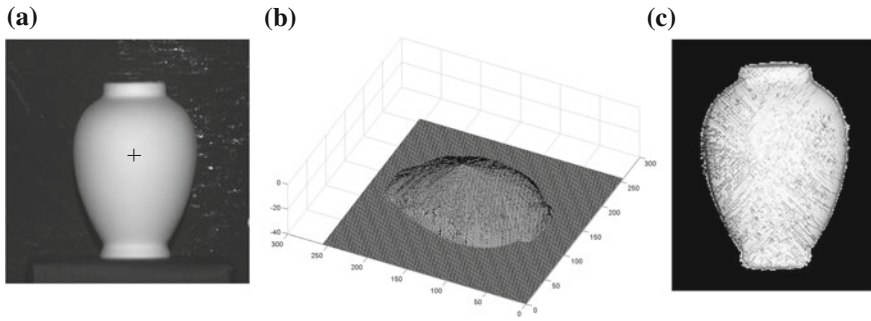


Fig. 3 a Original shaded image with minimum singular points. b Reconstructed depth map. c Shaded image generated from reconstructed depth map



**Fig. 4** **a** Original shaded image with minimum singular points. **b** Reconstructed depth map. **c** Shaded image generated from reconstructed depth map

the reconstructed depth maps are rendered as shown in Figs. 3c and 4c. The obtained shaded images are quite similar to the original images.

### 4.3 Error Analysis and Efficiency

In case of synthetic images, the error map is calculated by the absolute difference of true depth map and reconstructed depth map. The mean error and standard deviation error are calculated as shown in Table 1. All reconstruction processes are performed on a PC with Pentium Core 2 Duo 1.86 GHz and 1.00 GB memory. The algorithm is coded in C++ and MATLAB is used as a tool. The computation time is recorded for the sphere image of size  $8 \times 8$ ,  $16 \times 16$ ,  $32 \times 32$ ,  $64 \times 64$ ,  $128 \times 128$ ,  $256 \times 256$ , and  $320 \times 320$  in milliseconds as shown in Table 2.

**Table 1** Computed errors

Surfaces	Oblique	
	mean error	Std. error
Sphere	8.63	6.37
Vase	18.04	9.14

**Table 2** Computational time (in milliseconds) for sphere image

Size	FMM	MCC
$8 \times 8$	0	2
$16 \times 16$	15	31
$32 \times 32$	31	49
$64 \times 64$	94	212
$128 \times 128$	344	710
$256 \times 256$	1281	2809
$320 \times 320$	2046	4392

## 5 Conclusions

This paper has presented a fast and robust algorithm for SfS under oblique light source. The MCC method is used to solve the Hamilton Jacobi equation and the iterative variant of MCC is applied to deal with the images taken under the oblique light source direction. The orthographic projection and the most widely used Lambertian reflectance map have been used in SfS problem formulations. It can be observed that the present algorithm reconstructs the shapes in less computation time than the method proposed by Tankus et al. [4] which reconstructs the shape of the objects using Fast Marching Method. The computational time table indicates that as the size of image increases, the computing time in MCC is less as compared to FMM. The reported algorithm solves the problem with the time complexity of  $O(KN)$ , where,  $K$  is the ratio of maximum to minimum  $z$  values and  $N$  is the total number of pixels in the image. The method is guaranteed to obtain the solution provided the depth at local minimum singular points are given as it always freezes at least one grid point to the correct solution at each step. The effectiveness of the proposed algorithm has been demonstrated by experimental results. Experiments are conducted on various synthetic surfaces computed by formulae. The results suggested that the proposed algorithm successfully reduced the error and the reconstructed shapes are closely matched with the true data. However, the proposed scheme does not deal with the perspective projection and discontinuities due to occlusion in the surfaces. Furthermore, these problems may be discussed with the development of theory proposed in this paper and will be further refined in the future.

## References

1. Tankus, A., Sochen, N., Yeshurun, Y.: A new perspective on shape from shading. In: Proceeding of 9th ICCV, **2**, 862–869 (2003)
2. Tankus, A., Sochen, N., Yeshurun, Y.: Perspective shape from shading by fast marching. In: Proceedings of IEE Computer Society Conference on Computer Vision and, Pattern Recognition, (2004)
3. Tankus, A., Sochen, N., Yeshurun, Y.: Shape from shading under perspective projection. Int. J. Comp. Vision **63**(1), 21–43 (2005)
4. Tankus, A., Sochen, N., Yeshurun, Y.: Shape from shading by iterative fast marching for vertical and oblique light source, geometric properties for incomplete data, Springer, Netherlands **1**, 237–258 (2006)
5. Ascher, U.M., Carter, P.M.: A multigrid method for shape from shading. SIAM J. Numer. Anal. **30**(1), 102–115 (1993)
6. Cristiani, E., Fast marching and semi-lagrangian methods for hamilton-jacobi equations with applications, Ph.D. thesis, Dipartimento di Metodi e Modelli Matematici per le Scienze Applicate, SAPIENZA Universit' a di Roma, Rome, Italy (2007) [www.iac.rm.cnr.it/~cristiani/attach/ECristianiPhDthesis.pdf](http://www.iac.rm.cnr.it/~cristiani/attach/ECristianiPhDthesis.pdf)
7. Cristiani, E., Falcone, M., Seghini, A.: Some remarks on perspective shape-from-shading models. In: Proceedings 1st International conference Scale Space and Variational Methods in Computer Vision, Ischia, Italy, 2007, In: Sgallari, F., Murli, A., Paragios, N. (eds.) vol. 4485 of LNCS, 276–287

8. Prados, E., Faugeras, O.: Perspective shape from shading and viscosity solution. In: Proceedings of 9th ICCV, **2**, 826–831 (2003)
9. Prados, E., Soatto, S.: Fast marching method for generic shape from shading. In: Proceedings of VLISM'05. Third International Workshop on Variational Geometry and Level Set Method in Computer Vision, LNCS **3752**, 320–331 (2005)
10. Rouy, E., Tourin, A.: A viscosity solution approach to shape from shading. *SIAM J. Numer. Anal.* **29**(3), 867–884 (1992)
11. Horn, B.K.P., Brooks, M.J.: Shape from shading. The MIT Press, Cambridge (1989)
12. Bichsel, M., Pentland, A.P.: A simple algorithm for shape from shading. In: Proceedings of CVPR, 459–465 (1992)
13. Breu, M., Cristiani, E., Durou, J.-D., Falcone, M., Vogel, O.: Numerical algorithms for Perspective Shape from Shading, *Kybernetika*, **46**, 207–225 (2010). <http://www.kybernetika.cz/content/2010/2/207>
14. Dupis, P., Oliensis, J., Direct method for reconstructing shape from shading. In: Proceedings of CVPR, 453–458 (1992)
15. Kimmel, R., Sethian, J.A.: Optimal algorithm for shape from shading and path planning. *J. Math. Imaging Vision* **14**(3), 237–244 (2001)
16. Zhang, R., Tsai, P.S., Cryer, J.E., Shah, M.: Shape from shading: a survey. *IEEE Trans. Pattern Anal. Mach. Intell.* **21**(8), 690–706 (1999)
17. Yuen, S.Y., Tsui, Y.Y., Leung, Y.W., Chen, R.M.M.: Fast marching method for shape from shading under perspective projection. In: 2nd international Conference Visualization, Imaging and Image Processing, 584–589 (2002)
18. Yuen, S.Y., Tsui, Y.Y., Chow, C.K.: A fast marching formulation of perspective shape from shading under frontal illumination. *Pattern Recogn. Lett.* **28**, 806–824 (2007)
19. Sean, M.: Efficient algorithms for solving static Hamilton-Jacobi equations, Ph.D. thesis, California Institute of Technology Pasadena, California (2003)

# Enhancement of Mean Shift Tracking Through Joint Histogram of Color and Color Coherence Vector

M. H. Sidram and N. U. Bhajantri

**Abstract** Tracking of an object in a scene, especially through visual appearance is weighing much relevance in the context of recent research trend. In this work, we are extending the one of the approaches through which visual features are erected to reveal the motion of the object in a captured video. One such strategy is a mean shift due to its unfussiness and sturdiness with respect to tracking functionality. Here we made an attempt to judiciously exploit the tracking potentiality of mean shift to provide elite solution for various applications such as object tracking. Subsequently, in view of proposing more robust strategy with large pixel grouping is possible through mean shift. The mean shift approach has utilized the neighborhood minima of a similarity measure through bhattacharyya coefficient (BC) between the kernel density estimate of the target model and candidate. However, similar capability is quite possible through color coherence vectors (CCV). The CCV are derived in addition to color histogram of target model and target candidate. Further, joint histogram of color model and CCV is added. Thus, the resultant histograms are empirically less sensitive to variance of background which is not ensured through traditional mean shift alone. Experimental results proved to be better and seen changes in tracking especially in similar color background. This work explores the contribution and paves the way for different applications to track object in varied dataset.

**Keywords** Object tracking · CCV · Mean shift · Kernel · BC

---

M. H. Sidram (✉)

JSS Research Foundation, JSS Technical Institutions Campus,  
Mysore, Karnataka, India  
e-mail: mhsidram@gmail.com

N. U. Bhajantri

Department of CS and E, Government Engineering College Chamarajanagar,  
Chamarajanagar, Karnataka, India  
e-mail: bhajan3nu@gmail.com

## 1 Introduction

In an itinerary of tracking of the moving object in a capture sequence of real time is a blistering theme of research in the broad present scenario. Most of tracking algorithms assume that the object motion is smooth with no abrupt changes. Researchers can further mention the constraints of the object motion to be of invariable velocity or steady acceleration based on a priori information. In other words prior knowledge about the quantity and the size of objects, sometimes object appearance and shape, can also be used to simplify the predicament.

The plentiful approaches for object tracking have been proposed [1, 12, 15]. These are principally contradictory from each other based on the means they loom. Some-time tracking is accurate due to suitability of object representation or for a moment modeled motion, appearance, and shape of the object is appropriate. However, object tracking is posed with many problems like change in illumination, scale of object, occlusion of object, change in dynamism in the background, sudden movement of the objects, and cost of computation [15]. A large number of tracking methods have been proposed which attempt to counter these questions for a diversity of scenarios [2, 9, 10, 14]. The goal of this research work is to tracking the object based on appearance based features.

The suitability of apt strategy to track the object in surveillance is quite encouraging. In this work, we have attempted to do so through Mean shift tracking. It has an adequate amount of capability through its appearance-based features using probability density function (PDF) with nonparametric approach.

This approach proceeding with postulation such as the appearance and position of the object will not change drastically. The subsequent elite part of approach carried with brute force advance where previous spatial information available for estimating the object location in the next frame.

A suitable kernel is used to establish the relation between the color PDF and spatial information. In this path, joint histogram of color and CCV of the target model and target candidate are perhaps essential to supplement the precise results, which is shown with experimental evidence in Sect.4. The following milestones are used to assist the flow of the research article. Section 2 presents comprehension of contemporary effort and in Sect.3 substantiates the proposed criteria and also enhanced version of algorithm is illustrated. Experimental results are elaborated in Sect.4. The conclusion is given in Sect.5.

## 2 Comprehension of Related Effort

In the greater part of circumferences, selecting the appropriate features plays a decisive role in tracking. Thus, the most desirable property of a visual feature is its exceptionality so that the objects can be straightforwardly eminent in the feature space. On other hand feature assortment is closely related to the object depiction

such as color is used as a feature for histogram-based appearance representations. In this view, the following are the literature elaborated briefly.

Comaniciu et al. demonstrated the establishment of target model and candidate model to track the object [6, 7]. Ning et al. Experimented using color and texture jointly for target model [5, 10]. In this case texture features are exploited in addition to color histogram. The object is represented by texture using local binary pattern (LBP) [4, 11, 12]. Wang Yagi et al. worked with color and shape features jointly to create the target model and using mean shift object is tracked [2, 13, 14].

We propose more robust criteria to track the object especially in homogeneous background. However, we are motivated by the observation of above literature to erect the suitable model which is capable to produce accurate results. Thus, we have taken assistance of statistical attribute such as CCV. On the other hand, traditional mean shift strategy outcome also encouraged and along with the joint histogram of color and CCV supplemented our motivation.

### 3 Proposed Methodology

#### 3.1 Basic Mean Shift Tracking Method

Object tracking using mean shift is a nonparametric method and robust to the change in appearance of object. Object under consideration is cropped as a rectangle. In other words it is Template of object or Target model. Its weighted RGB color histogram using suitable number of bins is determined using Eq. 2,  $q_u$  as notation where  $u = 1 \dots m$  and  $\sum_{u=1}^m q_u = 1$ . A similar histogram of Candidate of object or Candidate model around the spatial information of previous frame is created using Eq. 3,  $p_u(y)$  as notation and  $\sum_{u=1}^m p_u(y) = 1$ . Weights are extracted using Eq. 7. The shift in the mean is calculated by using Eq. 8 and the spatial information  $y_1$  will be used as  $y_0$  for computing the next frame mean shift.

#### 3.2 RGB Color Histogram

To facilitate smooth weights which calculated through the similarity between the target PDF and candidate PDF, a kernel is used. The Epanecknikov kernel is one such approach. Due to its ellipsoidal region it performs better and gives more weights to the pixels nearer to the center of the kernel expressed in Eq. 1.

$$k(x) = \begin{cases} 1 - r & r \leq 1 \\ 0 & \text{otherwise} \end{cases} \tag{1}$$



$q_u$  is a PDF of the target model and  $p(y)$  is a PDF of candidate model at  $y$  location and same concept glimpses through Eq. 2 and Eq. 3.

$$q_u = C_1 \sum_{i=1}^n k(\|x_i^*\|)^2 \delta [c(x_i^*) - u] \tag{2}$$

$$p_u(y) = C_2 \sum_{i=1}^n k\left(\left\|\frac{(y-x_i)}{h}\right\|\right)^2 \delta [c(x_i^*) - u] \tag{3}$$

### 3.3 Color Coherence Vectors Histogram

The Color histogram is less capable to discriminate the objects clearly because dissimilar images can have similar histograms. Even though its computation is linear, determination of CCV resembles color histogram [1, 3, 4, 8, 13]. The color space of image is converted in to the number of bins using connected component analysis. The pixels of particular bin are classified based on threshold  $\tau$  Coherent and Incoherent pixels. The larger pixels group of a bin is called Coherent pixels and incoherence noticed by smaller group.

Let there be  $n$  number of bins. Therefore, number of Coherent pixels  $\alpha_i$  and Incoherent pixels  $\beta_i$  of  $i$ th bin. Hence CCV pair is given by  $(\alpha_i, \beta_i)$  and also Color Coherence vector is denoted by

$$(\alpha_1, \beta_1) (\alpha_2, \beta_2) \dots (\alpha_n, \beta_n) \tag{4}$$

Weighted histograms of CCV are  $c$  &  $d$  calculated using the kernel.

### 3.4 Joint Histogram

A joint histogram of color and CCV for target model and Target candidate calculated [14]. Joint histograms of target model  $q_u$  and target candidate  $p_u$  are as follows.

$$q_u = q_u \cdot * c \tag{5a}$$

$$p_u = p_u \cdot * c \tag{5b}$$

Bhattacharyya coefficient is extended to measure similarity as shown through Eqs. 6, 7.

$$\rho = \sum_{i=1}^m \sqrt{p_u(y), q_u} \tag{6}$$

$$w_i = \sum_{u=1}^m \sqrt{\frac{q_u}{p_u(y)}} \delta [b(x_i^*) - u] \quad (7)$$

$$Y_1 = \frac{\sum_{i=1}^{\text{nk}} x_i w_i g\left(\frac{\|y_0 - x_0\|^2}{h}\right)}{\sum_{i=1}^{\text{nk}} \left(\frac{\|y_0 - x_0\|^2}{h}\right)} \quad (8)$$

### 3.5 Proposed Algorithm

1. Convert the given avi video into number of frames. Declare variables and Kernel (Epanechnikov).
2. Read the first frame, select the object (Target Model or Template) to be tracked and store its spatial information such as  $X_0$ ,  $Y_0$ ,  $W$  and  $H$ .
3. Create the weighted histogram of color  $q_u$  and Compute the weighted histograms of CCV ( $c$  &  $d$ ).
4. Determine the Joint histogram of color and CCV ( $q_u = q_u \cdot c$ ).
5. Read the next frame and crop the object (Target Candidate) as per the spatial information from previous step ( $X_0$ ,  $Y_0$ ,  $W$  and  $H$ ).
6. Create the weighted histogram of color  $p_u$  and Compute the weighted histograms of CCV ( $c$  &  $d$ ).
7. Determine the Joint histogram of color and CCV ( $p_u = p_u \cdot c$ ) and  $w_i$  using Eq. 7.
8. Calculate the Target's new location  $Y_1$  using Eq. 8. Repeated five times for convergence by substituting  $Y_0 = Y_1$ .
9. Put the bounding box over the object using the spatial information from previous step ( $X_0$ ,  $Y_0$ ,  $W$  and  $H$ ).
10. If number of frames not equal to zero-proceed with step 5.

### 3.6 Computation of Weighted Histogram of CCV

1. Read the object (Target Model or Target Candidate or Template).
2. Color space of object is converted into number of bins.
3. Label the image using connected components theory.
4. Determine the centroids of the labeled regions and estimate the number of pixels in each labeled region.
5. Separate coherent pixels and incoherent pixels ( $\alpha$  and  $\beta$ ) for each bins using threshold.
6. Calculate weighted histograms ( $c$  &  $d$ ) using the above said Kernel.  $c$  is weighted histogram of coherent pixels and  $d$  is Weighted histogram of Incoherent pixels.
7. Normalize the histogram ( $c$  &  $d$ ).

**Table 1** Color histogram

SN	Dataset	TP*	FP**	FN***	DR+	FAR^^	Remarks
1	PETS2001	15	33	2	88	69	50 frames
2	dtneuWinter	21	16	3	87	43	40 frames

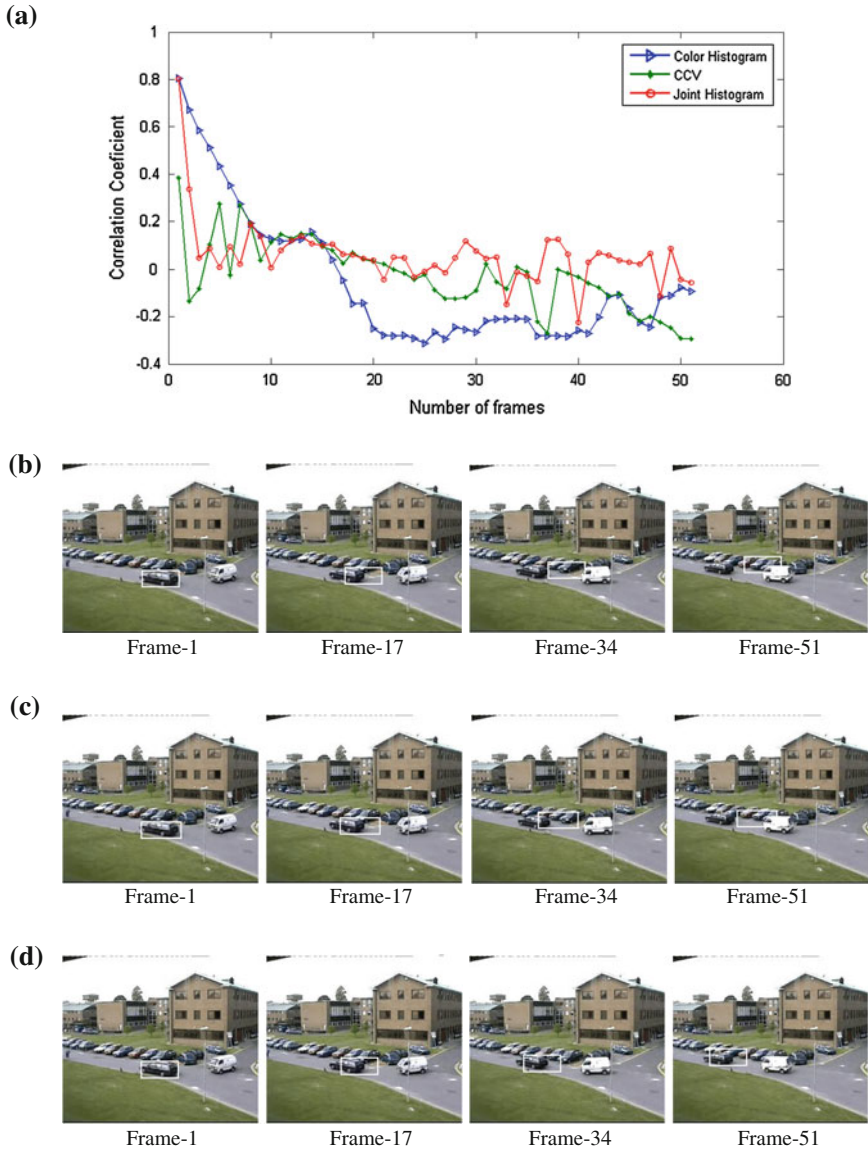
\* TP = True Positive, \*\*FP = False Positive, \*\*\*FN = False Negative, + DR = Detection Rate in %, ^^FAR = False Alarm Rate in %. Here, we attempted to narrate typical computation for the above said terminology.  $DR = (TP/(TP + FN)) * 100$ ,  $FAR = (FP/(TP + FP)) * 100$ ,  $DR = (15/(15 + 2)) * 100 = 88.23\% \approx 88\%$ ,  $FAR = (33/(15 + 33)) * 100 = 68.75\% \approx 69\%$

## 4 Experimental Results

Here, we address the difficulties by presenting a tracking algorithm that uses a simple symmetric similarity function between kernel density estimates of the template and target distributions in a joint spatial-feature space. Given sufficient samples, the kernel density estimation works well with both in low and high dimensions. The similarity measure is symmetric and the expectation of the density estimates centered on the model image over the target image. Using this similarity measure, we can derive a mean shift tracking algorithm with the histogram-based similarity measures. The proposed approach employed the information-theoretic similarity measure is more robust and more discriminative. An experiment on video sequence is conducted first with color histogram, second with CCV, and finally with joint histogram of color and CCV. We have conducted an experiment with different dataset to confirm the performance efficacy of the proposed mean shift approach. The computational aspects of the method occurred as the quadratic. The same is tested over the available machine Dual-core CPU of 2 GHz with MATLAB periphery.

In the first instance, we have conducted an experiment on PETS2001 (3) video sequence. Here the vehicle such as black car object is attempted to track as it has the dark background. It is observed that with color as feature the tracking fails and shown in Fig. 1a. With CCV histogram the result is better but with joint histogram of color and CCV outcome is best and robust which is portrayed through Fig. 1(b–d). Second an experiment leading via dtneuWinter (Traffic) multiple object video has been accomplished. Due to space limitation we are unable to include. Normally, single component such as color histogram is unable to discriminate the object of its same background color. As it can be observed in Fig. 1b, the bounding box is located other than the ground truth of the object. In other words, it may lead to mistrack. With CCV histogram the result (Fig. 1c) is better further with joint histogram the tracking is efficient. The bounding box is located over the object itself and can be seen in Fig. 1d.

Hence, it is quite possible through enhancement of traditional mean shift with the effort of statistical characteristics as exhibited by CCV which has extensively remarked through the experimental outcomes. In order to reveal the tracking performance, the following empirical metrics are considered such as True Positives and False Positives as shown in Tables 1, 2 and 3.



**Fig. 1** a Correlation coefficient versus number of frames. b PETS2001(3) sequence with color histogram. c PETS2001(3) sequence with CCV histogram. d PETS2001(3) sequence with joint histogram of color and CCV

**Table 2** CCV histogram

SN	Dataset	TP	FP	FN	DR	FAR	Remarks
1	PETS2001	46	1	3	94	2	50 frames
2	dtneuWinter	34	2	4	89	6	40 frames

**Table 3** Joint histogram

SN	Dataset	TP	FP	FN	DR	FAR	Remarks
1	PETS2001	48	1	1	98	2	50 frames
2	dtneuWinter	36	2	2	95	5	40 frames

**Table 4** Detection rate (DR)

SN	Dataset	DR for color hist	DR for CCV hist	DR for joint hist
1	PETS2001	88	94	98
2	dtneuWinter	87	89	95

From the Table 4 results such as DR helping to remark and increased monotonically through Color, CCV, and Joint histograms as an experimental evidences. The plot for CCV versus number of frames for PETS2001(3) dataset is shown in Fig. 1a. It witnessed the determination of correlation coefficient of template and candidate. On the other hand template and candidate extracted from first and subsequent frames, respectively. Further, color histogram, CCV histogram, and joint histogram of color and CCV are considered as the remarkable parameters to unearth the tracking outcome. In order to discriminate the correlation coefficient of three strategies through the appropriate distinct legends are quite essential. Hence, the experimental results of correlation coefficient represented through legends such as arrow, star, and circle are the correspondingly denoted. The three criteria said in the previous Para.

The performance of tracking algorithm through correlation coefficient for joint histogram of color and CCV has shown little supremacy over the color histogram and CCV histogram, which is exhibiting the accuracy of object tracking outcome. Furthermore, the same is demonstrated through the Fig. 1(b-d).

## 5 Conclusion

The proposed approach is simple symmetric similarity function between spatially smoothed kernel density estimates of the model and target distributions for object tracking. The resemblance measure is based on the expectation of the density estimates over the model or target image. Experimental results prove that they are precise, and reliable as compared to traditional methods.

To track the objects, the similarity function is maximized using the mean shift algorithm to iteratively find the local mode of the function. Since the similarity measure is an expectation taken over all pairs of the pixel between two distributions, the computational complexity is quadratic. The proposed method leads to a very efficient and robust nonparametric tracking algorithm has achieved better performance especially through the correlation coefficient of Target model and candidate.

## References

1. Ajay, M., Sanjeev, S., Venkatesh, M.: A novel color coherence vector based obstacle detection algorithm for textured environments. The 3rd international conference on machine vision (2010)
2. Birchfield, S.: Elliptical head tracking using intensity gradients and color histograms. In: Proceedings of the IEEE conference on computer vision and pattern recognition, 232–237 (1998)
3. Brian, V.: Funt, Graham, D., Finlayson.: Color constant color indexing. IEEE Trans. Pattern Anal. Mach. Intell. **17**(5), 522–529 (1995)
4. Chan Nguyen, V.: An efficient obstacle detection algorithm using color and texture. World Acad. Sci. Technol. **36**, 132–137 (2009)
5. Cheng, Y.: Mean shift, mode seeking, and clustering. IEEE Trans. Pattern Anal. Ma chine Intell. **17**, 790–799 (1995)
6. Comaniciu, D., Ramesh, V., Meer, P.: Real-time tracking of non-rigid objects using mean shift. In: Proceedings IEEE conference computer vision and pattern recognition **II**s 142–149 (2000)
7. Comaniciu, D., Ramesh, V., Meer, P.: PAMI. Kernel based object tracking **25**(5), 564–575 (2003)
8. Greg, P., Ramin, Z., Justin, M.: Comparing color images using color cohe rence vector. In: Proceedings 4th ACM international conference on multimedia (1997)
9. Han, B., Davis, L.: Object tracking by adaptive feature extraction. In: Proceedings of the IEEE conference on image processing, **3**, 1501–1504 (2004)
10. Ning, J., Zhang, L., Chengke W.: Robust object tracking using joint Co- lor\_Texture histogram. Int. J. Pattern Recogn. Artif. Intell. **23**(7), 1245–1263 (2009)
11. Li, X., Wu, F.: Convergence of a mean shift Algorithm. J. Softw. **16**(3), 365–374 (2005)
12. Ning, J., Zhang, L., Zhang, D.: Robust mean shift tracking with corrected background- weighted histogram. IET-CV, (2010)
13. Swain, M., Ballard, D.: Color indexing. Int. J. Comput. Vision **7**(1), 11–32 (1991)
14. Wang, J., Yagi, Y.: Integrating shape and color features for adaptive real-time object tracking. In: Proceedings international conference on robotics and biomimetics, Kunming. 1–6 (2006)
15. Yilmaz, A., Javed, O., Shah, M.: Object tracking. A survey. ACM Comput. Surv. **38**(4), 13, (2006). doi:[10.1145/1177352.1177355](https://doi.org/10.1145/1177352.1177355)

# A Rubric Based Assessment of Student Performance Using Fuzzy Logic

Meenakshi G. and Manisharma V.

**Abstract** Assessment of student performance is one of the important tasks in the teaching and learning process. It has great impact on the student approach to learning and their outcomes. Evaluation of student learning in different activities is the process of determining the level of performance of students in relation to individual activities. A rubric is a systematic scoring guideline to evaluate student performance (assignment, quiz, paper presentation, open and closed book test etc.) through the application of detailed description of performance standards. After giving the specific task the student should be explained about the criteria and evaluation points. This allows the students to be aware of the performance and they will try to improve the performance. In this paper the main focus is on student centered learning activities which are mainly based on multiple intelligences. This paper presents an integrated fuzzy set approach Lotfi et al. [2] to assess the outcomes of student-centered learning. It uses fuzzy set principles to represent the imprecise concepts for subjective judgment and applies a fuzzy set method to determine the assessment criteria and their corresponding weights.

**Keywords** Student centered learning · Fuzzy logic · Active learning · Passive learning · Multiple intelligences

---

G. Meenakshi (✉) · V. Manisharma  
Department of Computer Science, Nalla Malla Reddy Engineering College,  
Hyderabad, Andhra Pradesh, India  
e-mail: meena\_ganti@yahoo.com

V. Manisharma  
e-mail: manisharmavittapu@gmail.com

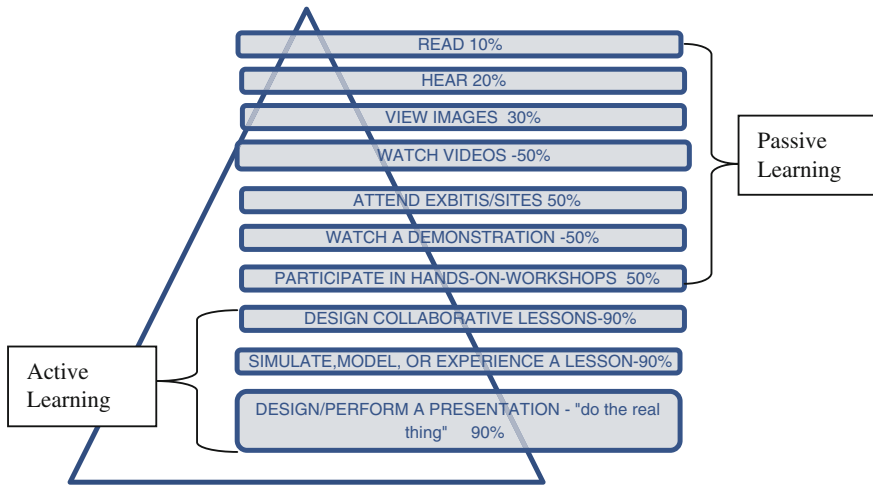


Fig. 1 The Cone of active and passive learning

## 1 Introduction

Currently the shortage of skilled people at work place is one of the major problems faced by the Indian economy. It was found that there was a large gap between the current education standards and employability skills. Several studies have shown that students prefer strategies promoting active learning to traditional lectures [5].

This is a passive method of teaching which results in less retention of knowledge by students as indicated in the cone of learning shown in the Fig. 1.

## 2 Proposed Methodology

Howard Gardner’s Multiple Intelligences (MI) theory has sparked a revolution in the educational field. According to him each person is unique and a blend of intelligences namely Linguistic, Logical -Mathematical, Spatial, Musical, Interpersonal, Intrapersonal, Naturalistic. People differ in the intelligences. According to multiple intelligence the course contents must be designed to meet the activity based activities so that the students can actively participate in the classroom [4] (Fig. 2).



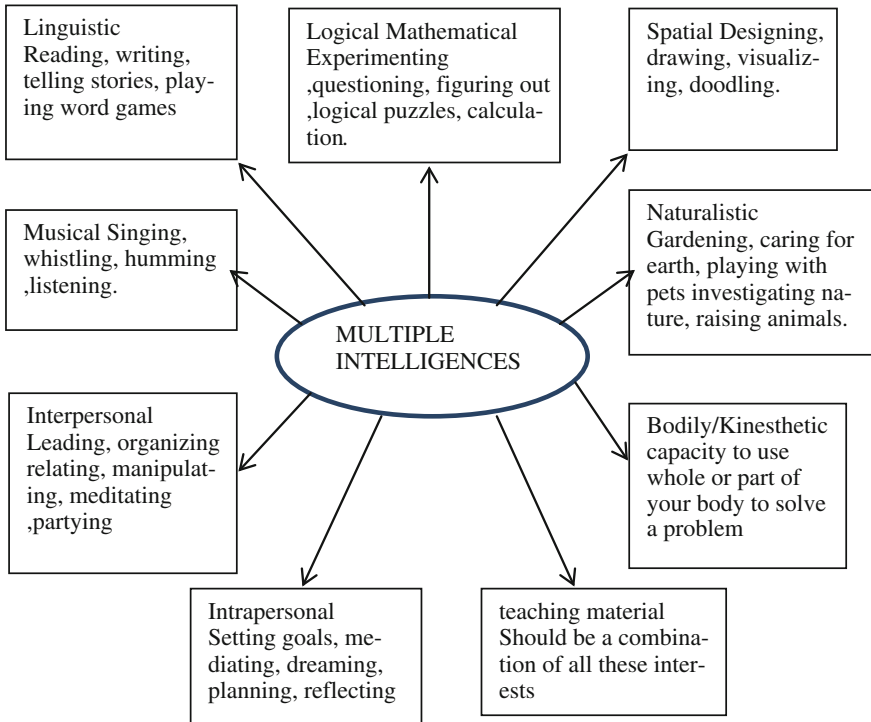


Fig. 2 Multiple intelligences

### 2.1 Student Assessment Model

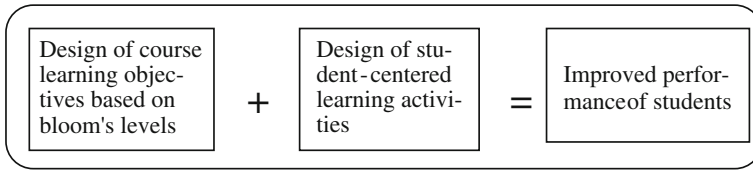
To improve and develop the student learning [3], staff are required to prepare a list of tasks to be implemented are prepared, different tasks are assigned to faculty members at the commencement of the year/semester the evaluation of the students in that particular period is evaluated [1].

### 2.2 Evaluating Steps: The Following Steps are Followed for Evaluating the Student Performance

Student assessment model can be implemented in academics also as shown in [6] Fig. 3.

Step 1: Normalize the marks

The marks obtained by each of the student have to be converted to the normalized values. Normalized value is referred to a value in a range of [0, 1]. It can be obtained



**Fig. 3** Student evaluation method

**Table 1** Normalized value

Criteria	Total marks	Mark obtained	Normalized value
Poster/chart presentation (C1)	100	70	0.70
Subject based quiz (C2)	100	80	0.80
Open book/closed book test (C3)	100	60	0.60
Power point presentation/seminars (C4)	100	80	0.80
Assignments (C5)	100	90	0.90

by dividing the mark for each criterion with the total mark. This will be the input value of this evaluation. Table 1 tabulates the example marks and the normalized values obtained by a student for all the criteria.

Step 2: Developed the graph of the Fuzzy Membership Function [2]

The graph of membership function is developed in order to execute the fuzzification process. In this process, the input value is mapped into the graph of membership function to obtain the fuzzy membership value of that particular input value. Each membership value will represent the level of satisfaction.

Table 2 shows five satisfaction levels that have proposed in this study. It is based on the linguistic term. The degree of satisfaction shows the range of marks for each satisfaction level which are based on some grading system. The maximum degree of satisfaction denoted by  $T(x_i)$  describes the mapping function for corresponding satisfaction level where  $T(x_i) \rightarrow [0,1]$ .

Step 3: calculate the degree of satisfaction

The degree of satisfaction of  $j$ th criteria which denoted by  $D(C_j)$  is evaluated by  $x$

$$D(C_j) = \frac{y_1 * T(x_1) + y_2 * T(x_2) + \dots + y_5 * T(x_5)}{y_1 + y_2 + \dots + y_5} \tag{1}$$

where  $y_i$  = degree of membership value for each satisfaction level,  $y_1$

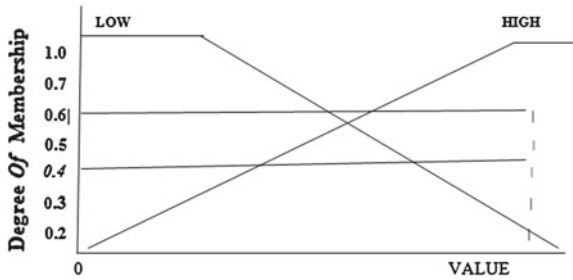
Step 4: Compute the final rank

The final mark for  $k$ th student denoted by  $F(S_k)$  is calculated using the formula below:

$$F(S_k) = \frac{w_1 * D(C1) + w_2 * D(C2) + \dots + w_5 * D(C5)}{w_1 + w_2 + \dots + w_5} \tag{2}$$

**Table 2** Satisfaction levels

Satisfaction levels (Xi)	Degrees of satisfaction	Maximum degrees of satisfaction T(xj)
Exemplary	80–100 % (0.8–1.0)	1.0
Accomplished	70–79 % (0.70–0.79)	0.79
Delveloping	60–69 % (0.6–0.69)	0.69
Beginning	40–59 % (0.4–0.59)	0.59
Fail	0–39 % (0–0.39)	0.39



**Fig. 4** Graph of membership function

where  $w_i$  = the total marks of  $i$ th criteria for  $i = 1, 2, \dots 5$ .

The result obtained is put into the fuzzy grade sheet (Table 3) in the appropriate columns.

**NUMERICAL EXAMPLE:** As an illustration, the example mark of a student is taken (as in Table 1). The student is evaluated based on procedure mentioned earlier. The graph of membership function is generated to execute the fuzzification process in step 2 is shown in Fig. 4.

Based on the Fig. 1 we can see the satisfaction level of ACCOMPLISHED and DEVELOPING that represent the degree of membership 0.4 and 0.6 respectively. The degree of satisfaction regarding criterion 1 is calculated as follows:

$$D(Ci) = (0.4 * 1.0 + 0.6 * 0.79) / (0.4 + 0.6) = 0.874$$

The same procedure is applied for calculating the  $D(C1), D(C2), \dots D(C5)$

Finally, the final mark earned by the student for all criteria is computed using (2).

$$\begin{aligned} F(S1) &= 100 * 0.874 + 100 * 0.752 + 100 * 0.960 + 100 * 0.704 \\ &\quad + 100 * 0.672 / 500 \\ &= 0.7924 = 0.79 \end{aligned}$$

Based on the final mark obtained, the student is awarded by the fuzzy linguistic terms of Accomplished at 0.19 (UAc) Exemplary at 0.83 (Uex = 0.81). These values are obtained from the graph of the membership function (as in Fig. 1). Besides that the

**Table 3** Final marks of a student

Student	Criteria	Fuzzy membership value					Degree of satisfaction	Final mark
		E	A	D	B	F		
1								0.801
	C1	0.4	0.6	0	0	0	0.874	
	C2	0	0.62	0.38	0	0	0.752	
	C3	0.81	0.19	0	0	0	0.960	
	C4	0	0.57	0.43	0	0	0.747	
	C5	0.2	0	0	0.8	0	0.672	

**Table 4** Comparison of fuzzy and non fuzzy

	Non-fuzzy method		Fuzzy-evaluation method	
	Final mark	Linguistic term	Final mark	Linguistic term
1	70	Accomplished	0.79	Exemplary at 0.4 Accomplished at 0.6
2	80	Exemplary	0.90	Accomplished at 0.62 Developing at 0.38
3	70	Accomplished	0.73	Exemplary at 0.17 and Accomplished at 0.83
4	40	Beginner	0.59	Developing at 0.43 and Accomplished at 0.57
5	60	Developing	0.71	Exemplary at 0.2 and Beginner at 0.8

final mark also can be valued as 78.69 (by multiplying with 100 %) which represent the linguistic term of Exemplary. The details of the fuzzy marks obtained from this evaluation procedure as shown in Table 3.

Since most of the computation used in fuzzy evaluation method is made as fuzzy sets with the range of [0, 1], therefore the results obtained from this method as shown in the Table 3 are in the range of [0, 1] only. The final mark earned by student 1 is 0.79, but after converted in terms of percentage, it will be 79 % Table 4.

### 3 Conclusion and Future Direction

Overdependence on lecturing and other instructor-centered learning strategies often fosters a passive learning attitude and mental disengagement during class. Effective instructors regularly utilize more student-centered strategies that are beneficial to students.

**Acknowledgments** I am heartily thankful to Dr. Mrs. Divya Nalla , Principal, Nalla Mallareddy Engineering College Whose encouragement and support resulted in the preparation of paper.I am thankful to our research Director Prof. Vara Prasad, Dept HOD and ASSOC. Prof. P.V.S Siva Prasad and Mr. Mani Sarma Assoc. Prof for their encouragement guidance and support from the initial to the final level.

## References

1. Jian, M., Duanning, Z.: Fuzzy set approach to the assessment of student-centered learning. *IEEE Trans. Educ.* **43**(2), 237 (2000)
2. Lotfi A. Zadeh, L.A.: *Fuzzy logic*. Berkeley
3. Chickering, A.W., Gamson, Z.F.: Seven principles of good practice. *AAHE Bull.* **39**, 3–7 (1987). (ED 282 491. 6 pp. MF-01; PC-01)
4. Lowman, J.: *Mastering the techniques of teaching*. Jossey-Bass, San Francisco (1984)
5. McKeachie, W.J., Pintrich P.R., Lin Y.-G., Smith, D.A.F.: *Teaching and learning in the college classroom: a review of the research literature*. Regents of The University of Michigan, Ann Arbor (1986). (ED 314 999. 124 pp. MF-01; PC-05)
6. Penner, J.G.: *Why many college teachers cannot lecture*. Charles C. Thomas, Springfield (1984)

# Representation and Classification of Medicinal Plants: A Symbolic Approach Based on Fuzzy Inference Technique

H. S. Nagendraswamy and Y. G. Naresh

**Abstract** In this paper, a method of representing shape of medicinal plant leaves in terms of interval-valued type symbolic features is proposed. Axis of least inertia of a shape and the fuzzy equilateral triangle membership function is exploited to extract features for shape representation. Multiple class representatives are used to handle intra class variations in each species and the concept of clustering is used to choose multiple class representatives. A simple nearest neighbor classifier is used to perform the task of classification. Experiments are conducted on the standard flavia leaf dataset to demonstrate the efficacy of the proposed representation scheme in classifying medicinal plant leaves. Results of the experiments have shown that the method is effective and has achieved significant improvement in classification accuracy when compared to the contemporary work related to leaf classification.

**Keywords** Axis of least inertia · Fuzzy equilateral triangle · Symbolic data · Shape classification · Shape representation

## 1 Introduction

Medicinal plants play an important role in Ayurvedic system of medicine. This system emphasizes not only on curing but also on the prevention of the recurrence of diseases. Certain diseases can be treated effectively using Ayurvedic medicine and it has been practiced since ancient years. Though several medicinal plants are available in our surrounding environment, we are not able identify and make use of them for preparation of simple house-hold medicines for common diseases in day-to-day life.

---

H. S. Nagendraswamy · Y. G. Naresh (✉)  
DoS in Computer Science, University of Mysore, Mysore, India  
e-mail: swamy\_hsn@yahoo.com

Y. G. Naresh  
e-mail: naresh.yg@gmail.com

Since the taxonomy of medicinal plants is very vast, even the experts may find it difficult to identify and classify them effectively. Even though there are many biological methods to identify the plant species, it is worth exploring image processing and pattern recognition techniques to create a knowledge base of medicinal plants and to provide an automated support for identification and classification of medicinal plants by analyzing the visual properties such as shape, texture, internal vein patterns, and color of the leaves.

## 2 Related Work

Shape of a plant leaf plays a major role in identifying and classifying the plant species. In the literature, both contour-based and region-based methods have been proposed to characterize the shape and experimented on leaf datasets.

In [1], the region-based morphological features of a leaf viz., aspect ratio, rectangularity, area ratio of convex hull, perimeter ratio of convex hull, sphericity, circularity, eccentricity, form factor, and invariant moments are used for its description. The concept of physiological width and physiological length of a plant leaf along with other geometric and region-based morphological features have been proposed in [2] for characterizing shape of a plant leaf. In [3], landmark points are considered for polygon approximation. Given any two points in the set of landmark points, Inner-distance between those two points as a replacement to Euclidean distance is computed to build shape descriptors, for classification. In [4], a method of characterizing a shape by modeling shape contour as a complex network through multiscale fractal dimension is proposed. In [5], Fuzzy equilateral triangle membership values have been proposed to describe a shape in terms of multiinterval-valued type features. In [6], Contour-based symbolic representation method has been proposed to describe the shape curve using string of symbols. In [7], symbolic representation in terms of multiinterval-valued type features has been proposed to characterize two dimensional shapes. In [9], Histogram of gradients is used as shape descriptors for characterizing leaf shape.

From the literature survey, it has been observed that several methods have been proposed to effectively represent shape of a plant leaf and to improve the accuracy of classification results. Despite several methods available for the task of classification of leaves, still there is a scope for exploring new methods to improve the accuracy of classification results through realistic and effective representation techniques. It has also been observed from the survey that the representation techniques based on the concept of fuzzy symbolic data have shown good performance when compared to the representation techniques based on conventional data. This is due to the fact that the symbolic data are more unified in terms of relationship and can capture the variations more effectively which is very much essential for most of the real-life objects and the concept of fuzzy theory is a natural choice for handling vagueness and uncertainty in representation. However, only few attempts [5, 7] have been made in this direction which motivated us to think of exploring the unconventional

representation technique for representing shape of medicinal plant leaves for their classification. Thus, in this work, we made an attempt to propose a representation technique based on the Fuzzy Inference Technique and the concept of symbolic data. The experimental study has revealed that the proposed representation technique has shown significant improvements in the accuracy of classification and is comparable with the contemporary work in this direction.

### 3 Proposed Method

Extracting relevant and discriminative features for characterizing a leaf shape is an important step in any recognition or classification task. In this section, a method of extracting interval-valued features adopting axis of least inertia of a shape and the concept of fuzzy equilateral triangle is explained.

#### 3.1 Feature Extraction

The color images of plant leaves are first converted into binary images. Then the contour of binary images is obtained by using a suitable contour extraction algorithm. The extracted closed contour serves as a shape curve of a plant leaf image.

The proposed feature extraction technique adopts the axis of least inertia of a shape to preserve the orientation of a shape curve which is very important to extract features invariant to geometric transformations (Rotation, translation, and scaling). The details regarding the computation of the axis of least inertia of a shape curve can be found in [7].

Once the axis of least inertia of a shape is computed, all the points of shape contour are projected onto the axis and the two farthest points are obtained. Figure 1 shows a shape with axis of least inertia and two extreme points  $E_1$  and  $E_2$ . Let  $PE_1$  and  $PE_2$  be the two contour points on the shape curve obtained by projecting the two extreme points  $E_1$  and  $E_2$  of the axis of least inertia as shown in the Fig. 1. The shape contour is traversed in clockwise direction keeping either  $PE_1$  or  $PE_2$  as the starting point. In order to identify this starting point, the Euclidean distance between the  $PE_1$  and the shape centroid and the distance between  $PE_2$  and the shape centroid are computed. The shortest distance among the two is considered as a starting point. In some cases, there is a possibility that these two distances may be same and leads to ambiguity in selecting the starting point. In such case, we resolve the conflict by considering the horizontal width of the shape at subsequent points on the axis starting from the two extreme points.

Keeping either  $PE_1$  or  $PE_2$  as a starting point and traversing in clockwise direction, the contour is split into ' $k$ ' equal number of segments. The centroid of each curve segment is obtained by taking the average of all the pixels of the curve segment. The centroids so obtained serve as feature points on the shape curve.



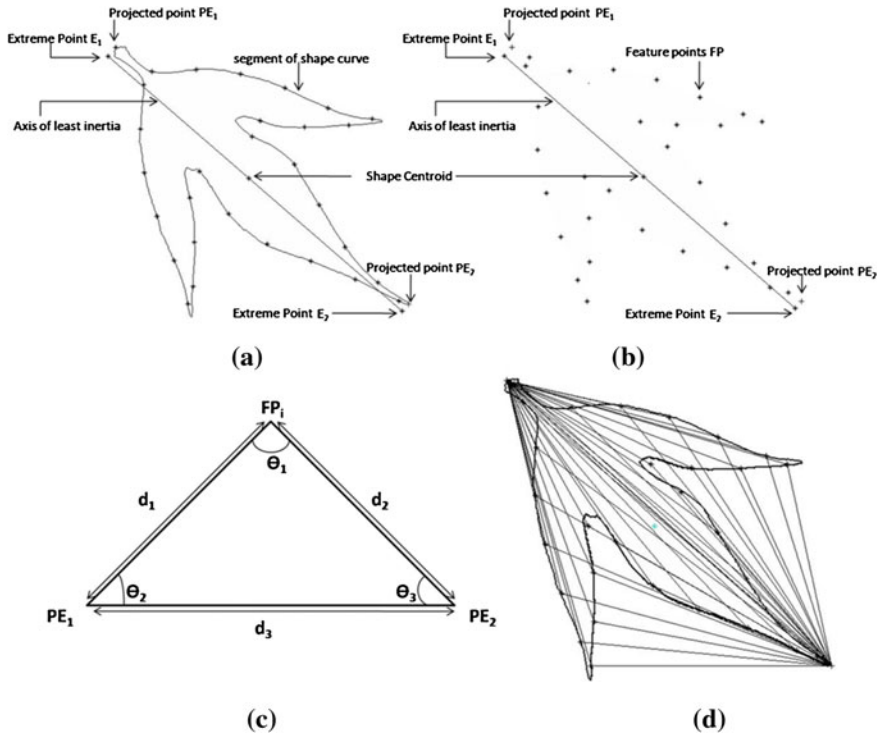


Fig. 1 Shape with axis of least inertia and two extreme points

The idea behind obtaining the local centroids of a shape curve is to take into consideration all the pixels information to define a feature point rather than considering a corner points or dominant points on the shape curve, which are not consistent and robust due to noise and shape transformation. Figure 1b shows the feature points obtained for a shape curve shown in Fig. 1a.

Once the feature points on the shape curve are obtained, we traverse the shape curve in clockwise direction and at every feature point  $FP_i$  for  $i = \{1, 2, 3, \dots, k\}$ , we form a triangle considering the two extreme points  $PE_1$  or  $PE_2$ . We use the fuzzy inference technique [10] to approximate the triangle as equilateral and the corresponding membership value is computed as follows.

Let  $\theta_1, \theta_2$  and  $\theta_3$  be the inner angles of the triangle in the order  $\theta_1 > \theta_2 > \theta_3$ . Let  $U$  be the universe of the triangle.

$$U = \{(\theta_1, \theta_2, \theta_3) / \theta_1 \geq \theta_2 \geq \theta_3 \geq 0; \theta_1 + \theta_2 + \theta_3 = 180^\circ\} \tag{1}$$

Let  $d_1, d_2, d_3$  be the Euclidean distances between  $PE_1$  and  $FP_i$ ,  $PE_2$  and  $FP_i$  and  $PE_1$  and  $PE_2$ , respectively as shown in the Fig. 1c. The inner angles of a triangle are computed as follows:

$$\theta_1 = \cos^{-1} \left( \frac{d_2^2 + d_3^2 - d_1^2}{2 * d_2 * d_3} \right) \quad (2)$$

$$\theta_2 = \cos^{-1} \left( \frac{d_1^2 + d_3^2 - d_2^2}{2 * d_1 * d_3} \right) \quad (3)$$

$$\theta_3 = \cos^{-1} \left( \frac{d_1^2 + d_2^2 - d_3^2}{2 * d_1 * d_2} \right) \quad (4)$$

The membership value of the triangle which approximates equilateral triangle is computed as

$$\mu(\theta_1, \theta_2, \theta_3) = 1 - \frac{1}{180} (\theta_1 - \theta_3) \quad (5)$$

The membership values  $\mu_i$  (for  $i = 1$  to  $k$ ) are computed and considered as feature values to describe a shape.

### 3.2 Feature Representation

Since the shape of leaves in a class may vary due to size, maturity, and other biological facts, there will be significant intraclass variations among the shapes. To handle this case, we propose to have multiple representatives for a class by grouping similar shapes into one group and choose a representative for that group within the class. We have used hierarchical clustering technique to group similar shapes in a class by utilizing inbuilt Matlab function. The natural groups in a class are identified using the inconsistency coefficient for each link of the hierarchical cluster tree yielded by the respective linkage. Once the natural groups are obtained for each plant species, we consider 60 % of the samples from each group to form a class representative to be stored in the knowledge base during training and remaining 40 % of the samples for testing. A representative feature vector for a particular group within the class is obtained by aggregating the corresponding features of the shapes in the group to form an interval-valued type feature. Thus, the feature vector representing a group within a class is of interval-valued type rather than crisp. Thus in the proposed approach, the shape of plant leaves in the knowledge base are represented in the form  $k$ -dimensional Interval-valued type feature vector.

Lower the intraclass variations in the class  $C_i$ , fewer the number of groups obtained and higher the intraclass variations, more the number of groups. Hence the number of groups in a class  $C_i$  is directly proportional to its intraclass variations.

Let  $[G_1, G_2, G_3 \dots, G_m]$  be the ' $m$ ' number of group formed in a class. Let  $[S_1, S_2, S_3 \dots, S_P]$  be the leaf shapes in the group. Each shape in  $S_i$  for  $i = \{1, 2, 3, \dots, P\}$  in a group is represented by feature vector of dimension  $k$  i.e.,  $S_i = \{F_{i1}, F_{i2}, F_{i3} \dots, F_{ik}\}$ . To form a group representative vector, we aggregate the

**Table 1** An example of  $k$ -dimensional Interval-valued feature vector representing a group in the knowledge base.

Shapes in a group	1	2	...	...	$k$
$S_1$	0.2204	0.1793	...	...	0.1542
$S_2$	0.1216	0.1503	...	...	0.1536
..	...	...	...	...	...
$S_p$	0.1246	0.1263	...	...	0.0899
Interval type feature value	[0.1216, 0.2204]	[0.1263, 0.1793]	...	...	[0.0899, 0.1542]

corresponding features of the shape  $S_i$  to form an interval by choosing the minimum and maximum of corresponding values feature values. Table 1 shows an example of  $k$ -dimensional interval-valued feature vector representing a group in the knowledge base as explained earlier.

### 3.3 Matching and Classification

Let  $TS = \{F_1, F_2, F_3, \dots, F_k\}$  be the  $k$ -dimensional feature vector representing the shape of a plant species to be classified. Let  $MS = \{[F_{si}^-, F_{si}^+]\}$  for  $s = \{1, 2, 3, \dots, N\}$  where  $N$  is the number of model shapes and  $i = \{1, 2, 3, \dots, k\}$  be the  $k$ -dimensional interval-valued feature vector representing  $j$ th model shape in the knowledge base pertaining to a particular class of a plant species.

We use the similarity measure proposed in [7] to find the similarity score between the test shape and the model shape as

$$\text{Sim}(TS, MS) = \frac{1}{K} \sum_{i=1}^K SV_i \tag{6}$$

where

$$SV_i = \left[ \begin{array}{l} 1 \quad \text{if } (F_{Si}^- \leq F_i \leq F_{Si}^+) \\ \text{else} \\ \frac{1}{2} \left[ \frac{1}{1 + \text{abs}(F_{Si}^- - F_i)} + \frac{1}{1 + \text{abs}(F_{Si}^+ - F_i)} \right] \end{array} \right]$$

The test leaf shape is compared with all the model (reference) shape of the plant species in the knowledge base. The label of model (reference) shape which possesses the highest similarity value is assigned to the test leaf shape.

## 4 Experimental Results

We have implemented our method using Matlab R2011b. We have conducted experiments on the dataset provided by [2]. All the plant species in the dataset have medicinal values. Thus we have called them as medicinal plant species. We considered 30 plant species for our experiments from the dataset [2]. In our experiments, the ‘complete’ linkage is chosen empirically for finding the compact groups in every class of leaf shape. The training and testing set of samples are considered as explained in the Sect. 3.2. The performance of the proposed method is evaluated in terms of accuracy, precision, recall, and  $F$ -measure for varying values of  $k$  and the values are tabulated in Table 2. From Table 2, it is observed that the proposed method has shown highest average Accuracy, Precision, Recall, and  $F$ -measure respectively for  $k = 40$ . The following Table 2 gives Average Accuracy, Precision, Recall, and  $F$ -measure, respectively, for various values of  $k$ .

Since we have used the same dataset used by [2], we are comparing the performance of the proposed methodology with that of [2]. The authors in [2] have obtained the overall classification accuracy of 90.13 % by observing the number of leaves correctly classified over the total number of leaves considered for experiment. Accordingly, the proposed method has shown the overall classification accuracy of 92.29 %. This reveals that the proposed methodology shows better performance compared to [2] Table 3.

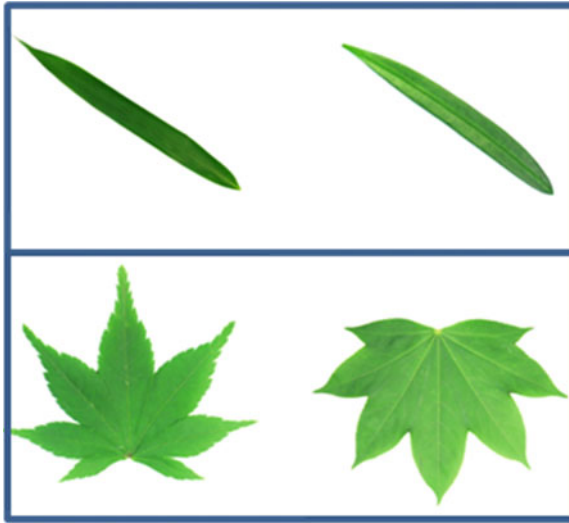
Figure 2 shows example leaves belonging to different species but possess similar shape structures. Thus it is very difficult to classify such leaves just by considering only shape information.

**Table 2** Performance measures of the proposed method

No. of features	Average accuracy	Average precision	Average recall	Average $F$ -measure
30	0.9919	0.9062	0.8792	0.8853
40	<b>0.9949</b>	<b>0.9315</b>	<b>0.9229</b>	<b>0.9246</b>
50	<b>0.9943</b>	<b>0.9242</b>	<b>0.9146</b>	<b>0.9157</b>
60	<b>0.9943</b>	<b>0.9275</b>	<b>0.9146</b>	<b>0.9172</b>
70	0.9928	0.9413	0.8917	0.9047
80	0.9931	0.9386	0.8958	0.9082
90	0.9924	0.9307	0.8854	0.8985

**Table 3** Comparison for the method proposed in [2]

Scheme	Classification accuracy %
Proposed scheme	92.29
Stephen et al. [2]	90.13



**Fig. 2** Leaves belonging to different species possessing similar shape structure

## 5 Conclusion

In this work, we proposed a novel method of representing medicinal plant leaves for classification. The method exploits the concept of fuzzy inference technique and symbolic data analysis for effective representation. Experiments are conducted on the standard database of considerably large size and the performance of the proposed method is evaluated in terms of standard performance evaluation measures. The results are more encouraging and comparable with that of state of the art work. However, the approach may fail to classify accurately the plant leaves belonging to different species possessing similar shape structure as shown in Fig. 2. So, we shall explore the texture-based representation techniques in such cases. Also, the multi-stage classifier techniques incorporating shape and texture features will be explored to further improve the classification accuracy.

## References

1. Du, Xiao-Feng Wang, Ji-Xiang, : Zhang, Guo-Jun: Leaf shape based plant species recognition. *Appl. Math. Comput.* **185**, 883–893 (2007)
2. Wu, S.G., Bao, F.S., Xu, E.Y., Wang, Y.-X., Chang, Y.-F., Shiang, C.-L.: A leaf recognition algorithm for plant classification using probabilistic neural network. In: *IEEE 7th International Symposium on Signal Processing and Information Technology*, Cairo, Egypt (2007).
3. Ling, H., Jacobs, D.W.: Shape classification using the inner distance. *IEEE Trans. Pattern Anal. Mach. Intell.* **29**(2), 286–299 (2007)

4. Backes, A.R., Bruno, O.M.: Shape classification using complex network and multi-scale fractal dimension. *Pattern Recogn. Lett.* **31**, 44–51 (2010)
5. Nagendraswamy, H.S., Guru, D.S.: A new method of representing and matching two dimensional shapes. *Int. J. Image Graphics* **7**(2), 337–405 (2007)
6. Daliri, M.R., Torre, V.: Robust symbolic representation for shape recognition and retrieval. *Pattern Recogn.* **41**, 1782–1798 (2008)
7. Guru, D.S., Nagendraswamy, H.S.: Symbolic representation of two dimensional shapes. *Pattern Recogn. Lett.* **28**, 144–155 (2007)
8. Tsai, D.M., Chen, M.F.: Object recognition by linear weight classifier. *Pattern Recogn. Lett.* **16**, 591–600 (1995)
9. Xiao, X., Hu, R., Zhang, S., Wang, X.: HOG-based approach for leaf classification. In: *ICIC*, vol. 2, pp. 149–155 (2010)
10. Ross, T.J.: *Fuzzy Logic with Engineering Applications*, 2nd edn. Wiley, Hoboken (2004)

# Fractal Image Compression Using Dynamically Pipelined GPU Clusters

Munesh Singh Chauhan, Ashish Negi and Prashant Singh Rana

**Abstract** The main advantage of image compression is the rapid transmission of data. The conventional compression techniques exploit redundancy in images that can be encoded. The main idea is to remove redundancies when the image is to be stored and replace it back when the image is reconstructed. But the compression ratio of this technique is quite insignificant, and hence is not a suitable candidate for an efficient encoding technique. Other methods involve removing high frequency Fourier coefficients and retaining low frequency ones. This method uses discrete cosine transforms(DCT) and is used extensively in different flavors pertaining to the JPEG standards. Fractal compression provides resolution-independent encoding based on the contractive function concept. This concept is implemented using attractors (seed) that are encoded/copied using affine transformations of the plane. This transformation allows operations such as, skew, rotate, scale, and translate an input image which is in turn is extremely difficult or impossible to perform in JPEG images without having the problem of pixelization. Further, while decoding the fractal image, there exist no natural size, and thus the decoded image can be scaled to any output size without losing on the detail. A few years back fractal image was a purely a mathematical concept but with availability of cheap computing power like graphical processor units (GPUs) from Nvidia Corporation its realization is now possible graphically. The fractal compression is implemented using MatLab programming interface that runs on GPU clusters. The GPUs consist of many cores that together give a very high computing speed of over 24 GFLOPS. The advantage of fractal compression

---

M. S. Chauhan

Research Scholar, Pacific University, Udaipur, Rajasthan, India  
e-mail: muneshchauhan@gmail.com

A. Negi

Department of CSE, G.B. Pant Engineering College, Uttarakhand, India  
e-mail: ashish.ne@gmail.com

P. S. Rana (✉)

Research Scholar, Department of ICT, IIITM, Gwalior, MP, India  
e-mail: psrana@gmail.com

can have varied usage in satellite surveillance and reconnaissance, medical imaging, meteorology, oceanography, flight simulators, extra-terrestrial planets terrain mapping, aircraft body frame design and testing, film, gaming and animation media, and besides many other allied areas.

**Keywords** GPU · Fractal · Attractor · Affine transformation · PIFS

## 1 Introduction

Image/video data constitute a major chunk that is transmitted over networks. Since image and video data consume more memory as compared to text data, they are generally transmitted in compressed form. The main aim for an efficient multimedia data transfer is to retrieve almost the same quality of the data at the receiver-end that was originally transmitted. Considering the availability of the present algorithms for multimedia data compression, it still remains a challenge. Some of the standards that are in vogue are JPEG [14] (still images), MPEG [20] (motion video images), H.261 [15] (Video telephony on ISDN lines), and H.263 [12, 18] (Video telephony on PSTN lines). All these formats compress data signals using Discrete Cosine Transform (DCT) [7]. Since all of these compressions standards are lossy, the image and video data do not retain the original quality. This is acceptable to an extent as human eye is not able to discern the pixels loss if it is limited to a certain threshold. The major issue arises, if the compressed image is scaled up. This leads to pixelization. Fractal images till recently have been researched in the domain of mathematics. Fractal images are derived exploiting a common property of a real image, i.e., self-similarity [8, 11]. Most partitions of a real image show extensive self-similarity. As a result, the original image can be represented as a finite set of contractive affine transformations using partitioned iterated function systems (PIFS).

## 2 Nature of Fractals

Fractal images are found in nature in great abundance [3]. Undulated coastlines, mountains chains, ferns, and also galaxies too represent a striking amount of self-similarity, which can be usually represented by fractals. Fractals have applications in gaming, animation, and science-fiction films where the terrains/landscapes are artificially created [16].

The major disadvantage of a fractal image is its encoding time. The time complexity of encoding a fractal image is  $O(n^4)$  [14, 19]. The decoding part is very efficient and almost instantaneous [17]. Moreover, the fractal images are resolution-independent and they do not show pixelization unlike JPEG images. The scaled up image contains the same level of details as in the original image.



### 3 Encoding Images Using Partitioned Iterated Function System (PIFS)

The mathematical equivalent of partitioned copying machine is termed as PIFS. The transformations in PIFS are affine transformations. These affine transformations consist of two spatial dimensions and a third dimension that is the grey level. In sum, the transformations  $w_i$  may be defined as in Eq. 1 where  $s_i$  denotes contrast and  $o_i$  the brightness.

$$w_i \begin{bmatrix} x \\ y \\ z \end{bmatrix} = \begin{bmatrix} a_i & b_i & 0 \\ c_i & d_i & 0 \\ 0 & 0 & s_i \end{bmatrix} \begin{bmatrix} x \\ y \\ z \end{bmatrix} + \begin{bmatrix} e_i \\ f_i \\ o_i \end{bmatrix} \tag{1}$$

Thus the spatial part  $v_i$  of the image may be defined as in Eq. 2.

$$v_i(x, y) = \begin{bmatrix} a_i & b_i \\ c_i & d_i \end{bmatrix} \begin{bmatrix} x \\ y \end{bmatrix} + \begin{bmatrix} e_i \\ f_i \end{bmatrix} \tag{2}$$

Different partitions of the image as shown in Fig. 1 are considered as  $D_i$  and  $R_i$  lying in the plane above the image. Each  $w_i$  is restricted to  $D_i \times I$  (the vertical space above  $D_i$ ).

Hence  $v_i(D_i = R_i)$ . Thus, we need  $W(f)$  as the image with the conditions as given in Eq. 3.

$$\begin{aligned} \bigcup R_i &= I^2 \\ R_i \cap R_j &= \emptyset \text{ when } i \neq j \end{aligned} \tag{3}$$

As shown in Eq. 3, we obtain single-valued function above each point of the square  $I^2$ . In addition to it each copy is nonoverlapping in terms of the copying machine metaphor.

According to Contractive Mapping Theorem [5], a fixed point (attractor) of a given image  $f$  is described as  $W(f) = f$ . We must guarantee that  $W$  has a unique fixed point in order for an image to be encoded. It has been found that for  $s_i < 1.2$  (where  $s_i$  is defined as the contrast factor) can be considered as a safe limit for an

**Fig. 1** The maps  $w_i$  map the graph above  $D_i$  to a graph above  $R_i$

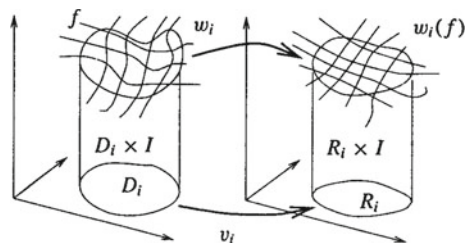


image to be contractive. Though there exists no surety of the contractiveness of an image for any given values of  $s_i$ .

Further, the copying machine metaphor, as defined for fractal image compression reduces contrast ( $s_i$ ) of a given image during each iteration of the feedback loop. This does not mean that the final image through successive iterations will be a homogenous grey. On the flip side, this produces increased levels of details in each of the successive iterations as found in fractals.

Though there are many views of fractal image compression as outlined below but we shall delve on a special case of IFS, i.e., PIFS.

1. Partitioned iterated function system (PIFS)
2. Self-vector quantization: It is based on VQ codebook approach.
3. Self-quantized wavelet subtrees: It uses a type of wavelet transform coding (Haar wavelet coefficient).
4. Convolution transform coding: Uses convolution operation while searching a matching image.

## 4 Applying PIFS on a Sample Image (Lenna Image)

The Lenna image consists of large chunks of homogeneous regions [4]. As a result, appropriate collage may be derived to encode large blocks. For regions of high contrast smaller blocks are selected for high quality. We apply *variable quadtree partition* approach to encode Lenna image. Variable partitioning provide users an option to specify image size and quality parameters according to their needs. The variable blocks in our experiment shall be of 4, 8, 16, and 32 pixels wide.

The image encoding is simulated on a GPU cluster simulated using 24 GPU machines with the host machine having ATI Radeon graphics hardware [6, 10]. The topology followed is *Dynamic Allocation with Circulating Pipeline Processing* as outlined in [1, 9].

As depicted in Fig. 2 each range block is circulated through a pipeline that traverses through nodes comprising of PEs (Processing Elements- GPUs [13]). Each PE is represented by a domain and thus each range is matched with it. Once a match is found the range exits the pipeline. If no match is obtained, the host  $PE_0$  subdivides the range into four sub-blocks and the process of matching continues through the pipeline till an appropriate match is found. The advantage of the pipeline approach is that the work is spread evenly among slave processors. In addition to this, less memory is used as each slave processor is required to save only part of the image (domain) and not the entire image. The pipeline topology scale evenly (linearly) as number of slave processors is increased. It is noted that the processor utilization efficiency is 95 % for the sample Lenna image.

The experimental results for encoding the Lenna image over the pipelined topology are outlined in Table 1.

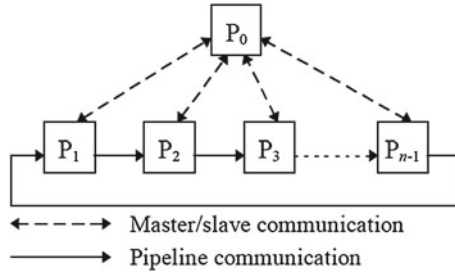


Fig. 2 Circulating pipeline configuration

Table 1 Encoding and compression time chart

Range	PSNR (dB)		Encoding time (s)	Compression ratio
	Collage	Attractor		
4 × 4	34.78	34.56	56.07	6.6
8 × 8	27.95	27.34	34.29	19.67
16 × 16	23.03	23.78	28.55	89.34
32 × 32	19.66	19.54	25.02	341.89

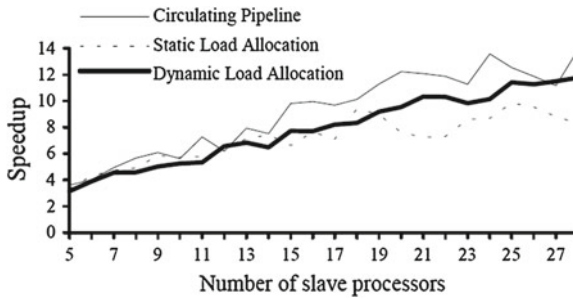


Fig. 3 Performance simulation for a GPU cluster



Fig. 4 Encoding results using PIFS partitioning scheme on GPU cluster (PSNR: 19.54, Compression ratio: 341.89 %)

The performance simulation graph [2] shown in Fig. 3 clearly shows performance gain in terms of speedup factor against the number of GPU PEs. The circulating pipeline approach is compared with the other conventional schemes like *static load allocation and dynamic load allocation*.

The results of the encoding using the PIFS approach with *PSNR* value 19.54 shows an impressive compression ratio of 341.89 % (refer Fig. 4).

## 5 Conclusion

The results obtained using PIFS scheme on a set of GPU cluster are promising. Though the computing time for this scheme still remains  $O(n^4)$  but the pipelining of slave GPU processing cores open new avenues of multithreading (inherent inside GPU cores) the image compression algorithms which till now have been implemented in uniprocessor architectures or selective simulations on SIMD machines. The pipelining approach is scalable and considering the GPU availability in the market on commodity rates it can be implemented using cheap processing power for computer intensive fractal image processing logic. The quality of the image (fidelity) still remains an open question as it has been observed that the PIFS approach creates degradation in the image fidelity in case the image is heterogenous and thus the range blocks need to be partitioned more frequently in each of the pipeline stage.

## References

1. Ahmed, N., Natarajan, T.: Discrete cosine transform. *IEEE Trans. Comput.* **23**, 90–93 (1974)
2. An Introduction to Fractal Image Compression. Literature Number: BPRA065, Texas Instruments Europe, October 1997.
3. Barnsley, M.F., Sloan, A.: Chaotic compression. *Comput. Graphics. World* **5**, 107–108 (1987)
4. Chady M.: Application of the Bulk Synchronous Parallel Model in Fractal Image Compression. School of Computer, Science (2004).
5. Erra, U.: Toward real time fractal image compression using graphics hardware. In: Proceedings of Advances in Visual Computing, LNCS, vol. 3804, Springer, pp. 723–728. 2005, doi:[10.1007/11595755\\_92](https://doi.org/10.1007/11595755_92).
6. Galabov, M.: Fractal image compression. In: International Conference on Computer System and Technologies - CompSysTech'2003 (1990).
7. Hockney, R.W.: Performance parameters and benchmarking of supercomputers. *Parallel Comput.* **17**, 1111–1130 (1991)
8. Hurtgen, B., Mols, P., Simon, S.F.: Fractal transform coding of color images. SPIE Conference on Visual Communications and Image Processing, Chicago, In (1994)
9. Jackson, D.J., Blom, T.: Fractal image compression using a circulating pipeline computation model. *Int. J. Comput. Appl.* (in review).
10. Jacquin, A.: Image coding based on a fractal theory of iterated contractive image transforms. In: SPIE, Visual Communications and Image Processing, vol. 1360 (1990).
11. Kominek, J.: Advances in fractal compression for multimedia applications. *Multimedia Systems*. Springer, New York (1997).

12. Line Transmission of Non-Telephone Signals. Video CODEC for AudioVisual Services, ITU-T Recommendation (H.261).
13. Mandelbrot, B.B.: *The Fractal Geometry of Nature*. W.H. Freeman and Company, San Francisco (1982). ISBN 0-7167-1186-9
14. Monro, D.M., Wooley, S.J.: Fractal image compression without searching. In: *Proceedings of ICASSP*, vol. 5, pp. 557–560 (1994).
15. MPEG-7 Whitepaper. Sonera MediLab, 13 October 2003.
16. Owens, J.D. et al.: A survey of general-purpose computation on graphics hardware. In: *Eurographics 2005, State of the Art Reports*, pp. 21–51, August 2005.
17. Ruhl, M., Hartenstein, H.: Optimal fractal coding is NP-hard. *Proceeding of IEEE Computer Society Washington, DC, USA, In* (1997)
18. Series H: Audiovisual and multimedia systems, infrastructure of audiovisual services - Coding of moving video. Video coding for low bit rate communication ITU-T, ITU-T Recommendation (H.263).
19. Sodora, A.: *Fractal Image Compression on the Graphics Card*. Johns Hopkins University, Baltimore (2010)
20. Wallace, G.K.: The JPEG still picture compression standard. *IEEE Trans. Consum. Electron.* **38**(1), 18–34 (1992)

# Person Identification Using Components of Average Silhouette Image

Rohit Katiyar, K. V. Arya and Vinay Kumar Pathak

**Abstract** Gait biometrics is one of the non-cooperative biometrics traits particularly in the situation of video surveillance. In the proposed method human knowledge is combined with gait information to get the better recognition performance. Here, individual contributions of different human components, namely head, arm, trunk, thigh, front-leg, back-leg and feet are numerically analyzed. The performance of the proposed method is evaluated by experimentally with CASIA dataset B and C. The effectiveness and impact of seven human gait components is analyzed by using Average Silhouette Image (ASI) under wide range of circumstances.

**Keywords** Biometrics · Human gait recognition · Average silhouette image · Human gait modeling · Visual surveillance.

## 1 Introduction

In visual surveillance some kind of biometric information is required to be extracted for human identification and verification. Majority of researchers focused on biometrics traits such as face, fingerprints, iris, handwriting etc but some of the most prominent are discussed below.

---

R. Katiyar (✉)  
CSE Department, H.B.T.I, Kanpur, India  
e-mail: rohit.katiyar@rediffmail.com

K. V. Arya  
AVB-Indian Institute of Information Technology and Management, Gwalior, India  
e-mail: kvarya@iiitm.ac.in

V. K. Pathak  
Uttarakhand Open University, Haldwani, India  
e-mail: vinaypathak.hbti@gmail.com

- (i) In visual surveillance, the distance between the cameras and the people under surveillance are often large and hence, it is very difficult (almost impossible) to get the detailed and accurate biometric information in above mentioned conventional biometric systems.
- (ii) The subject's cooperation often required to capture conventional biometric information. Therefore, the quality of input image is highly dependent on cooperation.
- (iii) People's attention in authentication and authorization: Human gait provides an interesting alternative for visual surveillance applications. A gait describes by the walking pattern of a person. It can be acquired at a distance and even without the cooperation or knowledge of the person.

Human gait is affected by the person's physical characteristics and some factors related to ambient. Tao et al. [1] have presented that carrying status of walking person and its clothes, shoes etc. affect the performance of human gait. In [2] Phillips et al. demonstrated that the effect of camera view point and elapsed time on the gait measurement and demonstrated that for visual surveillance the elapsed time should be as small as possible. It has been shown by Tanawongsuwan and Bobick [4] that walking speed, rhythm and surface bounciness are the inherent characteristics associated with gait and do affect the performance of gait recognition system. As identified by Liu et al. [5], the efforts are still required to resolve the issues like image quality, lighting condition, subject's familiarity of walking surface.

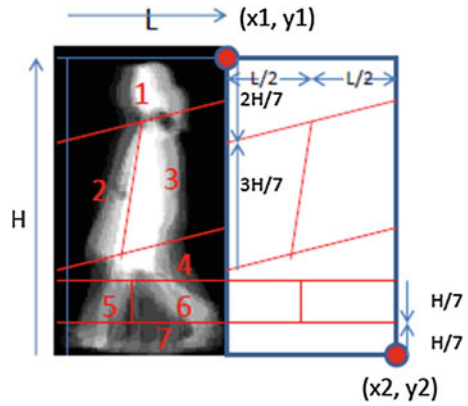
In this work, an effort is made to resolve some of the above mentioned issues. Here, human gait is first decomposed into seven components, and then, the person gait identification is carried out using average silhouette image of gait for each component. During experiments we have observed that the component based gait recognition system is capable of recognizing the people efficiently. Human gait shows the distinctive moving silhouette of a human body which also indicates the physical situation as well as psychological state of the walking person. Hence, the study of various components of the human silhouette along with their effect on human gait recognition process is studied in this work.

The rest of the paper is organized as follows. In Sect. 2 gait modeling scheme is presented along with ways of human silhouette decomposition into seven components also the process of Average Silhouette Image (ASI) generation is discussed. The details of gait dataset used for the experiments are given in Sect. 3. The proposed human gait recognition system is presented in Sects. 4 and 5 experimental results are described. Finally the paper is concluded in Sect. 6.

## 2 Scheme to Model Human Gait

In the module the human gait the averaged silhouette image partitioned into the seven components as described below using the partition shown in Fig. 1. These components are: (i) head (ii) arm includes shoulder, (iii) the trunk without chest, (iv) thigh including hip, (v) front leg (vi) back leg and (vii) the feet. The front-leg

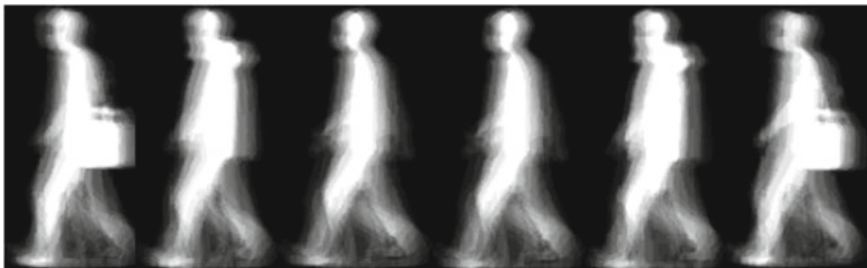
**Fig. 1** Human gait image partition model to get average image



and back-leg are included as separate components because of the bipedal walking style. During walking, the left-leg and the right-leg come to back and front one by one.

The three steps for preparing the averaged silhouette image described in [6] and reproduced below for sake of completing the study. A sample set of images for average gait is shown in Fig. 2.

- Step 1: For all the averaged silhouette images in a gallery set compute the average image (as shown in Fig. 1).
- Step 2: Mark all the six control points to locate head (2 points), the arm include shoulder (1 points), trunk (1 point) and one point is used to find thigh and feet location respectively reach.”
- Step 3: Use lines to connect the relevant pairs of points to partition the mean image into seven parts as shown in Fig. 1.



**Fig. 2** Average Silhouette Images (ASIs) in the gallery set.



### 3 The Proposed Human Gait Recognition Method

It is observed that different persons have different average silhouette images (ASIs), hence they can be used for gait recognition. Some examples for a gallery set of ASIs are shown in Fig. 2. The ASIs obtained by taking the average of silhouette images over a gait cycle within a series of images Liu and Sarkar [7] demonstrated that based on the gate period of length  $N_{\text{Gait}}$  sequence of images is partitioned into a series of cycles (subsequence). The ASIs are achieved by averaging the silhouette (binary images) over one subsequence and represented as follows [7].

$$\text{ASI}_i \Big|_{i=1}^{\lfloor T/N_{\text{Gait}} \rfloor} = \left( \sum_{k=iN_{\text{Gait}}}^{k=(i+1)N_{\text{Gait}}-1} S(k)/N_{\text{Gait}} \right) \quad (1)$$

where  $S(k)$  represents the  $k$  silhouette, as stated earlier, a binary image. ASI is very robust against errors in individual frames; the ASI is used to represent a gait cycle. Many ASIs are resulted from one sequence and their number depends the number of cycles contained in a sequence. In the proposed work the ASI act as the input data for gait recognition system. We have used the same definition as given in [7] for computer the distance between training sequence and test sequence and represented by (2).

$$\text{Dist} \left( \text{ASI}_P^{\text{Method}}, \text{ASI}_G^{\text{Method}} \right) = \text{Median}_{i=1}^{N_P} \left( \min_{j=1}^{N_G} \left\| \text{ASI}_P^{\text{Method}}(i) - \text{ASI}_G^{\text{Method}}(j) \right\| \right) \quad (2)$$

where  $\text{ASI}_P^{\text{Method}}(i) \Big|_{i=1}^{N_P}$  is the  $i$ th projected ASI in the probe data and  $\text{ASI}_G^{\text{Method}}(j) \Big|_{j=1}^{N_G}$  is the  $j$ th projected ASI in the gallery. Equation (2) uses the median of the Euclidean distances between the averaged silhouettes from the probe and the gallery sequences. The difference between (2) and the gait recognition measure developed in [7] is that here we select a template for recognition which is most closely related. The algorithm is described below and demonstration with respect to dataset images is shown in Fig. 3. First each sequence in the training set is segmented into a few subsequences consisting of a complete gait cycle. Then the averaged silhouette image is calculated for each subsequence and a component or its negative (or complement) is selected from each averaged silhouette image through a predefined template and the similar procedure is adopted for test image dataset. Finally, the acceptance or rejection decision is taken based on the similarity measure between stored training information from gallery and test sample of average silhouette image (ASI) from the probe set. We simply find the Euclidean distance between the test data and training data set and arrange the distances in descending order to find out the matching person.

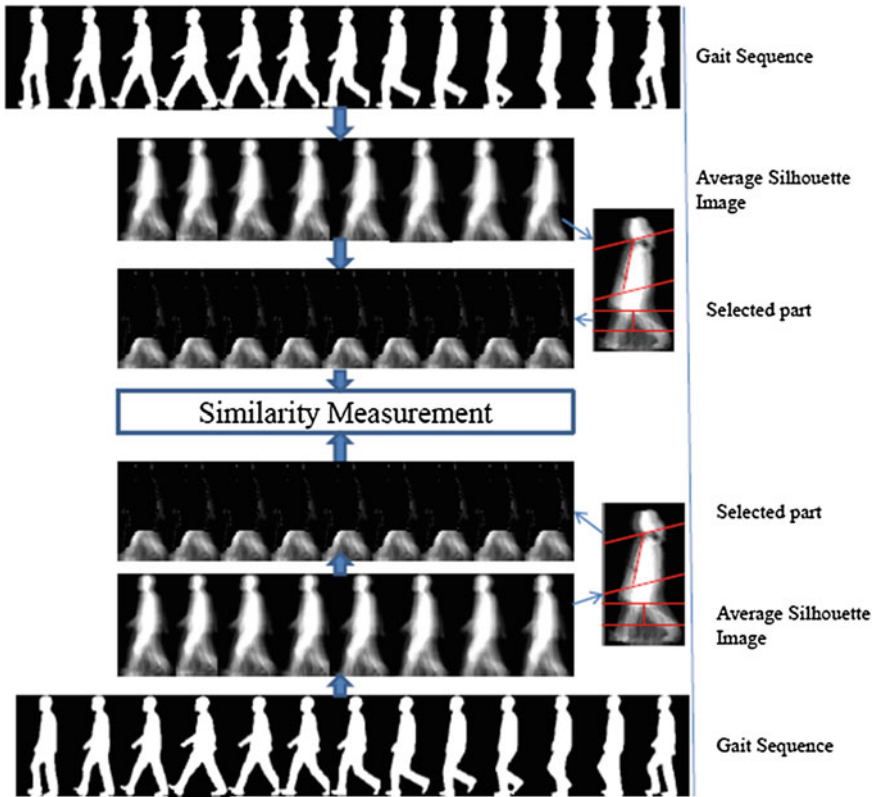


Fig. 3 Construction of the average silhouette image along with the similarity measure *vis-a-vis* the steps of the proposed method

### 4 Brief Review of CASIA Dataset

The performance of the proposed method is evaluated using the CASIA dataset B [8]. It is a large gait dataset that contains 124 subjects where 6 video sequences are recorded for each subject. Thus, a total of 744 ( $124 \times 6$ ) gait sequences are used in this experiment.

The dataset is partitioned into 2 groups. The first group contains 24 subjects and is used to construct gallery set for training the system are remaining 100 subjects behave as the probe set and used as training images in performance evaluation.

## 5 Experimental Results

The effectiveness of the averaged silhouette image as well as the components of the averaged silhouette image for gait recognition has been studied through experimental results. Here the contribution of different component of human Average Silhouette Image ASI in human gait recognition system is observed. The effect of individual component on gait recognition is evaluated and results of the experiments are shown in Table 1. The first column contains the identification of 12 subjects from training dataset and the remaining columns contain the recognition rates for using the different parts of the human body for gait recognition where M presents the averaged/mean silhouette images and h, a, t, th, fl, bl, and f respectively indicates the recognition of gait using head, arm, trunk, thigh, front-leg, back-leg and feet. Similarly the human gait recognition employing the averaged silhouette image without head, arm, trunk, thigh, front-leg, back-leg and feet is indicated by -h, -a, -t, -th, -fl, -bl, and -f respectively. In this analysis effect of the individual component is considered as positive if there is a significant reduction in the recognition rate after removing that component from the averaged silhouette image and similarly the effect is considered negative if the recognition rate increases after the component removal.

We presume that the component has little effect on the gait recognition in other case. As an example we can observe from Table 1 that the head has a positive effect for the training subject 1, as the recognition rate is reduced to 79 from 85 by removing the head from the averaged silhouette and the front-leg has a negative effect for the training subject 3, because the recognition rate is increasing to 70 from 67 without considering the trunk in averaged silhouette image. However, the trunk has little effect on the recognition rate for training subject 4 as the recognition rate is unchanged in case of with or without trunk.

**Table 1** Rank 1 experimental result for human gait recognition

IDs	M	h	-h	a	-a	t	-t	th	-th	fl	-fl	bl	-bl	f	-f
1	85	33	79	29	80	45	82	33	79	33	84	35	78	27	82
2	86	55	84	53	84	73	84	73	81	48	86	37	85	36	86
3	67	25	66	16	65	28	70	29	62	12	68	21	68	20	68
4	23	7	22	8	23	11	23	5	33	10	23	5	22	7	13
5	22	4	19	5	24	15	20	6	28	6	29	9	26	4	19
6	10	5	11	4	9	5	13	6	10	6	13	8	10	3	13
7	15	7	18	6	11	11	17	4	17	8	17	4	13	6	11
8	53	54	47	37	44	62	42	3	80	32	49	14	51	44	38
9	49	44	43	23	48	58	40	4	67	16	51	11	45	32	39
10	41	30	34	10	37	36	38	4	48	12	46	14	38	13	31
11	2	6	3	9	3	16	3	11	2	2	5	3	5	3	13
12	7	3	4	11	5	8	3	4	7	2	7	3	7	4	14

## 6 Conclusion

This paper presents a gait recognition method which uses the concept of average silhouette image for efficient gait recognition. The method is developed keeping in mind that the various parts of the human body play a significant role in the human gait recognition. After analyzing the experimental results it can be concluded that in human gait recognition system is not only affected by legs but also head, arm, trunk and hands plays the vital role for person recognition and consequently may contribute in improving the recognition accuracy. We find out the contribution of each body part in recognition rate and observed that dynamic areas affect more than the static parts of the human body. If we go through the Average Silhouette Image (Figs. 2 and 3) then it is almost clear that body part containing gray region which represents the dynamic information have the positive effect on recognition rate.

Our future work will focus on to derive such a image which only contains all the dynamic areas of whole body in a complete gait cycle, so that space required need to store it in gallery will be reduced and will find easy to extract the limited features from it.

## References

1. Tao, D., Li, X., Wu, X., Maybank, S.: Human carrying status in visual surveillance. *IEEE Comput. Vis. Pattern Recog.* **2**, 1670–1677 (2006)
2. Phillips, P., Sarkar, S., Robledo, I., Grother, P., Bowyer, K.: The gait identification challenge problem: datasets and baseline algorithm. *IEEE Int. Conf. Pattern Recog.* **1**, 385–388 (2002)
3. Tao, D., Li, X., Wu, X., Maybank, S.: Elapsed time in human gait recognition: A new approach. In: *Proceedings of IEEE ICASSP*, pp. 177–180 (2006)
4. Tanawongsuwan, R., Bobick, A.: Modelling the effects of walking speed on appearance-based gait recognition. *IEEE Comput. Vis. Pattern Recog.* **2**, 783–790 (2004)
5. Liu, Z., Malave, L., Sarkar, S.: Studies on silhouette quality and gait recognition. *IEEE Comput. Vis. Pattern Recog.* **2**, 704–711 (2004)
6. Sarkar, S., Phillips, P., Liu, Z., Vega, I., Grother, P., Bowyer, K.: The humanid gait challenge problem: data sets, performance, and analysis. *IEEE Trans. Pattern Anal. Mach. Intell.* **27**(2), 162–177 (2005)
7. Liu, Z., Sarkar, S.: Simplest representation yet for gait recognition: averaged silhouette. In: *Proceedings of International Conference on Pattern Recognition*, Cambridge, U.K., vol. 4, pp. 211–214 (2004)
8. CASIA Gait Database available at <http://www.cbsr.ia.ac.cn/english/Databases.asp>

# Modified LSB Method Using New Cryptographic Algorithm for Steganography

R. Boopathy, M. Ramakrishnan and S. P. Victor

**Abstract** Steganography is different from Cryptography, Steganography is the process of hiding the information so that no one will try to decrypt the information, where as in Cryptography it is obvious that the message is encrypted, so that any one will try decrypting the message. In this paper, we are suggesting new methods to improve the security in data hiding, perhaps by combining steganography and cryptography. In this work, we propose a new encryption method that provides the cipher text as the same size of the plain text. We also presented an extensive classification of various steganographic methods that have used in the field of Data Security. We analyze both security and performance aspects of the proposed methods by PSNR values and proved that in the cryptographic point of view. The proposed method is feasible in such a way that it makes to intricate the steganalyst to retrieve the original information from the Stego-image even if he detect the presence of digital steganography. An embedded message in this method is perceptually indiscernible under normal observation and thus our proposed method achieves the imperceptibility. The volume of data or message to be embedded in this method is comparatively large and proved in Experimental Results hence the high capacity is also achieved.

**Keywords** Encryption · Steganography · Data hiding · Cryptography

---

R. Boopathy (✉)

Research Scholar, Manonmaniam Sundaranar University, Tirunelveli, India  
e-mail: boopathy123@gmail.com

M. Ramakrishnan

Department of IT, Velammal Engineering College, Chennai, India  
e-mail: ramkrishod@gmail.com

S. P. Victor

Research Director, St. Xavier College, Palyamkottai, India  
e-mail: victorsp@rediffmail.com

## 1 Introduction

Steganography and watermarking [6] are the cardinal components of the fast escalating area of information security. Steganography and watermarking bring a wide range of very important techniques as to how one can hide important information in an imperceptible and/or irremovable way in an image and video data. Both Steganography and watermarking work toward secret communication. In the other hand, Cryptography hides the contents of the message from an attacker, but not the existence of the message. Steganography/watermarking even hide from the view of the message in communicating data. Cryptography is not concerned with hiding the existence of a message, but rather its meaning by a process called encryption. Generally, AES algorithms are not suitable for many digital video applications [18, 20]. In order to avoid many paper have been proposed [19].

Recently, a research paper was published [1] on how to improve existing methods of hiding secret messages, by combining Steganography and Cryptography in such a way to make it harder for the Steganalyst [7] to retrieve the plain text of a secret message from a Stego-object if cryptanalysis were not used. The prime intention of this paper is the combined approach of Cryptography and Steganography. Very often, a message is encrypted before being hidden in an image in order to achieve a better level of secrecy (which provides a basic model on how to combine Cryptography and Steganography). Steganography embeds the secret message in a harmless looking cover, such as a digital image file [5].

In [21] Esra Satir and Hakan Isik proposed a compression-based text Steganography method to improve the hiding capacity.

## 2 Related Works

Extensive Research has been carried out on Steganography and Steganalysis [8, 11]. Analysis of Least Significant Bit (LSB) and DCT methods were already proposed [2]. Jessica Fridrichetal [9] has discussed a reliable and accurate method for detecting LSB non-sequential embedding in digital images. The images can be hidden in DCT domain [10] also. The length of the messages can be acquired by inspecting the lossless capacity in the LSB and shifted LSB plane. The most accepted method for Steganography is the LSB encoding [4]. Using any digital image, LSB replaces the least significant bits of each byte by the hidden message bits. The message may also be dispersed at random throughout the image. There are numerous means of hiding information in digital media. Most common approaches are

- Least significant bit insertion
- Masking and filtering
- Redundant Pattern Encoding
- Encrypt and Scatter
- Algorithms and transformations

Every one of these techniques can be applied by varying the degrees of success.

*Least significant bit insertion*

In this paper, we have used LSB insertion method with little modification. It is a common and simple approach to embed information in an image file. In LSB insertion, the LSB of a byte is altered with an M's bit. This method is commonly used for any image, audio as well as video Steganography. When viewed by an HVS the resulting image resembles the cover object [16].

For example, in [4] an image Steganography, the letter A can be concealed in three pixels, assuming no compression. The raster data for 3 pixels, i.e., 9 bytes may be drawn as

```
00100111 11101001 11001000
00100111 11001000 11101001
11001000 00100111 11101001
```

The binary value for B is 01000011. Inserting the binary value for B in the three pixels would result in

```
(00100110 11101001 11001000)
(00100110 11001000 11101000)
(11001001 00100111 11101001)
```

The underlined bits are the only three actually changed data of the 8 bytes used. On an average, the LSB requires only half the bits in an image to be changed. We can hide data in the least and second least significant bits and still the human eye would not be able to discern it [15]. In [14] they have proposed method to verify whether the secret message was deleted or changed by hackers.

Our first implication in this paper is to get better Steganographic techniques by combining them to Cryptographic ones in a new way that is, as far as we know, not available in the literature. Indeed, most of the techniques that combine Cryptography and Steganography aid in encrypting the secret message before hiding its existence in a cover object. Usually applying an entrenched, common-purpose symmetric-key encryption algorithm to guarantee the privacy during video/image transmission [3] is a high-quality idea from a security point of view. Although numerous classifications of image encryption algorithms [17] have been formerly presented, we provide an extended and more comprehensive such classification. Finally, we show that our method allows for a new type of digital image Steganography where a given message is camouflaged with jpeg/bitmap cover image. We evaluated in both security and performance aspects of the proposed method and found that the method is efficient and adequate from a Cryptographic point of view. Our proposed method satisfies the following requirements.

*Imperceptibility*—The invisibility of a Steganographic algorithm is the most important and basic need, since the strength of Steganography lies in its ability to be unnoticed by the human eye. The moment one can see that an image has been altered, the algorithm is compromised.

*Payload capacity*—Steganography requires enormous embedding capacity, unlike watermarking which needs only a small capacity of copyright information.

*Robustness*—Our method is Robust against statistical attacks—Statistical Steganalysis is the practice of detecting hidden information through applying statistical tests on image data. Many Steganographic algorithms leave an impression when embedding information that can be easily detected through statistical analysis.

### 3 Proposed Model

High-quality encryption is a process that produces randomized information by the way compression efficiency [12] and is directly reliant on the presence of source data redundancy. The more the data is correlated, better the compression and vice versa [13]. This paper introduces a method of encrypting the text and image files in an image in order to test the accuracy and efficiency of encryption. This process enhances the transfer of information to the intended receiver without any potential risk. In this paper, the proposed method will help to secure the text content within the image and encryption of image file within the image will help to make the document much securer because, though the unauthorized person succeeds in hacking the image, the person will not be able to read the message as well as acquire the information in the image file. The proposed approach finds the suitable algorithm for embedding the data in an image using Steganography which provides a better security pattern for sending messages through a network. This paper deals with digital images acting as a cover medium to store secret data in such a manner that it becomes invisible. The Java software is used to extensively analyze the functions of the LSB algorithm in Steganography. Mat lab software is used to evaluate the PSNR values and to evaluate the performance of the proposed method.

#### 3.1 Overall View

The data hiding patterns using the Steganography technique in this paper can be explained using this simple block diagram. The block diagram for Steganography technique is as follows (Fig. 1).

#### 3.2 Implementation

Implementation section discusses about the different modules of this work and shows the methods of implementation. This work is implemented by using the following step by step procedure.

The Steganography process is implemented in different stages like:

- Encryption section
- Data transmission section
- Decryption section



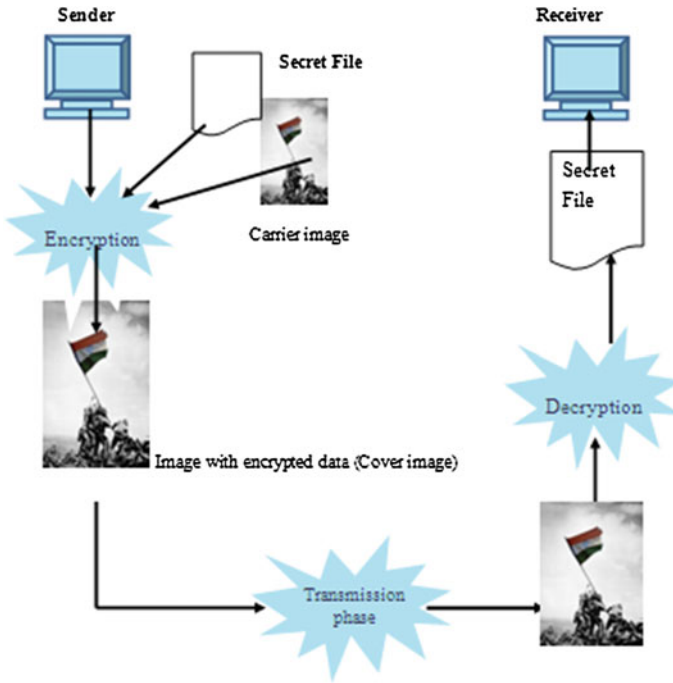


Fig. 1 Overall architecture diagram for proposed model

### 3.3 The Encryption Section

The encryption section of Steganography is the primary stage. In this stage, the sender sends the data as well as the image file which acts as a carrier image to transfer the data to the destination. In this paper, different images are used as carriers because all images are highly resistant for Steganalysis. In the encryption section, the text message (secret message) is encrypted by using a proposed new algorithm and then it will be embedded into the image file. The data is embedded into the image and the encryption is implemented using Java.

#### Proposed New Encryption Algorithm

This algorithm was written and coded by us specifically for this paper. The main advantage of this algorithm is that it provides the encrypted text, the same size as the original text.

#### Encryption Algorithm

- Step 1: Generate the ASCII value for every letter.
- Step 2: Generate the equivalent binary value of it.

[Binary value should be 8 digits, e.g., for decimal 14 binary number should be 1110]

Step 3: The resultant binary number should be reversed.

Step 4: Take a divisor having 4 digits length ( $\geq 1,000$ ) as the Key.

Step 5: Divide the resultant number already reversed with the divisor.

Step 6: Store the remainder in first 3 digits and quotient in next 5 digits (remainder and quotient wouldn't be more than 3 digits and 5 digits long respectively. If we find any of these digits are less than 3 and 5 respectively then we need to add required number of 0s (zeros) in the left-hand side. So, this would be the preprocessed text to be embedded. Now store the remnants in first 3 digits and quotient in next 5 digits.

Steps to embed a message into a Master file:

- Convert a Secret message into a character array.
- Create a byte array. The length of the binary array is equal to size of input file.
- Open input file and read all bytes into byte Array.
- Skip past OFFSET\_JPG bytes.
- Skip past OFFSET\_PNG bytes.
- Skip past OFFSET\_GIF\_BMP\_TIF bytes.
- The 32 bit input file size should be converted into byte array.
- 4 byte input File size array should be embedded into the master file.
- Write the remaining bytes.
- 3 byte version information should be embedded into the file.
- Write 1 byte for features.
- Compress the message from level 0 to 9.
- Get the result of compressed message byte array.
- Embed the 1 byte compression ratio into the output file.
- Encrypt the message based on proposed new Encryption algorithm.
- Convert the 32 bit message size into byte array.
- Embed 4 byte message size array into the master file.
- Embed the message.

### ***3.4 Data Embedding Section***

The embedding is done based on the well-known Least Significant Bit (LSB) algorithm with little modification. We used the last two significant bits of each pixel and replaced with the significant bits of the text document. The encrypted data is embedded into the cover image. Now the compression is done. The level of compression can be from 0 to 9. Using the modified approach the message bits are embedded properly in the place of Least Significant Bits of cover image, such that the image doesn't lose its resolution and hence the security will be robust. The encrypted image is protected with a secured symmetric key such that is used to avoid the damages caused due to hackers or unauthorized persons.

### 3.5 Decryption Section

In the decryption phase, the intended receiver receives the carrier image from sender through the transference medium. The intended receiver then sends the carrier image to the decryption phase. In the decryption phase, the same ‘Least Significant Algorithm’ is implemented for decrypting the LSB from the image and merge in an order to frame the original message bits. After successful completion of the process, the file is decrypted from the carrier file and accessed as an original text document.

### 3.6 Proposed Decryption Algorithm

- Step 1: Multiply last 5 digits of the encrypted text by Key value.
- Step 2: Add first 3 digits of the encrypted text with the result produced in the previous step.
- Step 3: If the result produced in the step 2 is not an 8-bit number then we need to make it as 8-bit number
- Step 4: Reverse the number to get the encrypted text.

## 4 Results and Discussion

We have chosen image Steganography because it is a simple and user friendly application. Though there are various applications for image hiding but the proposed approach is created using Java which is efficient for coding and the performance is better compared to other languages.

Comparing with paper [1] we have used two-bit stego instead of conventional one-bit stego, and even though the various encryption algorithms have been proposed already we have used our own encryption algorithm as proposed in Sect. 3. The advantage of algorithm is it will produce the cipher text with the same size of that plain text. The algorithm used in this paper falls under the classification of spatial domain.

This paper gave us good experience in dealing with the data security issues in theoretical as well as in technical domain and in Java programming. I performed the paper in a satisfactory level with the help and good guidance from my supervisor (Table 1).

#### *PSNR results*

PSNR—phrase peak signal-to-noise ratio, is defined as the ratio between the maximum possible power of a signal and the power of corrupting noise that affects the fidelity of its representation. As most signals have a wide and dynamic range, PSNR is usually denoted in terms of the logarithmic decibel scale. Imperceptibility has been calculated using PSNR between Original cover image (I) and Stego-Image (Js).

**Table 1** Comparison of different Steganography algorithms

Steganography algorithm	Speed	Quality of hiding	Security
LSB	High	Good	Strong
F5	Low	High up to 13.4 %	Strong
JSteg	Moderate	Embedding capacity up to 12 %	Less

**Table 2** Comparison of different sizes in jpeg images

Cover image name	Cover image size (KB)	Text file (KB)	Compressed file (KB)	Stego-image size (KB)
Cameraman.jpg	7.17	10.4	7.96	7.97
Cutepuppy.jpg	28.8	65.6	56.6	52.1
Flag.jpg	26.5	60.6	49.2	47.1
Windows.jpg	51.3	120	101.2	99.4
Barsilona.jpg	63.6	57.9	55.9	111
Cell.jpg	6.13	104	96.1	46.5

$$\text{PSNR} = 10 * \log (255 * 255/\text{MSE}) / \log (10) ;$$

In the equation, MSE is the mean square error between the original and the denoised image. The higher the PSNR in the restored image, the better is its quality. In testing, few images were experimented. The quantitative results have been given in the table for the six images (Table 2).

## 5 Conclusion

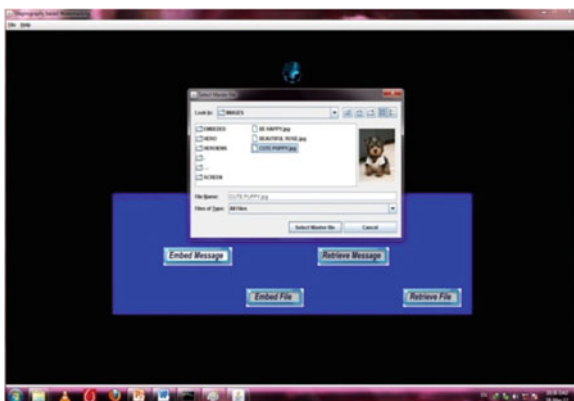
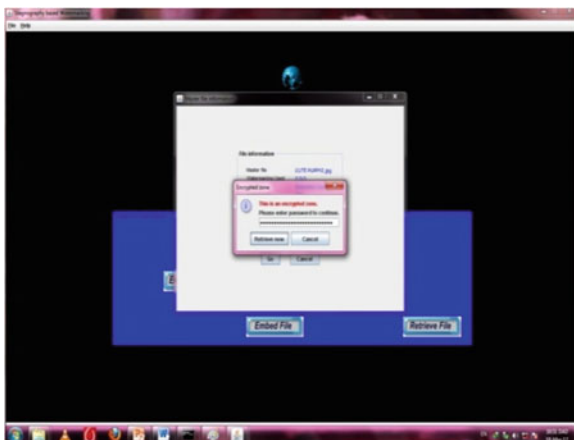
In this world, data transfers using Internet is rapidly growing because it is so easier as well as faster to transfer the data to the destination. Security is an important issue and transferring the data using Internet because any unauthorized individual can hack the data and make it useless or obtain information unintended to him.

The proposed approach in this paper uses a new combined approach of Encryption and Steganography. This creates a Stego-image in which the personal data is embedded and is secured with a symmetric key which is highly protective. The main contribution in this paper is the introduction of new encryption algorithm/approach for Steganography application that provides commendable security. The main advantage of this algorithm is that it provides the encrypted text in the same size as the plain text.

The proposed approach provides higher PSNR Value of 41db as an average. It has three levels of security. In the first level, the text file is compressed and zipped. In the second level, it is encrypted using proposed algorithm. In the final level a secret key is used to protect the message from Stego-attacks. The change in image resolution is negligible when we embed the message into the image and the image is concealed or secured with the personal password. And hence the data is protected from damage by any unintended user.

As future work, we plan to use the same concept in Frequency domain to increase the hiding capacity. We are aiming to use the different combination of frequency domain.

### SAMPLE SCREEN SHOTS



**Acknowledgments** We would like to express our gratitude to Velammal Engineering College in which where I am working, for providing to access all the resources . I would like to acknowledge Ms. Mary Elizabeth for her great support.

## References

1. Challita, K., Farhat, H.: Combining steganography and cryptography: new directions. In: IJC-NAA **1**(1), 199–208 (2012). The Society of Digital Information and Wireless Communication
2. Walia, E., Jain, P., Navdeep.: An analysis of LSB & DCT based steganography. Glob. J. Comput. Sci. Technol. **10**(1), 4–8 (2010)
3. Socek, D., Kalva, H., Magliveras, S.S., Marques, O., Culibrk, D., Furht, B.: New approaches to encryption and steganography for digital videos. *Multimedia Syst.* **13**(3), 191–204 (2007). (Springer)
4. Bandyopadhyay, S.K., Bhattacharyya, D., Ganguly, D., Mukherjee, S., Das: A tutorial review of steganography. In: IC3, pp. 105–114 (2008)
5. Dunbar B.: A detailed look at Steganographic techniques and their use in an open systems environment. Sans Institute InfoSec Reading Room (2002)
6. Katzenbeisser, S., Peticolas, F.A.P.: Information hiding techniques for steganography and watermarking. Artech House, Boston (2000)
7. Upham, D.: Steganographic algorithm JSteg. <http://zooid.org/paul/crpto/jsteg>
8. Zahedi Kermani, M.J.Z.: A robust steganography algorithm based on texture similarity using gabor filter. In: IEEE 5th International Symposium on Signal Processing and Information Technology (2005)
9. Fridrich, J., Goljan, M.: Detecting LSB steganography in color and grey scale images. *IEEE Multimedia Secur* **8**, 22–28 (2001)
10. Ashourian, M., Jain, R.C., Ho, Y.-S.: Dithered quantization for image data hiding in the DCT domain. In: Proceeding of IST, pp. 171–175 (2003)
11. Krenn, J.R.: Steganography and Steganalysis, January 2004
12. Hwang, R.-J., Shih, T.K., Kao, C.-H.: A lossy compression tolerant data hiding method based on JPEG and VQ. *J. Internet Technol.* **5**, 171–178 (2004)
13. Tseng, H.-W., Chang, C.-C.: High capacity data hiding in JPEG compressed images. *Informatika*, **15**, 127–142 (2004)
14. Park, Y., Kang, H., Yamaguchi, K., Kobayashi, K.: Integrity verification of secret information in image steganography. In: Symposium on Information Theory and its Applications. Hakodate, Hokkaido, Japan (2006)
15. Neeta, D., Snehal, K., Jacobs, D.: Implementation of LSB steganography and its evaluation for various bits. In: 2006 1st International Conference on Digital Information Management on 6 Jan 2007. doi:[10.11.09/ICDIM.2007.369349](https://doi.org/10.11.09/ICDIM.2007.369349) (2007)
16. Jain, A., Gupta, I.S.: A JPEG compression resistant steganography scheme for raster graphics images. In: IEEE Region 10 Conference TENCON 2007, vol. 2 (2007)
17. Furht, B., Muharemagic, E.A., Socek, D.: *Multimedia security: encryption and watermarking. Multimedia Systems and Applications*, vol. 28. Springer, Berlin (2005)
18. Li, S., Chen, G., Zheng, X.: Chaos-based encryption for digital images and videos. In: Furht, B., Kirovski, D (eds.) *Multimedia Security Handbook. Internet and Communications Series*, vol. 4, pp. 133–167. CRC Press, West Palm Beach (2004)
19. Li, S., Zheng, X., Mou, X., Cai, Y.: Chaotic encryption scheme for real-time digital video. In: *Real Time Imaging VI, Proceedings of SPIE*, vol. 4666, pp. 149–160. SPIE Publishers (2002)
20. Uhl, A., Pommer, A.: Image and video encryption: from digital rights management to secured personal communication. In: *Advances in Information Security*, vol. 15. Springer, New York (2005)
21. Esra S., Hakan I.: A compression-based text steganography method (2012). doi:[10.1016/j.jss.2012.05.027](https://doi.org/10.1016/j.jss.2012.05.027)

# TDAC: Co-Expressed Gene Pattern Finding Using Attribute Clustering

Tahleen A Rahman and Dhruva K Bhattacharyya

**Abstract** An effective unsupervised method (TDAC) is proposed for identification of biologically relevant co-expressed patterns. Effectiveness of TDAC is established in comparison to its other competing algorithms over four publicly available benchmark gene expression datasets in terms of both internal and external validity measures.

**Keywords** Cluster · Outlier · Core · Neighbour · Co-expressed

## 1 Introduction

Many clustering algorithms have been evolved and applied on gene expression data. The existing approaches for gene data clustering are categorised into three types: (a) Gene-based, where genes are treated as the objects, while the samples are as features; (b) Sample-based, where samples are generally related to various diseases or drug effects within a gene expression matrix; and, finally (c) Subspace clustering, which attempts to find subset of objects such that the objects emerge as a cluster in a subspace created by a subset of the features. Subspace clustering techniques are further classified into two subcategories, i.e. biclustering and triclustering. In biclustering, it attempts to cluster the gene expression data both row-wise as well as column-wise simultaneously [1]. Whereas, triclustering [2] aims to mine biologically relevant coherent clusters over a gene sample time (GST) domain for any gene expression datasets. In this paper, we propose a cost-effective attribute clustering method for finding co-expressed gene patterns that does not require discretisation. To avoid the restrictions caused due to the use of any proximity measure while expanding the cluster, it exploits the regulation information computed over the expression values.

---

T. A. Rahman (✉) · D. K. Bhattacharyya  
Tezpur University, Napaam, Assam 784028, India  
e-mail: dkb@tezu.ernet.in

## 2 TDAC: The Proposed Attribute Clustering Method

TDAC is basically a three step method. In *step 1*, the gene expression data matrix, i.e.  $G_{m \times n}$  of order  $m \times n$ , is normalised to have a mean 0, and standard deviation 1. In *step 2*, we find condition-wise neighbourhood for each expression value based on regulation information and proximity measure with the neighbouring expression values. To find neighbourhood based on expression value proximity, we use a linear density-based clustering that works based on  $L_1$  norm with reference to  $\beta$ , a user defined threshold. Similarly, to find similarity between a pair of genes based on regulation information, we use the angular deviation (i.e. +ve, -ve or *neutral*) computed based on the *arccos* formula given in [3]. It identifies the core gene groups for each condition based on the regulation information and proximity-based neighbourhood information with reference to  $\beta$ . *Step 3* performs two major tasks, i.e. identification of (i) outlier genes and (ii) co-expressed gene groups. The co-expressed gene group is a subset of genes having common neighbours  $\geq 2$ , over at least  $k$  conditions. Here, we assume that to form a co-expressed gene group or cluster, there must be at least 'two' neighbour genes over at least  $k$  conditions. An outlier gene is defined as a gene having neighbourhood  $< 2$  over  $\geq k$  conditions.

## 3 Algorithm

TDAC operates on a preprocessed gene expression dataset for simultaneous identification of both outlier as well as co-expressed genes based on regulation information and attribute/condition level proximity. The proposed TDAC is free from the restrictions of using (i) discretisation and (ii) specific proximity measure. Based on the regulation information and the expression-level proximity for each condition computed over the pre-processed gene matrix, a faster attribute clustering technique, i.e. *attrib\_clus* identifies the core genes. Here, *attrib\_clus* finds core genes based on the regulation information using the *arccos* expression given in [3] and finds expression-level dissimilarity using  $L_1$  norm. However, it is free from the restriction of using any proximity measure. Based on regulation, core genes and their connectivity information and by using the concepts given in the Definitions  $k$ -neighbour and Cluster, TDAC can identify the co-expressed gene groups as well as the outlier genes, with reference to a given user defined threshold. The basic steps of TDAC for finding co-expressed gene groups are stated next.

1. Preprocess  $G_{m \times n}$  with z-score normalization to obtain  $G'_{m \times n}$ .
2. Apply *attrib\_clus*() on  $G'_{m \times n}$  to obtain core\_gene groups for each condition;
  - a. Find neighbour gene (s) for a given gene  $g_i$  at condition, say  $C_a$  based on regulation information (with reference to its previous condition, i.e.  $C_{a-1}$ ) and  $L_1$  proximity with reference to  $\beta$ .
  - b. Identify  $g_i$  as core at  $C_a$  if satisfies the core gene conditions.



3. Identify the co-expressed gene groups across  $n$  conditions;
  - a. Find genes which are core over atleast  $k$  conditions.
  - b. From the subset of neighbour genes obtained, find genes which have the same nearest neighbours across atleast  $k$  conditions.
  - c. Find the set of  $k$ —neighbors for each gene based on the subsets obtained above.
  - d. Each gene in the list of genes obtained along with its respective nearest  $k$ —neighbours is assigned cluster ids and form clusters.
  - e. If there are common nearest neighbours between two such genes, i.e. some gene is assigned to more than one cluster, then the respective clusters are merged.

## 4 Performance Evaluation

Our technique was implemented in MATLAB running on a 1.73 GHz(2CPUs) Intel Pentium processor with 16GB RAM. We have compared the results of our work in terms of several internal and external validity measures with several other competing techniques Table 1.

*Homogeneity and Separation* We have used CVAP [4] to test the performance of TDAC in terms of homogeneity and separation measures. The clusters detected by our technique in Datasets 1, 2 and 3 are shown in Figs. 1 and 2 respectively. Average homogeneity [5] reflects the compactness of a cluster given by a clustering algorithm. It can be seen from the Table 2 that the proposed TDAC shows a better homogeneity than its other competing algorithms. Average separation [5] reflects the overall distance among the clusters given by a clustering algorithm. As it can be seen from the Table 2 that the proposed TDAC shows superior performance in terms of separation than its other competing algorithms. Silhouette Index [6] reflects the compactness and separation of clusters. As can be seen from the Table 3 that our work shows significant improvement in performance in comparison to its other competing algorithms [7] like MOGA-SVM, MOGA (without SVM), FCM, SOM, Average-linkage,  $k$ -means and DGC for most of the datasets.

**Table 1** List of datasets used and their sources

Dataset	Genes	Samples	Source
1. Yeast sporulation [9]	474	7	<a href="http://cmgm.stanford.edu/pbrown/sporulation/index.html">http://cmgm.stanford.edu/pbrown/sporulation/index.html</a>
2. Human fibroblasts [10]	517	19	<a href="http://genomewww.stanford.edu/serum/data/">http://genomewww.stanford.edu/serum/data/</a>
3. Arabidopsis thaliana	138	8	<a href="http://homes.esat.kuleuven.be/thijs/Work/Clustering.html">http://homes.esat.kuleuven.be/thijs/Work/Clustering.html</a>
4. Subset of yeast cell cycle [11]	384	17	<a href="http://yscdp.stanford.edu/yeast-cellcycle/fulldata.html">http://yscdp.stanford.edu/yeast-cellcycle/fulldata.html</a>

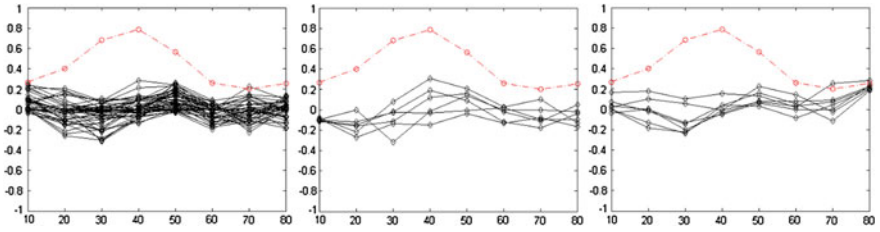


Fig. 1 An outlier gene with a cluster obtained from Dataset 3

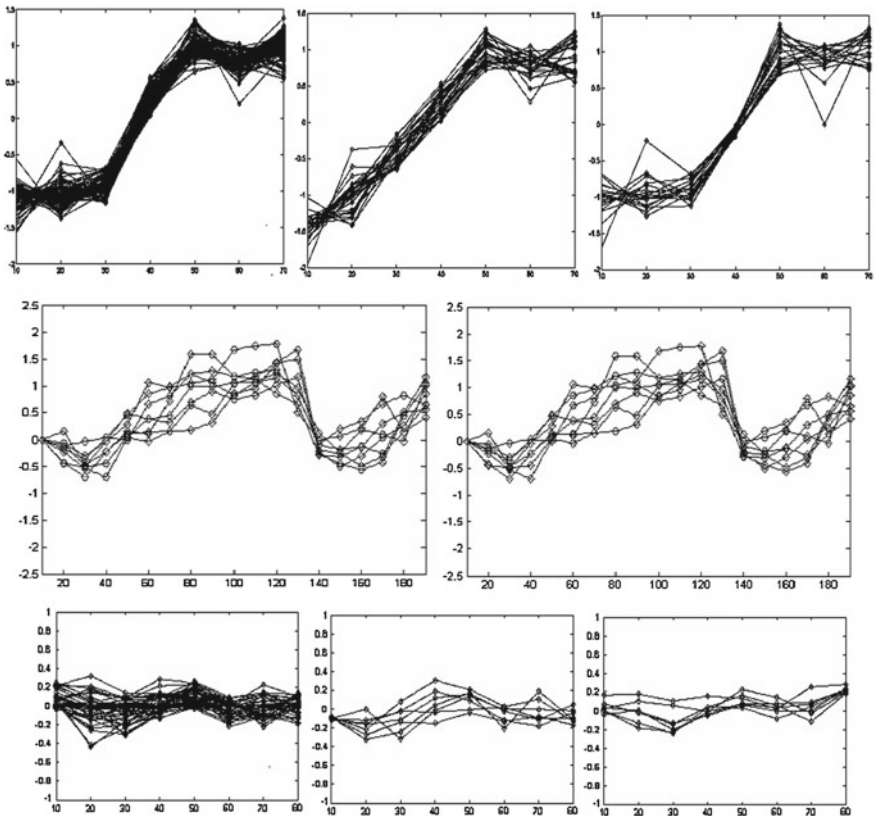


Fig. 2 Some of the clusters obtained from Dataset 1 and 2

*External Quality p-value:* We have obtained  $p$ -value [8] using the software FuncAssociate [8], which is a web-based tool that accepts as input a list of genes, and returns a list of GO attributes that are over-(or under-) represented among the genes in the input list. A low  $p$ -value indicates that the genes belonging to the enriched

**Table 2** Performance comparison in terms of Homogeneity and Separation

Dataset used	Method applied	Number of clusters	Homogeneity	Separation
Dataset 1	<i>k</i> -means	9	0.11047	0.40366
	TDAC	9	0.96915	0.12266
	SOM	9	0.11804	0.40898
Dataset 2	<i>k</i> -means	3	0.29568	0.46473
	TDAC	3	0.77574	0.18869
	SOM	3	0.29973	0.47346
	CLICK	3	0.750	0.107
	CAST	3	0.831	0.0166
Dataset 3	<i>k</i> -means	5	0.24113	0.39542
	TDAC	5	0.2243	0.20996
	SOM	5	0.24425	0.38723
Dataset 4	<i>k</i> -means	3	0.302	0.490
	TDAC	3	0.482	0.171
	SOM	3	0.300	0.512
	CLICK	3	0.349	0.212
	CAST	3	0.360	0.164

**Table 3** Performance comparison in terms of Silhouette Index

Dataset used	Method applied	Number of clusters	Silhouette index
Dataset 1	<i>k</i> -means	9	0.24752
	SOM	9	0.27703
	TDAC	4	0.29877
Dataset 2	SOM	6	0.3235
	MOGA-SVM (RBF)	6	0.4154
	MOGA (without SVM)	6	0.3947
	FCM	8	0.2995
	Average Linkage	4	0.3562
	DGC	16	0.6880
	TDAC	6	0.6909
Dataset 4	DGC	17	0.7307
	SOM	6	0.3682
	MOGA-SVM (RBF)	5	0.4426
	MOGA (without SVM)	5	0.4392
	FCM	6	0.3872
	Average Linkage	4	0.4388
	TDAC	6	0.7248

functional categories are biologically significant in the corresponding clusters. The enriched functional categories for Dataset 1 and Dataset 3 are listed in Tables 4 and 5 respectively. The cluster C1 in Dataset 1 contains several enriched GO categories. Two examples of highly enriched categories in C1 are ‘anatomical structure

**Table 4** *p*-values of dataset 1

Cluster	<i>p</i> value	GO number	GO category	
C1	1.187e-22	GO:0048646	Anatomical structure formation involved in morphogenesis	
	1.395e-21	GO:0010927	Cellular component assembly involved in morphogenesis	
	6.871e-19	GO:0030476	Developmental process	
	2.295e-18	GO:0032502	Ascospore wall assembly	
	2.295e-18	GO:0042244	Spore wall assembly	
	2.295e-18	GO:0071940	Fungal-type cell	
	3.373e-18	GO:0070726	Cell wall assembly	
	2.039e-17	GO:0048869	Cellular developmental process	
	2.464e-16	GO:0030435	Sporulation resulting in formation of a cellular spore	
	2.464e-16	GO:0030154	Cell differentiation	
	2.464e-16	GO:0043934	Sporulation	
	1.338e-15	GO:0003006	Developmental process involved in reproduction	
	1.534e-14	GO:0048610	Cellular process involved in reproduction	
	6.201e-13	GO:0022414	Reproductive process	
	C2	1.298e-21	GO:0002181	Cytoplasmic translation
		9.073e-20	GO:0003735	Structural constituent of ribosome
5.303e-17		GO:0022625	Cytosolic large ribosomal subunit	
7.408e-19		GO:0005840	Ribosome	
1.641e-16		GO:0005198	Structural molecule activity	
1.856e-16		GO:0006412	Translation	
5.072e-13		GO:0030529	Ribonucleoprotein complex	
6.726e-11		GO:0044267	Cellular protein metabolic process	
1.321e-10		GO:0043228	Nonmembrane-bounded organelle	
1.321e-10		GO:0043232	Intracellular nonmembrane-bounded organelle	
C3	7.389e-10	GO:0005622	Intracellular	
	4.230e-06	GO:0031145	Anaphase-promoting complex-dependent proteasomal ubiquitin-dependent protein catabolic process	

formation involved in morphogenesis' and 'cellular component assembly involved in morphogenesis' with *p*-values 1.187e-22 and 1.395e-21, respectively. Similarly, for Dataset 3, TDAC identifies several clusters with highly enriched GO categories of very low *p*-values. Cluster C1 in this dataset includes GO categories like 'response to stimulus' and 'response to chemical stimulus' with *p*-values 6.12e-08 and 1.19e-07, respectively.

**Table 5** *p*-values of dataset 3

Cluster	<i>p</i> value	GO number	GO category
C1	6.12e-08	GO:0050896	Response to stimulus
	1.19e-07	GO:0042221	Response to chemical stimulus
	2.04e-04	GO:0070887	Cellular response to chemical stimulus
	2.37e-04	GO:0010033	Response to organic substance
C2	1.68e-05	GO:0003857	05 3-hydroxyacyl-CoA dehydrogenase activity
	3.35e-05	GO:0004300	Enoyl-CoA hydratase activity
	2.09e-04	GO:0006629	Lipid metabolic process
	6.50e-04	GO:0006631	Fatty acid metabolic process

## 5 Conclusion and Future Work

A method for identification of biologically relevant co-expressed patterns based on regulation information and attribute clustering is reported. The proposed TDAC is established over four publicly available gene datasets in terms of both internal and external validity measures. Work is going on to extend the present TDAC toward handling of large number of gene expression datasets +ve, -ve and mixed-correlated gene patterns.

## References

- Jiang, D., Tang, C., Zhang, A.: Cluster analysis for gene expression data: a survey. *IEEE Trans. Knowl. Data Eng.* **16**(11), 1370–1386 (2004)
- Mahanta, P., Ahmed, H.A., Bhattacharyya, D.K., Kalita, J.K.: Triclustering in gene expression data analysis: A selected survey. In: *Proceedings of IEEE NCETACS*, pp 1–6 (2011)
- Sarma, S., Sarma, R., Bhattacharyya, D.K.: An effective density based hierarchical clustering technique to identify coherent patterns from gene expression data. In: *Proceedings of PAKDD 2011*, vol. 6634, pp. 225–236 (2011)
- Kaijun, Wang, Wang, Baijie, Peng, Liuqing: CVAP: validation for cluster analyses. *Data Sci. J.* **8**, 88–93 (2009)
- Sharan, R., Shamir, R.: CLICK: A clustering algorithm with applications to gene expression analysis. In: *Proceedings of the International Conference on Intelligent Systems for Molecular Biology*, pp. 307–316. AAAI Press, Menlo Park (2000)
- Rousseeuw, P.: Silhouettes: a graphical aid to the interpretation and validation of cluster analysis. *J. Comput. Appl. Math.* **20**, 153–165 (1987)
- Das, R., Bhattacharyya, D.K., Kalita, J.K.: Clustering gene expression data using an effective dissimilarity measure. *Int. J. Comput. Bio Sci. (Special Issue)* **1**(1), 55–68 (2011)
- Berriz, F.G., et al.: Characterizing gene sets with Funcassociate. *Bioinformatics* **19**, 2502–2504 (2003)
- Chu, S., DeRisi, J., Eisen, M., et al.: The transcriptional program of sporulation in budding yeast. *Science* **282**, 699–705 (1998)
- Iyer, V.R., Eisen, M.B., Ross, D.T., et al.: The transcriptional program in the response of the human fibroblasts to serum. *Science* **283**, 83–87 (1999)
- Cho, R.J., Campbell, M., Winzeler, E., Steinmetz, L., et al.: A genome-wide transcriptional analysis of the mitotic cell cycle. *Mol. Cell* **2**(1), 65–73 (1998)

# An Introduction to Back Propagation Learning and its Application in Classification of Genome Data Sequence

Medha J. Patel, Devarshi Mehta, Patrick Paterson  
and Rakesh Rawal

**Abstract** The gene classification problem is still active area of research because of the attributes of the genome data, high dimensionality and small sample size. Furthermore, the underlying data distribution is also unknown, so nonparametric methods must be used to solve such problems. Learning techniques are efficient in solving complex biological problems due to characteristics such as robustness, fault tolerances, adaptive learning and massively parallel analysis capabilities, and for a biological system it may be employed as tool for data-driven discovery. In this paper, some concepts related to cognition by examples are discussed. A classification technique is proposed in which DNA sequence is analyzed on the basis of sequence characteristics near breakpoint that occur in leukemia. The training dataset is built for supervised classifier and on the basis of that back propagation learning classifier is employed on hypothetical data. Our intension is to employ such techniques for further analysis and research in this domain. The future scope and investigation is also suggested.

**Keywords** Supervised classifier · Artificial neural network · Cancer classification

---

M. J. Patel (✉)  
Gujarat Technological University, Ahmadabad, India  
e-mail: medhapate0@gmail.com

D. Mehta  
GTU, Gujarat, India

P. Paterson  
Industrial Engineering Department, Texas Tech University, Lubbock, Texas, USA

R. Rawal  
Gujarat Cancer Research Institute, Gujarat, India

## 1 Introduction

To solve a problem on a computer, we need algorithm, but for some applications, we do not have algorithms. We know the inputs, sometimes we know what the output should be, but do not know how to transform input to the output. Human brain is adaptable to get some insight, i.e., cognition by examples for this kind of applications. But in modern scenario, the pressing need of rapid transformation from data to information and from information to knowledge and above all repeating this task a large number of times are ideally suited for machine—not humans. And so we want some combination of machine and learning. Learning is somewhat very subjective—can we make our machine to learn? The easier approach is to mechanize the process of learning. We can develop some learning algorithm which can make computers (machine) to extract automatically the hypothesis/rules from examples, than it is called machine learning [1]. Machine learning is programming computers to optimize performance criterion using example data or past experience. Machine learning uses the theory of statistics in building mathematical models, because the core task is making inference from samples. Artificial neural network (ANN) mimics the learning or adaptability of the biological system and thus provides a kind of machinery of learning.

## 2 Artificial Neural Network

ANN is an information processing system that has been developed as a generalization of the mathematical model of human cognition (ability to know). It consists of simple computational units called neurons that are highly interconnected and each connection has a strength that is expressed by a positive or negative number called weight. The connection of neurons are normally arranged in layers and executed in parallel. The connections are categorized as network topology. The size of the weight controls the influence that one neuron has on other, with a positive weight excite an element and negative weight inhibit. Overall the activation of an element is determined by a combination (summation) of excitatory and inhibitory influence it receives from its neighbors. The weights of the net are adaptable which store the experimental knowledge from task example through a process of learning. The information is stored in the connections and distributed throughout, so the network can function as a memory of brain. The memory is content addressable, in the sense that the information may be recalled by providing partial or even erroneous input pattern. The information is stored in association of other stored data, hence it is adaptable.

The network architecture determines how and which type of neurons can be connected and in which topology. The way nodes are connected determines how computations proceed. On the basis of the connection patterns (architecture) the ANNs can be grouped as (i) *feed forward*, in which there are no loops. Examples single layer perceptron, multi-layer perceptron (MLP), radial basis function (RBF) (ii) *recurrent* (feedback) in which loop occurs because of feedback connections. Examples are Hopfield network and adaptive resonance theory (ART) models [1].

**Learning Process** The issue of learning is central to the study and design of artificial neural network. Learning encodes pattern information into interneuronal connection strengths, i.e., free parameters or weights of network. The algorithms are developed according to well-defined learning rules which simulate the learning methodology of brain's mathematical models. The basic learning rules can be broadly categorized as error correction learning, memory based learning, Hebb postulate learning, competitive learning, and Boltzmann machine learning [2]. The learning paradigm can be supervised, unsupervised, and reinforcement according to the way by which the network is trained. If desired output is already available with sample data than the main work is to find the patterns in that data.

**Error correcting rules** The error correcting rules are fundamental building blocks of supervised learning. The general philosophy underlying most supervised learning is based on *principle of minimal disturbance*. 'Adapt to reduce the output error for the current training pattern, with minimum disturbances to the patterns already learnt.' The weights of the network can be altered by either presenting the linear error to reduce the error or gradient information to reduce the mean square error (MSE), usually averaged over all training patterns. Let us consider a single neuron ( $k$ ) of output layer which produce the output  $y_k$  for a particular sample  $n$  (or discrete time step for real time system). Now this output is compared with desired output  $d_k$  and consequently an error signal  $e_k$  is produced. Thus  $e_k = d_k - y_k$  error actuate a control mechanism, the purpose of which is to apply a sequence of corrective adjustment to the synaptic weights of neuron  $k$ . The corrective adjustments are designed to make the output signal  $y_k$  come closer to the desired response in a step by step manner. The objective here is to minimize the cost function defined in terms of error signal. This kind of learning process is used in delta rule, generalized delta rule ( $\alpha$ -LMS or widrow-hoff rule). According to delta rule the adjustment  $\Delta w_{kj}$  applied to weight  $w_{kj}$  is defined as

$$\Delta w_{kj} (n) = \eta \cdot e_k (n) x_j (n) \quad (1)$$

Here  $\eta$  is a positive constant that determines rate of learning. The rule can be stated as:

*The adjustment made to a synaptic weight of a neuron is proportional to the product of the error signal and the input signal [2].*

Back propagation is similar to LMS algorithm and is based on gradient descent: weights are modified in the direction that corresponds to the negative gradient of error measure. For successful application of this method differentiable node activation function is required. The major advance of back propagation over LMS and perceptron learning is in expressing how an error at a higher (outer) layer of a multilayer network can be propagated backwards to node at lower (inner) layers of the network. Back propagation learning has emerged as standard algorithm for the training of multi layer perceptron against which other networks are benchmarked. This algorithm has had a major impact on field of neural network and has been applied to a large number of problems in many disciplines. These ANNs have been applied to virtually all pattern recognition problems and are typically the first network tried on a new problem. The reason for this is the simplicity of the algorithm, and vast body of research that has studied these networks.



## 2.1 Why Machine Learning for Genome Data

Biological data is high dimensional, complex, not fully annotated, noisy, and voluminous. There are number of reasons why machine learning approaches are widely used in practice, especially in bioinformatics.

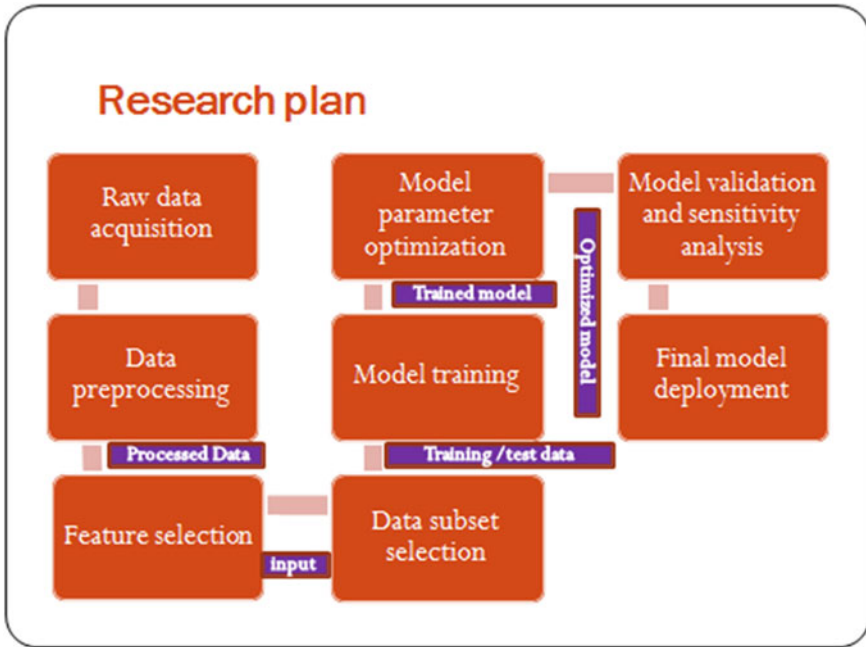
1. Systems often produce results different from desired ones, due to unknown properties of the inputs during designing the computational system. However, with the capacity to improve/learn dynamically, the machine learning can cope with such types of problems, often occurs in biological world.
2. Missing and noisy data is one of the characteristics of biological data. Though conventional techniques is unable to handle this, machine learning can do well.
3. In molecular biology research, new data and concepts are generated very often and replaces old one. Machine learning can easily adapt this change.
4. For biological data it is possible that some hidden relationship or correlation exist in the data. Machine learning techniques are able to extract such relationship voluminous data and supports for data driven knowledge discovery.
5. There are some biological problems in which experts can specify input/output pairs, but not the relationships between inputs and outputs. This can be addressed by machine learning to predict outputs for new inputs introduced to program, by generalization capabilities.

There are many practical issues to deal with when performing machine learning. This is especially true when it is applied to computational biology because the data sets are complex, high dimensional and not annotated, so inferring meaningful results require high accuracy and deep insight. Some points are narrated here. (1) Using more parameters may lead to more over fitting. For biological purpose we have high dimensional input data with comparatively less samples. So it is very difficult to learn all the parameters by given training sets. If features are more in data than it may be more likely that the classifier finds something that separates data just by chance. It also make difficult to draw conclusions from the parameters of a learned model. (2) If we have not enough input samples we cannot separate training sets and test sets, so cross validation technique is used.

## 3 A Classification Problem

**Philadelphia chromosome** or Philadelphia **translocation** is a specific chromosomal abnormality that is associated with chronic myelogenous leukemia (CML). It is the result of a reciprocal translocation between chromosome 9 and 22, and is specifically designated  $t(9; 22)(q34; q11)$  [3]. Chromosome translocations are very important in the initiation and/or progression of cancer; and consequently high numbers of translocation events have been reported in human genome. If high throughput data available than analyzing sequence features in the vicinity of translocation break-

points, may have major clinical role as: (1) Diagnostic markers (2) Response markers (3) Therapeutic markers.



**Reasons for selecting this problem** are (i) In 2007, cancers caused about 13 % of all human death worldwide (7.9 million) rates are rising as more people live to an old age. And (ii) In 2000 approximately 256,000 children and adults around world developed some form of leukemia and 209,000 died from it. About 90 % of all leukemia is diagnosed in adults [3].

### 3.1 Materials and Methods

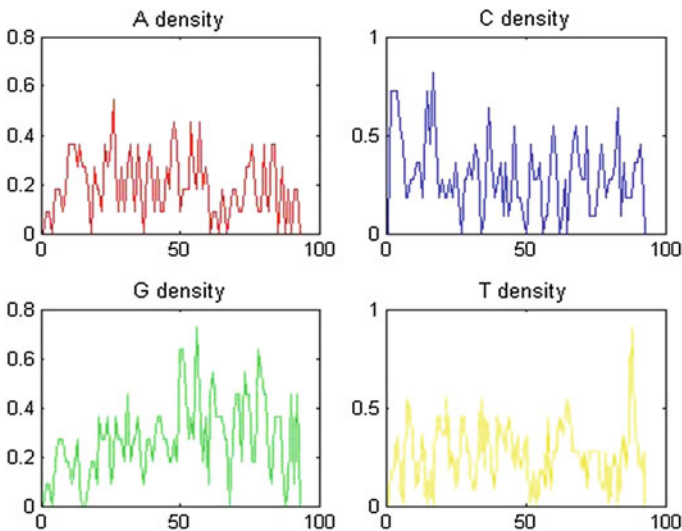
To address this issue the DNA sequence of BCR and ABL chromosomes with precise location of the break point which is involved in reciprocal translocation of leukemia were taken from various databases and further analysis were done. Data retrieval is done from publicly available database. Following databases:

1. Mitelman Database of chromosome aberration and gene fusion in cancer- (<http://cgap.nci.nih.gov/chromosomes/Mitelman>)
2. NCBI

The bioinformatics analyses are done by following method.

1. The 50 nucleotide base pair upstream and 50 downstream from breakpoint location of BCR and ABL is taken.

2. The occurrence of base pair in a sliding window of window size 3 is calculated and the factor of occurrence to window size is taken as frequency of the position. The graph of it with respect to position is as shown in figure.
3. The mean of frequency is taken as characteristics data for further analysis [4]. The above exercise is done for four nucleotide base pairs “A”, “C”, “G”, and “T” for 10 positive data samples and 5 negative data sample of housekeeping genes. The  $15 \times 4$  data matrix with 15 sample and four attributes are prepared.
4. For positive data the desired output is ranked as 0.95 instead of 1 and for negative data 0.05 instead of 0, because the activation functions is sigmoid. For sigmoid node function the output value will be 0 only if net input is  $-\infty$  and 1 only if net input is  $+\infty$  [5]. Since input signal is finite, we need weights of infinitely large magnitude. To avoid this desired out [2] put is taken as 0.95 and 0.05.
5. Data is introduced to the network for several epochs until the error is within desired tolerance.
6. The back propagation algorithm is implemented in MATLAB. A 4–3–1 network with hidden layer of three nodes is designed. Only three layers with one hidden layer are considered as per universal approximation theorem. Input layer neurons are linear while hidden and output layer neuron is sigmoid [6]. The weights are initialized randomly and values between  $-1$  to  $1$ . The frequency of the weight update is either “per pattern”. The value of “*learning rate*  $\eta$ ” is primarily taken as 1. The performance index used is MSE and the goal is to minimize it. The fast convergence of BP algorithm can be obtained by introducing momentum.
7. For testing purpose the weight matrix generated by training program for input to hidden nodes and hidden to output nodes are used to check the validity of the program. A new input vector is introduced in the output is checked.
8. The outputs of the data taken from training set give the correct answer. The output of unseen data not given in training set gives 95 % correct results.



### 3.2 *Future Scope and Conclusion*

With more sample data available, the result efficiency can be improved. Training model with cross validation technique for both positive and negative examples can be used for better efficiency. The design of architecture is optimized by network pruning. Optimizing the number of hidden nodes is still under process. The genome sequence can be characterized in two ways, mathematically and with biological perception. The sequence can be rich in content of its nucleotides A, C, T or G, it may have more GC content, fractal dimension of ACTG can be calculated. All this characteristics if related with biological characteristics like DNA bend ability, torsion of sequence and other parameters which can cause fragility is analyzed than gene annotation and classification or prognosis phase diagnosis of cancer can also be obtained. The learning rate can also be made adaptive by comparing the errors in two consecutive presentations of input samples. The motivation behind this work is to develop some supervised learners—artificial neural network, support vector machine, and thereby build an ensemble classifier. The gene annotation and diagnosis of cancer at prognosis phase is really a helpful outcome for medical field.

### References

1. Sushmita Mitra, E.: Introduction to Machine Learning and Bioinformatics. CRC Press, Boca Raton (2008)
2. Haykins, S.: Neural Networks a Comprehensive Foundation. Pearson Prentice Hall, Hamilton (2008)
3. Wikipedia, (n.d.)
4. Santosh, R., Uma, M.: Back propagation neural network method for predicting lac gene structures. *Int. J. Biotechnol. Mol. Biol. Res.* **2**(4), 61–72 (2011)
5. Mehrotra, K., Mohan, C.K., Ranka, S.: Elements of Artificial Neural Network. MIT Press, Cambridge (1997)
6. Kumar, S.: Neural Network a Classroom Approach. Tata McGraw Hill Education Private Ltd., Agra (2012)
7. Thompson, J.M.T.: An introduction to the mechanics of DNA. *The Roy. Soc.* vol. 362, (2004)

# Sobel-Fuzzy Technique to Enhance the Detection of Edges in Grayscale Images Using Auto-Thresholding

Jesal Vasavada and Shamik Tiwari

**Abstract** Images have always been very important in human life because humans are very much adapted in understanding images. Feature points or pixels play very important role in image analysis. These feature points include edge pixels. Edges on the image are strong intensity variations which show the difference between an object and the background. Edge detection is one of the most important operations in image analysis as it helps to reduce the amount of data by filtering out the less relevant information and if edge can be identified, basic properties of object such as area, perimeter, shape, etc can be measured. In this paper, a Sobel-Fuzzy technique using auto-thresholding is proposed by fuzzifying the results of first derivatives of Sobel in  $x$ ,  $y$  and  $xy$  directions. The technique automatically finds the six threshold values using local thresholding. Comparative study has been done on the basis of visual perception and edgel counts. The experimental results show the proposed Sobel-Fuzzy approach is more efficient in comparison to Roberts, Prewitt, Sobel, and LoG and produces better results.

**Keywords** Edge detection · Sobel edge detection · Image processing · Fuzzy logic

## 1 Introduction

Edge is defined by discontinuity in the gray levels of pixels. Edge detection is one of the most frequently used techniques in digital image processing [1]. Edge detection is

---

J. Vasavada (✉) · S. Tiwari  
Department of Computer Science and Engineering, Faculty of Engineering and Technology,  
Mody Institute of Technology and Science (Deemed University), Lakshmanagarh,  
Sikar, Rajasthan 332311, India  
e-mail: jesal.vasavada@gmail.com

S. Tiwari  
e-mail: tiwari@rediffmail.com

a preprocessing step to extract some low-level boundary features of an image, which are then used for higher level processing such as object finding and recognition. The Edge detection contains three steps namely Filtering, Enhancement, and Detection. The objective of Filtering is to remove noise from an image so that noise free image is obtained. Edge detection becomes difficult task in noisy images because both edges and noise contain high frequency content. Edge detection in noisy images sometimes give rise to the problems like missing true edges, false edge detection, false edge localization, etc. To filter the noise from an image, the nature and type of noise must be known in prior that helps to choose the correct filtering method [2]. Quality of digital image can be improved by Enhancement techniques. Edge detection identifies the edges by using thresholding. Thresholding can be categorized into global thresholding and local thresholding. Global thresholding is more appropriate in images with uniform contrast distribution of background and foreground like document images. Local thresholding is used when the background illumination is highly nonuniform. The main idea behind edge detection in an image is to find the places where the intensity of pixel changes rapidly, using one of the two general criterias. One of which is finding the places where the first derivative of the intensity is greater in magnitude than a specified threshold. Second is finding the places where the second derivative of the intensity has a zero crossing [3]. Edge detection using fuzzy logic has the advantage that fuzzy set theory and Fuzzy logic offer powerful tools to represent and process human knowledge in the form of fuzzy-if-then rules

Section 2 explains in brief fuzzy image processing. Section 3 explains fuzzy logic-based proposed method. Section 4 gives comparison between Roberts, Prewitt, Sobel, LoG, and proposed method. Finally the Sect. 5 is concluding the paper.

## 2 Fuzzy Image Processing

Fuzzy logic, one of the decision-making techniques of AI has many application areas. Fuzzy means “unclear”. Image data contains a lot of vagueness. Fuzzy logic helps to represent the uncertainties that exist in the image data. Fuzzy image processing is a collection of all approaches that understand, represent, and process images, their segments and features as fuzzy sets. Fuzzy image processing has three main steps:

- Image fuzzification
- Modification of membership values
- Image defuzzification as shown in Fig. 1

Fuzzy image processing is important to represent uncertainty in data. Fuzzy set theory and Fuzzy logic offer powerful tools to represent and process human knowledge in the form of fuzzy-if-then rules. Fuzzy logic is tolerant of imprecise data and can deal with uncertain data which helps to create a model for edge detection in image as presented in [4]. Several approaches on fuzzy logic-based edge detection have been proposed on fuzzy-if-then rules [5–8].

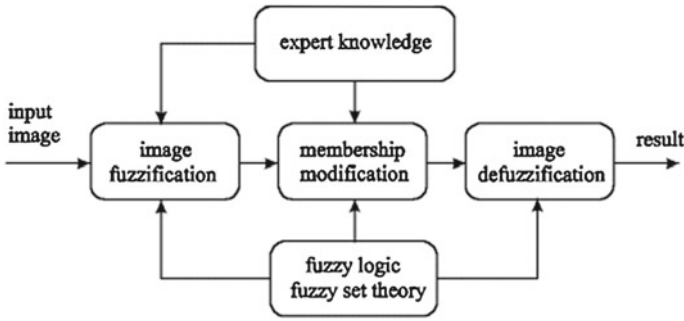


Fig. 1 General structure of fuzzy image processing

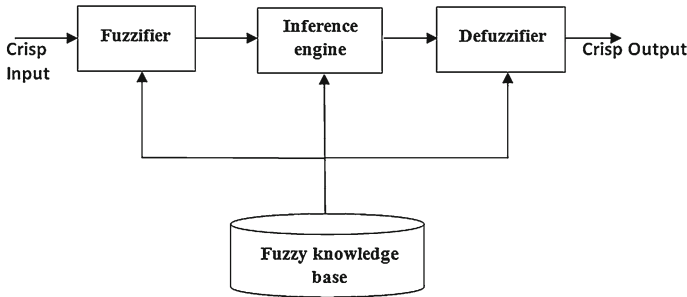


Fig. 2 Block diagram of fuzzy inference system

A *fuzzy inference system (FIS)* is a system that uses fuzzy set theory to map inputs (*features* in the case of fuzzy classification) to outputs (*classes* in the case of fuzzy classification). The block diagram is shown in Fig. 2.

The function of Fuzzifier is to convert the crisp input to a linguistic variable using the membership functions stored in the fuzzy knowledge base. The function of Inference Engine using If-Then type fuzzy rules is to convert the fuzzy input to the fuzzy output. Functioning of Inference Engine is shown in Fig. 3.

Defuzzifier converts the fuzzy output of the inference engine to crisp using membership functions analogous to the ones used by the fuzzifier. In an FIS, defuzzification is applied after aggregation. Five commonly used defuzzifying methods are Centroid of Area (COA), Bisector of Area (BOA), Mean of Maxima (MOM), Smallest of Maximum (SOM), and Largest of Maximum (LOM). Popular defuzzification methods include the Centroid of Area defuzzifier [9], and the Mean-of-Maxima defuzzifier [9]. The Centroid of Area defuzzifier is the best-known method, which is used to find the centroid of the area surrounded by the MF and the horizontal axis. There are three Fuzzy Models namely Mamdani Fuzzy models, Sugeno Fuzzy Models, and Tsukamoto Fuzzy models. All the models have same style for antecedents but different style for consequence. In the paper, Mamdani Fuzzy Model and COA defuzzifying method are used.

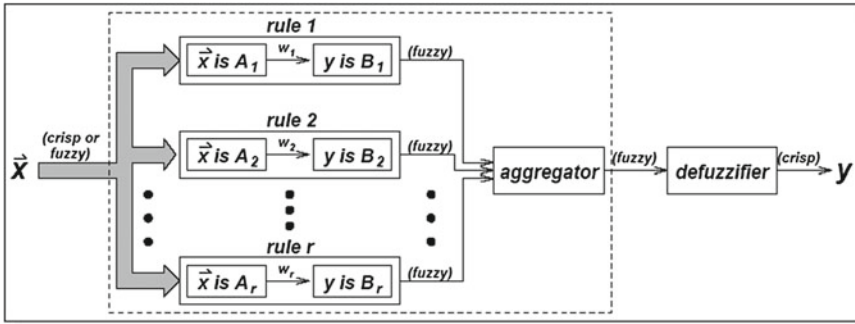


Fig. 3 Functioning of fuzzy inference engine

### 3 The Proposed Methodology

The block diagram of the algorithm to identify edges in image is given in Fig. 13. In the existing world, almost all the researchers use combined magnitude of Sobel gradients in  $x$  and  $y$  directions as one input along with one or more inputs like standard deviation, high pass filters, etc. These inputs are then fuzzified. In the paper, first derivatives of Sobel i.e.,  $G_x$ ,  $G_y$ , and  $G_{xy}$  are calculated in three different directions i.e., in  $x$ ,  $y$  and  $xy$  directions. The three inputs are then fuzzified. The proposed method contains four steps as follows:

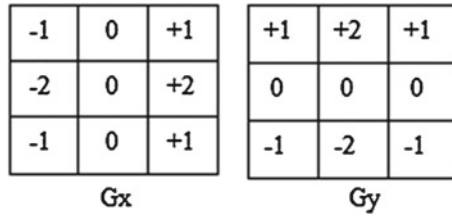
#### 3.1 Noise Identification and Filtering

The paper performs noise identification in the image under process and after knowing what type of noise is present, filters the noise and then detects edges using proposed method. At first the image to be processed goes through noise identification as given in [2]. If the image contains no noise then the proposed fuzzy method for edge detection is directly applied to image and if image contains it is filtered after knowing what type of noise it is [2].

#### 3.2 Fuzzification

Derivatives of Sobel  $G_x$ ,  $G_y$ , and  $G_{xy}$  are calculated in three different directions i.e., in  $x$ ,  $y$  and  $xy$  directions respectively. The first and the second inputs are calculated using the Sobel masks given in Fig. 4. The third input that is  $G_{xy}$  in 45 degree direction is calculated by the following equation given below where  $Y$  and





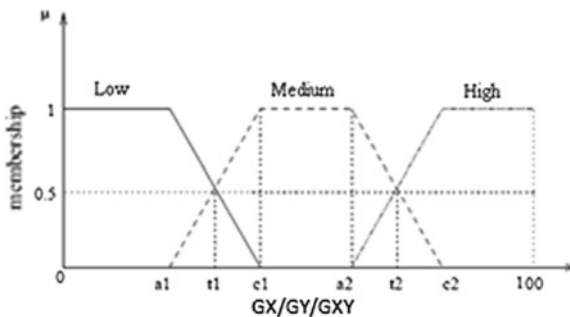
**Fig. 4** Sobel convolution masks

X are derivatives in the y and x direction. The equation allows the calculation of the derivative in any direction given by alpha.

$$G_{xy} = \sqrt{(Y \sin(\alpha))^2 + (X \cos(\alpha))^2}$$

Three computed values are used as fuzzy system inputs. Appropriate membership functions are defined for fuzzy system inputs. To apply these functions, first of all the three inputs are mapped to the range of [0–100]. The classification of mapped values is done into one of the following classes that is low, medium, or high. The Gx classes are shown by GX<sub>L</sub>, GX<sub>M</sub>, and GX<sub>H</sub> symbols, Gy classes are shown by GY<sub>L</sub>, GY<sub>M</sub> and GY<sub>H</sub> and The Gxy classes are shown by GXY<sub>L</sub>, GXY<sub>M</sub>, and GXY<sub>H</sub> symbols. To separate different Gx, Gy and Gxy classes four different thresholds a<sub>1</sub>, c<sub>1</sub>, a<sub>2</sub>, and c<sub>2</sub> are used are used. Such that if values of GX, GY, or GXY lies in the range of [0–c<sub>1</sub>], then, the corresponding pixel is classified to GX<sub>L</sub> or GY<sub>L</sub> or GXY<sub>L</sub> for the range of [a<sub>1</sub>–c<sub>2</sub>], the pixel is classified to GX<sub>M</sub> or GY<sub>M</sub> or GXY<sub>M</sub>, and finally for the range of [a<sub>2</sub>–100], pixel is classified to GX<sub>H</sub> or GY<sub>H</sub> or GXY<sub>H</sub>. The defined classes and membership functions are shown in Fig. 5.

If GX value of a pixel is equal to P, GY is equal to Q and GXY value of the pixel is R the fuzzy rules are defined as given in Table 1.



**Fig. 5** The defined classes and membership functions

**Table 1** Defined Fuzzy Rules

<b>P</b>	<b>Q</b>	<b>R</b>	<b>P<sub>edge</sub></b>
GX <sub>L</sub>	GY <sub>L</sub>	GXY <sub>L</sub>	E <sub>L</sub>
GX <sub>L</sub>	GY <sub>L</sub>	GXY <sub>M</sub>	E <sub>L</sub>
GX <sub>L</sub>	GY <sub>L</sub>	GXY <sub>H</sub>	E <sub>L</sub>
GX <sub>L</sub>	GY <sub>L</sub>	GXY <sub>L</sub>	E <sub>L</sub>
GX <sub>L</sub>	GY <sub>L</sub>	GXY <sub>M</sub>	E <sub>M</sub>
GX <sub>L</sub>	GY <sub>M</sub>	GXY <sub>H</sub>	E <sub>H</sub>
GX <sub>L</sub>	GD <sub>H</sub>	GXY <sub>L</sub>	E <sub>L</sub>
GX <sub>L</sub>	GY <sub>H</sub>	GXY <sub>M</sub>	E <sub>H</sub>
GX <sub>L</sub>	GY <sub>H</sub>	GXY <sub>H</sub>	E <sub>H</sub>
SX <sub>L</sub>	GY <sub>L</sub>	GXY <sub>L</sub>	E <sub>L</sub>
SX <sub>L</sub>	GY <sub>L</sub>	GXY <sub>M</sub>	E <sub>M</sub>
SX <sub>L</sub>	GY <sub>L</sub>	GXY <sub>H</sub>	E <sub>H</sub>
SX <sub>M</sub>	GY <sub>M</sub>	GXY <sub>L</sub>	E <sub>M</sub>
SX <sub>M</sub>	GY <sub>M</sub>	GXY <sub>M</sub>	E <sub>H</sub>
SX <sub>M</sub>	GY <sub>M</sub>	GXY <sub>H</sub>	E <sub>H</sub>
SX <sub>M</sub>	GD <sub>H</sub>	GXY <sub>L</sub>	E <sub>H</sub>
SX <sub>M</sub>	GY <sub>H</sub>	GXY <sub>M</sub>	E <sub>H</sub>
SX <sub>M</sub>	GY <sub>H</sub>	GXY <sub>H</sub>	E <sub>H</sub>
GX <sub>H</sub>	GY <sub>L</sub>	GXY <sub>L</sub>	E <sub>L</sub>
GX <sub>H</sub>	GY <sub>L</sub>	GXY <sub>M</sub>	E <sub>H</sub>
GX <sub>H</sub>	GY <sub>L</sub>	GXY <sub>H</sub>	E <sub>H</sub>
GX <sub>H</sub>	GY <sub>M</sub>	GXY <sub>L</sub>	E <sub>H</sub>
GX <sub>H</sub>	GY <sub>M</sub>	GXY <sub>M</sub>	E <sub>H</sub>
GX <sub>H</sub>	GY <sub>M</sub>	GXY <sub>H</sub>	E <sub>H</sub>
GX <sub>H</sub>	GD <sub>H</sub>	GXY <sub>L</sub>	E <sub>H</sub>
GX <sub>H</sub>	GY <sub>H</sub>	GXY <sub>M</sub>	E <sub>H</sub>
GX <sub>H</sub>	GY <sub>H</sub>	GXY <sub>H</sub>	E <sub>H</sub>

On the basis of fuzzy rules described in Table 1, the output of this fuzzy system is classified to one of the three classes  $E_L$ ,  $E_M$  and  $E_H$ . The classes  $E_L$ ,  $E_M$ , and  $E_H$  corresponds to pixels with low, medium, and high probability value, respectively, to belong to edge pixels set. Output membership functions are shown in Fig.6.

### 3.3 Defuzzification

Defuzzification is done by Centroid of Area method. This method was developed by Sugeno in 1985. This is the most common and accurate technique. This technique can be expressed as:

$$x^* = \frac{\int \mu_i(x) x dx}{\int \mu_i(x) dx}$$

where  $x^*$  is defuzzified output,  $\mu_i(x)$  is aggregated membership function and  $x$  is the output variable.

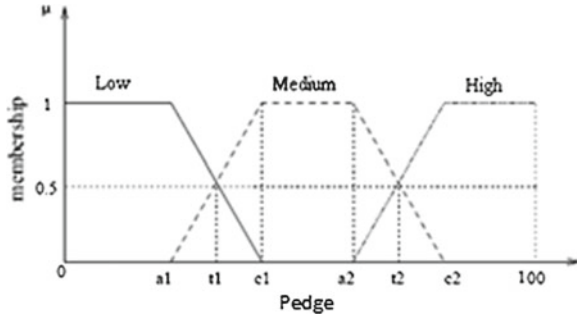


Fig. 6 Output membership functions



Fig. 7 Image divided into six parts

### 3.4 Auto-Thresholding

The concept of local thresholding is applied in the paper. The problem with global thresholding is that changes in illumination across the scene may cause some parts to be brighter (in the light) and some parts darker (in shadow) in ways that have nothing to do with the objects in the image. We can deal, at least in part, with such uneven illumination by determining thresholds locally. That is, instead of having a single

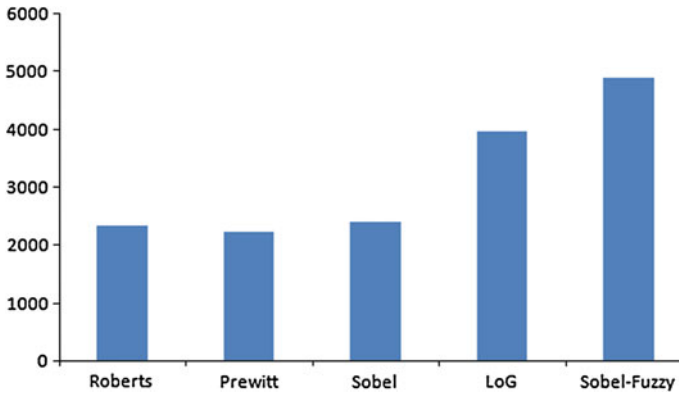


Fig. 8 Edgel counts of the image without noise using different operators

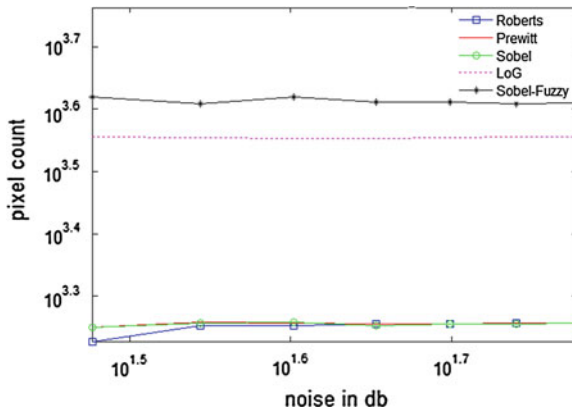


Fig. 9 Edgel counts after filtering speckle noise for different operators

global threshold, we allow the threshold itself to smoothly vary across the image. In the paper, image is divided into six parts as shown in Fig. 7 and then thresholding is applied to each part by taking mean of each part. In the first part if the pixel value is greater than T1 (threshold of 1st part) then it is considered as edge pixel else not. Similarly for the other parts T2, T3, T4, T5, T6 are calculated and edge pixels are found for each part, in the end all the parts are merged to form one complete image.

### 4 Performance Evaluation

This section compares the proposed method discussed above with the Roberts, Prewitt, Sobel, and LoG on the basis of their edge pixel count. The Fig. 8 compares the edgel count of Roberts, Prewitt, Sobel and LoG with proposed Sobel-fuzzy

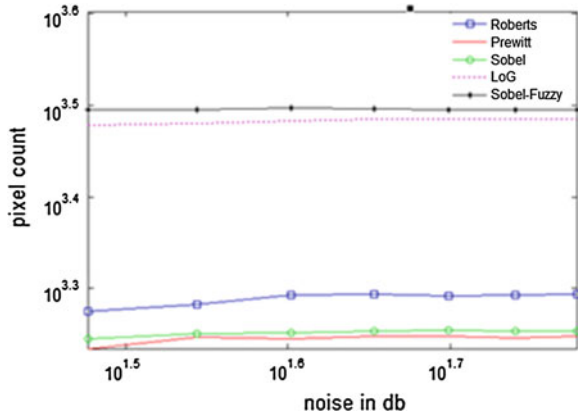


Fig. 10 Edgel counts after filtering Gaussian noise for different operators

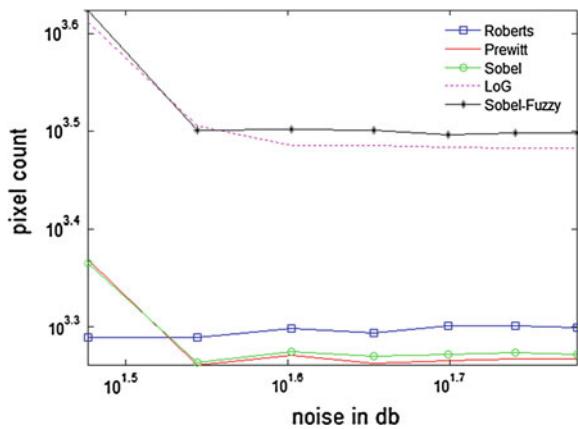
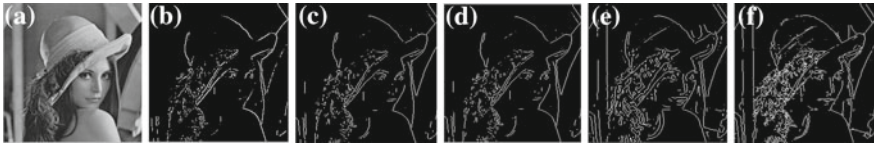
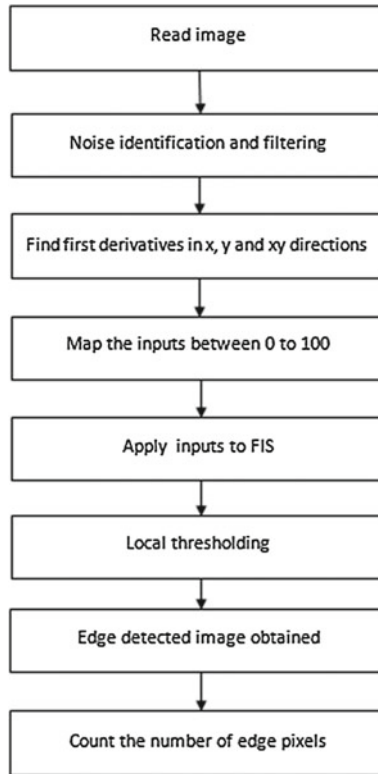


Fig. 11 Edgel counts after filtering salt and pepper for different operators

method for the image without noise. To know how the proposed method performs at different levels of noise, experiments are done with three types of noise, Gaussian noise, Speckle noise, and Salt and Pepper noise at noise levels from 30 to 60 db. Noise identification and filtering are done using the method given in [2]. For Salt and Pepper noise median filter is used, for Gaussian noise weiner filter is used, and for Speckle noise lee filter is used. Then all the techniques considered for comparison are applied to filtered image and edge pixels are counted. The results are shown in Figs. 9, 10 and 11. The evidence for the best detector type is judged by studying the edge maps relative to each other through statistical evaluation. For each edge map the number of edge pixels is count and compared. The proposed Sobel-fuzzy based method reports the higher detected edge pixels as shown in Figs. 8, 9, 10, and 11.



**Fig. 12** a Main image, b Roberts results, c Prewitt results, d Sobel results, e LoG results, and f Sobel-Fuzzy results



**Fig. 13** Block diagram of proposed method

Figure 12 shows the visual comparison of edge detection techniques. Although Sobel provides both differencing and smoothing but it detects only some part of edges. The Roberts operator fails to detect thin/fine edges. LoG is better than gradient-based operators because smoothing is performed before the application of the Laplacian in order to remove sensitivity to noise but still it is sensitive to noise and sometimes produces double edges. We find that Sobel and Prewitt give almost the same results. These operators are highly sensitive to noise. Sobel-Fuzzy based method produces best edge map which is proved in pixel count analysis of all operators with each other in Figs. 8, 9, 10, and 11.

## 5 Conclusion

In this paper, first different edge detection operators to the Lena image with different levels of noise and without noise are applied, afterward results are compared quantitatively and qualitatively. Performance is measured in presence of three types of noise, Salt and Pepper noise, Gaussian noise, and Speckle noise from 30 to 60 database are introduced and then image is filtered using appropriate filters namely median, weiner, and lee filters after noise classification. The classical edge detectors chosen for the comparison are Roberts, Sobel, and Prewitt and LoG. Analysis is done by comparing the edgel count of all the edge detectors with the proposed Sobel-Fuzzy based method. So the paper concludes that given Sobel-Fuzzy based method performs well in detecting the edges, when compared to other edge detectors.

## References

1. Senthilkumaran, N., Rajesh, R.: Edge detection techniques for image segmentation- a survey of soft computing approaches. *Int. J. Recent. Trends. Eng.* **1**(2), 250–254 (2009)
2. Tiwari, S., Kumar Singh, A., Shukla, V.P.: Statistical moments based noise classification using feedforward back propagation neural network. *Int. J. Comput. Appl.* **18**(2), 0975–8887 (2011)
3. Maini, R., Aggarwal, H.: Study and comparison of various image edge detection techniques. *Int. J. Image Process.* **3**(1), 1–12 (2010)
4. Stefno, B.D., Fuk's, H., Lawniczak A.T.: Application of fuzzy logic in CA/LGCA models as a way of dealing with imprecise and vague data. *Can. Conf. Electr. Comput. Eng.* **1**, 212–217 (2000)
5. Mendoza, O., Melin, P., Licea, G.: A new method for Edge Detection in Image Processing Using Interval Type-2 Fuzzy Logic. In: *IEEE International Conference Granular Computing*, 151–156 (2007)
6. Ur Rahman khan, A., Thakur, K.: An efficient fuzzy logic based edge detection algorithm for gray scale image. *Int.J. Emerg. Technol. Adv. Eng.* **2**(8), 2250–2459. <http://www.ijetae.com> (2012)
7. Ching-Yu, T., Wang, P.P.: Image processing-enhancement, filtering and edge detection using the fuzzy logic approach. In: *Second IEEE Conference Fuzzy Systems* **1**, 600–605 (1993)
8. Aborisade, D.O.: Novel fuzzy logic based edge detection technique. *Int. J. Adv. Sci. Technol.* **29**, 75–82 (2011)
9. Mamdani, E.H.: Application of fuzzy algorithms for control of a simple dynamic plant. *Proc. Inst. Electr. Eng.* **121**, 1585–1588 (1974)

**Part VI**  
**Soft Computing for Classification (SCC)**



# Hesitant k-Nearest Neighbor (HK-nn) Classifier for Document Classification and Numerical Result Analysis

Neeraj Sahu, R. S. Thakur and G. S. Thakur

**Abstract** This paper presents new approach Hesitant k-nearest neighbor (HK-nn)-based document classification and numerical results analysis. The proposed classification HK-nn approach is based on hesitant distance. In this paper, we have used hesitant distance calculations for document classification results. The following steps are used for classification: data collection, data pre-processing, data selection, presentation, analysis, classification process and results. The experimental results are evaluated using MATLAB 7.14. The Experimental results show proposed approach that is efficient and accurate compared to other classification approach.

**Keywords** Hesitant k-nearest neighbor · Hesitant distance · Classification · Data mining

## 1 Introduction

Document classification is the recent issue in text mining. Document classification areas are science, technology, social science, biology, economics, medicine, and stock market, etc. In past recent years, lot of research work has been done decodes some best contributions on Document classification are as follows: An Algorithm for a Selective Nearest Neighbor Decision Rule [1], Gradient-Based Learning Applied to Document Recognition [2], Condensed Nearest Neighbor Rule [3], Fast Nearest-Neighbor

---

N. Sahu (✉)

Singhania University Rajasthan, Jhunjhunu, India

e-mail: neerajsahu79@gmail.com

R. S. Thakur · G. S. Thakur

MANIT, Bhopal, India

e-mail: ramthakur2000@yahoo.com

G. S. Thakur

e-mail: ghanshyamthakur@gmail.com

Search in Dissimilarity Spaces [4], Branch and Bound Algorithm for Computing k-Nearest Neighbors [5], Finding Prototypes for Nearest Neighbor Decision Rule [6], An Algorithm for Finding Nearest Neighbors in Constant Average Time [7], Strategies for Efficient Incremental Nearest Neighbor Search [8], Accelerated Template Matching Using Template Trees Grown by Condensation [9], An Algorithm for Finding Nearest Neighbors [10], A Simple Algorithm for Nearest-Neighbor Search in High Dimension [11], A Fast k Nearest Neighbor Finding Algorithm Based on the Ordered Partition [12], Multidimensional Binary Search Trees Used for Associative Searching [13], Discriminant Adaptive Nearest-Neighbor Classification [14], Comparing Images Using Hausdorff Distance [15], Empirical Evaluation of Dissimilarity Measures for Color and Textures [16], A Multiple Feature/Resolution Approach to Hand printed Character/Digit Recognition [17], Representation and Reconstruction of Handwritten Digits Using Deformable Templates [18], Sparse Representations for Image Decompositions with Occlusions [19], A Note on Binary Template Matching [20], Classification with Non-metric Distances: Image Retrieval and Class Representation [21], Properties of Binary Vector Dissimilarity Measures [22], Nearest Neighbor Pattern Classification [23], Hesitant Distance Similarity Measures for Document Clustering [24], Classification of Document Clustering Approaches [25], Architecture-Based Users and Administrator Login Data Processing [26]. The above mentioned work suffers from lack of efficiency and accuracy. The low accuracy is still issue and challenge in the Classification. This motivates us to construct the new method for Classification. New Document Classification method we called Hesitant k-nearest neighbor (HK-nn). Hence we proposed new document classification approach HK-nn. The remaining paper is organized as follows: Sect. 1 describes introduction and review of literatures. Section 2 describes HK-nn and k-nn. In Sect. 3, methodology of document classification steps are described. In Sect. 4, experimental results are described. In Sect. 5, results Evaluation and measurement are described. Finally, we concluded and proposed some future directions in Conclusion Section (Fig. 1).

## 2 Calculations for Hesitant k-nn and General k-nn Classifier

In this calculation, we find k-nearest neighbor based on Hesitant distance (Hd) and General distance (Gd). Hesitant distance and General distance of each  $P_i$  to  $P_j$  (Tables 1, 2). Represent all distance calculated by Hd, Gd. Hesitant distance and General distance Cluster Point shown in Tables 3 and 4 with ascending order. This calculation shows hesitant distance-based accuracy percentages and General distance-based accuracy percentages Cluster Point show in Tables 5 and 6 (Fig. 2).

For computational model, we give tabulation form from Tables 1, 2, 3, 4, 5, and 6.

### 3 Methodology

In the classification of different document the steps are used. The steps are as follows:

- (A) **Data collection.** In this phase, collect relevant documents like e-mail, news, web pages, etc., from various heterogeneous sources. These text documents are stored in a variety of formats depending on the nature of the data. The datasets are downloaded from UCI KDD Archive. This is an online repository of large datasets and has wide variety of data types.
- (B) **Classification method.** Initial step is to complete review of literature in the field of data mining. Next step is a detailed survey of data mining and existing Algorithms for Classification. In this area some works are done by various researchers. After studying their work, it would be attempted to find the Classification algorithm.
- (C) **Classification process.** Algorithms develop for Classification Process. Classification Process means transform documents into a suitable determined in classes for the Classification task. In Classification Process, we performed Different tasks. Optimized classification will also be studied. The real data may be great source for the Classification.
- (D) **Classification results.** In this Experiment we calculate k-nearest neighbor based on Hesitant distance and General distance. Hesitant distance and General distance from Cluster Points  $P_i$  to  $P_j$  calculated and gives ascending order of the hesitant distance and General distance for tabulation. Hesitant Distance

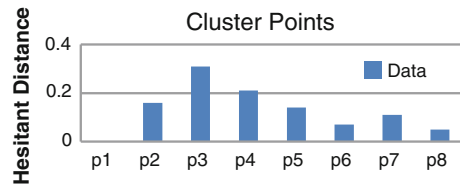
**Table 1** Hesitant distance from cluster point

Clusters points	Hesitant distance from cluster point $P_1(7, 4)$
$P_1(7, 4)$	0.00
$P_2(9, 6)$	0.16
$P_3(11, 4)$	0.31
$P_4(2, 3)$	0.21
$P_5(4, 5)$	0.14
$P_6(5, 6)$	0.07
$P_7(7, 9)$	0.11
$P_8(9, 8)$	0.05

**Table 2** General distance from cluster point

Clusters points	General distance from cluster point $P_1(7, 4)$
$P_1(7, 4)$	0.00
$P_2(9, 6)$	2.82
$P_3(11, 4)$	4.00
$P_4(2, 3)$	5.09
$P_5(4, 5)$	3.16
$P_6(5, 6)$	2.82
$P_7(7, 9)$	5.00
$P_8(9, 8)$	4.47

**Fig. 1** Hesitant distance from cluster point



accuracy percentages and General distance accuracy percentages from Cluster Point show in tabulation. This Experiment show hesitant distance-based accuracy percentages is efficient and accurate compared with General distance-based accuracy percentages (Fig. 3).

---

**Algorithm 1:** This Algorithm obtains Hesitant distance of a cluster from each cluster.

---

Step 1: Input eight clusters points.

Step 2: Initialize  $x_1, y_1$  for cluster point and  $x_2, y_2$  for each clusters points.

Step 3: Produce and compare hesitant distance one by one.

Step 4: Find minimum Hesitant distance Hd from clusters points say first.

Step 5: Arrange all hesitant distance in ascending order.

---



---

**Algorithm 2:** This Algorithm obtains General distance of a cluster from each cluster.

---

Step 1: Input eight clusters points.

Step 2: Initialize  $x_1, y_1$  for cluster point and  $x_2, y_2$  for each clusters points.

Step 3: Produce and compare General distance one by one.

Step 4: Find minimum General distance Gd from clusters points say first.

Step 5: Arrange all General distance in ascending order.

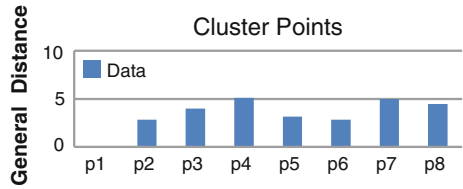
---

## 4 Experimental Results

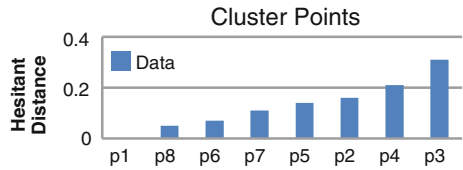
In this Experiment we calculate k-nearest neighbor based on Hesitant distance and General distance. Hesitant distance and General distance from Cluster Points  $P_1$  to  $P_8$  calculated and gives ascending order of the hesitant distance and General distance for tabulation describe in Tables 3 and 4. Hesitant Distance accuracy percentages and General distance accuracy percentages from Cluster Point are shown in Tables 5 and 6. This Experiment which shows hesitant distance-based accuracy percentages is efficient and accurate compared with General distance-based accuracy percentages (Fig. 4).

Figures 5 and 6 describe document classification results and accuracy % of classification process.

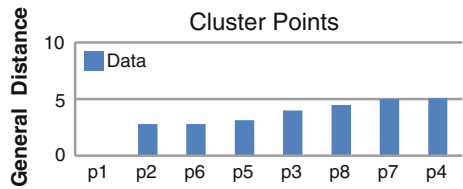
**Fig. 2** General distance from cluster point



**Fig. 3** Hesitant distance from cluster point in ascending order



**Fig. 4** General distance from cluster point in ascending order



**Table 3** Hesitant distance from Cluster Point in ascending order

Clusters points	Hesitant distance from cluster point $P_1(7, 4)$
$P_1(7, 4)$	0.00
$P_8(9, 8)$	0.05
$P_6(5, 6)$	0.07
$P_7(7, 9)$	0.11
$P_5(4, 5)$	0.14
$P_2(9, 6)$	0.16
$P_4(2, 3)$	0.21
$P_3(11, 4)$	0.31

**Table 4** General distance from cluster point in ascending order

Clusters points	General distance from cluster point $P_1(7, 4)$
$P_1(7, 4)$	0.00
$P_2(9, 6)$	2.82
$P_6(5, 6)$	2.82
$P_5(4, 5)$	3.16
$P_3(11, 4)$	4.00
$P_8(9, 8)$	4.47
$P_7(7, 9)$	5.00
$P_4(2, 3)$	5.09

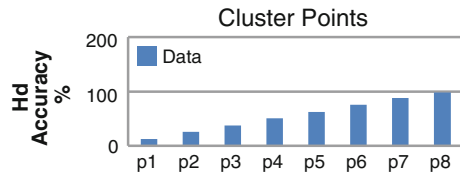
**Table 5** Hesitant distance accuracy percentages from cluster point

Clusters points	Accuracy percentages from cluster point %
$P_1(7, 4)$	12.48
$P_2(9, 6)$	25.63
$P_3(11, 4)$	37.59
$P_4(2, 3)$	50.37
$P_5(4, 5)$	62.22
$P_6(5, 6)$	75.29
$P_7(7, 9)$	87.67
$P_8(9, 8)$	97.99

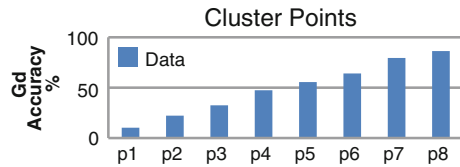
**Table 6** General distance accuracy percentages from cluster point

Clusters points	Accuracy percentages from cluster point %
$P_1(7, 4)$	10.34
$P_2(9, 6)$	22.34
$P_3(11, 4)$	32.45
$P_4(2, 3)$	47.45
$P_5(4, 5)$	55.45
$P_6(5, 6)$	64.34
$P_7(7, 9)$	79.45
$P_8(9, 8)$	86.45

**Fig. 5** Accuracy % from cluster point for Hesitant distance



**Fig. 6** Accuracy % from cluster point for general distance



**Acknowledgments** This work is supported by research grant from MPCST, Bhopal M.P., India, Endt.No. 2427/CST/R&D/2011 dated 22/09/2011.

## References

1. Ritter, G.L., Woodruff, H.B., Lowry, S.R., Isenhour, T.L.: An algorithm for a selective nearest neighbor decision rule. *IEEE Trans. Inf. Theory* **21**, 665–669 (1975)
2. LeCun, Y., Bottou, L., Bengio, Y., Haffner, P.: Gradient-based learning applied to document recognition. *Proc. IEEE* **81**(11), 2278–2324 (1998)
3. Hart, P.E.: Condensed nearest neighbor rule. *IEEE Trans. Inf. Theory* **14**, 515–516 (1968)
4. Farago, A., Linder, T., Lugosi, G.: Fast nearest-neighbor search in dissimilarity spaces. *IEEE Trans. Pattern Anal. Mach. Intell.* **15**(9), 957–962 (1993)
5. Fukunaga, K., Narendra, P.M.: A branch and bound algorithm for computing k-nearest neighbors. *IEEE Trans. Comput.* **24**(7), 750–753 (1975)
6. Chang, C.L.: Finding prototypes for nearest neighbor decision rule. *IEEE Trans. Comput.* **23**(11), 1179–1184 (1974)
7. Vidal, E.: An algorithm for finding nearest neighbors in (approximately) constant average time. *Pattern Recogn. Lett.* **4**(3), 145–157 (1986)
8. Broder, A.J.: Strategies for efficient incremental nearest neighbor search. *Pattern Recogn.* **23**(1/2), 171–178 (1986)
9. Brown, R.L.: Accelerated template matching using template trees grown by condensation. *IEEE Trans. Syst Man Cybern.* **25**(3), 523–528 (Mar. 1995)
10. Friedman, J.H., Baskett, F., Shustek, L.J.: An algorithm for finding nearest neighbors. *IEEE Trans. Comput.* **24**(10), 1000–1006 (1975)
11. Nene, S.A., Nayar, S.K.: A simple algorithm for nearest-neighbor search in high dimension. *IEEE Trans. Pattern Anal. Mach. Intell.* **19**(9), 989–1003 (1997)
12. Kim, B.S., Park, S.B.: A fast k nearest neighbor finding algorithm based on the ordered partition. *IEEE Trans. Pattern Anal. Mach. Intell.* **8**(6), 761–766 (1986)
13. Bentley, J.L.: Multidimensional binary search trees used for associative searching. *Commun. ACM* **18**(9), 509–517 (1975)
14. Hastie, T., Tibshirani, R.: Discriminant adaptive nearest-neighbor classification. *IEEE Trans. Pattern Anal. Mach. Intell.* **18**(6), 607–615 (1996)
15. Hunttenlocher, D., Klanderma, G., Rucklidge, W.: Comparing images using Hausdorff distance. *IEEE Trans. Pattern Anal. Mach. Intell.* **19**(1), 1–14 (1997)
16. Puzicha, J., Buhmann, J., Rubner, Y., Tomasi, C.: Empirical evaluation of dissimilarity measures for color and textures. In: *Proceedings of International Conference on Computer Vision*, pp. 1165–1172 (1999)
17. Favata, J.T., Srikantan, G.: A multiple feature/resolution approach to hand printed character/digit recognition. *Proc. Intl J. Imaging Syst. Technol.* **7**, 304–311 (1996)
18. Jain, A.K., Zongker, D.: Representation and reconstruction of handwritten digits using deformable templates. *IEEE Trans. Pattern Anal. Mach. Intell.* **19**(12), 1386–1391 (1997)
19. Donahue, M., Geiger, D., Hummel, R., Liu, T.: Sparse representations for image decompositions with occlusions. In: *Proceedings of the IEEE Conference on Computer Vision and Pattern Recognition*, pp. 7–12 (1996)
20. Tubbs, J.D.: A note on binary template matching. *Pattern Recogn.* **22**(4), 359–365 (1989)
21. Jacobs, D.W., Weinshall, D.: Classification with non-metric distances: image retrieval and class representation. *IEEE Trans. Pattern Anal. Mach. Intell.* **22**(6), 583–600 (June 2000)
22. Zhang, B., Srihari, S.N.: Properties of binary vector dissimilarity measures. In: *Proceedings of JCIS International Conference on Computer Vision, Pattern Recognition, and Image Processing* (2003)
23. Cover, T.M., Hart, P.E.: Nearest neighbor pattern classification. *IEEE Trans. Inf. Theory* **13**, 21–27 (1968)
24. Neeraj, S., Thakur, G.S.: Hesitant distance similarity measures for document clustering. In: *IEEE Conference World Congress on Information and Communication Technologies Mumbai, India*. ISBN: 978-1-4673-0125-1, 11–14 December 2011

25. Sahu, S.K., Sahu, N, Thakur, G.S.: Classification of document clustering approaches. *Int. J. Adv. Res. Comput. Sci. Softw. Eng. (IJARCSSE) ISSN (ONLINE): 2277 128X*, **2**(5), 509–513 (2012)
26. Sahu, B., Sahu, N., Thakur , G.S.: Architecture based users and administrator login data processing In: *International Conference on Intelligent Computing and Information System (ICICIS-2012)*, Pachmarhi, Piparia (MP). ISSN (ONLINE): 2249–071X, Oct. 27–28 2012



# Lower Bound on Naïve Bayes Classifier Accuracy in Case of Noisy Data

Karan Rawat, Abhishek Kumar and Anshuman Kumar Gautam

**Abstract** Classification is usually the final and one of the most important steps in most of the tasks involving machine learning, computer vision, etc., for e.g., face detection, optical character recognition, etc. This paper gives a novel technique for estimating the performance of Naïve Bayes Classifier in noisy data. It also talks about removing those attributes that cause the classifier to be biased toward a particular class.

**Keywords** Optimal statistical classification · Confusion matrix · ROC · Discriminant functions · Bayes theorem

## 1 Introduction

Naïve Bayes [1] classification is a generative machine learning algorithm that exploits the possible independence between attributes of data points. It is a special case of more general “**Optimal Statistical Classifier**” [2]. Although other techniques such as **Logistic Regression, Neural Networks, Gaussian Discriminant Analysis**, its special case, **Linear Discriminant Analysis** [3] are available, but the simplicity in design and implementation makes **NB** classification a popular choice for classification, provided its underlying assumption holds true to some extent. It has proved to be useful in large number of classification problems involving multivariate feature vectors.

---

K. Rawat (✉)  
IIT Allahabad, Allahabad, India  
e-mail: rawatkaran4@hotmail.com

A. Kumar · A. K. Gautam  
Government Engineering College, Ajmer, Rajasthan, India

## 2 Related Work

Accuracy of statistical classifiers can be measured using **Confusion Matrix** [4], **ROC** [5] curve, etc. However, these measures (a) estimate how well the assumed model fits the underlying data and (b) this too requires testing the classifier on another data set called “Test Data”. But, this paper does something different. It assumes that the data model chosen is correct. It checks the accuracy of the classifier against noisy inputs, i.e., to what extent noise in the input data vector is tolerable. The above-mentioned measures, however, test the accuracy of the data against a given test data and does not give any information about the noise handling capacity of the classifier.

## 3 Bayes Theorem

The concept of **Inverse probability** was first given by Thomas Bayes but published by Laplace who reached the same result independently and published it in a paper titled “**Théorie analytique des probabilités**” in 1812. It calculates the probability of the event that occurred on performing an experiment given the result (outcome) of the experiment. This is mathematically given as:

$$P(A|B) = P(B|A)P(A)/P(B).$$

In case the experiment is composed of  $n$  events,  $P(B)$  is given as:

$$P(B) = \sum_i (P(B|A_i)P(A_i)).$$

## 4 Discriminant Functions

These are the functions used that determine the class of a data point using one discriminant function [4] corresponding to each class.

The predicted class of a data vector  $\mathbf{x}$  is  $i$  if

$$d_i(\mathbf{x}) > d_j(\mathbf{x}) \quad \text{for all } j \neq i.$$

Decision Boundary between classes  $i$  and  $j$  is given by

$$d_{ij}(\mathbf{x}) = d_i(\mathbf{x}) - d_j(\mathbf{x}) = 0.$$

## 5 Optimal Statistical Classification

If a data vector  $\mathbf{x}$  is predicted to belong to class  $j$  when it actually belongs to class  $I$ , the loss incurred is, say,  $L_{ij}$ . Now,  $i$  could have been any possible class, therefore, the prediction that  $\mathbf{x}$  belongs to  $j$  incurs an expected loss:

$$r_j(\mathbf{x}) = \sum_i P(i|\mathbf{x})L_{ij}.$$

This is known as **Conditional Average Risk**.

Using Bayes Theorem, we have

$$r_j(\mathbf{x}) = (1/P(\mathbf{x})) \sum_i L_{ij} P(\mathbf{x}|i)P(i).$$

Since,  $P(\mathbf{x})$  is same for all  $i$ , we can define a new conditional average risk variable,

$$s_i(\mathbf{x}) = \sum_i P(\mathbf{x}|i)L_{ij}P(i).$$

Optimal Statistical Classification calculates  $s_1(\mathbf{x}), s_2(\mathbf{x}), \dots, s_w(\mathbf{x})$  and predicts the class with minimum CAR. Bayes Classifier minimizes the total CAR over all predictions by assigning a data vector  $\mathbf{x}$  to class  $i$  if

$$s_i(\mathbf{x}) < s_j(\mathbf{x}) \\ \sum_p P(\mathbf{x}|p)L_{pi}P(p) < \sum_q P(\mathbf{x}|q)L_{qj}P(q) \quad \text{for all } j \neq i.$$

Now, for a correct prediction, loss incurred should be 0 and a loss of unity is incurred in case of incorrect prediction.

$$L_{ij} = 1 - \delta(i, j)$$

where  $\delta$  is the Kronecker delta function.

$$\sum_p P(\mathbf{x}|p)P(p)(1 - \delta(p, i)) < \sum_q P(\mathbf{x}|q)P(q)(1 - \delta(q, j)). \\ P(\mathbf{x}) - P(\mathbf{x}|i)P(i) < P(\mathbf{x}) - P(\mathbf{x}|j)P(j) \\ P(\mathbf{x}|j)P(j) < P(\mathbf{x}|i)P(i) \quad \text{for all } j \neq i.$$

Hence, for Bayesian classification,

$$d_i(\mathbf{x}) = P(\mathbf{x}|i)P(i)$$

## 6 Naïve Bayes Assumption

The classifier assumes that the attributes of data are independent of each other, and hence, contribution of an attribute to the probability that a given data point belongs to a given class does not depend on the values assumed by other attributes. Formulating this mathematically:

$$P(x_1, x_2, \dots, x_n|C) = P(x_1|C)P(x_2|C) \dots P(x_n|C)$$

where  $C$  is a class label and  $x_i$  is the random variable corresponding to  $i$ th attribute.

## 7 Algorithm

1. After the calculation of means and variances for all the classes and for each attribute (to be used in NB classification), for each pair of classes,  $i, j$  and for each attribute,  $k$ ,  $x_{ij,k}^*$  is calculated using the following equation :

$$(\varphi_i)^{1/n} f_{i,k}(x_{ij,k}^*) = (\varphi_j)^{1/n} f_{j,k}(x_{ij,k}^*)$$

where  $\varphi_p$  is the prior probability of occurrence of class  $p$  and  $f_{p,q}(z)$  is the probability density function for class  $p$  and attribute  $q$  with random variable  $Z$ . Often, when  $f$  is not known,  $Z$  is assumed to follow Gaussian distribution and hence,

$$f_{p,q}(z) = (1/\sigma_{p,q}\sqrt{2\pi}) \exp(-(z - \mu_{p,q})^2/2\sigma_{p,q}^2)$$

where  $\mu_{p,q}$  and  $\sigma_{p,q}$  are mean and variance for class  $p$  and attribute  $q$ , respectively.

2. Using  $x_{ij,k}^*$ , find the intervals for which  $f_{i,k}(z) > f_{j,k}(z)$ . Find the c.d.f of  $f_{i,k}(z)$  over these intervals and obtain a value  $D_{i,k}$ .
3. Calculate  $D_{i,k}$  for all  $k$ .
4. The probability that a data vector belonging to class  $i$  comes from the intervals determined in step 2 is

$$\prod_k D_{i,k}$$

## 8 Working

By determining the value of  $t$  for classifier boundary between each pair of classes, we can calculate the confusion matrix and hence, find the accuracy. The principle behind the correctness of this method is that for any two classes,  $i, j$  a data vector is

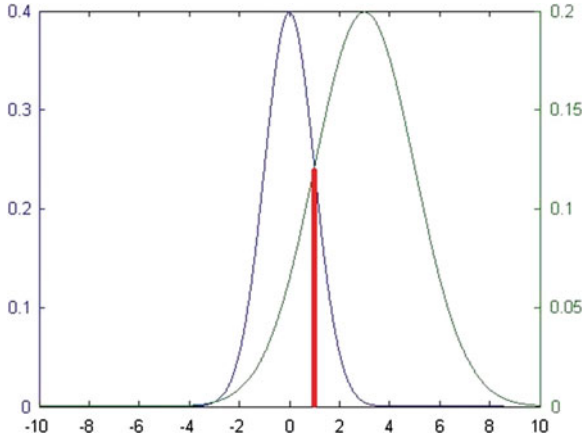


Fig. 1

assigned to class  $i$  if

$$d_i(\mathbf{x}) > d_j(\mathbf{x}).$$

And, this will happen for sure if

$$(\varphi_i)^{1/n} f_{i,k}(x_{ij,k}) > (\varphi_j)^{1/n} f_{j,k}(x_{ij,k}), \quad \text{for all } k.$$

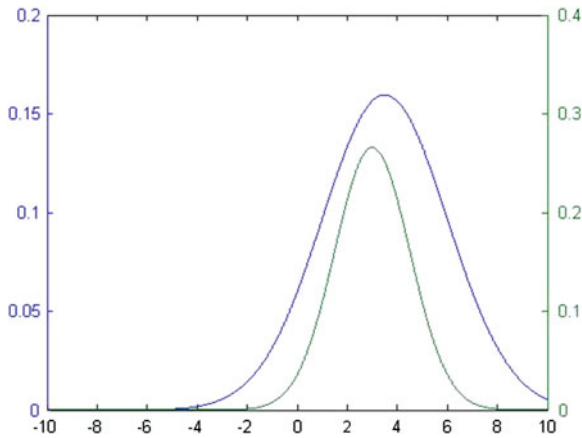
By determining the set of values for which these will hold and estimate of the relative frequency of data vectors that will fall within this set using c.d.f. of standard normal distribution.

### 9 Graphical Approach

Taking a two-class problem in which data vectors are two- dimensional, two graphs are shown corresponding to each attribute.

Prior probability of each class is taken to be 0.5. So, in Fig. 1 the red line shown is the dividing line  $x = x^*$ . There exists one more point because of the quadratic nature of Gaussian decision boundaries, however, Gaussian value at that point is quite low, therefore, it is not of concern.

Figure 2 tells us that Gaussian for class 1 has higher value than that for class 2 and that too includes large amount of neighborhood of mean of class 2. This tells that using second attribute for classification will not be a good idea as classifier would be biased toward class 1. Hence, we should reduce the dimensionality to 1 taking only first attribute.



**Fig. 2**

## 10 Conclusion

The accuracy of **NB** classifier can be estimated only from the parameters of discriminant functions, determined using training data. Hence, no further test data is required and thus, prior to training, data set does not need to be cross-validated and a larger data set can be used, resulting in higher accuracy. This method, however, assumes that NB assumption holds true and determines how the accuracy of prediction is affected when data points that are less likely to belong to a given class actually belong to that class.

## References

1. John, G.H., Langley, P.: Estimating continuous distributions in Bayesian classifiers. In: Proceedings of the Eleventh Conference on Uncertainty in Artificial Intelligence. Morgan Kaufmann Publishers, San Mateo (1995)
2. Gonzalez, R.C., Woods, R.E.: Digital Image Processing. Prentice Hall, New Jersey. ISBN-10:013168728X (2007)
3. Fisher, R.A.: The use of multiple measurements in taxonomic problems. *Ann. Eugenics* **7**, 179–188 (1936)
4. Ting, K.M.: Confusion Matrix. *Encyclopedia of Machine Learning*, 1st edn. Springer, Berlin, p. 209. ISBN-10: 0387307680 (2011)
5. Fawcett, T.: An introduction to ROC analysis. *Pattern Recogn. Lett.* **27**(2006), 861–874 (2006)

# A Neuro-Fuzzy Approach to Diagnose and Classify Learning Disability

Kavita Jain, Pooja Manghirmalani Mishra and Sushil Kulkarni

**Abstract** The aim of this study is to compare two supervised artificial neural network models for diagnosing a child with learning disability. Once diagnosed, then a fuzzy expert system is applied to correctly classify the type of learning disability in a child. The endeavor is to support the special education community in their quest to be with the mainstream. The initial part of the paper gives a comprehensive study of the different mechanisms of diagnosing learning disability. Models are designed by implementing two soft computing techniques called Single-Layer Perceptron and Learning Vector Quantization. These models classify a child as learning disabled or nonlearning disabled. Once diagnosed with learning disability, fuzzy-based approach is used further to classify them into types of learning disability that is Dyslexia, Dysgraphia, and Dyscalculia. The models are trained using the parameters of curriculum-based test. The paper proposes a methodology of not only detecting learning disability but also the type of learning disability.

**Keywords** Learning disability · Single-layer perceptron · Learning vector quantization · Fuzzy expert system

---

K. Jain (✉) · P. M. Mishra  
Department of Computer Science, University of Mumbai, Mumbai-98, India  
e-mail: cavita\_jain@yahoo.com

P. M. Mishra  
e-mail: pmanghirmalani@gmail.com

S. Kulkarni  
Department of Mathematics, Jai Hind College, Mumbai-20, India  
e-mail: sushiltry@gmail.com

## 1 Introduction

Learning disability [LD] denotes to a neurological condition which disturbs an individual's ability to think and remember. It is established in disorders of listening, thinking, reading, writing, spelling, or arithmetic [1]. These individuals are not attributed to medical, emotional, or environmental causes despite having normal intellectual abilities [2].

LD can be broadly classified into three types. They are difficulties in learning with respect to read (Dyslexia), to write (Dysgraphia) or to do simple mathematical calculations (Dyscalculia) [4] which are often termed as special learning disabilities. Kirk [3] stated that, children with special learning disabilities exhibit a disorder in one or more of the basic psychological processes involved in understanding or in using spoken or written language. These may be manifested in disorders of listening, thinking, talking, reading, writing, spelling, or arithmetic. They include conditions which have been referred to as perceptual handicaps, brain injury, minimal brain dysfunction, dyslexia, developmental aphasia, etc., and they do not include learning problems which are due primarily to visual, hearing, or motor handicaps, to mental retardation, emotional disturbance or to environmental deprivation.

For diagnosing LD, there does not exist a global method. Mostly detection is done using Wechsler Intelligence Scale for Children (WISC) test [5], conducted in the supervision of special educators and with the observation of parent and teachers. In this context, computational approach to detect LD is quite significant. Once LD is successfully diagnosed, there is no substantial work done to classify LD into its three types.

This paper proposes a model for diagnosis and classification of LD. Section 2 of this paper explores in detail different computational methods and models applied in or diagnosing LD. Having elaborately explored different approaches, we have found that there are still possible ways to improvise the entire diagnosing process. Section 3 describes the system parameters and Sect. 4 introduces the proposed models and compares their diagnosis results. Section 5 gives the system results based on accuracy, sensitivity, specificity for the diagnosing phase. Section 6 discusses the classification of LD which is done by applying a fuzzy-based approach and Sect. 7 gives the result for classification phase of the experiment. Finally Sect. 8 discusses the conclusion and future works by the authors.

## 2 Taxonomy of Computational Diagnosis of Learning Disability

The different computational methods and models used in detecting learning disability can be classified into four groups. The grouping is done based on the broader theoretical foundation and computational characteristics of the models and methods applied. The following subsections deal with such models and methods.



## ***2.1 Digital Signal Processing Methodologies***

Reitano [6] analyses and compares spoken words with prerecorded and properly pronounced phonemes. The mispronounced phonemes are indicated which led to the diagnosis of LD. Fonseca et al. [7] conducted electroencephalograms (EEG) to detect abnormalities related to electrical activity of the brain by studying different brainwaves. He concluded that there is a significant difference in brainwaves of normal and learning disabled children. Assecondi et al. [8] carried out Electroencephalograms while awake and resting and the values for absolute and relative powers were calculated. Children with severe reading/ writing disabilities had more delta activity in frontal-temporal regions and those with less intense disabilities had more theta activity and less relative alpha activity. A study of the relationship between quantitative EEG variables and IQ provided greater knowledge about the biological aspects related to LDs. Bonte et al. [9] compared the values of amplitude and latency of some peaks in Reading Related Potential (RRP) of the dyslexia children with the reference template of normal children. The amplitude and latencies in RRP are based on *Dynamic Time Warping Technique* and this technique is used in the speech processing to match 1-Dimensional signals [10]. This comparison indicated a valuable tool in understanding of dyslexia [11].

## ***2.2 Digital Image Processing (DIP) Methodologies***

Mico-Tormos et al. [12] inferred that eye movements of even an infant could indicate LD by analyzing the responses of the movement of eye through oculographic signals. From computer analysis of records, high correlation between the neural activity and eye response, as well as linear dependency of eye movement on stimulus velocity has been documented by numerous studies [13, 14]. Pavlidis [15] observed that erratic and strikingly large number of regressive eye movements pointed to dyslexia.

## ***2.3 Soft Computing Methodologies***

The various components of soft computing used to diagnose LD can be viewed as follows:

### **2.3.1 Artificial Neural Network (ANN)**

Jain et al. [16] proposed a simple perceptron based ANN model and it comprised of a single input layer with eleven units which correspond to different sections of a curriculum-based test and one output unit for diagnosing LD. Bullinaria [17] on

the other hand applied a multilayer feed forward perceptron to diagnose dyslexia where letter strings were mapped to phoneme strings in multisyllabic words. Wu et al. [18] proved that a multilayer perceptron with back propagation gave better results in diagnosing LD. He later attempted to diagnose LD using support vector machines [19]. Manghirmalani et al. [20] proposed a soft computing technique called Learning Vector Quantization. The model classifies a child as learning disabled or nonlearning disabled. Once diagnosed with learning disability, rule-based approach is used further to classify them into types of learning disability that is dyslexia, dysgraphia, and dyscalculia.

### **2.3.2 Fuzzy Systems (FS)**

Sanchez et al. [21] proposed a technique to deal with the vagueness of the data by analyzing the set of different granularities based on more flexible representation of polygons. Manghirmalani et al. [39] used fuzzy expert systems to classify the type of LD out of the correctly identified LD cases. Fuzzy expert system uses rules which are the most fundamental part for classification purpose and thus successfully classifying the LD cases into one of the seven types of LD.

### **2.3.3 Genetic Algorithms with Fuzzy Systems**

Georgopoulos et al. [22] put forth a strong mechanism to deal with the inputs whose information is not adequate by combining Fuzzy Cognitive Maps (FCM) and genetic algorithm (GA). This combination of FCM and GA led to better accuracy of diagnosing LD.

## ***2.4 Hybridized Computational Techniques***

Hybridized approaches in LD include attempts to apply video and signal processing techniques along with soft computing techniques. Salhi et al. [23] used both wavelet transforms and neural networks to diagnose LD from Pathological Voices. The results using the multilayer neural network (MNN) classifier gives the best correct classification. A feature vector based on wavelet coefficients was used for classification of normal and pathological speech data. The MNN with BP used as a classifier has been proved to be more efficient and more precise than the time-frequency analysis method. The MNN classifier represents a low cost, accurate, and automatic tool for pathological voice classification using wavelet coefficients. Using the MNN with BP the system gave the classification rate between 70–100 %. learner is as close as possible to learner is as close as possible to Novak et al. [24] have calculated a set of features from signals of horizontal and vertical eye movement using self-organizing map and genetic algorithm (GA). They concluded that the reading speed increased with the

probability of the patient being healthy. Wu et al. [25] combined different feature selection algorithms like brute-force, greedy, and GA along with ANN to improve the identification rate of LD. Macaš et al. [26] developed a system for extracting the features of eye movements from time and frequency domain. They concluded that back propagation-based classification gave better results than that offered by Bayes' and Kohonen network.

### 3 Collection of Parameters

A curriculum-based test was designed with respect to the syllabus of primary-level school going children. This test was conducted in schools for collecting non-LD and testing datasets. Historic data for LD cases were collected from LD Clinics of Government hospitals where the tests were conducted in real-time medical environments. The system was fed with 11 input units which correspond to 11 different sections of the curriculum-based test [16]. Dataset consists of 240 cases, out of which 160 are of normal children and 80 of LD children. The system was trained using 120 data items and the remaining was used to test the network.

### 4 Diagnosis Model

Single layer Perceptron and LVQ are supervised neural network algorithms. Both the soft computing models have been tested and trained using the same dataset and hence their comparison is of relevance with respect to the problem of diagnosing LD using artificial neural networks.

#### 4.1 Single Layer Perceptron

The proposed system is called Perceptron based Learning Disability Detector (PLEDDOR). PLEDDOR consists of one input layer and one output layer. The goal of the Perceptron algorithm is to find a combination of expert predictions such that the performance of the learner is as close as possible to the best combination of experts. The Perceptron maps an input vector  $x = [x_1, x_2, x_3, \dots, x_n]^T$  to a binary output  $y$ . The value of  $x$  and  $y$  is taken to be 0 and 1. Thus, the model could be looked as a simple two-class classifier [27]. In this manuscript, it is classifying the data set into 'Normal' and 'Learning Disabled,' that is, for taking the value 1 for Normal children and 0 for Learning Disabled children. A weight vector  $w = [w_1, w_2, w_3, \dots, w_n]^T$ , is used to train the network [28]. The model consists of one input layer and one output layer. In the input layer, the proposed model is fed in with 11 inputs corresponding

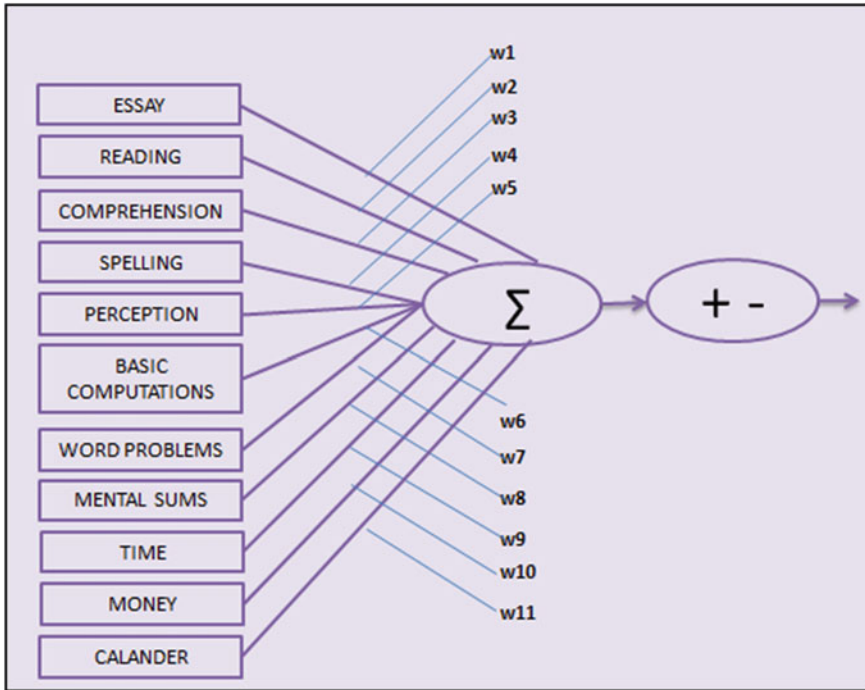


Fig. 1 Perceptron model with system parameters

to the 11 sections of the curriculum-based test as shown in Fig. 1. On these 11 inputs, 11 weight vectors ( $w_1 - w_{11}$ ) are applied.

---

**Algorithm**

---

1. Create a Perceptron with n inputs and n weights.
  2. Initialize the weights to random real values.
  3. Iterate through the training set, collecting all data misclassified by the current set of weights.
  4. If all the data is classified correctly, output the weights and quit.
  5. If output is low, increment weights for all inputs which are 1.
  6. If output is high, decrement weights for all the inputs which are 1.
- 

1. Applying Activation function

The activation function used in the system is given by:  $f(z) = 1$  if  $z - \theta \geq 0$ ;  $f(z) = 0$  if  $z - \theta < 0$  where  $z = w^T x$  and  $\theta$  is a threshold, which is called as 'LD threshold'. After experimental results, the value of LD threshold is fixed as 30.

2. Training of the network

The PLEDDOR is trained using the training pair  $\{x^1, d^1\}, \{x^2, d^2\}, \dots, \{x_m, d_m\}$ ; where  $x^k$  is the  $k$ th input vector and  $d^k = \{1, 0\}$  where  $1 \rightarrow$  Normal;  $0 \rightarrow$  Learning Disabled. The system is trained by adjusting the weight vector to make the output  $y^k$  corresponding to the input  $x^k$  match with the desired output  $d^k$ .

**4.2 Learning Vector Quantization (LVQ)**

The second proposed system is called Diagnosis & Classification using Learning Vector Quantization for Learning Disability (DICQOLD) applying the scheme proposed by Kohonen [29]. LVQ is a special case of artificial neural network (ANN) which applies a winner-take all Hebbian Learning-based approach [30]. Here one regulates the pattern for each data which is closest to the input vector agreeing to a Euclidian distance. The location of the winner prototype is thus computed.

This learning technique uses the class information to reposition the weight vectors ( $w_j$ ) slightly, so as to increase the quality of the classifier. The basic LVQ approach is quite intuitive. This allows us to use the known classification labels of the inputs to find the best classification label for each ( $w_j$ ). The objective of LVQ is the representation of a set of feature vectors  $x \in \chi \subset IR^n$  by a set of prototypes  $\nu = \{v_1, v_2 \dots v_c\} \subset IR^n$ . Thus, vector quantization can also be seen as a mapping from a dimensional Euclidean space into the finite set  $\nu \in IR^n$ , also referred to as the codebook [31]. The network consists of an input layer and an output layer. Each node in the input layer is connected directly to the cells, or nodes, in the output layer. A prototype vector is associated with each cell in the output layer [32].

---

**Algorithm:**

---

1. Initialize weights vectors (for the system it is  $w_1 - w_{11}$ ).
  2. Initialize learning rate ( $\alpha$ ), (for the system it is 0.8).
  3. For each training input vector  $x$  (for the system it is  $x_1$  to  $x_{11}$ ), do steps 4 to 5.
  4. Compute  $J$  using squared Euclidean distance:  $D(j) = \sum (w_{ij} - x_j) * D(j) = \sum (w_{ij} - x_j)$  Find  $j$  when  $D(j)$  is minimum. This leads to the classification of the entire dataset into two classes, one pertaining to LD and the other pertaining to the normal class.  $C_j$  indicates the class of LD;  $C_j = 0$  indicates that the child is suffering from LD and  $C_j = 1$  indicates the child is normal.
  5. Update  $W_j$  as follows: If  $t = C_j$ , then  $W_j(\text{new}) = W_j(\text{old}) + \alpha [x - W_j(\text{old})]$  If  $t \neq C_j$ , then  $W_j(\text{new}) = W_j(\text{old}) - \alpha [x - W_j(\text{old})]$
  6. Reduce  $\alpha$  by a small amount 0.01.
  7. System is tested for every new value of  $\alpha$  till the result shows redundancy. This is the stopping condition.
-

## 5 Results and Discussions–Diagnosing Phase

### 5.1 Detection Measures

The paper uses the following conventional detection measures as benchmarks to compare the performance of the proposed model with that of similar models.

- *Accuracy*: ratio of the number of correct classification of input-output data to the total number of training data.
- *Sensitivity*: ratio of the correctly classified LD cases to the total number of LD cases.
- *Specificity*: ratio of the correctly classified non-LD cases to the total number of non-LD cases.
  - a. System performance measures for PLEDDOR: Accuracy = 84 %, Sensitivity = 80 %, Specificity = 80 %.
  - b. System performance measures for DICQOLD: Accuracy = 91.8 %, Sensitivity = 84.5 %, Specificity = 84.5 %.

### 5.2 Comparison

It is observed that as the number of samples increases, the accuracy of the system also increases and then it tends to stabilize from the training dataset size 90 onwards. Testing is done using 100 samples. For PLEDDOR the accuracy of 84 % is achieved whereas for DICQOLD an accuracy of almost 92 % is achieved.

## 6 Classification Model

Once LD has been detected, the system further classifies the case into the type/s of LD. Classification is done using the fuzzy logic [33]. It consists of crisp input stage, fuzzy inference system, and a crisp output stage. The input stage maps inputs to apt membership functions and truth values. The processing stage invokes each suitable rule and generates a result for each, then combines the results of the rules. Finally, the output stage converts the combined result back into a specific control output value [34, 35]. This is done using ‘IF variable IS property THEN action’ rule [36].

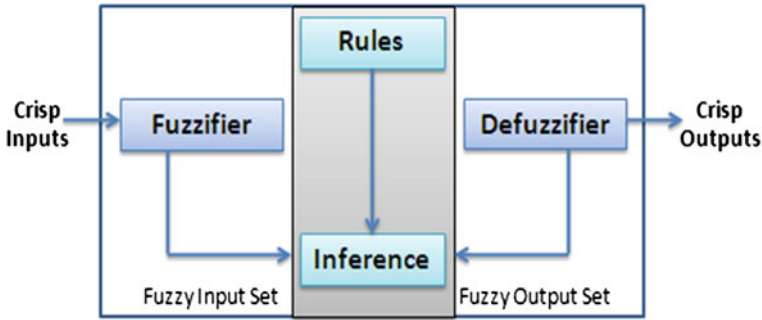


Fig. 2 Fuzzy inference system

## 6.1 Fuzzy Logic System

A fuzzy logic system (FLS) can be defined as the nonlinear mapping of an input data set to a scalar output data. A FLS consists of four main parts: fuzzifier, rules, inference engine, and defuzzifier. FLS is one of the most famous applications of fuzzy logic and fuzzy sets theory. They can be helpful to achieve classification tasks, offline process simulation, and diagnosis, online decision support tools and process control [37]. As shown in Fig. 2, a crisp set of input data are gathered and converted to a fuzzy set using fuzzy linguistic variables, fuzzy linguistic terms, and membership functions. This step is known as fuzzification. Afterward, an inference is made based on a set of rules. And lastly, the resulting fuzzy output is mapped to a crisp output using the membership functions, in the defuzzification step.

## 6.2 Fuzzy Modeling

As show in the Fig. 3, given below are the seven steps of fuzzy model applied to the data [38].

1. Define the linguistic variables and terms.
2. Construct the membership functions.
3. Construct the rule base.
4. Convert crisp input data to fuzzy values using membership functions.
5. Applying implication method.
6. Aggregating all output.
7. Convert the output data to nonfuzzy values.

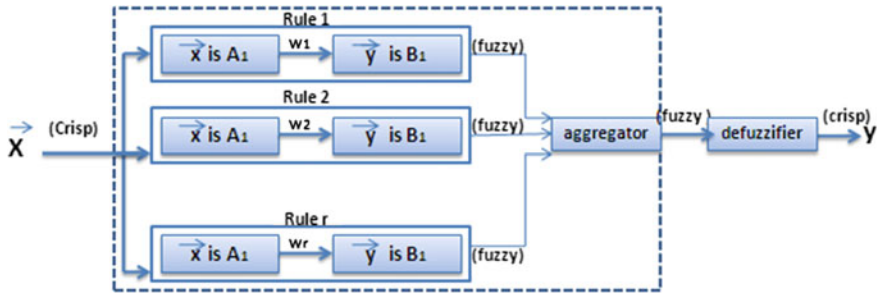


Fig. 3 Fuzzy expert system steps

### 6.3 Rules for Diagnosis

- Case-1: IF score low in essay, reading, comprehension, spelling, perception, solve, word problems, mental sums, time, money; THEN Dyslexia, Dysgraphia and Dyscalculia
- Case-2: IF low in of reading, comprehension, perception, word problem; THEN Dyslexia
- Case-3: IF low in of spelling, comprehension, essay; THEN Dysgraphia
- Case-4: IF low in of solve, mental sums, word problems, sums related to time, calendar, money; THEN Dyscalculia
- Case-5: IF low in of reading, comprehension, perception, word problem, spelling, essay; THEN Dyslexia and Dysgraphia

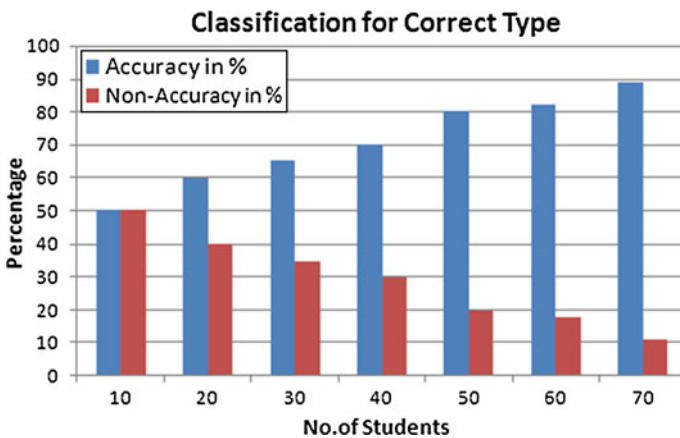
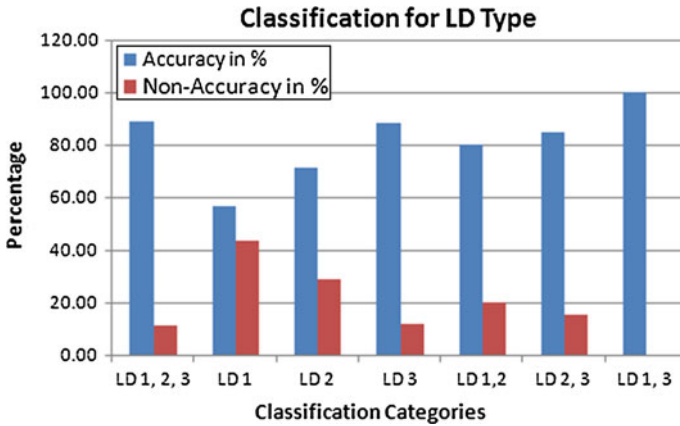


Fig. 4 Classification for correct type of LD showing the accuracy and the nonaccuracy during the training phase. accuracy and the nonaccuracy during the training phase





**Fig. 5** Classification for specific LD showing the accuracy and the nonaccuracy during the training phase. accuracy and the nonaccuracy during the training phase

Case-6: IF low in of reading, comprehension, perception, solve, mental sums, word problems, sums related to time, calendar and money; THEN Dyslexia and Dyscalculia

Case-7: IF low in of spelling, comprehension essay, solve, mental sums, word problems, sums related to time, calendar, money; THEN Dysgraphia and Dyscalculia.

## 7 Results and Discussions—Classification Phase

The classification system gives an accuracy of 90% Figs. 4 and 5.

## 8 Conclusion

We have presented a comparison between two supervised artificial neural network algorithms names Single-Layer Perceptron and Learning Vector Quantization. We have observe, when trained and tested with the same dataset, the accuracy measure between both these approaches is competitive. However, the model of LVQ has proved to be slightly more accurate with respect to the Single-Layer Perceptron. However, there is scope for further enhancement of system by finding a combination of algorithms so as to build up a model that is satisfactorily accurate. It is also seen that on increasing the number of data in the training set of the system, the overall accuracy in both the models shows a promising growth.

In future we intend to explore the possibility of parameter classification in order to distinguish irrelevant and superfluous variables which might lead to decrease in diagnosis and classification process time and increase in accuracy. This can be beneficial for the special educators, doctors, and teachers by providing suggestions that lead to the exclusion of redundant tests and saving of time needed for diagnosing LD. On the whole, the focus of our research is to identify early diagnosis of LD and to support special education community in their quest to be with mainstream.

## References

1. Kirk, S.A.: Educating exceptional children book. Wadsworth Publishing, ISBN: 0547124139
2. Weyandt, L.L.: The physiological bases of cognitive and behavioral disorders. Blausen Medical Communications, United States
3. Lerner, J.W.: Learning disabilities: theories, diagnosis, and teaching strategies. Houghton Mifflin, Boston ISBN 0395961149
4. Fletcher, J.M., Francis, D.J., Rourke, B.P., Shaywitz, B.A., Shaywitz, S.E.: Classification of learning disabilities: an evidencebased evaluation. (1993)
5. Kaplan, R.M., Saccuzzo, D.P.: Psychological testing: principles, applications, and issues, 7th edn. p. 262. Wadsworth, Belmont ISBN 978-0-495-09555-2 (citing Wechsler (1958) The Measurement and Appraisal of Adult Intelligence) (2009)
6. Carmen T.R.: System and method for dyslexia detection by analyzing spoken and written words. US Patent 6,535,853 B1, 18 Mar 2003
7. Fonseca, L.C., Tedrus, G.M.A.S., Chiodi, M.G., Cerqueira, J.N. Tonelotto J.M.F.: Quantitative EEG in children with learning disabilities. *Anal. Band power*. **64**(2-B):376–381 (2006)
8. Asseondi, S., Casarotto, S., Bianchi, A.M., Chiarenza, G.A., D'Asseler, Y., Lemahieu, I.: Automatic measurement of reading related potentials in dyslexia. In: IEEE Benelux EMBS Symposium, Belgian Day on Biomedical Engineering, 7–8 Dec 2006
9. Bonte, M.L.: Developmental dyslexia: ERP correlates of anomalous phonological processing during spoken word recognition. *Cognitive Brain Res.* **21**, 360–376 (2004)
10. Rath, T.M., Manmatha, R.: Word image matching using dynamic time warping. *Natl. Sci. Found.*
11. Chiarenza, G.A.: Motor-perceptual functions in children with developmental reading disorders: neuropsychophysiological analysis. *J. Learn. Disabil.* **23**(6), 375–385 (1990)
12. Pau, M-T., David, C-F., Daniel, N.: Early Dyslexia Detection Techniques by means of Oculographic Signals. In: 2nd European Medical and Biological Engineering Conference, Austria, Vienna (2002)
13. Merrill, C.E., Jordan, D.R.: Dyslexia in the classroom. pp.1–4. publishing Company, New York (1977)
14. Sheppard, R.: Why kids can't read. *Maclean's*. **111**(36), 40–48 (1998)
15. George T.P.: Eye movement in dyslexia: their diagnostic significance. *J. Learn. Disabil.* (2001)
16. Jain, K., Manghirmalani, P., Dongardive, J., Abraham, S.: Computational diagnosis of learning Disability. *Int. J. Recent Trends Eng.* **2**(3), (2009)
17. Bullinaria, J.A.: Neural network models of reading multi-syllabic words. In: 1993 International Joint Conference on Neural Networks
18. Wu, T-K., Meng, Y-R., Huang, S-C.: Application of ANN to the identification of students with LD. *IC-AI*: 162–168 (2006)
19. Wu, T-K., Meng, Y-R., Huang, S-C.: Identifying and diagnosing students with LD using ANN and SVM. In: IEEE International Joint Conference on Neural Networks, Vancouver (2006)
20. Manghirmalani, P., Panthaky, Z., Jain, K.: Learning disability diagnosis and classification-a soft computing approach. In: IEEE World Congress on Information and Communication Technologies (WICT), 2011 (doi:[10.1109/WICT.2011.6141292](https://doi.org/10.1109/WICT.2011.6141292))

21. Sanchez, L., Palacios, A., Suarez, M.R., Couso, I.: Graphical exploratory analysis of vague data in the early diagnosis of dyslexia.
22. Georgopoulos, V., Stylios, C.: Genetic algorithm enhanced fuzzy cognitive maps for medical diagnosis. In: IEEE 2008
23. Salhi, L., Talbi, M., Cherif, A.: Voice disorders identification using hybrid approach: wavelet analysis and multilayer neural networks. Proceedings of World Academy of Science, Engineering and Technology, **35**, ISSN 2070–374 (2008)
24. Novak, D., Kordk, P., Macas, M., Vyhnaek, M., Brzezny, R., Lhotska, L.: School children dyslexia analysis using self organizing maps. In: IEEE 26th Annual International Conference, San Francisco 2004
25. Wu, T-K., Meng, Y-R., Huang, S-C.: Effects of feature selection on the identification of students with LD Using ANN. Springer-Verlag, Heidelberg (2006)
26. Macaš, M., Lhotská, L., Novák, D.: Bioinspired methods for analysis and classification of reading eye movements of dyslexic children. In: Czech Republic NiSIs Symposium, Czech Technical University, Prague Department of Cybernetics (2005)
27. Chiarenza, G.A.: Motor-perceptual functions in children with developmental reading disorders: neuro psycho physiological analysis. *J. Learn. Disabil.* **23**(6), 375–385 (1990)
28. Bonte, M.L.: Developmental dyslexia: ERP correlates of anomalous phonological processing during spoken word recognition. *Cognitive Brain Research* **21**, 360–376 (2004)
29. Kohonen, T.: Self-Organization and Associative Memory, 3rd edn. Springer-Verlag, Berlin (1989)
30. Lerner, J.W.: Learning disabilities: theories, diagnosis, and teaching strategies. Houghton Mifflin, Boston (2000) ISBN 0395961149
31. Sivamanbam, S.N., Sumathi, S., Deepa, S.N.: Introduction to neural networks using MATLAB 6.0. ISBN 9780070591127
32. Karayiannis, N.B.: A Methodology for Constructing fuzzy algorithms for learning vector quantization. *IEEE Trans. Neural Networks* **8**(3), (1997). doi:[1045-9227\(97\)00466-9](https://doi.org/10.1045-9227(97)00466-9)
33. Yegnanarayana, B.: Artificial Neural Networks. Prentice Hall India, Publication (2006)
34. Zadeh, L.A.: Fuzzy sets and systems. In: Fox, J. (ed.) System Theory, pp. 29–39. Polytechnic Press, Brooklyn, NY (1965)
35. Zadeh, L.A.: Fuzzy sets. *Information and Control* **8**(3), 338–353 (1965)
36. Gerla, G.: Fuzzy Logic Programming and fuzzy control. *Studia Logica* **79**, 231–254 (2005)
37. Arjona, M.A.L., Escarela-Perez, R., Melgoza-Vázquez, E., Hernández, C. F.: Convergence improvement in two-dimensional finite element nonlinear magnetic problems—a fuzzy logic approach. *Finite Elements in Analysis and Design, Science, Direct* (2004) doi:[10.1016/S0168-874X\(02\)00165-8](https://doi.org/10.1016/S0168-874X(02)00165-8).
38. Yuan, G.J.K.: Fuzzy sets and fuzzy logic: theory and applications
39. Manghirmalani, P., More, D., Jain, K.: A fuzzy approach to classify learning disability. *Int. J. Adv. Res. Artif. Intell.* **1**(2), U.S ISSN:2165–4069(Online), U.S ISSN : 2165–4050(Print) (2012)

# A Review of Hybrid Machine Learning Approaches in Cognitive Classification

Shantipriya Parida and Satchidananda Dehuri

**Abstract** The classification of functional magnetic imaging resonance (fMRI) data involves many challenges due to the problem of high dimensionality, noise, and limited training samples. In particular, mental states classification, decoding brain activation, and finding the variable of interest by using fMRI data was one of the focused research topics among machine learning researchers during past few decades. In the context of classification, algorithms have biases, i.e., an algorithm perform better in one dataset may become worse in other dataset. To overcome the limitations of individual techniques, hybridization or fusion of these machine learning techniques proposed in recent years which have shown promising result and open up new direction of research. This paper reviews the hybrid machine learning techniques used in cognitive classification by giving proper attention to their performance and limitations. As a result, various domain specific techniques are identified in addition to many open research challenges.

**Keywords** Functional magnetic resonance imaging · Machine learning · General linear model · Genetic algorithm · Particle swarm optimization

## 1 Introduction

Since decade after decade, the complexity of brain has been the primary research of many studies and experiment. Although the advancement of technologies improve our understanding about brain, still far from being completely understood.

---

S. Parida (✉)

Carrier Software and Core Network, Huawei Technologies India Pvt Ltd, The Leela Palace,  
23 Airport Road, Bangalore, Karnataka 560008, India  
e-mail: shantipriya.parida@gmail.com

S. Dehuri

Department of Systems Engineering, Ajou University, San 5, Woncheon-dong,  
Yeongtong-gu suwon 443-749, South Korea  
e-mail: satchi@ajou.ac.kr

The cognitive neuroscience is evolving with the latest neuroimaging techniques combined with experimental methodologies which provide us images of the structure or function of the brain. The magnetic resonance imaging (MRI) uses a powerful magnetic field and radio waves to produce highly transparent images of the human body which shows injury, diseases process, or abnormal condition [1]. The fMRI is a technology to detect the localized changes in blood flow and blood oxygenation which occur in the brain in response to neural activity [2]. The classification techniques can identify many types of activation patterns within or shared across subjects [3].

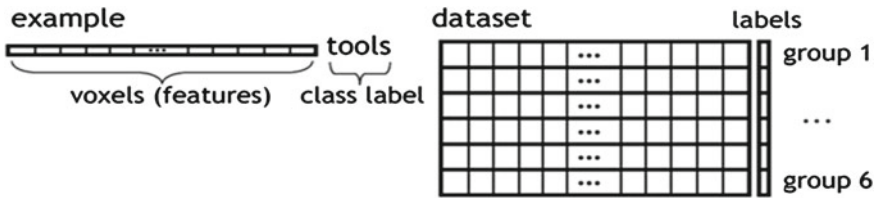
As a part of this review, this study focus on the challenges involved in the classification task and different machine learning approaches performing the classification activities and the requirement of hybrid classification. The various classification approaches for cognitive states discrimination developed under the umbrella of hybrid machine learning techniques have been reviewed.

The rest of the paper is set out as follows. In Sect. 2, the challenges in cognitive classification have been studied. Some of the popular machine learning approaches used for cognitive classification is discussed in Sect. 3. Hybrid techniques and their applications are reviewed in Sect. 4. Future perspectives and conclusions are derived in Sects. 5 and 6 respectively.

## 2 Challenges in Cognitive Classification

The fMRI involves many challenges starting from image acquisition to final data analysis, which the neuroscientists trying to make best use of the technique [4]. In cognitive neuroscience the key challenge is to identify the mapping between neural activity and mental representations [5]. The challenge in fMRI data analysis is due to the noisy and weakly activated voxel in the acquired images and may therefore go undetected [6]. The data obtained from fMRI neuroimaging are especially rich and complex [7] and fMRI generates vast amount of data which are handled using computer-based methods [8]. The main factors cause the fMRI data analysis so complex is as follows [9]: (i) extremely large feature to instance ratio; (ii) spatial relationship between features; (iii) low contrast to noise ratio; and (iv) redundancy in the feature set.

One of the major challenges is using multivariate classification techniques to decode cognitive states from fMRI images. The problem involved in this scenario is high intersubject variability in the spatial locations and functional activation degrees [10]. The multivariate pattern recognition (MPR) methods are becoming popular rapidly for fMRI data analysis as these methods detect activity patterns in brain regions which can collectively discriminate one cognitive or participant group from another. The performance of these methods often limited due to the challenge that the number of regions considered in the fMRI data (“features”) analysis is larger compared to the number of observations (“trials or participants”) [11]. The evolved of real-time fMRI classification opens new direction for interactive self-regulation, as in this technique, the brain response can be modeled better. The major challenges



**Fig. 1** An example where voxels are features as a row vector (*left*) and a dataset as matrix of such vectors (*right*) (extracted from [14])

in case of real-time fMRI is that the number of training instances comparative less and the classifier must be capable of perform within the time constraint [12].

### 3 Machine Learning Approaches in Cognitive Classification

One of the popular techniques used in recent development is machine learning classifiers for classifying cognitive states by analyzing the fMRI data. The trained classifier represents a function of the form [13]:

$$\Phi : fMRI (t, t + n) \rightarrow Y, \tag{1}$$

where  $fMRI (t, t + n)$  is the observed fMRI data during the interval from time  $t$  to  $t + n$ , and  $Y$  is a finite set of cognitive states to be discriminated.

$\Phi (fMRI (t, t + n))$  the classifier prediction regarding which cognitive state gave rise to the observed fMRI data  $fMRI (t, t + n)$ .

In case of neuroimaging [14], the voxel represent features and activation of subject denoted as class is shown in Fig. 1.

### 4 Hybrid Techniques and Application

The hybrid classifier tries to use the desirable properties of each individual classifier and emphasizes to improve the overall accuracy in the combined approach.

Anderson et al. [15], have proposed a hybrid SVM-Markov model to predict accurately the real-time cognitive states such as the subject is viewing a video while either resting or nicotine craving. The markov transition matrix contributed in improving the classification accuracy by effectively removing unlikely state transition and the transition matrix acts as high pass filter for SVM probability prediction.

Wang [16] has combined the advantages of both general linear model (GLM) and SVM to develop a hybrid technique for fMRI data analysis. The proposed technique used the power of SVM for data derive reference function and GLM for statistical

inference. His experimental study confirms that the combined approach shown better sensitive than the regular GLM for detecting the sensorimotor task.

Yang et al. [17], have proposed hybrid machine learning approach for classifying the schizophrenia and healthy control subjects. Their experimental result shows that the hybrid approach classification accuracy is promising and able to extract the discriminating information to classify schizophrenia efficiently.

Kharrat et al. [18] have proposed a hybrid machine learning approach based on genetic algorithm (GA) and SVM for fMRI brain tissues classification. The feature extraction is performed using spatial gray-level dependence method (SGLDM) and feature selection by GA-based global search method. The selected feature subset is given as input to the SVM for classification. The proposed method has shown very promising result for classifying the healthy and pathological brain.

Dahshan et al. [19], have proposed a hybrid method for classifying subjects as normal or abnormal using MRI images. The proposed technique consists of discrete wavelet transforms (DWT), the principal component analysis (PCA), feed forward artificial neural network (FP-ANN), and k-nearest neighbor (k-NN). The experimental result confirms that it is efficient in classifying the normal and abnormal brain.

Similarly, Zhang et al. [20], have developed a hybrid classifier to distinguish between the normal and abnormal of the brain using the MR images. In this approach the feature extraction performed using the wavelet transform and subsequently it applied the PCA to reduce the dimensions of the features. The reduced features input to the neural network (NN) and the parameters optimized by the chaotic particle swarm optimization (ACPSO). The k-fold cross validation has been used for enhancing the generalization.

Roussos et al. [21], have extended the ICA and propose a hybrid wavelet-ICA (W-ICA) model for transforming the signals into domain and apply the Bayesian inference. The directed acyclic graph (DAG) which is also known as Bayesian network structure represents the probabilistic dependence relationships. They applied this WICA model to fMRI data. This new approach showing great interest but further analysis required to find the comparative study with other hybrid techniques and its usefulness applying on neuroscientific data.

Kim et al. [22], have proposed a hybrid ICA-Bayesian approach for identifying the differences between the brain regions of normal and abnormal subject. The correlation between brain regions in one group versus another measured by the approximate conditional score (ACL) and its observed that ICA-filtered data significantly improved the magnitude of the ACL score. The ICA for filtering noise components from fMRI datasets is recommended as it plays more significant in determining higher level correlations which are more sensitive to noisy datasets.

Li et al. [23] have presented a hybrid approach for brain state classification based on both statistical data analysis and graphical information modeling (model-based). The proposed framework consists of three components. The first component includes image enhancement, event prediction and detection where the event prediction is performed using the temporal cluster analysis (TCA). The second component includes feature extractions and modeling where the linear predictive coding (LPC) used for feature extraction and variational bayesian gaussian mixture model (VBGMM) used

for event classification. The third component includes graphical model based inference using the probabilistic graphical model. The experimental result has shown that the neural activities can be detected and classified using this hybrid approach. As part of further study, other complex neural activities need to test with this hybrid approach.

Tohka et al. [24], have proposed a hybrid-GA algorithm for solving the challenging finite mixture model (FMM) optimization which arises in the neuroimaging classification. The hybrid algorithm tested with T1-weighted MR brain scans of healthy and mental disorder (Alzheimer's diseases (AD), schizophrenia) subject. The hybrid-GA algorithm compared with the other FMM optimization algorithm and found most consistent and accurate although in some case other algorithms recommended for computational reasons. It is recommended to use this hybrid algorithm in many FMM optimization task and automatic image analysis procedure for brain imaging.

Abraham et al. [25], have proposed hybrid schemes which involves particle swarm optimization (PSO) algorithm-based rough set reduction for SVM applied to cognitive state classification. The PSO algorithm can find optimal regions of complex search spaces through interaction of particle in a population of studies and it is converging fast. Based on fMRI experiment they shown that the proposed scheme is feasible for classification for single or multiple subjects.

Brodersen et al. [26] have proposed a hybrid generative-embedding approach to address the two major challenges with fMRI classification, i.e., first challenge due to high dimensionality and low sample size and second challenge is that popular discriminative method like SVM rarely affords mechanistic interpretability. The proposed approach combined the dynamic causal models (DCMs) and SVMs. It shows that the generative-embedding approach achieves 98% accurate classification and performs better compared with conventional activation-based and correlation-based methods.

Cheng et al. [27], have proposed a hybrid generative/discriminative framework for brain region classification. The hybrid framework consists of two major parts such as "generative part" and "discriminative part". The idea of generative part is to choose a generative model capable of considering all ROI at the same time along with the relations between them. The discriminative part contains the "fisher kernels" which allows an effective general way of mixing generative and discriminative models for classification. In this approach, the data is represented using Fisher Score Space and classification using SVM. The experimental result shows that the hybrid approaches successfully discriminating between the healthy and schizophrenic patients based on analysis of brain MRI scan.

Zhang et al. [28] (after inspired from their earlier model [20]), have proposed a hybrid model based on forward neural network (FNN) for classifying the normal and abnormal states based on MR brain image. The proposed approach consists of five stages: (1) in the first stage, it use DWT to extract feature; (2) then in the second stage, use PCA to reduce feature size; (3) third stage contain k-fold stratified cross validation to prevent over-fitting; (4) in the fourth stage, it contain the FNN to construct the classifier; (5) in the final stage, it uses scaled chaotic artificial bee colony



(SCABC) to train the FNN. The SCABC-FNN classifier obtains 100 % classification accuracy to distinguish between normal and abnormal MRIs of the brain.

Jafarpour et al. [29], have proposed a robust classification technique for classifying normal and abnormal brain MRI. The proposed approach consists of the following techniques: gray level co-occurrence matrix (GLCM), PCA, linear discriminant analysis (LDA), ANN, and K-NN. The three stages of their work includes: feature extraction, feature reduction, and classification. The methodology effectively used the image features and employed hybrid feature reduction technique to distinguish the normal, multiple sclerosis (MS), and tumorial brain MRIs. The experimental study shows 100 % accuracy for normal, 100 % accuracy for tumoral, and 92.86 % for MS images with both ANN and KNN classifiers.

## 5 Future Perspectives

The hybrid feature reduction [29] applied on T2-weighted images and future research can extend to other type of MRI and more kind of brain disease. The SCABC-FNN classifier [28] which successfully distinguishes normal and abnormal MRIs of the brain can further explore for multi class and specific MRIs disorder and advanced wavelet transforms can be applied for improved features. One of the future directions for hybrid generative/discriminative method [27] is to explore more complex probabilistic model and introducing clinical data with more variability. The proposed hybrid GA algorithm [24] for solving FMM optimization problem arise in neuroimaging can be further use to study how to fully automate many FMM optimization task to develop automatic brain image analysis procedure. The hybrid framework which is based on statistical data analysis and graphical information modeling [23] can be further extending to dealing with complex neural activities. The hybrid wavelet-ICA [21] model can be further extended to consider the residual dependencies in the wavelet coefficient to enhance separation and to better match the structure of signals it can explore to adapt the dictionary itself. The hybrid classification method based on ACPSO [20] can be further extended to apply on other type of MR images, reducing computation time, focusing specific brain MRI disorder. The hybrid technique classifying the normal and abnormal classes [19] can be further extended to processing pathological brain tissues (e.g., lesion, tumors).

## 6 Conclusion

In this paper, we have walked through the recent developments of the hybrid techniques for brain state classification and discussed their efficiency and limitations. It has been observed that the hybrid techniques outperform the non-hybrid one. Hence, this paper prescribes to use hybrid machine learning techniques for

fMRI classification. Alongside it recommends toward fine tuning of parameters for enhancing user understandability, and interestingness.

## References

1. McGowan, J.C.: Basic principles of magnetic resonance imaging. *Neuroimaging Clin. N. Am.* **18**(4), 623–636 (2008)
2. Savoy, R.L.: Functional magnetic resonance imaging (fMRI), *Encyclopedia of Neuroscience*, 2nd edn. Birkhauser, Boston, MA (1996)
3. Etzel, J.A., Gazzola, V., Keysers, C.: An introduction to anatomical ROI-based fMRI classification analysis. *Brain Res.* **1282**, 114–125 (2009)
4. Amaro Jr, E., Barker, G.J.: Study design in fMRI: basic principles. *Brain Cogn.* **60**(3), 220–232 (2006)
5. Norman, K.A., Polyn, S.M., Detre, G.J., Haxby, J.V.: Beyond mind-reading: multi-voxel pattern analysis of fMRI data. *Trends Cogn. Sci.* **10**(9), 424–430 (2006)
6. Friman, O., Borga, M., Lundberg, P., Knutsson, H.: Detection and detrending in fMRI data analysis. *NeuroImage* **22**(2), 645–655 (2004)
7. Horwitz, B., Tagamets, M., McIntosh, A.R.: Neural modeling, functional brain imaging, and cognition. *Trends Cogn. Sci.* **3**(3), 91–98 (1999)
8. Nielsen, F.A., Christensen, M.S., Madsen, K.H., Lund, T.E., Hansen, L.K.: fMRI Neuroinformatics. *IEEE Eng. Med. Biol. Mag.* **25**(2), 112–119 (2006)
9. Kuncheva, L.I., Plumpton, C.O.: Choosing parameters for random subspace ensembles for fMRI classification. *Lect. Notes Comput. Sci.* **2010**(5997), 54–63 (2010)
10. Fan, Y., Shen, D., Davatzikos, C.: Detecting cognitive states from fMRI Images by machine learning and multivariate classification. In: *Proceedings of Conference on Computer Vision and Pattern Recognition Workshop*, IEEE Computer Society, Washington, DC, USA (2006)
11. Ryali, S., Supekar, K., Abrams, D.A., Menon, V.: Sparse logistic regression for whole-brain classification of fMRI data. *NeuroImage* **51**(2), 752–764 (2010)
12. Plumpton, C.O., Kuncheva, L.I.: On-line fMRI data classification using linear and ensemble classifier”. In: *20th International Conference Pattern Recognition*, pp. 4312–4315 (2010)
13. Mitchell, T.M., Hutchinson, R., Just, M.A., Niculescu, R.S., Wang, X.: Classifying instantaneous cognitive states from fMRI data. In: *American Medical Informatics Association, Symposium*, pp. 465–469 (2003)
14. Pereira, F., Mitchell, T., Botvinick, M.: Machine learning classifiers and fMRI: a tutorial overview. *NeuroImage* **45**(1), S199–S209 (2009)
15. Anderson, A., Han, D., Douglas, P.K., Bramen, J., Cohen, M.S.: Real-time functional MRI classification of brain states using Markov-SVM hybrid models: Peering inside the rt-fMRI black box. In: *Neural Information Processing Systems* (2011)
16. Wang, Z.: A hybrid SVM-GLM approach for fMRI data analysis. *NeuroImage* **46**(3), 608–615 (2009)
17. Yang, H., Liu, J., Sui, J., Pearlson, G., Calhoun, V.D.: A hybrid machine learning method for fusing fMRI and genetic data: combining both improves classification for schizophrenia. *Frontiers Hum. Neurosci.* **4**, (2010)
18. Kharrat, A., Gasmı, K., Messaoud, M.B., Benamrane, N., Abid, M.: A hybrid approach for automatic classification of brain MRI using genetic algorithm and support vector machine. *Leonardo J. Sci.* **9**(17), 71–82 (2010)
19. Sayed, E.L., Dahshan, E.L., Salem, Abdul- Badeeh. M., Yousin, T.H.: A hybrid technique for automatic MRI brain images classification, vol. LIV. *Studia Univ. Babeş. Bolyai, Romania* (2009)
20. Zhang, Y., Wang, S., Wu, L.: A novel method for magnetic resonance brain image classification based on adaptive chaotic PSO. *Prog. Electromagnet. Res.* **109**, 325–343 (2010)

21. Roussos, E., Roberts, S., Daubechies, I.: Variational Bayesian learning for wavelet independent component analysis. In: 25th Int. Workshop on Bayesian Inference and Maximum Entropy Methods in Science and Engineering, vol. 803, 274–281 (2005)
22. Kim, D., Burge, J., Lane, T., Pearlson, G.D., Kiehl, K.A., Calhoun, V.D.: Hybrid ICA-Bayesian network approach reveals distinct effective connectivity differences in schizophrenia. *NeuroImage* **42**(4), 1560–1568 (2008)
23. Li, C., Hao, Q., Guo, W., Hu, F.: A hybrid approach for compressive neural activity detection with functional MR images. In: Proceedings of 31th IEEE Conference on Engineering in Medicine and Biology Society, pp. 4787–4790 (2009)
24. Tohka, J., Krestyannikov, E., Dinov, I.D., Graham, A.M., Shattuck, D.W., Ruotsalainen, U., Toga, A.W.: Genetic algorithms for finite mixture model based voxel classification in neuroimaging. *IEEE Trans. Med. Imaging* **26**(5), 696–711 (2007)
25. Abraham, A., Liu, H.: Swarm intelligence based rough set reduction scheme for support vector machines. In: IEEE International Conference on Intelligence and Security Informatics, pp. 200–202 (2008)
26. Brodersen, K.H., Schofield, T.M., Leff, A.P., Ong, C.S., Lomakina, E.I., Buhmann, J.M., Stephan, K.E.: Generative embedding for model-based classification of fMRI data”. *PLoS Comput. Biol.* **7**(6), e1002079 (2011)
27. Cheng, D. S., Bicego, M., Castellani, U., Cristani, M., Cerruti, S., Bellani, M., Rambaldelli, G., Aztori, M., Brambilla, P., Murino, V.: A hybrid generative/discriminative method for classification of regions of interest in schizophrenia brain MRI, In: Proceedings of MICCAI09 workshop on Probabilistic Models for, Medical Image Analysis (2009)
28. Zhang, Y., Wu, L., Wang, S.: Magnetic resonance brain image classification by an improved artificial bee colony algorithm. *Prog. Electromagnet. Res.* **116**, 65–79 (2011)
29. Jafarpour, S., Sedghi, Z., Amirani, M.C.: A robust brain MRI classification with GLCM features. *Int. J. Comput. Appl.* **37**(12), 1–5 (2012)

# “A Safer Cloud”, Data Isolation and Security by Tus-Man Protocol

Tushar Bhardwaj, Manu Ram Pandit and Tarun Kumar Sharma

**Abstract** Today cloud computing is well-known for touching all periphery of technology with its on-demand and elastic capability. Ever since it has come into picture, security has remained a major concern. VM model is already known to be vulnerable to various issues. We introduce Tus-Man protocol which will act in addition to existing system to make computing secure enough for both service provider as well as service consumers. In this protocol, we suggest a tunnel-based protocol to make data transfer not only secure but also safe enough against any malicious attack.

**Keywords** Cloud computing · Security in cloud computing · Tus-Man algorithm (Cloud computing security protocol)

## 1 Introduction

Today cloud computing is well-known for touching all periphery of technology with its on-demand and elastic capability. Ever since it has come into picture, security has remained a major concern. VM model is already known to be vulnerable to various issues. We introduce Tus-Man protocol which will act in addition to existing system to make computing secure enough for both service provider as well as service consumers. In this protocol, we suggest a tunnel-based protocol to make data transfer

---

T. Bhardwaj (✉)  
M.T.U Noida, Noida, India  
e-mail: tusharbhardwaj19@gmail.com

M. R. Pandit  
BITS Pilani, Pilani, India  
e-mail: manupandit123@gmail.com

T. K. Sharma  
IIT Roorkee, Roorkee, India  
e-mail: taruniitr1@gmail.com

not only secure but also safe enough against any malicious attack. This paper is divided into two main sections viz. Top threats to cloud computing followed by description of Tus-Man protocol.

## 2 Top Threats to Cloud Computing

Before getting into the business to secure the public cloud let us look into the security threats to the world of cloud computing. We have enlisted the threats which we have been undertaken before writing this paper [1].

1. *Insecure interfaces and APIs*: The interfaces and the different APIs are open to the users for the communication among the different services. The security and the availability of the services highly depend on these interfaces and APIs. There are many activities like encryption, authentication, and access control mechanism that are monitored by these APIs.
2. *Malicious Insiders*: This is a very common attack for any organization. The main cause is the lack of transparency among the customers and the system. The introduction of IT and the management tool under the same roof leads to this problem.
3. *Shared Technology Issues*: Several vendors deliver their services in a highly scalable way by sharing the infrastructure. It is quite obvious that the elements that incorporate this so-called infrastructure (e.g., CPU and GPUs) are not kept isolated to match with the multitenancy architecture.
4. *Data Loss or Leakage*: The data is open for all in the cloud. As this is the main advantage of cloud computing, it leads to the data compromise. It can be done due to several reasons like lack of authentication, authorization, and audit (AAA) control. It also amplifies due to the increase in the number of users day-to-day.
5. *Account or Server Hijacking*: There are many methods like phishing, fraud, and exploitation that still prevail to hijack any server and hence its services. Passwords and credentials are mostly repeated which supports this kind of attack.

## 3 Tus-Man Protocol

Earlier we have studied that are many threats to the world of cloud computing like malicious insiders, data loss or leakage, account or server hijacking, and insecure interfaces and APIs. All the above-mentioned loopholes of the existing system lead us to focus on this highly increasing demanding field of security. So, we have proposed a protocol for the same. This protocol is assumed to be injected to the transport layer of the cloud provider communication system. Our aim is to secure the access mechanism and authentication system.

So, this protocol has two distinct but important features:

1. A secure access mechanism.
2. Authentication system (Fig. 1).

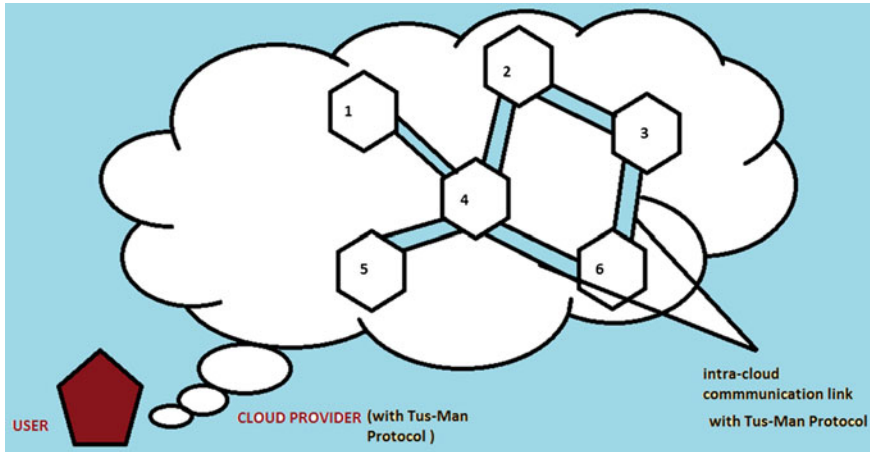


Fig. 1 Cloud communication channel injected with Tus-Man protocol

### 3.1 Introduction

When we talk about the access mechanism it is the user interaction with the system. It tells that how the user is able to access the data from the cloud. If the access mechanism is weak then any unauthorized user may enter the system and compromise the data. On the other authentication system means that only the authorized user should be allowed to enter the cloud and have access to it.

### 3.2 Basics

Before entering into the detail of the protocol let us brush up the basics of cloud computing. Whenever a user logs on with his/her user name and password, then he/she is able to access both the public and private data of his own cloud. In addition to that he/she can visualize the shared data (read only mode) of other users in that particular cloud. Consider the case of an organization where many employees are working and having their own private clouds. So, the main aim is to secure the access mechanism and authentication system as to prevent the malicious insiders and data loss attack of cloud computing [2, 3].

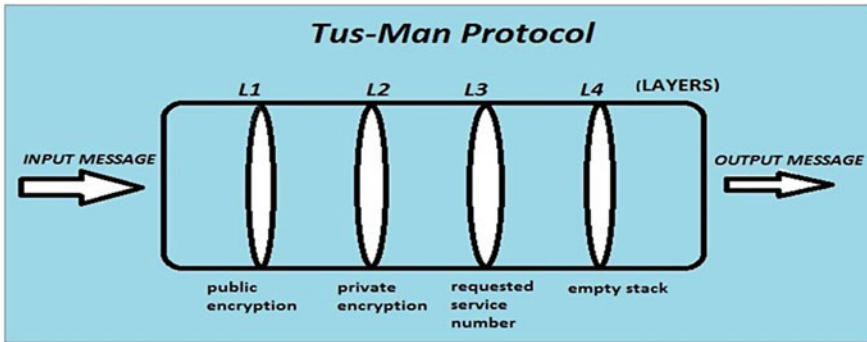


Fig. 2 Tus-Man protocol design

### 3.3 Design

Consider a tunnel with several layers. Each layer has a specific purpose attached with it. The tunnel has two ends one for input and other for output. There is a flow of data that have to pass from each subsequent layer to the destination, i.e., cloud. The system design is such that if at any layer the data halts or failed to fulfill the given criteria then the data flow will not be done. In other words the message that is traversing in the tunnel has to pass and qualify the necessary condition of each layer.

### 3.4 Working

In this section we will look into the structure of the protocol in detail (Fig. 2):

*Layer 1 (public key Encryption):* This is the first layer which contains the public information of the user. This layer authenticates the public credentials of the user and opens the gateway to the public data.

*Layer 2 (private key Encryption):* This is the second layer that deals with the private data. When the message gets traversed and passes the Layer 1, it means that an authentic user has entered the cloud. Next is the authentication for the private data. For this layer the password is required. Layer 2 has the collection of all the passwords for matching with the incoming request (message + credentials). This authentication is being done with a highly secure passion. This method of authentication will be discussed later (Fig. 3) [4].

*Layer 3 (Stack: requested service numbers):* All the services present in a particular cloud are given a random number. When a user passes the two layer of authentication, then he/she have to demand for that particular service. The user is unaware (as in most of cases today) of this random number methodology; he/she have performed the required operations. The main function of this layer is that whenever a user requests a service, the corresponding service number is passed to the layer 4 (Fig. 4).

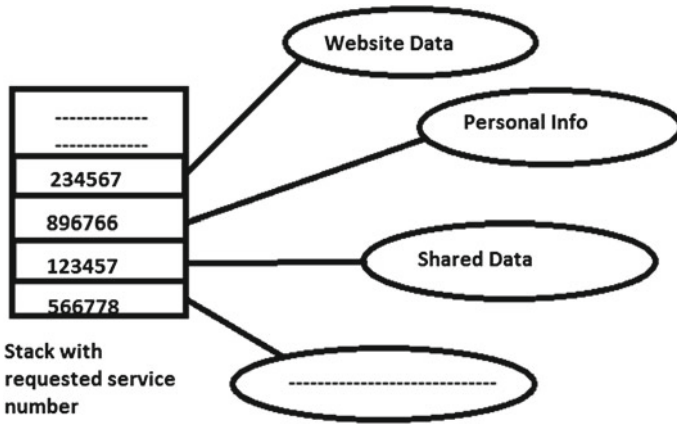


Fig. 3 Requested service mapping with random numbers

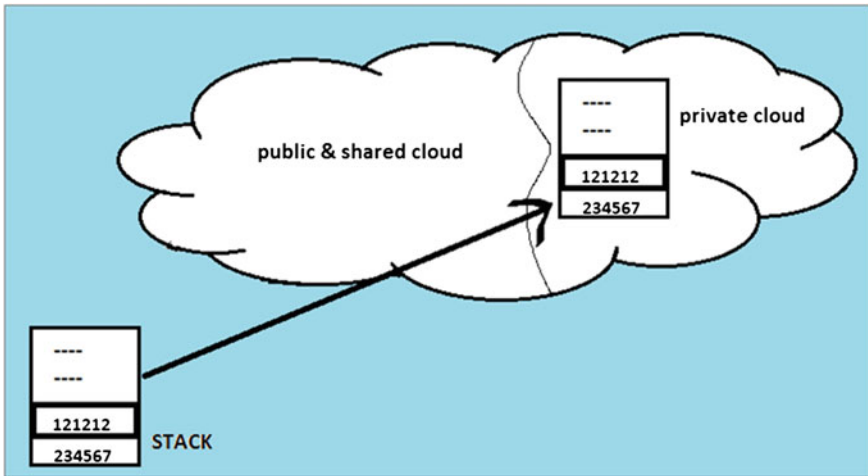


Fig. 4 Operation of layer 4

*Layer 4 (empty stack):* Next the message having the service number is passed to the layer 4. Here, we are having an empty stack on which the random number is updated. These stacks have all the services that have been requested by the user with a time stamp. This information is updated to the private area of that particular cloud. This feature helps for monitoring the activities done by the user.

*Monitoring:* The basic benefit of layer 3 and 4 is that the user can keep an eye on the service being used and accessed. In the private area of user’s cloud the stack is shown in the form of a database where instead of random numbers the corresponding service name is given [5].



### 3.5 Authentication and Key Exchange

The basic aim of Tus-Man protocol is to provide:

1. A secure access mechanism.
2. Authentication system.

In this section, we deal with the authentication and the key exchange mechanism used in the Tus-Man protocol.

#### 3.5.1 Security Model

The main aspects we have to guarantee are: (**Authentication and confidentiality**). Here we have **third party token provider (TPTP)**. It generates a **TOKEN** on demand of the client. The **TOKEN** is useful in making the transaction more secure and reliable between the client and the service provider.

##### 1. Theme

This algorithm has been designed on the basis of locking system used in the luxury cars now-a-days. In which there is a microchip built in the car's lock and the key used to unlock that key. Whenever the key is being put into the lock the data in the two chips are matched and car will be opened. On the other hand, when the car is being turned off, the data will be changed and stored both in the car's and key's microchip.

##### 2. Salient features

- The value of the token will be changed every time the user requests for the token from the service provider.
- It provides an extraordinary level of security to the data stored on the cloud.
- The regular change of the **TOKEN** value makes all attacks on the data just next to impossible.
- Encryption and decryption depends on the key's present values, which makes it very secure.
- The current value of **TOKEN** is not known to the user himself.

##### 3. Working

Step 1: The User's ID [ID<sub>USER</sub>] and TUS-MAN CODE is send to the third party token provider.

Step 2: The third party token provider generates a Token [T] and delivers it to both the client and the service provider.

Step 3: Client generates a three way hand shake protocol with the service provider to check that the data is being available and accessible to communicate.

Step 4: After confirmation, user sends the **TOKEN** and its TUS-MAN CODE to the service provider.

- Step 5: The service provider than matches the two TOKEN values and maps it with the particular TUS-MAN CODE.
- Step 6: When the two values of TOKEN are matched, the service provider fetches the data from the particular cloud and returns to the client.
- Step 7: When the data is being fetched than the user synchronizes with the third party token provider to inform that he/she has to sign out.
- Step 8: Than the values of the token will be changed and kept secret with the service provider.
- Step 9: Next time the same user logins with the same credentials the stored token value is now active and the same procedure is repeated.

## 4 Conclusion

Tus-Man protocol will provide capability to service providers and consumers to act seamlessly keeping security context in mind. This will act as a protocol which is to be used for providing secure services (viz. confidentiality, Access control) to both the service provider and service consumer. Salient feature that can be summarized are:

1. Tunnel-based security to hide network traffic.
2. Data Isolation from intercloud and intracloud communication.
3. A highly sensitive monitoring system for keeping track of requested services.

All the above-mentioned features help the secure transmission of data among the clouds as well as cloud-consumer network. The Tus-Man algorithm provides certain protocol that isolates and secure the personal data in the clouds. We are looking forward in making the cloud computing a better place to bank upon.

## References

1. Cloud computing security threats [<http://www.cloudsecurityalliance.org/topthreats/csathreats.v1.0.pdf> ]
2. Basics of public key encryption [[http://en.wikipedia.org/wiki/Public-key\\_cryptography](http://en.wikipedia.org/wiki/Public-key_cryptography)]
3. Top security thread to cloud [<http://h30458.www3.hp.com/ww/en/ent/954867.html>]
4. Basics of private key encryption [<http://searchsecurity.techtarget.com/definition/private-key>]
5. Working of kerberos [<http://searchsecurity.techtarget.com/definition/Kerberos>]

# Poem Classification Using Machine Learning Approach

Vipin Kumar and Sonajharia Minz

**Abstract** The collection of poems is ever increasing on the Internet. Therefore, classification of poems is an important task along with their labels. The work in this paper is aimed to find the best classification algorithms among the K-nearest neighbor (KNN), Naïve Bayesian (NB) and Support Vector Machine (SVM) with reduced features. Information Gain Ratio is used for feature selection. The results show that SVM has maximum accuracy (93.25 %) using 20 % top ranked features.

**Keywords** Poem · Classification · Ranked feature

## 1 Introduction

A poem is a piece of writing in which the expression of feelings and ideas is given intensity by particular attention to diction (sometimes involving rhyme), rhythm, and imagery [5]. It is generally meant to deliver expressions such as love, happiness, success, etc. Thus, poems of many category are available. However, an effort in automatic poem classification is rare. Usually, poems are as short textual paragraphs with little discriminative value of word features for automatic classification. Therefore, poem classification is a challenging task. Some text classification algorithms have been developed to categorize news [6], patent [7], etc. Many machine learning algorithms have been attempted for automatic text classification.

A poet may use any word for the poem. In fact, poems are often structured differently from normal text documents. Therefore, there is a necessity to identify an effective machine learning algorithm for poem classification. Three machine learning

---

V. Kumar (✉) · S. Minz  
JNU, New Delhi, India  
e-mail: rt.vipink@gmail.com

S. Minz  
e-mail: sona.minz@gmail.com

algorithms Naïve Bayesian (NB), k-Nearest Neighbor (KNN), and Support Vector Machine (SVM) are considered. For feature selection, Gain Ratio is used. The comparison of three machine learning algorithms with respect to poem classification is considered to identify the best suited one. The paper is structured as follows: Sect. 2 is on related work. Section 3 introduces poem data set. Implementation is described in Sect. 4. Section 5 contains experiment results and analysis. Finally, we present the conclusions and future work.

## 2 Related Work

Many types of statistical and machine learning algorithms are available to classify text documents such as k-Nearest Neighbor, Naïve Bayesian [8], and Support Vector Machine [9]. The effort in automatic classification of literary texts such as poetry is less. Malay poetry is classified using support vector machine. In this, Radial Basic Function (RBF) and linear kernel function are implemented to classify pantun by theme, as well as poetry and none poetry [10]. Logan and Kositsky [11] have done a comparison with the acoustic similarity technique and semantic text analysis technique for collecting lyrics from the Web to analyze artistic similarity.

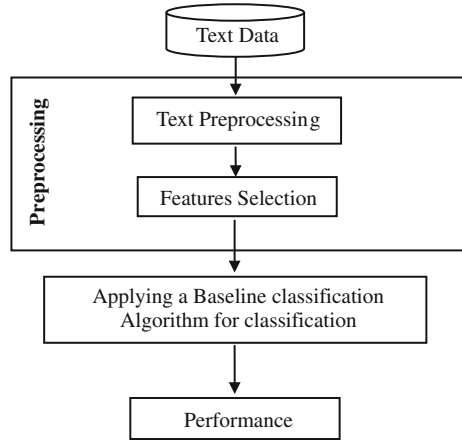
## 3 Data Set

A collection of 400 text documents from popular sites such as <http://www.poetseer.org>, <http://www.poetry.org>, and <http://www.poemhunter.com> has been considered for experiment. More than 225 numbers of labels of poem are available on the Internet. It is difficult to consider all labels for this research. Therefore, the data set includes only 8 labels as alone, childhood, god, hope, love, success, valentine, and world. Each label has 50 text documents and each text document has nearly the same length.

## 4 Implementation

Poem classification framework is presented in Fig. 1. RapidMiner5 [2], an open source data mining package has been used to model the NB, k-KNN, and SVM [4]-based classifiers. The preprocessing steps include two main components such as text preprocessing and feature selection. In the text preprocessing task, all poems are input and processed by transformation of upper case to lower case, tokenization, stop word removal, and stemming using WordNet [1]. The text preprocessing task transforms poems into term-document vector, where the vector represents the weight of terms in the documents. Therefore, in feature selection the weight of each term is based on the *tf-idf* weighting scheme as shown below:

**Fig. 1** Poem classification frameworks



$$w_{ij} = tf_{ij} \times \log \frac{N}{n_j}$$

where  $w_{ij}$  is the weight of term  $j$ ,  $N$  is the total number of poems, and  $n_j$  is the number of poems.

The feature selection scheme Gain Ratio (GR) is applied to the feature vector of the document to rank the features for feature reduction. It applies a kind of normalization to information gain using splitting information value defined analogously with  $\text{Info}(D)$  as

$$\text{SplitInfo}_A(D) = - \sum_{j=i}^v \frac{|D_j|}{|D|} \times \log_2 \left( \frac{|D_j|}{|D|} \right)$$

where  $D$  is data set into  $v$  partitions on attribute  $A$ . The Gain ratio is defined as

$$\text{Gain Ratio}(A) = \frac{\text{Gain}(A)}{\text{SplitInfo}(A)}$$

The attribute with the higher gain ratio is considered to have more relevance for classification.

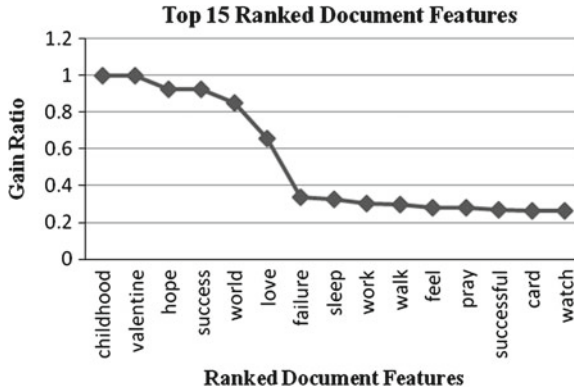
After the preprocessing task, baseline classifiers KNN, NB, and SVM are applied for respective percentage of ranked features, where accuracy is a key measure to evaluate the performance of the classifiers. It can be calculated from Table 1 using the formula:

$$\text{Accuracy} = \frac{(TP + TN)}{(TO + TN + FP + FN)}$$

The true positive, true negative, false positive, and false negative are also useful in assessing the costs benefits (or risk ad gain) associated with the classification model.

**Table 1** Confusion matrix for 2-class classification

Actual class	Predicted class	
	Positive	Negative
Positive	True positive (TP)	False positive (FP)
Negative	False negative (FN)	True negative (TN)



**Fig. 2** Top 15 Ranked features of documents

## 5 Results and Analysis

The objective of the research is to find out suitable machine learning classification algorithms. NB, KNN, and SVM, three classifiers are chosen for the desired objective. Evaluation of classifiers is based on the classification accuracy. The poem data set was partitioned into training and test data. Gain Ratio was used to rank the features of the documents. Classifiers were developed using the 10, 20, 30...90% and all features using the NB, KNN, and SVM. Ten-fold cross validation method was used to estimate the performances of all the classifiers.

### 5.1 Results

Gain Ratio was used to rank the document features in the experiment. To form the 3707 features, 15 top ranked features are shown in Fig. 2. It shows that childhood and Valentine features have 1 gain ratio. Hope, Success, World, Love, and Failure features are between 1.0 to 0.25 gain ratio.

Table 2 shows average accuracy of the classifiers using 10-fold cross validation with top ranked features. NB classifier has maximum accuracy using 10% top ranked features. Using 40% top ranked features, KNN yields maximum accuracy of 87.50%. SVM-based classifier has maximum 93.50% accuracy by using 20% top ranked features.

**Table 2** Accuracy of NB, KNN, and SVM classifiers

% of top ranked attribute	Classification accuracy (%)		
	NB	KNN	SVM
10	<b>80.00</b>	85.50	93.00
20	79.75	86.00	<b>93.25</b>
30	76.50	84.00	93.25
40	71.25	<b>87.50</b>	92.75
50	71.25	87.00	93.25
60	68.50	83.25	92.75
70	66.25	80.00	93.00
80	66.25	76.25	92.75
90	65.75	75.50	93.00
100	79.50	85.50	92.25

**Table 3** Accuracy of NB, KNN, and SVM classifiers using less than 10% ranked features

% of top ranked attribute	Classifiers accuracy (%)		
	NB	KNN	SVM
1	<b>82.00</b>	86.00	90.00
2	81.00	85.75	90.00
3	80.00	84.00	89.75
4	80.50	86.00	91.25
5	79.50	86.26	91.50
6	79.50	85.25	92.00
7	78.50	<b>86.50</b>	91.00
8	78.00	86.00	92.50
9	78.75	85.25	92.75
10	80.00	85.50	<b>93.00</b>

From Table 2, it can be observed that SVM does not have significant difference in accuracy using 10 and 20% top ranked features. The accuracy of KNN classifier does not have significant difference, with using 10 and 40% top ranked features. Therefore, 10% top ranked features are considered for the further reduced set of features.

Table 3 shows average accuracy of classifiers using 1, 2, 3... 10% top ranked selected features. NB, KNN, and SVM have maximum accuracy of 82.00, 86.50, and 93.00% using 1, 7 and 10% selected features respectively.

### 5.2 Analysis

The objective of this research is to identify an efficient machine learning algorithm (NB, KNN, and SVM) for poem classification with reduced features. From Fig. 2, it is observed that only 6 features have Gain Ratio more than 0.6 and others have

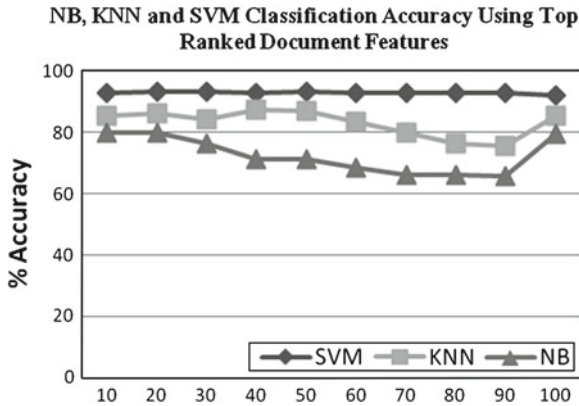


Fig. 3 NB, KNN, and SVM classification accuracy using top ranked document features

Gain Ratio less than 0.34. The top 6 features (childhood, valentine, hope, success, world, and love) are the same as labels mentioned in the data set. It means that these features (words) directly play a role in the poem classification task.

From Fig. 3 it can be easily analyzed that SVM classifier has the best performance for all percentage of ranked features and KNN has the second best performance. The performance of the classifiers displays decrease in accuracy as size of feature set increases except when 100% features are used to model the classifiers. NB, KNN, and SVM achieved best accuracies of 80.00, 87.50, and 93.25%, using 10, 40, and 20% of selected features. The best performances of KNN and SVM classifiers do not indicate a significant difference using 10% ranked features. Therefore, performance of the classifiers using 10% ranked features has been considered for comparison of the three machine learning algorithms.

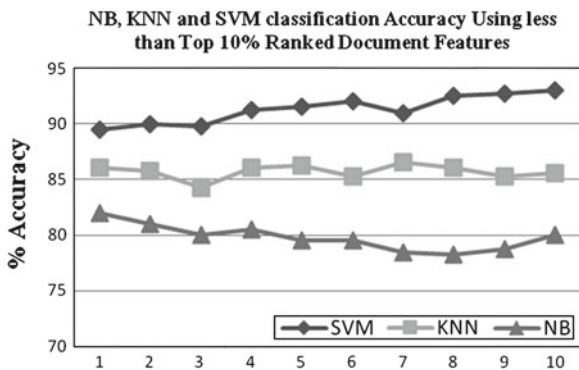


Fig. 4 NB, KNN, and SVM classification accuracy using less than 10% top ranked document features



Figure 4 exhibits that the performance of NB-based classifiers decreases whereas the size of feature set increases. It achieves best performance 82.00 %, using 1 % of top ranked features. SVM performance is decreasing with 10 to 1 % of top ranked; therefore SVM has best performance using 10 % top ranked features. KNN has best performance 86.50 %, using 7 % of ranked features.

## 6 Conclusion and Future Work

A large number of poem data sets are available on Internet. Therefore, labeling poems is an important task. This study has attempted to identify an effective machine learning algorithms (NB, KNN, and SVM). The experiment results show that SVM have best performance compared to the NB and KNN. It has 93.5 % using 20 % ranked features. The top 6 features (childhood, valentine, hope, success, world, and love) have played an important role in classifying the respective poem labels.

Gain Ratio has been used for features selection of the documents. Therefore, other feature selection techniques (Information gain, Gini Index...etc) can be used in the future for features ranking. SentiWordNet [3] is a lexical resource, which gives three sentiment scores of positivity, negativity, and objectivity at each synset. Extracted document features, using SentiWordNet can play the important role for poem classification task.

## References

1. Andrea, E., Sebastiani F.: SentiwordNet: a publicly available lexical resource for opinion mining. In: Proceedings of the 5th Conference on Language Resources and Evaluation (LREC 2006), Genova, IT, 2006, pp. 417–422 (2006).
2. <http://www.rapidminer.com>
3. Esuli., Sebastiani, F.: Sentiwordnet: a publicly available lexical resource for opinion mining. In: Proceedings from International Conference on Language Resources and Evaluation (LREC), Genoa (2006).
4. Chih-Chung, C., Chih-Jen, L.: LIBSVM: a library for support vector machines. In: ACM Transactions on Intelligent Systems and Technology, 2:27:127:27, (2011).
5. <http://oxforddictionaries.com/definition/english/poem>
6. Shih, L.K., Karger, D.R.: Learning classifiers: using URLs and table layout for web classification tasks. In: Proceedings of the 13th International Conference on World Wide Web, New York, NY, pp. 193–202 (2004).
7. Richter, G., MacFarlane, A.: The impact of metadata on the accuracy of automated patent classification. *World Patent Inf.* 37(3), 13–26 (March 2005)
8. Wang, B., Zhou, S., Hu, Y.: Naive bayes-based garual Chinese documents categorization. In: Proceedings of World Multi conference on Systems, Cybernetics and Informatics, 2, July, Orlando, pp. 516–521 (2001).

9. Noraini, J., Masnizah, M.: Shahrul Azman, N.: Poetry classification using support vector machines. *J. Comput. sci.* **8**(9), 1441–1446 (2012)
10. Logan, B., Kositsky, A., Moreno, P.: Semantic analysis of song lyrics. In: the Proceeding of IEEE Int. Conf. on Multimedia and Expo, 2, pp. 827–830 (2004).
11. Tizhoosh, H.R., Dara, R.: On poem recognition. *Pattern Anal. Appl.* **9**(4), 325–338 (2006)

# Novel Class Detection in Data Streams

Vahida Attar and Gargi Pingale

**Abstract** Data stream classification is challenging process as it involves consideration of many practical aspects associated with efficient processing and temporal behavior of the stream. Two such aspects which are well studied and addressed by many present data stream classification techniques are infinite length and concept drift. Another very important characteristic of data streams, namely, concept-evolution is rarely being addressed in literature. Concept-evolution occurs as a result of new classes evolving in the stream. Handling concept evolution involves detecting novel classes and training the model with the same. It is a significant technique to mine the data where an important class is under-represented in the training set. This paper is an attempt to study and discuss the technique to handle this issue. We implement one of such state-of-art techniques and also modify for better performance.

**Keywords** Novel class detection · Data stream classification · Concept evolution

## 1 Introduction

Advances in electronics and hardware technology have highly increased the capability to generate as well as to store enormous data in various forms. Mobile phones, laptops, easily available camera, the Internet are few among the various devices which generate huge amount of digital data. Though data mining provides with many good applications to mine this huge data, data stream classification is a major challenge for data mining community. With increasing volume of data it is no longer possible to process the data in multiple passes. Also the data stream may evolve over the time

---

V. Attar (✉) · G. Pingale  
College of Engineering Pune Shivaji Nagar, Pune, India  
e-mail: vahida.comp@coep.ac.in

G. Pingale  
e-mail: gargipingale04@gmail.com

period. Concept-evolution occurs when new classes evolve in the stream. Handling concept evolution involves detecting novel classes and training model with the same. When we are using continuous data stream for classification it is not possible to predict the class or type of data in advance that system is going to encounter. System should be able to detect an emergence of new class of data in stream.

Novel class detection is concerned with recognizing inputs that differ in some way from those that are usually seen or which already exist in the trained model. It is a significant technique to mine the data where an important class is under-represented in the training set. Traditional classifiers cannot detect presence of novel class. All the instances which belong to such class are misclassified by the algorithm unless there is some kind of manual intervention and model is trained with such a novel class. Novel class detection technique is immensely useful in medical sciences, intrusion detection, fraud detection, signal processing, and image analysis. Novel class detection refers to learning algorithms being able to identify and learn new concepts. In this case, the concepts to be detected and those to be learned correspond to an emerging pattern that is different from noise, or drift in previously known concepts. In simple words, systems detecting novel class must be able to identify new concept emerging in the stream and train the existing models with it so that in future instances belonging to that novel class can be correctly classified. Novelty class detection is now being under constant attention from researchers and academicians. Various approaches to detect the new concept as well as to learn the new concept have been devised.

In rest of the paper Sect. 2 describes about Novel class Detection. In Sect. 3, we explore different technique to handle this issue, Sect. 4 is about the implemented techniques and improvements over the same. Results of both the techniques are presented and compared in Sect. 5 and conclusion in Sect. 6.

## 2 Overview of Concept Evolution and Novel Class Detection

There are many algorithms in literature that address novelty detection. These algorithms can be divided into one-class approach and multi-class approach. In one class method [6, 7, 9], one class is able to detect a single class of data instances that is different from classes with which system is trained, however, multi-class method can detect more than one new class in training data set. These algorithms show different results for different data sets because their efficiency and accuracy depends on underlying method used and properties of data taken into consideration. Major challenge is to detect novel classes in presence of concept drift in data stream. There are broadly two approaches for novelty detection in data stream, Statistical and Neural Network approach.

**Neural networks** [6] are immensely used in Novelty Detection. In comparison to statistical methods some critical issues in neural networks are generalization of computational expense during training and expense involved in retraining. Some

of these methods are multi-layer perceptions, support vector machines, radial basis function networks, self-organizing maps, oscillatory networks, etc.

**Statistical Approach** uses the statistical properties of data for creating models. It further uses these models to estimate whether the given instance belongs to the existing class or not. There exist various techniques for novelty detection using this approach. To mention a few, building a density function for data of known class and then calculate the probability of the coming test instance belonging to existing class. Another technique can be finding mean distance of test instance under consideration from the center of nearest cluster of existing class first to detect it as outlier and if there are several such outliers close to each other considering some threshold value for closeness as a novel class. The distance measure can be a Euclidian distance or some other probabilistic distance. Further down there are two types of statistical approach, Parametric and Non-parametric approaches.

In **parametric approach** data distributions are assumed to be known and then the parameters such as mean, variance of model are estimated, the test data falling outside the estimated parameters of distribution are declared as novel. But the parametric approach does not have much practical implications as the distribution of real data is already not known. Some of the parametric methods for novelty detection are Hypothesis testing, Probabilistic/Gaussian mixture modeling.

**Non-parametric approach** involves estimation of density of data for training for example, Parzen window and K-Nearest Neighbor. The instances which fall out of certain threshold density are regarded as novel. These methods do not make any assumption regarding data distribution functions. Thus in a way they are more flexible. But they do have shortcomings in handling of noise in data. In KNN method, the normal data distribution is defined by a few numbers of spherical clusters formed by k-nearest neighbor technique. Novel class is identified by calculating distance of data point from the center of the clusters which fall beyond its radius. Parzen windows method is used for estimation of data density. It uses Gaussian function. In this method a threshold for detecting novelty is set which is being applied on the probability of test pattern.

### 3 Techniques for Novel Class Detection

Various papers to deal with the novel class detection are noted in the literature. Smola [5], proposes approach to this problem by trying to estimate a function  $f$  which is positive on  $S$  and negative on the complement. The functional form of  $f$  is given by a kernel expansion in terms of a potentially small subset of the training data; it is regularized by controlling the length of the weight vector in an associated feature space. It provides a theoretical analysis of the statistical performance of algorithm. The algorithm is a natural extension of the support vector algorithm to the case of unlabeled data. Given a small class of sets, the simplest estimator accomplishing this task is the empirical measure, which simply looks at how many training points fall into the region of interest. This algorithm does the opposite. It proposes an algorithm

which computes a binary function which is supposed to capture regions in input space where the probability density lives (its support), i.e., a function such that most of the data will live in the region where the function is nonzero. In doing so, it is in line with Vapnik's principle never to solve a problem which is more general than the one we actually need to solve. Moreover, it is applicable also in cases where the density of the data's distribution is not even well-defined, e.g., if there are singular components. It starts with the number of training points that are supposed to fall into the region, and then estimates a region with the desired property.

In [6], a new single class classification technique has been proposed that can detect novelty and handle concept drift. The proposed method uses clustering algorithm to produce the normal model. It relies on Discrete Cosine Transform (DCT) to build compact and effective generative models such that the closest model to a new instance will be an approximation of its  $K$  nearest neighbors. Also using the DCT coefficients it presents an effective method for discriminating normal concepts as well as detecting novelty and concept drift. The proposed method referred to as Discrete Cosine Transform Based Novelty and Drift Detection (DETECTNOD), consists of two phases. In the first phase, based on the normal data, it tries to generate an initial model with an effective and compact knowledge about the clusters. At the second phase, the testing data is divided into equal sized blocks whose size is limited only by the storage space. In this phase, using the previously obtained generative models, normal data is discriminated from novel classes and concept drift.

D. Martinez [8] introduced a neural competitive learning tree as a computationally attractive scheme for adaptive density estimation and novelty detection. This approach combines the unsupervised learning property of competitive neural networks with a binary tree-type structure. The initialization process can be performed with input data sampled either randomly from the training set (random initialization) or sequentially as data become available (sequential initialization) in case of an Independently Identically Distributed (IID) sequence and then nodes are splitting each at one time. To avoid this dependency of initialization process on particular data tree is built by taking into account entire dataset and splitting all nodes once. Thus, the learning rule provides an adaptive focusing mechanism capable of tracking time-varying distributions. The constructed tree from the training data serves as a reference tree. Another tree is built for the testing data and a novelty is detected when it differs too much from the reference tree.

Markos Markou [9] proposes a new model of "novelty detection" for image sequence analysis using neural networks. This model uses the concept of artificially generated negative data to form closed decision boundaries using a multi-layer perceptron. It uses novelty filter to classify data as known and unknown. One neural network is trained per class where samples are labeled as belonging (positive) or not belonging (negative) to class. Negative data is used for novelty detection. Neural Network with Random Rejects (NN-RR) novelty filter works on thresholding the neural network output activation in response to an input test pattern. Rejected samples are then collected in data storage called bin. Clustering is done using  $k$ -means clustering method. This helps in deciding which clusters should be used for retraining.

## 4 Implemented Technique and Proposed Up-Gradation

In real streaming environment where new classes evolve it is not the case that total number of classes is fixed for classification purpose. Masud et al. [4] propose an algorithm to detect emergence of novel class in the presence of concept drift by quantifying cohesion among unlabeled instances and separation of them from training instances. Traditional novelty detection schemes assume or build a model of normal data and identify outliers that deviate from normal points. This scheme not only detects single point which deviates from normal data but also to find if there is any strong bond among the points. This technique uses ensemble approach to handle concept drift. Data stream is divided into equal sized chunks. Each chunk is accommodated in memory and processed online and classification model is trained from each chunk. Newly trained model replaces original model. And the ensemble evolves representing most up-to-date concepts in the stream. This paper forms the platform of our work. We implement this technique and also propose some improvements in the algorithm.

Input data stream is divided into equal sized chunks. Each unlabeled chunk is given as input to the algorithm. It first detects presence of novel class. Instances belonging to the novel class are separated from the chunk and the remaining instances are classified normally. A new model is trained using the instances of the latest chunk. Finally the ensemble is updated by choosing the best  $M$  classifiers from  $M + 1$  classifiers. The base learners used are  $K$  Nearest Neighbors and Decision tree. Clusters of the training instances are built and hence store only cluster summaries. These clusters are called as Pseudo points. Any strong cohesion among the instances falling in the unused space indicates presence of a novel class. Novel class detection is a two step process. Initially the training data is clustered and stored as cluster summaries called Pseudopoints which are used to keep the track of used spaces. Later these Pseudopoints are used to detect outliers and if a strong cohesion exists among the outliers a novel class is declared. Every time the data chunk is clustered and the cluster centroid and relevant information is stored as Pseudopoints. Clustering is specific to each base learner. In case of decision tree at its each leaf node where as for KNN classifier the already existing Pseudopoints are used.  $K$  Means clustering approach is adapted for the same. The desired value of  $K$  parameter in  $K$  Means algorithm should be determined experimentally. We build  $K_i = (t_i/S)*K$  clusters in  $l_i$ , where  $t_i$  denoted number of training instances in the leaf node  $l_i$ ,  $S$  is the chunk size.

Cluster summary is stored in Pseudopoints which consist of Weight ( $W$ )—total number of instances in the cluster. Centroid ( $C$ ). Radius( $R$ )—maximum distance between the centroid and the data instances belonging to the cluster. Mean distance— it is the mean distance from each data instance to the cluster centroid. Once the Pseudopoints are formed the raw data is discarded. The union of regions covered by all Pseudopoints represents union of all the used spaces which forms a decision boundary.

R-Outlier is a data instance such that the distance between the centroid of the nearest Pseudopoint and the instance is greater than the radius of this Pseudopoint.

For KNN approach R-Outliers are determined by testing each data instance against all the Pseudopoints. For decision tree each data point is tested against only the Pseudopoints stored at the leaf node where the instance belongs. So any data instance outside the decision boundary is an R-Outlier for that classifier.

### **Up-Gradations: Early Novel Class Detection (ENCD)**

Sometimes test data instance may be considered as an R-outlier because of one or more reasons like: The test instance belongs to an existing class but it is a noise, shift in the decision boundary, Insufficient training data. To avoid an ordinary instance being declared as a novel class instance filtering is done. If a test instance is an R-Outlier to all the classifiers in the ensemble only then it is considered as filtered outlier that is F-Outlier. Rest all are filtered out. Hence being an F-Outlier is a necessary condition for being in a new class. Detection of novel class basically means to verify whether F-Outliers satisfy the two properties of a novel class that is separation and cohesion.  $\lambda_C$  neighborhood is the set of  $\eta$  nearest neighbours of  $x$  belonging to class  $C$  where  $\eta$  is user defined parameter. In the existing algorithm a new classifier is built only when the test chunk is completed. As soon as a new class is found a new classifier must be built, instead of waiting for the test chunk to finish, and then to train a classifier. Now we don't need to wait for the test chunk to complete, instead we train the new classifier with whatever part of test chunk at hand and this puts us in a position to detect and identify the forthcoming novel instances in that present chunk itself. To achieve this, we put an additional condition for building a classifier. During testing, whenever a new class is detected, a flag is set. Building or training of new classifier is done when this flag is set or when the test chunk is completed. We call this as Early Novel Class Detection (ENCD).

## **5 Experiments and Results**

### **5.1 Datasets**

10% of KDDCup 99 network intrusion detection [5] contains around 4,90,000 instances. Here different classes appear and disappear frequently, making the new class detection very challenging. There are 22 types of attacks, each record consists of 42 attributes. We have also used synthetically generated dataset from [4] which simulates both concept-drift and novel-class. The data size varies from 100 to 1000k instances, class label varies from 5 to 40 and data attributes from 20 to 80 (Fig. 1).

### **5.2 Implementation Environment**

The proposed algorithm is implemented in Java programming language on Linux platform. We have used MOA-Massive Online Analysis tool for all the experimen-



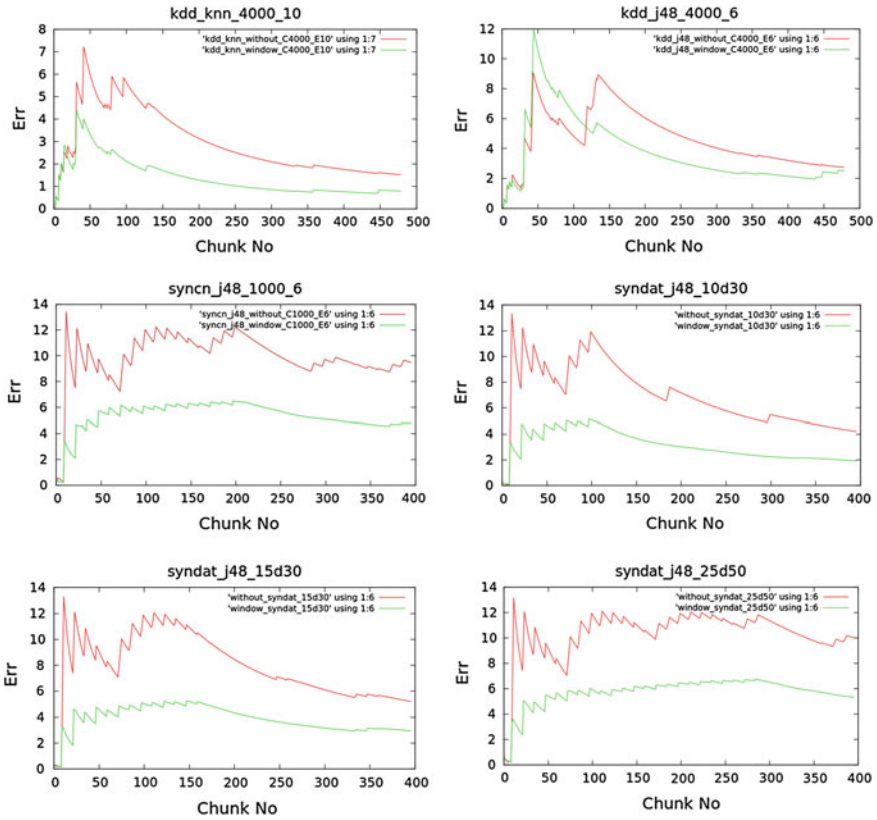


Fig. 1 Error rate versus Chunk No. for Datasets: KDD (KNN, DT), SyncCN ()

tation of the proposed approach. Performance existing algorithm is compared with ETNCD proposed by us. For plotting the graphs of chunk no. and error rate of the two algorithms, we used GNU plot version 4.2.

**Parameters-Error:** Whenever predicted class value of the instance under consideration is different from its actual class value error is noted. If an existing class instance is misclassified as a novel class instance error is incremented.

$$\text{Global Error} = (100 * \text{Err}) / \text{total no. of instances in dataset.}$$

**Chunk Size:** We have experimented with chunk size from 500 to 5,000 and selected 4,000 for real and 1,000 for synthetic dataset.

**Ensemble Size:** 10 for KNN and 6 for Decision tree classifier.

**Minimum Number of Points required to declare a novel class:** 50.

### 5.3 Results Based on Up-Gradations

Initially models are built with the first  $N$  chunks. From the  $N + 1$  chunk performance of each method is evaluated for that chunk and then the same chunk is used to update the existing models. We compared the proposed approach that is ENCD and the existing algorithm in [4]. We perform comparisons for all the mentioned datasets.

## 6 Conclusion and Future Work

Various techniques in novel class detection have been studied and analyzed. We propose early detection and identification of every new class. This improvement gives us an edge to classify the novel instances correctly. Experimental results show that the proposed up gradations improve the existing algorithm. The current technique does not take into consideration multiple-label instances. So we would also like to apply our technique to multiple-label instances.

## References

1. Mohammad, M.M., Jing, G., Latifur, K., Jiawei, H., Bhavani, M.T.: Classification and novel class detection in concept drifting data streams under time constraints. In: Preprints, IEEE Transactions on Knowledge and Data Engineering (TKDE), 2010.
2. Mohammad, M., Masud, J.G., Latifur, K., Jiawei, H.: Bhavani. Classification and novel class detection in data streams in a dynamic feature space, M.T. (2010)
3. Mohammad, M.M., Jing, G., Latifur, K., Jiawei, H.: Bhavani. Classification and novel class detection in data streams with active mining, M.T. (2010)
4. Mohammad, M.M., Jing, G., Latifur, K., Jiawei, H.: Bhavani. M.T, Integrating novel class detection with classification for concept drifting data streams (2009)
5. Smola, A.J., Shawe-T., Scholkopf, B.P., Williamson R.C.. Advances in neural information processing systems (1999).
6. Zi, M.H., Hashemi M.R.: A DCT based approach for detecting novelty and concept drift in data streams (2010).
7. Martinez, D.: Neural tree density estimation for novelty detection (1998).
8. Markos, M.: Sameer. A neural network-based novelty detector for image sequence, Analysis, S. (2006)
9. Stephen, D.B.: The UCI KDD archive. <http://kdd.ics.edu> 1999
10. Markou, M., Singh S.: Novelty detection: a review-part 1: statistical approaches part 2: neural network based approaches (2003).

# Analyzing Random Forest Classifier with Different Split Measures

Vrushali Y. Kulkarni, Manisha Petare and P. K. Sinha

**Abstract** Random forest is an ensemble supervised machine learning technique. The principle of ensemble suggests that to yield better accuracy, the base classifiers in the ensemble should be diverse and accurate. Random forest uses decision tree as base classifier. In this paper, we have done theoretical and empirical comparison of different split measures for induction of decision tree in Random forest and tested if there is any effect on the accuracy of Random forest.

**Keywords** Classification · Split measures · Random forest · Decision tree

## 1 Introduction

Random forest is an ensemble supervised machine learning technique. Ensembles use multiple classifiers and are always more accurate than individual classifiers. Random forest uses decision tree as base classifier. It is based on principle of bagging [1] and uses randomization in two ways: one in the selection of training data samples to train each base tree and another in the selection of attributes for induction of tree. The principle of ensemble suggests that to yield better accuracy, the base classifiers in the ensemble should be diverse and accurate [2].

---

V. Y. Kulkarni (✉)  
COEP, Pune, India  
e-mail: kulkarnivy@rediffmail.com

V. Y. Kulkarni  
MIT, Pune, India

M. Petare  
MIT, Pune, India

P. K. Sinha  
HPC and R&D, CDAC, Pune, India

In the original Random forest algorithm, Brieman has used Gini index as split measure to induce decision trees. Gini index particularly is not able to detect strong conditional dependencies among attributes [4]. There are various top-down decision tree inducers like ID3, C4.5 which work with split measures other than Gini index [5]. Robnik and Sikonja experimented with Random forest using five different attribute measures; each fifth of the trees in the forest is generated using different split measure (Gini index, Gain ratio, MDL, Myopic ReliefF, or ReliefF). This helped in decreasing correlation between the trees while retaining their strengths. In the literature survey related to Random forest [12], we found that there is very less work done related to attribute split measures in Random forest.

There are 29 different attribute split measures [6], we have selected the commonly used split measures for our work. In this paper we tested use of different split measures (Information gain, Gain ratio, Gini index, Chi square, and ReliefF) to induce decision trees for Random forest, how it is affecting the accuracy, is the strength of individual tree is increased by a specific split measure. For this, we have first done theoretical study of different measures and generated a comparison matrix. In [13] the authors have mentioned that for research related to decision tree induction, empirical comparisons are to be preferred. Hence these results are verified by empirical study and conclusions are derived.

This paper is organized in following way: Sect. 2 introduces in brief the Theoretical Foundations for this research work. They include Random forest and split measures used for experimentation. Section 3 explains methods and results. Section 4 gives concluding remarks.

## 2 Theoretical Foundations

### 2.1 Random Forest

*Definition:* A Random forest is a classifier consisting of a collection of tree-structured classifiers  $\{h(x, \theta_k) \mid k = 1, 2, \dots\}$  where the  $\{\theta_k\}$  are independent identically distributed random vectors and each tree casts a unit vote for the most popular class at input  $x$  [3]. Random forest generates an ensemble of decision trees. To classify a new object from an input vector, the input vector is run down each of the trees in the forest. Each tree gives a classification and each tree votes for the class. The forest chooses the classification having maximum votes. Each tree is grown in the following way: If the number of records in the training set is  $N$ , then  $N$  records are sampled at random but with replacement, from the original data, this is bootstrap sample. This sample will be the training set for growing the tree. If there are  $M$  input variables, a number  $m \ll M$  is selected such that at each node,  $m$  variables are selected at random out of  $M$  and the best split on these  $m$  is used to split the node. The value of  $m$  is held constant during forest growing. Each tree is grown to the largest extent possible. There is no pruning. The generalization error of Random forest is given as,

$$PE^* = P_{x,y} (mg(X, Y)) < 0$$

The margin function is given as,

$$mg(X, Y) = av_k I (h_k(X) = Y) - \max_{j \neq Y} av_k I (h_k(X) = j)$$

The margin function measures the extent to which the average number of votes at  $(X, Y)$  for the right class exceeds the average vote for any other class. Strength of Random forest is given in terms of the expected value of margin function as,

$$S = E_{X, Y} (mg(X, Y))$$

If  $\rho$  is mean value of correlation between base trees, an upper bound for generalization error is given by,

$$PE^* \leq \rho (1 - s^2) s^2$$

Hence, to yield better accuracy in Random forest, the base decision trees are to be diverse and accurate.

## 2.2 Split Measures for Decision Tree

In decision tree induction, split measures are used to generate splitting rules. A splitting rule is a one-ply look ahead heuristic used to guess the best test to make at the current node in the tree [11].

### 2.2.1 Information Gain

This attribute selection measure is based on Shannon’s information theory, which finds the value or information content of message. Hence for each splitting attribute, Information gain is calculated and the attribute with highest gain is chosen as splitting attribute. This attribute is such that it creates minimum impurity or randomness in the generated splits and hence it minimizes the information needed to classify the tuples. If  $D$  is the entire dataset, then information content of  $D$  or entropy of  $D$  is given as

$$\text{Info}(D) = - \sum_{i=1}^m (p_i \log p_i)$$

Here  $i = 1, 2, \dots, m$  are classes in dataset  $D$ .  $P_i$  is probability that an arbitrary tuple in  $D$  belongs to class  $C_i$ . Let  $A$  be an attribute in  $D$  and  $\{a_1, a_2, \dots, a_v\}$  are different values of attribute  $A$  in  $D$  such that  $\{D_1, D_2, \dots, D_v\}$  are partitions generated based on these values. These partitions are likely to be impure. How much more information

is still needed to arrive at an exact classification or pure partition is given as [10]:

$$\text{Info}_A(D) = \sum_{j=1}^v (|D_j|/|D|) * \text{Info}(D_j)$$

The smaller this additional information, the greater the purity of the partition.

$$\text{Gain}(A) = \text{Info}(D) - \text{Info}_A(D)$$

The attribute with highest Information gain is selected for splitting. Information gain is biased toward choosing attributes with a large number of values.

### 2.2.2 Gain Ratio

The Gain ratio attempts to overcome the bias toward multi-valued attributes. The less evenly spread its value, the less information in the attribute [7].

$$\text{SplitInfo}_A(D) = - \sum_{j=1}^v (|D_j| / |D|) * \log \frac{|D_j|}{|D|}$$

$$\text{Gain Ratio}(A) = \text{Gain}(A) / \text{SplitInfo}_A(A)$$

The attribute with maximum Gain ratio is selected for splitting.

### 2.2.3 Gini Index

It is known as generalized inequality index. If a dataset  $D$  contains examples from  $n$  classes, Gini Index,  $\text{Gini}(D)$  is defined as [10]:

$$\text{Gini}(D) = 1 - \sum_{j=1}^n p_j^2$$

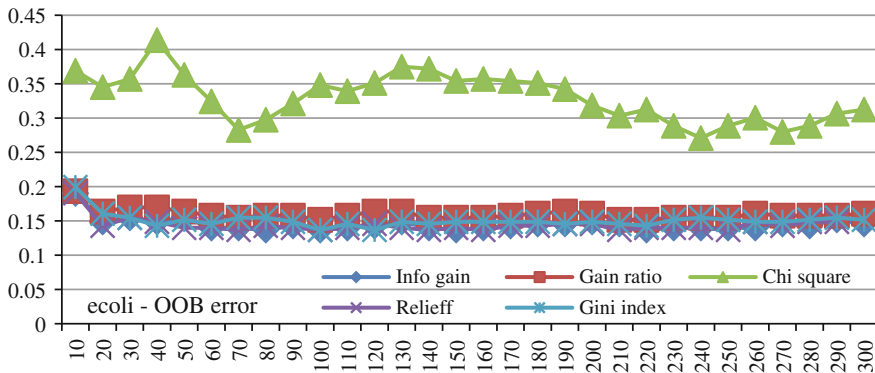
$p_j$  is the relative frequency of class  $j$  in  $D$ . Gini index considers binary split for each attribute. For attributes having more than two distinct values, subsets of attributes are considered. For binary split on partitions  $D$  into  $D_1$  and  $D_2$ , the Gini index of  $G$  is;

$$\text{Gini}_A(D) = \frac{|D_1|}{|D|} \text{Gini}(D_1) + \frac{|D_2|}{|D|} \text{Gini}(D_2)$$

The attribute with minimum Gini index is selected for splitting. The best split is the one with the largest decrease in diversity. Gini prefers split that put the largest class into one pure node, and all remaining classes into the other [9].

**Table 1** Comparison of different split measures

Measures issues	Information gain	Information gain ratio	Gini index	Chi square	Relief
Split type	Multiway	Multiway	Binary	Multiway	Binary
Splitting function	Entropy	Entropy	Gini coefficient	$\chi^2$ statistics	Diff( $A, I_1, I_2$ )
Target	Continuous, discrete	Continuous, discrete	Continuous, discrete	Discrete	Continuous, discrete
Predictors	Continuous, discrete	Continuous, discrete	Continuous, discrete	Discrete	Continuous, discrete
Algorithm	ID3	C4.5	CART	CHAID	RELIEFF family
Biasing	Biased toward multi-valued attributes	Helps to reduce biasing	Biased toward multi-valued attributes	Adjustment is possible to reduce biasing	Relief exhibits an implicit normalization effect to reduce biasing



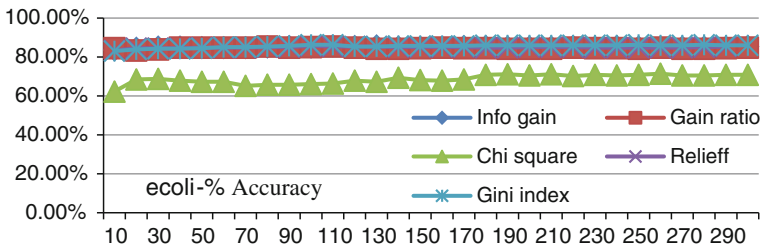
**Fig. 1** Graph showing comparative OOB error for ecoli dataset

### 2.2.4 Chi Square

Chi square test uses contingency matrix to test distribution of available data tuples into different classes. If  $(A_i, B_j)$  denote the events that attribute  $A$  takes on value  $a_i$  and attribute  $B$  takes on value  $b_j$  then Chi square value is computed as [10]:

**Table 2** Datasets used for analysis

Dataset	Instances	Attributes	Classes	Imbalanced ?	Attribute type
Hypothyroid	3772	30	4	yes	Numeric/nominal
Ionosphere	351	35	24	no	Numeric
kr-vs-kp	3196	37	2	no	Nomial
Sick	3772	37	2	yes	Numeric/nominal
Sonar	208	61	2	no	Numeric
Soybean	683	36	19	no	Nomial
Vehicle	846	19	4	no	Numeric
Anneal	898	39	5	yes	Numeric/nominal
Vote	435	17	2	no	Nomial
Audiology	226	70	24	no	Nomial
Vowel	990	14	11	no	Numeric/nominal
Waveform	5000	41	3	no	Numeric
Diebetes	768	9	2	no	Numeric
Breast cancer	286	10	2	no	Nomial
credit-g	1000	21	2	no	Numeric/nominal
segment	2310	20	7	no	Numeric/nominal
Splice	3190	62	3	no	Nomial
Car	1728	7	4	no	Nomial
Ecoli	336	8	8	no	Numeric
Glass	214	10	7	no	Numeric



**Fig. 2** Graph showing comparative % accuracy for ecoli dataset

$$X^2 = \sum_{i=1}^c \sum_{j=1}^r (o_{ij} - e_{ij})^2 / e_{ij}$$

where  $o_{ij}$  is observed frequency and  $e_{ij}$  is expected frequency,  $N$  is number of data tuples. The attribute that gives highest Chi square value is used as the best split.



**Table 3** Percentage accuracy values for different split measures

Trees	Measure	Sonar	Soybean	Vote	Vowel	BC	Diabetis	Ecoli
50	Info gain	87.50	94.00	96.09	98.18	69.23	75.26	84.82
	Gain ratio	85.10	93.70	96.09	97.98	70.63	75.00	84.82
	Chi square	85.10	91.51	96.32	97.78	67.83	74.61	67.26
	ReliefF	86.06	93.70	96.32	98.38	68.53	74.48	84.52
	Gini index	84.62	92.39	96.32	98.59	65.38	75.78	84.52
100	Info gain	85.58	93.41	96.32	98.48	69.58	75.91	85.12
	Gain ratio	86.54	93.85	96.32	98.38	70.98	75.65	85.12
	Chi square	86.54	91.65	96.78	98.59	66.78	74.87	66.07
	ReliefF	83.65	94.00	96.09	98.38	67.48	75.26	85.12
	Gini index	84.62	92.83	96.32	98.69	66.43	75.52	86.31
150	Info gain	85.58	93.41	96.55	98.48	70.63	75.91	85.12
	Gain ratio	87.02	93.27	96.55	98.48	70.28	75.78	84.52
	Chi square	86.06	91.36	96.32	98.59	66.70	74.87	68.15
	ReliefF	86.54	94.00	96.32	98.48	67.48	74.87	84.82
	Gini index	83.17	92.53	96.32	98.89	66.43	76.04	85.71
200	Info gain	87.98	93.56	96.55	98.48	70.98	75.26	85.12
	Gain ratio	87.02	93.12	96.55	98.59	70.63	75.26	84.23
	Chi square	87.02	91.51	96.55	98.89	66.43	75.13	70.54
	ReliefF	87.02	93.56	96.55	98.38	67.13	75.00	84.82
	Gini index	84.62	92.53	96.32	98.79	65.04	75.39	86.01
250	Info gain	86.06	93.70	96.55	98.59	69.23	75.00	85.12
	Gain ratio	87.98	93.12	96.55	98.59	70.63	75.13	84.23
	Chi square	88.46	91.22	96.55	98.69	65.38	75.13	70.83
	ReliefF	87.02	94.00	96.55	98.48	67.13	74.61	84.82
	Gini index	86.54	92.53	96.32	98.69	65.38	74.87	86.31
300	Info gain	84.62	93.70	96.55	98.59	69.23	75.30	85.42
	Gain ratio	87.02	93.12	96.55	98.59	70.98	75.00	84.82
	Chi square	88.46	91.36	96.55	98.38	65.38	75.13	70.83
	ReliefF	86.54	94.00	96.55	98.48	67.83	74.74	85.42
	Gini index	86.54	92.68	96.32	98.69	65.38	75.13	86.01

### 2.2.5 ReliefF

ReliefF is an attribute selection method that is based on attribute estimation. ReliefF is useful when there are strong inter dependencies among the attributes [8]. It assigns a relevance weight to each attribute. The attributes are estimated based on how well their values distinguish between the instances that are near to each other.

Given a randomly selected instance  $R$ , ReliefF searches for its two nearest neighbors: One from the same class called nearest hit  $H$ , and the other from a different class called nearest miss  $M$ . Then a quality estimation  $W[A]$  is updated for all attributes depending on their values for  $R$ ,  $M$ , and  $H$ . If the values of attribute  $A$  at instances  $R$  and  $H$  are different then attribute  $A$  separates two instances of the same class which is not desirable, and hence negative updation is added to quality estimation

$W[A]$ . If the values of attribute  $A$  at instances  $R$  and  $M$  are different then attribute  $A$  separates two instances with different class values which is desirable, and hence a positive update is done to quality estimate  $W[A]$ .

The process is repeated for  $m$  times where  $m$  is user-defined parameter.

$\text{Diff}(A, I1, I2)$  is a function which calculates difference between the values of attribute  $A$  for instances  $I1$  and  $I2$ .

For discrete attribute:

If  $\text{Diff}(A, I1, I2) = 0$  :  $\text{value}(A, I1) = \text{value}(A, I2)$ , 1 : Otherwise

For continuous attribute:

$\text{Diff}(A, I1, I2) = [\text{value}(A, I1) - \text{value}(A, I2)] / (\max(A) - \min(A))$ .

### 3 Methods and Results

The aim behind performing this experiment was to observe the effect of variation in attribute split measure on the accuracy of Random forest classifier. For this, we have generated five different Random forest classifiers each using different split measures (Info gain, Gain ratio, Chi square, Gini index, and ReliefF). For each of this measure, Random forest is generated with varying size, i.e., from 10 to 300 trees with a step of 10. The datasets used are all selected from UCI machine learning repository, and the selection is such that they are already used in different experiments related to Random forest classifier. The details of datasets used for analysis are given in Table 2. The accuracy values and OOB error [3] values are noted down. The accuracy reflects overall performance of Random forest classifier and the OOB error estimation is a measure of strength of individual tree in the forest. The OOB readings recorded here are average of OOB error values over all trees in the forest. The experimentation is done using 10-fold cross validation. The experiments were conducted on 20 datasets with variation in their size, but due to space limit we are presenting here the readings for 7 datasets (given in Table 3) and graphs for one of them. For all the graphs, values on X-axis show number of trees and values on Y axis show either OOB error or percentage accuracy.

### 4 Conclusion

The empirical results show that there is not much / significant variation in accuracy obtained except Chi square. Information gain and Gain ratio give comparable results for almost all datasets. Chi square is not suitable for Random forest classifier. ReliefF gives slightly better results as compared to Information gain or Gain ratio, but the time taken by Random forest with ReliefF is more. We are at present working on the time aspect of all the split measures where we will exclude Chi square from the experimentation. With most of the datasets, Gini index slightly lags in the results. Taking into consideration both theoretical and empirical comparisons, we conclude

that Gain ratio and ReliefF are better options, and considering the time aspect, Gain ratio is the best option.

As a future scope, we are working on generating Hybrid Decision Tree where individual decision tree of Random forest will be generated using different split measures and the effect on accuracy of Random forest will be observed.

## References

1. Breiman, L.: Bagging predictors, Technical report No 421, September (1994).
2. Opitz, David; Maclin, richard: popular ensemble methods: an empirical study. *J. Arti. Intel.* **11**, 169–198 (1999)
3. Brieman, Leo: Random forests. *Machine Learning*, **45**, 5–32 (2001)
4. Sikonja, M.R.: Improving random forests. In: Boulicaut, J.F., et al. (eds): *Machine Learning, ECML 2004 Proceedings, LNCS*, vol. 3201, PP. 359–370, Springer, Berlin (2004).
5. Rokach, Lior; Maimon, oded: top-down induction of decision trees classifiers-a survey. *IEEE trans. syst. man. cyber. part c: appli. rev.* **35**(4), 476–487 (2005).
6. Badulescu, L.A.: The choice of the best attribute selection measure in DecisionTree induction, *Annals of University of Craiova, Math. Comp. Sci. Ser. Vol. 34* (1) (2007).
7. Mingers, J.: An empirical comparison of selection measures for decision tree induction. *Mach. Learn.* **3**, 319–342 (1989)
8. Robnik-Sikonja, M., Kononenko, I.: Attribute dependencies, understandability, and split selection in tree based models, *Machine Learning: Proceedings of the 6th International Conference (ICML)*, 344–353 (1999).
9. Brieman, Leo: Technical note-some properties of splitting criteria. *Mach. Learn.* **24**, 41–47 (1996)
10. Han, J., Kamber, M.: *Data mining: concepts and techniques*, 2nd edn. Morgan Kaufmann Publisher, San Francisco (2006)
11. Buntine, Wray: Niblet, tim: a further comparison of splitting rules for decision tree induction. *Mach. learn.* **8**, 75–85 (1992)
12. Kulkarni, V.Y., pradeep, K.S.: Random forest classifiers: a survey and future research directions. *Int. J. Adv. Comput.* ISSN 2051–0845. **36**(1), 1144–1153 (2013).
13. Liu, W.Z., White, A.P.: The importance of attribute selection measures in decision tree induction. *Mach. Learn.* **15**, 25–41 (1994)

# Text Classification Using Machine Learning Methods-A Survey

**Basant Agarwal and Namita Mittal**

**Abstract** Text classification is used to organize documents in a predefined set of classes. It is very useful in Web content management, search engines; email filtering, etc. Text classification is a difficult task due to high-dimensional feature vector comprising noisy and irrelevant features. Various feature reduction methods have been proposed for eliminating irrelevant features as well as for reducing the dimension of feature vector. Relevant and reduced feature vector is used by machine learning model for better classification results. This paper presents various text classification approaches using machine learning techniques, and feature selection techniques for reducing the high-dimensional feature vector.

**Keywords** Text classification · Feature selection · Machine learning Algorithms

## 1 Introduction

Text mining means to extract relevant information from text and to search for interesting relationships between extracted entities. Text classification is one of the basic and important tasks of text mining. Text classification means automatically assign a document in some predefined categories of documents based on their contents. Text classification is a supervised learning model that can classify text documents according to their predefined categories. Web content for a search engine can be organized properly using text classification for efficient retrieval of Web documents. Text classification techniques are used for automatically email filtering, medical diagnosis,

---

B. Agarwal (✉) · N. Mittal  
Malaviya National Institute of Technology, Jaipur, India  
e-mail: thebasant@gmail.com

N. Mittal  
e-mail: mittalnamita@gmail.com

news group filtering, documents organization, indexing for document retrieval, word sense disambiguation by detecting the topics a document covers.

Main challenges for text classification are following:

1. High dimensionality, due to which it is difficult to create a classifier model because performance of the classifier degrades as feature vector increases for a classifier [1].
2. Not all features are important for classification, some features may be redundant or irrelevant and some may even misguide the classification result [1].
3. To remove redundancy and noisy features from the data.

In text classification, feature vector generally consist of thousands of attributes/features, that is why feature reduction methods has to be used for removing irrelevant features, in such a way that classifier accuracy does not affected. Efficiency and success of any machine learning algorithm depends on the quality of data. Automatic feature reduction methods are used for reducing the size of feature vector and removing irrelevant features. There are two methods for this purpose, (i) feature selection and (ii) feature transformation. In feature selection important features are identified and used for classification. In feature transformation feature vector is transformed into a new feature vector with selected lower dimensions.

The objective of this paper is to discuss, (i) filter-based feature selection methods, (ii) feature transformation techniques, and (iii) machine learning techniques used for text classification.

The remainder of the paper is organized as follows. Section 2 describes the text classification process, Sect. 2.4 discusses the evaluation methods used for text classification, and Sect. 3 concludes the paper.

## 2 Text Classification Process

In text classification process, initially documents are read from the collection, then preprocessing like stemming, removal of stop words takes place. After that, important features are selected from the feature vector. Lower dimensional feature vector is fed to the classifier. Common text classification methods include both supervised and unsupervised machine learning methods like Support Vector Machine (SVM) [9], K-Nearest Neighbour (KNN), Neural Network (NN), Naive Bayes [19] etc.

### 2.1 Preprocessing

The most common preprocessing task for text classification is that of stop-word removal and stemming. In stop-word removal, the common words in the documents which are not discriminatory to the different classes are removed from feature vector.

For example “a”, “the”, “that”, etc., are frequent words that do not help in classification, which occurs almost equally in all the documents.

In stemming, different forms of the same word are converted into a single word. For example, singular, plural, and different tenses are converted into a single word. Port stemmer algorithm is well-known algorithm for stemming [7].

## 2.2 Text Representation

For text classification using machine learning methods, each document should be represented in the form so that learning algorithm can be applied. So each document is represented as a vector of words/terms/feature. The values in the feature vectors are weighted to reflect the frequency of words in the documents and the distribution of words across the collection. The more times a word/term occurs in a document, the more it is relevant to the document. The more times the word occurs throughout all documents in the collection, the more poorly it discriminates between documents [15]. A popular weighting scheme is Term Frequency–Inverse Document Frequency (TF-IDF):  $w_{ij} = tf(ij) * idf(i)$ , where  $tf(ij)$  is the frequency of term  $i$  in document  $j$ , and  $idf(i)$  is the inverse document frequency, it measures if a term is common or rare across documents.  $IDF$  can be calculated by  $\log(N/F)$ , where  $N$  is total number of documents in the corpus,  $F$  is number of documents where term  $I$  appears.

The  $tf * idf$  weighting scheme does not consider the length of document,  $tfc$  weighting is similar to  $tf * idf$  weighting except, length normalization is used in  $tfc$  weighting. In addition, a logarithm-based weighting scheme is log-weighted term frequency that uses a logarithm of word frequency, reducing the effect of large number of term frequency in a document with big document length [19]. One method is word frequency weighting, i.e., to use the frequency of the term in the document [19]. Another method for text representation is to simply calculate binary feature values, i.e., a term either present or not in the document [14].

## 2.3 Feature Reduction

Feature reductions methods are used to remove the irrelevant features and reduce the dimensionality of feature space. Basically, there are two methods for feature reductions (1) Feature selection, and (2) Feature extraction/Feature transformation. Feature extraction means reduce the dimensionality by transformation/projection of all the features in subset features. It maps the high-dimensional data on lower dimensional space. New attributes are obtained by the combination of all the features, for e.g., Principal Component Analysis (PCA) [22], Singular Value Decomposition (SVD) [12]. Feature selection technique selects the important features/attributes from the high-dimensional feature vector using certain criteria for e.g. Information Gain (IG). Its main purpose is to reduce the dimensionality of the feature space, remove

the irrelevant features so that performance and accuracy of the machine learning algorithm can be improved and also algorithm can run faster.

Feature selection methods are basically of three types depending on how they select feature from the feature vector, i.e., filter approach, wrapper approach, and embedded approach [14, 22].

In filter approach [14, 22], all the features are treated independent to each other. Features are ranked according to their importance score of each feature, which is calculated by using some function. Filter approach-based methods does not depend on the classifier. Advantages of this approach are that they are computationally simple, fast, and independent to the classifier. Feature selection step is performed once and then reduced feature vector is used with any classifier can be used. Disadvantage of this approach is that it does not interact with the classifier. It assumes features are independent; it is possible that a feature performs well but performs worse with the combination of other feature, and similarly a lower scoring attribute can show good performance with the combination to other features [22]. However filter approach with some modification, included features dependency in multivariate filtering approach.

In wrapper approach [14, 22], a search procedure is defined to search the feature subset, and various subsets of features are generated and evaluated for a specific classifier. In wrapper approach features are treated dependant to each other, and model interacts with the classifier. As the number of features subset grows exponentially with increase in the number of features, hence heuristic search methods can be used for selecting feature subsets. Advantages of this approach are that it interacts with the classifier, and features dependencies are considered. Disadvantages are that there is a risk of over fitting, slow and classifier-dependant.

Filter approach is very fast compared to wrapper approach, wrapper approach is very efficient but specific for a classifier algorithm. It is time consuming. If size of dataset is high than it is very difficult to create wrapper.

### 2.3.1 Filter-based Feature Selection Methods

#### *Document Frequency*

Document Frequency (DF) is the number of documents in which a term appears. In document frequency thresholding, those terms are removed whose document frequency is less than a predefined value. This is an unsupervised feature selection method; it can be computed without class labels. Assumption is that rare terms are less informative for learning algorithms [3, 4], and frequent words have more chances that they will be present in future test cases.

#### *Information Gain*

Information gain measures decrease in entropy when the feature value is given, means number of bits of information obtained due to knowing the presence or absence of a term for prediction [4].

First, Information gain for each term is computed. Further, terms are removed from the feature vector whose value is below predefined threshold value [4].

#### *Mutual Information*

Mutual information of a term and class attribute is used for feature selection methods. Mutual information is used to quantitatively analyze the relationship between any two features or between a feature and a class variable. Mutual information compares the probability of occurring term  $t$  and class  $c$  together and probability of term and class individually [6, 22]. The mutual information of between term  $t$  and class  $c$  is defined as

$$I(t, c) = \log \frac{P(t, c)}{P(t)*P(c)} = \log \frac{P(t \wedge c)}{P(t)*P(c)} \quad (1)$$

If there is a relationship between term and class then joint probability  $P(t,c)$  will be greater than the  $P(t)*P(c)$ , and  $I(t,c) \gg 0$ . High value of mutual information of a feature with the class indicates higher importance of feature for classification. Threshold value can be set for selecting the features.

#### *Chi Square*

The chi squared measures the lack of independence between term  $t$  and class  $c$ . it can be used for testing independence or association between two variables. Chi squared statistic test tries to identify the best terms for the class  $c$  and are the ones which are distributed most differently in the sets of positive and negative examples of class  $c$  [1, 2].

#### *Odds Ratio*

Odds Ratio is a fraction of the word occurring in the positive class normalized by that of the negative class. It has been used for relevance ranking in information retrieval. It is based on the assumption that the distribution of features on the relevant documents is different from the distribution of features on the nonrelevant documents [17].

### **2.3.2 Feature Transformation**

Feature transformation techniques are used to reduce the feature vector size, it does not rank the features according to their importance but it transforms higher dimensional feature space on the lower dimensional feature space.

Singular value decomposition can be used for feature reduction for text classification. Latent Semantic Analysis (LSA) uses singular value decomposition method for mapping high-dimensional features to lower dimensional space that is latent semantic space [12].

Principal Component Analysis (PCA) is a common method for feature transformation. PCA seeks a linear projection of high-dimensional data into lower dimensional space in such way that maximum variance is extracted from the variables. These extracted variables are called principal components those are orthogonal to each other and uncorrelated. Principal Component Analysis rejects data with small variance [11].



Linear Discriminant Analysis (LDA) is one of the popular dimension reduction methods. It finds out the feature that has high-class discriminant capability. Discriminant features are identified by maximizing the ratio of the between-class to the within-class variance of a given data set. So a feature scattered more among different classes and less scattered within class is important for the classification. A novel text classification method is proposed which is based on LDA and SVM. High-dimensional feature vector is transformed into lower dimensional feature vector by LDA feature reduction technique. Then SVM classifier is used for text classification [15].

Independent Component Analysis (ICA) [16], on the other hand, is to identify independent components. ICA transforms the original high dimensional data into lower dimensional components that are maximally independent from each other. These independent components are not necessarily orthogonal to each other like PCA. For dimension reduction ICA finds  $k$  components that effectively contain maximum variability of the original data.

## 2.4 Classifier Models

There has been active research in text classification over the past few years. Most of the research work in text classification has focused on applying machine-learning methods to classify text based on words from a training set [1, 18, 19]. These approaches include Naïve Bayes (NB) classifiers, SVM, K-Nearest Neighbor (KNN), Decision Tree, Rocchio algorithm, etc., and also by combining approaches.

Naïve Bayes classifier assumes independence among attributes. NB approach's implementation is simple and learning time is less, however, its performance is not good for categories defined with very few features [21, 25]. It gives a good classification result of a text document provided there are a sufficient number of training instances of each category. Gini index-based weighted features is combined with NB classifier, this approach improved the performance for text classification [10]. Bayesian classifier is modified to handle one hundred thousand of variables. Experiment result shows that modified tree-like Bayesian classifier works with sufficient speed and accuracy [2]. Maximum entropy is used for a new text classifier proposed in [8], resulting in better performance in contrast to bayes classifier.

SVM produces good results for two class classification problems like text document belongs to a particular category or not, but it is difficult to extend to multiclass classification. To solve multiclass problems of SVM more efficiently, class incremental approach is proposed in [23]. SVM outperforms with KNN and naïve Bayesian classifier for text classification as proposed in [28]. Naïve Bayesian method was used as a preprocessor for dimensionality reduction followed by the SVM method for text classification [5].

A modified k-NN-based text classification is proposed, in which variants of the k-NN method with different decision functions,  $k$  values, and feature sets were evaluated to increase the performance of the algorithm [9]. An improved k-NN algorithm

is proposed in which unimportant documents are not considered, to increase the performance of the classification [13].

Decision Tree-based text classification does not assume independence among its features as in Naïve Bayesian. Decision tree performs well as a text classifier when there are very less number of features; however it becomes difficult to create a classifier for large number of feature [19].

In Rocchio Algorithm, text is indicated as an N-dimensional vector. N is the total number of features, and each feature item is weighted by TF-IDF algorithm. Training text dataset is expressed as a feature vector, and then generated the prototype vector for each class. At the time of classification, similarity between different class features vectors and feature vector of unknown text document is calculated, and the text is assigned to the class which has highest similarity [19].

Boosting and Bagging are two voting-based classifiers. In voting classifier, training samples are taken randomly from the collection multiple times, and different classifiers are learned. To classify a new sample, each classifier gives a different class label; the result of voting classifier is decided by the maximum votes earned for a particular class [29]. Main difference between bagging and boosting is in the way, they take the samples for training a classifier. In bagging, training samples are taken with equal weights randomly, and in boosting, more weightage are given to those samples which have been misclassified by previous classifiers. AdaBoost which is a boosting classifier outperforms rocchio when the training dataset contains a very large number of relevant documents [20].

Feature vector is fed to the inputs of the neural network and classification results come from the output of the network. Problem with the neural network is its slow learning. Performance of neural network-based text classification was improved by assigning the probabilities derived from Naïve Bayesian method as initial weights [24]. In [27], three neural networks, i.e. (i) the Competitive, (ii) the Back Propagation (BP), and (iii) the Radial Basis Function (RBF), in text classification are compared. The competitive network is an unsupervised and BP and RBF are supervised methods for learning. Experimental results show that BP works effectively for text classification, RBF network learns faster compare to others. BP and RBF perform better than competitive network. A modified back propagation neural network is proposed to improve the performance of traditional algorithm. SVD technique is used for reducing the dimension of the feature vector. Experimental results show that the modified neural network outperforms traditional back propagation NN [26].

There is a need to experiment with more such hybrid techniques in order to derive the maximum benefits from machine learning algorithms and to achieve better classification results. Different feature selection and reduction techniques are used in combination with different machine learning algorithm to increase the performance and accuracy of the classifier.

### 3 Conclusion

The commercial importance of automatic text classification applications has increased due to the number of blogs, Web contents, growth rate of Internet access. Therefore, much research is currently focused in this area. Performance of text classification can be increased using machine learning techniques. However preprocessing plays important role due to high-dimensional data, and feature selection and reduction techniques enhances the quality of training data for the classifier, resulting into improved classifier accuracy.

Text classification for regional language documents can be useful for several governmental and commercial projects. Multitopic text classification, identify contextual use of terms on blogs and use of semantics for better classifiers are some of the areas, where future research can be done.

### References

1. Sebastiani, F.: Machine learning in automated text categorization. *ACM Comput. Surv.* **34**(1), 1–47 (2002)
2. Al-Harbi, S., Almuhareb, A., Al-Thubaity, A., Khorsheed, M., Al-Rajeh, A.: Automatic Arabic text classification. In: *JADT'08*, France, pp. 77–83 (2008)
3. Forman, George: An extensive empirical study of feature selection metrics for text classification. *J. Mach. Learn. Res.* **3**, 1289–1305 (2003)
4. Yang, Y., Pedersen, J.O.: A Comparative study on feature selection in text categorization. In: *Proceedings of the Fourteenth International Conference on Machine Learning*, pp. 412–420, 08–12 July 1997
5. Isa, D., Lee, L.H., Kallimani, V.P., RajKumar, R.: Text document pre-processing with the Bayes formula for classification using the support vector machine. *IEEE Trans. Knowl. Data Eng.* **20**(9), 1264–1272 (2008)
6. Yan, X., Gareth J., Li J.T., Wang, B., Sun, C.M.: A study on mutual information-based feature selection for text categorization'. *J. Comput. Inf. Syst.* **3**(3), 1007–1012 (2007)
7. Porter, M.F.: An algorithm for suffix stripping. *Program* **14**(3), 130–137 (1980)
8. Nigam, K., Mccallum, A.K., Thrun, S., Mitchell, T.: Text classification from labeled and unlabeled documents using EM. *Mach. Learn.* **39**, 103–134 (2000)
9. Joachims, T.: A statistical learning model for text classification for support vector machines. In: *24th ACM International Conference on Research and Development in Information Retrieval (SIGIR)* (2001)
10. Dong, Tao, Shang, Wenqian, Zhu, Haibin: An improved algorithm of Bayesian text categorization. *J. Softw.* **6**(9), 1837–1843 (September 2011)
11. Kumar, C.A.: Analysis of unsupervised dimensionality reduction techniques. *Comput. Sci. Inf. Syst.* **6**(2), 217–227 (Dec. 2009)
12. Soon, C.P.: Neural network for text classification based on singular value decomposition. In: *7<sup>th</sup> International conference on Computer and Information Technology*, pp. 47–52 (2007)
13. Muhammed, M.: Improved k-NN algorithm for text classification. Department of Computer Science and Engineering University of Texas at Arlington, TX, USA
14. Ikonomakis, M., Kotsiantis, S., Tampakas, V.: Text classification using machine learning techniques. *IEEE Trans. Comput.* **4**(8) 966–974 (2005)
15. Wang, Z, Qian, X.: Text categorization based on LDA and SVM. In: *Computer Science and Software Engineering, 2008 International Conference*, vol. 1, pp. 674–677 (2008)

16. Kolenda, T., Hansen, L.K., Sigurdsson, S.: Independent components in text. In: Girolami, M. (ed.) *Advances in Independent Component Analysis*, Springer-Verlag, New York (2000)
17. Jia-ni, H.U., Wei-Ran, X.U. Jun, G., Wei-Hong, D.: Study on feature methods in chinese text categorization. *Study Opt. Commun.* **3**, 44–46 (2005)
18. Aggarwal, C.C., Zhai, C-X.: *A survey of text classification algorithms*. *Mining Text Data*. pp. 163–222, Springer (2012)
19. Aas, K., Eikvil, L.: *Text categorisation: A survey*™m Tech. rep. 941. Norwegian Computing Center, Oslo, Norway (1999)
20. Schapire, R.E., Singer, Y., Singhal, A.: Boosting and Rocchio applied to text filtering. In: *Proceedings of SIGIR-98 21st ACM International Conference on Research and Development in Information Retrieval*, pp. 215–223, ACM Press, New York US (1998)
21. Kim, S.B., Rim, H.C., Yook, D.S., Lim, H.S.: Effective Methods for Improving Naive Bayes Text Classifiers. *LNAI* **2417**, 414–423 (2002)
22. Saeyns, Y., Inza, I., Larranaga, P.: A review of feature selection techniques in bioinformatics. *Bioinformatics* **23**(19), 2507–2517 (2007)
23. Zhang, B., Su, J., Xu, X.: A class-incremental learning method for multi-class support vector machines in text classification. In: *Proceedings of the 5th IEEE international conference on Machine Learning and, Cybernetics*, pp. 2581–2585 (2006)
24. Goyal, R.D.: Knowledge based neural network for text classification. In: *Proceedings of the IEEE international conference on Granular, Computing*, pp. 542–547 (2007)
25. Meena, M.J., Chandran, K.R.: Naïve bayes text classification with positive features selected by statistical method. In: *Proceedings of the IEEE international conference on Advanced, Computing*, pp. 28–33 (2009)
26. Li, C.H, Park, S.C.: An efficient document classification model using an improved back propagation neural network and singular value decomposition. *J. Expert Syst. Appl.* **36**(2), pp. 3208–3215 (2009)
27. Wang, Z., He, Y., Jiang, M.: A comparison among three neural networks for text classification. In: *8th IEEE International Conference on, Signal Processing* (2006)
28. Zhijie, L., Lv, X., Liu, K., Shi, S.: Study on SVM compared with other text classification methods. In: *2<sup>nd</sup> International workshop on education technology and computer, science* (2010)
29. Freund, Y., Shapire, R.R.: Experiments with a new boosting algorithm. In: *Proceedings of 13th International Conference on, Machine learning*, pp. 148–156 (1996)

# Weka-Based Classification Techniques for Offline Handwritten Gurmukhi Character Recognition

Munish Kumar, M. K. Jindal and R. K. Sharma

**Abstract** In this paper, we deal with weka-based classification methods for offline handwritten Gurmukhi character recognition. This paper presents an experimental assessment of the effectiveness of various weka-based classifiers. Here, we have used two efficient feature extraction techniques, namely, parabola curve fitting based features, and power curve fitting based features. For recognition, we have used 18 different classifiers for our experiment. In this work, we have collected 3,500 samples of isolated offline handwritten Gurmukhi characters from 100 different writers. We have taken 60 % data as training data and 40 % data as testing data. This paper presents a novel framework for offline handwritten Gurmukhi character recognition using weka classification methods and provides innovative benchmark for future research. We have achieved a maximum recognition accuracy of about 82.92 % with parabola curve fitting based features and the multilayer perceptron model classifier. In this work, we have used C programming language and weka classification software tool. At this point, we have also reported comparative study weka classification methods for offline handwritten Gurmukhi character recognition.

**Keywords** Handwritten character recognition · Feature extraction · Classification · Weka · Tool

---

M. Kumar (✉)

Department of Computer Science, Panjab University Rural Centre,  
Kauni, Muktsar, Punjab, India  
e-mail: munishcse@gmail.com

M. K. Jindal

Department of Computer Science and Applications, Panjab University Regional Centre,  
Muktsar, Punjab, India  
e-mail: manishphd@rediffmail.com

R. K. Sharma

School of Mathematics and Computer Applications, Thapar University,  
Patiala, Punjab, India  
e-mail: rksharma@thapar.edu

# 1 Introduction

Offline Handwritten Character Recognition usually abbreviated as Offline HCR. Offline HCR is one of the oldest ideas in the history of pattern recognition by using the computer. In character recognition, the process commences by reading of a scanned image of character, determining its meaning, and finally, translates the image into a computer written text document. In recent times, Gurmukhi character recognition has become one of the fields of practical usage. OHCR involves activities like digitization, preprocessing, feature extraction, classification, and recognition. Recognition rate depends on the quality of features extracted from characters and effectiveness of the classifiers. For the past several years, many academic laboratories and companies are occupied with research on handwriting recognition. In the character recognition system, we need three things, i.e., preprocessing on digitized data, feature extraction, and decision-making algorithms. Preprocessing is the initial stage of character recognition. In this phase, the character image is normalized into a window of size  $100 \times 100$ . After normalization, we produce bitmap image of the normalized image. Afterwards, the bitmap image is transformed into a skeletonized image. In this work, we have used two efficient feature extraction techniques, namely, parabola curve fitting based features and power curve fitting based features for character recognition. Aradhya et al. [1] have presented a multilingual OCR system for South Indian scripts based on PCA. Bansal and Sinha [2, 3] have presented a technique for complete Devanagari script recognition. In this technique, they have recognized the character in two steps. In first step, that recognize the unknown characters and in the second step they recognize the character based on the strokes. Chaudhary et al. [4] have represented a technique for recognition of connected handwritten numerals. Gader et al. [6] have presented a handwritten word recognition system using neural network. Hanmandlu et al. [8] have presented a handwritten Hindi numeral recognition system using Fuzzy logic. Kumar [11] has proposed a AI based approach for handwritten Devanagari script recognition. Kumar et al. [12] have presented a review on OCR for handwritten Indian scripts. They have also proposed two efficient feature extraction techniques for offline handwritten Gurmukhi character recognition [13]. Lehal and Singh [14] have presented a printed Gurmukhi script recognition system, where connected components are initially segmented using thinning based approach. Pal et al. [18] have assimilated a comparative study of handwritten Devanagari character recognition using twelve different classifiers and four sets of features. Rajashekaradhya and Ranjan [20] have proposed zoning based feature extraction technique for Kannada script recognition. Roy et al. [21] have presented a script identification system for Persian and Roman script. Sharma et al. [22] have proposed a offline handwritten character recognition system using quadratic classifier. Pal et al. [16, 17] have come up with a technique for offline Bangla handwritten compound characters recognition. They have used modified quadratic discriminant function for feature extraction. They have also presented a technique for feature computation of numeral images. Classification is the most significant activity for character recognition. In the classification process, we required decision making algorithms. There



**Fig. 1** *Gurmukhi* script character set

have presented various kinds of decision making algorithms as: Baye's Net, DMNB Text, Naïve Baye's, multilayer perceptron model, etc [5, 7, 9, 10, 15, 19]. We have applied 18 different weka classification methods for offline handwritten Gurmukhi character recognition.

## 2 Gurmukhi Script and Data Collection

*Gurmukhi* script is the script used for writing in the Punjabi language and is derived from the old *Punjabi* term *Guramukhi*, which means “from the mouth of the Guru”. *Gurmukhi* script has three vowel bearers, thirty two consonants, six additional consonants, nine vowel modifiers, three auxiliary signs, and three half characters. The *Gurmukhi* script is the 12th most widely used script in the world. Writing style of *Gurmukhi* script is from top to bottom and left to right. In the *Gurmukhi* script, there is no case sensitivity. The character set of *Gurmukhi* script is given in Fig. 1. In the *Gurmukhi* script, most of the characters have a horizontal line at the upper part called, headline and the characters are connected with one another through this line.

For the present work, we have collected the data from 100 different writers. These writers were requested to write each Gurmukhi character. A sample of handwritten Gurmukhi characters by five different writers ( $W_1, W_2, \dots, W_5$ ) is given in Fig. 2.

Script Character	$w_1$	$w_2$	$w_3$	$w_4$	$w_5$
ੳ					
ਅ					
ੲ					
ਸ					
ਹ					

Fig. 2 Samples of handwritten *Gurmukhi* characters

### 3 Feature Extraction

In this phase, the features of input character are extracted. The performance of Offline HCR system depends on features, which are being extracted. The extracted features should be able to uniquely classify a character. In this work, we have used two efficient feature extraction techniques, namely, parabola curve fitting based features and power curve fitting based features.

#### 3.1 Parabola Curve Fitting Based Features

In this technique, initially, we have divided the thinned image of a character into  $n$  ( $=100$ ) zones. A parabola is fitted to the series of  $ON$  pixels in every zone by using the least square method. A parabola  $y = a + bx + c$  is uniquely defined by three parameters:  $a$ ,  $b$ , and  $c$ . This will give  $3n$  features for a given bitmap.

The steps that have been used to extract these features are given below.

- Step I: Divide the thinned image into  $n$  ( $=100$ ) number of equal sized zones.
- Step II: For each zone, fit a parabola using the least square method and calculate the values of  $a$ ,  $b$  and  $c$ .
- Step III: Corresponding to the zones that do not have a foreground pixel, the values of  $a$ ,  $b$ , and  $c$  are taken as zero.



### 3.2 Power Curve Fitting Based Features

In this technique also, we have divided the thinned image of a character into  $n$  ( $=100$ ) zones. A power curve is fitted to the series of  $ON$  pixels in every zone, using the least square method. A power curve of the form  $y = a$  is uniquely defined by two parameters:  $a$  and  $b$ . This will give  $2n$  features for a given bitmap.

The steps that have been used to extract these features are given below.

Step I: Divide the thinned image into  $n$  ( $=100$ ) number of equal sized zones.

Step II: In each zone, fit a power curve using least square method and calculate the values of  $a$  and  $b$ .

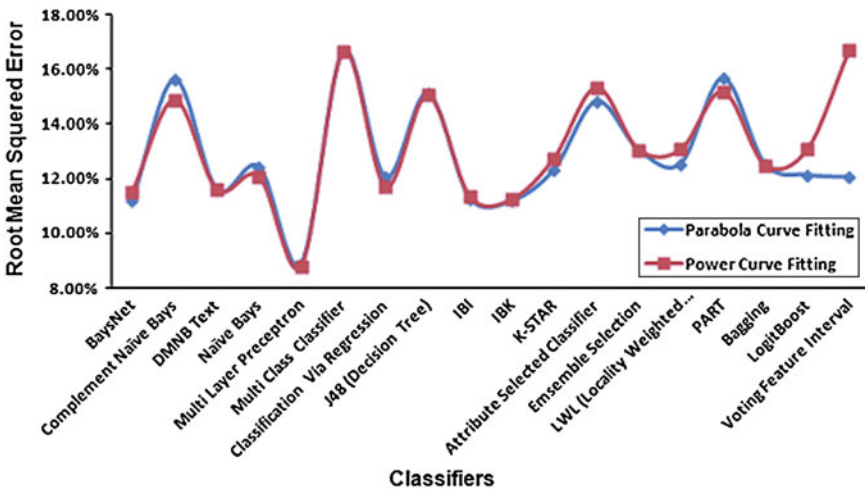
Step III: Corresponding to the zones that do not have a foreground pixel, the value of  $a$  and  $b$  is taken as zero.

**Table 1** Experimental results of parabola curve fitting based features

Classifier	Accuracy (%)	Root mean squared error (%)	Weighted average precision (%)	False rate (%)	Rejection rate (%)	Weighted F-measure average (%)
Baye's Net	72.78	11.18	74	0.80	26.20	73
Complement naïve bays	57.35	15.61	65.80	1.20	41.40	55.50
DMNB text	72.86	11.58	73.80	0.80	26.25	73
Naïve bays	71.29	12.41	74.30	0.80	27.90	71.70
Multi-layer perceptronl	82.92	8.88	83.40	0.50	16.60	82.90
Multi class classifier	60.86	16.64	65.70	1.10	38	61.80
Classification Via regression	65.57	12.03	66.70	1	33.40	65.60
J48 (decision tree)	55.64	15.11	56.7	1.30	43.10	55.60
IBI	77.85	11.25	79	0.60	20.40	78
IBK	77.86	11.16	80.00	0.60	21.40	78
K-Star	72.07	12.32	74.70	0.80	27.10	72.40
Attribute selected	57.07	14.81	58.80	1.20	41.70	57.30
Ensemble selection	58.07	13.03	59.40	1.20	40.70	57.60
LWL	66.07	12.53	68.70	1	32.90	66.60
PART	53.36	15.66	54.60	1.40	45.20	53.40
Bagging	63.42	12.50	64.60	1.10	35.50	63.30
LogitBoost	62.14	12.11	63.30	1.10	36.80	62.30
Voting feature interval	67.85	12.03	68.10	0.40	31.70	67

**Table 2** Experimental results of power curve fitting based features

Classifier	Accuracy (%)	Root mean squared error (%)	Weighted average precision (%)	False rate (%)	Rejection rate (%)	Weighted F-measure average (%)
Baye's Net	72.07	11.50	72.90	0.80	27.10	72.20
Complement naïve bays	61.28	14.87	66.80	1.10	37.60	60.40
DMNB text	72.86	11.58	73.80	0.80	26.30	72.80
Naïve bays	72.86	12.07	75.30	0.80	26.30	73.30
Multi-layer perceptron	82.86	8.80	83.50	0.50	16.60	82.60
Multi class classifier	65.78	16.64	69.30	1.00	33.20	66.60
Classification Via regression	67.85	11.68	68.10	1.00	31.10	67.70
J48 (decision tree)	55.50	15.04	57.10	1.30	43.20	55.60
IBI	77.57	11.32	79.40	0.60	21.80	77.60
IBK	77.57	11.23	79.40	0.60	21.85	77.60
K-Star	69.42	12.74	72.20	0.90	29.70	69.60
Attribute selected	53.14	15.32	54.60	1.40	45.50	53
Ensemble selection	59.42	13.04	60.60	1.20	39.40	59
LWL	64.50	13.05	66.90	1.00	34.50	64.60
PART	55.64	15.18	57.30	1.30	43.10	55.70
Bagging	64.07	12.47	65.10	1.00	34.90	63.80
LogitBoost	64.50	13.05	66.90	1.00	34.50	64.60
Voting feature interval	60.78	16.71	62.60	1.20	38.00	60.00



**Fig. 3** Recognition accuracy of diverse classification techniques

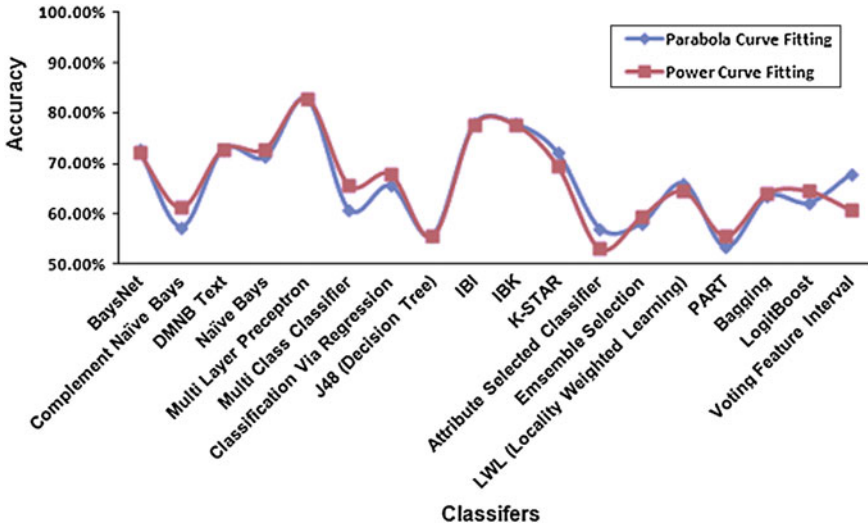


Fig. 4 Comparison of RMSE in various classification techniques

### 4 Classification

Classification phase is the decision-making phase of an OHCR engine. This phase uses the features extracted in the previous stage for deciding class membership. In this work, we have used 18 different classifiers based on *weka* namely, Baye’s Net, Complement Naïve Baye’s, Discriminative Multinomial Naïve Baye’s Text (DMNB

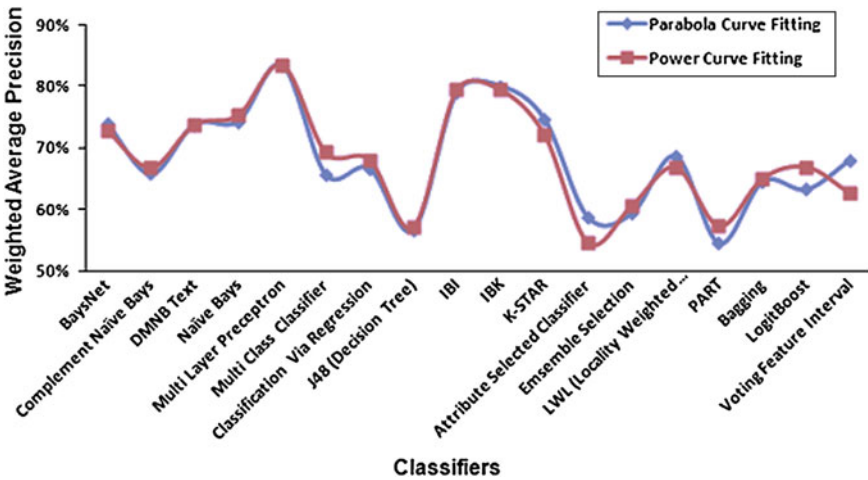


Fig. 5 Weighted average precision of divergent classification techniques

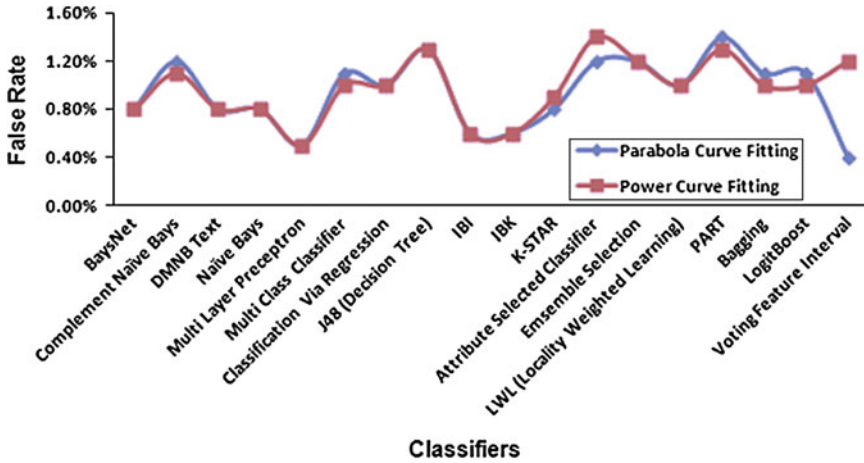


Fig. 6 Comparison of FPRate of different classifiers

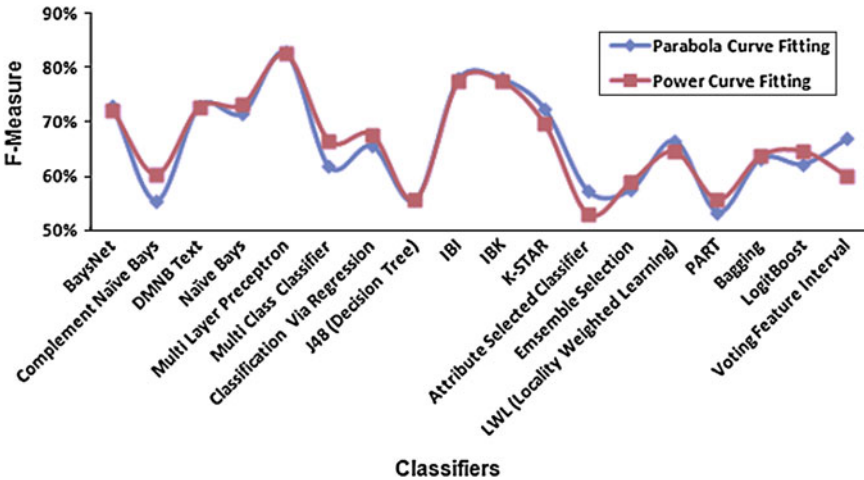


Fig. 7 F-Measure of diverse classification methods

Text), Naïve Baye’s, Multi-Layer Perceptron, Multi Class Classifier, Classification via Regression, Decision Tree, IBI, IBK, K-Star, Attribute Selected Classifier, Ensemble Selection, Locality Weighted Learning (LWL), PART, Bagging, Logit-Boost, and Voting Feature Interval classifier for offline handwritten *Gurmukhi* character recognition. Experimental results of these classifiers are presented in the next section.

## 5 Experimental Results

In this section, we have presented results of various *weka*-based classification methods. Table 1, depicts the results based on parabola curve fitting based feature extraction technique and Table 2 shows the power curve fitting based feature extraction results. In Fig. 3, we have presented recognition accuracy of various classification techniques for offline handwritten *Gurmukhi* character recognition. As such, we have seen that the multilayer perceptron model is the preeminent classifier for offline handwritten character recognition. We have achieved a maximum accuracy of about 82.92 % with parabola curve fitting based features and the multilayer perceptron model classifier.

In Fig. 4, we have presented the root mean squared error (RMSE) of various classification techniques, based on parabola curve fitting features and power curve fitting features. Figure 5, signifies the precision of different classification techniques. In Fig. 6, false rate (FP) of different classification techniques is depicted, graphically. Figure 7, describes the F-measure of various classifiers, considered in this work.

## 6 Conclusion

In present work, we have illustrated the effectiveness of various *weka*-based classification techniques for offline handwritten *Gurmukhi* character recognition. We have experimented on our own data set. We have collected 3,500 samples of isolated handwritten *Gurmukhi* characters from 100 different writers. After making a comparison of various classifiers for the recognition of character, we drew conclusion that the most appropriate classification technique is multilayer perceptron model. We obtained a maximum accuracy of about 82.92 % with parabola curve fitting based features and multilayer perceptron model classifier. The results of power curve fitting are also promising. A further study of the benefits of this technique can also be extended to offline handwritten character recognition of other Indian scripts.

## References

1. Aradhya, V.N.M., Kumar, G.H., Nousath, S.: Multilingual OCR system for south Indian scripts and English documents: an approach based on Fourier transform and principal component analysis. *Eng. Appl. Artif. Intell.* **21**, 658–668 (2008)
2. Bansal, V., Sinha, R.M.K.: Integrating knowledge sources in devanagari text recognition. *IEEE Trans. Syst. Man Cybern.* **30**(4), 500–505 (2000)
3. Bansal, V., Sinha, R.M.K.: Segmentation of touching and fused Devanagari characters. *Pattern Recogn.* **35**(4), 875–893 (2002)
4. Chaudhuri, B.B., Majumder, D.D., Parui, S.K.: A procedure for recognition of connected hand written numerals. *Int. J. Syst. Sci.* **13**, 1019–1029 (1982)
5. Friedman, N., Geiger, D., Goldszmidt, M.: Bayesian network classifiers. *Mach. Learn.* **29**, 131–163 (1997)

6. Gader, P.D., Mohamed, M., Chaing, J.H.: Handwritten word recognition with character and inter-character neural networks. *IEEE Trans. Syst. Man Cybern. Part B Cybern.* **27**(1), 158–164 (1997)
7. Genkin, A., Lewis, D., Madigan, D.: Large-scale Bayesian logistic regression for text categorization. *TECHNOME TRICS.* **49**(3), 291–304 (2004)
8. Hanmandlu, M., Grover, J., Madasu, V. K. and Vasikarla, S.: Input fuzzy for the recognition of handwritten Hindi numeral. In: *Proceedings of ITNG*, pp. 208–213 (2007)
9. Jomy, J., Parmod, K.V., Kannan, B.: Handwritten character recognition of south Indian scripts: a review. In: *Proceedings of Indian Language Computing*, pp. 1–6 (2011)
10. Kala, R., Vazirani, H., Shukla, A. and Tiwari, R.: Offline handwriting recognition using genetic algorithm. *Int. J. Comput. Sci. Issues* **7**(2,1), 16–25 (2010)
11. Kumar, D.: AI approach to hand written Devanagri script recognition. In: *Proceedings of 10th International conference on EC3-Energy, Computer, Communication and Control Systems*, **2**, 229–237 (2008)
12. Kumar, M., Jindal, M. K. and Sharma, R. K.: Review on OCR for handwritten Indian scripts character recognition. In: *Proceedings of DPPR*, pp. 268–276 (2011)
13. Kumar, M., Jindal, M.K., Sharma, R.K.: Efficient feature extraction technique for offline handwritten Gurmukhi character recognition. *Chaing Mai J. Sci.* (2012)
14. Lehal, G.S., Singh, C.: A Gurmukhi script recognition system. In: *Proceedings of 15th ICPR*, pp. 557–560 (2000)
15. McCallum, A., Nigam, K.: A comparison of event models for Naive Baye’s text classification. Paper presented at the workshop on learning for text categorization (1998)
16. Pal, U., Wakabayashi, T., Kimura, F.: Handwritten numeral recognition of six popular scripts. In: *Proceedings of ICDAR*, vol. **2**, pp. 749–753 (2007a)
17. Pal, U., Wakabayashi, T., Kimura, F.: A system for off-line Oriya handwritten character recognition using curvature feature. In: *Proceedings of 10th ICIT*, pp. 227–229 (2007b)
18. Pal, U., Wakabayashi, T., Kimura, F.: Comparative study of devanagari handwritten character recognition using different feature and classifiers. In: *Proceedings of 10th ICDAR*, pp. 1111–1115 (2009)
19. Patel, C.I., Patel, R., Patel, P.: Handwritten character recognition using neural network. *Int. J. Sci. Eng. Res.* **2**(4), 1–5 (2011)
20. Rajashekararadhya, S.V., Ranjan, S. V.: Zone based feature extraction algorithm for handwritten numeral recognition of Kannada script. In: *Proceedings of IACC*, pp. 525–528 (2009)
21. Roy, K., Alaei, A., Pal, U.: Word-wise handwritten Persian and Roman script identification. In: *Proceedings of ICFHR*, pp. 628–633 (2010)
22. Sharma, N., Pal, U., Kimura, F., Pal, S.: Recognition of off-line handwritten devanagari characters using quadratic classifier. In: *Proceedings of ICVGIP*, pp. 805–816 (2006)

**Part VII**  
**Soft Computing for Security (SCS)**

# An Efficient Fingerprint Indexing Scheme

Arjun Reddy, Umarani Jayaraman, Vandana Dixit Kaushik  
and P. Gupta

**Abstract** This paper proposes an efficient geometric-based indexing scheme for fingerprints. Unlike other geometric-based indexing schemes, the proposed indexing scheme reduces both memory and computational costs. It has been tested on IITK database containing 2,120 fingerprints of 530 subjects. Correct Recognition Rate is found to be 86.79 % at top 10 best matches. Experiments prove its superiority against well-known geometric-based indexing schemes.

**Keywords** Biometrics · Fingerprint indexing · Core point · Minutiae

## 1 Introduction

Fingerprint recognition system is used to recognize the identity of a subject. Identification can be done by searching all images in the database (henceforth termed as *models*) against a image (henceforth termed as *query*). To make an efficient process, there is a need of an efficient indexing technique. A fingerprint has the following characteristics:

---

A. Reddy (✉) · U. Jayaraman · P. Gupta  
Indian Institute of Technology, Kanpur, India  
e-mail: areddy@cse.iitk.ac.in

U. Jayaraman  
e-mail: umarani@cse.iitk.ac.in

P. Gupta  
e-mail: pg@cse.iitk.ac.in

V. D. Kaushik  
Harcourt Butler Technological Institute, Kanpur, India  
e-mail: vandanadixitk@yahoo.com



- Number of minutiae extracted from a fingerprint of a subject at any two time instants may not be same.
- There are too many minutiae in a fingerprint; some may be false.
- Number of minutiae of any two fingerprints may not be same.
- There may be partial occlusion in a fingerprint of a subject and it may overlap with some other subjects that are not present in the database.
- A query fingerprint may be rotated and translated with respect to the corresponding model fingerprints in the database.

Most of the available fingerprint indexing schemes can be classified on the basis of the features such as singular points [1], directional field [2], local ridge-line orientations [3], orientation image [4], minutiae [5], minutiae descriptor, multiple features, and SIFT features. Since most matching algorithms use minutiae, the use of minutiae is especially beneficial. These schemes derive robust geometric features from triplets of minutiae and use hashing techniques to perform the search.

A prominent geometric-based indexing technique for fingerprints is proposed by Germain et al. [6] in which geometric features from triplets are used with the help of Fast Look up Algorithm for String Homology (FLASH) hashing technique. It does clustering using transformation parameter where all the fingerprints in that bin represent a hypothesis match between the three points in the query fingerprint and those in the fingerprints of database. The best coordinate transformation that matches query triplet and model triplet is calculated with the information. The transformation should be such that squared distance between the points of query triplet and model triplet is minimum. This transformation parameter reduces false matches.

The scheme in [7] uses geometric features from minutiae triplets where the triplet features are maximum length of three sides, median and minimum angles, triangle handedness, type, direction and ridge count minutiae density. Since triangles are formed using all possible minutiae, this increases both memory and computational cost. A fast and robust projective matching for fingerprints has been proposed in [8]. It performs a fast match using a Geometric Hashing [9] which needs large computational time and memory.

Bebis et al. [10] have used the geometric features from Delaunay triangles formed on the minutiae for indexing the fingerprints, instead of all possible combination of triangles. It can be shown that for a given set of minutiae, the Delaunay triangulation produces linear number of triangles. This compares favorably to the number of all possible combinations of triangles/ bases pairs considered in approaches [6–8]. However, the major issue with Delaunay triangulation is that it is more sensitive to noise and distortion. For example, if some minutiae are missed or added (spurious minutiae), the structure of Delaunay triangulation gets affected.

This paper presents an efficient indexing scheme which uses geometric information from triangles formed on minutiae to index model fingerprints. It assumes that the uncertainty of feature locations associated with minutiae feature and shear does not affect the angles of a triangle arbitrarily. Triangles are invariant to translation and rotation. It reduces the number of possible triangles by taking minutiae to form triangles within the specified region  $R$  from its core point  $C$  and is inserted exactly

once into a hash table. So it effectively removes the use of all triangles/bases pairs used in [6–8] reducing memory and computational complexity.

The paper is organized as follows. Next section discusses feature extraction technique from a fingerprint image. Section 3 discusses the proposed indexing scheme. Experimental results are analyzed in the next section. Conclusions are given in the last section.

## 2 Feature Extraction

Feature extraction is a series of steps such as minutiae detection and core point detection [11]. Let  $M = \{m_1, m_2, \dots, m_o\}$  be the detected minutiae from each model fingerprint image. Each minutia  $m_i$  is a 4-tuple  $(x_{mi}, y_{mi}, \alpha_{mi}, T_{mi})$  which denotes their coordinates, direction, and type. Let  $C = (x_c, y_c, \alpha_c)$  be the core point, detected through [11] where  $(x_c, y_c)$  denote the coordinates and  $\alpha_c$  is the direction of the core point. The proposed indexing scheme overcomes some of the issues and constraints in [6, 7] by considering small number of possible triangles instead of all possible triangles. In a model fingerprint, it considers the minutiae to form triangles within the specific range  $R$  from its core point  $C$  reducing computational and memory cost. Further, it introduces some additional features to reduce false correspondences. The triplet features used in the proposed indexing scheme are:

1. Sides of the triangles  $s_1, s_2, s_3$ : Sides of the triangle is considered in certain order as the longest side, the medium side and the smaller side. If any two or three sides are similar, this system does not consider them because this type of triplets is negligible in number and their exclusion does not affect the results.
2. Regions of vertices  $r_1, r_2, r_3$ : Considering core point  $C$  as the center, concentric circles are drawn with radius  $r, 2r, 3r, 4r \dots$  till the circle's outer line is completely outside fingerprint boundary. The optimal value of  $r$  is found out with the help of experiments. Let  $p_1, p_2, p_3$  be three vertices of triplet and  $r_1, r_2, r_3$  be their respective regions of vertices and  $d_1, d_2, d_3$  be their respective distances from core point  $C$ . Then the value of  $r_i$  is given by  $r_i = \frac{d_i}{r} + 1, i = 1, 2, 3$ .
3. Triangle type  $\lambda$ : Each minutia is either termination or bifurcation. If  $\lambda_1, \lambda_2, \lambda_3$  are three vertices to indicate whether they are termination or bifurcation point, then  $\lambda$  for the triplet can be used as one more attribute for indexing component. Since  $\lambda_1, \lambda_2$  and  $\lambda_3$  can have values either 0 or 1, based on termination or bifurcation,  $\lambda$  can be any value between 0 and 7 and is calculated by  $\lambda = 4\lambda_1 + 2\lambda_2 + \lambda_3$ .
4. Orientation  $\varphi$ : Sometime all the above features may be same for triplets of two triangles. They can be differentiated by their orientation which can be calculated using cross-product between the longest side and the medium side. Orientation has two values, +1 or -1.

### 3 Proposed Indexing Scheme

The proposed indexing technique consists of two stages known as indexing and searching. During indexing, the model fingerprints in the database are indexed into a hash table. For any new fingerprint image, it can be added into a hash table without affecting the performance of the searching algorithm and without modifying the existing hash table. During searching, it recognizes the query fingerprint by searching only indexed hash bins.

#### 3.1 Indexing

For each model fingerprint consisting of core point  $C$  and minutiae, concentric circles are drawn with radius  $r, 2r, 3r, 4r\dots$  till the circle's outer line is completely outside fingerprint boundary. The value of  $r$  is found experimentally. All possible triangles within various circles are determined. The index  $I = (s_1, s_2, s_3, r_1, r_2, r_3\lambda, \varphi)$  is generated from each triangle to select an appropriate bin in hash table. At this bin, model fingerprint ID is added. At the time of indexing, it keeps track of number of triangles generated from each model fingerprint. Let  $T_i$  be the total number of triangles generated from a model  $M_i$  used for indexing. Steps for indexing are given in Algorithm 1.

---

##### Algorithm 1: Indexing

---

For each model fingerprint  $M_i$  do the following

1. Generate all possible triangles for minutiae of fingerprint.
  2. Consider only those triangles whose all sides are in the specifies range  $R$ .
  3. Store numbers of triangles considered in indexing and store it in  $T_i$  where  $T_i$  indicates total number of triangles of fingerprint  $M_i$  considered for indexing.
  4. For each triplet do the following
    - a) Generate index  $I = (s_1, s_2, s_3, r_1, r_2, r_3, \lambda, \varphi)$ .
    - b) Access appropriate bin of the hash table.
    - c) Add model fingerprint ID of the image to this bin.
- 

---

##### Algorithm 2: Searching

---

For the given query  $Q$  do the following

1. Generate all possible triangles from the minutiae of the query image.
  2. Consider only those triangles whose all sides are in the specified range  $R$ . Let there be  $T$  such triangles.
  3. For each triangle, do the following
    - a) Generate index  $I = (s_1, s_2, s_3, r_1, r_2, r_3, \lambda, \varphi)$ .
    - b) Access appropriate bin of the hash table.
    - c) Increment count  $C_i$  for all model fingerprints whose ID is in that bin.
    - d) Calculate  $S_i$ , score of image  $M_i$ , by formula  $S_i = \frac{C_i}{T_i}$ .
    - e) Obtain largest  $t$   $S_i$ 's that are to be considered for critical search.
-

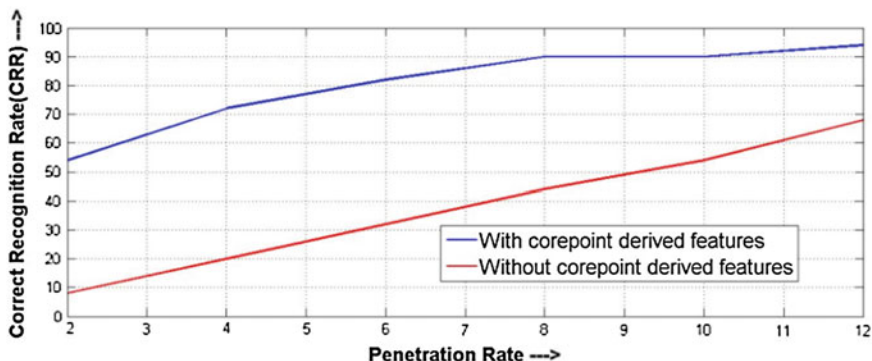


Fig. 1 Performance graph: effect of core point generated features

### 3.2 Searching

For a given query fingerprint, all possible triangles are generated using minutiae similar to indexing stage. Then only those triangles are considered whose all sides of triangle fall within the range  $R$ . Let there be  $T$  such triangles. From these triangles, an index  $I = (s_1, s_2, s_3, r_1, r_2, r_3, \lambda, \varphi)$  is generated to find an appropriate bin of hash table and to count each model fingerprint ID in that bin  $C_i$ . Same process is repeated for remaining query's triangles. Finally, score  $S_i$  is calculated by  $S_i = \frac{C_i}{T_i}$ ,  $i = 1, 2, \dots, N$  where  $N$  denotes the number of fingerprints in the database. Largest  $t$   $S_i$ 's which are considered for top  $t$  best matches are used for critical search to find out the exact match. Steps for searching are given in Algorithm 2.

## 4 Experimental Results

The proposed indexing scheme has been tested on IITK fingerprint database of 2,120 images acquired from 530 subjects. Every person has given four fingerprints of the same finger, at different instant of times. Four datasets have been created to carry out various experiments. DB1 contains 2120 fingerprints, DB2 has 1,336 fingerprints while DB3 and DB4 contains 668 fingerprints and 200 fingerprints respectively. In all these datasets, three impressions of each finger are used for indexing and remaining one impression is used for searching.

Figure 1 shows the performance of the proposed indexing scheme with respect to core point and database sizes. DB4 dataset is used for performing this experiment. The  $CRR$  is very high when core point is considered to obtain additional features from triangles. This  $CRR$ , when core point is used, is close to the  $CRR$  of the existing schemes like [6] and [7]. But the proposed scheme has achieved this performance without using transformation parameter cluster and imposing any geometrical

constraints. Experiments have also been conducted on all datasets DB1, DB2, DB3, DB4. It is found that there is no drastic difference in *CRR* for different datasets and as database size is increasing, *CRR* is coming down for a given *Penetration Rate*, slightly.

## 5 Conclusion

This paper has proposed a fingerprint-based indexing scheme which uses core point. This has helped to overcome various issues and constraints of well-known schemes. It has been tested on IITK database containing 2,120 fingerprints of 530 subjects. Accuracy is found to be 86.79 % at top 10 best matches. This accuracy has been achieved without using clustering based on transformation parameter and without imposing geometrical constraints as in existing schemes. However, it may not perform well when a fingerprint does not contain any core point.

## References

1. Liu, T., Zhu, G., Zhang, C., Hao, P.: Fingerprint indexing based on singular points. In: Proceedings of International Conference on Image Processing, pp. 293–296 (2005)
2. Cappelli, R., Maio, D., Maltoni, D.: Indexing fingerprint databases for efficient 1:N matching. In: Proceedings of International Conference on Control, Automation, Robotics and Vision (2000)
3. Alessandra, L., Dario, M., Davide, M.: Continuous versus exclusive classification for fingerprint retrieval. *Pattern Recogn. Lett.* **18**(10), 1027–1034 (1997)
4. Li, J., Yau, W.Y., Wang, H.: Fingerprint indexing based on symmetrical measurement In: Proceedings of International Conference on Pattern Recognition, pp. 1038–1041 (2006)
5. Liang, X., Asano, T., Bishnu, A.: Distorted fingerprint indexing using minutiae detail and delaunay triangle. In: Proceedings of the 3rd International Symposium on Voronoi Diagrams in Science and Engineering, pp. 217–223 (2006)
6. Germain, R.S., Califano, A., Colville, S.: Fingerprint matching using transformation parameter clustering. *IEEE Comput. Sci. Eng.* **4**(4), 42–49 (1997)
7. Bhanu, Bir, Tan, Xuejun: Fingerprint indexing based on novel features of minutiae triplets. *IEEE Trans. Pattern Anal. Mach. Intell.* **25**(5), 616–622 (2003)
8. Boro, R., Roy, S.D.: Fast and robust projective matching for fingerprints using geometric hashing. In: Proceedings of the 4th Indian Conference on Computer Vision, Graphics and Image Processing, pp. 681–686 (2004)
9. Haim, J.: Wolfson and Isidore Rigoutsos. Geometric Hashing: An overview, *IEEE Computational Science and Engineering* **4**(4), 10–21 (1997)
10. Bebis, G., Deaconu, T., Georgiopoulos, M.: Fingerprint identification using delaunay triangulation. In: Proceeding of IEEE International Conference on Intelligence, Information, and Systems, pp. 452–459 (1999)
11. Jain, A., Prabhakar, S., Hong, L.: A multichannel approach to fingerprint classification. *IEEE Trans. Pattern Anal. Mach. Intell.* **21**(4), 348–359 (1999)

# Gait Biometrics: An Approach to Speed Invariant Human Gait Analysis for Person Identification

Anup Nandy, Soumabha Bhowmick, Pavan Chakraborty  
and G. C. Nandi

**Abstract** A simple and a common human gait can provide an interesting behavioral biometric feature for robust human identification. The human gait data can be obtained without the subject's knowledge through remote video imaging of people walking. In this paper we apply a computer vision-based technique to identify a person at various walking speeds, varying from 2 km/hr to 10 km/hr. We attempt to construct a speed invariance human gait classifier. Gait signatures are derived from the sequence of silhouette frames at different gait speeds. The OU-ISIR Treadmill Gait Databases has been used. We apply a dynamic edge orientation histogram on silhouette images at different speeds, as feature vector for classification. This orientation histogram offers the advantage of accumulating translation and orientation invariant gait signatures. This leads to a choice of the best features for gait classification. A statistical technique based on Naïve Bayesian approach has been applied to classify the same person at different gait speeds. The classifier performance has been evaluated by estimating the maximum likelihood of occurrences of the subject.

**Keywords** Human gait · Orientation histogram · Naïve Bayesian · Speed invariance gait · OU-ISIR gait database

---

A. Nandy (✉) · S. Bhowmick · P. Chakraborty · G. C. Nandi  
Robotics and AI Lab, Indian Institute of Information Technology Allahabad, Allahabad, India  
e-mail: nandy.anup@gmail.com

S. Bhowmick  
e-mail: iro2011005@iiita.ac.in

P. Chakraborty  
e-mail: pavan@iiita.ac.in

G. C. Nandi  
e-mail: gcnandi@iiita.ac.in

# 1 Introduction

Bi-pedal locomotion is a complex task for a human. It requires a strong coordination of different joints of the human body which generates the rhythmic motion. A normal walking is involved with balancing ability and proper stability through the synchronous oscillations of different body joints of a person. The rhythmic motion [1] is called as gait which holds biometric signatures of the human behavioral walking pattern. Gait biometric has brought an enormous attention in security-related issues for detecting threats in controlled environments like Airports, Banks, Big Malls, and military installations. Johansson [2] has extracted the biological pattern of human gait by mounting Moving Lights Display (MLD) markers onto different major body parts of human subjects. Gait recognition from a video sequence signifies the gait as a potential biometric. It extends its advantages over the other biometrics traits like face, iris-scans, fingerprints, and hand scans for its unobtrusiveness properties, distance identification, and dealing with low resolution videos. Several gait review articles [3, 4] offer a general outline of the gait identification process. Morris [5] first started the wearable sensor-based gait recognition technique where motion recording sensors [6, 7] were attached on different locations of human body to record the acceleration of the gait which is utilized for identification purposes. The disadvantage of this system is that the full cooperation of the person is extremely required. Orr and Abowd [8] have shown the floor sensor-based gait recognition approach. It deals with force plates and an array of sensors deployed on the floor [8, 9] which enable to extract gait features from a person's walking on the floor. The Motion Vision-based gait recognition applies image and video processing techniques to extract gait features for identification from the video camera at a far distance. BenAbdelkader et al. [10] investigates individual identification and verification by calculating stride and cadence. Johnson and Bobick [11] applied a technique to measure static body parameters pertaining to distances among head and pelvis, height of the subject, maximum distance obtained between pelvis and feet, and distance among both the feet. These parameters are used for person recognition. It has been observed that maximum MV-based gait recognition works are based on the human silhouette [12, 13]. Liu and Sarkar [12] applied a technique to estimate the average silhouettes of a gait cycle and adopted a classification method called Euclidean distance to compare two averaged silhouettes for similarity measurements. A model-based approach is applied to determine gait features by evaluating the static and dynamic body parameters [14–16]. It is generally view and scale invariant which provides the advantage over the holistic approaches. The main disadvantage of this approach is low robustness and needs very high quality gait images and difficult capturing which requires proper camera calibration. Holistic approaches directly concentrate on gait sequences rather than any specific model for human body or parts of the human body. They are robust to the quality of human silhouettes and have low computational complexity [17, 18] which offers great advantages comparing to model-based approaches and are easy to implement with acceptable recognition rate. The major disadvantage of this model free approach is changing the shape of the silhouette with the effect

of occlusions, wearing different clothes and carrying of objects. Sarkar et al. [19] proposed the baseline algorithm which is directly used on gait silhouette images to extract features which are scaled and aligned before applying on classification techniques. A Radon Transform was applied by Boulgouris and Chi [20] on binary silhouette gait images to construct a template from binary gait sequences. The feature vector was constituted by Radon coefficients derived by applying subspace projections and linear discriminate analysis (LDA). Dimensionality reduction method was used in the context of gait analysis to capture most discriminative features.

The advantage of vision-based technique exposes that no person's physical cooperation is required. It also attracts the person's identification from a large distance with low resolution image where other biometrics modality perhaps fails to obtain good classification result. The overview of this paper is stated as follows:

In Sect. 2, the process of deriving gait signatures as a feature has been explained. Section 3 investigates the classification technique using Naïve Bayesian rule for speed invariant human identification. In Sect. 4, gait identification results together with the distribution of gait features using histogram bins have been addressed accordingly. The conclusion and the future work for enhancement of this research work have been added at the end of this paper.

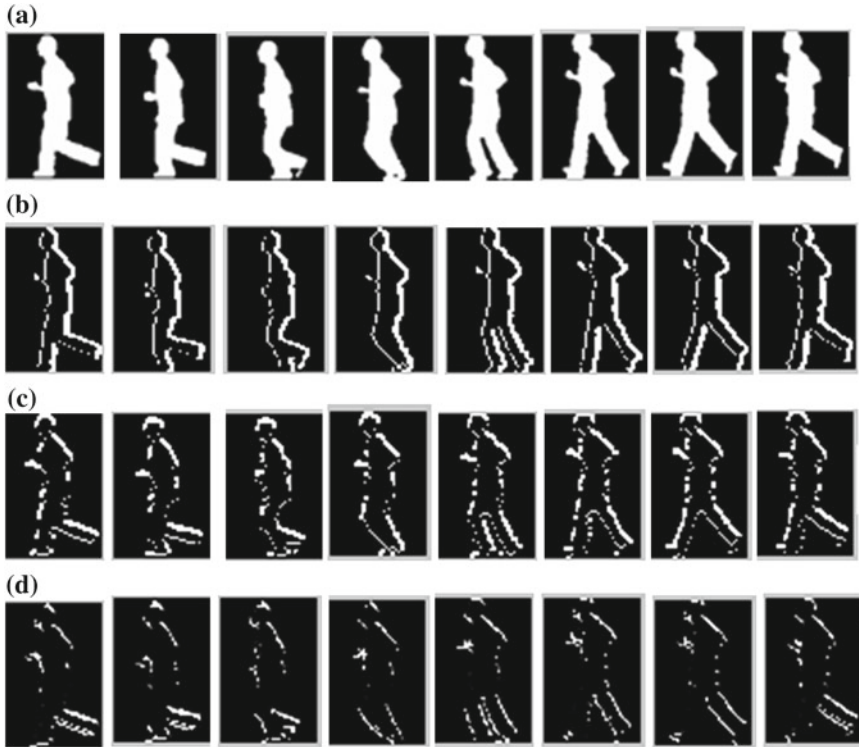
## 2 Method for Feature Extraction

As the human gait is purely a nonlinear time varying signal, hence selecting the best feature for speed invariant person identification is indeed a challenging job. The dynamic edge orientation histogram is chosen as a feature vector which appeals its robustness in orientation and translation invariant gait speeds. The orientation histogram computes the gradient by applying three tap derivative filter and subsequently produces the histogram in the desired orientations [21]. It has been investigated that the same person with different gait speeds will generate the similar feature vector. The algorithm for finding out the dynamic edge orientation histogram has been described in [22]. We have used OU-ISIR Gait Databases [23] for analyzing the human gait of 10 people at different gait speeds. The process of obtaining gait signatures at 10 km/hr gait speed has been depicted in Fig. 1.

## 3 Method for Gait Classification

In gait classification process, a Naïve Bayesian-based technique has been applied to identify a person walking at different speeds. Since the gait signal carries nonlinear characteristics, uncertainties are involved in classifying persons at various gait speeds. The statistical-based approach will allow us to differentiate different gaits at various speeds in order to achieve more accurate results for person identification. The Naïve Bayesian technique has been explained in the following section.





**Fig. 1** a Silhouette sequences at 10km/hr. b Edge derivative along X direction. c Edge derivative along Y direction, d Gradient of silhouette frames

### 3.1 Naïve Bayseian Technique

*Theory:* In naïve Bayesian classification technique, the probability density function at the feature point

$x = [x(1) \dots \dots \dots x(m)]^T \in R^m$  is required to be estimated by the given rule:

$$p(x) = \prod_{i=1}^m p(x(i))$$

It has been assumed that the features (attributes) of the constructed feature vector are statistically independent. This assumption has been made for the high-dimensional feature space to deal with the curse of dimensionality problem. It produces a great impact on a large number of training data points to compute a good estimation of multidimensional probability density function. Although the feature's

independence assumption is not true indeed, the performance of the naïve Bayesian classifier will still be satisfactory with fewer number sample points to obtain a reliable approximation of one-dimensional probability density function.

Naïve Bayesian classification technique based on the Bayes’ conditional probability theorem gives the probability of a hypothesis being true supported by the set of evidences. In the working formula of the Bayes’ theorem given underneath  $p(Hy_i|Ev)$  signifies the probability of the  $i$ th hypothesis being true supported by the evidences. Here each hypothesis is defined as the subject under test belongs to the  $i$ th class. In our analysis we have a set of nine evidences each corresponding to nine distinct speeds with which the subjects were walking.  $p(Evk|H_j)$  symbolizes that the evidence  $k$  supports  $i$ th hypothesis, whereas  $p(Hy_j)$  is the prior probability of  $j$ th hypothesis.

$$P(Hy_i|Ev) = \frac{\left(\prod_{k=1}^{\text{No of Evidence}} P(Evk|Hy_i) * P(Hy_i)\right)}{\sum_{j=1}^{\text{No of Subjects}} \left(\prod_{k=1}^{\text{No of evidence}} P(Evk|H_j)\right) * P(Hy_j)}$$

MaxLikelihood = Max ( $P(Hy_i|Ev)$ )  $\forall i = 1$  to No of subjects

We have taken the number of subjects to be ten where each of them was walking at a speed range of 2 km/hr to 10 km/hr with an interval of 1 km/hr. The hypothesis having the maximum likelihood is concluded as true.

### 4 Result Analysis and Discussion

We have applied Naïve Bayesian technique on ten subjects each walking on nine distinct and constant speeds. Separate datasets were used for training and testing purposes. The system was trained with features extracted from the silhouette images for each distinct speed. Once trained the classifier was tested for ten subjects each walking at nine different speeds. The classifier being a probabilistic one gave the maximum chance of resemblance of the pattern of the individual under test with each of the individuals present in the training database. The subject under test is classified to the corresponding subject in the training with which the likelihood of matching is maximum. In Fig. 2 is shown the graph for ten persons walking at nine different speeds and the percentage of maximum likelihood values in three different axes where one axis denotes the number of subjects, the second axis designates the speeds of walking, and the third axis symbolizes the percentage of maximum likelihood. For instance, the greater likelihood values, in case of person 2 or person 3 suggests the classifier classifying the test data set with a high confidence rate. It implies better probability of resemblance with the corresponding data in the training set. Figure 3 shows the polar plot of dynamic edge.

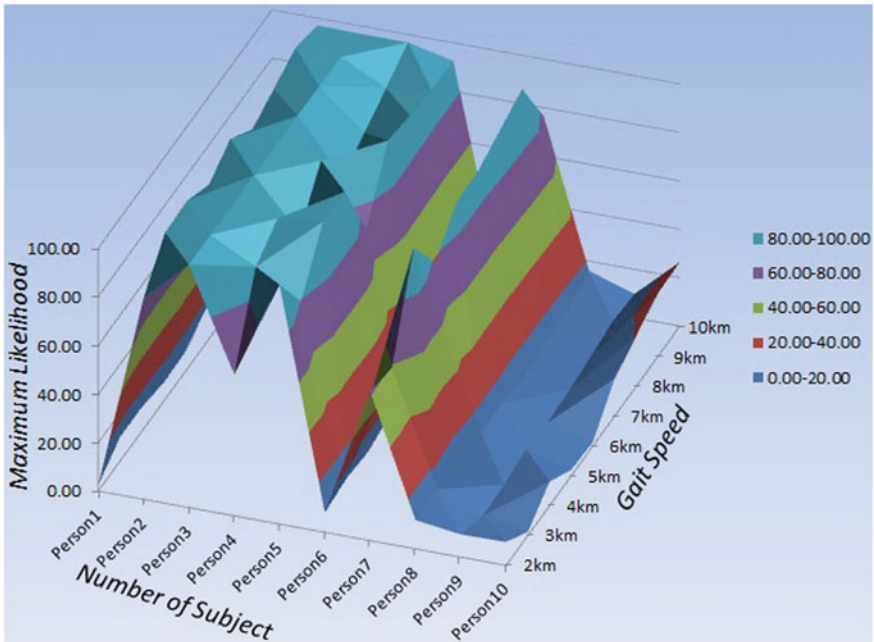
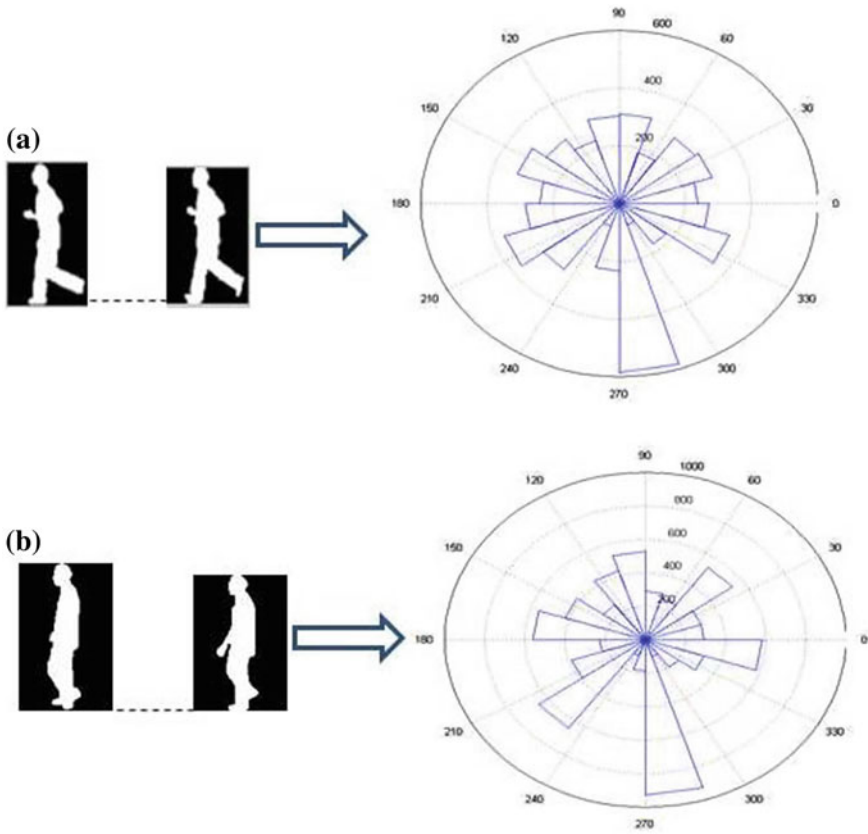


Fig. 2 3-D surface plot of Naïve Bayesian classification result

Orientation histogram at gait speed 10 and 2 km/hr. This plot implies the distribution of edge direction values clubbed together with respect to their magnitude range. Each group is collectively known as one histogram bin.

### 5 Conclusion and Future Work

It has been investigated and can also be concluded that data procurement is the most simple, as well as flawless, as the subject is freely walking on a treadmill at a constant speed. Moreover, as vision based has been taken as the subjects' Gait signature, it was free from any abnormalities that could have crept in if sensor-based data acquisition methods were applied. However the feature extraction process which needed to be applied for discriminating the individual subjects was quite a challenging job. The feature which was taken for the purpose of recognition should not only reduce the dimension of the dataset but also suffered from the risks of losing valuable information. Hence the performance of the classifiers can be significantly affected. We have after applying the analysis on a population of ten individuals come to the conclusion that the system could identify a person irrespective of its walking speed. We have used Naïve Bayesian technique for recognition purpose which provided the



**Fig. 3** Polar plot of orientation histogram for **a** 10km/hr and **b** 2km/hr gait speed

maximum likelihood for the resemblance of a person with the ones present in the training database.

Population size is a matter of concern as with the increase in the population size drastic change in the performance has been noted. The classifier starts misclassifying and a substantial drop of the likelihood has been observed. It would have been nice if rather selecting all the features the most significant ones could be identified which in course result in significant amendment of the classifier’s performance. Apart from it in lieu of incorporating one feature extraction technique ensemble of feature extraction techniques could be taken which may possibly embellish the classifier performance and better likelihood results could have been accomplished. Finally as the human gait is a purely nonlinear oscillatory pattern, Central Pattern Generator-based approach could be taken where from a mathematical model of the biped locomotion could be achieved which would subsequently ease the person identification process.

**Acknowledgments** We would like to express our warm gratitude to Prof Yasushi Yagi and his entire research team of Osaka University, Japan for providing us OU-ISIR Gait database to accomplish our research work.

## References

1. Taga, G., Yamaguchi, Y., Shimizu, H.: Self-organized control of bipedal locomotion by neural oscillators in unpredictable environment. In: *Biological Cybernetics* **65**(3), 147–159 (1991)
2. Johansson, G.: Visual perception of biological motion and a model for its analysis. In: *Perception and Psychophysics*, 14(2), 1973.
3. Boulgouris, N.V., Hatzinakos, D., Plataniotis, K.N.: Gait recognition: a challenging signal processing technology for biometric identification. In: *IEEE Signal Processing Magazine* **22**, 78–90 (2005)
4. Nixon, M.S., Carter, J.N.: Automatic Recognition by Gait. In: *Proceedings of the IEEE* **94**, 2013–2024 (2006)
5. Morris, S.J.: A shoe-integrated sensor system for wireless gait analysis and real time therapeutic feedback. PhD thesis, Harvard University-MIT Division of Health Sciences and Technology, 2004. <http://hdl.handle.net/1721.1/28601>
6. Ailisto, H.J., Lindholm, M., M antyj arvi, J., Vildjiounaite, E., M akel a, S.: Identifying people from gait pattern with accelerometers. In: *Proceedings of SPIE Volume: 5779; Biometric Technology for Human Identification II*, pages 7–14, 2005.
7. Gafurov, D., Snekkenes, E., Buvarp, T.E.: Robustness of biometric gait authentication against impersonation attack. In: *First International Workshop on Information Security (IS'06), OnThe-Move Federated Conferences (OTM'06)*, pages 479–488, Montpellier, France, Oct 30 - Nov 1 2006. Springer LNCS 4277.
8. Orr, R J., Abowd, G.D.:The smart floor: A mechanism for natural user identification and tracking. In: *Proceedings of the Conference on Human Factors in, Computing Systems*, 2000.
9. Suutala, J., Rning, J.:Towards the adaptive identification of walkers: Automated feature selection of footsteps using distinction sensitive LVQ. In: *Int. Workshop on Processing Sensory Information for Proactive Systems (PSIPS 2004)*, June 14–15 2004.
10. BenAbdelkader, C., Cutler, R., Davis, L.: Stride and cadence as a biometric in automatic person identification and verification. In: *Fifth IEEE International Conference on Automatic Face and Gesture Recognition*, pages 357–362, May 2002.
11. Johnson, A.Y., Bobick, A.F.: A multi-view method for gait recognition using static body parameters. In: *Third International Conference on Audio- and Video-Based Biometric Person Authentication*, pages 301–311, June 2001.
12. Liu, Z., Sarkar, S.: Simplest representation yet for gait recognition: Averaged silhouette. In: *International Conference on, Pattern Recognition*, pp. 211–214, 2004.
13. Liu, Z., Malave, L., Sarkar, S.: Studies on silhouette quality and gait recognition. In: *Computer Vision and, Pattern Recognition*, pp. 704–711, 2004.
14. Lee, L., Grimson, W.E.L.: Gait analysis for recognition and classification. In: *Proc. IEEE Int. Conf. Automatic Face and Gesture Recognition*, Washington, DC, May 2002, pp. 148–155.
15. Cunado, D., Nixon, M.S., Carter, J.N.: Automatic extraction and description of human gait models for recognition purposes. In: *Comput. Vis. Image Understand* **90**(1), 1–14 (2003)
16. Wagg, D.K., Nixon, M.S.: On automated model-based extraction and analysis of gait. In: *Proc. IEEE Int. Conf. Automatic Face and Gesture Recognition*, Seoul, Korea, May 2004, pp. 11–16.
17. Tafazzoli, F., Safabakhsh, R.: Model-based human gait recognition using leg and arm movements. In: *Engineering Applications of Artificial Intelligence* **23**(8), 1237–1246 (Dec. 2010)
18. Wang, J., She, M., Nahavandi, S., Kouzani, A.: A Review of Vision-Based Gait Recognition Methods for Human Identification. In: *2010 International Conference on Digital Image Computing: Techniques and Applications*, pp. 320–327, Dec. 2010.

19. Sarkar, S., Phillips, P., Liu, Z., Vega, I.R., Grother, P.: J., Bowyer, K.W.: The human ID gait challenge problem: data sets, performance, and analysis. In: *IEEE Transactions on Pattern Analysis and Machine Intelligence*, **27**, 162–177 (2005)
20. Boulgouris, N. V., Chi, Z. X.: Gait Recognition Using Radon Transform and Linear Discriminant Analysis. In: *IEEE Transactions on, Image Processing*, vol. 16, pp. 731–740, 2007.
21. Nandy, A., Prasad, J.S., Mondal, S., Chakraborty, P., Nandi, G.C.: Recognition of Isolated Indian Sign Language gesture in Real Time. In: *proceeding of BAIP 2010, Springer LNCS-CCIS*, Vol. 70, pp. 102–107, March 2010.
22. Hninn, T., Maung, H.: Real-Time Hand Tracking and Gesture Recognition System Using Neural Networks. In: *WASET 50*, 466–470 (2009).
23. OU-ISIR Gait Database <http://www.am.sanken.osaka-u.ac.jp/GaitDB/index.html>

# XML-Based Authentication to Handle SQL Injection

Nitin Mishra, Saumya Chaturvedi, Anil Kumar Sharma  
and Shantanu Choudhary

**Abstract** Structured Query Language (SQL) injection is one of the most devastating vulnerabilities to impact a business, as it can lead to the exposure of sensitive information stored in an application's database. SQL injection can compromise usernames, passwords, addresses, phone numbers, and credit card details. It is the vulnerability that results when an attacker achieves the ability to influence SQL queries that an application passes to a back-end database. The attacker can often leverage the syntax and capabilities of SQL, as well as the power and flexibility of supporting database functionality and operating system functionality available to the database to compromise the web application. In this article we demonstrate two non-web-based SQL injection attacks one of which can be carried out by executing a stored procedure with escalating privileges. We present XML-based authentication approach which can handle this problem in some way.

**Keywords** Web architecture · SQLIA · HTTP · XML · Web application · Web security · Authentication · Attacker

---

N. Mishra (✉) S. Chaturvedi · S. Choudhary  
Sangam University, Bhilwara, India  
e-mail: nitinmishra10@gmail.com

S. Chaturvedi  
e-mail: saumyachaturvedi5@gmail.com

S. Choudhary  
e-mail: shantunu.chintu@gmail.com

A. K. Sharma  
ITM Bhilwara, Bhilwara, India  
e-mail: anilsharma8423@gmail.com

# 1 Introduction

SQL Injection Attack (SQLIA) is considered one of the top five web application vulnerabilities by the Open Web Application Security Project (OWASP) in the year 2010. A database is an essential component that is necessary in modern web applications. Every web-based application that is developed and deployed over the Internet, requires the interaction of a database, thereby the application becomes fully database driven. It has been noted that, at an average, applications experience, 71 attempts an hour. Some applications experience aggressive attacks and at a peak, were attacked 800–1,300 times per hour.

An SQLIA involves the insertion or “injection” of a SQL query by an attacker via the input data from the client to the application. This injection in the SQL query involves inserting malicious input statements by an attacker. The execution of these malicious input statements by the web server at the database end results in unexpected behavior thus compromising the security of the database. The database just executes the input data provided by a client/attacker as it is. It does not have the ability to differentiate between a valid input string and/or a malicious/injected input string.

A successful SQL injection exploit can

- read sensitive data from the database
- alter database data (Insert/Update/Delete).

## 1.1 Modern Web Architecture

The diagram above shows the general web architecture. Any web-based architecture typically follows the Client-Server architecture. The client sends a HTTP request to the Web Server. This request will have the user input data. This input data will be sent to the database layer for processing the web server. At the database end, the SQL queries will be processed and the results will be sent to the web server. Hence, the entire web application is database-driven. The database server usually contains many databases, and in turn, each database contains many tables. The database is under huge threat to the attackers Fig. 1.

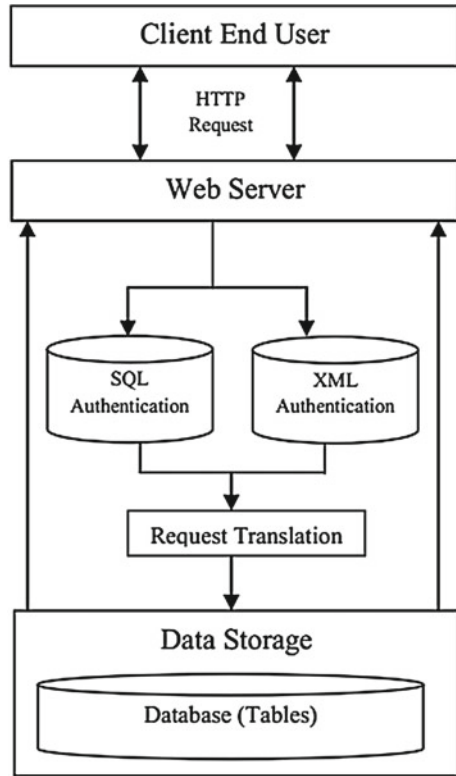
## 1.2 Intent

The attacker wants to access the resources of the system so he uses SQL injection for the same. When he gets access to the information of other authentic users of the system he can use the information as he likes. This also fails confidentiality and integrity of the system.

There are lot of users who use the web-based application and store lot of their personal data on it. Facebook is the very common example of web-based application



Fig. 1 Web architecture



which has large numbers of users. Most of the web-based applications, social websites, banking websites, and online shopping websites require a user to sign up for the system. Users fill their information and get username and password. A user is identified by the system based on his identity. This process of validating an individual based on a username and password is referred as authentication. The system identifies the user, and provides individual access to the system objects based on his/her identity. This process is referred as authorization. This user credential and other information is stored in the database, and accessing this database is the main goal of the attacker.

Attacker uses SQL injection with following aim in his mind

- Bypass authentication procedure (authentication is lost)
- Extract the existing data from the system (Confidentiality lost)
- Alter the existing data (Integrity lost).

Bypassing an authentication is a serious threat, as it allows an attacker to forge another authorized user identity, perform certain actions on behalf of the other user, and importantly access/modify confidential information that belongs to the user.

Our paper mainly focuses on how the attacker uses various injection techniques to bypass the authentication procedure in a system and presents method for prevention of such attacks.

## 2 Recent Similar Works

Below I am mentioning some of the recent works which focus on SQLIA. A lot of research has been done in detecting and preventing injection attacks and few approaches are discussed below.

The system proposed by Kiani, Clark, and Mohay [1] uses an anomaly based approach which utilizes the character distribution of certain sections of HTTP requests to detect previously unseen SQLIA. The advantage of the system proposed by Mehdi Kiani et al. is that it does not require any user interaction, or no modification of, or access to the backend database or the source code of the web application. The problem faced is the high rate of false alerts which had to be taken care while implementing the system in real-time environment. This is because of less information available on attacks to the administrator, thus making it difficult to differentiate between false alerts and the real attacks. Shanmughaneethi, Emilin Shyni, and Swamynathan [2] uses a methodology which make use of an independent web service which is intended to generalize the syntactic structure of the SQL query and validate user inputs. The SQL query inputs submitted by the user are parsed through an independent service and the correctness of the syntactic structure of the query is checked. The main advantage of this paper is that the error message generated doesn't contain any Metadata information about the database which could help the attacker. Since the web service is not integrated with the web application, any modification that should be done to the system should be done in such a way that it should be supported by the web service. Ezumalai, Aghila [3], proposed a combinatorial approach for shielding web applications against SQLIA. This combinatorial approach incorporates signature-based method, used to address security problems related to input validation and auditing based method which analyze the transactions to find out the malicious access. This approach requires no modification of the runtime system, and imposes a low execution overhead. It can be inferred from this approach that the public interface exposed by an application becomes the only source of attack. Kosuga, Kono, Hanaoka et al. [4] proposed a technique called Sania for detecting SQL injection vulnerabilities during the development and debugging phases of a web application. It identifies the vulnerable spots by analyzing the SQL queries issued in response to the HTTP requests in which an attacker can insert arbitrary strings. The main feature of Sania is the generation of attacks using the knowledge by this model, thus checking if the SQL injection vulnerabilities lie in the web application. Wei, Muthuprasanna, Kothari [5] proposed a technique to defend attacks against the stored procedures. This technique combines a static application code analysis with a runtime validation to eliminate injection attacks. In the static part, a stored procedure parser is designed, and for any SQL statement that depends

on user inputs, and use this parser to instrument the necessary statements in order to compare the original SQL statement structure to that including user inputs. The underlying idea of this technique is that any SQLIA will alter the structure of the original SQL statement and by detecting the difference in the structures, a SQLIA can be identified. Kai-Xiang Zhang, Chia-Jun Lin et al. [6] proposed a translation and validation (TransSQL)-based approach for detecting and preventing SQLIA. The basic idea of this approach relies on how different databases interpret SQL queries and those SQL queries with injection. After detailed analysis on how different databases interpret SQL queries, Kai-Xiang Zhang, et al. proposed an effective solution TransSQL, using which the SQL requests are executed in two different databases to evaluate the responses generated.

### 3 Overview of the System

SQL injection is a technique that exploits a security vulnerability occurring in the database layer of an application. The key behind this attack is that it alters the structure of the original SQL statement when malicious input statements are added along with the original query.

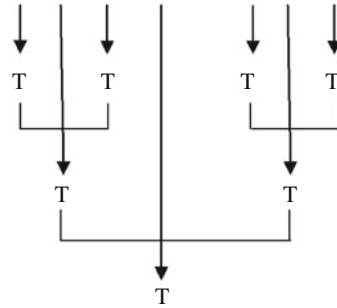
In this scenario, on bypassing authentication, the injection technique is carried out on login forms where a user has to provide a username and a password, and any other places that has to be provided with a user input. In this paper, we focus the attacker's concentration on a user login form in any web page. A typical login form will contain a username and a password field, and this is where the attacker keeps trying different injection techniques until he compromises the security of the database.

#### 3.1 Consequences of SQLIA

With SQL injections, attackers can take complete remote control of the database, and some of the impacts are:

- Insert a command to obtain access to all account details in the system, including usernames and passwords.
- With the username and password in attacker's hand, he can alter the password; change the privilege of the account.
- Forge an user identity.
- Shutdown a database.
- Upload files.
- Delete a database and its entire contents.

Fig. 2 Tautology



## 4 Types of SQLIA Techniques

### 4.1 Tautology

The general goal of a tautology based attack is to inject code in one or more conditional statements so that they always evaluate to true. The most common usages are to bypass the authentication pages and to extract the data. In this type of injection, an attacker exploits an injectable field that is used in query’s ‘where’ conditional. Typically, the attack is successful when the code either displays all of the returned records or performs some action if at least one record is returned.

A typical user authentication SQL statement at the database end will take the following form.

Example. Select name from users where name=‘\$name’ and pass=‘\$pass’;

In the case of a legitimate user, with username as ‘user1’ and password as ‘pass1’, the query will take the form,

Select name from users where name=‘user1’ and pass=‘pass1’; [ No Injection ]

And when these user credentials are validated by the database, the user is authenticated Fig. 2.

Now as an example of a tautology attack, the attacker submits the malicious code [‘ OR ‘1’=‘1’] as input for the username and password field, and the query takes the form,

select name from user where name= ‘ ‘OR ‘1’=’1’ and pass= ‘ ‘OR ‘1’=‘1 ’;

select name from users where  
name= ‘ ‘OR ‘1’= ‘1’ and pass=‘ ‘OR ‘1’=‘1’;

The code injected in the condition [‘ OR ‘1’=’1’] transforms the entire ‘where’ clause into a tautology. Since the conditional is a tautology, the query evaluates to a true for each row in the table and returns all of them, and finally the attacker will be authenticated into the system with the identity of the first record returned by the SQL query.

## 4.2 *Logically Incorrect Query*

This attack lets an attacker gather important information about the type and structure of the back-end database of a web application. The attack is considered to be an information gathering step for other types of attacks. The vulnerability leveraged by this attack is that the default error page returned by the application servers is often overly descriptive. Such error messages generated can often reveal vulnerable/injectable parameters to an attacker. When performing this attack, an attacker tries to inject statements that cause a syntax, or logical error into the database.

## 4.3 *Piggy Backed Query*

This kind of attack appends additional queries to the original query string. If the attack becomes successful, the database receives and executes a query string that contains multiple distinct queries. The first query is usually the original legitimate query, whereas the subsequent queries are the injected/malicious queries. This type of attack can be harmful because attackers can use it to inject virtually any type of SQL command.

Example. By using the other injection techniques discussed above, the attacker will have the name(s) of authorized user(s). For subsequent trials and in the case of Piggy Backed queries, he uses the authorized username as input for the user field, and uses the following malicious code for the password field,

```
pass = 'OR (SELECT COUNT(*) FROM user)=10 AND ''='
```

The entire SQL statement will take the form,

```
Select name from users where name='user1' and pass= '=' OR (SELECT COUNT(*) FROM user)=10 AND ''=' ;
```

If this query evaluates to true, then the attacker gains an insight that, there are exactly 15 users in the system. If it is evaluated to be false, then the condition is found to be incorrect and tries different possible techniques. Here, if the 'INSERT into' clause is used, and if the condition evaluates to be true, then the attacker can successfully insert data into the database.

# 5 Our Method

## 5.1 *Existing Technique*

In the existing web applications, authentication process takes place as follows. The user enters his assigned user name and password. The database checks if the particular user name, password combination exists in the database, and if it exists, authenticates the user. If we look at the tautology based attack, an attacker might be able to

break into the system even without entering a valid user name in the user field. This is the main issue in few of the existing web applications, that there is no proper authentication procedure. This necessitates the need for a strong user authentication procedure.

This algorithm presents an efficient user authentication procedure, in a way that, an input SQL statement will be processed by the database only if the user is found to be a valid user of the system. This totally isolates the database from such injection attacks. A user is validated against two different databases of the same system.

## ***5.2 Proposed Method***

The proposed methodology here is to provide two levels of User authentication at the database level.

1. SQL Authentication
2. XML Authentication

The HTTP request sent by the Client is passed to the Web server. The input user credentials entered in the form are passed to the web server for processing at the database end. Now, the Web server has to pass it to the database. In any form of a SQL-based database, Relational Database management system is used.

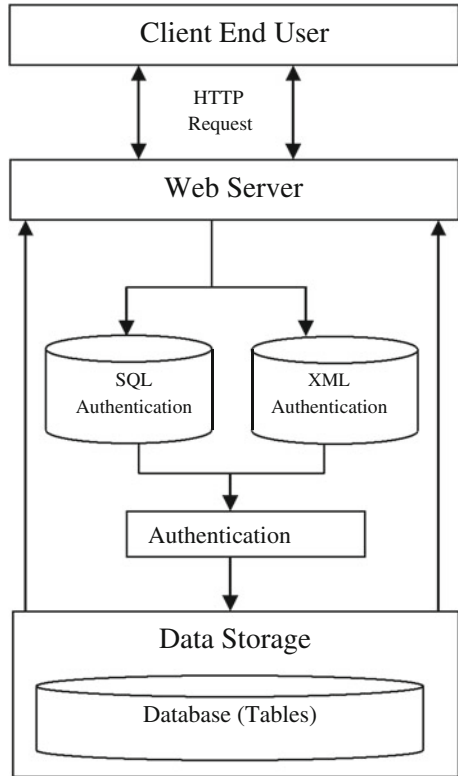
The problem faced here is that, the same SQL query no matter in which relational database it is executed, it does not have the ability to differentiate the response or result obtained from the query processed by the database. That is, if a particular SQL request is evaluated to be true in a database, then the same request would evaluate to true on all the other SQL-based databases, which happens because all of these databases work based on the relational database management systems Fig. 3.

Therefore, if the same malicious/injected SQL request is run on hierarchal based database management system, then the response would be different. In a relational database management system like Microsoft Access, SQL Server, MySQL, data is stored in the form of rows and columns in tables, whereas in a hierarchical database, data is stored in the hierarchical tree structures, with the bottom most nodes that store the value. Hence the way of data processing among relational and hierarchical database management will differ, and this is the core concept of this work.

### **5.2.1 Using XML**

Though XML is a widely used language for transportation of data in the web, there have many instances of using the XML language as a means of just storing the data, thus acting as a database. Also XML, stores data in hierarchical structures of trees, that stores data in terminal nodes, with each of the node constituting a root node. The major advantage of using XML is that, it is widely portable, platform independent, and can be integrated very easily into different web technologies. Other

**Fig. 3** Proposed system architecture



existing hierarchical database management systems like Microsoft Active Directory, Apache Directory Studio, Open LDAP for Windows are not as flexible as XML, and require a lot of overhead in initial configuration and, not totally reliable in terms of compatibility.

We can convert the database in XML format and then both SQL and XML can be used for authentication. Nowadays databases comes with tools that can convert database table into XML equivalent. XML also has a disadvantage that retrieval time in a hierarchical database is slow as compared to relational databases if the number of users of the system is high. This is because when data is searched in a XML or hierarchical database, all the nodes in present in the database from the beginning are searched and this consumes a lot of time. So we propose, instead of storing the entire user database in a single database file, a single XML file is created for every user of the system, and the corresponding password alone is stored in the XML file. This reduces the search complexity and search time to a large extent and also the size of individual file is of small size.

### 5.3 How Our System Works?

So, when a user tries to gain access to a system, initially, SQL authentication is done, which might evaluate to true, even in the case of an input by an attacker. But during the XML authentication, initially the corresponding XML database file is searched in the system, and if present the password is checked and only then is the user validated. So, the attacker can hack into a system only in the case of a authorized username. So in the case of an attacker input/injection, even if the SQL authentication evaluates to true, the XML authentication will fail and hence the request will not be processed by the database, thus preventing the direct access to the database. This is the method implemented in this work.

## 6 Conclusion and Future works

SQL injection is a common technique hackers used to attack these web based applications. SQLIA has also been specified under the top five web security threats by the OWASP in the year 2010. These attacks change the SQL queries, thereby altering the behavior of the program for the benefit of the hacker. In the work carried out, a method is put forward to detect and prevent SQL injection. The technique is based on the intuition that injection codes implicitly perform a different meaning from general queries. An elaborate environment based on XML for distinguishing between legitimate and malicious users has been presented. Here, the main idea is to secure the database from external users/attackers. Also this method helps us to achieve the same by allowing the web server to access the database only if both the levels of authentication have been satisfied. This is the unique functionality of this proposed method. And also there is no necessity to modify/update the legacy application code, as XML can be easily integrated into other languages. There are other various ways of detecting injection attacks and this is just one of them [7–9].

Further, our method can be extended by adding different levels of authentication within the same application.

## References

1. Kiani, M., Clark, A., Mohay G.: Evaluation of anomaly based character distribution models in the detection of SQL injection attacks. In: The third International Conference on availability, reliability and security, IEEE. 0–7695-3102-4/08 (2008)
2. Shanmughaneethi, V., Emilin Shyni, C., Swamynathan, S.: SBSQLID: securing web applications with service based SQL injection detection. In: 2009 International Conference on Advances in Computing, Control, and Telecommunication Technologies, IEEE . 978–0-7695-3915-7/09 (2009)



3. Ezumalai, R., Aghila, G.: Combinatorial approach for preventing SQL injection attacks. In: 2009 IEEE International Advance Computing Conference (IACC 2009) Patiala, India, 6–7 March 2009
4. Kosuga, Y., Kono, K., Hanaoka, M., Kohoku-ku, H., Yokohama, F., Hishiyama, M., Takahama, Y., Minato-ku, K.: Sania: syntactic and semantic analysis for automated testing against SQL injection. In: 23rd Annual Computer Security Applications Conference, 2007, 1063–9527/07, 2007 IEEE (2007)
5. Wei, K., Muthuprasanna, M., Kothari, S.: Preventing SQL injection attacks in stored procedures. In: Proceedings of the 2006 Australian, Software Engineering Conference (ASWEC'06) (2006)
6. Kai-Xiang, Z., Chia-Jun, L., Shih-Jen, C., Yanling, H., Hao-Lun, H., Fu-Hau, H.: TransSQL: A translation and validation-based solution for SQL- injection attacks. In: First International Conference on Robot, Vision and Signal Processing, IEEE (2011)
7. Lambert, N., Lin, K.S.: Use of query tokenization to detect and prevent SQL injection attacks. IEEE. 978–1-4244-5540-9/10/2010 (2010)
8. Sushila, M., Supriya, M.: Shielding against SQL injection attacks using ADMIRE model. In: 2009 First International Conference on Computational Intelligence, Communication Systems and Networks, IEEE. 978–0-7695-3743-6/09, 2009
9. Yeole, A.S., Meshram, B.B.: Analysis of different technique for detection of SQL injection. In: International Conference and Workshop on Emerging Trends in Technology (ICWET 2011)—TCET, Mumbai, India, ICWET' 11, 25–26 Feb 2011, Mumbai, Maharashtra, India, 2011 ACM (2011)

# Observation Probability in Hidden Markov Model for Credit Card Fraudulent Detection System

Ashphak Khan, Tejpal Singh and Amit Sinhal

**Abstract** The internet has taken its place beside the telephone and the television as an important part of people's lives. Consumers rely on the internet to shop, bank and invest online shoppers use credit card to their purchases. In electronic commerce, credit card has become the most important means of payment due to fast development in information technology around the world. Credit card will be most consentient way to do online shopping, paying bills, online movie ticket booking, fees pay etc., In case of fraud associated with it is also increasing. Credit card fraud come in several ways, Many techniques use for find out the credit card fraud detection. Hidden markov model (HMM) is the statistical tools for Engineering and scientists to solve various problems. In this project, we model the sequence of operations in credit card transaction processing using a HMM and show how it can be used for the detection of frauds.

**Keywords** Credit card · Hidden markov model · Online transaction · E-commerce · Clustering · Credit card fraud detecting system

## 1 Introduction

Credit cards are the most popular payment instrument on the internet. The first credit card was introduced decades ago. (Diner's club in 1949, American Express in 1958). These cards have been produced with the magnetic stripes with unencrypted and read-only information. But today many cards are smart cards with the hardware devices offering encryption and far greater storage capacity. The most interesting

---

A. Khan (✉) · T. Singh · A. Sinhal  
Department of Information Technology, Technocrats Institute of Technology,  
Bhopal, India  
e-mail: ashukhan30@gmail.com

T. Singh  
e-mail: tejpal1985@gmail.com

A. Sinhal  
e-mail: amit\_sinhal@rediffmail.com

event in the whole of this area has been the off again on-again liaison between Master card and Visa to produce what is becoming the de facto Internet standard for secure bankcard payments. Credit cards are by far the most common method of payment for online purchases—60 % of global online consumers used their credit card for a recent online purchase, while one in four online consumers chose PayPal. Of those paying with a credit card, more than half (53 %) used Visa. “Shopping on the Internet with the ease of a credit card is especially appealing to consumers in emerging markets who simply cannot find or buy items they want in their retail trade. Occurrence of credit card fraud is increasing dramatically due to the security weaknesses in contemporary credit card processing systems resulting in loss of billions of dollars every year credit cards can be used for doing shopping either offline or online. In offline transaction, the card must be physically present and is inserted in the payment machine in the merchant’s place for making the payment. However, in online transaction, only some of the card details like secure code, expiration date and card number etc., is needed to do the transaction as it is mostly done via phone or internet [1].

Credit card fraudsters employ a large number of techniques to commit fraud. To combat the credit card fraud effectively, it is important to first understand the mechanisms of identifying a credit card fraud. Over the years credit card fraud has stabilized much due to various credit card fraud detection and prevention mechanisms. Those have been suggestion by Benson Edwin Raj, Annie Portia [2]. In day-to-day life, online transactions have increased to purchase goods and services. According to Nielsen study conducted in 2007–2008, 28 % of the world’s total population has been using internet [1]. 85 % of total population today have used internet to make online shopping and the rate of making online purchasing has increased by 40 % from 2005 to 2008. In developed countries and in developing countries to some extent, credit card is most acceptable payment mode for online and offline transaction. As usage of credit card increases worldwide, chances of attacker to steal credit card details and then, make fraud transaction are also increasing. There are several ways to steal credit card details such as phishing websites, steal/lost credit cards, counterfeit cards, theft of card details, intercepted cards etc [3]. The total amount of credit card online fraud transaction made in the United States itself was reported to be \$1.6 billion in 2005 and estimated to be \$1.7 billion in 2006 [4].

In this paper, we show the credit card fraud detection at using statically model for this techniques show hidden markov model (HMM). Show the spending profile of each to be made by the credit card to show each transaction. Hidden markov model, in which the transition probability between hidden state and depend on the observations state.

## 2 Literature Survey

Credit card fraud detection has received an important attention from researchers in the world. Several techniques have been developed to detect fraud transaction using credit card which are based on neural network, genetic algorithms, data mining, clustering techniques, decision tree, Bayesian networks etc.

Ghosh and Reilly [6] have proposed a neural network method to detect credit card fraud transaction. They have built a detection system, which is trained on a large sample of labeled credit card account transactions. These sample contain example fraud cases due to lost cards, stealing cards, application fraud, stolen card details, counterfeit fraud etc. They tested on a data set of all transactions of credit card account over a subsequent period. Kokkinaki and other have proposed the technics of decision tree. This technics of decision tree are simple and easy to the implementation, decision trees is reduces misclassification of incoming transaction of data, but this is not for use dynamically adaptive of online transaction. A decision tree is defined recursively; it contains nodes and edges that are labeled with attribute names and with values of attributes, respectively [7]. Meas, Suggest of fraud detection technics using the bayesian network, in this technics, improving the fraud detecting by removing highly correlated attribute, ANN was found the credit card fraud predication faster of the testing phase, at using transaction profile. Bayesian algorithm is performed better result of fraud detection only on neural network [8].

Chan and Stalfo, have proposed the a technics of multi-classifier Meta learning issues of credit card transaction, it detecting the fraud detection 46% improving of overall fraud, to use for each tanning experiment are required to the best distribution determine [9]. Kim, method improving number fraud detection classifier and compare only on the neural network by using the unsupervised algorithm of data mining, this method is only able to find local minima in the error function [10]. Centralize fraudulent transaction from fraud investigation of increasing, accuracy of model a distributed dataset for higher fraud are show chiu and tsai, a web based knowledge sharing scheme using for rule-based algorithms. Since there are millions of transactions processed, every day and their data are highly skewed. The transactions are more legitimate than fraudulent. It requires highly efficient technique to scale down all data and try to identify fraud transaction not legitimate transactions [11]. Syeda has proposed improving the speed of data mining, discovery of knowledge in credit card fraud detection system (FDS) of transaction process using granular neural network. Credit card fraud detecting purpose this system has been implemented [12]. Establish logic rules capable of classifying transactions of credit card into suspicious and non-suspicious classes using Genetic algorithm. This algorithm based on genetic programming this concept suggest by Bentley [13].

Bolton and Hand et al. [14] it has proposed credit card detection using unsupervised method by frequency of transactions and observing abnormal spending behavior. Break point analysis and Group analysis techniques as unsupervised tools, Successful in detection local anomalies and can FDS of behavior in a continuous manner. Those accounts are treating as suspicious ones and fraud analysis is to be done only on these accounts. If break point analysis can identify suspicious behavior such as sudden transaction of high amount and high frequency, then card will be identified as fraudulent. Algorithms do not show differentiate between accounts it show the treats of all accounts equally. We propose in this system of credit card fraud detection using observation probability in HMM. HMM is statically model for best engineering practice. Hidden markov Model is best for using the FDS. Hidden markov process is double embedded random process means it performs transaction

of probability if state is “hidden” or state of transaction is “open” of two different levels. In this data mining technics we have divide the three sub categories method. We suggestion of present FDS to alternative sequence to spending profile show online transaction data generate of credit card system Credit card data set is not available to easily its most important part of banking system. Bank should not provide be provide, it is security part of any banking system. We use a dummy data set to credit card FDS; improve fraud-detecting accuracy of system. We propose the observation probabilistic in HMM to detecting “observation” state of cardholder they use the online transaction.

### 3 Use Hidden Markov Model

We are use application of HMM in credit card fraud detection. Hidden Markov Model is probably the simplest and easiest models, which can be used to model sequential data, i.e. data samples that are dependent from each other. Hidden Markov Model is probably the simplest and easiest models, which can be used to model sequential data, i.e. data samples that are dependent from each other. An HMM is a double embedded random process with two different levels, one is hidden and other is open to all. Hidden Markov Model does not directly use the states, which provide the external observation and gate use external observer find the visible state. Hidden Markov Model technics successfully apply for data mining, speech recognition, bio-information, robotics, artificial intelligence, voice recognition etc.

Hidden Markov Model’s characterizes by the following five traits:-

1. The number of  $N$  hidden states within the model. Each state corresponds to a unique state provide by the model. In the model, the states are defines by data set.
2. The amount of  $M$  unique observation per state. These symbols are denoted, as this can be trough of as the number of observation that fall in each data set.
3. State transition probability Matrix

$$A = \{a_{ij}\},$$

where

$$a_{ij} = P(q_{t+1} = S_j | q_t = S_i), \quad i \leq i, j \leq N$$

and

$$\sum_{k=1}^M b_j(k) = 1, \quad i \leq i \leq N \quad (1)$$

4. The emission probability Matrix in state  $j$ ,

$$B = \{b_j(k)\},$$

where

$$b_j = P(V_k, a_t = 1 | q_t = S_j), \quad 1 \leq i \leq N, 1 \leq j \leq M$$

and

$$\sum_{k=1}^M b_j(k) = 1, \quad 1 \leq j \leq N \tag{2}$$

5. The initial provability  $\pi = \{\pi_i\}$  of system being in state the observation where

$$\pi_i = P(q_1 = S_i); \quad 1 \leq i \leq N$$

Such that

$$\sum_{i=1}^N \pi_i = 1$$

Then we need the HMM in sequence of observation symbols:

$$\lambda = (A, B, \pi)$$

To denote an HMM with discrete probability distribution, while

$$\lambda = (A, C_{jm}, \mu_{jm}, \sum_{jm}, \pi)$$

where  $C_{jm}$  = Weighting Coefficients,  $\mu_{jm}$  = Mean Vector,

$$\sum_{jm} = \text{Covariance matrices}$$

## 4 Propose Fraud Detection System and Discussion

In this section, we present credit card FDS based on HMM, which does not require fraud signatures and still is able to detect frauds just by bearing in mind a cardholder’s spending habit. The important benefit of the HMM-based approach is an extreme decrease in the number of False Positives transactions recognized as malicious by a FDS even though they are genuine (Fig. 1).

Interstate transition in section. In this FDS, we consider four different spending profiles of the cardholder, which is depending upon range, named Card-I, Card-II, Card-III, Card-IV. In this set of symbols, we define  $V = \{C_1, C_2, C_3, C_4\}$  and  $M = 4$ . The price range of proposed symbols has taken as  $C_1$  (0, \$100],  $C_2$  (€101, €500],  $C_2$ (€501, €1000], and  $C_2$  (€1001, Limit of Credit Card], and after finalizing the state and symbol representations, the next step is to determine different components of the HMM, i.e. the probability matrices  $A, B,$  and  $I$  so that all parameters required

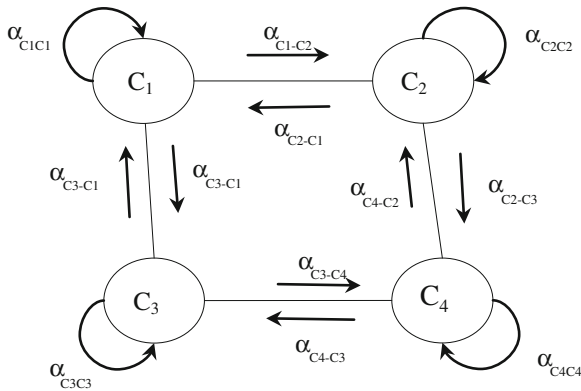


Fig. 1 Different transaction state

for the HMM is known. We show Fig. 2. That every states reach and show each other state, different states denoted and show online purchase, banking, e-cash, pay thought internet. it has been shown that probability of transition from one state to another (for example from  $C_1$  to  $C_2$  and vice versa, show as  $a_{C_1-C_2}$  and  $a_{C_2-C_1}$ , respectively) and also probabilities of transition from a particular state (1, 2, 3 and 4 ) to different spending  $C_1, C_2, C_3$  or  $C_4$  (for example,  $a_{C_1-C_2}, b_{C_1-C_2}$ , etc.,). After deciding HMM parameters, we will consider to form an initial sequence of the existing spending behavior of the cardholder. Let  $O_1, O_2, O_R$  be consisting of  $R$  symbols to form a sequence. This sequence is recorded from cardholder’s transaction till time  $t$ . We put this sequence in HMM model to compute the probability of acceptance. Let us assume be this probability is  $\alpha_1$ , which can be calculated as

$$\delta_1 = P(o_1, o_2, o_3, \dots o_R | \lambda),$$

Let  $O_{R+1}$  be new generated sequence at time  $t + 1$ , when a transaction is going to process. The total number of sequences is  $R + 1$ . To consider  $R$  sequences only, we will drop  $O_1$  sequence and we will have  $R$  sequences from  $O_2$  to  $O_{R+1}$ .

$$\delta_2 = P(o_2, o_3, o_4, \dots o_{R+1} | \lambda),$$

Let the probability of new  $R$  sequences be  $\alpha_2$  hence, we will find

$$\Delta\delta = \delta_1 - \delta_2,$$

If  $\Delta\alpha > 0$ , it means that HMM consider new sequence i.e.  $O_{R+1}$  with low probability and therefore, this transaction will be considered as fraud transaction if and only if percentage change in probability is greater than a predefined threshold value.

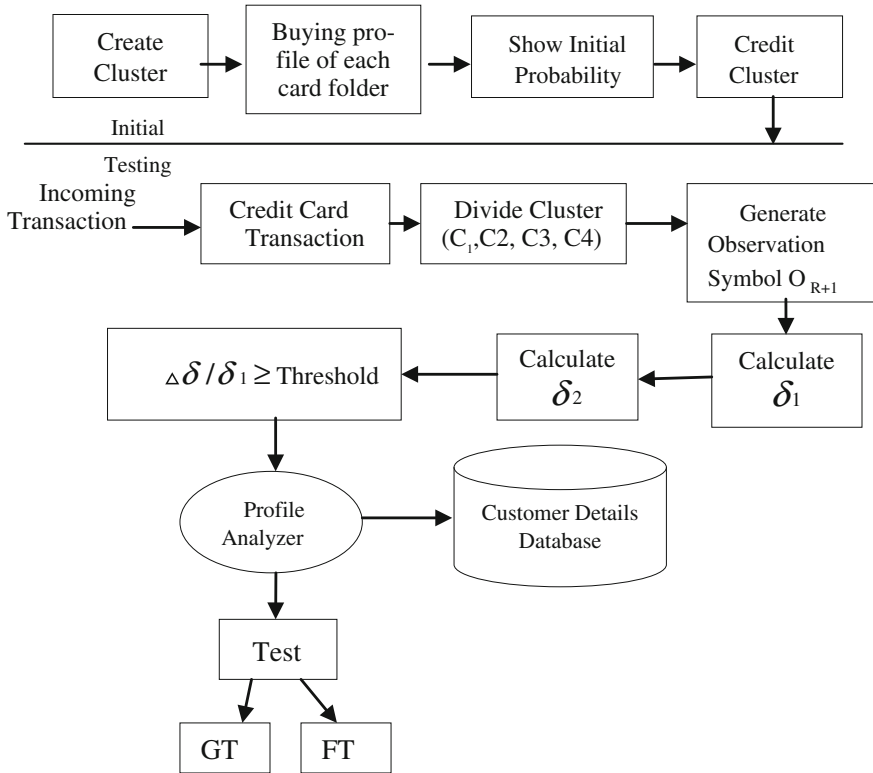


Fig. 2 Propose fraud detection system

$$\Delta\delta/\delta_1 \geq \text{Threshold value}, \tag{3}$$

The threshold value can be calculated empirically. This FDS if finds that the present transaction is a malicious, then credit card issuing bank will regret the transaction and FDS discard to add  $O_{R+1}$  symbol to available sequence. If it will be a genuine transaction, FDS will add this symbol in the sequence and will consider in future for fraud detection.

## 5 Experimental Result and Discussion

It is very difficult to do simulation on real time data set that is not providing from any credit card bank on security reasons. We calculate probability of each spending  $C_1, C_2, C_3$  and  $C_4$  of every category. Fraud detection of incoming transaction will be checked on last 20 transactions (Fig. 3).



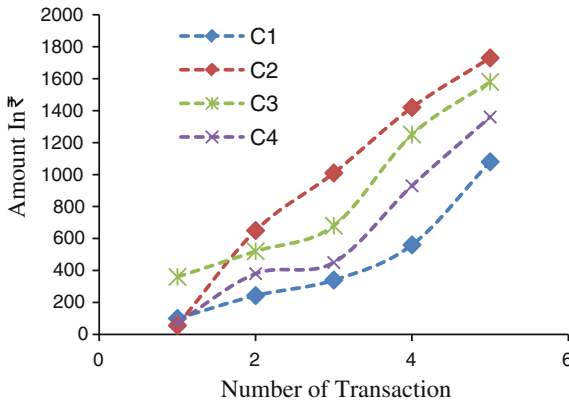


Fig. 3 Amount categories of different transaction

Table 1 All transactions happened until date

Transaction no	Category	Amount in €	Transaction no	Category	Amount in €
1st	C <sub>1</sub>	20	11th	C <sub>4</sub>	450
2nd	C <sub>3</sub>	10	12th	C <sub>3</sub>	680
3rd	C <sub>2</sub>	40	13th	C <sub>1</sub>	560
4th	C <sub>1</sub>	75	14th	C <sub>2</sub>	1420
5th	C <sub>4</sub>	28	15th	C <sub>4</sub>	930
6th	C <sub>2</sub>	115	16th	C <sub>3</sub>	1250
7th	C <sub>4</sub>	54	17th	C <sub>1</sub>	1080
8th	C <sub>3</sub>	110	18th	C <sub>4</sub>	1360
9th	C <sub>2</sub>	180	19th	C <sub>2</sub>	1730
10th	C <sub>1</sub>	119	20th	C <sub>3</sub>	1580

We have simulated several large data sets; one is shown in Table 1, in our proposed FDS and found out probability mean distribution of false and genuine transactions. When probability of genuine transaction is going down, correspondingly probability of false transaction going up and vice versa. If the percentage change in probability of false transaction will be more than threshold value, then alarm will be generated for fraudulent transaction and credit card bank will decline the same transaction (Fig. 4).

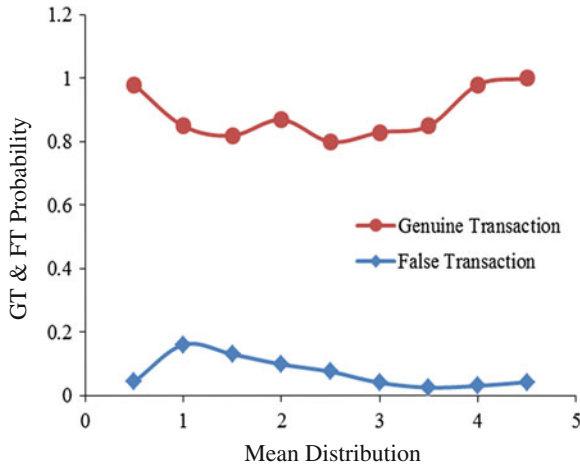


Fig. 4 Mean distribution of GT and FT

## 6 Conclusion

Credit card FDS is an utmost required for and card issuing bank or all type of online transaction that through using credit card. In this paper, we have implemented of HMM in credit card fraud detection. The very easily detect and remove the complexity for using in this HMM. It has also explained the HMM how can detect whether an incoming transaction is fraudulent or not comparative studies reveal that the accuracy to the system is also 90% over a wide variation in the input data. We are dividing the transaction amount in three categories that is grouping high, medium and low used on different ranges of transaction amount each group show the aberration symbols. In HMM methods is very low compare techniques using fraud detection rate. It also have been explained low the HMM can detecting whether an incoming transaction is fraudulent or not. The system is also scalable for handling large volumes of transaction.

## References

1. Internet usage world statistics. <http://www.ternetworldstats.com/stats.htm> (2011)
2. Benson Edwin Raj, S., Annie Portia, A.: Analysis on credit card fraud detection method. In: IEEE International Conference on Computer, Communication and, Electrical Technology ICCET2011 (2011)
3. Trends in online shopping, a global nelson consumer report. <http://www.nielsen.com/us/en/insights/reports-downloads/2010/global-trends-in-online-shopping-nielsen-consumer-report.html> (2008)

4. European payment cards fraud report, payments, cards and mobiles llp & author. [http://www.paymentscardsandmobile.com/payments-cards-mobile-affiliates/fraud-report/pcm\\_fraud\\_report\\_2010.pdf](http://www.paymentscardsandmobile.com/payments-cards-mobile-affiliates/fraud-report/pcm_fraud_report_2010.pdf)
5. Srivastava, A., Kundu, A., Sural, S., Majumdar, A.K.: Credit card fraud detection using hidden markov model. *IEEE Trans. Dependable Secure Comput.* **5**(1), 37–48 (2008)
6. Ghosh, S., Reilly, D.I.: Credit card fraud detection with a neural-network. In: *Proceedings Of 27th Hawaii International Conference on System Science: Information Systems, Decision Support and Knowledge-Based Systems*, vol. 3, pp. 621–630 (2004)
7. Kokkinaki, A.I.: On atypical database transaction: identification of probable using machine learning for using profiling. In: *IEEE Knowledge and Data Engineering Exchange Workshop*, pp. 107 (1997)
8. Maes, S., Tuyls, K., Vanschoenwinkel, B., Manderick, B.: Credit card fraud detection using bayesian and neural networks. In: *Proceedingd of 1st Naiso Congress on Neuro Fuzzy Technologies*, Hawana (2002)
9. Stolfo, S.J., Fan, D.W., Lee, W., Prodromidis, A.L., Chan, P.K.: Credit card fraud detection using meta-learning issues and iniitial result. In: *Proceedings of AAAI Workshop AI Methods in Fraud and Risk Management*, pp. 83–90 (1997)
10. Kim, M.J., Kim, T.S.: A neural classifier with fraud density map for effective credit card fraud detection. In: *Proceedings of International Conference on Intelligent Data Engineering and Automated, Learning*, pp. 378–383 (2002)
11. Chiu, C., Tsai, C.: A web services-based collaborative scheme for credit card fraud detection. In: *Proceedings of 2004 IEEE International Conference on e-Technology, e-Commerce and e-Service* (2004)
12. Syeda, M., Zjang, Y.Q., Pan, Y.: Parraller granular networks for fast credit card fraud detection. In: *Proceeding of IEEE International Confrence on Fuzzy System*, pp. 572–577 (2002)
13. Bentley, P.J., Kim, J., Jung, G.H., Choi, J.U.: Fuzzy darwinian detection of credit card fraud. In: *Proceeding of 14th Annual Fall Symposium of Korean Information Processing Society* (2000)

# Comparative Study of Feature Reduction and Machine Learning Methods for Spam Detection

Basant Agarwal and Namita Mittal

**Abstract** Nowadays, e-mail is widely used for communication over Internet. A large amount of Internet traffic is of e-mail data. A lot of companies and organizations use e-mail services to promote their products and services. It is very important to filter out spam messages to save users' precious time. Machine learning methods plays vital role in spam detection, but it faces the problem of high dimensionality of feature vector. So feature reduction methods are very important for better results from machine learning approaches. In this paper, Principal Component Analysis (PCA), Singular Value Decomposition (SVD), and Information Gain (IG) methods are used for feature reduction. Further, e-mail messages are classified as spam or ham message using seven different classifiers namely Naïve Baysian, AdaBoost, Random Forest, Support Vector Machine, J48, Bagging, and JRip. Comparative study of these techniques is done on TREC 2007 Spam e-mail Corpus with different feature size.

**Keywords** Spam classification · E-mail classification · Machine learning algorithms · Feature selection

## 1 Introduction

With the growth of Internet, e-mail is widely being used for communication over Internet due to fast, efficient, and economical way to communicate. That's why, large number of companies use e-mail facility to promote and advertise their products and services. These unwanted and unsolicited e-mails are known as spam e-mails [1]. Large part of the Internet traffic comprises of these spams. Users have to waste

---

B. Agarwal (✉) · N. Mittal  
Malaviya National Institute of Technology, Jaipur, India  
e-mail: thebasant@gmail.com

N. Mittal  
e-mail: nmittal@mnit.ac.in

a lot of time to read spam messages. These spam mail can cause damage to users' system and annoying individual user. That's why it is very important to automatically classify/filter the spam messages from legitimate messages.

Spam filtering is a text classification task. Text classification for spam is challenging due to huge features size and large number of texts [2]. High dimensionality data is a problem for classification algorithm because of the high computational cost and memory usage. So feature reduction methods are essential for better performance of the classification model [3].

Objective of this paper is to do comparative study of machine learning algorithm for building an efficient classifier that can determine if an e-mail message is spam or not. In addition, to analyze the effect of feature reduction methods and feature size on the performance of classifier.

The remainder of the paper is as follows: Sect. 2 discusses related work, Sect. 3 explains spam classification method process, Sect. 4 describes the results and discussions, and Sect. 5 concludes the paper with possible directions for future work.

## 2 Related Work

It has become necessary to have a filtering system that will classify the e-mails either as spam or ham/legitimate. Spam mails are the unwanted messages which are sent without the consent of the user. Researchers have applied different machine learning methods like Naïve Bayes (NB), Support Vector Machine (SVM), Neural Network (NN), etc., in automatically classifying spam messages from legitimate messages [4, 5]. Principal Component Analysis (PCA) is used for reducing the dimensionality of feature size and then NN is used for spam classification [6]. Latent Semantic Analysis (LSA) is used for anti-spam filtering system, results obtained from LSA is compared with naïve bayesian classifier [7].

Several variants of boosting algorithms are performed for e-mail classification and compared the results with naïve bayesian and decision tree [8]. Effect of PCA on three different classifier, i.e., C5.0, instance-based learner and naïve Bayes are analyzed [9]. Effect of PCA as pre-processing is analyzed on machine learning accuracy with high dimensional dataset [10]. Benefits of dimensionality reduction are explored with the context of latent semantic indexing for e-mail detection [11].

SVM is used for online spam filtering system on large dataset, a Relaxed Online SVM (ROSVM) System is proposed that gives performance comparable to traditional filtering system at reduced computation cost [12]. Performance of the Naïve Bayesian classifier is compared to an alternative memory based learning approach on spam filtering [13]. An anti-spam filtering system is proposed in which a NB classifier is used to detect spam messages considering the effect of attribute size, training dataset size [14].

### 3 Spam Classification Process

Spam classification is categorized as a problem of text classification. For this, incoming messages will be classified as spam or legitimate message. First, all the documents are pre-processed, after that feature vector will be constructed, then feature reduction techniques can be applied to reduce the feature size. This reduced feature vector is used for spam classification model.

#### 3.1 Pre-processing

Pre-processing tasks are in order to extract unique words which occur in spam e-mails. All the words are lower cased, and symbols like %, \$, @ etc. are removed. Further, stop words are removed and stemming is performed.

#### 3.2 Feature Vector Construction

Term Frequency-Inverse Document Frequency (TF-IDF) weighting scheme is used for creating feature vector; the dimensionality of this feature vector is in order of thousands of features [2]. TF-IDF can be calculated by TF-IDF:  $w_{ij} = tf_{ij} * idf_i$ , where  $tf_{ij}$  is the frequency of term  $i$  in e-mail  $j$ , and  $idf_i$  is the inverse document frequency, it measures if a term is common or rare across e-mails.

#### 3.3 Feature Reduction

Feature vector generated using words as a feature is huge in dimension. Therefore, it is required to reduce this feature vector size using dimension reduction techniques like IG, PVA, SVD, etc. Computation complexity of the classifier increases with the size of feature vector. So feature reduction methods are used for removing irrelevant and not important features from the feature vector [15].

IG is one of the important feature selection techniques. It measures the importance of feature globally and top ranked features can be selected based on reduction in the uncertainty after knowing the value of the feature for reducing the feature vector. This reduced feature set is used for better classification results [3]. PCA is a feature reduction technique that transforms high dimensional feature vector into lower dimensional such that maximum variance is extracted from the data. For reducing the size of the feature vector top  $k$  principal components are selected. SVD also transforms the high dimensional feature vector into lower dimensional space that is latent semantic space. For reducing the size of feature vector top  $k$  singular values are selected [16].

### ***3.4 Classification Methods***

Different machine learning algorithms are used for classification of spam messages. Naïve bayesian is based on probability and bayes theorem. This classifier assumes independence of feature vectors and tries to predict the probability of new instance.

Boosting and Bagging are two voting based classifiers. In voting classifier, training samples are taken randomly from the dataset multiple times, and different classifiers are learned. To classify a new sample, each classifier gives a different class label; the result of voting classifier is decided by the maximum votes earned for a particular class. Main difference between bagging and boosting is the way; they take the samples for training a classifier. In bagging, training samples are taken with equal weights randomly, and in boosting, more weightage are given to those samples which have been misclassified by previous classifiers.

A single J48 is a classifier based on C4.5 decision tree algorithm [17] and JRip is a java implementation of a propositional rule learner, called Repeated Incremental Pruning to Produce Error Reduction (RIPPER) [18]. Random forest (RF) [19] is an ensemble classifier that comprises of many decision trees and outputs the class that is the mode of the class's output by individual trees. Random forests are generally used when training datasets is huge and input is of the order of thousands of variables. A random forest model is normally composed of tens or hundreds of decision trees. SVM is a supervised learning method that represents input instances as points in space, mapped so that the instances of the separate categories are divided by a gap that is as wide as possible.

## **4 Results and Discussions**

The 2007 TREC Spam e-mail Corpus [20] contains 75,419 e-mail messages at the University of Waterloo. For the experiments, 2,500 sample messages are used for building the classifier out of which 25 % messages are spam messages and others are ham (not spam) messages. After processing of these messages (i.e., stop word removal, stemming,) size of feature vector is 1,400. The classification accuracy is determined using a 5-fold cross-validation.

### ***4.1 Effect of Feature Size and Feature Reduction Methods***

IG, PCA, and SVD methods are used for reducing the feature size. It is observed that as features size is reduced, accuracy of the classifier slightly decreases or it remains unchanged. There is not much variation in the performance of all the classifier with reduction of feature size as shown in Tables 1, 2, and 3. For example, using Bagging Technique with all features (without using any feature reduction technique),

**Table 1** Accuracy (%) of different classifiers with different feature size when SVD is used for feature reduction

Feature size	NB	Adaboost	Random forest	SVM	J48	Bagging	JRip
400	63	79	80.5	77.3	77.1	83.8	80.5
800	62.2	79.4	80.6	77.7	77.5	83.6	79.7
1100	63.4	79.7	80.4	78.6	76.6	83.2	78.3
1400	63.5	83.6	81.6	79.6	80	86.8	84

**Table 2** Accuracy (%) of different classifiers with different feature size when PCA is used for feature reduction

Feature size	Naïve Baysian	Adaboost	Random forest	SVM	J48	Bagging	JRip
400	56.4	80.1	79	77.1	72.8	83.7	77.8
800	58.2	80.2	79.8	77.9	70.2	84.3	80
1100	60.1	80.4	79.3	76.3	74	85.5	81
1400	63.5	83.6	81.6	79.6	80	86.8	84

**Table 3** Accuracy (%) of different classifiers with different feature size when IG is used for feature reduction

Feature size	Naïve Baysian	Adaboost	Random forest	SVM	J48	Bagging	JRip
400	56.6	83.7	83.9	82.9	83.3	85.7	80.5
800	57.8	83.7	82.3	81.2	84.5	85.1	79.7
1100	58.8	83.8	82.2	80.1	84.8	86.6	78.3
1400	63.5	83.6	81.6	79.6	80	86.8	84

i.e., 1,400 got accuracy is 86.8% while with feature size 400 (as shown in Table 3) we got the accuracy 85.7% (-1.26%). Similarly accuracy of Adaboost without any feature reduction technique gives the accuracy of 83.6% and with 400 features it gives accuracy of 83.7% as shown in Table 3. Therefore without compromising much with accuracy of the classifier, complexity of the model can be decreased and time required for building the model is also decreased.

Accuracies of seven different classifiers are given in Tables 1, 2, and 3 with different feature size when different feature reduction techniques are used, i.e., SVD, PCA, and IG. Experimental results show that information gain gives better results for spam classification when used for feature reduction than PCA and SVD methods as observed from Tables 1, 2, and 3. For example, performance of J48 and random forest slightly increases after reduction of features using information gain (Table 3). Also for all the classifiers information gain gives better accuracy than SVD and PCA as shown in Tables 1, 2, and 3. It is also observed from Tables 2 and 3 that SVD performs better as compared to PCA.



In term of time required for applying the feature reduction technique PCA takes maximum time to reduce the features. And information gain technique take minimum time to create the ranking of important features for reducing the feature size.

### 4.2 Effect of Machine Learning Algorithm

Different classification methods like Support Vector Machine classifier, Naïve Bayesian classifier, J48, Bagging, Random Forest, JRip are evaluated on TREC 2007 dataset to analyze the efficiency of different machine learning algorithm for spam detection.

Experimental results show that Naïve bayesian classifier performs worst among these seven classifiers and Bagging technique outperform all other 6 machine learning methods as shown in Figs. 1, 2, and 3 for all the feature size and feature reduction technique. For example, Bagging gives 86.8% accuracy when no feature reduction technique is used and after reducing feature size even then it gives good results as compare to others, i.e., 83.8% as shown in Table 1. It is observed from Figs. 1, 2, and 3 that except naïve bayesian classifier all other classifiers perform well. It is also observed that JRip, Adaboost, SVM, J48, and Random forest gives almost equal accuracy for all the feature size as shown in Figs. 1, 2, and 3.

### 4.3 Time Taken by the Machine Learning Algorithm

As features of spam data are reduced, time taken by each machine learning algorithm is also decreased as shown in Fig. 4. Naïve bayesian classifier takes minimum time among all the algorithms, whereas support vector machine and bagging takes maximum time for building the model. Time required for building the model increases very fast for support vector machine and bagging classifiers. Performance (in term of accuracy) and time taken to build the model are minimum for NB classifier. Bagging takes maximum time to build the model also gives maximum accuracy.

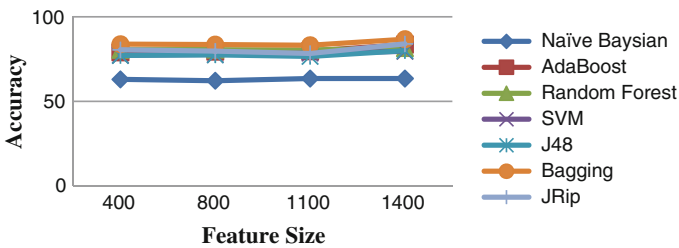


Fig. 1 Accuracy of classifiers with different feature size when SVD is used for feature reduction

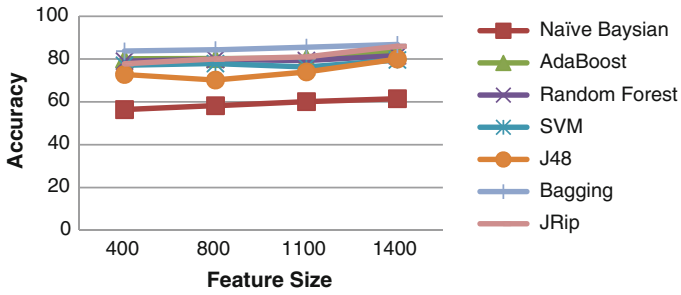


Fig. 2 Accuracy of classifiers with different feature size when PCA is used for feature reduction

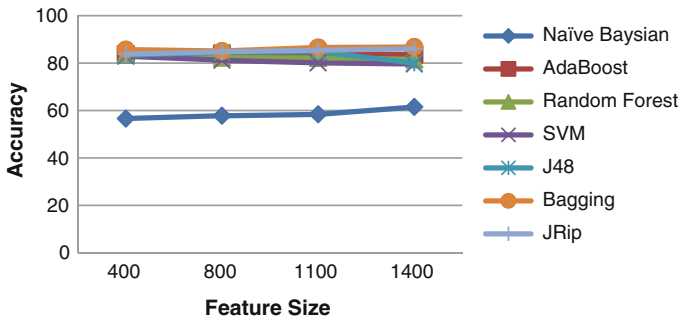


Fig. 3 Accuracy of classifiers with different feature size when information gain is used for feature reduction

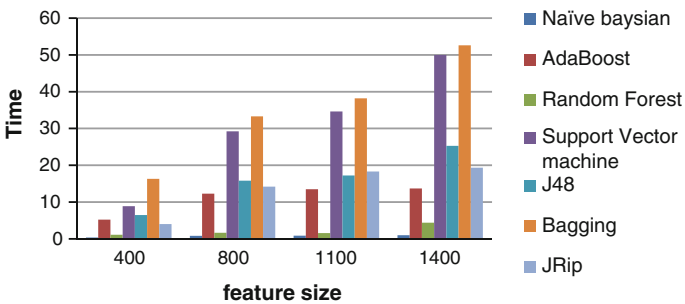


Fig. 4 Time taken by classifier for different feature size when PCA is used for feature reduction

If time is a constraint then random forest should be considered, it takes less time to build the model and performance of spam detection is also comparable with bagging technique, i.e., 81.6 and time taken is 4.4 s for building the model.

## 5 Conclusions

There are various anti-spam filtering systems which uses different kind of techniques. Therefore, comparative study of these techniques is performed in order to evaluate the performance of classification algorithms. Different algorithms are evaluated with different dataset size and varying feature size. Information gain, PCA, SVD are used for feature reduction methods and seven different machine learning algorithms are used for evaluating the performance for e-mail classification on 2,500 instances using TREC 2007 dataset. It is observed that reducing the feature size does not reduce the performance of classification, whereas information gain technique gives better results for feature reduction in terms of accuracy and time taken for building the model. It is also observed that bagging gives better classification accuracy compare to other machine learning algorithms.

## References

1. Cranor, L.F., LaMacchia, B.A.: Spam!. *Commun. ACM* **41**(8), 74–83 (1998)
2. Sebastiani, F.: Machine learning in automated text categorization. *ACM Comput. Surv.* **34**(1), 1–47 (2002)
3. Janecek, A., Gansterer, W.N.: On the relationship between feature selection and classification accuracy. In: *JMLR:Workshop and Conference Proceedings*, vol. 4, pp. 90–105 (2008)
4. Guzella, Thiago S., Caminhas, Waldir M.: A review of machinelearning approaches to Spam filtering. *Expert Syst. Appl.* **36**(7), 10206–10222 (2009)
5. Fawcett, T.: In vivo spam filtering: a challenge problem for data mining. In: *Proceedings of ninth KDD Explorations*, vol. 5, No. 2 (2003)
6. Cui, B., Mondal, A., Shen, J., Cong, G., Tan, K.: On effective email classification via neural networks. In: *Proceedings of DEXA*, pp. 85–94 (2005)
7. Gee, K.R.: Using latent semantic indexing to filter spam In: *Proceedings of the 2003 ACM Symposium on Applied Computing*, pp. 460–464. ACM press, New York (2003)
8. Carreras, X., Marquez, L.: Boosting trees for anti-spam email filtering. In: *Proceedings of RANLP-2001*, pp. 58–64, Bulgaria (2001)
9. Popelinsky, L.: Combining the principal components method with different learning algorithms. In: *Proceedings of the ECML/PKDD2001 IDDM, Workshop* (2001)
10. Howley, Tom, Madden, Michael G., O’Connell, Marie-Louise, Ryder, Alan G.: The effect of principal component analysis on machine learning accuracy with high-dimensional spectral data. *Knowl. Based Syst.* **19**(5), 363–370 (2006)
11. Gansterer, W.N., Janecek, A.G.K., Neumayer, R.: Spam filtering based on latent semantic indexing. In: *Survey of Text Mining II—Clustering, Classification, and Retrieval*, vol. 2, pp. 165–185. Springer (2008)
12. Sculley, D., Wachman, G.M.: Relaxed online SVMs for spam filtering. In: *Proceedings of the 30th Annual International ACM SIGIR Conference on Research and Development in, Information Retrieval SIGIR ’07*, pp. 415–422 (2007)
13. Androutsopoulos, I., Koutsias, J., Chandrinou, K.V., Spyropoulos, D.: Learning to filter spam e-mail: A comparison of a naïve bayesian and a memory-based approach. In: *4th PKDD’s Workshop on Machine Learning and Textual Information Access* (2000)
14. Androutsopoulos, I., Koutsias, J., Chandrinou, K.V., Spyropoulos, D.: An experimental comparison of naive bayesian and keyword based anti-spam filtering with personal e-mail messages. In: *Proceedings of the 23rd ACM SIGIR Annual Conference*, pp. 160–167 (2000)

15. Parimala, R., Nallaswamy, R.: A study of Spam E-mail classification using feature selection package. *Global J. Comput. Sci. Technol.* **11**(7) (2011)
16. Kumar, C.A.: Analysis of unsupervised dimensionality reduction techniques. *Comput. Sci. Inf. Syst.* **6**(2), 217–227 (2009)
17. Quinlan, R.J.: *C4.5: Programs for Machine Learning*. Morgan Kaufmann, Burlington (1993)
18. Cohen, W.W.: Fast effective rule induction. In: *Proceedings of the Twelfth International Conference on Machine Learning*, pp. 115–123. Morgan Kaufmann, Burlington (1995)
19. Breiman, Leo: Random forests. *Mach. Learn.* **45**, 5–32 (2004)
20. TREC 2007 Public Spam Corpus. <http://plg.uwaterloo.ca/gvcormac/treccorpus07/>

# Generation of Key Bit-Streams Using Sparse Matrix-Vector Multiplication for Video Encryption

M. Sivasankar

**Abstract** The contribution of stream ciphers to cryptography is immense. For fast encryption, stream ciphers are preferred to block ciphers due to their XORing operation, which is easier and faster to implement. In this paper we present a matrix-based stream cipher, in which a  $m \times n$  binary matrix single handedly performs the work of  $m$  parallel LFSRs. This can be treated as an equivalent way of generating LFSR-based stream ciphers through sparse matrix-vector multiplication (SpMV). Interestingly the output of the matrix multiplication can otherwise be used as a parallel bit/byte generator, useful for encrypting video streams.

**Keywords** Linear feedback shift registers · Permutations · Primitive polynomials · Sparse matrix-vector multiplication

## 1 Introduction and Background Study

### 1.1 Stream Ciphers

Cryptography is basically all about secure communication and broadly revolves around symmetric techniques (communicating parties possess the same key) and asymmetric techniques (communicating parties possess different keys). A key is a data used for encrypting/decrypting purpose. Further symmetric key cryptography is classified into stream ciphers and block ciphers. While block ciphers encrypt data in blocks of fixed size (64, 128 bits, etc.), stream ciphers do encryption in a bit-by-bit manner [1]. Elaborating further, in stream ciphers the data (plain text) is converted

---

M. Sivasankar (✉)  
Department of Mathematics, Amrita School of Engineering,  
Amrita Vishwa Vidyapeetham, Coimbatore, India  
e-mail: m\_sivasankar@cb.amrita.edu

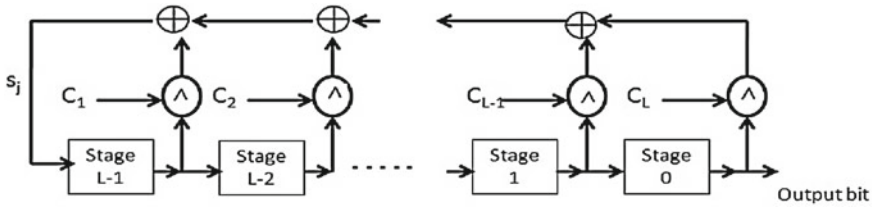


Fig. 1 An LFSR with L stages

into a stream of 0s and 1s and is XORed bit-by-bit with the bits of a bit stream generator. The result is the encrypted plain text called the cipher text.

The bit generator is initialized with a seed and it starts generating bits. The seed bits (called the key) and how the generator is using the present state to generate the next bit are kept secret with the encrypting/decrypting ends. Upon receiving the cipher text, the receiver generates the same bit stream and XORs it with the received cipher text; as XORing a bit with itself nullifies the effect, the plain text is retrieved. Also, as XORing requires less CPU and memory, stream ciphers are preferred when computational and storage overheads are to be minimized.

### 1.2 Linear Feedback Shift Registers

An LFSR of length L consists of L stages numbered 0, 1, ..., L- 1, each capable of storing one bit and having one input and one output; and a clock which controls the movement of data. During each unit of time the following operations are performed: (i) the content of stage 0 is output and forms part of the output sequence; (ii) the content of stage i is moved to stage i - 1 for each 1 ≤ i ≤ L- 1 and (iii) the new content of stage L - 1 is the feedback bit s which is calculated by adding together mod 2 the previous contents of a fixed subset of stages [1].

The LFSR < L, C(D)>, in Fig. 1 has the connection polynomial  $C(D) = 1 + c_1D + c_2D^2 + \dots + C_LD^L \in Z_2(D)$ . If the initial content is  $[s_{L-1}, \dots, s_1, s_0] \in \{0,1\}^L$  then the feed back to this LFSR is  $s_j = (c_1s_{j-1} \oplus c_2s_{j-2} \oplus \dots \oplus c_Ls_{j-L})$  for  $j \geq L$ . The period of a generated sequence  $s_0, s_1, s_2, \dots$  is p if  $s_i = s_{i+p}$  for all  $i \geq 0$ .

### 1.3 Irreducible and Primitive Polynomials

Consider the collection  $Z_2[X]$  of all polynomials in variable x of any degree, with coefficients from  $\{0,1\} = Z_2$ . A polynomial  $p(x) \in Z_2[X]$  is said to be irreducible if it cannot be factored into lower degree polynomials of  $Z_2[X]$ . A primitive polynomial is an irreducible polynomial that generates all elements of an extension field

from a base field. For a detailed introduction to primitive polynomials and extension fields the reader can refer [1, 9]. It is interesting to note that if  $C(D)$  is a primitive polynomial, then any of the  $2^L - 1$  nonzero initial state of the LFSR, produces an output sequence with maximum possible period  $2^L - 1$ , which is a requirement for secure communications [1].

### ***1.4 Combination Generators and Attacks on Stream Ciphers***

Due to the inherent linearity nature of an LFSR, the output of an LFSR is easily predictable. Berlekamp-Massey Algorithm [1, 9], can construct an LFSR for a given sequence. So it is advisable to combine the outputs of many LFSRs to introduce some sort of nonlinearity through a filter generator or through a clock controlled generator [3]. Another way of achieving nonlinearity is by using Boolean functions. A Multi-output Boolean function on  $n$  variables is a mapping from  $\{0,1\}^n$  into  $\{0,1\}^m$  and is denoted by  $f(x_1, x_2, \dots, x_n)$  [4].

Obviously the Boolean function used for inducing nonlinearity should be resistant to various possible attacks mounted on stream ciphers. In fact the Boolean function used should be capable of generating a secure stream cipher possessing the necessary properties of (i) Long period (ii) Large linear complexity (iii) Randomness [10]. A lot of valuable research contributions are available in designing immune Boolean functions [2–4]. These results stress that, Boolean functions should be balanced and possess immunity against fast algebraic attacks and correlation attacks. The linear complexity of the resulting key stream depends on the linear complexity of the constituent streams and it will be maximum if the lengths of individual LFSRs are relatively prime [1].

### ***1.5 Sparse Matrix-Vector Multiplication***

In general, matrices used in cryptography are bigger than available memory. Luckily, many of these matrices are sparse with a special case, binary sparse (entries being 0 or 1). Large binary matrices play an important role in computer science and in information theory. Efficient methods of handling sparse matrices, multiplying them with vectors are in need since their introduction. Due to the crucial requirements of SpMV in (i) Iterative methods for solving large linear systems  $Ax = b$  and (ii) Eigenvalue problems  $Ax = \lambda x$  it attracted many researchers and more efficient methods are being introduced [8, 13, 15].

## 2 Proposed Key Bit-Stream Generator

### 2.1 Binary Matrix Representation of Parallel LFSRs

We observe that the coefficients of a polynomial of degree  $n$ , belonging to  $Z_2[X]$  can be denoted by a 0 – 1 vector of length  $n$ . For example, the connection trinomial  $C(D) = 1 + D^3 + D^5$  can be represented as  $(0, 0, 1, 0, 1) \in \{0,1\}^5$ ; note that, the feedback coefficient 1 (which is always present in connection polynomials) of  $C(D)$ , is not used in the vector representation of  $C(D)$ . Evaluating this polynomial for a state vector  $(b_5, b_4, b_3, b_2, b_1)$  is simply the product  $(0, 0, 1, 0, 1) (b_5, b_4, b_3, b_2, b_1)^T = b_3 + b_1$ . This vector–vector multiplication (mod 2) is in fact the output bit of the LFSR for that state  $(b_5, b_4, b_3, b_2, b_1)$ . Hence shifting the present state vector by one bit and loading the output bit of the just previous vector–vector multiplication as the new entry, we get the next state vector of the LFSR. Continuing this we get the output bit stream of the LFSR. This idea can be extended to represent a set of  $m$  parallel LFSRs (i.e., connection polynomials), each having  $n$  states, in a binary matrix. The  $m$  parallel connection polynomials,  $C_i(D) = 1 + c_{i1}D + c_{i2}D^2 + \dots + c_{in}D^n$ ,  $1 \leq i \leq m$  can be represented by the binary matrix  $C = (c_{ij})$ ,  $i = 1$  to  $m$ ,  $j = 1$  to  $n$ .

### 2.2 Getting the Bit Stream

Using the matrix representation discussed in Sect. 2.1, the  $i$ th row of

$$\begin{pmatrix} c_{11} & c_{12} & \dots & c_{1n} \\ c_{21} & c_{22} & \dots & c_{2n} \\ & & \dots & \\ c_{m1} & c_{m2} & \dots & c_{mn} \end{pmatrix} \begin{pmatrix} b_n \\ b_{n-1} \\ \vdots \\ b_1 \end{pmatrix} = \begin{pmatrix} c_{11}b_n + c_{12}b_{n-1} + \dots + c_{1n}b_1 \\ c_{21}b_n + c_{22}b_{n-1} + \dots + c_{2n}b_1 \\ \dots \\ c_{m1}b_n + c_{m2}b_{n-1} + \dots + c_{mn}b_1 \end{pmatrix}$$

is the output bit of the  $i$ th LFSR,  $1 \leq i \leq m$ , for the state  $(b_n, b_{n-1}, \dots, b_2, b_1)$ . Let us denote this output vector by  $O_k = (o_{k1}, o_{k2}, \dots, o_{km})^T$ ,  $k$  being the iteration number. Now combining the bits of  $O_k$  using a Boolean function  $f$ , we get the key bit,  $\text{bit}_k = f(o_{k1}, o_{k2}, \dots, o_{km})$ . The generation process is continued as described below:

- The input vector  $(b_n, b_{n-1}, \dots, b_2, b_1)$  is shifted by one bit and the feedback of the first LFSR (i.e.,  $o_{k1}$ ) is loaded as the new entry.
- The Matrix-Vector multiplication is performed.
- The resulting vector  $O_{k+1}$  is fed into the Boolean function  $f$  to get  $\text{bit}_k$ .

This way of generation differs from existing schemes, in the randomness happening in loading of the next state of the LFSRs. At any iteration  $k$ , the output bit of the



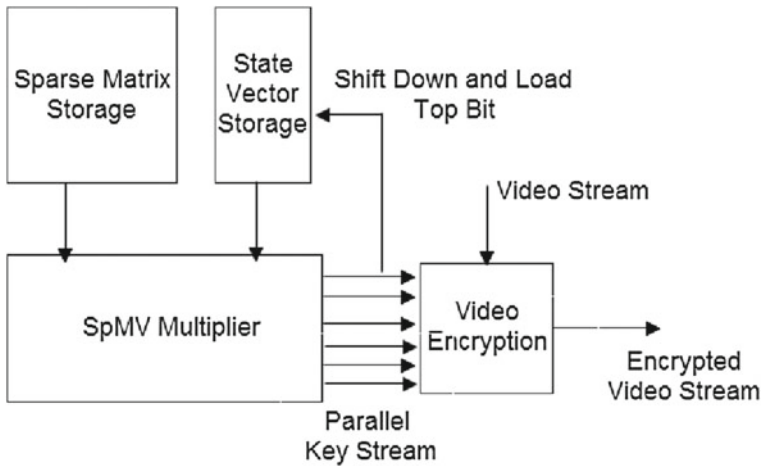


Fig. 2 Video encryption

first LFSR ( $o_{k1}$  of  $O_k$ ) only is used to load the next state. Hence, the first LFSR continues to get its states, according to its connection  $C_1(D)$ , whereas the other LFSRs are loaded with this state vector, leading to randomness in their states. Since  $C_1(D)$  is a primitive connection polynomial, the first LFSR goes through all the possible  $2^L - 1$  states and consequently all the other LFSRs also get these different possible states, the main difference (with the existing schemes) being in the order they get the states if they were standing alone (independent). The randomness in the order of acquiring the states has an effect similar to irregular clocking/random deletion and the periodicity of the sequence generated is not affected. Basically one more randomness to the input bits of Boolean function is introduced and it provides more security to the bit-stream generated.

### 2.3 Using the Stream for Video Stream Encryption

The security requirement in digital video streaming while maintaining efficiency and format compliance [14] can also be achieved by eliminating the nonlinear combinator Boolean function  $f$ , and instead using the output bits of the parallel LFSRs as such (Fig. 2). If byte encryption is required  $m$  can be set to 8 and for more security  $m$  can be set to 9 and the 8 bits excluding the first LFSR's output bit can be used.

## 3 Experimental Works on the Key Stream

Meier and Staffelbach proposed the idea of fast correlation attacks on nonlinear combination generators. In such attacks (i) few bits of the key bit-stream (ii) connection Polynomial of the individual LFSRs (iii) The  $m$ th order Boolean function  $f$

**Table 1** Partial edit distance matrix for the target LFSR

LFSR2↓ and LFSR3→	10101	11101	10111	11111	10001
10101	2	2	1	1	1
11101	2	1	1	1	2
10111	2	1	2	1	1
11111	2	1	2	1	1
10001	3	2	1	2	1

(iv) The correlation probability of the key stream with the output of the target LFSR are known to the attacker. A detailed study of this type of attack can be found in [7]. In our experimental work we perform another type of attack, the edit distance attack [5], (which is a known plain text attack), on the proposed stream cipher. Basically, stream ciphers generate the key bit-stream from a short key. For a secure stream cipher, it should not be possible to reconstruct the short key from the key stream sequence. The core idea behind edit distance attacks lies in guessing the initial state of the generator and then trying to determine whether the initial guess is consistent.

We proceed with three ( $m = 3$ ) 5 bit LFSRs with connection polynomials  $C_1(D) = 1 + D^2 + D^5$ ,  $C_2(D) = 1 + D + D^2 + D^3 + D^5$ ,  $C_3(D) = 1 + D^3 + D^5$ , with an initial state (10101) and the Boolean function  $f = x_1x_2 + x_3$ . The time taken for calculating the edit distance matrix is a crucial step in the attack time. Table 1 shows partial edit distance matrix obtained for various combinations of initial states of LFSR 2 and LFSR 3 with a fixed initial state of (10100) of LFSR 1. From the table it is observed that an increase in the number of known bits leads to a significant increase in the computation time; and comparing with the conventional way of generating the stream, we observe that required properties of the sequence are not compromised.

## 4 Implementation Issues

Usually, as the number of LFSRs increases the memory/hardware requirement also increases. Boolean function calculation also plays a role in implementation. But here since all the LFSRs are controlled by a Boolean matrix, sparse matrix multiplication implementation is crucial [16]. The number of variables involved in the generation decides the order of the matrix. The space required for LFSR implementation increases linearly with the number of variables and the space required for the Boolean function increases exponentially with the number of variables [11, 12]. Either we can directly implement the Boolean function or we can simplify to some extent so that the hardware requirement is optimized. The possible implementation of the case  $m = n$  (number of LFSRs and their number of stages are equal), leading to a square sparse matrix can be analyzed in future.

## 5 A Variant of SpMV Stream Cipher

### 5.1 Permutation Matrices

We observe that given a nonzero initial state, an irreducible polynomial makes the LFSR to visit all the possible  $2^L - 1$  nonzero states, and hence the LFSR gives out a binary sequence of maximum period possible. The order in which the states are visited is nothing but a permutation of the list of  $2^L - 1$   $L$ -bit strings. The possible number of permutations is, as we know  $(2^L - 1)!$ ; and an  $L$ -stage LFSR with an irreducible connection polynomial goes through the states in order, which is one order among the  $(2^L - 1)!$  ordered lists. This is in fact a combinatorial problem of listing down all the possible permutations of the  $2^L - 1$   $L$ -bit strings. It is interesting to note that a permutation of  $n$  elements has a matrix representation, the permutation matrix, which is a sparse matrix. A permutation  $\pi$  of  $n$  elements is a rearrangement of the  $n$  elements. The permutation matrix  $P$ , of a permutation is the square matrix of order  $n$  whose entries are 0 everywhere except in row  $i$ , where the entry  $\pi(i)$  is 1.

### 5.2 Generating Permutations

We can slightly vary the process discussed in Sect. 2.2, by permuting the output bits of the  $m$  LFSRs (that is the vector  $O_k$ ), before feeding it into  $f$ . While trying to list down all the possible permutations of a set of elements, we may be interested in whether they have to be listed systematically (with some specific ordering) or randomly. One way to generate all the permutations is using factorial number system and Lehmer codes. It suffers from a drawback of converting back and forth from the permutations to such a number system. Ways of systematically generating all the permutations may become infeasible for large  $n$ . An exhaustive list of such algorithms are discussed in [6].

### 5.3 Including Permutations in Generation

After having access to all possible permutations, we can select one of these permutations and can apply it to the output vector  $O_k$  of the SpVM unit. The permutation used is kept secret, adding one more level of diffusion to the key stream generated. Instead of one permutation, two or more permutations can also be applied. As permutation matrices are sparse in nature, we can use the same SpVM unit for performing the permutation. We observed more randomness after applying a permutation over the input before fed to  $f$ . This is supported by the partial edit distance matrix (Table 2) for the target LFSR under the same conditions of Sect. 3 except that a permutation

**Table 2** Partial edit distance matrix in the SpMV variant case

LFSR2↓ and LFSR3→	10101	11101	10111	11111	10001
10101	3	4	2	3	3
11101	4	2	2	3	4
10111	4	2	3	3	3
11111	3	2	3	3	3
10001	3	4	3	4	3

$C = \begin{pmatrix} 1 & 0 & 0 \\ 0 & 0 & 1 \\ 0 & 1 & 0 \end{pmatrix}$  is introduced. This is so, as the edit distance attack has no information about the permutation introduced in between.

## 6 Concluding Remarks

In this paper we have proposed a sparse matrix-vector multiplication-based bit/parallel stream cipher. A variant of the proposed scheme is also discussed in connection with the permutation of the output bits. As in binary matrix multiplication, the possibility of compatibility mismatch with devices never arises, this generator can be implemented in almost all devices. Since research on Boolean functions, Sparse matrix representation, and hardware architecture of multipliers is proceeding at a high pace, we can expect improved, more efficient type of stream cipher generators in the near future. SpMV implementation of the new class of FCSR (feedback carry shift register) can also be explored. The usage of polynomial/multivariate polynomial matrices can also be analyzed in stream cipher generation that will lead to a new class of stream ciphers for video encryption.

## References

1. Menezes, A.J., van Oorschot, P.C., Vanstone, S.A.: Handbook of Applied Cryptography. CRC Press LCC, Boca Raton (1996)
2. Dalai, D.K., Gupta, K.C., Maitra, S.: Results on algebraic immunity for cryptographically significant boolean functions. In: The Proceedings of Progress in Cryptology, INDOCRYPT 2004, vol. 3348, pp 92–106. Springer, LNCS (2004)
3. Ekdhal, P.: On LFSR based stream ciphers analysis and design, Ph.D. Thesis, Department of Information Technology, Lund University (2003)
4. Frederik, Armknecht: Matthias, Krause: Constructing Single and Multi-output Boolean Functions with Maximal Algebraic Immunity, In: The Proceedings of ICALP 2006, Venice, Italy vol. 4052. Springer, LNCS (2006)
5. Golic, J.: Edit distances and probabilities for correlation attacks on clock controlled combiners with memory. In: ACISP 96, Wollongong, Australia. IEEE Trans. Inf. Theory **47**(3), (2001)
6. Knuth, D.E.: The Art of Computer Programming, Combinatorial Algorithms, Part 1. Addison-Wesley Professional, New Jersey (2001)

7. Meier, W., Staffelbach, O.: Fast Correlation Attacks on Stream Ciphers. In: The Proceedings of Advances in Cryptography, EUROCRYPT'88, vol. 330, Springer, LNCS, Davos, Switzerland (1988)
8. Bell, N., Garland, M.: Efficient Sparse Matrix-Vector Multiplication on CUDA. NVIDIA Technical, Report, NVR-2008-004 (2008)
9. Lidl, R., Niederreiter, H.: Finite Fields, 2nd edn. Cambridge University Press, Cambridge (1997)
10. Rueppel, RA.: Analysis and Design of Stream Ciphers. Springer, Berlin (1986)
11. Sarkar, P: Efficient implementation of large stream cipher systems. In: The Proceedings of Cryptographic Hardware and Embedded Systems, CHES 2001, vol. 2162, pp. 319–332, Springer, LNCS, Paris, France (2001)
12. Sarkar, P., Maitra, S.: Efficient implementation of cryptographically useful large boolean functions. *IEEE Trans. Comput.* **52**, 410–417 (2003)
13. Williams, S., Oliker, L., Vuduc, R., Shalf, J., Yelick, K., Demmel, J.: Optimization of sparse matrix-vector multiplication on emerging multicore platforms. In: The Proceedings of ACM/IEEE Conference on Supercomputing (2007)
14. Wong, A., Bishop, W.: An efficient, parallel multikey encryption of compressed video streams. In: The proceedings of International Conference on Signal and Image Processing (2006)
15. Yousef, S.: Iterative Methods for Sparse Linear Systems, 2nd edn. SIAM (2003)
16. Yzelman, A.N.: Fast sparse matrix-vector multiplication by partitioning and reordering. Ph.D. dissertation, Utrecht University (2011)

# Steganography-Based Secure Communication

Manjot Bhatia, Sunil Kumar Muttoo and M. P. S. Bhatia

**Abstract** Security and scalability are important issues for secure group communication in a grid environment. Secure communication involves confidentiality and authenticity of the user and the message between group members. To transmit data in a secure way, a secure and authenticated key transfer protocol should be applied. Key transfer protocol needs an entity responsible for user authentication and secures session keys. Recently, many researchers have proposed secure group communication methods based upon various cryptographic techniques. In this paper, we propose a secure key transfer protocol that uses the concepts of soft dipole representation of the image and steganography to establish secure communication between group of authenticated users. Steganography hides the existence of group keys in images. This protocol is more secure as compare to previously proposed encryption based group communication protocols. This protocol uses a centralized entity key management center (KMC). KMC generates the group key using soft dipoles of the images of the group members and broadcast it securely to all the communicating group members.

**Keywords** Grid security · Key management protocol · Secure group communication · Soft dipole representation · Communication security

---

M. Bhatia (✉) · S. K. Muttoo  
Department of Computer Science, University of Delhi, New Delhi, India  
e-mail: manjot\_bhatia@hotmail.com

S. K. Muttoo  
e-mail: skmuttoo@cs.du.ac.in

M. P. S. Bhatia  
Department of Computer Engineering, Netaji Subhas Institute of Technology,  
New Delhi, India  
e-mail: bhatia.mps@gmail.com

## 1 Introduction

One of the most important issues in grid environment is security. Since grid environment is based on Internet, various active attackers repeatedly explore security holes existing in hardware, software, processes, or systems to steal information or to distribute the network services [2]. Grid environment is a form of distributed environment in which resources are geographically distributed and owned by different individuals with different technologies. For secure grid environment, grid systems and applications require security functions to (i) provide stronger authentication solutions to user and resources (ii) protect grid applications and data from local applications (iii) protect local policies of different administrative domains (iv) provide secure group communication to users to coordinate and secure their group activities [2]. From these security requirements we focused on secure authenticated group communication environment for authorized users in a secure manner. As we know, secure authenticated group communication is an environment in which members of a group interested in sharing some information in a secure way so that no other person outside the group should be able to perform an attack. The communication among users forming a group must be confidential; this brings the need of protocol for secure group communication [2]. The various applications where secure group communication plays an important role are cyber forensics, multiparty military actions, doctors discussions on serious medical issues, law enforcement practice, and government decisions on critical issues. Apart from these, secure group communications can be used in distributed interactive simulations, interactive games, and real-time information services [2]. Group key management is an important issue for secure group communication. The secure group communication needs to consider the following security functions [2]:

- Group key generation: The group key is generated for carrying out confidential communication among the group members of that specified group.
- Group Key confidentiality: Broadcasting group key to the group members securely, so that it could be recovered by the authorized group members only.
- Message confidentiality: To ensure that the message should be read only by the specified receiver.
- Message verification: Each user verifies the authenticity of the message to ensure that the message was sent by the authorized group member of its group.

Most of the secure group communication protocols presented by the various researchers are either implementing key generation and key confidentiality functions or message confidentiality and message authentication functions. Since group communication involves communication and information sharing among several members, so above listed security functions can be provided only by establishing a secure group key or secure session key among the group members for confidential communication [2]. The group key should be generated by the trusted Key management center and distributed to all the members of the communicating group. To send the group key securely to the group members, it can be encrypted using another secret

key. Once the group Key received, members of the group can communicate securely with each other. Several group key management protocols have been proposed by various researchers [2].

- (1) Centralized Group Key Management Protocol: A centralized single entity as key management center is responsible for generating group key for the entire group, reducing storage requirements and computational effort of the clients. The threat lies in the failure of the single entity.
- (2) Distributed Key Management Protocol: In distributed key management protocol there is no explicit KMC, the members of the group communicate with each other and can generate the group key themselves. They do not need to depend on the third party. Each member can contribute some information to generate the group key. So the security level has been raised but this method is suitable for a small group only. For large groups it is very time consuming to collect information from every user due to the scalability factor of the group users.
- (3) Decentralized Key Management Protocol: In a decentralized architecture the management of a large group is divided among subgroup managers, trying to minimize the problem of concentrating the work in a single place [7, 26].

This paper is an implementation of our previous work in [2] that explains the proposed protocol for user authentication and secure group communication.

## 2 Related Work

Many researchers have proposed various protocols for secure group communication between grid entities. Grid security infrastructure (GSI) above all provides confidentiality and security for transferring sensitive information on the Internet [10]. Most of the researchers have used centralized group key management protocols for secure group communication. Sudha et al. [21] have proposed secret keys multiplication protocol based on modular polynomial arithmetic (SKMP), which eliminates the need for the encryption/decryption during the group re-keying. Valli et al. [22] have proposed a new technique (SGKP-1), using hybrid key trees, has certain advantages like secure channel establishment for the distribution of the key material, reducing the storage requirements and burden at each member, minimization of time requirement to become a new member of a group. The computational complexity further reduced using both the combination of public and private key cryptosystems. The dual level key management protocol proposed by Zoua et al. (DLKM) [26] uses access control polynomial (ACP) and one-way functions that provides flexibility, security, and hierarchical access control. Researchers used encryptions to update the group key for forward and backward secrecy, Harney [11] group key management protocol based on encryptions is of  $O(n)$ , where  $n$  is the size of group. Zhenga et al. [25] used identity-based signature (IBS) scheme for grid authentication. Park et al. [18] have proposed an ID-based key distribution scheme which is secure against



session state reveal attacks and long-term key reveal attacks, this scheme offers the scalability, non-usage of additional cryptographic algorithms, and efficiency similar to those of the existing schemes. The distributed group key management protocol proposed by Steiner et al. [20], Burmester and Desmedt [3] are based on DH key agreement protocol. Li et al. [15] proposed a scalable service scheme using digital signatures and used Huffman binary tree to distribute and manage keys. Li et al. [16] have proposed an authenticated encryption mechanism for group communication in terms of the basic theory of threshold signature and the basic characteristics of group communication in grid. In this approach, each group member in the grid can verify the identity of the signer and hold the private key. Li et al. [17] have proposed the service infrastructure of middleware for pervasive grid. Ingle and Sivakumar [12] presented an extended grid security infrastructure (EGSI) that includes an authentication and access control scheme at virtual organization (VO) level for group communication in grid environment. EGSI introduced the concept of application class awareness in grid. This paper is organized as follows. We discuss introduction in Sect. 1 and related work in Sect. 2. In Sect. 3, we discuss model of our proposed protocol for secure group communication. Section 4 discusses security analysis of the proposed protocol.

### 3 Proposed Protocol: Secure Communication

The proposed architecture of secure protocol tries to fulfill the security constraints of the grid environment: single sign-on, secure group communication (Fig. 1).

#### 3.1 Model of the Proposed Protocol

We proposed a secure group communication protocol which consists of total of  $m$  users  $usr_i (i = 1, 2, \dots, m)$ . Our proposed protocol consists of the following phases (Table 1):

##### (i) Registration Process

Each user needs to register with one centralized authority, key management center. During registration, users need to submit their images  $I_i (i = 1, 2, \dots, m)$  to the KMC as the part of the registration process through the secured channel. KMC stores the images  $I_1, I_2 \dots I_n$  of users. KMC assigns a unique identification number (uid) and unique password (pw) to every user. Each user's password generated by the KMC is a soft dipole representation ( $S_I$ ) of user's image, i.e.,  $pw_i = S_{I(i)}$ , soft dipole representation of an image is a triple  $S_I(d, \alpha, \beta)$  that uniquely represents the image [27]. Password (pw) of each user is embedded into its corresponding image  $I$  using any embedding algorithm given by Neil and Stefan [14] and stego image (sp) is transferred to its corresponding user.

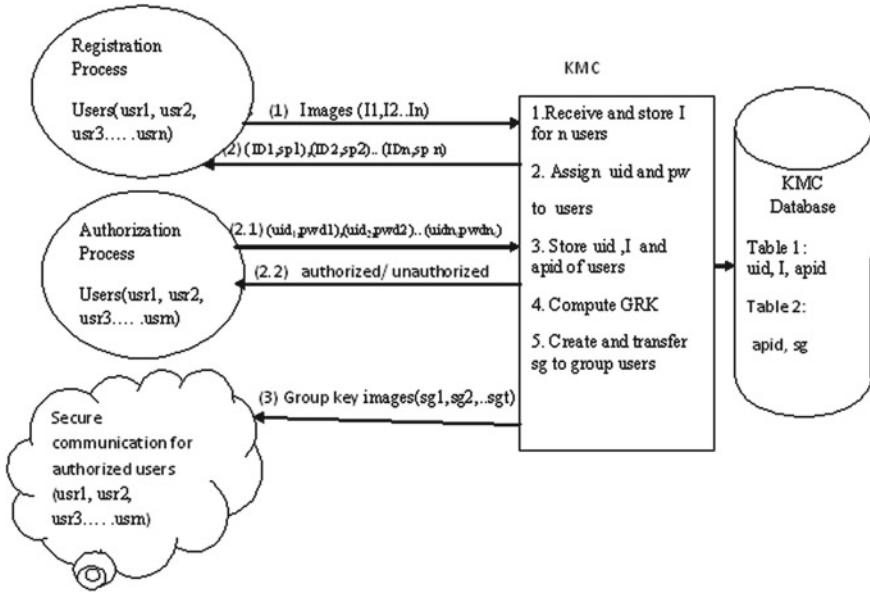


Fig. 1 Architecture of proposed model [2]

Table 1 Notations

$usr_i$	User
$I_i$	User's image
$uid_i$	Every registered user is assigned a unique identification number
$pwd_i$	Every registered user is assigned a password
$Ausr_i$	Authorized user
$S_I(i)$	Soft dipole representation for image of $i$ th user
$sp_i$	Stego-image transferred to each user with embedded password
$sg_i$	Stego-image transferred to each group member with embedded group key
$apid$	Unique application ID of applications required by users in groups
$m$	Total number of registered users
$t$	Total number of group members
$n$	nonce (number used only once)
GRK	Group key

**Process: registration**


---

```

KMC_Registration(int i)
{
  Get Ii
  uidi=generate_uid(int i)//using dicomuid function of matlab
  pw(i)=compute_ SI (image Ii)
  spi=embed(SI(i), Ii) // using any steganography technique
  store uidi, Ii into KMC DB
  return uidi,spi
}

```

---

**Process: password computation**

```

compute_ SI (image Ii)
{
  N= total no. of pixels in an image
  Pi= 3.14159, sigma=1, pw=0
  A=sum of color values of 1st pixel at (0,0) position of the image
  B=sum of color values of dth pixel
  For d=0 to m // where m can be any value ranging 0 to N-1
  {
    For r=0 to N-1-d
    {
      C=(sum of color values of rth pixel-A)
      E=(sum of color values of (r+d)th pixel - B)
      Gc=probability density function based on value of C
      Ge= probability density function based on value of E
      pw=∑(Gc*Ge)
    }
  }
  Return pw
}

```

---

## (ii) Authentication Process

For authentication process, KMC stores the uid and its corresponding image ( $I$ ) for every user. When user enters the uid and pw, KMC computes the  $S_I$  values of the user from the already stored  $I$ . As  $S_I$  value of user's image is used as password, KMC compares the computed  $S_I$  with pw entered by the user for authentication.

**Process: user login**


---

```

for all users (i=1..m)
{
  receive uidi, spi
  pwi=extract(spi) // using any extraction technique
}

```

---

**Process: user authentication**


---

```

user_authentication(int i)
{
  Get uidi
  Verify uidi from the KMC DB
  if exists(uidi)
  {
    get "password" , pwi
    retrieve Ii for uidi from KMC DB
    SI(i) = compute_ SI (image Ii)
    If pwi = SI(i)
    result = "authorized"
  }
  else
  result = "unauthorized"
}
else
result = "uidi unauthorized"
return result for uid
}

```

---

**(iii) Group Key Generation**

After the authentication process is over KMC computes the group key for group communication of the users with common application ID (apid). Groups are identified by the unique application ID (apid). The registered users have to go through the authentication process for secure group communication. At the initial set up, when all the registered users of any particular group authenticates with KMC, group key for that group is computed and distributed to all the members of that group.

$$GRK_j = \sum (S_{I(i)}) + n, k = (1, 2, \dots, t_j), \quad i \in k$$

where  $k$  denotes the number of group members of the group [2] under consideration and  $n$  represents nonce.

**(iv) Group Key Confidentiality**

The group key is transferred securely and confidentially to the group members by hiding it in such a way that does not allow any message trapper to even detect the presence of GRK. To conceal the existence of GRK while transferring it to group members we use steganography. The security of group key in our protocol is kept by hiding the GRK into user's image ( $I$ ) and transferring image  $I$  as GRK.

**(v) Password/Group Key Extraction**

Each group member  $usr_i$  knows the extraction method and can extract the password and group key from the received stego-image file using the extraction algorithm [14].

**Process P3:** Group Key generation

---

```

Group Key generation
{
select unique apid from KMC DB
for all apids
GRK(apid)=0;
for all user usri (i=1..m)
{
user_authentication (int i)
if result="authorized"
{
Select apid for uidi from KMC DB
GRK(apid)=GRK(apid)+SI(i)
}
unauthorized
}
}

```

---

**Process P3:** Group Key generation

---

```

for all apids from KMC DB
{
sg(apid)=embed (GRK(app_id), I(uid) ) //using any steganography technique
return sg(uid)
}

```

---

## 4 Security Analysis

Proposed protocol can handle following security attacks from two enemies: internal and external.



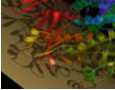

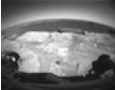
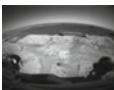














### 4.1 Insider Attack

Internal attack that a group member can extract the information from sg files of other group members. The sg files transferred to the t group members are protected with user's login password. Any jth user inside the group trying to gain access to the image file sg<sub>i</sub> of the i<sup>th</sup> user would not be able to do as sg<sub>1</sub>, sg<sub>2</sub>, . . . , sg<sub>m</sub> files for all the group users are locked with the unique password, i.e., pw.

### 4.2 Outsider Attack

KMC keeps the record of unique apid of every group ids of its corresponding group members in KMC database. Any other registered user sending the request for the group key needs to send the uid and apid of the application for which it is sending

**Table 2** User’s image, password computed and embedded, stego image, PSNR of IM and stego image, and password extracted

User’s image	Password computed	Stego image (stmp)	PSNR	Password extracted
	4911739		88.6851	4911739
	49695168		87.9885	49695168
	29602972		Infinity	29602972
	48341515		91.1411	48341515
	10548923		Infinity	10548923
	7280785		95.4008	7280785
	3635416		Infinity	3635416
	14759021		88.3967	14759021
	46550076		79.3712	46550076
	11089453		79.1484	11089453

the request. KMC checks the database for uids of the users for the received app\_id. If that uid is not in the list, KMC will not respond for that request.

## 5 Simulation Result

The above-proposed protocol is divided into three phases: (i) user registration, (ii) user authentication, (iii) generating group key.

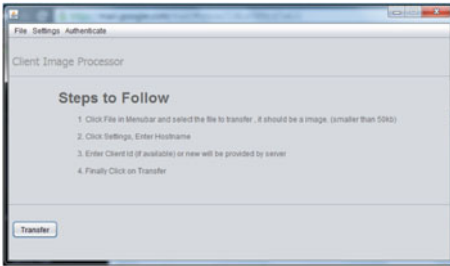
To simulate the first two phases of our protocol, we took the example of ten users: The simulation is done using java programming and Matlab. We used java for creating client and KMC server environment, submitting images to the KMC by the clients and computing passwords from the submitted images. Matlab programming is used for embedding and extracting password in user's image. After embedding password in original image, stego image is passed to the user as password. To compare the original images and the stego images, peak signal to noise ratio (PSNR) is calculated through Matlab code. The PSNR values in Table 2 shows that there is not any visible difference between the original and the stego images of the users.

## 6 Conclusion

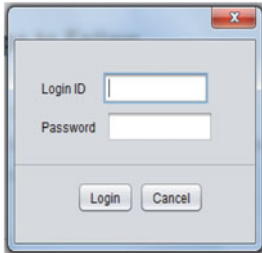
We have proposed a secure group key generation protocol for secure group communication where every user needs to register with an image with centralized entity KMC. KMC is responsible for generating passwords and group keys for the users. The security of the password and group key is achieved with steganography based embedding algorithm. Only group users can extract the group key. In future we will work on completing its implementation part and try to enhance security features of secure group communication.

## Appendix 1

Screen shots of simulation [28].



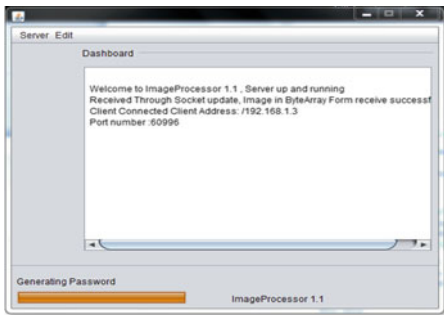
Client side screen



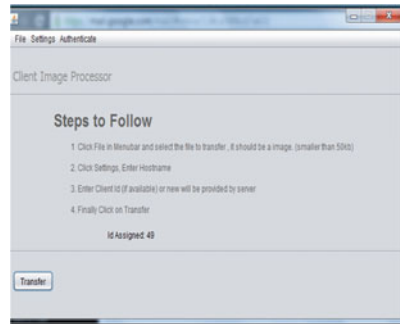
Login Screen

ID	IMAGE	APPID
16	01_00	5
17	01_00	5
18	01_00	5
19	01_00	374628
20	01_00	374628
21	01_00	374628
22	01_00	34
23	01_00	374628
24	01_00	5
25	01_00	5
26	01_00	5
27	01_00	5
28	01_00	5
29	01_00	5
30	01_00	5
31	01_00	5
32	01_00	5

Client table in KMC database



Server generating password



ID assigned to client side

## References

1. Aparna, R., Amberker, B.B.: Dynamic authenticated secure group communication. World Acad. Sci. Eng. Technol. **34** (2007)
2. Bhatia, M., Mutto, S.K., Bhatia, M.P.S.: Secure group communication protocol. Int. J. Adv. Eng. Sci. Technol. (2011)
3. Burmester, M., Desmedt, Y.G.: A secure and efficient conference key distribution system. In: Proceedings of Eurocrypt '94 Workshop Advances in Cryptology, pp. 275–286 (1994)
4. Chadramouli, R., Memon, N.: Analysis of LSB based image steganography techniques. IEEE (2001)
5. Chubb, C., Yellott, J.I.: Dipole statistics of discrete finite images: two visually motivated representation theorems. J. Opt. Soc. Am. A (2002)
6. Cody, E., Sharman, R., Rao, R.H., Upadhyaya, S., et al.: Security in grid computing: a review and synthesis. Decis. Supp. Syst. **44**(4), 749–764 (2008)



7. Foster, I., et al.: Grid services for distributed systems integration. *IEEE Comput. Soc.* **35**(6), 37–46 (2002)
8. Foster, I., et al.: *In the Grid: Blueprint for a New Computing Infrastructure*. Morgan Kaufmann, San Francisco (1999)
9. Foster, I., et al.: The anatomy of the grid: enabling scalable virtual organizations. *Int. J. High Perform. Comput. Appl.* ACM Digital Library, pp. 200–222 (2001)
10. Foster, I., Kesselman, C., Tsudik, G., Tuecke, S.: A security architecture for computational grids. In: *Proceedings of ACM Conference on Computers and Security* (1998)
11. Harnay, H., Muckenhirn, C., Rivers, T.: Group Key Management Protocol (GKMP), Architecture RFC2094 (1997)
12. Ingle, R., Sivakumar, G.: EGSI: TGKA based security architecture for group communication in grid. In: *Proceedings of the 10th IEEE/ACM International Conference on Cluster, Cloud and Grid Computing*, May 17–20, IEEE Computer Society, Australia, pp. 34–42 (2010). doi:[10.1109/CCGRID.2010.28](https://doi.org/10.1109/CCGRID.2010.28)
13. Johnson, N. F., Katzenbeisser Stefan, C.: *A Survey of Steganographic Techniques*. Artech House Books, London (2000)
14. Katzenbeisser, S., Petitcolas, F.A.P.: *Information Hiding Techniques for Steganography and Digital Watermarking*. Artech House, London (2000)
15. Li, Y., Jin, H., Zou, D., Liu, S., Han, Z.: A scalable service scheme for secure group communication in grid. In: *31st Annual International Computer Software and Applications Conference (COMPSAC 2007)*, pp. 31–38 (2007)
16. Li, Y., Xu, X., Wan, J., Jin, H., Han, Z.: An authenticated encryption mechanism for secure group communication in grid. In: *Proceedings of the International Conference on Internet Computing in Science and Engineering*, Jan. 28–29, USA, pp. 298–305 (2008). doi:[10.1109/ICICSE.2008.80](https://doi.org/10.1109/ICICSE.2008.80)
17. Li, Y., Jin, H., Han, Z., Liu, S., et al.: A secure mechanism of group communication for pervasive grid. *Int. J. Ad Hoc Ubiquitous Comput.* **4**, 344–353 (2009). doi:[10.1504/IJAHUC.2009.028662](https://doi.org/10.1504/IJAHUC.2009.028662)
18. Park, H., Yi, W.S., Lee, G.: Simple ID-based key distribution scheme. In: *Fifth International Conference on Internet and Web Applications and Services 2010*, 369–373 (2010)
19. *Steganographic techniques, a brief survey*. Department of computer science, Wellesley College
20. Steiner, M., Tsudik, G., Waidner, M.: Diffie-Hellman key distribution extended to group communication. In: *Proceedings of Third ACM Conference on Computer and Communication Security (CCS '96)*, pp. 31–37 (1996)
21. Sudha, S., Samsudin, A., Alia, M.A.: Group rekeying protocol based on modular polynomial arithmetic over Galois field GF (2n). *Am. J. Appl. Sci.* **6**, 1714–1717 (2009). doi:[10.3844/ajassp.2009.1714.1717](https://doi.org/10.3844/ajassp.2009.1714.1717)
22. Valli, V., Kumari, D., NagaRaju, V., Soumy, K., Raju, K.V.S.V.N.: Secure group key distribution using hybrid cryptosystem. In: *Proceedings of the 2nd International Conference on Machine Learning and Computing*, IEEE Computer Society, Washington, pp. 188–192 (2010). doi:[10.1109/ICMLC.2010.4110](https://doi.org/10.1109/ICMLC.2010.4110)
23. Wikipedia, Digital Image processing, available at: [http://en.wikipedia.org/wiki/Digital\\_image\\_processing](http://en.wikipedia.org/wiki/Digital_image_processing), accessed on March 2012
24. Xu, S.: On the Security of Group Communication Schemes
25. Zhenga, Y., Wanga, H.Y., Wang, R., et al.: Grid authentication from identity-based cryptography without random oracles. *J. China Univ. Posts Telecommun.*, Elsevier **15**(4), 55–59 (2008)
26. Zoua X., Dai Y.S., Rana X.: Dual-level key management for secure grid communication in dynamic and hierarchical groups. *Future Gen. Comput. Syst.*, Science Direct, **23**(6), 776–78 (2007)

**Part VIII**  
**Soft Computing and Web Technologies**  
**(SCWT)**

# Heirarchy of Communities in Dynamic Social Network

S. Mishra and G. C. Nandi

**Abstract** Discovering the hierarchy of organizational structure can unveil significant patterns that can help in network analysis. In this paper, we used Enron email data which is well-known benchmarked data set for this sort of research domain. We derive a hierarchical structure of organization by calculating the individual score of each person based on their frequency of communication via email using page rank algorithm. After that, a communication graph is plotted that shows power of each individual among themselves. Experimental results showed that this approach was very helpful in identifying primal persons and their persistent links with others over the period of months.

**Keywords** Dynamic social network analysis · Social network analysis · Hierarchal structure.

## 1 Introduction

A network structure is the perfect epitome that provides a formal way of representing data that emphasizes the association between entities. This representation has a substantial importance that gives the insight of knowledge into the data. Since for the work to be done many entities these days are interconnected and behaviors of individual entity reflect the function of whole system to a large extent. The entity could be people, organization [1], computer nodes [2]. Networks are primarily studied in mathematical framework, i.e., graph [3].

---

S. Mishra (✉) · G. C. Nandi  
Robotics and AI Lab, Indian Institute of Information Technology,  
Allahabad, India  
e-mail: seema.mishra6@gmail.com

G. C. Nandi  
e-mail: gcnandi@iiita.ac.in

In modern era, social network analysis is proliferated area of research, has been in existence for quite some time and experiencing a surge in popularity to understand the behavior of the users at individual and group level [1, 2]. Understanding the behavior of individual social networking methods assuage the analysts to revealing hidden patterns from social communication. In order to model the social network mathematically, most popular data structure typically known as graphs are used where the nodes depict the individual or group of person, or event or organization, etc, and each link/edge represents connection/relationship between two individual. Social network analysis attempts to understand the network and its components like nodes (social entities commonly known as actor or event) and connections (interconnection, ties, and links). It has main focus of analyzing individuals and their interdependent relationships among them rather than individuals and their attributes as we deal in conventional data structure.

## 2 Dynamic Network Analysis

Versatile power of social network is being applied to mining pattern of social interaction in wide ranging applications including: disease modeling [4] information transmission, behavior analysis [5, 6], and business management and behavior analysis. Network analysis also came in to picture as its practical applications in intelligence and surveillance [7] and has become popularized paradigm to uncover antisocial network such like criminal, terrorist, and fraud network majorly after the tragically event of September 11, 2001 which has shattered the whole world.

Social interaction could be in any form that depends on the type of data available [8]. It might be verbal or written communication (cell phones, emails, and blogs chatting), scientific collaboration (co-authorship network, citation network), browsed websites, and group of animals.

This mathematical network model is very successful in analysis of social network but major drawback is that it may miss the temporal aspect of interaction because social interaction is inherently dynamic in nature. The static model of interaction can give the information that could be inaccurate and decision made based merely on this contributed information might lead analyst to false position of analysis.

Several shortcomings can be highlighted when dealing with static model of social network that could forbid acknowledging the casual relationship of pattern of social interaction [8]:

- What is the rate of spreading diseases while modeling diseases and who is the central person whom should be vaccinated to control spread of it among group of person.
- What are the causes and consequences of social structure evolution?

Dynamic social network analysis is emerging research area that play a crucial role to fill gap between traditional social network analysis and time domain. Dynamic

study of network includes classical network analysis, link analysis, and multiagent systems.

Dynamic network analysis facilitates the analysis of multiple types of nodes (multinode) and multiple types of links (multiplex) simultaneously. On the contrary, static network analysis can only focus at most two mode data and analyze one type of link at a time. There are several characteristics of dynamic network:

- Nature of nodes are dynamic, there properties changes with respect to time.
- Deals with meta-network.
- Network evolution is consequent of agent-based modeling.

### 2.1 Community Detection

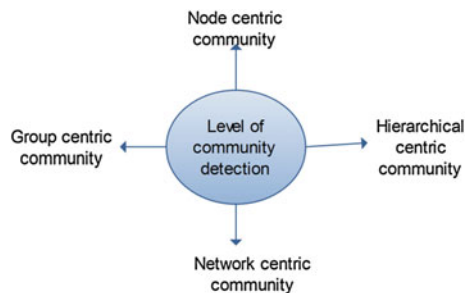
A community is subpart of whole network between which intercommunity interaction is relatively frequent and strong than intracommunity interaction. It can be in any form for example group, subgroup, and cluster. It may; (a) citation network represents related papers on single topics, (b) Web pages on related topics.

Community detection is a classical problem in social network analysis. Commonly, it can be the problem of identifying subgraphs of original graph and called vertex sparsifier [9]. These small networks uphold the relevant information of original group. Four levels of analyses are being conducted in community identification as shown in Fig. 1:

### 2.2 Analysis of Previous Work

Hierarchical methods for community detection falls into two categories: agglomerative and divisive. In former case each node is assumed to be a community and repetitively group together. Similarly, in later case initially whole network is considered as a community and divided subsequently into smaller one. Most methods

**Fig. 1** Level of analysis of community detection



are graph clustering and partition. Distance-based structural equivalence [10] uses distance metrics to identify similar entities. In graph partition methods several algorithms has been proposed [11, 12]. Newman-Girvan method and spectral clustering methods [13, 14] uses a notion of modularity and utilizes edge betweenness metric to divide into groups.

In analyzing dynamic pattern, many methods use the temporal snapshots of interaction over the times [15, 16].

### 2.3 Discovering Hierarchy of Group

Before analyzing community hierarchy we define several basic terminologies. Hierarchy of community provides the power of each individual in a group. If somehow we know this chain we can find the leader of group. Regarding this we used well-known algorithm Page Rank which calculate the individual score  $I\_score$  of each person to represent importance of person. Higher the score of person more powerful the person is.

**Definition 1** If  $P = \{p_1, p_2, \dots, p_k\}$  be the collection of person involved in a communication. For any member  $p_i$  and  $p_j$ , if  $I\_score(p_i) \geq I\_score(p_j)$  then  $p_i$  is more powerful than  $p_j$

#### A. Data Set

We performed the experiments on Enron data set. Since email communication data has become a practical source for research in network analysis like social network. Mostly the experiments are carried out on the artificial data due to the non-availability of real life communication data. The Enron email data set [17] has become a benchmark for this sort of research domain in network analysis. This data set was made public and posted on Web by the Federal Energy Regulatory Commission during its investigation for fraud happened in company, in order to make it test bed for validating and testing the efficacy of methodologies developed for counter-terrorism, fraud detection, and link analysis.

Data is about 150 users communication mostly senior managers organized into folder where nodes are people and edges are email communication between them. But this data set has still lots of issues regarding integrity issue and duplicate messages issue. We preprocessed the data sets in to socio matrix of 12 months from January to December and finally draw a graph of interaction over the months.

#### B. Experiments and Analysis

In this section, we evaluate the capability of the proposed approach on discovering organizational structure and to exploring evolution of organizational structure in a dynamic social network. The implementation was done in DEV C++. The experiments were conducted on a 2.1GHz PC with Core(TM)2 Dual-Core Pentium 4 processor with 2 GB RAM.

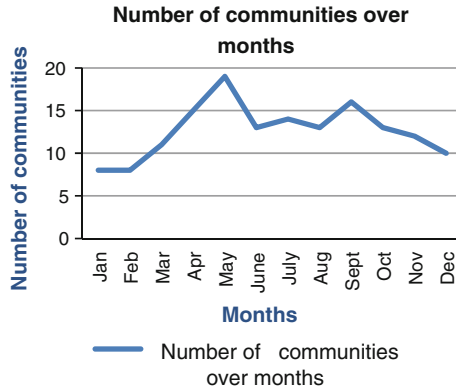


Fig. 2 Number of communities over months

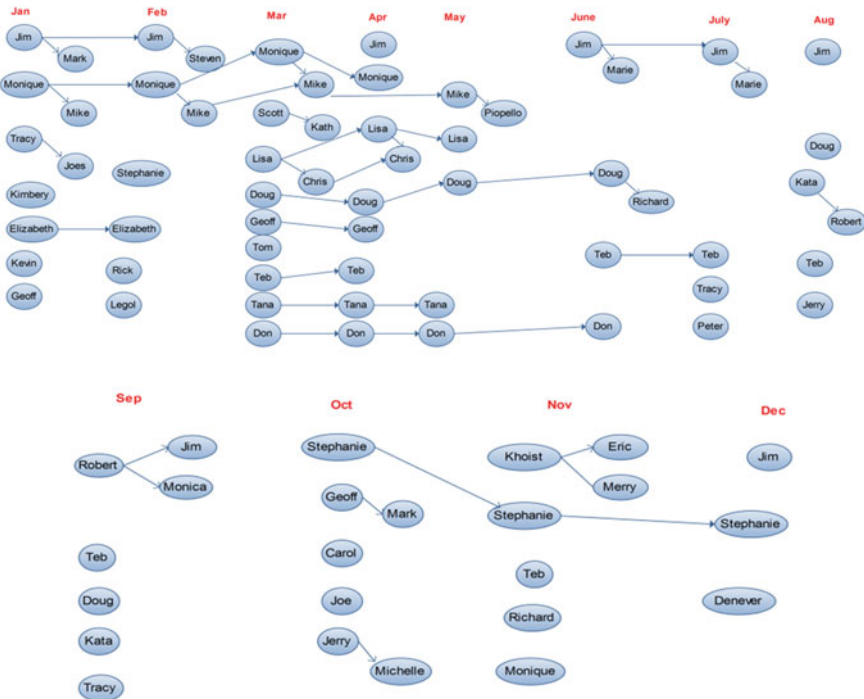


Fig. 3 Evolution of community from months Jan to Dec

On examining the results in Fig. 2, we analyzed the number of grouping in the month of May was maximum. Figure 3 shows that Jim was the person who headed the group from Jan to Feb. Monique was leader throughout the months form Jan to April.

### 3 Conclusion and Future Work

In this paper we introduced a concept of hierarchy of positions in group by taking temporal interaction data of 12 months in organization that shows how the position of group members changes when people joining and leaving the group. In future, we can also model the changes over time and detect event occurrences as consequence of this change. We also will improve the integrity issues of preprocessed Enron data results of experiments.

### References

1. Wasserman, S., Faust, K.: *Social Network Analysis: Methods Application*. Cambridge University Press, New York (1994)
2. Wellman, B.: Computer networks as social networks. *Sci. Mag.* **293**, 2031–2034 (2001)
3. Robert, A.H., Riddle, M.: *Introduction to Social Network Methods*. University of California, Riverside (published in digital form <http://faculty.ucr.edu/~hanneman/>) (2005)
4. Kretzschmar, M., Morris, M.: Measures of concurrency in networks and the spread of infectious disease. *Math. Biosci.* **133**, 165–195 (1996)
5. Baumes, J., Goldberg, M., Magdon-Ismael, M., Wallace, W.: *Discovering hidden groups in communication networks*. In: *Proceedings of the 2nd NSF/NIJ Symposium on Intelligence and Security Informatics* (2004)
6. Tyler, J., Wilkinson, D., Huberman, B.: *Email asspectroscopy: Automated discovery of community structure within organizations*. In: *Proceedings of the 1st International Conference on Communities and Technologies* (2003)
7. Baumes, J., Goldberg, M., Magdon-Ismael, M., Wallace, W.: *Discovering hidden groups in communication networks*. In: *Proceedings 2nd NSF/NIJ Symposium on Intelligence and Security Informatics* (2004)
8. Berger-Wolf, T.Y., Saia, J.: A framework for analysis of dynamic social networks. In: *Proceedings of the KDD'06*, pp. 523–528 (2006)
9. Moitra, A.: *Approximation algorithms for multicommoditytype problems with guarantees independent of the graph size*. In: *Proceedings of the FOCS*, pp. 3–12 (2009)
10. Santo, F., Castellano, C.: *Community structure in graphs*, chapter of *Springer's Encyclopedia of Complexity and System Science* (2008)
11. Chekuri, C., Goldberg, A., Karger, D., Levin, M., Stein, C.: *Experimental study of minimum cut algorithms*. In: *Proceedings of the 8th SAIM Symposium on Discreet Algorithm*, pp. 324–333 (1997)
12. Andrew, Y., Wu., et al.: *Mining scale-free networks using geodesic clustering*. In: *Proceedings of the KDD'04*, pp. 719–724 (2004)
13. Newman, M.E.J., Girvan, M.: *Finding and evaluating community structure in networks*. *Phys. Rev. E* **69**, 026113 (2004)
14. Newman, M.E.J.: *Modularity and community structure in networks*. *PNAS* **103**(23), 8577–8582 (2006)
15. Zhou, D., Councill, I., Zha, H., Lee Giles, C.: *Discovering temporal communities from social network documents*. In: *Proceedings of the ICDM'07*, pp. 745–750 (2007)
16. Tantipathananandh, C., Berger-Wolf, T., David Kempe, A.: *Framework for community identification in dynamic social networks*. In: *Proceedings of the KDD'07*, pp. 717–726 (2007)
17. The original dataset can be downloaded from William Cohen's web page <http://www-2.cs.cmu.edu/~enron/>



# SLAOCMS: A Layered Architecture of SLA Oriented Cloud Management System for Achieving Agreement During Resource Failure

Rajkumar Rajavel and Mala T

**Abstract** One major issue of cloud computing is developing Service Level Agreement (SLA)-oriented cloud management system, because situations like resource failures may lead to the violation of SLA by the provider. Several research works has been carried out regarding cloud management system were the impact of SLA is not properly addressed in the perspective of resource failure. In order to achieve SLA in such circumstance, a novel-layered architecture of SLA-oriented Cloud Management System (SLAOCMS) is proposed for service provisioning and management which highlight the importance of various components and its impacts on the performance of SLA- based jobs. There are two components such as Task Scheduler and Load Balancer which are introduced in SLA Management Framework to achieve SLA during resource failure. So, an SLA Aware Task Scheduling Algorithm (SATSA) and SLA Aware Task Load Balancing Algorithm (SATLB) are proposed in the above components to improve the performance of SLAOCMS by successfully achieving the SLA's of all the user jobs. The results of traditional and proposed algorithms are compared in the scenario of resource failure with respect to violations of SLA-based jobs. Moreover, SLA negotiation framework is introduced in application layer for supporting personalized service access through the negotiation between the service consumer and service provider.

**Keywords** Cloud management · SLA management · Task scheduling · Task load balancing · Achieving SLA

---

R. Rajavel (✉)

Anna Centenary Research Fellow, Department of IST, Anna University, Chennai, India  
e-mail: rajkumarprt@gmail.com

Mala T

Assistant Professor, Department of IST, Anna University, Chennai, India  
e-mail: malanehr@annauniv.edu

## 1 Introduction

Cloud Computing provides differentiated services to the users on demand with respect to the expectation of service quality on a pay for usage basis. One major issue in this area is cloud management which requires the management of services such as Infrastructure as a Service (IaaS), Platform as a Service (PaaS), Software as a Service (SaaS), and Storage as a Service in the specified layers. In cloud management several challenges such as scalability, multiple levels of abstraction, federation, sustainability, and dynamism are addressed to adapt in future [6]. A taxonomical spectrum of cloud computing framework describes the various components of cloud where SLA Management is addressed as one of the major component in the management service [11].

Existing cloud management systems does not support the SLA-based service provisioning with respect to all the available parameters of service. Because any malfunction such as resource failure and VM failure may lead to serious trouble for the providers to meet the SLAs of all the user jobs. The major challenges of SLA-oriented resource management such as architecture framework, SLA-based scheduling policies, and SLA resource allocators were addressed [3]. In the future perspective, cloud management seems to have most daunting and challenging issues, because improper management without any precautions will swipe out the customer data and leads to the provider's SLA violation. Supporting of SLAs with multiple objectives is addressed as one of the important requirement of future cloud management [4]. Above challenges, issues and requirements motivates our research work to develop a novel SLAOCMS for supporting SLA-based service provisioning and management in future trends of cloud.

Objective of this SLAOCMS is to provide SLA-based cloud service provisioning and management during the resource failure by using an efficient Task Scheduler and Task Load Balancer components. In order to test the efficiency of the proposed SLAOCMS, SLA-based jobs are submitted to unified resource layer by insisting resource failure (limited resource availability). As an impact of introducing the SATS and SATLB algorithms in the proposed system, the SLA is achieved for all jobs by rearranging its sequence within the resource in case of compatible deadline and migrating to other resources in case of incompatible deadline. In case of limited resource availability, only SATS algorithm can be effectively used to achieve the SLA of user jobs. This situation may impact the SATLB algorithm, to migrate only the moderate amount of workload to the free resource available in the environment. Hence, the achievement of jobs SLA during resource failure is probably in the hands of resource availability present at that moment. Moreover, the proposed research work of SLAOCMS system addresses various open research issues and challenges in specific to SLA Management activity.

## 2 Related Work

In this section, traditional model of cloud management systems, and its drawbacks are addressed such as IaaS, PaaS, SaaS, and Storage as a Service management. The SLA-based service virtualization architecture is proposed to avoid SLA violation under changing workload, system malfunction, hardware and software failure [8]. A service-oriented policy-driven IaaS Management system is proposed to improve the performance of services running on IaaS [14]. A market-oriented hierarchical scheduling strategy is proposed for SwinDeW-C cloud workflow system using the service-level scheduling algorithm and meta-heuristic-based scheduling algorithm [13]. One phase and two phase algorithms are proposed to overcome the problems of workflow scheduling in IaaS cloud [1].

An Analysis is made regarding the security mechanism and SLA for the development of geoprocessing services in cloud PaaS which helps to manipulate the geographic information [9]. A problem of limited resource capacity is considered to serve the SLA-based SaaS request for the cloud resource management. The knapsack problem model employs the virtual infrastructure to obtain the heuristic solution [2]. In order to effectively use the cloud resource an SLA-based admission control and scheduling algorithm is proposed for the benefit of SaaS provider [12]. Paper [4], discuss the importance of managing SLA activity in cloud where SLA Management is noted as one of the research challenge in future cloud management. In order to reduce the quality of service violation, an energy efficient resource management framework is proposed for cloud service provisioning [7]. In the previous research work hierarchical scheduling is used for prioritizing the deadline-based job in both cloud and cluster controller level [10]. Hence SLA management framework is included in application, platform and unified resource layers of proposed SLAOCMS where SLA aware scheduler and load balancer are highlighted as important component to manage the SLA of all the user jobs.

## 3 SLA-Oriented Cloud Management System

In this section, an SLAOCMS is introduced as shown in Fig. 1 to support the personalized service provisioning and achieving SLA in the future cloud. This cloud management system consists of four layers such as fabric, unified resource, platform, and application. A service layer is introduced as a sub layer of application layer which supports the consumer and provider to negotiate with respect to SLA parameters for providing personalized cloud service access. The service layer contains the components like SLA template, SLA negotiation framework, negotiation protocol, request handler, service classifier, and information manager. An SLA template is a pattern for creating agreement which contains the information like name of the service and parties, context, terms and negotiation constraints. A negotiation strategy is followed by the SLA negotiation framework for making communication with the consumer

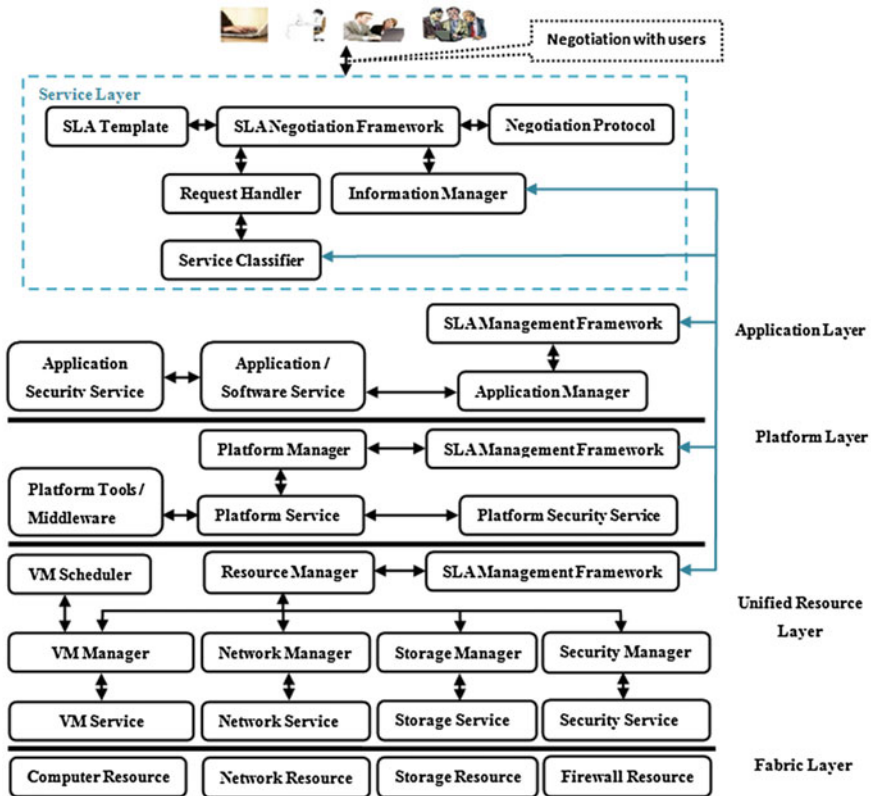


Fig. 1 Architecture of SLAOCMS

or broker by exploiting the negotiation protocol and SLA template. Moreover, the information manager is invoked during the negotiation process for collecting the service availability and its reservation information. The request handler will obtain the negotiated request and place it in the request handler queue for further processing. Then the request is periodically pulled by the service classifier, to identify its service type and forward the request to the SLA management framework of the concerned layer. The structure of the SLA management framework is shown in Fig. 2, which includes components such as service integrator and manager, task scheduler, task load balancer, SLA manager, agreement generator, service provisioner, dispatcher, SLA monitor, notification generator, SLA terminator, and utility manager.

This management framework contains the SLA Manager who is responsible for managing all the SLA-related activities of cloud services by using the above components in the lifecycle. The reservation queue is maintained in the reservation manager, which contains all the committed jobs to execute in the reserved time. In the existing system, this reservation queue follows the FCFS scheduling by executing the task one

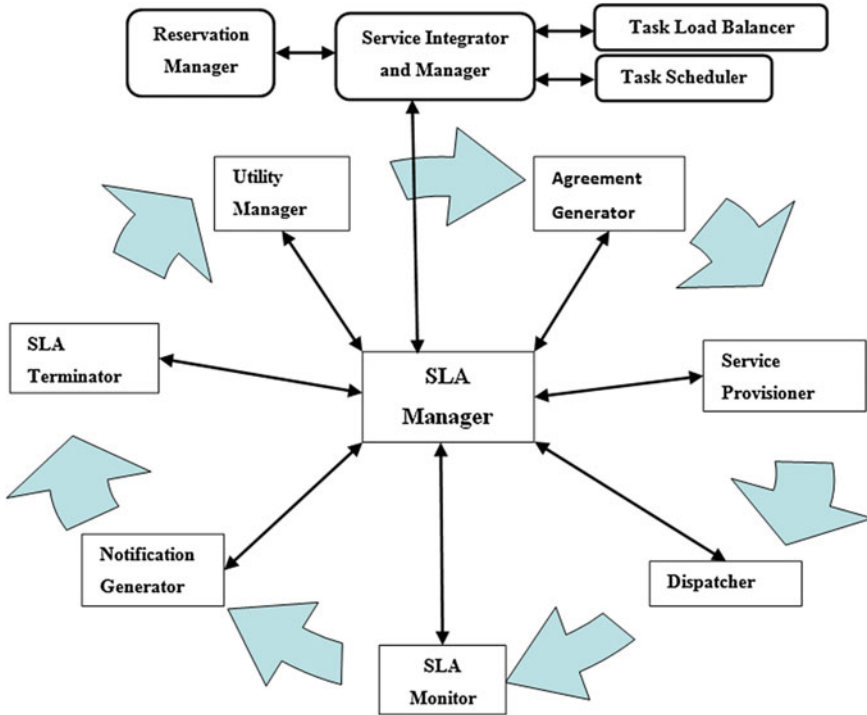


Fig. 2 Structure of SLA management framework in unified resource layer

by one in the same sequence as present in the queue. This type of system may lead to SLA violation of tasks during the VM failure in the Data Center (DC). Because of this failure, the scheduled task may be delayed due to shortage of VM available in the DC. In this scenario proposed SLAOCMS invokes the task scheduler and load balancer component to avoid the SLA violations of the submitted job which is present in the reservation queue. These two components exploit the SLA Aware Task Scheduling Algorithm (SATSA) and SLA Aware Task Load Balancing Algorithm (SATLBA) as shown in Algorithm 1 and 2. Here, the Estimated Completion Time (ECT) of any deadline-based jobs present in the Deadline Job List (DJL) size 'n' can be computed using the Eq. (1). This equation will compute the ECT of Deadline Job (DJ) at the position 'i' DJ<sub>i</sub> by summing of all the jobs Completion Time (CT) present in the DJL<sub>1to*i*</sub>.

$$ECT(DJL_i) = \sum CT(DJ_1) + CT(DJ_2) + \dots + CT(DJ_i) \tag{1}$$

**Algorithm 1** SLA Aware Task Scheduling Algorithm

```

Begin
  Get the set of Virtual Machine (VM) L from the Data Center DCi
  Assign the reserved deadline RD to each job
  Get the set of Jobs J from the Reservation Queue (RQ)
  for all VM  $l_i \in L$  do
    Ping the VM
    Add to Active Virtual Machine (AVM) set AL
  end for
  for all AVM  $al_i \in AL$  do
    if AL.length() == L.length() then
      Submit the job in FCFS fashion
    else if AL.length() < L.length()
      Get the set of Deadline based Job List (DJL)
      Compute the Estimated Completion Time (ECT) of DJL
      Align the DJL in the order in which the ECT is less as first
      for all  $djl_i \in DJL$  do
        if ECT( $djl_i$ ) > RD( $djl_i$ ) then
          Increment the position of  $djl_i$  from the RQ
          Compute the Estimated Completion Time (ECT) of DJLi
          if ECT(DJLi) > RD(DJLi) then
            Invoke Algorithm 2
          else
            Refresh the RQ position
          end if
        else if ECT( $djl_i$ ) <= RD( $djl_i$ )
          Keep the job in same position
        end if
      end for
    end if
  end for
end

```

**Algorithm 2** SLA Aware Task Load Balancing Algorithm

```

Begin
  Get the set of Available Data Center (ADC) in service provider side
  Get the DJLi from the Reservation Queue (RQ)
  for all  $adc_i \in ADC$  do
    Compute the ECT(DJLi) in the ADC
    if ECT( $djl_i$ ) < RD( $djl_i$ ) then
      Migrate to RQ of ADC
    end if
  end for
end

```

The main objective of the SATSA is to prioritizing the task present in the reservation queue based on the deadline specified in the agreement. At the maximum level, this algorithm will avoid the violation of task by prioritization. In case of more VM failure in the DC may be difficult to avoid the violation of the entire task. Because of the availability of VM in the DC, it is possible to prioritize only limited number of task. So to over such situation, SATLBA is invoked by this algorithm to migrate the extra task (which is not able to prioritize) to other DC which is capable of completing the task within the stipulated time.

### 4 Performance Evaluation

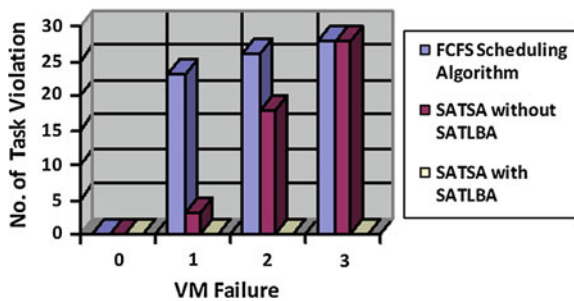
The simulation of cloud environment with the resource provisioning and management is implementation using the cloudsim toolkit [5]. For the sake of simplicity, experimental setup is simulated with 3 DC with 5 VM. Assume the tasks present in the DC1 with Reserved Deadline (RD) and Execution Time (ET) of each task is in the sequence as shown in Table 1.

The performance evaluation of proposed SATSA and SATLBA is evaluated in this experimental setup. Assume there is no task executed in the reservation queue of DC1 at the initial stage (all the VM are free). First the experiment is simulated for traditional FCFS scheduling algorithm, SATSA without SATLBA and SATSA with SATLBA in the unified resource layer without any resource failure. Similarly, the experiment is simulated with 1, 2, and 3 VM failures. The number of task violation is marked for all the simulated cases in the graph as shown in Fig. 3.

**Table 1** Task Information present in DC1 reservation queue

Task ID	ET (min)	RD (min)
1 – 5	30	30
6 – 10	30	60
11 – 15	30	NIL
16 – 20	30	NIL
21 – 25	30	150
26 – 30	30	180
31 – 35	30	NIL
36 – 40	30	NIL
41 – 45	30	270
46 – 50	30	300
51 – 55	30	NIL
56 – 60	30	NIL

**Fig. 3** Performance evaluation of FCFS, SATSA and SATSA



## 5 Conclusion and Future Work

Thus from the performance graph, it is clear that the proposed SATSA with SATLBS gives no SLA violation of task with respect to number of VM failures. The task violation gradually increases with respect to number of VM failures for the case of SATSA without SATLBA. But in the case of FCFS scheduling algorithm, number of task violation drastically increases with respect to number of VM failures. Hence the proposed SATSA with SATLBA in the SLAOCMS helps to achieve SLA during resource failure by migrating task from one DC to another.

In future, Automated Dynamic SLA Negotiation Framework will be proposed to support the personalized service access in the cloud environment. This framework constitutes the negotiation strategy of service provider, trusted third party broker and service consumer for describing the communication process involved between the negotiating parties. In addition, the framework derives the mathematical model using the game theory approach to providing optimal solution for bargaining between negotiation parties.

**Acknowledgments** We like to sincerely thank the Anna University, India for their financial support to this research work under the scheme of Anna Centenary Research Fellowship.

## References

1. Abrishami, S., Naghibzadeh, M., Epema, D.: Deadline-constrained workflow scheduling algorithms for IaaS Clouds. *Future Genera. Comput. Syst.* **29**, 158–169 (2012)
2. Aisopos, F., Tserpes, K., Varvarigou, T.: Resource management in software as a service using the knapsack problem model. *Int. J. Prod. Econ.* **141**, 465–477 (2011)
3. Buyya, R., Garg, S.K., Calheiros, R.N.: SLA-Oriented resource provisioning for cloud computing: challenges, architecture, and solutions. In: *IEEE International Conference on Cloud and Service, Computing*, pp. 1–10 (2011)
4. Cook, N., Milojevic, D., Talwar, V.: Cloud management. *J. Internet Serv. Appl.* **3**, 67–75 (2012)
5. Calheiros, R.N., Ranjan, R., Beloglazov, A., De Rose, C.A.F., Buyya, R.: CloudSim: a toolkit for modeling and simulation of cloud computing environments and evaluation of resource provisioning algorithms. *Softw. Pract. Experience* **41**(1), 23–50 (2011)
6. Forell, T., Milojevic, D., Talwar, V.: Cloud management: challenges and opportunities. In: *IEEE International Parallel and Distributed Processing, Symposium*, pp. 881–889 (2011)
7. Guazzone, M., Anglano, C., Canonico, M.: Energy-efficient re-source management for cloud computing infrastructures. In: *Third IEEE International Conference on Cloud Computing Technology and Science*, pp. 424–431 (2011)
8. Kertesz, A., Kecskemeti, G., Brandic, I.: An interoperable and self-adaptive approach for SLA-based service virtualization in heterogeneous cloud environments. In: Rana O., Corradi A. (eds.) *Special Issue of Future Generation Computer Systems on Management of Cloud Systems*, Elsevier (2012)
9. Ludwig, B., Coetzee, S.: Implications of security mechanisms and Service Level Agreements (SLAs) of Platform as a Service (PaaS) clouds for geoprocessing services. *Appl. Geomatics* **5**(1), 25–32 (2012)
10. Rajavel, R., Mala, T.: Achieving service level agreement in the cloud environment using job prioritization in hierarchical scheduling. In: *International Conference on Information Systems*



Design and Intelligent Applications, *Advances in Intelligent and Soft Computing*, vol. 132, pp. 547–554 (2012)

11. Rimal, B.P., Choi, E.: A service-oriented taxonomical spectrum, cloudy challenge and opportunities of cloud computing. *Int. J. Commun. Syst.* **25**, 796–819 (2012)
12. Wu, L., Garg, S.K., Buyya, R.: SLA-based admission control for a software-as-a-service provider in cloud computing environments. *J. Comput. Syst. Sci.* **78**, 1280–1299 (2012)
13. Wu, Z., Liu, X., Ni, Z., Yuan, D., Yang, D.: A market-oriented hierarchical scheduling strategy in cloud workflow systems. *J. Supercomput.* **63**(1), 256–293 (2013)
14. Xiao-xiang, L., Mei-na, S., Jun-de, S.: Research on service-oriented policy-driven IAAS management. *J. Chin. Univ. Posts Telecommun.* **18**(1), 64–70 (2011)

# Semantic Search in E-Tourism Services: Making Data Compilation Easier

Juhi Agarwal, Nishkarsh Sharma, Pratik Kumar, Vishesh Parshav,  
Anubhav Srivastava, Rohit Rathore and R. H. Goudar

**Abstract** After the advancement of the internet technology, user can get any information on tourism. Tourism is the world's largest and fastest growing industry. It contains so many things like accommodation, food, events, transportation package, etc. So information must be reliable because tourism product is intangible in nature. Customer cannot physically evaluate the service until he/she physically experienced but there are some areas where a greater measure of intelligence is required. The Semantic Web did a lot of work to enhance the Web by enriching its content with semantic data. E-Tourism is a good candidate for such enrichment, since it is an information-based business. In this paper, we are constructing E-Tourism ontology to provide intelligent tourism service. The algorithm is designed to integrate data from different reliable sources and structure properly in tourism knowledge base for efficiently searching the data.

**Keywords** Semantic web · Ontology · SPARQL

---

J. Agarwal (✉) · N. Sharma · P. Kumar · V. Parshav · A. Srivastava · R. Rathore · R. H. Goudar  
Graphic Era University, Dehradun, India  
e-mail: juhiagrawal@gmail.com

N. Sharma  
e-mail: nishkarsh4@gmail.com

P. Kumar  
e-mail: pratikkumar938@gmail.com

V. Parshav  
e-mail: vishparshav1@gmail.com

A. Srivastava  
e-mail: anubhav.v.sri@gmail.com

R. H. Goudar  
e-mail: rhgoudar@gmail.com

## 1 Introduction

After the advancement of the internet technology, user can get any information on tourism very easily. Tourism is a global information-intensive industry that has a long chain of stakeholders including service providers, marketers, managers, and consumers. So E-Tourism sites are making our journey comfortable but the tourism product is intangible in nature. Customer cannot physically evaluate the service until he/she physically experienced. So the information should be accurate and believable. The Semantic Web did a lot of work to enhance the Web by enriching its content with semantic data. E-Tourism is a good candidate for such enrichment, since it is an information-based business [1]. Semantic search uses ontology [2]. Ontology is a good approach. It is a formal conceptualization of a particular domain that is shared by a group of people [3]. Ontology is used in knowledge-based systems as conceptual frameworks for providing, accessing, and structuring information in a comprehensive manner [4]. Retrieval of keyword and text matching in the retrieval engine can be successful only through Semantic Web. In this paper, we are constructing E-Tourism ontology for intelligent tour service where we can search the data semantically using Semantic Search Engine. It can improve the process of searching for the perfect tourism package by analyzing the user interest with the help of ontology.

## 2 Ontology Creation for E-Tourism Service

### 2.1 Domain Ontology for Tourist Information

It could be observed that the tourism sector is an area in which ontology is playing very important role. Ontology essentially consists of a vocabulary of terms in a domain of interest and their meanings. This includes definition of concepts, the properties of the concepts, and the interrelationship between concepts [5, 6]. Ontology creation for E-Tourism service is given in Fig. 1. Figure 3 is an ER-diagram showing relationship and properties of the classes. The class hierarchy is as follows:

**Thing:** All the other classes are the sub class of this class. In other words, this is the Super Class containing all the other classes.

**Club:** The tourists may be interested in places like Clubs and Disco, etc., for night life, leisure activities. This class includes sub classes Casino, PubBar, and Disco.

**Shopping Place:** This class includes information about the shopping places available at a destination. It is further sub classed into Mall, Market, and Shop.

Object properties are used to link objects of different classes and tell about their relation. The object properties are as follows:

**Belongs to State:** This property links the objects of City class with the objects of State class to tell a particular city belongs to which State.



Fig. 1 E-tourism ontology

**Has Climate:** This property links the objects of Destination class with the Climate class. It tells about the climate that a particular place has Fig. 2.

## 2.2 Creation of Intelligent Tourist Information Service Using Semantic Search Engine

There are four phases for development and implementation of Intelligent Tourist Information Service using Semantic Search Engine, which are explained below:

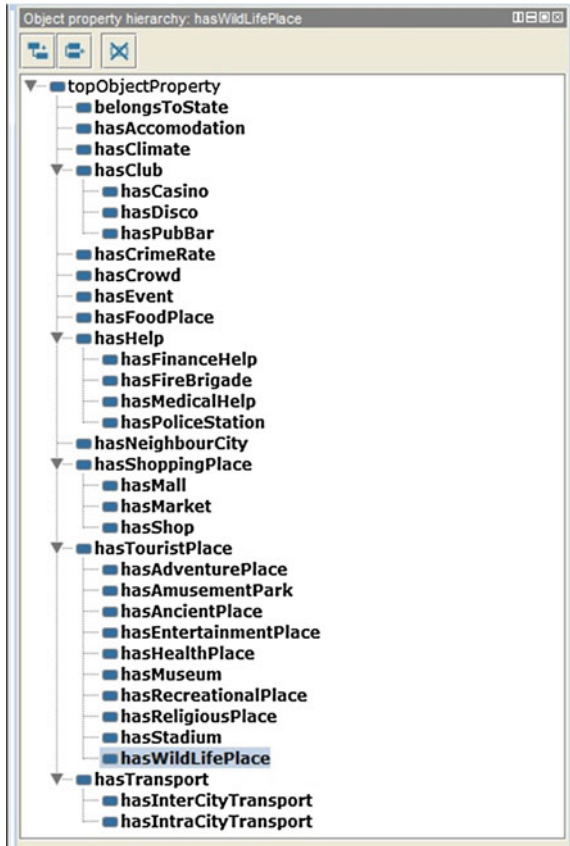


Fig. 2 Object properties

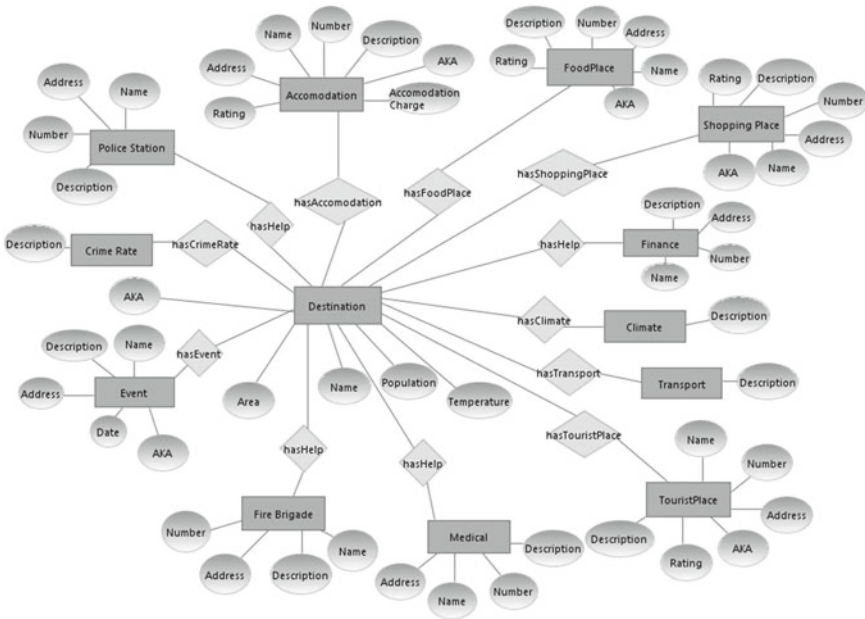
### 2.2.1 Prepare Backbone Structure for Capturing and Representing Knowledge in Tourism Domain. India Tourism Ontology Creation

- Identifying the concepts of the domain.
- Identify the attributes or properties of these concepts.
- Identify the relationship between these concepts and defining the properties for these relationships.
- Defining the rules or axioms for the domain on the basis of which inferences could be drawn.

### 2.2.2 Create the India Tourism Knowledge Base Using Ontology

This crucial phase will follow the given sequence of steps:

- Identify all the authentic sources of information available on the Web about the India Tourism.



**Fig. 3** ER-diagram for E-tourism. The destination is connecting different classes means it is showing relationship and properties from destination to different classes

- Identify additional sources of information to make the tourism information as rich as possible by the tourism department in various forms.
- Validating and integrating the information to populate the knowledge base Fig. 4.

**2.2.3 Create the Semantic Search Mechanism**

- User enters the search query in the normal English language, i.e., similar to the search query of keyword based search engines like Google.
- This keyword query needs to be expanded on the basis of the created Tourism ontology to add a number of semantically related terms to it.
- The expanded query will be converted to a semantic query.
- Semantic query will be fired and necessary information will return to user Fig. 5.

**2.2.4 Creating the User-Interface and the E-Tourism Portal**

- Out of the huge information possible for the tourism domain, the most important information should be presented to the user directly i.e., through the use of menus and tabs the broad classes of information will be available.

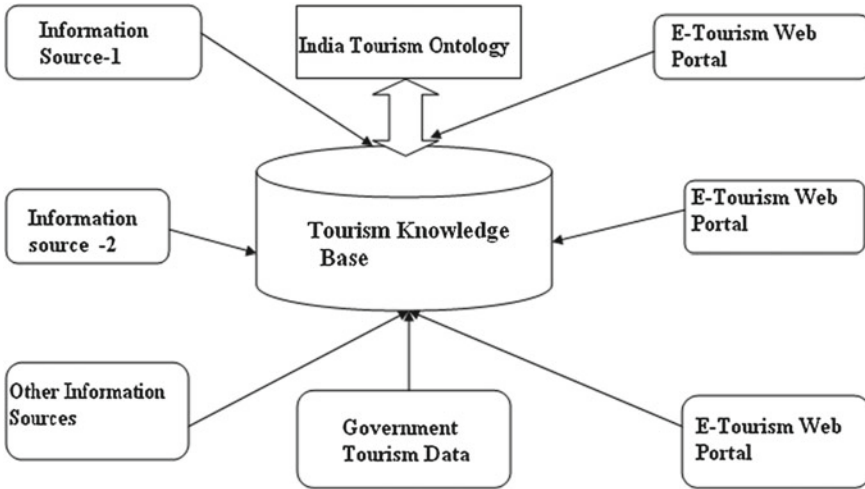


Fig. 4 Indian tourism knowledge base creation

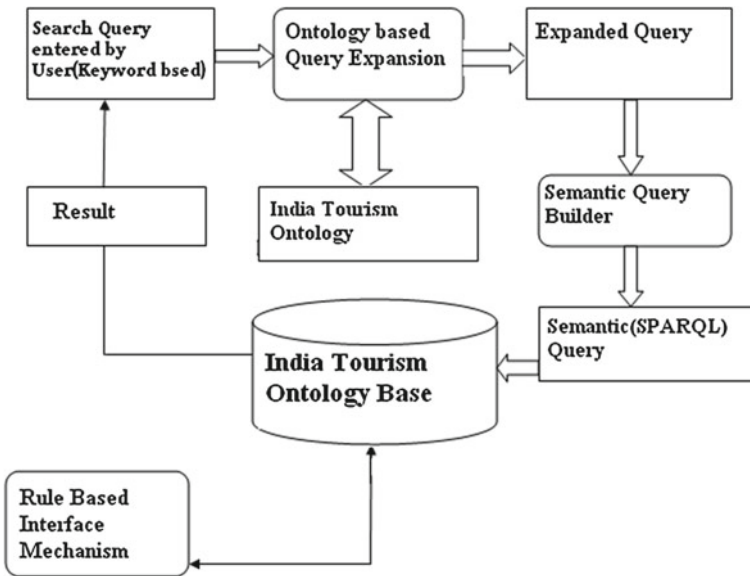


Fig. 5 Various semantic search steps to return the result to the user

- A semantic search interface will be presented to the user which will act as the gateway to the comprehensive India Tourism related information. The various links containing the information within the portal or referring to the other sites will be returned through this search.
- The facilities of booking will be provided through the web portal.

- The system will keep track of the type of users so that the information specific to the user interest could be provided. There will be a separate login for the tourism and the other players in the tourism domain like tour-guide.

### 3 Searching Algorithm

Example of searching:

- User enters the keyword “ Dehradoon ”.
- After parsing (removing spaces from the search query), the keyword becomes “Dehradoon”. The keyword is converted to lowercase.
- The keyword is then matched to the data element that is linked to the objects using has Name property in the ontology base.
- If the match is found (which is not true in this case), the SPARQL query is built upon the selection of the user using the keyword.
- If the match is not found (which is true in this case), the keyword is matched with the synonyms of all the objects. If again, the match is not found, user is displayed a message “No Records Found”.
- If the synonym match is found, then the SPARQL query is built upon the selection of the user using the keyword.
- The query is then executed and the result is displayed to the user (Figs. 6, 7, 8, 9).

### 4 Semantic Matching Algorithm Based on Mathematical Model

**Question:** Semantic Search

**Answer:** Let query=q

Parsed query=p

Let S be the set of Synonyms stored in O such that  $S = \{s_1, s_2, s_3 \dots \dots s_n\}$

Let the ontology dataset be O,

Let the result set be R.

$R \neq \phi$ , If  $p \in O$ , result found.

$R = \phi$ , if  $p \notin O$

If  $R = \phi$ , then

$R = \phi$ , if  $p \notin S$

$R \neq \phi$ , If  $p \in S$ , result found.

It searches data according to the keyword. If keyword matches with the ontology then it returns the result, but if the result set is null, then the search is performed according to the synonyms of the keyword, i.e., the keyword p is searched in the synonym set S. If p matches any keyword in S, it means keyword exists in the ontology base and the result is returned according to that matched synonym.



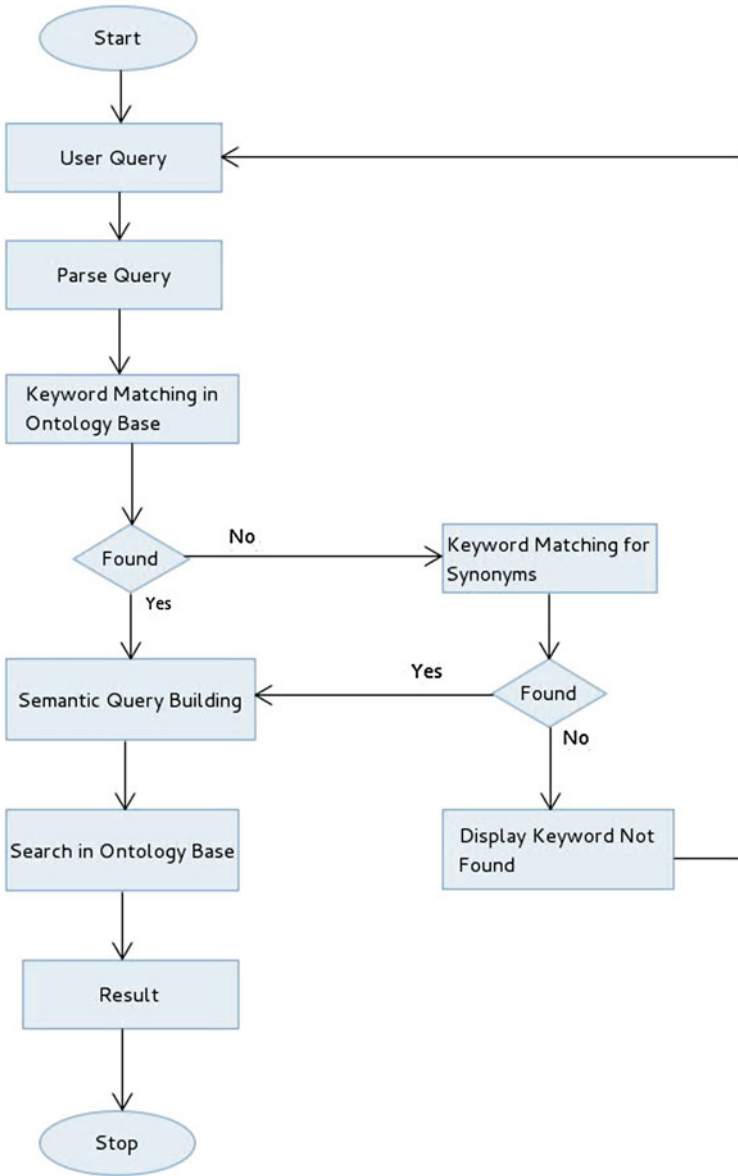


Fig. 6 Workflow of searching the data semantically

```

1. search()
2. { q ← read query;
3.   q ← parse(q);
4.   q ← tolower(q);
5.   match ← keyword_match_name(q);
6.   if(match==true)
7.     then
8.       build SPARQL query
9.       result ← execute_SPARQL_query(s);
10.      display result;
11.   else
12.     then
13.       match ← keyword_match_synonyms(q);
14.       if(match==true)
15.         then
16.           build SPARQL query
17.           result ← execute_SPARQL_query(s);
18.           display result;
19.       else
20.         then
21.           display "No records found"   }
```

**Fig. 7** Algorithm for searching data

```

1. boolean keyword_match_for_name(query q)
2. { triple ← "select ?subject
3.   where
4.     ?subject hasName q";
5.   res ← execute_SPARQL_query(triple);
6.   if(result_num_rows(res)>0)
7.     return true;
8.   else
9.     return false;   }
```

**Fig. 8** Algorithm for searching data according to keyword

```

1. boolean keyword_match_for_synonyms(query q)
2. { triple ← "select ?subject
3.   where
4.     ?subject AKA q";
5.   res ← execute_SPARQL_query(triple);
6.   if(result_num_rows(res)>0)
7.     return true;
8.   else
9.     return false;   }
```

**Fig. 9** Algorithm for searching data according to synonyms (semantically)

## 5 Conclusion

It could be observed that the tourism sector is an area in which ontology can be applied anywhere [7]. The tourism domain is a decent area for new information and communication technologies by assisting users and agencies with quick information

searching, integrating, recommending, and various intelligent E-Tourism services [8]. We introduced a creation of intelligent tourism information service using semantic search engine based on E-Tourism and Domain Ontology for Tourist Information for intelligent tourist information services. In addition, the ontology will play an important role as they promise a shared and common understanding of tourism and travel concepts that reaches across people and application systems. So semantic search is making searching very easier than keyword search [9]. Ontology based search can be made on tourism sites by constructing tourism ontology and information can be generated accurately according to the tourist interest using ontology.

## References

1. Yan, Z.: Ontology and semantic management system: state-of-the-arts analysis. In: Proceedings of the IADIS International Conference, ISBN: 978-972-8924-44-7, pp. 111–115 (2007)
2. Werther, H.: Intelligent systems in travel and tourism. *IEEE Intell. Syst.* **17**(6) (2003)
3. Park, H., Yoon, A., Kwon H.-C.: Task model and task ontology for intelligent tourist information service. *Int. J. u- e- Serv. Sci. Technol.* **5**(2), 47–58 (2012)
4. Cardoso, J.: Developing dynamic packaging systems using semantic web technologies. *Trans. Inf. Sci. Appl.* **3**(4), 729–736 (2006)
5. Mohsin, A.: Tourist attitudes and destination marketing—the case of Australia’s Northern Territory and Malaysia. *Tourism Manag.* **26**, 723–732 (2005)
6. Jun, S.H., Vogt, C.A., MacKay, K.J.: Relationships between travel information search and travel product purchase in pretrip contexts. *J. Travel Res.* **45**(3), 266–274 (2007)
7. Daramola, O., Adigun, M., Ayo, C.: Building an ontology-based framework for tourism recommendation services. *Information and Communication Technologies in Tourism*, Amsterdam, pp. 135–147 (2009)
8. Zhou, L., Zhang, D.: An ontology-supported misinformation model: toward a digital misinformation library. *IEEE Trans. Syst. Man Cybern. A. Syst. Humans* **37**(5), 804–813 (2007)
9. Damjanovic, D., Devedzic, V.: Applying Semantic Web to E-tourism. Chapter X, Springer, Berlin, pp. 243–263 (1993)

# Deep Questions in the “Deep or Hidden” Web

Sonali Gupta and Komal Kumar Bhatia

**Abstract** The Hidden Web is a part of the Web that consists mainly of the information inside databases, i.e., anything behind an interactive electronic form (search interfaces), which cannot be accessed by the conventional Web crawlers [1, 2, 8]. However, there have been well-defined, effective, and efficient methods for accessing Deep Web contents. One of these methods for accessing the Hidden Web employs an approach similar to ‘traditional’ crawling but aims at extracting the data behind the search interfaces or forms residing in databases. The paper brings insight into the various steps, a crawler must perform to access the contents in the Hidden Web. We structure the problem area and analyze what aspects have already been covered by previous research and what needs to be done.

**Keywords** WWW · Hidden web · Surface web · Hidden web crawler

## 1 Introduction

The growth of the World Wide Web (WWW) has been phenomenal over the years [8, 10, 11]. Surface Web refers to the abundant web pages that are static, typically having, outgoing links to other web pages, and incoming links which allow them to be reached from other pages, creating a spider-web like system of interconnected data; whereas the Hidden Web (HW) consists of unlinked data and refers to the Web pages created dynamically as the result of a specific search. The Hidden or Deep Web consists mainly of information inside databases, i.e., anything behind an

---

S. Gupta (✉) · K. K. Bhatia  
Department of Computer Engineering, YMCA University of Science and Technology,  
Faridabad, India  
e-mail: Sonali.goyal@yahoo.com

K. K. Bhatia  
e-mail: Komal\_bhatia1@rediffmail.com

interactive electronic search form interface with most of it elicited by the HTTP form submission. Examples of Hidden web content include directories and collection of patents, scientific and research articles, holiday booking interfaces, etc. Estimates of the size of the Hidden Web differ, but some place it at up to 500 times the size of the traditional surface Web [1, 3, 5, 7].

The Hidden Web though hidden and not accessible through traditional document-based search engines, is a huge and distributed repository of data lying in databases which has to be accessed by some means. Methods must exist to prove the expediency of the source [8]. There are two basic approaches to access the contents in the HW:

1. **Crawling/Trawling or Surfacing:** It refers to the crawler's activity of collecting in the background as much relevant, interesting fraction of the data as possible and updating the search engine's index. This approach has the main advantage of best fit with the conventional search engine technology.
2. **Virtual Data Integration:** It refers to the creation of vertical search engines for specific domains where APIs will be used to access Hidden Web sources at time and construct the result pages based on their responses. Since external API calls need to be made by the search engine, this approach is traditionally slower than crawling.

The major goal of the paper is to describe the research problems associated with Hidden Web crawlers and analyze the existing research in the context of the research problems so as to identify and bring outstanding issues to the forefront.

## 2 Background (Search Engines/Crawlers)

Finding or Searching information on the Web has become an important part of our daily lives and about 550 million Web searches are performed every day [10, 11]. The tools that have been used to find information on the Web are typically known as Web Search Engines [2, 10, 11]. Figure 1 illustrates the activities and the corresponding components or elements of a basic search engine.

The various activities performed by a search engine can be divided into: *Crawling* by which a search engine gathers pages from the WWW; *Indexing* which is building a data structure that will allow quick searching of the text [11]; or "the act of assigning index terms to documents" where an index term is a (document) word whose semantics helps in remembering the document's main themes [11]; *Query Processing* which includes receiving a query from the user, searching the index or database for relevant entries, and presenting the results to the user. The component responsible for the process of crawling is known as a Crawl Engine or more typically a Web crawler [2, 11], whereas the element responsible for building the search engine's index is termed as the Index Engine or typically as an Indexer.

The increasing prevalence of online databases has influenced the structure of the web crawlers and their capabilities for information access through search form

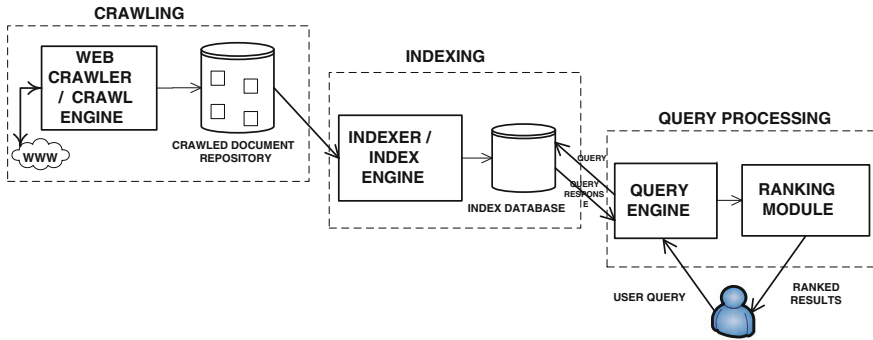


Fig. 1 Elements of a basic search engine

interfaces [2]. So, the paper discusses crawling, distinguishing on the basis of Surface and Hidden web crawl. The common belief is that over 1 million search engines currently operate on the WWW [7, 11] most of which cover only a small portion of the Web in their indices or databases. This coverage can be increased by either of the following means:

1. Employing multiple search engines: A search system that uses other search engines to perform the search and combines their search results is generally called a meta-search engine.
2. Enhancing the crawler’s Capability: Since the HW comprises a major part of the Web (almost  $\approx 80\%$ ) developing hidden Web crawlers has clearly become the next frontier for information access on the Web.

### 3 Hidden Web Crawler

Figure 2 illustrates the sequence of steps that take place when a user wants to access the contents in any Hidden Web resource. The user has to fill out a query form for retrieving documents that have been dynamically generated from the underlying database [3, 4].

Figure 3 illustrates the difference in the sequence of steps undertaken by any crawler to access the Hidden Web’s informational content.

A Hidden Web crawler starts the same as the Surface web crawler by downloading the required web page, but then later it requires a lot of analysis and intelligence to extract information from the hidden web. The Surface Web Crawlers can record the address of a search front page but can tell nothing about the contents of the database [1, 5, 8].

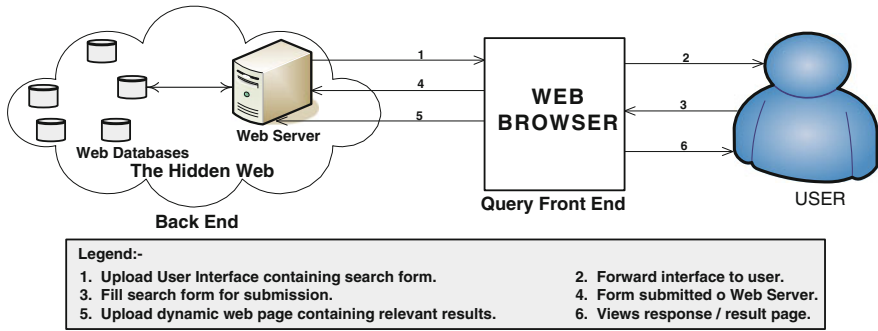


Fig. 2 User interaction with a search form interface

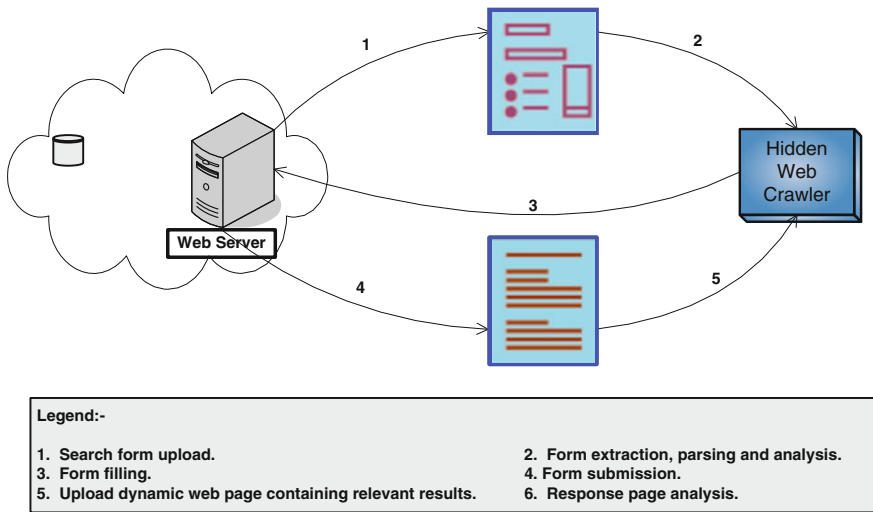


Fig. 3 A crawler interacting with the search form interface

### 4 Research Problems

Making a comprehensive crawl of the HW does not seem practical due to the two fundamental reasons [1, 3, 4, 8]: *Scale* The Hidden Web is unprecedented in many ways; unprecedented in size and content quality; unprecedented in the lack of coordination in its creation (distributed nature), and unprecedented in the diversity of backgrounds and motives of its participants. *Restricted Search form interfaces:* Access to the Hidden Web databases is provided only through restricted search interfaces, perceived to be used by humans [3, 4]. This raises the non-trivial problem of “training” the crawler for an appropriate use of the restricted interface to extract relevant content. Below are presented the two sub-problems or steps in the present scenario that suggest likely directions:

1. Resource discovery: In order to overcome the problem of Scale, the crawler must be trained to carry a crawl of only the relevant sources (effective crawling) rather than carrying a comprehensive crawl of the Hidden Web (exhaustive crawling) [3, 4, 8, 16, 17]. This requires the crawler to first locate the sites containing search form interfaces and then select the relevant subset from it. And as the Hidden Web data sources are growing continuously at a high rate, selecting the subset of relevant sources will prove not only cost-effective but also effective in time and make the crawler less prone to errors.
2. Content extraction: The task of harvesting information lying behind the form interfaces of the selected Hidden Web sources depends largely on the way, the crawler is able to understand and model the search form interface so as to come up with meaningful queries to issue to the search interface for probing the database behind it. The crawler must then be able to extract the data instances from the retrieved result pages. This problem of Content Extraction poses significant challenges and the solution lies in the three steps process comprising: Understanding the Search Form interfaces, automatically filling them and Information extraction.

The three steps together form the following basic modules of the system: *Form Analyzer* that will analyze each and every downloaded page to see if it can be used as a search page to retrieve information or not. It basically checks whether a web page is query able, has some form fields or not; *Form Parser* that extracts the fields from the search form and passes them on to the form processor for filling; *Form Processor* that fills in the various form fields by assigning appropriate values and finally submits the form for retrieving result pages; *Result Analyzer* that will analyze all the result pages obtained by the crawler after form execution, in order to get the required information.

## 5 The State of the Art in Hidden Web

In this section we discuss the previous work in the area grouped by the problem domains. Research on Hidden Web search can be dated back to the 1980s. Since then, substantial progress has been made in different sub-problems of crawling and accessing the Hidden Web.

### 5.1 Resource Discovery

The goal of any focused crawler is to select links that lead to documents that have been identified as relevant to the topic of interest and hence addresses the resource discovery problem, The work on focused crawling [14, 16, 17] describes the design of topic-specific crawlers for the Surface Web which complements our problem, as



same resource discovery techniques can be used to identify target sites for a Hidden Web crawler. The work in [14] discusses a best-first focused crawler which uses a page classifier to guide the search. Unlike an exhaustive crawler which follows each link in a page in a breadth first manner, this crawler gives priority to links that belong to pages classified as relevant. In domains that are not very narrow the number of irrelevant links can still be very high, the strategy can lead to suboptimal harvest rates and an improvement to which was proposed in [17].

An issue that remains with these focused crawlers is that they may miss relevant pages by only crawling pages that are expected to give immediate benefit. In order to address this limitation, certain strategies have been proposed that train a learner by collecting features from paths leading to a page, as opposed to just considering the contents of a page [17–19]. Reference [19] extends the idea in [14] and presents a focused crawling algorithm that builds a model for the context within which topically relevant pages occur on the Web. Another extension of the focused crawler idea is presented in [18] using a reinforcement learning algorithm to develop an efficient crawler for building domain-specific search engines.

Finally, it is worth pointing out that there are directories specialized on hidden-Web sources, e.g., [1, 20] that organize pointers to online databases in a searchable topic hierarchy and hence can be used as seed points for the crawl.

## 5.2 Content Extraction

Extracting content from the Hidden Web has received a lot of attention to date [3–6, 12, 15]. Most approaches to information retrieval in the Hidden Web are focused on understanding the various semantics associated with the form elements and automatically filling them as they are the only entry points to the Hidden Web.

Reference [3] presents an architectural model for a task-specific semi-automatic Hidden-Web crawler. The main focus of their work is to learn Hidden-Web query interfaces, not to generate queries automatically. A significant contribution of this work is the label matching approach that identifies elements of a form based on layout position, not proximity within the underlying HTML code. When analyzing forms, HiWE only associates one text to each form field according to a set of heuristics that take into account the relative position of the candidate texts with respect to the field (texts at the left and at the top are privileged), and their font sizes and styles. To learn how to fill in a form, HiWE matches the text associated with each form field and the labels associated to the attributes defined in its LVS. In this process, HiWE has the following restriction: it requires the LVS table to contain an attribute definition matching with each unbounded form field.

Many approaches exist that rely on filling forms [4, 6, 15] automatically. The main focus of the work in [4] is to generate queries automatically without any human intervention in order to crawl all the content behind a form. New techniques are proposed to automatically generate new search keywords from previous results, and to prioritize them in order to retrieve the content behind the form, using the minimum

number of queries. The problem of extracting the full content behind a form has been also addressed in [6]. They have proposed a domain-independent approach for automatically retrieving the data behind a given Web form. The approach to gather data is based on two phases: first the responses from the web site of interest are sampled and then if necessary methodically try all possible queries until either a fix point of retrieved data has arrived or all possible queries have exhausted. They have developed a prototype tool that brings the user into the process when an automatic decision becomes hard to make. These techniques focus on coverage, i.e., retrieve as big a portion of the site’s content as possible.

The hidden web can also be accessed using the meta-search paradigm instead of the crawling paradigm. This body of work is often referred to as meta-searching or database selection problem over the Hidden Web. In meta-search systems, a query from the user is automatically redirected to a set of underlying relevant sources, and the obtained results are integrated to return a unified response. Data integration is the problem of combining data from various web databases sources to provide the users with a unified view of data [8]. One of the main tasks to formalize the design of a data integration system is to establish the mapping between the Web database sources and a global schema. The meta-search approach is more lightweight than the crawling approach, since it does not require indexing the content from the sources. Nevertheless, the users will get higher response times since the sources are queried in real-time.

## 6 Open Issues in Hidden Web Crawling

A critical look at the available literature indicates that the following issues need to be addressed while designing the framework for any fully automatic crawler for the Hidden Web. Most of the research to date has focused on the last issue. Little attention has been made to the first two questions of scalability and synchronization:

1. There exists a variety of Hidden Web sources that provide information about the multitude of topics/domains [1, 7, 20]. The continuous growth of information about the WWW [8, 10] and hence the domain-specific information with ever-increasing number of domain areas pose a challenge to crawler’s performance. The crawl of the portion of the web for a particular domain must be completed within the expected time. This download rate of the crawler is limited by the underlying resources. An open challenge is the design a crawler that scales its performance according to the increase in the information on the WWW and number of domains. These scalability limitations stem from search engines’ attempt to crawl the whole Web, and to answer any query from any user.
2. Decentralizing the crawling process is clearly a more scalable approach and bears the additional benefit that crawlers can be driven by a rich context (topics, queries, user profiles) within which to interpret pages and select the links to be visited. However, a rigorous focus only on scalability can be costly; of course,

the system must also coordinate information coming from multiple sources, not all of which are under the control of the same organization. The pattern of communication is many-to-many, with each server talking to multiple clients and each client invoking program on multiple servers.

3. As the number of data sources is growing continuously at a very high rate, it is very tedious, time-consuming, and error-prone to process the search interfaces in web-based applications. An important objective of any Hidden Web crawler is to build an internal representation of these search forms [4–6] that supports efficient form processing and interface matching techniques so as to fully automate the process.

## 7 Conclusion and Future Work

A move in the Web structure from hyperlinked graph in the past to electronic form-based search interfaces of present day, represent the biggest challenge a Web crawler needs to tackle with. Despite the Web's great success as a technology and the significant amount of computing infrastructure on which it is built, it remains as an entity, surprisingly unstudied. Users need and want better access to the information on the Web. We believe that Hidden Web crawling is an increasingly important and fertile area to explore as such a crawler will enable indexing, analysis, and mining of Hidden Web content, akin to what is currently being achieved with the Surface Web. The paper provides a look at some of the technical challenges that must be overcome to model the Web as a whole, keep it growing and understand its continuing social impact. The topic of concerns as mentioned in the paper are further exacerbated by the rapid growth of Hidden Web content, fueled by the success of social networking online, the proliferation of Web 2.0 content and the profitability of the companies that steward in this new era. We look forward to continuing this promising line of research. One of the main objectives of our work will remain as the design of a crawler whose performance can be scaled up by adding additional low-cost processes and using them to run multiple crawls in parallel.

## References

1. Bergman, M.K.: The deep web: Surfacing hidden value. *J. Electron. Publ.* **7**(1), 1174–1175 (2001)
2. Sherman, C., Price, G.: *The Invisible Web: Uncovering Information Sources Search Engines Can't See*. CyberAge Books, Medford (2001)
3. Raghavan, S., Garcia-Molina, H.: Crawling the hidden web. In: *27th International Conference on Very large databases (Rome, Italy, September 11–14: VLDB'01)*, pp. 129–138. Morgan Kaufmann Publishers Inc., San Francisco (2001)
4. Ntoulas, A., Zerkos, P., Cho, J.: Downloading textual hidden web content through keyword queries. In: *5th ACM/IEEE Joint Conference on Digital Libraries (Denver, USA, Jun 2005)*

- JCDL05, pp. 100–109 (2005)
5. Barbosa, L., Freire, J.: Siphoning hidden-web data through keyword-based interfaces. In: SBBD, 2004, Brasilia, Brazil, pp. 309–321 (2004)
  6. Liddle, S.W., Embley, D.W., Scott, D.T., Yau, S.H.: Extracting data behind web forms. In: 28th VLDB Conference 2002, HongKong, China, pp. 38–49 (2002)
  7. Chang, K.C.-C., He, B., Li, C., Patel, M., Zhang, Z.: Structured databases on the web: Observations and implications. *SIGMOD Rec.* 33(3), 61–70 (2004)
  8. Gupta, S., Bhatia, K.: Exploring ‘hidden’ parts of the web: The hidden web. In: Lecture notes in Electrical Engineering, Proceedings of the International Conference ArtCom 2012, pp. 508–515, Springer, Heidelberg (2012)
  9. Gupta, S., Bhatia, K.: A system’s approach towards domain identification of web pages. In: Proceedings of the Second IEEE International Conference on Parallel, Distributed and Grid Computing (India, December 6–8, 2012) PDGC’12, IEEE Xplore
  10. Lawrence, S., Giles, C.L.: Accessibility of information on the web. *Nature* 400, 107–109 (1999)
  11. Baeza-Yates, R., Ribeiro-Neto, B.: *Modern Information Retrieval*, 2nd edn. Addison-Wesley-Longman, Boston (1999)
  12. Ipeirotis, P.G., Gravano, L., Sahami, M.: Probe, count, and classify: Categorizing hidden-web databases. In: Proceedings of the ACM SIGMOD International Conference on Management of Data, pp. 67–78, Santa Barbara, CA, USA, May (2001)
  13. Wang, W., Meng, W., Yu, C.: Concept hierarchy based text database categorization. In: Proceedings of International WISE Conference, pp. 283–290, China, June (2000)
  14. Chakrabarti, S., van den Berg, M., Dom, B.: Focused crawling: A new approach to topic-specific web resource discovery. In: Proceedings of the 8th International WWW Conference (1999)
  15. Zhang, Z., He, B., Chang, K.C.-C.: Light-weight domain-based form assistant: Querying web databases on the fly. In: Proceedings of the 31st Very Large Data Bases Conference (2005)
  16. McCallum, A., Nigam, K., Rennie, J., Seymore, K.: Building domain-specific search engines with machine learning techniques. In: Proceedings of the AAAI Spring Symposium on Intelligent Agents in Cyberspace (1999)
  17. Chakrabarti, S., Punera, K., Subramanyam, M.: Accelerated focused crawling through online relevance feedback. In Proceedings of WWW, pp. 148–159 (2002)
  18. Rennie, J., McCallum, A.: Using reinforcement learning to spider the web efficiently. In Proceedings of ICML, pp. 335–343 (1999)
  19. Diligenti, M., Coetzee, F., Lawrence, S., Giles, C.L., Gori, M.: Focused crawling using context graphs. In: Proceedings of the 26th International Conference on Very Large Databases, pp. 527–534 (2000)
  20. Profusion’s search engine directory. <http://www.profusion.com/nav>

# Combined and Improved Framework of Infrastructure as a Service and Platform as a Service in Cloud Computing

Poonam Rana, P. K. Gupta and Rajesh Siddavatam

**Abstract** Cloud computing is based on five attributes: multiplexing, massive scalability, elasticity, pay as you go, and self provisioning of resources. In this paper, we describe various cloud computing platforms, models, and propose a new combined and improved framework for Infrastructure as a Service (IAAS) and Platform as a Service (PAAS). As we know, that PAAS Framework has certain desirable characteristics that are important in developing robust, scalable, and hopefully portable applications like separation of data management from the user interface, reliance on Cloud Computing standards, an Integrated Development Environment, Life cycle management tools but it also has some drawbacks like the PAAS platform such as in Google Application engine, a large number of web servers catering to the platform are always running. This paper proposes an architecture which combines IAAS and PAAS framework and remove the drawbacks of IAAS and PAAS and describes how to simulate the cloud computing key techniques such as data storage technology (Google file system), data management technology, Big Table as well as programming model, and task scheduling framework using CLOUDSIM simulation tool.

**Keywords** PAAS · IAAS · Virtualization · Google application engine

---

P. Rana

KIET School of Engineering and Technology, Ghaziabad , UP 201206, India  
e-mail: doli238rana@gmail.com

P. K. Gupta (✉) · R. Siddavatam

Department of CSE and IT, Jaypee University of Information Technology,  
Waknaghat, Solan , HP 173234, India  
e-mail: pradeep1976@yahoo.com

R. Siddavatam

e-mail: srjesh@juit.ac.in

## 1 Introduction

A cloud computing platform dynamically configures, reconfigures the servers as needed. Virtualization is the key that enables cloud computing with increased utilization, compared with deploying, installing, and maintaining traditional forms of servers for on a task per server basis [1, 2]. Linux, Apache, and other programming languages like C++, Python, and Java as well as PHP have been widely adopted for Cloud Computing supported by many vendors. Cloud Computing delivers infrastructure, platform, and software as service in a pay as you go model to consumers. These services in industries are referred to as IAAS, PAAS, SAAS (Software as a service). IAAS [3, 4] is the capability provided to the consumer for processing storage networks and other fundamental computing resources where the consumer is able to deploy and run arbitrary software, which can include operating system and applications and limited control of select networking components. PAAS is the capability to deploy onto the cloud infrastructure consumer created or acquired using programming languages and tools supported by the provider [3, 4]. The consumer does not manage or control the underlying cloud infrastructure including network servers, operating system, or storage but has control over the deployed applications and possible application hosting environment, which can include operating systems and applications. Unlike server based application development, cloud based applications development is focused on splitting two things which is also required by every application too. First, every application needs computing power to manipulate the data. Second, data storage that can also be done at different levels: shared and nonshared.

## 2 Related Work

There are various service providers and various platforms or framework available for cloud computing. Anandasivam and Weinhardt [5] inspected the problem of how Cloud service providers would decide to accept or reject requests for services when the resources offering these services become scarce and proposed a decision support policy called Customized Bid-Price Policy (CBPP). Armbrust et al. [6] have redefined the cloud computing and reduces the confusion by clarifying the various terms. They have also quantified comparison between cloud computing and conventional computing and identified the top technical and non-technical obstacles and opportunities of cloud computing. Böhm et al. [7] have considered different point of view to look at the cloud computing from an IT provisioning perspective and further examined the evolution from outsourcing cloud computing as a new IT deployment paradigm. Buyya et al. [8] suggested that the cloud computing powers the next generation data centers and enables application service providers to lease data center capabilities for deploying applications. They have proposed an extensible simulation toolkit that enables modeling and simulation of cloud computing environment which is known as CLOUDSIM. In [9] Buyya et al. presented the vision of computing for twenty-first

century and delivered the vision of computing utilities. They have also stated the importance of cloud computing and provides the architecture for creating market-oriented clouds by leveraging technologies such as virtual machines. In [10] Yadav has presented the latest vision of cloud computing and identifies various commercially available cloud services promising to deliver the infrastructure on demand and provides architecture and description about various types of clouds.

There are number of companies that offer cloud computing services like Amazon [11, 12] offers something called Amazon Elastic Cloud (EC2). Amazon Web Services (AWS) provide infrastructure as a service offerings in the cloud for organizations requiring computing, power, storage, and other services. Kumar et al. [13] discusses about the various aspects of cloud computing and focuses on the security and trust to share the data for developing cloud computing applications in a distributed environment. They have also provided the concept of utility cloud to be used by the persons.

### 3 Cloud Models and Implementation Issues

The Google cloud also known as Google Application Engine (GAE) [14, 15], is a (PAAS) offering. Figure 1 describes PAAS offering which hides the actual execution environment from users. Instead a software platform is provided along with an SDK for users to develop applications and deploy them on the cloud [16, 17]. The PAAS platform is responsible for executing the applications including servicing external service requests, as well as running scheduled jobs in the applications. By making the actual execution servers transparent to the user, a PAAS platform is able to share application servers across users who need lower capacities, as well as automatically scale resources allotted to applications that experience heavy loads. Normally users upload their code in any programming language along with all required files and are stored with the GAE [18].

Resource usage for an application is measured in terms of web requests served and CPU hour actually spent on executing requests or batch jobs. The desirable characteristics of PAAS are [1, 18]:

- PAAS application can be made globally available  $24 \times 7$  but can change only when accessed.
- Deploying applications in GAE is free within usage limits, thus applications can be developed and tried out free and incurs cost only when actually accessed by a large volume of requests.
- The PAAS model enables GAE to provide such a free service because applications do not run in dedicated virtual machines. Deployed application which is not accessed merely, consumes storage for its code, data, and expands no CPU cycles.

GAE allows a user to run web applications written using the Python Programming language, other than supporting the Python standard library [19]. We have

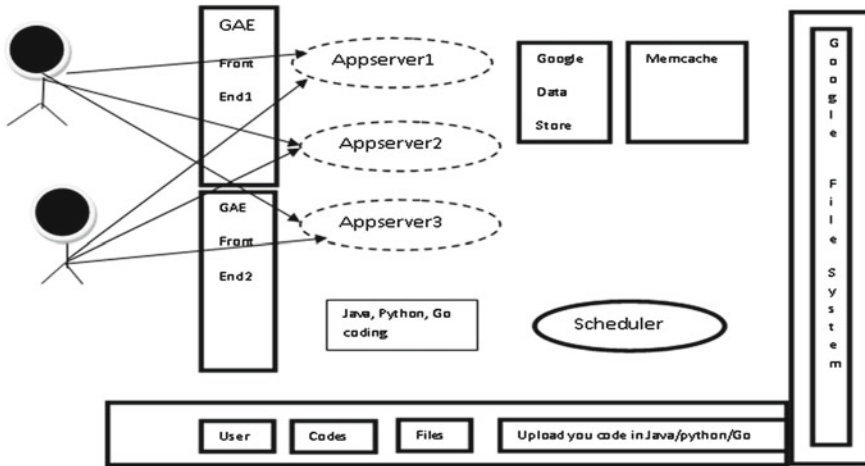


Fig. 1 Google application engine PAAS framework

developed our application using Java development tools and standard APIs. Our application interacts with the environment using the Java Servlet standard and common web application technologies such as Java Server Pages (JSP) [9]. Ease of use and supporting tools are advantages of GAE for Java and other cloud computing solutions. Google data store is a distributed object store where objects of all GAE applications are maintained and also provides a NOSQL schema-less object data store with a GQL query engine and atomic transactions. You have choice between two data storage options differentiated by their availability and consistency guarantees. Memcache [15, 20], provides your application with a high performance in memory key value cache that is accessible by multiple instances of your application. Memcache is useful for data that does not need the persistence transactional features of the data, stored as temporary data or data copied from the data, stored to the cache for high speed access.

### 4 Proposed Combined Framework of IAAS and PAAS

First, we have compared the existing IAAS and PAAS cloud models from an economic perspective. The PAAS model described by the Google Application Engine and Microsoft Azure cloud offerings can exhibit economic advantages as compared to an IAAS model for certain classes of applications. In Fig. 2, we have described the combined framework of IAAS and PAAS. We know that as far as the cloud computing is concerned, the cost factors also come into the account and there are various system matrices which measures the total cost. These measurements are an aggregate of one or more web servers in infrastructure capacity and measure the system level statistics.



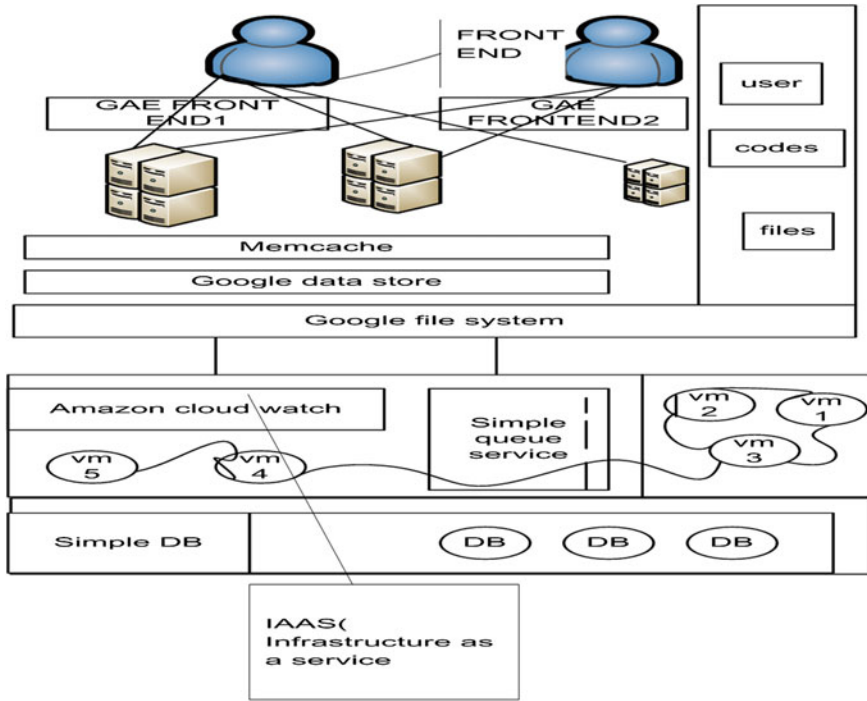


Fig. 2 Proposed combined framework of IAAS and PAAS

The PAAS model exemplified by the Google Application Engine and Microsoft Azure Cloud offerings can exhibit economic advantages as compared to an IAAS model for certain classes of application. Consider a web application that needs to be available  $24 \times 7$ , but where the transaction volume is highly unpredictable and can vary rapidly. With IAAS model a minimum number of servers would be provisioned at all times to ensure availability of the web service [21]. While in PAAS model such as Google Application Engine, deploying the application costs nothing. As usage increases beyond the free limits, charges begin to increase and a well-engineered application scale to meet the demand. So, both the IAAS and PAAS suffer from disadvantages. Further, taking additional servers for an application takes a finite amount of time, such as 15 or 20 min; the minimum capacity that needs in IAAS needs to account for this delay by organizing and paying for excess bandwidth capacity even in the cloud environment. But in the PAAS platform such as GAE, supports a large number of serving platforms, thus every users application code is available to all servers via the distributed file system. Sudden rises in demand are automatically routed to free web servers by the load balancer and ensures minimal performance degradation. The additional overhead induced is loading the code and data from the file system when such a web server handles a request to a new application for the first time.

## 5 Simulation of the Proposed Architecture

The simulation of the proposed framework in IAAS is being done by CLOUDSIM toolkit 3.0 released in Jan 2011 [8, 22]. CLOUDSIM is an extensible simulation toolkit that enables modeling and simulation of cloud computing environment for difficult applications and service models [21]. CLOUDSIM toolkit also supports modeling and creation of one or more virtual machines on a simulated node of a data center with jobs and their mappings to the virtual machines. For quantifying the scheduling performance and allocation policies in a real cloud environment, different applications and service models are available under different conditions [8]. An alternative is the utilization of the simulation tools that open the possibility of evaluating the hypothesis prior to software development in an environment where one can reproduce tests. Tests can be of various types. A machine instance (physical or virtual) is primarily defined by four essential resources (1) CPU (2) Memory (RAM) (3) Disk (4) Network connectivity. Each of these resources can be measured by tools that are operating system specific but for which tools that are their counterparts exists for all operating systems [8, 23]. Examining the four parameters, the server system metrics do not give you enough information to do meaningful capacity planning. Load testing gives an answer to many questions: (1) Maximum load that the current system can support. (2) Which resources represent the bottleneck in the current system that limits the system performances? This parameter is referred to as resource cutting depending upon a server's configuration. Now, what performance measurement tool should be used is the main goal to create a set of resource utilization curves.

## 6 Results

In simulation configuration, we tried to reconstruct virtual machines and cloudlet on a E-series Intel core 350m, processor 2.26 GHz, Window 7 Home Basic (64-bit), using Eclipse workbench and JDK 1.6 (standard edition). We tried to illustrate the proposed architecture using data centers with one host each and run the cloudlets on them. We have to describe various parameters with the help of CLOUDSIM toolkit for simulating our proposed architecture. The snapshots of the simulation are illustrated below in Table 1.

The Table 1 shows that our proposed architecture is successfully simulated and below are the results given for one of our executed scenario.

```
Starting CloudSimExample2...
Initializing...
Starting CloudSim version 3.0
Datacenter_0 is starting...
Broker is starting...
Entities started.
```

**Table 1** Results of proposed framework

S. No.	Scenario	Status	Result
1	Data center with one host and two cloudlets on it	Successful	71.2 ms
2	Data center with two hosts and two cloudlets on it	Successful	224.8 ms
3	Two Data centers with two hosts and run cloudlets of two users on them	Successful	35.6 ms of each user
4	Scalable simulation	Successful	6156.3 ms of each user
5	How to pause and resume the simulation	Successful	The simulation is paused for 5 s
6	How to create a simulation entity using global broker entity	Successfully created	–

```

0.0: Broker: Cloud Resource List received with 1 resource(s)
0.0: Broker: Trying to Create VM #0 in Datacenter_0
0.0: Broker: Trying to Create VM #1 in Datacenter_0
0.1: Broker: VM #0 has been created in Datacenter #2, Host #0
0.1: Broker: VM #1 has been created in Datacenter #2, Host #0
0.1: Broker: Sending cloudlet 0 to VM #0
0.1: Broker: Sending cloudlet 1 to VM #1
1000.1: Broker: Cloudlet 0 received
1000.1: Broker: Cloudlet 1 received
1000.1: Broker: All Cloudlets executed. Finishing...
1000.1: Broker: Destroying VM #0
1000.1: Broker: Destroying VM #1
Broker is shutting down...
Simulation: No more future events
CloudInformationService: Notify all CloudSim entities for shutting down.
Datacenter_0 is shutting down...
Broker is shutting down...
Simulation completed.....
    
```

## 7 Conclusion

In this paper, we have proposed a novel combined framework using the PAAS and IAAS to produce a hybrid architecture using Google Application Engine as front end and IAAS elastic compute service as back end and then simulate our architecture

using CLOUDSIM toolkit. As we know, that heavier application IAAS is better suited, so it is better if we combine them and get all the advantages of PAAS framework as well as IAAS framework. Therefore, we proposed an architecture that is combination of IAAS and PAAS architecture. Here PAAS provides the web front end and IAAS provides the power when needed. The performance statistics of the load balanced requests can also be monitored by cloud watch and used by auto scale to add or remove servers from the load balanced users. Using these tools the users can configure a scalable architecture that also adjusts resource consumption. The future work can be resource allocation and resource provisioning can be done, to develop such architecture which is economically lower as compared to the proposed hybrid architecture of IAAS and PAAS.

## References

1. Sosinky, B.: Cloud Computing Bible, pp. 1–528. Wiley, India (2011)
2. Roy, G.M., Saurabh, S.K., Upadhyay, N.M., Gupta, P.K.: Creation of virtual node, virtual link and managing them in network virtualization. In: IEEE 2011 World Congress on Information and Communication Technologies (WICT), pp. 738–742. Mumbai, India (2011)
3. Peter M., Timothy G.: The NIST Definition of Cloud Computing, Tech Report National Institute of Standards and Technology. pp. 1–7. (2011)
4. Info. Apps. Gov. : What are the Services. <http://info.apps.gov/content/what-are-services>
5. Anandasivam, A., Weinhardt, C.: Towards an Efficient Decision Policy for Cloud Service Providers. In: Proceedings of the ICIS, Paper 40 (2010)
6. Armbrust, M., Fox, A., Griffith, R., Anthony, D., Katz, R., Konwinski, A., Lee, G., Patterson, D., Rabkin, A., Stoica, I., Zaharia, M.: A view of cloud computing. *Commun. ACM* **53**(4), 50–58 (2010)
7. Böhm, M., Leimeister, S., Riedl, C., Krmar, H.: Cloud Computing - Outsourcing 2.0 or a new Business Model for IT Provisioning. Springer Application, Management. pp. 31–56. Gabler, GmbH (2011)
8. Buyya, R., Ranjan, R., Rodrigo, N.: Modelling and Simulation of scalable cloud computing environment and the cloudsim toolkit: challenges and opptuties. In: IEEE International Conference on High Performance computing & simulation, pp. 1–11. (2009)
9. Buyya, R., Yeo, C.S., Venugopal, S.: Market oriented cloud computing, vision hype and reality for delivering it services as computing utilities. In: The 10th IEEE conference on high performance computing and communications, pp. 5–13. (2008)
10. Yadav, S.S.: Cloud a computing Infrastructure on demand. In: International conference on computer engineering and technology (ICCET), pp. 423–426. (2010)
11. Mather, T., Kumaraswami, S., Latif, S.: Cloud Security and Privacy an Enterprise respective on Risks and Compliance. O’ Reilly Media, Inc, Canada (2009)
12. Amazon. : Amazon web services. <http://aws.amazon.com>
13. Pardeep, K., Sehgal, V.K., Chauhan, D.S., Gupta, P.K., Diwakar, M.: Effective ways of secure, private and trusted cloud computing. *IJCSI Int. J. Comput. Sci. Issues* **8**(3), 412–421 (2011)
14. Bedra, A.: Getting started with Google App Engine and Closure. *IEEE Internet Comput.* **14**(4), 85–88 (2010)
15. Malawski, M., Kuzniar, M., Wojcik, P., Bubak, M.: How to use Google App Engine for Free Computing. *IEEE Internet Comput.* **17**(1), 50–59 (2011)
16. Baiardi, F., Sgandurra, D.: Securing a community cloud. In: IEEE 30<sup>th</sup> International Conference on Distributed Computing Systems Workshops (ICDCSW), pp. 32–41. (2010)

17. Alexander, L., Klems, M., Nimis, J., Tai, S., Sandholm, T.: What's inside the Cloud? An architectural map of the cloud landscape. In: Proceedings of the, ICSE Workshop on Software Engineering Challenges of Cloud, Computing, pp. 23–31. (2009)
18. Gautam, S.: Enterprise Cloud Computing: Technology, Architecture. Applications. Cambridge University Press, Cambridge (2010)
19. Armando, F., Michael, A., Rean, G.: The Clouds: A Berkely View of Cloud, Computing, UC Berkeley, USA (2009)
20. Google Developers. : What is Google App Engine? <https://developers.google.com/appengine/docs/whatisgoogleappengine>
21. [www.cloudbus.org/](http://www.cloudbus.org/).
22. <https://developers.google.com/appengine/docs/>
23. Ekstrom, J., Bailey, M.: Teaching web deployment with OS-virtualization. In: Proceedings of 2009 ASEE Annual Conference and Exposition, pp. 1–8. (2009)

# Web Site Reorganization Based on Topology and Usage Patterns

R. B. Geeta, Shashikumar G. Totad and P. V. G. D. Prasad Reddy

**Abstract** The behavioral web users' access patterns help website administrator/web site owners to take major decisions in categorizing web pages of the web site as highly demanding pages and medium demanding pages. Human beings act as a spider surfing the web pages of the website in search of required information. Most of the traditional mining algorithms concentrate only on frequency/support of item sets (web pages set denoted as  $ps$  in a given web site), which may not bring considerably more amount of profit. The utility mining model focuses on only high utilities item sets ( $ps$ ). General utility mining model was proposed to overcome weakness of the frequency and utility mining models. General utility mining does not encompass website topology. This limitation is overcome by a novel model called human behavioral patterns' web pages categorizer (HBP-WPC) which considers structural statistics of the web page in addition to support and utility. The topology of the web site along with log file statistics plays a vital role in categorizing web pages of the web site. The web pages of the website along with log file statistics forms a population. Suitable auto optimization metric is defined which provides guidelines for website designers/owners to restructure the website based on behavioral patterns of web users.

**Keywords** Web mining · Reorganization · Log file · Web site topology

---

R. B. Geeta (✉)

Department of Information Technology, GMRIT, Rajam, AP, India  
e-mail: geetatotad@yahoo.co.in

S. G. Totad

Department of Computer Science, GMRIT, Rajam, AP, India  
e-mail: skumartotad@yahoo.com

P. V. G. D. Prasad Reddy

Department of CS and SE, Andhra University, Vizag, AP, India  
e-mail: prsadreddy.vizag@gmail.com

## 1 Introduction

Web is huge repository of information. There has been gigantic development of the world wide web. The information is available throughout the globe in the form of websites. Web mining is the application of data mining. Web mining is a process of extracting useful information from the Web. Yang and others [1] suggested that web mining forms universal set of web structure mining, web usage mining and web content mining. Web structure mining deals with how well the web pages in the web site can be organized, so that most demanding pages can be kept very near to home page.

## 2 Related Work

To perform any website evaluation, web visitor's information plays an important role, in order to assist this, many tools are available. Li et al. [2] expressed that web mining is a popular technique for analyzing website visitor's behavioral patterns in e-service systems. Jian et al. [3] found that web log mining helps in extracting interesting and useful patterns from the log file of the sever. Shen et al. [4] suggested that HTML documents contain more number of images on the WWW. Such documents' containing meaningful images ensures a rich source of images cluster for which query can be generated. The documents which are highly needed by users can be placed near to the home page of the website. Manoj and Deepak [5] suggested that the development of web mining techniques such as web metrics and measurements, web service optimization, process mining etc... will enable the power of WWW to be realized. Wang et al. [6] found that weakness of both frequency and utility can be overcome by general utility mining model. Miller and Remington [7] revealed that the structure of linked pages has decisive impact factor on the usability. Geeta et al. [8] suggested that the number of pages at a particular level, the number of forward links and the number of backward links to a particular web page reflect the behavior of visitors to a specific page in the website. However Garofalakis [9] pointed out that the number of hit counts calculated from log file is an unreliable indicator of page popularity. Geeta et al. [10] suggested that the topology of the website plays an important role in addition to log file statistics to help users to have quick response. Jia-Ching et al. [11] found that web usage mining helps in discovering web navigational patterns mainly to predict navigation and improve website management. Lee et al. [12, 13] proved that the web behavioral patterns can be used to improve the design of the website. These patterns also could help in improving the business intelligence.

### 3 Web Structure Mining

Web structure mining concentrates on link structure of the web site. The different web pages are linked in some fashion. The potential correlation among web pages makes the web site design efficient. This process assists in discovering and modeling the link structure of the web site. Generally topology of the web site is used for this purpose. The linking of web pages in the Web site is challenge for web structure mining. The page with in degree high indicates that the page is with valuable content.

### 4 Web Usage Mining

Web Usage mining helps in understanding the users’ behavior while interacting with the website. The main objective of web usage mining is to identify useful patterns and assist site adaption to better suit the users. Log file of server provides the various statistics such as the number of hits to a particular web page tells us about how well a particular web page is popular.

### 5 Proposed Work

Whenever a client/user requests for a server, communication takes place between client and server [14]. If user requesting page is at leaf level, the user has to go through all intermediary nodes to reach leaf node, meanwhile those many times communications take place between server and client using various resources like bandwidth, server’s processor time, client processor time and power spent at both client and server. If a particular web page is located at  $n$ th level, all  $(n - 1)$  entries will be entered into log file of the server. All these parameters can be mathematically modeled as follows. Time spent by server and client is denoted by TSC.

$t_s$  is the time spent by the server and  
 $t_c$  is time spent by the client.

Let CCSC represents how many times communication is carried out between client and server and SL denotes space required to store all log entries. The parameter  $n$  represents the level of the web page. BW is used to represent the bandwidth utilized. nbw stands for network bandwidth.

$$TSC = (n + 1)^* t_s + (n + 1)^* t_c \text{ units}$$

$$CCSC = (n + 1)^* (\text{msg\_generated\_by\_client} + \text{msg\_generated\_by\_server})$$

$$SL = (n + 1)^* b \text{ bytes}$$

$$BW = (n + 1)^* nbw$$



The main motto of this work is to minimize all above mentioned parameters, so that users will have quick response, bandwidth can be utilized efficiently, server time and client time can be used effectively and reduction of log file entries thereby saving memory space, reducing power supply and users will have quick response.

## 5.1 System Design

Whenever web user requests for a particular web page, he leaves the information in the log file. The web pages of the web site along with server's log file details forms the population which helps in decision making. The fitness function is to maximize the number of visitors to the web page/(s) and to minimize log file entries. This approach helps in satisfying users to have quick response.

We start with the formal definition of HBP-WPC as follows.

Let us consider a website of  $n$  pages  $\{w_p, g_p, t_p\}_{p=1,\dots,n}$  for binary categorization problem, where  $g_p \in \{\text{Excellent, Medium}\}$  and  $t_p \in (0, 1]$  is the degree of web page  $w_p$  belonging to  $g_p$ .

The HBP-WPC equation is defined with the following terms.

- $P = \{p_1, p_2, \dots, p_n\}$  is the web pages lookup table which contains mapping of acronyms for actual web page names  $\{w_1, w_2, \dots, w_n\}$ . The index  $n > 0$  and  $n$  is the total number of web pages for the given website.
- $L = \{T_1, T_2, \dots, T_n\}$  is a transactions database where each transaction  $T_i \in \text{Log File of the server}$ .
- $S(p_i)$  denotes the ratio of frequency of web page  $p_i$  to total frequency of all web pages in all transactions for a particular session threshold.
- $O(p_i)$  is the ratio of out degree of web page  $p_i$  to total number of links in the website.
- $I(p_i)$  denotes the ration of in degree of web page  $p_i$  to total number of links in the website.
- $D(p_i)$  denotes the ratio of  $p_i$  to total number of pages in the web site.
- $L(p_i) = \text{level of } p_i / \text{total number of pages in that level}$ .
- $\text{Sup}(w_i)$ , the support count of an web page  $w_i$ , is the frequency of occurrence of all transactions containing  $w_i$ , for a particular session threshold.
- $S$ , the total number of frequency of occurrences of web pages in all transactions.
- $U$ , the total time spent on different web pages by various transactions in a given threshold.
- $U(p_i)$  represents the ratio of utility of a web page  $p_i$  in all transactions over the given threshold to the total utility of all web pages for a given threshold.
- The HBP-WPC of a web page  $p_i$  denoted as  $\text{WC}(p_i)$ , is the linear combination of log file statistics and web site topology statistics as shown in Eq. 1

$$\text{WC}(p_i) = W(p_iL) + W(p_iS) \quad (1)$$

$W(p_i;S)$  denotes details of the web page such as in degree, out degree, level and number of pages in that level.  $\alpha$  and  $\beta$  are grading factors taking all possible values between 0 and 1 which help to assign different combination of weightages for Support and Utility.

- $W(p_i;L) = \alpha S(p_i) + (1 - \alpha) U(p_i)$
- $W(p_i;S) = \beta O(p_i) + (1 - \beta) I(p_i) + D(p_i) + L(p_i)$
- $G1(p_i, \alpha, \beta) = W(p_i;L) + W(p_i;S)$  for  $i = 1..n, \alpha = 0..1$  and  $\beta = 0..1$
- $Temp = Avg(G1(p_i, \alpha, \beta))$
- $G2(p_i, \alpha) = \min(\text{diff}(G1(p_i, \alpha, \beta), Temp))$
- Let  $C = Avg(G2)$ . The web page whose  $(G2) \geq C$ , such a page can be considered as highly demanding web page else it can be considered as low demanding web page.

### 5.2 Experimental Results

Figure 1 shows structure of the website. The website contains seven web pages A, B, C, D, E, F and G with support and utility for each web page. The page B has 2 forward links 1 backward link, the level of page is 2 and number of pages at level 2 is 3. The Page B has utility 5 and frequency 8 etc... total utility of the web site is 213 and total Support is 101.

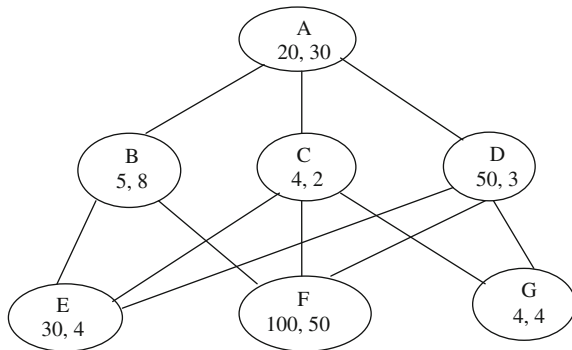
As per Garafalokis relative access (RA) is calculated using absolute access (AA) of each web page obtained from log file of server as shown in Eq. 2.

$$RA [i] \propto AA [i] \tag{2}$$

$i$  stands for index of web page. The Relative Access of web page is directly proportional to AA. The constant of proportionality is replaced with  $K$ .  $K$  is defined as follows

$$RA [i] = K [i] * AA [i]$$

**Fig. 1** Structure of the web-site with utility and support



$K [i] = d [i] + n [i] / [i]$  where d-depth of page, n-number of pages as level i and r-number of references to page i from other pages. The value of RA for each web page is shown in Table 3. The heap tree is generated based RA. Six nodes were swapped to obtain heap tree in 3 iterations. The web pages which should not be moved can be made stable. With the heap tree generation all demanding pages will be brought very near to home page. Geeta and others suggested constant of proportionality K in Eq. 2 as follows

$$GRA [i] = K [i] * AA [i] \tag{3}$$

$K [i] = L [i] + FL [i] / BL [i]$  where i-index of a web page, L-level of page i, FL[i]-number of forward links from web page i and BL[i]-number of backward links to page i. The value of GRA calculated for each web page is shown in Table 3. The heap tree is generated based on RA. The WC calculated for each web page using Eq. 1 is also shown in Table 3. Using this approach, the highest grade pages at 2nd level are compared with its successors and swapped. After this next highest grade web page is considered and compared with its children, the page with highest WC is swapped with parent and so on.

$\alpha$  is the grading factor for support  $\beta$  is the grading factor for in degree and out degree. When  $\alpha$  is 0 utility is given the importance, when  $\alpha = 1$  support is given the importance. When  $\beta$  is 0 in degree is given the importance and when  $\beta$  is 1 out degree is given the importance. For each page G is calculated for all possible values of  $\alpha$  and  $\beta$  ranging from 0 to 1 at the step of 0.1. Calculate G1 and G2 using the above formulas. The G1 for each web page is as shown in Table 1.

Table 2 shows values of G2 for each web page. Consider average of G2 of all web pages. The average G2 for above table is 0.14869. If  $G2 (p_i) >$  average of G2 consider the page as excellent/highly demanding web page and such a page can be moved near to the home page. To decide which pages are highly demanding and which pages are low demanding, fuzzy approach can be applied. This algorithm returns the values between 0 and 1. The web page whose G2 is greater than average (G2),

**Table 1** G1 for all web pages

A	B	C	D	E	F	G
1.3731	1.4455	1.4863	1.7022	1.7057	2.0344	1.5382
1.3934	1.4511	1.4864	1.6817	1.6956	2.0369	1.5403
1.4137	1.4566	1.4865	1.6612	1.6855	2.0395	1.5424
1.4340	1.4622	1.4866	1.6407	1.6754	2.0420	1.5445
1.4543	1.4678	1.4867	1.6202	1.6652	2.0446	1.5465
1.4746	1.4734	1.4868	1.5997	1.6551	2.0472	1.5486
1.4949	1.4789	1.4869	1.5792	1.6450	2.0497	1.5507
1.5153	1.4845	1.4870	1.5587	1.6349	2.0523	1.5528
1.5356	1.4901	1.4871	1.5382	1.6247	2.0548	1.5549
1.5559	1.4957	1.4872	1.5177	1.6146	2.0574	1.5570
1.5762	1.5012	1.4873	1.4972	1.6045	2.0599	1.5590

**Table 2** G2 for each web page

Web page	G2
A	0.1432
B	0.1364
C	0.1352
D	0.1361
E	0.1557
F	0.1978
G	0.1483

**Table 3** Values obtained using Eqs. 1, 2 and 3

Web Page	G2(HBP-WPC)	RA	GRA
A	Fixed	Stable	Fixed
B	0.1364	40-II	32-II
C	0.1352	10	8
D	0.1361	15	15-III
E	0.1557-II	16	12
F	0.1978-I	200-I	150-I
G	0.1483-III	18-III	12

such a web page can be treated as highly demanding web page, otherwise it will be medium demanding web page. With such an approach all highly demanding pages can be moved near to home page. The web pages E and F are moved to upper level. The web page F is interchanged with B and E is interchanged with C. This information can be provided to the web site administrator for reorganization of the website. The G2 values can be compared with the values obtained from Eqs. 2 and 3.

Table 3 shows ranking of web pages for all three approaches. HBP-WPC tries to scale all the values between 0 and 1 and accurate results can be obtained, whereas the values calculated using RA and GRA take all possible integer values. HBP-WPC gives importance for web pages whose in-degree is high compared to out degree. So HBP-WPC is efficient and provides accurate result compared to other two approaches. Based on this ranking web site owners/designers can go for reorganization of web pages of the web site.

## 6 Conclusion

The contributions of this paper are as follows. First, this model helps in best utilization of web sources such as client, server and communication media. Second, since the highly demanding pages are brought near to the home page, users will have quick response. The control messages generated between server and client to have communications are minimized along with power consumption. Third, whenever client requests for HTTP transaction the entry will be made in the log file. Since

most demanding pages are very near to home page, entries in log file are minimized. Client's and server's process time is minimized. Fourth, highly demanding pages can be kept in high speed servers', medium pages can be clustered and stored in low speed servers. This work aims to provide sophisticated metric, robust, useful techniques and fundamental basis for high conformity website reorganization routine and applications. In future work, we will investigate techniques for improvement in the metric and the procedure adopted.

## References

1. Yang, Q., Zhang, H.: Web-log mining for predictive caching. *IEEE Trans. Knowl. Data Eng.* **15**(4), 1050–1053 (2003)
2. Li, Y., Zhang, C., Zhang, H.: Cooperative strategy web-based data cleaning. *Appl. Artif. Intell.* **17**(5–6), 443–460 (2003)
3. Pei, J., Han, J., Mortazavi-Asl, B., Zhu, H.: Mining access patterns efficiently from web logs. In: *Pacific-Asia Conference on Knowledge Discovery and Data Mining (PAKDD'00)*, Kyoto, Japan, pp. 396–407, April 2000
4. Shen, H.T., Ooi, B.C., Tan, K.: Giving meanings to WWW, *ACM SIGM Multimedia, L.A.*, pp. 39–47 (2000)
5. Mano, M., Deepak, G.: Semantic web mining of un-structured data: challenges and opportunities. *Int. J. Eng.* **5**(3), 268–276 (2011)
6. Wang, J., Liu, Y., Zhou, L., Shi, Y., Zhu X.: Pushing frequency constraint to utility mining model. In: *ICCS, LNCS*, vol. 4489, pp. 685–692. Springer, Heidelberg (2007)
7. Miller, C.S., Remington, R.W.: Implications for information architecture. *Human Comput. Interact. J. IEEE Web Int.* **19**(3), 225–271 (2004)
8. Geeta, R.B., Shashikumar G.T., PrasadReddy, PVGD.: Optimizing user's access to web Pages, *RJooiJA. Trans. World Wide Web-Spring* **8**(1), 61–66 (2008)
9. Garofalakis, Web Site optimization using page popularity. *IEEE Int. Comput.* **3940**, 22–29 (1999)
10. Geeta, R.B, Shashikumar G.T., PrasadReddy PVGD.: In: *Conference, Topological Frequency Utility Mining Model Springer International. SocPros 11*, pp. 505–508 (2011)
11. Ying, J.-C., Tseng, V.S. Yu, P.S.: In: *IEEE International Conference on Data Mining Workshops. IEEE Computer Society* (2009)
12. Lee, Y.S., Yen, S.J., Hsiegh, M.C.: A lattice-based framework for interactively and incrementally mining web traversal patterns. *Int. J. Web Inf. Syst.* 197–207 (2005)
13. Lee, Y.S., Yen, S.J., Tu, G.H., Hsieh, M.C.: Mining traveling and purchasing behaviors of customers in electronic commerce environment. In: *Proceedings of the EEE'04*, pp. 227–230 (2004)
14. Geeta, R.B., Shashikumar G.T., PrasadReddy PVGD.: Manager-members distributed software development reference model. In: *IEEE International Advanced Computing Conference IACC 2009 Patiala*, 6–7 March 2009

# Web Search Personalization Using Ontological User Profiles

Kretika Gupta and Anuja Arora

**Abstract** In web, users with different interest and goal enter queries to the search engine. Search engines provide all these users with the same search results irrespective of their context and interest. Therefore, the user has to browse through many results most of which are irrelevant to his goal. Personalization of search results involves understanding the user's preferences based on his interaction and then re-ranking the search results to provide more relevant searches. We present a method for search engine to personalize search results leading to better search experience. In this method, a user profile is generated using reference ontology. The user profile is updated dynamically with interest scores whenever, he clicks on a webpage. With the help of these interest scores in the user profile, the search results are re-ranked to give personalized results. Our experimental results show that personalized search results are effective and efficient.

**Keywords** Personalization · Ontological user profile · Re-ranking

## 1 Introduction

The amount of information in world wide web has seen a phenomenal increase in the past years. In 1994, one of the first web search engines had to index 110,000 web pages approximately. Today, search engines need to deal with more than 25 billion documents. Search results retrieved by internet search engines display the same result irrespective of who has queried. A user looking for “apple” maybe interested in apple

---

K. Gupta (✉) · A. Arora  
Department of Computer Science, Jaypee Institute of Information Technology,  
Noida, India  
e-mail: kretika@hotmail.com

A. Arora  
e-mail: anuja.arora@jiit.ac.in

as a fruit instead of apple the company. A user has to go through irrelevant search results before he finds his required results. This irrelevant information is due to the one size fits all policy of the search engines [1]. Identical queries from different users with different interest generate same search results. Another main reason of irrelevant search results is ambiguity in query. Ambiguity can be attributed to polysemy, existence of many meanings for a single word, and synonymy, existence of many words with the same meaning. Ontology is defined as an explicit specification of conceptual categories and relationships between them [2]. Therefore, to personalize the search results, a user profile is required to map the user interest. Re-ranking of webpages is done using user profile. Many approaches have been developed to personalize web search. User preference based on the analysis of past click history was discussed in detail by Pretschner and Gauch [3] and Sugiyama et al. [4]. Short-term personalization based on a current user session was discussed by Sriram et al. [5].

## 2 Methodology

Reference ontology is built by using Open Directory project. A user profile is generated by annotating interest scores in the concepts provided by the reference ontology. The interest scores in the user profile created is updated dynamically whenever he clicks on a webpage. With the help of the user interest the search results are re-ranked.

### 2.1 User Profile Generation

The User profile is an instance of reference domain ontology. The reference domain ontology is created with the help of a web directory, Open Directory Project (ODP) [6]. A portion of ODP has been shown in Fig. 1. In this, the concepts are

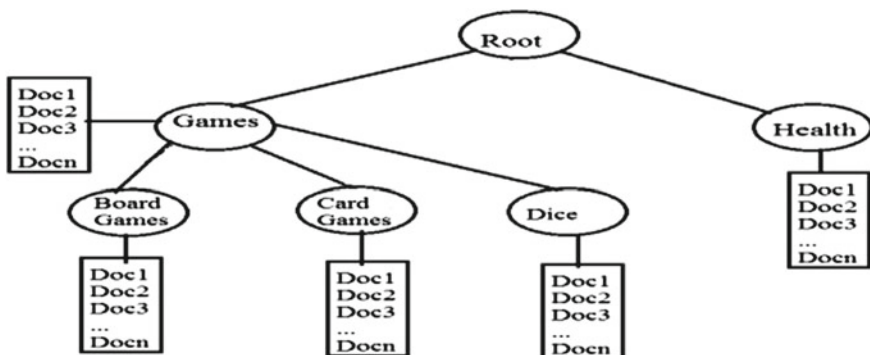


Fig. 1 Portion of an ontological profile. Each node has documents associated with it

annotated with an interest score which is updated dynamically each time the user clicks on a webpage. Open directory project is considered as the “largest human-edited directory of the web”. The data structure is organized in Directed Acyclic Graph. Each category has a set of documents associated with it which were used as a training set for classification. Text classification is required to find out under which category the content of the webpage lies in. For text classification, all the documents classified under one category in the ODP structure is merged under one super document. Whenever a user clicks on a webpage, a page vector is computed and then compared with each category’s vector in the DAG to calculate the similarities. Trajkova and Gauch [7] have calculated the similarity between Web pages visited by the user and the concepts in an ontology. The page vector is computed with the help of the title of the web page, Metadata Description Unigrams, and Metadata Keywords Unigrams associated with the webpage [8].

### 2.2 Updating User Profile

The User Profile for a given user saves his interests in the particular categories determined by the ODP structure. The user does not have to choose his interest areas explicitly [9]. This is automatically generated using various features which will be further discussed. The user profile is dynamic and keeps updating over time. As, whenever a user clicks on given link, the interest score is determined and updated. Since the profile is dynamically updated it takes into consideration the changing interests of a user.

Interest score is calculated with the help of the time spent, length, and subject similarity of the webpage. Time denotes the user’s duration of viewing the webpage, length denotes the number of characters in a webpage. Subject similarity denotes the similarity between the webpage’s content and the category defined by the ODP structure. As shown in Fig. 2.

$Sim(d, c_i)$  refers to the similarity of match between the content of document ( $d$ ) and category ( $c_i$ ) defined by ODP. Adjustment of the interest of a user in category ( $c_i$ ) is  $\delta(i, c_i)$ . The interest score is updated with the help of the following equation, according to [3].

$$\delta(i, c_i) = \log(\text{time} / (\log \text{length})) * Sim(d, c_i) \tag{1}$$

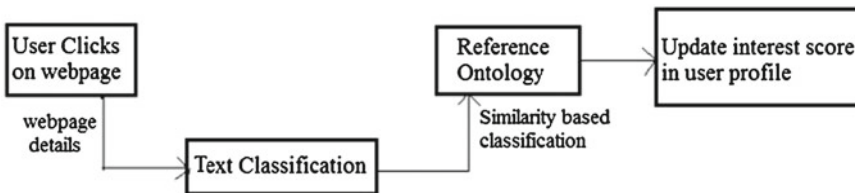


Fig. 2 Updating user profile



It can be noted that the above equation takes length into less consideration as the users can tell from a glance that the webpage is not relevant and move on to the next webpage swiftly irrespective of the length.

### 2.3 Re-ranking Search Results

Web search API: many commercial search engines have provided their API's so third party tools can access their search results (index). Google custom search API is used to retrieve search results for a query given by the user. These search results are retrieved with their index and are then used to re-rank web pages according to the interest scores in the generated user profile of that user.

The pages are re-ranked by a similarity matching function that computes the similarity of the retrieved result's document with each concept in the user profile's ontology to find the best matching concept.

$$\text{CSim}(\text{UserProfile}_i, \text{Result}_j) = \sum_{k=1}^N \text{wp}_{i,k} * \text{wd}_{j,k} \quad (2)$$

where,

$\text{Wp}_{i,k}$  represents the weight of concept  $k$  in the user profile,

$\text{Wd}_{j,k}$  represents the weight of concept  $k$  in the result  $j$ .

As Google applies its own PageRank algorithm, to rank websites based on their importance, we have incorporated Google's original ranking score as well. This will keep a check that we do not miss important webpages.

$$\begin{aligned} \text{FinalRank}(\text{UserProfile}_i, \text{Result}_j) \\ = \gamma * \text{CSim}(\text{UserProfile}_i, \text{Result}_j) + (1 - \gamma) \text{GRank}(\text{Result}_j) \end{aligned} \quad (3)$$

where GRank is the original rank.  $\gamma$  is used to combine the two ranking measures. We consider  $\gamma$  as 0.5 to give equal weightage to both the ranking mechanisms. If  $\gamma$  is 0, ranking will be done based on Google search results and if  $\gamma$  is 1 the ranking is done purely according to context. Each time, a user clicks on the links of the search results; the interest score is updated dynamically to determine the user's preferences. This has been represented in Fig. 3.

## 3 Experiments

To evaluate the effectiveness of personalized search results we need to find:

Research Question 1: (RQ1): Do the interest scores for individual concepts in ontological profile converge?

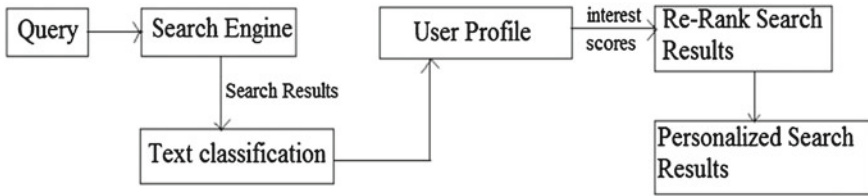


Fig. 3 Re-ranking results

Research Question 2: (RQ2): Can the interest scores maintained by the ontological profile be used to re-rank Web search to give personalized search results?

### 3.1 Experiment 1

With this experiment we want to evaluate RQ1, if the rate of increase in the user’s interest scores for all categories stabilizes over incremental updates [10]. The categories are defined by the user’s ontology. Each time the user clicks on a webpage the user interest are updated in the ontological user profile. Initially, the interest scores for the categories in the user profile will continue to change rapidly. However, once enough information has been collected and processed, the rate of change interest scores should decrease. Hence, we wanted to find out if over time the concepts with the highest interest scores would become relatively stable or not. For conducting the experiment, 15 users were asked to use the personalized search engines over a period of 20 days. Their user profile was monitored during these days. The number of categories the profiles converged to, changed according to the user, mainly it was in the range of 48 and 180. The Fig. 4 shows the convergence for a sample of 4 users. We can see that over time the user profile converges and becomes stable.

### 3.2 Experiment 2

In this experiment, we determined if the users found the personalized search results more relevant than standard web search results for RQ2. Experiment has been performed manually. To conduct this comparative experiment, whenever the user clicked on a given webpage for a query, we asked the user to mark the page as relevant or irrelevant. 15 users entered several queries over a period of 20 days. On a single search query, 12 webpages from each of the standard search engine and personalized search engine was randomly presented to the user. Few pages were marked as “both”, if they were common to both the search engines. By looking at the log of the user, it was determined how many relevant webpages the users clicked on from each.

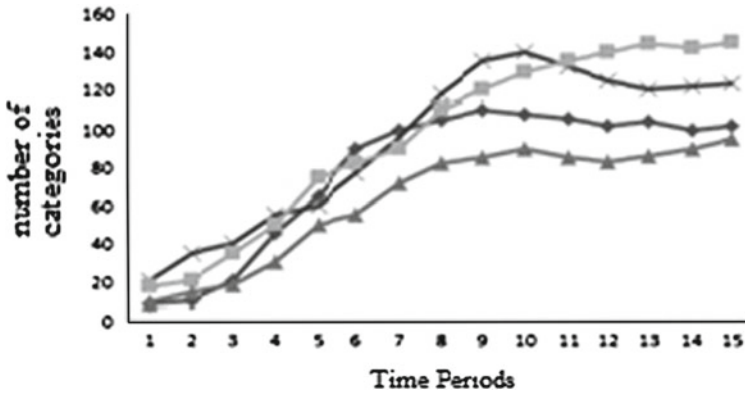


Fig. 4 Convergence of profiles

The proposed personalized search results were 55% more relevant than the normal search results for the user searches.

## 4 Conclusion

This paper proposed a method for a search engine to personalize search results based on a user's preferences. The user preferences were mapped to a user profile. It was shown with the help of experiments that over time, the interest got converged. With the help of the user profile, web search results can be re-ranked leading to more relevant results for the users. In future, we plan to optimize our search engine for more relevant results. We would also look into the location based information of user to provide better search results.

## References

1. Allan, J., et al.: Challenges in information retrieval and language modeling. *ACM SIGIR Forum* 37(1), 31–47 (2003)
2. Sieg, A., Mobasher, B., R. Burke.: Web search personalization with ontological user profiles. In: *Proceedings of CIKM* (2007)
3. Pretschner, A., Gauch, S.: Ontology based personalized search. In: *Proceedings of the 11th IEEE International Conference on Tools with Artificial Intelligence*. Chicago, IL, pp. 391–298. IEEE Computer Society (1999)
4. Sugiyama, K., Hatano, K., Yoshikawa, M.: Adaptive web search based on user profile constructed without any effort from user. In: *Proceedings of the 13th International Conference on World Wide Web*. New York, pp. 675–684. (2004)
5. Sriram, S., Shen, X., Zhai, C.: A session-based search engine. In: *Proceedings of SIGIR(2004)*
6. Open Directory Project - <http://dmoz.org>

7. Trajkova, J., Gauch, S.: Improving ontology-based user profiles. In: Proceedings of the Recherched'Information Assiste par Ordinateur, RIAO 2004, pp. 380–389. University of Avignon (Vaucluse), France, April (2004)
8. Chirita, P., Firan, C., Nejdl, W.: Summarizing local context to personalize global web search. In: Proceedings of the 15th ACM International Conference on Information and Knowledge Management, CIKM 2006, pp. 287–296. Arlington, VA, November (2006)
9. Teevan, J., Dumais, S., Horvitz, E.: Personalizing search via automated analysis of interests and activities. In: Proceedings of the 28th Annual International ACM SIGIR Conference on Research and Development in Information Retrieval, SIGIR 2005, pp. 449–456. Salvador, Brazil, August (2005)
10. Liu, F., Yu, C., Meng, W.: Personalized web search for improving retrieval effectiveness. *IEEE Trans. Knowl. Data Eng.* **16**(1), 28–40 (2004)

# Autonomous Computation Offloading Application for Android Phones Using Cloud

Mayank Arora and Mala Kalra

**Abstract** The usage of smartphones has increased hastily over the past few years. The number of smartphones being sold is much more than the number of PC's due to the smartphone's mobile nature and good connectivity. However, they are still constrained by limited processing power, memory, and Battery. In this paper, we propose a framework for making the applications of these smartphones autonomous enough, to offload their compute intensive parts automatically from the smartphone to the virtual image of the smartphones on the cloud, thus using the unlimited resources of the cloud and enhancing the performance of the smartphones. By using this framework the application developers will be able to increase the capabilities of the smartphones making them even more feature rich.

**Keywords** Smartphone · Offloading · Cloud · Android

## 1 Introduction

Cloud can be viewed as a great service which hosts everything, and it may be the data, applications, or any other running programs. A Cloud could be seen as an amorphous collection of computers and servers that could be accessed through the Internet[1–3]. Cloud computing has emerged as the great technology in term of scalability and portability. It has changed our view of carrying data and communication. Cloud services are also very much indulging into mobile networks as most of the smartphones have the capability to support cloud computing environment [4].

---

M. Arora (✉) · M. Kalra  
Computer Science and Engineering Department, NITTTR, Chandigarh, India  
e-mail: mayank.nitttr@gmail.com

M. Kalra  
e-mail: malakalra2004@yahoo.co.in

Smartphones are mobile phones with advanced computing capability, connectivity, and rich set of functionality. In a nutshell, a smartphone combines the functionalities of a phone, personal digital assistant (PDA), and a small computer. With the increasing popularity and a large number of developers developing applications for smartphones, the users of these phones have started using them for high end 3D gaming, to handle their finances, i.e., Internet banking and as their health and wellness managers (e.g., Eat This, Not That application for Android [5]). These new applications could be very resource exhaustive and the phones have a limited memory, computational power, and battery life. That's why it makes good sense to offload the heavy applications to the Virtual Smartphone running on the cloud, thus saving the actual phone's precious resources [6, 7].

A number of techniques have been proposed to offload the applications of smartphones to the cloud [8–14], including complete offloading of the applications as well as partial offloading of the applications. In these techniques used for offloading, the application is partitioned at the binary level and thus making this partitioning transparent for the application developer. But this has its drawbacks, i.e., first, this process is compute intensive. Second, to make changes at the binary level of an application needs changes in the application loader, which is difficult as well as leads to security vulnerabilities. Furthermore, in the proposed techniques an application called the application partitioner or off loader needs to be installed on the smartphone which makes the partitions and offloads the appropriate partition of other applications to the cloud. The application offloader makes the offloading decision for all the applications in the phone weather small or big in terms of computation required and thus become an overhead on the phone's resources. In this paper, we propose a framework for offloading an application partially, i.e., only the compute intensive, non-interactive part of an application is offloaded. The partitioning is done by the application developer at the time of development of the application and the offloading decision is taken by the application itself thus eradicating the need of making changes at the binary level and the need of application partitioner or offloader. These applications will offload their compute intensive part to the cloud autonomously.

The remainder of this paper is organized as follows. In Sect. 2, we describe the motivation behind the proposed architecture. Sections 3 and 4 outline the review of the proposed architectures in the related research and the challenges faced by the offloading techniques proposed. In Sect. 5 we describe the new offloading architecture to cater the challenges discussed in the above sections. Toward the end, we give the details about the working of our framework. In Sect. 6 the benefits of the proposed architecture are discussed and the paper is concluded in Sect. 7.

## 2 Motivation

The applications and features of smartphones are increasing day by day because the usage of these feature-rich phones is increasing. People are replacing their laptops and personal computers with these smartphones, thus the demand for processing and

memory is increasing. These phones use a battery as their power source which has a limited capacity as compared to plug in devices like personal computers.

Some of the major problems faced by the smartphone users are nowadays listed as follows. First, the applications using heavy graphics, memory, or CPU result in a lot of battery drainage. Second, due to the small size of the phones the processing power, memory, and battery are limited and these phones are not able to perform compute intensive tasks which our laptops or desktops could perform. The solution to these problems is either to increase the size of battery, processing power of the CPU and the size of memory which in turn results in increased size, and cost of the phone or to use the resources of the cloud to execute the heavy applications thus saving the phone's scarce resources.

Cloud computing on the other hand provides computing resources (hardware and software) as a service through Internet. We can use the resources such as memory, processing power in a pay per use environment.

The major motivation for this paper is to use the computing resources provided as a service by the cloud to run the resource exhaustive applications of the smartphones connected to the Cloud through Internet. In the past couple of years some techniques have been proposed to partially or completely offload the applications on to the cloud. We will be discussing those techniques in the next section and the challenges faced by the offloading techniques.

### 3 Review of Proposed Architectures in the Related Research

Quite a few approaches have been proposed for offloading applications from a smartphone to the cloud, which includes offloading the complete application, offloading an application partially. Related work in the field of offloading applications from android phones to the cloud have been discussed below [8–14].

In 1998, Alexey Rudenko et al. [8] proposed a scheme to enhance the battery life of a laptop through wireless remote processing of power costly tasks. They proposed that the battery life of a laptop could be increased by shifting the power costly tasks on to a server through wireless connectivity or the Internet. This powerful server will perform the tasks as required and send back the results to the laptop saving the laptop from processing the tasks itself and in the meanwhile the laptop will keep on performing the less power costly tasks. This research gave birth to a new idea of remote processing of power costly tasks of the smartphones using the resources of the cloud.

Year 2009 witnessed the proposal of Augmented Smartphone Applications Through Clone Cloud Execution by Byung-Gon Chun and Petros Maniatis [9]. This research proposed to augment the smartphone's capabilities by offloading an application partially or completely to a clone smartphone. A clone is a virtual system on the cloud running the same operating system as that of the phone using hardware from the cloud's pool of hardware. The application is offloaded partially because only the part of the application which is compute intensive is to be offloaded and thus reducing the load on the smartphone. While the compute intensive part is being

executed by the clone the actual phone executes the remaining application. After the clone is finished with the execution of the compute intensive part of the application it returns the results to the actual phone. The phone processes the results as required and provides the user with the results. The proposed architecture includes a Controller and a Replicator installed in the actual phone and an Augmenter and Replicator installed on the clone. The Replicator synchronizes the changes in the phone software and state to the clone. The controller offloads the application from the smartphone to the clone and merges back the results from the clone to the phone. The Augmenter running in the clone manages the local execution, and returns a result to the actual phone.

Following the vision provided by the above research, Byung-Gon Chun et al. [10] in the year 2011 implemented an architecture named Clone Cloud for offloading an application partially to its clone in the cloud. This scheme uses a partition analyzer which partitions the application to be offloaded for remote execution. The partition analyzer has a static analyzer which discovers the possible migration points and the constraints for migration and a dynamic profiler to build a cost model for execution and migration. The partition analyzer helps the migration unit to migrate and re-integrate the application at the chosen points. The migration unit comprises of a migrator, node manager, and a partition database. The migrator provides the part of application to be migrated to the node manager which migrates the part to the clone and an entry is made to the partition database which helps in re-integrating the partitioned application.

In the year 2011, a new approach of offloading the applications from android smartphone to the cloud was introduced by Eric Y. Chen and Mistutaka Itoh named Virtual Smartphone over IP [11]. In this approach, the complete application was offloaded from the android smartphone to the cloud. In this approach it was proposed to provide cloud computing environment specifically tailored for smartphone users. This architecture allows users of smartphones to create virtual smartphone images in the cloud and install and run their applications in these images remotely. The user can create a number of smartphone images using a dedicated server for each user.

In 2012, Eric Y. Chen et al. [12] introduced a framework for offloading heavy back-end tasks of a standalone android application to an android virtual machine in the cloud, which is an extension of Virtual Smartphone over IP. This architecture uses android interface definition language in order to offload without modifying the source code. This framework incorporates a dedicated server for each client to offload their application [11]. This architecture divides an application into two parts, i.e., GUI and a compute intensive component and it offloads only the compute intensive component to the android virtual machine. This framework comprises of basically three components a helper tool, a service offloader, and a virtual machine. The helper tool has to be integrated to the application code at the time of development by the developer. The service offloader has to be installed to the android phone by downloading it from the application market and each user needs to have at least one dedicated instance of the android virtual machine which is the virtual image of the phone hosted on the cloud. The helper tool generates two copies of the application, i.e., one for local execution and one for remote execution and calls the service offloader which then



analyzes the cost of remote execution and local execution. If the cost of remote execution is less than the cost of local execution then the service is offloaded otherwise it is not offloaded to the virtual android phone.

In 2010, Georgios Portokalidis et al. [13] proposed a new scheme named Paranoid Android to provide security to android phones by applying security checks on remote security servers that host exact replicas of the smartphones in virtual environments. As the remote servers are not constrained with battery or processing power, multiple detection schemes could be applied simultaneously. On the phone, a tracer records all information needed to accurately replay its execution. The recorded execution trace is transmitted to the cloud over an encrypted channel, where a replica of the phone is running on an emulator. On the cloud, a replayer receives the trace and faithfully replays the execution within the emulator.

Another system named MAUI was introduced in 2010 by Eduardo Cuervo et al. [14]. MAUI enables fine-grained energy aware offload of mobile's code to a cloud infrastructure. MAUI uses code portability to create two versions of a smartphone application, one of which runs locally on the smartphone and the other runs remotely in the infrastructure. Managed code enables MAUI to ignore the differences in the instruction set architecture between today's mobile devices (which typically have ARM-based CPUs) and servers (which typically have x86 CPUs). It uses programming reflection combined with type safety to automatically identify the remote able methods and extract only the program state needed by those methods. MAUI profiles each method of an application and uses serialization to determine its network shipping costs (i.e., the size of its state). MAUI combines the network and CPU costs with measurements of the wireless connectivity, such as its bandwidth and latency to construct a linear programming formulation of the code offload problem.

## 4 Challenges

The main problem which is identified in the previous architectures is that offloading a compute intensive application partially can improve the battery life of a smartphone, but the offloading system will incur some overhead on the phone especially if the offloading decision is taken for a large number of applications when only a few number of applications are actually required to be offloaded.

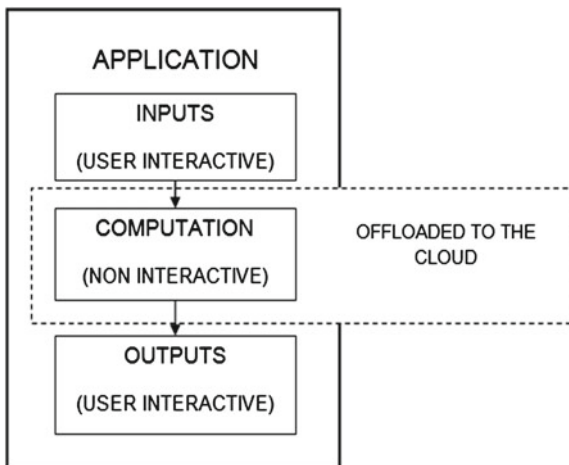
The architectures discussed in the above section need to make changes in the binary of the application at the time of execution, to make it offloadable. To make changes at the binary level, the program loader has to be changed which may result in security vulnerabilities and to analyze the binary of an application could be compute intensive thus imposing overhead on the phone.

## 5 Proposed Architecture

In this paper, we present a framework for automated offloading of compute intensive applications of android smartphones to the virtual image of the smartphone on the cloud. An offloading framework is proposed which if used by the developers of the application, will empower the application to offload its compute intensive, non interactive parts based on static analysis to the smartphone image on the cloud. The static analysis is done to make the decision-making more fast and light than the previous techniques.

This framework proposes to make an application autonomous for offloading itself from the smartphone to the smartphone image on the cloud. An application will be divided into two major parts, i.e., a user interactive part which takes the inputs from the user and provides the output to the user and a compute intensive non interactive part which does the computations as shown in the Fig. 1. This framework will empower the application to offload its compute intensive part to the cloud via Internet after analyzing the cost of offloading over the cost of running the application on the phone itself. The analysis will be done using parameters like input size and internet connectivity. By using this framework the developers will empower the applications to offload themselves without the need of some other application to analyze and offload parts of the application.

The Fig. 2 shows the working of the proposed architecture where the offloading decision is taken by the application itself after analyzing the parameters discussed above. According to the offloading decision the application is partially offloaded to the virtual phone on the cloud. The cloud performs the compute intensive tasks and returns the results to the phone. Thus saving the resources of the phone and increasing the capabilities of the phone.



**Fig. 1** Partitioning of applications into interactive and non-interactive parts

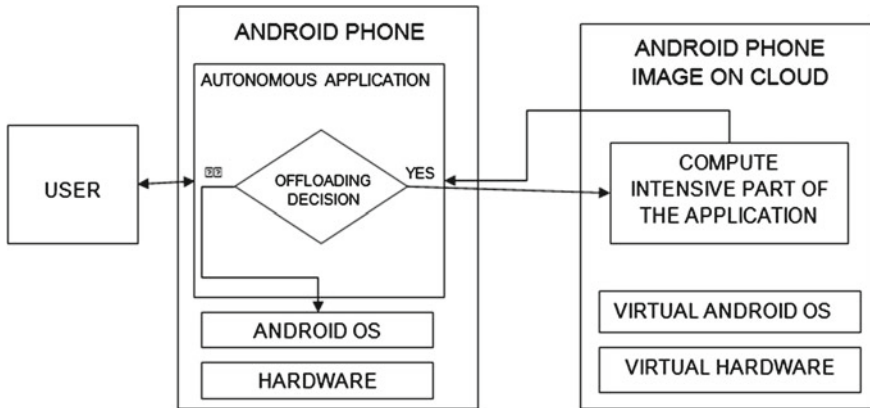


Fig. 2 Framework of autonomous computation offloading application for android phones

### 6 Advantages of the Proposed Architecture

The major advantage of using this framework is that the offloading decision will be taken by the application itself. This decision making will have to be inserted in the source code while writing the applications which is advantageous over the previous approaches in the following ways. First, the approaches discussed earlier modified the applications at binary level using modifications in the loader and thus increasing the security vulnerabilities. Second, they analyzed each application’s binary to offload it, but only a few compute intensive applications need to be offloaded thus causing an overhead on the phone’s resources. By using this technique the offloading decision will be taken only for the compute intensive applications which need to be offloaded and the application developers will not use this offloading framework for small applications. This technique will need to modify the applications at the development stage and will not modify the applications binary thus eradicating the need of changing the application loader.

### 7 Conclusion and Future Work

In this paper, we explored the design of a framework which makes an application autonomous to offload its compute intensive part to the cloud thus saving the resources of the android phone. This framework makes changes in the application at the development time thus eradicating the need to make changes in the application’s binary. The application will make the offloading decision using static analysis.

Our future work includes implementation and evaluation of this design, adding dynamic analysis to support the offloading decision and comparing the performance

of both frameworks using static analysis and the one using dynamic analysis. We are also planning to incorporate security, privacy, and trust related models [15–18], in the proposed framework.

## References

1. Peng, J., Zhang, X., Lei, Z., Zhang, B., Zhang, W., Li, Q.: Comparison of several cloud computing platforms. In: Proceedings of IEEE international conference on Information Science and Engineering, 23–27 (2009)
2. National Institute of Science and Technology.: The NIST definition of cloud computing. <http://csrc.nist.gov/publications/nistpubs/800-145/SP800-145.pdf> (2010)
3. Buyya, R., Broberg, J., Goscinski, A.: Introduction to cloud computing. In: Cloud Computing: Principles and Paradigms. Wiley Press [Online]. 1–44. [http://media.johnwiley.com.au/product\\_data/excerpt/90/04708879/0470887990-180.pdf](http://media.johnwiley.com.au/product_data/excerpt/90/04708879/0470887990-180.pdf) (2009)
4. SONG, W., SU, X.: Review of mobile cloud computing. In IEEE 3rd International Conference on Communication Software and Networks, 1–4 (2011)
5. Health and Wellness - Phone Apps. University of California. <http://wellness.ucr.edu/Wellness%20Apps%20Resources.pdf>
6. Saarinen, A., Siekkinen, M., Xiao, Y., Nurminen, J.K., Kempainen, M., Hui, P. Smartdiet: offloading popular apps to save energy. ACM SIGCOMM Conference, 297–298 (2012)
7. Android Open Source Project. Philosophy and Goals. Google. <http://source.android.com/about/philosophy.html> (2012)
8. Rudenko, A., Reiher, P., Popek, G.J., Kuenning, G.H.: Saving portable computer battery power through remote process execution. In: MCCR'98–ACM SIGMOBILE Mobile Computing and Communications Review Newsletter. Vol. 2, no. 1, 19–26 (1998)
9. Chun, B.G., Maniatis, P.: Augmented smartphone applications through Clone Cloud execution. In: Proceedings of 12th conference on Hot topics in operating systems, 8–8 (2009)
10. Chun, B.G., Ihm, S., Maniatis, P., Naik M., Patti, A.: Clonecloud: elastic execution between mobile device and cloud. In: Proceedings of 6th Conference on Computer Systems, 301–314 (2011)
11. Chen, E.Y., Itoh, M.: Virtual smartphone over IP. In: Proceedings of IEEE international conference on World of Wireless Mobile and Multimedia Networks, 1–6 (2010)
12. Chen, E., Ogata, S., Horikava, K.: Offloading android applications to the cloud. In: Proceedings of IEEE International Conference on Pervasive Computing and Communications Workshops (PERCOM Workshops), 788–793 (2012)
13. Portokalidis, G., Homburg, P., Anagnostakis K., Bos, H.: Paranoid android: versatile protection for smartphones. In: Proceedings of the 26th Annual Computer Security Applications Conference, 347–356 (2010)
14. Cuervo, E., Balasubramanian, A., Cho, D.K., Wolman, A., Saroiu, S., Chandra, R., Bahl, P.: MAUI: Making Smartphones Last Longer with Code Offload. In Proceedings of the 8th international conference on Mobile systems, applications, and services, 49–62 (2010)
15. Singh S., Bawa, S.: A privacy, trust and policy based authorization framework for services in distributed environments. *Inter. J. Comput. Sci.* **2**(1): 85–92 (2007)
16. Singh, S., Bawa, S.: A framework for handling security issues in grid environment using web services security specifications. In: Second International Conference on Semantics, Knowledge and Grid, : SKG'06, Guilin, China **68**(2008), (2006)
17. Singh, G., Singh, S.: A comparative study of privacy mechanisms and a novel privacy mechanism [Short Paper]. In: ICICS'09 Proceedings of the 11th International Conference on Information and Communication Security, Beijing, China. 346–358 (2009)
18. Singh, S.: Trust based authorization framework for grid services. *J. Emerg. Trends Comput. Inf. Sci.* **2**(3): 136–144 (2011)

# Optimizing Battery Utilization and Reducing Time Consumption in Smartphones Exploiting the Power of Cloud Computing

Variza Negi and Mala Kalra

**Abstract** Over the past few years, the usage and boost of handheld devices such as Personal Digital Assistants (PDAs) and smartphones have increased rapidly and estimates show that they will even exceed the number of Personal Computers (PCs) by 2013. Smartphones enable a rich, new, and ubiquitous user experience, but have limited hardware resources on computation and battery. In this paper, the focus has been made on enhancing the capabilities of smartphones by using cloud computing and virtualization techniques to shift the workload from merely a smartphone to a resource-rich computational cloud environment.

**Keywords** Cloud computing · Smartphone · Offloading

## 1 Introduction

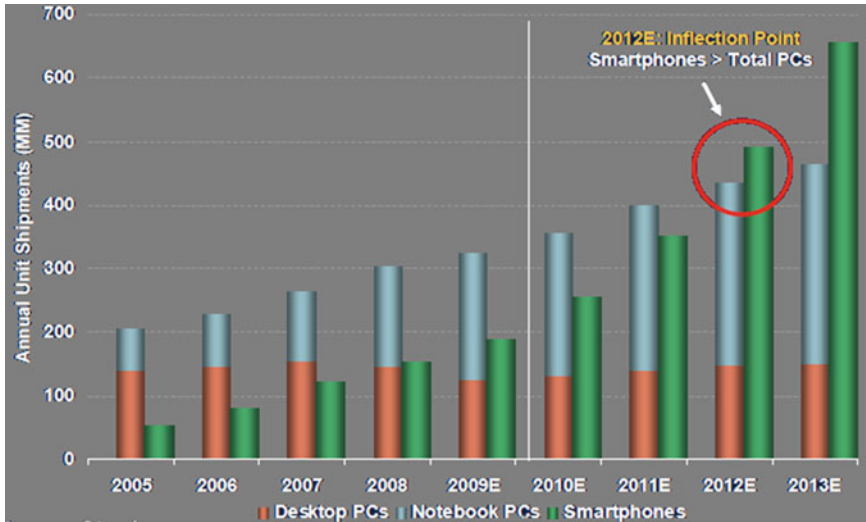
According to Morgan Stanley's Internet Trends Report, as shown in Fig. 1, smartphone is forecasted to be a dominant computing platform [2].

Smartphones have emerged as a type of mobile device providing "all-in-one" convenience by integrating traditional mobile phone functionality and the functionality of handheld computers. Now mobile users look up songs by audio samples; analyze, index, and aggregate their mobile photo collections; play games; capture, edit, and upload video; manage their personal health and wellness and also analyze their finances. Smartphones have every capability of a computer as smartphones are capable of producing great computing and processing output.

---

V. Negi (✉) · M. Kalra  
Computer Science and Engineering Department, NITTTR, Chandigarh, India  
e-mail: variza9@gmail.com

M. Kalra  
e-mail: malakalra2004@yahoo.co.in



**Fig. 1** Global unit shipments of desktop PCs, notebooks, and smartphones, 2005–2013E (estimation) [2]

However, power consumption by these devices is a prime factor when usage of these features comes into play. Power consumption increases dramatically while we are using different features like surfing Internet, watching videos, antivirus scanning, etc. Also the hardware capabilities of smartphones can be compared with or are similar to those of desktop PC’s of the mid-1990, many generations of hardware and software behind (see Table 1 vs. Table 2)

Furthermore, there are many APIs installed in smartphones that tend to consume limited battery resources, which in turn results in short battery life time for smartphones. Cloud computing is a rapidly accelerating revolution within IT and will become the default method of IT delivery moving into the future—organizations

**Table 1** Specifications of a few high-end smartphones

Phone	CPU (GHz)	RAM (MB)	Battery life (web-browsing)
Nokia lumia	1.4	512	4hr,10min
HTC one X	1.5	1024	4hr,18min
Samsung galaxy III	1.4	1024	5hr,17min

**Table 2** Specification of a commodity laptop and a desktop

Computer	CPU (GHz)	RAM (GB)
MAC book pro laptop	2.5, Quad-core	8/16
Origin genesis desktop	4.6, Quad-core	16

would be advised to consider their approach toward beginning a move to the clouds sooner, rather than later [8–10].

Cloud services could provide great means to save this type of power consumption. Much research has been done while considering this vision like Clone including [3–6]. All of the aforesaid papers lay emphasis on the basic idea of maintaining a replica or a mirror image of the smartphone on a Cloud computing infrastructure. With the help of a mirror, we can greatly reduce the workload and virtually expand the resources of the smartphones.

This paper has been organized as follows: The above section has introduced the general background of smartphones and Cloud computing. Also, limitations of smartphones have been pointed out. Next section provides an overlay of the various offloading techniques proposed in the past research studies. In Sect. “Paranoid Android Architecture”, the major concerns and issues related to the offloading in smartphones have been laid down. In Sect. “Augmented Smartphone”, the methodology to be used by in this particular research work has been discussed and finally a framework for migrating a compute-intensive Smartphone Application to the Cloud Computing Environment has been presented as the Proposed Architecture. Section “Clone Cloud Architecture” concludes as well as points out the future scope. Section “Mirroring Smartphone” presents the acknowledgements.

## 2 Related Work

### 2.1 *Paranoid Android Architecture*

Portokalidis et al. proposed Paranoid Android in [3]. This architecture aims at providing security as just another service to a smartphone by offloading security services on to the Cloud. The basic idea is to run a synchronized replica of the smartphone on a security server in a Cloud. As the server does not have the tight resource constraints of a phone, security checks can be performed on the Cloud that otherwise are too expensive to run on the phone itself. To achieve this, a minimal trace of the phone’s execution (enough to permit replaying only) is recorded, which is then transmit to the Cloud-server, where a replica of the phone is running on an emulator. Thus on the Cloud, a replayer receives the trace and faithfully replays its execution within the emulator.

This architecture focuses more on attack detection. The prototype implementation works on the Android platform and is specific to the Android architecture. This architecture can be used to provide offloading by implementing suitable security functions in the Cloud; but always requires an extra overhead of synchronization. This architecture assumes loose synchronization, as it is assumed that the smartphones cannot always be connected to the Internet. Therefore availability is affected, as the security functions in the Cloud are not always available to the smartphones.

## 2.2 *Augmented Smartphone*

Distribution of computation between the smartphones and the Cloud resources in the form of clone Cloud architecture has been suggested by Chun et al. [4]. The concept behind this architecture is to seamlessly offload execution from the smartphone to a cloud infrastructure. Resource intensive processes or portions of processes are performed by the smartphone clone in the Cloud and the results are then merged with the state of the smartphone which resumes execution. This process of splitting the computation between the smartphone and its clone is referred to as “augmentation”. This augmentation of computation is being done in four steps:

1. Creation of a clone of the smartphone in the Cloud;
2. Periodic or on-demand synchronisation of the smartphone and the clone;
3. Applications can be augmented (whole applications or augmented pieces of an application) automatically or upon request; and
4. Results obtained from the augmented segment of computation from the clone are synchronized with the smartphone.

Clone execution architecture for the smartphone aims at transforming a single machine’s execution into a distributed execution. The smartphone and the clone have a replicator which is responsible for synchronizing the clone state with the smartphone (on-demand or periodic) and a controller component on the smartphone that invokes augmented execution in the clone and integrates the results of the computation by the clone with the smartphone.

## 2.3 *Clone Cloud Architecture*

The Clone Cloud architecture presents an effective method for computation offloading from the mobile devices. A prototype implementation of the Clone Cloud is demonstrated in [5]. In the Clone Cloud prototype, an application is partitioned by the use of a static analyzer, dynamic profiler, and an optimization solver. The execution (migration and re-integration) points are defined where the application migrates part of its execution to the Cloud. This takes place at a thread level and when the compute intensive thread completes execution in the Cloud; its results are merged into the state of the smartphone. The other threads can still continue to run on the smartphone. Migration decisions are made based on criteria such as current network characteristics, CPU speed, and energy consumption at the smartphone.

The prototype implementation evaluation proves up to 20x speedup and 20x energy reduction. Again in this technique an extra overhead of synchronization comes into play and the phone has to be always kept synchronized with the clone. Furthermore, the details of how a smartphone and its clone are kept synchronized have not been discussed. Therefore, analysis of how a clone would be created and managed needs to be considered if this architecture is to be adopted.



## 2.4 Mirroring Smartphone

Zhao et al. [6] propose a framework to keep the mirrors of smartphones on a computing infrastructure in a telecommunications network thereby offloading heavy computations to the mirror. The mirror server in the telecommunications network is capable of hosting a large number of virtual machines. Synchronization between the smartphone and the mirror is achieved by replaying all the inputs to the smartphone in the same order at the mirror. Their framework is different from the others in the following two major aspects:

- The Cloud is located in the telecommunication service provider's infrastructure
- A smartphone is connected to its mirror through a 3G network

Modifications to the existing telecommunications network are necessary to enable the forwarding of all the incoming traffic of the smartphone to the mirror server. In this system design, it is considered that the changes in the state of the smartphone are triggered by user or network inputs which produce deterministic outputs. Thus they suggest that synchronisation can be achieved by replaying these inputs in the mirror in the order of their occurrence. Data caching applications and anti-virus scanning are the two services for smartphones that have been identified to benefit from this framework. However, this framework has not been implemented yet. Furthermore, this approach does not consider Wi-Fi and Bluetooth connections and caters only to the Internet connections through 3G.

## 3 Issues

The major problem identified in the above discussed techniques is that, to make a clone of the phone on the Cloud, the entire phone's data is required to be uploaded on to the Cloud which consumes a lot of bandwidth and time.

Second, whenever the phone's data is updated the same changes are required to be made in the clone and thus an extra overhead due to continuous monitoring and synchronization between the smartphone and the Smartphone's image/clone on the Cloud is leveraged on the phone. Also, for this constant synchronization, a smart phone always has to be connected to the Internet service.

In some of the previous researches, the detail of how a Smartphone and its clone are kept synchronized has not been discussed.

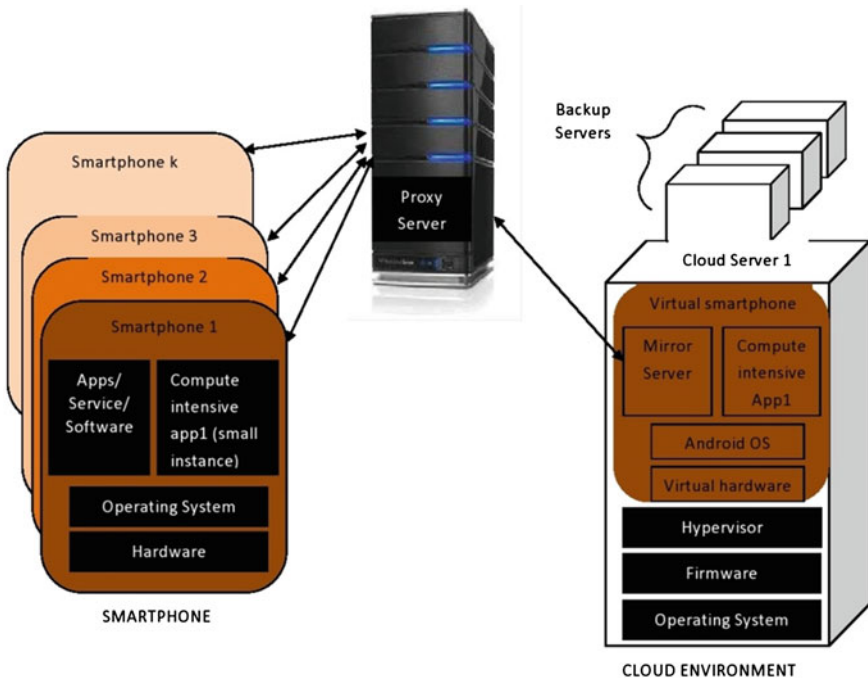
## 4 Proposed Architecture

In this research, all together a new approach has been proposed which focuses on optimizing the battery utilization and reducing the time consumption by the heavy applications in the smartphones, exploiting the power of Cloud computing. This can

be done by completely offloading the compute intensive applications on to the Cloud and thus unleashing the smartphone from doing heavy computational work. Also, there is no need to synchronize the smartphone and the Cloud continuously, which is a major drawback in all the other previously proposed offloading architectures.

CPU and battery consumption measurements will be performed by gadgets available for android in android market. Due to availability of resources, android will be chosen [7]. A compute intensive application in android will be developed. Further, analysis of the time taken and battery utilized by the application on the actual device will be made. These results will be further compared with the results when the application will be uploaded on the Cloud. This off-loading mechanism will benefit in saving battery and demonstrate the concept of API-as-a-service.

Figure 2 illustrates a high-level overview of the proposed system. On the smartphone's side, a small instance module of the actual compute intensive application is deployed within the smartphone's operating system (OS). This small instance collects the smartphone input data, including user keyboard inputs, and transmits them to the mirror server located on the Cloud. The compute intensive application and its workings are designed according to the specification provided by the Service Provider and the manufacturer.



**Fig. 2** Framework for migrating compute intensive smartphone application to the cloud computing environment

On the Cloud environment's side, the mirror server is a powerful application server maintaining one or more VMs. Each VM is a mirror to one of the smartphone. The Mirror Server on the Cloud receives the data from the Smartphone's application instance. The communication can be done using any of the communication techniques; here the communication is shown via Internet. The detailed designs and implementations of the other modules are out of the scope of this paper.

## 5 Conclusion and Future Scope

A detailed analysis of battery and time consumption in a smartphone on running a compute intensive application will be performed, based on measurements of a software tool. It will be shown how the battery drainage varies with increasing computational work. Focus will be on delivering all together a new method in which the whole application has been kept on the Cloud rather than on the phone.

Also the detailed measurements of the same application has been done for the VM running on Cloud, which has depicted lesser execution time and no issues of battery, as the Cloud is always connected to the mains directly. The ultimate aim of this work is to enable a systematic approach for improving power management of mobile devices. Presenting these analysis, future research can be done regarding how the offloading techniques can be made more intelligent and adaptive.

## References

1. Gartner: gartner research report. <http://www.gartner.com/technology/home.jsp> (2011)
2. Stanley: internet trends report (2010)
3. Portokalidis, P.H., Anagnostakis, H.B.: Paranoid android: versatile protection for smartphones, 26th annual computer security applications conference, pp. 347–356 (2010)
4. Chun, P.M: Augmented smartphone applications through clone cloud execution, 12th conference on hot topics in operating systems, pp. 8–8 (2009)
5. Chun, S.I., Manitis, M., Patti: Clonecloud: elastic execution between mobile device and cloud, 6th Conference on computer systems, pp. 301–314 (2011)
6. Zhao, Z.X., Chi, S.Z., Cao.: mirroring smartphones for good: a feasibility study, ZTE, communications (2011)
7. Wikipedia : android (Operating System) [http://en.wikipedia.org/wiki/Android\\_\(operatingsystem\)](http://en.wikipedia.org/wiki/Android_(operatingsystem)) (2012)
8. Kepes: understanding the cloud computing stack SaaS, Paas, IaaS. diversity limited (2011)
9. Sengupta, V.K., Sharma: cloud computing security- trends and research directions, IEEE World Congr Serv, pp. 524–531 (2011)
10. Dillon, C.W., Chang: Cloud computing: issues and challenges, 24th IEEE international conference on advanced information networking and applications, pp. 27–33 (2010)
11. Singh, S.B.: A privacy, trust and policy based authorization framework for services in distributed environments. *Int. J. Comput. Sci.* **2**(1), 85–92 (2007)
12. Singh, S.B.: Design of a framework for handling security issues in grids, international conference on information technology, ICIT'06, pp. 178–179 (2006)

13. Singh, S. B.: A framework for handling security issues in grid environment using web services security specifications, second international conference on semantics, knowledge and grid, 2006, SKG'06, Guilin, China, pp. 68 (2006)
14. Singh, S.B.: A privacy policy framework for grid and web services. *Inform. Technol. J.* (6), pp. 809–817 (2007)

**Part IX**  
**Algorithms and Applications (AA)**

# On Clustering of DNA Sequence of Olfactory Receptors Using Scaled Fuzzy Graph Model

Satya Ranjan Dash, Satchidananda Dehuri, Uma Kant Sahoo  
and Gi Nam Wang

**Abstract** Olfactory perception is the sense of smell that allows an organism to detect chemical in its environment. The first step in odor transduction is mediated by binding odorants to olfactory receptors (ORs) which belong to the heptahelical G-protein-coupled receptor (GPCR) super-family. Mammalian ORs are disposed in clusters on virtually all chromosomes. They are encoded by the largest multigene family (~1000 members) in the genome of mammals and *Caenorhabditis elegans*, whereas *Drosophila* contains only 60 genes. Each OR specifically recognizes a set of odorous molecules that share common molecular features. However, local mutations affect the DNA sequences of these receptors. Hence, to study the changes among affected and non-affected, we use unsupervised learning (clustering). In this paper, a scaled fuzzy graph model for clustering has been used to study the changes before and after the local mutation on DNA sequences of ORs. At the fractional dimensional level, our experimental study confirms its accuracy.

**Keywords** Olfactory receptors · Clustering · Fuzzy graph model · Fractional dimension

---

S. R. Dash (✉) · U. K. Sahoo  
School of Computer Application, KIIT University, Bhubaneswar 751024, India  
e-mail: satyaranjan.dash@gmail.com; sdashfca@kiit.ac.in

U. K. Sahoo  
e-mail: umakant.iitkqp@gmail.com

S. Dehuri  
Department of Systems Engineering, Ajou University, San 5, Woncheon-dong,  
Yeongtong-gu, Suwon 443-749, Republic of Korea  
e-mail: satch@ajou.ac.kr

G. N. Wang  
Department of Industrial Engineering, Ajou University, San 5, Woncheon-dong,  
Yeongtong-gu, Suwon 443-749, Republic of Korea  
e-mail: gnwang@ajou.ac.kr

## 1 Introduction

The olfactory system [13] has the notable capability to discriminate a wide range of odor molecules. In humans, smell is rather considered to be an esthetic sense in contrast to most other species, which rely on olfaction to detect food, predators, and mates. Terrestrial animals, including humans, smell air-borne molecules, whereas aquatic animals smell water-soluble molecules with low volatility, such as amino acids. Humans are thought to have a poor olfactory ability compared with other animals such as dog or rodents, and yet they can perceive a vast number of volatile chemicals. Of the millions of volatile molecular species that have been catalogued by chemists, hundreds of thousands of distinct odors can be detected by the human nose. Odorants, typically small organic molecules of less than 400 Da, can vary in size, shape, functional groups, and charge. They include a set of various alcohols, aliphatic acids, aldehydes, ketones and esters; chemicals with aromatic, alicyclic, polycyclic, or heterocyclic ring structures; and innumerable substituted chemicals of each of these types, as well as combinations of them. However, subtle differences in the structure of an odorant, even between two enantiomers, can lead to pronounced modifications in odor quality. In this paper our special focus is on to study the changes of OR before or after local mutations. Through clustering analysis on DNA sequences of OR this work can detect the changes.

Clustering has been a folklore problem in the area like Bioinformatics, data mining, pattern recognition, image analysis, etc. Clustering techniques used in many applications are either dominated by distance based or connectivity based. A few alike algorithms have been used in [3]. However, the other popular category of clustering based on graph theory approach also igniting many researchers for application in bioinformatics field.

Graph-based clustering is the task of grouping the vertices of the graph into clusters taking into consideration the edge structure of the graph in such a way that there should be many edges within each cluster and relatively few between the clusters.

Recent study [4] shows that the fuzzy graph [1, 3] approach is more powerful in cluster analysis than the usual graph theoretic approach due to its ability to handle the strengths of arcs effectively. Fuzzy graph models can be used to solve various practical issues in clustering analysis, network analysis, information theory, database theory, etc. [7]. Obviously, this relies on the fact that these problems should involve uncertainty to get better results. More about fuzzy graph theory can be obtained in [5, 6].

In this paper we have used the scaled version of fuzzy graph model for clustering of DNA sequences of OR. Based on their fractal dimensions, before or after mutations, we study the difference in the clustering of these receptors. To increase the compatibility of the data, instead of considering a 0–1 scale we considered a 0-max scale.

## 2 Background of the Research

### 2.1 Clustering

A cluster is a set of nodes. Clustering can be considered the most important unsupervised learning problem; so, as every other problem of this kind, it deals with finding a structure in a collection of unlabeled data. Clustering is the task of assigning a set of nodes into groups, so that the nodes in the equivalent cluster are more related to each other than to those in other clusters. Typical cluster models include:

Connectivity models: build models based on distance connectivity.

- Centroid models: symbolize every cluster by a distinct mean vector.
- Distribution models: clusters are modeled using statistic distributions.
- Density models: defines clusters as associated broad regions in the data space.
- Subspace models: clusters are modeled with both cluster members and relevant attributes.
- Group models: some algorithms do not offer a superior model for their results and just provide the combination in sequence.
- Graph-based models: a subset of nodes in graph such that every two nodes in the subset are connected by an edge can be considered as a prototypical form of cluster.

Clustering's can be roughly distinguished in hard clustering where each object belongs to a cluster or not and soft clustering where each object belongs to each cluster to a certain degree. When a clustering outcome is evaluated based on the records that was clustered itself, this is called internal evaluation. These methods usually assign the best score to the algorithm that produces clusters with high comparison within a cluster and low similarity between clusters. For more information reader may refer [8].

### 2.2 Fuzzy Graph Model

Fuzzy graph theory is interplay between graph theory and theory of fuzzy sets introduced by Zadeh [2]. Rosenfeld, in his paper Fuzzy Graphs, presented the basic structural and connectivity concepts, while Yeh and Bang introduced different connectivity parameters of a fuzzy graph and discussed their applications in the paper titled Fuzzy relations, Fuzzy graphs, and their applications to clustering analysis.

A graph is a pair  $G = (V, E)$  of sets such that  $E$  is a subset of  $V^2$ , thus, the elements of  $E$  are 2-elements subsets of  $V$ . If we associate weights  $w$  to each of the edges  $e_i$ , we get a weighted graph. A fuzzy graph is a pair of functions  $G(\sigma, \mu)$  where  $\sigma$  is a fuzzy subset of  $V$  and  $\mu$  is a symmetric fuzzy relation on  $\sigma$ . This has been studied in [4–6] (Figs. 1 and 2).



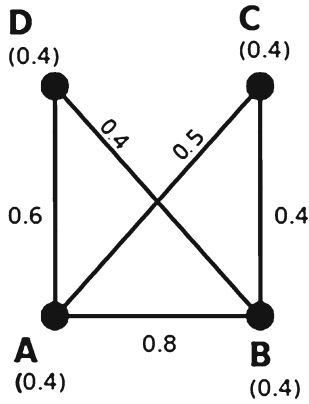


Fig. 1 Fuzzy Graph

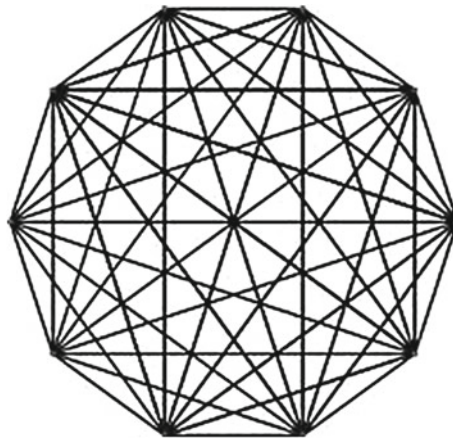


Fig. 2 Fuzzy graph of the Protein Sequence

What  $\sigma$  does is assign a number between 0 and 1 to each node and  $\mu$  assigns a number between 0 and 1 to each edge present in the fuzzy graph. The following diagram shows a fuzzy graph on 4 vertices and 5 edges with their respective  $\sigma$  and  $\mu$  values.

Fuzzy graph theory has numerous applications in various fields like clustering analysis, database theory, network analysis, information theory, etc. [7]. Research on this has witnessed an exponential growth in mathematics and its applications, since it fosters the possibility of interdisciplinary research.

### 2.3 Fractional Dimension

In topological geometry, we have dimension of a point, line, plane, and space as 0, 1, 2, and 3 respectively. This is called the topological dimension. Formally, we call an object as  $n$ -dimensional if it can be represented by  $n$  independent variables. When we deal with more than one objects grouped together, the dimension of such a collection is the maximum of dimensions of the individual objects. However if this collection is infinite, the dimension grows.

Topological dimensions take care of the issues with dimensionality of regular objects. Nevertheless, this cannot be used to describe the dimensionality of fractals. For example the Koch snowflake has a topological dimension of 1 but is no way just a curve. Also it is not a (part of) plane, hence should not have a dimension of 2. In a way, it seems that it is too big to have a dimension of 1 and small to have a dimension of 2. So, a number between 1 and 2 would be an appropriate indicator of its dimensionality. The formulation of the above idea was the inception of the concept of fractal dimension.

## 3 Dataset and Preprocessing

We collect the DNA sequences and protein sequences of various Olfactory receptors from the ORDB [9]. Then, we mutated the DNA sequences and converted it into protein sequences using a translator [10]. Now we processed the before and after protein sequences through the protein structure analysis of the Bioinformatics toolbox of MATLAB. Then we processed the obtained graphics files in BENOIT [11], a fractal analysis software. The resultant was a set of fractal dimensions of the various properties of the protein sequence.

## 4 Our Work

In the initial phase of this work we have prepared the data for cluster analysis. From the prepared dataset we collected the fractional dimensions of 10 OR DNA sequences. We selected the fractal dimensions of the nine properties of each of the proteins. Now each protein is represented by a vector ( $v_i$ ) with nine parameters.

$$v_i = (fd_1, fd_2, fd_3, fd_4, fd_5, fd_6, fd_7, fd_8, fd_9)$$

We now use the Euclidean transformation  $E: \mathbb{R}^9 \rightarrow \mathbb{R}$  to represent each protein vector  $v_i$  where,

$$E(v_i) = \text{length of the vector } v_i = \text{rms}[v_i]$$

This is done for each protein sequence before and after mutation. Now each protein sequence has two representative fractal dimensions, one before and one after the mutation. So now we have two representative fractal dimensions of each protein sequence. We then separated the before and after data. We applied the following techniques to both datasets.

First we formed a 10\*10 matrix  $A$ , such that  $A[i, j] = 10000 (fd_i - fd_j)$  where  $fd_i$  is the representative fractal dimension of  $v_i$ . The number 10,000 was multiplied to scale the small numbers  $(fd_i - fd_j)$  to a perceivable scale. We then found out the cohesive matrix  $matB$  from the matrix  $A$ . Note that the elements of  $A$  are not fuzzy parameters, but we use the same techniques to find  $matB$ , since scalability has no effect on relative clustering. We then found the  $\alpha$ -cut matrix. We store this  $\alpha$ -cut matrix as  $cut\ matB(\alpha)$

matrixBefore=

0	0.244396	0.455526	0.788137	1.22191	1.967	1.84422	2.49999	2.7113	4.04374
0.244396	0	0.21113	1.03253	1.46631	1.7226	2.08862	2.25559	2.4669	4.28814
0.455526	0.21113	0	1.24366	1.67744	1.51147	2.29975	2.04446	2.25577	4.49927
0.788137	1.03253	1.24366	0	0.433773	2.75514	1.05609	3.28812	3.49944	3.25561
1.22191	1.46631	1.67744	0.433773	0	3.18891	0.622312	3.7219	3.93321	2.82183
1.967	1.7226	1.51147	2.75514	3.18891	0	3.8112	0.532986	0.744302	6.01074
1.84422	2.08862	2.29975	1.05609	0.622312	3.81122	0	4.34421	4.55552	2.19952
2.49999	2.25559	2.04446	3.28812	3.7219	0.532986	4.34421	0	0.211315	6.54373
2.7113	2.4669	2.25577	3.49944	3.93321	0.744302	4.55552	0.211315	0	6.75504
4.04374	4.28814	4.49927	3.25561	2.82183	6.01074	2.19952	6.54373	6.75504	0

Similar technique is applied to the data obtained from after the mutation.

matrixAfter=

0	2.76695	3.19985	4.04418	3.4556	3.62222	4.49996	1.5668	1.77779	1.95573
2.76695	0	0.432901	1.27724	0.68865	0.855271	1.73301	1.20015	0.989153	0.81122
3.19985	0.432901	0	0.844335	0.255749	0.42237	1.30011	1.63305	1.42205	1.24412
4.04418	1.27724	0.844335	0	0.588586	0.421965	0.455776	2.47739	2.26639	2.08846
3.4556	0.68865	0.255749	0.588586	0	0.166621	1.04436	1.8888	1.6778	1.49987
3.62222	0.855271	0.42237	0.421965	0.166621	0	0.877741	2.05542	1.84442	1.66649
4.49996	1.73301	1.30011	0.455776	1.04436	0.877741	0	2.93316	2.72217	2.54423
1.5668	1.20015	1.63305	2.47739	1.8888	2.05542	2.93316	0	0.210997	0.38893
1.77779	0.989153	1.42205	2.26639	1.6778	1.84442	2.72217	0.210997	0	0.177934
1.95573	0.81122	1.24412	2.08846	1.49987	1.66649	2.54423	0.38893	0.177934	0

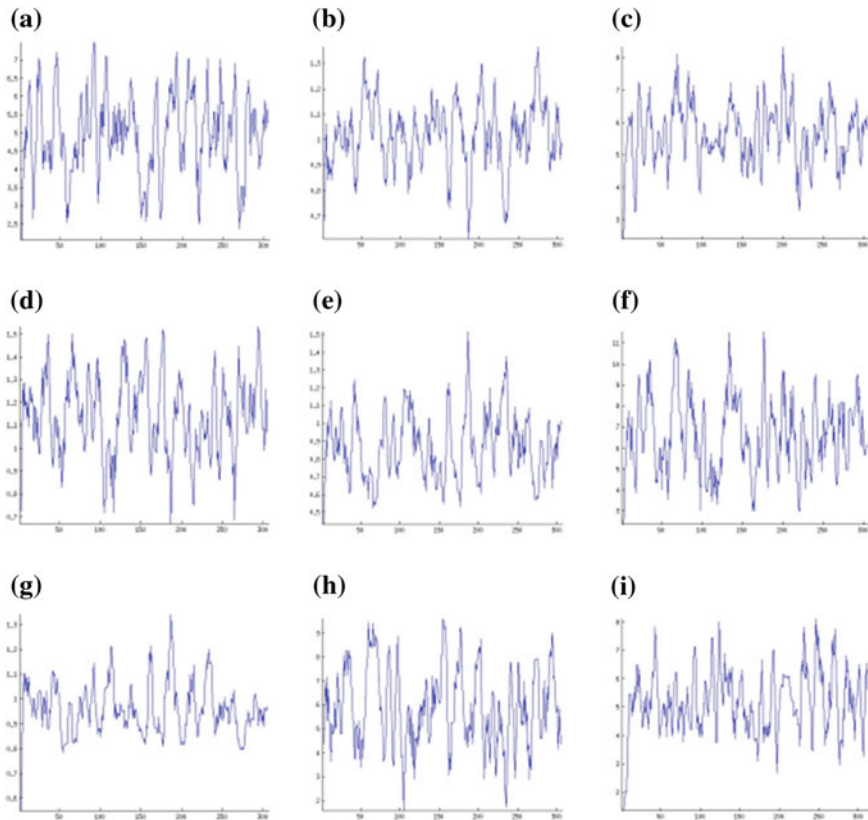
## 5 Simulation Results

In our simulation studies by varying the value of alpha, we found out the alpha cut matrix and then corresponding clusters. For  $\alpha = 4$ , we found that before mutation

the clusters were (1), (2), (3), (4), (5) and (6,7,8,9,10), whereas after clustering it turned out to be (1), (2), (3), (4), (5), (6), (7), (8), (9), and (10). The fuzzy clusters of all levels are summarized in Table 1 (for  $\alpha = 1$  to 7).

**Table 1** Clustering results for various  $\alpha$  cuts

$\alpha$ cut	Clustering before Mutation	Clustering after Mutation
1	(1, 2, 3, 4, 5, 6, 7, 8, 9, 10)	(1, 2, 3, 4, 5, 6, 7, 8, 9, 10)
2	(1, 2, 3, 4, 5, 6, 7, 8, 9, 10)	(1, 2, 3, 4, 5, 6, 7, 8, 9, 10)
3	(1, 2, 3, 4, 5, 6, 7, 8, 9, 10)	(3, 4, 5, 6, 7),(1),(2),(8),(9),(10)
4	(1, 2, 3, 6, 7, 8, 9, 10),(4),(5)	(4, 7),(1),(2),(3),(5),(6),(8),(9),(10)
5	(6, 7, 8, 9, 10),(1),(2),(3),(4),(5)	(1), (2), (3), (4), (5), (6), (7), (8), (9), (10)
6	(6, 7, 8, 9, 10), (1), (2), (3), (4), (5)	(1), (2), (3), (4), (5), (6), (7), (8), (9), (10)
7	(1), (2), (3), (4), (5), (6), (7), (8), (9), (10)	(1), (2), (3), (4), (5), (6), (7), (8), (9), (10)



**Fig. 3** Protein plot of an amino acid sequence properties (before mutation)

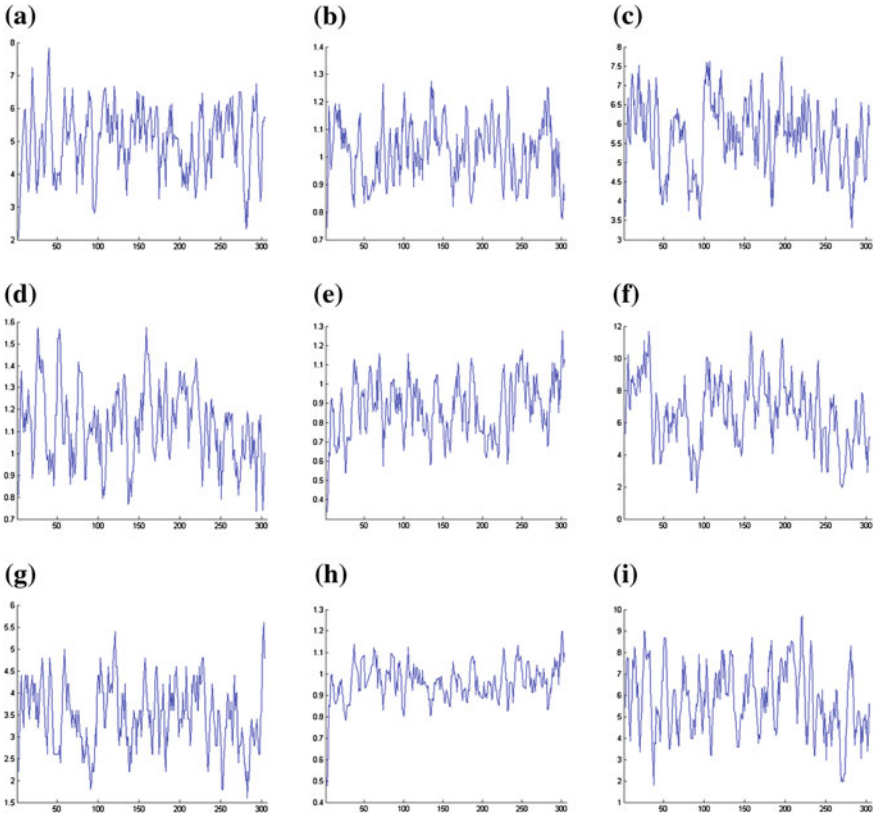


Fig. 4 Protein plot of an amino acid sequence properties (after mutation)

CutMatB (4) =

$$\begin{pmatrix} 0 & 0 & 0 & 0 & 0 & 0 & 0 & 0 & 0 & 0 \\ 0 & 0 & 0 & 0 & 0 & 0 & 0 & 0 & 0 & 0 \\ 0 & 0 & 0 & 0 & 0 & 0 & 0 & 0 & 0 & 0 \\ 0 & 0 & 0 & 0 & 0 & 0 & 0 & 0 & 0 & 0 \\ 0 & 0 & 0 & 0 & 0 & 0 & 0 & 0 & 0 & 0 \\ 0 & 0 & 0 & 0 & 0 & 1 & 1 & 1 & 1 & 1 \\ 0 & 0 & 0 & 0 & 1 & 0 & 1 & 1 & 1 & 1 \\ 0 & 0 & 0 & 0 & 1 & 1 & 0 & 1 & 1 & 1 \\ 0 & 0 & 0 & 0 & 1 & 1 & 1 & 0 & 1 & 1 \\ 0 & 0 & 0 & 0 & 1 & 1 & 1 & 1 & 0 & 1 \end{pmatrix}$$

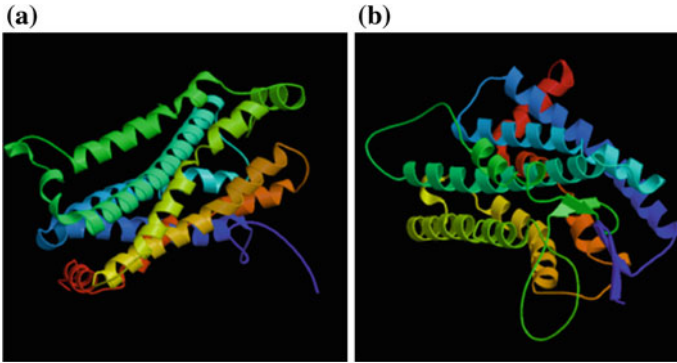


Fig. 5 3D Protein structure of an amino acid before and after mutation

CutMatA (4) =

$$\begin{pmatrix} 0 & 0 & 0 & 0 & 0 & 0 & 0 & 0 & 0 & 0 & 0 & 0 \\ 0 & 0 & 0 & 0 & 0 & 0 & 0 & 0 & 0 & 0 & 0 & 0 \\ 0 & 0 & 0 & 0 & 0 & 0 & 0 & 0 & 0 & 0 & 0 & 0 \\ 0 & 0 & 0 & 0 & 0 & 0 & 0 & 0 & 0 & 0 & 0 & 0 \\ 0 & 0 & 0 & 0 & 0 & 0 & 0 & 0 & 0 & 0 & 0 & 0 \\ 0 & 0 & 0 & 0 & 0 & 0 & 0 & 0 & 0 & 0 & 0 & 0 \\ 0 & 0 & 0 & 0 & 0 & 0 & 0 & 0 & 0 & 0 & 0 & 0 \\ 0 & 0 & 0 & 0 & 0 & 0 & 0 & 0 & 0 & 0 & 0 & 0 \\ 0 & 0 & 0 & 0 & 0 & 0 & 0 & 0 & 0 & 0 & 0 & 0 \\ 0 & 0 & 0 & 0 & 0 & 0 & 0 & 0 & 0 & 0 & 0 & 0 \\ 0 & 0 & 0 & 0 & 0 & 0 & 0 & 0 & 0 & 0 & 0 & 0 \end{pmatrix}$$

Figures 3 and 4 shows the difference in the fractal dimensions of the amino acid sequence properties. Figure 5 illustrates the structural changes of before and after local mutation of the Olfactory Receptors.

### 6 Conclusion

As a result of intensive interdisciplinary research to characterize the mechanisms underlying olfaction, the understanding of sensory systems has impressively grown in recent years. Without loss of generality the study of the changes of ORs before and after local mutation through fuzzy graph model, our simulation result confirms that a local mutation in the DNA sequence of olfactory receptors brings in a huge difference in their clustering. It is also evident from Figure 5 that there has been a change in the structure of the mutated protein.

## References

1. Rosenfeld, A.: Fuzzy graphs. In: Zadeh, L.A., Fu, K.S., Shimura, M. (eds.), *Fuzzy Sets and Their Applications to Cognitive and Decision Processes*, Academic Press, New York, pp. 77–95(1975).
2. Zadeh, L.A.: Fuzzy sets. *Inform. Control* **8**, 338–353 (1965)
3. Yeh R.T., Bang S.Y., Fuzzy relations, Fuzzy relations, fuzzy graphs and their applications to clustering analysis. In: Zadeh L.A., Fu K.S., Shimura M. (eds.), *Fuzzy Sets and Their Applications*, Academic Press, pp. 125–149(1975).
4. Mathew, S., Sunitha, M.S.: Node connectivity and arc connectivity of a fuzzy graph. *Inform. Sci.* **180**, 519–531 (2010)
5. Bhattacharya, P.: Some remarks on fuzzy graphs. *Pattern Recogn. Lett.* **6**, 297–302 (1987)
6. Bhattacharya, P., Suraweera, F.: An algorithm to compute the maxmin powers and a property of fuzzy graphs. *Pattern Recogn. Lett.* **12**, 413–420 (1991)
7. Mordeson, J.N.: Nair. *Fuzzy graphs and fuzzy hypergraphs*. Physica-Verlag, P.S. (2000)
8. Diday, E., Simon, J.C.: Clustering analysis. In: Fu, K.S. (ed.) *Digital Pattern Recognition*, pp. 47–94. NJ, Springer-Verlag, Secaucus (1976)
9. Olfactory Receptors Database. <http://senselab.med.yale.edu/ordb/>
10. DNA to protein translation. <http://insilico.ehu.es/translate/>
11. BENOIT. <http://www.trusoft-international.com/>
12. Protein Structure Prediction Server. <http://ps2.life.nctu.edu.tw/index.php>
13. Gaillard, I., Rauquier, S., Giorgi, D.: Olfactory Receptors. *ICMLS Cell. Mol. Life Sci.* **61**, 456–469 (2004)

# Linear Hopfield Based Optimization for Combined Economic Emission Load Dispatch Problem

J. P. Sharma and H. R. Kamath

**Abstract** In this paper a linear Hopfield model is used to solve the problem of combined economic emission dispatch (CEED). The objective function of CEED problem comprises of power mismatch, total fuel cost and total emission subjected to equality/inequality constraints. In proposed methodology, inclusion of power mismatch in objective function exhibits the ability of attaining power mismatch to any desirable extent and may be employed for large-scale highly constrained nonlinear and complex systems. A systematic procedure for the selection of weighting factor adopted. The proposed method employs a linear input-output model for neurons. The efficacy and viability of the proposed method is tested on three test systems and results are compared with those obtained using other methods. It is observed that the proposed algorithm is accurate, simple, efficient, and fast.

**Keywords** Economic dispatch · Emission · Power mismatch · Modified price penalty factor · Linear hopfield model

## 1 Introduction

Emissions produced by fossil-fueled electric power plants release many contaminants like sulfur oxides ( $\text{SO}_2$ ) and oxides of nitrogen ( $\text{NO}_x$ ) and directly effects on human beings, plants and animals etc. In recent years, due to strict environmental regulations, emission control has become one of the important operational objectives of power systems and as result of it thermal power plants cannot only be run at

---

J. P. Sharma (✉)

The Electrical Engineering, Department of JK, LakshmiPat University, Jaipur, India  
e-mail: jpsharma.cseb@gmail.com

H. R. Kamath

The Malwa Institute of Technology, Indore, India  
e-mail: rskamath272@gmail.com



absolute minimum fuel cost criterion. So, it become evitable to consider total fuel cost (operating cost) and total pollutant emission as objective function in power system optimization problems. In power system optimization problems, emissions can be considered either in the objective function or treated them as additional constraints, which is called combined economic emission load dispatch (CEED) and reliable and useful planning for power system optimization. The main aim of the combined economic emission load dispatch (CEED) problem is to find an optimal combination of the output power of all the online generating units that simultaneously minimizes both fuel cost and pollutant emissions, while satisfying unit constraints, equality and inequality constraints. The recent literature shows that many mathematical and different heuristic techniques such as Particle Swarm Optimization (PSO), Hopfield Neural Network, Ant Colony Optimization (ACO), Artificial Bee Colony (ABC), Genetic Algorithm (GA) and Differential Evolution (DE) gives solution very easily in terms of machine usage and time of computation etc. In this paper, objective function of CEED problem consists of three terms, power mismatch, total fuel cost and total emission cost. Each term is multiplied by a weighting factor, which represents the relative importance of that term. These weighting factors are named as A, B and C respectively. A systematic procedure for evaluating the value of weighting factors, associated with the various terms of the energy function is developed. This work focuses on emission of nitrogen oxides ( $\text{NO}_x$ ) only, because its control is a significant issue at the global level. The suitability of hopfield neural network [1] for a CEED problem is investigated and a linear function for neuron's input-output characteristics is proposed to reduce computational requirement. Because sigmoidal function for neuron's input-output characteristics utilizes the iterative procedures to solve the optimization problem gives large amount of computational requirement. The proposed method is applied to a three [2, 3] and six [3] generating unit system and the results obtained are compared with those obtained using Hybrid Cultural Algorithm [2], Genetic Algorithm [2], PSO [2], ABC [3], Conventional Method [3], Hybrid Genetic Algorithm [3], Hybrid GTA [3] and Simulated Annealing Algorithm [4]. The computational results reveal that Proposed Hopfield Method is simple, accurate, efficient and straightforward.

## 2 Multi-Objectives Combined Economic Emission Dispatch

### 2.1 Economic Objective

$$F_1 = \sum_{i=1}^n (a_i + b_i P_i + c_i P_i^2) \quad (1)$$

### 2.2 Environmental Objective

$$F_2 = \sum_{i=1}^n (\alpha_i + \beta_i P_i + \gamma_i P_i^2) \tag{2}$$

### 2.3 Problem Formulation

In this paper CEED problem is the combination of three single objective functions like power mismatch, total fuel cost and emission level and it is formulated as to minimize  $f(P_m, F_1, F_2)$  subject to the equality and inequality constraints.

$$E = \frac{A}{2} \left[ (P_D + P_L) - \sum_i^n P_i \right]^2 + \frac{B}{2} \left[ \sum_{i=1}^n (a_i + b_i P_i + c_i P_i^2) \right] + \frac{C}{2} \left[ \sum_{i=1}^n (\alpha_i + \beta_i P_i + \gamma_i P_i^2) \right]$$

$$E = \frac{A}{2} P_m^2 + \frac{B}{2} F_1 + \frac{C}{2} F_2 \tag{3}$$

#### 2.3.1 Equality Constraints

$$P_m = P_D + P_L - \sum_{i=1}^n P_i \tag{4}$$

where

$$P_L = \sum_{i=1}^n \sum_{j=1}^n P_i B_{ij} P_j \tag{5}$$

#### 2.3.2 Equality Constraints

$$P_{i \min} \leq P_i \leq P_{i \max} \tag{6}$$

The value of weighting factor ‘C’ is equal to modified price penalty factor (*h*). In this paper a modified price penalty factor [5, 6] is used for the particular load demand and calculated by following equation

$$Z = h_{i1} + \frac{(h_{i2} - h_{i1})}{(p_{\max 2} - p_{\max 1})} * (P_D - P_{\max 1}) \tag{7}$$

In this paper weighting factor ‘A’ is calculated using Eq. 21 by varying *B* from 0.4 to 1.25 along with calculated value of weighting factor ‘C’ by Eq. 7 at a particular load demand.

### 2.4 Mapping of CEED Problem on to Hopfield Model

In this paper, continuous Hopfield Neural Network is considered and dynamic characteristic of each neuron is described by the following equation [1].

$$\frac{dU_i}{dt} = \sum_j^n T_{ij} V_j + I_i \tag{8}$$

The energy function of continuous Hopfield model [1] is defined as

$$E = \left(-\frac{1}{2}\right) \sum_{i=1}^n \sum_{j=1}^n T_{ij} V_i V_j - \sum_{i=1}^n I_i V_i \tag{9}$$

By comparing Eq. 3 with Eq. 9, parameters for neurons in terms of weighting factors for aforesaid objective function are defined as follows

$$T_{ii} = -A - Bc_i - C\gamma_i \tag{10}$$

$$T_{ij} = -A \tag{11}$$

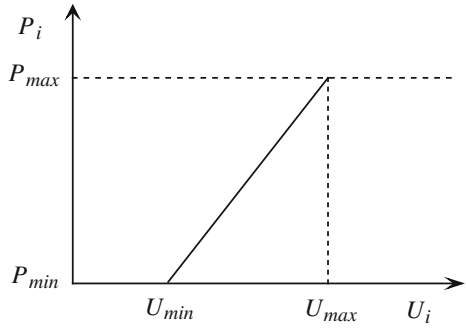
$$I_i = A (P_D + P_L) - \frac{B}{2} b_i - \frac{C}{2} \beta_i \tag{12}$$

### 2.5 Proposed Linear Hopfield Model

The neuron model chosen is a linear input output model as shown in Fig. 1, instead of conventional sigmoid model.

$$P_i = K_{1i} U_i + K_{2i} \forall U_{\min} \leq U_i \leq U_{\max} \tag{13}$$

**Fig. 1** The linear input-output function



where

$$K_{1i} = \frac{(P_i \max - P_i \min)}{(U_{\max} - U_{\min})} \tag{14}$$

$$K_{2i} = -K_{1i}U_{\min} + P_i \min$$

### 2.6 Computational Expressions for CEED Problem

The dynamic equation [1] of a neuron is

$$\frac{dU_i}{dt} = \sum_j^n T_{ij} P_j + I_i \tag{15}$$

After substituting different parameter from Eqs. 10, 11 and 12 in Eq. 15, dynamic equation of a neuron is as follows

$$\frac{dU_i}{dt} = AP_m - \frac{B}{2} \left( \frac{dF_1}{dP_i} \right) - \frac{C}{2} \left( \frac{dF_2}{dP_i} \right) \tag{16}$$

putting values from Eqs. 1, 2 and 13 in to Eq. 16, the dynamic Eq. 16 becomes

$$\begin{aligned} \frac{dU_i}{dt} &= AP_m - \frac{B}{2} [b_i + 2c_i (K_{1i}U_i + K_{2i})] - \frac{C}{2} [\beta_i + 2\gamma_i (K_{1i}U_i + K_{2i})] \tag{17} \\ &= K_{4i} + K_{3i}U_i \end{aligned}$$

where

$$K_{3i} = -K_{1i} (Bc_i + C\gamma_i) = -(Bc_i + C\gamma_i) \frac{(P_{i \max} - P_{i \min})}{(U_{\max} - U_{\min})}$$

$$K_{4i} = AP_m - \frac{B}{2}b_i - Bc_i K_{2i} - \frac{C}{2}\beta_i - C\gamma_i K_{2i}$$

Neurons input function  $U_i$  is obtained by solving Eq. 17 as follows

$$U_i = \left[ U_i^0 + K_{4i} \div K_{3i} \right] e^{K_{3i}t} - [K_{4i} \div K_{3i}] \tag{18}$$

By putting neurons input function  $U_i$  in Eq. 13, the neuron’s output function

$$P_i = \left[ \left[ K_{1i} U_i^0 + K_{2i} \right] - \left( \frac{2K_{AB} P_m - b_i - K_{CB} \beta_i}{2c_i + 2K_{CB} \gamma_i} \right) \right] e^{K_{3i}t}$$

$$+ \left( \frac{2K_{AB} P_m - b_i - K_{CB} \beta_i}{2c_i + 2K_{CB} \gamma_i} \right) \tag{19}$$

where  $K_{AB} = \frac{A}{B}$  and  $K_{CB} = \frac{C}{B}$

At  $t = \infty$  the steady state value of Eq. 19 give optimum power generation

$$P_i^* = \left( \frac{2K_{AB} P_m - b_i - K_{CB} \beta_i}{2c_i + 2K_{CB} \gamma_i} \right) \tag{20}$$

Optimum power generation does not depend on  $P_i^0$  and  $(U_{\max} - U_{\min})$ , which is reasonable and comprehensible. From Eqs. 13, 20 and 19, a more simple formula for  $K_{AB}$  can be written as

$$K_{AB} = \frac{\left[ (P_D + P_L) + \frac{1}{2} \sum_{i=1}^n \left\{ \frac{(b_i + K_{CB} \beta_i)}{(c_i + K_{CB} \gamma_i)} \right\} \right]}{\left[ P_m \sum_{i=1}^n \left\{ \frac{1}{(c_i + K_{CB} \gamma_i)} \right\} \right]} \tag{21}$$

### 3 Simulation Results

The applicability and validity of the proposed algorithm has been tested on three different test systems (test system-I [2], test system-II [3] and test system-II [3]) and results are presented in Tables 1, 2, 3, 4, 5, and 6.

**Table 1** Best compromise solution by proposed method for combined economic emission dispatch (CEED)-test system-I

Particulars	$P_D = 650\text{MW}$	$P_D = 700\text{MW}$	$P_D = 750\text{MW}$
Power mismatch factor (A)	458488.7621	469375.5820	477456.8377
Fuel cost factor (B)	0.60	0.56	0.52
Price plenty factor (h)	35.1840	33.7478	32.3117
$P_1$ (MW)	168.0304	181.4098	194.8724
$P_2$ (MW)	251.3413	271.1990	291.1563
$P_3$ (MW)	250.6923	270.7759	290.9497
Fuel cost (Rs/hr)	32885.40	35461.14	38094.31
Emission level (Kg/hr)	551.34	651.66	762.36
Total cost (Rs/hr)	52283.84	57453.20	62727.49
Power loss (MW)	20.0640	23.3848	26.9784
Total generation (MW)	670.0640	723.3847	776.9784
Escape time (sec)	0.842	0.606	0.66

**Table 2** Comparison of combined economic emission dispatch (CEED) results for test system-I

$P_D$	Performance	Hybrid CA [2]	Proposed method
650 MW	$P_1$ (MW)	157.5395	168.0304
	$P_2$ (MW)	248.7636	251.3413
	$P_3$ (MW)	264.0454	250.6923
	Fuel cost (Rs/hr)	32876.00	32885.40
	Emission level (Kg/hr)	553.9684	551.34
	Power loss (MW)	20.2448	20.0640
	Total generation (MW)	670.3485	670.0640
700 MW	$P_1$ (MW)	182.7369	181.4098
	$P_2$ (MW)	276.0215	271.1990
	$P_3$ (MW)	264.6389	270.7759
	Fuel cost (Rs/hr)	35466.00	35461.14
	Emission level (Kg/hr)	651.9255	651.66
	Power loss (MW)	23.3498	23.3848
	Total generation (MW)	723.5368	723.3847
750 MW	$P_1$ (MW)	192.8946	194.8724
	$P_2$ (MW)	292.1908	291.1563
	$P_3$ (MW)	291.9240	290.9497
	Fuel cost (Rs/hr)	38089.00	38094.31
	Emission level (Kg/hr)	762.5753	762.36
	Power loss (MW)	27.0066	26.9784
	Total generation (MW)	777.4081	776.9784

**Table 3** Comparison of results by different methods for combined economic emission dispatch (CEED) with a demand of 650 MW for test system-I

Performance	Hybrid CA [2]	GA [2]	PSO [2]	Proposed method
Fuel cost (Rs/hr)	32876.00	32888.6	32888.0	32885.40
Emission level (Kg/hr)	553.9684	551.299	551.274	551.34
Power loss (MW)	20.2448	20.0477	20.0466	20.0640

**Table 4** Comparison of combined economic emission dispatch (CEED) results for test system-II

$P_D$	Performance	Conventional [4]	SGA [4]	RGA [4]	SA [4]	ABC [3]	Proposed method
400 MW	Fuel cost (Rs/hr)	20898.83	20801.94	20801.81	20838	20838	20835.53
	Emission level (Kg/hr)	201.50	201.35	201.21	200.22	200.2211	200.27
	Total cost (Rs/hr)	29922	29820	29812	29804.17	29804.2	27024.07
	Power loss (MW)	7.41	7.69	7.39	7.41	7.5681	7.4085
	Escape time (sec)	–	–	–	4.945824	1.895377	1.17
500 MW	Fuel cost (Rs/hr)	25486.64	25474.56	25491.64	25495	25495	25484.50
	Emission level (Kg/hr)	312.00	311.89	311.33	311.16	311.1553	311.55
	Total cost (Rs/hr)	39458	39441	39433	39428.25	39428.3	30014.49
	Power loss (MW)	11.88	11.80	11.70	11.69	11.6937	11.7140
	Escape time (sec)	–	–	–	5.808751	2.340603	0.651
700 MW	Fuel cost (Rs/hr)	35485.05	35478.44	35471.48	35464	35464	35459.54
	Emission level (Kg/hr)	652.55	652.04	651.60	651.58	651.5775	651.59
	Total cost (Rs/hr)	66690	66659	66631	66622.52	66622.52	57450.21
	Power loss (MW)	23.37	23.29	23.28	23.37	23.3664	23.3485
	Escape time (sec)	–	–	–	5.174793	3.770030	0.639

**Table 5** Best compromise solution by proposed method for combined economic emission dispatch (CEED)-test system-II

Particulars	$P_D = 400\text{ MW}$	$P_D = 500\text{ MW}$	$P_D = 700\text{ MW}$
Power mismatch factor (A)	318544.5134	265374.9454	466933.7337
Fuel cost factor (B)	0.83	0.77	0.55
Price plenty factor (h)	30.9003	14.54038	33.7494
$P_1$ (MW)	101.4039	124.4383	181.4495
$P_2$ (MW)	154.2941	195.3598	271.1577
$P_3$ (MW)	151.7105	191.9158	270.7413
Total generation (MW)	407.4085	511.7140	723.3485

**Table 6** Comparison of combined economic emission dispatch (CEED) results for test system-III

$P_D$	Performance	Conventional [3]	RGA [3]	HGA [3]	Hybrid GTA [3]	SA [4]	ABC [3]	Proposed method
500MW	Fuel cost (Rs/hr)	27638.30	27692.1	27695	27613.4	27613	27613	27608.16
	Emission level (Kg/hr)	262.454	263.472	263.37	263.00	263.01	263.012	263.14
	Total cost (Rs/hr)	39159.5	39258.10	39257.5	39158.9	39156.9	39156.9	38620.37
	Power loss (MW)	8.830	10.172	10.135	8.930	8.943	8.9343	8.9550
	Escape time (sec)	–	–	–	–	4.887728	4.11105	0.667
900MW	Fuel cost (Rs/hr)	48892.90	48567.7	48567.5	48360.9	48351	47045.3	47950.14
	Emission level (Kg/hr)	701.428	694.169	694.172	693.570	693.79	693.791	705.05
	Total cost (Rs/hr)	82436.58	81764.5	81764.4	81529.1	81527.6	81527.6	67609
	Power loss (MW)	35.230	29.725	29.178	28.004	28.01	28.0087	28.5528
	Escape time (sec)	–	–	–	–	5.914351	3.94864	0.629

## 4 Conclusions

A linear Hopfield Neural model for the solution of CEED problem has been proposed and investigated. Proposed method exhibits the ability of attaining power mismatch to any desirable extent due to consideration of mismatch power in objective function, which is more meaningful for large scale generating system. For applying Hopfield neural network to CEED Problem, proper selection of weighting factors associated with the energy function are required, which is a cumbersome task. This paper employs a systematic procedure for evaluating the value of weighting factors, associated with the various terms of the energy function. The proposed method has been applied to three test systems and it’s applicability for solving multi objective generation dispatch problem is showed by obtained results, which is very comparable to the optimization algorithms, such as conventional method, RGA and SGA, Hybrid GA,PSO , ABC and SA algorithm. Thus, proposed algorithm is accurate, simple, efficient, and fast.



## References

1. Su, C.T., Chiou, G.J.: A fast-computation hopfield method to economic dispatch. *IEEE Trans. Power Syst.* **12**(4), 1759 (1997)
2. Bhattacharya, B., Mandal, K.K., Chakraborty, N.: A hybrid cultural approach for combined economic and emission dispatch. *Annual IEEE India Conference (INDICON)*, 16–18 (2011).
3. Gaurav Prasad, D., Hari Mohan, D., Manjaree, P., Panigrahi, B.K.: Artificial bee colony optimization for combined economic load and emission dispatch. *Second International Conference on Sustainable Energy and Intelligent System (SEISCON)*, 340–345 (2011).
4. Kaurav, M.S., Dubey, H.M., Manjaree, P., Panigrahi, B.K.: Simulated annealing algorithm for combined economic and emission dispatch. *UACEE Int. J. Adv. Electron. Eng.* **1**, 172–178 (2011)
5. Venkatesh, P., Gnanadass, R.: Narayana Prasad, P.: Comparison and application of evolutionary programming techniques to combined economic emission dispatch with line flow constraints. *IEEE Trans. Power Syst.* **18**(2), 688 (2003)
6. Gupta, A., Swarnkar, K.K., Wadhwani, S., Wadhwani, A.K.: Combined economic emission dispatch problem of thermal generating units using particle swarm optimization. *Int. J. Sci. Res. Publ.* **2**(7), 1 (2012)

# Soft Computing Approach for VLSI Mincut Partitioning: The State of the Arts

Debasree Maity, Indrajit Saha, Ujjwal Maulik and DariuszPlewczynski

**Abstract** Recent research shows that the partitioning of VLSI-based system plays a very important role in embedded system designing. There are several partitioning problems that can be solved at all levels of VLSI system design. Moreover, rapid growth of VLSI circuit size and its complexity attract the researcher to design various efficient partitioning algorithms using soft computing approaches. In VLSI partitioning, *netlist* is used to optimize the parameters like mincut, power consumption, delay, cost, and area of the partitions. Hence, the Genetic Algorithm is a soft computational meta-heuristic method that has been applied to optimize these parameters over the past two decades. Here in this paper, we have summarized important schemes that have been adopted in Genetic Algorithm for optimizing one particular parameter, called *mincut*, to solve the partitioning problem.

**Keywords** Genetic algorithm · Mincut · Netlist · Survey · VLSI circuit partitioning

---

D. Maity

Department of Electronics and Communication Engineering, MCKV Institute of Engineering, Howrah, Liluah 711204, India  
e-mail: debasree.maitysaha@gmail.com

I. Saha (✉) · U. Maulik

Department of Computer Science and Engineering, Jadavpur University, Kolkata 700032, India  
e-mail: indra@icm.edu.pl

D. Plewczynski

Interdisciplinary Centre for Mathematical and Computational Modelling, University of Warsaw, 02106 Warsaw, Poland  
e-mail: darman@icm.edu.pl

## 1 Introduction

With the rapid increment and development of modern electronic circuit technology and its fabrication make the very large-scale integration (VLSI) circuit so dense that a single silicon chip may contain millions of circuit modules, like transistors, resistors, capacitors, etc. The circuit modules are communicating with each other through physical connections. In order to decrease the complexity of VLSI circuits and improve the circuit delay characteristics, an effective method is the dividing and rule. Moreover, to speed up the design process it is necessary to split the circuit into many subcircuits so that each subcircuit can be designed independently. Minimization of the interconnections, area differences between the subcircuits, cost of the partitioning, delay, power consumption, and maximization of the module compactness in the circuit is the main objectives of circuit partitioning [1, 4].

VLSI is a vast field of electronics system. There are very complicated electronics circuitries made to perform different types of operations that are very effective to simulate before hardware design. The circuit needs partitioning [1, 2] to reduce the complexity of the large circuit, as it is divided into small independent parts. This will make the circuit more compact, reduce the area and fabrication cost [5, 13]. However, in circuit partitioning process, some points should be kept in mind that the individual area of the partitions is minimized to maximize the compactness and the number of interconnections between the partitions are also be minimum to reduce the delay, power consumption. These are the constraints considered as individual functions for partitioning problems. Moreover, the number of partitions is going to be made, depending on problem is more specifically termed as *k-way* or *multi-way* partitioning [6, 7].

To solve the VLSI partitioning problems the circuit description is very important. For this purpose, ISPD'98 [8] benchmark standard already exist for circuit description. In this benchmark, circuits are defined as *Netlist*, indicating the number of components/modules, I/O ports, and nuts, in the circuit. Hence, the circuit partitioning is also termed as *Netlist Partitioning* [9]. Netlist is considered as a hypergraph with vertices corresponding to cells (components/modules/gates) and edges corresponding to nets [2], where *Mincut* [10] indicates the possible minimum number of interconnections between partitions. Here, in this short review, we have considered *mincut* as an object that has been optimized by a well-known soft computing meta-heuristic method, called Genetic Algorithm (GA) [14], whereas other parameters, such as delay, power, and area are kept constant. However, the optimization of these parameters has also been reported in [28–31].

## 2 Mathematical Formulation of VLSI Mincut Problem

The problem of minimizing the interconnection, i.e., mincut, is considered here. Generally, an electronics circuit partitioning problem is just like a graph partitioning problem [11, 12]. A standard electronic circuit can be described by the circuit netlist

and the netlist can be represented by a hypergraph  $H(V, E)$  with  $m$  modules and  $n$  nets, where  $V$  is a set of nodes and  $E$  is a set of nets (connection lines). In a circuit, a net can connect all the modules in the same signal line. However, partitioning is required mainly to minimize the interconnections between the subcircuits. Let there is a circuit that contains  $m$  number of modules and  $n$  number of nets (connections). This circuit will be partitioned to a specified number of subset  $k$ , where  $k = 2$  as it is a bipartition problem, to assign the modules that satisfying the specified constraints. Now, if the subsets are denoted by  $V_1, V_2, \dots, V_k$  with  $S_1$  and  $S_2$  are the maximum and areas, then the constraints can be defined as follows:

$$V_1 \cup V_2 \cup \dots \cup V_k = V$$

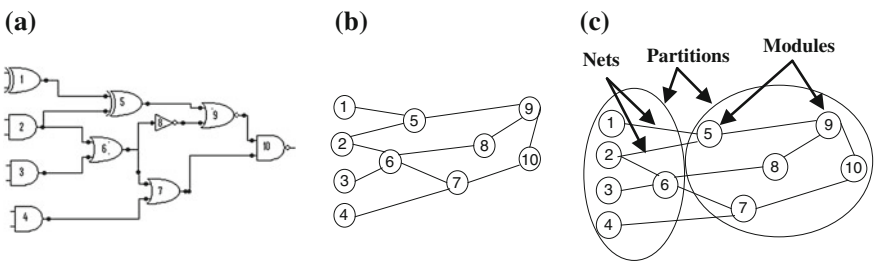
$$V_1 \cap V_2 = \varphi; S_2 \leq S(V_i) \leq S_1$$

where  $S(V_i)$  is the area of subset  $V_i, i = 1, 2, \dots, k$

The graphical representation of a digital circuit is shown in Fig. 1a, b. A possible two-way partitioning of the circuit with nets and modules is also shown in Fig. 1c. In this paper, for single objective partitioning, our aim is to minimize the number of interconnections between two or multipartitions, called *mincut*. Therefore, this partitioning can be modeled mathematically on the basis of *mincut*. The mathematical model for mincut is defined in [3, 10] as:

$$f_{\text{min cut}} = \left( \sum_{j=1}^n \sum_{k=1}^2 y_{jk} \right) \tag{1}$$

where, if net  $j$  is in block or subset of  $k$ , then  $y_{jk} = 1$ , otherwise  $y_{jk} = 0$ .



**Fig. 1** a A digital circuit, b Graphical representation of the digital circuit, c Possible two-way partitioning indicating nets, modules, and partitions

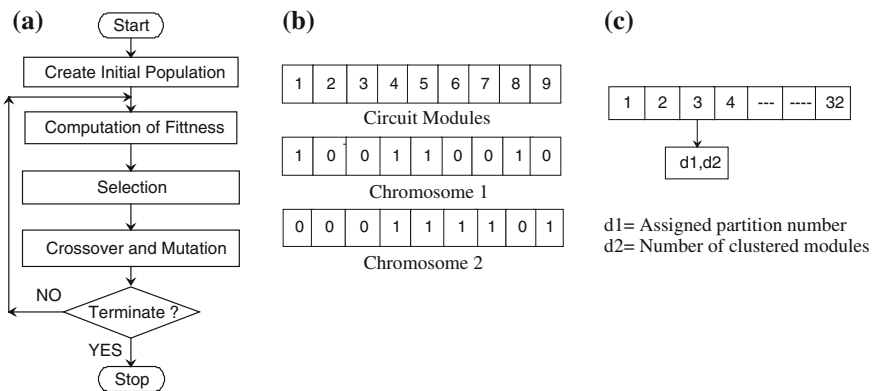
### 3 Genetic Algorithm for VLSI Mincut Circuit Partitioning

Genetic Algorithm (GA) [14] is a heuristic search algorithm based on the evolutionary concepts of genetics and natural selection. Figure 2a shows the different steps of GA in flow chart form. In VLSI domain, many different types of research based on GA have been done in past two decades. For example, mincut partitioning [3, 10, 15], multilevel partitioning [16], dynamic embedding partitioning [32], VLSI physical design [2, 4], network partitioning [7, 17], cell placement techniques [33], floor plan designing [34], channel routing [35], VLSI layout optimization [36], network flow-based partitioning [18, 19]. For partitioning the VLSI circuits using GA, different schemes have been observed and those are described in below.

#### 3.1 Initialization of Population

In GA, the population is initialized by different encoding schemes in different papers [3, 13, 20]. In [3], the encoding scheme, called 0-1 encoding, where the bi-partitioning problem allocates the circuit modules into a pair of disjoint blocks or subsets *A* and *B*. The 0 values of the genes represent the respective modules are assigned to subset *A* and when the value is 1, the respective modules are in subset *B*. Figure 2b shows its pictorial representation. Moreover, it has also been noticed that the integer encoding scheme is used in [3], where each chromosome is encoded with the module number. It is then divided into parts to create disjoint subsets of modules.

In [13], another integer encoding scheme is used, where the modules interconnection information as in the netlist is converted to an adjacency matrix first and then Breath First Search (BFS) search algorithm is applied on the matrix to traverse. Once the BFS order the modules, it is then used to form the chromosome for GA.



**Fig. 2** a Flow chart of genetic algorithm, b 0-1 Encoding based chromosome, and c 32-bit encoded chromosome

It is a 32 bit chromosome containing integers for each gene of the chromosome. Each integer value is encoded to represent the assigned partition number and number of elements clustered to make each chromosome element is shown in Fig. 2c. Using this encoding policy random population is generated with user defined population size. Then for each population cost is calculated.

Another different type of chromosome encoding for bi-partitioning of a circuit is depicted in [20]. Here, the chromosomes are in layered form. Depending on the number of partitions made in the circuit, the layers of the chromosome are formed. Figure 3a shows a 2-layer chromosome structure which represents each individual in the populations. It can be extended for the multi layer chromosomes (for the multi way partitioning).

### 3.2 Fitness Computation

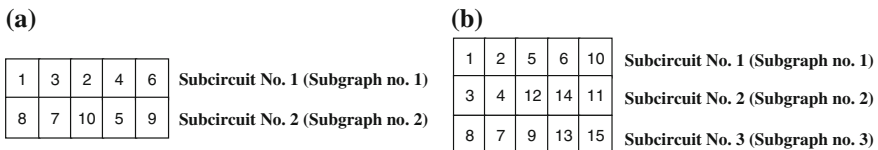
The fitness functions defined for the mincut partitioning problem that uses above mentioned encoding schemes are stated in Eq. 1–3. In [3], fitness function for binary encoding is defined as follows:

$$f_{\text{mincut}} = \left( \sum_{j=1}^n \sum_{k=1}^2 y_{jk} \right) \left( 1 - \frac{V_1 - V_2}{V_1 + V_2} \right)^{r_1} \tag{2}$$

where  $V_1$  and  $V_2$  are actual size of the two subsets or blocks,  $r_1$  is a factor that controls the ratio for cut partitioning ( $0 \leq r_1 \leq 2$ ),  $y_{jk}$  is defined in Eq. (1). However, for integer encoding, fitness function is same as Eq. (1). The fitness function reported in [20] is stated below:

$$f_{\text{mincut}} = \left( \frac{NG}{NSG} \right) \tag{3}$$

where,  $NSG$  = the number of all connections between the created subgraphs, i.e., external connections and  $NG$  = the number of all connections in the graph (constant).



**Fig. 3** a 2-layer chromosome representation of a bi-partitioned circuit, b 3-layer chromosome representation of a tri-partitioned circuit

### 3.3 Selection

In the selection process, mostly the Roulette Wheel selection strategy is used [3, 13]. In [20], fan selection (a modified Roulette Wheel selection) operations are used to find the best solution.

### 3.4 Crossover and Mutation

The crossover and mutation operations performed for the above mentioned encoded chromosomes are different. For 0-1 encoded chromosome, two parents are taken randomly to do the crossover operation with a crossover probability [3]. Here, two-point crossover is used to get a better offspring. In this scheme, according to the mutation probability, some bits are inverted in the binary chromosome randomly. The mutation probability is not constant and varies with the number of circuit modules. The mutation probability is defined in [3] as  $M_p = 2/m$ .

For integer encoded chromosome, if conventional crossover operation is used, then two problems can occur: (a) possibility of having the same module in both the blocks and (b) some modules may not be in any blocks. Hence, to avoid these problems, partial mapped crossover is used. This is illustrated in Fig. 4. Here, for this encoding policy, the general exchange mutation operation can't be performed, as it gives some invalid results. Therefore, an improved exchange mutation is used here. It first selects a random bit  $b_1$  and then a second bit  $b_2$  by the following formula:

$$b_2 = \begin{cases} \text{rand}(1, m_1) & b_1 > m_1 \\ \text{rand}((m_1 + 1), m) & b_1 \leq m_1 \end{cases} \quad (4)$$

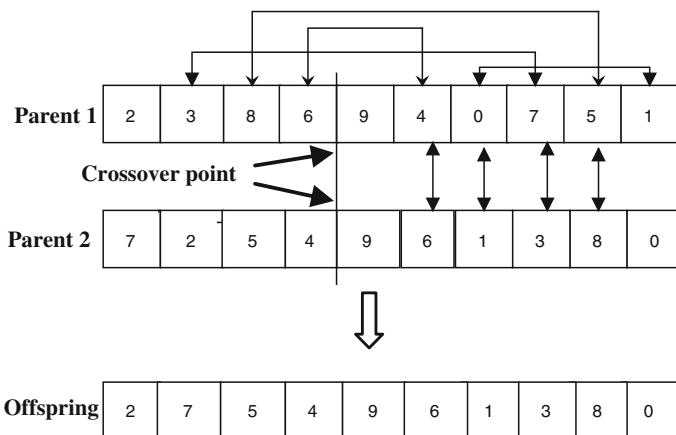


Fig. 4 General partial mapping crossover

where  $m_1$  is the number of modules which are in the first block or subset and  $m$  is the total number of modules. As this process is used for all the pool of chromosomes, the mutation probability is kept constant 0.02. In [13] also this type of crossover and mutation is noticed.

In [20], idea of the Partial Mapping Crossover (PMX) [21] operation is used. The crossover mainly has 3 steps. In first step, it selects parent chromosome and the crossover point as shown in Fig. 5a, and after this, the cross point is exchanged, as shown in Fig. 5b. In second step, non-colliding genes, those are not present still in the newly generated off-springs are copied into the respective blank places from the parents, as shown in Fig. 5c, for parent X these are '5' and '3' and for Y it is '3' and '5'. Finally, in third step, the rest blank places in each new off-spring are filled by the module values that are still not present in it, as depicted in Fig. 5d.

Here, mutation operation is done using two different operators. After selecting a gene for mutation, type of mutation operator is randomly selected with equal probability. In case of the first operator, two genes are selected randomly from the parent individual and are exchanged during mutation as shown in Fig. 6a. In second type of operation, a circulation is done on the randomly selected column, shown in Fig. 6b.

Moreover, except mincut optimization for VLSI circuit partitioning using GA, there are other soft computing meta-heuristic techniques have been noticed to solve the same problems using Ant Colony Optimization [22], Particle Swarm Optimization [25], Simulated Annealing [26], and Tabu Search [27].

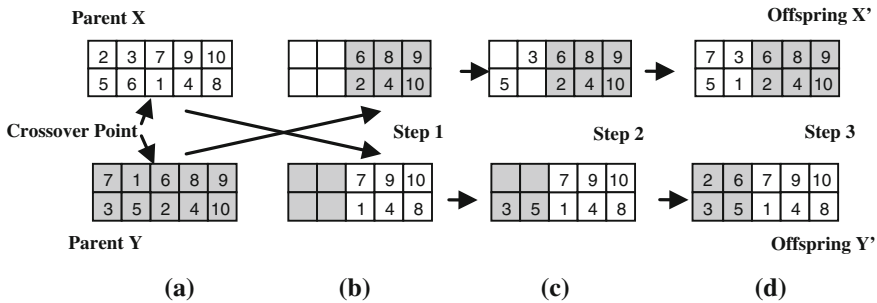


Fig. 5 Crossover operation of two-layered chromosomes

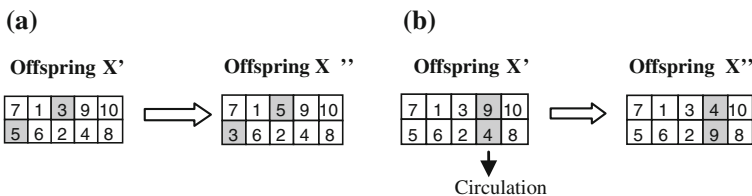


Fig. 6 a First mutation operation, b second mutation operation



## 4 Conclusion

In this survey paper, we have discussed the available genetic algorithms for VLSI circuit partitioning using mincut as an objective function. These methods adopt the hypergraph partitioning effectively to reduce the number of interconnections between two partitions in the circuit. It can also be applicable for multi-way partitioning. This short survey shows the different types of encoding, crossover, and mutation process that can be used to solve the mincut problems.

As a scope of further research, apart from mincut, other parameters like area, circuit delay, power consumption, etc., are also needed to study. Moreover, the application of different meta-heuristic methods can also be reviewed in context of single [36] and multiobjective optimization [23, 37] of different parameters of VLSI circuits. Authors are working in this direction.

**Acknowledgments** Mr. Saha is grateful to the All India Council for Technical Education (AICTE) for providing National Doctoral Fellowship (NDF) to support the work.

## References

1. Johannes, F.M.: Partitioning of VLSI circuits and systems. In: Proceedings 33rd ACM/IEEE International Conference on Design Automation, pp. 83–87 (1996).
2. Mazumder, P., Rudnick, E.M.: Genetic Algorithms for VLSI Design, Layout and Test Automation Partitioning. Prentice Hall, New Jersey (1999)
3. Nan, G.F., Li, M.Q., Kou, J.S.: Two novel encoding strategies based genetic algorithms for circuit partitioning. In: Proceedings of 3rd International Conference on Machine Learning and Cybernetics 4, pp. 2182–2188 (2004).
4. Sherwani, N.: Algorithms for VLSI Physical Design and Automation, 3rd edn. New Delhi, Springer (India) Private Limited (2005)
5. Bui, T.N., Moon, B.R.: A fast and stable hybrid genetic algorithm for the ratio-cut partitioning problem on hypergraphs. In: proceedings of 31st ACM/IEEE International Conference on Design Automation, pp. 664–669 (1994).
6. Tan, X., Tong, J., Tan, P., Park, N., Lombardi, F.: An efficient multi-way algorithm for balance partitioning of VLSI Circuits. In: Proceedings of International IEEE Conference on Computer Design: VLSI in Computers and Processors, pp. 608–613 (1997).
7. Sanchis, L.A.: Multiple-way network partitioning with different cost functions. IEEE Trans. Comput. **42**(12), 1500–1504 (1993)
8. Alpert, C.J.: The ISPD98 circuit benchmark suite. In: Proceedings of International Symposium on Physical Design, pp. 80–85 (1998).
9. Alpert, C.J., Khang, A.B.: Recent directions in netlist partitioning: a survey. Integr. VLSI J. **19**(1–2), 1–81 (1995)
10. Krishnamurthy, B.: An improved min-cut algorithm for partitioning VLSI networks. IEEE Trans. Comput **33**(5), 438–446 (1984)
11. Bui, T.N., Moon, B.R.: Genetic algorithm and graph partitioning. IEEE Trans. Comput. **45**(7), 841–855 (1996)
12. Andreev, K., Racke, H.: Balanced graph partitioning. In: Proceedings of 16th International Annual ACM Symposium on Parallelism in Algorithms and Architectures, pp. 120–124 (2004).
13. Gill, S.S., Chandel, R., Chandel, A.: Genetic algorithm based approach to circuit partitioning. Int. J. Comput. Electr. Eng. **2**(2), 196–201 (2010)

14. Chambers, L.D.: Practical Handbook of Genetic Algorithms. CRC Press, Inc. Boca Raton(1995).
15. Jiang, X., Shen, X., Zhang, T., Liu, H.: An improved circuit-partitioning algorithm based on min-cut equivalence relation. *Integr. VLSI J.* **36**(1–2), 55–68 (2003)
16. Alpert, C.J., Huang, J.H., Khang, A.B.: Multilevel circuit partitioning. In: proceedings of 34th ACM/IEEE International Conference on Design Automation, pp. 530–533 (1997).
17. Fiduccia, C.M., Mattheyses, R.M.: A linear time heuristic for improving network partitions. In: Proceedings of 19th International Conference on Design Automation, pp. 175–181 (1982).
18. Yang, H., Wong, D.F.: Efficient network flow based min-cut balanced partitioning. Proceedings of IEEE/ACM International Conference on Computer-Aided Design **15**(12), 1533–1540 (1996)
19. Liu, H., Wong, D.F.: Network-flow-based multiway partitioning with area and pin constraints. *IEEE Trans. Comput. Aided Des. Integr. Circuits Syst.* **17**(1), 50–59 (1998)
20. Slowik, A., Bialko, M.: Partitioning of VLSI circuits on subcircuits with minimal number of connections using evolutionary algorithm. In: Proceedings of International Conference AISC, pp. 470–478(2006).
21. Goldberg, D.E., Lingle, R.: Alleles, loci and the TSP. In: Proceedings of International Conference on Genetic Algorithms, pp. 154–159 (1985).
22. Gill, S.S., Chandel, R., Chandel, A.: Comparative study of ant colony and genetic algorithms for VLSI circuit partitioning. *Eng. Tech.* **28**, 890–894 (2009)
23. Sait, S.M., El-Maleh, A.H., Al-Abaji, R.H.: Evolutionary algorithms for VLSI multi-objective netlist partitioning. *Eng. Appl. Artif. Intell.* **19**(3), 257–268 (2005)
24. Peng, S., Chen, G.L., Guo, W.Z.: A discrete PSO for partitioning in VLSI circuit. In: Proceedings of International Conference on Computational Intelligence and, Software Engineering, pp. 1–4 (2009).
25. Kolar, D., Puksec, J.D., Branica, I.: VLSI circuit partitioning using simulated annealing algorithm. In: Proceedings of IEEE Melecon, pp. 12–15 (2004).
26. Lodha, S.K., Bhatia, D.: Bipartitioning circuits using TABU search. In: Proceedings of 11th IEEE Annual International Conference on ASIC, pp. 223–227 (1998).
27. Rajaraman, R., Wong, D.F.: Optimal clustering for delay minimization. In: Proceedings of 30th ACM/IEEE International Conference on Design Automation, pp. 309–314 (1993).
28. Yang, H., Wong, D.F.: Circuit clustering for delay minimization under area and pin constraints. *IEEE Trans. Comput. Aided Des. Integr. Circuits Syst.* **16**(9), 976–986 (1997)
29. Vaishnav, H., Pedram, M.: Delay optimal partitioning targeting low power VLSI circuits. *IEEE Trans. Comput. Aided Des. Integr. Circuits Syst.* **18**(6), 298–301 (1999)
30. Yang, H., Wong, D.F.: Optimal min-area min-cut replication in partitioned circuits. *IEEE Trans. Comput. Aided Des. Integr. Circuits Syst.* **17**(11), 1175–1183 (1998)
31. Kim, C.K., Moon, B.R.: Dynamic embedding for genetic VLSI circuit partitioning. *Eng. Appl. Artif. Intell.* **11**(1), 67–76 (1998)
32. Esbensen, H., Mazumder, P.: SAGA: A unification of the genetic algorithm with simulated annealing and its application to macro-cell placement. In: Proceedings of 7th International Conference on, VLSI Design, pp. 211–214 (1992).
33. Cohoon, J.P., Hegde, S.E., Martin, W.N., Richards, D.S.: Distributed genetic algorithms for the floorplan design problem. *IEEE Trans. Comput. Aided Des. Integr. Circuits Syst.* **10**(4), 483–492 (1991)
34. Lienig, J., Thulasiraman, K.: A genetic algorithm for channel routing in VLSI circuits. *Evol. Comput.* **1**(4), 293–311 (1993)
35. Schnecke, V., Vormberger, O.: An adaptive parallel genetic algorithm for VLSI layout optimization. In: Proceedings of 4th International Conference on Parallel Problem Solving from Nature III, pp. 859–868 (1996).
36. Maulik, U., Saha, I.: Modified differential evolution based fuzzy clustering for pixel classification in remote sensing imagery. *Pattern Recognit.* **42**(9), 2135–2149 (2009)
37. Saha, I., Maulik, U., Plewczynski, D.: A new multi-objective technique for differential fuzzy clustering. *Appl. Soft Comput.* **11**(2), 2765–2776 (2011)

# Multimedia Classification Using ANN Approach

Maiya Din, Ram Ratan, Ashok K. Bhateja and Aditi Bhateja

**Abstract** Digital multimedia data in the form of speech, text and fax is being used extensively. Segregation of such multimedia data is required in various applications. While communication of such multimedia data, the speech, text and fax data are encoded with CVSD coding, Murray code and Huffman code respectively. The analysis and classification of such encoded multimedia from unorganized and unstructured data is an important problem for information management and retrieval. In this paper we proposed an ANN based approach to classify text, speech and fax data. The normalized frequency of binary features of varying length and PCA criterion is considered to select effective features. We use selected features in Back-propagation learning of MLP network for multimedia data classification. The proposed method classifies data efficiently with good accuracy. The classification score achieved for encoded plain data is of the order of 91, 93 and 90 % for speech, text and fax respectively. Also for 30 % distorted data, the classification score obtained is of the order of 78, 80 and 72 % for speech, text and fax respectively.

**Keywords** Multimedia data · Binary features · PCA criterion · ANN classifier · MLP network · Back-propagation learning

---

M. Din (✉) · R. Ratan · A. K. Bhateja  
Defence Research and Development Organization, Scientific Analysis Group, Delhi, India  
e-mail: anuragimd@gmail.com

R. Ratan  
e-mail: ramratan\_sag@hotmail.com

A. K. Bhateja  
e-mail: akbhateja@gmail.com

A. Bhateja  
Ambedkar Institute of Advanced Communication Technologies and Research, Delhi, India  
e-mail: aditibhateja89@gmail.com

## 1 Introduction

With emergence of digital communication, most of the signals (speech, text or fax) are being sent over a channel in digital form. Nowadays digital multimedia data is being used extensively even by common people in their communication. In the age of Information Technology, the information flow in binary form between communicating and computing devices. The classification of multimedia data as speech, text and fax is very important before any further analysis in several applications such as steganography and cryptography in information security [1–5] and information indexing and categorization for efficient information management and retrieval systems [6]. For efficient communication or storage of data with adequate signal quality, the data should be encoded with appropriate encoding techniques. The speech is encoded in binary form by Continuously Variable Slope Delta (CVSD) coding is adopted apart from various existing encoding techniques due to its low bit rate and with reasonable speech quality [7]. The English text is converted into binary form using Murray code [8]. The fax messages are represented in binary form using Huffman encoding technique [9].

For classification of data, normally it is represented in pattern space by variety of multidimensional feature vectors. The components of feature vector may be frequency of binary words, correlation values or energy-based measurements etc. We apply N-gram features which have also been applied in pattern recognition problems such as classification of speech and text, and identification of speech encodings [10–12]. The Principal Component Analysis (PCA) helps to find independent features for their use in pattern recognition [13]. The conventional classifiers are less effective when data to be classified is ambiguous or vague and class boundaries are overlapped and not defined clearly. The artificial neural networks are found very suitable to tackle ambiguous situations efficiently [14–17]. In this paper, an ANN based approach is proposed to classify multimedia data. The approach uses normalized frequency of binary features of varying length and PCA criterion to identify and select effective features. We utilize effective features to train Multi Layer Perceptron (MLP) Network for classification using Back Propagation Learning [15]. The proposed method classifies multimedia data efficiently with higher classification accuracy.

The paper is organized as follows: We describe encoding for multimedia data in Sect. 2. The detail of data preparation and effective feature selection is discussed in Sect. 3. The Back-propagation learning and MLP network is described briefly in Sect. 4 and classification results obtained are presented in Sect. 5. The paper is concluded in Sect. 6.

## 2 Multimedia Data Encoding

We represent multimedia data in binary form for its classification. The speech is encoded in binary form by CVSD coding [7] apart from various existing encoding techniques due to its low bit rate and reasonable speech quality. The English Text is

converted into binary form using Murray code [8]. Fax data are represented in binary form using Huffman encoding technique [9].

## ***2.1 Speech Coding***

The speech is a time varying signal representing audio signals. The speech coding is carried out basically using Waveform coders and Voice coders. Pulse Code Modulation (PCM), Linear Predictive Coding (LPC) and CVSD are commonly used coding techniques in speech encodings [7, 18]. We consider CVSD encoding which represents speech data with adequate speech quality. The CVSD coding is a special type of Adaptive Delta Modulation coding where adaptation is considered at pitch period. It possesses remarkable degree of robustness to bit error rates of order of 1%. The CVSD encoded speech contains special sequence called idling binary pattern due to pause regions exist in speech utterances.

## ***2.2 Text Encoding***

There are various codes used for binary representation of text messages. The American Standard Code for Information Interchange (ASCII), Unicode and Murray Code are commonly used in computer and communication applications. We consider Murray code to represent English text messages in binary form with five-bit length fixed code [8]. Some of the monographs, digraphs and trigraphs of letters occur frequently and some occur rarely in plain English text. The linguistic characteristics are also exists in corresponding binary texts.

## ***2.3 Fax Encoding***

Fax is a 2-Dimensional data representing spatial variation of document. Huffman coding is used to encode fax messages in binary form [9]. It is a variable length binary coding scheme based on the probability of symbols. In this coding, the most frequent symbol is represented by least number of bits and least frequent symbol is represented by highest number of bits.

## **3 Effective Feature Selection**

The binary multimedia data is prepared from speech, text and fax messages. We consider 500 speech frames each of 2,500 bits, 500 text messages each of 500 characters and 50 fax messages each of 25,000 bits. These fax messages are divided into frames

**Table 1** Effective feature patterns used for classification

Effective features	Feature pattern
Bi-grams	01, 10
Tri-grams	101, 110
Four-grams	1101, 1110
Five-grams	10000, 00001, 00011, 00110
Six-grams	011001
Ten-grams	0000100101, 00110010100
Twelve-grams	000000000000, 111111111111
Thirteen-grams	0101010101010

each of 2,500 bits. This data is distorted randomly at 10, 20 and 30 % distortion levels for its classification study.

We consider 124 features (bi-gram to six-gram), two ten-gram (0000100101, 00110010100) features, two twelve-gram (000000000000, 111111111111) features and one thirteen-gram (0101010101010) binary feature of multimedia data. After careful study of speech, text and fax data and applying PCA criterion, following 15 binary effective feature patterns are identified as shown in Table 1.

### 4 MLP-ANN Based on Back-Propagation Learning

An artificial neural network is a computational model that is inspired by the structure and/or functional aspects of biological neural networks. It is also known as Neural Network (NN). An ANN consists of an interconnected group of artificial neurons, and it processes information using a connectionist approach. In general an ANN works as an adaptive system that changes its structure according to external or internal information flowing through the network during its learning process. Modern neural networks are applied as non-linear modeling of given data. ANNs are usually used to model complex relationships between inputs and outputs, finding hidden patterns in data and data mining applications.

A Multilayer Perceptron (MLP) Network [10] is a feed-forward artificial neural network that maps sets of input data onto a set of appropriate output. MLP is a modification of the standard linear perceptron, which can distinguish data that is not linearly separable. An MLP consists of multiple layers of nodes, with each layer fully connected to the next one. Except for the input nodes, each node is a neuron with a nonlinear activation function. An ANN having multi layers (Input layer, Hidden layers and Output layers) is called Multilayer ANN as shown in the Fig. 1. MLP utilizes a supervised learning technique for training the network.

There are several learning techniques used to train MLP-ANNs. Back-propagation learning technique is one out of these used to train the network [15]. In this learning, gradient search optimization technique is used to minimize cost function up to least mean square error between target and actual net outputs. An ANN based

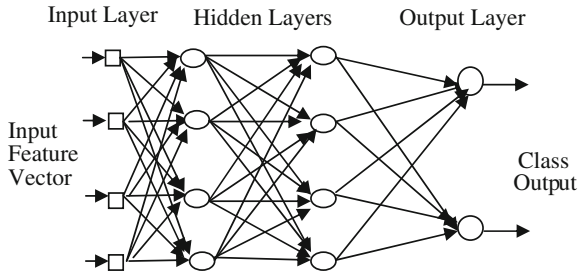


Fig. 1 Multilayer artificial neural network

classification approach is developed to classify speech, text and fax data. The normalized frequencies of 15 effective features are computed by dividing frame length, which are used in Back-propagation learning of Multilayer Perceptron (MLP) network having three layers. The number of neurons used in the network layers are 15, 7, 2 (Input layer to output layer respectively) based on Sigmoid Activation Function. The above effective features are used in training and testing of ANN. This network is trained using BP Learning on 900 feature vectors i.e. 300 vectors of each class consisting of clear and distorted data with 10, 20 and 30% distortion. The variable learning rate used is from 1.8 to 0.5 for achieving required error threshold level. The network is tested on different 150 feature vectors corresponding to clear data and 450 corresponding to distorted data consisting of 150 for each class with 10, 20 and 30% distortion level.

### 5 Classification Results

The proposed ANN classification method is applied on both training and test data sets. For test data, the classification results of speech, text and fax in clear and distorted domain is summarized in Table 2.

The classification score achieved through proposed approach for clear data is of the order of 91, 93 and 90% for speech, text and fax respectively and 78, 80 and 72% for corresponding 30% distorted data. The classification score for text data is higher than speech and fax data in clear as well as distorted domain. It is also observed from obtained results that as level of distortion increases the classification accuracy decreases.

Table 2 Classification results

Multimedia test data	Classification (%)		
	Speech	Text	Fax
Clear data	91	93	90
10% Distorted data	90	92	89
20% Distorted data	84	86	80
30% Distorted data	78	80	72

## 6 Conclusion

An ANN based method has been proposed for classification of plain and distorted multimedia data to segregate speech, text and fax data. The effective binary features of multimedia data have been utilized in the proposed method. The PCA criterion has been applied to select effective features that have been used in Back-propagation Learning of MLP network for efficient and effective classification. The classification score obtained for clear speech, text and fax data is of the order of 91, 93 and 90 % and for 30 % distorted speech, text and fax data is of the order of 78, 80 and 72 % respectively. The proposed ANN method could be used for segregation, analysis and interpretation of multimedia data in various multimedia applications.

## References

1. Katzenbeisser, S., Petitcolas, F.A.P.: Information hiding techniques for steganography and digital watermarking. Artech House, London (2000)
2. Ratan, R., Madhavan, V.C.E.: Steganography based information security. *IETE Tech. Rev.* **19**, 213–219 (2002)
3. Menezes, A., Van Oorschot, P., Vanstone, S.: *Handbook of Applied Cryptography*. CRC Press, USA (1996)
4. Stallings, W.: *Cryptography and Network Security*. Prentice Hall, Englewood Cliffs (2011)
5. Becker, H., Piper, F.: *Cipher Systems: The Protection of Communication*. Northwood Booker, London (1982)
6. Yates, R.B., Nieto, B.R.: *Information Retrieval*. Addison Wesley, England (1999)
7. Deller, J.R., Hansen, J.H.L., Proakis, J.G.: *Discrete-Time Processing of Speech Signals*. IEEE Press, New York (2000)
8. Beker, P.W.: *Recognition of Patterns: Using Frequency of Binary Words*. Springer, New York (1978)
9. Jain, A.K.: *Fundamentals of Digital Image Processing*. Prentice Hall, USA (1989)
10. Chelba, C., Acero, A.: Discriminative training of N-gram classifiers for speech and text routing. *Proceedings of the Eurospeech International Conference ISCA* (2003).
11. Maithani, S., Saxena, P.K.: Identification of coding in enciphered speech. *Proceedings of 6th International Conference on recent trends in Speech, Music and Allied, Signal Processing* (2001).
12. Maithani, S., Maiya, D.: Speech systems classification based on frequency of binary word features. *Proceedings of the IEEE International Conference SPCOM-04* (2004).
13. Jolliffe, I.T.: *Principal Component Analysis*. Springer-Verlag, New York (2002)
14. Katagiri, S. (ed.): *Hand Book of Neural Networks for Speech Processing*. Artech House, London (2000).
15. Haykin, S.: *Neural networks- a comprehensive foundation*. Macmillan, New York (2001)
16. Basu, J.K., Bhattacharyya, D., Kim, T.H.: Use of artificial network in pattern recognition. *Int. J. Softw. Eng. Appl.* **2**(2), 23–34 (2010)
17. Remeikis, N., Skucas, I., Melninkaite, V.: Text categorization using neural networks initialized with decision trees. *Informatica* **15**(4), 551–564 (2004)
18. Kondoz, A.M.: *Digital speech codings for low bit rate communications systems*. John Wiley and Sons, New York (1995)



# Live Traffic English Text Monitoring Using Fuzzy Approach

Renu, Ravi and Ram Ratan

**Abstract** Current communication systems are very efficient and being used conveniently for secure exchange of vital information. These communication systems may be misused by adversaries and antisocial elements by capturing our vital information. Mostly, the information is being transmitted in the form of plain English text apart from securing it by encryption. To avoid losses due to leakage of vital information, one should not transmit his vital information in plain form. For monitoring of huge traffic, we require an efficient plain English text identifier. The identification of short messages in which words are written in short by ignoring some letters as in mobile messages is also required to monitor. We propose an efficient plain English text identifier based on Fuzzy measures utilizing percentage frequencies of most frequent letters and least frequent letters as features and triangular Fuzzy membership function. Presented method identifies plain English text correctly even, the given text is decimated/discontinuous and its length is very short, and seems very useful.

**Keywords** Traffic analysis · Fuzzy approach · Linguistic features · Plain text · Random text · Information security

---

Renu

Defence Research and Development Organization, Defence Scientific Information and Documentation Center, Delhi, India  
e-mail: renu25686@gmail.com

Ravi

Guru Premsukh Memorial College of Engineering, Guru Gobind Singh  
Indraprastha University, Delhi, India  
e-mail: talk2ravi@yahoo.in

R. Ratan (✉)

Defence Research and Development Organization, Scientific Analysis Group, Delhi, India  
e-mail: ramratan\_sag@hotmail.com

## 1 Introduction

With the advancement in information technology, efficient communication systems such as mobile and internet are available and being used nowadays even by common people. While communication of sensitive or vital information, it should not be communicated in plain form in any case and should be protected by appropriate safety measures to avoid losses due to capturing of such information by adversaries. The English language is commonly used worldwide in exchange of information. There are following ways to achieve information security—spread-spectrum, steganography and cryptography [1–5]. The spread-spectrum techniques modulate given information over the carriers randomly within the available channel bandwidth. The steganographic techniques conceal the existence of information by hiding it in another ordinary data. The cryptographic techniques conceal the content of information by transforming it into unintelligible form. The cryptographic techniques are being used widely all over the Globe in the area of information security for achieving the confidentiality apart from other security issues. The encryption process transforms plain text into crypt text by distorting the linguistic characteristics. When the English text is encrypted by cryptographic techniques, the obtained crypt text appears as random and there remains no intelligibility of text. The frequency of each letter occurs almost equal in random or encrypted text but in English text some letters occur highly and some letters occur very rarely.

Identification of plain text from such encrypted or random text is required in monitoring of sensitive traffic. The careful monitoring and analysis of traffic for English text are the most important problem to safeguard the communication. Moreover, monitoring and analysis of text have a vital role in combating terrorist activities and cyber crimes. The monitoring of plain text is also required to manage sensitive data securely over computer network. The identification of short messages in which words are written in short by ignoring some letters is also required to monitor mobile messages and analysis of crypts. We should never keep such data in plain form and it should always be kept secure. For monitoring of such huge traffic, the identification method should perform the task with minimum efforts, i.e., minimum computing complexity, time, and memory requirements.

Text mining is a very important field that attempts to extract meaningful information automatically from huge volume of natural language text for particular use [6, 7]. The text mining problems involve assessing the similarity between different texts and grouping them. Automatic text categorization has many practical applications such as indexing for retrieval and organizing and maintaining large catalogs of Web resources. The language identification is a particular application of text categorization. The text categorization or classification is gaining momentum due to its diverse applications such as classification of sensitive text [8], cyber terrorism investigation [9] and E-mail filtering [10]. The  $n$ -grams or patterns of  $n$  consecutive letters and words are used to identify language of texts [11, 12]. It is seen that the linguistic characteristics of the language have a key role in analysis of English text [13, 14]. The conventional methods of identifying English text become inapplicable

specifically when the size of text is less or the text is not continuous and also due to the uncertainty or variability of the linguistic features occurred. A Fuzzy approach based on soft computing is most suitable to tackle such problems better in uncertain and ambiguous situations where lot of difficulties arises in taking right decisions and perform better than neural networks and traditional pattern recognition approaches [15–19]. The Fuzziness or degree of uncertainty pertains due to the inconsistency of linguistic properties appear in text when it is of special type such as discontinuous and its length is short.

In this paper, a Fuzzy method is proposed for identification of English text in which we utilize the percentage occurrence of most frequent and least frequent letters as features and triangular Fuzzy membership function. The triangular Fuzzy membership function has been applied successfully in various pattern recognition problems. The method is also tested for partial text which is discontinuous or decimated text of short length.

The paper is organized as follows: In Sect. 2, we present briefly the linguistic characteristics of English language useful in the analysis of English text. We present the Fuzzy approach for identification of English text in Sect. 3. The performance of proposed Fuzzy method is presented in Sect. 4. Finally, the paper is concluded in Sect. 5 followed by the references.

## 2 Letter Characteristics of English Text

The English language has 26 symbols/letters (excluding spaces, punctuation marks, etc.). The occurrences of letters, *n*-grams, digraphs and its reversals, left–right contacts of letters, percentage of vowels and consonants, etc. in the plain-text and in the crypt-text are the only statistical measures which may be helpful. The following most important facts [13] are observed from frequency distributions of letters:

1. Irregular appearance occurred due to the fact that some of the letters are most frequent and others are very rare.
2. Most prominent crests are marked by letters E T O A N I R S H and the most prominent troughs are marked by J K Q X Z.
3. The occurrences of vowels and consonants are as:

Vowels	A E I O U Y	40 %
Consonants		
High frequent	T S R N H	34 %
Medium frequent	D C L M P F W G B V	24 %
Low frequent	J K Q X Z	2 %

4. The relative order of letters according to decreasing order of frequencies is as E T O A N I R S H D L U C M P F Y W G B V K J X Z Q.
5. Not more than two consecutive vowels normally occur (except ‘ious’).
6. Not more than four consecutive consonants normally occur.

7. Most frequent digraph reversals normally have a vowel.
8. Less frequent letters mostly contact with vowels than with other consonants.
9. The most frequent digraphs according to frequencies are as  
TH ER ON AN RE HE IN ED ND HA AT EN ES OF OR  
NT EA TI TO IT ST IO LE IS OU AR AS DE RT VE.

Above facts have been successfully utilized in the analysis of linguistic properties of texts [11–14, 20, 21]. For online identification of English text, the features to be used should be simple and easy to compute for efficient and accurate results. Some measures such as  $n$ -grams [11], words [12], phi measure [13] joint mutual information [20] and index of garbledness [21] have been used in this regard. The frequency of letters,  $n$ -grams, words, digraphs, joint mutual information, and index of garbledness are not suited for English text identification when the length of given text is less and the text is discontinuous or decimated. In short and discontinuous English text, the linguistic properties are changed and become useless in categorization and language identification. In random English text, the properties of plain text do not remain and the alphabets appear uniformly.

In this paper, we consider the percentage frequencies of most frequent and least frequent letters for efficient identification of English text in live traffic analysis. Here, the letters *E T O A N I R S H* are taken as most frequent letters and the letters *J K Q X Z* are taken as least frequent letters whose approximately percentage frequencies are 73 and 2% respectively.

Conventionally, the text is identified as plain-text when  $P_{mf} \geq T_{mf}$  and  $P_{lf} \leq T_{lf}$ . The  $P_{mf}$  and  $P_{lf}$  are the computed and  $T_{mf}$  and  $T_{lf}$  are expected percentage values of most frequent and least frequent letters. The selection of proper thresholds is very difficult because of uncertainty in plain English text and we get incorrect results when the value of thresholds is not appropriate.

### 3 Fuzzy English Text Identification

As Fuzzy approach handles uncertain and redundant data more comfortably to solve ambiguous problems, we do not require the tuning of  $T_{mf}$  and  $T_{lf}$  exactly for identifying plain English text correctly in suggested method. The value of  $T_{mf}$  and  $T_{lf}$  is taken 73 and 2% respectively which are the expected percentage values of most frequent and least frequent letters as mentioned in Sect. 2 for English text. For a given English text, we compute the value of the  $P_{mf}$  and  $P_{lf}$  features.

For comparing a given pattern with reference pattern, the normal process is to compute the Hamming or the Euclidean distance and to use minimum criteria. Here, we use a triangular fuzzy membership function to obtain membership value ( $\mu$ ) for  $P_{mf}(u)$  feature as shown in Fig. 1.

The  $T_{mf}(r)$  is the reference value for plain English text and  $P_{mf}(u)$  is the computed value in given text to be identified. Similarly, the Fuzzy membership function is also defined for  $P_{lf}(u)$ . The values  $\mu(P_{mf}(u))$  and  $\mu(P_{lf}(u))$  lie between 0 and 1 and

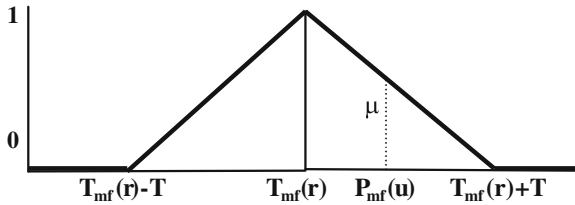


Fig. 1 Fuzzy membership function

is computed using triangular Fuzzy membership function as defined. The value of  $T$  used in membership function is chosen suitably. The value of  $\mu(P_{mf}(u))$  and  $\mu(P_{lf}(u))$  for English text is close to 1 and for random text is close to 0.

The similarity score of a given text with reference text is computed by using the concept of fuzzy intersection [16]. The similarity of a given pattern with the reference pattern is given by

$$S = \cap\{\mu(P_{mf}(u)), \{\mu(P_{lf}(u))\}. \tag{1}$$

According to the definition of fuzzy intersection, the similarity is the minimum value of  $\mu(P_{mf}(u))$  and  $\mu(P_{lf}(u))$ .

The overall similarity score can also be obtained by computing the average similarity as given by

$$S = 1/2[\mu(P_{mf}(u)) + \mu(P_{lf}(u))]. \tag{2}$$

The decision of identification is taken based on the similarity. The given text is identified as plain English text when the similarity score is near to 1 and it is identified as random or encrypted English text when the similarity score is near to 0.

## 4 Performance

The Fuzzy approach proposed is applied on various English text of varying length of normal plain text as well as decimated/discontinuous partial text to study the performance. For demonstrating the results obtained, we take normal English text in partial form by decimation of letters for identification. As an illustration, the plain English text, decimated texts, and short messages are given in Table 1.

Here, the decimated texts are unintelligible and look difficult to identify as part of plain English text. Identification of decimated texts is harder compare to normal plain English texts and mobile short messages. The space, punctuation marks, and non-English alphabet letters are excluded and only 26 alphabet letters are considered in identification of given English texts.

Proposed Fuzzy method identify given plain English text correctly with high confidence and almost 100% accuracy even when the text is discontinuous and its length is very short. The result of text identification for decimated English texts of

**Table 1** Plain english text, decimated text and short message

Plain text	The importance of the role played by repetitions in the analysis of cryptograms is well understood even by the amateur cryptanalyst repetitions in cryptographic text are basically of two sorts casual and accidental casual repetitions...
Decimated text (letter 1, 4, 7, ...)	TIOAETREADRETNNEASORTRSWL DSOVBHMECP...
Decimated text (letter 2, 5, 8, ...)	HMRNOHOPYBETISTALIFYOAIU ETDEYEURT...
Decimated text (letter 1, 8, 15, ...)	TRFEBINLCRERVERNEOYPTIFT LICEO...
Short message 1	Wish you a very happy and prosperous new year
Short message 2	Certainly SOCPROS 2012 is to be a grand successful event of JKLU

**Table 2** Identification of decimated plain english texts

Decimated text	Length of decimated text	Membership values $\mu(P_{mf}(u))$ and $\mu(P_{lf}(u))$	Similarity scores as (1) and (2)
TRFEBINLCRERVERNEOYPTIFTLICEO	29	0.87, 0.95	0.87, 0.91
HTTPYTTYRALSEACAPNPHACTSADAPN	29	0.87, 0.95	0.87, 0.91
EAHLRIHSYMLTNMRLESTIRAWCNEUES	29	0.92, 0.95	0.92, 0.94
INEAEOEIPSUOBAYYTIOCELOADNSTA	29	0.97, 0.95	0.95, 0.96
MCRYPNASTINOYTPSINGTBLSUATAI	28	0.86, 0.95	0.86, 0.91
PEDEESNOOSDDTETTTCREAYOSCALT	28	1.0, 0.95	0.95, 0.98
OOLDTIAFGWEEHUARIRAXSORACLRI	28	0.90, 0.96	0.90, 0.93
TIOAETREADRETNNEASORTRSWLD SOVBHMECPNYREOIRTRHTTESA	50	0.99, 0.98	0.98, 0.99
HMRNOHOPYBETISTALIFYOAIU IEUETDEYEURTASETNNYOAIUABIL	50	1.00, 1.00	1.00, 1.00
EPTCFELLEYPPIOIHNYSCPGMSLNRO ENTATRYALTPISCPGPCXRACL	50	0.99, 0.98	0.98, 0.99

short length is shown in Table 2. The performance shows that Fuzzy method presented is efficient for monitoring of traffic for detection and further analysis of plain English text of very short length even when such texts are discontinuous or decimated. The performance of the proposed Fuzzy method for identification of plain English text is not comparable with other methods [11–14] and [20, 21] as these are applicable on larger size of English text.

The presented method can meet the requirement of monitoring and analysis of live traffic sensitive texts and taking preventive measures accordingly to protect adversaries and criminal activities on mobile and internet.

## 5 Conclusion

The detection of plain English text is one of the most important requirements to monitor and analyze the traffic for preventing transmission of vital information through mobile and internet communication. Moreover, detection and analysis of plain English text are also in demand to intercept the communication of adversaries and antisocial elements for protecting terror and criminal activities by taking appropriate safety measures. The fuzzy method utilizing percentage frequency of most and frequent letters as features and triangular Fuzzy membership function has been proposed in the paper. As per simulation results shown, the proposed method is very efficient and can be applied for online monitoring of huge traffic for identification and further analyze of English text with high accuracy even when it is discontinuous and its length is very short. The Fuzzy method proposed has vast applications in various defence as well as civil applications such as monitoring and analysis of harmful and sensitive short messages being communicated through mobile and internet by adversaries and antisocial elements.

## References

1. Stephen, G.W.: Digital Modulation and Coding. Prentice Hall, New Jersey (1996)
2. Katzenbeisser, S., Petitcolas, F.A.P.: Information Hiding Techniques for Steganography and Digital Watermarking. Artech House, London (2000)
3. Ratan, R., Madhavan, V.C.E.: Steganography Based Information Security. IETE Tech. Rev. **19**(4), 213–219 (2002)
4. Menezes, A., Van Oorschot, P., Vanstone, S.: Handbook of Applied Cryptography. CRC Press, USA (1996)
5. Stallings, W.: Cryptography and Network Security. Prentice Hall, Englewood Cliffs (2011)
6. Han, J., Kamber, M.L.: Data Mining: Concepts and Techniques. Elsevier, Amsterdam (2006)
7. Sebastiani, F.: Machine learning in automated text categorization. ACM Comput. Surv. **34**(1), 1–47 (2002)
8. Wong, A.K.S., Lee, J.W.T., Yeung, D.S.: Using complex linguistic features in context - sensitive text classification techniques. Proceedings of the 4th IEEE International Conference on Machine Learning and Cybernetics **5**, 3183–3188 (2005)
9. Simanjuntak, D.A., Ipung, H.P., Lim, C., Nugroho, A.S.: Text classification techniques used to facilitate cyber terrorism investigation. Proceedings of the 2nd IEEE International Conference on Advances in Computing, Control and Telecommunication Technologies (ACT), 198–200 (2010).
10. Upasana, Chakrabarty, S.: A survey of text classification techniques for e-mail filtering. Proceedings of the 2nd IEEE International Conference on Machine Learning and Computing (ICMLC), 32–36 (2010).

11. Cavnar, W.B., Trenkle, J.M.: N-Gram based text categorization, pp. 161–175. Proceedings of the Symposium on Document Analysis and Information Retrieval. Las Vegas, NV pp (1994)
12. Grefenstette, G.: Comparing two language identification schemes. Proceedings of the International Conference on Statistical Analysis of Textual Data JADT-95 (1995).
13. Kullback, S.: Statistical Methods in Cryptanalysis. Aegean Park, CA (1976)
14. Friedman, W.F.: Elements of Cryptanalysis. Aegean Park, CA (1976)
15. Anderson, A., Rosenfield, E.: Neuro Computing. MIT Press, MA (1988)
16. Dubois, D., Prade, H.: Fuzzy Sets and Systems: Theory and Applications. Academic Press, New York (1980)
17. Bezdek, J.C., Pal, S.K.: Fuzzy Models for Pattern Recognition. IEEE Press, New York (1992)
18. Puri, S., Kaushik, S.: A technical study and analysis on fuzzy similarity based models for text classification. *Int. J. Data Min. Knowl. Manag. Process* 2(2), 1–15 (2012).
19. Ratan, R., Saxena, P.K.: Algorithm for the restoration of distorted text documents. Proceedings of the International Conference on Computational Linguistics, Speech and Document Processing (ICCLSDP) (1998)
20. Yang, H.H., Moody, J.: Feature selection based on joint mutual information. *J. Comput. Intell. Met. Appl. Int. Comput. Sci. Conv.* **13**, 1–8 (1999)
21. Saxena, P.K., Yadav, P., Mishra, G.: Index of garbledness for automatic recognition of plain english texts. *Defence Sci. J* **60**(4), 415–419 (2010)



# Digital Mammogram and Tumour Detection Using Fractal-Based Texture Analysis: A Box-Counting Algorithm

K.C. Latha, S. Valarmathi, Ayesha Sulthana, Ramya Rathan,  
R. Sridhar and S. Balasubramanian

**Abstract** Mammography and X-ray imaging of the breast are considered as the mainstay of breast cancer screening. In the past several years, there has been tremendous interest in image processing and analysis techniques in mammography. The fractal is an irregular geometric object with an infinite nesting of structure of different sizes. Fractals can be used to make models of any objects. The most important properties of fractals are self-similarity, chaos, and non-integer fractal dimension. The fractal dimension analysis has been applied to study the wide range of objects in biology and medicine and has been used to detect small tumors, microcalcification in mammograms, tumors in brain, and to diagnose blood cells and human cerebellum. Fractal theory also provides an appropriate platform to build oncological-related software program because the ducts within human breast tissue have fractal properties. Fractal analysis of mammogram was used for the breast parenchymal density assessment. The fractal dimension of the surface is determined by utilizing the Box-counting method. The Mammograms were collected from HCG Hospital, Bangalore. In this study, a method was developed in the Visual Basic for extracting the suspicious

---

S. Valarmathi · R. Sridhar · S. Balasubramanian  
DRDO-BU-CLS, Bharathiar University, Coimbatore, Tamil Nadu, India  
e-mail: valar28aadarsh@gmail.com

R. Sridhar  
e-mail: rmsridhar@rediffmail.com

S. Balasubramanian  
e-mail: director\_research@jssuni.edu.in

A. Sulthana (✉) · K. C. Latha  
Water and Health, JSS University, Mysore, Karnataka, India  
e-mail: ayeshasulthanaa@gmail.com

K. C. Latha  
e-mail: latha\_tanvi23@yahoo.com

R. Rathan  
JSS University, Anatomy, Mysore, Karnataka, India  
e-mail: ramirohith@ymail.com

region from the mammogram based on texture. The fractal value obtained through Box-counting method for benign and malignant breast cancer is combined into a set. An algorithm was used to calculate the fractal value for the extracted image of the mammogram using Box-counting method.

**Keywords** Fractal dimension Box-counting algorithm · Mammogram · Benign · Malignant · Range and pixel based algorithms

## 1 Introduction

Mammography and X-ray imaging have largely contributed for the early detection of breast cancer. However, the effectiveness and sensitiveness of digital mammography in detection of breast cancer is currently under investigation. The imaging modality separates image acquisition and image display. Therefore, radiologists have to optimize the efficiency of both processes for treatment or removal of the tumor. A series of heuristic techniques such as filtering and thresholding (texture analysis) automatically detect abnormalities. These methods suffered from lack of robustness when the number of images to be classified is large. Recently, several statistical methods are used to overcome such problems and the primary one is the fractal dimension which is widely applied in biology and medicine; especially this technique is used to detect small tumors and microcalcification in mammograms [1]. Several algorithms were used for fractal dimension in which the Box-counting method is applied to estimate the fractal value of an X-ray (mammogram) image, because the Box-counting dimension provides the information regarding the 3D objects of the tissue composition of the breast mammogram [2]. Hence fractal analysis may be useful as the strategy of the current study allows an algorithm which aims at assisting the radiologist toward fast detection and early diagnosis in the prediction of breast cancer. The fractal is an irregular geometric object with an infinite nesting of structure of different sizes. Fractals can be used to make models of any objects. The most important properties of fractals are self-similarity, chaos and non-integer fractal dimension.

Challenges in the use of fractal methods on images are the limitation of the possible range of power law behavior because the results have been hard to be reproduced by other researchers. Therefore, this approach has been questioned by the medical practitioners [3]. Nilsson and Georgsson have reported that the Box-counting method can be applied to estimate the fractal value of an X-ray (mammogram) image, because the Box-counting dimension provides the information regarding the 3D objects of the tissue composition of the breast mammogram [2].

Therefore, fractal analysis may be useful to evaluate mammographically discovered breast masses. The design and analysis strategy of the current study allows an algorithm which aims at assisting the radiologist towards fast detection and early diagnosis in the prediction of breast cancer. With this background, this study aims:

- (i) To develop an algorithm for extracting the abnormal region in the breast mammogram
- (ii) To calculate the fractal value for the extracted image from the mammogram using Box-counting method
- (iii) To clarify the usefulness of using the fractal features (as a texture scale-invariant features) and to classify benign and malignant region in the respective images.

## 1.1 Fractal Dimension

The concept of fractal was first introduced by Mandelbrot in 1967. Fractal geometry compares the irregular forms, even at different scales since the approximate measure of the dimension  $D$  is independent of the unit of measurement [4]. The term “fractal” means break or fragment and is a pattern that reveals greater complexity as it is enlarged. For fractals, the counterparts of the dimensions (0, 1, 2, and 3) are known as fractal dimensions (FD). When applied to a point, a line, a square, or a cube,  $D$  simply gives the number of ordinary dimensions needed to describe the object —0, 1, 2, and 3, respectively. The value of fractal dimension is between one to two for a curve and in between two to three for a surface. The larger the  $D$ , rougher is the surface. The fractal dimension indicates how the measures of the object change with generalization [5].

Fractal dimension quantifies the metric information in lines and surfaces. The shapes of fractal objects keep invariant under successive magnification or shrinkage of the objects. A variety of procedures, including Box-counting, fractal Brownian motion [6], and fractal interpolation function system have been proposed for estimating the fractal dimension of images.

The fractional Brownian motion model (FBM) with gray-scale variation has shown promise in the medical image texture [6]. The Brownian motion curve concepts was extended to the FBM curve  $I(x)$ , and  $|I(x_2) - I(x_1)|$  having a mean value proportional to  $|x_1 - x_2|^H$ . Thus, in the FBM there is only one parameter of interest, the Hurst coefficient, which can be described as texture features when applied to classify breast tumor images. Considering the topological dimension  $T_d$ , for images, the FD can be estimated from the Hurst coefficient  $H = T_d - D$ . Using this relationship, the FD can be applied for the medical images [7] as:

$$D = \log(n_2/n_1) / \log(s_1/s_2) \quad (1)$$

## 1.2 Box-Counting Method

The fractal dimension of the surface is determined by utilizing the Box-counting method. This method yields quantitative agreement with the line-segment method. In the Box-counting method, the Hausdorff-dimension was utilized, where the

number,  $N(\xi)$ , of squares of side-length ' $\xi$ ' is needed to cover a set of increases like  $N(\xi) \propto \xi^{-d}$  for  $\xi \leftarrow 0$  for a set of fractal Hausdorff dimension  $d$ . From  $d = -\log[N(\xi_1)/N(\xi_2)]/\log[\xi_1/\xi_2]$ , the fractal dimension can be obtained theoretically [8].

Box-counting method was applied to compute FD for measuring the structure of an object in a digital image and to analyze morphological changes within organs. Fractal analysis based on microcomputer studies of image systems provides many advantages to the understanding of the complex microscopical arrangement of natural objects [9]. The fractal-based computerized image analysis of mammographic parenchymal patterns was used to differentiate women at high risk and low risk for the development of breast cancer and this study was evaluated [10].

## 2 Data Preparation

The Marathon database (Digital Database for Screening Mammography) associated with South Florida (United States), contains approximately 2,500 studies, each one includes two images of each breast, along with the information of the associated patient (age at time of study, breast density, and abnormalities) and image information (scanner and spatial resolution). Images containing suspicious areas also have associated pixel-level "ground truth" information about the locations and types of suspicious regions. The database is further organized into cases and volumes. A case is a collection of images and information corresponding to one mammography. A volume is simply a collection of cases. Some cases contain more than one cancer in one breast, a cancer in each breast, or a cancer along with other abnormal/suspicious regions. The outlines of all the regions have been transcribed from markings made by an experienced radiologist [11].

## 3 Methodology

A method was developed in the visual basic for extracting the suspicious region from the mammogram based on texture. For the extracted image, the fractal dimension was calculated using Box-counting method.

### *3.1 Extraction of Breast Cancerous Surface: Marathon Database and HCG Hospital Bangalore Database*

The following steps were used for extracting the abnormal region from the mammogram.

- Step 1: Extraction of the boundary from the given mammogram by using an algorithm given in the Appendix I.
- Step 2: Find the centroid for a set of boundary points which was extracted through the previous step.
- Step 3: Determine the distance of each boundary point from the centroid and also find the highest and lowest distance.
- Step 4: With highest distance as a radius, to draw a circle which encompasses all the boundary points and to store all the points of circle.

### ***3.2 Fractal Dimension: Box-Counting Method***

The algorithm used to calculate the fractal value for the extracted image of the mammogram using Box-counting method is shown in Appendix II. The red pixels or white pixels in the image cover the border of the object. A well-spaced grid with multiple small boxes of a particular pixel length was superimposed on the cell. Thus the FD of an image can be calculated with the boxes (2, 4, 8, 16, 32, 64, and 128).

## **4 Results**

Computer-aided diagnosis techniques were used to improve the diagnostic accuracy and efficiency for screening the mammogram. For this several algorithms are used to separate the normal and the abnormal region from the mammogram. As mentioned earlier, the identification is a laborious process, while comparing the breast lesions with the normal report, two problems occur in the image processing which are as follows:

- (i) To locate the malignant region in the breast mammogram and
- (ii) To identify the area of the spread in different regions of the mammogram.

In addition to separate the malignancy from the breast mammogram through image processing, a need for an algorithm arises. Fractal dimension methods are applicable for image processing technique for which Mandelbrot formula was followed:

$$\text{Fractal Dimension} = \log N / \log (1/r) \quad (2)$$

The algorithm used for FD is based on the above equation where they have used the number of boxes and its length. In this study, images from the oncology institute HCG, Bangalore were obtained to identify a suspicious region in the mammogram, which was illustrated and marked by the radiologist. This image of the breast cancer is used to segment and analyze the fractal dimension. The image scanned from left to right and top to bottom is brought to the system as a JPEG file. The JPEG image

was used for further analysis. A method was proposed to extract cancer surface on an image of breast cancer and Box-counting method is used to calculate the fractal dimension for benign and malignant breast cancer.

### 4.1 Extraction of Breast Cancerous Surface: Marathon Database and HCG, Bangalore Database.

The desired images of the breast cancer mammogram in the JPEG format were opened as a picture file. An algorithm was employed for converting the given image into a black and white image by classifying each pixel with Red Green Blue (RGB) color and the respective positions were stored in an array. The mild abnormality includes, the calcification, well-defined or circumscribed masses, speculated masses, ill-defined masses, asymmetry, and the architectural distortion. The benign and malignant breast mammogram involved in this study was considered as group A and group B for calculating the fractal value. Thus, the image of breast cancer was processed using the above steps and the suspicious area was extracted, which is shown in the Fig. 1

### 4.2 Fractal Dimension: Box-Counting Method

The fractal value for the extracted breast cancer image from the Marathon Database is presented in Table 1.

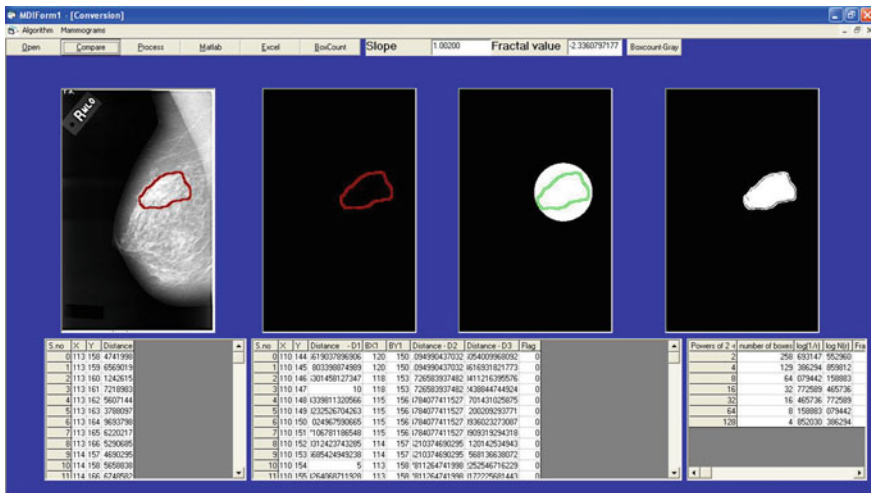


Fig. 1 Extraction of the abnormal region from the mammogram

**Table 1** Fractal value of an image—marathon database value for the breast

Powers of 2 <sup>f</sup>	Number of boxes	log(1/r)	log N(r)	Fractal value
2	264	-0.69315	5.575949	-8.0444
4	59	-1.38629	4.077537	-2.94132
8	12	-2.07944	2.484907	-1.19499

Usually the fractal value of an image obtained will be negative. The calculated fractal value for the eight benign and ten malignant breast mammograms using an algorithm is observed in the Table 2 in which the sample value 2.2297 (Malignant) is shown in the Fig. 2.

Similarly, the fractal values for the benign and malignant in the above table were calculated from their respective slope. With the benign and malignant fractal value, the mean and the standard deviation were calculated to find the significance of the results. The fractal value for the benign mammogram ranges from 2.2685 to 2.5850 and for malignant from 2.0922 to 2.4236. The fractal mean and standard deviation for the benign breast mammogram was found to be  $2.4621 \pm 0.11384$  and for malignant as  $2.3028 \pm 0.09454$ , respectively. The result obtained by the above method was used for classifying the unknown breast mammogram into benign or malignant.

The fractal value was calculated for ten benign and ten malignant mammograms based on the number of boxes using the Eq. 1. The fractal value for the benign and malignant mammograms ranges from 2.2759 to 2.6904 and 2.1771 to 2.4663, respectively. The Mean Fractal value for the benign and malignant tumor in the mammograms was found to be  $2.44834 \pm 0.16039$  and  $2.35554 \pm 0.077322$ , respectively. Similarly, the output obtained by this method was also used for classifying the mammogram into benign or malignant tumor.

**Table 2** Mean fractal value for the breast cancer mammograms—marathon database

S.No	n = 8	n = 10
	Benign	Malignant
1	2.5294	2.2297
2	2.3171	2.3068
3	2.5284	2.3767
4	2.4886	2.3342
5	2.4352	2.4236
6	2.5850	2.0922
7	2.5443	2.3317
8	2.2685	2.2458
9		2.3095
10		2.3774
Mean	2.4621	2.3028
SD	0.11384	0.09454

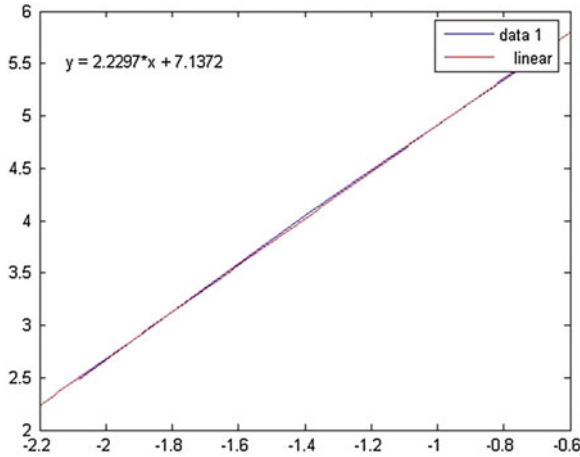


Fig. 2 Least square method of regression analysis — marathon database

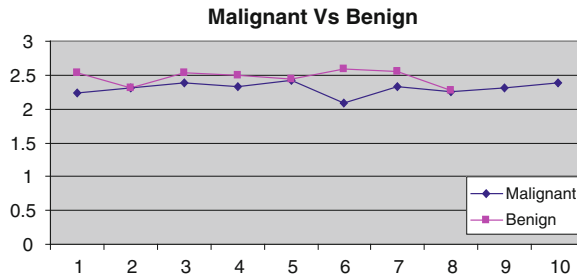


Fig. 3 Fractal value for the benign and malignant mammograms

### 4.3 Linear Regression and Statistical Method

Log(1/r) and log [N(r)] in X-axis Y-axis co-ordinates was used in MATLAB for the (n) number of boxes, marathon database and presented in Fig. 2. The number of boxes and dimension of boxes in the graph was observed as a straight line which was predicted using Least Square Method of Regression Analysis and the fractal dimension was obtained as the slope of the line as 2.2297. Statistical t-test was calculated between two independent samples of size eight and ten and was found to be as 3.2407. There was a significant difference between benign and malignant at 1% (2.95) level of significance, respectively. The fractal dimension of the benign and malignant was observed as  $2.4621 \pm 0.14$  and  $2.3028 \pm 0.09$  with 95% security coefficient in the Table 3.

Using the fractal values obtained from the benign and malignant breast cancer mammogram, a graph was drawn and shown in the Fig. 3



**Table 3** Statistical calculations for fractal dimension of benign and malignant

	Parameter	Benign	Malignant
	Mean	2.4621	2.3028
	Stdandard error of mean	0.04025	0.02990
	Median	2.5085	2.3206
	Mode	2.27	2.09
	Stdandar deviation	0.1138	9.454E-02
	Variance	1.296E-02	8.938E-03
	Skewness	-0.941	-1.195
	Standard error of skewness	0.752	0.687
	Kurtosis	-0.490	1.890
	Standard error of kurtosis	1.481	1.334
	Range	0.32	0.33
	Minimum	2.27	2.09
	Maximum	2.59	2.42
	Sum	19.70	23.03
Percentiles	25	2.3466	2.2418
	50	2.5085	2.3206
	75	2.5406	2.3769

Therefore, the methodology adopted above proves that the fractal dimension of benign is greater than malignant breast mammogram.

The FD values of the benign and malignant were subjected to ‘t’ test and found, there is a significant difference between benign and malignant at 1 % probability level, which will reveal that the FD of benign is greater than the malignant breast mammogram.

Determination of the Fractal Box-counting Dimension of a cell surface was applied to derive a quantitative measure for the raggedness of cells or small biological organisms [8]. Analysis of fractal dimension is used to find the roughness value and to locate the suspicious region in the mammogram of the breast cancer [5]. Sign of breast cancer is the appearance of clustered microcalcifications whose individual particles are less than 0.5 mm in diameter with irregular and heterogeneous shape [12]. Fractal properties are used to differentiate the tumor from healthy tissue and for the segmentation within an image, but it is not possible to compare fractal properties between images [13]. Fractal properties alone are not sufficient for effective texture segmentation and suggested the use of fractal features in texture classification [6, 10]. In the study of frequency distribution histogram, a large proportion of the lymphocytes of hairy cell leukemia patients had a fractal dimension exceeding 1.28 [8]. The fractal dimension calculated by applying the Box-counting method for the proximal convoluted tubule of the dog kidney was obtained as  $1.33 \pm 0.18$  with 95 % security coefficient [14]. The metastases of colorectal cancer with fractal dimensions greater than 1.35 were associated with poor survival rate [15].

Fractal dimensions of surface growth patterns in different grades of endometrial adenocarcinoma ranged from 2.318 to 2.383 [16]. These values were greater than the topological dimension of a surface, reflecting a three-dimensional structure. This concludes that the endometrial adenocarcinoma has a fractal structure, and that the Mean FD may differ according to histological grades. Fractal dimension analysis was used to identify the migration in breast cancer cell wound healing assay. In image intensity fluctuation, fractal dimension analysis can be used as a tool to quantify cell migration in terms of cancer severity and treatment responses [17]. Fractal analysis based on Chen's method for the tumor images, the slope of the benign and the malignant line was found to be 0.3644 and 0.3425, respectively [6]. Similar studies were applied for the smear of breast and cervical lesions where they calculated the fractal dimension values as  $0.8536 \pm 0.1120$  for malignant and  $0.8403 \pm 0.1115$  for benign [18]. The Mann-Whitney U test of these two samples shows significant difference at 5% probability level for cervix, whereas 2% probability level for breast cancer. Significant difference between the fractal dimension of benign and malignant cells at  $p = 0.006$  [19].

## 5 Conclusion

From the above study it is concluded that the measurement of fractal dimension is helpful in discriminating the malignant and benign breast lesions and to study the screening of classic image morphology based on Euclidean geometry. The algorithms proposed in this study extracted the similar suspicious area. Therefore, any one of the proposed methods can be adopted for easy extraction from breast cancer mammogram in advanced and benign cases.

In this study, fractal dimension has been applied to identify microcalcifications and tumors in the tissues of the body. Through this method, the size, location, and seriousness of the abnormality or suspicious regions are estimated for better diagnosis. However, a more intricate and higher level study, i.e., at cellular level is required for treatment of benign or malignant tumors.

## Appendix I

Algorithm for Boundary Extraction from the Mammogram.

---

```

For i = 0 To Picture1.ScaleWidth
For j = 0 To Picture1.ScaleHeight
tcol1 = GetPixel(Picture1.hdc, i, j)
r1 = tcol1 Mod 256
g1 = (tcol1 Mod 256) \ 256
b1 = tcol1 \ 256 \ 256
If r1 > 200 And g1 < 200 And b1 < 200 Then
tcol1 = vbRed
Else
tcol1 = vbBlack
End If
SetPixel Picture2.hdc, i, j, tcol1
Next j
Next i

```

---

## Appendix II

Algorithm for calculating the fractal value using Box-counting method.

---

```

Begin
Set  $N(\varepsilon) < -0$  for all values of  $\varepsilon$ 
For each pixel,  $S(x, y)$ , in the image
 $M = 0$ 
For each cell of size  $\varepsilon$ 
Center a cell of size  $\varepsilon$  on  $(x, y)$ 
If  $S(x - \varepsilon/2, y - \varepsilon/2)$  to  $S(x + \varepsilon/2, y + \varepsilon/2) \neq 0$  then
 $M = 1$ 
End if
End for
If  $m = 1$ , then increment  $N(\varepsilon)$  by 1
End for
Estimate  $D$  as the regression slope of  $\log(\varepsilon)$  versus  $\log(1/N(\varepsilon))$ 

```

---

## References

1. Buczko, W., Mikolajczak, D.C.: Shape analysis of MR brain images based on the fractal dimension. *Annales UMCS Informatica (AI)* **3**, 153–158 (2005)
2. Georgsson, F., Jansson, S., Olsen, C.: Fractal analysis of mammograms. In: Ersboll, B.K., Pedersen, K.S. (eds.) *SCIA, LNCS*, vol. pp. 92–101. 4522. Springer, Heidelberg (2007)
3. Baish, J.W., Jain, R.K.: Fractals and cancer. *Cancer Res.* **60**, 3683–3688 (2000)
4. Mandelbrot, B.B.: How long is the coast of Britain? statistical self-similarity and fractional dimension. *Science* **156**(3775), 636–638 (1967)
5. Rejani, Y.A.I., Thamaraiselvi, S.: Digital mammogram segmentation and tumour detection using artificial neural networks. *Int. J. Soft Comput. Medwell* **3**(2), 112–119 (2008)
6. Chen, C.C., Daponte, J.S., Fox, M.D.: Fractal feature analysis and classification in medical imaging. *IEEE Trans. Med. Imaging.* **8**(2), 133–142 (1990)
7. Mohamed, A.W., Kadah, M.Y.: Computer aided diagnosis of digital mammograms. *IEEE* **1**, 299–303 (2007). ISSN 4244–1366-4/07.
8. Bauer, W., Mackenzie, D.C.: Cancer detection via determination of fractal cell dimension. *Heavy Ion Phys.* **14**, 39–46 (2001)
9. Cross, S.S., Cotton, D.W.K.: The fractal dimension may be a useful morphometric discriminant in histopathology. *J. Path.* **166**, 409–411 (1992)
10. Lee, W.L., Chen, Y.C., Chen, Y.C., Hsieh, K.S.: Unsupervised segmentation of ultrasonic liver images by multiresolution fractal feature vectors. *Inf. Sci.* **175**(3), 177–199 (2005)
11. Rose, C., Turi, D., Williams, A., Wolstencroft, K., Taylor, C.: University of south florida digital mammography home page. IWDWM. <http://marathon.csee.usf.edu/Mammography/> Database.html, (2006)
12. Kopans, D.B.: *Breast Imaging Medicine*, Lippincott Williams and Wilkins, ISBN-10.PS, Philadelphia (1989).
13. Veeland, J., Grashuis, J.L., Van der Meer, F., Beckers, A.L.D., Gelsema, E.S.: Estimation of fractal dimension in radiographs. *Med. Phys.* **23**, 584–585 (1996)
14. Gil, J., Gimeno, M., Laborda, J., Nuviala, J.: Fractal dimension of dog kidney proximal convoluted tubuli sections by mean Box-counting algorithm. *Int. J. Morphol.* **24**(4), 549–554 (2006)
15. Metser, U.: 18 F-FDG PET in evaluating patients treated for Metastatic colorectal cancer: can we predict prognosis? *J. Nucl. Med.* **45**(9), 1428–1430 (2004)
16. Kikuchi, A., Kozuma, S., Yasugi, T., Taketani, Y.: Fractal analysis of surface growth patterns in endometrioid endometrial adenocarcinoma. *Gynecol. Obstet. Invest.* **58**(2), 61–67 (2004)
17. Sullivan, R., Holden, T., Jr Tremberger, G., Cheung, E., Branch, C., Burrero, J., Surpris, G., Quintana, S., Rameau, A., Gadura, N., Yao, H., Subramaniam, R., Schneider, P., Rotenberg, A., Marchese, P., Flamholz, A., Lieberman, D., Cheung, T.: Fractal dimension of breast cancer cell migration in a wound healing assay. *Eng. Technol.* **34**, 25–30 (2008). ISSN 2070–3740.
18. Ohri, S., Dey, P., Nijhawan, R.: Fractal dimension in aspiration cytology smears of breast and cervical lesions. *Anal. Quant. Cytol. Histol.* **26**(2), 109–112 (2004)
19. Dey, P., Mohanty, K.S.: Fractal dimensions of breast lesions on cytology smears. *Diagn. Cytopathol.* **29**(2), 85–86 (2003).
20. Snedecor, W.G., Cochran, G.W.: *Statistical Methods*, 7th edn. The IOWA State University Press, Ames (1980)

# Approaches of Computing Traffic Load for Automated Traffic Signal Control: A Survey

Pratishtha Gupta, G. N. Purohit and Adhyana Gupta

**Abstract** Traffic images captured using CCTV camera can be used to compute traffic load. This document presents a survey of the research works related to image processing, traffic load, and the technologies used to re-solve this issue. Results of the implementation of two approaches: morphology-based segmentation and edge detection using sobel operator, which are close to traffic load computation have been shown. Segmentation is the process of partitioning a digital image into its constituent parts or objects or regions. These regions share common characteristics based on color, intensity, texture, etc. The first step in image analysis is to segment an image based on discontinuity detection technique (Edge-based) or similarity detection technique (Region-based). Morphological operators are tools that affect the shape and boundaries of regions in the image. Starting with dilation and erosion, the typical morphological operation involves an image and a structure element. The edge detection consists of creating a binary image from a grayscale image where the pixels in the binary image are turned off or on depending on whether they belong to region boundaries or not. Image processing is considered as an attractive and flexible technique for automatic analysis of road traffic scenes for the measurement and data collection of road traffic parameters. Combined background differencing and edge detection and segmentation techniques are used to detect vehicles and measure various traffic parameters. Real-time measurement and analysis of road traffic flow parameters such as volume, speed and queue are increasingly required for traffic control and management.

---

P. Gupta (✉) · G. N. Purohit · A. Gupta  
Banasthali University, Banasthali, Rajasthan, India  
e-mail: pratishthal1@gmail.com

G. N. Purohit  
e-mail: gn\_purohitjaipur@yahoo.co.in

A. Gupta  
e-mail: adhyanagupta@gmail.com

**Keywords** Image processing · Simulation · Segmentation · Edge detection · Real time · Traffic load computation

## 1 Introduction

This study describes all the functions and specifications which can be used for Traffic Load Computation using traffic images, which can be further used for real-time image processing for traffic signal control. In this paper, after analyzing existing video object segmentation algorithms, it is found that most of the core operations can be implemented with simple morphological operations. Therefore, with the concepts of morphological image processing element array and stream processing, a reconfigurable morphological image processing accelerator is proposed, whereby the proposed instruction set, the operation of each processing element can be controlled, and the interconnection between processing elements can also be reconfigured.

Field Programmable Gate Array (FPGA) technology has become an alternative for the implementation of software algorithms. The unique structure of the FPGA has allowed the technology to be used in many applications from video surveillance to medical imaging applications. FPGA is a large-scale integrated circuit that can be reprogrammed.

This study comprises of eight sections including the present one, which provides an introduction and objectives of this brief survey same purpose. Section 7 compares the two approaches implemented in Sects. 5 and 6. Finally Sect. 2 presents various image processing approaches. Section 3 presents various research works aimed at computing traffic load. Section 4 presents various technologies used in this field. Section 5 implements one of the morphological approaches for traffic load computation purpose. Section 6 presents the implementation of an approach using sobel operator for the conclusion drawn in Sect. 8.

## 2 Image Processing Approaches

### 2.1 Image Segmentation

Shao-Yi Chien and Liang-Gee Chen [1] discussed in this paper, after analyzing existing video object segmentation algorithms, it is found that most of the core operations can be implemented with simple morphology operations. Therefore, with the concepts of morphological image processing element array and stream processing, a reconfigurable morphological image processing accelerator is proposed, whereby the proposed instruction set, the operation of each processing element can be controlled, and the interconnection between processing elements can also be reconfigured.

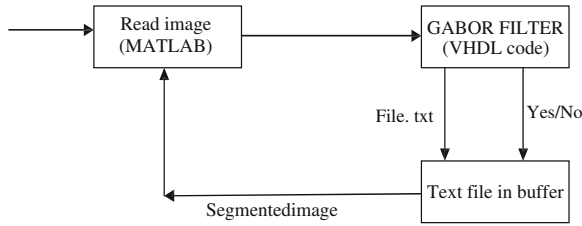


Fig. 1 Use of Gabor filter

Thakur et al. [2] explain tonsillitis, tumor, and many more skin diseases can be detected in its early state and can be cured. Image segmentation is the processes of partitioning a digital image into multiple segments that is sets of pixels Fig. 1.

Ramadevi et al. [3] discussed in this paper image segmentation is to partition an image into meaningful regions with respect to a particular application. Image segmentation is the process of partitioning/subdividing a digital image into multiple meaningful regions or sets of pixels regions with respect to a particular application. The three steps in edge detection process is: (a) filtering, (b) enhancement, and (c) detection. This paper focuses mainly on the Image segmentation using edge operators.

Salem Saleh Al-amri et al. [4] have proposed segmentation algorithms based on one of two basic properties of intensity values discontinuity and similarity. First category is to partition an image based on abrupt changes in intensity, such as edges in an image. Second category is based on partitioning an image into regions that are similar according to predefined criteria.

Bo Peng et al. [5] discussed image segmentation as an inference problem, where the final segmentation is established based on the observed image. In addition, a faster algorithm has been developed to accelerate the region merging process, which maintains a nearest neighbor graph (NNG) in each iteration.

## 2.2 Digital Image Segmentation

Haris Papasaika-Hanusch [6] explains a digital image differs from a photo in that the values are all discrete.

- **Image Enhancement:** Processing an image so that the result is more suitable for a particular application (sharpening or deblurring an out of focus image, highlighting edges, improving image contrast, or brightening an image, removing noise).
- **Image Restoration:** This may be considered as reversing the damage done to an image by a known cause (removing of blur caused by linear motion, removal of optical distortions).
- **Image Segmentation:** This involves subdividing an image into constituent parts, or isolating certain aspects of an image (finding lines, circles, or particular shapes in an image, in an aerial photograph, identifying cars, trees, buildings, or roads).

### **2.3 Edge Detection**

Allin Christe et al. [7] discussed in this paper focuses on processing an image pixel by pixel and in modification of pixel neighborhoods and the transformation that can be applied to the whole image or only a partial region.

Draper et al. [8] explain although computers keep getting faster and faster, there are always new image processing (IP) applications that need more processing than is available. Examples of current high-demand applications include real-time video stream encoding and decoding, real-time biometric (face, retina, and/or fingerprint) recognition, and military aerial and satellite surveillance applications.

### **2.4 Fuzzy Edge Detection**

Sriramakrishnan et al. [9] explain edge is a basic feature of image; edge detection is a process of identifying and locating edges in image which is vital for image segmentation. Distortion, noise, overlaps, and intensity variation are some of the factors, which contributes to edge extraction. Image identification and segmentation pose a challenge to image retrieval process.

## **3 Traffic Load Computation**

Gupta et al. [10] have also proposed a model capable of managing intelligent traffic system using CCTV cameras and WAN. The proposed model will make the traffic signaling dynamic and automatic as well. Besides this, it will generate the dynamic messages for the users on the message boards to avoid congestion, reduce waiting time, pollution control, accident control, and vehicle tracking. This brief survey presents various approaches for intelligent traffic systems.

Duan et al. [11] discussed due to a huge number of vehicles, modern cities need to establish effectively automatic systems for traffic management and scheduling. This method optimizes speed and accuracy in processing images taken from various positions.

Abhijit Mahalanobis et al. [12] explain the detection and tracking of humans as well as vehicles is of interest. The three main novel aspects of the work presented in this paper are (i) the integration of automatic target detection and recognition techniques with tracking, (ii) the handover and seamless tracking of objects across a network, and (iii) the development of real-time communication and messaging protocols using COTS networking components.

Siyal et al. [13] has presented real-time measurement and analysis of road traffic flow parameters such as volume, speed, and queue are increasingly required for traffic control and management. Many techniques have been proposed to speed up the analysis of road traffic images, and some intelligent approaches have been developed to compensate for the effects of variable ambient lighting, shadows, occlusions, etc., in the road traffic images.



Kastrinaki et al. in [14] present an overview of image processing and analysis tools used in these applications, and we relate these tools with complete systems developed for specific traffic applications. Image processing also finds extensive applications in the related field of autonomous vehicle guidance, mainly for determining the vehicle’s relative position in the lane and for obstacle detection.

Koutsia et al. [15] explain traffic control and monitoring using video sensors has recently drawn increasing attention, due to the significant advances in the field of computer vision. The paper presents a real-time vision system for automatic traffic monitoring based on a network of autonomous tracking units that capture and process images from one or more recalibrated cameras.

Ejaz [16] discussed manually configured traditional time-based traffic signals are not categorically efficient in controlling traffic and merely tend optimize a certain traffic condition, which may only occur at a specific time of day. By doing that it may also create a highly unoptimized situation for some other traffic conditions. Sensor-based approaches tend to provide only a limited number of parameters, which may prove to be incomplete for making fully context aware decisions for road signals. Large cities of developing countries face a huge rise in the total number of on-road vehicles over a period of last few years.

Bosman [17] discussed traffic loads are the most important variable actions to be accounted for in the design of road pavements and bridges. Axle mass is probably one of the main factors that determine the effect of traffic loads on pavements. In the case of bridges, it is not only the axle mass, but also the spacing between axles, that determines the effect of traffic loads on the different structural elements.

### 4 Technologies

Parker et al. [18] explain the goal of this project is to implement histogram equalization algorithm using MATLAB for a real-time processing system on a FPGA. The histogram equalization algorithm was implemented and tested using a known 4×4 array.

Chikalli et al. [19] discussed Histogram is used for automatically determining the threshold for different region in image. (Fig. 2) The histogram is a very important tool in image analysis.

Ali et al. [20] evaluated in Xilinx system generator is a very useful tool for developing computer vision algorithm. Image processing is used to modify the picture, extract information, and change their structure. This paper focuses in the processing

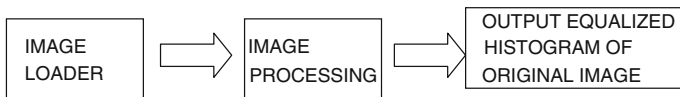


Fig. 2 Use of histogram tool

pixel to pixel of an image and in the modification of pixel neighborhoods and of course the transformation can be applied to the whole image or only a partial region.

Elamaram et al. [21] discussed a real-time image processing algorithm are implemented on FPGA. Implementation of these algorithm on a FPGA is having advantage of using large memory and embedded multipliers.

Chandrashekar et al. [22] discussed enhancing digital image to extract true image is a desired goal in several applications, such transformation is known as image enhancement. Performing the task automatically without human intervention is particularly hard in image processing. FPGA implemented result compared with Matlab experiments and comparisons to histogram equalization are conducted.

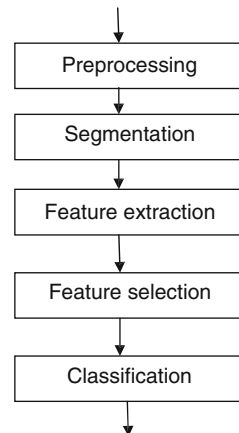
Acharya et al. [23] discussed an efficient FPGA-based hardware design for enhancement of color and gray scale image in image and video processing. The approach that is used is adaptive histogram equalization, which works very effectively for image captured under extremely dark environment as well as nonuniform lighting environment where bright regions are kept unaffected and dark object in bright background.

Gribbon et al. [24] explain FPGA as implementation platforms for real-time image processing applications because the structure allows them to exploit spatial and temporal parallelism. High level languages and compilers which automatically extract parallelism from the code do not always produce an efficient mapping to hardware.

Devika et al. [25] explain FPGA technology has become viable target for the implementation of real-time algorithms suited to video image processing applications. The FPGA technologies offer basic digital blocks with flexible interconnections to achieve high speed digital hardware realization Fig. 3.

Anusha et al. [26] discussed the image processing algorithms has been limited to software implementation which is slower due to the limited processor speed.

**Fig. 3** Typical steps in image processing algorithms



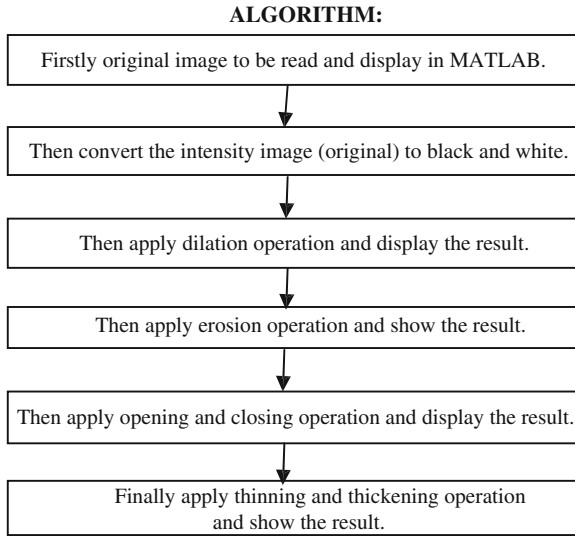
## 5 Implementation of Morphological Based Segmentation

FPGA technology has become viable target for the implementation of real-time algorithms suited to video image processing applications. The FPGA technologies offer basic digital blocks with flexible interconnections to achieve high speed digital hardware realization.

### 5.1 Morphological Operations

Morphological operators are defined as combinations of basic numerical operations taking place over an image A and a small object B, called a structuring element. B can be seen as a probe that scans the image and modifies it according to some specified rule. The shape and size of B, which is typically much smaller than image A, in conjunction with the specified rule, define the characteristics of the performed process. Binary mathematical morphology is based on two basic operators: Dilation, and erosion. Both are defined in terms of the interaction of the original image A to be processed, and the structuring element B. The Morphological operations are:

- (i) **Dilation Operation:** The basic effect of the operator on a binary image is to gradually enlarge the boundaries of regions of foreground *pixels* (i.e. white pixels, typically). Thus areas of foreground pixels grow in size while holes within those regions become smaller.
- (ii) **Erosion Operation:** The basic effect of the operator on a binary image is to erode away the boundaries of regions of foreground pixels (i.e. white pixels, typically). Thus areas of foreground pixels shrink in size, and holes within those areas become larger.
- (iii) **Opening Operation:** The basic effect of an opening is somewhat like erosion in that it tends to remove some of the foreground (bright) pixels from the edges of regions of foreground pixels. However it is less destructive than erosion in general. As with other morphological operators, the exact operation is determined by a *structuring element*.
- (iv) **Closing Operation:** It tends to enlarge the boundaries of foreground (bright) regions in an image (and shrink background color holes in such regions), but it is less destructive of the original boundary shape. As with other *morphological operators*, the exact operation is determined by a *structuring element*. The effect of the operator is to preserve background regions that have a similar shape to this structuring element, or that can completely contain the structuring element, while eliminating all other regions of background pixels.
- (v) **Thinning operation:** It is particularly useful for *skelitonization*. In this mode it is commonly used to tidy up the output of *edge detectors* by reducing all lines to single pixel thickness. Thinning is normally only applied to binary images, and produces another binary image as output. The thinning operation is related



**Fig. 4** Steps of morphological approach

to the *hit-and-miss transform*, and so it is helpful to have an understanding of that operator before reading on.

- (vi) **Thickening operation:** It has several applications, including determining the approximate *convex hull* of a shape, and determining the *skeleton by zone of influence*. Thickening is normally only applied to binary images, and it produces another binary image as output Fig. 4.

## 5.2 Experimental Results

The experimental results for Morphological based Segmentation in MATLAB are shown below:

Figure 5. Firstly original image to be read and display in MATLAB.

Figure 6. Then convert the intensity image (original) to black and white.

Figure 7. Then apply dilation operation and display the result.

Figures 8 and 9. Then apply erosion operation and show the result.

Figures 10 and 11. Then apply opening and closing operation and display the result.

Figures 12 and 13. Finally apply thinning and thickening operation and show the result.



Fig. 5 Original image

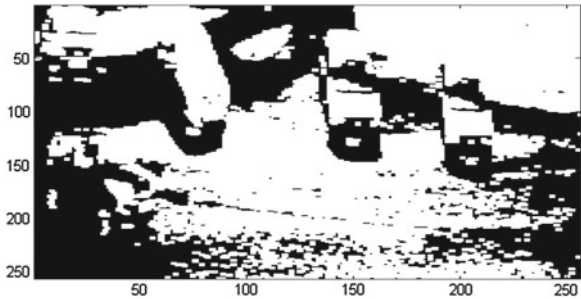


Fig. 6 Original image into black and white

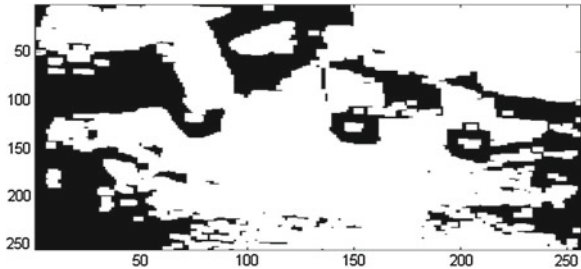


Fig. 7 Dilation operation

## 6 Implementation of SOBEL Edge Detection on FPGA

The proposed work presents FPGA based architecture for Edge Detection using Sobel operator and uses Histogram method for Segmentation. The data of edge detection is very large so the speed of image processing is a difficult problem. FPGA can overcome it. Sobel operator is commonly used in edge detection. Sobel operator has been researched for parallelism but Sobel operator locating complex edges are not accurate.

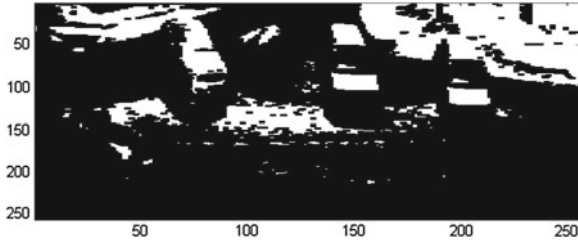


Fig. 8 Erosion operation

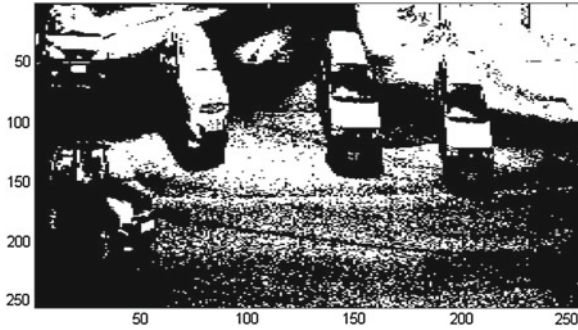


Fig. 9 Erosion operation

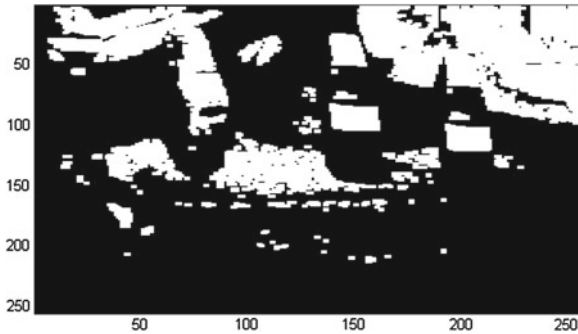


Fig. 10 Opening operation

**Edge detection**

Edge detection is a method of determining the discontinuities in gray level images. Conventional edge detection mechanisms examine image pixels for abrupt changes by comparing pixels with their neighbors. This is often done by detecting the maximal value of gradient such as Roberts, Prewitt, Sobel, Canny, and so on all of which are classical edge detectors.

**Sobel Edge Detection**

The Sobel operator is a classic first order edge detection operator computing an approximation of the gradient of the image intensity function. At each point in the

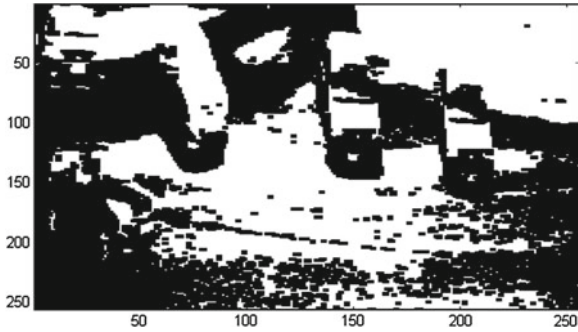


Fig. 11 Closing operation

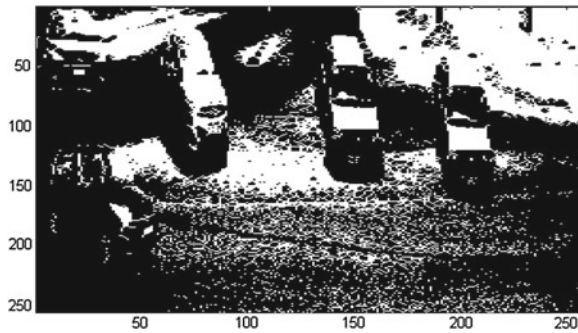


Fig. 12 Thinning operation

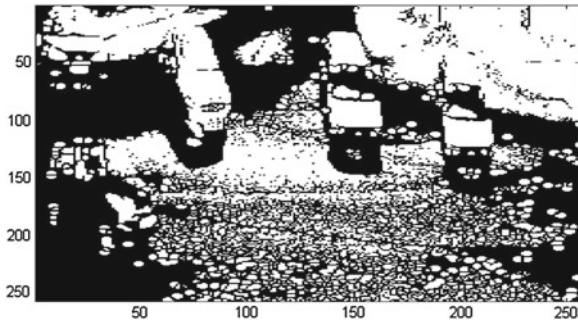


Fig. 13 Thickening operation

image, the result of the Sobel operator is the corresponding norm of this gradient vector. The Sobel operator only considers the two orientations which are 0 and 90 degrees convolution kernels as shown in Fig. 14.

These kernels can then be combined together to find the absolute magnitude of the gradient at each point. The gradient magnitude is given by:

**Fig. 14** Convolution kernels in X and Y direction

-1	-2	-1
0	0	0
1	2	1
Gy		

-1	0	1
-2	0	2
-1	0	1
Gx		

$$|G| = \sqrt{Gx^2 + Gy^2}$$

Typically an approximate magnitude is computed using:

$$|G| = |Gx| + |Gy|$$

This is much faster to compute.

The sobel operator has the advantage of simplicity in calculation.

But the accuracy is relatively low because it only used two convolution kernels to detect the edge of image.

### 6.1 Experimental Results

The experimental results for image edge detection in MATLAB are shown below:

Figure 15 is the original image for edge detection.

Figure 16 shows gray scale image for edge detection.

Figure 17 shows edge detection result using MATLAB. (Table 1)



**Fig. 15** Original image for edge detection



**Fig. 16** Gray scale for edge detection



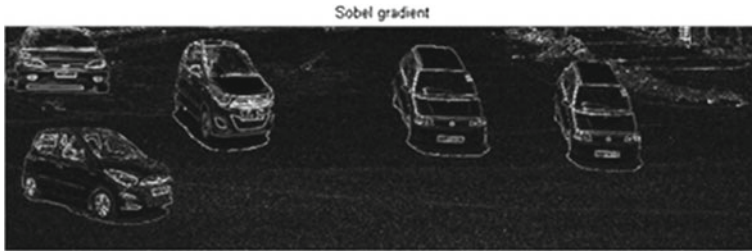


Fig. 17 Result of edge detection

## 7 Comparison

**Table 1** Comparison of morphological and sobel operator approaches

Morphological-based segmentation	SOBEL Edge Detection on FPGA
Segmentation could be also obtained using morphological operations	Sobel operator due to its property of less deterioration in high level of noise
Segmentation subdivides an image into its constituent regions or objects	Edge detection is used to check the Sudden change in images
Segmentation should stop when the objects of interest in an application have been isolated	It analysis and processing the image with the help sobel operator
For example, in the automated inspection of electronic assemblies, interest lies in analyzing images of the products with the objective of determining the presence or absence of specific anomalies, such as missing components or broken connection paths	The execution time for the entire program of edge detection for an image of size $256 \times 256$ is few seconds. The execution time for the entire program of edge detection for an image of size $256 \times 256$ is few seconds
Image processing algorithms are conventionally implemented in DSP processors and some special purpose processors	To improve the speed and efficiency pipelining can be further done in edge detection
In morphology we have performed erosion, dilation, opening, closing, thinning and thickening	The edge detection is a terminology in image processing particularly in the areas of feature extraction to refer to algorithms which aim at identifying points in a digital image at which the image brightness changes sharply

## 8 Conclusion

In this paper, we introduced the existing image processing algorithms suitable for real-time traffic load computation and analyzed their outputs. We implemented two important approaches edge detection and morphology based segmentation and provided a qualitative comparison of those two approaches for our requirement. After analyzing existing image object segmentation algorithms, it is found that most of the core operations can be implemented with simple morphology operations. Therefore, with the concepts of morphological image processing element array and stream processing, a reconfigurable morphological image processing accelerator is proposed, whereby the proposed instruction set, the operation of each processing element can be controlled, and the interconnection between processing elements can also be reconfigured.

In summary, the open issue in real-time traffic load computation is to find the most efficient algorithm to compute traffic load in real time. The research direction is that as technologies in hardware are advancing and becoming mature, digital image processing algorithms need to be developed so as to get the real-time benefits of these hardware technologies.

## References

1. Chien, S.-Y., Chen, L.-G.: Reconfigurable Morphological Image Processing Accelerator for Video Object Segmentation. *Signal. Process. Syst.* **62**(1), 77–96 (2011)
2. Thakur, R.R., Dixit, S.R., Dr.Deshmukh, A.Y.: VHDL design for image segmentation using gabor filter for disease detection. *Int. J. VLSI Design. Commun. Sys.* **3**(2), 211 (2012).
3. Ramadevi, Y., Sridevi, T., Poornima, B., Kalyani, B.: Segmentation and object recognition using edge detection techniques. *Int. J. Comp. Sci. Info. Technol.* **2**(6), 153–161 (2010)
4. Al-amri, S.S., Kalyankar, N.V., Khamitkar, S.D.: Image segmentation by using thershod techniques. *J. Comput.* **2**(5), ISSN 2151–9617 (2010).
5. Peng, B., Zhang, L., Zhang, D.: Automatic image segmentation by dynamic region merging. The Hong Kong Polytechnic University, Hong Kong (2010)
6. Papasaika-Hanusch, H.: Digital image processing using matlab. ETH Zurich, Zurich (1967)
7. Mrs. Allin Christe, S., Mr. Vignesh, M., Dr. Kandaswamy, A.: An efficient FPGA implementation of MRI image filtering and tumour characterization using Xilinx system generator. *Int. J. VLSI. Des. Comm. Sys.* **2**(4), (2011).
8. Draper, B.A.: Ross Beveridge, J., Willem Böhm, A.P., Ross, C., Chawathe, M.: Accelerated image processing on FPGAs. *IEEE Trans. Image Process.* **12**(12), 1543–1551 (2003)
9. Sriramakrishnan, C., Shanmugam, A.: Image Retrieval Optimization Using FPGA Based Fuzzy Segmentation, ISSN 1450–216X **63**(1) (2011).
10. Gupta, P., Purohit, G.N., Dadhich, A.: Approaches for intelligent traffic system: a survey. Banastahli University, Jaipur (2012)
11. Duan, T.D., Du Hong, T.L., Phuoc, T.V.: Hoang. Building an automatic vehicle license- plate recognition system. *Int. J. Adv. technol.* **N.V.** (2005)
12. Abhijit Mahalanobis, Jamie Cannon, S. Robert, Stanfill, Robert Muise, Lockheed Martin, Network video image pro-cessing for security, Surveillance, and Situational Awareness. *Digital. Wireless. Commun.* doi:10.1117/12.548981.

13. Siyal, M.Y., Fathi, M., Atiquzzaman, M.: A parallel pipeline based multiprocessor system for real-time measurement of road traffic parameters. *Int. J. Imaging. Sys. Technol.* **21**(3), 260–270 (2011)
14. Kastrinaki, V., Zervakis, M., Kalaitzakis, K.: A survey of video processing techniques for traffic applications. *Image. Vision. Comput.* **21**, 359–381 (2003)
15. Koutsia, A., Semertzidi, T., Dimitropoulos, K., Grammalidis, N.: Intelligent traffic monitoring and surveillance with multiple camras. In: *Proceedings of International Workshop on Content-Based Multimedia Indexing (CBMI '08)*, 125–132 (2008).
16. Ejaz, Z.: Morphological image processing based road traffic signal control system.
17. Bosman, J.: Traffic loading characteristics of south african heavy vehicles.
18. Parker, S.: Ladeji-Osias. Implementing a histogram equalization algorithm in reconfigurable hardware. J.K. (2009)
19. Ms. Chikkali, P S.: FPGA based Image edge detection and segmentation. *Int. J. Adv. Eng. Sci.* **9**(2), 187–192 (2011).
20. Ali, S.M., Mr. Naveen, Mr. Khayum.: FPGA based design and implementation of image architecture using XILINX system generator, *IJCAE*, **3**(1), 132–138 (2012).
21. Elamaran, V., Rajkumar, G.: FPGA implementation of point processes using Xilinx system generator **41**(2), (2012).
22. Chandrashekar, M., Naresh Kumar, U., Sudershan Reddy, K., Nagabhushan Raju, K.: FPGA implementation of high speed In: *Frared Image Enhancement*, ISSN 0975–6450 **1**(3), 279–285 (2009).
23. Acharya, A., Mehra, R., Takher, V.S.: FPGA based non uniform illumination correction in image processing applications *Int. J. Comp. Tech. Appl.* **2**(2), 349–358 (2009)
24. Gribbon, K. T., Bailey, D. G., Johnston, C.T.: Design patterns for image Processing Algorithm Development on FPGAs.
25. Devika, S.V., Khumuruddeen, S.K., Alekya.: Hardware implementation of Linear and Morphological Image Processing on FPGA. **2**(1), 645–650 (2012).
26. Anusha, G., Dr.JayaChandra Prasad, T., Dr.Satya Narayana, D.: Implementation of SOBEL edge detection on FPGA. **3**(3) (2012).

# Comparative Analysis of Neural Model and Statistical Model for Abnormal Retinal Image Segmentation

D. Jude Hemanth and J. Anitha

**Abstract** Artificial Neural Networks (ANN) are gaining significant importance in the medical field, especially in the area of ophthalmology. Though the performance of ANN is theoretically stated, the practical applications of ANN are not fully explored. In this work, the suitability of Back Propagation Neural Network (BPN) for ophthalmologic applications is highlighted in the context of retinal blood vessel segmentation. The neural technique is tested with Diabetic Retinopathy (DR) images. The performance of the BPN is compared with the k-Nearest Neighbor (k-NN) classifier which is a statistical classifier. Experimental results verify the superior nature of the BPN over the k-NN approach

**Keywords** Back propagation network · k-Nearest neighbor · Retinal images.

## 1 Introduction

Eye diseases are mostly gradual in nature which affects the human society to a high extent. The nature of the eye disease can be determined from the affected anatomical structures. Hence, detecting the anatomical structures like blood vessels is mandatory for treatment planning.

The literature survey reveals the variety of techniques available for blood vessel segmentation. Supervised methodologies are used for retinal vessel segmentation in [1]. Morphological approaches-based blood vessel segmentation is implemented in [2]. Blood vessel segmentation using functional and textural features are reported in [3, 4]. The combined approach of line operators and support vector machines

---

D. J. Hemanth (✉) · J. Anitha  
Department of ECE, Karunya University, Coimbatore, India  
e-mail: jude\_hemanth@rediffmail.com

J. Anitha  
e-mail: rajivee1@rediffmail.com

are used for segmentation in [5]. Fuzzy-based techniques are used for segmentation applications in [6]. Filtering approaches are also used for blood vessel extraction in [7]. Statistical approaches are also widely used for vascular detection in retinal images [8]. Ridge-based detection methods are reported in [9]. Wavelet-based segmentation methodologies are also available in the literature [10].

Though many techniques are available, the segmentation efficiency of such techniques is not very high which ultimately limits the practical applications of such systems. This drawback is overcome in this proposed approach in which the automated system is based on Artificial Intelligence (AI). BPN is the segmentation technique proposed in this work and the results are compared with the k-NN technique.

## 2 Proposed Methodology

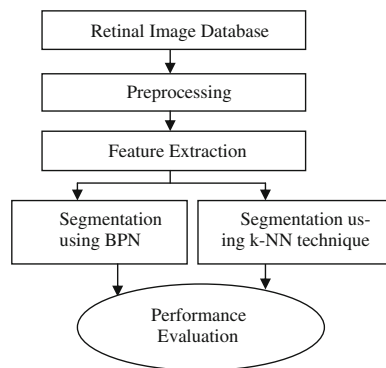
The automated system used for this application is shown in Fig. 1.

In this work, 40 retinal images provided by the DRIVE database are used for segmentation. It is then preprocessed by various methods which are followed by feature extraction process. These features are given to BPN for the training process. This trained network will be used to segment the retinal blood vessel from the retinal images. The same procedure is repeated with the k-NN technique except for the difference in the training methodology.

## 3 Image Pre-Processing

Retinal images usually have pathological noise and various texture backgrounds, light variations, and poor contrast which may cause difficulties in extraction. In order to reduce these imperfections and generate images more suitable for extracting the pixel features demanded in the classification step, a preprocessing comprising the

**Fig. 1** Flow diagram of the proposed work



following steps is applied: (1) green channel extraction, (2) gray scale conversion, (3) adaptive histogram equalization, (4) vessel central light reflex removal, and (5) background homogenization.

## 4 Feature Extraction

Feature extraction is a methodology of dimensionality reduction in which suitable features representing the blood vessel pixels and non-blood vessel pixels are extracted from the pre-processed images. The features used in this work are mean, standard deviation, skewness, kurtosis, energy, and entropy. These features are computed using the following equations prescribed by [11].

## 5 Segmentation Approaches

In this work, two segmentation techniques are employed. One is the neural technique and the other is the statistical technique.

### 5.1 *Back Propagation Neural Network*

BPN is a supervised neural network in which gradient descent method is used to minimize the total squared error of the output computed by the network. The proposed architecture consists of six neurons in the input layer, 15 neurons in the hidden layer, and two neurons in the output layer. Two set of weight matrices are involved in the architecture for the hidden layer and the output layer. In addition to the input vector and output vector, the target vector is given to the output layer neurons. Since BPN operates in the supervised mode, the target vector is mandatory. During the training process, the difference between the output vector and the target vector is calculated and the weight values are updated based on the difference value. After the segmentation process, a two-step post-processing is used: the first step is aimed at filling pixel gaps in detected blood vessels, while the second step is aimed at removing falsely detected isolated vessel pixels. A detailed algorithm is given in [12].

### 5.2 *k-NN Approach*

k-nearest neighbor (k-NN) classification makes the classification by getting votes of the k-nearest neighbors. Performance of k-NN classifier depends largely upon the efficient selection of k-nearest neighbors. Classification using an instance-based

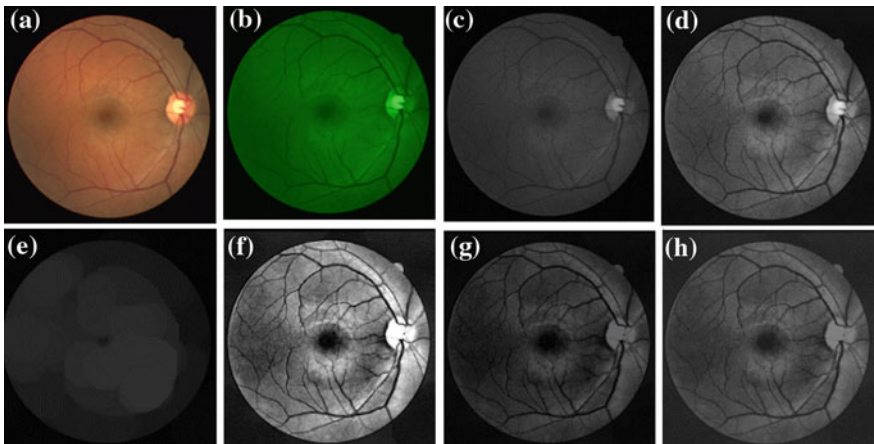
classifier can be a simple matter of locating the nearest neighbor in instance space and labeling the unknown instance with the same class label as that of the located (known) neighbor. This approach is often referred to as a nearest neighbor classifier. In the k-nearest neighbor (k-NN) algorithm, the classification of a new sample is determined by the class of its k-nearest neighbors. The value of k is selected randomly depending on the availability of the database and the nature of application. After segmentation, a thresholding operation is used as the post-processing step to extract the blood vessel region.

## 6 Experimental Results and Discussions

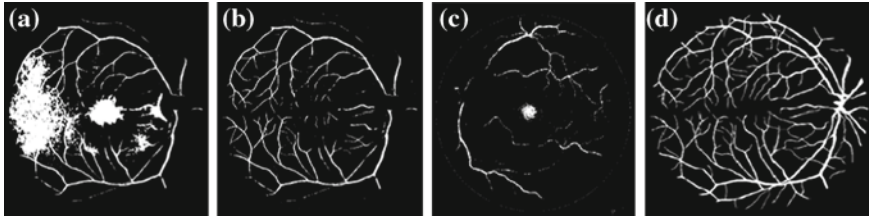
The software used for the implementation is MATLAB [13] and the processor specification is 1 GB RAM with 1.66 GHz clock frequency. Initially, the image pre-processing results are shown in Fig. 2.

Figure 2 illustrates the necessity for pre-processing steps. Figure 2h shows the pre-processed output which is much suitable for further processing than Fig. 2a. After pre-processing, the features are extracted from the images. The features are sufficiently different for the blood vessel category and non-blood vessel category. The segmented outputs for the two segmentation techniques are given in Fig. 3.

The qualitative results have verified the superior nature of the BPN over the statistical classifier. The blood vessels are clearly identified in the neural technique but it is hardly visible in the statistical technique. The orientation of k-NN classifier is given in a different direction. A quantitative analysis on the segmented images of



**Fig. 2** Illustration of preprocessing process: **a** RGB image, **b** Green channel of the RGB image, **c** Gray scale image, **d** Adaptive histogram equalized image, **e** Background image, **f** Vessel central light reflex removed image, **g** Shade-corrected image, **h** Homogenized image



**Fig. 3** Sample results: **a** BPN output before postprocessing, **b** BPN output after postprocessing, **c** k-NN output, **d** Target image

**Table 1** Performance measures of BPN

Input	Se	Npv	Acc
Image1	0.7474	0.9800	0.9811
Image2	0.5702	0.9591	0.9612
Image3	0.7105	0.9800	0.9809
Image4	0.5779	0.9546	0.9511
Image5	0.6344	0.9626	0.9649
Image6	0.6564	0.9696	0.9713
Image7	0.6662	0.9688	0.9706

the BPN technique is given in Table 1. The BPN algorithm is evaluated in terms of Sensitivity (Se), Negative predictive value (Npv), and Accuracy (Acc). These values are displayed for randomly selected images from DRIVE database.

The ideal values of these performance measures are unity and the values indicated in these tables are closely related to unity which indicates the superior nature of the proposed approach. Thus, the advantages of the neural technique for ophthalmologic applications are verified in this work. The quantitative analysis of the k-NN approach is shown in Table 2.

The quantitative analysis has clearly shown the superior nature of the neural method. Only sample results are shown here but the same procedure has been experimented on all the images. The values of Negative Predictive Value and Accuracy are very low for the statistical technique in comparison to the neural-based approach. The average accuracy of the BPN technique is 97% whereas the accuracy of the

**Table 2** Performance measures of k-NN

Input	Se	Npv	Acc
Image1	0.3271	0.5002	0.5121
Image2	0.3002	0.4772	0.4987
Image3	0.3910	0.4832	0.4952
Image4	0.2512	0.4705	0.4800
Image5	0.3067	0.4812	0.4832
Image6	0.3126	0.4728	0.4325
Image7	0.3775	0.4912	0.4873



conventional technique is only 48%. The other performance measures are also affected in the same manner. A 50% increase in efficiency is obtained for the neural-based technique over the conventional statistical technique. Thus, this work has explored the application of neural-based techniques for retinal image analysis.

## 7 Conclusion

In this work, effort has been taken in exploring the usage of neural network for retinal image segmentation. The proposed BPN method segments the blood vessels in an efficient way so that further processing of this segmented image will help the ophthalmologist to diagnose diseases like diabetic retinopathy and glaucoma. The superior nature of ANN over other conventional techniques is also verified in this work.

**Acknowledgments** The authors thank Dr. A. Indumathy, Lotus Eye Care Hospital, Coimbatore, India for her help regarding database validation. The authors also thank the Council of Scientific and Industrial Research (CSIR), New Delhi, India for the financial assistance towards this research (Scheme No: 22(0592)/12/EMR-II).

## References

1. Martin, D., Aquino, A., Arias, M.E.G., Bravo, J.M.: A new-supervised method for blood vessel segmentation in retinal images by using gray-level and moment invariants-based features. *IEEE Trans. Med. Imaging* **30**(1), 146–158 (2011)
2. Mendonca, A.M., Campilho, A.: Segmentation of retinal blood vessels by combining the detection of centerlines and morphological reconstruction. *IEEE Trans. Med. Imaging* **25**(9), 1200–1213 (2006)
3. Narasimha-Iyer, H., Beach, J.M., Khoobehi, B., Roysam, B.: Automatic identification of retinal arteries and veins from dual-wavelength images using structural and functional features. *IEEE Trans. Biomed. Eng.* **54**(8), 1427–1435 (2007)
4. Li, H., Chutatape, O.: Fundus image features extraction. In: *Proceedings of the 22nd Annual EMBS International Conference, Chicago IL, July 2000*, pp. 3071–3073.
5. Ricci, E., Perfetti, R.: Retinal blood vessel segmentation using line operators and support vector classification. *IEEE Trans. Med. Imaging* **26**(10), 1357–1365 (2007)
6. Kande, G.B., Savithri, T.S., Subbaiah, P.V.: Segmentation of vessels in fundus images using spatially weighted fuzzy c-means clustering algorithm. *IJCSNS Int. J. Comput. Sci. Netw. Secur.* **7**(12), 102–109 (2007)
7. Sofka, M., Stewart, C.V.: Retinal vessel centerline extraction using multiscale matched filters, confidence and edge measures. *IEEE Trans. Med. Imaging* **25**(12), 1531–1546 (2006)
8. Lam, B.S.Y., Yan, H.: A novel vessel segmentation algorithm for pathological retina images based on the divergence of vector fields. *IEEE Trans. Med. Imaging* **27**(2), 237–246 (2008)
9. Staal, J., Abramoff, M.D., Niemeijer, M., Viergever, M.A., Ginneken, B.V.: Ridge-based vessel segmentation in color images of the retina. *IEEE Trans. Med. Imaging* **23**(4), 501–509 (2004)
10. Soares, J.V.B., Jorge, J., Leandro, G., Roberto, M., Herbert, F., Jelinek, F., Cree, M.J.: Retinal vessel segmentation using the 2-D morlet wavelet and supervised classification. *IEEE Trans. Med. Imaging* **25**(9), 1214–1222 (2006)

11. Haralick, R.M.: Statistical and structural approaches to texture. *IEEE Trans. Syst. Man Cybern.* **67**, 86–804 (1979)
12. Freeman, J.A., Skapura, D.M.: *Neural Networks. Algorithms, Applications and Programming Techniques*, Pearson education, New York (2004)
13. *MATLAB: User's Guide*, The Math Works Inc., Natick (1994–2002).

# An Efficient Training Dataset Generation Method for Extractive Text Summarization

Esther Hannah and Saswati Mukherjee

**Abstract** The work presents a method to automatically generate a training dataset for the purpose of summarizing text documents with the help of feature extraction technique. The goal of this approach is to design a dataset which will help to perform the task of summarization very much like a human. A document summary is a text that is produced from one or more texts that conveys important information in the original texts. The proposed system consists of methods such as pre-processing, feature extraction, and generation of training dataset. For implementing the system, 50 test documents from DUC2002 is used. Each document is cleaned by pre-processing techniques such as sentence segmentation, tokenization, removing stop word, and word stemming. Eight important features are extracted for each sentence, and are converted as attributes for the training dataset. A high quality, proper training dataset is needed for achieving good quality in document summarization, and the proposed system aims in generating a well-defined training dataset that is sufficiently large enough and noise free for performing text summarization. The training dataset utilizes a set of features which are common that can be used for all subtasks of data mining. Primary subjective evaluation shows that our training is effective, efficient, and the performance of the system is promising.

**Keywords** Feature extraction · Dataset · Summarization · Pre-processing

---

E. Hannah (✉)

Department of Computer Science, Anna University, Chennai, India  
e-mail: hanmoses@yahoo.com

S. Mukherjee

Department of Information Science and Technology, College of Engineering,  
Anna University, Chennai, India

## 1 Introduction

The digital revolution has made digitized information easy to capture and fairly inexpensive to store. With the development of computer hardware and software, huge amount of data have been collected and stored in databases. The rate at which such data is stored is growing at a phenomenal rate. Several domains where large volumes of data are stored include the following: Financial investment, Health care, Manufacturing and Production, Telecommunication network, Scientific Domain and World Wide Web (WWW). The increasing availability of online information has necessitated intensive research in the area of automatic text summarization within the Natural Language Processing Community. Text summarization is a text reduction process, and a summary is a text that is produced from one or more texts, that convey important information in the original texts, and that is no longer than half of the original text.

## 2 Summarization Approaches

One of the very first works in automatic text summarization was done by Luhn et al. in 1958, demonstrates research work done in IBM, focused on technical documents [1]. Luhn proposed that the 'frequency of word' proves to be a useful measure in determining the significance factor of sentences. Words were stemmed to their roots having the stop words removed. Luhn generated a set of content words that helped to calculate the significance factor of sentences, which were then scored, and the top ranking sentences become the candidates to be part of the generated summary. In the same year, Baxendale et al. proved that the sentence position plays an important role in determining the significance factor of sentences [2]. He examined 200 paragraphs to find that in 85 % of the paragraphs the topic sentence came as the first one and in 7 % of the paragraphs it was the last sentence.

Edmundson in 1969 proposed a method for obtaining document extracts by using a linear combination of features such as cue words, keywords, title or heading, and sentence location [3]. Kupiec et al. in 1995, used human-generated abstracts as training corpus, from which he produced extracts, the feature set included sentence length, fixed phrases, sentence position in paragraph, thematic words, and uppercase words [4]. In 2004, Khosrow Kaikhah et al. proposed a new technique for summarizing news articles using a neural network that is trained to learn characteristics of sentences that should be included in the summary of the article. Rasim. M. Alguliev et al., in 2005 proposed a text summarization method that creates text summary by definition of the relevance score of each sentence by extracting sentences from the original documents [5].

Hsun-Hui Huang, Yau-Hwang Kuo, Horng-Chang Yang et al. in 2006, proposed to extract key sentences of a document as its summary by estimating the relevance of sentences through the use of fuzzy-rough sets [6]. The approach removes the problem

that sentences of the same or similar semantic meaning but written in synonyms being treated differently.

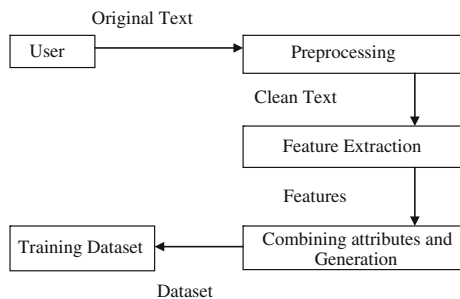
Huantong Geng, Peng Zhao, Enhong Chen, Qingsheng Cai in the year 2006, described summarization based on subject information from term co-occurrence graph and linkage information of different subjects [7]. In 2007, Amini and Usunier et al. came forward with a Contextual Query Expansion Approach that makes use of Term Clustering [8]. Ladda Suanmali et al. [9] in 2009 developed a system that generates extractive summaries based on a set of features that represent the sentences in a text.. A variation to this is brought out in a sentence-oriented approach [11]. Other approaches such as multivariate [10], classification-based approaches are currently exploited for various summarization purposes.

### 3 Proposed Work

The overall data flow of the system is shown in Fig. 1, various processes through which data is processed. The overall system can be split into three major processes namely:

- a. **Pre-processing:** Pre-processing is done as a means of cleaning the document by removing words that do not contain any information that uniquely identifies a sentence.
- b. **Feature Extraction:** The Feature Extraction includes 7 important features: Title Feature, Sentence Length, Term Weight, Sentence to sentence similarity, Proper Noun, Thematic Word, and Numerical Data.
- c. **Generate Training Dataset:** Training datasets help to train models that will perform tasks like classification, clustering, summarization, etc. The feature ‘class’ identifies whether the chosen sentence is part of the summary document or not. The ‘class’ is marked as ‘INT’ or ‘NOT\_INT’ based on its presence or absence in the summary document.

Fig. 1 Proposed system



The Fig. 1 shows the overall view of the system. The input text document is pre-processed, its features are extracted and the training dataset is generated from them. The following subsections discuss each of these subprocesses.

### ***3.1 Dataset and Pre-processing***

The system made use of 50 documents from DUC2002 to generate the training dataset for document summarization. Each document consists of 7–33 sentences with an average of 21 sentences. Each document in DUC2002 collection is supplied with a set of human generated summaries provided by two different experts.

There are four main activities performed as pre-processing : Sentence Segmentation, Tokenization, Removing Stop Word, and Word Stemming. Sentence segmentation is boundary detection and separating source text into sentence. Tokenization is separating the input document into individual words. Next, Removing Stop Words, stop words are the words which appear frequently in document but provide less meaning in identifying the important content of the document such as ‘a’, ‘an’, ‘the’, etc. The last step for pre-processing is Word Stemming; Word stemming is the process of removing prefixes and suffixes of each word.

### ***3.2 Sentence Features***

For any task of text mining, features play an important role. The features are attributes that attempt to represent the data used for the task. The proposed approach focuses on seven features for each sentence. Each feature is given a value between ‘0’ and ‘1’. Therefore, one can extract the appropriate number of sentences according to 30% compression rate. The features and the way they are extracted are as follows:

#### **3.2.1 Title Feature**

The number of title words in the sentence contributes to title feature. Titles contain group of words that give important clues about the subjects contained in the document. Therefore, if a sentence has higher intersection with the title words, the sentence is more important than others. Eq. (1) exhibits how the value is calculated.

$$\text{Score (S}_i\text{)} = \text{Number of Title words in S}_i / \text{Number of Words in Title} \quad (1)$$

### 3.2.2 Sentence Length

The number of words in sentence gives good idea about the importance of the sentence. This feature is very useful to filter out short sentences such as datelines and author names commonly found in articles. The short sentences are not expected to belong to the summary and the sentence length feature is calculated by the formula given in Eq. (2).

$$\text{Score (Si)} = \text{Numberof Words in Si} / \text{Numberof Words in longest sentence} \quad (2)$$

### 3.2.3 Term Weight

The term weight feature score is obtained by calculating the average of the Term frequency, Inverse sentence frequency (TF-ISF). Inverse term frequency helps to identify important sentences that represent the document. Term weight feature is calculated by the formula given in Eq. (3).

$$\text{Score (Si)} = \text{Sum of TF - ISF in Si} / \text{Max (Sum of TF - ISF)} \quad (3)$$

### 3.2.4 Sentence to Sentence Similarity

The score of this feature for a sentence is obtained by computing the ratio of the summation of sentence similarity of a sentence  $s$  with each of the other sentences over the maximum value sentence similarity as given in Eq. (4).

$$\text{Score (Si)} = \text{Sum of Sentence Similarity for Si} / \text{Max (Sum of Sentence Similarity)} \quad (4)$$

### 3.2.5 Proper Noun

The proper noun feature gives the score based on the number of proper nouns present in a sentence, or presence of named entity in the sentence. Usually sentences that contain proper nouns are considered to be important and these should be included in the document summary and is calculated by the formula given in Eq. (5).

$$\text{Score (Si)} = \text{Number of Proper nouns in Si} / \text{Length (Si)} \quad (5)$$

### 3.2.6 Thematic Word

The number of thematic word in sentence is an important feature because terms that occur frequently in a document are probably related to topic. Thematic words are

words that capture main topics discussed in a given document. We used the top 10 most frequent content word for consideration as thematic. The score for this feature is calculated by the formula given in Eq. (6).

$$\text{Score (Si)} = \text{Number of Thematic Words in Si} / \text{Length (Si)} \quad (6)$$

### 3.2.7 Numerical Data

This feature gives a score for the number of numerical data in a sentence. The contribution made by this feature to the weight given to a sentence is significant since a sentence that contains numerical data essentially contains important information. The score for this feature is calculated by the formula given in Eq. (7).

$$\text{Score (Si)} = \text{Number of Numerical Data in Si} / \text{Length (Si)} \quad (7)$$

## 3.3 Generation of Training Dataset

The dataset that can be used as a training dataset consists of seven attributes namely: Title Feature, Sentence Length, Term Weight, Sentence to Sentence Similarity, Proper Noun, Thematic Word, and Numerical Data. The ‘class’ identifies whether the chosen sentence is part of the summary document or not. The ‘class’ is marked as ‘INT’ or ‘NOT\_INT’ based on its presence or absence in the summary document. INT indicates that the sentence is *interesting* and hence is present in the model summary. NOT\_INT indicates that the sentence is *not\_so\_interesting* and hence not present in the model summary. Figure 2 shows a sample input document and Fig. 3 shows the corresponding model summary as provided by DUC 2002.

### 3.3.1 Corpus Used

The TIPSTER program with its two main evaluation style conference series TREC & Document Understanding Conference-DUC (now called as Text Analysis Conference-TAC) have shaped the scientific community in terms of performance, research paradigm, and approaches. 50 documents from DUC 2002 were used for generating the training dataset. The main features of the document corpus are: Each document has minimum of seven sentences and maximum of 33 sentences. The total number of sentences in the corpus is 980.



Yasser Arafat On Tuesday Accused The United States Of Threatening To Kill Plo Officials If Palestinian Guerrillas Attack American Targets. The United States Denied The Accusation. The State Department Said In Washington That It Had Received Reports The Plo Might Target Americans Because Of Alleged Us Involvement In The Assassination Of Khalil Wazir, The Plo's Second In Command. Wazir Was Slain April 16 During A Raid On His House Near Tunis, Tunisia. Israeli Officials Who Spoke On Condition They Not Be Identified Said An Israeli Squad Carried Out The Assassination. There Have Been Accusations By The Plo That The United States Knew About And Approved Plans For Slaying Wazir. Arafat, The Palestine Liberation Organization Leader, Claimed The Threat To Kill Plo Officials Was Made In A Us Government Document The Plo Obtained From An Arab Government. He Refused To Identify The Government. In Washington, Assistant Secretary Of State Richard Murphy Denied Arafat's Accusation That The United States Threatened Plo Officials. State Department Spokesman Charles Redman Said The United States Has Been In Touch With A Number Of Middle Eastern Countries About Possible Plo Attacks Against American Citizens And Facilities. He Added That Arafat's Interpretation Of Those Contacts Was Entirely Without Foundation . Arafat Spoke At A News Conference In His Heavily Guarded Villa In Baghdad, Where Extra Security Guards Have Been Deployed. He Said Security Also Was Being Augmented At Plo Offices Around The Arab World Following The Alleged Threat. He Produced A Photocopy Of The Alleged Document. It Appeared To Be Part Of A Longer Document With The Word Confidential Stamped At The Bottom. The Document, Which Was Typewritten In English, Referred To Wazir By His Code Name, Abu Jihad. It Read:You May Be Aware Of Charges In Several Middle Eastern And Particularly Palestinian Circles That The U.S. Knew Of And Approved Abu Jihad's Assassination. On April 18th (A) State Department Spokesman Said That The United States 'Condemns This Act Of Political Assassination, 'Had No Knowledge Of And 'Was Not Involved In Any Way In This Assassination. It Has Come To Our Attention That The Plo Leader Yasser Arafat May Have Personally Approved A Series Of Terrorist Attacks Against American Citizens And Facilities Abroad, Possibly In Retaliation For Last Month's Assassination Of Abu Jihad. Any Possible Targeting Of American Personnel And Facilities In Retaliation For Abu Jihad's Assassination Would Be Totally Reprehensible And Unjustified. We Would Hold The Plo Responsible For Any Such Attacks . Arafat Said The Document Reveals The Us Administration Is Planning, In Full Cooperation With The Israel Is, To Conduct A Crusade Of Terrorist Attacks And Then To Blame The Plo For Them. These Attacks Will Then Be Used To Justify The Assassination Of Plo Leaders . He Strongly Denied That The Plo Planned Any Such Attacks.

Fig. 2 Sample input document

Yasser Arafat On Tuesday Accused The United States Of Threatening To Kill PLO Officials If Palestinian Guerrillas Attack American Targets. The United States Denied The Accusation. The State Department Said In Washington That It Had Received Reports The PLO Might Target Americans Because Of Alleged Us Involvement In The Assassination Of Khalil Wazir, The PLO's Second In Command. Wazir Was Slain April 16 During A Raid On His House Near Tunis, Tunisia. Any Possible Targeting Of American Personnel And Facilities In Retaliation For Abu Jihad's Assassination Would Be Totally Reprehensible And Unjustified. We Would Hold The PLO Responsible For Any Such Attacks.

Fig. 3 Model summary document

Table 1 Feature categories

Feature_score	Class	Notation
0–0.2	Very low	VL
0.21–0.4	Low	L
0.41–0.6	Average	A
0.61–0.8	High	H
0.81–1.0	Very high	VH

### 3.3.2 Categories of Features

The feature are extracted and are categorized to five distinct classes as shown below: (Table 1).

A feature score of 0–0.2 is given a class name ‘very low’ a notation ‘VL’, score having values 0.21 till 0.4 is placed under the class low with a notation ‘L’. A score of 0.41–0.6 is given the class ‘average’ under the notation ‘A’ while a score of 0.61–0.8

is given a value ‘high’ and a notation ‘H’. The final delimit 0.8–1.0 having class name ‘very high’ is having a notation ‘VH’.

### 3.3.3 Sample Training Dataset

The system generated a dataset that can be used for training any system for the task of text summarization. The dataset consists of attributes F1, F2,...F7 that represents the feature values for a given sentence and the ‘class’ attribute is marked as ‘INT’ or ‘NOT\_INT’ based on the presence or absence of the sentence in the model summary document. INT indicates an *interesting* sentence and NOT\_INT indicates a *not\_so\_interesting* sentence. The following table shows a sample of the training dataset generated (Table 2).

In the above table, F1 represents the ‘title feature’, F2 represents the ‘sentence length’, F3 represents the ‘term weight’, F4 represents the ‘sentence to sentence similarity’, F5 represents the ‘proper noun’, F6 represents the ‘thematic word’, and F7 represents the ‘numerical data’ for a given sentence.

## 4 Conclusions and Future Work

The system titled ‘Generation of training dataset for document summarization’ has successfully generated training dataset for the task of summarization. The input text document was pre-processed and the important features for each sentence of the document such as title feature, sentence length, term weight, sentence to sentence similarity, proper noun, thematic word and numerical data was extracted, and the presence or absence of the sentence in the model summary given by DUC was utilized

The system is designed only for the English language. The System can be used only with well formatted documents with respect to the grammatical rules of the English language. System cannot understand an exhaustive set of mathematical and

**Table 2** Sample training dataset

Sentence #	F1	F2	F3	F4	F5	F6	F7	CLASS
1	VH	H	H	VL	L	VH	VL	NOT_INT
2	L	A	H	L	VL	H	VL	INT
3	VL	A	VH	VL	VL	VL	L	NOT_INT
4	VL	H	H	VL	L	VH	VL	NOT_INT
5	L	H	H	VL	VL	H	VL	NOT_INT
6	L	H	H	L	VL	H	H	INT
7	L	VH	H	VL	VL	VH	VL	NOT_INT

special symbols and considers them as individual strings; however the system accepts large text documents.

## References

1. Luhn, H.P.: The automatic creation of literature abstract. *IBM J. Res. Dev.* **2**, 159–165 (1958)
2. Kupiec, J., Pedersen, J., Chen, F.: “A Trainable document summarizer”. In *Proceedings of the Eighteenth Annual International ACM Conference on Research and Development in Information Retrieval (SIGIR)*, pp. 68–73. Seattle (1995).
3. Edmundson, H.P.: New methods in automatic extracting. *J. Assoc. Comput. Mach.* **16**(2), 264–285 (1969).
4. Baxendale, P.: Machine-made index for technical literature—an experiment. *IBM J. Res. Dev.* **2**, 354–361 (1958)
5. Rasim, M.: Alguliev, Effective summarization method of text documents. *Proceedings of IEEE International Conference on Web Intelligence*, In (2005)
6. Hsun-Hui, H., Yau-Hwang, K., Horng-Chang, Y.: Fuzzy-rough set aided sentence extraction summarization. *Proceedings of the first International Conference on Innovative Computing, Information and Control*, In (2006)
7. Huantong, G., Peng, Z., Enhong, C., Qingsheng, C.: A novel automatic text summarization study based on term co-occurrence. *Proceedings of ICCI*, In (2006)
8. Massih, R.: Amini and nicolas usunier, a contextual query expansion approach by term clustering for robust text summarization. *Proceedings of DUC*, In (2007)
9. Suanmali, L., Mohammed Salem, B., Salim, N.: Sentence features fusion for text summarization using fuzzy logic. In: *Proceedings of HIS 2009*, 142–146 (2009).
10. Esther, H., Saswati, M., Kumar, G.: An extractive text summarization based on multivariate approach. *ICACTE* **3**, 157 (2010)
11. Esther, H., Geetha T.V., Saswati M.: Automatic extractive text summarization based on fuzzy logic: a sentence oriented approach. *LNCS* 2011.

# Online Identification of English Plain Text Using Artificial Neural Network

Aditi Bhateja, Ashok K. Bhateja and Maiya Din

**Abstract** In online communication, most of the time plain English characters are transmitted, while a few are encrypted. Thus there is a need for an automatic recognizer of plain English text (based on the characteristics of the English Language) without using a dictionary. It works for continuous text without word break-up (text without blank spaces between words). We propose a very efficient artificial neural network-based technique by selecting relevant or important features using Joint Mutual Information for online recognition of English plain text which can recognize English text from English like or random data.

**Keywords** Feature vector · Joint mutual information · Artificial neural network · Back-propagation

## 1 Introduction

The identification of text whether it is plain or not is the first requirement for the analysis of online communication. The non-plain text may be garbage or an encrypted text, which appears as random. Identification of the text can be carried out by applying a suitable pattern recognition technique using appropriate features. Every language has some inherent characteristics in terms of occurrences of letters out of the alphabet set in words, which in turn constitutes sentences. Each language has its own grammar,

---

A. Bhateja (✉)

Ambedkar Institute of Advanced communication Technologies and Research, Delhi, India  
e-mail: aditibhateja89@gmail.com

A. K. Bhateja · M. Din

Defence Research and Development Organization, Scientific Analysis Group, Delhi, India  
e-mail: akbhateja@gmail.com

M. Din

e-mail: anuragimd@gmail.com

which defines the constraints on word spellings and syntax of sentences. In each language there are some “vowel” like letters, whereas others are “consonant” like, which are basically characterized by the phonetic properties. The English language has five vowels (‘Y’ also treated sometimes as 6th vowel) and 21 consonants. Some letters such as E, T, O, A, I occur more frequently, whereas others such as B, J, X, W, Z occur occasionally in any given English text [1]. There are certain letter combinations such as WX, ZX, BX (bigrams), which are very rare whereas combinations such as TH, ER, HE occur more frequently. Similarly certain combinations of three letters like THE, ING, AND, HER, DTH (trigrams) occur more frequently. Such characteristics and affinity of certain letters with some specific letters makes one language distinguishable from the other and also enables one to check if the given text is meaningful valid plain text of the language or it is a random text (sequence of letters occurring randomly). When random text is very close to English, it becomes difficult to recognize whether it is English text or not. Therefore it is required to extract the features which are relevant for recognizing the English text from a random text. The irrelevant features create problems in recognition. Thus our goal is to filter out random data and extract English data online. Joint Mutual Information (JMI) [2] is used in ordering the features according to their decreasing order of relevance. The optimal number of relevant (distinguishing) features is selected by cumulative insertion of the features in the input of a feed-forward network, and a reduced feature set is formed. Feed-forward back-propagation Artificial Neural Network [3] with the reduced feature vector as input, is trained for the classification of English plain text and a non-English text (which look like English or random text).

In this paper, we propose an efficient scheme for the identification of English text in online communication. This scheme performs well, with very high accuracy. Data preparation and feature extraction is explained in Sect. 2. Back-propagation learning based ANN is detailed in Sect. 3. Experimental results are presented in Sect. 4. Finally, Sect. 5 concludes the paper.

## 2 Data Preparation and Feature Extraction

We collected 2,000 texts of English each of size 500 characters after removing special characters, numerals, and blanks, i.e., the text has only 26 upper case alphabets. We then created 1,000 English-like texts of length 500 each, by replacing some bigram/trigram, in standard plain English text, with some random bigram/trigram (e.g. THE is replaced with CMU). Thousand random texts using true random number generator and 1,000 pseudo random sequences of alphabets (by using simple substitution, Playfair [4], Vigenere [5] encryption schemes and pseudorandom generator, 250 each) each of length 500 were generated. Features considered: 26 alphabets, 48 high frequent bigrams, and 36 high frequent trigrams [6] of plain English. We selected 48 bigrams because after 48 bigrams there is a sharp decrease in frequency of the bigrams. Similarly, in case of trigram there is a sharp decrease of frequency after 36 trigrams. Feature vectors (size 110) with these features were created for each of the 5,000 texts (2,000 English text, 1,000 very close to English, 1,000 pseudo

random, and 1,000 true random). For extracting the features which are relevant or important for identification of English text from non-English, JMI technique is used.

### 2.1 Joint Mutual Information

Filter techniques [7] are defined by a criterion ‘Relevance Index’ denoted by  $J$  which is intended to measure how potentially useful a feature may be when used in a classifier. An intuitive  $J$  would be some measure of correlation between the feature and the class label, i.e., the intuition being that a stronger correlation between these should imply a greater predictive ability when using the feature. For a class label  $Y$ , the ‘Mutual Information’ index for a feature  $X_k$  is as follows:

$$J_{\text{mim}}(X_k) = I(X_k; Y)$$

‘mim’, standing for *Mutual Information Maximization*. An important limitation is that this assumes that each feature is independent of all other features and effectively ranks the features in descending order of their individual mutual information content. However, where features may be interdependent, this is known to be suboptimal. In general, it is widely accepted that a useful and parsimonious set of features should not only be individually *relevant*, but also should not be *redundant* with respect to each other—features should not be highly correlated.

Battiti (1994) presented the ‘Mutual Information Feature Selection’ (MIFS) criterion:

$$J_{\text{mifs}}(X_k) = I(X_k, Y) - \beta \sum_{X_j \in S} I(X_k, X_j)$$

where  $S$  is the set of currently selected features. This includes the  $I(X_k; Y)$  term to ensure feature *relevance*, but introduces a penalty to enforce low correlations with features already selected in  $S$ . The  $\beta$  in the MIFS criterion is a configurable parameter, which must be set experimentally. Using  $\beta = 0$  would be equivalent to  $J_{\text{mim}}(X_k)$ , selecting features independently, while a larger value will place more emphasis on reducing inter-feature dependencies. In experiments, Battiti found that  $\beta = 1$  is often optimal, though with no strong theory to explain why. The MIFS criterion focuses on reducing *redundancy*; an alternative approach was proposed by Yang and Moody (1999), and also later by Meyer et al. (2008) using the *Joint Mutual Information* (JMI), to focus on increasing *complementary* information between features.

The JMI index for feature  $X_k$  is defined as:

$$J_{\text{jmi}}(X_k) = \sum_{X_j \in S} I(X_k X_j; Y)$$

This is the information between the targets and a joint random variable  $X_k X_j$ , defined by pairing the candidate  $X_k$  with each previously selected feature. The idea is that if the candidate feature is complementary with existing features, it should be included.

## 2.2 Formation of Reduced Feature Vector

JMI algorithm arranges all the features according to decreasing order of their relevance. We used cumulative insertion technique to find the number of important features. The method used for finding the number of relevant features is given below:

---

**Algorithm:** To extract the important/relevant features  
 Create a feature vector consisting of the frequencies of 26 alphabets, 48 high frequent bigrams, and 36 high frequent trigrams of plain English.  
 Apply JMI technique to find the rank of all the 110 features according to decreasing order of their relevance.  
 List of relevant features =  $\phi$ .  
 For  $k = 1$  to total number of features.  
 Select the most important feature from the list prioritized by JMI and delete it from the list.  
 Add this feature to the list of relevant features.  
 Train a three-layer ANN consisting of  $k$  number of neurons in input layer, 6 to 12 neurons in the hidden layer and 2 neurons in the output layer.  
 Test the performance of the network on test data.  
 If the performance decreases, then stop.  
 In this way we found that out of 110 only 20 features are important, which are used for actual classification.

---

## 3 Back-Propagation Learning-Based ANN

An Artificial Neural Network (ANN) is a mathematical model or computational model that is inspired by the structure and/or functional aspects of biological neural networks. A neural network consists of an interconnected group of artificial neurons, and it processes information using a connectionist approach to computation [8] (Fig. 1).

Standard back-propagation is a gradient descent algorithm, in which the network weights are moved along the negative of the gradient of the performance function. The term back-propagation refers to the manner in which the gradient is computed for nonlinear multilayer networks. Properly trained back-propagation networks tend to give reasonable answers when presented with inputs that they have never seen. Typically, a new input leads to an output similar to the correct output for input vectors used in training that are similar to the new input being presented. This generalization property makes it possible to train a network on a representative set of input/target

pairs and get good results without training the network on all possible input/output pairs.

The reduced feature vectors (feature vector consisting of relevant/important features) ranked by JMI algorithm are used as input for training and weights were stored which are used for classification of unknown text.

### 4 Results and Analysis

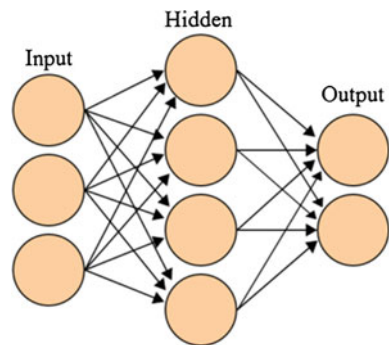
2,000 texts of English, 1,000 texts of close to English, 1,000 texts of pseudo Random, and 1,000 texts of true random, each of length 500 characters, were created. Out of these 5,000 text samples 70% of each category was used for training and the remaining 30% was used for testing the neural network.

For each of the texts the feature vector of size 110 consisting of frequencies of 26 alphabets (A to Z), frequencies of 48 high frequent English bigrams (TH, IN, ER, RE, AN, HE, AR, EN, TI, TE, AT, ON, HA, OU, IT, ES, ST, OR, NT, HI, EA, VE, CO, DE, RA, RO, LI, RI, IO, LE, ND, MA, SE, AL, IC, FO, IL, NE, LA, TA, EL, ME, EC, IS, DI, SI, CA, UN) and frequencies of 36 high frequent English trigrams (THE, ING, AND, ION, ENT, FOR, TIO, ERE, HER, ATE, VER, TER, THA, ATI HAT, ERS, HIS, RES, ILL, ARE, CON, NCE, ALL, EVE, ITH, TED, AIN, EST, MAN, RED, THI, IVE, REA, WIT, ONS, ESS), were formed.

JMI algorithm ranked these features in decreasing order of their relevance. A reduced list of features (list containing only the relevant features) is formed by adding one by one the most important feature from the ranked relevance list of features, and used as input vector to train a three-layer neural network. Performance of the network with increase in number of features is shown in Fig. 2.

It is clear from Fig. 2 that out of 110 features only 20 are the relevant features. Therefore a reduced feature vector of size 20 was created for all the texts. A three-layer neural network with 20 input neurons, 10 hidden neurons, and 2 output neurons was trained with the training data. The weights after training were stored in a file.

Fig. 1 Feed-forward neural network





**Fig. 2** Number of features versus identification performance



**Table 1** Performance analysis

Text type	Classification score	
	Training data (%)	Testing data (%)
Plain english	96.6	93.4
Close to english	88.9	82.7
Pseudo random	97.1	96.2
True random	99.3	98.7

Network of the same architecture and stored weights was used to test all the test samples. The performance of the network is shown in Table 1.

After a certain value of mean square error (over training) the performance of the network degrades. The neural network is more than 96 % classification score achiever when it is used to classify plain English text versus pseudo random or true random text.

## 5 Conclusion

Online identification of plain text is very important for the analysis of communication. Relevant features improve the performance of a classifier. Joint Mutual Information-based approach for ranking the features is very effective. We have used cumulative addition approach to extract the optimal number of relevant features. Using the relevant features, back-propagation neural network recognize English plain text very accurately and efficiently.

## References

1. Saxena, P.K., Pratibha, Y.: Girish, M: Index of garbledness for automatic recognition of plain english texts. *Defence Sci. J.* **60**(4), 415–419 (2010)
2. Yang, Howard Hua, Moody, John: Feature Selection based on Joint Mutual Information. *J Comput Intell Methods Appl. Int. Comput. Sci. Convention 13*, 1–8 (1999).

3. Haykin, S: Neural Networks- A Comprehensive Foundation, 2nd edn. Macmillan, New York.
4. [http://en.wikipedia.org/wiki/Playfair\\_cipher](http://en.wikipedia.org/wiki/Playfair_cipher)
5. [http://en.wikipedia.org/wiki/Vigen%C3%A8re\\_cipher](http://en.wikipedia.org/wiki/Vigen%C3%A8re_cipher)
6. <http://jnicholl.org/Cryptanalysis/Data/EnglishData.php>
7. Brown, Gavin, Pocock, Adam, Jhao, M.J., et al.: Conditional likelihood maximization: a unifying framework for information theoretic feature selection. *J. Mach. Lear. Res.* 13, 27–66 (2012).
8. [http://en.wikipedia.org/wiki/Artificial\\_neural\\_network](http://en.wikipedia.org/wiki/Artificial_neural_network)

# Novel Approach to Predict Promoter Region Based on Short Range Interaction Between DNA Sequences

Arul Mugilan and Abraham Nartey

**Abstract** Genomic studies have become one of the useful aspects of Bioinformatics since it provides important information about an organism's genome once it has been sequenced. Gene finding and promoter predictions are common strategies used in modern Bioinformatics which helps in the provision of an organism's genomic information. Many works has been carried out on promoter prediction by various scientists and therefore many prediction tools are available. However, there is a high demand for novel prediction tools due to low level of prediction accuracy and sensitivity which are the important features of a good prediction tool. In this paper, we have developed the new algorithm Novel Approach to Promoter Prediction (NAPPR) to predict eukaryotic promoter region using the python programming, which can meet today's demand to some extent. We have developed the parameters for Singlet ( $4^1$ ) to nanoplets ( $4^9$ ) in analyzing short range interactions between the four nucleotide bases in DNA sequences. Using this parameters NAPPR tool was developed to predict promoters with high level of Accuracy, Sensitivity and Specificity after comparing it with other known prediction tools. An Accuracy of 74 % and Specificity of 78 % was achieved after testing it on test sequences from the EPD database. The length of DNA sequence used as input has no limit and can therefore be used to predict promoters even in the whole human genome. At the end, it was found out that NAPPR can predict eukaryotic promoter with high level of accuracy and sensitivity.

---

A. Mugilan (✉)

Department of Bioinformatics, School of Health Science and Biotechnology,  
Karunya University, Coimbatore, India  
e-mail: bioinformaticsmugil@gmail.com

A. Nartey

Department of Theoretical and Applied Biology,  
Kwame Nkrumah University of Science and Technology,  
College of Science, Kumasi, Ghana  
e-mail: abrahamnart@gmail.com

**Keywords** Positional score value · Nanoplets · Short-range-interactions · Expected promoter region

## 1 Introduction

Promoters are responsible for the transcription regulation of the gene downstream of it. This is because, specific conserved pattern of nucleotides known as motifs are present in this promoter regions. Transcriptional factors therefore recognize these motifs and bind it to initiate the transcription of genes. Three distinguishing parts of the promoter region can be identified, namely; the Core promoter, the Proximal promoter and the Distal promoter. The part which contains the sequence necessary to bind transcription factors is the Core promoter [1]. This part mainly contains the transcription start site, the binding site for RNA polymerase and a conserved sequence region which binds with transcription factors. Different organisms have different genomic DNA contents and there is also a variation between the coding and non-coding genomes among them. Only small portion of the human genome for instance is coding whereas larger percentage (98 %) is non-coding [2]. The coding region has two boundaries at each end, it is bounded at the 5' end by a start codon and 3' end by a stop codon [3]. Non-coding region describes the components of an organism's DNA sequence that do not encode protein sequences. Though some DNA sequences are coded or transcribed but by the virtue of the fact that they do not encode protein, they classified as non-coding sequence. Transcriptional and translational regulations of the coding sequences are carried out by these non-coding DNA sequences. Human Genome Project has the list of all human genes fully annotated to improve biomedical research [4]. The outcome of this project has served a tremendous improvement in the field of biology [5]. The result of this project was made available to the public through databases and publications of which scientists can easily get access to it to carry out further projects. These databases come in different categories, from genes, Nucleotide sequences, promoters and through coding and non-coding regions of the genomic DNA.

The Frequency Distribution Analysed Feature Selection Algorithm (FDAFSA), in which the frequency of hexamers (adjacent triplet pairs) in a dataset are considered. The second approach is the Random Triplet Pair Feature Selecting Genetic Algorithm (RTPFSGA), where the genetic algorithm to find random triplet pairs (RTPs), that is non-adjacent triplets [6]. This method was used because it has been proven in previous researches that the distributions of triplet frequencies are very useful in serving as codons which play an important role in the protein's biological functionality [7, 8]. Based on four scoring criteria, genetic algorithm was developed for predicting the operon [9]. Furthermore, there are Neural Network Promoter Prediction tool and Promoter Scan. NNPP promoter prediction tool is a promoter prediction tool that uses artificial neural network in predicting promoters. It uses a time-delay architecture method to analyze the compositional and structural properties of promoter sequence [10]. Another prediction tool, Promoter scan (PROSCAN v1.7) is also showing a low

level of accuracy and specificity. It is a program that uses a weighted matrix for scoring a TATA box related sequence. It was built by using the densities of a transcription binding sites to derive a ratio between promoter and non-promoter sequence [11]. Even though a lot of works have been done on promoter predictions, there is a need to improve upon the accuracy and sensitivity of these prediction tools. There are numerous prediction tools available but their level of accuracy and specificity is low. In this research, a new promoter prediction algorithm has been introduced for eukaryotic promoter sequence known as the Novel Approach to Promoter Prediction (NAPPR).

## 2 Method of Promoter Prediction

### 2.1 Description of the Databases

We have collected 9710 (Last updated on 02 Mar. 2012) Eukaryotic promoter sequences from the Eukaryotic Promoter Database [12]. We have used 9700 promoters region (training set) for the preparation of parameters and randomly selected 10 promoter regions (test set) as the input sequences (not included in the training set). Python programming was used to count numbers of singlet ( $4^1$ ), doublets ( $4^2$ ), triplets ( $4^3$ ), tetraplets ( $4^4$ ), pentaplets ( $4^5$ ), hexaplets ( $4^6$ ), heptaplets ( $4^7$ ), octaplets ( $4^8$ ) and nanoplets ( $4^9$ ) from the above dataset (9700).

### 2.2 Statistical Analysis

The observed frequency values from the various observed count (singlet to nanoplets) were computed using the formula below [13, 14].

$$P(x) = \frac{\sum Ni(x)}{\sum Yi}$$

where  $X$  = individual nucleotide bases (acgt) for singlet, two consecutive bases (aa, ac...gg) for doublet ..... nine consecutive bases (aaaaaaaa, aaaaaaac..... gggggggg) for nanoplets.

$Ni$  = Number of count for  $x$  in the  $i$ th promoter sequence

$Yi$  = Total number of nucleotide bases.

$i$  varies from 1 to 9700.

Theoretical estimate for the nucleotide bases were calculated based on the singlet frequency of occurrence.

$$P(xy) = P(x) \times P(y)$$

$P(x)$  is the frequency of occurrence of singlet  $x$

$P(y)$  is the frequency of occurrence of singlet  $y$ .

Based on the above formula, we have calculated theoretical values up to nanoplets. The chi square value for nucleotide sequence singlet to nanoplets is calculated as follows

$$\chi^2(\mathbf{x}) = (\mathbf{P}_{\text{observed}}(\mathbf{x}) - \mathbf{P}_{\text{theoretical}}(\mathbf{x}))^2 / \mathbf{P}_{\text{theoretical}}(\mathbf{x})$$

If the observed value is greater than theoretical value, chi square value is assigned as positive (preferential selection) else it is negative (non-preferential selection) [13]. The chi square value are normalized by the below formula

$$\text{Normalized value } (N) = \frac{Xi - \sigma}{\omega - \sigma}.$$

where  $Xi$  is the chi square value for  $i$ th DNA base ( $i = a$  to  $g$  for singlet, aa to gg for doublets ..... aaaaaaaaaa to gggggggggg for nanoplet) is to be normalized,

$\sigma$  is the minimum value occurring within the group

$\omega$  is the maximum value occurring within the group [15].

Based on the above normalized value, we have developed the Normalized prediction parameter (NPP) for singlet, doublets, triplets, tetraplets, pentaplets, hexaplets, heptaplets, octaplets and nanoplets ( $4^1-4^9$ ).

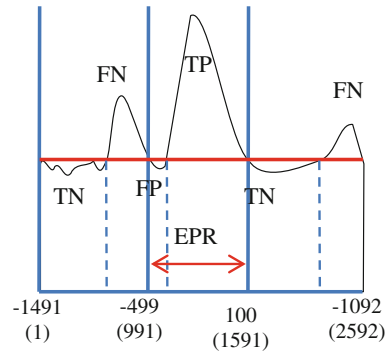
### 2.3 Positional Score Value

We have collected the test set (10) nucleotide sequence which has 2600 nucleotide length. The above test set was calculated starting from  $-1491$  to  $1092$  from the promoter region. We have subtracted 992 nucleotides from each side, the expected promoter region is  $-499(991)-100(1591)$ . Positional score value (PSV) has been determined for each nucleotide base in a test set promoter sequence and the region that shows the highest PSV's were predicted as the promoter region. A python program was written to associate the possible sequence with their respective frequency parameters. The PSV was counted along the entire length of the promoter sequence starting from the 9th position to the 2,590th position. Taking one nucleotide into account, the positional score value was calculated for all possible short-range interaction from singlet ( $4^1$ ) to nanoplets ( $4^9$ ). This is represented in the Table 1. An average score value of 0.5 was used as the minimum threshold value. Any PSV which is below this average value is considered as not predicted and values greater or equal to it is considered as predicted.

**Table 1** A table showing manual calculation of PSV along a promoter sequence

TGTTATCTTTGCTTTTCT		
	SRI(T)	F
Singlet	<b>T</b>	0.16166
Doublet	<b>TT</b>	0.32332
	<b>TT</b>	0.32332
Triplet	<b>CTT</b>	0.31486
	<b>TTT</b>	0.39708
	<b>TTG</b>	0.20395
Tetraplet	<b>TCTT</b>	0.28753
	<b>CTTT</b>	0.35425
	<b>TTTG</b>	0.27641
	<b>TTGC</b>	0.21244
Pentaplet	<b>ATCTT</b>	0.09707
	<b>TCTTT</b>	0.22329
	<b>CTTTG</b>	0.18753
	<b>TTTGC</b>	0.16021
	<b>TTGCT</b>	0.15619
Hexaplet	<b>TATCTT</b>	0.04444
	<b>ATCTTT</b>	0.08481
	<b>TCTTTG</b>	0.11645
	<b>CTTTGC</b>	0.12775
	<b>TTTGC</b>	0.12302
Heptaplet	<b>TTGCTT</b>	0.10790
	<b>TTATCTT</b>	0.03169
	<b>TATCTTT</b>	0.03334
	<b>ATCTTTG</b>	0.04186
	<b>TCTTTGC</b>	0.05681
	<b>CTTTGCT</b>	0.06638
	<b>TTTGCCT</b>	0.07236
Octaplet	<b>TTGCTTT</b>	0.07879
	<b>GTTATCTT</b>	0.00645
	<b>TTATCTTT</b>	0.01752
	<b>TATCTTTG</b>	0.01188
	<b>ATCTTTGC</b>	0.01390
	<b>TCTTTGCT</b>	0.02075
	<b>CTTTGCTT</b>	0.02256
	<b>TTTGCCTT</b>	0.04471
Nanoplet	<b>TTGCTTTT</b>	0.04250
	<b>TGTTATCTT</b>	0.00324
	<b>GTTATCTTT</b>	0.00324
	<b>TTATCTTTG</b>	0.00424
	<b>TATCTTTGC</b>	0.00349
	<b>ATCTTTGCT</b>	0.00474
	<b>TCTTTGCTT</b>	0.00648
	<b>CTTTGCTTT</b>	0.01122
	<b>TTTGCCTTT</b>	0.02592
	<b>TTGCTTTTC</b>	0.01745
	<b>PSV(T)</b>	4.05256

**Fig. 1** A sketch of graph showing the positions of TP, FP, TN and FN for a prediction tool



## 2.4 Method to Calculate Accuracy of Prediction

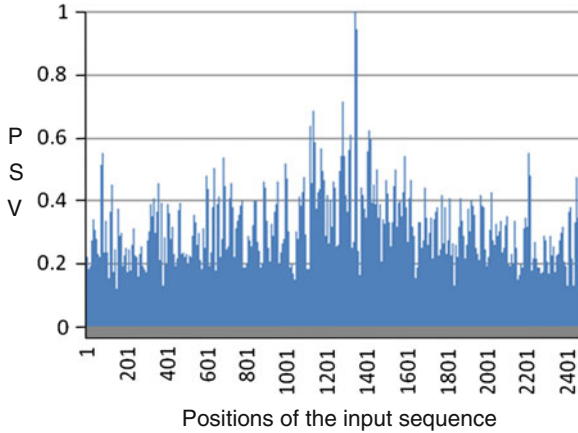
We have considered whether this predicted nucleotide is found in the Expected Promoter Region (EPR) or outside the region. The expected promoter region is the known promoter region as in the Eukaryotic Promoter Database. Any PSV found within the EPR which is greater or equal to the average PSV for the entire sequence was counted and recorded as number of True Positive (TP) while the PSV less than the average PSV for the entire sequence is also counted and recorded as False Positives (FP). Also, any PSV found outside the EPR which is greater or equal to the average PSV for the sequence is counted and recorded as False Negative (FN) whereas the PSV outside the EPR which are less than the average PSV for the sequence were also counted and recorded as True Negative (TN). These counting values were used to calculate for the accuracy (ACC), sensitivity (SN) and specificity (SP) for the NAPPR prediction tool. This is shown in Fig. 1.

The sequences used in our test set were submitted to the NNPP version 2.2. The minimum promoter score was set to 0.5 and all the 10 sequences were predicted. The results were then computed for true-positive and false-negative analysis in order to obtain the sensitivity, specificity and accuracy. For the comparative analysis we have submitted our test sequences to the web server promoter scan version 1.7 for prediction. It was able to predict only 7 out of 10 test sequences submitted. The results were then analyzed.

## 3 Prediction of Promoter Region

The test set DNA sequences were run on the following promoter sequences from the EPD; [A2LD1], [H3F3AP1], [N6AMT2], [S100BPB], [SAM12], [C10orf188],





**Fig. 2** Prediction of promoter region using NAPPR of H3F3AP1 gene

[CCDC51], [RAB11B], [P2RX69] and [WBP11]. Our NAPPR method is used to predict the promoter region within the above named promoter sequences. This is to test whether the proposed NAPPR method will be able to identify the promoter region with high level of accuracy and specificity. Figure 2 shows the outcomes of the predicted result of H3F3AP1. Position number 991–1591 has the experimental predicted area for promoter region. Figure 2 show that our method (NAPPR) also prepares the above promoter region.

The evaluation is then made of the number of true positives (TP), where the length and end sequence positions are correctly predicted, and the number of over-predicted positioned prediction or false positives (FP), True Negative (TN), under-predicted residues as misses or false-negative (FN) predictions. The following Accuracy calculations [16] are used:

1. The sensitivity of the method SN is given by true positives/actual Positives =  $TP / (TP + FN)$ .
2. The specificity by SP = true negatives/actual negatives which is;  $TN / (TN + FP)$ .
3. Accuracy ACC =  $(TP+TN) / (TP+TN+FP+FN)$ .

#### 4 Analysis of Promoter Prediction

According to our method, good prediction accuracy was achieved. Looking at it individually from Table 2, test sequence 2 (H3F3AP1) recorded the highest accuracy of 79 % followed by test set 5, 6 and 7 (SAM12,C10orf18&CCDC51) of 77 % accuracy. However, test set 9 (P2RX69), predicted with the least accuracy of 61 % of which on the average prediction was lowered to 74 % accuracy.

**Table 2** A table showing true-positive and true-negative calculations of the NAPPR method

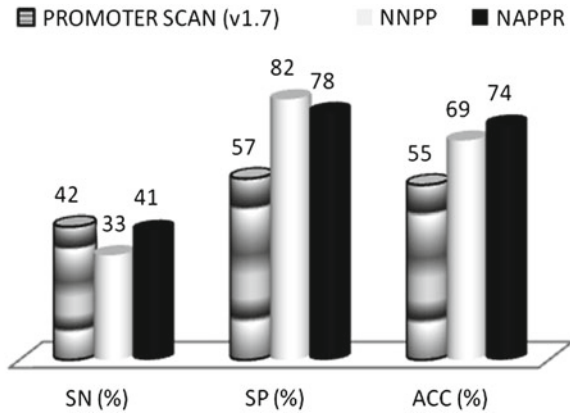
SN	Promoter ID	TP	FP	TN	FN	SN	SP	ACC
1	A2LD1	41	559	1941	51	0.45	0.78	0.76
2	H3F3AP1	56	544	1979	13	0.81	0.78	0.79
3	N6AMT2	173	427	1788	204	0.46	0.81	0.76
4	S100PBP	126	474	1765	227	0.36	0.79	0.73
5	SAMD12	67	533	1919	73	0.48	0.78	0.77
6	C10orf188	48	552	1945	47	0.51	0.78	0.77
7	CCDC51	22	578	1964	28	0.44	0.77	0.77
8	RAB11B	13	587	1917	75	0.15	0.77	0.74
9	P2RX69	175	425	1403	589	0.23	0.77	0.61
10	WBP11	76	524	1782	210	0.27	0.77	0.72
**	AVERAGE	80	520	1840	152	0.41	0.78	0.74

Furthermore, looking at the number of TP in test set 2 (H3F3AP1), predicted only 56 out 600 PP values and also it predicted the highest number of true negatives leading to the least false positive prediction (13) which all contributed to the high accuracy level for that sequence.

High numbers of false negatives predicted in test set 9 were due to single sequence repeat (SSR) of the nucleotide Adenine. This is because the stability of the DNA sequence is affected by SSRs depending of the length of repeat. There is also high mutation (deletion or insertion) in GC rich repeats [17, 18]. It consist of (13, 16) nt repeats from the position of (229–241, 541–555) respectively which are all outside the EPR therefore biasing the result. This bias was due to the fact that, our program was trained to predict short-range interactions between four different nucleotides which were not present in this region and hence it has nothing to predict. Also high PSV recorded can be interpreted as over prediction of SSRs of a given type of nucleotide and length since this type of repeats might have been over represented [19]. This kind of finding may be helpful in understanding the influence of SSRs and their effects on gene or promoter prediction. From this it was found out that when a particular region of the DNA sequence is made up of more than 10 nt SSR, the program cannot predict any useful short-range-interaction between the nucleotides. Notwithstanding, high number of TPs recorded were due to the high number of C and G nucleotides present in the EPR. This was confirmed in the normalized frequency values used in the parameters. The frequency for A, C, G and T were 0.2032, 0.2019, 0.2942 and 0.3007 respectively which confirm the high percentage of CpG islands in the promoter region [20, 21]. Based on this we expected the PSV to be very high within the EPR.

Figure 3 shows the comparison between PROMOTER SCAN, NNPP and NAPPR prediction tools. Now looking at the figure, promoter scan showed the highest level of sensitivity among the three prediction tools followed by our method, the NAPPR and the least sensitive is the NNPP prediction tool. Also comparing in terms of the rate of negative prediction, the NNPP showed the highest rate of negative predictions. Finally

**Fig. 3** Comparison between PROMOTER SCAN, NNPP and NAPPR



looking at the accuracy which is the most important feature of a good prediction tool, our method (NAPPR) has the highest level of accuracy followed by the NNPP and the least is the Promoter scan. Therefore despite the fact that promoter scan is more sensitive in prediction the level of accuracy is very low. Furthermore, the NNPP also is less sensitive and has the highest rate of negative prediction with medium level of accuracy and this does not qualify it as a good prediction tool.

## 5 Conclusion

Finally, NAPPR, the newly introduced prediction tool has the highest level of accuracy and medium level of both sensitivity and specificity and these qualities makes it an outstanding among the three methods compared. It can therefore be highly recommended to biologist as the most efficient and most reliable prediction tool. There has been a major achievement in this project that, the NAPPR method can predict with high level of accuracy and sensitivity.

**Acknowledgments** Glory be to God almighty for making it possible for us to come out with this kind of project. Much appreciation is also rendered to Karunya University for the support and provision of facilities toward this research project.

## References

1. Smale, S., Kadonaga, J.T.: The RNA polymerase II core promoter. *Ann. Rev. Biochem.* **72**, 449–479 (2003)
2. Elgar, G., Vavouri, T.: Tuning in to the signals, non-coding sequence conservation in vertebrate genomes. *Trends Genet.* **24**(7), 344–352 (2008)
3. Gene Structure. [[http://genome.wellcome.ac.uk/doc\\_WTD020755.html](http://genome.wellcome.ac.uk/doc_WTD020755.html)]

4. Lander, E.S.: The new genomics, global views of biology. *Science* **3**, 536–539 (1996)
5. Lander, E.S.: Initial sequencing and analysis of the human genome. *Nature* **409**, 860–921 (2001)
6. Azad, A.K.M., Saima, S., Nasimul, N., Hyunju, L.: Prediction of plant promoters based on hexamers and random triplet pair analysis. *Algorithms Mol. Biol.* **6**, 19 (2011)
7. Kornev, A.P., Taylor, S.S., Ten, E.L.F.: A helix scaffold for the assembly of active protein kinases. *Proc. Natl. Acad. Sci.* **105**(38), 14377–14382 (2008)
8. Ten, E.L.F., Taylor, S.S., Kornev, A.P.: Conserved spatial patterns across the protein kinase family. *Biochim. Biophys. Acta* **1784**(1), 238–243 (2008)
9. Shuqin, W., Yan, W., Wei, D., Fangxun, S., Xiumei, W., Yanchun, L., Chunguang, Z.: Proceedings of the 8th international conference on Adaptive and Natural Computing Algorithms ICANNGA '07, Pp. 296–305 (2007)
10. Resse, M.G.: Application of a time-delay neural network to promoter annotation in the *Drosophila melanogaster* genome. *Comput. Chem.* **26**, 51–56 (2001)
11. Prestridge, D.S.: Predicting Pol II promoter sequences using transcription factor binding sites. *J. Mol. Biol.* **249**, 923–932 (1995)
12. Christoph, D., Schmid, Viviane, P., Mauro, D., Rouaïda, P., Philipp, B.: *Nucl. Acids Res.* **32** (suppl 1), D82–D85. (2004). doi:[10.1093/nar/gkh122](https://doi.org/10.1093/nar/gkh122)
13. Arul, M.S.: Sequence, structure and conformational analysis of protein databases. *J. Adv. Bioinform. Appl. Res.* **2**, 183–192 (2011)
14. Mugilan, S.A., Veluraja, K.: Generation of deviation parameters for amino acid singlets, doublets and triplets from three-dimensional structures of proteins and its implications in secondary structure prediction from amino acid sequences. *J. Bioscience.* **5**, 81–91 (2000)
15. Doherty, K., Adams, R., Davey, N.: Non-Euclidean norms and data normalization. *Verleysen.* **6**, 181–186 (2004)
16. Óscar, B., Santiago, B.: CNN-PROMOTER, new consensus promoter prediction program based on neural networks. *Revista EIA* **15**, 153–164 (2011)
17. Callahan, J.L., Andrews, K.J., Zakian, V.A., Freudenreich, C.H.: Mutations in yeast replication proteins that increase CAG/CTG expansions also increase repeat fragility. *Mol. Cell. Biol.* **23**(21), 7849–7860 (2003)
18. Wang, G., Vasquez, K.M.: Models for chromosomal replication-independent non-B DNA structure-induced genetic instability. *Mol. Carcinog.* **48**(4), 286–298 (2009)
19. Kiran, J.A., Veeraraghavulu, P.C., Yellapu, N.K., Somesula, S.R., Srinivasan, S.K., Matcha, B.: Comparison and correlation of simple sequence repeats. *Bioinformatics* **6**(5), 179–182 (2011)
20. Gardiner, G.M., Frommer, M.: CpG islands in vertebrate genomes. *J. Mol. Biol.* **196**, 261–287 (1987)
21. Ioshikhes, I.P., Zhang, M.Q.: Large-scale human promoter mapping using CpG islands. *Nat. Benet.* **26**, 61–63 (2000)

# “Eco-Computation”: A Step Towards More Friendly Green Computing

Ashish Joshi, Kanak Tewari, Bhaskar Pant and R. H. Goudar

**Abstract** There has been continuously arising demand for more computational power and is increasing day by day. A lot of new and adaptable technologies are coming forth to meet the user requirements, e.g., include clusters, grids, clouds and so on each having advantages and disadvantages providing computation, resources, or services. The problem arising is that for large computation many participating entities in the decision system are required and thereby more power is consumed. This paper focuses on minimizing the computation power required by the task (computation task or problem statement) especially in homogeneous systems here we are calling it as a Decision System which require some form of data (may be structured) along with the problem statement and thus proving to be a green computing environment (reducing use of hazardous things and maximizing the energy efficiency).

**Keywords** Green computing · Computation · Homogeneous systems · Dimensionality reduction · Bio-Hazards · Rough set theory

---

A. Joshi (✉) · K. Tewari  
Research Scholar, Graphic Era University, Dehradun, India  
e-mail: a.joshicse1986@gmail.com

K. Tewari  
e-mail: kanak.tewari@gmail.com

B. Pant · R. H. Gounder  
Department Of CSE, Graphic Era University, Dehradun, India  
e-mail: rhgoudar@gmail.com

B. Pant  
e-mail: pantbhaskar2@gmail.com

## 1 Introduction

As we all know the demand for computing is increasing day by day, i.e., because the data is becoming more and more complex along with its availability. To achieve the task may require more and more computational power along with other resources. These days the scenario is quite common and more and more technologies have been adopted so far.

Major focus is on adopting Green IT or green computing methodologies in order to make our planet green. The main aim of Green Computing is to utilize the resources effectively and efficiently while maintaining the overall performance of the system. Intending to achieve the 3R's- (reduce, recycle, and reuse) goal of Green Computing measures are being taken. Recent studies have shown that the usage of compute-power exceeds 50 % of that of total energy cost of the organization. The unnecessary usage of the computation power leads to energy wastage. For utilizing energy more efficiently and effectively, its wastage needs to be minimized.

Apart from implementation in homogeneous system, current technologies like Cloud Computing and Grid Computing are continuously on the search of new measures and techniques that can be worked upon the heterogeneous platforms and architectures too. Eco-friendly methodologies in relation with Green IT are on the verge to bring upon new technologies that can lesser the hazardous effect made to the planet and thus enforcing them onto the current scenario. The compute power reduction certainly reduces the unnecessary energy consumption leading its usage in other important tasks, such that energy can be utilized effectively without its wastage.

## 2 Related Work

Prior work has been done toward enhancing the overall performance in publish/subscribe systems. These approaches, however, were further manipulated and improved with the proposal of a 3-phase scheme in order to reconfigure the publish/subscribe systems along with the experimentation on a cluster test bed and a high performance computing platform. The algorithm phase 1 gathers performance information from the network followed by phase 2 in which the subscriptions were allocated using the information gathered and the last phase place them onto the newly built broker overlay with the relocation algorithm GRAPE [1–3].

Another contribution related to grid project, focused on the energy efficient aspect of desktop-grid computing: the Green Desktop grid, as a task of the EUFP7 DEGISCO project, the primary motivation was to optimize the compute unit energy specific consumption while avoiding the usage of energy intensive air-condition [4, 5].

Irrespective of the earlier searches made to reduce the compute-power wastage; steps are being taken to develop such systems that can operate so efficiently leading to utilization of the energy in the environment. As with respect to the earlier work done,

the paper focuses on homogenous system providing measures so that the computation power usage can be minimized to such an extent to optimize the energy effectively and efficiently within the environment. Its implementation includes approach via Rough Set Theory following certain data mining techniques leading to the algorithm implementation

### 3 Proposed Work

In this paper, we proposed an adaptive functionality to facilitate green computing in the homogenous network. To accomplish this, present techniques of Data Mining are utilized: Classification algorithms, Discretization, Rough Set Theory concepts, etc., that proved to be quite effective in implementation.

#### 3.1 Problem Description

Suppose a large complex problem need to be solved requiring huge computation, the problem statement consists of a large database or the input in any other form may be in the form of structured data, etc. A brief module of the system is pictorially represented below:

Figure 1 show how a task is given to the system along with the data values. We know generally whenever a large and complex task is to be achieved it requires very large processing on the data and data sets. Afterward, the processing on the data is performed. This requires high powered system to work continuously for several hours and can carry for moreover days. This certainly increases the cost of electric consumption and makes temperature of the room or the organization high.

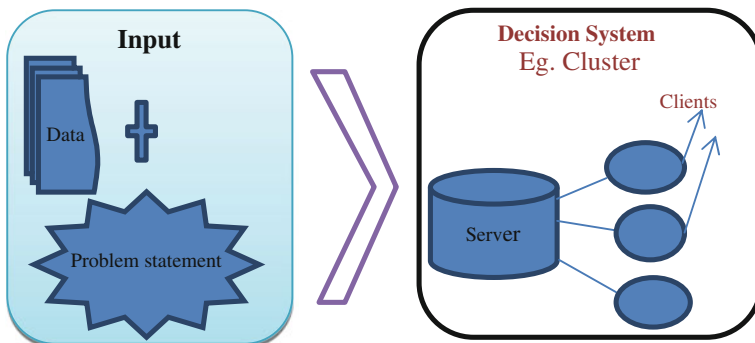


Fig. 1 A brief overview of the system

Sometimes, it happens that if there are 150 participating systems in our complex environment, it might be possible that 30 or 40 among all finishes the task within an hour of the given assignment, other 20 or 30 in the next 1 h, and so on. In general, these may have variation among them. However, if a task is assigned to 150 systems, they are all busy according to the server. But, actually the systems have finished the task, produced the output and are free. The objective of this paper focuses on reducing the amount of hours required on the processing time first, afterwards on saving the electricity measures.

The scenario taken in Fig. 1 is that of a generalized client-server approach which generally follows TCP protocol for the communication. The server may be any entity that holds the responsibilities of the clients and handling of the data with the problem statement in the system. In general, it is the first interaction to the system of the server along with performing general duties like load balancing, etc., in that specified region or portion. When the server has the task and the data, it processes the following steps:

The approach followed to simplify the problem is normally applied in relevance to the Rough Set Theory-based technique combining feature extraction and mining process through classification, Dimensionality Reduction, and Discretization. The tables in Rough set theory are termed as “Information Systems”, naming rows as “objects” and columns as “attributes” shown as:  $\tilde{A} = (U, A)$ , where  $U$  is a non-empty finite set of objects called the “universe” and  $A$  is a non-empty finite set of “attributes” such that  $a : U \rightarrow V_a$  for every  $a \in A$ . The set  $V_a$  is called the value set of  $a$ .

The data provided is minimized applying methods and techniques such that the resulted data set, i.e., “Reduct set” is having the same meaning as that of the original data. Applications of Rough Set Theory include Decision Support systems, Knowledge Discovery, medicine, finance, data mining, etc., as described in [5] that leads to the less power consumption and efficient usage.

In Discretization, various methods are applied on the continuous data to get the discretized data. The approach of rough set theory is mainly unable to tackle the continuous data. Thus, new techniques of Discretization were implemented. Some of them are: Boolean Reasoning, Equal Frequency Binning, and Entropy, etc. Now-a-days, it is widely used for obtaining the minimal set of attributes from the dataset following the supervised learning techniques [5].

In Data Mining, Dimensionality Reduction can be further divided into two parts: Feature Selection and Feature Extraction. The dataset available is highly dimensional. Principal Component Analysis (PCA) is one of the techniques of Feature Extraction. Thus, implementing any of these techniques on the given input dataset (structured) results into the reduced dataset that enable green computing facilities in the homogeneous environment which when followed by the trigger leads to the saving of computational power. Here, combination of all these techniques has been applied.

A generalized approach is shown in the flowchart in Fig. 2. It may be applied recursively to the system if there are certain changes in between the processing. The Fig. 2 shows the process of creation of reduct sets with relevance to the attribute selection process. The reduct set attributes when created are processed inside the



system. After the sets and all attributes have been clarified from the mining techniques and the processing has been done on the new refined attribute sets, reduced and refined data is obtained. Hence, the computation task is shrunk to a very large extent and thus less time is consumed in producing the desired output.

An algorithmic approach to the Fig. 2 is shown below:

Steps with explanation to algorithm

- 0: Consider a decision system of a server and associated entities or clients in the network. Where  $s = \text{server}$  and  $C = \{c_1, c_2, \dots, c_n\}$  are the clients on the decision system,  $n$  stands for total number. Input is the problem statement  $P$  and the data values  $D$ .
- 1: Server performs steps 2–5, 7, 8
- 2: Scan the Attributes of the data set in the decision system. And the problem statement, Total data set  $D = \{x_1, x_2, x_3, x_4, \dots, x_n\}$  where  $n$  stands for total no of attribute in the system.

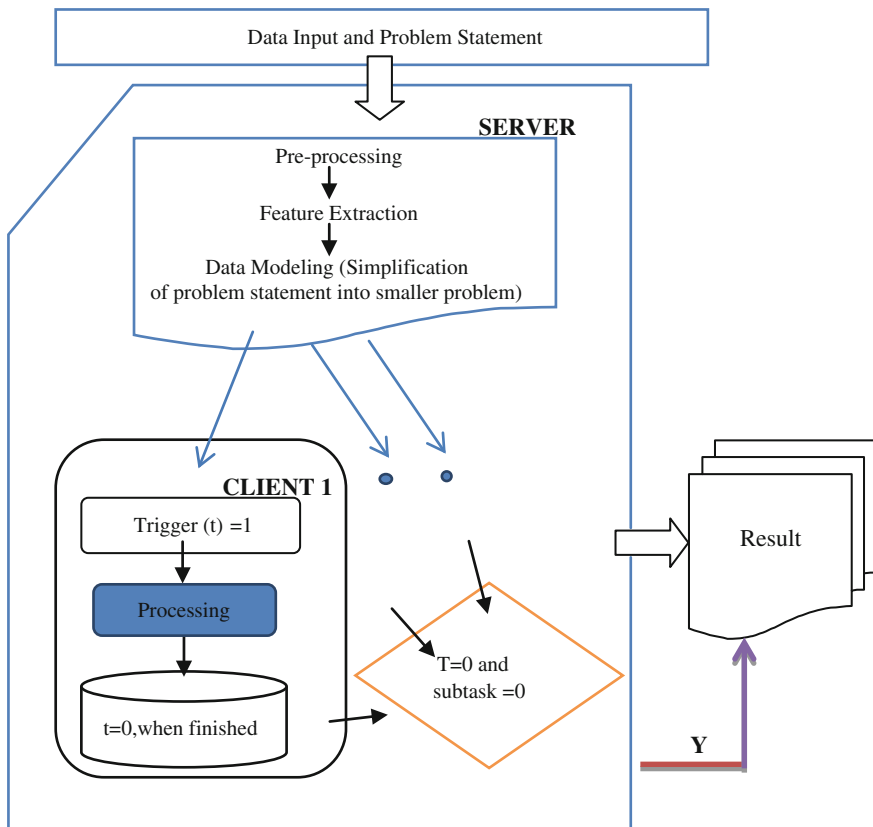


Fig. 2 Processing approach followed by task reduction step

---

```

Step 0:  $C \{c_1, c_2, \dots, c_n\}, t = 0$ 
Step 2:  $D \{x_1, x_2, x_3, x_4, \dots, x_n\}$ 
Step 3:  $R \{x_1, x_2, x_3, \dots, x_m\}$  where  $m < n$ 
Step 4:  $P = \{p_1, p_2, p_3, p_4, \dots, p_n\}$ 
Step 6: while( $i = 1$  to  $n$ )
{
  While( $t = 1$ ) {
     $C_i[i] = P_i$ 
    If( $P_i \neq D_j$ ) {
       $C_i[i] = P_i + D_j$ 
    }
    If( $P_i = 0$ ) \ \ refers to client finished its task
  }
  Step 6:  $T = 0$ ;
  Step 7: Shutdown();
}
Step 8: if( $p_1, \dots, p_n \neq 0$ )
For( $c = 1$  to  $n$ )
{ if (state= shutdown or  $p_i = 0$ )
  { wakeup();
     $C_i = P_i$ 
    Goto 6; }}

```

---

- 3: Apply the rough set-based approach to calculate the reduct set  $R = \{x_1, x_2, x_3, \dots, x_m\}$  where  $m < n$ .
- 4: Divide the problem into sub problems  $P = \{p_1, p_2, p_3, p_4, \dots, p_n\}$  where  $p_1, p_2, p_3, p_4, \dots, p_n$  are the sub problem of the main problem.
- 5: Distribute  $p_1, p_2, p_3, p_4, \dots, p_n$  among clients  $c_1, c_2, \dots, c_n$  with the data set  $R = \{x_1, x_2, x_3, \dots, x_m\}$ , and each client trigger value is set to 0 ( $t=0$ ) on which task has been assigned. If any data value is required by the processing side it is given as value of the data  $D_j$  means at particular position  $j$  in data set.
- 6: after the clients finishes its operation it puts the trigger value as 1,  $t = 0$ , (Done by the client).
- 7: Server on seeing the trigger value as 1 take results from clients and initiates the remote shutdown procedure for the client and puts trigger value as  $t = 1$ .
- 8: If the server needs the client again it initiates the remote wakeup procedure puts trigger  $t = 1$  and assigns the task.

A. Description:

After the new reduced task is received by the server it is then further subdivided into smaller subtasks and is distributed among the server subentities in the system and leads to a more precise decision system. After the subtasks have been created by the server side, it just follows either of the mechanisms given.

*Mechanism 1:* if it follows a general TCP for the communication, the general packet format as described in the RFC 793.

For this type of environment, we can modify TCP protocol. As we know that, some bits after Data offset values, i.e., from 3 to 9 bits are reserved for future use,

We can take 1 bit for the notification purpose for notifying the server and the clients in general. Thus, we can use 1 if the work is been assigned to the client by the server. After the processing, the client put the value back to 0. So, in this way, the server come to know whether the client or a particular entity has finished its task. After the server has the information, it initiates remote shut down procedure and the entity or the client move to the shutdown mode. Suppose, after the server has finished all the tasks, if it gets a new task and if client is needed to initiate the remote wakeup procedure, it again come to live and perform several activities. Similarly, in IP-based communication we can further add a trigger bit at the end of the datagram packet. Adding 1 bit does not modify the whole packet format.

*Mechanism 2:* A trigger is a form of the small code segment appended with the data at the end. When it starts processing its value is set to 1 and when the client finishes the task it puts the trigger value to 0. The results and the trigger value is sent to the server. On receiving the trigger and results value, server initiates the remote shutdown of the client system. If further action is requested by the same client again the trigger value for the intended client is set to 0 and the remote wakeup procedure is initiated for the intended client. Thus, leads to the preservation of overall computational power and electricity.

A scenario illustrates the processing problem, suppose an organization wishes to set up a new Enterprise between Delhi and New York and want to build six offices in between them, also connecting these offices. For this, they need to set up research and development laboratories. Thus, enquiring about the whole situation at different locations is required. The input to the problem statement in terms of data is quite huge. They have to gather information regarding every perspective including the policies, the climate, man power, cost, competition, etc., at different regions.

A simple program illustrates the problem further and provides the remedial solution to the problem. Consider a tcp connection established between the client and server the server and the clients are interacting through concurrent mechanism which defines that several clients can establish the connection to a single server. We are now writing the full code here the server takes the input from the client means whatever we write on the client is to be written on the server side too.

In this set of programs, we can call as much clients as we can; provided the port number should be same. We use a general approach that whatever we write

```

ashish-ashu@ashish-ashu-laptop: ~/Client Server Lab/intro
File Edit View Terminal Help
ashish-ashubashish-ashu-laptop:~$ cd Client\ Server\ Lab/
ashish-ashubashish-ashu-laptop:~/Client Server Lab/$ cd intro/
ashish-ashubashish-ashu-laptop:~/Client Server Lab/intro$ ls
ashish  day_clienttcp.c  echo_clienttcp  server_udp
server  day_clienttcp.c  echo_clienttcp.c  server_udp.c
server.c  day_clientudp.c  echo_servertcp  serverudp.c
serverudp.c  day_clientudp.c  echo_servertcp.c  test1.c
client  day_clientudp.c  echo_servertcp.c  test1.c
client.c  day_servertcp.c  mpar.c  test2.c
clienttcp.c  day_servertcp.c  mpar.c  test2.c
clientudp.c  day_serverudp.c  server2.c  test3.c
client_udp.c  day_serverudp.c  server2.c  tmp_read
client_udp.c  day_serverudp.c  servertcp  test3.c
ashish-ashubashish-ashu-laptop:~/Client Server Lab/intro$ gcc server.c -o ashish
gcc: server.c: No such file or directory
gcc: no input files
ashish-ashubashish-ashu-laptop:~/Client Server Lab/intro$ gcc server.c -o ashish
ashish-ashubashish-ashu-laptop:~/Client Server Lab/intro$ ./ashish 5000
Please enter the message: hello
ashish-ashubashish-ashu-laptop:~/Client Server Lab/intro$

```

```

ashish-ashu@ashish-ashu-laptop: ~/Client Server Lab/intro
File Edit View Terminal Help
ashish-ashubashish-ashu-laptop:~$ cd Client\ Server\ Lab/
ashish-ashubashish-ashu-laptop:~/Client Server Lab/$ cd intro/
ashish-ashubashish-ashu-laptop:~/Client Server Lab/intro$ ls
ashish  client_udp.c  day_serverudp  mpar.c  test1  test2  test3
ashish$  clienttcp.c  day_serverudp.c  server  test1.c
server.c  day_clienttcp.c  day_serverudp.c  server2  test2.c
serverudp.c  day_clienttcp.c  echo_clienttcp  server2.c  test3.c
client  day_clientudp.c  echo_clienttcp.c  servertcp  test3.c
client.c  day_clientudp.c  echo_servertcp  servertcp  tmp_read
clienttcp.c  day_servertcp.c  mpar.c  test2.c
clientudp.c  day_serverudp.c  server2.c  test3.c
client_udp.c  day_serverudp.c  servertcp  test3.c
ashish-ashubashish-ashu-laptop:~/Client Server Lab/intro$ gcc client.c -o ab
usage: ./ab hostname port
ashish-ashubashish-ashu-laptop:~/Client Server Lab/intro$ ./ab localhost 5000
Please enter the message: hello
I got your message
ashish-ashubashish-ashu-laptop:~/Client Server Lab/intro$

```

Fig. 3 Showing implementation part

---

Server code:

```

...newsockfd = accept(sockfd,(struct sockaddr *) &cli_addr,&clilen);
if (newsockfd < 0)
error("ERROR on accept");
bzero(buffer,256);
n = read(newsockfd,buffer,255);
if (n < 0) error("ERROR reading from socket");
printf("Here is the message: %s\n",buffer);
n = write(newsockfd,"I got your message",18);
if (n < 0) error("ERROR writing to socket");
close(newsockfd);
close(sockfd);
return 0;
}

```

---

Client's code:

```

....if (connect(sockfd,(struct sockaddr *) &serv_addr,sizeof(serv_addr)) < 0)
error("ERROR connecting");
printf("Please enter the message: ");
bzero(buffer,256);
fgets(buffer,255,stdin);
n= write(sockfd,buffer,strlen(buffer));
if (n < 0)
error("ERROR writing to socket");
bzero(buffer,256);
n = read(sockfd,buffer,255);
if (n < 0)
error("ERROR reading from socket");
printf("%s\n",buffer);
close(sockfd);
return 0;
}

```

---

on particular client is wrote remotely on the server side uses buffer concept for writing values. This Buffer will act as a semaphore or trigger in this case. But for large processing, a client will wait for the response from user side. In this type of programs, e.g., chat server for eco computing we need to save energy to much extent so whenever the client remains idle for few minutes it is automatically shut down and wakeup whenever required we can use a trigger as in case of this concept. Although we take example of client server here but the same applies to the large computation task whose data sets is first been reduced and afterwards the Eco computation facility is been provided in the system.

A screenshot of the applied mechanism is as shown below (Fig. 3).

## 4 Conclusion

This paper presented focuses on providing various methodologies to facilitate the green computing scenario using some of the known techniques of Data Mining on the provided dataset. Through this we are able to produce the desired results with a really good rate and make our environment quite green and reduce the environmental hazards caused to it by the unnecessary wastage of computational power with extra consumption of electricity too.

## References

1. Lo, C.T.D., Qian, K.: Green computing methodology for next generation computing scientist in Computer Software and Applications Conference (COMPSAC), 2010 IEEE 34th Annual, pp. 250–251, IEEE (2010)
2. Cheung, A. K. Y., & Jacobsen, H. A.: Dynamic load balancing in distributed content-based publish/subscribe pp. 141–161, Springer Berlin Heidelberg, (2006)
3. Cheung, A.K.Y., Jacobsen, H.-A.: Publisher placement Algorithm in content-based publish/subscribe, in ICDCS'10 (2005)
4. Schott, B., Emmen, A.: Green Methodologies in Desktop-Grid, in Proceedings of the 2010 International Multi conference on Computer Science and Information Technology (IMCSIT), pp. 671–676, IEEE (2010)
5. Komorowski, J., et al. Rough sets: A tutorial. Rough fuzzy hybridization: A new trend in decision-making, 3–98 (1999)
6. Cheung, A. K. Y., & Jacobsen, H. A.: Green resource allocation algorithms for publish/subscribe systems, in proceedings of 31st (ICDCS) International Conference on Distributed Computing Systems, pp. 812–823, IEEE (2011)
7. Gruber, R., Keller, V.: HPC@ Green it: Green high performance computing methods, Springer Publications, (2010)
8. Comer, Douglas E.: Internetworking con TCP/IP. Vol. 1. Pearson, (2006)

# A Comparative Study of Performance of Different Window Functions for Speech Enhancement

A. R. Verma, R. K. Singh and A. Kumar

**Abstract** In this paper, a speech enhancement technique proposed by Soon and Koh is examined and improved by exploiting different window functions for preprocessing of speech signals. In this method, instead of using two-dimensional (2-D) discrete Fourier transform (DFT), discrete cosine transform (DCT) is employed with a hybrid filter based on one-dimensional (1-D) Wiener filter with the 2-D Wiener filter. A comparative study of performance of different window functions such as Hanning, Hamming, Blackman, Kaiser, Cosh, and Exponential windows has been made. When compared, Cosh window gives the best performance than all other known window functions.

**Keywords** Cosh · Kaiser · Exponential · Hybrid filter · Wiener filter

## 1 Introduction

An explosive advances in recent years in the field of digital computing have provided a remarkable progress to the field of speech processing such as voice communication and voice recognition [1]. The presence of background noise in speech significantly reduces the intelligibility of speech as degrades the performance of the speech processing systems [1–3]. In early stage of research, many algorithms [4–7] were developed to suppress background noise and improve the perceptual quality

---

A. R. Verma (✉) · R. K. Singh · A. Kumar  
PDPM Indian Institute of Information Technology Design and Manufacturing  
Jabalpur, Jablpur, M.P 482005, India  
e-mail: agyaram06ei03@gmail.com

R. K. Singh  
e-mail: rahul09088@iiitdmj.ac.in

A. Kumar  
e-mail: anilkdee@gmail.com

of speech. These methods were developed with some perceptual constraints placed on noise and speech signals. They involve simple signal processing and some of the speech signal is distorted during enhancement process. Hence, these techniques have a tradeoff between amount of noise removal and speech distortions which was introduced because of processing of speech signal. In the past two decades, a substantial progress has been made in the field of speech processing. So far, several efficient speech enhancement techniques such as spectral subtraction, minimum mean-square error (MMSE) estimation, Wiener filtering (linear MMSE), and Kalman filtering and subspace methods have been reported in literature [6–8]. Most commonly exploited technique is the spectral subtraction method as it is relatively easy to understand and implement [8, 9]. This technique requires only DFT of noisy signal, application of gain function, the inverse DFT and based on minimal assumption of signal and noise. Therefore, many researchers [5, 6] have used this basic spectral subtraction technique and have developed several algorithms for speech enhancement. In all these algorithms, the basic technique varies subtraction of the noise spectrum over the entire speech spectrum. Then, wiener gain function or Wiener filtering has been employed for speech enhancement [8, 9]. Thereon, many techniques based on MMSE estimation have been proposed for the speech enhancement. In these techniques, an optimal MMSE and short-time spectral amplitude estimator (STSA) for speech enhancement was introduced [5]. To estimate clean speech, the short time Fourier coefficients for continuous frame which is independent Gaussian variables of noisy speech are statistically modeled. The authors in [10] have proposed a speech enhancement technique based on adaptive filtering such as Kalman filtering, while in [11, 12], the subspace method has been used for speech enhancement. Recently, several new techniques [12–15] have been developed for speech enhancement.

Speech signal is quasi-stationary in nature and possible to observe it is by in segments. Therefore, speech signal is divided into frame block. To maintain order of continuity of first and last frame, every frame is multiply by a window function to avoid discontinuities between frames. Hamming window is most commonly used for windowing of the speech signal [5–8]. This window function gives fairly good frequency resolution as compared to other window functions. However, in speech processing, one more important spectral parameter, called side lobe roll-off ratio ( $S$ ) is more essential as compared to other spectral characteristics of window function [16–19]. For the speech applications, higher side lobe ratio is required. Therefore, to improve the spectral characteristics, many window functions have been developed such as Kaiser, Saramaki, Cosh, and Exponential [16–19]. In above context, therefore, in this paper, an improved method based on DCT for speech enhancement using different window functions is presented from slight modification in Soon and Koh algorithm [7].

## 2 Overview of Different Windows

Window functions are widely used in digital signal processing for various applications of signal analysis [16–19]. A window is time-domain weighting function. In speech processing, because of quasi-periodic in nature and possible to observe this, a speech signal is segmented into different frames. To maintain order of continuity of first and last frame, every frame is multiplied by a window function [5, 7]. The performance of window function in different applications relies on the spectral characteristics of a window. For example, in digital filter design and image processing, the ripple ratio or main lobe to side lobe energy ratio (MSR) are more essential as compared to the side lobe roll-off ratio, while in speech processing, the side lobe roll-off ratio is more important [16–19].

In literature, a window function has been categorized in two ways: fixed length window and adjustable length window. In fixed length window, only window length controls the window’s main lobe width. In the adjustable windows, in addition to the window length, the window shape parameter is also exploited for controlling the spectral characteristics such as the main lobe width and ripple ratio [18]. The authors in [18, 19] have developed new window functions, named as exponential and Cosh windows which give better the side lobe roll-off ratio and also computationally efficient. In this research, a comparative study of performance of different window functions for speech enhancement is made. In this work, following window functions are used:

**Hamming Window:** In 2-D, Hamming window is defined as

$$h(j, k) = (0.54 - 0.46 \cos(\frac{2\pi j}{255})) (0.54 - 0.46 \cos(\frac{2\pi k}{15})), \tag{1}$$

for  $0 \leq j \leq 255, 0 \leq k \leq 15$

**Hanning Window:** It is defined as

$$h(j, k) = 0.5(1 - \cos(\frac{2\pi j}{255}))0.5(1 - \cos(\frac{2\pi k}{15})), \text{ for } 0 \leq j \leq 255, 0 \leq k \leq 15 \tag{2}$$

**Blackman window:** In 2-D, Blackman window is defined as

$$w(n) = (a_0 - a_1 \cos(\frac{2\pi j}{255}) + a_2 \cos(\frac{4\pi j}{255})) (a_0 - a_1 \cos(\frac{2\pi k}{15}) - a_2 \cos(\frac{4\pi k}{15})) \tag{3}$$

for  $0 \leq j \leq 255, 0 \leq k \leq 15$

where,

$$a_0 = \frac{1 - \alpha}{2}, a_1 = \frac{1}{2} \text{ and } a_2 = \frac{\alpha}{2}. \tag{4}$$



In Eq. (3),  $\alpha = 0.16$ .

**Kaiser window:** In DT domain, Kaiser Window is defined by [16]:

$$W(n) = \begin{cases} \frac{I_0(\alpha\sqrt{1-(\frac{2j}{255}-1)^2})}{I_0(\alpha)} \times \frac{I_0(\alpha\sqrt{1-(\frac{2k}{16}-1)^2})}{I_0(\alpha)} & \text{for } 0 \leq j \leq 255 \text{ and } 0 \leq k \leq 15 \\ 0 & \text{otherwise} \end{cases} \tag{5}$$

where  $\alpha$  is the adjustable parameter and  $I_0(x)$  is the modified Bessel function of the first kind of order zero which can be described by the power series expansion as

$$I_0(x) = 1 + \sum_{k=1}^{\infty} \left[ \frac{1}{k!} \left(\frac{x}{2}\right)^k \right]^2 \tag{6}$$

**Exponential window:** The authors in [17, 19] have used exponential function instead of Bessel function, and introduced a new window, called Exponential window, defined as

$$w(n) = \frac{e^{\left[\alpha\sqrt{1-(1-(2j/(255)))^2}\right]}}{e^\alpha} \times \frac{e^{\left[\alpha\sqrt{1-(1-(2k/(15)))^2}\right]}}{e^\alpha} \text{ for } 0 \leq j \leq 255 \text{ and } 0 \leq k \leq 15 \tag{7}$$

where  $\alpha$  is window shape parameter which controls ripple ratio. Exponential window provides better side lobe roll-off ratio.

**Cosh window:** Cosh window is defined as [18, 20]

$$w_c(n) = \begin{cases} \frac{\cosh(\alpha_c\sqrt{1-(\frac{2j}{255})^2})}{\cosh(\alpha_c)} \times \frac{\cosh(\alpha_c\sqrt{1-(\frac{2k}{16})^2})}{\cosh(\alpha_c)} & \text{for } 0 \leq j \leq 255 \text{ and } 0 \leq k \leq 15 \\ 0 & \text{otherwise} \end{cases} \tag{8}$$

where,  $\alpha_c$  and  $N$  are the adjustable parameters to control the window spectrum in terms of the ripple ratio and main lobe width.

### 3 DCT-Based Methodology for Speech Enhancement

The noise taken for speech enhancement is additive noise to model background noise and both are uncorrelated. The additive noise model for speech is defined as

$$y(t) = x(t) + n(t) \tag{9}$$

where,  $y(t)$  is the observed noisy speech,  $x(t)$  is the clean speech and  $n(t)$  additive background noise. The observed speech signal is divided into overlapping frame of 256 samples. The overlap taken between two consecutive frames is 75 %, which means each frame is shifted by previous frame by 64 samples [7]. To maintain the

order of continuity of first and last frame, every frame is multiplied by a window function. The product of window and block is called as windowed speech block. Then, 2-D DCT can be applied onto each windowed speech block. The forward 2-D DCT of windowed speech block is defined as [21].

$$W(u, v) = \alpha_u \alpha_v \sum_{j=0}^{255} \sum_{k=0}^{15} w(j, k) \cos\left(\frac{\pi(2m+1)u}{2M}\right) \cos\left(\frac{\pi(2n+1)v}{2N}\right), \quad (10)$$

$$\text{For } 0 \leq u \leq M - 1 \text{ and } 0 \leq v \leq N - 1$$

where,

$$\alpha_u = \begin{cases} \frac{1}{\sqrt{M}}, & u = 0 \\ \sqrt{\frac{2}{M}}, & 1 \leq u \leq M - 1 \end{cases} \quad \text{and} \quad \alpha_v = \begin{cases} \frac{1}{\sqrt{M}}, & v = 0 \\ \sqrt{\frac{2}{M}}, & 1 \leq v \leq M - 1 \end{cases} \quad (11)$$

In Eq. (13),  $M$  and  $N$  are the row and column size. The inverse 2-D DCT can be obtained with

$$w(j, k) = \sum_{u=0}^{M-1} \sum_{v=0}^{N-1} \alpha_j \alpha_k W(u, v) \cos\left(\frac{\pi(2m+1)u}{2M}\right) \cos\left(\frac{\pi(2n+1)v}{2N}\right) \quad (12)$$

where,  $0 \leq j \leq M - 1$  and  $0 \leq k \leq N - 1$ .  $\alpha_j$  and  $\alpha_k$  are defined as

$$\alpha_j = \begin{cases} \frac{1}{\sqrt{M}}, & j = 0 \\ \sqrt{\frac{2}{M}}, & 1 \leq j \leq M - 1 \end{cases} \quad \text{and} \quad \alpha_k = \begin{cases} \frac{1}{\sqrt{M}}, & k = 0 \\ \sqrt{\frac{2}{M}}, & 1 \leq k \leq M - 1 \end{cases} \quad (13)$$

## 4 Spectral Magnitude Subtraction

In this paper, 2-D speech enhancement technique given in [7] is modified using DCT and different window functions. In Soon and Koh algorithm [7], 2-D DFT is employed with magnitude spectral subtraction. In this method, magnitude of cosine transform coefficients which is less than particular threshold is used. These coefficients depend upon the expected noise magnitude [7]. Let “ $Y$ ” represents as transformed noisy speech block and  $\hat{X}$  represents enhanced speech block which is defined as

$$\left| \hat{X}(u, v) \right| = \max(|Y(u, v)| - E[|N(u, v)|], 0) \quad (14)$$

where,  $E[|N(u, v)|]$  is the expected mean of noise and noisy phase  $\theta_{Y(u, v)}$  is represented by

$$X(\hat{u}, v) = \left| X(\hat{u}, v) \right| \exp(i \theta_Y(u, v)) \tag{15}$$

Before taking inverse DCT, weaker coefficients can be combined with the noisy phase. By applying inverse 2-D DCT, the enhanced speech block in the time domain is obtained this equation.

$$x(j, k) = \sum_{u=0}^{M-1} \sum_{v=0}^{N-1} \alpha_j \alpha_k \hat{X}(u, v) \cos\left(\frac{\pi(2m+1)}{2M}\right) \cos\left(\frac{\pi(2n+1)}{2N}\right) \tag{16}$$

Finally, enhanced speech is obtained by reversing the blocking and framing process and is represented by this equation [12].

$$\hat{x}(t) = 0.25(f_L(j) + f_{L-1}(j + 64) + f_{L-2}(j + 128) + f_{L-3}(j + 192)) \tag{17}$$

where,

$$L = \left\lfloor \frac{t}{64} \right\rfloor \quad \text{and} \quad j = t - 64L \tag{18}$$

The hybrid filter not only shows 2-D wiener filter effect but also shows properties of 1-D filter to remove additive audible noise. By averaging the coefficients within the surrounding frame, the hybrid wiener filter shows correlation. Figure 1 shows a block diagram of a hybrid filter for speech enhancement using DCT [7]. Equation 17 shows standard wiener filter equation. The power and noise in the cleaned speech is being known for the construction of 1-D wiener filter and it is defined as.

$$W_{1D}(u, v) = \frac{\xi(u, v)}{\xi(u, v) + 1} \tag{19}$$

where, a-priori SNR is represented by

$$\xi(u, v) = \frac{E[X(u, v)^2]}{\lambda_N E[\cdot]} \tag{20}$$

and  $\lambda_N = E[N(u, v)^2]$  is the noisy expected mean. Priors SNR is nothing, but combination of posterior SNR and previous frame enhanced spectrum. In this work, value of  $\lambda_N$  is assumed to be known because during the pauses period in the speech signal, the background noise is easily estimated. The value of  $E[N(u, v)^2]$  is not known and should be estimated.

$$\xi(u, v) = \alpha \frac{X(u-1, v)^2}{\lambda_N} + (1 - \alpha) F \gamma(u, v) - 1 \tag{21}$$

The resulting speech filtered by 1-D Wiener filter is

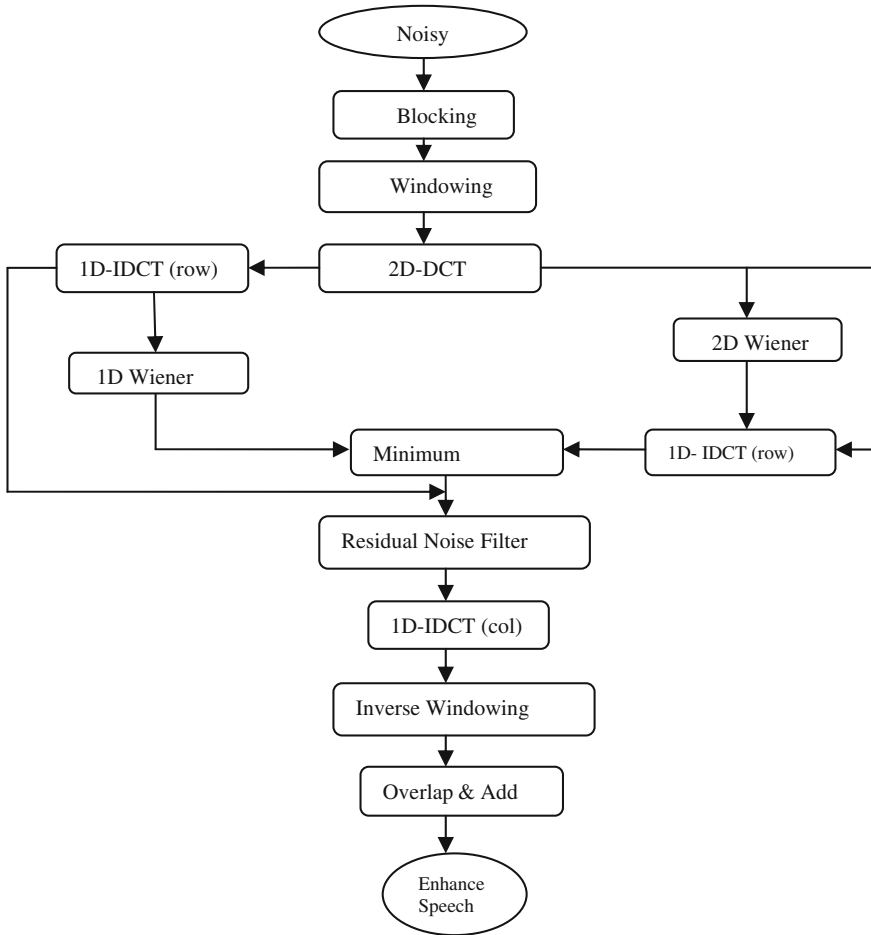


Fig. 1 Block diagram of 1-D and 2-D hybrid filter for speech enhancement [7]

$$\hat{X}_{1-D}(u, v) = \frac{\hat{\xi}(u, v)'}{\hat{X}(u, v)' + 1} Y(u, v) \tag{22}$$

where,  $\hat{X}(u - 1, v)$  is the estimated speech spectrum value of  $X(u, v)$  in the previous frame,  $\gamma(u, v) = Y(u, v)^2 / \lambda_N$  is the a-posteriori SNR,  $E[\cdot]$  denotes the half-wave rectification function.  $\alpha$  controls the behavior of the SNR estimator and value is normally set to 0.98. Basic method spectral magnitude subtraction does not show the 2-D properties in the 2D DFT [7]. By applying 2-D Wiener filter to speech signal, remove the mean noise magnitude level and reduce the instantaneous AC noise variation by coefficients to coefficients [7]. In this, 2-D Wiener filter is applied

to the DCT coefficient. Implementation part is accomplished using 2-D spectrum filtering; therefore at the outset 2-D noise model is introduced. There are two main parts in this model, namely, the DC component and the AC component:

$$N(u, v) = N_{AC}(u, v) + N_{DC}(u, v) \quad (23)$$

where, the DC component could be expressed as  $N_{DC}(u, v) = E[N(u, v)]$ . The variance of  $N_{AC}(u, v)$  is denoted as  $\sigma_{N_{AC}}(u, v)$  and can be obtained by Eq.(24):

$$\sigma_{N_{AC}}(u, v)^2 = E \left[ N(u, v)^2 \right] - N_{DC}(u, v)^2. \quad (24)$$

The 2-D Wiener filter is based on the maximum likelihood approach. if we know the noisy speech and the additive noise, then the 2-D noise model is used:

$$\hat{X}_{2-D}(u, v) = \frac{\sigma_Y(u, v)^2 - \sigma_{N_{AC}}(u, v)^2}{\sigma_Y(u, v)^2} \times (Y(u, v) - \overline{Y(u, v)}) + \overline{Y(u, v)} - N_{DC}(u, v) \quad (25)$$

where,  $\overline{X(u, v)}$  and  $\overline{Y(u, v)}$  are the local means of  $X(u, v)$  and  $Y(u, v)$ . “ $\sigma$ ” indicates the local variance. Hybrid filter is the combination of 1-D and 2-D Wiener filters, Fig. 1 describe the processing of noise speech spectrogram through the hybrid Wiener filter via two channels: the 1-D Wiener filter and the 2-D Wiener filter. The result of the hybrid Wiener filtering in Fig. 1 is by taking the minimum of Eqs. (24) and (25):

$$\hat{X}(u, v) = \min(X_{1-D}(u, v), X_{2D}(u, v)) \quad (26)$$

Based on the listening test, the enhanced speech obtained is compared with either the 1-D Wiener filtered speech or 2-D Wiener filtered speech.

## 5 Result and Discussion

Results included in Table 1 illustrate the performance of different windows based on DFT and Table 2 represents the performance of different windows in the speech enhancement based on DCT. For performance analysis, several fidelity parameters such as signal-to-noise ratio (*SNR*), maximum error (*ME*), and mean square error (*MSE*) given in [6] are computed. As it is evident from Tables 1 and 2, Cosh window gives better performance as compared to other windows in terms of SNR and other fidelity parameters.

**Table 1** Performance of different windows based on DFT

Windows	Input SNR (dB)	Output SNR (dB)	ME	MSE
Hamm	4.14	15.18	0.1045	0.2118
Hanning	4.14	9.11	15.45	0.5639
Kaiser	4.14	33.42	1.6225	0.0044
Blackman	4.14	21.26	2.5847	0.0022
Exponential	4.14	36.45\	0.1806	$1.09 \times 10^{-4}$
Cosh	4.14	39.45	0.1806	$1.43 \times 10^{-4}$

**Table 2** Comparative performance of different windows base on DCT

Windows	Input SNR (dB)	Output SNR (dB)	ME	MSE
Hamm	4.14	18.22	0.0306	0.0631
Hanning	4.14	15.12	6.857	0.0639
Kaiser	4.14	37.66	0.0825	0.0214
Blackman	4.14	24.30	1.5821	0.0032
Exponential	4.14	41.31	0.0481	$2.09 \times 10^{-5}$
Cosh	4.14	45.56	0.0806	$3.43 \times 10^{-6}$

## 6 Conclusions

In this paper, an improved method based on DCT is presented for the speech enhancement. A comparative study of performance of different window functions has been made. The simulation results included in this paper clearly shows better performance as compared to other window functions. The most effective result is obtained using Cosh window in the 2-D DCT domain for speech enhancement. The Cosh window gives signal to noise ratio (SNR) at output is 45.56 db. It is also evident that discrete cosine transform gives better results as compared to 2-DFT, and it is computationally efficient.

## References

1. Virag, N.: Single channel speech enhancement based on masking properties of the human auditory system. *IEEE Trans. Speech Audio Process.* **7**, 126–137 (1999)
2. Yang, L., Shuangtian, L.: DCT speech enhancement based on masking properties of human auditory System. In: *Proceeding Institute of Acoustics Chinese Academy of Science*, pp. 450–453 (2010)
3. Lei, S.F., Tung, Y.K.: Speech enhancement for nonstationary noises by wavelet packet transform and adaptive noise estimation. In: *Proceedings of Internation Symposium on Intelligent Signal Processing and Communication Systems*, pp. 41–44 (2005)
4. Chen, H., Smith, C.H., Fralick, S.: A fast computation algorithm for the discrete cosine transform. *IEEE Trans. Commun.* **25**, 1004–1009 (1997)

5. Ephraim, Y., Malah, D.: Speech enhancement using a minimum mean-square error short-time spectral amplitude estimator. *IEEE Trans. Acoust. Speech Signal Process. (ASSP)* **32**, 1109–1121 (1984)
6. Boll, S.F.: Suppression of acoustic noise in speech using spectral subtraction. *IEEE Trans. Acoust. Speech Signal Process.* **27**, 113–120 (1979)
7. Soon, I.Y., Koh, S.N.: Speech enhancement using 2D Fourier transform. *IEEE Trans. Speech Audio process.* **11**, 717–724 (2003)
8. Yuan, Z.X., Koh, S.N., Soon, I.Y.: Speech enhancement based on a hybrid algorithm. *Electron. Lett.* **35**, 1710–1712 (1999)
9. Vaseghi, S.V.: *Advanced Digital Signal Processing and Noise Reduction*, 2nd edn., pp. 270–290. Wiley, Hoboken (2000)
10. Paliwal, K.K., Basu, A.: A speech enhancement method based on Kalman filtering. In *Proceeding of International Conference Acoustics Speech, Signal Process.* pp. 177–180 (1987)
11. Ephraim, Y., Harry, L., Trees, V.: A signal subspace approaches for speech enhancement. *IEEE Trans. Speech Audio Process.* **3**(4), 251–266 (1995)
12. Huang, J., Zhao, Y.: A DCT-based fast signal subspace technique for robust speech recognition. *IEEE Trans. Speech Audio Process.* **8**(6), 747–751 (2000)
13. Oberle, S., Kaelin, A.: HMM-based speech enhancement using pitch period information in voiced speech segments. In: *International Symposium on Circuits and Systems ISCAS* vol. 27, pp. 114–120 (1997)
14. Makhoul, J.: A fast cosine transform in one and two dimensions. *IEEE Trans. Acoust. Speech Signal Process.* **28**(1), 27–34 (1980)
15. Mittal, U., Phamdo, N.: Signal/noise KLT based approach for enhancing speech degraded by colored noise. *IEEE Trans. Speech Audio Process.* **8**, 159–167 (2000)
16. Kaiser, J.F., Schafer, R.W.: On the use of the IO-sinh window for spectrum analysis. *IEEE Trans. Acoust. Speech Signal Process.* **28**, 105–107 (1980)
17. Avci, K., Nacaroglu, A.: A New Window Based on Exponential Function. In: *IEEE Conference on Research in Microelectronics and Electronics* pp. 69–72 (2008)
18. Kumar, A., Kuldeep, B.: Design of M-channel cosine modulated filter bank using modified exponential window. *J. Franklin Inst.* **349**, 1304–1315 (2012)
19. Avci, K., Nacaroglu, A.: Cosine hyperbolic window family with its application to FIR filter design. In: *3rd International Conference on Information and Communication Technologies: from Theory to Applications, ICTTA'08, Damascus, Syria* (2008)
20. Kumar, A., Singh, G.K., Anand, R.S.: An improved closed form design method for the cosine modulated filter banks using windowing technique. *Appl. Soft Comput.* **11**(3), 3209–3217 (2011)
21. Garello, R. (ed.): *Two-dimensional Signal Analysis*

# Methods for Estimation of Structural State of Alkali Feldspars

T. N. Jowhar

**Abstract** There is much interest in characterizing the variations in feldspar structures because of the abundance and importance of feldspars in petrologic processes and also due to their general significance in mineralogical studies of exsolution and polymorphism, especially order-disorder. With the appearance of new analytical and rapid methods of X-ray crystallographic study and computational techniques, the significance of feldspars in igneous and metamorphic rocks has increased tremendously. In this paper methods for estimation of structural state of alkali feldspars is reviewed and discussed.

**Keywords** Alkali feldspars · X-ray crystallography · Lattice parameters · Structural state · Al-Si distribution

## 1 Introduction

The alkali feldspars are major components of granites and granite pegmatites. The study of their structural state and composition has always been one of interesting researches in petrology and mineralogy [1–3]. Pioneering works by Barth (1969) [4] and Laves (1952) [5], where alkali feldspar composition and structure were correlated with the formation conditions, and the effect of ordering factors on crystal structure was demonstrated.

With the appearance of new analytical and rapid methods of X-ray crystallographic study and computational techniques, the significance of feldspars in igneous and metamorphic rocks has increased [1–3, 6–13]. In this paper methods for estimation of structural state of alkali feldspars is reviewed and discussed.

---

T. N. Jowhar (✉)

Wadia Institute of Himalayan Geology, Dehradun 248001, India  
e-mail: tnjowhar@rediffmail.com; tnjowhar@gmail.com



## 2 Feldspar Structure

In the feldspar structure, all the four oxygen atoms of  $\text{SiO}_4$  tetrahedron are shared with neighbouring tetrahedra, forming a three dimensional framework, giving a silicon oxygen ratio of 1:2. The ideal formula of a feldspar can be expressed as  $\text{MT}_4\text{O}_8$ . The M site is occupied by large atoms like K, Na and Ca with 9–10 coordination. T is a tetrahedral site which is occupied by small trivalent or tetravalent atoms (Al, Si). In the feldspar structure four, four membered rings of tetrahedra are joined with each other by sharing apical oxygens designated  $A_1$  and  $A_2$  to form eight membered rings of elliptical cross section. Each four membered ring consists of four tetrahedra, in which the central cation of two tetrahedra are of type  $T_1$  and two of type  $T_2$ . The four membered rings of tetrahedra are joined by oxygen atoms of type  $A_2$  on mirror plane and oxygens of type  $A_1$  on 2-fold axes, to form eight membered ring of elliptical cross section. The M atom occupies a four fold site on mirror planes.

The structure of the  $\text{KAlSi}_3\text{O}_8$  polymorphs can be described as the variants of the high-temperature sanidine structure. Each unit cell of sanidine contains  $4(\text{KAlSi}_3\text{O}_8)$  formula units and sanidine has space group symmetry  $C2/m$ . The (12 Si + 4 Al) atoms in the unit cell of sanidine are distributed randomly over two crystallographically distinct tetrahedral sites  $T_1$  and  $T_2$ . The four potassium atoms occupy special positions on mirror planes perpendicular to b-axis. The 32 oxygen atoms are located on both special positions (four on two fold axes; four on mirror planes) and on general positions.

Structure of the lower-temperatures polymorphs (maximum microcline, orthoclase) differ from that of sanidine due to the order-disorder relations of Si and Al atoms in tetrahedral sites. Ordering of Al in T site results in loss of a 2-fold axis of rotation and a mirror plane of symmetry and only the center of symmetry at the lattice plane persists, with a concomitant transition from monoclinic to triclinic symmetry. The two tetrahedral sites  $T_1$  and  $T_2$  of the monoclinic phase become four symmetrically distinct tetrahedral sites  $T_1\text{O}$ ,  $T_1\text{m}$ ,  $T_2\text{O}$  and  $T_2\text{m}$  in triclinic phase. In the structure of ideal orthoclase ( $\text{KAlSi}_3\text{O}_8$ ) space group  $C2/m$  aluminium is concentrated in the  $T_1$  sites and depleted from  $T_2$  and the probability being 50% that each  $T_1$  site will contain aluminium. Structural refinements of maximum microcline (Triclinic) space group  $C\bar{1}$  have shown that Al is strongly ordered into  $T_1\text{O}$  site [1, 3].

## 3 Structural State of Alkali Feldspars

The difference in symmetry of sanidine and microcline is due to order-disorder relations of Si and Al atoms over tetrahedral sites. The distribution of Al and Si in tetrahedral sites in maximum microcline (Low microcline) is of the highest degree of order and microcline has a lowest structural state. On the other hand, sanidine, with the highest structural state shows random Al-Si distribution in tetrahedral sites. In between these two end members maximum microcline and sanidine, several intermediate structural states e.g. orthoclase and intermediate microcline exist.

### 3.1 Determination of Al, Si Distribution in the Tetrahedral Sites of Alkali Feldspars

The Si-Al proportion in each tetrahedral site  $T_{10}$ ,  $T_{1m}$ ,  $T_{20}$  and  $T_{2m}$  of alkali feldspar is difficult to determine directly from X-ray diffraction methods because the scattering factors of Al and Si are very similar. But, the ionic radius of Al is  $\sim 0.14 \text{ \AA}$  larger than that of Si, therefore, it is possible to make correlations between mean T-O distances and Al content of tetrahedral sites. Multiple linear regression analyses of monoclinic K-feldspars by Phillips and Ribbe (1973) [14] have shown that the Al content of a tetrahedral site is the principle factor influencing individual T-O distances. Smith and Bailey (1963) [15], Jones (1968) [16] and Ribbe and Gibbs (1969) [17] has suggested a linear model relating the mean T-O bond length of a tetrahedron to its Al content. In a detailed study of Al-O and Si-O tetrahedral distances Smith and Bailey (1963) [15] found that the mean tetrahedral bond length in feldspars varies linearly with percentage of aluminium from  $1.61 \text{ \AA}$  for Si-O to  $1.75 \text{ \AA}$  for Al-O. They estimated that the average Al content of a tetrahedron can be predicted to  $\pm 5\%$ . This relationship determined from two and three dimensional refinements of feldspar structures has since been used to predict Al-Si distribution in feldspars and other framework structures, thereby permitting an estimate of the degree of long-range order or structural state.

### 3.2 X-ray Methods for Determining the Structural State of Alkali Feldspars

**Three peak method of Wright:** Wright (1968) [18] introduced a procedure for estimating composition and structural state of alkali feldspars from the  $2\theta$  positions of three reflections that depend principally on a single cell parameter. The reflections and the cell parameters upon which their  $2\theta$  value depends are  $\bar{2}01 - a$ ,  $060 - b$ , and  $\bar{2}04 - c$ . The reflections  $\bar{2}01$ ,  $060$  and  $\bar{2}04$  are of sufficient intensity and their  $2\theta$  values can be accurately measured. Curves relating the  $2\theta$  values to the appropriate cell dimensions are essentially linear and permit easy estimation of starting cell parameters for a complete refinement of the unit cell.

**130, 131 and 111 splittings:** In monoclinic feldspars, 130, 131 and 111 diffractions are represented by a single peak. However, in triclinic feldspars each of these (130, 131 and 111) splits into two diffractions. These splittings are useful for measuring the deviation from monoclinic geometry.

$$\text{Let } Q = \frac{1}{d^2} \quad \text{Then } Q(130) - Q(\bar{1}\bar{3}0) = 6a^*b^* \cos \gamma^* \quad (1)$$

$$Q(131) - (Q\bar{1}\bar{3}1) = 6a^*b^* \cos \gamma^* + 6b^*c^* \cos \alpha^* \quad (2)$$

Therefore, an estimate of  $\alpha^*$  and  $\gamma^*$  can be obtained from splitting of the 130 and 131 diffractions, since  $a^*$ ,  $b^*$  and  $c^*$  can be easily obtained.

Mackenzie (1954) [19] used the splitting of the 130 diffraction, whereas Goldsmith and Laves (1954) [20] used the splitting of the 131 diffraction for microcline. Goldsmith and Laves (1954) [20] defined triclinicity  $\Delta$  as:

$$\Delta = 12.5 [d(131) - d(\bar{1}\bar{3}1)] \quad (3)$$

The value of 12.5 is chosen so that  $\Delta$  reaches unity for maximum microcline.

When  $\Delta = 1$  feldspar is fully ordered (Maximum microcline)

When  $\Delta = 0$  feldspar is monoclinic.

For microcline, the 130 triclinic indicator is given by (Smith 1974a) [1]:

$$\Delta = 7.8 [d(130) - d(\bar{1}\bar{3}0)] \quad (4)$$

Mackenzie (1954) [19] and Goldsmith and Laves (1954) [20] have shown that many natural k-feldspars yield blurred 130 and 131 peaks that can be interpreted as the superposition of K-feldspars with different triclinic indicators. The concept of random disorder of a multitude of very small volumes each with a different degree of Si-Al order was introduced by Christie (1962) [21].

**Ragland parameters:** Ragland (1970) [22] defined parameters  $\delta$  and  $\delta'$  based upon the data of Wright (1968) [18]:

$$\delta = \frac{9.063 + 2\theta(060) - 2\theta(\bar{2}04)}{0.340} \quad (5)$$

$$\text{and } \delta' = \frac{9.063 + 2\theta(060) - 2\theta(\bar{2}04)}{0.205} \quad (6)$$

$\delta$  describes variations in structural state between the maximum microcline-low albite series and the orthoclase series.  $\delta$  varies from 1.00 for maximum microcline-low albite series to 0.00 for orthoclase series.  $\delta'$  describes the variations between the orthoclase and the sanidine-high albite series.  $\delta'$  varies from 0.00 for orthoclase series to -1.00 for high sanidine-high albite series. Thus a unique value from -1.00 to +1.00 can be calculated to define the structural state of any alkali feldspar. Ragland (1970) [22] also related parameters  $\delta$  and  $\delta'$  to estimate Al in the  $T_1$  sites by the following equations:

$$\text{Al } T_1 = \frac{\delta + 2.331}{3.33}; \quad \text{Al } T_1 = \frac{\delta' + 3.500}{5.0} \quad (7)$$

The above equations are based upon (i) that feldspars of the maximum microcline-low albite series are perfectly ordered ( $\delta = 1$ ;  $\text{Al } T_1 = 1$ ), (ii) that feldspars of the sanidine-high albite series are perfectly disordered ( $\delta' = -1$ ;  $\text{Al } T_1 = 0.5$ ).

**Phillips and Ribbe (1973) [14]** suggested the use of the following equations in estimating Al contents in monoclinic feldspars:

$$\text{Al } T_1 = 2.360(c - 0.4b) - 4.369 \quad (8)$$

$$\text{Al } T_2 = 2.256(c - 0.4b) - 4.658 \quad (9)$$

**Kroll method:** Kroll (1971, 1973, 1980) [23–25] has proposed a method to estimate Al, Si distribution of alkali feldspars from two lattice translations, called Tr [110] and Tr  $[1\bar{1}0]$ , which are the repeat distances in the [110] and  $[1\bar{1}0]$  directions. He has shown that the repeat distances in the [110] and  $[1\bar{1}0]$  directions were controlled by the distribution of Al atoms among the tetrahedral sites. The repeating sequence of the tetrahedra is along [110] :  $T_10$ ,  $T_20$ ,  $T_2m$  and along  $[1\bar{1}0]$  :  $T_1m$ ,  $T_20$ ,  $T_2m$ .

The differences in the repeat distance [110] and  $[1\bar{1}0]$  estimates the transfer of Al from  $T_1m$  to  $T_10$  sites, while the mean of the repeat distances measures the combined transfer of Al from  $T_2$  to  $T_1$  sites. This assumes that there is no interaction with the M site. However, there is an effect from the M site and Kroll prepared separate calibration curves for Na and K feldspar.

The translational distances in the two directions [110] and  $[1\bar{1}0]$  are designated by Tr [110] and Tr  $[1\bar{1}0]$ . They are related to the cell dimensions by:

$$\text{Tr [110]} = \frac{1}{2} \left( a^2 + b^2 + 2ab \cos \gamma \right)^{1/2} \quad (10)$$

$$\text{Tr } [1\bar{1}0] = \frac{1}{2} \left( a^2 + b^2 - 2ab \cos \gamma \right)^{1/2} \quad (11)$$

The changing site occupancies cause the repeat distances to change their lengths: Tr [110] increases, whereas Tr  $[1\bar{1}0]$  decreases during ordering of triclinic alkali feldspars.

For the K-rich and Na-rich alkali feldspars the following equations have been derived by Kroll (1980) [25] to estimate Al site occupancies:

For K-rich alkali feldspar ( $\text{Or}_{70} - \text{Or}_{100}$ ):

$$T_10 = 29.424 - 3.7962 \text{ Tr } [1\bar{1}0] + 0.5355 n_{\text{or}} \quad (12)$$

$$T_1m = 22.838 - 2.9362 \text{ Tr [110]} + 0.4265 n_{\text{or}} \quad (13)$$

For Na-rich alkali feldspars ( $\text{Or}_0 - \text{Or}_{30}$ ):

$$T_10 = 28.961 - 3.7594 \text{ Tr } [1\bar{1}0] + 0.8396 n_{\text{or}} \quad (14)$$

$$T_1m = 17.778 - 2.3049 \text{ Tr [110]} + 0.7356 n_{\text{or}} \quad (15)$$

where  $n_{\text{or}}$  = mole fraction  $\text{KAlSi}_3\text{O}_8$  (or). The  $n_{\text{or}}$  content can be determined from the cell volume using Stewart and Wright (1974) [26] method:

$$n_{\text{or}} = \left( 0.2962 - \sqrt{(0.953151 - 0.0013V)} \right) 0.18062 \quad (16)$$

or using the following equation of Kroll and Ribbe (1983) [27] for low-albite-maximum microcline series:

$$n_{\text{or}} = -1227.8023 + 5.35958 V - 7.81518 \times 10^{-3} V^2 + 3.80771 \times 10^{-6} V^3 \quad (17)$$

**Structural indicators**  $\Delta(\alpha^*\gamma^*)$ ,  $\Delta(b^*c^*)$ ,  $\Delta(bc)$  and  $\Delta(bc^*)$ :

The  $\alpha^*\gamma^*$  plot was first introduced in alkali feldspar studies by Mackenzie and Smith (1955) [28]. Subsequently, Smith (1968) [29] showed that from the quadrilateral of the end-members MF (Monoclinic Feldspars), LM (Low Microcline), LA (Low Albite) and HA (High Albite) plotted on the  $\alpha^*\gamma^*$  diagram, one can derive the  $\Delta(\alpha^*\gamma^*)$  indicator which measures the difference in Al content between the T<sub>10</sub> and T<sub>1m</sub> tetrahedral sites. All experimental data so far obtained by number of structure analyses confirm that the  $\alpha^*\gamma^*$  plot can be used for this purpose [1, 3, 8]. From the values of unit cell parameters b\* and c\*, or b and c, it is possible to obtain indicator  $\Delta(b^*c^*)$  [1, 29] or the structural indicator  $\Delta(bc)$  or  $\Delta(bc^*)$  [26, 30, 31].

Kroll and Ribbe (1987) [32] proposed the following linear equations for determining  $\Delta(bc^*)$  and  $\Delta(\alpha^*\gamma^*)$ :

$$\Delta(bc^*) = \text{Al}(T_{10} + T_{1m}) = \frac{b - 21.5398 + 53.8405c^*}{2.1567 - 15.8583c^*} \quad (18)$$

$$\Delta(\alpha^*\gamma^*) = \text{Al}(T_{10} - T_{1m}) = \frac{\gamma^* - 44.778 - 0.50246\alpha^*}{6.646 - 0.05061\alpha^*} \quad (19)$$

The b – c\* equations produce nearly linear plots for alkali-exchange series, a substantial improvement over the relationships involving b and c cell parameters.

The distribution of Al over the four tetrahedral sites in the alkali feldspar of any structural state can now be estimated using the following equations from Stewart and Ribbe (1969) [30]:

$$\text{Al } T_{10} = \frac{\Delta(bc) + \Delta(\alpha^*\gamma^*)}{2} \quad (20)$$

$$\text{Al } T_{1m} = \text{Al } T_{10} - \Delta(\alpha^*\gamma^*) \quad (21)$$

The Al in T<sub>2</sub> sites can be divided equally between T<sub>20</sub> and T<sub>2m</sub> sites because all available feldspar structure analyses show nearly equal T-O bond lengths for these sites.

$$\text{Al } T_{20} = \text{Al } T_{2m} = \frac{[1.0 - (\text{Al } T_{10} + \text{Al } T_{1m})]}{2} \quad (22)$$

**Jowhar Method (1981, 1989) [6, 7]:** Jowhar (1981) [6] described a procedure and made a computer program in FORTRAN IV for calculating lattice parameters and distribution of aluminium in tetrahedral sites T<sub>10</sub>, T<sub>1m</sub>, T<sub>20</sub> and T<sub>2m</sub> sites of alkali feldspars by using 4 X-ray reflections ( $\bar{2}01$ ), (002), (060) and ( $\bar{2}04$ ) and by making use of equations described by Wright (1968) [18], Wright and Stewart (1968) [33] and Orville (1967) [34]. This method however sometimes gives negative values of Al in

T sites, which is theoretically not possible. This is because of propagation of errors in estimation of lattice parameters  $\alpha$ ,  $\beta$  and  $\gamma$ . Jowhar (1989) [7] presented another rapid method for calculating lattice parameters and distribution of aluminium in tetrahedral sites  $T_10$ ,  $T_1m$ ,  $T_20$  and  $T_2m$  sites of alkali feldspars. This method is based on 2 $\theta$  values of 6 hkl planes ( $\bar{2}01$ ), (130), (002), ( $\bar{1}13$ ), (060) and ( $\bar{2}04$ ) which can be easily obtained on X-ray powder diffractometer. A computer program in FORTRAN 77 on WIPRO 286 computer system was also prepared for computations involved in the determination of lattice parameters and structural state of alkali feldspars.

**Coefficient of order:** Ribbe and Gibbs (1967) [35] defined coefficient of order as:

$$\text{Coefficient of order} = \frac{P - 0.25}{0.75} \quad (23)$$

where P is the fractional occupancy of Al in  $T_10$  site. Coefficient of order varies from 0 for sanidine to 0.33 for orthoclase to 1.0 for maximum microcline.

**Obliquity:** Obliquity,  $\phi$ , defined by Thompson and Hovis (1978) [36] is a direct measure of the departure of a triclinic feldspar from the dimensional requirements for monoclinic symmetry. The quantity  $1 - \cos \phi$  must vanish for monoclinic feldspars. In a monoclinic crystal it is necessary (but not sufficient) that the b axis and the pole  $b^*$ , to (010) coincide, and that:

$$b = \frac{1}{b^*} = d(010) \quad (24)$$

On the other hand, in a triclinic crystal b and  $b^*$  do not coincide. Thompson and Hovis (1978) [36] designated the angle between b and  $b^*$  as  $\phi$  and called it obliquity. Therefore,

$$d(010) = \frac{1}{b^*} = b \cos \phi \quad (25)$$

It is necessary for monoclinic symmetry that  $\phi = 0$  or  $\cos \phi = 1$ . However, it is possible that a triclinic crystal may also have  $\phi = 0$ . Therefore, the vanishing of the obliquity thus ensures that only the geometric form of the unit cell meets the requirements for monoclinic symmetry, and does not prove that the crystal is monoclinic. The quantity  $[d(131) - d(\bar{1}\bar{3}\bar{1})]$  must vanish when  $\phi$  vanishes, but the reverse is not true.

**Thompson ordering parameters:** Thompson (1969) [37] described ordering parameters X, Y and Z as:

$$X = N_{Al(T_20)} - N_{Al(T_2m)} \quad (26)$$

$$Y = N_{Al(T_10)} - N_{Al(T_1m)} \quad (27)$$

$$Z = [N_{Al(T_10)} + N_{Al(T_1m)}] - [N_{Al(T_20)} + N_{Al(T_2m)}] \quad (28)$$

where N is the fraction of each T site occupied by Al. The three ordering parameters X, Y, and Z, respectively show the deviation in the Al content of the  $T_2$  site from

monoclinic symmetry, the deviation from monoclinic symmetry of the T<sub>1</sub> site, and finally the amount of Al transferred from the T<sub>2</sub> sites into the T<sub>1</sub> sites. For completely disordered feldspars, all three ordering parameters are zero. For low microcline and low albite, Y and Z are both 1 but X is zero. Smith (1974a) [1] argued that alkali feldspar under equilibrium conditions would follow a one-step trend and that coherency between domains is responsible for the monoclinic symmetry at the early stages of ordering. In ideal one-step ordering path Al moves to the T<sub>10</sub> site at an equal rate from T<sub>1m</sub>, T<sub>20</sub> and T<sub>2m</sub> sites, whereas in the ideal two-step ordering path, the Al atoms first segregate into T<sub>1</sub> and T<sub>2</sub> sites preserving monoclinic symmetry by equal occupancy of 0 and m sub-sites, and the second stage of ordering proceeds with triclinic symmetry as Al moves from T<sub>1m</sub> to T<sub>10</sub>. In addition, there is an infinite number of ordering paths between the extreme ideal one-step and two-step ordering path [8, 12, 13].

### 4 Homogeneous Equilibria in Alkali Feldspars

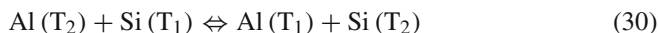
Estimates of maximum P-T conditions attained during metamorphism can be made relatively easily, but, the determination of the temperatures at which minerals re-equilibrate, following cooling, is more difficult to make (Jowhar 1994, 2005, 2012) [8, 38, 39].

Methods of thermodynamic analysis have been successful in dealing with the problem of homogeneous equilibria in crystals [37]. The intensive properties of an alkali feldspar are functions of P, T, N<sub>or</sub>, N<sub>An</sub> and of the ordering parameters X, Y and Z. For fully equilibrated feldspars, conditions of equilibrium are (Thompson 1969) [37]:

$$\left(\frac{\delta\bar{G}}{\delta X}\right)_{P,T,N_{or},N_{An},Y,Z} = \left(\frac{\delta\bar{G}}{\delta Y}\right)_{P,T,N_{or},N_{An},X,Z} = \left(\frac{\delta\bar{G}}{\delta Z}\right)_{P,T,N_{or},N_{An},X,Y} = 0 \quad (29)$$

where  $N_{or} = \frac{n_K}{n_K+n_{Na}+n_{Ca}}$  and  $N_{An} = \frac{n_{Ca}}{n_K+n_{Na}+n_{Ca}}$

For monoclinic alkali feldspar the ion exchange of Al and Si between T<sub>1</sub> and T<sub>2</sub> sites may be expressed by the following reaction:



Thompson (1969) [37] defined the quantity K'<sub>Z</sub> as:

$$K'_Z = \frac{N_{Al(T_1)}N_{Si(T_2)}}{N_{Si(T_1)}N_{Al(T_2)}} = \frac{(1+Z)(3+Z)}{(1-Z)(3-Z)} \quad (31)$$

K'<sub>Z</sub> has the form of an apparent equilibrium constant.

## 5 Determination of Lattice Parameters of Alkali Feldspars

Determination of direct lattice parameters  $a$ ,  $b$ ,  $c$ ,  $\alpha$ ,  $\beta$ ,  $\gamma$  of alkali feldspars is carried out by solving the following Eq. 32 for triclinic crystal system ( $a \neq b \neq c \neq \alpha \neq \beta \neq \gamma \neq 90^\circ$ ) for at least 6 hkl planes [7, 8, 13, 40–42]:

$$\frac{1}{d_{hkl}^2} = \frac{\frac{h^2}{a^2} \sin^2 \alpha + \frac{k^2}{b^2} \sin^2 \beta + \frac{l^2}{c^2} \sin^2 \gamma + \frac{2hk}{ab} (\cos \alpha \cos \beta - \cos \gamma) + \frac{2hl}{ac} (\cos \alpha \cos \gamma - \cos \beta) + \frac{2kl}{bc} (\cos \beta \cos \gamma - \cos \alpha)}{1 - \cos^2 \alpha - \cos^2 \beta - \cos^2 \gamma + 2 \cos \alpha \cos \beta \cos \gamma} \quad (32)$$

$d$  spacing as a function of reciprocal unit cell parameters is:

$$\frac{1}{d_{hkl}^2} = \sigma_{hkl}^2 = [h^2 a^{*2} + k^2 b^{*2} + l^2 c^{*2} + 2hka^* b^* \cos \gamma^* + 2klb^* c^* \cos \alpha^* + 2lhc^* a^* \cos \beta^*] \quad (33)$$

Unit cell volume is obtained by using the relation:

$$V = abc \sqrt{1 - \cos^2 \alpha - \cos^2 \beta - \cos^2 \gamma + 2 \cos \alpha \cos \beta \cos \gamma} \quad (34)$$

$$V^* = a^* b^* c^* \sqrt{1 - \cos^2 \alpha^* - \cos^2 \beta^* - \cos^2 \gamma^* + 2 \cos \alpha^* \cos \beta^* \cos \gamma^*} \quad (35)$$

## 6 Conclusions

The difference in symmetry of sanidine and microcline is due to order-disorder relations of Si and Al atoms over tetrahedral sites. The distribution of Al and Si in tetrahedral sites in maximum microcline (Low microcline) is of the highest degree of order and microcline has a lowest structural state. On the other hand, sanidine, with the highest structural state, shows random Al-Si distribution in tetrahedral sites. In between these two end members maximum microcline and sanidine, several intermediate structural states, e.g. orthoclase and intermediate microcline exist. In this paper methods for estimation of structural state of alkali feldspars is reviewed and discussed. Various ordering parameters have been used to designate the state of Al-Si distribution in alkali feldspars. Although the coefficient of order, the triclinicity, the Ragland parameter and obliquity indicate the structural state in quantitative manner, we can only draw broad generalizations with their help as regard to the actual physical environment during the formation of the alkali feldspar. On the other hand, Thompson X, Y and Z ordering parameters are more useful because it relates Gibbs function, entropy, enthalpy, etc., with the Al-Si distribution.

**Acknowledgments** Professor Ram S. Sharma and Professor V. K. S. Dave provided tremendous inspiration for this research work. The facilities and encouragement provided by Professor Anil K. Gupta, Director, Wadia Institute of Himalayan Geology, Dehradun, to carry out this research work is thankfully acknowledged.



## References

1. Smith, J.V.: Feldspar minerals. Crystal Structure and Physical Properties, vol. 1, p. 627. Springer, Berlin (1974a)
2. Smith, J.V.: Feldspar minerals. Chemical and Textural Properties, vol. 2, p. 690. Springer, Berlin (1974b)
3. Smith, J.V., Brown, W.L.: Feldspar minerals. Crystal Structures, Physical, Chemical and Microtextural Properties, vol. 1, Second revised and extended edition, p. 828. Springer, Berlin (1988)
4. Barth, T.F.W.: Feldspars, p. 261. John Wiley, New York (1969)
5. Laves, F.: Phase relations of the alkali feldspars I and II. *J. Geol.* **60**(436–450), 549–574 (1952)
6. Jowhar, T.N.: AFEL, a fortran IV computer program for calculating lattice parameters and distribution of aluminium in tetrahedral sites of alkali feldspars. *Comput. Geosci.* **7**, 407–413 (1981)
7. Jowhar, T.N.: Determination of lattice parameters and structural state of alkali feldspars—a rapid X-ray diffraction method. *Indian J. Earth Sci.* **16**, 173–177 (1989)
8. Jowhar, T.N.: Crystal parameters of K-feldspar and geothermometry of Badrinath crystalline complex, Himalaya, India. *Neues Jahrb. Mineral. Abh.* **166**, 325–342 (1994)
9. Jowhar, T.N.: Refinement of the alkali feldspar-muscovite geothermometer and its application to the Badrinath crystalline complex, Himalaya, India. *Indian Mineral.* **32**, 7–20 (1998)
10. Jowhar, T.N.: Geobarometric constraints on the depth of emplacement of granite from the Ladakh batholith, northwest Himalaya, India. *J. Mineral. Petrol. Sci.* **96**, 256–264 (2001)
11. Jowhar, T.N., Verma, P.K.: Alkali feldspars from the Badrinath crystalline complex and their bearing on the Himalayan metamorphism. *Indian Mineral.* **29**, 1–12 (1995)
12. Kaur, M., Chamyal, L.S., Sharma, N., Jowhar, T.N.: Geothermometry of the granitoids of eastern higher kumaun Himalaya, India. *J. Geol. Soc. India* **53**, 211–217 (1999)
13. Pandey, P., Rawat, R.S., Jowhar, T.N.: Structural state transformation in alkali feldspar: evidence for post-crystallisation deformation from a proterozoic granite kumaun Himalaya, India. *J. Asian Earth Sci.* **25**, 611–620 (2005)
14. Phillips, M.W., Ribbe, P.H.: The structures of monoclinic potassium-rich feldspars. *Am. Mineral.* **58**, 263–270 (1973)
15. Smith, J.V., Bailey, S.W.: Second review of Al-O and Si-O tetrahedral distances. *Acta Crystallogr.* **16**, 801–811 (1963)
16. Jones, J.B.: Al-O and Si-O tetrahedral distances in alumino-silicate framework structures. *Acta Crystallogr.* **B24**, 355–358 (1968)
17. Ribbe, P.H., Gibbs, G.V.: Statistical analysis and discussion of mean Al/Si-O bond distances and the aluminium content of tetrahedra in feldspars. *Am. Mineral.* **54**, 85–94 (1969)
18. Wright, T.L.: X-ray and optical study of alkali feldspar: II. An X-ray method for determining the composition and structural state from measurement of  $2\theta$  values for three reflections. *Am. Mineral.* **53**, 88–104 (1968)
19. Mackenzie, W.S.: The orthoclase-microcline inversion. *Mineral. Mag.* **30**, 354–366 (1954)
20. Goldsmith, J.R., Laves, F.: The microcline-sanidine stability relations. *Geochim. Cosmochim. Acta* **5**, 1–19 (1954)
21. Christie, O.H.J.: Feldspar structure and equilibrium between plagioclase and epidote. *Am. J. Sci.* **260**, 149–153 (1962)
22. Ragland, P.C.: Composition and structural state of the potassic phase in perthites as related to petrogenesis of a granitic pluton. *Lithos* **3**, 167–189 (1970)
23. Kroll, H.: Determination of Al, Si distribution in alkali feldspars from X-ray powder data. *Neues Jahrb. Mineral. Monatsh.* 91–94 (1971)
24. Kroll, H.: Estimation of the Al, Si distribution of feldspars from the lattice translations Tr [110] and Tr  $[\bar{1}\bar{1}0]$ . I. alkali feldspars. *Contrib. Miner. Petrol.* **39**, 141–156 (1973)
25. Kroll, H.: Estimation of the Al, Si distribution of alkali feldspars from the lattice translations Tr [110] and Tr  $[\bar{1}\bar{1}0]$ . Revised diagrams. *Neues Jahrb. Mineral. Monatsh.*, 31–36 (1980)

26. Stewart, D.B., Wright, T.L.: Al/Si order and symmetry of natural alkali feldspars and the relationship of strained cell parameters to bulk composition. *Bull. Soc. Franc. Miner. Cristall.* **97**, 356–377 (1974)
27. Kroll, H., Ribbe, P. H.: Lattice parameters, composition and Al, Si order in alkali feldspars. In: Ribbe, P. H. (ed.) *Feldspar Mineralogy*, Mineralogical Society of America, Reviews in Mineralogy, vol. 2, Second Edition, pp. 57–99 (1983)
28. Mackenzie, W.S., Smith, J.V.: The alkali feldspars I. orthoclase-microperthites. *Am. Mineral.* **40**, 707–732 (1955)
29. Smith, J. V.: Cell dimensions  $b^*$ ,  $c^*$ ,  $\alpha^*$ ,  $\gamma^*$  of alkali feldspar permit qualitative estimates of Si, Al ordering: albite ordering process (Abstract), Geological Society of America Meeting, Mexico, p. 283 (1968)
30. Stewart, D.B., Ribbe, P.H.: Structural explanation for variations in cell parameters of alkali feldspar with Al/Si ordering. *Am. J. Sci.* **267-A**, 444–462 (1969)
31. Blasi, A.: Different behaviour of  $\Delta(bc)$  and  $\Delta(b^*c^*)$  in alkali feldspar. *Neues Jahrb. Mineral. Abh.* **138**, 109–121 (1980)
32. Kroll, H., Ribbe, P.H.: Determining (Al, Si) distribution and strain in alkali feldspars using lattice parameters and diffraction peak positions: a review. *Am. Mineral.* **72**, 491–506 (1987)
33. Wright, T.L., Stewart, D.B.: X-ray and optical study of alkali feldspar: I. Determination of composition and structural state from refined unit-cell parameters and 2V. *Am. Mineral.* **53**, 38–87 (1968)
34. Orville, P.M.: Unit-cell parameters of the microcline-low albite and the sanidine-high albite solid solution series. *Am. Mineral.* **52**, 55–86 (1967)
35. Ribbe, P.H., Gibbs, G.V.: Statistical analysis of Al/Si distribution in feldspars. *Trans. Am. Geophys. Union* **11**, 229–230 (1967)
36. Thompson Jr, J.B., Hovis, G.L.: Triclinic feldspars: angular relations and the representation of feldspar Series. *Am. Mineral.* **63**, 981–990 (1978)
37. Thompson Jr, J.B.: Chemical reactions in crystals. *Am. Mineral.* **54**, 341–375 (1969)
38. Jowhar, T.N.: Computer programs for P-T calculations and construction of phase diagrams: Use of TWQ, WEBINVEQ and THERMOCALC. In: Rajan, S., Pandey, P.C. (eds.) *Antarctic Geoscience, Ocean-Atmosphere Interaction and Paleoclimatology*, National Centre for Antarctic and Ocean Research, Goa, pp.248–262 (2005)
39. Jowhar, T.N.: Computer programs for P-T history of metamorphic rocks using pseudosection approach. *Int. J. Comput. Appl. Technol.* **41**, 18–25 (2012)
40. Azaroff, L.V.: *Elements of X-ray Crystallography*. McGraw Hill Book Company, New York (1968)
41. Appleman, D.E., Evans, H.T., Jr.: Job 9214: Indexing and least-squares refinement of powder diffraction data. Document PB 216 188, National Technical Information Service, U. S. Department of Commerce, Springfield, Virginia (1973)
42. Benoit, P.H.: Adaptation to microcomputer of the appleman-evans program for indexing and least squares refinement of powder diffraction data for unit cell dimensions. *Am. Mineral.* **72**, 1018–1019 (1987)

# Iris Recognition System Using Local Features Matching Technique

Alamdeep Singh and Amandeep Kaur

**Abstract** Iris is one of the most trustworthy biometric traits due to its stability and randomness. In this paper, the Iris Recognition System is developed with the intention of verifying both the uniqueness and performance of the human iris, as it is a briskly escalating way of biometric authentication of an individual. The proposed algorithm consists of an automatic segmentation system that is based on the Hough transform, and can localize the circular iris and pupil region, occluding eyelids and eyelashes, and reflections. The extracted iris region is then normalized into a rectangular block. Further, the texture features of normalized image are extracted using LBP (Local Binary Patterns). Finally, the Euclidean distance is employed for the matching process. In this thesis, the proposed system is tested with the co-operative database such as CASIA. With CASIA database, the recognition rate of proposed method is almost 91 %, which shows the iris recognition system is reliable and accurate biometric technology.

**Keywords** Iris pre-processing · Normalization · Circular hough transform · LBP · Euclidean distance

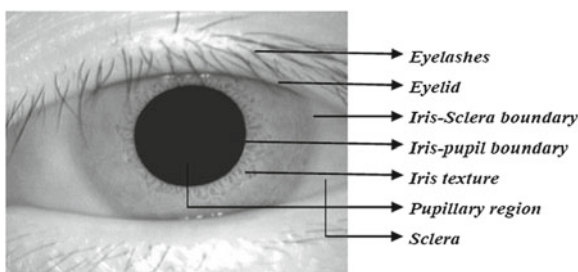
## 1 Introduction

A biometric system provides automatic recognition of an individual based on some sort of unique attributes or traits (such as fingerprints, facial features, voice, hand geometry, handwriting, the retina, and the iris) possessed by the individual. Biometric authentication has evolved from the demerits of traditional means of authentication.

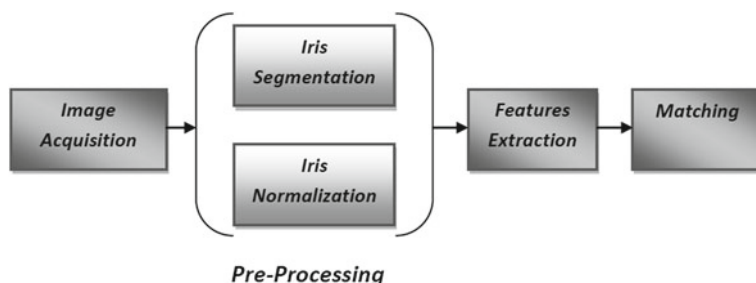
---

A. Singh (✉) · A. Kaur  
Department of Computer Science, Punjabi University, Patiala, India  
e-mail: bhinder.alam@gmail.com

A. Kaur  
e-mail: aman\_k2007@hotmail.com



**Fig. 1** Classification of human eye



**Fig. 2** Stages of iris recognition system

Biometric authentication is divided into two rudimentary categories such as: Physiological (or passive) and Behavioral (or active) biometrics. Physiological biometrics are based on parts of body like face, fingerprints palm print geometry, retina and iris recognition. While Behavioral biometrics are based on the actions taken by a person such as Voice recognition, keystroke dynamics and online/offline signatures. Iris, due to its permanence and ease of acquiring, plays a significant role among all the biometric traits. In these days Iris recognition is used as living passports, driving licenses and credit cards authentication, automobile ignition and unlocking, et cetera. Iris recognition is the process of automatically segregating people on the basis of information of an individual's iris image for biometric authentication system.

Pupil is the black circular shaped area in the eye image that controls the amount of light entering the eye by dilation and contraction. Iris is the circular shaped muscle that differentiates pupil from the sclera region. The Fig. 1 depicts the structure of the human eye.

Generally, Iris Recognition is mainly performed in four steps, as illustrated in Fig. 2: Image Acquisition, Image Pre-processing includes image segmentation and image normalization, Feature Extraction and Matching.

## 2 Literature Review

Since 2012, following are the main approaches for iris recognition:

At the outset, Flom and Safir [1] proposed the first mechanized biometrics system beneath extremely controlled conditions in 1987. They recommended the concept of practicing pattern recognition tools, including difference operators, edge detection algorithms, and the Hough transform, to extract iris descriptors, but no experimental results were scrutinized.

The first operational iris biometric system has been developed at University of Cambridge by Daugman [2–4]. Daugman put forwarded the concept of integro-differential operator with 2-dimensional Gabor filters and hamming distance. Contrariwise, Wildes [5], method involved computing a binary edge map followed by a Hough transform and then applied a Laplacian of Gaussian filter at multiple scales to generate a template and computed the normalized correlation as a similarity measure. Basit et al. [6] implemented an algorithm by representing eigen-irises after determining the centre of each iris and at last the recognition of irises was based on Euclidean distances. Chou, Chen and Weng [7] suggested a non-orthogonal view iris recognition system and proposed a circle rectification method to match iris images acquired at different off-axis angles. Hollingsworth et al. [8] offered a method of fusion of hamming distance and fragile bit distance. An independent component analysis method was used by Huang et al. [7] to condense the size of the iris feature without sacrificing the accuracy of iris recognition. Monro et al. [9] advised an iris coding method using differences of the discrete cosine transform coefficients that achieved highly accurate recognition results. Araghi et al. [10] proposed an Iris Recognition System based on covariance of discrete wavelet using Competitive Neural Network which discriminated noisy images very well. Bharadwaj et al. [11] proposed the Periocular biometrics as an alternative to iris recognition if the iris images were captured at a distance. They used GIST (global matcher) and complex local binary patterns (CLBP) for feature extraction with UBIRIS v2 database for recognition process.

Vatsa et al. [12] proposed a concept of curve evolution to effectively segment a non ideal iris image using the modified Mumford–Shah functional. An elastic iris blob matching algorithm was implemented by Zhenan et al. [13] to overcome the limitations of local feature based classifiers (LFC). Zhou et al. [14] used methods such as Two-dimensional Gabor wavelet method with Log–Polar coordinates and 1-D Log–Gabor wavelet method with Polar coordinates, automatically eliminated the poor-quality images, evaluated the segmentation accuracy, and measured if the iris image had sufficient feature information for recognition. Ojala et al. [15] presented a theoretically very simple, yet efficient, multi-resolution approach to gray-scale and rotation invariant texture classification based on local binary patterns and nonparametric discrimination of sample and prototype distributions with excellent experimental results.

The database surveyed was CASIA database version 1.0 [16] includes 756 iris images from 108 eyes.

## 3 Brief Background of Proposed Technique

### 3.1 Image Acquisition

Images are acquired through a standard database—CASIA dataset (The Chinese Academy of Sciences—Institute of Automation), contains 756 grey scale eye images with 108 unique eyes or classes and 7 different images of each unique eye.

### 3.2 Image Pre-processing

#### 3.2.1 Image Segmentation

The Circular Hough transform [17] is used to detect the iris/sclera boundary and iris/pupil boundary for making the circle detection process more efficient and accurate. After the completion of this process, six parameters are stored, the radius, and x (row) and y (column) centre coordinates for both circles according to the equation:

$$X_c^2 + Y_c^2 - r^2 = 0 \quad (1)$$

Afterwards, the Linear Hough Transform is used for isolation of eyelids. For segmentation of Iris, consider some general values according to *Masek's* approach for CASIA database as:

$$\begin{aligned} \text{Lower pupil radius} &= 28, & \text{Upper pupil radius} &= 75, \\ \text{Lower iris radius} &= 80, & \text{Upper iris radius} &= 150 \end{aligned}$$

Further, Canny edge detection is used to create an edge map, and only horizontal gradient information  $|G_x|$  is taken.

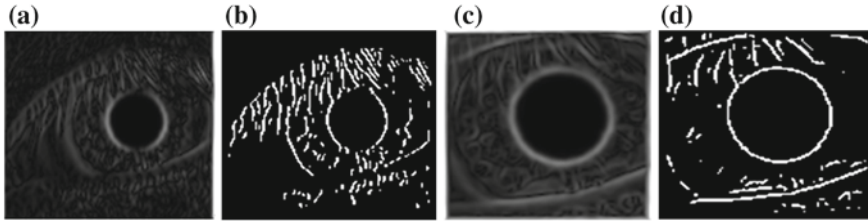
$$|G| = \sqrt{G_x^2 + G_y^2} \quad (2)$$

$$|G| = |G_x| + |G_y| \quad (3)$$

Where,  $G_x$  and  $G_y$  are the gradients in x and y direction. The direction of the edge can be determined and stored by using:

$$\theta = \arctan\left(\frac{|G_y|}{|G_x|}\right) \quad (4)$$

Then the Final edges are determined by suppressing all edges that are not connected to a very certain (strong) edge (Fig. 3).



**Fig. 3** Preprocessing stages: **a** Iris image after canny edge detection, **b** Iris image after hysteresis, **c** Pupil image after canny edge detection, **d** Pupil image after hysteresis

Now find circle by using circular Hough Transform (CHT). The mathematical equation for CHT is:

$$(x - a)^2 + (y - b)^2 = r^2 \quad (5)$$

Where, a and b are the centers of the circle in the x and y direction respectively and where r is the radius. The parametric representation of the circle is:

$$x = a + r \cos(\theta) \quad (6)$$

$$y = b + r \sin(\theta) \quad (7)$$

For each edge point, the algorithm draw circles of different radii. From these it finds the maximum in the Hough space that is considered as the parameters of the circle.

### 3.2.2 Image Normalization

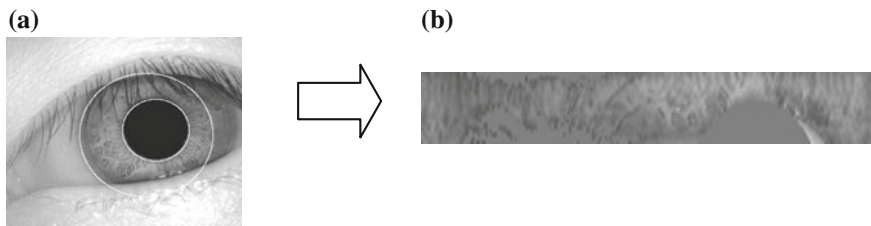
The segmented area is normalized to unwrap the iris region into polar coordinates by using Daugman Rubber Sheet Model [17]. The extracted iris region was then normalized into a rectangular block. This is given by:

$$r' = \sqrt{\alpha\beta^2 - \alpha - r^2} \quad (8)$$

$$\alpha = \alpha x^2 + \alpha y^2 \quad (9)$$

$$\beta = \cos\left(\pi - \arctan\left(\frac{O_y}{O_x}\right) - \theta\right) \quad (10)$$

Where, displacement of the centre of the pupil relative to the centre of the iris is given by  $O_x$ ,  $O_y$ , and  $r'$  is the distance between the edge of the pupil and edge of the iris at an angle,  $\theta$  around the region, and  $r_I$  is the radius of the iris (Fig. 4).



**Fig. 4** Image normalization: **a** Image after segmentation, **b** after normalization

### 3.3 Iris Features Extraction

In this phase, LBP (Local Binary Pattern) is used to extract the features of normalized iris image. LBP is a simple yet very efficient texture operator, which labels the pixels of an image by thresholding the neighborhood of each pixel and considers the result as a binary number. The formula to compute the local texture around  $(x_c, y_c)$  for normalized iris image obtained in the Normalization stage is:

$$LBP_{p,r}(x_c, y_c) = \sum_{p=0}^{p-1} s(g_p - g_c)2^p \tag{11}$$

Where coordinates of individual neighbor,  $g_p$  is given by:

$$x_c + R \cos \frac{2\pi p}{p}, y_c - R \sin \frac{2\pi p}{p}, \tag{12}$$

Where,  $(x_c, y_c)$  are coordinates of the center pixel. In the next step, a set of the histogram features is computed together for LBP to construct the feature vector. The feature vector is saved for matching process (Fig. 5).



**Fig. 5** Image after applying LBP on normalized iris image

### 3.4 Iris Matching

Finally, the Euclidean distance is employed for the matching process. An incredible feature of iris is the arbitrarily distributed irregular texture details in it. After getting



histograms from both test ( $H_1$ ) and training image ( $H_2$ ), calculate the Euclidean distance as:

$$H_3 = \text{sqrt} \left( \sum (H_1 - H_2)^2 \right) \quad (13)$$

The shortest distance gives the nearest match.

## 4 Proposed Algorithm

The algorithm used is as follows:

- Acquire images from CASIA database,
- Iris localization using Circular Hough Transform,
- Apply Daugman's Rubber Sheet Model to normalize the extracted region into rectangular block.
- Apply LBP to the normalized image to find the texture features which are, later on, saved in histogram,
- Finally, the Euclidean distance is used to recognize the applicable image.

## 5 Experimental Results

The CASIA database provided good segmentation, which undoubtedly tells apart the boundaries of iris pupil and sclera. The segmentation technique extracted the iris region of 624 out of 756 eye images, which connotes a success rate of around 83%. The normalization process is not capable of flawlessly restructuring the similar pattern from images with the variation of pupil dilation. Then after LBP features are extracted. LBP is faster and easy to implement. The classification results are given below in the Table 1:

The accuracy of the proposed algorithms is less than Daugman's method that is a benchmark for iris recognition, but the computation speed is faster than their method. The accuracy of the proposed method is better than Masek's approach.

**Table 1** Comparison of proposed method with other popular methods

Algorithm	Database	Recognition rate (%)
Daugman	CASIA	98.58
Masek	CASIA	83.92
Proposed method	CASIA	91.42

## 6 Conclusion

To conclude, the most complicated phase of the system is the preprocessing stage where the result of this stage is completely dependent upon the quality of the image. CHT is a popular and easy technique used to segment the iris pattern successfully from the eye image. The drawback of this method is that it still consumes enough time. After that, the iris image is normalized by the Daugman's Rubber Sheet model, which does not give the high-quality results due to the variation of pupil dilation. Then after, LBP and Euclidean Distance are used for features extraction and matching phase, which are easy to implement and gives first-rate results with 91.42 % accuracy.

## References

1. Flom, L., Safir, A.: Iris recognition system. U.S. Patent IEEE, PP. 4,641,394, ©(1987)
2. Daugman, J.: High confidence visual recognition of persons by a test of statistical independence. *IEEE Trans. Pattern Anal. Mach. Intell.* **15**(11), 1148–1161 (1993)
3. Daugman, J.: The importance of being random: statistical principles of iris recognition. *Pattern Recogn.* **36**(2), 79–291 (2003)
4. Daugman, J.: Biometric personal identification system based on iris analysis. U.S. Patent Number 5,291,560 1 March 1994
5. Wildes, R.: Iris recognition: an emerging biometric technology. *Proc. IEEE* **85**, 1348–1363 (1997)
6. Basit, A., Javed, M., Anjum, M.: Efficient iris recognition method for human identification. *Proc. WEC* **2**, 24–26 (2005)
7. Huang, Y., Luo, S., Chen, E.: An efficient iris recognition system. In: *International Conference on Machine Learning and Cybernetics*, vol. 1, pp. 450–454. Beijing (2002)
8. Hollingsworth, K.P., Bowyer, K.W., Flynn, P.J.: Improved iris recognition through fusion of hamming distance and fragile bit distance. *IEEE Trans. Pattern Anal. Mach. Intell.* **33**(12), (2011), [Epub ahead of print] [www.ncbi.nlm.nih.gov/pubmed/21576740](http://www.ncbi.nlm.nih.gov/pubmed/21576740)
9. Monro, D., Rakshit, S., Zhang, Y. et al.: DCT-based iris recognition. *IEEE Trans. Pattern Anal. Mach. Intell.* **29**(4), 586–596 (2007)
10. Araghi, L., Shahhosseini, H., Setoudeh, F.: IRIS recognition using neural network. In: *Proceedings of The International Multiconference of Engineers and Computer Scientists 2010*, vol. 1, pp. 338–340. IMECS, Hong kong (2010)
11. Bharadwaj, S., Bhatt, H., Vatsa, M., Singh, R.: Periocular biometrics: when iris recognition fails. In: *Proceedings of International Conference on Biometrics Theory, Applications and Systems*, Washington, DC, 978–1–4244–7580–3/10/\$26.00 © 2010 IEEE
12. Vatsa, M., Singh, R., Noore, A.: Improving iris recognition performance using segmentation, quality enhancement, match score fusion, and indexing. *IEEE Trans. Syst. Man Cybern.* **38**(4), 896–897 (2009)
13. Sun, Z., Wang, Y., Tan, T., Cui, J.: Improving iris recognition accuracy via cascaded classifiers. *IEEE Trans. Syst. Man Cybern.* **35**(3), 435–441 (2005)
14. Zhou, Z., Du, Y., Belcher, C.: Transforming traditional iris recognition systems to work in nonideal situations. *IEEE Trans. Ind. Electron.* **56**(8), 3203–3213 (2009)
15. Ojala, T., Pietikäinen, M., MañenpaEa, T.: Multiresolution gray-scale and rotation invariant texture classification with local binary patterns. *IEEE Trans. Pattern Anal. Mach. Intell.* **24**(7), 971–987 (2002)
16. CASIA iris image database. See <http://www.cbsr.ia.ac.cn/Databases.htm>

17. Masek, L., Kovesi P.: MATLAB Source Code for a Biometric Identification System Based on Iris Patterns. The School of Computer Science and Software Engineering, The University of Western Australia. [http://www.csse.uwa.edu.au/\\_pk/studentprojects/libor/sourcecode.html](http://www.csse.uwa.edu.au/_pk/studentprojects/libor/sourcecode.html) (2003).

**Part X**  
**Soft Computing for Image Analysis**  
**(SCIA)**

# Fast and Accurate Face Recognition Using SVM and DCT

Deepti Sisodia, Lokesh Singh and Sheetal Sisodia

**Abstract** The main problem of face recognition is large variability of the recorded images due to pose, illumination conditions, facial expressions, use of cosmetics, different hairstyle, presence of glasses, beard, etc., especially the case of twins' faces. Images of the same individual taken at different times, different places, different postures, different lighting, may sometimes exhibit more variability due to the aforementioned factors, than images of different individuals due to gender, age, and individual variations. So a robust recognition system is implemented to recognize an individual even from a large amount of databases within a few minutes. So in order to handle this problem we have used SVM for face recognition. Using this technique an accurate face recognition system is developed and tested and the performance found is efficient. The procedure is tested on ORL face database. Results have proved that SVM approach not only gives higher classification accuracy but also proved to be efficient in dealing with the large dataset as well as efficient in recognition time. Results have proved that not only the training performance, the recognition performance but also the recognition rate raises to 100 % using SVM.

**Keywords** Machine learning · Support vector machine · ORL face database

---

D. Sisodia · L. Singh  
Technocrats Institute Of Technology, Bhopal, M.P, India  
e-mail: chanchal.sisodia@gmail.com

L.Singh  
e-mail: lokeshsingh@gmail.com

S. Sisodia (✉)  
Samrat Ashok Technical Institute, Vidisha, M.P, India  
e-mail: sheetal.sisodia@gmail.com

## 1 Introduction

Learning theory helps give a researcher applying machine learning algorithms some rules of the thumb that tell how to best apply the algorithms. “Dr. Andrew Ng Likens” knowing machine learning algorithms to a carpenter acquiring a set of tools. However, the difference between a good carpenter and not so good one is the skill in using those tools. In choosing which one to use and how. In the same way Learning Theory gives a “machine-learnist” some intuitions about how an ML algorithm would work and helps in applying them better. A common problem that can be observed in many A.I. engineering applications is pattern recognition. The problem is as follows: given a training set of vectors, each belonging to some known category, the machine must learn, based on the information implicitly contained in this set, how to classify vectors of unknown type into one of the specified categories. SVMs provide one means of tackling this problem [1].

Therefore, using Support Vector Machine (SVM) for recognition/authentication of facial images in this paper. Face authentication is a two-class problem. As face recognition system is presented all about with a claimed identity and it is making decision whether the claimant is really that person or not.

Due to daily changes in facial images such as variations in gestures, pose, facial expressions, etc., face recognition becomes a difficult problem to be solved, especially the case of twins’ faces. It is difficult to recognize the difference between both faces. It is also a problem for detection of faces in images than detection of salient features within that facial image and finally which classification model to be used that identifies clearly whether the resultant image is the desired image or not. For solution to this obstacle if we use large training image set then it might increase the complexity and if we keep training set small then the performance of facial recognition system degrades. So the only option remains to solve this problem is to reduce the dimensionality [2].

## 2 Structure of Support Vector Machine

A support vector machine is a machine in the sense that it is given inputs that are processed by the machine to produce outputs. Support vector machines are general algorithms based on guaranteed risk bounds of SLT, i.e., “statistical learning theory”. Support vector machines are a type of state-of-the-art pattern recognition technique whose foundations stem from statistical learning theory. They have found numerous applications, such as in face recognition, character recognition, face detection, and so on [3]. The basic principle of SVM is to find an optimal separating hyperplane so as to separate two classes of patterns with maximal margin. It tries to find the optimal hyperplane making expected errors minimized to the unknown test data, while the location of the separating hyperplane is specified via only data that lie close to the decision boundary between the two classes, which are support vectors.

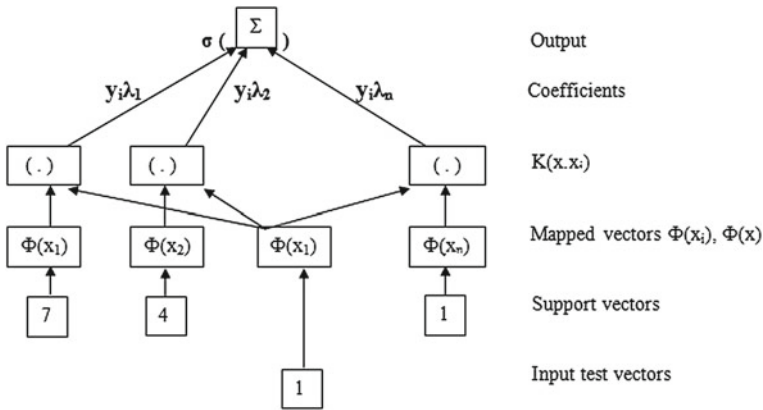


Fig. 1 SVM architecture [4]

SVM is a two-class classifier system. The SVM can be trained to classify both linearly separable and nonlinearly separable data. The SVM locates the most influential samples called SV, i.e., “support vectors”. These support vectors are samples (from both classes under consideration) found closest to the decision surface being constructed [4]. The idea behind the SVM is to create a hyperplane decision surface located equidistance between two decision boundaries. Each boundary is specified by the location of support vectors that satisfy.

$$y_j[w^T x_j + b] = 1; j = 1, N_{SV} \tag{1}$$

where  $N_{SV}$  is the number of support vectors. Locating the decision surface in such a way produces an optimal hyperplane decision surface between the samples of the two classes, and therefore minimum error in classification [4].

The SVM is trained to classify samples of only one specific class-of-interest at a time. All other samples which are not classified as the class-of-interest are considered to be outside the class-of-interest. Fig. 1 shows the architecture of an SVM used to realize the linear SVM decision boundaries of Eq. 1 during construction of a hyperplane decision function [4].

### 3 SVMs and Statistical Learning Theory

SVMs are trained as function approximators that can be used for classification or interpretation (i.e., regression) when one wants to understand the structure of an underlying system [4].

SVMs are based on statistical learning theory where learning machine models are constructed with the goal of finding a function approximator that estimates the

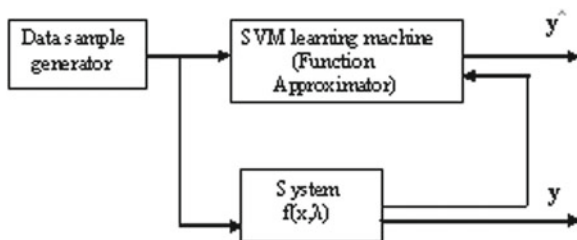


Fig. 2 SVM—learning machine model

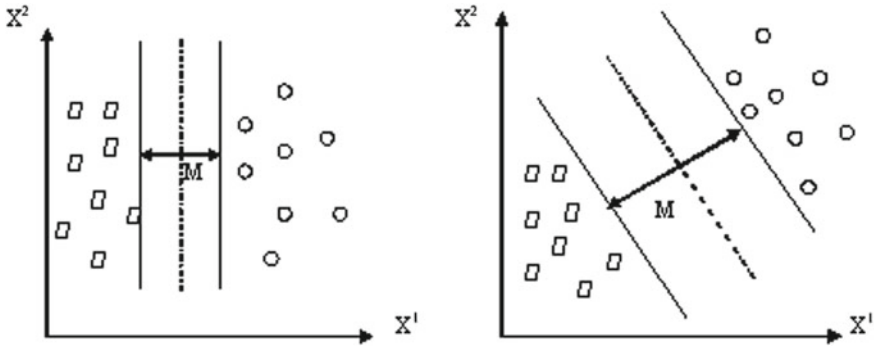
unknown input-output dependency of a system based on a set of observable samples as shown in Fig. 2. Once an SVM has been trained to capture the underlying system structure, it may be used to classify new unknown samples [4]. Multi-class classification is possible by specifying a different class as the class-of-interest each time the technique is applied. In our face detection application there are only two classes to be discriminated, i.e., faces versus non-faces [4].

Large margin classifiers are popular approaches to solve the supervised learning problems. Founded on Vapniks statistical learning theory, SVM is a representative large margin classifier that has played an important role in many areas due to its salient properties such as margin maximization and kernel substitution for classifying the data in a high-dimensional feature space [5]. As SVM considers training data as uncorrelated points, and thus is insensitive to the data distribution information, there is still room for further improvement in generalization ability. Inspired by the fact that linear discriminant analysis (LDA) and mini-max probability machine (MPM) discriminate between classes and employ the class structure into determining the classification boundary, Huang, proposed a large margin learning model: min-max margin machine (M4) that improves SVM by considering class structures into decision boundary calculation via utilizing Mahalanobis distance as the distance metric [5]. M4 does show better generalization ability in some applications, but as the true data structure is not captured, its performance sometimes is not as good as SVM [5].

It is the aim of support vector machine learning to classify data sets where the number of training data is small and where traditional use of statistics of large numbers cannot guarantee an optimal solution [6]. For example consider Fig. 3. Here two decision boundaries on the same data are seen. Both decision boundaries correctly classify the data with zero error. However, subjectively, the decision boundary on the figure on the right is a better choice [6]. The reason that this decision boundary is a better choice is because this decision boundary classifies the two classes with the maximum possible distance (the margin) between the nearest points of each class.

The goal of SVM learning applied to a classification problem is to find the maximum margin decision boundary. This is termed a maximal margin classifier. The formulation of SVM is based on the structural risk minimization (SRM) principle, whereas the empirical risk minimization (ERM) approach is commonly used in





**Fig. 3** *Left* Plot of two classes showing a small margin between classes defined by the decision boundary. *Right* The same plot but with the largest possible distance between opposite classes. SVM maximizes the margin M [6]

statistical learning (for example the classical batch learning for radial basis networks). This approach to SVMs gives a greater potential to generalize [6].

## 4 Approach Used

### *Discrete Cosine Transform*

The DCT has properties which make it suitable to SVM learning. The discrete cosine transform (DCT) helps separate the image into parts. It transforms a signal or image from the spatial domain to the frequency domain.

When the DCT is applied on large images, the rounding effects when floating point numbers are stored in a computer system result in the DCT coefficients being stored with insufficient accuracy. The result is a deterioration in image quality. As the size of the image is increased, the number of computations increases disproportionately. For these reasons an image is subdivided into 8\*8 blocks. Where an image is not an integral number of 8\*8 blocks, the image can be padded with white pixels (i.e., extra pixels are added so that the image can be divided into an integral number of 8\*8 blocks). The two-dimensional DCT is applied to each block so that an 8\*8 matrix of DCT coefficients is produced for each block. This is termed the “DCT Matrix”. The top left component of the DCT matrix is termed the “DC” coefficient and can be interpreted as the component responsible for the average background colour of the block (analogous to a steady DC current in electrical engineering). The remaining 63 components of the DCT matrix are termed the “AC” components as they are frequency components analogous to an electrical AC signal. The DC coefficient is often much higher in magnitude than the AC components in the DCT matrix.

Each component of the DCT matrix represents a frequency in the image. The further an AC component from the DC component the higher the frequency represented.

Since an image comprises hundreds or even thousands of  $8 \times 8$  block of pixels so for an  $8 \times 8$  block it results in this matrix. Now let us start with a block of image-pixel values. This particular block was chosen from a very upper left-hand corner of an image.

## *Quantization*

Our  $8 \times 8$  block of DCT coefficients is now ready for compression by quantization. After the quantization obtained matrix is ready for the final step of compression. Quantizing involves reassigning the value of the weight to one of limited number of values. To quantize the weights the maximum and minimum weight values (for the whole image) are found and the number of quantization levels are pre-defined. The 2-dimensional discrete cosine transform is applied to each block. After the DCT each block comprises 64 discrete cosine coefficients. The coefficients are comprised of one DC coefficients and 63 AC coefficients. The DC coefficients are separated and treated differently to the AC coefficients. Before the AC and DC coefficients are separated, the matrix of discrete cosine coefficients is divided by a quantization. The components of the quantization table are largest in the bottom-right corner. This will produce smaller AC coefficients for higher frequency components in the image.

The quantization table may be multiplied by an arbitrary number. This number is a user defined parameter which defines compression ratio. A larger number results in larger components in the quantization table which in turn results in smaller discrete cosine coefficients. The DC coefficients are Huffman encoded. The AC coefficients are mapped into a row of number using the zigzag mapping. The row of AC coefficients will tend to have nonzero coefficients at the beginning of the row while toward the end of the row, the coefficients are usually zero. Increasing the number by which the quantization matrix is multiplied will further increase the number of zeros. The row of AC coefficients is Huffman coded.

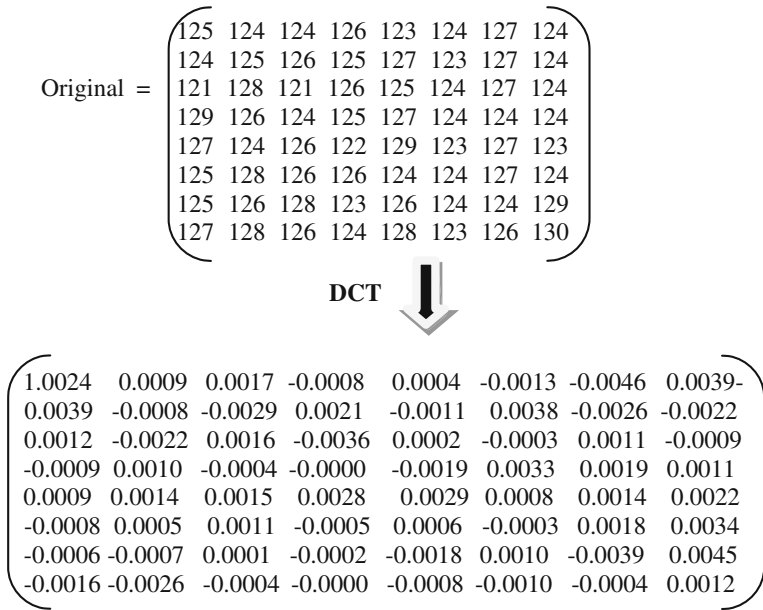
The elements of the matrix in Fig. 4 are mapped using the zig-zag sequence shown in Fig. 5 to produce a single row of numbers. That is a single row of numbers is collected as the zig-zag trail is followed in the DCT matrix. This will produce a row of 64 numbers where the magnitude tends to decrease traveling down the row of numbers [5].

In this research work the original size of each image was  $92 \times 112$  pixels, with 256 grey levels per pixel. But since we have divided images into  $8 \times 8$  block so we have scaled or resize the image size into  $96 \times 112$  pixels. After dividing the image into  $8 \times 8$  blocks, the total blocks of image becomes 168.

Following are the steps involved in the research work:

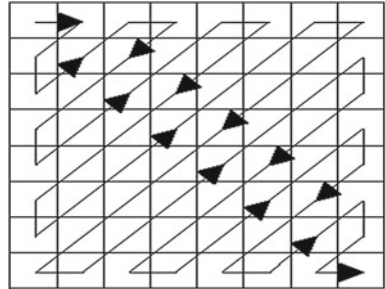
**Step-1** The image is broken into  $8 \times 8$  blocks of pixels.

**Step-2** Working from left to right and top to bottom, DCT is applied to each block.



**Fig. 4** DCT maps a block of pixel color values to the frequency domain

**Fig. 5** The zig-zag pattern applied to a block of DCT coefficients to produce a row of 64 coefficients



**Step-3** The zigzag pattern applied to a block of DCT Coefficients to produce a row of 64 coefficients.

**Step-4** DCT coefficients-Top left 3\*3 block, all other components discarded.

**Step-5** Support vector machine learning is applied to the absolute values of each row of AC terms.

The block diagram of proposed procedure is depicted in Fig. 7.



Fig. 6 Sample images from the ORL face database [7]

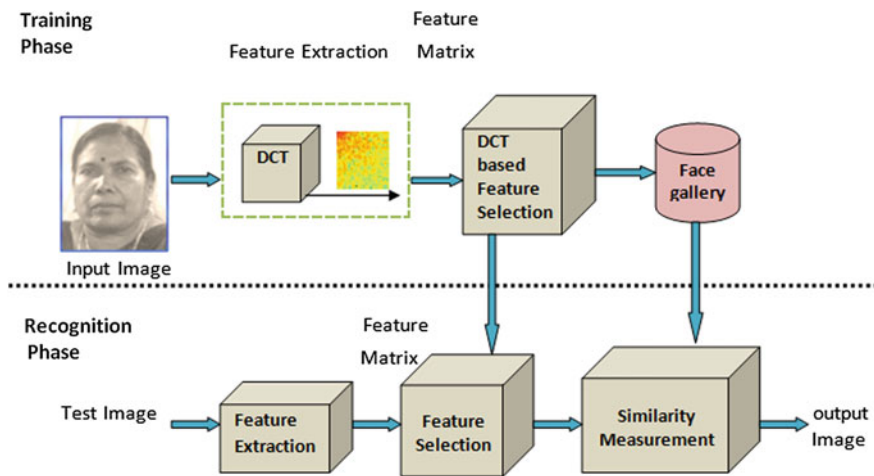


Fig. 7 Block diagram of the proposed face recognition system

## 5 Experiments and Results

### Motivation

In order to test the recognition system, lots of face images were required. There are so many standard face databases for testing and rating a face recognition system. A standard database of face imagery was essential to supply standard imagery to the recognition system and to supply a sufficient number of images to allow testing.

### Dataset

All the experiments here have been executed mainly on the face images provided by the ORL face database. The ORL Database of faces contains a set of face images taken between April 1992 and 1994 [7] as shown in Fig. 6.

There are ten different images of each of 40 distinct subjects. For some subjects, the images were taken at different times, varying the lighting, facial expressions

(open/closed eyes, smiling/not smiling) and facial details (glasses/no glasses). The image files are in PGM (portable gray map) format. The size of each image is 92\*112 pixels, with 256 grey levels per pixel. But since images are divided into 8\*8 block so images are scaled or resized into 96\*112 pixels. The images are organized in 40 directories (one for each subject), which have names of the form sX, where X indicates the subject number (between 1 and 40) i.e. s1–s40. In each of these directories, there are ten different images of that subject, which have names of the form Y.pgm, where Y is the image number for that subject (between 1 and 10) i.e. 1.pgm. The following figure shows image of one person from ORL face database.

For training, from the database 6 images of each subject is taken while the remaining 4 images is left for testing, means 240 images are used to training the database and the remaining 160 images are used for testing from the same database while some other images of the same format are also used for testing (not from the same database). Results after the experiments are shown in the Table.

Image data base	Images for training	Images for testing	SVM					
			Training time (sec)			Matching time(sec)		
			Iterations			Iterations		
			I	II	III	I	II	III
400	240	160	12.31	12.27	12.22	0.36	0.30	0.28
			18.23	18.41	18.35	1.13	1.10	1.06
			28.77	28.55	28.68	1.81	1.66	1.72
			39.75	39.58	39.69	2.43	2.50	2.54

*Recognition Rate*

The closer a system’s measurements to the accepted value, the more accurate the system is considered to be. Recognition rate means a rate which a face recognition system recognizes an individual by matching the input image against images of all users in a database and finding the best match.

$$\begin{aligned}
 \text{Recognition rate} &= \frac{\text{total no. of correct matches} * 100}{\text{Total no. of faces}} \\
 &= \frac{400 * 100}{400} \\
 &= 100 \%
 \end{aligned}$$

The following graph shows 100% recognition rate (Fig. 8).

*Training Performance*

The training performance of recognition system varies according to the system configuration. This recognition system has been implemented and tested in MATLAB version 7.5 under Microsoft Windows XP operating system. The training dataset is image database taken from ORL face database [7].

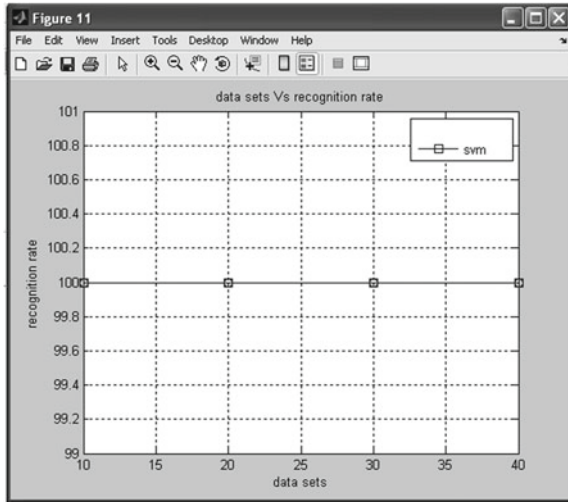


Fig. 8 Graph of recognition rate

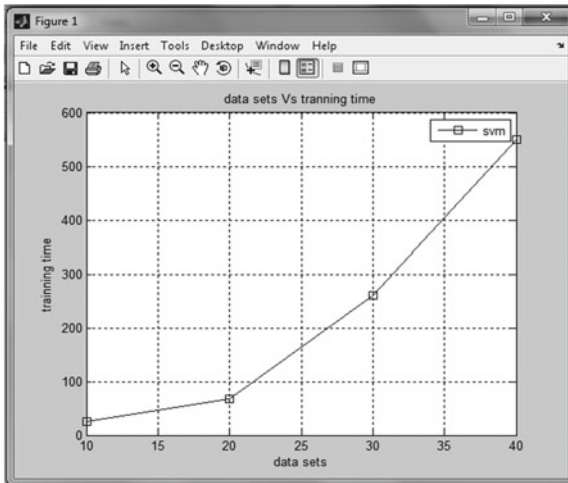


Fig. 9 Graph of training time

The following graph shows the training performance of the recognition system (Fig. 9).

*Matching Time Performance*

Likewise the training performance, the matching performance of the recognition system varies according to the system configuration. The following graph shows the matching performance of the recognition system (Fig. 10).

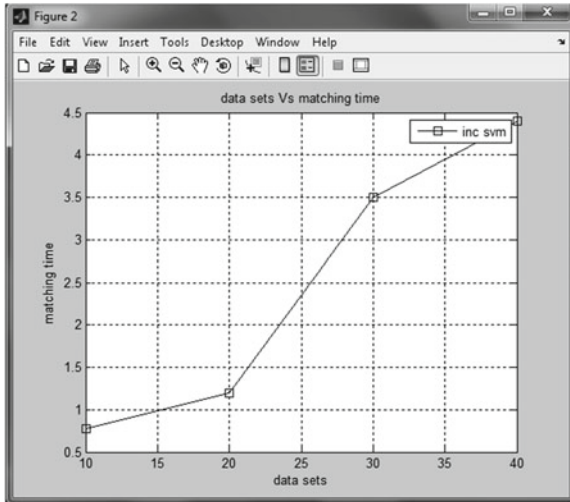


Fig. 10 Graph of matching time

## 6 Conclusion

By using the SVM in the DCT domain, not only the storage requirement is largely relaxed, but also the computational complexity is simplified. Some redundant information is removed by truncating the DCT coefficients so that the dimensionality of the coefficient vectors can be reduced. When the powerful features of the SVM, such as margin maximization and kernel substitution for classifying data in a high dimensional kernel space, are combined with the low dimensional DCT feature vector as described, a good compromise between the computational efficiency and performance accuracy is obtained upto 100%.

## 7 Future Work

In this paper we have used SVM and DCT for face recognition. Using this technique fast and accurate face recognition system is developed and tested and the performance found is 100%. Of course in future there can be some other ways to improve the overall performance of the face recognition such as “Incremental SVM” [8] and “Decremental SVM” [9] along with DCT [10].

## References

1. Palaniswami, M., Shilton, A., Ralph, D., Owen, B.D.: Machine learning using support vector machine. The University of Melbourne, Victoria -3101, Australia and University of Cambridge Trumpington, UK
2. Amine, A., Ghouzali, S., Rziza, M., Aboutajdine, D.: Investigation of feature dimension reduction based DCT/SVM for face recognition. In: IEEE Symposium on Computers and Communications Program, pp. 188–193. IEEE, Marrakech (2008)
3. Chen, Q.-Y., Yang, Q.: Segmentation of images using support vector machine. In: Proceedings of the Third International Conference on Machine Learning and Cybernetics, pp. 3304–3306. IEEE, Shanghai (2004)
4. Shavers, C., Li, R., Lebby, G.: An SVM based approach to face detection. In: Proceedings of the 38th Southeastern Symposium on System Theory Tennessee Technological University Cookeville, pp. 362–366. IEEE, TN (2006)
5. Wang, D.F., Yeung, D.S., Tsang, E.C.C., Wang, X.Z.: Structured large margin learning. In: Proceedings of the Fourth International Conference on Machine Learning and Cybernetics, pp. 4242–4248. IEEE, Guangzhou (2005)
6. Robinson, J.: The application of support vector machines to compression of digital images, Doctor of Philosophy, the University of Auckland, Feb (2004)
7. The database can be retrieved from the following link. [http://www.cl.cam.ac.uk/Research/DTG/attarchive:pub/data/att\\_faces.zip](http://www.cl.cam.ac.uk/Research/DTG/attarchive:pub/data/att_faces.zip) as a ZIP file of similar size
8. Yang, J., Li, Z.-W., Zhang, J.-P.: A training algorithm of incremental support vector machine with recombining method. In: Proceedings of the Fourth International Conference on Machine Learning and Cybernetics, pp. 4285–4288. IEEE, Guangzhou (2005)
9. Galmeanu, H., Andonie, R.: Incremental / decremental SVM for function approximation, optimization of electrical and electronic equipment. In: 11<sup>th</sup> International Conference on Digital Object Identifier, pp. 155–160. IEEE, Brasov (2008)
10. Khayam, S.A.: The Discrete cosine transform (DCT): theory and application, Department of Electrical and Computer Engineering Michigan State University, ECE 802–602 Information Theory and Coding, 10 Mar 2003



# Multi-Temporal Satellite Image Analysis Using Gene Expression Programming

J. Senthilnath, S. N. Omkar, V. Mani, Ashoka Vanjare and P. G. Diwakar

**Abstract** This paper discusses an approach for river mapping and flood evaluation to aid multi-temporal time series analysis of satellite images utilizing pixel spectral information for image classification and region-based segmentation to extract water covered region. Analysis of Moderate Resolution Imaging Spectroradiometer (MODIS) satellite images is applied in two stages: before flood and during flood. For these images the extraction of water region utilizes spectral information for image classification and spatial information for image segmentation. Multi-temporal MODIS images from “normal” (non-flood) and flood time-periods are processed in two steps. In the first step, image classifiers such as artificial neural networks and gene expression programming to separate the image pixels into water and non-water groups based on their spectral features. The classified image is then segmented using spatial features of the water pixels to remove the misclassified water region. From the results obtained, we evaluate the performance of the method and conclude that the use of image classification and region-based segmentation is an accurate and reliable for the extraction of water-covered region.

**Keywords** MODIS satellite image · Gene expression programming · Artificial neural network

---

J. Senthilnath (✉) · S. N. Omkar · V. Mani · A. Vanjare  
Department of Aerospace Engineering, Indian Institute of Science, Bangalore, India  
e-mail: snrj@aero.iisc.ernet.in

S. N. Omkar  
e-mail: omkar@aero.iisc.ernet.in

V. Mani  
e-mail: mani@aero.iisc.ernet.in

A. Vanjare  
e-mail: ashokav@aero.iisc.ernet.in

P. G. Diwakar  
Earth Observation System, ISRO Head Quarters, Bangalore, Karnataka, India  
e-mail: diwakar@isro.gov.in

## 1 Introduction

Multi-temporal time series analysis of satellite images plays an important role in discriminating areas of land surface changes between imaging dates. The data from NASA's MODIS satellite sensor have considerable potential for multi-temporal image analysis. The results of multi-temporal image analysis are very useful in hydrological applications such as flood detection and damage assessment. Although MODIS is a moderate resolution image sensor it does provide excellent between land and water discrimination [1]. Because of the moderate resolution of MODIS, some features such as river courses, canals, and roads appear in the images as linear segments, without additional details that would further complicate the automatic extraction of related features. Hence the complexity in extracting river networks and evaluating floods from MODIS image has attracted many researchers [1, 2]. In literature, many extraction techniques are devised based on pixel, region, and knowledge for a given image [1–6].

In this paper, we consider a combination of the pixel-based, region-based, and knowledge-based classification and segmentation methods that were used in earlier studies for the extraction of roads [3]. The same approach is used with Artificial Neural Network (ANN) and Gene Expression Programming (GEP) classifiers for this study. Multi-temporal MODIS images for the automatic extraction of river networks (before flood) and for evaluating floods (during flood) is presented. ANN and GEP classifiers are used to classify the similar spectral features of an image to differentiate water and non-water image pixels. As the classification uses only the spectral features, some misclassified water image pixels, which have spectral reflectance similar to the water, are also classified into the water group. This discrepancy between true water and misclassified water image pixels is resolved by using region-growing image segmentation and knowledge-based techniques to extract the shape and density of water-covered regions, based on the spatial features of the image. The extracted features are evaluated to differentiate water regions from non-water regions. Finally, the performance of these methods are evaluated and compared.

## 2 Image Classification

Optical satellite image data are often adversely affected by image “noise” due to clouds. It is therefore important to eliminate or minimize such noise before subsequent image classification and segmentation. In this study, we use a median-based switching filter, called Progressive Switching Median (PSM) filter, where both the impulse detector and the noise filter are applied progressively in iterative manner [7]. This technique is applied to remove all the cloud noise from MODIS images. In satellite imagery, the appearance of water strongly depends on the sensor's spectral sensitivity and spatial resolution. In this study, moderate-resolution gray-scale MODIS images (250 m per pixel) are used. The gray-scale intensity of any pixel in an

image depends on the reflectance properties of the object it depicts. Each pixels can therefore be classified into one of the two groups based on its specific intensity level of the pixels, i.e., water and non-water. The two supervised classification techniques such as Artificial Neural Network (ANN) [8–10] and Gene Expression Programming (GEP) [11] are used to classify water image pixels. In GEP unlike ANN, provides an efficient method for obtaining classification rules in the form of a mathematical expression for a given image. Initially, the water pixels and non-water pixels from two images (before and during flood) are picked randomly for training. For the given training data set, ANN generates weights where as GEP provides mathematical expression. Using these weights and mathematical expression all pixels of the image are extracted and evaluated.

### 3 Image Segmentation

The objective of image segmentation is to eliminate those pixels that are wrongly classified as water. However, as some non-water pixels in the image will have reflectance properties similar to water and hence these pixels may be misclassified into the water group. Because of this misclassified water pixels get classified into true-water pixels which are a hindrance in the classification. This hindrance is removed by segmentation using spatial features of the image. The image is first divided into regions and the geometrical parameters for every region are calculated. Then these regions are segmented as true-water and false-water regions. For this we use Shape Index (SI) and Density Index (DI) defined as [3]:

$$SI = \frac{P}{4 \cdot \sqrt{A}} \quad (1)$$

$$DI = \frac{\sqrt{A}}{1 + \sqrt{\text{VAR}(X) + \text{VAR}(Y)}} \quad (2)$$

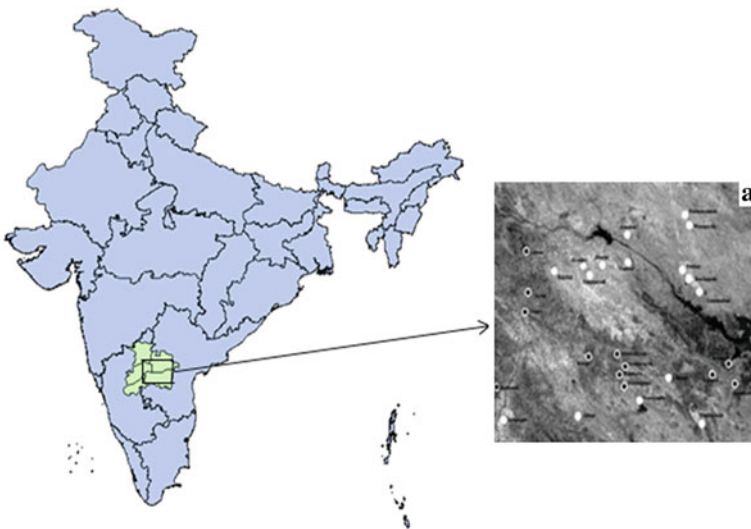
where  $P$  represents the perimeter of the region (the number of pixels on the boundary of the region),  $A$  represents the area of the region (the number of pixels of the region),  $\text{VAR}(X)$  represents variance of  $x$ -coordinates of all the pixels in the region,  $\text{VAR}(Y)$  represents variance of  $y$ -coordinates of all the pixels in the region, and the term  $\sqrt{\text{VAR}(X) + \text{VAR}(Y)}$  gives approximate radius of the region [3]. The river pixels have a high SI and a low DI, whereas non-river pixels have a low SI and a high DI. Thus, for segmentation purpose, threshold values are set for both indices: SI and DI. Regions having a SI greater than the SI threshold value and a DI less than the DI threshold value are segmented as water and non-water regions. Those regions which do not qualify as water are segmented as non-water. We see that the non-flooded regions are more than the flooded region in an image. The perimeter value of a non-flood region is greater than that of a flood region. This makes the ratio of perimeter to the area, a high value for non-flood region and a low value for

flood region. Thus, non-flood regions have a higher value of SI than flood regions. Thereby, the DI for flooded regions is higher than that of non-flooded regions. Thus, for segmenting purpose, threshold values can be set for both the indexes: SI and DI. Regions having a SI lower than the threshold value and DI higher than the threshold value are segmented as flooded regions.

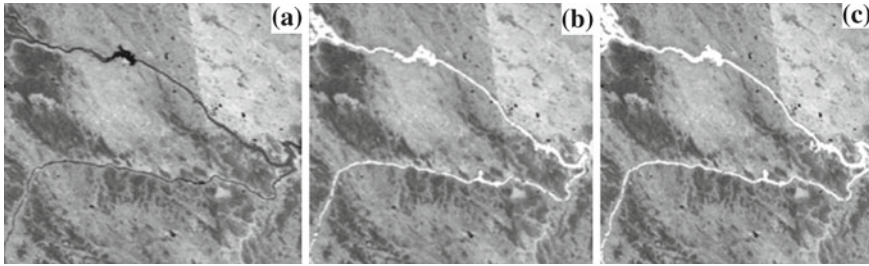
## 4 Results and Discussion

In this section, two classifier methods are used to extract the course of the Krishna river. Figure 1 shows the ground truth information of the flooded and non-flooded regions. All the flooded and non-flooded regions (cities) are shown in the map. The cities (regions) which were not affected by flood are represented by white dots whereas the cities which were affected by flood are represented by white dots with black dots in the center. The images cover an area of 18888.37 km<sup>2</sup> and districts like Kurnool, Mahaboobnagar, Bellary, Gulbarga, and Raichur. Figures 2a and 3a show the March 2009 image (i.e., before the flood) and September 2009 image (i.e., during the flood) MODIS satellite images. For both images, we have applied classification and segmentation technique to extract the river network (before flood) and flooded region (during flood).

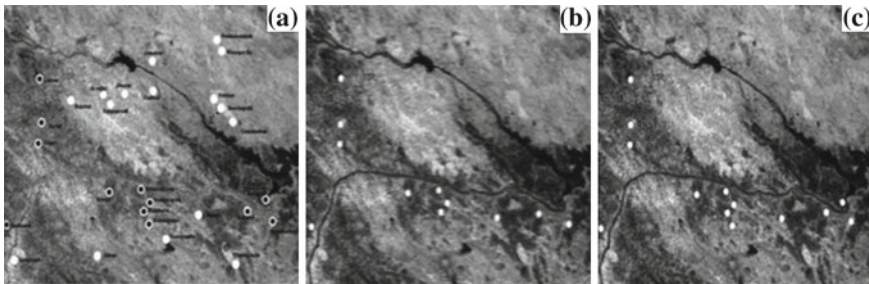
Two MODIS images [12] of the same region are used to classify and validate. The classifiers were trained using 20 randomly picked samples of two classes (water



**Fig. 1** Study area with flooded and non-flooded cities marked on MODIS image



**Fig. 2** a MODIS image of Krishna River before flood, b segmented image using ANN, c segmented Image using GEP



**Fig. 3** a MODIS during flood image with ground truth information: flooded and unflooded cities; b segmented Image using ANN (white points are identified as flooded cities); c segmented image using GEP (white points are identified as flooded cities)

**Table 1** Evaluating features based on ROC parameters during flood image

Methods	True positive rate	True negative rate	False positive rate	Accuracy
ANN	0.83	0.94	0.06	0.89
GEP	1	0.94	0.06	0.96

and non-water) [12]. Then the MODIS Band 2 image was tested using the trained classifiers.

The GEP expression tree generated for the training sample using before and during flood images are given in Eqs. (3) and (4) respectively.

$$M = (2 * B2) - 4.5 \tag{3}$$

$$N = 3.3 - (11.3 * B2) \tag{4}$$

where *B2* represent the Band 2 of the MODIS image. Each pixel in the image is classified as water or non-water image pixel using the above equations. If the value of *M* and *N* for a pixel is >0.5 then this pixel is classified as water; otherwise this pixel is classified as non-water pixel. However, their might be some misclassified pixels.

These misclassified water pixels are properly classified as non-water pixels using region-based segmentation. For segmentation purpose, we use two indices based on geometrical features—Shape Index (SI) and Density Index (DI), in order to differentiate the water pixels from non-water pixels, by thresholding the index values. The results of ANN and GEP method are compared in terms of the Root Mean Square Error (RMSE) [13] and Receiver Operating Characteristic (ROC) parameters [14].

Figure 2a and b shows river extracted image using ANN and GEP respectively. RMSE value is analyzed for before flood image. RMSE values for ANN and GEP are 0.126 and 0.1205, respectively. We can observe that, based on the RMSE values for before flood image, GEP results in less error in comparison with ANN.

Figure 3a and b shows the list of flooded and unflooded regions (cities) using ANN and GEP respectively. From Table 1, we can observe that true positive rate and accuracy during flood image is better in GEP. The performance of GEP is better than ANN for before and during flood images.

## 5 Conclusions

The tasks of river mapping and flood extraction are accomplished successfully by the procedure of pixel-based spectral information for classification, and shape information for segmentation, as discussed above. This has been found to be an efficient way to extract water regions from before and during flood satellite images. In the classification stage of extracting water and non-water groups, the gene expression programming classifier proved better than the artificial neural network classifier. The results of classification using spectral information are improved through region-growing image segmentation (based on spatial feature) using similarity criteria emphasizing shape information, resulting in an effective extraction of water-covered regions.

**Acknowledgments** This work is supported by the Space Technology Cell, Indian Institute of Science, Bangalore and Indian Space Research Organization (ISRO). We also acknowledge the MODIS mission scientists and associated NASA personnel for the production of the remote sensing data which is used in this paper.

## References

1. Brakenridge, R., Anderson, E.: MODIS-based flood detection, mapping and measurement: the potential for operational hydrological applications. *Transboundary Floods: Reducing Risks through Flood Management*. Springer-Verlag, pp. 1–12 (2006)
2. Khan, S.I., Hong, Y., Wang, J., Yilmaz, K.K., Gourley, J.J., Adler, R.F., Brakenridge, G.R., Policelli, F., Habib, S., Irwin, D.: Satellite remote sensing and hydrologic modeling for flood inundation mapping in Lake Victoria Basin: implications for hydrologic prediction in ungauged basins. *IEEE Trans. Geosci. Remote Sens.* **49**, 85–95 (2011)
3. Mingjun, S., Daniel, C.: Road extraction using SVM and image segmentation. *Photogram. Eng. Remote Sens.* **70**(12), 1365–1371 (2004)

4. Senthilnath, J., Rajeswari, M., Omkar, S.N.: Automatic road extraction using high resolution satellite image based on texture progressive analysis and normalized cut method. *J Indian Soc. Remote Sens.* **37**(3), 351–361 (2009)
5. Omkar, S.N., Senthilnath, J., Mudigere, D., Manoj Kumar, M.: Crop classification using biologically inspired techniques with high resolution satellite image. *J. Indian Soc. Remote Sens.* **36**(2), 172–182 (2008)
6. Senthilnath, J., Omkar, S.N., Mani, V., Tejovanth, N., Diwakar, P.G., Archana Shenoy, B.: Hierarchical clustering algorithm for land cover mapping using satellite images. *IEEE J. Sel. Topics Appl. Earth Obs. Remote Sens.* **5**(3), 762–768, (2012)
7. Wang, Z., Zhang, D.: Progressive switching median filter for the removal of impulse noise from highly corrupted images. *IEEE Trans. Circuits Syst.* **II**(46), 78–80 (1999)
8. Haykin, S.: *Neural Networks—A Comprehensive Foundation*, 2nd edn. Pearson Prentice Hall Publication, New Jersey (1994)
9. Omkar, S.N., Sivaranjani, V., Senthilnath, J., Mukherjee, S.: Dimensionality reduction and classification of hyperspectral data. *Int. J. Aerosp. Innov.* **2**(3), 157–163 (2010)
10. Omkar, S.N., Senthilnath, J.: Integration of Swarm Intelligence and Artificial Neural Network, Neural Network and Swarm Intelligence for Data Mining, Chapter 2. In: Dehuri, S., et al. World Scientific Press, Singapore, pp. 23–65 (2011)
11. Ferreira, C.: Gene expression programming: a new adaptive algorithm for solving problems. *Complex Syst.* **13**(2), 87–129 (2001)
12. Senthilnath, J., Shivesh, B., Omkar, S.N., Diwakar, P.G., Mani, V.: An approach to multi-temporal MODIS image analysis using image classification and segmentation. *Adv. Space Res.* **50**(9), 1274–1287 (2012)
13. Arvind, C.S.: Ashoka Vanjare, Omkar, S.N., Senthilnath, J., Mani, V., Diwakar, P.G.: Multi-temporal satellite image analysis using unsupervised techniques. *Adv. Comput. Inf. Technol. Adv. Intell. Syst. Comput.* **177**, 757–765 (2012)
14. Fawcett, T.: An introduction to ROC analysis. *Pattern Recogn. Lett.* **27**(8), 861–874 (2006)

# An Advanced Approach of Face Alignment for Gender Recognition Using PCA

Abhishek Kumar, Deepak Gupta and Karan Rawat

**Abstract** In this paper we have used principal component analysis (PCA) tool by adding mathematical rigor to provide explicit solution for gender recognition by extracting feature vector. We will implement face recognition system using PCA algorithm along with the application of kernel support vector machine for error minimization. In addition by using face-rec database. This is an Eigen face approach motivated by information theory using an images database of 545 images of male and female for improved efficiency. sometimes PCA mixes data points which lead to classification error. We are improving principal component analysis (PCA) by taking vector corresponding to  $k$  minimum error unlike conventional PCA.

**Keywords** Gender Recognition · Principal component analysis · Eigen faces · SVM · Euclidian distance

## 1 Introduction

The face is an important biometric feature of human beings. Faces are accessible ‘windows’ into the mechanisms that govern our emotional and social lives. A successful gender classification method has many potential applications such as human identification, smart human computer interface, computer vision approaches for monitoring people, passive demographic data collection, etc. This paper deals with gender classification based on frontal facial images we will deal with significant variation between faces that significant features are known as Eigen faces. A Principal Compo-

---

A. Kumar (✉) · D. Gupta  
Government Engineering College Ajmer, Ajmer, Rajasthan, India  
e-mail: abhishekkmr812@gmail.com

D. Gupta  
e-mail: gupta\_de@rediffmail.com

K. Rawat  
IIIT Allahabad, Allahabad, Uttar Pradesh, India  
e-mail: rawatkaran4@hotmail.com



Principal Component Analysis (PCA)-based image representation [1, 2] was used along with radial basis functions and preceptor networks investigated the use of SVMs for gender classification we will discuss the learning method back propagation as well for more efficient recognition rate. But a higher recognition rate is probably achieved due to excluding of negative feature. In general, all existing method or technique is appearance based, we have shown mathematical approach for feature analysis followed by structural risk minimization with the application of SVM [3]. As in order to get more accuracy a learning algorithm is needed so we have used back propagation. that is, they learn the decision boundary between male and female classes from training images, without extracting any geometrical features such as distances, face width, face length, etc. Almost all the modern face recognition algorithms use the PCA approach as the starting point for dimensionality reduction. We need to install image processing tool box, specifically we may use `imread`, `imresize`, etc., function in implementation phase. Principal Component Analysis proves to be the most robust and novel algorithm for face recognition and this can be verified by the fact that almost every other face algorithm such as the Linear Discriminant Analysis [4] and the Gabor filter approach [3, 5] make use of the PCA for dimensionality reduction. This technique classifies images in form of Eigen faces, explained further.

## 2 Principal Component Analysis

In this paper, we will implement a face recognition system using the PCA algorithm [6]. Automatic face recognition systems try to find the identity of a given face image according to their memory. The memory of a face recognizer is generally simulated by a training set. In this paper, our training set consists of the features extracted from known face images of different persons. Thus, the task of the face recognizer is to find the most similar feature vector among the training set to the feature vector of a given test image. Here, we want to recognize the identity of a person where an image of that person (test image) is given to the system. We will use PCA as a feature extraction algorithm in this paper. In the training phase, we should extract feature vectors for each image in the training set. Let  $\Omega_A$  be a training image of person A which has a pixel resolution of  $M * N$  ( $M$ rows,  $N$ columns). In order to extract PCA features of  $\Omega_A$  we will first convert the image into a pixel vector  $\odot A$  by concatenating each of the  $M$ rows into a single vector. The length (or, dimensionality) of the  $\odot A$  vector will be  $M * N$ . In this project, we will use the PCA algorithm as dimensionality reduction technique which transforms the vector  $\odot A$  to a vector  $\mathbf{w}_a$ , which has a dimensionality  $d$  where  $d \gg M * N$ . For each training image  $\mathbf{a}_i$ , we should calculate and store these feature vectors  $\mathbf{w}_i$ . In the recognition phase (or, testing phase), we will be given a test image  $\Omega_j$  of a known person. Let  $\alpha_j$  be the identity (name) of this person. As in the training phase, we should compute the feature vector of this person using PCA and obtain  $\mathbf{w}_j$ . In order to identify,  $\mathbf{a}_j$  we should compute the similarities between  $\mathbf{w}_j$  and all of the feature vectors  $\mathbf{w}_i$ s in the training set. The similarity between feature vectors can be computed using Euclidean distance. The identity of the most similar  $\mathbf{w}_i$  will be the output of our face recognizer. If  $i = j$ , it

means that we have correctly identified the person  $j$ , otherwise if  $i \neq j$ , it means that we have misclassified the person  $j$ . of computational resources. Thus, to sum up, the jobs which the PCA technique can do are prediction redundancy removal, feature extraction and data compression.

### 3 Mathematical Approach of the PCA

We are considering 2-D image for working so first of all it will get converted in to 1-D vector by concatenating rows and columns  $T$  Suppose we have  $M$  vectors each of size  $N$  (rows \* columns) representing a set of sampled images [7].

Let ' $=p_j$ ' represent the values of the pixels.

$$X_i = [p1, p2, p3, p4, \dots, pN]; i = 1, 2, 3, 4, \dots M. \tag{1}$$

then the images are mean centered when we subtract the mean image from each image vector. Let us suppose  $m$  as the mean image:

$$m = (1/M)^* (\Sigma X_i) \tag{2}$$

Let  $W_i$  be the mean centered image:

$$W_i = X_i - m \tag{3}$$

Ultimately, we have to find the values of  $e_i$ 's which have the largest possible projection onto each of the  $w_i$ 's. The purpose is to get  $M$  orthogonal vectors  $e_i$  for which the quantity

$$\Lambda_i = (1/M) \Sigma (e_{iT} * w_n)2 \tag{4}$$

is normalized with the orthogonality constraint:

$$e_{iT} * e_k = \delta_{lk} \tag{5}$$

The values of  $e_i$ 's and  $\lambda_i$ 's are calculated from the Eigen vectors and the Eigen values of the covariance matrix:

$$C = W * W_T \tag{6}$$

$W$  is a matrix formed by the column vectors  $w_i$  places side by side. The size of the covariance matrix is enormous ( $N * N$ ). It is not possible to solve for eigenvectors directly. In mathematics, there are areas where one needs to find the numbers  $\lambda$  and the vectors  $v$  that satisfy the equation where  $A$  is the square matrix:

$$Av = \lambda v \tag{7}$$



**Fig. 1** An example face under a fixed view and varying illumination

Any  $\lambda$  satisfying the above equation is the Eigen value of  $A$ . The vector  $v$  is called the eigenvector of  $A$ . The Eigen values and eigenvectors are obtained by solving the equation:

$$[A - \lambda I] = 0 \quad (8)$$

For every  $\lambda$ , we calculate the corresponding eigenvectors and then normalize them. The eigenvectors are then sorted in the ascending order. This gives us the final KL Transform matrix. The covariance matrix of the final transformed image will have the Eigen values as their diagonal elements. More over the mean of final image will be zero.

## 4 Statistical Projection Methods

The first step is to create a database of images of different people. The database considered in this case is the—Face Recognition Database, MIT, USA||. The images will exhibit different variations in the positioning of the head, the hair, the light content, the contrast, the skin color, and the expressions of the people (Fig. 1).

The variation of head pose or, in other words, the viewing angle from which the image of the face [8] was taken is another difficulty and essentially impacts the performance of automatic face analysis methods. For this reason, many applications limit themselves to more or less frontal face images or otherwise perform a pose-specific processing that requires a preceding estimation of the pose, like in multiview face recognition approaches. 2-D pose estimation approaches that have been presented in the literature. If the rotation of the head coincides with the image plane the pose can be normalized by estimating the rotation angle and turning the image such that the face is in an upright position. This type of normalization is part of a procedure called face alignment or face registration Fig. 2 shows some example face images with varying head pose. Fig. 3 is showing original images and their PCA pattern map.



Fig. 2 An example face under fixed illumination and varying pose

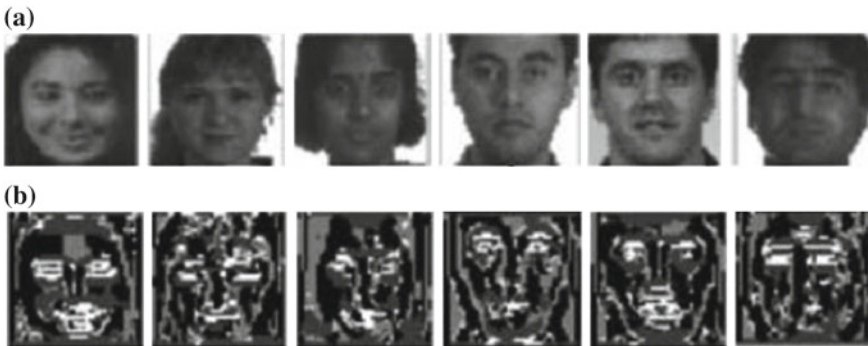


Fig. 3 Set of original images and PCA pattern maps

### 5 Support Vector Machines

The classification technique called Support Vector Machine (SVM) is based on the principle of Structural Risk Minimization. One of the basic ideas of this theory is that the test error rate, or structural risk  $R(\alpha)$ , is upper bounded by the training error rate, or empirical risk  $R_{emp}$  and an additional term called VC-confidence which depends on the so-called Vapnik-Chervonenkis (VC)-dimension  $h$  of the classification function. More precisely, with the probability  $1 - \eta$ , the following holds

$$R(\alpha) < R_{emp}(\alpha) + \sqrt{h(\log(2l/h) + 1) - \log(\eta/4)/L} \tag{9}$$

where  $\alpha$  are the parameters of the function to learn and  $l$  is the number of training examples. The VC-dimension  $h$  of a class of functions describes its—capacity—to classify a set of training data points. For example, in the case of a two-class classification problem, if a function  $f$  has a VC-dimension of  $h$  there exists at least one set of  $h$  data points that can be correctly classified by  $f$ , i.e., assigned the label  $-1$  or  $+1$  to it. If the VC-dimension is too high the learning machine will over fit and show poor generalization. If it is too low, the function will not sufficiently



**Fig. 4** Mean image for men and women created from the respective database images

approximate the distribution of the data and the empirical error will be too high. Thus, the goal of SRM is to find a  $h$  that minimizes the structural risk  $R(\alpha)$ , which is supposed to lead to maximum generalization (Fig. 4).

## 6 The Back Propagation Algorithm

We will focus on the Back propagation algorithm since it is the most common and maybe most universal training algorithm. In the context of NNs, the Back propagation (BP) algorithm has initially been presented by Rumelhart. It is a supervised learning algorithm defining an error function  $E$  and applying the gradient descent technique in the weight space in order to minimize  $E$ . The combination of weights leading to a minimum of  $E$  is considered to be a solution of the learning problem. In order to calculate the gradient of  $E$ , at each iteration, the error function has to be continuous and differentiable. Thus, the activation function of each individual perceptron. Mostly, a sigmoid or hyperbolic tangent activation function is employed, depending on the range of desired output values, i.e.  $[0, 1]$  or  $[-1, +1]$ . Note that BP can be performed in online or offline mode, i.e.,  $E$  represents either the error of one training example or the sum of errors produced by all training examples. In the following, we will explain the standard online BP algorithm, also known as Stochastic Gradient Descent, applied to MLPs [9]. There are two phases of the algorithm:

- the forward pass, where a training example is presented to the network and the activations of the respective neurons is propagated layer by layer until the output neurons.
- the backward pass, where at each neuron the respective error is calculated starting from the output neurons and, layer by layer, propagating the error back until the input neurons.

Now, let us define the error function as:

$$E = 1/2 \sum_{p=1}^n ||o_p - t_p||_2 \quad (10)$$

where  $P$  is the number of training examples,  $o_p$  are the output values produced by the  $NN$  having presented example  $p$ , and  $t_p$  are the respective target values. The goal is to minimize  $E$  by adjusting the weights of the  $NN$ . With online learning we calculate the error and try to minimize it after presenting each training example.

Thus,

$$E_p = 1/2 \sum ||o_p - t_p||_2 = 1/2 \sum_{k=1}^k (o_{pk} - t_{pk})^2 \tag{11}$$

where  $k$  is the number of output unit when minimizing this function by gradient descent, we calculate the steepest descent of the error surface in the weight space, i.e. the opposite direction of the gradient. In order to ensure convergence; the weights are only updated by a proportion of the gradient.

Thus,

$$\nabla E_p = (\partial E_p / \partial W_1, \dots, \partial E_p / \partial W_k)$$

In order to ensure convergence, the weights are only updated by a proportion of the gradient.

Thus,

$$\Delta W_k = -\lambda \partial E_p / W_k \tag{12}$$

Once we have analyze the images fixed illumination and varying pose now we will have to Eigen faces by conventional methods in order to get the corresponding Eigen vector as explained in section of PCA in above section. For the reconstruction of the test image we will need that the value of each Eigen faces. When we consider the entire training set for reconstructing the test image in Fig. 5 the reconstructed image resembles a lot with the test image shown in Fig. 5. We will analyze the performance using fuzzy logic, neural network, back propagation, and SVM. After these above step get completed, we will do the gender classification (Fig. 6).

Figures 7, 8, and 9 are showing the performance of different gender classification system on different dataset with different set of values for better analysis every time.

**Fig. 5** Test input image having same number of pixels as the database images



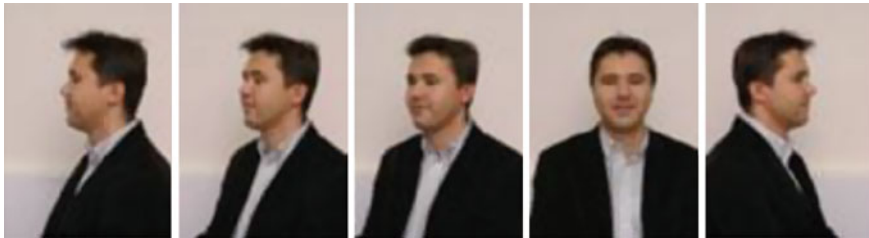


Fig. 6 Reconstructed image using men’s database

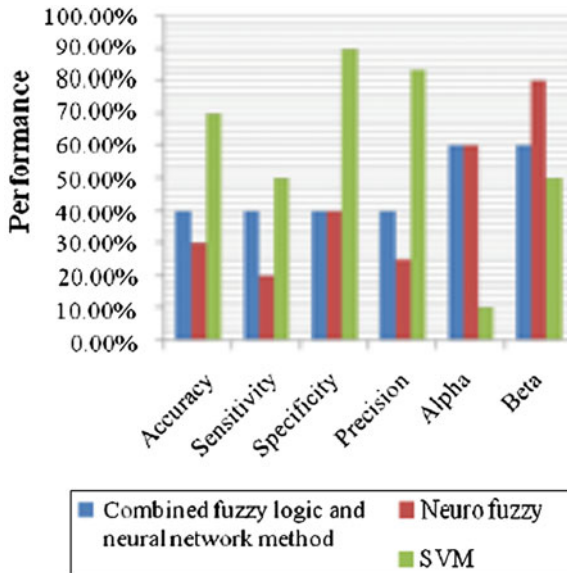


Fig. 7 Performance based on SVM, neuro fuzzy, and neural network method

On the basis of different values of threshold we have done the analysis. The different dataset is showing how at different value of threshold the accuracy is getting better each time we are altering the threshold values. The different dataset is showing not only the accuracy but sensitivity at the same time followed by specificity and precision. We have considered the value 0.1, 0.5, and 0.8 for the above dataset, respectively. So at the threshold value 0.1 SVM has achieved the accuracy of 70 % and the sensitivity of 45 % the specificity is much more than the sensitivity it is 88.72 % as shown in dataset 1f in Fig. 7. Now for the data set 2 we have the threshold value 0.5 in this case SVM has achieved the accuracy of 40 % and 25 % of sensitivity and specificity of 59.3 % similarly for the dataset 1, neuro fuzzy has achieved some different values as shown in respective figure. So through above given graph we could manage to calculate the performance of SVM, combined fuzzy logic, and neuro fuzzy in more analytical manner. As the different dataset are showing the percentage of accuracy precision, sensitivity, specificity, etc.

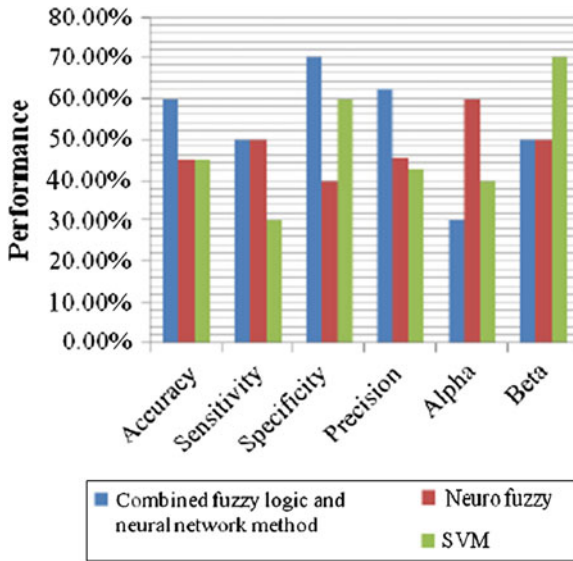


Fig. 8 Dataset 2

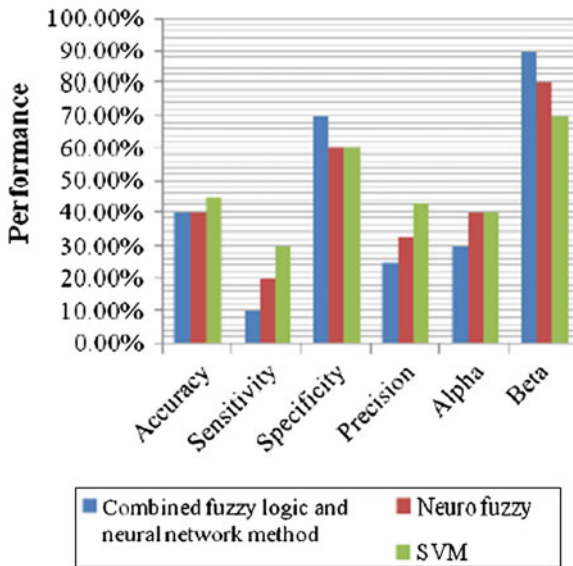


Fig. 9 Dataset 3



## 7 Analysis of Facial Feature With the Evaluation of Euclidian Distance

The above Fig. 10 is showing the analysis of facial feature in which it is very obvious to have different areas for the gender classification. So it is necessary to analyze facial feature in which area having more contribution for gender recognition. If we are processing on selective area the beneficial part will be the less bulky calculation and less complexity. So when we have the final test set and training set then we will go for the evaluations of Euclidian distance of that selective area of the face on which we were processing. In a mean while it evaluates how close the image from the test set is that from the training set. The consequences will be like the smaller the Euclidian distance the similarity of the face will be greater in that respect. At the same time higher recognition rate can be achieved due to excluding of the negative feature. We will divide the facial image in to smaller region as shown in the Fig. 10 in order to consider the shape information of the image. So the region around the moustache will be the specific area to go with further as the area we are going to consider is very sensitive as far as gender recognition is concerned using facial image. Women will have less intensity than men so we can calculate the brightness further to distinguish. This is how it plays an important role in gender classification as the feature analysis fig shows the frequencies of each region we are working on.

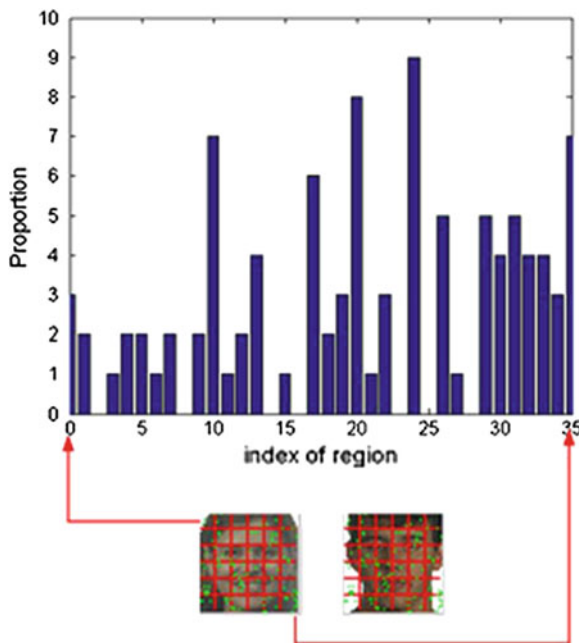


Fig. 10 Feature analysis

**Table 1** Illumination changes: principal component analysis + neural network and PCA + support vector machine

Training	Testing	Correct nearest neighbour (%)	Correct kernel SVM (%)	Correct radial basis SVM (%)
4, 5, 6, 7, 8, 21	10	97.34	72.05	100
4, 5, 6, 7, 8, 21	11	100	79.41	100
4, 5, 6, 7, 8, 21	12	58.82	48.17	98.52
4, 5, 6, 7, 8, 21	20	96.34	64.70	100

**Table 2** Pose changes: principal component analysis + neural network and PCA + support vector machine

Training	Testing	Correct nearest neighbor (%)	Correct kernel SVM (%)	Correct radial basis SVM (%)
1, 2, 3, 4, 6	8	83.82	33.82	76.47
1, 2, 3, 4, 6	9	97.05	98.52	100
2, 3, 4, 9	1	50	60.20	55.88
2, 3, 4, 9	6	27.94	30.88	33.82

In the next part we are going to show our experimental results with the neuro and SVM application for pose changed and illumination changed. We will show that how SVM approach along with PCA will show better classification results over conventional PCA. We are showing the experimental results by taking 60 images of men and women at one time then repeating the process for further results.

## 8 Experimental Results

Training samples have only uniform illumination. Testing samples have sharp illumination changes. Both training and testing samples have moderate and sharp illumination changes. We have the experimental results in Tables 1 and 2 which shows better classification above conventional PCA Use of SVM on both experiments gives more accuracy over conventional PCA in illumination changes and pose changed condition, respectively. Our aim is to reduce the classification error with advance approach of PCA by taking vector corresponding to k minimum classification error, unlike conventional PCA.

## 9 Conclusion

The PCA approach can effectively be used for the purpose of Face Recognition and Gender Recognition. We have used image basis function. The EIGEN FACE approach to gender recognition was motivated by information theory. It is fast relative simple but we have compared the performance using neuron network and SVM for purpose such as human computer interaction and security system. The characteristics of feature are comprehensively analyzed through the application to gender recognition performed on face image with different pose using MIT.CBCL DATABASE. Improved (PCA)-based gender detection with the application of (KERNAL SVM) shows robustness against different types of noises and external influences that face images can undergo in real world setting and result are more superior and efficient than other approaches we have given experimental results in Tables 1 and 2 with illumination change and pose change which is showing the improvement of this advance approach over conventional PCA. Further work can conspire improvement in accuracy and minimization of classification error as compare to classical and conventional approach of PCA.

## References

1. Jain, A. K. Ross, A. Prabhakar, S.: An introduction to biometric recognition. *IEEE Trans. Circ. Syst. Video Technol.* **14**(1), 4–20 (2004)
2. Yan, S., Xu, D., Zhang, B., Zhang, H.J.: Graph embedding and extensions: a general framework for dimensionality reduction. *IEEE Trans. Pattern Anal. Mach. Intell.* **29**(1), 40–51 (2007)
3. Mohammed, A.A., Minhas, R., Jonathan Wu, Q.M., Sid-Ahmed, M.A.: Evaluation of face recognition technique using PCA, wavelets and SVM. *Pattern Recognit. (Elsevier)* **44**(10–11), 6404–6408 (2011)
4. Zhao, D., Liu, Z., Xiao, R., Tang, X.: Linear laplacian discrimination for feature extraction. In: *Proceedings of the IEEE Conference on Computer Vision and Pattern Recognition* (2007)
5. Dagher, I., Nachar, R.: Face recognition using IPCA-ICA algorithm?. *IEEE Trans. Pattern Anal. Mach. Intell.* **28**, 996–1000 (2006)
6. Kekre, H.B., et al.: Face and gender recognition using principal component analysis. *Int. J. Comput. Sci. Eng. (IJCSE)* **02**(04), 959–964 (2010)
7. Anton, H.: *Elementary Linear Algebra 5e?*. Wiley, Hoboken. ISBN 0-471-85223-6 (1987)
8. Utah State University—Spring 2012 STAT 5570: Statistical Bioinformatics, Notes 2.4
9. Yang, W.: Laplacian bidirectional PCA for face recognition. *Neurocomputing (Elsevier)* **74**, 487–493 (2010)

# Analysis of Pattern Storage Network with Simulated Annealing for Storage and Recalling of Compressed Image Using SOM

Manu Pratap Singh and Rinku Sharma Dixit

**Abstract** In this paper, we are analyzing the SOM-HNN for storage and recalling of fingerprint images. The feature extraction of these images is performed with FFT, DWT, and SOM. These feature vectors are stored as associative memory in Hopfield Neural Network with Hebbian learning and Pseudoinverse learning rules. The objective of this study is to determine the optimal weight matrix for efficient recalling of the memorized pattern for the presented noisy or distorted and incomplete prototype patterns from the Hopfield network using Simulated Annealing. This process minimizes the effect of false minima in the recalling process.

**Keywords** Pattern storage network · SOM · FFT · DWT · Simulated annealing

## 1 Introduction

Pattern recognition has been implemented most commonly using the feedback neural networks. The key idea in pattern storage by feedback networks is the formation of basins of attraction in the energy landscape of the output state space. The number of basins of attraction depends only on the network, i.e., the number of processing units and their interconnection strengths. When the number of patterns to be stored is less than the number of basins of attraction, i.e., stable states then spurious stable states will exist, which do not correspond to any desired pattern. Determination of

---

M. Pratap Singh (✉)

Department of Computer Science, Institute of Engineering and Technology, Dr. B.R.Ambedkar University, Agra (Khandari), Uttar Pradesh, India  
e-mail: manu\_p\_singh@hotmail.com

R. Sharma Dixit

Manav Rachna College of Engineering, Sector-43, Aravali Hills, Surajkund—Badkal Road Faridabad, Haryana, India  
e-mail: rinkudixit.mrce@mrei.ac.in

the number and locations of the basins of attraction in the network is not normally possible, but it is possible to estimate the capacity of the network and the average probability of error in recall.

The standard Hopfield model uses a very simple weight matrix formed with one-shot hebbian learning that produces a network with relatively poor capacity and performance [1]. This capacity and performance can be enhanced by adopting the modified Pseudoinverse rule. Pattern storage for continuum features as the input data can be characterized with the self organizing map for dimension reduction and feature extraction with Hopfield energy function analysis [2]. Iterations of the competitive learning between the input and the feedback output layer reduce the neighboring region in the processing elements of feedback layer and at each learning iteration, the used activation dynamics of the feedback layer leads the network toward the stable state. The feedback layer, which behaves as the HNN, at the equilibrium stable state reflects the stored pattern at the minimum energy state. It reflects that we may explore the possibilities of mapping of the features from the pattern space to the feature space and simultaneously encode the presented patterns. This SOM-HNN combination can be used to enhance the capabilities of the HNN. However, the stable states may not necessarily correspond to the memorized pattern and this can be one of the major pitfalls of the SOM-HNN formulation. Since the energy surface comprises several basins of attraction, there may be many local minima and on presenting the memorized pattern there is an equal probability that the activation dynamics converges to some false minima instead of the memorized pattern. Error in pattern recall due to false minima can be reduced by using a *stochastic update* [3] of the state for each unit, instead of the deterministic update. This paper explores this strategy wherein noise is introduced into the network dynamics. In effect, the network will reach states of lower energy but will also occasionally jump to higher energy states. This extended dynamics can help the network to skip out of local minima of the energy function. This approach will be implemented through the process of simulated annealing controlled by the temperature parameter to check the recall of the memorized patterns. The appearance of false minima in the SOM-HNN networks can be formulated as an Optimization problem for optimizing the activation dynamics. Such network when presented a prototype input pattern or its noisy variant should move stochastically through the activation dynamics in such a way that the network settles only into the energy basin corresponding to the memorized pattern thus avoiding the convergence to some false minima. This has been implemented in the simulations in this paper.

## 2 Preprocessing for Feature Extraction

The feature extraction algorithms extract unique information from the images [4]. The pattern set, i.e., scanned fingerprint images of multiple individuals are pre-processed before converting them to suitable patterns. The scanned RGB images are converted to *Grayscale*, enhanced and made sharper using *histogram equalization*

and finally converted into a binary image by thresholding about the histogram peak. The efficiency of the feature extraction method decides to a great extent the quality of the image. Therefore, we are employing FFT and DWT for feature extraction to consider the pattern for storage.

The two-dimensional X-by-Y FFT and inverse X-by-Y FFT relationships are respectively given as

$$F(p, q) = \sum_{x=0}^{X-1} \sum_{y=0}^{Y-1} f(x, y) e^{-j2\pi px/X} e^{-j2\pi qy/Y} \quad \begin{matrix} p = 0, 1, \dots, X - 1 \\ q = 0, 1, \dots, Y - 1 \end{matrix} \quad (1)$$

$$f(x, y) = \frac{1}{XY} \sum_{p=0}^{X-1} \sum_{q=0}^{Y-1} F(p, q) e^{j2\pi px/X} e^{j2\pi qy/Y} \quad \begin{matrix} x = 0, 1, \dots, X - 1 \\ y = 0, 1, \dots, Y - 1 \end{matrix} \quad (2)$$

The values  $F(p, q)$  are the FFT coefficients of  $f(x, y)$ .

Wavelet analysis expresses the original image in terms of a sum of basis functions, which are the shifted and scaled versions of the original (or mother) wavelet [4] and can often compress or de-noise a signal without appreciable degradation. Each DWT is characterized by a transform function pair or set of parameters that define the pair. Transform functions also called the wavelets are obtained from a single prototype wavelet called mother wavelet by dilations and shifting as:

$$\psi_{a,b}(t) = \frac{1}{\sqrt{a}} \psi \frac{t - b}{a} \quad (3)$$

where,  $a$  is the scaling parameter and  $b$  is the shifting parameter. The transform functions can be represented by three separable 2-D wavelets, i.e.,  $\psi^H(x, y)$ ,  $\psi^V(x, y)$ ,  $\psi^D(x, y)$  and one separable 2-D scaling function, i.e.,  $\varphi(x, y)$ . The digitized binary images are subjected to FFT and DWT filtering and the refined and filtered images are obtained by Inverse FFT and DWT, respectively.

The filtered images are then converted to bipolar patterns. The general form of the  $l$ th pattern vector is  $x_l = [x_{l1}, x_{l2}, x_{l3}, \dots, x_{lN}]^T$  where  $N = 1$  to 900. All the  $L$  image pattern vectors are presented to the feedback network for storage in the form of a comprehensive matrix  $P$  of order  $N \times L$ .

### 3 Self Organizing Maps

Self-organizing maps can be used for feature mapping. The feature map can often be effectively used for the feature extraction from the input data for their recognition or, if the neural network is a regular two-dimensional array, to project and visualize high dimensional signal spaces on such a one or two dimensional display. It is used to deal for the patterns which represent the continuity in the feature space.

The features extracted from the SOM can be used as patterns for storing or encoding in the feedback neural network of Hopfield type. The associative memory feature of HNN for pattern storage and their recalling can be accomplished to incorporate symmetric feedback synaptic interconnection between the processing units with bipolar state of the output layer in self organizing map. Obviously, it is quite interesting to incorporate feedback connections among the processing units of grid in SOM for pattern recognition [2, 5, 6]. In this network, the processing elements of the feedback layer, i.e., grid of SOM are fully interconnected with the symmetric connection strength represented with weight vector  $M$ . The processing elements of the input layers are connected to each of the processing element of the feedback layer with connection strength represented with weight vector  $W$ . The presented input pattern to the network is  $K$ -dimensional with continuum features, applied one at a time. The network trained to map the similarities in the set of input patterns and at any given time only few of the input may be turned on. That is, only the corresponding links are activated to accomplish the aim of capturing the features in the space of input pattern and the connections are like soft wiring dictated by the unsupervised learning mode in which the network is expected to work [5]. There are several ways of implementing the feature mapping process. In one of the method, output layer is organized into predefined receptive fields, and the unsupervised learning should perform the feature mapping by activating the appropriate connections [7, 8]. Another method of implementing the feature mapping process is to use the architecture of a competitive learning network with on center off surround type of connections among units, but at each stage the weights are updated not only for the winning units, but also for the units in its neighborhood [9]. This neighborhood region may be progressively reduced during learning. The input pattern vector  $X = \{x_1, x_2, x_3, \dots, x_k\} \in R^n$  is applied to the processing elements of the input layer. The processing elements of the input layer are connected with each element in the SOM grid. This grid contains the feedback layer region. We associate connection strength  $W_i = [w_{i1}, w_{i2}, \dots, w_{in}]^T \in R^n$  to every processing element of the feedback layer. The initial value of  $W^T$  is selected randomly. Now the input pattern vector  $X$  is applied on the processing units of the input layer. The linear output of these processing units feed the weighted input through feed forward connection to the SOM grid. The activation of the  $j$ th process unit of the feed back layer can be represented as:

$$y_j = \sum_{i=1}^K w_{ij} x_i \quad (4)$$

where,  $j = 1$  to  $N$  (Number of units in the feed back layer.)

A winning unit, say  $P$  is selected among all the processing units of the feedback layer as:

$$y_p = \max_i(y_j)$$

$$W_p^T X \geq W_j^T X \text{ for all } j$$

Geometrically, the above relationship means that the input vector  $X$  is closest to the weight vector  $w_p$  among all  $w_i$  i.e.,

$$\sum_{i=1}^k (x_i - w_{pi}) \leq \sum_{i=1}^k (x_i - w_{ji}) \quad \text{for all } j \tag{5}$$

Hence, during learning, the nodes that are topographically close up to certain geometric distance will activate each other to learn from the same input vector  $X$  and the weights associated with the winning unit  $P$  and its neighboring units  $r$  are updated as:

$$w_{iP}(t + 1) = w_{iP}(t) + \lambda(P, r)[x_i(t) - w_{ij}(t)] \tag{6}$$

For  $i = 1$  to  $K$  and  $j = 1$  to  $N$ , here the  $\lambda(P, r)$  is the neighborhood function. The neighborhood region reduces in successive iterations of the training process. Therefore, with this mechanism of competitive learning, the SOM is able to learn in unsupervised mode the feature mapping of the input pattern with continuum feature space.

### 4 Hopfield Neural Network

The proposed Hopfield Model to store  $L$  of patterns each of order  $N \times 1$  consists of  $N$  processing units and  $N * N$  connection strengths. The state of the processing unit is considered bipolar with symmetric connection strength between the processing units. Each neuron can be in one of the two stable states, i.e.,  $\pm 1$ . Storage as patterns is accomplished with Hebbian rule and the Pseudoinverse Rule. The Hebbian Rule to store  $L$  patterns is given by the summation of correlation matrices for each pattern as:

$$\begin{aligned} W_{ij} &= \frac{1}{N} \sum_{l=1}^L x_{li} * l_j \quad \text{for } i \neq j \\ &= 0 \quad \text{for } i = j, 1 \leq i \leq N \end{aligned} \tag{7}$$

where  $N$  is the number of units/neurons in the network.

The standard pseudoinverse rule is known to be better than the hebbian rule in terms of the capacity ( $N$ ), recall efficiency and pattern corrections [10]. The Pseudoinverse Rule to store the pattern set  $P$  of Eq. (5) is given by

$$W = P P^\dagger \tag{8}$$

where  $P^\dagger$  is its pseudoinverse of  $P$  [11, 12]. But pseudoinverse rule is neither local nor incremental as compared to the hebbian rule. These problems can be solved by modifying the rule in such a way that some characteristics of hebbian learning are



also incorporated such that locality and incrementality is ensured. Hence the weight matrix is first calculated using hebbian rule stated in Eq. (7) then the pseudoinverse of the weight matrix can be obtained as:

$$W_{\text{pinv}}^L = (W^L)^\dagger (W^L * (W^L)^\dagger)^{-1} \quad (9)$$

where  $(W^L)^\dagger$  is the transpose of the weight matrix  $W^L$  and  $(W^L * (W^L)^\dagger)^{-1}$  is the inverse of the product of  $W^L$  and its transpose. After storing pattern set  $P$  in the HNN using either the Hebbian or the Pseudoinverse rule, the performance of the network needs be tested for the memorized patterns, their noisy variants and also for incomplete pattern information. For this, the process of recalling is considered, whereby a test pattern, which can be the memorized pattern or its noisy form, is input into the network and the network is allowed to evolve through its activation dynamics. The output state of the network is then tested for resemblance with one of the expected stable states.

## 5 Stochastic Recall using Simulated Annealing

In associative memory architectures, the memorized patterns act as attractors in the state space of the network. In effect as the memorized pattern is presented it moves to the attractor that it most closely resembles to. However there exist additional attractors that do not correspond to any memorized pattern and thus are unhelpful. These spurious attractors may lead to error in pattern recall. The addition of noise to the deterministic HNN can be beneficial in the elimination of the spurious minima because as the free energy landscape is changed, the spurious local minima of the energy function may no longer be stable and therefore the probability that the network converges to a memorized pattern is increased [13].

In the stochastic case the update rule is probabilistic instead of being deterministic. Whenever a unit is selected for updating, the energy either decreases or remains the same. It is possible to realize a transition to a higher energy state from a lower energy state by using a stochastic update [3] in each unit instead of the deterministic update of the output function. In this process the probability of firing for an activation value of  $y$  can be expressed as

$$P(s = 1/y) = 1/1 + e^{-(y-\theta)/T} \quad (10)$$

where  $T$  is the temperature of the network. At  $T = 0$  the stochastic update reduces to a deterministic update. As the temperature is increased, the uncertainty in making the update according to  $f(y)$  increases, giving thus a chance for the network to go to a higher energy state. Therefore the result of Hopfield energy analysis, i.e.  $\Delta V \leq 0$ , will be no longer true for nonzero temperatures. Finally when  $T = \infty$ , then the

update of the unit does not depend on the activation value  $y$  any more. The state of the network changes randomly from 1 to  $-1$  or vice versa.

The training and recall of patterns in a stochastic network use the process of annealing controlled by the temperature parameter. Simulated Annealing has been widely applied to solve optimization problems [14, 15]. The recall of the memorized patterns corresponding to the presented noisy prototype patterns from the HNN can also be formulated as an optimization problem. Here the criterion is to minimize the network energy in such a way that the network settles into the global minima corresponding to the memorized pattern and thus avoids getting trapped into any false minima. The annealing schedule, becomes critical in realizing the desired probability of states near  $T = 0$ . Thus, for recall, when a prototype input pattern or its noisy variant is presented, the network is allowed to evolve through its stochastic dynamics following an annealing schedule and reach an equilibrium state near  $T = 0$ . This will reduce the effects of local minima and thus reduces the probability of error in the recall. The temperature is initialized to a high value and then a neuron is randomly selected from the network for updating. The energy of the network for the state  $s$  is computed via the Hopfield energy function as

$$E(s) = -\frac{1}{2} \sum_i \sum_j w_{ij} s_i s_j \tag{11}$$

The state of the chosen neuron is flipped to generate a new configuration. The energy of the new configuration is again computed using Eq. (11). Change in energy for change of state in the unit  $k$  from 0 to 1, for example, is given by:

$$\Delta E = E(s_k = 1) - E(s_k = 0) = - \sum_j w_{kj} s_j = -x_k \tag{12}$$

If  $\Delta E$  is negative then the new configuration obtained as a result of flipping of the chosen neuron is considered as a better state and the new state is accepted. But if the change in energy is positive then the new state is accepted with a probability calculated as:

$$P(s_i) = \frac{1}{1 + \exp(\Delta E_i/T)} \tag{13}$$

The above procedure continues several times until a thermal equilibrium is reached. At this point the temperature is lowered and the procedure is repeated. This continues until the temperature reaches a very small value. A critical aspect here is the choice of initial temperature and the annealing schedule, specified as  $T_{k+1} = cT_k$ , where  $T_k$  is the current temperature,  $T_{k+1}$  is the new temperature and  $c$  is a constant with value ranging between 0 and 1, with actual working range 0.8–0.9 for gradual reduction of temperature and skipping of false minima.

## 6 Simulation Design and Results

In the simulation design and implementation the proposed HNN is designed with 900 processing units. This HNN is trained for pattern storage with two learning rules i.e. Hebbian and Pseudoinverse Rules. The patterns for storage have been preprocessed and filtered through FFT and DWT separately. In one implementation the preprocessed patterns are directly entered into the HNN while in other the preprocessed patterns are first fed into the SOM and the feature spaces generated thereafter are stored into the HNN. Thereafter the process of recalling is initiated for prototype input patterns and for the noisy prototype input patterns of already memorized patterns. The recall is evaluated with the standard Hopfield recall algorithm and with Simulated Annealing. The results show that the SOM-HNN when trained with FFT filtered patterns shows poor results as compared to the HNN. The storage capacity with hebbian rule is reduced to almost half i.e.  $\frac{1}{2} (N/2 \log_2 N)$  while that with Pseudoinverse rule is reduced to one-ninth i.e.  $N/9$ . But on the other hand the same network when trained with DWT filtered patterns shows enhanced storage capacity with both the learning rules. With hebbian rule the capacity increases to  $0.28N$  while with pseudoinverse rule the capacity is maintained at the maximum i.e.  $N$ . The Pattern recall ability of the SOM-HNN for the noisy variants of the FFT and DWT feature vectors is better with DWT filtered patterns as compared to the FFT filtered patterns. But it is also observed from the results that the occurrence of false minima is increased in this network as compared to a stand-alone HNN. But this drawback can also be taken care of by stochastic recalling of the patterns using Simulated Annealing, whereby the occurrence of false minima is been completely eliminated.

## 7 Conclusions

Efficiency of the Pattern Storage networks is dependent on preprocessing techniques, the learning methods adopted and the activation dynamics of the network. Modified Pseudoinverse learning rule can be used to enhance the network capabilities. The continuum feature spaces created by SOM when stored in the Hopfield network can lead to substantial enhancement in the capacity and recall efficiency but this mapping amplifies the occurrence of false minima, which can be eliminated by using stochastic update instead of deterministic update of the network units in the recall mechanism.

## References

1. Davey, N., Hunt, S.P., Adams, R.: High capacity recurrent associative memories. *Neurocomputing - IJON* **62**, 459–491 (2008). doi:[10.1016/j.neucom.2004.02.007](https://doi.org/10.1016/j.neucom.2004.02.007)
2. Gill, S., Sharma, N.K., Singh, M.P.: Study of pattern storage techniques in self organizing map using hopfield energy function analysis. In: *Proceedings of ADCOM–2006*, pp. 640–641. (1–4244-0716-8/06/2006/IEEE).

3. Stroeve, S., Kappen, B., Gielen, S.: Stimulus segmentation in a stochastic neural network with exogenous signals. In: Ninth International Conference on Artificial Neural Networks, 1999, ICANN 99, vol. 2, pp. 732–737 (1999)
4. Sandirasegaram, N., English, R.: Comparative analysis of feature extraction (2D FFT & wavelet) and classification (Lp metric distances, MLP NN & HNet) algorithms for SAR imagery. In: Proceedings Of SPIE **5808**, 314–325 (2005)
5. Kaski, S., Kangas, J., Kohonen, T.: Bibliography of self-organizing map (SOM) papers: 1981–1997. *Neural Comput. Surv.* **1**(3&4), 1–176 (1998)
6. Kohonen, T.: Self-organized formation of topologically correct feature maps. *Biol. Cybernet.* **43**, 59–69 (1982b)
7. Kohonen, T.: Self-organizing formation of topologically correct feature maps. *Biol. Cybern.* **43**, 59–69 (1982)
8. Hubel, D.H., Wiesel, T.N.: Receptive fields, binocular interaction, and functional architecture in the cat's visual cortex. *J. Physiol. London* **160**, 106–154 (1962)
9. Colin, M., Utku, S., Hugues, B.: Introduction of a Hebbian unsupervised learning algorithm to boost the encoding capacity of Hopfield networks, neural networks. In: Proceedings of the IEEE International Joint Conference on IJCNN '05. 2005, vol. 3, pp. 1552–1557 (2005)
10. Gorodnichy, D.O.: The influence of self connection on the performance of pseudoinverse autoassociative networks. In: Proceedings of CVPR Workshop on Face Processing in Video (FPIV '04) (2004)
11. Emmert-Streib, F.: Active learning in recurrent neural networks facilitated by a hebb-like learning rule with memory. *Neural Inf. Process. Lett. Rev.* **9**(2), 31–40 (2005)
12. Labiouse, C.L., Salah, A.A., Starikova, I.: The impact of connectivity on the memory capacity and the retrieval dynamics of hopfield-type networks. In: Proceedings of the Santa Fe Complex Systems Summer School, pp. 77–84 (2002)
13. Davey, N., Adams, R.G.: Stochastic dynamics and high capacity associative memories. In: Proceedings of the Ninth International Conference on Neural Information Processing, pp. 1666–1671 (2002)
14. Jeffrey, W., Rosner, R.: Optimization algorithms: simulated annealing and neural network processing. *Astrophys. J.* **310**(1), 473–481 (1986)
15. Salcedo Sanz, S.: A hybrid hopfield network-simulated annealing approach for frequency assignment in satellite communication systems. *IEEE Trans. Syst. Man Cybern. B: Cybern.* **34**(2), 1108–1116 (2004)

# Nonrigid Image Registration of Brain MR Images Using Normalized Mutual Information

Smita Pradhan and Dipti Patra

**Abstract** Registration is an advanced technique which maps two images spatially and can produce an informative image. Intensity-based similarity measures are increasingly used for medical image registration that helps clinicians for faster and more effective diagnosis. Recently, mutual information (MI)-based image registration techniques have become popular for multimodal brain images. In this chapter, normalized mutual information (NMI) method has been employed for brain MR image registration. Here, the intensity patterns are encoded through similarity measure technique. NMI is an entropy-based measure that is invariant to the overlapped regions of the two images. To take care of the deformations, transformation of the floating image is performed using B-spline method. NMI-based image registration is performed for similarity measure between the reference and floating image. Optimal evaluation of joint probability distribution of the two images is performed using parzen window interpolation method. The hierarchical approach to nonrigid registration based on NMI is presented in which the images are locally registered and nonrigidly interpolated. The proposed method for nonrigid registration is validated with both clinical and artificial brain MR images. The obtained results show that the images could be successfully registered with 95 % of correctness.

**Keywords** Medical image registration · Mutual information · Normalized mutual information · B-spline method

---

S. Pradhan

IPCV Laboratory, Department of Electrical Engineering, NIT, Rourkela, India  
e-mail: ssmitta.pradhan@gmail.com

D. Patra (✉)

Department of Electrical Engineering, NIT, Rourkela, India  
e-mail: DPATRA@nitrrkl.ac.in

## 1 Introduction

Image registration is the process of transforming different sets of data into one coordinate system. Registration methods can be classified by a number of characteristics, which include the type of transformation and the registration measure. Although it has applications in many fields, medical image registration is important among them. Medical image registration has a wide range of potential applications, but the emphasis is on radiological imaging. Modern three-dimensional treatment radiation planning is based on sequences of tomographic images. Computed tomography (CT) has the potential to quantitatively characterize the physical properties of heterogeneous tissue in terms of electron densities. Magnetic resonance (MR), is very often superior to CT, especially for the task of differentiating between healthy tissue and tumor tissue. Positron emission tomography (PET), single photo emission tomography (SPECT), and MRS (magnetic resonance spectroscopy) imaging have the potential to include information on tumor metabolism. They have specific properties and deliver complementary information. The images supply important information for delineation of tumor and target volume, and for therapy monitoring.

A widespread survey of image registration methods have been published by Brown and Zitova et.al. They have classified the image registration techniques as intensity-based methods and feature-based methods [1, 2]. In intensity-based methods, similarity measure has an important role, which quantifies the relationship of transformation between the images. The most commonly used similarity measures are based on intensity differences, intensity cross correlation, and information theory. Among them, mutual information (MI) has gained wide interest in the medical image registration field [3]. When the assumptions of corresponding intensities are not one-to-one related, maximization of mutual information (MMI) is widely applicable [4]. Pluim et al. proposed to combine MI with an image gradient-based term that favors similar orientation of edges in both images [5].

As MI is computed on voxel-by-voxel basis, it does not take the spatial information inherent to the original image. To overcome this drawback, variations of MI have been proposed. Pluim et al., suggested interpolation artifacts in similarity measures [6]. Likar et al. developed a hierarchical image subdivisions strategy, that decomposes the nonrigid matching problem into an elastic interpolation of numerous local rigid registration [7]. For overlapping sub regions of the image, a non-rigid registration scheme was proposed by extending the intensity joint histogram with a third channel representing a spatial label by Chen et al. [8]. Rueckert et al. employed for transformation modeling the multiresolution scheme [9]. Studholme et al. employed normalized mutual information (NMI) for nonrigid registration of serial brain magnetic resonance imaging (MRI) due to the local intensity changes, which are mainly caused by imaging distortions and biological changes of the brain tissue [10]. The optimization algorithm for nonrigid medical image registration based on cubic b-spline and maximization of MI is derived in [11].

MI faces difficulties for registration of small-sized images. To overcome this limitation, Andronache et al. used the MI for global registration and cross correlation to register the small image patches [12]. Besides the Shannon’s entropy, other divergence measures have been used such as Tsallis entropy by Khader et al. [13].

In image registration, finding homologous landmarks is a challenging task due to lack of redundancy in anatomical information, in different modalities. Intensity-based techniques circumvent these problems as they do not require any geometrical landmarks. Their basic principle is to search, the transformation that maximizes a criterion measuring the intensity similarity of corresponding voxels. In this chapter, the registration scheme has been proposed using similarity measure-based method by incorporating NMI. The NMI approach is a robust similarity measure technique used for multimodal medical image registration. Moreover, the NMI-based registration is less sensitive to the changes in the overlap of two images. Here, we propose a non-rigid image registration approach by optimizing the NMI as similarity measure and B-spline method for modeling the transformation of the deformation field between the reference and floating image pairs.

## 2 Problem Statement

Here the NMI-based similarity measure is used as a matching criterion to solve the image alignment problem.

Let A and B be two misaligned images to be registered where A is the reference image and B is the floating image. The floating image B is a deformed image with a deformation field. The deformation field is described by a transformation function  $T(r, \mu)$  where  $\mu$  is the set of transformation parameter to be determined. The image registration problem may be formulated as an optimization problem

$$\hat{\mu} = \arg \max_{\mu} NMI(A(r), B(T(r; \mu))) \tag{1}$$

For alignment of the transformed target image  $B(T(r; \mu))$  with the reference image A, we need the set of transformation parameters  $\hat{\mu}$  that maximizes the image cost function  $NMI(A(r), B(T(r; \mu)))$ .

## 3 Problem Formulation

### 3.1 Registration by Normalized Mutual Information

The notion of image registration based on MI has been proposed by Maintz et al. [3]. The MI of two images is a combination of the entropy values of the images. The entropy of an image can be computed by estimation of the probability distribution of the image intensities [5].

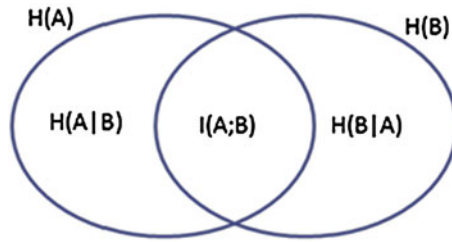


Fig. 1 Mutual Information of two images

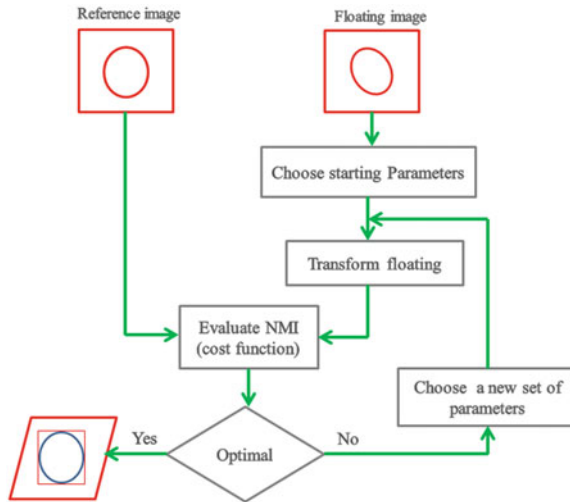


Fig. 2 Block diagram of NMI

If A and B are two random variables, then the amount of information that one variable contains about another is evaluated by MI (Fig. 1) which is given as

$$I_{(A:B)} = \sum_{a,b} p_{A,B}(a, b) \log \left( \frac{p_{A,B}(a, b)}{p_A(a)p_B(b)} \right) \tag{2}$$

where  $P_A(a)$  and  $P_B(b)$  are the marginal probability mass function and  $P_{AB}(a, b)$  is the joint probability mass function. MI is related to the entropies by

$$I(A, B) = H(A) + H(B) - H(A, B) \tag{3}$$

where  $H(A)$  and  $H(B)$  are the entropies of A and B and  $H(A, B)$  is the joint entropy defined as (Fig. 2)



$$\begin{aligned}
H(A) &= - \sum_a p_A(a) \cdot \log p_A(a) \\
H(B) &= - \sum_b p_B(b) \cdot \log p_B(b) \\
H(A, B) &= - \sum_{a,b} p_{a,b}(a, b) \cdot \log p_{a,b}(a, b)
\end{aligned} \tag{4}$$

The MI of two images determines the uncertainty of one of the images when the other is known. MI is assumed to be maximum when the images are registered. According to Studholme et al., the registration quality might decrease despite an increasing MI value whenever overlap between voxel occurs. At that time, MI is maximum but the quality of the registration is not optimal [10]. To counter the effect of increasing MI with decreasing registration quality NMI is considered. The transformation yielding the highest NMI value is assumed to be the optimal registration of two images. An estimate of the intensity distribution of the images is necessary to compute the NMI value. NMI is a well-established registration quality measure which can be defined in terms of image entropies,

$$NMI(A, B) = \frac{H(A) + H(B) - H(A, B)}{H(A, B)} \tag{5}$$

### 3.2 Optimization Using Parzen Window

To calculate the NMI between the reference image A and the floating image B using a transformation  $T(r; \mu)$ , the joint histogram  $H(a, b; \mu)$  has been taken. The popular Parzen window interpolation method is formulated to obtain the joint histogram. Parzen window places a kernel at a particular bin  $r$  and updates all the bins falling under the kernel with the corresponding kernel value. The parzen window joint histogram is given by;

$$H(a, b; \mu) = \sum_{r \in A} w_a(I_A(r_a) - a)w_b(I_B(T(r_a; \mu)) - b) \tag{6}$$

where  $I_A(r)$ : intensity of A,  $I_B(r)$  : intensity of B,  $T(r; \mu)$ , maps every reference position  $r_a$  to the corresponding floating position  $r_b = T(r_a; \mu)$  with a given set of parameters  $\mu$ .  $w_a$  and  $w_b$  are the Parzen window kernels used to distribute an intensity over the neighboring bins.

### 3.3 Transformation Model

The transformation model defines how one image can be deformed to match another; it characterizes the type and number of possible deformations. Several transformation models have been proposed for nonrigid image registration. In this chapter, we adopt the second order B-splines model for transformation of deformed image. By contrast, B-splines are only defined in the vicinity of each control point; perturbing the position of one control point only affects the transformation in the neighborhood of the point. Because of this property, B-splines are often referred to as having “local support”. B-spline based nonrigid registration techniques are popular due to their general applicability, transparency, and computational efficiency. The B-spline model is situated between a global rigid registration model and a local nonrigid model at voxel scale. Its locality or nonrigidity can be adapted to a specific registration problem by varying the mesh spacing and thus the number of degrees of freedom.

Let  $\Phi$  denote a  $r_x \times r_y$  mesh of control points  $\Phi_{i,j}$  with a uniform spacing  $\Delta$ . Then, the 2D transformation at any point  $r = [x, y]^T$  in the target image is interpolated using a linear combination of a B-spline convolution kernel as follows:

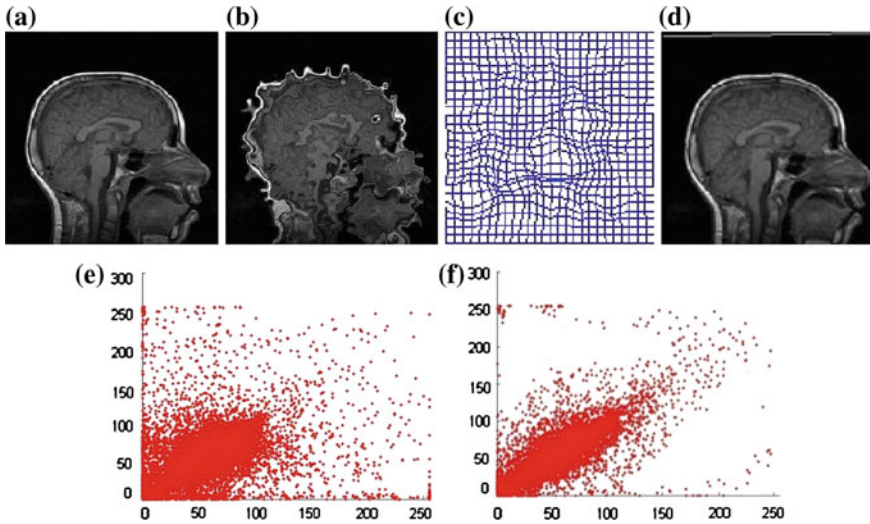
$$T(r; \mu) = \sum_{ij} \eta_{ij} \beta^2 \left( \frac{r - \phi_{ij}}{\Delta} \right) \quad (7)$$

where  $\beta^{(2)}(r) = \beta^{(2)}(x)\beta^{(2)}(y)$  is a separable B-spline convolution kernel, and  $\eta_{ij}$  are the deformation coefficients associated to the control points  $\Phi_{i,j}$ .

### 3.4 Simulation and Results

The optimization of nonrigid transformation using B-spline interpolation method leads to align the images. The time required for optimization steps to reach registration can be used as a measure of computational speed. The interpretation of NMI function is based on dispersion of the joint histogram, meaning the less dispersed the joint histogram, the better the two images are assumed to be registered. Under this interpretation, minimization of the dispersion of the joint histogram is related to maximization of NMI value.

The registrations were performed for a set of deformed brain MR images in our simulation. In the first set, a T1 weighted brain MR image and a deformed image that are considered as reference and floating images and, are shown in Fig. 3a, b respectively. The deformation field is shown in Fig. 3c. The registered image is shown in Fig. 3d. The joint histograms of the two images before registration and after registration are shown in Fig. 3e and f respectively. It can be seen that the histogram is not dispersed, rather focused after registration using NMI-based similarity measure. The dispersion shows the misalignment between the images with a



**Fig. 3** a Floating image b Reference image c Deformation field d Registered image e Joint histogram before registration f Joint histogram after registration

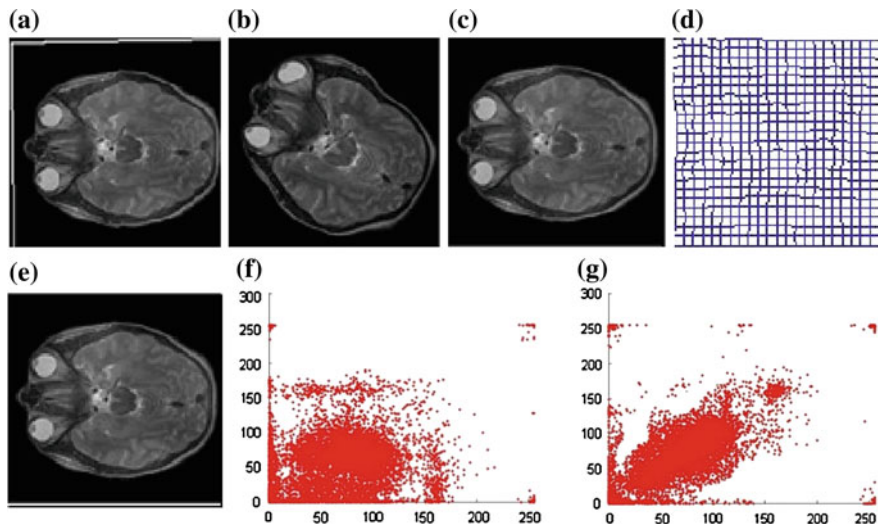
percentage of 4.009. The optimization timing or computational timing is recorded as 41.14 s.

Another set of MR images are taken, where Fig. 4a is the floating image which is deformed and rotated with an angle of 30%. The reference image is shown in Fig. 4b. The floating image is first rotated for best alignment with the reference one shown in Fig. 4c. The deformation field is presented in Fig. 4d. The joint histogram of Fig. 4a, b is shown in Fig. 4f, where it can be observed that the histogram is dispersed due to misalignment between the two images. But in case of Fig. 4g it can be seen that the histogram is very much focused after the registration process. The computation time for optimal registration is recorded as 18.51 s.

The optimized NMI value, the percentage of misregistration error (MRE), and the computational time for optimization metrics for both experiments are presented in Table 1. The normalized value signifies the alignment between the two images after registration process. The higher the value of NMI means more alignment of the images. MRE is misregistration error calculated by considering the registered image with respect to the reference images. Less value of MRE means best alignment of the images. Computational time is the time required for optimal registration. From

**Table 1** Calculated NMI value with % age of Mis-reg Error and comp. time

Image	NMI value	MRE (%)	Comp. timing (s)
Figure 3	0.2880	4.0090	18.51
Figure 4	0.3960	7.5041	41.14



**Fig. 4** a Floating image b Reference image c 30° rotated floating image d Deformation field e Registered image f Joint histogram before registration g Joint histogram after registration

the table, it can be concluded that the optimization process for aligning the images takes more time with a low percentage of misalignment and vice versa.

### 4 Conclusion

In this paper, intensity-based technique is applied for alignment problem as we can work directly with the volumetric data. We propose the registration scheme by optimizing the NMI as similarity measure. This measure produces accurate registration results on both artificial and clinical brain images that we have tested. B-spline method is used for modeling the nonrigid deformation field of the target image with respect to the reference image. Parzen window interpolation method is employed for joint histogram plot. Current attempts are made to register the image with multimodal images. This work can be extended towards multimodal brain image registration.

### References

1. Brown, L.G.R.: A survey of image registration techniques, *ACM Comput. Surv.* **24**(4), 325–376 (1992)
2. Zitova, Barbara, Flusser, Jan: Image registration methods: a survey. *Image Vis. Comput.* **21**, 977–1000 (2003)

3. Pluim, J., Maintz, J., Viergever, M.: Mutual-information-based registration of medical images: a survey. *IEEE Trans. Med. Imag.* **22**(8), 986–1004 (2003)
4. Viola, P., Wells, W.M.: Alignment by maximization of mutual information. In: *ICCV '95 Proceedings of the Fifth International Conference on Computer Vision*, IEEE Computer Society (1995)
5. Pluim, J., Maintz, J., Viergever, M.: Image registration by maximization of combined mutual information and gradient information. *IEEE Trans. Med. Imag.* **19**(8), 809–814 (2000)
6. Pluim, J.P.W., Maintz, J.B.A., Viergever, M.A.: Interpolation artefacts in mutual information-based image registration. *Comput. Vis. Image Understand.* **77**(2), 211–232 (2000)
7. Likar, B., Pernu, F.: A hierarchical approach to elastic registration based on mutual information. *Image Vis. Comput.* **19**(1–2), 33–44 (2001)
8. Chen, H.M., Varshney, P.K.: Mutual information-based CT-MR brain image registration using generalized partial volume joint histogram estimation. *IEEE Trans. Med. Imag.* **22**(9), 1111–1119 (2003)
9. Rueckert, D., Aljabar, P., Heckemann, R.A., Hajnal, J.V., Hammers, A.: Diffeomorphic registration using b-splines. *Medical Image Computing and Computer-Assisted Intervention, Lecture Notes Computer Science*, **4191**, 702–709. Springer, New York (2006)
10. Studholme, C., Drapaca, C., Iordanova, B., Cardenas, V.: Deformation-based mapping of volume change from serial brain MRI in the presence of local tissue contrast change. *IEEE Trans. Med. Imag.* **25**(5), 626–639 (2006)
11. Klein, S., Staring, M., Pluim, J.P.W.: Evaluation of optimization methods for nonrigid medical image registration using mutual information and B-splines. *IEEE Trans. Image Process.* **16**(12), 2879–2890 (2007)
12. Andronache, A., Siebenthal, M.v., Szekely, G., Cattin, P.: Nonrigid registration of multimodal images using both mutual information and cross-correlation. *Med. Image Anal.* **12**, 3–15 (2008)
13. Khader, M., Hamza, A.B., An entropy-based technique for nonrigid medical image alignment. In: *Proceedings of the 14th International Workshop Combinatorial Image, Analysis*, pp. 444–455 May 2011

**Part XI**  
**Soft Computing for Communication,**  
**Signals and Networks (CSN)**

# A Proposal for Deployment of Wireless Sensor Network in Day-to-Day Home and Industrial Appliances for a Greener Environment

Rajat Arora, Sukhdeep Singh Sandhu and Paridhi Agarwal

**Abstract** Wireless automation sensor communication network (WASCN) is the promising tool for energy conservation [1] according to the research work of this paper. This paper considers the two aspects of analyzing an appliance, i.e., at manufacturer level and user condition level of that appliance. At manufacturer level, the manufacturer company of the particular appliance will itself provide the concerned data of appliance and its effect on the environment, whereas at user level, these data may depend on the infrastructure or the environment of that particular appliance where it is being used. Now to analyze the 2nd impact we have environment and infrastructure manager (EIM). EIM will deploy WASCN [2] between various appliances to measure the effects of the appliance according to user, infrastructure as well as the environment in which it is being used. These data recorded by the EIM will be shared to analyze the effect of a particular appliance in various particular conditions which in turn will help the customers or an industry to choose the environment friendly products considering the cost too.

**Keywords** WASCN · EIM · Energy conservation

---

R. Arora  
Mechanical Engineering Department, IIT Kanpur, Kanpur, UP, India  
e-mail: rajat.arora9464@gmail.com

S. S. Sandhu (✉) · P. Agarwal  
Computer Science and Engineering Department, Gyan Vihar University, Jaipur, Rajasthan, India  
e-mail: sukhdeepsingh90@gmail.com

P. Agarwal  
e-mail: paridhi.agarwal1990@gmail.com

## 1 Introduction

One of the most common and of utmost concern in today's world is energy conservation, that too, environmental friendly. Today various companies are coming up with eco friendly appliances. The need of hour is to change the old devices with newer ones but for large-scale industries it is not possible to change them all one at a time. So, in this paper we discuss the alternative method for energy conservation in an environment friendly way. This paper argues on the fact that WASCN has all the potential to improve the energy efficiency of such devices allowing EIM to target more and more green purchases [3].

WASCN are low cost wireless sensors [4] that ensure the consumption of low power of radio technologies. WASCN promises the monitoring of appliances via a common EIM interface. Simultaneous monitoring of appliances via WASCN provides the path of identification of appliances requiring maintenance or replacement.

Refreshed data being generated after regular intervals creates an opportunity for a manufacturer to develop energy as well as environment friendly products considering infrastructure as well as the environment in which appliance will be used via detailed power profile being generated by EIM in this regard.

## 2 Proposed Architecture for Energy Conservation and a Step Ahead to Greener Environment

This section of our paper describes the components of our proposed architecture and how the same components will help in conserving energy [5] and ENVIRONMENT. The main thing is that to achieve our desired goal all these components should be entangled with each other via Internet services so as to share their data.

### 2.1 Executive Roles

We have identified different executive roles at different levels that are as follows:

- i> EIM
- ii> Manufacturers
- iii> End users

EIMs are the major proposed executive role in this system. EIMs are responsible for maintaining a power profile of a particular appliance working under some environmental conditions as well as space and area constraints. This power profile may be different from the ideal power profile of an appliance. Also, we may note here that power profile in one particular environment and area of the same appliance may differ from other power profile in some other area size and environment. This feature of EIM helps the customer to choose the most appropriate appliance according to his environment and area size which in turn helps customer saving energy and environment by choosing the appropriate appliance.



The second Executive role is that of the manufacturers. Manufacturers create the power profile of an appliance in ideal conditions which is compared to EIM's power profiles. Now as we have pointed earlier, all the executive role players are connected to each other in a network so a manufacturer can create one appliance for two different environments for, e.g., homemade appliances may have different environmental impacts and energy consumption than industries.

End users are the ones who help EIM to make a power profile of their appliances by deploying WASCN with each appliance of theirs. It is also the responsibility of the end user to check the power profile of appliances and choose the best appliance which will help in conserving energy and environment according to their available conditions.

## 2.2 WASCN and Its Features

WASCNs are the major proposed technology in our paper. According to our proposed architecture WASCN are small chips that are entangled with each appliance which in turn help in making the power profile. WASCN records the effect of appliance on the environment and vice versa and the energy consumed by that appliance in a particular area and environment. The sensed data is then sent to EIM. EIM is connected to WASCN which will record the data of all the appliances in a particular home or industry which may be helpful for the new customer to compare the profiles of one appliance of the same company being used by different end users situated at different areas having two different environmental conditions and select the eco friendly appliance.

Various features expected to be possessed by WASCN are:

- Low power: WASCN are small chips or sensors that consume very less operating power [6].
- Reliability: As the same WASCN will be applied in different areas having different environment therefore, it should work in any of the conditions without any failure or it must be reliable enough to be used.
- Low cost: There may be thousands of appliances at some places being used so the operating cost and the maintenance cost must be low and within the budget of the end user [7].
- Submission of manufacturer data: It is also expected that WASCN may be used by manufacturers also to record their profiles and share data. So, WASCN should fit into any conditions and may be used by any user.

### A. Power profiles.

Power profile [8] refers to the power consumed by the device in a particular area and environment and the worst-case will always be considered. Some areas may be hot while some areas may be cold so the behaviour of one particular appliance will be different in both the conditions. Also, some areas may be compact and some areas may be wide so the heat dissipated by the device in compact area will be more

which will disturb the environmental condition of that area. Thus here we choose the appliance which will dissipate the minimum heat. So, we conclude that both area as well as environmental condition somewhere has effect on appliance which may again have an adverse effect on our environment itself and may consume more energy. Therefore, this power profile helps in comparing data of different appliances [9] in same conditions, different appliances in different conditions, same appliances in same conditions and same appliances in different conditions.

### B. Assembling of various power profiles by different executive roles

Now the need of the hour says to gather all power profiles recorded by EIM and the manufacturers. All these profiles are shared online and data of different appliances in same conditions, different appliances in different conditions, same appliances in same conditions, and same appliances in different conditions is compared so that we can work upon the existing appliances which are a threat to the environment or it may also help in the case where we intend to replace the existing appliances with new ones or it may also work when we go on for buying new appliances.

### C. Power profile repository

Power profile repository [10] is like a database which stores various power profiles generated by EIMs and the manufacturers. This repository is not maintained at end user side, rather we make EIM and manufacturer responsible for holding the same, but at the same time we should also keep in mind that this repository should be accessible [11] by every executive role (Fig. 1).

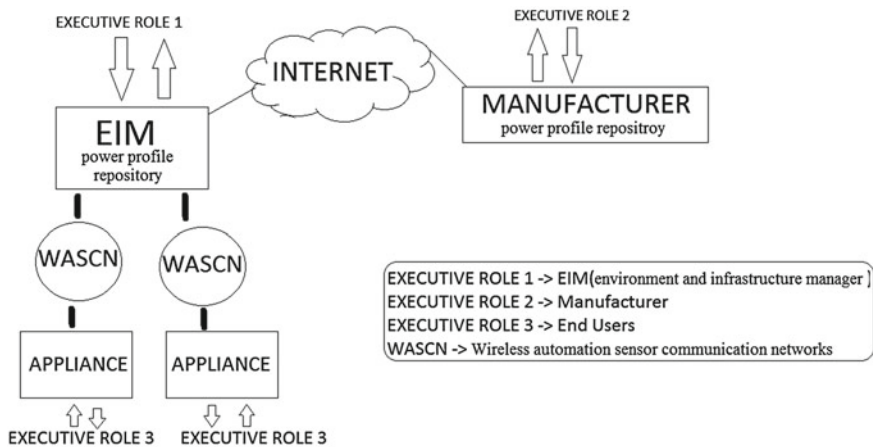


Fig. 1 Architecture of the proposed model

### 3 Working of our Proposed System

In the following section we explain the working of our proposed architecture:-

First, executive role 2, i.e., the manufacturer will develop an appliance and will make the power profile of the appliance in the ideal conditions. The power profile is then stored in the power profile repository which will in turn be shared on the Internet. Then comes the role of the executive role 3, i.e., end user of an appliance. Now in our proposed system executive role 3 is assigned the duty to deploy WASCN with every appliance they are using. Now according to the surroundings for, e.g., area, temperature, room space, weather conditions, etc., the sensors will record the effect an appliance on the environment and vice versa. Its power consumption also depends on the surrounding. So, according to the conditions its power profile will be recorded and will be stored in the repository of executive role 1, i.e., EIM. Now EIM is responsible for storing data of different appliances in same conditions, different appliances in different conditions, same appliances in same conditions, and same appliances in different conditions & is compared so that we can work upon the existing appliances which are threat to the environment or it may also help in the case where we intend to replace the existing appliances with new ones or it may also work when we go for buying new appliances. Likewise, it will be beneficial for end users to search for the best suitable appliance according to their surroundings which in turn will help us saving in the environment and reduce the electricity consumption hence, saving the energy too.

### 4 Conclusion

Through this paper we have tried to present an energy conservation model which will also help in making the present environment greener. Wireless sensors [12] introduced itself has a low power consumption and is environmental friendly which helps customer to go for an efficient purchase of an appliance which also cuts short the maintenance cost keeping in mind the green environment as its main aim.

### 5 Review

*A Review by*

*Mr DEEPAK SACHAN*

*Alumni IIT Roorkee Electronics and Communication Engineering.*

*MBA SungKyunKwan University Seoul, South Korea.*

*Manager Samsung Electronics Gurgaon*

“There is hope if people will begin to awaken that spiritual part of them, that heartfelt knowledge that we are caretakers of this planet.”—Brooke Medicine Eagle

According to the proposed idea if the research scientists really implement it in the practical life then it would change the whole current scenario and mind sets of people towards efficient use of home appliances leading to a greener environment. Till now whenever we talk about purchasing an appliance it's just the deal between an end user and manufacturer but both manufacturer as well as end user are least bothered about environmental aspects. If Executive role 1 and WASCN (according to the proposed idea) comes into picture then there is hope to save environment from the dangerous aspects of appliances. I'm moved by the idea and as a manager at Samsung Electronics Gurgaon we'll try to conduct research on the idea in our industry too.

## References

1. <http://info.iet.unipi.it/anastasi/papers/adhoc08.pdf>
2. <http://arri.uta.edu/acs/networks/WirelessSensorNetChap04.pdf>
3. <http://www.deepgreenrobot.org/using-green-technology-under-the-threat.html>
4. <http://www.sciencedaily.com/releases/2011/04/110412143123.htm>
5. <http://www.sciencedirect.com/science/article/pii/S1570870508000954>
6. Daabaj, K., Dixon, M.W. and Koziniec, T.: Adaptive transmission power control scheme for wireless sensor networks. In: 2011 MUPSA Multidisciplinary Conference, 29 Sept, Murdoch University, Murdoch (2011)
7. [http://cache.freescale.com/files/microcontrollers/doc/ref\\_manual/DRM094.pdf](http://cache.freescale.com/files/microcontrollers/doc/ref_manual/DRM094.pdf)
8. [http://www.ict-aim.eu/fileadmin/user\\_files/deliverables/AIM-D2-3v2-0.pdf](http://www.ict-aim.eu/fileadmin/user_files/deliverables/AIM-D2-3v2-0.pdf)
9. <http://www.ecnmag.com/articles/2012/08/designing-low-cost-wireless-sensor-networks-real-world-applications>
10. <http://researchrepository.murdoch.edu.au/4460/>
11. [http://doc.oracle.com/cd/E23507\\_01/Platform.20073/ATGPersProgGuide/html/s0401settingupacompositeprofilereposi01.html](http://doc.oracle.com/cd/E23507_01/Platform.20073/ATGPersProgGuide/html/s0401settingupacompositeprofilereposi01.html)
12. <http://www.sensor-networks.org/>

# Energy-Aware Mathematical Modeling of Packet Transmission Through Cluster Head from Unequal Clusters in WSN

Raju Dutta, Shishir Gupta and Mukul Kumar Das

**Abstract** Clustering techniques in wireless sensor networks (WSNs) compare to random selection techniques is less costly due to the saving of time in journeys, reduction in number of transmissions and receptions at each node, identification, contacts, etc., which are valuable for increasing the overall network life, scalability of WSNs. Clustering sensor nodes is an effective and efficient technique for achieving the requirement. The maximizing lifetime of network by minimizing energy consumption poses a challenge in design of protocols. Therefore, proper organization of clustering and orientation of nodes within the cluster becomes one of the important issues to extend the lifetime of the whole sensor network through Cluster Head (CH). We investigate the problem of energy consumption in CH rotation in WSNs. In this paper, CH selection algorithm has been proposed from an unequal cluster. The total energy and expected number of packet retransmissions in delivering a packet from the sensor node to other nodes have been mathematically derived. In this paper, we applied the approach for producing energy-aware unequal clusters with optimal selection of CH and discussed several aspects of the network mathematically and statistically. The simulation results demonstrate that our approach of re-clustering in terms of energy consumption and lifetime parameters.

**Keywords** WSN · Packet transmission · Unequal cluster · Cluster head · Lifetime

---

R. Dutta (✉)  
Narula Institute of Technology, Kolkata, India  
e-mail: rdutta80@gmail.com

S. Gupta · M. K. Das  
Indian School of Mines, Dhanbad, India  
e-mail: shishir\_ism@yahoo.com

M. K. Das  
e-mail: mkdas12@gmail.com

## 1 Introduction

Cluster schemes are hierarchical. Selection of sensor node as a CH in WSN greatly affects the power consumption efficiency of the network. In conventional clustering, the network is divided and sensor nodes are accumulated into groups, known as clusters and then one sensor node from cluster is selected to lead as clusterhead. The distribution of the clusterhead may be uneven. In unequal clusters size, the selection strategy of CH effects in uneven energy consumption of the network. For a given number of sampling units, cluster sampling is more convenient and less costly. The advantages of cluster sampling are

1. Within a cluster, all normal nodes send their data to the CH. The resulting absence of flooding scheme, multiple route which is energy saving.
2. The backbone network consists only of the CHs, which are fewer in number than all nodes in the entire network and therefore simpler.
3. the change of nodes within the cluster affects only that cluster but not the entire network.
4. collection of data for neighbouring elements is easier, cheaper, faster and operationally more convenient than observing units spread over a region.
5. It is less costly than simple random sampling due to the saving of time in journeys, identification, contacts, etc.
6. When a sampling frame of elements may not be readily available.

Energy conservation is always a challenging issue in wireless sensor networks. Lifetime of wireless network based on battery power, which has limited energy source. For increasing the lifetime of such network and nodes, it is important that one has to find the techniques either increasing the battery power or an alternative source of energy for the nodes. One of the methods for increasing the lifetime of nodes is by adjusting the transmission power of sensor node during transmission. However, adjusting the transmission power is not always sufficient to improve the battery power of sensor nodes and optimize the energy consumption. Now-a-days to increase in the network life time interference plays an important role for minimizing the energy consumption. Due to interference, the quality of service of wireless network to a great extent causing collision of packets, packet loss, and retransmission frequency. Decreasing interference level may save the node power by minimizing collision, retransmission and congestion. In this paper, we consider transmission and reception power of nodes for a good quality routing path for delivering the packets from source to destination. Our protocol minimizes the total energy consumption of routing path from source to destination and balances load among the nodes. We propose our protocol with shortest path routing.

## 2 Related Work

In this paper [1] proposed a distributed, randomized clustering techniques to find optimum cluster size and cost to organize the sensors in a wireless sensor network within clusters. In [2] it describes mathematical modeling of packet transmission through CH from unequal clusters in WSN. Low Energy Adaptive Clustering Hierarchy (LEACH) described in [3] the rotation of CH among the nodes and a cluster based data gathering in WSN. MECH [4] explains a communication range and sensor nodes select themselves as CH if satisfying the fixed node degree criterion. ACE-C [5] pointed out for even distribution of sensor nodes and avoid re-clustering in each round. Reconfiguration of the clusterhead explained in [6] and also avoid re-clustering technique power efficient routing protocol is given in [7] for selecting CH in power efficient at even distribution of CH. Power consumption and maximizing network lifetime during communication of sensor node in WSN has been discussed in [8]. In [9] efficient clustering techniques to optimize the system lifetime in wireless sensor network. In [10] topology control of wireless networks is achieved using link level interference. In [11] sender computes the potential interference of receivers and adjusts their transmission ranges to reduce the receiver interference using global information. The energy consumption pattern in an integrated interference-aware and confidentiality-enhanced multipath routing scheme for continuous data streams on Wi-Fi based multi-hop wireless ad hoc networks has also been proposed [11]. In [13, 14] dynamic virtual carrier sensing and interference aware routing protocol to select the optimum path based on two criteria, shortest path and interference of nodes, have been proposed. The sensor network is a wireless collection of portable devices that offers a variety of services, including area and wildlife monitoring, etc. [15]. A cluster-based approach is introduced in [16] using PSO, which was found to function better than Low-Energy Adaptive Clustering Hierarchy-Centralized (LEACH-C) [17] protocol in terms of energy efficiency. Another improved PSO has been proposed in [18] for improving the performance of the optimization technique. In [19] the research work evaluates a routing optimization method on the basis of graph theory and PSO.

## 3 Network Model and Assumptions

The assumptions made to describe our network scenario (Fig. 1).

- The sensor network is assumed to be a circular geographic region with the sink  $S$ , positioned at coordinate  $(x_0, y_0)$ , and radius  $R_s$ .
- The sensors are uniformly deployed in the sensing area  $A_s$ . Moreover, the number of sensor nodes is distributed according to 2-dimensional Poisson point process with  $\rho$  as the expected density of  $A_{ca}$ .
- The cluster covers circular area with its CH at the center  $o$  with radius  $R_{ca}$ .

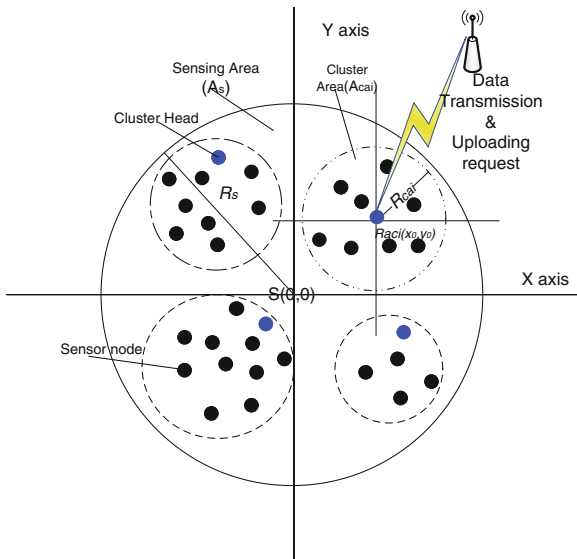


Fig. 1 Network model with data transmission from sensor node and uploading request from BS

- There are total  $k$  clusters in the sensor network. Further, owing to the uniform node deployment strategy, we can compute an approximation for the cluster radius,  $R_{ca}$ :

$$K \times A_{ca} = A_s \Rightarrow K \times \pi \times R_{ca}^2 = \pi \times R_s^2 \Rightarrow R_{ca} = \sqrt{\frac{R_s}{K}}$$

where  $K = \sum_{i=1}^k K_i$  and  $R_{ca} = \sum_{i=1}^k R_{cai}$

- The base station (or sink) periodically sends a request to the CH of unequal cluster size to upload samples collected by the sensors (Fig. 1). On receiving the request, the CH broadcasts a data-gathering-signal to all its cluster members.
- In our contribution we have applied unequal clustered sensor network, where the nodes are stationary. The basic aim is to find optimized position for CH from the base station, i.e., the distance is as close as possible to the base station. Such localization for CH would ultimately minimize the average distance covered by the sensors to transmit data to the CH and to the base station.



### 3.1 Power Consumption Schemes

The normal nodes in a cluster only transmit and relay their data to their CH. In addition to transmitting their data, the CHs are also receiving data from the normal nodes and transferring these data. The CHs therefore consume more power than other normal nodes and when the CHs run out of energy the cluster will break down. To avoid this situation and keep network healthy, we have implemented a Cluster Selection Efficient Protocol (CSEP), where clusters will be selected in the basis of few assumption.

- Here we consider a dynamic clustered network where clusters are unequal.
- There may not be even distribution of CH.
- In each cluster, the CH is selected by CH routing protocol.
- In each cluster, a node will be selected as a CH whose energy level is high than others node.
- The CH will be selected from the cluster if the variance within the cluster is less.
- The CH will be selected from the cluster if the distance from the base station is less. But if the closer cluster is unable to find CH then next closer distance cluster have opportunity to select CH.
- The sensor nodes which are in the boundary of the cluster consumes more energy than other node.
- CH rotation is associated with Re-clustering technique.

### 3.2 Cluster Head Selection Algorithm

In this section, CHs are selected. If  $E_{\text{residual}} > E_{\text{threshold}}$  satisfy then a sensor become KEY NODE then it broadcast the MESSAGE. Then each KEY NODE receives the MESSAGE within the range of the sensor node. If a node satisfies all the condition  $E_{\text{residual}} > E_{\text{threshold}}$  and  $d(n_j, \text{BS}) < d(n_k, \text{BS})$  and  $E_{\text{residual}} > E_{\text{any node}}$  simultaneously then it becomes CH otherwise re-clustering will be carried out.

**Lemma** *In every cluster, only one CH exists at a  $\text{Timer}_{\text{Phase}}$  within the radio range ( $R_{\text{range}}$ ) of the cluster.*

*Proof* Let us consider  $S$  be the set of all sensor node in a cluster of size  $M_i$ . Let us consider  $S = \{x, \text{ if } d(x, y) < R_{\text{range}}\}$ . Let  $p, q \in S$  then if we consider  $p$  is a CH, then by our algorithm of selecting of CH we can say  $p. E_{\text{residual}} > q. E_{\text{residual}}$ . Again if we take  $q$  as a CH then according to the algorithm we have  $p. E_{\text{residual}} > q. E_{\text{residual}}$ . Which is only possible if  $p = q$ . So In every cluster only one CH exists at a  $\text{Timer}_{\text{Phase}}$  within the radio range ( $R_{\text{range}}$ ) of the cluster.

---

**Algorithm 1** Clusterhead selection algorithm
 

---

/\*

 $\forall n_j \in M_i$ Timer  $p_{phase}$ , each node gets sufficient time to complete operation.

```

1. state  $\leftarrow$  NODE;
2. if ( $E_{residual} > E_{threshold}$ ) then
3.     state  $\leftarrow$  KEY NODE;
4.     broadcast MESSAGE;
5.     while (Timer phase not expired) do
6.         msg  $\leftarrow$  receive MESSAGE;
7.         if ( $(E_{residual} > E_{threshold}) \& d(n_j, BS) < d(nK, BS)$ 
             $\& (E_{residual} > E_{any\ node})$ ) then
8.             state  $\leftarrow$  CH;
9.         else if
10.            state  $\leftarrow$  NODE;
11.            break;
12.        end if
13.    end while
14. end if
15. if (state = KEY NODE) then
16.     state  $\leftarrow$  CH;
17. end if

```

---

## 4 Unequal Cluster Sampling and Sampling for Proportion

Estimator of Mean and its Variance. In many practical situations, cluster size vary. Suppose there are  $N$  clusters. Let the  $i$ th cluster consists of  $M_i$  elements ( $i = 1, 2, \dots, N$ ) and  $\sum_{i=1}^N M_i = M_0$ . The cluster population mean per element  $\bar{Y}$  is defined by

$$\bar{Y} = \frac{\sum_{i=1}^N \sum_{j=1}^{M_i} y_{ij}}{\sum_{i=1}^N M_i} = \frac{\sum_{i=1}^N M_i \bar{y}_i}{\sum_{i=1}^N M_i} = \frac{\sum_{i=1}^N M_i \bar{y}_i}{M_0} \text{ where } \bar{y}_i \text{ is the mean per element of the } i\text{th}$$

cluster. We may also defined the pooled mean  $\bar{Y}_N = \frac{\sum_{i=1}^N \bar{y}_i}{N}$

Suppose it is required to estimate the proportions of elements belongs to a specified classes when the population consists  $N$  clusters, each of size  $M$  and a random sample of  $n$  clusters is selected. Suppose the  $M$  elements in any cluster can be classified into two classes. Assuming that  $y_{ij} = 1$  if the  $j$ th elements of the  $i$ th cluster belongs to the class = 0, otherwise.

It can be easily seen that  $p_i = \frac{a_i}{M}$  is the true proportion in the  $i$ th cluster,  $a_i$  being the number of elements in the  $i$ th cluster belongs to the specified class. An

unbiased estimator of the population proportion  $P = \frac{\sum_{i=1}^N a_i}{NM} = \frac{\sum_{i=1}^N p_i}{N}$  is given by  $\hat{P}_c =$

$\frac{\sum_i^n p_i}{n} = \bar{p}$  where  $p_i$ , the proportion of elements is belongs to the specified class in the  $i$ th cluster of the sample. The sampling variance of  $\widehat{P}_c$  is given by [4]  $V(\widehat{P}_c) = \frac{N-n}{n} \frac{\sum_{i=1}^N (p_i - P)^2}{N-1} = \frac{(1-f)}{n} S_b^2$  is the variance between cluster proportions and is given by  $MS_b^2 = \sum_i^N \frac{(p_i - P)^2}{N-1} = \frac{N}{N-1} PQ$ , where  $Q = 1 - P$ . For large  $N$ , we have  $S^2 \cong S_b^2 + S_w^2 = PQ$  and the within variance  $S_w^2$  is given by  $\sum_i^N \frac{P_i Q_i}{N}$ . Hence the intraclass correlation coefficient  $\rho$  can be written as  $\rho = 1 - \frac{\sum_i^N MP_i Q_i}{(M-1)PQ}$  and the range of  $\rho$  is given by  $-\frac{1}{M-1} (-\frac{M_0-1}{M_0(M-1)} \leq \rho \leq \frac{(N-1)S_b^2}{NS^2}$  where  $S_b^2 = \sum_i^N \frac{M_i(M_i-1)(\bar{y}_i - \bar{Y})^2}{M(M-1)(N-1)}$  therefore, the sampling variance, in terms of the intraclass correlation coefficient can be expressed as

$$V(\widehat{P}_c) = \frac{(1-f)NPQ}{(N-1)nM} [1 + (M-1)\rho] \tag{1}$$

An estimation of total number of units belonging to the specified class, can be obtained by multiplying by  $\widehat{P}_c$  by  $NM$  and the expression for its sampling variance is  $N^2M^2$  times that given by Eq.(1). If Simple Random Sampling (SRS) of  $nM$  elements could be taken, the variance of the sampling proportions  $\widehat{P}$  would be obtained by binomial theory and is given by

$$V_{bin}(\widehat{P}) = (1-f) \frac{NPQ}{nM(NM-1)}$$

The efficiency of cluster sampling as compared to SRS, without replacement, can be obtained as

$$\frac{V(\widehat{P}_c)}{V_{bin}(\widehat{P})} = \frac{(MN-1)[1+(M-1)\rho]}{N-1} \tag{2}$$

And for large  $N$

$$\frac{V(\widehat{P}_c)}{V_{bin}(\widehat{P})} = M[1+(M-1)\rho]$$

If the cluster sizes  $M_i$  are variable, the estimate  $\widehat{P}_c = \frac{\sum_i^{a_i}}{\sum_i M_i}$  is a ratio estimate. Its variance is given by approximately by the formula (1),  $V(\widehat{P}_c) = \frac{N-n}{nM} \frac{\sum_{i=1}^N M_i^2 (p_i - P)^2}{N-1}$  if this sample is compared with a simple random sample of  $n\bar{M}$  elements, we find as a generalization of Eq. (2), by

$$\frac{V(\widehat{P}_c)}{V_{\text{bin}}(\widehat{P})} = \frac{(\bar{M}N - 1) [1 + (\bar{M} - 1)\rho]}{N - 1} \text{ where } \bar{M} = \frac{\sum M_i}{N} \tag{3}$$

### 5 Varying Probability Cluster Sampling

In many practical situations, cluster size is positively correlated with the variable under study. In these cases, it is advisable to select the clusters with probability proportional to the number of elements in the cluster of their sizes  $M_i$ . There are several applications in which size is not the number of elements in the cluster and some other measure is considered for probability selection. In this paper, we shall confine ourselves to discussion of the case where the probability of selection is proportional to cluster size  $M_i$ . Let  $p_i$  ( $0 < p < 1$ ) be the probability of selecting the  $i$ th cluster if size  $M_i$  ( $i = 1, 2, \dots, N$ ) at each draw with  $\sum_i^N p_i = 1$ . Suppose that  $z_{ij} = \frac{M_i y_{ij}}{M_0 p_i}$  for  $j = 1, 2, \dots, M_i$  and  $i = 1, 2, \dots, N$ , further suppose that  $n$  clusters are selected by pps with replacement so that  $z_{ij} = \frac{M_i \bar{y}_i}{M_0 p_i}$  for  $i = 1, 2, \dots, N$ . If clusters are selected with probabilities proportional to size  $p_i = \frac{M_i}{M_0}$  and with replacement, then an unbiased estimator of  $\bar{Y}$  is given by  $\bar{z}_n = \sum_i^n \frac{\bar{y}_i}{n}$  with variance

$$V(\bar{z}_n) = \sum_i^n \frac{M_i}{nM_0} (\bar{y}_i - \bar{Y})^2 \tag{4}$$

and unbiased estimator of the variance  $V(\bar{z}_n)$  is given by  $V(\bar{z}_n) = \frac{\sum_i^n (\bar{y}_i - \bar{Y})^2}{n(n-1)}$ .

The efficiency of sampling  $n$  unequal clusters with pps, without replacement as compared to Simple random sampling by taking  $n\bar{M}$  elements, can be obtained by Eq. (4) with the variance  $V_{SR}(\bar{y}) = \frac{S^2}{n\bar{M}}$  which can be expanded by introducing  $\bar{y}_i$  in the above relation. Thus,

$$\begin{aligned} V_{SR}(\bar{y}) &= \frac{1}{n\bar{M}} \frac{1}{n\bar{M}} \left[ \sum_i^N \sum_j^{M_i} (y_{ij} - \bar{y}_i)^2 + \sum_i^N M_i (\bar{y}_i - \bar{Y})^2 \right] \\ &= \frac{\sigma_w^2}{n\bar{M}} + V(z_n) \text{ where } \sigma_w^2 = \frac{1}{n\bar{M}} \sum_i^N \sum_j^{M_i} (y_{ij} - \bar{y}_i)^2 = \sum_i^N \frac{M_i \sigma_i^2}{n\bar{M}} \end{aligned}$$

Hence, the efficiency of cluster sampling is given by

$$E = \frac{V_{SR}}{V_{pps}} = \left[ \bar{M} \left( 1 - \frac{\sigma_i^2}{\sigma^2} \right) \right]^{-1} \quad (5)$$

It can be seen that  $E$  is always greater than 1.

## 6 Expected Number of Retransmission Attempts

Initially, we assume that an aggregation tree exists in every cluster with the CH as the root. Moreover, within the cluster, transmission of data to the CH follows the path in the aggregation tree. We assume that there are  $h$  hops or links between the source node and CH. Also, every link (between two sensors) possesses link failure probability ( $p_{LFP}$ ). Clearly, for a tree of  $m$  links, the number of transmissions required for one successful sending of data to CH is also  $m$ . Now, the probability of  $m$  successful transmission for one successful end-to-end data delivery (towards CH) is  $(1 - p_{LFP})^m$ . Also, the probability of at least one failed transmission, leading to failed data delivery, is  $[1 - (1 - p_{LFP})^m]$ . Let random variable  $Y$  which denotes the number of successful data delivery attempts. Further,  $(\mu - 1)$  failures followed by one successful attempt satisfy geometric distribution and is given by:  $p[Y = \mu] = [1 - (1 - p_{LFP})^m]^{(\mu-1)} \times (1 - p_{LFP})^m$

Therefore, the expected number of attempts leading to a successful delivery of data is:

$$E[\mu] = \sum_{\mu=1}^{\infty} \mu \times p[Y = \mu] = \sum_{\mu=1}^{\infty} \mu \times [1 - (1 - p_{LFP})^m]^{(\mu-1)} \times (1 - p_{LFP})^m = \frac{1}{(1 - p_{LFP})^m} \quad (6)$$

## 7 Energy Consumption Model

The radio energy dissipated by a sensor node is mainly in form of electronics and amplifier energy. Here  $E_{elec}$  is the energy dissipated per bit to run the radio electronics ( $E_{elec}$ ) largely depends on how efficiently the signal is encoded, modulated, and filtered and  $\xi_{amp}$  is the energy expended to run the power amplifier for transmitting a bit over unit distance. However, the energy dissipation rate in the radio amplifier ( $\varepsilon_{amp}$ ) is directly proportional to  $d^\lambda$ , where  $d$  is the distance between the source (member of the cluster) and destination node CH and  $\lambda$  is the path loss component. Therefore, the expected value of  $d^2$ , represented by  $E[d^2]$  is obtained as following:

$$\begin{aligned}
 E[d^2] &= \int \int [(x - x_0)^2 + (y - y_0)^2] \times \rho(x, y) dx dy \\
 &= \rho \int_{x_0}^p \int_{y_0}^{\sqrt{p^2 - x_0^2}} [(x - x_0)^2 + (y - y_0)^2] dx dy \\
 &= \frac{\rho}{3} (p - x_0) \left[ \begin{aligned} &2p^2 \left( \sqrt{p^2 - x_0^2} - 2y_0 \right) + \\ &2px_0 \left( y_0^2 - \sqrt{p^2 - x_0^2} \right) + y_0 \left( 2x_0^2 + y_0 \left( 3\sqrt{p^2 - x_0^2} - y_0 \right) \right) \end{aligned} \right]
 \end{aligned}$$

Where  $x \leq p \leq R_s$ ,  $\rho = \frac{\sum_{i=1}^k \rho_i}{K}$  and  $\rho_i = \frac{K_i}{\pi R_{cai}^2}$

To transmit an  $m$ -bit packet over a distance  $d$  the energy used by a sensor node is given by:

$$e_T = \begin{cases} m \times E_{elec} + m \times \epsilon_{amp} \times d_i^2 & d_i < v_0 \\ m \times E_{elec} + m \times \epsilon_{amp} \times D^4 & D \geq v_0 \end{cases} \tag{7}$$

In Eq. (7)  $v_0$  is the threshold distance and  $d_i$  denotes the distance between the  $(i + 1)$ th node and  $i$ th node in the cluster and  $D$  is the beyond threshold distance where the signal strength is affected by multi-path fading between the leader and the base station. In our approach, we have used both the free space (distance 2 power loss) and the multipath fading (distance 4 power loss) channel modes. In our model, we assume that inter-nodal distances are small compared to distance between the nodes and the Base Station (BS). Thus for communication among sensors, we take  $n = 2$ , and that between the leader and BS, we take  $n = 4$ , in Eq. (7). The energy spent in the receiving the packet is,  $e_R = m \times E_{elec}$ . Finally the total energy expended ( $E_{NODE}$ ) by a sensor node to support transmission—reception operation as well as in other energy consumption ( $E_{other}$ ) can be determined by the following equation:

$$\begin{aligned}
 E_{NODE} &= \lambda \times e_T + (1 - \lambda) \times e_R + E_{other} \\
 &= \lambda \times \left[ \begin{aligned} &mE_{elec} + m \epsilon_{amp} \times \frac{\rho}{3} (p - x_0) \left[ \begin{aligned} &2p^2 \left( \sqrt{p^2 - x_0^2} - 2y_0 \right) + \\ &2px_0 \left( y_0^2 - \sqrt{p^2 - x_0^2} \right) + \\ &y_0 \left( 2x_0^2 + y_0 \left( 3\sqrt{p^2 - x_0^2} - y_0 \right) \right) \end{aligned} \right] \end{aligned} \right] \\
 &\quad + (1 - \lambda) mE_{elec} + E_{other}
 \end{aligned}$$

where other energy consumption due to the environmental noise. Finally, the total energy in delivering a packet can be expressed as following:

$$\begin{aligned}
 E_{\text{TOTAL}} &= h \times E_{\text{NODE}} \times E[\mu] \\
 &= h \times \left[ \lambda \times \left[ mE_{\text{elec}} + m \epsilon_{\text{amp}} \times \frac{\rho}{3} (p - x_0) \left[ \begin{aligned} &2p^2 \left( \sqrt{p^2 - x_0^2} - 2y_0 \right) + \\ &2px_0 \left( y_0^2 - \sqrt{p^2 - x_0^2} \right) + \\ &y_0 \left( 2x_0^2 + y_0 \left( 3\sqrt{p^2 - x_0^2} - y_0 \right) \right) \end{aligned} \right] \right] \right. \\
 &\quad \left. + (1 - \lambda) mE_{\text{elec}} + E_{\text{other}} \right] \tag{8} \\
 &\quad \times \frac{1}{(1 - \text{PLFP})^m}
 \end{aligned}$$

where  $h$  hops or links between the source node and CH.

### 8 Simulation Results

Extensive simulation carried out, and the results of the distribution power consumption of sensors are shown in Fig. 2.

### 9 Conclusion

In this paper, we have considered unequal clustering techniques to minimize interference, transmission power, and reception power of nodes to derive a good quality routing path for delivering the packets from source to destination based on our pro-

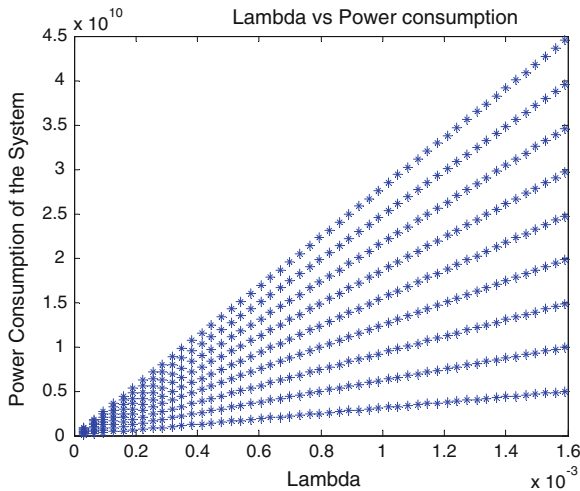


Fig. 2 Power consumption reduces according to the increase of lambda

posed algorithm. For a given source to destination pair in the network, there may exist more than one routing paths. But according to our proposed model only the optimum route will be considered based on our algorithm for cluster and CH selection. Figure 2 shows the power consumption according to the different values of lambda. We compared our protocol with other sampling and Eq. (5) shows that the efficiency of cluster sampling is always better than other sampling. Equation 3 conclude that the sampling variance  $\widehat{P}_c$  of unequal clustering gives better result if this sample is compared with a simple random sample of  $nM$  elements and if intracluster correlation coefficient  $\rho$  is small. Equation 8 gives the total energy consumption for delivering a data packet. At present, we are carrying further studies in this area.

## References

1. Dutta, R., Gupta, S., Das, M.K.: Mathematical modelling of packet transmission through cluster head from unequal clusters in WSN. In: IEEE International Conference Parallel, Distributed and Grid, Computing (PDGC-2012), University of Jaypee, Guna, 515–520 (2012)
2. Dutta, R., Gupta, S., Das, M.K.: Efficient statistical clustering techniques for optimizing cluster size in wireless sensor network. In: International Conference on Modeling, Optimization and Computing (ICMOC-2012) (Procedia Eng. J.), vol. 38, pp. 1501–1507. Elsevier, London (2012)
3. Heinzelman, W., Chandrakasan, A., Balakrishnan, H.: Energy-efficient communication protocol for wireless microsensor network. In: Proceedings of 33rd HICS **2**, 1–10 (2000)
4. Chang, R., Kuo, C.: An energy efficient routing mechanism for wireless sensor networks. In: Proceedings of International Conference in Advanced Information Networking and Applications (AINA '06), **5**(2) (2006)
5. Liu, C., Lee, C., Chun Wang, L.: Distributed clustering algorithms for datagathering in wireless mobile sensor networks, Elsevier science. J. Parallel Distrib. Comput. **67**, 1187–1200 (2007)
6. Kim, N., Heo, J., Kim, H., Kwon, W.: Reconfiguration of clusterheads for load balancing in wireless sensor networks, Elsevier science. J. Compos. Commun. **31**, 153–159 (2008)
7. Zhang, W., Linag, Z., Hou, Z., Tan, M.: A power efficient routing protocol for wireless sensor network. In: Proceedings of IEEE International Conference in Networking, Sensing and Control, London, 20–25 (2007)
8. Dutta, R., Gupta, S., Das, M.K.: Power consumption and maximizing network lifetime during communication of sensor node in WSN. Procedia Technology, vol. 4, pp. 158–162. Elsevier, London (2012)
9. Dutta, R., Saha, S., Mukhopadhyay, A.K.: Efficient clustering techniques to optimize the system lifetime in wireless sensor network. In: IEEE - International Conference on Advances in Engineering, Science and Management, IEEE Explore pp. 679–683.(2012)
10. Burkhart, M., Rickenbach, P., Wattenhofer, R., Zollinger, A.: Does topology control reduce interference?. In: Proceedings of ACM MobiHoc. (2004)
11. Krunz, M., Muqattash, A., Lee, S.: Transmission power control in wireless ad hoc networks: challenges, solutions, and open Issues. J. IEEE Netw. 8–14 (2004)
12. Lee, C.W.: Wireless transmission energy analysis for interference-aware and confidentiality-enhanced multipath routing. In: Proceedings of 8th IEEE International Symposium on Network Computing and Applications, (2009)
13. Lou, W., Liu, W., Fang, Y.: SPREAD: enhancing data confidentiality in mobile ad hoc networks. In: Proceedings of IEEE INFOCOM, 2404–2413 (2004)
14. Hou, K., Qin, Y.: A dynamic virtual carrier sensing and interference aware routing protocols in wireless mesh networks. In: Proceedings of IEEE ICCS, (2008)



15. Akyildiz, I.F., Su, W., Sankarasubramanian, Y., Cayirci, E.: Wireless sensor networks: a survey. *J. Comput. Netw.* **384**, 393–422 (2002)
16. Latiff, N.M.A., Tsemenidis, C.C., Sheriff, B.S.: Energy-aware clustering for wireless sensor networks using particle swarm optimization. In: The 18th Annual IEEE International Symposium on Personal, Indoor and Mobile Radio, Communications (PIMRC'07), 1–5 (2007)
17. Heinzelman, W.B., Chandrakasan, A.P., Balakrishnan, H.: An application-specific protocol architecture for wireless microsensor networks. *IEEE Trans. Wirel. Commun.* **14**, 660–670 (2002)
18. Yang, E., Erdogan, A.T., Arslan, T., Barton, N.: An improved particle swarm optimization algorithm for power-efficient wireless sensor networks. In: ECSIS Symposium on Bio-inspired, Learning, and Intelligent Systems for Security (BLISS), 76–82 (2007)
19. Cao, X., Zhang, H., Shi, J., Cui, G.: Cluster heads election analysis for multi-hop wireless sensor networks based on weighted graph and particle swarm optimization. In: Fourth International Conference on Natural Computation, 599–603 (2008)

# Evaluation of Various Battery Models for Bellman Ford Ad hoc Routing Protocol in VANET Using Qualnet

Manish Sharma

**Abstract** The present era in communication is the era of VANET which simply represents the communication between fast moving vehicles. The VANET is expanding day by day from planes to higher altitude, from metropolitan to towns etc. At higher altitude the performance of VANET becomes prime area of consideration. Because power consumption is more due to average QoS (Quality of Service). Everyday new functions like gaming, internet, audios, videos, credit card functions etc. are being introduced leading to fast CPU clock speed hence more battery consumption. Since energy conservation is main focus now days therefore in this paper we studied and compared various battery models for residual battery capacity taking Bellman Ford ad hoc routing protocol in to consideration along with various VANET parameters like nodes, speed, altitude, area etc. in real traffic scenario. The battery models Duracell AA(MX-1500), Duracell AAA(MN-2400), Duracell AAA(MX-2400), Duracell C-MN(MN-1400) are compared in hilly scenario using Qualnet as a simulation tool taking nearly equal real scenarios after a frequent study of that region. The performance of various battery models for residual battery capacity is compared so that right battery model shall be chosen in hilly VANET. Varying parameters of VANET shows that in the real traffic scenarios battery models AA (MX-1500) and C-MN (MN-1400) performs more efficiently for energy conservation.

**Keywords** VANET · Bellman ford · Duracell · Qualnet

## 1 Introduction

Vehicular Ad hoc Network (VANET) is a new communication mode by which fast moving vehicles communicate. The concept of VANETs is quite simple: by incorporating the wireless communication and data sharing capabilities, the vehicles can

---

M. Sharma (✉)

Department of Physics, Government College, Dhaliara, Himachal Pradesh 177103, India  
e-mail: manikambli@rediffmail.com

be turned into a network providing similar services like the ones with which we are used to in our offices or homes. VANETs are direct offshoot of Mobile Ad hoc Networks (MANETs) [1] but with distinguishing characteristics like, movement at high speeds, constrained mobility, sufficient storage and processing power, unpredictable node density and difficult communication environment with short link lifetime etc. It has been found that at higher altitude the mobile terminals in fast moving vehicles like cars, buses and trains are frequent signal breakdowns as compared to pedestrians leading to more battery consumption. Since we can't change geographical and physical conditions hence in order to improve QoS and energy conservation in fast moving vehicles various battery models and light weight routing protocols needed to be studied. So that right selection of the battery model along with routing protocol can be made. Now days more and more functions like gaming, internet, audios, videos, credit card functions etc. are being introduced leading to fast CPU clock speed hence more battery consumption. Therefore performance of battery models counts a lot in any scenario. Moreover, transmission speed of cellular networks is increasing exponentially. It has increased from few kbps to 10 several mbps, a third generation system in last 10 years. Unfortunately, battery capacity has been tripled in the last 10 years [2, 3] throughout the world. As the dependence on mobile is increasing day by day therefore offsetting the energy conservations of the mobile terminals is the formidable challenge and hence need immediate attention. In this paper we studied and compared various battery models for Bellman Ford [4] ad hoc routing protocol taking in to consideration various VANET parameters like nodes, speed, altitude, area etc. in real traffic scenario. The battery models [5] are compared in hilly scenario using Qualnet as a Simulation tool [6] taking almost real scenarios after a frequent study of that region and Potentials for optimizing the deployed transport and routing Protocols is investigated. These battery models are different in impedance, weight, ANSI and IEC. Special care is taken in to provide realistic scenarios of both road traffic and network usage. A micro simulation environment for road traffic supplied vehicle movement information, which is then fed in to an event-driven network simulation that congaed and managed a VANET model based on this mobility data. The protocols and their various parameters of the transport, network, data link, and physical layers is provided by well-tested implementations for the networks simulation tool, while VANET mobility is performed by our own implementation.

## 2 Ad hoc Routing Protocols

Routing protocol [7] is a standard that controls how nodes decide how incoming packets are routed between devices in a wireless domain and further distinguished in many types. There are mainly three types of routing protocols: Proactive [7], Reactive [8] and Hybrid [9]. These protocols are having different criteria for designing and classifying routing protocols for wireless ad hoc network. The factors which must be taken under considerations while choosing a protocol are multicasting, loop free,

multiple routes, unidirectional link support, power consumption etc. The selection of right protocol is the target for the fast moving vehicles so that QoS and power saving shall be improved [10, 11]. Routing protocols are always challenging in the fast moving nodes as their performance degrades and such type of network is difficult to manage as fast handoff, signal quality, Interference maximizes along with other geographical factors. In addition to mobility, the power availability to the mobile node is also a serious consideration. Unlike typical wired-link routers, the power source of mobile nodes comes from non-permanent power sources such as batteries. There are mainly three types of routing protocols [12]. In our work the chosen protocols is Bellman Ford ad hoc routing protocol which is proactive in nature and the simple reason behind choosing this protocol because it uses distance-vector algorithm.

## 2.1 Bellman Ford Routing Protocol

The term vector–distance, Ford–Fulkerson, Bellman–Ford, and Bellman are synonymous with distance–vector [4, 13], the last two are taken from the names of researchers who published the idea. The term distance–vector refers to a algorithms class where routers use to propagate routing information. The idea behind distance–vector algorithms is quite simple. The router keeps a list of all known routes in a table. When it boots, a router initializes its routing table to contain an entry for each directly connected network. Each entry in the table identifies a destination network and gives the distance to that network, usually measured in hops. For example, Fig. 1 shows an existing table in a router, *K*, and an update message from another router, *J*. Periodically, each router sends a copy of its routing table to any other router it can reach directly. When a report arrives at router *K* from router *J*, *K* examines the set of destinations reported and the distance to each. If *J* knows a shorter way to reach a destination, or if *J* lists a destination that *K* does not have in its table, or if *K* currently routes to a destination through *J* and *J*'s distance to that destination changes, *K* replaces its table entry. For example, Fig. 1 shows an existing table in a router, *K*, and an update message from another router, *J*.

Note that if *J* reports distance *N*, an updated entry in *K* will have distance  $N+I$  (the distance to reach the destination from *J* plus the distance to reach *J*). Of course, the routing table entries contain a third column that specifies a next hop. The next hop entry in each initial route is marked *direct delivery*. When router *K* adds or updates an entry in response to a message from router *J*, it assigns router *J* as the next hop for that entry.

## 3 Battery Models

Batteries are continued to power an increasing number of electronic systems, their life becomes a primary design consideration. By understanding both the source of energy

Destination	Distance	Route		Destination	Distance
Net1	0	Direct		Net1	2
Net2	0	Direct	→	Net4	3
Net4	8	Router L		Net17	6
Net17	5	Router M	→	Net21	4
Net24	6	Router J		Net24	5
Net30	2	Router Q		Net30	10
Net42	2	Router J	→	Net42	3

(a)
(b)

**Fig. 1** **a** An existing route table for a router *K*, and **b** an incoming routing update message from router *J*. The marked entries will be used to update existing entries or add new entries to *K*'s table

and the system that consumes it, the battery life can be maximized. There are basically two types of battery models alkaline or lechlanche cells. The zinc/potassium hydroxide/manganese dioxide cells, commonly called alkaline [5] or alkaline-manganese dioxide cells and the zinc-carbon cells are called as Lechlanche cells. The alkaline cells have a higher energy output than zinc-carbon (Lechlanche) cells. The use of an alkaline electrolyte, electrolytic ally prepared manganese dioxide, and a more reactive zinc powder contributes to a higher initial cost than zinc-carbon cells. However, due to the longer service life, the alkaline cell is actually more cost-effective based upon cost-per-hour usage, particularly with high drains and continuous discharge. The high-grade, energy-rich materials composing the anode and cathode, in conjunction with the more conductive alkaline electrolyte, produce more energy than could be stored in standard zinc carbon cell sizes. The product information and test data included in this section represent Duracell's newest alkaline battery products. Note that both these battery models have some common battery parameters Table 1.

**Table 1** Parameters of Duracell AA (MX-1500), Duracell AAA (MX-2400), Duracell AAA (MN-2400), Duracell C-MN (MN-1400)

Parameters	AA (MX-1500)	AAA (MX-2400)	AAA (MN-2400)	C-MN (MN-1400)
Nominal voltage	1.5 V	1.5 V	1.5 V	1.5 V
Operating voltage	1.6–0.75 V	1.6–0.75 V	1.6–0.75 V	1.6–0.75 V
Impedance	81 m-ohm @ 1 kHz	114 m-ohm @ 1 kHz	114 m-ohm @ 1 kHz	136 m-ohm @ 1 kHz
Typical weight	24 g (0.8 oz.)	11 g (0.4 oz.)	11 g (0.4 oz.)	139 g (0.4 oz.)
Typical volume	8.4 cm <sup>3</sup> (0.5 in <sup>3</sup> )	3.5 cm <sup>3</sup> (0.2 in <sup>3</sup> )	3.5 cm <sup>3</sup> (0.2 in <sup>3</sup> )	3.5 cm <sup>3</sup> (0.2 in <sup>3</sup> )
Storage temperature	–20–35 °C	–20–35 °C	–20–35 °C	–20–35 °C
Operating temperature	–20–54 °C	–20–54 °C	–20–54 °C	–20–54 °C
Terminals	Flat	Flat	Flat	Flat
ANSI	15 A	24 A	24 A	13 A
IEC	LR06	LR03	LR03	LR20

## 4 Simulation Tool

Network simulation [1] methodology is often used to verify analytical models, generalize the measurement results, evaluate the performance of new protocols that are being developed, as well as to compare the existing protocols. Actually Qualnet [6] is a comprehensive suite of tools for modelling large wired and wireless networks. It uses simulation and emulation to predict the behaviour and performance of networks to improve their design, operation and management. Qualnet is a commercial simulator that grew out of GloMoSim, which was developed at the University of California, Los Angeles, UCLA, and is distributed by Scalable Network Technologies [6]. The QualNet simulator is C++ based. All protocols are implemented in a series of C++ files and are called by the simulation kernel. QualNet comes with a java based graphical user interface (GUI). Here while creating scenario the mobility model selected is Random Waypoint Mobility Model [14] in which a mobile node begins the simulation by waiting a specified pause-time Table 2.

**Table 2** Simulation parameters

Parameters	Values
Simulator	Qualnet version 5.o.1
Terrain size	1500 × 1500
Simulation time	3000s
Number of nodes	15
Mobility	Random way point, Pause time = 0s
Speed of vehicles	Minimum = 5 m/s Maximum = 20 m/s
Routing protocols	Bellman Ford
Medium access protocol	802.11 MAC, 802.11 DCF
T × power	150dbm
Data size	512 bytes
Data interval	250ms
Number of sessions	5
Altitude	1500m
Weather mobility	100ms
Battery models	Duracell AA (MX-1500) Duracell AAA (MN-2400) Duracell AAA (MX-2400) Duracell C-MN (MN-1400)

## 5 Designing of Scenario

The scenario is designed in such a way that it undertakes the real traffic conditions as shown in Fig. 2. We have chosen 15 fast moving vehicles in the region of  $1500 \times 1500$  with the random way point mobility model. There is also well defined path for some of the vehicles, so that real traffic conditions can also be taken care of. It also shows wireless node connectivity of few vehicles using CBR application. The area for simulation is hilly area with altitude of 1500 meters. Weather mobility intervals is 100 ms. Pathloss model is two ray with max prop distance of 100m. The data size is 512 bytes and the data interval is 250 ms. The speed of the vehicles varies from 5 m/s to 20 m/s and for precision the numbers of sessions are five. Battery models are Duracell AA(MX-1500), Duracell AAA(MN-2400), Duracell AAA(MX-2400), and Duracell C-MN(MN-1400). The simulation is performed with different node mobility speed and CBR (Constant bit rate) traffic flow. CBR traffic flows with 512 bytes are applied. Simulations is made in different speed utilization with IEEE 802.11 Medium access control (MAC) and Distributed Coordination Function (DCF) ad hoc mode and the channel frequency is 2.4 GHz and the data rate 2 mbps.

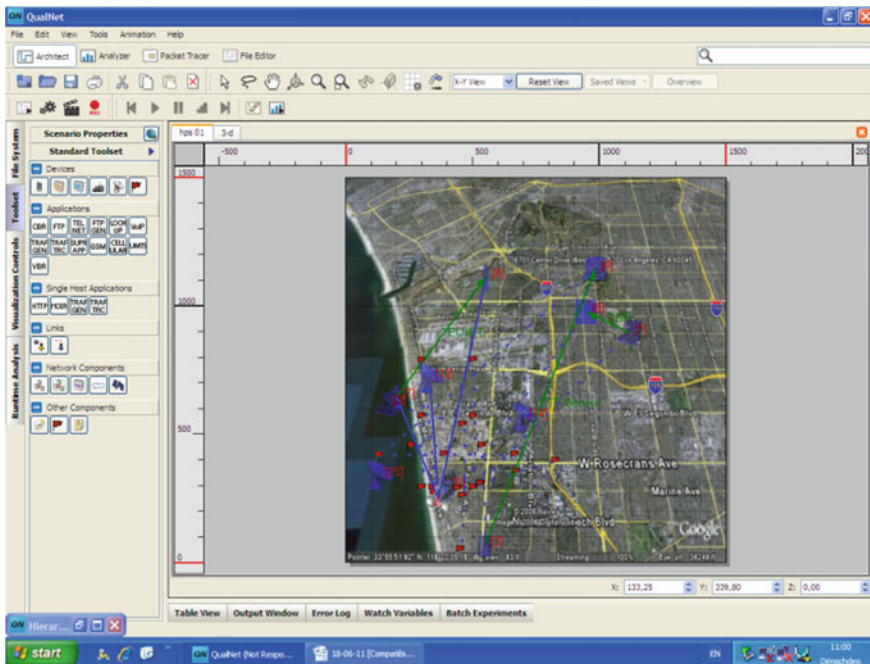


Fig. 2 Qualnet VANET scenario

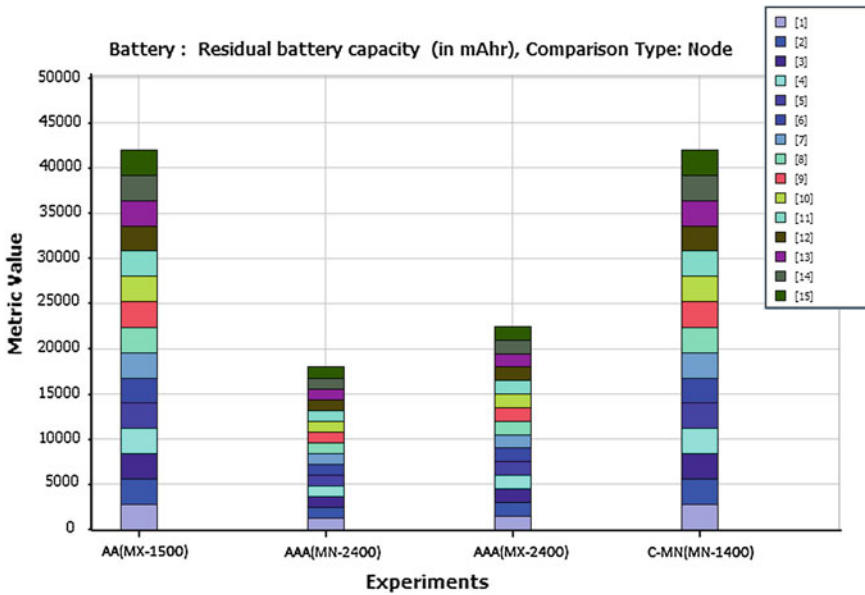


Fig. 3 Residual battery capacity for Bellman Ford routing protocol

## 6 Results and Discussions

The simulation result brings out some important characteristic differences between the various battery models as shown in Fig. 3. It has been found that the residual battery capacity for Duracell AA (MX-1500) and Duracell C-MN (MN-1400) is 4200mA/h is quite high as compared to other two. This is because they offer low impedance of 81 m-ohm @ 1 kHz and 136 m-ohm @ 1 kHz as compared to 250 m-ohm @ 1 kHz for Duracell AAA (MN-2400). Moreover ANSI values are 15 A and 13 A as compared to 24 A for both Duracell AAA (MN-2400) and Duracell AAA (MX-2400). The IEC values are LR6 and LR20 for Duracell AA (MX-1500) and Duracell C-MN (MN-1400) as compared to LR03 for other two. The typical weight values are also meant for considerations in hilly areas.

## 7 Conclusion

Evaluation of the feasibility and the expected quality of VANETs operated as per various battery models, shows significant results. It has been found that the battery models depending upon their impedance, volume, weight, various temperatures operating range show significant variations in performance. Since energy conservations is most required now days. Hence its study leads to solutions to many problems.



Note that performance of these battery models also depends upon routing protocols and other parameters like, number of times link broke, signal transmitted and received, throughput, IEEE 802.11 (MAC), IEEE 802.11 (DCF), IP, FIFO, broadcast received, time difference (Real time and simulation time) and power saving etc. Result shows that for comfort and safety applications in a V2V communication environment the significant requirements are high and reliable quality of service packet. In general, position-based routing is more promising than other routing protocols for VANETs because of the geographical constrains. These routing protocols would improve the traffic control management and provide the information in timely manner to the concern authority and drivers. From the result and analysis, we now look into further improving the use battery models and ad hoc routing protocols in the VANET communication of the vehicular environment [14]. The scope of this research on VANET would be a very vast for ad hoc routing protocol that is used for comfort and safety applications.

## References

1. Raw, R.S., Das, S.: Performance comparison of position based routing protocols in vehicle-to-vehicle (V2V) communication. *Intl. J. Eng. Sci. Technol.* **3**(1), 435–444 (2011)
2. Toor, Y., Laouiti, A., Muhlethaler, P.: Vehicular ad hoc network applications and related technical issues. *IEEE. Commun. Surv. Tutorials* **10**(3), 74–88 (2008)
3. Paradiso, J.A., Stamer, T.: Energy scavenging for mobile and wireless electronics. *IEEE. Pervasive. Comput.* **4**(1), 18–27 (2005)
4. Comer, D.,E.: *Internetworking with TCP/IP: Principles, Protocols and Architecture*, Vol. I, 4th edn. Prentice Hall, Upper Saddle River (2000)
5. <http://www.duracell.com/>
6. Qualnet simulator version 5.0.1. Scalable Network Technologies. <http://www.scalable-networks.com/>
7. Lason, T., Hedman, N.: *Routing Protocols in Wireless Ad Hoc Network*. Lulea University of Technology, Stockholm (1998)
8. Sommer, C., Dressler, F.: *The DYMO Routing Protocol in VANET Scenarios*. University of Erlangen-Nuremberg, Germany (2009)
9. Mustafa, B., Waqas Raja, U.: *Issues of routing in VANET*. Thesis MCS-2010-20, School of Computing, Blekinge Institute of Technology (2010)
10. IEEE, wireless LAN medium access control (MAC) and physical layer (PHY) specifications. IEEE Std. 802.11-1997
11. Forouzan, B., A.: *Data Communications and Networking*. Networking Series, Tata Mcgraw-Hill, India (2005)
12. Perkins, C., Royer, E., Das, S., Marina, K.: Performance comparison of two on-demand routing protocols for ad hoc network. *IEEE. Pers. Commun.* 16–28 (2001)
13. Kozierok C.M.: *The TCP/IP Guide Version 3*, No Starch Press, San Francisco (2005)
14. Khan, I.: *Performance evaluation of ad hoc routing protocols for vehicular ad hoc networks*. Thesis, Mohammad Ali Jinnah University

# A Comparative Analysis of Emotion Recognition from Stimulated EEG Signals

Garima Singh, Arindam Jati, Anwasha Khasnobish, Saugat Bhattacharyya, Amit Konar, D. N Tibarewala and R Janarathanan

**Abstract** This paper proposes a scheme to utilize the unaltered direct outcome of brain's activity viz. EEG signals for emotion detection that is a prerequisite for the development of an emotionally intelligent system. The aim of this work is to classify the emotional states experimentally elicited in different subjects, by extracting their features for the alpha, beta, and theta frequency bands of the acquired EEG data using PSD, EMD, wavelet transforms, statistical parameters, and Hjorth parameters and then classifying the same using LSVM, LDA, and kNN as classifiers for the purpose of categorizing the elicited emotions into the emotional states of neutral, happy, sad, and disgust. The experimental results being a comparative analysis of the different classifier performances equip us with the best accurate means of emotion recognition from the EEG signals. For all the eight subjects, neutral emotional state is classified with an average classification accuracy of 81.65 %, highest among the other three emotions. The negative emotions including sad and disgust have better average

---

G. Singh · A. Jati · S. Bhattacharyya · A. Konar · R. Janarathanan  
Department of Electronics and Telecommunication Engineering, Jadavpur University,  
Kolkata, India  
e-mail: garima201290@gmail.com

A. Jati  
e-mail: arindamjati@gmail.com

S. Bhattacharyya  
e-mail: saugatbhattacharyya@gmail.com

A. Konar  
e-mail: konaramit@yahoo.co.in

R. Janarathanan  
e-mail: srmjana\_73@yahoo.com

A. Khasnobish (✉) · D.N. Tibarewala  
School of Bioscience and Engineering, Jadavpur University, Kolkata, India  
e-mail: anweshakhasno@gmail.com

D.N. Tibarewala  
e-mail: biomed.ju@gmail.com

classification accuracy of 76.20 and 74.96 % as opposed to the positive emotion i.e., happy emotional state, the average classification accuracy of which turns out to be 73.42 %.

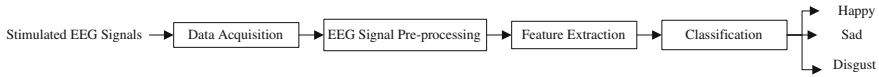
**Keywords** Emotion recognition · Electroencephalogram (EEG) · Power spectral density (PSD) · Wavelet transform (WT) · Empirical mode decomposition (EMD) · Statistical parameters (STAT) · Hjorth parameters · Linear discriminant analysis (LDA) · Linear support vector machine (LSVM) · K-nearest neighbor (kNN)

## 1 Introduction

In today's era, when no realm of science remains untouched by the miracles of artificial intelligence; 'Emotion,' no longer remains a terminology that solely defines human acts and performances, but is being incorporated to enhance the performance of emotionally challenged computers/machines as well [1, 2]. However, development of emotionally intelligent systems and devices, demand the recognition of the emotion as a vital step forward in this regard. The quality of performance of a system would improve with its ability to atone the negative emotional effects by the use of positive emotions accordingly. The act of emotion recognition may be achieved either through physiological signals or through external gestures and facial expressions of the individual. EEG signals, being the unmodified direct outcome of one's brain activity [3, 4] and independent of the hemodynamic of the brain, rather rely on the electrical potentials obtained from scalp due to various activities in brain and henceforth are not susceptible to voluntary suppression or modification. The procedure involves sending information regarding emotional changes, consciousness, and thinking to the frontal and prefrontal lobes of the cerebral cortex, which are then recorded by electrodes placed on the scalp above these regions. Raw EEG signals are needed to be processed and classified into different emotional categories, using different features and intelligent classifier algorithms.

Various strategies used for the purpose of feature extraction are power spectral densities, statistical parameters, wavelet transforms, Hjorth parameters, Fourier transforms, short time Fourier transforms (STFTs), empirical mode decompositions, higher order crossings, etc. [5–8] while the next step of emotion classification is done using Bayes' classifiers, support vector machines, fuzzy classifiers, genetic algorithms, K-means [9–14].

The aim of this research is to classify the emotional states experimentally elicited in the different subjects under consideration, by extracting the features from the alpha, beta, and theta frequency bands using power spectral density (PSD), empirical mode decomposition (EMD), Hjorth parameters, and wavelet transforms and then classifying the same using linear support vector machine (LSVM), linear discriminant analysis (LDA), and k-nearest neighbor (kNN) as classifiers. Thus categorizing the elicited emotions into the emotional states of neutral, happy, sad, and disgust are achieved in this work (Fig. 1).



**Fig. 1** The Approach

The paper is divided into six sections. The experimental setup and data organization is explained in Sect. 2. The feature extraction techniques and classifiers are mentioned in Sects. 3 and 4, respectively. Performance analysis of the classifiers is given in Sect. 5. Experimental results and conclusions are listed in Sect. 6.

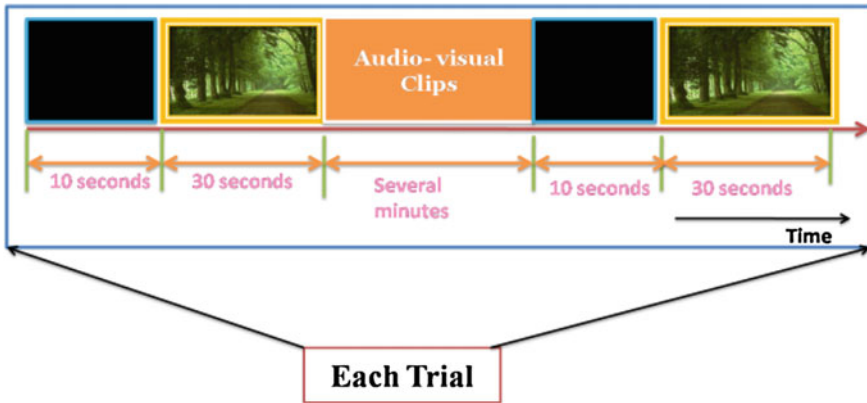
## 2 Experimental Data Description

It has been noted that among various modes to stimulate emotions in subjects under a controlled environment, audio-visual cues have the potential to elicit discrete emotions more effectively [15]. Keeping in mind these findings and the age group and cultural background of the subjects under study, after extensive search of movie clips, 20 movie clips are selected for eliciting happy, sad, and disgust emotions, 5 movie clips of each category. The movie clips were first shown to ten subjects, and based on their manual feedback which was recorded in the consent and feedback form, the final eight movie clips (two clips for each emotion) were selected for these discrete emotions. But these 10 subjects did not take part in the actual experiments.

The stimulus consisted of a blank screen for 10 seconds, followed by few soothing pictures of total 30 seconds duration. This was given to relax the subjects so that their neutral EEG baseline could be detected. This relaxing clip was followed by a movie clip first of the corresponding emotion, followed by the relaxing clip in the end (Fig. 2).

The experimental phase involved collection of EEG data from eight different subjects who were subjected to audio-visual stimulus relating to the four emotional states viz. neutral, happy, sad, and disgust. The subjects were given a brief introduction of the experimental procedure followed by filling up of consent form. The EEG signals were recorded using the NEUROWIN EEG amplifier of Nasan Medicals with a sampling rate of 250 Hz from electrodes positioned at F3, F4, Fp1 and Fp2, since they lie over the frontal and prefrontal lobe [16, 17]. Common reference montage was used for the recording purpose which represents the EEG signal as a difference of potentials of each electrode to one reference point that is placed on either ear lobe

To extract the EEG signals free from these artifacts, the raw signals were pre-processed in the MATLAB environment using an elliptical band pass filter of order 10 and bandwidth 4–32 Hz. The bandwidth of the filter is chosen as mentioned above since the required frequency bands are theta (4–7 Hz), alpha (8–12 Hz) and beta (13–32 Hz) that lie well within the chosen range.



**Fig. 2** Schematic representation of the stimulus

### 3 Feature Extraction

Five feature extraction techniques namely, power spectral density (PSD) [18, 19], Hjorth parameters, empirical mode decomposition (EMD), wavelet transform (WT) [20, 21], and the statistical parameters (STAT) [22, 23] of the wavelet coefficients have been employed to extract features from the preprocessed EEG signal.

### 4 Classification

Our ultimate goal is to classify the features extracted from the EEG signal related to various emotions into their respective classes with maximum attainable classification accuracy. For this job we have used three different classifiers (1) Linear Discriminant Analysis (LDA) [19, 22, 23], (2) Linear Support Vector Machine (LSVM) [22, 23] and (3) k-nearest neighbor (kNN) [22, 23].

### 5 Performance Analysis

Features were extracted from the preprocessed stimulated EEG signals that had been recorded from the subjects, using power spectral density (PSD), empirical mode decomposition (EMD), Hjorth parameters, statistical parameters, and wavelet coefficients. These features were then classified using LSVM (linear support vector machine), LDA (linear discriminant analysis), and kNN (k-nearest neighbor) classifies into the respective emotional states of neutral, happy, sad, and disgust. The overall classification results among all eight subjects for the four emotions using the

**Table 1** Classification accuracies of emotion classification

Emotions	Classifiers	Subjects								Classifier mean	Emotion mean
		01	02	03	04	05	06	07	08		
Neutral	LDA	84.5	80.23	76.7	77.43	80.6	77.07	73.0	74.61	78.05	81.65
	LSVM	83.18	84.88	78.5	78.56	88.4	80.07	77.9	81.86	81.67	
	kNN	84.87	86.77	82.6	82.87	92.4	81.67	81.7	88.56	85.2	
Happy	LDA	69.6	67.15	71.1	66.43	75.9	65.59	62.7	71.13	68.71	73.42
	LSVM	75.59	71.77	76.4	71.32	80.5	74.17	70.1	78.86	74.85	
	kNN	75.29	72.03	73.4	72.08	91.6	73.2	70.0	85.77	76.69	
Sad	LDA	75.31	70.93	71.2	69.44	77.0	63.59	66.4	75.51	71.18	76.20
	LSVM	82.03	78.34	77.3	73.72	81.7	74.74	72.5	81.02	77.68	
	kNN	80.71	79.63	72.9	74.45	91.7	75.53	73.6	89.37	79.75	
Disgust	LDA	67.51	67.97	69.8	65.21	84.0	72.5	64.6	79.60	71.42	74.96
	LSVM	74.95	72.47	77.0	69.55	83.1	75.91	70.7	80.71	75.56	
	kNN	75.92	71.39	75.5	70.52	96.1	74.43	71.2	88.15	77.91	

three classifiers and all the five features are enlisted in Table 1. For all the eight subjects, neutral emotional state is classified with an average classification accuracy of 81.65 %, highest among the four emotions under consideration. The negative emotions including sad and disgust have better average classification accuracy of 76.20 and 74.96 % than the positive emotion i.e., happy emotional state whose average classification accuracy is 73.42 %, being the lowest among the four emotions considered in this work. It is seen that with increase in average classification accuracy, the variance decreased. kNN proved to be classifying the emotional states from EEG signal better than LSVM followed by LDA when all the five features are considered together. Subject 05 showed the highest CAs with all the four emotions in all the different classifiers used. kNN was found out to be the most suitable classifier for emotion classification with the four emotions being classified from the stimulated EEG signals with an average classification accuracy of 76.6 %. Conclusively, A combination of PSD, Statistical features and kNN classifier is found to perform most efficiently for emotion classification.

## 6 Conclusion

This work presented a comparative study of classifying the different emotional states from the stimulated EEG signals. Recognition of the emotions elicited in different subjects with the usage of audio-visual stimuli has been a prerequisite for achieving our final goal of developing a complete emotionally adaptive intelligent system. Four emotions (viz. neutral, happy, sad, and disgust) were classified suitably by three classifiers (viz. LDA, LSVM, and kNN) from five extracted features

(viz. PSD, EMD, wavelet transforms, statistical parameters, and Hjorth parameters) of stimulated EEG signals. Performances of all the classifiers were compared and an overall classification accuracy of 76.6 % was found. PSD and statistical features were found to be better feature extractors among the other techniques used. kNN classified emotions with higher classification accuracy than the other classifiers when all the features are considered together.

With the utility of other modalities like speech, facial expressions etc., developing a multimodal emotion recognition system, that employs the emotional correlates of other physiological signals, research in the area can be extended further to develop an emotionally intelligent system lies.

## References

1. Chakraborty, A., Konar, A.: Emotional intelligence: a cybernetic approach, studies in computational intelligence. 1st (edn.), Springer, Hiedelberg (2009)
2. Cornelius, R.R.: Theoretical approaches to emotion. In: Proceedings of the ISCA Workshop on Speech and Emotion, Belfast (2000)
3. Pantic, M., Rothkrantz, L.J.M.: Toward an affect-sensitive multimodal human-computer interaction. In: Proceedings of the IEEE Invited Speaker, vol. 91, no. 9, September (2003)
4. Chanel, G., Kronegg, J., Grandjean, D., Pun, T.: Emotion assessment: arousal evaluation using EEG's and peripheral physiological signals. *Lect. Notes Comput. Sci.* vol. 4105, pp. 530 (2006)
5. Picard, R.W., Vyzas, E., Healey, J.: Toward machine emotional intelligence: analysis of affective physiological state. *IEEE Trans. Pattern Anal. Mach. Intell.* **23**(10), 1175–1191 (2001)
6. Jung, T.: Removing electroencephalographic artifacts by blind source separation. *J. Psychophysiol.* **37**, 163–178 (2000)
7. Gott, P.S., Hughes, E.C., Whipple, K.: Voluntary control of two lateralized conscious states: validation by electrical and behavioral studies. *Neuropsychologia* **22**, 65–72 (1984)
8. Murugappan, M., Rizon, M., Nagarajan, R., Yaacob, S., Zunaidi, I., Hazry, D.: EEG feature extraction for classifying emotions using FCM and FKM. *J. Comput. Commun.* **1**, 21–25 (2007)
9. Das S., Halder A., Bhowmik P., Chakraborty A., Konar A., Janarthan R.: A support vector machine classifier of emotion from voice and facial expression data. In: Proceedings of the IEEE 2009 World Congress on Nature and Biologically Inspired Computing (NaBIC 2009), Coimbatore, pp. 1010–1015 (2009)
10. Srinivasa, K.G., Venugopal, K.R., Patnaik, K.R.: Feature extraction using fuzzy C-means clustering for data mining systems. *Int. J. Comput. Scie. Netw. Secur.* **6**, 230–236 (2006)
11. Michael, S., Chambers J.A.: Brain computer interfacing. In: Proceedings of the EEG Signal Processing, pp. 239–265, Wiley, NJ (2007)
12. Lotte, F. et al.: A review of classification algorithms for EEG-based Brain-computer interfaces. *J. Neural. Eng.* **4**(2), (2007)
13. Rezaei, S., Tavakolian, K., Nasrabadi, A.M., Setarehdan, S.K.: Different classification techniques considering brain computer interface applications. *J. Neural. Eng.* **3**(2), 139–144 (Jun 2006)
14. Xu, W., Guan, C., Siong, C.E., Ranganatha, S., Thulasidas, M., Wu, J.: High accuracy classification of EEG signal. In: Proceedings of the 17th International Conference on Pattern Recognition (ICPR), vol. 2, 2004, pp. 391–394. Cambridge (2004)
15. Ledoux, J.: Brain mechanisms of emotion and emotional learning. *Curr. Opin. Neurobiol.* **2**, 191–197 (1992)
16. Davidson, R.I., Jackson, D.C., Kahn, N.H.: Emotion, plasticity, context, and regulation: perspectives from affective neuroscience. *Psychol. Bull.* **126**(6), 89–909 (2000)

17. Niemic, C.P.: Studies of emotion: a theoretical and empirical review of psychophysiological studies of emotion. *J. Undergrad. Res.* pp. 15–18 (2002)
18. Sanei, S., Chambers J.A.: Brain computer interfacing. In: *Proceedings of the EEG Signal Processing*, pp. 239–265, Wiley, NJ (2007)
19. Stoica, P., Moses, R.: *Introduction to spectral analysis*. Prentice Hall, NJ, USA (1997)
20. Proakis, J.G., Malonakis, D.G.: *Digital signal processing: principles, algorithm and applications*, 3rd (edn.), Prentice Hall, NJ, USA (1996)
21. Oppenheim, A., Schafer, R.: *Digital signal processing*. Prentice Hall, NJ, USA (1975)
22. Alpaydin, E.: *Introduction to machine learning*. MIT Press, Cambridge (2004)
23. Webb, A.R.: *Statistical pattern recognition*, 2nd edn. Wiley, Reprint (2004)



# Propagation Delay Analysis for Bundled Multi-Walled CNT in Global VLSI Interconnects

Pankaj Kumar Das, Manoj Kumar Majumder, B. K. Kaushik  
and S. K. Manhas

**Abstract** Multi-walled carbon nanotube (MWCNT) bundle potentially provided attractive solution in current nanoscale VLSI interconnects. This research paper introduces an equivalent single conductor (ESC) model for bundled MWCNT that contains a number of MWCNTs with different number of shells. A driver-interconnect-load (DIL) system employing CMOS driver is used to calculate the propagation delay. Using DIL system, propagation delay is compared for bundled CNT structures containing different number of MWCNTs. At global interconnect lengths, delay is significantly reduced for the bundled CNT containing more number of MWCNTs with lesser number of shells. It is observed that compared to the bundles containing lesser number of MWCNTs, the overall delay is improved by 9.89% for the bundle that has more number of MWCNTs.

**Keywords** Carbon nanotube (CNT) · Multi-walled CNT (MWCNT) · Propagation delay · Interconnect · Nanotechnology · VLSI

---

P. K. Das (✉) · M. K. Majumder · B. K. Kaushik · S. K. Manhas  
Microelectronics and VLSI Group, Department of Electronics and Computer Engineering,  
Indian Institute of Technology Roorkee, Roorkee 247667, India  
e-mail: pankaj\_jkd@yahoo.co.in

M. K. Majumder  
e-mail: manojbesu@gmail.com

B. K. Kaushik  
e-mail: bkk23fec@iitr.ernet.in

S. K. Manhas  
e-mail: samanfec@iitr.ernet.in

## 1 Introduction

In recent years, carbon nanotubes (CNT) have aroused a lot of research interest for their applicability as VLSI interconnects in future high speed electronics due to their extremely desirable electrical and thermal properties [1, 2]. CNTs have long mean free paths (MFPs) in the order of several micrometers that provide low resistivity and possible ballistic transport. CNTs are formally known as allotropes of carbon. They are made by rolling up graphene sheets in cylindrical form. Graphene is a monolayer sheet of graphite with  $sp^2$  bonding of carbon atoms arranged in honeycomb lattice structure. The  $sp^2$  bonding in graphene is stronger than  $sp^3$  bonds in diamond [2], making graphene the strongest material. CNTs have unique atomic arrangement as well as interesting physical properties that include large current carrying capability, long ballistic transport length, high thermal conductivity, and mechanical strength [1–3]. These remarkable properties make CNTs one of the most promising research materials for the future nanoscale technology. These extraordinary physical properties of CNTs make them exciting prospects for a variety of applications in the areas of microelectronics/ nanoelectronics, spintronics, optics, material science, mechanical, and biological fields [3, 4]. Particularly, in the area of nanoelectronics, CNTs and graphene nanoribbons (GNRs) show a lot of research interest in their applicability as energy storage (such as supercapacitors) devices, energy conversion devices (including thermoelectric and photovoltaic devices), field emission displays and radiation sources, nanometer semiconductor transistors, nano-electromechanical systems (NEMS), electrostatic discharge (ESD) protection, interconnects, and passives [1–4]. The unique physical properties are mainly due to the structure of CNTs that depends on the rolling up direction of graphene sheets. Depending on the number of rolled up graphene sheets, CNTs can be categorized as single-walled CNTs (SWCNTs) and multi-walled CNTs (MWCNTs).

MWCNTs have similar current carrying capabilities compared to metallic SWCNTs but are easier to fabricate than SWCNTs due to easier control of the growth process. In fact most of the CNT interconnect fabrication efforts have targeted multi-walled CNTs (MWCNTs) [5]. The typical diameter of SWCNT is about 1 nm and depending on its chirality, it can be either metallic or semiconducting [5, 6] in nature. MWCNT consists of several coaxial CNT shells and each shell can have different chirality depending on their rolled up direction. MWCNTs may have diameters in the range of a few to hundreds of nanometers. Initially, most experiments have indicated that only the outer shell in an MWCNT conducts. Recently, it has been confirmed that all shells can conduct if they are properly connected to contacts [6, 7]. Earlier experiments made contacts to outer shells only and the impact of inner shells is very small on overall conduction. This research paper analyzes the propagation delay for bundled MWCNT structures containing different number of shells. An equivalent single conductor (ESC) model is introduced to estimate the delay using driver-interconnect-load (DIL) system [7].

The paper is organized into four different sections. Section 1 provides details of the current research scenario and briefs about the works carried out. Section 2 describes

the geometry and ESC model of bundled MWCNT structure. Details of simulation setup and comparison of delay for different bundled MWCNT structures is discussed in Sect. 3. Finally, Sect. 4 concludes the paper.

## 2 Geometry and ESC Model of Bundled MWCNT

Consider the geometry of single and bundled MWCNT over ground plane as shown in Fig. 1. The diameters of MWCNT are considered as  $D_1, D_2, D_3, \dots, D_n$ , where  $D_1$  and  $D_n$  are the inner shell and outer shell diameters respectively.  $l$  is the nanotube length,  $S_i$  is intershell spacing, and  $H$  represents the distance between center of MWCNT and ground plane. It is assumed that the spacing between each shell is fixed, while diameter of outermost nanotube can change over a fixed interval. For current fabrication technology, intershell spacing  $S_i$  can be formulated as [6–8]

$$S_i = \frac{D_n - D_{n-1}}{2} \approx 0.34 \text{ nm} \tag{1}$$

Bundled MWCNT with width  $w$  and height  $h$  contains a number of MWCNTs with spacing of  $S_p$  as shown in Fig. 1b. The total number of metallic MWCNTs in bundle can be formulated as

$$N_{MWCNT} = \beta [N_h N_w - (N_h/2)] \tag{2}$$

where  $N_w$  and  $N_h$  are the number of MWCNTs in bundle at horizontal and vertical directions respectively. The center to center distance between adjacent MWCNTs in bundle can be expressed using the cross-section of bundle (Fig. 1b)

$$S_p = S_i + D_n \tag{3}$$

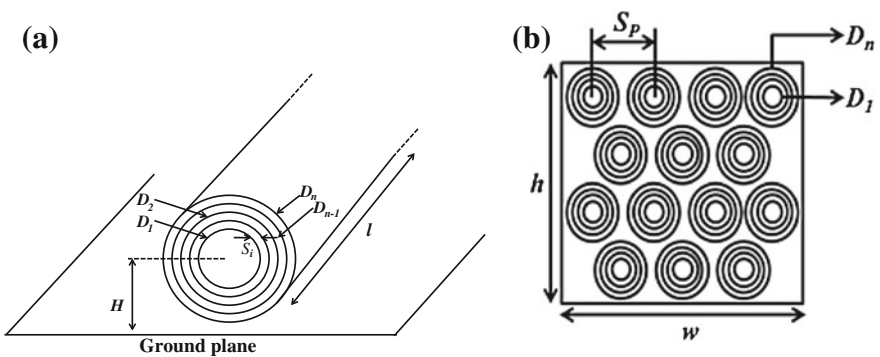


Fig. 1 Geometry of **a** single and **b** bundled MWCNT

where  $S_i = 0.34 \text{ nm}$  [7] is the spacing between MWCNTs in bundle that depends on the Vander Waals gap [8, 9]. Based on the geometry, ESC model of bundled MWCNT is presented in Fig. 2b that is simply developed on the basis of multi-conductor transmission line as shown in Fig. 2a.

For the ESC model, it is assumed that all the shells of MWCNTs are properly contacted. Assuming the metallic to semiconducting tube ratio as  $\beta$ , the approximate number of conducting channels per shell is given by [10]

$$N_{channel/shell}(d) \approx (ad + b)\beta, d > 4 \text{ nm}$$

$$\approx 2\beta, d < 4 \text{ nm} \tag{4}$$

where  $a = 0.1836 \text{ nm}^{-1}$  and  $b = 1.275$  [10]. Typical value of  $\beta$  can be defined as 1/3 for an MWCNT bundle [10]. The number of conducting channels per shell in any given shell  $j$  varies with respect to the shell diameter.

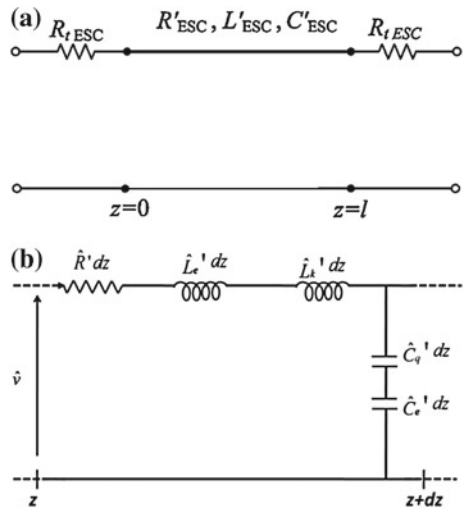
The ESC model of Fig. 2 exhibits *p.u.l.* resistance, capacitance, and inductances that can be expressed as [8–10]

$$\hat{R}' = \left[ \sum_{j=1}^s (2n_j/R') \right]^{-1} = R'/2n_{tot} \tag{5}$$

$$\hat{L}'_e = L'^{s, s}_e \text{ and } \hat{L}'_k = \left[ \sum_{j=1}^s (1/L'^{j, j}_k) \right]^{-1} = L'_k/2n_{tot} \tag{6}$$

$$C'_e = C'^{s, s}_e \text{ and } \hat{C}'_q \approx 2n_{tot}C'_q \tag{7}$$

**Fig. 2 a** Basic transmission line and **b** ESC model of MWCNT bundle interconnects



where  $n_{tot}$  is the total number of conducting channels in MWCNT that can be presented as

$$n_{tot} = n_1 + n_2 + \dots + n_j + \dots + n_s \tag{8}$$

Using the equations from (5–8), it is observed that the interconnect parasitics such as resistance, inductance and capacitance primarily depends on the number of MWCNTs in bundle and can be expressed as [8, 11]

$$L'_k = h/2e^2v_F, C'_q = 2e^2/hv_F, R' = h/2e^2v_F\tau \tag{9}$$

where  $v_F = 8 \times 10^5$  m/s is the Fermi velocity and  $\tau$  is the diffusion time of CNT. Apart from this, the ESC model considers terminal contact resistance  $R_{cj}$  of the  $j$ th shell of MWCNT [8]. This resistance accounts the effect of voltage drop at the metal-nanotube interface.

### 3 Performance Analysis

Propagation delay is compared using DIL system as shown in Fig. 3. A CMOS driver with supply voltage  $V_{dd} = 1V$  is used for accurate estimation of delay. The ESC model of bundled MWCNT represents interconnects line in the bus architecture. The interconnect line ranging from length 100 to 1,000  $\mu m$  is terminated by a load capacitance  $C_L$  of 10 aF [7].

Using the above-mentioned setup, propagation delay is compared for different bundled MWCNT structures. Figure 4 presents the variation of delay at different interconnect lengths. It is observed that the delay increases with interconnect lengths, whereas it reduces for the bundle containing more number of MWCNTs. The reason is that the delay primarily depends on interconnect parasitic such as resistance and capacitance that reduces for higher number of MWCNTs in bundle. With smallest value of parasitic associated, the bundle containing MWCNTs of four shells results in smaller delay as compared to other bundled MWCNTs that are presented in Fig. 5. Finally, Table 1 summarizes the percentage improvement in delay for the bundle containing MWCNTs of four shells that shows an overall improvement of 7.93 % compared to other bundles.

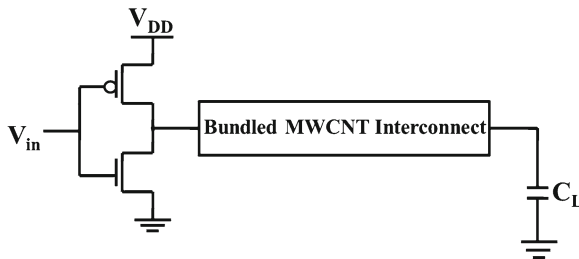


Fig. 3 Simulation setup for bundled MWCNT interconnects using DIL system

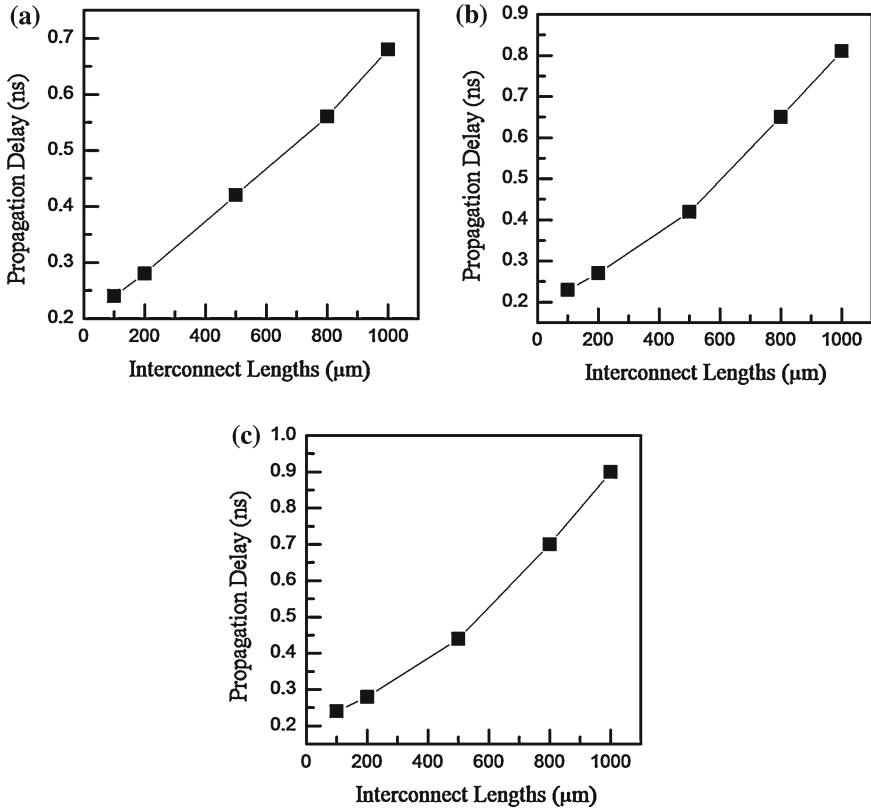
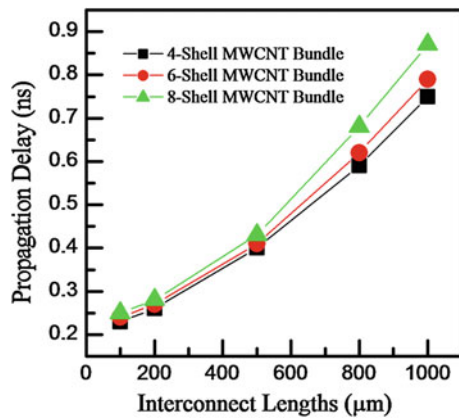


Fig. 4 Propagation delays for bundled CNTs containing a 4, b 6, c 8-shell MWCNTs

Fig. 5 Propagation delay with varying interconnect lengths for different bundled MWCNTs



**Table 1** Percentage improvement in delay *w.r.t.* 8-shell bundled MWCNT

Interconnect lengths ( $\mu\text{m}$ )	Bundle with MWCNT shell = 4	Bundle with MWCNT shell = 6
100	5.00	4.00
200	6.98	5.57
500	8.14	7.65
800	13.23	8.82
1,000	15.79	9.19

### 4 Conclusion

This research paper presents a comparative analysis between bundled CNT containing MWCNTs with different number of shells. Based on the number of shells and conducting channels, a generalized ESC model has been developed that primarily follows basic transmission line theory. Using the ESC model, propagation delay has been evaluated with the help of DIL system at different global interconnect lengths. It has been observed that the bundle containing more number of MWCNTs exhibits significant improvement in delay compared to other bundle structures. Therefore, from fabrication point of view, it is desirable to use a bundle containing lesser number of shells for future global VLSI interconnects.

### 5 Biography



**Pankaj Kumar Das** received his B. Tech degree in Electronics and Communication Engineering from SLIET, Longowal in the year of 2006. Currently, he is

working towards his M.Tech in Microelectronics and VLSI group at Indian Institute of Technology, Roorkee.

Since 2006, he has been served as Assistant Professor at Department of Electronics and Communication Engineering, Sant Longowal Institute of Engineering and Technology, Longowal. He has received best faculty and research award during his services. He has published more than five papers in national and international conferences. His current research area includes microelectronics-based VLSI circuits, circuit modeling, and analysis of carbon naotubes and nanowires.



**Manoj Kumar Majumder** (SM'11) received his B. Tech and M. Tech in the year of 2007 and 2009, respectively. Currently, he is working towards his Ph.D. in Microelectronics and VLSI group at Indian Institute of Technology, Roorkee.

From 2009 to 2010, he was associated with academic activities in electronics department in Durgapur Institute of Advanced Technology and Management (DIATM), West Bengal, India. His current research interest is Carbon Nanotube-based VLSI interconnects and circuit modeling. He has published more than 35 research papers in various international journals and conferences.

Mr. Majumder has obtained Graduate Aptitude Test Engineering (GATE) fellowship in 2007 and MHRD fellowship in 2010.





**Brajesh Kumar Kaushik** (M'10) received his Ph.D. in 2007 from Indian Institute of Technology, Roorkee.

In 1998, he joined as a lecturer at G.B.Pant Engineering College Pauri Garhwal, where he served as Assistant Professor till 2009. Since 2009, he has been working as Assistant Professor in VLSI group at IIT Roorkee. His current research area includes Electronic simulation, Low power VLSI Design. He has published more than 150 research papers in various international journals and conferences.

Dr. Kaushik has received many awards and recognitions from IBC, Cambridge such as top 100 scientists in World-2008 and International Educator of 2008.



**Sanjeev Kumar Manhas** (M'00) received his Ph.D. in 2003 from De Montfort University, Leicester UK.

In August, 2007 he joined the Indian Institute of Technology, Roorkee where he has served as Assistant Professor till now. His current research area includes silicon nanowire-based circuit design, parasitic evaluation and fabrication technologies, MOSFET modeling and reliability, DRAM leakage mechanism and refresh, VLSI technologies and OTFTs. He has both academic and industrial experience.

Dr. Manhas has received many academic awards such as Microelectronics best paper award in 2002, graduate merit award in 1991, and Indian National Research Scholarship award in 1993.

## References

1. Li, H., Xu, C., Srivastava, N., Banerjee, K.: Carbon nanomaterials for next-generation interconnects and passives: physics, status and prospects. *IEEE Trans. Electron. Devices* **56**(9), 1799–1821 (2009)
2. Javey, A., Kong, J.: *Carbon Nanotube Electronics*. Springer, New York (2009)
3. Majumder, M.K., Pandya, N.D., Kaushik, B.K., Manhas, S., K.: Analysis of crosstalk delay and area for MWNT and bundled SWNT for global VLSI interconnects. In: *Proceedings of the 13th IEEE International Symposium on Quality Electronic Design (ISQED 2012)*, pp. 291–294, Santa Clara (2012)
4. Avorious, P., Chen, Z., Perebeions, V.: Carbon-based electronics. *Nat. Nanotechnol.* **2**(10), 605–613 (2007)

5. Yu, M.F., Lourie, O., Dyer, M.J., Moloni, K., Kelly, T.F., Ruoff, R.S.: Strength and breaking mechanism of multiwalled carbon nanotubes under tensile load. *Science* **287**(5453), 637–640 (2000)
6. Naeemi, A., Meindl, J.D.: Compact physical models for multiwall carbon nanotube interconnects. *IEEE Electron. Device Lett.* **27**(5), 338–340 (2006)
7. Majumder, M.K., Pandya, N.D., Kaushik, B.K., Manhas, S.K.: Analysis of MWCNT and bundled SWCNT interconnects: impact on crosstalk and area. *IEEE Electron. Device Lett.* **33**(8), 1180–1182 (2012)
8. Sarto, M.S., Tamburrano, A.: Single-conductor transmission-line model of multiwall carbon nanotubes. *IEEE Trans. Nanotechnol.* **9**(1), 82–92 (2010)
9. Amore, M.D., Sarto, M.S., Tamburrano, A.: Fast transient analysis of next-generation interconnects based on carbon nanotubes. *IEEE Trans. Electromagn. Compat.* **52**(2), 496–503 (2010)
10. Subash, S., Kolar, J., Chowdhury, M.H.: A new spatially rearranged bundle of mixed carbon nanotube as VLSI interconnection. *IEEE Trans. Nanotechnol.* **7**, 1–10 (2011)
11. Burke, P.J.: Luttinger liquid theory as a model of the gigahertz electrical properties of carbon nanotubes. *IEEE Trans. Nanotechnol.* **1**(3), 129–144 (2002)

# Improvement in Radiation Parameters Using Single Slot Circular Microstrip Patch Antenna

Monika Kiroriwal and Sanyog Rawat

**Abstract** This paper investigates a new geometry of circular microstrip patch antenna using rectangular slot which can be used for WLAN and Wi-Max application. This geometry obtained bandwidth enhancement upto 9.58 % in comparison with conventional design and there is also improvement in other radiation parameters like gain, efficiency and return loss. For entire bandwidth the radiation pattern is stable and uniform.

**Keywords** Bandwidth · Circular microstrip patch antenna · Return loss · Coaxial probe feed · Radiation pattern

## 1 Introduction

Microstrip antennas are the most rapidly developing field in the last 20 years [1]. At present use of microstrip antennas are increasing day by day in wireless communication due to their low profile structure and also other advantage of low cost, light weight, ease of fabrication [2], conformable to mounting surface and being integrated in active devices [3]. Microstrip patch antenna may be square, rectangular, circular, elliptical, triangular and other desired configuration [4]. Coaxial probe fed microstrip antennas provide excellent isolation between the feed network and the radiating elements and yield very good front to back ratios [5]. Among the conventional microstrip antenna geometries, circular microstrip antenna is most widely analyzed antenna due to easy modeling and applicable boundary conditions [6]. The major drawback of circular microstrip patch antenna is narrow bandwidth and low gain especially at lower microwave frequencies [7]. Drawbacks which are responsible for the limited application in consumer world and it was realized that after doing

---

M. Kiroriwal (✉) · S. Rawat  
ASET, Amity University Rajasthan, Rajasthan, India  
e-mail: m.kiroriwal@rediffmail.com

some changes in the geometry of the conventional patch, these limitations may be removed [8]. To overcome this limitation, one of the methods is to cut slots in various shapes. For example in circular patch antenna bandwidth was increased up to 4.13 % of a skimmer shaped circular microstrip patch antenna [9] and in another example bandwidth is improved by 2.3 times of the conventional antenna bandwidth (1.4 %) using slots in circular microstrip patch antenna [10].

In this paper geometry is simulated using electromagnetic simulator, Zealand IE3D software [11]. This software works on method of moment. This circular microstrip patch antenna has good thermal, emissivity and mechanical properties: light weight, low profile, robust and it is easily constructed and it comes under the second band (5.15–5.825GHz) of IEEE802.11 WLAN and high band (5.25–5.85 GHz) of Wi-Max application. The Sect. 2 comprises of antenna geometry and in the Sect. 3 of this paper simulated and measured results are discussed followed by conclusion in the Sect. 4.

## 2 Antenna Configuration

Here conventional circular patch microstrip antenna is considered the reference antenna to compare the results of that simulated from single slot circular patch antenna.

### 2.1 Antenna Design

The geometry of the proposed antenna structure is shown in Fig. 1a. The patch has the diameter of 14 mm. A  $50 \Omega$  coaxial probe is used to connect the microstrip patch at coordinates and it is made fixed for both the conventional and the single slot circular microstrip patch antenna. The dimension of single slot is 0, –4 mm with 8 mm length and 2.75 mm width. Impedance bandwidth of about 9.38 % can be obtained from the above geometry.

### 2.2 Antenna Prototype

For validation of the proposed antenna geometry is fabricated as shown in Fig. 1b, on a supporting substrate FR4 with dielectric constant,  $\epsilon_t = 4.4$  and the thickness of the substrate,  $h = 1.59$  mm. Many simulations are done for optimizing the length; width and location of the slot and best result are obtained with defined length and width of the slot. Due to existence of the slot, the current distribution changed and another mode is excited, each mode has its own cut off frequency, so modified geometry has a new resonant frequency, which is less than the conventional patch resonant frequency.

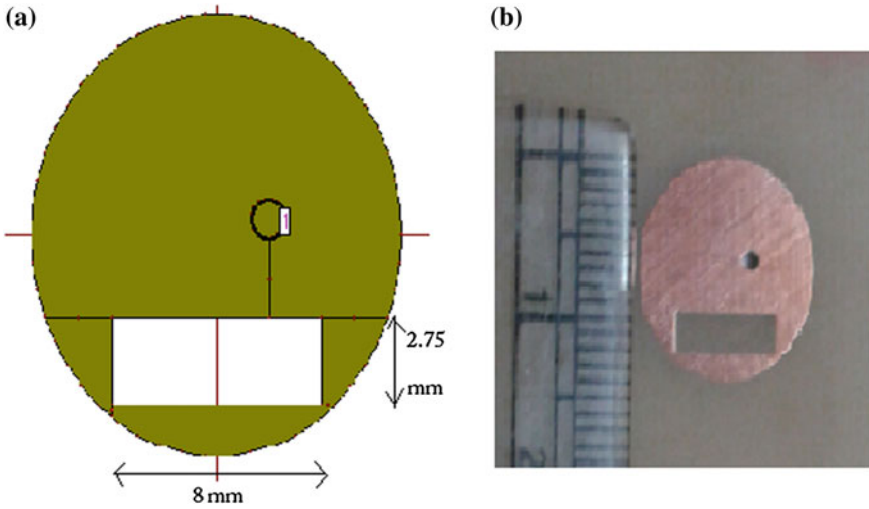


Fig. 1 a Proposed geometry of *circular* microstrip patch antenna. b Fabricated antenna prototype

### 3 Simulated and Measured Results

#### 3.1 Return Loss and Bandwidth

Return Loss is a measure of how much power is delivered from the source to a load and measured by  $S_{11}$  parameters. Bandwidth is the range of frequencies over which the antenna can operate effectively. Bandwidth can be calculated by going 10 dB down in return loss.

As shown in Fig. 2 simulated return loss of the single slot circular microstrip patch antenna is  $-38.3067$  dBi at resonating frequency 5.32 GHz and from the return loss curve the simulated bandwidth obtained is 9.38 % and measured bandwidth is 9.58 % with  $-35$  dBi return loss.

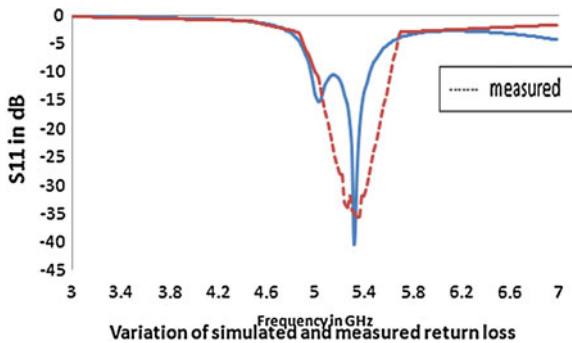


Fig. 2 Measured and simulated return loss for proposed *circular x* microstrip patch antenna

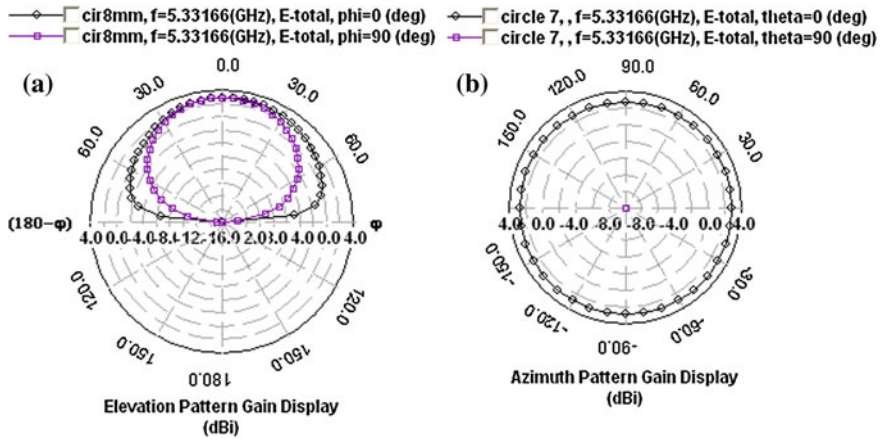


Fig. 3 a Computed elevation radiation pattern. b Azimuth radiation pattern for proposed circular microstrip patch antenna

### 3.2 Radiation Pattern

A plot through which it is visualizes where the antenna transmits or receives power. The microstrip antenna radiates normal to its patch surface. So, the elevation pattern for  $\phi = 0$  and  $\phi = 90$  degrees are important for the simulation. The simulated elevation and azimuth radiation pattern of proposed antenna is illustrated in Fig. 3a and b. Elevation radiation pattern is smooth and uniform over the band of frequencies and azimuth radiation pattern is omni directional.

### 3.3 Smith Chart

Smith Chart provides the information about polarization and the impedance match of the radiating patch. Figure 4 shows the smith chart for proposed antenna and the input impedance of  $49.68 \Omega - j2.129$  at resonant frequency 5.32 GHz. This smith chart shows that the antenna is circularly polarized with some impurity.

### 3.4 Gain

Gain is basically measure of the effectiveness of a directional antenna as compared to a standard non-directional antenna. The gain observed for the proposed circular patch antenna is shown in Fig. 5. The gain is found to be uniform over the whole the frequency band Tables 1 & 2.



**Table 1** Variation in antenna parameters with slot area

Sr. no.	Slot area (mm) <sup>2</sup>	Resonant frequency (GHz)	Return loss (dBi)	Gain (dBi)	Band-width (%)	Efficiency (%)
1.	20	5.45	-32.01	2.85	7.9	42.26
2.	20.3	5.30	-31.61	2.67	8.1	40.66
3.	20.54	5.35	-35.77	2.81	9.1	41.91
4.	22	5.32	-38.30	2.75	9.38	41.45
5.	24	5.31	-35.98	2.73	8.8	41.21

**Table 2** Comparison of conventional and proposed antenna

Sr.no.	Patch antenna	Resonant frequency (GHz)	Return loss (dBi)	Gain (dBi)	Band-width (%)	Efficiency (%)
1.	Conventional patch antenna	5.48	-27.43	1.28	2.53	29.99
2.	Proposed antenna	5.32	-35	2.75	9.58	41.45

## 4 Conclusion

In this paper, the radiation performance of single slot circular microstrip patch antenna is simulated by applying IE3D full-wave electromagnetic simulator and results are compared with conventional circular patch antenna. Using optimization it is observed that as we increase the slot area there is a decrement in the resonant frequency. Measured results indicate that the antenna exhibits bandwidth up to 9.56% by optimizing the length and width of the slot in antenna geometry. There is also improvement in radiation characteristics like gain 2.75 dBi and efficiency 41.45%. In radiation pattern, the direction of maximum radiation is normal to the patch geometry and also found to be stable over the entire bandwidth.

## References

1. El Aziz D.A., Hamad, R.: Wideband circular microstrip antenna for wireless communication Systems. 24th National Radio Science Conference (NRSC), Egypt, pp. 1–8 (2007)
2. sfahlani, S.H.S., Tavakoli, A., Dehkhoda, P.: A compact single layer dual-band microstrip antenna for satellite application. *IEEE Antennas Wirel. Propag. Lett.* **10**, 931–934 Piscataway, USA (2011)
3. Constantine A. B.: *Antenna Theory: Analysis and Design*. 3rd edn, Wiley, (ed.) New York May (2005)
4. Garg, R., Bhartia, P., Bhal, I.J., Ittipiboon, A.: *Microstrip antenna design book*. Artech House, New York (2001)
5. Pozar, D.M.: Microstrip antennas. In: *IEEE Proceedings* **80**, 79–91 (1992)



6. Surmeli, K., Turetken, B.: U-Slot stacked patch antenna using high and low dielectric constant material combination in S- Band. General Assembly and Scientific Symposium, URSI, Hiroshima pp. 1–4 (2011)
7. Singh, J., Singh, A.P., Kamal, T.S.: Design of circular microstrip antenna using artificial neural networks. In: Proceedings of the World Congress on Engineering, Vol 2, U.K. (2011)
8. Wong, K.L.: Compact and broadband microstrip antenna. John Wiley & Sons, New York (2002)
9. Ryu, M.R., Woo, J. M., Hu, J.: Skimmer shaped linear polarized microstrip antennas for miniaturization. International Conference on Advance Communication Technology, Vol. (1) pp. 758–762 (2006)
10. Wu, J. W., Jui H. L.: Slotted circular microstrip patch antenna for bandwidth enhancement. IEEE Proceeding Microwave Antennas Propagation, Vol. 2, pp. 272–275 (2003)
11. Huang, C. Y., Wu, J. Y., Wong, K.: LIE3D Software, Release 14.65 (Zeland Software Inc. Fremont, USA), April (2010)

# A $\Pi$ - Slot Microstrip Antenna with Band Rejection Characteristics for Ultra Wideband Applications

Mukesh Arora, Abha Sharma and Kanad Ray

**Abstract** Federal Communications Commission (FCC) revealed that a bandwidth of 7.5 GHz from 3.1 to 10.6 GHz is for Ultra Wideband (UWB) wireless communication. UWB is a rapidly advancing technology for high data rate wireless communication. The main challenge in UWB antenna design is achieving the very broad impedance bandwidth with compactness in size. The proposed antenna has the capability of operating between 1.1 and 11.8 GHz. In this paper, a rectangular patch antenna is designed with truncated corners at the ground as well as at the patch. A  $\Pi$ -shaped slot is cut out from the patch to get the complete UWB. After that two equal size of slits on sides of the  $\Pi$  shape are cut out from the patch which dispends the WLAN. The proposed antenna uses Rogers RT/duroid substrate with a thickness of 1.6 mm and relative permittivity of 2.2. The aperture coupled feed is used for excitation. The proposed antenna is simulated using HFSS 11 software.

**Keywords** Microstrip patch antenna · Ultra wide band · Dispend band · Aperture coupled feed · I slot · WLAN

## 1 Introduction

The UWB technology is one of the most demanding technologies which provides high data rate transmission. The FCC approved rules for the commercial use of UWB in 2002. UWB uses the unlicensed spectrum from 3.1 to 10.6 GHz allocated

---

M. Arora  
Department of Electronics and Communication, SKIT, Jaipur, Rajasthan, India

A. Sharma  
Department of Electronic and Communication, GCT, Jaipur, Rajasthan, India

K. Ray (✉)  
Institute of Engineering and Technology, JKLakshmiapat University, Jaipur, Rajasthan, India  
e-mail: kanadray@jklu.edu.in

by FCC [1, 2]. The FCC allocated a bandwidth of 7.5 GHz from 3.1 to 10.6 GHz for UWB applications. Low-cost UWB antennas are required for various applications such as wireless communications, medical imaging, parking radars, and other military applications and indoor positioning. It has many advantages over conventional wireless communication technology such as low power consumption, high speed transmission, and large impedance bandwidth. But within this range some other licensed narrowband systems exist for which the UWB causes the potential interference. Systems like WLAN for IEEE 802.11/a/b/g operate in 5.15–5.35 GHz and 5.725–5.825 GHz. This band interferes with the UWB system, so it is desirable to remove this band from ultra wideband [3]. In order to improve coexistence of UWB with other wireless standards, research has been done to devise mechanisms to reject certain bands within the pass band of the UWB [4].

One common and simple way to achieve this function is cutting a slot on the patch [5]. This slot adds an extra path to the antenna's current, eventually introducing, an additional resonance circuit. As the resonance frequency of the slot depends on its position and dimensions one can optimize them so that the rejected band can be adjusted to cover the WLAN band. But often it is difficult to achieve sharp and narrow stop band while the interference signals have narrow bandwidth usually.

According to Shannon- Nyquist criterion,

$$C = \mathcal{C} B \log_2 [1 + \text{SNR}] \text{ bits/sec.}$$

where  $C$  is the maximum transmission data rate,  $B$  denotes bandwidth of the channel, and  $\text{SNR}$  stands for the Signal-to-Noise ratio. The maximum achievable data rate or capacity for the ideal band limited additive white Gaussian noise (AWGN) channel is related to the bandwidth and the signal-to-noise ratio [6]. From above principle, the transmit data rate can be increased either by enhancing the bandwidth or transmission power. Since many portable devices are battery operated, the power cannot be easily increased, so a large frequency bandwidth is a better solution to achieve a high data rate.

Aperture coupled microstrip antenna couples patch to the feed line through a slot. In this technique the radiating microstrip patch element is etched on the top of the antenna substrate, and the microstrip feed line is etched on the bottom of the feed substrate [7] (Fig. 1).

In this paper, a compact microstrip patch antenna with band-rejection characteristics for UWB application is proposed. First, the ground as well as patch is truncated at all its four corners, which reduced the size of the antenna. Second, a  $\square$ -shaped slot is cut out from the patch which gives the continuous frequency band from 1.12 to 10.86 GHz covering the entire ultra wideband. To improve upon the sharpness of stop band we explore the combination of slots with the insertion of slits on the patch (another conventional method). After that two equal-sized rectangular slits are cut out on the sides of the  $\square$  shape in the patch which notches the band from 5.07 to 5.84 GHz covering the WLAN band. By removing this band from UWB, a major problem of interference associated with UWB band is resolved. The performance characteristics of the proposed antenna are simulated using HFSS 11 software.

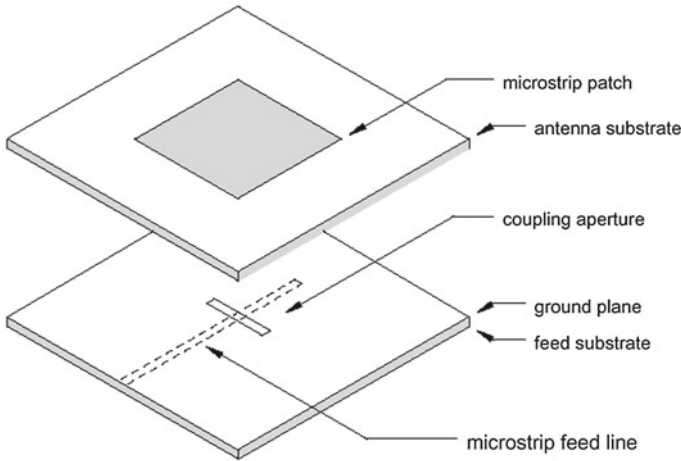


Fig. 1 Microstrip antenna with aperture coupled feed [8]

Table 1 Antenna dimension of Fig. 2

Length of trunk corner in ground (L1)	5.3 mm
Width of trunk corner in ground (W1)	5.7 mm
Length of trunk corner in ground (L2)	6.65 mm
Width of trunk corner in ground (W2)	7.4 mm
Length of trunk corner in patch (L3)	3 mm
Width of trunk corner in patch (W3)	3 mm
Length of trunk corner in patch (L4)	3 mm
Width of trunk corner in patch (W4)	4 mm

## 2 Antenna Geometry and Design

In this design, a Substrate of Rogers RT/duroid of relative permittivity 2.2 is used to design the antenna. The substrate dimension is  $22.8 \times 26.6 \times 1.6$  mm. A rectangular patch is used with dimensions of  $13.2 \times 17$  mm. The ground and patch is truncated at all its four corners. The aperture coupled feed is used for excitation. The geometry of proposed antenna is discussed in Table 1. The designed patch antenna is shown in Fig. 2.

## 3 Measured Results

The measured return loss is shown in Fig. 3 while the VSWR plot and radiation pattern are shown in Figs. 4 and 5. The measured return loss plot shows that there one resonant frequency band from 1.08 to 8.42 GHz with return loss of  $-43.72$  dB. The measured VSWR is also less than 2.

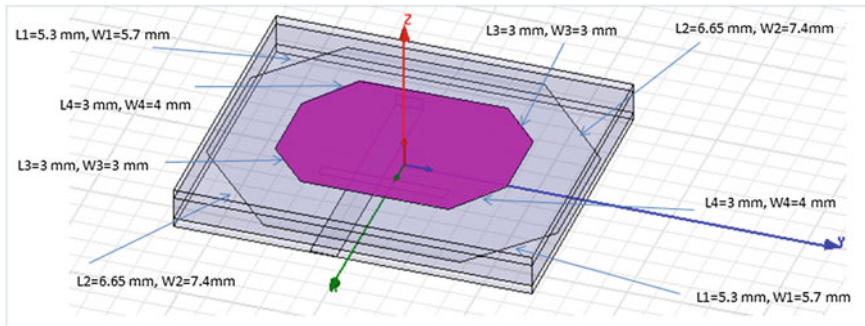


Fig. 2 Geometry of the antenna

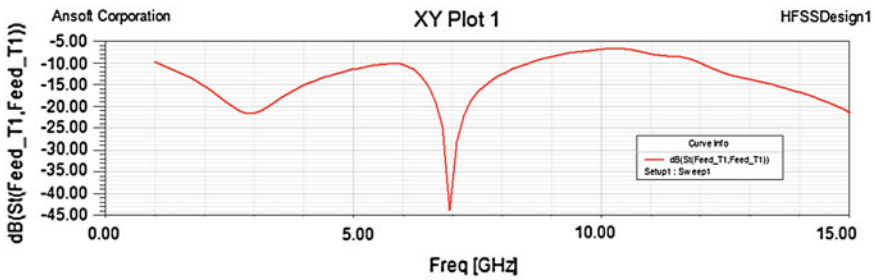


Fig. 3 Simulated return loss  $S_{11}$  V/s frequency

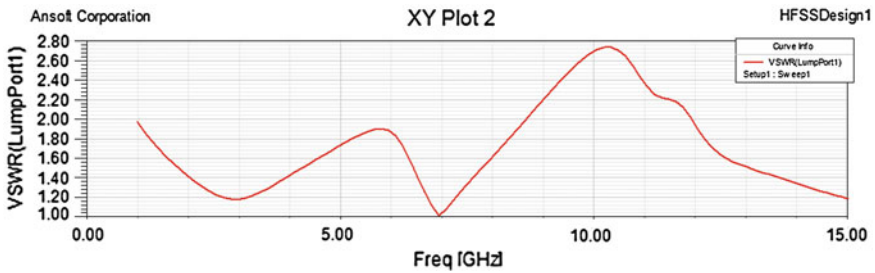


Fig. 4 The measured VSWR

### 4 UWB Antenna Geometry and Design

In this design, a  $\Pi$ -shaped slot is cut out from the truncated patch. This  $\Pi$ -shaped slot gives frequency band from 1.12 to 10.86 GHz which covers the entire UWB band. The dimensions of substrate and patch are the same as that used in the previous design. The geometry is shown in Fig.6. The dimensions of I slot are shown in Table 2.

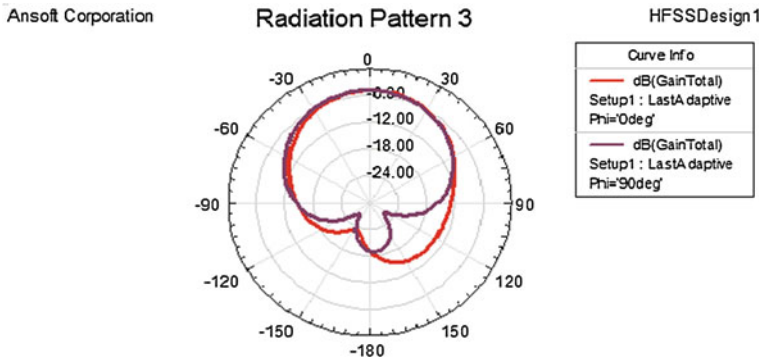


Fig. 5 Radiation pattern

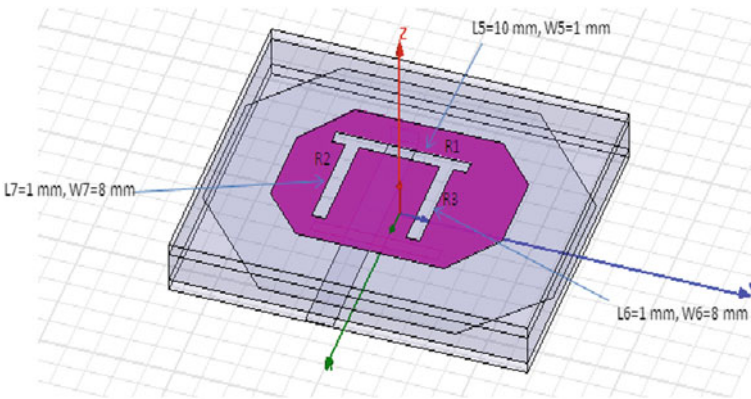


Fig. 6 Geometry of the antenna

Table 2 Antenna dimension of Fig. 6

Length of R1	10 mm
Width of R1	1 mm
Length of R2	1 mm
Width of R2	8 mm
Length of R3	1 mm
Width of R3	8 mm

## 5 Measured Results

The return loss plot gives the impedance bandwidth of 162.57% from 1.12 to 10.86 GHz which is less than -10 dB as shown in Figs. 7, 8 and 9 show the VSWR plot and radiation pattern for the proposed antenna.

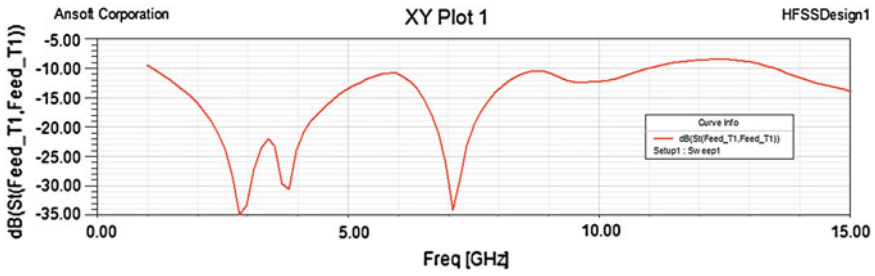


Fig. 7 Simulated return loss  $S_{11}$  V/sfsfrequency

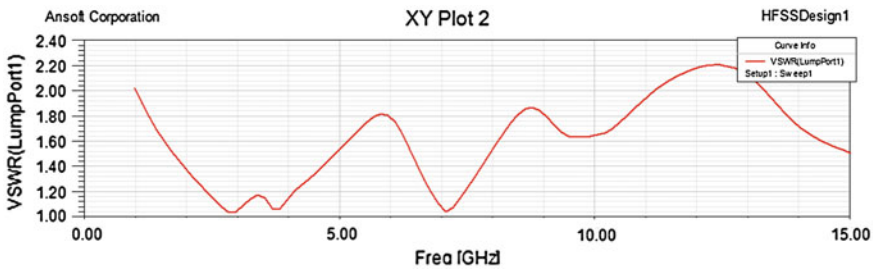


Fig. 8 The measured VSWR

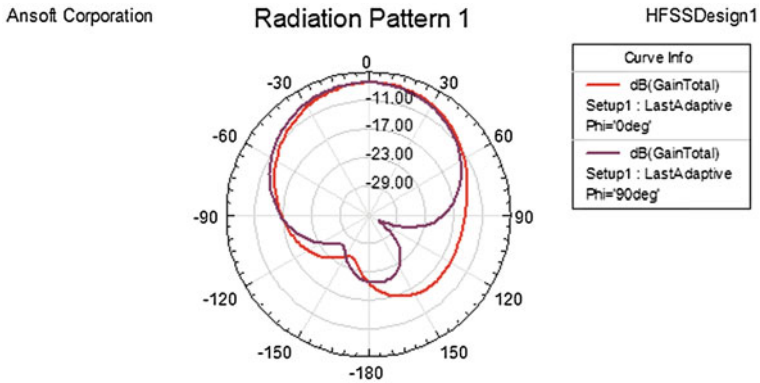


Fig. 9 Radiation pattern for UWB antenna

Figures 10, 11 and 12 show the current distributions at 3, 7, and 10 GHz frequencies respectively.

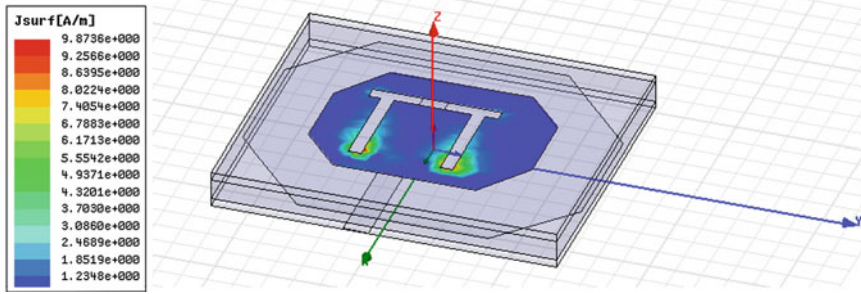


Fig. 10 Current distribution at 3 GHz

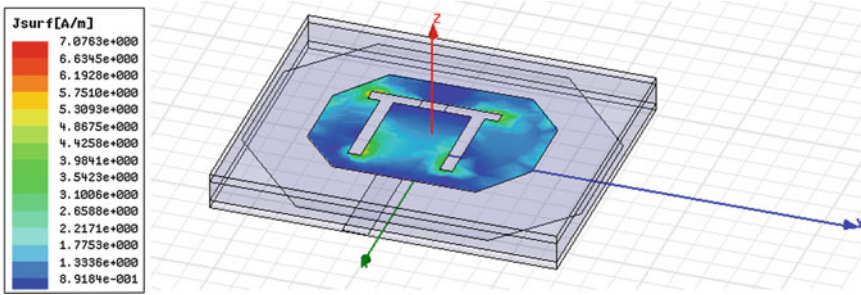


Fig. 11 Current distribution at 7 GHz

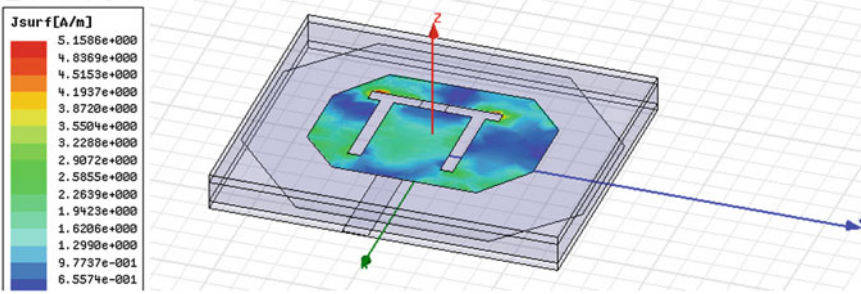


Fig. 12 Current distribution at 10 GHz

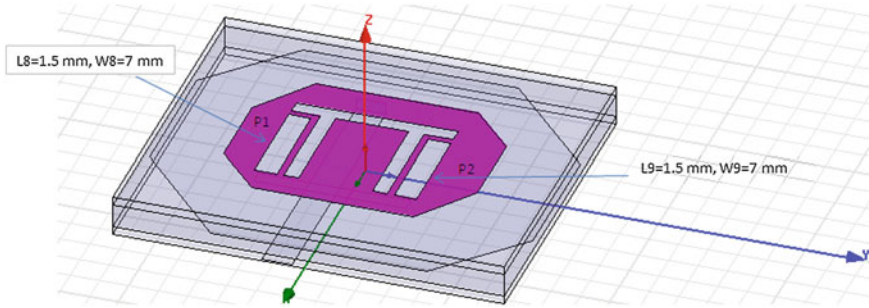
## 6 UWB Antenna with Band Notch

We have simulated and observed earlier that a  $\Pi$ -shaped slot cut out from the truncated patch gives a continuous band from 1.12 to 10.86 GHz covering the complete UWB. In this design we introduced two symmetric-sized rectangular slits P1 and P2. It depends a band from 5.07 to 5.84 GHz which covers WLAN. By removing

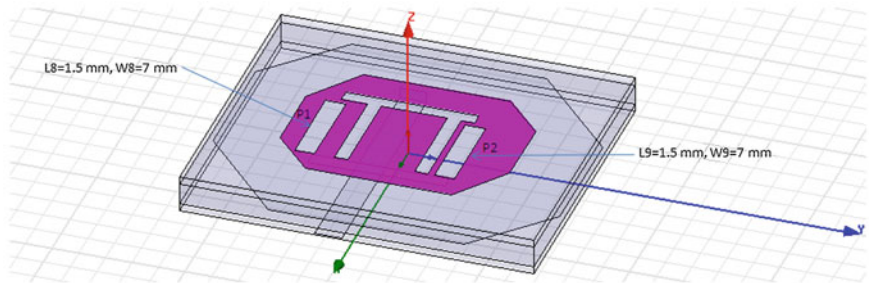


**Table 3** Antenna dimension of Fig. 13

Length of Rectangular Slit P1	1.5 mm
Width of Rectangular Slit P1	7 mm
Length of Rectangular Slit P2	1.5 mm
Width of Rectangular Slit P2	7 mm



**Fig. 13** Geometry of Notched UWB antenna



**Fig. 14** Geometry of completely WLAN dispended Notched UWB antenna

WLAN band from UWB band, interference problem associated with UWB band is resolved. The dimensions of rectangular slits are shown in Table 3.

In Fig. 13, two rectangular slits equidistant from  $\Pi$  slot are introduced. These rectangular slits at the present positions do not remove the band which covers the complete WLAN band, by properly optimizing them we have obtained a complete UWB —without WLAN band which resolves the interference problem. The completely WLAN dispended microstrip antenna is shown in Fig. 14.

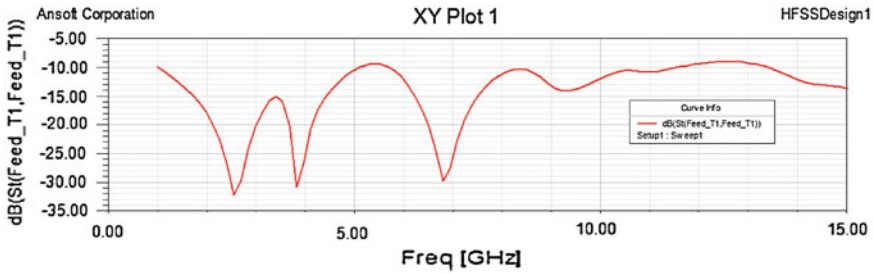


Fig. 15 Simulated return loss  $S_{11}$  V/S frequency

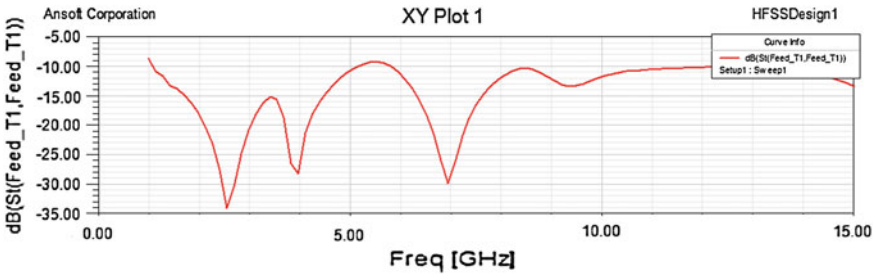


Fig. 16 Simulated return loss  $S_{11}$  V/S frequency

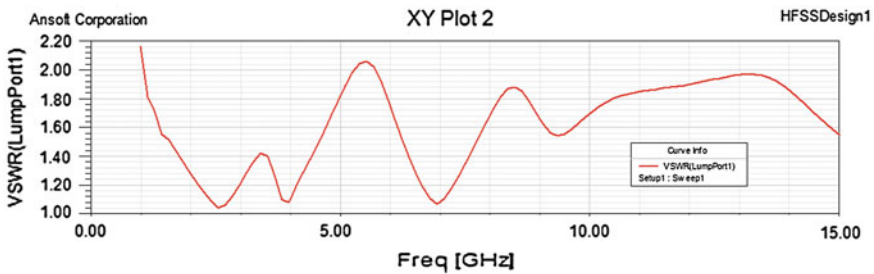
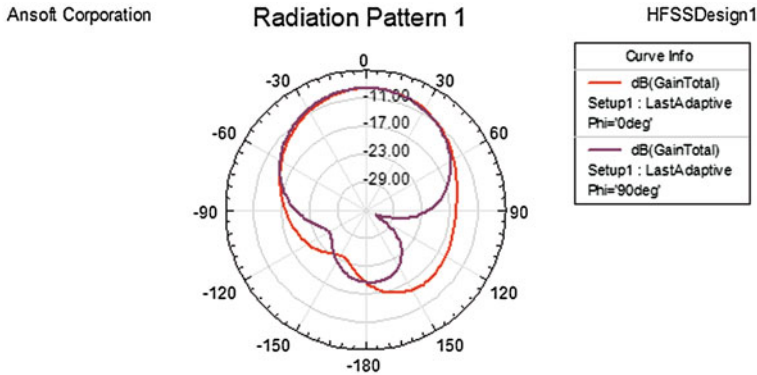


Fig. 17 Measured VSWR for UWB antenna

## 7 Measured Results

In the return loss plot shown in Fig. 15, two resonant bands exist. First, frequency band existing from 1.02 to 5.05 GHz resulted in impedance bandwidth of 132.81 % and another band— from 5.72 to 11.42GHz gives the bandwidth of 66.54 %. From the above analysis it is observed that it does not remove the complete WLAN.

From Fig. 16, it is observed that it covers the complete UWB along with the removal of the WLAN band. The first resonant band is from 1.08 to 5.07 GHz and the second band is from 5.84 to 11.82 GHz (Figs. 17 and 18).



**Fig. 18** Radiation pattern for completely WLAN despended Notched UWB antenna

## 8 Conclusion

A small-sized ultra wideband microstrip patch antenna with band rejection characteristics has been obtained and the results are simulated. These results are encouraging and it is expected to produce a suitable structure for ultra wideband applications. The proposed antenna resulted in wide bandwidth performance from 1.1 to 11.8 GHz. This designed antenna can be used in any compact handheld devices as well as in military applications, radar, etc., involving UWB applications without interference with WLAN.

In most of the antennas, designed incorporating slots, it is fairly difficult to create multiple frequency notches. We hope that the method will be helpful for creating multiple frequency notches as well as achieving sharp stop band.

## References

1. Federal Communications Commission, Washington, DC: FCC report and order on ultra wide-band technology (2002)
2. Schantz, H.G., Wolenc, G., Mysza, E.M.III.: Frequency notched UWB antennas. In: Proceedings of IEEE Conferences Ultra Wideband System Technology, 214–218 November 2003
3. Lim, E.G., Wang, Z., Lei, C.-U., Wang, Y., Man, K.L.: Ultra wideband antennas—past and present. *IAENG Int. J. Comput. Sci.* **37**:3 (2010)
4. Zhang, J., Xu, Y., Wang, W.: Microstrip-fed semi-elliptical dipole antennas for ultrawideband communications. *IEEE Trans. Antennas Propag.* **56**(1), 241–244 (2008)
5. Jang, J.W., Hwang, H.Y.: An improved band-rejection UWB antenna with resonant patches and a slot. *IEEE Antennas Wirel Propag. Lett.* **8**, 299–302 (2009)
6. Taub's Principles of Communication systems, Herberttaub, DonaldL: Schilling, GoutamSaha, TMH, 3rd edn. ISBN 0-07-064811-5 (2009)
7. Balanis, C.: *Antenna Theory*, 2nd edn. Chapter 14. ISBN 0-471-59268-4 Wiley (1997)
8. A Review of Aperture Coupled Microstrip Antennas: History, Operation, Development, and Applications. <http://www.ecs.umass.edu/ece/pozar/aperture.pdf>

# A Technique to Minimize the Effect On Resonance Frequency Due to Fabrication Errors of MS Antenna by Operating Dielectric Constant

Sandeep Kumar Toshniwal and Kanad Ray

**Abstract** This paper presents a method to minimize the effect on resonance frequency due to fabrication error of microstrip patch antenna. When a patch antenna is fabricated, dimension of the patch may be slightly different from its calculated value due to error in the fabrication operations, which causes into variation of its resonance frequency. To overcome this problem this paper presents a new technique to minimize the effect on resonance frequency due to fabrication error of MS antenna by operating dielectric constant. Effective dielectric constant of substrate is changed in such a way that the resonant frequency is set back to the calculated value.

**Keywords** Micro strip Antenna · Resonance frequency · Composite dielectric constant · Multilayer structure.

## 1 Introduction

The rapid growth of communication system developed a great demand of small antennas. The most commonly and popularly used small or miniature antenna is microstrip patch antenna [1].

Nowadays microstrip antennas are most popular antennas for HF applications. The microstrip patch antenna possesses a number of important advantages such as low profile, low weight, low manufacturing cost and having conformability. The main advantage of this antenna is that we can easily change the frequency, bandwidth and

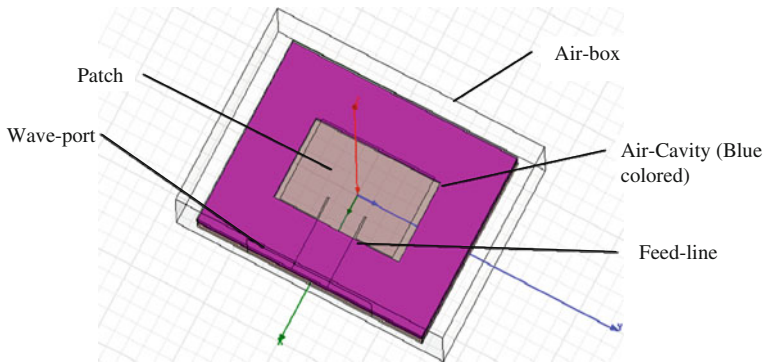
---

S. K. Toshniwal (✉)

Department of Electronics and Communication, Kautilya Institute of Technology and Engineering and School of Management, Jaipur, Rajasthan, India  
e-mail: toshniwal.sandeep@gmail.com

K. Ray

Institute of Engineering and Technology, JK Lakshmi pat University, Jaipur, Rajasthan, India  
e-mail: kanadray@jklu.edu.in



**Fig. 1** Layout of MS Antenna with air-cavity drawn by HFSS

gain by changing the parameters of MS antenna [2]. We can modify the frequency, bandwidth and gain by changing either the patch or dielectric width and length. This paper investigates the effect of frequency variation with respect to the change in dielectric constant [3]. For that we simply cut the material below the patch and consider it as an air-cavity [4]. The new effective dielectric constant gives the new value of resonance frequency. All analysis has been carried out using High Frequency Structural Simulator (HFSS). Change in resonance frequency has been plotted against area of cavity to take a broad view of the results. The paper is mainly divided into two sections. Section 2, describes the design methodology explained in brief. Section 3, describes results and discussion of the calculated parameters (Fig. 1).

## 2 Antenna Design and Simulation

Dimensions of antenna patch were calculated using standard equations. The essential parameters required for designing of MS antenna are  $f_0 = 2.4\text{GHz}$ ,  $\epsilon_r = 4.4$ ,  $h = 6.4\text{ mm}$ .

The length, width and other parameters related to designing of the MS antenna are calculated by EM Calculator.

Here are the calculated parameters:

$$W = 38.036\text{ mm}$$

$$\epsilon_{\text{reff}} = (\epsilon_r + 1/2) + (\epsilon_r - 1/2)[1 + 12h/w]^{-1/2}$$

$$L_{\text{eff}} = 32.5\text{ mm}, \Delta L = 2.8215\text{ mm}, L = 27\text{ mm}$$

Simulations have been done for two values of resonance frequency ( $f_0$ )—2 GHz and 2.4 GHz. For each value of resonance frequency ( $f_0$ ) two values of substrate

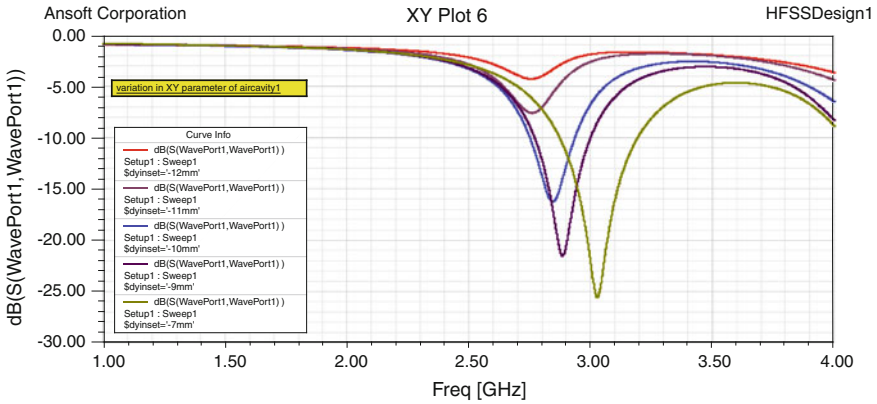


Fig. 2 Variation of resonance frequency ( $f_0$ ) with various values of area of air cavity1

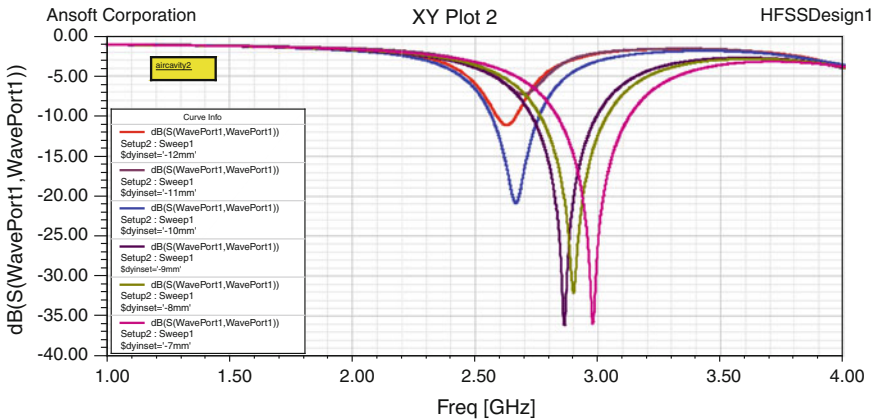


Fig. 3 Variation of resonance frequency ( $f_0$ ) with various values of area of air cavity2

height ( $h$ )–1.2 mm and 6.4 mm have been investigated. A cavity has been created in the antenna dielectric just below the patch. Various values of cavity area have been considered. HFSS simulations yielded the resonance frequency ( $f_0$ ) of the structure. Figures 2 and 3 are the simulation results which show variation in  $f_0$  with area of the air cavity 1 and air cavity 2 respectively.

### 3 Results and Discussion

Figures 4 and 5 shows dependence of resonance frequency with the area air cavity 1 (When we inserted air-cavity in only one layer of dielectric) and air cavity 2 (When we inserted air-cavity in two layers of dielectric).

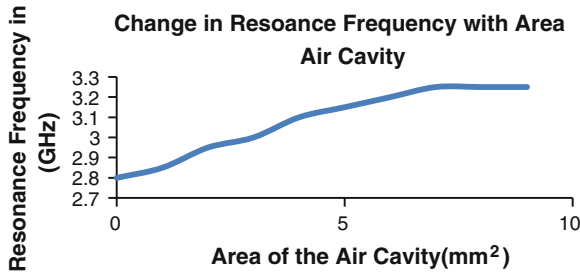


Fig. 4 Change in dimension of air cavity1 (vary in area)

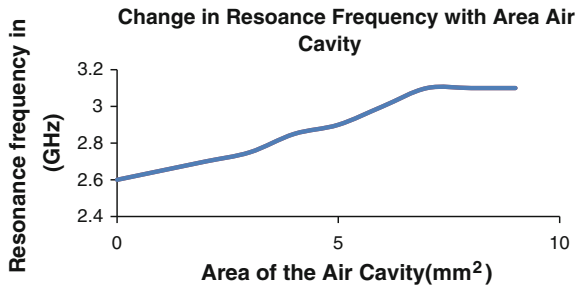


Fig. 5 Change in dimension of air cavity2 (vary in area)

Here we see the effects of change of area of cavity with respect to frequency, which is as in Table 1.

The result we are getting through inserting air-cavities in two layers is different from when we are inserting air-cavity in one layer because there is a variation in thickness of the air-cavity. Difference is only that the initial frequency is different in both of them. But both the frequencies linearly increased with area below 6 mm and after that frequency is constant.

Above results indicate that when a cavity is made in the antenna dielectric just below the patch, the resonance frequency  $f_0$  of the structure increases.

**Table 1** Effect of area of cavity with respect to frequency

Area	Frequency
$< 6\text{mm}^2$	Linearly increase
$\geq 6\text{mm}^2$	Constant

## 4 Conclusion

Through our simulation we conclude that, to enhance the range of frequencies, there is no need to change in the basic structure of the MS antenna, instead of that we can directly cut the material equal to the dimension of the air-cavity and find the change in the frequency. Effective dielectric constant of the substrate is changed in such a way that the resonance frequency is set back to the calculated value if change occurs due to error in fabrication process. Results indicate that when a cavity is made in the antenna dielectric just below the patch, the resonance frequency  $f_o$  of the structure increases.

These results are found here only for FR-4 epoxy but are equally valid for other dielectric materials (i.e. duroid, Rogers) also.

**Acknowledgments** The authors are thankful to the JKLU, Jaipur and KITE, Jaipur for encouragement to pursue this work and for providing the supporting materials.

## References

1. Garg, R., Bhartia, P., InderBahl and Ittipiboon, A.: Microstrip Antenna Design Handbook, pp. 1–68, 253–316. Artech House Inc., Norwood, MA (2001)
2. Kumar, G and Ray, K.P.: Broadband Microstrip Antenna. Artech House, London 2003.
3. Hoorfar, A., Perrotta, A.: An experimental study of microstrip antennas on very high permittivity ceramic substrates and very small ground planes. IEEE Trans. Antennas Propag. **49**(4), 838 (2001)
4. Lee, B. and Harackiewicz, F.J.: Miniature microstrip antenna with a partially filled high-permittivity substrate. IEEE Trans. Antennas Propag. **50**(8), 1160 (2002)



**Part XII**  
**Soft Computing for Industrial**  
**Applications (SCI)**

# Artificial Neural Network Model for Forecasting the Stock Price of Indian IT Company

Joydeep Sen and Arup K. Das

**Abstract** The central issue of the study is to model the movement of stock price for Indian Information Technology (IT) companies. It has been observed that IT industry has some promising role in Indian economy. We apply the artificial neural networks (ANNs) for modeling purpose. ANNs are flexible computing frameworks and its universal approximations applied to a wide range with desired accuracy. In the study, multilayer perceptron (MLP) models, which are basically feed-forward artificial neural network models, are used for forecasting the stock values of an Indian IT company. On the basis of various features of the network models, an optimal model is being proposed for the purpose of forecasting. Performance measures like  $R^2$ , standard error of estimates, mean absolute error, mean absolute percentage error indicate that the model is adequate with respect to acceptable accuracy.

**Keywords** Artificial neural network · Financial forecasting · Stock price · Indian IT companies · Multilayer perceptron.

## 1 Introduction

The study considers modeling the movement of stock price for Indian Information Technology (IT) companies. It has been observed that IT industry has some promising role in Indian economy. A number of profitable Indian companies today belong to the IT sector and a great deal of investment interest is now being focused. Companies in BSE IT index are those that have more than 50% of their turnover from IT

---

J. Sen (✉)

Population Studies Unit, Indian Statistical Institute, Kolkata, India  
e-mail: joydp.sen@gmail.com

A. K. Das

SQC and OR Division, Indian Statistical Institute, Kolkata, India  
e-mail: akdas@isical.ac.in

related activities like IT infrastructure, IT education, software training, telecommunication services, networking infrastructure, software development, hardware manufacture, vending, support and maintenance. BSE IT index constituents represent about 10.22% of the free float market capitalization.

In the literature, Box-Jenkins ARMA and ARIMA models [1] have respectively been adopted for financial forecasting. These traditional models do not learn immediately as the arrival of new data, instead they must be re-estimated periodically.

De Groot and Wurtz [2] analyzed univariate time series forecasting using feed-forward neural networks. Due to the inherently noisy, non-stationary and chaotic nature of financial time series, it is often difficult to forecast based on the restricted statistical models. Therefore, artificial neural networks (ANNs) have received an increasing attention in time series forecasting in recent years.

El-Hammday and Abo-Rizka [3] developed a recurrent neural network model trained by ARIMA analysis for forecasting stock price in Egyptian Stock Market. Zhang and Wu [15] proposed an improved bacterial chemotaxis optimization (IBCO), which is later integrated into back-propagation (BP) artificial neural network to develop an efficient forecasting model for predicting various stock indices. Panahian [9] used a multilayer perceptron (MLP) neural network to determine the relationship between some variables as independent factors and the level of stock price index (TEPIX) as a dependent element in Iranian stock market. Kara et al. [6] observed that the average performance of ANN model in predicting the daily Istanbul Stock Exchange (ISE) National 100 Index was found significantly better than that of SVM model.

Several attempts [7, 8, 13, 14] have been done to implement artificial neural network to model Indian financial indexes like BSE SENSEX and NIFTY. But only a few studies have been done for the different Indian IT companies. The purpose of the study is to model the stock price of Indian IT companies using artificial neural network and forecast the same.

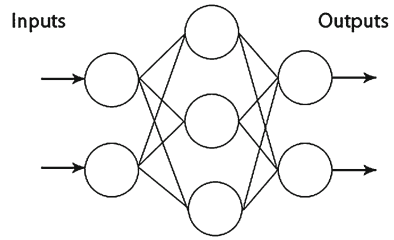
We organise the rest of this paper in the following way. In Sect. 2, a brief exposition of the methodology used in the study is discussed. Section 3 provides the analysis and results along with discussion. A conclusion of the study is presented in Sect. 4.

## 2 Methodology

Artificial neural networks are computational structures modeled on the gross structure of human brain. Neural network can model the behavior of known systems without being given any rule or models. Moreover neural networks may be considered as flexible nonlinear non-parameterized models where the parameters may be adopted according to the available data.

As the design is based on the human brain, they are made to obtain knowledge through learning. The process of learning for a neural network consists of regulating the weights of each of its node considering the input of the neural network and its expected output.

Fig. 1 Multilayer Perceptron



The model is characterized by a network of three layers (viz. input, hidden and output) of simple processing units connected by acyclic links. The relationship between the output ( $y_t$ ) and the inputs ( $y_{t-1}, \dots, y_{t-p}$ ) has the following mathematical representation :

$$y_t = w_0 + \sum_{j=1}^q w_j g \left( w_{0j} + \sum_{i=1}^p w_{i,j} y_{t-i} \right) + e_t$$

where  $w_{i,j} (i = 0, 1, 2, \dots, p; j = 1, 2, \dots, q)$  and  $w_j (j = 0, 1, 2, \dots, q)$  are model parameters often called connection weights,  $p$  is the number of input nodes,  $q$  is the number of hidden nodes. Identity, sigmoid, tanh, logistic, exponential functions are used as the hidden layer activation function and output activation function. The choice of  $q$  is data dependent and no systematic, well-accepted rule exists in deciding  $q$ . Experiments are conducted to find  $p$ .

MLP is one of the most popular network architectures used today, due to Rumelhart and McClelland [11]. Each performs a biased weighted sum of inputs and passes this activation level through a transfer function to produce the outputs, and the units are arranged in a layered feed-forward topology. The network thus has a simple interpretation in a form of input–output model with weights and thresholds (biases) as the free parameters of the model. Such networks can model functions of almost arbitrary complexity. MLPs are variable tools when one has less knowledge about the form of the relationship between inputs and outputs. The architecture of a MLP is shown in Fig. 1.

To adjust weights properly, we apply a general method for non-linear optimization, called Broyden–Fletcher–Goldfarb–Shanno (BFGS) algorithm. Sum of squares (SOS) is used as error function.

The accuracy of the prediction for each ANN model has been compared by the indexes of training performance and the testing perfection. The efficiency of ANN models varies with the number of input layers ( $p$ ) and hidden layers ( $q$ ). The residual of the proposed ANN model is tested for the presence of autocorrelation and white noise property.

**Table 1** Summary of the selected ANN model for INFOSYS limited

Network name	MLP 6-7-1
Training perfection	0.99762
Training error	0.00013
Testing perfection	0.99772
Testing error	0.00014
Algorithm	BFGS 26
ERROR function	SOS
Hidden activation function	Tanh
Output activation function	Identity

### 3 Analysis and Results

To analyze the stock market price, we consider the daily data of consecutive five financial years from 2006 to 2011 of the stock-values of INFOSYS Limited. The data is collected at a particular time interval on every working day. On Saturday, Sunday and other national holidays, Bombay Stock Exchange remains closed and also there is no transaction in stock exchange market.

The closing price represents the most up-to-date valuation of a security until trading commences again on the next trading day. Closing prices provide a useful marker for investors to assess changes in stock prices over time. The closing price of a day can be compared to the previous closing price in order to measure market sentiment for a given security over a trading day. So we consider only closing price of the stock for our analysis.

The accuracy of prediction for each ANN model has been compared by the indexes of training performance and the testing performance. The efficiency of ANN models vary with the number of input layers ( $p$ ) and hidden layers ( $q$ ).  $p$  and  $q$  are chosen based on experimentation.

The whole data set is being divided into three groups as 80, 15 and 5% of the total observations for the purpose of training, testing and validation to develop the ANN model. For having the least training performance and testing performance, the multilayer perceptron model with six input nodes, seven hidden nodes and one output node (i.e. MLP 6-7-1 model) is chosen to model and forecast the daily stock price of INFOSYS Limited. Summary of the selected ANN model is depicted in Table 1.

The actual close-price and the predicted close-price obtained by using the selected ANN model are shown in Fig. 2. The weight of the network parameters of MLP 6-7-1 is presented in Table 2.

The Var1 indicates the actual close-price and 2.MLP 6-7-1 indicates the predicted close price based on the ANN model of MLP 6-7-1.

Following the similar methodology discussed earlier, we apply the multilayer perceptron model for forecasting the daily stock prices of two other Indian IT companies: Tata Consultancy Services Ltd. (TCS Ltd.) and WIPRO Ltd. A performance summary of the optimum multilayer perceptron model for each of these three Indian IT companies is given in Table 3.

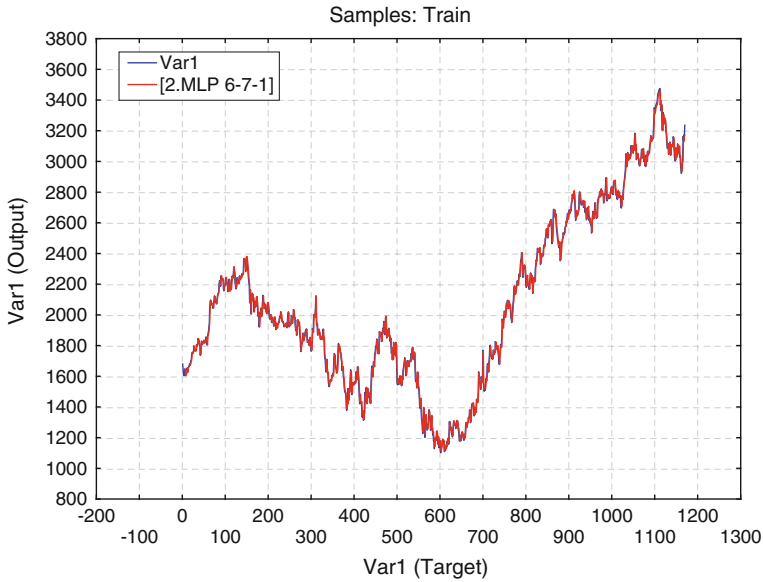


Fig. 2 Actual and predicted (by MLP 6-7-1) closing stock price of INFOSYS Limited

Table 2 Network weights of MLP 6-7-1

Serial number	Connections (MLP 6-7-1)	Weight values (MLP 6-7-1)
1	Input bias → hidden neuron 1	0.137006
2	Input bias → hidden neuron 2	0.144430
3	Input bias → hidden neuron 3	-0.178096
4	Input bias → hidden neuron 4	-0.340784
5	Input bias → hidden neuron 5	-0.058491
6	Input bias → hidden neuron 6	-0.264130
7	Input bias → hidden neuron 7	-0.072084
8	Hidden neuron 1 → Var1	-0.323277
9	Hidden neuron 2 → Var1	0.327605
10	Hidden neuron 3 → Var1	0.290812
11	Hidden neuron 4 → Var1	0.710852
12	Hidden neuron 5 → Var1	0.191150
13	Hidden neuron 6 → Var1	0.151419
14	Hidden neuron 7 → Var1	-0.610038
15	Hidden bias → Var1	0.292043

Fisher’s  $Kappa = 7.352384$  (for Infosys Ltd.) indicates that the MLP residual of Infosys Ltd. is white noise. We obtain similar results for the TCS Ltd. and WIPRO Ltd. Performance measures presented in Table 3 show that MLP models provide excellent prediction and these models are adequate for modeling the stock price.

**Table 3** Performance summary of INFOSYS Ltd., TCS Ltd. and WIPRO Ltd

Indian IT company	Infosys Ltd.	TCS Ltd.	WIPRO Ltd.
Fitted model	MLP 6-7-1	MLP 5-6-1	MLP 6-6-1
Standard error of the fitted model	39.55929	22.57515	28.46415
R <sup>2</sup> of the fitted model	0.99531	0.99135	0.99395
MAE of the fitted model	29.91343	14.67768	18.653321
MAPE of the fitted model	0.01547	0.01831	0.02303

## 4 Conclusion

The present study is designed to model the stock price for the Indian IT companies using artificial neural network for the purpose of prediction. We observe that artificial neural network performs well to model stock price. This phenomenon is true in the sense that ANN may capture the non-linear and chaotic behavior as compared to other conventional time series models. Our experiment has shown that the multilayer perceptron model is capable of predicting the stock price with acceptable accuracy. In this study it has been observed that multilayer perceptron model has ability to explain the time series pattern of the stock market data.

## References

1. Box, G.E.P., Jenkins, G.M.: Time series analysis: forecasting and control. Holden-day Inc., San Francisco (1976)
2. De Groot, C., Wurtz, D.: Analysis of univariate time series with connectionist nets: a case study of two classical examples. *Neurocomputing* **3**, 177–192 (1991)
3. El-Hammady, A.H., Abo-Rizka, M.: Neural network based stock market forecasting. *IJCSNS* **11**(8), 204–207 (2011)
4. Freeman, J.A., Skapura, D.M.: Neural network algorithms, application and programming techniques. Addison Wesley (1991)
5. Hornick, K., Stinchcombe, M., White, H.: Universal approximation of an unknown mapping and its derivatives using multilayer feedforward networks. *Neural Netw.* **3**, 551–560 (1990)
6. Kara, Y., Boyacioglu, M.A., Baykan, O.K.: Predicting direction of stock price index movement using artificial neural networks and support vector machines: the sample of the Istanbul stock exchange. *Expert Syst. Appl.* **38**, 5311–5319 (2011)
7. Manjula, B., Sarma, S.S.V.N., Naik, R.L., Shruthi, G.: Stock Prediction using Neural Network. *IJAEST*. **10**(1), 13–18 (2011)
8. Merh, N., Saxena, V.P., Pardasani, K.R.: A comparison between hybrid approaches of ANN and ARIMA for Indian stock trend forecasting. *Bus. Int. J.* **3**(2), 23–43 (2010)
9. Panahian, H.: Stock market index forecasting by neural networks models and nonlinear multiple regression modeling: study of Iran's capital market. *Am. J. Sci. Res.* **18**, 35–51 (2011)
10. Qi, M., Zhang, G.P.: An investigation of model selection criteria for neural network time series forecasting. *Eur. J. Operat. Res.* **132**(3), 666–680 (2001)
11. Rumelhart, D.E., McClelland, J.L., The PDP Research Group: Parallel distributed processing: explorations in the microstructure of cognition, vols. 1–2. MIT Press, Cambridge (1986)

12. Schoneburg, E.: Stock price prediction using neural network: a project report. *Neurocomputing* **2**(1), 17–27 (1990)
13. Thenmozhi, M.: Forecasting stock index returns using neural networks. *DBR* **7**(2), 59–69 (2006)
14. Vashisth, R., Chandra, A.: Predicting stock returns in nifty index: an application of artificial neural network. *IRJFE* **49**, 15–23 (2010)
15. Virli, F., Freisleben, B.: Neural network model selection for financial time series prediction. *Comput. Stat.* **16**(3), 451–463 (2001)
16. Zhang, Y., Wu, L.: Stock market prediction of S&P 500 via combination of improved BCO approach and BP neural network. *Expert. Syst Appl.* **36**(5), 8849–8854 (2009)



# V/f-Based Speed Controllers for an Induction Motor Using AI Techniques: A Comparative Analysis

Awadhesh Gupta, Lini Mathew and S. Chatterji

**Abstract** This paper presents a comparative analysis of speed controllers for three-phase induction-motor scalar speed control. The control strategy consists in keeping constant the voltage and frequency ratio of the induction-motor supply source. First, a conventional control loop including a PI controller is realized. Then a fuzzy-control system is built on a MATLAB platform, which uses speed and difference in speed variation to change both the fundamental voltage amplitude and frequency of a sinusoidal pulse width modulated inverter. An alternative optimized method using Genetic Algorithm is also proposed. The controller performance, in relation to reference speed and step change of speed variations with constant load-torque, is evaluated by simulating it on a MATLAB platform. A comparative analysis of these with conventional proportional-integral controller is also presented.

**Keywords** Artificial intelligence (AI) · Adjustable speed drives (ASDs) · Proportional-integral (PI) · Fuzzy Logic Controller (FLC) · Genetic Algorithm (GA)

## 1 Introduction

Adjustable speed drives (ASDs) are the essential and endless demand of industries and researchers. These are widely used in industries to control the speed of conveyor systems, blower speeds, machine tool speeds, and other applications that require adjustable speeds. In many industrial applications, traditionally, dc motors were the workhorses for the ASDs due to their excellent speed and torque response [1, 2]. These however have the inherent disadvantage of commutator and mechanical

---

A. Gupta (✉)  
EED, MNNIT, Allahabad, India  
e-mail: awadhesh.g@rediffmail.com

L. Mathew · S. Chatterji  
EED, NITTTR, Chandigarh, India  
e-mail: lenimathew@yahoo.com

brushes, which undergo wear and tear with the passage of time [3]. An induction machine is the most widely used motor in the industry because of its high robustness, reliability, low cost, high efficiency, and good self-starting capability. In spite of these capabilities induction motors suffer from two disadvantages. First, the standard motor is not a true constant-speed machine; its full load slip varies from less than 1 % (in high horse power motors) to more than 5 % (in fractional horse power motors). Second, it is not inherently capable of providing variable-speed operation. These limitations can be solved through the use of adjustable speed controllers [4]. The basic action involved in adjustable speed control of induction motor is to apply a variable voltage magnitude and variable frequency to the motor so as to obtain variable speed operation. Voltage source inverter can be used to meet the aforesaid purpose. Induction motors offer a very challenging control problem due to its nonlinearity of dynamical system, motor parameter variation, and difficulty in measuring rotor variables. Moreover, the widely used PID controller does not offer satisfactory results when adaptive algorithms are required [5–8]. This problem can be solved by using artificial intelligent control techniques such as neural network, fuzzy logic, genetic algorithms, and particle swarm optimization techniques which can enhance the performance of the system to a great extent without requiring an exact model of induction motor.

## 2 Controller Design

The conventional closed loop PI control scheme is developed using the MATLAB/SIMULINK for V/f-based speed control of induction motor which is shown in Fig. 1. The various parameters required for the model of Fig. 1 saved in an m-file is

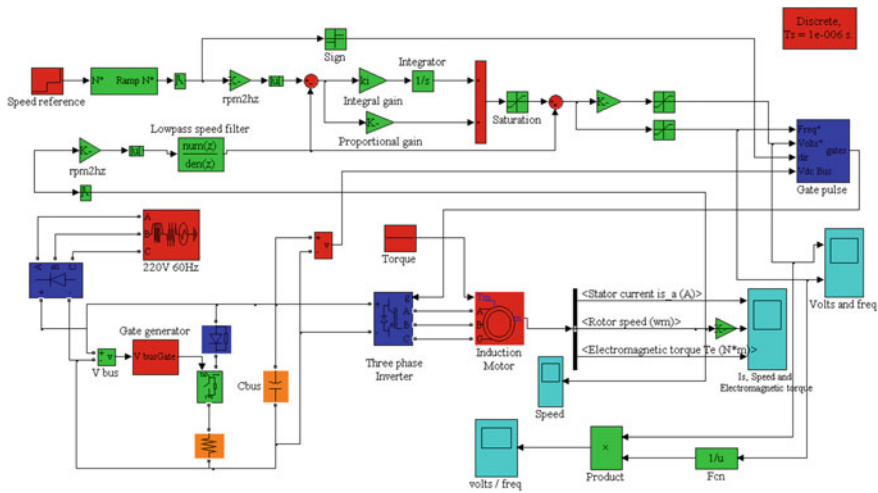


Fig. 1 SIMULINK model of IMD with PI controller

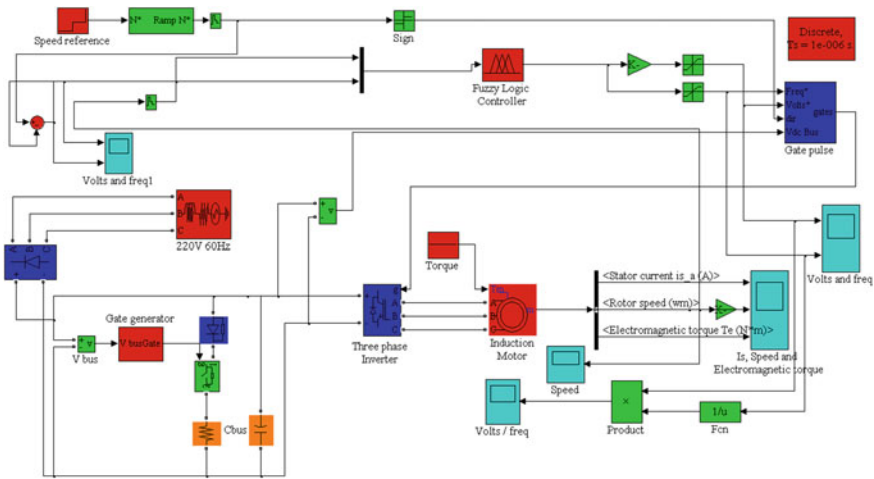


Fig. 2 SIMULINK model of IMD with Fuzzy Logic Controller

run first. Then SIMULINK model of Fig. 1 is run to get the response of conventional P-I controller. Another approach namely Fuzzy Logic Controller design is shown in Fig. 2. The actual speed of the induction motor is sensed and is compared with the reference speed. The error so obtained is processed in a P-I controller and its output sets the inverter frequency. The synchronous speed, obtained by adding actual speed  $\omega_m$  and the slip speed  $\omega_{slip}$  determines the inverter frequency. The reference signal for closed loop control of machine terminal voltage is generated from the frequency.

### 3 Results and Discussions

The induction motor drive system has been simulated with P-I controller and then a fuzzy controller is employed in place of P-I controller. After that the P-I controller parameters have been optimized using genetic algorithm. The optimum value of  $K_p$  and  $K_i$  have been chosen for the controller. All the controllers are tested for speed tracking with constant load torque conditions. Results obtained by employing the different controllers have been finally compared. The drive is subjected to operate at different speeds with constant load torque to test the robustness of the different controllers. The rating and parameters of the three-phase induction motor which has been considered as the test case is given in Table 1.

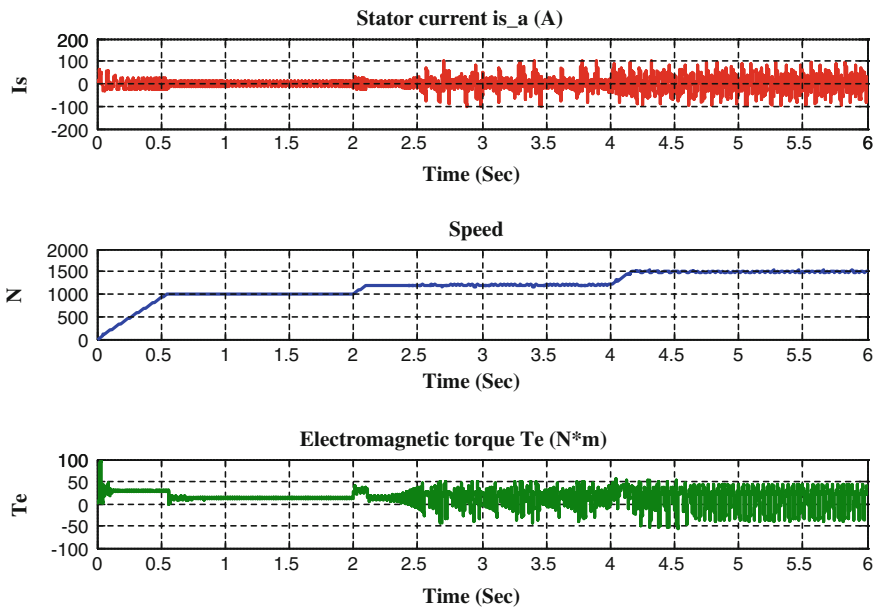
Different cases under which the simulation tests have been carried out are

- (i) Step change in reference speed.
- (ii) Tracking of reference speed.
- (iii) Robustness test against constant load torque.

**Table 1** Induction motor parameters

Rated value	Power (P)	3,730 VA
	Voltage (V)	460 V
	Frequency (f)	60 Hz
	Speed (N)	1,760 rpm
	Pole pairs	2
Constants	Stator resistance (Rs)	1.115 Ω
	Rotor resistance (Rr)	1.083 Ω
	Stator inductance (Ls)	0.005974 H
	Rotor inductance (Lr)	0.005974 H
	Mutual inductance	0.2037 H
	Inertia constant (J)	0.02 kg m <sup>2</sup>
	Damping constant (B)	0.005752 Nm/s

The simulation responses of the drive system with P-I controller, Fuzzy controller and Genetic Algorithm (GA) optimized P-I controller are shown in Figs. 3, 4 and 5, respectively. The reference speed is changed from 1,000 to 1,200 rpm at time,  $t = 2$  s, and again from 1,200 to 1,500 rpm at time,  $t = 4$  s and after that the motor is continued to run at this speed till,  $t = 6$  s. The load torque is kept constant. The responses of stator current, speed, and electromagnetic torque are also shown in Figs. 3, 4 and 5. It can be seen from the response of Fig. 3 that the current ripples and



**Fig. 3** Simulation results with PI controller

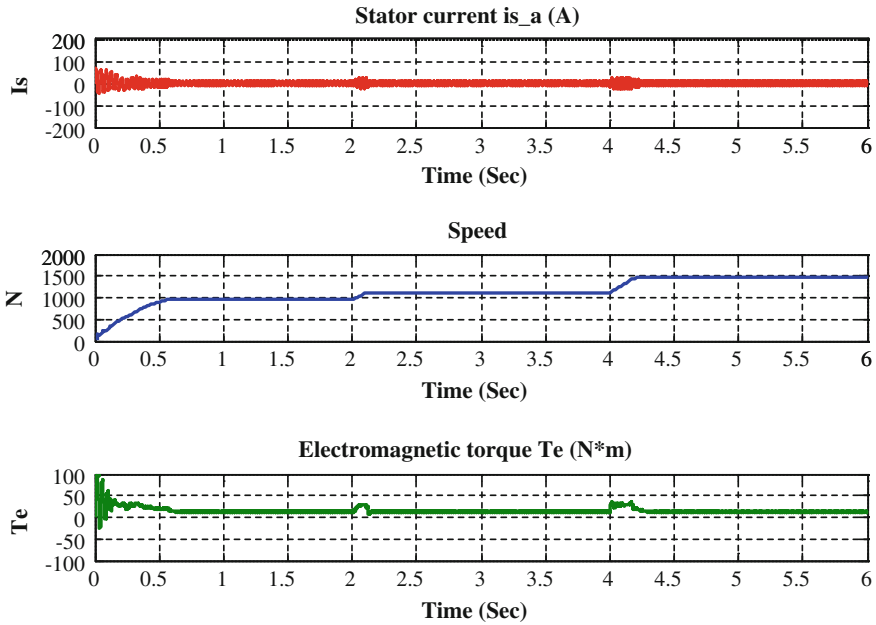


Fig. 4 Simulation results with fuzzy controller

torque ripples at 1,200 and 1,500rpm are quite high while at 1,000rpm the ripples are less. From Figs. 3 and 4, it is clear that, in case of fuzzy controller, the speed response is smoother than P-I controller. Also, the torque ripples and current ripples are minimized with fuzzy controller. From Figs. 3, 4 and 5, it is clear that, in case of GA optimized P-I controller the speed response is further smoother than P-I controller and fuzzy controller. The torque ripples and current ripples are also greatly minimized.

The simulation response of the drive system with P-I and GA optimized P-I controller at different set points are shown in Figs. 6 and 7. In case of P-I controller, it is observed that the reference speed is changed from 1,500 to 1,000rpm at time,  $t = 2$  s, and again from 1,000 to 1,200rpm at time,  $t = 4$  s and after that the speed reference of motor is changed from 1,200 to 900rpm at  $t = 5$  s. In case of GA optimized P-I controller, it is observed that the reference speed is changed from 1,500 to 1,200rpm at time,  $t = 2$  s and again from 1,200 to 1,000 rpm at time,  $t = 3$  s and after that the speed reference of motor is changed from 1,000 to 600rpm at  $t = 5$  s. The load torque is kept constant in both the cases. The response of stator current, speed and electromagnetic torque are also shown in Figs. 6 and 7. From Figs. 6, 4 and 7, it is clear that the induction motor has run up to 900rpm with P-I controller, up to 1,000rpm with fuzzy controller and up to 600rpm with GA optimized P-I controller. Thus the speed control range has been increased with GA optimized P-I controller.

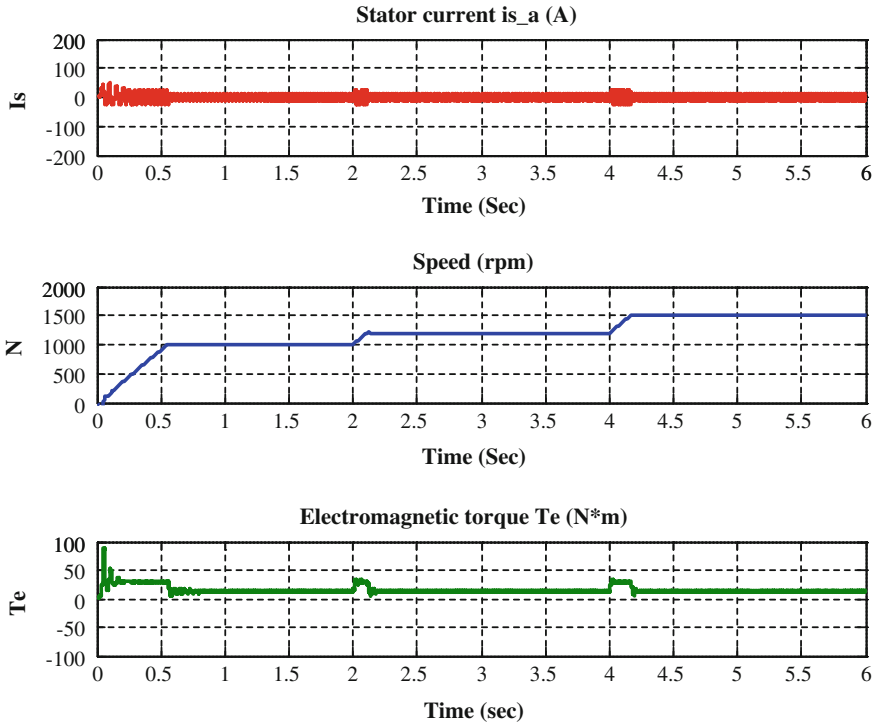


Fig. 5 Simulation results with GA optimized controller

### 4 Comparative Analysis of Results

The different controllers were tested for their speed response at different set points. The results obtained for the drive with P-I controller, Fuzzy controller, and GA optimized P-I controller are shown in Figs. 8, 9 and 10, respectively. For all the three controllers the reference speed is changed from 1,000 to 1,200rpm at time,  $t = 2$  s, and again from 1,200 to 1,500rpm at time,  $t = 4$  s and after that the motor is continued to run at this speed till,  $t = 6$  s.

The speed response of the drive with conventional controller shows the rise time of 0.6 s as shown in Fig. 8. The overshoot value at 1,000rpm is within reasonable limits but at 1,200 and 1,500 rpm, there exists sustained oscillations. The steady-state response of the drive is found to be poor. This could be due to the improper choice of integral gain. Table 2 shows the parameters of the P-I Controller.

The speed response of the drive with fuzzy controller as shown in Fig. 8 shows smoother response as compared to the conventional controller. Comparing Figs. 8 and 9, it is observed that the speed ripples are suppressed to a great extent but the steady-state error of the drive is found to be poor. Although the drive shows smoother response it generates appreciable offset. The speed ripples in the steady-state as well

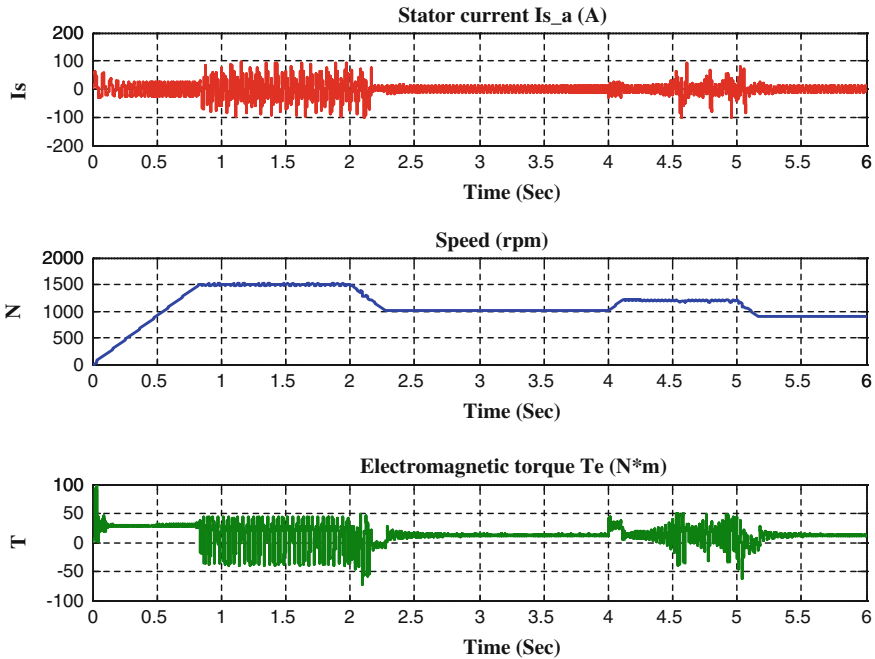


Fig. 6 Simulation results with PI controller with different set points

as in dynamic conditions are found to be reduced. This offset error can be resolved by making the fuzzy rule base more exhaustive.

The speed response of the drive with GA optimized controller as shown in Fig. 10 shows much smoother response as compared to the conventional controller and fuzzy controller. The speed ripples are greatly suppressed with respect to the other controllers' response mentioned earlier. The steady-state error of the drive at speeds 1,000, 1,200, and 1,500 rpm is almost negligible, depicted in Fig. 10. In case of GA optimized controller, the steady-state response as well as dynamic response is considerably improved with no torque ripples, as compared to the other controllers, thus, making the drive robust. Table 3 shows the parameters of the P-I controller which is obtained by the optimization process with the help of GA toolbox of MATLAB software with IATE considered as objective function.

## 5 Comparison Among Controllers

Table 4 shows the summary of comparative assessment of all the controllers considered here.

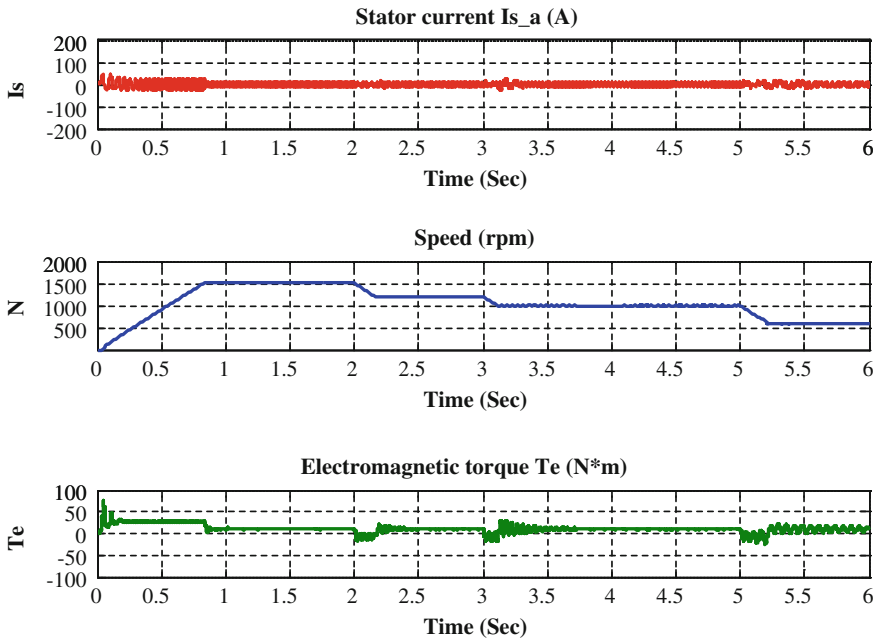


Fig. 7 Simulation results with GA optimized controller with different set points

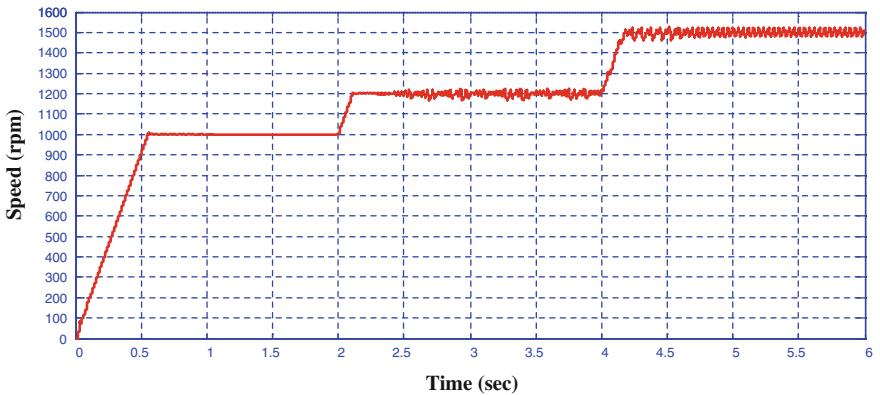


Fig. 8 Speed response with P-I controller

In view of the above discussions, it is clear that the transient as well as dynamic performance of the GA Optimized P-I controller is far superior to the conventional and fuzzy controllers. The speed control range obtained is also more as compared to the other controllers mentioned. The torque ripples and current ripples have also been minimized. Thus, GA-Optimized P-I controller is inferred as the best choice.



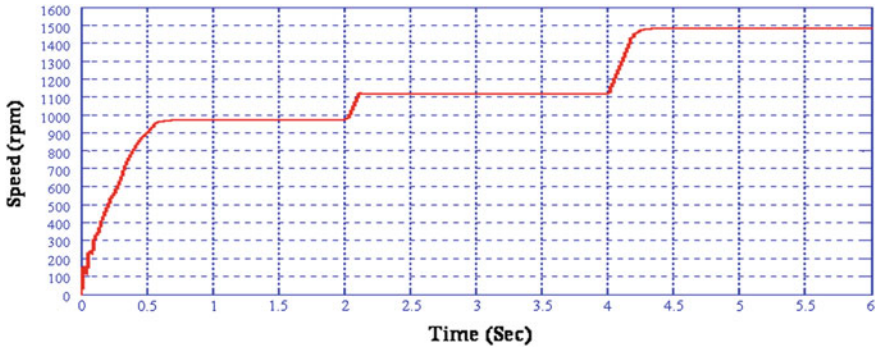


Fig. 9 Speed response with fuzzy controller

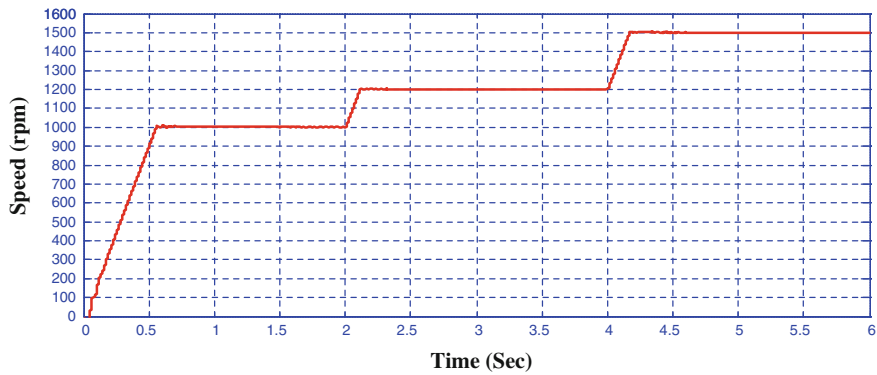


Fig. 10 Speed response with GA optimized controller

Table 2 P-I controller parameters

Sr. No.	Parameter	Value
1.	$K_p$	39
2.	$K_i$	50

Table 3 GA optimized P-I controller parameter

Sr. No.	Parameters	Value
1.	$K_p$	09
2.	$K_i$	10

Table 4 Comparative assessment of the controllers

Property	Conventional P-I	Fuzzy controller	GA-optimized P-I
Starting transient performance	Poor	Good	Very Good
Steady-state performance	Poor	Poor	Very Good
Speed-control range	Up to 900 rpm	Up to 1,000 rpm	Up to 600 rpm
Robustness	Average	Good	Very Good

## 6 Conclusion

In this work, artificial intelligence-based scalar speed control for an induction motor has been examined. First, a PI algorithm was thoroughly explored. After this, fuzzy and GA control system have been investigated to cope better with the dynamic conditions. The main conclusions are listed below:

- (i) Conventionally, P-I controller is suited for the speed control of induction motor.
- (ii) The unique characteristics of the proposed GA-based tuning technique are found to be completely model independent.
- (iii) This study demonstrates that GA technique can solve tuning problem of the controller more efficiently.
- (iv) The conventional PID control mechanism performs poorly. If the system has to be controlled without assumption and linearization, the heuristic search algorithm, especially GA is found to be the best choice.
- (v) Unlike the other methods, the GA technique is simple, fast, and easy to implement in a variety of control loops and yields much better results as compared to the currently available conventional tuning methods.
- (vi) The simulation results have shown that the performance of the system under dynamic conditions have improved significantly which is the main drawback of the scalar speed control.
- (vii) The simulation results have shown that the speed control range is considerably increased by using the GA optimization technique to the P-I controller.
- (viii) The dynamic response with the Fuzzy controller shows much more improvement but at the same time the offset error is not completely eliminated.
- (ix) In the simulation response with the GA optimization, the offset error is eliminated considerably.

The investigator attempts to modernize the V/f control strategy, which already exists in various industries, by incorporating artificial intelligent control techniques such as Fuzzy Logic and GA, so as to give good dynamic performance along with the steady-state performance.

## References

1. Javadi, S.: Induction motor drive using fuzzy logic. In: Proceedings of the 7<sup>th</sup> WSEAS International Conference on System Theory and Scientific Computation, Athens, Greece, August 2007
2. Bose, B.K.: Modern Power Electronics and AC Drives, A Text Book , 4th edn. Pearson Education, New York (2004)
3. Singh, B., Ghatak Choudhuri, S.: DSP based implementation of vector controlled induction motor drive using fuzzy pre-compensated proportional integral speed controllers. IEEMA J. **17**(4), 77–84 (2007)

4. Koreboina, V.B., Magajikondi, S.J., Raju, A.B.: Modeling, simulation and PC based implementation of a closed loop speed control of VSI fed induction motor drive. In: Proceedings of the IEEE International Conference on Power Electronics, Bangalore, January 2011
5. Muthuselvan, N.B., Dash, S.S., Somasundaram P.: A high performance induction motor drive system using fuzzy logic controller. In: Proceedings of the IEEE International Conference on Power Electronics, Chennai, November 2006
6. Yang, L., Li, Y., Chen, Y., Li, Z.: A novel fuzzy logic controller for indirect vector control induction motor drive. In: Proceedings of the 7<sup>th</sup> World Congress on Intelligent Control and Automation, pp. 24–28, Beijing, China, June 2008
7. Zerikat, M., Mechernene, A., Chekroun, S.: High-performance sensorless vector control of induction motor drives using artificial intelligent technique. In: Proceedings of the International Conference on Methods and Models in Automation and Robotics, pp. 67–75, Oran, Algeria, August 2010
8. Chaudhary, P.S., Patil, P.M., Patil, S.S., Kulkarni, P.P., Holmukhe, R.M.: Comparison of performance characteristic of a squirrel cage induction motor by three phase sinusoidal and PWM inverter supply using MATLAB digital simulation. In: Proceedings of the Third International Conference on Emerging Trends in Engineering and Technology, pp. 362–367, Pune, India, November 2010

**Part XIII**  
**Soft Computing for Information**  
**Management (SCIM)**

# Enhanced Technique to Identify Higher Level Clones in Software

S. Mythili and S. Sarala

**Abstract** Code copy and reuse are the most common way of programming practice. Code duplication occurs in every software program. A function, a module, or a file is duplicated for various reasons. The copied part of the source code with or without modification is called a code clone. Several tools have been designed to detect duplicated code fragments. These simple code clones assists to identify the design level similarities. Recurring patterns of simple clones indicate the presence of design level similarities called higher level clones. In this work we describe a new technique using fingerprinting to find higher level clones in software. Initially the simple clones are found, and then using LSH, we compare the fingerprints to find recurring patterns of method level, file level, and directory level clones. Finally, experiments and results shows that the proposed method finds all higher level clones in the software.

**Keywords** Software clones · Clone detection · Similarity hashing · Fingerprinting

## 1 Introduction

Recent research suggests that most of the codes in large software system are duplicated. Programmers normally clone the software by simple copy and paste method. After copying, the original code is modified according to the programmer's need.

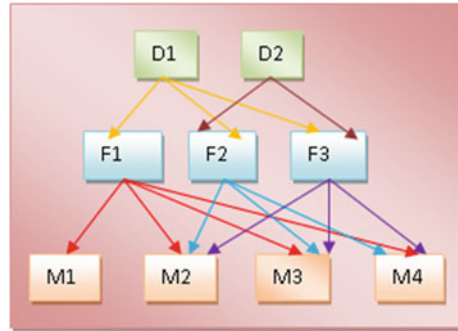
---

S. Mythili (✉)

Research Scholar, Department of Information Technology,  
Bharathiar University, Coimbatore 46, India  
e-mail: smythili78@gmail.com

S. Sarala

Department of Information Technology, School of Computer Science and Engineering,  
Bharathiar University, Coimbatore 46, India  
e-mail: sriohmau@yahoo.co.in

**Fig. 1** Higher level clones

This copy and paste programming practice often creates exactly matched or similar portion of the code, which are called as code clones. Several tools are available to find these code clones. DECARD [1], Cp-Miner [2], CCFinder [3] and CloneDR [4] are some of the best clone detection techniques to find clones in the software and the Web applications. The drawback of most of the clone detection tools are that they concentrate on finding simple clones and do not concentrate on a wider picture looking for design level similarities. Simple clones are lower level clones with similar code fragments. These lower level clones when combined to form design level similarities are called as Higher Level Clones. Examples of higher level clones are shown in Fig. 1.

## 2 Literature Review

This section describes the various categorizations of code clones that have been proposed by different authors.

One of the first categorizations of clones in software was proposed by Mayrand et al. [5]. This categorization classifies candidate code clones according to the types and degrees of differences between code segments. The type of differences considered are function names, layout, expressions, and control flow. Using these attributes, clones are categorized in to eight types.

Balazinska et al. [6] created a schema for classifying various cloned methods based on the differences between the two functions that are cloned. The differences are accounted in five groups. These categories are used by Balazinska et al. to produce software-aided reengineering systems for code clone elimination.

Major limitations of the above categorizations are that they concentrate only on function clones. These function clones will cover only 30–50% of the cloning activity. As an improvement to this a new taxonomy was designed by Cory Kapser [7] and the new scheme is based on different attributes of the clone including similarity, locality within the software system, scope of the cloned code, degree of similarity of regions the clones exist in, and the type of region the clone occurs in. This taxonomy is

a hierarchical classification of code clones which helps in finding Same File Clones, Same Region Clones, Function to Function Clones, Structure Clones, Macro Clones, Heterogeneous Clones, and Misc. Clones.

Koschke et al. [8] define another clone classification using only the types of differences between clones. In this classification only three types of clones are considered, as described above for its use in the Bellon benchmark. Basit et al. [9] have produced a clone classification scheme that groups clones according to higher level structures such as files or classes. The data mining techniques “market basket analysis” is used for searching frequently co-occurring clones.

### 3 Proposed Model for Finding Higher Level Clones

Figure 2 represents an idea of the new technique for finding the higher level clone patterns in the software system. The software system taken into consideration is a sample java system. The first step in the above technique is the preprocessing and formattings. It accepts the source code to be compared and preprocesses. This involves *white space* removal, *comment* removal and converting the lines of code into general format. In the general format conversion the source code is traversed for data types and variable names. Then the data types and the variable names are converted into a general format for, e.g., `void sum(int a, int b) → void sum($v, $v);`

The next step of the above technique is to split the source code considered into tokens. After tokenizing the tokens of the arbitrary length are converted into fingerprints using the *Message Digest Algorithm*. Most of the clone detection methods uses various algorithms which compares the literals and the identifiers for finding the clones. The proposed technique finds the code clones using fingerprinting technique.

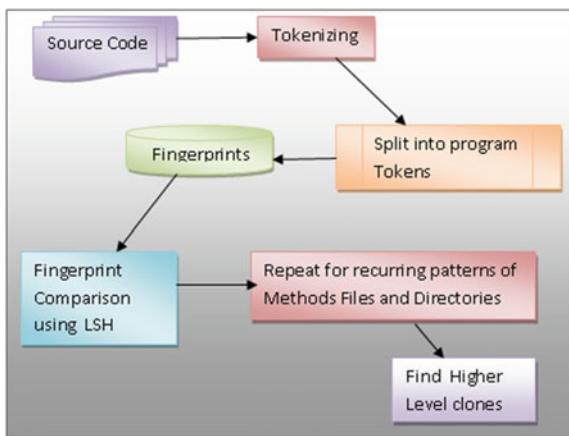


Fig. 2 Proposed technique

Id	Path	Method	Fingerprint
174	Formatsrc\java3\UsingLayoutManag...	publicvoidwindowClosing(WindowEv...	11010011010111000101100101110...
175	Formatsrc\java3\UsingLayoutManag...	publicstaticvoidmain(Stringargv[])	11001011101011100011110011100...
176	Formatsrc\java3\WalkingText.java	publicvoidinit()	11001111100011000111100011110...
177	Formatsrc\java3\WalkingText.java	publicvoidstop()	11011011001101110001100101110...
178	Formatsrc\java3\WalkingText.java	publicvoidstart()	11010011000111000101110011110...
179	Formatsrc\java3\WalkingText.java	publicString[]getParameterInfo()	1100101110011100011101111001...
180	Formatsrc\java3\WalkingText.java	publicvoidrun()	11000111101001100001111000110...
181	Formatsrc\java3\WalkingText.java	publicvoidpaint(Graphicsg)	11000101100001110011110010011...

Fig. 3 Fingerprints for the methods

Figure 3, shows the fingerprints generated for the methods. In the same way fingerprints are generated for files and directories.

The major idea of our proposed technique is to find the similarity using fingerprints. One of the advantages of this technique is to map a large dataset of arbitrary length into a same bit sequence. We use the *Message Digest Algorithm* [10] for this purpose. Fingerprints are computed for every token at the method level, file level, and the directory level. The *Message Digest Algorithm* generates unique fingerprints for every token. At the method level the fingerprints are calculated for the tokens and the similar tokens will have the similar fingerprint. At the file level fingerprints are calculated for the sequence of statements and similar files will have similar fingerprints which gives the File Level clones. And at the directory level fingerprints are calculated for the group of file in the same directory and such similar directories will have similar fingerprints.

The next step in the above process is to find the similarity between the fingerprints. The similarity is calculated using a hash function called Locality Sensitive Hashing. A LSH function is a hash function which hashes for vectors such that the probability that two vectors having the same hash value is strictly decreasing function of their corresponding distance. In other words we can say that two vectors having the smaller distance will have the higher probability of having the same hash code. Let a hashing family be defined as

$$h_i = (p_i) \text{ where } p_i = \text{ith bit of } p.$$

$$\Pr_H [h(p) \neq h(q)] = \frac{\|p, q\|_H}{d}. \tag{1}$$

$$\Pr_H [h(p) = h(q)] = 1 - \frac{\|p, q\|_H}{d}. \tag{2}$$



When similar points collide Pr must be  $\geq 1 - \left(1 - \frac{1}{p^l}\right)^K$

When dissimilar points collide Pr must be  $\leq P_2^K$

The LSH function [11] is used to hash the fragments into smaller sets called buckets based on their hash code. The cloned fragments having similar hash codes are mapped into same buckets. LSH similarity comparison is computed using the formula Fig. 2. After finding the similarity the values are compared with a threshold value to classify them as *Exactly Similar Clones*, *Most Similar Clones* and *Least Similar Clones*. Under each threshold value method level, file level, and directory level are identified. The last process is to form clone pairs and form the clone set. The clones which come under the same classification are compared to form clone pairs. From the clone pairs method level, file level and directories level clone sets are formed.

### 3.1 Algorithm for Finding Higher Level Clones

## 4 Implementation and Evaluation

Experiments were carried over on the Sample Java System given in Table 2. The system includes the following contents.

**Table 1** Detection algorithm

---

Algorithm for finding Higher-Level Clones

---

1. For every file in the software
    - a. Find for files
    - b. Find for directories
  2. For every file in the directory
    - a. Collect all the methods
  3. Generate the Fingerprints for methods, files, and directories
  4. Find the similarity using LSH
  5. Find the ClonePair and CloneSets for recurring patters of methods, files, and directories.
- 

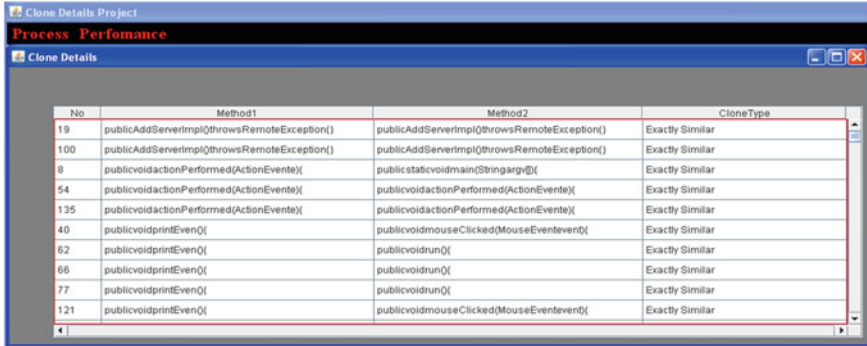
The algorithm for finding higher level clone is given in Table 1

Our main aim is to find the cloned code in terms of higher level patterns, i.e., methods, files and directories. In the method level two similar methods of the same content will have the same fingerprints and will be identified as method level clones. Similarly, the file level and the Directory level clones are identified. The new technique proposed by us enables to find the Clone Pairs and their corresponding CloneSets for a particular threshold value. Figure 4. shows the Clone Pairs identified for the exactly similar clones at the method level.

To find the exactly similar clones the threshold (Th) values are varied from 1.0, 0.9, and 0.8. To find the *Most Similar Clones* the Th values are 0.6, 0.7, and 0.75.

**Table 2** Sample Java system

Sample Java System	Contents
No of files	129
No of methods	181
No of directories	3



**Fig. 4** Clone pairs for exactly similar clones

**Table 3** Exactly and most similar clone pairs

Threshold value		Methods		Files		Directory	
ES	MS	ES	MS	ES	MS	ES	MS
0.8	0.6	221	814	76	1	4	0
0.9	0.7	89	451	70	2	4	0
1.00	0.75	57	170	62	2	4	0

**Table 4** Exactly and most similar clone sets

Threshold value		Methods		Files		Directory	
ES	MS	ES	MS	ES	MS	ES	MS
0.8	0.6	57	57	110	0	2	0
0.9	0.7	54	42	99	3	2	0
1.00	0.75	53	43	90	3	2	0

The same process is continued to find the *Least Similar Clones*. By changing the threshold values the following Clone Pairs and the Clone Sets are detected and the results are shown in Tables 3 and 4. The graph for the *Exactly Similar Clone* pairs and clone sets are shown in Figs. 5, 6.

## 5 Conclusion and Future Work

In this work, a technique has been presented to detect the higher level clones in the softwares such as File Level, Method level, and the Directory level clones. This technique uses Message Digest Algorithm to find out the fingerprints and uses LSH

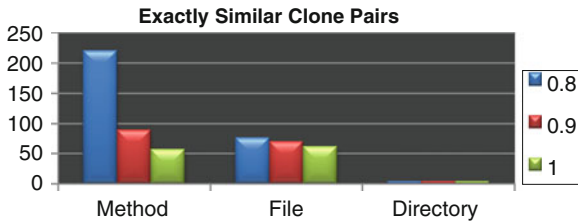


Fig. 5 Exactly similar clone pairs

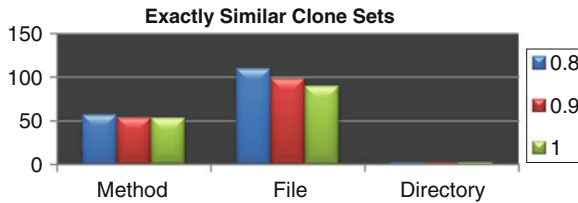


Fig. 6 Exactly similar clone sets

to compare it. The output produced by this system is a group of Clone pairs and Clone sets for Files, Methods and Directories. From the clone sets the number of Methods, Files, and directories which belong to the *Exactly Similar*, *Most Similar* and the *Least Similar* category are identified. The algorithm is tested using a sample java system. According to our sample system 53 out of 181 methods, 90 out of 129 files, and 2 out of 3 directories are cloned. In future, clone pairs can be clustered using the clustering techniques and the structural similarities can be found. Further the algorithm can be extended to detect clones in other data structures.

## References

1. Jiang, L., Misherghi, G., Su, Z., Glondu, S.:Deckard: scalable and accurate tree-based detection of code clones. In: Proceedings of International Conference on Software Engineering, pp. 96–105, (2007)
2. Li, Z., Lu, S., Myagmar, S., Zhou, Y.: CP-miner: a tool for finding copy-paste and related bugs in operating systemcode. In: Proceedings of the Symposium Operating System Design and Implementation, pp. 289–302, (2004)
3. Kamiya, T., Kusumoto, S., Inoue, K.: CCFinder: a multilinguistic token-based code clone detection system for large scale source code. In: IEEE Transaction on Software Engineering, pp. 654–670, (2002)
4. Baxter, I.D., Yahin, A., Moura, L., Sant’Anna, M., Bier, L.:Clone detection using abstract syntax trees. In: International Conference on Software Maintenance, pp. 368-378, (1998)
5. Mayrand, J., Leblanc, C., Merlo, E.: Experiment on the automatic detection of function clones in a software system using metrics. In: International Conference on Software Maintenance, pp. 244–253, (1996)

6. Balazinska, M., Merlo, E., Dagenais, M., Lague, B., Kontogiannis K.: Measuring clone based reengineering opportunities. In: IEEE Symposium on Software Metrics, pp. 292–303, (1999)
7. Kapsner, C.: Toward a taxonomy of clones in source code: a case study. In: Evolution of Large Scale Industrial Software Architectures, pp. 67-78, (2003)
8. Koschke, R., Falke, R., Frenzel, P.: Clone detection using abstract syntax suffix trees. In: Working Conference on Reverse Engineering, pp. 253–262, (2006)
9. Basit, H.A., Jarzabek, S.: Detecting higher-level similarity patterns in programs. In: Proceedings of the 10th European Software Engineering Conference held Jointly with 13th ACM SIGSOFT, International Symposium on Foundations of Software Engineering, pp. 156–165, (2005)
10. Rivest, R.: The MD5 message digest algorithm. RFC1321, Network Working Group. [www.ietf.org/rfc/rfc1321.txt](http://www.ietf.org/rfc/rfc1321.txt). (1992)
11. Gionis, A., Indyk P., Motwani, R.: Similarity search in high dimensions via hashing. In: Proceedings of the 25th International Conference on Very Large Data Base, 518–529, (1999)

# Privacy Protected Mining Using Heuristic Based Inherent Voting Spatial Cluster Ensembles

R. J. Anandhi and S. Natarajan

**Abstract** Spatial data mining i.e., discovery of implicit knowledge in spatial databases, is very crucial for effective use of spatial data. Clustering is an important task, mostly used in preprocessing phase of data analysis. It is widely recognized that combining multiple models typically provides superior results compared to using a single, well-tuned model. The idea of combining object partitions without accessing the original objects' features leads us to knowledge reuse termed as cluster ensembles. The most important advantage is that ensembles provide a platform where vertical slices of data can be fused. This approach provides an easy and effective solution for the most haunted issue of preserving privacy and dimensionality curse in data mining applications. We have designed four approaches to implement spatial cluster ensembles and have used these for merging vertical slices of attribute data. In our approach, we have brought out that by using a guided approach in combining the outputs of the various clusterers, we can reduce the intensive distance matrix computations and also generate robust clusters. We have proposed hybrid and layered cluster merging approach for fusion of spatial clusterings and used it in our three-phase clustering combination technique. The major challenge in fusion of ensembles is creation and manipulation of voting matrix or proximity matrix of order  $n^2$ , where  $n$  is the number of data points. This is very expensive both in time and space factors, with respect to spatial data sets. We have eliminated the computation of such expensive voting matrix. Compatible clusterers are identified for the partially fused clusterers, so that this acquired knowledge will be used for further fusion. The apparent advantage is that we can prune the data sets after every  $(m-1)/2$  layers. Privacy preserving has become a very important aspect as data sharing between organizations is also difficult. We have tried to provide a solution for this problem. We have obtained clusters

---

R. J. Anandhi (✉)

Department of Computer Science and Engg, The Oxford College of Engineering, Bangalore, India  
e-mail: rjanandhi@hotmail.com

S. Natarajan

Department of Information Science and Engineering, PESIT, Bangalore, India  
e-mail: snatarajan\_44@gmail.com

from the partial datasets and then without access to the original data, we have used the clusters to help us in merging similar clusters obtained from other partial datasets. Our ensemble fusion models are tested extensively with both intrinsic and extrinsic metrics.

**Keywords** Cluster ensembles · Degree of agreement · Performance metrics · Spatial attribute data

## 1 Introduction

Clustering ensembles can be applied in various application environments and can be summarized based on the final clusters formed. The foremost utility of cluster ensembles is its ability to cluster categorical data. A noteworthy capability of clustering ensembles is that it provides a very natural and elegant way to cluster categorical data without any external labeling and uses the underlying data structure. Let us consider a data set with tuples  $t_1, ..t_n$  over a set of categorical attributes  $A_1...A_m$ . The basic idea here is to view each attribute  $A_j$  as a way of producing a simple clustering of the data. If  $A_j$  contains  $k_j$  distinct values, then it is considered as  $A_j$  partitions the data into  $k_j$  clusters, one cluster for each value. Then, clustering fusion considers all those  $m$  clusterings produced by the  $m$  attributes and tries to find a consensus clustering that agrees as much as possible with all of them. Cluster ensemble approaches for fusing clusterings can also be extended to incorporate domain knowledge along with human guidance, when available. The clustering ensembles framework provides several ways for dealing with missing values in categorical data. One of the most important features of the usage of clustering ensembles is that there is no need to specify the number of clusters in the result. The formulation of clustering ensembles or aggregation [1] gives one inherent way of automatically selecting the number of clusters. If majority of the input clusterings place two objects in the same cluster, then it will not be beneficial for a clustering fusion solution to split these two objects.

Privacy-preserving data mining is a most studied subject in the last decade. There can be a common situation where a database table is vertically split and different attributes are maintained in different sites. For such cases, ensembles offer a natural model for clustering. the data maintained in all sites as a whole and also in a privacy-preserving manner. The only information revealed is which tuples are clustered together and no information is revealed about data values of any individual tuples. This becomes a welcome boom for the privacy preserving related issues.

The rest of the paper is organized as follows. The related work is in Sect. 2. The proposed knowledge guided fusion ensemble technique and its application in vertical slices merging, thereby favoring privacy protected data mining, is discussed in Sect. 3. In Sect. 4, we present experimental test platform and results with discussion. Finally, we conclude with a summary and our planned future work in this area of research.

## 2 Literature Survey

### 2.1 Work Done in Cluster Ensembles

The goal of cluster ensemble is to combine the clustering results of multiple clustering algorithms to obtain better quality and robust clustering results. Even though many clustering algorithms have been developed, not much work is done in cluster ensembles in data mining and machine learning community. There are few special categories of consensus function such as Voting Approach, Hyper graph Partitioning, Mutual Information Algorithm, Finite Mixture model and Co-association based functions, all of which we have studied and consolidated during our literature survey.

Strehl and Ghosh [2] have considered three different consensus functions for ensemble clustering. The **C**luster based **S**imilarity **P**artitioning **A**lgorithm (CSPA) and **H**yper**G**raph **P**artitioning **A**lgorithm (HGPA) proposed by them has a computing complexity of  $O(kn^2H)$  and  $O(knH)$ . Their proposed algorithms improved the quality and robustness of the solution, but their greedy approach is the slowest and often is intractable for large  $n$ . Moreover all their algorithms are based on static approaches, in the sense they do not reuse the gained knowledge during fusion.

Azimi et al. [5], proposed a new clustering ensemble method, that generates a new feature space from initial clustering outputs. Multiple runs of an initial clustering algorithm like k-means generate a new feature space, which is significantly better than pure or normalized feature space and also reduces the local maxima effect. Then, applying a simple clustering algorithm on this generated feature space can obtain the final partition significantly better than pure data or the initial clusterings. Fischer and Buhmann [6], and also Dudoit and Fridlyand [4], have implemented a combination of partitions by re-labeling and voting. Their works practiced direct re-labeling approaches to the correspondence problem. A re-labeling can be done optimally between two clusterings using the Hungarian algorithm as in basic voting approaches. Topchy et al. [7] have developed a different consensus function based on information theoretic principles, using generalized Mutual Information (MI). Fred [3] proposed to summarize various clustering results using a co-association matrix. The rationale of his approach is to weigh associations between sample pairs by the number of times they co-occur or repeat in a cluster from the set of data partitions produced by independent runs of clustering algorithms.

### 2.2 Motivation for the Current Work in Ensembles

Many clustering algorithms are capable of producing different partitions of the same data because they capture various distinct aspects of the data. Due to the lowest computational complexity in mutual information based clustering ensembles technique and simplicity in voting technique we have a hybrid combination of both of these, resulting in a new heuristic algorithm called **H**ybrid **I**nherent **V**oting **E**nsamble

Fusion technique [8–10]. We have tried to find answers for which clusterers to merge first, how to merge and how to reuse the gained intelligence during merge in an effective way [12].

### **3 Proposed Hybrid Inherent Voting Spatial Cluster Ensembles**

#### ***3.1 Motivation and Challenges***

To achieve compromise between individual yet conflicting clusterings is an important aim of cluster ensembles. The problem of combination of multiple clusterings brings its own new and tough challenges. The major difficulty is in arriving at a consensus partition from the various output partitions of different clustering algorithms. Unlike supervised classification and the classifier ensembles, here the patterns are unlabeled. This implies that there is no explicit correspondence of label information that is available from different clusterings. An extra complexity arises when different partitions contain different numbers of clusters, often resulting in an intractable label correspondence problem. This results in either under fitting or over fitting the data. Most of the existing methods consider all generated partitions, for deciding the concluding clusters. This may not be the optimal solution because some ensemble members are less accurate than others and these in turn may have detrimental effects on the final performance. It is to be noted that technique we have used are fundamentally different from the existing methods because we aim to design and employ heuristics for selection of ensemble members, without considering the characteristics of the data sets and the clusterings. Our goal is to select ensembles based on the underlying implicit clusters of the data set and also to make use of the various approaches available in the clustering algorithm themselves.

#### ***3.2 The Inherent Voting Approach in Spatial Cluster Ensembles***

The hybrid inherent Voting approach has two phases, ensemble initialization process and the fusion process. Basically, there are two basic possibilities for fusion namely static and dynamic approaches. In the static approach, all the compatible pairs for fusion are found using methods like co-association and then the actual merge takes place. The second method does not have that kind of clear cut demarcation between the merging pairs ahead of the fusion process. This dynamic approach follows the simultaneous select and fuse process, so that any added knowledge gained during the fusion process can further guide in selection of better fusion points. Our approach is based on the dynamic fusion method. The layer based merging uses the clusterers as layers and selects two layers at a time for the fusion. This technique avoids the need for generation of the costly distance matrix, thereby exploiting the inherent



voting advantages. We felt that the knowledge gained during the intermediate merge stages, is not at all considered nor utilized till now in any of the existing work. None of the existing approaches use the merged knowledge to guide the fusion of the remaining clusterers. But, we had an intuition that this knowledge can actually help in guiding the fusion process and will be very useful in an unsupervised clustering scenario. Combination of approaches like voting model, mutual information model and co-association model might lead to overcome the weakness of each one of them. Hence we have tried a hybrid combination of all these approaches, resulting in a new heuristic algorithm called Hybrid Inherent Voting Ensemble Fusion technique.

We have used Shannon entropy measure to calculate the entropy between all the clusterers and form a **Clusterer Compatibility Matrix (CCM)** of the order  $m \times m$ , where 'm' is the number of clusterers. The corresponding  $i$  and  $j$  values for the maximum 'CCM( $i,j$ )'th value indicates that these two clusterers ( $i$  and  $j$ ), if selected as initial clusterers for fusion, will provide a stronger base information for guiding further fusions. We have built two fusion models using the above mentioned CCM technique termed as **Slice and Dice Ensemble Model** [8] and other without using CCM technique, as in **Inherent Voting Depth First Merge** and **Cyclic Merge** [11].

Selecting the best clusterer pair with whom the fusion can commence, based on the clusterer compatibility has given the initial head start for the whole fusion process resulting in more accurate clusters. Extra knowledge about the underlying data structure is already available in the form of label vectors. Hence highly computational intensive methods like normalized mutual information computation or counting the number of all the co associations or checking for complete majority votes are not needed for selection of fusion joints. The merge and purge technique, where we keep purging the input data set once their confidence levels are above a threshold, along with the process of merging the data points, helps in fast convergence of the algorithm as well as leads to the effective use of the memory resources. Validation of the ensemble fusion results of clusters, generated in this unsupervised manner has been done using both intrinsic and extrinsic metrics.

We have formulated four greedy and heuristics approaches [8–12] to exploit the hidden knowledge in the spatial data clusterings.

During the second phase of fusion, we have framed four models for fusing the clusterings formed in first phase, using the dynamic approach. This phase comprises of activities like **(i)** computation of clusterer compatibility matrix, **(ii)** finding the initial fusion seed from clusterer compatibility matrix using partition entropy. Then, the fusion joints are identified, for those clusterings of the clusterers, selected by the fusion seed component, using the proposed similarity measures. The main component of the ensemble fusion model is the consensus functions based on the various heuristic models like **Inherent Voting Depth First merge model**, **Cyclic Merge model**, **Slice and Dice Ensemble Merge model** and the **Nebulous Pool merge model**. Framing different similarity measures for finding the fusion joints, elegant but effortless approximation base methods for identifying the prime fusion seed, i.e., clusterer compatibility identification, usage of different consensus techniques are the key techniques in this work. We have also categorized the experimental data sets into

small, medium and large based on the number of instances, number of dimensions and number of underlying classes.

### 3.3 Parameters and Definitions for the Hybrid Fusion

**Fusion Joint Set— $FJ_{ij}$ :** Set of probable matching pairs of  $i$ th clusterer with the  $j$ th clusterer, based on the maximum entropy factor or maximum degree of overshadow factor. The cardinality of this fusion set is equal to the maximum number of clusters in  $i$  or  $j$ . This set will be used for deciding where the fusion, if happens, will most likely yield optimal information gain in the resultant clusters.

**Clusterer Compatibility Matrix— $CCM(m \times m)$ :** Symmetric matrix where  $m$  is the total number of clusterers considered for fusion.  **$CCM(i, j)$ :** An integer value representing the Shannon entropy between  $i$ th clusterer and  $j$ th clusterer. The maximum value in a cell of the matrix, say  $CCM(i, j)$ , indicates that there is maximum partition entropy between clusterer 'i' and 'j', indicative of probable profitable fusion. This value forms the seed for the fusion.

**Degree of Agreement (DoA factor):** Cumulative ratio of the index of the merging level to the total number of clusterers.

### 3.4 Proposed Models for the Hybrid Fusion

**Inherent Voting Depth First Merge (IVDFM)** algorithm is framed with the notion that if normally a clustering with maximum number of data points is handled properly then the convergence of such fusion will happen faster. This is seen even during manually clustering objects, where we tend to handle the bigger components first by intuition. And also the clusterings with comparatively lesser number of data points will tend to disturb the bigger clusterings' co-occurrence measure. Another feature of this model is that we will not be explicitly building the complete static voting matrix though we will rely on majority opinions. The IVDFM fusion model starts with the first clusterer's clustering which has maximum data points ( $L_{max1}$ ). The selection of the order of the clusterer goes with the way input is provided. That is, we have considered first come first serve basics during selection of clusterers. The IVDFM model uses both the similarity measures i.e., MeCos co-efficient based on, Minimum enclosing circle's overshadow and the measure based on partition entropy, separately, for finding the compatible clustering fusion joint. In **Cyclic Merge Model (CycM)**, the clustering ensembles are combined in sliced pair, called **Matching Groups set**,  $MG_{mk}$ , using clusterer compatibility matrix. The main difference between this model and the IVDFM model is that equal and fair chances are given to all the clusterings in the first layer to choose their fusion joints. The layered **Slice and Dice Ensemble Merge model (SDEM)** is an enhanced model from the earlier IVDFM and CycM, in the sense that it incorporates heuristics in selection of clusterers as well as clusterings

for the fusion. And also it tries to make the model more efficient both in the terms of run time as well as space complexity. During the merge phase, fusion joint sets are formed by using either MeCos coefficient or the partition entropy between the data elements of the clusterings. The usage of similarity between core points is a normally used approach, which is very sensitive to the presence of outliers. The co-association based approach is computationally intensive with regard to spatial data. Instead we have found that the usage of cardinality of set intersection in association with partition entropy performs better in respect to identifying the concluding cluster partitions as well as resolves the label naming issues very easily and elegantly.

During the merging phase, initially, for each data point in the clusterer in focus, the **Degree of Agreement (DoA)** is calculated. There are two types of merge that we have used in the fusion step. Normal merge takes place between two clusterers when the DoA value is less than the threshold. Pruned Merge occurs when the DoA value is equal to or greater than the threshold DoA value. This ensures that once, certain data points have the marginal majority, they can be placed in the corresponding concluding clusters. This type of pruned merge helps to drastically reduce the data points half way through the fusion process. Spatial data with spatial auto correlated elements tends to benefit from this pruned merging approach.

## 4 Experimental Platform, Results and Inferences

### 4.1 Metrics Used in the Study

In the study of the hybrid inherent voting ensembles, we have used intra cluster density, inter cluster density and Dunn indices from the group of intrinsic measures as metrics. Dunn’s index is a metric of, how well a set of clusters represent compact separated clusters. The Dunn index defines the ratio between the minimal inter cluster distances to maximal intra cluster distance. The Dunn index is limited to the interval [0, 1] and should be maximized. Dunn’s index ( $\alpha$ ) for a partition U is defined as in Eq. (1)

$$\alpha(c, U) = \frac{\min_{1 \leq q \leq c} \min_{1 \leq r \leq c, r \neq q} \text{dist}(C_q, C_r)}{\max_{1 \leq p \leq c} \text{diam}(C_p)} \tag{1}$$

These metrics measure the goodness of a clustering structure without referring to any external information and depends on the under lying data structure itself. Inter cluster density, an intrinsic metric is based on how distant are the data elements in one cluster from elements in other clusters. This metric comes under More-The-Better category of factor values in the performance study. Intra cluster density, an intrinsic metric is based on proximity of elements are within one cluster to each other.

## ***4.2 The Experimental Test Platform***

In the test platform, both homogeneous as well as heterogeneous ensembles are considered. For the clusterings in homogeneous ensembles, we have used k-means with different values of k. For the heterogeneous ensembles, we have created the ensemble clusters using k-means, CLARA, Average Link agglomerative algorithm, fuzzy clustering and Wards divisive algorithms. The entire ensembles are from different clustering techniques; hence we have made the test platform with as much diversity as possible. The resources needed for executing the above process is a PC with Pentium Dual Core processor with 4 GB RAM and the code for implementing the ensemble fusion models is written using Matlab 7.0.

## ***4.3 Data Sets Used in the Experiments***

The cluster ensemble applications were tested on both real and synthetic data-sets. The data sets were downloaded from University of California, Irvine (UCI) Machine Learning repository and <http://www.Strehl.com>. As an indication of the impact of the archive, it has been extensively cited, making it one of the top 100 most cited "papers" in all of Computer Science research. These data sets serve as a benchmark for most of the algorithm verification and validation in Data Mining. We have collected the experimental data sets in such way that it includes as much diversity as possible. Based on the properties of the data sets, we have categorized them into small, average and large groups. This will help us to get the insight of which ensemble fusion approach will be more suitable for a particular data set. We have also chosen data sets with more number of dimensions and instances and classes, which reflects the basic traits of spatial data.

## ***4.4 Experimentation Results and Inferences***

The input for the ensemble algorithms are from base clusterers. Each of these algorithms was executed at least 15 times to see that no discrepancy due to the base algorithm is passed on as inputs. To check how useful homogenous ensembles can be, while handling huge dimensions in data set and to verify the quality and robustness of the final clusters, metrics like Cluster Purity and Dunn Indices were used. Initially the data set is divided vertically, simulating partial attributes and clusterings are formed for ensembles, using k-means clustering algorithm. This way the availability of partial attributes is simulated and homogenous base clusterers are formed based on different disjoint attributes of the same data set and is used for base clusterers' formation. The clusterings are merged using the hybrid fusion model. A

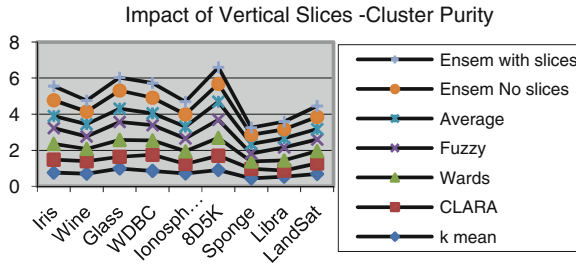


Fig. 1 Validation with cluster purity

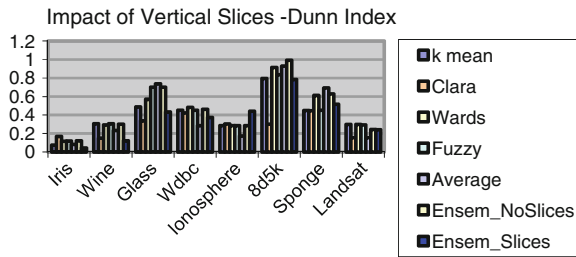


Fig. 2 Validation with dunn indices

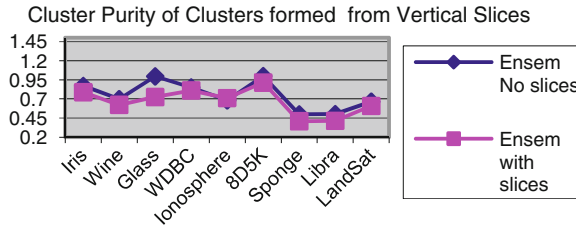
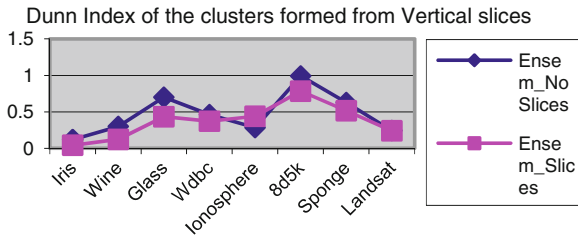


Fig. 3 Behavior of vertical slices ensemble fusion: cluster purity

comparison of the base clusterers’ values against the fused clusters generated from partial view data sets is done to check for the deviations between them.

The graphs shown in the Figs. 1 and 2 bring out the deviations of the Cluster Purity and Dunn Index values between the clusters formed from the complete data set and clusters formed from partial view of data. We can see that the purity of the clusters has been reduced in the cases where the dimensions are low. In data sets like Ionosphere (34 D), Sponge (45 D), Libra (91 D) and Landsat (36 D), we have achieved almost the same purity. Similarly, the Dunn indices are 38 % better in Ionosphere data set, revealing that robust clusters can also be formed from having partial view of the data set attributes using our fusion process. This is graphically shown in Figs. 3 and 4.



**Fig. 4** Behavior of vertical slices ensemble fusion: dunn index

## 5 Conclusion and Future Work

The concept of fusion of clusters derived from different clustering algorithms ensures that we have robust, novel and compact cluster outputs. And also clustering is an important functionality and also most of the times it used as pre processing step in the field of Data Mining. First, we have tested several non-spatial datasets which are normally used as bench marks for data clustering. Then we tested how our layer based methodology can work with spatial data. We have evaluated our work incorporating spatial feature spaces. The proposed automated layered merge approach was able to provide the acceptable accuracy with more efficiency both in space constraint and in computations. The results of the fusion of vertically sliced attribute data against the clusters derived from complete data was promising and proves that cluster compactness of the fused clusters derived from partial data is also in acceptable margin, when the dimensions are large. This is a promising result for data analysts who are concerned about the privacy of data attributes and who are deprived of some fields in their data due to privacy issues. However, more work should be carried out to provide support for more real life data from satellites and incomplete data. Future work in the short term will focus on how to acquire such datasets, and continue with more testing, in spite of current security concerns in distributing such data.

## References

1. Gionis, A., Mannila, H., Tsaparas, P.: Clustering aggregation. *J. ACM Trans. Knowl. Disc. Data (TKDD)* **1**(1), (2007). doi:[10.1145/1217299.1217303](https://doi.org/10.1145/1217299.1217303)
2. Strehl, A., Ghosh, J.: Cluster ensembles - a knowledge reuse framework for combining multiple partitions. *J. Mach. Learn. Res.* **3**, (2002)
3. Fred, A.L.N.: Finding consistent clusters in data partitions. In: *Proceedings of Second International Workshop on Multiple Classifier Systems*, pp. 309–318. Springer-Verlag, London (2001)
4. Dudoit, S., Fridyand, J.: Bagging to improve the accuracy of a clustering procedure. *Oxford J. Bioinform.* **19**(9), 1090–1099 (2003). doi:[10.1093/bioinformatics/btg038](https://doi.org/10.1093/bioinformatics/btg038)

5. Azimi, J., Abdoos, M., Analoui, M.: A new efficient approach in clustering ensembles, LNCS, **4881**, pp. 395–405 (2007)
6. Fischer, B., Buhmann, J.M.: Bagging for path-based clustering. *IEEE Trans. Pattern Anal. Mach. Intell.* **25**(11):1411–1415 (2003)
7. Topchy, A., Jain, A.K., Punch, W.: Combining multiple weak clusterings. *Proceeding of the Third IEEE International Conference on Data Mining*, pp. 331–338 (2003). ISBN :0-7695-1978-4 doi:[10.1109/ICDM.2003.1250937](https://doi.org/10.1109/ICDM.2003.1250937)
8. Anandhi, R.J., Natarajan, S.: Efficient consensus function for spatial cluster ensembles: An heuristic layered approach. *Proceedings of International Symposium on Computing, Communication and Control*, Singapore (2009). ISBN 978-9-8108-3815-7
9. Anandhi, R.J., Natarajan, S.: A novel method for combining results of clusters in spatial cluster ensembles: A layered depth first merge approach with inherent voting. *Int. J. Algorithms, Comp. Math.* **2**(4), 53–58 (2009). ISSN 0973–8215
10. Anandhi, R.J., Natarajan, S.: An enhanced clusterer aggregation using nebulous pool. *Proceedings of ACM -w International Conference of Celebration of Women in Computing, India, ACM Digital, Library* (2010). 978–1-4503-0194-7
11. Anandhi, R.J., Natarajan, S.: A robust-knowledge guided fusion of clustering ensembles. *Int. J. Comput. Sci. Inf. Sci.* ISBN 1947-5500 **8**(4), LJS Publisher and IJCSIS Press, Pennsylvania, USA (2010)
12. Anandhi, R.J., Natarajan, S.: Efficient and effortless similarity measures for spatial cluster ensembles. *CiiT Int. J. Artif. Intell. Syst. Mach. Learn. Pr.* ISSN 0974–9667 and Online: ISSN 0974–9543, doi:[AIML112010010](https://doi.org/10.1109/AIML112010010), **2**(11), pp. 359–365 (2010)

# Smart Relay-Based Online Estimation of Process Model Parameters

Bajarangbali and Somanath Majhi

**Abstract** This paper presents online estimation of unstable and integrating time delay process model parameters using a smart relay. The describing function (DF) approximation of relay not only results in simpler analytical expressions but also enables one to estimate the model parameters with significant accuracy. Measurement noise is an important issue during estimation of process model parameters. The smart relay is capable of emulating the dynamics of a conventional relay and also of rejecting the ill effects of measurement noise. Simulation results show the usefulness of the identification technique.

**Keywords** Relay · Hysteresis · Smart relay · Process model

## 1 Introduction

Industrial controllers are tuned offline or online depending upon the ways process model parameters are estimated. In online identification, relay is connected in parallel with a controller to extract the process information from the measurements made on the limit cycle output. A sustained oscillatory output can be obtained from relay feedback test. Several authors have used the describing function analysis for estimation of integrating and unstable time delay process model parameters. Since Relay is a nonlinear device it is approximated by an equivalent gain using describing function technique. Initially, Åström and Hägglund [1] proposed the use of relay feedback technique combined with describing function approximation to determine the

---

Bajarangbali (✉) · S. Majhi  
Department of Electronics and Electrical Engineering, Indian Institute  
of Technology, Guwahati 781039, India  
e-mail: bajarangbali@iitg.ernet.in

S. Majhi  
e-mail: smajhi@iitg.ernet.in



ultimate gain and frequency. Later Luyben [2] pioneered the use of relay feedback with describing function analysis for process identification. Accurate process model parameters cannot be estimated because of the measurement noise, which may even fail the test. Sources of measurement noise are many subsystems those do not possess low-pass characteristics. Using a relay with hysteresis, the effect of measurement noise can be reduced [1]. Majhi [3] proposed relay-based identification of integrating process model parameters by state space technique. Recently Panda et al. [4] proposed estimation of integrating and time delay processes using single relay feedback test. Liu and Gao [5] derived exact relay response expressions for integrating and unstable processes by using Newton-Raphson iteration method. Estimation of parameters of unstable processes with time delays is a difficult task. Because the limit cycle exists only when the ratio of time delay to unstable time constant is less than 0.693 [6, 7]. Majhi and Atherton [8] proposed online tuning of process controllers for an unstable first order plus time delay systems by using single relay feedback test and state space technique. Li et al. [9] used two relay tests for estimation of stable and unstable process model parameters. But in their method the use of an additional relay test is tedious and time consuming. Later some authors improved relay auto-tuning by using Fourier analysis or by exact analysis. These improvements do not get rid of the practical constraints of relay-based estimation. The conventional relay method is an offline identification method. But sometimes offline identification may be dangerous since it affects the operational process regulation which may not be acceptable for certain critical applications. Therefore, the tuning under tight continuous closed loop control often known as online tuning is preferred. Marchetti et al. [10] developed identification method for open-loop unstable processes by using two relay tests. But the above-mentioned methods are not simple and straightforward like the describing function method, and also they are time consuming. It becomes extremely difficult to obtain simple explicit expressions for unstable and integrating process model parameters by exact analysis methods.

This paper, proposes a smart relay and a straightforward method to estimate the process model parameters. The mathematical analyses of the authors' recent publication [11] have been extended here to estimate online parameters of unstable and integrating time delay process models. This paper is organized as follows. Section 2 describes the proposed identification methods and estimation of process model parameters. Simulation examples are presented in Sect. 3. And conclusions are given in Sect. 4.

## 2 Proposed Identification Methods

This section presents the procedure for online estimation of unstable and integrating process model parameters by relay-based closed loop tests.

The conventional online identification scheme is shown in Fig. 1. Here it can be seen that relay is connected in parallel with a PID controller  $G_c(s)$  in the loop. Figure 2 shows equivalent representation of Fig. 1. For the purpose of identification,

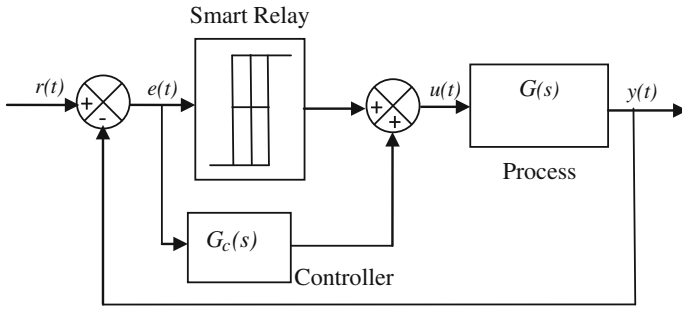


Fig. 1 Online identification scheme

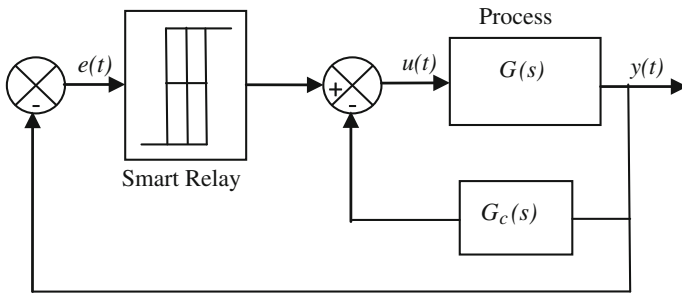


Fig. 2 Equivalent representation of Fig. 1

reference input in Fig. 2 is considered to be zero. The process gets stabilizing signal from the inner feedback controller  $G_c(s)$  thereby improving its stability during identification.

Switching function such as ideal symmetrical relay encounters practical problems under real-time implementation. Multiple switching of relay may occur due especially to the measurement noise. Rustamov et al. [12] have proposed a method for synthesis of a relay regulator with fuzzy switching times on the basis of a macro-variable. A smart relay to overcome the problems associated with multiple switching is implemented with the help of fuzzy rules. The smart relay is assumed to have a nonlinear gain,  $M$ , expressed as

$$M = \frac{4h(\sqrt{A^2 - \varepsilon^2} - j\varepsilon)}{\pi A^2} \tag{1}$$

where  $h$  and  $\varepsilon$  are parameters of the relay and  $A$  is the amplitude of the relay input signal.

### 2.1 Unstable FOPDT Process Model

Let the dynamics of  $G(s)$  be represented by the unstable FOPDT transfer function model

$$G_m(s) = \frac{K_1 e^{-\theta_1 s}}{T_1 s - 1} \tag{2}$$

Here, the model has three unknown parameters  $K_1$ ,  $T_1$  and  $\theta_1$ . where  $K_1$ ,  $T_1$  and  $\theta_1$  are the steady-state gain, time constant, and the time delay respectively. Let the form of the PID controller be

$$G_c(s) = K_p \left( 1 + \frac{1}{T_i s} + \frac{T_d s}{\gamma T_d s + 1} \right) \tag{3}$$

where  $K_p$ ,  $T_i$ ,  $T_d$  and  $\gamma$  are proportional gain, integral time constant, derivative time constant and derivative filter constant respectively. Since  $\gamma$  is very small, the derivative filter term in Eq. (3) is neglected in the following analysis.

#### 2.1.1 Estimation of $T_1$ and $\theta_1$

Here  $T_1$  and  $\theta_1$  of the process model are estimated online from the measurements of peak amplitude ( $A$ ) and time period ( $P$ ) of the limit cycle output signal, for any non-zero settings of the relay height and hysteresis, i.e.,  $h \neq 0$  and  $\varepsilon \neq 0$ . The following condition should be satisfied for a periodic solution to correspond to a stable limit cycle,

$$M \bar{G}_m(j\omega) = -1 \tag{4}$$

where  $\omega = \frac{2\pi}{P}$  and

$$\bar{G}_m(j\omega) = \frac{G_m(j\omega)}{1 + G_c(j\omega) G_m(j\omega)} \tag{5}$$

Then, Eq. (4) can be written as

$$G_m(j\omega) [M + G_c(j\omega)] = -1 \tag{6}$$

Substitution of  $G_m(j\omega)$ ,  $M$  and  $G_c(j\omega)$  in Eq. (6) and solving gives

$$\frac{K_1 e^{-j\omega\theta_1}}{j\omega T_1 - 1} (a + jb) = -1 \tag{7}$$

where

$$a = \frac{4h\sqrt{A^2 - \varepsilon^2}}{\pi A^2} + K_p$$

$$b = K_p\omega T_d - \frac{K_p}{\omega T_i} - \frac{4h\varepsilon}{\pi A^2}$$

The steady-state gain  $K_1$  can be estimated by several methods. Equating the magnitude and phase angle of both sides of Eq. (7), gives

$$T_1 = \frac{\sqrt{K_1^2(a^2 + b^2) - 1}}{\omega} \quad (8)$$

$$\theta_1 = \frac{\tan^{-1}\left(\frac{b}{a}\right) + \tan^{-1}(\omega T_1)}{\omega} \quad (9)$$

$T_1$  and  $\theta_1$  are estimated using Eqs. (8) and (9), respectively.

## 2.2 Integrating SOPDT Process Model

Next, let the dynamics  $G(s)$  be represented by an integrating SOPDT process model transfer function as

$$G_m(s) = \frac{K_2 e^{-\theta_2 s}}{s(T_2 s + 1)} \quad (10)$$

The model parameters are  $K_2$ ,  $T_2$  and  $\theta_2$ .

### 2.2.1 Estimation of $T_2$ and $\theta_2$

The steady-state gain  $K_2$  can be estimated by several methods. Measurements of peak amplitude ( $A$ ) and time period ( $P$ ) made on the limit cycle output signal for any non-zero settings of the relay height and hysteresis, i.e.,  $h \neq 0$  and  $\varepsilon \neq 0$  are used to estimate the model parameters. Repeating the procedure given in Sect. 2.1 the loop gain is expressed as

$$\frac{K_2 e^{-j\omega\theta_2}}{j\omega(j\omega T_2 + 1)} (a + jb) = -1 \quad (11)$$

where

$$a = \frac{4h\sqrt{A^2 - \varepsilon^2}}{\pi A^2} + K_p$$

$$b = K_p\omega T_d - \frac{K_p}{\omega T_i} - \frac{4h\varepsilon}{\pi A^2}$$

Equating the magnitude and phase angle of both sides of Eq. (11), gives

$$T_2 = \frac{\sqrt{\frac{K_2^2(a^2+b^2)}{\omega^2} - 1}}{\omega} \quad (12)$$

$$\theta_2 = \frac{\frac{\pi}{2} + \tan^{-1}\left(\frac{b}{a}\right) - \tan^{-1}(\omega T_2)}{\omega} \quad (13)$$

Thus the parameters  $T_2$  and  $\theta_2$  are estimated from Eqs. (12) and (13) respectively.

### 2.3 Initial PID Controller Parameters

The relay induces stable limit cycle output when the fictitious process model  $\bar{G}_m(s)$  satisfies the condition in Eq. (3). Extensive simulation studies show that the choice of initial controller parameters  $K_p = 0.01$ ,  $T_i = 1$  and  $T_d = 0.25$ , results in a stable limit cycle output. The relation  $T_i = 4T_d$  is maintained for good transient response of the closed loop system.

## 3 Simulation Results

### Example 1

Consider the unstable FOPDT process transfer function [10]

$$G(s) = \frac{e^{-0.4s}}{s - 1}$$

The smart relay with the parameters  $(h, \varepsilon) = (1, 0.1)$  induces the limit cycle output as shown in Fig. 3. Substituting the peak amplitude and time period of the output signal in Eqs. (8) and (9), the model parameters are estimated as  $T_1 = 0.8293$  and  $\theta_1 = 0.4285$ . Initial PID controller parameters chosen are  $K_p = 0.01$ ,  $T_i = 1$  and  $T_d = 0.25$ . To validate the proposed method, Nyquist plots of actual process transfer function, and the identified model are shown in Fig. 4. It is evident from the plots that

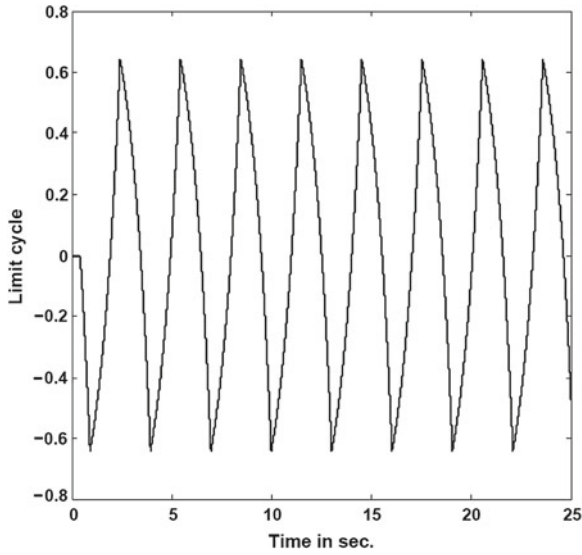


Fig. 3 Limit cycle output for Example 1

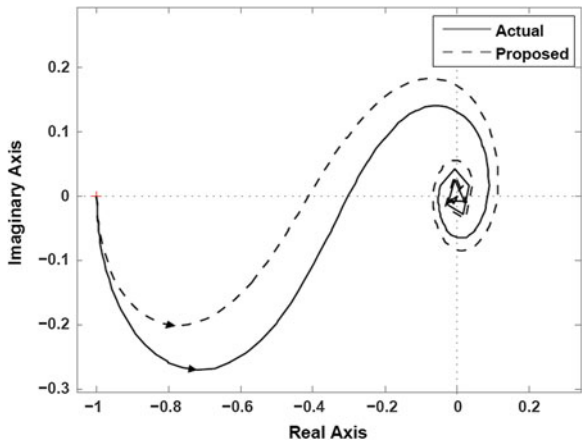


Fig. 4 Nyquist plots for Example 1

the proposed method can be used to estimate online the process model parameters of unstable FOPDT systems.

**Example 2**

Consider the integrating SOPDT process transfer function [3]

$$G(s) = \frac{e^{-1.5s}}{s(5s + 1)}$$

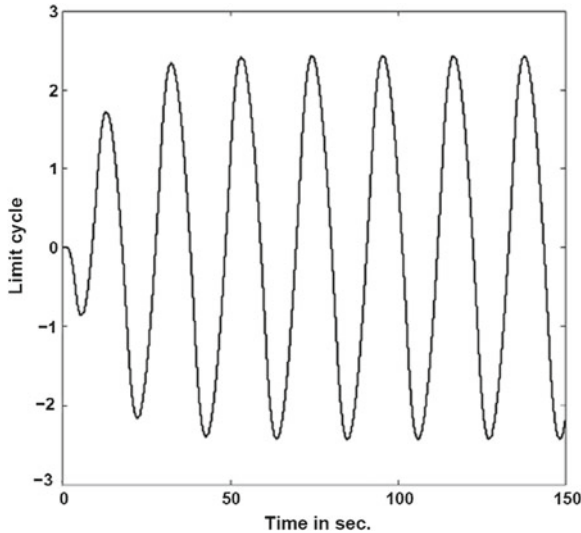


Fig. 5 Limit cycle output for Example 2

The peak amplitude and time period are measured from the limit cycle output shown in Fig. 5 resulting from the autotuning test with the relay parameters  $(h, \varepsilon) = (1, 0.1)$ . Substituting the measured values in Eqs. (12) and (13), the model parameters  $T_2 = 5.0344$  and  $\theta_2 = 1.636$  are estimated.  $K_2$  is assumed to be known a priori. Initial PID controller parameters chosen are  $K_p = 0.01$ ,  $T_i = 1$ , and  $T_d = 0.25$ . The Nyquist plots of actual process transfer function, and that of the process model are compared in Fig. 6. It can be concluded from the proximity of the plots that the proposed method can be used to estimate the process model parameters of integrating SOPDT systems online.

## 4 Conclusion

Online estimation technique for process model parameters of integrating and unstable processes with time delay is presented. A smart relay is used to overcome the difficulties associated with the conventional symmetrical relay. Two examples, one each for an integrating process and unstable process, are considered to validate the proposed method and results are compared using Nyquist plots. Automatic tuning of the controllers, as and when required, can be done employing the smart relay that induces sustained oscillatory output.

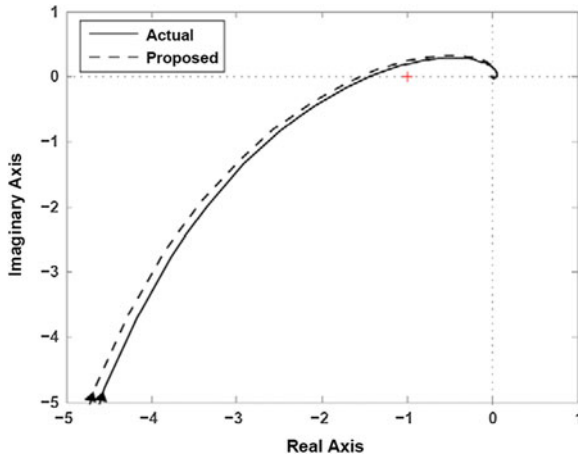


Fig. 6 Nyquist plots for Example 2

## References

1. Åström, K.J., Hägglund, T.: Automatic tuning of simple regulators with specifications on phase and amplitude margins. *Automatica* **20**, 645–651 (1984)
2. Luyben, W.L.: Derivations of transfer functions for highly non-linear distillation columns. *Ind. Eng. Chem. Res.* **26**, 2490–2495 (1987)
3. Majhi, S.: Relay based identification of processes with time delay. *J. Process Control* **17**, 93–101 (2006)
4. Panda, R.C., Vijayan, V., Sujatha, V., Deepa, P., Manamali, D., Mandal, A.B.: Parameter estimation of integrating and time delay processes using single relay feedback test. *ISA Trans.* **50**, 529–537 (2011)
5. Liu, T., Gao, F.: Identification of integrating and unstable processes from relay feedback. *Comput. Chem. Eng.* **38**, 3038–3056 (2008)
6. Atherton, D.P.: Improving accuracy of autotuning parameter estimation. In: *Proceedings of the IEEE International Conference on Control Applications*, pp. 51–56, Hartford (1997)
7. Atherton, D.P., Majhi, S.: Plant parameters identification under relay control. In: *Proceedings of the IEEE Conference on Decision and Control*, pp. 1272–1277, Tampa (1998)
8. Majhi, S., Atherton, D.P.: Online tuning of process controllers for an unstable FOPDT. *IEEE Proc. Control Theory Appl.* **147**(4), 421–427 (2000)
9. Li, W., Eskinat, E., Luyben, W.L.: An improved auto tune identification method. *Ind. Eng. Chem. Res.* **30**, 1530–1541 (1991)
10. Marchetti, G., Scali, C., Lewin, D.R.: Identification and control of open-loop unstable processes by relay methods. *Automatica* **37**, 2049–2055 (2001)
11. Bajarangbali, Majhi, S.: Relay based identification of systems. *IJSER* 3(6)ISSN. 2229–5518 (2012)
12. Rustamov, G.A., Namazov, M.B., Misrikhanov, L.M.: Synthesis of a relay regulator with fuzzy switching times on the basis of a macro-variable. *Autom. Control Comput. Sci.* **41**(3), 158–163 (2007)



# Software Cost Estimation Using Similarity Difference Between Software Attributes

Divya Kashyap and A.K. Misra

**Abstract** The apt estimate of the software cost in advance is one of the most challenging, difficult and mandatory task for every project manager. Software development is a critical activity which requires various considerable resources and time. A prior assessment of software cost directly depends on the expanse of these resources and time, which in turn depends in the software attributes and its characteristics. Since there are many precarious and dynamic attributes attached to every software project, the accuracy in prediction of the cost will rely on the prudential treatment of these attributes. This paper deals with the methods of selection, quantification and comparison of different attributes related to different projects. We have tried to find the similarity difference between project attributes and then consequently used this difference measurement for creating the initial cost proposals of any software project that has some degree of correspondence with the formerly completed projects whose total cost is fairly established and well known.

**Keywords** Software development cost · Software attributes · Cost estimation · k-nearest neighbor classifier · Analogy and similarity difference

## 1 Introduction

Accurate software cost approximation is a widely researched issue related to every industry engaged in software design and development. Despite many estimation models that have been proposed till date, there is a continuous requirement of new

---

D. Kashyap (✉)

Department of Computer Science and Engineering, MNNIT, Allahabad, India  
e-mail: div.kashyap@gmail.com

A. K. Misra

Department of Computer Science and Engineering, MNNIT, Allahabad, India  
e-mail: akm@mnnit.ac.in

systems to forecast the software cost because of continuous and swift changes occurring in the sphere of information technology and software development life cycle. A prototype is always needed that span through all the factors or attributes that are consequent with the project and consequently forms precise development cost estimate. “Cost estimation is a critical and arduous job which is mandatorily required to silhouette the future software development activities” [1]. It is also required for software overall project management, contract negotiations, scheduling, resource allocation and project planning [2, 3]. Thus it may be informed that the timely production of fully-functional and quality software directly depends on the initial estimates of the required cost, effort and resources.

All of the cost prediction models [4], proposed till date, fall in one of the two categories:

- (a) Parametric or Algorithmic models.
- (b) Non-Algorithmic methods.

Tables 1 and 2 lists various models/methods belonging to these categories.

Algorithmic models [4] are based on the mathematical formulas and depend on the measurements and processing of certain project attributes. Most of the algorithmic models are of the form of:

**Table 1** Parametric or algorithmic models

1	COCOMO-II [4–6]
2	Function points [7, 8]
3	Putnam slim [9]
4	SEER SEM [10]
5	SLOC [11]
6	The Doty model [12]
7	Price-S model [13]
8	Walston-Felix multiplicative model [14]
9	Estimacs [15, 16]
10	Checkpoint [17]

**Table 2** Non-algorithmic methods

1	Analogy costing [18–20]
2	Expert judgment [21, 22, 24, 25]
3	Parkinson method [26–28]
4	Price-to-win [29]
5	Bottom-up approach [30]
6	Top-down approach [30]
7	Delphi [31]
8	Machine learning [32]

$$\begin{aligned}\text{Size (KLOC)} &= f(\text{cost affecting factors}) \\ \text{Effort (person months)} &= f(\text{size}) \\ \text{Software cost (INR)} &= f(\text{Effort})\end{aligned}$$

Cost factors are the variables or project attributes, numerous in numbers that simultaneously effect the software development and the form of function  $f$  varies from model to model.

Non-Algorithmic models are the proposed heuristics that requires a considerable reasoning, logic and a large knowledge base. These methods are generally based on the terminologies like “*learning by experience*” or “*trial by case studies*”. Non-algorithmic methods are based on discovery while algorithmic methods focus on calculation.

Algorithmic methods are good because they have fixed and well defined step by step procedure to deliver out the estimate.

Non-Algorithmic models are good because they do not require extraneous parameters that require tuning or calibration according to the measurement environment. In this paper combined both of these approaches in order to enjoy the benefits of both strategies.

A previously completed software project may shed some light on the cost estimation of the current project if both of them have similar attributes and characteristics. Although there exists many factors that describe software project; tried to sort out some the essential nominal, linguistic and numerical attributes [33–35] that prominently affect the software development effort. Then, to find the cost of new software, we find the previously completed projects that have a least similarity difference with the new project in terms of these attributes. To collect these similar projects we have used clustering algorithm to create a cluster of similar projects. Then, we have tried to deliver out the possible cost range of the new project based on the costs of these clustered projects. The flow of our paper goes in the following manner: In section two we have discussed various types of attributes and the operation that can be applied on them. In section three we have proposed an algorithm to create a cluster of projects that has a least similarity difference. Later on in section four we have tried to figure out the performance of our algorithm on some predefined project datasets.

## 2 Software Attributes

Obviously, the similarity between the bygone projects and the current project is gauged on the basis of some parameters or project characteristics. To find out these cost affecting attributes is a separate area of research in itself and researchers have proposed various factors that potentially affect the software development cost. For more information on software attributes we redirect the reader to [36–38].

To establish a correspondence between two projects we have divided various attributes into three categories, nominal attributes, linguistic attributes and numerical

attributes. The following sub-section describes these categories and the attributes of interest covered under each category.

## 2.1 Nominal Attributes (No)

A nominal scale is the lowest level of measurement scale. The attributes covered under this category are categorical. This scale is used to classify a measurement into one of the predetermined class [34, 39]. The attributes covered under this category are:

Name: Implementation programming language.

Values: C, C++, Java, .Net, Scripting, PL/SQL or PHP

Name: Development platform.

Values: Mainframe, mid-range, personal computer or mobile.

Name: Type of software.

Values: System software, application software, programming software, operating system or embedded system.

Name: Existence of overall schedule or plan.

Values: Yes or no.

Name: Use of modern programming practices.

Values: Yes or no.

Name: Software development model in practice.

Values: Waterfall model, prototype model, spiral model, agile development or iterative model.

Name: Project priority.

Values: High or low.

Name: Risks associated with the project.

Values: Low, medium or high.

Name: Type of software release.

Values: Firsthand release or next version.

Similarity difference  $D_{no}$  between two projects  $P1$  and  $P2$  in the nominal attributes space on any nominal attribute ( $No_i$ ) is calculated as below:

$$D_{no}(P1 \rightarrow No_i \cdot P2 \rightarrow No_i) = \begin{cases} \text{if } (P1 \rightarrow No_i \cdot \text{value} = P2 \rightarrow No_i \cdot \text{value}) \\ \text{then } 0 \\ \text{else } 1 \end{cases}$$

In this category each attribute can have a predefined fixed value or we may say that it belong to a fix class. So to calculate the similarity difference on the basis of some attribute belonging to this category, we directly compare their values. If their values are identical i.e. they can be mapped to same class, the similarity difference between the projects is 0 otherwise the similarity difference would be 1.

### 2.2 Linguistic Attributes ( $L_i$ )

Some software attributes neither have a concrete class, into which they can be classified nor have a fix numerical value. These attributes are known as linguistic attributes and these can be measured on a relative scale, like: (*very low, low, medium, high, and very high*) [40, 41]. Although this scale is partial and imprecise but it is quick, easy and less efforts are made to optimize it. For maintaining standards we have taken all the COCOMO-II [29] cost drivers under this category. It uses 17 cost drivers [5, 30, 42] named as: *RELY, CPLX, DOCU, DATA, RUSE, TIME, PVOL, STOR, ACAP, PCON, PCAP, PEXP, AEXP, LTEX, TOOL, SCED, SITE* and five scaling factors named as: *Precedentedness (PREC), Development Flexibility (FLEX), Risk Resolution (RESL), Team Cohesion (TEAM), Process maturity (PMAT)*. Out of these five scale factors four will be assumed nominal, while the remaining fifth (PMAT) rating will based on the development process maturity level, and hence, will vary according to the rating of process maturity level.

Similarity difference  $D_{L_i}$  between two projects  $P1$  and  $P2$  in the linguistic attributes space on any linguistic attribute ( $L_i$ ) is calculated as below:

$$D_{L_i}(P1 \rightarrow L_i, P2 \rightarrow L_i) = \begin{cases} \text{if } (P1 \rightarrow L_i, \text{value} = P2 \rightarrow L_i, \text{value}) \\ \quad \text{then } 0 \\ \text{elseif } (P1 \rightarrow L_i, \text{value} = P2 \rightarrow L_i, \text{value}, \pm 1) \\ \quad \text{then } 0.5 \\ \quad \text{else } 1 \end{cases}$$

In this category each attribute is measured on a relative scale varying from 1 to 5. If the compared attribute have the same value then the similarity difference between projects is 0. Or if according to attribute values, they belong to neighbor classes (*very low and low* or *low and medium* or *medium and high* or *high and very high*) their similarity difference is 0.5. Otherwise the similarity difference is 1.

### 2.3 Numerical Attributes ( $Nu$ )

Software attributes for which we can associate a fix and precise numerical value, can be termed as numerical attributes. Some of the software numerical attributes that we have considered are as follows:

Name: Functions points [7, 8]  
 Name: Quality index [43, 44]  
 Name: Project duration (in months)  
 Name: Team size  
 Name: Number of consultants.  
 Name: Number of intended users.

Similarity difference  $D_{nu}$  between two projects  $P1$  and  $P2$  in the numerical attributes space on any numeric attribute ( $Nu_i$ ) is calculated as below:

$$D_{nu}(P1 \rightarrow Nu_i, P2 \rightarrow Nu_i) = \begin{cases} \text{if } (P1 \rightarrow Nu_i, \text{value} = P2 \rightarrow Nu_i, \text{value}) \\ \quad \text{then } 0 \\ \text{elseif } (P1 \rightarrow Nu_i, \text{value} = P2 \rightarrow Nu_i, \text{value} \pm 5\%) \\ \quad \text{then } 0.25 \\ \text{elseif } (P1 \rightarrow Nu_i, \text{value} = P2 \rightarrow Nu_i, \text{value} \pm 10\%) \\ \quad \text{then } 0.5 \\ \text{elseif } (P1 \rightarrow Nu_i, \text{value} = P2 \rightarrow Nu_i, \text{value} \pm 20\%) \\ \quad \text{then } 0.75 \\ \text{else } 1 \end{cases}$$

In this category each attribute can have any numerical value. If the value of the attribute of the source project and the target project is same then the similarity difference between the projects would be 0 otherwise the similarity difference would be 0.25 or 0.5 or 0.75 if the target projects attribute value lies in the range of  $\pm 5\%$  or  $\pm 10\%$  or  $\pm 20\%$  target projects attribute value respectively. In the absence of both of the above cases the similarity difference would be 1.

### 3 Similarity Difference Measurement

Hitherto, we have the target software described in the form of various attributes and we have a set of bygone software projects whose cost is properly established and these projects also have the required set of attributes. Now we have to find the projects from the database that are similar to target software on the basis of these attributes. Apparently we are estimating the cost using analogy. Although human intelligence is the best live example of analogy based reasoning, lot of software tools like ANGEL [45], ESTOR [46], DD-EbA [47], ANALOGY-X [48] and Fuzzy classification [34] are also present in the market for software cost estimation. By combining the results from various algorithms that are using analogy and some latest researches on improving these results in presence of imprecisions, noise and outliers [49], we are in a position to say that these methods have outperformed many of the parametric and non-algorithmic methods we quote in Sect. 1.

Our algorithm is a further improvement over the other methods because all the existing methods have not explored various categories of attributes. So, they didn't have separate methods to map attributes belonging to different categories. Also, we have used  $k$ -nearest neighbor [50] classifier [49] to form a cluster of  $k$ -similar projects

in the attribute space. These projects form a set of  $k$  closest projects which have the least similarity difference. Finally the cost of target project is proposed according to the cost of these  $k$  similar projects. The following paragraphs we have discussed the mathematical model of the problem.

Any entity  $SP (No_{1...i}, Li_{1...j}, Nu_{1...p})$  is defined as a software project  $SP$ , described on the basis of three categories of attributes i.e. Nominal attributes ( $No$ ), Linguistic attributes ( $Li$ ) and Numerical attributes ( $Nu$ ).  $No_x, Li_y$  and  $Nu_z$ , specifies the value of  $x$ th,  $y$ th and  $z$ th attribute in the respective category. In context to the above statement the following algorithm tends to find out the cost estimate of a target software project  $SP^T$  according to the cost of  $k$  most similar projects from the database of  $n$  old projects  $SP_{1...n}$ . The value  $D_{tn}$  is the similarity difference between the target software project and the  $n$ th old project present in the database and it is calculated according to the following algorithm.

**Algorithm 1:** Finding k-similar projects.

After execution of Algorithm 1, we get a cluster of  $k$  existing projects in the similarity difference space. This cluster contains the projects that are most similar to the target project when the projects are compared against the set of attributes describes in the previous section. And the cost of target project  $SP^T (No_{1...i}, Li_{1...j}, Nu_{1...p})$  can be estimated cost as the average cost of a project that belongs to the formed cluster, and this relationship can be mathematically expressed as:

$$\text{Cost} (SP^T) = \frac{1}{k} \sum_{i=1}^k \text{Cost} (SP_i) \tag{1}$$

### 4 Performance Analysis

To scrutinize the performance of our model, we have used Mean Magnitude Relative Error (MMRE) [51], as a benchmark.

$$\text{MMRE} = \frac{1}{I} \sum_{i=1}^I \frac{|\text{Actual\_cost}_i - \text{Etimated\_cost}_i|}{\text{actual\_cost}_i} \tag{2}$$

$i$  is the total number of fitness cases.  $\text{Actual\_cost}_i$  and  $\text{Etimated\_cost}_i$  represent the value of actual cost and model calculated cost respectively for the  $i$ th project. To set up the test-bed we have used 120 sample projects from ISBSG data repository [52]. Out of these 120 projects, 20 (the value for  $I$  is 20) are used as the target projects for which we only know the attributes and rest 100 are used as the data repository of old projects for which the cost as well as the value of software attributes is well known. To recognize importance of number of old projects, we increase the number of old projects gradually in our test from 50 to full 100 with an interval of 5. And from the results we can conclude that MMRE of the similarity difference method is very less and it decreases with an increase in the number of old projects (Fig. 1). It can also be clinched that given a very large database of old projects, MMRE may

**Parameters:****Inputs:**

$i$ : Total number of Nominal Attributes ( $No$ ).

$j$ : Total number of Linguistic Attributes ( $Li$ ).

$p$ : Total number of Numerical Attributes ( $Nu$ ).

$No_x$ : Value of  $x^{th}$  Nominal Attributes;  $1 \leq x \leq i$ .

$Li_y$ : Value of  $y^{th}$  Linguistic Attributes;  $1 \leq y \leq j$ .

$Nu_z$ : Value of  $z^{th}$  Numerical Attributes;  $1 \leq z \leq p$ .

$SP^T(No_{1..i}, Li_{1..j}, Nu_{1..p})$ : Target Software Project.

$SP_{1..n}(No_{1..i}, Li_{1..j}, Nu_{1..p})$ :  $n$  old projects.

$k$ : Variable;  $k \ll n$ .

**Output:**

Set  $SP^S$  of  $k$  most similar projects.

**Local variables:**

$D_{no}$ : Similarity difference in nominal attributes space

$D_{li}$ : Similarity difference in linguistics attributes space

$D_{nu}$ : Similarity difference in numerical attributes space

$D_{tn}$ : Total Similarity difference between  $SP^T$  and  $SP_n$

**Procedure:**

Step 1. set  $SP^S = \{\emptyset\}$

Step 2. for each project  $pr$  in database ( $1 \dots n$ )

set  $D_{no} = 0$

set  $D_{li} = 0$

set  $D_{nu} = 0$

for each nominal attribute  $at$  ( $1 \dots i$ )

set  $D_{no} += D_{no}(SP^T \rightarrow No_{at}, SP_{pr} \rightarrow No_{at})$

end for

for each linguist attribute  $at$  ( $1 \dots j$ )

set  $D_{li} += D_{li}(SP^T \rightarrow Li_{at}, SP_{pr} \rightarrow Li_{at})$

end for

for each numerical attribute  $at$  ( $1 \dots p$ )

set  $D_{li} += D_{li}(SP^T \rightarrow Nu_{at}, SP_{pr} \rightarrow Nu_{at})$

end for

set  $D_{tn} = D_{no} + D_{li} + D_{nu}$

end for

Step 3. sort  $SP_n$  on the values of  $D_{tn}$  in increasing order

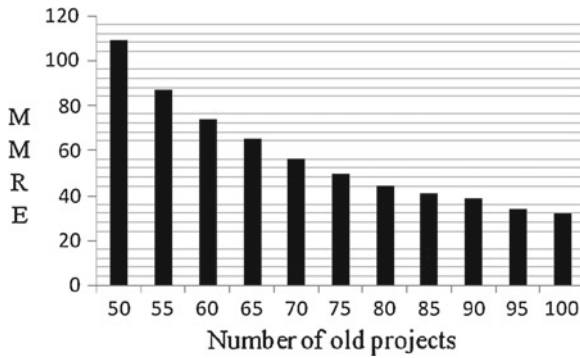
Step 4. move the top  $k$  elements into set  $SP^S$

Step 5. return  $SP^S$

---

cease to trifle value. In our executions we have taken the value of parameter  $k$  as five i.e. we have estimated the cost of a project from the cost of its five nearest neighbors.





**Fig. 1** Performance of cost estimation algorithm based on similarity difference measurement

## 5 Conclusion and Future Work

Despite of the presence of various software estimation models, software project managers are still encountering the complications and challenges in predicting the cost of forth coming software. It is so because of inherent vitality in the software attributes and wide dimensions of software development methodology. In our present paper we have described a method based on ‘similarity difference measure’ to estimate the cost of a software project. To calculate the similarity difference between softwares we have defined any software on the basis of three aspects, namely Nominal Attributes, Linguistic Attributes and Numerical Attributes. We have described the methods to calculate the similarity difference for each category. Then we have used this difference to find out  $k$  most similar projects or nearest neighbors in the similarity difference space. We have also tried to validate this procedure using MMRE as the error benchmark.

To extend this model in future we are trying the find out more cost affecting attributes in each category, to increase the precision of the model. Secondly we are also trying to reframe the similarity difference measurement procedure by assigning the weights to attributes

## References

1. Gray, R., MacDonell, S.G., Shepperd, M.J.: Factors systematically associated with errors in subjective estimates of software development effort: the stability of expert judgment, IEEE 6<sup>th</sup> Metrics Symposium, IEEE Computer Society, pp. 216–227, Los Alamitos (1999)
2. Nolan, A., Abrahao, S.: Dealing with cost estimation in software product lines: experiences and future directions. Software Product Lines: Going Beyond, pp. 121–135. LNCS, Springer, Berlin (2010)
3. Leung, H., Fan, Z.: Software Cost Estimation. Hong Kong Polytechnic University, Handbook of Software Engineering (2002)

4. Ma, J., and Mu, L.: Comparison Study on methods of software cost estimation, supported by Hebei Provincial Construction of Science and Technology Research Program, 2010 IEEE
5. Boehm, B.W.: Software engineering economics. *IEEE Trans. Softw. Eng.* **10**(1), 4–21 (1981)
6. Boehm, B. W., Valerdi, R.: Achievements and challenges in cocomo-based software resource estimation, *IEEE Softw* **25**(5), 74–83. doi:10.1109/MS, 2008
7. Zheng, Y., Wang, B.: Estimation of software projects effort based on function point, Proceedings of 4th International Conference on Computer, Science and Education 2009
8. Fu, Y. -F., Liu, X.-D., Yang, R. -N., Du, Y. -L., Li, Y. -J.: A software size estimation method based on improved FPA. Second WRI World Congress on, Software Engineering (2010)
9. Kemerer, C.F.: An empirical validation of software cost estimation models. *Commun. ACM* **30**(5), 416–429 (1987)
10. GalorathandM. D.D., Evans, W.: Software Sizing, Estimation, and Risk Management: When Performance is Measured Performance Improves. Auerbach, Boca Raton (2006)
11. Pressman, R.S.: Software Engineering: A Practitioner's Approach, 6th edn. McGraw-Hill, New York (2005). ISBN 13: 9780073019338
12. Herd, J.R., Postak, J.N., Russell, W.E., Steward, K.R.: Software cost estimation study—Study results, Final technical report, RADC-TR77-220, vol. I. Doty Associates Inc., Rockville (1977)
13. The PRICE software model user's manual. Moorestown, PRICE Systems (1993)
14. Walston, C.E., Felix, C.P.: A method of programming measurement and estimation. *IBM Syst. J.* **16**(1), 54–73 (1977)
15. Rubin, H.A.: Macroestimation of software development parameters: the ESTIMACS system, In: SOFTFAIR Conference on Software Development Tools, Techniques and Alternatives (Arlington, July 25–28) , pp. 109–118. IEEE Press, New York (1983)
16. Robin, H.A.: Using ESTIMACS E. Management and Computer Services, Valley Forge (1984)
17. Checkpoint for Windows User's Guide, version 2.3.1. Burlington, Software Productivity Research (1996)
18. Walkerden, F., Jeffery, R.: An empirical study of analogy-based software effort estimation. *Empirical Softw. Eng.* **4**, 135–158 (1999). Kluwer Academic Publishers, Boston
19. Kocaguneli, E., Bener, A.B.: Exploiting the essential assumptions of analogy-based effort estimation. *IEEE Trans. Softw. Eng.* **38**(2), 425–438 (2012)
20. Keung, J.: Software development cost estimation using analogy: A review. Australian, software engineering conference, 2009
21. Cuadrado-Gallego, J. J., Rodríguez-Soria, P., Martín-Herrera, B.: Analogies and differences between machine learning and expert based software project effort estimation. 11th ACIS international conference on software engineering, artificial intelligence, networking and parallel/distributed, computing (2010)
22. Jorgensen, M.: Practical guidelines for expert-judgment-based software effort estimation. *IEEE Softw.* **22**(3), 57–63 (2005)
23. Jorgensen, M., Shepperd, M.: A Systematic review of software development cost estimation studies. *IEEE Trans. Softw. Eng.* **33**(1), 33–53 (2007)
24. Hughes, R.T.: Expert judgment as an estimating method. *Inf. Softw. Technol.* **38**, 67–75 (1996)
25. Parkinson, G.N.: Parkinson's Law and Other Studies in Administration. Houghton-Mifflin, Boston (1957)
26. Leung, H.: Fan . Software Cost Estimation, *IEEE Transactions on Software Engineering*, **Z.** (1984)
27. Heemstra, F.J.: Software cost estimation. *Inf. Softw. Technol.* **34**(10), 627–639 (1992)
28. Putnam, L. H., Fitzsimmons, A.: Estimating software cost. *Datamation* (1979)
29. Boehm, B.W.: Software Cost Estimation Using COCOMO II. Prentice-Hall, Englewood Cliffs (2000)
30. Albrecht, A.J., Gaffney, J.E.: Software function, source lines of codes and development effort prediction: a software science validation. *IEEE Trans. Softw. Eng.* **9**, 639–648 (1983)
31. Alkoffash, M.S., Bawanehand, M.J.: Al Rabea, Ai: Which software cost estimation model to choose in a particular project. *J. Comput. Sci.* **4**(7), 606–612 (2008)

32. Khatibi, V., Jawawi, D.N.A.: Software cost estimation methods: a review. *J. Emerg. Trends Comput. Inf. Sci.* **2**(1), 21–29 (2011)
33. Idri, A., Abran, A., Khoshgoftaar, T. M.: Estimating software project effort by analogy based on linguistic values metrics. Eighth IEEE international symposium on software metrics (METRICS'02), pp. 21, 2002
34. Idri, A., Abran, A., Khoshgoftaar, T.M.: Fuzzy case-based reasoning models for software cost estimation. *Soft Computing in Software Engineering*, pp. 64–96. Springer-Verlag, Berlin (2004)
35. Morasca, S., Briand, L. C.: Towards a theoretical framework for measuring software attributes. In: *Proceedings of the Fourth International Symposium on Software Metrics*, Albuquerque, November 1997, pp. 119–126. IEEE Computer Society (1997)
36. Sommerville, I.: *Software Engineering*, 7th edn. Addison-Wesley, Boston (2004)
37. Clarke, P., O'Connor, R.V.: The situational factors that affect the software development process: Towards a comprehensive reference framework. *J. Inf. Softw. Technol.* **54**(5), 433–447 (2012)
38. Lagerström, R., von Würtemberg, L.V., Holm, H., Luczak, O.: Identifying factors affecting software development cost. *Proceedings of the Fourth International Workshop on Software Quality and Maintainability (SQM)*, March, In (2010)
39. Raschia, G., Mouaddib, N.: SAINTETIQ: a fuzzy set-based approach to database summarization. *Fuzzy Sets Syst.* **129**, 137–162 (2002)
40. Zadeh, L.A.: Fuzzy set. *Inf. Control* **8**, 338–353 (1965)
41. Zadeh, L.A.: A computational approach to fuzzy quantifiers in natural languages. *Comput. Math.* **9**, 149–184 (1983)
42. Khatibi, V., Jawawi, D.N.A.: Software cost estimation methods: A review. *CIS J.* **2**, 21–29 (2011)
43. McCall, J. A., Richards, P. K., Walters, G. F.: *Factors in software quality*. Technical report RADC-TR-77-369. U.S. Department of Commerce, Washington, DC (1977)
44. Pressman, R.S.: *Software Engineering: A Practitioner's Approach*, 5th edn. McGraw-Hill series in computer science, New York (2001)
45. Shepperd, M., Schofield, C.: Estimating software project effort using analogies. *IEEE Trans. Softw. Eng.* **23**(12), 736–743 (1997)
46. Mukhopadhyay, T., Vicinanza, S., Prietula, M.J.: Examining the feasibility of a case-based reasoning model for software effort estimation. *MIS Quart.* **16**(2), 155–171 (1992)
47. Kostli, M. V., Mittas, N., Angelis, L.: DD-EbA: An algorithm for determining the number of neighbors in cost estimation by analogy using distance distributions, 3rd artificial intelligence techniques in software engineering workshop, Larnaca, 7 October 2010
48. Keung, J.W., Kitchenham, B.A., Jeffery, D.R.: Analogy-X: Providing statistical inference to analogy-based software cost estimation. *IEEE Trans. Softw. Eng.* **34**(4), 471–484 (2008)
49. Shepperd, M., Kadoda, G.: Using simulation to evaluate predictions systems. In: *Proceedings of the 7th International Symposium on Software Metrics*, England, pp. 349–358. IEEE Computer Society (2001)
50. Coomans, D., Massart, D.L.: Alternative k-nearest neighbour rule in supervised pattern recognition: Part 1. k-nearest neighbour classification by using alternative voting rules. *Anal. Chim. Acta* **136**, 15–27 (1982). doi:[10.1016/S0003-2670\(01\)95359-0](https://doi.org/10.1016/S0003-2670(01)95359-0)
51. Shin, M., Goel, A.L.: Empirical data modeling in software engineering using radial basis functions. *IEEE Trans. Softw. Eng.* **26**, 567–576 (2000)
52. ISBG: Online data repository. <http://www.isbsg.org/>. Accessed 28 Feb 2012

# Mining Knowledge from Engineering Materials Database for Data Analysis

Doreswamy and K. S. Hemanth

**Abstract** With growing science and technology in manufacturing industry, an electronic database as grown in a diverse manner. In order to maintain, organizing and analyzing application-driven databases, a systematic approach of data analysis is essential. The most succeeded approach for handling these problems is through advanced database technologies and data mining approach. Building the database with advance technology and incorporating data mining aspect to mine the hidden knowledge for a specific application is the recent and advanced data mining application in the computer application domain. Here in this article, association rule analysis of data mining concepts is investigated on engineering materials database built with UML data modeling technology to extract application-driven knowledge useful for decision making in different design domain applications.

**Keywords** Data mining · Object-oriented · Advanced engineering materials · Association rule

## 1 Introduction

Advancement in sensing and digital storage technologies and their dramatic growth in the applications ranging from market analysis to scientific data explorations have created many high-volume and high-dimensional data sets. Most of the data stored in electronic media have influenced the development of efficient mechanisms of maintaining and automatic information retrieval for data analysis and data summarize.

---

Doreswamy · K. S. Hemanth (✉)

Department of Computer Science, Mangalore Univeristy, Mangalagangotri,  
Mangalore, Karnataka 574199, India  
e-mail: doreswamyh@yahoo.com

K. S. Hemanth

e-mail: reachhemanthmca@gmail.com

In order to maintain and efficiently analyze the high-dimensional data, the advanced DBMS and the data analysis methods respectively contribute the data organizing methods and knowledge discovery from large database. To represent the concept of both technologies a growing advance engineering materials property database is considered. Increasing engineering technology in civil construction, automobiles, and aerospace, etc., emerges with new engineering materials with new features. This leads complexity in maintaining the database through relational data model. This motivates for the construction of an advanced object-oriented database model (OODM) for engineering materials data [1]. By constructing the OODM for materials data, it is possible to maintain and extract the information from the large database in an efficient manner. Extracting knowledge from the OODM database for the selection of materials for different applications required an efficient and modern technology. Most popular and effective method for extracting hidden knowledge from the complicated database is by using data mining technique [2]. Construction of highly effective data mining rules for the selection of materials is investigated. Quantitative association rules are built on performance of mechanical behavior of materials. These rules filter the materials according to the application and support to process of selection of materials.

The remaining sections in the paper are organized as follows: in Sect. 2 a brief review of advanced engineering materials database and construction of a database is discussed. Extraction of relevant information through mining concept is presented in Sect. 3. Implementation and experimental results are discussed in the Sect. 4. And the conclusion is discussed in the Sect. 5.

## 2 Advanced Engineering Materials' Database

An engineering materials database is a database used to store empirical data of materials in such a way that they can be retrieved efficiently by humans or computer programs. Engineering materials databases are the basis of materials informatics [3], manufacturing industries [4], and the related disciplines [3]. Design and development of materials databases are done to enrich the availability and accessibility of materials data to materials scientist, researcher, and design engineers in manufacturing industries [5, 6].

Materials database consist of a variety of information about materials behaviour and manufacturing process [7]. Currently, in the market a few major online materials' databases provide rich information about material properties and manufacturing processes in an ad hoc manner. The major advantages of materials database are to provide information about materials behavior to engineer while selecting the material for engineering applications.

Thus, it is an important task in engineering materials field (Material Informatics), especially in informatics to investigate searchability and comparability in existing knowledge. Developing an advanced database, which supports for knowledge system, is the core task of the research in computer application.

One of the most promising approaches to advanced database support for engineering applications is the concept of advanced object-oriented database management systems (AOODBMS) [8]. Due to the object-oriented nature of the database model, it is much simpler to approach a problem with these needs in terms of objects. Code can be directly applied to a database, and thus saves time and money in development and maintenance [9].

The main intention of developing an object-oriented database models for advance engineering materials data is to (1) increase searchable and comparable of existing knowledge about materials data in large databases, (2) increase availability of information and expandability of database for future, and (3) expanding the knowledge on proper application of estimation methods of material behavior and mainly for mining prospective.

An object-oriented database model for advanced engineering materials is implemented in C#.Net technology. A GUI model is designed for accessing and analyzing the data without interacting the back end database, the database can be retrieved; updated and new data can be inserted from the GUI module. Complete process of construction of object-oriented database is explained in the form of UML class diagram. The class diagram consists of 12 classes (Engineering materials (), Reinforcement Materials (), Matrix Materials (), Thermal\_Prop (), Environment\_Prop (), Mechanical\_Prop (), Electrical\_Prop (), Chemical\_Prop (), Optical\_Prop (), Magnetic\_Prop (), Manufacturing\_Prop (), and Acoustical\_Prop (). Engineering materials class is the main class where the information of requested materials is being retrieved. Engineering materials class is associated with metric and reinforcement class, therefore objects of reinforcement and matrix class can be described through engineering materials class. Engineering materials class is also associated with Thermal\_Prop, Environment\_Prop, Mechanical\_Prop, Electrical\_Prop, Chemical\_Prop, Optical\_Prop, Magnetic\_Prop, Manufuretring\_Prop, and Acoustical\_Prop classes. Similar to the other class, certain objects can be desirable through engineering materials class. The class diagram of the object-oriented data model for engineering materials is shown in Fig. 1.

### 3 Extraction of Relevant Information Through Quantitative Association Rules Mining

Selection of materials for application requirement is purely depending on the performance and the cost of materials. Here, we consider the performance-based selection through quantitative association rule mining. Usually materials are analyzed by their performance like strength, toughness, rigidity, durability, and formability [4, 6]. This performance is analyzed by their experimental results stored in the database as different features (Table 1). The availability of detailed information on materials experimental values has led to the development of techniques that automatically look for association between each behavior that are quantitatively stored in the database [10, 11].

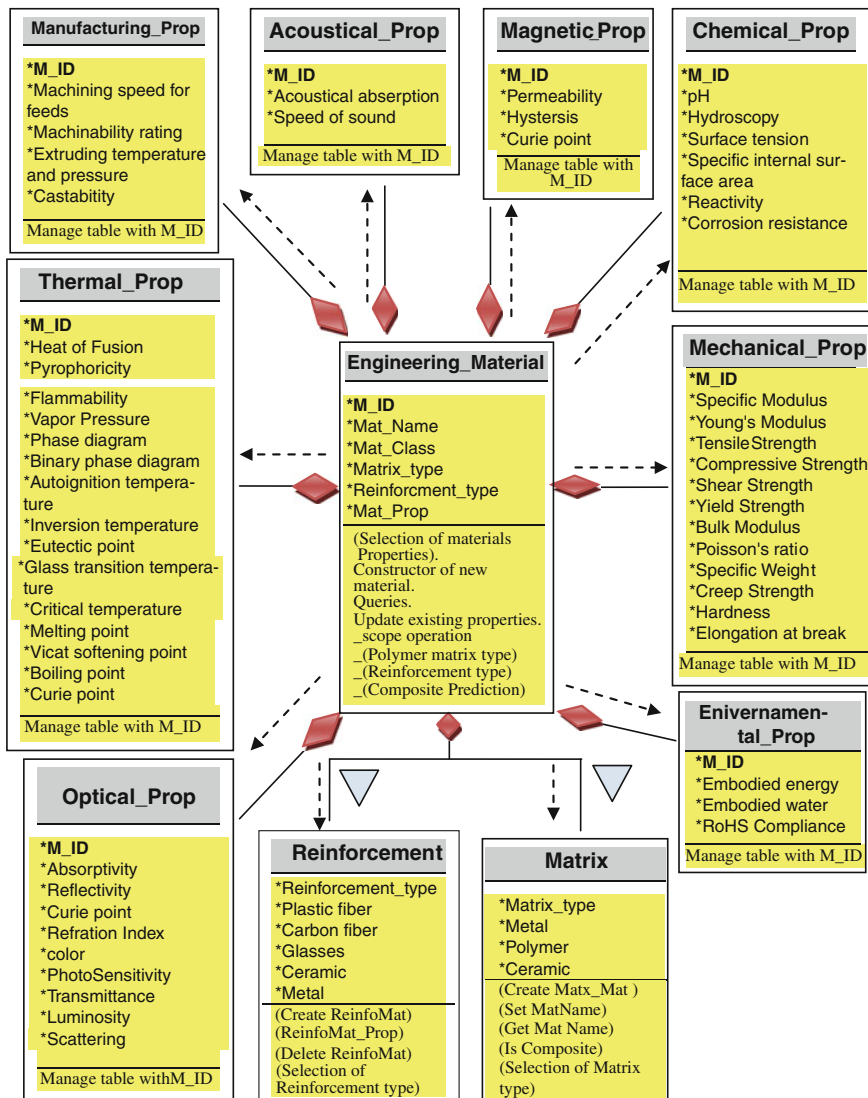


Fig. 1 The static structure of classes in the system with its relationship through UML notation

### 4 Implementation and Experimental Results

In this article an advanced object-oriented engineering material database is implemented in C# .Net technology. Materials data are collected from website and hand-books of engineering materials and materials science books and blogs [6, 12–14]. Mainly engineering materials data supporting for Civil engineering, Automobiles,

**Table 1** The database samples

Mat_type	bM	cS	eB	sS	sM	tS	yS	yM	Hrds
Polymer	0	0	2	0.004	0.015	0.9	11.24	0.016	1,165
Polymer	0	0	8	1.2	0.147	11	12.3	0.14	1,035
Ceramic	15	23.47	0	1.7	3	421.1	0	10.2	905
Ceramic	23	42.11	0	5.6	5.95	463.1	0	32.1	775
Metal	0	0	4.3	5.1	1.6	19.6	1.3	3.1	645
Composite	0.0018	0	255	2	41.6	200	90	20	385
Composite	235	950	0	10	45.3	1500	0	250	255

Minimum support = 50 % and Minimum Confidence = 60 %

Where *bM* Bulk Modulus, *cS* Compressive Strength, *eB* Elongation at Break, *sS* Shear strength, *sM* Specific Modulus, *tS* Tensile Strength, *yS* Yield Strength, *yM* Young Modulus Strength, *Hrds* Hardness

**Table 2** Representation of qualitative association rules constructed for selecting the materials for different application requirements

Rules	Support (%)	Confidence (%)
<b>Strength</b> => <Material(), tS :1000..1500> And <Material(), yS:500..1000> And <Materials(), sS:0.1..100> And <Materials(),cS:18..200>	50	100
<b>Strength</b> => <Material(), tS:...> And <Materials(),yS:...>	50	70
<b>Rigidity</b> =><Materials(),yM:10..100> And <Materials(),sM:0.1..100>	50	100
<b>Rigidity</b> =><Materials(),yM:10..100>	50	50
<b>Formability</b> =><Materials(),eB:100..500> And <Materials(),Dsty;0.1..3>	50	100
<b>Formability</b> =><Materials(), Dsty:0.1..3>	50	50
<b>Toughness</b> =><Materials(),eB:100..500> And <Materials(),yS:0.85..70>	50	100
<b>Toughness</b> => <Materials(),eB:100..500>	50	50
<b>Durability</b> => <Materials(),Hrds:1000..2000> And <Materials(),tS:0.85..200>	50	100
<b>Durability</b> => <Materials(),tS:0.85..200>	50	50

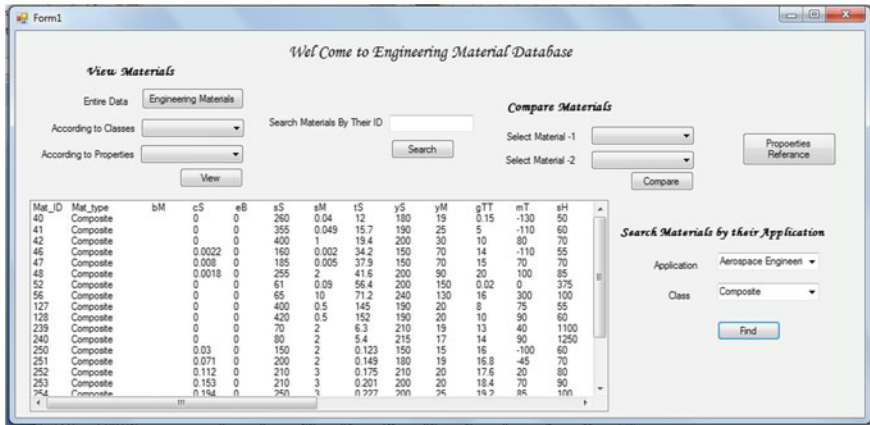
and Aerospace applications are collected. The database consists of 1,299 materials dataset with eight properties tables. Total of 32 behaviors are considered and organized in eight property tables, which are related to Engineering applications. In this experiment performance criteria are depend on mechanical properties. In mechanical property table, nine behaviors (attribute) are used to construct the rules. Each time different application is selected through the GUI and the corresponding materials are analyzed. The Table 3 shows the percentage of materials selection under different classes for different applications.s

Experimental results are shown in Table 2 which represent materials which satisfy the qualitative association rules that supports the required performance by a different



**Table 3** The percentage of materials satisfying QA rules under different classes' database for different applications

Materials class	Civil engineering materials (%)	Aerospace engineering materials (%)	Automobiles engineering materials (%)
Polymer	5	68	30
Ceramic	30	2.5	00
Metal	58	20	35
Composite	10	70	62



**Fig. 2** A GUI model for QA rule analysis

application. A GUI interface for selecting materials for engineering application is represented in Fig. 2.

### 5 Conclusion

In this paper advanced object-oriented data model for advanced engineering materials data is constructed in order to maintain and summarizing the materials data effectively and user friendly. Through data mining approach, quantitative association rules are investigated on materials datasets for selecting the materials based on their performance for different engineering applications. The model is compatible with effective data analysis rules. The proposed quantitative association rules can be used for the retrieval of effective information from the large application-driven engineering materials database.

## References

1. Walls, M.D.: Data Modeling, 2nd Revised edn. URISA, Park Ridge (2007)
2. Han, J., Kamber, M., Pie, J.: Data Mining: Concepts and Techniques, 3rd edn. Morgan Kaufmann, Burlington (2012)
3. Rajan, K.: Materials informatics. *Mater. Today* **8**(10), 38–45 (2005)
4. Ashby, M.F.: Materials Selection in Mechanical Design, 3rd edn. Pergamon Press, Oxford (2005)
5. Doreswamy, Manohar, M.G., Hemanth, K.S.: Object-oriented database model for effective mining of advanced engineering materials data sets. In: The Second International Conference on Computer Science Engineering and Applications (CCSEA-2012), pp. 129–137 (2012)
6. Budinski, K.G.: Engineering Materials Properties and Selection, 5th edn. Prentice Hall Publishing, New York (2000)
7. Callister, W.D Jr.: Materials Science and Engineering, 5th edn. Wiley, New York (2000)
8. Umoh, U.A., Nwachukwu, E.O., Eyoh, I.J., Umoh, A.A.: Object oriented database management system: a UML design approach. *Pacific J. Sci. Technol.* **10**(2), 355–365 (2009)
9. Satheesh, A., Patel, R.: Use of object-oriented concepts in databases for effective mining. *Int. J. Comput. Sci. Eng.* **1**(3), 206–216 (2009)
10. Srikant, R., Agrawal, R.: Mining quantitative association rules in large relational tables. In: Proceedings of the ACM-SIGMOD: Conference on Management of Data, Montreal, Canada, June 1996
11. Watanabe, T., Takahashi, H.: A study on quantitative association rules mining algorithm based on clustering algorithm. *Biomed. Soft Comput. Hum. Sci.* **16**(2), 59–67 (2011)
12. Online database for materials' properties. <http://www.makeitfrom.com/> (2012)
13. Online material data obtained from literature research and from experiments performed during work on projects and doctoral thesis. <http://www.matdat.com/> (2012)
14. Online materials properties database. <http://www.matweb.com/> (2012)

# Rule Based Architecture for Medical Question Answering System

Sonal Jain and Tripti Dodiya

**Abstract** As the wealth of online information is increasing tremendously, the need for question-answering systems is evident. Current search engines return ranked lists of documents to the users query, but they do not deliver the precise answer to the queries. The goal of a question-answering system is to retrieve answers to questions rather than full documents or best-matching passages, as most information retrieval systems currently do. Patients/Medical students have many queries related to the medical terms, diseases, and its symptoms. They are inquisitive to find these answers using search engines. But due to keyword search used by search engines it becomes quite difficult for them to find the correct answers for the search item. This paper proposes the architecture of question-answering system for medical domain and discusses the rule-based question processing and answers retrieval. Rule formation for retrieval of Answers has also been discussed in the paper.

**Keywords** Question answering · Question processing · Document processing · Answer processing

## 1 Introduction

Internet has made a tremendous wealth of information available which is accessible through information retrieval (IR) search engines. The search engines return ranked lists of documents to the users query, but they do not deliver the precise answer to the queries. Question-answering (QA) systems are a step ahead of

---

S. Jain (✉)

J K Laksmipat University, Jaipur, India  
e-mail: drsonalamitjain@gmail.com

T. Dodiya

GLS Institute of Computer Applications, Ahmedabad, India  
e-mail: triptidodiya@glsica.org

Information retrieval systems [3]. The goal of a question-answering system is to retrieve answers to questions rather than full documents or best-matching passages, as most information retrieval systems currently do. They take as input a natural language question (e.g., “*what is the capital of India?*”) and return a short passage or the precise text (e.g. “*New Delhi*”) that provide the answer. They combine techniques from the Information Retrieval (IR), Information Extraction (IE), and more broadly Natural Language Processing (NLP) fields [3].

Research and development of QA systems have been evaluated since 1999 in the yearly TREC (text retrieval conference) evaluations conducted by NIST and have been supported in the U.S by AQUAINT program. QA systems are also evaluated by two other workshops namely CLEF and NTCIR.

Patients/Medical students have many questions related to the medical terms, diseases, and its symptoms. They frequently need to seek answers for their questions. Medical information retrieval systems (e.g., PubMed) are used by physicians and medical students to retrieve information [2]. But studies indicate that as the average time taken to find the answer is more, the question is likely to be abandoned. Also, it has been surveyed in [8] that most of the current QA systems though found to be useful to obtain information, showed some limitations in various aspects which can be resolved for the user satisfaction. QA systems in the medical field can bring significant time saving to the patients as well as students who are often unhappy with the complexity of the IR systems.

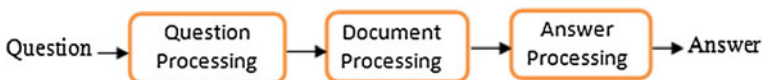
## 2 Process Model

Most of the QA systems contain three process modules namely question processing, document processing, and answer processing [2, 4–7] as shown in the Fig. 1.

### 2.1 Question Processing

Question processing is performed to understand the question posed by the user. It can be further classified into (a) Question Analysis and Classification and (b) Query Reformulation.

Question analysis and classification require several steps such as parse the question, classify the question on one of the following types such as who, what, when,



**Fig. 1** Three main process models of QA systems

which, why, and where [4]. It is used to find the type of question and the expected answer which further helps in searching the right passages from a large number of documents. For answer extraction from large documents, patterns should be provided by the system to find the correct answer and then send the query for further document processing [5].

Query reformulation transforms input question to a set of queries which acts as input to a document retrieval engine. Thus syntax and the semantic relations between the words in the question can be used [5]. A very important part of the system “usage knowledge” database saves the previously asked questions and their answers. If a new question matches a previously asked question then the answer can be extracted from the usage knowledge and presented to the user. But if there is some difference between the user question and the saved question in terms of name, adverb, adjective, or preposition then the system searches the ontology to find the similarity between the words. Usage knowledge helps in reducing the time to search the answer.

## ***2.2 Document Processing***

Document processing relies on the extraction of the documents keeping in focus the question. The query generated from the question processing module acts as an input to a document retrieval engine. A set of relevant documents are selected from which the candidate answer passages are extracted containing the relevant text. These candidate answers will act as input to the answer processing module.

## ***2.3 Answer Processing***

The answer processing module consists of (a) answer matching and ranking (b) user answer voting.

In answer matching the candidate answers extracted from the document processing modules are matched against the type of expected answer generated in the question processing module. Some of the passages will be removed from the collected candidate answers and the most relevant ones will be further sent for ranking. The ranking component classifies the answers and gives each of them a priority number. The answers are ranked based on the distance of the keywords, answer type and the answer repetition in the candidate answers [5]. The answers ranked as highest to lowest will be displayed as the answer list to the users for further voting.

In answer voting, the users will be shown the list of answers generated from the answer matching and ranking component. The users will vote the best answer generated by the system. If the users vote for the topmost answer, then the question-answer pair will be saved in the usage knowledge for further use. A validation grade will be assigned to the [q, a] pair. The next time [q, a] pair is selected by the user, the system increments the validation grade. If the user does not find any of the answers

relevant to be voted from the list, then the system asks for a new question with some additional information and sends it back to question processing module.

A detailed architecture of the medical QA system is described in the next section. This architecture has used the process model outlined in this section.

### 3 Medical QA System Architecture

Figure 2 shows the architecture of our system. Each module in the system is described in further section.

1. *Query Interface* In this part the user will input the question using the interface. A list of questions will be presented in the interface to give idea on how to formulate questions. If the user question matches the one in the list he can select it and the answer is retrieved from the usage knowledge. Also, if the question is similar to the one that is saved in the usage knowledge, the highest ranked answers are extracted and presented. If the user is not satisfied with the answer he/she can reformulate the question.
2. *Query Analyser* It segments the question into subjects, verb, adjectives, prepositional phrases, and objects. The type of words and their synonyms are searched in the WordNet lexical database and domain specific ontology. The subjects form as the keywords and are used in query reformulation.

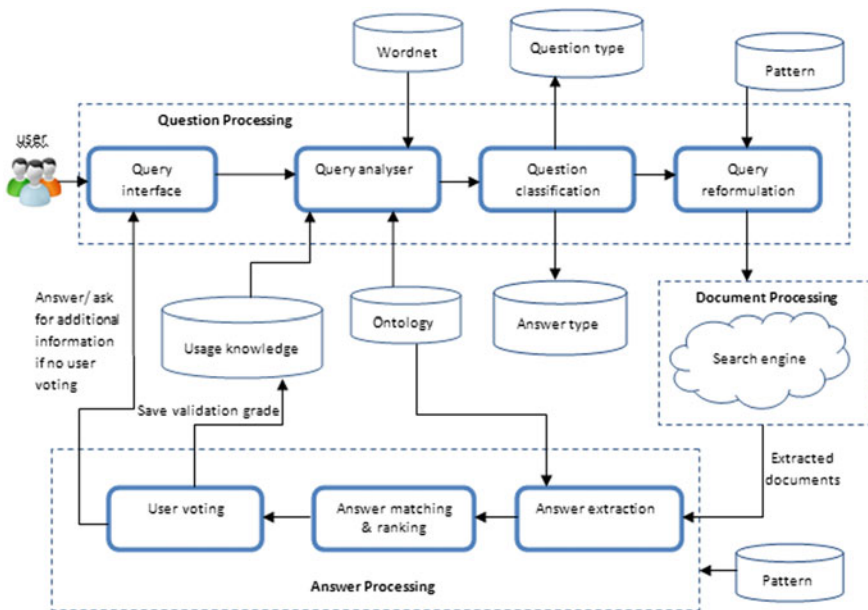


Fig. 2 Architecture for medical question answering system

3. *WordNet* This part acts like a dictionary containing all the words that are in related domains and used to search the type of words and their synonyms. It will be used as lexical database whose building block is synset, a set of synonym words representing the underlying lexical concept [9].
4. *Ontology* This part helps in surveying the questions and the answers semantically. Ontology for medical domain will be created for semantic analysis of the questions and answers.
5. *Usage knowledge* It acts like FAQ and is domain specific. First, the user question will be searched in usage knowledge. If the question structure is the same as the one in usage knowledge, the answer is presented to the user. If there are differences between the words, then domain ontology will be searched to find the synonyms. For example, the two questions will seem to be different if the new question uses the word “operation” and the saved question uses “surgery”. But if in the domain ontology they both are saved as synonyms, then the system consider the two questions and the type of their answers as same.
6. *Question classification* This part will be used to find the type of question and answers. The question is classified according to the type like *who*, *what*, *when*, *which*, *why*, and *where*. In some cases the type of question does not clearly indicate the expected answer. For example, the type of answer for questions starting with “*when*” will be “date” but for questions starting with “*what*” the expected answer can be a definition, number or procedure. Table 1 shows the question classification and the answer type.
7. *Question reformulation* The user question (Q) will be reformulated to (Q') by using the rules. The input question will be transformed to a set of keyword queries which acts as input to a document retrieval engine. The keywords from the question can be words that are noun, adverbs, objects, subject, or words in quotation. To find the correct answer, the system uses patterns. Also use of syntax relations, semantic relations, and usage knowledge are important for question reformulation.
8. *Search engine* It searches for the documents based on the set of keywords in the reformulated query and the answer patterns.
9. *Answer extraction* The documents from the search engine will be sent to answer extraction module which will extract the information satisfying the reformulated question (Q') from the collected documents.
10. *Answer matching and ranking* In this part the candidate answers extracted will be matched against the answer type and the co-occurrence patterns. Rule-base will be designed for the answer retrieval as shown in Table 2. Irrelevant passages will be removed and the most relevant ones will be ranked. Answer ranking can be based on keywords distance and rate of keywords in the answer. The answers will be listed and shown to the user from the highest to the lowest rank.
11. *User voting* Here the user will check the listed answers and give a validation answer grade to them. This will be further saved in the usage knowledge. If the user does not find the answer to be relevant and gives no validation grade, then the system will ask for a new question or to give more information about the question asked which will be again passed to the question processing module.

**Table 1** Question classification and answer type

Question classification	Sub classification	Answer type	Example
What	With preposition	Procedure	What is the procedure/process for kidney stone removal?
		Definition	What is the meaning of pancreas?
		Advantages/ Disadvantages	What are advantages of chemoprophylaxis?
		Digits	What is length of large intestine?
When	Without preposition	Definition	What is obesity?
		Date	When was penicillin invented?
Which	Which-when	Date	Which date is celebrated as world cancer day?
	Which-what	Methods	Which are the methods for kidney stone treatment?
	Which	List	Which are the reproductive organs of the body?
Who		Person/ Authority	Who received noble prize for Prostate cancer treatment? Who did first kidney transplant?
How		Procedure	How to calculate BMI?
Where		Place	Where is thyroid gland? Where is mayo clinic?
How many		Digits	How many bones are there in human body? How many teeth does an adult have?
Other than 'Wh' questions	With or without preposition	Procedure/Process	Procedure/Process for kidney stone removal
		Date	World cancer day
		Define	Define obesity
		List	List of salivary glands
		Rules	Rules of murphy
		Benefits	Benefits of exercise
		Hazards	Hazards of smoking
		Difference	Difference between constipation and diarrhea
		Describe	Describe peripheral smear



**Table 2** Rules for answer retrieval

Pattern type picked up from question	Answer retrieval	Examples of answer
Definition/ Define/ Defining/ Mean/ Meaning	<p><i>a. Subject is.....</i></p> <p><i>i. Obesity is.....</i></p> <p><i>b. Subject is defined as</i></p> <p><i>i. Obesity is defined as .....</i></p> <p><i>c. Subject called .....</i></p> <p><i>i.Obesity called</i></p> <p><i>d. Subject known as .....</i></p> <p><i>i. Obesity is known as.....</i></p> <p><i>e. Subject means.....</i></p> <p><i>i.Obesity means ...</i></p> <p><i>f. ....is called subject .....is called obesity</i></p> <p>Sentence containing the said pattern will be displayed. In addition sentence in continuation will be checked, if it starts with pronoun, it is presumed that it is related with the sentence containing pattern and hence will be displayed. The process of displaying sentence would be stopped once a sentence starting with noun is fetched</p>	<p>Obesity is defined as the body mass index greater than 28</p>
Benefits/ Advantages/ Merits and Demerits/ Disadvantages	<p><u>Advantages</u></p> <p><i>a. Advantages of subject....</i> (include further)</p> <p><i>b. It/Subject helps in....</i></p> <p><i>c. It/Subject benefits in....</i></p> <p><i>d. It/Subject can/would help to ....</i></p> <p><i>e. It/Subject use in.....</i></p> <p><u>Disadvantages</u></p> <p><i>a. Disadvantages of subject....</i></p> <p><i>b. It/Subject can't help in....</i></p> <p><i>c. It/Subject can't use in....</i></p> <p><i>d. It Restricts to.....</i></p> <p><i>e. It can't apply to.....</i></p> <p>Sentence containing the said pattern will be displayed. In addition sentence in continuation will be checked, if it starts with pronoun, it is presumed that it is related with the sentence containing pattern and hence will be displayed. The process of displaying sentence would be stopped once a sentence starting with noun is fetched. Here "It" in the sentence is considered as subject</p>	<p>Advantages of regular exercise</p> <ol style="list-style-type: none"> <li>1. Stay fit</li> <li>2. Strengthen muscles and bones</li> <li>3. Improves digestion</li> </ol>

(continued)

**Table 2** (continued)

Pattern type picked up from question	Answer retrieval	Examples of answer
Date	Sentence should contain subject and any combination of below: -Day/Day of month -Month -Year	Date of penicillin invention
Describe	Apply All the rules for definition, characteristics, process, advantages and disadvantages	1. Definition 2. Characteristics 3. Process 4. Advantages and disadvantages
Key phrase	Follow the rules as discussed in describe	

## 4 Conclusion and Future Work

The medical QA system addresses patients' and medical students' information needs. Corresponding to the growth of medical information there is a growing need of QA systems that can utilize the ever-accumulating information. In this paper, we have described the architecture for medical QA system. The question classification and the rule-base for answer retrieval are designed. Answers to medical questions should be searched in the most reliable data available. Also, answers to complex medical questions often need to span more than one sentence. The extraction of the answers can be performed from single documents or from multiple documents. Building the usage knowledge improves the system performance to a great extent. Also, continued research on using semantic knowledge in the QA systems is required.

The medical domain poses a particular challenge for QA with its highly complex terminology. As the first step toward building the proposed system, we have constructed the rules for question type and expected answer. We envisage the following tasks ahead for the development of the medical QA system.

- Construction of medical ontology.
- Development of more sophisticated techniques for natural language question analysis and classification.
- Development of effective methods for answer generation.
- Extensive utilization of semantic knowledge throughout the QA process.
- Incorporation of logic and reasoning mechanism.

## References

1. Demner-Fushman, Dina, Lin, Jimmy: Answering clinical questions with knowledge-based and statistical techniques. *Comput. Linguist.* **33**(1), 63–103 (March 2007)
2. Hong, Yu., Lee, Minsuk, Kaufman, David, Ely, John, Osheroff, Jerome A., Hripcsak, George, Cimino, James: Development, implementation, and a cognitive evaluation of a definitional question answering system for physicians. *J. Biomed. Inform.* **40**, 236–251 (2007)
3. Pierre, J., Zweigenbaum, P.: Towards a medical question-answering system: a feasibility study. In: *Medical Informatics Europe, Studies in Health Technology and Informatics*, vol. 95, pp. 463–468. IOS Press, Amsterdam (2003)
4. Vargas-Vera, Maria, Motta, Enrico, Domingue, John: AQUA: an ontology-driven question answering system. In: Maybury, M. (ed.) *New directions in question answering*. AAAI Press, Menlo Park (2003)
5. Kangavari, M.R., Samira, G., Manak, G.: Information retrieval: improving question answering systems by query reformulation and answer validation. *World Acad. Sci. Eng. Technol.* **48**, 303–310 (2008)
6. Minsuk, L., James, C., Hai Ran, Z., Carl, S., Vijay, S., John, E., Hong Y.: Beyond information retrieval—medical question answering, *AMIA Annu. Symp Proc.* 469–473 (2006)
7. Athenikosa, S.J., Hanb, H.: Biomedical question answering: a survey. *Comput. Methods Programs Biomed.* **99**, 1–24 (2010)
8. Dodiya, T., Jain, S.: Comparison of question answering systems. *Adv. Intell. Syst. Comput.* ISBN 978-3-642- 32063-7. vol. 182, 99–107 Springer
9. <http://wordnet.princeton.edu/>

**Part XIV**  
**Soft Computing for Clustering (SCCL)**

# Adaptive Mutation-Driven Search for Global Minima in 3D Coulomb Clusters: A New Method with Preliminary Applications

S. P. Bhattacharyya and Kanchan Sarkar

**Abstract** A single-string-based evolutionary algorithm that adaptively learns to control the mutation probability ( $p_m$ ) and mutation intensity ( $\Delta_m$ ) has been developed and used to investigate the ground-state configurations and energetics of 3D clusters of a finite number ( $N$ ) of ‘point-like’ charged particles. The particles are confined by a harmonic potential that is either isotropic or anisotropic. The energy per particle ( $E_N/N$ ) and its first and second differences are analyzed as functions of confinement anisotropy, to understand the nature of structural transition in these systems.

**Keywords** 3D Coulomb clusters · Genetic algorithm · Simulated annealing · Mutation probability · Mutation intensity

## 1 Introduction

Coulomb clusters, having concentric multi-shell structures, are observed in laser-cooled trapped ion systems. Three-dimensional (3D) multi-shell structures of dust particles under spherically symmetric potential have been extensively investigated [1–4] partly because of their analogy to other physically interesting systems, e.g., cold ionic systems, classical artificial atoms, and one or multi-component plasmas. Dust grains, or solid particles of  $\mu\text{m}$  to sub- $\mu\text{m}$  sizes, are observed in various low-temperature laboratory plasmas such as process plasmas, dust plasma crystals, space plasmas (e.g., planetary rings, comets, noctilucent clouds), ‘plasma crystals,’ or

---

S. P. Bhattacharyya (✉)  
IIT Bombay, Mumbai 400076, India  
e-mail: pcspb@chem.iitb.ac.in

K. Sarkar  
Indian Association for the Cultivation of Science, Jadavpur, Kolkata 700032, India  
e-mail: pcks@iacs.res.in

Coulomb lattices of charged dust grains in a plasma. The massive dust grains are generally highly charged. Dust grains that are immersed in plasma and/or radiative environments are electrically charged owing to processes such as plasma current collection, photoemission, or secondary emission. The first experimental realization of a spherical 3D cloud of monodisperse dust particles was achieved [2] by clever manipulation of thermophoretic forces and the plasma-induced field to counter the action of gravity, and the application of lateral external potential resulting in parabolic confinement.

It is important to understand how the global (local) minimum energy configurations emerge in such systems, how their energetics, stabilities, and other attributes change as functions of varying strength and symmetry of the confining potential, number and types of particles trapped, etc. Some theoretical investigations of structural properties and melting behavior in 3D Coulomb clusters have been very recently reported in [5]. The minimum energy structure of an assembly of cold charged particles depends on the delicate balance between inter-ionic Coulomb energy (two body) and the confining potential (one body). Since many local minima are possible, it is always challenging to locate the lowest energy structure. It is possible to invoke a population ( $n_{\text{pop}}$ ) based method like the genetic algorithm (GA) [6] to handle the problem. GA has been very successful and popular among the cluster physics community [7, 8]. The use of a population of strings makes the search thorough, although the necessity of evaluating  $n_{\text{pop}}$  number of configurations in every generation could make the search costly relative to a single-string method (e.g., simulated annealing method) unless the GA hits the solution at least  $n_{\text{pop}}$  times faster than any method using a single string. Parallelization of the string evaluations step can make the GA more efficient [9]. For problems with rugged energy landscapes, simulated annealing (SA) [10] may encounter what has been known as the ‘freezing’ problem [11], because the escape rate from local minimum diverges with decreasing temperature (can be amended at the expense of introducing additional parameters). It could be profitable to develop a single-string-based evolutionary strategy [12–15] that could, in principle, outperform a GA-based search through the complex potential energy landscape. We propose an adaptive mutation-only algorithm and evaluate its performance vis-a-vis that of GA and SA in the context of search for the global minimum on the potential energy surfaces of Coulomb clusters.

## 2 The Method

The configuration of the system of  $N$ –confined charges is completely defined by a geometry string  $S$  containing the Cartesian coordinates  $(x_i, y_i, z_i)$  of the  $N$  charges ( $q_i$ ):

$$S_k = s(x_1^k, y_1^k, z_1^k; x_2^k, y_2^k, z_2^k; \dots; x_N^k, y_N^k, z_N^k) \equiv (\xi_1^k, \xi_2^k, \dots, \xi_{3N-1}^k, \xi_{3N}^k) \quad (1)$$

The initial coordinate values are generated randomly within a specified range. The fitness ( $f_k$ ) of  $S_k$  is determined by computing the potential energy  $V_k(\xi_1, \dots, \xi_{3N})$  for the  $k$ th configuration of charges encoded by  $S_k$  as follows:

$$f_k = \frac{1}{(V_k - V_L^k)^2 + \delta} \quad (2)$$

where,

$$V_k = \sum_{i=1}^{N-1} \sum_{j>i}^N \frac{q_i q_j}{(r_{ij})_k} + \frac{1}{2} K \sum_{i=1}^N (r_i^2)_k \quad (3)$$

and

$$\begin{aligned} (r_{ij})_k &= \sqrt{(x_i^k - x_j^k)^2 + (y_i^k - y_j^k)^2 + (z_i^k - z_j^k)^2} \\ (r_i)_k &= \sqrt{(x_i^k)^2 + (y_i^k)^2 + (z_i^k)^2} \end{aligned} \quad (4)$$

$V_L^k$  is an updatable lower bound to the current potential energy  $V_k$ .  $\delta$  is a small constant ( $\approx 10^{-12}$ ) that takes care of exponential overflow. We start with a randomly chosen geometry string  $S_0$  ( $k = 0$ ) and allow it to undergo a mutation in geometry with a current mutation probability  $P_m^k$  and intensity  $\Delta_m^k$ . Supposing that the  $p$ th coordinate ( $\xi_p$ ) in  $S_k$  has been selected for mutation, the mutated coordinate becomes

$$\xi_p^{k+1} = \xi_p^k + (-1)^M \Delta_m^k r \quad (5)$$

where  $M$  is a random integer, and  $r$  is a uniformly distributed random number in the range  $(0, 1)$ .  $\Delta_m^k$  is the current mutation intensity. The mutated-geometry string  $S_{k+1}$  is used to compute  $V_{k+1}$  and the fitness  $f_{k+1}$ . If  $f_{k+1} \geq f_k$  the mutation is retained; if not, it is rejected and another mutation is attempted. The current mutation intensity is automatically determined from the experience so far by the following heuristics. If more than 20% of the mutations were accepted in the last 100 trials, we set  $\Delta_m^l = \Delta_m^{l-1} \times (1 + r)$ , where  $r$  is a random number in the range  $(0, 1)$ . If less than 10% of the trials were accepted during the same span, we set  $\Delta_m^l = \Delta_m^{l-1} \times \frac{1}{1+r}$ . In all other cases,  $\Delta_m^l = \Delta_m^{l-1}$ ,  $\Delta_m^0$  being set equal to 0.5.

The adaptive adjustment of  $P_m$  is also done following a similar logic:

$$P_m^l = P_m^{l-1} \times \frac{1}{1+r} \quad (6)$$

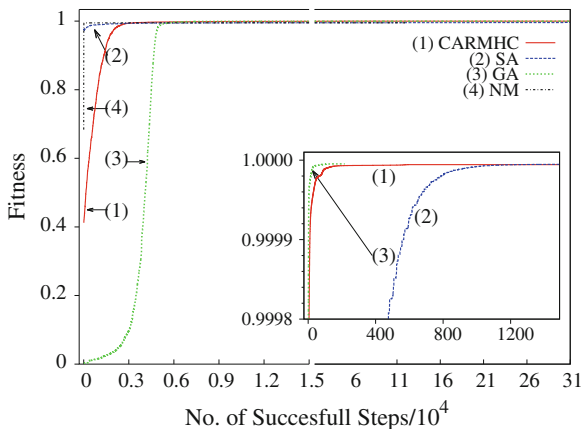
if less than 10 % of the trials led to successful mutation during the last 100 generation, else

$$P_m^l = P_m^{l-1} \times (1 + r) \tag{7}$$

if more than 30 % of the trials produced successful mutations. Otherwise,  $P_m^l$  is set equal to  $P_m^{l-1}$ .  $P_m^0$  is chosen to have an initial value between  $\frac{1}{3}$  and  $\frac{1}{4}$  randomly. The value of  $P_m^k$  is kept fixed once it is  $\leq \frac{1}{3N}$ ,  $N$  being the number of charges in the cluster. The logic of adaptive control of  $\Delta_m^k$  and  $P_m^k$  can be found in the fact that if a large number of trials are producing successful mutations (fitness-increasing mutations), then it would be reasonable to allocate higher values of probability and intensity of mutation. If too few trials are leading beneficial mutations, both  $\Delta_m^k$  and  $P_m^k$  should be reduced from their current values.

### 3 Results and Discussion

We consider a 3D cluster of 200 unit charges randomly distributed in space. Values of  $\Delta_m^0$  and  $P_m^0$  are chosen to be 0.5 and 0.25, respectively. Initially,  $V_L$  is approximately chosen and lowered if  $(V_k - V_L) \leq \epsilon$ , ( $\epsilon = 10^{-2}$ ). The confinement is harmonic and isotropic with  $k = 1.0$ .



**Fig. 1** Comparison of fitness evolution profiles for 200 unit positive charges confined in a harmonic trap obtained in CARMHC, NM, SA, and GA. The evolution in the GM region in an expanded scale has been shown in the inset. Compared to the CARMHC, SA requires much longer run (with multiple cooling and heating) in order to reach the desired optimum. NM ends up in a relatively higher energy structure. GA reaches the GM in a fewer number of ‘generations,’ each generation involving 20–30 fitness evaluation



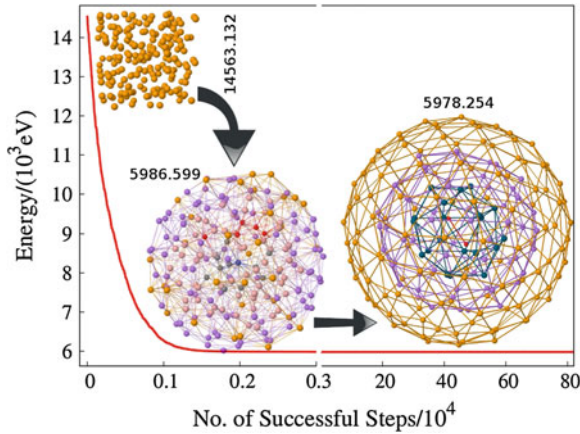


Fig. 2 Energy and structural evolution in CARMHC as the search proceeds to locate the GM

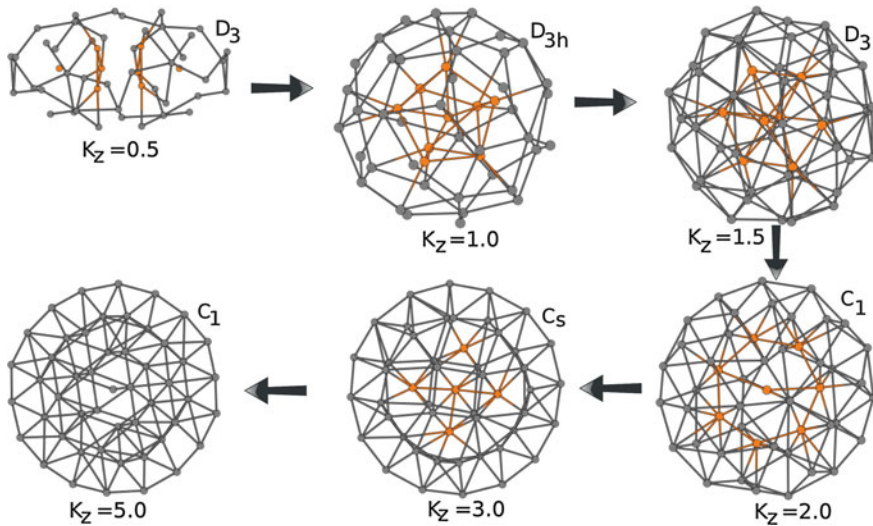
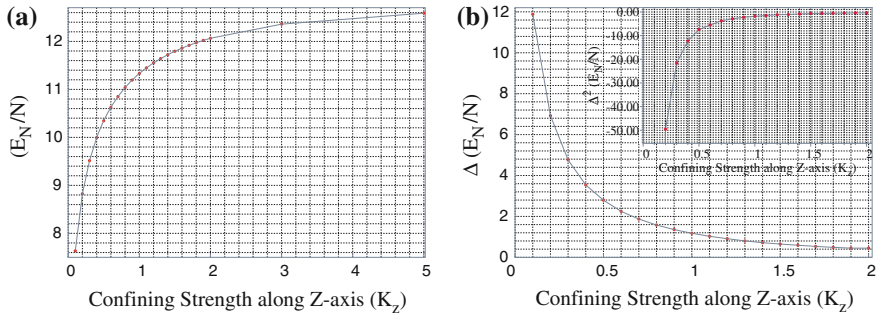


Fig. 3 Structural evolution for a system consisting of 50 charged particles with varying confinement strength along the z-axis ( $K_z$ ). The point symmetry of each structure is also displayed

Figure 1 shows the growth of fitness as a function of the number of the successful trials (generations), while Fig. 2 displays the energy evolution profile along with snapshots of the mutated structures at different stages of evolution. For comparison, we have also included the GA energy evolution profile for the best string in a population of size (30) using tournament selection, arithmetic mutation, and BLX- $\alpha$  crossover. The crossover probability was kept fixed at  $p_c = 0.7$ , while the mutation probability  $p_m$  was set at 0.05. The initial mutation intensity used is  $\Delta_m = 0.02$ . It is clear that our single-string adaptive random mutation hill climbing method performs



**Fig. 4** **a** Energy evolution profile for a system consisting of 50 charged particles with varying confinement strength along the z-axis ( $K_z$ ) and **b** first and second differences in energy

better than the GA as far as the rate of convergence to the global minimum is concerned. We have also compared the performance of our CARMHC method with that of simulated annealing (SA) applied to the same problem. SA as usual takes longer time as well as several heating and cooling schedules to reach the final structure, often requiring multiple starts.

Figure 3 displays the structural evolution in a Coulomb cluster with  $N = 200$  when  $k_x = k_y \neq k_z$ . The anisotropy destroys the symmetry of the structures that were produced in isotropic confinement. The optimal energy ( $E_n$ ) and the first and second differences of energy have been analyzed as functions of  $k_z$  (Fig. 4a, b). Apparently, there is a continuous structural phase transition as  $K_z$  attains a high value.

We are extending these studies to monodisperse clusters of much larger sizes and looking into the effects of charge anisotropy in polydisperse clusters on the possibility of structural phase transition.

**Acknowledgments** K. Sarkar thanks the CSIR, Government of India, New Delhi, for the award of senior research fellowship, and S.P.B. thanks the DAE, Government of India, for the award of Raja Ramanna Fellowship.

## References

1. Zuzic, M., et al.: Phys. Rev. Lett. **85**, 4064 (2000)
2. Arp, O., Block, D., Piel, A., Melzer, A.: Phys. Rev. Lett. **93**, 165004 (2004)
3. Kählert, H., Bonitz, M.: Phys. Rev. Lett. **104**, 015001 (2010)
4. Buluta, I.M., Hasegawa, S.: Phys. Rev. A **78**, 042340 (2008)
5. Apolinario, S.W.S., Peeters, F.M.: Phys. Rev. E **83**, 041136 (2011)
6. Holland, J.H.: Adaptation in Natural and Artificial Systems: An Introductory Analysis with Applications to Biology, Control and Artificial Intelligence. MIT Press, Cambridge, MA, USA (1992)
7. Sobczak, P., Kucharski, L., Kamieniarz, G.: Comput. Phys. Commun. **182**, 1900 (2011)
8. Ali, M., Smith, R., Hobday, S.: Comput. Phys. Commun. **175**, 451 (2006)

9. Nandy, S., Sharma, R., Bhattacharyya, S.P.: *Appl. Soft Comput.* **11**, 3946 (2011)
10. Kirkpatrick, S., Gelatt, C.D., Vecchi, M.P.: *Science* **220**, 671 (1983)
11. Li, Z., Scheraga, H.A.: *Proc. Nat. Acad. Sci.* **84**, 6611 (1987)
12. Mitchell, M., Holland, J.H., Forrest, S.: When will a genetic algorithm outperform hill climbing?. In: *Advances in Neural Information Processing Systems*, vol. 6, pp. 51–58, Morgan Kaufmann, (1993)
13. Sharma, R., Bhattacharyya, S.P.: Direct search for wave operator by a genetic algorithm (ga): route to few eigenvalues of a hamiltonian. In: *IEEE Congress on, Evolutionary Computation*, pp. 3812–3817, (2007)
14. Sarkar, K., Sharma, R., Bhattacharyya, S.P.: *J. Chem. Theory Comput.* **6**, 718 (2010)
15. Sarkar, K., Sharma, R., Bhattacharyya, S.P.: *Int. J. Quantum Chem.* **112**, 1547 (2012)

# A New Rough-Fuzzy Clustering Algorithm and its Applications

Sushmita Paul and Pradipta Maji

**Abstract** Cluster analysis is a technique that divides a given data set into a set of clusters in such a way that two objects from the same cluster are as similar as possible and the objects from different clusters are as dissimilar as possible. A robust rough-fuzzy  $c$ -means clustering algorithm is applied here to identify clusters having similar objects. Each cluster of the robust rough-fuzzy clustering algorithm is represented by a set of three parameters, namely, cluster prototype, a possibilistic fuzzy lower approximation, and a probabilistic fuzzy boundary. The possibilistic lower approximation helps in discovering clusters of various shapes. The cluster prototype depends on the weighting average of the possibilistic lower approximation and probabilistic boundary. The reported algorithm is robust in the sense that it can find overlapping and vaguely defined clusters with arbitrary shapes in noisy environment. The effectiveness of the clustering algorithm, along with a comparison with other clustering algorithms, is demonstrated on synthetic as well as coding and non-coding RNA expression data sets using some cluster validity indices.

**Keywords** Cluster analysis · Robust rough-fuzzy · C-means clustering algorithm

## 1 Introduction

Cluster analysis is one of the important problems related to a wide range of engineering and scientific disciplines such as pattern recognition, machine learning, psychology, biology, medicine, computer vision, web intelligence, communications, and remote sensing. It finds natural groups present in a data set by dividing the data set

---

S. Paul (✉) · P. Maji  
Machine Intelligence Unit, Indian Statistical Institute, Kolkata, India  
e-mail: sushmita\_t@isical.ac.in

P. Maji  
e-mail: pmaji@isical.ac.in

into a set of clusters in such a way that two objects from the same cluster are as similar as possible and the objects from different clusters are as dissimilar as possible. Hence, it tries to mimic the human ability to group similar objects into classes and categories [5].

A number of clustering algorithms have been proposed to suit different requirements [5, 6]. One of the most widely used prototype based partitional clustering algorithms is Hard *C*-Means (HCM) [10]. The hard clustering algorithms generate crisp clusters by assigning each object to exactly one cluster. When the clusters are not well defined, that is, when they are overlapping, one may desire fuzzy clusters. In this regard, the problem of pattern classification is formulated as the problem of interpolation of the membership function of a fuzzy set in [2], and thereby a link with the basic problem of system identification is established. A seminal contribution to cluster analysis is Ruspini's concept of a fuzzy partition [12]. The application of fuzzy set theory to cluster analysis was initiated by Dunn and Bezdek by developing fuzzy ISODATA [4] and Fuzzy *C*-Means algorithms (FCM) [3].

The FCM relaxes the requirement of the HCM by allowing gradual memberships [3]. In effect, it offers the opportunity to deal with the data that belong to more than one cluster at the same time. It assigns memberships to an object those are inversely related to the relative distance of the object to cluster prototypes. Also, it can deal with the uncertainties arising from overlapping cluster boundaries. Although the FCM is a very useful clustering method, the resulting membership values do not always correspond well to the degrees of belonging of the data, and it may be inaccurate in a noisy environment [7]. However, in real data analysis, noise and outliers are unavoidable. To reduce this weakness of the FCM, and to produce memberships that have a good explanation of the degrees of belonging for the data, Krishnapuram and Keller [7] proposed Possibilistic *C*-Means (PCM) algorithm, which uses a possibilistic type of membership function to describe the degree of belonging. However, the PCM sometimes generates coincident clusters [1].

Rough set theory is a new paradigm to deal with uncertainty, vagueness, and incompleteness. It is proposed for indiscernibility in classification or clustering according to some similarity [11]. In this regard, a rough-fuzzy clustering algorithm, termed as *robust Rough-Fuzzy C-Means* (rRFCM) [9], is applied in the current study. It integrates judiciously the merits of rough sets, and probabilistic and possibilistic memberships of fuzzy sets. While the integration of both membership functions of fuzzy sets enables efficient handling of overlapping partitions in noisy environment, the concept of lower and upper approximations of rough sets deals with uncertainty, vagueness, and incompleteness in cluster definition. Each cluster is represented by a set of three parameters, namely, a cluster prototype or centroid, a possibilistic lower approximation, and a probabilistic boundary. The cluster prototype depends on the weighting average of the possibilistic lower approximation and probabilistic boundary. Integration of probabilistic and possibilistic membership functions avoids the problems of noise sensitivity of the FCM and the coincident clusters of the PCM. The reported algorithm is robust in the sense that it can find overlapping and vaguely defined clusters with arbitrary shapes in noisy environment. The effectiveness of the

reported algorithm, along with a comparison with other clustering algorithms, is demonstrated on synthetic as well as coding and non-coding RNA expression time-series data sets using some standard cluster validity indices.

## 2 Robust RFCM Algorithm

This section reports a new  $c$ -means algorithm, termed as rRFCM. Let  $X = \{x_1, \dots, x_j, \dots, x_n\}$  be the set of  $n$  objects and  $V = \{v_1, \dots, v_i, \dots, v_c\}$  be the set of  $c$  centroids, where  $x_j \in \mathfrak{R}^m$  and  $v_i \in \mathfrak{R}^m$ . Each of the clusters  $\beta_i$  is represented by a cluster center  $v_i$ , a lower approximation  $\underline{A}(\beta_i)$  and a boundary region  $B(\beta_i) = \{\overline{A}(\beta_i) \setminus \underline{A}(\beta_i)\}$ , where  $\overline{A}(\beta_i)$  denotes the upper approximation of cluster  $\beta_i$ . According to the definitions of lower approximation and boundary of rough sets, if an object  $x_j \in \underline{A}(\beta_i)$ , then  $x_j \notin \underline{A}(\beta_k), \forall k \neq i$ , and  $x_j \notin B(\beta_i), \forall i$ . That is, the object  $x_j$  is contained in  $\beta_i$  definitely. Hence, the memberships of the objects in lower approximation of a cluster should be independent of other centroids and clusters. Also, the objects in lower approximation should have different influence on the corresponding centroid and cluster. From the standpoint of “compatibility with the cluster prototype”, the membership of an object in the lower approximation of a cluster should be determined solely by how far it is from the prototype of the cluster, and should not be coupled with its location with respect to other clusters. As the possibilistic membership  $v_{ij}$  depends only on the distance of object  $x_j$  from cluster  $\beta_i$ , it allows optimal membership solutions to lie in the entire unit hypercube rather than restricting them to the hyperplane given by FCM. Whereas, if  $x_j \in B(\beta_i)$ , then the object  $x_j$  possibly belongs to cluster  $\beta_i$  and potentially belongs to another cluster. Hence, the objects in boundary regions should have different influence on the centroids and clusters, and their memberships should depend on the positions of all cluster centroids. So, in the rRFCM, the membership values of objects in lower approximation are identical to the PCM, while those in boundary region are the same as the FCM, and are as follows:

$$\mu_{ij} = \left[ \sum_{k=1}^c \left( \frac{d_{ij}^2}{d_{kj}^2} \right)^{\frac{1}{m_1-1}} \right]^{-1} ; v_{ij} = \left[ 1 + \left\{ \frac{d_{ij}^2}{\eta_i} \right\}^{\frac{1}{(m_2-1)}} \right]^{-1}$$

subject to  $\sum_{i=1}^c \mu_{ij} = 1, \forall j$ , and  $0 < \sum_{j=1}^n \mu_{ij} < n, \forall i$ ,

also  $0 < \sum_{j=1}^n v_{ij} \leq n, \forall i$ ; and  $\max_i v_{ij} > 0, \forall j$ ;

where  $\eta_i$  is the scale parameter. The centroid for the rRFCM is computed as:

$$v_i = \begin{cases} w\mathcal{C}_1 + (1 - w)\mathcal{D}_1 & \text{if } \underline{A}(\beta_i) \neq \emptyset, B(\beta_i) \neq \emptyset \\ \mathcal{C}_1 & \text{if } \underline{A}(\beta_i) \neq \emptyset, B(\beta_i) = \emptyset \\ \mathcal{D}_1 & \text{if } \underline{A}(\beta_i) = \emptyset, B(\beta_i) \neq \emptyset \end{cases} \tag{1}$$

$$\text{where } \mathcal{C}_1 = \frac{\sum_{x_j \in \underline{A}(\beta_i)} (v_{ij})^{m_2} x_j}{\sum_{x_j \in \underline{A}(\beta_i)} (v_{ij})^{m_2}}; \quad \mathcal{D}_1 = \frac{\sum_{x_j \in B(\beta_i)} (\mu_{ij})^{m_1} x_j}{\sum_{x_j \in B(\beta_i)} (\mu_{ij})^{m_1}}.$$

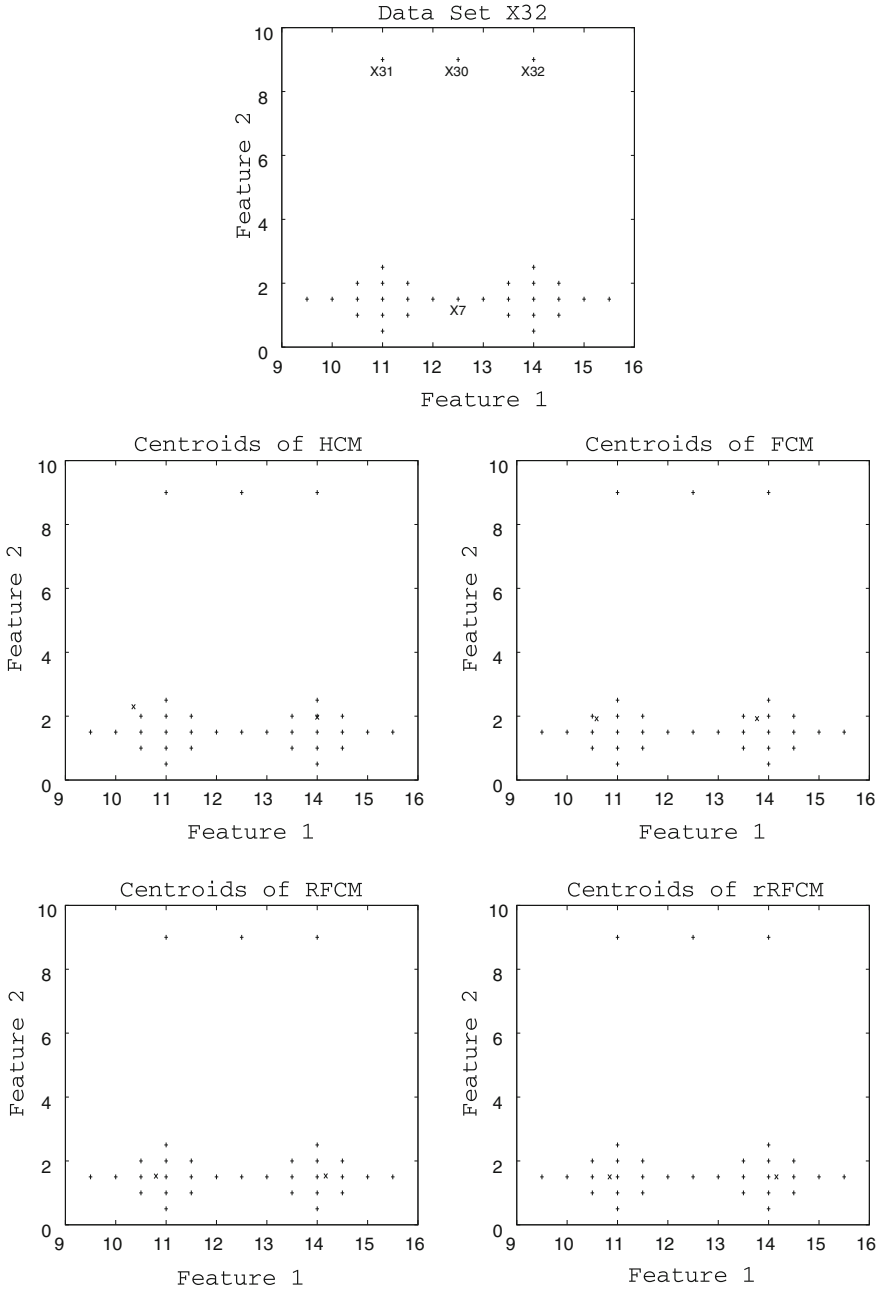
The process starts by choosing  $c$  objects as the initial centroids of the  $c$  clusters. The possibilistic memberships of all the objects are calculated. Let  $v_i = (v_{i1}, \dots, v_{ij}, \dots, v_{in})$  represents the possibilistic cluster  $\beta_i$  associated with the centroid  $v_i$ . After computing  $v_{ij}$  for  $c$  clusters and  $n$  objects, the values of  $v_{ij}$  for each object  $x_j$  are sorted and the difference of two highest memberships of  $x_j$  is compared with a threshold value  $\delta_1$ . Let  $v_{ij}$  and  $v_{kj}$  be the highest and second highest memberships of  $x_j$ . If  $(v_{ij} - v_{kj}) > \delta_1$ , then  $x_j \in \underline{A}(\beta_i)$ , otherwise  $x_j \in B(\beta_i)$  and  $x_j \in B(\beta_k)$  if  $v_{ij} > \delta_2$ . After assigning each object in lower approximations or boundary regions of different clusters based on the thresholds  $\delta_1$  and  $\delta_2$ , the probabilistic memberships  $\mu_{ij}$  for the objects lying in the boundary regions are computed. The new centroids of different clusters are computed as per (1). The thresholds  $\delta_1$  and  $\delta_2$  control the size of granules of rough-fuzzy clustering. In practice, the following definitions work well:

$$\delta_1 = \frac{1}{n} \sum_{j=1}^n (v_{ij} - v_{kj}) \quad \delta_2 = \frac{1}{\acute{n}} \sum_{j=1}^{\acute{n}} v_{ij} \tag{2}$$

where  $n$  is the total number of objects,  $v_{ij}$  and  $v_{kj}$  are the highest and second highest memberships of object  $x_j$ . On the other hand, the objects with  $(v_{ij} - v_{kj}) \leq \delta_1$  are used to calculate the threshold  $\delta_2$ ; where  $\acute{n}$  is the number of objects those do not belong to lower approximations of any cluster and  $v_{ij}$  is the highest membership of object  $x_j$ .

### 3 Experimental Results and Discussions

The performance of the rRFCM algorithm is compared extensively with that of different  $c$ -means algorithms on 1 synthetic ( $X32$ ), 1 mRNA, and 1 miRNA expression data sets, which are downloaded from *Gene Expression Omnibus* ([www.ncbi.nlm.nih.gov/geo/](http://www.ncbi.nlm.nih.gov/geo/)) with accession numbers GDS1013, and GSE9449. The synthetic data set  $X32$  consists of  $n = 32$  objects in  $\mathfrak{R}^2$  with two clusters. The object  $x_{30}$  is outlier or noise, and the object  $x_7$  is the so called inlier or bridge. The objects belong to either of two groups and both the clusters are overlapping in nature.



**Fig. 1** Example data set X32 and clusters prototypes of different *c*-means algorithms



The algorithms compared are HCM [5, 10], FCM [3], and rough-fuzzy  $c$ -means (RFCM) [8]. The input parameters used, which are held constant across all runs, are values of fuzzifiers  $\hat{m}_1 = 2.0$  and  $\hat{m}_2 = 2.0$ , value of  $w$ , used in the rRFCM algorithm is set to 0.99. For expression data sets the value of  $c$  for each data set is decided by using the cluster identification via connectivity kernels (CLICK) algorithm [13].

Two randomly generated initial centroids, along with two scale parameters and the final prototypes of different  $c$ -means, are reported in Table 1 for the synthetic data set. Fig. 1 depicts the scatter plot of the X32 synthetic data set. Fig. 1 also represents the scatter plots of X32 synthetic data set along with the clusters prototypes obtained using different  $c$ -means algorithms. The objects of synthetic data sets are represented by +, while  $\times$  depicts the positions of cluster prototypes.

Finally, Table 2 presents the performance of different  $c$ -means algorithms for optimum values of  $\lambda$ . The results are presented for one synthetic data set, one mRNA and one miRNA expression data sets with respect to Silhouette index, DB index, Dunn index, and  $\beta$  index. All the results reported in this table establish the fact that the rRFCM algorithm is superior to other  $c$ -means clustering algorithms, irrespective of the cluster validity indices and data sets used.

**Table 1** Cluster prototypes of different  $c$ -means for data set X32

Different algorithms	X32	
	Centroid 1	Centroid 2
Initial	11.088 2.382	14.100 2.000
Scale	$\eta_1 = 7.090$	$\eta_2 = 7.090$
HCM	10.353 2.294	14.000 1.969
FCM	10.585 1.919	13.770 1.924
RFCM	10.798 1.525	14.168 1.530
rRFCM	10.844 1.500	14.156 1.500

**Table 2** Performance of different  $c$ -means algorithms on different data sets

Different data sets	Different algorithms	Cluster validity indices			
		Silhouette index	DB index	Dunn index	$\beta$ index
Synthetic	HCM	0.408	1.306004	0.993485	1.376322
	FCM	0.416	1.779841	0.907058	1.366696
	RFCM	0.416	1.667268	0.987276	1.301975
	rRFCM	0.628	0.131575	13.862039	19.259300
mRNA	HCM	0.240	0.771935	0.001268	22.379993
	FCM	0.250	1.432223	0.002458	22.454958
	RFCM	0.255	0.769563	0.001619	22.666529
	rRFCM	0.580	0.364647	0.154374	263.586884
miRNA	HCM	0.256	0.907291	0.199289	2.745963
	FCM	0.192	4.979097	0.005345	2.007121
	RFCM	0.345	0.816723	0.103278	2.427899
	rRFCM	0.427	0.595101	1.030297	6.110056

## 4 Conclusion

In this paper, the application of the rRFCM algorithm on three different types of data has been demonstrated. Integration of the merits of rough sets, fuzzy sets, and  $c$ -means algorithm generates better results as compared to other  $c$ -means algorithms. The effectiveness of the rRFCM algorithm, along with a comparison with other algorithms, is demonstrated on one synthetic data set, one mRNA, and one miRNA microarray data sets.

**Acknowledgments** This work is partially supported by the Indian National Science Academy, New Delhi (Grant No. SP/YSP/68/2012). The work was done when one of the authors, S. Paul, was a Senior Research Fellow of Council of Scientific and Industrial Research, Government of India.

## References

1. Barni, M., Cappellini, V., Mecocci, A.: Comments on a possibilistic approach to clustering. *IEEE Trans. Fuzzy Syst.* **4**(3), 393–396 (1996)
2. Bellman, R.E., Kalaba, R.E., Zadeh, L.A.: Abstraction and pattern classification. *J. Math. Anal. Appl.* **13**, 1–7 (1966)
3. Bezdek, J.C.: *Pattern Recognition with Fuzzy Objective Function Algorithm*. Plenum, New York (1981)
4. Dunn, J.C.: A fuzzy relative of the ISODATA process and its use in detecting compact, Well-separated clusters. *J. Cybern.* **3**, 32–57 (1974)
5. Jain, A.K., Dubes, R.C.: *Algorithms for Clustering Data*. Prentice Hall, Englewood Cliffs (1988)
6. Jain, A.K., Murty, M.N., Flynn, P.J.: Data clustering: a review. *ACM Comput. Surv.* **31**(3), 264–323 (1999)
7. Krishnapuram, R., Keller, J.M.: A possibilistic approach to clustering. *IEEE Trans. Fuzzy Syst.* **1**(2), 98–110 (1993)
8. Maji, P., Pal, S.K.: RFCM: a hybrid clustering algorithm using rough and fuzzy sets. *Fundamenta Informaticae* **80**(4), 475–496 (2007)
9. Maji, P., Paul, S.: Rough-fuzzy clustering for grouping functionally similar genes from microarray data. In: *Proceedings of the 10th Asia Pacific Bioinformatics Conference*, pp. 307–320, Australia (2012)
10. McQueen, J.: Some methods for classification and analysis of multivariate observations. In: *Proceedings of the 5th Berkeley Symposium on Mathematics, Statistics and Probability*, 281–297 (1967)
11. Pawlak, Z.: *Rough Sets: Theoretical Aspects of Reasoning About Data*. Kluwer, Dordrecht (1991)
12. Ruspini, E.H.: Numerical methods for fuzzy clustering. *Info. Sci.* **2**, 319–350 (1970)
13. Shamir, R., Sharan, R.: CLICK: a clustering algorithm for gene expression analysis. In: *Proceedings of the 8th International Conference on Intelligent Systems for Molecular Biology*, 2000

# A Novel Rough Set Based Clustering Approach for Streaming Data

Yogita and Durga Toshniwal

**Abstract** Clustering is a very important data mining task. Clustering of streaming data is very challenging because streaming data cannot be scanned multiple times and also new concepts may keep evolving in data over time. Inherent uncertainty involved in real world data stream further magnifies the challenge of working with streaming data. Rough set is a soft computing technique which can be used to deal with uncertainty involved in cluster analysis. In this paper, we propose a novel rough set based clustering method for streaming data. It describes a cluster as a pair of lower approximation and an upper approximation. Lower approximation comprises of the data objects that can be assigned with certainty to the respective cluster, whereas upper approximation contains those data objects whose belongingness to the various clusters is not crisp along with the elements of lower approximation. Uncertainty in assigning a data object to a cluster is captured by allowing overlapping in upper approximation. Proposed method generates soft-cluster. Keeping in view the challenges of streaming data, the proposed method is incremental and adaptive to evolving concept. Experimental results on synthetic and real world data sets show that our proposed approach outperforms Leader clustering algorithm in terms of classification accuracy. Proposed method generates more natural clusters as compare to k-means clustering and it is robust to outliers. Performance of proposed method is also analyzed in terms of correctness and accuracy of rough clustering.

**Keywords** Clustering · Streaming data · Cluster approximation · Rough set

---

Yogita (✉) · D. Toshniwal  
Indian Institute of Technology, Roorkee, India  
e-mail: thakranyogita@gmail.com

D. Toshniwal  
e-mail: durgafec@iitr.ernet.in

## 1 Introduction

Digital data is increasing enormously in the present times. Applying data analysis techniques to such huge data repositories is thus very important currently. Data mining aims to extract useful information and patterns from huge quantities of data and can be applied on a variety of data types.

Nowadays many applications are generating streaming data for an example real-time surveillance, medical systems, internet traffic, online transactions and remote sensors. Data streams and streaming data are synonymous. Data streams are temporally ordered, fast changing, massive, and potentially infinite sequence of data objects [6]. Unlike traditional data sets, it is impossible to store an entire data stream or to scan through it multiple times due to its tremendous volume. New concepts may keep evolving in data streams over time. Evolving concepts require data stream processing algorithms to continuously update their models to adapt to the changes.

Clustering is an important data stream mining technique. Inherent uncertainty involved in real worlds streaming data increases the challenge of cluster analysis of data streams.

Rough set theory was introduced by Pawlak [10]. Rough sets have its application across a wide range of fields such as: data mining, medical data processing, information retrieval, machine learning, knowledge based systems etc. Rough set can be used to deal with uncertainty and vagueness involved in real world cluster analysis [5, 11]. It describes a cluster by a pair of two crisp set one is lower approximation and another is upper approximation. Lower approximation comprises of the data objects that are the sure members of a cluster. Upper approximation contains those data objects whose belongingness to clusters is uncertain along with the elements of lower approximation. In Rough Set based clustering [5, 8] an object must satisfy the following properties:

1. An object can be part of at most one lower approximation.
2. For a cluster  $C$  and object  $x$ , if  $x$  belongs to lower approximation of cluster  $C$ , then  $x$  also belongs to upper approximation of  $C$ .
3. If an object is not part of any lower approximation, then it belongs to two or more upper approximations.

There are many algorithms in literature for clustering of static and stored data sets which are based on a variety of approaches like Partitioning approach, hierarchical approach, density based approach, model based approach. Most of existing clustering methods require multiple scanning. Such methods cannot be used for clustering streaming data. Though some research work has been done on clustering of streaming data [1, 2, 4] but most of these methods do not deal with the uncertainty involved due to the lake of information.

In this paper we have proposed a novel rough set based clustering method for streaming data. This method uses rough sets for handling the uncertainty involved in clustering. It describes a cluster as a pair of lower approximation and an upper approximation. As oppose to most of existing clustering methods, keeping in view the

streaming data environment proposed clustering method is incremental and adaptive to evolving concepts of data.

The rest of this paper is organized as follows: Section 2 discusses related work. Section 3 describes proposed method. Section 4 presents experimental results. Section 5 concludes the paper.

## 2 Related Work

Several clustering methods for streaming data have been proposed recently. A brief description of some of them is given here. STREAM [9] is very first algorithm for data stream clustering. It scans data once and organise them in buckets. Median of each bucket is taken and weighted by number of objects in a bucket. In next step these weighted medians are clustered. CluStream is proposed by Aggarwal et al. [2]. It divides the clustering process in online phase and offline phase. Summary statics are stored in online phase and based on that clustering is done in offline phase. HPStream is proposed in [1] it uses a fading function and dimation projection for high dimensional data. It performs better then CluStream and STREAM. Cao et al. has proposed DenStream [4]. It is a density-based clustering algorithm. DenStream also involves two phase clustering. It uses the concept of micro-cluster to store an approximate representation of the data points. DenStream is able to identify clusters with arbitrary shapes. E-Stream is introduced by Udommanetanakit in [13] for data stream clustering. It supports the concept evolution of data over time.

Pawlak has proposed the rough sets [10]. Rough- $K$ -means is proposed by Lingras in [8]. It is rough set based extension of  $K$ -means clustering algorithm. Represent a cluster by lower and upper approximation. Zhou et al. has suggested an approach for adapting the parameters of rough- $K$ -means based on the number of iterations [15]. Wang in [5] has proposed a new type of adaptive weights based on the rough accuracy relating to different rough clusters and a new hybrid threshold by combining the difference and distance thresholds, refine the algorithm for assigning objects into lower and upper approximations. Asharaf et al. in [3] proposed a incremental approach for clustering interval data by employing rough set to deal with uncertainty involved in clustering. Yogita et al. in [14] has proposed a rough set based framework for exception discovery. Joshi et al. in [7] has presented interval- $K$ -mean and compared the Rough- $K$ -mean, Fuzzy- $K$ -mean and interval- $K$ -means.

## 3 Proposed Method Rough Set Based Clustering Approach for Streaming Data

In this section preliminary concepts and proposed scheme is described. Abstract pictorial representation of proposed technique is given in Fig. 1.

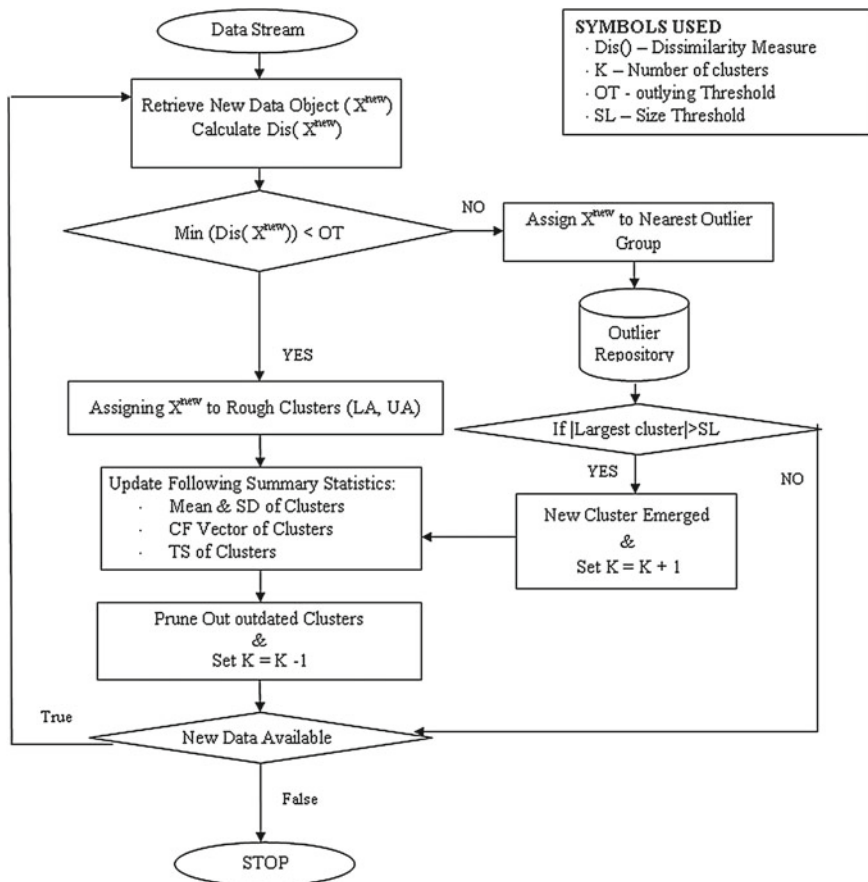


Fig. 1 Block diagram—rough set based data stream clustering

### 3.1 Preliminary Concepts

- Data Stream—A DataStream  $DS = x_1, x_2, \dots, x_n$  is a unbounded sequence of data objects. Object  $x_i = (x_{1i}, x_{2i}, \dots, x_{mi})$  is characterize by a set of  $m$  attributes.
- Rough Cluster It is represented by a pair of lower approximation and upper approximation.
- Lower Approximation  $(LA(C_i))$  Lower approximation of a cluster comprises of the data objects that definitely belongs to that cluster.
- Upper Approximation  $(UA(C_i))$  UA of a cluster contains those data objects whose belongingness to that cluster is not crisp along with the elements of LA.
- Mean of LA Mean of the LA of a cluster  $C_i$  is represented by  $MLA(C_i)$ . Its value is the average of the all elements of  $LA(C_i)$

- Mean of UA Mean of the UA of a cluster  $C_i$  is represented by  $MUA(C_i)$ . Its value is the average of the all elements of  $UA(C_i)$
- Mean of Cluster Mean of a cluster  $C_i$  is the weighted sum of  $MLA(C_i)$  and  $MUA(C_i)$  as given by following Eq. [15]

$$\text{Mean of Cluster}(C_i) = W_l \times MLA(C_i) + W_u \times MUA(C_i)$$

with  $W_l + W_u = 1$ .  $W_l$  and  $W_u$  specifies the importance of LA and UA in cluster mean calculation.

- Standard Deviation of Cluster ( $SD(C_i)$ )- It is the standard deviation of LA of a cluster. We have considered only definite members of cluster for calculation of value of ( $SD(C_i)$ ).
- Cluster Feature Vector (CF-Vector) It is a six tuple vector defined as  $\langle nl, sl, ssl, nu, su, ssu \rangle$  where  $nl$  is the number of data objects in LA,  $sl$  is the sum of all the data objects of LA in each dimension,  $ssl$  is the sum of square of all the data objects in each dimension,  $nu$  is the number of data objects in UA,  $su$  is the sum of all the data objects of UA in each dimension,  $ssu$  is the sum of square of all the data objects in each dimension U.
- Time Stamp of Cluster ( $TS(C_i)$ ) It represent the last time a data object is assigned to the lower approximation of a cluster.

### 3.2 Proposed Technique Phases

Proposed method comprises of the following steps:

Initial cluster can be generated by any static clustering algorithm on a small fraction of data. At that time LA is equal to UA and CF vector is stored and then following steps starts.

- Step1: Data stream is input to this phase. It retrieves the new data object from data stream and calculates the dissimilarity of new object to all the clusters using Euclidean measure.
- Step 2: In this phase, minimum dissimilarity of new data object out of all clusters is found and compared to a threshold (OT). If minimum dissimilarity is to nearest cluster is smaller than OT then go to Step 3 otherwise go to Step 4.
- Step 3: In this phase, new data object is assigned to LA and UA of cluster based on following conditions: Let  $d(x, C_i)$  be the dissimilarity between new object  $x$  and the cluster  $C_i$ . The difference between  $d(x, C_i) - d(x, C_j)$ ,  $1 \leq i, j \leq K$ ,  $k$  is the number of clusters, is used to determine the membership of  $x$  as follows:
  - If  $d(x, C_i) - d(x, C_j) \leq \text{threshold}$ , then  $x \in UA(C_i)$  and  $x \in UA(C_j)$ . Furthermore,  $x$  will not be a part of any LA.
  - Otherwise,  $x \in LA(C_i)$ , such that  $d(x, C_i)$  is the minimum for  $1 \leq i \leq K$ . In addition,  $x \in UA(C_i)$ .

Go to Step 7 by skipping Steps 4, 5 and 6.

- Step 4: In Step 2 if minimum dissimilarity of new object is to nearest cluster is larger than threshold (OT) than control flow directly jump to this step. Because such new object can be an outlier or it may be a member of new emerging cluster that appear as outlier currently. Outlying objects are stored as groups in outlier repository. New object is assigned to most similar outlier group. Go to Step 5.
- Step 5: In this phase, size of largest group is compared to user specified size if it is greater then got to Step 6 otherwise go to Step 9.
- Step 6: Largest group from outlier repository is considered as new emerged cluster [13] and number of clusters is increased by one. Let  $K$  is the number of clusters the  $K = K + 1$ .
- Step 7: It is the updation phase. It updated in following manner:
  - If new object is assigned to  $LA(C_i)$  then update MLA, MUA, complete CF vector, Time stamp, Mean and SD of corresponding cluster.
  - If new object is assigned to UA of two or more cluster then update MUA, only  $\langle nu, su, ssu \rangle$  portion of CF vector, Mean of all clusters.
  - If new cluster has emerged then initialise its summary statistics that are MLA, MUA, CF vector, Time stamp, Mean and SD. Her  $LA = UA$  is assumed.
- Step 8: In streaming data some clusters may disappear over the time as no new data is assigned to them. Such clusters represent the disappearing concepts of data [13]. To keep a track of such clusters a time stamp is associated with cluster and updated whenever a data object is assigned to LA of that cluster. If time stamp of a cluster is older than an allowed time then that cluster is considered as obsolete cluster and it discarded and number of clusters decreased.
- Step 9: If more streaming data is available then for processing that go to Step 1 otherwise stop.

### ***3.3 Difference Between Proposed Clustering Technique and Rough K-Means***

- Proposed clustering technique is incremental in nature as oppose to Rough K-means which is iterative in nature.
- Proposed clustering technique performs well on streaming data as proved by results in Sect. 4 and it requires only single scan of data. But Rough K-means requires multiple scanning of data which is not possible in case of streaming data.
- Proposed clustering technique is adaptive to concept evolution as it focuses on new upcoming clustering and discards the obsolete clusters. But there is no such feature in Rough K-means as it is meant for static data.
- Rough K-means is sensitive to outliers that can worsen its performance as oppose to this Proposed clustering technique is robust to outliers.



## 4 Experimental Results

We have done all implementation in matlab R2010a. We have compared our results with Leader clustering algorithm which is an incremental method of clustering. In next coming subsection we will focus on performance analysis of proposed method.

### 4.1 Data Sets

Experiments are conducted on synthetic as well as real data sets (Table 1). Real data sets were taken from UCI machine learning repository [12].

There are total 10 classes in yeast data that are following: CYT, NUC, MIT, ME3, ME2, ME1, EXC, VAC, POX, and ERL. These classes represent the localization site of protein. Out of these classes we have not considered ERL as a cluster instead consider as outliers because its size is very small. Sequence number attribute of yeast dataset is not used as it is not relevant. In abalone data set there are in all 29 classes that corresponds to the age of abalone. In our experiments only large sized 20 classes are taken as clusters others are of very small size assumed as outliers. In synthetic data there are five clusters each having 2,000 samples and 20 outlier. This data is generated by a mixture of normal distribution and then based on statistical characteristics like mean, standard deviation, class distribution outliers are planted. In all experiments  $Wl = 0.75$ ,  $Wu = 0.25$ ,  $OT = 2 * SD$ ,  $ST = 5$  for yeast data set,  $ST = 9$  for abalone and  $ST = 10$  for synthetic data set.

### 4.2 Comparison of Proposed Method with K-Means Clustering

In this section, we will analyse the result of proposed clustering method and  $K$ -means clustering. For visual representation, we have used a synthetic data consisting of total 150 samples. Original data set is shown in Fig. 2.

There are clusters in the data set. From Figs. 3 and 4. It is clear the proposed method gives more natural clusters as compare to  $K$ -means method because proposed

**Table 1** Characteristics of the data sets

Data set name	Number of instances	Number of attributes	Number of clusters	Outliers
Yeast	1,484	8	9	5
Abalone	4,177	8	20	24
Synthetic dataset	10,020	6	5	20

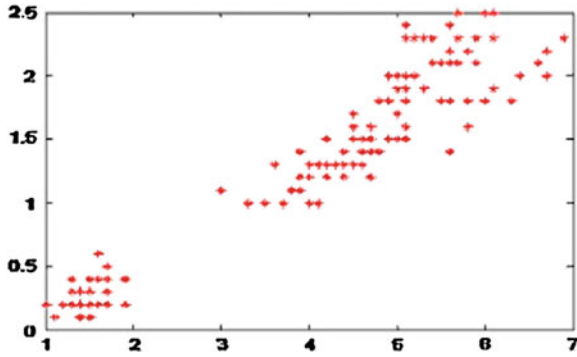


Fig. 2 Original data

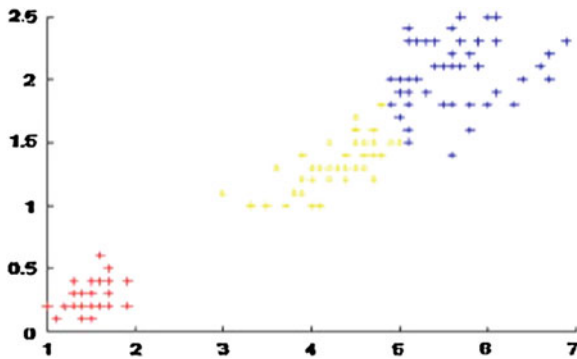


Fig. 3 K-means clustering results (Red, Blue, yellow colored are clusters and it does not give any overlapping points)

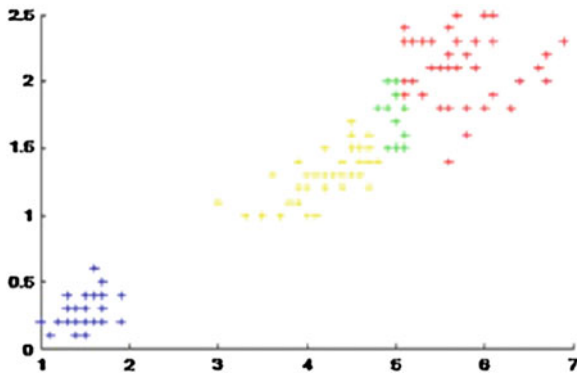


Fig. 4 Proposed method clustering results (Red, Blue, yellow colored are clusters and green color represent the overlap of yellow and red cluster)

method can handle uncertainty of belongingness of a data objects by allowing overlapping cluster( see Fig.4) which is not allowed in *K*-means.

### 4.3 Effect of Outlier on Proposed Method and *K*-Means Clustering

In this section, we will analyse the effect of outlier on proposed clustering method and *K*-means clustering. For visual representation, we have used a synthetic data consisting of total 158 samples. Out of which 8 are outliers other 150 represent 3 clusters. Original data set is shown in Fig.5.

From Fig. 6, it is concluded that due to the presence of outliers *K*-means clusters centers are get distorted because *K*-mean clustering algorithm cannot handle outliers and assign them to clusters. Proposed method is robust to outliers so it can be seen from Fig. 7 that cluster centers are more natural.

It is concluded the proposed method generates more intuitive and better quality clusters as compare to *K*-means.

### 4.4 Performance Comparison in terms of Classification Accuracy

In this section classification accuracy of proposed and leader clustering algorithm is compared on all three data sets. For this datasets are divided in a ration of 70 % for cluster generation training and 30% for testing. Cluster prototypes (Center of clusters) are used for nearest neighbour classifier.

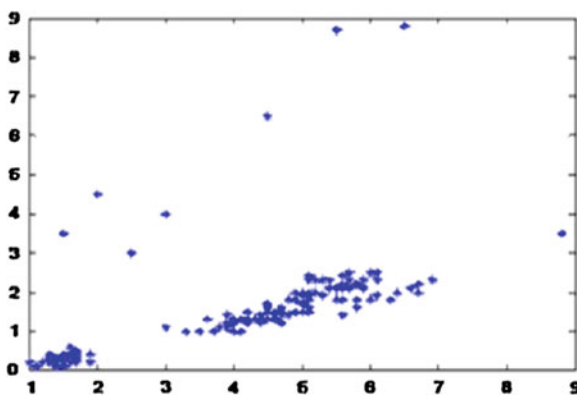
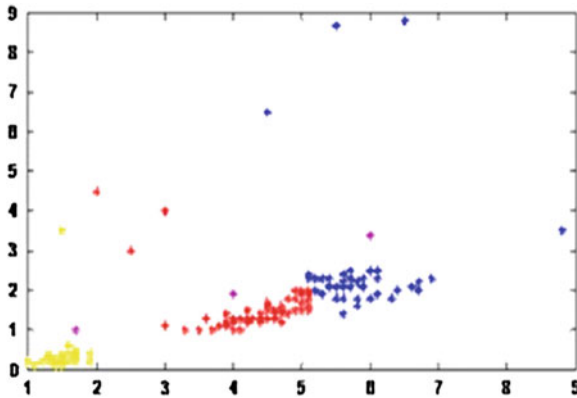
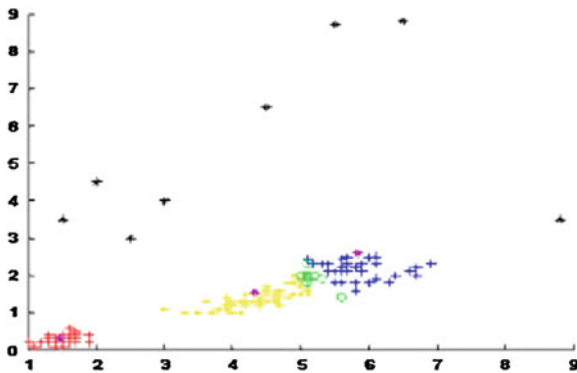


Fig. 5 Original data with outliers



**Fig. 6** K-means clustering results in presence of outliers (Red, Blue, yellow colored are clusters and magenta color represent the centers of clusters)



**Fig. 7** Proposed method clustering results in presence of outliers (Red, Blue, yellow colored are clusters and green color represent the overlap of yellow and blue cluster, black color are outliers, magenta color cluster centers )

Figure 8 shows that classification accuracy of proposed method is much better than the leader clustering algorithm. It is because proposed scheme allow the overlap and more importance is given to sure members in finding the prototype of clusters.

### 4.5 Performance Analysis of Proposed Method

In this section, the performance of proposed method is analysed in the terms of correctness and accuracy. The correctness of rough clustering is defined as the correct rate of lower approximations, because the objects in the lower approximation of a rough cluster are the representative members of this cluster [5].

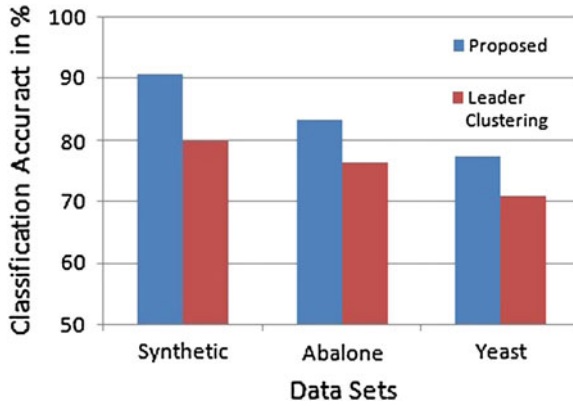


Fig. 8 Classification accuracy

Table 2 Performance of proposed method in terms of accuracy and correctness

Data set name	Correctness in %	Accuracy in %
Yeast	76.11	70.67
Abalone	79.84	68.89
Synthetic dataset	88.91	91.3

The correctness of rough clustering:

$$Correctness = \frac{\sum_{j=1}^K |LA(C_j) \cap A(C_j)|}{\sum_{j=1}^K |LA(C_j)|} \times 100$$

The accuracy of rough clustering describes the classification ability of rough clustering. A rough clustering with higher correctness and accuracy is better than that with lower values.

The accuracy of rough clustering:

$$Accuracy = \frac{\sum_{j=1}^K |LA(C_j)|}{\sum_{j=1}^K |UA(C_j)|} \times 100$$

In above equations K number of clusters and A(C<sub>j</sub>) is the set of objects of that are actually labelled as class C<sub>j</sub>.

The higher the value of correctness and accuracy better is the performance of rough clustering. It can be analysed from Table 2 that the performance of proposed

method is good on all three data sets. Correctness and accuracy both are highest for synthetic data sets.

## 5 Conclusion

In this paper, we have presented a rough set based clustering technique for streaming data. Rough set is employed to capture the inherent uncertainty involved in cluster analysis. To face the challenges of data stream processing our proposed scheme is incremental and dynamic in nature. Proposed clustering method is robust to outliers and generates soft-clusters.

Experimental results show that the proposed method generates more meaningful clusters as compare to K-mean. Its performance is better than leader clustering in terms of classification accuracy on all three datasets. Performance of proposed method is also good in terms of correctness and accuracy of rough clustering on all used data sets.

Thus the results show that the proposed technique is very promising for clustering streaming data. Further analysis of the performance of the proposed method is being further examined by using more real world and larger datasets.

## References

1. Aggarwal, C., Han J., Wang J., Yu P.S.: A framework for projected clustering of high dimensional data streams. In: Proceedings of the 30th VLDB Conference (2004)
2. Aggarwal, C., Han, J., Wang, J., Yu, P.S.: A framework for clustering evolving data streams. In: Proceedings of 2003 International Conference on Very Large Data Bases (VLDB03), Berlin (2004)
3. Asharaf, S., Narasimha Murty, M., Shevade, S.K.: Rough set based incremental clustering of interval data. *Pattern Recogn. Lett.* **27**(6), 515–519 (2006)
4. Cao, F., Ester, M., Qian, W., Zhou, A.: Density-based clustering over evolving data stream with noise. In: Proceedings of the 6th SIAM International Conference on Data Mining (SIAM 2006), pp. 326–337 (2006)
5. Hailiang, W., Mingtian, Z.: A refined rough k-means clustering with hybrid threshold. *Rough Sets and Current Trends in Computing. Lecture Notes in Computer Science*, vol. 7413, pp. 26–35 (2012)
6. Jiawei, H., Micheline, K.: *Data Mining, Concepts and Techniques*. 2nd edn. Morgan Kaufmann, Massachusetts (2006)
7. Joshi, M., Yiyu, Y., Lingras, P., Virendrakumar, C.B.: Rough, fuzzy, interval clustering for web usage mining. In: Proceedings of 10th International Conference on Intelligent Systems Design and Applications (ISDA), pp. 397–402 (2010)
8. Lingras, P.: Rough set clustering for web mining. In: Proceedings of 2002 IEEE International Conference on Fuzzy Systems, pp. 1039–1044 (2002)
9. OCallaghan, L., Mishra, N., Meyerson, A., Guha, S.: Streaming data algorithms for high-quality clustering. In: Proceedings of ICDE Conference, pp. 685–704 (2000)
10. Pawlak, Z.: Rough Sets. *Int. J. Inf. Commun. Comp.Sci.* **11**, 145–172 (1982)
11. Pawlak, Z.: Some Issues on rough sets. *Trans. Rough. Sets.* **3100**, 1–58 (2004)

12. UCI Machine Learning Repository Irvine: CA University of California, School of Information and Computer, Irvine, CA (2010)
13. Udommanetanakit, K., Rakthanmanon, T., Waiyamai, K.: E-Stream. In: Evolution-Based Technique for Stream Clustering, pp. 605–615. Springer, Heidelberg (2007)
14. Yogita, Saroj, Kumar, D., Pal, V.: Rules + Exceptions: automated discovery of comprehensible decision rules. In: Proceedings of IEEE International Advance Computing Conference, pp. 1479–1484, TIET Patiala, India (2009)
15. Zhou, T., Zhang, Y.N., Lu, H.L.: Rough k-means cluster with adaptive parameters. In: 6th International Conference Machine on Learning and Cybernetics, pp. 3063–3068 (2007)

# Optimizing Number of Cluster Heads in Wireless Sensor Networks for Clustering Algorithms

Vipin Pal, Girdhari Singh and R P Yadav

**Abstract** Clustering of sensor nodes is an energy efficient approach to extend lifetime of wireless sensor networks. It organizes the sensor nodes in independent clusters. Clustering of sensor nodes avoids the long distance communication of nodes and hence prolongs the network functioning time. The number of cluster heads is an important aspect for energy efficient clustering of nodes because total intra-cluster communication distance and total distance of cluster heads to base station depends upon number of cluster heads. In this paper, we have used genetic algorithms for optimizing the number of cluster heads while taking trade-off between total intra-cluster distance and total distance of cluster heads to base station. Experimental results show that proposed scheme can efficiently optimize the number of cluster heads for clustering of nodes in wireless sensor networks.

## 1 Introduction

Wireless sensor networks [1, 2] are application specific and consist of large number of sensor nodes deployed in a harsh environment/area. Sensor nodes sense area and send information to base station located outside/inside of area via single or multi-hop. Lifetime of network depends upon limited battery power of nodes. Due to harsh working area, it is not possible to change or replace battery of nodes. Hence, energy efficiency is critical issue for wireless sensor networks.

---

V. Pal (✉) · G. Singh  
Malaviya National Institute of Technology, Jaipur, India  
e-mail: vipinrwr@yahoo.com

G. Singh  
e-mail: girdharisingh@rediffmail.com

R. P. Yadav  
Rajasthan Technical University, Kota, India  
e-mail: rp\_yadav@yahoo.com



Clustering of nodes is an energy efficient approach for wireless sensor networks. Clustering approaches [3, 4] increases energy efficiency of network by avoiding long distance communication of nodes. Nodes are organized in independent sets or clusters. At least one cluster head is selected for each cluster. Clustering algorithms apply data aggregation techniques [5] which reduce the collected data at cluster head in the form of significant information. Cluster heads then send the aggregated data to base station.

For energy efficiency in wireless sensor network, the number of cluster heads is an important issue for clustering algorithms. Value of total intra-cluster communication distance and total distance of cluster heads to base station depends upon number of cluster heads. If numbers of cluster heads are less, total distance of cluster heads to base station decreases, while total intra-cluster communication distance increases. When numbers of cluster heads are more, total intra-cluster communication distance decreases, but there is increase in total distance of cluster heads to base station.

In this paper, genetic algorithm is applied for finding optimal number of cluster head while taking trade-off of total intra-cluster communication distance and total distance of cluster heads to base station. Experimental results show that proposed solution is effective to optimize number of cluster heads.

Rest of paper is organized as: Sect. 2 describes related work for energy efficient clustering algorithms. Section 3 describes genetic algorithm to optimize number of cluster heads. Section 4 describes results, and Sect. 5 concludes the work of paper.

## 2 Related Work

Low energy adaptive cluster hierarchy (LEACH) [6] is fully distributed algorithm. In setup phase cluster heads selection, cluster formation and TDMA scheduling are performed. In steady phase, nodes send data to cluster head and cluster head aggregate the data. Aggregated data are sent to base station. After a fix round time, re-clustering is performed. Role of cluster head is rotated to all the sensor nodes to make the network load balance. LEACH scheme does not guarantee about equal number of cluster heads in each round and number of nodes in each cluster.

LEACH-C [7] is centralized algorithm to form cluster and to assign duty of cluster heads. During setup phase, nodes send information about respective location and energy level to BS. BS formulates clusters using simulated annealing algorithm [8]. Algorithm provides CHs such that nodes minimize their transmission distance and conserve energy. After the formation of clusters and cluster heads, BS broadcasts a message that contains the information of CH ID for each node. The steady phase is same as of LEACH.

Adaptive decentralized re-clustering protocol (ADRP) [9] selects a cluster head and set of next heads for upcoming few rounds based on residual energy of each nodes and average energy of cluster. A round of ADRP has two phases: initial phase and cycle phase. In the initial phase, nodes send status of their energy and location to base station. Base station partitions the network in clusters and selects a cluster

head for each cluster along with a set of next heads. In the cycle phase, cluster head aggregates the data and sends to the base station. In the re-cluster stage, nodes transit to cluster head from set of next heads without any assistance from base station. If the set of next heads is empty, initial phase is executed again. Re-clustering energy consumption is avoided for few rounds, but node death from next cluster head list makes network unbalanced.

References [10–13] applies genetic algorithm to clustering algorithm to find better cluster formation. All these approaches combined effect of total intra-cluster communication distance and total distance of cluster heads to base station. Two adverse factors are combined in one factor for fitness function. So, work of this paper takes effect of these two papers independently to find optimal number of cluster heads.

### 3 Genetic Algorithm to Optimize Number of Cluster Head

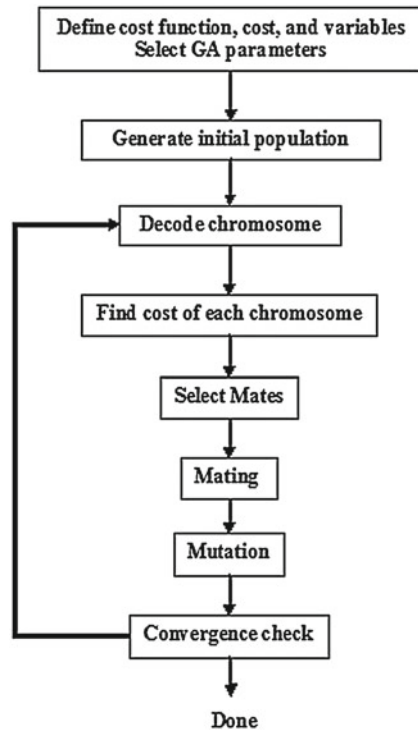
Genetic algorithms are heuristic search-based algorithms and are useful for searching and optimizing problems. GAs are based on theory of survival of the fittest. GA has population of individuals, and each individual represents a solution. Fitness value of each individual is calculated, and best-valued individual always has better chance of survival. Survived individuals go under genetic transformations, crossover, and mutation. Then, there is new population of individuals that is fitter to previous one. Procedure of GA is shown in Fig. 1.

- Population: Population consists of various individual solutions for the problem. Larger the size of population, higher is the accuracy of algorithm. Length of individual depends upon number of nodes in network as a 1 in individual represents node as cluster head, while a 0 means nodes is member node. Initial population is generated randomly.
- Fitness Function: Survivability of an individual depends upon its fitness value. Fitness value of each individual is calculated according a fitness function. In our work, fitness function consists of following three parameters.
  - Number of cluster heads (CH)
  - Total intra-cluster communication distance (IC)
  - Total distance from cluster heads to base station (BSD)

Value of last to parameters depends upon first. Less number of cluster heads has less total distance from cluster heads to base station but has high total intra-cluster communication distance. While high number of cluster heads has less total intra-cluster communication distance but has more total distance from cluster heads to base station. After scaling the fitness function, we have fitness function as:

$$\text{Fitness} = (N - \text{CH}) + \frac{\text{IC}}{100} + \frac{\text{BSD}}{100}$$

Fig. 1 Genetic algorithm



where  $N$  is total number of nodes in network. Fitness function shows that there is more emphasis on decreasing total distance from cluster heads to base station.

- Selection: Selection is the process of choosing individuals from current population for new population. The purpose of the selection process in a genetic algorithm is to give more reproductive chances to those population members that are better fit. The selection procedure may be implemented in a number of ways like roulette wheel selection, tournament selection, Boltzmann selection, rank selection, and random selection. In this work, roulette wheel selection procedure is applied to select chromosomes for generating new population.
- Crossover: In this paper, one-point crossover method is used. The crossover operation takes place between two chromosomes with probability specified by crossover rate. These two chromosomes exchange portions that are separated by the crossover point. The following is an example of one-point crossover.

Individual 1	0	1	1	1	0	0	1	1	1	0	1	0
Individual 2	1	0	1	0	1	1	0	0	1	0	1	0

After crossover, two offsprings are created as below:

Offspring 1	0	1	1	1	0	1	0	0	1	0	1	0
Offspring 2	1	0	1	0	1	0	1	1	1	0	1	0

- **Mutation:** The mutation operator is applied to each bit of a chromosome with a probability of mutation rate. After mutation, a bit that was 0 changes to 1 and vice versa.

Before mutation	0	1	1	1	0	0	1	1	1	0	1	0
After mutation	0	1	1	0	0	0	1	1	1	0	1	0

### 4 Results

Genetic algorithm for optimizing number of cluster heads is first implemented in C++ language. Sensor network topologies of 50 nodes over  $50 \times 50 \text{ m}^2$  are generated. Base station is located outside the field (100, 25).

Figure 2 shows best fitness values and average fitness values for 100 simulations. The best fitness graph represents average of best fitness value of each iteration of a simulation, while average fitness graph shows average of fitness value of each chromosome of each iteration of a simulation. Random topology is generated for

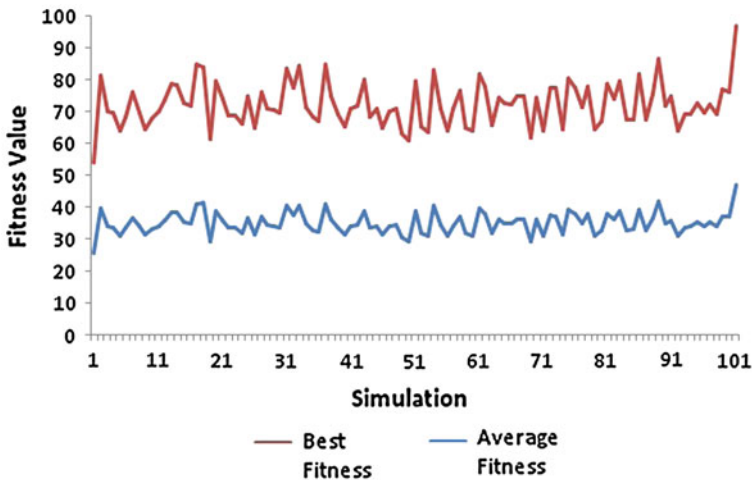


Fig. 2 Fitness for various simulations

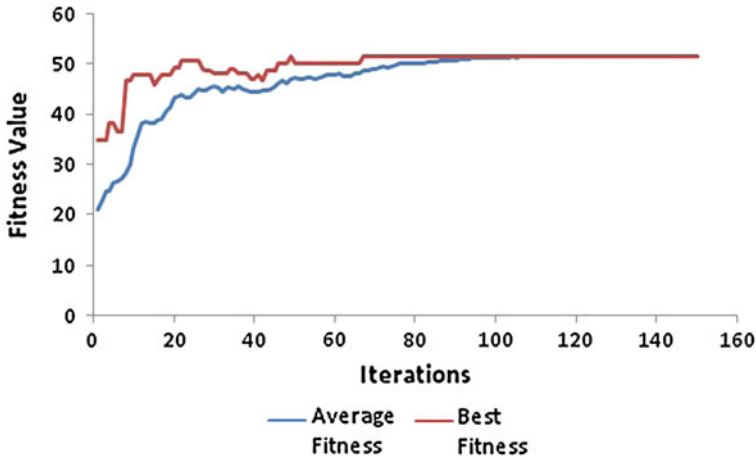


Fig. 3 Fitness with respect to generations

each simulation. There is significant difference between best fitness and average fitness values for each simulation

Figure 3 shows change in average fitness value and best fitness value over increase in generations. There is increase in both average fitness value and best fitness value as iterations increases. Both converge at one point after 120 iterations. That shows that fitness function is successful to converge the solution for finding optimal number of cluster heads in network.

Figure 4 shows number of cluster heads in network as iterations increases. At first, there are 30 cluster heads, while as iterations increased number of clusters are decreased and after 115 iterations it is constant, i.e., it optimized. So, the suggested fitness function is effective to optimize the solution.

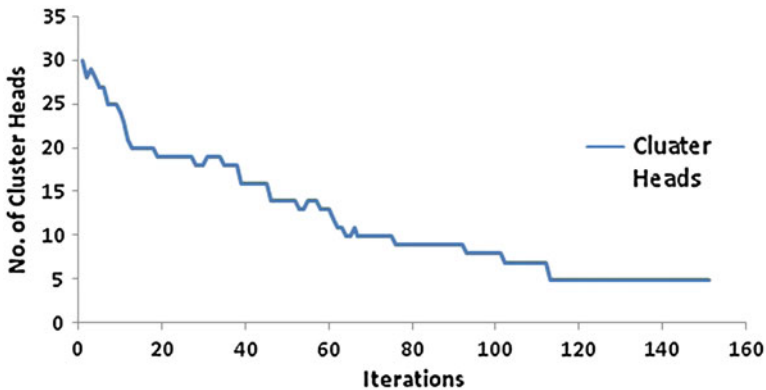


Fig. 4 Number of cluster heads over iterations

## 4.1 Proposed Scheme for Wireless Sensor Network

Nodes are deployed randomly in field. Nodes are considered to be location aware. Nodes send their information about location and remaining energy to base station. Genetic algorithm is applied to optimize number of cluster heads and their respective cluster formation at base station. Base station broadcasts complete information about cluster heads, member nodes of cluster heads, and data transmission/receive schedule of nodes to network. All nodes in network receive the broadcasted message and update their status; Setup phase is completed. Nodes send sensed data to cluster heads. Cluster heads performs aggregation. Reduced data are then sent to base station. After completion of current round, nodes send their updated information to base station for new cluster head selection and cluster formation.

## 5 Conclusion and Future Work

The number of cluster heads is a critical issue for energy efficient clustering of sensor nodes in wireless sensor networks. Work of this paper has optimized the number of cluster heads for clustering while taking trade-off of inter-cluster communication distance and cluster heads to base station distance. Results show that proposed scheme has effectively optimized the cluster heads.

Based on the work of this paper, we have also proposed a framework for centralized clustering of wireless sensor network. In future, we will implement the proposed framework and will compare the performance of proposed scheme with other existing clustering scheme.

## References

1. Akyildiz, I., Su, W., Sankarasubramanian, Y., Cayirci, E.: Wireless sensor networks: a survey. *Comput. Netw.* **38**(4), 393–422 (2002)
2. Estrin, D., Govindan, R., Heidemann, J.S., Kumar, S.: Next century challenges: scalable coordination in sensor networks. In: *MOBICOM*. pp. 263–270 (1999)
3. Younis, O., Krunz, M., Ramasubramanian, S.: Node clustering in wireless sensor networks: recent developments and deployment challenges. *IEEE Network Mag.* **20**, 2025 (2006)
4. Abbasi, A.A., Younis, M.: A survey on clustering algorithms for wireless sensor networks. *Comput. Commun.* **30**(14–15), 2826–2841 (2007)
5. Karl, H., Willig, A.: *Protocols and Architectures for Wireless Sensor Networks*. Wiley, England (2007)
6. Heinzelman, W.R., Chandrakasan, A., Balakrishnan, H.: Energy efficient communication protocol for wireless microsensor networks. In: *Proceedings of the 33rd Hawaii International Conference on System Sciences*, pp. 10–20 (2000)
7. Heinzelman, W., Chandrakasan, A., Balakrishnan, H.: An application-specific protocol architecture for wireless microsensor networks. *IEEE Trans. Wireless Commun.* **1**(4), 660–670 (2002)

8. Murata, T., Ishibuchi, H.: Performance evaluation of genetic algorithms for flowshop scheduling problems. In: *Proceeding First IEEE Conference on IEEE World Congress on Computational Intelligence, Evolutionary Computation*, pp. 812–817 (1994)
9. Bajaber, F., Awan, I.: Adaptive decentralized re-clustering protocol for wireless sensor networks. *J. Comput. Syst. Sci.* **77**(2), 282292 (2011)
10. Heidari, E., Movaghar, A.: An efficient method based on genetic algorithms to solve sensor network optimization problem. *Int J. GRAPH-HOC* **3**(1), 18–32 (2011)
11. Sajid, H., Abdul, W.M., Obidul, I.: Genetic algorithm for hierarchical wireless sensor networks. *J. Netw.* **2**(5), 87–97 (2007)
12. Jin, F., Parish, D.J.: Using a genetic algorithm to optimize the performance of a wireless sensor network. In: *Proceeding PGNNet*, (2007)
13. Jenn-Long, L., China, V.R.: LEACH-GA: genetic algorithm-based energy-efficient adaptive clustering protocol for wireless sensor networks. *Int. J. Mach. Learn. Comput.* **1**(1), 79–85 (2011)

# Data Clustering Using Cuckoo Search Algorithm (CSA)

P. Manikandan and S. Selvarajan

**Abstract** Cluster Analysis is a popular data analysis in data mining technique. Clusters play a vital role for users to organize, summarize and navigate the data effectively. Swarm Intelligence (SI) is a relatively new subfield of artificial intelligence which studies the emergent collective intelligence of groups of simple agents. It is based on social behavior that can be observed in nature, such as ant colonies, flocks of birds, fish schools and bee hives. SI technique is integrated with clustering algorithms. This paper proposes new approaches for using Cuckoo Search Algorithm (CSA) to cluster data. It is shown how CSA can be used to find the optimally clustering N object into K clusters. The CSA is tested on various data sets, and its performance is compared with those of K-Means, Fuzzy C-Means, Fuzzy PSO and Genetic K-Means clustering. The simulation results show that the new method carries out better results than the K-Means, Fuzzy C-Means, Fuzzy PSO and Genetic K-Means.

**Keywords** Clustering · Swarm Intelligence (SI) · CSA · K-Means · Fuzzy C-Means · Fuzzy PSO · Genetic K-Means

## 1 Introduction

Clustering analysis identifies and groups the data, where each cluster consists of similar objects and dissimilar to objects of other clusters. For high quality clusters, the inter-cluster similarity is low and the intracluster similarity is high [15, 17, 24].

---

P. Manikandan (✉)  
Paavaai Group of Institutions, Namakkal, Tamilnadu, India  
e-mail: mani.p.mk@gmail.com

S. Selvarajan  
Muthayammal Technical Campus, Rasipuram, Tamilnadu, India  
e-mail: asselvarajan@rediffmail.com



Swarm Intelligence (SI) [1, 6] is the collective behaviour which has no definite organized system but it has a self-organized system, which may be natural or artificial. The expression was introduced by Gerardo Beni and Jing Wang in 1989.

A survey of the clustering algorithms can be found in [13, 17]. Genetic algorithms are used in [3, 5, 14, 19, 21, 23] while an analytical review of the use of neural networks in clustering is given in [12]. Clustering algorithms based on Ant Colony Optimization are used in [2, 4, 8, 10, 26]. While in [7, 9, 16, 18] clustering algorithms based on Particle Swarm Optimization are applied.

This paper aims to propose Cuckoo Search Algorithm (CSA) to solve the clustering problem. The proposed CSA is applied for optimally clustering  $N$  object into  $K$  clusters. The CSA is tested on various data sets, and its performance is compared with those of  $K$ -Means, Fuzzy C-Means, Fuzzy PSO and Genetic  $K$ -Means clustering. The simulation results illustrate that this algorithm not only has a better response but also converges more quickly than the ordinary evolutionary methods. The rest of the paper is organized as follows: Proposed technique of CSA for Data Clustering is described in Sect. 2. The detailed result and discussion is discussed in Sect. 3. Conclusion and Future Research is described in Sect. 4.

## 2 The Proposed Cuckoo Search Algorithm for Clustering

### 2.1 Cuckoo Breeding Behaviour

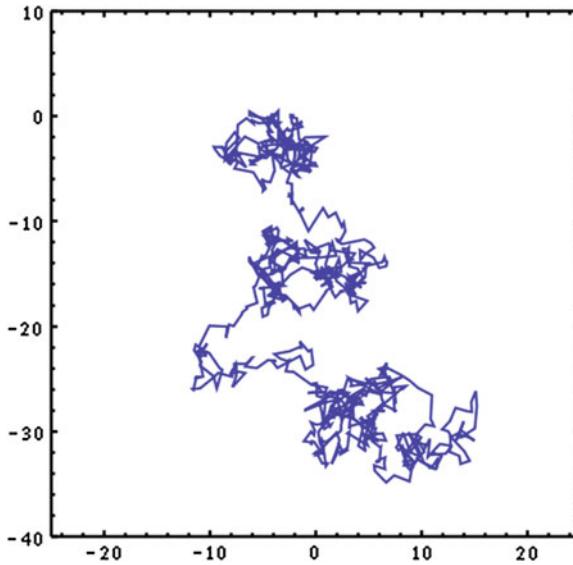
Cuckoo birds attract attention because of their unique aggressive reproduction strategy. Cuckoos engage brood parasitism in which a bird lays and discards its eggs in the nest of another species. Species lay their eggs in shared nests.

While flying, some animals and insects follow the path of long path with sudden 900 turns shared with short, random movements. This random walk is called Levy flight and it describes foraging patterns in natural systems, such as systems of ants, bees and bumbles. These flights can also be noticed in the movements of chaotic fluids. One example of Levy flight paths is depicted on Fig. 1.

Levy-style search behavior [22] and random search in general has been applied to optimization and implemented in many search algorithms [11, 20]. One of such algorithms is CSA [25]. Preliminary results show its promising capability.

### 2.2 Description of the Cuckoo Search Algorithm

Cuckoo Search Algorithm (CSA) is population based stochastic global search meta-heuristics. It is based on the general random walk system which will be briefly discussed in this paper.



**Fig. 1** Possible Levy flight path

In CSA, Nature's systems are complex and thus, they cannot be modeled by computer algorithms in its basic form. Simplification of natural systems is necessary for successful implementation in computer algorithms.

One approach is to simplify CSA through three below presented approximation rules:

- Cuckoos chose random location (nest) for laying their eggs. Artificial cuckoo can lay only one egg at a time.
- Elitist selection process is applied, so only the eggs with highest quality are passed to the next generation.
- Host nests number is not adjustable. Host bird discovers cuckoo egg with probability  $pd \in [0, 1]$ . If cuckoo egg is disclosed by the host, it may be thrown away, or the host may abandon its own nest and commit it to the cuckoo intruder.

To make the things even simpler, the last assumption can be approximated by the fraction of  $pd$  of  $n$  nests that are replaced by new nests with new random solutions. Considering maximization problem, the quality (fitness) of a solution can simply be proportional to the value of its objective function. Other forms of fitness can be defined in a similar way; the fitness function is defined in genetic algorithms and other evolutionary computation algorithms.

A new solution  $x^{(t+1)}$  for cuckoo  $i$  is generated using a Levy flight according to the following equation:

$$x_i(t+1) = x_i(t) + \alpha \wedge Levy(\lambda), \quad (1)$$

Where  $\alpha (\alpha > 0)$  represents a step scaling size. This parameter should be related to the scales of problem the algorithm is trying to solve. In most cases,  $\alpha$  can be set to the value of 1 or some other constant. The product  $\wedge$  represents entry-wise multiplications.

Equation (2) states that described random walk is a *Markov chain*, whose next location depends on two elements: current location (first term in Eq. 2) and transition probability (second term in the same expression).

The random step length is drawn from a Levy distribution which has an infinite variance with an infinite mean:

$$Levy \sim u = t - \lambda \quad (2)$$

Where  $\lambda \in [0, 3]$ .

### 3 Computational Results

#### 3.1 Dataset Description

The performance of the proposed methodology is tested on four benchmark instances taken from the UCI Machine Learning Repository (<http://archive.ics.uci.edu/ml/datasets.html>). The datasets are chosen to include a wide range of domains and their characteristics. The data sets are wine, blood-transfusion, breast cancer Wisconsin and Space.

#### 3.2 Experimental Results

Data clustering as one of the important data mining techniques is a fundamental and widely used method to achieve useful information about data. In face of the clustering problem, clustering methods still suffer from trapping in a local optimum and cannot often find global clusters. In order to overcome the shortcoming of the available clustering methods, this paper presents efficient clustering algorithms based on CSA. The obtained experimental results such as, Fitness values of various iterations for wine, Blood-Transfusion, Breast Cancer-Wisconsin and Space dataset are shown in Tables 1, 2, 3 and 4.

#### 3.3 Comparative Analysis

In this section, the scope is to compare the CSA clustering algorithm with several typical algorithms including K-Means, Fuzzy C-Means, Fuzzy PSO and Genetic K-Means. Four data sets have been used. The performance analysis has been made by

**Table 1** Fitness values of various iterations for wine dataset

Iterations	Fitness value				
	CSA	K-Means	F C-Means	Fuzzy PSO	G K-Means
1	17958.31	16556.18	40063.98	19593.3	18318.59
2	16618.49	16556.18	39079.49	19593.3	17552.52
3	16580.31	18295.45	40098.22	18754.42	17275.87
4	16580.31	16556.18	22331.47	17951.09	17189.49
5	16580.31	18295.45	19146.47	17951.09	17055.54
Average	16721.93	16904.03	24464.64	18351.02	17058.94

**Table 2** Fitness values of various iterations for blood-transfusion dataset

Iterations	Fitness				
	CSA	K-Means	F C-Means	Fuzzy PSO	G K-Means
1	297053.7	325565.5	700113.2	308098.6	340869.2
2	297053.7	366406.4	651359.1	308098.6	312919.2
3	297053.7	325565.5	440347.1	308098.6	308862.5
4	297053.7	366406.4	436916.4	307469.5	295575.1
5	297053.7	325565.5	413273.8	291531.3	295575.1
Average	295006.5	333733.7	411692.1	298095.3	303167.7

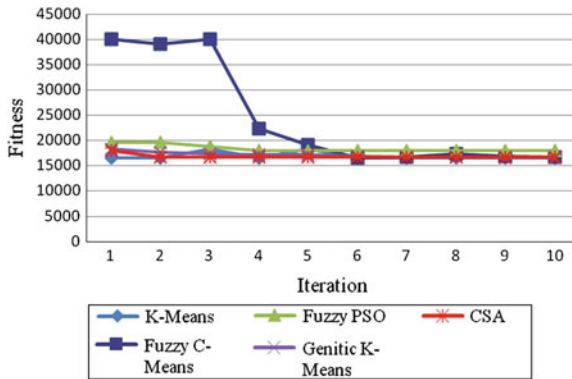
**Table 3** Fitness values of various iterations for breast cancer-Wisconsin dataset

Iterations	Fitness				
	CSA	K-Means	F C-Means	Fuzzy PSO	G K-Means
1	73676602	75011185	161000000	78837480	80818812
2	73676602	72714041	141000000	78837480	74635073
3	72308694	72714041	130000000	73974520	74635073
4	72308694	72714041	76971891	73974520	74635073
5	72308694	72714041	80138269	73470934	74635073
Average	72582276	74453340	96231713	74644960	75253447

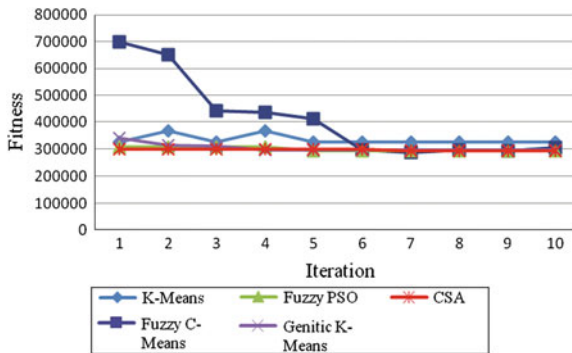
plotting the graphs. By analyzing the plotted graph, the performance of the proposed technique has significantly improved compared with other techniques. Figures 2, 3, 4 and 5 shows the graph which is plot between iteration and fitness value for our proposed technique as well as other algorithms. In Figs. 2, 3, 4 and 5, our proposed technique (plotted in orange color) shows better performance when compared to the other techniques.

**Table 4** Fitness values of various iterations for space dataset

Iterations	Fitness				
	CSA	K-Means	F C-Means	Fuzzy PSO	G K-Means
1	158.2374	232.5886	1218.797954	161.3488	201.6643
2	158.2374	143.5048	436.3725051	161.3488	200.3161
3	158.2374	143.5048	268.5698966	161.3488	200.3161
4	158.2374	238.0524	260.0512394	161.3488	200.3161
5	158.2374	238.0524	143.3624333	161.3488	200.3161
Average	155.4592	208.049	318.8903314	160.3235	200.4509



**Fig. 2** Iteration versus fitness value of wine dataset.



**Fig. 3** Iteration versus fitness value of blood-transfusion dataset

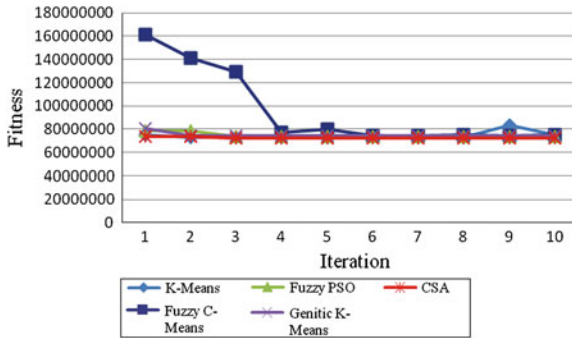


Fig. 4 Iteration versus fitness value of breast cancer Wisconsin dataset

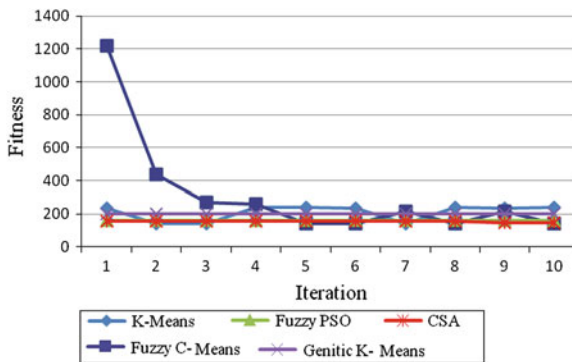


Fig. 5 Iteration versus fitness value of space dataset

### 4 Conclusion and Future Research

A CSA to solve clustering problems has been developed in this paper. To evaluate the performance of the CSA, it is compared with other stochastic algorithms viz. K-Means, Fuzzy C-Means, Fuzzy PSO and Genetic K-Means clustering algorithms on several well known data sets. The experimental results indicate that the proposed clustering algorithm is comparable to the other algorithms in terms of fitness function. The result illustrates that the proposed CSA algorithm can be considered as a viable and an efficient heuristic. In future CSA clustering algorithm which has been discussed can be hybrid with Swarm Intelligence or some conventional clustering algorithms for achieving optimal results.

## References

1. Abraham, A., Guo, H., Liu, H.: *Swarm Intelligence: Foundations, Perspectives and Applications*, *Swarm Intelligence in Data Mining*. Springer, Germany (2006)
2. Azzag, H., Venturini, G., Oliver, A., Gu, C.: A hierarchical ant based clustering algorithm and its use in three real-world applications. *J. Oper. Res.* **179**, 906–922 (2007)
3. Babu, G., Murty, M.: A near-optimal initial seed value selection in k-means algorithm using a genetic algorithm. *Pattern Recogn. Lett.* **14**(10), 763–769 (1993)
4. Chen, L., Tu, L., Chen, H.: A novel ant clustering algorithm with digraph. In: Wang, L., Chen, K., Ong, Y.S. (eds.) LNCS, pp. 1218–1228. Springer, Berlin (2005)
5. Cowgill, M., Harvey, R., Watson, L.: A genetic algorithm approach to cluster analysis. *Comput. Math. Appl.* **37**, 99–108 (1999)
6. Bonabeau, E., Dorigo, M., Theraulaz, G.: *Swarm Intelligence: From Natural to Artificial Systems*. Oxford University Press, New York (1999)
7. Nie, F., Tu, T., Pan, M., Rong, Q., Zhou, H.: *Advances in Intelligent and Soft Computing*, vol. 139, pp. 67–73. Springer, Heidelberg (2012)
8. He, Y., Hui, S.C., Sim, Y., et al.: A novel ant-based clustering approach for document clustering. In: Ng, H.T. (ed.) LNCS, pp. 537–544. Springer, Berlin (2006)
9. Janson, S., Merkle, D., et al.: A new multi-objective particle swarm optimization algorithm using clustering applied to automated docking. In: Blesa, M.J. (ed.) LNCS, pp. 128–141. Springer, Berlin (2005)
10. Kao, Y., Cheng, K., et al.: An ACO-based clustering algorithm. In: Dorigo, M. (ed.) LNCS, pp. 340–347. Springer, Berlin (2006)
11. Ozdamar, L.: A dual sequence simulated annealing algorithm for constrained optimization. In: *Proceedings of the 10th WSEAS International Conference on, Applied Mathematics*, pp. 557–564 (2006)
12. Liao, S.-H., Wen, C.-H.: Artificial neural networks classification and clustering of methodologies and applications - literature analysis from 1995 to 2005. *Expert Syst. Appl.* **32**, 1–11 (2007)
13. Verma, M., Srivastava, M., Chack, N., Kumar Diswar, A., Gupta, N.: A comparative study of various clustering algorithms in data mining. *Int. J. Eng. Res. Appl. (IJERA)* **2** 1379–1384 (2012)
14. Meng, L., Wu, Q.H., Yong, Z.Z., et al.: A faster genetic clustering algorithm. In: Cagnoni, S. (ed.) LNCS, pp. 22–33. Springer, Berlin (2000)
15. Mirkin, B.: *Mathematical Classification and Clustering*. Kluwer, Dordrecht (1996)
16. Paterlini, S., Krink, T.: Differential evolution and particle swarm optimization in partitionial clustering. *Computational Statistics and Data Analysis* **50**, 1220–1247 (2006)
17. Rokach, L., Maimon, O.: Clustering methods. In: Maimon, O., Rokach, L. (eds.) *Data Mining and Knowledge Discovery Handbook*, pp. 321–352. Springer, New York (2005)
18. Shen, H.-Y., Peng, X.-Q., Wang, J.-N., Hu, Z.-K.: A mountain clustering based on improved PSO algorithm. In: Wang, L., Chen, K., Ong, Y.S. (eds.) LNCS, pp. 477–481. Springer, Berlin (2005)
19. Sheng, W., Liu, X.: A genetic it k-medoids clustering algorithm. *J. Heuristics* **12**, 447–466 (2006)
20. Chen, T.Y., Cheng, Y.L.: Global optimization using hybrid approach. *WSEAS Trans. Math.* **7**(6), 254–262 (2008)
21. Tseng, L., Yang, S.: A genetic approach to the automatic clustering problem. *Pattern Recogn.* **34**, 415–424 (2001)
22. Viswanathan, G.M., Raposo, E.P., da Luz, M.G.E.: Lévy flights and superdiffusion in the context of biological encounters and random searches. *Phys. Life Rev.* **5**(3), 133–150 (2008)
23. Wu, F.-X., Zhang, W.J., Kusalik, A.J.: A genetic k-means clustering algorithm applied to gene expression data. In: Xiang, Y., Chaib-draa, B. (eds.) LNAI, pp. 520–526. Springer, Berlin (2003)

24. Xu, R., Wunsch II, D.: Survey of clustering algorithms. *IEEE Trans. Neural Networks* **16**(3), 645–678 (2005)
25. Yang, X.S., Deb, S.: Engineering Optimisation by Cuckoo Search. *Int. J. Math. Model. Numer. Optim.* **1**(4), 330–343 (2010)
26. Yang, Y., Kamel, M.S.: An aggregated clustering approach using multi-ant colonies algorithms. *Pattern Recogn.* **39**, 1278–1289 (2006)



# Search Result Clustering Through Expectation Maximization Based Pruning of Terms

K. Hima Bindu and C. Raghavendra Rao

**Abstract** Search Results Clustering (SRC) is a well-known approach to address the lexical ambiguity issue that all search engines suffer from. This paper develops an Expectation Maximization (EM)-based adaptive term pruning method for enhancing search result analysis. Knowledge preserving capabilities of this approach are demonstrated on the AMBIENT dataset using Snowball clustering method.

**Keywords** Information retrieval · Clustering · FPtree · Expectation maximization

## 1 Introduction

Due to enormous growth of information available on the Web, search engine users are swamped with millions of search results, especially in case of broad and ambiguous queries. Ambiguity arises from the low number of query words [7]. Users typically give short queries with an average query length of three words per query [12]. Many search engines use diversification techniques to avoid duplicate results on the first pages of the results. This approach enables quick retrieval of one relevant result per subtopic, but may not facilitate retrieval of more results of user interest [13].

Search Results Clustering (SRC) is a solution to address the lexical ambiguity issue [2]. This approach is especially useful in case of polysemous queries. Search Results Clustering partitions the results obtained in response to a query into a set of labeled clusters. Each cluster corresponds to a subtopic of the query. Therefore, the user need not accurately predict the words used in the documents that best satisfy his

---

K. Hima Bindu (✉) · C. Raghavendra Rao  
Department of Computer and Information Sciences, University of Hyderabad,  
Hyderabad, Andhra Pradesh, India  
e-mail: himagopal@gmail.com

C. Raghavendra Rao  
e-mail: cracs@uohyd.ernet.in

or her information needs. Instead, the user can start with a generic or broad query and quickly navigate to relevant subtopic. Further, user can grasp the semantic structure in the search results or refine the queries by using the cluster labels.

Search Results Clustering has specific challenges in contrast to traditional clustering methods. These include quick response time (as this is an online activity), ephemeral clustering (clustering happens when the user issues a query), meaningful cluster labels (must be human readable), and no fixed number of clusters.

A Frequent Itemset-based document clustering technique [4] can generate meaningful cluster labels and does not require the number of clusters as an input parameter. However, identification of frequent itemsets is a complex and time-consuming task and also involves subjectivity. Hence, we used Expectation Maximization (EM) [3] to prune the irrelevant terms to make our approach meet search result analysis challenges, in particular the SRC requirements. Snowball clustering proposed by [6] develops clusters starting with highest score (fitness) to least score. Hence, we have chosen to build a clustering method based on these approaches.

The outline of this paper is as follows. Section 2 briefly discusses the search results acquisition procedure and the preprocessing methods. The objective term pruning approach based on EM is presented in Sect. 3. Section 4 briefs the clustering and labeling algorithm. Section 5 shows our experimental results and the comparison with other popular data centric algorithms used for SRC. We conclude the paper in Sect. 6.

## 2 Search Results Acquisition and Preprocessing

The search results of a search engine are acquired by using the search engine's API by sending HTTP requests. All major search engines provide APIs with restrictions on the number of queries per day as a free service and as a paid service without such limitations. By sending a RESTful (Representational State Transfer) request to the public search engine APIs, the results are available in either JSON or XML format. Usually, the first 100 results are considered.

The title of each search result along with one or two lines summary of the web page (called as snippet) forms a search result document. These search results are usually preprocessed by tokenization, stemming (Porter Stemmer) and stopword removal. Stop words are frequently occurring words, which do not carry semantics. We used the stop word list of 571 words from SMART<sup>1</sup> system. Then, the words are stemmed by Porter's suffix stripping algorithm<sup>2</sup>. By using Vector space model, each result is represented as a TF-IDF vector [8]. The terms of a result's title and snippet after these steps form the features.

---

<sup>1</sup> <http://www.lextek.com/manuals/onix/stopwords2.html>

<sup>2</sup> <http://tartarus.org/~martin/PorterStemmer/>

### 3 Term Pruning with Expectation Maximization

Expectation Maximization is frequently used for data clustering in Machine learning, as it can handle latent variables in the data. Expectation Maximization method is developed for characterizing the population characteristics, which is a mixture of finite fundamental factors. Each factor will have its own uncertainty model characterized by associated probability distribution. The characteristics of the population will obey an uncertainty model characterized by mixed distribution, which is generalization of fundamental factors. This mixture model will have set of parameters, namely mixing proportions, and the parameters of fundamental factor distributions. If one assumes that the population is a mixture of  $k$  fundamental factors, and each factor obeys normal distribution, when the characteristic under study is one-dimensional, then the mixture model will have parameter's mixing proportions  $\pi_1, \pi_2, \dots, \pi_k$ ;  $\left(\pi_i > 0 \text{ and } \sum_{i=1}^k \pi_i = 1\right)$  and  $(\mu_i, \sigma_i)$  as the mean and standard deviation of  $i$ th fundamental factor. Estimation process of these parameters is addressed by EM [3] based on the sample.

The terms occurring in each preprocessed search result constitute the population for the analysis. However, some of the terms are relevant and some are not relevant for building the knowledge. Thus, the distribution of the TF-IDF values of the terms can be viewed as a mixture of relevant and irrelevant terms (i.e., as a mixture of two distributions). The simpler way of representing it is by using Gaussian distribution,  $f(x) = \pi_1 f_1(x|\mu_1, \sigma_1) + \pi_2 f_2(x|\mu_2, \sigma_2)$ , where  $f_1$  is the probability distribution function of TF-IDF values of relevant terms with mean  $\mu_1$  and standard deviation  $\sigma_1$ ,  $f_2$  is the probability distribution function of TF-IDF values of non-relevant terms with mean  $\mu_2$  and standard deviation  $\sigma_2$ ;  $\pi_1$  and  $\pi_2$  are the mixing proportions. These parameter estimates must have the property that  $\mu_1 > \mu_2$ . Based on the parameters obtained for the mixture model, the threshold on TF-IDF values is  $\frac{\pi_1 \mu_1 + \pi_2 \mu_2}{\pi_1 + \pi_2}$ , from [14]. Any term with TF-IDF value more than this threshold is classified as relevant term, otherwise irrelevant term.

### 4 The Clustering and Labeling Algorithm

Search Results Clustering algorithms must be faster to have minimum latency between query submission and cluster presentation. Our algorithm performs clustering and labeling on the fly by processing only the search results without using external knowledge, hence, it is a lightweight approach. It labels the clusters automatically by using only the text concepts (frequent termsets) available in the search results.

The frequent termsets are identified by FPGrowth [5], by considering the relevant terms retained after the EM based term pruning, snowball clustering method [6] has been applied to arrive at the clusters along with the labels. The size of the relevant

terms set due to EM makes the frequent itemset analysis manageable, though it is a tedious task.

## 5 Results and Analysis

An illustration of EM-based term pruning is provided here, by considering the first ten results of the query “Beagle,” from the AMBIENT<sup>3</sup>. dataset.

### 5.1 Terms Extraction

The first 10 results after tokenization (using white space as delimiter) resulted in 189 terms, are shown in Sect. 5.1.1. With the preprocessing by stemming and stop-word removal as discussed in the Sect. 3, 118 terms are retained, these are shown in Sect. 5.1.2. The TF-IDF vectors are constructed for these terms. When EM algorithm is run, the threshold on TF-IDF values is obtained as 1.17, based on the method described in Sect. 4. It is observed that 28 terms’ TF-IDF satisfy this threshold. These are treated as relevant terms, which are given in Sect. 5.1.3.

#### 5.1.1 Terms Obtained After Tokenization

(EC), (software), -, -, ..., 2, 3, 5, :, A, ANSI/ISO, American, Apple, Architecture, BEAGLE, Beagle, Beagle, Beagle-type, Beagle, Beagles, Breed, Britannica, British, C++, C++, CenterÂ®, Club, Computation, Consortium, Debian, Desktop, Dog, Download, Earth, Encyclopaedia, English, Evolutionary, Files, GNOME, God’s, Google, Group, Guide, Head, Hound, Information, Information, Kennel, Linux, Main, Mars, Open, Owner’s, PSSRI, Package, Page, Pillinger, Professor, Profile:, Search, Size, Spotlight, Standard, Storage, The, There’s, University-based, University, Unix, W3, Wikipedia, Windows, a, all, also, among, an, and, any, architectures, are, article, as, at, available, be, beagle, beagle, blog-post, breed, built, but, by, can, centuries, child, coat, code, coded, color, come, compliant, critters, cutest, data, dog, dog, dogs, easy-care, encyclopedia, enhance, entirely, existed, experience, exploration, fairly, for, framework, free, get, good, gotten, green, group, has, have, head, heavy, hound, idea, in, indexing, industrial, is, its, led, long, medium, member, modern, not, of, on, or, other, over, overwhelmed, pack, page, partners, people, personal, pet, point, post, power, product, puppies, puppy, reference, researchers, search, short, should, similar, simplicity, single, sized, skull, sleek, small, solidly, sporty, standard, system, the, their, this, to, together, tool, website, where, which, will, with, you, your, â€.

<sup>3</sup> AMBIGUOUS ENTRIES : <http://credo.fub.it/ambient>.

### 5.1.2 Terms After Pre Processing by Stemming and Stop-Word Removal

american, ansiiso, appl, architectur, articl, avail, beagl, beagletyp, blogpost, breed, britannica, british, built, center, centuri, child, club, coat, code, color, come, compliant, comput, consortium, critter, cutest, data, debian, desktop, dog, download, earth, easycar, ec, encyclopaedia, encyclopedia, english, enhanc, entir, evolutionari, exist, experi, explor, fairli, file, framework, free, gnome, god, good, googl, gotten, green, group, guid, head, heavi, hound, idea, index, industri, inform, kennel, led, linux, long, main, mar, medium, member, modern, open, over, overwhelm, owner, pack, packag, page, partner, peopl, person, pet, pilling, point, post, power, product, professor, profil, pssri, puppi, refer, research, search, short, similar, simplic, singl, size, skull, sleek, small, softwar, solidli, sporti, spotlight, standard, storag, system, togeth, tool, univers, universitybas, unix, w3, websit, wikipedia, window.

### 5.1.3 Terms After EM-Based Term Pruning

american, architectur, britannica, british, club, code, debian, desktop, download, encyclopaedia, encyclopedia, explor, free, guid, inform, kennel, led, main, mar, open, owner, page, profil, puppi, search, softwar, w3, wikipedia.

## 5.2 Analysis

For the query “Beagle”, by considering the first 100 search results, the number of terms after stemming and stop-word removal is 840. With term pruning, the number of terms is 230. The tokenized termset size is not reported as it not the interest of researchers.

The average terms set size for all the 44 queries of AMBIENT dataset, resulted without term pruning as 865.18 (with standard deviation 74.06), and with term pruning as 274.22 (with standard deviation 72.22). The percentage of reduction in terms set size is 68.30.

The associated FP Trees of pre and post term pruning have been constructed and the corresponding estimates of the size (obtained by multiplying the maximum depth and maximum width) are derived and reported in Fig. 1. For the 44 datasets of AMBIENT, the Mean (Standard Deviation) of FPTree sizes before and after term pruning are 2486.48 (SD = 286.12) and 962.82 (SD = 243.29), respectively. The percentage of reduction in FP tree sizes is 61.28.

The “degree of knowledge representation” (Kappa) developed in the Rough Set theory [10] which quantifies the knowledge representation in considered features is employed, treating the terms as features. It is observed that pre pruning produced mean Kappa as 1 (SD = 0), indicating that the pre pruned termset possess hundred percent knowledge about the ground truth. Whereas post pruning term set has mean Kappa 0.95 (SD = 0.04) indicates that, the knowledge representation by post pruned

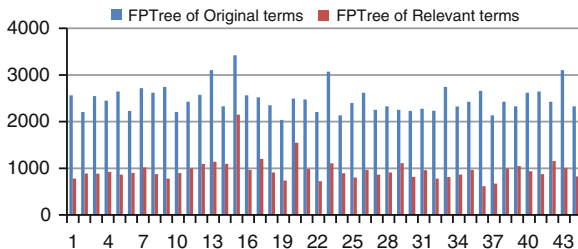


Fig. 1 FP Tree sizes of the AMBIENT dataset

term set will possess the knowledge about the ground truth from 0.8 to 1 (with mean 0.95). The relevant terms set may lead at the most 20% loss in knowledge representation, 68.02% gain by reduction in term set size and with 61.28 gain by FPTrees size reduction. This suggest that the relevant term set obtained by EM-based term set pruning can be employed in search result analysis in Web Mining.

The search result clustering method discussed in Sect. 4 has been considered for demonstrating the effectiveness of the recommended method. The distribution of the no of clusters with and without pruning is given in Fig. 2. The term pruning approach resulted in more specific clusters, so the number of clusters has increased.

RandIndex (RI) [11] is used as the evaluation measure, to compare our approach against the ground truth. The Rand Index values of each query when the clustering method is run with and without term pruning, are reported in Fig. 3. With term pruning, every query’s RI value improved (statistically significant from our experiments).

When the Snowball clustering algorithm is run on the AMBIENT datasets, without term pruning, the average Rand Index has a low value of 58.83. When the term pruning is performed, RI value raised to 61.72. Comparison of our approach against some of the data centric SRC approaches, which do not use external resources is presented in Table 1. Lingo [9] uses Singular Value Decomposition, STC [15] uses Suffix trees and KeySRC [1] is based on Key Phrases.

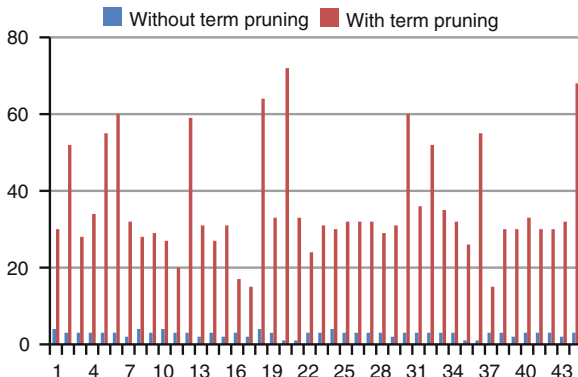


Fig. 2 Number of clusters with and without term pruning

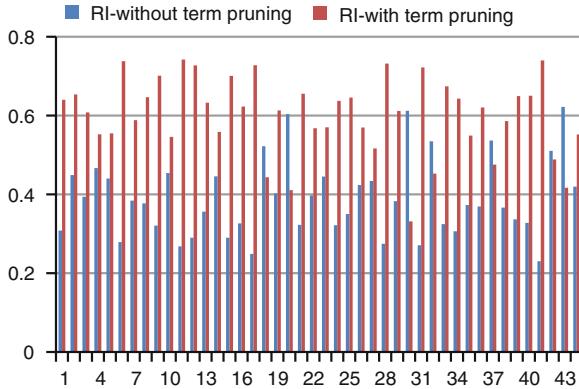


Fig. 3 RI values with and without term pruning

Table 1 Average rand index

Clustering method	Rand index
Lingo	62.75
STC	61.48
KeySRC	66.49
Snowball without term pruning	58.83
Snowball with EM based term pruning	61.72

## 6 Conclusion

The data centric SRC is effective due to the pruning of terms beyond well-defined stop words, through the EM algorithm. The search results are clustered and labeled with Snowball clustering method, without any human interaction or even external knowledge. As the threshold computed by EM algorithm is adaptive, the recommended method is adaptive machine learning technique. EM based term pruning has shown two benefits—overcome the curse of dimensionality and less runtime memory (FP Tree sizes are low).

## References

1. Bernardini, A., Carpineto, C., D’Amico, M.: Full-subtopic retrieval with keyphrase-based search results clustering. In: Proceedings of Web Intelligence 2009, IEEE Computer Society, pp. 206–213 Milan (2009)
2. Carpineto, C., Osinski, S., Romano, G., Weiss, D.: A survey of web clustering engines. ACM. Comput. Surv. (CSUR) **41**(3) (2009). Article No. 17. ISSN:0360–0300
3. Dempster, A.P., Laird, N.M., Rubin, D.R.: Maximum likelihood from incomplete data via the EM algorithm. J. Roy. Stat. Soc.: Ser. B (Methodol.) **39**(1), 1–38 (1977)
4. Fung, B., Wang, K., Ester, M.: Hierarchical document clustering using frequent itemsets. In: Proceedings of SIAM International Conference on Data Mining, pp. 59–70 (2003)

5. Han, J., Pei, J., Yin, Y.: Mining frequent patterns without candidate generations. In: Proceedings of ACM SIGMOD International Conference on Management of Data, Dallas, TX, USA (2000)
6. Hima Bindu K., Raghavendra Rao C.: Association rule centric clustering of web search results. In: Proceedings of MIWAI'11, Vol. 7080/2011, pp. 159–168, Hyderabad (2011). doi:[10.1007/978-3-642-25725-4\\_14](https://doi.org/10.1007/978-3-642-25725-4_14)
7. Kamvar, M., Baluja, S.: A large scale study of wireless search behavior: google mobile search. In: Proceedings of CHI'06, pp. 701–709, New York (2006)
8. Manning, C. D., Raghavan, P., Schütze, H.: Introduction to Information Retrieval. Cambridge University press, New York, USA (2008)
9. Osinski, S., Stefanowski, J., Weiss, D.: Lingo: Search results clustering algorithm based on singular value decomposition. In: Proceedings of the International Intelligent Information Processing and Web Mining Conference. Advances in Soft Computing, Springer, 359–368 (2004)
10. Pawlak, Z.: Rough Sets—Theoretical Aspects of Reasoning about Data. Kluwer, Boston (1991)
11. Rand, W. M.: Objective criteria for the evaluation of clustering methods. *J. Am. Stat. Assoc.* **66**(336), 846–850 (1971)
12. Scaiella, U., Ferragina, P., Marino, A., Ciaramita, M.: Topical clustering of search results. In: Proceedings of WSDM 2012, pp. 223–232. ACM, New York (2012)
13. Taghavi, M., et al.: An analysis of web proxy logs with query distribution pattern approach for search engines. *Comput. Stand. Interfaces.* 162–170 (2011). doi:[10.1016/j.csi.2011.07.001](https://doi.org/10.1016/j.csi.2011.07.001)
14. Wajahat Ali, M. S., Raghavendra Rao, C., Bhagvati, C., Deekshatulu, B. L.: EMTrain++: EM based incremental training algorithm for high accuracy printed character recognition system. *Int. J. Comput. Intell. Res.* **5**(46), 365–371 (2010)
15. Zamir, O. And Etzioni, O.: Web document clustering: A feasibility demonstration. In: Proceedings of the 21st International ACM SIGIR Conference on Research and Development in Information Retrieval. ACM Press, 46–54 (1998)



# Intensity-Based Detection of Microcalcification Clusters in Digital Mammograms using Fractal Dimension

P. Shanmugavadivu and V. Sivakumar

**Abstract** This paper presents a novel method to locate and segment the microcalcification clusters in mammogram images, using the principle of fractal dimension. This proposed technique detects the edges using the intensities of the regions/objects in the image, the Fractal dimension of the image, which is image-dependent in such a way that leads to the segmentation of microcalcification clusters in the image. Hence this fractal dimension based detection of microcalcifications is proved to produce excellent results and the location of the detected microcalcifications clusters complies with the specifications of dataset of the mini-MIAS database accurately, which substantiate the merit of the proposed technique.

**Keywords** Fractal dimension · Edge detection · Mammogram · Microcalcifications · Image segmentation

## 1 Introduction

The recent advancements in Digital Image Processing (DIP) have broadened its application horizons in Medical Image Processing, and thus have added a new dimension in the diagnosis of medical images. Image segmentation, an element of DIP, deals with subdividing an image into its constituent regions/objects and the level of segmentation is determined by the requirements of the problem domain. This technique has gained popularity in many areas including medical imaging, satellite imaging and under-water imaging, as it provides a platform to segment and retain the vital

---

P. Shanmugavadivu (✉) · V. Sivakumar  
Department of Computer Science and Applications, Gandhigram Rural Institute–Deemed University, Gandhigram, Tamil Nadu 624302, India  
e-mail: psvadivu67@gmail.com

V. Sivakumar  
e-mail: sivakumar.vengusamy@gmail.com

objects/regions of interest (RoI) and ignore the insignificant details of an image, which has to pay-off on reduced computation time and storage space, during the subsequent phases like image analysis and image registration. Edge detection is a subprocess of image segmentation using which the prospective pixels that constitute contour/boundary of RoI are identified [1, 2].

Breast cancer is one of the primary causes of early mortality among women in both developed and developing countries [3]. Recently mammography has emerged as the most popular and reliable source for the early detection of breast cancer and other abnormalities in the breast tissues. The texture, shape and dimension of breast tissues play a significant role in the detection of breast cancer which is made up of lobules, the glands for milk production and the ducts that connect lobules to the nipple. According to the radiologists' version, a patient is confirmed to have breast cancer if certain types of masses or calcifications which appear as small white specks are identified in the mammogram [4]. Generally, a mass is explained as a 'spot' or 'density' that may appear in the mammogram and calcifications are described as deposits of calcium into various tissues within the breast [5, 6]. As the breast tissues very much possess self-similar property of fractal objects, fractal-based techniques can be extended to mammograms for the diagnosis and analysis of mammograms [6–10].

The rough geometric shapes which can be subdivided into discrete parts, each of which replicates the structure of whole object, are termed as Fractals. Every fractal object is characterized by its fractal dimension, which is an important parameter that measures the fractal property of an object. It has got wider applications in the fields of image segmentation and shape recognition [6, 7, 10–14]. This paper projects the potential of combining the potential of edge intensities and fractal dimension, using which, the microcalcifications present in the input images are precisely segmented.

In this paper, Sect. 2 describes the basics of edge detection as well as fractal dimension and the computational methodology of the segmentation of microcalcifications clusters presented in Sect. 3. The results and discussion and the conclusions are presented in Sects. 4 and 5 respectively.

## **2 Basics of Techniques Used in the Proposed Work**

### ***2.1 Edge Detection***

Due to the limitations in the image acquisition mechanism and its dependent attributes, the edges may get blurred, and thus the pixels constituting the edges may not appear distinct with respect to neighbours, which in turn may misguide the process of edge detection. Moreover, the rate of sampling and quantization also adds a new dimension to the problem. Hence, it is important to enhance the quality of any input image, prior to the application of image segmentation [2]. An edge is a vector variable with two components, magnitude and direction. The edge magnitude

is the magnitude of the gradient and the edge direction is rotated with respect to the gradient direction by  $-90^\circ$ . The gradient direction gives the direction of maximum growth of the function. The first-order derivatives in an image are computed using the Gradient and the second-order derivatives are obtained using the Laplacian.

Sobel is a powerful edge detection technique that uses the doubled center coefficient of mask to give more importance for the center point. For computation of the gradient of an image, sobel operators provide both a differencing and a smoothing effect [1, 2]:

$$\begin{aligned} G_x &= (z_7 + 2z_8 + z_9) - (z_1 + 2z_2 + z_3) \\ G_y &= (z_3 + 2z_6 + z_9) - (z_1 + 2z_4 + z_7) \end{aligned} \quad (1)$$

The sobel mask for computing x-derivative is anti-symmetry with respect to the y-axis. It has the positive sign on the right side and negative sign on the left side. It should be noted that the sum of all coefficients is equal to zero to make sure that the response of a constant intensity area is zero. The sobel operator is often used as a simple detector of horizontality and verticality of edges [1, 2].

## 2.2 Fractal Dimension

Fractals are the geometric primitives that are self-similar and irregular in nature. Self-similarity is defined as a property where a subset is indistinguishable from the whole, when magnified to the size of the whole. In 1982, Mandelbrot introduced the *Fractal geometry* to the world of research. Fractals are of rough geometric shapes which can be subdivided in parts, each of which is reduced to similar of the whole [11, 12].

Fractal objects are characterized by their fractal dimension (defined as D) which is an important characteristic of fractals as it has got information about their geometric structure. In the fractal world, the fractal dimension of an object, need not be an integer number and is normally greater than its topological dimension (i.e.  $D \geq d$ ) [11–13].

In Euclidean n-space, the bounded set X is said to be self-similar when X is the union of  $N_r$  distinct non-overlapping copies of itself, each of which is similar to X scaled down by a ratio r. Fractal dimension D of X can be derived from the relation [11], as

$$D = \frac{\log(N_r)}{\log(\frac{1}{r})} \quad (2)$$

## 3 Methodology

The proposed work initially finds the fractal dimension, D for a given input mammo-gram image by box counting method using Eq. (2). Then, the input image undergoes image enhancement process that maps the intensity values of the input grayscale

image A to new values in B by compressing the low end and expanding the high end such that 1% of data is saturated at low and high intensities of A. This increases the contrast of the input image.

Further, edges are detected for enhanced input image B using the sobel operator and those edge intensities are noted. Now those edge intensities are compared with the fractal dimension of the image and the pixels for which the fractal dimension value is greater than those edge intensities are noted and marked separately in the image that leads to the segmentation of microcalcifications clusters in the given input mammogram image. As, in the images of mini-Mammographic Image Analysis Society (MIAS) database several types of noises and imaging artifacts are present, by default the detected image consists of the entire frame that the image acquires which contains even the chest wall behind portion, high intensity rectangular labels and low intensity labels too. The proposed methodology aims to exclude such high intensity noises in the detected image. To omit such unwanted noise areas and to acquire the required portion of the frame, the concept of region of interest is considered to set the desired region. This gives the projection of microcalcifications part alone that results in exact segmented image. The algorithm for the above methodology is given as follows.

---

Algorithm : Detection of microcalcification clusters from a mammogram image

**Aim :** To detect microcalcification clusters

**Input :** A 2-dimensional mammogram image, A

**Output :** Segmented portions of microcalcifications in A

Step 1: Read a 2-dimensional input mammogram image A

Step 2: Enhance the input image A to acquire B

Step 3:  $[M, N] \leftarrow \text{IMSIZE}[B]$

Step 4: If  $M > N$  then  $r \leftarrow M$

Else  $r \leftarrow N$

Step 5: Compute fractal dimension D using Eq.(2).

Step 6: Detect the edges of objects in B to C using sobel operator

Step 7: Note the edge intensities  $b(i, j)$  of C

Step 8: Compare D with  $b(i, j)$  of C

Step 9: Plot the pixels for which  $D > b(i, j)$  of B in D

Step 10: Considering only the region of interest in D that results in the segmented image.

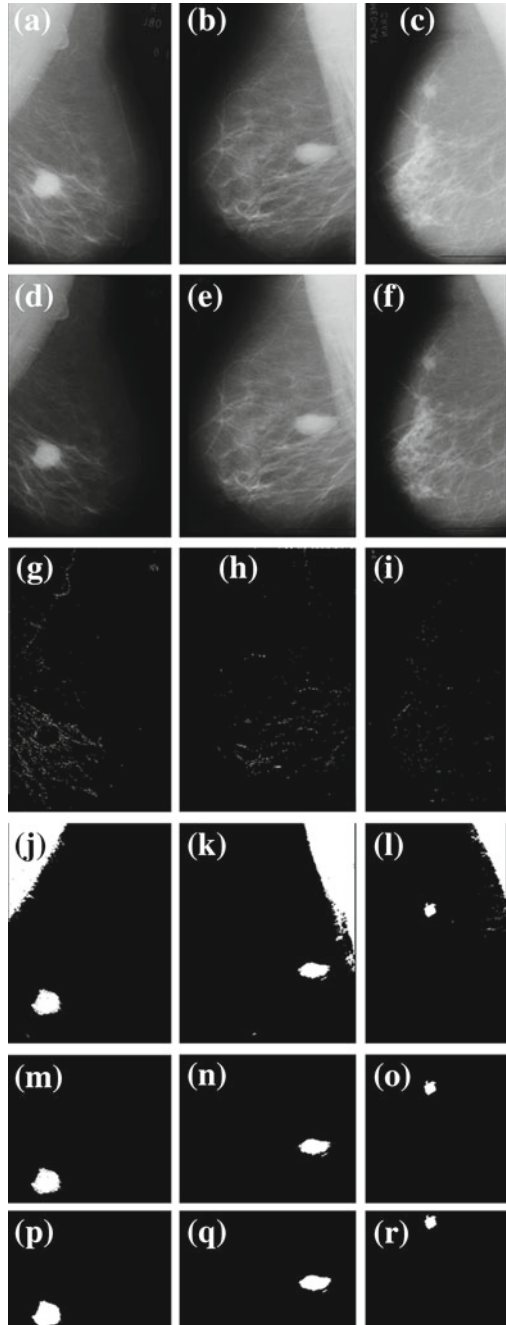
Step 11: Stop.

---

## 4 Results and Discussion

The proposed procedure was implemented using Matlab 7.8. to ascertain the merit of the proposed method, different mammogram images were collected from the mini-mammographic database of the MIAS from the Pilot European Image Processing Archive (PEIPA) at the University of Essex (<ftp://peipa.essex.ac.uk/ipa/pix/mias/>). As per the principle of the proposed methodology, the input image has been enhanced

**Fig. 1** **a-c** Original images. **d-f** Enhanced images of **(a-c)**. **g-i** Intensity values of edges of **(d-f)**. **j-l** Detected images of **(g-i)**. **m-o** Artifacts cleared images of **(j-l)**. **p-r** Segmented mass of **(m-o)**



by adjusting the contrast values. Then the edges are detected for the enhanced image using sobel operator and those edge intensities are recorded in another image. For illustrative purpose, the results of three mammograms (mdb028.pgm (image1), mdb023.pgm (image2), mdb025.pgm (image3)) are depicted in Fig.1a–r. The original images and the corresponding enhanced images for the input mammograms are depicted in Fig.1a–c and Fig.1d–f respectively.

The recorded intensity values of edges that are detected using sobel operator are depicted in Fig.1g–i. After finding the fractal dimension of the input images, it is compared with those edge intensities and the pixels whose Fractal dimension value is greater than those edge intensities are recorded and marked separately in an image that leads to the detection of microcalcifications which is depicted in Fig.1j–l.

Fig.1j–l shows that it contains the pectoral muscle portion of the breast and such unwanted areas are removed by considering only the region of interest so that the desired region is acquired which is depicted in Fig.1m–o. Dilation and erosion are done on the artifacts cleared images as post-processing methods to smoothen the image so that the interior gaps are filled which results in the segmentation of microcalcification clusters which are shown in Fig.1p–r. As the validation process, finally the location of the coordinates of the detected mass in the final segmented image is verified and very much complies with the location specified in the mini-MIAS dataset. Hence, it is clearly understood that the proposed work using fractal dimension is proved to be precise and robust in detection of microcalcification clusters in a digital mammogram.

## 5 Conclusions

This method proposes an edge intensity based novel method for the detection of microcalcifications in the mammogram images, using fractal dimension, that enables the early diagnosis of breast cancer. This paper provides a framework that seems to make segmentation easier by considering the optimal RoI in the detected masses in order to avoid the inclusion of pectoral muscle portion. As per the mini-MIAS database, the location of the (x,y) image-coordinates of centre of circumscribed mass abnormalities for the input images mdb023, mdb025 and mdb028 are (538, 681), (674, 443) and (338, 314) respectively which substantiates the microcalcifications detected by the proposed method that vouches its merit. The future scope of the study covers the classification of the detected masses, either as benign or malignant, using texture analysis.

## References

1. Gonzalez, R.C., Woods, R.E.: Digital Image Processing, Second edition. Prentice Hall, New York (2009)
2. Sonka, M., Hlavac, V., Boyle, R.: Digital Image Processing and Computer Vision. Cengage Learning, Stamford (2008)
3. Kom, G., Tiedeu, A., Kom, M.: Automated detection of masses in mammogram by local adaptive thresholding. *Comput. Biol. Med.* **37**, 37–48 (2007)
4. Maitra, I.K. et al.: Technique for preprocessing of digital mammogram. *Comp. Meth. Programs Biomed.* **107**, 175–188 (2012)
5. Stojic, Tomislav, et al.: Adaptation of multifractal analysis to segmentation of microcalcifications in digital mammograms. *Physica A* **367**, 494–508 (2006)
6. Shanmugavadivu, P., Sivakumar, V.: Fractal approach in digital mammograms: a survey, NCSIP-2012, pp. 141–143, ISBN: 93-81361-90-8, (2012)
7. Shanmugavadivu, P., Sivakumar, V.: Fractal dimension-based texture analysis of digital images. *Procedia Eng.* **38**, 2981–2986, ISSN: 1877–7058, (Elsevier-Scidirect) (2012)
8. Cheng, H.D., Cai, X., Chen, S., Hu, L., Lou, X.: Computer-aided detection and classification of microcalcifications in mammograms: a survey. *Pattern Recogni.* **36**, 2967–2991 (2003)
9. Claudio, M., Mario, M., D’Elia, C., Tortorella, F.: A computer-aided detection system for clustered microcalcifications. *Artif. Intell. Med.* **50**, 23–32 (2010)
10. Mohamed, W.A., Alolfe, M.A., Kadah, Y.M.: Fast fractal modeling of mammograms for microcalcifications detection. In: 26th National Radio Science Conference, Egypt (2009)
11. Addison, P.S.: *Fractals and Chaos*. IOP Publishing, Bristol (2005)
12. Welstead, S.: Fractal and wavelet image compression techniques. In: *Tutorial Texts in Optical Engineering*, Vol. TT40. SPIE Press (<http://www.spie.org/bookstore/tt40/>) (1999)
13. Lopes, R., Betrouni, N.: Fractal and multifractal analysis: a review. *Med. Image Anal.* **13**, 634–649 (2009)
14. Vuduc, R.: Image segmentation using fractal dimension. Report on GEOL 634, Cornell University (1997)

**Part XV**  
**General Soft Computing**  
**Approaches and Applications**



# Palmprint Recognition Using Geometrical and Statistical Constraints

Aditya Nigam and Phalguni Gupta

**Abstract** This paper proposes an efficient biometrics system based on palmprint. Palmprint ROI is transformed using proposed local edge pattern (LEP). Corner like features are extracted from the enhanced palmprint images as they are stable and highly discriminative. It has also proposed a distance measure that uses some geometrical and statistical constraints to track corner feature points between two palmprint ROI's. The performance of the proposed system is tested on publicly available PolyU database consisting of 7,752 and CASIA database consisting of 5,239 hand images. The feature extraction as well as matching capabilities of the proposed system are optimized and it is found to perform with CRR of 99.97 % with ERR of 0.66 % for PolyU and CRR of 100 % with ERR of 0.24 % on CASIA databases respectively.

**Keywords** Biometrics · Palmprint · Local Binary Pattern (LBP) · Phase only Correlation (POC) · Optical Flow

## 1 Introduction

Reliable human identification and authentication in real time is a huge challenge and one of the most desirable tasks of our society. Hence researchers got motivated to design an efficient, effective, robust and low cost personal authentication systems. Biometrics can be an alternative to the token-based traditional methods as they are easier to use and harder to circumvent. Authentication systems based on biometrics are extensively used in computer security, banking, law enforcement etc. Exponential increase in the computational power and society driven business, guides biometrics

---

A. Nigam (✉) · P. Gupta  
Indian Institute of Technology, Kanpur, India  
e-mail: naditya@cse.iitk.ac.in

P. Gupta  
e-mail: pg@cse.iitk.ac.in

**Table 1** Trait-wise challenges and issues

	Challenges	Issues
Face	Pose, expression, illumination, aging, rotation, translation and background	Too many challenges
Finger	Rotation and translation	Acceptance
Iris	Segmentation and illumination	Acquisition, cooperation, acceptance
Palm	Illumination, rotation and translation	–

research so as to meet the practical real field challenges. Behavioral as well as physiological biometrics based characteristics (such as face [12, 15, 16], fingerprint [20], iris [8], knuckleprint [7, 17], gait, voice, vein patterns *etc.*) are used to develop robust, accurate and highly efficient personal authentication systems. But every biometric trait has its own challenges (like occlusion, pose, expression, illumination, affine transformation) and trait specific issues (such as user acceptance, cooperation) as shown in Table 1. Hence one cannot consider any trait to be best for all applications.

Hand based biometric recognition systems (e.g. palm print [5], fingerprint [20] and finger knuckleprint [17]) have gathered attraction over past few years because of their good performance and inexpensive acquisition sensors. The inner part of the hand is called palm and the extracted region of interest in between fingers and wrist is termed as palmprint. Pattern formation within this regions are suppose to be stable as well as unique even monozygotic twins are found to have different palmprint patterns. Hence one can consider it as a well discriminative biometrics trait.

Palmprint's prime advantages over fingerprint includes its higher acceptance socially because it is never being associated with criminals and larger ROI area as compared to fingerprint images. Larger ROI ensures abundance of structural features including principle lines, wrinkles, creases and texture pattern even in low resolution palmprint images, that enhances system's speed, accuracy and reduces the cost. Some other factors favoring palmprint includes its lesser user cooperation, non-intrusive and cheaper acquisition sensors.

Huge amount of work has been reported on palmprint based authentication systems because of the above mentioned advantages. Developed systems have adopted either structural or statistical features analysis.

- **Structural Features:** Morphological operations are applied on sobel edges [10] to extract line-like features from palmprints. Isolated points as well as some points along principle line are considered as features for palmprint authentication [9].
- **Statistical Features:** Several systems are developed that transform palmprint features into higher dimensional space where they are considered as a points using PCA, LDA, ICA and their combinations. Direction based filtering using gabor is performed to obtained *palmcode* [22], *compcode* [11] and *ordinalcode* [21]. Moments like Zernike [6] and transforms like Stockwell [4] and Fourier [5] are applied on palmprint low resolution images to achieve better results.
- **Combined:** System proposed in [3] uses Kernal PCA and ICA gabor filter response to extract the kernal principle components of gabor features.

This paper proposes a transformation technique as well as a distance measure which is robust against illumination and slight amount of local non-rigid distortions. The performance of the system is studied on publicly available PolyU and CASIA datasets where the hand image are obtained under varying environment. The rest of the paper is organized as follows. Section 2 discusses mathematical basis of the proposed system. Section 3 presents the proposed palmprint based recognition system. Experimental results are analyzed in Sect. 4. Conclusions are presented in the last section.

## 2 Mathematical Basis

### 2.1 LBP based Image Enhancement

In Ref. [18], LBP (Local Binary Pattern) is proposed that assumes pixel's relative gray value with respect to its eight-neighborhood pixels can be more stable than its own gray value. In Ref. [16] *gt*-transformation is proposed that can also preserve the distribution of gray level intensities in facial images. It also helps to address the problems like robustness against illumination variation and local non-rigid distortions.

### 2.2 Phase Only Correlation (POC)

It has been used for image registration and alignment purposes. Let  $f$  and  $g$  are  $M \times N$  images such that  $m = -M_0 \dots M_0 (M_0 > 0)$  and  $n = -N_0 \dots N_0 (N_0 > 0)$ . Also  $M = 2M_0 + 1$  and  $N = 2N_0 + 1$ .  $F$  and  $G$  are the DFT of  $f$  and  $g$  images and  $F$  can be defined as:

$$F(u, v) = \sum_{m=-M_0}^{M_0} \sum_{n=-N_0}^{N_0} f(m, n) e^{-j2\pi(\frac{mu}{M} + \frac{nv}{N})} \quad (1)$$

$$= A_F(u, v) e^{j\theta_F(u, v)} \quad (2)$$

$$G(u, v) = \sum_{m=-M_0}^{M_0} \sum_{n=-N_0}^{N_0} g(m, n) e^{-j2\pi(\frac{mu}{M} + \frac{nv}{N})} \quad (3)$$

$$= A_G(u, v) e^{j\theta_G(u, v)} \quad (4)$$

Cross Phase Spectrum between  $G$  and  $F$  is defined as:

$$R_{GF}(u, v) = \frac{G(u, v) \times F^*(u, v)}{|G(u, v) \times F^*(u, v)|} = e^{j(\theta_G(u, v) - \theta_F(u, v))} \quad (5)$$

Phase Only Correlation is the IDFT of  $R_{GF}(u, v)$  defined as:

$$P_{gf}(m, n) = \frac{1}{MN} \sum_{u=-M_0}^{M_0} \sum_{v=-N_0}^{N_0} R_{GF}(u, v) e^{j2\pi(\frac{mu}{M} + \frac{nv}{N})} \quad (6)$$

Phase Only Correlation can be obtained by taking the IDFT of  $R_{GF}(u, v)$ . If two images are ‘‘Same’’ the POC function  $P_{gf}(m, n)$  becomes kronecker delta function  $\delta(m, n)$ . If two images are ‘‘Similar’’ POC function gives a distinct sharp peak otherwise the peak value drops significantly. Hence peak height of  $P_{gf}(m, n)$  can be considered as a similarity measure.

### 2.3 Lukas Kanade Tracking

Sparse optical flow between two images can be estimated using Lukas Kanade tracking algorithm [13]. Let there be some feature at location  $(x, y)$  at time instant  $t$  with intensity  $I(x, y, t)$  and this feature has moved to the location  $(x + \delta x, y + \delta y)$  at time instant  $t + \delta t$ . LK Tracking [13] make use of three assumptions to estimate the optical flow.

- **Brightness Consistency:** Little variation in brightness for small  $\delta t$ .

$$I(x, y, t) \approx I(x + \delta x, y + \delta y, t + \delta t) \quad (7)$$

- **Temporal Persistence:** Small feature movement for small  $\delta t$ . One can estimate  $I(x + \delta x, y + \delta y, t + \delta t)$  by applying Taylor series on Eq. (7) and neglecting the high order terms to get

$$\frac{\delta I}{\delta x} \delta x + \frac{\delta I}{\delta y} \delta y + \frac{\delta I}{\delta t} \delta t = 0 \tag{8}$$

Dividing both sides of Eq. (8) by  $\delta t$  one gets

$$I_x V_x + I_y V_y = -I_t \tag{9}$$

where  $V_x, V_y$  are the respective components of the optical flow velocity for feature at pixel  $I(x, y, t)$  and  $I_x, I_y$  and  $I_t$  are the local image derivatives in the corresponding directions.

- Spatial Coherency:** It assumes local constant flow (i.e. a patch of pixels moves coherently) to estimate the optical flow vector  $\widehat{\mathbf{V}}$  ( $2 \times 1$  matrix) for any corner. A non-iterative method that assume constant flow vector ( $V_x, V_y$ ) within  $5 \times 5$  neighborhood (i.e. 25 neighboring pixels) around the current feature point (center pixel) is used to estimate its optical flow. Hence, an overdetermined linear system of 25 equations is obtained which can be solved using least square method as

$$\underbrace{\begin{pmatrix} I_x(P_1) & I_y(P_1) \\ \vdots & \vdots \\ I_x(P_{25}) & I_y(P_{25}) \end{pmatrix}}_C \times \underbrace{\begin{pmatrix} V_x \\ V_y \end{pmatrix}}_V = - \underbrace{\begin{pmatrix} I_t(P_1) \\ \vdots \\ I_t(P_{25}) \end{pmatrix}}_D \tag{10}$$

where rows of the matrix  $C$  represent the derivatives of image  $I$  in  $x, y$  directions and those of  $D$  are the temporal derivative at 25 neighboring pixels. The  $2 \times 1$  matrix  $\widehat{\mathbf{V}}$  is the estimated flow of the current feature point determined as

$$\widehat{\mathbf{V}} = (C^T C)^{-1} C^T (-D) \tag{11}$$

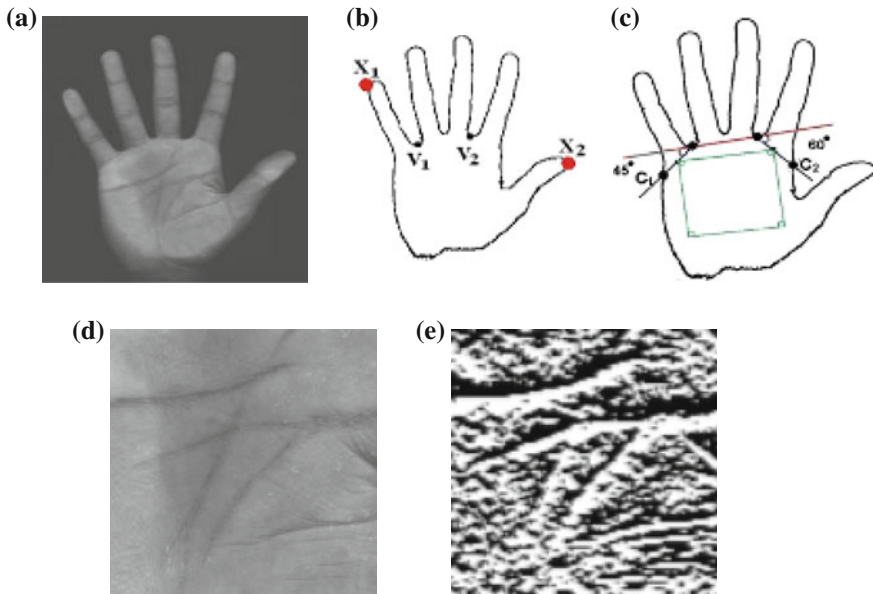
The final location  $\widehat{\mathbf{F}}$  of any feature point can be estimated using its initial position vector  $\widehat{\mathbf{I}}$  and the estimated flow vector  $\widehat{\mathbf{V}}$  by

$$\widehat{\mathbf{F}} = \widehat{\mathbf{I}} + \widehat{\mathbf{V}} \tag{12}$$

The tracking performance depends on how well these three assumptions are satisfied.

### 3 Proposed System

The proposed authentication system works in four phases: ROI extraction, image enhancement, feature extraction and finally feature level matching. In first phase ROI is extracted from palmprint images using the method suggested in Ref. [5] and shown in Fig. 1. In second phase extracted ROI is transformed so as to achieve better



**Fig. 1** Palmprint ROI extraction and transformation [5]. **a** Original. **b** Contour. **c** Key points. **d** Palmprint ROI. **e** Transformed

and robust feature representation using proposed local edge pattern (LEP) method. Corner features are extracted in third phase. Finally, matching between features is performed using proposed *UTC* dissimilarity measure. Tasks performed in each phase are explained as follows.

**[A] Palmprint ROI Extraction [5]:** Hand images are thresholded to obtain binarized image from which hand contour is extracted. Four key-points ( $X_1$ ,  $X_2$ ,  $V_1$ ,  $V_2$ ) are obtained on the hand contour as shown in Fig. 1b. Then two more key-points are obtained,  $C_1$  that is the intersection point of hand contour and the line passing from  $V_1$  with a slope of  $45^\circ$  and  $C_2$  that is the intersection point of line passing from  $V_2$  with a slope of  $60^\circ$  as shown in Fig. 1c. Finally the midpoints of the line segment  $V_1C_1$  and  $V_2C_2$  are joined which is considered as one side of the required square ROI. The final extracted palmprint ROI is shown in Fig. 1d. The ROI extracted palmprints are normalized to  $100 \times 100$  size.

**[B] Local Edge Pattern (LEP) Based Transformation:** Palmprint images have abundant texture information including wrinkles, principle line, creases, ridges, minutia that can be useful for recognition purposes. In order to achieve illumination invariance *edgemaps* are extracted and worked on. Sobel edge detector uses pure central difference operator to reduce artifacts, but it lacks perfect rotational symmetry. Scharr operators are obtained by optimized minimization of weighted mean squared angular error in Fourier domain under the condition that resulting filters are numerically consistent. Hence Scharr kernels are better derivative kernels

than usual sobel kernels. To achieve robust features  $x$ -derivative of palmprint ROI is convolved with  $3 \times 3$  Scharr kernel. The proposed *local edge pattern* (LEP) based transformation calculates *scharr\_code* for each pixel from the obtained derivative image. Every palmprint ROI is transformed into its *lep\_code* (as shown in Fig. 1e) that is robust to illumination and local non-rigid distortions. Any palmprint ROI,  $P$  is transformed by applying the  $x$ -direction scharr filter to obtain derivative image  $P^d$ . The *lepcode* can be obtain by evaluating *scharr\_code* for every pixel  $P_{j,k}$  using the derivative image  $P^d$ . The *scharr\_code* for any pixel is a 8 bit binary number whose  $i$ th bit is defined as

$$scharr\_code_i = \begin{cases} 1 & \text{if } (Neigh[i] > 0) \\ 0 & \text{otherwise} \end{cases} \quad (13)$$

where  $Neigh[i]$ ,  $i = 1, 2, \dots, 8$  are the  $x$ -direction scharr gradient of eight neighboring pixels centered at pixel  $P_{j,k}$  obtained from  $P^d$ .

In *lepcode* (as shown in Fig. 1e), every pixel is represented by its *scharr\_code* which is an encoding of edge pattern in its *eight-neighborhood*. The *scharr\_code* of any pixel retains only the sign of the derivative in its neighborhood hence any sudden change in the illumination cannot affect *scharr\_code* much because the edge pattern near the pixel (within a neighborhood) remains to be more or less same. This property ensures robustness of the proposed system in illumination varying environments.

**[C] Feature Extraction:** Corners can be an ideal candidate for features because they are robust to illumination variations and can be tracked accurately. Corner features can provide enough information for tracking because they possess strong derivative in two orthogonal directions. In order to find corners, eigen analysis of structure tensor is done. The structure tensor of second-order is a common tool for local orientation estimation. It is defined as Cartesian product of the gradient vector  $(I_x, I_y)^T$  with itself. Any image  $I$  can be seen as a function represented as a discrete array of samples  $I[P]$ , where  $P$  corresponds to any pixel. The 2D structure tensor at any pixel  $P$  at  $i$ th row and  $j$ th column can be defined as

$$\begin{pmatrix} I_x^2(P) & I_x(P).I_y(P) \\ I_x(P).I_y(P) & I_y^2(P) \end{pmatrix} \quad (14)$$

where  $I_x(P)$  and  $I_y(P)$  are the partial derivatives sampled at pixel  $P$  that are estimated using finite difference formula by considering all the pixels within  $(2K + 1) \times (2K + 1)$  window ( $N$ ) centered at pixel  $P$ . The value of  $K$  is empirically chosen to be five. The above matrix can have two eigen values  $\lambda_1$  and  $\lambda_2$  such that  $\lambda_1 \geq \lambda_2$  with  $e_1$  and  $e_2$  as the corresponding eigenvectors. Like [19], all pixels having  $\lambda_2 \geq T$  (smaller eigen value greater than a threshold) are considered as corner feature points.

**[D] Feature Matching:** Let  $A$  and  $B$  are two palmprint ROI that are to be matched and  $P_a, P_b$  are their corresponding *lepcode*. In order to make the decision on match-

ing between  $A$  and  $B$ , LK tracking has been used (as discussed in Sect. 2). A dissimilarity measure UTC (Unsuccessfully Tracked Corners) is defined that tries to quantify the performance of LK tracking using some geometrical as well as statistical constraints. It is assumed that the tracking performance of LK algorithm will be good between features of same subject while degrades substantially for others. The tracking performance depends on how well the three assumptions brightness consistency, temporal persistence and spatial coherency (as discussed in Sect. 2) are satisfied. The geometrical and statistical constraints that has to be satisfied in order to consider any feature at  $a(i, j)$  to be successfully tracked are defined below.

### Geometric and Statistical Constraints

- The euclidean distance between  $a(i, j)$  and its estimated tracked location should be less than or equal to a pre-assigned threshold  $T_d$ .
- The tracking error defined as pixel-wise sum of absolute difference between a local patch centered at  $a(i, j)$  and that of its estimated tracked location patch should be less than or equal to a pre-assigned threshold  $T_e$ .
- The phase only correlation (as discussed in Sect. 2) [14] between a local patch centered at  $a(i, j)$  and that of its estimated tracked location patch should be more than or equal to a pre-assigned threshold  $T_p$ .

However all tracked corners may not be the true matches, because of noise, local non-rigid distortions in iris and less difference in inter class matching as compared with intra class matching. Hence a notion of consistent optical flow is introduced .

---

#### Algorithm 1 $UTC(P_a, P_b)$

---

**Require:** The *lepcode*  $P_a, P_b$  of transformed palmprint ROI images.

$N_a$  and  $N_b$  are the number of corners in  $P_a, P_b$  respectively.

**Ensure:** Return the symmetric function  $UTC(P_a, P_b)$ .

- 1: Track all the corners of *lepcode*  $P_a$  in *lepcode*  $P_b$  using LK tracking algorithm.
  - 2: Calculate the number of successfully tracked corners (i.e.  $stc_{ab}$ ) that have their tracked spatial location with in  $T_d$ , their local patch dissimilarity under the  $T_e$  and have their phase only correlation more than  $T_p$ .
  - 3: Similarly calculate successfully tracked corners of *lepcode*  $P_b$  in *lepcode*  $P_a$  (i.e.  $stc_{ba}$ ).
  - 4: Quantize optical flow directions into eight directions and find out the consistent direction that have maximum number of successfully tracked features.
  - 5: Calculate the number of corners that are successfully tracked and have consistent optical flow (i.e.  $cof_{ab}$  and  $cof_{ba}$ ).
  - 6:  $utc_{ab} = 1 - \frac{cof_{ab}}{N_a}$ ;
  - 7:  $utc_{ba} = 1 - \frac{cof_{ba}}{N_b}$ ;
  - 8: **return**  $UTC(P_a, P_b) = \frac{utc_{ab} + utc_{ba}}{2}$ ;
-



### 3.1 Consistent Optical Flow

The direction of optical flow at any feature at  $a(i, j)$  can be calculated by determining the slope of the line joining  $a(i, j)$  and its tracked location estimated using LK tracking algorithm. It can be noted that true matches have the optical flow which can be aligned with the actual affine transformation between the two images. The estimated optical flow direction is quantized into eight directions and the most consistent direction is selected as the one which has most number of successfully tracked features. Any pair of matching corners other than the most consistent direction is considered as false matching pair.

In Algorithm 1, two *lepcodes*  $P_a$  and  $P_b$  are matched. Successfully tracked corners of *lepcode*  $P_a$  in *lepcode*  $P_b$  and vice-versa are calculated using constraints as defined above. The consistent optical flow direction is evaluated and finally the number of unsuccessfully tracked corners of  $P_a$  in  $P_b$  and vice-versa is calculated. The  $UTC(P_a, P_b)$  measure is made symmetric by taking the average of  $utc_{ab}$  and  $utc_{ba}$ .

#### Some properties of UTC distance measure

1.  $UTC(A, B) = UTC(B, A)$ .
2.  $UTC(A, A) = 0$ .
3.  $UTC(A, B)$  always lies in the range  $[0, 1]$ .

## 4 Experimental Results

This section analyses the performance of the proposed system. The performance of the system is measured using correct recognition rate ( $CRR$ ) in case of identification and equal error rate ( $EER$ ) for verification.  $CRR$  of the system is defined by

$$CRR = \frac{N_1}{N_2} \tag{15}$$

where  $N_1$  denotes the number of correct (Non-False) top best match of palmprint ROI and  $N_2$  is the total number of palmprint ROI in the query set.

At a given threshold, the probability of accepting the impostor, known as false acceptance rate ( $FAR$ ) and probability of rejecting the genuine user known as false rejection rate ( $FRR$ ) are obtained.  $EER$  is the value of  $FAR$  for which  $FAR$  and  $FRR$  are equal.

$$EER = \{FAR|FAR = FRR\} \tag{16}$$

The proposed system is tested on two publicly available benchmark palmprint databases CASIA [1] and PolyU [2]. All possible genuine as well as imposter matching are considered to evaluate the performance of the system. The CASIA palmprint database have 5,502 palmprint images taken from 312 subjects (i.e. 624 distinct

**Table 2** Parameterized analysis

Parameters			PolyU			Casia		
$T_p$	$T_d$	$T_e$	$d'$	CRR	EER	$d'$	CRR	EER
0.15	150	600	2.137	100	0.7913	2.3121	99.97	0.2604
0.25	200	600	2.140	100	0.6665	2.3166	99.97	0.2459
0.35	200	600	2.235	100	0.6626	2.3168	99.97	0.2757
0.45	200	600	2.32	100	0.9035	2.224	99.97	0.3435
0.4	290	600	2.287	100	0.6834	2.3070	99.97	0.2907

**Table 3** Performance analysis

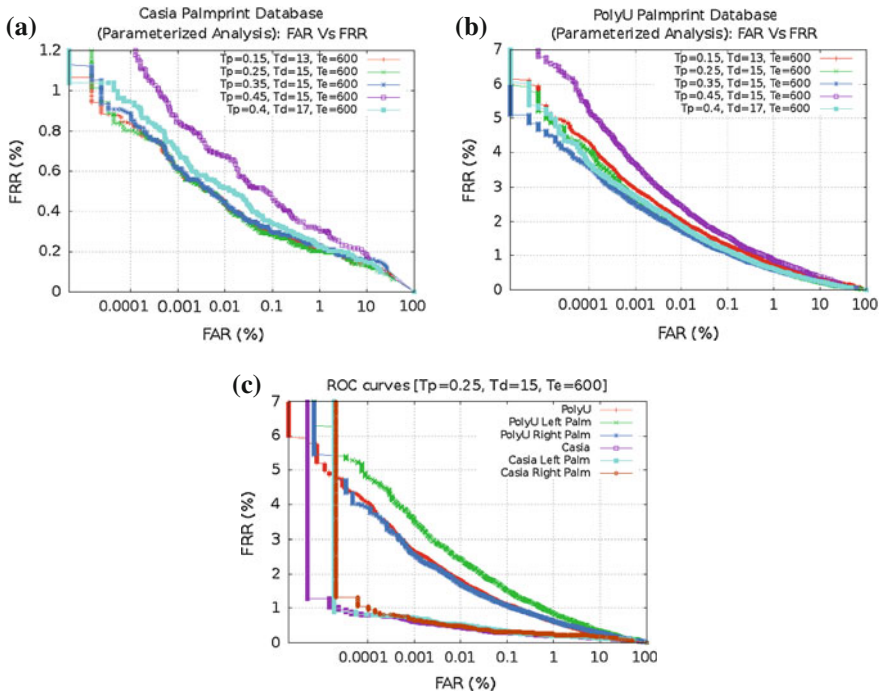
Systems	CASIA	PolyU
	CRR/ERR (%)	CRR/ERR (%)
PalmCode [22]	99.619/3.6730	99.916/0.5338
CompCode [11]	99.716/2.0130	99.964/0.3082
OrdinalCode [21]	99.843/1.7540	100.00/0.709
Zernike moments [6]	99.75/2.003	100.00/0.2939
Stockwell transform [4]	100/1.1606	100.00/0.1
<i>Proposed</i>	99.97/0.245	100.00/0.6626

palms). From each subject eight images are collected from left as well as right hand. Hence the total matching possible are 20,498,256 out of which 31,696 matching are genuine while rest are imposter matching. The PolyU palmprint database have 7, 752 palmprint images taken from 193 subjects (i.e. 386 distinct palms). From each subject 20 images are collected from left as well as right hand palm in two sessions (10 images per session). Hence the total matching possible are 59,590,680 out of which 146,680 matching are genuine while rest are imposter matching. There are some palms in both databases with incomplete or missing data such palms are discarded for this experiment.

#### 4.1 Parameterized Analysis

The proposed *UTC* dissimilarity measure is primarily parameterized by three parameters  $T_e$ ,  $T_p$  and  $T_d$ . Our system is tested using these parameters as input and their values are fixed so as to maximize the performance of the system. The parameterized analysis for some parameter sets on both databases are shown in Table 2 and the corresponding Receiver Operating Characteristics curves are drawn in Fig. 2a, b.

The proposed system has been compared with state of the art palmprint systems [11, 21, 22]. It is found that the *CRR* of the proposed system is more than 99.95% for both databases. The *CRR/ERR* of other systems are shown in Table 3. Further, *EER* of the proposed verification system is 0.245% for CASIA database which



**Fig. 2** The ROC curves for various experiments. **a** Parameterized analysis—CASIA. **b** Parameterized analysis—polyU. **c** ROC curves for all databases

is better than the reported systems and that for PolyU is 0.6626% which is also comparable to the reported systems.

For each database, ROC curves which plots  $FRR$  against  $FAR$  is shown in Fig. 2c for best parameters. In another experiment both databases are divided into left and right palms. It has been found as also shown in Fig. 2c that right palm’s performance is marginally better than the left palm for both databases. Also, by classifying query palm into left or right, matching will only be performed with either left or right training set. This will reduce the computational cost hugely with out loosing much on performance.

## 5 Conclusion

This paper has proposed a dissimilarity measure termed as Unsuccessfully Tracked Corners ( $UTC$ ) to compare structural features in palmprint ROI’s. Further, a palmprint based user authentication system is designed using it. In order to address the issue of varying illumination conditions edge-maps are extracted and worked on. The proposed palmprint system first transformed ROI, extracted from palmprint images

using proposed *LEP* method then extract the corner features. Finally, proposed *UTC* measure is used for matching to achieve the appearance based comparison on palmprint ROI's. Rigorous experimentation shows that *UTC* can work effectively and efficiently under environments, having slight amount of variations in illumination, rotation and translation. The system has been tested on publicly available PolyU as well as CASIA databases of palmprint images. It has achieved *CRR* of more than 99.9 % for the top best match, in case of identification for both databases and *EEER* of 0.24 and 0.66 % for CASIA and PolyU respectively, in case of verification. The proposed system has been compared with well known palmprint based systems [11, 21, 22] and is found to perform better.

## References

1. Casia database. <http://www.cbsr.ia.ac.cn>
2. Polyu database. <http://www.comp.polyu.edu.hk/biometrics>
3. Aykut, M., Ekinici, M.: Kernel principal component analysis of gabor features for palmprint recognition. In: ICB, pp. 685–694 (2009)
4. Badrinath, G.S., Gupta, P.: Stockwell transform based palm-print recognition. *Appl. Soft Comput.* **11**(7), 4267–4281 (2011)
5. Badrinath, G.S., Gupta, P.: Palmprint base phase-difference information. *Future Gen. Comp. Syst.* **28**(1), 287–305 (2012)
6. Badrinath, G.S., Kachhi, N.K., Gupta, P.: Verification system robust to occlusion using low-order zernike moments of palmprint sub-images. *Telecommun. Sys.* **47**(3–4), 275–290 (2011)
7. Badrinath, G.S., Nigam, A., Gupta, P.: An efficient finger-knuckle-print based recognition system fusing sift and surf matching scores. In: International Conference on Information and Communications Security, ICICS, pp. 374–387 (2011)
8. Bendale, A., Nigam, A., Prakash, S., Gupta, P.: Iris segmentation using improved hough transform. In: International Conference on Intelligent Computing, ICIC, pp. 408–415 (2012)
9. Duta, N., Jain, A.K., Mardia, K.V.: Matching of palmprints. *Pattern Recogn. Lett.* **23**(4), 477–485 (2002)
10. Han, C.C., Cheng, H.L., Lin, C.L., Fan, K.C.: Personal authentication using palm-print features. *Pattern Recogn.* **36**(2), 371–381 (2003)
11. Kong, A.W.K., Zhang, D.: Competitive coding scheme for palmprint verification. In: ICPR(1), pp. 520–523 (2004)
12. Kumar, J., Nigam, A., Prakash, S., Gupta, P.: An efficient pose invariant face recognition system. In: International Conference on Soft Computing for Problem Solving, SocProS (2), pp. 145–152 (2011)
13. Lucas, B.D., Kanade, T.: An iterative image registration technique with an application to stereo vision. In: IJCAI, pp. 674–679 (1981)
14. Miyazawa, K., Ito, K., Aoki, T., Kobayashi, K., Nakajima, H.: An effective approach for iris recognition using phase-based image matching. *IEEE Trans. Pattern Anal. Mach. Intell.* **30**(10), 1741–1756 (2008)
15. Nigam, A., Gupta, P.: A new distance measure for face recognition system. In: International Conference on Image and Graphics, ICIG, pp. 696–701 (2009)
16. Nigam, A., Gupta, P.: Comparing human faces using edge weighted dissimilarity measure. In: International Conference on Control, Automation, Robotics and Vision, ICARCV, pp. 1831–1836 (2010)
17. Nigam, A., Gupta, P.: Finger knuckleprint based recognition system using feature tracking. In: Chinese Conference on Biometric Recognition, CCBR, pp. 125–132 (2011)

18. Ojala, T., Pietikäinen, M., Mäenpää, T.: Multiresolution gray-scale and rotation invariant texture classification with local binary patterns. *IEEE Trans. Pattern Anal. Mach. Intell.* **24**(7), 971–987 (2002)
19. Shi, J., Tomasi: Good features to track. In: *Computer Vision and, Pattern Recognition*, pp. 593–600 (1994). doi:[10.1109/CVPR.1994.323794](https://doi.org/10.1109/CVPR.1994.323794)
20. Singh, N., Nigam, A., Gupta, P., Gupta, P.: Four slap fingerprint segmentation. In: *International Conference on Intelligent Computing, ICIC*, pp. 664–671 (2012)
21. Sun, Z., Tan, T., Wang, Y., Li, S.Z.: Ordinal palmprint representation for personal identification. In: *CVPR* (1), pp. 279–284 (2005)
22. Zhang, D., Kong, W.K., You, J., Wong, M.: Online palmprint identification. *Pattern Anal. Mach. Intell.* **25**(9), 104–1050 (2003). doi:[10.1109/TPAMI.2003.1227981](https://doi.org/10.1109/TPAMI.2003.1227981)

# A Diversity-Based Comparative Study for Advance Variants of Differential Evolution

Prashant Singh Rana, Kavita Sharma, Mahua Bhattacharya,  
Anupam Shukla and Harish Sharma

**Abstract** Differential evolution (DE) is a vector population-based stochastic search optimization algorithm. DE converges faster, finds the global optimum independent to initial parameters, and uses few control parameters. The exploration and exploitation are the two important diversity characteristics of population-based stochastic search optimization algorithms. Exploration and exploitation are compliment to each other, i.e., a better exploration results in worse exploitation and vice versa. The objective of an efficient algorithm is to maintain the proper balance between exploration and exploitation. This paper focuses on a comparative study based on diversity measures for DE and its prominent variants, namely JADE, jDE, OBDE, and SaDE.

**Keywords** Diversity measures · Stochastic search · Exploration–exploitation · Differential evolution · Comparative study

## 1 Introduction

Differential evolution (DE), proposed by Rainer Storn and Ken Price in 1995, is a popular evolutionary algorithm (EA) and exhibits good results in a wide variety of problems from diverse fields [20]. Like other EAs, DE uses mutation, crossover, and selection operators at each generation to move its population toward the global optimum. The performance of DE mainly depends on two components: One is its offspring vector generation strategy (i.e., mutation and crossover operators) and the

---

P. S. Rana (✉) · M. Bhattacharya · A. Shukla · H. Sharma  
ABV—Indian Institute of Information Technology and Management, Gwalior,  
Madhya Pradesh, India  
e-mail: psrana@gmail.com

K. Sharma  
Government Polytechnic College, Kota, Rajasthan, India  
e-mail: k\_sharma28@rediffmail.com

other is its control parameters (i.e., population size NP, scaling factor F, and crossover control rate CR).

Researchers are continuously working to improve the performance of DE. Some of the recently developed variants of DE with appropriate applications can be found in [1, 4, 6, 17, 27]. Experiments over several numerical benchmark problems [29] show that DE performs better than the genetic algorithm (GA) [11] and particle swarm optimization (PSO) [12]. DE has successfully been applied to various areas of science and technology, such as chemical engineering [15], signal processing [5], mechanical engineering design [26], machine intelligence, and pattern recognition [19]. DE outperforms in nonlinear, non-convex, multi-model, constrained, and discrete optimization problems. The results indicate that DE has the advantage of fast convergence and low computational consumption of function evaluations. But it is found that DE easily trapped in local optimum [14, 16, 21] due to its greedy updating process and intrinsic differential property results in a premature convergence.

Diversity has a significant effect on the performance of an algorithm [9]. It shows the behavior of the algorithm during the global optimum search process. A large value of diversity implies more exploration, while low implies more exploitation. It is expected that an optimization algorithm retains high diversity in the early stage of the search process and proportionally decreases diversity as search progresses. The performance of an algorithm can be ranked on the basis of their diversity measures. There are many diversity measures in the literature [2, 9, 10, 13, 24, 28]. A good study on diversity measures for PSO process is given in [18], and the presented study is based on this study.

In this paper, seven important diversity measures (Listed in Table 1) have been used to quantify the diversity of DE and its prominent variants such as JADE [30], jDE [3], OBDE [23], and SaDE [22]. The Table 2 lists the benchmark problems that are taken into consideration for diversity measures to quantify the dispersion of individuals in the population. Further, effect of outliers has been analyzed over the diversity measures.

Rest of the paper is organized as follows: Sect. 2 describes various diversity measures. In Sect. 3, importance and behavior of diversity measures are discussed. Experimental results are shown in Sect. 4. Finally, in Sect. 5, paper is concluded.

**Table 1** Diversity measure

S.no.	Diversity measure
1	Population diameter
2	Population radius
3	Average distance around the population center
4	Geometric average distance around the population center
5	Normalized average distance around the population center
6	Average of the average distance around all individuals in the population
7	Population coherence

**Table 2** Test problems

Test problem	Objective function	Search range	I	Acceptable error
Ackley	$f_1(x) = -20 + e + \exp\left(-\frac{0.2}{T}\sqrt{\sum_{i=1}^I x_i^3}\right) - \exp\left(\frac{1}{I}\sum_{i=1}^I \cos(2\pi x_i x_i)\right)$	$[-1, 1]$	30	$1.0E - 15$
Griewank	$f_2(x) = 1 + \frac{1}{4000}\sum_{i=1}^I x_i^2 - \prod_{i=1}^I \cos\left(\frac{x_i}{\sqrt{i}}\right)$	$[-600, 600]$	30	$1.0E - 15$
Rosenbrock	$f_3(x) = \sum_{i=1}^I (100(x_{i+1} - x_i^2)^2 + (x_i - 1)^2)$	$[-30, 30]$	30	$1.0E - 15$
Sphere	$f_4(x) = \sum_{i=1}^I x_i^2$	$[-5.12, 5.12]$	30	$1.0E - 15$

## 2 Diversity Measures

There are many diversity measuring strategies available in the literature [18]. Most of the diversity measures are based on the distance metric of individuals. Diversity measures are also differed in terms of normalization of parameters or distance metric. Further, the measures are differed based on the choice of population center which may be global best solution found so far or may be spatial. In this section, seven different diversity measures (Listed in Table 1) based on the Euclidean distance metric are discussed. Further, global best population center is used in this paper wherever required opposed to a spatial population center. Generally, spatial population center and global best population center can be considered equivalent where the global best is not necessarily centered position in the population. Further, for normalization of parameters, the population diameter is used, instead of the radius of population.

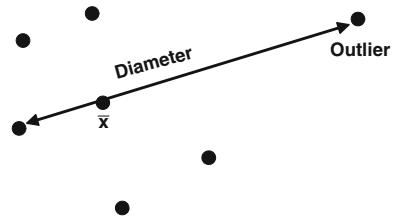
### 2.1 Population Diameter

The population diameter is defined as the distance between two farthest individuals, along any axis [25], of the population as shown in Fig. 1.

The diameter  $D$  is calculated using Eq. (1):

$$D = \max_{(i \neq j) \in [1, N_p]} \left( \sqrt{\sum_{k=1}^I (x_{ik} - x_{jk})^2} \right) \tag{1}$$

**Fig. 1** Population diameter





where  $N_p$  is the population size,  $I$  is the dimensionality of the problem, and  $x_{ik}$  is the  $k$ th dimension of the  $i$ th individual position.

In Fig. 1, an outlier individual is also shown. In a population, a significantly deviated individual from the remaining individuals is often termed as *outlier*. From Fig. 1, it can be seen that the presence of an outlier can significantly affect the diameter of a population.

### 2.2 Population Radius

The radius of a population is defined as the distance between the population center and the individual in the population which is farthest away from it [25], as shown in Fig. 2.

The population radius is calculated using Eq. (2):

$$R = \max_{i \in [1, N_p]} \left( \sqrt{\sum_{k=1}^I (x_{ik} - \bar{x}_k)^2} \right) \tag{2}$$

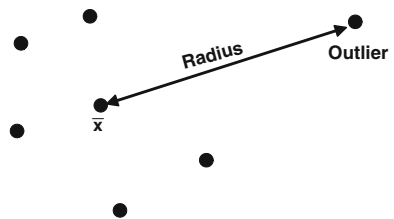
where the parameters have same meaning as for the population diameter.  $\bar{x}$  is the position of population center, and  $\bar{x}_k$  represents the  $k$ th dimension of  $\bar{x}$ .

Now, it is evident that the population diameter ( $D$ ) and radius ( $R$ ) are two important diversity measures. A large value of  $D$  or  $R$  exhibits exploration of the search region, while low value exhibits exploitation. However, both are badly affected with outliers.

### 2.3 Average Distance around the Population Center

The average distance from the population center,  $D_A$ , can be defined as the average of distances of all individuals from the population center. This measure is given in [13] and defined in Eq. (3)

Fig. 2 Population radius



$$D_A = \frac{1}{N_p} \sum_{i=1}^{N_p} \left( \sqrt{\sum_{k=1}^I (x_{ik} - \bar{x}_k)^2} \right) \tag{3}$$

where the notations have their usual meaning. A low value of this measure shows population convergence around the population center, while a high value shows large dispersion of individuals from the population center.

### 2.4 Geometric Average Distance around the Population Center

Geometric average is not significantly affected by outliers in the population on the high end. The geometric average distance around the population center is defined in Eq. (4).

$$D_{GM} = \left( \prod_{i=1}^{N_p} \sqrt{\sum_{k=1}^I (x_{ik} - \bar{x}_k)^2} \right)^{\frac{1}{N_p}} \tag{4}$$

### 2.5 Normalized Average Distance around the Population Center

This diversity measure is almost the same as the average distance of all individuals from the population center. The only difference is that the average distance is normalized using the population diameter. This normalization can also be done by the radius of the population. This diversity measure is given in [25] and described by Eq. (5):

$$D_N = \frac{1}{N_p \times D} \sum_{i=1}^{N_p} \left( \sqrt{\sum_{k=1}^I (x_{ik} - \bar{x}_k)^2} \right) \tag{5}$$

### 2.6 Average of the Average Distance around all Individuals in the Population

In this measure, first the average distances, considering each individual as a population center, are calculated, and then, an average of all these average distances is taken. It is described by Eq. (6).

$$D_{all} = \frac{1}{N_p} \sum_{i=1}^{N_p} \left( \frac{1}{N_p} \sum_{j=1}^{N_p} \sqrt{\sum_{k=1}^I (x_{ik} - x_{jk})^2} \right) \tag{6}$$

This diversity measure shows average dispersion of every individual in the population from every other individual in the population.

## 2.7 Population Coherence

This diversity measure is given in [10] and described by Eq. (7):

$$S = \frac{s_c}{\bar{s}} \quad (7)$$

where  $s_c$  represents the step size of population center which is defined in Eq. (8):

$$s_c = \frac{1}{N_p} \left\| \sum_{i=1}^{N_p} \tilde{s}_i \right\|_2 \quad (8)$$

where  $\tilde{s}_i$  is the vector of step size for  $i$ th individual as indicated in Eq. (9) and  $\bar{s}$  shows the average individual step size in the population and is defined by Eq. (10).  $\|\cdot\|_p$  is the Euclidean  $p$ -norm.

$$\tilde{s}_i = F \times (x_{i_1} - x_{i_2}) \quad (9)$$

Here,  $F$  is a scaling factor and  $x_{i_1}, x_{i_2}$  are randomly selected individuals from the population such that  $i_1 \neq i_2$ . This equation is used in the mutation process of DE.

$$\bar{s} = \frac{1}{N_p} \sum_{i=1}^{N_p} \|\tilde{s}_i\|_2 \quad (10)$$

This diversity measure is calculated by averaging the step sizes of all the individuals in a population with respect to population center.

The dispersion of the individuals in DE and its prominent variants such as SaDE, jDE, OBDE, and JADE could be quantified, using the various diversity measures described in this section. The diversity measures show a trend of exploration or exploitation of the population and helps to analyze the behavior of the population-based algorithms.

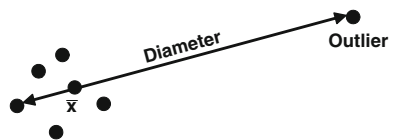
## 3 Discussion

The two important diversity characteristics of population-based stochastic search optimization algorithms are exploration and exploitation. Exploration capability explores the solution search space to find the possible solution region, whereas

exploitation capability exploits a particular region for a better solution. Exploration and exploitation are compliment to each other, i.e., a better exploration results in worse exploitation and vice versa. The main objective of an efficient algorithm is to maintain a proper balance between exploration and exploitation in the population. High value of diversity measure shows the exploration, whereas low value exhibits exploitation. A decreasing diversity measure through iterations represents the transition of exploration to exploitation. On the basis of these characteristics, the following conclusions have been drawn:

- The population diameter presents a required decrease by iterations, as  $(x_{ik} - x_{jk})^2$  (refer Eq. (1)) tends to zero for all the individuals as the population converges to a solution. The same behavior is shown by the population radius as the distance between each individual and population center decreases as the population converges with iterations. Further, it is clear from the Eqs. (1) and (2) that the population diameter and population radius both are very sensitive to the outlier individual. Considering Figs. 1 and 3, it can be shown that the diverse behavior of the current population shown in Figs. 1 and 3 is same, if population radius or population diameter is the diversity measure, while in Fig. 1, the individuals are more diversified than in Fig. 3.
- The diversity measure  $D_A$ , which is shown in Eq. (3), is robust measure as compared to the population diameter and population radius because it is based on the average distance of all individuals in the population from the population center. Hence, this diversity measure is considered less affected due to the outliers as compared to the population diameter and population radius. But an extreme farthest outlier may skew the individual's dispersion significantly in the population. Further,  $(x_{ik} - \bar{x}_k)^2 \rightarrow 0$  (refer Eq. (3)) for all individuals in the population as population converges. The same behavior is shown by the diversity measure  $D_{all}$  given by Eq. (6) because for all individuals in the population, the component  $(x_{ik} - x_{jk})^2$  also approaches to zero as population converges.
- The diversity measure  $D_{GM}$  shown in Eq. (4) is again a robust measure for measuring diversity. In statistics, geometric average is relatively less affected from outliers.
- The diversity measure  $D_N$  shown in Eq. (5) is the ratio of the average distance  $D_A$  to the population diameter  $D$ . Here, diameter is considered as a normalization parameter used to normalize the average distance around the population center. In this measure of dispersion, as population converges,  $D_N$  and  $D$  both approaches to zero with iterations. Further, in this dispersion, as the normalization is done by the population diameter or the population radius, it is significantly influenced by

Fig. 3 Population diameter and outlier



the outlier individuals. Therefore,  $D_A$  and  $D_{all}$  still may be considered as a better choice for measuring diversity of the population.

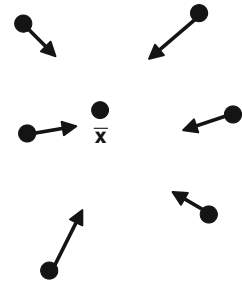
- The diversity measure  $S$ , which is shown in Eq. (7), is the ratio of the absolute step size of the population center to the average step size of all individuals in the population. A high value of the population center step size implies that all the individuals in the population are moving in the same direction. Further, a low value implies that most of the individuals are moving to opposite directions. A high value of average individual's step size in population implies that the solutions are significantly changing the positions, which implies exploration of the search space, while a low value shows the convergence in the population, i.e., exploiting the solution search space found so far. Thus,  $S$  could be used to analyze the diversity behavior of the algorithm.

Figures 4 and 5 show a large population diversity for small population coherence and large population coherence, respectively. The individuals are dispersed in the search space, whereas the step size of population center is relatively low and relatively high, respectively.

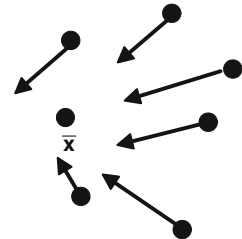
Further, by analyzing Figs. 6 and 7, it is clear that the value of  $S$  does not depend completely on the diversity of population. Therefore, it could be concluded that the population coherence is not proportional to population diversity of individuals in the DE and its prominent variants are not a true measure of diversity.

The outcome of the above discussion is that the effect of outlier is significant in most of the diversity measures and it biases the measure of dispersion. However, the effect of outliers could be minimized; it cannot be ignored completely.

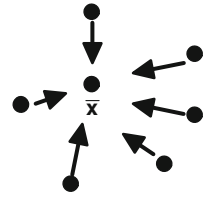
**Fig. 4** High individuals' diversity and small population coherence



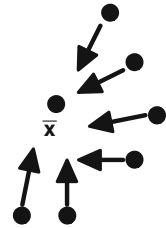
**Fig. 5** High individuals' diversity and large population coherence



**Fig. 6** Low individuals' diversity and small population coherence



**Fig. 7** Low individuals' diversity and large population coherence



### 4 Experimental Setting and Results

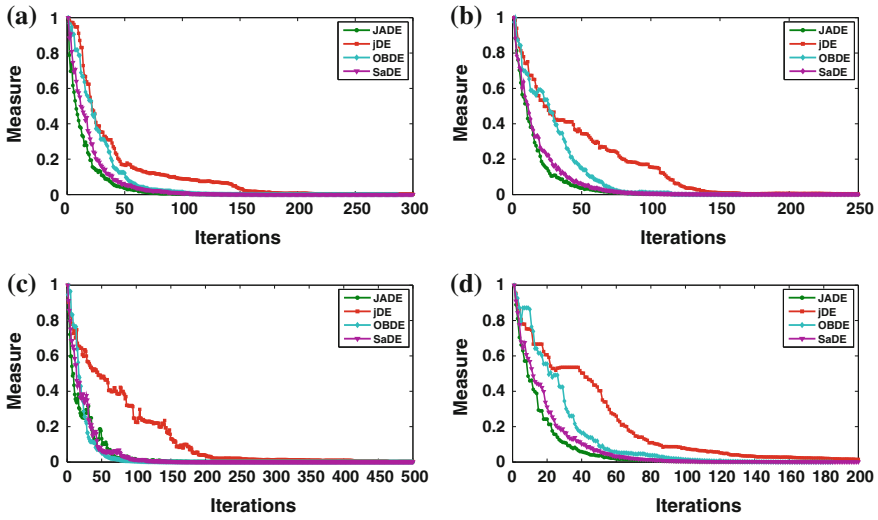
To analyze the various diversity measures for DE and its prominent variants, experiments have been carried out on four well-known benchmark test problems (Listed in Table 2). For these experiments, the following experimental setting is adopted:

- Population size  $NP = 50$  [7, 8],
- $F = 0.5$ ,
- $CR = 0.9$ ,
- The stopping criterion is either the maximum number of function evaluations (which is set to be 200000) is reached or the acceptable error (mentioned in Table 2) has been achieved,
- The number of runs = 100, and graphs are plotted using the mean of each run.
- Scaling, which is used to construct the graph outputs to the interval  $[0, 1]$ , is shown below:

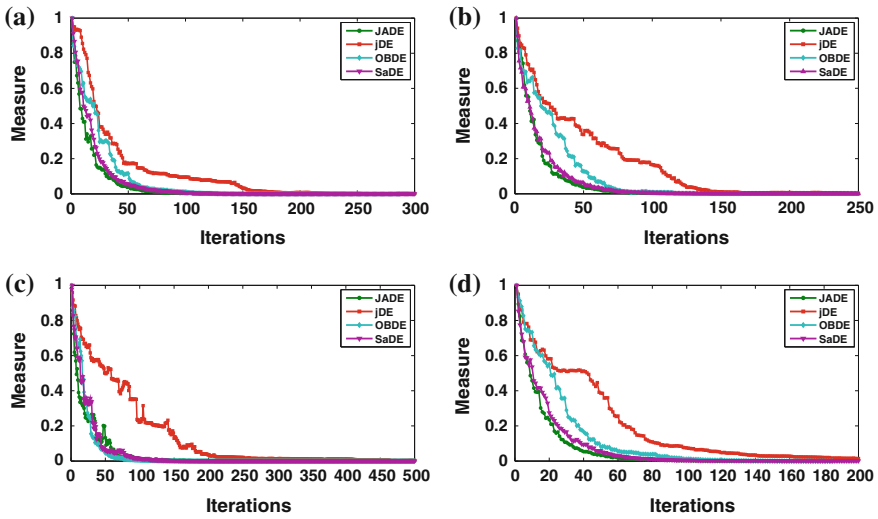
$$\bar{y} = \frac{\bar{y} - \min(\bar{y})}{\max(\bar{y}) - \min(\bar{y})}$$

This is done to make comparisons of all measures in the same range.

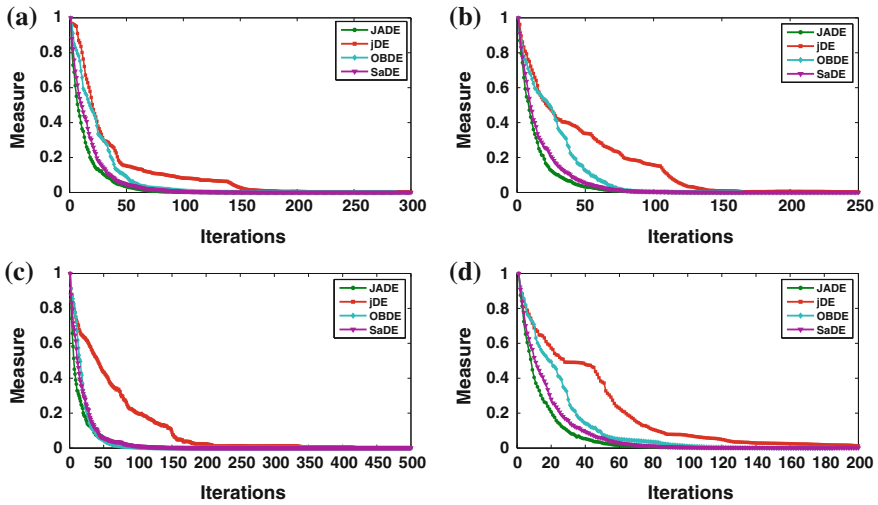
Figures 8, 9, 10, 11, 12, 13, and 14 show the diversity measures based on diameter, radius, average distance around the population center, geometric average distance, normalize average distance, average of the average distance around all individuals in the population, and population coherence for the considered advance variant of DE, respectively. It is clear from these figures that, in terms of diversity in population, jDE is better, while in terms of convergence speed, JADE is better, among considered DE variants.



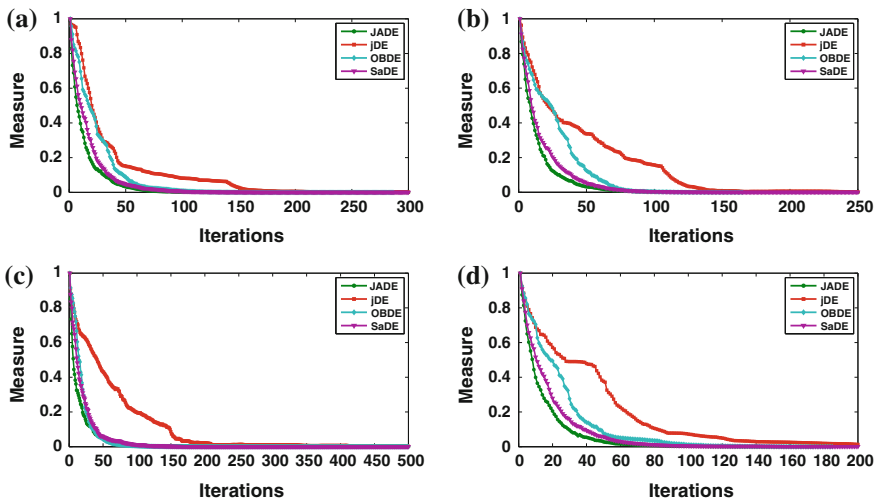
**Fig. 8** Diversity measure for population diameter. **a** Diameter for Ackley function. **b** Diameter for Griewank function. **c** Diameter for Rosenbrock function. **d** Diameter for sphere function



**Fig. 9** Diversity measure for radius. **a** Radius for Ackley function. **b** Radius for Griewank function. **c** Radius for Rosenbrock function. **d** Radius for sphere function

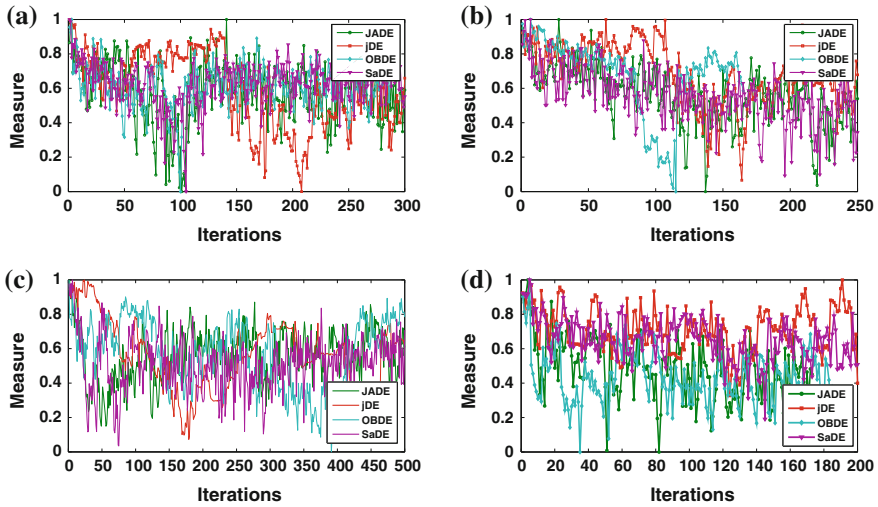


**Fig. 10** Diversity measure for average distance around population center. **a** Average distance for Ackley function. **b** Average distance for Griewank function. **c** Average distance for Rosenbrock function. **d** Average distance for sphere function

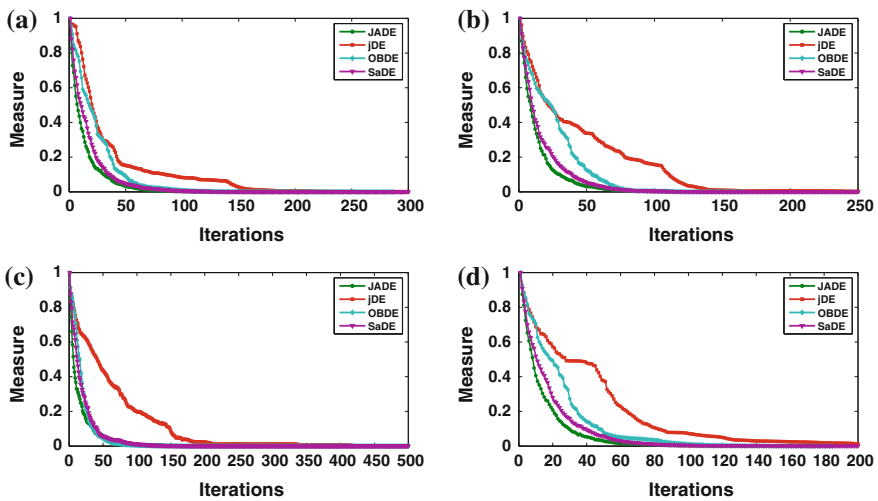


**Fig. 11** Diversity measure for geometric average distance. **a** Geometric average distance for Ackley function. **b** Geometric average distance for Griewank function. **c** Geometric average distance for Rosenbrock function. **d** Geometric average distance for sphere function

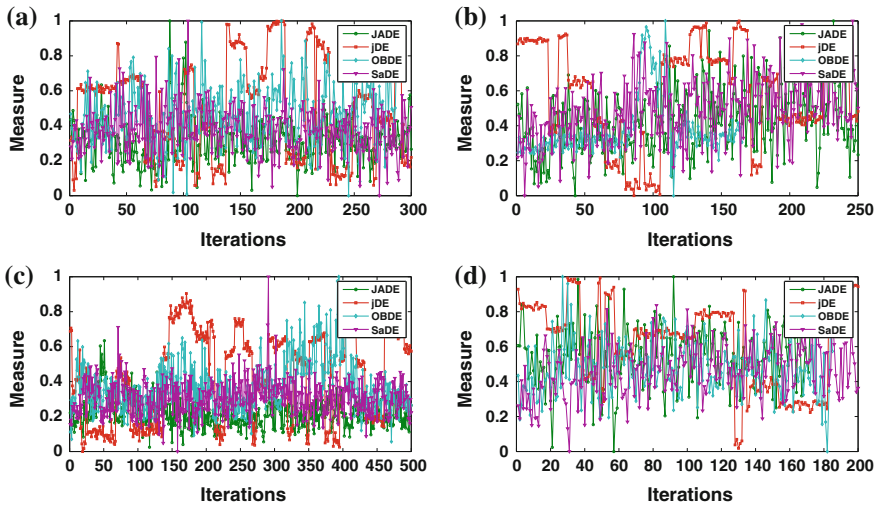




**Fig. 12** Diversity measure for normalized average distance. **a** Normalized average distance for Ackley function. **b** Normalized average distance for Griewank function. **c** Normalized average distance for Rosenbrock function. **d** Normalized average distance for sphere function



**Fig. 13** Diversity measure for average of the average distance around all individuals in the population. **a** Average of average distance for Ackley function. **b** Average of average distance for Griewank function. **c** Average of average distance for Rosenbrock function. **d** Average of average distance for sphere function



**Fig. 14** Diversity measure for coherence. **a** Coherence for Ackley function. **b** Coherence for Griewank function. **c** Coherence for Rosenbrock function. **d** Coherence for sphere function

## 5 Conclusion

In this paper, various diversity measures are studied and analyzed to measure the dispersion in the population of prominent DE variants, namely JADE, jDE, OBDE, and SaDE. In population-based algorithms, diversity measures are used to investigate the exploration and exploitation characteristics. Further, the diversity measures are analyzed on four well-known benchmark problems. The outcome of the experiments shows that the value of diversity measures proportionally decreases with the iterations. Further, it is found that the diversity measures are more or less affected by the outliers in the population. Diversity measures like the average distance around the population center, the geometric mean average distance around the population center, and the average of average distance around the population center are less affected by the outliers and could be used for analyzing the exploration and exploitation of the solution search space in the population. The considered DE variants are compared on the basis on these diversity measure, and it is found that diversity of jDE algorithm is better, while convergence speed of JADE algorithm is better among considered algorithms.

## References

1. Bansal, J.C., Sharma, H.: Cognitive learning in differential evolution and its application to model order reduction problem for single-input single-output systems. *Memetic Comput.* 1–21, (2012)

2. Blackwell, T.M.: Particle swarms and population diversity i: Analysis. In GECCO, pp. 103–107, 2003.
3. Brest, J., Greiner, S., Boskovic, B., Mernik, M., Zumer, V.: Self-adapting control parameters in differential evolution: A comparative study on numerical benchmark problems. *Evolutionary Computation, IEEE Transactions on* **10**(6), 646–657 (2006)
4. Chakraborty, U.K.: *Advances in differential evolution*. Springer, Berlin (2008)
5. Das, S., Konar, A.: Two-dimensional IIR filter design with modern search heuristics: A comparative study. *Int. J. Comput. Intell. Appl.* **6**(3), 329–355 (2006)
6. Das, S., Suganthan, P.N.: Differential evolution: A survey of the state-of-the-art. *IEEE Trans. Evol. Comput.* **99**, 1–28 (2010)
7. Diwold, K., Aderhold, A., Scheidler, A., Middendorf, M.: Performance evaluation of artificial bee colony optimization and new selection schemes. *Memetic Comput.*, 1–14 (2011).
8. El-Abd, M.: Performance assessment of foraging algorithms vs. evolutionary algorithms. *Inf. Sci.* (2011).
9. Engelbrecht, A.P.: Fundamentals of computational swarm intelligence. *Recherche* **67**, 02 (2005)
10. Hendtlass, T., Randall, M.: A survey of ant colony and particle swarm meta-heuristics and their application to discrete optimization problems, pp. 15–25. In: *Proceedings of the Inaugural Workshop on Artificial Life* (2001).
11. Holland, J.H.: *Adaptation in natural and artificial systems*. The University of Michigan Press, Ann Arbor (1975)
12. Kennedy, J., Eberhart, R.: Particle swarm optimization. In: *Proceedings of IEEE International Conference on Neural Networks* **4**, 1942–1948 (1995)
13. Krink, T., Vesterström, J.S., Riget, J.: Particle swarm optimisation with spatial particle extension. In: *Proceedings of the 2002 Congress on Evolutionary Computation, CEC'02*, pp. 1474–1479 (2002)
14. Lampinen, J., Zelinka, I.: On stagnation of the differential evolution algorithm. In: *Proceedings of MENDEL*, pp. 76–83. Citeseer (2000).
15. Liu, P.K., Wang, F.S.: Inverse problems of biological systems using multi-objective optimization. *J. Chin. Inst. Chem. Eng.* **39**(5), 399–406 (2008)
16. Mezura-Montes, E., Velázquez-Reyes, J., Coello Coello, C.A.: A comparative study of differential evolution variants for global optimization. In: *Proceedings of the 8th annual conference on Genetic and evolutionary computation*, pp. 485–492. ACM (2006).
17. Neri, F., Tirronen, V.: Recent advances in differential evolution: a survey and experimental analysis. *Artif. Intell. Rev.* **33**(1), 61–106 (2010)
18. Olorunda, O., Engelbrecht, A.P.: Measuring exploration/exploitation in particle swarms using swarm diversity. In: *Evolutionary Computation (IEEE World Congress on Computational Intelligence)*, pp. 1128–1134 (2008).
19. Obran, M.G.H., Engelbrecht, A.P., Salman, A.: Differential evolution methods for unsupervised image classification. In: *The 2005 IEEE Congress on Evolutionary Computation* **2**, 966–973 (2005)
20. Price, K.V.: Differential evolution: A fast and simple numerical optimizer. In: *Fuzzy Information Processing Society. NAFIPS, Biennial Conference of the North American, IEEE*, pp. 524–527 (1996).
21. Price, K.V., Storn, R.M., Lampinen, J.A.: *Differential evolution: a practical approach to global optimization*. Springer, Berlin (2005)
22. Qin, A.K., Huang, V.L., Suganthan, P.N.: Differential evolution algorithm with strategy adaptation for global numerical optimization. *IEEE Trans. Evol. Comput.* **13**(2), 398–417 (2009)
23. Rahnamayan, S., Tizhoosh, H.R., Salama, M.M.A.: Opposition-based differential evolution. *IEEE Trans. Evol. Comput.* **12**(1), 64–79 (2008)
24. Ratnaweera, A., Halgamuge, S., Watson, H.: Particle swarm optimization with self-adaptive acceleration coefficients. In: *Proceedings of 1st International Conference on Fuzzy System Knowledge. Discovery*, pp. 264–268 (2003).
25. Riget, J., Vesterstrøm, J.S.: A diversity-guided particle swarm optimizer—the ARPSO. *Dept. Comput. Sci., Univ. of Aarhus, Aarhus, Denmark. Tech. Rep* **2**, 2002 (2002)

26. Rogalsky, T., Kocabiyik, S., Derksen, R.W.: Differential evolution in aerodynamic optimization. *Can. Aeronaut. Space J.* **46**(4), 183–190 (2000)
27. Sharma, H., Bansal, J., Arya, K.: Dynamic scaling factor based differential evolution algorithm. In: *Proceedings of the International Conference on Soft Computing for Problem Solving (SocProS 2011)* Dec 20–22, 2011, pp. 73–85. Springer (2012).
28. Vesterstrom, J.S., Riget, J., Krink, T.: Division of labor in particle swarm optimisation. In: *IEEE proceedings of the 2002 Congress on Evolutionary Computation, CEC'02.*, 2, pp. 1570–1575 (2002)
29. Vesterstrom, J., Thomsen, R.: A comparative study of differential evolution, particle swarm optimization, and evolutionary algorithms on numerical benchmark problems. In: *IEEE Congress on Evolutionary Computation, CEC2004*, 2, pp. 1980–1987, 2004.
30. Zhang, J., Sanderson, A.C.: Jade: adaptive differential evolution with optional external archive. *IEEE Trans. Evol. Comput.* **13**(5), 945–958 (2009)

# Computing Vectors Based Document Clustering and Numerical Result Analysis

Neeraj Sahu and G. S. Thakur

**Abstract** This paper presents new approach analytical results of document clustering for vectors. The proposed analytical results of document clustering for vectors approach is based on mean clusters. In this paper we have used six iterations  $I_1$  to  $I_6$  for document clustering results. The steps Document collection, Text Pre-processing, Feature Selection, Indexing, Clustering Process and Results Analysis are used. Twenty news group data sets are used in the experiments. The experimental results are evaluated using the numerical computing MATLAB 7.14 software. The experimental results show the proposed approach out performs.

**Keywords** Mean clusters · Clustering technique · Vectors and iterations

## 1 Introduction

Document clustering is an important issue in text mining. Clustering has been widely applicable in different areas of science, technology, social science, biology, economics, medicine and stock market. Clustering problem appears in other different field like pattern recognition, statistical data analysis, bio-informatics, etc. There exist many clustering methods in the literature. In last recent years lot of research work has been done on document clustering. Some contributions are as follows: Approximation Schemes for Euclidean k-median and Related Problems [1], Multi-dimensional Binary Search Trees Used for Associative Searching [2], Refining Initial Points for k-means Clustering [3], Geometric Clusterings [4], Learning Mixtures of

---

N. Sahu (✉)  
Singhania University Rajasthan, Rajasthan, India  
e-mail: neerajsahu79@gmail.com

G. S. Thakur  
MANIT, Bhopal, India  
e-mail: ghanshyamthakur@gmail.com

Gaussians [5], Centroidal Voronoi Tessellations: Applications and Algorithms [6], Exact and Approximation Algorithms for Clustering [7], Pattern Classification and Scene Analysis [8], Clustering and the Continuous k-means Algorithm [9], Approximate Range Searching, Computational Geometry: Theory and Applications [10], Cluster Analysis of Multivariate Data: Efficiency versus Interpretability of Classification [11], Advances in Knowledge Discovery and Data Mining [12], Introduction to Statistical Pattern Recognition [13], Some Fundamental Concepts and Synthesis Procedures for Pattern Recognition Pre-processors [14], A Two-Round Variant of EM for Gaussian Mixtures [15], An Introduction to Probability Theory and its Applications [16], An Efficient k-means Clustering Algorithm [17], Optimal Algorithm for Approximate Nearest Neighbour Searching [18], Convergence Properties of the k-means Algorithms, Advances in Neural Information Processing Systems 7 [19], A Spatial Filtering Approach to Texture Analysis [20], A Database Interface for Clustering in Large Spatial Databases [21], Hesitant Distance Similarity Measures for Document Clustering [22], Classification of Document Clustering Approaches [23], Architecture Based Users and Administrator Login Data Processing [24].

The paper is organized as follows. Section 1 describes the introduction and review of literature. In Sect. 2, the methodology of document clustering is described. In Sect. 3, the numerical results analysis of document clustering for computing vectors is described. In Sect. 4, experimental results are described. In Sect. 5, evaluation measurement is described. Finally, we concluded and proposed some future directions in the conclusion section.

## 2 Methodology

In the document clustering different the steps are used. The steps are as follows:

### 2.1 Document Collection

In this phase we collect relevant documents like e-mail, news, web pages etc. from various heterogeneous sources. These text documents are stored in a variety of formats depending on the nature of the data. The datasets are downloaded from the UCI KDD archive. This is an online repository of large datasets and has wide variety of data types.

### 2.2 Text Pre-processing

Text pre-processing means transforming documents into a suitable representation for the clustering task. The text documents have different stop words, punctuation marks, special character and digits and other characters. Algorithm 1 is removed

HTML tags and stop words from the text documents. After removing stop words, word stemming is performed. Word stemming is the process of suffix removal to general word stems. A stem is a natural group of words with similar meaning. In text-pre-processing we performed the following task: Removal of HTML tags and special character, stop words and word stemming. Algorithm 1 is proposed for text pre-processing. The proposed algorithm removes special characters and stop words from the document.

---

Algorithm1: This algorithm obtain to remove stop words & special characters

Input: A document Data Base D and List of Stop words L

$D = \{d_1, d_2, d_3, \dots, d_k\}$ ; where  $1 \leq k \leq i$

$t_{ij}$  is the  $j$ th term in  $i$ th document

Output: All valid stem text term in D

for (all  $d_i$  in D) do

for (1 to  $j$ ) do

Extract  $t_{ij}$  from  $d_i$

If( $t_{ij}$  in list L)

Remove  $t_{ij}$  from  $d_i$

End for

End for

---

### 2.3 Dimension Reduction

High dimension is the greatest challenge of document clustering, so dimension reduction became major issue of clustering. This module performs two functions- indexing and feature selection. In indexing method we assign the value to the terms in the documents. After indexing, feature selection method is applied. Feature selection is the process of removing indiscriminate terms from the documents to improve the document clustering accuracy and reduce the computational complexity. Algorithm 2 is proposed for indexing and feature selection.

---

Algorithm 2: Basic algorithm obtain for feature selection

Input: A document DataSet D and  $y$  minimum threshold value, N is the counter

$D = \{d_1, d_2, d_3, \dots, d_k\}$ ; where  $1 \leq k \leq i$

$t_{ij}$  is the  $j$ th term in  $i$ th document

Output: Documents Dataset D after feature selection

for (all  $d_i$  in D) do

for (1 to  $j$ ) do

Count total occurrence of  $t_{ij}$  in document  $d_i$

Assign the total occurrence of  $t_{ij}$  in N

If ( $N < y$ )

Remove  $t_{ij}$  from the document  $d_i$

End for

End for

---

Algorithm 2 removes all low frequency terms from the documents. This improves clustering effectiveness and reduces the computational complexity. The document clustering Algorithm 3 is developed. In this algorithm the formulae from  $I_1$  to  $I_6$  are used to calculate the similarities.

---

Algorithm 3: k-mean algorithm obtains to final cluster of each vector for each Iteration.  
 Step 1: Input eight vectors and three initial Clusters ( $k=3$ ) form of vector coming from input vectors.  
 Step 2: initialize  $x_1, y_1, z_1$  for each vector and  $d_1, d_4, d_7$  for each initial clusters vector  
 Step 3: Produce and compare  $\cos\theta_1$  one by one.  
 Step 4:  $\cos\theta_1$  maximum value from each vector final cluster of each vector for first Iteration.  
 Step 5: After first Iteration find new mean cluster for each Iteration.  
 Step 6: Repeat step 2 to step 5 for all Iteration until all final clusters vector are not same for next Iterations.

---

### 3 Vector Representation of Text Document

Text document representation is a challenging issue in text mining. After performing text pre-processing, feature selection and dimension reduction the text documents can be represented as a vector form. Illustrative example I: Let  $D$  be a set of documents  $D = \{d_1, d_2, d_3, d_4, d_5, d_6, d_7, d_8\}$  where  $D$  is a documents set and  $d_i$  are the text documents  $i \leq 1 \leq 8$ . The documents  $d_1$  to  $d_8$  is represented in vector form.  $d_1 = (2, 7, 10)$ ,  $d_2 = (2, 3, 5)$ ,  $d_3 = (8, 3, 5)$ ,  $d_4 = (5, 3, 8)$ ,  $d_5 = (7, 3, 5)$ ,  $d_6 = (6, 4, 7)$ ,  $d_7 = (11, 2, 3)$ ,  $d_8 = (4, 3, 9)$ . Here the tables are Tables 1 and 2. Clustering algorithm K-mean in my algorithm we choose  $k=3$  and centres are  $d_1, d_4, d_7$ .

**Table 1** Final clusters in iteration I to VI

Iteration → Vectors ↓	I	II	III	IV	V	VI
$d_1$	1	1	1	1	1	1
$d_2$	3	1	1	1	1	1
$d_3$	3	3	3	3	3	3
$d_4$	2	2	2	3	2	2
$d_5$	3	2	2	2	2	2
$d_6$	2	3	2	2	2	2
$d_7$	2	3	3	3	3	3
$d_8$	2	2	2	2	2	2



**Table 2** Document clustering results percentages

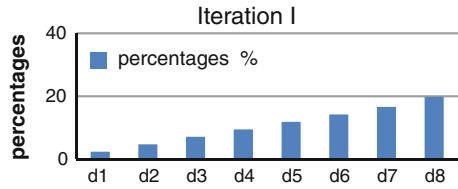
Iteration vectors	Accuracy percentages	Iteration vectors	Accuracy percentages
I <sub>1</sub> V <sub>a</sub>	2.37	I <sub>3</sub> V <sub>e</sub>	51.31
I <sub>1</sub> V <sub>b</sub>	4.75	I <sub>3</sub> V <sub>f</sub>	53.68
I <sub>1</sub> V <sub>c</sub>	7.12	I <sub>3</sub> V <sub>g</sub>	56.05
I <sub>1</sub> V <sub>d</sub>	9.50	I <sub>3</sub> V <sub>h</sub>	59.43
I <sub>1</sub> V <sub>e</sub>	11.87	I <sub>4</sub> V <sub>a</sub>	61.80
I <sub>1</sub> V <sub>f</sub>	14.25	I <sub>4</sub> V <sub>b</sub>	64.18
I <sub>1</sub> V <sub>g</sub>	16.62	I <sub>4</sub> V <sub>c</sub>	66.55
I <sub>1</sub> V <sub>h</sub>	19.82	I <sub>4</sub> V <sub>d</sub>	68.93
I <sub>2</sub> V <sub>a</sub>	21.37	I <sub>4</sub> V <sub>e</sub>	71.33
I <sub>2</sub> V <sub>b</sub>	23.75	I <sub>4</sub> V <sub>f</sub>	73.67
I <sub>2</sub> V <sub>c</sub>	26.12	I <sub>4</sub> V <sub>g</sub>	76.05
I <sub>2</sub> V <sub>d</sub>	28.50	I <sub>4</sub> V <sub>h</sub>	79.45
I <sub>2</sub> V <sub>e</sub>	30.87	I <sub>5</sub> V <sub>a</sub>	81.82
I <sub>2</sub> V <sub>f</sub>	33.25	I <sub>5</sub> V <sub>b</sub>	84.19
I <sub>2</sub> V <sub>g</sub>	35.62	I <sub>5</sub> V <sub>c</sub>	86.59
I <sub>2</sub> V <sub>h</sub>	39.44	I <sub>5</sub> V <sub>d</sub>	88.99
I <sub>3</sub> V <sub>a</sub>	41.81	I <sub>5</sub> V <sub>e</sub>	91.39
I <sub>3</sub> V <sub>b</sub>	44.19	I <sub>5</sub> V <sub>f</sub>	93.79
I <sub>3</sub> V <sub>c</sub>	46.56	I <sub>5</sub> V <sub>g</sub>	96.16
I <sub>3</sub> V <sub>d</sub>	48.94	I <sub>5</sub> V <sub>h</sub>	98.56

## 4 Experimental Results

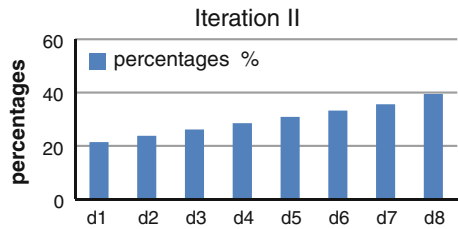
In this paper the unstructured datasets are used. The datasets are downloaded from UCI KDD Archive [4]. This is an online repository of large datasets with wide variety of data types. This repository has twenty newsgroups dataset for text analysis. This data set consists of 20,000 messages taken from Usenet newsgroup. The subset of twenty newsgroups is mini newsgroup. We have done our experiments on 20 newsgroup datasets. Each category contains 1,000 documents, so there are 20,000 documents for experiments. The five categories Computer Hardware, Computer Graphics, Medical, Sports and Automobile are used in first experiment. The experimental results are shown in Figs. 1, 2, 3, 4, 5, 6, 7, 8, 9, 10, 11 and 12 with eight vectors d<sub>1</sub> to d<sub>8</sub>.

The document clustering results percentages show accuracy of clustering process. Here percentages are increases iteration by iterations.

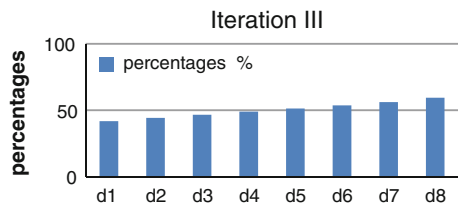
**Fig. 1** Accuracy percentages for iteration I



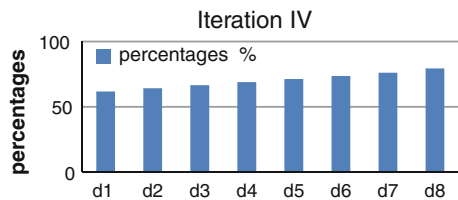
**Fig. 2** Accuracy percentages for iteration II



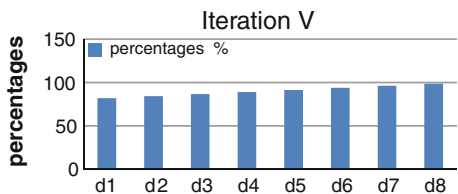
**Fig. 3** Accuracy percentages for iteration III



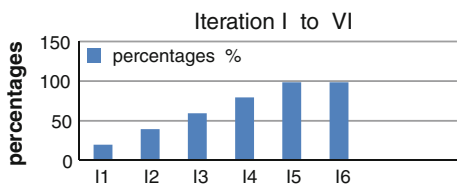
**Fig. 4** Accuracy percentages for iteration IV



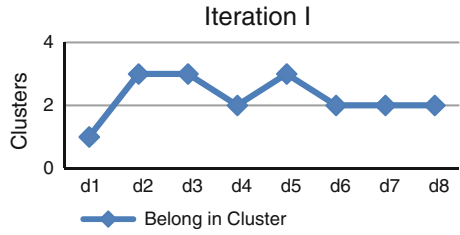
**Fig. 5** Accuracy percentages for iteration V



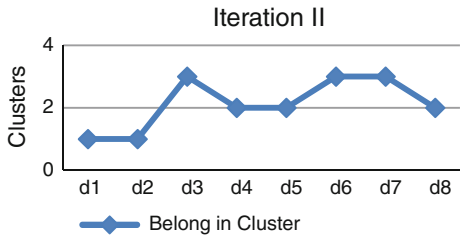
**Fig. 6** Accuracy percentages from I to VI



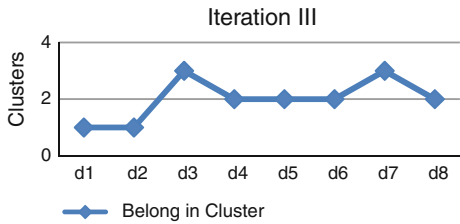
**Fig. 7** final clusters for iteration I



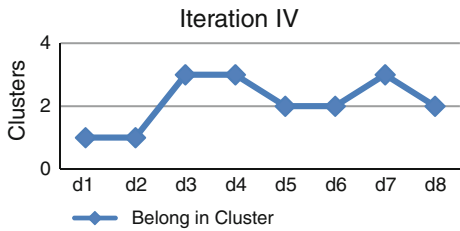
**Fig. 8** final clusters for iteration II



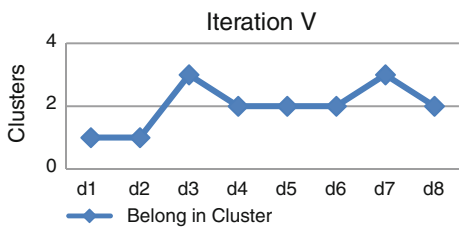
**Fig. 9** final clusters for iteration III



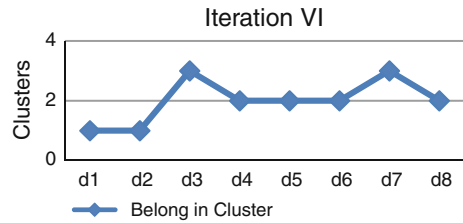
**Fig. 10** final clusters for iteration IV



**Fig. 11** final clusters for iteration V



**Fig. 12** final clusters for iteration VI



The graphical representations of the results are shown in Figs. 1, 2, 3, 4, 5, 6, 7, 8, 9, 10, 11, 12. We performed our experiments on five newsgroups—Computer graphics, Computer hardware, Automobile, Sports and Medical. In this research the 80% dataset is used as the training dataset and 20% dataset as the test dataset.

## 5 Conclusions

This paper analyzed document clustering using computing vectors. The experimental results of document clustering are efficient and accurate. The proposed approach works efficiently. The accuracy is best as compare to other existing algorithm of the document clustering.

**Acknowledgments** This work is supported by research grant from MPCST, Bhopal M.P., India, Endt.No. 2427/CST/R&D/2011 dated 22/09/2011.

## References

1. Arora, S., Raghavan, P., Rao, S.: Approximation schemes for Euclidean k-median and related problems. In: Proceedings of the 30th Annual ACM Symposium on Theory of Computing, May 1998, pp. 106–113
2. Bentley, J.L.: Multidimensional binary search trees used for associative searching. *Comm. ACM* **18**, 509–517 (1975)
3. Bradley, P.S., Fayyad, U.: Refining initial points for k-means clustering. In: Proceedings of the 15th International Conference on Machine Learning, 1998, pp. 91–99
4. [www.kdd.ics.uci.edu](http://www.kdd.ics.uci.edu)
5. Dasgupta, S.: Learning mixtures of Gaussians. In: Proceedings of the 40th IEEE Symposium on Foundations of Computer Science, Oct 1999, pp. 634–644
6. Du, Q., Faber, V., Gunzburger, M.: Centroidal Voronoi tessellations: Applications and algorithms. *SIAM Rev.* **41**, 637–676 (1999)
7. Agarwal, P.K., Procopiu, C.M.: Exact and approximation algorithms for clustering. In: Proceedings of the Ninth Annual ACM-SIAM Symposium on Discrete Algorithms, Jan 1998, pp. 658–667
8. Duda, R.O., Hart, P.E.: *Pattern Classification and Scene Analysis*. Wiley, New York (1973)
9. Faber, V.: Clustering and the continuous k-means algorithm. *Los Alamos Sci.* **22**, 138–144 (1994)

10. Arya, S., Mount, D.M.: Approximate range searching. *Comput. Geom. Theor. Appl.* **17**, 135–163 (2000)
11. Forgy, E.: Cluster analysis of multivariate data: efficiency versus interpretability of classification. *Biometrics* **21**, 768 (1965)
12. Fayyad, U.M., Piatetsky-Shapiro, G., Smyth, P., Uthurusamy, R.: *Advances in Knowledge Discovery and Data Mining*. AAAI/MIT Press, Cambridge (1996)
13. Fukunaga, K.: *Introduction to Statistical Pattern Recognition*. Academic Press, Boston (1990)
14. Ball, G.H., Hall, D.J.: Some fundamental concepts and synthesis procedures for pattern recognition preprocessors. In: *Proceedings of the International Conference on Microwaves, Circuit Theory, and Information Theory*, Sept 1964
15. Dasgupta, S., Shulman, L.J.: A two-round variant of EM for Gaussian mixtures. In: *Proceedings of the 16th Conference on Uncertainty in Artificial Intelligence (UAI-2000)*, June 2000, pp. 152–159
16. Feller, W.: *An Introduction to Probability Theory and Its Applications*, 3rd edn. Wiley, New York (1968)
17. Alsabti, K., Ranka, S., Singh, V.: An Efficient k-means clustering algorithm. In: *Proceedings of the First Workshop High Performance Data Mining*, Mar 1998
18. Arya, S., Mount, D.M., Netanyahu, N.S., Silverman, R., Wu, A.Y.: An optimal algorithm for approximate nearest neighbor searching. *J. ACM* **45**, 891–923 (1998)
19. Bottou, L., Bengio, Y.: Convergence properties of the k-means algorithms. In: *Tesauro, G., Touretzky, D. (eds.) Advances in Neural Information Processing Systems 7*, pp. 585–592. MIT Press, Cambridge (1996)
20. Coggins, J.M., Jain, A.K.: A spatial filtering approach to texture analysis. *Pattern Recognit. Lett.* **3**, 195–203 (1985)
21. Ester, M., Kriegel, H., Xu, X.: A database interface for clustering in large spatial databases. In: *Proceedings of the First International Conference on Knowledge Discovery and Data Mining (KDD-95)*, 1995, pp. 94–99
22. Neeraj, S., Thakur, G.S. : Hesitant distance similarity measures for document clustering. In: *IEEE Conference—2011 World Congress on Information and Communication Technologies Mumbai*, 11–14 Dec 2011. ISBN: 978-1-4673-0125-1
23. Sahu, S.K., Sahu, N., Thakur, G.S.: Classification of document clustering approaches. *Intl. J. Comput. Sci. Softw. Eng.* **2**(5), 509–513 (2012). ISSN (Online): 2277 128X
24. Sahu, B., Sahu, N., Thakur, G.S.: Architecture based users and administrator login data processing. In: *International Conference on Intelligent Computing and Information System (ICICIS-2012)*, Pachmarhi, Piparia, 27–28 Oct 2012. ISSN (Online): 2249–071X
25. Bradley, P.S., Fayyad, U., Reina, C.: Scaling clustering algorithms to large databases. In: *Proceedings of the Fourth International Conference on Knowledge Discovery and Data Mining*, 1998, pp. 9–15

# Altered Fingerprint Identification and Classification Using SP Detection and Fuzzy Classification

Ram Kumar, Jasvinder Pal Singh and Gaurav Srivastava

**Abstract** Fingerprint recognition is one of the most commonly used biometric technology. Even if fingerprint temporarily changes (cuts, bruises) it reappears after the finger heals. Criminals started to be aware of this and try to fool the identification systems applying methods from ingenious to very cruel. It is possible to remove, alter, or even fake fingerprints (made of glue, latex, silicone), by burning the fingertip skin (fire, acid, other corrosive material), by using plastic surgery (changing the skin completely, causing change in pattern—portions of skin are removed from a finger and grafted back in different positions, like rotation or “Z” cuts, transplantations of an area from other parts of the body like other fingers, palms, toes, and soles). This paper presents a new algorithm for altered fingerprints detection based on fingerprint orientation field reliability. The map of the orientation field reliability has peaks in the singular point locations. These peaks are used to analyze altered fingerprints because, due to alteration, more peaks as singular points appear with lower amplitudes.

**Keywords** Fingerprints · Alteration · Image enhancement · Reliability · Singular points

---

R. Kumar

M.Tech Scholar in R.K.D.F Institute of Technology and Science, Bhopal, India  
e-mail: hr.coet@gmail.com

J.P. Singh and G. Srivastava

Assistant Professor in Computer Science and Engineering in R.K.D.F Institute of Technology and Science, Bhopal, India  
e-mail: jasvinder162@gmail.com

G. Srivastava

e-mail: gashr83@gmail.com



**Fig. 1** A fingerprint altered by switching two parts of a ‘Z’ shaped cut [2]

## 1 Introduction

Fingerprint alteration is not a new phenomenon. As early as in 1934, John Dillinger, the infamous bank robber and a dangerous criminal, applied acid to his fingertips [1]. Since then, there has been an increase in the reported cases of fingerprint alteration. In 1995, a Criminal was found to have altered his fingerprints by making a “Z” shaped cut into the finger and switching the finger skin the two parts (see Fig. 1). In 2009, a Chinese woman successfully deceived the Japan immigration fingerprint system by performing surgery to swap fingerprints on her left and right hands [3]. Fingerprint alteration has even been performed at a much larger scale involving multiple individuals. Hundreds of asylum seekers have cut, abraded, and burned their fingertips to prevent identification by EURODAC, a European Union fingerprint system for identifying asylum seekers [2]. Additional cases of fingerprint alteration have been compiled in [2].

The primary purpose of fingerprint alteration [4] is to evade identification using techniques that vary from abrading, cutting, and burning fingers to performing plastic surgery.

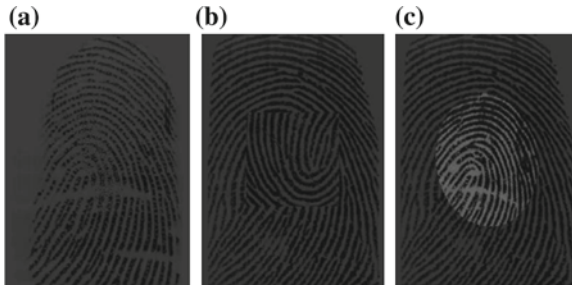
Fingerprint alteration constitutes a serious “attack” against a border control fingerprint identification system since it defeats the very purpose for which the system was deployed in the first place, i.e., to identify individuals on a watch-list.

The goal of this work is to introduce the problem of fingerprint alteration and to develop methods to automatically detect and classify altered fingerprints.

## 2 Type of Altered Fingerprint

According to the changes made to the ridge patterns, fingerprint alterations may be categorized into three types:

- i. Obliteration
- ii. Distortion
- iii. Imitation (see Fig. 2).



**Fig. 2** Three types of altered fingerprints. **a** Obliterated fingerprint **b** distorted fingerprint, and **c** imitated fingerprint

For each type of alteration, its characteristics and possible countermeasures are described.

### 3 Methodology

In this section, we consider the problem of automatic detection of alterations and classification based on analyzing singular point reliability map of orientation field.

A set of features is first extracted from the ridge orientation field of an input fingerprint and then a fuzzy classifier is used to classify it into natural or altered fingerprint and its alteration type.

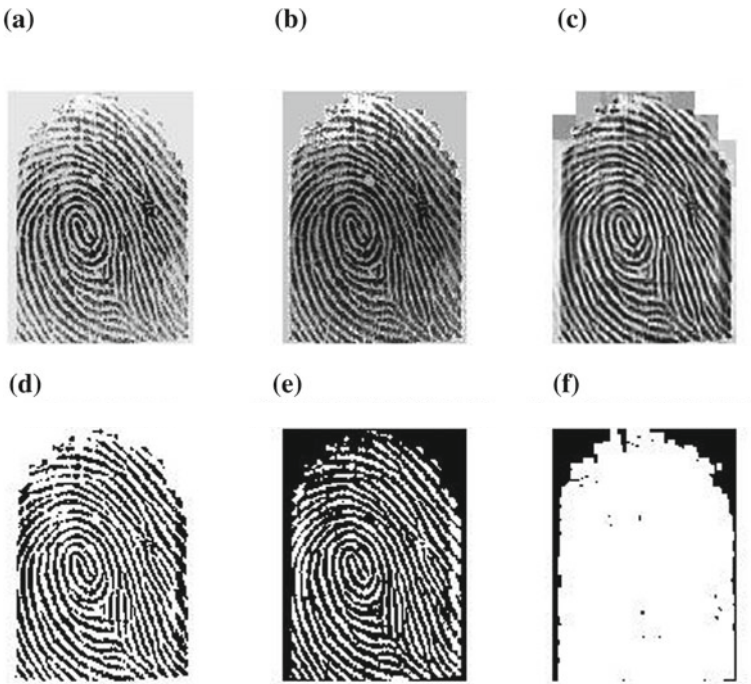
#### 3.1 Fingerprint Database

Due to lack of altered fingerprint data, I use constructed database synthetically from the original fingerprints. I collect more than 100 original fingerprints of my friends to analyze the proposed system. After collecting the original fingerprint, I altered those fingerprint by the three different techniques of fingerprint alteration named obliteration, distortion, and imitation respectively. For analyzing the system, we use 49 images for all type of alteration.

#### 3.2 Preprocessing on Fingerprint

The aim of the image preprocessing stage is to increase both the accuracy and the interpretability of the digital data during the image processing stage. The preprocess-





**Fig. 3** Preprocessing steps: **a.** Real altered fingerprint image; **b.** Image obtain after Histogram Equalization; **c.**Image obtained after FFT; **d.** Binary image; **e.** Distance transform image; **f.** Region of interest.

ing takes place prior to any principal component analysis. The main steps for pre-processing are enhancement, binarization, distance transform, and segmentation.

### ***3.3 Image Enhancement***

The fingerprint input image is enhanced in the spatial domain by applying the Histogram Equalization technique, for a better distribution of the pixel values. Considering the real altered fingerprint from Fig. 3a, the result image is represented in Figs. 3b and 4)

### ***3.4 Histogram Equalization***

The histogram of a digital image with gray levels in the range  $[0, L-1]$  is a discrete function:

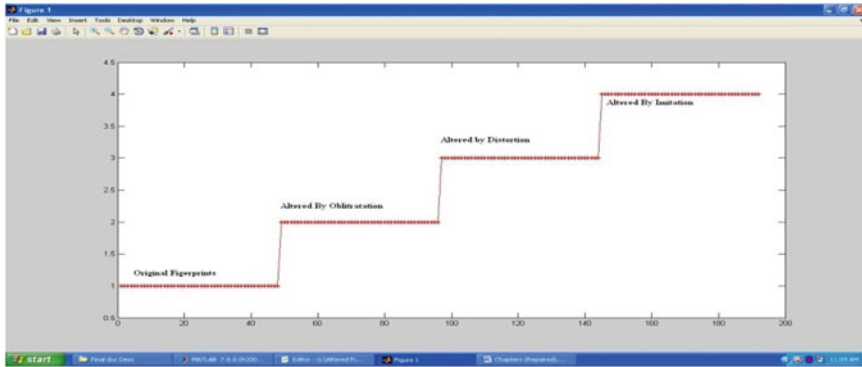


Fig. 4 Classification of fingerprint using fuzzy classification

$$p(r_k) = \frac{n_k}{n}; \tag{1}$$

where  $r_k$  represents the  $k$ 'th gray level,  $n_k$  is the number of pixels in the image with that gray level,  $n$  represents the total number of pixels in the image,  $k = 1, 1, \dots, L, L = 256$ .

### 3.5 Binarisation

Most minutiae extraction algorithms operate on basically binary images where there are only two levels of interest: The black pixels represent ridges, and the white pixels represent valleys. Binarisation [4] converts a greylevel image into a binary image. This helps in improving the contrast between the ridges and valleys in a fingerprint image, and consequently facilitates the extraction of minutiae.

## 4 Singular Point Detection

Singular point detection is the most challenging task; it is an important process for fingerprint image alignment, fingerprint classification, and fingerprint matching. In the following subsections, we propose orientation reliability and singular point position methods.

## 5 Orientation Field Reliability Map

The fingerprint image is made up of pattern of ridges and valleys; they are the replica of the human fingertips. The fingerprint image represents a system of oriented texture and has very rich structural information within the image. This flow-like pattern forms an orientation field extracted from the style of valleys and ridges. In the large part of fingerprint topologies, the orientation field is quite smooth, while in some areas, the orientation appears in a discontinuous manner. These regions are called singularity or singular points, including core and delta and are defined as the centers of those areas. In addition, the reference point is defined here as the point with maximum curvature on the convex ridge. The reliability of the orientation field describes the consistency of the local orientations in a neighborhood along the dominant orientation is used to locate the unique reference point constantly for all types of fingerprints.

## 6 Experiment Result

In this paper, the singular point is defined as the point with maximum curvature on the convex ridge. In natural fingerprints, the reliability orientation image generally has one or two sharp point, while in altered fingerprints more points are detected with smaller values. Starting from this observation, the altered fingerprint analysis can be done using the density and the count of the singular points.

The proposed algorithm for fingerprint analysis based on the estimation of orientation field and the computation of the reliability was tested with real altered fingerprint and simulated altered fingerprint obtained from natural fingerprint images by using synthetic method due to unavailability of altered fingerprint database.

For the classification, we capture 49 fingerprints of friends and altered them synthetically. On training, it will be classified according to the type of alteration. The graph will show the classification .

## 7 Conclusion and Future Scope

The proposed system design will be tested using altered fingerprints synthesized in the way typically observed in operational cases with good performance.

This paper proposes a method to consistently and precisely locate the singular points (core and delta) in fingerprint images. The method applied is based on the enhanced fingerprint image orientation reliability. Classification of three different types of altered fingerprint using fuzzy clustering method, the false acceptance rate is 16.7 % and false rejection rate is 13.8 % of 192 fingerprint database. In context with K-Mean classification on the same database, the false acceptance rate is 20.7 %

and false rejection rate is 13.4 %. Classification using fuzzy clustering is better for false acceptance rate and 0.4 % less for false rejection rate.

The current altered fingerprint detection algorithm can be improved along the following directions:

1. Reconstruct altered fingerprints. For some types of fingerprints where the ridge patterns are damaged locally or the ridge structure is still present on the finger but possibly at a different location, reconstruction is indeed possible.
2. Match altered fingerprints to their unaltered mates. A matcher specialized for altered fingerprints can be developed to link them to unaltered mates in the database utilizing whatever information is available in the altered fingerprints.

In this paper, we use the synthetic fingerprints due to the unavailability of public databases, but this method will give a way for researcher to do in the fields of altered fingerprint recognition.

## References

1. Jain, A.K., Yoon, S., Feng, J.: Altered fingerprints: analysis and detection. *IEEE Trans. Pattern Anal. Mach. Intell.* **34**, 451–464 (2012)
2. Singh, K.: Altered Fingerprints. <http://www.interpol.int/Public/Forensic/fingerprints/research/alteredfingerprints.pdf> (2008)
3. Jain, A.K.: Surgically altered fingerprints help woman evade immigration. <http://abcnews.go.com> (2009)
4. Cummins, H.: Attempts to alter and obliterate fingerprints. *J. Am. Inst. Crim. Law Criminol.* **25**, 982–991 (1935)

# Optimal Advertisement Planning for Multi Products Incorporating Segment Specific and Spectrum Effect of Different Medias

Sugandha Aggarwal, Remica Aggarwal and P. C. Jha

**Abstract** A large part of any firm's investment goes in advertising and therefore planning of an appropriate media for advertisement is the need of today so as to achieve the best returns in terms of wider reach over potential market. In this paper, we deal with a media planning problem for multiple products of a firm in a market which is segmented geographically into various regional segments with diverse language and cultural base. As such each of these regional segments responds to regional advertising as well as national advertising which reaches them with a fixed spectrum. The objective is to plan an advertising media (national and regional media) for multiple products in such a way that maximizes the total reach which is measured through each media exclusively as well as through their combined impact. The problem is formulated as a multi-objective programming problem and solved through goal programming technique. A real life case is provided to illustrate the applicability of the proposed model.

**Keywords** Multiple products · Market segmentation · National advertising · Regional advertising · Spectrum effect · Media planning · Mathematical programming

---

S. Aggarwal (✉) · P. C. Jha  
Department of Operational Research, University of Delhi, Delhi, India  
e-mail: sugandha\_or@yahoo.com

R. Aggarwal  
Department of Management, Birla Institute of Technology and Science, Pilani, India  
e-mail: remica\_or@rediffmail.com

P. C. Jha  
e-mail: jhpc@yahoo.com

## Abbreviations

- . Max-maximize
- . Min-minimize
- . s.t.-subject to
- . GP-goal programming

## 1 Introduction

Companies ranging from large multinational corporations to small retailers rely on different forms of promotion to market their products and services. Advertising is one of the most important forms and is done through various media sources such as print media and electronic media. Planning a suitable media source includes appropriate selection of advertising media and development and allocation of advertising budget. Selection of media largely depends on the target potential market in which product needs to be advertised. The target market could be a single/sole market or may be divided into several segments based on certain criteria. These criteria are defined either geographically, psycho-graphically, sociologically, etc. Take for example geographic segmentation of target market. Here, market is segmented according to geographic criteria—nations, states, regions, countries, cities, neighborhoods, zip codes, population density, or climate. This paper considers a geographically segmented market in which two types of advertising is done, national advertising and regional advertising. National advertising simultaneously reaches all the geographically segmented regions of the country. Various sources of national advertising include national newspapers, national television channels, magazines, websites, etc. Whereas regional advertising targets a specific regional segment of the country through regional newspapers, regional radio channels, regional TV channels, etc.

Regional advertising targets a more concentrated customer base while national advertising has the potential to bring in larger amounts of customers. As national advertisement reaches masses it creates an effectiveness segment-spectrum, which is distributed over various regional segments of the country. Thus, in each region, people get affected by regional advertisements as well as national advertisements with a spectrum effect. Such concept of advertising holds well in a country like India which has a large cultural and language base. Companies advertise their products in Indian market by giving ad messages in national language as well as people belonging to a particular region are emotionally targeted by regional advertising in their native language. In this way they relate themselves with the product in a better way. For example, Hindustan Unilever Limited (HUL), India's largest consumer goods company prepares different versions of ads for its consumable products. They advertise their products in Hindi language national television channels such as Zee TV, Doordarshan, Star Plus, Life OK, etc., to create a mass demand all over the country. Advertisements floating on these channels create a spectrum effect in several regions

of country as it is viewed by people all over India. Along with it, the same advertisement is dubbed in various state dominant regional languages, such as Gujarati, Telugu, Tamil, Kannada, Punjabi, Marathi, etc., and telecasted in regional channels also. In this way they try to reach maximum number of people all over the country.

In this chapter, both national as well as regional media are considered as a source of advertising multiple products in different regions. A media planning problem is formulated for allocating total budget available among several national and regional media that are found suitable for advertising the products, maximizing total reach in all the regions where each region's people get affected by regional advertisement corresponding to that region as well as national advertisement with a fixed spectrum. Goal programming technique is used to solve the formulated problem.

The chapter is organized as follows: Section 2 gives a brief literature review. Section 3 formulates the media planning problem for multiple products. Solution procedure for the formulated problem has been given in Sect. 4. A real life case problem is presented in Sect. 5 which clearly illustrates solution methodology. Concluding remarks are made in Sect. 6.

## 2 Literature Review

A plethora of work has been done on media planning problems. Charnes et al. [1] introduced a GP model for media selection to address problems associated with the critical advertising measurement of frequency and reach. A similar kind of problem was introduced by Lee [2] as well. De Kluyver [3] proposed the more realistic use of hard and soft constraints for linear programming model used in media selection. An integer GP model was developed by Keown and Duncan [4] to solve media selection problems and improved upon sub-optimal results produced by linear programming and non-integer GP models. Some of the prominent literature relating multi-criteria decision making with media selection includes the works by Moynihan et al. [5] and Fruchter and Kalish [6]. They contended that the mathematical requirements of the MCDM model for media selection force the media planner to create an artificial structuring of the media selection criteria. An information resource planning using an analytic hierarchy process based GP model was developed by Lee and Kwak [7]. Mihiotis and Tsakiris [8] discussed the best possible combination of placements of commercial with the goal of the highest rating subject to constrained advertisement budgets. Kwak et al. [9] presented a case study that considers two options: Industrial and consumer products. In order to resolve the strategic decision making about dual market high technology products, a mixed integer GP model is developed to facilitate the advertising media selection process. A chance constraints GP model for the advertising planning media problem was proposed by U.K. Bhattacharya [10] to decide the number of advertisement in different advertising media and the optimal allocation of the budget assigned to the different media so as to maximize the total reach. Jha et al. [11, 12] formulated a media planning problem for allocating the available budget among the multiple media that are found suitable for the advertising of single/multiple products considering marketing segmentation aspect of advertising. Spectrum effect

of an advertising channel has been discussed recently by Burrato et al. [13] assuming that an advertising channel has an effectiveness segment-spectrum, which is distributed over potential market segments and solutions to deterministic optimal control problems were obtained. However, the above models have not included the segment specific and spectrum effect of different media in media allocation problems. In the following section, a model has been developed which deals with optimal allocation of budget for multiple products advertised through different regional and national media in order to maximize national and regional reach considering the spectrum effect of national media in the regional segments.

### 3 Model Development

The model is based on an Indian company which manufactures a range of consumable products. It advertises its products through national and regional media in four geographically segmented regions. The media considered are print media (different types of newspapers) and different channels of television. The total budget ( $A$ ) available is fixed. It is desired to find optimal number of advertisements of different products to be allocated to different national and regional media that would maximize the total advertising reach of all products in each segment of the market, under cost budget and frequency constraints. The advertisements is carried through a national newspaper and a national channel of television alongwith two regional newspapers and two regional channels of each region. Each of these media (regional as well as national) have many suboptions, i.e., advertisements can be given in front page (FP) or other pages (OP) of a newspaper. Similarly considering a television channel, advertising can be done in prime time (PT) as well as in other time (OT).

$p_{is_c j k_{ij}}^r C_{ij k_{ij} l_{ij}}^r X_{ij k_{ij}}^r P_{is_c j k_{ij}} \underline{C}_{ij k_{ij} l_{ij}} C_{ij k_{ij} l_{ij}} C_{ij k_{ij} l_{ij}} \forall i = 0, 1, \dots, 4$  Let is the total circulation/average number of viewers of national (for  $i = 0$ ) and  $i$ th regional segment's  $j$ th media,  $k_{ij}$ th media option and  $l_{ij}$ th slot respectively (where  $j = 1$  represents newspaper,  $j = 2$  represents television;  $k_{ij} = 1, 2 \forall i = 1, 2, \dots, 4$ ;  $j = 1, 2$  as in case of regional segments, for each media two media options is considered in each region;  $k_{0j} = 1$  for national media as only one type of national newspaper and TV channel is considered;  $l_{ij} = 1, 2 \forall i = 0, 1, \dots, 4$ ;  $j = 1, 2$  represents slots, i.e., front page and other page in newspapers and prime time and other time in television). Let  $\underline{C}_{ij k_{ij} l_{ij}}$  is circulation common to national media for  $i$ th regional segment's  $j$ th media,  $k_{ij}$ th media option,  $l_{ij}$ th slot. It is assumed that media chosen for advertisement for all the products is same. Let  $C_{ij k_{ij} l_{ij}}^r$  is advertisement cost of inserting one advertisement for  $r$ th product in national/ $i$ th regional segment's  $j$ th media,  $k_{ij}$ th media option and  $l_{ij}$ th slot. It has been assumed that the cost of advertisements at any pages other than the front page is the same. The readership profile/viewership profile represents the percentage of people in different criteria who are reading or viewing the advertisement.  $p_{is_c j k_{ij}}^r$  is percentage of people for  $r$ th product who fall under  $s_c$ th criteria and read/view national/ $i$ th regional segment's  $j$ th media,  $k_{ij}$ th media option, and  $l_{ij}$ th slot.



Let  $p_{-1s_cjk_{ij}}^r$  is percentage of people common to national media for  $r$ th product who fall under  $s_c$ th criteria and read/view national/ $i$ th regional segment's  $j$ th media,  $k_{ij}$ th media option, and  $l_{ij}$ th slot. Different criteria for specifying the target population to whom the advertisement should reach can be age, income, education, etc. Let  $w_{cj}$  be the weight corresponding to  $s_c$ th criteria,  $j$ th media. Let  $\alpha_{ij}$  be the spectrum effect of  $j$ th national media on  $i$ th regional segment.

Also let  $x_{ijk_{ij}l_{ij}}^r$  be decision variable corresponding number of advertisements of  $r$ th product in national/ $i$ th regional segment's  $j$ th media,  $k_{ij}$ th media option, and  $l_{ij}$ th slot. Let  $Z_0$  be reach objective corresponding to national media and  $Z_i$  (for  $i = 1, 2, \dots, 4$ ) be exclusive reach objective for  $i$ th segment's regional media. Exclusive as in each region, there are common people who read/view both national and regional media and these people get subtracted from the total reach of that region as they are already included in the total national reach objective. Thus, problem for finding optimal number of advertisements of different products to be allocated to different media that would maximize advertising reach at national and regional level under cost–budget and advertisement frequency constraint can be formulated as:

$$\text{Max} \left\{ \begin{aligned}
 Z_0 &= \sum_{r=1}^2 \sum_{j=1}^2 \sum_{l_{0j}=1}^2 \alpha_{1j} \left[ \left( \sum_{c=1}^q w_{cj} p_{0j1l_{0j}}^r \right) C_{0j1l_{0j}} \right] x_{0j1l_{0j}}^r \\
 &+ \sum_{r=1}^2 \sum_{j=1}^2 \sum_{l_{0j}=1}^2 \alpha_{2j} \left[ \left( \sum_{c=1}^q w_{cj} p_{0j1l_{0j}}^r \right) C_{0j1l_{0j}} \right] x_{0j1l_{0j}}^r \\
 &+ \sum_{r=1}^2 \sum_{j=1}^2 \sum_{l_{1j}=1}^2 \alpha_{3j} \left[ \left( \sum_{c=1}^q w_{cj} p_{0j1l_{0j}}^r \right) C_{0j1l_{0j}} \right] x_{0j1l_{0j}}^r \\
 &+ \sum_{r=1}^2 \sum_{j=1}^2 \sum_{l_{1j}=1}^2 \alpha_{4j} \left[ \left( \sum_{c=1}^q w_{cj} p_{0j1l_{0j}}^r \right) C_{0j1l_{0j}} \right] x_{0j1l_{0j}}^r \\
 Z_1 &= \sum_{r=1}^2 \sum_{j=1}^2 \sum_{k_{1j}=1}^2 \sum_{l_{1j}=1}^2 \left[ \left( \sum_{c=1}^q w_{cj} p_{1s_cjk_{1j}l_{1j}}^r \right) C_{1jk_{1j}l_{1j}} \right. \\
 &\quad \left. - \left( \sum_{c=1}^q w_{cj} p_{1s_cjk_{1j}l_{1j}}^r \right) \underline{C}_{1jk_{1j}l_{1j}} \right] x_{1jk_{1j}l_{1j}}^r \\
 Z_2 &= \sum_{r=1}^2 \sum_{j=1}^2 \sum_{k_{2j}=1}^2 \sum_{l_{2j}=1}^2 \left[ \left( \sum_{c=1}^q w_{cj} p_{2s_cjk_{2j}l_{2j}}^r \right) C_{2jk_{2j}l_{2j}} \right. \\
 &\quad \left. - \left( \sum_{c=1}^q w_{cj} p_{2s_cjk_{2j}l_{2j}}^r \right) \underline{C}_{2jk_{2j}l_{2j}} \right] x_{2jk_{2j}l_{2j}}^r \\
 Z_3 &= \sum_{r=1}^2 \sum_{j=1}^2 \sum_{k_{3j}=1}^2 \sum_{l_{3j}=1}^2 \left[ \left( \sum_{c=1}^q w_{cj} p_{3s_cjk_{3j}l_{3j}}^r \right) C_{3jk_{3j}l_{3j}} \right. \\
 &\quad \left. - \left( \sum_{c=1}^q w_{cj} p_{3s_cjk_{3j}l_{3j}}^r \right) \underline{C}_{3jk_{3j}l_{3j}} \right] x_{3jk_{3j}l_{3j}}^r \\
 Z_4 &= \sum_{r=1}^2 \sum_{j=1}^2 \sum_{k_{4j}=1}^2 \sum_{l_{4j}=1}^2 \left[ \left( \sum_{c=1}^q w_{cj} p_{4s_cjk_{4j}l_{4j}}^r \right) C_{4jk_{4j}l_{4j}} \right. \\
 &\quad \left. - \left( \sum_{c=1}^q w_{cj} p_{4s_cjk_{4j}l_{4j}}^r \right) \underline{C}_{4jk_{4j}l_{4j}} \right] x_{4jk_{4j}l_{4j}}^r
 \end{aligned} \right.$$

$$\begin{aligned}
 \text{s.t. } & \sum_{r=1}^2 \sum_{j=1}^2 \sum_{l_{0j}=1}^2 c_{0j1l_{0j}}^r x_{0j1l_{0j}}^r + \sum_{r=1}^2 \sum_{i=1}^4 \sum_{j=1}^2 \sum_{k_{ij}=1}^2 \sum_{l_{ij}=1}^2 c_{ijk_{ij}l_{ij}}^r x_{ijk_{ij}l_{ij}}^r \leq A \quad (\text{P1}) \\
 & \sum_{r=1}^2 \sum_{j=1}^2 \sum_{l_{0j}=1}^2 c_{0j1l_{0j}}^r x_{0j1l_{0j}}^r \geq vA \\
 & \left. \begin{aligned} x_{0j1l_{0j}}^r &\geq t_{0j1l_{0j}}^r, x_{0j1l_{0j}}^r \leq u_{0j1l_{0j}}^r \\ x_{0j1l_{0j}}^r &\geq 0 \text{ and integers} \end{aligned} \right\} \forall r = 1, 2; j = 1, 2; l_{0j} = 1, 2 \\
 & \left. \begin{aligned} x_{ijk_{ij}l_{ij}}^r &\geq t_{ijk_{ij}l_{ij}}^r, x_{ijk_{ij}l_{ij}}^r \leq u_{ijk_{ij}l_{ij}}^r \\ x_{ijk_{ij}l_{ij}}^r &\geq 0 \text{ and integers} \end{aligned} \right\} \forall r = 1, 2; i = 1, 2, \dots, 4; \\
 & \qquad \qquad \qquad j = 1, 2; l_{ij} = 1, 2; k_{ij} = 1, 2
 \end{aligned}$$

where  $v$  is the minimum proportion of the total budget required to be allocated to national media  $t_{ijk_{ij}l_{ij}}^r$  is the minimum number of advertisements of  $r$ th product in national/ $i$ th regional segment's  $j$ th media,  $k_{ij}$ th media option, and  $l_{ij}$ th slot, respectively. Similarly  $u_{ijk_{ij}l_{ij}}^r$  is the maximum number of advertisements of  $r$ th product in national/ $i$ th regional segment's  $j$ th media,  $k_{ij}$ th media option, and  $l_{ij}$ th slot.

The optimal value of  $Z_0, Z_1, Z_2, Z_3, Z_4$  obtained on solving the above problem can be set as individual aspiration level to be achieved from different segments. Problem (P1) can then be written as a multi-objective programming problem.

$$\text{Max } \left\{ \begin{aligned}
 Z_0 &= \sum_{r=1}^2 \sum_{j=1}^2 \sum_{l_{0j}=1}^2 \alpha_{1j} \left[ \left( \sum_{c=1}^q w_{cj} p_{0j1l_{0j}}^r \right) C_{0j1l_{0j}} \right] x_{0j1l_{0j}}^r \\
 &\quad + \sum_{r=1}^2 \sum_{j=1}^2 \sum_{l_{0j}=1}^2 \alpha_{2j} \left[ \left( \sum_{c=1}^q w_{cj} p_{0j1l_{0j}}^r \right) C_{0j1l_{0j}} \right] x_{0j1l_{0j}}^r \\
 &\quad + \sum_{r=1}^2 \sum_{j=1}^2 \sum_{l_{1j}=1}^2 \alpha_{3j} \left[ \left( \sum_{c=1}^q w_{cj} p_{0j1l_{0j}}^r \right) C_{0j1l_{0j}} \right] x_{0j1l_{0j}}^r \\
 &\quad + \sum_{r=1}^2 \sum_{j=1}^2 \sum_{l_{1j}=1}^2 \alpha_{4j} \left[ \left( \sum_{c=1}^q w_{cj} p_{0j1l_{0j}}^r \right) C_{0j1l_{0j}} \right] x_{0j1l_{0j}}^r \\
 Z_1 &= \sum_{r=1}^2 \sum_{j=1}^2 \sum_{k_{1j}=1}^2 \sum_{l_{1j}=1}^2 \left[ \left( \sum_{c=1}^q w_{cj} p_{1scjk_{1j}l_{1j}}^r \right) C_{1jk_{1j}l_{1j}} \right. \\
 &\quad \left. - \left( \sum_{c=1}^q w_{cj} p_{1scjk_{1j}l_{1j}}^r \right) \underline{C}_{1jk_{1j}l_{1j}} \right] x_{1jk_{1j}l_{1j}}^r \\
 Z_2 &= \sum_{r=1}^2 \sum_{j=1}^2 \sum_{k_{2j}=1}^2 \sum_{l_{2j}=1}^2 \left[ \left( \sum_{c=1}^q w_{cj} p_{2scjk_{2j}l_{2j}}^r \right) C_{2jk_{2j}l_{2j}} \right. \\
 &\quad \left. - \left( \sum_{c=1}^q w_{cj} p_{2scjk_{2j}l_{2j}}^r \right) \underline{C}_{2jk_{2j}l_{2j}} \right] x_{2jk_{2j}l_{2j}}^r \\
 Z_3 &= \sum_{r=1}^2 \sum_{j=1}^2 \sum_{k_{3j}=1}^2 \sum_{l_{3j}=1}^2 \left[ \left( \sum_{c=1}^q w_{cj} p_{3scjk_{3j}l_{3j}}^r \right) C_{3jk_{3j}l_{3j}} \right. \\
 &\quad \left. - \left( \sum_{c=1}^q w_{cj} p_{3scjk_{3j}l_{3j}}^r \right) \underline{C}_{3jk_{3j}l_{3j}} \right] x_{3jk_{3j}l_{3j}}^r \\
 Z_4 &= \sum_{r=1}^2 \sum_{j=1}^2 \sum_{k_{4j}=1}^2 \sum_{l_{4j}=1}^2 \left[ \left( \sum_{c=1}^q w_{cj} p_{4scjk_{4j}l_{4j}}^r \right) C_{4jk_{4j}l_{4j}} \right. \\
 &\quad \left. - \left( \sum_{c=1}^q w_{cj} p_{4scjk_{4j}l_{4j}}^r \right) \underline{C}_{4jk_{4j}l_{4j}} \right] x_{4jk_{4j}l_{4j}}^r
 \end{aligned} \right.$$

$$\begin{aligned}
 \text{s.t. } & \sum_{r=1}^2 \sum_{j=1}^2 \sum_{l_{0j}=1}^2 c_{0j1l_{0j}}^r x_{0j1l_{0j}}^r + \sum_{r=1}^2 \sum_{i=1}^4 \sum_{j=1}^2 \sum_{k_{ij}=1}^2 \sum_{l_{ij}=1}^2 c_{ijk_{ij}l_{ij}}^r x_{ijk_{ij}l_{ij}}^r \leq A \quad (\text{P2}) \\
 & \sum_{r=1}^2 \sum_{j=1}^2 \sum_{l_{0j}=1}^2 c_{0j1l_{0j}}^r x_{0j1l_{0j}}^r \geq vA \\
 & Z_0 \geq Z_0^*, Z_1 \geq Z_1^*, Z_2 \geq Z_2^*, Z_3 \geq Z_3^*, Z_4 \geq Z_4^* \\
 & \left. \begin{aligned} x_{0j1l_{0j}}^r &\geq t_{0j1l_{0j}}^r, x_{0j1l_{0j}}^r \leq u_{0j1l_{0j}}^r \\ x_{0j1l_{0j}}^r &\geq 0 \text{ and integers} \end{aligned} \right\} \forall r = 1, 2; j = 1, 2; l_{0j} = 1, 2 \\
 & \left. \begin{aligned} x_{ijk_{ij}l_{ij}}^r &\geq t_{ijk_{ij}l_{ij}}^r, x_{ijk_{ij}l_{ij}}^r \leq u_{ijk_{ij}l_{ij}}^r \\ x_{ijk_{ij}l_{ij}}^r &\geq 0 \text{ and integers} \end{aligned} \right\} \forall r = 1, 2; i = 1, 2, \dots, 4; \\
 & \hspace{15em} j = 1, 2; l_{ij} = 1, 2; k_{ij} = 1, 2
 \end{aligned}$$

Problem (P2) leads to an infeasible solution. GP approach has been used to obtain a feasible compromised solution to the problem.

### 4 Solution Methodology: GP

In a simpler version of GP, management sets goals and relative importance (weights) for different objectives. Then an optimal solution is defined as one that minimizes both positive and negative deviations from set goals simultaneously or minimizes the amount by which each goal can be violated. First, we solve the problem using rigid constraints only and then the goals of objectives are incorporated depending upon whether priorities or relative importance of different objectives are well defined or not. The problem (P2) can be solved in two stages as follows:

#### Stage 1

$$\begin{aligned}
 \text{Min } g_0(\eta, \rho, X) &= \rho_1 + \eta_2 + \sum_{r=1}^2 \sum_{j=1}^2 \sum_{l_{0j}=1}^2 \eta_{0j1l_{0j}}^r + \sum_{r=1}^2 \sum_{i=1}^4 \sum_{j=1}^2 \sum_{k_{ij}=1}^2 \sum_{l_{ij}=1}^2 \eta_{ijk_{ij}l_{ij}}^r \\
 &+ \sum_{r=1}^2 \sum_{j=1}^2 \sum_{l_{0j}=1}^2 \rho_{0j1l_{0j}}^r + \sum_{r=1}^2 \sum_{i=1}^4 \sum_{j=1}^2 \sum_{k_{ij}=1}^2 \sum_{l_{ij}=1}^2 \rho_{ijk_{ij}l_{ij}}^r \\
 \text{s.t. } & \sum_{r=1}^2 \sum_{j=1}^2 \sum_{l_{0j}=1}^2 c_{0j1l_{0j}}^r x_{0j1l_{0j}}^r + \sum_{r=1}^2 \sum_{i=1}^4 \sum_{j=1}^2 \sum_{k_{ij}=1}^2 \sum_{l_{ij}=1}^2 c_{ijk_{ij}l_{ij}}^r x_{ijk_{ij}l_{ij}}^r + \eta_1 - \rho_1 = A \\
 & \hspace{25em} (\text{P3})
 \end{aligned}$$

$$\begin{aligned}
 & \sum_{r=1}^2 \sum_{j=1}^2 \sum_{l_0j=1}^2 c_{0j1l_0j}^r x_{0j1l_0j}^r + \eta_2 - \rho_2 = vA \\
 & \left. \begin{aligned}
 x_{0j1l_0j}^r + \eta_{0j1l_0j}^r - \rho_{0j1l_0j}^r &= t_{0j1l_0j}^r, x_{0j1l_j} + \eta_{0j1l_0j}^r - \rho_{0j1l_0j}^r = u_{0j1l_j} \\
 x_{0j1l_0j}^r &\geq 0 \text{ and integers} \\
 \eta_{0j1l_0j}^r, \rho_{0j1l_0j}^r, \eta_{0j1l_0j}^r, \rho_{0j1l_0j}^r &\geq 0
 \end{aligned} \right\} \\
 & \qquad \qquad \qquad \forall r = 1, 2; j = 1, 2; l_0j = 1, 2 \\
 & \left. \begin{aligned}
 x_{ij^r k_{ij} l_{ij}} + \eta_{ij^r k_{ij} l_{ij}} - \rho_{ij^r k_{ij} l_{ij}} &= t_{ij^r k_{ij} l_{ij}}^r, x_{ij^r k_{ij} l_{ij}} + \eta_{ij^r k_{ij} l_{ij}}^r - \rho_{ij^r k_{ij} l_{ij}}^r = u_{ij^r k_{ij} l_{ij}}^r \\
 x_{ij^r k_{ij} l_{ij}} &\geq 0 \text{ and integers} \\
 \eta_{ij^r k_{ij} l_{ij}}^r, \rho_{ij^r k_{ij} l_{ij}}^r, \eta_{ij^r k_{ij} l_{ij}}^r, \rho_{ij^r k_{ij} l_{ij}}^r &\geq 0,
 \end{aligned} \right\} \\
 & \eta_1, \rho_1, \eta_2, \rho_2 \geq 0 \\
 & \qquad \qquad \qquad \forall r = 1, 2; j = 1, 2; l_{ij} = 1, 2; k_{ij} = 1, 2
 \end{aligned}$$

where  $\eta$  and  $\rho$  are the over and under achievement (positive and negative deviational) variables of the goals for their respective objective/constraint function.  $g_0(\eta, \rho, X)$  is the goal objective function corresponding to rigid constraints. Let  $(\eta^0, \rho^0, X^0)$  be the optimal solution for the problem (P3) and  $g_0(\eta^0, \rho^0, X^0)$  be the corresponding objective function value then final problem can be formulated using the optimal solution of the problem (P3) through the problem (P2).

**Stage 2**

$$\text{Min } g(\eta, \rho, X) = \lambda_0 \eta_0 + \sum_{i=1}^4 \lambda_{si} \eta_{si}$$

$$\text{s.t. } \sum_{r=1}^2 \sum_{j=1}^2 \sum_{l_0j=1}^2 c_{0j1l_0j}^r x_{0j1l_0j}^r + \sum_{r=1}^2 \sum_{i=1}^4 \sum_{j=1}^2 \sum_{k_{ij}=1}^2 \sum_{l_{ij}=1}^2 c_{ij^r k_{ij} l_{ij}}^r x_{ij^r k_{ij} l_{ij}}^r + \eta_1 - \rho_1 = A \tag{P4}$$

$$\begin{aligned}
 & \sum_{r=1}^2 \sum_{j=1}^2 \sum_{l_0j=1}^2 c_{0j1l_0j}^r x_{0j1l_0j}^r + \eta_2 - \rho_2 = vA \\
 & Z_0 + \eta_0 - \rho_0 = Z_0^*, Z_i + \eta_{si} - \rho_{si} = Z_i^* \quad \forall i = 1, 2, \dots, 4 \\
 & \left. \begin{aligned}
 x_{0j1l_0j}^r + \eta_{0j1l_0j}^r - \rho_{0j1l_0j}^r &= t_{0j1l_0j}^r, x_{0j1l_j} + \eta_{0j1l_0j}^r - \rho_{0j1l_0j}^r = u_{0j1l_j}^r \\
 x_{0j1l_0j}^r &\geq 0 \text{ and integers} \\
 \eta_{0j1l_0j}^r, \rho_{0j1l_0j}^r, \eta_{0j1l_0j}^r, \rho_{0j1l_0j}^r &\geq 0
 \end{aligned} \right\} \\
 & \qquad \qquad \qquad \forall r = 1, 2; j = 1, 2; l_0j = 1, 2
 \end{aligned}$$

$$\left. \begin{aligned} x_{ijk_{ij}l_{ij}}^r + \eta_{ijk_{ij}l_{ij}}^r - \rho_{ijk_{ij}l_{ij}}^r &= t_{ijk_{ij}l_{ij}}^r, x_{ijk_{ij}l_{ij}}^r + \eta_{ijk_{ij}l_{ij}}^r - \rho_{ijk_{ij}l_{ij}}^r = u_{ijk_{ij}l_{ij}}^r, \\ x_{ijk_{ij}l_{ij}}^r &\geq 0 \text{ and integers} \\ \eta_{ijk_{ij}l_{ij}}^r, \rho_{ijk_{ij}l_{ij}}^r, \eta_{ijk_{ij}l_{ij}}^{rr}, \rho_{ijk_{ij}l_{ij}}^{rr} &\geq 0, \end{aligned} \right\}$$

$$g_0(\eta, \rho, X) = g_0(\eta^0, \rho^0, X^0)$$

$$\forall r = 1, 2; i = 1, 2, \dots, 4; j = 1, 2; l_{ij} = 1, 2; k_{ij} = 1, 2$$

$$\eta_0, \rho_0, \eta_1, \rho_1, \eta_2, \rho_2 \geq 0$$

$$\eta_{si}, \rho_{si} \geq 0 \quad \forall i = 1, 2, \dots, 4$$

$g(\eta, \rho, X)$  is objective function of the problem (P3). Goal programming is used to find a compromise solution.

### 5 Case Problem

A company is considered which has to advertise its two types of consumable products, targeting middle income group people in its four selected regions. Advertisement is done in national as well as regional newspapers and television channels. The fixed budget available for advertising is ₹ 2,50,00,000. It is desired to allocate at least a minimum of 35 % of the total budget in national media. Data corresponding to circulation figures for newspapers, average number of viewers for TV channels, advertisement costs in various newspapers, and TV channels are given below in Tables 1, 2, 3, and 4, respectively. Readership profile and Viewership profile matrix based on random sample of size 200 is listed in Tables 5 and 6. Finally, the minimum and maximum number of advertisements in various Newspapers and Television

**Table 1** Circulation figure for Newspapers (‘10000)

NN	Region 1		Region 2		Region 3		Region 4									
	RNP1		RNP2		RNP1		RNP2									
	T	C	T	C	T	C	T	C								
180	52	17	45	15	36	12	25	6	42	15	41	13	34	13	32	9

**Table 2** Circulation figure for TV channels (‘100000)

NCH	Region 1				Region 2				Region 3				Region 4				
	RCH1		RCH2		RCH1		RCH2		RCH1		RCH2		RCH1		RCH2		
	T	C	T	C	T	C	T	C	T	C	T	C	T	C	T	C	
PT	600	110	40	100	30	140	60	130	40	110	40	130	50	120	50	150	70
OT	400	80	30	60	28	90	40	80	35	70	20	90	30	70	25	100	40

**Table 3** Advertisement cost (per 100 column cm) in Newspapers

		NN	Region 1		Region 2		Region 3		Region 4	
			RNP1	RNP2	RNP1	RNP2	RNP1	RNP2	RNP1	RNP2
P1	FP	1900	820	750	480	450	690	650	400	410
	OP	1300	550	400	225	200	400	380	220	210
P2	FP	1800	700	630	450	410	640	580	390	350
	OP	1100	460	350	210	200	340	320	175	170

**Table 4** Advertisement cost (per 10 seconds spot) in TV Channels (‘1000)

		NCH	Region 1		Region 2		Region 3		Region 4	
			RCH1	RCH2	RCH1	RCH2	RCH1	RCH2	RCH1	RCH2
P1	PT	120	36	32	41	40	37	39	37	45
	OT	80	16	17	20	18	18	20	14	20
P2	PT	108	33	29	37	36	34	36	34	41
	OT	72	15	16	18	17	17	18	13	18

**Table 5** Readership profile matrix for newspapers

		NN	Region 1				Region 2				Region 3				Region 4			
			RNP1		RNP2		RNP1		RNP2		RNP1		RNP2		RNP1		RNP2	
			T	C	T	C	T	C	T	C	T	C	T	C	T	C	T	C
P1	FP	0.52	0.49	0.27	0.45	0.22	0.5	0.28	0.45	0.2	0.46	0.21	0.44	0.22	.46	0.22	0.43	0.16
	OP	0.34	0.33	0.2	0.31	0.14	0.33	0.21	0.32	0.13	0.33	0.16	0.33	0.16	0.34	0.14	0.29	0.1
P2	FP	0.45	0.46	0.23	0.42	0.21	0.45	0.23	0.42	0.14	0.43	0.19	0.4	0.2	0.44	0.21	0.41	0.19
	OP	0.28	0.3	0.14	0.26	0.15	0.3	0.16	0.26	0.1	0.26	0.13	0.25	0.12	0.28	0.16	0.22	0.13

**Table 6** Viewership profile matrix for television

		NCH	Region 1				Region 2				Region 3				Region 4			
			RCH1		RCH2		RCH1		RCH2		RCH1		RCH2		RCH1		RCH2	
			T	C	T	C	T	C	T	C	T	C	T	C	T	C	T	C
P1	PT	0.56	0.48	0.28	0.45	0.25	0.47	0.23	0.5	0.21	0.49	0.25	0.43	0.2	0.44	0.23	0.52	0.29
	OT	0.35	0.32	0.16	0.29	0.15	0.31	0.14	0.34	0.15	0.33	0.17	0.29	0.14	0.29	0.16	0.35	0.2
P2	PT	0.42	0.47	0.29	0.43	0.27	0.45	0.22	0.45	0.2	0.42	0.2	0.54	0.3	0.45	0.21	0.4	0.19
	OT	0.33	0.37	0.23	0.35	0.2	0.33	0.15	0.36	0.15	0.31	0.16	0.22	0.13	0.3	0.17	0.22	0.1

Channels and the spectrum effect of national media on different regional segments are given in Tables 7, 8, and 9, respectively.

Using the above given data we solve (P1) with each objective subject to constraints individually. The optimal values so obtained for each objective is then set as aspiration level to be achieved for reach corresponding to national media and each of the four segment’s regional media. The multi-objective programming problem combining all the objectives and incorporating the individual aspirations obtained can be written as:

**Table 7** Minimum and maximum number of advertisements in various Newspapers

		NN	Region 1		Region 2		Region 3		Region 4	
			RNP1	RNP2	RNP1	RNP2	RNP1	RNP2	RNP1	RNP2
P1	FP	[12,20]	[10,16]	[7,12]	[6,15]	[4,12]	[7,15]	[6,15]	[6,12]	[4,15]
	OP	[7,12]	[4,12]	[3,7]	[6,12]	[6,9]	[5,14]	[4,12]	[4,6]	[2,6]
P2	FP	[10,16]	[12,15]	[9,12]	[7,15]	[6,12]	[7,15]	[6,16]	[3,12]	[3,15]
	OP	[7,12]	[7,12]	[3,9]	[3,12]	[3,7]	[7,14]	[3,12]	[3,7]	[2,7]

**Table 8** Minimum and maximum advertisement in various TV channels

		NCH	Region 1		Region 2		Region 3		Region 4	
			RCH1	RCH2	RCH1	RCH2	RCH1	RCH2	RCH1	RCH2
P1	PT	[3,12]	[2,8]	[1,6]	[1,9]	[1,5]	[3,8]	[2,10]	[1,8]	[2,6]
	OT	[1,6]	[2,4]	[1,3]	[1,4]	[0,2]	[2,6]	[1,5]	[0,3]	[1,4]
P2	PT	[2,10]	[2,12]	[1,3]	[2,9]	[2,5]	[1,8]	[1,7]	[1,6]	[1,6]
	OT	[1,7]	[3,7]	[1,6]	[2,7]	[0,4]	[2,5]	[0,5]	[0,4]	[0,4]

**Table 9** Spectrum effect of national media on different regional segments

	Region 1	Region 2	Region 3	Region 4
National Newspaper	0.27	0.21	0.25	0.22
National Channel	0.21	0.26	0.23	0.27

$$\begin{aligned}
 & \left[ \begin{aligned}
 Z_0 &= \{0.95(936000x_{0111}^1 + 612000x_{0112}^1 + 810000x_{0111}^2 + 504000x_{0112}^2) \\
 &\quad + 0.97(3360000x_{0211}^1 + 1400000x_{0212}^1 + 2520000x_{0211}^2 + 1320000x_{0212}^2)\} \\
 Z_1 &= \{208900x_{1111}^1 + 137600x_{1112}^1 + 169500x_{1121}^1 + 118500x_{1122}^1 \\
 &\quad + 416000x_{1211}^1 + 208000x_{1212}^1 + 375000x_{1221}^1 + 132000x_{1222}^1 \\
 &\quad + 200100x_{1111}^2 + 132200x_{1112}^2 + 157500x_{1121}^2 + 94500x_{1122}^2 \\
 &\quad + 401000x_{1211}^2 + 227000x_{1212}^2 + 349000x_{1221}^2 + 154000x_{1222}^2\} \\
 Z_2 &= \{146400x_{2111}^1 + 93600x_{2112}^1 + 100500x_{2121}^1 + 72200x_{2122}^1 \\
 &\quad + 520000x_{2211}^1 + 223000x_{2212}^1 + 566000x_{2221}^1 + 219500x_{2222}^1 \\
 &\quad + 134400x_{2111}^2 + 88800x_{2112}^2 + 96600x_{2121}^2 + 59000x_{2122}^2 + 498000x_{2211}^2 \\
 &\quad + 237000x_{2212}^2 + 505000x_{2221}^2 + 235500x_{2222}^2\} \\
 Z_3 &= \{161700x_{3111}^1 + 114600x_{3112}^1 + 151800x_{3121}^1 + 114500x_{3122}^1 \\
 &\quad + 439000x_{3211}^1 + 197000x_{3212}^1 + 459000x_{3221}^1 + 219000x_{3222}^1 \\
 &\quad + 152100x_{3111}^2 + 89700x_{3112}^2 + 138000x_{3121}^2 + 86900x_{3122}^2 + 382000x_{3211}^2 \\
 &\quad + 185000x_{3212}^2 + 552000x_{3221}^2 + 159000x_{3222}^2\} \\
 Z_4 &= \{127800x_{4111}^1 + 97400x_{4112}^1 + 123200x_{4121}^1 + 83800x_{4122}^1 \\
 &\quad + 413000x_{4211}^1 + 163000x_{4212}^1 + 577000x_{4221}^1 + 270000x_{4222}^1 \\
 &\quad + 122300x_{4111}^2 + 74400x_{4112}^2 + 114100x_{4121}^2 + 58700x_{4122}^2 + 435000x_{4211}^2 \\
 &\quad + 167500x_{4212}^2 + 467000x_{4221}^2 + 180000x_{4222}^2\}
 \end{aligned} \right]
 \end{aligned}$$

Max

$$\begin{aligned}
& \text{s.t. } 1900x_{0111}^1 + 1300x_{0112}^1 + 120000x_{0211}^1 + 80000x_{0212}^1 + 820x_{1111}^1 + 550x_{1112}^1 \\
& + 750x_{1121}^1 + 400x_{1122}^1 + 36000x_{1211}^1 + 16000x_{1212}^1 + 32000x_{1221}^1 \\
& + 17000x_{1222}^1 + 480x_{2111}^1 + 225x_{2112}^1 + 450x_{2121}^1 + 200x_{2122}^1 + 41000x_{2211}^1 \\
& + 20000x_{2212}^1 + 40000x_{2221}^1 + 18000x_{2222}^1 + 690x_{3111}^1 + 400x_{3112}^1 + 650x_{3121}^1 \\
& + 380x_{3122}^1 + 37000x_{3211}^1 + 18000x_{3212}^1 + 39000x_{3221}^1 + 20000x_{3222}^1 \\
& + 400x_{4111}^1 + 220x_{4112}^1 + 410x_{4121}^1 + 210x_{4122}^1 + 37000x_{4211}^1 + 14000x_{4212}^1 \\
& + 45000x_{4221}^1 + 20000x_{4222}^1 + 1800x_{0111}^2 + 1100x_{0112}^2 + 108000x_{0211}^2 \\
& + 72000x_{0212}^2 + 700x_{1111}^2 + 460x_{1112}^2 + 630x_{1121}^2 + 350x_{1122}^2 + 33000x_{1211}^2 \\
& + 15000x_{1212}^2 + 29000x_{1221}^2 + 16000x_{1222}^2 + 450x_{2111}^2 + 210x_{2112}^2 + 410x_{2121}^2 \\
& + 200x_{2122}^2 + 37000x_{2211}^2 + 18000x_{2212}^2 + 36000x_{2221}^2 + 17000x_{2222}^2 \\
& + 640x_{3111}^2 + 340x_{3112}^2 + 580x_{3121}^2 + 320x_{3122}^2 + 34000x_{3211}^2 + 17000x_{3212}^2 \\
& + 36000x_{3221}^2 + 18000x_{3222}^2 + 390x_{4111}^2 + 175x_{4112}^2 + 350x_{4121}^2 + 170x_{4122}^2 \\
& + 34000x_{4211}^2 + 13000x_{4212}^2 + 41000x_{4221}^2 + 18000x_{4222}^2 \leq 25000000 \\
& 1900x_{0111}^1 + 1300x_{0112}^1 + 120000x_{0211}^1 + 80000x_{0212}^1 + 1800x_{0111}^2 + 1100x_{0112}^2 \\
& + 108000x_{0211}^2 + 72000x_{0212}^2 \geq .35 \times 25000000 \\
& Z_0 \geq 71181200, Z_1 \geq 23458500, Z_2 \geq 18629800, Z_3 \geq 23455000, \\
& Z_4 \geq 15999600 \\
& x_{0111}^1 \geq 12, x_{0112}^1 \geq 7, x_{0211}^1 \geq 3, x_{0212}^1 \geq 1, x_{1111}^1 \geq 10, x_{1112}^1 \geq 4, x_{1121}^1 \geq 7, \\
& x_{1122}^1 \geq 3, x_{1211}^1 \geq 2, x_{1212}^1 \geq 2, x_{1221}^1 \geq 1, \\
& x_{1222}^1 \geq 1, x_{2111}^1 \geq 6, x_{2112}^1 \geq 6, x_{2121}^1 \geq 4, x_{2122}^1 \geq 6, x_{2211}^1 \geq 1, x_{2212}^1 \geq 1, \\
& x_{2221}^1 \geq 1, x_{2222}^1 \geq 0, x_{3111}^1 \geq 7, x_{3112}^1 \geq 5, \\
& x_{3121}^1 \geq 6, x_{3122}^1 \geq 4, x_{3211}^1 \geq 3, x_{3212}^1 \geq 2, x_{3221}^1 \geq 2, x_{3222}^1 \geq 1, x_{4111}^1 \geq 6, \\
& x_{4112}^1 \geq 4, x_{4121}^1 \geq 4, x_{4122}^1 \geq 2, x_{4211}^1 \geq 1, \\
& x_{4212}^1 \geq 0, x_{4221}^1 \geq 2, x_{4222}^1 \geq 1, x_{0111}^2 \geq 10, x_{0112}^2 \geq 7, x_{0211}^2 \geq 2, x_{0212}^2 \geq 1, \\
& x_{1111}^2 \geq 12, x_{1112}^2 \geq 7, x_{1121}^2 \geq 9, x_{1122}^2 \geq 3, \\
& x_{1211}^2 \geq 2, x_{1212}^2 \geq 3, x_{1221}^2 \geq 1, x_{1222}^2 \geq 1, x_{2111}^2 \geq 7, x_{2112}^2 \geq 3, x_{2121}^2 \geq 6, \\
& x_{2122}^2 \geq 3, x_{2211}^2 \geq 2, x_{2212}^2 \geq 2, x_{2221}^2 \geq 2, \\
& x_{2222}^2 \geq 0, x_{3111}^2 \geq 7, x_{3112}^2 \geq 7, x_{3121}^2 \geq 6, x_{3122}^2 \geq 3, x_{3211}^2 \geq 1, x_{3212}^2 \geq 2, \\
& x_{3221}^2 \geq 1, x_{3222}^2 \geq 0, x_{4111}^2 \geq 3, x_{4112}^2 \geq 3, \\
& x_{4121}^2 \geq 3, x_{4122}^2 \geq 2, x_{4211}^2 \geq 1, x_{4212}^2 \geq 0, x_{4221}^2 \geq 1, x_{4222}^2 \geq 0, x_{0111}^1 \leq 20, \\
& x_{0112}^1 \leq 12, x_{0211}^1 \leq 12, x_{0212}^1 \leq 6, \\
& x_{1111}^1 \leq 16, x_{1112}^1 \leq 12, x_{1121}^1 \leq 12, x_{1122}^1 \leq 7, x_{1211}^1 \leq 8, x_{1212}^1 \leq 4, x_{1221}^1 \leq 6, \\
& x_{1222}^1 \leq 3, x_{2111}^1 \leq 15, x_{2112}^1 \leq 12,
\end{aligned}$$



$$\begin{aligned}
 &x_{2121}^1 \leq 12, x_{2122}^1 \leq 9, x_{2211}^1 \leq 9, x_{2212}^1 \leq 4, x_{2221}^1 \leq 5, x_{2222}^1 \leq 2, x_{3111}^1 \leq 15, \\
 &x_{3112}^1 \leq 14, x_{3121}^1 \leq 15, x_{3122}^1 \leq 12, \\
 &x_{3211}^1 \leq 8, x_{3212}^1 \leq 6, x_{3221}^1 \leq 10, x_{3222}^1 \leq 5, x_{4111}^1 \leq 12, x_{4112}^1 \leq 6, x_{4121}^1 \leq 15, \\
 &x_{4122}^1 \leq 6, x_{4211}^1 \leq 8, x_{4212}^1 \leq 3, \\
 &x_{4221}^1 \leq 6, x_{4222}^1 \leq 4, x_{0111}^2 \leq 16, x_{0112}^2 \leq 12, x_{0211}^2 \leq 10, x_{0212}^2 \leq 7, x_{1111}^2 \leq 15, \\
 &x_{1112}^2 \leq 12, x_{1121}^2 \leq 12, x_{1122}^2 \leq 9, \\
 &x_{1211}^2 \leq 12, x_{1212}^2 \leq 7, x_{1221}^2 \leq 3, x_{1222}^2 \leq 6, x_{2111}^2 \leq 15, x_{2112}^2 \leq 12, x_{2121}^2 \leq 12, \\
 &x_{2122}^2 \leq 7, x_{2211}^2 \leq 9, x_{2212}^2 \leq 7, \\
 &x_{2221}^2 \leq 5, x_{2222}^2 \leq 4, x_{3111}^2 \leq 15, x_{3112}^2 \leq 14, x_{3121}^2 \leq 16, x_{3122}^2 \leq 12, x_{3211}^2 \leq 8, \\
 &x_{3212}^2 \leq 5, x_{3221}^2 \leq 7, x_{3222}^2 \leq 5, \\
 &x_{4111}^2 \leq 12, x_{4112}^2 \leq 7, x_{4121}^2 \leq 15, x_{4122}^2 \leq 7, x_{4211}^2 \leq 6, x_{4212}^2 \leq 4, x_{4221}^2 \leq 6, \\
 &x_{4222}^2 \leq 4 \\
 &x_{0j1l_0j}^r \geq 0 \text{ and integers } \forall r = 1, 2; j = 1, 2; l_0j = 1, 2 \\
 &x_{ijk_l ij}^r \geq 0 \text{ and integers } \forall r = 1, 2; i = 1, 2, \dots, 4; j = 1, 2; l_{ij} = 1, 2; k_{ij} = 1, 2
 \end{aligned}$$

This problem gives an infeasible solution when solved mathematically. Hence GP technique is used to obtain a compromised solution to the problem.

### 5.1 Solution Procedure: GP

#### Stage 1

$$\begin{aligned}
 \text{go } (\eta, \rho, X) = &\rho_1 + \rho_2 + \eta_{0111}^1 + \eta_{0112}^1 + \eta_{0211}^1 + \eta_{0212}^1 + \eta_{0111}^2 + \eta_{0112}^2 \\
 &+ \eta_{0211}^2 + \eta_{0212}^2 + \eta_{1111}^1 + \eta_{1112}^1 + \eta_{1121}^1 + \eta_{1122}^1 + \eta_{1211}^1 + \eta_{1212}^1 + \eta_{1221}^1 + \eta_{1222}^1 \\
 &+ \eta_{1221}^2 + \eta_{1222}^2 + \eta_{2111}^1 + \eta_{2112}^1 + \eta_{2121}^1 + \eta_{2122}^1 + \eta_{2211}^1 + \eta_{2212}^1 + \eta_{2221}^1 + \eta_{2222}^1 + \eta_{2211}^2 \\
 &+ \eta_{2212}^2 + \eta_{2221}^2 + \eta_{2222}^2 + \eta_{3111}^1 + \eta_{3112}^1 \\
 &+ \eta_{3121}^1 + \eta_{3122}^1 + \eta_{3211}^1 + \eta_{3212}^1 + \eta_{3221}^1 + \eta_{3222}^1 + \eta_{3111}^2 + \eta_{3112}^2 \\
 \text{Min } &+ \eta_{3121}^2 + \eta_{3122}^2 + \eta_{3211}^2 + \eta_{3212}^2 + \eta_{3221}^2 + \eta_{3222}^2 + \eta_{4111}^1 + \eta_{4112}^1 \\
 &+ \eta_{4121}^1 + \eta_{4122}^1 + \eta_{4211}^1 + \eta_{4212}^1 + \eta_{4221}^1 + \eta_{4222}^1 + \eta_{4111}^2 \\
 &+ \eta_{4112}^2 + \eta_{4121}^2 + \eta_{4122}^2 + \eta_{4211}^2 + \eta_{4212}^2 + \eta_{4221}^2 + \eta_{4222}^2 + \rho_{0111}^1 \\
 &+ \rho_{0112}^1 + \rho_{0211}^1 + \rho_{0212}^1 + \rho_{0111}^2 + \rho_{0112}^2 + \rho_{0211}^2 + \rho_{0212}^2 + \rho_{1111}^1 \\
 &+ \rho_{1112}^1 + \rho_{1121}^1 + \rho_{1122}^1 + \rho_{1211}^1 + \rho_{1212}^1 + \rho_{1221}^1 + \rho_{1222}^1 + \rho_{1111}^2 \\
 &+ \rho_{1112}^2 + \rho_{1121}^2 + \rho_{1122}^2 + \rho_{1211}^2 + \rho_{1212}^2 + \rho_{1221}^2 \\
 &+ \rho_{1222}^2 + \rho_{2111}^1 + \rho_{2112}^1 + \rho_{2121}^1 + \rho_{2122}^1 + \rho_{2211}^1 + \rho_{2212}^1
 \end{aligned}$$

$$\begin{aligned}
 &+ \rho_{2221}^1 + \rho_{2222}^1 + \rho_{2111}^2 + \rho_{2112}^2 + \rho_{2121}^2 + \rho_{2122}^2 + \rho_{2211}^2 + \rho_{2212}^2 + \rho_{2221}^2 \\
 &+ \rho_{2222}^2 + \rho_{3111}^1 + \rho_{3112}^1 + \rho_{3121}^1 + \rho_{3122}^1 + \rho_{3211}^1 + \rho_{3212}^1 + \rho_{3221}^1 \\
 &+ \rho_{3222}^1 + \rho_{3111}^2 + \rho_{3112}^2 + \rho_{3121}^2 + \rho_{3122}^2 + \rho_{3211}^2 + \rho_{3212}^2 + \rho_{3221}^2 \\
 &+ \rho_{3222}^2 + \rho_{4111}^1 + \rho_{4112}^1 + \rho_{4121}^1 + \rho_{4122}^1 + \rho_{4211}^1 + \rho_{4212}^1 + \rho_{4221}^1 \\
 &+ \rho_{4222}^1 + \rho_{4111}^2 + \rho_{4112}^2 + \rho_{4121}^2 + \rho_{4122}^2 + \rho_{4211}^2 + \rho_{4212}^2 + \rho_{4221}^2 + \rho_{4222}^2
 \end{aligned}$$

**s.t.**  $1900x_{0111}^1 + 1300x_{0112}^1 + 120000x_{0211}^1 + 80000x_{0212}^1 + 1800x_{0111}^2$   
 $+ 1100x_{0112}^2 + 108000x_{0211}^2 + 72000x_{0212}^2 + \eta_2 - \rho_2 = 0.35 \times 25000000$

$$\begin{aligned}
 x_{0111}^1 + \eta_{0111}^1 - \rho_{0111}^1 &= 12, x_{0112}^1 + \eta_{0112}^1 - \rho_{0112}^1 = 7, \\
 x_{0211}^1 + \eta_{0211}^1 - \rho_{0211}^1 &= 3, x_{0212}^1 + \eta_{0212}^1 - \rho_{0212}^1 = 1, \\
 x_{1111}^1 + \eta_{1111}^1 - \rho_{1111}^1 &= 10, x_{1112}^1 + \eta_{1112}^1 - \rho_{1112}^1 = 4, \\
 x_{1121}^1 + \eta_{1121}^1 - \rho_{1121}^1 &= 7, x_{1122}^1 + \eta_{1122}^1 - \rho_{1122}^1 = 3, \\
 x_{1211}^1 + \eta_{1211}^1 - \rho_{1211}^1 &= 2, x_{1212}^1 + \eta_{1212}^1 - \rho_{1212}^1 = 2, \\
 x_{1221}^1 + \eta_{1221}^1 - \rho_{1221}^1 &= 1, x_{1222}^1 + \eta_{1222}^1 - \rho_{1222}^1 = 1, \\
 x_{2111}^1 + \eta_{2111}^1 - \rho_{2111}^1 &= 6, x_{2112}^1 + \eta_{2112}^1 - \rho_{2112}^1 = 6, \\
 x_{2121}^1 + \eta_{2121}^1 - \rho_{2121}^1 &= 4, x_{2122}^1 + \eta_{2122}^1 - \rho_{2122}^1 = 6, \\
 x_{2211}^1 + \eta_{2211}^1 - \rho_{2211}^1 &= 1, x_{2212}^1 + \eta_{2212}^1 - \rho_{2212}^1 = 1, \\
 x_{2221}^1 + \eta_{2221}^1 - \rho_{2221}^1 &= 1, x_{2222}^1 + \eta_{2222}^1 - \rho_{2222}^1 = 0, \\
 x_{3111}^1 + \eta_{3111}^1 - \rho_{3111}^1 &= 7, x_{3112}^1 + \eta_{3112}^1 - \rho_{3112}^1 = 5, \\
 x_{3121}^1 + \eta_{3121}^1 - \rho_{3121}^1 &= 6, x_{3122}^1 + \eta_{3122}^1 - \rho_{3122}^1 = 4, \\
 x_{3211}^1 + \eta_{3211}^1 - \rho_{3211}^1 &= 3, x_{3212}^1 + \eta_{3212}^1 - \rho_{3212}^1 = 2, \\
 x_{3221}^1 + \eta_{3221}^1 - \rho_{3221}^1 &= 2, x_{3222}^1 + \eta_{3222}^1 - \rho_{3222}^1 = 1, \\
 x_{4111}^1 + \eta_{4111}^1 - \rho_{4111}^1 &= 6, x_{4112}^1 + \eta_{4112}^1 - \rho_{4112}^1 = 4, \\
 x_{4121}^1 + \eta_{4121}^1 - \rho_{4121}^1 &= 4, x_{4122}^1 + \eta_{4122}^1 - \rho_{4122}^1 = 2, \\
 x_{4211}^1 + \eta_{4211}^1 - \rho_{4211}^1 &= 1, x_{4212}^1 + \eta_{4212}^1 - \rho_{4212}^1 = 0, \\
 x_{4221}^1 + \eta_{4221}^1 - \rho_{4221}^1 &= 2, x_{4222}^1 + \eta_{4222}^1 - \rho_{4222}^1 = 1, \\
 x_{0111}^2 + \eta_{0111}^2 - \rho_{0111}^2 &= 10, x_{0112}^2 + \eta_{0112}^2 - \rho_{0112}^2 = 7, \\
 x_{0211}^2 + \eta_{0211}^2 - \rho_{0211}^2 &= 2, x_{0212}^2 + \eta_{0212}^2 - \rho_{0212}^2 = 1, \\
 x_{1111}^2 + \eta_{1111}^2 - \rho_{1111}^2 &= 12, x_{1112}^2 + \eta_{1112}^2 - \rho_{1112}^2 = 7, \\
 x_{1121}^2 + \eta_{1121}^2 - \rho_{1121}^2 &= 9, x_{1122}^2 + \eta_{1122}^2 - \rho_{1122}^2 = 3, \\
 x_{1211}^2 + \eta_{1211}^2 - \rho_{1211}^2 &= 2, x_{1212}^2 + \eta_{1212}^2 - \rho_{1212}^2 = 3, \\
 x_{1221}^2 + \eta_{1221}^2 - \rho_{1221}^2 &= 1, x_{1222}^2 + \eta_{1222}^2 - \rho_{1222}^2 = 1, \\
 x_{2111}^2 + \eta_{2111}^2 - \rho_{2111}^2 &= 7, x_{2112}^2 + \eta_{2112}^2 - \rho_{2112}^2 = 3, \\
 x_{2121}^2 + \eta_{2121}^2 - \rho_{2121}^2 &= 6, x_{2122}^2 + \eta_{2122}^2 - \rho_{2122}^2 = 3, \\
 x_{2211}^2 + \eta_{2211}^2 - \rho_{2211}^2 &= 2, x_{2212}^2 + \eta_{2212}^2 - \rho_{2212}^2 = 2,
 \end{aligned}$$

$$\begin{aligned}
 x_{2221}^2 + \eta_{2221}^2 - \rho_{2221}^2 &= 2, x_{2222}^2 + \eta_{2222}^2 - \rho_{2222}^2 = 0, \\
 x_{3111}^2 + \eta_{3111}^2 - \rho_{3111}^2 &= 7, x_{3112}^2 + \eta_{3112}^2 - \rho_{3112}^2 = 7, \\
 x_{3121}^2 + \eta_{3121}^2 - \rho_{3121}^2 &= 6, x_{3122}^2 + \eta_{3122}^2 - \rho_{3122}^2 = 3, \\
 x_{3211}^2 + \eta_{3211}^2 - \rho_{3211}^2 &= 1, x_{3212}^2 + \eta_{3212}^2 - \rho_{3212}^2 = 2, \\
 x_{3221}^2 + \eta_{3221}^2 - \rho_{3221}^2 &= 1, x_{3222}^2 + \eta_{3222}^2 - \rho_{3222}^2 = 0, \\
 x_{4111}^2 + \eta_{4111}^2 - \rho_{4111}^2 &= 3, x_{4112}^2 + \eta_{4112}^2 - \rho_{4112}^2 = 3, \\
 x_{4121}^2 + \eta_{4121}^2 - \rho_{4121}^2 &= 3, x_{4122}^2 + \eta_{4122}^2 - \rho_{4122}^2 = 2, \\
 x_{4211}^2 + \eta_{4211}^2 - \rho_{4211}^2 &= 1, x_{4212}^2 + \eta_{4212}^2 - \rho_{4212}^2 = 0, \\
 x_{4221}^2 + \eta_{4221}^2 - \rho_{4221}^2 &= 1, x_{4222}^2 + \eta_{4222}^2 - \rho_{4222}^2 = 0, \\
 x_{0111}^1 + \eta_{0111}^1 - \rho_{0111}^1 &= 20, x_{0112}^1 + \eta_{0112}^1 - \rho_{0112}^1 = 12, \\
 x_{0211}^1 + \eta_{0211}^1 - \rho_{0211}^1 &= 12, x_{0212}^1 + \eta_{0212}^1 - \rho_{0212}^1 = 6, \\
 x_{1111}^1 + \eta_{1111}^1 - \rho_{1111}^1 &= 16, x_{1112}^1 + \eta_{1112}^1 - \rho_{1112}^1 = 12, \\
 x_{1121}^1 + \eta_{1121}^1 - \rho_{1121}^1 &= 12, x_{1122}^1 + \eta_{1122}^1 - \rho_{1122}^1 = 7, \\
 x_{1211}^1 + \eta_{1211}^1 - \rho_{1211}^1 &= 8, x_{1212}^1 + \eta_{1212}^1 - \rho_{1212}^1 = 4, \\
 x_{1221}^1 + \eta_{1221}^1 - \rho_{1221}^1 &= 6, x_{1222}^1 + \eta_{1222}^1 - \rho_{1222}^1 = 3, \\
 x_{2111}^1 + \eta_{2111}^1 - \rho_{2111}^1 &= 15, x_{2112}^1 + \eta_{2112}^1 - \rho_{2112}^1 = 12, \\
 x_{2121}^1 + \eta_{2121}^1 - \rho_{2121}^1 &= 12, x_{2122}^1 + \eta_{2122}^1 - \rho_{2122}^1 = 9, \\
 x_{2211}^1 + \eta_{2211}^1 - \rho_{2211}^1 &= 9, x_{2212}^1 + \eta_{2212}^1 - \rho_{2212}^1 = 4, \\
 x_{2221}^1 + \eta_{2221}^1 - \rho_{2221}^1 &= 5, x_{2222}^1 + \eta_{2222}^1 - \rho_{2222}^1 = 2, \\
 x_{3111}^1 + \eta_{3111}^1 - \rho_{3111}^1 &= 15, x_{3112}^1 + \eta_{3112}^1 - \rho_{3112}^1 = 14, \\
 x_{3121}^1 + \eta_{3121}^1 - \rho_{3121}^1 &= 15, x_{3122}^1 + \eta_{3122}^1 - \rho_{3122}^1 = 12, \\
 x_{3211}^1 + \eta_{3211}^1 - \rho_{3211}^1 &= 8, x_{3212}^1 + \eta_{3212}^1 - \rho_{3212}^1 = 6, \\
 x_{3221}^1 + \eta_{3221}^1 - \rho_{3221}^1 &= 10, x_{3222}^1 + \eta_{3222}^1 - \rho_{3222}^1 = 5, \\
 x_{4111}^1 + \eta_{4111}^1 - \rho_{4111}^1 &= 12, x_{4112}^1 + \eta_{4112}^1 - \rho_{4112}^1 = 6, \\
 x_{4121}^1 + \eta_{4121}^1 - \rho_{4121}^1 &= 15, x_{4122}^1 + \eta_{4122}^1 - \rho_{4122}^1 = 6, \\
 x_{4211}^1 + \eta_{4211}^1 - \rho_{4211}^1 &= 8, x_{4212}^1 + \eta_{4212}^1 - \rho_{4212}^1 = 3, \\
 x_{4221}^1 + \eta_{4221}^1 - \rho_{4221}^1 &= 6, x_{4222}^1 + \eta_{4222}^1 - \rho_{4222}^1 = 4, \\
 x_{0111}^2 + \eta_{0111}^2 - \rho_{0111}^2 &= 16, x_{0112}^2 + \eta_{0112}^2 - \rho_{0112}^2 = 12, \\
 x_{0211}^2 + \eta_{0211}^2 - \rho_{0211}^2 &= 10, x_{0212}^2 + \eta_{0212}^2 - \rho_{0212}^2 = 7, \\
 x_{1111}^2 + \eta_{1111}^2 - \rho_{1111}^2 &= 15, x_{1112}^2 + \eta_{1112}^2 - \rho_{1112}^2 = 12, \\
 x_{1121}^2 + \eta_{1121}^2 - \rho_{1121}^2 &= 12, x_{1122}^2 + \eta_{1122}^2 - \rho_{1122}^2 = 9, \\
 x_{1211}^2 + \eta_{1211}^2 - \rho_{1211}^2 &= 12, x_{1212}^2 + \eta_{1212}^2 - \rho_{1212}^2 = 7, \\
 x_{1221}^2 + \eta_{1221}^2 - \rho_{1221}^2 &= 3, x_{1222}^2 + \eta_{1222}^2 - \rho_{1222}^2 = 6, \\
 x_{2111}^2 + \eta_{2111}^2 - \rho_{2111}^2 &= 15, x_{2112}^2 + \eta_{2112}^2 - \rho_{2112}^2 = 12,
 \end{aligned}$$

$$\begin{aligned}
 x_{2121}^2 + \eta_{2121}^2 - \rho_{2121}^2 &= 12, x_{2122}^2 + \eta_{2122}^2 - \rho_{2122}^2 = 7, \\
 x_{2211}^2 + \eta_{2211}^2 - \rho_{2211}^2 &= 9, x_{2212}^2 + \eta_{2212}^2 - \rho_{2212}^2 = 7, \\
 x_{2221}^2 + \eta_{2221}^2 - \rho_{2221}^2 &= 5, x_{2222}^2 + \eta_{2222}^2 - \rho_{2222}^2 = 4, \\
 x_{3111}^2 + \eta_{3111}^2 - \rho_{3111}^2 &= 15, x_{3112}^2 + \eta_{3112}^2 - \rho_{3112}^2 = 14, \\
 x_{3121}^2 + \eta_{3121}^2 - \rho_{3121}^2 &= 16, x_{3122}^2 + \eta_{3122}^2 - \rho_{3122}^2 = 12, \\
 x_{3211}^2 + \eta_{3211}^2 - \rho_{3211}^2 &= 8, x_{3212}^2 + \eta_{3212}^2 - \rho_{3212}^2 = 5, \\
 x_{3221}^2 + \eta_{3221}^2 - \rho_{3221}^2 &= 7, x_{3222}^2 + \eta_{3222}^2 - \rho_{3222}^2 = 5, \\
 x_{4111}^2 + \eta_{4111}^2 - \rho_{4111}^2 &= 12, x_{4112}^2 + \eta_{4112}^2 - \rho_{4112}^2 = 7, \\
 x_{4121}^2 + \eta_{4121}^2 - \rho_{4121}^2 &= 15, x_{4122}^2 + \eta_{4122}^2 - \rho_{4122}^2 = 7, \\
 x_{4211}^2 + \eta_{4211}^2 - \rho_{4211}^2 &= 6, x_{4212}^2 + \eta_{4212}^2 - \rho_{4212}^2 = 4, \\
 x_{4221}^2 + \eta_{4221}^2 - \rho_{4221}^2 &= 6, x_{4222}^2 + \eta_{4222}^2 - \rho_{4222}^2 = 4,
 \end{aligned}$$

$$\left. \begin{aligned}
 x_{0j1l_{0j}}^r &\geq 0 \text{ and integers} \\
 \eta_{0j1l_{0j}}^r, \rho_{0j1l_{0j}}^r, \eta_{0j1l_{0j}}^r, \rho_{0j1l_{0j}}^r &\geq 0
 \end{aligned} \right\} \forall r = 1, 2; j = 1, 2; l_{0j} = 1, 2 \quad (*)$$

$$\left. \begin{aligned}
 x_{ijk_{ij}l_{ij}}^r &\geq 0 \text{ and integers} \\
 \eta_{ijk_{ij}l_{ij}}^r, \rho_{ijk_{ij}l_{ij}}^r, \eta_{ijk_{ij}l_{ij}}^r, \rho_{ijk_{ij}l_{ij}}^r &\geq 0,
 \end{aligned} \right\} \forall r = 1, 2; j = 1, 2; l_{ij} = 1, 2; k_{ij} = 1, 2$$

$$\eta_1, \rho_1, \eta_2, \rho_2 \geq 0$$

**Stage 2**

$$\text{Ming}(\eta, \rho, X) = \lambda_0 \eta_0 + \lambda_{s1} \eta_{s1} + \lambda_{s2} \eta_{s2} + \lambda_{s3} \eta_{s3} + \lambda_{s4} \eta_{s4}$$

$$\text{s.t. } Z_0 + \eta_0 - \rho_0 = 71181200, Z_1 + \eta_{s1} - \rho_{s1} = 23458500,$$

$$Z_2 + \eta_{s2} - \rho_{s2} = 18629800,$$

$$Z_3 + \eta_{s3} - \rho_{s3} = 23455000, Z_4 + \eta_{s4} - \rho_{s4} = 15999600$$

$$\eta_0, \eta_{s1}, \eta_{s2}, \eta_{s3}, \eta_{s4}, \rho_0, \rho_{s1}, \rho_{s2}, \rho_{s3}, \rho_{s4} \geq 0$$

together with constraints of problem (\*).

Giving equal weightage to national and regional segments, a satisfactory advertising reach is received from both the national media as well as each of the regional media of Regions 1,2,3, and 4 given as 68271200, 18926500, 13617800, 18621000, and 11318600, respectively. The budget allocated to the national media is ₹ 1159600 and for Regions 1, 2, 3, and 4 is ₹ 367250, ₹ 315690, ₹ 406740, ₹ 247875 respectively.

The total reach thus generated given the total budget as ₹ 2,50,00,000 all the media is 130755100. The number of advertisements to be allocated to different media for

**Table 10** Advertisement of different products allocated to different media

National Media	Region 1's Media	Region 2's Media	Region 3's Media	Region 4's Media
$x_{0111}^1$ 20	$x_{1111}^1$ 16	$x_{2111}^1$ 15	$x_{3111}^1$ 15	$x_{4111}^1$ 12
$x_{0112}^1$ 12	$x_{1112}^1$ 12	$x_{2112}^1$ 12	$x_{3112}^1$ 14	$x_{4112}^1$ 6
$x_{0211}^1$ 4	$x_{1121}^1$ 12	$x_{2121}^1$ 12	$x_{3121}^1$ 15	$x_{4121}^1$ 15
$x_{0212}^1$ 1	$x_{1122}^1$ 7	$x_{2122}^1$ 9	$x_{3122}^1$ 12	$x_{4122}^1$ 6
$x_{0111}^2$ 16	$x_{1211}^1$ 2	$x_{2211}^1$ 1	$x_{3211}^1$ 3	$x_{4211}^1$ 1
$x_{0112}^2$ 12	$x_{1212}^1$ 2	$x_{2212}^1$ 1	$x_{3212}^1$ 2	$x_{4212}^1$ 0
$x_{0211}^2$ 4	$x_{1221}^1$ 1	$x_{2221}^1$ 1	$x_{3221}^1$ 2	$x_{4221}^1$ 2
$x_{0212}^2$ 1	$x_{1222}^1$ 1	$x_{2222}^1$ 0	$x_{3222}^1$ 1	$x_{4222}^1$ 1
	$x_{1111}^2$ 15	$x_{2111}^2$ 15	$x_{3111}^2$ 15	$x_{4111}^2$ 12
	$x_{1112}^2$ 12	$x_{2112}^2$ 12	$x_{3112}^2$ 14	$x_{4112}^2$ 7
	$x_{1121}^2$ 12	$x_{2121}^2$ 12	$x_{3121}^2$ 16	$x_{4121}^2$ 15
	$x_{1122}^2$ 9	$x_{2122}^2$ 7	$x_{3122}^2$ 12	$x_{4122}^2$ 7
	$x_{1211}^2$ 2	$x_{2211}^2$ 2	$x_{3211}^2$ 1	$x_{4211}^2$ 1
	$x_{1212}^2$ 3	$x_{2212}^2$ 2	$x_{3212}^2$ 2	$x_{4212}^2$ 0
	$x_{1221}^2$ 1	$x_{2221}^2$ 2	$x_{3221}^2$ 1	$x_{4221}^2$ 1
	$x_{1222}^2$ 1	$x_{2222}^2$ 0	$x_{3222}^2$ 0	$x_{4222}^2$ 0

both the products in different slots are given below in Table 10 products in different slots are given. Problem is solved using optimization software LINGO 11.0 (Thiriez [14]).

## 6 Conclusion

In this paper, a media planning problem is considered for advertising multiple products of a firm in a segmented market at both national and regional level. The objective is to allocate the advertisements so as to capture maximum advertising reach from all media. Problem is formulated as a multi-objective programming problem and a compromise solution is achieved using GP approach.

## References

1. Charnes, A., Cooper, W.W., DeVoe, J.K., Learner, D.B., Reinecke, W.: A goal programming model for media planning. *Manag. Sci.* **14**, 422–430 (1968)
2. Lee, S.M.: *Goal Programming for Decision Analysis*. Auerbach Publishers, Philadelphia (1972)

3. De Kluyver, C.A.: Hard and soft constraints in media scheduling. *J. Advertisement Res.* **18**, 27–31 (1978)
4. Keown, A.J., Duncan, C.P.: Integer goal programming in advertising media selection. *Decis. Sci.* **10**, 577–592 (1979)
5. Moynihan, G.P., Kumar, A., D'Souza, G., Nockols, W.G.: A decision support system for media planning. *Comput. Ind. Eng.* **29**(1), 383–386 (1995)
6. Fruchter, G.E., Kalish, S.: Dynamic promotional budgeting and media allocation. *EJOR* **111**(1), 15–27 (1998)
7. Lee, C.W., Kwak, N.K.: Information resource planning using AHP-based goal programming model. *J. Oper. Res. Soc.* **51**, 1–8 (1999)
8. Mihiotis, A., Tsakiris, I.: A mathematical programming study of advertising allocation problem. *Appl. Math. Comput.* **148**(2), 373–379 (2004)
9. Kwak, N.K., Lee, Chang Won, Kim, Ji Hee, et al.: An MCDM model for media selection in the dual consumer/industrial market. *EJOR* **166**, 255–265 (2005)
10. Bhattacharya, U.K.: A chance constraints goal programming model for the advertising planning problem. *EJOR* **192**, 382–395 (2009)
11. Jha, P. C., Aggarwal, R. and Gupta, A.: Optimal Media Selection of Advertisement Planning in a Segmented Market. Om Parkash (Ed.), *Advances in Information Theory and Operations Research: interdisciplinary trends*, VDM Verlag, Germany, 248–268 (2010)
12. Jha, P.C., Aggarwal, R., Gupta, A.: Optimal Media Planning for Multi-product in Segmented Market. *Applied Mathematics and Computation*. Elsevier. **217**(16), 6802–6818 (2011)
13. Buratto, A., Grosset, L., Viscolani, B.: Advertising a new product in a segmented market. *EJOR*. **175**, 1262–1267 (2006)
14. Thiriez, H.: OR software LINGO. *EJOR*. **12**, 655–656 (2000)

# Two Storage Inventory Model for Perishable Items with Trapezoidal Type Demand Under Conditionally Permissible Delay in Payment

S R Singh and Monika Vishnoi

**Abstract** This article develops a two warehouse deterministic inventory model for deteriorating items with trapezoidal type demand under conditionally permissible delay in payments. A rented warehouse is used when the ordering quantity exceeds the limited capacity of the owned warehouse, and it is assumed that deterioration rates of items in the two warehouses may be different. In contrast to the traditional deterministic two-warehouse inventory model with shortages at the end of each replenishment cycle, an alternative model in which each cycle begins with shortages and ends without shortages is proposed. Deterioration rate is taken to be time-dependent. Shortages are allowed and fully backlogged. Then a solution procedure is shown to find the optimal replenishment policy of the considered problem. At last, article provides numerical example to illustrate the developed model. Sensitivity analysis is also given with respect to major parameters.

**Keywords** Two warehouse · Trapezoidal type demand · Shortages · Deterioration · Conditionally permissible delay in payments

## 1 Introduction

Demand is the most volatile of all the market forces, as it is the least controlled by management personnel. Even a slight change in the demand pattern for any particular item causes a lot of havoc with the market concerned. Overall, it means that every time the demand for any commodity goes a noticeable change, the inventory manager has to reformulate the complete logistics of management for that item. Here, one thing

---

S. R. Singh (✉) · M. Vishnoi  
D.N. (P.G.) College, Meerut, C.C.S. University, Meerut 250002, U.P, India  
e-mail: shivrajpundir@gmail.com

M. Vishnoi  
e-mail: monikavishnoi11@gmail.com

becomes very apparent, even if the firm is able to take the jolt of changed customer's preference, it will not be able to take the sweep of formulating a new inventory management theory every time. Previously, two types of time dependent demands, i.e., linear and exponential have been studied. The main limitation in linear time-dependence of demand rate is that it implies a uniform change in the demand rate per unit time. This rarely happens in the case of any commodity in the market. On the other hand, an exponential rate of change in demand is extraordinarily high and the demand fluctuation of any commodity in the real market cannot be so high. It concludes that demand rate never been constant or an increasing function or decreasing function of time. To observe these fluctuation in demand pattern, ramp-type demand rate taken into consideration.

Trapezoidal type demand pattern is more realistic in comparison to ramp-type demand in many cases like fad or seasonal goods coming to market. The demand rate for such items increases with the time up to certain time and then ultimately stabilizes and becomes constant, and finally the demand rate approximately decreases to a constant or zero, and the begins the next replenishment cycle. Hill [4] first proposed a time dependent demand pattern by considering it as the combination of two different types of demand such as increasing demand followed by a constant demand in two successive time periods over the entire time horizon and termed it as ramp-type time dependent demand pattern. Wu [11] further investigated the inventory model with ramp-type demand rate such that the deterioration followed the Weibull distribution deterioration and partial backlogging. Giri et al. [3] extended the ramp-type demand inventory model with Weibull deterioration distribution. Manna and Chaudhuri [5] have developed a production inventory model with ramp-type two time periods classified demand pattern where the finite production rate depends on the demand.

The effect of deterioration of physical goods in stock is very realistic feature of inventory control. For more details about deteriorating items one can see the review paper of Goyal and Giri [2]. In the past few decades, inventory problems for deteriorating items have been widely studied. In general, deterioration is defined as the damage, spoilage, dryness, vaporization, etc., that result in decrease of usefulness of the original one. In 2006, the Wu et al. [12] defined a new phenomenon as non-instantaneous deteriorating and considered the problem of determining the optimal replenishment policy for such items with stock dependent demand. Soon, Ouyang et al. [6] further developed an inventory model for non-instantaneous deteriorating items with permissible delay in payment.

Generally, when suppliers provide price discounts for bulk purchases or the products are seasonal, the retailers may purchase more goods than can be stored in his own warehouses (OW). Therefore, a rented warehouse (RW) is used to store the excess units over the fixed capacity  $W$  of the own warehouse. Usually, the rented warehouse is to charge higher unit holding cost than the own warehouse, but to offer a better preserving facility resulting in a lower rate of deterioration for the goods than the own warehouse. To reduce the inventory costs, it will be economical to consume the goods of RW at the earliest. Consequently, the firm stores goods in OW before RW, but clears the stocks in RW before OW. Chung and Huang [1] proposed



a two-warehouse inventory model for deteriorating items under permissible delay in payments, but they assume that the deteriorating rate of two warehouses are the same. Rong et al. [7] developed an optimization inventory policy for a deteriorating item with imprecise lead time, partially/fully backlogged shortages, and price dependent demand under two-warehouse system. Vishnoi and Shon [8] presented a two-warehouse production inventory model for deteriorating items with inflation induced demand and partial backlogging. Singh and Vishnoi [9] developed optimal replenishment policy for deteriorating items with time dependent demand under the learning effect. Vishnoi and Shon [10] explored an economic order quantity model for non-instantaneous deteriorating items with stock dependent demand, time varying partial backlogging under permissible delay in payments and two warehouses.

So far it seems none has tried to investigate this important issue with the assumptions of two warehouse, trade credit, deterioration, and shortages. The whole combination is very unique and very much practical. We think that our work will provide a solid foundation for the further study of this kind of important models with trapezoidal type demand rate. In this paper, we proposed the work as follows:

- (i) We introduce a trapezoidal type demand rate, with its variable part being linear function of time.
- (ii) Variable rate of deterioration.
- (iii) Shortages are allowed.
- (iv) Infinite planning horizon consider in this model.
- (v) This paper divides in two sections
  - (a) Model 1. When shortages occur at the end of the cycle with conditionally permissible delay in Payments
  - (b) Model 2. When shortages occur at the beginning of the cycle without permissible delay in Payments

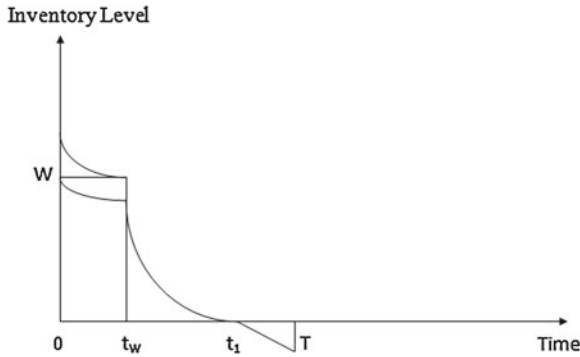
## 2 Assumptions and Notations

### 2.1 Assumptions

The mathematical model of the economic order quantity problem here is based on the following assumptions:

- The trapezoidal type demand rate,  $D(t)$ , which is positive and consecutive, is assumed to be a trapezoidal type function of time, that is,

$$D(t) = \begin{cases} a_1 + b_1t, & t \leq t_W \\ D_1, & t_W \leq t \leq t_1 \\ a_2 - b_2t, & t_1 \leq t \leq T \end{cases} \quad \text{and} \quad D(t) = \begin{cases} a_3 - b_3t, & t \leq T' \\ D_2, & T' \leq t \leq t'_W \\ a_4 + b_4t, & t'_W \leq t \leq t'_1 \end{cases}$$



**Fig. 1** Graphical representation of a two warehouse inventory system

where  $t_W$  is the time at which demand is changing from the linearly increasing demand to constant demand and  $t_1$  is time at which demand is changing from the constant demand to the linearly decreasing demand for Model 1. (See Fig.1) and  $a_1, a_2 > b_1, b_2$  and  $T'$  is the time at which demand is changing from the linearly decreasing demand to constant demand, and  $t'_W$  is time at which demand is changing from the constant demand to the linearly increasing demand for Model 2. (See Fig. 3) and  $a_3, a_4 > b_3, b_4$ .

- Shortages are allowed and fully backlogged.
- There is no repair or replenishment of deteriorated units during the period.
- Deterioration rate is  $\theta_1(t) = \theta_1 t$ , for RW and  $\theta_2(t) = \theta_2 t$  for OW, which is a continuous function of time
- Deteriorated items are neither replaced nor repaired.
- A single item inventory is considered over the prescribed period.
- Planning horizon is infinite and lead-time is zero.
- The retailer can accumulate revenue and earn interest after his/her customer pays for the amount of purchasing cost to the retailer until the end of the trade credit period offered by the supplier.

## 2.2 Notations

The following notations are used in the proposed study:

$W$	Capacity of the OW
$C_{h1}$	The holding cost per unit per unit time in OW
$C_{h2}$	The holding cost per unit per unit time in RW
$C_D$	The purchasing cost per unit
$C_S$	Shortage Cost per unit per unit time
$C_0$	Fix amount of the replenishment costs per \$ per order
$p$	The purchasing cost per unit.

$c$	The selling price per unit.
$I_p$	The capital opportunity cost in stock per \$ per year.
$I_e$	The interest earned per \$ per year.
$t_W$	The time at which the inventory level reaches zero in RW for Model.1
$t_1$	The time at which the inventory level reaches zero in OW for Model.1
$T$	The time at which the shortage reaches the lowest point in the replenishment cycle for Model.1
$T'$	The time at which the shortage occur for Model.2
$t'_W$	The time at which the inventory level reaches zero in RW for Model.2
$t'_1$	The time at which the inventory level reaches zero in OW for Model.2
$q_1(t)$	The level of positive inventory in RW at time $t$ for Model.1
$q_2(t), q_3(t)$	The level of positive inventory in OW at time $t$ for model.1
$q_4(t)$	The level of negative inventory at time $t$ for Model.1
$q_1(t)$	The level of negative inventory at time $t$ for Model.2
$q_2(t)$	The level of positive inventory in RW at time $t$ for Model.2
$q_3(t)$	The level of positive inventory in OW at time $t$ for Model.2
$q_4(t)$	The level of positive inventory in OW at time $t$ for Model.2
$TC_i$	The present value of the total relevant cost per unit time for Model $i$ , $i = 1, 2$

### 3 Formulation and Solution of the Model

There are two storage shortage models under the assumptions described in previous section, i.e., one is the traditional model and another is starting with shortage model so far can be found in literature. The traditional model is depicted graphically in Fig. 1. It starts with an instant replenishment and ends with shortages. It has been studied in several papers. In contrast, we propose the other shortage model in which the demand will be met at the end of cycle. In fact, the inventory level in our proposed model starts with shortages and ends without shortages. The proposed shortage model is depicted graphically in Fig. 3.

#### 3.1 Shortages Occur at the End of the Cycle with Permissible Delay in Payment (Model 1)

In this section, we discussed the deterministic inventory model for deteriorating items with the traditional two warehouse model where shortage occur at the end of the cycle at time  $t = 0$ , a lot size of certain units enters the system from which a portion is backlogged toward previous shortages,  $W$  units are kept in OW, and the rest is stored in RW. The goods of OW are consumed only after consuming the goods kept in RW. During the interval  $(0, t_W)$ , the inventory in RW gradually decreases due

to deterioration and linearly increasing demand and it vanishes at  $t = t_W$ . At OW, the inventory W remains same in the interval  $(0, t_W)$ . During the interval  $(t_W, t_1)$  the inventory level is depleted due to constant demand and deterioration. By the time  $t_1$ , both warehouses are empty and thereafter the shortages are allowed to occur with linearly decreasing function of time. The shortage quantity is supplied to customers at the beginning of the next cycle. By the time  $t_2$ , the replenishment cycle restarts. The objective of the traditional model is to determine the timings of  $t_W, t_1$ , and T, so that the total relevant cost (including holding, deterioration, shortage, and ordering costs) per unit time of the inventory system is minimized when in between retailer get some trade credit privilege.

Mathematically, the system can be represented by the following system of differential equations:

$$q_1'(t) + \theta_1(t)q_1(t) = -(a_1 + b_1t), \quad 0 \leq t \leq t_W \tag{1}$$

$$q_2'(t) + \theta_2(t)q_2(t) = 0, \quad 0 \leq t \leq t_W \tag{2}$$

$$q_3'(t) + \theta_2(t)q_3(t) = -D_1, \quad t_W \leq t \leq t_1 \tag{3}$$

$$q_4'(t) = -(a_2 - b_2t), \quad t_1 \leq t \leq T \tag{4}$$

With the boundary conditions  $q_1(t_W) = 0, q_2(0) = W, q_3(t_1) = 0, q_4(t_1) = 0$ , one can arrive the following equations

$$q_1(t) = a_1(t_W - t) + \frac{a_1\theta_1}{6}(t_W^3 - t^3) + \frac{b_1}{2}(t_W^2 - t^2) + \frac{b_1\theta_1}{8}(t_W^4 - t^4) - \frac{a_1\theta_1}{2}(t_W t^2 - t^3) - \frac{b_1\theta_1}{4}(t_W^2 t^2 - t^3), \quad 0 \leq t \leq t_W \tag{5}$$

$$q_2(t) = W e^{-\frac{\theta_2 t^2}{2}} = W - W \frac{\theta_2 t^2}{2}, \quad 0 \leq t \leq t_W \tag{6}$$

$$q_3(t) = D \left[ (t_1 - t) + \frac{\theta_2}{6}(t_1^3 - t^3) - \frac{\theta_2}{2}(t_1 t^2 - t^3) \right], \quad t_W \leq t \leq t_1 \tag{7}$$

$$q_4(t) = a_2(t_1 - t) + \frac{b_2}{2}(t_1^2 - t^2), \quad t_1 \leq t \leq T \tag{8}$$

i **Ordering Cost** Since replenishment is done at the start of the cycle, the ordering cost per cycle is given by

$$A = C_0/T \tag{9}$$

ii **Holding Cost for RW** The inventory holding cost in RW per cycle can be derived as

$$HC_{RW} = \frac{C_{h2}}{T} \left[ \int_0^{t_W} q_1(t) dt \right] = \frac{C_{h2}}{T} \left( \frac{a_1}{2} t_W^2 + \frac{b_1}{3} t_W^3 + \frac{a_1\theta_1}{12} t_W^4 + \frac{b_1\theta_1}{15} t_W^5 \right) \tag{10}$$

iii **Holding Cost for OW** The inventory holding cost in OW per cycle can be derived as

$$\begin{aligned}
 HC_{OW} &= \frac{C_{h1}}{T} \left[ \int_0^{t_w} q_2(t)dt + \int_{t_w}^{t_1} q_3(t)dt \right] \\
 &= \frac{C_{h1}}{T} \left[ \left( Wt_w - \frac{W\theta_2}{6} t_w^3 \right) + D \left\{ \left( \frac{t_1^2}{2} - t_1 t_w + \frac{t_w^2}{2} \right) \right. \right. \\
 &\quad \left. \left. + \frac{\theta_2}{6} \left( \frac{3t_1^4}{4} - t_1^3 t_w + \frac{t_w^4}{4} \right) + \frac{\theta_2}{6} \left( \frac{3t_1^4}{4} - t_1^3 t_w + \frac{t_w^4}{4} \right) \right\} \right] \quad (11)
 \end{aligned}$$

iv **Deterioration Cost** The deterioration cost per cycle can be derived as

$$\begin{aligned}
 DC &= \frac{C_D}{T} \left[ \int_0^{t_w} \theta_1(t)q_1(t)dt + \int_0^{t_w} \theta_2(t)q_2(t)dt + \int_{t_w}^{t_1} \theta_2(t)q_3(t)dt \right] \\
 &= \frac{C_D}{T} \left[ \theta_1 \left( \frac{a_1}{6} t_w^3 + \frac{b_1}{8} t_w^4 + \frac{a_1\theta_1}{120} t_w^5 + \frac{b_1\theta_1}{48} t_w^6 \right) + \theta_2 \left( W - W \frac{\theta_2}{8} t_w^4 \right) \right. \\
 &\quad \left. D\theta_2 \left\{ \left( \frac{t_1^3}{6} + t_1 \frac{t_w^2}{2} + \frac{t_w^3}{3} \right) + \frac{\theta_2^2}{6} \left( \frac{3t_1^5}{10} - t_1^3 \frac{t_w^2}{2} + \frac{t_w^5}{5} \right) - \frac{\theta_2^2}{2} \left( \frac{t_1^5}{20} - t_1 \frac{t_w^4}{4} + \frac{t_w^5}{5} \right) \right\} \right] \quad (12)
 \end{aligned}$$

v **Shortage Cost** The shortage cost per cycle can be derived as

$$SC = C_S \left[ \int_{t_1}^{t_2} [-q_4(t)] dt \right] = \frac{C_S}{T} \left[ a_2 \left( \frac{t_1^2}{2} - t_1 T + \frac{T^2}{2} \right) + \frac{b_2}{2} \left( \frac{2t_1^3}{3} - t_1^2 T + \frac{T^3}{3} \right) \right] \quad (13)$$

vi **The interest payable opportunity cost** There are three cases depicted as Fig. 2.

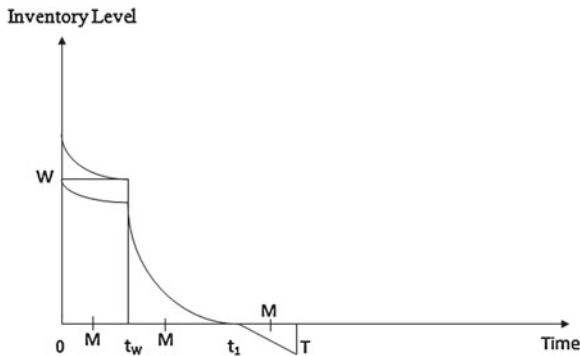


Fig. 2 Different cases of trade credit period M

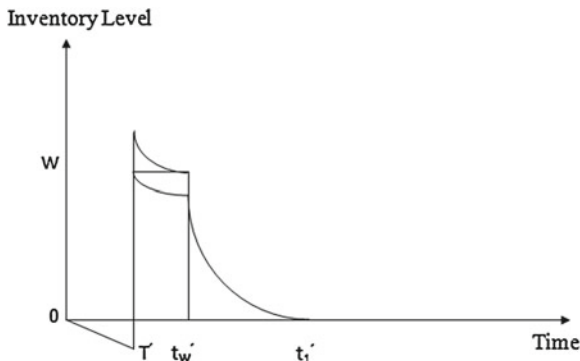


Fig. 3 Graphical representation of a two warehouse inventory system

**Case 1**  $M \leq t_w < T$  or  $0 < M \leq t_w$  In this case, the annual interest payable is

$$\begin{aligned}
 IP_1 &= \frac{cIP}{T} \left[ \int_M^{t_w} q_1(t)dt + \int_M^{t_w} q_2(t)dt + \int_{t_w}^{t_1} q_3(t)dt + \int_{t_1}^T q_4(t)dt \right] \\
 IP_1 &= \frac{cIP}{T} \left[ a_1 \left( \frac{t_w^3}{2} + t_w M + \frac{M^2}{2} \right) + \frac{a_1 \theta_1}{6} \left( \frac{3t_w^4}{4} + t_w^3 M + \frac{M^4}{4} \right) \right. \\
 &\quad + \frac{b_1}{2} \left( \frac{2t_w^3}{3} + t_w^2 M + \frac{M^3}{3} \right) + \frac{b_1 \theta_1}{8} \left( \frac{4t_w^5}{5} - t_w^4 M + \frac{M^5}{5} \right) \\
 &\quad - \frac{a_1 \theta_1}{2} \left( \frac{t_w^4}{12} - t_w \frac{M^3}{3} + \frac{M^4}{4} \right) - \frac{b_1 \theta_1}{4} \left( \frac{2t_w^5}{5} - t_w^4 \frac{M^3}{3} + \frac{M^5}{5} \right) \\
 &\quad + \left( Wt_w - \frac{W\theta_2}{6} t_w^3 - WM + \frac{W\theta_2}{6} M^3 \right) + D \left\{ \left( \frac{t_1^2}{2} - t_1 t_w + \frac{t_w^2}{2} \right) \right. \\
 &\quad + \frac{\theta_2}{6} \left( \frac{3t_1^4}{4} - t_1^3 t_w + \frac{t_w^4}{4} \right) - \frac{\theta_2}{2} \left( \frac{t_1^4}{12} - t_1 \frac{t_w^3}{3} + \frac{t_w^4}{4} \right) \left. \right\} \\
 &\quad + a_2 \left( \frac{t_1^2}{2} - t_1 T + \frac{T^2}{2} \right) + \frac{b_2}{2} \left( \frac{2t_1^3}{3} - t_1^2 T + \frac{T^3}{3} \right) \left. \right] \tag{14}
 \end{aligned}$$

**Case 2**  $t_w < M \leq T$  In this case, the annual interest payable is

$$\begin{aligned}
 IP_2 &= \frac{cIP}{T} \left[ \int_M^{t_1} q_3(t)dt + \int_{t_1}^T q_4(t)dt \right] \\
 &= \frac{cIP}{T} \left( \frac{t_1^2}{2} - t_1 M + \frac{M^2}{2} \right) + \frac{\theta_2}{6} \left( \frac{3t_1^4}{4} - t_1^3 M + \frac{M^4}{4} \right)
 \end{aligned}$$

$$\begin{aligned}
 & - \frac{\theta_2}{2} \left( \frac{t_1^4}{12} - t_1 \frac{M^3}{3} + \frac{M^4}{4} \right) \Bigg\} + a_2 \left( \frac{t_1^2}{2} - t_1 T + \frac{T^2}{2} \right) \\
 & + \frac{b_2}{2} \left( \frac{2t_1^3}{3} - t_1^2 T + \frac{T^3}{3} \right) \Bigg] \tag{15}
 \end{aligned}$$

**Case 3**  $M > t_1$  In this case, no interest charges are paid for the items.

vii **The opportunity interest earned** There are two cases as follows:

**Case 1**  $0 < M \leq t_W$  or  $M \leq T$  In this case, the annual interest earned is

$$IE_1 = \frac{pI_e}{T} \left[ \int_0^M (a_1 + b_1 t) t dt \right] = \frac{pI_e}{T} \left[ a_1 \frac{M^2}{2} + b_1 \frac{M^3}{3} \right] \tag{16}$$

**Case 2**  $t_W < M \leq t_1$  In this case, the annual interest earned is

$$\begin{aligned}
 IE_2 &= \frac{pI_e}{T} \left[ \int_0^{t_W} (a_1 + b_1 t) t dt + \int_{t_W}^M D_1 t dt \right] \\
 &= \frac{pI_e}{T} \left[ a_1 \frac{t_W^2}{2} + b_1 \frac{t_W^3}{3} + D_1 \frac{M^2}{2} - D_1 \frac{t_W^2}{2} \right] \tag{17}
 \end{aligned}$$

**Case 3**  $M > t_1$  In this case, the annual interest earned is

$$\begin{aligned}
 IE_3 &= \frac{pI_e}{T} \left[ \int_0^{t_W} (a_1 + b_1 t) t dt + \int_{t_W}^{t_1} D_1 t dt \right] \\
 &= \frac{pI_e}{T} \left[ \left\{ \left( a_1 \frac{t_W^2}{2} + b_1 \frac{t_W^3}{3} \right) + \frac{D_1}{2} (t_1^2 - t_W^2) + \left( a_2 \frac{M^2}{2} - b_2 \frac{M^3}{3} - a_2 \frac{t_1^2}{2} + b_2 \frac{t_1^3}{3} \right) \right\} \right. \\
 &\quad \left. + (M - t_1) \left\{ \left( a_1 \frac{t_W^2}{2} + b_1 \frac{t_W^3}{3} \right) + \frac{D_1}{2} (t_1^2 - t_W^2) + \left( a_2 \frac{M^2}{2} - b_2 \frac{M^3}{3} - a_2 \frac{t_1^2}{2} + b_2 \frac{t_1^3}{3} \right) \right\} \right] \tag{18}
 \end{aligned}$$

viii **Total Cost**

Therefore, the annual total relevant cost for the retailer can be expressed as:

$$\begin{aligned}
 TC(t_W, t_1, T) &= \text{ordering cost} + \text{Inventory holding cost in RW} \\
 &\quad + \text{Inventory holding cost in OW} + \text{deteriorating cost} \\
 &\quad + \text{shortage cost} + \text{interest payable opportunity cost} \\
 &\quad - \text{opportunity interest earned.} \tag{19}
 \end{aligned}$$

### 3.2 Shortage Occurs at the Beginning of the Cycle Without Permissible Delay in Payments (Model 2)

In this section, we discussed the deterministic inventory model for deteriorating items with the two warehouse model where shortage occurs at the beginning of the cycle is discussed. At time  $t = 0$ , it starts with zero inventory. At the time interval  $(0, T')$  shortages are allowed to occur with linearly decreasing function of time. At time  $t = T'$ , excess quantity of lot size enters to remove the previous shortages. It is assumed that the management owns a warehouse with fixed capacity and any quantity exceeding this should be stored in RW, which is assumed to be available with abundant space. Deterioration starts by the time  $T'$  and also it is the time for changing the demand pattern from decreasing trend to constant trend. The goods of OW are consumed only after consuming the goods kept in RW. During the time interval  $(T', t'_W)$ , the inventory in RW gradually decreases due to joint effect of constant demand and deterioration it vanishes at  $t = t'_W$ . At OW, the inventory is only depleted by the effect of deterioration. During  $(t'_W, t'_1)$  the inventory is depleted due to linearly increasing demand and deterioration.

Mathematically, the system can be represented by the following system of differential equations:

$$q'_1(t) = -(a_3 - b_3t), \quad 0 \leq t \leq T' \tag{20}$$

$$q'_2(t) + \theta_1(t)q_2(t) = -D_2, \quad T' \leq t \leq t'_W \tag{21}$$

$$q'_3(t) + \theta_2(t)q_3(t) = 0, \quad T' \leq t \leq t'_W \tag{22}$$

$$q'_4(t) + \theta_2(t)q_4(t) = -(a_4 + b_4t), \quad t'_W \leq t \leq t'_1 \tag{23}$$

With the boundary conditions  $q_1(0) = 0, q_2(t'_W) = 0, q_3(T') = W, q_4(t'_1) = 0$ , one can arrive the following equations

$$q_1(t) = -\left[ a_3t - \frac{b_3}{2}t^2 \right], \quad 0 \leq t \leq T' \tag{24}$$

$$q_2(t) = D_2 \left[ (t_W t - t) + \frac{\theta_1}{6} (t'^3_W - t^3) - \frac{\theta_1}{2} (t'_W t^2 - t^3) \right], \quad T' \leq t \leq t'_W \tag{25}$$

$$q_3(t) = W e^{\frac{\theta_2}{2}(T'^2 - t^2)}, \quad t'_W \leq t \leq t'_1 \tag{26}$$

$$q_4(t) = \left[ a_4 (t'_1 - t) + \frac{\theta_2 a_4}{6} (t'^3_1 - t^3) + \frac{b_4}{2} (t'^2_1 - t^2) + \frac{\theta_2 a_4}{8} (t'^4_1 - t^4) - \frac{\theta_2 a_4}{2} (t'_1 t^2 - t^3) - \frac{\theta_2 b_4}{4} (t'^2_1 t^2 - t^4) \right], \quad t'_W \leq t \leq t'_1 \tag{27}$$

i **Ordering Cost** Since replenishment is done at the start of the cycle, the ordering cost per cycle is given by

$$A = C_0/t_1, \tag{28}$$



ii **Holding Cost for RW** The inventory holding cost in RW per cycle can be derived as

$$\begin{aligned}
 HC_{RW} &= \frac{C_{h2}}{t'_1} \left[ \int_{T'}^{t'_W} q_2(t) dt \right] \\
 &= \frac{C_{h2}}{t'_1} \left[ \left( \frac{t'^2_W}{2} - t'_W T' + \frac{T'^2}{2} \right) + \frac{\theta_1}{6} \left( \frac{3t'^2_W}{4} - t'^3_W T' + \frac{T'^4}{4} \right) \right. \\
 &\quad \left. - \frac{\theta_1}{6} \left( \frac{t'^4_W}{12} - t'_W T'^3 + \frac{T'^4}{4} \right) \right] \tag{29}
 \end{aligned}$$

iii **Holding Cost for OW** The inventory holding cost in OW per cycle can be derived as

$$\begin{aligned}
 HC_{OW} &= \frac{C_{h1}}{t'_1} \left[ \int_{T'}^{t'_W} q_3(t) dt + \int_{t'_W}^{t'_1} q_4(t) dt \right] \\
 &= \frac{C_{h1}}{t'_1} \left[ \left\{ W (t'_W - T') + \frac{W\theta_2}{6} \left( T'^2 t'_W - \frac{t'^3_W}{3} - \frac{2T'^3}{3} \right) \right\} \right. \\
 &\quad + a_4 \left( \frac{t'^3_1}{2} + t'_1 t'_W + \frac{t'^2_W}{2} \right) + \frac{a_4 \theta_4}{6} \left( \frac{3t'^4_1}{4} + t'^3_1 t'_W + \frac{t'^4_W}{4} \right) \\
 &\quad + \frac{b_4}{4} \left( \frac{2t'^3_1}{3} + t'^2_1 t'_W + \frac{t'^3_W}{3} \right) + \frac{b_4 \theta_2}{8} \left( \frac{4t'^5_1}{5} - t'^4_1 t'_W + \frac{t'^5_W}{5} \right) \\
 &\quad \left. - \frac{a_4 \theta_2}{2} \left( \frac{t'^4_1}{12} + t'_1 \frac{t'^3_W}{3} + \frac{t'^4_W}{4} \right) - \frac{b_4 \theta_2}{4} \left( \frac{2t'^5_1}{15} - t'^2_1 \frac{t'^3_W}{3} + \frac{t'^5_W}{5} \right) \right] \tag{30}
 \end{aligned}$$

iv **Deterioration Cost** The deterioration cost per cycle can be derived as

$$\begin{aligned}
 DC &= \frac{C_D}{t'_1} \left[ \int_{T'}^{t'_W} \theta_1 t \cdot q_2(t) dt + \int_{T'}^{t'_W} \theta_2 t \cdot q_3(t) dt + \int_{t'_W}^{t'_1} \theta_2 t \cdot q_4(t) dt \right] \\
 &= \frac{C_D}{t'_1} \left[ \left\{ D_2 \theta_1 \left( \frac{t'^3_W}{6} + t'_W \frac{T'^2}{2} + \frac{T'^3}{3} \right) + \frac{\theta_1}{6} \left( \frac{3t'^5_W}{10} + t'^3_W \frac{T'^2}{2} + \frac{T'^5}{5} \right) \right. \right. \\
 &\quad \left. \left. - \frac{\theta_1}{2} \left( \frac{t'^5_W}{20} + t'_W \frac{T'^4}{4} + \frac{T'^5}{5} \right) \right\} \right. \\
 &\quad \left. + \theta_2 W \left\{ \frac{1}{2} (t'^2_W - T'^2) + \frac{\theta_2}{2} \left( T'^2 \frac{t'^2_W}{2} - \frac{t'^4_W}{4} - \frac{T'^4}{4} \right) \right\} \right]
 \end{aligned}$$

$$\begin{aligned}
 &+ \theta_2 \left\{ \left( \frac{t_1'^3}{6} + t_1' \frac{t_W'^2}{2} + \frac{t_W'^3}{3} \right) + \frac{\theta_2 a_4}{6} \left( \frac{3t_1'^5}{10} + t_1'^3 \frac{t_W'^2}{2} + \frac{t_W'^5}{5} \right) \right. \\
 &+ \frac{b_4}{2} \left( \frac{t_1'^4}{4} + t_1'^2 \frac{t_W'^2}{2} + \frac{t_W'^4}{4} \right) + \frac{\theta_2 b_4}{8} \left\{ \left( \frac{2t_1'^6}{6} + t_1'^4 \frac{t_W'^2}{2} + \frac{t_W'^6}{6} \right) \right. \\
 &\left. \left. - \frac{\theta_2 a_4}{2} \left( \frac{t_1'^5}{20} - t_1' \frac{t_W'^4}{4} + \frac{t_W'^5}{5} \right) - \frac{\theta_2 b_4}{4} \left( \frac{t_1'^6}{12} + t_1'^2 \frac{t_W'^4}{4} + \frac{t_W'^6}{6} \right) \right\} \right\} \quad (31)
 \end{aligned}$$

v **Shortage Cost** The shortage cost per cycle can be derived as

$$SC = \frac{C_S}{t_1'} \left[ \int_0^{T'} [-q_1(t)] dt \right] = \frac{C_S}{t_1'} \left[ \frac{a_3}{2} T'^2 - \frac{b_3}{6} T'^3 \right] \quad (32)$$

vi **Total Cost** Therefore, the annual total relevant cost for the retailer can be expressed as:

$$\begin{aligned}
 TC(t_W', t_1', T') = & \text{orderingcost} + \text{stockholdingcost in RW} \\
 & + \text{stockholdingcost in OW} + \text{deterioratingcost} + \text{shortagecost} \quad (33)
 \end{aligned}$$

### 4 Appendix

To minimize total average cost per unit time ( $TC_i$ ),  $i = 1, 2$  for both of **Model 1**. and **Model 2**. The optimal values of  $t_W, t_1$  and  $T$  for Model 1 and  $t_W', t_1'$  and  $T'$  for Model 2 can be obtained by solving the following equations simultaneously from the equations

$$\frac{\partial TC_i}{\partial t_W} = 0, \frac{\partial TC_i}{\partial t_1} = 0, \frac{\partial TC_i}{\partial T} = 0, \quad (34)$$

$$\frac{\partial TC_i}{\partial t_W'} = 0, \frac{\partial TC_i}{\partial t_1'} = 0, \frac{\partial TC_i}{\partial T'} = 0, \quad (35)$$

Provided, they satisfy the following conditions

$$\frac{\partial^2 TC_i}{\partial t_W^2} > 0, \frac{\partial^2 TC_i}{\partial t_1^2} > 0, \frac{\partial^2 TC_i}{\partial T^2} > 0, \quad (36)$$

$$\frac{\partial^2 TC_i}{\partial t_W'^2} > 0, \frac{\partial^2 TC_i}{\partial t_1'^2} > 0, \frac{\partial^2 TC_i}{\partial T'^2} > 0, \quad (37)$$

### 5 Solution Procedure

We use the classical optimization techniques for finding the minimum value of the total cost. The Eq. (34) consists of different equations for both cases of Model 1 and Eq. (35) consists of different equations for both cases of Model 2 are highly nonlinear in the continuous variable  $t_w, t_1, T$  for Model 1 and  $t'_w, t'_1, T'$  for Model 2. We have used the mathematical software *MATLAB 7.0.1*. to arrive at the solution of our system. We obtained the optimal values. With the use of these optimal values Eqs. (19) and (33) provides minimum total average cost per unit time of the system in consideration. Here, numerical illustration is to be given from 1st to 5th replenishment.

### 6 Numerical Illustrations and Analysis

To elucidate, by the preceding theory the following numerical data is given by:

**Example 1**  $W = 500$  units,  $C_0 = \$100$  per setup,  $C_{h1} = \$0.3, C_{h2} = \$0.6, C_D = \$0.5$ per unit,  $C_S = \$3/$  unit/unit time,  $a_1 = 200, b_1 = 5, I_P = \$0.15$  unit/year,  $I_e = \$0.12$  unit/year,  $c = \$ 10/$  unit,  $p= \$15/$  unit,  $a_2 = 220, b_2 = 10, D_1 = 500$  units,  $a_3 = 220, b_3 = 10, a_4 = 200, b_4 = 5, D_2 = 500$  unit,  $\theta_1 = 0.002, \theta_2 = 0.005$ . Tables 1 and 2.

**Table 1** Optimal solution for model 1

N	$t_w$	$t_1$	T	Total cost (TC)
1	6.32754	11.3479	14.7978	835.124
2	6.32754	11.3479	14.7978	835.113
3	6.32754	11.3479	14.7978	835.065
4	6.32754	11.3479	14.7978	835.043
5	6.32754	11.3479	14.7978	835.022

**Table 2** Optimal solution for model 2

N	$T'$	$t'_w$	$t'_1$	Total cost (TC)
1	0.28193	1.36414	3.49076	169.856
2	0.28163	1.36618	3.46629	169.325
3	0.28145	1.36763	3.46474	169.186
4	0.28131	1.36423	3.46313	169.087
5	0.28124	1.36193	3.46190	169.056

## 7 Sensitivity Analysis

In Tables 3 and 4 some sensitivity analysis of the model is performed by changing the parameter values  $-50\%$ ,  $-25\%$ ,  $25\%$ , and  $50\%$ , taking one at a time and keeping the remaining unchanged. The analysis is performed based on the adjusted results obtained in Tables 1 and 2. Some simple characteristics of parameter’s impact on total cost (Figs. 4, 5).

### 7.1 Sensitivity Analysis for Model 1

### 7.2 Observations for Model 1

The following observations are made based on the above findings: The values of percentage variation in total costs are the highly sensitive to the following parameters:  $\theta_1$ ,  $a_1$  and  $a_2$ ,  $b_1$ ,  $b_2$ . The values of percentage variation in total costs are quite sensitive to the parameters  $D_1$ . The values of percentage variation in total costs are not so sensitive to the following parameters:  $a_1$ ,  $\theta_2$ , and  $W$ .

**Table 3** Sensitivity analysis of optimal solution for model 1

Parameter	-50 % Changed		-25 % Changed		+25 % Changed		+50 % Changed	
	N	PCV	N	PCV	N	PCV	N	PCV
W	1	0.05	1	0.02	1	-0.03	1	-0.05
$a_1$	1	0.32	1	0.16	1	-0.17	1	-0.33
$a_2$	1	-12.95	1	-6.48	1	6.47	1	12.94
$b_1$	1	-22.17	1	-11.08	1	11.08	1	22.16
$b_2$	1	-21.07	1	-10.54	1	10.52	1	21.05
$D_1$	1	-3.42	1	-1.71	1	1.69	1	3.40
$\Theta_1$	1	11.64	1	5.82	1	-5.82	1	-11.64
$\Theta_2$	1	-0.75	1	-0.37	1	0.37	1	0.74

**Table 4** Sensitivity analysis of optimal solution for model 2

Parameter	-50 % Changed		-25 % Changed		+25 % Changed		+50 % Changed	
	N	PCV	N	PCV	N	PCV	N	PCV
$\theta_1$	1	-0.37	1	-0.19	1	0.19	1	0.38
$\theta_2$	1	0.16	1	0.08	1	-0.08	1	-0.16
$a_4$	1	-1.28	1	-0.64	1	0.64	1	1.28
$b_4$	1	-20.31	1	-10.15	1	10.15	1	20.31
$a_3$	1	-1.35	1	-0.67	1	0.67	1	1.35
$b_3$	1	-1.36	1	-0.68	1	0.68	1	1.36
$D_2$	1	5.15	1	2.57	1	-1.93	1	-4.51
W	1	0.05	1	0.02	1	-0.02	1	-0.05

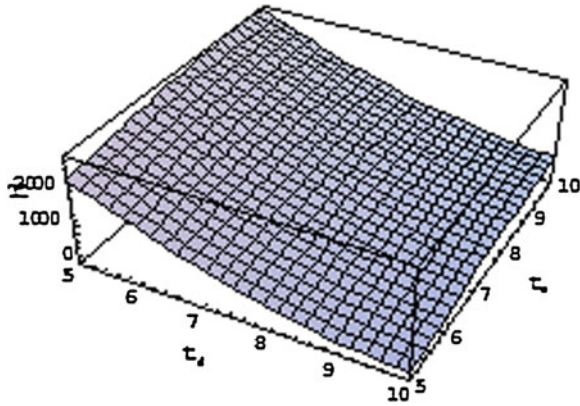


Fig. 4 Convexity of the total cost for model.1 when  $tW$  fixed

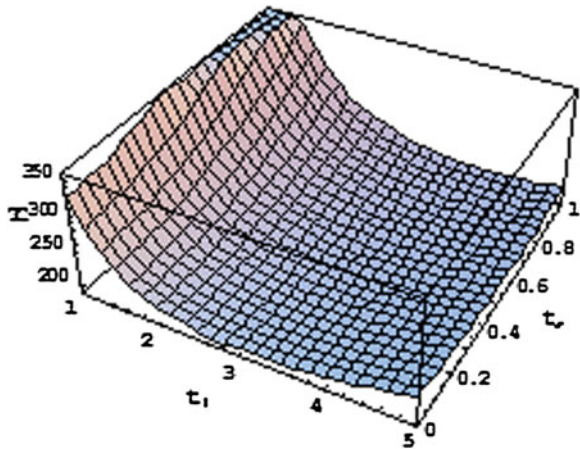


Fig. 5 Convexity of the total cost function when  $t'_W$  fixed

### 7.3 Sensitivity Analysis for Model 2

#### 7.4 Observations for Model 2

The following observations are made based on the above findings: The values of percentage variation in total costs are the highly sensitive to the parameters ' $b_4$ '. The values of percentage variation in total costs are quite sensitive to the following parameters: ' $D_2$ ', ' $a_4$ ', ' $a_3$ ', ' $b_3$ '. The values of percentage variation in total costs are not so sensitive to the following parameters:  $\theta_1$ ,  $\theta_2$ , and  $W$ .

## 8 Concluding Remarks

In this paper, we successfully provide a rigorous and efficient method to derive the optimal solution for the inventory models with deteriorating items and trapezoidal type demand rate under the permissible delay in payments. We study two alternative inventory models for determining the optimal replenishment schedule for two warehouse inventory problem under shortages, in which the inventory deteriorates at a variable rate over time. In this model deterioration rate at any item is assumed to time dependent.

The nature of demand of seasonal and fashionable products is increasing-steady-decreasing and becomes asymptotic. The demand pattern assumed here is found to occur not only for all types of seasonal products but also for fashion apparel, computer chips of advanced computers, spare parts, etc. The procedure presented here may be applied to many practical situations. Retailers in supermarket face this type of problem to deal with highly perishable seasonal products. Thus, to make a better combination of increasing- steady-decreasing demand pattern for perishable seasonal products.

In addition to the above mentioned facts, we have also tried to establish two possible shortage models. For each model the optimal policy is obtained. In general, Model 2 is less expensive to operate than Model 1 if the factors of trapezoidal type demand rate, shortages, deterioration, and permissible delay in payments are considered. A numerical assessment of the infinite planning horizon theoretical model has been done to illustrate the theory. The solution obtained has also been checked for sensitivity with the result that the model is found to be quite suitable and stable and discussed some interesting and important facts where the company's management need to take proper attention. The variations in the system statistics with a variation in system parameters have also been illustrated graphically.

### Author Biographies



**S.R. Singh** Faculty of Mathematics in D.N. (P.G.) College Meerut (U.P.), has experience of 18 years in academics and research. His Ph.d. is from C.C.S. University, Meerut (U.P.). His areas of specialization are inventory control, supply chain management, cryptography and fuzzy set theory. He has attended various seminars/conferences and presented his research papers. Fifteen students have been awarded PhD under his supervision. He has published more than hundred research papers in reputed national and international journals. His research papers have been published in *Opsearch*, *International Journal of Operational Research*, *Fuzzy Sets and Systems* and *International Journal of Operations and Quantitative Management*. He is author/co-author of seven of books.



**Monika Vishnoi** has Ph.d. in Mathematics. She has completed her research in the field of Inventory Management. She has communicated several research papers to journals of international repute. Several of her papers have been published in journals of national and international repute, while a few are under review at journals of international repute.

## References

1. Chung, K.J., Huang, T.S.: The optimal retailer's ordering policies for deteriorating items with limited storage capacity under trade credit financing. *Int. J. Prod. Econ.* **106**, 127–145 (2007)
2. Goyal, S.K., Giri, B.C.: Recent trends in modeling of deteriorating inventory. *Eur. J. Oper. Res.* **134**(1), 1–16 (2001)
3. Giri, B.C., Jalan, A.K., Chaudhuri, K.S.: Economic order quantity model with Weibull deterioration distribution, shortage and ramp-type demand. *Int. J. Syst. Sci.* **34**(4), 237–243 (2003)
4. Hill, R.M.: Optimal EOQ models for deteriorating items with time-varying demand. *J. Oper. Res. Soci.* **47**, 1228–1246 (1995)
5. Manna, S.K., Chaudhuri, K.S.: An EOQ model with ramp type demand rate, time dependent deterioration rate, unit production cost and shortages. *Eur. J. Oper. Res.* **171**, 557–566 (2006)
6. Ouyang, L.Y., Wu, K.S., Yang, C.T.: A study on an inventory model for non-instantaneous deteriorating items with permissible delay in payments. *Comput. Ind. Eng.* **51**, 637–651 (2006)
7. Rong, M., Mahapatra, N.K., Maiti, M.: A two warehouse inventory model for a deteriorating item with partially/fully backlogged shortage and fuzzy lead time. *Eur. J. Oper. Res.* **189**, 59–75 (2008)
8. Vishnoi, M., Shon, S.: An EPQ model with flexible production rate, inflation induced demand with partial backorder for two warehouses. *Int. Trans. Appl. Sci.* **2**(2), 211–224 (2010)
9. Singh, S.R., Vishnoi, M.: Optimal replenishment policy for deteriorating items with time dependent demand under the learning effect. *Int. Trans. Math. Sci. Comput.* **4**(2), 171–186 (2011)
10. Vishnoi, M., Shon, S.: Two levels of storage model for non-instantaneous deteriorating items with stock dependent demand, time varying partial backlogging under permissible delay in payments. *Int. J. Oper. Res. Optim.* **1**(1), 133–147 (2010)
11. Wu, K.S.: An EOQ model for items with Weibull distribution deterioration, ramp-type demand rate and partial backlogging. *Prod. Plann. Control* **12**(8), 787–793 (2001)
12. Wu, K.S., Ouyang, L.Y., Yang, C.T.: An optimal replenishment policy for non-instantaneous deteriorating items with stock dependent demand and partial backlogging. *Int. J. Prod. Econ.* **101**, 369–384 (2006)

# Development of an EOQ Model for Multi Source and Destinations, Deteriorating Products Under Fuzzy Environment

Kanika Gandhi and P. C. Jha

**Abstract** Business in the present highly competitive scenario emphasises the need to satisfy customers. Generally, uncertainty in demand is observed from customer side when products are deteriorating in nature. This uncertain demand cannot be predicted precisely, which causes fuzziness in related constraints and cost functions. Synchronizing inventory, procurement, and transportation of deteriorating natured products with fuzzy demand, and fuzzy holding cost at source and destination becomes essential in supply chain management (SCM). The current study demonstrates a fuzzy optimization model with an objective to minimize the cost of holding, procurement, and transportation of multi products from multi sources to multi destinations (demand point) with discount policies on ordered and weighted transportation quantity. A case study is illustrated to validate the model.

**Keywords** Supply chain management · Discount models · Transportation models · Deteriorating products · Fuzzy logics

## 1 Introduction

Deteriorating products are common in daily life. However, the academia has not reached a consensus on the definition of the deteriorating products. Deteriorating products can be classified into two categories. The first category refers to the products that become decayed, damaged, or expired through time, like meat, vegetables, fruit, medicine, etc; the other category refers to products that lose part or total value through

---

K. Gandhi (✉) · P. C. Jha

Department of Operational Research, Faculty of Mathematical Sciences, University of Delhi, Delhi 110007, India

e-mail: gandhi.kanika@gmail.com

P. C. Jha

e-mail: jhapc@yahoo.com



time because of new technology or the introduction of alternatives, like computer chips, mobile phones, fashion, and seasonal goods. Both the categories have the characteristic of short life cycle. For the first category, products have a short natural life cycle. After a specific period, the natural attributes of products will change and then lose useable value and economic value; for the second category, products have a short market life cycle. After a period of popularity in the market, the products lose the original economic value due to the changes in consumer preference, product upgrading, and other reasons. In the supply chain, decisions related to delivering ordered products in time become critical, as delivery or consumption delay leads to reduction in product's value. Because of the deteriorating nature of the products, demand of such products becomes highly volatile and cannot be forecasted precisely. Imprecision in demand forces total cost and holding costs to be imprecise and creates a fuzzy environment.

Many authors in the past have discussed concepts on deteriorating products and fuzzy environment due to fuzzy demand and cost. Initial discussion is with the assumption that the lifetime of a product is infinite while it is in storage. On the same lines, Silver and Meal [1] developed an approximate solution technique of a deterministic inventory model with time varying demand. Donaldson [2] first developed an exact solution procedure for products with a linearly increasing demand rate over a finite planning horizon. All these models are based on the assumption that there is no deterioration effect on inventory. But in reality, deterioration also depends on preserving facilities and environmental conditions of storage. So, due to deterioration effect, a certain fraction of the available quantity is either damaged or decayed and are not in a perfect condition to satisfy the future demand of customers for good items. Deterioration for such items is continuous and constant or time-dependent and is dependent on the on-hand inventory. A number of research papers have already been published on the above type of items by [3–5].

Due to deterioration, the demand of such products is uncertain, which develops a fuzzy environment. To convert fuzzy environment into crisp, Zimmermann [6] used the concept of fuzzy set in decision-making processes by considering the objective and constraints as fuzzy goals. He first applied fuzzy set theory with suitable choice of membership functions and derived a fuzzy linear programming problem. Lai and Hwang [7, 8] described the application of fuzzy sets to several operation research problems in two well-known books. Fuzzy set theory has also been used in few inventory models. Sommer [9] applied fuzzy dynamic programming to an inventory and production-scheduling problem. Kacprzyk and Staniewski [10] considered a fuzzy inventory problem in which, instead of minimizing the total average cost, they reduced it to a multi-stage fuzzy-decision-making problem and solved by a branch and bound algorithm. Lam and Wang [11] solved the fuzzy model of joint economic lot size problem with multiple price breaks. Roy and Maiti [12] solved the classical EOQ model in a fuzzy environment with fuzzy goal, fuzzy inventory costs, and fuzzy storage area by FNLP method using different types of membership functions for inventory parameters.

In the current study, a specific division of SCM is explained, where deteriorating natured multiple products are ordered to multi supplier by many buyers. The

problem is faced by the suppliers not being able to forecast demand because of the deteriorating nature of the products. In the process, the buyer at demand point plays a major role, which provides a holistic approach by integrating all the holding, procurement, inspection, and transportation activities such that holding cost; ordered quantity to suppliers and its purchase cost; inspection cost on ordered quantity; transported weights and its freight cost. He would also take care of the holding cost at suppliers, because suppliers cannot keep goods in the warehouse for a long time. As the capacity of warehouse is limited and may incur more cost that may further affect the selling price. The paper presents a fuzzy optimization model, which integrates inventory, procurement, and transportation mechanism to minimize all the costs discussed above. The total cost of the model becomes fuzzy because of fuzzy holding cost and demand. The study also includes the aspect of discounts that benefits the buyer to avail discounts on bulk purchase and transported weights.

## 2 Problem Statement and Assumptions

The current study develops a fuzzy model which shows flow of deteriorating multi products from multi sources to multi demand points (destinations) with fuzzy demand and holding cost at source and destination. In this coordination, the cost is associated at every stage like purchase cost, distribution cost, inspection cost, and fuzzy holding cost. The objective of the current study is to minimize the total costs discussed above by integrating procurement and distribution phase with incorporating quantity discount policies at the time of purchase and freight discount at the time of transportation and maximum reduction in vagueness of the fuzzy environment. At the time of model development the following assumptions were taken:

- Demand is uncertain.
- Supply is instantaneous.
- Initial inventory of each product for the beginning of planning horizon is zero.
- Constant rate of deterioration, as a percentage of stored units.
- Constant inspection rate.

## 3 Proposed Model Formulation

### 3.1 Sets

Product set with cardinality  $P$  and indexed by  $i$ , whereas periods set with cardinality  $T$  and indexed by  $t$ , price discount break point set with cardinality  $L$  and indexed by  $l$ , and freight discount break point with cardinality  $K$  and indexed by  $k$ . Destination set with cardinality  $M$  indexed by  $m$ , and source set with cardinality  $J$  indexed by  $j$ .

### 3.2 Parameters

$\tilde{C}$  is fuzzy total cost,  $C_0$  and  $C_0^*$  are the aspiration and tolerance level of fuzzy total cost respectively.  $\tilde{h}_{ijt}$  and  $\bar{h}_{ijt}$  are fuzzy and defuzzified holding cost per unit of product  $i$  in period  $t$  at source  $j$ .  $\tilde{h}_{imt}$  and  $\bar{h}_{imt}$  are fuzzy and defuzzified holding cost per unit of product  $i$  in period  $t$  at destination  $m$ .  $\varphi_{ijmt}$  is the unit purchase cost for product  $i$  from source  $j$  to destination  $m$  in period  $t$ .  $d_{ijmkt}$  is the discount factor is valid if more than  $a_{ijmkt}$  unit are purchased,  $0 < d_{ijmkt} < 1$ .  $\beta_{jmt}$  is the weight freight cost in  $t$ th period from source  $j$  to destination  $m$ .  $f_{jmkkt}$  is the transportation freight discount factor from source  $j$  to destination  $m$  in period  $t$  at freight break  $k$ .  $\tilde{D}_{imt}$  and  $\bar{D}_{imt}$  are fuzzy and defuzzified demand for product  $i$  in period  $t$  from  $m$ th destination.  $\bar{D}_0^*$  and  $\bar{D}_0$  are the aspiration and tolerance level of defuzzified demand, where  $\bar{D}_0^* = \sum_{t=1}^T \sum_{m=1}^M \bar{D}_{imt}$ .  $CR_{imt}$  is the consumption at destination  $m$  of product  $i$  in period  $t$ .  $a_{ijmkt}$  is the limit beyond which  $l^{th}$  price break becomes valid for destination  $m$  availed from source  $j$  in period  $t$  for product  $i$ .  $b_{jmkkt}$  is the limit beyond which  $k^{th}$  freight break becomes from source  $j$  to destination  $m$  valid in period  $t$ .  $w_i$  is per unit weight of  $i$ th product.  $IN_{ij1}$  and  $IN_{im1}$  are initial inventory of the planning horizon at source  $j$  and destination  $m$  resp. for product  $i$ .  $\lambda_{ijmkt}$  is per unit inspection cost of  $i^{th}$  product in terms of quantity ordered.  $\eta$  is percentage of defective items of the stored units.

### 3.3 Decision Variables

$X_{ijmkt}$  is the amount of product  $i$  ordered in period  $t$  from source  $j$  for destination  $m$ .  $R_{ijmkt}$  is the binary variable, which is 1 if the ordered quantity falls in  $l$ th price break, otherwise zero.  $I_{ijt}$  and  $I_{imt}$  are inventory level at source  $j$  and destination  $m$  for product  $i$  at the end of period  $t$ .  $Z_{jmkkt}$  is the binary variable, which is 1 if the weighted quantity transported falls in  $k^{th}$  price break, otherwise zero.  $L_{jmt}$  is the total weighted quantity transported in period  $t$  from source  $j$  to destination  $m$ .

### 3.4 Fuzzy Optimization Model Formulation

In many real problems, input information is incomplete or unreliable to develop a crisp mathematical model, which can quantify uncertain parameters. This enables to employ fuzzy optimization methods and fuzzy parameters that provide more adequate solution of real problem for uncertain and vague environment. Therefore, we formulate fuzzy optimization model for vague aspiration levels on total cost, demand, and holding cost, the decision maker may decide his aspiration levels on the basis of past experience.

$$\begin{aligned} \text{Min } \tilde{C} = & \sum_{t=1}^T \sum_{j=1}^J \sum_{i=1}^P \left[ \tilde{h}_{ijt} I_{ijt} + \sum_{m=1}^M \left\{ \left( \sum_{l=1}^L R_{ijmkt} d_{ijmkt} \right) \varphi_{ijmt} X_{ijmt} + \lambda_{ijmt} X_{ijmt} \right\} \right] \\ & + \sum_{t=1}^T \sum_{m=1}^M \left[ \tilde{h}_{imt} I_{imt} + \sum_{j=1}^J \left\{ \left( \sum_{k=1}^K Z_{jmkt} f_{jmkt} \right) \beta_{jmt} L_{jmt} \right\} \right] \end{aligned} \tag{1}$$

Subject to

$$I_{ijt} = I_{ij(t-1)} + \sum_{m=1}^M X_{ijmt} - \sum_{m=1}^M \tilde{D}_{imt} \quad i = 1, \dots, P; j = 1, \dots, J; t = 2, \dots, T \tag{2}$$

$$I_{ij1} = IN_{ij1} + \sum_{m=1}^M X_{ijm1} - \sum_{m=1}^M \tilde{D}_{im1} \quad i = 1, \dots, P; j = 1, \dots, J \tag{3}$$

$$\sum_{t=1}^T I_{ijt} + \sum_{t=1}^T \sum_{m=1}^M X_{ijmt} \gtrsim \sum_{t=1}^T \sum_{m=1}^M \tilde{D}_{imt} \quad i = 1, \dots, P; j = 1, \dots, J \tag{4}$$

$$I_{imt} = I_{im(t-1)} + \tilde{D}_{imt} - CR_{imt} - \eta I_{imt} \quad i = 1, \dots, P; m = 1, \dots, M; t = 2, \dots, T \tag{5}$$

$$I_{im1} = IN_{im1} + \tilde{D}_{im1} - CR_{im1} - \eta I_{im1} \quad i = 1, \dots, P; m = 1, \dots, M \tag{6}$$

$$(1 - \eta) \sum_{t=1}^T I_{imt} + \sum_{t=1}^T \tilde{D}_{imt} \gtrsim \sum_{t=1}^T CR_{imt} \quad i = 1, \dots, P; m = 1, \dots, M \tag{7}$$

$$X_{ijmt} \geq \sum_{l=1}^L a_{ijmkt} R_{ijmkt} \quad i = 1, \dots, P; j = 1, \dots, J; m = 1, \dots, M; t = 1, \dots, T \tag{8}$$

$$\sum_{l=1}^L R_{ijmkt} = 1 \quad i = 1, \dots, P; j = 1, \dots, J; m = 1, \dots, M; t = 1, \dots, T \tag{9}$$

$$L_{jmt} = \sum_{i=1}^P \left[ w_i X_{ijmt} \sum_{l=1}^L R_{ijmkt} \right] \quad j = 1, \dots, J; m = 1, \dots, M; t = 1, \dots, T \tag{10}$$

$$L_{jmt} \geq \sum_{k=1}^K b_{jmkt} Z_{jmkt} \quad j = 1, \dots, J; m = 1, \dots, M; t = 1, \dots, T \tag{11}$$

$$\sum_{k=1}^K Z_{jmk t} = 1 \quad j = 1, \dots, J; m = 1, \dots, M; t = 1, \dots, T \quad (12)$$

$$X_{ijm t}, I_{im t}, I_{ijt}, L_{jmt} \geq 0 \quad R_{ijm t} = 0 \text{ or } 1, \quad Z_{jmk t} = 0 \text{ or } 1$$

In the proposed model, Eq. (1) is the Fuzzy objective function to minimize the cost incurred in holding ending inventory at source, cost of purchasing the products, and cost of inspection on ordered quantity by destination  $m$  in period  $t$  reflected by the first term of the objective function; the combination of transportation cost from the source to the destination, and holding cost at destination is the second term. The cost is calculated for the duration of the planning horizon. The ordering cost is a fixed cost and is not affected by the ordering quantities and therefore is not the part of objective function. Constraints (2–7) are the balancing equations for sources and destinations where Eq. (2) finds total ending inventory at source  $j$  of  $i$ th product in  $t^{th}$  period is found by reducing the fuzzy demand of all the destinations from total of ending inventory of previous period and ordered quantity at  $t^{th}$  period of all the destinations. Equation (3) finds total ending inventory at source  $j$  of  $i^{th}$  product in the first period by reducing the fuzzy demand of all the destinations from the total of initial inventory if the planning horizon and ordered quantity is at first period of all the destinations. Equation (4) shows that total fuzzy demand in all periods from all destinations is less than or equal to the total ending inventory and ordered quantity at source  $j$  in all periods, i.e., shortages are not allowed. Equation (5) calculates ending inventory at  $m^{th}$  destination for  $t^{th}$  period by reducing consumption rate and fraction of deteriorated ending inventory of the same destination from the combination of ending inventory of previous period and fuzzy demand of at  $m^{th}$  destination. Equation (5) calculates ending inventory for the first period at  $m^{th}$  destination by reducing consumption and fraction of deteriorated ending inventory of the same destination from the combination of initial inventory of planning horizon and fuzzy demand of  $m^{th}$  destination. Equation (7) shows that the total consumption in all the periods at  $m^{th}$  destination is less than or equal to the total ending inventory and fuzzy demand at destination  $m$  in all the periods, i.e., shortages are not allowed. Equations (8–9) find out the order quantity of all products in period  $t$  which may exceed the quantity break threshold and avails discount on ordered quantity at exactly one quantity discount level. Equation (10) is the integrator for procurement Eqs. (2–9) and transportation Eqs. (11–12), which calculates per product weighted quantity to be transported from source  $j$  to destination  $m$ . Equations (11–12) find the weighted transport quantity of all products in period  $t$  which may exceed the freight break threshold, and avail discount on transportation quantity at exactly one freight discount break.

### 3.5 Price Breaks

As discussed above, variable  $R_{ijm}l_t$  specifies the fact that when the order size at period  $t$  is larger than  $a_{ijm}l_t$  it results in discounted prices for the ordered items for which the price breaks are defined as; Price breaks for ordering quantity are:

$$d_f = \begin{cases} d_{ijm}l_t & a_{ijm}l_t \leq X_{ijm}t \leq a_{ijm}(l+1)t \\ d_{ijm}L_t & X_{ijm}t \geq a_{ijm}L_t \end{cases}$$

$i = 1, \dots, P; j = 1, \dots, J; t = 1, \dots, T; l = 1, \dots, L; m = 1, \dots, M$

Freight breaks for transporting quantity are:

Here  $b_{jmk}t$  is the minimum required quantity to be transported

$$d_f = \begin{cases} f_{jmk}t & b_{jmk}t \leq L_{jmt} \leq b_{jm(k+1)t} \\ f_{jmK}t & L_{jmt} \geq b_{jmK}t \end{cases}$$

$j = 1, \dots, J; m = 1, \dots, M; t = 1, \dots, T$

## 4 Fuzzy Solution Algorithm

The following algorithm [7] specifies the sequential steps to solve the fuzzy mathematical programming problems.

**Step 1.** Compute the crisp equivalent of the fuzzy parameters using a defuzzification function. The same defuzzification function is to be used for each of the parameters. Let  $\bar{D}_{imt}$  be the defuzzified value of  $\tilde{D}_{imt}$  and  $D_{imt}^1, D_{imt}^2, D_{imt}^3$  be triangular fuzzy numbers then,  $\bar{D}_{imt} = (D_{imt}^1 + 2D_{imt}^2 + D_{imt}^3)/4, i = 1, \dots, P; t = 1, \dots, T; m = 1, \dots, M$

$\bar{D}_{imt}$  and  $C_0$  are defuzzified aspiration levels of model's demand and cost. Similarly,  $\bar{h}_{ijt}$  and  $\bar{h}_{imt}$  are defuzzified aspiration levels of holding cost at source and destination.

**Step 2.** Employ extension principle to identify the fuzzy decision, which results in a crisp mathematical programming problem and on substituting the values for

$\bar{D}_{imt}$  as  $\tilde{D}_{imt}; \bar{h}_{imt}$  as  $\tilde{h}_{imt}; \bar{h}_{ijt}$  as  $\tilde{h}_{ijt}$ , the problem becomes:

$$\text{Min } \bar{C} = \sum_{t=1}^T \sum_{j=1}^J \sum_{i=1}^P \left[ \bar{h}_{ijt} I_{ijt} + \sum_{m=1}^M \left\{ \left( \sum_{l=1}^L R_{ijm}l_t d_{ijm}l_t \right) \varphi_{ijm} X_{ijm}t + \lambda_{ijm} X_{ijm}t \right\} \right]$$

$$+ \sum_{t=1}^T \sum_{m=1}^M \left[ \bar{h}_{imt} I_{imt} + \sum_{j=1}^J \left\{ \left( \sum_{k=1}^K Z_{jmk}t f_{jmk}t \right) \beta_{jmt} L_{jmt} \right\} \right]$$

$$\text{Subject to } X \in S = \{X \mid I_{ijt} = I_{ij(t-1)} + \sum_{m=1}^M X_{ijmt} - \sum_{m=1}^M \bar{D}_{imt} \quad \forall i, j, t = 2, \dots, T$$

$$I_{ij1} = IN_{ij1} + \sum_{m=1}^M X_{ijm1} - \sum_{m=1}^M \bar{D}_{im1} \quad \forall i, j; I_{imt} \\ = I_{im(t-1)} + \bar{D}_{imt} - CR_{imt} - \eta I_{imt} \quad \forall i, m, t$$

$$I_{im1} = IN_{im1} + \bar{D}_{im1} - CR_{im1} - \eta I_{im1} \quad \forall i, m; X_{ijmt} \geq \sum_{l=1}^L a_{ijmlt} R_{ijmlt} \quad \forall i, j, m, t$$

$$\sum_{l=1}^L R_{ijmlt} = 1 \quad \forall i, j, m, t; L_{jmt} = \sum_{i=1}^P \left[ w_i X_{ijmt} \sum_{l=1}^L R_{ijmlt} \right] \quad \forall j, m, t$$

$$L_{jmt} \geq \sum_{k=1}^K b_{jmkt} Z_{jmkt} \quad \forall j, m, t \quad \sum_{k=1}^K Z_{jmkt} = 1 \quad \forall j, m, t$$

$$\sum_{t=1}^T I_{ijt} + \sum_{t=1}^T \sum_{m=1}^M X_{ijmt} \geq \sum_{t=1}^T \sum_{m=1}^M \bar{D}_{imt} \quad \forall i, j;$$

$$(1 - \eta) \sum_{t=1}^T I_{imt} + \sum_{t=1}^T \bar{D}_{imt} \geq \sum_{t=1}^T CR_{imt} \quad \forall i, m$$

$$\bar{C}(X) \leq C_0$$

$$X_{ijmt}, I_{ijt}, I_{imt}, L_{jmt} \geq 0 \text{ and integer, } R_{ijmlt}, Z_{jmkt} \in \{0, 1\}, \theta \in [0, 1]$$

$$i = 1, \dots, P; j = 1, \dots, J; m = 1, \dots, M; t = 1, \dots, T; l = 1, \dots, L$$

**Step 3.** Define appropriate membership functions for each fuzzy inequalities as well as constraints corresponding to the objective function. The membership function for the fuzzy is given as

$$\mu_C(X) = \begin{cases} 1 & ; C(X) \leq C_0 \\ \frac{C_0^* - C(X)}{C_0^* - C_0} & ; C_0 \leq C(X) < C_0^* \\ 0 & ; C(X) > C_0^* \end{cases}$$

where  $C_0$  is the restriction and  $C_0^*$  is the tolerance levels to the fuzzy total cost.

$$\mu_{I_{ijt}}(X) = \begin{cases} 1 & ; I_{ijt}(X) \geq \bar{D}_0^* \\ \frac{I_{ijt}(X) - \bar{D}_0}{\bar{D}_0^* - \bar{D}_0} & ; \bar{D}_0 \leq I_{ijt}(X) < \bar{D}_0^* ; \\ 0 & ; I_{ijt}(X) > \bar{D}_0 \end{cases}$$

$$\mu_{I_{imt}}(X) = \begin{cases} 1 & ; I_{imt}(X) \geq \bar{D}_0^* \\ \frac{I_{imt}(X) - \bar{D}_0}{\bar{D}_0^* - \bar{D}_0} & ; \bar{D}_0 \leq I_{imt}(X) < \bar{D}_0^* \\ 0 & ; I_{imt}(X) > \bar{D}_0 \end{cases}$$

where  $\bar{D}_0^* = \sum_{m=1}^M \sum_{t=1}^T \bar{D}_{imt}$  is the aspiration and  $\bar{D}_0$  is the tolerance level to inventory constraint.

**Step 4.** Employ extension principle to identify the fuzzy decision. While solving the problem its objective function is treated as constraint. Each constraint is considered to be an objective for the decision maker and the problem can be looked as crisp mathematical programming problem

**Max**  $\theta$  subject to:  $\mu_c(X) \leq \theta$ ;  $\mu_{I_{ijt}}(X) \geq \theta$ ;  $\mu_{I_{imt}}(X) \geq \theta$ ;  $X \in S$  can be solved by the standard crisp mathematical programming algorithms.

## 5 Case Study

A dried fruit may deteriorate by oxidation, due to atmospheric oxygen and by water uptake. The oxidation may cause loss of color and undesirable odor changes. The case considers the influence of water on deterioration of dried fruits. Here, discussing the problems of a dried fruit company “Cocco” mainly visible in Gujarat (India). They purchase loose dried fruits from small wholesalers, pack, and brand them and further sell in their retail shops. The material is purchased from eight small wholesalers and shipped to their 18 retail shops. In the case, a tiny problem is explained with two wholesalers and three retail shops in Anand city (Gujarat), three products [Cashew Nuts (CN), Dry Dates (DD), and Dry Coconut (DC)] with packet size of 500gms, 1 kg, and 1.5 kg, respectively, and 3 months period during rainy season (June, July, and August). In Anand city wholesale shops are located in Akriti Nagar (AN), and Chavdapura (CP) and retail shops are located at Swastik Vatika (SV), Adarsh Colony (AC), and Govardhan Nagar (GN). The company faces problems like uncertain (fuzzy) demand which leads to fuzzy inventory carrying cost; deterioration of ending inventory (at constant rate i.e. 6%); inspection of each received packet at stores (₹3 for CN; ₹5 for DD and ₹7 for DC). Because of the company’s basic problems, they desire to find out the optimum order quantity from different wholesalers so that they keep low inventory at shops. This decision is able to keep cost at optimum level. The cost to company at retail shops includes cost of purchasing, inspection cost, transportation cost, inventory carrying cost at retail shops, and inventory carrying cost of wholesalers as they don’t keep big quantity. As far as the uncertain demand is concerned, the Co. has past idea of quantity demand, so it fixes three possible demands for each product. They also considered Aspired



**Table 1** Holding cost at wholesale shop (source) (₹)

Period		June		July		August	
PDT	Source	Fuzzy	DF	Fuzzy	DF	Fuzzy	DF
CN	AN	30,25,16.4	24.1	27,30,26.6	28.4	30,24,30.8	27.2
	CP	30,25,24.4	26.1	27,25,27.8	26.2	26,27,21.2	25.3
DD	AN	15,14,9.4	13.1	19,18,18.2	18.3	16,15,22.8	17.2
	CP	20,17,18.8	18.2	16,18,12.8	16.2	19,14,13.4	15.1
DC	AN	18,16,14.4	16.1	21,22,19.8	21.2	20,21,18.4	20.1
	CP	22,23,16.8	21.1	20,21,15.2	19.3	20,21,10.8	18.2

where *PDT* Product Type; *DF* Defuzzified

**Table 2** Holding cost at retail shop (destination) (₹)

Period		June		July		August	
PDT	Destination	Fuzzy	DF	Fuzzy	DF	Fuzzy	DF
CN	SV	26,25,21.6	24.4	25,26,27	26	35,34,39	35.5
	AC	30,28,29.6	28.9	25,26,19	24	22,20,24.4	21.6
	GN	28,27,28.4	27.6	23,25,15.8	22.2	26,25,23.2	24.8
DD	SV	27,28,23.8	26.7	23,25,17.4	22.6	33,31,35.8	32.7
	AC	27,25,30.6	26.9	27,25,30.6	26.9	25,26,21	24.5
	GN	26,27,23.6	25.9	21,22,18.2	20.8	25,26,22.2	24.8
DC	SV	24,26,18	23.5	26,24,29.6	25.9	16,15,17.2	15.8
	AC	24,24,30.8	25.7	20,19,15.6	18.4	14,13,14.8	13.7
	GN	15,16,11.4	14.6	17,16,17.4	16.6	24,23,24.4	23.6

Total Cost as ₹ 2692015 and Tolerance Cost as ₹ 3092015. Wholesellers provide quantity discounts on bulk purchase as well as transportation discounts are availed from the private carriage company. The data of the case are as follows (Tables 1, 2, 3, 4, 5, 6, 7, 8 and 9):

A LINGO code is generated to solve the proposed mathematical model by employing the case data. The total cost of the system is ₹ 2809260.605, which is comprising of ₹ 2359.5 as holding cost at all whole sellers, ₹ 2635993 as purchase cost, ₹ 85299 as inspection cost at retail stores, ₹ 81706.46 as transportation cost, and ₹ 3902.645 as holding cost at retail stores. We are discussing a small part of the results and the remaining results are shown in tubules in Tables 10, 11, 12, and 13. Ending inventory at Wholesale shop ‘AN’ is 0 pack of CN, 0 and 19 packs of DD and DC resp. Ending inventory at Retail store ‘SV’ are 2, 5, and 0 packs for product CN, DD, and DC resp. From wholesale shop AN, in the month of June, Co. ordered for retail store SV, and AC as 850 and 0 packs of CN with quantity discounts of 5 and 0% resp. 960 and 0 packs of DD with quantity discount of 6 and 0% for each. Transportation is done in weights (in kg). From wholesale point AN, 1692.5 and 501 kg is transported to retail store SV and AC each, 600 kg is transported to GN with transportation discount of 10, 0, and 0% respectively. As far as vagueness is concerned, Co. is able to minimize the uncertainty nearby 71%.

**Table 3** Demand at retail shop (destination) (pack)

Period		June		July		August	
PDT, aspiration	Destintination	Fuzzy	DF	Fuzzy	DF	Fuzzy	DF
CN, 2765	SV	240,270,300	270	290,340,290	315	290,340,310	320
	AC	280,290,340	300	340,390,440	390	210,240,190	220
	GN	240,270,340	280	300,310,440	340	300,310,400	330
DD, 3100	SV	210,240,150	210	300,310,480	350	430,460,450	450
	AC	380,390,440	400	380,390,160	330	330,350,330	340
	GN	380,390,240	350	460,490,480	480	200,170,220	190
DC, 2690	SV	200,170,180	180	340,380,340	360	380,390,400	390
	AC	380,390,360	380	240,270,260	260	230,220,250	230
	GN	380,390,280	360	280,290,300	290	240,230,260	240

Demand tolerance is always less than the aspired demand, which may vary.

**Table 4** Consumption at retail shop (destination) for each product (in pack)

June		July			August				
Destination	CN	DD	DC	CN	DD	DC	CN	DD	DC
SV	268	205	180	300	349	360	320	450	388
AC	298	396	378	387	325	255	216	340	227
GN	276	342	358	333	480	288	327	190	240

**Table 5** Purchase cost per pack (₹)

Period		June		July		August	
PDT	Destination	AN	CP	AN	CP	AN	CP
CN	SV	241	261	284	262	272	253
	AC	254	221	233	263	214	201
	GN	352	323	212	241	232	243
DD	SV	131	182	183	162	172	151
	AC	153	124	131	164	113	104
	GN	253	221	112	141	132	141
DC	SV	161	212	212	193	201	182
	AC	183	154	164	191	143	134
	GN	282	251	142	173	161	172

**Table 6** Transportation cost per weight (₹)

Period		June		July		August	
Destination		Source					
		AN	CP	AN	CP	AN	CP
SV		3	6	5	7	4	6
AC		6	5	7	6	8	7
GN		3	4	4	4	5	5

**Table 7** Quantity threshold and discount factor by source AN

CN		DD		DC	
Quantity threshold	Discount factor	Quantity threshold	Discount factor	Quantity threshold	Discount factor
0–100	1	0–200	1	0–205	1
100–200	0.97	200–320	0.98	205–310	0.92
200–320	0.96	320–480	0.96	310–400	0.87
320 and above	0.95	480 and above	0.94	400 and above	0.82

**Table 8** Quantity threshold and discount factor by source CP

CN		DD		DC	
Quantity threshold	Discount factor	Quantity threshold	Discount factor	Quantity threshold	Discount factor
0–120	1	0–190	1	0–150	1
120–250	0.90	190–300	0.9	150–300	0.95
250–360	0.84	300–450	0.86	300–410	0.88
360 and above	0.79	450 and above	0.8	410 and above	0.8

**Table 9** Weight threshold and discount factor

June		July		August	
Weight Threshold	Discount Factor	Weight Threshold	Discount Factor	Weight Threshold	Discount Factor
500–1000	1	600–900	1	600–1050	1
1000–1200	0.94	900–1400	0.91	1050–1500	0.9
1200 and above	0.9	1400 and above	0.87	1500 and above	0.85

**Table 10** Ending inventory at wholesale shop (in packs)

Period	June		July			August	
	AN	CP	AN	CP	AN	CP	
CN	0	0	0	0	0	0	
DD	0	1	0	0	0	0	
DC	19	90	0	0	0	7	

**Table 11** Ending inventory at wholesale shop (in packs)

Period	June			July			August		
	SV	AC	GN	SV	AC	GN	SV	AC	GN
CN	2	2	4	16	5	10	15	8	12
DD	5	4	8	5	8	7	5	7	8
DC	0	2	2	0	5	4	2	9	4

**Table 12** Ordered quantity/discount % age from wholesale shop to retail store

Period		June		July		August	
PDT	Destination	Source					
		AN	CP	AN	CP	AN	CP
	SV	850/5	0	0	0	0	0
CN	AC	0	850/21	0	0	870/5	870/21
	GN	0	0	1045/5	1045/21	0	0
	SV	960/6	1/0	600/6	0	0	0
DD	AC	0	529/20	0	560/20	380/4	789/20
	GN	0	431/14	560/6	559/20	600/6	191/10
SV	205/8	333/12	400/18	0	400/18	410/20	
DC	AC	334/13	631/20	0	410/20	460/18	184/5
	GN	400/18	46/0	491/18	410/20	0	273/5

**Table 13** Transported weights/discount % age from wholesale shop to retail shop

Period		June			July			August	
Source	SV	Destination							
		AC	GN	SV	AC	GN	SV	AC	GN
AN	1692.5/10	501	600	600	600	1819/13	600	1,505/15	600
CP	500.5	1900.5/10	500	600	615	1696.5/13	615	1,500/15	600.5

## 6 Conclusion

Although there are many studies reported for procurement-distribution models, very few of them have incorporated fuzzy environment on deteriorating natured products. The objective of minimizing total incurred fuzzy cost during holding at sources and destinations, procurement, transportation with fuzzy demand and fuzzy holding cost in a supply chain network with both quantity and transportation discounts has not been addressed so far. So, the current study proposed a mathematical model for the literature gap identified and mentioned in this study. The proposed model was validated by applying to the real case study data, where the study is trying to reduce vagueness in fuzzy environment which converts the model in crisp form.

**Acknowledgments** Kanika Gandhi (Lecturer, Quantitative Techniques and Operations) is thankful to her organization “Bharatiya Vidya Bhavan’s Usha and Lakshmi Mittal Institute of Management” to provide her opportunity for carrying research work.

## References

1. Silver, E.A., Meal, H.C.: A heuristic for selecting lot-size quantities for the case of a deterministic time varying demand rate and discrete opportunities for replenishment. *Prod. Invent. Manag.* **14**, 64–74 (1973)

2. Donaldson, W.A.: Inventory replenishment policy for a linear trend in demand- an analytical solution. *Oper. Res. Q.* **28**, 663–670 (1977)
3. Sachan, R.S.: On (T, Si) policy inventory model for deteriorating items with time proportional demand. *J. Oper. Res. Soc.* **35**, 1013–1019 (1984)
4. Goswami, A., Chowdhury, K.S.: An EOQ model for deteriorating items with shortages and linear trend in demand. *J. Oper. Res. Soc.* **42**, 1105–1110 (1991)
5. Kang, S., Kim, I.: A study on the price and production level of the deteriorating inventory system. *Int. J. Prod. Res.* **21**(6), 899–908 (1983)
6. Zimmermann, H.J.: Description and optimization of fuzzy systems. *Int. J. Gen. Syst.* **2**, 209–215 (1976)
7. Lai, Y.J., Hwang, C.L.: *Fuzzy mathematical programming, methods and applications*. Springer, Heidelberg (1992)
8. Lai, Y.J., Hwang, C.L.: *Fuzzy multiple objective decision making*. Springer, Heidelberg (1994)
9. Sommer, G.: Fuzzy inventory scheduling. In: Lasker, G. (ed.) *Applied Systems and Cybernetics*, vol. VI. Academic Press, New York (1981)
10. Kacprzyk, J., Staniewski, P.: Long term inventory policy making through fuzzy decision making models. *Fuzzy Sets Syst.* **8**, 117–132 (1982)
11. Lam, S.M., Wang, D.C.: A fuzzy mathematical model for the joint economic lot-size problem with multiple price breaks. *Eur. J. Oper. Res.* **45**, 499–504 (1996)
12. Roy, T.K., Maiti, M.: A fuzzy inventory model with constraints. *OPSEARCH* **32**(4), 287–298 (1995)

# A Goal Programming Model for Advertisement Selection on Online News Media

Prerna Manik, Anshu Gupta and P. C. Jha

**Abstract** Promotion plays an important role in determining success of a product/service. Out of the many mediums available, promotion through means of advertisements is most effective and is most commonly used. Due to increasing popularity of the Internet, advertisers yearn for placing their ads on web. Consequently, web advertising has become one of the major sources of income for many websites. Several websites provide free services to the users and generate revenue by placing ads on its webpages. Advertisement for any product/service is placed on the site considering various aspects such as webpage selection, customer demography, product category, page, slot, time, etc. Further, different advertisers bid different costs to place their ads on a particular rectangular slot of a webpage, that is, many ads compete with each other for their placement on a specific position. Hence, in order to maximize the revenue generated through the ads, optimal placement of ads becomes imperative. In this paper, we formulate an advertisement planning problem for web news media maximizing their revenue. Mathematical programming approach is used to solve the problem. A case study is presented in the paper to show the application of the problem.

**Keywords** Advertisement planning · Revenue maximization · Online news web

---

P. Manik (✉) · P. C. Jha  
Department of Operational Research, University of Delhi, Delhi, India  
e-mail: prernamanik@gmail.com

P. C. Jha  
e-mail: jhpc@yahoo.com

A. Gupta  
SBPPSE, Dr. B. R. Ambedkar University, Delhi, India  
e-mail: anshu@aud.ac.in

## 1 Introduction

Advertising is an indispensable component of the marketing strategy for any firm. A well-designed advertisement campaign attracts a huge customer base, creates a brand name for the product and thereby enhances sales. Firms spend a large amount of capital to create effective exposure for its products by means of advertisements (ads). Today we see various media for advertising, starting from hoardings to television commercials, print ads to web media, and many more. Companies generally use a mix of various ad media to create maximum exposure for their products. Amongst all kinds of advertising media, the Internet has become the most famous and adopted media by the advertisers as well as consumers. And its popularity is increasing as information technology is reaching more and more people in the world and consumers stay connected to web for long hours. Other reasons for popularity of web advertising over other traditional media include traceability, cost effectiveness, reach, interactivity, etc. It is also capable of providing the dual features of both print and television media. The study in this paper focuses on a web ad scheduling problem where the objective is to maximize the revenue generated from placing ads on the multiple pages of a website. Maximization is achieved by selecting the ads on a slot from various competing ads in such a way that all the slots on every webpage under consideration are full at every time instant throughout the planning horizon. The proposed model surmounts one of the major limitations of the literature in the area.

Web ads commonly known as “banner ads” are devoted to promote, market, sell, or provide specific information about a product, service, or commercial event on web. Television and radio ads are expensive, short lived, and people tend to ignore them. However, in the case of web ads, customers have a choice as to whether or not they want to read or click on a web ad, while the ads may create an impression on the web users irrespective of their choice.

Though banner ads are the most popular ads on the web and constitute a major proportion of web advertising, there are also other ads that have been adopted by the advertisers such as are pop-up and pop-under ads, floating ads, unicast ads, etc. However, scope of this paper is limited to banner ads only. A banner ad is a small, typically rectangular, graphic image, which is linked to a target webpage. Many different types of banners with different sizes are being used in web advertisement. Rectangular-shaped banner ads are the most common type of banner ads. These banners usually appear on the side, top, or bottom of a screen as a distinct, clickable image [9]. For e.g., in Fig. 1, [www.newswebsite.com](http://www.newswebsite.com) displays a top banner ad of IBEF and two side banner ads of Artha Villas and CRAZEAL.

Due to constantly increasing popularity and power of web advertising, more and more websites and blogs are evolving that provide free services to their users. For e.g., websites such as Download.com, soft32, softpedia provide free software download facilities to the users. Also there are websites such as ApnaCircle and LinkedIn which help millions of professionals to connect and share their ideas for free. Then there are also websites such as hindustantimes.com and timesofindia.com, which provides their users a free service of e-paper, that is, a reader can read the newspaper



Fig. 1 Banner Ads on www.newswebsite.com (Date clicked: September 15, 2012)

online. Such websites generate major portion of their revenue by placing ads on their webpages. Hence, for such sites, optimal placement of ads on their webpages becomes imperative.

Many researchers have been working in the area of scheduling ads on web from past few years. One of the major focuses of the work has been on the effectiveness of web ads. Yager [14] described a general framework for the competitive selection of ads at web sites. A methodology was described in the paper for the use of intelligent agents to help in the determination of the appropriateness of displaying a given ad to a visitor at a site using very specific information about potential customers. Fuzzy system modeling was used for the construction of these intelligent agents. Dreze and Zufryden [3], Intern.com Corp. [5], Kohda and Endo [6], Marx [8] and Ridsen et al. [11] tackled the issue of increasing the effectiveness of web ads. Intern.com Corp. [5], McCandless [9], and Novak and Hoffman [10] described web advertising theories and terminologies. Researchers viz. Aggarwal et al. [2], Adler et al. [1], Kumar et al. [7] considered the issue of optimizing the ad space on the web. Aggarwal et al. [2] described a framework and provided an overview of general methods for optimizing the management of ads on web servers. They described a minimum cost flow model in order to optimize the assignment of ads to the predefined standard sizes of slots on webpages. Adler et al. [1] provided a heuristic called SUBSET-LSLF.

A major contribution in the area of ad scheduling has been done by Kumar et al. [7] and Gupta et al. [4]. Kumar et al. [7] addressed the problem of scheduling ads on a webpage in order to maximize revenue, for which they maximized the utilization of space available to place the ads. They used genetic algorithms to solve the problem. The major limitations of the model are that it considers only a particular side banner space on a specific page whose width is fixed and length can vary. The rectangular dimensions can thus be reduced to single dimension as the other dimension, i.e., width was assumed to be of unit size. All or some ads that can fit in this banner should therefore have the width of unit size. However, in practice banner ads that compete to be placed on a rectangular slot may be of varying rectangular dimensions. Second, in reality, the varying dimension of the slot for the banner can be a real value and need



not necessarily be an integral multiple of the defined unit slot length. Therefore, the problem that maximizes the space utilization may not be the true representative of the revenue maximization problem. Gupta et al. [4] overcame the limitations of the model formulated by Kumar et al. [7]. They considered the set of ads competing to be placed on various rectangular slots (that may have varying rectangular dimensions) in a given planning horizon on various webpages of a news website in order to maximize the revenue, where the revenue is generated from the costs different advertisers pay to place their ads on the website. One of the limitations of the model formulated by Gupta et al. [4] is that it allows an ad to appear more than once on the same webpage. For instance, suppose that a webpage  $W_1$  has three rectangular slots and suppose that an ad  $A_1$  has appeared in slot 1 of this webpage at time period  $T_1$ . Then according to this model this ad  $A_1$  can also appear in slot 2 and/or slot 3 of webpage  $W_1$  at the same time period  $T_1$ .

In this paper, we formulate a web ad scheduling problem considering sets of ads competing to be placed on various rectangular slots (which may have different rectangular dimensions) in a given planning horizon on different webpages of a news website in order to maximize the revenue. The revenue is generated from the costs different advertisers pay to place their ads on the website. The proposed model restricts the selection of an ad on the same webpage more than once at any instant of time. We also discuss the solution methods for the proposed model, which is a 0-1 linear programming model. The model can be programmed and solved on LINGO [13] software. Depending on the available data the model may or may not be feasible. As the number of constraints increase the feasible area reduces and may tend to infeasibility. In this case, we use goal programming approach (GPA) [12] to obtain a compromised solution. The goal model of the problem can also be programmed and solved on LINGO [13].

The rest of the paper is organized as follows. In Sect. 2, we discuss the mathematical model formulation. A Case study has been discussed in Sect. 3. Section 4 concludes the paper.

## 2 Model Formulation

### Notations

- $n$  : total number of webpages
- $m_j$  : number of rectangular slots on  $j$ th webpage
- $K$  : total number of ads
- $P$  : total number of time units in a day
- $Q$  : total number of days in a planning horizon
- $T$  : total number of time units over the planning horizon, where  $T = P \times Q$
- $C_{ijk}$  : cost of  $k$ th ad competing for  $i$ th rectangular slot on  $j$ th webpage
- $S$  : set of  $K$  ads
- $S_{ij}$  : set of ads which compete for  $i$ th rectangular slot on  $j$ th webpage;  $S_{ij} \subseteq S \forall i, j$

- $A_k$  :  $k$ th ad  
 $w_k$  : minimum required time units for which  $k$ th ad appears in any rectangular slot  
 $W_k$  : maximum time units for which  $k$ th ad appears in all the rectangular slots  
 $D$  : total number of rectangular slots over a planning horizon (= Total number of rectangular slots on all the webpages  $\times$  Length of planning horizon)

## 2.1 Web Ad Scheduling Problem

Web service providers endeavors to generate maximum revenue from the ads that are displayed on the webpages of their website. Therefore, optimal selection of the ads from the available sets of ads that compete to be placed on different rectangular slots of different webpages becomes critical.

We consider a set of  $K$  ads,  $S = \{A_1, A_2, \dots, A_K\}$  that compete to be placed on different rectangular slots of various webpages of a website in a planning horizon. The problem is formulated for a website consisting of  $n$  webpages, where  $j$ th webpage consists of  $m_j$  number of rectangular slots. A subset of ads  $S_{ij}$  competes to be placed on  $i$ th rectangular slot of  $j$ th webpage over a planning horizon. An advertiser  $k$ , where  $A_k \in S_{ij}$ , pays cost  $C_{ijk}$  to place his ad on  $i$ th rectangular slot of  $j$ th webpage with minimum frequency  $w_k$  and maximum frequency  $W_k$ .

Web ads are scheduled daily, fortnightly, weekly, monthly, or quarterly and so on depending on to the time units allocated to the ads. An ad which appears at any location stays there for some time and is then replaced by another ad. Consider for example, the minimum time for which an ad appears in any rectangular slot is one minute then, there will be  $60 \times 24 = 1440$  time slots/units ( $P$ ) in a day. And if the scheduling is to be done for say one week (i.e.,  $Q = 7$  days) then there will be a total of  $1440 \times 7 = 10080$  time slots, i.e., the planning horizon would be  $T = P \times Q = 1440 \times 7 = 10080$  time units.

Over a planning horizon, for each rectangular slot, web service provider selects ads which maximize their revenue and the unscheduled ads may compete for space in the next planning horizon with new ads. The set of ads assigned to all the slots for this time period is seen by the visitors who visit the site during that time interval and then the ads are updated according to their schedule. Now consider that we have in total  $\sum_{j=1}^n m_j$  number of rectangular slots and a total of  $T = P \times Q$  time units in the planning horizon, which can be considered as a scheduling problem of  $D = T \times \sum_{j=1}^n m_j$  slots. Minimum frequency  $w_k$  represents the number of time units for which the ad  $A_k$  must appear when selected for some slot and maximum frequency  $W_k$  represents the number of time units for which the ad  $A_k$  must appear in all the rectangular slots over a planning horizon.

The problem to maximize the revenue generated by placing ads on the website over a planning horizon, which depends heavily on the costs different companies pay for placing their ads on  $i$ th rectangular slot of  $j$ th webpage is as follows:

$$\begin{aligned}
 \text{Maximize } R &= \sum_{i=1}^{m_j} \sum_{j=1}^n \sum_{k \in S_{ij}} \sum_{t=1}^T C_{ijk} x_{ijkt} \\
 \text{Subject to } \sum_{t=1}^T x_{ijkt} &\geq w_k z_{ijk} \quad \forall i, j, k \in S_{ij} \\
 \sum_{i=1}^{m_j} \sum_{j=1}^n \sum_{t=1}^T x_{ijkt} &\leq W_k \quad \forall k \in S_{ij} \\
 \sum_{i=1}^{m_j} \sum_{j=1}^n \sum_{k \in S_{ij}} \sum_{t=1}^T x_{ijkt} &\leq D \tag{1} \\
 \sum_{i=1}^{m_j} x_{ijkt} &= 1 \quad \forall j, k \in S_{ij}, t \\
 \sum_{k \in S_{ij}} x_{ijkt} &\leq 1 \quad \forall i, j, t \\
 \sum_{k \in S_{ij}} z_{ijk} &\geq 1 \quad \forall i, j
 \end{aligned}$$

$$\begin{aligned}
 \text{where } x_{ijkt} &= \begin{cases} 1, & \text{if } k\text{th ad is chosen to be placed on } i\text{th rectangular slot of } j\text{th} \\ & \text{webpage at } t\text{th time unit} \\ 0, & \text{otherwise} \end{cases} \\
 z_{ijk} &= \begin{cases} 1, & \text{if } k\text{th ad is placed on } i\text{th rectangular slot of } j\text{th webpage} \\ 0, & \text{otherwise} \end{cases}
 \end{aligned}$$

In the above problem  $t = 1, \dots, P \times Q = T$ . Time slots are arranged in the ordinal manner i.e. the 1st  $P$  time units will correspond to 1st day, next  $P$  for 2nd day and so on.

Here, first constraint ensures that  $k$ th ad is assigned to at least  $w_k$  time slots. Second constraint guarantees that  $k$ th ad is assigned to not more than  $W_k$  number of slots over the planning horizon. Next constraint ensures the fullness of total number of rectangular slots over the planning horizon. Fourth constraint guarantees that if an ad is selected to be placed on any rectangular slot of a webpage at any given time period then that ad cannot appear on any other rectangular slot of that webpage at the same time unit. Next constraint ensures that at a particular time unit, on each rectangular slot on a webpage, not more than one ad can be placed. Last constraint ensures that number of times ad  $k$  appears on a particular rectangular slot over the planning horizon can be one or more than one.

Problem (1) can be solved using LINGO [13] software if a feasible solution to the problem exists. Otherwise for an infeasible solution, GPA [12] can be used to obtain a compromised solution.

### 2.2 Goal Programming Approach

In a simpler version of goal programming approach (GPA), management sets goals and relative importance (weights) for different objectives. Then an optimal solution is defined as one that minimizes both positive and negative deviations from set goals simultaneously or minimizes the amount by which each goal can be violated. First we solve the problem using rigid constraints only and then the goals of objectives are incorporated depending upon whether priorities or relative importance of different objectives are well defined or not. Problem (1) can be solved in two stages as follows:

$$\begin{aligned}
 \text{Minimize } g_0(\eta, \rho, x, z) &= \sum_{i=1}^{m_j} \sum_{j=1}^n \sum_{k \in S_{ij}} \eta_{ijk}^1 + \sum_{k \in S_{ij}} \rho_k^2 + \rho^3 \\
 &+ \sum_{j=1}^n \sum_{k \in S_{ij}} \sum_{t=1}^T (\eta_{jkt}^4 + \rho_{jkt}^4) + \sum_{i=1}^{m_j} \sum_{j=1}^n \sum_{t=1}^T \rho_{ijt}^5 \\
 &+ \sum_{i=1}^{m_j} \sum_{j=1}^n \eta_{ij}^6 \\
 \text{Subject to } &\sum_{t=1}^T x_{ijkt} + \eta_{ijk}^1 - \rho_{ijk}^1 = w_k z_{ijk} \quad \forall i, j, k \in S_{ij} \\
 &\sum_{i=1}^{m_j} \sum_{j=1}^n \sum_{t=1}^T x_{ijkt} + \eta_k^2 - \rho_k^2 = W_k \quad \forall k \in S_{ij} \\
 &\sum_{i=1}^{m_j} \sum_{j=1}^n \sum_{k \in S_{ij}} \sum_{t=1}^T x_{ijkt} + \eta^3 - \rho^3 = D \tag{2} \\
 &\sum_{i=1}^{m_j} x_{ijkt} + \eta_{jkt}^4 - \rho_{jkt}^4 = 1 \quad \forall j, k \in S_{ij}, t \\
 &\sum_{k \in S_{ij}} x_{ijkt} + \eta_{ijt}^5 - \rho_{ijt}^5 = 1 \quad \forall i, j, t \\
 &\sum_{k \in S_{ij}} z_{ijk} + \eta_{ij}^6 - \rho_{ij}^6 = 1 \quad \forall i, j \\
 &\eta, \rho \geq 0
 \end{aligned}$$

where,  $x_{ijkt}$  and  $z_{ijk}$  are as defined above and  $\eta$  and  $\rho$  are over-and under-achievement (positive- and negative-deviational) variables from the goals for the objective/constraint function and  $g_0(\eta, \rho, x, z)$ , is Goal objective function corresponding to rigid constraints.

The choice of deviational variable in the goal objective functions which has to be minimized depends upon the following rule. Let  $f(X)$  and  $b$  be the function and its goal respectively and  $\eta$  and  $\rho$  be the over and under achievement variables then

- if  $f(X) \leq b$ ,  $\rho$  is minimized under the constraints  $f(X) + \eta - \rho = b$ ,
- if  $f(X) \geq b$ ,  $\eta$  is minimized under the constraints  $f(X) + \eta - \rho = b$ ,
- if  $f(X) = b$ ,  $\eta + \rho$  is minimized under the constraints  $f(X) + \eta - \rho = b$ .

Let  $(\eta^0, \rho^0, x^0, z^0)$  be the optimal solution for the problem (2) and  $g_0(\eta^0, \rho^0, x^0, z^0)$  be its corresponding objective function value then finally GP problem can be formulated using optimal solution of the problem (2) through the problem (1) as follows:

$$\begin{aligned}
 &\textbf{Minimize} \quad g(\eta, \rho, x, z) = \eta^7 \\
 &\textbf{Subject to} \quad \sum_{t=1}^T x_{ijkt} + \eta_{ijk}^1 - \rho_{ijk}^1 = w_k z_{ijk} \quad \forall i, j, k \in S_{ij} \\
 &\quad \quad \quad \sum_{i=1}^{m_j} \sum_{j=1}^n \sum_{t=1}^T x_{ijkt} + \eta_k^2 - \rho_k^2 = W_k \quad \forall k \in S_{ij} \\
 &\quad \quad \quad \sum_{i=1}^{m_j} \sum_{j=1}^n \sum_{k \in S_{ij}} \sum_{t=1}^T x_{ijkt} + \eta^3 - \rho^3 = D \\
 &\quad \quad \quad \sum_{i=1}^{m_j} x_{ijkt} + \eta_{jkt}^4 - \rho_{jkt}^4 = 1 \quad \forall j, k \in S_{ij}, t \\
 &\quad \quad \quad \sum_{k \in S_{ij}} x_{ijkt} + \eta_{ijt}^5 - \rho_{ijt}^5 = 1 \quad \forall i, j, t \\
 &\quad \quad \quad \sum_{k \in S_{ij}} z_{ijk} + \eta_{ij}^6 - \rho_{ij}^6 = 1 \quad \forall i, j \\
 &\quad \quad \quad \sum_{i=1}^{m_j} \sum_{j=1}^n \sum_{k \in S_{ij}} \sum_{t=1}^T C_{ijk} x_{ijkt} + \eta^7 - \rho^7 = R^* \\
 &\quad \quad \quad g_0(\eta, \rho, x, z) = g_0(\eta^0, \rho^0, x^0, z^0) \\
 &\quad \quad \quad \eta, \rho \geq 0
 \end{aligned} \tag{3}$$

where  $R^*$  is the aspiration level desired by the management on revenue and  $g(\eta, \rho, x, z)$  is objective function of the problem (3). Problem (3) is solved using LINGO [13].

### 3 Case Study

In case of online news services, users spend long time on sites for reading news. In case of such websites, ads are updated periodically during this period, which is taken to be 1 h (length of one time slot) here.

We consider a news website which consists of five webpages. These pages have 3, 4, 2, 3, and 3 rectangular slots, respectively. A set of sixty ads,  $S = \{A_1, A_2, \dots, A_{60}\}$  compete to be placed on webpages of a news website in a planning horizon, which is taken as 1 week. Now, a week consists of 7 days and each day consists of 24 h. Since ads are updated every hour on the webpages, we refer to each hour as a time unit. Thus, in this case, we have  $168 (= 24 \times 7)$  time units to schedule ads. Ads need to be placed in  $D = \sum_{j=1}^5 m_j \times T (= 3 + 4 + 2 + 3 + 3) \times 168 = 2520$  slots. Sets of ads competing for  $i$ th rectangular slot on  $j$ th webpage and corresponding costs are as follows:

- $S_{11} = \{A_1, A_3, A_6, A_8, A_{10}, A_{13}, A_{15}, A_{18}, A_{20}, A_{23}, A_{25}, A_{27}, A_{29}, A_{32}, A_{33}, A_{36}, A_{38}, A_{40}, A_{43}, A_{44}, A_{46}, A_{49}, A_{51}, A_{54}, A_{57}, A_{59}\}; C_{11k} = 2,500 \quad \forall k \in S_{11}$
- $S_{21} = \{A_2, A_4, A_6, A_9, A_{11}, A_{13}, A_{14}, A_{16}, A_{19}, A_{22}, A_{24}, A_{26}, A_{28}, A_{31}, A_{33}, A_{35}, A_{37}, A_{39}, A_{42}, A_{44}, A_{47}, A_{49}, A_{50}, A_{52}, A_{54}, A_{56}, A_{57}, A_{60}\}; C_{21k} = 2,300 \quad \forall k \in S_{21}$
- $S_{31} = \{A_1, A_2, A_5, A_8, A_{10}, A_{12}, A_{14}, A_{17}, A_{18}, A_{20}, A_{23}, A_{24}, A_{26}, A_{28}, A_{29}, A_{31}, A_{34}, A_{36}, A_{37}, A_{38}, A_{40}, A_{42}, A_{43}, A_{45}, A_{47}, A_{50}, A_{51}, A_{53}, A_{55}, A_{58}, A_{59}\}; C_{31k} = 2,000 \quad \forall k \in S_{31}$
- $S_{12} = \{A_2, A_3, A_5, A_7, A_9, A_{11}, A_{13}, A_{15}, A_{17}, A_{19}, A_{21}, A_{22}, A_{24}, A_{25}, A_{27}, A_{30}, A_{32}, A_{35}, A_{36}, A_{38}, A_{39}, A_{41}, A_{43}, A_{44}, A_{46}, A_{47}, A_{49}, A_{52}, A_{54}, A_{56}, A_{60}\}; C_{12k} = 1850 \quad \forall k \in S_{12}$
- $S_{22} = \{A_1, A_3, A_4, A_6, A_8, A_{11}, A_{14}, A_{16}, A_{18}, A_{19}, A_{21}, A_{23}, A_{26}, A_{27}, A_{28}, A_{29}, A_{33}, A_{34}, A_{37}, A_{39}, A_{41}, A_{44}, A_{45}, A_{47}, A_{48}, A_{50}, A_{51}, A_{54}, A_{55}, A_{57}, A_{59}\}; C_{22k} = 1800 \quad \forall k \in S_{22}$
- $S_{32} = \{A_1, A_2, A_5, A_6, A_9, A_{12}, A_{15}, A_{17}, A_{18}, A_{20}, A_{22}, A_{24}, A_{25}, A_{26}, A_{28}, A_{30}, A_{34}, A_{35}, A_{38}, A_{40}, A_{42}, A_{46}, A_{48}, A_{51}, A_{55}, A_{58}\}; C_{32k} = 1700 \quad \forall k \in S_{32}$
- $S_{42} = \{A_3, A_4, A_6, A_7, A_{10}, A_{12}, A_{14}, A_{16}, A_{17}, A_{19}, A_{22}, A_{25}, A_{27}, A_{29}, A_{30}, A_{32}, A_{35}, A_{36}, A_{37}, A_{40}, A_{42}, A_{45}, A_{46}, A_{47}, A_{48}, A_{50}, A_{52}, A_{54}, A_{56}, A_{58}, A_{60}\}; C_{42k} = 1600 \quad \forall k \in S_{42}$
- $S_{13} = \{A_1, A_2, A_4, A_5, A_8, A_9, A_{11}, A_{13}, A_{15}, A_{17}, A_{18}, A_{20}, A_{21}, A_{23}, A_{24}, A_{28}, A_{31}, A_{33}, A_{35}, A_{37}, A_{39}, A_{41}, A_{43}, A_{45}, A_{48}, A_{51}, A_{52}, A_{53}, A_{54}, A_{55}, A_{57}, A_{59}\}; C_{13k} = 1500 \quad \forall k \in S_{13}$
- $S_{23} = \{A_2, A_3, A_5, A_6, A_7, A_{10}, A_{12}, A_{14}, A_{16}, A_{18}, A_{19}, A_{21}, A_{23}, A_{26}, A_{28}, A_{29}, A_{31}, A_{34}, A_{36}, A_{38}, A_{40}, A_{42}, A_{44}, A_{46}, A_{49}, A_{53}, A_{54}, A_{58}, A_{60}\}; C_{23k} = 1400 \quad \forall k \in S_{23}$
- $S_{14} = \{A_3, A_4, A_8, A_{10}, A_{11}, A_{14}, A_{17}, A_{22}, A_{24}, A_{25}, A_{26}, A_{29}, A_{32}, A_{34}, A_{38}, A_{41}, A_{44}, A_{46}, A_{49}, A_{51}, A_{53}, A_{56}, A_{59}\}; C_{14k} = 1300 \quad \forall k \in S_{14}$
- $S_{24} = \{A_2, A_4, A_7, A_9, A_{12}, A_{14}, A_{16}, A_{18}, A_{21}, A_{23}, A_{26}, A_{28}, A_{29}, A_{31}, A_{33}, A_{35}, A_{37}, A_{39}, A_{42}, A_{45}, A_{47}, A_{49}, A_{52}, A_{54}, A_{56}, A_{59}, A_{60}\}; C_{24k} = 1200 \quad \forall k \in S_{24}$
- $S_{34} = \{A_2, A_3, A_5, A_7, A_{10}, A_{13}, A_{15}, A_{17}, A_{19}, A_{22}, A_{25}, A_{26}, A_{29}, A_{32}, A_{33}, A_{36}, A_{38}, A_{40}, A_{43}, A_{44}, A_{46}, A_{48}, A_{51}, A_{53}, A_{55}, A_{58}, A_{60}\}; C_{34k} = 1100 \quad \forall k \in S_{34}$
- $S_{15} = \{A_1, A_5, A_6, A_8, A_9, A_{11}, A_{12}, A_{16}, A_{18}, A_{20}, A_{22}, A_{23}, A_{25}, A_{27}, A_{30}, A_{34}, A_{35}, A_{39}, A_{41}, A_{43}, A_{45}, A_{46}, A_{47}, A_{48}, A_{51}, A_{54}, A_{55}, A_{57}, A_{59}\}; C_{15k} = 1000 \quad \forall k \in S_{15}$
- $S_{25} = \{A_2, A_4, A_6, A_8, A_{10}, A_{13}, A_{15}, A_{17}, A_{19}, A_{21}, A_{24}, A_{26}, A_{28}, A_{31}, A_{33}, A_{35}, A_{36}, A_{38},$

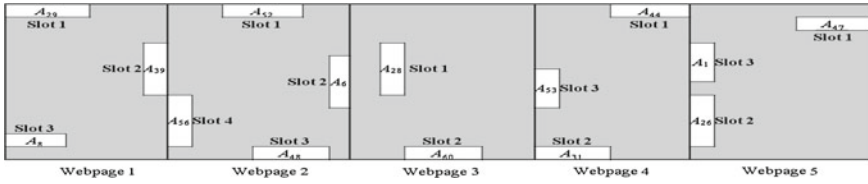


Fig. 2 Display of ads on the news website at time unit  $t = 66$

$$A_{40}, A_{42}, A_{44}, A_{46}, A_{47}, A_{49}, A_{50}, A_{53}, A_{56}, A_{58}, A_{59}; C_{25k} = 850 \quad \forall k \in S_{25}$$

$$S_{35} = \{A_1, A_3, A_5, A_7, A_9, A_{11}, A_{12}, A_{14}, A_{18}, A_{20}, A_{21}, A_{23}, A_{25}, A_{27}, A_{30}, A_{32}, A_{34}, A_{37},$$

$$A_{39}, A_{41}, A_{43}, A_{45}, A_{48}, A_{50}, A_{52}, A_{54}, A_{57}, A_{59}\}; C_{35k} = 800 \quad \forall k \in S_{35}$$

Although different companies may pay different costs for placing their ads on a particular rectangular slot of a specific webpage but for the sake of simplicity, cost for all the ads competing to be placed on any rectangular slot is taken to be same here. Further, minimum and maximum frequencies of the ads are tabulated in Table 1.

When problem (1) is solved using the above data, we get an infeasible solution and hence it is imperative to use GPA to obtain a compromised solution. Aspiration desired on revenue is taken to be ₹ 40,00,000. The compromised solution obtained after applying GPA is given in Table 2.

The revenue generated by this placement of ads comes out to be ₹ 38,47,200. It can be seen from Table 2 that when users access webpage 3 of news website at 18th hour of day 3 i.e., at  $t = 66$ , ad  $A_{60}$  appears in second slot of that webpage. To give a clear picture of how the ads are actually displayed to the users in accordance with the schedule obtained in Table 2, a pictorial representation of the selected ads on the news website at time unit  $t = 66$  is shown in Fig. 2.

**Table 1** Frequency table

Ads ( $A_k$ )	Min. freq. ( $w_k$ )	Max. freq. ( $W_k$ )	Ads ( $A_k$ )	Min. freq. ( $w_k$ )	Max. freq. ( $W_k$ )	Ads ( $A_k$ )	Min. freq. ( $w_k$ )	Max. freq. ( $W_k$ )	Ads ( $A_k$ )	Min. freq. ( $w_k$ )	Max. freq. ( $W_k$ )	Ads ( $A_k$ )	Min. freq. ( $w_k$ )	Max. freq. ( $W_k$ )	Ads ( $A_k$ )	Min. freq. ( $w_k$ )	Max. freq. ( $W_k$ )
A <sub>1</sub>	6	50	A <sub>11</sub>	6	68	A <sub>21</sub>	5	55	A <sub>31</sub>	5	50	A <sub>41</sub>	5	50	A <sub>51</sub>	7	50
A <sub>2</sub>	7	62	A <sub>12</sub>	5	50	A <sub>22</sub>	6	60	A <sub>32</sub>	4	48	A <sub>42</sub>	7	55	A <sub>52</sub>	5	45
A <sub>3</sub>	6	55	A <sub>13</sub>	4	52	A <sub>23</sub>	7	55	A <sub>33</sub>	6	52	A <sub>43</sub>	6	52	A <sub>53</sub>	4	44
A <sub>4</sub>	5	60	A <sub>14</sub>	6	50	A <sub>24</sub>	6	52	A <sub>34</sub>	5	50	A <sub>44</sub>	7	60	A <sub>54</sub>	8	65
A <sub>5</sub>	7	60	A <sub>15</sub>	4	45	A <sub>25</sub>	7	60	A <sub>35</sub>	7	62	A <sub>45</sub>	6	55	A <sub>55</sub>	5	50
A <sub>6</sub>	6	58	A <sub>16</sub>	5	52	A <sub>26</sub>	7	55	A <sub>36</sub>	6	58	A <sub>46</sub>	8	62	A <sub>56</sub>	4	48
A <sub>7</sub>	5	55	A <sub>17</sub>	7	68	A <sub>27</sub>	5	60	A <sub>37</sub>	6	55	A <sub>47</sub>	7	58	A <sub>57</sub>	4	50
A <sub>8</sub>	5	60	A <sub>18</sub>	8	70	A <sub>28</sub>	7	60	A <sub>38</sub>	7	60	A <sub>48</sub>	5	50	A <sub>58</sub>	3	40
A <sub>9</sub>	6	62	A <sub>19</sub>	6	60	A <sub>29</sub>	6	55	A <sub>39</sub>	6	55	A <sub>49</sub>	6	52	A <sub>59</sub>	7	56
A <sub>10</sub>	5	60	A <sub>20</sub>	4	50	A <sub>30</sub>	4	52	A <sub>40</sub>	6	58	A <sub>50</sub>	5	48	A <sub>60</sub>	5	60



**Table 2** Ads allocated to rectangular slot  $i$  of web page  $j$  at time unit  $t$

Time slots	Rectangular slots																						
	Slot 11	Slot 21	Slot 31	Slot 12	Slot 22	Slot 32	Slot 42	Slot 13	Slot 23	Slot 14	Slot 24	Slot 34	Slot 15	Slot 25	Slot 35								
1	A59	A26	A12	A3	A26	A34	A32	A51	A18	A11	A54	A32	A11	A40	A39								
2	A33	A39	A5	A52	A59	A51	A30	A48	A14	A44	A52	A26	A9	A38	A37								
3	A59	A35	A1	A47	A55	A35	A29	A45	A12	A41	A49	A22	A8	A36	A34								
4	A1	A49	A59	A44	A51	A17	A27	A43	A10	A38	A14	A15	A6	A35	A32								
5	A59	A16	A55	A41	A48	A12	A25	A41	A7	A53	A45	A13	A5	A33	A30								
6	A40	A33	A51	A19	A51	A6	A22	A39	A6	A49	A39	A10	A1	A28	A27								
7	A29	A24	A47	A35	A41	A2	A19	A37	A5	A46	A37	A7	A16	A26	A11								
8	A33	A16	A43	A30	A37	A22	A17	A35	A3	A49	A35	A5	A57	A24	A23								
9	A18	A26	A40	A25	A33	A17	A16	A33	A42	A38	A33	A3	A55	A21	A27								
10	A43	A9	A37	A22	A3	A9	A14	A31	A38	A29	A31	A2	A54	A19	A20								
11	A25	A2	A34	A19	A47	A26	A12	A28	A34	A24	A29	A60	A51	A17	A18								
12	A57	A50	A29	A13	A39	A58	A10	A39	A29	A17	A28	A58	A48	A15	A14								
13	A59	A49	A37	A9	A29	A48	A7	A35	A26	A11	A26	A55	A47	A13	A12								
14	A40	A47	A31	A2	A19	A40	A6	A39	A40	A8	A56	A53	A46	A10	A11								
15	A23	A44	A24	A27	A59	A34	A4	A31	A34	A3	A52	A51	A45	A8	A9								
16	A51	A42	A18	A60	A54	A25	A3	A21	A28	A59	A47	A55	A1	A6	A7								
17	A10	A39	A26	A54	A48	A20	A60	A15	A19	A53	A23	A48	A59	A4	A5								
18	A44	A37	A5	A49	A44	A15	A58	A33	A14	A49	A21	A44	A57	A2	A3								
19	A40	A35	A29	A46	A37	A6	A56	A31	A7	A44	A18	A43	A55	A59	A27								
20	A54	A60	A55	A43	A29	A2	A54	A28	A2	A41	A16	A40	A54	A58	A23								
21	A27	A56	A37	A39	A23	A55	A52	A55	A60	A22	A14	A38	A51	A56	A20								
22	A57	A52	A34	A36	A21	A46	A50	A5	A53	A34	A12	A36	A48	A53	A14								
23	A18	A49	A29	A32	A21	A38	A48	A51	A44	A32	A9	A33	A47	A50	A11								

(continued)

**Table 2** (continued)

Time slots	Rectangular slots														
	Slot 11	Slot 21	Slot 31	Slot 12	Slot 22	Slot 32	Slot 42	Slot 13	Slot 23	Slot 14	Slot 24	Slot 34	Slot 15	Slot 25	Slot 35
24	A1	A22	A40	A27	A18	A30	A47	A45	A40	A29	A4	A32	A46	A49	A7
25	A57	A39	A36	A49	A14	A24	A46	A41	A34	A26	A2	A29	A45	A47	A1
26	A3	A33	A51	A21	A14	A18	A45	A37	A6	A25	A60	A26	A43	A46	A59
27	A43	A28	A50	A2	A11	A12	A58	A33	A28	A24	A59	A25	A41	A15	A54
28	A57	A24	A40	A54	A8	A51	A56	A24	A21	A38	A56	A22	A39	A13	A50
29	A36	A16	A31	A49	A6	A58	A54	A21	A2	A17	A54	A19	A35	A10	A41
30	A49	A13	A18	A46	A4	A6	A52	A18	A60	A14	A52	A17	A34	A8	A37
31	A46	A9	A8	A43	A3	A5	A50	A15	A58	A11	A49	A15	A30	A6	A32
32	A54	A4	A1	A39	A8	A2	A48	A11	A49	A4	A47	A10	A27	A4	A21
33	A46	A2	A55	A38	A4	A12	A47	A8	A44	A8	A45	A7	A25	A2	A21
34	A44	A60	A45	A35	A1	A6	A46	A4	A42	A10	A4	A5	A23	A59	A18
35	A43	A57	A42	A32	A3	A26	A45	A51	A36	A3	A39	A33	A22	A58	A12
36	A40	A56	A38	A30	A54	A55	A42	A55	A31	A59	A37	A2	A20	A56	A9
37	A38	A54	A34	A27	A51	A2	A40	A52	A28	A56	A35	A60	A18	A53	A5
38	A44	A52	A17	A25	A59	A40	A37	A43	A23	A53	A33	A58	A16	A50	A1
39	A36	A50	A26	A24	A55	A35	A36	A37	A18	A51	A31	A55	A12	A49	A59
40	A32	A49	A23	A22	A50	A30	A35	A31	A14	A49	A29	A53	A11	A47	A57
41	A27	A47	A18	A21	A47	A25	A32	A23	A10	A46	A28	A51	A9	A46	A3
42	A27	A44	A14	A19	A44	A35	A30	A18	A6	A44	A26	A58	A8	A44	A52
43	A25	A42	A10	A17	A41	A28	A29	A13	A5	A41	A56	A44	A6	A42	A50
44	A23	A39	A5	A15	A39	A20	A27	A9	A3	A38	A52	A43	A5	A40	A48
45	A40	A37	A2	A13	A37	A15	A25	A5	A54	A34	A47	A40	A1	A38	A45
46	A36	A4	A58	A11	A34	A6	A22	A2	A49	A32	A42	A38	A59	A36	A43

(continued)

**Table 2** (continued)

Time slots	Rectangular slots														
	Slot 11	Slot 21	Slot 31	Slot 12	Slot 22	Slot 32	Slot 42	Slot 13	Slot 23	Slot 14	Slot 24	Slot 34	Slot 15	Slot 25	Slot 35
47	A32	A33	A53	A9	A33	A1	A19	A54	A19	A29	A37	A36	A57	A35	A41
48	A27	A31	A50	A7	A29	A58	A17	A48	A40	A10	A33	A3	A55	A33	A39
49	A20	A28	A45	A5	A28	A51	A16	A41	A36	A25	A29	A32	A54	A31	A37
50	A15	A16	A51	A3	A27	A55	A14	A35	A31	A24	A23	A29	A51	A28	A34
51	A10	A13	A38	A24	A26	A42	A12	A45	A28	A53	A18	A26	A48	A26	A32
52	A51	A9	A36	A21	A33	A35	A10	A39	A2	A49	A14	A25	A16	A24	A30
53	A49	A6	A31	A17	A16	A28	A7	A33	A21	A44	A9	A22	A12	A21	A27
54	A54	A4	A28	A21	A23	A12	A6	A24	A38	A38	A4	A19	A11	A19	A25
55	A43	A2	A50	A11	A19	A22	A4	A20	A31	A32	A2	A17	A9	A17	A50
56	A33	A60	A45	A5	A16	A18	A3	A15	A26	A25	A52	A15	A8	A15	A45
57	A13	A57	A42	A17	A26	A15	A60	A9	A16	A22	A49	A13	A6	A13	A41
58	A13	A56	A38	A56	A29	A9	A58	A1	A10	A14	A47	A10	A5	A10	A37
59	A3	A54	A36	A47	A27	A5	A56	A59	A54	A10	A45	A7	A1	A8	A32
60	A20	A52	A31	A43	A21	A1	A54	A54	A49	A4	A42	A5	A59	A6	A27
61	A6	A50	A28	A38	A18	A58	A6	A52	A46	A29	A21	A3	A57	A2	A21
62	A44	A49	A24	A11	A16	A51	A4	A48	A40	A56	A26	A2	A55	A59	A18
63	A40	A47	A18	A7	A14	A48	A3	A43	A36	A51	A49	A60	A54	A33	A12
64	A25	A44	A17	A2	A11	A46	A60	A39	A31	A49	A45	A58	A51	A31	A9
65	A10	A42	A12	A56	A8	A42	A58	A33	A2	A46	A35	A55	A48	A28	A5
66	A29	A39	A8	A52	A6	A48	A56	A28	A60	A44	A31	A53	A47	A26	A1
67	A46	A37	A1	A47	A4	A38	A54	A31	A53	A41	A28	A51	A46	A24	A41
68	A32	A35	A59	A44	A3	A35	A52	A21	A44	A38	A26	A53	A45	A21	A39
69	A15	A57	A55	A41	A8	A30	A50	A17	A38	A34	A49	A46	A43	A19	A37

(continued)

**Table 2** (continued)

Time slots	Rectangular slots														
	Slot 11	Slot 21	Slot 31	Slot 12	Slot 22	Slot 32	Slot 42	Slot 13	Slot 23	Slot 14	Slot 24	Slot 34	Slot 15	Slot 25	Slot 35
70	A1	A54	A37	A38	A4	A40	A48	A11	A29	A32	A45	A44	A41	A17	A34
71	A57	A50	A47	A36	A1	A22	A47	A9	A23	A4	A39	A43	A39	A15	A32
72	A3	A22	A43	A35	A57	A12	A46	A5	A18	A26	A33	A40	A35	A13	A30
73	A43	A19	A40	A32	A54	A34	A45	A1	A12	A59	A29	A38	A34	A10	A27
74	A38	A31	A37	A30	A51	A28	A42	A59	A58	A53	A28	A36	A30	A8	A25
75	A33	A37	A31	A27	A59	A26	A40	A55	A53	A49	A21	A32	A27	A6	A50
76	A27	A24	A28	A25	A4	A55	A37	A53	A46	A44	A14	A29	A25	A4	A45
77	A23	A26	A24	A24	A50	A48	A36	A2	A42	A38	A12	A26	A23	A2	A41
78	A18	A14	A20	A22	A47	A34	A35	A45	A38	A32	A4	A25	A22	A59	A37
79	A13	A11	A17	A21	A44	A38	A32	A43	A34	A25	A2	A22	A20	A58	A32
80	A6	A2	A12	A19	A41	A34	A30	A41	A29	A22	A59	A19	A18	A56	A27
81	A3	A4	A8	A17	A39	A25	A29	A39	A26	A14	A26	A17	A16	A53	A21
82	A29	A6	A2	A15	A37	A24	A27	A37	A60	A10	A52	A13	A12	A50	A18
83	A54	A60	A59	A13	A34	A20	A25	A35	A53	A4	A49	A10	A11	A49	A12
84	A44	A57	A55	A11	A33	A17	A22	A39	A44	A3	A47	A7	A9	A47	A1
85	A38	A56	A51	A9	A29	A12	A19	A37	A23	A56	A45	A5	A8	A46	A3
86	A32	A54	A47	A7	A28	A6	A17	A35	A31	A51	A42	A3	A6	A44	A1
87	A23	A52	A43	A5	A27	A2	A16	A33	A28	A49	A60	A2	A5	A42	A59
88	A15	A39	A40	A3	A26	A6	A12	A31	A21	A46	A56	A60	A30	A40	A57
89	A8	A35	A2	A22	A29	A5	A10	A28	A18	A44	A52	A58	A27	A38	A54
90	A1	A56	A59	A19	A27	A1	A7	A24	A14	A41	A16	A55	A25	A36	A3
91	A59	A52	A55	A15	A8	A51	A6	A23	A10	A38	A39	A53	A23	A35	A50
92	A51	A49	A24	A11	A55	A48	A4	A21	A6	A34	A35	A51	A22	A33	A48
93	A43	A24	A47	A7	A1	A46	A3	A20	A3	A32	A31	A48	A20	A31	A45

(continued)

**Table 2** (continued)

Time slots	Rectangular slots															
	Slot 11	Slot 21	Slot 31	Slot 12	Slot 22	Slot 32	Slot 42	Slot 13	Slot 23	Slot 14	Slot 24	Slot 34	Slot 15	Slot 25	Slot 35	
94	A36	A39	A43	A2	A57	A42	A60	A51	A42	A51	A28	A46	A18	A26	A43	
95	A49	A33	A40	A60	A54	A55	A14	A28	A36	A26	A44	A44	A16	A24	A41	
96	A27	A26	A37	A24	A50	A48	A12	A39	A29	A59	A18	A43	A12	A21	A39	
97	A25	A24	A34	A21	A47	A40	A10	A31	A21	A25	A16	A40	A11	A19	A37	
98	A23	A19	A29	A17	A44	A35	A7	A20	A16	A24	A14	A38	A9	A17	A34	
99	A43	A14	A26	A13	A39	A30	A6	A11	A10	A22	A12	A36	A8	A47	A32	
100	A20	A11	A51	A9	A34	A18	A4	A57	A6	A17	A9	A33	A6	A46	A30	
101	A32	A9	A45	A5	A29	A25	A3	A54	A3	A14	A2	A32	A5	A44	A27	
102	A27	A6	A40	A2	A27	A26	A60	A52	A31	A11	A37	A29	A1	A42	A25	
103	A20	A4	A36	A56	A23	A22	A58	A45	A28	A10	A33	A26	A59	A40	A50	
104	A15	A2	A29	A52	A19	A20	A56	A41	A23	A8	A60	A25	A57	A38	A45	
105	A10	A60	A24	A47	A16	A18	A54	A37	A21	A4	A59	A22	A55	A36	A18	
106	A6	A57	A17	A44	A11	A17	A52	A33	A58	A3	A56	A19	A54	A35	A11	
107	A1	A56	A10	A41	A6	A15	A50	A20	A54	A59	A54	A17	A51	A33	A5	
108	A29	A54	A1	A38	A1	A12	A48	A23	A53	A56	A52	A15	A48	A31	A1	
109	A57	A52	A59	A36	A59	A9	A47	A20	A49	A53	A49	A13	A47	A28	A57	
110	A54	A50	A53	A35	A55	A15	A46	A17	A46	A51	A9	A10	A46	A26	A52	
111	A51	A49	A47	A32	A51	A12	A45	A13	A6	A49	A45	A7	A45	A24	A50	
112	A49	A47	A40	A30	A59	A9	A42	A9	A26	A46	A42	A5	A43	A21	A48	
113	A49	A44	A36	A27	A55	A6	A40	A5	A40	A44	A29	A3	A41	A19	A45	
114	A44	A42	A29	A25	A50	A1	A37	A2	A38	A41	A49	A2	A39	A17	A43	
115	A40	A39	A23	A24	A47	A35	A36	A57	A36	A38	A45	A58	A35	A15	A41	
116	A36	A37	A26	A22	A44	A30	A35	A53	A34	A34	A37	A55	A34	A13	A39	
117	A32	A35	A14	A21	A41	A58	A32	A41	A10	A32	A33	A53	A30	A10	A37	

(continued)

Table 2 (continued)

Time slots	Rectangular slots														
	Slot 11	Slot 21	Slot 31	Slot 12	Slot 22	Slot 32	Slot 42	Slot 13	Slot 23	Slot 14	Slot 24	Slot 34	Slot 15	Slot 25	Slot 35
118	A25	A54	A10	A19	A39	A55	A29	A39	A40	A3	A29	A51	A27	A8	A34
119	A20	A50	A5	A17	A37	A25	A27	A37	A36	A46	A26	A53	A25	A6	A32
120	A15	A24	A2	A15	A34	A48	A25	A35	A29	A51	A23	A46	A23	A2	A30
121	A8	A42	A58	A11	A33	A46	A22	A33	A5	A8	A21	A40	A22	A59	A27
122	A3	A37	A53	A11	A29	A42	A19	A31	A19	A41	A18	A43	A20	A58	A25
123	A36	A31	A18	A7	A28	A58	A17	A28	A18	A34	A16	A40	A18	A56	A52
124	A27	A26	A14	A5	A27	A24	A16	A24	A16	A29	A14	A38	A46	A53	A48
125	A20	A22	A10	A3	A48	A18	A14	A23	A14	A24	A12	A33	A45	A50	A43
126	A13	A39	A5	A25	A44	A38	A12	A21	A12	A17	A9	A32	A43	A49	A39
127	A6	A16	A2	A22	A37	A34	A10	A20	A10	A11	A7	A29	A41	A47	A34
128	A1	A31	A58	A19	A29	A28	A7	A18	A7	A8	A4	A26	A39	A46	A30
129	A54	A24	A53	A15	A23	A26	A22	A17	A6	A3	A2	A25	A35	A44	A23
130	A46	A19	A50	A39	A18	A51	A19	A15	A5	A59	A60	A22	A34	A42	A20
131	A40	A14	A45	A36	A11	A46	A17	A13	A3	A53	A59	A19	A30	A40	A14
132	A33	A11	A42	A32	A4	A30	A16	A11	A58	A51	A56	A17	A27	A38	A11
133	A25	A6	A38	A27	A1	A38	A14	A9	A53	A49	A54	A15	A25	A36	A7
134	A20	A2	A36	A22	A57	A34	A12	A8	A46	A46	A54	A13	A23	A35	A3
135	A13	A60	A31	A19	A54	A25	A10	A5	A42	A44	A52	A10	A22	A2	A5
136	A1	A56	A28	A15	A48	A24	A7	A4	A38	A41	A49	A7	A20	A2	A1
137	A3	A52	A23	A11	A44	A20	A6	A2	A14	A38	A47	A5	A18	A2	A57
138	A54	A49	A20	A7	A41	A17	A4	A17	A12	A34	A45	A3	A16	A2	A52
139	A43	A44	A17	A2	A37	A12	A3	A13	A10	A32	A42	A2	A12	A2	A50
140	A49	A39	A12	A60	A33	A6	A48	A9	A6	A29	A39	A60	A11	A2	A48
141	A46	A35	A8	A54	A28	A2	A58	A53	A5	A26	A37	A58	A9	A2	A45
142	A44	A47	A1	A49	A26	A6	A56	A1	A3	A59	A35	A55	A8	A2	A43
143	A43	A39	A59	A46	A21	A1	A54	A59	A6	A3	A33	A53	A6	A44	A1

(continued)

**Table 2** (continued)

Time slots	Rectangular slots														
	Slot 11	Slot 21	Slot 31	Slot 12	Slot 22	Slot 32	Slot 42	Slot 13	Slot 23	Slot 14	Slot 24	Slot 34	Slot 15	Slot 25	Slot 35
144	A40	A31	A55	A43	A18	A55	A52	A55	A2	A3	A31	A51	A5	A42	A1
145	A38	A26	A36	A39	A14	A51	A50	A53	A3	A26	A29	A48	A1	A40	A9
146	A36	A22	A47	A38	A8	A48	A60	A51	A54	A3	A28	A46	A59	A38	A3
147	A33	A16	A43	A36	A4	A20	A47	A2	A53	A3	A26	A44	A57	A36	A1
148	A32	A13	A38	A35	A3	A42	A46	A43	A49	A3	A23	A43	A55	A35	A1
149	A29	A11	A26	A32	A57	A58	A45	A41	A46	A8	A21	A40	A54	A33	A1
150	A57	A9	A45	A30	A50	A1	A42	A48	A44	A3	A18	A38	A51	A31	A1
151	A51	A6	A40	A25	A44	A58	A37	A45	A26	A59	A16	A36	A48	A26	A1
152	A46	A4	A34	A24	A39	A20	A36	A43	A49	A53	A14	A33	A47	A24	A25
153	A1	A2	A28	A22	A33	A34	A35	A41	A44	A49	A12	A32	A46	A21	A9
154	A32	A60	A23	A21	A28	A24	A32	A39	A40	A44	A9	A29	A45	A19	A18
155	A43	A57	A17	A19	A34	A55	A30	A37	A36	A38	A4	A26	A43	A17	A12
156	A36	A56	A10	A17	A27	A42	A29	A35	A31	A32	A2	A25	A41	A15	A9
157	A29	A54	A12	A15	A21	A46	A27	A33	A29	A25	A60	A22	A39	A13	A5
158	A20	A52	A10	A13	A14	A34	A25	A31	A28	A22	A59	A19	A35	A10	A1
159	A54	A50	A5	A11	A44	A28	A22	A28	A26	A14	A56	A15	A34	A8	A57
160	A51	A49	A1	A9	A41	A30	A19	A24	A23	A10	A54	A60	A59	A6	A52
161	A59	A47	A58	A7	A3	A24	A17	A23	A21	A4	A52	A55	A57	A4	A48
162	A57	A44	A53	A5	A33	A18	A16	A21	A19	A3	A49	A53	A55	A2	A43
163	A10	A42	A50	A3	A29	A15	A32	A20	A18	A56	A47	A51	A54	A59	A39
164	A36	A35	A45	A49	A28	A9	A30	A18	A16	A51	A45	A48	A51	A58	A34
165	A13	A33	A42	A46	A27	A5	A29	A17	A14	A26	A42	A46	A48	A56	A30
166	A23	A31	A38	A43	A26	A1	A27	A15	A12	A41	A39	A44	A47	A53	A25
167	A15	A28	A34	A38	A48	A55	A25	A13	A10	A34	A37	A43	A46	A50	A32
168	A13	A26	A29	A35	A44	A2	A22	A11	A2	A29	A35	A40	A45	A49	A23

(continued)

## 4 Conclusion

In this paper, we have formulated a web ad scheduling problem to determine an optimal placement of ads that compete to be placed on rectangular slots in a given planning horizon on the various webpages of a news website in order to maximize the revenue generated from ads. The optimization model is a 0-1 linear programming model and restricts selection of an ad on the same webpage more than once at any instant of time. Problem is programmed on LINGO software to get the optimal solution. In case the problem results in an infeasible solution, goal programming method is used to solve the problem. A case study is presented in the paper to show the application of the problem.

## References

1. Adler, M., Gibbons, P.B., Matias, Y.: Scheduling space-sharing for internet advertising. *J. Sched.* **5**(2), 103–119 (2002)
2. Aggarwal, C. C., Wolf, J. L., Yu, P.S.: A framework for the optimizing of WWW advertising. *Trends in Distributed Systems for Electronic Commerce*, pp. 1–10 (1998)
3. Dreze, X., Zufryden, F.: Testing web site design and promotional content. *J. Advertising Res.* **37**(2), 77–91 (1997)
4. Gupta, A., Manik, P., Aggarwal, S., Jha, P. C.: Optimal advertisement planning on online news media. In: Handa, S. S., Uma Shankar, Ashish Kumar Chakraborty (eds.) *Proceedings of International Congress on Productivity, Quality, Reliability, Optimization and Modelling*, vol. 2, pp. 963–978. Allied Publishers, New Delhi (2011)
5. Intern.com Corp.: Theories and methodology. <http://webreference.com/dev/banners/theories.html> (1997)
6. Kohda, Y., Endo, S.: Ubiquitous advertising on the WWW: merging advertisement on the browser. *Comput. Netw. ISDN Syst.* **28**, 1493–1499 (1996)
7. Kumar, S., Jacob, V.S., Sriskandarajah, C.: Scheduling advertisements on a web page to maximize revenue. *Eur. J. Oper. Res.* **173**, 1067–1089 (2006)
8. Marx, W.: Study shows big lifts from animated ads. *Business Marketing*, vol. 1 (1996)
9. McCandless, M.: Web advertising. *IEEE Intell. Syst.* **13**(3), 8–9 (1998)
10. Novak, T.P., Hoffman, D.L.: New metrics for new media: Toward the development of web measurement standards. *World Wide Web*, **2**(1), 213–246 (Winter, 1997)
11. Risdien, K., Czerwinski, M., Worley, S., Hamilton, L., Kubinieć, J., Hoffman, H., Mickel, N., Loftus, E.: Internet advertising: patterns of use and effectiveness. In: *CHI' 98, Proceedings of the SIGCHI Conference on Human Factors in, Computing Systems*, pp. 219–224 (1998)
12. Steuer, R.E.: *Multiple Criteria Optimization: Theory Computation and Application*. Wiley, New York (1986)
13. Thiriez, H.: OR software LINGO. *Eur. J. Oper. Res.* **12**, 655–656 (2000)
14. Yager, R.R.: Intelligent agents for World Wide Web advertising decisions. *Int. J. Intell. Syst.* **12**, 379–390 (1997)



# An Integrated Approach and Framework for Document Clustering Using Graph Based Association Rule Mining

D. S. Rajput, R. S. Thakur and G. S. Thakur

**Abstract** Growth in number of documents increases day by day, and for managing this growth the document clustering techniques are used document clustering is a significant tool to allocating web search engines for data mining and knowledge discovery. In this paper, we have introduced a new framework graph-based frequent Term set for document clustering (GBFTDC). In this study, document clustering has been performed for extraction of useful information from document dataset based on frequent term set. We have generated association rules to perform pre-processing and then have applied clustering approach.

**Keywords** Document clustering · Text document · Association rule · Pre-processing

## 1 Introduction

Every day a huge number of document, reports, e-mails, and web pages are generated from different sources, such as Biomedical Software, Online media, Marketing, Academics, and Government Organizations, etc. This has resulted in demand for well-organized tools for turning data into important knowledge. To fulfill this necessity, researchers from several technological areas, like information retrieval [11], information extraction [17], Association Rule Mining [10, 35], pattern recognition

---

D. S. Rajput (✉) · R. S. Thakur · G. S. Thakur  
Department of Computer Applications, M.A.N.I.T., Bhopal 462051, India  
e-mail: dharm\_raj85@yahoo.co.in

R. S. Thakur  
e-mail: ramthakur2000@yahoo.com

G. S. Thakur  
e-mail: ghanshyamthakur@gmail.com

[21], machine learning [16], data visualization [16], neural networks [21] etc., are using well-known approaches for knowledge discovery from different databases.

All these approaches have ushered us into resulted in an effective research area know as Data Mining [16, 17]. Data Mining is extraction of hidden predictive information from large databases; it is a powerful technology with great potential to help organizations focus on the most important information in their Data Warehouses [5, 11, 16, 21, 28]. It is popularly known as Knowledge Discovery in Databases (KDD), [11, 12, 21, 35] is the nontrivial extraction of implicit, previously unknown and potentially useful information from data in databases [11, 12]. Though, data mining and knowledge discovery in databases are frequently treated as synonyms. It is divided into two models [12, 18, 21, 24, 28, 31]; Predictive Model and Descriptive Model. In predictive model makes prediction about unknown data values by using the known values. Like classification [11], regression [16], time series analysis [24], prediction [16], etc. In descriptive model identifies the patterns or relationships in data and explores the properties of the data examined. like clustering [29], summarization [35], association rule [11], sequence discovery, etc.

The repeated existing property of internet, which allows textual documents to be shared over the cyber space, is remarkable. However, it also makes users face the information-overloading problem. When users create queries to WWW search engines, they usually confusingly receive a small number of relevant web pages combined with a large number of irrelevant web pages. To valuably manage the result of a search engine query, it is the motivation to the use of document clustering [2, 6].

Document clustering is an unsupervised technique [18, 22] for discovering valuable knowledge from data. It is the common data mining technique for finding hidden patterns in data. It is an important issue in the analysis and exploration of data. Document clustering in textual data is a progressively more significant research field, since the requirement of attaining knowledge from the massive amount of textual documents. It has become an increasingly important technique for enhancing search engine results, web crawling, unsupervised document organization, and information retrieval or filtering. It is widely applicable areas of science, technology, social science, biology, economics, medicine, and stock market. Clustering engage dividing a set of documents into a particular number of groups. A few familiar clustering methods are partitioning method [16, 20], hierarchical methods [3], density and grid-based clustering method [11].

Among the technique developed for data and text mining, association rule mining [23, 34, 37, 39] is one of the useful and successful techniques for discovering interesting rules. Rules generation for textual databases has been an important application area. Yet, its application on text databases still seems to be more promising, owing to the difference in characteristics of transaction databases with textual databases [1, 8, 21]. In this case, rules are deduced on the co-occurrences of terms in texts and therefore able to return semantic relations among the terms [41]. Rule generation using graph-based approach [10, 36] requires only one pass of database scan and it doesn't require costly candidate key generation method for creating new candidates as like Apriori [33, 38]. The graph theoretic algorithm takes less memory space for

storing adjacency matrix. It also reduces I/O time and CPU overhead. Therefore, in this framework, we are using graph theoretic [10] algorithm to rule generation.

## 2 Literature Review

Document clustering [14] is a specialized data clustering problem, where the objects are in the form of documents. The objective of the clustering process is to group the documents which are similar in some sense like type of document, contents of document, etc., into a single group (cluster) [16]. The difficult part is to learn from a dataset, actually how many classes of such groups exist in the collection. Formally, a corpus of  $N$  unlabeled documents is given and a solution  $C = \{C_j : j = 1, \dots, k\}$  is searched that partitions the document into  $k$  disjoint clusters document clustering aims to discover natural grouping among documents in such a way that documents within a cluster are similar (high intra cluster similarity) to one another and are dissimilar to documents in other clusters (low inter cluster similarity). Exploring, analyzing, and correctly classifying the unknown nature of data in a document without supervision is the major requirement of document clustering method [30].

Traditionally, document clustering algorithm features like words, phrases, and sequences from the documents to perform clustering [14, 15, 20, 40]. Over the past few decades, several effective document clustering algorithms have been proposed to mitigate the hassle, including the K-means, Bisecting k-means [23], hierarchical agglomerative clustering (HAC) [32], and unweighted pair group method with arithmetic mean (UPGMA) [4]. K-means algorithm [18] for document clustering is easy to be implemented and works quickly in most situations, Table 5 shows the result of K-Mean Clustering for example of Table 2. Here the algorithm suffers from two major drawbacks, which make it incompatible for many applications. One is sensitivity to initialization and the other is convergence to local optima. To deal with the limitations that exist in traditional partition clustering methods especially K-means, recently new concepts and techniques have been entered into document clustering. In clustering of large document sets, it often concerned to some learning methods like optimization technique, which mostly intended to the lack of orthogonality (Table 1).

As pointed out by the literature survey [19–27], there are still challenges in improving the clustering quality, which are listed as follows: [6, 7]

1. Many document clustering algorithms work well on small document sets, but fail to deal with large document sets efficiently.
2. Some document clustering algorithms require users to specify the number of clusters as an input parameter. Though it seems complex to determine the number of clusters in advance. It doesn't provide good clustering accuracy.
3. Absence of Meaningful cluster labels is basic problem in document clustering.

**Table 1** Literature review

Author	Proposed method	Overlapping	Cluster label	Semantic discovery	Cluster quality	Cluster efficiency
K. Lin. et al. in 2001 [27]	A word-based soft clustering algorithm for documents	Yes	No	No	–	Yes
F. Beil et al. in 2002 [13]	Frequent term-based text clustering	Yes	Yes	No	–	Yes
B. Fung et al. in 2003 [3]	Hierarchical document clustering using frequent Itemsets	No	Yes	No	Yes	Yes
D. R. Recupero in 2007 [9]	A new unsupervised method for document clustering by using WordNet lexical and conceptual relations	No	No	Yes	Yes	No
C. L. Chen et al. in 2009 [7]	An integration of fuzzy association rules and WordNet for document clustering	No	Yes	Yes	No	No
C. L. Chen et al. in 2010 [6]	Fuzzy-based multi-label document clustering (FMDC)	Yes	Yes	Yes	–	–

## 2.1 Existing Clustering Methods Using Frequent Itemsets

Most of the researchers worked in the area of finding association rules from textual data by using Apriori, FP growth, pincer, and many other algorithms and some of researchers have worked with clustering algorithms also they have solved many problems. A number of existing clustering methods using frequent itemsets are available for document clustering.

HFTC: frequent term-based clustering [26] has been a first algorithm in this regard. But it doesn't work with high dimensional document data and method isn't scalable.

FIHC: this method uses the notion of frequent itemsets, which comes from association rule mining, for document clustering. The drawbacks of FIHC are like it has a number of frequent itemsets which may be very large and redundant. This method used hard clustering approach, and wasn't comparable with previous methods.

**Table 2** Document matrix

Document id	Word sequence
D <sub>1</sub>	1,2,5,6,7
D <sub>2</sub>	2,4,7
D <sub>3</sub>	4,5
D <sub>4</sub>	2,3,6,7
D <sub>5</sub>	5,6
D <sub>6</sub>	2,3,4,7
D <sub>7</sub>	1,2,6,7

**Table 3** Boolean representation of Table 2 after pre processing

Document id	Document vector
D <sub>1</sub>	{1,1,0,0,1,1,1}
D <sub>2</sub>	{0,1,0,1,0,0,1}
D <sub>3</sub>	{0,0,0,1,1,0,0}
D <sub>4</sub>	{0,1,1,0,0,1,1}
D <sub>5</sub>	{0,0,0,0,1,1,0}
D <sub>6</sub>	{0,1,1,1,0,0,1}
D <sub>7</sub>	{1,1,0,0,0,1,1}

There are many other methods like FIHC, FTC, CMS, and CFWS, etc. Table 2 shows textual dataset  $D = (D_1, D_2, D_3, D_4, D_5, D_6, D_7)$  with their term set.

Table 3 is Document representation using Boolean Matrix for Table 2.

Frequent term set extracted from document in Table 2 and their corresponding documents (Minimum Support = 2) using graph-based approach (Table 4).

Document Clustering produced by K-Mean with different number of clusters in Table 5.

**Table 4** Frequent termset sets using graph based approach

Frequent termset	List of document
{1,2}, {1,6}, {1,7}, {1,2,6}, {1,2,7}, {1,6,7}, {1,2,6,7}	D <sub>1</sub> , D <sub>7</sub>
{2,3}, {3,7}, {2,3,7}	D <sub>4</sub> , D <sub>6</sub>
{2,4}, {4,7}, {2,4,7}	D <sub>2</sub> , D <sub>6</sub>
{2,6}, {2,7}, {2,6,7}	D <sub>1</sub> , D <sub>4</sub> , D <sub>7</sub>
{5,6}	D <sub>1</sub> , D <sub>5</sub>

**Table 5** Document clustering using K-mean

Number of clusters	Document in clusters
2	{ 3,5} {1, 4, 6, 7}
3	{3, 5} {1, 7} {4, 6}
4	{3} {5} {1, 7} {4, 6}

### 3 Proposed Method

This section proposed, a new framework for document clustering using frequent term set. Figure 1 shows the proposed framework which consist three modules, namely Document Pre-processing Module, Frequent Term extraction Module and Frequent Term based Cluster Extraction Module as discussed in Sects. 3.1–3.3, respectively. The proposed framework will received document dataset as input and document preprocessing module will perform pre-processing operation on document dataset and extract the select key termset, after that in second module apply graph-based rule mining technique to mine the document and find the frequent term set, finally the last module will use the frequent term set to design the similarity matrix and find the document clusters.

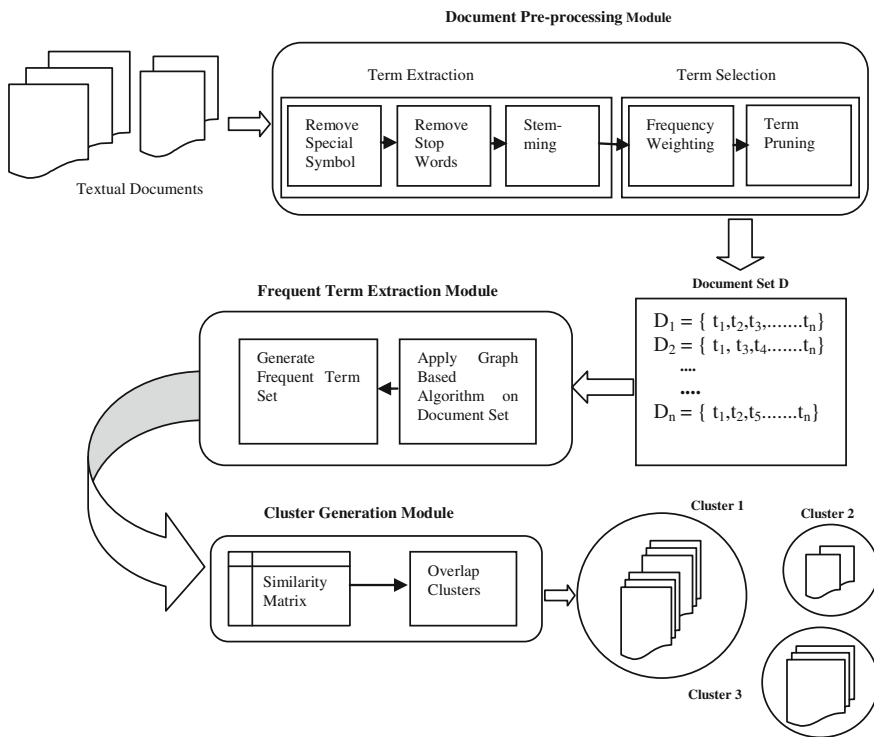


Fig. 1 Document clustering using graph based framework

### 3.1 Document Pre-Processing Module

Document Pre-processing Algorithms are specially designed for the properties of document data. Each document set has numerous stop words, special marks, punctuation marks, and spaces, first we remove all stop words and stemming, etc., and constructed term matrix for generating frequent term set. There are four steps, which are carried out when the document is provided to the pre-processing module of the system.

#### 3.1.1 Stop Words and Special Symbol Elimination

Stop words are the words which don't have meaning with respect to the classification [10, 16, 40]. So these words are removing when the term matrix is created for the classification purpose. In short, the words are removed from the documents which are not necessary for the next stage. it removed all prepositions, conjunction and articles from dataset  $D$ .

---

Algorithm1: To remove stop words & special characters

---

**Input:** A Document database  $D$  and a well defined stop words list  $L$ .

$D = \{d_1, d_2, d_3, \dots, d_n\}$  ; where  $1 \leq n \leq i$

$t_{ij}$  is the  $j^{\text{th}}$  term in  $i^{\text{th}}$  document

**Output:** All valid text term in  $D$

**START**

- 1: for (all  $d_i$  in  $D$ ) do
- 2: for (1 to  $j$ ) do
  - a. Extract  $t_{ij}$  from  $d_i$
  - b. If( $t_{ij}$  in database  $d_i$ )
  - c. Remove  $t_{ij}$  from  $d_i$
- 3: End for
- 4: End for

**END**

---

#### 3.1.2 Stemming

A stemming is a computational procedure which reduces all words with the same root (or, if prefixes are left untouched, the same stem) to a common form, usually by stripping each word of its derivational and inflectional suffixes [10, 25]. It is useful in many areas of computational linguistics and information-retrieval work. Researchers from the fields of Computational linguistics and information retrieval find it as, one of the necessary step to fulfill their research needs. It helps to decrease the size of the dictionary file.

---

Algorithm2: To remove the stemming word.

---

**Input:** A Document database  $D$  and List of stemming word list

$D = \{d_1, d_2, d_3, \dots, d_n\}$  ;where  $1 \leq n \leq i$

**START**

1. Determine where on ending list to begin searching for a match so that stem is at least two characters long.
2. Search ending list for a match to the last part of the word being stemmed.
3. If (ending is found) Then
4. {
5. if context sensitive rule is satisfied
6. Remove ending
7. Recoding Procedure ();
8. Else
9. Go to step 3
10. }
11. Else
12. Recoding Procedure();

**END**

The Recoding procedure used by Stemming Algorithm is given below

Recoding Procedure ()

**START**

1. {
2. Undoable final consonant of stem, if applicable
3. Search list of transformations for match on remaining stem
4. If (match== found) Then
5. {
6. Recode stem according to rule
7. Output stem
8. }
9. Else (no rule applies)
10. Output stem
11. }

**END**

---

### 3.1.3 Feature Set Selection

In text classification, the important term selection is critical task for the classifier performance. With increasing number of documents, number of features also increases and to reduce the size of the dictionary, the threshold feature set reduction methods is used.

In this method, lower thresholds are decided according to the number of words in the dictionary. The term which below lower threshold are extracted from the document.



**Table 6** BMM representation

Document id	Term 1	Term 2	.....	Term n
D <sub>1</sub>	0	1	...	1
D <sub>2</sub>	1	0	...	1
...	...	...	...	...
D <sub>3</sub>	0	0	...	1

Algorithm 3: Algorithm for feature selection

**Input:** A Document dataset  $D$  and  $y$  lower threshold value  $N$  is the counter  
 $D = \{d_1, d_2, d_3, \dots, d_n\}$  ;where  $1 \leq n \leq i$   
 $t_{ij}$  is the  $j^{\text{th}}$  term in  $i^{\text{th}}$  document  
**Output:** Documents Dataset  $D$  after feature selection  
**START**  
 1: for (all  $d_i$  in  $D$ ) do  
 2: for (1 to  $j$ ) do  
     a. Count total occurrence of  $t_{ij}$  in document  $d_i$   
     b. Assign the total occurrence of  $t_{ij}$  in  $N$   
     c. If ( $N < y$ )  
     d. Remove  $t_{ji}$  from the document  $d_i$   
 3: End for  
 4: End for  
**END**

### 3.1.4 Document Term Matrix and Normalization

The main principle of the pre-processing phase is to organize the document term matrix that will provide appropriate input to the next phase of the system. After selection process, we have limited terms in each document. Suppose we have  $n$  documents and maximum  $m$  steem words in a document. The binary matrix  $M$  is represented as [12, 14, 17] (Table 6).

$$M[d_i * w_j] = \begin{cases} 1 & \text{if } w_i \text{ in present in } d_i \\ 0 & \text{otherwise} \end{cases}$$

Where  $i = 1, 2, 3 \dots n$  and  $j = 1, 2, 3 \dots m$ .

### 3.2 Frequent Term Extraction Module

After Sect. 3.1 we get structured vector, which will be treated as input for frequent term extract module. In this module, the graph-based algorithm [10, 36] is applied to generate the frequent termsets from term matrix. It reduces the CPU time because we are scanning only two times the preprocessed dataset and no need to generate candidate set like Apriori [16].

---

**Algorithm 4: Graph Based Association Rule Mining Algorithm (GBARMA)**


---

**Input:** The set of different Textual document  $D$  or BMM Table.

**Output:** Frequent Term Set.

1. Scan document table  $D$  and create directed graph  $G$ .
  2. Create Adjacency Matrix  $A$  of  $G$ .
  3. Update Value of each element  $A_{ij}$  list and  $A_{ij}$  count of matrix  $A$ .
  4. Delete corresponding row and column of an element  $A_{ij}$  count=0 only for diagonal elements.
  5. Read each element  $A_{ij}$  of matrix  $A$  if  $A_{ij}$  count < minimum Support then set  $A_{ij}$  Count =0
  6. Find 1- Frequent termset and 2- frequent termset from matrix.
  7. Calculate other  $k$ -termsets from each column using logical AND operator.
  8. END
- 

Algorithm 4 generates frequent term sets based on predefined minimum support value  $\ominus$  the minimum support of the frequent term set is usually in the range of 5–15%. From a large textual document set. When the minimum support is too large, the total number of frequent terms would be very small, so that the resulting compact documents would not have enough information about the original dataset. In this case, a lot of documents will not be processed because they do not support any frequent word, and the final clustering result will not cover these documents.

### 3.3 Frequent Term-Based Cluster Generation Module

The objective of this module is to assign each document to multiple clusters and determine labels and assign them to document. If we are having the confidence to achieve these goals by some automatic process, we would completely bypass the expense of having humans assign labels, but the process known as document clustering is less than perfect. Document clustering assigns each of the documents in a collection to one or more smaller groups called clusters. Examinations show that the clusters should contain similar documents. The initial collection is a single cluster. After processing, the documents are distributed among a number of clusters, where ideally each document is very similar to the other documents in its cluster and much less similar to documents in other clusters.

We define a similarity matrix of all documents using frequent term set. We are providing frequent term set as an input is the matrix of similarities  $S$ . where  $S(i, j)$  is the similarity matrix and  $1 \leq i \leq n - 1$  and  $1 \leq j \leq n$ . The preferences should be placed on the half diagonal of the matrix.

---

 Algorithm 5: Graph based Frequent Term Set based Document Clustering (GBFTDC)
 

---

**Input:** All Frequent Term Set of dataset D.

**Output:** Find clusters.

**START**

**Step 1:-** Construct Similarity Matrix S using all frequent term set they have in common.

**Step 2:-** Find minimum number in similarity matrix excluding zero.

**Step 3:-** Find Maximum value in S, and then finding all document pairs of unclustered Documents with the maximum value.

**Step 4: If** (Maximum value = Minimum value) **then**

All documents in corresponding document pairs which do not attach to any cluster are used to construct a new cluster.

**Else**

All found document pairs with the maximum value, the following process is conducted. For all document pairs with maximum value, subsequent processes are conducted. First, for each document pair, if the documents are not belonging to any clusters, then they would be grouped together to form a document cluster. In other approach if one document of the pair belongs to an existing cluster, then the other unattached document will also be included in the same, finally similarities of found document pairs set to zero.

**Step 5:-** Go to step 3.

**Step 6:-** If there are any documents which do not attach to any cluster, then each of these documents is used to construct a new cluster.

**END**

---

### 3.4 An Illustrative Example

The working process of algorithms applies in document database and performs pre-processing face, finally we have Table 2. After that we find frequent termset using graph-based algorithm from Table 2, now apply frequent termset-based document clustering. Figures 2, 3 and 4 basically, shows the clustering procedure by similarity values between documents within clusters. It prefers to create new cluster other than adding documents to existing clusters in order to balance the amount of documents in a cluster. There is no overlap among document clusters produced by this method.

Step 1: Construct Similarity Matrix S using, frequent term set. (All frequent term set which are common in all document sets).

Step 2: finding minimum value of S when  $S \geq 1$ .

Step 3: Document pair (1, 7) has largest similarity as 15, clustered pair (1, 7) set similarity as 0. Unclustering document set {2, 3, 4, 5, 6}.

Step 4: Document Pair (1, 4) (2, 6), (4, 6) (4, 7) are having largest similarity as 7, and sets Pair (1, 4) (2, 6), (4, 6) (4, 7) similarity is 0. Now add (2,4,6) with cluster (1, 7) and get (1,2,4,6,7) as new clustered pair. The unclustered document set is {3, 5}.

Now select the most frequent documents with maximum length for each cluster as its document topic (Table 7).

**Fig. 2** Similarity matrix S using frequent term set

1	.					
2	3	.				
3	1	1	.			
4	7	1	0	.		
5	3	0	1	1	.	
6	3	7	1	7	0	.
7	15	3	0	7	1	3
	1	2	3	4	5	6

**Fig. 3** Similarity matrix after step 3

1	.					
2	3	.				
3	1	1	.			
4	7	1	0	.		
5	3	0	1	1	.	
6	3	7	1	7	0	.
7	0	3	0	7	1	3
	1	2	3	4	5	6

**Fig. 4** Similarity matrix after step 4

1	.					
2	3	.				
3	1	1	.			
4	0	1	0	.		
5	3	0	1	1	.	
6	3	0	1	0	0	.
7	0	3	0	0	1	3
	1	2	3	4	5	6

**Table 7** Clustering results

Cluster id	Documents topics	List of documents
1	2, 6, 7	{ 1, 2, 4, 6, 7 }
2	5	{3, 5}

Document topic reductions; if one frequent term belong in more than one cluster id (it is contained in the assigned topics of other clusters) then the frequent term should be eliminated from the document topics of the cluster. In this example, there are no document topic belonging to in more than one cluster so this step is not required here.

**Table 8** Dataset description

Data set	Documents	Classes
20 newsgroup dataset	20000	20
Reuter’s text categorization	8654	52

## 4 Experimental Evaluation

F-measure [16, 29] is employed to estimate performances of the proposed clustering methods. Further, clustering results are normalized into a fixed number of predefined clusters. The F-measure can be used to balance the contribution of false negatives by weighting recall through a parameter. F-measure compares the results to the pre-classified classes. Let precision and recall is defined as follows: The formula of F-measure is depicted as equations.

Precision: This is the percentage of retrieved documents that are in fact relevant to the query. It is calculated as:

$$P_i = TP/TP + FP \tag{1}$$

Recall: This is the percentage of documents that are relevant to the query and were, in fact, retrieved. It is calculated as

$$R_i = TP/TP + FN \tag{2}$$

We can calculate F-Measure by using to the formula

$$F = 2 * P_i * R_i/P_i + R_i \tag{3}$$

To test and compare proposed clustering algorithms, the pre-classified sets of documents are used. We have used 20 newsgroup dataset and Reuter’s dataset, which are widely used in many publications. A summary description of these datasets is given in Table 8. The experiments were performed on an Intel core 2 Duo, 2.94 GHz system running Windows 7 professional with 2 GB of RAM.

We treat each cluster as, it were the result of a query and each class as if it were the relevant set of documents for a query. The proposed approach used these dataset as input and finally we get 20 clusters as result. For each cluster, we have computed the precision, Recall and F-measure with the help of Eqs. 1–3. The experimental results are shown in Table 9.

In this research study, we have choose some parameters to compare Performa of our proposed approach with other existing algorithms like K-mean, HFTC, FIHC. Therefore, the final comparison of these three algorithms are shown in Table 10.

Figures 5 and 6 shows overall F-Measure values for proposed GBFTDC and other existing algorithms with 20 newsgroup dataset and Reuter’s dataset respectively. For both dataset we choose the Minimum threshold from the elements in { 10, 15, 20, 25, and 30% }.

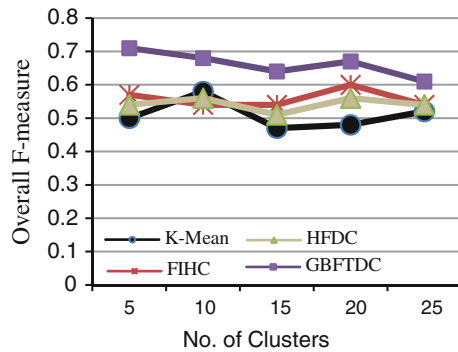
**Table 9** Clustering performances obtained on 20 newsgroup dataset

Cluster	Precision	Recall	F-measure	Cluster	Precision	Recall	F-measure
C <sub>1</sub>	0.8	0.5333	0.639976	C <sub>11</sub>	0.17	0.65	0.26951
C <sub>2</sub>	1	0.5	0.666667	C <sub>12</sub>	0.9	0.7	0.7875
C <sub>3</sub>	0.6666	0.1333	0.222172	C <sub>13</sub>	0.63	1	0.7730
C <sub>4</sub>	0.514	1	0.67899	C <sub>14</sub>	0.5	0.4	0.4444
C <sub>5</sub>	0.3333	0.0909	0.142843	C <sub>15</sub>	0.231	0.745	0.35265
C <sub>6</sub>	1	0.587	0.73976	C <sub>16</sub>	1	0.0714	0.133284
C <sub>7</sub>	0.51	0.29	0.36975	C <sub>17</sub>	0.75	0.25	0.375
C <sub>8</sub>	0.6	0.2784	0.38032	C <sub>18</sub>	1	0.5	0.66667
C <sub>9</sub>	0.84	0.45	0.58604	C <sub>19</sub>	0.3333	0.0909	0.142843
C <sub>10</sub>	0.744	0.12	0.21156	C <sub>20</sub>	0.9285	1	0.962925

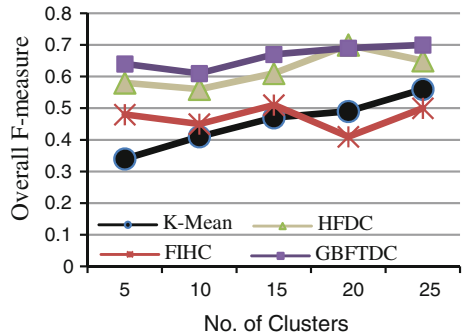
**Table 10** Parameters list for our approach and the other three approaches

Parameter name	GBFTDC	K-means	HFTC	FIHC
Dataset	20 newsgroup, Reuter's	20 newsgroup, Reuter's	20 newsgroup, Reuter's	20 newsgroup, Reuter's
Stop word removal	Yes	Yes	Yes	Yes
Stemming	Yes	Yes	Yes	Yes
Length of smallest term(threshold)	5(Five)	5(Five)	5(Five)	5(Five)
Cluster count k	5, 10, 15, 20	Depend on value of k	–	–
Overlapping	No	Yes	Yes	No
Work with high dimensional data	Yes	No	Yes	Yes
Scalibility	Yes	No	No	Yes

**Fig. 5** Overall F-measure comparison for 20 newsgroup dataset



**Fig. 6** Overall F-measure comparison for Reuter’s dataset



### 5 Conclusion

This paper presents a new framework design for document clustering using graph based frequent term set. First we review many papers and present a review method of document clustering using frequent termset. We take 20 news group data for document clustering and we do our pre-processing algorithm and find the frequent term set.

Advantage of this method is that it removes the overlapped clusters, and it reduces the CPU time because we are scan the original document set only twice to find the frequent term set and don’t need to generate the candidate set. The method is applicable on large document databases. It uses half similarity matrix to find the similarity this save more memory.

Experiments have been conducted to evaluate the performance of proposed approach over the other methods like as HFTC and FIHC. The experimental results show that this method performs better because other methods follow apriori algorithm to find the frequent itemsets. As the Apriori algorithm have few disadvantages: like as generates candidate sets, and scans the dataset more number of time. HFTC isn’t scalable and it doesn’t work with high dimensional data. The FIHC method also works based on hard clustering approach.

A result shows the proposed method will perform well with high dimensional document data and no overlapping. With the above analysis, we may conclude that it has constructive quality in clustering documents using graph-based frequent term sets.

**Acknowledgments** This work is supported by research grant from MANIT, Bhopal, India under Grants in Aid Scheme 2010-11, No. Dean(R&C)/2010/63 dated 31/08/2010.

## References

1. Kongthon, A.: A text mining framework for discovering technological intelligence to support science and technology management. Technical Report, Georgia Institute of Technology (2004)
2. Kalogeratos, A., Likas, A.: Document clustering using synthetic cluster prototypes. *Data Knowl. Eng.* **70**, 284–306 (2011)
3. Fung, B., Wang, K., Ester, M.: Hierarchical document clustering using frequent itemsets. In: *Proceeding of SIAM International Conference on Data Mining (SDM'03)*, pp. 59–70 (2003)
4. Michenerand, C.D., Sokal, R.R.: A quantitative approach to a problem in classification. *Evolution* **11**, 130–162 (1957)
5. Chapman, P., Clinton, J., Kerber, R., Khabaza, T., Reinartz, T., Shearer, C., Wirth, R.: CRISP-DM 1.0 : Step-by-step data mining guide, NCR Systems Engineering Copenhagen (USA), DaimlerChrysler AG, SPSS Inc. (USA) and OHRA Verzekeringen Bank Group B.V (Netherlands), (2000)
6. Chen, C.L., Frank, S.C.T., Liang, T.: An integration of wordnet and fuzzy association rule mining for multi-label document clustering. *Data Knowl. Eng.* **69**, 1208–1226 (2010)
7. Chen, C.L., Tseng, F.S.C., Liang, T.: An integration of fuzzy association rules and WordNet for document clustering. In: *Proceeding of the 13th Pacific-Asia Conference on Knowledge Discovery and Data Mining (PAKDD-09)*, pp. 147–159 (2009)
8. Cutting, D.R., Karger, D.R., Pedersen, J.O., Tukey, J.W.: Scatter/Gather: A Cluster-based approach to browsing large document collections. In: *Proceedings of the Fifteenth Annual International ACM SIGIR Conference*, pp. 318–329, June 1992
9. Recupero, D.R.: A new unsupervised method for document clustering by using WordNet lexical and conceptual relations. *Inf. Retrieval* **10**(6), 563–579 (2007)
10. Rajput, D.S., Thakur, R.S., Thakur, G.S.: Rule generation from textual data by using graph based approach. In: *International Journal of Computer Application (IJCA) 0975–8887*, New york, ISBN: 978-93-80865-11-8, Vol. 31, No.9, pp. 36–43, Oct 2011
11. Dunham, M.H., Sridhar, S.: *Data mining: introductory and advanced topics*. Pearson Education, New Delhi, ISBN: 81-7758-785-4, 1st edn. (2006)
12. Fayyad, U., Piatetsky-Shapiro, G., Smyth, P.: From data mining to knowledge discovery in databases. *AI Magazine*, American Association for Artificial Intelligence (1996)
13. Beil, F., Ester, M., Xu, X.: Frequent term-based text clustering. In: *Proceeding of International Conference on Knowledge Discovery and Data Mining (KDD'02)*, pp. 436–442 (2002)
14. Fung, B.C.M., Wang, K., Ester, M.: Hierarchical document clustering using frequent itemsets. In: *Proceedings of SIAM International Conference on Data Mining (2003)*
15. Hammouda, K.M., Kamel, M.S.: Efficient phrase-based document indexing for web document clustering. *IEEE Trans. Knowl. Data Eng.* **16**, 1279–1296 (2004)
16. Han, I., Kamber, M.: *Data Mining Concepts and Techniques*, pp. 335–389. M. K. Publishers, Berlin (2000)
17. Haralampos, K., Christos, T., Babis, T.: An approach to text mining using information extraction. In: *Proceeding Knowledge Management Theory Applications Workshop, (KMTA 2000)*, pp. 165–178. Lyon, Sept 2000
18. Hartigan, J.A., Wong, M.A.: A K-means clustering algorithm. *Appl. Stat.* **28**, 126–130 (1979)
19. Hotho, A., Staab, S., Stumme, G.: Wordnet improves text document clustering. In: *Proceeding of SIGIR International Conference on Semantic Web, Workshop, (2003)*
20. Hung, C., Xiaotie, D.: Efficient phrase-based document similarity for clustering. *IEEE Trans. Knowl. Data Eng.* **20**, 1217–1229 (Sept 2008)
21. *Introduction to Data Mining and Knowledge Discovery*, 3rd edn. ISBN: 1-892095-02-5, Two Crows Corporation, 10500 Falls Road, Potomac, MD 20854, U.S.A., (1999)
22. Jain, A.K., Murty, M.N., Flynn, P.J.: Data clustering: a review. *ACM Comput. Surv.* **31**(3), 264–323 (1999)
23. MacQueen, J.B.: Some methods for classification and analysis of multivariate observations. In: *Proceedings of 5th Berkeley Symposium on Mathematical Statistics and Probability*, pp. 281–297 (1967)



24. Jensen, C.S.: Introduction to Temporal Database Research. <http://www.cs.aau.dk/csj/Thesis/pdf/chapter1.pdf>
25. Lovins, J.B.: Development of a stemming algorithm. *Mech. Transl. Comput. Linguist.* **11**(1, 2), 22–31, June 1968
26. Kiran, G.V.R., Ravi Shankar, Vikram Pudi: Frequent itemset based hierarchical document clustering using wikipedia as external knowledge. *KES 2010, Part II, LNAI 6277*, pp. 11–20. Springer, Berlin (2010)
27. Lin, K., Kondadadi, R.: A word-based soft clustering algorithm for documents. In: *Proceedings of Computers and Their Applications*, pp. 391–394. Seattle (2001)
28. Larose, D.T.: *Discovering knowledge in data: an introduction to data mining*, Wiley, Inc., 2005. *International Journal of Distributed and Parallel systems (IJDPDS)* Vol. 1, No. 1, (2010)
29. Steinbach, M., Karypis, G., Kumar, V.: A comparison of document clustering techniques. *KDD-2000 Workshop on Text Mining*, pp. 109–110 (2000)
30. Rafi, Muhammad, Shahid Shaikh, M., Farooq, Amir: Document clustering based on topic maps. *Int. J. Comput. Appl.* **12**(1), 32–36 (2010)
31. Nasukawa, T., Nagano, T.: Text analysis and knowledge mining system. *IBM Syst. J.* **40**(4), 967–984 (2001)
32. Willett, P.: Recent trends in hierarchic document clustering: a critical review. *Inf. Process. Manage.* **24**(5), 577–597 (1988)
33. Lin, K., Kondadadi, R.: A word-based soft clustering algorithm for documents. In: *Proceeding Computers and Their Applications*, pp. 391–394 (2001)
34. Agrawal, R., Imielinski, T., Swami, A.: Mining association rules between sets of items in large databases. In: *Proceedings of ACM SIGMOD International Conference on Management of Data*, pp. 207–216 (1993)
35. Richards, A.L., Holmans, P., O’Donovan, M.C., Owen, M.J., Jones, L.: A comparison of four clustering methods for brain expression microarray data. *BMC Bioinform.* **9**, pp. 1–17 (2008)
36. Thakur, R.S., Jain, R.C., Pardasani, K.R.: Graph theoretic based algorithm for mining frequent patterns. In: *IEEE World Congress on Computational Intelligence*, pp. 629–633. Hong Kong (2008)
37. Thakur, R.S., Jain, R.C., Pardasani, K.R.: Fast algorithms for mining multi-level association rules in large databases. *Asian J. Inf. Manage. USA* **1**(1), 19–26 (2008)
38. Thakur, R.S., Jain, R.C., Pardasani, K.R.: MAXFP: a multi-strategy algorithm for mining maximum frequent pattern and their support counts. *Trends Appl. Sci. Res.* **1**(4), 402–415 (2006)
39. Vishnu Priya, R., Vadivel, A., Thakur, R.S.: Frequent pattern mining using modified CP-Tree for knowledge discovery. *Advanced Data Mining and Applications, LNCS-2010, Vol. 6440*, pp. 254–261. Springer, Berlin (2010)
40. Soon, M.C., John, D.H., Yanjun, L.: Text document clustering based on frequent word meaning sequences. *Data Knowl. Eng.* **64**, 381–404 (2008)
41. Valentina, C., Sylvie, D.: Text mining supported terminology construction. In: *Proceedings of the 5th International Conference on Knowledge Management*, pp. 588–595. Graz, Austria (2005)

# Desktop Virtualization and Green Computing Solutions

Shalabh Agarwal and Asoke Nath

**Abstract** Greecomputing is now more than just being environmentally responsible. It is also the exercise of utilizing optimal IT resources in a more efficient way. It is realized by the computer professionals and also by the Scientists that one of the key enablers of Green computing is virtualisation. Virtual computing and management will enable toward environmentally sustainable ICT infrastructure. The desktop virtualisation enables to utilise the untapped processing power of today's high-power PCs and storage devices. The same or improved performance can be delivered with reduced operating expenses, a smaller carbon footprint and significantly curtailed greenhouse gas emissions. In this work the authors have made a complete study on Desktop virtualisation, Thin client architecture, and its role in Green computing.

**Keywords** Green computing · Virtualisation · ICT · Greenhouse gas · Thin client

## 1 Introduction

In the present scenario one cannot think of living without computers. At the same time it is important to find ways to use the computers in a way that can sustain the environment. Currently, personal computers (PC) consume far too much electricity and generate too much e-waste to be considered an eco-friendly solution by today's standards. With a typical PC taking approximately 110–240 W to run, and with well over 1 billion of them on the planet, it is easy to understand the carbon footprint and Green House Emissions generated by these PCs. E-waste is another issue that is the

---

S. Agarwal (✉) · A. Nath  
St. Xavier's College [Autonomous], Kolkata WB 700016, India  
e-mail: shalabh@sxccal.edu

A. Nath  
e-mail: asokejoy1@gmail.com

fastest growing part of the waste stream and is harming the planet in more than one ways [1–3].

Today's PCs are so powerful that we no longer need one PC per person. We can utilise the excess capabilities in one PC and share it with many users. Desktop virtualisation thin client devices do just that and use just 1–5 W, last for a more than 10 years, and generate very little e-waste. Not only is this a simple solution to a complex problem, it is also very efficient. Desktop virtualisation saves 75% on hardware, and since they draw very less power, we can reduce nearly 90% energy footprint per user. These devices produce practically no heat, reducing the need for air-conditioning, which in turn saves power consumed by such cooling solutions.

Today, the biggest driving force for IT companies to adopt thin client desktop virtualisation is major savings. What has made server-based computing easier is that many desktop virtualisation solutions integrate seamlessly with existing virtualisation infrastructure and even use the same management tools, enabling IT managers to get started and feel comfortable with their new solution right away—realising benefits from day one [4]. Once deployed, desktop virtualisation solutions centralise management and enable easy software updates and security and patch rollouts. They also improve security and provide users with options like self-help and desktop mobility. Although the draw for IT to implement desktop virtualisation is often not green, more and more organisations have realised that with virtualisation, green benefits often correlate with cost savings. In turn, these cost savings result in a significant environmental impact that will lower an organisation's carbon footprint and e-waste volume while changing the future of green computing.

## 2 Green Computing

According to San Murugesan, the field of green computing is “the study and practice of designing, manufacturing, using, and disposing of computers, servers, and associated subsystems—such as monitors, printers, storage devices, and networking and communications systems—efficiently and effectively with minimal or no impact on the environment”. It is about environmentally friendly use of computers and related technologies. Efforts to reduce the energy consumption associated with PC are often referred to as “green computing,” which is the practice of using computing resources efficiently and in an environmentally sensitive manner. “Green IT” refers to all IT solutions that save energy at various levels of use. These include (i) hardware, (ii) software and (iii) services [1–3].

Green is used in everyday language to refer to environmentally sustainable activities. Green computing encompasses policies, procedures and personal computing practices associated with any use of information technology (IT). People employing sustainable or green computing practices strive to minimise green house gases and waste, while increasing the cost-effectiveness of IT, such as computers, local area networks and data centres. More directly it means using computers in ways that save the environment, save energy, and save money.

The greenhouse effect is a process by which thermal radiation from a planetary surface is absorbed by atmospheric greenhouse gases, and is re-radiated in all directions. Since part of this re-radiation is back towards the surface and the lower atmosphere, it results in an elevation of the average surface temperature above what it would be in the absence of the gases. Particularly since the arrival of industrialisation, the human race has intensified this effect, as combustion processes and other industrial processes release greenhouse gases which, with their increased concentration, influence the Earth's radiation balance and thus influence the greenhouse effect. Possible measures for reduction of greenhouse gas emissions include increasing the energy efficiency of machinery, e.g. via intelligent control programs, or replacing energy-intensive computer architectures with low-carbon, solutions. Here, green IT or server-based computing can make a significant contribution by using energy more efficiently than conventional IT equipment and thus saving greenhouse gases.

### 3 Thin Client Desktop Virtualisation

Wikipedia's definitions of a thin client is: A thin client (sometimes also called a lean or slim client) is a client computer or client software in client-server architecture networks which depends primarily on the central server for processing activities, and mainly focuses on conveying input and output between the user and the remote server. In contrast, a thick or fat client does as much processing as possible and passes only data for communications and storage to the server [4–8].

Consultants have been saying for a long time that thin clients are the future. Today, thin client technology finally has caught up with the vision. A few years ago, most companies had two or three models of thin clients, but today there are many models to choose from with varying CPU speeds, memory capacities, storage capacities and operating systems. Besides being more secure and easier to deploy, manage and maintain (than their PC counterparts) thin clients boast a longer life expectancy because they have no moving parts, small footprint on the desktop, lower power consumption and server-centralized data storage.

Desktop virtualisation is an implementation of thin client concept and is defined as a computing environment in which some or all components of the system, including operating system and applications, reside in a protected environment, isolated from the underlying hardware and software platforms. The virtualisation layer controls interactions between the virtual environment and the rest of the system. Essentially, servers host desktop environments specific to each user and stream applications and operating systems to the desktop (Fig.1).

Desktop virtualisation separates software from the basic hardware that provides it, putting the focus on what is being delivered, making the user unaware and unconcerned about how it is being delivered or from where it is coming. Virtualisation separates the fundamental operating system, applications and data from an end user's device and moves these components into the central server where they can be secured and centrally managed. This approach allows users to access their "virtual desktop" with a full personal computing experience across devices and locations. Desktop

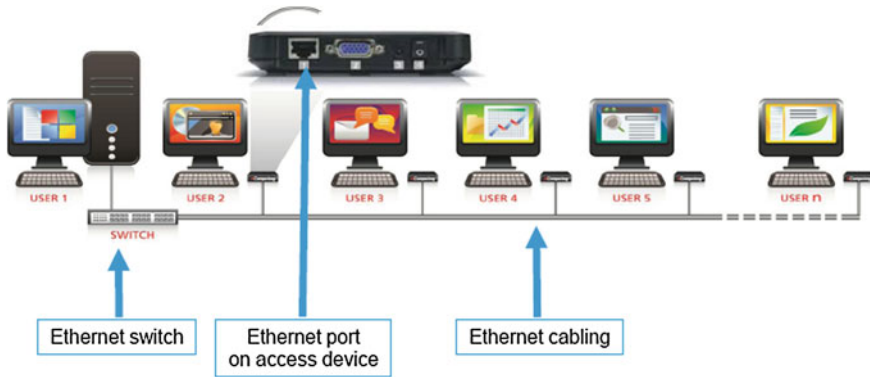


Fig. 1 Desktop virtualisation using N-computing. (Source: <http://www.ncomputing.com>)

virtualisation takes the efficiencies offered through a centralized processing environment and merges it with the flexibility and ease of use found in a traditional PC. It is the concept of isolating a logical operating system instance from the client that is used to access it.

There are several different conceptual models of desktop virtualisation, which can broadly be divided into two categories based on whether or not the operating system instance is executed locally or remotely. It is important to note that not all forms of desktop virtualization involve the use of virtual machines which lead to more efficient use of computing resources, both in terms of energy consumption and cost-effectiveness.

Host-based forms of desktop virtualisation require that users view and interact with their desktops over a network by using a remote display protocol. Because processing takes place in a server, client devices can be thin clients, zero clients, smartphones and tablets.

Client-based types of desktop virtualisation require processing to occur on local hardware; the use of thin clients, zero clients, and mobile devices is not possible.

In this chapter, all the references to desktop virtualisation are related to host-based forms of desktop virtualisation where the client does not require any processor, memory or storage facilities. The solution can be implemented in a LAN as well as WAN environment. Whereas in the WAN scenario, the bandwidth and the speed becomes an important driving factor.

## 4 Virtualisation Benefits

### 4.1 Affordable to All

With virtualisation, the investment on PCs can be maximised by adding users for a small fraction of the cost. The client access devices are mostly thin or zero computing

devices which are nearly three times cheaper than a PC. Hence 50–70% increase in the number of computing seats can be implemented for the same budget. The savings enables to improve computer upgrade cycles, expand access or invest extra funds in other technology upgrades.

## ***4.2 Compatible***

The implementation of desktop virtualisation supports multiple operating system platforms like Microsoft Windows and Linux. So, the current applications can be used in the same environment without the need of any migration of technology.

## ***4.3 Easy to Manage***

Once deployed, desktop virtualisation solutions centralise management and enable easy software updates and security and patch rollouts. They also improve security and provide users with options like self-help and desktop mobility. Desktop virtualisation, creates a single “golden” image of the OS on a server and each user takes advantage of the same golden image. So, in effect, there is a need to manage only a single image, not hundreds or thousands. It is also a simple matter to create multiple such images for different groups, each setup with the applications that users in that group need.

## ***4.4 Efficient to Operate***

The efficiency of the virtualisation solution goes beyond getting more from the PC resources. The virtual desktop devices save space in the work area and save electricity by drawing substantially less power than a typical PC.

## ***4.5 Simple to Deploy***

Every virtualisation software and hardware product is designed to be easy to set up, secure and maintain by people with basic PC skills. The virtual desktops require no maintenance and do not contain sensitive components such as hard drives and fans. And with fewer PCs to manage, there will be fewer support issues.

## 5 Virtualisation Green Advantage

One of the best ways to reduce energy consumption is to consider the use of thin client technology. This is similar to server virtualisation in that one physical computer runs several workstations in the same way that several server instances can run on one physical server box using virtualisation tools [1].

This approach has been made possible by the increased power of modern computers. Processors are faster, they often have multicores, can run in 64 bit mode, and may be arranged in pairs or fours within a single machine. Memory has reduced in price considerably and, using 64 bit systems, is able to be addressed in more than 4 GB memory configurations thus dramatically increasing the performance of systems. Graphics and sound have also improved greatly with on board sound and graphics now more capable than the average user requires. These computer hardware improvements continue delivering a faster and richer experience to the user. The increased potential of modern PCs and the need to become more environmentally responsible has provided an option to run many workstations from one computer base unit.

The average person uses less than 5% of the capacity of their PC. The rest is simply wasted. The Desktop Virtualisation solution is based on this simple fact that today's PCs are so powerful that the vast majority of applications only use a small fraction of the computer's capacity. Virtualisation tap this unused capacity so that it can be simultaneously shared by multiple users—maximizing the PC utilisation. Each user's monitor, keyboard, and mouse connect to the shared PC through a small and highly reliable virtualisation access device. These access devices use the concept of thin client or zero client. The zero client access device has no CPU, memory, or moving parts. Electricity consumption of a thin/zero client is less than 10% that of a PC. A standard PC consumes 150–200 W compared to 5–15 W by thin/zero clients. Hence, virtualisation can reduce electricity consumption as well as cooling requirements, thus reducing both carbon emissions and cost.

Virtualisation reduces carbon emissions and have a significantly smaller footprint, with some solutions using less than one twentieth of the materials required for a traditional PC, which results in far less e-waste filling landfills. The elimination of the physical desktop PC lessens the landfill issues as zero-clients contain no processor, memory or other moving elements like hard disks [1–3].

Additionally, zero-client desktop virtualisation solutions can have a useful life more than twice the length of a traditional PC because they do not have an operating system, software or moving parts on the device which can fail or quickly become outdated or obsolete. As long the desktop device is capable of handling the software updates made on the server, the solution continues to work. Zero-clients can last for 8–10 years as opposed to 3–4 years of a conventional PC. Hence in case of Desktop virtualisation, e-waste reduction, as opposed to e-waste recycling, is definitely a grand step towards greener environment. PCs typically weigh about 10 kg and are disposed of in landfills after 3–5 years. Desktop virtualisation access devices weighs about 150 g, and easily last 5 years or more, for a 98% reduction in electronic waste. So there's less to transport and less e-waste that will find its way to a landfill.

In addition to reduced energy use, emissions are also reduced dramatically with the concept of virtualisation. For example, 26 physical servers and a network would produce 210,269 pounds of carbon dioxide per year compared to a private cloud hosting solution that has the capacity of 35 servers and produces only 27,903 pounds of carbon dioxide per year. The Verdantix report, the result of a study, has found that if companies adopt cloud computing (which is an advanced implementation of virtualisation), they can reduce the energy consumption of their IT and save money on energy bills. The report, created by research firm Verdantix and sponsored by AT&T, estimates that cloud computing could enable companies to save \$12.3 billion off their energy bills. That translates into carbon emission savings of 85.7 million metric tons per year by 2020 [4, 6, 7].

**Virtualisation Green Benefits**

**Less energy consumption**

Personal computers draw about 110W of electricity, whereas virtual desktops only draw 1–5 W. The energy footprint per user declines by as much as 98 %.

**Air-conditioning**

Consume less energy and produces less heat as air-conditioning is not compulsory. Less air- conditioning compounds the savings on your electricity and releases less carbon footprint.

**E-waste**

The solutions are also the most eco-friendly on earth, and not just because of how little electricity they consume: they generate a negligible amount of e-waste, reducing contribution to the e-waste stream (Fig. 2).

**Environmental impact**

Because the products deliver green computing and cost less to buy and operate, they address the triple bottom line perfectly. That is, they save money while they help reduce climate change and hazardous e-waste.

As PC adoption grows globally, it is estimated that there will be more than two billion PCs in use by 2015. It took 30 years to reach one billion but will only take three more years to double that number. With this trend, something needs to change. If desktop virtualisation access systems are used at a ratio of 6 devices to each PC:

- Energy use would decline by over 143 billion kilowatt hours per year
- CO<sub>2</sub> emissions would decrease by 114 million metric tons. That’s like planting 550 million trees!
- E-waste would be reduced by 7.9 million metric tons



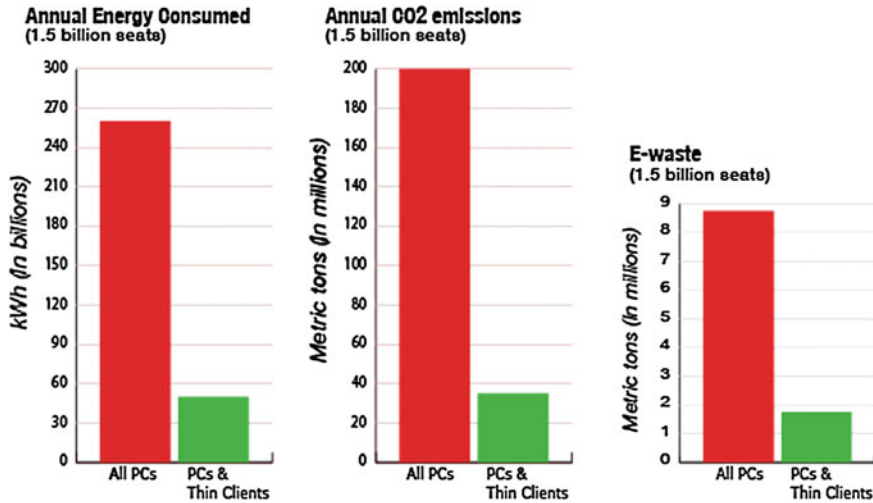


Fig. 2 Energy consumed, emissions and E-waste comparison of PCs and thin clients. (Source: <http://www.ncomputing.com/company/green-computing>)

## 6 The Global Warming Potential Effect

According to Wikipedia, Global-warming potential (GWP) is a relative measure of how much heat a greenhouse gas traps in the atmosphere. It compares the amount of heat trapped by a certain mass of the gas in question to the amount of heat trapped by a similar mass of carbon dioxide. A GWP is calculated over a specific time interval, commonly 20, 100 or 500 years. GWP is expressed as a factor of carbon dioxide (whose GWP is standardized to 1). For example, the 20 year GWP of methane is 72, which means that if the same mass of methane and carbon dioxide were introduced into the atmosphere, that methane will trap 72 times more heat than the carbon dioxide over the next 20 years [2, 3].

The GWP depends on the following factors:

- the absorption of infrared radiation by a given species
- the spectral location of its absorbing wavelengths
- the atmospheric lifetime of the species

Thus, a high GWP correlates with a large infrared absorption and a long atmospheric lifetime. The dependence of GWP on the wavelength of absorption is more complicated. Even if a gas absorbs radiation efficiently at a certain wavelength, this may not affect its GWP much if the atmosphere already absorbs most radiation at that wavelength. A gas has the most effect if it absorbs in a “window” of wavelengths where the atmosphere is fairly transparent.

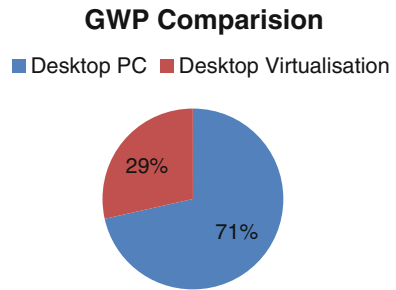
**Table 1** Global warming potential in kg CO<sub>2</sub>eq

Phase	Desktop PC	Desktop virtualisation
Production phase	117.33	3.67
Manufacturing phase	21.04	0.66
Distribution phase	25.25	0.79
Operation phase	529.67	271.55
Total	693.29	276.67

According to a study “Thin Clients 2011—Ecological and economical aspects of virtual desktops”, conducted by Fraunhofer Institute of Environmental, Safety and Energy Technology UMSICHT, compared to Desktop virtualisation, a Desktop PC user has nearly 2.5 times GWP. The following table shows the GWP at various phases.

As it is clear from Table 1, virtualisation has substantially less impact on global warming. This leads to a lots of savings in terms of CO<sub>2</sub> emissions. The following pie-chart shows the comparison (Fig. 3).

**Fig. 3** Comparison of GWP of a desktop PC and virtualisation



## 7 Challenges of Virtualisation

However, desktop Virtualisation is not without drawbacks and challenges. Users that require multitasking, interaction with multimedia applications or support for local peripherals may not experience satisfactory performance. Traditional desktop virtualisation solutions are designed to support the “lowest common denominator” client device, often sacrificing user experience for improved access. In general thin client technology and desktop virtualisation is used in open access areas such as learning centres and libraries or general purpose classrooms. It is not used for activities requiring significant processing power such as graphics and audio editing tasks or data manipulation activities. For general purpose computing (word processing, e-mail, Web browsing) the user experience is unaffected. Some of the disadvantages relate to the reliability of the server, network bandwidth issues, less flexibility and being unsuitable for certain tasks such as multimedia.

As anyone who has undertaken a virtualisation project quickly discovers, many applications and hardware devices are not amenable to easy virtualisation; therefore, a detailed assessment of applications and hardware in use is a key prerequisite to successful virtualisation. Even if virtualisation is technically feasible, many vendors offer limited support for virtual instances of their software, and some even refuse to honor warranties and maintenance contracts if their apps are running in a virtual environment.

## 8 Conclusion

The specific recommendation for IT decision-makers is to consider thin clients as an alternative to the desktop PCs. This operating model offers ecological and economic advantages over conventional Client-Server models. In order to minimise the consumption of materials and energy, the IT infrastructure should be designed to suit the actual needs of the end-users and not just implement a heavily loaded solution in which the infrastructure is not utilised to the fullest capacity. Traditional terminal servers can be combined with desktop virtualisation solutions to provide each user equipment tailored to their specific requirements so as to optimise the capacity utilisation of the hardware.

Any organisation using for more than one PC should seriously consider the advantages of moving to desktop virtualisation. By taking advantage of today's low-cost yet ever-more-powerful computers, even the smallest organisation can appreciate immediate benefits without the high expense of mainframe computing or the complexity and performance limitations of server-based computing. Desktop virtualisation makes computing available to more people within the organisation for less cost. Best of all, it saves a lot of energy and minimises e-waste, thus contributing the sustainability of the environment.

## References

1. Agarwal, S., Nath, A.: Green computing—a new horizon of energy efficiency and electronic waste minimization: a global perspective. In: Proceedings of IEEE CSNT-2011 held at SMVDU (Jammu), pp. 688–693, 3–6 June 2011
2. Agarwal, S., Nath, A.: Cloud computing is an application of green computing—a new horizon of energy efficiency and its beyond. In: Proceedings of International conference ICCA 2012 held at Pondechery, 27–31 Jan 2012
3. Agarwal, S., Nath, A., Chowdhury, D: Sustainable approaches and good practices in green software engineering. *Int. J. Res. Rev. Comp. Sci.* **3**(1), 2079–2557 (2012)
4. Knorr, E.: What desktop virtualization really means—depending on whom you talk to, desktop virtualization is either the hottest trend in IT or an expensive notion with limited appeal
5. Thin Clients 2011—Ecological and Economical Aspects of Virtual Desktops, a Study Conducted by Fraunhofer Institute of Environmental, Safety and Energy Technology UMSICHT
6. Chitnis, N., Bhaskaran, R., Biswas, T.: Going Green with Virtualisation. *Setlabs Briefings*, **9**(1), 31–38 (2011)

7. Desktop Virtualisation in Higher Education. A Strategy Paper from Centre for Digital Education, 1-8
8. A. Orady, Going Green with Desktop Virtualisation
9. Freedman, R.: Investing in Virtualization has Green IT Payoffs

# Noise Reduction from the Microarray Images to Identify the Intensity of the Expression

S. Valarmathi, Ayesha Sulthana, K. C. Latha, Ramya Rathan,  
R. Sridhar and S. Balasubramanian

**Abstract** Microarray technique is used to study the role of genetics involved in the development of diseases in an early stage. Recently microarray has made an enormous contribution to explore the diverse molecular mechanisms involved in tumorigenesis. The end product of microarray is the digital image, whose quality is often degraded by noise caused due to inherent experimental variability. Therefore, noise reduction is a most contributing step involved in the microarray image processing to obtain high intensity gene expression results and to avoid biased results. Microarray data of breast cancer genes was obtained from National Institute of Animal Science and Rural Development Administration, Suwon, South Korea. Two algorithms were created for noise reduction and to calculate the intensity of gene expression of breast cancer susceptibility gene 1 (BRCA1) and breast cancer susceptibility gene 2 (BRCA2). The new algorithm successively decreased the noise and the expression value of microarray gene image was efficiently enhanced.

---

S. Valarmathi (✉) · R. Sridhar · S. Balasubramanian  
DRDO-BU-CLS, Bharathiar University, Coimbatore, Tamil Nadu, India  
e-mail: valar28aadarsh@gmail.com

R. Sridhar  
e-mail: rmsridhar@rediffmail.com

S. Balasubramanian  
e-mail: director\_research@jssuni.edu.in

A. Sulthana · K. C. Latha  
Department of Water and Health, JSS University, Mysore, Karnataka, India  
e-mail: ayeshasulthanaa@gmail.com

K. C. Latha  
e-mail: latha\_tanvi23@yahoo.com

R. Rathan  
Department of Anatomy, JSS University, Mysore, Karnataka, India  
e-mail: ramirohith@ymail.com

**Keywords** Noise reduction · Image processing · Microarray · Algorithm · Gene expression · Breast cancer

## 1 Introduction

Thousands of individual DNA sequences are printed in parallel on a glass microscope slide of cDNA microarrays [19]. Microarray slide consists of a rectangular array of subgrids, each subgrid printed by one pin of the contact-printer. A subgrid consists of an array of spots, each spot containing a single cDNA probe. The hybridized arrays are imaged using a scanner and the output stored as 16-bit image files. Different dyes were used to visualize the image clearly. In the analysis of cDNA microarray images, the most important task involved is the gridding of the spots [9]. For this multiple methods related to array recognition; spot segmentation and measurement extraction have emerged over past several years [12]. Large numbers of commercial tools have been developed in microarray image processing. Microarrays measure expression levels of tens of thousands of genes simultaneously and suffer from the presence of inherent experimental noise. Detection of random noise causes inconsistencies in the image processing [15]. The noise generally results during the phases of sample preparation, hybridization, and scanning [16]. The sample preparation noise results from the process of RNA amplification, and the hybridization noise refers to the randomness in the process of RNA binding to the probes. The sources of scanning noise include leak of external light, variations in laser intensity, and presence of dirt [4]. Many types of distortions limit the quality of digital images during image acquisition, formation, storage, and transmission. Often, images are corrupted by impulse noise, thereby causing loss of image details. It is important to eliminate noise in images before using them for image processing techniques like edge detection, segmentation, and registration [13]. Removal of noise in the microarray technique involves three steps; gridding (addressing each spot), segmentation (separating spot pixels from background pixels), and quantification (putting spot intensity data into numerical form for comparison) [5]. Noise reduction framework enables efficient filtering of large and color images in real-time application with the preservation of their textural features [14]. An extensive quantitative measure of the efficiency of the noise estimation determines the quality of the JPEG file. Several authors have developed and discussed denoising methods in microarray data [3, 18].

Gene expression analysis were carried out using microarray for simultaneous interrogation of the expression of genes in a high-throughput fashion and offers unprecedented opportunities to obtain molecular signatures of the activity of diseased cells [10]. Stanford University was the first to describe and use microarray to study gene expression in various diseases including cancer [17]. Gene expression in cancer by microarray is fast gaining popularity in providing better prognostic and predictive information on the disease. Microarray-based gene expression profiling is used as a tool for Breast Cancer Management, in identifying genes whose expression has changed in response to pathogens or other organisms by comparing gene

expression of infected to that of uninfected cells or tissues [1]. Heritable mutation influences the gene-expression profile of the breast cancer with BRCA1 and BRCA2 mutations [6]. Gene expression profiles evaluated by microarray-based quantification of RNA are used in studies of differential diagnosis and prognosis in cancer. Microarray data were evaluated using both unsupervised, and supervised multivariate statistical methods [8]. Differential gene expression was analyzed for gene oncology to identify important functional categories [2].

Our study is involved in developing an algorithm for the processing of microarray images with the following objectives:

- I To reduce noise from a microarray image of breast cancer gene\*.
- II To identify the intensity of gene expression from a microarray image of a breast cancer gene.

## 2 Data and Methodology

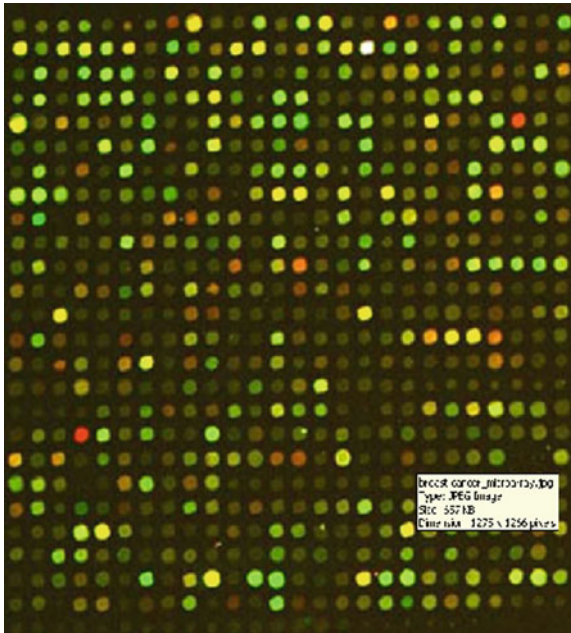
For the present study the microarray data was obtained from National Institute of Animal Science and Rural Development Administration, Suwon, South Korea and was used to test our algorithm integrated with MATLAB. The main aim is to reduce the noise and to calculate the intensity of gene expression of BRCA1 and BRCA2 genes in the microarray image, rather to give interpretation on gene expression in microarray images of breast cancer genes. A fully automated method that removes the existing impulse of noise from the microarray plate with virtually no required user interaction or external information, greatly increasing efficiency of the image analysis was developed. For image processing of microarray data, two algorithms were developed in Visual Basic and integrated with MATLAB (Appendixes I and II):

- (i) Algorithm for Noise reduction
- (ii) Algorithm to calculate intensity of gene expression

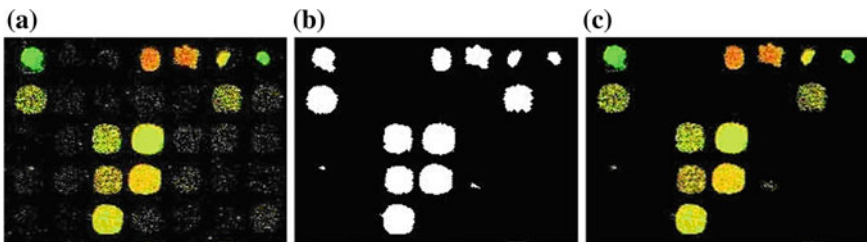
## 3 Results

### 3.1 Removal of Noise in the Microarray Image

The proposed approach was used to test microarray image of the Breast Cancer Patient containing thousands of spots (Fig. 1). A section from the microarray image (Fig. 1) was cropped and it was named as original image (Fig. 2a). The noise from the microarray image was removed by using algorithm (i). Initially the original image (Fig. 2a) was converted into gray image. Using Otsu method (reduction of a gray level image to a binary image) the graythresh value [11] for the image was calculated. Using this graythresh value the image was then converted into Black and White image. From the image, the objects which have fewer than P pixels were removed and used to create a new structural binary image. This step was performed



**Fig. 1** Microarray image of the breast cancer patient



**Fig. 2** Removal of noise from the microarray image **a** Original image **b** Black and White after Filtering **c** Image after noise removal

repeatedly until all the fewer objects from the image were removed. To this image, a flood-fill operation was performed to fill the background pixels and the output image was obtained (Fig. 2b).

The image obtained after filtering was compared with the original image (Fig. 2a) to produce the final image (Fig. 2c) using MATLAB environment. Thus the noise from the original image was removed and the obtained image can be used for calculating the intensity of gene expression and to find the level of risk of breast cancer using microarray. This method achieves an accuracy of more than 95 % and it outperforms the existing methods.



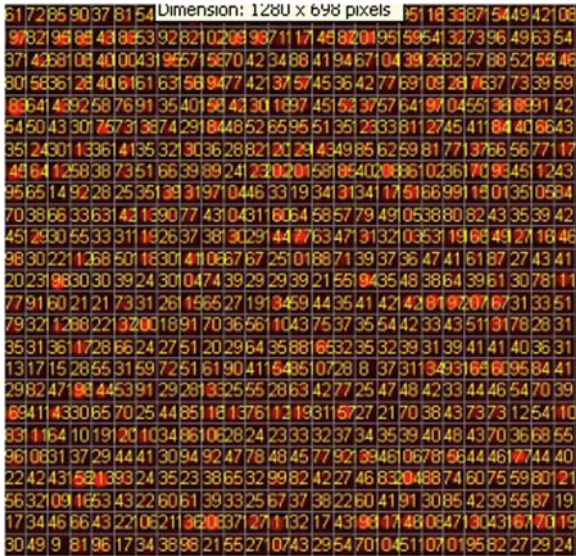


Fig. 3 Red intensity image of microarray plate

### 3.2 Gene Expression Analysis

The intensity was calculated from the ‘noise removed microarray image’ to find the gene expression value for each spot in the plate using algorithm (ii). The red intensity and green intensity in the microarray image was obtained based on the fluorescent tag used in the experimental analysis and are shown in the Figs. 3 and 4. The red spot (Cy5 fluorescent) indicates the expression value of the defective gene and the green spot (Cy3 fluorescent) indicates the expression value of the normal gene. The overall gene expression of a microarray plate was obtained by merging the image of the red and green intensity and is shown in the Fig. 5. In this image, the intensity of green spot shows that the expression of the gene is repressed. The red intensity spot shows that the gene expression is induced in the microarray plate, due to the presence of defective gene. The yellow (mixture of green and red) color spot in the image shows that gene expression is unchanged (normal and abnormal gene is equally expressed). This provides knowledge to the molecular biologist and particularly to oncologist in the diagnosis of defective genes. Therefore, the developed algorithm is a new attempt to predict the expression value of any microarray gene images.



## 4 Conclusion

Microarray image quality is distorted by various source of noise like inherent technical variations and biological sample variations. Therefore the most critical aspect is to reduce the noise from microarray image to avoid the misinterpretation of results. In this study, the microarray image of a breast cancer patient was used to reduce the noise using the proposed algorithm developed in Visual Basic and integrated with MATLAB. Noise reduction of microarray image was achieved successfully without generating any negative effect on the data. The algorithm developed to identify the intensity of gene expression was implied on a noise reduced microarray image to identify the expression of the gene based on the intensity of the spot in the image. These algorithms can be used further to reduce noise in microarray images and to enhance the intensity of gene expression, this will lead to better analysis and interpretation of microarray images.

## Appendix I

### Algorithm for Noise Removal from the Microarray Plate

- Step 1 : Read an RGB Microarray Image.
- Step 2 : Convert the given image to gray.
- Step 3 : Calculate the graythresh value of the given image using Otsu Method.
- Step 4 : Convert the gray image to BW image using graythresh value.
- Step 5 : Remove from a binary image all connected components (objects) that have fewer than P pixels, producing another binary image.
- Step 6 : Create morphological structuring element.
- Step 7 : Perform morphological closing on the binary image obtained from step 4 with the structuring element created in the step 6.
- Step 8 : Perform a flood-fill operation on background pixels of the input binary image obtained from step 7. The output is saved as Picture 1.
- Step 9 : The Picture 1 is compared with original image from which the final image is produced based on the white pixel shown in the Picture 1.

### Algorithm to Convert RGB Image to Gray Image

```

For i = 0 To Picture1.ScaleWidth
    For j = 0 To Picture1.ScaleHeight
        tcol = GetPixel(Picture1.hdc, i, j)
        r = tcol Mod 256
        g = (tcol / 256) Mod 256
        b = tcol / 256 / 256
        colour = r * 0.3 + g * 0.59 + b * 0.11
        SetPixel Picture2.hdc, i, j, RGB(colour, colour, colour)
    Next
Next
Next
    
```

Algorithm for Obtaining Graythresh Value

Otsu shows that minimizing the intraclass variance is the same as maximizing inter-class variance which is expressed in terms of class probabilities  $\omega_i$  and class means  $\mu_i$  which in turn can be updated iteratively. This idea yields an effective algorithm.

- Step 1 : Compute histogram and probabilities of each intensity level
- Step 2 : Set up initial  $\omega_i(0)$  and  $\mu_i(0)$
- Step 3 : Step through all possible thresholds maximum intensity
- Step 4 : Update  $\omega_i$  and  $\mu_i$
- Step 5 : Compute Desired threshold corresponds to the maximum

Algorithm to convert Gray Image to Black and White image using Graythresh Value

```

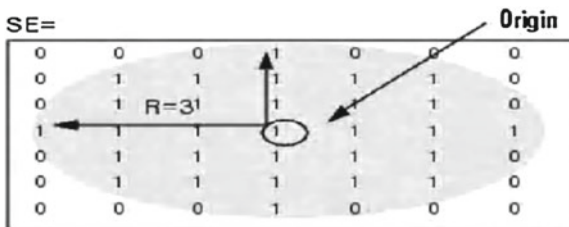
For i = 0 To Picture1.ScaleWidth
  For j = 0 To Picture1.ScaleHeight
    tcol = GetPixel(Picture1.hdc, i, j)
    if tcol > graythresh_value then
      SetPixel Picture2.hdc, i, j, RGB(255, 255, 255)
    else
      SetPixel Picture2.hdc, i, j, RGB(0, 0, 0)
    endif
  Next
Next
    
```

Algorithm to Remove Small Objects

- Step 1: Determine the connected components for BW image using 4-Connected Neighbourhood.
- Step 2: Compute the area of each component which are expressed in terms of Pixel.
- Step 3: Consider the only components whose pixels are greater than 10.

Create Morphological Elements using MATLAB

$SE = \text{strel}('disk', R, N)$  creates a flat, disk-shaped structuring element, where R specifies the radius. R must be a nonnegative integer. N must be 0, 4, 6, or 8. When N is greater than 0, the disk-shaped structuring element is approximated by a sequence of N periodic-line structuring elements. When N equals 0, no approximation is used, and the structuring element members consist of all pixels whose centers are no greater than R away from the origin. If N is not specified, the default value is 4.



Algorithm for Black and White Image to RGB

Step 1:

```

For i = 0 To Picture1.ScaleWidth
  For j = 0 To Picture1.ScaleHeight
    tol = GetPixel(Picture2.hdc, i, j)
    If tol = 0 Then
      Grid2.TextMatrix(i, j) = 0
    Else
      Grid2.TextMatrix(i, j) = 1
    End If
  Next
Next

```

Step 2:

```

Picture3.BackColor = vbBlack
Picture3.height = Picture1.height
Picture3.width = Picture1.width
For i = 0 To Picture1.ScaleWidth
  For j = 0 To Picture1.ScaleHeight
    If Grid2.TextMatrix(i, j) = 1 Then
      SetPixel Picture3.hdc, i, j, val(Grid1.TextMatrix(i, j))
    End If
  Next
Next

```

**Appendix II**

Algorithm for Calculating Expression Value for each spot  
in Microarray Plate

```

x = imread('MicroArraySlide.JPG');
  %x = imread('microarray_test6_agri.JPG');
  %x = imread('Composite-s416-.jpg');
  %x = imread('dna_microarray.JPG');
  %x = imread('t1.JPG');
  %x = imread('t9.jpg')
  %x = imread('t5.jpg')
  %x = imread('t10.jpg')
  %x = imread('microarray_test1_agri_rice.JPG');
  %x = imread('t4.JPG');
imageSize = size(x)
screenSize = get(0,'ScreenSize')
iptsetpref('ImshowBorder', 'tight')

```

```
imshow(x)
title('original image')
```

#### Crop Specified Region

```
%y = imcrop(x, [622 2467 220 227]);
[y,RECT] = imcrop(x) %, [398 449 218 214]);
    %y = imcrop(x, [398 449 218 214]);
    f1 = figure('position', [40 46 285 280]);
imshow(y)
```

#### Display Red and Green Layers

```
f2 = figure('position', [265 163 647 327]);
subplot(121)
    redMap = gray(256);
    redMap(:, [2 3]) = 0;
    t = subimage(y(:, :, 1), redMap)
axis off
title('red (layer 1)')
subplot(122)
    greenMap = gray(256);
    greenMap(:, [1 3]) = 0;
subimage(y(:, :, 2), greenMap)
axis off
title('green (layer 2)')
```

#### Convert RGB Image to Grayscale for Spot Finding

```
z = rgb2gray(y);
figure(f1)
imshow(z)
```

#### Create Horizontal Profile

```
xProfile = mean(z);
f2 = figure('position', [39 346 284 73]);
plot(xProfile)
title('horizontal profile')
axis tight
```

#### Estimate Spot Spacing by Autocorrelation

```
ac = xcov(xProfile);
f3 = figure('position', [-3 427 569 94]);
plot(ac)
s1 = diff(ac([1 1:end]));
```

```

s2 = diff(ac([1:end end]));
maxima = find(s1>0 & s2<0);
estPeriod = round(mean(diff(maxima)))
hold on

plot(maxima,ac(maxima), 'r^')
hold off

title('autocorrelation of profile')
axis tight

Remove Background Morphologically

seLine = strel('line', estPeriod, 0);

%seLine = strel('disk', 2);
xProfile2 = imtophat(xProfile,seLine);
f4 = figure('position', [40 443 285 76]);
plot(xProfile2)
title('enhanced horizontal profile')
axis tight

Segment Peaks

level = graythresh(xProfile2/255)*255

bw = im2bw(xProfile2/255, level/255);
L = bwlabel(bw);
f5 = figure('position', [40 540 285 70]);
plot(L)
axis tight

title('labelled regions')

Locate Centers

stats = regionprops(L);

centroids = [stats.Centroid];
xCenters = centroids(1:2:end)

figure(f5)
hold on

plot(xCenters, 1:max(L), 'ro')
hold off

title('region centers')

Determine Divisions between Spots

gap = diff(xCenters)/2;
first = abs(xCenters(1) - gap(1));
xGrid = round([first xCenters(1:end) + gap([1:end end])])

Transpose and Repeat

```

```

yProfile = mean(z');
    ac = xcov(yProfile);
    p1 = diff(ac([1 1:end]));
    p2 = diff(ac([1:end end]));
    maxima = find(p1>0 & p2<0);
    estPeriod = round(mean(diff(maxima)))
    seLine = strel('line', estPeriod, 0);
%seLine = strel('disk', 2);
    yProfile2 = imtophat(yProfile, seLine);
    level = graythresh(yProfile2/255);
    bw = im2bw(yProfile2/255, level);
    L = bwlabel(bw);
    stats = regionprops(L);
    centroids = [stats.Centroid];
    yCenters = centroids(1:2:end)
    gap = diff(yCenters)/2;
    first = abs(yCenters(1)-gap(1));

```

#### List Defining Vertical Boundaries between Spot Regions

```

yGrid = round([first yCenters(1:end) + gap([1:end end])])
    f7 = figure('position', [52 94 954 425]);
    ax(1) = subplot(121);
subimage(y(:, :, 1), redMap)
    title('red intensity')
    ax(2) = subplot(122);
subimage(y(:, :, 2), greenMap)
    title('green intensity')
    f8 = figure('position', [316 34 482 497]);
ax(3) = get(imshow(y, 'notruesize'), 'parent');
    title('gene expression')
for i=1:3
    axes(ax(i))
    axis off
    line(xGrid'*[1 1], yGrid([1 end]), 'color', 0.5*[1 1 1])
    line(xGrid([1 end]), yGrid'*[1 1], 'color', 0.5*[1 1 1])
end

[X, Y] = meshgrid(xGrid(1:end-1), yGrid(1:end - 1));
[dX, dY]= meshgrid(diff(xGrid), diff(yGrid));
ROI = [X(:) Y(:) dX(:) dY(:)];

```

#### Segment Spots from Background by Thresholding



```
fSpots = figure('position', [265 163 647 327]);
subplot(121)
imshow(z)
title('gray image')
subplot(122)
    bw = im2bw(z, graythresh(z));
imshow(bw)
title('global threshold')
```

Apply Logarithmic Transformation then Threshold Intensities

```
figure(fSpots)
subplot(121)
    z2 = uint8(log(double(z) + 1)/log(255)*255);
imshow(z2)
title('log intensity')
subplot(122)
    bw = im2bw(z2, graythresh(z2));
imshow(bw)
title('global threshold')
```

Try local Thresholding Instead

```
figure(fSpots)
subplot(122)
    bw = false(size(z));
    for i=1:length(ROI)
        rows = round(ROI(i, 2)) + [0:(round(ROI(i, 4))-1)];
        cols = round(ROI(i, 1)) + [0:(round(ROI(i, 3))-1)];
        spot = z(rows, cols);
        bw(rows, cols) = im2bw(spot, graythresh(spot));
    end
imshow(bw)
title('local threshold')
```

Logically Combine Local and Global Thresholds

```
figure(fSpots)
subplot(121)
    bw = im2bw(z2, graythresh(z2));
    for i=1:length(ROI)
        rows = round(ROI(i, 2)) + [0:(round(ROI(i, 4))-1)];
        cols = round(ROI(i, 1)) + [0:(round(ROI(i, 3))-1)];
        spot = z(rows, cols);
        bw(rows, cols) = bw(rows, cols) | im2bw(spot, graythresh(spot));
    end
imshow(bw)
    title('combined threshold')
```

```

subplot(122)
imshow(z)

    title('linear intensity')
        Fill Holes to Solidify Spots

figure(fSpots)
subplot(121)

    for i=1:length(ROI)
        rows = round(ROI(i, 2)) + [0:(round(ROI(i, 4))-1)];
        cols = round(ROI(i, 1)) + [0:(round(ROI(i, 3))-1)];
        end
        bw(rows, cols) = imfill(bw(rows, cols), 'holes');
seDisk = strel('disk', round(estPeriod));
L = zeros(size(bw));

    for i=1:length(ROI)
        rows = ROI(i, 2) + [0:(ROI(i, 4)-1)];
        cols = ROI(i, 1) + [0:(ROI(i, 3)-1)];
        rectMask = L(rows, cols);
        spotMask = bw(rows, cols);
        rectMask(spotMask) = i;
        L(rows, cols) = rectMask;
    end
spotData = [ROI zeros(length(ROI), 5)];

    for i=1:length(ROI)
        spot = imcrop(y, ROI(i, :));
        spot2 = imtophat(spot, seDisk);
        mask = imcrop(L, ROI(i, :))==i;
        for j=1:2
            layer = spot2(:, :, j);
            intensity(j) = double(median(layer(mask)));
            text(ROI(i, 1) + ROI(i, 3)/2, ROI(i, 2) + ROI(i, 4)/2, sprintf('%0.0f',
            intensity(j)),...
            'color', 'y', 'HorizontalAlignment', 'center', 'parent', ax(j))
            rawLayer = spot(:, :, j);
            rawIntensity(j) = double(median(layer(mask)));
        end
        expression = log(intensity(1)/intensity(2));
        text(ROI(i, 1) + ROI(i, 3)/2, ROI(i, 2) + ROI(i, 4)/2, sprintf('%0.2f',
        expression),...
        'color', 'w', 'HorizontalAlignment', 'center', 'parent', ax(3))
        drawnow
        spotData(i, 5:9) = [intensity(:)' expression rawIntensity(:)'];
    end
    xlswrite('microarray.xls', spotData)

```

## References

1. Adomas, A., Heller, G., Olson, A., Osborne, J., Karlsson, M., Nahalkova, J., Vanzyl, L., Sederoff, R., Stenlid, J., Finlay, R., Asiegbu, F.O.: Comparative analysis of transcript abundance in *Pinus sylvestris* after challenge with a saprotrophic pathogenic or mutualistic fungus. *Tree Physiol.* **28**(6), 885–897 (2008)
2. Birnie, R., Bryce, D.S., Roome, C., Dussupt, V., Droop, A., Lang, H.S., Berry, A.P., Hyde, F.C., Lewis, L.J., Stower, J.M., Maitland, J.N., Collins, T.A.: Gene expression profiling of human prostate cancer stem cells reveals a pro-inflammatory phenotype and the importance of extracellular matrix interactions. *Genome Biol.* **9**(R83), 1–13 (2008)
3. Cai, X., Giannakis, G.B.: Identifying differentially expressed genes in microarray experiments with model-based variance estimation. *IEEE Trans. Signal Process.* **54**(6), 2418–2426 (2006)
4. Dror, R.: Noise models in gene array analysis. Report in fulfillment of the area exam requirement in the MIT Department of Electrical Engineering and Computer Science (2001)
5. Greenblum, S., Krucoff, M., Furst, J., Raicu, D.: Automated image analysis of noisy microarrays. Department of Biomedical Engineering and School of Computer Science, Telecommunications and Information systems, IL, USA (2006)
6. Hedenfalk, I., Duggan, D., Chen, Y., Radmacher, M., Bittner, M., Simon, R., Meltzer, P., Gusterson, B., Esteller, M., Kallioniemi, O.P., Wilfond, B., Borg, A., Trent, J., Raffeld, M., Yakhini, Z., Ben-Dor, A., Dougherty, E., Kononen, J., Bubendorf, L., Fehrl, W., Pittaluga, S., Gruvberger, S., Loman, N., Johannsson, O., Olsson, H., Sauter, G.: Gene-expression profiles in hereditary breast cancer. *N. Engl. J. Med.* **344**, 539–548 (2001)
7. Jain, A.N., Tokuyasu, T.A., Snijders, A.M., Segraves, R., Albertson, D.G., Pinkel, D.: Fully automatic quantification of microarray image data. *Genome Res.* **12**, 325–332 (2002)
8. Jochumsen, K.M., Tan, Q., Dahlgaard, J., Kruse, A.T., Mogensen, O.: RNA quality and gene expression analysis of ovarian tumor tissue undergoing repeated thaw–freezing. *Exp. Mol. Pathol.* **82**(1), 95–102 (2007)
9. Larese, M.G., Gomez, J.C.: Automatic spot addressing in cDNA microarray images. *JCS&T* **8** (2008)
10. Macgregor, F.P., Squire, A.J.: Application of microarrays to the analysis of gene expression in cancer. *Clin. Chem.* **48**(8), 1170–1177 (2002)
11. Otsu, N.: A threshold selection method from gray-level histograms. *IEEE Trans. Sys. Man. Cyber.* **9**, 62–66 (1979)
12. Petrov, A., Shams, S.: Microarray image processing and quality control: genomic signal processing. *J. VLSI Signal Process.* **38**(3), 211–226 (2004)
13. PhaniDeepti, G., Maruti, V.B., Jayanthi, S.: Impulse noise removal from color images with Hopfield neural network and improved vector median filter. In: Proceedings of the 6th Indian Conference on Computer Vision, Graphics and Image Processing, pp. 17–24. IEEE Computer Society (2008)
14. Smolka, B., Lukac, R., Plataniotis, K.N.: Fast noise reduction in cDNA microarray images. In: Proceedings of the 23rd Biennial Symposium, pp 348–351. IEEE Xplore (2006)
15. StanislavSaic, B.M.: Using noise inconsistencies for blind image forensics. *Image Vis. Comput.* **27**(10), 1497–1503 (2009)
16. Tu, Y., Stolovitzky, G., Klein, U.: Quantitative noise analysis for gene expression microarray. *Proc. Natl. Acad. Sci.* **99**(22), 14031–14036 (2002)
17. Uma, S.R., Rajkumar, T.: DNA microarray and breast cancer-A review. *Int. J. Hum. Genet.* **7**(1), 49–56 (2007)
18. Vikalo, H., Hassibi, B., Hassibi, A.: A statistical model for microarrays, optimal estimation algorithms, and limits of performance. *IEEE Trans. Signal Process.* **54**(6), 2444–2455 (2006)
19. Yin, W., Chen, T., Zhou, X.S., Chakraborty, A.: Background correction for cDNA microarray images using the TV + L1. *Advaced Access*, publication February 22, 2005

# A Comparative Study on Machine Learning Algorithms in Emotion State Recognition Using ECG

Abhishek Vaish and Pinki Kumari

**Abstract** Human-Computer-Interface (HCI) has become an emerging area of research among the scientific community. The uses of machine learning algorithms are dominating the subject of data mining, to achieve the optimized result in various areas. One such area is related with emotional state classification using bio-electrical signals. The aim of the paper is to investigate the efficacy, efficiency and computational loads of different algorithms scientific comparisons that are used in recognizing emotional state through cardiovascular physiological signals. In this paper, we have used Decision tables, Neural network, C4.5 and Naïve Bayes as a subject under study, the classification is done into two domains: *High Arousal and Low Arousal*.

**Keywords** PCA · Emotion classification · ECG and data mining algorithms

## 1 Introduction

Emotion is a psycho-physiological process triggered by conscious and unconscious perception of an object or situation and is often associated with mood, temperament, personality and disposition and motivation [1]. Emotions play an important role in human communication and can be expressed either verbally or by non-verbal cues such as tone of voice, facial expression, gesture and physiological behavior.

Interestingly, it has been observed through past researches that various fields are utilizing this as a key signal for system development in different context and some of the most applied areas are:

*In the area of medical science* many physiological disorders exists those are directly correlated with the one of the different class of emotions. According to the prior art of healthcare, numerous study has been conducted to recognize the early stage of stress to prevent the human's life before entering in danger zone. The outputs

---

A. Vaish (✉) · P. Kumari  
Indian Institute of information Technology Allahabad, Allahabad, India  
e-mail: abhishek@iitaa.ac.in

of the studies are some kind of tools and algorithms which helps to detect the early stage of mental illness which is a manifestation of the fact that classification through machine learning is important.

*In area of Multi-modal authentication system* various bio-signals (ECG, EEG and SC etc.) are fused and interpreted for generation of unique identification factors. These factors have the capability like unique and robust and are strong enough to be cracked. This system could be used in securing highly sensitive areas like defense and banking section etc.

*In the area of affective gaming* the different levels of emotions are used to make the gaming software more affective and easy to use. For example the famous is NPC (Non-player character) in which each and character associated with the different emotions.

In view of above described areas of emotional state classification, the accuracy of a prediction is the only thing that really matters. Here, we are proposing an alternative method that will increase the efficacy and efficiency of the system using machine learning algorithms of data mining. The scope of the study has considered four machine learning algorithms among top 10 algorithms of data mining: Decision tables, neural network, C4.5 and Naïve Bayes and applied over the ECG data corpus with full features dataset and with reduced features datasets and examined the result's effect due to highly contained features. The ultimate contribution of the research work is related with analysis of the known classifiers and observed their performance. This would help the researchers to use the best model in the area of emotion classified through ECG data set.

## 2 Literature Review

A copious number of researches are present in the literature for recognizing human's emotions from the physiological signals. Recently, among researches, a great deal of attention has been received on the efficacy improvement. In this section, we would like to briefly review the dynamics of the ECG signal followed by the current state of the scientific contribution in the subject under study.

Electrocardiography is a tool which measures and records the electrical potentials of the heart. A complete ECG cycle can be represented in a waveform and is known as PQRST interval. A close analysis of the same reveals that two major orientations exist i.e. the positive orientation and the negative orientation, PRT is a positive orientation and QS is a negative orientation in a given PQRST interval and the same can be seen in Fig. 1. The description of ECG waves and intervals are vital to catch the state of emotions present in human body how he/she is feeling as negative feeling and stress feeling leads the dangers state of life Fig. 2.

Jang et al. [2] have compared few data mining algorithm such as SVM, CART, SOM and Naïve Bayes over few Bio-signals like ECG, EDA and SKT and got the accuracy like 93.0, 66.44, 74.93 and 37.67%. Chang et al. [3] used two modal to classify the emotional state of human, one is facial expression and another is

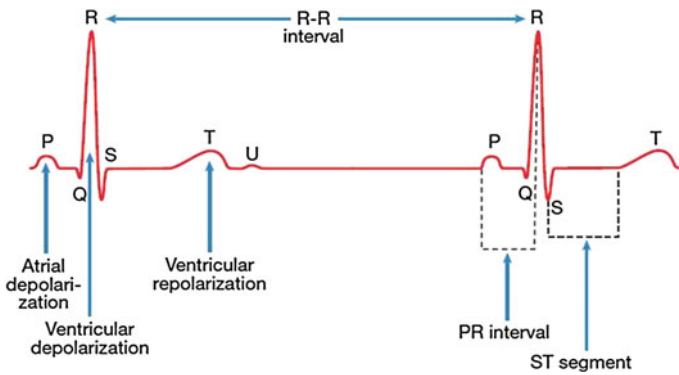


Fig. 1 ECG waveform generation from electrical activities of the heart

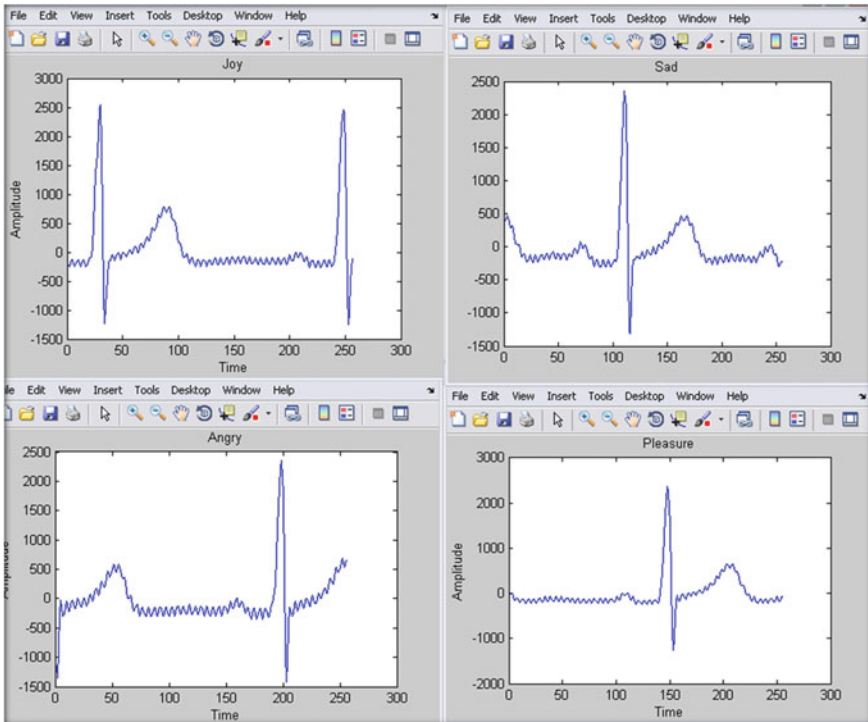


Fig. 2 Sample signals from AuBT data corpus

physiological signals of various subjects and then applied classification algorithm to recognize the different emotional state and got the accuracy somewhere around 88.33% with the physiological signals. Gouizi et al. [4] have used support vector machine and obtained a result of 85% recognition rate.

Li and Chen's [5] paper proposed to recognize emotion using physiological signals such as ECG, SKT, SC and respiration, selected to extract features for recognition and achieved accuracy such as 82% with 17 features, 85.3% with 22 features and same accuracy with 20 features. Siraj et al. [6], the presented paper says about classification of emotion of subjects in two classes i.e. active arousal and passive arousal using ECG pattern and achieved the accuracy around 82%.

Li and Lu [7] described how emotion could be classified through EEG signals. They considered two types emotions: Happiness and sadness. Using common spatial patterns (CSP) and linear SVM classification has been done and achieved the satisfied accuracy. Murugappan [8] presents Electromyogram (EMG) signal based human emotion classification using K Nearest Neighbor (KNN) and Linear Discriminant Analysis (LDA). Five most dominating emotions such as: happy, disgust, fear, sad and neutral are considered and these emotions are induced through Audio-visual stimuli (video clips).

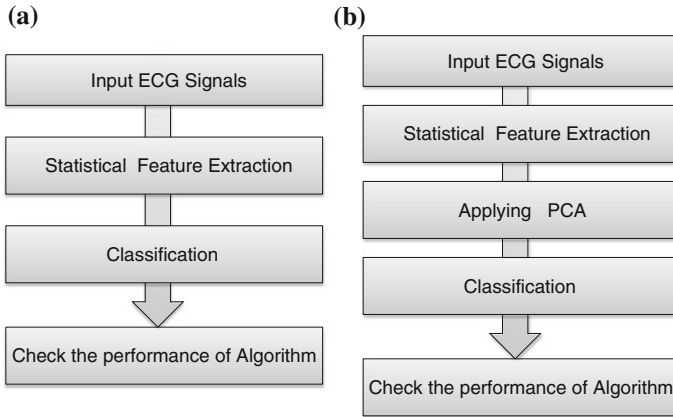
Sun [1], in this paper, we evaluate these tools' classification function in authentic emotion recognition. Meanwhile, we develop a hybrid classification algorithm and compare it with these data mining tools. Finally, we list the recognition results by various classifiers. Ma and Liu [9], wavelet transform was applied to accurately detect QRS complex for its advantages on time-frequency localization, in order to extract features from raw ECG signals. A method of feature selection based on Ant Colony System (ACS), using K-nearest neighbor for emotion classification, was introduced to obtain higher recognition rate and effective feature subset.

These research articles provide support for the conclusion that Bio-electrical signals carries generic information about the human behavior or different human emotions. There is however limited research which considers computational time effect by reducing the dimensionality of features of heart rhythms.

In the proposed article, we are trying to analyze the performance of the data mining algorithms with high feature dataset and reduced feature dataset.

### 3 Research Methodology

Person emotion recognition has lately evolved as an interesting research area. Physiological signals such as ECG, EEG, EMG and respiration rate are successfully utilized by quite a few researchers to attain the emotion classification [4]. In this research we have used simulative research design using quantitative data that has been collected using four bio-sensors. In this section, we would be highlighting the schematic diagram in Sect. 3.1 (Fig. 3) that has been followed to extract the results and also to make sure that the contamination in the research design could be avoided. Additionally, the description of data corpus in Sect. 3.2.



**Fig. 3** Schematic diagram of proposed work. **a** Efficacy with high dimensionality. **b** Efficacy with reduced dimensionality

### 3.1 High Level Schematic Diagram

The whole of this high level diagram is categorized into three main steps. These are as follows:

- Extraction of statistical features—Help us to extract the maximum number of feature from the raw data set. Features are those data point that has potential information for output.
- Applying the PCA for Feature Reduction—Helps in extracting the best fit feature that without compromising the results improves the system performance.
- Classification algorithm to check the efficacy—Helps in the decision making system for accurate results.

### 3.2 Description of Subject

Each subject (participant) selects four favorite songs reminiscent of their certain emotional experiences corresponding to four emotion categories. Signals were collected with 25 subjects with four emotions within 25 days.

### 3.3 Mode of Collection Data

The physiological data were recorded through biosensor and the length of the recordings depends on the length of the songs, but was later cropped to a fixed length of the two minutes and ECG was sampled at 256Hz.



### 3.4 Research Procedure

In the field of automatic emotion recognition probably the most often used features are based on statistically such as Mean, Median, Standard deviation, max min of all waves of ECG i.e. PQRST waveform which represents complete ECG cycle. For the feature extraction and feature selection of ECG signal in time domain we have used *Analysis of variance (ANOVA)* Method. After collecting the statistical features of cardiac signal then performed the different classification to investigate the efficacy of the classification algorithms of data mining such as Decision table, Neural network, Naïve Bayes and C4.5.

## 4 Experimental Results

In this section, the results are presented, the result are presented into different phases i.e. the feature selection and the classification of emotions, feature extraction with reduced dimensionalities and their classification, finally the computational load of each classification algorithm is presented.

### Phase I

Figure 4 depicts the classification accuracy of different algorithms. The total numbers of feature extracted by inbuilt use of ANOVA were 82. It can be seen that multilayer perceptron is giving the best result among the four with approximately 60% and Naïve Bayes is showing a response of 53% which is considered to be the least. It can be interpreted with the result that the FAR is low and FRR is high.

### Phase II

In order to optimize the result depicted in Fig. 4, we have used a dimensional reduction scheme and the most prevailing technique is the principle component analysis. It is pertinent to briefly discuss the equation used in PCA.

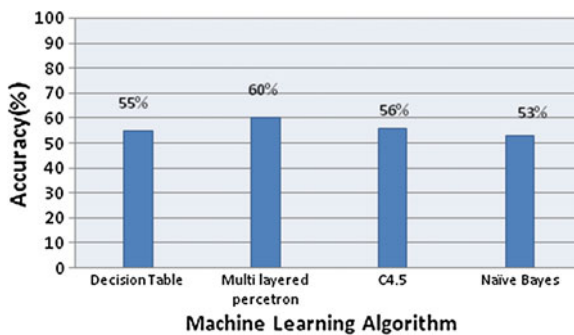


Fig. 4 Performance of machine learning algorithms with full features

Given the data, if each datum has N features represented for instance by  $x_{11}$   $x_{12} \dots x_{1N}$ ,  $x_{21}$   $x_{22} \dots x_{2N}$ , the data set can be represented by a matrix  $X_{n \times m}$ .

The average observation is defined as:

$$\mu = \frac{1}{n} \sum_{i=1}^n x_i \tag{1}$$

The deviation from the average is defined as:

$$\Phi_i = X_i - \mu \tag{2}$$

Using Eqs. 1 and 2, we have extracted the following results as depicted in Table 1. The total numbers of extracted feature were 13 out of 82. The accuracy post extraction is depicted in Fig. 5. In this case C4.5 is giving us the most optimized result. So it can be inferred that the combination of PCA + C4.5 in the given data set is the maximum. However, if we look at the more modest form, it can be seen that performance of all classification algorithm has gone up to the average of 20 % using Eq. 3

$$\text{Impact of post PCA} = (\text{Post PCA} - \text{Pre PCA}) \tag{3}$$

Table 2 depicted in this section give the specific of the scalar value of the classification algorithm. The tabulation has been arranged with row and column. The first column is populating with the machine learning algorithm and corresponding rows has the statistical measures like True-positive rate, precision, F-measures and ROC area. The classes are labeled as High Arousal, Low Arousal and same can be correlated with Fig. 5.

**Phase III**

This section is interesting for the readers and researchers because the most fundamental question with development of decision making system lies with cost of decision and accuracy. The latter has been discussed in this phase. In Fig. 6 it can

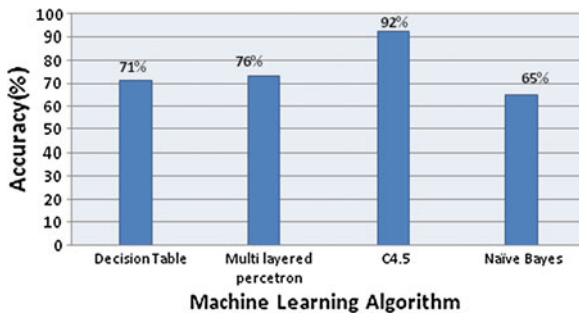


Fig. 5 Performance of machine learning algorithms with reduced features

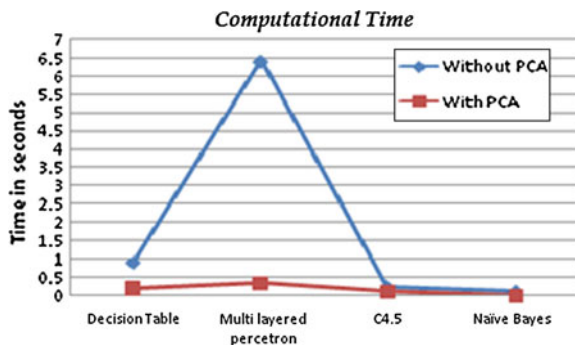
**Table 1** Reduced data corpus with 13 features

	Number of reduced features
1	ecgQ-mean
2	ecgS-range
3	ecgQS-max
4	ecgT-std
5	ecgSampl-std
6	ecgSampl-mean
7	ecgPQ-range
8	ecgHrvDistr-triind
9	ecgQS-std
10	ecgHrv-specRange1
11	ecgHrvDistr-min
12	ecgHrv-specRange1
13	ecgHrv-pNN50

**Table 2** Efficacy of Machine Learning Algorithms for emotion classification

ML's algorithms	Class	TP Rate	Precision	F-Measure	ROC Area
C4.5	High Arousal	1	0.097	0.985	0.988
	Low Arousal	0.859	1	0.984	0.986
	<b>Avg. weighted</b>	<b>0.9295</b>	<b>0.985</b>	<b>0.984</b>	<b>0.987</b>
Neural network	High Arousal	0.722	0.885	0.898	0.812
	Low Arousal	0.807	0.912	0.886	0.823
	<b>Avg. weighted</b>	<b>0.7645</b>	<b>0.8985</b>	<b>0.892</b>	<b>0.8175</b>
Naïve Bayes	High Arousal	0.64	0.867	0.65	0.924
	Low Arousal	0.67	0.594	0.596	0.806
	<b>Avg. Weighted</b>	<b>0.655</b>	<b>0.7305</b>	<b>0.623</b>	<b>0.865</b>
Decision table	High Arousal	0.712	0.867	0.74	0.864
	Low Arousal	0.722	0.512	0.596	0.796
	<b>Avg. weighted</b>	<b>0.717</b>	<b>0.6895</b>	<b>0.668</b>	<b>0.83</b>

**Fig. 6** Comparison of computational load with and without feature reduction



be seen that time taken to perform the task is categorizing in the domains i.e. with PCA and without PCA. The result is highly encouraging. Without PCA the time is reduced drastically. However, an important point worth observing that MLP is more computationally expensive among four in both the domains.

## 5 Conclusion and Future Works

The work aimed at showing the possibility of recognizing the two levels of emotional state: *High Arousal and Low Arousal*. We have presented an alternative method to investigate the performance of data mining algorithms to raise the efficacy of the emotional recognition system and also give solution the question how dimensionality reduction can save the burden of computing. The recognition rates increased after applying proposed methods are: 16 % with Decision table; 12 % with neural network; 36%, with C4.5 and 12 % with Naïve Bayes. All experiments have done with openly available tool (WEKA) for data mining and machine learning algorithms for data classification. There are few challenges we have faced which is the lack of data corpus quantum. In future, we would like to explore another data corpus available in this domain. Furthermore, we would like to work on investigation of those classification algorithms which have been used for ECG classification in two different levels of emotional states with other physiological signals such as EMG, EEG, SC and respiration. Another future work may be explored in area of affective computing like to automatically detect the stages of mental illness with good recognition rates through bio-signals. Bio-signals may also be fruitful in the area of multimodal authentication system or cognitive biometrics.

## References

1. Sun, Y., Li, Z., Zhang, L., Qiu, S., Chen, Y.: Evaluating data mining tools for authentic emotion classification in Intelligent Computation Technology and Automation (ICICTA). 2010 International Conference, vol. 2, pp. 228–232 (2010)
2. Jang, E.-H., Park, B.-J., Kim, S.-H., Eum, Y., Sohn, J.-H.: Identification of the optimal emotion recognition algorithm using physiological signals. 2011 International Conference on Engineering and Industries (ICEI), 2011, pp. 1–6
3. Chang, C.-Y., Tsai, J.-S., Wang, C.-J., Chung, P.-C.: Emotion recognition with consideration of facial expression and physiological signals in computational intelligence in bioinformatics and computational biology. CIBCB '09 IEEE Symposium, 2009, pp. 278–283
4. Gouizi, K., Reguig, F.B., Maaoui, C.: Analysis physiological signals for emotion recognition in Systems, Signal processing and their Applications (WOSSPA). 2011 7th International Workshop , 2011, pp. 147–150.
5. Li, L., Chen, J.-H.: Emotion recognition using physiological signals from multiple subjects in intelligent information hiding and multimedia signal processing. IHH-MSP '06 International Conference, 2006, pp. 355–358
6. Siraj, F., Yusoff, N., Kee, L. C.: Emotion classification using neural network. International Conference on Computing and Informatics ICOCI '06, 2006, pp. 1–7

7. Li, M., Lu, B. -L.: Emotion classification based on gamma-band EEG in engineering in medicine and biology society. Annual International Conference of the IEEE, 2009, pp. 1223–1226
8. Murugappan, M.: Electromyogram signal based human emotion classification using KNN and LDA in System Engineering and Technology (ICSET). IEEE International Conference, 2011, pp. 106–110
9. Ma, C.-W., Liu, G.-Y.: Feature extraction, feature selection and classification from electrocardiography to emotions in computational intelligence and natural computing. CINC '09 International Conference, vol. 1, pp. 190–193 (2009)
10. Wagner, J., Kim, J., Andre, E.: Signals, from physiological, to emotions: Implementing and comparing selected methods for feature extraction and classification. IEEE International Conference in multimedia and expo (ICME), 2005, pp. 940–943

# Fault Diagnosis of Ball Bearings Using Support Vector Machine and Adaptive Neuro Fuzzy Classifier

Rohit Tiwari, Pavan Kumar Kankar and Vijay Kumar Gupta

**Abstract** Bearing faults are one of the major sources of malfunctioning in machinery. A reliable bearing health condition monitoring system is very useful in industries in early fault detection and to prevent machinery breakdown. This paper is focused on fault diagnosis of ball bearing using adaptive neuro fuzzy classifier (ANFC) and support vector machine (SVM). The vibration signals are captured and analyzed for different types of defects. The specific defects consider as inner race with spall, outer race with spall, and ball with spall. Statistical techniques are applied to calculate the features from the vibration data and comparative experimental study is carried using ANFC and SVM. The results show that these methods give satisfactory results and can be used for automated bearing fault diagnosis.

**Keywords** Fault diagnosis · Condition monitoring · Adaptive neuro fuzzy classifier · Support vector machine

## 1 Introduction

Rotating rolling element bearing is widely used in industrial machines. Bearing fault diagnosis is an even more challenging task in condition monitoring especially when the machine is operating in a noisy environment. For diagnosis of all types of fault either localized or distributed vibration analysis can be employed. A vibration

---

R. Tiwari (✉) · P. K. Kankar · V. K. Gupta  
PDPM Indian Institute of Information Technology, Design and Manufacturing,  
Jabalpur, India  
e-mail: 1110508@iiitdmj.ac.in

P. K. Kankar  
e-mail: kankar@iiitdmj.ac.in

V. K. Gupta  
e-mail: vkgupta@iiitdmj.ac.in

signal-based fault diagnosis can be performed in time domain [6], frequency domain [8]. Artificial neural network [10], and support vector machines (SVM) [11] methods are also being used. Abasiona and Rafsanjani [1] have carried out multi-fault detection in such system with wavelet analysis and SVM.

This study is mainly focused on bearing fault classification using two methods, SVM and neuro-fuzzy, as both are capable in nonlinear classification. Four defects considered for the study includes inner race with spall, outer race with spall, ball with spall, and combined bearing component defect. Statistical methods are used to extract the features from the time domain signal. Selected features with their known class are used for training and testing of SVM and ANFC.

### 2 Support Vector Machines

SVM based on the statistical learning theory is a supervised machine learning method. It is used for classification of two or multi-class of data. The performance of SVM is not influenced by the dimension of feature space, which is why it is more efficient in large classification problem. Cristianini and Shawe-Taylor [3] have used SVM for pattern recognition and classification.

A simple example of two-class problem is shown in Fig. 1. In Fig. 1, square and triangles show two classes of sample points. These two classes are separated by hyper plane  $H$ . Planes passing through the sample points and nearest to  $H$  are given by  $H_1$  and  $H_2$  (shown by dashed line). SVM creates linear boundary in such a way that the margin between classes  $H_1$  and  $H_2$  will be maximum. This reduces the generalization error. Support vectors are the nearest data point used to define the margin.

### 3 Adaptive Neuro Fuzzy Classifier

The neuro fuzzy classifier is an adaptive network-based system in which fuzzy parameters are adapted with neural networks. In fuzzy classification feature space is

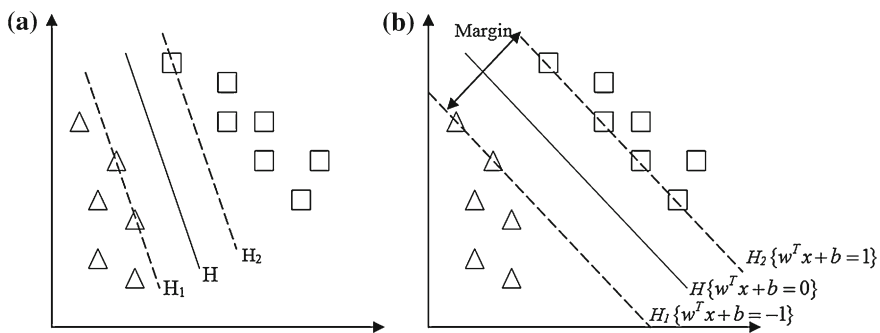
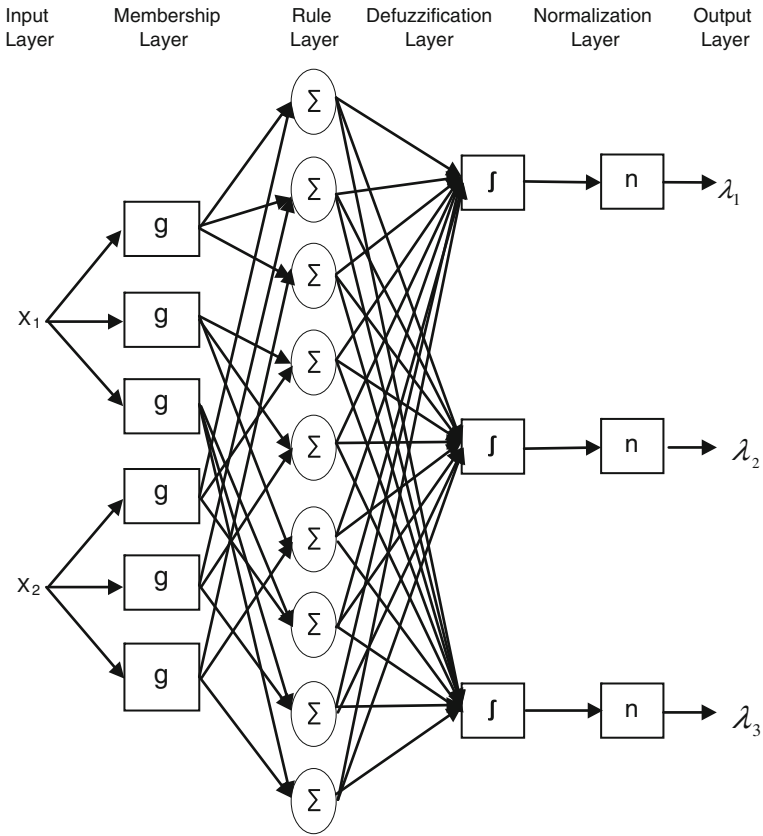


Fig. 1 Hyper plane classifying two classes: a small margin, b large margin



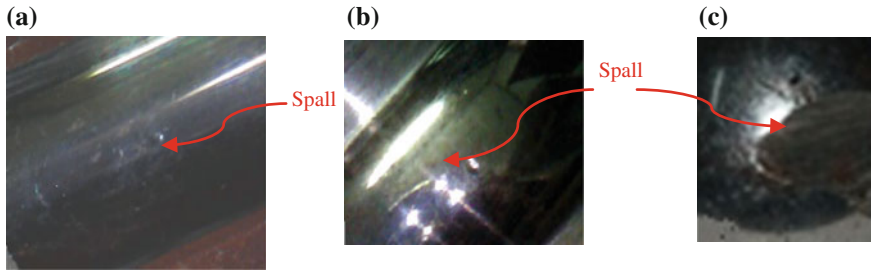
**Fig. 2** Architecture of adaptive neuro fuzzy classifier

divided in to fuzzy classes. Sun and Jang [9] have applied fuzzy rules to control each fuzzy region. Cetisli [2] has developed an adaptive neuro fuzzy classifier using linguistic hedges and applied for different classification problems. Du and Er [4] have applied neuro fuzzy classifier for fault diagnosis in air-handling unit system.

In this study the proposed neuro fuzzy classifier is described by zero-order surgeon fuzzy model. Output level is a constant for a zero order surgeon model and weighted average operator [5] will gives the crisp output from the fuzzy rules. To initialize fuzzy rules k-mean algorithm is used. Fuzzy relation between variable are often created by fuzzy clustering [12]. In this architecture shown in Fig. 2, the first layer measures membership grade of each input to specified fuzzy region. Gaussian function is employed as membership function (MF).

The next layer is known as rule layer. This layer is responsible to calculate the firing strength of fuzzy rules using the membership value of the inputs. The third layer in architecture calculates the weighted outputs. Each class is decided according to the maximum firing strength of the rules.





**Fig. 3** Bearing components with faults induced in them. **a** Outer race with spall, **b** inner race with spall, **c** Ball with spall

After calculating the rule weights the next layer function is to normalize network output because the summation of the weight should not be more than 1.

After the normalization output layer is calculated the class labels. There are many methods for network parameter optimization. In this paper, scale conjugate gradient (SCG) method is used to adapt antecedent parameters [7].

## 4 Experimental Setup and Data Acquisition

Training and testing data sets are generated by the experimental test on a test rig. The rig is connected with the data acquisition system. At various speeds different faults are simulated on the bearing as shown in Fig. 3. Vibration data for healthy bearing operation is used as baseline data. These data can be used for comparison with faulty bearing signature data. Features are extracted from the vibration signal. These data are compiled to form a feature vector which is given as input to ANFC/SVM for training. Faults introduced in bearings are outer race with spall, inner race with spall, ball with spall, and combined faults in all bearing components. For acquiring training data from the data acquisition system cases considered are healthy bearing (HB), inner race defect (IRD), outer race defect (ORD), ball fault in bearing (BFB), and combined bearing component defect (CBD).

## 5 Results

Statistical features such as mean, standard deviation, skewness, kurtosis, min, max, and range are calculated from the vibration data. This will reduce the dimensionality of original vibration features. 9 attribute are selected including statistical features, speed, and loader.

After calculation of features, classification of faults is done using machine learning techniques, i.e., ANFC/SVM. Input features are compiled and given as input. The

**Table 1** Confusion matrix

BFB		MFB		HB		ORD		IRD		Classified as
ANFC	SVM	ANFC	SVM	ANFC	SVM	ANFC	SVM	ANFC	SVM	
4	9	1	0	0	0	4	0	0	0	BFB
2	2	5	7	0	0	2	0	0	0	MFB
1	2	0	0	2	1	0	0	0	0	HB
0	3	1	2	0	0	8	4	0	0	ORD
0	0	0	0	0	0	0	0	10	10	IRD

**Table 2** Evaluation of the success of the numeric prediction

Parameters	Values (ANFC)	Values (SVM)
Correctly classified instances	29 (72.50%)	31 (77.50%)
Incorrectly classified instances	11 (27.50%)	9 (22.50%)

defects classified using ANFC/SVM are shown in Table 1. A total of 40 cases are considered for testing in which 9, 9, 3, 9, 10 cases of ball with spall, combined bearing component defects, healthy bearing, inner race with spall, and outer race with spall are taken.

Table 1 shows that ANFC has correctly classified 4, 5, 2, 8, and 10 cases, while SVM has predicted 9, 7, 1, 4, and 10 cases correctly for ball with spall combined bearing component defect, healthy bearing, inner race with spall, and outer race with spall respectively. Values of correctly and incorrectly classified instances with percentage accuracy are given in Table 2. Table 2 shows that SVM gives better classification efficiency of 77.5% than the ANFC.

## 6 Conclusions

In this study, bearing fault detection has been done by classifying them using two methods, ANFC and SVM. Statistical techniques are used to calculate the features from the time-domain vibration signals. It is observed that ANFC has less accuracy to predict the ball fault in bearing while SVM is not accurate to predict outer race defect in bearing. SVM has a better classification accuracy than ANFC. Results show that these methods can be apply to develop a reliable condition monitoring system and used to predict defect in early stage. This can avoid the machinery breakdown and reduce operating cost.

## References

1. Abbasiona, S., Rafsanjani, A.: Rolling element bearing multi fault classification based on wavelet denoising and support vector machine. *Mech. Syst. Signal Process.* **2**, 2933–2945 (2007)
2. Cetisli, B.: Development of adaptive neuro-fuzzy classifier using linguistic hedges: Part-1. *Expert Syst. Appl.* **37**, 6093–6101 (2010)
3. Cristianini, N., Shawe-Taylor, N.J.: An introduction to support vector machines. Cambridge University press, Cambridge (2000)
4. Du, J., Er, M.J.: Fault diagnosis in air—handling unit system using dynamic fuzzy neural network. In: *Proceeding of the 6th International FLINS Conference*, pp. 483–488 (2004)
5. Jang, J.S.R., Sun, C.T., Mizutani, E.: *Neuro-Fuzzy and Soft Computing*. Upper Saddle River, prentice Hall (1997)
6. Kankar, P.K., Sharma, S.C., Harsha, S.P.: Fault diagnosis of ball bearings using machine learning methods. *Expert Syst. Appl.* **38**, 1876–1886 (2011)
7. Moller, M.F.: A Scaled conjugate gradient algorithm for fast supervised learning. *Neural Netw.* **6**(4), 525–533 (1993)
8. Robinson, J.C., Canada, R.G., Piety, K.R.: Peak vue analysis—new methodology for bearing fault detection. *Sound Vib.* **30**(11), 22–25 (1996)
9. Sun, C.T., Jang, J.S.: A neuro-fuzzy classifier and its applications. In: *Proceedings of the IEEE International Conference on Fuzzy System*, San Francisco, pp. 94–98 (1993)
10. Vyas, N.S., Satish kumar, D.: Artificial neural network design for fault identification in a rotor bearing system. *Mech. Mach. Theory* **36**, 157–175 (2001)
11. Widodo, A., Yang, B.S.: Review on support vector machine condition monitoring and fault diagnosis. *Mech. Syst. Signal Process.* **21**, 2560–2574 (2007)
12. Zio, E., Baraldi, P.: Evolutionary fuzzy clustering for the classification of transients in nuclear components. *Prog. Nucl. Energy* **46**(3–4), 282–296 (2005)

# Designing a Closed-Loop Logistic Network in Supply Chain by Reducing its Unfriendly Consequences on Environment

Kiran Garg, Sanjam, Aman Jain and P. C. Jha

**Abstract** This paper examines the relationship between the operations of forward and reverse logistics and the environmental performance measures like CO<sub>2</sub> emission in the network due to transportation activities in closed-loop supply chain network design. A closed-loop structure in the green supply chain logistics and the location selection optimization was proposed in order to integrate the environmental issues into a traditional logistic system. So, we present an integrated and a generalized closed-loop network design, consisting four echelons in forward direction (i.e., suppliers, plants, and distribution centers, first customer zone) and four echelons in backward direction (i.e., collection centers, dismantlers, disposal centers, and second customer zone) for the logistics planning by formulating a cyclic logistics network problem. The model presented is bi objective and captures the trade-offs between various costs inherent in the network and of emission of greenhouse gas CO<sub>2</sub>. Numerical experiments were presented, and the results showed that the proposed model and algorithm were able to support the logistic decisions in a closed loop supply chain efficiently and accurately.

**Keywords** Environmental performances · Cradle to cradle principle · Closed loop supply chain network · Trade off · Greenhouse gas

---

K. Garg · P. C. Jha (✉)

Department of Operational Research, University of Delhi, Delhi, India

e-mail: jhac@yahoo.com

K. Garg

e-mail: mittalkiran12@gmail.com

Sanjam · A. Jain

Faculty of Management Science, University of Delhi, Delhi, India

e-mail: sanjam.s13@fms.edu

A. Jain

e-mail: aman.j13@fms.edu

## 1 Introduction

Supply chain consists of set of activities such as transformation and flow of goods, services, and information from the sources of materials to end-users. Due to the government legislation, environmental concern, social responsibility, and customer awareness, companies have been forced by customers not only to supply environmentally harmonious products but also to be responsible for the returned products. So, interest in supply chains lies in the recovery of products, which is achieved through processes such as repair, remanufacturing and recycling, which, combined with all the associated transportation and distribution operations, are collectively termed as *Reverse Chain activities*. In reverse logistics there is a link between the market that releases used products and the market for “new” products. When these two markets coincide, it is called *Closed Loop Network*. Thus the supply chain in which forward and reverse supply chain activities are integrated is said to be closed-loop, and research on such chains have given rise to the field of closed-loop supply chains (CLSCs) and Supply chain network design concerned with environmental issues, collectively named as *Green Supply Chain*.

At present, researcher’s emphasis on green supply chain due to global warming and wants to minimize the waste at landfills. A closed-loop logistics management ensures the least waste of the materials by following the cradle to cradle principle and conservation law along the life cycles of the materials. In reverse logistics used products, either under warranty or at the end of use or at the end of lease are taken back, so that the products or its parts are appropriately disposed, recycled, reused, or remanufactured. Beside it they explicitly focus on significant sources of greenhouse gas emission, and one of those sources is transportation. CO<sub>2</sub> is very prominent in its hazardous consequences on human health. Transport is the second-largest sector of global CO<sub>2</sub> emission. CO<sub>2</sub> constraints in logistics markets will need to be realized in the near future as it was enforced by protocols, and a shift in freight transportation could be expected to reduce the CO<sub>2</sub> emissions within the reasonable cost and time constraints.

In this study, we model and analyze a CLSC for its operational and environmental performances, i.e., a multi-echelon forward–reverse logistics network model is described for the purpose of design with the reflection of the effects on environment of greenhouse gas emission. Objectives of the model is to maximize the total expected profit earned and minimizing CO<sub>2</sub> emission due to transporting material in forward and reverse logistics networks with the use of different type of vehicles for transport, each of which has its own emission rates and transportation costs. Using the proposed model and a numerical illustration result of computational experiments shed light on the interactions of various performance indicators, primarily measured by cost and then captures the environmental aspects.

## 2 Literature Review

This section presents a brief overview of the existing literature on closed loop supply chain (CLSC). Beamon [1] describes the challenges and opportunities facing the supply chain of the future and describes sustainability and effects on supply chain design, management and integration. Network chain members of a CLSC can be classified into two groups [2]: Forward logistics chain members and Reverse logistics chain members. But designing the forward and reverse logistics separately results in suboptimal designs with respect to objectives of supply chain; hence the design of forward and reverse logistics should be integrated [3–5]. This type of integration can be considered as either horizontal or vertical integration [6]. Manufacturers and demand nodes (i.e., customers) could be seen as ‘junction’ points where the forward and the reverse chains are combined to form the CLSC network. A closed-loop logistics model for remanufacture has been studied in [7], in which decisions relevant to shipment and remanufacturing of a set of products, as well as establishment of facilities to store the remanufactured products are taken into consideration [8]. Consider a reverse logistics network design problem which analyzes the impact of product return flows on logistics networks. A strategic and tactical model for the design and planning of supply chains with reverse flows was proposed by [9]. Authors considered the network design as a strategic decision, while tactical decisions are associated to production, storage and distribution planning. A general reverse logistics location allocation model was developed in [10] in a mixed integer linear programming form. The model behavior and the effect of different reverse logistics variables on the economy of the system were studied. Demand in this proposed model is deterministic. The problem of consolidating returned products in a CLSC has been studied in [11]. Kannan et al. [12] developed a multi-echelon, multiperiod, multi-product CLSC network model for product returns, in which decisions are made regarding material procurement, production, distribution, recycling, and disposal. For an excellent review of methodological and case study-based papers in reverse and closed-loop logistics network design, the reader is referred to [13].

Meixell and Gargeya [14] focused on the design of supply chains of production, purchasing, transportation, and profit and has neglected the environmental aspects. Given recent concerns on the harmful consequences of supply chain activities on the environment, and transportation in particular, it has become necessary to take into account environmental factors when planning and managing a supply chain. The list of environmental performance metrics of a supply chain includes emissions, energy use and recovery, spill and leak prevention, and discharges is discussed in [15]. A comprehensive survey of the field is provided by [16]. Sarkis [17] provides a strategic decision framework for green supply chain management, in which he investigates the use of an analytical network process for making decisions within the GrSC. Sheu et al. [18] present a multiobjective linear programming model for optimizing the operations of a green supply chain, composed of forward and reverse flows, including decisions pertaining to shipment and inventory [19]. Consider environmental issues within CLSCs and examine a supply chain design problem for refrigerators,

offer a comprehensive mathematical model that minimizes costs associated with distribution, processing, and facility set-up, also takes into account the environmental costs of energy and waste.

The remainder of the paper is structured as follows. In Sect. 3 a CLSC model is proposed for single product, with the underlying assumptions. In Sect. 4, used methodology of goal programming is described. In Sect. 5, we present a numerical implementation in order to highlight the features of the proposed model. The paper ends with concluding remarks.

### 3 Model Description

The CLSC problem discussed in this paper is an integrated multiobjective multi-echelon problem in a forward/reverse logistic network, which requires more efforts to analyze than both forward and backward logistic simultaneously. Here we are considering the flow of a product in the network. The model considers modular product structure and every component of the product has an associated recycling rate, specifying the rate at which the component can be recycled. For instance, a rate of 100 % indicates that the used product can be fully recovered or transformed into a new one, whereas a rate of 50 % denotes that the product can only be partially recovered.

In the network suppliers are responsible for providing components to manufacturing plants. The new products are conveyed from plants to customers via distribution centers (d/c) to meet their demands. Returned products from customers are collected at collection centers where they are inspected. After testing in collection centers, the repairable and recyclable products are shipped to plants and dismantlers respectively, after completing the demand of secondary market of used products. At plant repairable used products are repaired and supplied back to distribution centers as new product. Dismantled components at dismantlers are drives back to suppliers if they are repairable else to disposal site to be disposed of.

The purpose of this paper is to evaluate a forward/reverse logistic system with respect to given objectives in order to determine the facility locations and flows between facilities using which type of transport. The transportation operations from one layer to another can be realized via a number of options. These options consist of different types of transport alternatives, e.g., different models of trucks. The proposed model considers the following assumptions and limitations:

1. Supplier and customer locations are known and fixed.
2. The demand of product is deterministic and no shortages are allowed.
3. The potential locations of manufacturing facilities, distribution centers, collection centers, and dismantlers are known.
4. The flow is only permitted to be transported between two consecutive stages. Moreover, there are no flows between facilities at the same stage.
5. The numbers of facilities that can be opened are restricted.

6. The other costs (i.e., operational costs and transportation costs) are known.
7. The estimated emission rate of CO<sub>2</sub> for all type of vehicle available is known.

**Notations:**

**Sets:**

- S* set of component’s suppliers index by *s*, *s* = 1, 2, . . . , *S*
- P* set of manufacturing plants index by *p*, *p* = 1, 2, . . . , *P*
- K* set of distribution centers (d/c) index by *k*, *k* = 1, 2, . . . , *K*
- E* set of first market customer zones index by *e*, *e* = 1, 2, . . . , *E*
- C* set of collection centers (CC) index by *c*, *c* = 1, 2, . . . , *C*
- M* set of dismantlers (d/m) position index by *m*, *m* = 1, 2, . . . , *M*
- H* set of second market customer zones index by *h*, *h* = 1, 2, . . . , *H*
- F* set of disposal sites (d/p) index by *f*, *f* = 1, 2, . . . , *F*
- A* set of subassemblies index by *a*, *a* = 1, 2, . . . , *A*
- N* set on nodes in the network ( $N = S \cup P \cup K \cup E \cup C \cup M \cup H \cup F$ )

**Parameters:**

- SC<sub>sa</sub>* Unit purchasing cost of sub assembly *a* by supplier *s*
- PC<sub>p</sub>* Unit production cost of product at manufacturing plant *p*
- OC<sub>k</sub>* Unit operating cost of product at d/c *k*
- IC<sub>c</sub>* Unit inspection cost of product at collection center *c*
- RPC<sub>p</sub>* Unit repairing cost of used product at manufacturing plant *p*
- DMC<sub>m</sub>* Unit dismantling cost of product at d/m position *m*
- RCC<sub>sa</sub>* Unit recycling cost of sub assembly *a* at supplier *s*



- $D_e$  Demand of product at first customer  $e$
- $D_h$  Demand of used product at second customer  $h$
- $TPC^t$  Unit transportation cost per mile of product or component shipped from one node to another via type of truck  $t$
- $D_{ij}$  Distance between any two nodes  $i, j \in N$  of given CLSC network
- $CAP_{sa}$  Capacity of supplier  $s$  for sub assembly  $a$
- $PCAP_p$  Production capacity of plant  $p$
- $KCAP_k$  Capacity of distribution center  $k$
- $CCAP_c$  Capacity of collection center  $c$
- $MCAP_m$  Capacity of dismantler  $m$
- $FCAP_f$  Disposal capacity of disposal site  $f$
- $RPCAP_p$  Repairing capacity of plant  $p$
- $RCCAP_s$  Recycling capacity of supplier  $s$
- $PF_a$  Unit profit made in the network from recycling component  $a$
- $PF$  Unit profit made in the network from repairable product
- $PR_e$  Unit price of product at customer  $e$
- $PR_h$  Unit price of product at customer  $e$
- $ER^t$  Per mile emission rate of CO<sub>2</sub> gas from the type of transport  $t \in T$
- $Rr$  Return ratio at the first customers
- $Rc_a$  Recycling ratio of component  $a$

$R_p$  Repairing ratio

$W$  Weight of product in kg

$W_a$  Weight of component  $a \in A$  in kg

$U_a$  Utilization rate of component  $a \in A$

**Decision variables:**

$x_{ija}^t$  Quantity of component  $a$  shipped from node  $i$  to node  $j, i, j \in N$  in the network via transport of type  $t \in T$

$x_{ij}^t$  Quantity of product shipped from node  $i$  to node  $j, i, j \in N$  in the network via transport of type  $t \in T$

$W_{ij}^t$  Weighted quantity transported from node  $i$  to node  $j, i, j \in N$  in the network via transport of type  $t \in T$

$$X_i = \begin{cases} 1, & \text{if facility } i, (i \in P \cup K \cup C \cup M) \text{ is opened} \\ 0, & \text{otherwise} \end{cases}$$

$$L_{ij}^t = \begin{cases} 1, & \text{if a transportation link is established between any two locations} \\ & i \text{ and } j, i, j \in N \text{ via mode } t \\ 0, & \text{otherwise} \end{cases}$$

**Model**

**Maximize,  $Z_0 =$**  
$$\sum_k \sum_e \sum_t x_{ke}^t P R_e + \sum_c \sum_h \sum_t x_{ch}^t P R_h + \sum_m \sum_s \sum_a \sum_t P F_a x_{msa}^t$$

$$+ \sum_c \sum_p \sum_t P F x_{cp}^t - \left( \sum_s \sum_p \sum_a \sum_t x_{spa}^t S C_{sa} + \sum_p \sum_k \sum_t x_{pk}^t P C_p \right.$$

$$+ \sum_k \sum_e \sum_t x_{ke}^t O C_k + \sum_e \sum_c \sum_t x_{ec}^t I C_c + \sum_c \sum_p \sum_t x_{cp}^t R P C_p$$

$$+ \sum_c \sum_m \sum_t x_{cm}^t D M C_m + \sum_m \sum_s \sum_a \sum_t x_{msa}^t R C C_{sa}$$

$$+ \sum_m \sum_f \sum_a \sum_t x_{mfa}^t D P C_f + \sum_s \sum_p \sum_t T P C^t D_{sp} x_{sp}^t$$

$$+ \sum_p \sum_k \sum_t T P C^t D_{pk} x_{pk}^t + \sum_k \sum_e \sum_t T P C^t D_{ke} x_{ke}^t$$

$$+ \sum_e \sum_c \sum_t T P C^t D_{ec} x_{ec}^t + \sum_c \sum_p \sum_t T P C^t D_{cp} x_{cp}^t$$

$$+ \sum_c \sum_m \sum_t T P C^t D_{cm} x_{cm}^t + \sum_c \sum_h \sum_t T P C^t D_{ch} x_{ch}^t$$

$$\left. + \sum_m \sum_s \sum_a \sum_t T P C^t D_{ms} x_{msa}^t + \sum_m \sum_f \sum_a \sum_t T P C^t D_{mf} x_{mfa}^t \right)$$

**Minimize,  $Z_1 =$**  
$$\sum_t E R^t \left( \sum_s \sum_p D_{sp} L_{sp}^t W_{sp}^t + \sum_p \sum_k D_{pk} L_{pk}^t W_{pk}^t + \sum_k \sum_e D_{ke} L_{ke}^t W_{ke}^t \right.$$

$$+ \sum_e \sum_c D_{ec} L_{ec}^t W_{ec}^t + \sum_c \sum_p D_{cp} L_{cp}^t W_{cp}^t$$

$$+ \sum_c \sum_m D_{cm} L_{cm}^t W_{cm}^t + \sum_c \sum_h D_{ch} L_{ch}^t W_{ch}^t + \sum_m \sum_s D_{ms} L_{ms}^t W_{ms}^t$$

$$\left. + \sum_m \sum_f D_{mf} L_{mf}^t W_{mf}^t \right)$$

**Subject To**

**(Flow balancing constraints)**

$$\sum_s \sum_t x_{spa}^t + \sum_c \sum_t x_{cp}^t * U_a = \sum_k \sum_t x_{pk}^t * U_a \quad \forall p, a \tag{1}$$

$$\sum_p \sum_t x_{pk}^t = \sum_k \sum_e x_{ke}^t \quad \forall k \tag{2}$$

$$\sum_k \sum_e x_{ke}^t \geq D_e \quad \forall e \tag{3}$$

$$\sum_c \sum_t x_{ec}^t = R_r * D_e \quad \forall e \tag{4}$$

$$\sum_c \sum_t x_{ch}^t \leq D_h \quad \forall h \tag{5}$$

$$\sum_p \sum_t x_{cp}^t = Rp * \left( \sum_e \sum_t x_{ec}^t - \sum_h \sum_t x_{ch}^t \right) \quad \forall c \tag{6}$$

$$\sum_m \sum_t x_{cm}^t = (1 - Rp) * \left( \sum_e \sum_t x_{ec}^t - \sum_h \sum_t x_{ch}^t \right) \quad \forall c \tag{7}$$

$$\sum_s \sum_t x_{msa}^t = Rca * Ua * \sum_c \sum_t x_{cm}^t \quad \forall m, a \tag{8}$$

$$\sum_f \sum_t x_{mfa}^t = (1 - Rca) * Ua * \sum_c \sum_t x_{cm}^t \quad \forall m, a \tag{9}$$

**Capacity constraints**

$$\sum_s \sum_t x_{spa}^t \leq CAP_{sa} \quad \forall s, a \tag{10}$$

$$\sum_k \sum_t x_{pk}^t \leq PCAP_p * X_p \quad \forall p \tag{11}$$

$$\sum_e \sum_t x_{ke}^t \leq KCAP_k * X_k \quad \forall e \tag{12}$$

$$\sum_e \sum_t x_{ec}^t \leq KCAP_k * X_k \quad \forall c \tag{13}$$

$$\sum_c \sum_t x_{cp}^t \leq RPCAP_p * X_p \quad \forall p \tag{14}$$

$$\sum_c \sum_t x_{cm}^t \leq MCAP_m * X_m \quad \forall m \tag{15}$$

$$\sum_m \sum_t x_{msa}^t \leq RCCAP_s \quad \forall s, a \tag{16}$$

$$\sum_m \sum_a \sum_t x_{mfa}^t \leq FCAP_s \quad \forall f \tag{17}$$

$$w_{sp}^t = \sum_a x_{spa}^t * wa \quad \forall s, p, t \tag{18}$$

$$w_{pk}^t = x_{pk}^t * w \quad \forall p, k, t \tag{19}$$

$$w_{ec}^t = x_{ec}^t * w \quad \forall e, c, t \tag{20}$$

$$w_{ke}^t = x_{ke}^t * w \quad \forall k, e, t \tag{21}$$

$$w_{cp}^t = x_{cp}^t * w \quad \forall c, p, t \tag{22}$$

$$w_{ch}^t = x_{ch}^t * w \quad \forall c, h, t \quad (23)$$

$$w_{cm}^t = x_{cm}^t * w \quad \forall c, h, t \quad (24)$$

$$w_{ms}^t = \sum_a x_{msa}^t * w_a \quad \forall s, m, t \quad (25)$$

$$w_{mf}^t = \sum_a x_{mfa}^t * w_a \quad \forall m, f, t \quad (26)$$

### Maximum number of activated locations constraints

$$\sum_p X_p \leq P \quad (27)$$

$$\sum_k X_k \leq K \quad (28)$$

$$\sum_c X_c \leq C \quad (29)$$

$$\sum_m X_m \leq M \quad (30)$$

### Linking–shipping constraints

$$L_{sp}^t \leq \sum_a x_{spa}^t \quad \forall s, p, t \quad (31)$$

$$L_{pk}^t \leq x_{pk}^t \quad \forall p, k, t \quad (32)$$

$$L_{ke}^t \leq x_{ke}^t \quad \forall k, e, t \quad (33)$$

$$L_{ec}^t \leq x_{ec}^t \quad \forall e, c, t \quad (34)$$

$$L_{cp}^t \leq x_{cp}^t \quad \forall c, p, t \quad (35)$$

$$L_{ch}^t \leq x_{ch}^t \quad \forall c, h, t \quad (36)$$

$$L_{cm}^t \leq x_{cm}^t \quad \forall c, m, t \quad (37)$$

$$L_{ms}^t \leq \sum_a x_{msa}^t \quad \forall s, m, t \quad (38)$$

$$L_{mf}^t \leq \sum_a x_{mfa}^t \quad \forall m, f, t \quad (39)$$

**Shipping linking constraints**

$$\sum_a x_{spa}^t \leq MI * L_{sp}^t \quad \forall s, p, t \tag{40}$$

$$x_{pk}^t \leq MI * L_{pk}^t \quad \forall p, k, t \tag{41}$$

$$x_{ke}^t \leq MI * L_{ke}^t \quad \forall k, e, t \tag{42}$$

$$x_{ec}^t \leq MI * L_{ec}^t \quad \forall e, c, t \tag{43}$$

$$x_{cp}^t \leq MI * L_{cp}^t \quad \forall c, p, t \tag{44}$$

$$x_{cm}^t \leq MI * L_{cm}^t \quad \forall c, m, t \tag{45}$$

$$x_{ch}^t \leq MI * L_{ch}^t \quad \forall c, h, t \tag{46}$$

$$\sum_a x_{msa}^t \leq MI * L_{ms}^t \quad \forall s, m, t \tag{47}$$

$$\sum_a x_{mfa}^t \leq MI * L_{mf}^t \quad \forall m, f, t \tag{48}$$

$$x_{ija}^t, x_{ij}^t \geq 0$$

$$X_i, L_{ij}^t \in \{0, 1\}$$

The first objective is to maximize the total profit including the total income and profit obtained by introducing recycled materials back into the (forward) supply chain (which is used as an incentive for the companies to choose and use recyclable products) minus the total cost which includes cost of purchasing components from suppliers, production cost incurred at plants, operating costs incurred at d/c, inspection cost for the returned products in collection centers, remanufacturing cost of recoverable products in plants, dismantling cost in dismantling the product, recycling cost at supplier and disposal costs for scrapped products. Second objective is to minimize the CO<sub>2</sub> emission by choosing various available type of transport.

Constraints are divided in five sets: first set is consisting of flow balancing constraints. Constraint (1) assures that the flow entering in the manufacturing plant is equal to the flow exit from it. Constraint (2) is for d/c. Constraint (3) insures that demands of all first customers are satisfied. Constraint (4) insures the flow entering in collection center through a customer will be equal to demand of the customer multiplied by return ratio. Constraint (5) insures that flow entering to each second customer from all collection centers does not exceed the second customer demand. Constraint (6) and (7) imposes that, the flow exiting from each collection center to all plants and dismantler is equal to the amount remaining at each collection

center after satisfying second customer demand multiplied by the repairing ratio and (1-repairing ratio ) respectively. Constraint (8) and (9) shows that, the flow exiting from each dismantler to supplier and disposal sites are equal to the flow entering from all CC multiplied by recycling ratio and (1-recycling ratio) respectively. Constraint (10–17) insures that flow either exiting or entering at any facility does not exceed the respective facility capacity. Constraints (27–30) limit the number of activated locations, where the sum of binary decision variables which indicate the number of activated locations, is less than the maximum limit of activated locations. Constraints (31–39) insure that there are no links between any locations without actual shipments during all periods. Constraints (40–48) ensure that there is no shipping between any non-linked locations.

### 4 Multiobjective Methodology: Goal Programming

The basic approach of **goal programming** is to establish a specific numeric goal for each of the objectives, formulate an objective function for each objective, and then seek a solution that minimizes both positive and negative deviations from set goals simultaneously or minimizes the amount by which each goal can be violated. There is a *hierarchy of priority levels* for the goals, so that the goals of primary importance receive first priority attention, those of secondary importance receive second-priority attention, and so forth.

Generalized model of goal programming is:

$$\begin{aligned} \min a &= \{g_1(\bar{\eta}_1, \bar{\rho}_1), \dots, g_k(\bar{\eta}_2, \bar{\rho}_2)\} \\ \text{s.t. } f_i(\bar{x}) + \eta_i - \rho_i &= b_i \quad \forall i = 1, 2, \dots, m \\ \bar{x}, \bar{\eta}, \bar{\rho} &\geq 0; \end{aligned}$$

$x_j$  is the  $j$ th decision variable,  $a$  is denoted as the achievement function; a row vector measure of the attainment of the objectives or constraints at each priority level,  $g_k(\bar{\eta}, \bar{\rho})$  is a function (normally linear) of the deviation variables associated with the objectives or constraints at priority level  $k$ ,  $K$  is the total number of priority levels in the model,  $b_i$  is the right-hand side constant for goal (or constraint)  $i$ ,  $f_i(\bar{x})$  is the left-hand side of the linear goal or constraint  $i$ .

We seek to minimize the non-achievement of that goal or constraint by minimizing specific deviation variables. The deviation variables at each priority level are included in the function  $g_k(\bar{\eta}, \bar{\rho})$  and ordered in the achievement vector, according to their respective priority. Algorithm of sequential goal programming:

**Step 1:** Set  $k = 1$  ( $k$  represents the priority level and  $K$  is the total of these).

**Step 2:** Establish the mathematical formulation as discussed above using positive and negative deviations for priority level  $k$  only.

**Step 3:** Solve this single-objective problem associated with priority level  $k$  and the optimal solution of  $g_k(\bar{\eta}, \bar{\rho})$  is  $a^*$ .

**Step 4:** Set  $k = k + 1$ . If  $k > K$ , go to Step 7.

**Step 5:** Establish the equivalent, single objective model for the next priority level (level  $k$ ) with additional constraint  $g_k(\bar{\eta}, \bar{\rho}) = a_s^*$ .

**Step 6:** Go to Step 3.

**Step 7:** The solution vector  $x^*$ , associated with the last single objective model solved, is the optimal vector for the original goal programming model.

## 5 Numerical Illustration

In this section, a numerical example is presented in order to demonstrate the applicability of the model. In considered CLSC, a product which is made up of six components say 1, 2, 3, 4, 5, and 6 with respective utilization rate of 1, 4, 1, 2, 1, and 3 and recycling rate of 1, 0.5, 7.5, 1, 0.3 and 0 flows between various facilities. In forward direction, there is a set of three suppliers that can provide components to two potential locations of manufacturing plants. Three potential location of d/cs are there in the network to cater the demand of 2000, 2700, 3250, 2550, and 2700 units from respective 5 zones of first customer market at a unit selling price of 11000, 10500, 10000, 10750, and 10500. In backward direction, potential locations of CC, dismantlers and disposal sites are 3, 2, and 1 respectively. Beside its demand of 500, 350, and 550 units of used product from respective three zones of second customers can be satisfied at unit selling price of 7500, 8000, and 7000. As for transportation, road-based transportation is used to carry out the shipping operations, for which there are three types of trucks available which are 0–3, 4–7, and 8–11 years old, respectively. We assume that the older the trucks, the cheaper their rental fees, but, at the same time, the greater their CO<sub>2</sub> emissions, due to decreasing engine efficiency. Unit transportation costs for the different types of trucks used are 1, 0.85 and 0.70 for truck types 1, 2, and 3, respectively. Emission rate of CO<sub>2</sub> found to be 1.3, 2.8, and 3.1 g/mi for truck types 1, 2 and 3 respectively. Profit raised in the network by repairing the product is 5500/unit and by recycling a unit of component 1, 2, 3, 4, and 5 are 250, 50, 90, 55, and 300 respectively.

Other parameters are set as follows:  $Rr = 0.60$ ,  $Rp = 0.25$ , and  $Rc_a = (1, 1, 1, 1, 1, 0)$ . Set of unit purchasing costs of components (in order) from supplier 1, 2, and 3 are (460, 0, 190, 125, 0, 80), (480, 120, 200, 150, 650, 100) and (470, 95, 0, 0, 620, 90), respectively. Unit recycling costs of components (in order) at supplier 1, 2, and 3 are (20, 0, 60, 10, 0, 0), (25, 90, 55, 20, 390, 0) and (0, 65, 0, 0, 380, 0), respectively. Price 0 means that component service is not provided by respective supplier. 2500 and 3000 are unit production cost, and 1500 and 2200 are unit repairing costs of the product at plant 1 and 2, respectively. Unit operating costs at d/c 1, 2, and 3 are 500, 550, and 600 respectively. Unit Inspection costs at collection centers 1, 2, and 3 are 100, 100, and 120 respectively. Unit dismantling



cost at d/m 1 and 2 are 125 and 110 respectively. Unit disposal cost of component 6 is 15.

Data on capacities at various facilities are as follows: Supplier 1 can supply at most of 8000, 0, 9000, 12000, 0, and 14000 units of component 1, 2, 3, 4, 5, and 6 respectively. Capacity of supplier 2 and 3 of components are (7500, 40000, 5000, 27000, 7700, 15000) and (0, 20000, 0, 0, 7500, 1400) respectively. Recycling capacities of supplier 1, 2 and 3 are (3000, 0, 2900, 4000, 0, 0), (2000, 15000, 2000, 6000, 2500, 0) and (0, 8000, 0, 0, 2500, 0) respectively. Production capacities of plants are 8000, 7500 and repairing capacities are 2000, 1800 respectively. Capacities of d/c's are 4800, 5000 and 5500, of CC's are 3500, 3000 and 2500; of dismantlers are 5000, 5000 and of disposal site is 250000.

Data on distance (in miles) between any two facilities is as follows:

$$D_{ij} = \{D_{11}, D_{12}, D_{13}, \dots, D_{21}, D_{22}, D_{23}, \dots\}$$

$$D_{sp} = \{200, 190, 310, 350, 290, 280\},$$

$$D_{pk} = \{120, 100, 135, 170, 190, 200\},$$

$$D_{ke} = \{24, 17, 22, 21, 18, 29, 19, 21, 20, 31, 33, 25, 28, 15, 28\},$$

$$D_{ec} = \{6, 9, 8, 8.5, 7, 10, 11, 12, 13, 9, 8, 9.5, 11, 9, 8\},$$

$$D_{cp} = \{150, 120, 135, 110, 130, 100\}$$

$$D_{cm} = \{8.5, 9, 11, 12, 10, 11\},$$

$$D_{ch} = \{15, 21, 19, 24, 16, 18, 20, 22, 21\}$$

$$D_{ms} = \{100, 150, 120, 95, 154, 130\},$$

$$D_{mf} = \{80, 75\}$$

The above data is employed to validate the proposed model. A LINGO code for generating the proposed mathematical models of the given data was developed and solved using LINGO11.0 [20]. Problem is solved individually with each objective subject to given set of constraints. Thus, Profit and amount of CO<sub>2</sub> emission would be 66625630 and 252121600 respectively. Which are set as the aspiration levels for profit and emission functions. Then multiobjective programming problem combining all the objectives and incorporating the individual aspirations is solved which results in infeasible solution hence goal programming technique has been used to obtain a compromise solution to the above problem. Giving weight age 0.5 and 0.5 to profit and CO<sub>2</sub> objective respectively, a compromised solution of allocation of facilities and transporting vehicle is obtained. Total profit thus generated in the network is Rs. 54, 240, 470 and amount of CO<sub>2</sub> emitted is 543, 833, 100. The flow between facilities using different type vehicles is given below.

$$x_{spa}^t : x_{111}^3 = 3016, \quad x_{113}^3 = 4016, \quad x_{114}^3 = 12000, \quad x_{121}^2 = 4984, \quad x_{123}^2 = 4984,$$

$$x_{126}^1 = 14000, \quad x_{211}^2 = 3570, \quad x_{212}^2 = 12860, \quad x_{213}^2 = 2570, \quad x_{214}^2 = 1172,$$

$$x_{215}^2 = 4070, \quad x_{216}^2 = 5758, \quad x_{222}^1 = 19080, \quad x_{224}^1 = 9968, \quad x_{226}^1 = 952,$$

$$x_{312}^3 = 13484, \quad x_{315}^3 = 2516, \quad x_{316}^3 = 14000, \quad x_{322}^1 = 856, \quad x_{325}^1 = 4984$$

$$\begin{aligned}
x_{pk}^t : x_{11}^3 &= 1086, & x_{13}^2 &= 5500, & x_{21}^3 &= 3714, & x_{22}^2 &= 2900 \\
x_{ke}^t : x_{13}^1 &= 450, & x_{14}^1 &= 1650, & x_{15}^1 &= 2700, & x_{21}^1 &= 2000, & x_{24}^1 &= 900, \\
& & x_{32}^3 &= 2700, & x_{33}^3 &= 2800 \\
x_{ec}^t : x_{13}^3 &= 1200, & x_{21}^1 &= 150, & x_{22}^3 &= 1470, & x_{31}^2 &= 1950, & x_{42}^3 &= 1530, \\
& & x_{51}^3 &= 1400, & x_{53}^3 &= 220 \\
x_{cp}^t : x_{12}^3 &= 525, & x_{22}^1 &= 750, & x_{32}^3 &= 355 \\
x_{cm}^t : x_{11}^3 &= 1575, & x_{22}^1 &= 2250, & x_{32}^1 &= 1065 \\
x_{ch}^t : x_{11}^1 &= 500, & x_{12}^2 &= 350, & x_{13}^2 &= 550 \\
x_{msa}^t : x_{121}^3 &= 1575, & x_{122}^3 &= 6300, & x_{123}^3 &= 1575, & x_{124}^3 &= 3150, & x_{125}^3 &= 1575, \\
& & x_{211}^2 &= 2890, & x_{214}^3 &= 3780, & x_{221}^3 &= 425, & x_{222}^2 &= 8700, \\
& & x_{223}^3 &= 425, & x_{224}^2 &= 2850, & x_{225}^3 &= 925, & x_{232}^1 &= 4560, & x_{235}^1 &= 2390 \\
& & x_{mfa}^t : x_{116}^3 &= 4725, & x_{216}^2 &= 9945
\end{aligned}$$

## 6 Conclusions

One of the important planning activities in supply chain management (SCM) is to design the configuration of the supply chain network. Besides, due to the global warming recently attention has been given to reverse logistic in SCM. Modeling of a CLSC network design problem can be a challenging process because there is large number of components that need to be incorporated into model. Here in this paper, trade-offs between operational and environmental performance measures of shipping product were investigated. Due to global warming, this paper focused on CO<sub>2</sub> emissions, One of the main findings of this paper is that, costs of environmental impacts are still not as apparent as operational measures, as far as their relative importance in a emission rate function are concerned. Operational costs of handling products, both in forward and reverse networks, seem to be dominant ignoring emissions rate. Another interesting result is relevant to the promotion of reusable products, the use of which seems to lessen the operational costs of the chain, but places a burden on the environmental costs.

## References

1. Beamon, B.M.: Sustainability and the future of supply chain management. *Oper. Supply Chain Manag.* **1**(1), 4–18 (2008)
2. Zhu, Q.H., Sarkis, J., Lai, K.H.: Green supply chain management implications for “closing the loop”. *Transp. Res. Part E* **44**(1), 1–18 (2008)
3. Fleischmann, M., Beullens, P., Bloemhof-ruwaard, J.M., Wassenhove, L.: The impact of product recovery on logistics network design. *Product. Oper. Manag.* **10**, 156–173 (2001)
4. Lee, D., Dong, M.: A heuristic approach to logistics network design for end-of-lease computer products recovery. *Transp. Res. Part E* **44**, 455–474 (2008)
5. Verstrepren, S., Cruijssen, F., de Brito, M., Dullaert, W.: An exploratory analysis of reverse logistics in Flanders. *Eur. J. Trans. Infrastruct. Res.* **7**(4), 301–316 (2007)
6. Pishvae, M.R., Farahani, R.Z., Dullaert, W.: A memetic algorithm for bi-objective integrated forward/reverse logistics network design. *Comput. Oper. Res.* **37**(6), 1100–1112 (2010)
7. Jayaraman, V., Guide Jr, V.D.R., Srivastava, R.: A closed-loop logistics model for remanufacturing. *J. Oper. Res. Soc.* **50**(5), 497–508 (1999)
8. Fleischmann, M., Beullens, P., Bloemhof-Ruwaard, J.M., Wassenhove, L.: The impact of product recovery on logistics network design. *Prod. Oper. Manag.* **10**(3), 156–173 (2001)
9. Salema, M.I., Barbosa-Póvoa, A.P., Novais, A.Q.: A strategic and tactical model for closed-loop supply chains, (pp. 361–386). EURO Winter Institute on Location and Logistics, Estoril (2007a)
10. El Saadany, Ahmed M. A., El-Kharbotly, Amin, K.: Reverse logistics modeling. In: 8th International Conference on Production Engineering and Design for Development, Alexandria, Egypt (2004)
11. Min, H., Ko, C.S., Ko, H.J.: The spatial and temporal consolidation of returned products in a closed-loop supply chain network. *Comput. Ind. Eng.* **51**(2), 309–320 (2006)
12. Kannan, G., Sasikumar, P., Devika, K.: A genetic algorithm approach for solving a closed loop supply chain model: a case of battery recycling. *Appl. Math. Model.* **34**(3), 655–670 (2010)
13. Aras, N., Boyaci, T., Verter, V.: Designing the reverse logistics network. In: Ferguson, M.E., Souza, G.C. (eds.), *Closed-loop Supply Chains: New Developments to Improve the Sustainability of Business Practices*, pp. 67–97. CRC Press, Taylor & Francis, Boca Raton (2010)
14. Meixell, M.J., Gargeya, V.B.: Global supply chain design: a literature review and critique. *Transp. Res. Part E* **41**(6), 531–550 (2005)
15. Hervani, A.A., Helms, M.M., Sarkis, J.: Performance measurement for green supply chain management. *Benchmarking: An International Journal* **12**(4), 330–353 (2005)
16. Srivastava, S.K.: Green supply-chain management: a state-of-the-art literature review. *Int. J. Manag. Rev.* **9**(1), 53–80 (2007)
17. Sarkis, J.: A strategic decision framework for green supply chain management. *J. Cleaner Prod.* **11**(4), 397–409 (2003)
18. Sheu, J.B., Chou, Y.H., Hu, C.: An integrated logistic operational model for green supply chain management. *Transp. Res. Part E* **41**(4), 287–313 (2005)
19. Krikke, H., Bloemhof-Ruwaard, J., Van Wassenhove, L.: Concurrent product and closed-loop supply chain design with an application to refrigerators. *Int. J. Prod. Res.* **41**(16), 3689–3719 (2003)
20. Thiriez, H.: OR software LINGO. *Eur. J. Oper. Res.* **12**, 655–656 (2000)

# Optimal Component Selection Based on Cohesion and Coupling for Component-Based Software System

P. C. Jha, Vikram Bali, Sonam Narula and Mala Kalra

**Abstract** In modular-based software systems, each module has different alternatives with variation in their functional and nonfunctional properties, e.g., reliability, cost, delivery time, etc. The success of such systems largely depends upon the selection process of commercial-off-the shelf (COTS) components. In component-based software (CBS) development, it is desirable to choose the components that provide all necessary functionalities and at the same time optimize nonfunctional attributes of the system. In this paper, we have discussed the multiobjective optimization model for COTS selection in the development of a modular software system using CBSS approach. Fuzzy mathematical programming (FMP) is used for decision making to counter the effects of unreliable input information.

**Keywords** Commercial-off-the shelf (COTS) · Components-based software system (CBSS) · Fuzzy mathematical programming (FMP) · Intra-modular coupling density (ICD)

---

P. C. Jha (✉) · S. Narula  
Department of Operational Research, University of Delhi, Delhi, India  
e-mail: jhpc@yahoo.com

S. Narula  
e-mail: sonam.narula88@gmail.com

V. Bali  
Rayat Bahra Institute of Engineering and Bio-Technology, Mohali, Punjab, India  
e-mail: vikramgcet@gmail.com

M. Kalra  
National Institute of Technical Teachers Training and Research, Chandigarh, India  
e-mail: malakalra2004@yahoo.co.in

## 1 Introduction

With the growing need of complex software systems, the use of commercial off-the-shelf (COTS) products has grown steadily. COTS products as a way of managing cost, developing time, and effort [1] requires less code that needs to be designed and implemented by the developers. Compared with traditional software development, COTS-based system development promises faster delivery with lower resource cost. However, the use of COTS products in software development can require a considerable integration effort [2].

In recent years, component-based approach to software development has become more and more popular [3]. Component-based software systems (CBSS) development focuses on the decomposition of a software system into functional and logical components with well-defined interfaces. It allows a software system to be developed using appropriate and suitable software components that are available in COTS components' market. The vendor of the COTS supplier provides information about cost and delivery time of the COTS products. The software development using CBSS approach has reduced significantly the software development time and also facilitates system with better maintainability. Optimization problems of optimum selection of COTS components are widely studied by many researchers in the literatures such as Belli and Jedrzejowicz [4], Berman and Ashrafi [5], Berman and Kumar [6], Cortellesa et al. [7], Gupta et al. [8, 9], Jha et al. [10], Kapur et al. [11], Kumar [12], Kwong et al. [13, 14], and Neubauer and Stummer [15]. The models proposed by the authors have been used to achieve the different attributes of quality along with the objective of minimizing the cost or keeping cost to a budgetary level.

CBSS development employs modular approach for the development of the software system. It also improves the flexibility and comprehensibility of the software [16]. In the development of modular-based conventional software systems, the criteria of minimizing the coupling and maximizing the cohesion of software modules were commonly used [16–19]. Coupling is about the measure of interactions among software modules while cohesion is about the measure of interactions among the software components which are within a software module. A good software system should possess software modules with high cohesion and low coupling. A highly cohesive module exhibits high reusability and loosely coupled systems enable easy maintenance of a software system [20].

In the previous studies of COTS selection discussed above it is assumed that COTS components within the set of alternative software components are often regarded to have the same functions in CBSS development. Since the COTS components are provided by multiple suppliers, functions performed by these components could be different from each other. Therefore, the functional contributions of the software components toward the functional requirements of a CBSS should be considered. Kwong et al. [21] presented a methodology for optimal selection of software components for CBSS development based on the criteria of simultaneously maximizing functional performance and intra-modular coupling density (ICD).

In this paper, we devise a multiobjective optimization model for COTS selection in the development of a modular software system using CBSS approach. The formulated model simultaneously maximizes the functional performance and also intra-modular coupling density which in turn maximizes cohesion and minimizes coupling in CBSS. The selection of COTS components is constrained using minimum threshold on the intra-modular coupling density and maximum allowable limit on budget and delivery time of acquiring all the COTS components for CBSS development. The proposed research can be considered as an extension of the optimization model proposed in [21]. The authors in their work have not considered budget and delivery time for the selection of COTS components. We cannot always have software system with highly cohesive and loosely coupled modules because of the limitations on budget and delivery time. The delivery time of the COTS component is the time of acquiring and integrating the components within and amongst the modules of the software system. The total delivery time includes integration and system testing. Similarly, we cannot spend as much as we want on component selection because in real life situation we have limitations on budget. Therefore, there is a need to maintain a trade-off between a highly cohesive software system and its cost. Moreover, in our work, we have also incorporated issue of compatibility amongst the components of the modules.

## 2 COTS Selection in CBSS

CBSS development starts with identification of modules in the software and each module must contain at least one COTS component. In order to select COTS components for modular software systems, the following criteria may be used.

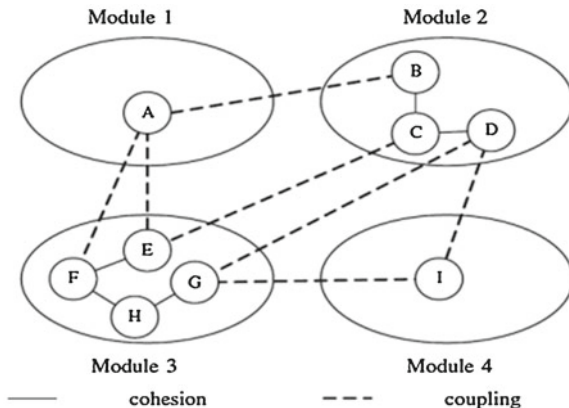
### 2.1 Intra-modular Coupling Density

In this research, we have employed Abreu and Gaulao's [17] approach which yields the quantitative measures of cohesion and coupling. The authors in their work presented intra-modular coupling density (ICD) to measure the relationship between cohesion and coupling of modules in design of modular software system and is given as follows:

$$ICD = \frac{CI_{IN}}{CI_{IN} + CI_{OUT}} \quad (1)$$

where,  $CI_{IN}$  is the number of class interactions within modules, and  $CI_{OUT}$  is the number of interactions between classes of distinct modules.

Referring to Eq. (1), the ratio of cohesion to all interactions within the  $j$ th module can be expressed as  $ICD_j$ . However, it can be found if any module contains only one component, the values of ICD for that module becomes zero. To make up for the



**Fig. 1** Cohesion and coupling

deficiency 1 is added to the numerator of Eq. (1) to form another measure of ICD as follows:

$$ICD = \frac{(CI_{IN})_j + 1}{(CI_{IN})_j + (CI_{OUT})_j} \tag{2}$$

where,  $ICD_j$  is the intra-modular coupling density for the  $j$ th module;  $(CI_{IN})_j$  is the number of component interactions within the  $j$ th module; and  $(CI_{OUT})_j$  is the number of component interactions between the  $j$ th module and other modules. Figure 1 (replicated from [21]) shows diagrammatic depiction of cohesion and coupling of software modules in the development of modular software system.

## 2.2 Functional Performance

Functionality of the COTS components can be defined as the ability of the component to perform according to the specific needs of the customer/organization requirements. The functional capabilities of the COTS components are different for different components as they are provided by different suppliers in the COTS market. We use functional ratings of the COTS components to the software module as coefficients in the objective function corresponding to maximizing the functional performance of the modular software system. These ratings are assumed to be given by the software development team.

### ***2.3 Cost***

Cost is the major factor in determining the selection of COTS components. Cost is one of the constraints in our proposed model. We have considered cost based on procurement and adaptation costs of COTS components.

### ***2.4 Delivery Time***

The delivery time of the COTS component is the time of acquiring and integrating the components within and amongst the modules of the software system. The total delivery time includes integration and system testing.

### ***2.5 Compatibility***

In the development of software system, sometimes the COTS product for one module is incompatible with the alternative COTS products for other modules due to problem such as implementation technology, interfaces, and licensing. Therefore, the issue of compatibility is also incorporated in the optimization model for COTS selection.

## **3 Formulation of Optimization Model for CBSS**

Generally, a CBSS is developed based on a top-down approach. Based on this approach, functional/customer requirements are first identified. The number and nature of software modules are then determined. The next task is to integrate software components for modules. The selection of components should be in such a way so as to have maximum interactions of components within the software modules and minimum interactions of software components amongst the software modules.

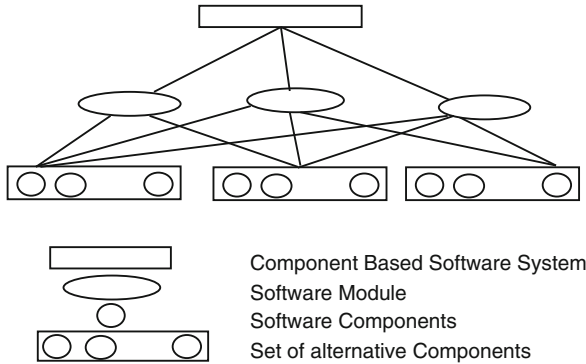
Let  $S$  be a software architecture made of  $M$  modules, with a maximum number of  $N$  components available for each module. Figure 2 shows how CBSS can be developed using software components.

### ***3.1 Notations***

$M$  the number of software modules

$N$  the number of software components





**Fig. 2** A CBSS system

$Sc_i$  the  $i$ th software component;  $i = 1, 2, \dots, N$

$m_j$  the  $j$ th software module;  $j = 1, 2, \dots, M$

$S_k$  a set of alternative software components for the  $k$ th functional requirement of a CBSS. Only one software component in  $S_k$  is selected to implement the  $k$ th requirement;  $k = 1, 2, \dots, L$

$i \in S_k$  denotes that  $Sc_i$  belongs to the  $k$ th set

$r_{ii'}$  the number of interactions between  $Sc_i$  and  $Sc_{i'}$ ;  $i, i' = 1, 2, \dots, N$  as the coupling and cohesion are undirected relations,  $r_{ii'} = r_{i'i}$

$f_{ij}$   $f_{ij}$  are real numbers ranging from 0 to 1 depicting the function rating of  $Sc_i$  to  $m_j$ ;  $i = 1, 2, \dots, N$ ;  $j = 1, 2, \dots, M$

$H$  a threshold value of  $ICD_j$  of each module that needs to be set by decision makers.

$C_{ij}$  cost of  $i$ th component available for  $j$ th module

$d_{ij}$  delivery time of  $i$ th component available for  $j$ th module

$B$  maximum budget limit set by the decision makers

$T$  maximum threshold given on delivery time of a component

$Sc_{ij}$  the  $i$ th software component of  $j$ th software module, s.t.  $Sc_{ij} = Sc_{i'j} = Sc_i$  for all  $j, j' = 1, 2, \dots, M$

$$x_{ij} \quad \text{binary variable} \begin{cases} 1, & \text{if } Sc_i \text{ is selected for } m_j \\ 0, & \text{otherwise} \end{cases}$$

### 3.2 Assumptions

1. At least one component is supposed to get selected from each module.
2. A threshold value of  $ICD_j$ , budget and delivery time are set by the decision makers.
3. Redundancy not allowed i.e. exactly one software component in  $S_k$  may get selected to implement  $k$ th requirement.
4. The cost and delivery time of COTS components are given.
5. Interaction data for components is exactly same for all modules, irrespective of the selection happened.
6. Interaction associated is set by the software development team.

### 3.3 Optimization Model

The multiobjective optimization model for COTS selection using CBSS development can be formulated as follows:

$$\text{Max ICD} = \frac{\sum_{j=1}^M \sum_{i=1}^{N-1} \sum_{i'=i+1}^N r_{ii'} x_{ij} x_{i'j}}{\sum_{i=1}^{N-1} \sum_{i'=i+1}^N r_{ii'} \left( \sum_{j=1}^M x_{ij} \right) \left( \sum_{j'=1}^M x_{i'j'} \right)} \tag{3}$$

$$\text{Max F} = \sum_{j=1}^M \sum_{i=1}^N f_{ij} x_{ij} \tag{4}$$

Subject to  $X \in S = \left\{ x_{ij} \text{ is binary variable/} \right.$

$$\frac{\sum_{i=1}^{N-1} \sum_{i'=i+1}^N r_{ii'} x_{ij} x_{i'j} + 1}{\sum_{i=1}^{N-1} \sum_{i'=i+1}^N r_{ii'} x_{ij} \sum_{j'=1}^M x_{i'j'}} \geq H; \quad j = 1, 2, \dots, M, \quad j' = 1, 2, \dots, M \tag{5}$$

$$\sum_{j=1}^M \sum_{i=1}^N C_{ij} x_{ij} \leq B \tag{6}$$

$$\sum_{i \in S_k} \sum_{j=1}^M d_{ij} x_{ij} \leq T ; k = 1, 2, \dots, L \tag{7}$$

$$\sum_{i \in S_k} \sum_{j=1}^M x_{ij} = 1 ; k = 1, 2, \dots, L \tag{8}$$

$$\sum_{i=1}^N x_{ij} \geq 1 ; j = 1, 2, \dots, M \tag{9}$$

$$x_{ij} \in \{0, 1\} ; i = 1, 2, \dots, N ; j = 1, 2, \dots, M \tag{10}$$

$$x_{rs} - x_{ukh} \leq \bar{M} y_k \tag{11}$$

$$\sum_{k=1}^z y_k = z - 1 \tag{12}$$

$$y_k \in \{0, 1\} ; k = 1, 2, \dots, z \} \tag{13}$$

The objective function (3) is based on maximizing cohesion within software modules and minimizing coupling among software modules. Objective function (4) maximizes the functional performance of a software system to be developed. Constraint (5) shows the minimum threshold on ICD value. Constraint (6) is budget limitation. Constraint (7) is restriction on delivery time. Equation (8) denotes that only one software component can be selected from a set of alternative software components for a particular software module. Constraint (9) refers to the software module that contains at least one software component. Constraint (10) shows selection or rejection of a particular COTS product. Constraints (11)–(13) are used to deal with incompatibility amongst COTS components. The incompatibility constraint can be denoted by  $x_{rs} \leq x_{u1t}$ , that is if the module  $s$  chooses COTS component  $r$ , then the module  $t$  must choose the COTS component  $u1$ . This decision is called contingent decision constraint [22]. Suppose that there are two contingent decisions in the model, such as the COTS alternative for the module is only compatible with the COTS products  $u1$  and  $u2$  for the module  $t$ , i.e., either  $x_{u1t} = 1$  if  $x_{rs} = 1$  or  $x_{u2t} = 1$  if  $x_{rs} = 1$ , these constraint can be represented as either  $x_{rs} \leq x_{u1t}$  or  $x_{rs} \leq x_{u2t}$ . Since the presence of “either-or” constraint makes the optimization problem nonlinear, it can be linearized by binary variable  $y_k$  as follows:

$$y_k = \begin{cases} 0, & \text{if } k\text{th constraint is active} \\ 1, & \text{if } k\text{th constraint is inactive} \end{cases}$$

Thus, only one out of  $z$  contingent decision constraints for any COTS products between two modules is guaranteed to be active if  $\bar{M}$  is sufficiently large.

### 4 Fuzzy Approach for Solving Multiobjective Optimization Problem

Conventional optimization methods assume that all parameters and goals of an optimization model are precisely known. But for many practical problems there are incompleteness and unreliability of input information. This caused us to use fuzzy multiobjective optimization method with fuzzy parameters. Following steps are required to perform for solving fuzzy multiobjective optimization problem [9].

**Step 1:** Construct multiobjective optimization problem. Refer problem (P1)

**Step 2:** Solve multiobjective optimization problem by considering first objective function. This process is repeated for all the remaining objective functions. If all the solutions (i.e.  $X^1 = X^2 = \dots = X^k = x_{ij}, i = 1, \dots, N; j = 1, \dots, M$ ) are same, select one of them as an optimal compromise solution and stop. Otherwise, go to step 3.

**Step 3:** Evaluate the  $k$ th objective function at all solutions obtained and determine the best (worst) lower bound ( $L_k$ ) and best (worst) upper bound ( $U_k$ ) as the case may be.

**Step 4:** Define membership function of each objective of optimization model. The membership function for ICD is given as follows:

$$\mu_{ICD}(x) = \begin{cases} 1, & \text{if } ICD(x) \geq ICD_u, \\ \frac{ICD(x)-ICD_l}{ICD_u-ICD_l}, & \text{if } ICD_l < ICD(x) < ICD_u, \\ 0, & \text{if } ICD(x) \leq ICD_l \end{cases}$$

where  $ICD_l$  is the worst lower bound and  $ICD_u$  is the best upper bound of ICD objective function.

The membership function for functionality is given as follows.

$$\mu_F(x) = \begin{cases} 1, & \text{if } F(x) \geq F_u, \\ \frac{F(x)-F_l}{F_u-F_l}, & \text{if } F_l < F(x) < F_u, \\ 0, & \text{if } F(x) \leq F_l \end{cases}$$

where  $F_l$  is the worst lower bound and  $F_u$  is the best upper bound of functionality objective function.

**Step 5:** Develop fuzzy multiobjective optimization model.

Following Bellaman-Zadeh’s maximization principle [23] and using the above defined fuzzy membership functions, the fuzzy multiobjective optimization model for COTS selection is formulated as follows:

$$\begin{array}{ll}
 \max & \lambda \\
 \text{subject to} & \lambda \leq \mu_{\text{ICD}(x)} \\
 & \lambda \leq \mu_{F(x)} \\
 & 0 \leq \lambda \leq 1 \\
 & X \in S
 \end{array}$$

Solve the above model. Present the solution to the decision maker. If the decision maker accepts it, then stop. Otherwise, evaluate each objective function at the solution. Compare the upper (lower) bound of each objective function with new value of the objective function. If the new value is lower (higher) than the upper (lower) bound, consider it as a new upper (lower) bound. Otherwise, use the old values as it is. If there are no changes in current bounds of all the objective functions then stop otherwise go to step 4.

The solution process terminates when decision maker accepts the obtained solution and considers it as the preferred compromise solution which is in fact a compromise feasible solution that meets the decision maker's preference.

## 5 Case Study

A case study of CBSS development is presented to illustrate the proposed methodology of optimizing the selection of COTS components for CBSS development. A local software system supplier planned to develop a software system for small and medium size manufacturing enterprises. In this case, a software system is decomposed into three modules  $M_1$ ,  $M_2$  and  $M_3$ . A total of 20 software components ( $Sc_1$ – $Sc_{20}$ ) are available in market to make up ten sets of alternative software component ( $S_1$ – $S_{10}$ ) for each module. Total components available for selection are sixty and total twenty components are available for selection per module and may be represented as ( $Sc_1$ – $Sc_{20}$ ). Exactly one software components in each set of alternatives may get selected for a particular software module for fulfilling functional requirements. For example,  $Sc_1$ ,  $Sc_2$ ,  $Sc_3$  and  $Sc_4$  all belong to the set of alternative software components  $S_1$ . Hence, only one of the four components will be selected for fulfilling the  $S_1$  functional requirement.

Individual functional requirements and their corresponding alternative software components, as well as the function ratings of software components corresponding to software modules, are shown in Table 1. The function ratings describe the degree of functional contributions of the software components toward the software modules. The function ratings range from 0 to 1 where 1 refers to a very high degree of contribution while 0 indicates zero degree of contribution.

Table 2 shows the degrees of interaction among software components. The range of the degrees is 1–10. The degree '1' means a very low degree of interaction while the degree '10' refers to a very high degree of interaction.

In Table 3, Cost ( $C_{ij}$  for all  $i, j$ ) in 100\$ unit; and delivery time ( $d_{ij}$  for all  $i, j$ ) in days associated with COTS components is given.

**Table 1** Example description and functionality of COTS components

Functional requirements	$S_k$	Software components	Module1 (Front office)	Module2 (Back office)	Module3 (Finance)
Inventory control and management	$S_1$	$Sc_1$	0.68	0.51	0.00
		$Sc_2$	0.22	0.63	0.01
		$Sc_3$	0.15	0.79	0.00
		$Sc_4$	0.23	0.87	0.00
Payment collection and authorization	$S_2$	$Sc_5$	0.94	0.10	0.55
		$Sc_6$	0.75	0.45	0.22
Sales	$S_3$	$Sc_7$	0.08	0.94	0.01
Automatic updates	$S_4$	$Sc_8$	0.10	0.22	0.00
		$Sc_9$	0.00	1.00	0.20
		$Sc_{10}$	0.20	0.45	0.05
		$Sc_{11}$	0.00	0.98	0.20
E-commerce	$S_5$	$Sc_{12}$	0.00	0.31	0.10
		$Sc_{13}$	0.11	0.12	0.31
Financial reporting	$S_6$	$Sc_{14}$	0.05	0.07	0.71
		$Sc_{15}$	0.22	0.02	0.42
Business rules and protocol	$S_7$	$Sc_{16}$	0.30	0.02	0.00
Shift wise reporting statistics	$S_8$	$Sc_{17}$	0.80	0.10	0.00
		$Sc_{18}$	0.00	0.70	0.32
		$Sc_{19}$	0.00	0.06	0.78
Accounts	$S_9$	$Sc_{20}$	0.00	0.00	0.18
Finance	$S_{10}$				

## 6 Solution

*Steps 1, 2 and 3* After forming multiobjective programming using the above data, the solution of each single objective problem is found and hence upper and lower bounds are obtained as follows:

	$X^1$	$X^2$
<b>ICD</b>	0.653	0.581
<b>F</b>	1.17	7.35

where  $X^1 = (Sc_{201}, Sc_{142}, Sc_{152}, Sc_{192}, Sc_{33}, Sc_{53}, Sc_{63}, Sc_{103}, Sc_{113}, Sc_{173})$   
 $X^2 = (Sc_{51}, Sc_{61}, Sc_{161}, Sc_{32}, Sc_{92}, Sc_{112}, Sc_{143}, Sc_{153}, Sc_{193}, Sc_{203})$

**Table 2** Interactions among COTS components

		S <sub>1</sub>		S <sub>2</sub>		S <sub>3</sub>		S <sub>4</sub>		S <sub>5</sub>		S <sub>6</sub>		S <sub>7</sub>		S <sub>8</sub>		S <sub>9</sub>		S <sub>10</sub>	
		Sc <sub>1</sub>	Sc <sub>2</sub>	Sc <sub>3</sub>	Sc <sub>4</sub>	Sc <sub>5</sub>	Sc <sub>6</sub>	Sc <sub>7</sub>	Sc <sub>8</sub>	Sc <sub>9</sub>	Sc <sub>10</sub>	Sc <sub>11</sub>	Sc <sub>12</sub>	Sc <sub>13</sub>	Sc <sub>14</sub>	Sc <sub>15</sub>	Sc <sub>16</sub>	Sc <sub>17</sub>	Sc <sub>18</sub>	Sc <sub>19</sub>	Sc <sub>20</sub>
S <sub>1</sub>	Sc <sub>1</sub>	0	0	5	3	0	4	9	6	3	6	8	5	2	1	0	0	0	0	0	3
	Sc <sub>2</sub>	0	0	3	1	0	4	5	3	7	8	5	3	4	2	0	0	1	0	0	2
	Sc <sub>3</sub>	5	3	0	4	1	3	3	0	2	7	10	2	0	1	0	4	3	1	0	1
	Sc <sub>4</sub>	3	1	4	0	2	2	7	8	6	9	2	3	0	0	0	0	0	2	1	1
S <sub>2</sub>	Sc <sub>5</sub>	0	0	1	2	0	10	1	2	3	2	1	2	0	0	0	0	0	2	1	2
S <sub>3</sub>	Sc <sub>6</sub>	4	4	3	2	10	0	1	2	2	2	2	0	0	0	0	8	7	1	1	2
S <sub>4</sub>	Sc <sub>7</sub>	9	5	3	7	1	1	0	0	3	7	3	2	2	1	0	0	0	1	2	1
	Sc <sub>8</sub>	6	3	0	8	2	2	0	0	2	6	2	1	2	3	0	1	0	2	2	2
	Sc <sub>9</sub>	3	7	2	6	3	2	3	2	0	4	10	7	2	1	0	0	0	2	1	1
	Sc <sub>10</sub>	6	8	7	9	2	2	7	6	4	0	10	7	4	2	1	3	4	2	1	3
S <sub>5</sub>	Sc <sub>11</sub>	8	5	10	2	1	2	3	2	10	10	0	2	3	2	3	0	0	4	2	4
	Sc <sub>12</sub>	5	3	2	3	2	0	2	1	7	7	2	0	4	1	2	0	0	3	1	5
S <sub>6</sub>	Sc <sub>13</sub>	2	4	0	0	0	0	2	2	2	4	3	4	0	0	8	1	0	10	7	10
	Sc <sub>14</sub>	1	2	1	0	0	0	1	3	1	2	2	1	0	0	6	3	0	4	3	3
S <sub>7</sub>	Sc <sub>15</sub>	0	0	0	0	0	0	0	0	0	1	3	2	8	6	0	0	0	9	10	10
S <sub>8</sub>	Sc <sub>16</sub>	0	0	4	0	0	8	0	1	0	3	0	0	1	3	0	0	2	2	0	0
	Sc <sub>17</sub>	0	1	3	0	0	7	0	0	0	4	0	0	0	0	0	2	0	0	0	0
S <sub>9</sub>	Sc <sub>18</sub>	0	0	1	2	2	1	1	2	2	2	4	3	10	4	9	2	0	0	1	10
	Sc <sub>19</sub>	0	0	0	1	1	1	2	2	1	1	2	1	7	3	10	0	0	1	0	4
S <sub>10</sub>	Sc <sub>20</sub>	3	2	1	1	2	2	1	2	1	3	4	5	10	3	10	0	0	10	4	0

The value of D, H, and B are assumed as 9, 0.4, and 80, respectively.

Owing to the compatibility condition third module of second component is found to be compatible with the fifth component of first module.

**Steps 4 and 5** Then fuzzy multiobjective is developed and solved using the LINGO software [24]. The following components are selected.

$X = (Sc_{51}, Sc_{61}, Sc_{161}, Sc_{32}, Sc_{92}, Sc_{112}, Sc_{143}, Sc_{153}, Sc_{193}, Sc_{203})$ . The objective function values are:  $\lambda = 0.919$ ,  $ICD = 0.649$  and  $F = 6.85$ .

## 7 Conclusion

In this paper a fuzzy multiobjective optimization model is proposed for selection of components for CBSS development. The selection of components is based on the criteria of having maximum cohesion between components of modules and minimum coupling amongst the components of module. The model is also based on maximizing the function ratings of various COTS components. Compared with the previous studies on CBSS development, the model incorporates constraints on cost, delivery time and compatibility. To obtain the optimal solution a fuzzy algorithm

**Table 3** Cost and delivery time data set of COTS components

Cost						Delivery time					
Module 1		Module2		Module3		Module 1		Module2		Module3	
C <sub>11</sub>	10	C <sub>12</sub>	9	C <sub>13</sub>	8	d <sub>11</sub>	3	d <sub>12</sub>	5	d <sub>13</sub>	6
C <sub>21</sub>	9	C <sub>22</sub>	8	C <sub>23</sub>	9	d <sub>21</sub>	4	d <sub>22</sub>	6	d <sub>23</sub>	4
C <sub>31</sub>	8	C <sub>32</sub>	7	C <sub>33</sub>	6	d <sub>31</sub>	6	d <sub>32</sub>	7	d <sub>33</sub>	9
C <sub>41</sub>	8	C <sub>42</sub>	10	C <sub>43</sub>	7	d <sub>41</sub>	6	d <sub>42</sub>	4	d <sub>43</sub>	7
C <sub>51</sub>	7	C <sub>52</sub>	7	C <sub>53</sub>	8	d <sub>51</sub>	7	d <sub>52</sub>	7	d <sub>53</sub>	6
C <sub>61</sub>	9	C <sub>62</sub>	8	C <sub>63</sub>	9	d <sub>61</sub>	5	d <sub>62</sub>	6	d <sub>63</sub>	4
C <sub>71</sub>	6	C <sub>72</sub>	9	C <sub>73</sub>	6	d <sub>71</sub>	8	d <sub>72</sub>	4	d <sub>73</sub>	8
C <sub>81</sub>	7	C <sub>82</sub>	6	C <sub>83</sub>	7	d <sub>81</sub>	7	d <sub>82</sub>	8	d <sub>83</sub>	7
C <sub>91</sub>	8	C <sub>92</sub>	10	C <sub>93</sub>	10	d <sub>91</sub>	6	d <sub>92</sub>	3	d <sub>93</sub>	3
C <sub>101</sub>	10	C <sub>102</sub>	8	C <sub>103</sub>	8	d <sub>101</sub>	3	d <sub>102</sub>	6	d <sub>103</sub>	6
C <sub>111</sub>	9	C <sub>112</sub>	8	C <sub>113</sub>	7	d <sub>111</sub>	4	d <sub>112</sub>	6	d <sub>113</sub>	7
C <sub>121</sub>	9	C <sub>122</sub>	9	C <sub>123</sub>	9	d <sub>121</sub>	4	d <sub>122</sub>	5	d <sub>123</sub>	5
C <sub>131</sub>	10	C <sub>132</sub>	7	C <sub>133</sub>	8	d <sub>131</sub>	4	d <sub>132</sub>	7	d <sub>133</sub>	6
C <sub>141</sub>	8	C <sub>142</sub>	6	C <sub>143</sub>	9	d <sub>141</sub>	6	d <sub>142</sub>	8	d <sub>143</sub>	4
C <sub>151</sub>	7	C <sub>152</sub>	8	C <sub>153</sub>	6	d <sub>151</sub>	7	d <sub>152</sub>	6	d <sub>153</sub>	8
C <sub>161</sub>	6	C <sub>162</sub>	9	C <sub>163</sub>	7	d <sub>161</sub>	9	d <sub>162</sub>	4	d <sub>163</sub>	7
C <sub>171</sub>	7	C <sub>172</sub>	7	C <sub>173</sub>	10	d <sub>171</sub>	7	d <sub>172</sub>	7	d <sub>173</sub>	3
C <sub>181</sub>	8	C <sub>182</sub>	8	C <sub>183</sub>	7	d <sub>181</sub>	6	d <sub>182</sub>	6	d <sub>183</sub>	7
C <sub>191</sub>	9	C <sub>192</sub>	9	C <sub>193</sub>	8	d <sub>191</sub>	5	d <sub>192</sub>	4	d <sub>193</sub>	6
C <sub>201</sub>	9	C <sub>202</sub>	10	C <sub>203</sub>	6	d <sub>11</sub>	3	d <sub>202</sub>	3	d <sub>203</sub>	8

was developed to get an optimal solution for selection of COTS components. A case study of manufacturing system is also discussed.

### References

1. Gupta, P., Mehlatat, M., Mittal, G., Verma, S.: COTS Selection Using Fuzzy Interactive Approach, pp. 273–289. Springer (2010)
2. Ruiz, M., Ramos, I., Toro, M.: Using Dynamic Model and Simulation to Improve the COTS Software Process, pp. 568–581. Springer, Berlin (2004)
3. Szyperski, C., Pfister, C.: Component-oriented programming: WCOP’96 workshop report (Special issues in object-oriented programming). In: Workshop Reader of the 10th European Conference on Object-Oriented Programming, pp. 127–130 (1996)
4. Belli, F., Jadrzejowich, P.: An approach to reliability optimization of software with redundancy. IEEE Trans. Softw. Eng. **17**(3), 310–312 (1991)
5. Berman, O., Ashrafi, N.: Optimization models for reliability of modular software systems. IEEE Trans. Softw. Eng. **19**(11), 1119–1123 (1993)
6. Berman, O., Kumar, U.D.: Optimization models for recovery block schemes. Eur. J. Oper. Res. **115**, 368–379 (1999)
7. Cortellessa, V., Marinelli, F., Potena, P.: An optimization framework for “build-or-buy” decisions in software architecture. Comput. Oper. Res. (Elsevier Sci.) **35**(10), 3090–3106 (2008)



8. Gupta, P., Verma, S., Mehlawat, M.K.: A membership function approach for cost-reliability trade-off of COTS selection in fuzzy environment. *Int. J. Reliab. Qual. Safety Eng.* **18**(6), 573–595 (2011)
9. Gupta, P., Mehlawat, M.K., Verma, S.: COTS selection using fuzzy interactive approach. *Opt. Lett.* **6**(2), 273–289 (2012)
10. Jha, P.C., Kapur, P.K., Bali, S., Kumar, U.D.: Optimal component selection of COTS based software system under consensus recovery block scheme incorporating execution time. *Int. J. Reliab. Qual. Safety Eng.* **17**(3), 209–222 (2010)
11. Kapur, P.K., Bardhan, A.K., Jha, P.C.: Optimal reliability allocation problem for a modular software system (OPSEARCH). *J. Oper. Res. Soc. India* **40**(2), 133–148 (2003)
12. Kumar, U.D.: Reliability analysis of fault tolerant recovery blocks (OPSEARCH). *J. Oper. Res. Soc. India* **35**(4), 281–294 (1998)
13. Tang, J., Mu, L.F., Kwong, C.K., Luo, X.: An optimization model for software component under multiple applications development. *Eur. J. Oper. Res.* **212**, 301–311 (2011)
14. Wu, Z., Kwong, C.K., Tang, J., Chan, J.: Integrated models for software component selection with simultaneous consideration of implementation and verification. *Comput. Oper. Res. (Elsevier)* **39**, 3376–3393 (2012)
15. Neubauer, T., Stummer, C.: Interactive decision support for multiobjective COTS selection. In: *Proceedings of the 40th Annual Hawaii International Conference on System Sciences (HICSS' 07)*. IEEE (2007)
16. Parsa, S., Bushehrian, O.: A framework to investigate and evaluate genetic clustering algorithms for automatic modularization of software systems. In: *Lecture Notes in Computer Science*, pp. 699–702 (2004)
17. Britoe Abreu, F., Goulao, M.: Coupling and cohesion as modularization drivers: are we being over-persuaded? In: *Proceedings of the 5th European Conference on Software Maintenance and Reengineering* (2001)
18. Carlo, G., Mehdi, J., Dino, M.: *Fundamentals of Software Engineering*. Prentice-Hall, Upper Saddle River (2001)
19. Ian, S.: *Software Engineering*. Addison-Wesley Longman, Reading (2001)
20. Seker, R., van der Merwe, A.J., Kotze, P., Tanik, M.M., Paul, R.: Assessment of coupling and cohesion for component-based software by using Shannon languages. *J. Integr. Des. Process Sci.* **8**(4), 33–43 (2004)
21. Kwong, C.K., Mu, L.F., Tang, J.F., Luo, X.G.: Optimization of software components selection for component-based software system development. *Comput. Ind. Eng.* **58**, 618–624 (2010)
22. Jung, H.W., Choi, B.: Optimization models for quality and cost of modular software systems. *Eur. J. Oper. Res.* **112**(3), 613–619 (1999)
23. Bellman, R.E., Zadeh, L.A.: Decision-making in a fuzzy environment. *Manage. Sci.* **17**(4), B141–B164 (1970)
24. Thiriez, H.: OR software LINGO. *Eur. J. Oper. Res.* **124**, 655–656 (2000)

# Some Issues on Choices of Modalities for Multimodal Biometric Systems

Mohammad Imran, Ashok Rao, S. Noushath and G. Hemantha Kumar

**Abstract** Biometrics-based authentication has advantages over other mechanisms, but there are several variabilities and vulnerabilities that need to be addressed. No single modality or combinations of modalities can be applied universally that is best for all applications. This paper deliberates different combinations of physiological biometric modalities with different levels of fusion. In our experiments, we have selected Face, Palmprint, Finger Knuckle Print, Iris, and Handvein modalities. All the modalities are of image type and publicly available, comprising at least 100 users. Proper selection of modalities for fusion can yield desired level of performance. Through our experiments it is learnt that a multimodal system which is considered just by increasing number of modalities by fusion would not yield the desired level of performance. Many alternate options for increased performance are presented.

**Keywords** Multimodal · Feature level · Score level · Decision level · Fusion

## 1 Introduction

During the recent decades, identity theft has been dramatically increasing at an exponential rate. Cyber-crime is difficult to be prevented and traced. Hence, people are exploring reliable and authentic forms of identity security. Techniques that reliably

---

M. Imran (✉) · G. Hemantha Kumar  
DoS in Computer Science, University of Mysore, Mysore, India  
e-mail: emraangi@gmail.com

G. Hemantha Kumar  
e-mail: ghk.2007@yahoo.com

A. Rao  
Freelance Academician, 165, 11th main, S.Puram, Mysore, India  
e-mail: ashokrao.mys@gmail.com

S. Noushath  
Department of Information Technology, College of Applied Sciences Sohar, Sohar, Oman  
e-mail: noushath.soh@cas.edu.om

identify people play a critical part in our everyday social and commercial activities. Within a scheme of access control to secure system, authorized users should be allowed with high levels of precision while unauthorized users should be denied [1]. Example of such an application includes physical access control to a secure facility as in, e-commerce which provides access to computer networking and welfare distribution. The primary task in an identity management system is in determining an individual's identity. Some of the traditional methods are password-based (knowledge) and ID card-based (token) [2]. In case of the password-based identification system most of us use obvious or randomly guessable passwords such as "password" or our pet names which are insecure and hackers can attack easily. The problem with ID card-based system is that it can be lost or stolen; therefore, they are unsuitable for identity verification in the modern world [3]. Only biometrics can solve all these problems by requiring an additional credential which is something associated with the person's own body traits. The advantages of biometrics over the traditional methods are the following: identification of the rightful owner, user convenience, elimination of repudiation claims, difficulty in being copied or forged, enhanced security, as well as the fact that it cannot be lost, forgotten, or transferred [4].

A number of biometric modalities are being used in various applications. Each biometric trait has its own pros and cons and, therefore the choice of a biometric trait for a particular application depends on a variety of issues besides its recognition rate. In general, several factors must be considered to determine the suitability of a physical or a behavioral trait to be used in a biometric application. When it comes to multimodal biometric systems, a number of issues arise such as how many modalities need to be fused to get 100% GAR? Which are the modalities to be fused? Specifically, which combination of biometric traits gives the best accuracy? These subjective issues are the focus of investigation in this work.

## 2 Review of Literature

Poh et al. [5] in their study, carried out within the framework of the BioSecure DS2 (Access Control) evaluation campaign, organized by the University of Surrey that involved face, fingerprint and iris biometrics for person authentication, targeting the application of physical access control in a medium-size establishment with 500 persons. While multimodal biometrics is a well-investigated subject in the literature, there exists no benchmark for a fusion algorithm comparison. Working to achieve this objective, they designed two sets of experiments: quality-dependent and cost-sensitive evaluation. Loris Nanni et al. [6] presents a novel trained method for combining biometric matchers at the score level. This method is based on a combination of machine learning classifiers trained using the match scores from different biometric approaches as features. The parameters of a finite Gaussian mixture model are used for modeling the genuine and impostor score densities during the fusion.

Ajay Kumar et al. [7] investigated an information theoretic approach for formulating performance indices for the biometric authentication. Initially, they formulate the constrained capacity, as a performance index for biometric authentication system for the finite number of users. Like Shannon capacity, constrained capacity is formulated using signal-to-noise ratio, which is estimated from known statistics of users' biometric information in the database. Lorene Allano et al. [8] addressed the problem of measuring the dependency of multibiometric system scores using Kolmogorov-Smirnov and Mutual Information criteria and studying the validity of performance evaluation on chimeric persons on the NIST-BSSR1 database. Multi-biometric systems can be evaluated on random chimeric persons. It shows that this is not valid for dependent scores and proposed protocol for building cluster-based chimeric persons maintaining the level of dependency between scores. Mingxing He et al. [9] proposed a new robust normalization scheme (Reduction of High-scores Effect normalization) which is derived from the Min–Max normalization scheme. They also show performance of sum rule-based score level fusion and support vector machines (SVM)-based score level fusion. Three biometric traits considered in this are fingerprint, face, and fingervein. Experiments on four different multimodal databases suggest that integrating the proposed scheme, in sum rule-based fusion and SVM-based fusion consistently leads to high accuracy.

Xin Geng et al. [10] proposed context-aware multi-biometric fusion, which can dynamically adapt the fusion rules to the real-time context. As a typical application, the context-aware fusion of gait and face for human identification in video are investigated. Two significant context factors that may affect the relationship between gait and face in the fusion are considered, i.e., view angle and subject-to-camera distance. Fusion methods adaptable to these two factors based on either prior knowledge or machine learning are proposed and tested.

### 3 Proposed Method

The performances of multimodal biometric systems generally give marginal to significant improvement over a unimodal system. This means some more additional information about that person is available that enable improved recognition. Experience shows that improvement in recognition rate ranges from Marginal to Significant. We use this to define the following [11]:

Complementary information: The information available in a multibiometric system that enables significant improvement in recognition rate over a unimodal system.  
Supplementary information: The information available in a multibiometric system that enables marginal improvement in recognition rate over a unimodal system [12].

While it is not a rule, it does imply relying on single (to elicit supplementary information) or heterogeneous (multiple) sensors (to elicit complementary information). For example in Images, Raw Image data can be seen as Supplementary information, whereas the texture data of the same can be seen as Complementary information of the same modality [13]. One of the challenges in multibiometric system seems to

hinge on using just the required information for a given application. These can also be called as Weak (Supplementary) and Strong (Complementary) modalities [11].

Thus, many situations warrant a single sensor from which the supplementary information may be just adequate to get the desired FAR/FRR and it will be a low cost, easy to deploy system. The other extreme is the case of using multiple sensors to get enough Complementary information to get the desired FAR/FRR. These would be complex, expensive, extremely secure access situations like access to Nuclear Reactor site/Defense Laboratories, etc. These are difficult to deploy everywhere solutions [14].

Much of the current work in multimodal are based on fixed number of modalities since it is easy to adopt and yet flexible. There are some issues in multimodal which are still to be answered:

1. How many modalities are needed from the user to identify 100 % correctly?
2. How many acquisition devices we need, to collect the user modalities?
3. Does same feature extractor works on all the modalities which we have taken from user, since some trait performs well to local features (ex: Fingerprint, Iris etc.) others perform well to global features (ex: Face, Palmprint etc.)
4. What mix and in what sequence the modalities that provide Complementary (strong biometric) or Supplementary (weak biometric) are needed to achieve a particular level of FRR/FAR
5. How to solve the curse of dimensionality problem especially at feature level fusion? Particularly so in multibiometric situation?

And some general issues like cost of deployment, enrollment time, throughput time, expected error rate, user habituation, etc., these issues really need to be solved in multimodal biometric systems. We will be answering some of these in this paper.

### ***3.1 Feature Extraction***

A number of feature extraction algorithms for biometrics have been used in research for identification like PCA, KICA, Gabor filter, SIFT features, etc. Every feature extraction algorithm has its own advantages and disadvantages depending on its usage on biometric modality. In our work, we have organized the vast range of biometric feature extraction algorithms into two different levels of features: (a) Appearance based and (b) Textures based, feature extraction algorithms.

In appearance-based feature extraction algorithms, we have used Principal Component Analysis (PCA), Linear Discriminant Analysis (LDA), Locality Preserving Projections (LPP), and Independent Component Analysis1 (ICA1) [15]. In texture-based feature extraction algorithms, we have used Local Binary Patterns Variance (LBPV), Local Phase Quantization (LPQ) and Gabor [16]. The above-mentioned feature extraction algorithms are well known to all and a lot of research has been done on extracting the features using these efficiently. Our main aim is to represent each

modality in the optimal and informative form which is invariant to the deformations that are unavoidably present during extraction of these features.

### 3.2 *Biometrics Fusion Strategies*

Fusion of biometric systems, algorithms and/or traits is a well-known solution to improve authentication performance of biometric systems. Researchers have shown that multi-biometrics, i.e., fusion of multiple biometric evidences, enhances the recognition performance [12]. In biometric systems; fusion can be performed at different levels; Sensor Level, Feature Level, Score Level, and Decision Level Fusion [4].

**Sensor Level Fusion:** Entails the consolidation of evidence presented by multiple sources of raw data before they are subjected to feature extraction. Sensor level fusion can benefit multi-sample systems which capture multiple snapshots of the same biometric.

**Feature Level Fusion:** In feature-level fusion, the feature sets originating from multiple biometric algorithms are consolidated into a single feature set by the application of appropriate feature normalization, transformation, and reduction schemes. The primary benefit of feature-level fusion is the detection of correlated feature values generated by different biometric algorithms and, in the process, identifying a salient set of features that can improve recognition accuracy [14].

**Score Level Fusion:** The match scores output by multiple biometric matchers are combined to generate a new match score (a scalar).

**Decision Level Fusion:** Fusion is carried out at the abstract or decision level when only final decisions are available, this is the only available fusion strategy which fuses the output decision of matcher/classifier.

## 4 Experimental Results

The main objective of an evaluation is to provide consequences of level of fusion under different strategies of multimodal system. We have chosen Face, Palmprint (Pp), Handvein (Hv), and Finger Knuckle Print (FKP) modalities [17–20] and its corresponding best feature extraction algorithm which gives good performance. In all of our experiments, performance of levels of fusion is measured in terms of False Acceptance Rate (FAR) at values 0.01, 0.1 and 1%, its related values of Genuine Acceptance Rate (GAR in %). First, we measure the performance of unimodal biometric system. Further, we evaluate the results for multimodal biometric system; Results obtained from all experiments are tabulated.

### 4.1 Performance Evaluation of Unimodal Systems

We have considered Face, Palmprint (Pp), Handvein (Hv), and Finger Knuckle Print (FKP) as physiological modalities. The performance analyses of the above-mentioned physiological modalities are obtained and tabulated.

Table 1 shows the performance of face modality with respect to appearance- and texture-based algorithms. Among distinct appearance-based feature extraction an algorithm, ICA1, performs relatively well on the face modality with highest values of GAR% for different values FAR%. The LDA also performs better for face modality compared to other feature extraction algorithms like LPP and PCA. The PCA gives lowest GAR% for different values of FAR%; it performs poorly among the appearance based algorithms. From Table 1, it can be observed that LPQ feature extraction algorithm gives the best performance on the face modality with highest GAR% for distinct values of FAR 0.1 and 1 %. Typically, Gabor performs healthier for the face modality compared to appearance-based feature extraction method. The LBPV feature extraction algorithm performs worst compared to all other feature extraction algorithms, with lowest GAR% for different values of FAR%.

Performance of palmprint with respect to both appearance and texture based algorithms are shown in Table 2, ICA1 feature extraction algorithm gives the best performance to the palmprint modality with highest GAR% for distinct values of FAR 0.1 and 1 %. Typically, the LDA also performs healthier for the palmprint modality in comparison to other appearance-based feature extraction methods. The LPP feature extraction algorithm performs worst among other appearance-based methods, with lowest GAR% for different values of FAR%. The performance of Palmprint modality with respect to texture-based algorithms. It can be seen from Table 2 that, among distinct texture-based feature extraction algorithms, LPQ performs relatively well to the Palmprint modality with highest values GAR% for different values of FAR%. The Gabor also performs best for Palmprint modality compared to other feature extraction algorithms.

The performance of appearance- and texture-based algorithms on the handvein modality is summarized in Table 3. It can be seen that PCA feature extraction method

**Table 1** Performance of face modality on different appearance and texture-based feature extraction algorithms

Modality	Feature extraction algorithms	GAR%		
		0.01 %FAR	0.1 %FAR	1 %FAR
Face	PCA	26.0	40.5	56.0
	LDA	26.0	69.5	91.0
	LPP	28.5	46.0	73.0
	ICA1	67.5	81.0	91.5
	LBPV	7.5	9.0	28.5
	Gabor	48.5	65.0	80.5
	LPQ	32.0	80.5	92.0

**Table 2** Performance of palmprint modality on different appearance- and texture-based feature extraction algorithms

Modality	Feature extraction algorithms	GAR%		
		0.01 %FAR	0.1 %FAR	1 %FAR
Palmprint	PCA	27.5	52.0	76.5
	LDA	–	58.5	69.5
	LPP	46.5	50.0	62.0
	ICA1	–	65.5	78.0
	LBPV	27.0	42.0	78.5
	Gabor	86.0	87.5	95.5
	LPQ	61.7	55.5	72.5

**Table 3** Performance of handvein modality on different appearance- and texture-based feature extraction algorithms

Modality	Feature extraction algorithms	GAR%		
		0.01 %FAR	0.1 %FAR	1 %FAR
Handvein	PCA	21.5	34.0	54.0
	LDA	13.0	16.0	30.0
	LPP	3.0	6.0	13.5
	ICA1	32.5	46.0	60.5
	LBPV	5.0	17.0	37.0
	Gabor	33.5	54.0	74.5
	LPQ	26.5	38.0	55.0

performs slightly better than other methods with highest GAR% for different values of FAR%, but the LPP gives worst performance among all methods for handvein. It can be observed in Table 3 that Gabor feature extraction method performs better than other methods with highest GAR% for different values of FAR%, but the LBPV gives worst performance among all texture-based algorithms for handvein.

Table 4 shows the performance of various appearance and texture-based methods on the FKP. Initially at 0.01 and 0.1 %FAR LDA feature extraction algorithm outperforms the handvein modality with highest GAR%. The ICA1 also performs better for FKP modality among other feature extraction algorithms at 1 %FAR. LPP feature extraction algorithm underperforms with lowest GAR% for different values of FAR%. From the results listed in Table 4 that LPQ feature extraction algorithm outperforms on the handvein modality with highest GAR%. The Gabor also performs better for FKP modality among other feature extraction algorithms at 1 %FAR. LBPV feature extraction algorithm underperforms with lowest GAR% for different values of FAR%.



**Table 4** Performance of FKP modality on different appearance and texture based feature extraction algorithms

Modality	Feature extraction algorithms	GAR%		
		0.01 %FAR	0.1 %FAR	1 %FAR
FKP	PCA	50.0	69.5	84.0
	LDA	73.5	78.0	85.0
	LPP	55.0	61.5	74.5
	ICA1	73.0	77.5	86.0
	LBPV	10.0	19.5	40.0
	Gabor	83.0	86.0	90.5
	LPQ	84.0	88.5	92.0

## 4.2 Performance Evaluation of Multimodal Systems

In this section, we have emphasized on comparative analysis of different levels of fusion in multimodal approach on fusion of two, three, and four modalities. The comparison is on sensor, feature, score, and decision level fusion with their relevant fusion rules. Each of the performance is measured in terms of False Acceptance Rate (FAR) at values 0.01, 0.1, 1 %, and its related values of Genuine Acceptance Rate (GAR in %) have been tabulated and discussed in details.

Table 5 shows the different levels of fusion and its strategies on fusion of Face and Palmprint modalities. When we compare each level of fusion, the sum rule in score level fusion outperforms with top GAR% for distinct values of FAR%. Further, the OR rule of decision level fusion perform relatively better; the sensor level fusion under performs with least GAR% for different values of FAR%. At feature level fusion, normalization rules such as, Min–max, Z-score, Median, and

**Table 5** Comparative analysis on performance of different levels of fusion with different rules on fusion of Face (ICA1) and Palmprint (LPQ) in multimodal systems

Fusion	Rules	GAR%		
		0.01 %FAR	0.1 %FAR	1 %FAR
Sensor level	Wavelet based	35.0	48.5	70.5
Feature level	Min–Max	91.0	94.0	95.0
	Z-score	89.5	93.5	98.5
	Tanh	91.0	94.0	95.0
	Median	89.5	93.5	98.5
Score level	Min	85.0	89.5	97.0
	Max	93.8	94.5	99.0
	Sum	95.0	99.0	100
Decision level	OR	94.0	94.5	99.5
	AND	85.0	89.0	97.0

**Table 6** Comparative analysis on performance of different levels of fusion with different rules on fusion of Face (ICA1), Palmprint (LPQ) and FKP (LPQ) in multimodal systems

Fusion	Rules	GAR%		
		0.01 %FAR	0.1 %FAR	1 %FAR
Sensor level	Wavelet based	16.0	39.5	65.5
Feature level	Min–Max	92.0	93.5	97.0
	Z-score	92.5	97.0	99.0
	Tanh	92.5	96.5	97.5
	Median	91.0	96.5	97.5
Score level	Min	95.0	89.5	93.5
	Max	99.5	94.5	99.5
	Sum	99.5	99.0	100
Decision level	OR	95.5	96.0	99.5
	AND	16.0	39.5	65.5

Tanh perform equally well. Hence, all levels of fusion which we have considered perform well compared to their unimodal case, except the sensor level fusion in multimodal approach on fusion Face and Palmprint.

A performance assessment of the results on different levels of fusion of three modalities namely Face, Palmprint, and Finger Knuckle Print is presented in Table 6. The result for each levels of fusion is as follows: at feature level fusion the normalization rules Min–Max, Z-score, Median, and Tanh achieve healthy GAR% for distinct values FAR%. The sum rule of score level fusion gives among the best GAR% for different values of FAR 0.01, 0.1 and 1 % are 99.5, 99 and 100 % respectively. The other rules of score level fusion perform equally better compared to their prior version of fusion of two modalities. At Decision level fusion OR and AND rules also perform well. Sensor level fusion is the only one fusion method which performs poorest amongst all the levels of fusion and also compared to its earlier fusion of two modalities.

Table 7 summarizes the overall performances of different levels of fusion and its fusion rules on fusion of four modalities namely Face, Palmprint, FKP, and Handvein. Each level of fusion can be compared in Table 7, wavelet base image fusion rule of sensor level is the only fusion scheme which is most abominable on fusion of the above-mentioned modalities. The other fusion schemes are as follows: at feature level there is no significant improvement in performance when compared to its previous fusion of three modalities with respect to its normalization schemes explicitly, Min–Max, Z-score, Median, and Tanh. The score level fusion sum rule achieves best GAR% of 99.5, 100, and 100 with distinct values of FAR% of 0.01, 0.1, and 1 respectively. The other rules of score level fusion, viz., Min and Max rules perform better for GAR% at values FAR% of 0.1 and 1. In decision level fusion both AND and OR rules execute less GAR% for different values of FAR% compared to its previous case fusion of three modalities.

**Table 7** Comparative analysis on performance of different levels of fusion with different rules on fusion of Face (ICA1), Palmprint (LPQ), FKP (LPQ), and Handvein (Gabor) in multimodal systems

Fusion	Rules	GAR%		
		0.01 %FAR	0.1 %FAR	1 %FAR
Sensor level	Wavelet based	11.0	20.0	43.0
Feature level	Min–Max	92.0	96.5	97.0
	Z-score	92.5	97.0	99.0
	Tanh	92.5	96.5	97.5
	Median	92.5	96.5	97.5
Score level	Min	87.0	92.0	95.0
	Max	93.8	94.5	99.0
	Sum	99.5	100	100
Decision Level	OR	94.5	95.0	99.5
	AND	87.5	91.5	93.5

## 5 Conclusion

From the analysis of experimental results and observations one can conclude:

1. Choice of modality is application and context dependent.
2. Performance of the feature extraction algorithm is significantly subjective on the choice of biometric modality.
3. Although all the chosen modalities are of image type (Face, Palmprint, Finger Knuckle Print, and Handvein), the performance variation is quite significant. The worst being (handvein) and the best being (Finger Knuckle Print) in unimodal case.
4. While improved performance is available with increasing additional modalities, their choice and number are very critical.
5. One observes significant change from unimodal to biomodal case. However, further addition of modalities does not yield comparable improvement. There is tendency toward saturation with every additional modality.
6. Performance of multimodal system depends on the level of fusion.
7. In general, for two or more modalities under fusion the performance in decreasing order is as follows: score level, feature level, decision level, and sensor level.
8. Too much is too bad: It is necessary to recognize that, by simply increasing the number of modalities to be fused to get a desired level of performance is poor strategy. A proper selection of lesser number of modalities efficient feature extraction, levels of fusion and fusion rules all constitute to desire level of performance, even if the modalities are few.

**Acknowledgments** The research leading to these results has received Research Project Grant Funding from the Research Council of the Sultanate of Oman Research Grant Agreement No [ORG MoHE ICT 10 023].

## References

1. Nandakumar, K., Jain, A.K., Ross, A.: Introduction to Biometrics. Springer, New York (2011)
2. Ross, A., Jain, A.K., Prabhakar, S.: An introduction to biometric recognition. *IEEE Trans. Circuits Syst. Video Technol.* **14**, 44–48 (2004)
3. Jain, A.K., Flynn, P.J., Ross, A.: Handbook of Biometrics. Springer, New York (2008)
4. Kumar, A., Zhang, D.: Combining fingerprint, palmprint and hand-shape for user authentication. *ICPR* **4**, 549–552 (2006)
5. Poh, N., Bourlai, T., Kittler, J., Allano, L., Alonso-Fernandez, F., Ambekar, O., Baker, J.P., Dorizzi, B., Fatukasi, O., Fiérrez-Aguilar, J., Ganster, H., Ortega-García, J., Maurer, D.E., Ali Salah, A., Scheidat, T., Vielhauer, C.: Benchmarking quality-dependent and cost-sensitive score-level multimodal biometric fusion algorithms. *IEEE Trans. Inf. Forensics Sec.* **4**(4), 849–866 (2009)
6. Nanni, L.: Lumini, Alessandra, Brahnam, Sheryl: likelihood ratio based features for a trained biometric score fusion. *Expert Syst. Appl.* **38**(1), 58–63 (2011)
7. Bhatnagar, J., Kumar, A.: On estimating performance indices for biometric identification. *Pattern Recognit.* **42**(9), 1803–1815 (2009)
8. Allano, L., Dorizzi, B., Garcia-Salicetti, S.: A new protocol for multi-biometric systems' evaluation maintaining the dependencies between biometric scores. *Pattern Recognit.* **45**(1), 119–127 (2012)
9. He, M., Horng, S.-J., Fan, P., Run, R.-S., Chen, R.-J., Lai, J.-L.: Muhammad Khurram Khan, Kevin Octavius Sentosa: Performance evaluation of score level fusion in multimodal biometric systems. *Pattern Recognit.* **43**(5), 1789–1800 (2010)
10. Geng, X.: Smith-Miles, K., Wang, L., Li, M., Qiang, W.: Context-aware fusion: a case study on fusion of gait and face for human identification in video. *Pattern Recognit.* **43**(10), 3660–3673 (2010)
11. Imran, M., Rao, A., Hemanthakumar, G.: Extreme subjectivity of multimodal biometrics solutions: role of strong and weak modalities/features information. In: Proceedings of IICAI 2011, pp. 1587–160
12. Kittler, J., Fumera, G., Roli, F., Muntoni, D.: An Experimental Comparison of Classifier Fusion Rules for Multimodal Personal Identity Verification System. Springer, Berlin (2002)
13. Yang, F., Ma, B.: A new mixed-mode biometrics information fusion based-on fingerprint, hand-geometry and palm-print. Fourth International Conference on Image and Graphics, 2007, ICIG 2007, 22–24 Aug 2007, pp. 689–693
14. Sim, T., Zhang, S., Janakiraman, R., Kumar, S.: Continuous verification using multimodal biometrics. *IEEE Trans. Pattern Anal. Mach. Intell.* **29**(4), 687–700 (April 2007)
15. Rao, A., Noushath, S.: Subspace methods for face recognition. *Comput. Sci. Rev.* **4**(1), 1–17 (2010)
16. Ojansivu, V., Heikkilä, J.: Blur insensitive texture classification using local phase quantization. In: ICISP, pp. 236, 243 (2008)
17. Zhu, L.-q., Zhang, S.-y.: Multimodal biometric identification system based on finger geometry, knuckle print and palm print. *Pattern Recogn. Lett.* **31**(12), 1641–1649 (2010)
18. [http://rv11.ecn.purdue.edu/~aleix/aleix\\_face\\_DB.html](http://rv11.ecn.purdue.edu/~aleix/aleix_face_DB.html)
19. [www.comp.polyu.edu.hk/~biometrics](http://www.comp.polyu.edu.hk/~biometrics)
20. Heenaye-Mamode Khan, M., Subramanian, R.K., Mamode Khan, N.A.: Low dimensional representation of dorsal hand vein features using principle component analysis (pca). World Academy of Science, Engineering and Technology, vol. 49, pp. 1001–1007 (2009)

# An Adaptive Iterative PCA-SVM Based Technique for Dimensionality Reduction to Support Fast Mining of Leukemia Data

Vikrant Sabnis and Neelu Khare

**Abstract** Primary Goal of a Data mining technique is to detect and classify the data from a large data set without compromising the speed of the process. Data mining is the process of extracting patterns from a large dataset. Therefore the pattern discovery and mining are often time consuming. In any data pattern, a data is represented by several columns called the linear low dimensions. But the data identity does not equally depend upon each of these dimensions. Therefore scanning and processing the entire dataset for every query not only reduces the efficiency of the algorithm but at the same time minimizes the speed of processing. This can be solved significantly by identifying the intrinsic dimensionality of the data and applying the classification on the dataset corresponding to the intrinsic dataset only. Several algorithms have been proposed for identifying the intrinsic data dimensions and reducing the same. Once the dimension of the data is reduced, it affects the classification rate and classification rate may drop due to reduction in number of data points for decision. In this work we propose a unique technique for classifying the leukemia data by identifying and reducing the dimension of the training or knowledge dataset using Iterative process of Intrinsic dimensionality discovery and reduction using Principal Components Analysis (PCA) technique. Further the optimized data set is used to classify the given data using Support Vector Machines (SVM) classification. Results show that the proposed technique performs much better in terms of obtaining optimized data set and classification accuracy.

---

V. Sabnis (✉)

Maulana Azad National Institute of Technology, Bhopal, India  
e-mail: vikrant\_sabnis@rediffmail.com

N. Khare

VIT University Vellore, Vellore, Tamilnadu, India  
e-mail: neelu.khare@vit.ac.in

**Keywords** Principle component analysis · Support vector machine · Dimensionality reduction · Eigen value · Local PCA

## 1 Introduction

Leukemia [8] is a type of cancer of the blood or bone marrow characterized by abnormal increase of white blood cells. Leukemia is a broad term covering a spectrum of diseases. It is generally detected from the blood cell structure and is the cause of significant increase in WBC (white blood Cells). It is generally categorized into two broader categories: Chronic and Acute. In this work we classify a given pattern into one of the acute Leukemia types, i.e., Acute lymphoblastic leukemia (ALL) and Acute myelogenous leukemia (AML). We use dataset of Leukemia provided by [7] for data training and classification.

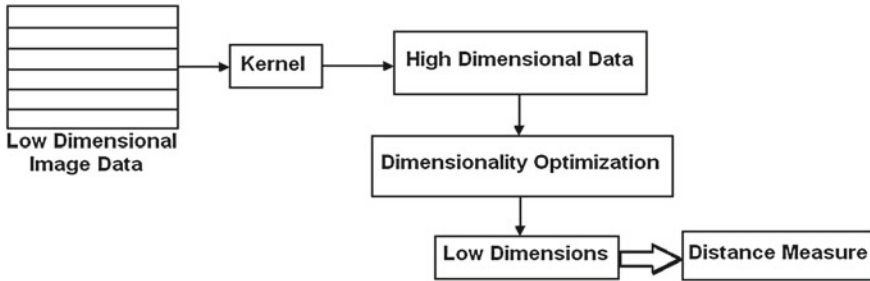
The dataset has 7,200 dimensions for each pattern. Mining through entire dataset with such a huge number of dimension not only consumes time but at the same time reduces the efficiency of the classification to a great deal due to correlated and irrelevant data in the training and classification process.

Therefore, we adopt dimensionality reduction to mark the optimum dimensions and columns such that training and classification is fast and accurate.

One of the most common approach of representing the underneath pattern in any dataset is through certain kernels which are linear or nonlinear machines that can represent a dataset as a set of functional models and model coefficients [5]. The kernel techniques are nothing but mapping low-dimensional data with many columns into a high-dimensional feature space with fewer columns which are essentially model parameters for these functions. The higher the accuracy desired for patterns the higher would be dimensional plane of representation.

A unique way to efficiently deal with highly dense dataset is to reduce the number of dimensions obtained through a kernel through a mapping function such that the low dimensions retain the same information as their high-dimensional counterpart. The low dimensionality brings down computational complexity as well as spatial requirement. The concept is represented by Fig. 1.

High-dimensional data are difficult to visualize and therefore deriving an appropriate distance measure between two points in high dimensional datasets are difficult. For example, the distance between two points in  $x$ - $y$  plane can be easily obtained through Euclidean distance but the distance between the same points over  $x$ ,  $y$  and  $z$  plane are difficult to represent. This anomaly stands through for any type of dimensions representing any type of features. Therefore, a distance measure in the high dimensional data space stands a risk of returning a null set. The solution to the problem is known as multidimensional scaling [5] which is nothing but dimension reduction technique. The dimensionality reduction technique is further divided into two types (1) Linear mapping (2) Nonlinear mapping. A linear mapping is



**Fig. 1** Dimensionality mapping from high to low through Kernel-based technique

a method of transforming data objects from one dimension to another dimension through a linear quadratic equation or a direct mapping function or some look up tables. Real-time objects and the data are rarely bounded by linearity measures. Had it been so, there would not have any requirement for enhancing the dimension itself. Therefore, we assume that dimensional scaling or reduction is a nonlinear approach.

## 2 Methodology

### 2.1 Overall Technique

Identified intrinsic dataset and the reduced data do not always reciprocate the actual data behavior. Therefore, we use an iterative process to first dividing the entire dataset into two hypothetical parts. We use a part as training and another as testing. We calculate the intrinsic dimension of the training data and minimize the dataset using PCA to number of intrinsic dimension obtained. Now we apply the classification to the test dataset. The efficiency is calculated. If the efficiency is bellowing the desired threshold of 90%, we increase the dimension in the step of 1. This process is continued till the desired accuracy is obtained. Once the accuracy is obtained, we increase the hypothetical training data by 50% by migrating 50% of the test data and measure the efficiency once more. This process is continued till the optimum solution is reached. The iteration is stooped for optimum solution and the parameters are globally accepted as the trusted parameters for the classification process.

The training dataset is reduced with the number of dimension achieved through the above process and test data is classified against the reduced data.

## 2.2 MLE-Based Intrinsic Dimensionality Identification

The existing approaches to estimating the intrinsic dimension can be roughly divided into two groups: eigenvalue or projection methods, and geometric methods. Eigen value methods, from the early proposal of to a recent variant are based on a global or local PCA, with intrinsic dimension determined by the number of eigenvalues greater than a given threshold. Global PCA methods fail on nonlinear manifolds, and local methods depend heavily on the precise choice of local regions and thresholds. The eigenvalue methods may be a good tool for exploratory data analysis, where one might plot the eigenvalues and look for a clear-cut boundary, but not for providing reliable estimates of intrinsic dimension.

We first estimate intrinsic dimension of a dataset derived by applying the principle of maximum likelihood to the distances between close neighbors. We derive the estimator by a Poisson process approximation, assess its bias and variance theoretically and by simulations, and apply it to a number of simulated and real datasets. We also show it has the best overall performance compared with two other intrinsic dimension estimators.

Here, we derive the maximum likelihood estimator (MLE) of the dimension  $m$  from i.i.d. observations  $X_1, \dots, X_n$  in  $\mathbb{X}^p$ . The observations represent an embedding of a lower dimensional sample, i.e.,  $X_i = g(Y_i)$ , where  $Y_i$  are sampled from an unknown smooth density  $f$  on  $\mathbb{R}^m$ , with unknown  $m \leq p$ , and  $g$  is a continuous and sufficiently smooth (but not necessarily globally isometric) mapping. This assumption ensures that close neighbors in  $\mathbb{R}^m$  are mapped to close neighbors in the embedding.

The basic idea is to fix a point  $x$ , assume  $f(x) \approx \text{const}$  in a small sphere  $S_x(R)$  of radius  $R$  around  $x$ , and treat the observations as a homogeneous Poisson process in  $S_x(R)$ . Consider the inhomogeneous process  $\{N(t, x), 0 \leq t \leq R\}$ ,

$$N(t, x) = \sum_{i=1}^n 1\{X_i \in S_x(t)\} \quad (1)$$

which counts observations within distance  $t$  from  $x$ . Approximating this binomial (fixed  $n$ ) process by a Poisson process and suppressing the dependence on  $x$  for now, we can write the rate  $\lambda(t)$  of the process  $N(t)$  as;

$$\lambda(t) = f(x)V(m)mt^{m-1} \quad (2)$$

This follows immediately from the Poisson process properties since  $V(m)mt^{m-1} = \frac{d}{dt} [V(m)t^m]$  is the surface area of the sphere  $S_x(t)$ . Letting  $\theta = \log f(x)$ , we can write the log-likelihood of the observed process  $N(t)$  as



$$L(m, \theta) = \int_0^R \log \lambda(t) dN(t) - \int_0^R \lambda(t) dt \tag{3}$$

This is an exponential family for which MLEs exist with probability  $\rightarrow 1$  as  $n \rightarrow \infty$  and are unique. The MLEs must satisfy the likelihood equations

$$\frac{\partial L}{\partial \theta} = \int_0^R dN(t) - \int_0^R \lambda(t) dt = N(R) - e^\theta V(m) R^m = 0 \tag{4}$$

$$\frac{\partial L}{\partial m} = \left( \frac{1}{m} + \frac{V'(m)}{V(m)} \right) N(R) + \int_0^R \log t dN(t) - e^\theta V(m) R^m \left( \log R + \frac{V'(m)}{V(m)} \right) = 0 \tag{5}$$

Substituting (5) in (6) gives the MLE for  $m$ :

$$\hat{m}_R(x) = \left[ \frac{1}{N(R, x)} \sum_{j=1}^{N(R,x)} \log \frac{R}{T_j(x)} \right]^{-1} \tag{6}$$

In practice, it may be more convenient to fix the number of neighbors  $k$  rather than the radius of the sphere  $R$ . Then the estimate in (7) becomes

$$\hat{m}_k(x) = \left[ \frac{1}{k-1} \sum_{j=1}^{k-1} \log \frac{T_k(x)}{T_j(x)} \right]^{-1} \tag{7}$$

Note that we omit the last (zero) term in the sum in (6) and divide by  $k - 1$  rather than  $k$  since that makes the estimator approximately unbiased, as we show below. Also note that the MLE of  $\theta$  can be used to obtain an instant estimate of the entropy of  $f$ .

### 2.3 PCA-Based Dimension Reduction

Once the exact hidden dimension is obtained through maximum likelihood intrinsic dimensionality finding technique, the data needs to be reduced using PCA.

One of the most common forms of dimensionality reduction is PCA [6]. Given a set of data, PCA finds the linear lower dimensional representation of the data such

that the variance of the reconstructed data is preserved. Intuitively, PCA finds a low-dimensional hyperplane such that, when we project our data onto the hyperplane, the variance of our data is changed as little as possible. A transformation that preserves variance seems appealing because it will maximally preserve our ability to distinguish between beliefs that are far apart in Euclidean norm. As we will see below, however, Euclidean norm is not the most appropriate way to measure distance between beliefs when our goal is to preserve the ability to choose good actions.

We first assume we have a data set of  $n$  beliefs  $\{b_1, \dots, b_n\} \in \mathbb{B}$ , where each belief  $b_i$  is in  $\mathbb{B}$ , the high-dimensional belief space. We write these beliefs as column vectors in a matrix  $B = [b_1 | \dots | b_n]$ , where  $B \in \mathbb{R}^{|S| \times n}$ . We use PCA to compute a low-dimensional representation of the beliefs by factoring  $B$  into the matrices  $U$  and  $\tilde{B}$ ,

$$B = U\tilde{B}^T. \quad (8)$$

In Eq. (8),  $U \in \mathbb{R}^{|S| \times l}$  corresponds to a matrix of bases that span the low-dimensional space of  $l < |S|$  dimensions.  $\tilde{B} \in \mathbb{R}^{n \times l}$  represents the data in the low-dimensional space. From a geometric perspective,  $U$  comprises a set of bases that span a hyperplane  $\tilde{B}$  in the high-dimensional space of  $\mathbb{B}$ ;  $\tilde{B}$  are the co-ordinates of the data on that hyperplane. If no hyperplane of dimensionality  $l$  exists that contains the data exactly, PCA will find the surface of the given dimensionality that best preserves the variance of the data, after projecting the data onto that hyperplane and then reconstructing it. Minimizing the change in variance between the original data  $B$  and its reconstruction  $U\tilde{B}^T$  is equivalent to minimizing the sum of squared error loss:

$$L(B, U, \tilde{B}) = \left\| B - U\tilde{B}^T \right\|_F^2 \quad (9)$$

## 2.4 Pre-Classification

Once the training or the knowledge data is reduced, the test dataset is classified. Now most important thing to notice here is that once a dataset is reduced to high dimension or fewer columns, these columns are no more linearly associated with the exact data values. Therefore, number of columns in the test data and the actual knowledge data and their dimensions will also be different. Therefore a normal data cannot be classified against a reduced dataset.

Therefore first the given test data needs to be considered as the part of the knowledge data and the entire set of knowledge data and one test data is subjected to dimensionality reduction as a single set. Once the reductionality is achieved, the test data is separated and is classified.

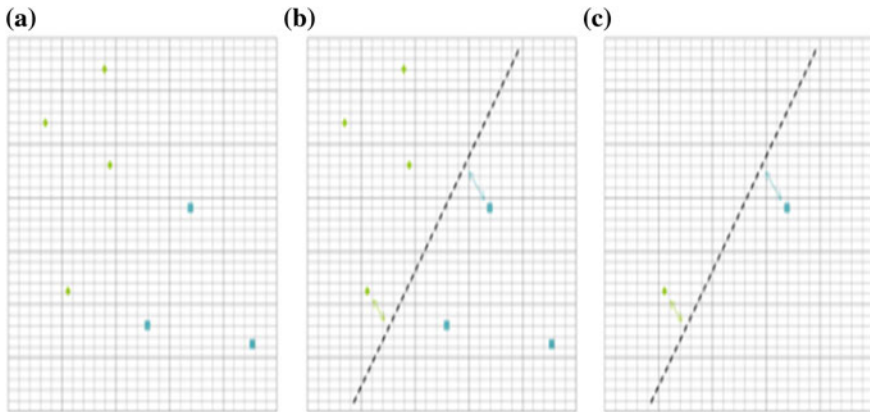


Fig. 2 Support vector machine as a maximum margin classifier

### 2.5 Support Vector Machine as Classification

SVMs is a supervised learning method which can be used for both classification and regression. In its simplest form, given two set of data points with same dimensions, SVM can form a decision model so that a new set of points can be classified as either of the two input points. If the examples are represented as points in space, a linear SVM model can be interpreted as a division of this space so that the examples belonging to separate categories are divided by a clear gap that is as wide as possible. New examples are then predicted to belong to a category based on which side of the gap they fall on (as explained in Fig. 2).

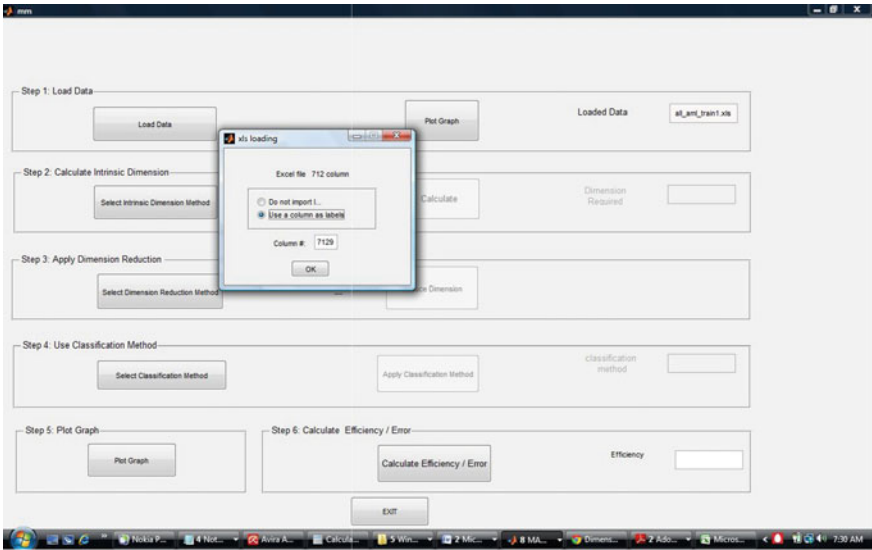
The (A) shows a decision problem for two classes, blue and green. (B) Shows the hyperplane which has the largest distance to the nearest training data points of each class. (C) Shows that only two data points are needed to define this hyperplane. Those will be taken as support vectors, and will be used to guide the decision process of new input data which needs to be classified.

A linear support vector machine is composed of a set of given support vectors  $\mathbf{z}$  and a set of weights  $\mathbf{w}$ . The computation for the output of a given SVM with  $N$  support vectors  $z_1, z_2, \dots, z_N$  and weights  $w_1, w_2, \dots, w_N$  is then given by:

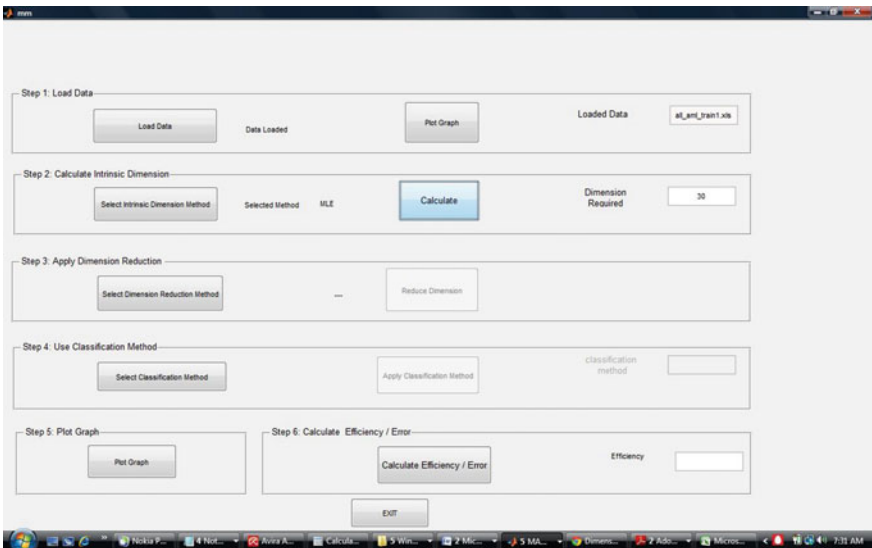
$$F(x) = \sum_{i=1}^N w_i \langle z_i, x \rangle + b \tag{10}$$

A decision function is then applied to transform this output in a binary decision. Usually,  $\text{sign}(\cdot)$  is used, so that outputs greater than zero are taken as a class and outputs lesser than zero are taken as the other.

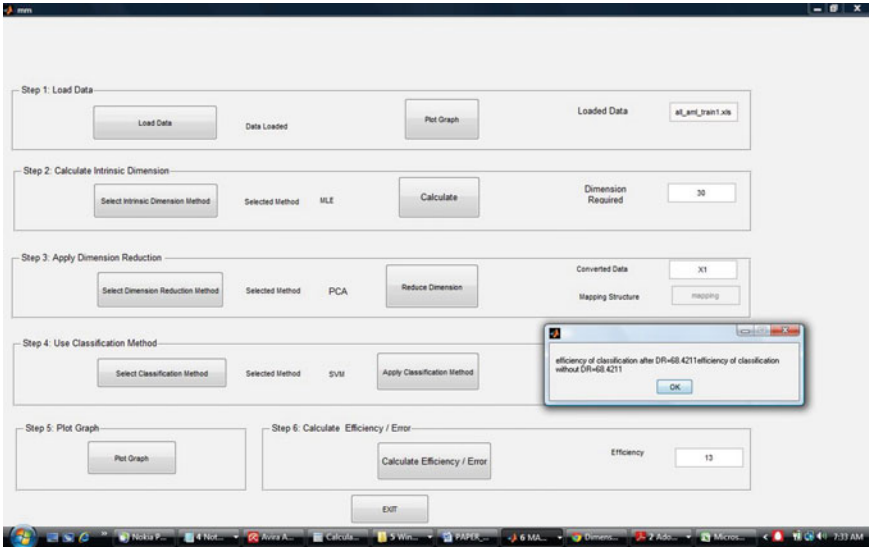
### 3 Results and Discussion



Loading of dataset with huge number of columns



Intrinsic Dimension Obtained by MLE. 7,200 column of data is reduced to 30 Columns



Classification Step

### 4 Graphs

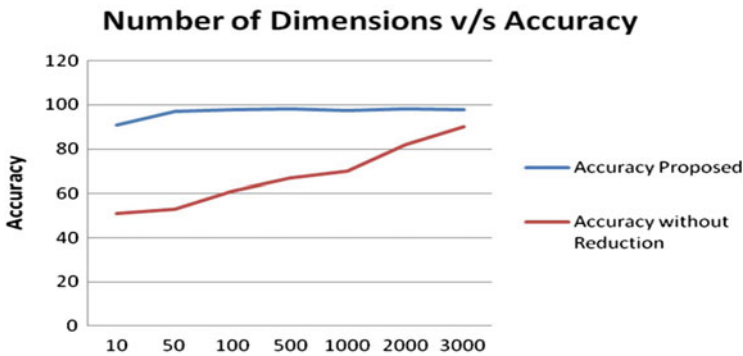
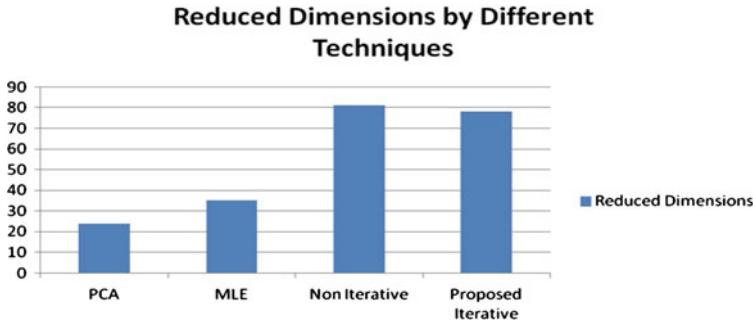


Figure shows that higher number of dimensions results in better accuracy only in the case of linear mapping where numbers of dimensions are linearly dependent on each other. But once the data is reduced by a nonlinear mapping fewer number of data has as much accuracy as higher number of dataset.



Shows that PCA and MLE finds out the optimum dimensions in a dataset. But the efficiency of the system for both is extremely low (69%). Hence it can be concluded that though PCA and MLE together can resolve the intrinsic dimensionality of the data, they cannot identify the dimensionality which will result in better accuracy.

## 5 Conclusion

Dimensionality reduction in data mining is not a new task. Conventionally various techniques are being proposed toward this direction that reduces the data before processing. But in features data such as any medical patterns, dimensionality reduction may result in loss of accuracy in overall mining process due to the inherent relationship among the data set. Applying dimension reductionality must be combined with appropriate recognition rate in order to achieve good accuracy. The technique finds out the intrinsic dimensionality based on the MLE and by checking the efficiency of the system at each iteration. Therefore, the method not only succeeds to minimize the dimensionality for speeding up the processing but also preserves the accuracy of the recognition. A medical database was chosen to prove the theory due to sensitiveness of the data in such a database. Results show significant performance consistency over different iterations. Results also show that for optimum intrinsic dimensionality, the accuracy is better than nonreduced dataset. But the experiments also shows that due to nonlinear mapping of the dataset, linear kernels cannot be applied and polynomial kernels with appropriate optimization is better suited for the task. Another major observation was that the test vectors independently cannot be used to derive the data dependency and therefore needs to be processed with the knowledge data or the training vectors in order to acquire the dimensions of the test vectors also. Therefore a future work can be designed to obtain the actual mapping function for the knowledge data which can then be used to extract the needed dimensions from the test set without test set being simulated with the knowledge base for extracting the intrinsic dimensions of the test set.

## References

1. <http://en.wikipedia.org/wiki/Leukemia>
2. [http://en.wikipedia.org/wiki/Microarray\\_databases](http://en.wikipedia.org/wiki/Microarray_databases)
3. <http://www.ncbi.nlm.nih.gov/geo/>
4. Jing, L., Shuzhong, L., Ming, L., Jianyun, N.: Application of dimensionality reduction analysis to fingerprint recognition. In: Proceedings of 2008 International Symposium on Computational Intelligence and Design, iscid, vol. 2, pp. 102–105 (2008)
5. Lespinats, S., Verleysen, M., Giron, A., Fertil, G.: DD-HDS: a method for visualization and exploration of high-dimensional data. *IEEE Trans. Neural Netw.* **18**(5), 1265–1279 (2007)
6. Segall, R. S., Pierce, R. M.: Data mining of Leukemia cells using self-organized maps. In: Proceedings of 2009 ALAR Conference on Applied Research in Information Technology, 13 February (2009)
7. Segall, R. S.: Data mining of microarray databases for the analysis of environmental factors on corn and maize. In: Proceedings of the 2005 Conference of Applied Research in Information Technology, Sponsored by Acxiom Laboratory for Applied Research (ALAR), University of Central Arkansas, 18 February (2005)
8. Segall, R.S.: Data mining of microarray databases for the analysis of environmental factors on plants using cluster analysis and predictive regression. In: Proceedings of the Thirty-sixth Annual Conference of the Southwest Decision Sciences Institute, vol. 36, no. 1, Dallas, TX, 3–5 March (2005)

# Social Evolution: An Evolutionary Algorithm Inspired by Human Interactions

R. S. Pavithr and Gursaran

**Abstract** Inherent intelligent characteristics of humans, such as human interactions and information exchanges enable them to evolve more rapidly than any other species on the earth. Human interactions are generally selective and are free to explore randomly based on the individual bias. When the interactions are indecisive, individuals consult for second opinion to further evaluate the indecisive interaction before adopting the change to emerge and evolve. Inspired by such human properties, in this paper a novel social evolution (SE) algorithm is proposed and tested on four numerical test functions to ascertain the performance by comparing the results with the state-of-the-art soft computing techniques on standard performance metrics. The results indicate that, the performance of SE algorithm is better than or quite comparable to the state-of-the-art nature inspired algorithms.

**Keywords** Society and civilization · Social evolution · optimization

## 1 Introduction

Nature inspired computing is one of the main branches of natural computing techniques and an emerging computational paradigm for solving large-scale complex and dynamic real-world problems. Nature inspired computing builds on the principles of emergence, self-organization, and complex systems [1]. One of the main objectives of the nature inspired computing paradigm is to provide alternative stochastic, nature inspired search-based techniques to problems that have not been

---

R. S. Pavithr (✉) · Gursaran  
Dayalbagh Educational Institute, Dayalbagh, Agra, India  
e-mail: rspavithr@ieee.org

Gursaran  
e-mail: gursaran.db@gmail.com



(satisfactorily) resolved by traditional deterministic algorithmic techniques, such as linear, nonlinear, and dynamic programming, etc [2].

Some of the interesting algorithms inspired by the natural phenomena are:

- Algorithms inspired by biology
- Algorithms Inspired by the behavior of groups of agents (Swarm)
- Algorithms inspired by human interactions and beliefs in the society.

For the past two decades, the research in the nature inspired evolutionary algorithms has been focused upon algorithms inspired by biological processes [3–7] and intelligent foraging behavior of social insects such as ants, birds, bees. For example, in the natural ant system, ants interact with each other indirectly by sharing the Pheromone trails. Swarm intelligence can be defined as “a property of a system of unintelligent agents of limited individual capabilities exhibiting collective intelligent behavior” [8]. Inspired by natural ant system, artificial ant colony optimization was designed and successfully implemented for many practical complex applications. Mimicking the behavior of flying birds, Kennedy and Ebergart [9] introduced another popular swarm-based evolutionary algorithm called particle swarm optimization. Artificial bee colony (ABC) algorithm is another stochastic search-based technique that belongs to class of swam intelligence-based algorithms, which is inspired by the intelligent behavior of the honeybees [10].

In 1994, Reynolds, designed a new algorithm called Cultural algorithm inspired by human interactions and beliefs and he argued that, “the cultural evolution enables the societies to evolve or adapt to their environments at rates that exceed that of biological evolution based on genetic inheritance only” [11]. Cultural algorithms are a class of computational models of cultural evolution that support dual inheritance, from belief space and individual interactions. This model of dual-inheritance is the key feature of Cultural Algorithms which is built on the principles of Renfrew’s THINKS model [11] and which allows for a two-way system of learning and adaptation to take place. Reynolds and his team observed that, various knowledge sources like topographic knowledge, situational knowledge, and the fine-grained knowledge interact at the cultural level representing the Cultural Swarm, i.e., swarming behavior [12–14]. The early cultural evolution was modeled and studied based on single agent and multiagents to explore the impact of decision-making methods and resource sharing methods on population survival [15, 16].

Ray and Liew [17], inspired by nature’s complex intra- and intersociety interactions, proposed an algorithm called society and civilization algorithm (SCA), in which, the artificial societies are build and the leader of the society is identified. The individuals collaborate with the leader and other individuals in the society to evolve. The leader will extend collaboration and communication with the other society leaders, in the civilization in order to improve. This may lead to migration of leaders and individuals to better performing societies. The SCA was implemented on engineering optimizations problems to demonstrate effectiveness of the algorithm.

Nature inspired evolutionary algorithms that emulate the behavior of living organisms and species integrated interactions among the agents for generating the next

generation solution space. The outcome of these, interactions are either positive or negative based a random value compared with the algorithm specific control parameter. What if, the outcome of these interactions is indecisive? Indecisive interactions are also one of the outcomes of an interaction which may also need an attention to be accounted in the evolution process. Humans are intelligent species and are capable of withholding the information from the indecisive interaction in the memory and further evaluate, before adopting the change. The indecisive interactions drive the individual to seek a second opinion to build on the exchanged information from the previous interaction to emerge and evolve which is a common behavior with the people in the society.

In a society, in the process of evolution, individuals interact and exchange information. Human's interactions are generally selective and are free to explore randomly based on the individual bias. The individuals initially extend the interactions within the neighborhood because of affinity and trust worthiness. But, the interactions, does not get limited to neighborhood only. The individual is free to extend the interactions with the society in the process of evolution, particularly, when these interactions does not offer better prospects for growth or purely based on personal choice.

Motivated by such human characteristics, this paper introduces social evolution (SE) algorithm that employs the concept of second opinion and freedom of interactions to enable the individual's evolution leading to social evolution.

## 2 Social Evolution Algorithm

The pseudo code of SE algorithm is presented below:

### 1. Initialization:

- Initialize Control parameters
  - Maximum Cycle Number (MCN)
  - Neighborhood Cooperation factor (NCR)
  - Quality of Interaction (QI)
  - Indecisive Factor (IFD)
  - Second Opinion (Neighbor Best)–NB
  - Second Opinion (Average Best)–AB
  - Second Opinion (Society Best)–SB
- Initialize the population

### 2. Evaluation Phase:

- Evaluate the fitness of each individual
- Calculate the probability of each individual and average solution
- Store the best solution in the community

### 3. Cycle = 0

### 4. REPEAT when Cycle < Maximum cycle number

5. Interaction Phase:

REPEAT (for all the individuals in the society)

- Allow Individuals to interact based on their ability to interact (probabilistically).
- Freedom of interaction:
  - Identify the neighbors based on von Neumann architecture
  - Store the best in the neighborhood
  - Choose between the random neighbor and a random individual based on the cooperation factor and fitness
- Produce the new solution  $v_i$  for each individual using (1)

$$V_{ij} = X_{ij} + \emptyset_{ij}(X_{ij} - X_{kj}) \quad \text{if } R_j < \text{QI},$$

*Otherwise, evaluate IDF* (1)

$[\emptyset_{ij}]$ — is a Emotion Quotient—a random number in the range  $[-1, 1]$ .  $k \in \{1, 2, \dots, \text{SN}\}$  (SN: Number of individuals in a society) is randomly chosen index within the neighborhood/society of the individual. Although  $k$  is determined randomly, it has to be different from  $i$ .  $R_j$  is a randomly chosen real number in the range  $[0, 1]$  and  $j \in \{1, 2, \dots, \text{D}\}$  (D: Number of dimensions in a problem). [QI, Quality of interaction, is a control parameter].

- Process of second opinion
  - Evaluate the Indecisive Factor (IDF)
    - If  $\text{Rand}() > \text{IDF}$ , –  $V_{ij} = X_{ij}$
    - If  $\text{Rand}() < \text{IDF}$  – Look out for second opinion
  - Seek Second opinion and build on the previous interaction
    - If  $\text{Rand}() < \text{NB}$

$$V_{ij} = V_{ij} + \emptyset_{ij}(V_{ij} - X_{ij}) \tag{2}$$

$1 \in \{1, 2, \dots, \text{SN}\}$  is index of the neighborhood best

- If  $\text{Rand}() < \text{AB}$

$$V_{ij} = V_{ij} + \emptyset_{ij}(V_{ij} - A_j) \tag{3}$$

A is the average individual and  $j \in \{1, 2, \dots, \text{D}\}$

- If  $\text{Rand}() < \text{SB}$

$$V_{ij} = V_{ij} + \emptyset_{ij}(V_{ij} - X_{mj}) \tag{4}$$

$m \in \{1, 2, \dots, \text{SN}\}$  is index of the best in the society.

- Evaluate the fitness of the individual before and after interaction and consider the best for next generation

6. UNTIL for all the individuals in the society are processed
7. Calculate the probability if each individual and average solution
8. Store the best solution in the society
9. Cycle = Cycle + 1

#### 10. UNTIL (Maximum cycle number—The termination criteria is satisfied).

In the initialization phase, the basic control parameters such as number of maximum cycle number, quality of interaction, indecisive factor, second opinion ranges are initialized and the random population of individuals are generated. In the evaluation phase, each individual's fitness and its probability is calculated along with the average fitness of the individuals.

In the interaction phase, individuals interact with the neighbors probabilistically. In this algorithm, von Neumann neighborhood architecture is adopted for building the neighborhood. The individual first identifies the neighborhood individuals and randomly identifies a neighbor to interact. Before interaction, the individual evaluates the neighbor based on the cooperation factor and the ability or productivity of the neighbor. Based on the analysis or simply based on individual's bias, individual may interact with the identified neighbor or may consider a random individual in the society for an interaction. The individual interaction operator is inspired by the artificial bee colony optimization algorithm's employee/onlooker bee operator [10] as this operator exhibits the human interactions model. In the interaction operator, unlike the bee agents in ABC, the individual will not interact with any random solution in the society instead, they may interact more with the random neighbor in the von Neumann neighborhood architecture because of affinity and trust worthiness, but they are free to explore the society based on NCF. Also, once the individual is selected for the interaction, the individual solution interacts with the selected individual for all the dimensions of the problem unlike the operator used in ABC algorithm [10]. Once the interaction is performed, individual evaluate the quality of interaction (QI). If the quality of interaction is inferior, interaction's indecisive factor IDF is evaluated to decide on the interaction as negative or indecisive. All the indecisive interactions will undergo a second opinion process.

In the second opinion process, the individual can consult an expert either from the neighborhood or from the society or a non-existing individual with the average capabilities to further evaluate the indecisive interaction before adopting the change to emerge and evolve. After the interaction phase, evaluate the fitness of the updated solutions and compare with the respective original solution to consider the best for next generation. Before the above process is repeated until a termination condition (maximum cycle number), calculate the probabilities of the individuals, average solution the best in the society for the next generation.

The proposed SE algorithm is applied on four numerical benchmark problems and three to test the effectiveness and adoptability of the algorithm.

**Table 1** Experimental parameters

Parameter	values
Population	100
Maximum cycle number (MCN)	10,000
Neighborhood cooperation factor (NCR)	0.75
Quality if interaction	0.8
Indecisive factor	0.5
Second opinion (Neighbor best)–NB	< 0.3
Second opinion (Average best)–AB	< 0.5
Second opinion (Best)–SB	< 1.0

### 3 Experiments

#### 3.1 Unconstrained Benchmark Optimization Problems

Initially, the performance of the algorithm is tested on four standard numerical benchmark problems given in Table 2 using the experimental parameters presented in Table 1. Sphere is a convex, separable, unimodal function which has no local minimum except the global one. Schwefel is a multi model, non-separable function whose surface is composed of a great number of peaks and valleys. For this problem, many search algorithms get trapped in to the second best minimum far from the global minimum. Rastrigin is a multimode separable function, which was constructed from Sphere adding a modulator term. Its contour has a large number of local minima whose value increases with the distance to the global minimum. Dixon-Price is multimode, non-separable, and non-symmetric function.

**Table 2** Benchmark functions

Function name	Interval	Function
Sphere	$[-100, 100]^n$	$\text{Min } F = \sum_{i=1}^n x_i^2$
Schwefel	$[-500, 500]^n$	$\text{Min } F = \sum_{i=1}^n \{-x_i \sin(\sqrt{ x_i })\}$
Dixon-price	$[-10, 10]^n$	$\text{Min } F = (x_1 - 1)^2 + \sum_{i=2}^n i(2x_i^2 - x_{i-1})^2$
Rastrigin	$[-5.12, 5.12]^n$	$\text{Min } F = \sum_{i=1}^n \{(x_i^2 - 10 \cos(2\pi x_i) + 10)\}$

**Table 3** Results (Mean of the best values) of PSO, DE and ABC and SE algorithms on unconstrained numerical benchmark problems

Function name	PSO [18]	DE [18]	ABC [18]	SE
Sphere	0	0	0	0
Schwefel	-2654.030	-4177.990	-4189.830	-4189.830
Dixon-price	0.666	0.666	0	4.67E-01
Rastrigin	7.363	0	0	0

The social evolution algorithm executed 30 independent runs, to ascertain the performance of the algorithm on each of the listed problems with 10 dimensions. For easy comparisons, the experimental parameters population size and the maximum number of cycles are defined as per the parameters defined for DE, PSO, and ABC algorithms [18]. The mean of the best values for each of the problems is reported in Table 3 and compared against some of the evolutionary algorithms such as, differential evolution (DE), particle swarm optimization (PSO) and artificial bee colony optimization (ABC). The reported results suggest that, the algorithm finds the global optimum values for the three functions Sphere, Schwefel, and Rastrigin successfully. When compared with individual algorithms, the ABC algorithm performed better than SE on one function and SE performed better than PSO on three functions and better than DE on two functions.

## 4 Conclusions

This paper proposes a novel social evolution (SE) algorithm that mimics the human interactions, behavior, and their biases. This algorithm adopts two basic human characteristics. First, individual's ability and bias to evaluate the neighbor before establishing the interaction to evolve. Second, the ability that discriminate the quality of interaction and identifying indecisive interactions and further seeking a second opinion from an expert before adopting the change to emerge and evolve. The proposed algorithm mimics such characteristics of humans tested on four numerical test functions and compared the results with the state-of-the-art nature inspired algorithms. The results indicate that the proposed social evolution algorithm is better than or quite comparable to the existing state-of-the-art algorithms.

**Acknowledgments** Authors gratefully acknowledge the inspiration and guidance of the Most Revered Prof. P. S. Satsangi, the Chairman, Advisory Committee on Education, Dayalbagh, Agra, India.

## References

1. Yoshida, Z.: *Nonlinear Science: the Challenge of Complex Systems*. Springer, Heidelberg (2010)
2. de Castro L.N.: *Fundamentals of natural computing: an overview*. *Phys. Life Rev.* **4**(1), 1–36 (2007)
3. Goldberg, D.E.: *Genetic Algorithms in Search, Optimization and Machine Learning*. Kluwer Academic Publishers, Boston, MA (1989)
4. Fogel, D.B.: *Evolutionary computation: toward a new philosophy of machine intelligence* (3rd edn). IEEE Press, Piscataway, NJ (2006)
5. Beyer, H.-G., Schwefel, H.-P.: *Evolution strategies: a comprehensive introduction*. *J. Nat. Comput.* **1**(1), 3–52 (2002)

6. Banzhaf, W., Nordin, P., Keller, R.E., Francone, F.D.: *Genetic Programming: An Introduction: On the Automatic Evolution of Computer Programs and Its Applications*. Morgan Kaufmann, Heidelberg (1998)
7. Korns, Michael: *Abstract Expression Grammar Symbolic Regression*, in *Genetic Programming Theory and Practice VIII*. Springer, New York (2010)
8. White, T., Pagurek, B.: Towards multi-swarm problem solving in networks. In: *Proceedings of the 3rd International Conference on Multi-Agent Systems (ICMAS-98)*, pp. 333–40, (1998)
9. Kennedy, J., Eberhart, R.C.: Particle swarm optimization. In *Proceedings of 1995 IEEE International Conference Neural Networks IV*, pp. 1942–1948, (1995)
10. Karaboga, D., Basturk, B.: A powerful and efficient algorithm for numerical function optimization: artificial bee colony (ABC) algorithm. *J. Global Optim.* **39**, 459–471 (2007)
11. Reynolds, R.G.: An introduction to cultural algorithms. In: *Proceedings of the Third Annual Conference on Evolutionary Programming*, pp. 131–139. San Diego, California (1994)
12. Reynolds, R.G., Peng, B., Brewster, J.J.: Cultural swarms: knowledge-driven problem solving in social systems. *IEEE Int. Conf. Syst. Man Cybern.* **4**, 3589–3594 (2003)
13. Reynolds, R.G., Peng, B., Brewster, J.: Cultural swarms. *Congr. Evol. Comput.* **3**, 1965–1971 (2003A)
14. Reynolds, R.G., Jacoban, R., Brewster, J.: Cultural swarms: assessing the impact of culture on social interaction and problem solving. In: *Proceedings of the 2003 IEEE Swarm Intelligence Symposium*, pp. 212–219 (2003b)
15. Reynolds, R.G., Kobti, Z., Kohler, T.: The effect of culture on the resilience of social systems in the village multi-agent simulation. In: *Proceedings of IEEE International Congress on Evolutionary Computation*. Portland, OR, vol. 24, pp. 1743–1750, June 19 (2004)
16. Reynolds, R.G., Whallon, R., Mostafa, Z.A., Zadegan, B.M.: Agent-based modeling of early cultural evolution. *IEEE Congress on Evolutionary Computation*. pp. 1135–1142 (2006)
17. Ray, T., Liew, K.M.: Society and civilization: an optimization algorithm based on the simulation of social behavior. *IEEE Trans. Evol. Comput.* **7**(4), 386–396 (2003)
18. Akay B., Karaboga D.: Artificial bee colony algorithm for large-scale problems and engineering design optimization. *J. Intel. Manuf.* pp. 1–14 (2010). DOI: 10.1007/s10845-010-0393-4

# A Survey on Filter Techniques for Feature Selection in Text Mining

Kusum Kumari Bharti and Pramod kumar Singh

**Abstract** A large portion of a document is usually covered by irrelevant features. Instead of identifying actual context of the document, such features increase dimensions in the representation model and computational complexity of underlying algorithm, and hence adversely affect the performance. It necessitates a requirement of relevant feature selection in the given feature space. In this context, feature selection plays a key role in removing irrelevant features from the original feature space. Feature selection methods are broadly categorized into three groups: filter, wrapper, and embedded. Filter methods are widely used in text mining because of their simplicity, computational complexity, and efficiency. In this article, we provide a brief survey of filter feature selection methods along with some of the recent developments in this area.

**Keywords** Text mining · Text categorization · Text clustering · Feature extraction · Feature selection · Filter methods

## 1 Introduction

It is difficult to extract relevant information in time from a heap of digital information, which is growing leap and bound with rapid development of Internet technology. It necessitates a need to organize available information in a well-structured format in order to facilitate quick and efficient retrieval of relevant information in time. Text mining is a key step to achieve this task. It discovers previously unknown information

---

K. K. Bharti (✉) · P. K. Singh

Computational Intelligence and Data Mining Research Lab, ABV-Indian Institute of Information Technology and Management Gwalior, Morena Link Road, Gwalior, Madhya Pradesh, India  
e-mail: kkusum.bharti@gmail.com

P. K. Singh

e-mail: pksingh@iiitm.ac.in



by automatically extracting useful information from huge corpus. It is widely used in various areas, e.g., information technology, Internet, banks, business analytics, market analysis, pharmaceutical, healthcare.

Text classification and text clustering are two subfields of text mining. Text classification is a form of supervised learning where a new document is assigned to one of the predefined classes based on a defined model whereas text clustering is an example of unsupervised learning where the classes are not known apriori. Before organizing the documents based on their intrinsic characteristics, documents are represented into a common format, known as vector space model [22], where each dimension corresponds to a single term. It increases the number of dimensions of representation model unmanageably. It necessitates a requirement of relevant feature selection as a lot of features are irrelevant, redundant, and noisy which adversely affect the efficacy and efficiency of the underlying algorithm and sometimes even misguide them. Moreover, high-dimensional feature space also makes it difficult to apply computationally intensive algorithm on all datasets. In this context, dimension reduction plays a key role in reducing the number of features.

The primary aim of the dimension reduction methods is to generate low-dimensional feature space from high-dimensional space without scarifying the performance of the underlying algorithm. Feature selection and Feature transformation are two subcategories of dimension reduction methods. A brief overview of these methods is presented in Table 1.

**Table 1** Comparative analysis of dimension reduction methods

Name	Key concept	Advantages	Disadvantages	Examples
Feature extraction (FE)	Summarize the dataset by creating linear combinations of the features	Preserves the original, relative distance between objects	Less effective in case of large number of irrelevant features	Principal component analysis [18]
		Covers latent structure	Sometime may be very difficult to interpret in the context of the domain	Latent semantic indexing [6]
Feature selection (FS)	Select a subset of relevant features based on defined criteria	Robust against irrelevant features	Feature selection criteria are hard to define	Information gain (IG) [21]
			May generate redundant features	Mutual information (MI) [5] Document frequency (DF) [12]

It can be observed from Table 1 that FE methods do not work well in case of high irrelevant features space. On the other hand, FS methods are more robust against irrelevant terms as selection of terms is not affected by irrelevant features. The FS methods efficiently reduce the high-dimensional irrelevant feature space into low-dimensional relevant subspace and hence increase performance of the underlying algorithm. Therefore, FS methods are more preferred for dimension reduction. These methods are broadly classified as filter, wrapper, and embedded. A brief description of these methods in terms of key concept, advantages, disadvantages, and examples is given in Table 2.

**Table 2** Comparative analysis of feature selection methods

	Key concept	Advantages	Disadvantages	Examples
Wrapper	Use classifier for selecting features subset	Simple Consider interaction with classifiers Less prone to generate local optimal solution	Computationally expensive	Sequential forward Selection [20] Sequential backward elimination [20]
Filter	Use intrinsic properties of the data	Fast Scalable Computationally efficient than wrapper methods	No guarantee to generate discriminative set of features Ignore interaction with classifiers	MI [5] IG [21] DF [12] Term variance (TV) [12]
Embedded	Facilitate interaction between classifier and feature selection methods	Facilitate interaction with classifier Computationally less expensive than wrapper methods	Computationally expensive than filter methods Classifier dependent selection	Bayesian logistic Regression [2] Sparse logistic regression [24]

Filter methods evaluate quality of features based on intrinsic properties of the documents without iteratively testing them with classifier (refer, Table 2). This property makes it considerably less computational expensive to other methods. Therefore, they are prominently used for feature selection (dimension reduction) in text mining. In this paper, we present a brief summary of various traditional filter feature selection methods along with some recent developments in this area.

## 2 Filter Methods for Feature Selection

Based on the literature survey of filter FS methods for text mining, we propose taxonomy of such methods as shown in Fig. 1. These methods are categorized as ranking methods and space search methods based on the strategy they use to select features subset. The ranking and search methods are further subcategorized into two groups, supervised, and unsupervised methods, based on the fact that whether they use class label information or not for quantifying the relevancy of terms. A brief summary of supervised and unsupervised filter FS is mentioned in Table 3.

### 2.1 Ranking Methods

These methods rank every feature individually using defined scoring function and then sort features in decreasing order based on their relevance score. Scoring/ranking of these features is performed either on the basis of class label information (known as supervised ranking methods) or on the basis of intrinsic properties (known as unsupervised ranking methods) of documents. Finally, the top score features are selected while the rest are discarded.

Summary of ranking supervised filter feature selection methods is given in Table 4.

Summary of ranking unsupervised filter feature selection methods is given in Table 5.

### 2.2 Space Search Methods

These methods work on the concept of optimizing some defined objective function as used in wrapper and embedded methods. The objective functions are defined in terms of feature interaction and/or feature class interaction. In supervised filter feature

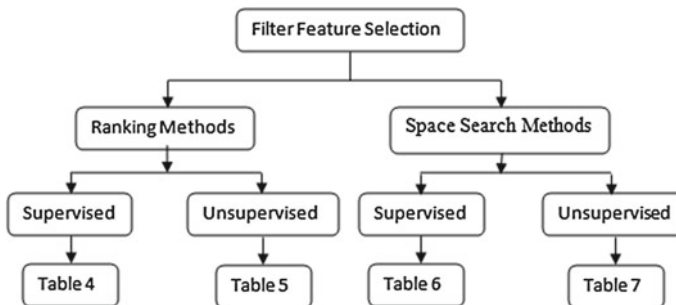


Fig. 1 Overview of proposed taxonomy

**Table 3** Comparative analysis of supervised and unsupervised filter FS

Method	Key concept	Advantage	Disadvantages	Examples
Supervised FS	Use class label information for quantifying the relevancy of terms	Simple	May suffer from over fitting	IG [21]
			Require ground truth information	MI [5]
Unsupervised FS	Quantify the relevancy of terms based on the intrinsic properties of the document	Do not need ground truth information, i.e., class label	Less efficient than supervised FS	DF [12]
				TV [12]

selection methods the objective function works on the concept of feature to class interaction whereas in unsupervised filter feature selection methods the objective function works on feature to feature interaction.

Summary of space search supervised filter feature selection functions is given in Table 6.

Summary of space search unsupervised filter feature selection functions is given in Table 7.

Having covered here prominent traditional approaches for filter feature selection, we discuss some of the recent developments in this area in next section.

### 3 Recent Development in Filter Feature Selection

In this section, we discuss some of the recent developments in the area of filter feature selection methods. Based on the methodology, we categories the available literature as genetic algorithm (GA)-based feature selection methods, particle swarm optimization (PSO)-based feature selection methods, and Hybrid feature selection methods.

#### 3.1 Genetic Algorithm-Based Feature Selection Methods

Chuang et al. [4] combine a filter FS method correlation-based feature selection (CFS) and a wrapper FS method taguchi-genetic algorithm (TGA) to form a new hybrid method for dimension reduction in gene analysis. They use k-nearest neighbor (KNN) with leave-one-out cross-validation (LOOCV) method as a classifier to judge the efficacy of their proposed method and observe that their proposed method

**Table 4** Summary of ranking supervised filter feature selection methods

Name	Description	Main idea	Mathematical form	Remark
IG [21]	Information gain	Quantifies relevancy of terms with respect to the class	$\sum_{j=1}^c P(w c_j) \log \frac{P(w c_j)}{c_j} + \sum_{j=1}^c P(\bar{w} c_j) \log \frac{P(\bar{w} c_j)}{c_j}$	Considers presence and absence of terms in observed category
CC [17]	Correlation coefficient	Quantifies the positive dependency between term and class	$\sum_{j=1}^c \frac{\sqrt{\pi} (P(w c_j) P(\bar{w} c_j) - P(w) P(\bar{w})) P(\bar{w} c_j)}{\sqrt{P(w) P(\bar{w}) P(c_j) P(\bar{c}_j)}}$	Get affected by size of the category
MI [5]	Mutual information	Measures dependency between target variable	$\sum_{j=1}^k P(c_j, w) \log \frac{P(c_j w)}{P(c_j)}$	Considers only positivity of term with respect to the class
MOR [1]	Multiclass odd ratio	Variant of MC-OR	$\sum_{j=1}^c \left  \log \frac{P(w c_j)(1-P(w \bar{c}_j))}{P(w \bar{c}_j)(1-P(w c_j))} \right $	Considers both positivity and negativity of term with respect to the class
CDM [1]	Class discriminating measure	Simplified form of MOR	$\sum_{j=1}^c \left  \log \frac{P(w c_j)}{P(w \bar{c}_j)} \right $	Considers both positivity and negativity of term with respect to the class

(continued)

**Table 4** (continued)

Name	Description	Main idea	Mathematical form	Remark
GINI[23]	Gini index	Considers document frequency for quantifying relevancy of the terms	$\sum_{j=1}^c \left( \frac{A_j}{M_j} \right)^2 \left( \frac{A_j}{A_j+B_j} \right)^2$ <p>Where <math>A_i</math>, number of documents with word <math>w</math> and belong to category  <math>B_i</math>, number of documents with word <math>w</math> and do not belong to category  <math>C_i</math>, number of document without word <math>w</math> and belong to category  <math>D_i</math>, number of documents without word <math>w</math> and do not belong to category</p>	Considers only document frequency of terms; ignores term frequency

**Table 5** Summary of ranking unsupervised filter feature selection methods

Name	Description	Main idea	Formula	Remark
DF [12]	Document frequency	Frequent terms are more informative than non frequent terms.	$df$ Total number of documents in which term appears	Easily biased by those common terms which have high document frequency but uniform distribution over different classes.
TV [12]	Term variance	Uses frequency of terms for quantifying the relevancy of terms	$\frac{1}{n} \sum_{j=1}^n (X_{ij} - \bar{X}_i)^2$	Measure deviation from mean
MM [8]	Mean median	Absolute difference between mean and median	$ \bar{X}_i - median(X_i) $	Measure dispersion

**Table 6** Summary of space search supervised filter feature functions

Name	Description	Formula	Remark
GCC [9]	Group correlation coefficient	$\frac{k r_{cf}}{\sqrt{k+k(k-1)r_{ff}}}$  $r_{cf}, r_{ff}$ - the average feature to class/feature to feature correlation	Higher value is more preferable
MID [7]	Mutual information difference	$I(w, c) - \frac{1}{ \Omega_s } \sum_t I(w_i, w_t)$  $I(w_i, w_t)$ the mutual information between feature $w_i \in \Omega_s$ and feature $w_t \in \Omega_s$	Need discretized feature inputs
MIQ [7]	Mutual information quotient	$\frac{I(w_i, c)}{\frac{1}{ \Omega_s } \sum_t I(w_i, w_t)}$  $I(w_i, c)$ - the mutual information between feature $w_i \in \Omega_s$ and class label $c$ $I(w_i, w_t)$ the mutual information between feature $w_i \in \Omega_s$ and feature $w_t \in \Omega_s$	Need discretized feature inputs

outperforms other competitive methods on 10 out of 11 classification profiles. Song and Park [25] propose, GAL, a genetic algorithm method based on LSI, for text clustering. As GA is computationally expensive for high dimensional space, the authors reduce the dimension of representational model using LSI. Additionally, they propose a variable string length GA which automatically evolves appropriated number of clusters for the given dataset. They show the superiority of their approach GAL

**Table 7** Summary of space search unsupervised filter feature functions

Function	Formula	Remark
Maximum information compression index [16]	$\frac{var(w_i) + var(w_t) - \sqrt{(var(w_i) + var(w_t))^2 - 4var(w_i)var(w_t)(1 - \rho(w_i, w_t))^2}}{2}$	Its zero value indicates that the features are linearly dependent.
Correlation coefficient [16]	$\frac{cov(w_i, w_t)}{\sqrt{var(w_i)var(w_t)}}$	Its zero value indicates that the features are linearly related.
Absolute cosine [8]	$\left  \frac{w_i \cdot w_t}{ w_i   w_t } \right $	Its zero value indicates that the features are orthogonal.

over conventional GA applied in VSM model for Reuter-21,578 document clustering results.

Li et al. [11] use ReliefF in stage one to evaluate the quality of each individual feature and obtain sequential feature sets based on the marks evaluated by ReliefF. Further, they use cross validation technique to obtain candidate feature set from the sequential sets. In second stage, they use genetic algorithm to search a more compact feature set based on the candidate set. They use three different classifiers linear discriminant (LD), KNN, and naïve bayes (NB) to evaluate their proposed method. The results to the real gear fault diagnosis show that the proposed method obtains a higher performance with a small size feature set. Yang et al. [30] hybridize a filter method IG and a wrapper method GA for feature selection in microarray datasets. Initially, they rank each feature using IG to select discriminative feature subsets and then use GA to further reduce the dimensions of representation model. They use KNN with LOOCV to show the efficacy of their proposed model. Experimental results demonstrate that the proposed method simplify the number of gene expression level efficiently and obtain higher accuracy to other competitive feature selection methods.

Summary of the literature belonging to genetic algorithm-based feature selection methods is given in Table 8.

### 3.2 Particles Swarm Optimization-Based Feature Selection Methods

PSO has been widely studied for dimension reduction. Liu et al. [13] use PSO to select feature subset for classification task and train radial basis function (RBF) neural network simultaneously. They experiment with four datasets from UCI Repository of machine learning databases image segmentation, page-blocks, ionosphere, and wine to show that their method effectively selects features with high accuracy as well as small feature subset size. Tu et al. [26] show the use of PSO to implement feature selection. They use support vector machines (SVMs) with the one-versus-rest method



**Table 8** Summary of the literature belonging to GA based feature selection

Authors	Key concept	Measures	Algorithms used	Remark
Chuang et al. [4]	CFS and TGA are combined to select discriminative features	CFS, TGA	KNN	Selects features highly correlated with class yet uncorrelated with each other
Song and Park [25]	Explore latent semantic structure along with decreasing the number of dimensions of representation model	LSI	GA	Creates appropriate number of clusters of documents without specifying them
Li et al. [11]	Use two step procedure for selecting discriminative set of features	Relieff, GA	KNN, NB LDC	Improves the accuracy of classification with reduced feature set compared to original feature set
Yang et al. [30]	Use a hybrid approach for feature selection	IG GA	KNN	Effectively reduces the number of features and achieves a good classification accuracy

as a fitness function in PSO for the problem. The proposed method is applied to five classification problems vowel, wine, WDBC, ionosphere, and sonar from the UCI Repository of machine learning databases. They observe that their method simplifies features effectively, obtains higher classification accuracy, and requires minimum computational resources than the other competitive feature selection methods.

Liu et al. [14] modify PSO and name it modified multi-swarm PSO (MSPSO); it holds a number of subswarms scheduled by the multi-swarm scheduling module. The multi-swarm scheduling module monitors all the subswarms, and gathers the results from the subswarms. Further, they propose a two stage method improved feature selection (IFS) consisting of MSPSO, SVM, and F-score. In the stage one, both the SVM parameter optimization and the feature selection are dynamically executed by MSPSO. In the second stage, SVM performs classification using these optimal values and selects feature subsets via tenfold cross validation. The designed objective function also consists of two parts: one is classification accuracy rate and the other is the F-score. Both are summed to form a single objective function by linear weighting. Experimental results on 10 different datasets from the UCI machine learning and StatLog databases show the efficacy of the proposed method IFS.

Chuang et al. [3] propose an algorithm catfish binary particle swarm optimization (CatfishBPSO). In CatfishBPSO, a new particle initialized at extreme points in the search space, known as catfish particle, replaces the worst fit individual to

**Table 9** Summary of the literature belonging to PSO based feature selection

Authors	Key concept	Measures	Algorithm used	Remark
Liu et al. [13]	Feature selection and neural network training are done simultaneously in each iteration	PSO	RBF Neural Network	Effectively selects features with high accuracy as well as small feature subset size
Tu et al. [26]	PSO is used to implement a feature selection, and SVM with the one-versus-rest method is used as evaluator for the PSO fitness	PSO	SVM	Obtains a good classification accuracy
Liu et al. [14]	Integrate multi-swarm PSO, SVM with F-score for selecting discriminative features	Multi-swarm PSO F-Score	SVM	A modified Multi-Swarm PSO to solve discrete problems
Chuang et al. [3]	Replace particles with the worst fitness by the catfish particle initialized at extreme points in the search space	CatfishBPSO	KNN	CatfishBPSO is effective in dimension reduction and/or classification accuracy
Uner et al. [29]	Use MI to weigh the bit selection probabilities in the discrete PSO	MI Discrete PSO	SVM	Consider feature-feature interaction for removing redundant features

avoid premature convergence if the gbest particle has not improved for a number of consecutive iterations. The experimental results on 10 different datasets from UCI machine learning database show that the proposed method efficiently reduces the dimension in the representation model and achieves highest accuracy in comparison to the other feature selection methods.

Uner et al. [29] propose a hybrid method maximum relevance minimum redundancy PSO (mr<sup>2</sup>PSO) for feature selection. In this, they integrate filter method mutual information within wrapper method PSO for selecting the informative features set. Instead of just removing irrelevant features they also remove redundant features from original feature space. The experimental results show that the proposed model is effective and efficient in terms of classification accuracy and computational complexity to the competing methods.

Summary of literature belonging to particle swarm optimization based feature selection is given in Table 9.

### 3.3 Hybrid Approaches for Feature Selection Methods

Here, we discuss the literature, which hybrids filter-filter methods, filter-wrapper methods, and FS-FE methods to reduce the dimensions of representation model. Uguz [28] proposes two-stage filter-wrapper (IG-GA) and FS-FE method (IG-PCA) methods for dimension reduction to improve the performance of text categorization. First, each term in the document is ranked on the basis of its importance for classification using IG. In the second stage, a FS method (GA) and a FE method (PCA) is applied separately to reduce the dimension of representation model. To evaluate the effectiveness of both the two-stage methods, the author uses KNN and C4.5 decision tree algorithm on Reuters-21,578 and Classic3 datasets collection for text categorization. The experimental results show that the proposed methods are effective in terms of precision, recall and F-measure. A similar approach has been used by Uguz [27] for Doppler signal selection.

Meng et al. [15], also use a two-stage procedure to gradually reduce the high dimensional space into a low dimensional subspace. First, they apply feature contribution degree (FCD) to select relevant features, and then construct low semantic space from relevant feature space using feature extraction method latent semantic indexing (LSI). They show effectiveness of the proposed model on spam database categorization.

Hsu et al. [10] propose a two-stage hybrid feature selection method, which combines filter and wrapper methods to take advantage of both. In stage one, they apply computationally efficient filter methods IG and F-score to select candidate features subset. In the second stage, they refine the subspace using wrapper method inverse sequential floating search; here, first sequential backward search (SBS), and then sequential forward search (SFS) is applied to select discriminative features subset. They experiment with two bioinformatics problems protein disordered region prediction and gene selection in microarray cancer data and show that equal or better prediction accuracy can be achieved with a smaller feature set also.

Sometime identification of only relevant features do not help much in improving accuracy of the classifiers as there may be some redundant features in the given features space, which adversely affect performance of the underlying algorithm. Thus, it is necessary to remove redundant features also along with irrelevant features. One of the initial works based on this concept is due to Peng et al. [19]. They propose a method called maximum relevance and minimum redundancy (mRMR). Here, they use feature selection measure MI [5] to select relevant features and remove redundant features.

Summary of literature belonging to hybrid methods is given in Table 10.

**Table 10** Summary of literature belonging to hybrid methods

Authors	Key concept	Measures	Algorithms used	Remark
Uguz [28]	Removes irrelevant features using two two-stage methods	IG PCA GA	KNN C4.5	Automatically selects number of dimensions in case of PCA
Uguz [27]	Hybridizes FS and FE methods for dimension reduction	IG PCA	SVM	Improves accuracy of underlying algorithm
Meng et al. [15]	Quantify the relevance by considering positivity of terms with respect the class.	FCD	SVM	Statistically derive conceptual indices to replace the individual terms.
Hsu et al. [10]	Utilize computational efficiency and accuracy of classifier for selecting discriminative set of features.	LSI IG  F-Score SBS SFS	SVM	Use two filter models for remove the most redundant or irrelevant features.

## 4 Conclusion and Future Works

Identification of relevant feature subset in text mining is utmost important as irrelevant features not only increase the computational complexity but also adversely affect performance of the underlying algorithm. In this context, feature selection is considered as a prominent preprocessing step to remove irrelevant, redundant and noisy terms. Feature selection methods are broadly classified into three categories: filter, wrapper, and embedded. This survey states a brief summary of various filter feature selection methods as they are the most widely used methods in the text mining because of their simplicity, computational complexity and efficiency. In addition, we present a brief introduction to recent developments in the area, e.g., nature-inspired algorithms, hybrid methods, present in the literature.

Though feature selection is widely explored in the literature, maximum number of features, threshold value and minimum similarity in case of redundant term removal are still an open and challenging research problems.

## References

1. Chen, J., Huang, H., Tian, S., Qu, Y.: Feature selection for text classification with Naïve Bayes. *Expert Syst. Appl.* **36**(3), 5432–5435 (2009)
2. Chen, X.: An improved branch and bound algorithm for feature selection. *Pattern Recogn. Lett.* **24**(12), 1925–1933 (2003)
3. Chuang, L.Y., Tsai, S.W., Yang, C.H.: Improved binary particle swarm optimization using catfish effect for feature selection. *Expert Syst. Appl.* **38**(10), 12699–12707 (2011)
4. Chuang, L.Y., Yang, C.H., Wu, K.C., Yang, C.H.: A hybrid feature selection method for DNA microarray data. *Comput. Biol. Med.* **41**(4), 228–237 (2011)
5. Church, K.W., Hanks, P.: Word association norm, mutual information and lexicography. *J. Comput. Linguist.* **27**(1), 22–29 (1990)
6. Deerwester, S.: Improving information retrieval with latent semantic indexing. In: *Proceedings of the 51st Annual Meeting of the American Society for Information Science*, Vol. 25, pp. 36–40 (1988)
7. Ding, C., Peng, H.: Minimum redundancy feature selection from microarray gene expression data. *J. Bioinf. Comput. Biol.* 185–205 (2005)
8. Ferreira, A.J., Figueired, M.A.T.: Efficient feature selection filters for high-dimensional data. *Pattern Recogn. Lett.* **33**(13), 1794–1804 (2012)
9. Hall, M.A.: Correlation-based feature selection for machine learning. Ph.D. Thesis. Department of Computer Science, University of Waikato (1999)
10. Hsu, H.H., Hsieh, C. W., Lu, M.D.: Hybrid feature selection by combining filters and wrappers. *Expert Syst. Appl.* **38**(7), 8144–8150 (2011)
11. Li, B., Zhang, P., Ren, G., Xing, Z.: A two stage feature selection method for gear fault diagnosis using reliefF and GA-wrapper. In: *Proceedings International Conference on Measuring Technology and Mechatronics Automation*, pp. 578–581 (2009)
12. Liu, L., Kang, J., Yu, J., Wang, Z.: A comparative study on unsupervised feature selection methods for text clustering. In: *Proceedings of Natural Language Processing and Knowledge, Engineering*, pp. 59–601 (2005)
13. Liu, Y., Qin, Z., Xu, Z., He, X.: Feature selection with particle swarms. In: *Computational and Information Science*, pp. 425–430. Springer, Heidelberg (2004)
14. Liu, Y., Wang, G., Chen, H., Dong, H., Zhu, X., Wang, S.: An improved particle swarm optimization for feature selection. *J. Bionic Eng.* **8**(2), 191–200 (2011)
15. Meng, J., Lin, H., Yu, Y.: A two-stage feature selection method for text categorization. *Knowl.-Based Syst.* **62**(7), 2793–2800 (2011)
16. Mitra, P., Murthy, C., Pal, S.: Unsupervised feature selection using feature similarity. *IEEE Trans. Pattern Anal. Machine Intell.* **24**(3), 301–312 (2002)
17. Ng, H. T., Goh, W. B., Low, K. L.: Feature selection, perception learning, and a usability case study for text categorization. In: *Proceedings of the 20th ACM International Conference on Research and Development in, Information Retrieval*, pp. 67–73 (1997)
18. Pearson, K.: On lines and planes of closest fit to systems of points in space. *Phil. Mag.* **1**(6), 559–572 (1901)
19. Peng, H., Long, F., Ding, C.: Feature selection based on mutual information: criteria of max-dependency, max-relevance, and min-redundancy. *IEEE Trans. Pattern Anal. Mach. Intell.* **27**(8), 1226–1238 (2005)
20. Pudil, P., Novoviciva, J., Kittler, J.: Floating search methods in feature selection. *Pattern Recogn. Lett.* **15**(11), 1119–1125 (1994)

21. Quinlan, J.R.: Induction of decision tree. *Mach. learn.* **1**(1), 81–106 (1986)
22. Salton, G., Wong, A., Yang, C. S.: A vector space model for automatic indexing. *Commun. ACM***18**(11), 613–620 (1975)
23. Shang, W., Huang, H., Zhu, H., Lin, Y., Qu, Y., Wang, Z.: A novel feature selection algorithm for text clustering. *Expert Syst. Appl.* **33**(1), 1–5 (2007)
24. Shevade, S., Keerthi, S.: A simple and efficient algorithm for gene selection using sparse logistic regression. *Bioinformatics* **19**(17), 2246–2253 (2003)
25. Song, W., Park, S.C.: Genetic algorithm for text clustering based on latent semantic indexing. *Comput. Math. Appl.* **57**(11–12), 1901–1907 (2009)
26. Tu, C.J., Chuang, L.Y., Chang, J.Y., Yang, C.H.: Feature selection using PSO-SVM. In: *Proceedings of Multiconferenc of Engineers*, pp. 138–143 (2006)
27. Uguz, H.: A hybrid system based on information gain and principal component analysis for the classification of transcranial Doppler signals. *Comput. Methods Programs Biomed.* **107**(3), 598–609 (2012)
28. Uguz, H.: A two-stage feature selection method for text categorization by using information gain, principal component analysis and genetic algorithm. *Knowl. Based. Syst.* **24**(7), 1024–1032 (2011)
29. Unler, A., Murat, A., Chinnam, R.B.: mr<sup>2</sup>PSO: A maximum relevance minimum redundancy feature selection method based on swarm intelligence for support vector machine classification. *Inf. Sci.* **181**(20), 4625–4641 (2011)
30. Yang, C.H., Chuang, L.Y., Yang, C.H.: IG-GA: a hybrid filter/wrapper method for feature selection of microarray data. *J. Med. Biol. Eng.* **30**(1), 23–28 (2009)

# An Effective Hybrid Method Based on DE, GA, and K-means for Data Clustering

Jay Prakash and Pramod Kumar Singh

**Abstract** Clustering is an unsupervised classification method and plays essential role in applications in diverse fields. The evolutionary methods attracted attention and gained popularity among the data mining researchers for clustering due to their expedient implementation, parallel nature, ability to search global optima, and other advantages over conventional methods. However, conventional clustering methods, e.g., K-means, are computationally efficient and widely used local search methods. Therefore, many researchers paid attention to hybrid algorithms. However, most of the algorithms lag in proper balancing of exploration and exploitation of solutions in the search space. In this work, the authors propose a hybrid method DKGK. It uses DE to diversify candidate solutions in the search space. The obtained solutions are refined by K-means. Further, GA with heuristic crossover operator is applied for fast convergence of solutions and the obtained solutions are further refined by K-means. This is why proposed method is called DKGK. Performance of the proposed method is compared to that of Differential Evolution (DE), genetic algorithm (GA), a hybrid of DE and K-means (DEKM), and a hybrid of GA and K-Means (GAKM) based on the sum of intra-cluster distances. The results obtained on three real and two synthetic datasets are very encouraging as the proposed method DKGK outperforms all the competing methods.

**Keywords** Evolutionary algorithm · Data clustering · Differential algorithm · Genetic algorithm · K-means

---

J. Prakash (✉) · P. K. Singh  
Computational Intelligence and Data Mining Research Laboratory, ABV-Indian Institute of Information Technology and Management, Gwalior, India  
e-mail: jayprakash.iiitm@gmail.com

P. K. Singh  
e-mail: pksingh@iiitm.ac.in

## 1 Introduction

Clustering has been approached by many disciplines in the past few decades because of its wide applications. The clustering classifies or groups the objects of an unlabeled dataset on the basis of their similarity. Each group, known as cluster, consists of objects such that the objects belonging to the same cluster have more similarity than the objects belonging to the other clusters. Though several similarity measures, e.g., Manhattan distance, Euclidean distance, cosine distance, Mahalanabis distance, are available in the literature, the most widely used distance measure is the Euclidean distance [22].

Clustering can be performed in two different modes fuzzy or Hard [11]. In fuzzy clustering, each object may belong to each cluster with a certain fuzzy membership grade. In hard clustering, the clusters are disjoint and each object belongs to exactly one cluster. We can mathematically represent hard partitioning of a data set  $X$ , based on the description in [5] as follows. Consider  $X = \{x_1, x_2, \dots, x_N\}$ , where every data point  $x_i$  in  $X$  corresponds to a  $n$ -dimensional feature vector. Then, hard partitioning of  $X$  is a collection  $C = \{C_1, C_2, \dots, C_k\}$  of  $K$  number of nonempty and nonoverlapping groups of data such that

$$C_i \neq \phi \quad I = 1, \dots, K \quad \text{and} \quad (1)$$

$$C_i \cap C_j = \phi \quad i, j = 1, \dots, K \quad \text{and} \quad i \neq j \quad (2)$$

Though conventional clustering algorithms exhibit fast convergence and are computationally efficient, they have many problems, e.g., they are quite sensitive to the initialization of prototypes, they do not provide any guarantee to the global optimality rather they easily stuck into the local minima [10]. Specifically, for these reasons, powerful metaheuristics such as evolutionary algorithms offer to be more effective methods to overcome the deficiencies of the conventional clustering methods as they possess several desired key features, e.g., upgradation of the candidate solutions iteratively based on objective function (fitness function), decentralization, parallel nature, flexibility, robustness, no need of prior information about domain knowledge, self organizing behavior [21]. Consequently, many researchers found that hybridization of metaheuristics within and with conventional algorithms increases the efficiency and accuracy of the clustering. Kwedlo [13] proposes a method DEKM that combines DE and K-means to obtain clusters based on the sum of squared error (SSE) criterion when number of cluster is known. Here, DE is a global search algorithm with slow convergence and K-means is local search algorithm with fast convergence. Tvrd'ik and Křiv'ý [20] empirically find that DE hybridized with K-means performs comparatively superior to the DE based on optimizing two basic criteria trace of within scatter matrix and variance ratio criterion. Tian et al. [19] use K-Harmonic mean in the place of K-means with DE when number of clusters is fixed. Here also the number of clusters is known *a priori*. As K-means is very sensitive toward the



choice of initial centers, Laszlo and Mukharjee [14] use GA to obtain initial cluster centers for K-means.

Das et al. [6] propose a method to determine proper number of clusters during run time. They modify classical DE by tuning parameters in two different ways to improve its slow convergence property. First, the scale factor is changed in random manner in the range (0.5, 1); it helps to retain diversity as the search progresses. Second, the crossover rate (Cr) linearly decreases from maximum to minimum of crossover rate with iterations during the run. He et al. [9] propose a two-stage genetic clustering algorithm TGCA that Initially focuses on finding best number of clusters, and then gradually moves finding global optimal cluster centers. Chang et al. [2] develop a GA for automatic clustering based on dynamic niching with niche migration to overcome the downsides of the fitness sharing approach. However, exploration and exploitation capabilities of these algorithms are not up to the mark.

In this work, we present a novel hybrid algorithm DKGK, which takes advantage of characteristics of DE, GA, and K-means. Here, DE is used to provide diversity in the search space. The obtained candidate solutions are fine tuned using k-means. Further, heuristic crossover [17] in GA is applied for fast convergence of the solutions and the obtained solutions are again refined by K-means. We experiment on three real datasets from UCI machine learning databases and two synthetic datasets to judge the efficacy of the proposed method. The results are very encouraging; the proposed method outperforms all the competing methods in all the datasets.

Rest of the paper is organized as follows. Section 2 presents a brief introduction to the evolutionary algorithms DE and GA, a most widely used conventional clustering method K-means, and hybrid algorithms DEKM and GAKM. Section 3 presents the proposed hybrid method DKGK. Results and discussions are included in Sect. 4. Finally, Sect. 5 concludes with a hint on possible future research directions.

## 2 Algorithms Background

In this section, we present a brief introduction to the Differential Evolution (DE), Genetic Algorithm (GA), K-means and hybrid algorithms DEKM and GAKM.

### 2.1 Differential Evolution

Storn and Price [18] propose DE, an evolutionary algorithm for global optimization for continuous-valued problem. The basic DE strategy can be described as the notation DE/x/y/z, where  $x$  is the vector to be mutated (a random vector or the best vector),  $y$  is the number of difference vectors, and  $z$  is the crossover scheme [18]. Some of the more frequently used strategies comprise DE/rand/2/bin, DE/best/1/bin, and DE/best/2/bin. In each generation, for each individual  $X_1$  in the current population, a mutation operator generates a mutant parameter vector  $T_1$  by mutating a

target vector  $X_2$  with difference vector of two individuals  $X_3$  and  $X_4$ , making sure that all these four individuals are different as shown in equation (3).

$$T_{1j} = X_{2j} + \beta(X_{3j} - X_{4j}) \quad (3)$$

Here,  $j$  represents dimension of an individual and  $\beta$  is a scaling factor, which manages the magnification of difference vector. For smaller values of  $\beta$ , the algorithm converges slowly but it can be used to explore search in local area, whereas a larger value of  $\beta$  assists greater diversity in search space but it may cause the algorithm to escape good solutions. Therefore, the value of  $\beta$  requires a careful balancing. It has been shown empirically that solutions often converge prematurely for large values of  $\beta$  and population size [3] whereas  $\beta = 0.5$  generally exhibits good performance [1, 18]. The generated trial vector by crossover operator through implementing a discrete recombination of the mutant vector  $T_1$  and the parent vector  $X_1$  is compared with the corresponding parent vector and the one with the higher fitness value is selected for the next generation. It is gaining attention of researchers, for solving optimization problems, as it is easy to implement, simple in design, and requires tuning of few parameters.

## 2.2 Genetic Algorithm

GA is a stochastic optimization method that mimics the process of natural evolution [7]. In GA, a solution to the problem is represented by a chromosome; a set of chromosomes is called a population. Typically, solutions of initial population are generated randomly and then three genetic operators crossover, mutation, and selection are applied on solutions of current generation to produce new candidate solutions. The candidate solutions are selected for the next generation based on their fitness value. The crossover, which usually operates on two parents and produces two offsprings with some crossover probability, is primarily responsible for diversification of solutions in the entire search space. The mutation alters the gene of a chromosome to find solutions near it with a very small probability. Selection operator selects solutions from current generation for next generation based on some selection strategy. This process of applying genetic operators to produce candidate solutions for next generation continues till termination criteria meets. GA provides optimal or near optimal solutions to a vast range of optimization problems as they are efficient, robust, self-adaptive, and parallel in nature. As GA is more suitable for discrete optimization problems, it is suitable for the problem.

## 2.3 K-means Algorithm

K-means [10] is a widely used local search clustering algorithm, which is computationally efficient and easy to implement. Since similarity among data points is measured using Euclidian distance, a data point having a smaller distance from a

particular cluster center is associated with that cluster. Most popularly, K-means minimizes a measure SSE to determine the quality of solution [15]. The k-means is described below.

Step 1: Randomly initialize centroids  $\{m_1, m_2, \dots, m_k\}$  of the  $k$  clusters.

Step 2: Repeat steps (i) to (iii) until a stopping criteria is satisfied.

- (i) Compute Euclidian distance of each data point to the centroid of each cluster and associate the data points with the clusters where they have minimum Euclidian distance.

$$ED(x_p, m_i) = \sqrt{\sum_{j=1}^d (x_{pj} - m_{ij})^2} \tag{4}$$

Here,  $x_p$  denotes  $p$ th data point of the dataset consisting of  $n$  instances (data points);  $m_i$  denotes centroid of  $i$ th cluster;  $d$  indicates number of dimensions in the dataset.

- (ii) Evaluate fitness value of the solution.
- (iii) Recompute the centroids of clusters by taking average of all corresponding dimensions of data points belonging to that cluster.

$$m_i = \frac{1}{n_i} \sum_{x_p \in c_i} x_p \tag{5}$$

Here,  $n_i$  is the number of data points in cluster  $c_i$ .

The termination criterion of K-means algorithm is based on user-specified parameter. However, in proposed algorithm, K-means algorithm is iterated single time after each of two algorithms DE and GA.

### 2.4 Hybrid Algorithms DEKM and GAKM

Since DE is a global search algorithm with slow convergence and K-means is local search algorithm with fast convergence, Kwedlo [13] proposes a method DEKM that combines DE and K-means to obtain clusters based on sum of SSE criterion. They use K-means twice before and after the DE; first, initial population for the DE is created using K-means and then, the best solution obtained by DE is refined by K-means. Although DEKM algorithm described in this paper is similar to the algorithm in [13], k-means is used only once to refine the solutions obtained by DE. Here, DE is used to perform clustering in global search space whereas K-means is used to refine the candidate solutions as local search heuristic. We run DE for user specified number of iterations and refine the obtained solutions by K-means in isolated single iteration.

Few researchers, e.g., [14], [12], hybridize GA and K-means; first, they run GA with random initial population to explore the search space and obtain good solutions,

then they refine the fittest solution using K-means to exploit the search space locally to obtain the (near-) optimal solution. In this work, in GAKM, we use randomly generated initial population and heuristic crossover [17] in GA and refine the obtained solutions using K-means. Here, GA is run for user specified number of iterations and K-means is run in isolated single iteration.

### 3 DKGK Based Clustering

This section presents a description of the proposed algorithm DKGK. Here, we explain encoding scheme, initial population generation, fitness function, avoiding invalid solutions, and different steps of the DKGK.

#### 3.1 Chromosome Representation

A chromosome is a representation of a solution in the evolutionary algorithms. In this work, we follow a chromosome representation as described in [13]. It is shown in Fig. 1. Every chromosome or candidate solution contains  $k \times d$  dimensions (genes) where  $k$  represents the number of clusters and  $d$  indicates the number of dimensions in the data points.

Here,  $m_{ij}$  represents centroid of the  $j$ th cluster and  $i$  indicates  $i$ th dimension in the cluster's centroid.

#### 3.2 Initialization of DE Population

Cluster centroids for initial population are randomly selected from the dataset. It means,  $k$  data points are selected to represent centroids of  $k$  clusters in a chromosome. For every algorithm, number of chromosomes for initial population is assigned 20 and remains fixed for every generation.

#### 3.3 The Fitness Function

As sum of distances has a profound impact on the error rate, we use sum of intra-cluster distances as the fitness function [4]. Its lower value indicates a better quality



Fig. 1 Chromosome representation

of solution and is represented as follows:

$$SICD = \sum_{i=1}^k \sum_{\forall x_p \in c_i} \|x_p - m_i\| \tag{6}$$

Here,  $x_p$  denotes  $p$ th data point of the dataset,  $m_i$  denotes centroid of the  $i$ th cluster,  $c_i$  denotes  $i$ th cluster and  $k$  denotes the number of clusters.

### 3.4 Avoiding Erroneous Particle

As data points are selected randomly from the dataset, there is a possibility that a data point, which is an outlier, is selected as centroid of a cluster. It is observed that a cluster represented by such a centroid generally does not consist of any data point or consists of too few data points to be regarded as a meaningful cluster. To overcome such a problem, respective chromosome is replaced a by new chromosome, which is created by taking average computation of  $n/k$  data points for each of the  $k$  clusters.

### 3.5 DKGK Algorithm

The DKGK algorithm is summarized in the following steps.

Inputs:

- (a) Evolutionary algorithmic parameters
- (b)  $n \times d$  dataset, where  $n$  is the number of instances of data points and  $d$  is the dimension
- (c) K-number of clusters

Output:

A set of K clusters.

Algorithm:

- (i) Select initial chromosomes from the dataset randomly.
- (ii) Run this step (DE) for  $3/4 * (\text{total iterations})$  to obtain diverse solutions
  - (a) Select three chromosomes  $X_{2j}, X_{3j}, X_{4j}$  randomly from population for chromosome  $T_{1j}$ , making sure that all four  $T_{1j}, X_{2j}, X_{3j}, X_{4j}$  are different. Then, evaluate  $T_{1j}$  as follows:

$$T_{1j} = X_{2j} + \beta(X_{3j} - X_{4j})$$

Here,  $\beta = R_1 (R_2 + R)$  is self-adaptive scaling factor used to evaluate mutant vector  $C_1$ ,  $R_1$  and  $R_2$  are user defined constants, and  $R$  is random number between 0 and 1.

- (b) Perform crossover with some crossover rate.
- (c) Fitter solution in  $C_1$  and  $X_1$  is selected for further operations.
- (iii) Refine the solutions obtained in step (ii) by K-means. The number of isolated iterations of K-means is subject to user-defined parameter (experimental study is based on single iteration).
- (iv) Run this step (GA) for  $1/4 * (\text{total iterations})$  for converging solutions
  - (a) Randomly select two different parents from the population and perform following heuristic crossover operation.

$$\text{Offspring1} = \text{Best\_Parent} + r(\text{Best\_Parent} - \text{Worst\_Parent}) \quad (7)$$

$$\text{Offspring2} = \text{Best\_Parent}. \quad (8)$$

Here,  $r = R_3 (R_4 + R)$  is self-adaptive random number used to evaluate offspring1;  $R_3$  and  $R_4$  are user defined constant;  $R$  is random number between 0 and 1.

- (b) Perform crossover with some crossover rate.
- (c) Candidate solutions move on to the next generation based on some selection strategy.
- (v) Refine the solutions obtained in step (iv) by K-means algorithm. The number of isolated iterations for K-means is subject to user-defined parameter (experimental study is based on single iteration).

In DKGK algorithm, DE is used to provide diversity of solutions in global search space. The DE runs for  $(3 * \text{total\_iteration} / 4)$  iterations, where  $\text{total\_iteration}$  is a user-defined parameter, which defines total number of iterations in DKGK. The solutions obtained by DE are refined by K-means in isolated single iteration. Further, using heuristic crossover [17] in GA, the solutions converge toward the quality solutions in last  $(\text{total\_iteration} / 4)$  iterations. Thereafter, K-means is applied to the solutions for single isolated iteration to get final partitions in the dataset. As it is known empirically that  $\beta = 0.5$  generally exhibits good performance, in our experiment,  $\beta$  varies from 0.25 to 0.75 randomly with mean value 0.50. Similarly,  $r$  also varies from 0.25 to 0.75 randomly with mean value 0.50. Note that inner-steps in steps (ii) and (iv) themselves execute 20 (size of population) times for one iteration of step (ii) and (iv) respectively.

## 4 Experimental Result and Discussions

This section presents experimental setup, datasets, and results and discussion. The experiments have been performed on a system with core *i5* processor and 2 GB RAM in Windows 7 environment using programs written in C language.

### 4.1 Parameters Setup

As results of the nature-inspired algorithms are influenced by number of control parameters, these values should be chosen carefully. Here, we experiment with different sets of values and present the results for following set of parametric values as it produces the best results. These values are same for the GA, DE, DEKM, GAKM, and the proposed method DKGK for a fair comparison. It is shown in Table 1.

### 4.2 Datasets Descriptions

The datasets are in matrix of size  $n \times d$  with real-valued elements and are partitioned into  $k$  nonoverlapping clusters. We consider three real datasets Iris, Vowel, Wisconsin Breast cancer (WBC) from the UCI machine learning repository [16] and two synthetic datasets 2d4c, 10d4c, which are generated from two generators developed by Handl and Knowles [8] and can be downloaded from <http://personalpages.manchester.ac.uk/mbs/Julia.Handl/generators.html>. A brief summary of these datasets is presented in Table 2. As WBC consists of 16 samples with some missing features, we remove them from the dataset and use only 683 samples out of originally 699 samples.

**Table 1** Control parameters for GA, DE, DEKM, GAKM, and DKGK

Name of parameters	Value
Population size	20
Number of iterations	100
Number of independent runs	100
Scaling Factor of DE( $\beta$ )	Self adaptive
Random number (r) in heuristic crossover of GA	Self adaptive
Crossover rate of DE	1
Crossover rate of GA	1
$R1, R2, R3, R4$	0.5

**Table 2** Datasets descriptions

Name of dataset	Number of clusters	Number of dimensions	Number of instances
Iris	3	4	150
Vowel	6	3	871
WBC	2	9	683
2d4c	4	2	1572
10d4c	4	10	1289

**Table 3** Best results obtained by different methods in 100 independent runs

Dataset	DE	GA	DEKM	GAKM	DKGK
Iris	97.65	98.97	97.07	97.06	96.99
Vowel	158521.75	159288.85	152281.03	150341.59	149227.54
WBC	3016.92	3011.45	2978.71	2978.50	2975.73
2d4c	3341.95	3348.88	3313.63	3319.67	3312.96
10d4c	18863.20	18752.88	17348.63	17340.57	17245.45

### 4.3 Experimental Results

The obtained results (sum of intra-cluster distances of the final clusters) by DE, GA, DEKM, GAKM, and the proposed method DKGK are shown in Table 3. The presented results are the best results obtained in 100 independent runs for each algorithm. The results have been generated by running all the algorithms with same initial population, on same set of parametric values as shown in Table 1, and on same fitness function for every test problem for a fair comparison. As it is a minimization problem, a minimum value of sum of intra-cluster distances represents a better solution. It is clear that DKGK consistently outperforms its competitive algorithms. A primary reason for better performance of proposed algorithm DKGK is separate choice of algorithms where DE takes care of exploration of solutions in the search space and the heuristic crossover of GA is responsible to converge to high quality solution. In addition, k-means does the refinement to obtain (near-) optimal solution.

## 5 Conclusion

As nature-inspired algorithms are more versatile and look for global optimal solutions in comparison to conventional algorithms for clustering, which usually look for local optimal solutions, they are increasingly attracting attention from researchers in diverse areas. In this paper, we propose a new hybrid algorithm DKGK, which maintains proper balance of exploration and exploitation of solutions in the search space taking advantages of DE, GA, and K-means. The empirical results on three



real and two synthetic datasets suggest that performance of the proposed DKGK is comparatively superior to DE, GA, DEKM, and GAKM.

We wish to extend this humble beginning in various possible ways. This algorithm works when the number of clusters is known *a priori*; it may be adapted to decide proper number of clusters on its own instead of it being a user defined parameter. As a vast array of nature-inspired algorithms are available with different philosophical base and features, the DE and GA may be replaced by other algorithms, e.g., evolutionary and swarm, to provide better exploration and exploitation capability in search space. Further, the most frequently used K-means to hybridize nature-inspired algorithms may be replaced with a better conventional local search method.

## References

1. Ali, M.M.; Törn, A.: Population set-based global optimization algorithms: Some modifications and numerical studies. *Comput. Oper. Res.* **31**(10), 1703–1725 (2004)
2. Chang, D., Zhang, X., Zheng, C., Zhang, D.: A robust dynamic niching genetic algorithm with niche migration for automatic clustering problem. *Pattern Recogn.* **43**, 1346–1360 (2010)
3. Chiou, J.-P., Wang, F.-S.: A hybrid method of differential evolution with application to optimal control problems of a bioprocess system, In: *IEEE World Congress on Computational Intelligence, Proceedings of the IEEE International Conference on Evolutionary Computation*, pp. 627–632. (1998)
4. Chuang, L.Y., Hsiao, C.J., Yang, C.H.: Chaotic particle swarm optimization for data clustering. *Expert Syst. Appl.* **38**, 14555–14563 (2011)
5. Cura, T.: A particle swarm optimization approach to clustering. *Expert Syst. Appl.* **39**, 1582–1588 (2012)
6. Das, S., Abraham, A., Konar, A.: Automatic clustering using an improved differential evolution algorithm. *IEEE Trans. Syst. Man Cybern. Part A: Syst. Hum.* **38**(1), 218–237 (2008)
7. Goldberg, D.E.: *Genetic Algorithms-in Search, Optimization and Machine Learning*. Addison-Wesley Publishing Company Inc., London (1989)
8. Handl, J., Knowles, J.: Improving the scalability of multiobjective clustering. In: *Proceedings of the Congress on Evolutionary Computation*, vol. 3, pp. 2372–2379 (2005)
9. He, H., Tan, Y.: A two-stage genetic algorithm for automatic clustering. *Neurocomput.* **81**, 49–59 (2012)
10. Jain, A.K., Dubes, R.C.: *Algorithms for Clustering Data*. Prentice-Hall, Engle-wood Cliffs, NJ (1988)
11. Jain, A.K., Murty, M.N., Flynn, P.J.: Data clustering: a review. *ACM Comput. Surv.* **31**(3), 264–323 (1999)
12. Kwedlo, W., Iwanowicz, P.: Using genetic algorithm for selection of initial cluster centers for the K-Means method. In: *Proceedings of 10<sup>th</sup> International Conference on Artificial Intelligence and Soft Computing. Part II, LNAI 6114*, pp. 165–172, (2010)
13. Kwedlo, W.: A clustering method combining differential evolution with the K-means algorithm. *Pattern Recogn. Lett.* **32**, 1613–1621 (2011)
14. Laszlo, M., Mukharjee, S.: A genetic algorithm that exchanges neighboring centers for k-means clustering. *Pattern Recogn. Lett.* **28**, 2359–2366 (2007)
15. MacQueen, J.: Some methods for classification and analysis of multivariate observations. In: *Proceedings of the Fifth Berkeley Symposium on Mathematical Statistics and Probability*, Vol. 1, 281–297, (1967)
16. Murphy, P., Aha, D.: UCI repository of machine learning data bases. (1995). URL <http://www.sgi.com/tech/mlc/db>

17. Peltokangas, R., Sorsa, A.: Real-coded genetic algorithms and nonlinear parameter identification. University of Oulu Control Engineering Laboratory Report, vol. 34, pp. 1–32 (2008)
18. Storn, R., Price, K.: Differential evolution—a simple and efficient heuristic for global optimization over continuous spaces. *J. Global Optim.* **11**(4), 341–359 (1997)
19. Tian, Y., Liu, D., Qi, H.: K-harmonic means data clustering with differential evolution. In: Proceedings International Conference on Future BioMedical Information, Engineering, pp. 369–372, (2009)
20. Tvrđík, J., Křivý, I.: Differential evolution with competing strategies applied to partitional clustering. In: Proceedings Symposium on Swarm Intelligence and Differential Intelligence, LNCS 7269. pp. 136–144 (2012)
21. Velmurugan, T., Santhanam, T.: A survey of partition based clustering algorithms on data mining: an experimental approach. *Int. Technol. J.* **10**, 478–484 (2011)
22. Xu, R., Wunsch II, D.: Survey of clustering algorithms. *IEEE Trans. Neural Networks* **16**(3), 645–678 (2005)

# Studies and Evaluation of EIT Image Reconstruction in EIDORS with Simulated Boundary Data

Tushar Kanti Bera and J. Nagaraju

**Abstract** Simulated boundary potential data for Electrical Impedance Tomography (EIT) are generated by a MATLAB based EIT data generator and the resistivity reconstruction is evaluated with Electrical Impedance Tomography and Diffuse Optical Tomography Reconstruction Software (EIDORS). Circular domains containing subdomains as inhomogeneity are defined in MATLAB- based EIT data generator and the boundary data are calculated by a constant current simulation with opposite current injection (OCI) method. The resistivity images reconstructed for different boundary data sets and images are analyzed with image parameters to evaluate the reconstruction.

**Keywords** EIT · Simulated boundary data · EIDORS · Image reconstruction · Resistivity images · Image parameters.

## 1 Introduction

Electrical Impedance Tomography (EIT) [1–6] is an image reconstruction technique in which a constant current is injected to the domain under test (DUT) and the electrical conductivity or resistivity distribution of the DUT is reconstructed from the boundary potentials using an image reconstruction algorithm [7–11]. EIT is a computed tomographic imaging modality which is being used in different fields of science and engineering due to its several advantages [12] over other conventional tomographic techniques [13]. Being a fast, portable, noninvasive, nonradiating, nonionizing, and inexpensive methodology, electrical impedance tomography has been extensively researched in medical diagnosis [14–18], biomedical

---

T. K. Bera (✉) · J. Nagaraju  
Department of Instrumentation and Applied Physics, Indian Institute of Science,  
Bangalore, Karnataka 560012, India  
e-mail: tkbera77@gmail.com

engineering [19] and biotechnology [20]. Studying the image reconstruction process in EIT is essential to test, calibrate, and assess the system performance. Design and development of EIT instrumentation [21–26] as well as the practical phantoms [2, 27, 28, 30, 31] are very crucial in EIT as the improper design parameters of the instrumentation and phantoms adversely affect the boundary data. Hence, the development of the instrumentation and practical phantoms and the image reconstruction studies [2, 5, 6, 21, 26–28, 30–33] on practical phantoms and their boundary data obtained in real EIT systems becomes difficult in real case. Computer simulation [34, 35] in science and engineering is a study of a particular problem by developing its mathematical model in personal computer. Computer simulation is conducted to obtain the preliminary solution before studying the problem with practical experiments. The simulation studies on EIT [36–38] are required to avoid the design and development works required in practical phantom studies or to reduce the errors in boundary data produced by phantoms and instrumentation. Studies on boundary data simulation and their EIT image reconstruction using standard reconstruction algorithm help the researchers to understand the physics and mathematics of EIT and its image reconstruction process.

In this paper, simulated data are generated with an EIT data generator and the resistivity reconstruction is studied with standard image reconstruction algorithm. In this direction, circular domains containing single or multiple circular subdomains are simulated as phantoms and the boundary data are generated in a MATLAB-based EIT data generator. The resistivity imaging in EIT is studied with simulated data using Electrical Impedance Tomography and Diffuse Optical Tomography Reconstruction Software (EIDORS) [39]. The resistivity reconstruction is conducted with Levenberg-Marquardt Regularization (LMR) technique [40]. A constant current injection is simulated with opposite current injection method in circular simulated domains and the simulated boundary data are calculated in PC. Simulated boundary data are generated for different domain geometries and the resistivity images are reconstructed. The image parameters are calculated from the reconstructed images and the images are studied to evaluate the reconstruction and boundary data quality.

## 2 Materials and Methods

### 2.1 Boundary Data Generation and Image Reconstruction

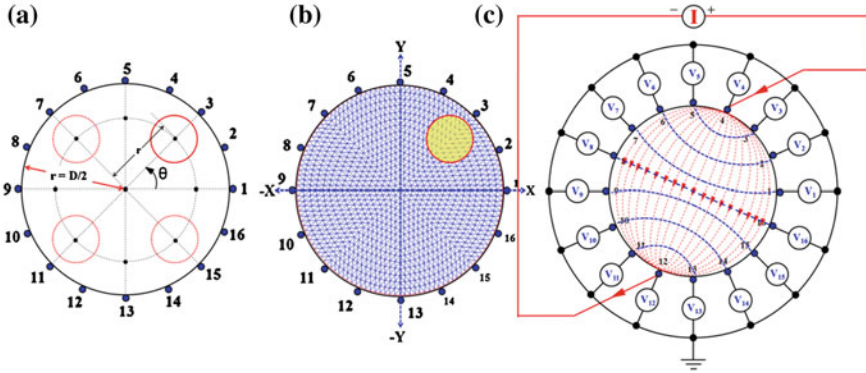
Circular simulated regions are simulated (Fig. 1a) as the DUT ( $\Omega$ ) in a MATLAB boundary data generator and a constant current injection is simulated to generate the boundary data. The circular DUTs (diameter  $D$ ) are discretized with a finite element (FE) mesh (Fig. 1b) and the boundary nodes are separated to define the nodes at the electrode positions called the electrode nodes. The elements inside the inhomogeneity and the background are identified and the background and inhomogeneity elements are defined with two different resistivities. Inhomogeneity of required shape and size

(diameter  $d_i = 30$  mm, 40 mm, 50 mm etc..) is made at different electrode positions inside the simulated domain by defining its center (P) with a polar co-ordinate ( $r, \theta$ ) as shown in Fig. 1a. Different circular DUTs are defined containing a single or multiple subdomains (diameter  $d$ ) as the inhomogeneities near different electrode nodes. The elements within the inhomogeneity are assigned with a particular resistivity ( $\rho_i = 50 \Omega\text{m}$ ) while the rest of the elements in the surrounding region called background are assigned with a different resistivity ( $\rho_b = 1.724 \Omega\text{m}$ ). A constant current injection is simulated in circular domains defined as simulated phantoms in MATLAB and the simulated boundary data are calculated in PC using opposite current injection (OCI) method. Changing the value of  $r$  and  $\theta$ , a number of phantom geometry can be obtained easily to generate the corresponding boundary data set.

1 mA 50 kHz constant current injection is simulated to the DUT boundary through the electrode nodes called current electrode nodes (CEN) and the voltages are calculated on the electrode nodes called voltage electrode nodes (VEN) using OCI protocol. In OCI method (Fig. 1c), the current is simulated through two opposite CEN and the electrode potentials are calculated on VEN. The potentials of all the FEM mesh nodes are calculated and the boundary node potentials are separated. The electrode node potentials are again separated from the boundary node potentials. The electrode node potentials are calculated for all the 16 current projections and the 256 electrode node potential data are saved as a .txt file in PC for the analysis and image reconstruction. As the boundary data for first eight current projections are sufficient to produce impedance image (due to reciprocity principle) and that is why the other eight current projections are not required [28]. For opposite current injection methods, the boundary potentials ( $V_1, V_2, V_3, \dots, V_{15}, V_{16}$ ) developed on the electrodes ( $E_1, E_2, E_3, \dots, E_{15}, E_{16}$  respectively) are collected for each current projection. Hence, in opposite current pattern (Fig. 1c), the boundary potentials on all the electrodes are measured for first eight current projections and the voltage data set containing 128 voltage data is obtained and it is then saved in a .txt file in PC for computation. Boundary potential data are generated for different phantom configurations and the resistivity images are reconstructed in EIDORS. The EIDORS discretizes the circular domains ( $D = 150$  mm) with a FEM mesh containing 1,968 triangular elements and 1,049 nodes [28] to solve the forward problem and inverse problem. EIDORS reconstructs the resistivity from the simulated data sets using regularized Gauss-Newton method with LMR regularization [5]. The mean inhomogeneity resistivity ( $IR_{\text{Mean}}$ ) [24], maximum inhomogeneity resistivity ( $IR_{\text{Max}}$ ), contrast to noise ratio (CNR) [24], percentage of contrast recovery (PCR) [24], coefficient of contrast (COC) [24], and diametric resistivity profile (DRP) [24, 27] of the reconstructed images are studied to evaluate the reconstruction.

### 3 Results and Discussion

Result shows that the resistivity is successfully reconstructed from the boundary data generated by the the data generator with a circular domain (Fig. 2) using OCI.

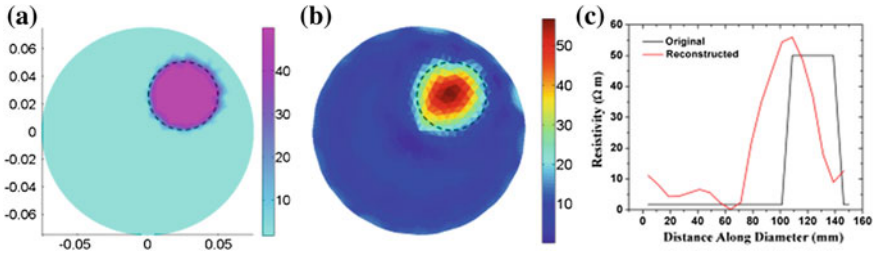


**Fig. 1** **a** A two-dimensional circular domain ( $\Omega$ ) with inhomogeneity defined by the Cartesian and polar co-ordinates with a particular radius ( $r = D/2$ ) in MATLAB, **b** Domain discretized by a FE mesh with triangular elements and the electrode nodes are located on boundary, **c** Boundary potential measurement for OCI in projection 4

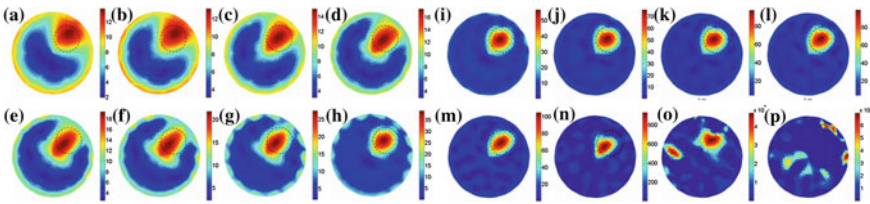
It is observed that the reconstruction quality depends on the boundary data accuracy which depends on the geometric accuracy of the domain. Figure 2a shows the original resistivity distribution of the simulated domain with a single circular inhomogeneity near electrode number-3 ( $D = 150$  mm,  $\eta_{mr} = 4$ ,  $d = 50$  mm,  $r = 37.5$  mm,  $\theta = 45^\circ$ ,  $\rho_i = 50 \Omega\text{m}$ ,  $\rho_b = 1.724 \Omega\text{m}$  and  $I = 1$  mA). Figure 2b, c show the resistivity image and DRP respectively.

Results show that the CNR of the reconstructed images for the inhomogeneity near electrodes 3 (Fig. 2a) is 5.1390 which indicates an efficient image reconstruction ( $\text{CNR} > 3$ ) [17, 22]. PCR and COC of the reconstructed image for the domain with inhomogeneity near electrode 3 (Fig. 2a) are 57.9489% and 4.6199 respectively.  $\text{IR}_{\text{Mean}}$ ,  $\text{BR}_{\text{Mean}}$  and  $\text{IR}_{\text{Max}}$  of the reconstructed image for the same domain are 35.7509  $\Omega\text{m}$ , 7.7385  $\Omega\text{m}$  and 56.7176  $\Omega\text{m}$  respectively. DRP (Fig. 2c) of the reconstructed images (Fig. 2b) for the domain with circular inhomogeneity near electrodes 3 is following the DRP of the original resistivity distribution. Results show that the reconstructed shape of the inhomogeneity is similar to that of the original one (Fig. 2a) and the reconstructed resistivity profile in Fig. 2c is almost similar to that of the original object in Fig. 2a.

Resistivity imaging of the simulated domain ( $D = 150$  mm,  $\eta_{mr} = 4$ ,  $d = 50$  mm,  $r = 37.5$  mm,  $\theta = 45^\circ$ ,  $\rho_i = 50 \Omega\text{m}$ ,  $\rho_b = 1.724 \Omega\text{m}$  and  $I = 1$  mA) with a circular inhomogeneity near electrode number 3 is studied (Fig. 3) in different iterations and all the images are evaluated in each steps. Results show that the image reconstruction starts with a poor quality image (Fig. 3a) and gradually it improves as the iteration goes on. It is observed that, in different iterations (Fig. 3a–p) the reconstructed image gradually becomes more localized and the resolution is improved. It is also observed that in each step the images are improved with a reduction in reconstruction errors appeared by the red color in the region of interface between the inhomogeneity and the background are minimized as the iterations goes on up to



**Fig. 2** **a** Domain with a circular inhomogeneity ( $D = 150$  mm,  $r = 37.5$  mm,  $\theta = 45^\circ$ ,  $d = 50$  mm,  $\rho_i = 50 \Omega\text{m}$ ,  $\rho_b = 1.724 \Omega\text{m}$ ,  $\eta_{mr} = 4$ ,  $I = 1$  mA), **b** Resistivity image reconstructed from boundary data collected through opposite method of current injection, **c** DRP



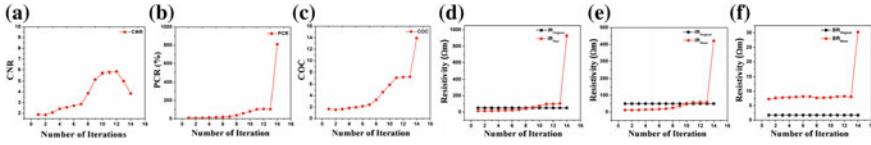
**Fig. 3** Reconstructed images of a circular domain with a circular inhomogeneity ( $D = 150$  mm,  $r = 37.5$  mm,  $\theta = 45^\circ$ ,  $d = 50$  mm,  $\rho_i = 50 \Omega\text{m}$ ,  $\rho_b = 1.724 \Omega\text{m}$ ,  $\eta_{mr} = 4$ ,  $I = 1$  mA) near electrode 3 for different numbers of iterations in inverse solver in EIDORS: **a** 1st iteration, **b** 2nd iteration, **c** 3rd iteration, **d** 4th iteration, **e** 5th iteration, **f** 6th iteration, **g** 7th iteration, **h** 8th iteration, **i** 9th iteration, **j** 10th iteration, **k** 11th iteration, **l** 12th iteration, **m** 13th iteration, **n** 14th iteration, **o** 15th iteration, **p** 16th iteration

12th iteration (Fig. 3a–l). Results show that, though the shape and resolution of all the reconstructed images in 9–12th iterations (Fig. 3i, j) are almost similar to that of the original object (shown by dotted circles in Fig. 3), but the resistivity is optimally reconstructed in 9th iteration (Fig. 3i).

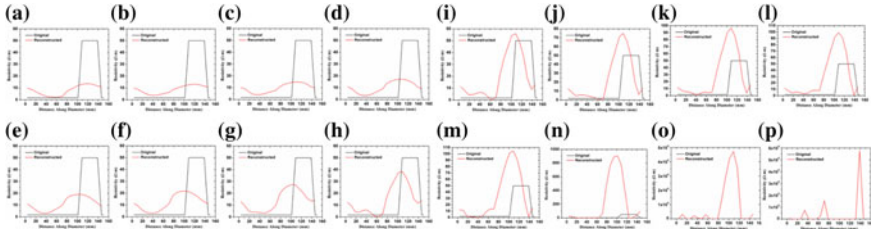
Image parameter study (Fig. 4a–f) shows that the CNR (Fig. 4a), PCR (Fig. 4b) and COC (Fig. 4c) of the reconstructed images for the inhomogeneity near electrodes 3 (as shown in Fig. 3) are poor in 1st iteration and they get improved as the iteration goes on. The  $IR_{Max}$  (Fig. 4d),  $BR_{Mean}$  (Fig. 4e) and  $IR_{Mean}$  (Fig. 4f) of the resistivity images are also improved as iteration goes but become over estimated after 9th iteration.

The DRPs of the reconstructed images (Fig. 5a–p) shows that the resistivity profile remains under estimated till the 8th iteration (Fig. 5a–h) and it becomes over estimated after 9th iteration (Fig. 5j–p). Therefore, it is observed that the reconstructed resistivity profile similar to that of the original is obtained only in the 9th iteration (Fig. 5i) and hence the 9th iteration is found as optimum iteration.

In 10–14th iterations (Fig. 5j–n) the resistivity is over estimated and the images are destroyed after 14th iteration (Fig. 5o, p). PCR becomes abnormal ( $>100\%$ ) after 11th iteration because of the over estimation of resistivity. In 15th iteration



**Fig. 4** Image parameters of the images obtained at different iterations as shown in Fig. 3 **a** CNR, **b** PCR, **c** COC, **d** IR<sub>Max</sub>, **e** IR<sub>Mean</sub>, **f** BR<sub>Mean</sub>



**Fig. 5** DRP of the reconstructed images (shown in the Fig. 3) of the simulated domain ( $D = 150$  mm,  $\eta_{mr} = 4$ ,  $d = 50$  mm,  $r = 37.5$ , mm,  $\theta = 45^\circ$ ,  $\rho_i = 50 \Omega\text{m}$ ,  $\rho_b = 1.724 \Omega\text{m}$  and  $I = 1$  mA) with a circular inhomogeneity near electrode number-3 in different iterations

the resistivity image is started to destroy (Fig. 5o) and in 16th iteration the image is completely lost (Fig. 5p). Hence the resistivity imaging studies with simulated boundary data show that boundary data generated by MatLAB-based boundary data generator is suitable for image reconstruction. Using simulated boundary data the resistivity imaging is successfully studied and evaluated using EIDORS. Image resistivity parameters and the image contrast parameters are calculated from the resistivity profiles of the reconstructed images and the image reconstruction process is studied and understood with image evaluation studies.

### 4 Conclusion

The EIT image reconstruction is studied and evaluated with simulated data generated by a MatLAB-based boundary data generator. Simulated boundary data are generated with circular domains for different configurations and the resistivity image reconstruction is studied in EIDORS. Results show that the resistivity images are successfully reconstructed from the simulated boundary data generated for all the domain configurations. Resistivity images reconstructed for simulated data are analyzed with their IR<sub>Mean</sub>, IR<sub>Max</sub>, CNR, PCR, COC and DRP. Results show that all the inhomogeneities are successfully reconstructed with their proper inhomogeneity and background profiles as well as with proper shapes and positions. Resistivity image reconstruction process is studied at different iterations and the results show that the reconstructed image quality varies with iteration steps and at a particular iteration



the optimum reconstruction is obtained. It is observed that the resistivity images are easy to analyze and evaluate by image parameters to identify the suitable iteration step in the reconstruction process. Hence, it is concluded that the resistivity imaging is successfully studied and evaluated using EIDORS using simulated boundary data.

## References

1. Webster, J.G.: *Electrical Impedance Tomography*. Adam Hilger Series of Biomedical Engineering, Adam Hilger, New York (1990)
2. Holder, D.S., Hanquan, Y., Rao, A.: Some practical biological phantoms for calibrating multifrequency electrical impedance tomography. *Physiol. Meas.* **17**, A167–77 (1996)
3. Denyer, C.W.L., *Electronics for real-time and three-dimensional electrical impedance tomographs*, PhD Thesis, Oxford Brookes University (1996)
4. Bera, T. K., Nagaraju, J.: Studies on thin film based flexible gold electrode arrays for resistivity imaging in Electrical Impedance Tomography. *Measurement* **47** 264–286 (2014)
5. Bera, T.K., Nagaraju, J.: Studying the resistivity imaging of chicken tissue phantoms with different current patterns in Electrical Impedance Tomography (EIT). *Measurement* **45**, 663–682 (2012)
6. Bera, T.K., Nagaraju, J.A.: Multifrequency Electrical Impedance Tomography (EIT) system for biomedical imaging. In: *Proceedings of International Conference on Signal Processing and Communications (SPCOM 2012)*, pp. 1–5. India, IISc - Bangalore, Karnataka, India (2012)
7. Thomas, J.Y., John, G.W., Willis, J.T.: Comparing reconstruction algorithms for Electrical Impedance Tomography. *IEEE Trans. Biomed. Eng. BME*-**34**(11), 843–852 (1987)
8. Bera, T.K., Biswas, S.K., Rajan, K., Nagaraju, J.: Improving conductivity image quality using Block Matrix-based Multiple Regularization (BMMR) technique in EIT: a simulation study. *J. Electr. Bioimpedance* **2**, 33–47 (2011)
9. Jing L., Liu S., Zhihong L., Meng S., An image reconstruction algorithm based on the extended Tikhonov regularization method for electrical capacitance tomography Original Research Article. *Measurement*, **42**(3), 368–376 (2009)
10. Bera, T.K., Biswas, S.K., Rajan, K., Nagaraju, J.: Improving image quality in Electrical Impedance Tomography (EIT) using Projection Error Propagation-Based Regularization (PEPR) Technique: a simulation study. *J. Electr. Bioimpedance*. **2**, 2–12 (2011)
11. Lionheart, W.R.B.: EIT reconstruction algorithms: pitfalls, challenges and recent developments, REVIEW ARTICLE. *Physiol. Meas.* **25**, 125–142 (2004)
12. Metherall, P.: *Three dimensional electrical impedance tomography of the human thorax*. PhD Thesis, University of Sheffield. January (1998)
13. Bushberg, J. T., Seibert, J. A., Leidholdt Jr. E. M., Boone, J. M.(eds.): *The Essential Physics of Medical Imaging*, 2nd edn. Lippincott Williams and Wilkins, Philadelphia (2001)
14. David, H. (ed.): *Clinical and Physiological Applications of Electrical Impedance Tomography*, 1st edn. Taylor and Francis, UK (1993)
15. Li, Ying et al.: A novel combination method of Electrical Impedance Tomography inverse problem for brain imaging. *IEEE Trans. Magn.* **41**(5) (2005)
16. Bagshaw, A.P., et al.: Electrical impedance tomography of human brain function using reconstruction algorithms based on the finite element method. *NeuroImage* **20**, 752–764 (2003)
17. Murphy, D., Burton, P., Coombs, R., Tarassenko, L., Rolfe, P.: Impedance imaging in the newborn. *Clin. Phys. Physiol. Meas. Suppl. A*, **8**, 131–40 (1987)
18. Hope, T. A., Iles, S. E.: Technology review: the use of electrical impedance scanning in the detection of breast cancer. *Breast. Cancer. Res.* **6**, 69–74 (2004)
19. Brown, B. H.: Medical impedance tomography and process impedance tomography: a brief review. *Meas. Sci. Technol.* **12**, pp. 991–996 (2001)

20. Linderholm, Pontus et al.: Cell culture imaging using Microimpedance Tomography. *IEEE Trans. Biomed. Eng.* **551** (2008)
21. Bera, T. K., Nagaraju, J. A.: Multifrequency constant current source for medical Electrical Impedance Tomography. In: Proceedings of the IEEE International Conference on Systems in Medicine and Biology 2010, pp. 278–283. Kharagpur, India (2010)
22. Bera, T.K., Nagaraju, J.: Surface electrode switching of a 16-Electrode wireless EIT system using RF-based digital data transmission scheme with 8 channel encoder/decoder ICs. *Measurement* **45**, 541–555 (2012)
23. Manuehr, S.: Electrical impedance tomography system: an open access circuit design. *Bio-Med. Eng. OnLine.* **5**(28), 1–8 (2006)
24. Bera, T.K., Nagaraju, J.: Switching of a sixteen electrode array for wireless EIT system using a RF-based 8-Bit digital data transmission technique. *Commun. Comput. Inform. Sci.* **269**, 202–211 (2012)
25. Tong, I.O., Hun, W., Do, Y.K., Pil, J.Y., Eung J.W.: A fully parallel multi-frequency EIT system with flexible electrode configuration: KHU Mark2. *Physiol. Meas.* **32**(7), 835–49 (2007)
26. Bera, T.K., Nagaraju, J.: Switching of the surface electrodes array in a 16-electrode EIT system using 8-bit parallel digital data. In: Proceedings of IEEE World Congress on Information and Communication Technologies, pp. 1288–1293. Mumbai, India (2011)
27. Bera, T.K., Nagaraju, J.A.: Chicken tissue phantom for studying an Electrical Impedance Tomography (EIT) system suitable for clinical imaging, sensing and imaging. *Int. J.* **12**( 3–4), 95–116 (2011)
28. Bera, T.K., Nagaraju, J.: Resistivity imaging of a reconfigurable phantom with circular inhomogeneities in 2D-Electrical Impedance Tomography. *Measurement* **44**(3), 518–526 (2011)
29. Bera, T.K., Nagaraju, J.: A reconfigurable practical phantom for studying the 2 D Electrical Impedance Tomography (EIT) using a FEM based forward solver. In: Proceedings of the 10th International Conference on Biomedical Applications of Electrical Impedance Tomography (EIT 2009), Manchester (2009)
30. Bera, T.K., Nagaraju, J. A.: Study of practical biological phantoms with simple instrumentation for Electrical Impedance Tomography (EIT). In: Proceedings of IEEE International Instrumentation and Measurement Technology Conference (I2MTC2009), pp. 511–516. Singapore (2009)
31. Bera, T.K., Nagaraju, J.A.: Simple instrumentation calibration technique for Electrical Impedance Tomography (EIT) Using A 16 Electrode Phantom. In: Proceedings of the 5th Annual IEEE Conference on Automation Science and Engineering, pp. 347–52. Bangalore (2009)
32. Bera, T. K., Nagaraju, J.: Studying The 2D Resistivity reconstruction of stainless steel electrode phantoms using different current patterns of Electrical Impedance Tomography (EIT). In: Proceedings of the International Conference on Biomedical Engineering, Biomedical Engineering, Narosa Publishing House, India, pp. 163–169 (2011)
33. Bera, T.K., Nagaraju J.: Studying the 2D-image reconstruction of non biological and biological inhomogeneities in Electrical Impedance Tomography (EIT) with EIDORS. In: Proceedings of the International Conference on Advanced Computing, Networking and Security: ADCONS 2011. India, NITK—Surathkal, India, 132–136 (2011)
34. Jochen, H., Leonard, M., Reindl.: A computer simulation platform for the estimation of measurement uncertainties in dimensional X-ray computed tomography, *Measurement.* **45**(8), 2166–2182 (2012)
35. Harvey, G., Jan, T., Wolfgang, C.: *An Introduction to Computer Simulation Methods: Applications to Physical Systems* (3rd Edn.), Addison-Wesley (January 19, 2006)
36. Tushar, K.B., Nagaraju, J.: A MATLAB Based Boundary Data Simulator for Studying The Resistivity Reconstruction Using Neighbouring Current Pattern, *J. Med. Eng.* vol. 2013, Article ID 193578, p. 15
37. Zlochiver, S., Radai, M.M., Abboud, S., Rosenfeld, M., Dong, X.Z., Liu, R.G., You, F.S., Xiang, H.Y., Shi, X.T.: Induced current electrical impedance tomography system: experimental results and numerical simulations. *Physiol. Meas.* **25**(1), 239–255 (2004)

38. Sadleir, R.J., Sajib, S.Z., Kim, H.J., Kwon, O.I., Woo, E.J.: Simulations and phantom evaluations of magnetic resonance electrical impedance tomography (MREIT) for breast cancer detection. *J. Magn. Reson.* **230**, 40–9 (2013)
39. Vauhkonen, M., Lionheart W.R.B., Heikkinen, L. M., Vauhkonen, P. J., Kaipio, J. P.: A MATLAB package for the EIDORS project to reconstruct two dimensional EIT images. *Physiol. Meas.* **22**, 107–111 (2001)
40. Bera, T.K., Biswas, S.K., Rajan,K., Nagaraju, J.: Image reconstruction in Electrical Impedance Tomography (EIT) with Projection Error Propagation-based Regularization (PEPR). In: *A Practical Phantom Study, Lecture Notes in Computer Science: ADCONS 2011*, vol. 7135/2012, pp. 95–105. Springer (2012)

# Coverage of Indoor WLAN in Obstructed Environment Using Particle Swarm Optimization

LeenaArya and S. C.Sharma

**Abstract** Wireless communications is the fastest growing segment of the communications industry and over the recent years, it has rapidly emerged in the market providing users with network mobility, scalability, and connectivity. It is a flexible data communication system implemented as an extension to or as an alternative for, a wired LAN [1]. The placement of access points (AP) can be modeled as a nonlinear optimization problem. The work explores the measured data in terms of signal strength in the indoor WLAN 802.11 g at Malviya Bhavan, Boys Hostel Building, Indian Institute of Technology, Roorkee, Saharanpur Campus coverage using optimization technique. In the present study, an application of particle swarm optimization (PSO) is shown to determine the optimal placement of AP.

**Keywords** Wireless LAN · Access point · Path loss model · Obstructed environment · Particle swarm optimization.

## 1 Introduction

Wireless LANs enable users to access network resources and applications securely anytime and anywhere a wireless network is deployed [2]. Access points can nowadays be found in our daily environment, e.g., in many office buildings, public spaces, and in urban areas [1]. In the corporate enterprise, wireless LANs are usually employed as the final link between the existing wired network and a group of client computers, giving these users wireless access to the full resources and services of

---

L. Arya (✉)

Electronics and Communication Department, Lingaya's University, Faridabad, India  
e-mail: leenaarya18@gmail.com

S. C. Sharma

Electronics and Computer Engineering Discipline Department, IIT Roorkee, UT, India  
e-mail: scs60fpt@iitr.ernet.in

the corporate network across a building or campus [3]. WLAN networks have become very popular means for providing a wireless networking facility for home users, educational institutions, companies etc. due to their ease of installation and their high data rate provision, apart from providing, although limited, mobility to users [2].

If the APs are placed too far apart, they will generate a coverage gap; but if they are too close to each other, this will lead to excessive co-channel interferences and increases the cost unnecessarily [5]. In this paper, we use PSO to determine location in such a WLAN. In the indoor environment, the propagated electromagnetic signal can undergo the necessary three mechanisms of electromagnetic wave propagation—reflection, diffraction, and scattering.

The basic structure of a WLAN is called a Basic Service Set (BSS) which comes in two categories: Infrastructure BSSs and Independent BSSs. In infrastructure mode, the wireless network consists of at least one access point connected to the wired network infrastructure and a set of wireless end stations. In an independent BSSs (IBSS), stations communicate directly with each other and are usually composed of a small number of stations setup for a short period of time [3]. IBSSs are often referred to as ad hoc networks.

The rest of the paper is organized as follows: Notations are given in Sect. 2. Section 3 provides the mathematical model description and path loss model. Section 4 shows the working of PSO. Section 5 describes the method of testing, setup, and methodology. Analysis of results for obstructed environment on the first floor and measurements and analysis taken inside rooms with soft and hard partitions are presented in Sect. 6. Finally, Sect. 7 concludes the paper.

## 2 General Notations

Throughout this paper, the following notations are used:

- $a_j$   $j = 1 \dots N$  Access point (AP)
- $r_i$   $i = 1 \dots M$  Receiver/user
- $d(a_j, r_i)$  Distance between AP and receiver
- $g(a_j, r_i)$  Path loss from  $i_{th}$  user to access point  $j$
- $g_{\max}$  Maximum tolerable path loss
- $P_t$  Transmit power
- $P_r$  Received power
- $R_{th}$  Receive threshold
- $Ap$  Position of AP

It should be noted that  $a_j$  represents the unknown coordinates of APs. Their number  $N$  is not known either. The coordinates of users  $r_i$  are assumed to be known and these users can be distributed in design area according to the design specifications.

In the present analysis, the distance function assumed to be Euclidean, hence on the plane, the distance ( $d$ ) between an AP  $a_j$  and a receiver  $r_i$  is given by [5]:

$$d(a_j, r_i) = \sqrt{(r_i^1 - a_j^1)^2 + (r_i^2 - a_j^2)^2}$$

where  $a_j = a_j(a_j^1, a_j^2)$ , and  $r_i = r_i(r_i^1, r_i^2)$

### 3 Model Description

The aforementioned problem can be modeled as an optimization problem for which the objective function is to minimize the path loss. Mathematically it may be given as:

$$\min g(a_j, r_i) \leq g_{\max} \forall i = 1, \dots, M \tag{1}$$

Constraint (1) states that path loss is evaluated against the maximum tolerable path loss  $g_{\max}$ . This ensures that the quality of coverage at each receiver location is above the given threshold. This given value,  $g_{\max}$  can be calculated by subtracting receiver threshold ( $R_{th}$ ) from transmitter power ( $P_t$ ).

$$g_{\max} = P_t - R_{th} \tag{2}$$

The above inequality (1) can be expressed in the equality form as:

$$(\min_j g(a_j, r_i) - g_{\max})^+ = 0, \tag{3}$$

#### 3.1 Path Loss Model

The propagation of radio waves is characterized by several factors: (a) free space loss. (b) Attenuated by the objects on the propagation path such as windows, walls, table, chair, and floors of building. (c) The signal is scattered and can interfere with itself [7]. The basic propagation model is based on free space propagation. In general, the power received by an antenna that is separated from the transmitting antenna by the distance  $d$  in free space is given by [5, 6]:

$$P_r(a_j, r_i) = \frac{P_t G_t G_r \lambda^2}{(4\pi)^2 d(a_j, r_i)^2} \tag{4}$$

where  $P_t$  is the transmitted power,  $G_t$  and  $G_r$  are the transmitter and receiver antenna gain,  $d$  is the distance between transmitter and receiver, and  $\lambda = c/f$  is the wavelength of the carrier frequency,  $c$  is the speed of light ( $3 \times 10^8$  m/s), and  $f$  is the frequency of radio carrier in hertz. The path loss, which represents signal attenuation between the transmitted and the received power and is measured in dB (decibels), in free space environments, is given by [5, 6]:

$$g(a_j, r_i)[dB] = -10 \log \left[ \frac{G_t G_r \lambda^2}{(4\pi)^2 d(a_j, r_i)^2} \right]$$

The above equation does not hold when points  $a_j$  and  $r_i$  are very close to each other. Therefore, large-scale propagation models use a close-in distance,  $d_0$  which is known as the received power reference distance point. Therefore, path losses at reference distance assuming transmit and receive antenna with unity gain as described in [5, 6] can be calculated from:

$$g(a_j, r_i) = g(d_0)[dB] = 20 \log \frac{4\pi d_0 f}{c} \quad (5)$$

Therefore, path loss function in free space at a distance greater than  $d_0$  is given by

$$g(a_j, r_i)[dB] = g(d_0)[dB] + 10 \log \left( \frac{d(a_j, r_i)}{d_0} \right)^2 \quad (6)$$

The RF (radio frequency) path between transmitter and receiver is affected by the distance between the two terminals and the type and number of obstacles (walls, doors, windows, furniture, etc). Thus, including loss caused by partitions in path loss model, Eq. (6) can be written as [5, 6]:

$$g(a_j, r_i)[dB] = g(d_0)[dB] + \log \left( \frac{d(a_j, r_i)}{d_0} \right)^2 + \Sigma n_{SP} l_{SP} + \Sigma n_{HP} l_{HP} \quad (7)$$

where  $n_{SP}$  represents the number of soft partitions of a particular type and  $l_{SP}$  represents the loss in dB attributed to a particular soft-type partitions,  $n_{HP}$  represents the number of hard partitions related to a particular type and  $l_{HP}$  represents the loss in dB associated with a particular hard-type partitions. The soft partition consists of movable objects like furniture, users etc. While hard partitions comprises of fixed objects like walls, doors, window etc. A move around corner of the building or a wall can cause the received signal to drop suddenly.

## 4 Working of PSO

For a D-dimensional search space, the position of the  $i$ th particle is represented as  $X_i = (x_{i1}, x_{i2}, \dots, x_{id}, \dots, x_{iD})$ . Each particle maintains a memory of its previous best position  $P_i = (p_{i1}, p_{i2}, \dots, p_{id}, \dots, p_{iD})$ . The best one among all the particles in the population is represented as  $P_g = (p_{g1}, p_{g2}, \dots, p_{gd}, \dots, p_{gD})$ . The velocity of each particle is represented as  $V_i = (v_{i1}, v_{i2}, \dots, v_{id}, \dots, v_{iD})$ , is clamped to a maximum velocity  $V_{\max} = (v_{\max,1}, v_{\max,2}, \dots, v_{\max,d}, \dots, v_{\max,D})$  which is specified by the user. During each generation, each particle is accelerated toward the particle's previous best position and the global best position. The two

basic equations which govern the working of PSO are that of velocity vector and position vector given by:

$$v_{id} = \omega^* v_{id} + c_1 r_1 (p_{id} - x_{id}) + c_2 r_2 (p_{gd} - x_{id}) \quad (8)$$

$$x_{id} = x_{id} + v_{id} \quad (9)$$

here  $c_1$  and  $c_2$  are acceleration constants.

## 5 Method of Testing

### 5.1 Setup for AP

We performed our experiment in first case without an obstacle and in the second case with obstacle in the design area which has the dimensions of 64 m x 60 m and has 400 users. It has 100 rooms and part of corridors. The data collection site building and google map of the site is given in Fig. 1. The layout of the floor is shown in Fig. 2. The entire wing of the first floor is covered by 10 access points installed at the locations indicated by red symbols in Fig. 2. Ten locations of measurement are chosen on the first floor of the Malviya Bhavan building as shown in Fig. 2 denoted as A, B, C, D, E, F, G, H, I, and J. The specification of the model of Access point is LINK (DWL-3200AP) and IEEE 802.11g standard are used to test the model. We conducted our experiments at the first and second floor of the Malviya Bhavan, IIT Roorkee, Saharanpur Campus. Our data collection system comprised of a laptop, running Windows 2007, an MSA 338 handheld spectrum analyzer, and an M304 omnidirectional dipole antenna.

### 5.2 Methodology

Once the priority area has been identified, the data has been collected nearby access points which require a connection to the wired LAN and a source of power. The signal strength has been measured using 3.3 GHz Spectrum Analyzer with omnidirectional dipole antennas at a number of points around the access point. The coverage and location of access points has been checked using optimization technique in those priority areas that are within range. While in other places the aim was to identify the points where the available bandwidth is likely to drop below the theoretical maximum, typically where the signal strength falls below  $-70$  dBm [8].

The received signal strength calculated using the spectrum analyzer is shown in Fig. 3 and similarly signal strength have been calculated using spectrum analyzer for



**Table 1** Optimal placement of APs for 100 users on first floor with  $P_t = 21$  dBm

Locations of access points	Received signal strength $R_{th}$ (dBm)	Actual placement of access point coordinates	Access point coordinates by PSO
Location A	-38.4	(18.90, 10.93)	(22.16, 11.32)
Location B	-37.2	(24.72, 2.51)	(27.34, 4.54)
Location C	-27.1	(35.90, 1.59)	(38.25, 1.09)
Location D	-40.4	(42.19, 12.92)	(38.98, 10.25)
Location E	-32.4	(38.97, 26.24)	(40.54, 24.25)
Location F	-20.2	(41.88, 43.70)	(40.98, 44.72)
Location G	-41.6	(36.36, 52.43)	(32.22, 50.35)
Location H	-23.2	(26.10, 25.94)	(25.12, 24.23)
Location I	-42.0	(30.54, 12.00)	(32.45, 10.26)
Location J	-29.6	(33.60, 25.94)	(30.25, 24.31)

obstructed environment. The optimal placement of access points for 100 users on first floor with transmitter power of 21 dBm is shown in Table 1. The actual placement of access point coordinates is shown in Fig. 4 and the distribution of access point coordinates by using particle swarm optimization is shown in Fig. 5.

**Fig. 1** Data collection site building



**Fig. 2** Plan of the floor where the experiment was conducted. Readings were collected in the corridors

## 6 Analysis of Results for Obstructed Environment on First Floor

Results for obstructed environment on the first floor have been analyzed by using the optimization technique. The analysis of each is described in the following subsections:

For the present analysis, we consider the obstacles in indoor environment such as brick walls, wooden doors, windows, furniture, and moving human being. Reported available data for these obstructions is taken at 2.4 GHz as shown in Table 2.

**Table 2** Signal attenuation through various obstructions at 2.4 GHz

Obstructions	Reported Signal Attenuation through various obstructions (dB)
Metal frame glass wall into building	6
Brick wall	6
Wooden block wall	4
Metal door in brick wall	12.4
Brick wall next to metal door	3
Window in a brick wall	2
Human	4

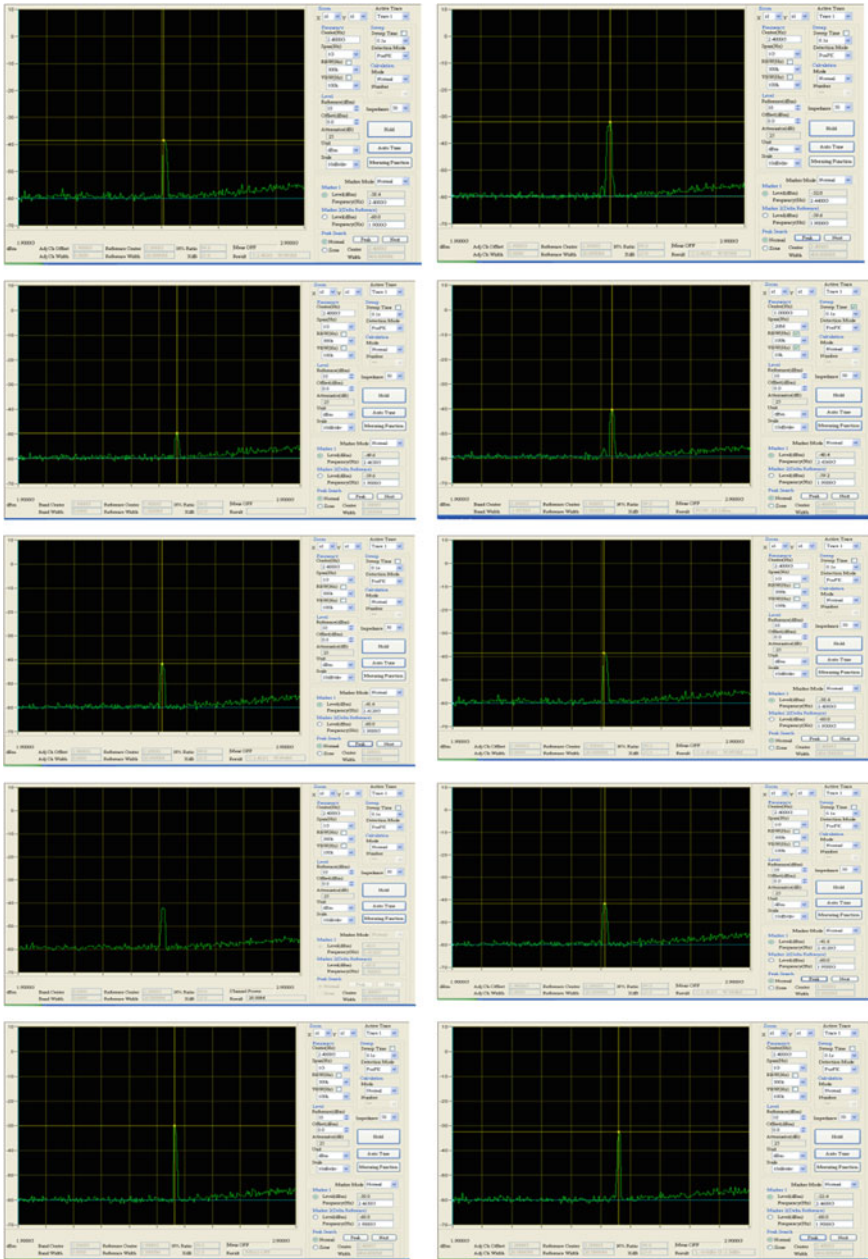


Fig. 3 Received signal strength calculated using spectrum analyser

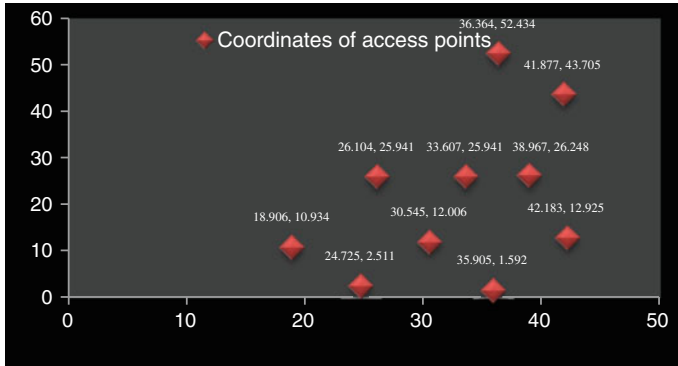


Fig. 4 Actual placement of access points

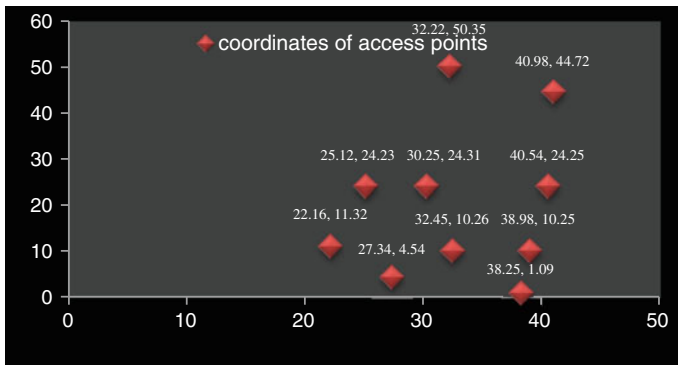


Fig. 5 Distribution of access points by using PSO

### 6.1 Measurements and Analysis Taken Inside Rooms with Soft and Hard Partitions on First Floor

Measurements taken inside rooms where the presence of a human being, desk, and table is possible and these are soft partitions, then

$$n_{SP} = \text{number of soft partitions human being, desk, table} = 1 \text{ each}$$

$l_{SP}$  = loss due to soft partitions human being, desk, table = 4 dB, 4 dB and 4 dB (as given in Table 2)

$$n_{SP}l_{SP} = (1 + 1 + 1) * (4 + 4 + 4) = 36 \text{ dB}$$

$$n_{HP} = \text{number of hard partitions wall, glass window, almirah, and door} = 1 \text{ each}$$

$l_{HP}$  = loss due to hard partitions wall, glass window, almirah, and door = 6 dB, 2 dB, 4 dB and 4 dB (as given in Table 2)

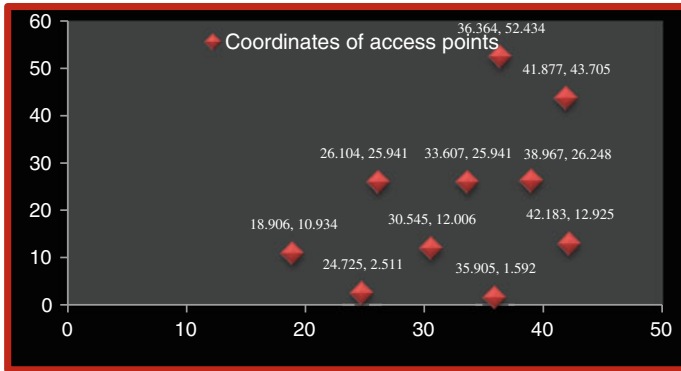


Fig. 6 Actual placement of access points

$$n_{HP}l_{HP} = (1 + 1 + 1 + 1) * (6 + 2 + 4 + 4) = 64 \text{ dB}$$

Now from the Eq. (6)

$$g(a_j, r_i)[dB] = g(d_o)[dB] + 10 \log \left( \frac{d(a_j, r_i)}{d_o} \right)^2$$

$$n_{SP}l_{SP} + n_{HP}l_{HP} = 36 + 64 = 100 \text{ dB}$$

Now from the Eq. (7)

$$g(a_j, r_i)[dB] = g(d_o)[dB] + 10 \log \left( \frac{d(a_j, r_i)}{d_o} \right)^2 + 100 \text{ dB}$$

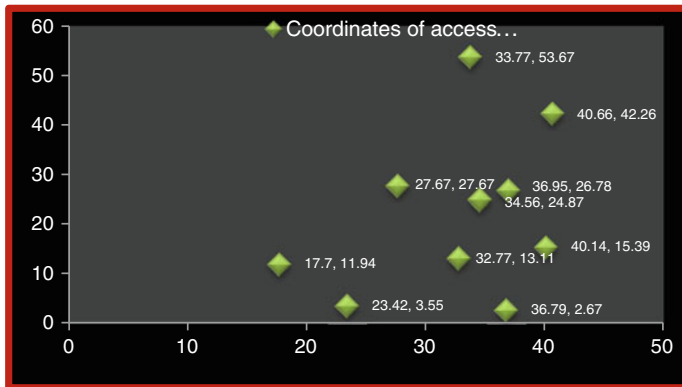
The received signal strength calculated using the spectrum analyzer is shown in Fig. 6. Table 3 shows the measurements taken inside rooms taking wall, human, desk, table, almirah etc. as obstructions and closed door for different access points. The actual placement of access point coordinates is shown in Fig. 6 and the distribution of access point coordinates by using particle swarm optimization is shown in Fig. 7. Similarly, the results have been taken for the second floor as well as for the ground floor where there is no access point installed but due to floor attenuation factor (FAF) some access of the network is found on the staircase near ground floor.

## 7 Conclusion

In this paper, we have presented particle swarm optimization to predict the signal strength in indoor environments. It is observed that the size of the design area and the

**Table 3** Measurements taken inside rooms with soft and hard partitions for different access points

S.No	Access point location	Positions	Distance between T-R separation in (m)	Signal (dBm)	Strength	Actual placement of access point coordinates	Access point coordinates by PSO
1	Location A	Inside room A-200, human, desk, door open	4.41	-54.0		(18.90, 10.93)	(17.70, 11.94)
2	Location B	Inside room A-232, human, desk, door open	4	-54.0		(24.72, 2.51)	(23.42, 3.55)
3	Location C	Inside room A-249, on bed, door open	5.83	-50.0		(35.90, 1.59)	(36.79, 2.67)
4	Location D	Inside room A-254, table, almirah, human	4	-54.4		(42.19, 12.92)	(40.14, 15.39)
5	Location E	Inside room A-267, table, almirah, door closed	8.7	-54.8		(38.97, 26.24)	(36.95, 26.78)
6	Location F	Inside room A-277, table, almirah, human, door closed	4	-54.4		(41.88, 43.70)	(40.66, 42.26)
7	Location G	Inside room A-280, table, bed, almirah, human, door closed	7.19	-54.8		(36.36, 52.43)	(33.77, 53.67)
8	Location H	Inside room A-219, table, almirah, human, door open	4.41	-51.2		(26.10, 25.94)	(27.67, 27.67)
9	Location I	Inside room A-226, desk, human, door open	4.41	-54.4		(30.54, 12.00)	(32.77, 13.11)
10	Location J	Inside room A-266, desk, human, door open	4.41	-54.8		(33.60, 25.94)	(34.56, 24.87)



**Fig. 7** Distribution of access points by using PSO

number of users and their locations have an effect on the location and the number of APs needed to cover users and path loss increases as a function of distance between the transmitter and user. This paper provides the results of comparison between the actual location of access points and the locations obtained by PSO in obstructed environment. The coverage area was varying between scenarios and there were different levels of signal strength for each receiver location depends on the obstacles between the receiver and the transmitter in the non-line of sight (NLOS) environment. It has been observed that the number of access points can be reduced so as to save the cost of installation of access points.

## References

1. Traoré, Soungalo, Renfa, Li, Fanzi, Zeng: Evaluating and Improving Wireless Local Area Networks Performance. *International Journal of Advancements in Computing Technology* **3**(2), 156–164 (2011)
2. Wireless LAN Solutions At-A-Glance - Cisco [www.cisco.com/web/AP/wireless/pdf/WirelessLAN.pdf](http://www.cisco.com/web/AP/wireless/pdf/WirelessLAN.pdf), United States (2012)
3. IEEE 802.11b Wireless LANs [http://www.3com.com/other/pdfs/infra/corpinfo/en\\_US/50307201.pdf](http://www.3com.com/other/pdfs/infra/corpinfo/en_US/50307201.pdf)
4. Particle Swarm Optimization (PSO) [www23.homepage.villanova.edu/varadarajan.komanduri/PSO\\_meander-line.ppt](http://www23.homepage.villanova.edu/varadarajan.komanduri/PSO_meander-line.ppt)
5. Kouhbor, S., Ugon, J., Kruger, A., Rubinov, A.: Optimal placement of access point in WLAN based on a new algorithm. In: proceedings of the International Conference on Mobile Business-IEEE/ICMB, pp. 592–598, Jul 2005
6. Shahnaz, K.: Physical security enhancement in WLAN systems. In: ISSNIP-IEEE, pp. 733–738 (2007)
7. Li, B., Dempster, A., Rizos, C., Barnes, J.: Hybrid method for localization using WLAN. In: Spatial Sciences Conference, [www.gmat.unsw.edu.au/snap/publications/lib\\_et al2005c.pdf](http://www.gmat.unsw.edu.au/snap/publications/lib_et al2005c.pdf) (2005)
8. GD/JANET/TECH.: Surveying wireless networks, [www.ukema.ac.uk/documents/.../technical../](http://www.ukema.ac.uk/documents/.../technical../) (2008)

# Stereovision for 3D Information

Mary Ann George and Anna Merine George

**Abstract** Stereovision is a technique aimed at inferring depth from two or more cameras. It plays an important role in computer vision. Single image has no depth or 3D information. Stereovision takes two images of a scene from different viewpoints usually referred to as left and right images using two cameras. Stereovision is similar to the binocular (two-eyed) human vision capturing two different views of a scene and brain processing and matching the similarity in both the images and the differences allow the brain to build depth information. OpenCV Library is used to compute the output of stereovision process—disparity and depth map.

**Keywords** Calibration · Disparity · Rectification · Stereo-correspondence · Triangulation

## 1 Introduction

Vision begins with the detection of light from the world. Humans and most animals have two eyes with overlapping regions. Stereovision helps to perceive depth in the overlapping region. Perception, lighting and shadows make a 2D image look real. More than one 2D image reveals 3D information. Modern computer vision stereo algorithms are capable of producing real-time results which are accurate enough for simple applications.

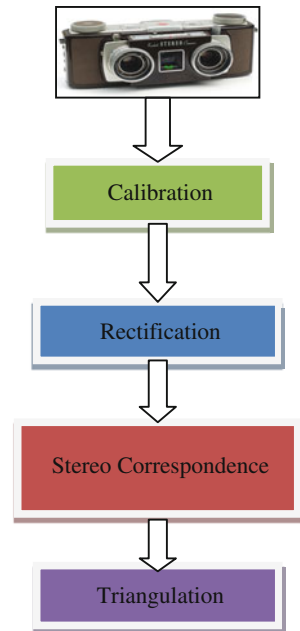
Stereovision process involves four main steps namely Calibration, Rectification, Stereo-correspondence or Stereo Matching, and Triangulation. Camera calibration is important for relating camera measurements with measurements in the real,

---

M. A. George (✉) · A. M. George  
M.I.T, Manipal 576104, India  
e-mail: starmaryann1247@yahoo.com

A. M. George  
e-mail: anna\_thanku@yahoo.com



**Fig. 1** Stereovision system

three-dimensional world. Rectification is a process of adjusting angle and distance between the cameras. Stereo-correspondence is a process of finding the same features in the left and right images. The output of this step is a disparity map. Disparity is the difference in x-coordinates on the image planes of the same feature viewed in the left and right cameras. Triangulation aims at calculating the depth or 3D position of points in the images from the disparity map and the geometry of the stereo setting. The output of this process is a depth map.

OpenCV stands for Open Source Computer Vision Library. It is an Intel-based library containing a collection of C and C++ functions to implement Image Processing and computer vision algorithms [1] (Fig. 1).

## 2 Overview of Stereovision System

### 2.1 Calibration

The camera calibration deals with both intrinsic and extrinsic parameters of the camera. Intrinsic parameters include both camera geometry and distortion model of the lens. For simplicity of analysis, we consider a pinhole camera model.

In a pinhole model, we do not consider the lens as a whole but only consider the camera as a point (optical center). Using this model, we calculate the focal length and form the camera intrinsic matrix.

There are two types of distortion namely tangential and radial distortion. Radial distortion arises as a result of the shape of lens, this distortion is zero at the (optical) center of the imager or image plane and increases as we move toward the periphery. Tangential distortions arise from the assembly process of the camera as a whole [2]. This distortion is due to manufacturing defects resulting from the lens not being exactly parallel to the imaging plane. Both these distortions are mathematically removed during the calibration process resulting in undistorted images. Extrinsic parameter deals with translation vector and rotational matrix. This is used to convert 3D object coordinates in meters  $(x, y, z)$  to camera coordinates in pixels  $(x, y)$ .

For calibration we generally use a chess board as a calibration object. This pattern of alternating black and white squares ensures that there is no bias toward one side or the other in measurement. We take multiple views of this planar object.

### 2.2 Rectification

The basic geometry of a stereo imaging system is referred to as epipolar geometry. Here we consider two pin hole models one for each camera. Rectification process takes into account epipolar constraint. Given a feature in one image the corresponding feature in the other image will lie along the epipolar line. Epipolar constraint makes two-dimensional search for matching features across two imagers to a one-dimensional search along the epipolar lines leading to faster computation [2].

The Fig. 2 shows the epipolar geometry. The points  $P$  (actual viewed point),  $O_1$  and  $O_r$  (Center of projections) forms the epipolar plane and this plane intersects the left

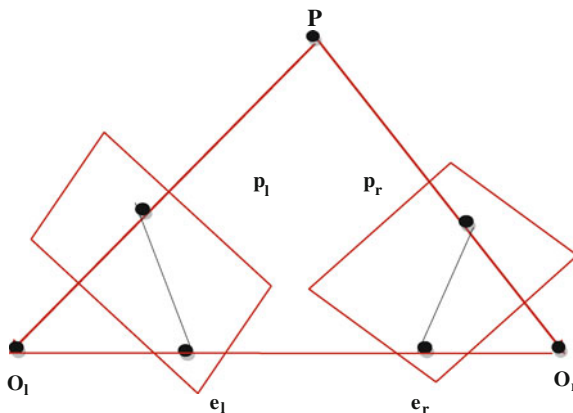


Fig. 2 Epipolar geometry

and right image planes and form lines called the epipolar lines ( $p_l - e_l$  and  $p_r - e_r$ ).  $p_l$  and  $p_r$  are the projection of  $P$  on the left and right image plane respectively.  $e_l$  and  $e_r$  are called the epipoles. The image of the center of projection  $O_l(O_r)$  on the other image plane is an epipole<sub>r</sub> ( $e_l$ ).

### 2.3 Stereo Matching

Stereo Matching or Stereo-correspondence aims at finding the homologous points in the two images of the same scene taken using two different cameras. Given a point A in the left image there will be a corresponding point B in the right image. The difference in the position between the corresponding points (A and B) in the two images is termed as the disparity. The output of this step is a disparity map. A pair of left and right image of the same scene taken using a stereo-camera is called a stereo-pair. There are two main classes of correspondence algorithm namely correlation-based and feature-based algorithm. In correlation-based method correspondence is achieved by matching the image intensities. This results in dense disparity map [2]. In feature-based method correspondence is achieved by matching image features like edges. This technique is faster and insensitive to illumination changes and produce sparse disparity map. Some challenges in stereo matching are color inconsistencies, untextured region, and occlusion problem.

### 2.4 Triangulation

It is the process of recovering the 3D position from the disparity map and geometry of the stereo setting. Triangulation is also called as reconstruction. In stereovision 3D location of any point is the intersection of two lines passing through their center of projection and projection of the point in each image.

In triangulation we are actually finding the depth from disparity. The depth and disparity are inversely related.

Figure 3 shows the depth calculation. P is the point in the 3D space with coordinates  $(X, Y, Z)$ . This point is projected to left and right image plane as  $P_l$  and  $P_r$  with coordinates  $(x_l, y_l)$  and  $(x_r, y_r)$  respectively.  $x_l - x_r$  is the disparity.  $x_l$  and  $x_r$  are measured from the corresponding left and right optical axis. B is the base length and  $f$  is the focal length. Focal length is the distance from the optical center to the image plane. Considering the similar triangles in Fig. 2 and we derive an expression for depth Z as shown in Eq. 1

$$Z = \frac{Bf}{x_l - x_r} \quad (1)$$

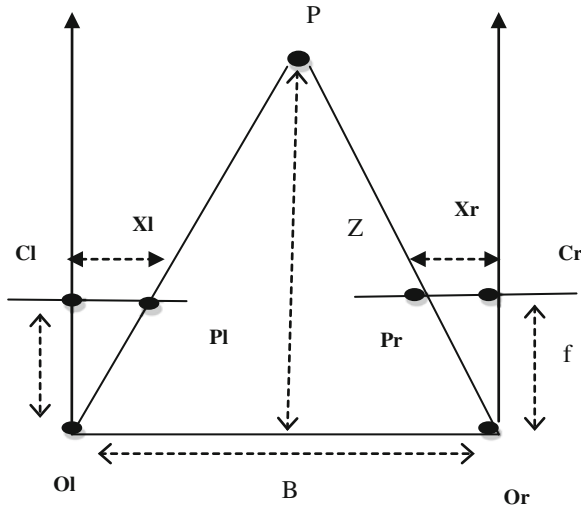


Fig. 3 Depth calculation

### 3 OpenCV

OpenCV means Intel® Open Source Computer Vision Library. It contains C and C++ functions for high speed implementation of image processing and computer vision applications. It is Optimized and intended for real-time applications and Provides interface to Intel’s Integrated Performance Primitives (IPP) with processor specific optimization (Intel processors).

Its key features include structural analysis, motion analysis, image processing, camera calibration, object recognition, etc. OpenCV module has CV, HighGUI, CXCORE, CvAux, CvCam, and ML libraries [1].

Important OpenCV Functions used for stereovision are cvFindChessboardCorners() to find the chessboard corners, cvCalibrateCamera2() for calibration, cvStereoRectify() for rectification, cvFindStereoCorrespondenceBM() for stereo matching, and cvReprojectImageTo3D() for depth map.

### 4 Experimental Results

OpenCV 2.1 Software was used for stereovision. Figure 4 shows the input images (chess board patterns), such 10 pairs were used. Figure 5 shows images after corner detection. Figure 6 shows the rectified images. Figure 7 shows the disparity map and Fig. 8 shows the depth map.

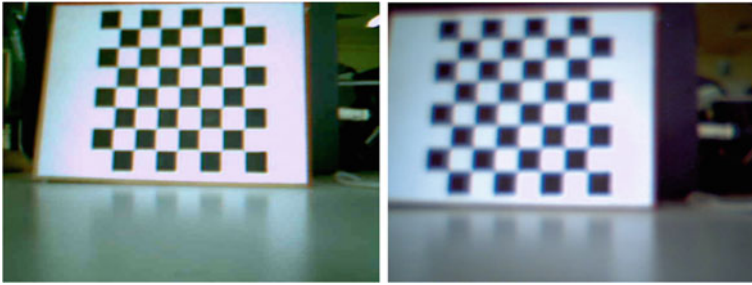


Fig. 4 Input images

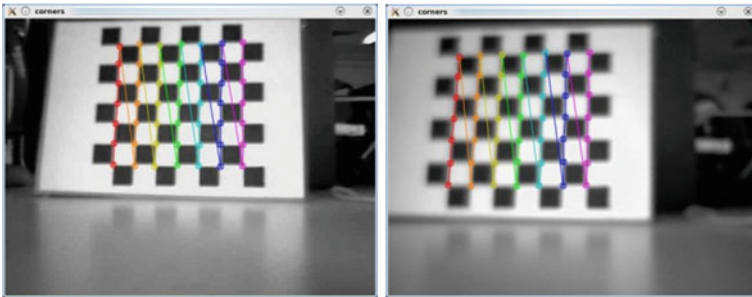


Fig. 5 Corner detected images

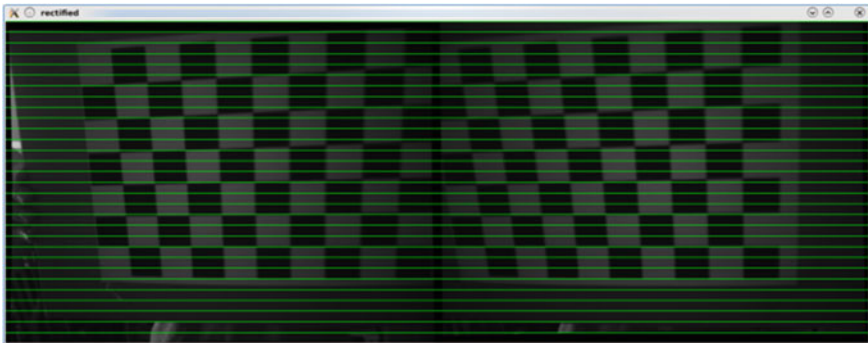


Fig. 6 Rectified images

Figure 9 shows the scale for the depth map. Red region shows the deeper region and Magenta region shows the less deep region.

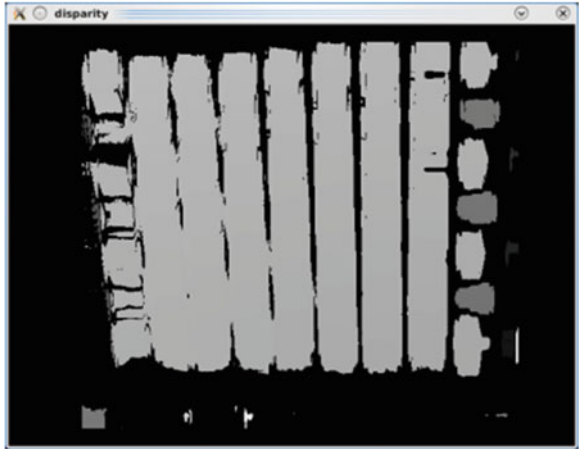


Fig. 7 Disparity map

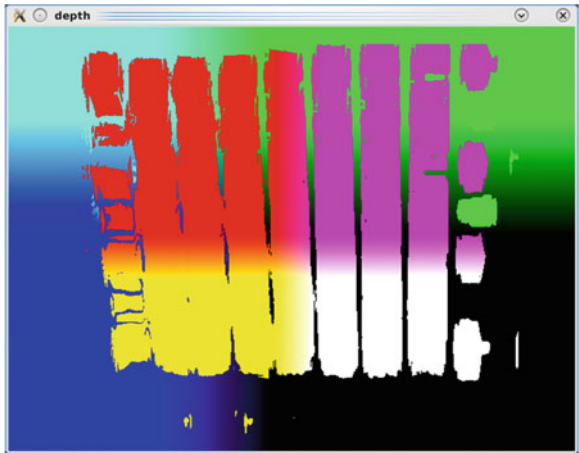


Fig. 8 Depth map



Fig. 9 Scale

## 5 Conclusion

Stereovision is of great importance in the field of machine vision, robotics, and image analysis. It is used to inspect infrastructure in human-inaccessible tunnels and pipes, and long sections of road and bridges. Stereovision can play an important role in

the medical procedures like anthropometry and plastic surgery for capturing and reproducing 3D information about the human body. It can be used in mining where depth information is of greater importance. It is used by automobile manufacturers to automate driving and navigation of road vehicles. It can be used to extend capabilities of security monitoring systems, and improve human face-recognition and tracking algorithms. Research is also being done to create human-wearable Stereo Vision systems to assist the blind. In Energy harvesting and control applications stereovision can be used to replace occupancy sensors and photo sensors.

**Acknowledgments** This work has been carried out as a part of summer internship at NITK. The authors would like to acknowledge the support and guidance of Professor Ramesh. M. Kini.

## References

1. Bradski, G., Kaehler, A.: O'Reilly learning OpenCV. 1st (edn), ISBN: 978-0-596-51613-0. O'Reilly Media Inc., NY, USA (2010).
2. Xu, G., Zhang, Z.: Epipolar geometry in stereo, motion and object recognition. Kluwer, Dordrecht (1996)
3. [OpenCV Wiki] Open Source Computer Vision Library Wiki. <http://opencvlibrary.sourceforge.net/>. Accessed 1 Oct 2008

## About the Editors

Dr. B.V. Babu is the Director of IET at JK Lakshmi Pat University and prior to that he was with BITS Pilani. He has over 28 years of teaching, research, consultancy, and administrative experience. He did his Ph.D. from IIT Bombay. He held various administrative positions such as Dean of various divisions during over 15 years of his tenure at BITS Pilani. His research interests include Evolutionary Computation, Environmental Engineering, Biomass Gasification, Energy Integration, Artificial Neural Networks, Nanotechnology, and Modeling and Simulation. He is Editorial Board member of six International Journals, has published six books, and has around 220 research publications in International and National Journals and Conference Proceedings.

Professor Atulya K. Nagar holds the Foundation Chair, as Professor and Head of Mathematics and Computer Science at Liverpool Hope University. He is an internationally recognized scholar working at the cutting edge of theoretical computer science, natural computing, applied mathematical analysis, operations research, and systems engineering and his work is underpinned by strong complexity-theoretic foundations. He received a prestigious Commonwealth Fellowship for pursuing his Doctorate (D.Phil) in Applied Non-Linear Mathematics, which he earned from the University of York in 1996. He holds B.Sc. (Hons.), M.Sc., and M.Phil (with Distinction) from the MDS University of Ajmer, India.

Dr. Kusum Deep is a full-time Professor with the Department of Mathematics, Indian Institute of Technology Roorkee, India. She earned her Ph.D. from IIT Roorkee in 1988 and carried out Post Doctoral Research at Loughborough University, UK during 1993–1994. She has co-authored a book entitled “Optimization Techniques” and has 75 research publications in refereed International Journals and 60 research papers in International/National Conferences. She is on the editorial board of a number of International and National Journals. She is the Founder President of Soft Computing Research Society, India and the secretary of Forum of Interdisciplinary Mathematics. Her areas of specialization are numerical optimization and their applications to engineering, science, and industry.

Dr. Millie Pant is an Associate Professor in the Department of Applied Science and Engineering, Saharanpur Campus of IIT Roorkee. She did her Ph.D. from math-



ematics department of IIT Roorkee. She has supervised five Ph.D. theses and at present four Ph.D. students are working under her guidance. She has to her credit more than 100 research papers in various journals and conferences of national and international repute. Also she has completed sponsored projects of DST and MHRD. Dr. Millie Pant is a member of editorial board of 'International Journal of Mathematical Modeling, Simulation and Applications' and an executive editor of International Journal of Swarm Intelligence (IJSI).

Dr. Jagdish Chand Bansal is an Assistant Professor at South Asian University New Delhi. Dr. Bansal has obtained his Ph.D. in Mathematics from IIT Roorkee. He is the Editor-in-Chief of "International Journal of Swarm Intelligence (IJSI)" published by Inderscience. His Primary area of interest is Nature Inspired Optimization Techniques. He has published 42 research papers in various international journals/conferences.

Dr. Kanad Ray is an Associate Professor in Physics at Institute of Engineering and Technology of JK Lakshmipat University, Jaipur. He obtained his Doctoral Degree in Physics from Jadavpur University, Kolkata. In his academic career spanning over 19 years, he has published and presented research papers in several national and international journals and conferences in India and abroad. He has authored a book on Electromagnetic Field Theory. Dr. Ray's current research areas of interest include applied physics, communication, and cognitive neurodynamics.

Dr. Umesh Gupta is working as an Associate Professor in Mathematics at Institute of Engineering and Technology of JK Lakshmipat University, Jaipur. He has 13 years of teaching and research experience. He did his Ph.D. from University of Rajasthan. His areas of research are Fluid Mechanics, Optimization and Statistics. He has number of research publications in International and National Journals and Conference Proceedings to his credit. He has authored textbooks on Engineering Mathematics and Research Methods in Management. He has presented his papers in various conferences held in India and abroad.